F1103

ACADÉMIE DE LA RÉPUBLIQUE SOCIALISTE DE ROUMANIE

REVUE ROUMAINE DE CHIMIE

TOME 25
N° 1
Janvier 1980

EDITURA ACADEMIEI REPUBLICII SOCIALISTE ROMÂNIA
Rev. Roumaine Chim.
RRCHAX, 25, *1*, p. 1–172 (1980), Bucarest

59

ACADÉMIE DE LA RÉPUBLIQUE SOCIALISTE DE ROUMANIE

COMITÉ DE RÉDACTION

Rédacteur en chef :

I. G. MURGULESCU, membre de l'Académie de la République Socialiste de Roumanie

Rédacteurs en chef adjoints :

A. T. BALABAN et V. EM. SAHINI, membres correspondants de l'Académie de la République Socialiste de Roumanie

Collège de rédaction :

EM. BRATU, ELENA CEAUŞESCU, ECATERINA CIORĂNESCU-NENITZESCU, CR. SIMIONESCU, membres de l'Académie de la République Socialiste de Roumanie; P. SPACU, membre correspondant de l'Académie de la République Socialiste de Roumanie; MARGARETA AVRAM, M. BANCIU, I. HAIDUC, D. I. MARCHIDAN, I. MOLDOVAN, G. NIAC et D. SĂNDULESCU

La Revue Roumaine de Chimie paraît 10 fois par an. Toute commande de l'étranger pour les travaux parus aux Editions de l'Académie de la République Socialiste de Roumanie sera adressée à ILEXIM, — Departamentul Export-Import Carte (Livres)/Departamentul Export-Import Presă (Revues) P.O.B. 136 — 137, télex 11226, 3, str. 13 Decembrie, 70116 Bucarest, Roumanie

Les manuscrits, les livres et les revues proposés en échange, ainsi que toute correspondance seront envoyés à la rédaction :

REVUE ROUMAINE DE CHIMIE

125, Calea Victoriei, 71021 Bucarest Roumanie, téléphone 50 76 80

EDITURA ACADEMIEI REPUBLICII SOCIALISTE ROMÂNIA
125, Calea Victoriei, 71021 Bucarest, Roumanie, téléphone 50 76 80

REVUE ROUMAINE DE CHIMIE

Tome 25, N° 1 Janvier 1980

Prof ION ATANASIU *(in memoriam)* 3
JOSETTE WEINBERG and V. EM. SAHINI, Xylidine isomers. VI. CNDO calculations on 2,4- and 2,6-xylidine 9
TATIANA ONCESCU and LIDIA DIMOFTE, Kinetics and mechanism of the reaction between 5-chloro-2-pentanone and diethylamine. I. Solvent effect 15
TATIANA ONCESCU and LIDIA DIMOFTE, Kinetics and mechanism of the reaction between 5-chloro-2-pentanone and diethylamine. II. Influence of the nucleophilic reagents 23
SOFIA MARCHIDAN, IULIANA VARTIRES and N. D. TOTIR, Determination of trace quantities of the group V—A elements by anodic stripping voltammetry. I. Trace analysis of arsenic 33
EDUARDO A. CASTRO, Application of an approximate calculation for the total energy of the hydrogen molecule-ion 41
C. E. MOROŞANU and E. SEGAL, Nondestructive thickness determination of silicon nitride films deposited on silicon 47
M. I. VASS and CR. CONŢESCU, Studies of alloy formation and surface properties in Ni—Cu systems 55
S. GRIGORAŞ, ANCA MEDEŞAN, ILEANA RUSU and Ş. MOLDOVEANU, A theoretical study of the hydration and hydration effects on some substituted benzoic acid molecules. II.The calculation of the substituent effect by semiempirical MO methods 67
EDUARDO A. CASTRO and ALICIA H. JUBERT, RRKM calculation of the unimolecular decomposition of trifluoromethyl hypofluorite 75
PARBATI PAL and ASHOK KR. CHAKRABORTY, Investigation of some thermodynamical properties of 2 — 1 electrolytes in solution 81
O. RADOVICI and M. V. POPA, The influence of the structure and the type of alloy on stress corrosion cracking in hydrochloric acid solutions 87
CONST. GH. MACAROVICI and E. CHIŞ, Synthesis and physico-chemical investigation of neutral salts of 4,4′-diaminodiphenylmethane-N,N′-tetraacetic acid with mono, di-, tri- and tetravalent metal ions (in German) 95
NAJMA SULTANA, IRSHAD A. KHAN, and S.R.R. NAQVI, Chemical and spectroscopic properties of silver-phosphine complexes containing oxine . . . 105
S. SOLACOLU, MARIA ZAHARESCU and MARINA DOROBANŢU, Thermal phase equilibria in the system $BaO-ZnO-Fe_2O_3$ with application to magnetoceramics 111
M. S. SUBHANI, Thermodynamic stability constants and other related thermodynamic properties for Cu(II) — PMBP complex 121

Revue Roumaine Chimie

25, *1,* 1 — 172 (1980) Bucarest

A. F. FAHMY, M. M. MOHAMED, A. A. AFIFY, M. Y. EL KADY and M. A. EL HASHASH, Base-catalyzed Michael addition of active methylene compounds on arylidene malonates and arylidene barbituric acids 125

LUMINIŢA VLĂDESCU and HENRY HURWITZ, On the combined ion exchange system-solvents extraction. II. A theoretical approach. (in French) 135

I. PETRARIU, MARIA ROTARU and STELA DRĂGAN, Quaternary ammonium polyelectrolytes. II. Quaternization reaction of some tertiary amines with chloromethylated polystyrene 145

R. Z. TUDOSE and C. NĂFORNIŢĂ, An experimental study of liquid flow in thin films on inclined plates at angles greater than 90° 155

BOOK REVIEWS 165

ION ATANASIU

1894 – 1978

Emeritus Professor Ion Atanasiu, Ph. D., D. Sc., was the founder of the Romanian school of electrochemistry and the first to teach this discipline in Romania. His remarkable humanistic and intellectual qualities secured him an outstanding place among the spiritual élite of this country.

The Professor succeeded to combine masterfully his teaching ability with the clearsightedness of the scientific discoverer, breaking new ground in the science to which he had devoted his whole life.

Professor Ion Atanasiu was born in 1894 in Galați, where he attended the "V. Alecsandri" secondary school; after graduation, in 1913, he enrolled in the Faculty of Sciences, Department of Physics and Chemistry of the Bucharest University. Having been severely wounded in the First World War he could not stand for his final examinations in 1920. And yet, perhaps that very struggle between life and death made of him an exceptional man.

His remarkable qualities showed up in both his didactic and scientific work. In what follows we shall highlight on the outstanding contributions made by Ion Atanasiu to the development of the electrochemical and electroanalytical sciences. He produced original experimental works, and guided his coworkers in the elaboration of doctoral theses as well as in other researches initiated and directed by himself.

He began his scientific activity at the Institute of Technological Chemistry of the Bucharest University being appointed assistant lecturer at the chair of Professor Dănăilă (1st of January 1921); there he worked together with well-known colleagues: T. Ionescu, A. Steopoe, I. Blum, A. Velculescu, N. Popa, D. Buttescu, C. Belcot, A. Braniski, E. Georgeacopol, M. Davidescu, M. Goruneanu, Gh. Pandele, A. Andrei, E. Melinescu, V. Stoenescu, V. Constantinescu, V. Atanasiu, D. Ionescu Bujor, C. Candea, M. Babor, V. Ștefănescu.

Ion Atanasiu's doctoral thesis was a fundamental study "On the displacement of the hydrolysis equilibrium in the systems: TiR_4-H_2O" (Soc. roumaine des sciences de Bucharest, *Bull. de Chimie*, XXVII; Nos. 4–6, 1924). Ion Atanasiu approached his preferential field: electrochemistry by means of conductiometric methods. In that period there was nobody in Romania capable to guide him in the area. The only source available at the time was bibliographic documentation, scarce as it was and only his own imagination and intuition helped him devise the instrumentation and the working method needed to obtain significant results for the solution of the problem under study. By conductiometric measurements Ion Atanasiu succeeded to characterize important hydrolysis parameters : equilibrium constants of the dissociation reactions, hydrolysis degree, dissociation degree, reaction order, etc. The original results obtained fitted well in the reasonable range of measured values, allowing for a rational discussion and interpretation.

Professor Atanasiu was a very modest man and he remained so despite his successful activity and renown. He was always wondering if his working method was accurate enough for the results scored to be rigorously scientific. Because of these doubts he went to France where he continued his studies in electrochemistry (1924—1926), under a grant from the Nancy University (Professor A. Guntz). The French laboratories were well equipped and an intense scientific activity was being carried on therein. He no longer doubted his results and possibilities : "I saw", he told later, "that my working method was not essentially different from the methods employed in the French laboratories of that time".

Professor Guntz of Nancy drew his attention to the fact that the rare earth elements had not been studied sistematically by electrochemical methods and that this aspect was worth being taken into account. The results of researches carried out in France were presented in the paper "On the electrotitrimetry of some elements on the way of precipitation", published in *Journal de Chimie Physique*, 23, 501 (1926). The first system investigated was the electrometric titration of the cerous ion with potassium ferrocyanide.

He returned to Romania in 1926,and was promoted chief of department at the Institute of Chemical Technology of the Bucharest University. At that time he worked on and published his first study concerning the "Cerric salts as oxidants in electrometry", *Bulletin de Chimie pure et appliquée*, 30, 73 (1927). This was actually the first work in the world which laid the bases of *cerimetry* as a quantitative analysis method for determining the end point potentiometrically. That Professor Ion Atanasiu was the founder of cerimetry is acknowledged also in a series of specialised publications. For instance Ferenc Szabadvary in "History of Analytical Chemistry" (*Pergamon Press*, *Oxford*, *London*), 1966, p. 267, wrote : "One of the most important new redox (methods, our note) was cerimetry, which today is as important as permanganatometry or chromatometry. Willard and Young (*J. Amer. Chem. Soc.*, 50, 1322 (1928)) applied this method in 1928 to the titration of iron (II) and oxalate, using diphenylamine as indicator. They subsequently published a series of papers on the use of this standard solution for the determination of other substances. It should be mentioned that Atanasiu had used cerium (IV) sulphate as standard solution in potentiometric titrations earlier (*Bull. Soc. Chim. Romane*, 30, 73 (1927))".

Later, I. Atanasiu published another paper on this subject in collaboration with V. Ștefănescu (*Ber. dtsch. Chem. Ges.*, 61, 1343 (1928)), in which the application of cerric salts is extended from the titration of the nitrite ion, to the oxalate, ferrocyanide, Fe(II), As(III), Sn(II), Ti(III) ions and hydroperoxides. Both papers are largely cited in a series of works published during 1930—1960 The citations begin with the work by N. H. Furman ("Potentiometric Titrations", *Ind. Eng. Chem.*, 2, 213 (1930)) which is a review on the subject. From the context and the bibliography there unquestionably follows that Professor Ion Atanasiu is the founder of the cerimetric method.

A comprehensive book for the period, it was printed in I. M. Kolthoff and N. Howell Furman's "Potentiometric Titrations. A Theoretical and Practical Treatise", *John Wiley and Sons, Inc., London*, 1949, which cites seven papers by Atanasiu and coworkers. In chapter XI, p. 280 "Oxidation with cerric sulphate" one reads : "I. A. Atanasiu and V. Ştefănescu (*Bull. Soc. roum. Chim.*, 30, 1 (1927) ; *Ber. dtsch. chem. Ges.*, 61 B, 1343 (1928)) were apparently the first to begin a systematic study of the applications of cerric sulphate in the potentiometric field. At about the same time Furman and Willard and Young (Furman, *J. Amer. Chem. Soc.*, 50, 755 (1928) ; Willard and Young *ibid.*, 50, 1322 (1928) commenced similar studies. Atanasiu and Ştefănescu studied the titration of oxalic acid, ferrous iron, hydrogen peroxide, ferrocyanide, and trivalent arsenic (cf. Willard and Young). Good results were obtained. In regard to the practical applications, the authors mention the titration with cerric sulphate of ferrocyanide (p. 287), hydrogen peroxide (p. 288), ferrous ion (p. 290), nitrite (p. 291) and also the determinations of lanthanum, cerium and thorium (p. 332), cerrous cerium (p. 332) and uranyl (p. 333).

Extended citations of the works by I. A. Atanasiu and coworkers, especially those concerning the discovery of cerimetry, can also be found in "Neuere massanalytische Methoden", a volume authored by several scientists, well known for their contributions to the development of chemistry : K. Fajans, N. H. Furman, R. Lang, H. Stamm, (*Ferdinand Enke Verlag*), Stuttgart, 1951. On page 80 they write : "The use of Ce(IV) sulphate in the quantitative analysis has been investigated systematically by Atanasiu (*Bull. chem. pur. aplicată*, 30, 73 (1927) ; and V. Ştefănescu, *Ber. dtsch. chem. Ges.*, 61, 1343 (1928)), Willard and Young (*J. Amer. Chem. Soc.*, 50, 1322 (1928)) and their coworkers. On page 93, the use of Ce (IV) is cited for the titration of the ferrous ion and ferrocyanide, and also hydrogen peroxide (p. 100), all these with reference to I. A. Atanasiu's publications*.

An overview of Professor Atanasiu's activity reveals that his didactic and scientific work focused on electrochemistry. He taught this discipline as lecturer (until 1945) and professor (from 1945 to 1964). In 1964, after his retirement, he was granted the title of emeritus professor, which he fully deserved.

Beside Atanasiu's works in electrochemistry, he carried out also other valuable pioneering studies.

---

* A surprise offers the five-volume book "Standard Methods of Chemical Analysis", *D. Van Nostrand Company Inc.*, Priceton, New Jersey, Toronto, London, New York 1962, edited by N. Howell Furman which, by omitting I.A.Atanasiu's name, suggests to the non-advised reader that cerimetry begins with Willard and Young, who published the results of their studies on cerric salts one year after I.A. Atanasiu. The same of other comprehensive books of analytical chemistry, edited by I.M.Kolthoff, although the latter together with N.H. Furman, had recognised in the 1949 edition of the above-mentioned book that I.A.Atanasiu was the father of cerimetry.

Of major importance are the series of works on the electrochemical oxidation of paraffins and mineral oils published during 1928–1933. These works deal with technological applications of great practical importance. Peculiar to the method used is the electrochemical oxidation of paraffin at normal pressure and at temperature below 100°. An important role in this process is played by cerium salts. An expert in the redox properties of this element, Professor Atanasiu realized that cerium salts can 'catalyse' the reactions with charge transfer, as intermediates in electrochemical oxidation processes. The interest aroused by his works is revealed also by their being referred to in a series of chemical speciality treatises.

Another important group of works concern the nuclear elements, e.g. uranium and thorium determination, and the electrochemical separation of lanthanum and thorium from organic solvents. In the treatise on the history of the development of radiochemistry, Professor Atanasiu is cited with these works by Irène Curie, among some other 30 scientists who had initiated radiochemistry works until the 1930's.

A substantial group of works is devoted to the electrical nitration of the aromatic hydrocarbons, as well as to other organic syntheses by electrochemical means and to the electrodeposition of some metals.

Even in the early period of his investigations, Professor Atanasiu rallied around him several coworkers, initiating a national school of electrochemical research. In his capacity of consultant professor he was called to guide and direct research works for doctoral dissertations and research programmes. Alike to all great teachers, Professor Atanasiu was also the founder of a school. Simultaneously with the introduction of several thousands of students in the knowledge of electrochemistry, electroanalysis and corrosion, he continued his researches by guiding dozens of doctorands and close coworkers, who further developed his approaches.

Among the works carried out under Professor Atanasiu's direct guidance and with his collaboration we shall mention some which focus upon several directions in electrochemistry.

A field of theoretical and practical importance is the use of the wavy current in electrochemical processes. I. Atanasiu and coworkers published a series of studies on the hindrance of oxidation reactions of the methyl and ethyl alcohols, the electrolysis of alkaline acetates and anodic dissolution of manganese and its alloys in direct and wavy current.

Other works continued Professor Atanasiu's older preoccupations in the field of organic synthesis. Among these, the studies on the electrolytic reduction of *p*-nitrophenol, p-nitrophenetol and the electrochemical chlorination of paraffins are cited in the review paper : K. Micka, *Chem. Listy*, 55 (1961).

During the past 24 years Professor Atanasiu studied electrochemical kinetics and corrosion elucidating in the almost 50 works published the mechanisms of several electrode processes, e.g., the mechanism of electrochemical formation of oxidated chlorine compounds on the graphite rotating electrode and electrochemical reductions on rotating cathodes. Mention should be made of his works on the electrodeposition and formation mechanism of nickel-phosphorus alloys (published in Romanian), which were cited on ten pages by Abner Brenner in the book "Electrodeposition of Alloys", *Academic Press*, New York and London, 1963, pp. 458 — 483. The group of works on the electrodeposition and formation mechanism of electrolytical powders was also largely cited in the specialised literature : N. Ibl in "Advances in Electrochemistry and Electrochemical Engineering", *Interscience*, New York, London, 1962, pp. 49—141; R. A. Despić and K. I. Popov in "Modern Aspects of Electrochemistry". Vol. 7, Chap. 4, *Plenum Press*, New York, 1972, pp. 199 – 313 ; N. Ibl and K. Schadeg, *J. Electrochem. Soc.*, *114*, 58 (1967) ; N. Ibl, *Chem. Ing. Technik*, *36*, 601—(12 (1964) ; F. Sauerwald, *Neue Hütte*, *8*, 274 (1963) ; S. G. Christov, *Proc. Australian Conf. Electrochem.*, Sydney 1963, Pergamon, Oxford, 1965, p. 273, etc.

Later, the works on the electrodeposition and formation mechanism of metal powders, initiated by Professor I. Atanasiu, were continued and confirmed by studies carried out in the "J. Heyrovsky" Institute of Prague. These works were extensively cited in the book by A. Călușaru, one of his coworkers, "Electrodeposition of Metal Powders" *Elsevier Publishing Company*, Amsterdam, Oxford, New York, 1979, thereby largely introducing them in the international scientific circulation.

The considerable diversity of the subjects approached by Professor Atanasiu is due also to his numerous coworkers. Some of his latest publications are the corrosion of iron and its alloys, electrolytic extraction of iodine, electrochemical oxidation of the oxalic acid, corrosion resistance of nickel and stainless steel, electrochemical oxidation of methanol on brittle platinum electrodes, the effect of some anions on the pitting corrosion of stainless steel, etc.

The life and activity of Emeritus Professor Ion Atanasiu stand out as a model of devotion to science. As a professor, investigator and scientist he has contributed to the creation of the Romanian school of electrochemistry, making important contributions by his applied studies to the development of electrochemistry-based Romanian industry.

None of his former students shall ever forget Professor Atanasiu's masterful courses and all of them, together with his coworkers, shall always think of him with affection and esteem.

His death on 19 December 1978 is an overwhelming loss for those who had known and appreciated him as well as for Romanian science and higher education at large.

June 21, 1979 EM. BRATU and A. CĂLUȘARU which were cited on ten pages by Abner Brenner in the book "Electrodeposition of Alloys", *Academic Press*, New York and London, 1963, pp. 158 – 183. The group of works on the electrodeposition and formation mechanism of electrolytical powders was also largely cited in the specialised literature: N. Ibl in "Advances in Electrochemistry and Electrochemical Engineering", *Interscience*, New York, London, 1962, pp. 49–141; R. A. Despić and K. I. Popov in "Modern Aspects of Electrochemistry", Vol. 7, Chap. 4, *Plenum Press*, New York, 1972, pp. 199 – 313; N. Ibl and K. Schadeg, *J. Electrochem. Soc.*, *114*, 38 (1967); N. Ibl, *Chem. Ing. Tech.*, *36*, 601 – (12 (1964); F. Sauerwald, *Neue Hütte*, *8*, 271 (1963); S. G. Christov, *Proc. Australian Conf. Electrochem.*, Sydney 1963, Pergamon, Oxford, 1965, p. 273, etc.

Later, the works on the electrodeposition and formation mechanism of metal powders, initiated by Professor I. Atanasiu, were continued and confirmed by studies carried out in the "J. Heyrovsky" Institute of Prague. These works were extensively cited in the book by A. Călușaru, one of his coworkers, "Electrodeposition of Metal Powders" *Elsevier Publishing Company*, Amsterdam, Oxford, New York, 1979, thereby largely introducing them in the international scientific circulation.

The considerable diversity of the subjects approached by Professor Atanasiu is due also to his numerous coworkers. Some of his latest publications are the corrosion of iron and its alloys, electrolytic extraction of iodine, electrochemical oxidation of the oxalic acid, corrosion resistance of nickel and stainless steel, electrochemical oxidation of methanol on brittle platinum electrodes, the effect of some anions on the pitting corrosion of stainless steel, etc.

The life and activity of Emeritus Professor Ion Atanasiu stand out as a model of devotion to science. As a professor, investigator and scientist he has contributed to the creation of the Romanian school of electrochemistry, making important contributions by his applied studies to the development of electrochemistry-based Romanian industry.

None of his former students shall ever forget Professor Atanasiu's masterful courses and all of them, together with his coworkers, shall always think of him with affection and esteem.

His death on 19 December 1978 is an overwhelming loss for those who had known and appreciated him as well as for Romanian science and higher education at large.

Revue Roumaine de Chimie, 25, 1, 9 – 13 (1980)

XYLIDINE ISOMERS. VI[1].

CNDO CALCULATIONS ON 2,4-AND 2,6- XYLIDINE

JOSETTE WEINBERG* and V. EM. SAHINI **
* Centre of Physical Chemistry, Splaiul Independenţei 202, Bucharest, Romania
** Physical Chemistry Laboratory, Bdul. Republicii 13, Bucharest, Romania

Received February 9, 1979

The results of CNDO/2 calculations for 2,4- and 2,6- xylidine are described. The coplanarity of the NH_2 group with the ring for a number of about six values of the dihedral angle θ between the plane of the CH_3 groups and the ring plane was considered. The dipole moments yielded by calculations are in a very good agreement with the experimental ones for the 2,4-xylidine at a 60° dihedral angle of the planes of CH_3 groups. The result confirms the coplanarity of the NH_2 group with the aromatic cycle for 2,4-xylidine. The equilibrium conformations and the variation of π and σ-electron densities to all the atoms in the molecule are discussed for the two isomers.

The aim of the present paper is a theoretical study of the most probable conformation for two isomers : 2,4- and 2,6-xylidine. These isomers are considered as most representative of the series both as physical-chemical and hepatotoxic properties [2]. This study was achieved by the CNDO/2 method [3]. The plane of the NH_2 group was assumed to maintain a zero degree dihedral angle with respect to the ring plane in order to optimize electronic interactions with the π system. *Ab initio* calculations have shown that this conformation is the most favorable [4]. At the same time, several values of the dihedral angle θ between the plane of the CH_3 groups and the ring plane were assumed and conformations of various energies were obtained for them (Fig. 1).

The computer program was Pople and Segal's FORTRAN program [5].

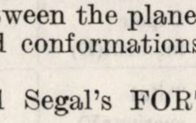

Fig. 1. — Schematic representation of the dihedral angle θ between the plane of the CH_3 group and the ring plane.

RESULTS AND DISCUSSION

Table 1 shows the dipole moments calculated for the two isomers, as compared to those obtained experimentally [6]. The following conclusions can be drawn from this table : a very good agreement between the theoretical and the experimental dipole moments is obtained in the case of the 2,4-xylidine by considering this molecular geometry. However, for 2,6-xylidine, the dipole moment is much too low (0.8 D) due to a cancelling out of the π contribution by a very strong, entirely in-plane, σ moment. The conformation change of NH_2 group plane with respect to the ring plane would yield a better agreement with the experimental dipole moment data in this case. We emphasize that in 2-6-xylidine the NH_2 group is not in the same plane with the aromatic cycle and an attenuation of the resonance between the nitrogen lone pair electrons and the π-electrons from the cycle results ; 2,4-xylidine has the NH_2 group in the phenyl plane and the result is an increase of the resonance and stability of this isomer. In Table 2 and in Figures 2—3, the total energy and the dipole moment for the two isomers at several dihedral angles (θ) of both CH_3 groups with respect to the ring plane are presented. The equilibrium conformation is obtained at a dihedral angle of 60° of CH_3 groups plane with the ring plane, for both isomers. The preferential rotamers and the rotational energies are presented in Table 3.

TABLE 1

The dipole moments for the two isomers

Isomer	μ calculated(D)				μexper.(D)
	μ_x	μ_y	μ_z	μ_{tot}	
2,4-xylidine	−1.3391	−0.4045	0.2405	1.4194	1.41
2,6-xylidine	−0.0337	0.7751	−0.2055	0.8026	1.67

TABLE 2

The total energy and the dipole moment at several dihedral angles

Isomer	θ	0°	60°	90°	120°	150°	180°
2,4-Xylidine	Total energy(eV)	−76.40	−76.46	−76.45	−76.42	−76.40	−76.42
	Dipole moment(D)	0.75	1.53	1.42	0.83	0.82	1.28
2,6-Xylidine	Total energy(eV)	−76,39	−76.45	−76.44	−76.41	−76.39	−76.41
	Dipole moment(D)	0.38	0.80	0.70	0.29	0.39	0.60

The energy difference between the isomers is not noticeable (0.3kcal/ /mole to equilibrium conformation), the 2,4-xylidine being more stable.

The charge distributions obtained for 2,6-xylidine under the assumptions that the NH_2 group and the cycle are either coplanar or noncoplanar are almost identical [7]. Therefore we further made use of the distributions calculated under the assumption of coplanarity of the NH_2 group with the cycle.

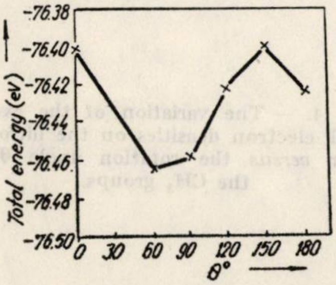

Fig. 2. — The total energy variation at several dihedral angles (θ) of the plane of both CH_3 groups for 2,4-xylidine.

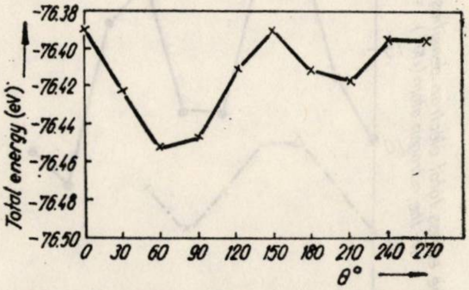

Fig. 3. — The total energy variation at several dihedral angles (θ) of the plane of both CH_3 groups for 2,6-xylidine.

TABLE 3

The preferential rotamers and the rotational energies

Isomer	Preferential rotamer[a]	Total energy (kcal/mole) to the equilibrium conform.	Rotation barrier[b]
2,4-Xylidine	90°	−1763.14	1.29
2,6-Xylidine	60°	−1762.98	1.43

a. The dihedral angle (degrees) between the ring plane and CH_3 groups plane.

b. The difference (kcal/mole) between the least stable and the most stable rotamer.

In Figure 4, the variation of the excess total electron densities on the nitrogen atom versus the rotation angle of the CH_3 groups is represented. The maximum excess of electronic density ($\sigma + \pi$), for both isomers, is obtained for equilibrium conformation. The excess density ($\sigma + \pi$) on nitrogen atom in the 2,6-xylidine with respect to 2,4-xylidine is noticeable.

The electron density on the nitrogen atom, on the carbon atoms from the cycle and on the CH_3 group and H_3 group, at the equilibrium conformation is presented in Tables 4—6.

Examination of Table 4 shows that the methyl substitution decreases the nitrogen π density and increases the nitrogen σ density.

Table 5 shows a polarization in both σ and π frameworks. It is worth mentioning that the amino group seems to polarize the ring electron density and this polarization is transmitted through the substituent carbons to the hydrogen atoms.

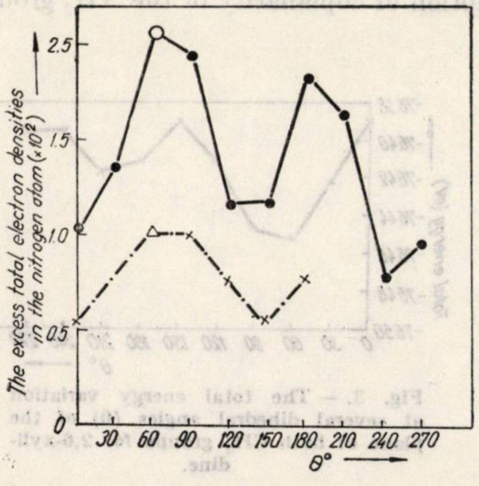

Fig. 4. — The variation of the excess total electron densities on the nitrogen atom *versus* the rotation angle θ of the CH_3 groups.

TABLE 4

The electron density on the nitrogen atom at the equilibrium conformation

Isomer	q^N_{tot}	q^N_σ	q^N_π
2,4-Xylidine	4,0101	2.0682	1.9419
2,6-Xylidine	4.0206	2.0819	1.9388

TABLE 5

The electron density on the carbon atoms from the aromatic cycle at the equilibrium conformation

	q_{C_1}	q_{C_2}	q_{C_3}	q_{C_4}	q_{C_5}	q_{C_6}
			2,4-Xylidine			
q_σ	1.9381	2.0430	1.9583	2.0588	2.0125	1.9517
q_π	0.9491	1.0155	1.0367	0.9743	1.0134	1.0639
q_{tot}	2.8872	3.0585	2.9950	3.0331	3.0259	3.0156
			2,6-Xylidine			
q_σ	1.9272	2.0470	2.0034	2.0100	1.9727	1.9998
q_π	0.9578	1.0047	1.0162	1.0277	1.0219	1.0244
q_{tot}	2.8850	3.0517	3.0196	3.0377	2.9946	3.0242

TABLE 6

The electron density on the CH_3 group and H_3 group at the equilibrium conformation

Isomer	$q^{tot}_{CH_3}$	$q^{tot}_{H_3}$	$\Delta q^{tot}_{CH_3}$	$\Delta q^{tot}_{H_3}$
2,4-Xylidine	12.1195	6.3234	-0.1195	-0.3234
2,6-Xylidine	12.1245	6.3287	-0.1245	-0.3287

REFERENCES

[1] Previous paper: J. Weinberg and V. E. Sahini (in print)

[2] G. Magnusson, N. O. Bodin, and E. Hansson, *Acta Path. Microbiol. Scand.*, *Section A* **79**, 639 (1971).

[3] J. A. Pople, D. P. Santry and G. A. Segall, *J. Chem. Phys.*, **43**, 129, 136 (1965).

[4] W. J. Hehre, L. Radom and J. A. Pople, *J. Amer. Chem. Soc.* **94**, 1496 (1972).

[5] J. A. Pople and D. L. Beweridge "Approximate Molecular Orbital Theory" Mc Graw-Hill, New York, 1970.

[6] V. E. Sahini and J. Weinberg, *Rev. Roumaine Chim.*, **18**, 1493 (1973).

[7] J. E. Bloor and D. L. Breen, *J. Phys. Chem.*, **72**, 716 (1968).

Revue Roumaine de Chimie, 25, 7, 15 – 21 (1980)

KINETICS AND MECHANISM OF THE REACTION BETWEEN 5-CHLORO-2-PENTANONE AND DIETHYLAMINE. I

SOLVENT EFFECT

TATIANA ONCESCU* and LIDIA DIMOFTE**

* Physical Chemistry Department, Institute of Chemical Technology, Bd. Republicii 13, Bucharest, Romania

** Institute of Chemical Pharmaceutical Research, Calea Vitan 112, Bucharest, Romania

Received November 10, 1977
Revised June 13, 1979

This paper deals with the kinetics and mechanism of the reaction between 5-chloro-2--pentanone and diethylamine in various solvents. The activation parameters are calculated and discussed in connection with the suggested reaction mechanism.

1. INTRODUCTION

The synthesis of 5-diethylamine-2-pentanone, known also as novalketone (NK), from the reaction between 5-chloro-2-pentanone (5ClP) and diethylamine (DEA) is indicated in three patents.[1-3] The secondary reaction product, acetylcyclopropane (ACP) results from an γ elimination reaction.

The present paper deals with the kinetics and mechanism of this reaction, in various solvents for which bibliographical data are missing.

2. EXPERIMENTAL

The reagents used are:

- 5-chloro-2-pentanone (5ClP) prepared according to a Romanian patent.[4]
- diethylamine (DEA) — LOBA — Austranal purum.
- benzene — Reactivul — dried on sodium and distilled before each experiment.
- acetone-Reactivul-dried on Na_2CO_3 sicc, and distilled.
- acetonitrile — U.C.B.
- propionitrile, prepared by catalytic hydrogenation of the acrylonitrile and distilled.
- nitrobenzene — C. Erba.

The experimental procedure used for the kinetic measurements were the same as those described in a previous paper[5] which dealt with the reaction between 5-bromo-2-pentanone (5BrP) and DEA. We determined by gas chromatography the disappearance of 5ClP and the formation of NK and ACP at different reaction moments. For the determination of diethylamine hydrochloride (DHCl) we used the argentometric titration.

3. RESULTS

The reaction system 5ClP—DEA consists of parallel processes, namely, nucleophilic substitution (1) and γ elimination (3). We proposed in this case a similar reaction mechanism suggested in the previous paper :[5]

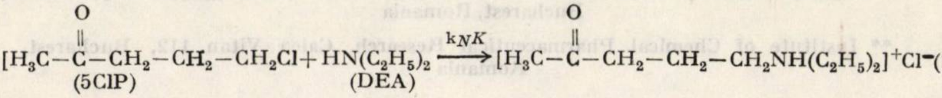

$$\underset{(5ClP)}{H_3C-\overset{\overset{O}{\|}}{C}-CH_2-CH_2-CH_2Cl} + \underset{(DEA)}{HN(C_2H_5)_2} \xrightarrow{k_{NK}} [H_3C-\overset{\overset{O}{\|}}{C}-CH_2-CH_2-CH_2NH(C_2H_5)_2]^+Cl^- \quad (1)$$

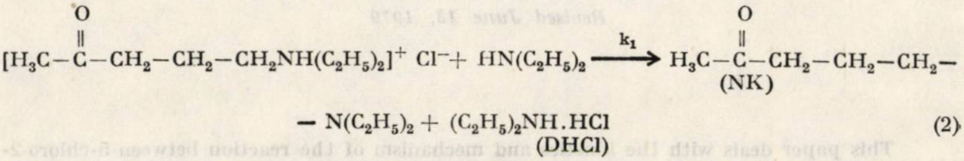

$$[H_3C-\overset{\overset{O}{\|}}{C}-CH_2-CH_2-CH_2NH(C_2H_5)_2]^+\ Cl^- + HN(C_2H_5)_2 \xrightarrow{k_1} \underset{(NK)}{H_3C-\overset{\overset{O}{\|}}{C}-CH_2-CH_2-CH_2-}$$
$$-N(C_2H_5)_2 + \underset{(DHCl)}{(C_2H_5)_2NH.HCl} \quad (2)$$

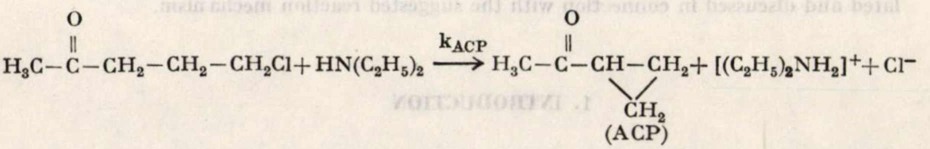

$$H_3C-\overset{\overset{O}{\|}}{C}-CH_2-CH_2-CH_2Cl + HN(C_2H_5)_2 \xrightarrow{k_{ACP}} \underset{(ACP)}{H_3C-\overset{\overset{O}{\|}}{C}-CH-CH_2\ (CH_2)} + [(C_2H_5)_2NH_2]^+ + Cl^- \quad (3)$$

$$[(C_2H_5)_2NH_2]^+ + Cl^- \xrightarrow{k_1'} (C_2H_5)_2\,NH.HCl \quad (4)$$

k_1 and k_1' are the rate constants of the processes in which DHCl forms much faster than k_{NK} and k_{ACP}, respectively.

The overall rate constant, either k_{5ClP} with respect to the disappearance of 5ClP, or k_{DHCl} with respect to the formation of DHCl, verifies a kinetic equation of second order. The rate constants k_{NK} and k_{ACP} verify also the same reaction order.

These rate constants were calculated plotting $\lg \dfrac{b-x}{a-x}$ versus time, where a and b are the initial concentrations of 5ClP and DEA, respectively and x is either the concentration diminution of 5ClP or the concentration of DHCl formed at time t.

Figure 1 presents the kinetic behaviour for the disappearance of 5ClP as well as of NK and ACP formation in benzene at 100°.

The rate constants values obtained at different work temperatures are given in Table 1.

Experiments carried out with other concentrations of the reagents, keeping constant their ratio, are illustrated in Table 2. The rate constants are practically the same, but the reaction rate decreases with decreasing concentration, in agreement with a second kinetic order (compare the last column of Tables 1 and 2).

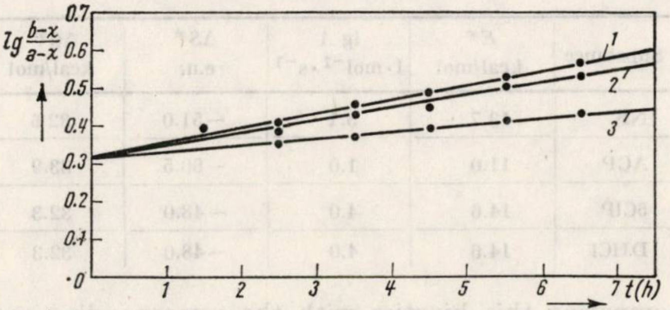

Fig. 1. — Plotting $\lg \frac{b-x}{a-x}$ vs time for :

a = 5ClP 1M and b = DEA 2.1M in benzene at 100°;
1 — 5ClP ; 2 — NK ; 3 — ACP

TABLE 1

Rate constants at different temperatures in benzene

$c_{5ClP} = 1M$; $c_{DEA} = 2.1M$

$T°$	$l \cdot mol^{-1} \cdot s^{-1} \times 10^4$				k_{NK}/k_{5ClP}	k_{ACP}/k_{5ClP}	Conversion after 2 hrs
	k_{5ClP}	k_{NK}	k_{ACP}	k_{DHCl}			
90	0.11	0.066	0.031	0.13	0.60	0.26	14
100	0.20	0.12	0.051	0.21	0.60	0.26	20
110	0.32	0.18	0.070	0.33	0.60	0.22	37
120	0.40	0.29	0.096	0.42	0.65	0.24	43

TABLE 2

Rate constants at different temperature in benzene

$c_{5ClP} = 0.67M$; $c_{DEA} = 1.4M$

$T°$	$l \cdot mol^{-1} s^{-1} \times 10^4$			Conversion after 4 hrs
	k_{5ClP}	k_{NK}	k_{ACP}	
90	0.09	0.056	0.026	9
100	0.22	0.130	0.049	21.1
110	0.29	0.190	0.060	37.2

The obtained kinetic data allowed the calculation of the activation parameters (Table 3) :

TABLE 3

Activation parameters of the reaction between 5ClP and DEA, in benzene

Substance	$E^{\neq}$ kcal/mol	lg A $l \cdot mol^{-1} \cdot s^{-1}$	$\Delta S^{\neq}$ e.u.	$\Delta G^{\neq}$ kcal/mol
NK	13.7	3.1	−51.0	32.6
ACP	11.0	1.0	−60.5	33.9
5ClP	14.6	4.0	−48.0	32.3
DHCl	14.6	4.0	−48.0	32.3

By comparing this kinetics with the corresponding reaction kinetics of 5BrP[5] one notices that the present values are lower than the first one. On the other hand, the ratio k_{NK}/k_{ACP} is only 2.4, whereas with 5BrP as reagent it rises to about 40. At the same time, the formation of other secondary reaction products, evidenced by thin layer chromatography, is favored so that equation (5) verified in the case of 5BrP, holds no longer on :

$$k_{NK} + k_{ACP} = k_{5ClP} \tag{5}$$

We investigated this reaction kinetics in other solvents with various dipole moment μ because our suggested mechanism [6] considers that the transition state has a structure characterized by charge separation.

Tables 4 and 5 show the results obtained with these solvents.

TABLE 4

Rate constants values at different temperatures in acetone

$c_{5ClP} = 1M; \quad c_{DEA} = 2.1M$

$T°$	$l \cdot mol^{-1} \cdot s^{-1} \times 10^4$				k_{NK}/k_{5ClP}	k_{ACP}/k_{5ClP}	Conversion after 2 hrs
	k_{5ClP}	k_{NK}	k_{ACP}	k_{DHCl}			
90	0.20	0.11	0.077	0.21	0.55	0.38	31
100	0.46	0.23	0.16	0.47	0.50	0.35	50
110	0.75	0.33	0.24	0.79	0.49	0.32	75

By comparing these data with those in Table 1, one notices that at each temperature the overall rate constants as well as the conversions increase with the solvent polarity. On the other hand, also the amount of ACP increases, so that in acetonitrile it becomes the preponderent reaction product.

TABLE 5

Rate constants values at different temperatures in acetonitrile

$c_{5ClP} = 1M$; $c_{DEA} = 2.1M$

$T°$	$l \cdot mol^{-1} \cdot s^{-1} \times 10^4$				k_{NK}/k_{5ClP}	k_{ACP}/k_{5ClP}	k_{NK}/k_{ACP}	Conversion after 2 hrs
	k_{5ClP}	k_{NK}	k_{ACP}	k_{DHCl}				
80	0.61	0.042	0.34	0.57	0.07	0.56	0.12	45
90	0.87	0.056	0.47	0.92	0.07	0.54	0.12	60
100	1.40	0.100	0.67	0.40	0.07	0.48	0.14	81

Tables 6 and 7 point out the activation parameters obtained from the kinetic data for these two solvents.

TABLE 6

Activation parameters of the reaction : 5 ClP + DEA in acetone

Substance	$E^{\neq}$ kcal/mol	lg A $l \cdot mol^{-1} \cdot s^{-1}$	$\Delta s^{\neq}$ e.u.	$\Delta G^{\neq}$ kcal/mol
NK	16.9	5.3	−41.5	31.6
ACP	14.6	3.8	−48.5	32.0
5ClP	19.6	7.1	−33.1	31.2
DHCl	19.6	7.1	−33.1	31.2

TABLE 7

Activation parameters of the reaction : 5ClP + DEA in acetonitrile

Substance	$E^{\neq}$ kcal/mol	lg A $l \cdot mol^{-1} s^{-1}$	$\Delta S^{\neq}$ e.u.	$\Delta G^{\neq}$ kcal/mol
NK	11.0	2.6	−53.8	29.8
ACP	9.1	1.2	−60.2	30.3
5ClP	11.0	2.6	−53.8	29.8
DHCl	11.0	2.6	−53.8	29.8

The negative value of the NK activation entropy can be explained as in a previous paper[6] by the formation of an activated complex with charge separation. The more negative value of ACP activation entropy is due moreover to a cyclic transition state formed from noncyclic products, what is to be expected since free rotatiton about the single bonds becomes restricted during cyclisation.

The activation energy of the reaction in acetonitrile is lower than that obtained in benzene due to the polarity of the solvent which increases the solvation of the transition state[7-9]. But the data of the reaction occurring in acetone do not show the same behaviour. Probably, the acetone forms condensation products with the ketones from the reaction system, especially under our experimental conditions : in closed ampoules, at temperatures much higher than the boiling point of acetone ($\sim 100°$). This assumption is supported by the thin layer chromatogram obtained, in which besides the usually synthesis products, 4 — 5 ketones were separated.

All the activation parameters are higher than the values obtained from the corresponding reaction with 5BrP regarding the NK formation and 5BrP disappearance.

We complete our kinetic measurements by experiments carried out in propionitrile and nitrobenzene. Table 8 presents comparatively the main characteristic of the reaction in all the solvents used.

TABLE 8

Overall rate constants and the ratio of the partial rate constants in solvents of various polarity (T = 100°)

Solvent	μ, Debye	k_{5ClP} $1 \cdot mol^{-1} \cdot s^{-1}$	k_{NK}/k_{ACP}
Benzene	0	0.20×10^{-4}	2.4
Acetone	2.72	0.46×10^{-4}	1.5
Propionitrile	3.34	0.13×19^{-3}	0.15
Acetonitrile	3.37	0.14×10^{-3}	0.15
Nitrobenzene	3.99	0.11×10^{-3}	0.60

The higher the polarity of the solvent, the greater the total rate constant k_{5ClP}. At the same time the k_{NK}/k_{ACP} ratio decreases with the increasing of the solvent dipole moment which favores the formation of the secondary product ACP.

It can be noticed that in the series of the solvents used, propionitrile and acetonitrile, with very near values of the dipole moment μ, give close values also for the rate constant and the k_{NK}/k_{ACP} ratios. Nitrobenzene excepts from this regularity. The data presented in Table 6 suggest that the basicity of the amine must be different in the series of these solvents, a fact that can be significant. So DEA can be a stronger base in acetonitrile than in nitrobenzene, which favors the formation of ACP.

The data obtained in this paper point out the same influence of the solvent on the reaction rate found in the case of 5BrP. These results lead to the conclusion that to obtain a higher yield in the synthesis of NK it is necessary to use a nonpolar solvent.

REFERENCES

[1] S. E. Former, U. S. Industrial Chemicals Inc. Br. U.S.A. 2419250 (1947); *Chem. Abstr.*, **41**, 4509 (1947).
[2] S. E. Former, U. S. Industrial Chemicals Inc. Br. Brit. 604884 *Chem Abstr.*, **43**, 668 (1949).
[3] N. Rădulescu, A. Maza, I. Ambrus, H. Aftalion, L. Dimofte and R. Simionovici, Romanian patent nr. 62682/21.V, 1976.
[4] N. Rădulescu, M. Iulian, I. Ambruş, H. Aftalion, and L. Dimofte, Romanian patent nr. 63128/22.VII, 1976.
[5] T. Oncescu and L. Dimofte, *Rev. Chim.*, (*Bucureşti*), **27**, 1029 (1976).
[6] T. Oncescu and L. Dimofte, *Rev. Chim.* (*Bucureşti*), **28**, 1139 (1977).
[7] E. A. Moelwyn-Hughes, "The Kinetics of Reaction in Solution", Oxford-University Press, 1969.
[8] C. Reinchard, "Lösungsmittel Effekte in der organischen Chemie", Verlag Chemie, Berlin, 1969, p. 63.
[9] H. Grim, H. Ruf and H. Wolff, *Z. phys. Chem.* **13**, 301 (1931).

Revue Roumaine de Chimie, 25, 1, 23 — 31 (1980)

KINETICS AND MECHANISM OF THE REACTION BETWEEN 5-CHLORO-2-PENTANONE AND DIETHYLAMINE. II[1]

INFLUENCE OF THE NUCLEOPHILIC REAGENTS

TATIANA ONCESCU * and LIDIA DIMOFTE**

* Physical Chemistry Department, Institute of Chemical Technology, Bd. Republicii 13, Bucharest, Romania

** Institute of Chemical-Pharmaceutical Research, Sos. Vitan 112, Bucharest, Romania

Received March 31, 1978

The reaction kinetics of 5-chloro-2-pentanone with diethylamine in high excess and of chloro-2-pentanone with various amines in benzene was studied. The results are in good agreement with the reaction mechanism proposed.

1. INTRODUCTION

In a previous paper [1] we determined the rate constants and the activation parameters of the reaction between 5-chloro-2-pentanone (5ClP) and diethylamine (DEA) for the ratio 1/2 of the reactant concentration in various solvents. The present paper deals with the study of the same reaction with DEA in excess, serving at the same time as solvent. We studied also this reaction with different amines like : diethylamine, dipropylamine and dibutylamine in benzene when 5-amino-2-pentanones, intermediates of interest in the synthesis of some drugs, were obtained.

As we showed in our previous paper [1] this reaction consists of a nucleophilic substitution process (SN) accompanied by a γ elimination (E) in which acetylcyclopropane (ACP) is formed. At the same time we studied the SN/E γ competition as a function of the nucleophilic reagent.

2. EXPERIMENTAL

We used the following reagents for our experiments :

5-chloro-2-pentanone (5ClP) prepared according to a Romanian patent ;[2] diethylamine (DEA), dipropylamine (DPA) and dibutylamine (DBA), LOBA-Austranal purum, distilled before each experiment.

benzene-Reactivul, anhydrized on metallic Na and then distilled.

The rate constants were determined by using the same technique described in the previous papers.[1,3,4] For the determination of 5-amino-2-pentanones characterized by different vapour pressures, we used gas chromatography under the conditions mentioned in another paper.[5]

For the separation and identification of the secondary reaction products we carried out the reaction between 5ClP and DEA at 100° in the absence of the solvent. The ensuing reaction mass was treated with benzene, the diethylamine hydrochloride was filtered and then the novalketone (NK) was extracted with an aqueous solution of 25 % HCl. The benzenic layer was dried on K_2CO_3 and then the fraction between 60° — 80°/10 mm was collected by fractioned distillation. Separately, 0.01 ml of this fraction and the same volume of each different standard solutions were applied to the chromatoplate (Silicagel Stahl) activated at 110°. We used as eluent benzene : ethylacetate (3 : 1) and developed the chromatogram with dinitrophenylhydrazine.Two ketones were present which could not be identified. Figure 1 shows such a chromatogram.

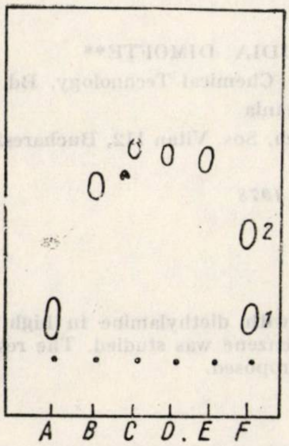

Fig. 1. — Thin layer chromatogram of the standard solutions and of the sample isolated form the fraction 60°— 80°/lomm Hg; $A =$ novalketone ($R_F = 0.14$); $B =$ acetylcyclopropane ($R_F = 0.46$); $C =$ 5-chloro-2-pentanone ($R_F = 0.52$); $D =$ cyclopentanone ($R_F = 0.52$); $E =$ methylallylketone ($R_F = 0.50$); $F =$ the unidentified products from the sample ($R_{F1} = 0.20$ and $R_{F2} = 0.36$).

It can be noticed that the R_F values obtained from the separated fractions are different from those of 5ClP, NK, ACP and also from methylallylketone and cyclopentanone assumed as possible reaction products. The same fraction obtained as above was introduced into a Silicon SE 30 column of a gas chromatograph[3] and two peaks were observed with the $T_R$values ($T_{R1} = 1'.15''$ and $T_{R2} = 1'.52''$) differing from those of 5ClP ($T_R = 46''$), ACP ($T_R = 21''$), NK ($T_R = 3'$), methylallylketone ($T_R = 33''$) and cyclopentanone ($T_R = 32''$). These results are in agreement with the behaviour obtained by thin layer chromatography. Figure 2 shows such a gas chromatogram.

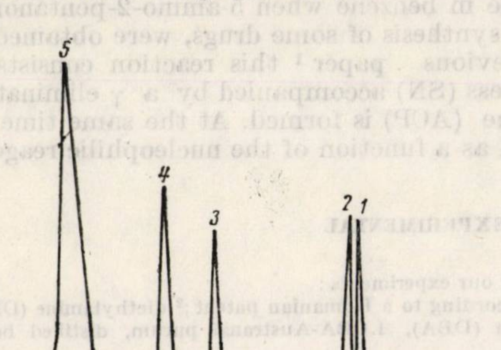

Fig. 2. — Gas chromatogram of the secondary products isolated from the fraction 60° — 80° /lomm Hg(*1* — ACP ; $T_R = 21''$; *2* — 5ClP, $T_R = 46''$; *3*—*4* unidentified products $T_R = 1'55'' - 2'20''$; *5* — NK, $T_R = 3'$)

The elementary analysis does not show the presence of Cl and N in the structure of these secondary compounds.

3. RESULTS AND DISCUSSION

We studied for the first time the reaction kinetics between 5ClP and DEA in the absence of the solvent using the following concentrations :

$$c_{5ClP} = 1.5\ \mathrm{M}, \quad c_{DEA} = 7.9\mathrm{M} \text{ and } \quad c_{5ClP} = 1\mathrm{M}, \quad c_{DEA} = 8.5\ \mathrm{M}$$

The suggested mechanism[3] is the same as that proposed in previous papers, [1-5] namely :

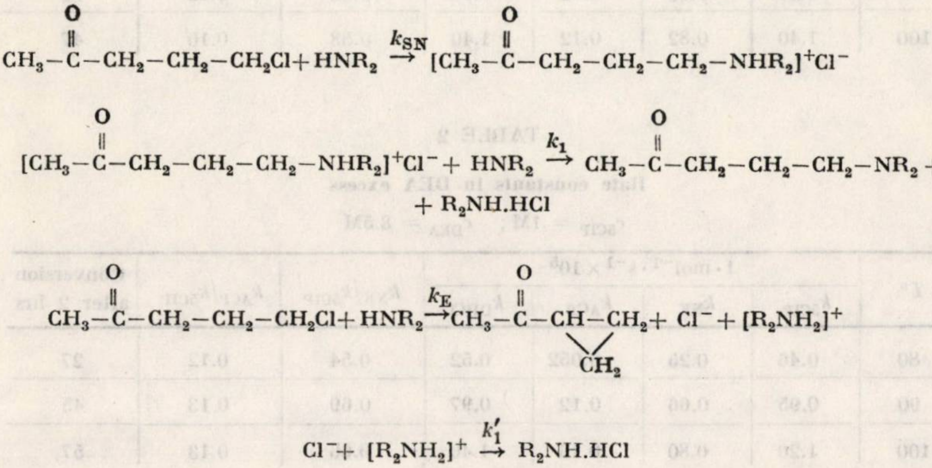

$$CH_3-\overset{\overset{O}{\|}}{C}-CH_2-CH_2-CH_2Cl + HNR_2 \xrightarrow{k_{SN}} [CH_3-\overset{\overset{O}{\|}}{C}-CH_2-CH_2-CH_2-NHR_2]^+Cl^- \qquad (1)$$

$$[CH_3-\overset{\overset{O}{\|}}{C}-CH_2-CH_2-CH_2-NHR_2]^+Cl^- + HNR_2 \xrightarrow{k_1} CH_3-\overset{\overset{O}{\|}}{C}-CH_2-CH_2-CH_2-NR_2 + R_2NH.HCl \qquad (2)$$

$$CH_3-\overset{\overset{O}{\|}}{C}-CH_2-CH_2-CH_2Cl + HNR_2 \xrightarrow{k_E} CH_3-\overset{\overset{O}{\|}}{C}-\underbrace{CH-CH_2}_{CH_2} + Cl^- + [R_2NH_2]^+$$

$$Cl^- + [R_2NH_2]^+ \xrightarrow{k_1'} R_2NH.HCl \qquad (3)$$

Where R can be : CH_3-CH_2- ; $CH_3-CH_2-CH_2-$; $CH_3CH_2-CH_2-CH_2-$ (4)

As we found in the previous paper [1] the rate constants with respect to 5ClP, NK and ACP verify a second order kinetic equation. Figure 3 presents our data obtained at 80° for the molar ratio (5ClP : DEA) 8.5.

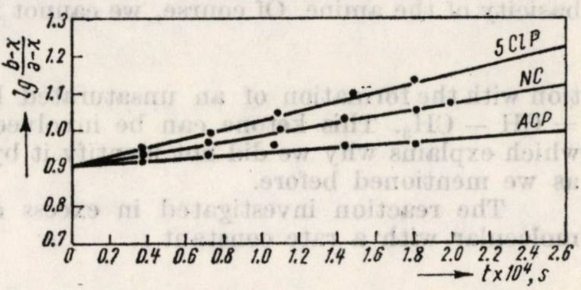

Fig. 3. — The second order kinetics obtained for the 8.5 molar concentration ratio c_{DEA}/c_{5ClP} at $T = 80°$

The values of rate constants at all the reaction temperatures are given in Tables 1 and 2.

It can be seen that the rate constant values are similar in both cases, but the conversion increases with the increase of the amine concentration.

TABLE 1

Rate constants in DEA excess

$c_{DEA} = 7.9M$; $c_{5ClP} = 1.5M$

$T°$	k_{5ClP}	$l \cdot mol^{-1} \cdot s^{-1} \times 10^5$			k_{NK}/k_{5ClP}	k_{ACP}/k_{5ClP}	Conversion after 2 hrs
		k_{NK}	k_{ACP}	k_{DHCl}			
80	0.42	0.26	0.06	0.48	0.62	0.14	15
90	0.99	0.63	0.12	0.90	0.63	0.12	35
100	1.40	0.82	0.12	1.40	0.58	0.10	47

TABLE 2

Rate constants in DEA excess

$c_{5ClP} = 1M$; $c_{DEA} = 8.5M$

$T°$	$l \cdot mol^{-1} \cdot s^{-1} \times 10^5$				k_{NK}/k_{5ClP}	k_{ACP}/k_{5ClP}	Conversion after 2 hrs
	k_{5ClP}	k_{NK}	k_{ACP}	k_{DHCl}			
80	0.46	0.25	0.052	0.52	0.54	0.12	27
90	0.95	0.66	0.12	0.97	0.69	0.13	45
100	1.20	0.80	0.16	1.40	0.66	0.13	57

If one compares these results with those obstained in benzene[1] one observes that the yield of NK formation measured by the k_{NK}/k_{5ClP} ratio is the same, but the conversion is much faster in excess of DEA. In exchange, the ACP yield is lowered to a half denoting the formation of other secondary products evidenced by thin layer chromatography. This behaviour can be ascribed to ACP self-condensation favoured by the basicity of the amine. Of course, we cannot rule out a β elimination reaction with the formation of an unsaturated ketone like $CH_3-\overset{\overset{O}{\|}}{C}-CH_2=CH-CH_3$. This ketone can be involved in a condensation reaction which explains why we did not identify it by thin layer chromatography, as we mentioned before.

The reaction investigated in excess of DEA becomes pseudounimolecular with a rate constant :

$$k = \frac{2,303}{bt} \lg \frac{a}{a-x} \tag{5}$$

$$\text{in which : } k = \frac{k_1}{b} \text{ ; } a = c_{5ClP} \text{ and } b = c_{DEA} \tag{6}$$

We exemplify this kinetics at 80° in Figure 4.

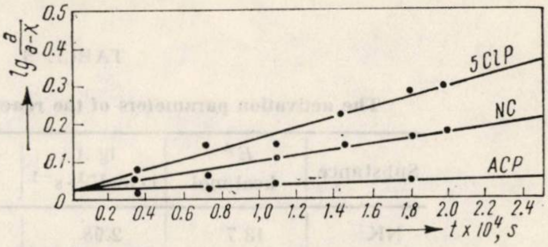

Fig. 4. — The pseudofirst order kinetics obtained for the 8.5 molar concentration ratio c_{DEA}/c_{5ClP}, at $T = 80°$.

In the same manner in Table 3 we calculated the first order rate constants for both molar ratios used at all working reaction temperatures.

TABLE 3

First order rate constant values (s^{-1})

	5ClP		NK		ACP	
	$k_1 \times 10^4$		$k_1 \times 10^4$		$k_1 \times 10^5$	
T° \ c_{DEA}/c_{5ClP}	5.2	8.5	5.2	8.5	5.2	8.5
80	0.30	0.38	0.20	0.22	0.48	0.51
90	0.68	0.67	0.47	0.52	0.86	0.89
100	1.00	0.95	0.57	0.72	1.30	1.20

By using these data and equation (6) we found a good agreement between the pseudounimolecular rate constant k and the second order rate constant k_2.

TABLE 4

Comparative values of pseudounimolecular and second order rate constants ($l \cdot mol^{-1} \cdot s^{-1}$)

T°	c_{DEA} (M)	5ClP		NK		ACP	
		$k \times 10^5$	$k_2 \times 10^5$	$k \times 10^5$	$k_2 \times 10^5$	$k \times 10^5$	$k_2 \times 10^5$
80	7.9	0.38	0.42	0.25	0.26	0.06	0.06
90	7.9	0.86	0.99	0.59	0.63	0.11	0.12
100	7.9	1.20	1.40	0.72	0.82	0.16	0.16
80	8.5	0.44	0.46	0.26	0.25	0.06	0.05
90	8.5	0.78	0.95	0.62	0.66	0.10	0.12
100	8.5	1.10	1.20	0.84	0.80	0.14	0.16

The activation parameters using the second order rate constant k_2, were calculated at the DEA : 5ClP molar ratio 8.5.

TABLE 5

The activation parameters of the reaction in excess of DEA

Substance	$E^{\neq}$ kcal/mol	lg A $l \cdot mol^{-1} \cdot s^{-1}$	$\Delta S^{\neq}$ e.u.	$\Delta G^{\neq}$ kcal/mol
NK	13.7	2.98	−52.0	31.9
ACP	11.6	1.02	−60.9	33.1
5ClP	14.7	3.72	−48.6	31.6
DHCl	14.7	3.72	−48.6	31.6

We investigated also the role of the amine nature of the α on the kinetics of the reaction between 5ClP and various amines in benzene solutions. Thus, when the nucleophile is changed with DPA or DBA, the 5ClP conversion is slower than that obtained with DEA. At the same time, the nucleophilic substitution reaction with formation of DPAP (5-dipropylamino-2-pentanone) and DBAP (5-dibutylamino-2-pentanone) as well as the γ elimination reaction with ACP formation, have also slower conversions.

Tables 6 and 7 present our experimental data obtained with DPA and DBA.

TABLE 6

The rate constants of the reaction with DPA in benzene, at different temperatures

$c_{5ClP} = 1M \quad c_{DBA} = 2.1M$

T_0	$l \cdot mol^{-1} \cdot s^{-1} \times 10^4$				k_{DPAP}/k_{5ClP}	k_{ACP}/k_{5ClP}	Conversion after 2 hrs	
	k_{5ClP}	k_{DPAP}	k_{ACP}	k_{DHCl}			DPA	DEA
110	0.17	0.09	0.05	0.17	0.54	0.30	0.28	37
120	0.28	0.16	0.08	0.35	0.51	0.32	35	43
130	0.40	0.20	0.13	0.40	0.50	0.32	54	—

The results show that the overall rate constants k_{5ClP} and k_{DHCl}, as well as the nucleophilic substitution rate constant k_{DPAP}, respectively k_{DBAP} are lower than the corresponding k_{NK}, whereas the γ elimination rate constant k_{ACP} is practically the same.

Apparently, the overall rate constant as well as the conversion value decrease in the series of these three amines, and especially more from the first to the second one.

TABLE 7

Rate constants of the reaction with DBA in benzene at different temperatures and same concentrations

$T°$	$l \cdot mol^{-1} \cdot s^{-1} \times 10^4$				k_{DBAP}/k_{5ClP}	k_{ACP}/k_{5ClP}	Conversion after 2 hrs.
	k_{5ClP}	k_{DBAP}	k_{ACP}	k_{DHCl}			
110	0.14	0.07	0.05	0.10	0.50	0.36	23
120	0.24	0.13	0.09	0.23	0.53	0.38	30
130	0.35	0.17	0.12	0.36	0.49	0.34	43

TABLE 8

Rate constants of the reaction of 5ClP with different nucleophilic reagents at $T = 110°$

Nucleophilic reagents	$l\ mol^{-1} \cdot s^{-1} \times 10^4$			Conversion after 2 hrs	k_{SN}/k_E
	$k_{overall}$	k_{SN}	k_E		
DEA	0.32	0.18	0.07	37	2.57
DPA	0.17	0.09	0.05	28	1.80
DBA	0.14	0.07	0.05	23	1.50

The substitution rate constant k_{SN} decreases with the increase of the amine catene whereas the elimination rate constant is the same leading to a decrease of the k_{SN}/k_E ratio. This ratio is a measure of the decrease of the amine nucleophilic capacity.

From the plots on Figure 5 an activation energy of 14.6 Kcal/mol was calculated for the overall reaction between 5 ClP and the three amines DEA, DPA and DBA.

An activation energy of 13.7 Kcal/mol and 11.0 Kcal/mol respectively, was determined in the same manner for both nucleophilic substitution and elimination reaction.

Table 9 presents the preexponential factor values.

With the help of these data the activation entropies were calculated as in Table 10.

From these two tables it results that the preexponential coefficients as well as the activation entropies decrease monotonically in the series : DEA, DPA, DBA.

In contrast to these values those referring to the γ elimination reaction are the same for the three amines.

The slow value of the determined activation energy for the nucleophilic substitution reaction as well as the negative activation entropy values plead for an SN_2 nucleophilic substitution. This affirmation is also supported by the fact that the ratio between the main reaction products changes with the nature of the nucleophilic reagent. This behaviour is similar to that of 5BrP, observed by us in a previous paper[5].

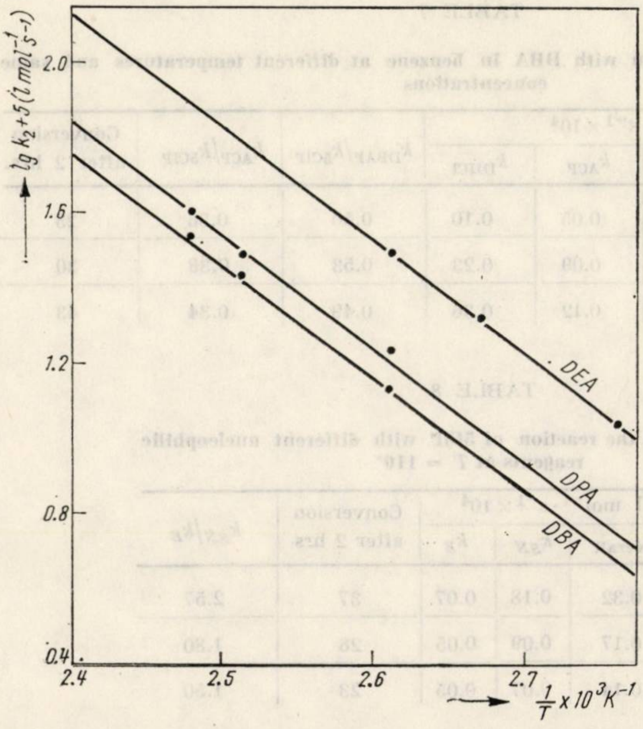

Fig. 5. — Plotting $1gk_2$ vs $1/T$ for the computation of activation energies in the case of the three amines used for the consumption of 5ClP.

TABLE 9

Preexponential coefficients (lg A) of the reaction between 5ClP and different amines

Amines / Reaction	DEA	DPA	DBA
5ClP	3.86	3.60	3.49
DHCl	3.86	3.60	3.49
SN	3.12	2.80	2.71
E	1.12	1.03	1.03

TABLE 10

Activation entropies (u.e.) of the reaction between 5ClP and different amines

Reaction \ Amines	DEA	DPA	DBA
5ClP	−48.0	−49.0	−49.8
DHCl	−48.0	−49.0	−49.8
SN	−51.0	−52.9	−53.3
E	−60.5	−61.0	−61.0

REFERENCES

[1] T. Oncescu and L. Dimofte, *Rev. Roumaine Chim.*, 25,15 (1980).

[2] N. Rădulescu, M. Iulian, I. P. Ambruș, H. A. Aftalion and L. Dimofte Romanian patent, nr. 62682/21.V, 1976.

[3] T. Oneescu, and L. Dimofte, *Rev. Chim.* (*București*), **12**, 1029 (1976).

[4] T. Oncescu, and L. Dimofte, *Rev. Chim.* (*București*), **11**, 1046 (1977).

[5] T. Oncescu and L. Dimofte, *Rev. Chim.* (*București*), **12**, 1139 (1977).

Revue Roumaine de Chimie, **25**, *1*, 33 – 39 (1980)

DETERMINATION OF TRACE QUANTITIES OF THE GROUP V–A ELEMENTS BY ANODIC STRIPPING VOLTAMMETRY. I

TRACE ANALYSIS OF ARSENIC

SOFIA MARCHIDAN, IULIANA VARTIRES and N. D. TOTIR
Centre of Physical Chemistry, Splaiul Independenţei 202, Bucharest 77208, Romania

Received June 4, 1977
Revised: May 10, 1979

A new method for determination of arsenic in the $10^{-6} - 10^{-9}$ M concentration range, with a variation coefficient less than 5% has been developed. Good sensibility and reproducibility for both arsenic (III) and arsenic (V) analysis on gold electrode, using 1 M H_2SO_4 as supporting electrolyte, have been obtained. The most satisfactory procedure for reducing the electrochemically inactive arsenic (V) to arsenic (III) was found to be the heating of the sample with Na_2SO_3 in acid solution. It has been established that large amounts of Ni, Cd, Zn, Fe and Pb do not disturb the stripping analysis of arsenic. Only Cu, even at the same level of concentration, interferes with arsenic (III) analysis.

During the last decade the anodic stripping voltammetry has become one of the most important physico-chemical methods for the determination of small quantities of elements. [1]

Anodic stripping voltammetry has been employed by many authors for the determination of arsenic, antimony, and bismuth in different samples.

Arsenic produces reduction waves only when present in the (III) valency state. Arsenic (V) cannot be analysed by anodic stripping voltammetry because in most supporting electrolytes it is not electrochemically reducible.

By using a stationary Pt electrode and 1 M HCl, Truscina and Kaplin [2] have analysed concentrations of arsenic as low as 2×10^{-7} M. In order to increase the sensitivity, a graphite electrode has been applied by Kaplin and coworkers. [3] The same electrode has been used for a simultaneous deposition of arsenic with other elements.[4-6] The rotating platinum electrode has also been used. [7]

Recently, by using a platinum or gold electrode in hydrochloric or perchloric acid as supporting electrolyte, Forsberg[8,9] has reached a detection limit of 10^{-10} M As.

In this paper a method is described by using a new supporting electrolyte, H_2SO_4, avoiding in this way a very tedious pretreatment of the solid working electrode.

EXPERIMENTAL

APPARATUS

An adequate description of the instrumentation and quartz cell used in this work was given in a previous paper.[10]

WORKING ELECTRODE

It is well known that the mercury electrode cannot be used for arsenic analysis by anodic stripping voltammetry. Instead, both platinum and gold are appropriate as working electrodes.

The platinum electrode was a wire of spectral purity, having 0.25 mm in diameter and an apparent surface of 8.0 mm^2, sealed into a soft glass tube.

The gold electrode was made in the same way from spectral purity wire of 0.25 mm in diameter with an apparent surface equal to 9.4 mm^2.

A platinum wire was used as a counter electrode. A saturated calomel electrode was used as a reference electrode.

REAGENTS

All the reagents used were high purity Merck-made chemicals without further purification. Standard solutions of arsenic (III) and arsenic (V) were prepared by dissolving As_2O_3 and $HNa_2As\cdot O_4 7H_2O$ respectively, in a few milliliters of 0.1 N NaOH and then acidified with sulphuric acid. Subsequent dilutions of these stock solutions were made only when required. Standard solutions for Cu, Ni, Zn, Fe, Cd and Pb were obtained from tetradistilled water and p.a. reagents. As reducing agent for arsenic (V) solutions, Na_2SO_3 of analytical grade was used. All the solutions were prepared just before measurements and stored in a Pyrex glass vessel.

PROCEDURE

In all the experiments we used 1 M H_2SO_4 as supporting electrolyte considering that in this solution the best polarographic waves for As(III) could be recorded.[11] Good results were obtained by using the same sulphuric acid solution for the pretreatment of the solid electrode instead of 0.1 M $HClO_4$ as is recommended in the literature.[12] In this way the pretreatment of the electrode is made directly in the supporting electrolyte from the cell, just before arsenic analysis.

Before measurements the quartz cell was thoroughly cleaned with 1 : 1 concentrated nitric acid and sulphuric acid and then rinsed with bi, three, and tetradistilled water.

The solid electrode, kept previously in 6 N HNO_3, was rinsed thoroughly with tetradistilled water and then placed in a cell containing the supporting electrolyte. The oxygen was removed from the solution by passing purified argon bubbles for 30 minutes before the pretreatment of the working electrode. After that the working electrode was polarized at 0.0 volts (SCE) between 10 and 30 minutes until the current reached a steady value of about 1 μA, then the stripping voltammogram of the supporting electrolyte was recorded.

The potential employed for the cathodic deposition step was usually − 200 mV vs. SCE.

By adding into the cell a certain amount of arsenic (III) solution and repeating the determination, the concentration of an unknown sample was determined after standard addition.

For electrochemically inactive arsenic (V) analysis, the reduction to arsenic (III) was realised by adding a fresh Na_2SO_3 solution in large excess to the sample dissolved in 1 M H_2SO_4, heated for 30 minutes at 100° for complete reduction and SO_2 removal. The standard solution of arsenic (V) should be prepared in the same manner for avoiding additional errors.

RESULTS AND DISCUSSION

In order to determine the trace quantities of arsenic by anodic stripping voltammetry it was necessary to establish the proper experimental conditions for obtaining a dissolution current, i_p, as large as possible and reproducible. For example, connected with the voltage scan rates it was found that for a value of 100 mV/sec one could obtain an adequate sensitivity for arsenic trace analysis. All the experiments were carried out using this sweep rate.

Our results have shown that the platinum electrodes can be used only with arsenic concentrations higher than 1×10^{-6}M. At lower concentrations the simultaneous evolution of hydrogen during arsenic deposition was significant, disturbing the arsenic deposition.

Gold has proven to be a more suitable working electrode because the hydrogen overvoltage was higher on gold than it was on platinum. In addition to this, the peak currents on gold are much clearer than on platinum, as can be seen in Figure 1.

As supporting electrolyte, 1 M H_2SO_4 was used without further purification. In the previous papers both 1 M HCl and 1 M $HClO_4$ were used by different authors as supporting electrolyte. But for using these electrolytes it was necessary an initial purification by repeated distillation in a quartz apparatus. On the other hand, by using HCl as supporting electrolyte during arsenic (V) reduction with Na_2SO_3 at 100°, some amount of the hydrochloric acid was volatilized and therefore the concentration of the solution was changed.

The dependence of peak current, i_p, of arsenic (III) on deposition potential, E_d, is given in Figure 2. The peak current is linearly dependent on potential and it decreases as the potential becomes more positive.

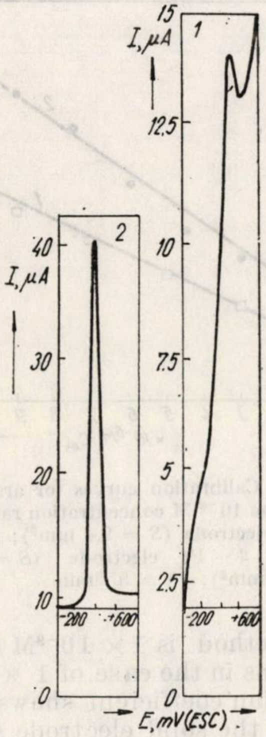

Fig. 1. — Dependence of peak current, i_p, on the type of electrode used: *1.* Pt electrode (S = 8.0 mm²); *2.* Au electrode (S = 9.4 mm²); $C_{As} = 3.0 \times 10^{-6}$M; $\tau = 5$ min.

Fig. 2. — Dependence of peak current, i_p, on deposition potential, E_d; Au electrode; $C_{As} = 5.0 \times 10^{-7}$ M; $\tau = 5$ min.

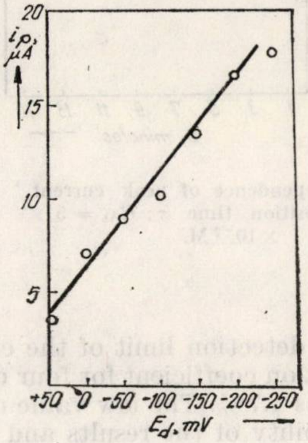

For good sensitivity and reproducibility the proper value of deposition potential is −200 mV (SCE).

At lower potential values than −300 mV, hydrogen evolution begins, followed by its adsorption which does not allow to obtain peak currents for arsenic.

The influence of deposition time, τ, on peak current is given in Figure 3. For 10^{-7} M concentration range of arsenic (III), the proper deposition time is five minutes. In this concentration range, for higher deposition time, there is no linear dependence between i_p and τ. It follows that for arsenic (III) concentrations higher than 10^{-7} M the proper deposition time is lower than five minutes and only for a concentration lower than 10^{-7} M As a longer deposition time will be necessary.

There is a linear dependence between arsenic concentration and the intensity of the peak current. The calibration curves for the concentration range 10^{-6} M of arsenic on gold and platinum electrodes are given in Figure 4. In Figure 5 the calibration curves for the gold electrode in the concentration range 10^{-7}—10^{-8} M As are presented. The same proportionality was found in the 10^{-9} M concentration range of arsenic.

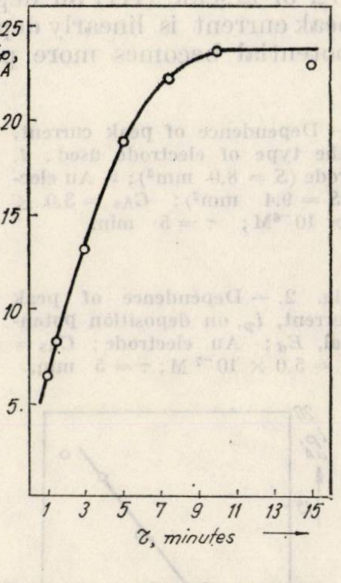

Fig. 3. — Dependence of peak current, i_p, on deposition time τ; $C_{As} = 5 \times \times 10^{-7}$ M.

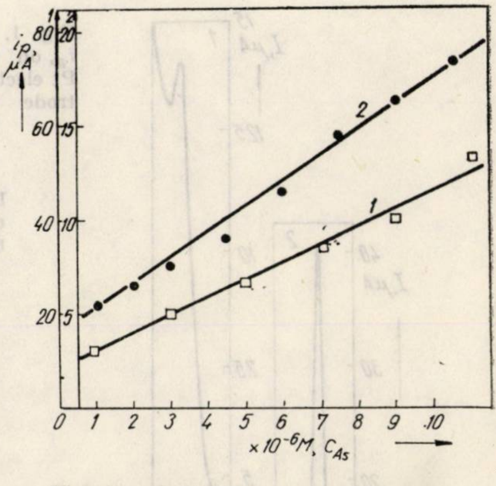

Fig. 4. — Calibration curves for arsenic (III) in the 10^{-6} M concentration range: *1* — Au electrode ($S = 9.4$ mm^2); $\tau = 3$min; *2* — Pt electrode ($S = 8.0$ mm^2); $\tau = 5$ min.

The detection limit of the elaborated method is 1×10^{-9}M arsenic. The variation coefficient for four determinations in the case of 1×10^{-7} M arsenic was 4.7%. The low value of the variation coefficient shows a good reproducibility of the results and therefore of the solid electrode surface.

In order to determine the interference of other cations, the influence of Cd^{2+}, Pb^{2+}, Zn^{2+}, Cu^{2+}, Ni^{2+}, and Fe^{3+} in the ratios As : cations equal to 1 : 1 ; 1 : 10 and 1 : 100 was studied. The stripping voltammogram of arsenic in the presence of large amounts of nickel is given in Figure 6. As can be seen, even for concentrations of the above cation one hundred times higher than arsenic, there is no interference. From the voltammograms shown in Figure 7 one can notice that Cd^{2+}, Pb^{2+}, Zn^{2+}, and Fe^{3+} ions did not interfere.

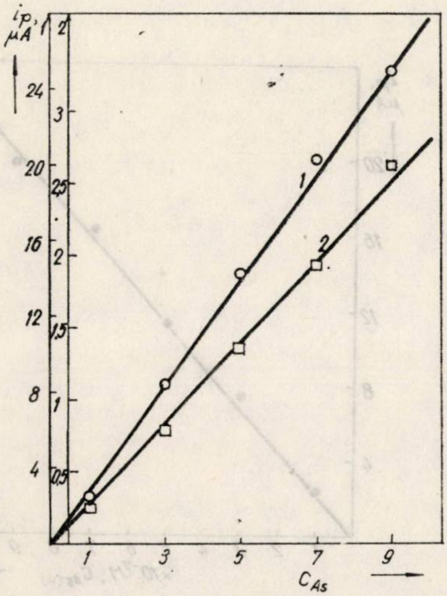

Fig. 5. — Calibration curves for arsenic (III) on gold electrode, in the concentration range $10^{-7} - 10^{-8}$ M : 1 — $C_{As} = 10^{-7}$ M ; $\tau = 5$ min ; 2 — $C_{As} = 10^{-8}$ M ; $\tau = 5$ min.

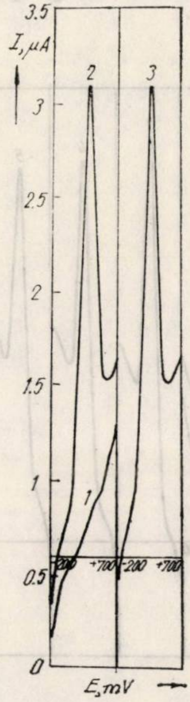

Fig. 6. — Stripping voltammograms of arsenic, on gold electrode, in the presence of nickel : 1. 1 M H_2SO_4 ; 2. 1 × 10^{-7} M As ; 3. 1 × 10^{-7}M As + 1 × 10^{-5} M Ni (As : Ni = 1 : 100), $\tau = 5$ min.

Copper is the only cation which disturbs the stripping analysis of arsenic even for the same concentration, because it has a dissolution peak in the same region with arsenic (+ 280 mV).

Arsenic (V) is electrochemically inactive and therefore it is necessary to reduce it chemically to arsenic (III) prior to stripping analysis. The reducing agent must be of high purity and the chemical reaction must be complete. We found that the best reducing agent is sodium sulfite which in large excess, As(V) : $Na_2SO_3 \geqslant 1 : 10^5$, allows the complete reduction of arsenic (V) to arsenic (III) in acid solution by decomposition of Na_2SO_3 to SO_2 after heating at 100° for 30 minutes.

By using such a procedure, to reduce solutions of 10^{-7} M arsenic (V), the values of i_p given in Figure 8, were obtained in terms of As(V) concentration. This shows that arsenic (V) can be determined by anodic stripping voltammetry after previous chemical reduction to arsenic (III). Comparing the results on Figure 5, obtained for the same concentration range of As(III), we found that there is a good agreement between both . The difference of about 10% for arsenic (V) appears probably because of incomplete reduction by sulfite and therefore the standard solution of As(V) should be prepared in the same conditions.

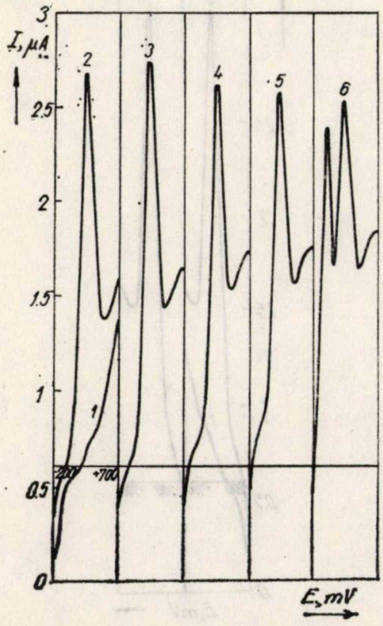

Fig. 7. — Stripping voltammograms of arsenic, on gold electrode, in the presence of iron, cadmium, zinc and lead : *1.* 1 M H_2SO_4 ; *2.* 1×10^{-7} M As ; *3.* sample $2 + 1 \times 10^{-5}$ M Fe ; *4.* sample $3 + 1 \times 10^{-5}$ M Cd ; *5.* sample $4 + 1 \times 10^{-5}$ M Zn ; *6.* sample $5 + 3 \times 10^{-6}$ M Pb ; $\tau = 5$ min.

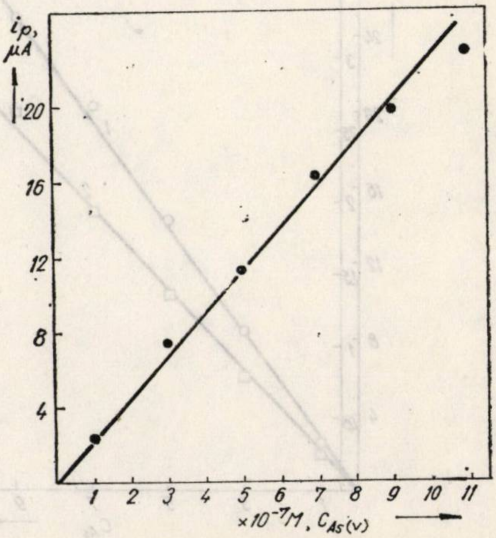

Fig. 8. — Calibration curve for arsenic (V) on gold electrode, after chemical reduction with Na_2SO_3 ; $C_{As(V)} : C_{Na_2SO_3} = 1 : 1 \times 10^5$; $\tau = 5$ min.

In this way by using anodic stripping voltammetry it was possible to analyse not only the total amount of arsenic from a solution, but to determine arsenic (III) and arsenic (V) independently. This is very important taking into account the different toxicity of either arsenic ion.

The newly developed method can be used for anodic stripping trace analysis of arsenic (V) and arsenic (III) in different organic and inorganic reagents of electronic grade or other ultrapure chemicals.

REFERENCES

[1] F. P. J. Cahill and G. W. Van Loon, *Internat. Lab.*, **July/Aug.**, 11 (1976).
[2] L. F. Truscina and A. A. Kaplin, *Zhur. analit. Khim.*, **25,** 1616 (1970).
[3] A. A. Kaplin, N. A. Veiţ and A. G. Stromberg, *Zhur. analit. Khim.*, **28,** 2192 (1973).
[4] E. Ia. Neiman and G. B. Ponomarenko, *Zhur. analit. Khim.*, **30,** 1132 (1975).
[5] T. Ia. Belova, I. B. Berengard and B. Ia. Kaplin, *Zavodskaya Lab.*, **41,** 1314 (1975).
[6] T. A. Krapivkina, E. M. Roizenblat, V. V. Nosaceva, L. S. Zareţkii and V. S. Utenko, *Zhur. analit. Khim.*, **29,** 1818 (1974).
[7] T. Kuwabara, S. Suzuki and S. Araki, *Bull. Chem. Soc. Japan*, **46,** 1690 (1973).
[8] G. Forsberg, J. W. O'Laughlin, R. G. Megargle and S. R. Koirtyohann, *Analyt. Chem.*, **47,** 1586 (1975).
[9] G. Forsberg, "The Determination of Arsenic by Stripping Analysis", Dissertation, Ph. D., 1975, University of Missouri, Columbia, U.S.A.
[10] N. Totir and Iuliana Vartires, *Rev. Roumaine Chim.*, **20,** 23 (1975).
[11] I. M. Kolthoff and J. J. Lingane, "Polarography", vol. II, Interscience Publ., New York, 1952, p. 542.
[12] I. M. Kolthoff and N. Tanaka, *Analyt. Chem.*, **26,** 632 (1954).

Revue Roumaine de Chimie, 25, 1, 41 – 45 (1980)

APPLICATION OF AN APPROXIMATE CALCULATION FOR THE TOTAL ENERGY OF THE HYDROGEN MOLECULE-ION

EDUARDO A. CASTRO
Instituto de Investigaciones Fisicoquïmicas Teóricas y Aplicadas, Sección Quïmica Teórica
Sucursal 4, Casilla de Correo 16, La Plata 1900, Argentina

Received July 11, 1978

The paper presents a calculation for the total energy of H_2^+ in the whole range of the internuclear distance. A previously proposed approximate formulation is applied and the results are coincident with the exact ones.

INTRODUCTION

Various approximations for the total molecular energy have been recently suggested.[1-3] Such approximations permit the expression of the total energy of a molecule as a function of the orbital energies ε_k. According to this, Ruedenberg [3] proposed the following identity

$$E = 1.55 \sum_k \nu_k \varepsilon_k \tag{1}$$

where ν_k is the orbital occupation number. Eq. (1) was applied for all the molecules included by Snyder and Basch in their compendium of SCF wavefunctions[4] in terms of Gaussian basis set of approximately double-zeta quality. The results obtained[5] showed that the identity (1) is satisfied up to 3%. A similar equation for atoms and molecules was derived by Politzer [1] on the basis of the screening function $\O(r, Z)$ with a fundamental and unifying nature, [6] because either for a free atom or for an atom in a molecule, such quantity plays a key role in determining the total energy. Politzer's relation was applied with good results to atoms and molecules, although it does not represent a good approximation for positive atomic ions.[7] March[9] provided some justification for Ruedenberg and Politzer's results from the first principles on the basis of the Thomas-Fermi statistical theory, which can be regarded as the simplest possible SCF method valid for a large number of electrons.[9] Anno and Sakai[10] have shown that Ruedenberg and Politzer's like molecular relations are justified only when the molecule is in its equilibrium state because any quantity defined as a multiple of $\sum_k \nu_k \varepsilon_k$ does not show a minimum, at least along a stretching coordinate, within a molecule. Often, the simple additive relation

$$E \simeq \sum_k \nu_k \varepsilon_k \tag{2}$$

is postulated and used for various purposes, such as Walsh rules, Woodward-Hoffmann correlation diagrams, Hückel methods, etc. So it would be interesting to try to find an approximate additive equation based on theoretical grounds which should give rationalization to the previous procedures. Working on this line, Schaad *et al.*[2] suggested the approximation

$$E_{\mathrm{elect}}(Z, R) = 0.25 \sum_k \nu_k \ \varepsilon_k(2Z, \ R/2) \tag{3}$$

where the electronic SCF energy of a molecule is replaced by 1/4 times the sum of the orbital energies of a scaled system obtained by doubling each nuclear charge and halving each internuclear distance in the original molecule. Nuclear repulsion is added to give the total SCF energy. The approximation is shown to give a rigorous upper bound to the Hartree-Fock energy.[2] Eq. (3) was derived using a Z^{-1} perturbation method for isoelectronic series and an analogous procedure was previously applied for atoms.[11]

The importance of Eq.(3) lies in the fact that it is not restricted to equilibrium bond lengths, but it is valid for all nuclear configurations. Hence, a reasonable foundation of schemes such as Walsh rules, Woodward-Hoffmann correlation diagrams and Hückel methods might lie in Eq. (3). In order to test their equation for total energy, Schaad *et al.*[2] calculated the scaled model for H_2 employing incomplete data of Fraga and Ransil's He_2^{2+} SCF orbital energies.[12] Unfortunately, the available data did not allow them to carry the total energy curve through the bonding region of H_2, and in general, molecular examples are not easy to be found in the literature since the highly charged molecules have not been of interest so far. Eq. (3) was tested for atoms employing Clementi's results[13] and good values were found (see Table I in Ref. 2).

RESULTS AND DISCUSSION

It would be of interest to study a case where the total energy curve could be carried over all internuclear distances. In the present work we shall show that the application of Eq. (3) gives results identical with the exact calculation when it is aplied to the H_2^+ molecule-ion in the LCAO-MO approximation. The calculation for H_2^+ using a variation function

$$\varphi = c_1 \ \psi_{1sa} + c_2 \ \psi_{1sb} \tag{4}$$

was first carried out by Finkelstein and Horowitz[14] and complemented by Coulson.[15] ψ_{1s} denotes a hydrogenic 1*s* AO with an effective nuclear charge K, which depends on the internuclear distance R. We shall use the explicit formulation given by the author *et al.* in a previous paper.[16] The scaled model for H_2^+ with bond length R is the He_2^{3+} molecule-ion, with bond length $R/2$. The total electronic energy for this model is

$$W_{1,2} = -0.5K^2 + \\ + \frac{K^2 - 2K - 2R^{-1}(1 + KR)\exp(-2KR) \pm K(K-4)(1 \pm KR)\exp(-KR)}{1 \pm (1 + KR + K^2R^2/3)\exp(-KR)} \tag{5}$$

where W_1 and W_2 are the energies corresponding to the $\sigma_g(1s)$ and $\sigma_u^*(1s)$ states respectively. The variational integrals W_1 and W_2 can be written as

$$W_1 = K^2f(t) + Kg(t), \ W_2 = K^2p(t) + Kq(t) \tag{6}$$

where :

$$t = KR \tag{7}$$

$$\left.\begin{aligned}
f(t) &= (1 - 0.5A(t) + (1 + t)\exp(-t))/A(t) \\
g(t) &= 2(-1 - t + (1 + t)\exp(-2t) - 2(1 + t)\exp(-t))/tA(t) \\
p(t) &= (1 - 0.5B(t) - (1 + t)\exp(-t))/B(t) \\
q(t) &= 2(-1 - t + (1 + t)\exp(-2t) + 2(1 + t)\,t\exp(-t))/tB(t) \\
A(t) &= 1 + \exp(-t)(1 + t + t^2/3) \\
B(t) &= 1 - \exp(-t)(1 + t + t^2/3)
\end{aligned}\right\} \tag{8}$$

Inserting these formulas into the minimization conditions

$$\partial W_1/\partial_k \text{ and } \partial W_2/\partial_K \tag{9}$$

and solving for K_1 and K_2, we obtain

$$K_1 = -(g(t) + tg'(t))/(2f(t) + tf'(t)) \tag{10}$$

$$K_2 = -(q(t) + tq'(t))/(2p(t) + tp'(t)) \tag{11}$$

where

$$r'(t) \equiv \mathrm{d}r/\mathrm{d}t \text{ for } r = f, g, q, p. \tag{12}$$

Comparing Eqs.(8) with the analogous formulas for H_2^+ : [16]

$$\begin{aligned} F(t) &= f(t) \\ G(t) &= g(t)/2 \\ P(t) &= p(t) \\ Q(t) &= q(t)/2 \end{aligned} \tag{13}$$

Then

$$K_1 = 2k_1,\ K_2 = 2k_2,\ \ 2R_{\mathrm{He}_2^{3+}} = R_{\mathrm{H}_2^+},\ t_{\mathrm{He}_2^{3+}} = t_{\mathrm{H}_2^+} \tag{14}$$

The approximate formula (3) for the He_2^{3+} model at $R/2$ gives

$$\left.\begin{aligned} E_1(\mathrm{He}_2^{3+}) &= 0.25\ (K^2 f(t) + K g(t)) + 2/R_{\mathrm{He}_2^{3+}} \\ E_2(\mathrm{He}_2^{3+}) &= 0.25\ (K^2\, p(t) + K\, q(t)) + 2/R_{\mathrm{He}_2^{3+}} \end{aligned}\right\} \tag{15}$$

Employing Eqs. (14) in Eqs.(15) we obtain

$$\left.\begin{aligned} E_1(\mathrm{He}_2^{3+}) &= k_1^2 F(t) + k_1 G(t) + 1/R_{\mathrm{H}_2^+} \\ E_2(\mathrm{He}_2^{3+}) &= k_2^2 P(t) + k_2 Q(t) + 1/R_{\mathrm{H}_2^+} \end{aligned}\right\} \tag{16}$$

and it shows that

$$E_{1,2}(\mathrm{He}_2^{+}) = E_{1,2}\,(H_2^+) \tag{17}$$

which is the desired result.
From Eqs (10) and (11) we can see that the limiting behaviour of the effective nuclear charge K for the states $\sigma_g\ (1s)$ and $\sigma_u^*\ (1s)$ is

$$\left.\begin{aligned} &\lim_{R\to 0} K_1 = 4, \quad \lim_{R\to\infty} K_1 = 2 \\ &\lim_{R\to 0} K_2 = 0.8, \ \lim_{R\to\infty} K_2 = 2 \end{aligned}\right\} \tag{18}$$

This limiting behaviour is the correct one because for $R \to 0$ we get the Be^{3+} ion and for $R \to \infty$ we get the He^+ ion, and furthermore[15] $\sigma_g\ (1s)$ correlates with the ground states $(1s)$ of Be^{3+} and $\sigma_u^*(1s)$ correlates with the excited atomic state $2p_z$ of Be^{3+}.

The results obtained are interesting enough to support the continuation of the investigations on semiempirical scaled Hückel methods based on the approximation of Eq(3)[2] and hence to reach a quantitatively sound rationalization of a number of approximate rules[17,18] which are so useful for a better understanding of the chemical phenomena.

REFERENCES

[1] P. Politzer, *J. Chem. Phys.*, **64**, 4239 (1976).
[2] L. J. Schaad, B. H. Robinson and B. A. Hess, Jr., *J. Chem. Phys.*, **67**, 4616 (1977).
[3] K. Ruedenberg, *J. Chem. Phys.*, **66**, 375 (1977).
[4] L. C. Snyder and H. Basch, "Molecular Wave Functions and Properties", Wiley-Interscience, New York, 1972.
[5] E. A. Castro, *Int. J. Quantum Chem.* (in press)
[6] P. Politzer and R. G. Parr, *J. Chem. Phys.*, **61**, 4258 (1974).
[7] E. B. Priestly and S. Fraga, *Canad. J. Phys.*, **44**, 1933 (1966).
[8] N. H. March, *J. Chem. Phys.*, **67**, 4618 (1977).
[9] N. H. March, *Adv. Phys.*, **7**, 1 (1957).
[10] T. Anno and Y. Sakai, *J. Chem. Phys.*, **67**, 4771 (1977).
[11] B. H. Robinson and L. J. Schaad, *J. chem. Phys.*, **59**, 6189 (1973).
[12] S. Fraga and B. J. Ransil *J. Chem. Phys.*, **35**, 1967 (1961); **37**, 1112 (1962).
[13] E. Clementi, *IBM J. Res. Dev. Suppl.*, **9**, 2 (1965).
[14] B. N. Finkelstein and G. E. Horowitz, *Z. Physik*, **48**, 118 (1928).
[15] C. A. Coulson, *Trans. Faraday Soc.*, **33**, 1479 (1937).
[16] E. A. Castro, C. Ferro and V. Amorebieta, *Amer. J. Phys.*, **42**, 612 (1974).
[17] G. Klopman, "Chemical Reactivity and Reaction Paths", Wiley-Interscience, New York, 1974.
[18] R.G. Pearson, "Symmetry Rules for Chemical Reactions", Wiley— Interscience, New York, 1976.

Revue Roumaine de Chimie, **25**, *1*, 47 – 54 (1980)

NONDESTRUCTIVE THICKNESS DETERMINATION OF SILICON NITRIDE FILMS DEPOSITED ON SILICON

CONSTANTIN-EUGEN MOROȘANU* and EUGEN SEGAL **

* Chemical Vapor Deposition Group, Research Institute for Electronic Components, ICCE, Str. Erou Iancu Nicolae 32B, R 72996, Bucharest, Romania

** Chair of Physical Chemistry and Electrochemical Technology, Polytechnic Institute of Bucharest, Bd. Republicii 13, Romania

Received October 14, 1977

The thickness of the silicon nitride thin films deposited on the silicon substrates can be determined by using infrared transmission and reflectance spectra. The absorption band half-width, the peak optical density and the absorption band area, obtained from the transmission spectrum, depend linearly on the Si_3N_4 thickness. The minimum wavelength due to the interference phenomenon and some parameters characterizing the extremes from the Si—N bond absorption region, obtained from the reflection spectrum, can be correlated with Si_3N_4 thickness.

INTRODUCTION

Among the various techniques for determining the thickness of the thin films deposited on silicon substrates, the methods based on transmission (absorption) and reflection spectra in the infrared range, have been widely used.

A. TECHNIQUES BASED ON TRANSMISSION (ABSORPTION) SPECTRA

Infrared absorption technique has been used for the measurement of the thickness of silicon dioxide films deposited on silicon substrates.[1,2] By using the infrared absorbance bands of silicon dioxide films at 9.2μ and 12.1μ, it has been shown that the optical density (at 9.2 or 12.1μ) depends linearly in SiO_2 film thickness deposited on silicon. Pliskin and Esch [3] used infrared transmission spectra for the measurement of SiO_2 films on silicon wafers. Mogab [4] suggested the measurement of film thickness from lattice absorption bands according to the formulas given by classical dispersion theory.

THEORETICAL BASIS

As previously shown, either transmission or absorption infrared spectra are useful in the determination of the thickness of the thin films deposited on silicon substrates.

In the case of either absorption or transmission spectra, the Lambert law gives the dependence of the optical density (extinction E) on the deposited thickness (d) : $E = kd$, where k is the extinction coefficient and the extinction is given by the following relationship :[3]

$$E = \log \frac{T_{0\bar{\nu}}}{T_{\bar{\nu}}}$$

$T_{\bar{\nu}}$ being the transmission corresponding to the absorption maximum and $T_{0\bar{\nu}}$ the transmission corresponding to the base level at the same wavenumber (Fig. 1).

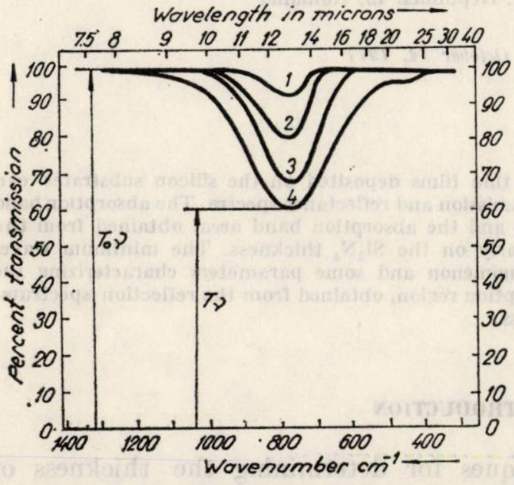

Fig. 1. — Infrared transmission spectra for silicon nitride films of various thickness deposited on silicon substrates. *1.* **2000 Å Si_3N_4 ;** *2.* **3000 Å Si_3N_4 ;** *3.* **4000 Å Si_3N_4 ;** *4.* **5000 Å Si_3N_4.**

Pliskin and Esch [3] pointed out that, the integrated band intensity (the area A under a plot of optical density vs. wavenumber), rather than the peak optical density, is a linear function of SiO_2 thickness :

$$A = E(\bar{\nu})\,d\bar{\nu} = d \int k(\bar{\nu})\,d\bar{\nu} = \int \log \frac{T_{0\bar{\nu}}}{T_{\bar{\nu}}} d\bar{\nu} = \frac{1}{2.3} \int \ln \frac{T_{0\bar{\nu}}}{T_{\bar{\nu}}} d\,\bar{\nu}$$

B. TECHNIQUES BASED ON REFLECTANCE SPECTRA

Using the reflectance spectra in the infrared range, the thicknesses of SiO_2 films deposited in Si,[5] of epitaxial Si deposited on Si[6-13] and of polycrystalline Si deposited on oxidized silicon,[14] were measured.

THEORETICAL BASIS

The reflectance spectrum is plotted as reflectance (ratio of reflected radiation intensity to incident radiation intensity) vs. wavenumber.

The reflectance can be calculated as a function of film thickness d, refractive index n_1 and extinction coefficient k_1 of the film, refractive index n_2, extinction coefficient k_2 of the substrate and the angle of incidence θ.

Indeed, the reflectance of an air-film-substrate system is given by :[11]

$$R = \frac{r_1^2 + r_2^2 - 2r_1r_2\cos(\delta - \emptyset)}{1 + r_1^2r_2^2 - 2r_1r_2\cos(\delta - \emptyset)} \qquad (1)$$

where

$$r_1^2 = [(n_1 - 1)^2 + k_1^2] \;/\; [(n_1 + 1)^2 + k_1^2]$$

$$r_2^2 = [(n_2 - n_1)^2 + k_2^2]/[(n_2 + n_1)^2 + k_2^2]$$

$$\delta = (4\pi n_1 d/\lambda)\,[1 - (1/n_1^2)\sin^2\theta]^{1/2}$$

$$\emptyset = \tan^{-1}[2n_1k_2/(n_1^2 - n_2^2 - k_2^2)]$$

Here, R is the reflectance, r_1 and r_2 are the amplitudes of the reflectance, δ is the optical phase difference in reflection, $\emptyset$ represents the phase shift on reflection at the film-substrate interface, θ is the angle of incidence on the infrared radiation, d is the film thickness, λ is the wavelength of the infrared radiation, n_1 and k_1 are the refractive index and the extinction coefficient of the thin film, n_2 and k_2 are the refractive index and the extinction coefficient of the silicon substrate.

Thus, as a rule, the thickness d could be determined from the rather complicated formulas discussed above.

In practice, it is easier to use the two characteristic zones of the reflectance-wavenumber curve :

— a region corresponding to the interference phenomenon of the reflected beams ;

— a region corresponding to the absorption phenomenon due to the resonance vibration of the Si—N or Si—O bond.

The variations in the reflection spectrum due to the interference and absorption can be correlated with the thickness of dielectric film deposited on silicon.

1°. Thickness determination from interference data

The thickness of the deposited film can be evaluated using the usual equation, which expresses the condition of interference :

$$d = \frac{P \cdot \lambda_{\min}}{2(n_1^2 - \sin^2\theta)^{1/2}} \qquad (2)$$

where :

d = the thickness of the deposited film

n_1 = the refractive index of the film

θ = the angle of incidence

λ_{min} = the wavelength corresponding to the minimum in reflectivity, where a destructive interference appears

P = the order number, which is 1/2 for the first minimum of the destructive interference.

2°. Thickness determination by using the absorption phenomenon

In the region of the resonance vibration of the Si—N bond (9 — 16μ, maximum absorption at near 12μ), the refractive index n and the extinction coefficient K_1 reach a maximum. According to formula (1), in this region, the reflectance will show a maximum.[5]

This variation of the reflectance can be correlated with the deposited film thickness. With the help of the obtained calibration curves (the dependence of the maximum reflectivity R_{max}, the wavelength corresponding to the reflection maximum $\lambda_{R\,max}$, or minimum reflectivity R_{min} as a function of the thickness of Si_3N_4 films), an unknown thickness can be determined.

In the present work, the thickness of the silicon nitride films deposited on silicon substrates is determined from the infrared transmission and reflection spectra.

EXPERIMENTAL

The measurements were made using a Beckman Acculab 6 double beam infrared spectrophotometer working in the range 4 000 — 250 cm^{-1} (2.5 — 40μ).

In the reflectance measurements, the instrument is provided with the specular reflectance attachment.

The transmission spectra were recorded against an uncovered silicon wafer.

The depositions of the silicon nitride films on doped silicon were performed at 700°, from N gas (1% silane + 99% ammonia) in an induction-heated horizontal reactor described earlier.[15]

The thickness of the silicon nitride films were measured with the Talysurf IV instrument.

RESULTS AND DISCUSSION

The transmission spectra (Fig. 1) were recorded in the absorption region corresponding to the resonance vibration of the Si—N bond (9 — 16μ), for various silicon nitride thicknesses, in the useful range 1000 — 5 000 Å.

Each of the following values calculated from the obtained spectra is proportional to Si_3N_4 film thickness :

1. Half-width (the width of the band at half maximum absorbance, Fig. 2).

2. Extinction (optical density) calculated according to the relation $E = \lg(T_{0\bar{\nu}}/T_{\bar{\nu}})$ (Fig. 3).

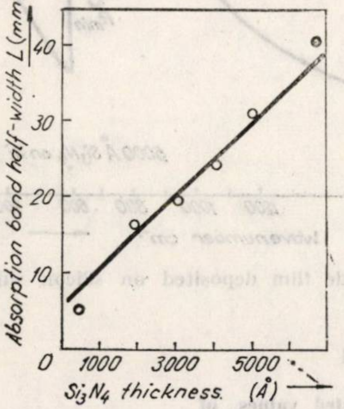

Fig. 2. Absorption band half-width vs. Si_3N_4 film thickness.

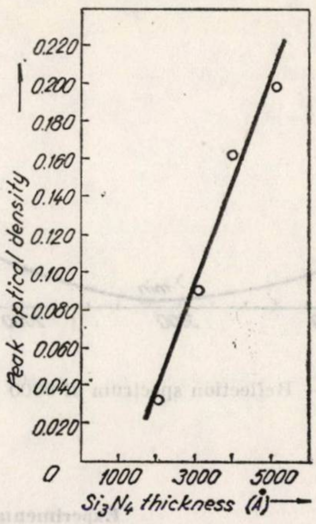

Fig. 3. — Peak optical density vs. Si_3N_4 film thickness.

3. The area under the absorption band (Fig. 4).

The reflection spectra were recorded in the range 2.5 — 40μ (Fig. 5).

— The existence of a minimum reflectance whose position is varying with thickness of the Si_3N_4 film is confirmed experimentally. Indeed, using the formula (2), where $P = 1/2$, $n_1 = 1.95$, $\theta = 30°$, reading λ_{min} on the graph, we can calculate d.

Table 1 includes the experimental and calculated values of λ_{min}. A good agreement between the two sets of data can be noticed.

— The reflection spectrum of the silicon nitride film deposited on single crystal silicon wafers shows, in the region corresponding to Si—N absorption, according to the previous theoretical considerations, the following characteristic values : R_{max}, (maximum reflectivity), $\lambda_{R_{max}}$ (the wavelength corresponding to maximum reflectivity), R_{min} (minimum reflectivity). These values (R_{max}, $\lambda_{R_{max}}$, R_{min}) and the difference ($R_{max} - R_{min}$) depend on the thickness of the silicon nitride film.

Variation of R_{max} with thickness **is presented in Figure 6. As thickness increases, R_{max} also increases.**

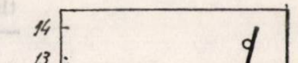

Fig. 4. — Area under the absorption band vs. Si_3N_4 film thickness.

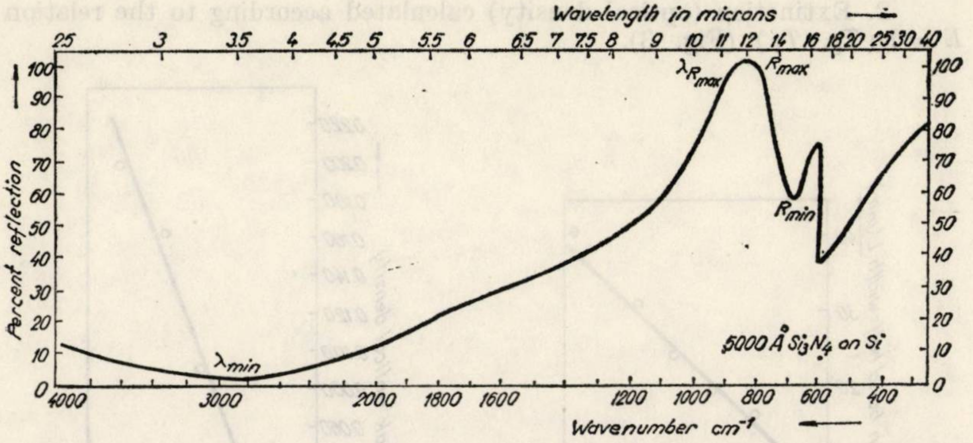

Fig. 5. — Reflection spectrum of 5000 Å silicon nitride film deposited on silicon substrate.

TABLE 1

Experimental and calculated values of the wavelength corresponding to the minimum reflectivity (λ_{min}), for various Si_3N_4 thickness

Si_3N_4 thickness (Å)	λ_{min} (calc) (μ)	λ_{min} (exp) (μ)
5 000	3.80	3.6
4 000	3.04	3.12
3 000	2.28	2.5
2 000	1.52	—

Variation of R_{min} with thickness is shown in Figure 7. R_{min} decreases with increasing thickness.

Variation of the difference ($R_{max} - R_{min}$) with thickness. As shown in Figure 8, the difference between maximum and minimum reflectivity is directly proportional to the thickness.

Variation of $\lambda_{R\,max}$ with thickness. It has been found that $\lambda_{R\,max}$ decreases with increasing thickness (Fig. 9).

The results obtained by using transmission and reflection spectra for the measurement of Si_3N_4 film thickness are in satisfactory agreement (within ± 5%) in almost all cases (Table 2).

CONCLUSION

The transmission and reflection spectra in the infrared, has been found useful for nondestructive determination of the thickness of thin silicon nitride films deposited on silicon substrates.

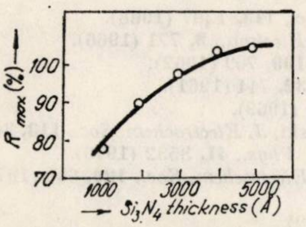

Fig. 6. — Maximum reflectivity (R_{max}) vs. Si_3N_4 film thickness.

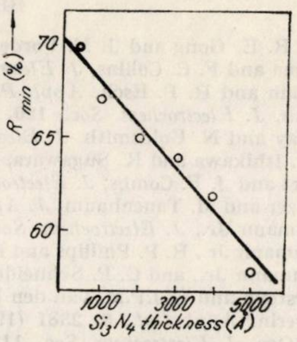

Fig. 7. — Minimum reflectivity (R_{min}) vs. Si_3N_4 film thickness.

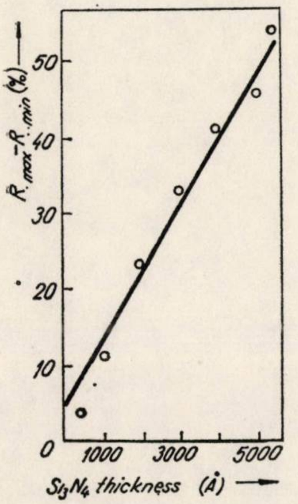

Fig. 8. The difference (R_{max}—R_{min}) vs. Si_3N_4 film thickness.

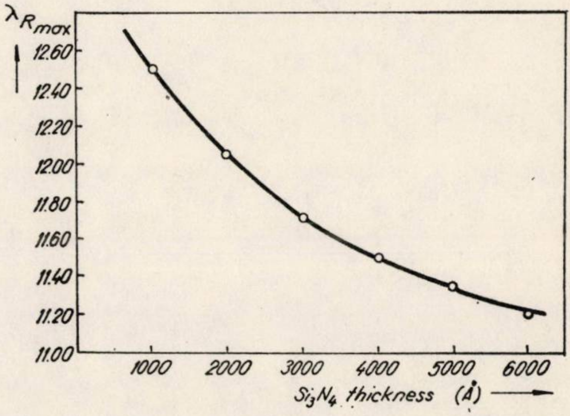

Fig. 9. — The dependence of the wavelength corresponding to the maximum reflectivity ($\lambda_{R\ max}$) on Si_3N_4 thickness.

TABLE 2

A comparison of the Si_3N_4 thickness measurements by using infrared transmission and reflection spectra

Si_3N_4 thickness (Å) measured using:		
Tallysurf IV instrument	IR transmission spectra	IR reflection spectra
1 500	1 400	1 460
2 500	2 540	2 480
3 500	3 450	3 600
4 500	4 700	4 650

REFERENCES

[1] J. E. Dial, R. E. Gong and J. N. Fordemwalt, *J. Electrochem. Soc.*, **115**, 326 (1968).
[2] T. Nakayama and F. C. Collins, *J. Electrochem. Soc.*, **113**, 706 (1966).
[3] W. A. Pliskin and R. P. Esch, *Appl. Phys. Lett.*, **11**, 257 (1967).
[4] C. J. Mogab, *J. Electrochem. Soc.*, **120**, 932 (1973).
[5] L. A. Murray and N. Goldsmith, *J. Electrochem. Soc.*, **113**, 1297 (1966).
[6] K. Sato, Y. Ishikawa and K. Sugawara, *Solid-State Electron.*, **9**, 771 (1966).
[7] M. P. Albert and J. F. Combs, *J. Electrochem. Soc.*, **109**, 709 (1962).
[8] W. G. Spitzer and M. Tanenbaum, *J. Appl. Phys.*, **32**, 744 (1961).
[9] P. A. Schumann Jr., *J. Electrochem. Soc.*, **116**, 409 (1969).
[10] P. A. Schumann Jr., R. P. Phillips and P. J. Olshefski, *J. Electrochem. Soc.*, **113**, 368 (1966).
[11] P. A. Schumann Jr., and C. P. Schneider, *J. Appl. Phys.*, **41**, 3532 (1970).
[12] F. C. Eversteyn and G.J.P.M. van den Heuvel, *J. Electrochem. Soc.*, **120**, 699 (1973).
[13] P. J. Severin, *Appl. Opt.*, **9**, 2381 (1970).
[14] C. J. Dell'Oca, *J. Electrochem. Soc.*, **119**, 108 (1972).
[15] C. E. Moroşanu and E. Segal, *Rev. Roumaine Chim.*, **23**, 515 (1978).

Revue Roumaine de Chimie, **25**, *1*, 55 – 65 (1980)

STUDIES OF ALLOY FORMATION AND SURFACE PROPERTIES IN Ni – Cu SYSTEMS

M.I. VASS, and CR. CONȚESCU
Institute of Physical Chemistry Bucharest, Splaiul Independenței 202, Romania

Received April : 22, 1978

Bimetallic Ni – Cu catalysts have been studied by means of magnetic, adsorption and catalytic activity measurements. A model for the structure of metallic particles in these catalysts was advanced.

1. INTRODUCTION

The study of bimetallic Ni – Cu type catalysts has been the object of many investigations. However, the relations between the structure, composition, surface properties and catalytic behaviour of these catalysts are not thoroughly understood.

For the reaction of ethylene hydrogenation, the literature offers many experimental results which can be divided, according to the variation of catalytic activity with Ni content, in the following three groups : (i) linear variation as expected by the band theory ;[1] (ii) higher activity for alloys in the middle range of composition ;[2–4] (iii) smaller activity than pure Ni, but constant for a wide range of Ni concentration.[4–6]

Understanding of the catalytic phenomena makes necessary the knowledge of the real structure and composition of the surface, which may be different from the bulk ones. For thin films, Sachtler[6,7] proved that the surface of Ni–Cu alloys shows a constant composition for a large range of Ni concentrations. The same author showed[8] that the so called "cherry" model applies to laminated or thin layer alloys, but is inadequate for very small particles. On the other hand, it is well known that the introduction of Cu or CuO in Ni catalysts enhances the NiO reduction and decreases the required temperature.[9–11]

The aim of the present work is to point out the influence of Cu on the NiO reducibility, and the magnetic, adsorptive and catalytic properties of Ni catalysts. The properties of a large series supported and unsupported catalysts of NiCu were systematically investigated. A new model of metallic particles in these systems is advanced, as it results from our data.

2. EXPERIMENTAL METHODS

2.1. CATALYSTS PREPARATION

Two groups each of 10 NiCu catalysts, with Cu contents between 0 and 90 % were prepared. The former is formed by NiCu catalysts, supported on kieselgur with metal loading of 50 % wt. The latter contains unsupported NiCu samples. The supported catalysts were prepared by coprecipitation of Ni and Cu hydroxides in a suspension of kieselgur under a vigurous stirring. The precipitates were filtered, washed and dried at 120°, then calcinated at 350° for 3 hours.

The reduction with hydrogen of all the supported samples was carried out at 400° (4 hours) and 1000° (4 hours); in this way the "normal" and "alloyed" series were respectively obtained.

The unsupported samples were prepared in the same manner. They have been used for the study of the reduction kinetics at 225° by means of a magnetic method. The grains of 0.3 — 0.8 mm size were used for our studies. The kieselgur used as support has 6.95 m^2/g surface area.

2.2. MEASUREMENT OF SPECIFIC MAGNETIZATION AND REDUCTION OF NiO.

The specific saturation magnetization of nickel was used both for the study of reduction kinetics of NiO in unsupported samples and for the magnetic characterization of NiCu alloy. The values of the saturation magnetization of different samples were used to check the NiCu solid solutions formation and to determine the degree of reduction for Ni.

The kinetics of NiO reduction was measured only for unsupported samples. The study of reduction for supported catalysts by magnetic method was not possible because the reduction temperatures were higher than the Curie temperature for Ni. After an activation *in situ* with hydrogen at 300°, for 1.5 h, the NiCu/kieselgur catalysts from the "normal" and "alloyed" series were tested at room temperature and the specific saturation magnetizations were measured. The mixed oxide samples were reduced with hydrogen *in situ* in an a.c. permeameter, previously described.[12,13] The reduction temperature was 225°, and the flow rate of purified hydrogen was 0.8 ml/s. Samples of 2—3 g were used.

At constant temperature, the degree of NiO reduction α is given by the ratio between the specific magnetization at time t, $\sigma_s(t)$, and the same value for the complete reduced sample $\sigma_s(t_\infty)$:

$$\alpha(t) = \frac{\sigma_s(t)}{\sigma_s(t_\infty)} \qquad (1)$$

The reduction isotherms at 225° for all unsupported oxide samples were plotted. For the NiCu/kieselgur catalysts, the magnetization curves at room temperature and fields up to 800 Oe were also plotted.

2.3. DETERMINATION OF ADSORBED HYDROGEN AMOUNT

In order to obtain information on the surface composition of NiCu supported cataylsts, hydrogen chemisorption at 25° was measured, in the equilibrium pressure range of 0,2 — 20 torr. A high vacuum volumetric apparatus previously described[14,15] was used. The reduced samples of 2 g catalysts were outgased in high vacuum at 400°, and again reduced *in situ* at the same temperature, for 1 h. The high purity hydrogen for reduction and chemisorption was obtained by the selective desorption from spongious Pd.

2.4. DETERMINATION OF CATALYTIC ACTIVITY

The catalytic activity of NiCu/kieselgur catalysts in the test reaction of ethene hydrogenation was measured at normal pressure and 100° using a dynamic flow microreactor. The amount of catalyst was 0.5 cm^3 (0.2 g), the contact time was in the 0.20 — 0.55 s range and the initial $C_2H_4 : H_2$ ratio was 1 : 1 . The process was proved to take place in kinetic conditions.

The reaction products were analysed by means of a Pye Unicam gas chromatograph, using the thermal-conductibility detector. Before the reaction all the samples were activated in the reactor with hydrogen at 120° for 1.5 h.

3. RESULTS

3.1. NiO REDUCTION

It is well known that the reduction of supported NiO proceeds more difficultly than free NiO. In order to decrease the influence of support, different amounts of other metals and oxides are added[9-11] to NiO, favorizing the reduction conditions.

We have studied the influence of adding variable amounts of CuO on the NiO reduction. The appearance of metallic Ni (ferromagnetic) during the reduction of oxides mixture was made evident by magnetic measurements. The reduction isotherms at 225° for NiO + CuO samples, with the Cu increasing amounts are shown in Figure 1.

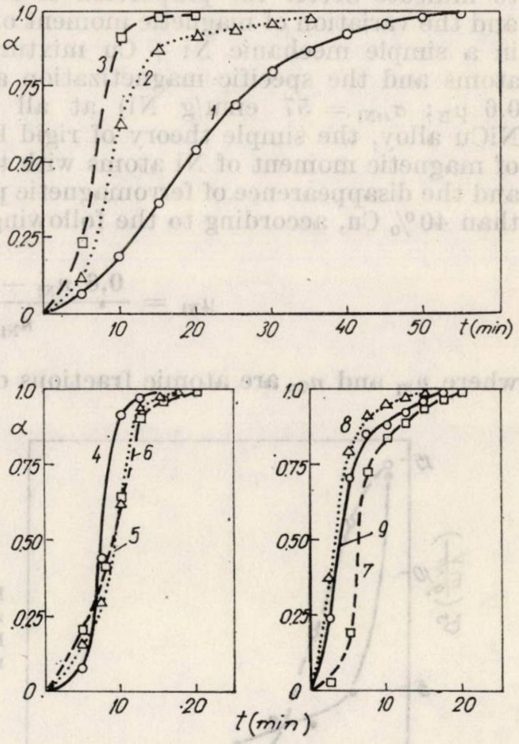

Fig. 1. — Reduction isotherm at 225° for NiO in the presence of variable Cu amounts. Sample composition : *1* — 100 % Ni ; *2* — 90 % Ni ; *3* — 80 % Ni ; *4* — 70 % Ni ; *5* — 60 % Ni ; *6* — 50 % Ni ; *7* — 40 % Ni ; *8* — 30 % Ni ; *9* — 20 % Ni.

The typical "S" shaped curves are characteristic for a self-accelerated process. In the linear portion of the reduction curves ($\alpha_{\min} < \alpha < \alpha_{\max}$), the variation of the reduction degree α in time, can be expressed by the following kinetic equation :

$$\alpha = k_{\bullet}(t - t_i) \tag{2}$$

The reduction process is described by two kinetic parameters : rate constant k_e and induction time t_i.

In the same figure an important increase of the reducibility by addition of 20% wt. Cu in metallic phase, can be observed. The reduction isotherms of samples with a higher Cu content are practically superposed, showing that the addition of Cu above a certain limit has not a cumulative effect.

3.2. SPECIFIC SATURATION MAGNETIZATION OF Ni

For the reduced samples the specific saturation magnetization σ_s depends on the number of the reduced Ni atoms, N_{Ni}, and on the magnetic moment of Ni atoms, μ_{Ni} :

$$\sigma_s = N_{Ni}\mu_{Ni} \tag{3}$$

The measured values for the saturation magnetization can be used to indicate better the proportion of Ni atoms formed during reduction and the variation of magnetic moment of Ni produced by alloying. Indeed, in a simple mechanic Ni + Cu mixture, the magnetic moment for Ni atoms and the specific magnetization at saturation are constant ($\mu_{Ni} = 0.6\ \mu_B$; $\sigma_{s,Ni} = 57$ emu/g Ni) at all compositions. When forming the NiCu alloy, the simple theory of rigid bands requires the linear decrease of magnetic moment of Ni atoms with the increasing of Cu concentration and the disappearence of ferromagnetic properties at concentrations higher than 40% Cu, according to the following equation

$$\mu_{Ni} = \frac{0,6\ n_{Ni} - 0.4\ n_{Cu}}{n_{Ni}}\,\mu_B \tag{4}$$

where n_{Ni} and n_{Cu} are atomic fractions of the both metals in the alloy.

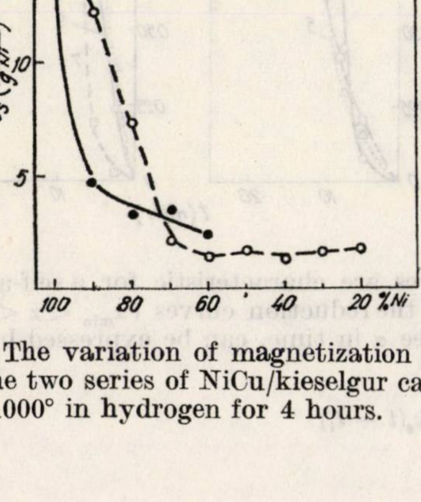

Fig. 2. — Specific saturation magnetization for Ni in NiCu/kieselgur catalysts. Continuous line — "normal" series ; dotted line — "alloyed" series.

The variation of magnetization at saturation is shown in Figure 2 for the two series of NiCu/kieselgur catalysts reduced respectively at 400° and 1000° in hydrogen for 4 hours.

For the same composition the values of the specific magnetization at saturation are lower for catalysts reduced at 400° than for those reduced at 1000°. This difference is likely due to the incomplete reduction of NiO at 400°. The straight line variation of σ_s and the zero value at room temperature for 40 % Cu, is a proof for NiCu alloy formation by reduction at 1000°.

3.3. HYDROGEN CHEMISORPTION

The chemisorption of hydrogen at 25° was studied for all supported catalysts obtained both at 400° and 1000°. The variation of chemisorption at saturation, versus Ni and Cu content, for both the "normal" and "alloyed" series is presented in Figure 3.

In the "normal" series (Fig. 3a) the maximum adsorbed amount is on the Cu — free catalyst. When adding 10 % Cu, the chemisorptive capacity decreases with 20 %. By further adding Cu in catalysts the adsorption at saturation linearly decreases and cancels at zero Ni concentration as expected.

For the catalysts reduced at 1000° ("alloyed" series) (Fig. 3b), the adsorptions are nearly one order of magnitude smaller, certainly because some sinterisation takes place. Two regions of variation of adsorbing capacity with Cu content can be observed. In the first one there is a pronounced decrease till 70 % Ni, followed in the second region by a much slower decrease. The slope changing in Fig. 3b is a first signal that the structure of surface for the "alloyed" catalysts modifies beginning from 70 % Ni (30 % Cu).

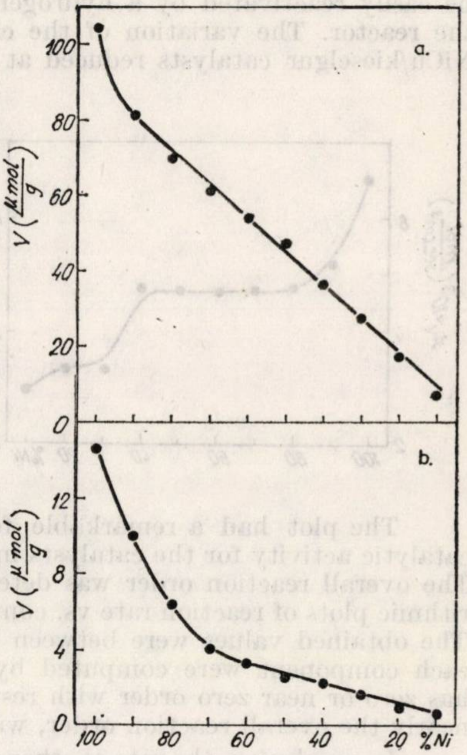

Fig. 3. — Hydrogen chemisorption at 25° at saturation on NiCu/ kieselgur catalysts : (a) "normal" series ; (b) "alloyed" series.

3.4. THE CATALYTIC ACTIVITY FOR ETHENE HYDROGENATION

The catalytic activity ($A_{v,m}$) in the reaction of ethene hydrogenation was expressed by the ratio between the reaction rate (for the same contact time) and the volume or mass unity of catalysts

$$A_v = \frac{c^0_{C_2H_4}}{V} \cdot \frac{dx}{dt} \; ; A_m = \frac{c^0_{C_2H_4}}{m} \cdot \frac{dx}{dt} \qquad (5)$$

where :

$c^0_{C_2H_4}$ = initial ethene concentration (moles/cm^3)

V, m = the volume (cm^3) and mass (g)

x = conversion (%) at contact time $t(s)$.

The stability to oxidation of catalysts from "normal" series is very low and their reactivation with hydrogen at 120° inside the microreactor was not sufficient. All these catalysts exhibited low activities, decreasing with Ni content ($4 \cdot 10^{-4}$ moles/s. cm^3 for the catalyst containing 50% Ni). A more detailed study was made on the catalysts from the "alloyed" series. They had a remarkable stability to oxidation and could be easily reactivated by a hydrogen pretreatment at 120° (1.5 h) inside the reactor. The variation of the catalytic activity with Ni content in NiCu/kieselgur catalysts reduced at 1000° is presented in Figure 4.

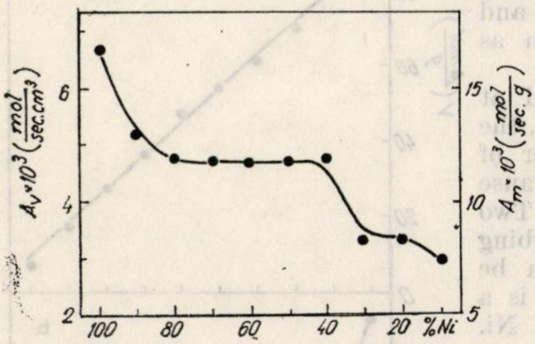

Fig. 4. — Catalytic activity of catalysts in "alloyed" series.

The plot had a remarkable feature, namely the constant value of catalytic activity for the catalysts in the range of 80 — 40% Ni contents. The overall reaction order was determined from the slope of semilogarithmic plots of reaction rate vs. conversion for 1 : 1 ratio of the reactants. The obtained values were between 0.55 and 0.80. The reaction orders for each component were computed by the Ostwald method. The reaction has zero or near zero order with respect to C_2H_4 and a fractionary order, nearly the overall reaction order, with respect to H_2.

In conclusion, the rate of ethene hydrogenation reaction on catalysts of the "alloyed" series can be written as follows :

$$-\frac{dp_{C_2H_4}}{dt} = k\,p^{m}_{H_2}\,p^{n}_{C_2H_4} \qquad (6)$$

where $n \approx 0$ and $0.55 < m < 0.80$ This expression of the rate equation supports an Eley-Rideal mechanism.[16]

4. DISCUSSIONS

Our results concerning the reduction of NiO + CuO with H_2 at 220° presented in Figure 1, showed that introduction of 20% Cu in the oxide mixture has an accelerating effect. This behaviour is better illustrated when comparing the values of kinetic constants k_e and of corresponding induction times t_i. In Figure 5 we present the values of induction time for NiO reduction in the NiO + CuO mixture. There are also presented the values $t_{0.25}$ and $t_{0.5}$ which are the times when the reduction degree becomes 0.25 and 0.5 respectively.

The values of apparent rate constant k_e for NiO reduction are presented in Figure 6.

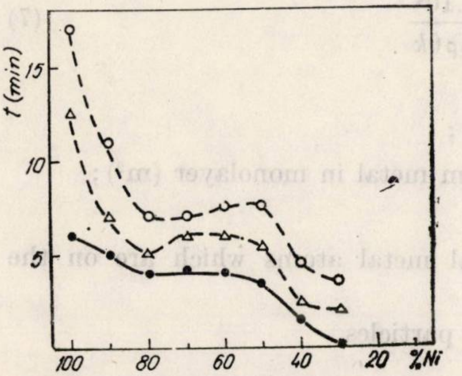

Fig. 5. — The influence of Cu addition on the reduction of NiO with hydrogen. The values of induction time t_i(.) and of $t_{0.25}$ (△); $t_{0.5}$ (○) are presented.

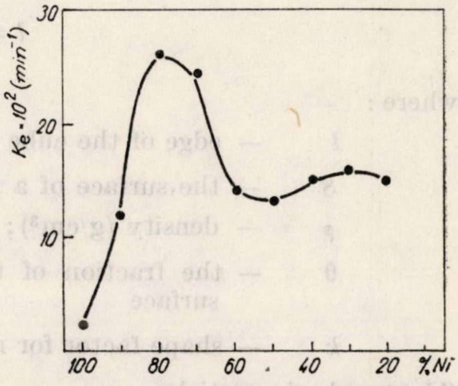

Fig. 6. — The influence of Cu addition on the NiO reduction. The values for the apparent rate constant k_e are presented.

By examining the both figures it results that the addition of Cu causes the decrease of the induction time t_i and of $t_{0.5}$, $t_{0.25}$ times. Practically the reduction of NiO does not need any induction time for an excess larger than 70% Cu. The reduction takes place with maximum rate for 20 — 30% Cu, where the rate constant k_e is 13 times greater than in the absence of Cu. At higher Cu contents the rate constant has intermediate values, lower than those for 20 — 30% Cu, but still higher than those for free NiO. In our work conditions, the two oxides do not simultaneously reduce. The free Gibbs energy for CuO reduction is $\Delta G^\circ = -24.2$ kcal/mole and for NiO reduction $\Delta G^\circ = -2.9$ kcal/mole. This difference shows the greater reducibility of CuO. The reduction of NiO starts after CuO has been completely reduced and takes place in contact with the previously formed metallic Cu.

The mechanism of the accelerating action of Cu in the reduction of NiO has not yet been sufficiently clarified. However, the mechanism advanced by Charcosset and Delmon [17] is valuable to explain our results. According to this mechanism, on the surface of metallic Cu active hydrogen species with high mobility occur. They reach the surface of NiO grains by spill over effects. These active species create metallic Ni nuclei and form the reaction interface Ni/NiO by whose advancement all the oxide phase will be completely reduced. We therefore conclude that catalytic action of Cu in reduction of NiO + CuO mixture is maximum for 20 — 30% Cu in metallic phase.

The size of active metal particles is an important parameter to characterize catalysts. The dispersion of metal particles was computed using the hydrogen selective chemisorption on the Ni component in catalysts. In this method the shape of metallic particles must be approximated as a cube [18] or a sphere. [19] In these cases the particle sizes can be expressed as follows :

(a) for cubic particles :

$$l = \frac{5.10^4}{S\rho\theta k} \tag{7}$$

where :

l — edge of the cube (Å) ;

S — the surface of a gram metal in monolayer (m^2) ;

ρ — density (g/cm^3) ;

θ — the fraction of total metal atoms which are on the surface

k — shape factor for real particles.

(b) for spheric particles :

$$\text{Ø} = \frac{6.10^{24}\,G}{A\rho d^2 k} \tag{8}$$

where :

Ø — diameter of the sphere (Å) ;

G — sample weight (g) ;

A — the number of H atoms chemisorbed on G grams of sample ;

d — lattice constant of metal (Å).

These two hypotheses introduce an idealizing factor because the actual shape of particles may be different from these simple models. In both methods the computation uses the amount of hydrogen chemisorbed at saturation on the active component (Ni), which is proportionally related to the Ni area on the metal particle surface. Taking into account that the surface of these particles also contains Cu atoms, which are inactive for hydrogen adsorption, it follows that the real particle size is greater than that presented. For NiCu/kieselgur catalysts in the "normal" series, the particle sizes computed from the adosrbed hydrogen amount was $90 Å < \tau < 110$ Å, respectively $85 Å < Ø < 104°$ Å. The metal particle size has a rather small variation with Cu content. Magnetic granulometry measurements following Dietz [20] led to values between 95 and 130Å. The shape factor $k = 5$ in formulae (7) and (8) was magnetically determined.

The hydrogen adsorption at saturation for the catalysts in the "alloyed" series is smaller (Fig. 3b) because of sintering during the treatment at 1000°. The particle size is much larger than that corresponding to catalysts in the "normal" series. The increasing of Cu content influences the size of adsorbant particles, which increases from 665Å to 2375 Å in the series. These results cannot be confirmed by magnetic granulometry since the method used in calculating the size of superparamagnetic particles does not apply to alloys where the Ni atomic magnetic moment depends on Cu content.

In order to explain the activity data for ethene hydrogenation on catalysts belonging to the "alloyed" series, the knowledge of Ni area, active in catalytic process, is necessary. To make clear the contribution of Ni to the active surface, a new parameter is defined, namely $s_{Ni}(m^2/g\,Ni) = S_{Ni}$ $(m^2/g$ catalyst) / (Ni content in samples). It is proportional to the θ value from Eq.(7), or in other words, to the fraction of Ni atoms which are on the surface from the total number of Ni atoms (considering that at saturation each Ni atom on the surface bonds one chemisorbed H atom). The variation of S_{Ni} with composition is given in Figure 7. After an initial decrease, s_{Ni} remains constant in the range of 70 — 30% Ni and then a new decrease follows.

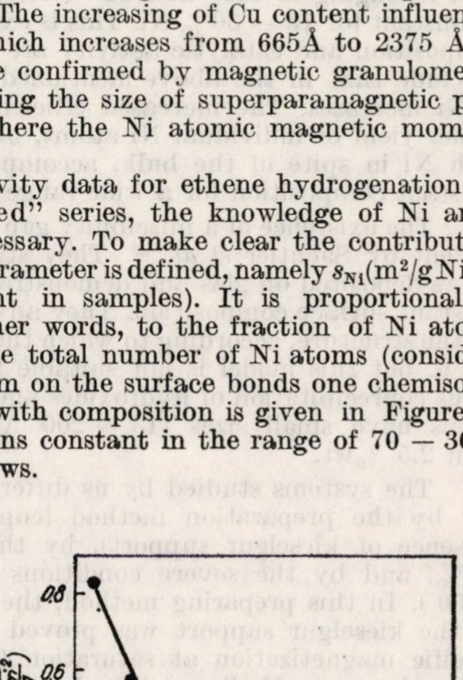

Fig. 7. — Variation of specific Ni area in the "alloyed" series.

By comparing the variation of Ni specific area, s_{Ni}, (Fig. 7) with the catalytic activity shown in Figure 4, their evident resemblance can be remarked. For catalysts belonging to the middle of series (70 — 30% Ni), both catalytic activity and specific Ni surface area are constant.

This behaviour could be explained considering that the catalytic action of surface Ni atoms in the ethene hydrogenation reaction is not influenced by alloying with Cu. This statement has a wider character; it applies to reactions involving C—H bonds, but not to reactions in which C—C bonds are formed or broken. [21] The more recently investigations on bimetallic alloy type catalysts led to the general conclusion that the most important factor which determines the catalytic activity and the adsorption properties is the real composition of the surface.

This conclusion is confirmed by our results, which can be understood in terms of the interval of constant composition of NiCu alloy surface under a large range of Ni and Cu content. Figure 7 shows that for catalysts belonging to the "alloyed" series, the surface exhibited by 1 g Ni is constant for 70 — 30% Ni. This is exactly the range where both surface composition and catalytic activity are constant. From this behaviour we conclude that in the above-mentioned composition range the usefulness of Ni increases. The increased efficiency could not be interpreted as a higher yield of individual Ni atoms, but as an enrichment of the surface with Ni in spite of the bulk, accompanied by the maintenance of this constant composition for a wide range of concentrations.

The existence of a miscibility gap in NiCu alloys was firstly rendered evident by Sachtler *et al.* [22] They studied NiCu alloys in form of thin layers deposited on glas and demonstrated the occurrence of a range with constant surface composition. They advanced the so called "cherry" model for the structure, according to which the core is richer in Ni and the surface in Cu, but this model is not suitable for catalysts obtained by simultaneous coprecipitation of hydroxides and support (SiO_2) where the metallic grains have small sizes (13 — 200 Å) and the Ni content is smaller than 2.5 %wt.

The systems studied by us differ from those investigated by Sachtler by the preparation method (coprecipitation of hydroxides in the presence of kieselgur support), by the high content of metallic phase (50%) and by the severe conditions of reduction and heat treatment (1000°). In this preparing method, the forming of an alloyed phase even on the kieselgur support was proved by the regulate decreasing of Ni specific magnetization at saturation (Fig. 2) and also by some X-rays diffraction tests. If alloy will be homogeneous for all catalysts in the series, then specific saturation magnetization will cancel at 60% Ni concentration. Our results showed on the contrary that even at smaller Ni content the "alloyed" samples keep magnetic properties and the saturation magnetization (for 1 g Ni) has constant values for all catalysts in the 70 — 30% Ni range (Fig. 2). This feature certainly indicates that within the above composition range the metallic grains in catalysts still contain domains of alloy with at least 60% Ni, which are responsible for the observed magnetization even for samples with a lower Ni content. Since the values of specific magnetization at saturation of these samples with low Ni content correspond well to the value for 70% Ni catalyst, we suppose that these samples contain magnetic domains of alloy with a constant composition, nearly 70% Ni.

On the other hand, the mentioned statements concerning the catalytic activity and the specific surface area of Ni in the "alloyed" series led us to assume the existence of a range of constant surface composition within 70 — 30%Ni. We conclude therefore that the surface of metallic grains in the range 70 – 30% Ni has an almost constant composition, approximately 70% Ni.

The forming of metallic grains on kieselgur support can be imagined according to the following model : in the range 100 – 70% Ni the metallic grains are formed by a homogeneous alloy, in which the surface composition and the bulk composition are the same. This fact is related to the linear decrease of specific saturation magnetization, Ni area and catalytic activity. Between 70–30% Ni the grains are composed by two alloy phases, where the surface phase maintanis a constant composition of approximately 70% Ni and the core is richer in Cu. This is supported by the constant values of specific magnetization, specific Ni surface and catalytic activity. Finally, at low Ni concentrations the Ni content in surface decreases.

The advanced model differs from Sachtler's "cherry" model both in the distribution of the two alloy phases in bulk and on the surface and in their supposed composition. These differences are ascribed to the preparation method and especially to the action of the kieselgur support, which modifies the thermodynamic premises which fundamentates Sachtler's model.

The nature of metal-metal and metal-support interactions in supported bimetallic catalysts, represents the field of an increasing interest, promising for further works.

REFERENCES

[1] T. Takeuki, M. Sagakuki, I. Myoshi and T. Takaleatake, *Bull. Chem. Soc. Japan*, **35**, 1390 (1962).
[2] R. J. Best and W. W. Russell, *J. Amer. Chem. Soc.*, **76**, 838 (1954).
[3] W. K. Hall and P. H. Emmett, *J. Phys. Chem.*, **63**, 1102 (1959).
[4] T. Takeuki, Y. Teuzuka and O. Takayasu, *J. Catalysis*, **14**, 126 (1969).
[5] G. M. Schwab and W. Brennecke, *Z. phys. Chem. (Frankfurt)*, **24**, 393 (1933).
[6] W. M. H. Sachtler and C. J. M. Dorgelo, *J. Catalysis*, **4**, 654 (1965).
[7] W. M. H. Sachtler and J. Jongepier, *J. Catalysis*, **4**, 665 (1965).
[8] S. D. Robertson, S. C. Kloet and W. M. H. Sachtler, *J. Catalysis*, **39**, 234 (1975).
[9] H. Charcosset, R. Frety, P. Grange and Y. Trambouze, *Compt. rend. Ser. C.*, **267**, 1746 (1968).
[10] H. Charcosset, R. Frety, A. Soldat and Y. Trambouze, *J. Catalysis*, **22**, 204 (1971).
[11] A. Roman and B. Delmon, *Compt. rend. Ser. C.*, **273**, 94 (1971).
[12] T. Chirulescu, *Studii şi Cercetări Chim. Acad. R.S.R.*, **22**, 169 (1974).
[13] T. Chirulescu, *Studii şi Cercetări Chim. Acad. R.S.R.*, **16**, 105 (1968).
[14] D. Cismaru and Al. Fruma, *Rev. Roumaine Chim.*, **14**, 1489 (1969).
[15] I. V. Nicolescu, Al. Fruma and I. Suciu, *Rev. Roumaine Chim.*, **16**, 91 (1971).
[16] C. C. Bond "Catalysis by Metals", Academic Press, New York, 1962.
[17] H. Charcosset and B. Delmon, *Ind. chim. belge*, **38**, 481 (1971).
[18] L. Spenadel and M. Boudart, *J. Phys. Chem.*, **64**, 204 (1960).
[19] Al. Fruma, *Internat. Chem. Engineering*, **12**, 503 (1972).
[20] R. E. Dietz and P. W. Selwood, *J. Chem. Phys.*, **35**, 270 (1961).
[21] V. Ponec and W. M. H. Sachtler, "Proc. 5-th Intern. Congress on Catalysis", Acad. Press, New York, 1972.
[22] W. M. H. Sachtler, G. J. M. Dorgelo and R. Jongepier, *J. Catalysis*, **4**, 100 (1969).

grains in the range 70 — 30% Ni has an almost constant composition, approximately 70% Ni.

The forming of metallic grains on kieselgur support can be imagined according to the following model : in the range 100 — 70% Ni the metallic grains are formed by a homogeneous alloy, in which the surface composition and the bulk composition are the same. This fact is related to the linear decrease of specific saturation magnetization, Ni area and catalytic activity. Between 70—30% Ni the grains are composed by two alloy phases, where the surface phase maintains a constant composition of approximately 70% Ni and the core is richer in Cu. This is supported by the constant values of specific magnetization, specific Ni surface and catalytic activity. Finally, at low Ni concentrations the Ni content in surface decreases.

The advanced model differs from Sachtler's "cherry" model both in the distribution of the two alloy phases in bulk and on the surface and in their supposed composition. These differences are ascribed to the preparation method and especially to the action of the kieselgur support, which modifies the thermodynamic premises which fundamentates Sachtler's model.

The nature of metal-metal and metal-support interactions in supported bimetallic catalysts, represents the field of an increasing interest, promising for further works.

REFERENCES

[1] T. Takeuki, M. Sagakuki, I. Myoshi and T. Takahatake, *Bull. Chem. Soc. Japan*, **35**, 1390 (1962).
[2] R. J. Best and W. W. Russell, *J. Amer. Chem. Soc.*, **76**, 838 (1954).
[3] W. K. Hall and P. H. Emmett, *J. Phys. Chem.*, **63**, 1102 (1959).
[4] T. Takeuki, Y. Tezuka and O. Takayasu, *J. Catalysis*, **14**, 126 (1969).
[5] G. M. Schwab and W. Brennecke, *Z. phys. Chem.* (*Frankfurt*), **24**, 393 (1933).
[6] W. M. H. Sachtler and G. J. M. Dorgelo, *J. Catalysis*, **4**, 654 (1965).
[7] W. M. H. Sachtler and J. Jongepier, *J. Catalysis*, **4**, 665 (1965).
[8] S. D. Robertson, S. C. Kloet and W. M. H. Sachtler, *J. Catalysis*, **39**, 234 (1975).
[9] H. Charcosset, R. Frety, P. Grange and Y. Trambouze, *Compt. rend. Ser. C.*, **267**, 1746 (1968).
[10] H. Charcosset, R. Frety, A. Soldat and Y. Trambouze, *J. Catalysis* **22**, 204 (1971).
[11] A. Roman and B. Delmon, *Compt. rend. Ser. C.*, **273**, 94 (1971).
[12] T. Chirulescu, *Studii și Cercetări Chim. Acad. R.S.R.*, **22**, 169 (1974).
[13] T. Chirulescu, *Studii și Cercetări Chim. Acad. R.S.R.*, **16**, 105 (1968).
[14] D. Gismaru and Al. Pruna, *Rev. Roumaine Chim.*, **14**, 1459 (1969).
[15] I. V. Nicolescu, Al. Pruna and I. Suciu, *Rev. Roumaine Chim.*, **16**, 91 (1971).
[16] G. C. Bond "Catalysis by Metals". Academic Press, New York, 1962.
[17] H. Charcosset and B. Delmon, *Ind. chim. belge*, **38**, 481 (1971).
[18] L. Spenadel and M. Boudart, *J. Phys. Chem.*, **64**, 204 (1960).
[19] Al. Pruna, *Internat. Chem. Engineering*, **12**, 593 (1972).
[20] R. E. Dietz and P. W. Selwood, *J. Chem. Phys.*, **35**, 270 (1961).
[21] V. Ponec and W. M. H. Sachtler, "Proc. 5-th Intern. Congress on Catalysis". Acad. Press, New York, 1972.
[22] W. M. H. Sachtler, G. J. M. Dorgelo and R. Jongepier, *J. Catalysis*, **4**, 100 (1965).

Revue Roumaine de Chimie, **25**, *7*, 67–73 (1980)

A THEORETICAL STUDY OF THE HYDRATION AND HYDRATION EFFECTS ON SOME SUBSTITUTED BENZOIC ACID MOLECULES. II

THE CALCULATION OF THE SUBSTITUENT EFFECT BY SEMIEMPIRICAL MO METHODS

S. GRIGORAŞ*, ANCA MEDEŞAN*, ILEANA RUSU* and Ş. MOLDOVEANU**
* Clinical Hospital Fundeni, Fundeni Street 37, Bucharest, Romania
** I.P.B., Faculty of Chemical Technology, Analyt. Chem. Dept., Splaiul Independenţei 202, Bucharest, Romania

Received October 25, 1978

This paper aims to obtain, by means of semiempirical MO calculations, the Hammett constants for several substituted benzoic acids. The results of this study prove the necessity to introduce the solvent effect and, also, the importance of the precision by which the electronic energy of the molecules considered is calculated.

INTRODUCTION

The influence of a substituent X on the aromatic ring of the benzoic acid upon the acidity of the latter, that is the influence of a substituent upon the reaction

$$AH \overset{K}{\rightleftarrows} A^{\bullet} + H^{\bullet} \qquad \text{(a)}$$

where A is $X - C_6H_4-COO$, is a problem much investigated, both experimentally and theoretically.[1–2]

The particular interest for the reaction (a) resides in the fact that if the COOH group is considered as a reaction centre, the effect of different substituents in *meta* or *para* upon this centre is observed to be proportional to the effect upon other reaction centres.

This observation led to the formulation of the Hammett equation, well-known in the organic chemistry :[3]

$$\lg \frac{K_X}{K_H} = \rho \sigma_X \qquad (1)$$

in which σ_X is the Hammett constant and ρ is a coefficient of proportionality which shows to what extent the effect of the substituent upon a reference reaction is transmitted to the reaction centre in the compared reaction.

The aim of the present paper is to try, by MO methods applied to substituted benzoic acids, to calculate the Hammett constant σ_X, for different substituents, namely CH_3, C_2H_5, NO_2, NH_2, OH, CN situated in *meta* or *para*, without or with the solvent influence.

Since, as a standard reaction for the Hammett equation, the ionization of the *m* and *p* substituted benzoic acids, that is, reaction (a) was arbitrarily chosen, it results $\rho = 1$ in equation (1) in this case, and thus :

$$\sigma_X = \log \frac{K_{X-C_6H_4-COOH}}{K_{C_6H_5-COOH}} \tag{2}$$

The calculation of the constants K could be done with the relation :

$$K = \exp\,(-\Delta G/RT) \tag{3}$$

ΔG being the variation of the free enthalpy in the reaction (a).

Even assuming, however, that the ΔG values for $X - C_6H_4 - COOH$ and C_6H_5COOH are corectly computed, in order to be in accord with the experiment the solvent effects have to be considered.

Thus, it was observed[4-5] that if the dissociation constants of the *m* and *p* substituted benzoic acids considered as reference, are determined in a solvent different from water, the coefficient ρ in equation (1) can be no more considered unity. For instance, if DMSO is taken as solvent, $\rho = 2.5$.

In order to analyse the solvent effect upon the reacting molecules we shall consider the following thermodynamic cycle :

$$\begin{tikzcd}
AH(g) \arrow[r, "\Delta G\text{ ionization}(g)"] \arrow[d, "\Delta G(s)(AH)"'] & A^-(g) \arrow[d, "\Delta G(s)(A^-)"'] & + \; H^+(g) \arrow[d, "\Delta G(s)(H^+)"] \\
AH(s) \arrow[r, "\Delta G\text{ ionization}(s)"] & A^-(s) & + \; H^+(s)
\end{tikzcd}$$

in which ΔG ionization is the free enthalpy of the ionization reaction, while the index (g) or (s) refers to the gazeous or the solution phase.

Considering this cycle, we have :

$$\Delta G\text{ ionization }(s) = \Delta G\text{ ionization}(g) -$$
$$- \Delta G(s)(AH) + \Delta G(s)\,H^+ + \Delta G(s)\,A^- \tag{4}$$

ΔG ionization (g) being given by the relation (the standard notation was employed) :

$$\Delta G\text{ ionization }(g) = \Delta H\text{ ionization }(g) - T\,\Delta S\text{ ionization }(g) \tag{5}$$

and neglecting the entropic term (which is relatively small[6]), it results that we can evaluate ΔG ionization (s) required in equation (3) if the variations of the enthalpies, ΔH ionization (g), and, also, $\Delta G(s)\mathrm{A}^-$ and $\Delta G(s)$ AH are known. $\Delta G(s)\mathrm{H}^+$ vanishes. The values of ΔH ionization (g) can be well approximated by the energy variations ΔW ionization (g) (at constant volume).

The attempts to correlate the Hammett constant with : $D_{\mathrm{H}}^{\mathrm{X}}(\Delta W)g = \Delta W$ ionization $\mathrm{X{-}C_6H_4COOH}(g) - \Delta W$ ionization $\mathrm{C_6H_5COOH}(g)$ alone showed that the quantities $\Delta G(s)\mathrm{A}^-$ and $\Delta G(s)\mathrm{AH}$ cannot be neglected, since there is no good correlation between σ_{X} and $D_{\mathrm{H}}^{\mathrm{X}}(\Delta W)g$ (see further).

This fact led to the attempt to evaluate ΔG ionization (s) directly or, to be more specific (on account of such considerents as those presented above), to the attempt to correlate the values of σ_{X} with $D_{\mathrm{H}}^{\mathrm{X}}(\Delta W)s$, where :

$$D_{\mathrm{H}}^{\mathrm{X}}(\Delta W)s = \Delta W \text{ ionization } \mathrm{X{-}C_6H_4{-}COOH}(s) - \\ - \Delta W \text{ ionization } \mathrm{C_6H_5COOH}(s) \qquad (7)$$

In the present paper, several approaches were used to this purpose, each of them and the corresponding results being presented below.

METHOD

The calculation of ΔW requires to know the values of the total energies for the compounds implied in reaction (a). Since in the relations (6) and (7) only the differences of ΔW values are considered, the energy of H^+ need not be calculated because the corresponding term would vanish, anyhow.

Thus, the energy of the neutral form, W_n, and the energy of the ionic form, W_i, remain to be computed.

When the hydration was not considered, the total energies of the molecules, W_n and W_i, were computed by means of the semiempirical MO methods EHT[7] and/or CNDO/2,[8] taking for the molecules the standard or optimized geometries as given in.[9]

The values of $D_{\mathrm{H}}^{\mathrm{X}}(\Delta W)g$ computed by the two methods differ (since the approximations used are essentially different), the CNDO/2 method being more trustworthy in these calculations.

There are several possibilities for the evaluation of $W_n(s)$ and $W_i(s)$, partly studied in this work, partly described elsewhere.[10] Thus, a first possibility is to use the supermolecule model for the hydrated molecules $\mathrm{X{-}C_6H_4{-}COOH \cdot 2H_2O}$, $\mathrm{X{-}C_6H_4{-}COO^- \cdot 2H_2O}$, where $\mathrm{X{=}H, CH_3, C_2H_5, NH_2, NO_2, OH, CN}$, for which the energies W_n and W_i to be evaluated as in the case of $W_i(g)$, $W_n(g)$, that is by means of a MO method, these energies being considered as $W_n(s)$ and $W_i(s)$. In these calculations, the standard and optimum geometries found in part I of this paper were used.[9]

A different approach consists of the calculation of the interactions with the solvent considering a simple model suggested by Born,[11] in spite of the fact that criticisms have been formulated against the use of this model in the case of non-ionic compounds.[12]

In the Born model (in the form proposed by Hoytink,[13] the solvation energy for a molecule in the solvent and considered as made up of a system of centres bearing the charges q_A, is given by (8) :

$$W\text{solv} = -\left[\sum_{A} \frac{q_A^2}{R_A} + \sum_{A} \sum_{B>A} \frac{q_A q_B}{R_{AB}}\right]\left(1 - \frac{1}{\varepsilon_s}\right) \tag{8}$$

where R_{AB} are the interatomic distances, R_A is the effective radius of the centre A and ε_s is the dielectric constant of the solvent.

The quantities q_A, which are the net changes on the centres of the molecule can be evaluated only by means of a MO method. In this paper, both the method EHT and the method CNDO/2 have been employed for this purpose.

In order to obtain a better agreement with the experiment of the charges computed by the method EHT, the calculated values were scaled with a coefficient of 0.43.[14]

The effective radius R_A corresponds, in the theory of Born, to the radius of the spherical cavity which contains the centre A, the creation of this cavity in the solvent leading to a variation of the energy given by the following relation :

$$\Delta W = -\frac{q_A}{2R_A}\left(1 - \frac{1}{\varepsilon_s}\right) \tag{9}$$

In the frame of a quantum method this cavity could be assimilated to a sphere of radius R_A in which there is a probability P to find the electrons belonging to the considered atom. It was considered that 0.95 would be a reasonable value for P.

According to,[13] P is given by :

$$P = 1 - \exp(-y) \cdot \sum_{N=0}^{2n} \frac{y^N}{N!} \tag{10}$$

with

$$y = 2(\xi_A + kq_A) \cdot R_A \tag{10'}$$

ξ_A being the Slater exponent for the last occupied atomic orbital in the atom A, n- the principal quantum number for the last shell occupied with electrons in A, and k — a shielding constant which is 0.3 for $n = 1$, and 0.35 for other values of n.

With the values of W solv and ΔW ionization(g) the values of ΔG ionization(s) can be calculated.

As W solv can be calculated also for the supermolecules $X-C_6H_4-COOH \cdot 2H_2O$, $X - C_6H_4-COO^- \cdot 2H_2O$, one can try to correlate σ_X with the energy of some molecules both hydrated and imbedded in the solvent.

RESULTS AND DISCUSSIONS

The results of the present study are summarized in table 1, in which the correlation coefficients between the constants σ_{X} in the *meta* and *para* series and the calculated values of the energies $D_{\mathrm{H}}^{\mathrm{X}}(\Delta W)$ (g) of the nonhydrated molecules, and $D_{\mathrm{H}}^{\mathrm{X}}(\Delta W)$ (g) of the molecules hydrated with 2 water molecules, with a standard or an optimized geometry (as presented in [9]), and $D_{\mathrm{H}}^{\mathrm{X}}(\Delta W)(s)$ of the nonhydrated, and $D_{\mathrm{H}}^{\mathrm{X}}(\Delta W)(s)$ of the already hydrated molecules are presented.

TABLE 1

The correlation coefficients values $\sigma_{\mathrm{X}} - D_{\mathrm{H}}^{\mathrm{X}}(\Delta W)$

Type of method and geometry	Substitution place	Type of molecule	Non-hydrated	Hydrated
EHT	*para*	Ideal gas	0.916197	0.942570
		solvated	0.913573	0.552764
	meta	Ideal gas	0.160789	0.358495
		solvated	0.992838	0.991683
CNDO/2 standard geometry	*para*	Ideal gas	0.475820	0.070775
		solvated	0.708841	0.053970
	meta	Ideal gas	0.952943	0.397499
		solvated	0.820097	0.038778
CNDO/2 optimizated geometry	*para*	Ideal gas	0.876037	0.713049
		solvated	0.351770	0.174334
	meta	Ideal gas	0.820251	0.355879
		solvated	0.154547	0.711889

In this table (in which the EHT and the CNDO/2 data are presented separately) one can see that, in order to get consistent results (correlation coefficients $r = 0.992831$ in the *meta* series and $r = 0.913565$ in the *para* series), the only reliable method is to employ the Born solvation model with charges calculated by the EHT method, all the other data remaining unsatisfactory.

This result cannot be, however, considered as satisfactory in what concerns the possibility of calculating the Hammett constants.

Indeed, if only solvation were considered and its effect as calculated with the model of Born, according to relation (8), it would imply that changing the solvent would exclusively influence by means of the factor $\left(1 - \frac{1}{\varepsilon_s}\right)$.

Calculating with the correlation linear dependence

$$\sigma_X = b + a\, D_H^X(\Delta W)$$

with $a = 3.52$ and $b = -0.07$ in the *para* series and $a = 5.9545$ $b = 0.036$ in the *meta* series and, taking $\varepsilon_{\text{water}} = 81$, the σ_X values obtained are given in table 2.

The values of σ_X for $\varepsilon = 43$, that is for $\varepsilon_{\text{DMSO}}$, using the same *a* and *b* are also presented in table 2.

TABLE 2

The values of Hammett constants and the calculated values for water and DMSO solvation

Substituent	Hammett constant	Calculated constant	
		H_2O	DMSO
p−OH	−0.370	−0.150	−0.149
p−CH_3	−0.170	−0.171	−0.170
p−C_2H_5	−0.151	−0.270	−0.268
p−MO_2	+0.778	+0.950	+0.940
p−NH_2	−0.660	−0.510	−0.500
p−CM	+0.660	+0.310	+0.310
m−OH	−0.121	−0.091	−0.090
m−CH_3	−0.069	−0.022	−0.022
m−C_2H_5	−0.070	−0.070	−0.069
m−NO_2	+0.710	+0.680	+0.673
m−NH_2	−0.160	−0.200	−0.200
m−CM	+0.560	+0.581	+0.574

It can be noticed that the two sets of σ_X values do not differ by the 2.5 factor, as given by the experiment,[4,5] a fact that shows that the solvent effect is not reduced to the one accountable to Born's.

However, the result of the study concerning the solvation energy in the model of Born with net charges given by the EHT is encouraging (see the good correlation), since it proves that this part of the total energy is correctly calculated (the values of the total electronic energies *W*(*g*) computed with the EHT affect the calculation but to a small extent since they are much underevaluated)

The calculation with the CNDO/2 data do not agree with the experiment, probably because, on the one hand, the charges are less correctly given than by the EHT, and, on the other, the electronic energy is not calculated well enough and has, at the same time, a greater weight.

REFERENCES

[1] O. Chalvet, M. J. Huron and F. Paradejordi, *Compt. rend.*, **259,** 1631 (1964).
[2] P. Birner, H. J. Kohler and C. Weiss, *Chem. Phys. Letters*, **27,** 347 (1974).
[3] L. P. Hammett, *J. Amer. Chem. Soc.*, **59,** 96 (1937).
[4] P. Letellier and R. Gaboriaud, *Bull. Soc. chim. France*, **1976,** 753.
[5] J. C. Halle and R. Schaal, *Analyt. Chim. Acta*, **60,** 197 (1972).
[6] D. H. Aue, H. M. Webb and M. T. Bowers, *J. Amer. Chem. Soc.*, **98,** 318 (1976).
[7] QCPE Catalog, vol. X, 1974, No. 64.
[8] J. A. Pople and D. L. Beveridge, "Approximate Molecular Orbital Theory" Mc.Graw-Hill Co., New York, 1970.
[9] S. Grigoraş, A. Medeşan, I. Rusu and S. Moldoveanu, *Rev. Roumaine Chim.*, **24,** 1431 (1979).
[10] A. Botrel and C. R. Guerillot, *J. Chim. phys.*, **71,** 974 (1974).
[11] J.O.M. Bochris and A. K. H. Reddy, "Modern Electrochemistry", Plenum Press, New York, 1970.
[12] R. Gaboriaud, *J. Chim. phys.*, **66,** 18 (1969).
[13] G. T. Hoytink, E. De Boer, P. H. Van der Meij and W. P. Weyland, *Rec. Trav. chim.*, **75,** 487 (1956).
[14] A. Botrel and C. R. Guerillot, *J. Chim. phys.*, **71,** 1240 (1974).

Revue Roumaine de Chimie, **25**, *1*, 75–79 (1980)

RRKM CALCULATION OF THE UNIMOLECULAR DECOMPOSITION OF TRIFLUOROMETHYL HYPOFLUORITE

EDUARDO A. CASTRO and ALICIA H. JUBERT
Instituto de Investigaciones Fisicoquimicas Teóricas y Aplicadas, Sucursal 4, Casilla de Correo 16, La Plata 1900, Argentina

Received May 6, 1978

The RRKM theory is applied to the unimolecular decomposition of the CF_3OF. An adjustment in the de-energization rate constant is made through the parameter λ and the frequencies of the activated complex were taken like those of the normal molecule because the infra-red spectrum of the CF_3O radical is not known. Theoretical results are compared with the available experimental values for different temperatures and a good agreement is found.

INTRODUCTION

By studying the kinetics of the thermal decomposition of CF_3OF in the presence of SO_3, Czarnowski *et al.*[1] were able to determine the specific rate constant of the unimolecular decomposition of CF_3OF. No direct reaction occurred between the two molecules. The CF_3OF decomposed in a unimolecular reaction, forming CF_3O radicals and F atoms. The F atoms reacted rapidly with SO_3 giving FSO_3 (in equilibrium with its dimer $F_2S_2O_6$) and the CF_3 radical reacted with FSO_3 forming CF_3OOSO_2F or with another CF_3O radical, forming the peroxide $(CF_3O)_2$. With a sufficiently high concentration of FSO_3, which could be obtained by adding beforehand a certain amount of $F_2S_2O_6$, the formation of $(CF_3O)_2$ could be almost completely suppressed. At 200 — 300 ° with SO_3 pressures from 10 to 70 torr and CF_3OF pressures from 50 to 600 torr, were needed 20—40 torr of $F_2S_2O_6$. The only product formed under these conditions was CF_3OOSO_2F. By extrapolation to infinite pressure the values of k_∞ for the reaction at 202.8, 203.7 and 234.1 were obtained

$$k_\infty = 2.50 \times 10^{14} \exp\left(-43.500 \pm 500/RT\right) \mathrm{sec}^{-1} \qquad (1)$$

In order to determine the energy content of the energized CF_3OF and to discuss the structure of the activated complex, a model which permits the calculation of the specific rate constant as a function of the energy is necessary. We will use the RRKM theory[2,3] which gives the specific rate constant as

$$k_\varepsilon = \frac{1}{\hbar} \, \frac{Z_1^+}{Z_1^*} \, \frac{\Sigma P(\varepsilon_{vr}^+)}{N^*(\varepsilon_{vr})} \tag{2}$$

where Z_1^+ and Z_1^* are the products of the partition functions of the adiabatic degrees of freedom of the activated complex and molecule, respectively; $P(\varepsilon_{vr}^+)$ is the total sum of the degeneracies of all the possible energy eigenstates of the active degrees of freedom of the complex at total energy ε_{vr}^+; $N^*(\varepsilon_{vr})$ is the number of eigenstates per unit energy of the active degrees of freedom for the molecule at energy ε_{vr}; $\hbar$ is the Planck's constant; ε_0 is the minimum energy necessary for the reaction and $\varepsilon_{vr}^+ = \varepsilon_{vr} - \varepsilon_0$. We will compare the theoretical results for k_{uni} with the experimental ones for different temperatures.

CALCULATION METHOD

We used in all cases, for the calculation, the computer program number 234 of the Quantum Chemistry Program Exchange.[4] The program was carried out in an IBM/360 computer and 106 K units of memory were required. The time needed for each run was nearly ten minutes of CPU time.

SPECIFICATIONS FOR THE POSTULATED MODEL OF THE REACTION

The assumed geometric parameters for CF_3OF were taken from the literature.[5] The configuration was taken as non-planar with a C_s symmetry.

The used value for the molecular diameter was 3Å and was calculated by means of the Van der Waals radii of atoms.[6] The unimolecular decomposition of CF_3OF involves simple bond breaking and yields a radical and an atom, so that the reverse reaction of association requires no formal activation energy.

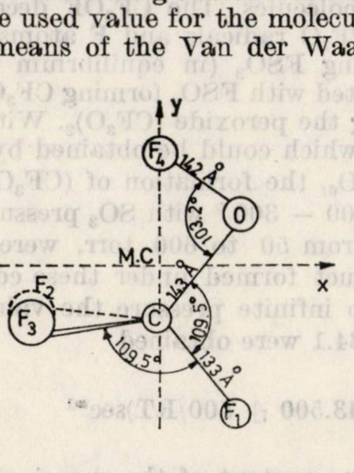

Fig. 1. — Assumed geometric parameters for CF_3OF.

This corresponds to the Type 1 reactions in the Forst's classification scheme,[7] with a loose transition state characterized by a high preexponential factor A_∞ ($\log A_\infty = 14$) which, in the thermodynamic interpretation of reaction rates, implies a high entropy of activation, i.e. one that is an appreciate fraction of the total entropy of the reaction. A high entropy of activation implies a transition state which is more like the final state (products) than like the reactants. Then we could expect that in the activation complex the distance between the center of gravity of the CF_3O radical and the F atom $\langle r_m \rangle$ would be relatively long. This was confirmed considering a potential which depends only on the distance $\langle r_m \rangle$ calculated as (see Ref. 7, p. 360)

$$\langle r_m \rangle = r_e(3D_e/kT)^{1/4} \tag{3}$$

For the activated complex we considered a non planar structure and assumed that it was formed by a CF_3O radical and the F atom in which it was possible that one of the internal degrees of freedom was available by the rotation of the CF_3O radical with respect to the straight line determined by the atoms C and F. The CF_3O radical kept the same geometric parameters as in the normal molecule. As the infra-red spectrum of the CF_3O radical is not known up to now, the frequencies of the activated complex were taken like those of the normal molecule.[5] As reaction coordinate was taken the stretching frequency O—F (947.3 cm^{-1}) and the lowest frequency (56.0 cm^{-1}) were changed in the activated complex to an appropriate value by means of an entropy adjustment. [8] The reaction path degeneracy was taken as unitary, the overall rotations were considered as adiabatic and a collisional deactivation efficiency $\lambda =$ $= 0.1$ was taken.

RESULTS AND DISCUSSION

The Arrhenius equation obtained by Czarnowski *et al.*[1] was verified with the experimental data because incorrect values of A_∞ and E_∞ may be a common source of difficulties in correlating the RRKM theory to experimental observations since the fall-off curves are quite sensitive to the values of these parameters.[9] As a preliminary calculation we performed the determination of k_{uni} at 234.1° in the range of pressures 140 — 2,000 torr, taking all the internal degrees of freedom of the activated complex as vibrations with $\sigma = 3Å$ and $\lambda = 0.1$. We studied two cases : I) the sums and densities of the active vibrational energy states were evaluated by the Whitten-Rabinovitch's method [10] and II) the direct count procedure was employed to calculate sums and densities. The results obtained were the following :

TABLE 1

Theoretical and experimental results of k_{uni} for the unimolecular decomposition of CF_3OF at 234.1°

p torr	$k_{exp} \times 10^5$ s.$^{-1}$	Case I $k_{calc} \times 10^5$ s.$^{-1}$	Case II $k_{calc} \times 10^5$ s.$^{-1}$
2 000	4.08	3.76	8.09
1 000	4.01	3.53	7.59
666.66	3.94	3.36	7.22
500	3.78	3.23	6.92
400	3.73	3.12	6.68
333.33	3.62	3.02	6.47
250	3.52	2.86	6.12
200	3.46	2.73	5.84
166.66	3.39	2.62	5.60
142.86	3.33	2.53	5.39

As the results showed a good agreement for Case I, we used the same approximation method to calculate k_{uni} at other temperatures. In Figure 2 we show the theoretical and experimental results.

In this calculation it was necessary to make an adjustment in the de-energization rate constant λZ by means of λ (see Ref. 8, p. 178).

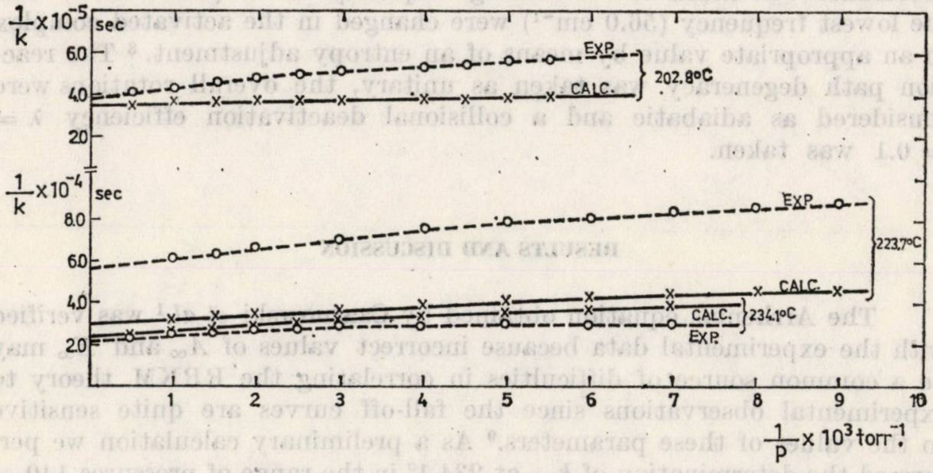

Fig. 2. — Theoretical and experimental results of k_{uni} for the unimolecular decomposition of CF_3OF at 202.8°, 203.7° and 234.1°.

This term appears in the expression for k_{uni} only as the product λZp, so that a change in λZ simply causes an inversely proportional change in the pressure required to produce a given value of k_{uni}. Thus, the plot of k_{uni}/k_∞ vs log p is shifted horizontally by a distance equal to the change in log λZ without any change in shape of the curve. By means of a λ adjustment we got a good agreement between experimental and calculated results at two temperatures : 202.8 and 234.1°, but for 223.7° it was not so good, as we can see in Figure 2. The feature of this particular result should not mask the fact that λZ is an important variable parameter, and many authors have freely introduced values between 0.1 and 1.0 (see Ref. 8, Chapter 6) to obtain agreement with their numerical results. Strictly, a failure of the strong collision assumption requires a more sophisticated treatment than the mere introduction of a corrective factor λ, but it emerges from the general treatment of the RRKM theory that this simple correction is adequate to our purposes. Taking the vibrations of the activated complex like those of the normal molecule, as it was our case, we must point out that the choice does not affect, in general, in a relevant form the theoretical results,[8] so that from the absence of information on the frequencies of the activated complex, the assignment performed is a reasonable one.

REFERENCES

[1] J. Czarnowski, E. Castellano and H. J. Schumacher, *Z. phys. Chem. (Frankfurt)*, **65**, 225 (1969).

[2] R. A. Marcus and C. K. Rice, *J. Phys. Colloid. Chem.*, **55**, 894 (1951).

[3] R. A. Marcus, *J. Chem. Phys.*, **20**, 359 (1952).

[4] W. L. Hase and D. L. Bunker, *QCPE*, **10**, 234 (1973).

[5] P. M. Wilt and E. A. Jones, *J. Inorg. Nuclear Chem.*, **30**, 2933 (1968).

[6] A. J. Hopfinger, "Conformational Properties of Macromolecules", Academic Press, New-York, 1973, Chapter 2.

[7] W. Forst, "Theory of Unimolecular Reactions", Academic Press, New-York, 1973, Chapter 3.

[8] P. J. Robinson and K. A. Holbrook, "Unimolecular Reactions", Wiley, New-York, 1972, Chapter 6.

[9] E. A. Castro and A. H. Jubert, *React. Kinet. Catal. Lett.*, **9**, 53 (1978).

[10] G. Z. Whitten and B. S. Rabinovitch, *J. Chem. Phys.*, **38**, 2466 (1963).

Revue Roumaine de chimie, **25**, *1*, 81–85 (1980)

INVESTIGATION OF SOME THERMODYNAMICAL PROPERTIES OF 2–1 ELECTROLYTES IN SOLUTION

PARBATI PAL* and ASHOK KR. CHAKRABORTY**

* S. N. Bose Institute of Physical Sciences, Calcutta University 92, Acharya Prafulla Chandra Road, Calcutta-700009, India

** Bankim Sardar College & S. N. Bose Institute of Physical Sciences, Calcutta University 92, A. P. C. Road, Calcutta-700009, India

Received May 11, 1978

Some thermodynamical properties of strong electrolytes in solution have been investigated, by using a special case of the distribution formula of Dutta [1], with a special value of its parameter in a paper of Pal.[1] In a subsequent paper of Pal [3] investigations have been made by using the general formula in case of 1–1 electrolytes in solution. Here the case for 2–1 electrolytes in solution are considered.

INTRODUCTION

From the papers of Dutta and Sengupta [4] and Sengupta [5,6] it has been found that the distribution formula of Dutta and Bagchi [7] and others can not be applied in the case of a concentrated solution as in some cases nb becomes greater than one, where *n* is the density number and *b*, the exclusion volume. In Pal's paper [3] it has been shown that the difficulty of taking $nb \geqslant 1$ can be avoided if the distribution formula of Dutta [1] is taken into account. In that paper satisfactory results have been obtained in the case of $1-1$ electrolytes in solution. In this paper we try to investigate to what extent these results are satisfactory in the case of $2-1$ electrolytes in solution.

The formula of Dutta [1] was deduced from the cell model but it will be shown in Section A that this formula holds good for the lattice model also.

SECTION A

According to Lennard-Jones and Devonshire [8] the structure of normal liquid is similar to that of an alloy composed of atoms and holes. The essential difference between the picture of the liquid and that of the solid is that in the solid there is a long distance-order whereas in the liquid the long-distance order disappears completely. Dutta [9] has shown that the properties of real gases and the distribution of ions of strong electrolytes in solution might be deduced from lattice structures. Later on many authors (Ruelle[10]; Fisher[11]) have worked on the similar type of model and they called it "lattice gas".

In a subsequent note Dutta[22] showed the equivalence of cell model and lattice model. In the paper of Dutta[1], he considered a cell to be either vacant or occupied by $r > 1$ particles only, where the maximum value of r is the number in the close packing. Thus, if one considers that a lattice point is either vacant or occupied by a complex of particles, where in the complex there may be 1, 2, . . . r particles, then exactly the same distribution formula as that of Dutta[1] can be obtained.

CALCULATIONS

According to Dutta[1], the distribution formula for an assembly of charged particles is given by

$$n_{\pm} = \frac{1}{b}\left[\frac{1}{\exp(\nu_{\pm} + z_{\pm}e_{\pm}\psi/kT)-1} - \frac{(r_{\pm}+1)}{\exp\{(r_{\pm}+1)(\upsilon_{\pm}+z_{\pm}e\psi/kT)\}-1}\right] \tag{1}$$

where $n_{\pm}$ are the number densities of positively and negatively charged particles with charges $z_+ e_+$ and $z_- e_-$ respectively at a point where the mean electric potential is ψ.

The charge density ρ at any point in the solution is given by

$$\rho = -\frac{e^2}{DkT}\,\Sigma A_i z_i^2 \psi, \text{ when } \frac{e\psi}{kT} \ll 1$$

where

$$A_i = (r_i + 1)\,B_i - B_i^2 + \frac{2B_i - r_i}{c_i - 1},$$

$$B_i = n_i^0 b$$

and c_i satisfies

$$\sum_{n=0}^{r} c_i^n B_i = \sum_{n=1}^{r} n c_i^{r-n}$$

n_i^0 being the stoichiometric number density of the ith ion in solution.

The solution of the Poisson equation when $\frac{e\psi}{kT} \ll 1$, as given in Pal[2,3] is

$$\lambda_{\pm} = \frac{z_{\pm}}{DkT}\,\frac{e^2 k e^{\xi_{a\pm}}}{i + \xi_{a\pm}}\,\frac{e^{-\xi}}{\xi},$$

where

$$\xi = kr,\ \lambda_{\pm} = \frac{e_{\pm}\psi}{kT}$$

According to the papers of Dutta and Sengupta,[4] and Sengupta,[5,6] the mean activity coefficient $f_\pm$ is given by

$$\ln f_\pm = -\frac{e^2}{DkT}\frac{z_+ + z_-}{\Sigma z_i}\left[(1-s)\,\Sigma z_i\theta_i + \frac{S}{2}\Sigma\frac{z_i}{i+ka_i}\right],$$

where

$$S = n_+M_+ + n_-M_-,$$

$$M_\pm = \frac{z_\pm^2\left(\dfrac{\partial A_\pm}{\partial n_\pm}\right)^2}{\Sigma A_i Z_i^2},$$

$$\theta_i = \left[\frac{(ka_i)^2}{2} - ka_i + \ln(1+ka_i)\right]\frac{1}{(ka_i)^3}$$

EXPERIMENTAL VERIFICATION

Numerical values of $-\log f_\pm$ calculated at 25° ($D = 78.6$), taking the volume of a cell to be given by $b = r\cdot(4/3)\pi a^3$, are given in table 1 and for comparison both the experimental values (cf. Harned and Owen[13]), and the calculated values of 2 — 1 electrolytes in solution are shown in figure.

TABLE 1

$-\log f_\pm$ for 2 — 1 electrolytes

m molarity	.1	.2	.5	.7	1	2	2.6	3
		$r_+=r_-$	$=3$					
$-\log f_\pm$		$a_+=a_-$	$=3.6$Å					
	.346	.426	.532	.565	.594	.614	.600	
		$a_+=a_-$	$=4$Å					
	.334	.408	.498	.523	.541	.526	.481	
		$r_+=r_-$	$=4$					
		$a_+=a_-$	$=2$Å					
	.413	.529	.709	.782	.860	1.0123		1.0922
		$r_+=r_-$	$=5$					
		$a_+=a_-$	$=2$Å					
	.414	.531	.714	.788	.870	1.029		1.113

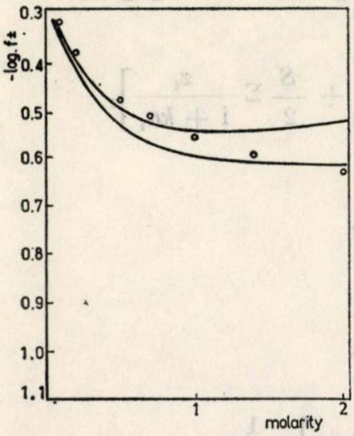

Fig. 1. — — log $f_{\pm}$ vs. concentration curves for $2-1$ electrolytes, for $r=3(a_+=a_-=4\text{Å}$ for the upper, $a_+=a_-=3.6\text{Å}$ for the lower). Dots correspond to the experimental value of Sr $(NO_3)_2$.

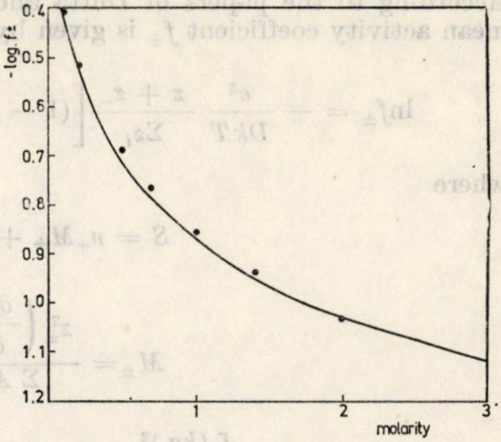

Fig. 2. — — log $f_{\pm}$ vs. concentration curve for $r=4$, $a_+=a_-=2\text{Å}$. Dots are experimental values of $Pb(NO_3)_2$.

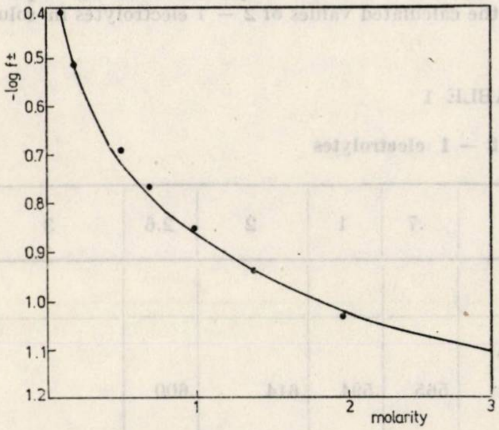

Fig. 3. — — log $f_{\pm}$ vs. concentration curve for $r=5$, $a_+=a_-=2\text{Å}$. Dots are experimental values of $Pb(NO_3)_2$.

CONCLUSION

Different curves have been drawn for different values of the ionic radii and different values of r. From the figures it is obvious that two $2-1$ electrolytes in solution correspond to the curves obtained. But the agreement obtained here is not so good as in the case of $1-1$ electrolytes in solution, earlier obtained.

ACKNOWLEDGEMENTS. The authors express their earnest gratitude to Professor M. Dutta, Centre of Advanced Study in Applied Mathematics, and Professor-in-Charge of S.N. Bose Institute of Physical Sciences, Calcutta University, for his valuable suggestions and guidance at every stage of the work.

REFERENCES

[1] M. Dutta, *Indian J. Phys.*, **60**, 422 (1966).
[2] P. Pal, *Indian J. Phys.*, **52B**, (1978).
[3] P. Pal, unpublished data.
[4] M. Dutta and M. Sengupta, *Proc. Nat. Inst. Sci. India*, **20**, 1 (1954).
[5] M. Sengupta, *Proc. Nat. Inst. Sci. India*, **22**, 13 (1956).
[6] M. Sengupta, *J. Indian Chem. Soc.*, **45**, 1133 (1968).
[7] M. Dutta and S. N. Bagchi, *Indian J. Phys.*, **24**, 61 (1950).
[8] Lennnard-Jones and Devonshire, *Proc. Roy. Soc.*, **169**, 31 (1939) ; **170**, 465 (1939).
[9] M. Dutta, *Proc. Nat. Inst. Sci. India*, **19**, 183 (1953).
[10] D. Ruelle, "Statistical Mechanics, Rigorous Results", W. A. Benjamin, Inc., New York, 1969.
[11] M. E. Fisher, *Commun. Math. Phys.*, **26**, 6 (1972).
[12] M. Dutta, *Bull. Cal. Math. Soc.*, **57**, 123 (1965).
[13] H. S. Harned and Owen, "Physical Chemistry of Electrolytic Solutions" 3rd Edn., Reinhold Pub. Corp. New York, 1958.

Revue Roumaine de Chimie, **25**, *1*, 87–93 (1980)

THE INFLUENCE OF THE STRUCTURE AND THE TYPE OF ALLOY ON STRESS CORROSION CRACKING IN HYDROCHLORIC ACID SOLUTIONS

O. RADOVICI and M. V. POPA

ICECHIM, Centre of Physical Chemistry, Bucharest, Spl. Independenţei 202, Romania

Received November 27, 1978

The influence of structure of some low-carbon high-strength steels and stainless steels on stress corrosion cracking (SCC) susceptibility in hydrochloric acid solutions was studied. The influence of some types of organic inhibitors on the SCC susceptibility of these alloys has been also studied.

INTRODUCTION

It is generally known that stainless steels [1] as well as low carbon steels[2] are susceptible to SCC in hydrochloric acid solutions. Different hydrochloric acid media have been utilized for the study of SCC :

— for austenitic stainless steels : 0.1N $HCl + 1\%\ FeCl_3.6H_2O$ at room temperature [1,3,4], $MgCl_2 + HCl$, $3\% NaCl + HCl$, $3\%\ NaCl + + 0.005\%$, $HCl + Na_2Cr_2O_7.\ 2H_2O$ at boiling point,[5]

— for high strength steels : $18\%\ HCl$, $18\%\ HCl + 1\%\ SeO_2$, $4\%\ HCl + 3\%\ NaCl + 20$ mg/l As at room temperature. [6–8]

Also some organic inhibitors has been used for reducing the susceptibility of high strength steels to SCC.[9–11]

In this paper we have studied the influence of the structure and the nature of the alloy and the efficiency of some organic inhibitors on the susceptibility to SCC of high strength low carbon steels and stainless steels in hydrochloric acid solutions, using the electrochemical testing method initiated by Suzuki and co-workers.[12,13]

EXPERIMENTAL

The experiments were carried out on low carbon steels API grade J-55, C-75, N-80, P-105 and on stainless steesls W. I. 4541, W.1.4571, W.1.4301, W.1.4306, W.1.4841, W.1.4021 with the chemical compositions and tensile strength (σ_r) shown in table 1.

TABLE 1

Chemical analyses, strutural and tensile strength of the high strength studied steels

Type of steel	Chemical analyses (%)									
	C	Mn	Si	P	S	Cr	Ni	Mo	V	Ti
Grade J-55	0.42	1.07	0.37	0.029	0.019	0.13	—	0.01	—	—
Grade C-75	0.37	1.48	0.29	0.014	0.016	0.14	—	0.07	—	—
Grade N-80	0.33	1.34	0.29	0.011	0.013	0.16	—	0.05	—	—
Grade P-105	0.40	1.59	0.33	0.012	0.012	0.57	—	0.20	0.09	—
W.1.4541	0.09	1.25	0.50	0.031	0.015	17.24	10.45	—	—	0.59
W.1,4571	0.045	1.86	0.62	0.040	0.024	17.30	10.65	2.15	—	0.25
W.1.4301	0.040	1.06	0.74	0.025	0.007	17.38	9.69	—	—	—
W.1.4306	0.046	0.92	0.63	0.027	0.009	17.35	9.31	—	—	—
W.1.4841	0.10	0.64	1.94	0.017	0.004	25.23	19.76	—	—	—
W.1.4821	0.25	0.42	0.23	0.018	0.014	14.50	—	—	—	—

Type of steel	Structure	Tensile strength
Grade J-55	perlite + ferrite	5.933 $10^8 N/m^2$
Grade C-75	troostite	7.355 $10^8 N/m^2$
Grade N-80	sorbite	7.463 $10^8 N/m^2$
Grade P-105	bainite + sorbite	9.365 $10^8 N/m^2$
W.1.4541	austenite	5.972 $10^8 N/m^2$
W.1.4571	austenite	5.540 $10^8 N/m^2$
W.1.4301	austenite	5.982 $10^8 N/m^2$
W.1.4306	austenite	6.120 $10^8 N/m^2$
W.1.4841	austenite + ferrite	6.050 $10^8 N/m^2$
W.1.4021	martensite	6.472 $10^8 N/m^2$

The testing specimens were obtained from a steel bar, 3 mm in diameter, which were sealed with Teflon tape, epoxy resin, as shown in Figure 1, where the working glass cell used in these experiments is presented too.

Before testing, the specimens were mechanically polished on SiC paper to grade 800, degreased in boiling benzene (5 min) and cleaned in acetone.

The specimens were constantly stressed at $\sigma = 2.456 \; 10^8 N/m^2$, with a Unisteel Stress Corrosion Machine-Distington.

The electrochemical testing method for SCC, initiated by Suzuki and co-workers,[12,13] is based on the fact that the dissolution rate accompanying crack propagation can be measured in a potentiostatic assembly, (Figure 2), of a stressed microelectrode A with an unstressed macroelectrode B, both of them made from the same metallic material.

The ratio between macroelectrode B surface (S) and microelectrode A surface (s) was 90 : 1.

The HCl solutions were prepared with reagent grade chemicals and double-distilled water. The temperature in the working cell was kept at 75° approximately ± 1°.

The tests were carried out in 18 % HCl solution for studying the influence of structure and the type of steels in susceptibility to SCC and in 20 % HCl solution in the presence or absence of 0.5 % organic inhibitors for studying the influence and efficiency of these inhibitors on SCC.

The organic inhibitor used in this paper were: ACOR-42 (aliphatic amine), aniline, hexamethylenimine, urea and thiourea.

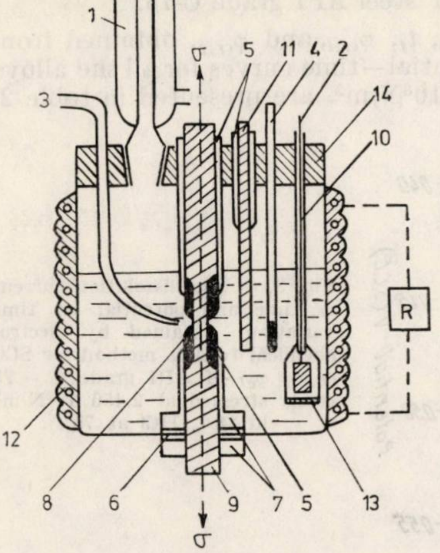

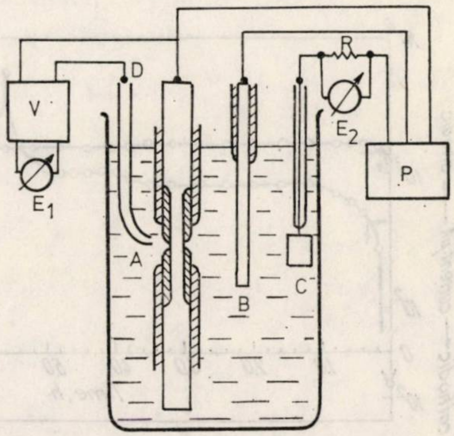

Fig. 1. — The working glass cell used in electrochemical testing method for SCC.

1. reflux condenser; 2. Pt counter electrode; 3. Haber-Luggin capillary; 4. control termometer; 5. teflon seal tape; 6. rubber set; 7. metallic nut; 8. epoxi resin; 9. metallic probe; 10. glass tube; 11. macro-electrode; 12. heating resistance; 13; glass frite; 14. rubber stopper.

Fig. 2. — The experimental scheme of electrochemical testing method for SCC. *A.* stressed microelectrode ; *B.* unstressed macroelectrode ; *C.* Pt counter electrode ; *D.* SCE. *R.*—resistance. E_1 and E_2.—recorders. *V.* — electronic voltmeter. *P.* — Wenking potenriostat.

RESULTS AND DISCUSSIONS

From the dissolution current-time and potential-time curves, recorded simultaneously when the stressed microelectrode was made anode and was set at the same potential as the unstressed macroelectrode made cathode ($\varphi_a = \varphi_c$), using the potensiostatic assembly, we can precisely estimate :

— the incubation time for crack initiation — t_i — which represents the time when dissolution current begins to increase,

— the crack propagation time — t_p — which represents the time when the dissolution current is continuously increasing,

— the time of failure — t_f — which represents the maximum value recorded in the dissolution current-time curve,

— the critical potential for crack initiation — $\varphi_{cr,i}$ — and respectively for crack propagation — $\varphi_{cr,p}$ — which represents the corespondents of t_i and t_p from the potential-time curve.

Because the shape of the dissolution current-time and the potential—time curves, in 18% HCl and 28% HCl solutions in the presence or the absence of organic inhibitors, is the same for all the steels studied, we present în figure 3 these results only for steel API grade C-75.

The experimental values for t_i, t_p, t_f, $\varphi_{cr,i}$, and $\varphi_{cr,p}$, obtained from the dissolution current—time and potential—time curves for all the alloys in 18% HCl solution at 75° and 2.456 $10^8 N/m^2$, are presented in table 2.

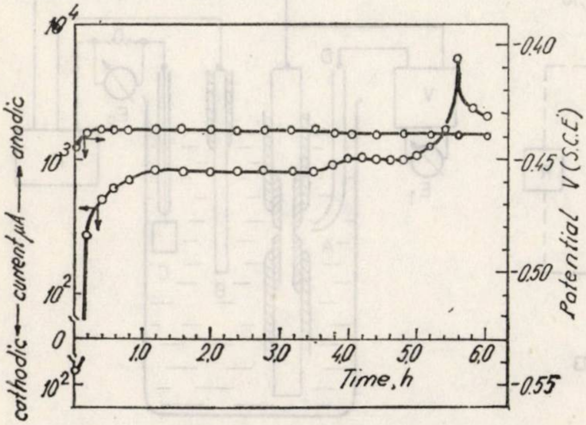

Fig. 3. — The dissolution current *vs.* time and potential *vs.* time variation, obtained by electrochemical testing method for SCC ($\varphi_a = \varphi_c$) of API grade C — 75 steel, stressed at 2.456 $10^8 N/m^2$ in 18% HCl at 75°.

We can see from the data of table 2 that t_f, t_i and t_p values rise with the increasing of the tensile strength of low carbon steels and the $\varphi_{cr,i}$ and $\varphi_{cr,p}$ values rise too, in electropositive sense, with the rising of the tensile strength of these steels namely in the sense :

$$\text{J-55} < \text{C-75} < \text{N-80} < \text{P-105}$$

TABLE 2

The experimental values for t_f, t_i, t_p, $\varphi_{cr,i}$, $\varphi_{cr,p}$, obtained by electrochemical testing method ($\varphi_a = \varphi_c$), for studied steels in 18% HCl solution at 75° and 2.456,$10^8 N/m^2$

Type of steel	t_f, h	t_i, h	t_p, h	$\varphi_{cr,i}$, V	$\varphi_{cr,p}$, V
grade J-55	4.92	3.20	1.72	−0.440	−0.442
grade C-75	5.60	3.55	2.05	−0.437	−0.439
grade N-80	6.22	4.00	2.22	−0.426	−0.430
grade P-105	10.21	7.50	2.71	−0.418	−0.422
W.1.4541	2.70	1.60	1.10	−0.362	−0.364
W.1.4571	4.50	3.25	1.25	−0.320	−0.323
W.1.4301	5.10	3.50	1.60	−0.342	−0.345
W.1.4306	2.03	1.05	0.98	−0.380	−0.384
W.1.4841	7.00	5.80	1.20	−0.351	−0.353
W.1.4021	0.82	0.50	0.32	−0.458	−0.460

For the stainless steels, we can also see from the data of table 2, that t_f and t_i values decrease in the sense :

$$W.1.4841 > W.1.4301 > W.1.4571 > W.1.4541 > W.1.4306 > W.1.4021.$$

In conclusion, on the basis of the results for t_f presented in table 2, we can appreciate that the susceptibility to SCC of the alloys depends on the structure and the type of the steel, under the same conditions of tensile stress, HCl concentration and temperature : for low carbon steels, the susceptibility increases in the following manner : bainit + sorbite < sorbite < troostite < perlite + ferrite, respectively : P-105 < N-80 < < C-75 < J-55,
and for stainless steels : austenoferritic < austenitic < martensitic, respectively : W.1.4841 < W.1.4301, W.1.4571, W.1.4541, W.1.4306 < < W.1.4021.

These conclusions are better illustrated by the data of table 3, which contain the values of the failure rate (V_f), the rate of crack initiation (V_i) and the rate of crack propagation (V_p).

TABLE 3

The experimental V_f, V_i, V_p, values obtained by electrochemical testing method ($\varphi_a=\varphi_c$) for studied steels in 18% HCl solution at 75° and 2.456 10^8N/m²

Type of steel	$V_f.10^3$, mm/min	$V_i.10^3$, mm/min	$V_p.10^3$, mm/min
grade J-55	10.16	15.82	29.07
grade C-75	8.92	14.08	24.39
grade N-80	8.04	12.50	22.52
grade P-105	4.89	6.66	18.45
W.1.4021	60.97	100.00	156.25
W.1.4306	24.63	47.62	51.02
W.1.4541	18.51	31.52	45.45
W.1.4571	11.11	15.30	40.00
W.1.4301	9.80	14.28	31.25
W.1.4841	7.14	8.62	41.66

The values in this table were obtained from the data included in table 2 with the help of the equation :

$$V_f = l_0/t_f = l_0/(t_i + t_p) = (V_i + V_p)(t_i + t_p)/t_f^2.$$

where : l_0 is the diameter of metallic probe (3 mm).

Based on the data presented in table 3 as well as in table 2, we can conclude that the API grade P-105 is less susceptible to SCC than all the other high strength steels and the austenoferritic stainless steel W.1.4841 is less susceptible to SCC than other studied stainless steels, in the same conditions of tensile stress, concentration and temperature of HCl solution.

TABLE 4

The φ_M experimental values obtained from the potential vs. time variation for unstrered studied steels in 18% HCl solution at 75°

Type of steel	φ_m, V
grade J-55	−0.413
grade C-75	−0.413
grade N-80	−0.405
grade P-105	−0.400
W.1.4021	−0.418
W.1.4541	−0.354
W.1.4571	−0.315
W.1.4301	−0.340
W.1.4306	−0.371
W.1.4841	−0.348

According to the electrochemical testing method for SCC[13], the steel is susceptible to this corrosion form when the mixed potential of unstressed specimen (φ_M) is nobler than the critical potential for crack propagation ($\varphi_{cr,p}$).

The values of φ_M for unstressed steels, presented in table 4, obtained from the potential-time curves in 18% HCl solution at 75°, show that these steels are susceptible to SCC in this corrosive solution.

The influence of the organic inhibitors in 0.5% concentration, on the susceptibility to SCC of some ferrous alloys, was studied starting from current-time and potential-time curves obtained by electrochemical method ($\varphi_a = \varphi_c$).

The experimental values for t_f, t_i, t_p, $\varphi_{cr,i}$ and $\varphi_{cr,p}$, in 28% HCl solution, in the presence of some organic inhibitors, at 75° and 2.456 10^8 N/m^2, are presented in table 5.

TABLE 5

The experimental values for t_f, t_i, t_p, $\varphi_{cr,i}$, $\varphi_{cr,p}$ obtained by electrochemical testing method ($\varphi_a = \varphi_c$) for studied steels in 28% HCl solution in the presence or absence of 0.5% organic inhibitors at 75° and 2.456.10^{8}N/m^2

Type of steel	Solution	t_f, h	t_i, h	t_p, h	$\varphi_{cr,i}$, V	$\varphi_{cr,p}$, V
grade J-55	28% HCl	1.34	1.14	0.20	−0.445	−0.445
W.1.4541		1.55	0.95	0.60	−0.385	−0.385
W.1.4841		2.46	1.70	0.76	−0.392	−0.392
W.1.4021		0.13	0.13	0	−0.490	−0.490
grade C-75	28% HCl + 0.5%ACOR-42	3.65	3.00	0.65	−0.424	−0.424
W.1.4541		3.50	2.90	0.60	−0.376	−0.376
W.1.4841		4.50	3.50	1.00	−0.386	−0.386
W.1.4021		0.45	0.37	0.08	−0.464	−0.464
grade C-75	28% HCl + hexamethylenimine 0.5%	2.15	1.70	0.45	−0.428	−0.428
W.1.4841		2.02	1.65	0.37	−0.380	−0.380
W.1.4541		3.50	2.60	0.90	−0.388	−0.388
W.1.4021		0.35	0.30	0.05	−0.465	−0.465
grade C-75	28% HCl + 0.5% aniline	2.11	1.85	0.25	−0.432	−0.432
W.1.4541		1.80	1.60	0.20	−0.382	−0.382
W.1.4841		3.15	2.70	0.45	−0.390	−0.390
W.1.4021		0.32	0,32	0	−0.468	−0.468
grade C-75	28% HCl + 0.5% tiourea	1.97	1.62	0.35	−0.435	−0.435
W.1.4541		1.76	1.46	0.30	−0.383	−0.383
W.1.4841		2.98	2.10	0.88	−0.390	−0.390
W.1.4021		0.25	0.25	0	−0.480	−0.480
grade C-75	20% HCl + ureea 0.5%	1.66	1.42	0.24	−0.440	−0.440
W.1.4541		1.60	1.40	0.20	−0.385	−0.385
W.1.4841		2.57	2.17	0.40	−0.390	−0.390
W.1.4021		0.20	0.20	0	−0.485	−0.485

For comparison we present the values reached by this method in 28% HCl solution at 75° and 2.456 $10^8 N/m^2$ in the absence of organic inhibitors, for the same low carbon steel API grade C-75 and stainless steels W.1.4541, W.1.4841 and W.1.4021.[14]

The data presented in table 5 show that t_f, t_i and t_p values rise in the presence of organic inhibitors. These values depend on the nature of the inhibitor, for all types of steels and decrease in the following order :

ACOR$-$42 > hexamethylenimine > aniline > thiourea > urea.

CONCLUSIONS

Our study concerning the SCC susceptibility of some high-strength carbon steels and stainless steels in HCl solutions shows that the susceptibility of low carbon steels in HCl 18% solution increases in the sense : P-105 < N-80 < C-75 < J-55 and for stainless steels, in the sense : W.1.4841 < W.1.4301 < W.1.4571 < W.1.4541 < W.1.4306 < W.1.4021.

From the structural point of view it was established that the structure of steels influences on SCC in 18% HCl solution that is for low carbon steels the best resistent structure is bainite + sorbite, and for stainless steels is austenoferritic structure.

Our results on the efficiency of organic inhibitors in 28% HCl solution on reducing the susceptibility to SCC of high strength steels showed that the best efficient inhibitor is the aliphatic amine ACOR-42.

REFERENCES

[1] G. Bianchi, F. Mazza and S. Torchio, "Proceedings of 5th International Congress on Metallic Corrosion", NACE, Houston, 1974, p. 380.
[2] A. W. Coulter, *Materials protection*, **7,** 23 (1968).
[3] M. B. Strauss and M. C. Bloom, *Corrosion*, **16,** 553 t (1974).
[4] E. G. Haney, P. Fugassi and D. B. Christner. *Corrosion*, **28,** 17 (1972).
[5] H. L. Logan "The Stress Corrosion of Metals", J. Wiley, New York, 1966.
[6] D. Van Rooyen, "1st International Congress on Metallic Corrosion", Butterworths, London, 1961, p. 134.
[7] "Stress Corrosion Testing", ASTM, Special Technical Publ., no. 425, ASTM, Baltimore 1967.
[8] M. G. Fontana and R. W. Staehle, "Proceedings of 7th World Petroleum Congress", Elsevier Publ., Mexico, 1967.
[9] H. Mazzille and H. H. Uhlig, *Corrosion*, **28,** 427 (1972).
[10] R. L. Martin, *Materials performance*, **13,** 19 (1974).
[11] O. Radovici and M. V. Popa, *Rev. Chim.* (*București*), **27,** 49 (1976).
[12] T. Suzuki and Y. Kitamura, *Corrosion*, **28,** 1 (1972).
[13] T. Suzuki, M. Yamabe and Y. Kitamura, *Corrosion* **29,** 70 (1973).
[14] M. V. Popa, *Rev. Chim.* (*București*), to be published.

Revue Roumaine de Chimie, **25**, *1*, 95–103 (1980)

EIN NEUES REAGENZ VOM EDTA-TYPUS. V[1]

SYNTHESE UND PHYSIKALISCH-CHEMISCHE UNTERSUCHUNG DER NEUTRALEN SALZE DER 4,4′-DIAMINODIPHENYLMETHAN–N,N′–TETRAESSIGSÄURE MIT I–, II–, III– UND IV– WERTIGEN METALLIONEN

CONSTANTIN GH. MACAROVICI* and EUGEN CHIŞ**
* Fakultät für Technologische Chemie der "Babeş-Bolyai" Universität Cluj-Napoca, Rumänien
** Fakultät für Mathematik, Abteilung Physik-Chemie, Universität aus Braşov, Rumänien

Eingegangen am 5. Juni 1978

Synthetisiert wurden neutrale Salze der 4,4′-Diaminodiphenylmethan-N,N′-tetraessigsäure, H_4RA, mit I-, II-, III- und IV-wertigen Metallionen, $M_4[RA_4]_n$, wo A : $-CH_2COO^-$ und R : $= N-C_6H_4-CH_2-C_6H_4-N =$, darstellen. Auf Grund der chemischen Analyse wurde ihre Zusammensetzung festgestellt, die (indirekt) auch durch die thermogravimetrische Analyse bestätigt werden konnte. Die Untersuchung der IR-Spektren, die diffusen Elektronenreflexionsspektren als auch die magnetischen Messungen ermöglichten das Aufstellen wahrscheinlicher Strukturschemen. Die geringe Löslichkeit der Salze in Wasser, sowie die Färbung und die Stabilitätskonstanten einiger Salze eröffnen die Möglichkeit ihrer Anwendung in der analytischen Chemie.

The neutral salts of 4,4′-diaminodiphenylmethane-N,N′-tetraacetic acid, H_4RA_4, with mono-, di-, tri- and tetravalent metals, by $M_4[RA_4]_n$-type, where R : $= N-C_6H_4-CH_2-C_6H_4-N =$ and A : $-CH_2COO-$, have been synthesized. On the basis of the chemical analysis, proved (indirectly) by the thermogravimetrical analysis, their composition have been established. The study of the IR spectra, of electronic diffuse spectra and magnetic measurement data, have enabled to set out some schemes of the probable structure. The reduced solubility of water, stability constants of some salts, their colour open the possibility of their application in analytical chemistry.

In einigen, im Druck befindlichen Berichten wurde die Synthese der in der Fachliteratur unbekannten 4,4′-Diaminodiphenylmethan-N,N′-tetraessigsäure[1], H_4RA_4, sowie ihre Synthese und die Untersuchung ihrer sauren Salze $M_2[H_2RA_4]_n$ beschrieben.[2]

In der vorliegenden Arbeit wird die Synthese der neutralen Salze $M_4[RA_4]_n$, (M = I-, II-, III- und IV-wertige Metallionen) und ihre wahrscheinliche Struktur beschrieben.

EXPERIMENTELLER TEIL UND ERGEBNISSE

Die wasserlöslichen Alkali- und Erdalkalimetalle-Salze der 4,4'-Diaminodiphenylmethan-N,N'-tetraessigsäure, H_4RA_4, werden durch die Mischung einer alkoholischen Lösungen der H_4RA_4 Säure und des Metallhydroxydes, in stöchiometrischen Mengenverhältnissen (1 Mol H_4RA_4 Säure : 4 Mols Alkalihydroxyd, bzw. 1 Mol H_4RA_4 Säure : 2 Mols Erdalkalihydroxyd) erhalten. Die auf diese Weise synthetisierten, in Alkohol unlöslichen Salze sondern sich in Form weißer Niederschläge ab. Nach 1 — 2 stündigem Stehen (im Falle der Erdalkalisalze benötigt es noch einer geringen Erwärmung) wird der ausgefällte Niederschlag filtriert, mit Alkohol (mit möglichst niedrigem Wassergehalt), und dann mit wenig Äther nachgewaschen und im Exikator auf P_2O_5 oder im Trockenschrank bei 35 — 40° getrocknet.

Die in Wasser unlöslichen $M_4[RA_4]_n$ Salze mit Metallionen der dritten und vierten Hauptgruppe des Periodischen Systems (Al^{3+} In^{3+}, Pb^{2+}) sowie die Salze der I-, II-, III- und IV-wertigen Übergangsmetalle, können durch Mischung in stöchiometrischen Mengenverhältnissen des neutralen Natriumsalzes Na_4RA_4 und der wasserlöslichen Metallsalze synthetisiert werden. Um neutrale Salze zu erhalten darf der pH-wert der Lösung nur zwischen 5 — 6 schwanken. Nach 1 — 2 Stunden werden die entstandenen komplexen Salze durch Filtrieren abgesondert, mit destilliertem Wasser bis zur gänzlichen Entfernung des Anions des reaktanten Salzes gewaschen und anschließend mit wenig Schwefeläther nachgespült. Das erhaltene Salz kann in Exikator auf Silikagel oder im Trockenschrank bei 35 — 40° getrocknet werden.

Die Alkali- und Erdalkalisalze der H_4RA_4 Säure sind in Wasser leicht löslich, in Alkohol und anderen organischen Lösungsmitteln unlöslich.

Die Salze der H_4RA_4 Säure mit Metallionen der dritten und vierten Hauptgruppe des Periodischen Systems, sowie jene der Übergangsmetalle sind in Wasser oder organischen Lösungsmitteln wenig löslich. Mit Ausnahme jener, die gefärbte Ionen enthalten, sind alle anderen komplexen Salze weiß. Die Salze verfärben sich in Kontakt mit der Luft bei Raumtemperatur nach mehreren Tage bläulich. Die Färbe vertieft sich nach leichter Erwärmung. Bei starkem Erhitzen werden die Salze braun, wobei die meisten nicht schmelzen (Tabelle 1).

TABELLE 1

Farbe und Löslichkeit einiger Salze M_4 $[RA_4]_n$ der H_4RA_4 Säure

Synthetisierte Salze	Mn^{2+}	Co^{2+}	Ni^{2+}	Cu^{2+}	Cd^{2+}	Al^{3+}	Cr^{3+}	Fe^{3+}	La^{3+}
Farbe	weiß	rosa	hellgrün	dunkelgrün	weiß	weiß	graugrün	braun	vei
Löslichkeit g/10 ml Lösung	0,0027	0,0121	0,0451	0,0042	0,0008	0,0003	0,0008	0,0008	0,0004

$$R: = N - C_6H_4 - CH_2 - C_6H_4 - N = \;; A: - CH_2COO^- ;$$

Die Ergebnisse der Elementaranalyse der erhaltenen Komplexverbindungen sind in Tabelle 2 enthalten.

Zwecks weiterer Informationen zur Strukturbestimmung der synthetisierten Salze wurden folgende Analysen durchgeführt. Die thermogravimetrischen Analysen wurden mit Hilfe eines Derivatographen (F. Paulik, J. Paulik, L. Erdely) im Temperaturbereich bis 1000° ausgeführt (Tabelle 3).

Die IR-Spektren wurden mit einem Perkin-Elmer Spektrophotometer ausgeführt, unter Benützung von KBr-Pastillen (Tabelle 4)

TABELLE 2

Chemische Analyse einiger Salze $M_4[RA_4]_n$ der H_4RA_4 Säure

Synthetisierte Substanz	% C		% N		% M		% H_2O	
	Ber.	Gef.	Ber.	Gef.	Ber.	Gef.	Ber.	Gef.
$Li_4RA_4 \cdot 4H_2O$	47,93	48,12	5,32	5,18	5,27	4,84	13,69	13,51
$Na_4RA_4 \cdot 4H_2O$	42,72	42,83	4,74	4,63	15,58	15,52	12,20	12,12
$Ca_2RA_4 \cdot 4H_2O$	43,59	43,48	4,84	4,79	13,85	13,91	12,45	12,52
$Ba_2RA_4 \cdot 4H_2O$	32,62	32,51	3,62	3,71	35,53	35,42	9,32	9,27
$Mn_2RA_4 \cdot 4H_2O$	41,46	41,54	4,60	4,28	18,04	17,89	11,89	11,92
$Co_2RA_4 \cdot 6H_2O$	38,67	38,59	4,29	4,18	18,07	17,85	16,57	16,72
$Ni_2RA_4 \cdot 6H_2O$	38,69	38,58	4,30	4,18	18,01	18,18	16,59	16,76
Cd_2RA_4	38,73	38,67	4,31	4,22	34,52	34,38	—	—
$Al_4[RA_4]_3 \cdot 10H_2O$	48,28	48,34	5,36	5,24	6,69	6,74	11,49	11,36
$La_4[Ra_4]_3 \cdot 10H_2O$	37,55	37,43	4,17	4,24	27,58	27,63	8,94	9,13
$Cr_4[RA_4]_3$	50,88	50,79	5,65	5,72	13,99	14,02	—	—
$Fe_4[RA_4]_3 \cdot 4H_2O$	48,05	48,13	5,33	5,21	19,19	19,08	4,59	4,61
$ThRA_4 \cdot 8H_2O$	34,53	34,46	3,48	3,92	31,80	31,69	9,86	9,74

$R: = N - C_6H_4 - CH_2 - C_6H_4 - N = ;\quad A = -CH_2COO^- ;$

TABELLE 3

Thermische Zersetzung einiger Salze $M_4[RA_4]_n$ der H_4RA_4 Säure

Komplexe Substanz	Molmasse	Temperaturbereich in dem die exothermen Effekte stattfinden	Nach der thermischen Zersetzung zurückgebliebene Substanz		
			Zusammensetzung	Gehalt %	
				Ber.	Gef. TG
$Li_4RA_4 \cdot 4H_2O$	526,21	100—850	Li_2CO_3	32,54	32,72
$Na_4RA_4 \cdot 4H_2O$	590,42	220—850	Na_2CO_3	35,90	35,75
$Ca_2RA_4 \cdot 4H_2O$	578,61	180—800	$CaCO_3$	34,60	34,74
$Ba_2RA_4 \cdot 4H_2O$	773,13	180—780	$BaCO_3$	51,05	51,16
$Co_2RA_4 \cdot 6H_2O$	652,36	100—540	CoO	22,97	23,00
$Ni_2Ra_4 \cdot 6H_2O$	651,93	140—580	NiO	22,92	22,36
$Al_4[RA_4]_3 \cdot 10H_2O$	1 567,24	100—940	Al_2O_3	12,90	12,86
$La_4[RA_4]_3 \cdot 10H_2O$	2 015,01	160—680	La_2O_3	32,34	32,14
$Cr_4[RA_4]_3$	1 487,31	200—485	Cr_2O_3	20,43	20,01
$Fe_4[RA_4]_3 \cdot 4H_2O$	1 574,63	130—680	Fe_2O_3	20,28	20,10
$ThRA_4 \cdot 8H_2O$	1 460,99	100—910	ThO_2	36,15	36,25

$R: = N - C_6H_4 - CH_2 - C_6H_4 - N = ;\quad A = -CH_2COO^- ;$

TABELLE 4

Zuordnung der in den IR-Spektren der synthetisierten Substanzen erschienenen Banden

Zugeordnete Banden Substanz	$\nu - CH_2 -$	$\nu - CH_2COOH$	$\nu - COO^-$	$\nu - C - H$	$\nu - COO^-$	$\nu - CH_2COOH$	$\nu Ar - N =$	$\nu Ar - N =$	$\nu - C - N$	$\nu - CH_2COOH$	$\nu - C_6H_4 -$
H_4RA_4	2 920 s	1 720 s	1 615 ss	1 520 ss	1 430 m	1 380 ss	1 330 s	1 235 s	1 190 ss	925 m	800 s
$Li_4RA_4 \cdot 4H_2O$	2 930 s	—	1 605 ss	1 520 ss	1 420 s	—	1 320 s	1 225 s	1 190 m	—	810 ss
$Na_4RA_4 \cdot 4H_2O$	2 930 s	—	1 610 ss	1 520 ss	1 425 s	—	1 340 s	1 230 s	1 195 ms	—	810 ss
$Ca_2RA_4 \cdot 4H_2O$	2 930 s	—	1 620 s	1 520 ss	1 425 s	—	1 325 s	1 210 m	1 195 ms	—	805 s
$Ba_2RA_4 \cdot 4H_2O$	2 940 s	—	1 620 s	1 520 ss	1 425 s	—	1 320 s	1 235 s	1 190 ms	—	810 s
$Mn_2RA_4 \cdot 4H_2O$	2 925 s	—	1 618 s	1 520 ss	1 425 s	—	1 330 m	1 230 s	1 195 m	—	805 m
$CO_2RA_4 \cdot 6H_2O$	2 930 s	—	1 615 s	1 520 ss	1 428 m	—	1 338 m	1 230 m	1 193 m	—	810 m
$Ni_2RA_4 \cdot 6H_2O$	2 930 s	—	1 618 s	1 520 s	1 425 m	—	1 335 m	1 233 m	1 195 m	—	806 m
$Cu_2RA_4 \cdot 2H_2O$	2 930 s	—	1 620 s	1 515 s	1 430 m	—	1 330 m	1 230 m	1 190 m	—	800 m
$Al_4[RA_4]_3 \cdot 10H_2O$	2 930 s	—	1 610 ss	1 520 ss	1 415 m	—	1 335 s	1 235 s	1 190 s	—	805 s
$La_4[RA_4]_3 \cdot 10H_2O$	2 940 s	—	1 620 ss	1 520 ss	1 415 s	—	1 325 s	1 230 s	1 195 s	—	810 s
$Cr_4[RA_4]_3$	2 940 s	—	1 620 ss	1 520 ss	1 415 s	—	1 330 s	1 235 s	1 195 s	—	810 s
$Fe_4[RA_4]_3 \cdot 4H_2O$	2 940 s	—	1 620 ss	1 520 ss	1 420 s	—	1 325 m	1 230 m	1 195 s	—	810 s
$ThRA_4 \cdot 8H_2O$	2 930 s	—	1 620 s	1 525 s	1 410 s	—	1 330 s	1 230 s	1 190 s	—	805 s

R: $= N - C_6H_4 - CH_2 - C_6H_4 - N =$; A $= - CH_2COO^-$; ss = sehr stark; s = stark; m = mäßig; ms = mäßig stark.

Die Reflexionselektronenspektren wurden mit einem Carl-Zeiss VSU-2P Spektrophotometer im Bereich 320 — 1 300 nm aufgenommen (Tabelle 5)

Für die magnetischen Suszeptibilitätbestimmungen gelangt die Faraday Methode, unter Benützung der Standarde $Co[Hg(SCN)_4]$ zur Anwendung (Tabelle 6).

TABELLE 5

Diffuse Elektronenreflexionsspektren einiger neutraler Salze der H_4RA_4 Säure

Synthetisierte Substanz	ν_1 cm^{-1}	ν_2 cm^{-1}	ν_3 cm^{-1}
$Co_2RA_4 \cdot 6H_2O$	$4_{T_{2g}} - 4_{T_{1g}}$ 8 000	$4_{T_{2g}} - 4_{T_{1g}}$ 15 800	$4_{T_{1g}}$ (P)$-4_{T_{1g}}$ (F) 19 000
$Ni_2RA_4 \cdot 6H_2O$	$3_{T_{2g}} - 3_{A_{2g}}$ 8 800	$3_{T_{1g}} - 3_{A_{2g}}$ 15 750	$3_{T_{1g}}$ (P)$-3_{A_{2g}}$ (F) 25 200
$Cr_4[RA_4]_3$	$4_{T_{2g}} - 4_{A_{2g}}$ 14 900	$4_{T_{1g}} - 4_{A_{2g}}$ 16 400	$4_{T_{1g}}$ (P)$-4_{A_{2g}}$ (F) 25 300

$R: = N - C_6H_4 - CH_2 - C_6H_4 - N =$; $A: - CH_2COO^-$;

TABELLE 6

Magnetische Eigenschaften einiger neutraler Salze der H_4RA_4 Säure

Synthetisierte Substanz	T°K	$\chi g.10^6$	$\chi_{M \cdot cor} \cdot 10^6$	μ BM
$Co_2RA_4 \cdot 6H_2O$	296	28,29	9 347	4,72
$Ni_2RA_4 \cdot 6H_2O$	296	12,73	4 035	3,10
$Cr_4[RA_4]_3$	296	16,17	6 136	3,83

$R: = N - C_6H_4 - CH_2 - C_6H_4 - N =$; A ; $- CH_2COO^-$;

DISKUSSION

Die chemische Analyse der synthetisierten komplexen Salze (Tabelle 2) bestätigt das Verhältnis Metall : Ligand (4 : 1 für M^I, 4 : 2 oder 2 : 1 für M^{II}, 4 : 3 für M^{III}, 4 : 4 oder 1 : 1 für M^{IV}).

Aus den thermogravimetrischen Diagrammen der Metall-Salze geht hervor, daß die Veränderungen, die während der Erwärmung der Proben bis auf 1000° stattfinden, sich nicht mit hinreichender Klarheit in der Gestalt der TG-Kurven widerspiegeln. Außer den Inflexionen im Temperaturbereich zwischen 100 — 160° die einen, dem Wassergehalt der Proben entsprechenden Gewichtsverlust andeuten konnten keine anderen Intervalle festgestellt werden, die klar abgegrenzten Veränderungen entsprechen würden, entsprechend den Zersetzungsprodukten von CO, CO_2, NH_3 die zu erwarten gewesen wäre. Die Temperaturbereiche, in denen diese Veränderung sattfinden überlagern sich wobei die Zersetzungsprodukte gleichzeitig anfallen. Der Abschluß dieser Veränderung wird durch eine horizontale Strecke angedeutet, die quantitativ dem Produkt entspricht, das nach der thermischen Zersetzung jeder Probe zurückbleibt.

Die IR-Spektren der synthetisierten festen neutralen Salze bestätigten die Substitution der vier Protonen aus dem Molekül der freien H_4RA_4 Säure durch Metallionen. Vergleichende Untersuchungen der IR-Spektren (Tabelle 4) bestätigen das Vorhandensein der $-COOM$ Gruppe und die völlige Abwesenheit der entsprechenden freien Säurefunktionen ($-CH_2COOH$ Gruppen). Die Anwesenheit der bisubstituierten Arylamine ($Ar-N=$) sowie aller Übrigen, auch in der Ausgangssubstanz enthaltenen Gruppen (wie : $-CH_2-$, $-C_6H_4-$, $-C-N$, $-CH$), konnten ebenfals durch die IR-Spektren bestätigt werden. Es konnten keine Gesetzmäßigkeiten bezüglich der Verschiebung der Frequenzen in Abhängigkeit des enthaltenen Metallions im Slaz festgestellt werden.[3]

Die diffusen Elektronenreflexionsspektren mancher synthetisierter Salze weisen eine Hexakoordinierung mit oktaedrisch verzerrter Symmetrie auf. Als Folge der Verzerrung erscheint z.B. im Spektrum des Chromsalzes bei 14 900 cm^{-2} eine Schwelle die auf die Aufhebung der partiellen Steigung der Degenerierung des Termes $^4T_{2g}$ (F) zurückzuführen ist.[4,5] Diese Tatsache wurde durch Bestimmung der magnetischen Momente bestätigt. Aus Tabelle 6 geht hervor, daß das magnetische Moment für Ni(II)-Chelat einen größeren Wert hat, als der nur dem Spin (2,83 BM) entsprechende, sowie es für das Ni^{2+}-Ion in oktaedrischer Konfiguration mit dem $^3A_{2g}$ Siglett-Grundterm zu erwarten wäre. Anderseits bestätigt das magnetische Moment (4,27 BM) für das Co(II) Salz die Anwesenheit eines den oktaedrischen Komplexverbindungen entsprechenden $^4T_{2g}$ Grundtermes. Der größere Wert des magnetischen Moments wird bedingt durch die Spin-Bahn Kopplungen aus dem Inneren des $^4T_{1g}$ und der gleichzeitigen Kopplung mit dem nächsten höher angeregten Term.

SCHLUßBEMERKUNGEN

Die Ergebnisse der chemischen und thermogravimetrischen Untersuchungen der synthetisierten neutralen Salze der H_4RA_4 Säure ermöglichten das Aufstellen folgender wahrscheinlichster Strukturschemen :

a. für die Salze der H_4RA_4 Säure mit Alkalimetallen :

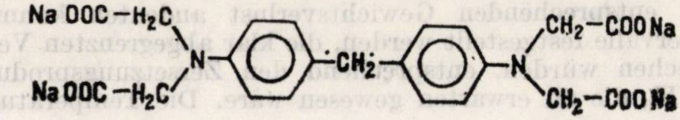

b. für die neutralen Salze der H_4RA_4 Säure mit Erdalkalimetallen:

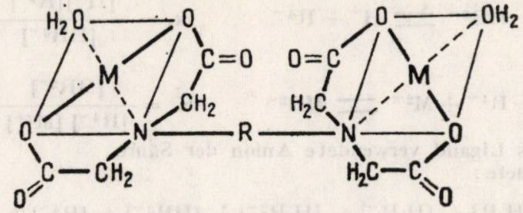

c. für die neutralen Salze von Co(II), Ni(II), eine dimere Struktur:

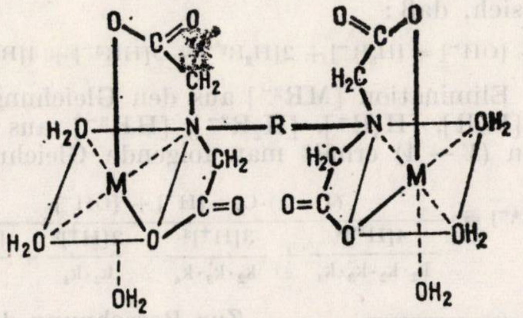

Für die neutralen Salze der H_4RA_4 Säure mit I-, II-, III- und IV-wertigen Metallionen sind räumliche polymere Strukturen möglich, die schwieriger darzustellen sind.

BESTIMMUNG DER STABILITÄTSKONSTANTEN

Um die Differenzierung der Salze nach ihrer Stabilität durchführen zu können, und eventuelle Vergleiche mit ähnlichen komplexen Verbindungen anderer Komplexonen vornehmen zu können, wurden Berechnungen der Stabilitätskonstanten einiger synthetisierten komplexen Verbindungen (Cu^{2+}, Co^{2+}, Cd^{2+}) mit der von Schwarzenbach, Freitag, Courtney, Chabereck Jr., Martell A.$^{6-9}$ beschriebenen algebraischen Methode bei EDTA und anderen analogen Säure durchgeführt.

Bei der Durchführung dieser Berechnung haben wir jene Gleichgewichte in Betracht genommen die wir auch im Falle der H_4RA_4-Säure als anwesend betrachteten und die wir auch mit H_4R bezeichnen können:

$$H_4R \rightleftharpoons H^+ + H_3R^- \qquad k_1 = \frac{[H^+][H_3R^-]}{[H_4R]} \qquad (1)$$

$$H_3R^- \rightleftharpoons H^+ + H_2R^{2-} \qquad k_2 = \frac{[H^+][H_2R^{2-}]}{[H_3R^-]} \qquad (2)$$

$$H_2R^{2-} \rightleftharpoons H^+ + HR^{3-} \qquad k_3 = \frac{[H^+][HR^{3-}]}{[H_2R^{2-}]} \tag{3}$$

$$HR^{3-} \rightleftharpoons H^+ + R^{4-} \qquad k_4 = \frac{[H^+][R^{4-}]}{[HR^{3-}]} \tag{4}$$

$$R^{4-} + M^{2+} \rightleftharpoons MR^{2-} \qquad K = \frac{[MR^{2-}]}{[R^{4-}]\,[M^{2+}]} \tag{5}$$

R^{4-} = das als Ligand verwendete Anion der Säure.
Man bezeichnete:

$$C_R = [H_4R] + [H_3R^-] + [H_2R^{2-}] + [HR^{3-}] + [R^{4-}] + [MR^{2-}] \tag{6}$$

$$C_M = [M^{2+}] + [MR^{2-}] \tag{7}$$

bzw., C_R = die Molarkonzentration der Säuretypen; C_M = die Molarkonzentration der Typen mit Metallionen. Aus der Elektroneutralitätsbedingung ergibt sich, daß:

$$aC_R + [H^+] + [OH^-] = [H_3R^-] + 2[H_2R^{2-}] + 3[HR^{3-}] + 4[R^{4-}] + 4[MR^{2-}] \tag{8}$$

Durch die Elimination $[MR^{2-}]$ aus den Gleichung (5), (6) und die Substituierung $[H_4R]$, $[H_3R^-]$, $[H_2R^{2-}]$, $[HR^{3-}]$, aus den entsprechenden Gleichungen (1 — 4) erhält man folgende Gleichung für $[R^{4-}]$:

$$[R^{4-}] = \frac{(4-a)\cdot C_R - [H^+] + [OH^-]}{\dfrac{4[H^+]^4}{k_1\cdot k_2\cdot k_3\cdot k_4} + \dfrac{3[H^+]^3}{k_2\cdot k_3\cdot k_4} + \dfrac{2[H^+]^2}{k_3\cdot k_4} + \dfrac{[H^+]}{k_4}} \tag{9}$$

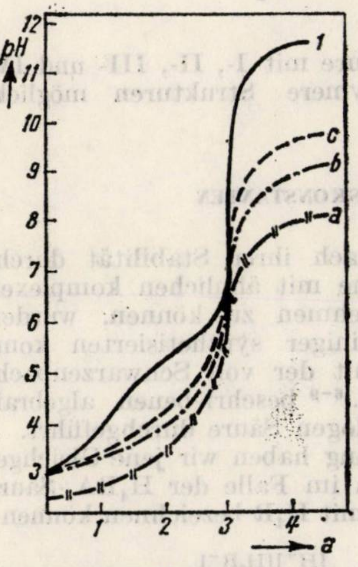

Abb.1. — Potentiometrische Titrationskurve der H_4RA_4 Säure mit NaOH 0,1 N in Gegenwart von ächivalenten Mengen der Ionen Cu^{2+}, Co^{2+}, Cd^{2+}.

Zur Berechnung der Stabilitätskonstante K verwendet man nächstfolgende Gleichung (10) die meßbare, aus den Ergebnisse erhaltene Größen umfaßt; diese dienten zur Festlegung der potentiometrischen Titrationskurve (Abb. 1) der liganden Säure (H_4RA_4, in unserem Fall) mit NaOH 0,1 N in Anwesenheit der Metallionen des Salzes, das sich im Verhältnis M : L bildet:

$$K = \frac{C_R - y[R^{4-}]}{[R^{4-}]\,C_M + y[R^{4-}] - C_R} \tag{10}$$

eine Gleichung zu der man als Folge der Elimination $[M^{2+}]$ und $[MR^{2-}]$ aus der Gleichung (5), durch Verwendung der Gleichungen (6), (7) und Substituierung in den Gleichungen (1—4) für $[H_4R]$, $[H_3R^-]$, $[H_2R^{2-}]$, $[HR^{3-}]$, gelangte und wo:

$$y = \frac{[H^+]^4}{k_1\cdot k_2\cdot k_3\cdot k_4} + \frac{[H^+]^3}{k_2\cdot k_3\cdot k_4} + \frac{[H^+]^2}{k_3\cdot k_4} + \frac{[H^+]}{k_4} + 1 \tag{11}$$

Da die Konzentration [OH^-] klein war, wurde sie vernachlässigt. Die Berechnungen wurden mit Hilfe des elektronischen Digitalrechners „Wang 2200 B" an der Universität aus Braşov durchgeführt.

Parallel mit den unter Berücksichtigung der Titrationskurve der EDTA Säure mit NaOH 0,1 N ausgeführten Berechnungen in Anwesenheit derselben Ionen, bzw. Cu^{2+}, Co^{2+}, Cd^{2+} wurden folgende Werte der Stabilitätskonstanten (bzw. pK-Werte) für die von uns synthetisierten Salze erhalten (Tabelle 7)

TABELLE 7

Stabilitäts-pK einiger Äthylendiaminotetraessigsäure (EDTA), Äthylendiaminodiessigdipropionsäure (EDDADP), Äthylendiaminotetrapropionsäure (EDTP) und 4,4′ diaminodiphenylmethan-N,N′-tetraessigsäure (H_4RA_4) Salze mit Cu^{2+}, Co^{2+}, Cd^{2+}

	Dissoziations-pK				Stabilitäts-pK			
	pk_1	pk_2	Pk_3	pk_4	Cu	Co	Cd	Lit.
EDTA	2,00	2,67	6,13	10,26	18,3	16,4	16,3	6
EDDADP	3,00	3,79	5,98	9.83	16,3	14,9	11,8	8
EDTP	3,00	3,83	6,77	9,60	15,4	7,6	6,0	9
H_4RA_4	3,35	4,80	5,70	11,15	15,00	13,14	12,93	–

R: $=N-C_6H_4-CH_2-C_6H_4-N=$; A: CH_2COO^- ;

Aus dem Vergleich der in der Tabelle 7 vorhandenen Daten ergibt sich auch für die H_4RA_4 Säure dieselbe Reihenfolge für die Stabilität der Cu-, Co-, Cd-Chelate wie auch im Falle anderer als Liganden verwendeter Aminotetracarboxylsäuren.

Die Tatsache, daß die Werte der Stabilitätskonstanten der Salze (Chelate) der H_4RA_4-Säure mit Cu^{2+}, Co^{2+}, Cd^{2+} kleiner sind, als die der anderen betrachteten Säuren, läßt sich durch die Natur des organischen Radikals zwischen den Aminodiessiggruppen erklären, das sie stark voneinander trennt. Die kleine Stabilität der Chelate mit RA_4^{4-} als Ligand wird auch praktisch bestätigt. Im Falle des Kupferkomplexonates z. B. wurde diese Tatsache leicht an der Farbänderung bemerkt : das Kupferkomplexonat der H_4RA_4 Säure ist in Wasser unlöslich und hat eine intensiv grüne Farbe. Beim Hinzufügen einer Na-EDTA oder EDTA Lösung, löst sich der intensiv grüne Niederschlag auf und die Farbe wird blau, dem Kupferchelat der EDTA entsprechend. Dieser Stabilitätsunterschied zwischen den Chelaten der von uns synthetisierten H_4RA_4 Säure und der EDTA Säure oder anderen Säuren (Komplexonen) eröffnet die Möglichkeit der Verwendung der freien H_4RA_4 Säure, und vor allem ihrer löslichen Salze als Sequestrierungsmittel für bestimmte Metallionen, bei pH-Werte, und der Dosierung des Metalls mit EDTA.

LITERATUR

[1] Part. IV. Const. Gh. Macarovici und E. Chiş, *Rev. Roumaine Chim.*, **11 – 12**, 1457 (1979).
[2] Const. Gh. Macarovici und E. Chiş, *Rev. Roumaine Chim.*, Im Druck.
[3] K. Nakamoto, Y. Morimoto und A. E. Martell, *J. Amer. Chem. Soc.*, **84**, 2081 (1967).
[4] B. N. Figgis, „Introduction to Ligand Fields", Interscience Ind. Ed., New York, 1967, S. 257.
[5] A. D. P. Lewer, "Inorganic Electronic Spectroscopy", Elsevier, Amsterdam, 1967, S. 249–265.
[6] G. Schwarzenbach und G. Freitag, *Helv. Chim. Acta*, **34**, 1503 (1951).
[7] S. Chaberek Jr. und A. E. Martell, *J. Amer Chem. Soc.*, **74**, 5052 (1952).
[8] G. Schwarzenbach, C. Courtney und A. E. Martell, *J. Amer. Chem. Soc.*, **74**, 6228 (1952).
[9] S. Chaberek Jr., C. Courtney und A. E. Martell, *J. Amer. Chem. Soc.*, **74**, 4814(1953).

Revue Roumaine de Chimie 25, 7, 105 – 109 (1980)

CHEMICAL AND SPECTROSCOPIC PROPERTIES OF SILVER-PHOSPHINE COMPLEXES CONTAINING OXINE

NAJMA SULTANA*, IRSHAD A. KHAN* and S.R.R.NAQVI**

* Department of Pharmaceutical Chemistry, Faculty of Pharmacy, University of Karachi, Karachi — 32, Pakistan

** Department of Chemistry, University of Karachi, Karachi — 32, Pakistan

Received January 16, 1978

Silver(I) complexes of the type $[AgX(PPh_3)_y(HOx_z]_n$ ($X = Br^-$, I^-, NO_3^- or SCN^-; PPh_3 = triphenylphosphine; HOx = 8-hydroxyquinoline) have been prepared. The variation in stoichiometry and the probable structure of these complexes have been discussed in view of their chemical and spectral data; these complexes have been suggested to have dimeric structure and the experimental data are in support of the bridging of halides, nitrate or thiocyanate group between the two silver atoms.

INTRODUCTION

Silver forms four types of complexes with ligand metal ratio 1 : 1, 2 : 1, 3 : 1, and 4 : 1 having a tetrahedral configuration. The mixed ligand complexes of the type $[CuNO_3(PPh_3)(biL)]$[1] and $[CuI(PPh_3)(Py)]$[2] have been reported where biL is 1, 10-phenenthroline or 2,2-biquinolyl. We have extended this study to the incorporation of 8-hydroxyquinoline into triphenylphosphine complexes with their synthesis, characterization and spectral studies. This paper deals with the study of complexes of triphenylphosphine and 8-hydroxyquinoline with silver bromide, iodide, nitrate and thiocyanate. 8-Hydroxyquinoline forms different compounds with silver triphenylphosphine with the ratio 1 : 1 and 2 : 1. The infrared spectral studies in the region 4000 — 700 cm^{-1} suggest that silver (I) has the coordination numbers 4, 5 and 6 in these complexes. They are sparingly soluble in most of the organic solvents consistent with a polymeric character.

RESULTS AND DISCUSSION

The analytical data of the complexes (Table 1) are compatible with the proposed stoichiometry and structures. These compounds are generally sparingly soluble in common organic solvents, thus prohibiting the measurement of their N.M.R. spectra and electrical conductivity. The property

TABLE 1

Elemental analysis and melting point [a]

Compound	C%	H%	N%	X%	P%	Ag%	M.P.	Colour
$[AgBr(PPh_3)(HOx)_2]_2.2H_2O$	55.80 (55.67)	4.02 (4.25)	3.71 (3.61)	10.10 (10.31)	3.80 (3.99)	13.80 (13.91)	154°	Yellow
$[AgBr(PPh_3)_2(HOx)_2]_2 \cdot H_2O$	63.21 (63.53)	4.54 (4.51)	2.68 (2.75)	7.68 (7.84)	5.98 (6.07)	10.23 (10.58)	160°	Yellow
$[AgBr(PPh_3)(HOx)]_2$	54.10 (54.45)	3.47 (3.69)	2.10 (2.35)	13.10 (13.44)	4.98 (5.21)	17.97 (18.15)	240°	Yellow
$[AgI(PPh_3)_2(HOx)]_2 \cdot 2H_2O$	58.23 (58.56)	4.39 (4.44)	1.38 (1.51)	13.31 (13.77)	6.45 (6.72)	11.48 (11.71)	190°d	Pale yellow
$[AgI(PPh_3)(HOx)]_2$	50.37 (50.46)	3.29 (3.43)	2.09 (2.18)	19.41 (19.78)	4.65 (4.82)	16.38 (16.82)	260°	Yellow
$[AgI(PPh_3)_2(HOx)_2]_2$	62.31 (61.77)	4.34 (4.19)	2.41 (2.67)	12.08 (12.11)	5.70 (5.91)	10.06 (10.29)	140°	Yellow
$[AgNO_3(PPh_3)_2(HOx)]_2$	64.73 (64.36	4.81 (4.41)	3.23 (3.33)	— —	7.10 (7.38)	12.38 (12.87)	235°d	Pale yellow
$[AgSCN(PPh_3)_2(HOx)]_2 \cdot H_2O$	64.81 (64.71)	4.80 (4.57)	3.10 (3.28)	3.52 (3.75)	7.08 (7.27)	12.38 (12.66)	240°	Pale yellow

[a] Calculated values are given in parentheses.

suggests that ionic species are unlikely. Anionic bridged dimers may be assumed to show distorted octahedral, tetrahedral and pentagonal structures. The magnetic susceptibility measurements proved these compounds to be diamagnetic and further support the position of the metal atom.

In halo—bis-(triphenylphosphine) and halo-tetrakis-(triphenylphosphine)silver (I) complexes, there are three coordination groups in the monomeric formula which do not complete square coordination of silver and hence the bridged structures have to be assumed for them. [3] The tetrakis-halo(triphenylphosphine)silver(I) complexes give different products when treated with equimolar ratios of 8-hydroxyquinoline. The reaction of tetrakis-bromo(triphenylphosphine)silver(I) with oxine in equimolar ratio gave the compound of the type $[AgBr(PPh_3)(HOx)_2]_2 \cdot .H_2O$; whereas the iodo complex gave the compounds having the form ulae $[AgI(PPh_3)_2(HOx)]_2.2H_2O$. When the concentration of the ligand 8-hydroxyquinoline increased twice, the compounds bearing the general formula $[AgX(PPh_3)_2(HOx)_2]_2$ were obtained. When di-μ-halo-bis (triphenylphosphine)silver(I) (where $X=Br^-$ or I^-) were treated with 8-hydroxyquinoline in equimolar ratio the compounds of the type $[AgX(PPh_3)(HOx)]_2$ were obtained. The complexes are pale-yellow and diamagnetic in character. By doubling the ratio of the ligand (HOx) in the above reactions, the complexes $[AgBr(PPh_3)(HOx)_2]_2$ and $[AgI(PPh_3)_2(HOx)_2]_2$ were obtained respectively. The halogen was knocked out if the ratio of the ligand (HOx) increased four times.

The sensitive modes of P—C stretching vibrations of triphenylphosphine complexes are at 1089 and 698 cm^{-1}. [4] The shift in the region 1098—1105 cm^{-1} has been observed in all the mixed ligand complexes prepared in this laboratory. According to Sheldon and Tyree [5] a band is observed near 720 cm^{-1} whenever phosphine acts as a donor or it is in the four-coordinated state. This band in our complexes occurs in association with the band of 698 cm^{-1} in the form of a doublet at 706 cm^{-1}- The two absorptions around 1098 and 1037 cm^{-1} in our complexes are very. intense whereas the other absorptions are of weak intensity.

The spectrum of 8-hydroxyquinoline shows the peaks at 1504 and 1580 cm^{-1} which are generally assigned to C = C and C ≡ N vibrations. The complexes show the former peak slightly shifted to a higher frequency, around 1507 cm^{-1}, whereas the latter occurs in the same position with an increase in intensity. The peaks observed around 1000 — 1200 cm^{-1} and 782 cm^{-1} are attributed to ring vibrations and C—H deformations. In metal chelates a peak is observed in the region 850 — 870 cm^{-1} which is assigned to a diatomic vibration, possibly to the C—O bond or to an M—O stretching frequency. [6] This band is absent in these complexes indicating the presence of free oxine. The strucural formulae of the compounds $[AgX(PPh_3)(HOx)]_2$ are supposed to be dimeric with halogen bridging, having distorted tetrahedral structures. The dimeric nature of these compounds is further on supported by the magnetic susceptibility measurements showing them to be diamagnetic.

The reaction of 8-hydroxyquinoline with tetrakisnitrato(triphenylphosphine)silver(I) in equimolar ratio gave the compound $[AgNO_3(PPh_3)_2(HOx)]_2$. The i.r. spectrum of the compound records the peak at 782 cm^{-1} indicating the presence of the ligand oxine. The presence of coordinated bidentate nitrato group is consistent with the peak recorded at 1288 cm^{-1}.[7] The bridged structure of the compound is further supported on the basis of i.r. spectra of $CuNO_3(PPh_3)_2$ and $CuNO_3(PPh_3)_3$ and X-ray crystallographic study of the former one which has shown it to be tetrahedrally coordinated copper (I) with a bidentate nitrato group.[8] The mono- and bidentate nitrato groups have been distinguished on the basis of the magnitude of the splitting as observed in the complexes $CuNO_3(PPh_3)_2$ and $CuNO_3(PPh_3)_3$.[8] The former has a splitting of 120 cm^{-1} and the latter of 200 cm^{-1}. It is therefore deduced that the nitrato group in our complexes is bridging the silver (I) atoms.

The reaction between di-μ-thiocyanato-bis-(triphenylphosphine)silver(I) and 8-hydroxyquinoline in equimolar ratio gave the compound $[AgSCN(PPh_3)_2(HOx)]_2.H_2O$. The structure of the compound is difficult to ascertain. It seems likely that the answer could only be obtained by X-ray analysis, but the nature of the SCN group may be ascertained on the basis of i.r. spectroscopy. The i.r. spectrum of the compound regarding bridge forming thiocyanato group between two metal atoms is consistent with the sharp band at 2103 cm^{-1}.

Chatt and coworkers[9] and later on Vallarino[10] have shown that the $C = N$ stretching frequency is at higher wave number 2150 — 2182 cm^{-1} when SCN group is bridging and in the range 2100 — 2150 cm^{-1} when it acts as a monodentate ligand. The complex $[AgSCN(PPh_3)_2(HOx)]_2.H_2O$ under study has a value somewhat at a lower wave number. This may be due to the unsymmetrically bonded thiocyanate, as stated in the case of $(NH_4)_4[Cd(NCS)_4.2H_2O$[11] or due to the presence of two ligands having a large difference in basicity and in π-bonding ability towards the silver(I) atoms. Similar results were obtained by Toeindiskoetter and Solomon[12] when examining the several complexes of N-heterocyclic amines with copper(I) and copper(II) thiocyanates.

EXPERIMENTAL

$[AgBr(PPh_3)(HOx)_2]_2.2HO$. was obtained by refluxing 8-hydroxy quinoline and tetrakis-bromo(triphenylphosphine)silver(I)[3] in benzene in equimolar ratio for 4—5 hours and crystallizing the solution at room temperature. If the ratio of 8-hydroxyquinoline was doubled in this reaction, the compound $[AgBr(PPh_3)_2(HOx)_2]_2.H_2O$ was obtained.

$[AgBr(PPh_3)(HOx)]_2$: was prepared by refluxing equimolar quantities of 8-hydroxyquinoline and di-μ-bromobis-(triphenylphosphine)=silver(I)[3] in benzene for about 4 hours; yellow crystals were obtained. By increasing the ratio of 8-hydroxyquinoline to 2 moles in the above reaction the compound $[AgBr(PPh_3)(HOx)_2]_2.2H_2O$ was obtained.

$[AgI(PPh_3)_2(HOx)]_2.2H_2O$: was prepared by refluxing equimolar quantities of 8-hydroxyquinoline and tetrakis-iodo(triphenyl-phosphine)silver(I)[3] in benzene for about 4—5 hours; pale yellow crystals were obtained. By doubling the ratio of 8-hydroxyquinoline in this reaction, yellow crystals of the compound $[AgI(PPh_3)_2(HOx)_2]_2$ were obtained.

$[AgI(PPh_3)(HOx)]_2$: was prepared by reflexing equimolar quantities of 8-hydroxyquinoline and di-μ-iodobis-(triphenylphosphine)silver(I)[3] in benzene for 4—5 hours. If the concentration of 8-hydroxyquinoline increased twice the compound $[AgI(PPh_3)_2(HOx)_2]_2$ was obtained.

$[AgNO_3(PPh_3)_2(HOx)]_2$: was prepared by refluxing equimolar ratio of 8-hydroxyquinoline and tetrakis-nitrato(triphenylphosphine)-silver(I)[3] in ethanol for about 5 hours; pale yellow crystals were obtained.

$[AgSCN(PPh_3)_2(HOx)]_2.H_2O$: was prepared by refluxing 8-hydroxyquinoline and di-μ-thiocyanato-bis-(triphenylphosphine) silver(I) in chloroform in equimolar ratio for about four hours; pale yellow crystalls were obtained.

I.R. spectra were recorded on a Perkin Elmer Model 237 Spectrophotometer using KBr pellets. Magnetic susceptibility measurements were made on powdered samples using a Newport Single Temperature Guoy Balance system Type C. We are indebted to P.C.S.I.R. Laboratories Karachi for using this Guoy Balance.

REFERENCES

[1] F. H. Jardine, A. G. Vohra and T. J. Young, *J. Inorg. Nuclear Chem.*, **33**, 2941 (1971).

[2] A. G. Vohra and T. Jannat, *Pak. J. Sci. Ind. Res.*, **16**, 164 (1973).

[3] A. G. Vohra, *Ph. D. thesis, University of London*, (1969).

[4] D. B. Deacon and J. H. S. Green, *Chem. Ind.*, **1965**, 1031.

[5] B. Sheldon and S. Y. Tyree, *J. Amer. Chem. Soc.*, **80**, 2117 (1958).

[6] R. G. Charles, H. Freiser, R. Friedel, L. E. Hillard and W. D. Johnston, *Spectrochim Acta.*, **1**, 8 (1956).

[7] N. F. Curtis and Y. M. Curtis, *Inorg. Chem.*, **4**, 804 (1965).

[8] G. G. Messmer and C. J. Palenik, *Canad. J. Chem.*, **47**, 1440 (1969); *Inorg. Chem.*, **8**, 2750 1969).

[9] J. Chatt and L. A. Duncanson, *Nature*, **178**, 997 (1965).

[10] L. Vallarino, *J. chem. Soc.*, **1957**, 2473.

[11] P. C. H. Mitchel and R.R.J. Wilkains, *J. Chem. Soc.*, **1960**, 1912.

[12] R. H. Toeniskoetter and S. Solomon, *Inorg. Chem.*, **7**, 617 (1968).

Revue Roumaine de Chimie, 25, 1, 111 – 120 (1980)

THERMAL PHASE EQUILIBRIA IN THE SYSTEM $BaO-ZnO-Fe_2O_3$ WITH APPLICATION TO MAGNETOCERAMICS

S. SOLACOLU, MARIA ZAHARESCU and MARINA DOROBANŢU

Bucharest, Center of Physical Chemistry – ICECHIM, Splaiul Independenţei 202, Romania

Received February 23, 1977

Revised March 23, 1979

Subsolidus thermal phase equilibria of the $BaO-ZnO-Fe_2O_3$ system have been studied, paragenesis subsystems have been established, and the formation mechanism of the defined compounds has been elucidated.

1. INTRODUCTION

Hexagonal ferrites are a class of magnetic materials having useful properties in the high frequency range, firstly noted by Jonker, Wijn and Braun.[1]

These materials can be described in terms of compositions belonging to systems of the $BaO-MeO-Fe_2O_3$ type, where Me = Co, Cu, Ni, Zn, Mg, Fe^{2+}, and Mn^{2+}.[2]

A scientific foundation of the study of these materials has been initiated by thermal phase equilibria investigation. This work deals with the ternary system $BaO-ZnO-Fe_2O_3$.

The binaries of this system have been previously studied. The binary $BaO-Fe_2O_3$ has been studied by some investigators,[3-5] chiefly because of the practical importance of the $BaO \cdot 6Fe_2O_3$ as a permanent magnet.[6] The thermal phase equilibrium diagram shows three compounds : $2BaO \cdot Fe_2O_3$, $BaO \cdot Fe_2O_3$ and $BaO \cdot 6Fe_2O_3$, and two eutectics: between $2BaO \cdot Fe_2O_3$ and $BaO \cdot Fe_2O_3$ at 41 mole % Fe_2O_3 and 1330°, and between $BaO \cdot Fe_2O_3$ and $BaO \cdot 6Fe_2O_3$ at 60 mole % Fe_2O_3 and 1370°. The presence of a narrow field of solid solutions near $BaO \cdot 6Fe_2O_3$ is noted, whose composition varies between 18.2 mole % BaO : 81.8 mole % Fe_2O_3 at 1350°, and 16.7 mole % BaO : 83.3 mole % Fe_2O_3 at 800°. Recently, Shirk[7] has synthetized a metastable compound $2BaO \cdot 3Fe_2O_3$, by solid phase reaction, and Okamoto *et al.*[8] obtained $BaO \cdot 2Fe_2O_3$ under hydrothermal conditions. The compounds in this system crystallize as follows : $2BaO \cdot Fe_2O_3$ in the cubic system,[9] $BaO \cdot Fe_2O_3$ is orthorhombic and has the superstructure of hexagonal $BaO \cdot Al_2O_3$,[10] and $BaO \cdot 6Fe_2O_3$ is hexagonal, with the structure of magnetoplumbite.[11]

Mori[12] noted the formation of a $BaFeO_x$ phase ($x = 2.5 - 3.0$), which can exist in some structural forms, depending on the amount of oxygen (x), namely, either as a hexagonal phase similar to $BaO \cdot TiO_2$, or as perowskite-type phases. Meriani[13] noted the existence of three polymorphs of $BaO \cdot Fe_2O_3$, by high-temperature diffractometry, namely $\gamma-BaO \cdot Fe_2O_3$ (orthorhombic), stable up to 800°, $\beta-BaO \cdot Fe_2O_3$ (orthorhombic pseudohexagonal), stable between 800° and 1 000°, and $\alpha-BaO \cdot Fe_2O_3$ (hexagonal), stable above 1 000°. By annealing the β—phase at room temperature, an orthorhombic, metastable β'—phase is obtained. The two points of polymorphic transformation had been previously determined by Ziolowski,[14] using the differential thermal analysis.

The formation mechanism of the defined chemical compounds in the $BaO-Fe_2O_3$ system by solid-phase reaction has been studied by Erchak *et al.*,[15] Suchet,[16] and Wullkopf.[17-18]

Thermal phase equilibria in the system $ZnO-Fe_2O_3$ have been studied by Toropov and Borisenko.[19-20] In this system a compound is formed, the zinc ferrite, which crystallizes in the cubic system, with a normal spinel-type structure. Up to 1100° the system is stable; above this temperature the Fe_2O_3 dissociation and ZnO volatilization are observed. Under the given experimental conditions, the presence of a continuous series of solid solutions between $ZnO \cdot Fe_2O_3$ and Fe_2O_3 is noted, between the limits 66.24—83.07 weight % Fe_2O_3.

There are available detailed studies dealing with the ZnO thermal decomposition.[21-22] Dulin and Rase[21] established that the volatilization of powdered ZnO, maintained for 24 hours at 1 300° has values between 0.51 and 1.22 weight %. The solid-phase reaction between ZnO and Fe_2O_3 with the formation of $ZnO \cdot Fe_2O_3$ has been studied by Parker *et al.*,[23] who confirmed the mechanism proposed by Reijen[24] for this reaction. By measurements of solubility in HNO_3, Wolski and Politanska[25] established that the reaction between ZnO and $\alpha-Fe_2O_3$, which results in $ZnO \cdot Fe_2O_3$ is completed at 1000°. The transfer of matter accompanying the formation of $ZnO \cdot Fe_2O_3$ from ZnO and $\alpha-Fe_2O_3$ was studied by Schnitt and Kleinert.[26]

No compounds are noted in the binary ZnO—BaO.[27]

Thermal phase equilibria in the ternary system $BaO-ZnO-Fe_2O_3$ have not been studied. There are, however detailed researches referring to the formation and properties of ternary ferrites in this system.[28] In the considered ternary system, the formation of five ternary compounds is mentioned, arbitrarily noted W, X, Y, Z, U, where: $W = BaO \cdot 2ZnO \cdot 8Fe_2O_3$; $X = BaO \cdot ZnO \cdot 7Fe_2O_3$; $Y = BaO \cdot ZnO \cdot 3Fe_2O_3$; $Z = 3BaO \cdot 2ZnO \cdot 12Fe_2O_3$; $U = 2BaO \cdot ZnO \cdot 9Fe_2O_3$. As the literature and our own data show that reduction of Fe_2O_3 and volatilization of ZnO occur above 1200°, our studies investigated the subsolidus range of temperatures.

2. EXPERIMENTAL

The substances used were Fe_2O_3, ZnO and $BaCO_3$, all of analytical purity grade. The dry homogenization of mixtures was mechanically effected. Then we calcined them for two hours at 900° in order to decompose $BaCO_3$ and obtain a preliminary reaction between the components. Afterwards, the prereacted mixtures were ground and then pressed in the shape of cylinders, and calcined thereafter at temperatures between 1 150° and 1 300° for a good sintering.

On the sintered samples the following measurements were made :

2.1. *Measuring of porosity,* by the liquid absorption method, in order to establish the stage of sintering.

2.2. *Determination of chemical composition,* by classical methods, in order to establish the volatilization degree of ZnO and the stage of the Fe^{3+} to Fe^{2+} reduction.

2.3. *Phase composition determination :* it was accomplished in two ways :

— using the Debye-Scherrer method, on a TUR M-60 diffractometer, using the $Mo_{k\alpha}$ radiation.

— microscopically, on polished sections in reflected light, using a research microscope MC-1 IOR type.

2.4. *The reaction mechanism of the formation of compounds in the system* was studied using the differential thermal and gravimetric analysis on an OD-102, MOM Budapest Paulik-Paulik Erdey type derivatograph, with a heating rate of 10°/min., up to 1000°.

3. RESULTS

3.1. COMPOUND FORMATION MECHANISM

In order to establish the temperature limits of formation and stability of binary and ternary compounds, their formation mechanism has been studied using differential thermal analysis and thermal gravimetric analysis. The results are shown in Figure 1.

On the thermodifferential curve of $BaCO_3$ two endothermic effects at 810° and 960° appear, corresponding to the polymorphous transformation from the rhombohedral to the hexagonal and from the hexagonal to the cubic structures, respectively. The thermodifferential curve of Fe_2O_3 has a weak endothermic effect at 675°, which is due to the two magnetic phase transitions corresponding to the Curie point and Néel point.[18,29] In the case of ZnO and of an equimolar mixture of composition $ZnO \cdot Fe_2O_3$ no thermal effect is noted, thus pointing at the absence of any structural transformation in the first case, or of a solid phase reaction between ZnO and Fe_2O_3 up to 1000°, resulting in zinc ferrite ($ZnO \cdot Fe_2O_3$) in the second case. For the four cases mentioned above, no weight losses were noted on the thermogravimetric curves.

The thermal differential analysis curves for the mixtures with compositions corresponding to the formation of the other compounds are also characterized by an endothermic effect at 675°. Two other endothermic effects are noted, at 810° and about 870°. On the thermogravimetric curves these effects are accompanied by weight losses corresponding to a total conversion of $BaCO_3$ into BaO and CO_2. In Figure 2 are shown thermodifferential and thermogravimetric curves of a mixture with the composition of the compound $BaO \cdot ZnO \cdot 3Fe_2O_3$(Y). The thermogravimetric curves show that $BaCO_3$ conversion begins at about 700°. The endothermic peak at 810° might be the effect of a polymorphous transformation of incompletely decomposed $BaCO_3$. The flattened peak at about 870° is considered the result of a superposition of effects caused by the

$BaCO_3$ decomposition and the solid phase reaction between resulted BaO, ZnO and Fe_2O_3.

These results are in good agreement with those obtained by other investigators [16-18] concerning formation kinetics of $BaO \cdot 6Fe_2O_3$; according to these results, the solid phase reaction is governed by the $BaCO_3$ decomposition; Ba hexaferrite is formed up to 1 000°.

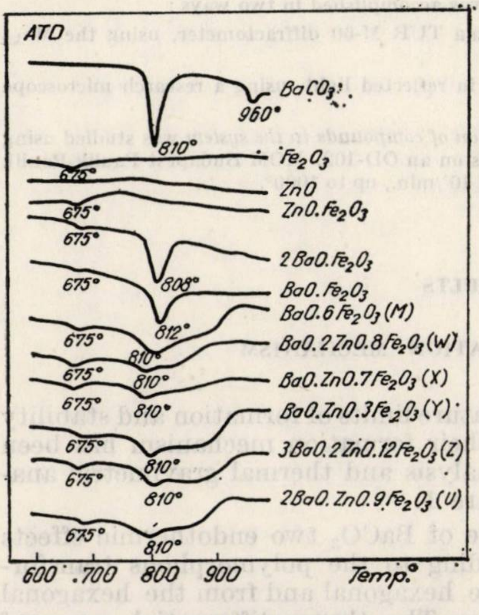

Fig. 1. — Differential thermal analysis curves of the pure substances and of the studied samples.

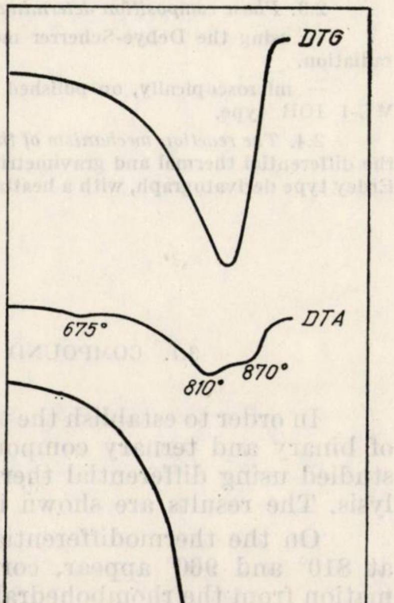

Fig. 2. — Thermodifferential and thermogravimetric curves of the $BaO.ZnO.3Fe_2O_3$ (Y) mixture.

On the other hand, the X-ray analysis made on thermally analyzed samples supports the idea that up to 1 000° the binary and ternary compounds are formed ($ZnO \cdot Fe_2O_3$ excepted); no intermediary compounds, as those noted by Winkler,[28] under isothermal treatment conditions, were identified.

TABLE 1

Sample compositions and porosities at some thermal treatment temperatures

Sample	Oxidic composition (weight %)			Porosity, %, at thermal treatment temperatures of			X-ray identified phases
	BaO	ZnO	Fe_2O_3	1150°	1200°	1300°	
$2BaO.Fe_2O_3$	65.76	—	34.24	6.4	—	—	$2BaO.Fe_2O_3$
(F) $BaO.Fe_2O_3$	48.99	—	51.01	17.8	14.4	8.4	(F) $BaO.Fe_2O_3$
(M) $BaO.6Fe_2O_3$	13.79	—	86.21	18.8	10.7	2.8	(M) $BaO.6Fe_2O_3$
(S) $ZnO.Fe_2O_3$	—	33.76	66.24	—	5.1	—	(S) $ZnO.Fe_2O_3$
(W) $BaO.2ZnO.8Fe_2O_3$	9.62	10.21	80.17	21.3	16.7	7.3	W
(X) $BaO.ZnO.7Fe_2O_3$	11.34	6.01	82.65	22.3	18.6	8.1	X
(Y) $BaO.ZnO.3Fe_2O_3$	21.48	11.39	67.13	11.7	4.1	—	Y
(Z) $3BaO.2ZnO.12Fe_2O_3$	18.11	6.40	75.49	20.3	13.5	5.8	Z
(U) $2BaO.ZnO.9Fe_2O_3$	16.81	4.45	78.74	21.0	14.1	6.7	U
Mixture 1	12.50	3.30	84.20	23.3	19.3	9.8	X + M
Mixture 2	14.60	6.10	79.20	23.8	15.8	7.0	W + U
Mixture 3	14.60	8.10	77.30	23.2	12.4	3.6	W + Z
Mixture 4	15.20	11.00	73.80	22.5	15.4	3,0	Z + S
Mixture 5	34.10	3.10	62.80	16.9	13.5	6.8	F + Z
Mixture 6	19.50	20.30	60.20	14.8	5.6	—	F + S
Mixture 7	38.80	20.70	40.50	8.3	—	—	F + ZnO
Mixture 8	55.60	15.20	29,20	0.1	—	—	$2BaO.Fe_2O_3$ + ZnO

3.2. THERMAL PHASE EQUILIBRIA RELATIONS IN THE $BaO-ZnO-Fe_2O_3$ SYSTEM

The study of the thermal phase equilibria in the subsolidus range of the ternary system $BaO-ZnO-Fe_2O_3$, involves the determination of the coordination between its compounds. All the possible coordination lines were traced, and by usual procedure both the defined compounds and the compositions situated in the intersection points of the hypothetical coordination lines were synthetized. The composition of the studied mixtures, in oxide weight %, thermal treatment temperatures and samples porosity are shown in table 1.

It was established, by chemical analysis, that at the thermal treatment temperatures used the volatilization of ZnO and reduction of Fe^{3+} to Fe^{2+} are very small (0.1 and 0.2 weight %, respectively), and do not affect the chemical composition of the studied samples.

X-ray diffraction phase analysis (Table 1) confirms the formation and stability of the defined compounds, in the temperature range studied, the results being correspondingly identical at the three thermal treatment temperatures. Differences are noted only in the crystallization degree of the compounds, which increases with the thermal treatment temperature. Figure 3 shows microscopic images of the sintered compounds, confirming the results of the phase analysis.

Fig. 3. — Sintered compounds micrography (×825) : *1*— W(1 300°); *2* — X(1 300°); *3* — Y(1 200°); *4* — Z(1 300°); *5* — U(1 300°); *6* — $2BaO.Fe_2O_3$(1 150°); *7*— $BaO.Fe_2O_3$(1 300°); *8* — $BaO.6Fe_2O_3$(1 300°); *9* — $ZnO.Fe_2O_3$(1 300°).

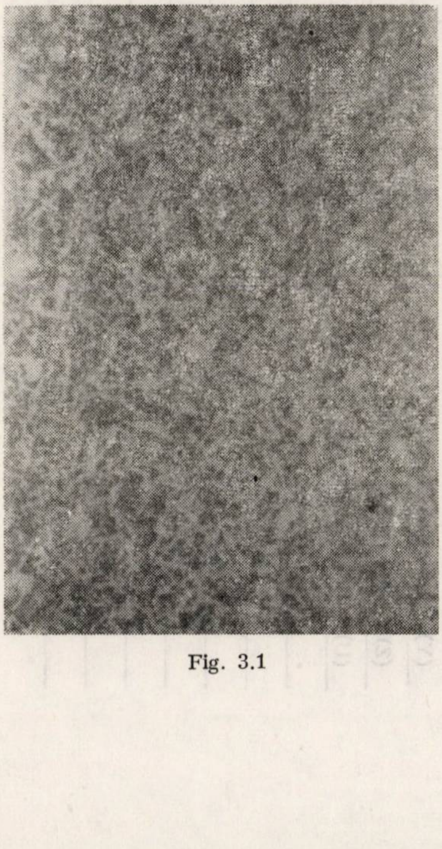

Fig. 3.1

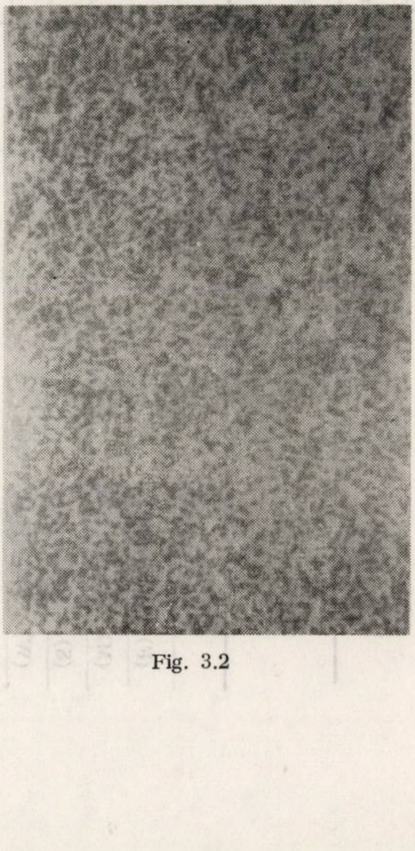

Fig. 3.2

Fip. 3.3

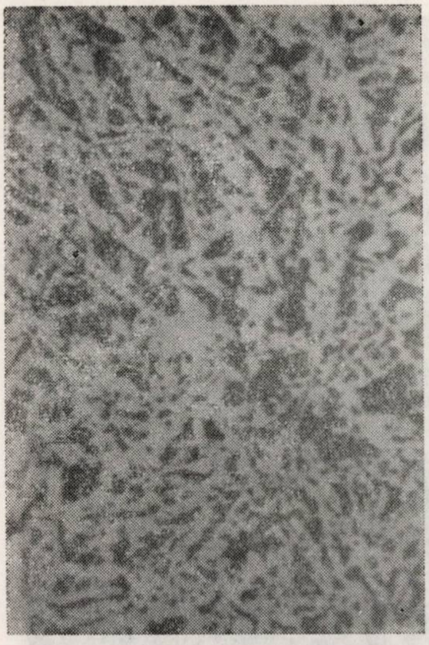

Fig. 3.4

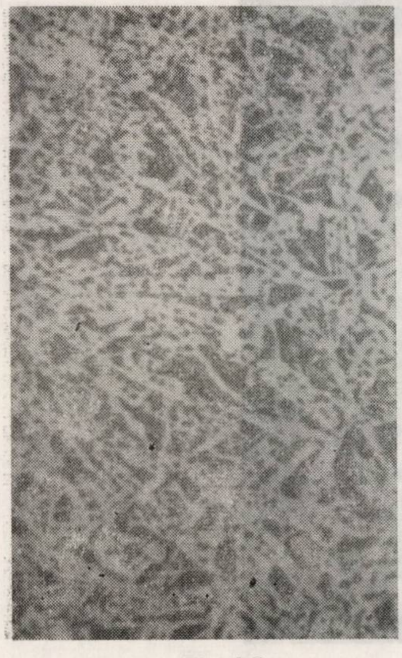

Fig. 3.5

Fig. 3.6

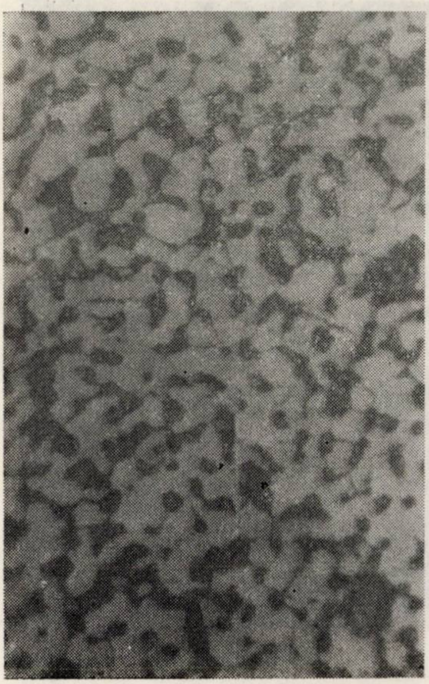

Fig. 3.7

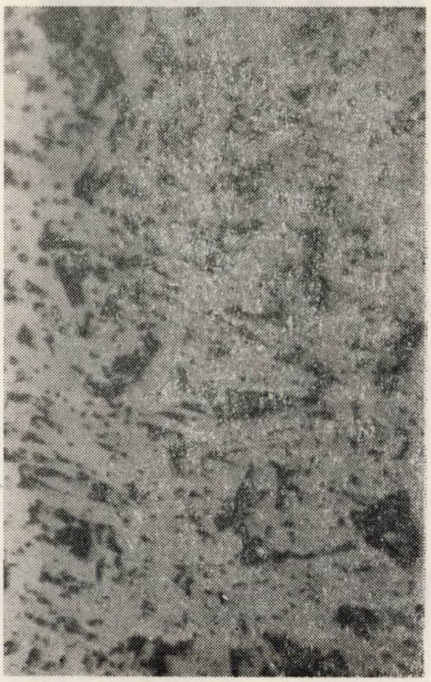

Fig. 3.8

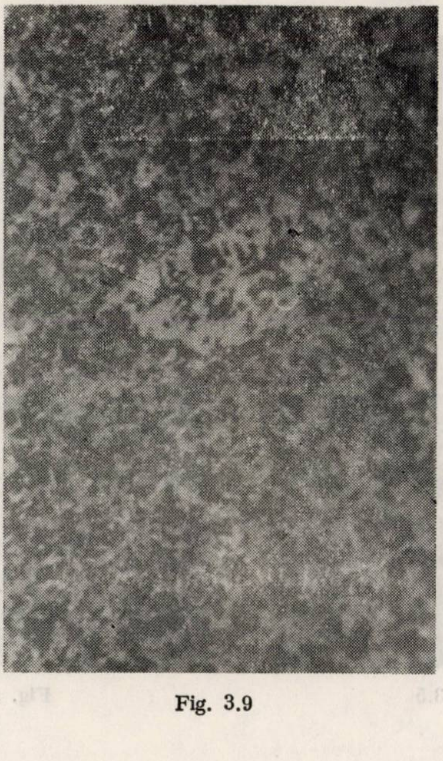

Fig. 3.9

Phase analysis results allowed us to determine the real coordination in the system (see Fig. 4). The ternary system $BaO-ZnO-Fe_2O_3$ is divided into 15 ternary paragenesis subsystems.

The ternary compounds W, X, Y, Z, U are situated in the Fe_2O_3 — rich zone, above the $BaO \cdot Fe_2O_3$ — $ZnO.Fe_2O_3$ coordination line, along which

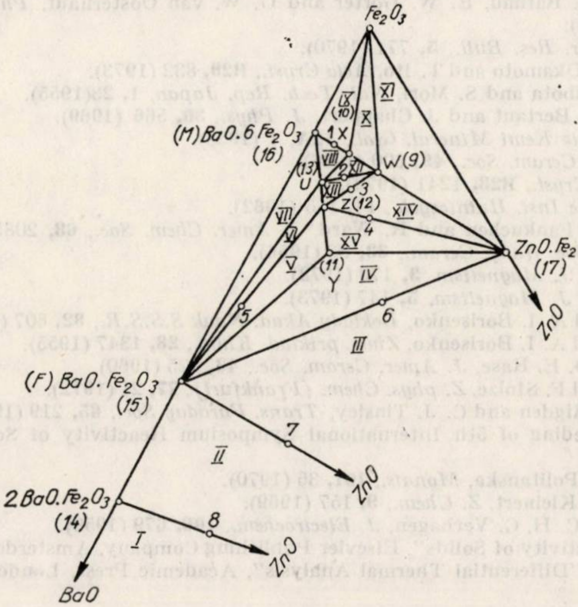
Fe_2O_3
IX
(10)
XI
X
(M) $BaO.6Fe_2O_3$
(16)
1 X
VIII
(13)
2
XII
W(9)
U
XIII
3
Z(12)
XIV
VII
4
VI
XV
$ZnO.Fe_2O_3$ (S)
(17)
V
(11)
Y
IV
5
6
ZnO
III
(F) $BaO.Fe_2O_3$
(15)
7
II
ZnO
$2BaO.Fe_2O_3$
(14)
8
I
ZnO
BaO

Fig. 4.—**Thermal phase equilibria in the system $BaO-ZnO-Fe_2O_3$: *I* $BaO - ZnO - 2BaO.Fe_2O_3$; *II* $2BaO.Fe_2O_3-ZnO-BaO.Fe_2O_3$; *III* $BaO.Fe_2O_3-ZnO-ZnO.Fe_2O_3$; *IV* $BaO.Fe_2O_3-ZnO.Fe_2O_3-Y$; *V* $BaO.Fe_2O_3-Y-Z$; *VI* $BaO.Fe_2O_3-Z-U$; *VII* $BaO.Fe_2O_3-U-BaO.6Fe_2O_3$; *VIII* $U-X-BaO.6Fe_2O_3$; *IX* $BaO.6Fe_2O_3-X-Fe_2O_3$; X Fe_2O_3-X-W; *XI* $Fe_2O_3-W-ZnO.Fe_2O_3$; *XII* $U-X-W$; *XIII* $U-Z-W$; *XIV* $Z-W-ZnO.Fe_2O_3$; *XV* $Z-Y-ZnO.Fe_2O_3$;**

the Fe_2O_3 content is of 50 mole %. This part of the system is of a great interest, because of the magnetic properties of the ternary compounds mentioned above, and also of $BaO.6Fe_2O_3$ and $ZnO \cdot Fe_2O_3$.

4. CONCLUSIONS

Thermal phase equilibria relations in the subsolidus range of the $BaO-ZnO-Fe_2O_3$ system have been studied.

The above mentioned system has been divided into paragenesis subsystems. The formation mechanism of the defined compounds has been elucidated.

REFERENCES

[1] G. H. Jonker, H. P. J. Wijn and P. B. Braun, *Philips Tech. Rev.*, **18**, 145 (1956—57).

[2] I. Gordon, R. L. Harvey and R. A. Braden, *J. Amer. Ceram. Soc.*, **45**, 297 (1962).

[3] Y. Goto and T. Takada, *J. Amer. Ceram. Soc.*, **43**, 150 (1960).

[4] P. Batti, *Ann. Chim.* (*Ital.*), **50**, 1461(1960).

[5] H. J. van Hook, *J. Amer. Ceram. Soc.*, **47**, 579 (1964).

[6] J. J. Went, G. W. Rathau, E. W. Gorter and G. W. van Oosterhaut, *Philips Tech. Rev.*, **13**, 194 (1951—52).

[7] B. T. Shirk, *Mater. Res. Bull.*, **5**, 771 (1970).

[8] S. Okamoto, S. I. Okamoto and T. Ito, *Acta Cryst.*, **B29**, 832 (1973).

[9] T. Okazaki, T. Kubota and S. Mori, *Nat. Tech. Rep. Japan*, **1**, 23(1955).

[10] C. Do-Dihn, E. F. Bertaut and J. Chappert, *J. Phys.*, **30**, 566 (1969).

[11] V. Adelsköld, *Arkiv Kemi Mineral, Geol.*, **12A**, 1 (1938).

[12] S. Mori, *J. Amer. Ceram. Soc.*, **49**, 600 (1966).

[13] S. Meriani, *Acta Cryst.*, **B28**, 1241 (1972).

[14] Z. Ziolowski, *Prace Inst. Hutniczych.*, **14**, 155 (1962).

[15] M. Erchak Jr., I. Fankuchen and R. Ward, *J. Amer. Chem. Soc.*, **68**, 2085 (1946).

[16] J. Suchet, *Bull. Soc. franç. Ceram.*, **33**, 33 (1956).

[17] H. Wullkopf, *Int. J. Magnetism*, **3**, 179 (1972).

[18] H. Wullkopf, *Int. J. Magnetism*, **5**, 147 (1973).

[19] N. A. Toropov and A. I. Borisenko, *Doklady Akad. Nauk S.S.S.R.*, **82**, 607 (1952).

[20] N. A. Toropov and A. I. Borisenko, *Zhur. priklad. Khim.*, **28**, 1347 (1955).

[21] F. H. Dulin and D. E. Rase, *J. Amer. Ceram. Soc.*, **43**, 125 (1960).

[22] W. Hirschwald and F. Stolze, *Z. phys. Chem. (Frankfurt)*, **77**, 21 (1972).

[23] R. Parker, C. J. Rigden and C. J. Tinsley, *Trans. Faraday Soc.*, **65**, 219 (1969).

[24] P. Reijen "Proceeding of 5th International Symposium Reactivity of Solids", München, 1964, p. 562.

[25] W. Wolski and U. Politanska, *Monats.*, **101**, 36 (1970).

[26] G. Schnitt and P. Kleinert, *Z. Chem.*, **9**, 157 (1969).

[27] H. Koelmans and C. H. C. Verhagen, *J. Electrochem.*, **106**, 679 (1959).

[28] G. Winkler, "Reactivity of Solids", Elsevier Publishing Company, Amsterdam, 1965, p. 572.

[29] R. C. Mackenzie, "Differential Thermal Analysis", Academic Press, London, 1970, p. 274.

Revue Roumaine de Chimie, 25, 1, 121 – 124 (1980)

THERMODYNAMIC STABILITY CONSTANTS AND OTHER RELATED THERMODYNAMIC PROPERTIES FOR Cu(II)-PMBP COMPLEX

M. S. SUBHANI
Department of Chemistry, University of Nigeria, Nsukka, Nigeria

Received June 14, 1978

The thermodynamic stability constants and other related thermodynamic properties for the complex formed between Cu(II) and I phenyl-3-methyl-4-benzoyl-pyrazolone-5 have been determined over the temperature range 5° to 45° in isoamyl alcohol phase.

INTRODUCTION

I-Phenyl-3-methyl-4-benzoyl-pyrazolone-5(PBBP) has been used as an efficient extracting agent.[1-8] The study of various thermodynamic constants for the formation of chelates during the extractions of various elements with PMBP is therefore of significant interest. In the present paper the work on Cu(II) —PMBP chelate is presented.

EXPERIMENTAL

All the chemicals used were of analaR grade or otherwise purified by recrystallization. Triply distilled water was used for making solutions for the metal ions of required concentration. PMBP was synthesized as described in the literature.[9] The methods for the measurements of percentage extraction and for the analysis of the samples were similar to those reported in the literature.[10] The pH measurements were made using the 23A model (Electronic instruments limited) and a thermostat bath HAAKE NK22 model was used to obtain the required temperature for the experiment. The partition coefficients measurements were made using the method described elsewhere.[11] The pK measurements for PMBP were made spectro-photometrically using zolon red as reagent for indicating the concentrations of the ionized and unionized species of PMBP. Absorption was measured at wavelength 420 nm and 480 nm.[12]

RESULTS AND DISCUSSIONS

The extraction constants (K_{ex}) for Cu(II) with PMBP were measured over the temperature range 5° to 45° using isoamyl alcohol as an extracting medium from aqueous solution of the element. The values thus obtained are reported in table 1. The extractions were carried out over a pH range 1.1 to 2.5 and it was observed that the values of K_{ex} were independent of hydrogen ion concentration in this pH range.

The log $-$ log plot for the percentage extraction in isoamyl alcohol phase (E) and hydrogen ion concentration gave rise to a slope of 1.98 indicating thereby that two hydrogen ions are liberated during the formation of complex. These results are similar to those reported elsewhere.[10] Thus the reaction can be written as follows,

$$Cu^{2+} + HA \underset{}{\overset{K_1}{\rightleftharpoons}} H^+ + CuA^+ \qquad (1)$$

$$CuA^+ + HA \underset{}{\overset{K_2}{\rightleftharpoons}} H^+ + CuA_2 \qquad (2)$$

where HA is PMBP and K_1 and K_2 are the first step and the second step stability constants respectively. The extraction constants can be written as

TABLE 1

The extraction constants for Cu(II) $-$ PMBP chelate at various temperatures

Temperature (T°C)	Log K_{ex}
5	2.260
15	1.832
25	1.430
35	1.148
45	0.760

$$K_{ex} = (CuA_2)\,(H^+)^2\,(Cu^{2+})^{-1}\,(HA)^{-2} \qquad (3)$$

The extraction constants of the complex CuA_2 can be expressed through overall stability constant (B_2) of the complex, the distribution constant of the complex (P_{CuA_2}), dissociation constant of the reagent (K_{HA}) and the distribution constant of the reagent (P_{HA}) as

$$K_{ex} = B_2\, K_{HA}^2\, P_{HA}^{-2}\, P_{CuA_2} \qquad (4)$$

Thus, for the evaluation of overall stability constants and the other two stability constants K_1 and K_2, the partition coefficients and distribution coefficients for the metal complex and reagent and the dissociation constants for the reagent were determined under the experimental conditions employed. The values are shown in table 2.

TABLE 2

Experimentally determined values for pK_{HA}, log P_{HA} and log P_{CuA2} over a range of temperature 5° to 45°

T° C	5	15	25	35	45
pK_{HA}	4.039	4.040	4.040	4.038	4.036
logP_{HA}	2.311	2.320	2.331	2.346	2.358
logP_{CuA2}	2.692	2.703	2.715	2.728	2.737

The values for the stability constants for step (1) and step (1) were obtained by the method reported in the literature[13] with the help of computer analysis. The values thus obtained for logB_2, logK_1 and logK_2 are summarized in table 3.

TABLE 3

The values obtained for the thermodynamic stability constants $\log B_2$ $\log K_1$ and $\log K_2$ at different temperatures

$T°C$	5	15	25	35	45
$\log B_2$	12.269	11.849	11.455	11.088	10.711
$\log K_1$	6.822	6.588	6.369	6.165	5.955
$\log K_2$	5.447	5.261	5.086	4.923	4.756

The tendency of a metal ion to take up ligand is proportional to the number of vacant sites.

For the type of ligand PMBP, coulombic attraction is more for Cu^{2+} as compared to CuA^+. Thus $\log K_1 - \log K_2$ is expected to be positive.[14] The values reported in table 3 are in agreement with it.

From the data on stability constant the standard free energy changes ($\Delta G°$) for the formation of the complexes which were evaluated at various temperatures and are shown in table 4. Standard heats of formation ($\Delta H°$) were also evaluated from the slope of the plot of $\log K$ or $\log B$ against $\frac{I}{T}$ which were fairly good straight lines over the temperature range studied. The values are also reported in table 4. From the data on $\Delta G°$ and $\Delta H°$ (see Table 4) at different temperatures the values for the state function entropy of formation ($\Delta S°$) of the complex were also calculated and the results are reported in table 4.

TABLE 4

The values of the thermodynamic properties ΔH°, ΔG° and ΔS° obtained from thermodynamic stability constants (see table 3)

$T°C$	5	15	25	35	45
$\Delta G^0_{B_2}(^{KJ}/_M)$	−234.52	−226.49	−218.96	−211.95	−204.74
$\Delta G^0_{K_1}(^{KJ}/_M)$	−130.40	−125.93	−121.74	−117.84	−113.83
$\Delta G^0_{K_2}(^{KJ}/_M)$	−104.12	−100.56	− 97.22	− 94.11	− 90.91
$\Delta H^0_{B_2}(^{KJ}/_M)$	− 70.15	− 70.15	− 70.15	− 70.15	− 70.15
$\Delta H^0_{K_1}(^{KJ}/_M)$	− 35.80	− 35.80	− 35.80	− 35.80	− 35.80
$\Delta H^0_{K_2}(^{KJ}/_M)$	− 34.35	− 34.35	− 34.35	− 34.35	− 34.35
$\Delta S^0_{B_2}(^{J}/_{MT})$	−591.26	542.85	499.36	460.39	423.24
$\Delta S^0_{K_1}(^{J}/_{MT})$	340.28	312.95	288.34	266.36	245.35
$\Delta S^0_{K_2}(^{J}/_{MT})$	250.98	229.90	211.02	194.03	177.89

ACKNOWLEDGEMENT. Author thanks Dr. M. K. Nageryal, Department of Electrical Engineering University of Leeds for the assistance in computer analysis.

REFERENCES

[1] Yu. A. Zolotov, V. G. Lambrev, M. K. Chmutova and N. T. Sizonenko, Doklady Akad. Nauk S.S.S.R., **165,** 117 (1965).

[2] Yu. A. Zolotov, M. K. Chmutova and P. E. Palei, *Zhur analit. Khim.,* **21,** 1217 (1966).

[3] L. I. Moseev and B. V. Monalhov, *Radiokhimiya,* **10,** 309 (1968).

[4] Yu. A. Zolotov and L. N. Gavzilova, *J. Inorg. Nuclear Chem.,* **31,** 3613 (1969).

[5] Yu. A. Zolotov, N. T. Sizonenko, E. S. Zolotovitiskaya and E. I. Yakovenko, *Zhur analit. Khim.,* **24,** 20 (1969).

[6] N. T. Sizonenko and Yu. A. Zolotov, *Zhur analit. Khim.,* **24,** 1341 (1969)

[7] Yu. A. Zolotov, A. O. Kiseleva, N. V. Shakhova and V. A. Lebedov, *Analyt. Chim. Acta,* **79,** 237 (1975).

[8] O. Navratil and B. S. Jensen, *J. Radioanal. Chem.,* **5,** 315 (1970)

[9] B. S. Jensen, *Acta Chem. Scand.,* **13,** 1668 (1959).

[10] Yu. A. Zolotov and N. T. Sizonenko, *Zhur analit. Khim.,* **25,** 54 (1970).

[11] H. Irving and C. F. Bell, *J. Chem. Soc.,* **1952,** 1216.

[12] A. M. Qureshi, A. N. Patel, M. S. Subhani, Submitted for publication (Pak. J. Sci. Ind. Res.)

[13] S. H. Matheson and A. Khalique, *J. Nat. Sci.,* **14,** 41 (1972).

[14] "Stability Constants of Metal Complexes", Part 1, The Chemical Soc., London, 1957.

Revue Roumaine de Chimie, **25**, *7*, 125–133, (1980)

BASE-CATALYZED MICHAEL ADDITION OF ACTIVE METHYLENE COMPOUNDS ON ARYLIDENE MALONATES AND ARYLIDENE BARBITURIC ACIDS

A.F.FAHMY, M. M. MOHAMED, A. A. AFIFY, M. Y. EL KADY
and M. A. EL HASHASH

Faculty of Science, Ain Shams University, Abbassia, Cairo, Egypt

Received May 30, 1978

Base-catalyzed Michael addition of active methylene compounds, namely malononitrile, benzyl phenyl ketone, ethyl benzoylacetate, cyanoacetic acid, *p*-chlorobenzylcyanide, ethyl cyanoacetate, ethyl acetoacetate and cyclohexanone on the olefinic double bond of arylidene malonates 1a and 1b or on the exocyclic double bond in 5-arylidene barbituric acids 2a and 2b has been described.

In the present investigation it has been found out that diethyl arylidene malonates,[1] **1a** and **1b** react with malononitrile at 100° in the presence of ammonium acetate to give a mixture of two products, namely arylidene malononitrile **3a** or **3b** and nicotinamide **4a** or ethyl nicotinate derivatives **4b** respectively.

On the other hand, 5-benzylidene barbituric acid,[2] (**2a**) reacts with malononitrile under the same conditions affording [α-(hexahydro-2,4,6-trioxo-5-pyrimidinyl)-benzyl]-malononitrile (**5**) and β-(dicyanomethyl)-hydrocinnamamide (**6**).

The structure of compounds **3, 4, 5** and **6** was supported by their infrared spectra. Compounds **3** show $\nu C=C$ at 1610 – 1 620 cm^{-1} and $\nu C\equiv N$ at 2200 cm^{-1}. Also, compounds **4** show $\nu C\equiv N$ at 2200 cm^{-1}, νCONH at 1690 – 1650 cm^{-1}, νNH or νNH with chelated νOH at 3460 – 3200 cm^{-1} and νCO of ester (for compound **4b**) at 1720 cm^{-1}. Similarly, compounds **5** and **6** have $\nu C\equiv N$ at 2260 – 2200 cm^{-1}, νCONH at 1680 – 1665 cm^{-1} and νNH or νNH with chelated νOH at 3400 – 3200 cm^{-1}.

Base-catalyzed Michael addition of benzylphenylketone to **1a** in the presence of sodium ethoxide gives a mixture of two products, namely diethyl-(2-benzoyl-1,2-diphenylethyl)-malonate (**7**) and ethyl hydrogen (2-benzoyl-1,2-diphenylethyl)-malonate (**8**). However, **1b** under the same conditions, gives with benzylphenylketone two products, namely 4-(dimethylamino)-α-phenylchalcone (**9**) and 3-[*p*-(dimethylamino)phenyl]-1,2,4,5,-tetraphenyl-1,5-pentanedione (**10**). This reaction is analogous with a recently reported one.[3]

Ethyl benzoylacetate and cyanoacetic acid react with **1a** to give 2-benzoyl-3-phenyl glutaric acid (**11a**) and 3-phenyl glutaric acid (**11b**) respectively. The reaction may involve the addition to the double bond followed by hydrolysis and then decarboxylation. The I.R. spectra of compounds **7**, **8**, **9**, **10** and **11** are presented in table 1.

TABLE 1

I.R. Spectral data of compounds 7, 8, 9, 10, 11, 12 and 18 (cm^{-1})

Compd.	ν(C=O) of ester and/or acid	ν(C_6H_5CO)	ν(OH bonded)	ν(C=C)	ν(C≡N)
7	1 725	1 680	—	—	—
8	1 720 ; 1 700	1 690	3 240—3 180	—	—
9	—	1 680	—	1 610	—
10	—	1 690	—	—	—
11a	1 700	1 690	3 220—3 170	—	—
11b	1 700	—	3 230—3 200	—	—
12a	—	—	—	1 600	2 220
12b	—	—	—	1 620	2 220
18a	1 700	—	3 120	1 610	2 220
18b	1 720	—	—	1 620	2 220
18c	1 720	—	—	1 620	2 220

Reaction of **1a** and **1b** with *p*-chlorobenzylcyanide in sodium ethoxide gives arylidene-*p*-chlorobenzylcyanide **12a** and **12b** respectively, probably via Michael reaction, followed by elimination of diethyl malonate.

The N.M.R. spectrum of compound **12a** shows the following signals when run in $(CD_3)_2SO$:

— at δ 5.35 ppm (s) corresponding to one proton ($-CH=\overset{|}{C}-CN$), at δ[7.40(s), δ7.50(d), and 7.58(d)] corresponding to five aromatic protons of the phenyl group and at δ[7.73(s), 7.80(s), 7.90(m) and 8.20(s)] corresponding to four aromatic protons of the substituted phenyl group.

Similarly, the N.M.R. spectrum of compound **12b** shows the following signals when run in $(CD_3)_2SO$:

— at δ 5.04 ppm(s) corresponding to one proton ($-CH=\overset{|}{C}-CN$), at δ 3.32 ppm(s) corresponding to six protons of the $[-N(CH_3)_2]$ group, two doublets at δ 6.78 ppm and δ 7.65 ppm corresponding to four aromatic protons of the substituted phenyl group 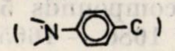 and another two doublets at δ 7.44 ppm and δ 7.82 ppm corresponding to the other four aromatic protons of the substituted phenyl group 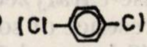.

Bond forming reactions which occur in the decomposition of some α,β-unsaturated esters and nitriles upon electron impact were recently described.[4]

In this study, compound **12a** is selected as a representative example of the prepared arylidene *p*-chlorobenzylcyanides to give a further proof of their structure and to demonstrate the general behaviour of arylidene *p*-chlorobenzylcyanides under electron impact.

The mass spectrum of **12a** indicated that the molecular ion (M^+) gives rise to a peak at m/e 240 which agrees with the molecular formula $C_{15}H_{10}NCl$. The spectrum shows also peaks at m/e 205 due to the loss of chlorine ion giving an ion **13**, at m/e 204 due to the loss of hydrogen ion from the ion **13** to give another one (**14**) and at m/e 178 due to the loss of cyanide ion from the ion **14** to give **15**. The spectrum shows appreciable peaks at m/e 89 corresponding to the ion $(C_7H_5)^{\cdot}$ **17**.

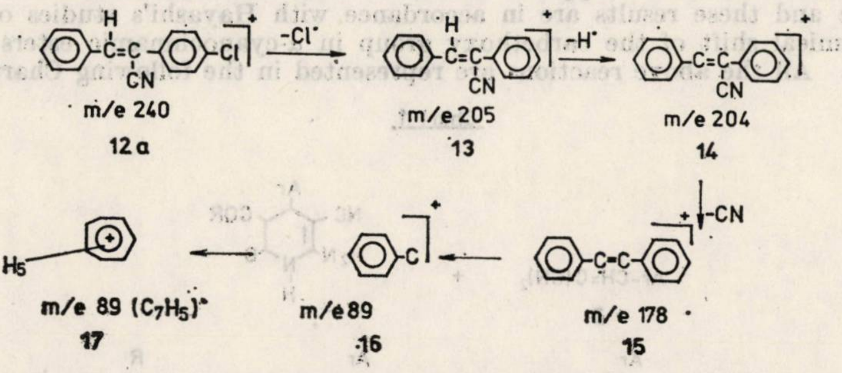

Compound **1b** reacts with cyanoacetic acid in the presence of ammonium acetate to give α-cyano-(*p*-dimethylamino) cinnamic acid (**18a**).

On the other hand, ethyl cyanoacetate reacts with **1b** in the presence of ammonium acetate and ethanol to give the *trans* ethyl-[α-cyano-*p*-dimethylamino] cinnamate (**18b**), while in the presence of ammonium acetate and *n*-butanol it gives the *cis*-isomer **18c**.

This reaction is still under further investigation.

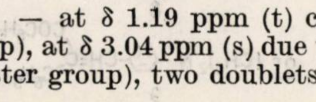

18a

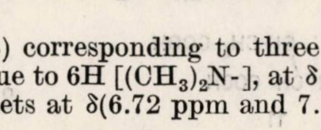

trans **18b**

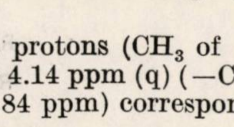

cis **18c**

The I.R. spectra of compounds **12** and **18** are presented in table 1.

The N.M.R. spectrum of compound **18b** shows the following signals when run in CD_3CN :

— at δ 1.19 ppm (t) corresponding to three protons (CH_3 of ester group), at δ 3.04 ppm (s) due to 6H [$(CH_3)_2N$-], at δ 4.14 ppm (q) ($-CH_2-$ of ester group), two doublets at δ(6.72 ppm and 7.84 ppm) corresponding to four aromatic protons of the substituted phenyl group 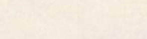, and at δ 8.03 ppm (s) corresponding to one olefinic proton ($-CH = \overset{|}{C}-CN$).

On the other hand, the N.M.R. spectrum of compound **18c** shows the following signals when run in CD_3CN ;

— at δ 0.9 ppm (*t*) corresponding to three protons (CH_3 of ester group), at δ 3.08 ppm (s) due to 6H [$(CH_3)_2N$-], at δ 4.16 ppm (q) ($-CH_2-$ of ester group), two doublets at δ (6.75 ppm and 7.89 ppm) corresponding to four aromatic protons of the substituted phenyl group $(-\overset{|}{N}-\bigcirc-C)$ and at δ 8.07 ppm (s) corresponding to one olefinic proton $(-CH=\overset{|}{C}-CN)$.

The N.M.R. data show that the signal for the carbethoxy group of the *trans*-isomer **18b** appears at a lower field than that of the *cis*-isomer **18c** and these results are in accordance with Hayashi's studies on the chemical shift of the carbethoxy group in α-cyanocinnamic esters.[5]

All the above reactions are represented in the following Chart 1.

Chart 1

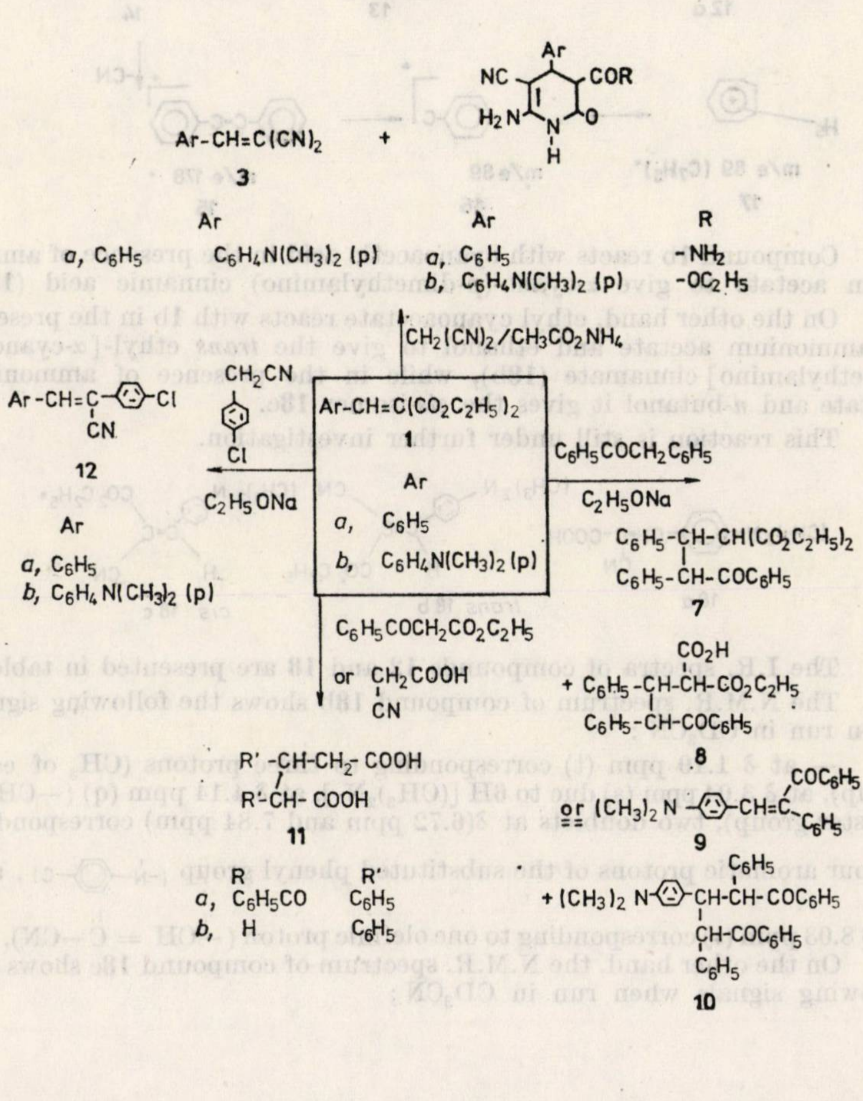

Ar-CH=C(CN)₂
3
+
Ar
NC
COR
H₂N
N
H
O
Ar
a, C₆H₅
C₆H₄N(CH₃)₂ (p)
Ar
a, C₆H₅
b, C₆H₄N(CH₃)₂ (p)
R
-NH₂
-OC₂H₅
CH₂(CN)₂/CH₃CO₂NH₄
Ar-CH=C-C₆H₄-Cl
CN
12
Ar
a, C₆H₅
b, C₆H₄N(CH₃)₂ (p)
CH₂CN
Cl
C₂H₅ONa
Ar-CH=C(CO₂C₂H₅)₂
1
Ar
a, C₆H₅
b, C₆H₄N(CH₃)₂ (p)
C₆H₅COCH₂C₆H₅
C₂H₅ONa
C₆H₅-CH-CH(CO₂C₂H₅)₂
C₆H₅-CH-COC₆H₅
7
C₆H₅COCH₂CO₂C₂H₅
or CH₂COOH
CN
CO₂H
+ C₆H₅-CH-CH-CO₂C₂H₅
C₆H₅-CH-COC₆H₅
8
R'-CH-CH₂-COOH
R-CH-COOH
11
R R'
a, C₆H₅CO C₆H₅
b, H C₆H₅
COC₆H₅
or (CH₃)₂N-C₆H₄-CH=C
C₆H₅
9
C₆H₅
+ (CH₃)₂N-C₆H₄-CH-CH-COC₆H₅
CH-COC₆H₅
C₆H₅
10

5-Arylidene barbituric acids **2a** and **2b** react with ethyl acetoacetate in the presence of ammonium acetate and *n*-butanol to give colourless products, namely ethyl 5-acetyl-1,4-dihydro-6-hydroxy-2-methyl-4-arylnicotinates (**19a** and **19b**) and barbituric acid. This reaction is analogous to the recently reported reactions.[6,7]

When 5-(*p*-chlorobenzylidene) barbituric acid **2b** reacts with cyclohexanone in the presence of sodium methoxide, it gives the Michael adduct 5-[1-*p*-chlorophenyl-1-(2-cyclohexanone)methyl] barbituric acid (**20**).

The N.M.R. spectrum of compound **19b** shows the following signals when run in CD_3CN :

— at δ 1.2 ppm (t) corresponding to 3H (CH_3 of ester), at δ 2.16 ppm(s) corresponding to 3H ($-C-CH_3$), at δ 2.26 ppm (s) corresponding to 3H (CH_3CO), at δ 3.86 (q) corresponding to two protons of ($-CH_2-$ of ester), at δ 4.81 ppm (s) corresponding to one proton ($-\overset{}{\underset{|}{C}}H-$), a broad absorption centered about δ 6.94 ppm due to NH proton, and two doublets at δ 7.55 ppm and δ 7.86 ppm corresponding to four protons of the substituted phenyl group 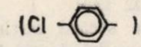 .

The IR spectra of compounds **19** show $\nu COCH_3$ at 1670—1660 cm^{-1}, νCO of ester at 1720 cm^{-1}, νNH chelated with νOH at 3380— 3240 cm^{-1} and νCH at 3000 — 2900 cm^{-1}.

Chart 2

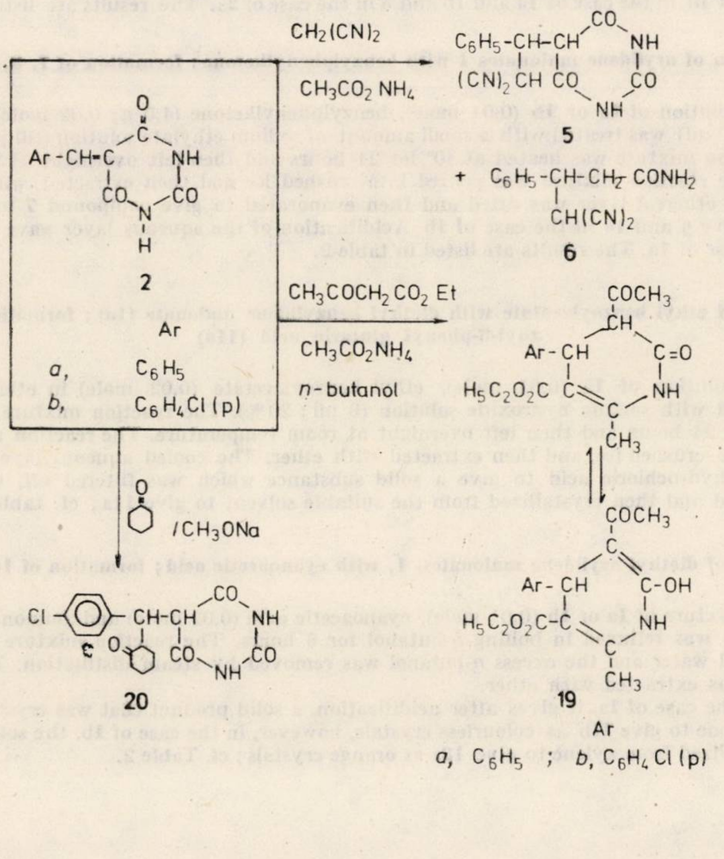
CH2(CN)2
CH3CO2 NH4
C6H5-CH-CH
(CN)2 CH CO
CO
NH
5
+ C6H5-CH-CH2-CONH2
CH(CN)2
6
Ar-CH=C
NH
CO
N
H
2
Ar
a, C6H5
b, C6H4Cl (p)
CH3COCH2CO2 Et
CH3CO2NH4
n-butanol
COCH3
CH
Ar-CH
C=O
H5C2O2C C
NH
CH3
/CH3ONa
COCH3
C
Ar-CH
C-OH
H5C2O2C-C
NH
CH3
19
Ar
a, C6H5 ; b, C6H4Cl (p)
Cl
CH-CH
O
20

Similarly, the I.R. spectrum of compound **20** shows νCONH at 1665 cm $^{-1}$, νCO of cyclohexanone at 1720 cm $^{-1}$, νNH chelated with νOH at 3230 cm $^{-1}$ and νCH at 2960 – 2920 cm $^{-1}$.

The reactions of 5-arylidene barbituric acids **2** with malononitrile, ethyl acetoacetate and cyclohexanone are given in Chart 2.

EXPERIMENTAL

The infrared absorption spectra were determined with a Unicam SP 1200 spectrophotometer using KBr wafer technique. The NMR spectra were recorded with a Varian VN 1009 (S-60 T) instrument, and the position of peaks is expressed in δ-values (ppm). All the melting points are uncorrected.

Reaction of arylidene malonates 1a and 1b or 5-benzylidene barbituric acid (2a) with malononitrile; formation of 3 and 4 or 5 and 6

A mixture of malononitrile (1.32 g; 0.02 mole), **1** or **2a** (0.01 mole) and ammonium acetate (2.31 g; 0.03 mole) was heated on the steam bath for 6 hours, and then cooled. The yellow oil obtained was washed with water, dried and then treated with ethanol or acetone. It separated into two parts, an ethanol or acetone soluble part (A) and an insoluble part (B). The ethanol or acetone soluble part (A) was concentrated and the solid that separated was fractionally crystallized from the suitable solvent to give **3a** and **3b** in the case of **1a** and **1b** or to give **6** in the case of **2a** respectively.

The ethanol or acetone insoluble part (B) was crystallized from glacial acetic acid to give **4a** and **4b** in the case of **1a** and **1b** and **5** in the case of **2a**. The results are listed in table 2

Reaction of arylidene malonates 1 with benzylphenylketone; formation of 7, 8, 9 and 10

A solution of **1a** or **1b** (0.01 mole), benzylphenylketone (4.0 g; 0.02 mole) in absolute ethanol (20 ml) was treated with a small amount of sodium ethylate solution (till just alkaline). The reaction mixture was heated at 40° for 24 hours and then left overnight at room temperature. The reaction mixture was poured into crushed ice and then extracted with ether.

The ethereal layer was dried and then evaporated to give compound **7** in the case of **1a** or to give **9** and **10** in the case of **1b**. Acidification of the aqueous layer gave the product **8** in the case of **1a**. The results are listed in table 2.

Reaction of ethyl benzoylacetate with diethyl benzylidene malonate (1a); formation of 2-benzoyl-3-phenyl glutaric acid (11a)

A solution of **1a** (0.01 mole), ethyl benzoylacetate (0.02 mole) in ethanol (30 ml) was treated with sodium hydroxide solution (6 ml; 20%). The reaction mixture was heated at 100° for 24 hours and then left overnight at room temperature. The reaction mixture was poured into crushed ice, and then extracted with ether. The cooled aqueous layer was acidified with hydrochloric acid to give a solid substance which was filtered off, washed with water, dried and then crystallized from the suitable solvent to give **11a**; cf. table 2.

Reaction of diethyl arylidene malonates, 1, with cyanoacetic acid; formation of 11b and 18a

A mixture of **1a** or **1b** (0.01 mole), cyanoacetic acid (0.02 mole) and ammonium acetate (0.03 mole) was refluxed in boiling *n*-butanol for 6 hours. The reaction mixture was poured into 200 ml water and the excess *n*-butanol was removed by steam distillation. The aqueous medium was extracted with ether.

In the case of **1a**, it gives after acidification, a solid product that was crystallized from chlorobenzene to give **11b** as colourless crystals, however, in the case of **1b**, the solid separated was crystallized from xylene to give **18a** as orange crystals; cf. Table 2.

TABLE 2

Characterisations of the organic compounds (3 – 20)

Compd.	m.p.° colour	Solvent yield (%)	Formula	Analysis % Calcd./Found		
				C	H	N
3a	81 colourless	P.E. (80–100°) 33	$C_{10}H_6N_2$	77.90 77.65	3.89 4.00	18.10 18.00
3b	179–180 red	P.E. (100–120°) 48	$C_{12}H_{11}N_3$	73.07 73.20	5.62 5.70	21.31 21.50
4a	over 300 yellowish-brown	A.A. 35	$C_{13}H_{12}N_4O_2$	60.93 60.90	4.72 4.60	21.87 21.60
4b	over 300 yellowish-brown	A.A. 42	$C_{17}H_{21}N_4O_3$	62.00 62.40	6.40 6.50	17.02 17.30
5	215 (dec.) yellowish-brown	A.A. 53	$C_{14}H_{10}N_4O_3$	59.57 59.90	3.57 3.80	19.85 19.50
6	117 colourless	toluene 26	$C_{12}H_{11}N_3O$	67.59 67.80	5.20 5.40	19.71 19.90
7	165 colourless	P.E. (100–120°) 65	$C_{28}H_{28}O_5$	75.65 75.70	6.35 6.40	— —
8	100 colourless	P.E. (60–80°) 24	$C_{26}H_{24}O_5$	74.98 75.00	5.81 5.80	— —
9	165 yellow	ethanol 67	$C_{23}H_{21}NO$	84.37 84.40	6.47 6.50	4.28 4.30
10	245 pale yellow	toluene 34	$C_{37}H_{33}NO_2$	84.86 84.90	6.35 6.40	2.68 2.56
11a	77 colourless	P.E. (80–100°) 72	$C_{18}H_{16}O_5$	69.22 69.40	5.16 5.20	— —
11b	140 colourless	chlorobenzene 84	$C_{11}H_{12}O_4$	63.45 63.50	5.81 5.90	— —
12a	100 red	P.E. (80–100°)	$C_{15}H_{10}NCl$	75.15 75.20	4.17 4.10	5.84 5.80
12b	186 yellow	benzene 68	$C_{17}H_{15}N_2Cl$	72.21 72.20	5.30 5.30	9.91 9.90

Table 2 (continued)

Compd.	m.p.° colour	Solvent yield (%)	Formula	Analysis % Calcd./Found		
				C	H	N
18a	147	xylene	$C_{12}H_{12}O_2N_2$	66.65	5.59	12.96
	orange	74		66.70	5.60	13.10
18b	126	ethanol	$C_{14}H_{16}N_2O_2$	68.83	6.60	11.47
	orange	96		68.90	6.60	11.50
18c	78	P.E.	$C_{14}H_{16}N_2O_2$	68.83	6.60	11.47
	yellowish-orange	(60—80°)		68.90	6.70	11.69
		68				
19a	150	benzene	$C_{17}H_{19}NO_4$	67.76	6.36	4.65
	colourless	89		67.90	6.40	4.60
19b	140	benzene	$C_{17}H_{18}NO_4Cl$	60.80	5.36	4.17
	colourless	75		60.80	5.30	4.20
20	125	xylene	$C_{17}H_{17}N_2O_4Cl$	58.53	4.87	8.03
	pale yellow	82		58.60	4.80	8.30

P.E. = petroleum ether ; A.A. = glacial acetic acid

Reaction of diethyl arylidene malonates 1a and 1b with p-chlorobenzylcyanide ; formation of 12a and 12b

To a solution of **1a** or **1b** (0.01 mole) and *p*-chlorobenzylcyanide (0.02 mole) in absolute ethanol (30 ml) a small amount of sodium ethylate was added (till just alkaline). The reaction mixture was heated at 40° for 24 hours, left overnight at room temperature and then extracted with ether. The ethereal layer was evaporated at room temperature. The solid product was filtered off and then crystallized from the proper solvent to give **12a** or **12b** ; cf. Table 2.

Reaction of 1b with ethyl cyanoacetate

a) *Formation of* trans-*ethyl(α-cyno-p-(dimethylamino)]-cinnamate* (**18b**) :

A mixture of **1b** (0.01 mole), ethyl cyanoacetate (0.02 mole) and ammonium acetate (0.03 mole) was refluxed in boiling ethanol for four hours. The solid separated from the reaction mixture was filtered off and crystallized from ethanol to give **18b** as yellowish orange crystals. The results are listed in table 2.

b) *Formation of* cis-*ethyl[α-cyano-p-(dimethylamino)] -cinnamate* (**18 c**) ;

A mixture of **1b** (0.01 mole), ethyl cyanoacetate (0.02 mole), and ammonium acetate (0.03 mole) was refluxed in boiling *n*-butanol for 6 hours. The reaction mixture was poured into 200 ml water and the excess *n*-butanol was removed by steam distillation. The aqueous medium was treated with ether and the ethereal layer was left to evaporate at room temperature. The solid separated was crystallized from petroleum ether (b.p. 60 — 80°) to give **18c** as yellowish orange crystals. The results are listed in table 2.

Reaction of 5-arylidene barbituric acids 2a and 2b with ethyl-acetoacetate

A mixture of ethyl acetoacetate (0.02 mole), arylidene barbituric acids **2a** or **2b** (0.01 mole) and ammonium acetate (0.03 mole) in *n*-butanol was refluxed for 6 hours. The excess *n*-butanol was removed by steam distillation. The reaction mixture was treated with ether and the ethereal layer was left to evaporate at room temperature. The solid separated was crystallized from benzene to give the products **19a** or **19b** as colourless crystals. The results are listed in table 2.

Reaction of 5-(p-chlorobenzylidene) barbituric acid (2b) with cyclohexanone

A mixture of 5-(*p*-chlorobenzylidene) barbituric acid (**2b**) (0.01 mole) and cyclohexanone (0.02 mole) in ethanol (50 ml) was treated with a small amount of sodium methylate (till just alkaline) and then set aside at room temperature for 24 hours. The reaction mixture was poured into crushed ice and the solid separated was filtered off, dried and then crystallized from xylene to give **20** as pale yellow crystals. The results are listed in table 2.

REFERENCES

[1] I. V. Melnichenko, T. S. Boiko and A. V. Yasnikov, *Ukr. Khim. Zhur.*, **37**, 561 (1971); *Chem. Abstr.*, **75**, 87759 (1971).

[2] M. L. Tamayo, J. M. Gamboa, and E. F. Alvarez, *Anales real Soc. españ. Fis. Quim.*, **48B**, 889 (1952); *Chem. Abstr.*, **48**, 1278 (1954).

[3] I. M. V. Ionescu and O. G. Popescu, *Bull. Soc. chim. France*, **51**, 1215 (1932).

[4] D. H. Williams, R. G. Cooks, J. H. Bowie, P. Madsen, G. Schroll and Seven-Olov Lawesson, *Tetrahedron*, **23**, 3173 (1967).

[5] T. Hayashi, *J. Org. Chem.*, **31**, 3253 (1966).

[6] O. Bredt, *Ber. dtsch. chem. Ges.*, **24**, 603 (1891).

[7] P. E. Rapadakis, *J. Amer. Chem. Soc.*, **67**, 1799 (1945).

Revue Roumaine de Chimie, **25**, *1*, 135 – 143 (1980)

SUR LE SYSTÈME COMBINÉ D'ÉCHANGE IONIQUE – EXTRACTION AUX SOLVANTS. II[1]

DISCUSSION THÉORIQUE

LUMINIŢA VLĂDESCU * et HENRY HURWITZ **

*** Institut National de Chimie, Laboratoire de Chimie Analytique, 202, Splaiul Independenţei, 77208 Bucarest, Roumanie**

**** Université Libre de Bruxelles, Laboratoire de Thermodynamique-Electrochimie, Belgique**

Reçu le 20 avril 1978

Les auteurs du présent travail font une analyse des facteurs qui agissent sur les équilibres d'échange ionique et de formation des complexes, en présence des solvants organiques de diverses classes. Basés sur des résultats expérimentaux et sur la discussion faite dans la Ière partie de l'article on donne une explication du processus combiné d'échange ionique – extraction aux solvants.

In this work an analysis of the factor which acts upon the equilibrium of the ion exchange and of the complex formation in the presence of different kinds of organic solvent, is presented.

Based on the experimental results and on the discussion performed in the first part of this work, an explanation on the Combined Ion Exchange – Solvent Extraction is given.

Pour pouvoir expliquer le comportement différent de certains ions à l'échange ionique en présence des solvants organiques et des acides minéraux, il faut prendre en considération leur action sur tous les facteurs qui interviennent dans les phases solution et résine.

PHÉNOMÈNES QUI ONT LIEU DANS LES PHASES SOLUTION À L'INTÉRIEUR ET À L'EXTÉRIEUR D'UNE RÉSINE ÉCHANGEUSE D'IONS, EN PRÉSENCE DES SOLVANTS MIXTES

Les échangeurs d'ions gonflés peuvent être considérés des solutions concentrées contenant un cation, ou un anion polyvalent et des contre-ions échangeables. La pression osmotique à l'intérieur de la resine se modifie en fonction de l'ionisation des groupements fonctionnels. Le gonflement est dû aux solvatations des groupements fonctionnels et des contre-ions de l'échangeur.[2,3] Il dépend des caractéristiques chimiques du solvant et de la constante diélectrique qui influence les interactions électrostatiques entre les ions individuels et les groupements ioniques dans la résine.

La distribution des macrocomposants (solvant, acide, trouvés dans la résine en quantité plus grande que les ions métalliques) entre la phase échangeur et celle de la solution extérieure se déroule différemment dans les cas des électrolytes et des non-électrolytes.

En général, les phénomènes liés à la pénétration des électrolytes dans la résine sont ceux propres aux équilibres de membrane. Ils sont réglés par l'équilibre des tendances opposées qui contrôlent la diffusion des ions inégalement chargés, due au gradient de concentration et au potentiel d'interface. Cela signifie que la formation des paires ioniques est un facteur important qui agit dans la distribution des électrolytes entre des solvants mixtes et la résine.[4]

La pénétration des non-électrolytes est, en essence, gouvernée par les caractéristiques physico-chimiques du non-électrolyte et de l'échangeur. Cela conduit à une pénétration plus importante d'un composant du solvant mixte, dans la résine, de sorte que la solution de l'intérieur de l'échangeur soit différente de celle de l'extérieur.[5,6] La concentration des macrocomposants dans la solution mixte détermine les propriétés diélectriques et la force ionique de celle-ci qui sont responsables de l'activité chimique du microcomposant (l'ion étudié) dans la solution.[7]

La modification du gonflement de la résine déterminée par les changements de la solution extérieure, la pression du gonflement et le volume molaire de l'électrolyte influencent également la pénétration du microcomposant dans l'ionit, parce que tous ces facteurs agissent sur la valeur de son potentiel chimique dans la phase échangeur.[7]

L'étude [8] concernant le gonflement des résines échangeuses d'anions dans des solvants mixtes eau-alcool éthylique et eau-acétone, en l'absence ou en présence de l'acide chlorhydrique, a relevé des faits importants pour l'élucidation du problème abordé. Ainsi, on a constaté, dans les deux cas, que, au fur et à mesure que la quantité du solvant dans le mélange augmente, sa proportion dans la résine augmente également. Mais, tandis que dans les mixtures eau-éthanol, le gonflement de la résine est comparable à celui dans l'eau étant un peu plus petit seulement pour les valeurs plus grandes que 90% éthanol, dans le cas des solvants mixtes eau-acétone un gonflement maximal pour 50% acétone est observé suivi de sa baisse et étant plus petit que dans l'eau (tableau 1).

La présence de l'acide chlorhydrique détermine, en général, la baisse du gonflement des résines, pour les deux types des mélanges eau-éthanol et eau-acétone, notamment quand le taux de solvant organique est de 90%, des différences plus grandes surgissant dans le cas des solutions acétoniques. La pénétration de l'électrolyte dans la résine par l'équilibre Donnan détermine l'élimination d'une quantité d'eau pour égaliser la pression de membrane. Un comportement particulier est présenté par les résines en solutions contenant 90% d'acétone, dont le gonflement est plus grand en présence de l'acide chlorhydrique qu'en l'absence de celui-ci. Il est intéressant que la variation du gonflement est accompagnée de la diminution de la quantite d'acétone absorbée et de la pénétration, en grande quantité, de l'acide dans la résine.

La solution à l'intérieur de l'anionit introduit dans des mélanges de 90% acétone contient une proportion plus grande d'eau, l'acide chlorhydrique passe en grande quantité dans la résine, mais pour égaliser la pression on n'élimine plus de l'eau, mais de l'acétone. Dans ces conditions, on forme des paires ioniques entre les groupements cationiques fixes et les contre-ions échangeables de l'ionit.

TABLEAU 1

Distribution des solvants et de l'acide chlorhydrique entre les solutions de l'extérieur et de l'intérieur d'une résine échangeuse d'anions, en fonction des proportions des composés dans le mélange [8]

Solvant organique %	HCl M	V_e cm³	Fractions molaires du solvant organique		Molarité de HCl	
			en solution	en résine	en solution	en résine
—	—	162,3	—	—	—	—
—	1	167,1	—	—	1,02	0,91
40	—	164,7	0,161	0,112	—	—
75	—	166,7	0,419	0,272	—	—
90	—	153,4	0,614	0,355	—	—
Ethanol 100	—	116,1	—	—	—	—
40	1	167,1	0,154	0,119	1,01	0,73
75	1	159,9	0,422	0,297	1,15	0,88
90	1	133,0	0,620	0,373	1,19	1,22
40	—	171,9	0,133	0,095	—	—
75	—	155,3	0,380	0,123	—	—
90	—	107,8	0,638	0,140	—	—
Acétone 100	—	15,4	—	—	—	—
40	1	150,8	0,134	0,096	1,08	0,55
75	1	132,0	0,388	0,124	1,14	1,52
90	1	117,3	0,625	0,130	1,19	4,81

Note: V_e—la variation du volume de la résine à l'équilibre

Dans des mélanges eau — alcool, les différences entre la composition des solutions à l'extérieur et à l'intérieur de la résine, sont plus petites en ce qui concerne les deux solvants et l'acide chlorhydrique en particulier.

A ces conclusions on ajoute la constatation que la pénétration de l'eau dans des résines échangeuses d'anions dépend de la nature des contreions, elle augmente dans l'ordre des formes ioniques : $ClO_4^- < NO_3^- < Cl^- < SO_4^{2-}$ et elle est plus grande pour des mélanges acétone-eau que pour ceux d'alcool-eau, surtout pour une grande teneur en solvant organique.[9] La pénétration du méthanol dans diverses formes ioniques de la résine est du même ordre que dans l'eau, ainsi que l'arrangement des contre-ions : $ClO_4^- < NO_3^- < Cl^- < SO_4^{2-}$. La quantité de l'acétone entrée dans la résine est très réduite et l'ordre des formes ioniques est opposé par rapport à l'ordre observé dans l'eau et le méthanol.[9]

Les résines échangeuses de cations préfèrent également les alcools à l'acétone, mais la pénétration de celle-ci est plus importante que dans le cas des résines échangeuses d'anions.[9]

Les résines échangeuses d'anions en forme Cl^- introduites dans des mélanges eau-dioxanne éliminent le solvant organique et retiennent préférentiellement de l'eau. Dans le cas d'une solution dans laquelle la fraction molaire du dioxanne est de 0,8 le taux de solvant dans la phase résine représente 1/2 — 1/3 seulement de cette valeur.[10] Le gonflement des résines échangeuses de cations en forme Na^+ baisse quand la proportion de dioxanne dans le mélange augmente, pendant que, dans le cas de la forme H^+, il reste inchangé.[11-12]

Une fois établies les conditions trouvées par le fer(III) à sa mise en contact avec des résines échangeuses d'ions en présence de solvants mixtes eau — solvant organique et d'acide chlorhydrique, nous essayerons d'expliquer le comportement mis en évidence dans le cadre du processus C.I.E.S.E.

L'EXPLICATION DU COMPORTEMENT DU FER (III) EN SYSTÈMES EAU – SOLVANT ORGANIQUE – HCl – RÉSINES ÉCHANGEUSES D'IONS

Les spectres d'absorption optique représentés dans les figures 2 — — 5, 7, 8[1] montrent l'existence des chloro-complexes du fer (III) en présence des solvants mixtes pour des concentrations de HCl qui ne déterminent pas leur apparition en solutions purement aqueuses.

a) SYSTÈMES D'ÉCHANGE CATIONIQUE

Dans le cas de la mise en contact de telles solutions avec une résine échangeuses de cations, les coefficients de partage du fer, seront d'autant plus bas que la proportion des combinaisons complexes, ayant le volume plus grand et la charge plus petite que les cations Fe^{3+}, augmentera et ils seront nuls quand dans la solution il existe des complexes $FeCl_3$ et $[FeCl_4]^-$. Ce comportement est commun à tous les systèmes d'échange cationique, quand la modification de l'affinité relative de la résine pour certains cations est déterminée par la formation des complexes supérieurs, soit qu'elle est réalisée par l'augmentation de la concentration de l'agent de complexation, soit par le remplacement graduel de l'eau par un solvant organique.

$$(\mathrm{Fe}^{3+})_{\mathrm{R}} + (\mathrm{H}^{+})_{\mathrm{S}} \rightleftharpoons (\mathrm{Fe}^{3+})_{\mathrm{S}} + (\mathrm{H}^{+})_{\mathrm{R}} \qquad \text{(I)}$$

$$\xrightarrow{+\ \mathrm{X}^{-}\ \text{ou solvant organique}} \text{des combinaisons complexes stables dans la solution}$$

Sous l'action conjointe de ces deux facteurs, l'équilibre (I) se déplacera de gauche à droite, donc vers le maintien du fer dans la solution, où il trouve des conditions supérieures de stabilisation.

Dans le cas d'échange cationique, l'influence des solvants organiques se manifeste plutôt par la favorisation de la formation des combinaisons complexes supérieures et par leur stabilisation, que par l'action sur les résines qui conservent inaltérées leurs propriétés d'échange ionique.

Donc, il existe, dans le cas des résines échangeuses de cations introduites en solvants mixtes, un processus combiné d'échange ionique et d'extraction aux solvants, très bien décrit par le sigle de « C.I.E.S.E. ».

Quand le système d'échange cationique contient plusieurs ions qui peuvent former des combinaisons complexes avec un anion complexant, la concentration de celui-ci et la teneur du solvant organique agiront dans la même direction, dans les deux cas.

D'après la relation :

$$\Delta\,(\log K_{12}) = \Delta \log \left(1 + \frac{C_x}{k_1} + \frac{C_x^2}{k_1 k_2} + \cdots + \frac{C_x^n}{k_1 k_2 \ldots k_n} \right) \tag{1}$$

où Δ (log K_{12}) représente la variation de la différence de l'affinité entre deux cations M_1 et M_2 ; K_{12} = la constante de l'équilibre d'échange ionique :

$$(M_1)_R + (M_2)_S \rightleftharpoons (M_1)_S + (M_2)_R \tag{II}$$

C_x = la concentration de l'anion complexant et

$k_1 \ldots k_n$ = les constantes d'instabilité des équilibres successifs de complexation), la différence d'affinité de la résine pour deux ions dépendra de la stabilité de leurs combinaisons complexes.

C'est le cation qui formera les complexes supérieurs les plus stables, qui passera dans la solution, en quantité plus grande.

L'approche du problème de ce point de vue permet d'expliquer la constatation expérimentale concernant le passage du cobalt en solution des mélanges 90% acétone — 10% HCl 6M en l'absence du fer et sa fixation dans le cationit quand dans la solution il y a des ions Fe^{3+}. D'après les spectres d'absorption,[1] le fer forme des anions complexes $[FeCl_4]^-$ en solutions qui contiennent 75 — 90% solvant organique (dioxanne, ou acétone) et acide clorhydrique 0,5 M. Les données de la littérature [13] montrent que, dans des solutions à 90% solvant organique, le cobalt existe seulement comme complexes $CoCl_2$ et $[CoCl]^+$, en milieu éthanolique, ainsi qu'acétonique, dans le dernier la proportion de $CoCl_2$ étant plus grande. En l'absence du fer, les équilibres de formation des chlorocomplexes du cobalt seront déplacés, par l'action du solvant organique, vers la formation des complexes cationiques et neutres, ce qui déterminera sa désorption du cationit. En présence du fer, qui forme des chlorocomplexes plus stables que les complexes du cobalt, les équilibres de réaction se déplaceront vers la formation des complexes supérieurs du fer, la complexation du cobalt étant régressée. Le fer reste dans la solution sous forme d'anions complexes ou de molécules neutres, exclus par une résine échangeuse de cations, et les cations Co^{2+} passent dans le cationit.

b) SYSTÈMES D'ÉCHANGE ANIONIQUE

Dans le cas des anionits, les solvants organiques agissent par leurs caractéristiques sur les propriétés d'échange ionique de ceux-ci. Ils déterminent le mode de gonflement de la résine, la composition, plus ou moins différente, des solutions à l'intérieur et à l'extérieur de l'ionit et la formation des paires ioniques à l'intérieur de l'échangeur.

Dans des solvants mixtes eau — alcools il n'existe pas de grandes différences entre la composition des phases solution et résine.

Quand la teneur en alcool augmente apparaissent dans la solution les complexes $FeCl_3$ et $[FeCl_4]^-$. L'échange ionique peut avoir lieu par les équilibres suivants :

$$(FeCl_3)_S \rightleftharpoons (FeCl_3)_R$$

$$(FeCl_3)_R + (Cl^-)_R \rightleftharpoons (FeCl_4^-)_R \qquad (III)$$

$$(FeCl_4^-)_S + (Cl^-)_R \rightleftharpoons (FeCl_4^-)_R + (Cl^-)_S \qquad (IV)$$

$$(H_SFeCl_4)_S \rightleftharpoons (H_SFeCl_4)_R \qquad (V)$$

où H_S représente le proton solvaté.

Il y a des conditions pour la pénétration des espèces neutres $FeCl_3$ ou H_SFeCl_4 dans l'ionit, parce que dans les mélanges eau-alcool la résine subit un gonflement analogue à celui des solutions purement aqueuses et la différence entre la concentration de l'acide chlorhydrique dans la solution à l'intérieur et à l'extérieur de la résine n'est pas trop grande. De même, les alcools ayant une structure semblable à celle de l'eau, les ions Cl^- pourront quitter la résine, permettant la fixation des anions complexes $[FeCl_4]^-$, parce qu'ils trouveront dans la solution, un milieu semblable comme propriétés et composition au milieu de l'intérieur de la résine.

La présence des alcools en grande quantité favorise la formation des complexes neutres et anioniques du fer avec l'acide chlorhydrique, mais elle ne modifie pas les propriétés d'échange ionique des anionits, ce qui conduit à l'augmentation des coefficients de partage.

Les solvants mixtes eau-solvant organique de la classe des cétones ou des éthers déterminent l'existence des complexes supérieurs, ainsi qu'un comportement nettement différent des résines échangeuses d'anions. Dans ces milieux, la phase résine peu gonflée est une solution fortement concentrée, prédominante aqueuse, dans laquelle les ions ne sont pas libres, mais associés en paires ioniques, ce qui rend plus difficile le développement de l'équilibre d'échange ionique (IV). Pour déplacer l'équilibre (IV) de gauche à droite, il faut que les anions $[FeCl_4]^-$ remplacent les ions Cl^- qui, d'une part sont immobilisés dans la resin eà cause de l'association avec les groupements ioniques fixes, et d'autre part, ils préfèrent la phase résine plus riche en eau que la solution extérieure concentrée en solvant organique.

A cause de la grande constante diélectrique de la solution extérieure, il est à prévoir que les ions $[FeCl_4]^-$ y existent essentiellement associés. Dans les solvants mixtes, le proton est solvaté avec des molécules d'eau et de solvant organique. La paire ionique $[O(H \ldots \ldots OC_4H_8O)_3]^+ [FeCl_4]^-$ aura donc un volume moléculaire beaucoup plus grand que l'anion $[FeCl_4]^-$, ce qui pourrait constituer un argument en défaveur de l'existence de l'équilibre (V). Ce point de vue peut expliquer, également, les coefficients de partage entre des anionits et la solution, toujours plus petits en i-alccools qu'en n-alcools.[14]

Bien que la pénétration des cations dans des résines échangeuses d'anions se produise le plus facilement quand ils se trouvent sous forme de composés neutres, ni dans ce cas le fer n'est pas fixé dans l'anionit. Outre les facteurs d'empêchement stérique, responsable de ce comportement est la modification de la phase résine. La très grande concentration d'acide chlorhydrique de la solution intérieure et le taux élevé de solvant organique de la solution exterieure déterminent des valeurs de la pression du gonflement qui ne permettent pas l'entrée de nouvelles molécules dans la résine, sans l'élimination des autres. La pénétration de grands agrégats $[O(H \ldots OC_4H_8O)_3]^+[FeCl_4]^-$ pourrait être accomplie seulement au compte du passage de nombreuses molécules d'acide chlorhydrique dans la solution (le volume de l'acide tétrachloroférrique $\gg$ le volume de HCl), mais éxpérimentalement on a constaté que celui-ci préfère nettement la phase résine plus riche en eau. Donc, le développement de l'équilibre (V) est aussi beaucoup défavorisé par les conditions de travail.

En regardant le problème de ce point de vue, on peut expliquer la rétention du fer dans des anionits des solutions avec 60% acétone et 1,2M HCl, parce que dans telles solutions la résine est suffisamment gonflée, la composition entre les deux phases est moins différente, les quantités d'acide chlorhydrique à l'intérieur et à l'extérieur sont comparables et donc, l'échange ionique peut avoir lieu. De même, le fait que les résines échangeuses d'anions sont plus gonflées quand se trouvent sous forme ionique NO_3^- que sous forme de Cl^-, explique la rétention partielle des éléments qui forment des complexes anioniques en solutions de tétrahydrofuran — acide azotique.

Dans les systèmes étudiés le taux de fer est plus ou moins élevé, comme complexe neutre $FeCl_3$. Ses chances de pénétrer dans l'anionit sont plus grandes, parce que son volume moléculaire est plus petit que celui de l'agrégat de l'acide tétrachloroferrique (on connait l'existence en solutions anhydres d'un composé 1 : 1 $FeCl_3$: dioxanne,[15] dont la présence a été aussi mise en évidence en solvants mixtes avec une teneur réduite en eau[16]). Mais dans la phase résine il existe un milieu différent de la solution extérieure qui était, grâce à la teneur élevée en solvant organique, favorable à la stabilisation des complexes supérieurs. Les complexes inférieurs, à charge électrique positive et les cations Fe^{3+} sont exclus par une résine échangeuse d'anions.

Cette différence entre la composition de ces deux phases peut expliquer la sorption dans l'anionit, en conditions similaires, des éléments qui forment des chlorocomplexes supérieurs, même en solutions aqueuses de faibles concentrations d'acide chlorhydrique : Ag, Hg, Zn, Bi, Tl, Au, parce qu'ils seront stables également, dans les conditions de l'intérieur de la résine. Les valeurs des coefficients de partage sont, également dans ce cas, plus petites qu'en présence des solvants organiques,[17] ce qui este justifié compte tenu des phénomènes décrits ci-dessus.

L'étude du comportement du fer (III) à l'échange ionique en présence de thiocyanate de potassium, et des solvants mixtes eau-acétone, a montré qu'à partir de 70% acétone le fer est complètement exclu par une résine échangeuse de cations et il est entièrement fixé sur une résine échangeuse d'anion. Si on travaille avec des solutions plus concentrées en acétone et avec des résines gonflées dans l'eau, les complexes sont fixés, mais, ils commencent à quitter la résine à un lavage à la solution de travail.[18]

Il y a ici un processus combiné d'échange ionique — extraction aux solvants, bien que le complexe existant en solution ne soit pas anionique. Le fer entre dans l'anionit, même aux grandes concentrations d'acétone, parce que dans les conditions données en solution existent des complexes neutres $Fe_2(SCN)_6$,[15] dont la pénétration dans la résine ne se fait pas par échange ionique, mais par équilibre Donnan. Dans la solution à l'intérieur de la résine, la concentration d'acétone est plus petite qu'à l'extérieur et les conditions n'étant plus favorables à l'existence de ce complexe, le fer quitte la résine. A la suite des équilibres qui ont lieu, le fer se trouvera finalement dans la phase dans laquelle la stabilité de ses combinaisons complexes sera maximale : la phase solution extérieure.

La différence entre la constitution des solutions à l'intérieur et à l'extérieur d'une résine échangeuses d'anions peut apparaître, également, dans des processus d'échange ionique en solutions purement aqueuses. Ainsi s'explique le fait que le fer(III) n'est pas retenu dans des résines échangeuses d'anions des solutions d'acide sulfosalicylique de pH 4,5 — — 10.[18] Les anions complexes, dont l'existence est prouvée dans la solution, peuvent pénétrer dans la résine, mais les conditions n'y sont plus favorables à leur stabilité, ils se décomposent et les cations Fe^{3+} sont obligés de quitter la résine.

Tous les phénomènes antérieurement décrits commencent à se faire sentir dans le cas des solvants mixtes eau-alcool seulement aux concentrations beaucoup plus grades du solvant organique ($> 95\%$), quand, pour les mêmes raisons, les coefficients de partage baissent.

CONCLUSIONS

Des faits expérimentaux décrits, on peut conclure que le processus C.I.E.S.E. est un phénomène complexe, ayant une sphère d'action beaucoup plus large. Il ne doit pas être limité seulement à l'échange ionique en présence des solvants organiques. Son apparition est liée à l'existence de certaines conditions qui déterminent l'apparition de fortes différences entre la solution à l'intérieur et celle à l'extérieur de la résine échangeuse d'ions. L'espèce étudiée sera répartie préférentiellement dans la phase dans laquelle sa stabilité sera maximale. Simultanément pourront se produire des phénomènes rencontrés dans l'échange ionique et dans l'extraction aux solvants, ou dans des conditions qui ne permettent pas la réalisation d'échange ionique, la résine fonctionne seulement comme support de la phase aqueuse et le processus essentiel reste celui de l'extraction aux solvants.

Il résulte que, bien que, en général, les résines échangeuses d'ions se comportent d'une manière analogue en solutions aqueuses et en solvants mixtes, les solvants organiques agissent par leurs propriétés particulières sur les équilibres chimiques de la solution extérieure, ainsi que sur la phase résine, en modifiant le gonflement et la composition de la solution interne et par cela, les propriétés d'échange ionique. Pour ces raisons, dans la discussion des processus d'échange ionique en solvants mixtes, il faut prendre en considération tous les facteurs qui interviennent.

Leur connaissance permet d'expliquer des phénomènes qui apparaissent et également la détermination des paramètres optimaux pour la réalisation de certaines séparations dans des conditions meilleures qu'en solutions aqueuses.

BIBLIOGRAPHIE

[1] Ire partie : L. Vlădescu et H. Hurwitz, *Rev. Roumaine Chim.*, **24**, 1353 (1979).
[2] T. Sasaki et H. Kakihana, *Bull. Chem. Soc. Japan*, **28**, 217 (1955).
[3] T. Sasaki, *Bull. Chem. Soc. Japan*, **28**, 220 (1955).
[4] H. P. Gregor, D. Hobel et M. H. Gottlieb, *J. Phys. Chem.*, **59**, 10 (1955).
[5] H. Rückert et O. Samuelson, *Acta. Chem. Scand.*, **11**, 303 (1957).
[6] R. Arnold et S. C. Churms, *J. Chem. Soc.*, **1965**, 325.
[7] R. G. Fessler et H. A. Stroebel, *J. Phys. Chem.*, **67**, 2562 (1963).
[8] M. Fojtik et V. Koprda, *Chem. Zvesti*, **27**, 32 (1973).
[9] S. Lasztity et T. A. Beliavskaia, *J. Chromatog.*, **102**, 293 (1974).
[10] C. H. Jensen et R. M. Diamond, *J. Phys. Chem.*, **75**, 79 (1971).
[11] O. D. Bonner et J. V. Morefield, *J. Phys. Chem.*, **8**, 555 (1954).
[12] H. Ohtaki, *Z. phys. Chem.*, (Frankfurt) **21**, 224 (1959) et **27**, 209 (1961).
[13] M. Fojtik et V. Koprda, *Chem. Zvesti*, **27**, 193 (1973).
[14] E. Klakl et J. Korkisch, *Talanta*, **16**, 1177 (1969).
[15] P. A. McCusker et S. M. Scholastica Kennard, *J. Amer. Chem. Soc.*, **81**, 2974 (1959).
[16] P. A. McCusker et S. M. Scholastica Kennard, *J. Amer. Chem. Soc.*, **81**, 2976 (1959).
[17] J. M. Peters et G. Del Fiore, *Radiochem. Radioanal. Lett.*, **21**, 11 (1975)
[18] G. Popa et L. Vlădescu, *Rev. Roumaine Chim.*, **22**, 725 (1977).

Revue Roumaine de Chimie, 25, 1, 145 – 154 (1980)

QUATERNARY AMMONIUM POLYELECTROLYTES. II[1]

QUATERNIZATION REACTION OF SOME TERTIARY AMINES WITH CHLOROMETHYLATED POLYSTYRENE

I. PETRARIU, MARIA ROTARU and STELA DRĂGAN

Institute of Macromolecular Chemistry "Petru Poni", Aleea Gr. Ghica Vodă No. 41 A,
6 600 Jassy, Romania

Received November 19, 1976
Revised February 10, 1979

The amination of chloromethylated polystyrene with triethylamine, tributylamine, trihexylamine and pyridine, was investigated. The influence of the solvent, amine and halogenated compound, as well as the molecular weight of chloromethylated polystyrene on the quaternization reaction was followed.

Ammonium quaternary polyelectrolytes constitute a category of macromolecular compounds that have acquired in the last years a greater and greater practical importance. For instance they can be successfully applied to the purification of water used by the energetics industry, to hydrometallurgy (flotation of ores), textile industry (modification of textile surface), as oil additives, oil refining products, soaps, shampoo, cosmetic products, etc.

Amination of chloromethylated polystyrene with different hydroxyalkyl tertiary amines has been the object of some previous researches.[1–2]

This paper deals with the best synthesis conditions of an ammonium quaternary polyelectrolyte of the type $(R_4N)^+X^-$, where R may represent aliphatic or benzylic radicals, either identical or different in comparison with some organic ammonium quaternary compounds of the benzyl and naphthyl chloride type.

Synthesis of ammonium quaternary polyelectrolytes through polystyrene chloromethylation and its amination with tertiary amines may be outlined as follows :

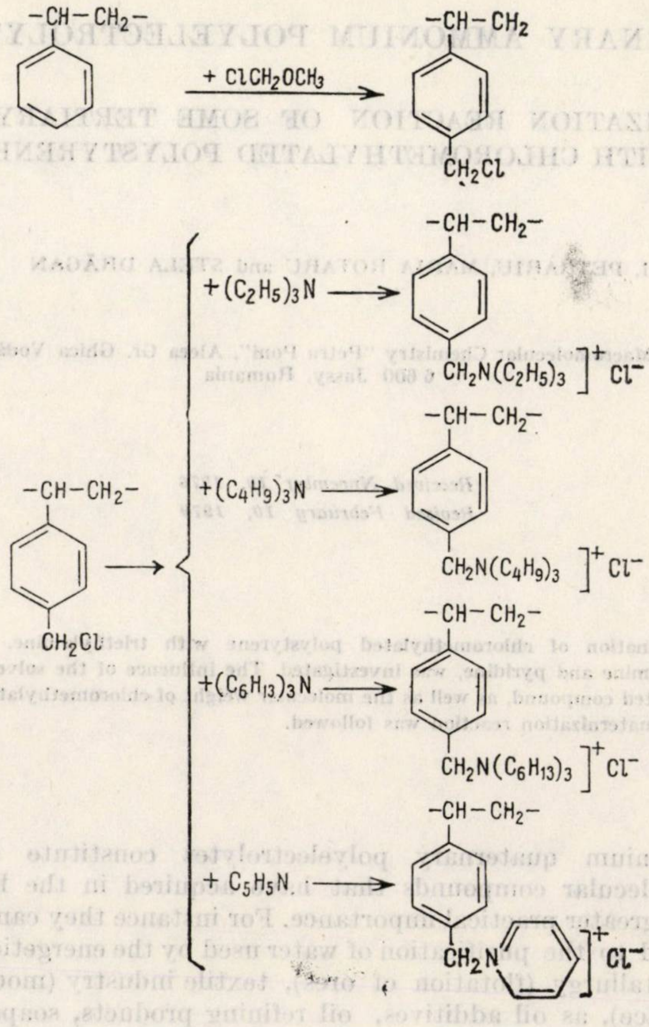

-CH-CH2-
+ ClCH2OCH3
CH2Cl
+(C2H5)3N
CH2N(C2H5)3]+ Cl−
+(C4H9)3N
CH2N(C4H9)3]+ Cl−
+(C6H13)3N
CH2N(C6H13)3]+ Cl−
+ C5H5N
CH2N]+ Cl−

EXPERIMENTAL

Polystyrene with $M_w = 8 \cdot 10^3$ was used for all chemical modifications. To study the influence of the chloromethylated polystyrene molecular weight in the amination reaction with triethylamine, there were prepared two samples of polystyrene possessing different molecular weights, respectively $M_w = 3 \cdot 10^4$ and $M_w = 1.1 \cdot 10^5$.

Polystyrene samples were obtained by the suspension polymerization technique,[3] purified twice in dioxan and methanol.

Chloromethylation of polystyrene was carried out with monochlorodimethyl ether.[4]

The chlorine amount caught by chloromethylated polystyrene was of 23.55 % Cl, which represents a 100 % *para* conversion of benzene ring, and a negligible percentage in *ortho* position.

In order to make a comparative study, certain halogenated organic aromatic compounds, such as benzyl chloride and naphthyl chloride, were used in some amination reactions.

All tertiary amines and solvents used have been previously distilled.

Amination of chloromethylated polystyrene was carried out according to the process described in a previous paper.[1]

The following tertiary amines were used: triethylamine, tributylamine, trihexylamine and pyridine. The molar ratio of chloromethylated polystyrene to amine was one to three.

In order to study the solvent effect as a function of its dielectric constant the following solvents were chosen: dimethylformamide (DMF), dioxan (DOX), tetrahydrofuran (THF), benzene (B), as well as solvent mixtures of the benzene-acetone type.

RESULTS AND DISCUSSION

To find the optimal conditions of amination we investigated the influence on the chemical conversion degree, k, of the following factors: the solvent and amine nature, the chloromethylated polystyrene-amine molar ratio, as well as the chloromethylated polystyrene molecular weight.

SOLVENT NATURE

It is well known that the quaternization reaction of a halogenated compound with a tertiary amine is strongly influenced by the solvent nature.[5–8]

In order to study this factor, the quaternization reaction of chloromethylated polystyrene with triethylamine was carried out in a molar ratio 1 : 3, at 80° for five hours in solvents with a different dielectric constant, such as DMF, DOX, THF and B.

In table 1 is given the conversion degree, k (after five hours) depending on the dielectric constants of solvents, and in Figure 1 the amination kinetics in the same solvents.

TABLE 1

Conversion degree, k, of chloromethylated polystyrene and benzyl chloride with triethylamine after five hours at 80° in organic solvents having different dielectric constants

Solvent nature	Dielectric constant 20°	k %	
		Chloromethylated polystyrene	Benzyl chloride
Dimethylformamide	38.42	89.40	77.29
Dioxan	2.22	18.98	8.40
Tetrahydrofuran	7.61	13.10	4.64
Benzene	2.28	5.18	—

The data in Figure 1 reveal that the amination reaction of chloromethylated polystyrene with triethylamine attains to an increased conversion degree in DMF comparatively with other solvents whose dielectric constant values are much lower.

In the case of DMF, a sudden increase of the conversion degree occurs within three hours of reaction, after which the quaternization velocity records a less marked increase.

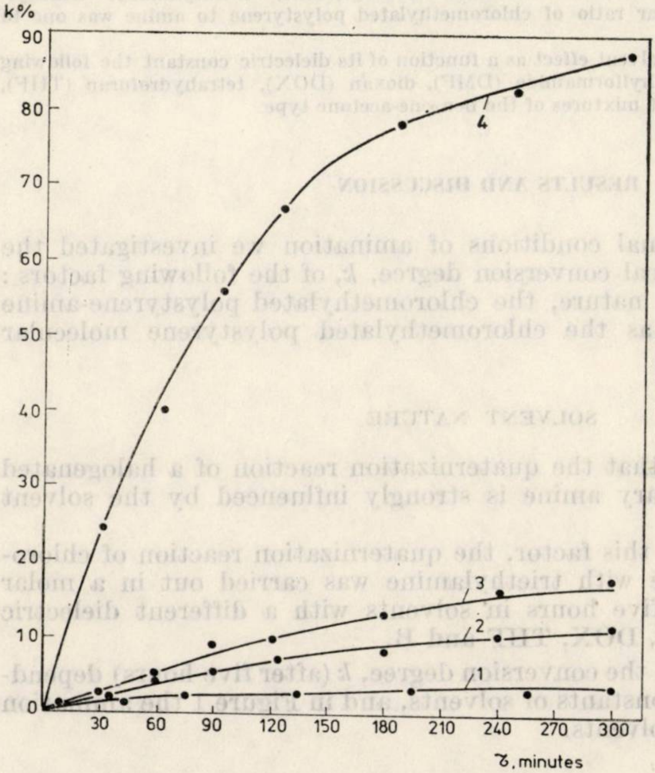

Fig. 1. — Influence of the solvent nature on the amination of chloromethylated polystyrene with triethylamine, at 80°.

1 — Benzene; *2* — tetrahydrofuran; *3* — dioxan; *4* — dimethylformamide.

A similar kinetics was obtained by using benzyl chloride instead of chloromethylated polystyrene (Table 1; Figure 2).

In this case, one can observe the same dependence upon the conversion degree *k'* and the solvent nature, except that the conversion degree records lower values when an organic halogenated compound with a small molecule of benzyl chloride is used.

In another experimental series we investigated the quaternization kinetics of chloromethylated polystyrene as well as of benzyl chloride with triethylamine for a molar ratio of one to three, at 50°, by using as a reaction medium a solvent mixture of the benzene-acetone type (Table 2, Figures 3 and 4). In this mixture, acetone was a strong polar solvent, while benzene a nonpolar one.

It was ascertained that at 50° the quaternization reaction in benzene does not take place.

If acetone is added to the quaternization reaction the quaternization velocity increases, because acetone has a higher dielectric constant.

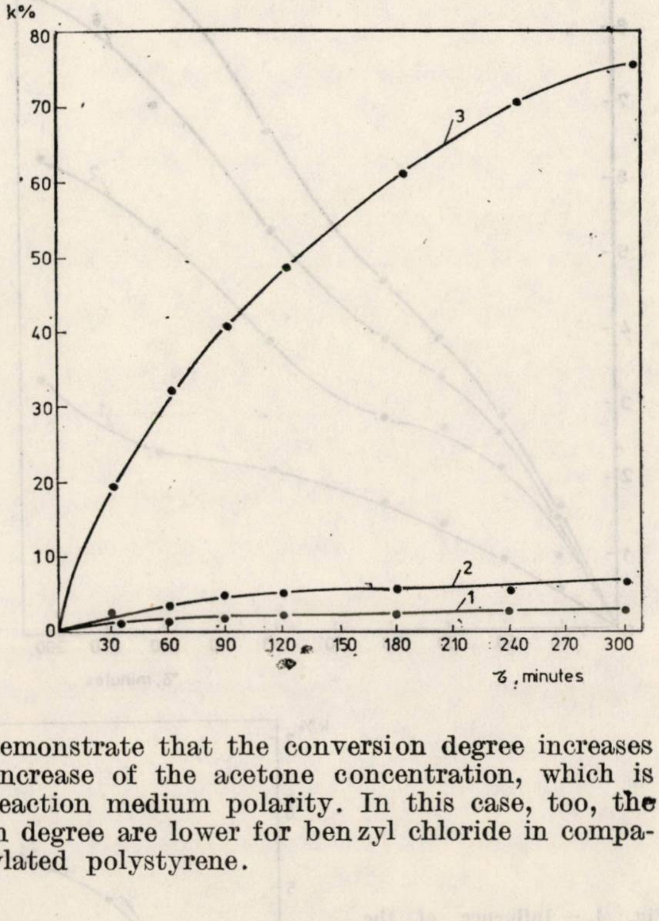

Fig. 2. — Influence of the solvent nature on the amination of benzyl chloride with triethylamine, at 80°.

— Tetrahydrofuran ; 2 — dioxan ; 3 — dimethylformamide.

The above data demonstrate that the conversion degree increases proportionally to the increase of the acetone concentration, which is accounted for by the reaction medium polarity. In this case, too, the values of the conversion degree are lower for benzyl chloride in comparison with chloromethylated polystyrene.

TABLE 2

Conversion degree, *k*, of chloromethylated polystyrene and benzyl chloride with trimethylamine after five hours at 50° in benzene-acetone mixture

Composition of the reaction mixture, Wt. %, benzene	*k* %	
	Chloromethylated polystyrene	Benzyl chloride
0	9.62	7.00
10	8.62	5.07
40	6.41	4.37
80	3.45	1.57

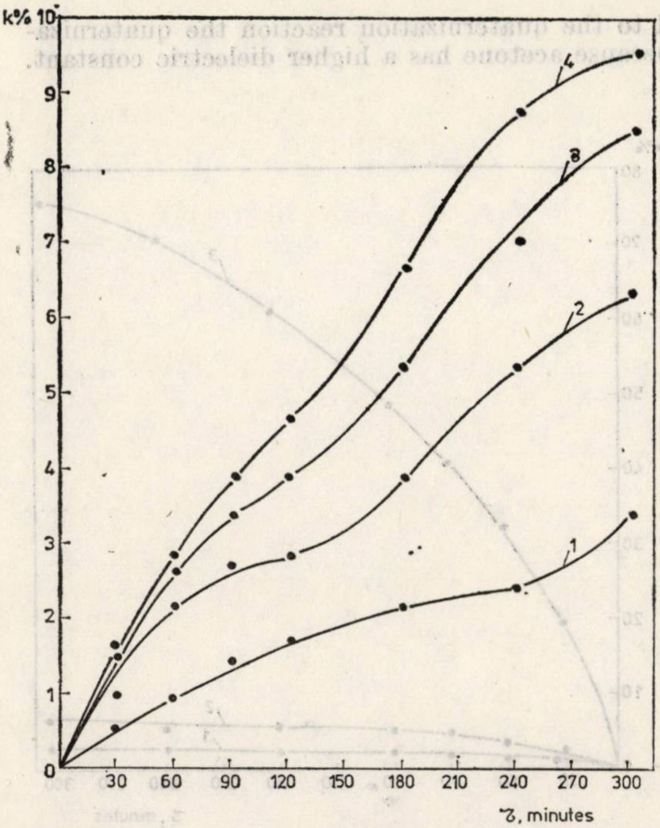

Fig. 3. — Influence of the solvent mixture on the amination of chloromethylated polystyrene with triethylamine, at 50°.

1 — Acetone (20%) + benzene (80%);
2 — acetone (60%) + benzene (40%);
3 — acetone (90%) + benzene (10%);
4 — acetone (100%).

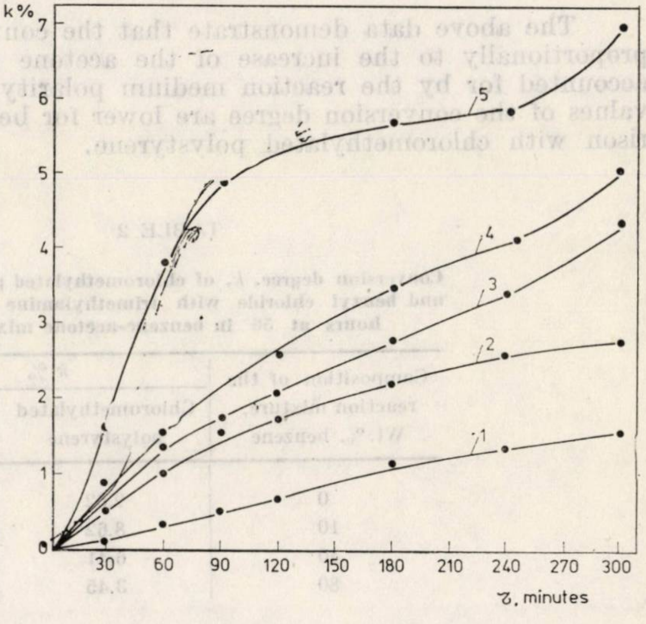

Fig. 4. — Influence of the solvent mixture on the amination of benzyl chloride with triethylamine, at 50°.

1 — Acetone (20%) + benzene (80%);
2 — acetone (40%) + benzene (60%);
3 — acetone (60%) + benzene (40%);
4 — acetone (90%) + benzene (10%);
5 — acetone (100%).

NATURE OF THE AMINE

In another experimental series we studied the amination reaction kinetics for a few tertiary amines with chloromethylated polystyrene (Figure 5).

It was ascertained that amine reactivity decreases proportionally to the increase of the aliphatic radical.

The amine reaction capacity may be correlated both with its basicity, i.e. with the density of electrons that surround the tertiary nitrogen atom, and with its steric effect produced by the size of radicals bounded to this atom.

The lower reactivity of pyridine in comparison with triethylamine and to a certain degree also with tributylamine is due to the fact that the two non-participant electrons of nitrogen conjugate with electrons of the aromatic ring and are less available for a nucleophilic attack.

Simultaneously we followed the conversion degree of chloromethylated polystyrene with benzyl dimethylamine, as well as with tertiary amines which have a large hydrocarbon radical, such as decyldimethylamine, myristyldimethylamine, lauryldimethylamine and cetyldimethylamine in DMF, at 80° (Table 3 ; Figure 6).

In this case the reactivity of these amines is much greater in comparison with trialkylamines where alkyl radicals are identical (compare Figures 5 and 6).

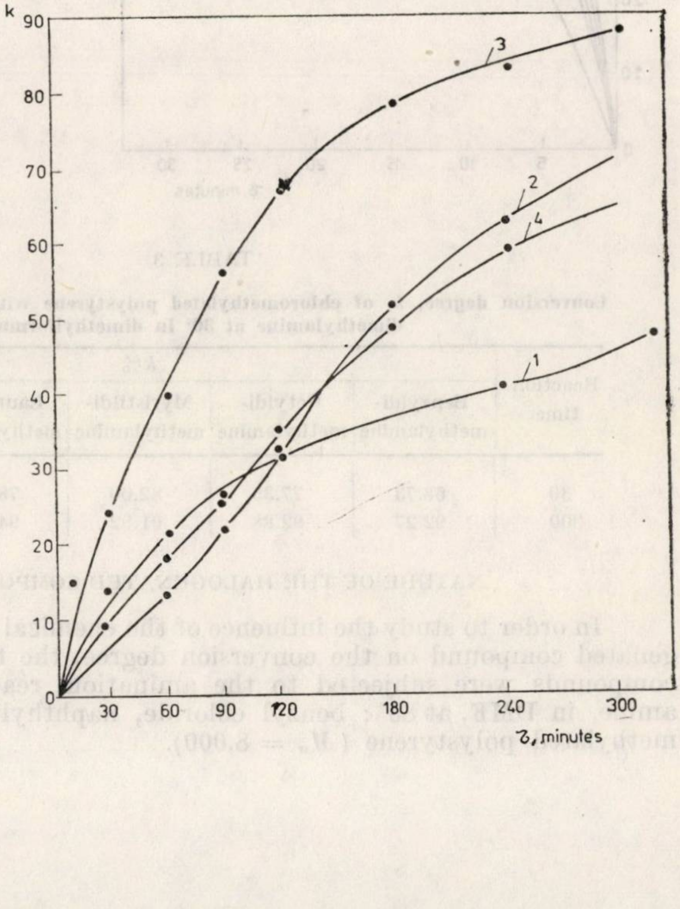

Fig. 5. — Influence of the amine nature on the amination of chloromethylated polystyrene in dimethylformamide for a chloromethylated/amine molar ratio of 1: 3, at 80°.

1 — Trihexylamine ; *2* — tributylamine ; *3* — triethylamine ; *4* — pyridine.

It was also ascertained that over 68 % of the quaternization reaction for amines of the alkyldimethylamine type occurs within the first thirty minutes, up to the 120th minute the values of the conversion degree increase by just a few percents, while between 120 and 300 minutes they remain practically unchanged.

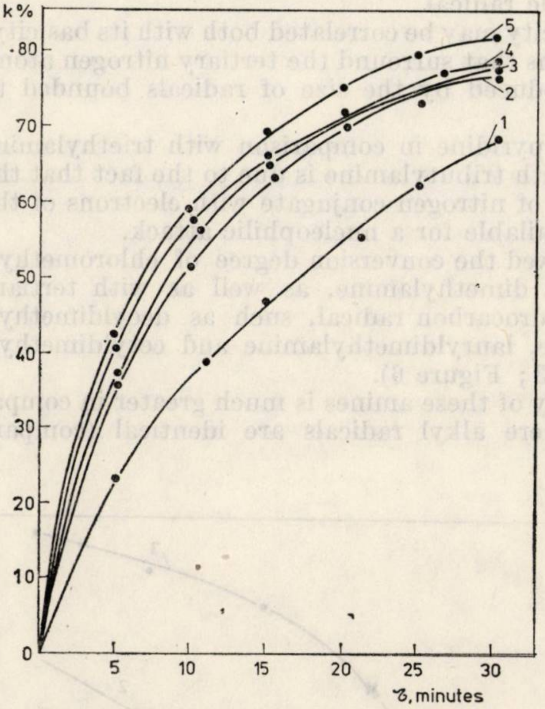

Fig. 6. — Amination of chloromethylated polystyrene with tertiary amines of the R-dimethylamine type, in dimethylformamide for chloromethylated polystyrene/amine molar ratio of 1 : 3, at 80°.

1 — R=benzyl; 2 — R= cetyl; 3 — R=lauryl; 4 — R = decyl; 5 — R = myristil.

TABLE 3

Conversion degree, k, of chloromethylated polystyrene with alkyl and benzyldimethylamine at 80° in dimethylformamide

Reaction time	k%				
	Benzyldimethylamine	Cetyldimethylamine	Myristildimethylamine	Lauryldimethylamine	Decyldimethylamine
30	68.73	77.35	82.00	78.13	77.97
300	92.27	92.88	91.92	94.24	96.32

NATURE OF THE HALOGENATED COMPOUND

In order to study the influence of the chemical structure of the halogenated compound on the conversion degree, the following halogenated compounds were subjected to the amination reaction with triethylamine, in DMF, at 80° : benzyl chloride, naphthylchloride, and chloromethylated polystyrene ($M_w = 8{,}000$).

The experimental data plotted in Figure 7 show that distinctions between the conversion degrees appear after the first 30 minutes of the reaction. The transformation degree decreases in the sequence : chloromethylated polystyrene > benzyl chloride > naphthyl chloride.

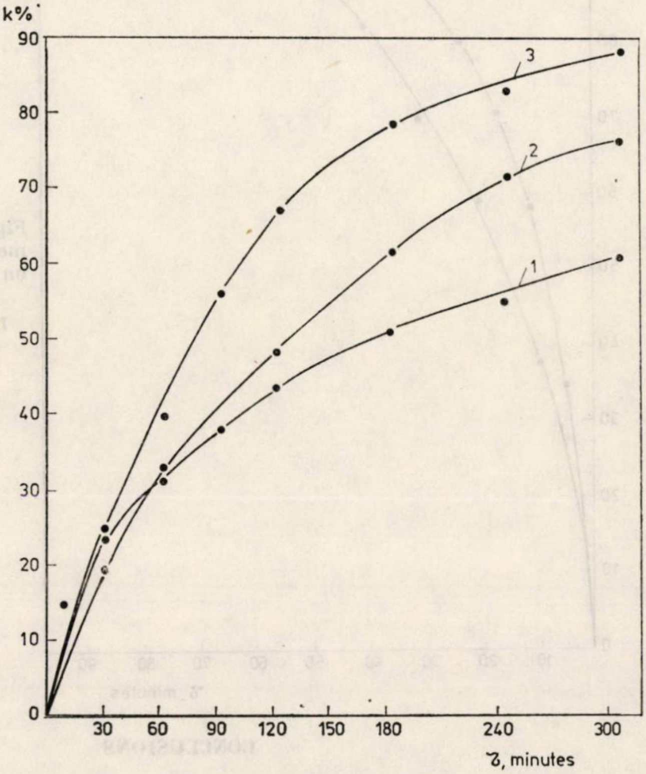

Fig. 7. — Influence of the halogenated compound nature on the conversion degree *k*.

1 — Naphthyl chloride; *2* — benzylchloride; *3* — chloromethylated polystyrene.

MOLECULAR WEIGHT OF CHLOROMETHYLATED POLYSTYRENE

With a view to setting up the influence of the chloromethylated polystyrene molecular weight on the amination reaction, two chloromethylated polystyrene samples were used, having nearly the same percentage of chlorine (23.2 %; 23.5 %) but different molecular weights, respectively $M_w = 110{,}000$ and $M_w = 30{,}000$. Both samples were aminated with triethylamine at 80°, for 90 minutes. From the experimental data plotted in Figure 8 it ensues that the amination kinetics of chloromethylated polystyrene ($M_w = 110{,}000$) increases suddenly within the first 50 minutes, after which it remains practically constant. The values of the conversion degree for chloromethylated polystyrene ($M_w = 30{,}000$) register an uninterrupted increase over the whole period of amination.

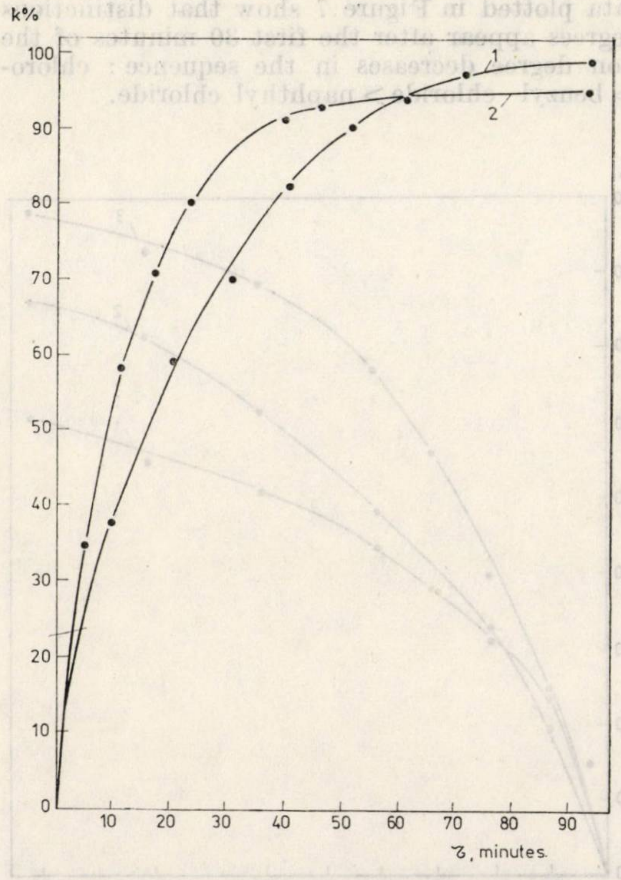

Fig. 8. — Influence of the chloromethylated polystyrene weight on the amination reaction with triethylamine at 80°.
1 — M_w = 30,000 ; 2 — M_w = 110,000.

CONCLUSIONS

1) The kinetics of the amination of chloromethylated polystyrene with four tertiary amines (triethylamine, tributylamine, trihexylamine and pyridine) in dimethylformamide, dioxan, tetrahydrofuran, benzene, as well as solvent mixtures of the benzene-acetone type was studied. The amination of benzyl-chloride and naphthylchloride with the four amines in dimethylformamide was followed.

2) It was found that the increased dielectric constant of the solvent favorably influences the reaction rate.

REFERENCES

[1] S. Drăgan, I. Petrariu and M. Dima, *J. Polymer Sci.*, **10**, 3077 (1972).
[2] I. Petrariu, C. Luca, Ig. Poinescu and M. Dima, *Rev. Roumaine Chim.*, **18**, 493 (1973).
[3] I. Petrariu and J. Stamberg., *Coll. Czech. Chem. Comm.*, **32**, 798 (1967).
[4] G. D. Jones, *Ind. Eng. Chem.*, **44**, 2688 (1952).
[5] N. Menschutkin, *Z. phys. Chem.*, **6**, 41 (1890).
[6] E. Tommila and P. Kauranen, *Acta Chem. Scand.*, **8**, 1152 (1954).
[7] E. Tommila, A. Koivisto, J. P. Lyyra, K. Antell and S. Heimo, *Ann. Acad. Sci. Fennicae*, **AII**, 47 (1952).
[8] I. Petrariu, C. Luca, M. Maftei and Z. Alistar, Roum. Pat. 71124, Dec. 18, 1974.

Revue Roumaine de Chimie, **25**, *1*, 155 – 163 (1980)

AN EXPERIMENTAL STUDY OF LIQUID FLOW IN THIN FILMS ON INCLINED PLATES AT ANGLES GREATER THAN 90° *

R. Z. TUDOSE and C. NĂFORNIŢĂ

"Petru Poni" Institute of Macromolecular Chemistry, 41A, Aleea Gr. Ghica Vodă, Iaşi, Romania

Received March 16, 1977

The paper studies the modifications in the structure of a thin water film flowing down on an inclined plate at angles greater than 90°, when the direction of gravity is changed, by measuring the frequency and amplitude of the waves. The flow develops into four different zones : waveless, transition (with regular waves), stabilization and stabilized.

INTRODUCTION

The flow of thin liquid films occurs in nature as well as in industry. The last 20 years have been a period of spectacular extension of the film applications in chemical industry, in rocket technologies, in controlling soil erosion, etc. Mention should be made of chemical engineering where the films are applied in heat exchangers, evaporators, mass transfer columns and reactors.

Various experiments have pointed out an intensification of the heat transfer of 100 %[1-3] and of a mass transfer of 250 %.[4-6] The mechanism of intensifying the heat and mass transfer is due to a specific structure of the film. The existence of waves on the free surface provides a perfect blending of the liquid mass, thus enabling the transfer by a convective mechanism. The waving of the surface leads also to an increase in the interface area.

The flow of liquids in thin films is extremely complex and it has been intensively studied theoretically and experimentally. Earlier papers trated the Newtonian liquid films[7-18] and it was only after 1960 that a restricted number of studies[19-21] dealt with the non-Newtonian films. Fulford [22] offered in 1964 a survey of this field.

Almost all the experimental investigations have been done with vertical cylindrical pipes, with interior and exterior films, or with plane vertical plates, inclined at various angles, ranging from 0 to 90°. The characteristics of the films are greatly influenced by the position of the border

---

[*] Presented at the Vth National Conference on General and Applied Physical Chemistry, Bucharest, September 1 – 4, 1976.

line, on which the flow takes place, versus the horizontal plane. By changing the angles, the structure and characteristics of the film are altered. These conclusions have led to the idea of studying the thin films flow on inclined planes at angles greater than 90°. Under particular circumstances and for angles greater than 90° a component of gravity tends to detach the film from the solid border, altering in another way the characteristics of the film. The aim of the present paper is to investigate the liquid flow under these conditions.

EXPERIMENTAL

The scheme of the experimental installation is shown in Figure 1. Its main part, that is plane 1 on which the liquid film is flowing, was of methylpolymethacrylate 2,000 mm long and 300 mm wide. When building the respective plane we took into account the fact that marginal effects may appear up to distances of 50 mm, so that its width had to be greater than 100 mm. In order to further underline the modifications and characteristics noticed in the film structure, a larger length of the plane was required. In order to measure the inclination of the angle, a measuring device (2) provided with a fastner was attached to the plane of flowing. The angle could be varied slowly from 90° — 165°. The upper part of the plane is provided with tank 3 having a capacity of 70 l and split into three separate compartments meant to diminish the turbulency created by the supplying liquid. The liquid comes into the smoothing tank *4* and then into the main tank provided with a baffle *5*.

In order to eliminate all the vibrations of the plane, produced by a centrifugal pump *6*, the plane is tied to all the other additional devices by elastic hoses *7*, *8*. Thus, the liquid reaches the overflow level of plane *1* after having eliminated all the generators of turbulency and vibrations, which consequently would lead to a nonuniform distribution along the width, and would create other kinds of waves at the surface of the film.

Plane *1*, is longitudinally strengthened by means of ribs *9* and thus the whole block-tank leans against the metallic frame *10* provided at the base with several screws *11* enabling the overflowing leading-edge of the liquid to become horizontal.

Measurements of the thickness of the film and the frequency of the waves were made by means of a pick-up needle attached to the micrometrical screw *12*. The whole measuring system is moving on its metallic frame, up and down the length and the width of the plane, so that measurements could be done in any place of the film surface.

The liquid on plane *1*, is captured by tank *13* or, after the flow had been measured, by funnel *14*, which is moving horizontally, the liquid being collected in a graduated container.

The centrifugal pump *6* is carrying the liquid from tank *13* to the constant level tank *16* through coiling coil *15*. The latter is provided with the heating and thermostating device *17*, and also with overflow *18*. The pipes and taps *19*, *20*, *21*, are made of stainless steel.

The installation for measuring the characteristics of the film of the liquid consists of micrometer, *12*, provided with a pick-up needle, a transformer and impulse amplifier *22*, impulse counter *23*, and electrode *24*. The source of energy is of 220 V.

The experiments were carried out at a temperature of 21.2° with distilled water in a constant flow, corresponding to the Reynolds number equal to 5500 according to Portalski.[23]

Before the experiments, the plane was cleaned with a solution of alcohol (50 % ethanol in water), then the leading-edge of the overflowing liquid was brought in to a horizontal plane. The check up of the above mentioned position followed the results obtained after measuring the thickness of the film along the width of the plate. After setting the installation into operation and establishing the working conditions, the measurements were performed at 36 different points placed along the central line of the plane. In all the 36 points the minimum and maximum thickness of the film was established, as well as the variations of the waves frequency versus the distance from the wall. The measurements were repeated at other angles : 90, 105, 120, 125°.

The frequency of the waves, in certain flowing conditions, reaches 60Hz. In order to ensure correct measurements, the pick-up needle was waxed to make it waterproof. The electric circuit was closed by de-waxing the point of the pick-up needle.

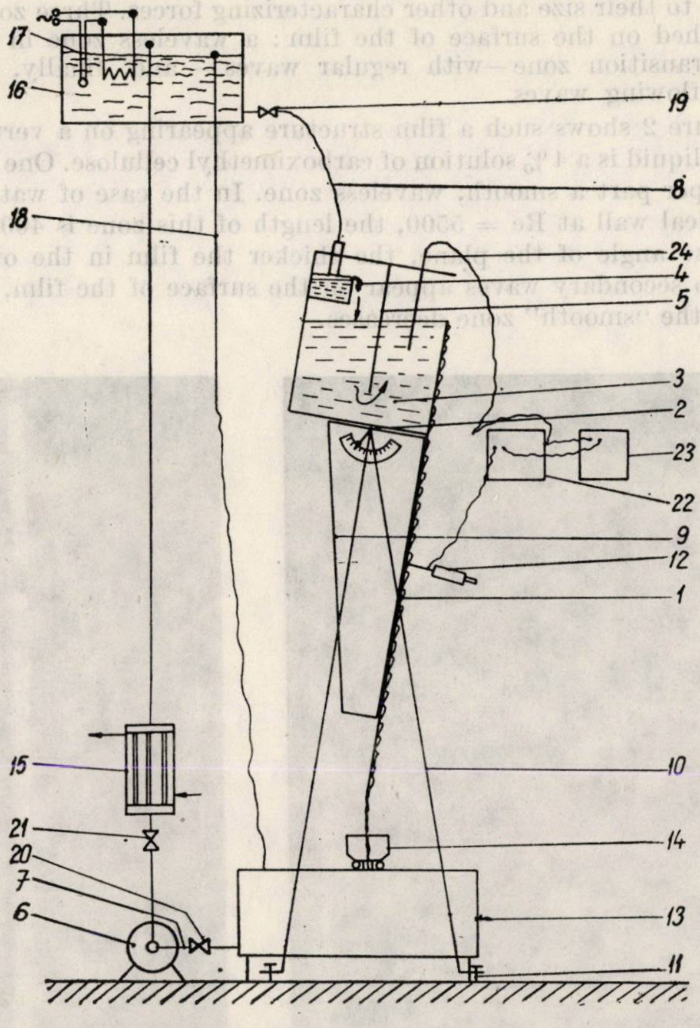

Fig. 1. — Schematic diagram of the experimental apparatus.

1. Plate; *2.* Inclining device; *3.* Tank; *4.* Smoothing tank; *5.* Baffle; *6.* Centrifugal pump; *7 – 8.* Elastic hose; *9.* Strenghthening frame; *10.* Backing frame; *11.* Screws; *12.* Micrometric screw; *13.* Tank; *14.* Funnel; *15.* Cooling coil; *16.* Constant level tank; *17.* Thermostat; *18.* Overflow; *19, 20, 21.* Throttling valves; *22.* Impulse amplifier; *23.* Impulse counter; *24.* Electrode.

RESULTS

In what follows a qualitative description of the structure of the film and of frequency and thickness measurements is given.

It is unanimously accepted that, in the absence of tensioactive elements at Re > 25, waves appear on the surface of the film; they may be gravitational (first-rate waves), or capillary (second-rate waves), according to their size and other characterizing forces. Three zones can be distinguished on the surface of the film : a waveless zone in the upper part, a transition zone —with regular waves — and, finally, a zone of irregular flowing waves.

Figure 2 shows such a film structure appearing on a vertical plane wall. The liquid is a 4 % solution of carboximethyl cellulose. One can notice in the upper part a smooth, waveless zone. In the case of water flowing on a vertical wall at Re = 5500, the length of this zone is 400 mm. The greater the angle of the plane, the thicker the film in the overflowing zone. Also secondary waves appear on the surface of the film, while the length of the "smooth" zone decreases.

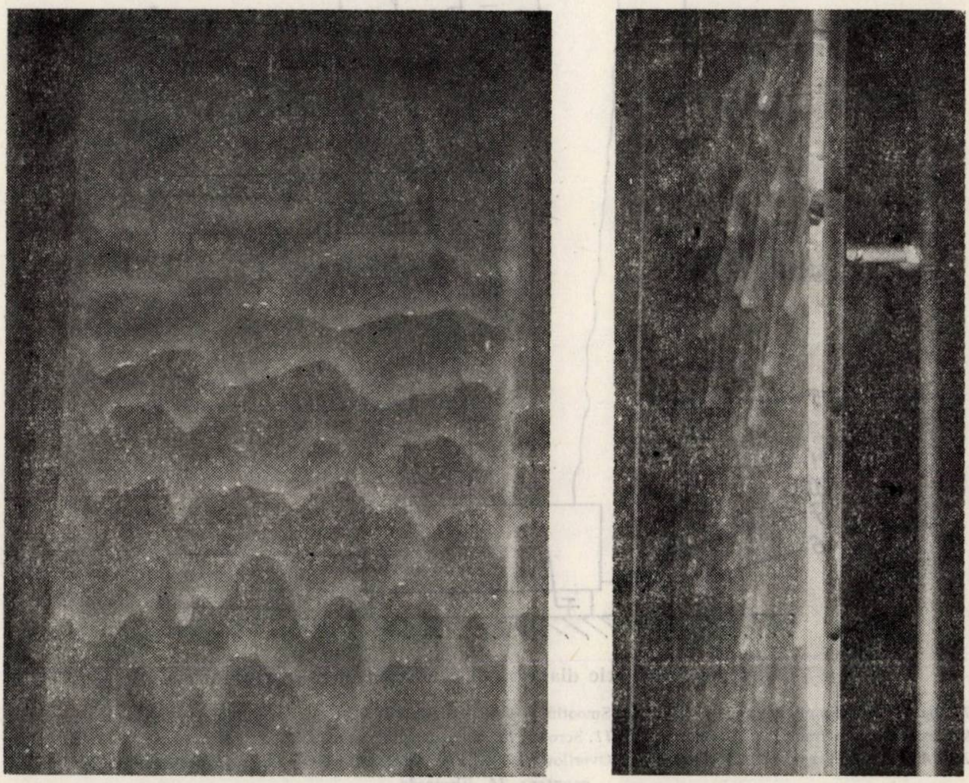

Fig. 2. — Structure of a film flowing on a vertical plane.

The transition zone starts with the first "primary" wave. We could not be very precise about the other part of the zone. The waves move normal to the flowing direction and are quite regular from the point of onset. At the distance of 2—3 wavelengths from the onset point, a certain lack of homogeneity in the flowing speed of the wave, can be noticed which changes into an irregular set of the "arrow" type (Figure 2 a). At the peak of the "arrow" wave a greater

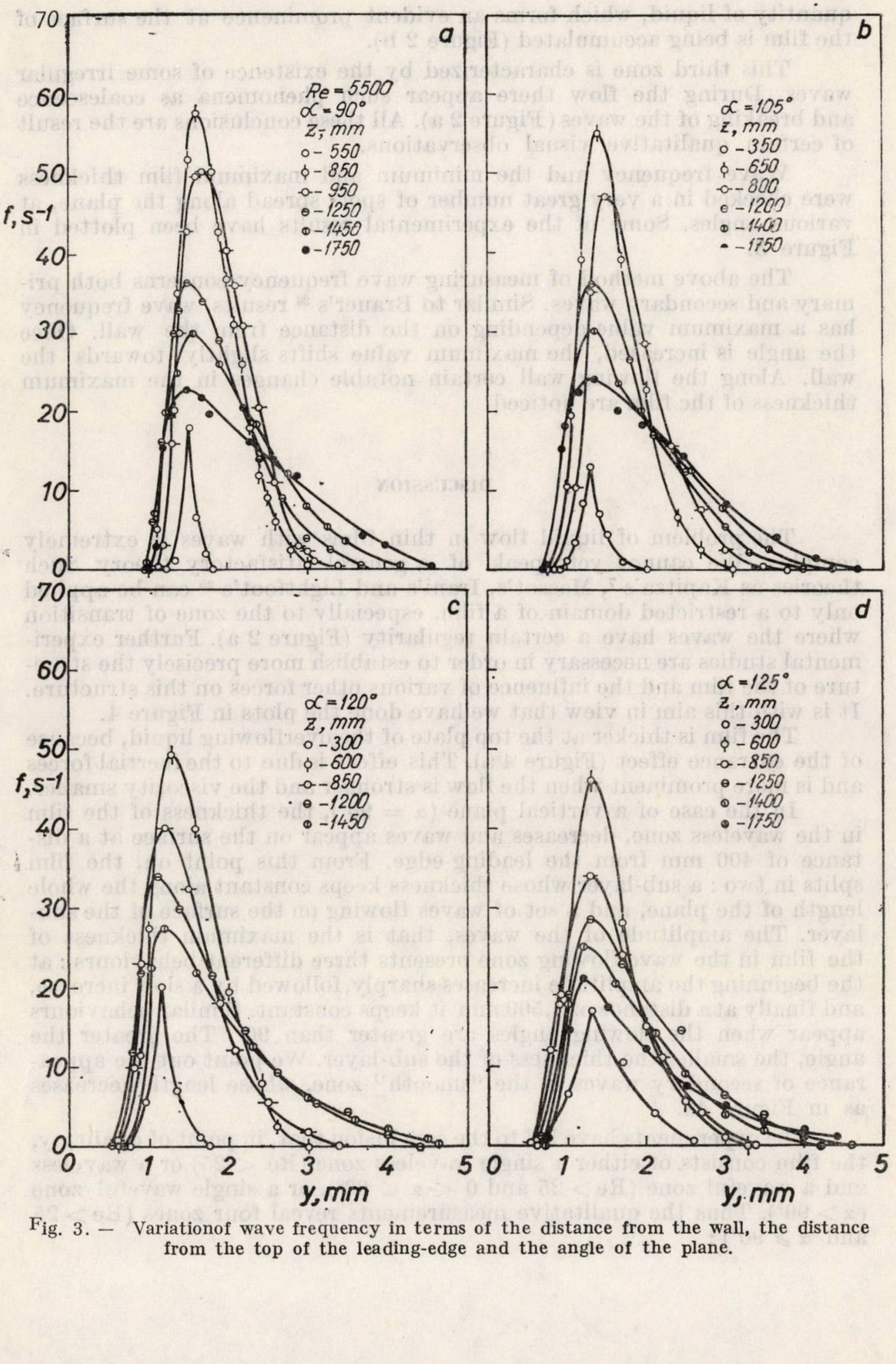

Fig. 3. — Variationof wave frequency in terms of the distance from the wall, the distance from the top of the leading-edge and the angle of the plane.

quantity of liquid, which forms an evident prominence at the surface of the film is being accumulated (Figure 2 b).

This third zone is characterized by the existence of some irregular waves. During the flow there appear such phenomena as coalescence and breaking of the waves (Figure 2 a). All these conclusions are the result of certain qualitative visual observations.

Wave frequency and the minimum and maximum film thickness were checked in a very great number of spots spread along the plane, at various angles. Some of the experimental results have been plotted in Figure 3.

The above method of measuring wave frequency concerns both primary and secondary waves. Similar to Brauer's [24] results, wave frequency has a maximum value depending on the distance from the wall. Once the angle is increased, the maximum value shifts slightly towards the wall. Along the flowing wall certain notable changes in the maximum thickness of the film are noticed.

DISCUSSION

The problem of liquid flow in thin films with waves is extremely complex. We cannot yet speak of a general satisfactory theory. Such theories as Kapitza's [7], Massot's, Irani's and Lightfoot's [25] can be applied only to a restricted domain of a film, especially to the zone of transition where the waves have a certain regularity (Figure 2 a). Further experimental studies are necessary in order to establish more precisely the structure of the film and the influence of various other forces on this structure. It is with this aim in view that we have done the plots in Figure 4.

The film is thicker at the top plate of the overflowing liquid, because of the entrance effect (Figure 4 a). This effect is due to the inertial forces and is more prominent when the flow is stronger and the viscosity smaller.

In the case of a vertical plane ($\alpha = 90°$), the thickness of the film in the waveless zone, decreases and waves appear on the surface at a distance of 400 mm from the leading-edge. From this point on, the film splits in two : a sub-layer whose thickness keeps constant along the whole length of the plane, and a set of waves flowing on the surface of the sub-layer. The amplitude of the waves, that is the maximum thickness of the film in the wave flowing zone presents three different behaviours : at the beginning the amplitude increases sharply, followed by a slow increase, and finally at a distance of 1.500 mm it keeps constant. Similar behaviours appear when the flowing angles are greater than 90°. The greater the angle, the smaller the thickness of the sub-layer. We point out the appearance of secondary waves in the "smooth" zone, whose length decreases as in Figure 4a.

The experiments have led to the conclusion that, in point of qualitaty, the film consists of either a single waveless zone ($Re < 25$) or a waveless and a waveful zone ($Re > 25$ and $0 < \alpha \leqslant 90°$), or a single waveful zone ($\alpha > 90°$). Thus the qualitative measurements reveal four zones ($Re > 25$ and $\alpha \geqslant 90°$) :

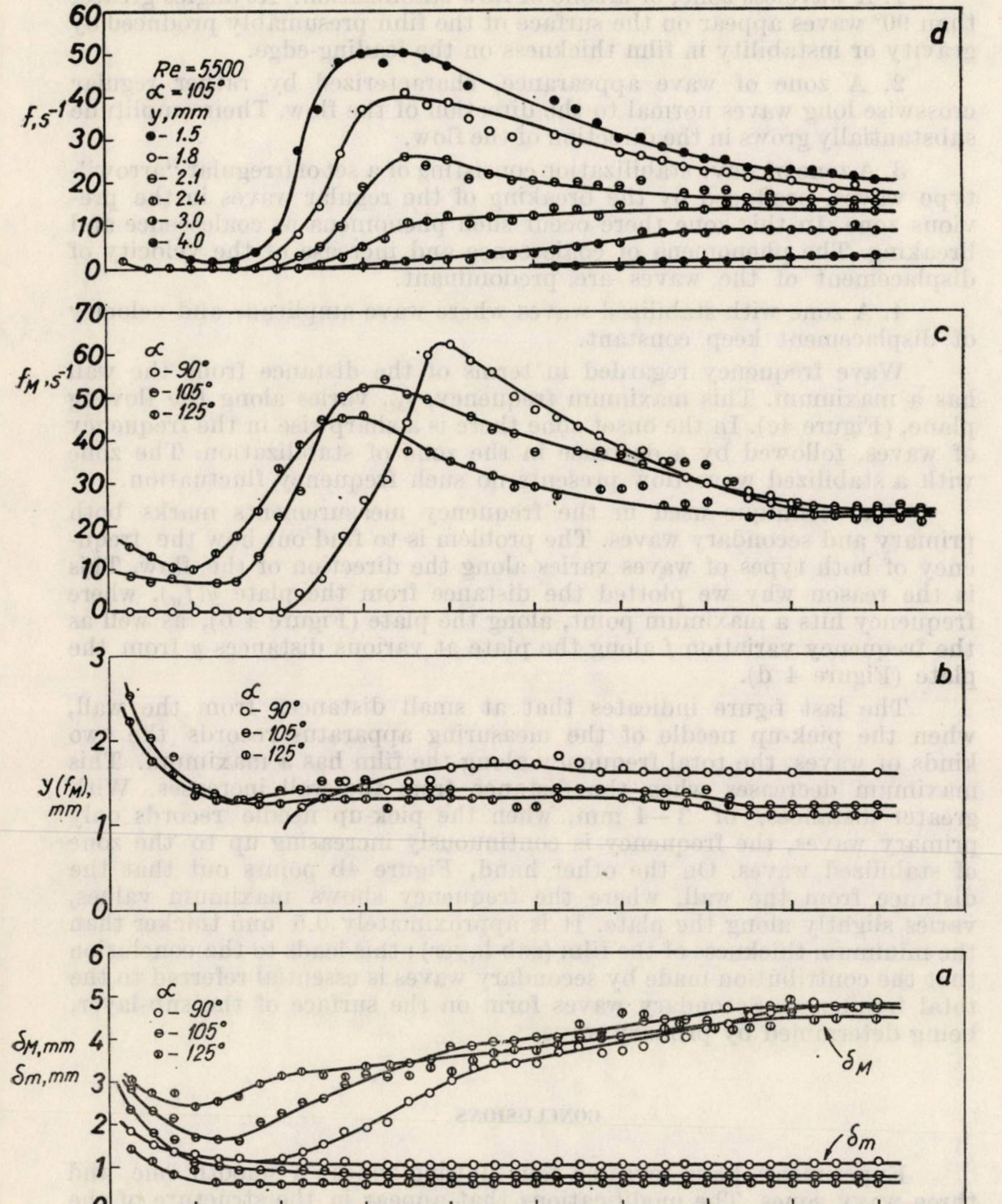

Fig. 4. — Variations of characteristics δ_M, δ_m, $y(f_M)$, f_M and f along the flowing plane.

1. A waveless zone, or a zone of flow stabilization. At angles greater than 90° waves appear on the surface of the film presumably produced by gravity or instability in film thickness on the leading-edge.

2. A zone of wave appearance, characterized by rather regular crosswise long waves normal to the direction of the flow. Their amplitude substantially grows in the direction of the flow.

3. A zone of wave stabilization consisting of a set of irregular "arrow"-type waves, produced by the breaking of the regular waves in the previous zone. In this zone there occur such phenomena as coalescence and breaking. The phenomena of coalescence and increase of the velocity of displacement of the waves are predominant.

4. A zone with stabilized waves where wave amplitude and velocity of displacement keep constant.

Wave frequency regarded in terms of the distance from the wall has a maximum. This maximum frequency, f_M, varies along the flowing plane, (Figure 4c). In the onset zone there is a sharp rise in the frequency of waves, followed by a decrease in the zone of stabilization. The zone with a stabilized wave flow presents no such frequency fluctuation.

The technique used in the frequency measurements marks both primary and secondary waves. The problem is to find out how the frequency of both types of waves varies along the direction of the flow. This is the reason why we plotted the distance from the plate $y(f_M)$, where frequency hits a maximum point, along the plate (Figure 4 b), as well as the frequency variation f along the plate at various distances y from the plate (Figure 4 d).

The last figure indicates that at small distances from the wall, when the pick-up needle of the measuring apparatus records the two kinds of waves, the total frequency along the film has a maximum. This maximum decreases when the distance from the wall increases. With greater distances, of 3—4 mm, when the pick-up needle records only primary waves, the frequency is continuously increasing up to the zone of stabilized waves. On the other hand, Figure 4b points out that the distance from the wall, where the frequency shows maximum values, varies slightly along the plate. It is approximately 0.5 mm thicker than the minimum thickness of the film (sub-layer); this leads to the conclusion that the contribution made by secondary waves is essential referred to the total frequency. Secondary waves form on the surface of the sub-layer, being determined by primary waves.

CONCLUSIONS

Experiments have revealed four flowing zones : a smooth one and three wavy zones. The modifications that appear in the structure of the waves are essential to passing from one zone to the next. When the flowing plane has angles greater than 90°, there appears a component of gravity tending to detach the film from the solid boundary. It also seems that the length of the wave stabilizing zone increases, while the thickness of the sub-layer decreases.

Our experiments led to the conclusion that gravity plays an essential role in the process of primary waves formation.

Our experimental techniques record the presence of both primary and secondary waves. Their frequency fluctuates nonuniformly along the flowing plane. The frequency of secondary waves is predominant in those zones where waves are formed and stabilized.

ACKNOWLEDGEMENTS. The authors express their deep gratitude to G Ioanid and I. Ibănescu for their assistance in preparing this work.

NOMENCLATURE

z — current distance, in the direction of the flow, from the leading-edge of the liquid.
y — current distance from the wall.
$y(f_M)$ — distance from the wall with maximum wave frequency.
f — wave frequency.
f_M — maximum frequency of waves.
δ_M — maximum thickness of the wave.
δ_m — minimum thickness of the wave.
α — inclination of the plane.
$Re = \frac{4Q}{\nu}$ Reynolds' number.
Q — flow of liquid per unit of wet perimeter.
ν — kinematic viscosity of the liquid.

REFERENCES

[1] W. Unterberg and D. K. Edwards, *AIChE Journal*, **11**, 1073 (1965).
[2] G. S. Bays and W. H. Mcadams, *Ind. Eng. Chem.*, **29**, 1240 (1937).
[3] R. Chand and H. F. Rosson, *Ind. Eng. Chem. Fund.*, **4**, 356 (1965).
[4] R. E. Emmert and R. L. Pigford, *Chem. Eng. Progr.*, **50**, 87 (1954).
[5] J. C. Jepsen, D. K. Crosser and R. H. Perry, *AIChE Journal*, **12**, 186 (1966).
[6] D. R. Oliver and T. E. Athrinos, *Chem. Eng. Sci.*, **23**, 525 (1968).
[7] P. L. Kapitza, *Zhur. Exsp. Teor. Fiz.*, **18**, 3 (1948).
[8] M. I. Jacskon, R. J. Johnson and N. H. Ceaglske,*Proc. Midwest Conf. Fluid Dynamics*, **1950**, 226.
[9] J. O. Wilkes and R. M. Nedderman, *Chem. Eng. Sci.*, **17**, 177 (1972).
[10] S. Portalski, *Chem. Eng. Sci.*, **19**, 575 (1964).
[11] B. Atkinson and P. A. Caruthers, *Trans. Inst. Chem. Eng.*, **43**, T33 (1965).
[12] F. Goodridge and G. Gartside, *Trans. Inst. Chem. Eng.*, **43**, T62 (1965).
[13] S. R. Tailby and S. Portalski, *Trans. Inst. Chem. Eng.*, **40**, 114 (1962).
[14] L. O. Jones and S. Whitaker, *AIChE Journal*, **12**, 525 (1966).
[15] W. J. Strobel and S. Whitaker, *AIChE Journal*, **15**, 527 (1969).
[16] S. R. Tailby and S. Portalski, *Trans. Inst. Chem. Eng.*, **38**, 324 (1960).
[17] S. R. Tailby and S. Portalski, *Trans. Inst. Chem. Eng.*, **39**, 328 (1961).
[18] D. F. Bruley, *AIChE Journal*, **11**, 945 (1965).
[19] G. Astarita, G. Marucci and G. Palumbo, *Ind. Eng. Chem. Fund.*, **3**, 333 (1964).
[20] N. D. Sylvester, J. S. Tyler and A. H. P. Skelland, *Canad. Journal Chem. Eng.*, **4**, 418 (1973).
[21] R. Z. Tudose and I. Ibănescu, *Rev. Chim. (București)*, **6**, 512 (1974).
[22] G. D. Fulford, Advances in Chemical Engineering, vol. 5, Academic Press, New York, 1964.
[23] S. Portalski, *AIChE Journal*, **6**, 1244 (1973).
[24] H. Brauer, *V.D.I.Forschungsh.*, **457** (1956).
[25] C. Massot, F. Irani and E. N. Lighfoot, *AIChE Journal*, **12**, 445 (1966).

Revue Roumaine de Chimie, **25**, *1*, 165 — 172 (1980)

BOOK REVIEWS

S. SUNNER and M. MANSSON (editors), *Combustion Calorimetry*, Experimental Chemical Thermodynamics, Vol 1. (IUPAC). Pergamon Press, Oxford, 1979, 428 p.

Even a casual reading of the contents of this book will reveal the valuable and authoritative condensation of the literature together with the most modern expertise concerning the calorimetry of combustion reactions, which it embodies. In addition, the adjuvant aspects of the presentation of such data to ensure that it may be critically evaluated are also heralded. This is important in an era in which an increasing fraction of the thermochemical data is produced by scientist not to thermodynamics *per se* and in which global energy problems underline the macroscopic — but not the microscopic — concerns of molecular and crystalline energies.

Molecular mechanics calculations are advancing step by step. Today, the energy of many hydrocarbons and simple compounds containing some hetero atom can be estimated in a satisfactory way. Quantum mechanical computations of varying complexity can also give reasonable results on molecular energies. Any semiempirical procedure, however, must have its roots in good experiments and only precise experimental results can determine the success of truly ab initio calculations. In this area, very important for our future, the highly accurate combustion calorimetric result is indispensable and it will not be in the nearest future that calculations will outgrow experiments. The future of combustion calorimetry must be judged to be bright. Several reasons can be given for such a point of view. We are still awaiting the real break-through for micro methods. The safe encapsulation of volatile materials in milligram quantities, without jeopardizing a high reproducibility of the results, is still a problem that has not been fully solved. Neither has an efficient marriage between moving bomb calorimetry and micro methods yet been achieved. Once these technical problems have been solved, attacks can be planned on successfully exploring the energetics of a vast number of organic, organo-metallic and inorganic compounds, which can be obtained only in minute amounts and which are of great interest in theory as well as in practice.

The first volume of Experimental Thermochemistry (1956) has been out of print for several years and today there is no detailed, fully authoritative presentation of the whole field of combustion calorimetry available to those who need it, whether they are already active in the field or intend to start such work. This in itself has given enough impetus to the editors, to the authors, and hopefully also to the publisher for producing this book.

This book is the result of coordinated efforts by its 26 authors :

1. Units and physical constants, F. D. Rossini.
2. Basic principles of combustion calorimetry, S. Sunner.
3. Calibration of combustion calorimeters, C. Mosselman and K. L. Churney.
4. Test and auxiliary substances in combustion calorimetry, J. D. Cox.
5. Strategies in the calculation of standard-state energies of combustion from the experimentally determined quantities, M. Mansson and W. N. Hubbard.
6. Assignment of uncertainties, G. Olofsson.
7. Presentation of combustion calorimetric data in the primary literature, E. F. Westrum jr.
8. General techniques for combustion of liquid/solid organic compounds by oxygen bomb calorimetry, A. J. Head, W. D. Good and C. Mosselman.
9. Combustion of liquid/solid organic compounds with non-metallic hetero-atoms, A. J. Head and W. D. Good.
10. Combustion calorimetry of metals and simple metallic compounds, Ch. E. Holley jr. and E. J. Huber jr.
11. Combustion calorimetry of organometallic compounds, H. A. Skinner.
12. Combustion in fluorine and other halogens, W. N. Hubbard, G. K. Johnson and V. Ya. Leonidov.
13. Bomb combustion of gaseous compounds in oxygen, V. P. Kolesov.
14. Oxygen flame calorimetry, G. Pilcher.
15. Fluorine flame calorimetry, G. T. Armstrong and R. C. King.
16. Combustion calorimetry as a technological service, O. Riedel and H. Vogl.
17. Trends in combustion calorimetry.

17.1. Aneroid bomb combustion calorimetry, A. S. Carson.
17.2. Miniaturization of bomb combustion calorimetry, M. Mansson.

17.3. The use of the Tian-Calvet microcalorimeter for combustion measurements, M. Laffitte.
18. From the history of combustion calorimetry, E. S. Domalski.

The book is intended for chemists and chemical engineers, biochemists, research staff and graduate students, highly qualified specialists in various fields.

D. I. Marchidan

M. E. GREEN and A. TURK, *Safety in working with chemicals*, London, Macmillan Publishing Co, 1979, 166 p.

Unlike many other books of the kind, in the present one the two authors report their personal experience with research laboratories in teaching establishments (the two authors are at the faculty of Chemistry Department of City University of New York). Most of the data they present as well as their findings are original and outstandingly interesting for the reader. Although a small book, it covers most of the problems one faces in chemistry laboratory and teaches the reader the very useful precautions. The content of the eight chapters is as follows :

Chapter 1, the introduction gives a classification of acute and chronical risks pertinent to chemistry laboratories. Many ailments chemists may suffer from, are due to inadequate handling of chemicals. This problem is ever more complicated due to synthetization of new chemicals whose action upon human organism is not known but just inferred by comparison with similar substances. There are at present about 1500 chemical compounds with potential cancerous action. At the end of this chapter the authors emphasize the responsibility all those involved have to assume in observing safety rules for handling of the chemicals.

Chapter 2, lists the main precautions one has to take in chemistry laboratories with handling glassware and chemicals ; keeping laboratories clean and tiny is recommended and so are individual protection means (glasses, masks, overalls). Special attention is awarded to individual protection and to utilization of labels with special accident-preventing warnings.

Chapter 3, deals with hazards associated to utilization of laboratory equipment. Hazards brought about by operation of devices with cooling water, high pressure gas cylinders, vacuum lines and electrical equipment. The danger of explosions caused by electric sparks and static electricity is discussed.

Chapter 4, deals with the dangers of some reactions, with ignition and explosion limits of chemical substances. In order to avoid these dangers, the authors present the adequate procedure for assembling devices and for preventing fires. Tables are supplied which specify the ignition limits of substances. Means are also reviewed of extinguishing fires ; a classification of possible fires according to substances involved is also available. Prevention of explosions is discussed by analysing their causes. Recommendations are issued regarding storage of solvents and other flammable substances as well as regarding the danger that their vapour catch fire or explode on transfering them from one container to another.

Chapter 5, is the most consistent as it comprises a description of toxic and corrosive substances. After presentation of the access ways, descriptions of specific actions and a table listing the limiting concentrations not chanceous for operators follow (the table has over 400 entries of substances of common laboratory use). Common and individual protection methods and methods for removing chemical substances in case of spillage are presented.

Chapter 6, specializes in a presentation of the physical hazards from a chemistry laboratory e.g. ionizing and nonionizing radiation (X rays, radiotracers, U.V. visible IR, laser radiation), microwave radiation, noise, heat and cold, their effects upon human body and protection against their effects. Special attention is given to ^{3}H, ^{14}C, ^{90}Sr, ^{40}K, ^{35}S, ^{32}P and ^{131}I, more frequently employed.

Chapter 7, refers to cleaning and maintenance of a chemistry laboratory including to removal of toxic or corrosive substances. Examples are given of flammable substances which turn explosive on lasting storage.

Chapter 8, refers to the official procedure in the case of an accident, to periodic inspection of laboratories and the briefing to which every laboratory worker must be subjected. The need to update information regarding determinations on newly synthetized chemicals whose physiologic action is not known is emphasized.

The book supplies a good deal of references on the matter. It is meant for high school students and undergraduates, for the teaching staff in high schools and universities, for researchers and chemists, specialists of high qualification, persons in charge with the safety of research and for all those who are regularly or only occasionally affiliated with chemistry laboratories.

D. I. Marchidan

Proceedings of the 1976 International Conference on Modern Trends in Activation Analysis, Vol. I-II, Akadémiai Kiadó, Budapest, 1977, 1958 pp.

The two volumes of the proceedings of the 1976 International Conference on modern trends in activation analysis issued by Akadémiai Kiadó-Budapest offers the reader the recent original work done in this rapidly developing field in the period 1972—1976. The book collects, in 1958 pages, 173 contributions of authors throughout the world published in the volumes 37, 38 and 39 (1977) of the Journal of Radioanalytical Chemistry.

The first volume organized as part 1 (956 pp) groups in four chapters the lectures of the Conference and a series of important communications of fundamental and technical developments as well as contributions on biological, biomedical, environmental and ecological applications. The lectures refer to relevant subjects such as: "Activation analysis and radiochemistry, comments to their interactions" (by H. -J. Born), "Medical significance of the essential biological metals" (by I. J. T. Davies), "The discovery and study of the nuclear reactor in Oklo" (by E. Roth), "Chemical fractionation in the solar system" (by J. W. Morgan) and "Analytical methods applied to water pollution" (by G. Baudin).

The second volume (1002 pp) sectioned as parts 2 and 3 groups in seven chapters some other important areas of this vast analytical domain. Part 2 deals with material sciences and industrial applications and with applications in geo- and cosmo-sciences. Part 3 is devoted to the applications in archaeology, art and forensic sciences, accuracy and precision, standard materials, sampling and homogeneity control. A discussion on the representative sampling follows the contributions. A list of participants and an author index end the volume.

This accurately printed and excellently edited book is a very useful collection of information for analytical chemists and radiochemists working in analytical and other related fields.

V. Drăguţan

Laser-Induced Processes in Molecules, K. L. KOMPA and S. D. SMITH (editors), Springer-Verlag, Berlin, Heidelberg, New York, 1979, XIV+368 pp.

The volume 6 of Springer Series in Chemical Physics, "Laser-Induced Processes in Molecules", edited by K.L. Kompa and S. D. Smith, presents the proceedings of the European Physical Society Divisional Conference at Heriot-Watt University Edinburgh, Scotland held in September 20 — 22, 1978. The book collects 95 communications (including 16 invited lectures) on the physics and chemistry of laser-induced processes in molecules reported by more than 200 participants working in this exciting field. The papers are grouped in five parts; an index of contributors and an information on the Quantum Electronics Division of European Physical Society end the book.

This very interesting volume of Springer Series offers the reader the progress that has been made on laser-induced processes in molecules all over the world. The papers deal with a great variety of aspects of this intensively investigated subject such as laser techniques suitable for applications in chemistry, spectroscopic studies with laser, multiphoton excitation, dissociation and ionization, laser control of chemical reactions and molecular relaxation.

The first part groups 9 papers referring to the study of lasers and related techniques suitable for applications in chemistry and spectroscopy. Among these the papers on rare gas halogen lasers, laser-induced intermolecular and intramolecular energy transfer processes, kinetic and thermodynamic aspects on the time evolution of chemical laser systems are of great interest. In the second part a number of 21 papers presents the spectroscopic studies with and related to lasers. Here the reader will find a wide range of laser applications in spectroscopic area. Multiphoton excitation, dissociation and ionization are the topics dealt with in about 30 papers of the part 3 ; a variety of applications of laser techniques in unimolecular and bimolecular processes is illustrated.

Part 4 grouping 22 contributions is devoted to laser-induced chemical reactions. The examples cover inorganic and organic reactions including theoretical considerations too.

The last part of the book treats some aspects of molecular relaxation and the use of laser technique in relaxation phenomena.

This volume is a very useful collection of recent information for molecular physicists working in laser-induced processes as well as for theoretical, inorganic or organic chemists interested in laser-induced phenomena.

V. Drăguţan

Structure and Bonding, vol. 34, Novel Aspects, Springer-Verlag, Berlin, Heidelberg, New York, 1978, 220 pp.

Volume 34 of Springer Series, Structure and Bonding, contains five contributions on inorganic and complex chemistry written by leading authorities in the field.

The first paper by S. Hubert, M. Hussonnois and R. Guillaumont is devoted to the measurement of complexing constants by radiochemical methods. The authors present a new radiochemical procedure for the determination of complexing constants based on solvent extraction method. The procedure is exemplified for the measurement of the formation constant β for the citric complex of all the lanthanides and transuranium elements from Am to Fm.

A very attractive discussion on the predictable quarkonium chemistry will be found in the second paper written by C. K. Jorgensen. Herein, the opportunities for concentrating and detecting quarks and the properties of adducts of atoms, ions and molecules with quarks are discussed. The existence of a pronounced difference between positive quarks located in the outer valence regions or in the conduction electrons of metals and negative quarks which are firmly bound to nuclei is outlined too. In the discussion analogies are drawn with neutrons, muons and other well-established particles.

The third contribution, by R. A. Bulman, deals with the chemistry of plutonium and the transuranics in biosphere. The paper reveals the fact that there are many complexing agents in the biosphere which could form stable complexes with the actinides and such complexes could alter the transport of the actinides in microenvironments. A special attention is paid to the concentration and to the transport of actinides through the biosphere to human body.

In the next paper J. W. Buchler, W. Kokisch and P. D. Smith review the available data on *cis*, *trans* and *meta* effects in transition metal porphyrins. The knowledge of these effects will help to sort out the essential electronic parameters that govern the specific action of the heme proteins in biologic oxygen transport and redox processes. Some perspectives that may serve as a guide to further research work are included as well.

The final paper, by D. K. Koppikar, P. V. Sivapullaiah, L. Ramakrishnan and S. Soundararajan, focuses on complexes of the lanthanides with neutral oxygen donor ligands. The paper offers the reader some general aspects from the coordination chemistry of lanthanide complexes with neutral oxygen donor ligands including their formation, classification, stoichiometry and geometrical parameters. The data obtained by various physical methods such as vibrational, electronic absorption, fluorescence emission, proton NMR and X-ray diffraction spectra as well as conductance and molecular weight measurements are largely discussed.

The volume presented here upholds the high standards of the well-known Springer Series Structure and Bonding. It is an useful source of up-to-date information for inorganic and bioinorganic chemists working in the complex chemistry as well as for theoretical and organic chemists interested in modern developments of structural and biological chemistry.

V. Drăguţan

Synergetics, Far from Equilibrium, A. PACAULT and C. VIDAL (editors), Springer-Verlag, Berlin, Heidelberg, New York, 1979, X + 176 pp.

The third volume of Springer Series in Synergetics, "Far from Equilibrium", edited by A. Pacault and C. Vidal collects lectures and communications presented at the meeting held in Bordeaux, France in September 1978 on physical and chemical phenomena that occur far from equilibrium. As the book fully illustrates, this meeting covered a broad area of topics including irreversible thermodynamics, bifurcation analysis of reaction diffusion equations, fluctuation theory, quantum optics, oscillating reactions, solid state chemistry, electro-chemical processes and hydrodynamics. It is a special merit of Springer-Verlag to provide the most recent information reported on these exciting trends of natural phenomena.

In the first part the volume gathers papers on subjects such as dissipative structures, bifurcation diagram of model chemical reactions, nonequilibrium phase transitions and instability hierarchy of the laser. The reader can find further some attractive discussions on chemical oscillations, noise induced transition phenomena, stability in chemical systems and membrane potentials. Soret-driven instability and Reyleigh-Benard instability are dealt with in two subsequent papers. The next contribution is a review of scaling theory of transient phenomena near the instability point including applications to transient laser radiation and chemical reactions. In the final part of the book various aspects of the instability concept such as chemical evolution far from equilibrium, instability in solid-gas reactions, origin of chemical and hydrodynamic instability are tackled.

The book represents an excellent up-to-date collection of information on the progress that has been made in the recent years on phenomena occurring far from equilibrium. It provides a deep insight on the physics, thermodynamics and chemistry of far from equilibrium processes and will be very useful to physicists and chemists interested in the theoretical and experimental aspects of these fields.

V. Drăguţan

Topics in Applied Physics, vol. 27, "Photoemission in Solids" II, "Case Studies", L. LEY and M. CARDONA (editors), Springer-Verlag, Berlin, Heidelberg, New York, 1979, XVIII + 402 pp.

Published as a continuation of Volume 26 of the series Topics in Applied Physics (Photoemission in Solids I), the present volume deals with the photoelectron spectra of some specific types of materials offering the information that can be obtained from such spectra about electronic structure.

The book contains seven contributions by well-known authorities in the field. After a short introduction by L. Ley and M. Cardona, the photoelectron spectroscopy as applied to semiconductors is extensively discussed in chapter 2. Photoemission in transition metals and their compounds and of rare earths and their compounds are the subjects discussed in the next two chapters. The last chapters treat photoemission from organic molecular crystals, synchrotron radiation and simple metals. An appendix with the table of core-level binding energies, an additional references section and a subject index end the book.

In chapter 2 L. Ley, M. Cardona and R. A. Pollak treat photoemission in semiconductors, a type of materials of large applicability which have been extensively studied and their electronic bands are well known. After a historical outlook on semiconductors and a discussion of their band structures, the testing capabilities of the photoemission techniques are illustrated on semiconductors, especially those of diamond-zincblende structure. A comprehensive discussion of amorphous semiconductors and the relationship between ionicity, core shifts and variations in the valence bands are considered. Methods complementary to photoelectron spectroscopy are also presented. This chapter offers the reader a complete treatment of the photoemission in semiconductors and constitutes a source of key references on various aspects of the subject.

Chapter 3, by S. Hüfner, reviews the photoelectron energy distribution curves (EDC) of transition metals and their compounds and the relation of these energy distribution curves to band structure. A special attention is paid to the problem of energy band structure and hybridization between the *d* and other levels. Alloys and intermetallic compounds are included as well.

Chapter 4, by M. Campagna, C. K. Wertheim and Y. Baer, is devoted to photoemission process in rare earth metals, their compounds and alloys. The authors discuss the positions of the $4f$ multiplets and the valence of the rare earth atom, including the cases of mixed valence or valence fluctuations. The $4s$ and $5s$ multiplet splittings of this type of atoms, due to exchange interaction with the corresponding core spectra of the $3d$ and $4d$ electrons, are also discussed.

Photoemission from organic molecular crystals is subsequently dealt with by W. D. Grobman and E. E. Koch in chapter 5. After a detailed presentation of various experimental aspects of photoelectron spectroscopy in organic molecular crystals, the typical solid-state effects for tetrathiofulvalenium-tetracyanoquinodimethane (TTF—TCNQ) and polymer $(SN)_x$ are emphasized. Both valence bands and core level spectra are discussed, in particular the relation between core shift and charge transfer in such compounds.

Synchrotron radiation as applied to photoelectron spectroscopy is developed further in chapter 6 by C. Kunz. After an extensive presentation of the properties of electromagnetic radiation emitted by synchrotrons and storage rings, the applications to synchrotron radiation are illustrated. The chapter also includes photoemission experiments which require the properties of synchrotron radiation, in particular its tunability and polarization, such as constant initial-state spectroscopy, constant final-state spectroscopy and yield spectroscopy.

The final chapter, by P. Steiner, H. Höchst and S. Hüfner, treats photoelectron spectroscopy of simple metals such as Na, Al, Be, and Mg. The XPS spectra of the valence band are also included. Besides the existent literature the authors furnish a considerable amount of unpublished material.

In conclusion, the book is clearly and concisely written, well documented and conceived. The material exposed in the book will be very useful for spectroscopists working in photoemission spectroscopy. It will be also a valuable source of information for physicists and theoretical chemists interested in electronic structure of solids.

V. Drăguţan

Hydrogen in Metals. II. Applications — Oriented Properties, edited by G. ALEFELD and J. VÖLKL, Springer-Verlag, Berlin, Heidelberg, New York, 1978, 387 + XXII, 162 figures.

This book is the 29th volume in the series entitled *Topics in Applied Physics* founded by H. K. V. Lotsch and gathers contributions by H. Wagner (Elastic interaction and phase transitions in coherent metal-hydrogen alloys), H. Peisl (Lattice strains due to hydrogen in metals), T. Springer (Investigation of vibrations in metal hydrides by neutron spectroscopy), A. C. Switendick (The change in electronic properties of hydrogen alloying and hydride formation), F. E. Wagner and G. Wortmann (Mössbauer studies of metal-hydrogen systems), W. E. Wallace (Magnetic properties of metal hydrides and hydrogenated intermetallic compounds), K. W. Kehr (Theory of the diffusion of hydrogen in metals), R. M. Cotts (Nuclear magnetic resonance in metal-hydrogen systems), K. Sköld (Quasielastic neutron scattering studies of metal hydrides) H. Kronmüller (Magnetic after effects of hydrogen isotopes in ferromagnetic metals and alloys), J. Völkl and G. Alefeld (Diffusion in metals) and A. Seeger (Positive muons as light isotopes of hydrogen).

There is a large number of areas of immediate or potential applications of the metal-hydrogen systems: purification of hydrogen (hydrogen filters), hydrogen embrittlement in powder metallurgy, metal hydrides used in nuclear technology as moderator, reflector, shielding or control material; isotopes separation using isotope-dependent properties of metal hydrides, hydrogen technology (water, water-methane splitting etc.), fusion technology, electric utility load leveling, heat storage using metal hydrides, energy cascading, i.e. topping cycles for power-generation stations using metal-hydrogen systems. This list is not complete but demonstrates the great variety of these applications treated in the above-mentioned chapters. The first volume of the book deals with theoretical features concerning metal hydrides.

Due to the extended areas these subjects are not completely treated, but covers concepts and methods of investigation new as compared to an earlier period neutron scattering, Mössbauer effect and new theoretical considerations concerning phase transitions.

Gh. Drăgan

H. H. KAUSCH, *Polymer Fracture*, Springer-Verlag, Berlin, Heidelberg, New York, 1978, 332 + X, 180 figures.

This volume continues the series *Chemie, Physik und Technologie der Kunststoffe in Einzeldarstellungen*, now entitled *Polymers, Properties and Applications*. Professor Hans Henning Kausch from Laboratoire des Polymères Departement des Matériaux, Ecole Polytechnique Fédérale de Lausanne, Suisse, is well known in the field of the polymer fracture, a tackled domain in the actual literature. As the author mentions, this book might be called "Kinetic Theory of Polymer Fracture", because a fracture process is discussed in detail in association with molecular motions which govern it. This aspect may be splitted into two stages : the molecular motion in normal material, and during the fracture process, respectively. The latter one which is the main purpose of the book, refers to the kinetic formation of the free radicals, and can be used as a measuring system for amplitude of fracture process. This subject is well synthesized and involves the morphological aspect of deformation as well as statistical aspects, continuous mechanics, rate process theories of fracture and detailed aspects of the strength of chemical bonds, both in theoretical and phenomenological terms, covalent bonds, bond energies, form of binding potential mechanical excitation and scission of a chain, identification by means of ESR spectra of the mechanically induced free radicals, phenomenology of free radical formation and of relevant radical reactions, the role of the chain scission in homogeneous deformation and fracture, and molecular chains in heterogeneous fracture. An important role in fracture phenomenology has by the initiation and propagation of crazes and cracks in many present studies.

An important deficiency of the monograph is the absence of the first aspect above-mentioned of this subject. It is well established, by phenomenological facts, that molecular motions in normal material detected by mechanical or dielectric losses govern the nature and amplitude of the fracture mechanism. This fact may be used as an important tool in diagnosis of the polymer thoughness.

Gh. Drăgan

E. PRETSCH, T. CLERC, J. SEIBL and W. SIMON, *Tabellen zur Strukturaufklärung organischer Verbindungen mit spektroskopischen Methoden*, Springer-Verlag, Berlin—Heidelberg—New York, 1976

The five main physical methods for the elucidation of organic chemical structures are nowadays part of the curriculum in all university programs for chemists or chemical engineers. The book under discussion is of considerable assistance to any chemist using these methods, because it contains practically all essential data for structure elucidation of unknowns, or for correlations between spectra and chemical structure.

The tables constituting the book present these five methods in the following order : ^{13}C—NMR, ^{1}H—NMR, IR, MS, UV—VIS. Under each method, the tables are arranged according to the chemical functions in the molecules. These five sections contain the main detailed information provided in the book, ordered first according to the method, and secondly according to the functions. The initial section which precedes the above five sections contains in condensed form the most sallient data, ordered first according to the main chemical functions (alkanes, alkenes including cyclic analogues, alkynes, aromatics, heteroaromatics, haloderivatives, hydroxy derivatives, ethers, amines, nitro derivatives, thiols, thioethers, aldehydes, carboxylic acids, esters, lactones, amides, lactams) and secondly, within the same table, according to the physical method. This initial section starts with Colthup-type illustrations of the ranges in which various characteristic absorptions occur.

Several peculiarities of the book deserve special mention : in order to avoid printing errors, the book is reproduced photographically from typewritten script ; the pages are numbered in an original way to allow in future editions supplemental tables to be included ; it was attempted to make each page complete by itself, with self-explanatory formulas and as little text as possible, so that even for those who cannot read German the use of the tables is easy.

The authors have taught for ten years the topic under discussion at the Eidgenossische Technische Hochschule, Zürich; Drs. Clerc and Pretsch have authored several books on NMR methods, Dr. Seibl a book on mass spectrometry, and Professor Simon is a well-known specialist in chemistry and optical spectroscopic methods. They have produced a reference book enabling chemists and chemistry students to locate rapidly vital information without scanning the enormous literature published in this field. The book is user-oriented, as proved by much useful information on the spectra of the main classes of compounds, or of the common solvents.

The section on $^{13}C-NMR$ includes data on the additivity rules for correlating structures with calculated chemical shifts. Coupling constants are also discussed. The section on $^{1}H-NMR$ is the most extensive in the book. The section on infrared spectroscopy contains, in addition to the tables, illustrations for the substituted benzenoids in the 1600–2000 cm^{-1} range. The section on mass spectroscopy contains an extensive table for mass correlations, an interesting illustration followed by a detailed table, both on isotopic abundances, as well as other useful tables and illustrations such as the combinations of halogens, or the diagnostic peaks. The section on electronic absorption spectra (UV/VIS) presents, in addition to tabular data, the Woodward rules with all generalizations, as well as a collection of reference spectra.

The authors motivate in their preface why no detailed literature survey is included, by the facts that the references are too numerous and that many data originate from the authors' laboratories. Three suggestions may be made for future editions, namely to include data for further classes of the main types of heterocycles, to add information on solvents for infrared spectroscopy, and to append data on relaxation in $^{13}C-NMR$ spectroscopy.

This impressive and extremely useful collection of spectral data in accessible format and very condensed form should be available to all chemical laboratories using the five physical methods discussed here. Students in chemical faculties and their teaching staff will also benefit from having, for the first time, a reference book with data obtained by all five methods, since in most other books $^{13}C-NMR$ and/or MS are absent.

A. T. Balaban

NOTE POUR LES AUTEURS

La Revue Roumaine de Chimie publie des articles en anglais, français, russe, allemand ou espagnol. Les auteurs sont priés d'envoyer des articles et des comptes rendus inédits.

Les manuscrits seront dactylographiés à deux intervalles. La bibliographie, les tableaux et la légende des figures seront placés après le texte.

Si l'article fait partie d'une série numérotée, le titre de la partie précédente sera indiqué dans une note au bas de la première page.

Chaque article sera précédé d'un résumé comprenant quinze lignes au maximum.

Les références bibliographiques dans le texte seront faites par des exposants sans parenthèse et paraîtront comme des notes au bas de chaque page.

Les publications périodiques mentionnées dans la bibliographie seront présentées suivant les prescriptions internationales : le nom de l'auteur précédé de l'initiale du prénom, le titre du périodique abrégé conformément à Chemical Abstracts et souligné par une ligne, le numéro du tome, indiqué par des chiffres arabes et souligné par deux lignes, suivi de la première page de l'article ; à la fin, l'année de la parution sera placée entre parenthèses. Le numéro de la revue ne sera pas indiqué si les pages du volume sont numérotées consécutivement. Pour les revues dont les tomes ne sont pas numérotés (par ex. Bull. Soc. Chim. France, etc.), l'année de la parution soulignée par deux lignes précèdera l'indication de la page.

Les textes des livres inclueront : les noms des auteurs, les initiales du prénom, le titre du livre entre guillements et sans être souligné, le numéro du tome précédé par l'abréviation « vol. » (ou « Bd. »), le numéro de l'édition, les éditions (the publisher), la localité de la parution et la page de la référence précédée par l'abréviation « p. » (ou « S. »).

Les brevets seront indiqués comme suit : l'auteur ou la firme, le pays et le numéro du brevet, la date et la revue (Chem. Abstr.). Par ex. M. Jones (to Union Carbide co.), Brit. Pat. 601 238, 2 sept. 1959, Chem. Abstr., 54, 12808 (1960).

Si la référence n'a pas étélue en original, on indiquera aussi la revue de références consultée.

Les diagrammes seront tracés à l'encre de Chine sur papier calque. Les tableaux et les figures (en nombre strictement nécessaire) seront numérotés par des chiffres arabes et leur explication sera donnée dans la légende des figures. Prière de ne pas inscrire les mêmes données dans les tableaux et dans les figures. Chaque tableau aura un titre. On indiquera dans le texte la place approximative des tableaux et des figures. Les formules chimiques seront incluses dans le texte ; en outre, elles seront transcrites sur papier calque, à l'encre de Chine.

Les auteurs sont priés d'indiquer les caractères italiques (en soulignant les lettres au crayon), ainsi qur tout autre caractère spécial ; les préfixes *ortho, meta, para, cis, trans,* etc. seront soulignés pour indiquer leurs caractères italiques et ne seront jamais écrits avec des majuscules.

Aucune correction à la main ne sera admise sur le manuscrit. Les corrections seront frappées à la machine. Les lettres grecques ou d'autres symboles spéciaux seront insérés à la main à l'encre clairement.

Le manuscrit sera signé par l'auteur.

Le colonne-titre aura 50 lettres au maximum.

L'entière responsabilité du contenu des articles appartient aux auteurs.

Pour détails voir le n° 2 (1980).

PRINTED IN ROMANIA

TRAVAUX PARUS AUX EDITIONS DE L'ACADÉMIE DE LA RÉPUBLIQUE SOCIALISTE DE ROUMANIE

A. T. BALABAN, L. GĂLĂŢEANU, G. GEORGESCU, LIGIA SIMIONESCU, **Compuşi marcaţi şi radioformaceutici cu aplicaţii în medicina nucleară** (Composés marqués et radiopharmaceutiques à application en médecine nucléaire), 1979, 495 p.

I. G. MURGULESCU, E. SEGAL, **Introducere în chimia fizică**, vol. II. 1, **Teoria molecular cinetică a materiei** ((Introduction à la chimie physique, IIe vol. 1. 5 La théorie moléculaire-cinétique de la matière), 1979, 1003 p.

I. E. TEODORESCU, MARIA FITI, **Iradierea tehnologică** (L'Irradiation technologique), 1979, 216 p.

S. STERNBERG, FL. DANEŞ, **Termodinamica chimică aplicată** (La thermodynamique chimique appliquée), 1978, 400 p.

I. G. MURGULESCU, V. EM. SAHINI, **Introducere în chimia fizică**. Vol. I.2. **Structura şi proprietăţile moleculelor** (Introduction à la chimie physique, Vol. I, 2. La structure et les propriétés des molécules), 1978, 604 p.

C. DRĂGULESCU, E. PETROVICI, **Chimie structurală modernă. Chimia coordinanţei 8** (La chimie structurale moderne. La chimie de la coordinence 8), 1977, 947 p.

D. PURDELA (sous la direction de), **Nomenclatura chimiei anorganice** (La nomenclature de la chimie inorganique), 1977, 153 p.

I. ZUGRĂVESCU, MAGDA PETROVANU, **Y-ylid chemistry**, 1977, 396 p.

D. NEGOIU, ANGELA KRIZA, **Poluanţi anorganici în aer** (Polluants inorganiques dans l'air), 1977, 220 p.

I. G. MURGULESCU, **Introducere în chimia fizică. Vol. I. Atomi, molecule, legătură chimică** (Introduction à la Chimie Physique, Ier vol. 1. Atomes, molécules, liaison chimique), 1976, 560 p.

E. P. BALTĂ, E. BALTĂ, **Introduction to the physical chemistry of the vitreous state**, coédition avec Abacus Press, 1976, 287 p.

H. I. GĂLĂŢEANU, **Radiochimia aplicată. Metode şi probleme** (La radiochimie appliquée. Méthodes et problèmes), 1976, 307 p.

CONST. V. UGLEA, **Cromatografia pe gel permeabil. Noi domenii de aplicare** (La chromatographie sur gel perméable. Nouveaux domaines d'application), 1976, 123 p.

FRANCISC A. GOTHARD, **Echilibre lichid-vapori. I. Baze teoretice şi metode de calcul** (Equilibres liquide-vapeurs, I. Bases théoriques et méthodes de calcul), 1975, 263 p. 2 pl.

CONST. GH. MACAROVICI, D. MACAROVICI, **Chimia oxizilor dubli şi utilizările lor** (La chimie des oxydes doubles et leur utilisation), 1975, 195 p.

ELENA CEAUŞESCU, **Research work on synthesis and characterization of macromolecular compounds. Contributions**, 1974, 251 p.

CR. SIMIONESCU, VIORICA RUSAN, V. POPA, **Chimia algelor marine** (La chimie des algues marines). 1974, 212 p., 1 pl.

I. P. INFORMAŢIA c. 1623

43 426

Lei 25

$ 50 (pour un abonnement annuel)

F1103

ACADÉMIE DE LA RÉPUBLIQUE SOCIALISTE DE ROUMANIE

[illegible]

REVUE ROUMAINE DE CHIMIE

TOME 25
N° 2
Février 1980

EDITURA ACADEMIEI REPUBLICII SOCIALISTE ROMÂNIA

Rev. Roumaine Chim.

RRCHAX, 25, 2, p. 173–304 (1980), Bucarest

ACADÉMIE DE LA RÉPUBLIQUE SOCIALISTE DE ROUMANIE

COMITÉ DE RÉDACTION

Rédacteur en chef :

I. G. MURGULESCU, membre de l'Académie de la République Socialiste de Roumanie

Rédacteurs en chef adjoints :

A. T. BALABAN et V. EM. SAHINI, membres correspondants de l'Académie de la République Socialiste de Roumanie

Collège de rédaction :

EM. BRATU, ELENA CEAUŞESCU, ECATERINA CIORĂNESCU-NENITZESCU, CR. SIMIONESCU, membres de l'Académie de la République Socialiste de Roumanie; P. SPACU, membre correspondant de l'Académie de la République Socialiste de Roumanie; MARGARETA AVRAM, M. BANCIU, I. HAIDUC, D. I. MARCHIDAN, I. MOLDOVAN, G. NIAC et D. SĂNDULESCU

La Revue Roumaine de Chimie paraît 10 fois par an. Toute commande de l'étranger pour les travaux parus aux Editions de l'Académie de la République Socialiste de Roumanie sera adressée à ILEXIM, Departamentul Export-Import Carte (Livres)/Departamentul Export-Import Presă (Revues), P.O.B. 136—137, télex 11226, 3, str. 13 Decembrie, 70116 Bucarest, Roumanie

Les manuscrits, les livres et les revues proposés en échange, ainsi que toute correspondance seront envoyés à la rédaction :

REVUE ROUMAINE DE CHIMIE

125, Calea Victoriei, 71021 Bucarest, Roumanie, téléphone 50 76 80

EDITURA ACADEMIEI REPUBLICII SOCIALISTE ROMÂNIA

125, Calea Victoriei, 71021 Bucarest, Roumanie, téléphone 50 76 80

REVUE ROUMAINE DE CHIMIE

Tome 25, Nº 2 Février, 1980

MARIA TOMOAIA-COTIŞEL, E. CHIFU, V. TĂMAŞ and VIRGINIA MĂRCULEŢIU, Behaviour of some apocarotenoid derivatives at the air/water interface 175–180

C. E. MOROŞANU and E. SEGAL, Kinetics of silicon nitride deposition on silicon from N-Gas . . . . 181–188 R

JOSETTE WEINBERG, ALEXANDRINA DONESCU and MIHAELA OLTEANU, Decomposition mechanism of sodium merthiolate in aqueous solutions at various pH values 189–194

M. S. SUBHANI, The effect of the solvent and ionic strength on the kinetics of reactionbetween I_2^- and IO^- 195–200

R. P. VARMA, P. BAHADUR and R. DAYAL, Conductivity studies of alkaline earth metal soaps in methanol 201–206

SILVIA BARBU and CONST. GH. MACAROVICI, Metallic complexes of nicotinealdehyde-thiocarbohydrazone. (in French) 207–214

K. N. JOHRI and K. A. VENUGOPALAN, Thermogravimetric investigation of the decomposition of certain metal dithiocarbamates . . . . 215–222 R

D. NEGOIU and J. CAMUS, Electron transfer reactions in some complex compounds of Hg(II), Co(II) and Cu(I) with quinoxalinic and naphtoquinonic ligands 223–229

ANA NIMARĂ and I. JULEAN, Basic salts of bismuth. I. Formation and properties of the basic bismuth chlorates 231–236

M. M. MOHAMED, M. A. EL HASHASH, M. Y, EL KADY and M. A. HASSAN, Some reactions with arylidene malonic acid and diethyl arylidene malonate 237–244

C. SÂRBU, NORA RĂDULESCU, MARIANA IONESCU, SOFIA NEGRIŢESCU, CORNELIA IOAN, NICULINA BOEŞTEANU and M. SIMIONOVICI, New indole derivatives with biological activity 245–251

M. M. OMARA, F. I. ABDEL-HAY, A. A. EL-BARBARY, M. BADAWI and M. M. ABDEL HAMID, Organophosphorus derivatives of expected biological activity. I. Reaction of phenols with N-arylhexachlorocyclodiphosphazanes 253–259

DOINA OŞIANU, ELENA NICOARĂ and C. BODEA, Inchain epoxides of carotenoids. VII. Astacene 9,10- and 11,12-epoxides 261–265

LUMINIŢA VLĂDESCU and DĂNUŢA VOICU, Utilisation of sodium hydroxide in separation of tin(II) with ion exchange resins. I. Cation-exchange behavior of tin (II) . . . . 267–272 R

S. GOCAN and C. KONNERT, Resolution in thin-layer chromatography with orthogonal temperatures gradient in S-chamber (in German) 273–276

CR. SIMIONESCU, I. MAZILU, LUCIA TĂTARU and TATIANA LIXANDRU, Ferrocene polymers as polymerization initiators. II. Polymerization of some *p*-alkylated chloroformylated vinyl monomers 277–283

DEMETRA DRĂGAN and A. CARPOV, Chemical modification of polymers. I. Reaction of vinyl chloroacetate copolymers with some herbicidal sodium phenoxides 285–293

D. C. RUPAINWAR and K. K. KAKKAR, A modified reversion technique for the spectrophotometric determination of thallium 295–300

BOOK REVIEWS 301–303

Revue Roumaine de Chimie, **25**, *2*, 175–180 (1980)

BEHAVIOUR OF SOME APOCAROTENOID DERIVATIVES AT THE AIR/WATER INTERFACE

MARIA TOMOAIA-COTIŞEL*, E. CHIFU*,
V. TĂMAŞ** and VIRGINIA MĂRCULEŢIU*

* "Babeş-Bolyai" University, Department of Physical Chemistry, str. Arany János nr. **11**, 3400 Cluj-Napoca, Romania

** Institute of Agronomy, Department of Biochemistry, str. Mănăştur nr. 3, 3400 Cluj-Napoca, Romania

Received May 30, 1979

Insoluble monolayers of some apocarotenoid derivatives : the β-apo-8′-carotenyliden-oxazolone, the diethylamide of the β-apo-7′-benzoylamino-6′-carotenoic acid, the retinyliden-oxazolone and the diethylamide of the β-apo-15′-benzoylamino-14′-carotenoic acid, were studied at the air/water interface by means of the compression isotherms (surface pressure *vs.* area). The experimental values of the limiting molecular area, collapse area, collapse pressure and surface compressional modulus were discussed in terms of the rotating rigid plate model of carotenoid molecules previously proposed by us.

As a sequel of the previously published papers,[1-9] in the present work we report new data on the behaviour of carotenoids at fluid interfaces, namely of insoluble monolayers of some apocarotenoid derivatives at the air/water interface. The structure of the apocarotenoid derivatives studied is shown in figure 1.[10-12] It is to be mentioned that the compounds I and III, respectively II and IV, have one and the same polar end group, whereas the structure and length of the hydrophobic chain are identical at compounds I and II, respectively III and IV.

The experimental results obtained in studying these substances as a monomolecular film are correlated with the molecular dimensions given by the rotating rigid plate model, formerly proposed by us[13] for the carotenoid molecules.

EXPERIMENTAL

The behaviour of carotenoids, in the form of insoluble monolayer at the air/water interface, was examined by means of the compression isotherms : surface pressure (π, dyn/cm)-area (*A*, Å^2/molecule) at room temperature (22 ± 2°).

The details concerning the experimental procedure have been described elsewhere.[1]

The surface pressure was measured by the Wilhelmy method, with an error of ±0.5 dyn/cm and the π-*A* curves were reproducible within 2 ÷ 4Å^2/molecule. The compression of the film started 1 ÷ 10 minutes after spreading, and so it was demonstrated that evaporation of the solvent did not appreciably affect the results. A complete isotherm was obtained in 5 ÷ 10 minutes, the compression rate being maintained constant (approximately 8 cm^2/min). The compression was discontinuous, so that the experimental points on the isotherms always correspond to the internal equilibrium in the film. Every isotherm below was selected from a number of 10 ÷ 20 experiments.

The apocarotenoid derivatives studied were synthetic products[10-12] of chromatographic purity and were utilized without previous purification. Though, by taking into account the sensitivity of carotenoid pigments, especially to light, their purity was checked in the course of the experiments, by thin layer chromatography.

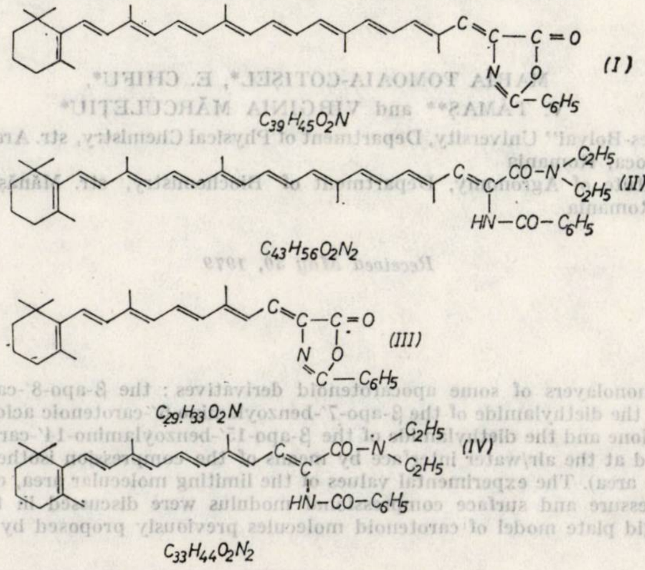

Fig. 1. — Structure of some apocarotenoid derivatives : β-apo-8′-carotenyliden-oxazolone (I), diethylamide of the β-apo-7′-benzoylamino-6′-carotenoic acid (II), retinyliden-oxazolone (III), diethylamide of the β-apo-15′-benzoylamino-14′-carotenoic acid (IV).

As a support for films, doubly distilled water, freshly prepared, was used. The spreading liquid was benzene for the substances I and III ; for the substances II and IV, whose solubility in benzene is reduced, a mixture of benzene : chloroform in the 4 : 1 volumetric ration was used. The benzene and the chloroform were of p.a. purity, produced at "Reactivul"-Bucureşti.

RESULTS AND DISCUSSION

The compression experimental isotherms : surface pressure vs. molecular area, for the insoluble monolayers of compounds I and II are shown in figure 2. Similarly, the isotherms for compounds III and IV are drawn in figure 3. We point out that the isotherms of compounds II and IV were reproducible only at relatively large spreading surface densities. The fact that isotherms at high molecular areas, respectively at low surface pressures, are not reproducible has been pointed out by other authors as well[14] and it is probably connected with structure-transforming phenomena in the film.

By extrapolating, at zero surface pressure, the linear portion at high pressures of the isotherms, the limiting molecular areas A_0 have been evaluated for each case.

There have also been determined the collapse pressures π_c, as the highest pressures to which the monolayer could be compressed; they are illustrated on the isotherms by the change of the slope at high pressures. Molecular areas of collapse A_c correspond to the collapse pressures.

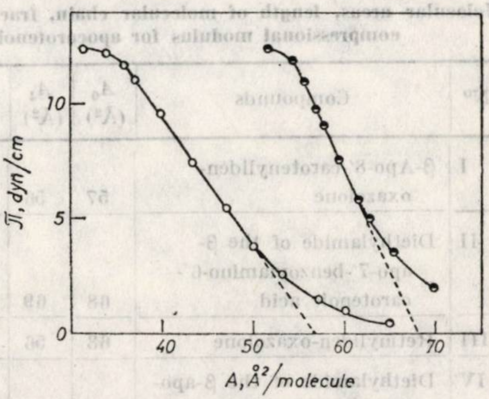

Fig. 2. — The compression isotherm: surface pressure vs. area for monomolecular film of compounds I(○) and II(●).

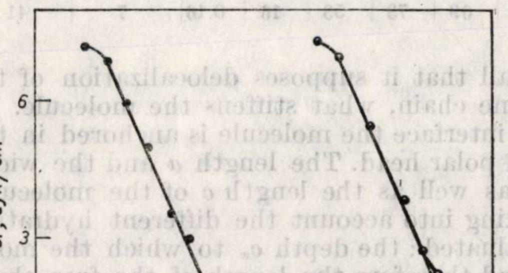

Fig. 3. — Surface pressure vs. area curve for film of substances III(●) and IV(●).

Finally, the surface compressional moduli C_s^{-1} have been evaluated, by making use of the linear portions of the isotherms at high pressures, with the aid of the well-known relationship [15]:

$$C_s^{-1} = -A\left(\frac{\partial \pi}{\partial A}\right)_T$$

where A stood for A_0.

The values of the magnitudes A_0, A_c, π_c and C_s^{-1}, obtained for the four studied compounds are listed in table 1.

The experimental data above can be correlated with those obtained by applying the geometric model for the molecules of carotenoid compounds previously proposed by us[13]. Without taking again the detailed description of the model, we shall recall that it supposes delocalization of the system of π-bonds of the polyene chain, what stiffens the molecule. In the monolayer, at the air/water interface the molecule is anchored in the aqueous phase with its hydrated polar head. The length a and the width b of the hydrated polar group, as well as the length c of the molecular chain have been calculated. Taking into account the different hydration possibilities, there have been evaluated : the depth c_w to which the molecule is immersed in the water and therefore the length of the free chain remained in the air phase $c_f = c - c_w$. Correspondingly, a fraction immersed $\alpha = \frac{c_w}{c}$ has been introduced.

TABLE 1

Molecular areas, length of molecular chain, fraction immersed, collapse pressure and surface compressional modulus for apocarotenoid derivatives monomolecular films

N°	Compounds	A_0 (Å²)	A_4 (Å²)	A_c (Å²)	A_p (Å²)	c_f (Å)	α	π_c (dyn/cm)	C_s^{-1} (dyn/cm)
I	β-Apo-8′-carotenyliden-oxazolone	57	56	36	31	26	0.21	12	35
II	Diethylamide of the β-apo-7′-benzoylamino-6′-carotenoic acid	68	69	54	53	26	0.10	12	59
III	Retinyliden-oxazolone	63	56	48	30	15	0.32	7	30
IV	Diethylamide of the β-apo-15′-benzoylamino-14′-carotenoic acid	88	69	73	53	16	0.16	7	41

The rigid plate-like molecule, of parallelipipedic form (sizes a, b, c), is supposed to perform a free rotation around the axis of its chain, rotation supposed to be perpendicular to the water surface ; this rotation can be equivalent to a random dynamical orientation of the polar group axis, so that the average space necessity of the molecule should be a vertical cylinder. If we admit a compact tetragonal packing of the molecular cylinders in the monolayer, the area necessity for a molecule would be $A_4 = a^2$.

If the same rigid plates are now oriented parallelly and closely packed in the monolayer, the area per molecule would be $A_p = a\,b$.

In table 1 the values A_4, A_p, c_f and α, defined and calculated as above have also been listed for the studied compounds.

It can be seen that the experimental areas A_0 and those calculated, A_4, are in a very good agreement for compounds I and II. We can thus consent to a compact tetragonal packing of the rotating rigid molecules in the insoluble film at the value A_0 of the molecular area.

In the case of compounds III and IV the A_0 values are larger than the calculated A_4. Since the free chains of these compounds are much shorter than those of compounds I and II (in accordance with values c_f in table 1), the intermolecular forces, mainly the dispersion forces of London type, are not strong enough to assure the orientation of the molecular chains axes perpendicular to the air/water interface. Therefore, their random orientation can explain the higher values of the experimental areas A_0. The area dissemination is larger when one compares compound II with IV — both having the same polar head-group; it is smaller when compound I is compared with III. The fact could be explained by the much larger value of the fraction immersed α in the latter case (see Table 1), which favours the tendency of vertical orientation of the molecular chains.

In what the experimental collapse areas A_c are concerned, it can be seen that the agreement with the calculated values A_p is satisfactory for the first two products; the collapse of the film arises then in this case at the moment the parallel orientation of the rigid molecular plates is achieved in a compact monolayer. Again, the experimental values are larger than those calculated, at compounds III and IV. To the same effect, the values of the collapse pressures π_c are low in the case of the short-chained molecules (compounds III and IV) as compared with molecules having longer chains (compounds I and II), where the stability of the film is higher.

The values of the surface compressional modulus C_s^{-1} for compounds I—IV, studied in the present work ($30 \div 60$ dyn/cm) lie between the limits admitted for the state of expanded liquid film.[15] They are much smaller than those reported by us before, for other carotenoid pigments (echinenone,[1] canthaxanthin,[1] isozeaxanthin,[3] β-apo-8′-carotenal[2]), when values of C_s^{-1} ($150 \div 100$ dyn/cm) indicated the state of condensed liquid.[15]

The fact could be mainly explained by the difference in structure of the polar head-groups. Whilst at the compounds I—IV the polar groups, bulky and deformable, lead to the expanded liquid type of film, in the case of other carotenoid pigments (echinenone ÷ carotenal) the polar head-group is rigid and the values of C_s^{-1} are higher, leading to the condensed liquid film.

Furthermore, it is obvious that the values of the C_s^{-1} will also depend on the orientation of the free molecular chain, which is immediately seen from the data in table 1: for compounds I and II the values are larger than for compounds III and IV, the free molecular chains of the latter being much shorter. If the compounds having the same polar head-group are compared, one realizes that the difference in the values of C_s^{-1} is relatively small in the case of compounds I and III, the molecules of which are strongly anchored into the water; on the other hand, the difference is large for the compounds II and IV, where the fraction immersed is low and thus the situation is similar to that of the limiting molecular areas A_0.

REFERENCES

[1] E. Chifu, M. Tomoaia and A. Ioanette, *Gaz. chim. Ital.*, **105**, 1225 (1975).

[2] M. Tomoaia, A. Ioanette and E. Chifu, "Proceedings International Conference Colloid and Surface Science", vol. 1, Akadémiai Kiadó, Budapest, 1975, p. 559.

[3] E. Chifu, M. Tomoaia, E. Nicoară and A. Olteanu, *Rev. Roumaine Chim.*, **23**, 1163 (1978).

[4] E. Chifu, M. Tomoaia-Cotişel, Z. Andrei and E. Bonciu, *Gazz. chim. Ital.*, **109**, 365 (1979).

[5] M. Tomoaia-Cotişel and E. Chifu, *Gazz. chim. Ital.*, **109**, 371 (1979).

[6] E. Chifu, M. Tomoaia-Cotişel and A. Ioanette, *Gazz. chim. Ital.*, **109**, 397 (1979).

[7] E. Chifu and M. Tomoaia-Cotişel, *Rev. Roumaine Chim.*, **24**, 979 (1979).

[8] E. Chifu, M. Tomoaia-Cotişel and Z. Andrei, *Stud, Univ. Babeş-Bolyai Chem.* **24**, 63 (1979).

[9] M. Tomoaia-Cotişel, I. Albu and E. Chifu, *Stud. Univ. Babeş-Bolyai, Chem.*, **24**, 68 (1979).

[10] V. Tămaş, V. Ciurdaru and C. Bodea, *Rev. Roumaine Chim.*, **18**, 1409 (1973).

[11] V. Tămaş and C. Bodea, *Rev. Roumaine Chim.*, **19**, 701 (1974),

[12] V. Tămaş, "Abstracts Contributed Papers of Fifth International Symposium on Carotenoids", Madison, Wisconsin, USA, July 23—28, 1978, p. 59.

[13] J. Zsakó, E. Chifu and M. Tomoaia-Cotişel, *Gazz chim. Ital.*, in press.

[14] H. D. Cook and H. E. Ries, Jr., *J. Phys. Chem.*, **60**, 1533 (1956).

[15] J. T. Davies and E. K. Rideal, "Interfacial Phenomena", Acad. Press, New York, 1963, p. 265.

Revue Roumaine de Chimie, **25**, *2*, 181–188 (1980)

KINETICS OF SILICON NITRIDE DEPOSITION ON SILICON FROM N-GAS

CONSTANTIN-EUGEN MOROȘANU* and EUGEN SEGAL**

* Chemical vapor deposition group, Research Institute for Electronic Components ICCE, str. Erou Iancu Nicolae 32B, Bucharest R72996, Romania

** Chair of Physical Chemistry and Electrochemical Technology, Polytechnic Institute of Bucharest, Bulevardul Republicii 13, Romania

Received October 14, 1977

The rate of silicon nitride deposition on silicon substrates, from N-Gas (mixture 1 % silane, 99 % ammonia), was investigated as a function of total gas flow rate, reactant gas concentration, temperature, time ,nature of dilution gas, nature of substrate, reactor geometry, type of heating. The kinetic parameters of the nucleation of Si N film on silicon substrates were determined.

INTRODUCTION

The use of a mixture instead of separate silane and ammonia gases provides many important advantages. Indeed, the reactants being premixed, it is not necessary to take precautions for a complete mixing in the equipment. The film thickness can be controlled more accurately because only a single flow has to be adjusted.

In silicon semiconductor technology the following premised gases are used :

— Oxygen containing 1 — 10 % hydrogen chloride used to obtain SiO_2 films with improved electrical properties.

— Binary mixture of tetrafluoromethane (CF_4) and 2 % oxygen used for dry plasma etching of SiO_2 and Si_3N_4 films.

— Ternary mixtures (3 — 10 % SiH_4 + 0.01 — 1 % PH_3 + argon or 3—10 % SiH_4 + 0.01 — 1 % B_2H_6 + argon) used for depositing phosphorus or boron doped silicon dioxide films.

— Mixture 1 % silane, 99 % carbon dioxide (0-Gas) used for the chemical vapor deposition of silicon dioxide.

— Mixture 1 % silane, 99 % ammonia (N-Gas) used for the chemical vapor deposition of silicon nitride.

The purpose of the present work was to studay the effect of various deposition parameters (total gas flow rate, reactant gas concentration, nature of dilution gas, nature of substrate, temperature, time, reactor geometry, type of heating) on the rate of formation of Si_3N_4 films deposited on polished silicon wafers, from N-Gas.

EXPERIMENTAL

The equipment for depositing Si_3N_4 films (induction heated horizontal reactor) was described in a previous paper.[1] N-Gas used was obtained from Matheson Gas Products ; the dilution gas was nitrogen. The deposition rate was measured using the infrared interference method[1] (Figure 1).

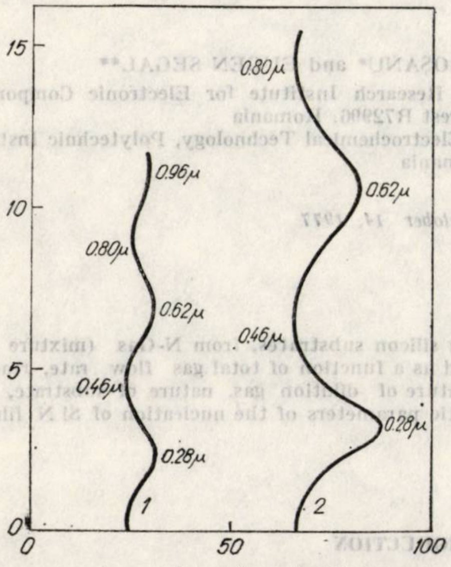

Fig. 1.— Infrared interference wave pattern when Si_3N_4 was deposited on *1.* silicon wafer and *2.* molibdenum substrate, from N-Gas. Deposition conditions : *1.* $T = 750°$, $F_{N_2} = 16$ l/min, $F_{\text{N-Gas}} = 1.125$ l/min, $d = 850$ Å/min ; *2.* $T = 750°$, $F_{N_2} = 16$ l/min, $F_{\text{N-Gas}} = 1.125$ l/min, d = 550 Å/min.

RESULTS AND DISCUSSION

1. Influence of the total gas flow rate

To determine whether the deposition rate of Si_3N_4 is limited by the surface chemical reaction or mass transfer, an experiment was performed in which the nitrogen flow rate was varied. The deposition temperature and N-Gas flow rate were kept constant. Figure 2 shows the results,

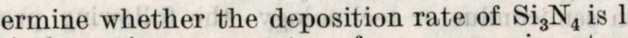

Fig. 2. — Deposition rate of Si_3N_4 film vs. total flow rate. (Deposition conditions : $t = 720°$, $F_{\text{N-Gas}} = 1.125$ l/min).

with the deposition rate plotted against the flow rate. At low total flow rates, the deposition rate is a function of the flow rate (diffusion range), but is independent of it for gas flow rates higher than 16 l/min (kinetic range). The flow rate at which the reaction ceased to be gas transport controlled, was used in all the subsequent experiments.

2. Comparison of premixed to separate gas depositions in the same experimental conditions

The two experiments summarized in table 1 were carried out under identical experimental conditions ($t = 720°$, $F_{N_2} = 16$ l/min), except that the reactant gas was N-Gas in one and ammonia and silane in the same ratio as in premixed gas (1 : 99) in the other. The deposition rates obtained were the same, within the limits of the experimental errors (400 Å/min).

TABLE 1

A comparison of N-gas and separate gas depositions

Reactant gas flow rates F(cm³/min)	Deposition rate (Å/min)
$F_{SiH_4} = 5.6$, $F_{NH_3} = 555$	430
$F_{N\text{-}Gas} = 555$	400

Deposition conditions : $t = 720°$, $F_{N_2} = 16$ l/min.

3. Influence of N-Gas concentration

The dependence of the Si_3N_4 deposition rate on N-Gas flow rate is shown in figure 3, at two different temperatures (700 and 740°) and a nitrogen flow rate of 20 l/min. In both cases, the rate increases linearly with N-Gas flow rate.

4. Influence of temperature

In figure 4 the logarithms of the deposition rate values were plotted against reciprocal values of absolute temperature. The Arrhenius plot lg $d - 1/T$ is a straight line. From its slope and intercept, the following values for the activation energy and preexponential factor were obtained; in the temperature range 700—900°, $E = 22.23$ kcal/mole and $A = 4.10^{10}$ Å/min, in the temperature range 900—1100°, $E = 6$ kcal/mole and $A = 4 \cdot 6 \cdot 10^7$ Å/min.

By comparing the values of the kinetic parameters in the two temperature ranges, a compensation effect was found.[2] The formation of silicon-nitrogen complexes on silicon surface at high temperatures[3] determining a blocking of active centers is probably responsible for the decrease of the preexponential factor. The decrease of the activation energy in the high temperature range compared to the low temperature one, can be explained by a structural (phase) change of the superficial silicon layer near the temperature of 900°.[4] According to the relation log

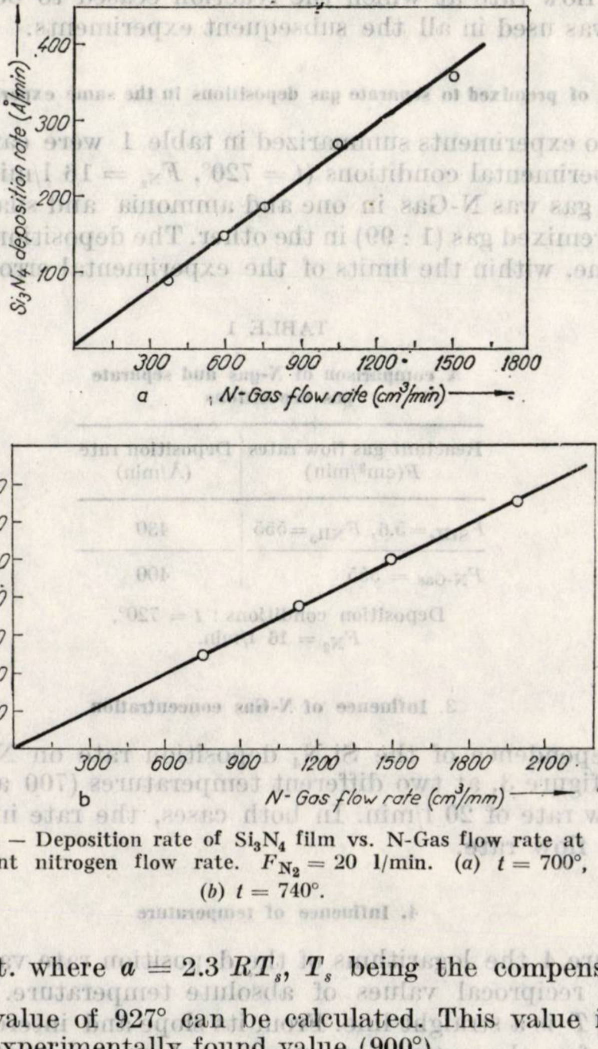

Fig. 3. — Deposition rate of Si_3N_4 film vs. N-Gas flow rate at constant nitrogen flow rate. $F_{N_2} = 20$ l/min. (*a*) $t = 700°$, (*b*) $t = 740°$.

$A = \frac{E}{a} +$ const. where $a = 2.3\,RT_s$, T_s being the compensation temperature, a T_s value of 927° can be calculated. This value is in agreement with the experimentally found value (900°).

5. Influence of the deposition time

The obtained experimental data show that the deposition thickness increases linearly with deposition time i.e. the deposition rate is constant along the period of deposition. In figure 5 this dependence is illustrated for a temperature of 740°, N-gas flow rate $F_{\text{N-Gas}} = 375$ cm³/min, nitrogen flow rate $F_{N2} = 20$ l/min for deposition time 5–60 minutes, the deposition rate being constant at 100Å/min.

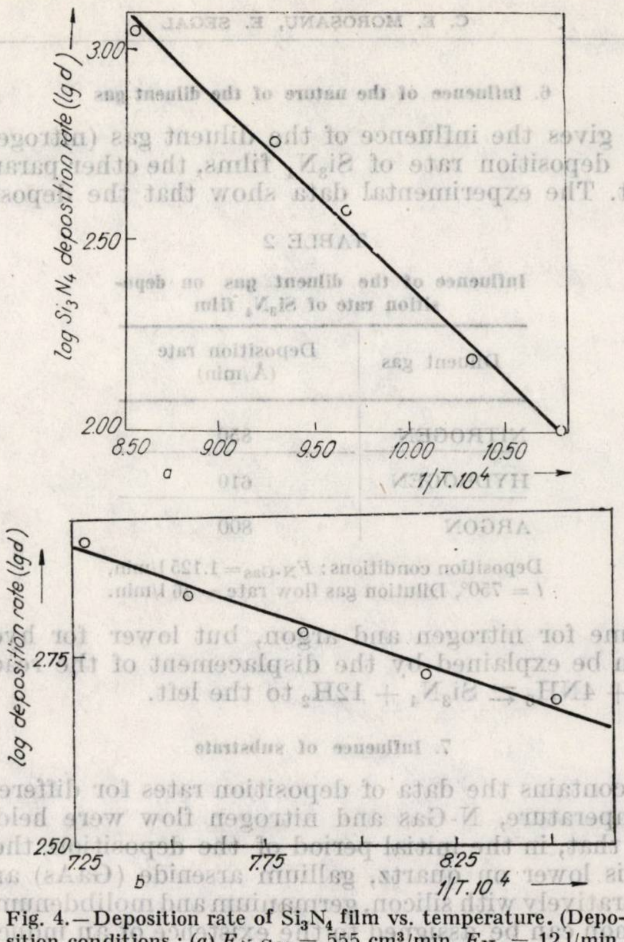

Fig. 4.—Deposition rate of Si_3N_4 film vs. temperature. (Deposition conditions : (*a*) $F_{\text{N-Gas}} = 555$ cm³/min, $F_{N_2} = 12$ l/min, $t = 700-900°$; (*b*) $F_{\text{N-Gas}} = 300$ cm³/min. $F_{N_2} = 10.87$ l/min, $t = 900-1100°$).

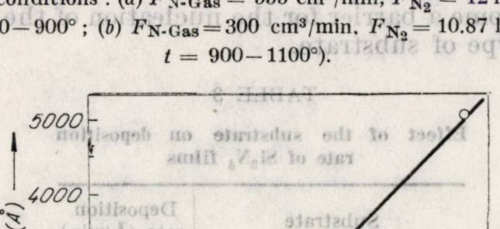

Fig. 5. — Time dependence of Si_3N_4 film thickness. (Deposition conditions : $t = 740°$, $F_{\text{N-Gas}} = 375$ cm³/min, $F_{N_2} = 20$ l/min).

6. Influence of the nature of the diluent gas

Table 2 gives the influence of the diluent gas (nitrogen, hydrogen or argon) on deposition rate of Si_3N_4 films, the other parameters being kept constant. The experimental data show that the deposition rate is nearly the same for nitrogen and argon, but lower for hydrogen. The latter case can be explained by the displacement of the reaction equilibrium $3SiH_4 + 4NH_3 \rightleftarrows Si_3N_4 + 12H_2$ to the left.

TABLE 2

Influence of the diluent gas on deposition rate of Si_3N_4 film

Diluent gas	Deposition rate (Å/min)
NITROGEN	850
HYDROGEN	610
ARGON	800

Deposition conditions: $F_{N\text{-}Gas} = 1.125$ l/min, $t = 750°$, Dilution gas flow rate = 16 l/min.

7. Influence of substrate

Table 3 contains the data of deposition rates for different substrates, when temperature, N-Gas and nitrogen flow were held constant. It is observed that, in the initial period of the deposition, the deposition rate of Si_3N_4 is lower on quartz, gallium arsenide (GaAs) and alumina (Al_2O_3), comparatively with silicon, germanium and molibdenum substrates. This phenomenon can be assigned to the existence of an induction period necessary to overcome a barrier for the nucleation of the film. This period depends on the type of substrate.

TABLE 3

Effect of the substrate on deposition rate of Si_3N_4 films

Substrate	Deposition rate (Å/min)
Silicon (Si)	850
Germanium (Ge)	500
Molibdenum (Mo)	550
Alumina (Al_2O_3)	200
Gallium Arsenide (GaAs)	300
Quartz (SiO_2)	100

Deposition conditions: $F_{N_2} = 16$ l/min, $F_{N\text{-}Gas} = 1.125$ l/min, $t = 750°$

8. Influence of the reactor geometry

The experimental data show that using quartz reactors with rectangular or circular cross section of the same area (e.g. 72 × 34 mm and 56 mm diameter reactors, respectively), in identical deposition conditions, the deposition rate is not influenced.

9. Influence of the type of heating

The use of the three types of heating (radiant, resistive or inductive), in the same deposition conditions, has no significant effect on the deposition rate.

Determination of the kinetic parameters of the nucleation of Si_3N_4 films on silicon substrates

In the initial stages of the deposition of Si_3N_4 films on silicon from N-Gas, the existence of an induction period t_i was found. This short period is necessary to overcome a barrier for film nucleation. Its value depends on the temperature and on the silane concentration, according to the relationship :

$$\frac{1}{t_i} = K\,X^0_{SiH_4} \cdot \exp(-E_a/RT) \text{ or}$$

$$t_i \cdot X^0_{SiH_4} = \frac{1}{K} \exp(E_a/RT),$$

where K is a constant and E_a is the activation energy of the nucleation.

The plot of $\lg(t_i \cdot X^0_{SiH_4})$ as a function of $1/T$ is a straight line with the slope $m = E_a/2.303$ R.

Table 4 gives the induction periods for the formation of Si_3N_4 films on silicon at different temperatures and identical nitrogen, silane and N-gas flow rates.

TABLE 4

Nucleation of Si_3N_4 films on silicon substrates

Temperature (°C)	1/T	t_i (sec)	$t \cdot \frac{F_{SiH_4}}{F_{total}}$	$\lg\left(t\frac{F_{SiH_4}}{F_{total}}\right)$
700	$1.03.10^{-3}$	25	10.10^{-3}	−2
790	$0.94.10^{-3}$	15	6.10^{-3}	−2.22
870	$0.87.10^{-3}$	10	4.10^{-3}	−2.40
925	$0.83.10^{-3}$	7.5	3.10^{-3}	−2.52

Deposition conditions : $F_{N\text{-}Gas} = 750$ cm³/min,

$$F_{N_2} = 18.62 \text{ l/min}, \quad \frac{F_{SiH_4}}{F_{total}} = 4.10^{-4}$$

Figure 6 illustrates the dependence lg $(t_i \cdot X^0_{SiH_4})$ against $1/T$. From the slope and intercept of the straight line, the following values of E_a and K were calculated : $E_a = 11.80$ kcal/mole and $K = 4 \cdot 5 \cdot 10^4$ sec^{-1}.

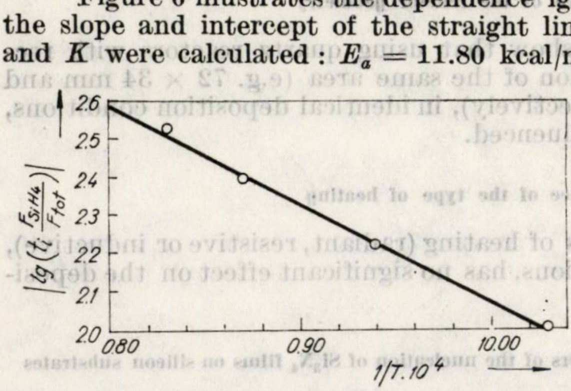

Fig. 6.—The dependence $|lg(t_i \cdot X^0_{SiH_4})|$ vs. $1/T$.

CONCLUSIONS

The kinetics of the deposition and the nucleation of Si_3N_4 films on silicon substrates from N-Gas have been studied as a function of various deposition parameters.

REFERENCES

[1] C.-E. Morosanu and E. Segal, *Rev. Roumaine Chim.*, **23**, 515 (1978).
[2] E. Cremer, *Adv. Catalysis*, **7**, 75 (1955).
[3] K. V. Ravi and C. J. Varker, *J. Electrochem. Soc.*, **119**, 236c (1972).
[4] S. Horiuchi, *Solid-State Electron.*, **18**, 1111 (1975).

Revue Roumaine de Chimie, **25**, *2*, 189–194 (1980)

DECOMPOSITION MECHANISM OF SODIUM MERTHIOLATE IN AQUEOUS SOLUTIONS AT VARIOUS pH VALUES

JOSETTE WEINBERG*, ALEXANDRINA DONESCU* and MIHAELA OLTEANU**

* ICECHIM, Centre of Physical Chemistry, Spl. Independenței 202, Bucharest, Romania

** National Institute of Chemistry, Department of Physical Chemistry, Bd. Republicii 13, Bucharest, Romania

Received February 9, 1979

The decomposition reactions of sodium merthiolate in aqueous solutions at different pH values and several concentrations of Na^+ and Ca^{2+} were studied. One may notice two reaction mechanisms, the behaviour of merthiolate in either acid or alkaline solution being different. The HgS formation by merthiolate decomposition leads to some colloidal solutions.

Sodium merthiolate (sodium ethyl-mercuri-thiosalicylate) is an organomercuric compound with a wide antibacterial activity domain.[1] The literature data[1] attribute this activity to the partial ionization of merthiolate with formation of ethyl-mercuric ions which block enzymatic processes.

The ionization reaction is:

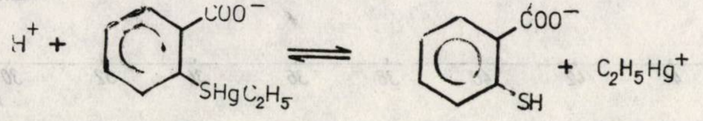

Polarographic studies[2] reveal the formation of ethyl-mercuric radicals, a process subsequently leading to the corresponding hydrocarbon and metallic mercury.

A recent work[3] studies the chemical behaviour of merthiolate at various pH values by thin layer chromatography and spectrophotometry. The results account for the different behaviour in alkaline and acid media but the decomposition mechanisms are not formulated.

The purpose of this work is to establish the decomposition mechanism of merthiolate as a function of pH values.

EXPERIMENTAL

Only p.a. grade reagents were employed.

Six aqueous solutions of 0.0524 g/l merthiolate at different pH-values were prepared. The behaviour of these solutions was studied spectrophotometrically within the 200—350 nm range with a UV—VIS Specord spectrophotometer.

The concentration variation in free mercury of this solution was evaluated, based on reversion procedure,[4] by spectrophotometric method with dithizone.

The time variation of the turbidity of the same solutions was determined by a SPEKOL turbidimeter.

RESULTS AND DISCUSSIONS

The ultraviolet spectra of aqueous solutions of merthiolate at different pH values in the preparation moment are presented in figure 1.

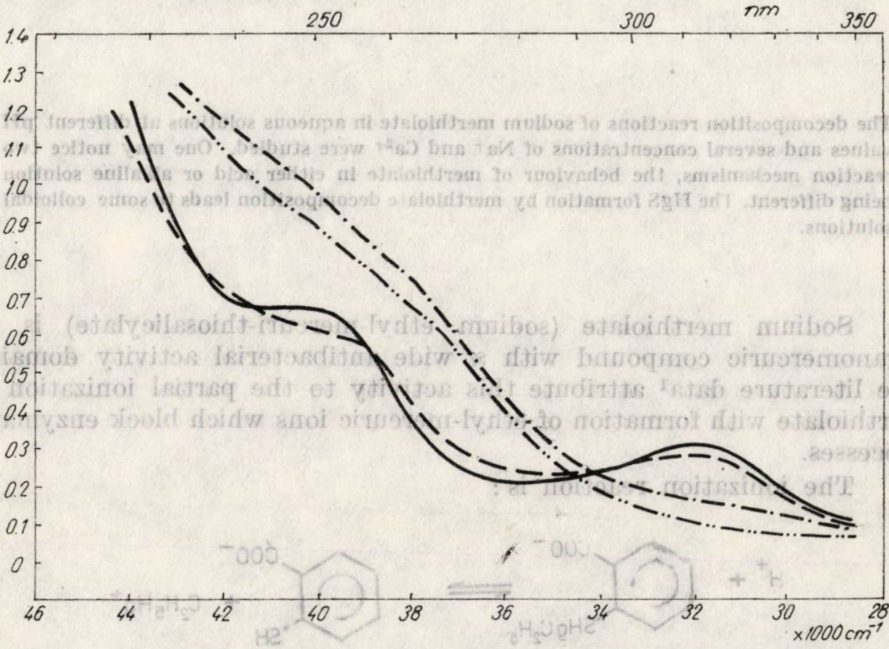

Fig. 1. — Absorption spectra of aqueous merthiolate solutions at few pH values (———— pH = 1.9, — — — — pH = 3.1, —.—.— pH = 8.5, —..—.. pH=10.9)

The different behaviour of aqueous solutions of merthiolate in alkaline and acid media is obvious in figure 1: the band at 312 nm present in the acid solution does not appear in alkaline solutions.

Thiosalicylic acid has an absorption band at 312 nm and thiophenol at ~286 nm.[5] Consequently, the band of 312 nm for merhiolate in acid medium may be attributed to the SH group, that is, the merthiolate decomposes to thiosalicylic acid in acid solutions. The literature data[3] indicate that the merthiolate at pH = 1 has two absorption bands:

at 312 nm and 247 nm. This layer chromatography confirms that the merthiolate and sodium thiosalicylate at pH = 1 leads to the same compounds.

The time variation of the band intensity at 312 nm is presented in table 1.

TABLE 1

Extinction coefficient variation of merthiolate solutions in time

pH values of merthiolate solutions (0.0524 g/l)	Extinction coefficient after :			
	initial moment	seven days	twenty days	fifty days
1.9	0.31	0.22	0.16	0.11
3.1	0.29	0.19	0.10	0.10
8.5	0.16	0.06	0.06	0.06
10.9	0.10	0.06	0.06	0.06

The band decrease intensity down the complete cancellation in time suggests a gradual liberation of the SH group from merthiolate molecule. In alkaline solutions, the decomposition is spontaneous due to the elimination of $-SHgC_2H_5$ group. NaOH acts on Hg^{2+} from thiosalts and forms Na_2S and (HgS_2).[2-6]

In table 2 the variation in time of free mercury content of merthiolate solutions is presented. (Mercury present as HgS and organic compounds is not determined by this method).

TABLE 2

The variation in time of free mercury content of merthiolate solutions

pH value of the sample	Free mercury γ/ml (± 0.06) after :			
	initial moment	eight days	twenty days	fifty days
1.9	12.75	13.30	13.50	18.90
3.1	10.25	8.91	10.30	15.08
5.7	10.75	10.43	9.08	7.08
7.5	11.00	9.31	8.33	9.25
8.5	10.33	7.50	9.41	10.53
10.9	9.93	10.25	8.73	10.58

The data presented in this table revealed that :

— merthiolate solution at pH = 1.9 has a concentration in free mercury relative constant ~13.30 γHg/ml in the first 20 days, which then goes up to 18.90 γHg/ml after 50 days (The total concentration in Hg is 25 γ/ml) ;

— merthiolate solution at pH = 3.1 presents a diminution of free mercury in the first 8 days, followed by a continuous increase ;

— merthiolate solution at pH = 5.7 has a relatively constant concentration in free mercury in the first 8 days, followed by a continuous decrease ;

— merthiolate solution at pH=7.5 presents a free mercury decrease after 20 days, followed by a raise. On the 50th days the concentration in free mercury is the same as that after 8 days (~ 9.25 γ Hg/ml).

— merthiolate solution at pH = 8.5 in the first 8 days presents an important decrease in free mercury concentration (from 10.33 to 7.50 γ/ml), then the concentration increases. After 50 days the concentration reaches the initial concentration of 10.53γ/ml ;

— merthiolate solution at pH = 10.9 presents an irregular variation of free mercury concentration. After 50 days this concentration is somewhat greater than the initial value.

In table 3 the variation of turbidity of these solutions is presented

TABLE 3

The variation in time of turbidity of merthiolate solutions

pH of the sample	Turbidity (versus water) % after :			
	initial moment	eight days	twenty days	fifty days
1.9	47	118	164	100
3.1	49	176	170	136
5.7	10	10	10	66
7.5	10	10	10	45
8.5	10	10	10	22
10.9	10	10	10	23

— the solution at pH = 1.9 has a maximum of turbidity after 20 days followed by a decrease ;

— the solution at pH = 3.1 reaches this maximum after 8 days then the turbidity decreases ;

— the solutions at pH = 5.7 ; 7.5 ; 8.5 and 10.9 present in the first 20 days a low turbidity, followed by a continuous increase afterwards.

The presented data pointed out the different behaviour of the merthiolate in alkaline and acid media :

a) At acid pH values, aqueous solutions of merthiolate are step by step decomposed to form thiosalicylic acid and $C_2H_5Hg^+$ ion. The diminution of the absorption band intensity at 312 nm confirms the gradual loss in the —SH group from molecule. The growth in time of the free mercury concentration emphasizes the validity of the proposed decomposition mechanism. The turbidity variation indicates the formation of a precipitate which disperses in time with forming a colloid solution.

b) At alkaline pH values, aqueous solution of merthiolate is entirely decomposed forming the $-SHgC_2H_5$ group. Absence of the band at 312 nm is a fact standing for this mechanism.

As above stated, NaOH acts on Hg^{2+} to form Na_2S from thiosalts with the subsequent formation of $(HgS_2)^{2-}$ ion. According to this mechanism one part of mercury is blocked as HgS and the other remains as free or metallic Hg. The concentration in free mercury is generally constant, the existing fluctuations being due to the partial solubility of HgS in NaOH.[6]

The HgS lyophobic colloid rapidly forms aggregates in the presence of other ions.[7] This explains the rapid increase of the turbidity of merthiolate solution after 50 days from preparation. In order to support this assertion two aqueous solutions of merthiolate (A and B) at pH = 8.5 with different concentration in Na^+ and Ca^{2+} were prepared; namely the concentration in Na^+ and Ca^{2+} ions is 10 times greater in solution B.

TABLE 4

The concentration variation in total and free mercury in the presence of Na^+ and Ca^{2+} ions

Sample	Total mercury γ/ml		Free mercury γ/ml		
	initial moment	after filtration	after filtration	on the 15th days after filtration	on the 30th days after filtration
A	19.33	17.30	10.67	8.05	8.55
B	18.52	6.95	4.10	3.05	3.55

The concentration variation in free mercury over a 40 days period was determined. After 10 days, in solution B appeared a precipitate which was filtrated. The determination of mercury concentration established that by this operation a great amount of mercury was removed from the system.

The concentration in free mercury in solution A is smaller than the total concentration in mercury. A black precipitate appeared after 45 days in solution A. X-ray study established that the precipitate was HgS.

As previously pointed out, the HgS and $(HgS_2)^{2-}$ are present in the alkaline solution of merthiolate. The $(HgS_2)^{2-}$ ion is adsorbed to HgS to form a colloid solution. The proposed structure of micelle is :

$$\{m\mathrm{HgS}\, n(\mathrm{HgS_2})^{2-}\ 2(n-x)\,\mathrm{Na}^+\}^{2-}\ 2x\mathrm{Na}^+$$

m stands for the number of HgS molecules forming the nucleus; *n* for the number of $(HgS_2)^{2-}$ ions adsorbed.

The presence of a great concentration of Na^+ or of cations with superior valences (Ca^{2+}), in the system (solution B), leads to a destruction of diffuse layer and a lyophobic micelle coagulation.

REFERENCES

[1] S. P. Beri and D. S. Shivdekar, *J.N.K.V.V. Research J.*, **4**, 1 (1970).
[2] R. Benesch and R. E. Benesch, *J. Amer. Chem. Soc.*, **73**, 3391 (1951).
[3] H. Moller, *Dermatologica*, **145**, 280 (1972).
[4] E. B. Sandell, "Colorimetric Determination of Trace of Metals" Interscience, New York, 3 rd Edition, 1959, p. 635.
[5] L. Lang, "Absorption Spectra in the Ultraviolet and Visible Region", Akad. Kiado Budapest, 1969.
[6] D. A. Beardsley, G. E. Briscoe and E. R. Clark, *Mikrochim. Acta*, **6**, 1287 (1970).
[7] P. H. Cox, *Radioisotopy*, **12**, 997 (1971).

Revue Roumaine de Chimie, **25**, *2*, 195–199 (1980)

THE EFFECT OF THE SOLVENT AND IONIC STRENGTH ON THE KINETICS OF REACTION BETWEEN I_2^- AND IO^-

M. S. SUBHANI
Department of Chemistry, University of Nigeria, Nsukka, Nigeria

Received June 14, 1979

Investigations were carried out using different dielectric media and various ionic strengths for the reaction between IO^- and I_2^- in solution. From the plot of $\mathrm{Log}k_0$ and $1/D$ the values of $r^{\neq}$ and r_{AB} were obtained for the activated complex $(I_2-IO)^{2-}$. In comparison with the theoretical results for the radii, the double sphere model was found to be the most suitable model for the activated state formed in reaction.

Electrostatic contributions to the changes in thermodynamic functions $\Delta G^{\neq}_{es}$, $\Delta S^{\neq}_{es}$ and $\Delta H^{\neq}_{es}$ in the formation of transition state were also evaluated.

INTRODUCTION

Various studies have been carried out to see the effect of dielectric constant and ionic strength on the reaction between stable inorganic ions[1-8] but little is known about the reaction between radicalanions and stable ions. A number of models have been proposed for the transition state formed during the course of reaction due to the rearrangement of the total charge of the reactants on the activated complex formed.[9-11]

Expressions relating the rate constant at zero ionic strength (k_0) to the dielectric constant (D) for a single sphere model and that of double sphere model are as follows

$$\mathrm{Log}k_0 = \mathrm{Log}k_i - \left[\frac{e^2}{4.606DKT}\frac{(Z_A+Z_B)^2}{r^{\neq}} - \frac{Z_A^2}{r_A} - \frac{Z_B^2}{r_B}\right] \quad (1)$$

$$\mathrm{Log}k_0 = \mathrm{Log}k_i - \frac{Z_A Z_B e^2}{2.303DKT\,r_{AB}} \quad (2)$$

The electrostatic contributions to the thermodynamic functions such as free energy of activation in a single and double sphere and a double sphere model are given in the literature[10,11] and in equations (3) and (4) too.

$$\Delta G^{\neq}_{es} = \frac{Ne^2}{D}\left[\frac{(Z_A+Z_B)^2}{r^{\neq}} - \frac{Z_A^2}{r_A} - \frac{Z_B^2}{r_B}\right] \quad (3)$$

$$\Delta G^{\neq}_{es} = \frac{N Z_A Z_B e^2}{D r_{AB}} \tag{4}$$

k_i is the rate constant at infinite dielectric constant, k, the Boltzman constant, Z_A, Z_B, r_A and r_B are the charges and radii of ions A and B respectively. $r^{\neq}$ and r_{AB} are the radii of the activated complex in single and double sphere models respectively.

Electrostatic contributions to entropy of activation or enthalpy of activation can be calculated using equations (3) and (4) and other standard thermodynamic relationships reported in the literature.[10]
In the present paper the work carried out on reaction between IO^- and I_2^- is presented. This reaction is found to be of a second order and the rate determining step can be written as:

$$I^- + IO^- \rightarrow IO + 2I^- \tag{5}$$

reported in the literature [12]

EXPERIMENTAL

All chemicals used were of Anala R grade and were used without further purification. Dilute solutions of Na(10^{-3} M to 10^{-4} M) were prepared by rapidly dissolving solid I_2 in solution containing 10^{-1} M NaOH.

All solutions were prepared in triply distilled water just before the experiment and were saturated with Ar gas by the usual bubbling procedure described elsewhere.[13] All measurements were made at room temperature.

Flash photolysis set up was similar to that described in the literature.[14] The technique of kinetic spectroscopy was used to the decay kinetics of I_2^- at wavelength 370 nm where I_2^- has its maximum absorption.[12]

Dielectric constant measurements for various systems (10% to 45% alcohol/water mixtures) were made by the method described elsewhere.[7]

RESULTS AND DISCUSSIONS

The observed values for the rate constant measured on flash photolysis of Ar saturated IO^- solution containing equal molar concentration of I^- at various ionic strengths and different dielectric constants are given in table 1.

From the observed rate constant for the reaction (5) the values for the specific rate constant at zero ionic strength (k_0) were determined from the plots of graph between Log$k$ and square root of ionic strength ($\sqrt{\mu}$), at a given dielectric constant. The intercept at zero ionic strength obtained on extra-polation gives value of Logk_0 as expected from equation (6)

$$\mathrm{Log}k = \mathrm{Log}k_0 + A Z_A Z_B \sqrt{\mu} \tag{6},$$

TABLE 1

The experimentally observed values for the specific rate constant (K) for the reaction between I_2^- and IO^- as a function of ionic strength and dielectric constant. $T = 298K$; $(IO^-) = 10^{-3}M$, $(I^-) = 10^{-3}M$

$K \times 10^7$ (M^{-1} Sec^{-1})	μ	D
5.08	0.01	79.8
5.36	0.015	79.8
5.60	0.02	79.8
6.04	0.03	79.8
6.43	0.04	79.8
6.79	0.05	79.8
4.50	0.01	72.1
4.79	0.015	72.1
5.04	0.02	72.1
5.50	0.03	72.1
5.92	0.04	72.1
6.31	0.05	72.1
3.95	0.01	65.5
4.25	0.015	65.5
4.52	0.02	65.5
5.00	0.03	65.5
5.43	0.04	65.5
5.85	0.05	65.5
3.15	0.01	56.3
3.48	0.015	56.3
3.75	0.02	56.3
4.26	0.03	56.3
4.73	0.04	56.3
5.19	0.05	56.3
2.55	0.01	49.2
2.85	0.015	49.2
3.11	0.02	49.2
3.63	0.03	49.2
4.14	0.04	49.2
4.63	0.05	49.2

where A is a constant at a given temperature and dielectric constant of the system. The values of Logk_0 thus obtained are shown in table 2. A graph was plotted between Logk_0 and reciprocal of dielectric constant ($1/D$) and a fairly good straight line was thus obtained (See figure 1), which satisfies equations (1) and (2).

From the slope of the straight line, the values of $r^{\neq}$ and r_{AB} were evaluated using equations (1) and (2). The values are given in table 3.

TABLE 2

The values for the rate constants at zero ionic strength (k_0) and reciprocal of dielectric constant for the reaction between I_2^- and IO^- in solution. $T = 298$ K.

$\log k_0$	$1/D \times 10^3$
7.604	12.53
7.533	13.87
7.460	15.27
7.329	17.76
7.195	20.32

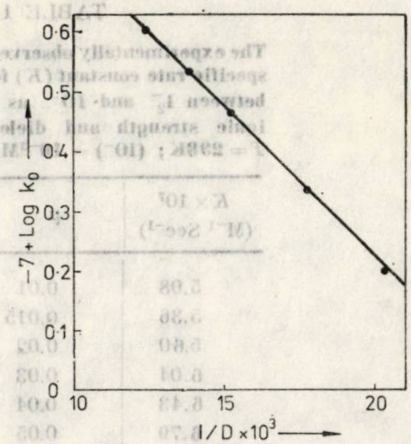

Fig. 1. — Dependence of $\text{Ln}k_0$ on reciprocal of dielectric constant ($1/D$) of the medium.

TABLE 3

The values for the radii for the activated complex formed between IO^- and I_2^- ions

	Theoretical values	Experimental values
	(Å)	(Å)
$r^{\neq}$	3.01	3.13
r_{AB}	4.71	4.66

Theoretical values for $r^{\neq}$ and r_{AB} were obtained by the method described in the literature,[3,5] using data for the various ionic radii reported in the literature.[15-17] The values are given in table 3. When comparing the theoretical values of $r^{\neq}$ and r_{AB} with those of the experimentally obtained values (See table 3) it was found out that the most probable shape of the activated complex formed in the reaction is of double sphere type.

The data obtained for r_{AB} were further used to calculate electrostatic contributions to the changes in free energy of activation ($\Delta G^{\neq}_{es}$), entropy of activation ($\Delta S^{\neq}_{es}$) and enthalpy of activation ($\Delta H^{\neq}_{es}$) for the activated state formed during the course of reaction. The values are summarized in table 4.

The negative sign and magnitude for the change in electrostatic contributions to the entropy of activation can be interpreted in terms of the description of the initial state of reactants and that of the activated state. IO^- and I_2^- are both singly negatively charged spheres before the start of the reaction when they are regarded at infinite distance from each other. In the activated state the sphere is doubly negatively charged $(IO - IO)^{2-}$.

Thus, the solvent molecules in the neighbourhood of these ions are acted upon by electrostrictions. More electrostriction is expected in the activated state than in the initial state of the reactants. This results in the decrease in electrostatic contributions to the entropy of activation.

TABLE 4

The values for the electrostatic contributions to the changes in the thermodynamic functions, $\Delta G^{\neq}_{es}$, $\Delta S^{\neq}_{es}$ and $\Delta H^{\neq}_{es}$ for the formation of the transition state in the reaction between I_2^- and IO^-

	$\Delta G^{\neq}_{es}$ XM(cal)$^{-1}$	$\Delta S^{\neq}_{es}$ XMT(cal)$^{-1}$	$\Delta H^{\neq}_{es}$ XM(cal)$^{-1}$
Theoretical values	883.9	−4.067	−328.1
Experimetal values	893.4	−4.111	−331.7

REFERENCES

[1] A. A. Frost and R. G. Pearson, "Kinetics and Mechanism", Wiley Inc., New York, 2nd Ed., 1961, p. 74.

[2] D. T. Y. Chem and K. J. Laidlar, *Canad. J. Chem.*, **37,** 599 (1959).

[3] K. J. Laidlar and H. Eyring, *Ann. New York Acad. Sci.*, **39,** 303 (1940).

[4] K. J. Laidlar, "Chemical Kinetics", McGraw Hill, New York, 2nd Ed., 1965, p. 221.

[5] M. S. Subhani and T. Kausar, *Pakistan J. Sci. Ind.* Res., **18,** 208 (1975).

[6] M. S. Subhani, *Rev. Roumaine Chim.*, **25** (1980) in press.

[7] M. S. Subhani and M.N.H. Lacewala, J. Sci.Math. **1,** 41 (1974)

[8] M. S. Subhani (Submitted for publication *Pakistan J. Sci. Ind. Research*)

[9] G. Scatchard, *Chem. Rev.*, **10,** 229 (1932).

[10] K. J. Laidler, "Chemical Kinetics", McGraw Hill, 2nd Ed., 1965, p. 212 and p. 217.

[11] E. S. Amis and J. E. Petts, *J. Amer Chem. Soc.*, **63,** 2883 (1941).

[12] L. I. Grossweiner and M. S. Matheson, *J. Phys. Chem.*, **61,** 1089 (1957).

[13] M. S. Subhani and T. Kausar, *Rev. Roumaine Chim.*, **25** (1980) in press.

[14] G. V. Buxton and M. S. Subhani, *J. Chem. Soc. Faraday Trans.* **68,** 958 (1972).

[15] J. Kleinberg, W. J. Arger Singer and E. Griswold, "Inorganic Chemistry", D. C. Health Co., Boston, 1965, p. 74.

[16] J. Moeler, "Inorganic Chemistry", Wiley Inc., New York, 1965, p. 140.

[17] A. F. Kapusttnsku, *Quart. Rev.*, **10,** 283 (1965).

Revue Roumaine de Chimie, **25**, *2*, 201–206 (1980)

CONDUCTIVITY STUDIES OF ALKALINE EARTH METAL SOAPS IN METHANOL

R. P. VARMA, P. BAHADUR and R. DAYAL
Chemistry Department, D.A. V. College, Muzaffarnagar-251001, India

Received June 28, 1976
Revised June 21, 1979

The conductance of barium, strontium and calcium soap solutions was studied in methanol at 35–50°. The c.m.c. of soaps was obtained and was not found to depend on temperature. The value of c.m.c. increases with atomic number of the metal and decreasing chain length of fatty acid in the soap. The conductance behaviour of soap solutions at various temperatures is exhibited by an equation : $\log \lambda M = A + B \log C$, where A and B are constants and C is the concentration of soap in g moles/litre. The constant A increases with temperature and chain length of barium and strontium soaps. The constant B does not depend on either of these parameters. Kraus and Bray's type expression was used to evaluate dissociation constant, molecular conductivity at infinite dilution, and heat of dissociation.

INTRODUCTION

Alkaline earth metal soaps have acquired considerable importance because of their use as catalyst,[1,2] corrosion inhibiting agents,[3,4] driers, fungicides and stabilizers.[5] These soaps are useful for a specific purpose on the basis of their fundamental properties. The following investigation has been undertaken to secure accurate data on the conductivity of soap solutions in methanol particularly those of alkaline earth metal soaps which have been given thorough investigation in water[6,7] and in various aqueous alcohols used as a solvent.[8,9]

The conductance data have been analysed in order to determine the micellar behaviour, dissociation constant, K, molecular conductivity at infinite dilution, λ_∞, and the heat of dissociation, $\Delta H°$ of soaps in methanol at 35–50°.

EXPERIMENTAL

The chemicals were purified and the soaps were prepared by the method described in the previous communication.[8] A conductivity bridge (Philips ; PR 9500, India) and a dipping type conductivity cell with platinized electrodes were used for measuring the conductance of the soap solutions in a thermostat at a constant temperature (± 0.05°). All data were obtained by concentration runs. Solvent was added into clean dry cell and its conductance measured. Several measurements were made to ascertain the reproducibility of results.

RESULTS AND DISCUSSION

The specific conductivity, *k* of soap solution has been measured at several temperatures (35—50°). The plots (Figure 1) of the specific conductivity *vs* concentration of soap are characterized by an intersection of two straight lines at a definite concentration (Table 1) probably indicating the formation of micelles.[10] It may be due to the fact that the long chain ion associates above c.m.c. to form aggregates and the number of free ions does not increase as rapidly as at a concentration less than c.m.c. The c.m.c. of these soaps is independent of temperature but decreases with atomic number of the metal and increasing chain length of fatty acid in the soap.

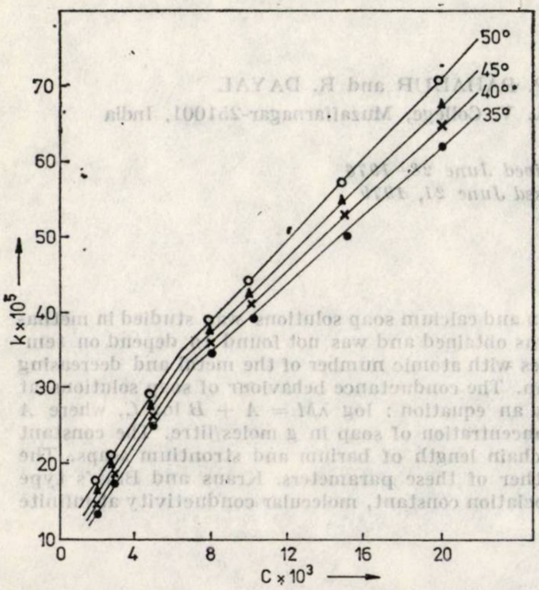

Fig. 1. — Plots of specific conductivity, k in $\text{ohm}^{-1}\ \text{cm}^{-1}$ *vs.* concentration C of strontium caprylate.

TABLE 1

Values of c.m.c. and heat of dissociation, $\Delta H°$ in methanol at 35—50°

Soap	c.m.c.	ΔH_0 in kcals. mole^{-1}
Calcium caprylate	0.004 M	9.20
Calcium caproate	0.010	8.28
Calcium valerate	0.012	7.90
Strontium caprylate	0.007	5.11
Strontium caproate	0.010	5.76
Strontium valerate	0.015	8.06
Barium caproate	0.012	7.55
Barium valerate	0.015	7.89

The molecular conductivity of the soap solution decreases with the increasing concentration of the soap. The plots (Figure 2) of λ_M vs. $C^{\frac{1}{2}}$ are upwardly concave maybe due to the weak electrolyte behaviour of soaps.

From the nature of the plots (Figure 3) of $\log\lambda_M$ vs. $\log C$, it is observed that the conductivity can be related to the concentration of soap by the equation :

$$\log\lambda_M = A + B \log C \tag{i}$$

Where A and B are constants.

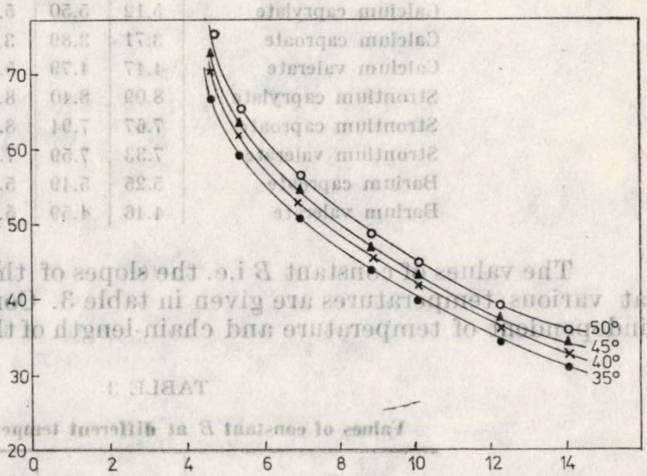

Fig. 2. — Plots of molecular conductivity, λ_M in cm² mole^{-1} ohm^{-1} *vs.* square root of concentration, $C^{\frac{1}{2}}$ for strontium caprylate.

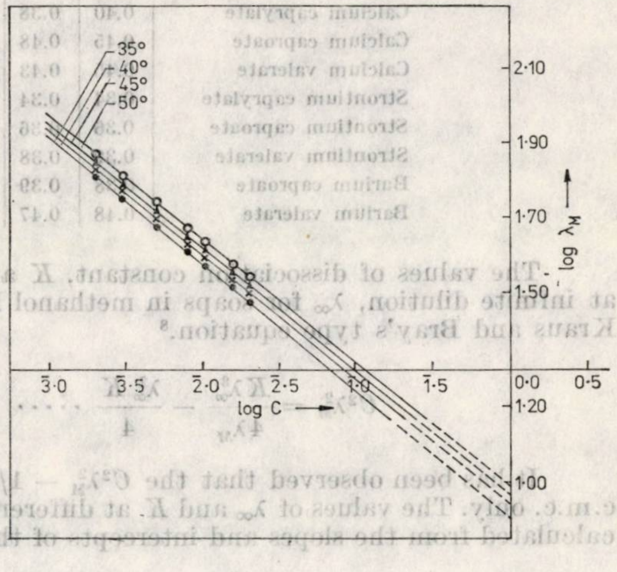

Fig. 3. — Plots of log λ_M *vs.* log C for strontium caprylate

The values of log λ_M for zero values of log C of 1 M solutions have been found by extrapolation. The values of λM of 1 M solutions at various temperatures recorded in table 2, show an increase with increasing temperature and chain length of the barium and strontium soaps.

TABLE 2

Extrapolated values of $\lambda M = 1$ at different temperatures

Soap	35°	40°	45°	50°
Calcium caprylate	5.12	5.50	5.75	6.03
Calcium caproate	3.71	3.89	3.98	4.17
Calcium valerate	4.47	4.79	5.13	5.62
Strontium caprylate	8.09	8.40	8.71	9.12
Strontium caproate	7.67	7.94	8.41	8.81
Strontium valerate	7.33	7.59	7.79	7.94
Barium caproate	5.25	5.49	5.75	5.89
Barium valerate	4.46	4.59	5.01	5.13

The values of constant B i.e. the slopes of the plots for all the soaps at various temperatures are given in table 3. Constant B is found to be independent of temperature and chain-length of the fatty acid in the soap.

TABLE 3

Values of constant B at different temperatures

Soap	35°	40°	45°	50°
Calcium caprylate	0.40	0.38	0.40	0.40
Calcium caproate	0.45	0.48	0.50	0.48
Calcium valerate	0.45	0.43	0.43	0.43
Strontium caprylate	0.34	0.34	0.34	0.34
Strontium caproate	0.36	0.36	0.35	0.36
Strontium valerate	0.39	0.38	0.39	0.39
Barium caproate	0.38	0.39	0.39	0.40
Barium valerate	0.48	0.47	0.48	0.48

The values of dissociation constant, K and molecular conductivity at infinite dilution, λ_∞ for soaps in methanol have been determined by Kraus and Bray's type equation.[8]

$$C^2\lambda_M^2 = \frac{K\lambda_\infty^3}{4\lambda_M} - \frac{\lambda_\infty^2 K}{4} \quad \cdots\cdots \quad \cdots\cdots \qquad \text{(ii)}$$

It has been observed that the $C^2\lambda_M^2 - 1/\lambda_M$ plots are linear below c.m.c. only. The values of λ_∞ and K at different temperatures have been calculated from the slopes and intercepts of the linear plots.

As may be seen from table 4 the molecular conductivity at infinite dilution of soaps increases with increasing temperature. This occurs due to the decrease in viscosity of the solvent. In other words, rise in temperature causes increase in ionic mobility despite of the fact that the addition of soap enhances the viscosity of solvent. It is observed that the value of λ_∞ for strontium soaps decreases with decreasing chain-length of the fatty acids in the soap whereas the calcium and barium soaps do not show such a trend. This indicates that both the fatty acids and the cations in the soap play a definite role.

TABLE 4

Values of λ_∞ at different temperatures

Soap	35°	40°	45°	50°
Calcium caprylate	82.60	85.70	100.00	110.50
Calcium caproate	61.50	67.80	73.10	80.78
Calcium valerate	68.10	76.90	81.81	86.30
Strontium caprylate	79.68	84.40	89.40	93.46
Strontium caproate	77.61	83.70	87.10	91.54
Strontium valerate	71.01	75.66	79.10	82.90
Barium caproate	61.38	66.37	70.47	76.47
Barium valerate	122.50	134.10	145.40	153.00

The dissociation constant decreases with the increase in temperature. Comparison of the values of K (Table 5) shows that at diferent temperatures they are in the following order:

barium caproate ⟩ barium valerate ⟩ strontium valerate ⟩ calcium caproate ⟩ strontium caproate ⟩ calcium valerate ⟩ strontium caprylate ⟩ calcium caprylate.

A plot of log. K *vs.* 1/T is found to be linear for various soaps. The heat of dissociation, Δ HO has been calculated from the slopes of the

TABLE 5

Values of dissociation constant $K \times 10^4$ at different temperatures (35—50°)

Soap	35°	40°	45°	50°
Calcium caprylate	0.270	0.229	0.160	0.124
Calcium caproate	1.650	1.220	0.971	0.797
Calcium valerate	0.949	0.862	0.657	0.590
Strontium caprylate	0.775	0.640	0.562	0.490
Strontium caproate	1.118	0.942	0.817	0.704
Strontium valerate	2.396	2.020	1.758	1.564
Barium caproate	3.044	2.492	2.109	1.741
Barium valerate	2.614	2.092	1.694	1.435

plots and is given in table 1. The trend in the change of ΔHO indicates that the system changes gradually from caprylate to valerate. However such change has also been observed in the value of c. m. c. of the soap. The results confirm that the c. m. c. remains unaffected by temperature in the range 35–50°.

ACKNOWLEDGEMENT. The authors are indebted to Dr. K. N. Mehrotra, Reader in the Department of Chemistry, University of Jodhpur, Jodhpur, for valuable criticism and college authorities for providing laboratory facilities.

REFERENCES

[1] E. S. Lower *Ind. Perfum.*, **2,** 319 (1947).
[2] M. P. Bespyatov and V. I. Polstyanoi, *Maslov-Zhur, Prom.*, **28,** 14 (1962).
[3] J.E.O. Mayne and D. V. Rooyen, *J. Appl. Chem. (Lond.)*, **4,** 384 (1954).
[4] W. C. Johnson, U. S. 2, 858, 285 Aug. 13, (1958), *Chem. Abstr*, **53,** 3733 (1959).
[5] A. J. Lehman *Assoc. Food and Drug Officials U. S. Quart. Bull.*, **15,** 82 (1951).
[6] R. P. Varma and P. Bahadur, *Indian J. Chem.*, **10,** 1189 (1972).
[7] R. P. Varma and R. Dayal, *J. Amer, Oil Chemists' Soc.*, **53,** 39 (1976).
[8] R. P. Varma and P. Bahadur, *Cellulose Chem. Technol.*, **8,** 27 (1974).
[9] K. N. Mehrotra and R. P. Varma, *J. Amer. Oil Chemists' Soc.*, **45,** 673 (1968).
[10] B. D. Flockhart and H. Graham, *J. Colloid Sci.*, **8,** 105 (1953).

Revue Roumaine de Chimie, 25, 2, 207–214 (1980)

COMPLEXES MÉTALLIQUES DE LA NICOTINEALDÉHYDE — THIOCARBOHYDRAZONE

SILVIA BARBU* et CONST. GH. MACAROVICI**
* Faculté de Pharmacie, 12, str. I. Creangă, Cluj-Napoca
** Faculté de Chimie, 11, str. Arany Janos, Cluj-Napoca
ROUMANIE

Reçu le 2 février 1978

On a synthétisé des complexes métalliques de la nicotinealdéhyde-thiocarbohydrazone avec des ions des métaux de transition ; Fe(III), Co(II), NI(II), Zn(II), Hg(II), et Pd(II). Les combinaisons complexes, de type $MLCl_2$, $ML_2(SCN)_2$ et $MLSO_4$, ont été isolées à l'état solide et l'on a enregistré des spectres électroniques et en IR. Plusieurs des composés synthétisés ont été étudiés par la méthode dérivatographique et magnétique.

The metallic complexes of nicotinaldehyde-thiocarbohydrazone with the ions of the transition metals ; Fe(III), Co(II), Ni(II), Zn(II), Hg(II), Pd(II) were studied. The complex combinations of the type $MLCl_2$, $ML_2(SCN)_2$ and $MLSO_4$ were isolated in solid state. The electronic and IR spectra were obtained. Some complexes synthesized were studied by the derivatographic and magnetic method.

Dans le cadre de nos recherches concernant les propriétés coordinatives des composés de la classe des thiocarbohydrazones nous avons étudié les conditions de synthèse et les propriétés physico-chimiques de certaines combinaisons complexes de la nicotinealdéhyde-thiocarbohydrazone (N-TCH) avec des ions des métaux de transition

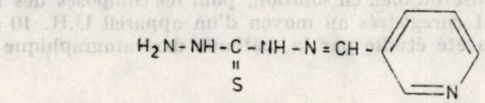

N-TCH

Les complexes métalliques de la nicotinealdéhyde-thiocarbohydrazone correspondent à la formule générale $MLCl_2$, $ML_2(SCN)_2$ et $MLSO_4$, où le rapport de combinaison métal-ligand est de 1 :1. respectivement 1 :2. (M = Fe(III), Co(II), Ni(II), Zn(II), Hg(II), Pd(II).

PARTIE EXPÉRIMENTALE

La nicotinealdéhyde-thiocarbohydrazone, utilisée comme ligand, a été préparée par la réaction de condensation de la nicotinealdéhyde et la thiocarbohydrazide[1].

Les synthèses des combinaisons complexes ont été réalisées par mélange, sous agitation, des solutions hydroalcooliques de chlorure ou de sulfate métallique, respectivement de solution

alcoolique de thiocyanates métalliques, avec une solution alcoolique de N-TCH en rapport molaire de 1 :2, maintenues au bain-marie pendant 30 minutes, après quoi l'on refroidit. On sépare les thiocyanates métalliques complexes par refroidissement du milieu alcoolique, mais pour les chlorures et les sulfates complexes on ajoute une solution à 5 % d'acétate de sodium, jusqu'à la séparation du précipité.

Excepté les thiocyanates, la purification des combinaisons complexes a été effectuée par recristallisation de l'alcool. Les données expérimentales concernant l'analyse élémentaire, le rapport de combinaison et certaines propriétés sont données au tableau 1.

TABLEAU 1

Analyse chimique et étude magnétique

Composé	Couleur	N %		S %		M %		Cl %		Étude magnétique	
		calc.	*trouvé*	*calc.*	*trouvé*	*calc.*	*trouvé*	*calc.*	*trouvé*	$\chi_{M.cor.} \cdot 10^{-6}$	μMB
$Fe(N-TCH)Cl_2$	brun	21,75	21,42	9,95	9,43	17,34	17,07	22,02	22,15		
$Co(N-TCH)Cl_2$	brun	21,54	22,02	9,86	9,40	18,06	18,48	21,80	21,16		
$Ni(N-TCH)Cl_2$	brun	21,56	21,03	9,87	9,57	18,07	17,65	21,82	21,53		
$Zn(N-TCH)Cl_2$	jaune	21,12	20,60	9,69	10,00	19,71	19,23	21,40	21,07		
$Hg(N-TCH)Cl_2$	jaune	14,99	15,41	6,86	6,20	42,98	42,51	15,20	14,82		
$Pd(N-TCH)Cl_2$	orange	18,79	18,43	8,60	8,09	28,55	28,91	19,05	18,60		
$Co(N-TCH)_2(SCN)_2$	brun	29,71	29,30	22,67	22,32	10,42	10,28	—	—	9 252	4,70
$Ni(N-TCH)_2(SCN)_2$	jaune	29,73	29,30	22,68	22,95	10,38	9,89	—	—	3 876	3,04
$Ni(N-TCH)SO_4$	brun	20,01	20,30	18,32	18,42	16,77	16,33	—	—		
$Zn(N-TCH)SO_4$	jaune verdâtre	19,63	19,28	17,97	18,32	18,33	18,12	—	—		

La susceptibilité magnétique a été déterminée à la température ambiante au moyen d'une balance de type Faraday, calibrée à l'aide de $Hg[Cd(SCN)_4]$.

Les spectres électroniques ont été enregistrés par un spectrophotomètre Carl Zeiss Jena VSU-2P en réflexion diffuse ou bien en solution, pour les composés des métaux avec des ions d^{10} ; les spectres IR étant enregistrés au moyen d'un appareil U.R. 10 Carl Zeiss Jena. Le comportement thermique a été étudié par la méthode dérivatographique par un appareil Érdely-Paulik M.O.M.

RÉSULTATS ET DISCUSSIONS

Les combinaisons complexes de la thiocarbohydrazone-nicotinealdéhyde synthétisées sont insolubles dans l'eau, peu solubles dans l'alcool, facilement solubles dans des solvants d'un caractère basique (DMF,Py).

Poursuivant au moyen de la dérivatographie la décomposition thermique de la combinaison $Ni(N\text{-}TCH)_2\ (SCN)_2$ (tabl. 2) on remarque les mêmes étapes de décomposition que pour la décomposition thermique du ligand libre[1]. A des températures au-dessous de 500°, le reste hydrazonique est détruit, tandis que la pyrolyse du reste aldéhydique se produit à une température au-dessus de 500°.

TABLEAU 2

La pyrolyse du $Ni(N\text{-}TCH)_2(SCN)_2$

Composé	Température °C	Effets thermiques à		Perte en poids %		Phénomène
		Endo	Exo	*Calc.*	*Trouvé*	
$Ni(N-TCH)_2(SCN)_2$	200	120 205	—	9,19	9,09	Elimination du CN
	400	—	240	10,97	10,91	Elimination du reste hydrazinique
	500	—	410 445	36,08	36,37	Elimination S et du reste de chaîne
	600	—	505			Pyrolyse du reste de molécule avec formation de NiS et finalement NiO
	800	795	—	13,17	12,81	

Le résidu obtenu à la suite de la pyrolyse est l'oxyde de nickel, dont la quantité se trouve en concordance avec le résultat de l'analyse élémentaire.

Dans certains cas, pour les complexes des ions aux orbitales incomplètes, les spectres électroniques ont été effectués en réflexion, en pastilles mélangées de MgO. Les paramètres des spectres électroniques (tabl. 3) relèvent l'existence de certaines géométries de coordination octaédrique pour les complexes des ions Co(II) et Ni(II)[2]. La présence de certaines bandes fendues, remarquées notamment pour le spectre des thiocyanates métalliques complexes, suggère l'existence des distorsions de la structure octaédrique [3].

Quant au spectre de la combinaison $Pd(N\text{-}TCH)Cl_2$, la présence de la bande située à 26100 cm^{-1} peut être attribuée à une transition de spin admise, dont l'attribution est incertaine, compte tenu que dans ce domaine les bandes peuvent interférer aux bandes dues aux transitions intraligand.[1,4,5]

La bande présentant une énergie faible, située à 16000 cm^{-1}, peut être estimée comme étant due à une transition de spin interdite[4].

En ce qui concerne les combinaisons complexes des ions ayant la configuration d^{10}, on a enregistré des spectres électroniques en ultraviolet par l'utilisation de solutions méthanoliques. Les résultats de l'étude spectrale, portés sur le tableau 4, indiquent des déplacements hypsochromes de la bande $\pi - \pi^*$ pour les complexes de l'ion Hg(II) et des modifications batochromes, par rapport au spectre des ligands libres[1], pour tous les complexes.

Afin d'établir les groupements électrono-donneurs de la molécule du ligand, impliqués dans la liaison coordinative, on a poursuivi les modifications susceptibles d'apparaître dans le spectre des combinaisons complexes, comparativement au spectre des ligands libres.

Les spectres IR suggèrent la participation des groupements thioliques et hydraziniques à la liaison coordinative par l'azote terminal, les domaines où ces groupements se manifestent présentant les modifications

TABLEAU 3

Spectres électroniques

Composé	ν cm^{-1}/Attribution							
$Fe(N-TCH)Cl_2$	26100 25000 d		19200	18500	16400			
$Co(N-TCH)Cl_2$	25000 ν_3	18870é			16400 ν_2		10603 1	
$Ni(N-TCH)Cl_2$	25000 3		20400é		16600 ν_2		10000 ν_1	
$Pd(N-TCH)Cl_2$	26100 $^1E_g \leftarrow {}^1A_{1g}$		25000			16000 cm^{-1} $^3E_g \leftarrow {}^1A_{1g}$		
$Co(N-TCH)_2(SCN)_2$	24000 22200	20000 ν_3	18870é	12200é	15100 ν_2	11700	11480	9300 ν_1
$Ni(N-TCH)_2(SCN)_2$	25000 ν_1				15100 ν_2	11400	9610 ν_1	
$Ni(N-TCH)SO_4$	25600 ν_3				14900 ν_2		10400 ν_1	

é = épaule

TABLEAU 4

Spectres électroniques des complexes avec des ions d^{10}

Composé	$\pi - \pi^*$		Autres bandes	
	λnm	ε	λnm	ε
$Zn(N-TCH)Cl_2$	320	23800	290	8100
$Hg(N-TCH)Cl_2$	310	18600	370	6800
$Zn(N-TCH)SO_4$	380	20850	285	9200

les plus significatives[1,6] (tabl. 5,6). Le domaine de la vibration de valence du groupement azometinique, où se manifeste également la déformation du groupement NH_2 situé à environ 1600 cm^{-1}, présente, par rapport au spectre des ligands libres, des modifications insignifiantes. Tout cela exclut la participation du groupement azométinique à liaison métal-ligand, la vibration de déformation « scissoring » n'étant pas affectée par la liaison coordinative.

La liaison de l'anion thiocyanique est réalisée par l'intermédiaire de l'azote dans le cas du complexe de l'ion Co(II), et par pont pour le complexe de l'ion Ni(II).[7]

Vu les données obtenues à la suite de l'étude de plusieurs complexes métalliques de la thiocarbohydrazone-nicotinealdéhyde, on peut supposer les formules probables de structure :

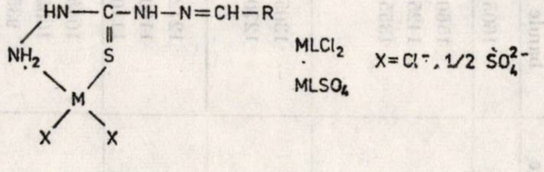

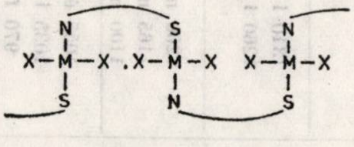

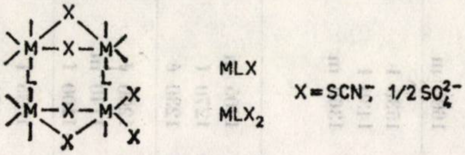

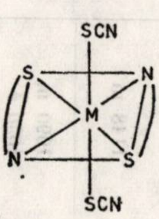

M = ion metallique

TABLEAU 5

Spectres IR des chlorures métalliques complexes

$Fe(N-TCH)Cl_2$	$Co(N-TCH)Cl_2$	$Ni(N-TCH)Cl_2$	$Pd(N-TCH)Cl_2$	$Zn(N-TCH)Cl_2$	$Hg(N-TCH)Cl_2$	Attribution	
bande large	bande large	bande large	bande large	bande large	bande large	νNH	νNH_2
1600 m	1600 m	1600 é	1605 é	1600 i	1603 i	νC=N	δNH_2
1535 i	1535 i	1555 i	1560 i	1535 i	1560 i	WNH	νC−N
1420 m	1430 i	1430 i	1425 i	1490 é	1430 i	νC−N	WNH
1375 f	1360 m	1360 f	1355 i	1425 m	1360 i		
				1390 m			
				1370 m			
1305 i	1305 m	1310 i	1305 i	1305 i	1305 i	νC−N	νC=S
1265 fd	1270 f	1260 i	1270 i	1265 i	1272 i		
1230	1230 é						
	1200 é	1200 m	1212 m	1225 i	1230 i	ρNH_2	
1148 m	1140 m	1165 m	1160 m	1190 é	1180 m		
	1100 f	1100 m	1110 m	1135 m	1120 m		
1090 m	1035 i	1055 é	1045 é	1090 m	1055 m	δNCS	
1030 é	970 m	1035 i	1005 é	1025 m	1020 m	WNH_2	
965 f	940 f	970 f	935 f	965 f	945 f	νCNN	
940 f	910 f	925 f	890 f	940 f	925 f	νC−N	
915 f	815 i	890 m	822	910 m			
815 f		815 m		885 m			
715 i	710 i	705 i	715 i	815 m	715 i	νC=S	νC−N
				710 i			

é = épaule i = intense ; m = moyen ; f = faible ; fd = fendu.

TABLEAU 6

Spectres IR des thiocyanates et des sulfates métalliques

$Co(N-TCH)_2(SCN)_2$	$Ni(N-TCH)_2(SCN)_2$	$Ni(N-TCH)SO_4$	$Zn(N-TCH)SO_4$	Attribution
bande large	bande large	bande large	bande large	νNH_2 νNH
2075 i	2098 i	—	—	$\nu C \equiv N$
1603 m	1610 m	1610–1640 é	1645	$\nu C=N$ δNH_2
1545 i 1495 é 1435 m 1345 m	1545 i 1495 i 1435 m	1565 m.i 1425 m.f 1360 é	1545	$WNH+\nu C-N$ $\nu C-N+WNH$
1315 m 1265 é	1310 m 1260 m	1315 m	1320 é 1280 é	$\nu C-N$ $\nu C=S$
1200 m 1110 f	1230 m 1200 m 1155 m 1110 f	1200 é	1145 f	ρHN_2 $\nu_3 SO_4^{2-}$
1035 m 960 f 945 f 888 f	1072 f 1040 f 970 f 950 t.f 915 t.f	1100 i 985 f 900 f	1075 t.f 965 f 870 f	δNCS WNH_2 νCNN $\nu C-N$
815 m 710 m	820 m 710 m	810 m 710 i	805 m 705 m	$\nu C=S$ $\nu C-N$

é = épaule ; i = intense ; m = moyen ; f = faible ; t.f. = très faible.

BIBLIOGRAPHIE

[1] S. Barbu et C. Gh. Macarovici, *Rev. Roumaine Chim.*, **23**, 1243 (1978).

[2] A. B. P. Lever, « Inorganic Electronic Spectroscopy », Elsevier Publishing Company, Amsterdam, 1968.

[3] A.B.P. Lever, *Inorg Chem.*, **4**, 1042 (1965).

[4] H. B. Gray et G. J. Ballhausen, *J. Amer. Chem. Soc.*, **85**, 260 (1963).

[5] D. S. Martin et M. A. Tucker, *Inorg. Chem.*, **5**, 1298 (1964).

[6] M. Mashima, *Bull. Chem. Soc. Japan*, **37**, 974 (1964).

[7] S. Arhland, J. Chatt et N. R. Davies, *Quart. Rev.*, **12**, 265 (1958).

Revue Roumaine de Chimie, **25**, *2*, 215–222 (1980)

THERMOGRAVIMETRIC INVESTIGATION OF THE DECOMPOSITION OF CERTAIN METAL DITHIOCARBAMATES

K. N. JOHRI and K. A. VENUGOPALAN
Department of Chemistry, University of Delhi, Delhi 110007, India

Received November 24, 1977
Revised July 5, 1979

The complexes of Cu(II), Zn(II), Cd(II), Co(II), Ni(II), Sn(II), VO(IV) and UO_2(VI) with ammonium N,N′-bis(dithiocarboxy)-*o*-phenylenediamine have been prepared. The mode of co-ordination of the ligand has been ascertained on the basis of analytical studies, room temperature magnetic susceptibility measurements, near and far infrared spectral studies. The systematic thermal decomposition studies of the complexes have been carried out under non-isothermal temperature conditions.

INTRODUCTION

Dithiocarbamates have shown considerable promise as excellent analytical reagents so far as their ease of formation and coordinating ability with various metal ions is concerned.[1,2]

In the present study, we have examined the complexation reactions of ammonium N,N′-bis (dithiocarboxy)-*o*-phenylenediamine (I), henceforth referred to as $(NH_4)_2$ DPD, and its possible use as an analytical reagent. The mode of coordination of the ligand and the stereochemistry of the complexes have been established. A survey of literature revealed that antifungal activity of the di-sodium salt is well established and documented.[3]

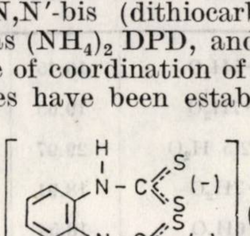

I

As a result of the considerable interest in the thermal behaviour of metal dithiocarbamates in recent years, a systematic thermoanalytical investigation of the complexes of $(NH_4)_2$DPD has been carried out, in order to confirm the purity of the precipitated products, to determine suitable drying conditions for the complexes, limit of initial horizontal stretch, mode of decomposition and nature of the final product of decomposition.

EXPERIMENTAL

Materials

Synthesis of $(NH_4)_2DPD$ *(I)*. Into a 250 ml two-necked R.B. flask fitted with a powerful mechanical stirrer, 20 ml of liquor ammonia (sp. gr. 0.88) and 7.6 ml of pure carbon disulphide were introduced. The flask was cooled in a freezing mixture and maintained at about 0° throughout the synthesis. To the well-stirred, chilled mixture, was added, in small quantities, freshly crystallized and powdered o-phenylenediamine (5.4 g) during about 20—30 min. Stirring was continued for the next 30 min. The solution was kept in refrigerator overnight. The bulky precipitate of I was quickly filtered at the pump, washed successively with small quantities of pure ethanol and ether. The crude product was crystallized from absolute alcohol. The light yellow shining crystallized product thus obtained was stored in a vacuum desicator over P_2O_5. Freshly prepared aqueous solution of the ligand was employed for each synthesis.

Metal ion solutions. Prepared from analytical grade salt of the respective metals (B.D.H. or AnalaR). Oxovanadium salt, used for the preparation of DPD complex, was prepared by reducing sodium meta-vanadate with Na_2SO_3/HCl, neutralized with NH_4OH and excess ammonia being boiled off. The starting metal salts used for preparing the complexes are summarized in table 1.

Synthesis of complexes. Of the various methods that have been suggested for the synthesis of metal dithiocarbamates, [2] the following general method was adopted for the synthesis of the complexes of Cu(II), Zn(II), Cd(II), Co(II), Ni(II), VO(IV) and UO_2(VI).

Into a neutral aqueous solution of the respective metal salts, a solution of I was added in small portions with vigorous stirring, at room temperature. As far as possible, the

TABLE 1

Physical and analytical data

Complex	Colour	Starting metal salt	% Metal		μ_{eff} (B.M.)
			Found	Calculated	
CuDPD	Brown	$CuSO_4 \cdot 5H_2O$	19.45	19.74	1.60 (301 °K)
ZnDPD	White	$ZnSO_4 \cdot 7H_2O$	19.63	20.19	dia
CdDPD	Yellow	$CdCl_2 \cdot 2.5\ H_2O$	29.97	30.33	dia
CoDPD	Deep green	$CoSO_4 \cdot 7H_2O$	18.91	18.57	4.77 (297°K)
NiDPD	Greenish yellow	$NiSO_4 \cdot 6H_2O$	18.54	18.51	dia
SnDPD	Bright yellow	$SnCl_2 \cdot 2H_2O$	30.82	31.49	dia
(VO) DPD	Greenish yellow	$NaVO_3 \cdot 4H_2O$	14.89	15.66	1.66 (298°K)
(UO_2)DPD	Reddish orange	$(NH_4)_2U_2O_7$	45.70	45.07	—

DPD = $C_8H_6N_2S_4$

access of oxygen into the reaction flask was avoided. The reaction mixture was stirred for 2–3 min. The precipitate was filtered through a medium porosity sintered glass crucible and washed with water to remove the unreacted starting materials. The precipitate was dried at room temperature over P_2O_5 in a vacuum desiccator.

For preparing the Sn(II) complex, a slightly acidic medium was employed, otherwise an essentially similar procedure, as detailed above, was adopted.

Measurements

The TG curves were recorded on a manual FCI thermobalance in a self-produced atmosphere using platinum crucible. Sample sizes ranged from 250 to 350 mg; a heating rate of $7.5 \pm 0.5° \mathrm{min}^{-1}$ was employed. Infrared spectra were recorded in KBr phase on a Perkin-Elmer 621 Infracord. Gouy's method[4] was employed for magnetic susceptibility measurements of the solid complexes using $\mathrm{Hg[Co(SCN)_4]}$ as calibrant.

RESULTS AND DISCUSSION

$(NH_4)_2$DPD and its complexes were found to be soluble in coordinating solvents. The complexes decompose uniformly in mineral acids, yielding colloidal sulphur. $(NH_4)_2$DPD was highly soluble in water, while the complexes were insoluble. Table 1 summarizes the physical and analytical data for the complexes. The observed IR frequencies and band assignments for the complexes are set out in table 2. The IR

TABLE 2

Observed IR frequencies (values in cm^{-1}) and band assignments of the ligand and the complexes

Assignments	$(NH_4)_2$DPD	CuDPD	ZnDPD	CdDPD	CoDPD	NiDPD	SnDPD	(VO)DPD	(UO_2)DPD
ν(C=C)	1610	1615	1610	1600	1615	1612	1610	1615	1610
δ(N–H) asym	1550	1510	1510	1520	1545	1520	1550	1525	1510
$\nu(\mathrm{C}\overset{\cdots}{-}\mathrm{N})$	1492	1495	1490	1505	1500	1495	1507	1505	1490
δ(C–N)	1450	1460	1460	1465	1460	1450	1465	1465	1445
δ(C–H) in plane	1380	1345	1350	1350	1355	1355	1357	1355	1355
$\nu(\mathrm{C}\overset{\cdots}{-}\mathrm{S})$	1030 995	1000	998	1010	1005	1000	1013	1020	1020
	740	740	740	740	740	745	742	740	760
ν(C–S) asym	680	655	640	660	665	660	660	655	660
ν(C–S) sym	625	645	600	635	640	635	635	630	645
ν(M–S) + ring deformn.	580	—	585	580	590	585	580	580	590
ν(M–S)	—	360	400	385	360	375	405	405	370
Specific	—	—	—	—	—	—	—	ν(VO)970	$\nu(UO_2)$890

studies enabled to establish the mode of linkage of the ligand with the metal ions. A summary of thermal stability data for the complexes is included in table 3. The table also includes the percent weight loss values.

TABLE 3

Summary of TGA data

Complex	Weight taken (g)	Decomposition range (°C)	% Weight loss	
			Found	Calcd.
$(NH_4)_2DPD$	0.3164	80−640	100.0	100.0
CuDPD	0.2978	60−800	74.1	75.2
ZnDPD	0.3490	50−870	74.0	74.8
CdDPD	0.2430	50−855	65.9	65.4
CoDPD	0.2645	60−830	73.1	74.7
NiDPD	0.2176	50−760	79.4	79.8
SnDPD	0.2964	70−735	59.5	60.0
(VO)DPD	0.2990	50−670	70.9	72.0
$(UO_2)DPD$	0.2852	65−760	45.8	46.9

DPD = $C_8H_6N_2S_4$

Estimation of $(NH_4)_2DPD$. The method of Shankaranarayana and Patel[5] for the volumetric estimation of water soluble dithiocarbamates was found to be suitable for the present investigation. The results are summarized in table 4.

TABLE 4

Results of estimation of $(NH_4)_2$ DPD normality of H_2SO_4 = 0.5 N

Wt. of $(NH_4)_2DPD$ taken (g)	Vol. of H_2SO_4 consumed (ml)	Mol. wt. of $(NH_4)_2DPD$		Error %
		Found	Calcd.	
0.5225	14.0	298.6	294.4	+1.43
0.4950	13.5	293.4	294.4	−0.34

Magnetic studies. The magnetic susceptibility measurements revealed the probable stereochemistry of the metal complexes.

The magnetic moment of 1.60 B.M., corresponding to one unpaired electron, for the Cu(II) complex suggests a tetra coordinate (sp^3) structure. Most of the Zn(II) and Cd(II) complexes mentioned in literature are tetrahedral[6]. The complexes are diamagnetic, therefore, the tetrahedral arrangement of the ligand molecules around Zn(II) and Cd(II)are assigned to these complexes. The much expected departure of the magnetic moment value of 4.77 B.M., for the Co(II) complex, from the 'spin-only value' is under the influence of the 'spin-orbit coupling', arising from the intrinsic orbital degeneracy of the ground electronic state, giving a substantial orbital contribution to the moment. At room temperature, magnetic moment values for octahedral Co(II) and quadricovalent planar, spin-free complexes have been found to lie between 4.8—5.2 B.M.[7] and for tetrahedral Co(II) complexes between 4.4—4.8 B.M.[8] The lower values for the tetrahedral complexes is due to a lesser orbital contribution. Thus, the composition of the CoDPD complex and the tetradentate behaviour of the ligand permit a tetra coordinated structure. A tetrahedral stereochemistry may, therefore, be proposed. The Ni(II) complex is diamagnetic. The diamagnetism is a very strong indication that the spatial arrangement of the ligand molecules around the nickel ion is square planar (dsp^2). Corresponding to the presence of one unpaired electron ($3d^1$), the value of the magnetic moment for the oxovanadium complex was found to be 1.66 B.M. A quadrivalent state of the central metal ion is, therefore, inferred. Most quadrivalent vanadium compounds contain the vanadyl ion.[1] Thus, a five-coordinated square-pyramidal structure with the vanadium-oxygen double bond (vide-infra) is suggested for this complex. Tin forms a diamagnetic complex in the lower oxidation state.

Infrared studies. The IR spectra of the ligand and metal dithiocarbamates show a strong absorption band in the region 1505—1490cm $^{-1}$, characteristic of the 'thioureide ion'. Chatt et al.[9] consider the only possible assignment to this absorption band to be to a polar $C \dashrightarrow N$ partial double bond. The presence of only one strong band around 1000 cm^{-1}, corresponding to the $C \dashrightarrow S$ stretching vibration, strongly supports chelation of the dithio- ligand.[10] A doublet was observed in the 1000 ± 70 cm^{-1} region in the case of unchelated ligand molecule.[11] In addition to other absorption bands, the IR spectra of the oxovanadium (IV) and the dioxouranium (VI) complexes show medium intensity absorptions at 970 and 890 cm^{-1}, assignable to $\nu(VO)$[12] and $\nu(UO_2)$[13] stretching modes respectively. Conclusive evidence of the metal-to-sulphur bond is provided by medium intensity bands observed in the far infrared region of the spectrum in the range 405—360 cm^{-1}.

Thermal studies. The TG curve (Figure 1) for the ligand and its complexes has been briefly discussed below. The temperatures referred to are 'procedural decomposition temperatures' at the heating rate indicated.

$(NH_4)_2DPD$. The ligand is thermally stable up to 80°. The decomposition which follows takes place in a single-step. Initially, there is a slow decomposition, which gets accentuated after a loss of nearly 15% of the ligand at 230°. The process is complete at 640°, where the crucible is entirely empty.

CuDPD. This complex is stable up to 60° as seen from the thermogram. Beyond 60°, a single-step decomposition of the complex sets in, which accelerates after a loss of nearly 8% of the initial weight of the complex around 250°. During a small temperature interval, covering about 60°, in the range 300—360°, there is a slight arrest in the rate of decomposition, probably due to some oxidation. The final phase of decomposition of the residual organic matter sets in at about 360° and continues thus, until the black residue corresponding to cupric oxide is obtained at about 800°, indicated by a horizontal in the TG curve.

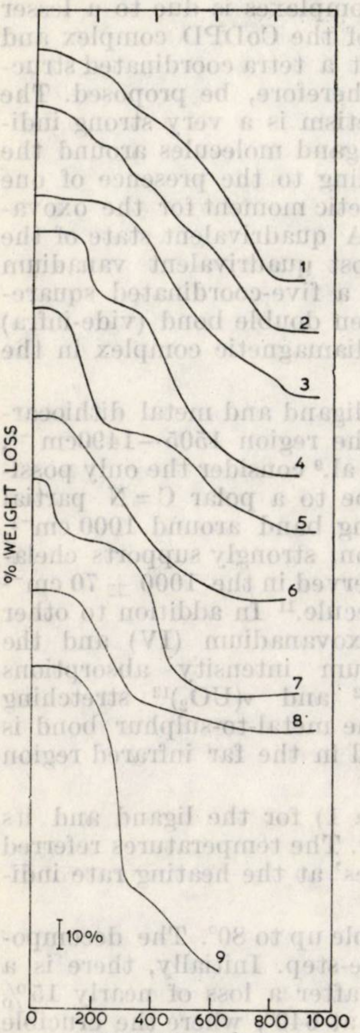

Fig. 1. — TG curves of N,N′-bis (dithiocarboxy)-o-phenylenediamine complex of *1* Cu(II), *2* Co(II), *3* Cd(II), *4* Ni(II), *5* Zn(II), *6* Sn(II), *7* VO(IV), *8* UO_2(VI) and *9* ligand.

ZnDPD. This complex was found to be thermally stable only up to 50°. The decomposition accelerates after a loss of nearly 8 % of the initial weight at 140° and proceeds unabated. The decomposition rate slows down after nearly 40 % of the complex has been decomposed, which can be attributed to the simultaneous oxidation of the sulphide formed, to the sulphate and the decomposition. No transitory intermediate level was observed. A perfectly horizontal level corresponding to white zinc oxide appears at 870°.

CdDPD. The initial loss in weight up to 110° for this complex was apparently due to the escape of adherent moisture present in the test sample. Beyond 190°, the TG curve descends slowly with the destruction of the organic matter. The decomposition rate picks up gradually with rise in temperature. The simultaneous destruction of the organic matter and the reoxidation of the sulphide and metal formed to sulphate and oxide respectively, resulted in a slight arrest in the decomposition rate of the complex. A yellowish-brown residue, presumably of the oxide, CdO, yielded a perfectly horizontal level from 855°.

CoDPD. This complex starts decomposing at 60°. The TG curve reveals an appreciable loss of mass due to a sudden and deep-seated decomposition. The organic matter burns off almost linearly as far as 830°, when the horizontal level corresponding to the oxide, Co_3O_4, appears.

NiDPD. The nickel complex starts decomposing from 50°. Except for a slight slackening in the weight loss curve between 200–380°, the one-step decomposition of the complex proceeds regularly up to 760°. Thereafter, a perfectly horizontal level, extending as far as 1000°, corresponding to black NiO appears. The slackening observed may be due to some oxidation of the elemental metal and sulphide formed during decomposition.

SnDPD. The thermolysis curve of this product is quite regular and follows a one-step decomposition. The decomposion once set in at 70° proceeds unabated up to 735°, when a horizontal due to white oxide, SnO_2, appears.

A slight arrest in the decomposition rate around 400° may be attributed to some oxidation.

(VO)DPD. The TG curve of the oxovanadium complex shows a loss of weight starting at 50° and continuing upto 670°. When about 20% of the organic matter has been burnt off at 150°, there is an appreciable arrest in the decomposition rate, but the curve is far from being horizontal. This can be attributed to the oxidation process. The oxidation of metallic vanadium probably occurs in the 500 –670° temperature range also, as revealed by a slackening in the weight loss curve. The horizontal of the residual product begins at 670° and accords with the oxide, V_2O_5.

(UO_2)DPD. The complex starts decomposing around 65°. The organic matter decomposes with an appreciable weight loss. The decomposition rate decreases near 300°, when probably the residue UO_3 is being approached, and in its turn loses oxygen. The olive-green oxide, U_3O_8, is obtained from 760°. Its level continues in essentially horizontal fashion upto 945°.

CONCLUSIONS

$(NH_4)_2$DPD acts as a tetradentate ligand with S_4 coordination unit. The stoichiometry (metal ligand ratio) of the complexes was found to be ML. According to the structure of $(NH_4)_2$DPD and on the basis of the chemical composition and other physico-chemical studies, the following tentative structure is proposed for the metal complexes with bivalent metals, including those of oxovanadium and dioxouranium.

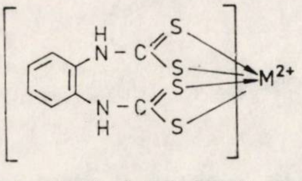

(where M = Cu(II), Zn(II), Cd(II), Co(II), Ni(II), Sn(II), VO(IV) or UO_2(VI)

The thermograms of complexes showed common features. All the complexes investigated proved to be highly thermally unstable, with the initial inflection on the TG curve appearing around 50°. Furthermore, the TG curve consistently showed one-step weight loss. Although none of the complexes includes an initial horizontal level, a well-defined plateau corresponding to the respective metal oxides was obtained, as final product of all the decompositions. The ligand was found to be completely volatile, in that no residue was left after its decomposition.

ACKNOWLEDGEMENTS. We are grateful to Dr. (Mrs) G. K. Sandhu, Research Officer, Department of Chemistry, G.N.D. University, Amritsar for permitting the generous use of the thermobalance. The author (K.A.V.) is thankful to University Grants Commission, New Delhi, India for the award of a research fellowship.

REFERENCES

[1] A. Hulanicki, *Talanta*, **14**, 1371 (1967).

[2] R. J. Magee, *Rev. Anal. Chem.*, **1**, 333 (1973).

[3] A. M. Shah and J. W. Jones, *J. Amer. Pharm. Assoc.*, **47**, 399 (1958).

[4] B. N. Figgis and J. Lewis, "Modern Coordination Chemistry", Interscience, New York, 1960.

[5] M. L. Shankaranarayana and C. C. Patel, *Analyt. Chem.*, **33**, 1398 (1961).

[6] F. A. Cotton and G. Wilkinson, "Advanced Inorganic Chemistry", 3 Edn., Wiley Eastern Limited, New Delhi, 1976.

[7] F. A. Cotton and R. H. Holm, *J. Amer. Chem. Soc.*, **82**, 2979 (1967).

[8] B. N. Figgis and J. Lewis, *Prog. Inorg. Chem.*, **6**, 180 (1964).

[9] J. Chatt, L. A. Duncanson and L. M. Venanzi, *Nature*, **177**, 1042 (1956).

[10] R. M. Golding, A. D. Rae, B. J. Ralph and L. Sulligoi, *Inorg. Chem.*, **13**, 2499 (1974)

[11] F. Bonati and R. Ugo, *J. Organometal Chem.*, **10**, 257 (1967).

[12] K. Nakamoto "Infrared Spectra of Inorganic and Coordination Compounds", 2 Edn., Wiley-Interscience, 1970.

[13] K. W. Bagnall and M. W. Wakerley, *J. Inorg. Nuclear Chem.*, **37**, 329 (1975).

Revue Roumaine de Chimie, 25, 2, 223–229 (1980)

ELECTRON TRANSFER REACTIONS IN SOME COMPLEX COMPOUNDS OF Hg(II), Co(II) AND Cu(I) WITH QUINOXALINIC AND NAPHTOQUINONIC LIGANDS

D. NEGOIU and J. CAMUS
National Institute of Chemistry,
Department of Chemical Technology
1, Polizu Street, 78126-Bucharest, Romania

Received February 12, 1979

The complex compounds of Hg(II), Co(II) and Cu(I) of the $(MO_4)^{z-}$ and $(MN_2S_2)^{z-}$ type with quinoxalinic and naphtoquinonic ligands were investigated. It was shown that these complexes can undergo electron transfer proceses. The compounds were analysed and characterized by molar conductivity measurements, electrochemical and spectroscopic methods. The parameters of the ESR spectra were estimated.

The redox properties of the complex compounds containing dithiols were discovered in 1963[1]. Since then, the concept of electron transfer series has been introduced in literature and extended to other bis-chelate species containing five-atom cyles with groups of oxygen, nitrogen and selenium atoms as donor atoms.[2] A peculiar feature of these combinations is that they do not modify their coordination geometry when participating in reversible electron transfer reactions. The data published so far emphasize the important part played in electron transfer processes by nitrogen, oxygen and sulfur-containing heterocyclic ligands.[3]

It is to be mentioned that the classical concept of formal oxidation state cannot describe adequately these compounds[4]. The combinations involved can be interconverted chemically or electrochemically by redox monoelectronic reactions, giving rise to an electron transfer series. The metal-ligand bond is covalent and the unpaired electrons of the paramagnetic species are strongly delocalized. The electron transfer reactions in which these complexes participate, either chemically or electrochemically, result in ionic species having the charge $z = 0, \pm 1, \pm 2$.

RESULTS AND DISCUSSION

Mercury complex compounds which are able to participate in electron transfer reactions are scantly reported in literature. Mureşan[5] succeded in preparing four complexes of this type, with dithiols as ligands.

In this work we synthesized $(MO_4)^z$ -type complexes of mercury with the ligands 2,3-dihydroxyquinoxaline (abbreviated 2,3-DHQ), 6-nitro- and 6,7-dinitro-2,3-dihydroxyquinoxaline (6-N-2,3-DHQ and 6-7-DN-2,3-DHQ, respectively) and $(MN_2S_2)^z$ — type complexes with the 2-amino-3-mercaptomethyl-1,4-naphtoquinone (2-A-3-MM-1,4-NQ) ligand. Four complexes of mercury with naphtoquinonic and quinoxalinic ligands were obtained.

Four complex combinations of copper were also synthesized; the starting materials were Cu(I) compounds. It was noticed that beside obtaining other species, than with Cu (II), the use of Cu(I) salts favors the formation of crystalline precipitates with a better yield than Cu(II).

The Co(II) complexes are obtained with more difficulty and at room temperature they do not have paramagnetic properties. No ESR signal could be obtained in our working conditions. The precipitates are very finely grained, filterable only with difficulty. The complex with dihydroxyquinoxaline could not be separated; a [Co(2,3-DHQ)] — type complex salt could only be obtained.

Elemental chemical analysis of the resulting combinations suggests the following compositions:

$[(C_4H_9)_4N][Cu(2,3\text{-DHQ})_2]$; $[(C_4H_9)_4N]_2[Cu(6\text{-N-}2,3\text{-DHQ})_2]$;
$[Cu(6,7\text{-DN-}2,3\text{-DHQ})_2]$; $[Cu(2\text{-A-}3\text{-MM-}1,4\text{-NQ})_2]$
$[Co(2,3\text{-DHQ}])$; $[Co(6\text{-N-}2,3\text{-DHQ})_2]$;
$[(C_4H_9)_4N][Co(6,7\text{-DN-}2,3\text{-DHQ}]$; $[Co(2\text{-A-}3\text{-MM-}1,4\text{-NQ})_2]$;
$[(C_4H_9)_4N][Hg(2,3\text{-DHQ})_2]$; $[(C_4H_9)_4N]\ [Hg(6\text{-N-}2,3\text{-DHQ})_2]$;
$[(C_4H_9)_4N][Hg(6,7\text{-DN-}2,3\text{-DHQ})_2]$; $[Hg(2\text{-A-}3\text{-MM-}1,4\text{-NQ})_2]$

Owing to the low solubility of the mercury complexes, their molar electric conductivity was measured in various solvents. The results (Table 1) are in good agreement with the formulas given above. In DMSO, the conductivity of the 1 : 1 electrolytes, ranges between 24 and 42 $cm^2.mole^{-1}$.

TABLE 1

Molar conductivity

Nr.	Compound	Type	λM $cm^2 \cdot mol^{-1} \cdot ohm^{-1}$	Solvent
1.	$[Bu_4N]\ [Hg(2,3\text{-DHQ})_2]$	$[HgO_4]^-$	32.5	DMSO
2.	$[Bu_4N]\ [Hg(6\text{-N-}2,3\text{-DHQ})_2]$	$[HgO_4]^-$	38.0	DMSO
3.	$[Hg(2\text{-A-}3\text{-MM-}1,4\text{-NQ})_2]$	$[HgN_2S_2]^{\circ}$	30.0	DMF
4.	$[Bu_4N]\ [Hg(6,7\text{-DN-}2,3\text{-DHQ})_2]$	$[HgO_4]^-$	68.0	DMF
5.	$[Bu_4N]_2\ [Cu(6\text{-N-}2,3\text{-DHQ})_2]$	$[CuO_4]^{2-}$	130.5	DMF
6.	$[Bu_4N]\ [Cu(2,3\text{-DHQ})_2]$	$[CuO_4]^-$	90.0	DMF
7.	$[Cu(2\text{-A-}3\text{-MM-}1,4\text{-NQ})_2]$	$[CuN_2S_2]^{\circ}$	16.5	DMF
8.	$[Co(6\text{-N-}2,3\text{-DHQ})_2]$	$[CoO_4]^{\circ}$	29.2	DMF
9.	$[Bu_4N]\ [Co(6,7\text{-DN-}2,3\text{-DHQ})_2]$	$[CoO_4]^-$	65.0	DMF
10.	$[Co(2\text{-A-}3\text{-MM}-1,4\text{-NQ})_2]$	$[CoN_2S_2]^{\circ}$	22.0	DMF

ohm^{-1},[6] which is of the same order as that of the combinations prepared by us. The $[HgS_2S_2]^\circ$ — type complexes have a conductivity in DMF of 30 $cm^2.mole^{-1}.ohm^{-1}$, which again is typical of a neutral species. The low values of the molar conductivity Λ_M ($22-29$ $cm^2.mole^{-1}.ohm^{-1}$ in DMF) of the cobalt complexes are in good agreement with their non-electrolyte character. The minimum value which would allow characterization as 1 : 1 electrolyte (65 $cm^2.mole^{-1}.ohm^{-1}$ in DMF) was obtained for the 6,7-dinitro-2,3-dihydroxyquinoline complex.

A good agreement was also noticed between the composition of the copper complexes and the type of ionic dissociation. Thus, the molar electric conductivity is 130.5 $cm^2.mole^{-1}.ohm^{-1}$ for the $R_2[CoO_4]$ — type combination, 90 $cm^2.mole^{-1}.ohm^{-1}$ for the $R_2[CuO_4]$ — type combination and 16.5 $cm^2.mole^{-1}.ohm^{-1}$ for the $[CuN_2S_2]^\circ$ — type combination. All measurements were carried out in DMF.

In all cases, the mercury complexes have easily measurable and reproducible polarograms. The polarograms of the quinoxalinic complexes have two waves. The first wave was assigned to the reduction of the complex species :

$$(\text{complex})^- \rightleftharpoons (\text{complex})^{2-}$$

The half-wave potential $E_{1/2}$ is -0.35 V in the case of $[Hg(2,3\text{-}DHQ)_2]^-$, and -0.99 V and -0.73 V in the case of the complexes with 6-nitro- and 6,7-dinitro-2,3-dihydroxyquinoxaline, respectively. The second wave is due to the ligand reduction in all three cases[7]. In the case of the $[HgN_2S_2]^\circ$ — type combinations the first two waves appear at $E_{1/2} = -0.31$ V and -0.64 V. They were assigned to the reduction of the complex species :

$$(\text{complex})^\circ \rightleftharpoons (\text{complex})^-$$

and

$$(\text{complex})^- \rightleftharpoons (\text{complex})^{2-}$$

The third wave was assigned to the reduction of quinone.

The complexes of copper with the unsubstituted DHQ have two waves : the first, at $E_{1/2} = -0.04$ V, was assigned to the reduction of the monoanionic complex species to the neutral species. The neutral complex obtained with 6,7-dinitro-2,3-dihydroxyquinoxaline has three reduction waves. The first wave appears at $E_{1/2} = 0.05$ V and was assigned to the reduction of the neutral complex species to the monoanionic species. The second wave appears at $E_{1/2} = -0.36$ V and was assigned to the reduction of the monoanionic species to the dianionic species. The third wave appears at $E_{1/2} = -0.63$ V and was assigned to the reduction of the nitro group.

The $[CuN_2S_2]^\circ$ — type complex has three reduction waves. The first appears at $E_{1/2} = -0.28$ V and was assigned to the reduction of the neutral species to the monoanion, the second, at -0.74 V, was assigned to the reduction of the monoanion to the dianion, and the third, at -1.17 V, to the reduction of quinone at the dripping mercury electrode.

The complex of cobalt with the 6-nitro-substituted quinoxaline has three waves ; the first two waves appear at $E_{1/2} = 0.15$ V and -0.36 V and were assigned to the reduction of the neutral complex to the monoanion and to the dianion, respectively ; the last reduction step, which appears at $E_{1/2} = -1.81$ V, was assigned to the reduction of the nitro group. The dinitro-substituted monoanionic combination has a first wave at $E_{1/2} = -0.46$ V, which was assigned to the reduction of the dianion, and two other waves at $E_{1/2} = -1.36$ V and -1.181 V, assigned to the reduction of the nitro groups.

The $[CoN_2S_2]^\circ$ — type complex is reduced at $E_{1/2} = -0.28$ V, which is assigned to the process :

$$(\text{complex})^\circ \rightleftharpoons (\text{complex})^-$$

Analysis of the infrared spectra offered some information concerning the way in which the ligands are coordinated. In particular, we examined the frequencies assigned to the vibration of the $-OH$, $-SCH_3$ and $-NH_2$ groups. The wide bands corresponding to the vibration modes of the $-OH$ groups disappear after complexation, and we assigned, therefore, this modification to the process of binding the central atom through the oxygen atom. The complexes with 2-amino-3-mercaptomethyl-1,4-naphtoquinone have bands characteristic to the $-NH_2$ group which are weakened and shifted to 3330 and 3350 cm^{-1} in the case of cobalt and copper complexes, respectively ; this suggests that the sulphur atom takes part in the coordination process.

The visible and ultraviolet spectra are presented in table 2. The assignment of the observed peaks is given.

TABLE 2

Electronic spectra

Complex combination	Vibration bands ν cm^{-1}	Assignment
$[Bu_4N]$ $[Hg(6\text{-}N\text{-}2,3\text{-}DHQ)_2]$	29,500 i	nitro
	22,300 sh	CT
$[Bu_4N]$ $[Hg(6,7\text{-}DN\text{-}2,3\text{-}DHQ)_2]$	26,200 i	nitro
	22,600 w	CT + ligand
$[Hg(2\text{-}A\text{-}3\text{-}MM\text{-}1,4\text{-}NQ)_2]$	18,600 i	quinone
$[Co(6\text{-}N\text{-}2,3\text{-}DHQ)_2]$	26,000 i	nitro + CT
	16,000 w	d−d
	1,100 vi	
$[Co(2-A-3-MM-1,4-NQ)_2]$	19,000 i	quinone
	16,000 sh, w	d−d
$[Bu_4N]$ $[Co(6,7\text{-}DN\text{-}2,3\text{-}DHQ)_2]$	24,500 sh	nitro + CT
	16,000 w	d−d
	1,100 vi	
$[Bu_4N]$ $[Cu(2,3\text{-}DHQ)_2]$	29,400 sh	CT
	25,800 sh	d−d
	15,800 w	
$[Bu_4N]_2$ $[Cu(6\text{-}N\text{-}2,3\text{-}DHQ)_2]$	27,700 sh, w	nitro
	24,500 i	CT
	16,000 w	d−d
$[Cu(6,7\text{-}DN\text{-}2,3\text{-}DHQ)_2]$	27,700 i	nitro
	24,400 sh	CT
	15,900 w	d−d
$[Cu(2\text{-}A\text{-}3\text{-}MM\text{-}1,4\text{-}NQ)_2]$	21,000 i	quinone

i = intense, sh = should, vi = very intense, w = week

The complexes of Cu(I) give strong ESR spectra, generally similar but not identical with those of the analogous Cu(II) complexes. The ESR spectra of the Cu(I) complexes, recorded with crystalline powder samples, are shown in figure 1. The respective ESR parameters are given in table 3. The best resolution of the component perpendicular to the direction of the external field, compared to the case of other monovalent or divalent copper complexes, was obtained for the 6-nitro-substituted compound.

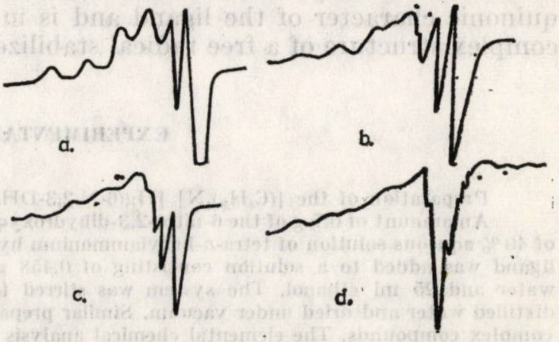

Fig. 1. — ESR spectra. *a.* $[Cu(2,3\text{-}DHQ)_2]^-$ *b.* $[Cu(6\text{-}N\text{-}2,3\text{-}DHQ)_2]^{2-}$ *c.* $[Cu(6,7\text{-}DN\text{-}2,3\text{-}DHQ)_2]^-$ *d.* $[Cu(2\text{-}A\text{-}3\text{-}MM\text{-}1,4\text{-}NQ)_2]$.

TABLE 3

ESR parameters

Complex	$A_{\parallel}$	$A_{\perp}$	$g_{\parallel}$	$g_{\perp}$	$A_{\top}$
$[Bu_4N]$ $[Cu(2,3\text{-}DHQ)_2]$	182.19	38.41	2.2420	2.0710	628.18
$[Bu_4N]_2$ $[Cu(6\text{-}N\text{-}2,3\text{-}DHQ)_2]$	183.28	34.96	2.2445	2.0647	623.00
$[Bu_4N]$ $[Cu(6,7\text{-}DN\text{-}2,3\text{-}DHQ)_2]$	168.46	33.88	2.4091	2.0689	785.11
$[Cu(2\text{-}A\text{-}3\text{-}MM-1,4\text{-}NQ)_2]$	33.48	81.58	2.1657	2.0386	368.71

Although the Hg^{2+} has the d^{10} electronic configuration, thus having no unpaired electrons, ESR signals were nevertheless obtained for the $[Hg(2,3\text{-}DHQ)_2]^-$ and $[Hg(6\text{-}N\text{-}2,3\text{-}DHQ)_2]^-$ complexes (Figure 2). In the first case only a singlet was observed, with $g = 2.0044$ and a line width of 19.07 gauss. The g value, which is close to that of the free electron, as well as the relatively small width of the line as compared to the spectra of other complexes, suggest a more pronounced electron density delocalization on the ligands, through the Hg(II) ion which is larger in size and hence more polarizable. A non-isotropic spectrum (with

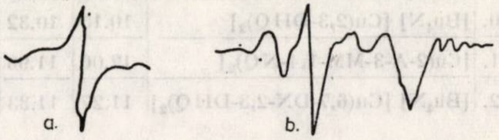

Fig. 2. — ESR spectra. *a*). $[Hg(2,3\text{-}DHQ)_2]^-$ *b*). $[Hg(6\text{-}N\text{-}2,3\text{-}DHQ)_2]^-$.

axial symmetry) was obtained in the case of the nitro-substituted complex, with $g = 2.0495$ and a total width of 95.36 gauss. The observed hyperfine structure is difficult to interpret. It may be the result of the interaction with the ^{199}Hg nucleus ($I = 1/2$), which amounts to 16.86% in natural mercury. The obtained signal is however a proof of the semiquinonic character of the ligand and is in agreement with ascribing the complex structure of a free radical stabilized through the cation.

EXPERIMENTAL

Preparation of the $[(C_4H_9)_4N]$ $[Hg(6\text{-}N\text{-}2,3\text{-}DHQ)_2]$ complex :

An amount of 0.7 g of the 6-nitro-2,3-dihydroxyquinoxaline ligand was dissolved in 5 ml of 40% aqueous solution of tetra-*n*-butylammonium hydroxide. After complete dissolution, the ligand was added to a solution consisting of 0.458 g of mercuric chloride in 5 ml distilled water and 25 ml ethanol. The system was stirred for 2 hours, then filtered, washed with distilled water and dried under vacuum. Similar preparation methods were used for the other complex compounds. The elemental chemical analysis results ar given in table 4.

TABLE 4

Elemental chemical analysis

Nr.	Compound	Analysed element							
		M%		C%		H%		N%	
		Calcd	Found	Calcd	Found	Calcd	Found	Calcd	Found
1.	$[Bu_4N]$ $[Hg(2,3\text{-}DHQ)_2]$	26.29	26.10	50,37	50.42	5.76	6.01	9.17	9.24
2.	$[Bu_4N]$ $[Hg(6\text{-}N\text{-}2,3\text{-}DHQ)_2]$	23.52	22.96	45.06	45.56	4.92	4.85	11.49	11.75
3.	$[Hg(2\text{-}A\text{-}3\text{-}MM\text{-}1,4\text{-}NQ)_2]$	30.21	29.98	39.79	39.84	2.41	3.11	4.22	4.31
4.	$[Bu_4N]$ $[Hg(6,7\text{-}DN\text{-}2,3\text{-}DHQ)_2]$	21.27	21.12	40.76	40.23	4.24	5.06	13.36	13.54
5.	$[Co(6\text{-}N\text{-}2,3\text{-}DHQ)_2]$	12.56	12.80	40.97	40.23	1.28	2.10	17.91	17.98
6.	$[Bu_4N]$ $[Co(6,7\text{-}DN\text{-}2,3\text{-}DHQ)_2]$	7.35	7.54	47.97	47.12	4.99	5.03	15.73	15.81
7.	$[Co(2\text{-}A\text{-}3\text{-}MM\text{-}1,4\text{-}NQ)_2]$	11.28	10.98	50.59	50.03	3.06	3.28	5.36	5.74
8.	$[Co(2,3\text{-}DHQ)_2]$	26.91	27.24	43.87	42.90	2.83	2.36	12.78	12.14
9.	$[Bu_4N]_2$ $[Cu(6\text{-}N\text{-}2,3\text{-}DHQ)_2]$	6.63	6.84	60.17	59.96	8.14	8.23	11.69	11.60
10.	$[Bu_4N]$ $[Cu(2,3\text{-}DHQ)_2]$	10.15	10.32	61.41	60.59	7.03	6.99	11.18	11.28
11.	$[Cu(2\text{-}A\text{-}3\text{-}MM\text{-}1,4\text{-}NQ)_2]$	12.06	11.96	50.15	51.02	3.03	2.85	5.31	6.04
12.	$[Bu_4N]$ $[Cu(6,7\text{-}DN\text{-}2,3\text{-}DHQ)_2]$	11.27	11.33	34.09	34.25	0.70	1.67	19.87	19.79

Measurements. The electronic spectra were recorded with a Zeiss Jena VSU-1 spectrophotometer, using spectral grade solvents and a 1 cm silica cell. The infrared spectra were obtained with a Zeiss Jena UR-10 spectrophotometer, the samples being pelleted in anhydrous KBr.

The polarograms were recorded with an Orion KTS Modell 7—77—4/b polarograph. The half-wave potentials were measured at room temperature, using a calomel electrode and, as measuring electrode, the dripping mercury electrode. 10^{-3} *M* solutions of the complexes were used; a $0.1M$ solution of tetra-*n*-butylammonium perchlorate was used as supporting electrolyte.

The electron spin resonance spectra were recorded with an IFA Bucureşti ART-5 spectrometer, working in the X band (9060 MHz) and having a 100 KHz modulation of the magnetic field. The spectra were obtained at room temperature using a Mn^{2+} standard ($g_3 = 2.03584$, $g_4 = 1.98040$, $H_3 = 3179.5$, $H_4 = 3268.5$).

REFERENCES

[1] A. Davison, N. Edelstein, R. H. Holm and A. H. Maki, *J. Amer. Chem. Soc.*, **85,** 2029 (1963).

[2] J. A. McCleverty, *Progr. Inorg. Chem.*, **10,** 49 (1968).

[3] A. Davison, M. Edelstein, R. H. Holm and A. H. Maki, *Inorg. Chem.*, **3,** 814 (1964).

[4] S. I. Shupack, E. Billig, R. J. H. Clark, R. Williams and H. B. Gray, *J. Amer. Chem. Soc.*, **86,** 4594 (1964).

[5] N. Mureşan, Thesis, National Institute of Chemistry, Faculty of Chemical Technology, Bucharest 1975.

[6] W. J. Geary, *Coord. Chem. Rev.*, **7,** 81 (1971).

[7] J. Camus and D. Negoiu, *Rev. Roumaine Chem.*, **24,** 673 (1979).

Revue Roumaine de Chimie, **25**, *2*, 231–236 (1980)

BASIC SALTS OF BISMUTH. I

FORMATION AND PROPERTIES OF THE BASIC BISMUTH CHLORATES

ANA NIMARĂ and I. JULEAN
Chemical Research Center, Bd. Mihai Viteazul 24, Timişoara Romania

Received June 5, 1978

The formation and the properties of the basic bismuth chlorates were followed by radiometric titration. In solution, three compounds were identified, having the combination ratio : Bi/OH/ClO$_3$ = 6/0/6 ; 6/2/4 and /6/3/3, and in the solid state only the first two were separated. On the basis of the chemical analysis and of the thermogravimetric study these compounds were formulated as : $Bi_6O_6(ClO_3)_6 \cdot 2H_2O$ and $Bi_6O_6(OH)_2(ClO_3)_4 \cdot 3H_2O$ respectively.

The hydrolysis mechanism of the bismuth ion and the structure of the basic bismuth compounds are problems which have not been completely elucidated up to now. If the latest investigations on the first stage of the hydrolysis are in agreement and lead to a polycation with a condensation degree six, the opinions regarding its composition and its structure are still divided [1-6].

As regards the concordance between the structure of the hexacondensed polycation in solution and in solid state, recent studies confirm that for certain basic salts of bismuth as perchlorates and nitrates, the hexacondensed structure existing in solution could be maintained in solid state too [7,8].

Continuing our research in the field of the bismuth ion hydrolysis, we have studied the series of the basic chlorates, which normally should have the same hexacondensed structure, considering the solubility of bismuthyl chlorate.

In literature, there is no indication about the existence of any preparation method or about the properties of the neutral or basic chlorates of bismuth. Wachter's attempts [9] to prepare bismuth chlorate starting from bismuth oxide and chloric acid failed because of the thermic decomposition of the chloric acid.

To avoid this inconvenience we used the double exchange reaction between the bismuthyl perchlorate and potassium chlorate. The reaction conditions have been thus chosen as to avoid the precipitation of the potassium perchlorate beside the basic bismuthyl chlorate.

EXPERIMENTAL

Reagents and apparatus

Bismuthyl perchlorate—$BiOClO_4 \cdot H_2O$ was prepared following the described procedure.[10] The marked bismuthyl perchlorate was prepared starting from Bi_2O_3, marked with ^{210}Bi.

Potassium chlorate — $KClO_3$ was the reagent grade. The solutions of $KClO_3$ were standardized by ClO_3^- determination.

Electronical counter "Vakutronik VAM — 16D" with "VAZ 410" G. M. tubes, pH-meter "Radiometer" with a glass electrode G 202 C and Derivatograph E. Paulik, S. Paulik and L. Erdey were used.

RESULTS AND DISCUSSION

The addition of $KClO_3$ into a bismuthyl perchlorate solution of 0.02 M concentration, slightly decreases from a pH value of 2.41 to a 2.16 reaching a ratio of $ClO_3/Bi = 0.35$ and after that the pH slightly increases. Performing the reaction between $BiOClO_4$ and $KClO_3$ in more concentrated solutions (0.1 M), but still below the concentration level at which $KClO_4$ would precipitate, a bulky precipitate separates, after a time, from solution. An analogous compound is obtained during a shorter period of time by adding NaOH into an equimolecular solution of $BiOClO_4$ and $KClO_3$.

The combination ratio was established determining the acidity resulted from reaction and the concentration of the bismuth and chlorate ions in the solution remained after the precipitation process.

The total acidity was determined from the pH-metric titration with NaOH until the first break of pH, as can be seen in figure 1.

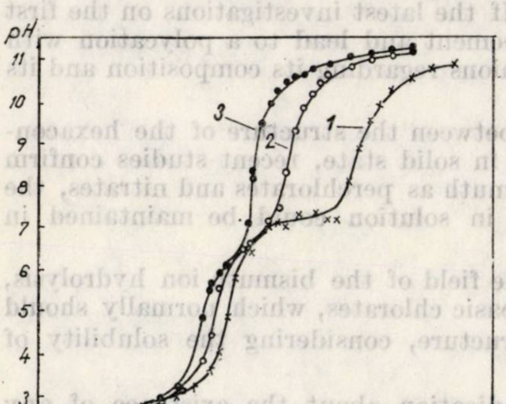

Fig. 1. — The pH-metric determination of the total acidity resulted at the separation of the basic bismuth chlorate
1 — in the moment of mixing; 2 — after 24 h; 3 — after 5 d

The number of the OH groups, Z, and the concentration of the chlorate ion, y in this basic compound related to one bismuth ion, has been calculated with the relations :

$$Z = \frac{h - 0.46\, b}{B - b}; \quad y = \frac{A - a}{B - b}$$

where h = the total hydrogen ion concentration in solution, determined from the pH-metric titration (Figure 1); 0.46 b = the acidity resulted by hydrolysis;[11,12] B = the initial concentration of bismuth; b = the free concentration of bismuth left in solution; A = the initial concentration of chlorate ion; a = the final concentration of chlorate ion.

The average values were $Z = 0.34 \pm 0.01$ and $y = 0.66 \pm 0.01$. The basic chlorate separated from solution, formulated on the basis of the above calculations corresponded to $Bi_6O_6(OH)_2\,(ClO_3)_4 \cdot n\ H_2O$.

The pH effect on the composition of the precipitate which separates from the solution was followed by radiometric titration. The results are presented in figures 2 and 3.

At 0.2 M $HClO_3$ a neutral chlorate separates from the solution with the combination ratio $BiO/OH/ClO_3 = 6/0/6$, and with increasing pH the basic compounds are formed with the ratio 6/2/4 and 6/3/3 respectively.

In solid state the neutral chlorate $Bi_6O_6(ClO_3)_6 \cdot 2H_2O$ and the basic chlorate $Bi_6O_6(OH)_2(ClO_3)_4 \cdot 3H_2O$ were isolated; the number of the crystallization water molecules was established from the thermogravimetric curves. The results of the chemical analysis are presented in table I.

TABLE 1

Chemical analysis of basic bismuth chlorates

Product	% Bi		% ClO_3	
	Theor.	Exp.	Theor.	Exp.
$Bi_6O_6(ClO_3)_6 \cdot 2H_2O$	66.45	60.86	26.55	26.48
$Bi_6O_6(OH)_2(ClO_3)_4 \cdot 3H_2O$	70.80	69.87	18.72	17.82

The deviations from the theoretical value might be due to some impurities of $KClO_4$.

The thermic behaviour of the two chlorates is presented in figures 4 and 5.

The T.G. and D.T.A. curves permitted to establish the decomposition steps and the intermediary compounds which were formed.

The decomposition of the neutral chlorate begins at 60° when it loses the crystallization water, at 180° a strong endothermic effect follows, and the chlorate decomposes forming a basic bismuth chloride which finally passes into the bismuth oxide and bismuth chloride:

$$Bi_6O_6(ClO_3)_6 \cdot 2H_2O \rightarrow Bi_6O_6(ClO_3)_6 \rightarrow Bi_6O_6Cl_6 \rightarrow 2Bi_2O_3 + 2BiCl_3$$

The basic chlorate loses the crystallization water at 60°, at 120° it loses the constitution water and a 280° at strong endothermic effect forming a stable product — basic bismuth chloride takes place.

$$Bi_6O_6(OH)_2(ClO_3)_4 \cdot 3H_2O \rightarrow Bi_6O_6(OH)_2(ClO_3)_4 \rightarrow Bi_6O_7(ClO_3)_4 \rightarrow Bi_6O_7Cl_4$$

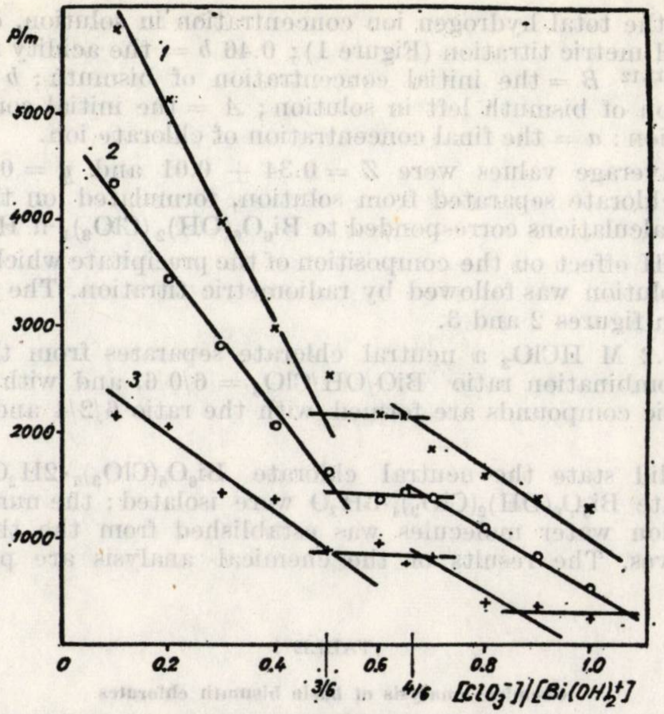

Fig. 2. — Radiometric titration 0.2 M $BiOClO_4$, with 0.2 M $KClO_3$, pH = 2.5

1 — 3 hrs ; 2 — 24 hrs ; 3 — 5 d

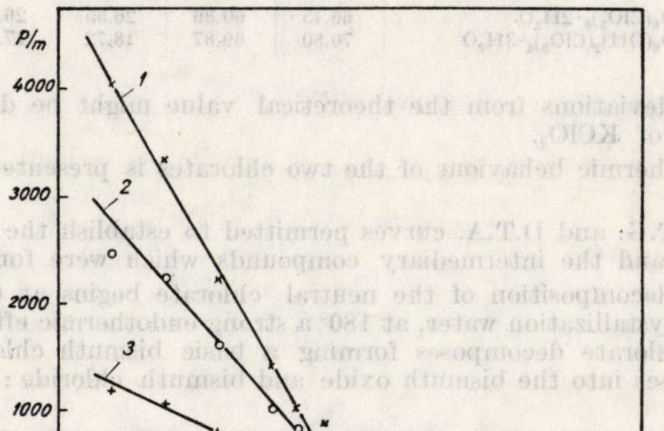

Fig. 3. — Radiometric titration 0.2 M $BiOClO_4$ with 0.2 M $KClO_3$, pH = 2.87.

1 — 2 hrs ; 2 — 24 hrs ; 3 — 5 d

In conclusion the basic products of the bismuth polycation hydrolysis both in solution and in solid state can be obtained. In solid state the basic salts are insoluble in water.

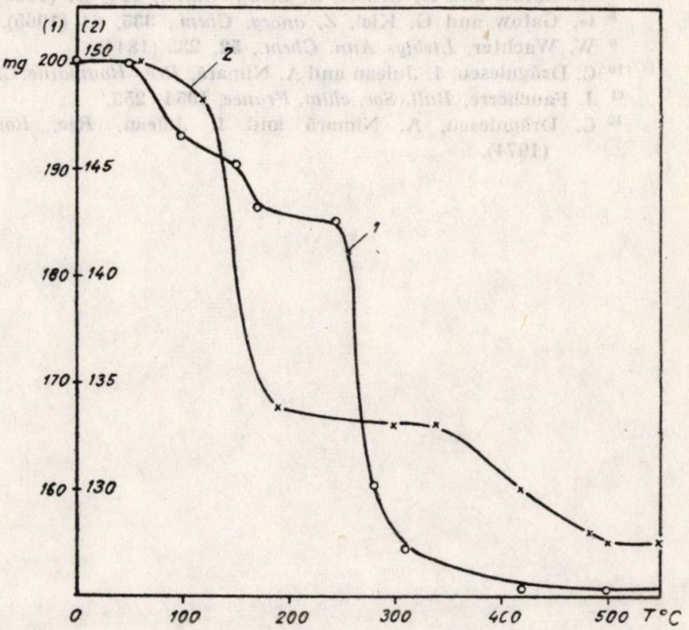

Fig. 4. — Thermogravimetric curves
1 — $Bi_6O_6(OH)_2(ClO_3)_4 \cdot 3H_2O$;
2 — $Bi_6O_6(ClO_3)_6 \cdot 2H_2O$.

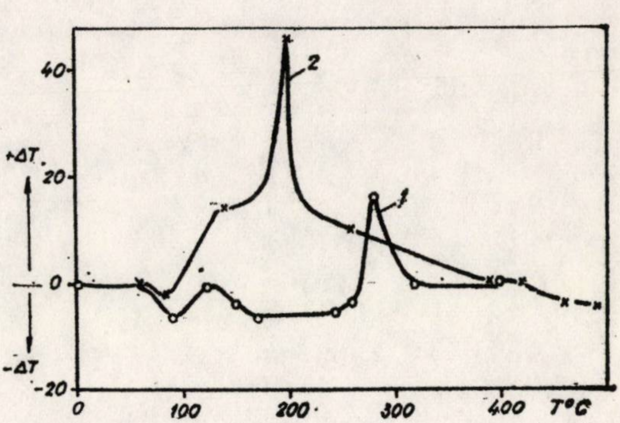

Fig. 5. — Diferential thermal analysis curves
1 — $Bi_6O_6(OH)_2(ClO_3)_4 \cdot 3H_2O$;
2 — $Bi_6O_6(ClO_3)_6 \cdot 2H_2O$.

REFERENCES

[1] A. Olin, *Acta Chem. Scand.*, **11**, 1445 (1957).
[2] H. A. Levy, M. D. Danforth and P. A. Agron, *J. Chem. Phys.*, **31**, 1458 (1959).
[3] V. A. Maroni and T. G. Spiro, *J. Amer. Chem. Soc.*, **88**, 1410 (1966), *Inorg. Chem.*, **7**, 1 (1968).

[4] R. S. Tobias, *J. Amer. Chem. Soc.*, **82**, 1070 (1959) ; **82**, 3244 (1960).
[5] R. W. Holmberg, K. A. Kraus and J. S. Johnson, *J. Amer. Chem. Soc.*, **78**, 506 (1956).
[6] J. S. Johnson, G. Scatchard and K. A. Kraus, *J. Phys. Chem.*, **63**, 787 (1959).
[7] G. Gatow and D. Schott, *Z. anorg. Chem.*, **324**, 31 (1963).
[8] G. Gatow and G. Kiel, *Z. anorg. Chem.*, **335**, 61 (1965).
[9] W. Wachter, *Liebigs Ann. Chem.*, **52**, 233 (1844).
[10] C. Drăgulescu, I. Julean and A. Nimară, *Rev. Roumaine Chim.*, **14**, 189 (1969).
[11] J. Faucherre, *Bull. Soc. chim. France*, **1954**, 253.
[12] C. Drăgulescu, A. Nimară and I. Julean, *Rev. Roumaine Chim.*, **19**, 1455 (1974).

Revue Roumaine de Chimie, **25**, *2*, 237–244 (1980)

SOME REACTIONS WITH ARYLIDENE MALONIC ACID AND DIETHYL ARYLIDENE MALONATE

M. M. MOHAMED, M. A. EL HASHASH, M. Y. EL KADY and M. A. HASSAN

Faculty of Science, Ain Shams University, Cairo, Abbassia, Egypt

Received December 5, 1977

Acid **1**a reacted with malononitrile, ethyl cyanoacetate, cyanoacetic acid and ethyl acetoacetate and gave the compounds **2, 3, 4** and **5**. Diethyl arylidene malonates **1**(b–e) reacted with hydrazine hydrate, phenylhydrazine and semicarbazide hydrochloride and gave the corresponding azines **6**(a–d) and malonic acid dihydrazide **7**; aldehyde phenylhydrazone **8**(a–d) and β, β-malonyl-α-phenylhydrazine (**9**); aldehydes semicarbazones **10** (a–d) and dicarbamoylmalonic acid dihydrazide (**11**) respectively. The effect of compounds **2, 3, 6–10**, on the growth of some pathogenic micro-organisms has been investigated.

On analogy of the recently reported reaction of chalcones with malononitrile[1], acid **1**a condenses with malononitrile in the presence of ammonium acetate at 100° yielding 6-amino-5-cyano-2-oxo-4-phenyl-1,2,3,4-tetrahydronicotinamide (**2**).

Structure **2** was proved from the following :

i) Its infrared spectrum showed $\nu(C = O)$ of primary amide at 1650 cm^{-1}, $\nu(C \equiv N)$ at 2240 cm^{-1} and $\nu(NH)$ with chelated $\nu(OH)$ in the region 3300–3200 cm^{-1}.

ii) The N.M.R. spectrum of 2 in $(CD_3)_2SO$ showed signals at δ 1.2 ppm (d) for one proton, δ 1.8 ppm (d) for another proton, a broad absorption centered about δ 4.4 ppm for 3 NH protons, δ 4.9 ppm(s) for two protons of $CONH_2$ and δ 7.4 ppm (m) for the five aromatic protons.

Acid **1**a reacts with ethyl cyanoacetate in the presence of ammonium acetate and boiling *n*-butanol yielding α-cyanocinnamamide (**3**). Structure **3** was proved from the following :

i) Its infrared spectrum showed $\nu(C = O)$ of primary amide at 1650 cm^{-1}, $\nu(C = C)$ at 1600 cm^{-1} and $\nu(C \equiv N)$ at 2230 cm^{-1}.

ii) The N.M.R. spectrum of compound **3** in $(CD_3)_2SO$ showed a broad absorption centered about δ 3.4–3.5 ppm corresponding to two protons of the $CONH_2$ group, the olefinic proton at δ 7.55 ppm (s) and a multiplet at δ 7.25 ppm corresponding to the five aromatic protons.

On the other hand, the reaction of acid **1**a with cyanoacetic acid in the presence of ammonium acetate and boiling *n*-butanol afforded an oily product which on hydrolysis with alcoholic potassium hydroxide yielded 3-phenylglutaric acid (**4**). The reaction can be explained by assuming initial Michael addition of cyanoacetic acid to the olefinic double bond of **1a** followed by hydrolysis and then by decarboxylation.

Structure **4** was confirmed from the following:

i) Compound **4** is soluble in aqueous sodium carbonate solution.

ii) The infrared spectrum of **4** showed ν(C=O) of acid at 1700 cm^{-1} and ν(OH) (bonded) at 3100—2890 cm^{-1}.

Similarly, ethyl acetoacetate added to acid **1a** in the presence of ammonium acetate and boiling *n*-butanol yielding 2-methyl-6-oxo-4-phenyl-1,4,5,6-tetrahydronicotinamide (**5**).

One possible approach to explain the formation of **5** *via* the action of ethyl acetoacetate on **1a** is the assumption that the reactants underwent Michael addition followed by cyclisation.

The infrared spectrum of **5** showed bands attributable to ν(C = O) of primary amide at 1640 cm^{-1} and ν(NH) chelated with ν(OH) at 3240—3140 cm^{-1}.

The N.M.R. spectrum of **5** shows the following signals when run in $(CD_3)_2SO$: at δ 0.9 ppm (s) corresponding to three protons of CH_3 group, δ 1.3 ppm (t) of the methine proton, at δ 2.1 ppm (d) corresponding to two protons of the methylene group, a broad absorption centered about δ 4.8 ppm corresponding to two protons of the NH_2 group and at δ 7.5 ppm (m) corresponding to the five aromatic protons.

On the analogy of the recently reported reaction of diethyl arylidene malonates and hydrazines,[2,3] diethyl arylidene malonates **1**(b—e) react iwith excess hydrazine hydrate in ethanol at room temperature and give the corresponding azines **6**(a—d) and malonic acid dihydrazide (**7**).

Structures **6** were established from the following assignments:

i) Their infrared spectra revealed the presence of ν(C = N) at 1640 cm^{-1}.

ii) Compounds **6**(a—d) were also obtained by the reaction of the corresponding aldehyde with hydrazine hydrate which was identified by melting points and mixed melting points.

Similarly, structure **7** was established by the reaction of hydrazine hydrate with diethyl malonate which was, then, identified by melting points and mixed melting points.

Phenylhydrazine reacts with diethyl arylidene malonates **1**(b—e) in ethanol at room temperature to give a mixture of the corresponding aldehyde phenylhydrazone **8**(a—d), and β,β-malonyl-α-phenylhydrazine (**9**). Structures **8** were established from the following:

i) The infrared spectra of compounds **8** showed absorption bands attributable to ν(C = N) at 1660 cm^{-1} and ν(NH) at 3340 cm^{-1}.

ii) Compounds **8** were also obtained by the reaction of the corresponding aldehyde with phenylhydrazine and then by comparison of the melting points and mixed melting points of the resulting products with those of compounds **8**.

Compound **9** was also prepared by the reaction of phenylhydrazine with diethyl malonate and was identified by melting points and mixed melting points.

Semicarbazide hydrochloride reacts with diethyl arylidene malonates **1**(b—e) in pyridine and give a mixture of the corresponding aldehyde semicarbazone **10**(a—d) and dicarbamoyl malonic acid dihydrazide (**11**).

Structures **10** and **11** were proved from the following evidence :

i) The infrared spectra of **10** exhibit strong absorption bands due to ν(C = N) at 1650–1640 cm^{-1}, ν(C=O) at 1670–1660 cm^{-1} and ν (NH) at 3400–3350 cm^{-1}. On the other hand, the infrared spectrum of **11** revealed absorption bands attributable to ν(C = O) at 1680–1660 cm^{-1} and to ν(NH) at 3400–3350 cm^{-1}.

ii) Compounds **10** and **11** were prepared by reaction of the corresponding aldehyde or diethyl malonate with semicarbazide hydrochloride and then identified by melting points and mixed melting points.

All the above reactions are represented in the following chart.

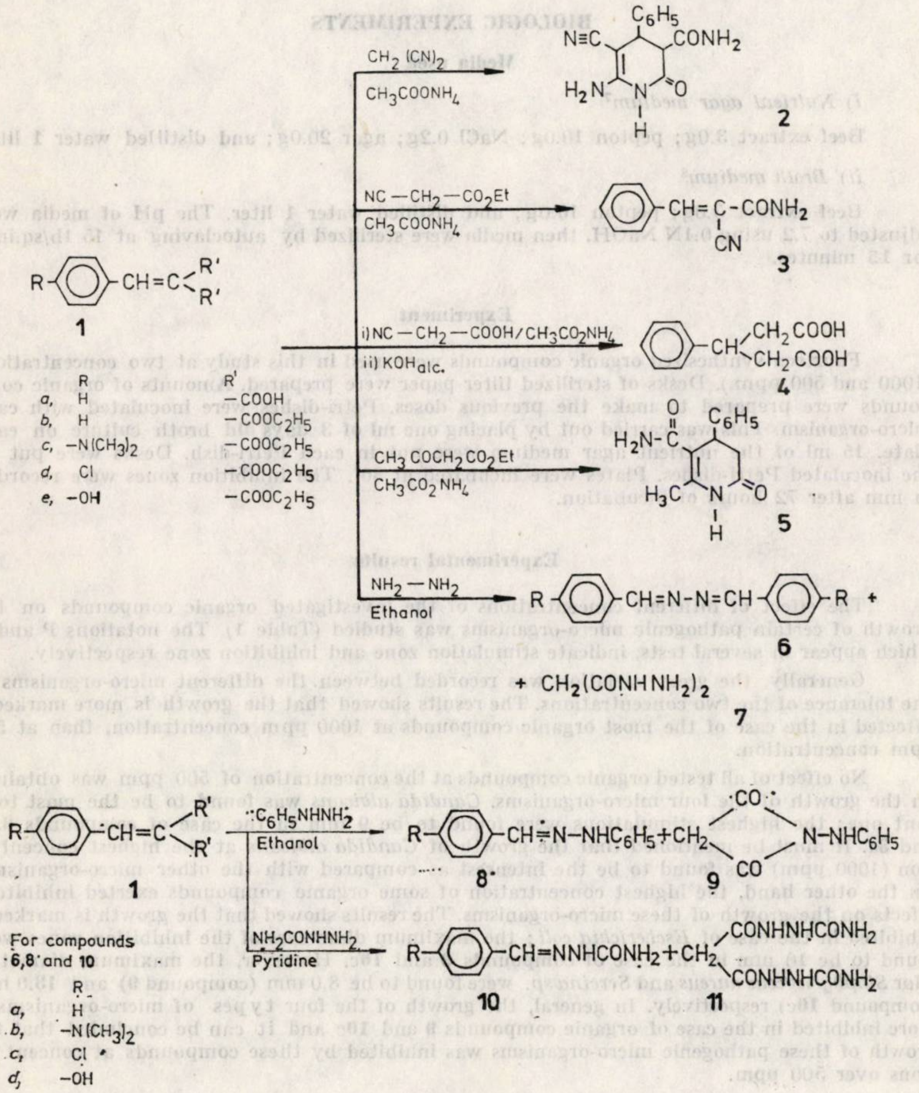
CH2 (CN)2
CH3COONH4
2
NC—CH2—CO2Et
CH3COONH4
3
1
i) NC—CH2—COOH/CH3CO2NH4
ii) KOH alc.
4
R R'
a, H —COOH
b, H —COOC2H5
c, —N(CH3)2 —COOC2H5
d, Cl —COOC2H5
e, —OH —COOC2H5
CH3COCH2CO2Et
CH3CO2NH4
5
NH2—NH2
Ethanol
6
+ CH2(CONHNH2)2
7
C6H5NHNH2
Ethanol
1
8
9
NH2CONHNH2
Pyridine
10
11
For compounds 6,8 and 10
R
a, H
b, —N(CH3)2
c, Cl
d, —OH

Effect of certain synthesized compounds on the growth of some pathogenic micro-organisms.

Recently, arylidene malonic acid esters have become compounds of increasing importance due to their antibatic action against *Aspergillus onyzae*, *Willia anomala* and *Saccharomyces cerevisiae*.[4] Several benzylidene and related compounds were tested for toxicity towards parasitic fungitoxicity.[5] In this study, we try to report the effect of certain synthesized organic compounds (**2**, **3**, **6**—**10**) on the growth of some pathogenic micro-organisms,[6] namely: *Staphylococcus aureus*, *Escherichia coli*, *Candida albicans* and *Sarcina sp.*

BIOLOGIC EXPERIMENTS

Media used

i) Nutrient agar medium[7]

Beef extract 3.0g; pepton 10.0g; NaCl 0.2g; agar 20.0g; and distilled water 1 liter.

ii) Broth medium[8]

Beef extract 5.0g; pepton 10.0g; and distilled water 1 liter. The pH of media were adjusted to 7.2 using 0.1N NaOH, then media were sterilized by autoclaving at 15 1b/sq.inch for 15 minutes.

Experiment

Fourteen synthesized organic compounds were used in this study at two concentrations (1000 and 500 ppm.). Desks of sterilized filter paper were prepared. Amounts of organic compounds were prepared to make the previous doses. Petri-dishes were inoculated with each micro-organism. This was carried out by placing one ml of 3 days old broth culture on each plate. 15 ml of the nutrient agar medium were put in each Petri-dish. Desks were put on the inoculated Petri-dishes. Plates were incubated at 30°. The inhibition zones were recorded in mm after 72 hours of incubation.

Experimental results

The effect of different concentrations of the investigated organic compounds on the growth of certain pathogenic micro-organisms was studied (Table 1). The notations P and I, which appear in several tests, indicate stimulation zone and inhibition zone respectively.

Generally, the great variation was recorded between the different micro-organisms in the tolerance of the two concentrations. The results showed that the growth is more markedly affected in the case of the most organic compounds at 1000 ppm concentration, than at 500 ppm concentration.

No effect of all tested organic compounds at the concentration of 500 ppm was obtained on the growth of the four micro-organisms. *Candida albicans* was found to be the most tolerant one; the highest stimulations were found to be 9 mm in the case of compounds **3**,**6c** and **8a**. It must be mentioned that the growth of *Candida albicans* at the highest concentration (1000 ppm) was found to be the intensest as compared with the other micro-organisms. On the other hand, the highest concentration of some organic compounds exerted inhibitory effects on the growth of these micro-organisms. The results showed that the growth is markedly inhibited in the case of *Escherichia coli*; the maximum diameters of the inhibition zones were found to be 10 mm in the case of compounds **9** and **10c**. However, the maximum diameters I for *Staphylococcus aureus* and *Sercina sp.* were found to be 8.0 mm (compound **9**) and 13.0 mm (compound **10c**) respectively. In general, the growth of the four types of micro-organisms is more inhibited in the case of organic compounds **9** and **10c** and it can be concluded that the growth of these pathogenic micro-organisms was inhibited by these compounds at concentrations over 500 ppm.

TABLE 1

Effect of certain synthetic organic compounds on the growth of some pathogenic micro-organisms

Org. Compd.	Pathogenic micro-organisms							
	Staphylococcus aureus		*Escherichia coli*		*Candida albicans*		*Sercina sp.*	
	Organic compounds concentrations, ppm							
	1000	500	1000	500	1000	500	1000	500
	Average of inhibition and stimulation zones in mm*							
2	—	—	—	—	I 7.0	—	—	—
3	—		—	—	P 9.5	—	—	—
6a	P 6.0	—	—	—	—	—	—	—
6b	—	—	—	—	—	—	—	—
6c	—	—	—	—	P 9.0	—	I 6.0	—
7	—	—	—	—	—	—	—	—
8a	—	—	—	—	P 9.0	—	—	—
8b	—	—	—	—	P 7.0	—	—	—
8c	—	—	—	—	—	—	—	—
9	I 8.0	—	I 10.0	—	P 7.0	—	—	—
10a	I 6.0	—	I 7.0	—	—	—	I 6.0	—
10b	—	—	—	—	—	—	—	—
10c	—	—	I 10.0	—	P 5.5	P 11.0	I 13.0	—
10d	—	—	—	—	P 5.5	—	—	—

*** P = stimulation zone ; I = inhibition zone.**

EXPERIMENTAL

The infrared absorption spectra were determined with a Unicam SP 1200 Spectrophotometer using KBr Wafer technique ; the NMR spectra were determined with a Varian VN 1009 (s— 60 T) instrument ; positions of peaks are expressed in δ values (ppm) from TMS as internal standard.

Condensation of acid **1**a *with malononitrile. Formation of 6-amino-5-cyano-2-oxo-4-phenyl-1,2,3,4-tetrahydronicotinamide* (**2**).

A mixture of the acid **1**a (1.93 g; 0.01 mole), malononitrile (1.32 g; 0.02 mole) and ammonium acetate (2.31g; 0.03 mole) was heated at 100° on a water bath for 6 hours, and then allowed to cool. The product obtained was washed with water, dried and then crystallized from acetic acid to give **2** as yellowish brown crystals; m.p. 250°; yield 46%. Found : C, 60.90 ; H, 4.60 ; N,21.60 ; $C_{13}H_{12}N_4O_2$ requires : C, 60.93 ; H,4.72 ; N, 21.87%.

Condensation of acid **1**a *with ethyl cyanoacetate. Formation of α-cyanocinnamamide* (**3**).

A solution of the acid **1**a (1.93g ; 0.01 mole) in 50 ml *n*-butanol was heated with ethyl cyanoacetate (2.26 g; 0.02 mole) and ammonium acetate (2.31 g; 0.03 mole) for 5 hours. The excess *n*-butanol was removed by steam distillation. The reaction mixture was treated with ether and the ethereal layer was left to evaporate at room temperature. The solid separated was crystallized from benzene to give **3** as colourless crystals; m.p. 123°; yield 73%. Found : C, 69.60 ; H,4.60 ; N, 16.00 ; $C_{10}H_8N_2O$ requires : C, 69.76 ; H, 4.65 ; N, 16.27%

Condensation of acid **1a** *with cyanoacetic acid. Formation of 3-phenyl glutaric acid* **(4)**.

A mixture of the acid **1a** (1.93g; 0.01 mole), cyanoacetic acid (1.70 g; 0.02 mole) and ammonium acetate (2.31 g; 0.03 mole) was refluxed in boiling *n*-butanol (50 ml) for 6 hours. The reaction mixture was poured into 200 ml water and the excess *n*-butanol was removed by steam distillation. The aqueous medium was treated with ether and the ethereal layer was left to evaporate at room temperature. The residual oil formed was treated with alcoholic potassium hydroxide (20%) and refluxed for an hour. The reaction mixture was poured into crushed ice and acidified with hydrochloric acid. The solid obtained was filtered off, dried and then crystallized from chlorobenzene to give **4** as colourless crystals; m.p. 140°; yield 80%. Found : C, 63.50 ; H, 5.90 ; $C_{11}H_{12}O_4$ requires : C, 63.45 ; H, 5.81%.

Condensation of acid **1a** *with ethyl acetoacetate. Formation of 2-methyl-6-oxo-4-phenyl-1,4,5,6-tetrahydronicotinamide* **(5)**.

A mixture of the acid **1a** (1.93g; 0.01 mole), ethyl acetoacetate (2.60 g; 0.02 mole) and ammonium acetate (2.31g; 0.03 mole) in *n*-butanol (50 ml) was refluxed for 6 hours. The excess *n*-butanol was removed by steam distillation. The reaction mixture was treated with ether and the ethereal layer was left to evaporate at room temperature. The solid separated was crystallized from light petrol (100—120°) to give **5** as colourless crystals; m.p. 152°; yield 51%. Found : C, 67.80 ; H, 6.10 ; N, 12.20 ; $C_{13}H_{14}N_2O_2$ requires : C, 67.81 ; H, 6.13 ; N, 12.17 %.

Reaction of diethyl arylidene malonates **1** *(b—e) with hydrazine hydrate. Formation of the azines* **6** *(a—d) and malonic acid dihydrazide* **(7)**.

To a solution of each **1b**, **1c**, **1d**, or **1e** (0.01 mole) in ethanol (20 ml), hydrazine hydrate (2 ml; 85%) was added and the mixture was left at room temperature (20°) for one hour. The solids separated were filtered off and fractionally crystallized from the suitable solvent to give the corresponding azines, **6** a—d, as yellow crystals and malonic acid dihydrazide **(7)** as colourless crystals.

Preparation of the authentic samples of **6a**—*d*.

Solutions of benzaldehyde, *p*-dimethylaminobenzaldehyde, *p*-chlorobenzaldehyde or *p*-hydroxybenzaldehyde (0.01 mole) in ethanol (10 ml) were treated with hydrazine hydrate (1.60 g; 0.05 mole), the mixtures were heated on water bath for one hour. The solids separated after cooling were crystallized from the suitable solvent to give crystals, identified as **6a**, **6b**, **6c**, and **6d** by m.p. and mixed m.p. determinations. The results are listed in table 2.

Preparation of the authentic sample of **7**.

A solution of diethyl malonate (0.01 mole) in ethanol (10 ml) was treated with hydrazine hydrate (0.02 mole), the reaction mixture was refluxed on a water bath for one hour. The solid separated on cooling was filtered off and crystallized from light petrol (60—80°) to give crystals, identified as **7**, by melting point and mixed melting point determinations. The results are listed in table 2.

Aldehyde phenylhydrazones **8**(*a—d*) *and* β,β*-malonyl-*α*-phenylhydrazine* **(9)**.

A solution of each of the diethyl arylidene malonate **1**(b—e) (0.01 mole) in ethanol (20 ml) was treated with phenylhydrazine (2.16g; 0.02 mole). The solution was left at room temperature (20°) for one hour. The solid separated was filtered off and fractionally crystallized from the suitable solvent to give the corresponding aldehyde phenylhydrazone **8** (a—d). The results are listed in table 2.

Preparation of the authentic samples of **8**(a—d).

Solutions of benzaldehyde, *p*-dimethylaminobenzaldehyde, *p*-chlorobenzaldehyde or *p*-hydroxybenzaldehyde (0.01 mole) in ethanol (10 ml) were treated with phenylhydrazine (1.08g; 0.01 mole). The mixtures were heated on water bath for one hour. The solids separated on cooling were crystallized from the suitable solvent to give crystals identified as **8** (a—d) by melting point and mixed melting point determinations. The results are listed in table 2.

Preparation of the authentic sample of **9**.

A solution of diethyl malonate (1.60 g; 0.01 mole) in ethanol (10 ml) was treated with phenylhydrazine (2.16g; 0.02 mole). The mixture was left at room temperature for one hour. The solid separated was filtered off and crystallized from the suitable solvent to give crystals, identified as **9** by melting point and mixed melting point determinations. The results are listed in table 2.

Reaction of diethyl arylidene malonate **1** *(b–e) with semicarbazide hydrochloride. Formation of aldehyde semicarbazones* **10** *(a–d) and dicarbamoyl malonic acid dihydrazide* **(11).**

A solution of each diethyl arylidene malonate **1** (b–e) (0.01 mole) in pyridine (30 ml) was treated with semicarbazide hydrochloride (2.23g; 0.02 mole). The mixture was heated for two hours, cooled and then poured into ice/HCl mixture. The solid separated was filtered off, washed several times with water and then fractionally crystallized from the suitable solvent to give the corresponding aldehyde semicarbazone **10** (*a–d*) and dicarbamoyl malonic acid dihydrazide **(11).** The results are listed in table 2.

TABLE 2

Products from the reaction of hydrazines and semicarbazide hydrochloride with 1 (b-e)

Compound	m.p.° *	Colour	Yield %
6a	90	colourless	57
6b	249	yellow	55
6c	192–3	yellow	69
6d	239–40	colourless	73
7	154	colourless	22
8a	158	colourless	57
8b	148	yellow	59
8c	127	colourless	52
8d	130	colourless	55
9	128	colourless	32
10a	224	colourless	66
10b	222	colourless	71
10c	232–3	colourless	70
10d	223–5	colourless	54
11	55	colourless	18

* Recrystallization solvent : ethanol

Preparation of the authentic samples of **10** *(a–d) and* **11.**

Solutions of benzaldehyde, *p*-dimethylaminobenzaldehyde, *p*-chlorobenzaldehyde and *p*-hydroxybenzaldehyde or diethyl malonate (0.01 mole) in pyridine (20 ml) were heated for two hours with semicarbazide hydrochloride (0.01 mole). The mixtures were poured into ice/HCl mixture and the solids separated were filtered off, washed several times with water and then crystallized from the suitable solvent to give crystals identified as **10** (a–d) and **11** by melting point and mixed melting point determinations. The results are listed in table 2.

REFERENECES

[1] A. Sammour, Y. Akhnoukh and H. Jahine, *U.A.R.J. Chem.*, **13**, 421 (1970).

[2] W. Gustowski and J. Lange, *Roczniki Chem.*, **36**, 163 (1962); *Chem. Abstr.*, **57**, 14995 (1962).

[3] H. Braeuniger and K. Breuer, *Pharm. Zentralh*, **1968**, 107 57983 (Ger.); *Chem. Abstr.*, **70**, 77477 (1969).

[4] K. Nakamura, *Rikagaku Kenkysho Hakoku* **35**, 151 (1959); *Chem. Abstr.*, **54**, 21336 (1960).

[5] J. D. Edwards and M. Pianka, *J. Sci. Food Agr.*, **14**, 55 (1963); *Chem. Abstr.*, **59**, 5048 (1963).

[6] O. V. Allen, "Experimentals in Soil Bacteriology", Burgess Publ. Co., 1961.

[7] "Difco Manual of Dehydrated Culture Media and Reagents", *9th* Ed: 32. Difco Laboratories, Detroit, Michigan, U.S.A, 1972.

[8] J. B. Walter and M. S. Israel, "General Pathology", *4th* Edition, Churchill Livingstone, Edinburgh, 1974.

Revue Roumaine de Chimie, **25**, *2*, 245–251 (1980)

NEW INDOLE DERIVATIVES WITH BIOLOGICAL ACTIVITY

C. SÂRBU, NORA RĂDULESCU, MARIANA IONESCU, SOFIA NEGRIȚESCU,
CORNELIA IOAN, NICULINA BOEŞTEANU and M. SIMIONOVICI
Central Chemical Research Institute,
Chemical and Pharmaceutical Research Institute,
Bucharest, Sos. Vitan, 112, Romania

Received September 27, 1977
Revised July 2, 1979

A number of new 2-methyl-3-ethyl-substituted indoles have been obtained by Fischer synthesis. 5-Dialkylamino-2-pentanones, 5-methoxy-2-pentanone as well as 2-methyl-2-(3′-methoxy-propyl)1,3-dioxolan were used as carbonyl containing components while phenylhydrazine hydrochloride and 4-chloro-benzoic acid-2-formyl-1-(4-methoxy-phenyl) hydrazide were used as phenylhydrazinic components. Data concerning the preparation method, the properties, the U.V. and I.R. spectra of the compounds are presented. The new compounds showed anticholinergic, analgesic, peripheral vasodilatory and antiinflammatory activity.

2-Methyl-3-ethyl substituted indoles of the general formula (I) have various and interesting pharmacological properties.

Y = H ; Hlg ; alkyl ; aryl ; alcoxy ; acyl
R_1 = amino ; carboxyl
R_2 = H ; alkyl ; acyl

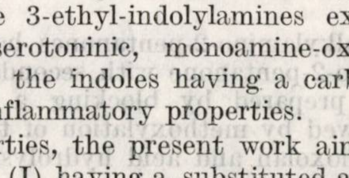

I

The substituent in position 3 decides to a great extent the type of the pharmacological activity. Thus the 3-ethyl-indolylamines exhibit especially tranquilising, sedative, antiserotoninic, monoamine-oxidase inhibitory, hypotensive activities, while the indoles having a carboxyl group reveal antipyretic, analgesic, antiinflammatory properties.

Concerning these interesting properties, the present work aims to synthesize new indole derivatives of type (I) having a substituted amino group or a methoxy group as R_1.

The new derivatives have been prepared by Fischer synthesis which implies the reaction of a carbonylic compound with phenylhydrazinic derivatives followed by cylisation of the arylhydrazone in acid catalysis :

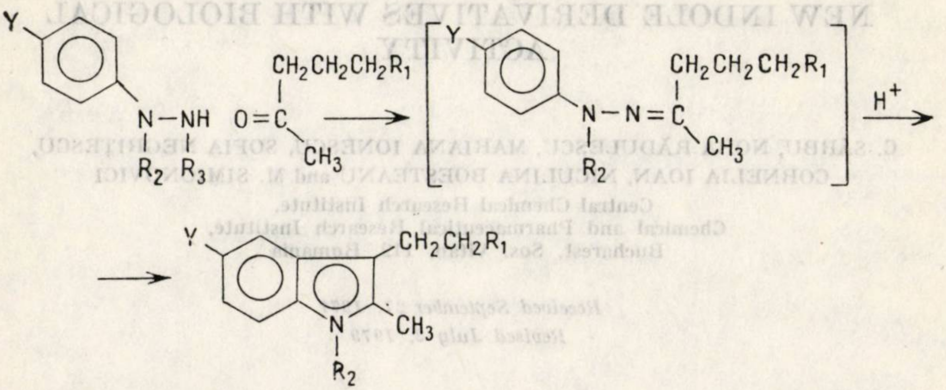
Y
N−NH
R2 R3
O=C
CH2CH2CH2R1
CH3
N−N=C
R2
H+
CH2CH2R1
N
CH3

$Y = H ; OCH_3$

$R_1 = N(C_2H_5)_2 ; \quad N(nC_3H_7)_2 ; \quad N(nC_4H_9)_2 ; \quad NC_2H_5(CH_2CH_2OH) ; \quad OCH_3$

$R_2 = H ; \ p-Cl-C_6H_4-CO$

$R_3 = H ; CHO$

The carbonylic derivatives have been obtained starting from 5-halo-2-pentanone by the following sequence of reactions :

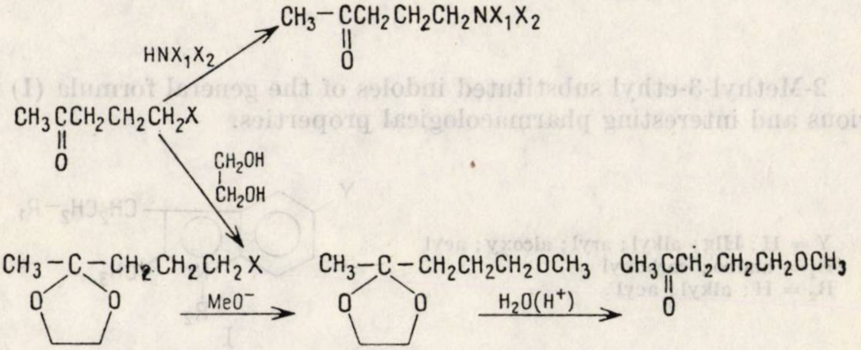
CH3−CCH2CH2CH2NX1X2
O
HNX1X2
CH3CCH2CH2CH2X
O
CH2OH
CH2OH
CH3−C−CH2CH2CH2X
MeO−
CH3−C−CH2CH2CH2OCH3
H2O(H+)
CH3CCH2CH2CH2OCH3
O

$X = Cl ; Br$

$X_1,X_2 = CH_3 ; C_2H_5 ; CH_2CH_2OH ; nC_3H_7 ; nC_4H_9$

5-Dialkylamino-2-pentanones have been prepared by the reaction of a 5-halo-2-pentanone with secondary amines while 5-methoxy-2-pentanone was prepared by blocking a 5-halo-2-pentanone with ethylene-glycol followed by methoxylation of the resulting 2-methyl-2-(3′-chloro-propyl) 1,3-dioxolan and acid hydrolysis of 2-methyl-2-(3′-methoxy-propyl) 1,3-dioxolan.

Phenylhydrazine hydrochloride and 4-chloro-benzoic acid 2-formyl-1-(4-methoxy-phenyl) hydrazide were used as phenylhydrazinic components.

Table 1 presents phenylhydrazinic and carbonylic components, the formula of the new indole derivatives, some short indications concerning reaction conditions, the method used for the separation of the products and the yields.

Some properties of the indole derivatives namely melting points, t.l.c. R_f values, the absorption maxima (λ_{max}) and the molar extinction coefficients (log ε) in electronic spectra are given in table 2.

The new compounds were analysed for the C, H, N, Cl content and the results agree within $\pm$ 0.4% with the calculated values. The compounds marked with an asterisk in table 2 are mentioned in the literature[1–5] but only few data concerning physical constants are available and the preparation method is different.

The I.R. spectra of the indole derivatives are in good agreement with the assigned formula. Table 3 presents the most important characteristic vibrations of I.R. spectra.

The N—H stretching vibration observed at 3200 cm^{-1} in the compounds of the A type, the associated O—H stretching vibrations at 3300 to 3400 cm^{-1} in the compounds A_2, C_2, the symmetrical and antisymmetrical stretching vibrations of the methyl group at 2900 cm^{-1} in all of the compounds, the characteristic stretching vibration of $C = O$ bond at 1690 cm^{1-} in the compounds of the C type, the bands which occurred at 1590 to 1630 cm^{-1} proving the aromaticity of the indolic nucleus in all derivatives are only some of the I.R. characteristic vibrations[6,7] which confirm the proposed structure of the new compounds.

The eleven synthesized indoles have been submitted to a primary pharmacological screening which emphasized anticolinergic, analgesic, peripheral vasodilatory and antiinflammatory activities.

EXPERIMENTAL

5-Chloro-2-pentanone and *5-bromo-2-pentanone* were prepared starting from α-acetyl-γ-butyrolactone and aq. hydrochloric or hydrobromic acid using a method established in our laboratory[8,9]: 5-chloro-2-pentanone b.p. 80—82°/30 mm, 5-bromo-2-pentanone b.p. 83—84°/15—16 mm.

2-Methyl-2-(3′-chloro-propyl)1,3 dioxolan was prepared from 5-chloro-2-pentanone with ethylene-glycol in benzenic soln and acid catalysis[10]: b.p. 80—82°/12 mm, n_{D}^{22} 1.4490[11,12].

2-Methyl-2-(3′-methoxy-propyl)1,3-dioxolan was prepared starting from 2-methyl-2-(3′-chloro-propyl) 1,3-dioxolan and sodium methoxide; b.p. 81—85°/15—17 mm, n_{D}^{24} 1.4265.

5-Methoxy-2-pentanone was obtained by acid hydrolysis of 2-methyl-2-(3′-methoxy-propyl) 1,3-dioxolan in a similar way to that described for other 5-alkoxy-2-pentanones:[13] b.p. 97°/35 mm, n_{D}^{20} 1.4148, semicarbazone m.p. 119° [14].

5-Diethylamino-2-pentanone and *5-ethyl-(β-hydroxyethyl)-amino-2-pentanone* were prepared from 5-chloro-2-pentanone and the corresponding amines by a convenient method established in our laboratory:[15,16] 5-diethylamino-2-pentanone b.p. 55—57°/3 mm, n_{D}^{22} 1.4362;[17] 5-ethyl-(β-hydroxyethyl) amino-2-pentanone: b.p. 98—100° /0.6 mm, n_{D}^{24} 1.4589.[18]

5-Dipropylamino-2-pentanone: b.p. 127—130°/30 mm, *5-Dibutylamino-2-pentanone* b.p. 119—123°/7—8 mm and *5-methyl-cyclohexylamino-2-pentanone:* b.p. 134—136°/10—11 mm were prepared starting from 5-bromo-2-pentanone and the corresponding amines.

Phenylhydrazine hydrochloride m.p. 225° and *4-chlorobenzoic acid 2-formyl-1-(4-methoxy-phenyl)hydrazide*, m.p. 100—104° intermediates in synthesis of other antiinflammatory drugs were used without further purifications.

TABLE 1

Reaction and separation conditions

Reaction partners		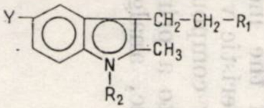			Reaction conditions			Method for product separation	Yield %
Ph-hydrazinic component	Carbonylic component	Y	R_1	R_2	Solvent	time h	temp. °C		
$C_6H_5-NH-NH_2\cdot HCl$	$CH_3CO(CH_2)_3N(C_2H_5)_2$	H	$-N(C_2H_5)_2$	H	EtOH	8	78	precipitation as hydrochloride	50
	$CH_3CO(CH_2)_3N\begin{smallmatrix}CH_2CH_2OH\\C_2H_5\end{smallmatrix}$	H	$-N\begin{smallmatrix}CH_2CH_2OH\\C_2H_5\end{smallmatrix}$	H	EtOH	8	78	—,,—	41
	$CH_3CO(CH_2)_3N(nC_3H_7)_2$	H	$-N(nC_3H_7)_2$	H	*i*PrOH	2	97	—,,—	70
	$CH_3CO(CH_2)_3N(nC_4H_9)_2$	H	$-N(nC_4H_9)_2$	H	*i*PrOH	2	97	—,,—	65
	$CH_3CO(CH_2)_3N\begin{smallmatrix}C_6H_{11}\\CH_3\end{smallmatrix}$	H	$-N\begin{smallmatrix}C_6H_{11}\\CH_3\end{smallmatrix}$	H	*i*PrOH	2	97	—,,—	74
	$CH_3CO(CH_2)_3-OCH_3$	H	$-OCH_3$	H	*i*PrOH	2	97	sepn. on neutral Al_2O_3 chrom. col.	20
$pCH_3O-C_6H_4-N(-NHCHO)-CO-C_6H_4-pC$	$CH_3CO(CH_2)_3N(C_2H_5)_2$	$-OCH_3$	$-N(C_2H_5)_2$	$pClC_6H_4CO$	EtOH	8	78	precipitation as hydrochloride	55
	$CH_3CO(CH_2)_3N\begin{smallmatrix}CH_2CH_2OH\\C_2H_5\end{smallmatrix}$	$-OCH_3$	$-N\begin{smallmatrix}CH_2CH_2OH\\C_2H_5\end{smallmatrix}$	$pClC_6H_4CO$	EtOH	8	78	—,,—	40
	$CH_3CO(CH_2)_3N(nC_3H_7)_2$	$-OCH_3$	$-N(nC_3H_7)_2$	H	*i*PrOH	2	97	—,,—	55
	$CH_3CO(CH_2)_3N(nC_4H_9)_2$	$-OCH_3$	$-N(nC_4H_9)_2$	H	*i*PrOH	2	97	—,,—	50
	$CH_3CO(CH_2)_3-OCH_3$ 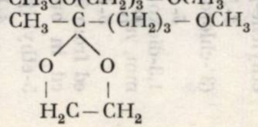	$-OCH_3$	$-OCH_3$	$pClC_6H_4CO$	*i*PrOH	2	97	sepn. on neutral Al_2O_3 chromat. col.	10 40

TABLE 2

Indole derivatives

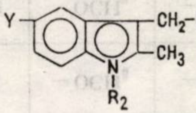			Formula	M.p °C (solvent)	t.l.c.** Rf value		Abs. maxima in electronic spectra (ethanolic soln)					
Y	R_1	R_2			syst. 1	syst. 2	λ_1 (nm)	lg ε	λ_2 (nm)	lg ε	λ_3 (nm)	lg ε
*H	$-N(C_2H_5)_2$	H	$C_{15}H_{22}N_2 \cdot HCl^{1-3}$	210–211 (MeOH)	0.3	0.5	226	4.32	284	3.83	290	3.76
H	$-N\Big\langle\genfrac{}{}{0pt}{}{CH_2CH_2OH}{C_2H_5}$	H	$C_{15}H_{22}N_2O \cdot HCl$	151–152 (*i*PrOH)	0.3	0.6	226	4.34	284	3.84	290	3.76
*H	$-N(nC_3H_7)_2$	H	$C_{17}H_{26}N_2 \cdot HCl^4$	211–212 (H_2O)	0.4	0.8	226	4.37	283	3.85	291	3.78
H	$-N(nC_4H_9)_2$	H	$C_{19}H_{30}N_2 \cdot HCl$	200–203 (H_2O)	0.6	0.8	226	4.39	283	3.85	291	3.79
H	$-N\Big\langle\genfrac{}{}{0pt}{}{C_6H_{11}}{CH_3}$	H	$C_{18}H_{26}N_2 \cdot HCl$	218–220 (*i*PrOH)	0.6	0.8	226	4.38	284	3.84	291	3.78
H	$-OCH_3$	H	$C_{12}H_{15}NO$	51–53	0.9	0.9	226	4.48	284	3.81	291	3.75
$-OCH_3$	$-N(nC_3H_7)_2$	H	$C_{18}H_{28}N_2O \cdot HCl$	201–203 (*i*PrOH)	0.3	0.9	226	4.35	284	3.88	294	3.85
$-OCH_3$	$-N(nC_4H_9)_2$	H	$C_{20}H_{32}N_2O \cdot HCl$	205–207 (*i*PrOH)	0.7	0.9	226	4.34	284	3.85	296	3.83
$-$*OCH_3	$-N(C_2H_5)_2$	$pClC_6H_4CO$	$C_{23}H_{27}ClN_2O_2HCl^5$	187–189 (*i*PrOH)	0.3	0.6	226	4.29	250	4.25	320	3.79
$-OCH_3$	$-N\Big\langle\genfrac{}{}{0pt}{}{CH_2CH_2OH}{C_2H_5}$	–,,–	$C_{23}H_{27}ClN_2O_3$ HCl	170–172 (*i*PrOH)	0.3	0.7	226	4.29	250	4.24	320	3.78
$-OCH_3$	$-OCH_3$	–,,–	$C_{20}H_{20}NO_3Cl$	75–76 (MeOH)	0.8	0.8	230	4.63	270	4.50	320	4.00

* mentioned in literature
** t.l.c. on DS 5 Camag Silicagel

System 1 : *n*BuOH : AcOH :H_2OC 4 :1 :5
System 2 : *i*PrOH : NH_4OH : H_2O 10 : 1 : 1 identificatuo by iodinəi vapours

TABLE 3

Characteristic vibrations in I.R.

Type	Nr.	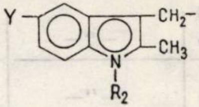			Domain ν (cm^{-1}) (s = strong, m = medium w = weak)				
		Y	R_1	R_2	3400 – 2800	1700 – 1600	1500 – 1400	1290 – 1010	850 – 700
A	1	H	$-N(C_2H_5)_2$	H	3220 m 2980 m 2920 m	1630 w	1470 s	1230 w 1020 m	760 s
	2	H	$-N{<}^{CH_2CH_2OH}_{C_2H_5}$	H	3380 s 3290 s 2980 m	1630 w	1480 s	1240 w 1040 m 1010 m	770 s 760 s
	3	H	$-N(nC_3H_7)_2$	H	3150 s 2970 s 2930 s	1630 w	1480s 1440 s	1240 w 1040 m 1010 m	760 s 710 s
	4	H	$-N(nC_4H_9)_2$	H	3180 s 2950 s	1630 w	1470 s 1450 s	1230 m 1010 m	740 s
	5	H	$-N{<}^{C_6H_{11}}_{CH_3}$	H	3230 s 2960 s 2870 s	1630 w	1470 s	1230 m 1030 s 1020 s	770 s 760 s 700 m
	6	H	$-OCH_3$	H	3400 s 2930 w 2870 w	1630 w 1590 w	1470 s 1450 m	1240 s 1230 m 1030 s	770 s 760 m 700 s
B	1	$-OCH_3$	$-N(nC_3H_7)_2$	H	3250 s 2960 s 2880 m	1630 m 1600 m	1490 s 1460 s	1220 s 1070 m 1040 m	830 m 810 m
	2	$-OCH_3$	$-N(nC_4H_9)_2$	H	3250 s 2960 s 2880 m	1630 m 1600 m	1490 s 1460 s	1220 s 1110 m 1070 m	830 m 810 m
C	1	$-OCH_3$	$-N(C_2H_5)_2$	$pClC_6H_4CO$	2980 m 2930 m	1690 s 1610 s	1430 s 1450 s	1250 s 1230 s 1030 m	850 m 850 m 760 s
	2	$-OCH_3$	$-N{<}^{CH_2CH_2OH}_{C_2H_5}$	$pClC_6H_4CO$	3330 m	1690 s 1600 s	1490 s 1450 s	1230 m 1090 m 1070 m	840 m 820 m 760 w
	3	$-OCH_3$	$-OCH_3$	$pClC_6H_4CO$	2920 m 2830 m	1690 s 1630 m 1590 m	1470 s 1440 s	1290 m 1270 m 1110 s	860 m 850 m 760 s

Fischer synthesis : to 0.01 M phenylhydrazinic derivative in an alcoholic soln. of 15–20% hydrochloric acid, 0.01 M carbonylic compound was added with stirring. The mixture was heated at the reflux temperatures for various times. The resulting ammonium chloride was filtered and the indole derivatives were isolated by various means. The indications concerning the reaction conditions, the separation methods and the yields are given in table 1. Tables 2 and 3 present some properties of the obtained indole derivatives.

The I.R. spectra have been realized in KBr pellets using a U.R. 10 Carl-Zeiss Jena spectrophotometer in the 4000–400 cm^{-1} domain.

The electronic spectra have been recorded in ethanolic solutions using a Pye Unicam 1800 spectrophotometer.

REFERENCES

[1] G. Bendz, C. C. Culvenor, L. J. Goldworthy and R. Robinson, *J. Chem. Soc.* **1950**, 1130.

[2] V. I. Shvedov, L. B. Altukhova, L. A. Kernyshova and A. N. Grinev, *Zhur. org. Khim.*, **5**, *2*, 221 (1969).

[3] R. Lenard and J. Borsy, *Acta Chim. Acad. Sci. Hung.*, **34**, 439 (1962).

[4] R. B. Barlow and J. Khan, *Brit. J. Pharmacol.*, **14**, 99 (1959).

[5] Merck & Inc. Neth. Appl. 6508553, 1964 ; *Chem. Abstr.*, **65**, 691 (1966).

[6] M. Avram and G. D. Mateescu, "Spectroscopia în Infraroșu", Editura tehnică, București, 1966.

[7] L. B. Bellamy, "The Infrared Spectra of Complex Molecules", Wiley, New-York 1960.

[8] N. Rădulescu, M. Iulian, I. P. Ambrus and V. Tamaș, R. S. Romania, Pat. 77626, 1974.

[9] N. Rădulescu and C. Sârbu, *Rev. Roumaine. Chim.*, **23**, 197 (1978).

[10] Y. Inoue and Y. Ban, *J. Chem. Soc. C.*, **1970**, 602.

[11] N. V. Kuznetsov and R. A. Myrsina, *Khim. Str. Stvoistva, Reactivnost org. Soedin.* **1969**, 75.

[12] P. Roffey and M. V. Sargent, *J. Chem. Soc. C.*, **1967**, 2328.

[13] Unilever Ltd, Brit. Pat. 1016516 (1966) ; *Chem. Abstr.*, **64**, 14095 (1966).

[14] O. S. Stepanova, *Zhur obshchei, Khim.*, **32**, 3295 (1962).

[15] N. Rădulescu, A. Maza, I. P. Ambruș, H. Aftalion, I. M. Popescu-Dimofte and R. Simionovici, R. S. Romania Pat. 62682, 1976.

[16] N. Rădulescu, M. Iulian, I. P. Ambruș, V. Tamaș, H. Aftalion and R. Simionovici, R. S. Romania Pat. 62680, 1976.

[17] P. A. Cruickshank and I. C. Sheenan *J. Amer. Chem. Soc.*, **83**, 2891 (1961).

[18] Sterling Drug. Inc. USA Pat. 25456658 (1951) ; *Chem. Abstr.*, **45**, 7155 (1951).

Revue Roumaine de Chimie, 25, 2, 253–259 (1980)

ORGANOPHOSPHORUS DERIVATIVES OF EXPECTED BIOLOGICAL ACTIVITY. I

REACTION OF PHENOLS WITH N-ARYLHEXACHLOROCYCLODIPHOSPHAZANES

M. M. OMARA, F. I. ABDEL-HAY, A. A. EL-BARBARY, M. BADAWI
and M. M. ABDEL HAMID *
Faculty of Science, Tanta University, Tanta, Egypt
* Microbiology Unit, National
Research Centre, Dokki, Cairo, Egypt

Received July 1, 1978

Some new hexachlorocyclodiphosphazanes have been prepared and reacted with phenol and substituted phenols. The reaction products were subjected to structural and mechanistic investigations. NMR, UV and IR spectra of the products are discussed. The prepared compounds have been found to possess activity against *Bacillus Subtilis, Escherichia coli, Candida albicans* and *Sarcina Lutea.*

Phosphorus compounds have long attracted attention for their patent biological activity.[1–3] It seemed therefore of interest to synthesize some new organophosphorus compounds. Such compounds are expected to possess biological activities, since they contain moieties of well known biological activity such as the pyridine and quinoline moieties.

It has been reported that primary amines react with phosphorus pentachloride to give the corresponding hexachlorocyclodiphosphazanes of the dimeric structure (I).[4–8]

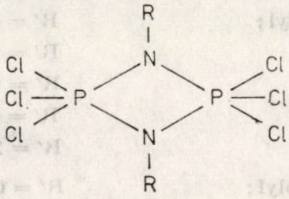

(I)

a ; R = $C_6H_4 - COOC_2H_5$ (*p*–) ;
b ; R = *p*-anisidyl
c ; R = 2-pyridyl
d ; R = 5-quinolyl

Pursuing this line of research, a new series of N-arylhexachlorocyclodiphosphazanes of the type (I) were prepared by reacting phosphorus pentachloride in cold dry benzene with *p*-aminoethylbenzoate, *p*-anisidine, 2-amino-pyridine and 5-aminoquinoline to give 1,3-di(*p*-ethylbenzoate) Ia, 1,3-di (*p*-anisidyl) Ib, 1,3-di(2-pyridyl) Ic and 1,3-di(5-quinolyl)2,2,2,4, 4,4-hexachlorocyclodiphosphazane Id, respectively.

Compounds (Ia—d) were allowed to react with phenols, namely, phenol, *o*- and *p*-chlorophenols, *p*-bromophenol, *m*- and *p*-cresols, *o*-nitrophenol and 2-naphthol in the presence of dry pyridine. The reaction was found to proceed smoothly with the precipitation of pyridine hydrochloride. In all the experiments, products other than the expected hexaphenoxy derivatives are separated.

Molecular weight determination and elemental analysis, indicate that these products correspond to orthophosphoro-monoamidates of the structure (II)

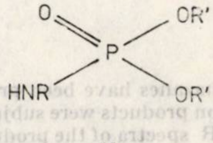

II

IIa ; R = $C_6H_4-COOC_2H_5(p\text{-})$; R′ = C_6H_5

b ; R = „ R′ = C_6H_4-Cl-*o*-

c ; R = „ R′ = C_6H_4Cl-*p*-

d ; R = „ R′ = C_6H_4Br-*p*-

e ; R = „ R′ = $C_6H_4CH_3$-*p*-

f ; R = „ R′ = $C_6H_4NO_2$-*o*-

g ; R = „ R′ = $2-C_{10}H_7$

IIh ; R = *p*-anisidyl ; R′ = C_6H_4Cl-*p*-

i ; R = „ R′ = C_6H_4Br-*p*-

j ; R = „ R′ = $C_6H_4CH_3$-*p*-

k ; R = „ R′ = $2-C_{10}H_7$

IIl ; R = 2-pyridyl ; R′ = C_6H_5

m ; R = „ R′ = C_6H_4Cl-*o*-

n ; R = „ R′ = C_6H_4Br-*p*-

o ; R = „ R′ = $C_6H_4CH_3$-*p*-

p ; R = „ R′ = $2-C_{10}H_7$

IIq ; R = 5-quinolyl ; R′ = C_6H_5

r ; R = „ R′ = C_6H_4Cl-*p*-

s ; R = „ R′ = C_6H_4Br-*p*-

t ; R = „ R′ = $C_6H_4CH_3$-*m*

u ; R = „ R′ = $C_6H_4CH_3$-*p*

v ; R = „ R′ = $2-C_{10}H_7$

The following tentative mechanisms can be postulated for their formation.

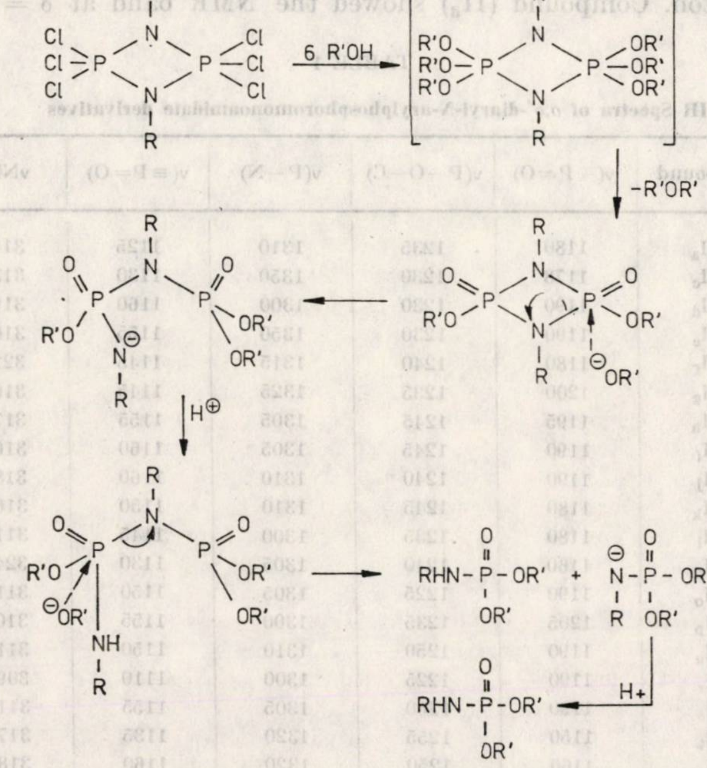

Besides, molecular weight determination and elemental analysis, the identities of the obtained products were also confirmed by the following spectroscopic measurements.

a) IR spectra of all the products ($II_a - II_v$) showed the band corresponding to $P = O$ stretching frequency in the region 1180—1200 cm^{-1}, a very strong absorption band at 1225—1260 cm^{-1} characteristic for the $P-O-C-$ aromatic stretching frequency, the band at 1310—1337 cm^{-1} characteristic for $P-N$ stretching frequency, the $N-H$ stretching vibration band in the region 3160—3180 cm^{-1} and a band in the region 1110—1160 cm^{-1} characteristic for the tetra coordinate phosphorus.[10,11] (cf. Table 1).

b) The UV spectra of these compounds do not show up the band at 270—290 nm corresponding to an n-π^* transition within the four membered ring structure,[12] thus indicating ring cleavage of the dimeric structure of cyclodiphosphazane.

c) The ^{1}H-NMR spectrum of compound (II_c) showed the following band assignments: $\delta = 1.5$ (3 H, triplet for the methyl group protons of the $COOCH_2CH_3$ moiety), $\delta = 4.58$ (2H, quartet for the CH_2 group protons of the $COOCH_2CH_3$), $\delta = 7.00-7.50$ (12 H, multiplet, for the aromatic protons) and $\delta = 8.18$ (1 H, doublet $J = 7$ c/s for the NH group-proton. Compound (II_d) showed the NMR band at $\delta = 1.6$ (3H, triplet for the $COOCH_2CH_3$) $\delta = 4.6$ (2H, quartet for the $COOCH_2-CH_3$), $\delta = 7.00-7.50$ (12 H, multiplet for the aromatic protons) and $\delta = 8.18$ (1H, doublet, $J = 7$ c/s, for the NH-group proton.

TABLE 1

IR Spectra of *o,o'*-diaryl-N-arylphosphoromonoamidate derivatives

Compound	ν(−P=O)	ν(P−O−C)	ν(P−N)	ν(≡P=O)	νNH
II_a	1180	1235	1310	1125	3140
II_c	1178	1230	1350	1130	3130
II_d	1190	1230	1300	1160	3190
II_e	1190	1230	1350	1155	3160
II_f	1180	1240	1315	1145	3225
II_g	1200	1235	1325	1145	3160
II_h	1195	1245	1305	1155	3170
II_i	1190	1245	1305	1160	3160
II_j	1190	1240	1310	1160	3180
II_k	1180	1245	1310	1150	3160
II_l	1180	1235	1300	1145	3110
II_m	1160	1240	1305	1130	3240
II_o	1190	1225	1305	1150	3110
II_p	1205	1235	1300	1155	3100
II_q	1190	1250	1310	1150	3110
II_r	1190	1225	1300	1110	3090
II_s	1190	1260	1305	1155	3110
II_t	1150	1255	1320	1135	3170
II_u	1160	1250	1320	1160	3180
II_v	1165	1250	1315	1145	3170

Compound (II_e) showed bands at $\delta = 1.45$ (3H, triplet for the $COOCH_2CH_3$), $\delta = 4.45$ (2H, quartet for the $COOCH_2 \cdot CH_3$), $\delta = 7.00-7.42$ (12 H, multiplet for the aromatic protons) and $\delta = 8.18$ (1 H, $J = 7$ Hz, for the NH group proton).

Also the presence of signals at $\delta = 2.38$ (6 H, singlet, for the methyl group-protons), $\delta = 3.96$ (3 H singlet, for the methoxyl group-protons) and at $\delta = 7.00-7.48$ (12 H multiplet, for the aromatic protons) was characteristic of the ^1H-NMR spectrum of compound (II_j).

The NMR spectrum of (II_0) showed the bands at $\delta = 2.40$ (singlet, for the methyl group-protons), the aromatic and pyridyl protons at $\delta = 7.00-7.80$ and at $\delta = 8.21$ (1 H, $J = 7$ c/s, for the NH group-proton). The proton-ratio-value was 6 : 12 : 1.

In addition, the NMR spectrum of compound (II_p) showed the pyridyl and naphthyl group-protons as a complex pattern in the $\delta = 7.20 - 8.0$ region. The NH group-proton gave a doublet at $\delta = 8.25$ ($J = 7$ Hz). The proton-ratio-value was 18 :1.

BIOLOGICAL ACTIVITY

The above prepared compounds were tested as antibacterial, using a modified cup test assay technique.[13,14] It was found that the majority of them showed activity against *Bacillus Subtillis*, *Escherichia Coli*, *Candida Albicans* and *Sarcina Lutea*.

EXPERIMENTAL

M.ps are uncorrected. Microanalyses were done by Microanalytical laboratory N.R.C., Cairo, Egypt. U.v. spectra were measured in ethanol using a Carl Zeiss Spectrophotometer Type PMQ II and I.R. spectra (KBr) were determined using a Carl Zeiss Jena spectrophotometer Model UR 10. The n.m.r. spectra were measured using a Varian A—60 spectrophotometer (in CF_3 COOH).

Preparation of 1,3,diaryl-2,2,2,4,4,4-hexachlorocyclo-diphosphazanes

General method

A solution of the primary amine (1 mole) in dry benzene (100 ml) was added dropwise to phosphorous pentachloride (1 mole) in dry benzene (200 ml) at 15°. The reaction mixture was heated under reflux for 3 hrs under anhydrous conditions. The reaction mixture was cooled to room temperature and the formed solid was filtered, washed several times with dry ether to give compounds (I_{a-d}) listed in table 2.

TABLE 2

1,3-Diaryl-2,2,2,4,4,4-hexachlorocyclodiphosphazane

Compound	M.P. °C	Compound	M.P. °C
I_a	130	I_c	178—9
I_b	193	I_d	182—3

Reaction of hexachlorocyclodiphosphazanes with phenols

General Method

To a solution of 1,3-diaryl-2,2,2,4,4,4-hexachloro-cyclodiphosphazane (0.01 mole) in dry benzene (150 ml.) containing 5 ml of pyridine was added dropwise with constant stirring (0.09 mole) of phenol in dry benzene (150 ml.). The reaction mixture was refluxed under anhydrous conditions for six hours, then kept overnight at room temperature. The formed pyridine hydrochloride was filtered off and the filtrate was evaporated under vacuo, the residue was washed with ethanol to remove the unreacted phenol. Recrystallization of the remaining solid from the appropriate solvent gave the corresponding *o*, *o'*-diaryl-N-phenylphosphoromonoamid ate. The products are listed in table 3.

TABLE 3

0,0′-Diaryl-N-phenylphosphoromonoamidate

Compound	M.P. °C (solvent)*	Formula	Calculated/Found				
			% C	% H	% N	% P	% halogen
II_a	155 (A)	$C_{21}H_{20}NO_5P$	63.47 63.61	5.03 5.11	3.52 3.55	7.80 7.40	
II_b	142 (A)	$C_{21}H_{18}Cl_2 \cdot NO_5P$	54.07 54.28	3.86 3.98	3.00 2.87	6.65 6.83	15.23 (Cl) 15.10
II_c	150 (B)	$C_{21}H_{18}Cl_2 \cdot NO_5P$	54.07 54.20	3.86 4.17	3.00 3.12	6.65 6.30	15.23 (Cl) 15.00
II_d	178 (B)	$C_{21}H_{18}Br_2 \cdot NO_5P$	45.41 45.52	3.24 3.48	2.52 2.31	5.59 5.89	28.82 (Br) 28.70
II_e	158 (B)	$C_{23}H_{24}NO_5P$	64.94 65.38	5.64 5.80	3.29 3.12	7.29 7.87	
II_f	152 (B)	$C_{21}H_{18}N_3O_9P$	51.74 51.82	3.69 3.65	8.62 7.95	6.36 6.70	
II_g	196 (B)	$C_{29}H_{24}NO_5P$	70.02 70.40	4.82 5.00	2.81 2.72	6.23 6.24	
II_h	160 (B)	$C_{19}H_{16}Cl_2 \cdot NO_4P$	53.77 53.42	3.77 3.66	3.31 3.19	7.31 7.81	16.74 16.57
II_i	177 (B)	$C_{19}H_{16}Br_2 \cdot NO_4P$	44.44 44.56	3.12 3.48	2.73 2.61	6.04 6.08	31.19 30.98
II_j	176 (B)	$C_{21}H_{22}NO_4P$	65.80 66.43	5.74 6.00	3.66 3.42	8.09 8.11	
II_k	165 (B)	$C_{27}H_{22}NO_4P$	71.21 70.98	4.84 4.62	3.08 2.93	6.81 7.02	
II_l	147 (C)	$C_{17}H_{15}N_2O_3P$	62.58 62.55	4.60 4.95	8.59 8.94	9.51 8.98	
II_m	186 (B)	$C_{17}H_{13}Cl_2 \cdot N_2O_3P$	51.65 51.72	3.29 3.18	7.09 6.82	7.85 7.75	17.97 17.62
II_n	116 (B)	$C_{17}H_{13}Br_2 \cdot N_2O_3P$	42.15 42.32	2.69 2.64	5.79 5.38	6.40 6.38	33.06 33.61
II_o	175 (B)	$C_{19}H_{19}N_2O_3P$	64.40 64.90	5.37 5.79	7.91 8.06	8.76 8.91	
II_p	183 (B)	$C_{25}H_{19}N_2O_3P$	70.42 70.36	4.46 4.68	6.57 6.83	7.28 7.31	
II_q	148 (D)	$C_{21}H_{17}N_2O_3P$	67.02 67.22	4.52 4.41	7.45 7.23	8.24 7.91	
II_r	125 (B)	$C_{21}H_{15}Cl_2 \cdot N_2O_3P$	56.62 56.44	3.37 3.35	6.29 6.01	6.97 7.31	15.96 15.68
II_s	191 (B)	$C_{21}H_{15}Br_2 \cdot N_2O_3P$	47.19 47.50	2.81 3.12	5.24 5.41	5.81 5.72	29.96 29.81
II_t	155 (D)	$C_{23}H_{21}N_2O_3P$	68.32 68.21	5.20 5.09	6.93 6.72	7.67 7.32	
II_u	135 (D)	$C_{23}H_{21}N_2O_3P$	68.32 68.14	5.20 5.34	6.93 7.09	7.67 8.01	
II_v	159 (A)	$C_{29}H_{21}N_2O_3P$	73.10 72.98	4.41 4.62	5.88 5.72	6.51 6.40	

* A, Benzene – pet. ether (b.p. 60 – 80°C) ; B, Ethanol ; C, Benzene ; D, aqueous methanol.

REFERENCES

[1] J. A. Hendry, F. L. Rose and A. I. Walpole, *Brit. J. Pharm.*, **6**, 201 (1951).

[2] E. Usdin "Anticholinesterase Agents (International Encyclopedia of pharmacology and Therapeutics" Vol. I, Pergamon Press, New York, 1970, p. 151.

[3] D. F. Heath, "Organophosphorous Poisons-Anticholinsterase and Related Compounds" Pergamon Press, New York, 1961.

[4] I. N. Zhmurova and A. V. Kirsanov, *Zhur. Obshchei Khim.*, **30**, 3044 (1960); *Chem. Abstr.*, **55**, 17551 (1961).

[5] A. C. Chapman, N. L. Padock and H. T. Searle, *J. Chem. Soc.*, **1961**, 1825.

[6] R. A. Shaw and E. H. M. Ibrahim, *Angew. Chem.*, **6**, 556 (1967).

[7] R. A Shaw, E. H. M. Ibrahim and B. C. Smith, *Tetrahedron Letters*, **36**, 3061 (1969).

[8] M. Becke-Goehring, L. Leichner and B. Scharf, *Z. anorg. Chem.*, **343**, 154 (1966).

[9] A. V. Kirsanov, *Zhur. obshchei Khim.*, **32**, 2576 (1962); *Chem. Abstr.*, **49**, 13161 (1955).

[10] R. A. Shaw, B. W. Fitrstimmans and B. C. Smith, *Chem. Rev.*, **62**, 267 (1962).

[11] L. J. Bellamy, "Infrared Spectra of Complex Molecules", Methuen, London, 1966.

[12] S. Trippett, *J. Chem. Soc.*, **1962**, 4731.

[13] T. Yamagushi, T. Kashida, K. Netwa, T. Yajma, T. Miyagishima, Y. Ito and T. Okuda, *J. Antibiotics*, **23**, 373 (1970).

[14] A. A. Abou-Zeid, M. M. Abdel-Hamid, and Y. M. Shehata, *Z. allg. Microbiologie*, **16**, 337 (1976).

Revue Roumaine de Chimie, **25**, *2*, 261–265 (1980)

INCHAIN EPOXIDES OF CAROTENOIDS. VII[1]

ASTACENE 9,10- AND 11,12-EPOXIDES

DOINA OŞIANU, ELENA NICOARĂ and C. BODEA
Institute of Agronomy, "Dr. Petru Groza", Department of Chemistry and Biochemistry,
Str. Mănăştur 3, Cluj-Napoca, Romania

Received March 13, 1979

Buffered epoxidation of astacene with perbenzoic acid affords, as main reaction products, 9,10-epoxy-(II), 11,12-epoxy-(III) and 9,12-oxy-astacene (IV). The structure of these new compounds was deduced by spectroscopic properties, deepoxidation, selective reductions, rearrangements and metal chloride-complexes.

Treatment with peracids of the keto-carotenoid canthaxanthin provided inchain-epoxides described in previous papers.[2–4]

Another keto-carotenoid with similar structure, frequently found in nature, is astaxanthin known to be rapidly converted into astacene (3,4-3′,4′-tetra-keto-β,β-carotene) during the isolation process. In solution as well as in crystalline state astacene exists in the form of tautomeric diosphenol (3,3′-dihydroxy-2,3,2,3′-tetrahydro-β,β-caroten-4,4′-dione), I.[5]

Astacene used in the present investigations was isolated from flowers of *Adonis aestivalis*.[6]

Acting with perbenzoic acid upon astacene in normal and buffered conditions we obtained hitherto unknown inchain-epoxides of astacene. Under normal conditions the main reaction product is 9,10-epoxy-astacene, II, accompanied by 11,12-epoxide, III, while epoxidation in the presence of sodium benzoate results in formation of the 11,12-epoxide, III as principal product, which is accompanied by the corresponding furanoid oxide (9,12-oxy-astacene), IV and by 9,10-epoxy-astacene, II (see scheme 1).

SCHEME 1

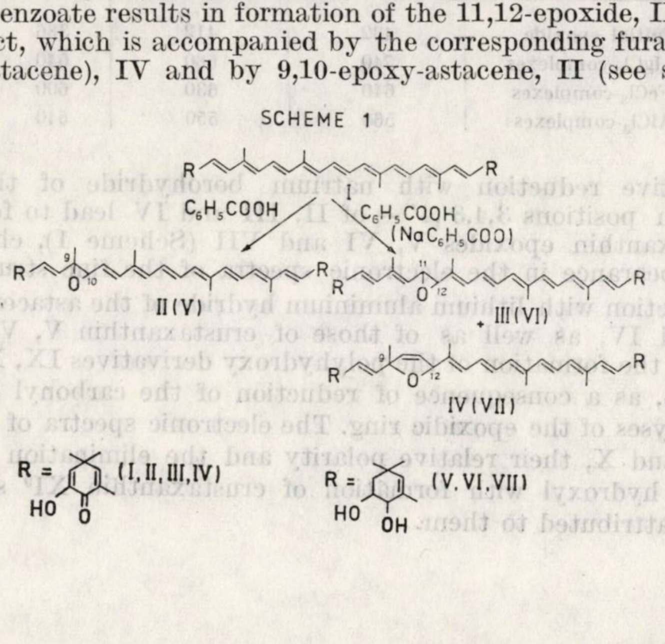

The structure of the astacene inchain-epoxides was established by spectroscopic methods and by means of transformation reactions, such as complexes with metal-chlorides, selective reduction with metal hydrides, de-epoxidation and isomerisation by acids and alkalies.

In the electronic spectra the epoxides II and III show, in ultraviolet and visible light, two absorption maxima corresponding to the two polyene fragments resulting from the interruption of the conjugated chain due to the fixation of the epoxidic oxygen at one of the inchain double bonds.[7] The position of the absorption maxima shown by the two polyene fragments permits to assign the double bond which underwent epoxidation.

The IR spectra of II and III revealed the diosphenolic structure showing peaks at 1630 cm^{-1},[8] and at 3440–3400 cm^{-1} characteristic for the carbonyl and the associated hydroxyl group respectively and besides it, bands at 1225 and 875 cm^{-1} attributed to the vibrations of the epoxy ring. In the IR spectrum of the inchain furanoid oxide IV bands at 1130–1100 cm^{-1} are assigned to vibrations of the furanoid ring.

With metal chlorides like $HgCl_2$, $FeCl_3$ and $AlCl_3$, the epoxides II and III and the furanoid oxide IV form complexes coloured from green to violet. Absorption maxima shown by these complexes are presented in table 1. On splitting the complexes of II and III by polar solvents the free epoxide is accompanied by astacene due to de-epoxidation of the epoxide.

TABLE 1

Visible light absorption maxima of metal-chloride complexes of astacene inchain-epoxides

	λ max (nm) in benzene		
	9,10-epoxide	11, 12-epoxide	9, 12-oxide
Initial epoxide	432	412	386
$HgCl_2$-complexes	740	680	640
$FeCl_3$-complexes	640	630	600
$AlCl_3$-complexes	560	550	540

Selective reduction with natrium borohydride of the carbonyl group from positions 3,4,3′,4′ – of II, III and IV lead to formation of the crustaxanthin epoxides V, VI and VII (Scheme 1), characterized by the appearance in the electronic spectra of the fine structure.

Reduction with lithium aluminium hydride of the astacene epoxides II, III and IV, as well as of those of crustaxanthin V, VI and VII, resulted in the formation of the polyhydroxy derivatives IX, X and VIII (Scheme 2), as a consequence of reduction of the carbonyl groups and hydrogenolyses of the epoxidic ring. The electronic spectra of compounds VIII, IX and X, their relative polarity and the elimination reaction of the allylic hydroxyl with formation of crustaxanthin XI[9] support the structures attributed to them.

SCHEME 2

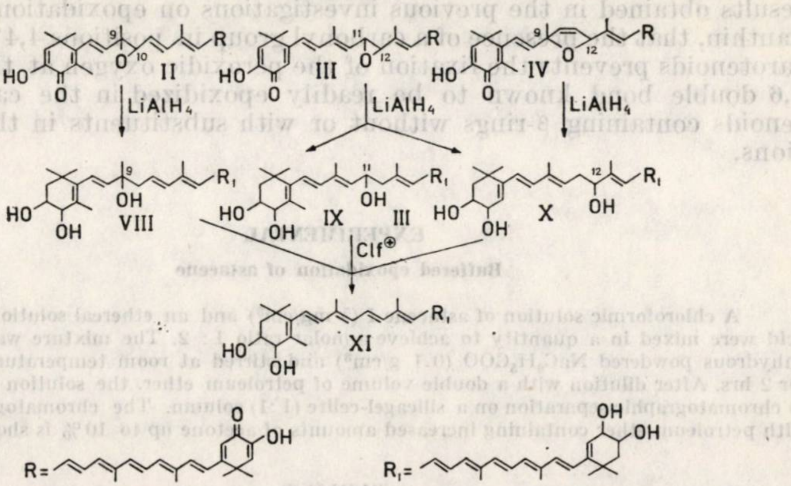
II
III
IV
LiAlH₄
LiAlH₄
LiAlH₄
VIII
IX
III
X
Clf⊕
XI
R=
R₁=

In diluted solutions of $HClO_4$ or NaOH the epoxides II and III as well as the furanoid oxide IV are converted into the compounds XII and XIII, explained by the isomerization of the epoxy- and furanoid rings into carbonyl groups. These inchain ketones have been characterized by their electronic spectra, relative polarity and reduction reaction with sodium borohydride leading to compounds X and XIV (Scheme 3). It is to be noticed that under the action of $HClO_4$ the epoxide III is converted into the same keto derivative XII as in the case of epoxide II and in the furanoid oxide IV; a behaviour similar to that of canthaxanthin-11,12-epoxide described in a former paper.[1]

SCHEME 3

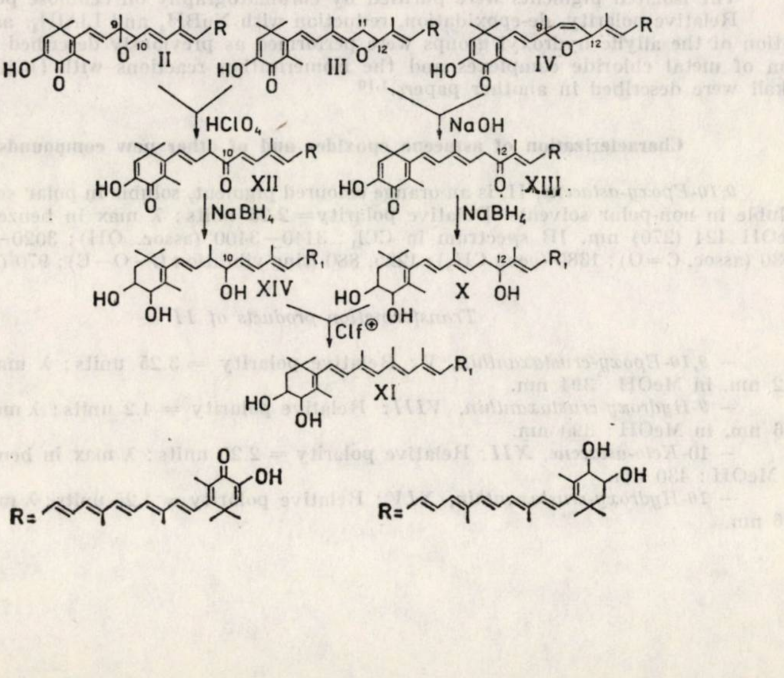
II
III
IV
HClO₄
NaOH
XII
XIII
NaBH₄
NaBH₄
XIV
X
Clf⊕
XI
R=
R=

The study of the action of peracids upon astacene confirms the results obtained in the previous investigations on epoxidation of canthaxanthin, that the presence of a carbonyl group in positions 4,4′ of β,β-type carotenoids prevents the fixation of the peroxidic oxygen at the adjacent 5,6 double bond known to be readily epoxidized in the case of carotenoids containing β-rings without or with substituents in the 3,3′-positions.

EXPERIMENTAL

Buffered epoxidation of astacene

A chloroformic solution of astacene I (5 mg/cm^3) and an ethereal solution of perbenzoic acid were mixed in a quantity to achieve a molar ratio 1 : 2. The mixture was treated with anhydrous powdered NaC_6H_5COO (0.1 g/cm^3) and stirred at room temperature, in the dark for 2 hrs. After dilution with a double volume of petroleum ether, the solution was submitted to chromatographic separation on a silicagel-celite (1 :1) column. The chromatogram developed with petroleum ether containing increased amounts of acetone up to 10% is shown in table 2.

TABLE 2

Chromatogram of buffered epoxidation of astacene

Zone	Colour	λ max (nm) in benzene	Pigment
5	yellow	386	9,12-oxy-astacene IV
4	deep-yellow	412	11,12-epoxy-astacene, III
3	red-violet	486	astacene, I
2	yellow	432	9,10-epoxy-astacene, II
1	pale yellow	<360	unidentified

The isolated pigments were purified by chromatography on cellulose powder.

Relative polarity, de-epoxidation, reduction with $NaBH_4$ and $LiAlH_4$, as well as elimination of the allylic hydroxyl groups were performed as previously described. [2] The preparation of metal chloride complexes and the isomerisation reactions with $HClO_4$ and alcoholic alkali were described in another papers.[1,10]

Characterization of astacene epoxides and of other new compounds

9,10-Epoxy-astacene, II, is an orange coloured pigment, soluble in polar solvents, slightly soluble in non-polar solvents. Relative polarity = 2.25 units; λ max in benzene 432 nm, in MeOH 424 (270) nm. IR spectrum in CCl_4 : 3440–3400 (assoc. OH); 3020–2820 (C–H); 1630 (assoc. C=O); 1380 (gem. CH_3); 1225, 880 (ring vibration C–O–C); 970 (all trans) cm^{-1}.

Transformation products of II

— *9,10-Epoxy-crustaxanthin, V:* Relative polarity = 3.25 units; λ max in benzene: 402 nm, in MeOH : 394 nm.

— *9-Hydroxy-crustaxanthin, VIII:* Relative polarity = 4.2 units; λ max in benzene: 396 nm, in MeOH : 390 nm.

— 10-*Keto-astacene, XII:* Relative polarity = 2.20 units; λ max in benzene : 438 nm, in MeOH : 430 nm.

— *10-Hydroxy-crustaxanthin, XIV:* Relative polarity = 4.25 units; λ max in benzene : 396 nm.

11,12-Epoxy-astacene, III, is a deep yellow pigment, soluble in alcohols, acetone and chloroform, slightly soluble in non-polar solvents; Relative polarity = 2.25 units; λ max in benzene: 412 nm, in MeOH; 400 (278) nm. IR spectrum in CCl_4 : 3440–3400 (assoc. OH); 3020–2820 (C–H); 1630 (assoc. C=O); 1470, 1440 (CH_2, C–CH_3); 1380, 1340 (gem. CH_3); 1225, 875 (ring vibration C–O–C); 970 (all trans) cm^{-1}.

Transformation products of III

— *11,12,-Epoxy-crustaxanthin, VI:* Relative polarity =2.95 units; λ max in benzene: 388 nm, in MeOH : 376 nm.

— *11-Hydroxy-crustaxanthin, IX:* Relative polarity = 4.60 units; λ max in benzene: 382 nm, in MeOH : 374 nm.

— *12-Hydroxy-crustaxanthin, X:* Relative polarity =4.80 units; λ max in benzene: 384 nm, in MeOH : 376 nm.

— *12-Keto-astacene, XIII:* Relative polarity =2.40 units; λ max in benzene: 420 nm, in MeOH : 414 nm.

9,12-Oxy-astacene, IV: is a yellow pigment, soluble in polar solvents.

Relative polarity = 2.20 units; λ max in benzene: 386 nm, in MeOH : 380 nm. IR spectrum in CCl_4 : 3580–3380 (assoc. OH); 1630 (assoc. C=O); 1480–1420 (CH_2, C–CH_3); 1340 (gem. CH_3); 1130, 1110, 1100 (cyclic C–O–C); 980 (all trans) cm^{-1}.

Transformation products of IV

— *9,12-Oxy-crustaxanthin, VII:* λ max in benzene: 370 nm

— *12-Hydroxy-crustaxanthin, X:* as above.

— *12-Keto-astacene, XIII:* as above.

REFERENCES

[1] Part VI. D. Oșianu, E. Nicoară and C. Bodea, *Rev. Roumaine Chim.*, **23,** 573 (1978).

[2] E. Nicoară, D. Oșianu and C. Bodea, *Rev. Roumaine Chim.*, **15,** 965 (1970).

[3] D. Oșianu, E. Nicoară and C. Bodea, *Rev. Roumaine Chim.*, **16,** 925 (1971).

[4] D. Oșianu, E. Nicoară and C. Bodea, *Rev. Roumaine Chim.*, **22,** 1085 (1977).

[5] A. Seybold and T. W. Goodwin, *Nature*, **184,** 1714 (1959).

[6] G. Neamțu, V. Tămaș and C. Bodea, *Rev. Roumaine Biochem.*, **3,** 309 (1966).

[7] Y. Ogata, K. Tomizawa and K. Tagagi, *Tetrahedron*, **29,** 47 (1973).

[8] A. J. Aasen and S. L. Jensen, *Acta. Chem. Scand.*, **20,** 1970 (1966).

[9] E. Nicoară, Gh. Illyes, M. Suteu and C. Bodea, *Rev. Roumaine Chim.*, **12,** 547 (1967).

[10] D. Oșianu, E. Nicoară and C. Bodea, *Rev. Roumaine Chim.*, **19,** 1203 (1974).

Revue Roumaine de Chimie, 25, 2, 267–272 (1980)

UTILISATION OF SODIUM HYDROXIDE IN SEPARATION OF TIN (II) WITH ION EXCHANGE RESINS. I

CATION – EXCHANGE BEHAVIOR OF TIN (II)

LUMINIȚA VLĂDESCU and DĂNUȚA VOICU
National Institute of Chemistry, Laboratory of Analytical
Chemistry, Splaiul Independenței 202, Bucharest, Romania

Received March 15, 1979

In the present study, the influence of sodium hydroxide upon the cation – exchange behavior of tin(II) has been approached. The equilibria of ion exchange, precipitation and complex combinations formation are numerous and shifted in one sense or another depending on many parameters pertinent to working conditions : hydroxide concentration, type of resin and the ionic form it assumes in the working medium, length of column, temperature and the nature of ions present and their concentration in the system.

The numerous utilisations of metallic tin in very different fields have required analytical procedures to separate it and its compounds from impurifying elements.

The ion exchange resins have allowed to find simple and rapid solutions of some difficult quantitative separation problems.

Studies regarding the ion exchange behaviour of tin in aqueous solutions in the presence of complexing agents, both inorganic : HCl,[1–6] HCl + HF,[4] HF,[7,8] HCl + $HClO_4$,[9,10] H_2SO_4,[11–16] HNO_3,[17] NH_4SCN,[18] sodium polysulphide,[19] and organic : acetic acid,[20] malonic acid,[15] oxalic acid[3,14,21–24] tartaric acid,[25] are available in literature. Likewise, alkali hydroxides were employed for the elution of tin retained in an anion exchange resin from various complexing media.[19,26]

Given the strong tin (II) tendency of reacting with alkali hydroxides to form stannous hydroxide and stannites, compounds in which tin preserves best the 2^+ oxidation state, in the present study the influence of sodium hydroxide upon the cation exchange behavior of tin (II) has been approached.

EXPERIMENTAL

Strongly acid cation exchange resins Dowex-50, X2, Merck I and Vionit CS-3 have been used.

The following chemicals were also employed : $SnCl_2 \cdot 2H_2O$ pro analysis and technical grade, NaOH, HCl, NH_3, $KBrO_3$, KI and starch, both p.a. grade.

Tin(II) was determined quantitatively by titration with potassium bromate solution in the presence of potassium iodide and starch [27]

Use has been made for ionic exchange studies of glass columns, 20 cm long, 1 cm in diameter provided with a stopcock at the bottom and with a dropping funnel with ground glass joint at the top.

Known amounts of cation exchanger swollen in water, purified and activated in ionic H^+ form were packed in the columns.

RESULTS

In order to establish the optimal working conditions, the influence of the type of resin, of sodium hydroxide and Sn^{2+} concentrations, of the degree of loading of the resin with Sn^{2+} ions and of column length upon the cation-exchange behavior of tin(II) was studied.

The influence of the type of resin. Three types of strongly acid cation exchangers were employed (Dowex-50,X2, Merck I and Vionit CS-3) in which the same amount of tin(II) ions was fixed quantitatively. Elution with 0,5N NaOH solution has yielded the curves shown in figure 1.

The differences between elution curves are due to the differences in affinity of resins toward Sn^{2+}, which evidences the influence of resin characteristics on the competitive equilibria of ion exchange, precipitation and complex combinations formation.

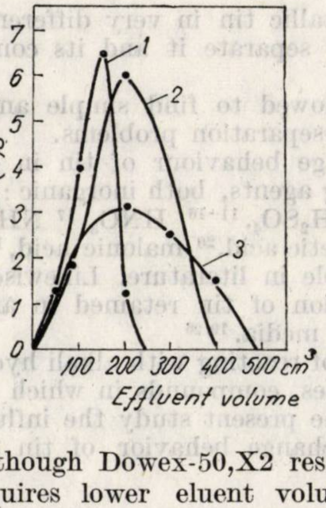

Fig. 1. — The influence of the type of resin upon tin(II) elution : 1-Dowex-50, X2 ; 2-Merck I ; 3-Vionit CS-3.

Although Dowex-50,X2 resin ensures a better exchange kinetics and requires lower eluent volumes, the cationic resin Merck I was preferred since its colour is darker and allows visual observation in the column of precipitation-dissolution processes (the exchange rate is also favourable).

The influence of sodium hydroxide solution concentration upon elution of tin (II) from Merck I cationic resin was studied for four concentrations i.e. : 0.1, 0.5, and 2N.

The elution curves in figure 2a show that the faster tin is eluted, the higher the concentration of sodium hydroxide is.

Curves in figure 2b show that above 1N NaOH, the increase of elution efficiency with increasing concentration of hydroxide approaches a limit such that the decisive factors are the column length and the amount of resin employed. It is not recommended to work in strongly basic media since they favour the air oxidation of tin (II).

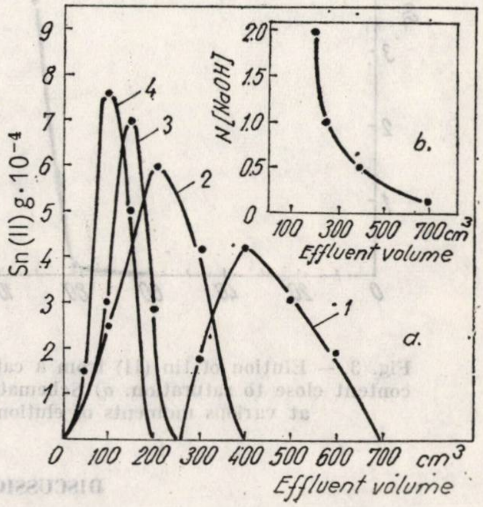

Fig. 2. — The influence of the NaOH concentration upon the tin (II) elution : *a*) Elution curves : 1—0.1N ; 2—0.5N ; 3—1 N ; 4—2N. *b*) Effluent volume — NaOH concentration dependence.

The influence of tin (*II*) *amount retained in resin on its elution with sodium hydroxide.* Use has been made both of cation exchange resins with tin(II) content close to saturation and of cationites in which tin occupies only a small part of the resin activated groups.

In both cases a front of tin(II) hydroxide migrates through the column. The elution curve in Figure 3b, yielded by a column which contained an amount of tin(II) close to maximum capacity, shows that tin is present in effluent in large amounts after 80 cm^3 of NaOH 1N solution has passed through the column. The small amount of tin that emerges from the column between 10 and 80 cm^3 effluent corresponds to its displacement by Na^+ in the regions of resin at the end of the column.

It has also been found out that up to 90 cm^3 the effluent contains no OH^- ions ; they appear only after the tin hydroxide front starts to flow out of column.

Figure 3a shows the schematic diagram of $Sn(OH)_2$ front at various moments of elution ; figure 3b presents the elution curve plotted in this case.

When the amount of tin (II) fixed in the resin is ten times smaller the elution curve is similar to that in figure 3b.

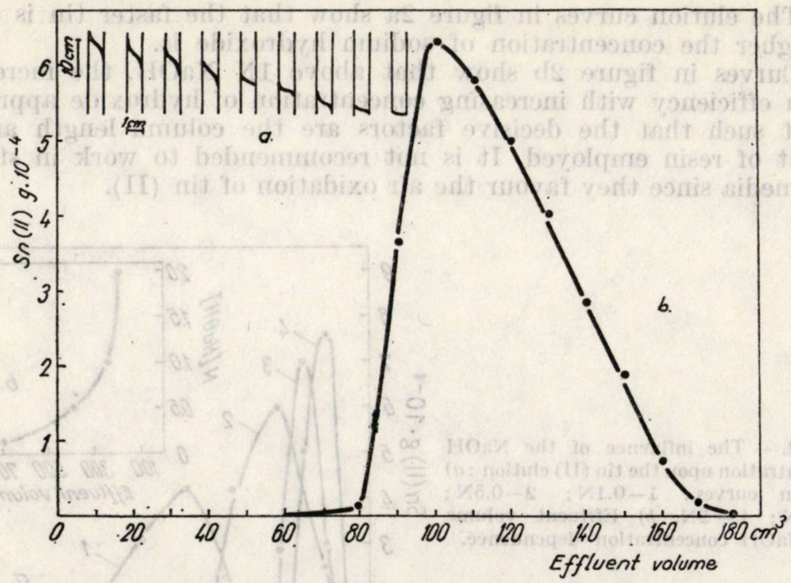

Fig. 3. — Elution of tin (II) from a cation exchange resin with tin (II) content close to saturation. *a*) Schematic diagram of the $Sn(OH)_2$ front at various moments of elution ; *b*) Elution curve.

DISCUSSION

To explain experimental data, all equilibria involved in the solution inside as well as in that outside the cation exchange resin must be considered.

The passing of a sample containing Sn^{2+} ions in acid solution through an H^+ form cation exchange resin makes tin be fixed according to the equilibrium :

$$(Sn^{2+})_S + 2(H^+)_R \rightleftharpoons (Sn^{2+})_R + 2(H^+)_S \tag{1}$$

where R and S refer to resin and external solution phases.

Subsequent introduction of sodium hydroxide alters the apparent affinity of the resin in two ways : the displacement of Sn^{2+} and H^+ ions existing in the cationite by the Na^+ ions, and the complexing action of HO^- anions left into the solution outside the resin.

The following equilibria may occur : Na^+ cations may penetrate into the solution inside the resin :

$$(Na^+)_{S_{ext}} \rightleftharpoons (Na^+)_{S_{int}} \tag{2}$$

where they replace H^+ and Sn^{2+} ions which neutralize the fixed ionic groups of the cationite and release them into the solution inside resin :

$$(Sn^{2+})_R + 2(Na^+)_{S_{int}} \rightleftharpoons (Sn^{2+})_{S_{int}} + 2(Na^+)_R \tag{3}$$

$$(H^+)_R + (Na^+)_{S_{int}} \rightleftharpoons (H^+)_{S_{int}} + (Na^+)_R \tag{4}$$

(S_{ext} and S_{int} indicate the solution phases outside and inside the resin particle, respectively).

Sn^{2+} ions react with water inside resin particle according to the equilibria :[28]

$$3(Sn^{2+})_{S_{int}} + 4(H_2O)_{S_{int}} \rightleftharpoons ([Sn_3(OH)_4]^{2+})_{S_{int}} + 4(H^+)_{S_{int}} \qquad (5)$$

$$2(Sn^{2+})_{S_{int}} + 2(H_2O)_{S_{int}} \rightleftharpoons [(Sn_2(OH)_2]^{2+})_{S_{int}} + 2(H^+)_{S_{int}} \qquad (6)$$

However, water inside resin may ionize and Sn^{2+} reacts with OH^- ions :

$$(Sn^{2+})_{S_{int}} + 2(HO^-)_{S_{int}} \rightleftharpoons (Sn(OH)_2)_{S_{int}} \qquad (7)$$

since $K_{S_0} = 10^{-27}\ mol \cdot l^{-1}$[29]

H^+ ions may act upon tin hydroxocomplexes to shift equilibria (5, 6) towards the formation of Sn^{2+} cation, and equilibrium (8) on the right :

$$(Sn(OH)_2)_{S_{int}} + (H^+)_{S_{int}} \rightleftharpoons [(Sn(OH)]^+)_{S_{int}} + H_2O \qquad (8)$$

with $K_2 = 10^{-429}\ mol \cdot l^{-1}$[30]

The H^+ ions formed in the solution inside the resin following various reactions may also leave the resin.

$$\begin{array}{l} (H^+)_{S_{int}} \rightleftharpoons (H^+)_{S_{ext}} \\ \qquad\qquad\quad | \\ \qquad\qquad\quad | + (HO^-)_{S_{ext}} \\ \qquad\qquad\quad \longrightarrow H_2O \end{array} \qquad (9)$$

This equilibrium, favoured by water formation, accounts for the absence of HO^- ions from the effluent until tin leaves the column.

Thus, as long as there are H^+ ions in the resin, the equilibria in which tin participates are shifted towards the existence of Sn^{2+} cations. As the amount of hydrogen in the resin is replaced with Na^+ ions, the weight of tin hydroxocomplex formation equilibria increases.

This entails the formation of tin (II) hydroxide in the solution inside the resin, hydroxide which takes part in the following equilibrium :

$$(Sn(OH)_2)_{S_{int}} \rightleftharpoons (Sn(OH)_2)_{S_{ext}} \qquad (10)$$

to an extent which depends on the resin's degree of crosslinking and porosity and $Sn(OH)_2$ front advances into the column.

When the whole resin is saturated with Na^+ ions, the sodium hydroxide excess determines the formation of higher tin (II) hydroxocomplexes :

$$Sn(OH)_2 + NaOH \rightleftharpoons [Sn(OH)_3]^- + Na^+ \qquad (11)$$

To displace tin from the cationite according to the equilibrium (3) it is necessary to work with concentrated solution of sodium hydroxide since, in dilute solutions the resin fixes preferentially the higher charge ion, while in concentrated solutions the lower charge one.

Thus, in the case of tin, an asymmetric elution curve is obtained (Figure 3b) with a front of maximum concentration and a wing toward higher effluent volumes. This curve points out to the presence of large tin amounts in the effluent after 80 cm^3 1 N NaOH is passed through the resin what agrees with the discussion on the equilibrium competition (5–8) and proves that the process occurs mostly according to the equilibria discussed.

The equilibria of ion exchange, precipitation and complex combinations formation are numerous and shifted in one sense or another depending on many parameters pertinent to working conditions.

The establishment of optimal operation parameters ensures concentration and separation of tin(II) fixed in a cation exchange resin, by elution with sodium hydroxide.

REFERENCES

[1] R. Kuroda, K. Ishida and T. Kiriyama, *Analyt. Chem.*, **40**, 1502 (1968).
[2] F. B. Marti and C. A. Herrero, *Chim. analyt.*, **48**, 602 (1966).
[3] W. G. Georges and W. M. Rieman, *Analyt. Chim. Acta*, **27**, 113 (1962).
[4] M. Ariel and E. Kirowa, *Talanta*, **8**, 214 (1961).
[5] F. Nelson, R. Rush and K. A. Kraus, *J. Amer. Chem. Soc.*, **82**, 339 (1960).
[6] N. N. Karnaukhova, *Zavododskaya Lab.*, **36**, 1047 (1970).
[7] Y. D. Smith, *Analyt. Chim. Acta*, **57**, 371 (1971).
[8] B. R. Chamberlain and R. I. Leech, *Talanta*, **14**, 597 (1967).
[9] M. D. Seymour and J. S. Fritz, *Analyt. Chem.*, **45**, 1394 (1973).
[10] C. I. Stronski and W. H. Rybskov, *Chem. Analit.*, **4**, 877 (1959).
[11] F. W. Strelow and C. J. C. Bothwa, *Analyt. Chem.*, **39**, 595 (1967).
[12] L. Danielsson, *Acta. Chem. Scand.*, **19**, 670 (1968).
[13] S. A. Reinolds, Analyst, **82**, 46 (1957).
[14] G. W. Smith and S. A. Reinolds, *Analyt. Chim. Acta*, **12**, 151 (1955).
[15] J. Dawson and R. J. Magee, *Mikrochim. Acta*, **3**, 325, (1958).
[16] V. A. Khalizova, A. Y. Alekseeva and A. Y. Smirnova, *Zhur. analit. Khim.*, **25**, 1525 (1970).
[17] F. Iehikowa, S. Uruno and H. Imai, *Bull. Chem.Soc. Japan*, **34**, 952 (1961).
[18] B. Dymond, *Analyt. Chem.*, **40**, 919 (1968).
[19] R. Klement and A. Kuhn, *Z. analyt. Chem.*, **152**, 146 (1956).
[20] W. Husain and M. Gulabi, *Separ. Sci.*, **6**, 737 (1971).
[21] M. L. Allant, *Chem. Rev.*, **61**, 213 (1961).
[22] T. Nazaki, O. Hiraiwa, C. Heumi and K. Kashiba, *Bull. Chem. Soc. Japan*, **42**, 245 (1969).
[23] B. K. Preobrajenski and L. H. Moskinin, *Radiokhimiya*, **3**, 309 (1961).
[24] B. K. Preobrajenski and I. P. Saikov, *Radiokhimiya*, **2**, 68 (1960).
[25] F. W. E. Strelow and T. V. van der Wolt, *Analyt. Chem.*, **47**, 2275 (1975).
[26] K. Shimizu and N. Ogata, *Bunseki Kagaku*, **12**, 526 (1963).
[27] C. Liteanu, "Chimie analitică cantitativă — Volumetria", Editura didactică şi pedagogică, Bucureşti, 1969.
[28] W. Feitknech and P. Schindler, *Pure Appl. Chem.*, **6**, 130 (1963).
[29] P. N. Novalenko, *Zhur. neorgan. Khim.*, **3**, 1065 (1958).
[30] A. B. Garret and S. Heiks, *J. Amer. Chem. Soc.*, **63**, 562 (1941).

Revue Roumaine de Chimie **25**, *2*, 273–276 (1980)

DIE AUFLÖSUNG IN DER DÜNNSCHICHTCHROMATOGRAPHIE MIT ORTHOGONALEM TEMPERATURGRADIENTEN BEI EINER S-KAMMER

S. GOCAN und C. KONNERT

Lehrstuhl für Analytische Chemie der Universität Cluj-Napoca, Str. Arany János Nr. 11,
Rumanien

Eingegangen am 28. Dezember 1978

Es werden die Vorteile der Dünnschichtchromatographie mit orthogonalem Temperaturgradienten gegenüber der konventionellen Technik in einer S-Kammer gezeigt. Ebenso werden die Faktoren die zu einer besseren Auflösung führen, diskutiert. Aus den experimentellen Ergebnissen ist festzustellen, daß bei der Trennung eines Systems von 6 Aminosäuren die Anwendung eines kleineren Temperaturgradienten als vorteilhaft erscheint welcher aber im Bereich der höheren Temperaturen gelagert ist (40°−35°)/3 mm = = 1,66°/mm.

In this paper, the advantages of orthogonal temperature gradient development *versus* the conventional development in S-chamber are shown. The contributory factors, through which orthogonal temperature gradient enhaces the resolution, are discussed. From experimental data, one can see that in the case of separation of a mixture of 6 aminoacids, the use of a small orthogonal temperature gradient placed in high temperature region is preferred (40°−35°)/3 mm = 1.66°/mm.

Die Vorteile der Entwicklung in der S-Kammer mit orthogonalem Temperaturgradienten (0-Temperaturgradient) wurden erstmals von Niederwieser [1] gezeigt. Als Folge des o-Temperaturgradienten entsteht ein antiparalleler Fließmittelgradient (der Fließmittelfluß fällt von der Frontlinie zur Eintauchlinie). Im Falle eines mehrkomponentigen Fließmittels ändert sich auch dessen Zusammensetzung. An Stelle des von der Schicht verdampften Fließmittels wird ein zusätzliches Fließmittelvolumen ΔV erzeugt, welches die Schicht durchsetzt. All diese Faktoren führen zur Erhöhung und Differenzierung der R_f-Werte der Komponenten [2].

Nicht zu vernachlässigen ist der Temperatureinfluß [3,4] auf die Trennergebnisse, da bei Entwicklung im o-Temperaturgradienten die Dünnschicht bei einer höheren Temperatur als die Raumtemperatur gehalten wird. Der o-Temperaturgradient bewirkt auch eine Verminderung der mittleren Trennstufenhöhe, H.

EXPERIMENTELLER TEIL

Die S-Kammer mit Möglichkeit zur Entwicklung im 0-Temperaturgradient wurde von Niederwieser beschrieben.

Die Platte mit der Dünnschicht (die gleichzeitig eine Wand der S-Kammer ist) wird bei einer Temperatur t_2 gehalten, die höher ist als die Temperatur t_1 der Gegenplatte. Der o-Temperaturgradient wurde nach folgender Beziehung berechnet:

$$\text{o-grad.}\, t = (t_2 - t_1)/d \qquad (°\text{C/mm}),$$

wo *d* die Distanz zwischen den beiden Platten darstellt.

Die Trennung des Gemisches gebildet aus 1. Histidin, 2. Glycin, 3. Glutaminsäure, 4. Alanin, 5. Valin und 6. Leucin wurde auf einer Schicht von mikrokristalliner Cellulose (Merck), Schichtdicke 0,2 mm, durchgeführt. Zur Entwicklung wurde folgendes Fließmittelsystem verwendet[5]: n-Butanol/Aceton/Essigsäure/Wasser (35 :35 :10 :20 v/v). Die Sichtbarmachung der Aminosäuren erfolgte durch Besprühen der Platten mit einer Ninhydrinlösung (0,2 % Ninhydrin in 2 % Essigsäure in Butanol) und anschließendem Trocknen im Trockenschrank bei 110°.

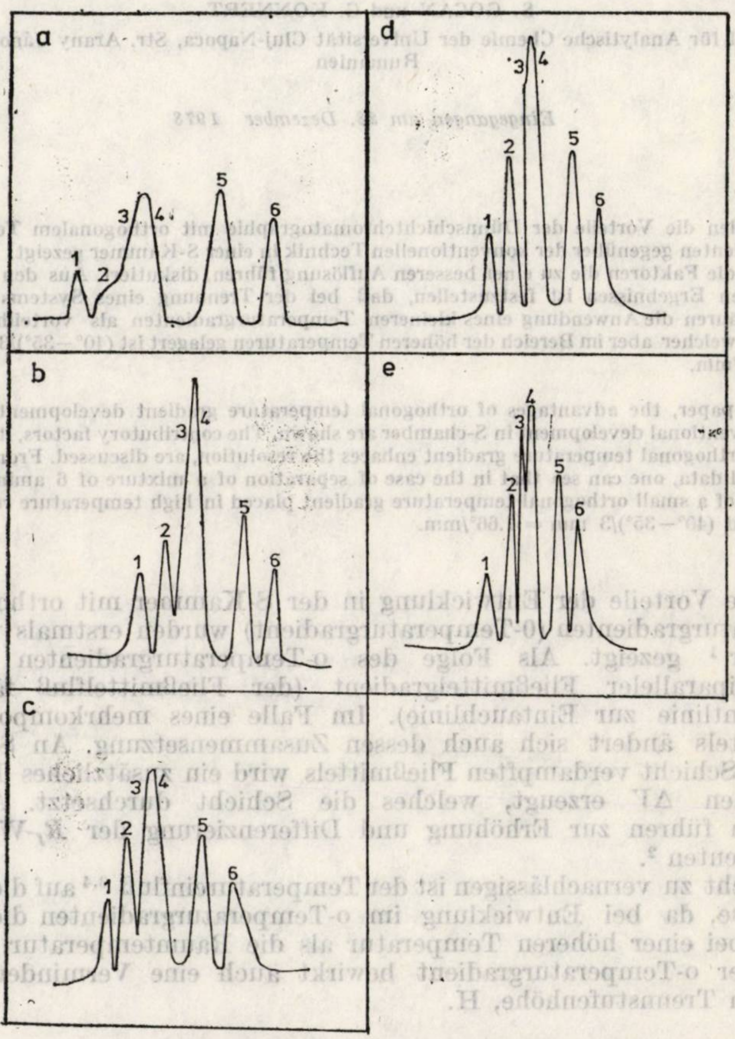

Abb. 1 — Densitogramme des Aminosäurengemisches: *1*. Histidin, *2*. Glycin, *3*. Glutaminsäure, *4*. Alanin, *5*. Valin, *6*. Leucin.

a) isotherme Entwicklung bei $t_1 = 20°$, Entwicklungszeit: 1 Stunde;
b) Entwicklung bei o-grad. $t = (25-20)/3 = 1{,}66$°C/mm, 1 Stunde;
c) Entwicklung bei o-grad. $t = (30-20)/3 = 3{,}33$°C/mm, 1 Stunde;
d) Entwicklung bei o-grad. $t = (35-20)/3 = 5{,}00$°C/mm, 1 Stunde;
e) Entwicklung bei o-grad. $t = (45-20)/3 = 6{,}66$°C/mm, 1 Stunde.

Die Abbildungen 1—3 zeigen die erhaltenen Densitogramme. Die Densitogramme aus Abbildung 1 zeigen die Trennung des angeführten Aminosäurengemisches bei verschiedenen o-Temperaturgradienten und konstanter Entwicklungszeit (60 Minuten).

Wenn man diese Densitogramme analysiert, so stellt man eine klare Verbesserung der Trennung mit wachsendem o-Temperaturgradienten fest. Auch die Auflösung wächst, obwohl die Entfernung Startlinie-Frontlinie bei einem o-grad.t=6,66°/C/mm ungefähr dreimal kleiner ist als unter isothermen Bedingungen. Größtenteils ist diese Verbesserung der Auflösung auf das Fallen der mittleren Trennstufenhöhe zurückzuführen, was eine Verengung der Zonen bewirkt (die Zonen werden strichförmig).

Wenn man den Einfluß eines konstanten Temperaturgradienten der aber in verschiedenen Bereichen der Temperaturskala gelagert ist untersucht, so stellt man fest, daß sich die Auflösung verbessert je höher die Temperatur der Dünnschicht ist.

Bei einem o-grad.t = (25—20)/ /3°C/mm wurden Chromatogramme bei einer Entwicklungszeit von 1, 2 und 3 Stunden erhalten. Die Ergebnisse sind in Abbildung 2 wiedergegeben.

Dasselbe Studium (Entwicklungszeit 1—3 Stunden) wurde bei einem o-grad. t = (40—35)/3°C/mm durchgeführt und die dafür erhaltenen Densitogramme in Abbildung 3 veranschaulicht. In diesem Fall wird die vollständige Trennung des Gemisches schon nach 2 Stunden verwirklicht.

Der o-Temperaturgradient, angewendet bei einer S-Kammer, hat einen positiven Einfluß auf die Trennung einiger Systeme deren Trennung mit der konventionellen Technik nicht möglich ist. Die Verwendung eines kleinen o-Temperaturgradienten, der aber in höheren Bereich der Temperaturskala gelagert ist, erscheint als vorteilhaft.

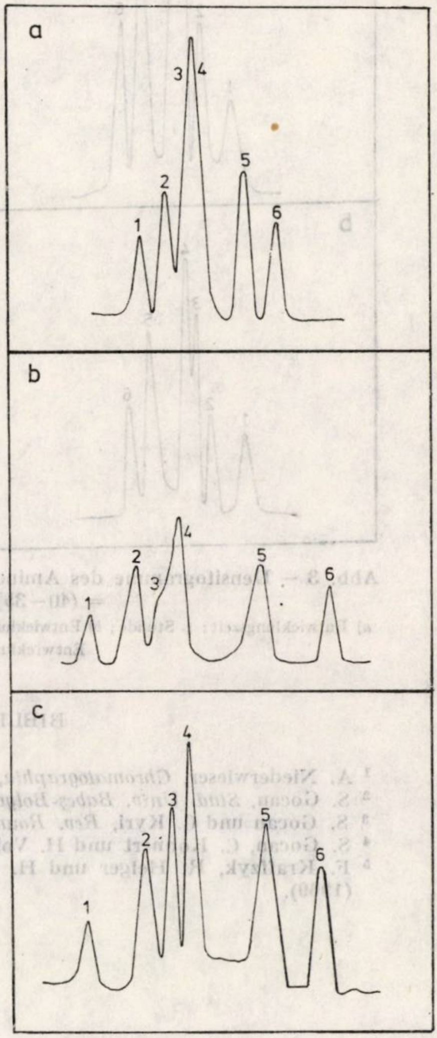

Abb. 2 — Densitogramme des Aminosäurengemisches aus Abb. 1 bei o-grad. $t = (25-20)/3 = 1{,}66$°C/mm;
a) Entwicklungszeit: 1 Stunde; *b*) Entwicklungszeit: 2 Stunden; *c*) Entwicklungszeit: 3 Stunden.

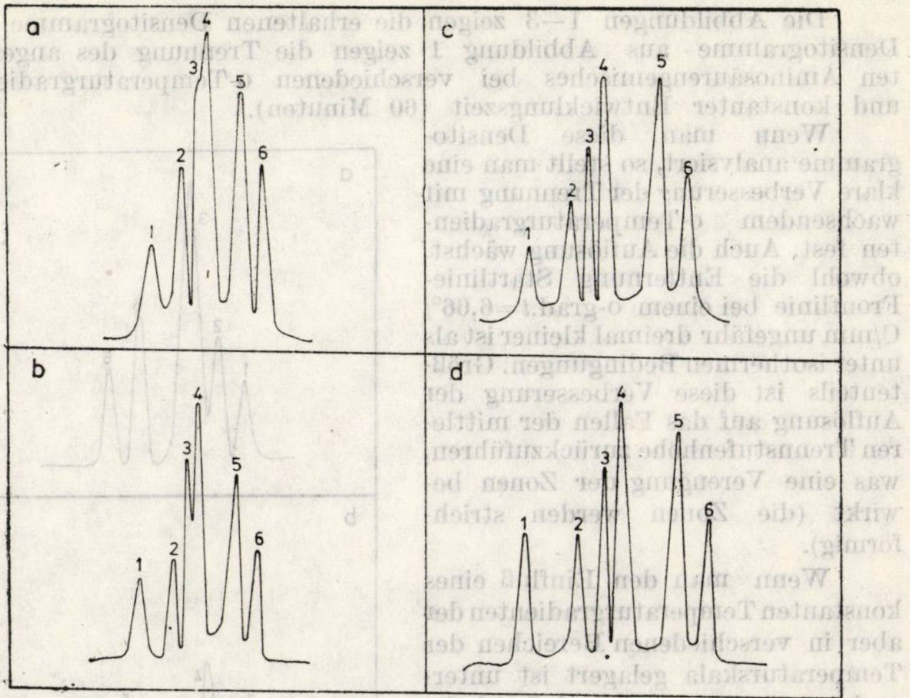

Abb. 3 — Densitogramme des Aminosäurengemisches aus Abb. 1 bei o-grad.t = = (40−35)/3 = 1,66°C/mm ;

a) Entwicklungszeit : 1 Stunde ; *b*) Entwicklungszeit : 1,5 Stunden ; *c*) Entwicklungszeit : 2 Stunden ; Entwicklungszeit : 3 Stunden.

BIBLIOGRAPHIE

[1] A. Niederwieser, *Chromatographia*, **2**, 362 (1969).

[2] S. Gocan, *Stud. Univ. Babeş-Bolyai, Chem.*, **20**, 33 (1975).

[3] S. Gocan und C. Kyri, *Rev. Roumaine Chim.*, **19**, 1957 (1974).

[4] S. Gocan, C. Konnert und H. Voik, *Rev. Roumaine Chim.*, **23**, 133 (1978).

[5] F. Kraffzyk, R. Helger und H. Lang, *Z. klin. Chemie und klin. Biochem.*, **7**, 521 (1969).

Revue Roumaine de Chimie, **25**, *2*, 277–283 (1980)

FERROCENE POLYMERS AS POLYMERIZATION INITIATORS. II[1]

POLYMERIZATION OF SOME *p*-ALKYLATED CHLOROFORMYLATED VINYL MONOMERS

CR. SIMIONESCU, I. MAZILU, LUCIA TĂTARU and TATIANA LIXANDRU
Department of Organic Chemistry,
Polytechnic Institute of Jassy,
Str. 23 August, No. 11, Jassy, Romania

Received May 5, 1979

In the present paper the results obtained in testing ferrocene polymers in polymerization of *p*-substituted chloroformylated vinylic monomers are reported. Using MO calculations in Hückel approximation, a series of molecular characteristics of the monomers used were estimated. The resulted products are oligomers with average polymerization degree between 3 and 14 showing thermal stability up to 300–400°.

INTRODUCTION

Ferrocene polymers and pyropolymers were studied for their catalytic action.[2–6] They were found to be efficient in the dehydrating and dehydrogenating reactions of alcohols.[7–9] Simionescu and coworkers tested recently a series of ferrocene polymers as redox initiators for polymerization of *p*-substituted chloroformylated vinylic monomers.[1]

In the present paper the polymerization of other *p*-substituted chloroformylated vinylic monomers in the presence of initiators is reported.

EXPERIMENTAL

The polymerization was carried out by the block procedure, in sealed glass vials, in inert medium, at an initiator concentration of 0.1–1.0%. The obtained products were soluble in common organic solvents. They were purified by dissolution in benzene followed by filtration of the initiator and precipitation with acidified methanol. The conversion was estimated gravimetrically.

The IR spectra were recorded on a SPECORD-71 apparatus. The thermograms were obtained by means of a MOM (J. Paulik, F. Paulik, L. Erdey — Budapest) apparatus.

RESULTS AND DISCUSSION

In the previous studies the polymers obtained from α-chloro-β-formyl-*p*-ferrocenylstyrene at 180° (A) and *p*-ferrocenylphenyl-acetylene at 200° (B) were found to be satisfactorily efficient as redox initiators in the polymerization of *p*-substituted chloroformylated vinylic monomers. Their efficiency is more evident in the case of the less reactive monomers, at temperatures below 150° at which the thermal polymerization does not proceed. The catalytic action of these polymers is probably due to the ion pair existing in the molecule which behaves as redox initiator under the reaction conditions.[1]

The polymerizations of *p*-methyl and *p*-ethyl-α-chloro-β-formylstyrene[10] in the presence of the initiators A and B were studied. The influence of the *p*-substituents on the monomer reactivity was appreciated on the basis of MO calculation in Hückel approximation. The parameters used for the coulombian (α) and resonance (β) integrals were those given in literature for the same bonds in similar compounds.[11–13] The molecular diagrams were drawn (Figure 1).

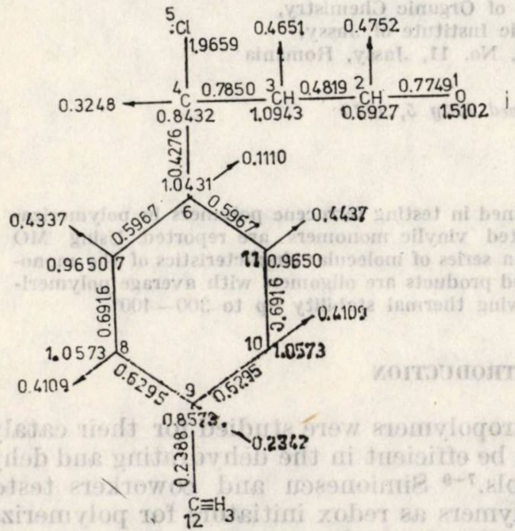
5
:Cl
0.4651
0.4752
1.9659
4
C
0.7850
3
CH
0.4819
2
CH
0.7749
1
O
0.3248
0.8432
1.0943
0.6927
1.5102
0.4276
0.1110
1.0431
0.4337
0.5967
6
0.5967
0.4437
0.9650
7
11
0.9650
0.6916
0.6916
0.4109
10
1.0573
1.0573
8
0.4109
0.6295
9
0.6295
0.8573
0.2342
0.2388
C≡H
12
3

Fig. 1. — The molecular diagram of α-chloro-β-formyl-*p*-methyl-styrene.

In table 1 the data on the molecular characteristics of the monomers under study as well as of other chloroformylated vinylic monomers are given.

TABLE 1

Molecular characteristics of some *p*-substituted chloroformylated vinylic derivatives

Monomer	Total energy (β)	Resonance energy (β)	F	P
α-Chloro-β-formyl-styrene	19.5634	9.5634	0.3977	0.7941
α-Chloro-β-formyl-*p*-bromostyrene	24.3663	9.4664	0.4477	0.7940
α-Chloro-β-formyl-*p*-chlorostyrene	24.6642	12.1642	0.3948	0.7911
α-Chloro-β-formyl-*p*-methylstyrene	23.5436	13.1436	0.3944	0.7850
α-Chloro-β-formyl-*p*-ethylstyrene	23.5492	13.1375	0.3874	0.7809

F = free valence index
P = π electronic bond order

It can be seen from the values of the resonance energies and free valence indices of the sp² vinylic carbon that the alkyl groups increase the stabilization energy through resonance leading to a decrease of the monomer reactivity.

The thermal polymerization failed at 140° and proceeded in very low yields at 180°. In the presence of the initiators A and B the polymerization proceeded even at 140° in an yield of about 20 %.

By following the influence of the temperature and of the two initiators on the conversion degree of the p-methylated monomer (Figure 2) the initiator synthesized at 180° was found to be more efficient. Its structure is less crosslinked and promotes the electronic interchange in the redox system.[1]

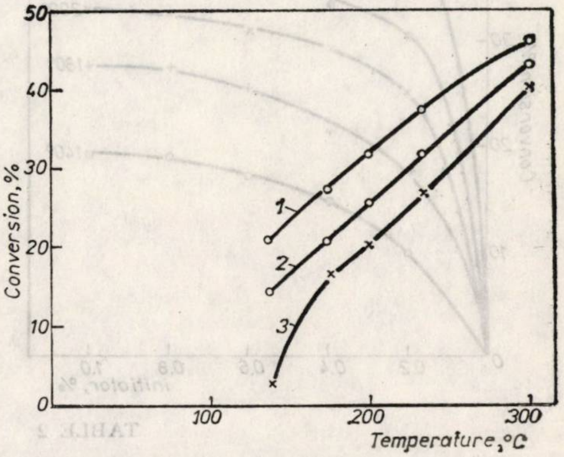

Fig. 2. — Variation of the polymer yield with temperature, initiator 1 % : *1.* polymerization with the initiator A ; *2.* polymerization with the initiator B ; *3.* thermal polymerization.

With this initiator (A) the influence of its concentration and of the temperature on the yield was followed. In figure 3 the yield variation is plotted *versus* initiator concentration at different temperatures for polymerization of the p-methylated monomer.

At a constant temperature a polymer yield increase with increasing of the initiator concentration is noticed up to 1 %, after that the yield increase is unsignificant. The yield increases gradually with the reaction duration up to 10 hours, remaining then almost constant. For this reason all runs were carried out at the optimum reaction time of 10 hours.

The data on the thermal polymerization as well as on the polymerization with initiators for these two monomers are given in table 2.

The data in table 2 demonstrate the initiator efficiency at temperatures between 140° and 230° for both monomers. The differences in the yield value for the two monomers are small owing to their close reactivities as results from both HMO calculation and experimental data. At temperatures above 230° the yields are about as high as those obtained by thermal polymerization.[10]

The average polymerization degree varies between 3 and 14. The lowest value (3) was obtained for the oligomer synthesized at 300°. At this temperature the polymerization is probably competing with the depolymerization to trimer.

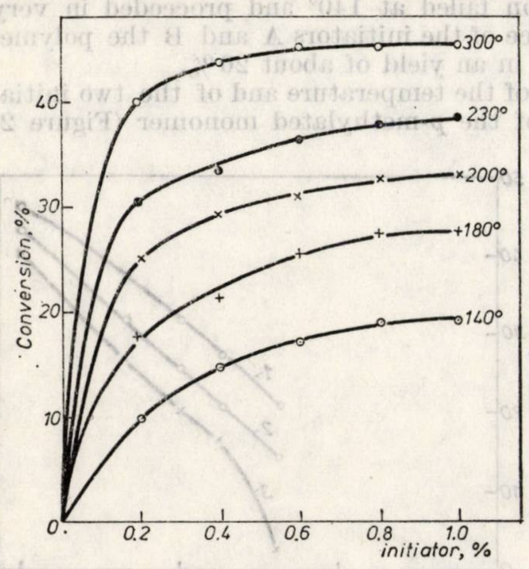

Fig. 3. — Yield *versus* initiator concentration.

TABLE 2

Temperature influence on the conversion and on the polymerization degree. (Initiator concentration 1 %; reaction time 10 hours).

Polymer [a]	Temperature, °	Conversion, %	Polymerization degree	Melting point, °
Me	140	5	—	
Me[b]	140	19.2	6	255
Me	180	18.5	6	256
Me[b]	180	27.5	6	255
Me	200	27.8	7	245
Me[b]	200	32.1	6	250
Me	230	31.8	14	256
Me[b]	230	37.3	14	256
Me	300	41.8	3	250
Me[b]	300	43.6	3	250
Et	140	—	—	—
Et[b]	140	11.3		
Et	180	15.6	6	195
Et[b]	180	22.7	6	195
Et	200	17.8	6	195
Et[b]	200	25.4	6	195
Et	230	21.2	7	190
Et[b]	230	26.5	6	185
Et	300	37.0	3	200
Et[b]	300	41.5	3	195

[a] Me = product obtained by thermal polymerization of α-chloro-β-formyl-*p*-methylstyrene; Et = product obtained by thermal polymerization of α-chloro-β-formyl-*p*-ethylstyrene.
[b] — product obtained by polymerization with initiators.

Characterization of the polymers

The synthesized polymers were characterized by means of elemental and thermodifferential analyses as well as by IR spectral measurements. The IR spectra of the polymers obtained at different temperatures and initiator concentrations are identical. Figure 4 presents the spectra of the *p*-methylated monomer (1) and of the corresponding polymer obtained at 230° and initiator concentration of 1 % (2).

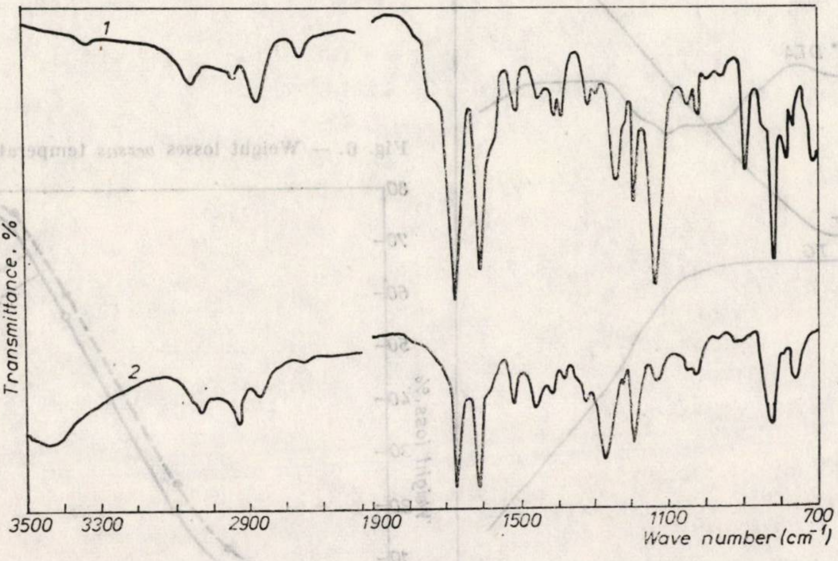

Fig. 4. — IR spectra of the *p*-methylated monomer (1) and of the polymer synthesized at 230°, initiator 1 %(2).

The monomer spectrum shows the absorption bands characteristic of the aromatic ring and of the functional groups ν(CO) 1675 cm^{-1}, ν(CH_3 sym) 2880 cm^{-1}, ν(CH_3 asym) 2913 cm^{-1}. The absorptions of the ethylenic double bond and of the halogen attached to the vinylic sp^2 carbon are superposed on those of the aromatic ring. However, the band at 720 cm^{-1} may be attributed to the chlorine attached to the vinylic sp^2 carbon.[14]

In the spectrum of polymer (2) all bands characteristic of the monomer, but of lower intensity, are to be found excepting for the absorption at 720 cm^{-1} which is absent due to the chlorine removal during polymerization.

The thermal stability was appreciated on the basis of the thermodifferential analysis data. In Figure 5 the thermograme of the polymer obtained from α-chloro-β-formyl-*p*-methylstyrene at 230° with initiator (1 %) is given.

The weight losses of the *p*-methylated (1) and *p*-ethylated (2) derivatives *versus* temperature are shown in figure 6.

The synthesized compounds show a particular thermal stability. The weight losses begin above 400° reaching 84% at 900°.

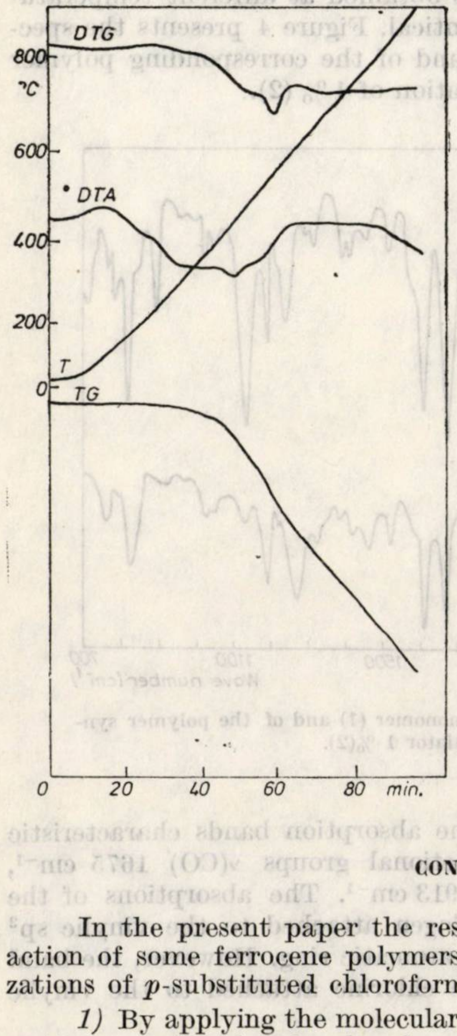

Fig. 5. — Thermogram of the *p*-methylated polymer synthesized at 230°, initiator 1 %.

Fig. 6. — Weight losses *versus* temperature

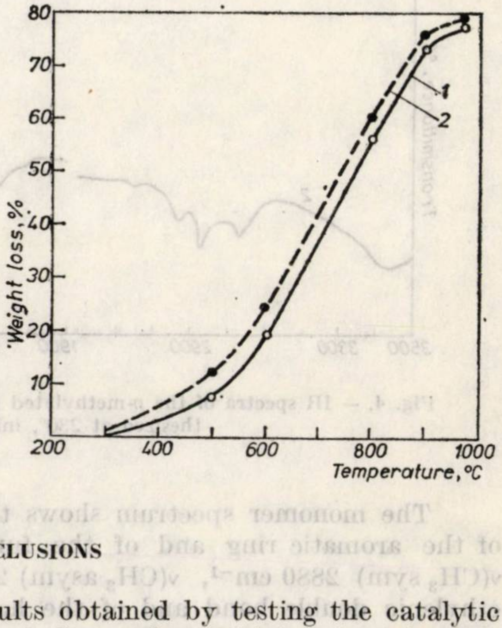

CONCLUSIONS

In the present paper the results obtained by testing the catalytic action of some ferrocene polymers used as redox initiators in polymerizations of *p*-substituted chloroformilated vinylic monomers are reported.

1) By applying the molecular orbital calculation in Hückel approximation, a series of molecular characteristics of the monomers were determined.

2) The initiated polymerizations of *p*-methyl and *p*-ethyl-α-chloro-β-formylstyrene were achieved in higher yields than in the case of thermal polymerization, under similar conditions. The obtained products are oligomers with average polymerization degree between 3 and 14.

3) The synthesized oligomers show a good thermal stability up to about 400°.

REFERENCES

[1] PartI : Cr. Simionescu and I. Mazilu, *Rev. Roumaine Chim.*, **22**, 753 (1977).

[2] K. H. Keier and I. Astofiev, *Kinetica i kataliz*, **3**, 364 (1962).

[3] J. Manassen and J. Wallach, *J. Amer. Chem. Soc.*, **87**, 2671 (1965).

[4] A. A. Slinkin, A. A. Dulov. I. M. Glavteva and L. M. Rutenstein, *Kinetica i kataliz*, **8**, 136 (1967).

[5] J. Gallard, Th. Lacaderlich, R. Salle and Ph. Fraynard, *Bull. Soc. chim. France*, **10**, 2204 (1963).

[6] J. Gallard, M. Nechtschein, M. Sontif and Ph. Fraynard, *Bull. Soc. chim. France*, **10**, 2209 (1963).

[7] M. A. Voronina, T. P. Vishnyakova, Ya. M. Paushkin. M. A. Bojilova and L. A. Aliev, *Vysokomol. Soedineniya*, **11**, 882 (1969).

[8] Ya. M. Paushkin, "5th International Conference on Organometallic Chemistry", vol. 2, Moscow, 1971, p. 577.

[9] Ya. M. Paushkin, T. P. Vishnyakova, A. F. Lunin and C. A. Nizova, "Organicheskie polimernyie polyprovodnike", Izd. Khim. Moscow, 1971, ch. IV and V.

[10] T. Lixandru, L. Tătaru, I. Mazilu and I. Cocîrlă, *Bul. Inst. Polit. Iași*, **22 (26)**, fasc. 1–2, 55 (1976).

[11] P. Purcell and J. Singer, *J. Amer. Eng. Data*, **12**, 235 (1967).

[12] A. Streitwieser, Jr., "Molecular Orbital Theory for Organic Chemists", Wiley, New York, 1961, ch. II and V.

[13] T. Lixandru, C. Ghirvu, L. Tătaru and I. Mazilu, *Bul. Inst. Polit. Iași*, **23 (27)**, fasc. 1–2, 65 (1977).

[14] M. Avram and G. D. Mateescu, "Infrared Spectroscopy", Wiley-Interscience, New York, 1966.

Revue Roumaine de Chimie, 25, *2*, 285–293 (1980)

CHEMICAL MODIFICATION OF POLYMERS. I

REACTION OF VINYL CHLOROACETATE COPOLYMERS WITH SOME HERBICIDAL SODIUM PHENOXIDES

DEMETRA DRĂGAN and A. CARPOV
"P. Poni" Institute of Macromolecular Chemistry, Jassy, Aleea Grigore Ghica
Vodă 41 A, Romania

Received July 11, 1978

Vinyl chloroacetate copolymers prepared by chloroacetylation of poly(vinyl alcohol) react with sodium salts of some herbicidal phenols in dipolar aprotic solvents by a bimolecular nucleophilic displacement mechanism yielding polymers with alkylaryl ether linkages in the side groups. The reactivity of the phenoxide anions is discussed as a consequence of electronic and steric effects of the substituents in the ring. The polymers were characterized by elemental analysis and IR spectra.

The controlled release of pesticides from polymeric systems uses the potential of pesticide-polymer combinations as a means of securing the localized, continuous release of a pesticide in the correct amount over an appropriate time period.

In recent years a lot of pesticide-polymer formulations have been proposed. A comprehensive review on controlled release of bioactive compounds, including herbicides is the recent paper of G. G. Allan et al.[1]

There have been so far known two synthetic routes to polymeric herbicides having halogeno(alkyl)aryloxyalkyl carboxylic ester units as pendent substituents to the vinyl polymer backbone : a) reaction of poly (vinyl alcohol) with the respective acid chlorides[2,3] and b) synthesis and polymerization of the respective vinyl halogeno (alkyl) aryloxyalkyl carboxylic esters.[4]

In the present paper another way of attaching side groups of aryloxyalkyl carboxylic ester type of the vinyl polymer backbone by means of the Williamson reaction was investigated. The chemical modification of the vinyl chloroacetate copolymers bearing displaceable chlorine with the sodium salts of some herbicidal phenols was used.

EXPERIMENTAL

The following herbicidal phenols were used : 2-sec-butyl-4-chlorophenol, 2-methyl-4-chlorophenol, 4-chlorophenol ($[H^+]_{25^\circ} = 3.60 \times 10^{-10}$),[5] 2,4-dichlorophenol ($[H^+]_{25^\circ} = 1.80 \times 10^{-8}$),[6] 2,4,5-trichlorophenol ($[H^+]_{25^\circ} = 1.00 \times 10^{-6}$),[7] pentachlorophenol ($[H^+]_{25^\circ} = 5.50 \times 10^{-6}$),[8] 2-sec-butyl-4,6-dinitrophenol and 2,4-dinitrophenol ($[H^+]_{25^\circ} = 1.10 \times 10^{-4}$).[9] Technical products were recrystallized for several times from the appropriate solvents.

The respective phenoxides were prepared : sodium 2-sec-butyl-4-chlorophenoxide (NaBCP), sodium 2-methyl-4-chlorophenoxide (NaMCP), sodium 4-chlorophenoxide (NaCP), sodium 2,4-dichlorophenoxide (NaDCP), sodium 2,4,5-trichlorophenoxide (NaTCP), sodium pentachlorophenoxide (NaPCP), sodium 2-sec-butyl-4,6-dinitrophenoxide (NaBDNP), and sodium 2,4-dinitrophenoxide (NaDNP).

They are synthesized either by azeotropic removal of water from an equimolar mixture of concentrated aqueous solution of sodium hydroxide and the respective phenol in xylene or by interaction of phenol and sodium in anhydrous ethanol.

Precautions must be taken in the case of air- and watersensitive phenoxides such as the first three products listed above. These phenoxides were prepared in an inert atmosphere.

All the other chemicals used were of a reagent grade.

The vinyl chloroacetate-vinyl acetate-vinyl alcohol copolymers (I) were prepared by chloroacetylation of various samples of poly(vinyl alcohol) (PVA) and are presented in table 1. Polymers A_1 — G were synthesized with chloroacetyl chloride in anhydrous N-methylpyrolidone[10]. Polymer A_2 was prepared by acid catalyzed esterification with chloroacetic acid.[11]

TABLE 1

Samples of vinyl chloroacetate copolymers used

Code	Type of PVA used*	Degree of polymerization of PVA[12]	Cl, % in the modified polymer	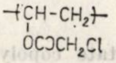 $-\!(\underset{OCOCH_2Cl}{\underset{\mid}{CH}}-CH_2)\!-$ (mole, %)	Molar conversion (% of the theoretical value)
A_1	N 30—88	350—450	26.50	85.62	97.29
B	N 50—88	500—600	26.36	84.57	96.10
C	N 70—88	1700—1800	26.28	83.98	95.43
D	N 30—98	500—600	28.65	94.85	96.78
E	N 50—98	—	28.44	93.05	94.94
F	N 70—98	1700—1800	28.18	90.88	92.73
G	N 90—98	2400—2500	28.30	91.85	93.72
A_2	N 30—98	350—450	21.67	56.34	64.02

* The PVA samples (Mowiol) were kindly supplied by Hoechst AG, Frankfurt (M) ; 30, 50, 70, 90 designate the Fikentscher constants and 88, 98, the hydrolysis degree, respectively.

The catalysts used were anhydrous sodium iodide (NaI) and triethylmethylammonium iodide (TEMAI).

The solvents were N,N-dimethylformamide (DMF), N-methylpyrolidone (NMP), hexamethylphosphorotriamide (HMPTA) and dimethyl-sulphoxide (DMSO).

All the syntheses were carried out in homogeneous media. Equal volumes of solutions (50 ml) of the starting copolymer (21.80 mmoles) and of the sodium phenoxide in a slight excess (5—10%), with or without a catalyst, were stirred at 25—80°, for the appropriate time intervals.

The crude polymers were purified by repeated precipitations of a DMF solution into large amounts of water and then dried in vacuo.

The actual composition of the modified polymers was determined by elemental analysis and IR spectra.

The molar conversions of polymers were estimated from analytical data (Cl, % ; N, %) by using the theoretical curves of conversions.

The IR spectra (KBr) were recorded on a UNICAM SP-200 spectrophotometer.

RESULTS AND DISCUSSION

The reaction of vinyl chloroacetate units from the starting copolymer (I) with various sodium phenoxides (II) in the above mentioned dipolar aprotic solvents leading to soluble copolymers (III) has been examined :

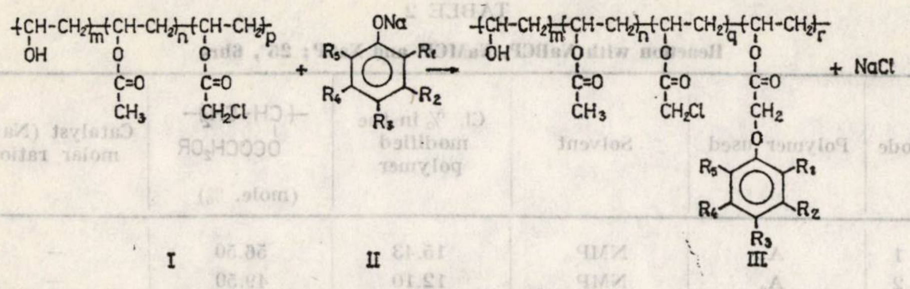

where, III-1 R_1 = sec-butyl ; R_2, R_4, R_5 = H ; R_3 = Cl
III-2 $R_1 = CH_3$; R_2, R_4, R_5 = H ; R_3 = Cl
III-3 R_1, R_2, R_4, R_5 = H ; R_3 = Cl
III-4 R_1, R_3 = Cl ; R_2, R_4, R_5 = H
III-5 R_1, R_3, R_4 = Cl ; R_2, R_5 = H
III-6 R_1, R_2, R_3, R_4, R_5 = Cl
III-7 R_1 = sec-butyl ; R_2, R_4 = H ; R_3, $R_5 = NO_2$
III-8 R_1, $R_3 = NO_2$; R_2, R_4, R_5 = H

The Williamson synthesis of ethers thus allows the preparation of a large variety of such copolymers with different substituents in the ring which cannot be prepared by direct polymerization (or only with difficulty).

It is well known that the reaction between reactive polymeric or non-polymeric organic halogen derivatives and alkaline phenoxides proceeds smoothly in homogeneous media of dipolar aprotic solvents of a relatively high dielectric constant and affords 0-alkylation products by a typical bimolecular nucleophilic displacement (SN_2 reaction) of the reactive halogen with the phenoxide anions. [12–15]

A complete conversion by chemical modification of pendent reactive groups on polymers is generally difficult to achieve though, in some cases, as in the present paper, satisfactory conversions are attainable. Steric inaccessibility and the low reactivity of the nucleophiles is very likely to contribute to the small extents of the reactions.

The rate enhancement of reactions involving negative ions and organic molecules caused by dipolar aprotic solvents has been generally ascribed both to an increased reactivity of the ions as a result of their reduced solvation, and to an increased solvation of the transition state which has an extended charged structure.[16] The tight solvation of the cation promotes the dissociation of the phenoxides to a "bare phenolate anion", which is a labile species and therefore a very active nucleophile.

Tables 2—6 show the results of reaction between the sodium phenoxides listed in the experimental part and the vinyl chloroacetate copolymers given in table 1 affording the modified copolymers with pendent alkylaryl ether linkages.

Although the substitutions are markedly reversible in homogeneous media the precipitation of the sodium chloride exerts a strong suppression on the back reaction.

Several attempts were made to determine the reaction extent and velocity in the presence of a catalyst.

It is also known that the dipolar aprotic solvents (DMF, DMSO, HMPTA) favour the replacement of chlorine by iodine in mixtures of

TABLE 2

Reaction with NaBCP, NaMCP and NaCP; 25°, 6hrs

Code	Polymer used	Solvent	Cl, % in the modified polymer	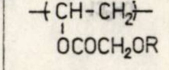 $-(\underset{OCOCH_2OR}{CH}-CH_2)-$ (mole, %)	Catalyst (NaI) molar ratio
1	A_1	NMP	15.43	56.50	—
2	A_2	NMP	12.10	49.50	—
3	A_2	NMP	12.46	46.50	1 :0.50
4	A_2	DMSO	12.47	46.50	—
5	A_2	NMP	14.20	46.00	—
6	A_1	NMP	15.73	74.70	—
7	A_1	DMF	16.00	71.30	—
8	A_1	DMSO	16.18	68.80	—
9	A_1	DMSO	18.00	52.00	1 :1
10	A_1	DMF	16.00	81.60	—
11	A_1	DMSO	16.20	79.00	—
12	A_1	DMSO	16.40	76.50	1 :1
13	A_1	NMP	15.80	84.50	—
14	A_2	NMP	15.60	53.00	—

1–4 R = 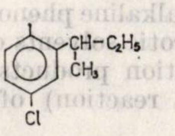

5–9 R = 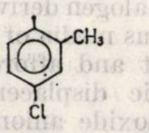

10–14 R = 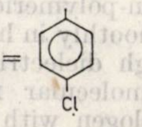

a reactive alkyl chloride and a strong electrolyte like an alkaline iodide or a tetraalkylammonium iodide according to the Finkelstein reaction.[17,18]

Therefore, it may be expected that the starting polymeric substrate partially substituted with iodine becomes more reactive in the nucleophilic substitution under consideration.

For this reason, various amounts of such a catalyst (NaI, TEMAI) were added to the reaction media at the appropriate temperature before the addition of the corresponding phenoxide.

The amount of catalyst, reported in the last column of tables 2–6, ranges from 1 : 0.25 to 1 : 1 molar ratio of I to the catalyst.

The presence of a soluble iodide in the medium has a positive effect (a catalytic effect) only in the reactions of the less reactive phenoxides in the series (tables 3, 5, 6). With the phenoxides in table 2 which provide strong nucleophilicities, a decreased extent of the respective reactions was observed, according to a secondary salt effect in the bimolecular nucleophilic displacements.[19]

The various examples in tables 2–6 are consistent with the electronic effects and the size of the substituents in the phenoxide anions. The extent of conversion to polymers III is also determined by the affinity and the accessibility of the anionic species to the electrophilic center in the polymeric substrate and by the strength of the arising C–O bond.

TABLE 3

Reaction with NaDCP and NaTCP; 6 hrs

Code	Polymer used	Solvent	Temperature (°C)	Cl, % in the modified polymer	$-\!(\underset{\text{OCOCH}_2\text{OR}}{\text{CH}}-\text{CH}_2)\!-$ (mole, %)	Catalyst (molar ratio)	
						NaI	TEMAI
15	A_1	NMP	40	27.08	69.00	—	—
16	A_1	NMP	25	27.15	65.50	1 :0.25	—
17	A_2	NMP	25	24.13	44.00	—	—
18	A_2	NMP	40	24.37	53.00	—	—
19	A_2	DMSO	25	24.09	44.50	—	—
20	A_2	DMF	80	32.33	52.00	—	—
21	A_2	NMP	80	32.40	52.50	—	—
22	A_2	NMP	40	31.42	44.00	—	—
23	A_2	NMP	40	32.42	52.50	—	1 :0.50
24	A_1	NMP	80	34.25	56.00	—	—
25	A_1	HMPTA	80	32.15	34.00	—	—
26	A_2	NMP	25	32.30	51.50	1 :0.50	—

15—19 R =

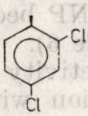

20—26 R =

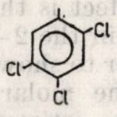

TABLE 4

Reaction with NaTCP; 6hrs, 80°, without a catalyst, in NMP

Code	Polymer used	Cl, % in the modified polymer	$-\!(\underset{\text{OCOCH}_2\text{OR}}{\text{CH}}-\text{CH}_2)\!-$ (mole, %)	Molar conversion (% of the theoretical value)
27	A_1	34.25	56.00	65.39
28	A_2	32.40	52.50	93.18
29	B	33.97	54.00	58.53
30	C	33.57	49.00	58.35
31	D	35.60	59.50	62.73
32	E	34.97	53.50	57.49
33	F	34.44	47.00	51.71
34	G	35.10	55.00	59.88

R=

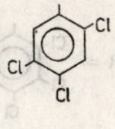

Like in the low-molecular alkyl α-halomethyl esters the replacement of chlorine is facilitated by the vicinity of the ester group but in the copolymer I the accessibility of the phenoxide anions to the reaction center is considerably restricted due to the proximity of the latter to the polymer backbone.

Dispersal of charge by electron-withdrawing groups ($-NO_2$) as in NaBDNP and NaDNP produces large anions stabilized through resonance (charge delocalization). This effect, in connection with the significant steric interactions with the polymeric substrate make these phenoxide anions behave as weak nucleophiles (Table 6).

Conversely, the other phenoxide anions with chlorine and alkyl substituents in the ring, having a much greater electronic density on the phenoxydic oxygen are proved to be relatively strong nucleophiles. With the latter phenoxides the steric interactions with the polymer are also less important and therefore, higher conversions to the final polymer are achieved (tables 2—5).

Generally, with increasingly bulky substituent in the 2-position of the phenoxide anions, steric hindrance becomes predominant as against the polar effects. For instance, with NaBCP, NaMCP, NaCP as the series of substituents hydrogen, methyl, sec-butyl is ascended, ether formation will become increasingly difficult (table 2).

This effect is the greatest with NaBDNP because of the two bulky substituents in the 2— and 6-positions (table 6).

In order to show the differencies in reactivity with various polymeric substrates the molar conversions in reaction with NaTCP, without a catalyst, were estimated (table 4).

The highest conversion with A_2 can be explained in that the vinyl chloroacetate units in the polymer are apart from each other and therefore the steric impediments in the substitution reaction are of little importance.

TABLE 5

Reaction with NaPCP; 6hrs

Code	Polymer used	Solvent	Temperature (°C)	Cl, % in the modified polymer	$-\!\!\left(\underset{\substack{\vert \\ OCOCH_2OR}}{CH}-CH_2\right)\!\!-$ (mole, %)	Catalyst (TEMAI) molar ratio
35	A_1	HMPTA	80	36.89	21.00	—
36	A_1	DMF	80	44.31	53.50	—
37	A_1	DMSO	80	42.91	45.00	—
38	A_1	NMP	80	45.62	61.50	—
39	A_1	NMP	60	45.45	61.00	1 :0.65
40	A_1	NMP	40	34.46	13.50	—
41	A_2	NMP	80	42.97	46.00	—

R =
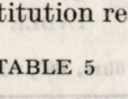

With the other samples of copolymers I quite similar values of conversions were obtained.

The eight phenoxides tested in the above nucleophilic displacement reaction can be divided into three groups:

a) phenoxides which easily react at 25°;
b) phenoxides which react at 40°;
c) phenoxides which react significantly only at 80°.

TABLE 6

Reaction with NaBDNP and NaDNP; 80°

Code	Polymer used	Solvent	Time (h)	N, % in the modified polymer	$-\!\left(\underset{\mathrm{OCOCH_2OR}}{\mathrm{CH}}-\mathrm{CH_2}\right)\!-$ (mole, %)	Catalyst (NaI) (molar ratio)
42	A_1	DMF	12	0.88	4.00	—
43	A_1	NMP	12	1.37	6.50	1 :0.50
44	A_1	DMSO	12	2.56	13.00	1 :0.50
45	A_2	DMF	12	0.97	3.80	—
46	A_1	NMP	6	1.05	4.50	—
47	A_1	NMP	12	3.86	20.00	—
48	A_1	NMP	12	6.25	38.00	1 :0.50
49	A_2	NMP	6	1.91	8.50	—
50	A_2	NMP	12	2.09	9.50	—
51	A_2	NMP	12	5.56	28.00	1 :0.50

42−45 R =

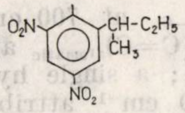

46−51 R =

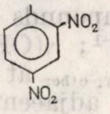

From the extent of reaction the following sequences of reactivity were found:

group a) NaCP > NaMCP > NaBCP
group b) NaDCP > NaTCP
group c) NaPCP > NaDNP > NaBDNP

It has been thus found that this reactivity of the phenoxides does not generally parallel the order of the decreasing basicity i.e. the order of the decreasing nucleophilic power of the respective anions.

Very similar effects on conversions were found with DMF, NMP, DMSO. With HMPTA, the strongest donor of electrons in the series,[20] relatively stable donor-acceptor adducts with the electrophilic center in the polymer are likely to be formed. Accordingly, smaller conversions to polymers III are to be expected. The data in tables 3 and 5 are consistent with this assumption.

All the chemically modified polymers are soluble in DMF, NMP, DMSO, HMPTA but are insoluble in water and in lower aliphatic alcohols. The polymers with a high chlorine content (III-6) are also soluble in chlorinated hydrocarbons.

In all experiments good yields of polymers (70–90 %) — which were white to light-brown powders — were obtained.

The analytical data of some selected samples reported in table 7 are in a satisfactory agreement with the supposed structure of the respective polymers.

The IR spectra of copolymers III show some absorption bands characteristic of the starting copolymer I together with some specific bands brought about by pendent phenolic moieties and the new C–O bond formed. This is also in accordance with the supposed chemical modification.

TABLE 7

Some analytical data of copolymers III

Code	C, %		H, %		Cl, %		N, %	
	calcd.	found	calcd.	found	calcd.	found	calcd.	found
2	60.34	59.71	6.50	6.35	—	12.10	—	—
7	56.45	56.63	4.92	4.88	—	16.00	—	—
11	55.71	55.40	4.45	4.31	—	16.20	—	—
18	49.35	49.66	4.02	3.98	—	24.37	—	—
20	43.76	43.21	3.28	3.22	—	32.33	—	—
38	35.82	36.04	1.99	1.95	—	45.62	—	—
45	44.95	44.65	5.22	5.02	18.64	17.93	—	2.56
51	45.38	45.96	4.23	4.50	7.54	8.11	—	3.86

Compounds I: $\nu(C-Cl)_{CH_2-Cl}$ at 695 cm^{-1}; $\nu(C=O)_{ester}$ at 1735 cm^{-1}; $\nu(OH)$ at 3420–3460 cm^{-1};

Compounds III–1: $\nu(C-Cl)_{CH_2-Cl}$ at 700 cm^{-1}; $\nu(C=O)_{ester}$ at 1735 cm^{-1}; $\nu(OH)$ at 3440 cm^{-1}; $\nu(C=C)_{aromatic}$ at 1590, 1480 cm^{-1}; $\nu(C-O)_{aryl\ ether}$ at 1240 cm^{-1} (shoulder); a single hydrogen at 875 cm^{-1} and two adjacent hydrogens at 820 cm^{-1} attributable to aromatic 1, 2, 4-trisubstitution.

Compounds III-2: $\nu(C-Cl)_{CH_2-Cl}$ 710 cm^{-1}; $\nu(C=O)_{ester}$ at 1730 cm^{-1}; $\nu(OH)$ at 3440 cm^{-1}; $\nu(C=C)_{aromatic}$ at 1590, 1480 cm^{-1}, $\nu(C-O)_{aryl\ ether}$ at 1235 cm^{-1}; a single hydrogen at 875 cm^{-1} and two adjacent hydrogens at 800 cm^{-1} attributable to aromatic 1,2,4-trisubstitution.

Compounds III-3: $\nu(C-Cl)_{CH_2-Cl}$ at 690 cm^{-1}; $\nu(C=O)_{ester}$ at 1735 cm^{-1}; $\nu(OH)$ at 3430 cm^{-1}; $\nu(C=C)_{aromatic}$ at 1580–1590, 1485 cm^{-1}; $\nu(C-O)_{aryl\ ether}$ at 1235 cm^{-1}; two adjacent hydrogens (aromatic 1,4-disubstitution) at 820 cm^{-1}.

Compounds III-4: $\nu(C-Cl)_{CH_2-Cl}$ at 695 cm^{-1}; $\nu(C=O)_{ester}$ at 1740 cm^{-1}; $\nu(OH)$ at 3490 cm^{-1}; $\nu(C=C)_{aromatic}$ at 1580, 1475 cm^{-1}; $\nu(C-O)_{aryl\ ether}$ at 1230 cm^{-1}; a single hydrogen at 870 cm^{-1} and two adjacent hydrogens at 820 cm^{-1} attributable to aromatic 1,2,4-trisubstitution.

Compounds III-5; $\nu(C-Cl)_{CH_2-Cl}$ at 680 cm^{-1}; $\nu(C=O)_{ester}$ at 1735 cm^{-1}; $\nu(OH)$ at 3450 cm^{-1}; $\nu(C=C)_{aromatic}$ at 1580, 1475 cm^{-1}; $\nu(C-O)_{aryl\ ether}$ at 1240 cm^{-1}; a single hydrogen (aromatic 1,2,4,5-tetrasubstitution) at 870 cm^{-1}.

Compounds III-6: $\nu(C-Cl)_{CH_2-Cl}$ at 710 cm^{-1}; $\nu(C=O)_{ester}$ at 1740 cm^{-1}; $\nu(OH)$ at 3450 cm^{-1}; $\nu(C-O)_{aryl\ ether}$ at 1240 cm^{-1}.

Compounds III-7 : $\nu(C-Cl)_{CH_2-Cl}$ at 690 cm^{-1}; $\nu(C=O)_{ester}$ at 1735 cm^{-1}; $\nu(OH)$ at 3440 cm^{-1}; $\nu(C=C)_{aromatic}$ at 1590, 1480 cm^{-1}; $\nu(C-O)_{aryl\ ether}$ at 1235 cm^{-1}; a single hydrogen (aromatic 1,2,4,6-tetrasubstitution) at 870 cm^{-1} (shoulder); $\nu(NO_2)$ at 1340 and 1530 cm^{-1} (shoulder).

Compounds III-8 : $\nu(C-Cl)_{CH_2-Cl}$ at 700 cm^{-1}; $\nu(C=O)_{ester}$ at 1735 cm^{-1}; $\nu(OH)$ at 3440 cm^{-1}; $\nu(C=C)_{aromatic}$ at 1600, 1485 cm^{-1}; $\nu(C-O)_{aryl\ ether}$ at 1240 cm^{-1}; a single hydrogen at 875 cm^{-1} (shoulder) and two adjacent hydrogens at 835 cm^{-1} attributable to aromatic 1,2,4-trisubstitution, $\nu(NO_2)$ at 1340 cm^{-1} and 1530 cm^{-1} (shoulder).

CONCLUSIONS

The Williamson reaction of vinyl chloroacetate copolymers with some herbicidal sodium phenoxides in dipolar aprotic solvents was investigated.

The process provides a new route of attaching aryloxyalkyl carboxylic ester type side groups with different substituents in the ring to the vinyl polymeric backbone.

A sequence of reactivity of the tested sodium phenoxides was established. The electronic and steric effects of the substituents in the respective phenoxides are discussed.

Soluble copolymers which are potential herbicidal polymeric compositions can thus be prepared by the stoichiometric control of the extent of reaction.

The actual composition of the polymers was determined by elemental analysis and IR spectra.

REFERENCES

[1] G. G. Allan, J. F. Friedhoff, W. J. Mc Connell and J. C. Powell, *J. Macromol. Sci., Chem.*, **A 10**, 223 (1976).

[2] G. G. Allan, C. S. Chopra, A. N. Neogi and R. M. Wilkins, *Nature*, **234**, 349 (1971).

[3] M. Dima, A. Carpov and S. Maxim, *Rev. Roumaine Chim.*, **13**, 485 (1968).

[4] F. W. Harris and L. K. Post, *J. Polym. Sci., Polym. Lett. Ed.*, **13**, 225 (1975).

[5] M. Z. Mizutani, *Z. physik. Chem. (Leipzig)*, **118**, 318 (1926).

[6] J. W. Murray and N. E. Gordon, *J. Amer. Chem. Soc.*, **57**, 110 (1935).

[7] A. Hantzsch, *Ber. dtsch. chem. Ges.*, **35**, 210 (1902).

[8] G. J. Tiessens, *Rec. Trav. chim.*, **50**, 112 (1931).

[9] J. M. Kolthoff, *Biochem. Z.*, **162**, 289 (1925).

[10] A. Carpov, D. Drăgan, *Angew. Makromol. Chem.*, **24**, 101 (1972).

[11] G. G. Zhilyaev, I. N. Faizullin, R. I. Ivanova, and V. A. Ezhova, *Plast. Massy*, **5**, 18 (1969).

[12] M. K. Lindemann in "Encyclopedia of Polymer Science and Technology", vol. 14, Ed. N. M. Bikales, Interscience, New York, 1971. p. 157.

[13] N. Kornblum and A. P. Lurie, *J. Amer. Chem. Soc.*, **81**, 2705 (1959).

[14] H. W. Gibson and F. C. Bailey, *J. Polym. Sci., Polym., Chem. Ed.*, **12**, 2141 (1974).

[15] H. Kamogawa, K. Kitahora, H. Hanawa and M. Nanasawa, *J. Polym. Sci., Polym. Chem. Ed.*, **14**, 1235 (1976).

[16] A. J. Parker, *Chem. Rev.*, **6**, 1 (1969).

[17] A. Roedig in Houben-Weyl "Methoden der Organischen Chemie", V/4 Bd., IV Aufl., Georg Thieme Verlag Stuttgart, 1960, S. 595.

[18] H. Tiedtke, G. Bühling and R. Kinne, Germ. Offen, 2 065 418 (to Nippon Oil Seal Industry Co., Ltd.) 10 Dec. 1970; *Chem. Abstr.*, **80**, 4214 (1974).

[19] F. Badea, "Mecanisme de reacţie în chimia organică", ed. II, Editura ştiinţifică, Bucureşti, 1973, p. 165.

[20] D. Martin, A. Weise and H. Y. Niclas, *Angew. Chem.*, **79**, 340 (1967).

Revue Roumaine de Chimie, **25**, *2*, 295–299 (1980)

A MODIFIED REVERSION TECHNIQUE FOR THE SPECTROPHOTOMETRIC DETERMINATION OF THALLIUM

D. C. RUPAINWAR* and K. K. KAKKAR**

* Applied Chemistry Section, Institute of Technology, Banaras Hindu University,
Varanasi-221005, India

** Chemistry Department, Lucknow University, Lucknow-226007

Received July 27, 1977

A modified reversion method has been developed for the determination of microgram quantities of thallium using dithizone as a reagent. The method is more accurate than the commonly employed mixed colour method.

INTRODUCTION

In recent years a number of colour reactions of thallium has been used to determine the metal by colorimetric method.[1–7] The interactions of dithizone, the well-known analytical reagent, with thallium have shown that while thallium (I) forms a 1 :1 red complex (pH range 9–12) extractable from carbontetrachloride or chloroform[8–9] the reaction with thallium (III) is quite complicated and the reagent is oxidized to give a series of oxidation products.[10] The spectrophotometric determination of thallium (I) using dithizone has been described by Clarke and Cuttitta.[8] However, the determination of thallium is based on the mixed colour method which depends on the constancy of standard solutions of dithizone. It has been recently shown[10–13] that dithizone solutions in chloroform are notoriously unstable and undergo ready oxidation especially when in contact with buffers of higher pH values. It has also been shown[12–13] that the oxidation products of dithizone absorb significantly in the region of the maximum absorption of the thallium (I) dithizone complex ; consequently, due to the presence of these adventitious light absorbing species the so-called mixed color methods are open to question.

To mitigate the instability of the reagent a reversion method previously reported by Irving[14] has been utilized. Thus, the details for the spectrophotometric determination of thallium (I) with dithizone have been worked out and the results are communicated in this paper.

---

* To whom all correspondence should be addressed

EXPERIMENTAL

Dithizone (Dz H_2) used was purified as described earlier.[14]

Preparation of thallium solution

Thallium metal (Johnson and Mathey's spectrographically pure) was dissolved in dilute nitric acid to get a solution of thallous nitrate. This solution was standardized by iodate titration and diluted with redistilled water to the desired concentration. The buffer solutions used were purified by shaking them with a dilute solution of dithizone in chloroform.

Spectrophotometric measurements for reversion procedure

The absorption spectra and absorbances were taken using Beckmann DU and SP. 500-spectrophotometers. The aqueous solution containing the desired amount of thallium and NH_4Cl-NH_4OH buffer of pH 10.2 was made up to 20 ml and then equilibrated for 2 minutes with a 20 ml solution of dithizone of the desired concentration (10^{-6} to 10^{-5}M) in chloroform. After settling, a portion of the organic phase was withdrawn through a dry pledget of cotton wool and its absorbance Am was measured at 505 nm using 1 cm cuvettes and chloroform in the reference cell. A further portion (about 10 ml) was withdrawn into another separating funnel and reverted by shaking for 2 minutes with an equal volume of 0.5N sulphuric acid. After the layers had separated, a portion of the organic phase was withdrawn as described above and its absorbance Ar was then measured.

DISCUSSION AND RESULTS

The formation and complete extraction of thallium 1 : 1 complex, at the pH employed, can be represented by

$$H_2Dz + Tl^+ \rightleftharpoons Tl(HDz) + H^+ \qquad (1)$$

If C_r is the (fixed) original concentration of the reagent and C_c the concentration of the complex formed, the absorbance of the organic phase measured in a cell of 1 cm will be given by

$$A_m = \varepsilon_c C_c + \varepsilon_r (C_r - C_c) \cdot k \qquad (2)$$

where ε_c and ε_r are the molar extinction coefficients of the complex and reagent respectively at the wavelength used. The factor k accounts for the partition of the dithizone between the two phases.

In the usual procedures i.e. the mixed colour method as the one used by Clarke[8] when the varying amounts of metal are shaken with a fixed (and excess) amount of the reagent – other factors being identical, a series of values of A_m is obtained. A calibration or standard curve plotted between the values of A_m and the initial metal content can then be interpolated to work out the metal concentrations of the unknown samples.

However, when dithizone is used as a reagent its solubility in the aqueous phase at higher pH values and its ready oxidation and re-extraction back into the organic layer can not be overlooked, which will obviously change the values of C_r and k in the equation (2) above. Now If C_i is the concentration of the extractable impurities (oxidation products) present in the organic layer, equation (2) should be amended to

$$\mathrm{A_m} = \mathrm{A}_c C_c + \mathrm{A}_r (C_r - C_c - x) \cdot k + \sum \varepsilon_i C_i \tag{3}$$

where A_i is the molar extinction coefficient of the impurity and x the amount of the reagent lost.

Now given the absorbance $\mathrm{A_m}$ of a mixed colour organic extract in a 1 cm cell with concentration of the complex C_c, the excess reagent C_r and C_i for various impurities is given by

$$\mathrm{A_m} = (\varepsilon_r C_r + \varepsilon_c C_c + \sum \varepsilon_i C_i) \tag{4}$$

If the organic phase is shaken with a reagent which decomposes only the metal complex TIHDz and thus permits the return of the metal ion into the aqueous layer and liberates an equivalent amount C_c of the reagent in the organic layer the new value of absorbance A_r is given by

$$A_r = (\varepsilon_r C_r + \varepsilon_r C_c + \varepsilon_i C_i) \tag{5}$$

This process is known as reversion and the change in absorbance which is termed as the reversion value, R, is given by

$$R = A_r - A_m = (\varepsilon_r - \varepsilon_c)\, C_c \tag{6}$$

It follows that a plot of the reversion value against the amount of the metal extracted should be linear. This curve is independent of the actual concentration of the reagent used and the presence of other light absorbing components. However, it must be emphasized that this is applicable only when (i) composition of the complex remains unchanged over the range of values of C_c involved, (ii) Beer's law is obeyed by the reagent and also its metal complex, and (iii) the reversion reagent is very specific.

The absorption spectra of the thallium dithizone mixed color system using chloroform in the solvent show two strong absorptions at 505 nm and 605 nm corresponding to the thallium complex and the ligand respectively. Thus, the absorption measurements for $\mathrm{A_m}$ and $\mathrm{A_r}$ were done at 505 and 605 nm and the reversion value $A_r - A_m$ was evaluated for different initial concentrations of thallium.

Figure 1 shows a plot of the reversion value against the initial amount of metal taken and is linear. Thus, unknown samples were worked out and the results are within ± 0.5 % error as shown in table I.

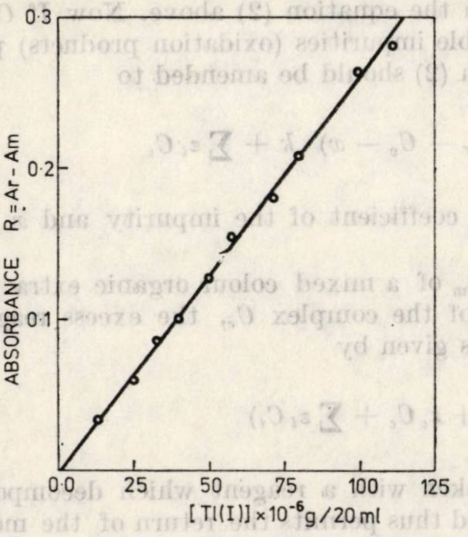

Fig. 1. — Calibration curve for Tl(I) determination by the reversion method.

TABLE 1

Analyses of thallium (I) samples with dithizone by the reversion method

S. No.	Tl (I) Taken $\times 10^{-6}$ gm/20 ml	Tl(I) Found $\times 10^{-6}$ gm/20 ml
1.	12.2	12.2
2.	24.4	24.5
3.	36.6	36.4
4.	48.8	49.0
5.	61.0	60.8

The method has proved useful and convenient for the analysis of thallium in its ores and minerals and is more reliable than the previously reported mixed colour method.

ACKNOWLEDGEMENTS. The authors are thankful to the Director of the Institute of Technology, Banaras Hindu University and Head of the Chemistry Department, Lucknow University for providing laboratory facilities.

REFERENCES

[1] C. Constantinescu and G. Constantinescu, *Rev. Roumaine Chim.*, **21**, 571 (1976).
[2] A. Serbanescu, *Rev. Chim. (Bucureşti)*, **26**, 771 (1975).
[3] E. Uhlemann and B. Schuknecht, *Analyt. Chim. Acta.*, **69**, 79 (1974).
[4] V. Zh. Artsruni and V. M. Tarayan, *Arm. Khim. Zhur.*, **27**, 106 (1974).

[5] A. Şerbănescu, *Chim. Anal.*, **1**, 84 (1973).

[6] Gr. Popa, C. Patroescu G. Constantinescu, *Chem. Anal.*, **2**, 243 (1972).

[7] A. Aleksandrov and A. Dimitrov, *Nauk. Tr, Plovdivski Univ. Mat. Fiz., Khim., Biol.*, **11**, 79 (1973).

[8] R. S. Clarke Jr and F. Cuttitta and references therein, *Analyt. Chim. Acta.*, **19**, 555 (1958).

[9] D. C. Rupainwar, Ph. D. Thesis, Univ. of Leeds, 1969.

[10] D. C. Rupainwar and H.M.N.H. Irving, *Proc. Soc. for Anal. Chem. (U.K.)* **6**, 188 (1969).

[11] H. Irving, A. M. Kiwan, D. C. Rupainwar and S. S. Sahota, *Analyt. Chim. Acta.*, **56**, 205 (1971).

[12] H. Irving, U. S. Mahnot and D. C. Rupainwar, *Aanlyt. Chim. Acta.*, **49**, 261 (1970).

[13] H. Irving and D. C. Rupainwar, *Analyt. Chim. Acta.*, **48**, 187 (1969).

[14] H. Irving, E. J. Risdon and G. Andrew, *J. Chem. Soc.*, **1949**, 537.

Revue Roumaine de Chimie, **25**, *2*, 301–303 (1980)

COMPTES RENDUS

Topics in Current Physics, vol. 11. "Raman Spectroscopy of Gases and Liquids", editor A. Weber, Springer Verlag, Berlin, Heidelberg, New York, 1979, 318 pages.

This book is being published on the occasion of the 50th anniversary of the discovery of the Raman effect. Numerous interesting researches have been carried out from the beginning but the introduction of lasers constituted a real breakthrough, expressed today by the denomination of "Laser Raman Spectroscopy".

The present volume is intended to bring in one book the results of modern researches (after 1973) on Raman spectroscopy of gases and liquids.

After a short introduction (by A. Weber) chapters 2 and 3 are devoted to high resolution Raman studies of low pressure gases and vapors. A modern theory of rotational Raman scattering is included in chapter 2 (written by S. Brodersen) beside some details concerning the experimental technique. The most important part of this chapter contains a review of the high resolution rotation — vibrational Raman spectra obtained in recent years. It is known that at present Raman spectra cannot be obtained with a resolution comparable to the best IR instruments. Nevertheless, Raman spectra afford more accurate values for molecular constants and consequently such data are detailed in chapter 2.

From chapter 3 (by A. Weber) we note the interesting problems of instrumentation and technique (e.g. scattering cells, the spectrograph, the photoelectron setting principle) and a rich collection of data concernig molecular characteristics of various molecules (starting from stable diatomic ones and going up to rather complex poliatomic ones e.g. dimethyldiacetylene, *sym*-triazine, *trans*-butadiene etc.).

In chapter 4 (by H. W. Schrötter and H. W. Klöckner) a critical review of Raman scattering cross section measurements in gases and liquids is presented. The results of the determinations with pre-laser techniques are included and reevaluated with the newer laser-derived results.

Chapter 5 (by R. P. Srivastava and H. R. Zaidi) describes, mainly theoretically, the effects of intermolecular forces (which become important on increasing gas density) on spectral shapes.

In chapter 6 (by D. L. Rousseau, J. M. Friedman and P. F. Williams) the basic mechanisms by which resonant Raman scattering could occur are described. Some illustrative examples e.g. iodine, porphyrine compounds (which are "without question the clearest and most beautiful example of scattering by the Herzberg — Teller mechanism") are also included.

The last chapter 7, (by J. W. Nibler and G. V. Knighten) is devoted to Coherent Anti-Stokes Raman Scattering (CARS), a nonlinear optical technique used to obtain a great coherence and signal strength, retaining, at the same time, the general applicability of spontaneous Raman spectroscopy. This phenomenon was observed in 1963 but developed to its real value only after the introduction of lasers in Raman spectroscopy. The subject of this chapter seems to be the most actively investigated one in this field.

In conclusions, this valuable book brings a lot of new and interesting results in the domain of laser Raman spectroscopy. Even dedicated mainly to physicists many parts of the book are very useful for chemists also.

M. Banciu

Academy of the Socialist Republic of Romania, "Memoriile secţiilor ştiinţifice" (Proceedings of the Scientific Sections), Fourth Series, Volume 1, 1977—1978, Editura Academiei R. S. România, Bucharest, 1979, 400 pages.

The *Proceedings of the Scientific Sections* of the Romanian Academy reappear with this new, fourth, series after a 30 year interruption. As set forth by Academician Prof. Cristofor Simionescu in his introductory remarks, one of the chief aims of the new series is to publish survey studies in frontier areas of various sciences in which original research has been carried out within the eight scientific sections of the Academy, as well as various authoritative contributions from the Academy's members and other specialists. There would be no overlap with the other regular publications of the Academy : the papers published in the *Proceedings* would be larger in scope and would express more comprehensive points of view than ordinary research communications.

The first volume includes 17 such survey and specialist reports, communicated within the plenary sessions of the Academy during 1977—78, three of which are dedicated to physics and chemistry subjects : "Researches on the properties of some spinel ferrites" by E. Luca, N. Rezlescu and E. Rezlescu (Center of Technological Physics, Jassy), "Researches on the precursors of the living matter" by C. Simionescu and E. Schneider (Institute of Macromolecular Chemistry, Jassy), and "The role of chemistry in the technico-scientific revolution in Romania" by M. Florescu (Ministry of Chemical Industry, Bucharest). All these papers are published in full and contain all the data to make them self-contained.

In the opinion of the reviewer, a major drawback of this first volume is that only part of the material is published in foreign languages, thus preventing potentially interested readers from abroad from properly understanding the arguments. It is hoped that in the future volumes a larger part of the papers will be published in English or French.

The Romanian Academy's tradition of publishing its proceedings goes back to 1867 and this has played a significant part in the dissemination of culture and science all along. The initiation of the new series is thus most welcome.

Alex. Butucelea

R. BARBUCCI (editor), "Calorimetry", Publishing Company : Edizioni Scuola Universitaria, Firenze, 1979, 238 p.

The aim of this book is to present the lectures given at the International School on Calorimetry held in Ischia (Naples), on May 1977. This school is a logical continuation of the Summer School on Stability Constants, held in Bivigliano (Florence), on June, 1974. Both of them, in turn, are to be considered as a part of the scientific and educational activity of the "Italian Group of the Thermodynamics of Complexes", founded in 1972.

Presently, several calorimeters may be found on the market and most of them are easy to use. However, there is a lack of information concerning both the data which may be obtained from these instruments and their interpretation. Since Calorimetry is a science requiring a strict control of the experimental conditions, it is imperative to instruct young scientists to have a correct approach towards it, hoping that one day they will surpass their masters. The contributions may be divided as follows : in the first part, papers concerning calorimetry in solution, namely those of Christensen, Tyrrell, Wadsö, Cabani and Paoletti are collected. The second part is devoted to Differential Scanning Calorimetry (Mortimer), and Combustion Calorimetry (Pilcher). Finally, Staveley relates about calorimetry at low temperature, which calls for instruments and techniques different from those usually known. Needless to say, the lecturer's names are too well known all over the world to need presentations.

I hope that the main purpose of this book, to present a coherent and rigorous approach to Calorimetry has been at least partly fulfilled.

Rolando Barbucci

"PLASMACHEMIE, Prozesse der chemischen Stoffumwandlung unter Plasma-Bedingungen", Akademie-Verlag-Berlin, 1978, von Helmut Drost (Berlin), 420 Seiten mit 91 Abbildungen, 32 Tabellen und 589 Literaturzitaten.

Die vorliegende Monographie behandelt, als zentrales Thema, die chemischen Vorgänge und Erscheinungen die durch ein Plasma verursacht und allgemein als ,,Plasmachemie" oder ,,Stoffumwandlung in Plasma" bezeichnet werden. Demzufolge befaßt sich der Hauptteil der Ausführungen mit der Durchführung chemischer Stoffumwandlungen in Plasma.

In einem einleitenden Kapitel (Kap.1) wird dieses Sachgebiet vorgestellt und die Entwicklungsgeschichte der Plasmachemie kurz skizziert. Indem die Unterschiede zwischen thermischer und nichtthermischer Plasmachemie, bzw. das Gemeinsame plasmathermischer und plas-

maelektrischer Vorgänge besprochen werden, ergibt sich eine Übersicht der spezifischen Besonderheiten dieser beiden Disziplinen.

Das zweite Kapitel behandelt jene physikalischen Grundlagen der Plasmachemie, deren Kenntnis Voraussetzung für die Beschäftigung mit plasmachemischen Vorgängen ist. Dabei werden folgende Bereiche ausführlich behandelt: Eigenschaften des Plasmas, plasmaphysikalische Elementarprozesse, plasmabildende elektrische Entladungsformen, Plasmadiagnostik und Methoden zur Bestimmung von Plasmaparametern.

Kapitel 3 beschäftigt sich mit dem chemischen Aspekt der Plasmachemie, d.h. mit den zahlreichen Bemühungen zur Realisierung der verschiedenen plasmachemischen Stoffsynthesen, die durch Angabe der Synthesebedingungen und der Prozeßparameter charakterisiert werden. Dabei sind die Grundtypen der mit der chemischen Stoffumwandlung im thermischen Plasma verknüpften Reaktionen, sowie Beispiele für jeden Reaktionstyp angeführt. So werden die Azetylen-Synthese, die Stickstoff-Fixierung, die plasmathermische Halogenierung und Kohle-Vergasung, wie auch sonstige plasmathermische Stoffumwandlungen besprochen.

Da das nichtthermische Plasma, im Vergleich zum thermischen, einige spezifischen Eigenschaften aufweist, die sich auf die darin durchgeführten Stoffumwandlungen auswirken, werden diese charakterisiert und die dem nichtthermischen Plasma eigenen Reaktionstypen besprochen. Als Beispiele werden die Synthese einfacher Moleküle, höhermolekularer sowie ,,ungewöhnlicher'' an organischer Verbindungen, die Plasmachemie organischer Substanzen, plasmaelektrische Schichtbildung und Oberflächenaktivierung als auch sonstige plasmaelektrische Stoffumwandlungen angeführt.

Die angegebenen Informationen sollen einen Überblick über den derzeitigen Stand, die Möglichkeiten und die praktische Durchführung plasmachemischer Stoffumwandlungen vermitteln. Die mit der Stoffumwandlung zusammenhängenden Reaktionsmechanismen, ohnehin meist unbekannt oder lediglich als hypothetische Deutungsansätze vorliegend, erhalten in diesem Zusammenhang nureine geringe Aufmerksamkeit.

Der physikalisch-chemische Aspekt, d.h. die theoretischen Grundlagen der Plasmachemie werden im 4. Kapitel einheitlich dargestellt. Unter Bezugnahme auf den plasmachemischen Prozeß als Gegenstand der Monographie, werden insbesondere thermodynamische und reaktionskinetische Untersuchungsergebnisse im Rahmen folgender Unterkapitel erläutert: Thermodynamik und Kinetik der Plasmareaktionen und kinetische Probleme plasmachemischer Reaktionen.

Eines der Unterkapitel befaßt sich mit dem gegenwärtigen Stand der Modellierung plasmachemischer Reaktionen unter Anwendung der Nichtgleichgewichtskinetik, ein Gebiet dem in letzter Zeit große Beachtung geschenkt wird. Ein relativ breiter Raum ist auch den speziellen plasmachemischen Phänomenen — der sogenannten Plasma-Katalyse — gewidmet (Sensibilisierung plasmachemischer Stoffumwandlungen). Dabei treten nicht nur die mit diesem Begriff verknüpften Effekte in den Vordergrund, sondern auch die von der Plasma-Kartalyse her zum Mechanismus plasmachemischer Prozesse erbrachten zahlreichen Informationen.

Die technische Nutzung, d.h. die verschiedenen Arten der chemischen Plasmatechnologien behandelt das 5. Kapitel. Da von den zahlreichen, in Kapitel 3 erörterten plasmathermischen Stoffumwandlungen bisher lediglich die Azetylen-Synthese und Plasma-Metallurgie technische Bedeutung erreicht haben, befaßen sich die Ausführungen hauptsächlich mit den technischen Verfahren zur Azetylen-Synthese, die im Detail beschrieben und anhand ihrer Prozeßparameter charakterisiert werden. Es werden weiterhin einige neuere Anwendungen plasmachemischer Stoffumwandlung besprochen; plasmaelektrische Polymerisation, Veraschung, Oberflächen-Ätzung, Anwendungen in der Halbleiter-Industrie, Aktivierung von Festkörper-Oberflächen, obwohl nur wenige dieser Anwendungen als ausgereifte ,,technische Verfahren'' angesehen werden können. Eines der Unterkapitel befaßt sich eben mit den wesentlichen technischen Problemen der plasmachemischen Stoffumwandlung, die sich aus den Besonderheiten dieses Prozesses ergeben.

Im sechsten Kapitel werden chemische Reaktionen in nichtelektrischen Plasmen erläutert, wobei die Aufmerksamkeit vor allem auf Reaktionen in Flammenplasmen, in Stoßwellenplasmen, in strahleninduzierten und in laser-induzierten Plasmen gerichtet ist. Ganz kurz werden auch die Prozesse in Tribo-Plasem gestreift. Besondere Beachtung verdient der Ausblick im letzten Kapitel. Hier werden die Komplexität der Plasmachemie als Forschungs und Arbeitsgebiet, ihr multidisziplinärer Charakter und das offensichtliche Mißverhältnis zwischen den derzeitigen bescheidenen Möglichkeiten plasmachemischer Stoffumwandlungen und den hohen Erwartungen die an die Plasmachemie als einem neuen Wirkprinzip in der chemischen Technologie geknüpft werden näher besprochen.

Abschließend wäre zu bemerken, daß vorliegende Monographie ein gründliches Spiegelbild des jetzigen Standes der ,,Plasmachemie'' darstellt und den interessierten Lesern nur empfohlen werden kann.

Erna Schneider

NOTE POUR LES AUTEURS

La Revue Roumaine de Chimie publie des articles en anglais, français, russe, allemand ou espagnol. Les auteurs sont priés d'envoyer des articles et des comptes rendus inédits.

Les manuscrits seront dactylographiés à deux intervalles. La bibliographie, les tableaux et la légende des figures seront placés après le texte.

Si l'article fait partie d'une série numérotée, le titre de la partie précédente sera indiqué dans une note au bas de la première page.

Chaque article sera précédé d'un résumé comprenant quinze lignes au maximum.

Les références bibliographiques dans le texte seront faites par des exposants sans parenthèses et paraîtront comme des notes au bas de chaque page.

Les publications périodiques mentionnées dans la bibliographie seront présentées suivant les prescriptions internationales ; le nom de l'auteur précédé de l'initiale du prénom, le titre du périodique abrégé conformément à « Chemical Abstracts » et souligné par une ligne, le numéro du tome indiqué par des chiffres arabes et souligné par deux lignes, suivi de la première page de l'article; à la fin, l'année de la parution sera placée entre parenthèses. Le numéro de la revue ne sera pas indiqué, si les pages du volume sont numérotées consécutivement.

Les textes des livres ou traités inclueront : les noms des auteurs, les initiales du prénom, le titre du livre entre guillemets et sans être souligné, le numéro du tome précédé par l'abréviation « vol. » (ou « Bd. »), le numéro de l'édition, les éditions (the publisher) la localité de la parution du livre, l'année de la parution et la page de la référence précédeé(s) par l'abréviation «p. » (ou « S. »).

Les brevets seront indiqués comme suit : l'auteur ou la firme, le pays et le numéro du brevet, la date et la revue (Chem. Abstr.). Par ex. : M. Jones (to Union Carbide Co), Brit. Pat. 601—238, 2 Sept. 1959, *Chem Abstr.*, 54, 12808 (1970).

Les diagrammes seront tracés à l'encre de Chine sur papier calque. Les tableaux et les figures (en nombre strictement nécessaire) seront numérotés par des chiffres arabes. Les courbes dans les figures seront numérotées par des chiffres arabes et leur explication sera donnée dans la légende des figures. Prière de ne pas inscrire les mêmes données dans les tableaux et les figures. Chaque tableau aura un titre. On indiquera dans le texte la place approximative des tableaux et des figures. Les formules chimiques seront incluses dans le texte ; en outre, elles seront transcrites sur papier calque, à l'encre de Chine.

Les auteurs sont priés d'indiquer les caractères italiques (en soulignant les lettres au crayon), ainsi que tout autre caractère spécial ; les préfixes *ortho*, *meta*, *para*, *cis*, *trans*, etc. seront soulignés pour indiquer leurs caractères italiques et ne seront jamais écrits avec des majuscules.

Aucune correction à la main ne sera admise sur le manuscrit. Les corrections seront frappées à la machine. Les lettres grecques ou autres symboles spéciaux seront insérés à la main à l'encre clairement.

Le manuscrit sera signé par l'auteur.

Le colonne-titre aura 50 lettres au maximum.

L'entière responsabilité du contenu des articles appartient aux auteurs.

PRINTED IN ROMANIA

TRAVAUX PARUS AUX ÉDITIONS DE L'ACADÉMIE DE LA RÉPUBLIQUE SOCIALISTE DE ROUMANIE

ELENA CEAUŞESCU, **Participări la manifestări ştiinţifice** (Participations aux manifestations scientifiques), 1979, 208 p.

A. T. BALABAN, L. GĂLĂŢEANU, G. GEORGESCU, LIGIA SIMIONESCU, **Compuşi marcaţi şi radiofarmaceutici cu aplicaţii în medicina nucleară** (Composés marqués et radio pharmaceutiques à application en médecine nucléaire),1979, 495 p.

I. G. MURGULESCU, E. SEGAL, **Introducere în chimia fizică,** vol. II. 1. **Teoria molecular cinetică a materiei** (Introduction à la chimie physique, IIe vol. 1. La théorie moléculaire-cinétique de la matière), 1979, 1003 p.

I. E. TEODORESCU, MARIA FITI, **Iradierea tehnologică** (Iradiation technologique), 1979, 216 p.

S. STERNBERG, FL. DANEŞ, **Termodinamica chimică aplicată** (La thermodynamique chimique appliquée), 1978, 400 p.

I. G. MURGULESCU, V. EM. SAHINI, **Introducere în chimia fizică, Vol. I, 2. Structura şi proprietăţile moleculelor** (Introduction à la chimie physique, Ier vol. 2. La structure et les propriétés des molécules), 1978, 604 p.

C. DRĂGULESCU, E. PETROVICI, **Chimie structurală modernă, Chimia coordinanţei 8** (La chimie structurale moderne. La chimie de la coordinence 8), 1977, 947 p.

D. PURDELA (sous la direction de), **Nomenclatura chimiei anorganice** (La nomenclature de la chimie inorganique), 1977, 153 p.

I. ZUGRĂVESCU, MAGDA PETROVANU, **N-ylid chemistry**, coédition avec McGraw-Hill, 1977, 396 p.

D. NEGOIU, ANGELA KRIZA, **Poluanţi anorganici în aer** (Polluants inorganiques dans l'air), 1977, 220 p.

I. G. MURGULESCU, **Introducere în chimia fizică. Vol. I. Atomi, molecule, legătură chimică** (Introduction à la Chimie Physique, Ier vol. 1. Atomes, molécules, liaison chimique), 1976, 460 p.

E. P. BALTĂ, E. BALTĂ, **Introduction to the physical chemistry of the vitreous state**, coédition avec Abacus Press, 1976, 287 p.

M. I. GĂLĂŢEANU, **Radiochimia aplicată. Metode şi probleme** (La radiochimie appliquée. Méthodes et problèmes), 1976, 307 p.

CONST. V. UGLEA, **Cromatografia pe gel permeabil. Noi domenii de aplicare** (La chromatographie sur gel perméable. Nouveaux domaines d'application), 1976, 123 p.

FRANCISC, GOTHARD, **Echilibre lichid-vapori. I. Baze teoretice şi metode de calcul** (Equilibres, liquide-vapeurs. I. Bases théoriques et méthodes de calcul), 1975, 263 p., 2 pl.

CONST. GH. MACAROVICI, D. MACAROVICI, **Chimia oxizilor dubli şi utilizările lor** (La chimie des oxydes doubles et leur utilisation), 1975, 195 p.

ELENA CEAUŞESCU, **Research work on synthesis and characterization of macromolecular compounds. Contributions**, 1974, 251 p.

CR. SIMIONESCU, VIORICA RUSAN, V. POPA, **Chimia algelor marine** (La chimie des algues marines), 1974, 212 p., 1 pl.

I. P. Informaţia c. 1682

43 426

Lei 25.—

$50 (price per year)

F1103 [illegible]

ACADÉMIE DE LA RÉPUBLIQUE SOCIALISTE DE ROUMANIE

REVUE ROUMAINE DE CHIMIE

TOME 25
Nº 3
Mars 1980

EDITURA ACADEMIEI REPUBLICII SOCIALISTE ROMÂNIA

Rev. Roumaine Chim.
RRCHAX, **25**, *3*, p. 305–446 (1980), Bucarest

ACADÉMIE DE LA RÉPUBLIQUE SOCIALISTE DE ROUMANIE

COMITÉ DE RÉDACTION

Rédacteur en chef:

I. G. MURGULESCU, membre de l'Académie de la République Socialiste de Roumanie

Rédacteurs en chef adjoints:

A. T. BALABAN et V. EM. SAHINI, membres correspondants de l'Académie de la République Socialiste de Roumanie

Collège de rédaction:

EM. BRATU, ELENA CEAUŞESCU, ECATERINA CIORĂNESCU-NENITZESCU, CR. SIMIONESCU, membres de l'Académie de la République Socialiste de Roumanie; P. SPACU, membre correspondant de l'Académie de la République Socialiste de Roumanie; MARGARETA AVRAM, M. BANCIU, I. HAIDUC, D. I. MARCHIDAN, I. MOLDOVAN, G. NIAC et D. SĂNDULESCU

La Revue Roumaine de Chimie paraît 10 fois par an. Toute commande de l'étranger pour les travaux parus aux Editions de l'Académie de la République Socialiste de Roumanie sera adressée à ILEXIM, Departamentul Export-Import Carte (Livres)/ Departamentul Export-Import Presă (Revues), P.O.B. 136—137, télex 11226, 3, str. 13 Decembrie, 70116 Bucarest 12, Roumanie

Les manuscrits, les livres et les revues proposés en échange ainsi que toute correspondance seront envoyés à la redaction:

REVUE ROUMAINE DE CHIMIE

125, Calea Victoriei, 71021 Bucarest, Roumanie, téléphone 50 76 80

EDITURA ACADEMIEI REPUBLICII SOCIALISTE ROMÂNIA
125, Calea Victoriei, 71021 Bucarest, Roumanie, téléphone 50 76 80

ORSZÁGOS MŰSZAKI KÖNYVTÁR ÉS DOKUMENTÁCIÓS KÖZPONT 1983

REVUE ROUMAINE DE CHIMIE

Tome 25, N° 3 Mars, 1980

AGNETA CARAGHEORGHEOPOL, H. CĂLDĂRARU, I. I. BĂDILESCU and V. E. SAHINI, An electron spin resonance study of the iminoxy radicals of 1-benzoxepin-5-one derivatives 307–313

C.-E. MOROȘANU and E. SEGAL, Deposition kinetics of Si_2N_4 films by the radiofrequency glow discharge and low pressure CVD methods 315–322

J. PRASHAD, Comparative studies of corona pressure effect. *Joshi* effect and thermionic analogue of *Joshi* effect in argon under semi-ozonizer discharge 323–326

M. S. SUBHANI, An investigation of the reaction between tellurite and chlorite ions in solution 327–331

M. S. SUBHANI, Thermochemical studies on solutions of monobromo-, dibromo- and tribromo-acetic acids in water and chloroform . . . . 333–337 R

SILVIA BARBU and CONST. GH. MACAROVICI, Complex combinations of thiocarbohydrazine of isonicotinealdehyde and thiphene-2-carbaldehide (in French) 339–347

D. NEGOIU, J. CAMUS and N. MUREȘAN, Electron transfer in some vanadium complexes with quinoxalinic and naphtoquinonic ligands . . . . 349–354 R

KEEMTI LAL, Complexes of copper (II), nickel (II), cobalt (II), iron (II) and manganese (II) with Schiff bases derived from sulphamethoxypyridazine 355–360

DUMITRA VĂCĂRESCU, Contributions to the chemistry of quaternary ammonium complexes. N-Cetyl-β-picolinium salts of halogen- and thiocyanate complex ions of Zn (II) and Cd (II) 361–370

DUMITRA VĂCĂRESCU, Study of some N-cetyl-β-picolinium halogen and thiocyanatomercurates (II) 371–378

G. RICART, Synthesis of [(5-Hydroxypentylamino)-1-n-Alkyl]-Aziridines (in French) 379–391

I. E. KHAWAD and G. M. ISKANDER, Favorskii reactions of α-halo-α, β-unsaturated monocyclic ketones 393–395

Y. AHMAD, S. A. SHAMSI and M. I. QURESHI, Studies in intramolecular interaction of aromatic nitro-group with *ortho* side-chain. II. Further syntheses of quinoline N-oxide derivatives 397–402

C. I. CHIRIAC, Dehydrations with chlorosulfonic acid in pyridine. A convenient method for the synthesis of amides 403–405

H.-J. TIMPE, V. SCHRÖDER and R. WORSCHECH, *s*-Triazolium-4N-ylide (in German). 407–414

M. M. ABD ALLA, E. A. SOLIMAN and M. W. OSMAN, Reactions of some arylidenefuranones 415–424

Revue Roumaine Chim. 25, *3*, 305–446 (1980) Bucarest

DEMETRA DRĂGAN and "A. CARPOV, Chemical modification of polymers. II. Reaction of poly(vinyl α-chloroacetophenone) with some herbicidal sodium phenoxides 425–433

A. O. FULEA, On "A correction technique for fractionation data and its application to the fractionation of polyethylene terephthalate" . . . . 435–437 R

S. N. KAPOOR and N. MISRA, Analytical aspects of some organic acids. II. Gravimetric determination of thorium by *o*-phenylene trioxytriacetic acid 439–442

BOOK REVIEWS 443–445

Revue Roumaine de Chimie, **25**, *3*, 307–313 (1980)

AN ELECTRON SPIN RESONANCE STUDY OF THE IMINOXY RADICALS OF 1-BENZOXEPIN-5-ONE DERIVATIVES*

AGNETA CARAGHEORGHEOPOL*, H. CĂLDĂRARU*, I. I. BĂDILESCU*** and
V. E. SAHINI**

* Institute of Physical Chemistry, Splaiul Independenței, 202, Bucharest, Romania
** Department of Physical Chemistry, Bd. Republicii 13, Bucharest, Romania
*** Department of Chemistry, Pedagogical Institute, Pitești, Romania

Received April 4, 1979

Iminoxy radicals (A) and α-keto-iminoxy radicals (B) derived from 2,3-dihydro-1-benzoxepin-5 (4*H*)-one and its sulphur analogue have been studied by ESR. In the Z isomer of (A) the proton hyperfine splittings (*hf*s) have been assigned using substitutions and deuteration. Use has been made of the previously established angular dependence of the α-anti proton *hf*s and of comparison with model compunds with known geometry to get information about the molecular geometry; the conclusion has been reached that the seven-membered ring in A adopts a rigid chair-like conformation. On the contrary, in the spectra of both E— and Z—isomers of B pairs of equivalent protons appear, a fact which indicates the flipping of the involved ring.

INTRODUCTION

Following previous works on the conformation of bicyclic and heterocyclic iminoxy radicals [2–4] obtained mostly on six-membered rings, we report now the results of the ESR investigation of heterocyclic seven-membered rings. Previous results regarding the dependence of proton hyperfine splittings on molecular geometry [5, 6] justify the extension of the ESR study to such systems.

In this work two types of radicals (Formulae A and B), having the iminoxy group in the 5— or 4-position, respectively, obtained from 2,3-dihydro-1-benzoxepin-5(4*H*)-one, its derivatives (Ia-Ih) and from 2,3-dihydro-1-benzthiepin-5(4*H*)-one (II) have been studied.

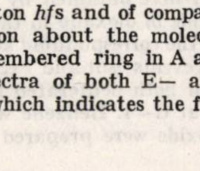

A.

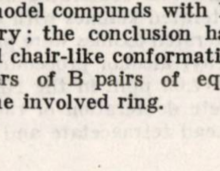

B.

*This paper represents Part VI of the series : Heterocyclic Compounds. [1]

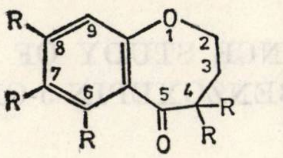

Ia $R_4 = R_6 = R_7 = R_8 = H$
Ib $R_4 = R_6 = H, R_7 = R_8 = Me$
Ic $R_4 = R_6 = R_7 = H, R_8 = Me$
Id $R_4 = R_6 = R_8 = H, R_7 = Me$
Ie $R_7 = R_4 = H, R_6 = R_8 = Me$
If $R_6 = R_7 = R_8 = H, R_4 = D$
Ig $R_6 = R_7 = R_8 = H, R_4, R_4 = -(CH_2)_4-$
Ih $R_6 = R_8 = Me, R_7 = H, R_4 = D$

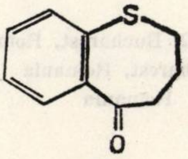

II

EXPERIMENTAL

Materials. The ketones (Ia—Ih, II) and the corresponding oximes were prepared as previously described. [7] The deuterated ketones (If, Ih) were obtained by refluxing (for about 50 hours) the undeuterated ketones with deuterium oxide in dioxane in the presence of NaOD as catalyst. The deuterated oximes were prepared from the corresponding ketones by the hydroxylamine-pyridine-ethyl alcohol procedure, [8] which prevents isotopic exchange. The absence of the signal at $\tau = 7{,}05$ ppm in the NMR spectra of both deuterated ketones and oximes indicated the complete deuteration of the methylene at C—4. Benzene was dried on sodium wire and distilled. Lead tetraacetate and nitrogen dioxide were prepared as described in the literature. [9]

Radicals. The 5-oximino radicals (III—VIII) were generated in the sample tube by adding benzene to the oxime lead tetraacetate mixture ; the 5-keto-4-oximino radicals (IX, X) were prepared by adding a saturated solution of nitrogen dioxide in benzene over the ketone in the sample tube.

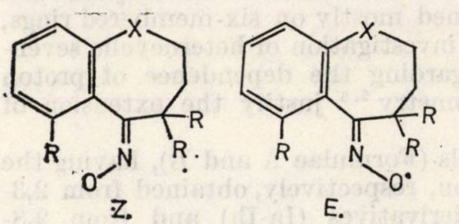

III, X = O $R_4 = R_6 = H$
IV, X = O $R_6 = H$; $R_4 = D$
V, X = O $R_6 = H$; $R_4, R_4 = -(CH_2)_4-$
VI, X = O $R_4 = H$; $R_6 = Me$
VII, X = O, $R_4 = D$; $R_6 = Me$
VIII, X = S $R_4 = R_6 = H$

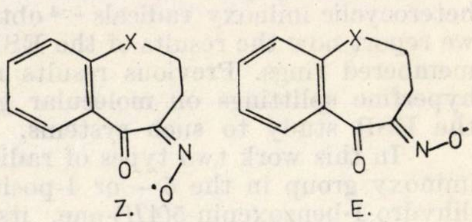

IX, X = O
X, X = S

ESR spectra. Both stereoisomers E and Z of the iminoxy group were observed in the spectra of all investigated compounds. In the case of radicals III—VIII the a_N and g values for the E and Z isomers are very close and a significant overlapping of the lines occurs. Therefore we do not report the precise values of a_N and g of these radicals. The approximate values of these parameters ($a_N \sim 30$ G and $g \sim 2.006$) are characteristic of iminoxy radicals. In all

the cases one of the isomers, which proved to be the Z one, prevails, the corresponding lines being clearly identified. The lines of the E isomers were partly hidden, and the hfs parameters indicated in Table 1, which are based on the overall width, distances and intensity ratio of the remaining lines (in both *X* and *K* bands) are tentative.

In α-keto iminoxy radicals (IX, X) the low and high field lines of the nitrogen triplet in E and Z isomers do not overlap.

The ESR parameters of the studied radicals are given in Tables 1 and 2. Since the spectra of the iminoxy radicals obtained from compounds Ia—Id are almost identical, their ESR parameters are not presented separately in Table 1.

TABLE 1

Proton *hf* splittings in 5-oximino radicals

Radical	a_H, G		Radical	a_H, G		
Z—III	2.0 (1)	1.5 (1)	E—III	3.0 (1)	1.5 (2)	0.7 (1)
Z—IV	2.1 (1)					
Z—V	2.1 (1)					
Z—VI		1.4 (1)	E—VI	2.7 (1)	1.4 (5)	
Z—VII	—					
Z—VIII	2.1 (1)	1.3 (1)	E—VIII	2.3 (1)	1.5 (1)	0.7 (2)

TABLE 2

ESR parameters of the 5-keto-4-oximino radicals

Radical	a_N, G	a_H, G		Radical	a_N, G	a_H, G	
Z—IX	28.2	1.1 (2)		E—IX	33.7	2.2 (2)	1.6 (2)
Z—X	28.2	1.0 (1)	0.9 (1)	E—X	33.0	1.2(2)	0.6(2)

The ESR spectra were recorded at room temperature on a JES—3B (JEOL) spectrometer with 100 kHz modulation using *X* and *K* bands. The *hfs* constants and *g* factors were measured in comparison with potassium peroxylaminedisulphonate ($a_N = 13.0$ G, $g = 2.0055$). For measurements at low and high temperatures the variable temperature cavity and the corresponding units were used.

RESULTS AND DISCUSSION

(i) 5—Iminoxy radicals

Assignment of the hf splittings. In the series of radicals III—VIII deuteration and other substitutions of both C—4 protons and/or the C—6 proton led to the following consistent assignment of the proton *hf* splittings :

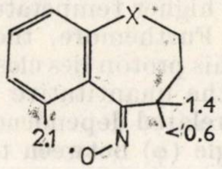

The number of protons involved in the *hf* interaction and the 2.1 G splitting for the C−6 proton (as compared with the corresponding value in radicals XI and XII[10]) are indications that these parameters have to be assigned to the Z isomer.

By analogy the same *hfs* assignment has been extended to radical Z−VIII.

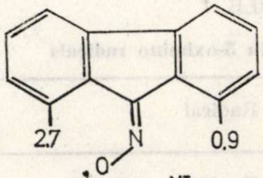

XI

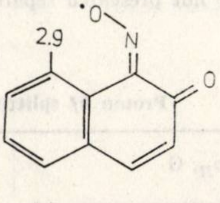

XII

Conformation of the seven-membered ring. The 2.1 G *hf* splitting of the C−6 proton compared with the corresponding values (2.7−2.9 G) in planar radicals (XI, XII[10]) points to a non-planar conformation for the phenyl-CNO fragment involved in the *hf* interaction. The non-planarity angle however, is unknown. A 2.4 G *hf* splitting has been found for the corresponding proton in the iminoxy radical obtained from dibenzosuberenone oxime.[11] The X-ray data available[12] for the corresponding ketone indicate a ~35° angle between the iminoxy plane and the phenyl plane. The absence of the *hf* splitting of methyl protons at C−6 is also an indication of the non-planarity of the above-mentioned fragment.[13]

The following discussion concentrates on the information contained in the *hfs* of *α-anti* geminal protons of Z isomers, as their angular dependence is best understood. In a previous paper[4] we have found — on the basis of available experimental data — this dependence to be:

$$a_{\mathrm{H}} = 0.6 + 1.6 \cos^2 \theta \qquad (1)$$

where θ is the angle defined in Figure 1a.

Thus, the *hf* splittings of the geminal protons provide information regarding the mobility of the ring involved. In our case the assigned *hf* splittings for the *α-anti* geminal protons are:

$$a_{\mathrm{H}_1} \leqslant \text{line width} \sim 0.6 \text{ G}$$

$$a_{\mathrm{H}_2} = 1.3 - 1.5 \text{ G}$$

The non-equivalence of these protons indicates that the seven-membered ring does not flip, adopting a preferential fixed conformation on the ESR time scale (measurements at higher temperatures (up to 60°) did not show any change in the spectra). Furthemore, the very small value of one of the two protons shows that this proton lies close to the plane of the iminoxy group.[5] Equation 1 allows the quantitative treatment of this information. Figure 1b shows the correlated dependence of the *hfs* of *α-anti* geminal protons vs. the dihedral angle (φ) between the $C_{im}-C_{\alpha}-H$ plane and σ plane. One observes that the pair of experimental *hfs* values corresponds to four values of the angle. Two of them, $\varphi = 50°$ and $\varphi = 190°$, are not possible in a seven-membered ring.

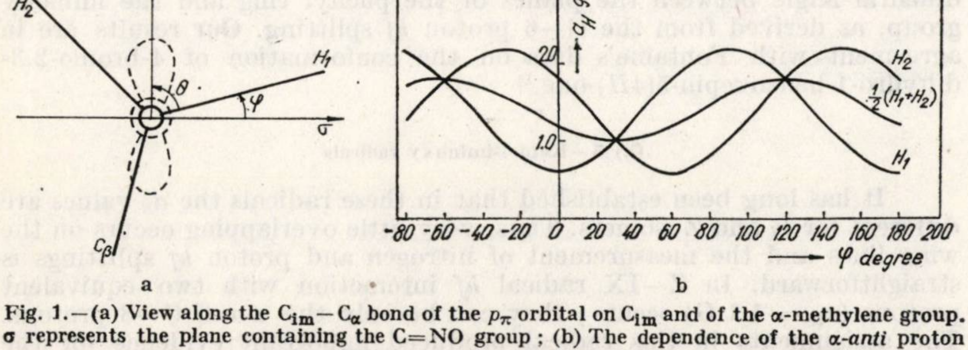

Fig. 1.—(a) View along the $C_{im}-C_\alpha$ bond of the p_π orbital on C_{im} and of the α-methylene group. σ represents the plane containing the C=NO group ; (b) The dependence of the α-*anti* proton *hf* splittings vs. the dihedral angle φ.

The other two, $\varphi = 10°$ and $\varphi = 230°$, represent symmetrical situations. So, we are further concerned with those conformations in which $\varphi = 10°$ (not $-10°$!). Examination of the Dreiding models indicates three conformations in which this angle can be achieved :

(a) a fixed chair-like conformation of the seven-membered ring in which all methylene groups are staggered and the angle between the planes of the iminoxy group and the phenyl ring is ~70° (XIII).

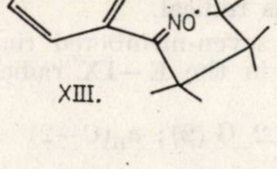

XIII.

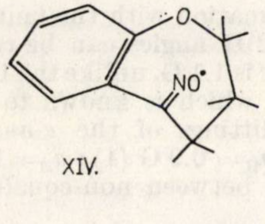

XIV.

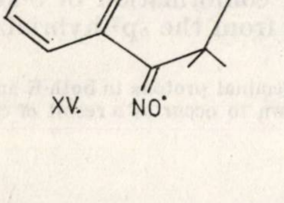

XV.

(b) two flexible boat conformations (XIV and XV). The non-equivalence of the α-geminal protons, as well as the non-dependence of their *hf* splittings on temperature, rules out such flexible conformations. Thus, we are led to assign the fixed chair-like conformation to the seven-membered ring in these radicals. This assignment is in agreement with the dihedral angle between the planes of the phenyl ring and the iminoxy group, as derived from the C—6 proton *hf* splitting. Our results are in agreement with Fontaine's data on the conformation of 4-bromo-2,3-dihydro-1-benzoxepin-5(4*H*)-one.[14]

(ii) 5—Keto-4-iminoxy radicals

It has long been established that in these radicals the a_N values are different for E and Z isomers. Thus, very little overlapping occurs on the wing lines and the measurement of nitrogen and proton *hf* splittings is straightforward. In Z—IX radical *hf* interaction with two equivalent protons ($a_H = 1.1$ G) occurs; they can be only the α-*anti* C—3 protons. The assignments in this radical produced important evidence for the recognition of the part played by α-*anti* protons in the *hf* interaction of iminoxy radicals.[15] The fact that three pairs of protons are equivalent rules out the possibility of accidental coincidence and represents an indication of the flipping of the seven-membered ring between limiting conformations which are equally probable. * In this case the arithmetical mean rule holds. Thus, the splittings of α-*anti* C—3 protons in the Z isomer, $a_H = 1.1$ G (2), point out to conformations with dihedral angles $\varphi = 10°$ or $\varphi = 50°$ as limiting conformations. For these angles eq. 1 and Figure 1 give: $a_{H_1} = 0.65$ G, $a_{H_2} = 1.55$ G; $a_H = 1/2\,(0.65 + 1.55) = 1.1$ G. From these angles $\varphi = 50°$ is not possible in the seven-membered ring; so, a limiting conformation with $\varphi = 10°$ is found to fit the experimental *hf* splittings of this radical.

The flipping of the seven-membered ring obviously requires the following *hf*s assignments in the E—IX radical:

$$a_H(C-3) = 2.2\ \text{G}\,(2);\ a_H(C-2) = 1.6\ \text{G}\,(2)$$

A fixed planar conformation with the iminoxy group plane bisecting the H(C—3)H and H(C—2)H angles can be ruled out, since the *hf*s of C—3 protons in the Z isomer is 1.1 G, unlike the 1.8 G value in the analogous radical of cyclopentanone, which is known to be planar.[5,16] The slight difference between the splittings of the α-*anti* protons in the sulphur analogous radical (Z—X) ($a_H = 0.9$ G (1); $a_H = 1.0$ G (1)) could be an indication that flipping occurs between non-equally probable conformations or at a lower rate.

In conclusion, the ESR data on the investigated series evidence a remarkable difference between the fixed conformation of 5-iminoxy radicals and the flipping conformation of 5-keto-4-iminoxy radicals, the higher mobility resulting from the sp^2-hybridization of one more C-atom.

---

* The equivalence of all geminal protons in both E and Z isomers of the α-keto-iminoxy radical of cyclohexanone is known to occur as a result of chair-chair interconversion.[5]

REFERENCES

[1] Part V, I. I. Bădilescu, *Rev. Roumaine Chim.*, **20,** 1077 (1975).
[2] H. Căldăraru, A. Caragheorgheopol and V. E. Sahini, *J. Magn-Resonance,* **11,** 335 (1973).
[3] H. Căldăraru and M. Moraru, *J. Amer. Chem. Soc.*, **96,** 149 (1974).
[4] H. Căldăraru and M. Moraru, *Rev. Roumaine Chim.*, **20,** 1219 (1975).
[5] H. Căldăraru, A. Caragheorgheopol, M. Moraru and V. E. Sahini, *J. Phys. Chem.*, **79,** 646 (1975).
[6] G. A. Russell and A. Mackor, *J. Amer. Chem. Soc.*, **96,** 145 (1974).
[7] I. I. Bădilescu, *Rev. Roumaine Chim.*, **20,** 761 (1975).
[8] W. E. Bachmann and M. X. Barton, *J. Org. Chem.*, **3**, 307 (1938)
[9] G. Brauer, "Handbook of Preparative Inorganic Chemistry", Academic Press, New York, London, 1963, p. 488, 767.
[10] B. C. Gilbert and R. O. C. Norman, *J. Chem. Soc.* (*B*), **1967,** 981.
[11] A. Caragheorgheopol, unpublished results.
[12] H. Shimanouchi, T. Hata and Y. Sasada, *Tetrahedron Letters*, **32,** 3573 (1968).
[13] B. C. Gilbert and R. O. C. Norman, *J. Chem. Soc.* (B), **1968**, 123.
[14] G. Fontaine, *Ann. Chim.* (*France*), **3,** 178 (1968).
[15] A. Caragheorgheopol, H. Căldăraru and V. E. Sahini, *Rev. Roumaine Chim.*, **18**, 1497 (1973).
[16] W. M. Fox, J. A. McRae and M. C. R. Symons, *J. Chem. Soc.* (*A*), **1967,** 1773.

Revue Roumaine de Chimie, **25,** *3,* 315–322 (1980)

DEPOSITION KINETICS OF Si_3N_4 FILMS BY THE RADIOFREQUENCY GLOW DISCHARGE AND LOW PRESSURE CVD METHODS

C.-E. MOROŞANU* and E. SEGAL**

*** ICCE, str. Erou Iancu Nicolae 32B, R–72996 Bucharest 30, Romania**

**** Chair of Physical Chemistry and Electrochemical Technology, National Institute of Chemistry, Polytechnic Institute of Bucharest, Bulevardul Republicii 13, R-70031 Bucharest, Romania.**

Received April 17, 1979

The aim of the present work is to evaluate the kinetics parameters of Si_3N_4 film deposition processes in the SiH_4-NH_3 system by radiofrequency glow discharge (in plasma) as well as in the SiH_4-NH_3 or $SiH_2Cl_2-NH_3$ systems using a reactor for chemical vapor depositions at low pressure.

INTRODUCTION

The method of obtaining Si_3N_4 thin films by means of the reaction between silane and ammonia stimulated by a glow discharge produced by radiofrequency currents,[1-18] shows a lot of important advantages in comparison with the pyrolitic deposition. Among these, we may quote the following : the use of low deposition temperature, including the room temperature, achievement of film depositions with amorphous structure on various substrates, etc.

The method of obtaining thin films of Si_3N_4 with the help of a heterogeneous deposition reaction of silane and ammonia or dichlorosilane and ammonia at low pressure[19-20] offers a lot of important advantages, too. Among these the following must be noted :

— the deposition rate is determined only, by the surface chemical reaction, the mass transfer being negligible under working conditions at low pressure (0.5–1 torr) ;

— the deposition occurs in the absence of a dilution gas (N_2, H_2, He or Ar) ; consequently the concentrations of the reactant gases are relatively high ;

— the deposition rates, although the process is taking place under low pressure conditions, are only several times lower than those obtained in the case of normal pressure depositions.

— the deposition process is more economical from all points of view (investments, labour, energy and gases) in comparison with the conventional process at normal pressure.

Since the silicon nitride films obtained by means of these methods present mechanical, optical, electrical and chemical properties similar with those obtained with the help of pyrolitic method and may therefore be used for the passivation of the semiconductor devices, a detailed study of the deposition kinetics has been considered useful.

EXPERIMENTAL

The Si_3N_4 film deposition equipment by radio-frequency glow discharge in the SiH_4-NH_3 system is similar to that of the pyrolytic deposition, containing in addition a system of producing and measuring the vacuum (Figure 1).

The chemical vapour deposition systems at low pressure of Si_3N_4 thin films by the silane or dichlorosilane reactions with ammonia consist of the following parts : a gas distribution panel, a horizontal quartz reactor heated by a resistance furnace (or an induction coil, the glow discharge being switched off by means of a magnet), a vacuum rotary pump and a vacuum gauge of Pirani type (Figure 1.).

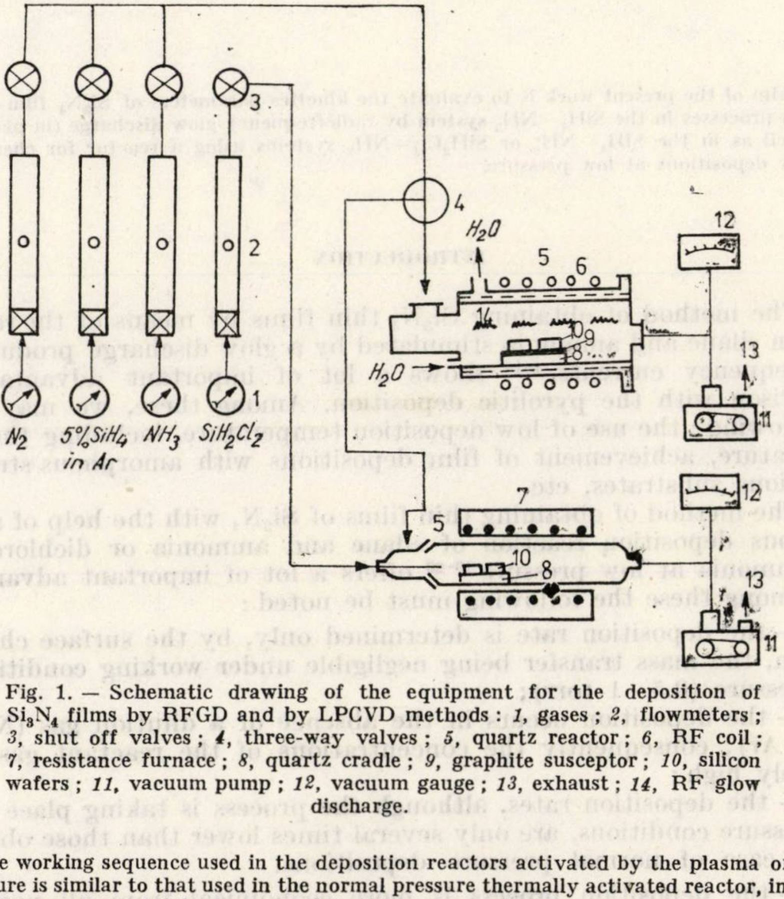

Fig. 1. — Schematic drawing of the equipment for the deposition of Si_3N_4 films by RFGD and by LPCVD methods : *1*, gases ; *2*, flowmeters ; *3*, shut off valves ; *4*, three-way valves ; *5*, quartz reactor ; *6*, RF coil ; *7*, resistance furnace ; *8*, quartz cradle ; *9*, graphite susceptor ; *10*, silicon wafers ; *11*, vacuum pump ; *12*, vacuum gauge ; *13*, exhaust ; *14*, RF glow discharge.

The working sequence used in the deposition reactors activated by the plasma or under low pressure is similar to that used in the normal pressure thermally activated reactor, including a stage of evacuation at 0.1—1 torr or 0.5—1 torr, respectively.

The conditions for obtaining the amorphous Si_3N_4 thin films by means of plasma activation method or working under low pressure are shown in Table 1 .

TABLE 1

Deposition conditions for amorphous Si_3N_4 thin films

Deposition technique Deposition parameter	RF glow discharge	Low pressure CVD
Reaction gases	5 % SiH_4 in Ar – NH_3	5 % SiH_4 in Ar – NH_3
SiH_4 Flow (cm³/min)	35–350	35–350
SiH_2Cl_2 Flow (cm³/min)	—	30–150
NH_3 Flow (cm³/min)	150–1800	150–1800
RF power (W)	500–1000	—
Pressure (torr)	0.1–20 (0.1–1)	0.5–1
Substrate temperature (°C)	25–650°	700–900°
Substrate	Silicon	Silicon
Deposition time (min)	5–60	5–60
Deposited film thickness (μ)	0.1–1	0.1–1
Deposition rate (Å/min)	50–5000	10–1000

RESULTS AND DISCUSSIONS

A. Deposition kinetics of silicon nitride films obtained by RF glow discharge method in the SiH_4-NH_3 system

The experimental data obtained by working either in a horizontal or in a vertical reactor, RF glow discharge taking place in a rarefied mixture of 5% SiH_4 in Ar and NH_3, show the influence of the following parameters on the deposition process : deposition time, silane flow rate, reactor total pressure, substrate temperature and RF energy.

1. *Influence of the deposition time*

Experimental results (Figure 2) show the existence of a linear relationship between film thickness and deposition time i.e. the deposition rate is constant during deposition (5–60 min).

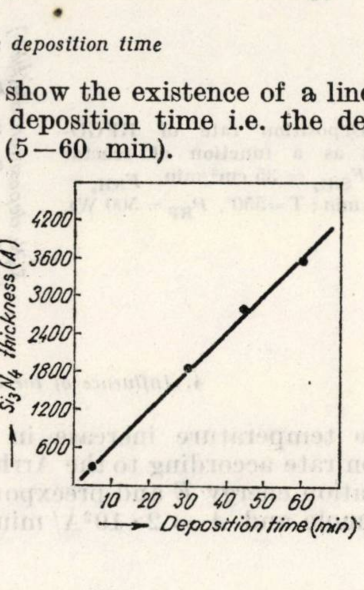

Fig. 2. — RFGD — Si_3N_4 films thickness as a function of deposition time ($F_{SiH_4} = 35$ m³/min ; $F_{NH_3} = 300$ cm³/min ; $p = 1$ torr ; T = 550° ; $P_{RF} = 500$ W).

2. *Influence of the silane concentration*

The relationship between deposition rate and silane concentration in the gas mixture is shown graphically in Figure 3. The linear dependence between the deposition rate and silane concentration means that the reaction is first order with respect to SiH_4. The rate constant value at 550° is $k_{550} = 640$ Å/ min.

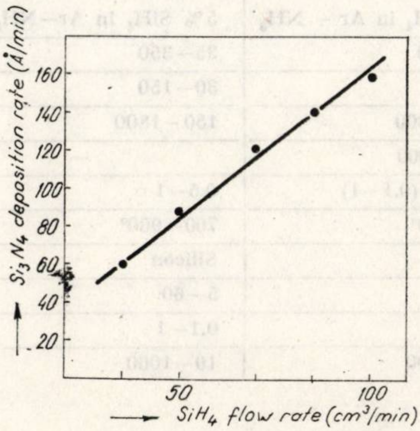

Fig. 3. — Deposition rate of RFGD — Si_3N_4 film as a function of SiH_4 flow rate ($F_{NH_3} = 300$ cm³/min ; $P = 1$ torr, $T = 550°$, $P_{RF} = 500$ W).

3. *Influence of the reactor total pressure*

The influence of the reactor total pressure (0.1 — 1 torr) on the deposition rate is shown in Figure 4. The deposition rate gradually decreases, while the reactor total pressure increases. This dependence may be explained by the decrease of the number of active species (radicals, ions, atoms, excited molecules) in the plasma, due to various types of collisions between them taking place more frequently at relatively higher pressures.

Fig. 4. — Deposition rate of RFGD-Si_3N_4 film as a function of reactor pressure ($F_{SiH_4} = 35$ cm³/min, $F_{NH_3} = 300$ cm³/min ; T = 550°, $P_{RF} = 500$ W).

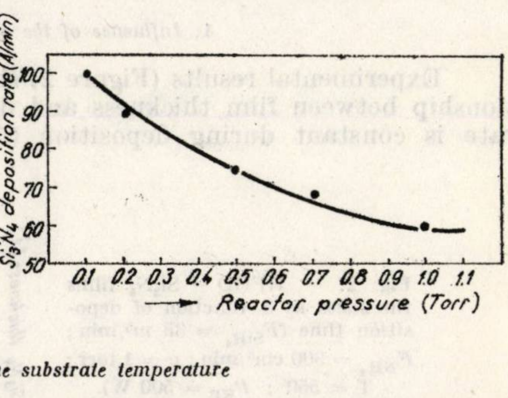

4. *Influence of the substrate temperature*

The temperature increase in the range 200—550° enhances the deposition rate according to the Arrhenius equation. The following values for activation energy E and preexponential factor A were obtained : $E = 1.4$ kcal/mole and $A = 2 \cdot 10^3$ Å/ min (Figure 5).

The results obtained, mainly the small value for the activation energy, can be explained with the help of a reaction mechanism in RF glow discharge. Due to the collisions of the electrons, induced by gas ionization under the influence of the electric field, with the gas molecules, excitation and dissociation of the molecules in free radicals takes place.

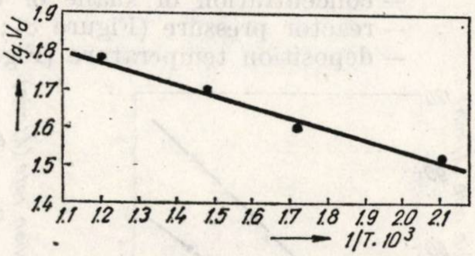

Fig. 5. — Deposition rate of RFGD-Si_3N_4 film as a function of deposition temperature ($F_{SiH_4} = 35$ cm³/min ; $D_{N_2} = 300$ cm³/min ; $P = 1$ torr ; $P_{RF} = 500$ W).

This mechanism of free radical formation is very likely to occur when the dissociation energy of the reactants is relatively small, as in the case of SiH_4 and NH_3 (7.3 kcal/mole and 11 kcal/mole, respectively).

The free radicals will react between them both in the gas phase and at the surface of the silicon layer.

Indeed, in the case of chemical vapor depositions promoted by a RF glow discharge, the existence of a homogeneous reaction in the gas phase together with the heterogeneous reaction occurring under the activation conditions of the substrate by electron or ion impacts, was put into evidence.

This homogeneous-heterogeneous mechanism, with a very high percentage of the homogeneous reaction, should also be applied to the SiH_4-NH_3 system, thus explaining the small value of the obtained activation energy.

5. *Influence of the RF power*

As expected, in the case of plasma stimulated reactions, the experimental results (Figure 6) show an important growth of the deposition rate with the increase of the plasma exciting power on the full range (500—1000 W).

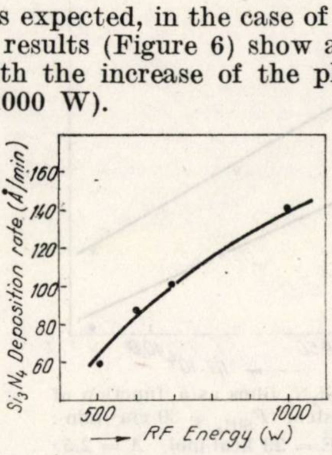

Fig. 6. — Deposition rate of RFGD-Si_3N_4 film as a function of RF power ($F_{SiH_4} = 35$ cm³/min, $F_{NH_3} = 300$ cm³/min, $P = 1$ torr, $T = 550$°C).

Indeed, an increasing RF electric field will increase the free electron energy in the plasma, consequently their collisions with gas molecules will be more efficient.

B. Kinetics of silicon nitride depositions at low pressure from SiH_4-NH_3 and $SiH_2Cl_2-NH_3$

The experimental data obtained in a heated resistive reactor (or in an inductive reactor in the absence of a glow discharge) show the influence of the following parameters on the deposition process :

- concentration of silane or dichlorosilane (Figure 7) ;
- reactor pressure (Figure 8) ;
- deposition temperature (Figure 9).

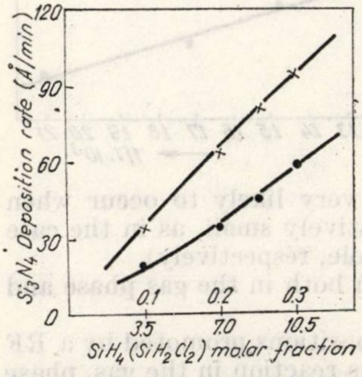

Fig. 7. — Deposition rate of LPCVD-Si_3N_4 film as a function of SiH_4 and SiH_2Cl_2 concentration : · SiH_4—NH_3 system (F_{NH_3} = 300 cm³/min ; T = 700° ; P = 0.5 torr) ; × SiH_2Cl_2—NH_3 system (F_{NH_3} = 300 cm³/min ; T = 700° P = 0.5 torr).

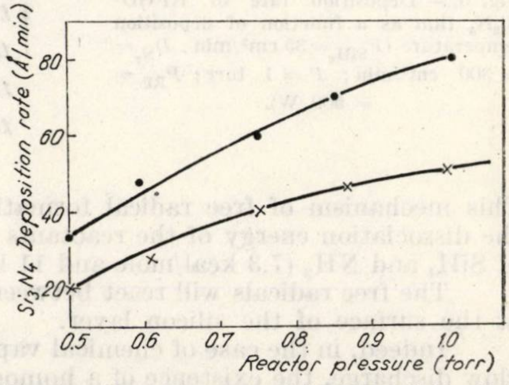

Fig. 8. — Deposition rate of LPCVD — Si_3N_4 film as a function of reactor pressure : (· SiH_4 — NH_3 system (F_{SiH_4} = 30 cm³/min ; F_{NH_3} = 300 cm³/min ; T = 700°C) ; × SiH_2Cl_2 — NH_3 system ($F_{SiH_2Cl_2}$ = 35 cm³/min ; F_{NH_3} = 300 cm³/min ; T = 700°).

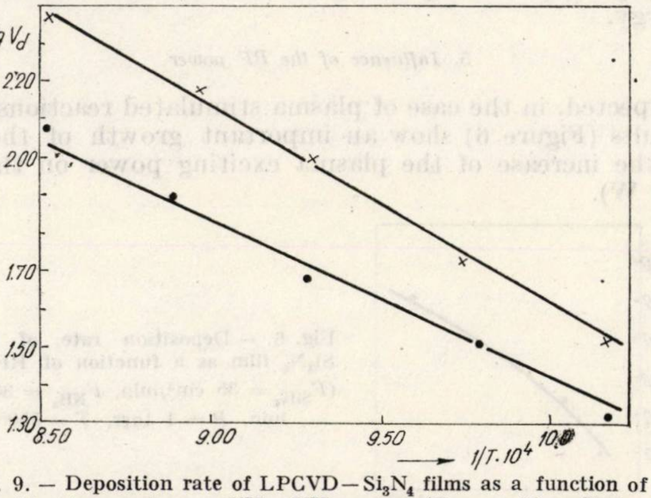

Fig. 9. — Deposition rate of LPCVD — Si_3N_4 films as a function of deposition temperature : · SiH_4 — NH_3 system (F_{SiH_4} = 30 cm³/min ; F_{NH_3} = 300 cm³/min ; P = 0.5 torr). E = 23 kcal/mol, $A = 2.5 \cdot 10^7$ Å/min ; × SiH_2Cl_2 — NH_3 system ($F_{SiH_2Cl_2}$ = 35 cm³/min ; F_{NH_3} = 300 cm³/min ; P = 0.5 torr) E = 20 kcal/mol, $A = 4.47 \cdot 10^7$ Å/min.

By analyzing the experimental data it turns out that the deposition rate is proportional to the concentration of SiH_4 or SiH_2Cl_2 in the gas mixtures, i.e. the reaction is first order with respect to these reactants. The rate constants obtained for 700° are $k_{700} = 1{,}000$ Å/min and $k_{700} = 300$ Å/min, respectively.

The influence of the reactor pressure was studied in the range 0.5—1 torr. The deposition rate increased with total pressure in the reactor.

The investigation of the temperature influence on the deposition rate in the range of 700—900° leads to the following values of the activation energy and preexponential factor :

$E = 20$ kcal/mole, $A = 2.5 \times 10^7$ Å/min for the SiH_4—NH_3 system and

$E = 23$ kcal/mole, $A = 4.5 \times 10^7$ Å/min for the SiH_2Cl_2—NH_3 system.

It is evident from the figure that the deposition rate increases with increasing temperature according to the Arrhenius equation.

A similar relation has also been found for RF glow discharge and normal pressure depositions. However, the values of the activation energies are higher in the case of LPCVD.

The relatively high activation energy obtained for LPCVD can be explained by considering the reaction mechanism. Indeed, in the case of LPCVD, due to the rarefaction of the gas mixture the homogeneous reaction in the gas phase between the nonactivated molecules is very unlikely to occur. The reaction proceeds via a heterogeneous mechanism under the activation conditions of the substrate by heating.

This heterogeneous mechanism explains the high values of the obtained activation energies.

CONCLUSIONS

The kinetic study of silicon nitride film deposition by plasma stimulated (RF glow discharge) reaction between silane and ammonia shows that the deposition rate is constant in time.

— the deposition rate is directly proportional to silane concentration in the gas mixture;

— the deposition rate decreases with total pressure increase in the reactor;

— the deposition rate increases with the excitation energy of the plasma and with the substrate temperature.

The kinetic investigation of silicon nitride film deposition at low pressures using SiH_4—NH_3 and SiH_2Cl_2—NH_3 leads to similar results, namely :

— the linear dependence of the deposition rate on the molar fraction of silane or dichlorosilane, the reaction with respect to SiH_4 or SiH_2Cl_2 being of the first order;

— the increase of the deposition rate with the total pressure in the reactor;

— the validity of the Arrhenius equation for the deposition rate.

REFERENCES

[1] H. F. Sterling and R. C. G. Swann, *Solid State Electron,* **8,** 653 (1965).
[2] H. F. Sterling, J. H. Alexander and R. J. Joyce, *Vide,* **21,** 80 (1966).
[3] R. J. Joyce, H. F. Sterling and J. H. Alexander, *Thin Solid Films,* **1,** 481 (1967/68).
[4] R. C. G. Swann, R. R. Mehta and T. P. Cauge, *J. Electrochem. Soc.,* **114,** 713 (1967).
[5] M. Parnell and H. F. Sterling, *Electrical Comm.,* **43,** 63 (1968).
[6] Y. Kuwano, *Japan J. Appl. Phys.,* **7,** 88 (1968).
[7] Y. Kuwano, *Japan J. Appl. Phys.* **8,** 876 (1968).
[8] P. S. Schaffer and B. Swaroop, *Am. Ceram. Soc. Bull.,* **49,** 536 (1970).
[9] E. A. Taft, *J. Electrochem. Soc.,* **118,** 713 (1967).
[10] Y. Shima, T. Miyazaki, N. Nakamura, E. Adachi and T. Tokuyama, *Japan. J. Appl. Phys.* **12,** 309 (1973).
[11] R. Gereth and W. Scherber, *J. Electrochem. Soc.,* **119,** 1248 (1972).
[12] C. Weissmantel, P. Morzeck, and G. Reisse, *Wiss. Z. Tech. Univ. Dresden,* **24,** 57 (1975)
[13] C. Weissmantel, *Thin Solid Films,* **32,** 11 (1976).
[14] R. S. Rosler, W. C. Benzing and J. Baldo, *Solid State Technol.,* **19**(6), 45 (1976).
[15] G. Turban and Y. Catherine, *Vide, Suppl.,* **182,** 51 (1976).
[16] G. Turban and Y. Catherine, *Thin Solid Films,* **35,** 179 (1976).
[17] Y. Catherine and G. Turban, *Thin Solid Films* **41,** L57 (1977).
[18] R. L. Bersin, *Solid State Electron.,* **19,** 31 (1976).
[19] R. S. Rosler, *Solid State Technol.,* **20** (4), 63 (1977).
[20] M. Hammond and R. Gieske, Presented at Semicon West, May 27, 1976.

Revue Roumaine de Chimie, **25,** *3,* 323–326 (1980)

COMPARATIVE STUDIES OF CORONA PRESSURE EFFECT, *JOSHI* EFFECT AND THERMIONIC ANALOGUE OF *JOSHI* EFFECT IN ARGON UNDER SEMI-OZONIZER DISCHARGE

JAGDISH PRASHAD,
Chemistry Department, Meerut College, Meerut–250001, India

Received September 7, 1978

Studies of the corona pressure effect Δp, Joshi effect Δi_L and the thermionic analogue of Joshi effect Δi_T have been carried out in argon under semi-ozonizer excitation. Three important results have been obtained : (i) The inversion of $+\Delta i_T$ into $-\Delta i_T$ with increased thermionic emission, which is similar to the inversion of $+\Delta i_L$ into $-\Delta i_L$ with increased light intensity ; (ii) potential inversion of $+\Delta i_T$ into $-\Delta i_T$, similar to the potential inversion of $+\Delta i_L$ into $-\Delta i_L$ and (iii) the co-occurrence of Δp, Δi_L and Δi_T. The co-occurrence of Δp, Δi_L and Δi_T in a limited potential range showed that the negative Joshi effect is accompanied by a decrease in the ionic mobility. The results support Joshi theory for Δi_L.

INTRODUCTION

The Joshi theory [1] for the phenomenon Δi_L — a photovariation of the discharge current, contemplates the formation of the negative space charge consisting of ions, electrons and excited particles. Argon is an electron-free gas and negative ion formation is improbable. Hence in order to study and correlate the corona pressure effect Δp, the Joshi effect Δi_L and the thermionic analogue of Joshi effect Δi_T in an electron-free gas, the present study was carried out in argon under semi-ozonizer discharge.

EXPERIMENTAL

To remove the traces of the adsorbed air on the glass walls and also on the platinum wire, the tube was continuously evacuated under discharge for 12 hours. The central platinum wire was heated to yellowish-white after every one hour during evacuation. [2] The first flow from the reservoir of spectroscopically pure argon into the discharge tube was removed under evacuation. After repeated washings with argon, the discharge tube was re-evacuated under discharge. The mode of excitation of the tube and measurement of the discharge current i and the corona pressure Δp were similar to those reported earlier [3] (Figure 1).

The measurements of Δi_L, Δi_T and Δp were carried out in the pressure range 28–308 mm Hg 30°C. The central platinum wire of the semi-ozonizer was heated to thermionic emission

by d.c. obtained from the battery. During the measurements of Δp under light from a 200 watt 220 volt bulb, a cell containing the alum solution was interposed in between the discharge tube and the source of irradiation, to minimize the heat effects.

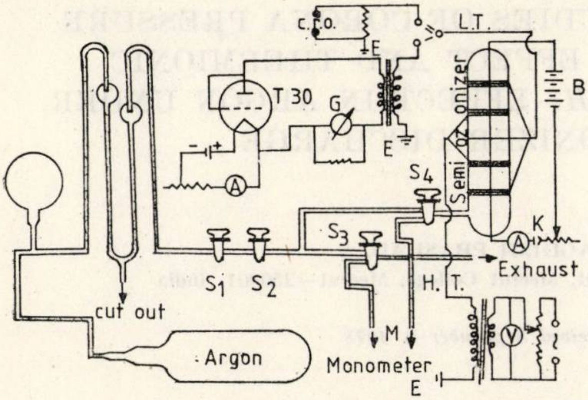

Fig. 1. — Comparative studies of corona pressure effect, Joshi effect and thermionic analogue of Joshi effect in argon under semi-ozonizer discharge.

RESULTS AND DISCUSSION

At the threshold potential V_m, the bluish glow appeared near the H.T. sleeves. It was ring-like and surrounded the central wire. The bright blue beads were observed only on the part of the wire which formed a conducting path for the discharge to pass. No measurable Δp was observed below $pA = 185$ mm. The results reveal that in the pressure range 2—308 mm, a large positive Joshi effect $+\Delta i_L$ was observed at $V < V_m$. This was followed by the initiation of a few h.f. pulses on the sinusoidal current trace. The positive effect increased at $V < V_m$ and changed into the negative effect $-\Delta i_L$ with further increase in the applied potential V. The magnitude of $-\%\Delta i$ decreased at higher potentials. At $V < V_m$, a large $+\Delta i_T$ was also observed under thermionic emission in the same potential range. This is similar to $+\Delta i_L$. With an increase in V, it first increased and then decreased precipitously and changed its sign to give $-\Delta i_T$. At higher potentials, it changed its sign to give a small positive effect. The curves at various applied potentials for $pA = 102$ mm show that with an increase in the value of i_F from 2 to 6 A, i.e., increased thermionic emission, $+\Delta i_T$ first increased, then decreased abruptly and finally changed to $-\Delta i_T$ (cf. Figure 2). The possibility that this cannot be attributed to ordinary heat effect is considered negligible as reported earlier.[3]

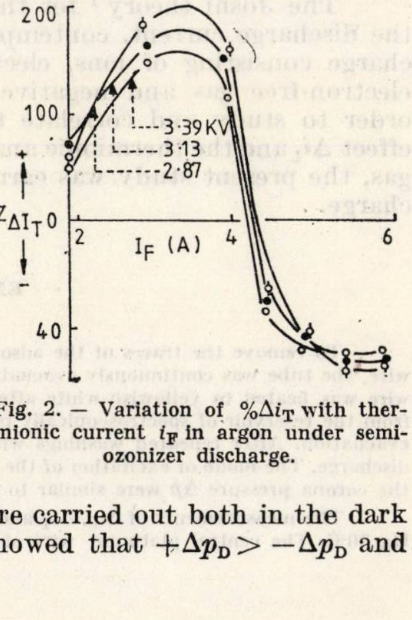

Fig. 2. — Variation of $\%\Delta i_T$ with thermionic current i_F in argon under semi-ozonizer discharge.

The measurements of Δp and Δi_L were carried out both in the dark and under light. The respective values showed that $+\Delta p_D > -\Delta p_D$ and

$+\Delta p_L > -\Delta p_L$. The maximum value of $+\Delta p_D$ was 0.45 and the minimum was 0.35 at $pA = 308$ mm Hg 30°C.

Δp values at different applied potentials kV both in the dark and under light showed that Δp increased with kV, when there was appreciable difference in between the two applied fields to cause some change in Δp, e.g.,

kV	$+\Delta p_D$	$+\Delta p_L$	k_D	k_L	$-\%\Delta i$
5.74	0.35	0.25	29.61	28.64	31
6.26	0.40	0.31	29.82	29.16	27
6.78	0.40	0.35	32.82	31.82	15
7.31	0.42	0.37	36.00	32.00	21
7.83	0.45	0.40	36.24	34.80	15
8.35	0.50	0.45	39.77	38.90	12

The above data show that : (i) $+\Delta p_D > +\Delta p_L$; (ii) Δp increases with kV ; (iii) ionic mobility in dark k_D or under light k_L increases with the applied potential ; (iv) $k_D > k_L$.

The increase of the discharge current i due to thermo-electrons $+\Delta i_T$ increases initially with an increase in the applied potential V ($< V_m$) to a maximum at V_m. Then, it decreases precipitously and changes sign to the negative effect $-\Delta i_T$, i.e. suppression of i due to thermo-electrons, at an inversion potential V_i^I. Beyond V_i^I, $-\Delta i_T$ first increases rapidly to a maximum and diminishes slowly thereafter. A second inversion from $-\Delta i_T$ into $+\Delta i_T$ was obtained at 308 mm with $i_F = 4.5$ A at higher applied potentials at V_i^{II}.

The initial $+\Delta i_T$ at $V < V_m$, and its enhancement with V, is ascribed to the release of thermo-electrons (at low i_F and applied field, at which field emission may occur), which should cause electron emission from the momentary cathode of field diminished work function. At V_m, when the nonselfmaintained discharge becomes selfmaintained, enhanced electron-emission causes formation of slowly moving negative ions and i is decreased. This is true for $-\Delta i_L$ or $-\Delta i_T$ in halogens,[4] oxygen[4] and perhaps hydrogen,[5] where negative ion formation is reported. But no negative ion formation is reported in the case of argon. Hence, certain additions are made to the Joshi theory.[1] It is assumed that the electrons may be considered to be the simplest and extreme case of negative ions and may cause the current reduction, as a space charge effect[6]. Δi_L or Δi_T can thus be explained, not only in the case of halogens, but also in electron-free gases like He, Ne and Ar.

Under light, the electrons are emitted from the walls or/and electrodes of the discharge tube, whereas under thermionic emission, the electrons are emitted from the metal surface. Before reaching the walls, the released electrons ionise the gas molecules and a tail of positive ions is left behind. The intense positive ion space charge formed near the anode retards the growth of the electron avalanches as a result of which the current decreases. This suggestion also supports the above view.

$+\Delta i_T$ is again observed beyond V_i^{II}. At higher potentials, β and γ mechanisms take place in the discharge space and at the cathode, respectively and give rise to secondary electrons. The continuous copious supply of thermo-electrons from the Pt surface and the secondary electrons produced in the discharge space escape collisions, mainly contributing to the increase in the current. It is well known that in a gas discharge, metastable atoms play an important role as a source of secondary ionization. The importance of the action of metastables in the gas phase and also at cathode has been emphasized.[7]

Considering the mobility in the dark and under light for different values of applied V, calculated from Tyndall's equation, it is found that $k_D > k_L$. At these potentials, 20 – 30 % negative effect is observed. This reveals that $-\Delta i_L$ is associated with a decrease in k and supports the Joshi theory for the phenomenon Δi_L.

ACKNOWLEDGEMENT. Thanks are due to Dr. R.J. Galagali for his valuable suggestions.

REFERENCES

[1] S. S. Joshi, *Curr. Sci.*, **16**, 19 (1947).
[2] I. Langmuir, *J. Amer Chem. Soc.*, **38**, 2221 (1916).
[3] J. Prashad, *Bol. Soc. Quim. Peru*, (1978) — Communicated.
[4] J. Prashad, *Rev. Roumaine Chim.*, **18**, 1075 (1973).
[5] J. Prashad, *Acta Ciencia Indica*, **1**, 13 (1974).
[6] J. Prashad, Ph.D. Thesis, Banaras Hindu University, 28 (1961).
[7] L. B. Loeb, *Rev. Mod. Phys.*, **8**, 26 (1936).

Revue Roumaine de Chimie, **25**, *3*, 327–331 (1980)

AN INVESTIGATION OF THE REACTION BETWEEN TELLURITE AND CHLORITE IONS IN SOLUTION

M. S. SUBHANI
Department of Chemistry, University of Nigeria, Nsukka, Nigeria

Received July 11, 1978

The rate of reaction between TeO_3^{2-} ion and ClO_2^- ion was studied in solution using different ionic strengths. The reaction was found to be a second order process with (a) $ClO_2^- + TeO_3^{2-} \rightarrow TeO_4^{2-} + ClO^-$(a) as the rate determining process. The energy of activation was evaluated. Investigations were also made on the rate of reaction using different dielectric media. A single sphere model is predicted for the activated state. The radius and the thermodynamic properties of the activated state are determined.

INTRODUCTION

The study of the reaction in solution has been the subject of research by various workers.[1-6] A number of mechanisms have been proposed. Effects of solvent and conic strength have also been studied.[5-9] Two models, the single and double sphere, have been proposed for the activated state formed during the reaction. Mathematical relationships, between specific rate constants at zero ionic strength (k_0) and radii of the activated complex ($r^{\ddagger}$ or r_{AB}) for the single and double sphere at a given dielectric of the medium (D), are suggested (see equations (1) and (2)).

$$\ln k_0 = \ln k_i - \frac{e^2}{2DkT}\left(\frac{(Z_A + Z_B)^2}{r^{\ddagger}} - \frac{Z_A^2}{r_A} - \frac{Z_B}{r_B}\right) \tag{1}$$

$$\ln k_0 = \ln k_i - \frac{e^2 Z_A Z_B}{DkT r_{AB}} \tag{2}$$

where k_i is the rate constant at infinite dielectric of the medium, e, the charge on the election, Z_A, Z_B, r_A, r_B are the valences and radii of the ions A and B, respectively and k is the Boltzman constant. The thermodynamic properties related to the activated state can also be evaluated using various relationships reported in the literature.[9,10,11]

The reaction between chlorite ion and sulphite ion has been reported in the literature,[12-13] but no work on the reaction between tellurite ion and chlorite ion.

In the present paper, the reaction between chlorite ion and tellurite ion in solution is reported.

EXPERIMENTAL

All chemicals used were of analaR grade. All solutions were prepared using triply distilled water just before the experiment. All experiments were carried out in inert atmosphere using nitrogen gas to avoid any areal oxidation of TeO_3^{2-} ion in solution. Pye Unicam SP 8000 spectrophotometer with thermostat attachment HAKE mode NK22 was used for the measurement of the concentration of ClO_2^- in the reaction mixture at a given time interval at known temperature. Absorption measurements were made at wavelength 260 nm using previously an experimentally determined extinction coefficient at a given temperature. Tellurite ion was found not absorbing at the wavelength. Dielectric constant measurements for various dielectric media (10 % to 45 % alcohol/ water mixture (V/V) were obtained by the method described elsewhere.[14]

RESULTS AND DISCUSSIONS

Linear plots were made only when second order integrated form of relationship, relating the concentration at any time t to that of time t for the reactant tellurite ion and chlorite ions in reaction mixture at a given temperature, dielectric constant and ionic strength, thus indicating the reaction as a second order process in solution. The most probable mechanism which can account for the above-mentioned observation would be an atom transfer from ClO_2^- to TeO_3^{2-} ion in the rate determining step 3 analogous to that proposed for the sulphitehalite ion reaction in solution.[12,13]

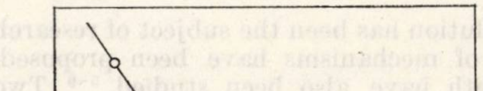

Fig. 1. — The plot logarithmic function of specific rate constant against reciprocal of temperature.

The mechanism can be written as follows:

$$ClO_2^- + TeO_3^{2-} \rightarrow (O_2TeO_3)^{3-} TeO_4^{2-} + ClO^- \text{ (slow)} \qquad (3)$$

$$ClO^- + TeO_3^{2-} \rightarrow TeO_4^{2-} + Cl^- \text{(fast)} \qquad (4)$$

Measurements of rate constants at various temperatures ranging from 5° to 50° were made and a plot between $\log k_{obs}$ and $1/T$ was linear (see Figure 1) and from the slope a value of 58.3 kJ/Mole for the activation energy of the reaction was evaluated. To observe the effect of dielectric constant and ionic strength studies were carried out using various ionic strengths in different dielectric media. The values of the rate constants obtained are summarized in Table 1.

TABLE 1

The observed rate constants ($k_{obs.}$) at various ionic strengths in different dielectric media

$T = 298$ K $(TeO_3^{2-}) = 10^{-2} - 10^{-3}$M, $(ClO_2^-) = IO^{-2} - 10^{-3}$M			$T = 298$ K $(TeO_3^{2-}) = 10^{-2} - 10^{-3}$M, $(ClO_2^-) = IO^{-2} - 10^{-3}$ M			$T = 298$ K $(TeO_3^{2-}) = 10^{-2} - 10^{-3}$M, $(ClO_2^-) = IO^{-2} - 10^{-3}$M		
log. $k_{obs.}$	D	U	log. $k_{obs.}$	D	U	log. $k_{obs.}$	D	U
$\bar{2}.6384$	79.9	0.02	$\bar{2}.6462$	65.1	0.05	$\bar{2}.6553$	49.2	0.08
$\bar{2}.7032$	79.9	0.03	$\bar{2}.7053$	65.1	0.06	$\bar{2}.7279$	49.2	0.09
$\bar{2}.7580$	79.9	0.04	$\bar{2}.7597$	65.1	0.07	$\bar{2}.7963$	49.2	0.10
$\bar{2}.8060$	79.9	0.05	$\bar{2}.8105$	65.1	0.08	$\bar{2}.0238$	45.2	0.02
$\bar{2}.8496$	79.9	0.06	$\bar{2}.8582$	65.1	0.09	$\bar{2}.1772$	45.2	0.03
$\bar{2}.8894$	79.9	0.07	$\bar{2}.9031$	65.1	0.10	$\bar{2}.3045$	45.2	0.04
$\bar{2}.9268$	79.9	0.08	$\bar{2}.2520$	56.8	0.02	$\bar{2}.4179$	45.2	0.05
$\bar{2}.9620$	79.9	0.09	$\bar{2}.3602$	56.8	0.03	$\bar{2}.5200$	45.2	0.06
$\bar{2}.9950$	79.9	0.10	$\bar{2}.4514$	56.8	0.04	$\bar{2}.6234$	45.2	0.07
$\bar{2}.5059$	70.36	0.02	$\bar{2}.5317$	56.8	0.05	$\bar{2}.7017$	45.2	0.08
$\bar{2}.5845$	70.36	0.03	$\bar{2}.6014$	56.8	0.06	$\bar{2}.7842$	45.2	0.09
$\bar{2}.6506$	70.36	0.04	$\bar{2}.6708$	56.8	0.07	$\bar{2}.8519$	45.2	0.10
$\bar{2}.7088$	70.36	0.05	$\bar{2}.7331$	56.8	0.08			
$\bar{2}.7614$	70.36	0.06	$\bar{2}.7916$	56.8	0.09	$\bar{3}.8229$	41.3	0.02
$\bar{2}.8098$	70.36	0.07	$\bar{2}.8467$	56.8	0.10	$\bar{3}.9974$	41.3	0.03
$\bar{2}.8550$	70.36	0.08				$\bar{2}.1445$	41.3	0.04
$\bar{2}.8974$	70.36	0.09	$\bar{2}.0581$	49.2	0.02	$\bar{2}.2740$	41.3	0.05
$\bar{2}.9374$	70.36	0.10	$\bar{2}.1924$	49.2	0.03	$\bar{2}.3909$	41.3	0.06
			$\bar{2}.3056$	49.2	0.04	$\bar{2}.4985$	41.3	0.07
$\bar{2}.4187$	65.1	0.02	$\bar{2}.4052$	49.2	0.05	$\bar{2}.5989$	41.3	0.08
$\bar{2}.5064$	65.1	0.03	$\bar{2}.4952$	49.2	0.06	$\bar{2}.6933$	41.3	0.09
$\bar{2}.5808$	65.1	0.04	$\bar{2}.5780$	49.2	0.07	$\bar{2}.7822$	41.3	0.10

In all the cases fairly linear plots were obtained between log k_{obs} and U in a given dielectric medium. The values of log k_0 obtained from the extrapolation of linear plots to zero ionic strength are shown in Table 2.

A plot of log k_0 against $1/D$ is linear (see Figure 2)

The linear plot (see Figure 2) between log k_0 and $1/D$ satisfies relationships (1) and (2). From the slope the values of $r^{\neq}$ and r_{AB} were evaluated and are shown in Table 3.

Theoretical values of $r^{\neq}$ and r_{AB} were calculated by the method reported in the literature, [5,7] using data for the various ionic radii available in the literature. [15-18] The values are also shown in Table 3. By comparing the theoretical values of $r^{\neq}$ and r_{AB} with those experimentally obtained (see table 3) it was concluded that the most probable shape of the activated complex formed during the reaction is of single sphere.

The values obtained for $r^{\neq}$ were used to calculate electrostatic contributions to the thermodynamic properties of the activated state. The values of the electrostatic free energy of activation, ($\Delta G^{\neq}_{es}$), entropy of activation, ($\Delta S^{\neq}_{es}$), and those of enthalpy of activation, ($\Delta H^{\neq}_{es}$), are summarized in Table 4.

TABLE 2

The values of log k_0 and the reciprocal of dielectric of the media

log k_0	$1/D + 10^3$
$\bar{2}.350$	12.52
$\bar{2}.157$	14.21
$\bar{2}.026$	15.36
$\bar{3}.771$	17.60
$\bar{3}.461$	20.32
$\bar{3}.346$	22.12
$\bar{3}.047$	24.21

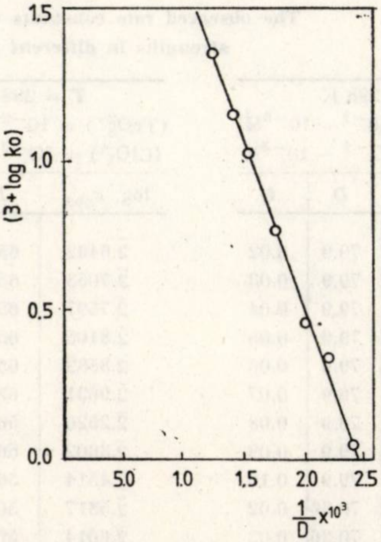

Fig. 2. — The plot of logarithmic function of specific rate constant at zero ionic strength against reciprocal of dielectric of the medium.

TABLE 3

The theoretical and experimental values of the radii $r^{\neq}$ and r_{AB} for the single and double sphere shape, respectively

	Experimental, values Å	Theoretical values Å
$r^{\neq}$	2.900	2.933
r_{AB}	4.27	4.63

TABLE 4

The values of the electrostatic contributions to the thermodynamic properties, $\Delta G^{\neq}_{es}$, $\Delta H^{\neq}_{es}$ and $\Delta S^{\neq}_{es}$ of the activated state

	$\Delta G^{\neq}_{es}$ (kJ/M)	$\Delta H^{\neq}_{es}$ (kJ/M)	$\Delta S^{\neq}_{es}$ (J/MT)
Theoretical value	8.14	−3.16	−37.94
Experimental value	8.98	−3.33	−41.31

The sign and magnitude of the changes in the entropy of activation (electrostatic), $\Delta S^{\neq}_{es}$ can be best explained in terms of the description of the initial state of the reactants and that of the activated state. TeO_3^{2-} and ClO_2^- can be regarded as doubly and single negatively charged spheres in their reactant states before the start of the reaction where the activated state is a triply negatively charged sphere $(ClO_2-TeO_3)^{3-}$ with greater charge density. The solvent molecules in the neighbourhood of these charge spheres are acted upon by electrostriction. Stronger electrostriction is expected in the activated state as compared to that in the initial state. Thus, a decrease in entropy of activation is expected. A similar interpretation can be put forth for the case of other thermodynamic properties mentioned earlier.

REFERENCES

[1] K. J. Laidler, "Reaction Kinetics", Pergamon, Oxford, 1963 p. 10.
[2] C. T. Burris and K. J. Laidler, *Trans. Faraday Soc.*, **51,** 1497 (1955).
[3] K. J. Laidler and D. T. Y. Chen, *Trans. Faraday Soc.*, **54,** 1026 (1958).
[4] D. T. Y. Chen and K. J. Laidler, *Canad. J. Chem.*, **37,** 599 (1959).
[5] M. S. Subhani and M. N. H. Laeewala, *J. Sci Math.*, **1,** 41 (1974).
[6] M. S. Subhani, *Rev. Roumaine Chim.* (accepted for publication).
[7] K. J. Laidler and H. Eyring, *Ann. New York Acad. Sci.*, **39,** 303 (1940).
[8] E. S. Amis, *J. Chem. Educ.*, **29,** 337 (1952).
[9] K. J. Laidler, "Chemical Kinetics" McGraw Hill, New York, 1965, p. 212, p. 217.
[10] E. S. Amis and J. E. Petts, *J. Amer. Chem. Soc.*, **63,** 2883 (1941).
[11] S. Arrhenius, *Z. phys. Chem.*, **4,** 226 (1889).
[12] A. C. Nixon and K. B. Krauskople, *J. Amer. Chem. Soc.*, **54,** 4606 (1932).
[13] J. Helperin and H. Taube, *J. Amer. Chem. Soc.*, **74,** 380 (1952).
[14] M. S. Subhani and I. Kausar, *Pakistan J. Sci. Ind. Res.*, India **18,** 208 (1975).
[15] G. S. Scatchard, *J. Chem. Phys.*, **7,** 657 (1939).
[16] J. Kleinberg, W. J. Argersinger and E. Griswold, "Inorganic Chemistry", D. C. Heath Co. Boston, 1965, p. 74.
[17] T. Moeler, "Inorganic Chemistry", Wiley, New York, 1960, p. 140.
[18] A. F. Kapusttnsky, *Quart. Rev.*, **10**, 283 (1956).

Revue Roumaine de Chimie, 25, 3, 333–337 (1980)

THERMOCHEMICAL STUDIES ON SOLUTIONS OF MONOBROMO-, DIBROMO- and TRIBROMO-ACETIC ACIDS IN WATER AND CHLOROFORM

M. S. SUBHANI*
Department of Chemistry, University of Nigeria, Nsukka, Nigeria

Received September 13, 1978

Enthalpies of mixing (ΔH_m) monobromo-, dibromo- and tribromo-acetic acids with water and chloroform have been evaluated using an isothermal phase-change calorimeter. The exothermicity of mixing decreases in the order of monobromo- $\lessdot$ dibromo- $\lessdot$ tribromo-acetic acid.

INTRODUCTION

Studies on the determination of enthalpies of mixing for the bromo substituted acid are not seen to be reported in the literature. In the present work an attempt has been made to evaluate the thermochemal properties of the solutions of these acids in water and chloroform.

EXPERIMENTAL

All the chemicals used were of analaR grade. All aqueous solutions were prepared in triply distilled water. The enthalpies of mixing for various systems were determined using an isothermal phase-change calorimeter reported in the literature. [1]

RESULTS AND DISCUSSIONS

The enthalpies of mixing (ΔH_m) for solutions of different compositions of monobromo-, dibromo- and tribromo-acetic acids in water and chloroform were determined and are summarized in Tables 1 and 2, respectively.

Since bromo-acetic acids do not interact with the solvents to form new chemical species, the heat effects accompanying the mixing of these acids with water and chloroform may be considered to arise from one or more of the factors namely, lattice energy, change in the degree of dime-

---

* Present address: Faculty of Science, PO Box 9480, Benghazi, Libya.

TABLE 1

Enthalpies of mixing for the bromoacetic acid-water system 25.0 ± 0.01°

A = Monobromoacetic acid,
B = Dibromoacetic acid and
C = Tribromoacetic acid

Acid water system	Mole fraction	ΔH_m (kJ/mole)
A	0.01	0.150
	0.04	0.608
	0.07	1.078
	0.10	1.560
	0.17	2.550
	0.28	4.144
	0.38	5.016
	0.50	5.700
B	0.01	−0.074
	0.06	−0.192
	0.08	−0.064
	0.13	0.286
	0.15	0.450
	0.19	0.722
	0.30	1.320
	0.39	1.482
	0.48	1.344
	0.62	0.744
C	0.02	−0.200
	0.04	−0.352
	0.07	−0.476
	0·09	−0.522
	0.12	−0.576
	0.18	−0.684
	0.42	−0.756
	0.54	−0.540
	0.66	−0.528
	0.83	−0.166
Chloroform system		
A	0.01	0.238
	0.02	0.452
	0.025	0.540
	0.03	0.618
	0.04	0.784
	0.05	0.920
	0.08	1.344
	0.14	2.240
	0.24	3.744

TABLE 2

Enthalpies of mixing of bromoacetic acid-chloroform system at 25.0 ± 0.01°

A = Monobromoacetic acid
B = Dibromoacetic acid and
C = Tribromoacetic acid

Acid water system	Mole fraction	ΔH_m (kJ/mole)
A	0.01	15.0
	0.04	15.2
	0.07	15.4
	0.10	15.6
	0.17	15.0
	0.28	14.8
	0.38	13.2
	0.50	11.4
B	0.01	−7.4
	0.06	−3.2
	0.08	−0.8
	0.13	2.2
	0.15	3.0
	0.19	3.8
	0.30	4.4
	0.39	3.8
	0.48	2.8
	0.62	1.2
C	0.02	−10.0
	0.04	−8.8
	0.07	−6.8
	0.09	−5.8
	0.12	−4.8
	0.18	−3.8
	0.42	−1.8
	0.54	−1.0
	0.66	−0.8
	0.83	−0.2
Chloroform system		
A	0.01	23.8
	0.02	22.6
	0.025	21.6
	0.03	20.6
	0.04	19.6
	0.05	18.4
	0.08	16.8
	0.14	16.0
	0.24	15.6

Table 1 (continued)

Acid water system	Mole fraction	ΔH_m (kJ/mole)
	0.33	5.882
	0.40	6.120
	0.46	6.992
	0.50	7.500
	0.53	8.162
B	0.04	0.624
	0.16	2.368
	0.26	3.744
	0.41	5.822
	0.50	7.000
	0.61	8.662
	0.70	10.080
	0.79	11.534
	0.87	12.963
C	0.03	0.360
	0.05	0.570
	0.06	0.672
	0.12	1.272
	0.16	1.600
	0.26	2.496
	0.38	3.800
	0.46	4.600
	0.51	5.304
	0.61	6.344
	0.70	7.140
	0.78	7.800
	0.93	9.114

Table 2 (continued)

Acid water system	Mole fraction	ΔH_m (kJ/mole)
	0.33	15.4
	0.40	15.3
	0.46	15.2
	0.50	15.0
	0.53	15.4
B	0.04	15.6
	0.16	14.8
	0.26	14.4
	0.41	14.2
	0.50	14.0
	0.61	14.2
	0.70	14.4
	0.79	14.6
	0.87	14.9
C	0.03	12.0
	0.05	11.4
	0.06	11.2
	0.12	10.6
	0.16	10.0
	0.26	9.6
	0.38	10.0
	0.46	10.0
	0.51	10.4
	0.61	10.4
	0.70	10.2
	0.78	10.0
	0.93	9.8

rization, change in the degree of ionization, solvation and hydrogen bonding. The heats of solution ΔH_s ($\Delta H_s = \Delta H_m / X_2$) in each solvent are in the order of $BrCH_2COOH > Br_2CHOOH > Br_3CHOOH$

Since ΔH_s values for the solutions of these acids are largely determined by the lattice energy of the acids (the values of the heat of fusion of monobromo-, dibromo- and tribromo-acetic acid are: 13.00 ± 0.3, 7.60 ± 0.06 and 5.85 ± 0.05 kJ/mole, respectively).[2] The expected order of ΔH_s values is the same as that obtained experimentally.

In aqueous system, heats of solution of bromoacetic acids were determined (see Figure 1).

It can be seen in Figure 1 that the value of ΔH_s at low solute concentration increases steeply with increase of bromoacetic acid concentration. Since acids are considered to be completely ionized forms in dilute solutions, the steep rise in the values of ΔH_s may be attributed to the change in their degree of ionization. The values of ΔH_s at infinite dilution, obtained by extrapolation of ΔH_s values to zero concentration, are reported in Table 3.

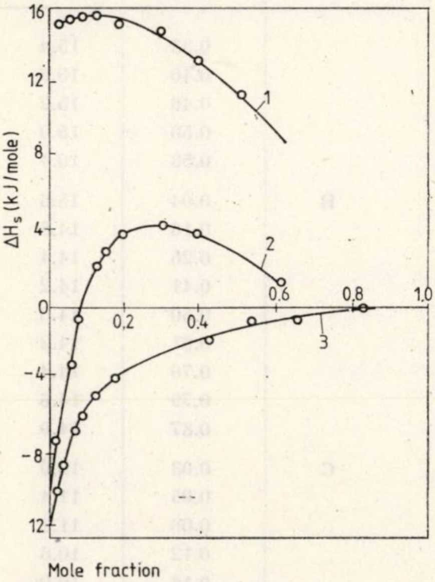

Fig. 1. — A plot of ΔH_s versus mole fraction of bromoacetic acid in water: 1 — monobromoacetic acid; 2. — dibromoacetic acid; 3 — tribromoacetic acid.

TABLE 3

Values of the heat of solution of the bromoacetic acids in water at infinite dilution (ΔH_s)

Acid	ΔH_s(kJ/mole)
Monobromoacetic acid	14.96 ± 0.01
Dibromoacetic acid	12.15 ± 0.01
Tribromoacetic acid	10.87 ± 0.01

There can be a variety of factors which may account for the exothermic and endothermic contributions to ΔH_s. The exothermic contributions are due to hydrogen bonding between the molecules of the acids and water and hydration of the ionic species of the acids. The endothermic contributions, on the other hand, are due to lattice energy (nearly equal to heat of fusion), ionization of the acid molecules to unhydrated ions and dissociation of dimer molecules to monomer species.

The values of percentage ionization obtained on the basis of ionization constant for the mono-, di- and tribromoacetic acids are 3.80, 21.62 and 39.36 in their pure state, respectively. [3] In aqueous solution at infinite dilution, not only do the ions (already present in pure solute) get hydrated but the acids get further ionized with subsequent hydration of ions. It is obvious now that the more ionized a solute in its pure state is, the more exothermic the net contribution from ionization of acid and hydration of ions to the heat of solution at infinite dilution. In view of the electron withdrawing character of bromine atoms, the heat of ionization of the bromoacetic acids is expected to be small as compared to the heat of ionization of acetic acid. It follows that the greater the number of bromine atoms in the acid molecule, the larger the difference in magnitude of heats of ionization and hydration. Hence the exothermic trend in the ΔH_s values of the acid solutions is expected to increase from monobromoacetic acid to tribromacetic acid. This is seen to be true from the values of ΔH_s at infinite dilution (see Table 3).

Since the extent of contributions from various factors to ΔH_s are not known, any further attempt to explain the results can be of no significant interest.

CHLOROFORM SYSTEM

The values of ΔH_s at infinite dilution determined from the plot of ΔH_s against mole fraction of acids (see Figure 2) and extrapolation to zero mole fraction are summerized in Table 4.

TABLE 4

The values for the heat of solutions of bromoacetic acids in chloroform at infinite dilution

Acid	ΔH_s (at infinite dilution) (kJ/mole)
Monobromoacetic acid	25.2±0.02
Dibromoacetic acid	15.84±0.02
Tribromoacetic acid	12.95±0.03

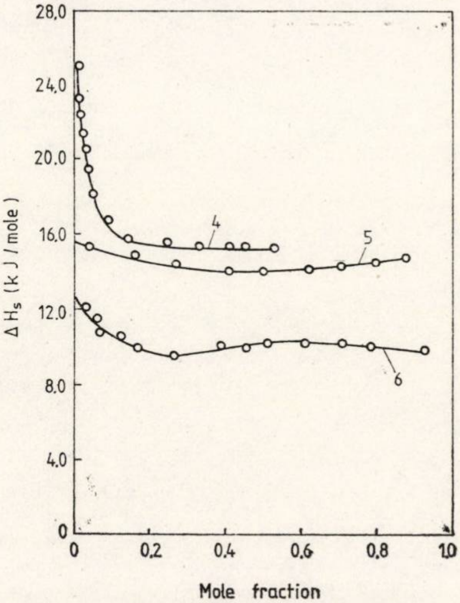

Fig. 2. — A plot of ΔH_s versus mole fraction of bromoacetic acids in chloroform : 4 — monobromoacetic acid ; 5 — dibromoacetic acid ; 6 — tribromoacetic acid.

These acids are known to dimerize in organic solvents. From the data reported in the literature, the extent of dimerization in chloroform was calculated to be between 80% to 90% even for dilute solutions.[4] Since the heat of dimerization is usually of the order of 42 kJ/mole, the value of ΔH_s (ranging from 0 to 21 kJ/mole) can be explained by postulating that the acids in their pure state are also sufficiently dimerized. Unlike the solutions of acids in water the ΔH_s values for chloroform solutions are found to decrease, in general, with the increase of acids concentration.

The decrease in ΔH_s is appreciable in solutions of monobromoacetic acid, less in solutions of dibromoacetic acid and almost negligible in the case of tribromoacetic acid. The above observations support the conclusion that the acids are not ionized in chloroform. The decrease in the values of ΔH_s may be assigned to an increase in the dimerization of the acids with the increase of the concentration of acids. It is also observed that ΔH_s values of bromoacetic acids are almost independent of the composition of higher acid concentration.

REFERENCES

[1] M. L. Lakhanpal, M. Lal and R. K. Sharma, *Indian J. Chem.*, **3**, 547 (1965).

[2] "International Critical Tables of Numerical Data : Physics, Chemistry and Technology", McGraw Hill, New York, 1929, p. 132.

[3] R. T. Morrison and R. N. Boyd, "Organic Chemistry", Prentice-Hall, New York, 1969, p. 600.

[4] C. P. Brown and A. R. Mathieson, *J. Phys. Chem.*, **58**, 1057 (1954).

Revue Roumaine de Chimie, **25**, *3*, 339–347 (1980)

COMBINAISONS COMPLEXES DES THIOCARBOHYDRAZONES ISONICOTIANEALDÉHYDE ET DU THIOPHÉNE-2-CARBALDÉHYDE

SILVIA BARBU* et CONST. GH. MACAROVICI**
*** Faculté de Pharmacie, 12, str. I. Creangă, Cluj-Napoca**
**** Faculté de Chimie, 11, str. Arany Janos, Cluj-Napoca**

Roumanie

Reçu le 2 février 1978

Les auteurs synthétisent et étudient des combinaisons complexes d'isonicotinealdéhyde-thiocarbohydrazone et de thiophène-2-carbaldéhyde-thiocarbohydrazone avec certains ions des métaux de transition ; Co (II), Ni (II), Zn (II), Cd (II), Hg (II), Pd (II). Les combinaisons complexes ont la formule générale $MLCl_2$; $MLCl_2 \cdot 2H_2O$ et $ML_2(SCN)_2$. Les combinaisons isolées à l'état solide sont étudiées au moyen de la dérivatographie, spectrophotométrie en U.V., V et I.R. et magnétique.

Complex combinations of isonicotine-aldehyde thiocarbohydrazones and of thiophene-2-carbaldehyde thiocarbohydrazones with ions of the transition metals : Co (II), Ni (II), Zn (II), Cd (II), Hg (II), Pd (II) were synthetized. Complex combinations with the general formula $MLCl_2$, $MLCl_2$. $2H_2O$ and $ML_2(SCN)_2$ were isolated in solid state and were studied by physico-chemical methods : derivatography, electronic and IR spectrophotometry and magnetically.

Poursuivant les propriétés coordinatives de certaines thiocarbohydrazones hétérocycliques, on a étudié plusieurs complexes métalliques de la thiocarbohydrazone isonicotinealdéhyde (I—TCH) et de la thiophène 2-carbaldéhyde (T—TCH), qui n'ont pas encore été mentionnés dans la littérature. Dans ce but on a synthétisé et isolé à l'état solide des combinaisons complexes correspondant aux formules $MLCL_2$, $MLCl_2 \cdot 2H_2O$ et $ML_2(SCN)_2$ où le rapport de combinaisons métal-ligand est de 1 : 1, respectivement 1 : 2. Comme ions métalliques générateurs des complexes on a utilisé certains ions des métaux de transition ayant la configuration $3d^7$, $3d^8$, $3d^{10}$, et $4d^8$.

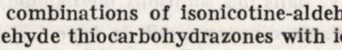

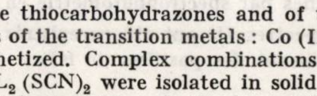

T-TCH

PARTIE EXPERIMENTALE

Les thiocarbohydrazones hétéroaromatiques, utilisées comme ligands, ont été préparées suivant la réaction de condensation de la thiocarbohydrazide avec les aldéhydes respectives. Leur purification a été réalisé par recristallisation de l'alcool. Les chlorures ont été préparés par le mélange d'une solution hydroalcoolique de chlorure métallique et d'une solution alcoolique de ligand, en rapport molaire de 2M : 1L. Le mélange, maintenu pendant environ 30 minutes au bain-marie est ensuite amené au pH = 6 par une solution d'acétate de sodium 5 % et l'on ajoute de l'eau jusqu'à ce que le précipité soit formé.

Les thiocyanates métalliques complexes ont été préparés par mélange d'une solution alcoolique de thiocyanate de Co (II) ou de Ni (II) et d'une solution alcoolique de ligand en rapport molaire de 1M : 2L. Le mélange, maintenu pendant 15 minutes au bain-marie est refroidi, ensuite, les thiocyanates métalliques complexes sont séparés de la solution par filtrage. La combinaison Co $(T-TCH)_2 (SCN)_2$ est isolée à l'état solide par addition d'eau jusqu'à la formation d'un précipité. Les précipités séparés sont filtrés et lavés à un mélange d'eau-alcool 1 : 1. Les complexes obtenus sont purifiés par recristallisation de l'alcool, séchés à la température ambiante. Le rapport de combinaison métal-ligand est de 1 : 1 pour les chlorures et de 1 : 2 pour les thiocyanates (tableau 1).

On a enregistré les dérivatogrammes des combinaisons Ni $(I-TCH)_2 (SCN)_2$ et Ni $(T-TCH)_2 (SCN)_2$, au moyen d'un dérivatographe M.O.M. de type Erdely-Paulik-Paulik.

Les déterminations magnétiques ont été effectuées au moyen d'une balance Faraday.

Les spectres électroniques des combinations complexes des ions métalliques à orbitales d'incomplètes ont été enregistrés en réflexion diffuse à un spectrophotomètre VSU—2P, utilisant des pastilles de substance qui, pour certains complexes ont été obtenues par mélange avec de l'oxyde de magnésium. Les chlorures complexes des ions ayant la configuration électronique d^{10} ont été étudiés par spectrophotométrie en U.V. dans des solutions méthanoliques.

Les spectres IR ont été enregistrés à l'aide d'un appareil de type UR—10 Carl-Zeiss Jena, en utilisant des pastilles de KBr.

RÉSULTATS ET DISCUSSIONS

Les combinaisons complexes synthétisées sont insolubles dans l'eau, peu solubles dans les solvants organiques, solubles dans les solvants de caractère basique (DMF, Py, hydroxydes alcalins).

Le comportement thermique des thiocyanates complexes (tableau 2) présente les mêmes étapes de décomposition que pour la décomposition thermique du ligand libre [1]. Par la pyrolyse de la molécule de thiocarbohydrazone à la première étape est détruit le reste hydrazonique, à des températures inférieures à 500°, suivie de la destruction du radical hétéroaromatique, à des températures comprises entre 500° et 600°. Le résidu de la pyrolyse est l'oxyde de nickel.

Les valeurs des moments magnétiques correspondent à la géométrie octaédrique dans le cas des complexes de l'ion de Co(II). [2,3]

Le terme fondamental de l'ion de Ni (II), scindé en champ octaédrique dans un singlet et deux sets de triplets, ne présente pas une dégénérescence orbitale à l'état fondamental, ce qui fait que les moments magnétiques aient des valeurs voisines à celle de spin. La différence par rap-

TABLEAU 1

Analyse chimique et étude magnétique

Composé	Couleur	N %		S %		M %		Cl%		Etude magnétique	
		calc.	*trouvé*	*calc.*	*trouvé*	*calc.*	*trouvé*	*calc.*	*trouvé*	$\chi_{M_{ac}}^{10-6}$	μ_{MB}
$Co(I-TCH)Cl_2$	brun	21,54	21,19	9,86	10,35	18,06	17,63	21,80	21,51		
$Ni(I-TCH)Cl_2$	brun	21,56	20,98	9,86	9,31	18,07	17,65	21,82	21,53		
$Zn(I-TCH)Cl_2$	jaune	21,12	20,82	9,69	9,90	19,71	19,25	21,40	20,91		
$Cd(I-TCH)Cl_2 . 2H_2O$	brun	16,89	17,31	7,73	7,05	27,0	26,83	17,12	17,63		
$Hg(I-TCH)Cl_2$	jaune	14,99	14,52	6,86	6,32	42,98	42,51	15,20	15,55		
$Pd(I-TCH)Cl_2$	jaune	18,79	19,08	8,60	7,98	28,55	28,06	19,05	18,75		
$Co(I-TCH)_2(SCN)_2$	brun	29,71	29,30	22,67	22,05	10,42	10,72	—	—	9 852	4,85
$Ni(I-TCH)_2(SCN)_2$	jaune	29,73	29,30	22,68	22,37	10,38	10,72	—	—	3 679	2,96
$Co(T-TCH)_2(SCN)_2$	brun	24,33	24,53	33,41	32,91	10,23	9,92	—	—	9 450	4,75
$Ni(T-TCH)_2(SCN)_2$	jaune	24,34	24,13	33,43	33,52	10,20	9,89	—	—	3 571	2,92

port à la valeur de spin est due au couplage spin-orbite entre l'état singlet et l'état triplet immédiatement supérieur. [4,5]

L'attribution des bandes des spectres électroniques aux complexes de l'ion Co(II) a été faite suivant le diagramme des niveaux énergétiques de Tanabe et Sugano [6] (tableau 3).

Comme il résulte du tableau 3, les bandes caractéristiques des trois types de transition de spin admis, sont généralement résolues pour tous les complexes.

TABLEAU 2

Pyrolyse du Ni(I-TCH$_2$) (SCN) et Ni(T-T$_2$)CH (SCN)$_2$

Composé	Température °C	Effets thermiques °C		Perte en poids %		Phénomène
		endo	exo	*cal.*	*trouvé*	
Ni(I−TCH)$_2$(SCN)$_2$	200	125	—	9,20	9,08	Elimination CN
	300	—	240	10,97	11,62	Pyrolyse reste hydrazinique
	500	—	400 463	35,76	36,60	Elimination 1S et pyrolyse reste de la chaîne d'atomes
	600	—	520	27,62	27,40	Pyrolyse reste molécule
	800	740	—	5,67 13,17	4,90 12,50	Brûlement et formation de NiO
Ni(T−TCH)$_2$(SCN)$_2$		200	—	9,04	8,61	Elimination en CN
	300	—	255	29,59		Pyrolyse de la chaîne d'atomes
		—	338	11,14	9,90	
	400	—	390	11,14	11,90	Elimination en 2S
	600	—	500 540	23,30	20	Pyrolyse reste molécule Formation de NiS
		—	770	5,57 12,95	5,45 11,50	Décomposition de NiS —NiO

L'attribution de la bande est incertaine dans plusieurs cas, vu la possibilité de son interférence avec les bandes intra-ligand [1] ou bien avec celles dues à certaines transitions de transfert de charge du type M—L. [7]

TABLEAU 3

Spectres électroniques de diffusion des combinaisons complexes avec les ions d incomplets

Composé	cm^{-1}/Attribué à									
Co(I−TCH)Cl$_2$	26000 ν_3				16300 u ν_2					
Ni(I−TCH)Cl$_2$	26900 é	20820 ν_3	19000			16100 ν_2			9800	
Pd(I−TCH)Cl$_2$	28200 é	25200	19000 é							
Co(I−TCH)$_2$(SCN)$_2$	23200 é	20400			13800 é	12200 e ν_2	11250 d 10700	9600 d 8400	1	8600
Ni(I−TCH)$_2$(SCN)$_2$	27800 ν_3	23200 é		15150 ν_3					9540	
Co(T−TCH)$_2$(SCN)$_2$	24400 ν_3		19000 é				11700 ν_2		10600 é	
Ni(T−TCH)$_2$(SCN)$_2$	2800 é ν_3	25000	22200 é			16600 u ν_2	15100 é		9280	

é = épaule

La présence de certaines épaules ou de plusieurs pics suggère des distorsions.[8]

Les spectres des complexes de l'ion de nickel (II) comportent les trois transitions de spin admises, sur les niveaux $^3T_{2g}$, $^3T_{1g}$ (F) et $^3T_{1g}$ (P) caractéristiques de la géométrie octaédrique. Dans ce cas, on suppose également l'interférence de la bande ν_3 avec la transition intra-ligand, ce qui explique, la position du pic respectif pour des nombres d'onde plus grands que 27 000 cm^{-1} quant aux thiocyanates.

Certains pics supplémentaires de certaines épaules pourraient être attribués aux transitions de spin interdites sur le niveau $^1T_{1g}$.[9]

Les transitions de spin admises $^2A_{A_{1g}} \rightarrow {}_1A_{A_{2g}}$ et $^1A_{1g} \rightarrow {}^1E_g$, caractéristiques de l'ion de palladium (II), situé en champ tétragonal plan, se manifestent dans le spectre du complexe Pd (I—TCH)Cl_2, dans le domaine dû aux transitions intra-ligand. Leur attribution est difficile à cause de la superposition des bandes de transition intra-ligand et aux bandes de transfert de charge.[10]

Comparativement au spectre de la molécule de ligand libre[1] la participation de la thiocarbohydrazone à la liaison coordinative entraîne des déplacements hyperchromes et hypochromes de la bande dus à la transition $\pi - \pi^*$ pour les complexes de l'ion Cd(II) et Hg(II). Ces modifications n'apparaissent pas dans les spectres du complexe de l'ion Zn (II) (tableau 4), fait probablement dû au phénomène de polarisation moins marqué dans le cas du zinc (II), ion moins susceptible d'être déformé.

Les paramètres des spectres I.R. (tableaux 5 et 6) indiquent la participation du groupement C=S et de celui hydrazinique à la liaison coordinative, la molécule de thiocarbohydrazone fonctionnant comme ligand bidenté.[11]

Par la position de la bande due au mode de vibration ν C≡N, on peut estimer que la liaison de l'anion thiocyanique est réalisée par l'azote pour les complexes de l'ion Co (II) et par pont pour les complexes de l'ion Ni (II).[12]

TABLEAU 4

Spectres électroniques des complexes comportant des ions d^{10}

Composé	Π — Π*		Autres bandes	
	λnm	ε	λnm	ε
Zn(I—TCH)Cl_2	330	30 000	292	11 900
Cd(I—TCH)$Cl_2 \cdot 2H_2O$	312	20 500	380	10 800
Hg(I—TCH)Cl_2	308	12 800	375	9 600

Les résultats de l'étude physico-chimique quant aux combinaisons complexes de la thiocarbohydrazone isonicotinealdéhyde et thiophène-2-

TABLEAU 5

Spectres I.R. des chlorures métalliques complexes

$Co(I-TCH)Cl_2$	$Ni(I-TCH)Cl_2$	$Zn(I-TCH)Cl_2$	$Cd(I-TCH)Cl_2.2H_2O$	$Hg(I-TCH)Cl_2$	$Pd(I-TCH)Cl_2$	Attribué à
			3480			
bande large	bande large	bande large	3180	bande large	bande large	νNH_2 νNH
			bande large			
1605 f	1600 é	1625 m	1600 i	1610 m	1650 é	$\nu C=N$ δNH_2
1560 m	1555 i	1545 m	1540 i	1545 i	1580 m	WNH + $\nu C-N$
1425 m	1500 é	1505 é	1430 i	1420 i	1400 é	$\nu C-N$ + WNH
1355 m	1420 m	1432 m				
	1360 m					
	1330 m					
1305 f	1300 m	1300 m				
	1255 é		1285 m	1335 m	1315	$\nu C-N$ $\nu C=S$
1280 f	1245 m	1270 m				
1215 f	1210 m	1210 m	1200 m	1230 é	1210	ρNH_2
1165 f	1170 é	1160 m	1155 m	1185 i	1135	
1110 f	1115 é		1105 m			
1045 f	1045 m	1060 m	1065 m	1060 m	1000 m	δNCS WNH_2
825 i	1025 m	1035 m	975 f		980 f	
	1005 m	945 m	955 f		950 f	
	920 f	925 f	895 m		880 m	νCNN $\nu C-N$
	890 f	830 m	825 i			
		820 i				
720 m	720 m	795	795 m	820 i	798 m	$\nu C=S$ $\nu C-N$
			705 i			

i = intense ; m = moyen ; f = faible ; é = épaule

TABLEAU 6

Spectres IR des thiocyanates métalliques complexes

$Co(I-TCH)_2(SCN)_2$	$Ni(I-TCH)_2(SCN)_2$	$Co(T-TCH)_2(SCN)_2$	$Ni(T-TCH)_2(SCN)_2$	Attribué à
bande large	bande large	bande large	bande large	νNH_2 νNH
2077 i	2100 i	2078 m	2095 m	$\nu C \equiv N$
1610 m	1620 m	1580 é	1595 m	$WC=N$ δNH_2
1555 m 1510 é 1430 m 1350 m	1540 i 1505 é 1425 s 1400 s 1350 é	1550 m 1420 m 1355 é	1550 m 1470 m 1420 m 1360 m	WNH $\delta C-N$ $\nu C-N$ WNH
1305 m	1305 m 1265 m	1330 m 1255 é	1323 m 1280 é 1255 m	$\nu C-N$ $\nu C=S$
1250 m 1200 m	1210 m 1155 f	1230 m 1205 é	1230 f 1180 m	ρNH_2
1060 é 1040 m 965 é 925 f	1070 f 1028 f 935 é 900 é	1100 m 1070 m 1030 f 935 f 850 m	1100 é 1070 m 1005 m 900 f 860 m	$\delta NHCS$ νCNN WNH_2 $\nu C-N$
825 m 720 f	830 i 745 m	792 f 725 m	799 f 728 m	$\nu C=S$ $\nu C-N$

i = intense ; m = moyen ; f = faible ; é = épaule.

carbaldéhyde permettent l'établissement probable des schémas de structure suivants :

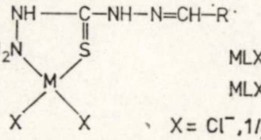
MLX_2

MLX

$X = Cl^-, 1/_2SO_4^{2-}$

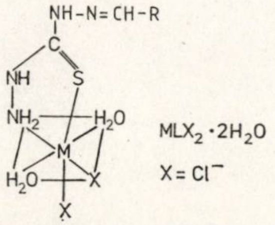
$MLX_2 \cdot 2H_2O$

$X = Cl^-$

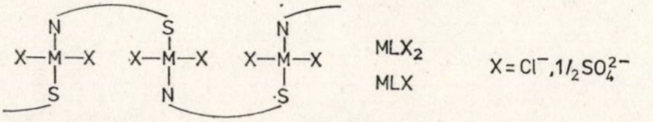
MLX_2

MLX

$X = Cl^-, 1/_2SO_4^{2-}$

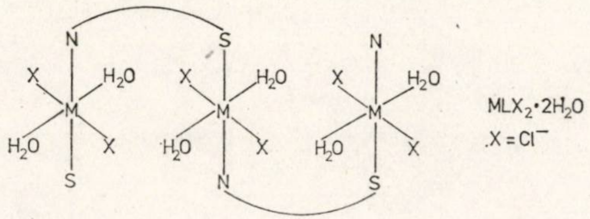
$MLX_2 \cdot 2H_2O$

$X = Cl^-$

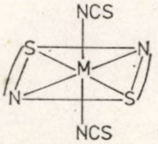

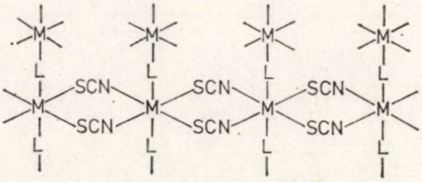

M = ion métalique

BIBLIOGRAPHIE

[1] S. Barbu et C. Gh. Macarovici, *Rev. Roumaine Chim.*, **23,** 1243, (1978).

[2] F. H. Burstall et R. S. Hyholm, *J. Chem. Soc.*, **1959,** 3570.

[3] H. James Weder, *Inorg. Chem.*, **6,** 258 (1967).

[4] A. B. P. Lever, *Inorg. Chem.* **4,** 764 (1965).

[5] F. A. Cotton et D. M. L. Goodgame, *J. Amer. Chem. Soc.*, **82,** 5771 (1960).

[6] Y. Tanabe et S. Sugano, *J. Phys. Soc. Japan.*, **9,** 753 (1954).

[7] A. B. P. Lever, "Inorganic Electronic Spectroscopy", Elsevier Publishing Company, 1968.

[8] J. Ferguson, *J. Chem. Phys.*, **32,** 533 (1960).

[9] G. O. Holmes et D. S. McClure, *J. Chem. Phys.*, **26,** 1686, (1957).

[10] H. B. Gray et G. J. Ballhausen, *J. Amer. Chem. Soc.*, **85,** 260 (1963).

[11] A. Yamaguchi, R. B. Penland, S. Mizushima, T. J. Lane, Columba Curran et I. V. Guagliano, *J. Amar. Chem. Soc.*, **80,** 527 (1958).

[12] M. Brezeanu et P. Spacu, "Chimia Combinaţiilor Complexe", Ed. didactică şi pedagogică, Bucarest, 1974.

Revue Roumaine de Chimie, 25, *3*, 349–354 (1980)

ELECTRON TRANSFER IN SOME VANADIUM COMPLEXES WITH QUINOXALINIC AND NAPHTOQUINONIC LIGANDS

D. NEGOIU*, J. CAMUS* and N. MUREŞAN**

* National Institute of Chemistry, Department of Chemical Technology 1, str. Polizu, 78126—Bucharest, Romania

** University of Craiova, Department of Natural Sciences 13, str. A. I. Cuza, 1100—Craiova, Romania

Received March 9, 1979

$[MO_4]^{z-}$, $[MO_2S_2]^{z-}$, $[MN_4]^{z-}$ and $[MN_2S_2]^{z}$-type complexes of vanadium with quinoxalinic and naphtoquinonic ligands, taking part in electron transfer reactions, were synthesized. The complexes were analyzed and characterized by molar conductivity measurements, electronic spectra and polarographic determinations. The parameters of the ESR spectra were estimated.

INTRODUCTION

Complex compounds of the dioxo-vanadium ion with maleonitrile dithiol, were synthesized and investigated by Atherton and Winscom, [1,2] but they did not point out that these complexes participate in electron transfer reactions, a process common to all other complexes with maleonitrile dithiol. [3] It is well known that the complex compounds of vanadium give all strong ESR spectra. Since these spectra have a good hyperfine resolution, the ESR parameters and the degree of covalency of the metal-ligand bond can be readily estimated. [4]

RESULTS AND DISCUSSION

The purpose of our work was to investigate the possibility of complexing the dioxo-vanadium ion with quinoxalinic and naphtoquinonic ligands in order to obtain $[MO_4]^{z-}$, $[MO_2S_2]^{z-}$, $[MN_4]^{z-}$ and $[MN_2S_2]^{z-}$ type complexes, capable of electron transfer reactions.

Five crystalline complexes, namely with 2,3-dihydroxyquinoxaline (abbreviated as 2,3-DHQ), 6-nitro-2,3-dihydroxyquinoxaline (6-N-2,3-DHQ), 6,7-dinitro-2,3-dihydroxyquinoxaline (6,7-DN-2,3-DHQ), 2-amino-3-mercaptomethyl-1,4-naphtoquinone (2-A-3-MM-1,4-NQ) and 2-hydroxy-3-mercaptomethyl-1,4-naphtoquinone (2-H-3-MM-1,4-NQ) and a semisolid complex with 2,3-diamino-1,4-naphtoquinone (2,3-DA-1,4-

NQ) were obtained. Based on elemental analysis results, dioxovanadium complex compounds can be written as follows: $[Bu_4N][VO(2,3\text{-}DHQ)_2]$, $[Bu_4N][VO(6\text{-}N\text{-}2,3\text{-}DHQ)_2]$, $[Bu_4N]_2[VO(6,7\text{-}DN\text{-}2,3\text{-}DHQ)_2]$, $[VO(2\text{-}H\text{-}3\text{-}MM\text{-}1,4\text{-}NQ)_2]$, $[Bu_4N][VO(2\text{-}A\text{-}3\text{-}MM\text{-}1,4\text{-}NQ)_2]$, $[VO(2,3\text{-}DA\text{-}1,4\text{-}NQ)_2]$.

Polarographic measurements have revealed several waves corresponding to the reduction of the complex species. The complex $[Bu_4N]$ $[VO(2,3\text{-}DHQ)_2]$ has one reduction wave, due to the process:

$$(\text{complex})^- + e^- \rightleftharpoons (\text{complex})^{2-}$$

at the half wave potential $E_{1/2} = 0.01$ V. The complex $[Bu_4N]$ $[VO(6\text{-}N\text{-}2,3\text{-}DHQ)_2]$ has three reduction waves at $E_{1/2} = -0.06$ V, -1.12 V and 1.36 V. The last two half-wave potentials are due to the reduction of the nitro-group. As in the preceding case, the first wave is due to the reduction of the monoanionic species to the dianionic species. The neutral complex $[VO(2\text{-}H\text{-}3\text{-}MM\text{-}1,4\text{-}NQ)_2]$ is reduced at the dripping mercury electrode to the monoanionic species. The second wave observed was assigned to the reduction of quinone. The two half-wave potentials are $E_{1/2} = -0.3$ V and -1.01 V, respectively.

Conductivity measurements confirmed the presence of ionic species in the solution. Thus, the complex $[Bu_4N]$ $[VO(6\text{-}N\text{-}2,3\text{-}DHQ)_2]$ behaves as a 1 : 1 electrolyte ($75\ cm^2 \cdot ohm^{-1} \cdot mole^{-1}$), corresponding to a monoanionic character. The complex $[Bu_4N]_2$ $[VO(6,7\text{-}DN\text{-}2,3\text{-}DHQ)_2]$ dissociates as a 2 : 1 electrolyte ($120\ cm^2 \cdot ohm^{-1} \cdot mole^{-1}$), whereas the complex $[Bu_4N]$ $[VO(2\text{-}A\text{-}3\text{-}MM\text{-}1,4\text{-}NQ)_2]$ has a conductivity value ($65\ cm^2 \cdot ohm^{-1} \cdot mole^{-1}$) typical of a 1 : 1 electrolyte.

The way in which the ligands are coordinated to dioxovanadium ion was deduced from the shift of the ligand vibration bands. Modification or disappearance of the absorption band due to the vibration of the O-H bond in the spectrum of the complex proves that the coordination takes place through the two oxygen atoms in the *ortho* position of the quinoxalinic ligands (Figure 1). Thus, the bands appearing around 3160 cm^{-1} in the spectra of the quinoxalinic ligands are no longer present in the spectra of the complexes. In the case of the ligands containing sulfur and nitrogen as donor atoms, the coordination was confirmed by the modification of the bands characteristic of the vibrations of the $-NH_2$ and $-SCH_3$ groups, which appear in the spectra of the free ligands at 3380 and 3470 cm^{-1} for the first group, and at 660 and 692 cm^{-1} for the second. These bands change their intensity in the spectra of the complexes and are shifted to 3308, 3412, 670 and 705 cm^{-1}, respectively. A supplementary

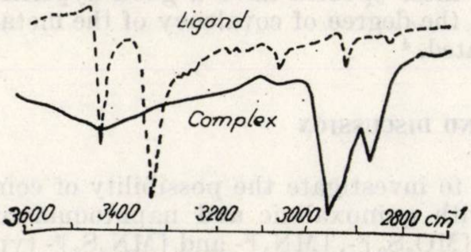

Fig. 1. — IR spectra: Ligand [2—A—3—MM—1,4—NQ]; Complex $[VO\ (2-A-3-MM-1,4-NQ)_2]^-$

proof of the coordination is the presence between 985−1000 cm^{-1} of a band typical of the V−O bond, which is slightly shifted, depending upon the nature of the ligand. Thus, for the $[VON_2S_2]^-$-type complex this band appears at 1000 cm^{-1} for $[VOO_2S_2]$ at 992 cm^{-1}, for $[VOO_4(6,7)]^{2-}$ at 995 cm^{-1}, for $[VOO_4(6)]^-$ at 990 cm^{-1}, and for $[VOO_4]^-$ at 985 cm^{-1}.

TABLE 1

Electronic spectra

Compound	$\bar{\nu}_{max}$, KK	Assignment
$[VO(2,3-DHQ)_2]$	47.00 vi 43.20 i 42.00 i 38.30 m	$\pi \rightarrow \pi^*$ (arom)
	36.20 w 33.40 sh 32.00 i 30.70 i 29,20 sh	$\pi \rightarrow \pi^*$ (quin)
	24.20 w	d−d or CT
	18.20 w	d−d
	16.10 w	d−d
$[VO(6-N-2,3-DHQ)_2]^-$	47.00 vi 42.00 sh 35.00 i	$\pi \rightarrow \pi^*$ (arom. + quin.)
	27.70 i	$n \rightarrow \pi^*$ (NO_2) + CT
	17.85 sh	d−d
	16.40 w	d−d
$[VO(6,7-DN-2,3-DHQ)_2]^{2-}$	47.00 vi 38.70 m	$\pi \rightarrow \pi^*$ (arom)
	34.60 i	$\pi \rightarrow \pi^*$ (quin)
	28.30 i	$n \rightarrow \pi^*$ (NO_2)
	25.50 sh	L → M (CT)
	21.80 sh	intramol. -L (CT)
	16.10 sh	d−d
$[VO(2-A-3-MM-1,4-NQ)_2]^-$	35.70 vi	$\pi \rightarrow \pi^*$ (arom)
	25.60 i	$n \rightarrow \pi^*$ (C−S+CT)
	21.70 w	$n \rightarrow \pi^*$ (quin)
	16.10 w	d−d
$[VO(2-H-3-MM-1,4-NQ)_2]$	21.70 i	$n \rightarrow \pi^*$ (quin)
	18.55 w	d−d
	14.92 w	d−d

vi = very intense, i = intense, m = medium, w = weak, sh = shoulder

The electronic spectra of the dioxo-vanadium ion complexes with quinoxalinic and naphtoquinonic ligands were recorded in acetonitrile solutions. As seen in Table 1, the ultraviolet range comprises absorption bands characteristic of electronic transitions in the ligands, slightly modified in position and intensity by complexation. As in the case of other dioxo-vanadium complexes, the visible spectrum consists of three weaker bands. These are assigned to the $^2B_{2g} \rightarrow {}^2E_g$, $^2B_{2g} \rightarrow {}^2B_{1g}$ and $^2B_{2g} \rightarrow {}^2A_{1g}$ d-d transitions. Consideration of the fine structure of the absorption bands at low temperatures [5] suggested that all *d-d* transitions would be located below 20,000 cm^{-1}. As expected, the transitions of the dioxo-vanadium complexes correspond to a square-planar conformation. The bands appearing above 20,000 cm^{-1} may be assigned to the ligands. These partially overlap the crystal field bands.

TABLE 2

ESR spectra. Non-isotropic values

Compound	$g_{\|\|}$	$g_{\perp}$	$A_{\|\|}$	$A_{\perp}$	A_T
$[VOO_4]^-$	1.9509	1.9724	171.40	58.41	1193.25
$[VOO_4(6)]^-$	1.9509	1.9724	167.45	68.10	1180.07
$[VOO_4(6,7)]^{2-}$	1.9984	2.0447	178.00	58.19	1232.30
$[VON_2S_2]^-$	1.9397	1.9680	181.42	71.88	1266.54
$[VOS_2O_2]$	1.9778	1.9936	63.49	20.88	458.35

The VO^{2+} ion complexes have unusually strong ESR spectra, with a good hyperfine resolution. The non-isotropic values of the tensors $g_{||}$, $g_{\perp}$, $A_{||}$ and $A_{\perp}$ were determined on polycrystalline powder samples (Table 2), and the isotropic ones in DMF (Table 3). Both measurements were carried out at room temperature. Since the unpaired electron of the VO^{2+} ion is in the b_{2g}^* (d_{xy}) orbital, it is mainly localized on the metal and a hyperfine splitting due to ligands is not expected. In all the cases the $g_{||}$ value was smaller than the $g_{\perp}$ value, and both these non-isotropic parameters were smaller than the free electron g value ($g = 2.0023$). Well-resolved ESR spectra were recorded for those complexes in which the VO^{2+} ion is bonded to the ligands through their oxygen atom. A pronounced anisotropy was observed in the ESR spectra of these complexes. This was assigned to the interaction between the magnetic moment of the odd electron and the nuclear magnetic moment of the central ion placed in a square-planar (D_{4h}) crystal field with axial symmetry. This anisotropy, as well as the large value of the total width of the ESR spec-

TABLE 3

ESR spectra. Isotropic values

Compound	g_I	A_I	A_T
$[VOO_4]^-$	1.9846	95.6	650.38
$[VOO_4(6)]^-$	1.9846	95.76	653.8
$[VOO_4(6,7)]^{2-}$	1.9908	89.0	650.38
$[VON_4]$	$g_{izo} = 1.9567$	$A_{izo} = 1.07$	

trum (over 1100 gauss), suggests that the highest occupied molecular orbital has a considerable metal character. The narrowing of the spectrum in the case of the [VOO_2S_2]-type complex and its poorer resolution indicate an increase of the covalent character of the metal-ligand bond. This fact is still more evident in [VON_4]-type complexes, for which the anisotropy vanishes. In this case, the ESR signal consists of a single, extremely narrow line ($A = 1.07$ gauss), characteristic of the donor-acceptor interactions present in typical charge transfer complexes (Figure 2).

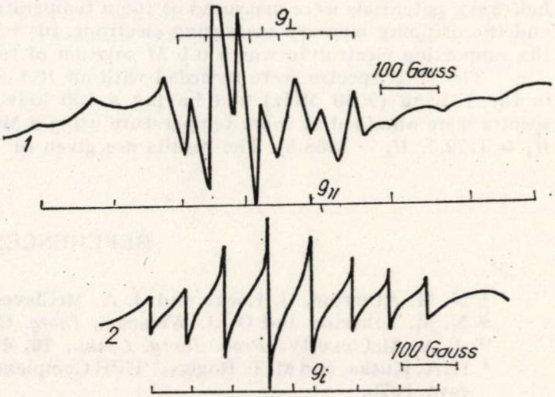

Fig. 2. — ESR spectra:
1. [VO (2–A–3–MM–1,4–NQ)$_2$]$^-$;
2. [VO(6–N–2,3–DHQ)$_2$]$^-$

EXPERIMENTAL

Preparation

A solution containing 0.70 g of 2,3-dihydroxyquinoxaline dissolved in 6.40 ml of a 40% aqueous solution of tetra-*n*-butyl-ammonium hydroxide was added under stirring to a solution containing 0.39 g of dioxo-vanadium sulfate dissolved in 5 ml water and 25 ml ethanol. After 2 hours of continuous stirring a gray-colored, crystalline precipitate was formed. It was filtered, washed two times with 15 ml of water and dried under vacuum. The other complex combinations were obtained similarly. The elemental chemical analysis results for the compounds prepared are listed in Table 4.

TABLE 4

Elemental chemical analysis

Compound	C%		H%		V%	
	Calcd.	Found	Calcd.	Found	Calcd.	Found
[Bu_4N] [Vo(2,3–DHQ)$_2$]	61.03	61.27	6.99	6.39	10.64	10.73
[Bu_4N] [VO(6–N–2,3–DHQ)$_2$]	53.39	53.02	5.84	6.10	9.30	9.03
[Bu_4N]$_2$ (VO(6,7–DN–2,3–DHQ)$_2$]	54.79	54.94	7.23	7.39	6.37	6.54
[Bu_4N] [VO(2–A–3–MM–1,4–NQ)$_2$]	59.04	60.32	6.73	6.04	8.64	8.75
[VO(2–H–3–MM–1,4–NQ)$_2$]	52.02	52.00	3.15	2.43	13.20	13.36
[VO(2,3–DA–1,4–NQ)$_2$]	54.66	54.68	2.73	3.02	11.60	11.72

Measurements

The electronic spectra were recorded with a Zeiss Jena VSU-1 spectrophotometer, using spectral grade solvents and a 1-cm silicacell. The infrared spectra were run on a Zeiss Jena UR—10 spectrophotometer, the samples being pelleted in anhydrous KBr. The data are given in Table 1.

The polarograms were obtained with an Orion KTS, model 7-77-4/b device. The half-wave potentials were measured at room temperature, using the calomel reference electrode and the dripping mercury measuring electrode. 10^{-3} *M* solutions of the complexes were used; the supporting electrolyte was a 0.1 *M* solution of tetra-*n*-butylammonium perchlorate.

The ESR spectra were recorded with an IFA-Bucureşti ART-5 spectrometer working in the X-band (9060 MHz) and having a 100 kHz modulation of the magnetic field. The spectra were obtained at room temperature using a Mn^{2+} standard ($g_3 = 2.03584$, $g_4 = 1.98040$, $H_3 = 3179{,}5$, $H_4 = 3268.5$). The results are given in Tables 3 and 4.

REFERENCES

[1] N. M. Atherton, J. Locke and J. A. McCleverty, *Chem. Ind. (London)*, **1965**, 1300.
[2] N. M. Atherton and O. J. Winscom, *Inorg. Chem.*, **12**, 383 (1970).
[3] J. A. McCleverty, *Prog. Inorg. Chem.*, **10**, 49 (1968).
[4] H. A. Kuska, and M. T. Rogers, "EPR Complexov perehodnyk metallov", Mir, Moscow, 1970.
[5] J. Selbin, T. R. Ortolano and F. J. Smith, *Inorg. Chem.*, **2**, 1315 (1962).

Revue Roumaine de Chimie, **25**, *3*, 355–360 (1980)

COMPLEXES OF COPPER(II), NICKEL(II), COBALT(II), IRON(II) AND MANGANESE(II) WITH SCHIFF BASES DERIVED FROM SULPHAMETHOXYPYRIDAZINE

KEEMTI LAL
Chemistry Department, D. N. College, Meerut–250002, India

Received September 29, 1978

Copper(II), nickel (II), cobalt(II), iron(II) and manganese(II) complexes of bidentate Schiff bases derived from sulphamethoxypyridazine, and salicylaldehyde (SMPSA) or *o*-hydroxyacetophenone (SMPHA) have been isolated and characterised. Based on elemental analysis, magnetic susceptibility and electronic absorption spectra, square-planar structure for Cu (II) complexes and tetrahedral structure for Ni (II), Co (II), Fe (II) and Mn (II) complexes are suggested. Infrared studies show that the metal is bonded through the nitrogen atom of the imine group and the oxygen atom of the phenolic group in the complexes.

INTRODUCTION

A variety of Schiff base complexes of transition metal ions have received considerable attention and some have been shown to exhibit reversible oxygenation behaviour. [1,2] Schiff bases formed from sulpha-drugs and salicylaldehyde have been found to be good bacteriostatic, [3,4] as well as chelating agents. [5,6] In continuation of the studies [7] on the sulpha-drugs-complexes, the present work embodies the preparation and characterisation (elemental analysis, magnetic moment, electronic and infra-red spectral data) of Cu(II), Ni(II), Co(II), Fe(II) and Mn(II) complexes with Schiff bases derived from sulphamethoxypyridazine, and salicylaldehyde (SMPSA) or *o*-hydroxyacetophenone (SMPHA).

EXPERIMENTAL

Standard solutions of the bivalent metal ion were prepared from AnalaR (B.D.H.) samples in doubly distilled water and standardized by usual methods.[8]

Magnetic measurements, infrared and electronic spectra were carried out as reported earlier. [9]

Preparation of ligands

The Schiff bases SMPSA and SMPHA were synthesised by condensing ethanolic solution of sulphamethoxypyridazine and salicylaldehyde or *o*-hydroxyacetophenone in 1 : 1 ratio. The product obtained was crystallized from acetone, m.p. 235° and 242° were observed for SMPSA and SMPHA, respectively.

Preparation of complexes

To an aqueous solution of metal (II) chloride or sulphate was added a solution of SMPSA or SMPHA in acetone in 1 : 2 ratio. The reaction mixture was stirred for 3–4 hrs when the colour of the solution gradually changed yielding crystals of the complexes. These were filtered off and recrystallized from ethanol and dried in the oven at 110–120°.

RESULTS AND DISCUSSION

Elemental analysis

The metal ions in the complexes were estimated by the usual methods.[8] The nitrogen was estimated by Dumas' method. The results of the elemental analysis are shown in table 1. The elemental analysis shows that the general formula for the complexes is $M(C_{18}H_{15}N_4SO_4)_2$ with SMPSA and $M(C_{19}H_{17}N_4SO_4)_2$ with SMPHA where M = Cu(II), Ni(II), Co(II), Fe(II) and Mn(II).

Magnetic susceptibility

The magnetic moments of all the complexes (Gouy's method using Hg $[Co(NCS)_4]$ as standard) were determined at room temperature (27°) (Table 1). The magnetic data show that all the complexes are paramagnetic.

TABLE 1

Analytical data and magnetic moment of SMPSA and SMPHA and their complexes

Compound	N(%)		M(%)		Magnetic moment (B.M.)
	Found	Cald.	Found	Cald.	
SMPSA	14.49	14.58	—	—	—
CuL_2	13.38	13.50	7.52	7.66	1.77
NiL_2	13.64	13.58	7.00	7.12	3.30
CoL_2	13.42	13.57	7.23	7.14	4.36
FeL_2	13.44	13.62	7.00	6.80	4.95
MnL_2	13.50	13.64	6.54	6.69	5.52
SMPHA	14.25	14.11	—	—	—
CuL'_2	13.00	13.09	7.56	7.42	1.78
NiL'_2	13.00	13.16	7.04	6.90	3.34
CoL'_2	13.30	13.16	6.74	6.92	4.33
FeL'_2	13.05	13.21	6.42	6.59	4.97
MnL'_2	13.40	13.22	6.62	6.48	5.53

$L = C_{18}H_{15}N_4SO_4$ (Deprotonated SMPSA)
$L' = C_{19}H_{17}N_4SO_4$ (Deprotonated SMPHA)

Infra-red spectra

The important frequencies of the ligands and their complexes are shown (Table 2). The ligands consist of methoxypyridazine, sulphamilamido ($=N-C_6H_4-SO_2NH-$) and salicyl ($OH-C_6H_4-COH$) or *o*-hydroxyacetophenyl ($OH-C_6H_4-COCH_3$) groups. These groups are expected to be observe din the infra-red spectra.

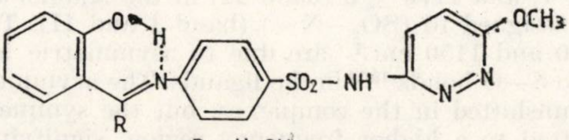

• R = H, CH$_3$

TABLE 2

Some important infra-red frequencies (in cm^{-1}) of the ligands and their complexes

Compound	ν(OH) chelated	ν(C=N)	ν(C–O) (phenolic)	ν(M–O)	ν(M–N)
				Coupled with ligand frequencies	
SMPSA	3250b 2700b	1650vs	1260vs	—	—
CuL$_2$	—	1630s	1300s	550m	500m
NiL$_2$	—	1635s	1300s	555m	510m
CoL$_2$	—	1640s	1305s	550m	510m
FeL$_2$	—	1640s	1305s	565m	505m
MnL$_2$	—	1642s	1310s	560m	515m
SMPHA	3250b 2650b	1645vs	1275vs	—	—
CuL$'_2$	—	1630s	1300s	550m	505m
NiL$'_2$	—	1632s	1305s	560m	518m
CoL$'_2$	—	1638s	1300s	565m	515m
FeL$'_2$	—	1635s	1310s	565m	520m
Mn$_2$	—	1640s	1310s	560m	515m

VS = very strong, S = strong, m = medium, b = broad
(L = Deprotonated SMPSA)
(L′ = Deprotonated SMPHA)

The intramolecularly hydrogen bonded[10,11] ν(OH) occurs around 3250 and 2700 cm^{-1} in the ligands and disappears in all the complexes indicating the formation of metal-oxygen bond. An absorption band of varying intensity at 3100 ± 10 cm^{-1} is observed in the ligands, as well as in the complexes, which may be assigned to the ($-SO_2-NH-$) part of the molecule showing that this group is not taking part in complexation.

The free ligands show ν(C=N) in the region 1645–1650 cm^{-1}; on complexation, it is shifted to the lower frequency side, indicating coordination through imine nitrogen.[12–14] However, the reduction in this frequency does no longer occur because of extended conjugation in the free ligands.[15,16] Further more the extent of decrease is lower in SMPHA complexes indicating that the steric hindrance in these complexes is comparatively greater than SMPSA.

The shift in ν(C—O) frequency observed in the free ligands around 1260 cm^{-1} to higher frequencies viz, 1310—1300 cm^{-1} in the complexes, is further indicative of the coordination of phenolic —OH.[10,17] The bands at 1320 $\pm$ 5 (band I) and 1170 $\pm$ 5 (band II) in the ligands and their complexes may be assigned to (SO_2—N=) (band I and II). Two prominent bands near 1350 and 1150 cm^{-1} are due to asymmetric and symmetric vibrations of two S—O bonds [18,19] in the ligands. The asymmetric vibrations are practically unshifted in the complexes, but the symmetric vibrations are slightly shifted to a higher frequency region, signifying the absence of any interaction between the sulphone group and the metal ions.

Katritsky [20] has discussed the infra-red spectra of hetero-aromatic nucleus in the region of 1600—1350 cm^{-1} and concluded that :

(a) The bands near 1605, 1575, 1480 and 1430 cm^{-1} are observed in the six-membered heterocyclic aromatic ring. The intensity varies widly depending upon the electronic nature of the substituents.

(b) The bands near 1590, 1490 and 1400 cm^{-1} generally appear in the five membered heterocyclic compounds.

In the present case, ligands and complexes show the frequencies at 1615 $\pm$ 8, 1570 $\pm$ 5, 1480 $\pm$ 5 and 1435 $\pm$ 5 cm^{-1} showing a six-membered methoxypyridazine group (heterocyclic aromatic ring).

The bands near 890 $\pm$ 5 and 760 cm^{-1} may be assigned to ν (S—N) and ν (C—S) frequency, respectively [21] in the ligands and the chelates.

It is worth mentioning that according to Ueno and Martell [10] the region of the ν (M—O) and ν (M—N) bond, in the complexes of the Schiff base, are 640—500 cm^{-1} and 500—430 cm,$^{-1}$ respectively. The assignment is made difficult because of their conjugation between the M—O, O—C and C—C bonds, a "pure" ν (M—O) and ν (M—N) which makes vibration actually not be expected. Therefore, bonds in the regions 560 $\pm$ 10 cm^{-1} and 510 $\pm$ 10 cm^{-1} may be attributed to ν (M—O) and ν (M—N), respectively which may also be coupled with the ligand bands.[22,23]

Taking into account the above observations, the following structure may be assigned to the complexes.

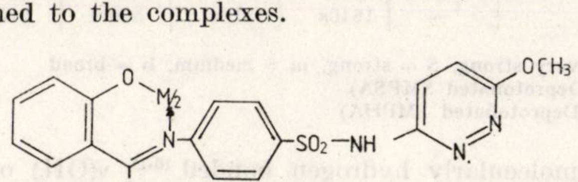

Electronic absorption spectra

The electronic absorption spectra of the ligands show four absorption bands at 238, 272, 305 and 345 nm in methanol. The aryl group exhibits two absorption bands at 200—220 nm and 240—270 nm in the U.V.

region, which are assigned to $\Pi-\Pi^*$ transition and are termed as K and B bands, respectively.[24,25] On substitution in the benzene ring, the K band shifts towards benzoid B region, while the B band is displaced to 270—285 nm (as observed in these ligands). The absorption bands at 305 and 345 nm are attributable to $n-\Pi^*$ transitions arising from —CH and —C=N in an extensively conjugated Π-electron system.

Electronic spectra of the metal complexes were recorded and $d-d$ transitions are discussed in brief along with ligand field parameters. The magnetic moment values of Cu(II) complexes are very close to spin — only the value for one unpaired electron (1.73 B.M.), which indicates that the orbital contribution is almost quenched by the crystalline field. The electronic spectra of the complexes show only three bands ~ 14600 cm^{-1}($^2B_g \rightarrow {}^2A_{1g}$), ~20000 cm^{-1}($^2B_g \rightarrow {}^2E_g$) and 25000 cm^{-1} (charge transfer). Tetrahedral Cu(II) complexes are expected to give a single broad band in the near infrared region and no absorption between 10000 cm^{-1} and 20000 cm^{-1}. The $d-d$ bands for Cu(II) complexes for which a square-planar structure has been proposed[26,27] to occur in the range 14000—18000 cm^{-1}. Hence the above information is consistent with an essentially square-planar structure.

The magnetic moments of the remaining metal complexes (Table 1) indicate the tetrahedral structure.[28] The electronic spectra of the Ni(II) complexes show two bands at 8800 cm^{-1}($^3T_1(F) \rightarrow {}^3A_2(F)$), and 17500 cm^{-1} ($^3T_1(F) \rightarrow {}^3T_1(P)$) transitions. The values of the ligand field parameters 10 D_q, B and β are calculated according to Figgis[28] and found to be 4700 cm^{-1}, 950 cm^{-1} and 0.90, respectively. The electronic spectra of Co(II) complexes show two bands at 7300 cm^{-1}($^4A_2(F) \rightarrow {}^4T_1(F)$) and 16000 cm^{-1}($^4A_2(F) \rightarrow {}^4T_1(P)$) transitions. The values of 10 D_q, B and β are found to be 4000 cm^{-1}, 920 cm^{-1} and 0.91, respectively. A broad band in the near IR region ~ 4500 cm^{-1} may be assigned to $^5E \rightarrow {}^5T_2$ transition for Fe(II) complexes.[29,30] Two bands at ~ 20500 cm^{-1} and 21400 cm^{-1} are observed for $^6A_1 \rightarrow {}^4E(G)$ and $^6A_1 \rightarrow {}^4A_1(G)$, respectively for Mn(*II*) complexes under study.

ACKNOWLEDGEMENT. **The author is grateful to U.G.C., New Delhi, India for financial assistance and M/s Cyanamide India Ltd. Bulsar India for supplying the pure sample of sulphamethoxypyridazine.**

REFERENCES

[1] R. H. Holm, G. W. Everett and A. Chakravorthy, *Progr. in Inorg. Chem.*, **7**, 83 (1966).

[2] G. Mclenden and A. E. Martell, *Coord. Chem. Revs.*, **19**, 1 (1976).

[3] T. Tsukamato and K. Yuhi, *Yakugaku Zasshi*, **78**, 706 (1958); *Chem. Abstr.*, **52**, 18293 (1958).

[4] T. Tsukamato, Takeda Pharmaceutical Industries Ltd. Japan, 5766 (1960); *Chem. Abstr.*, **55**, 5879 (1961).

[5] P. Jain and K. K. Chaturvedi, *J. Indian. Chem. Soc.*, **52**, 805; 1220 (1975); *J. Inorg. Nuclear Chem.*, **38**, 799 (1976); *Def. Sci. J.*, **27**, 91 (1977).

[6] R. R. Gupta and R. Kaushal, *J. Indian Chem. Soc.*, **51**, 385 (1974); **53**, 552 (1976).

[7] K. Lal, *Acta Ciencia Indica*, **4**, 242 (1978); *Chem. Era*, **14**, 170 (1978); *Acta Chim. Acad. Sci. Hung.* (In Press) (1979).

[8] A. I. Vogel, "A Text Book of Quantitative Inorganic Analysis", Longmans Green, London, 1971.

[9] K. Lal, J. Singh and S. P. Gupta, *J. Inorg. Nuclear Chem.*, **40,** 359 (1978) ; *Acta Chim. Acad. Sci. Hung.*, **95,** 233 (1977).

[10] K. Ueno and A. E. Martell, *J. Phys. Chem.*, **59,** 998 (1955) ; **60,** 1270 (1956).

[11] L. J. Bellamy, "Infrared Spectra of Complex Molecules" Wiley, New-York, 1954, p. 105.

[12] N. Nakamoto, "Infrared Spectra of Inorganic and Coordination Compounds" Wiley, New-York, 1963.

[13] J. E. Kavacic, *Spectr. Chim. Acta.*, **23A,** 183 (1967).

[14] J. Csaszar and L. Kiss, *Acta Chim. Acad. Sci. Hung.*, **78,** 17 (1973).

[15] L. W. Lane and L. T. Taylor, *J. Coord. Chem.*, **2,** 295 (1973).

[16] C. T. Spencer and L. T. Taylor, *Inorg. Chem.*, **10,** 2407 (1971).

[17] R. N. Prasad and J. P. Tondon, *J. Inorg. Nuclear Chem.*, **35,** 1473 (1974).

[18] C. N. R. Rao, "Application of Infrared Spectroscopy" Academic Press, New-York, 1963, p. 305.

[19] J. N. Baxter, J. Cymerman-Craig and J. B. Willis, *J. Chem. Soc.*, **1955,** 669.

[20] A. R. Katritzky, *Quart. Rev.*, **13,** 358 (1959).

[21] J. Brandmueller and M. Wahe, *Spectrochim. Acta*, **23A,** 2465 (1967).

[22] S. Pinches, B. C. Silver and I. Lanlicht, *J. Chem. Phys.*, **46** (1506 (1967).

[23] B. Hutchinson, D. Eversdyk and S. Olbricht, *Spectrochim. Acta.*, **30A,** 1605 (1974).

[24] J. R. Platt and H. B. Klevens, *Chem. Revs.*, **41,** 307 (1947) ; *J. Chem. Phys.*, **16,** 832 (1948).

[25] A. Burawoy, *Tetrahedron*, **2,** 122 ; 403 (1958).

[26] L. Sacconi and M. Ciampolini, *J. Chem. Soc.*, **1964,** 276.

[27] U. Doraswamy and P. K. Bhattacharya, *J. Inorg. Nuclear Chem.*, **37,** 1665 (1975).

[28] B. N. Figgis and J. Lewis, *Progr. in Inorg. Chem.*, **6,** 37 (1964).

[29] B. N. Figgis, "Introduction to Ligand Field" Wiley, New-Delhi, 1966.

[30] P. Day and C. K. Jorgenson, *J. Chem. Soc.*, **1964,** 6226.

Revue Roumaine de Chimie, 25, 3, 361–370 (1980)

CONTRIBUTIONS TO THE CHEMISTRY OF QUATERNARY AMMONIUM COMPLEXES

N-CETYL-β-PICOLINIUM SALTS OF HALOGEN- AND THIOCYANATE COMPLEX IONS OF Zn(II) AND Cd(II)

DUMITRA VĂCĂRESCU
Polytechnic Institute, Department of Technological Chemistry, Splaiul Independenţei, 202, Bucharest, Romania

Received January 29, 1977
Revised June 28, 1979

Eleven new zinc and cadmium complex compounds were synthesized, corresponding to the general formulas : [N-cetyl-β-pic]$_2$ [M^{II}X$_4$] and [N-cetyl-β-pic] [M^{II}X$_3$], where M^{II} = Zn and Cd and X = Cl, Br, I, SCN. The properties of the new substances were investigated and compared with those of analogous N-cetyl-α-picolinium and N-cetyl-γ-picolinium compounds previously studied. Conclusions were drawn on the influence exerted by the position of the methyl radical in the pyridine ring of the N-cetyl-pyridine cation, as well as the influence of the ligand nature on the behaviour of such substances.

I. INTRODUCTION

A series of previous works [1,2] have reported the properties and the methods for obtaining complex compounds resulted from zinc and cadmium halides and sulphocyanides with N-cetyl-γ-picolinium and N-cetyl-α-picolinium sulphocyanide.

The present paper includes contributions to the knowledge of N-cetyl-β-picolinium salts of halogen- and thiocyanate complex ions of Zn(II) and Cd(II) :

[N-cetyl-β-pic]$_2$[M^{II}X$_4$]
and
[N-cetyl-β-pic] [M^{II}X$_3$]

where M^{II} = Zn and Cd
X = Cl, Br, I, SCN

A comparison of some properties of the new substances with the properties of analogous N-cetyl-γ-picolinium and N-cetyl-α-picolinium compounds previously studied [1,2] has permitted conclusions to be drawn on the influence exerted by the position of the methyl radical in the pyridine ring of the N-cetyl-picolinium cation.

A problem which we have been studying for a long time refers to the complex halides and sulphocyanides of elements in subgroup II, hence of elements with a d^{10} configuration, corresponding to the general formula :

$$[N-R-Y\text{-picolinium}]_{m-2n}[M_nX_m]$$

in which :

M = Zn, Cd, Hg

X = Cl, Br, I, SCN

Y = α, β, γ,

R = an alkyl with a large number of carbon atoms (cetyl, octadecyl[7] etc.).

In the present stage of investigation, N-cetyl-β-picolinium halogen- and thiocyanatozincates were synthesized of the form : [N-cetyl-β-picolinium]$_2$ [ZnX_4], and also N-cetyl-β-picolinium halogeno- and thiocyanatocadmiates of the form :

[N-cetyl-β-picolinium][CdX_3] and [N-cetyl-β-pic]$_2$ [CdX_4].

The properties of these compounds are presented comparatively with those of the corresponding N-cetyl-α-picolinium and N-cetyl-γ-picolinium compounds analysed in the above-mentioned previous works.

The methyl position in the pyridine ring has been found to influence the obtention conditions, the stability and the type of compound being formed. Thus, unlike [N-cetyl-α-pic]^2 [ZnI_4], which could not be obtained in alcoholic medium from the stoichiometric amounts of the components, compound [N-cetyl-β-pic]$_2$ [ZnI_4] could be obtained in an alcoholic medium from the stoichiometric amounts of components (zinc iodide and N-cetyl-β-picolinium iodide). By recrystallization it will not decompose.

The influence of the position of methyl radical is more evident in the case of thiocyanatocadmiates. In a previous note [1] we have shown that only N-cetyl-γ-picolinium trithiocyanatocadmiate could be obtained by direct addition or by double-exchange reaction, in alcoholic or aqueous medium, regardless of the stoichiometric ratio of components. This is in agreement with some older works of Grossmann [3] on pyridinium thiocyanatocadmiate. In turn, in the case of N-cetyl-β-picolinium or of N-cetyl-α-picolinium trithiocyanatocadmiate could not be obtained in pure state. It has been analytically determined that a mixture of tetra- and trithiocyanate is formed, which has been totally converted to tetrathiocyanate by recrystallization from alcohol.

In contrast to N-cetyl-γ-picolinium trichlorocadmiate, which could not be obtained as a unitary product, [1] N-cetyl-β-picolinium trichlorocadmiate could be readily synthesized, working in an alcoholic medium, from $CdCl_2$ and N-cetyl-β-picolinium chloride, taken in stoichiometric ratio.

The influence of the methyl group in the pyridine ring on the melting points of the compounds was further investigated. Table 1 shows that, in general, the melting points of N-cetyl-β-picolinium compounds are lower than those of N-cetyl-α-picolinium compounds, yet they are higher than in the case of N-cetyl-γ-picolinium compounds. A similar behaviour was also recorded in the analogous compounds of mercury (II).

TABLE 1

Melting temperatures (in °C) of N-cetyl-α, β- and γ-picolinium halogen- and thiocyanate complexes of zinc and cadmium

Type of compound	M = Zn			M = Cd		
	X = α	X = β	X = γ	X = α	X = β	X = γ
[N-cetyl-X-pic]$_2$ [MCl$_4$]	94—95	85—96	64—67	86—87	80—83	69—72
[N-cetyl-X-pic]$_2$ [MBr$_4$]	72—75	?	62—63	98	57—61	70—73
[N-cetyl-X-pic]$_2$ [MI$_4$]	?	53	61—62	62—64	49—52	62—64
[N-cetyl-X-pic]$_2$ [M(SCN)$_4$]	65—66	34	39—40	61	56—59	—
[N-cetyl-X-pic] [MCl$_3$]	—	—	—	?	?	—
[N-cetyl-X-pic] [MBr$_3$]	—	—	—	103—104	67—68	60—62
[N-cetyl-X-pic] [M(SCN)$_3$]	—	—	—	?	—	81—82

Like in N-cetyl-γ-picolinium and N-cetyl-α-picolinium compounds, it is observed that the melting points are not clear, they extend over a temperature interval of 1—3°C. An analogous behaviour can also be found in other quaternary ammonium salts mentioned in the literature.[4]

Among the zinc compounds, chlorides present the higher melting temperatures, and among cadmium compounds with the coordination number 4, the highest melting points are again found in chlorides, in contrast to similar compounds studied by M. K. Aliavia.[5] The compound [N-cetyl-β-pic] [CdCl$_3$] melts over a temperature interval of 113—150, which would plead for a polymer structure in which cadmium may have the coordination number 4.

The solubilities of the new substances in water and in different organic solvents are in general similar to N-cetyl-α and N-cetyl-γ-picolinium compounds. Quantitative determinations were performed in ethanol (table 2) for compounds with the coordination number 4 and 3. The solubility in alcohol at 23°C is found to vary relative to the ligand nature. For the zinc compounds, this variation occurs in the following sense: $I > SCN > Br > Cl$, chloride being the most insoluble one. For cadmium compounds, an entirely different solubility variation is observed $Cl > > I > Br >> SCN$, thiocyanatocadmiate being the most insoluble.

To characterize the compounds, UV absorption spectra were also determined in the wavelengths domain ranging within 220—240 nm. It was worked with alcoholic solutions of $10^{-4} - 10^{-5}$ M concentration on a Universal Zeiss Jena VSU$_1$ spectrophotometer. The spectra of N-cetyl-β-picolinium halides and sulphocyanide were first performed (Figure 1). All the halides within the studied domain present one single absorption maximum at 266 nm, shifted to longer wavelengths as against that of

TABLE 2

Solubilities in ethanol of N-cetyl-α-, β- and γ-picolinium halogen- and thiocyanate complexes of zinc and cadmium expressed in moles/1 at 23°C

Type of compound	M = Zn			M = Cd		
	X = α	X = β	X = γ	X = α	X = β	S = γ
[N-cetyl-X-pic]$_2$ [MCl$_4$]	$3.21 \cdot 10^{-2}$	$2.93 \cdot 10^{-2}$	$5.48 \cdot 10^{-2}$	$1.25 \cdot 10^{-2}$	$7.243 \cdot 10^{-2}$	$2.56 \cdot 10^{-2}$
[N-cetyl-X-pic]$_2$ [MBr$_4$]	$3.40 \cdot 10^{-2}$	$3.33 \cdot 10^{-2}$	$3.37 \cdot 10^{-2}$	$6.41 \cdot 10^{-3}$	$4.67 \cdot 10^{-3}$	$6.86 \cdot 10^{-3}$
[N-cetyl-X-pic]$_2$ [MI$_4$]	$3.84 \cdot 10^{-2}$	$5.81 \cdot 10^{-2}$	$2.87 \cdot 10^{-2}$	$4.22 \cdot 10^{-3}$	$3.234 \cdot 10^{-2}$	$5.36 \cdot 10^{-3}$
[N-cetyl-X-pic]$_2$ [M(SCN)$_4$]	$4.5 \cdot 10^{-3}$	$5.27 \cdot 10^{-2}$	v. v. soluble	$1.40 \cdot 10^{-2}$	$1.45 \cdot 10^{-3}$	?
[N-cetyl-X-pic] [MCl$_3$]					$6.929 \cdot 10^{-2}$	
[N-cetyl-X-pic] [MBr$_3$]					$1.93 \cdot 10^{-3}$	
[N-cetyl-X-pic] [MI$_3$]					$3.89 \cdot 10^{-3}$	
[N-cetyl-X-pic] [M(SCN)$_3$]						

N-cetyl-γ-picolinium halides ($\lambda_{max} = 256$ nm) and towards shorter wavelengths as against that of N-cetyl-α-picolinium halides ($\lambda_{max} = 268$ nm). The change of the methyl radical from the γ position into β has therefore

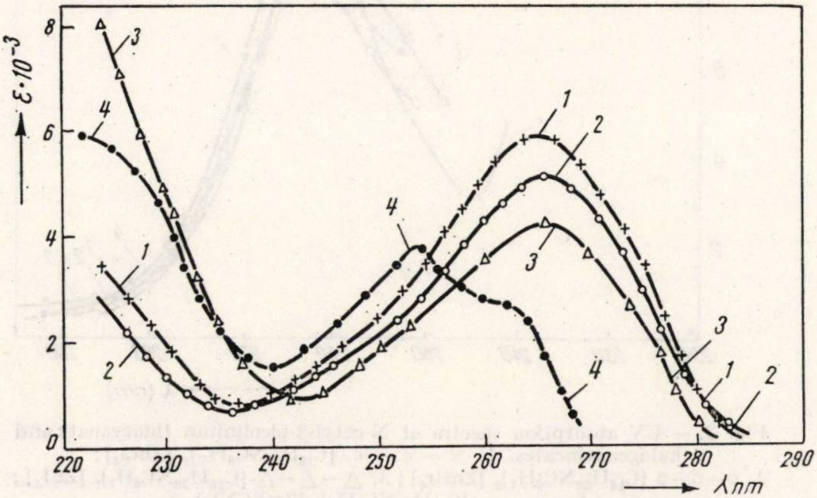

Fig. 1. — UV absorption spectra of N-cetyl-β-picolinium halides and sulphocyanide. 1. ×—×—× $[C_{16}H_{33}NC_6H_7]Cl$; 2. o—o—o $[C_{16}H_{33}NC_6H_7]Br$; 3. △—△—△ $[C_{16}H_{33}NC_6H_7]I$: 4. .—.—. $[C_{16}H_{33}NC_6H_7]SCN$.

a bathochromic effect, while it has a hypsochromic effect relative to the α position. The absorption maximum of N-cetyl-β-picolinium sulphocyanide is situated at $\lambda = 254-255$ nm, therefore at a shorter wavelength than that of halides. Similar influences were also recorded in the case of the new synthesized complexes.

Most of them present an absorption maximum comprised between 262—264 nm, characteristic of the organic cation (Figure 2—4). The N-cetyl-β-picolinium triiodocadmiate and the N-cetyl-α-and γ-picolinium triiodocadmiate absorbs continuously (Figure 4, curve 3).

While almost all compounds present an absorption maximum situated at approx. the same wavelength ($\lambda = 262-264$ nm), there are, on the contrary, fluctuations of the extinction coefficient (ε) as a function of the nature of the complex anion. For the zinc compounds, the extinction coefficient varies in the order : Cl > I > SCN > Br, and in the cadmium compounds with the coordination number 4, the extinction coefficient varies as follows :

$$I > Br > Cl > SCN.$$

The extinction coefficient of the N-cetyl-β-picolinium cadmium compounds with the coordination number 3 varies in the order : $\varepsilon_\beta < \varepsilon_\alpha \ll \varepsilon_\gamma$

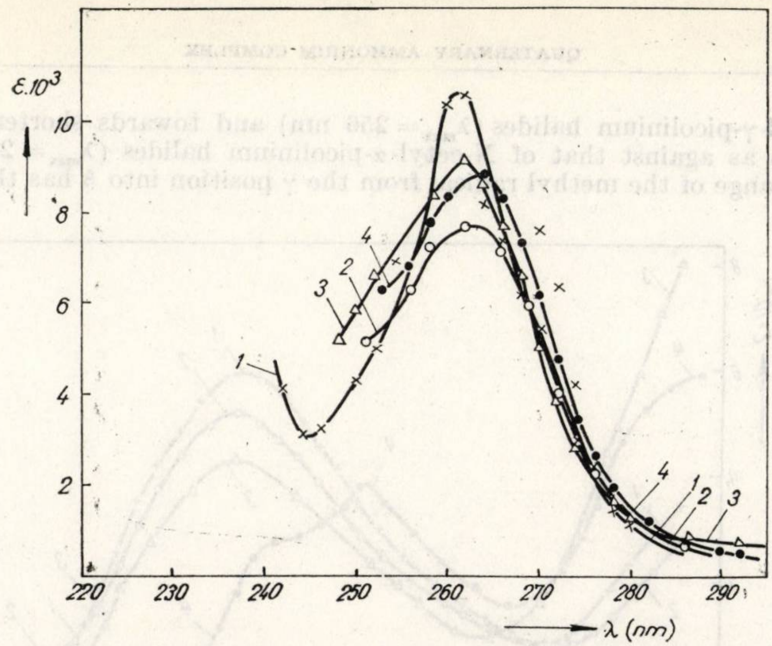

Fig. 2. — UV absorption spectra of N-cetyl-β-picolinium thiocyanate and halogenozincates. 1. × — × — × $[C_{16}H_{33}NC_6H_7]_2\ [ZnCl_4]$; 2. o—o—o $[C_{16}H_{33}NC_6H_7]_2\ [ZnBr_4]$; 3. △—△—△ $[C_{16}H_{33}NC_6H_7]_2\ [ZnI_4]$; 4. .—.—. $[C_{16}H_{33}NC_6H_7]_2\ [Zn(SCN)_4]$.

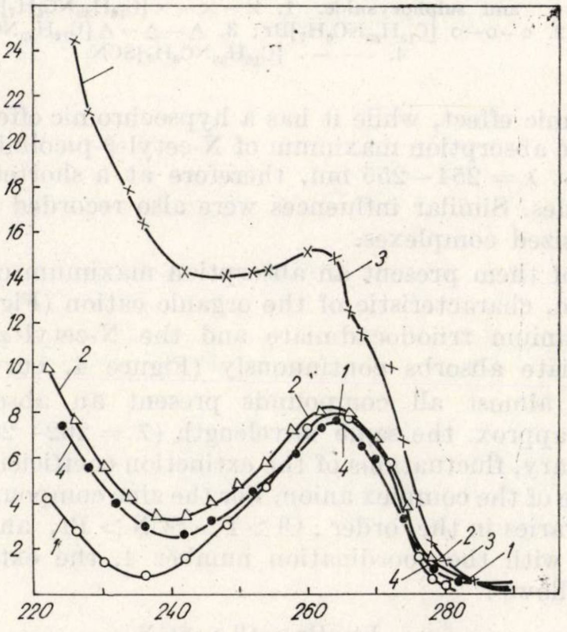

Fig. 3. — UV absorption spectra of N-cetyl-β-picolinium tetrathiocyanate and tetrahalogenocadmiates.
1. o—o—o $[C_{16}H_{33}NC_6H_7]_2[CdCl_4]$;
2. △—△—△ $[C_{16}H_{33}NC_6H_7]_2[CdBr_4]$;
3. × — × — × $[C_{16}H_{33}NC_6H_7]_2[CdI_4]$;
4. .—.—. $[C_{16}H_{33}NC_6H_7]_2[Cd(SCN)_4]$.

Fig. 4. — UV absorption spectra of N-cetyl-β-picolinium trihalogenocadmiates.
1. × — × — × $[C_{16}H_{33}NC_6H_7][CdCl_3]$;
2. o — o — o $[C_{16}H_{33}NC_6H_7][CdBr_3]$;
3. · — · — · $[C_{16}H_{33}NC_6H_7][CdI_3]$.

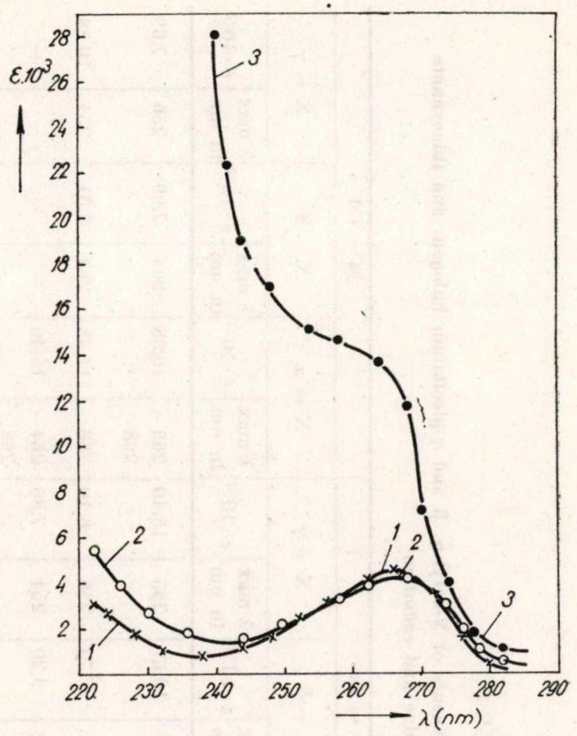

II. EXPERIMENTAL

1. *N-cetyl-β-picolinium tetrachlorozincate*. To an alcoholic solution obtained by dissolving 0.36 g $ZnCl_2 \cdot 2^{1/2}H_2O$ in 10 ml ethanol, one adds dropwise a solution containing 1.41 g N-cetyl-β-picolinium chloride. On mixing the two solutions, an opalescence will appear. It is filtered. From the clear solution, crystals will appear at room temperature. For a complete separation, the mixture is cooled on ice and then filtered and air-dried.

Hexagonal, elongated, very well-shaped crystals are obtained by slow recrystallization from ethanol, at room temperature.

The substance is extremely soluble in the cold in chloroform and acetone. In benzene, xylene and dioxan it dissolves on heating, while a gelatinous precipitate separates in the cold. It is insoluble in ether and carbon tetrachloride. The alkaline solutions decompose it. Calculated for: $C_{16}H_{33}NC_6H_7\ ZnCl_4$: Zn = 7.75 %; Cl = 16.90 %. Found: Zn = 7.75 %; Cl = 16.76 %.

2. *N-cetyl-β-picolinium tetrabromozincate*. 0.45 g $ZnBr_2$ are dissolved in 20 ml ethnaol and 1.592 g N-cetyl-β-picolinium bromide are also dissolved in 20 ml ethanol. The solutions are mixed. Crystals appear at room temperature. With a view to a complete separation, it is cooled in a mixture of ice and ammonium chloride and then filtered under reduced pressure. Small, agglomerated crystals will separate on recrystallization from alcohol.

The substance is very readily soluble in the cold in chloroform and acetone. In xylene and benzene, it dissolves on heating. It is insoluble in the cold and on heating in ether, carbon tetrachloride and benzene. It decomposes in an alkaline medium. Calculated for: $[C_{16}H_{33}NC_6H_7]_2[ZnBr_4]$: Zn = 6.41 %; Br = 31.30 %; Found: Zn = 6.20 %; Br = 31.49 %.

3. *N-cetyl-β-picolinium tetraiodozincate*. 0.32 g ZnI_2 are introduced into a glass and dissolved in 10 ml ethanol, adding them to a solution obtained by dissolving 0.89 g N-cetyl-β-picolinium iodide in 10 ml ethanol. It is cooled in a refrigerant mixture formed of ice and ammonium chloride. It is filtered under reduced pressure. In the filtering funnel the substance turns

TABLE 3

Absorption maxima in the UV domain and the extinction coefficients of N-cetyl-α, β and γ-picolinium halogen- and thiocyanate compounds of zinc and cadmium

Type of compound	M = Zn						M = Cd					
	X = α		X = β		X = γ		X = α		X = β		X = γ	
	λ max in nm	$\varepsilon \cdot 10^{-3}$	λ max in nm	$\varepsilon \cdot 10^{-3}$	λ max in nm	$\varepsilon \cdot 10^{-3}$	λ max in nm	$\varepsilon \cdot 10^{-3}$	λ max in nm	$\varepsilon \cdot 10^{-3}$	λ max in nm	$\varepsilon \cdot 10^{-3}$
[N-cetyl-X-pic]$_2$ [MCl_4]	266	10.86	262	10.61	255	15.40	266—268	10.38	264	7.99	256	7.69
[N-cetyl-X-pic]$_2$ [MBr_4]	266	16.48	264	7.73	256	8.10	266	11.48	264	8.31	254	10.86
[N-cetyl-X-pic]$_2$ [MI_4]	266	12.07	262	9.20	254	7.86	264—266	15.40	—	—	—	—
[N-cetyl-X-pic]$_2$ [$M(SCN)_4$]	266	14.61	264	8.84	256	8.47	266	11.60	264	7.63	—	—
[N-cetyl-X-pic] [MCl_3]							266	6.61	266	4.52	—	—
[N-cetyl-X-pic] [MBr_3]							266	5.31	264	4.28	233 256	12.07 4.36
[N-cetyl-X-pic] [MI_3]							—	—	256 264	—	—	—
[N-cetyl-X-pic] [$M(SCN)_3$]											256	5.60

slightly yellow on the top. Acicular crystals separate by recrystallization. Many of them appear in clusters. The substance is less stable than chloride and bromide. It is soluble in the cold in dioxan, chloroform and acetone. It is insoluble in carbon tetrachloride and ether and oily drops appear in xylene and benzene. The sodium hydroxide solution decomposes it. Calculated for : $[C_{16}H_{33}NC_6H_7]_2$ $[ZnI_4]$: Zn = 5.41 %; I = 41.28 %. Found : Zn = 5.37 %; I = 41.25 %.

4. *N-cetyl-β-picolinium tetrathiocyanatozincate*. The substance can be obtained in aqueous medium by a double-exchange reaction. 0.43 g $ZnSO_4 \cdot 7H_2O$ and 1.16 g KSCN are dissolved in the cold in 20 ml distilled water. A clear $Na_2[Zn(SCN)_4]$ solution is obtained to which one adds a solution obtained by dissolving 0.708 g N-cetyl-β-picolinium chloride in 20 ml cold water. The N-cetyl-β-picolinium chloride solution is added to the first solution under constant stirring. The occurrence of a white-pink precipitate is observed. 40 ml cold water are added allowing the precipitate to settle. It is filtered. It recrystallizes from alcohol. The substance is very soluble in the cold in dioxan, sylene, carbon tetrachloride, chloroform, benzene, acetone and ether. The sodium hydroxide solution decomposes it. Calculated for : $[C_{16}H_{33}NC_6H_7]_2[Zn(SCN)_4]$: Zn = 7.60 %; SCN = 24.85 %; Found : Zn = 7.26 %; SCN = 24.96.

5. *N-cetyl-β-picolinium tetrachlorocadmiate*. In contrast to the $[N\text{-cetyl-}\alpha\text{-pic}]_2$ $[CdCl_4]$ compound which could be obtained in a medium of ethyl alcohol, the synthesis of compound $[N\text{-cetyl-}\beta\text{-pic}]_2$ $[CdCl_4]$ was possible only by working in a HCl 2n medium. Thus, 0.22 g $CdCl_2 \cdot 2H_2O$ were dissolved in 10 ml HCl 2n adding a solution obtained by dissolving 0.76 g N-cetyl-β-picolinium chloride in 12 ml HCl 2n. The mixture is stirred and then it is heated and allowed to stand for the formed precipitate to settle. It is filtered. It is allowed to dry on the filter paper. The substance appears under the form of acicular, white, shiny crystals. It is very soluble in the cold in chloroform and acetone and on warming it dissolves in dioxan xylene and benzene. The substance is sparsely soluble in ether and insoluble in carbon tetrachloride. The sodium hydroxide solution decomposes it. Calculated for : $[C_{16}H_{33}NC_6H_7]_2[CdCl_4]$: Cd = 12.63 %; Cl = 15.95 % Found : Cd = 13.04 %; Cl = 15.87 %.

6. *N-cetyl-β-picolinium tetrabromocadmiate*. To a solution containing 0.34 g $CdBr_2 \cdot 4H_2O$ dissolved in 20 ml ethanol on heating one adds a solution obtained by dissolving 0.79 g N-cetyl-β-picolinium bromide in 10 ml ethanol. On mixing the two solutions, a faint precipitate appears in the cold. Alcohol is added to reach a 100 ml volume. It is brought to boil and then filtered. The solution is cooled on ice. The substance appears under the form of large rectangular, regular, well-shaped crystals. It is readily dissolved in chloroform acetone and benzene in the cold. It is insoluble in xylene, carbon tetrachloride and ether. The sodium hydroxide solution decomposes it. Calculated for : $[C_{16}H_{33}NC_6H_7]_2$ $[CdBr_4]$: Cd= 10.53 %; Br = 29.33 %; Found : Cd = 10.30 %; Br = 29.28 %.

7. *N-cetyl-β-picolinium tetraiodocadmiate*. A solution containing 0.72 g CdI_2 in 20 ml ethanol is mixed with a solution containing 1.78 g N-cetyl-β-picolinium iodide in 60 ml ethanol. It is cooled on ice and the formed precipitate is filtered under reduced pressure. After recrystallization from alcohol, thin, asbestiform crystals, under the form of long threads, are obtained. The substance is soluble in chloroform, acetone and benzene in the cold and it is dissolved in dioxan on heating. It is insoluble in xylene, carbon tetrachloride and ether. The sodium hydroxide solution decomposes it. Calculated for : $[C_{16}H_{33}NC_6H_7]_2$ $[CdI_4]$: Cd = 8.95 %; I = 40.42 %; Found : Cd = 9.17 %; I = 40.51 %.

8. *N-cetyl-β-picolinium tetrathiocyanatocadmiate*. In maximum 5 ml water we dissolve 0.46 g $CdCl_2 \cdot 2^1/_2$ H_2O and 1.28 g KSCN adding to it a solution obtained by dissolving 1.4 g N-cetyl-β-picolinium chloride in 25 ml water. It is stirred. A pink precipitate appears. It is filtered by routine procedure. The precipitate is dissolved in ethyl alcohol and placed on ice with ammonium chloride. Crystals under the form of polygonal plates, less regular, readily soluble in the cold in dioxan, xylene and benzene have been obtained on recrystallization from alcohol. The substance is insoluble in carbon tetrachloride, acetone and ether. Calculated for : $[C_{16}H_{33}NC_6H_7]_2$ $[Cd(SCN)_4]$: Cd = 11.46 %; SCN = 23.66 %. Found : Cd = 11.20 %; SCN = 23.53 %.

9. *N-cetyl-β-picolinium trichlorocadmiate* was obtained in alcoholic medium, mixing the solution obtained by dissolving 0.22 g $CdCl_2 \cdot 2^1/_2$ H_2O in 10 ml ethanol with a solution of 0.38 g N-cetyl-β-picolinium chloride in 10 ml ethanol. A white, flocculated precipitate appears at room temperature. The substance recrystallized from alcohol appears under the form of long, asbestiform, white crystals. The substance dissolves in benzene on heating and in acetone in the cold. In carbon tetrachloride, chloroform and ether it is insoluble. Calculated for : $[C_{16}H_{33}NC_6H_7]$ $[CdCl_3]$: Cd = 20.94 %; Cl = 19.82 %; Found : Cd = 21.10 %; Cl = 20.19 %.

10. *N-cetyl-β-picolinium tribromocadmiate*. 1.388 g $CdBr_2 \cdot 4H_2O$ together with 0.45 g N-cetyl-β-picolinium bromide are dissolved in 60 ml ethanol. When needed, it is heated. It

is filtered if needed and allowed to concentrate by evaporation at room temperature for approx. 48 hrs. The product separated at room temperature is stirred and filtered under reduced pressure. The substance appears under the form of white, prismatic crystals. The filtrate is cooled and a different product is separated. According to their behaviour on heating, both products seem to be the same substance. After recrystallization from acetonitrile or ethyl alcohol, the substance appears under the form of white acicular, shiny crystals. The substance is very soluble in the cold in acetone and chloroform while on heating, it dissolves only in dioxan. It is insoluble in xylene, carbon tetrachloride and ether. Calculated for : $[C_{16}H_{33}NC_6H_7]$ $[CdBr_3]$: Cd = 16.76 % ; Br = 35.77 %. Found : Cd = 17.10 % ; Br = 36.27 %.

11. *N-cetyl-β-picolinium triiodocadmiate* is obtained in an analogous manner with tribromocadmiate. 1.1 g CdI_2 and approx. 0.45 g N-cetyl-β-picolinium iodide are separately dissolved in 15 ml ethanol each. The solutions are filtered if needed and they are mixed, allowing them to concentrate by evaporation at room temperature for 48hrs. Acicular, white shiny crystals separate. The compound obtained is filtered and the filtrate is cooled on ice. It is filtered. Two products are thus obtained. By recrystallization from acetonitrile, the products change totally into tetraiodocadmiate. Thus the substance behaves like an addition product between CdI_2 and tetraiodocadmiate, of the form : $[\text{N-cetyl-}\beta\text{-pic}]_2$ $[CdI_4] \cdot CdI_2$. The substance is very soluble in dioxan, xylene, chloroform, benzene and acetone. It is sparsely soluble in carbon tetrachloride and insoluble in ether. Calculated for: $CdI_2 \cdot [CdI_4]$ $[C_{16}H_{33}NC_6H_7]_2$: Cd = 13.86 % ; I = 46.94 % ; Found : Cd = 13.39 % ; I = 46.83 %.

REFERENCES

[1] M. Stan and R. Zelingher, *Z. anorg. Chem.*, **340**, 86 (1965).
[2] M. Stan and D. Văcărescu, *Analele Univ. Buc. Seria Ştiinţele naturii, Chimie*, **2**, 101(1967).
[3] H. Grossmann, *Ber. dtsch. chem. Ges.*, **37**, 366 (1904).
[4] S. F. Babak and I. A. Kondraşev, *Zhur. obscchei Khim.*, **29**, 3148 (1959).
[5] M. K. Aliavia, *Zhur. neorg. Khim.*, **6**, 1608 (1961).

Revue Roumaine de Chimie **25**, *3*, 371–378 (1980)

STUDY OF SOME N-CETYL-β-PICOLINIUM HALOGEN AND THIOCYANATOMERCURATES(II)

DUMITRA VĂCĂRESCU

Polytechnic Institute, Department of Technological Chemistry, Splaiul Independenţei, 202, Bucharest, Romania

Received January 29, 1977
Revised June 28, 1979

A number of previous papers have presented the properties and the methods of preparation of some N-cetyl-α-picolinium and N-cetyl-γ-picolinium halogen- and thiocyanatomercurates (II). This paper makes a new contribution to completing the study of N-cetyl-picolinium halogen- and thiocyanatomercurates (II) by extending the investigation of such complex compounds with N-cetyl-β-picolinium. Since a significant number of halogen- and thiocyanatomercurates of the three isomers (α, β and γ) of N-cetyl-picolinium has been obtained so far, it is possible to make a comparative analysis of the properties of such substances, so as to reveal the influence of the position of the methyl radical in the pyridine ring of the N-cetyl-picolinium cation. New quaternary ammonium salts of halogen- and thiocyanatocomplex acids of mercury (II) of the type M $[HgX_3]$; M_2 $[HgX_4]$ have been synthesized in this research stage. The substances were characterized by their physical and chemical properties and also by UV absorption spectra.

INTRODUCTION

A large number of quaternary halogen- and pseudohalogen complexes of mercury (II) have been described in the literature [1–8] belonging mainly to the following types : M $[HgX_3]$; $M_2[HgX_4]$; $M[Hg_2X_5]$; $M_2[Hg_3X_8]$ in which X = F, Cl, Br, I, SCN and M = organic cation of the type pyridinium, α, β, γ-picolinium, quinolinium, lutidinium, methylammonium, dimethylammonium, tetramethylammonium, tetramethylphosphonium, etc.

The properties and methods for obtaining quaternary complex ammonium compounds resulted from the halides and the sulphocyanide of mercury (II) and N-cetyl-α-picolinium and N-cetyl-γ-picolinium halides and sulphocyanides have been described in two previous papers. [9–10]

Among the N-cetyl-β-picolinium salts of the complex acids of mercury (II) the following substances have been prepared and described:

$[\text{N-cetyl-}\beta\text{-pic}][HgCl_3]$ $[\text{N-cetyl-}\beta\text{-pic}]_2[HgCl_4]$
$[\text{N-cetyl-}\beta\text{-pic}][HgBr_3]$ $[\text{N-cetyl-}\beta\text{-pic}]_2[HgBr_4]$
$[\text{N-cetyl-}\beta\text{-pic}][HgI_3]$ $[\text{N-cetyl-}\beta\text{-pic}]_2[HgI_4]$
$[\text{N-catyl-}\beta\text{-pic}]_2[Hg(SCN)_4]$

These compounds were prepared in alcoholic or aqueous medium by one of the following methods :

— direct addition of N-cetyl-β-picolinium halide to the mercury (II) halide or by :

— the double-exchange reaction between the halogenomercurate (II) of an alkaline metal and a N-cetyl-β-picolinium halide.

The trihalogen compounds of mercury were obtained only in alkaline medium [8] by the reaction between mercury (II) halide with an appropriate quantity of N-cetyl-β-picolinium halide (mole/mole).

It must be observed that N-cetyl-β-picolinium trithyocyanatomercurate (II) could not be obtained in a pure state, regardless of the reactants ratio and of the reaction medium. The analysis of each resulted compound has indicated a mixture of tetra- and trithyocyanatomercurate(II).

N-cetyl-β-picolinium tetrahalogenomercurates and tetrathyocyanatomercurate could be synthesized only in aqueous medium except for tetraiodomercurate (II) which can be obtained in alcoholic medium. It has been again confirmed that the compounds with the coordination number 4, except for N-cetyl-β-picolinium tetraiodomercurate, could be obtained only in aqueous solution and not in alcoholic medium.

The mercury (II) compounds with the coordination number 4 change to the corresponding trihalogen derivatives by recrystallization from alcohol. They were purified without decomposition, by recrystallization from acetonitrile.

It is clearly proved, like in the previous papers [9,10] that the alcoholic medium favours the formation of complex compounds with coordination number 3 and that the aqueous medium and the acetonitrile medium favours the formation of complex compounds with coordination number 4.

N-cetyl-β-picolinium tetrachloromercurate and tetrabromomercurate are decomposed in an alcoholic medium according to reaction :

$$[\text{N-cetyl-}\beta\text{-pic}]_2\,[HgX_4] \rightarrow [\text{N-cetyl-}\beta\text{-pic}]\,[HgX_3] + [\text{N-cetyl-}\beta\text{-pic}]X$$

a fact that could be proved both chemically and conductometrically.

All the attempts to obtain compounds of the form : $[Hg_3X_8]$ $[\text{N-cetyl-}\beta\text{-pic}]_2$ as those obtained in the case of N-cetyl-γ-picolinium compounds, have failed. The β position of the methyl radical in the pyridine ring of picolinium probably constitues a steric hindrance in the formation of such compounds.

All the compounds prepared are crystalline, white substances except for tetraiodide and triiodide which form yellow, shiny crystals.

The new compounds of mercury (II) with N-cetyl-β-picolinium have relatively low melting points, they melt over a temperature interval of 1—3° C, analogously with the compounds of N-cetyl-α-and γ-picolinium.

Table 1 gives the melting points of N-cetyl-β-picolinium halogens and thiocyanatomercurates (II), comparatively indicating also those of N-cetyl-α and γ-picolinium analogous compounds.

It must be remarked that the melting points of the new compounds are lower than the melting points of N-cetyl-α-picolinium corresponding compounds and that, both in compounds with coordination number 3 and in those with coordination number 4, they vary as a function of the ligand nature, as follows : Cl > Br > I. It must also be observed that the melting points of N-cetyl-β-picolinium compounds are in general lower than in the case of N-cetyl-α-picolinium compounds and somewhat higher than

TABLE 1

Melting temperatures (in °C) of N-cetyl-α, β- and γ-picolinium halogen- and thiocyanatomercurates (II)

Type of compound	M = Hg		
	X = α	X = β	X = γ
[N-cetyl-X-pic][$HgCl_3$]	79–87	68–70	56–58
[N-cetyl-X-pic] [$HgBr_3$]	76–77	58–59	60–61
[N-cetyl-X-pic] [HgI_3]	62–63	53–54	69–70
[N-cetyl-X-pic] [$Hg(SCN)_3$]	44–47	not isolated	31–34
[N-cetyl-X-pic]$_2$ [$HgCl_4$]	82–83	77–77.5	64–65
[N-cetyl-X-pic]$_2$ [$HgBr_4$]	67–69	63–66	58–61
[N-cetyl-X-pic]$_2$ [HgI_4]	67–68	58–59	58–59
[N-cetyl-X-pic]$_2$ [$Hg(SCN)_4$]	35–37	—	29–30

those of N-cetyl-γ-picolinium compounds. We can state that, with a few exceptions, they vary as a function of the nature of the position of methyl radical as follows : $\alpha > \beta > \gamma$.

N-cetyl-β-picolinium halogen- and thiocyanatomercurates (II) are extremely soluble in acetone and chloroform. They are soluble in the warm in dioxan and in carbon sulphide except for tetrachloro- and tetrathiocyanatomercurates which form an emulsion with carbon sulphide.

The solubilities in ethanol were quantitatively determined and compared with those of N-cetyl-α- and γ-picolinium corresponding compounds. The results are given in Table 2.

Table 2 shows that among N-cetyl-β-picolinium compounds, similar to N-cetyl-γ-picolinium compounds, iodide is the most sparsely soluble, whereas in N-cetyl-α-picolinium compounds, bromide is the least soluble.

TABLE 2

Solubilities in ethanol of N-cetyl-α, β- and γ-picolinium halogen- and thiocyanatomercurates(II) expressed in moles/1 at 23°C

Type of compound	M = Hg		
	X = α	X = β	X = γ
[N-cetyl-X-pic] [$HgCl_3$]	$5.81 \cdot 10^{-3}$	$8.32 \cdot 10^{-3}$	$1.83 \cdot 10^{-2}$
[N-cetyl-X-pic] [$HgBr_3$]	$2.32 \cdot 10^{-3}$	$6.03 \cdot 10^{-3}$	$6.93 \cdot 10^{-3}$
[N-cetyl-X-pic] [HgI_3]	$3.36 \cdot 10^{-3}$	$4.45 \cdot 10^{-3}$	$2.89 \cdot 10^{-3}$
[N-cetyl-X-pic] [$Hg(SCN)_3$]	$1.85 \cdot 10^{-1}$	not isolated	v. v. soluble
[N-cetyl-X-pic]$_2$ [$HgCl_4$]	$5.81 \cdot 10^{-3}$	$1.07 \cdot 10^{-2}$	$1.36 \cdot 10^{-2}$
[N-cetyl-X-pic]$_2$ [$HgBr_4$]	$4.08 \cdot 10^{-3}$	$4.47 \cdot 10^{-3}$	$6.31 \cdot 10^{-3}$
[N-cetyl-X-pic]$_2$ [HgI_4]	$3.02 \cdot 10^{-3}$	$2.60 \cdot 10^{-3}$	$2.88 \cdot 10^{-3}$
[N-cetyl-X-pic]$_2$ [$Hg(SCN)_4$]	practically insoluble	very soluble	very soluble

The solubilities in alcohol of tetrahalogen and trihalogen derivatives of mercury (II) with N-cetyl-β-picolinium decrease in the following order : $Cl > Br > I$.

From a physico-chemical point of view, the constitution of compounds was confirmed by the study of UV spectra in the domain of wavelengths included within 220—400 nm, by a Universal Zeiss Jena VSU_1 spectrophotometer, using alcoholic solutions of $10^{-4}-10^{-5}$ M concentration. Accordingly, the spectrum of N-cetyl-β-picolinium halides and sulphocyanide was first performed, the spectrum of the new compounds being performed thereafter. All the compounds present an absorption maximum around 264 nm which is characteristic of the organic cation (N-cetyl-β-picolinium). The iodinated compounds make an exception, presenting a second maximum at 300 nm which is characteristic of anion $[HgI_3]^-$ and $[HgI_4]^{2-}$. The values found by us for iodomercurates agree with those found by Deacon [8] for similar pyridine and tetramethylphosphonium compounds.

Tetrathiocyanate presents a maximum at 252 nm, which is also observed in N-cetyl-β-picolinium sulphocyanide (254 nm) while a slightly marked maximum appears at 268 nm (Figure 1 — curve 4).

It should be mentioned that the band proper to the organic cation of N-cetyl-β-picolinium compounds is shifted towards longer wavelengths compared to those of N-cetyl-γ-picolinium compounds and towards shorter wavelengths compared to those of N-cetyl-α-picolinium compounds.

The methyl radical in β position of the pyrydine cycle acts bathochromally relative to the γ position of the radical and hypsochromally relative to the α position of methyl radical.

In the series of compounds with the coordination number 4 it can be observed that the absorption intensity is maximum in the complex with iodine (Figure 2, curve 3) and minimum in that with thiocyan (Figure 2, curve 4).

In the series of trihalogenomercurates, the molar extinction is maximum in triiodomercurate (Figure 3, curve 3) and minimum in trichloromercurate (Figure 3, curve 1).

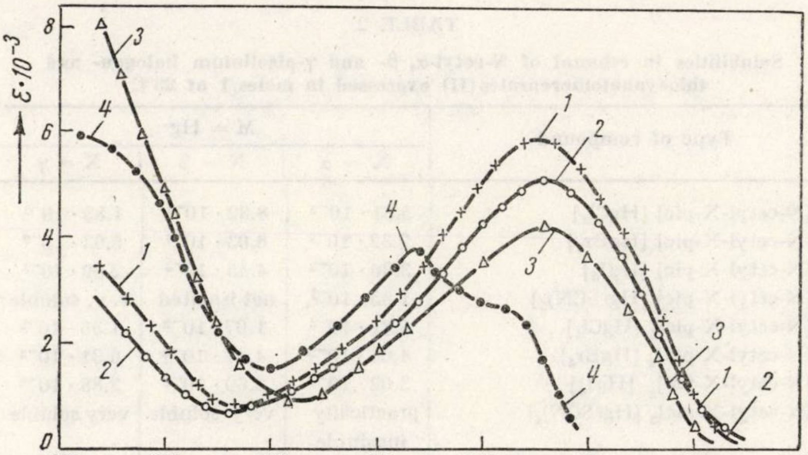

Fig. 1. — UV absorption spectra of N-cetyl-β-picolinium halides and sulphocyanide : 1. $[C_{16}H_{33}NC_6H_7]Cl$; 2. $[C_{16}H_{33}NC_6H_7]Br$; 3. $[C_{16}H_{33}NC_6H_7]I$; 4. $[C_{16}H_{33}NC_6H_7]SCN$.

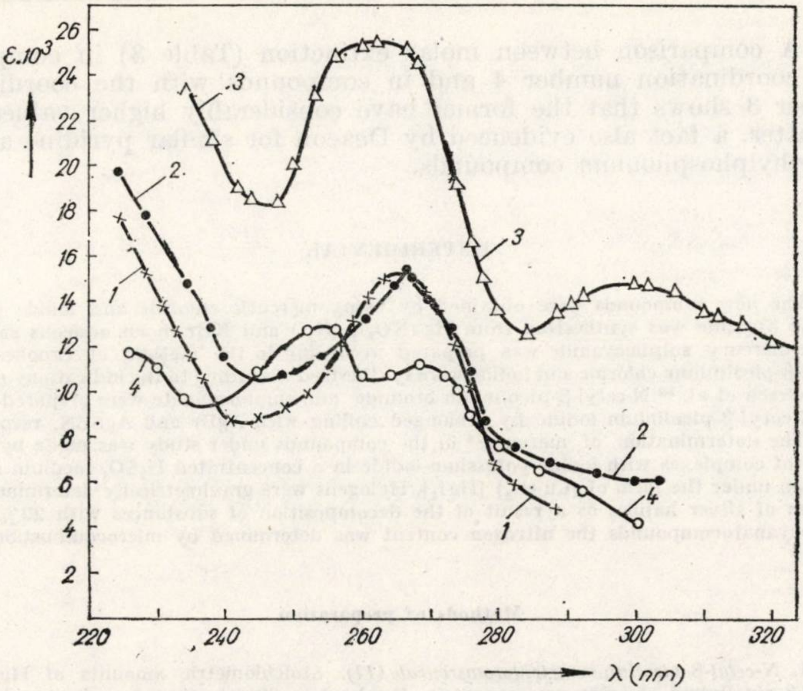

Fig. 2. — UV absorption spectra of N-cetyl-β-picolinium tetracyanato- and tetrahalogenomercurates (II) : 1. $[C_{16}H_{33}NC_6H_7]_2$ $[HgCl_4]$; 2. $[C_{16}H_{33}NC_6H_7]_2$ $[HgBr_4]$; 3. $[C_{16}H_{33}NC_6H_7]_2$ $[HgI_4]$; 4. $[C_{16}H_{33}NC_6H_7]_2[HgSCN_4]$.

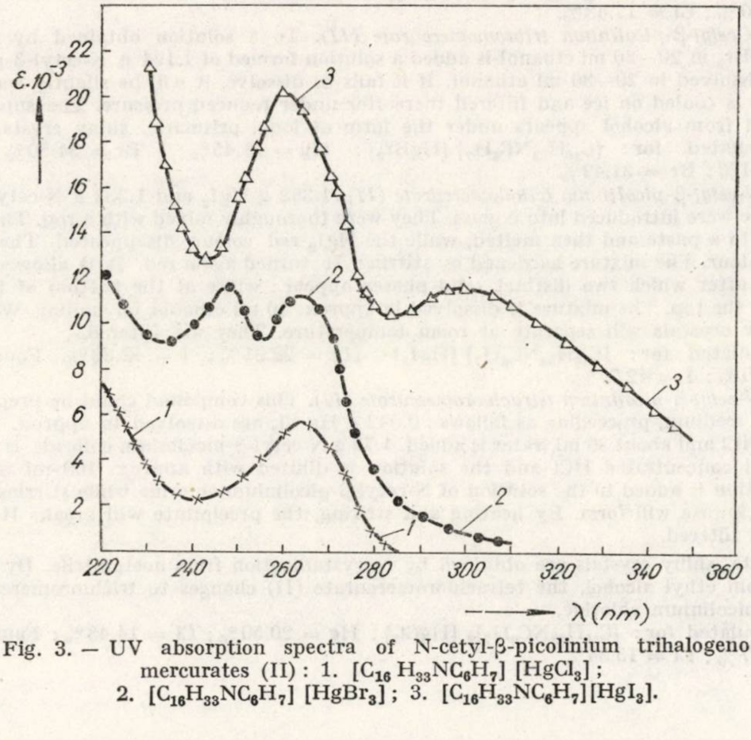

Fig. 3. — UV absorption spectra of N-cetyl-β-picolinium trihalogenomercurates (II) : 1. $[C_{16}H_{33}NC_6H_7]$ $[HgCl_3]$; 2. $[C_{16}H_{33}NC_6H_7]$ $[HgBr_3]$; 3. $[C_{16}H_{33}NC_6H_7][HgI_3]$.

A comparison between molar extinction (Table 3) in compounds with coordination number 4 and in compounds with the coordination number 3 shows that the former have considerably higher values than the latter, a fact also evidenced by Deacon for similar pyridine and tetramethylphosphonium compounds.

EXPERIMENTAL

The new compounds were obtained by using mercuric chloride and iodide p.a. The mercuric bromide was synthesized from Hg $(NO_3)_2 \cdot H_2O$ and KBr in an aqueous solution [11] and the mercury sulphocyanide was prepared according to the method of Crookes. [12] The N-cetyl-β-picolinium chloride and iodide were synthesized according to the indications given by E. Angelescu et al. [13] N-cetyl-β-picolinium bromide and sulphocyanate were prepared starting from N-cetyl-β-picolinium iodide by prolonged boiling with AgBr and AgSCN, respectively.

The determination of mercury[14] in the compounds under study was made by disintegration of complexes with iodine-potassium-iodide in a concentrated H_2SO_4 medium and precipitation under the form of $[Cu\ en_2]\ [HgI_4]$. Halogens were gravimetrically determined under the form of silver halides as a result of the decomposition of substances with 20% NaOH. In thiocyanatocompounds the nitrogen content was determined by microcombustion.

Methods of preparation

1. *N-cetyl-β-picolinium trichloromercurate (II).* Stoichiometric amounts of $HgCl_2$ and N-cetyl-β-picolinium chloride are separately dissolved in 20 ml ethanol each. A solution of N-cetyl-β-picolinium chloride is added to the first solution. It is cooled on ice. It is filtered. The substance recrystallized from alcohol has a white colour. On the microscope, small agglomerated crystals appear, whose shape cannot be clearly distinguished.

Calculated for: $[C_{16}H_{33}NC_6H_7]\ [HgCl_3]$: Hg = 32.10% ; Cl = 17.02%. Found: Hg = 32.30% ; Cl = 17.43%.

2. *N-cetyl-β-picolinium tribromomercurate (II).* To a solution obtained by dissolving 1.080 g $HgBr_2$ in 20—30 ml ethanol is added a solution formed of 1.194 g N-cetyl-β-picolinium bromide dissolved in 20—30 ml ethanol. If it fails to dissolve, it will be slightly warmed and filtered. It is cooled on ice and filtered thereafter under reduced pressure. The substance recrystallized from alcohol appears under the form of long, prismatic, shiny crystals.

Calculated for: $[C_{16}H_{33}NC_6H_7]\ [HgBr_3]$: Hg = 26.45% ; Br = 31.50% ; Found: Hg = 26.84% ; Br = 31.42%.

3. *N-cetyl-β-picolinium triiodomercurate (II).* 1.362 g HgI_2 and 1.333 g N-cetyl-β-picolinium iodide were introduced into a glass. They were thoroughly mixed with a rod. The mixture changed into a paste and then melted, while the HgI_2 red colour disappeared. The melt has a yellow colour. The mixture hardened by stirring. It turned again red. It is allowed to stand for 24 hr, after which two distinct solid phases appear: white at the bottom of the vessel and red on the top. The mixture is dissolved in approx. 80 ml ethanol on boiling Well-shaped pale yellow crystals will separate at room temperature. They are filtered.

Calculated for: $[C_{16}H_{33}NC_6H_7]\ [HgI_3]$: Hg = 22.31% ; I = 42.33%. Found: Hg = 23.00% ; I = 42.77%.

4. *N-cetyl-β-picolinium tetrachloromercurate (II).* This compound could be prepared only in aqueous medium, proceeding as follows: 0.542 g Hg Cl_2 are dissolved in approx. 2 ml concentrated HCl and about 30 ml water is added. 1.72 g N-cetyl-β-picolinium chloride is dissolved in 3—4 ml concentrated HCl and the solution is diluted with approx. 100 ml water. The $HgCl_2$ solution is added to the solution of N-cetyl-β-picolinium chloride while stirring. A gelatinous precipitate will form. By heating and stirring, the precipitate will break. It is cooled on ice and filtered.

White, shiny crystals are obtained by recrystallization from acetonitrile. By recrystallization from ethyl alcohol, the tetrachloromercurate (II) changes to trichloromercurate and N-cetyl-β-picolinium chloride.

Calculated for: $[C_{16}H_{33}NC_6H_7]_2\ [HgCl_4]$: Hg = 20.50% ; Cl = 14.48% ; Found: Hg = 20.67% ; Cl = 15.35%.

TABLE 3

Absorption maxima in the ultraviolet domain and the extinction coefficients of N-cetyl-α, β, and γ-picolinium halogen- and thiocyanatomercurates (II)

Type of compound	M = Hg											
	X = α				X = β				X = γ			
	λ_1	$\varepsilon \cdot 10^{-3}$	λ_2	$\varepsilon \cdot 10^{-3}$	λ_1	$\varepsilon \cdot 10^{-3}$	λ_2	$\varepsilon \cdot 10^{-3}$	λ_1	$\varepsilon \cdot 10^{-3}$	λ_2	$\varepsilon \cdot 10^{-3}$
[N-cetyl-X-pic] [$HgCl_3$]	266	5.61	—	—	264	5.66	—	—	256—258	5.6	—	—
[N-cetyl-X-pic] [$HgBr_3$]	266—267	8.05	—	—	264	11.28	248	11.65	255—257	4.0	—	—
[N-cetyl-X-pic] [HgI_3]	264—266	13.91	306—308	6	300—260	20.2	300	11.75	255—256	12.4	302—304	9.5
[N-cetyl-X-pic] [$Hg(SCN)_3$]	266	8.5	282—312	4.15	not isolat.				—	—	—	—
[N-cetyl-X-pic]$_2$ [$HgCl_4$]	266	9.37	—	—	266	15.2	—	—	256	9.8	—	—
[N-cetyl-X-pic]$_2$ [$HgBr_4$]	266	11.08	—	—	266	15.2	—	—	255—257	21.0	—	—
[N-cetyl-X-pic]$_2$ [HgI_4]	263—264	15.85	304—306	—	262	25.58	300	14.81	256—258	25.7	304	12.07
[N-cetyl-X-pic]$_2$ [$Hg(SCN)_4$]	266	12.05	243	8.75	268	11.19	252	12.88	254—256	21.3	—	—

5. *N-cetyl-β-picolinium tetrabromomercurate (II).* It could be prepared only in aqueous medium, as follows : to a solution of 0.72 g $HgBr_2$ dissolved in 20 ml water is added 2 ml HBr (d = 1.49) and subsequently 0.63 g KBr. To this solution one adds the solution obtained by dissolving 1.6 g N-cetyl-β-picolinium bromide in approx. 100 ml water and then 2 ml HBr (d = 1.49). A precipitate will appear. It is filtered and recrystallized from acetonitrile. The substance appears under the form of white crystals.

By recrystallization from alcohol, the substance is transformed into tribromomercurate and N-cetyl-β-picolinium bromide.

Calculated for : $[C_{16}H_{33}NC_6H_7]_2\,[HgBr_4]$: Hg = 17.35 % ; Br = 27.65 % ; Found : Hg = 17.29 % ; Br = 28.29 %.

6. *N-cetyl-β-picolinium tetraiodomercurate (II).* It is obtained in ethanol medium from 0.98 g HgI_2 dissolved in 110 ml ethanol and 1.8 g N-cetyl-β-picolinium iodide dissolved in 20 ml ethanol. An asbestiform precipitate formed of acicular, silky, pale yellow crystals will form on mixing the two solutions. It is filtered and the product obtained is recrystallized from alcohol.

Calculated for : $[C_{16}H_{33}NC_6H_7]_2\,[HgI_4]$: Hg = 14.93 % ; I = 37.77 % ; Found : Hg = 15.01 % ; I = 38.04 %.

7. *N-cetyl-β-picolinium tetrathiocyanatomercurate (II).* This compound was obtained only in aqueous medium by a double-exchange reaction between :

$$K_2[Hg(SCN)_4] + 2\,[C_{16}H_{33}NC_6H_7]Cl = [C_{16}H_{33}NC_6H_7]_2\,[Hg(SCN)_4] + 2KCl$$

For this reaction, a solution of $K_2[Hg(SCN)_4]$ is prepared by dissolving 0.306 g $Hg(SCN)_2$ and 0.388 g KSCN in 10 ml water. To this is added a solution obtained by dissolving 0.706 g N-cetyl-β-picolinium chloride in 50 ml warm water. A white melt appears which will solidify by cooling on ice. It is filtered in the cold under reduced pressure.

White crystals will be obtained by recrystallization from minimum 10 ml ethyl alcohol.

Calculated for : $[C_{16}H_{33}NC_6H_7]_2\,[Hg(SCN)_4]$: Hg = 18.73 % ; N = 7.86 %. Found : Hg = 18.73 % ; N = 7.61 %.

REFERENCES

[1] M. Straumanis and A. Cirulis, *Z. anorg. Chem.*, **244,** 17 (1937).

[2] G. S. Jamieseon and E. T. Wherry, *J. Amer. Chem. Soc.*, **42,** 136 (1920).

[3] G. Ellendt and K. Cruse, *Z. phys. Chem.*, Leipzig, **201,** 130 (1952).

[4] H. Grossmann and B. Schück, *Z. anorg. Chem.*, **50,** 465 (1906).

[5] H. Grossmann and F. Hünseler, *Z. anorg. Chem.*, **46,** 365 (1905).

[6] A. Hesekiel, *Ber. dtsch. chem. Ges.*, **18,** 3093 (1885).

[7] A. W. Hofmann, *Liebigs Ann. Chem.*, **78,** 273 (1851).

[8] G. B. Deacon and B. O. West, *J. Chem. Soc.*, 3929 (1965).

[9] M. Stan and R. Zelingher, *Analele Univ. Buc., Seria Științele naturii, Chimie,* 2 (1964).

[10] M. Stan and D. Văcărescu, *Analele Univ. Buc., Seria Științele naturii, Chimie,* **2,** 15 (1968).

[11] P. Pascal, "Traite de Chimie minérale", vol. 3, Paris 1933, p. 995.

[12] W. Crookes, *Liebigs, Ann. Chem.*, **78,** 183 (1851).

[13] E. Angelescu, A. Nicolescu and Em. Bărbulescu, *Studii și Cercet. Chim.*, 2, 357 (1961).

[14] D. Pirtea and I. Albescu, *Studii și Cercet. Chim.*, **1,** 137 (1959).

Revue Roumaine de Chimie, **25**, *3*, 379–391 (1980)

SYNTHÈSE D'[(HYDROXY-5-PENTYLAMINO)-n-ALKYL-1] AZIRIDINES*

GUY RICART
Université des Sciences et Techniques de Lille
Laboratoire de Chimie Organique I
B.P. 36 59650 Villeneuve D'Ascq, France

Reçu le 27 octobre 1978

La facilité d'addition des aziridines secondaires sur les nitriles α-éthyléniques diminue quand le degré de substitution de l'hétérocycle azoté augmente. La réduction catalytique, en milieu basique, des aziridines N-cyanoalkylées *1* donne les (aziridinyl-1) alkylamines primaires *2*. La condensation de ces amines avec le diméthyl-amino-2 tétrahydropyranne permet l'accès aux amines secondaires N-tétrahydropyrannylées *3* qui se présentent en faible pourcentage sous la forme iminoalcool ; leur réduction sur nickel de Raney conduit aux [(hydroxy-5-pentylamino) alkyl]-1 aziridines *4* que l'on peut cycliser en pipéridines de type *5*.

1-Unsubstituted aziridines add to a variety of α-olefinic nitriles forming 1-cyanoalkylaziridines *1* : the reaction is subject to various steric effects. Catalytic reduction in weakly alkaline media of compounds *1* lead to (1-aziridinyl) alkylamines *2*. Primary amines *2* react with 2-dimethylamino-tetrahydropyran to furnish 1 [N-(2-tetrahydropyranyl) aminoalkyl] aziridines *3* which are in equilibrium with iminoalcohol form (about 8 %). Hydrogenolysis of products *3* occurs under mild conditions on Raney nickel and results in cleavage of the tetrahydropyran ring between the oxygen and substituted carbon atoms with survival of the aziridine ring. The cyclisation of amino-alcohols *4* gives N- [(1-aziridinyl) alkyl] piperidines *5*.

Le but de ce travail est de présenter une synthèse relativement aisée d'aminoalcools-1,5 à fonction amine secondaire où le N-substituant comporte un cycle aziridine greffé sur la chaîne par l'atome d'azote. La séquence adoptée pour leurs préparations est la suivante ; cyanoalkylation des aziridines secondaires, hydrogénation de ces produits cyanoalkylés, passage aux (aziridinyl-1)-n N-(tétrahydropyrannyl)-2) alkylamines qui par réduction catalytique conduisent aux composés désirés.

I. – ÉTUDE DE LA CYANOALKYLATION DES AZIRIDINES SECONDAIRES : OBTENTION DES PRODUITS 1

a) *A partir de l'acrylonitrile:* Bien que la condensation de certaines aziridines secondaires sur le nitrile acrylique soit connue [2] un complément d'étude a été néanmoins nécessaire.

---

* Ce travail fait partie de la thèse de Doctorat d'Etat de G. RICART (nº 355, Université de Lille, juillet 1976). Il a fait l'objet d'une note préliminaire [1] et d'un exposé aux Journées d'études sur la chimie des aziridines (Toulouse, septembre 1976).

Cette réaction, aisée pour l'éthylènimine, devient plus difficile quand le degré de substitution de l'hétérocycle azoté augmente et la catalyse devient indispensable. L'agent catalysant utilisé est l'éthylate de sodium ou encore le chlorure de triméthylbenzylammonium (TMBAC) en solution aqueuse (l'hydroxyde quaternaire (triton B) accélère autant la polymérisation du nitrile éthylénique que la cyanoéthylation et n'est donc jamais employé). L'introduction d'un net excès de nitrile dans les cas difficiles n'améliore en rien le rendement de la réaction.

La stéréochimie des aziridines intervient aussi sur la réactivité. Le triméthyl-2, 4, 4 aza-7 bicyclo (4.1.0) heptane *cis* s'additionne plus rapidement que le produit à géométrie *trans*. [3] De même la benzyl-2 méthyl-3-aziridine *érythro* réagit plus vite que l'isomère *thréo* ; cette différence de comportement entre aziridines isomères peut s'expliquer en se basant sur des considérations stériques : pour l'éthylènimine de configuration R*S*, l'addition doit se faire préférentiellement à partir de l'invertomère

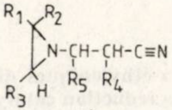
R1
R2
N-CH-CH-C≡N
R5
R4
R3
H

1

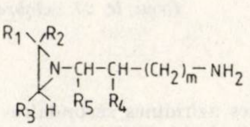
R1
R2
N-CH-CH-(CH2)m-NH2
R3
H
R5
R4

2

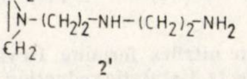
CH2
N-(CH2)2-NH-(CH2)2-NH2
CH2

2'

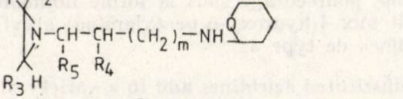
R1
R2
N-CH-CH-(CH2)m-NH
R5
R4
R3
H

3

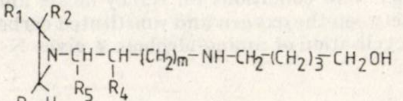
R1
R2
N-CH-CH-(CH2)m-NH-CH2-(CH2)3-CH2OH
R5
R4
R3
H

4

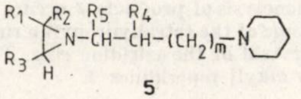
R1
R2
R5
R4
N-CH-CH-(CH2)m-N
R3
H

5

	a	b	c	d	e	f, g(*)	h(**)	i
R1	H	H	H	H	CH_3	$C_6H_5CH_2$		H
R2	H	H	H	H	CH_3	H	H	H
R3	H	H	H	C_2H_5	H	CH_3		H
R4	H	H	CH_3	H	H	H	H	H
R5	H	CH_3	H	H	H	H	H	H
m					1			0

(*)f : isomère *cis* ; g : isomère *trans*. (**) $R_1 + R_3 = -CH_2(CH_3)_2-CH_2-CH(CH_3)-$ (*cis* + *trans*) ayant le doublet libre de l'atome d'azote du côté le moins encombré, c'est-à-dire situé en *syn* par rapport aux hydrogènes aziridiniques ; il n'y a donc pas d'interactions stériques entre les substituants du cycle et le groupement cyanoéthyle ; par contre, dans l'aziridine de configuration R* R*, l'approche de la molécule d'acrylonitrile de l'un ou l'autre des invertomères est stériquement gênée (schéma 1). Cette différence de réactivité peut être mise à profit pour éliminer des traces d'aziridine *cis* contenues dans une benzyl-2-méthyl-3 aziridine *trans*.

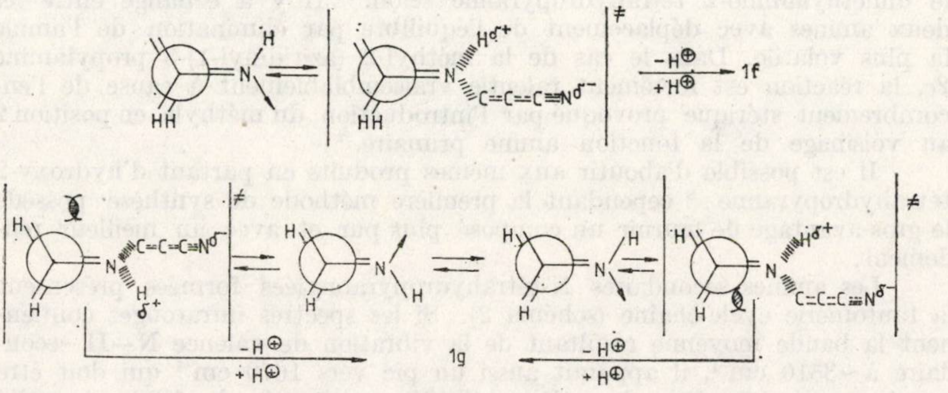

Schéma 1

b) *A partir du méthacrylonitrile:* Ce nitrile éthylénique est peu réactif ; sa mise en œuvre a nécessité une mise au point pour obtenir une transformation convenable. Le TMBAC ne catalyse plus suffisamment la réaction et se trouve avantageusement remplacé par l'éthoxyde de sodium ; la dilution du milieu avec la triéthylamine inhibe la réaction. Le taux de transformation du réactif en défaut est nettement plus élevé en travaillant avec un excès d'aziridine.

c) *A partir du nitrile crotonique:* sa réactivité avec l'éthylènimine se situe entre celles des deux nitriles éthyléniques précédemment étudiés : le TMBAC et l'éthylate de sodium catalysent la réaction.

II. — SYNTHÈSE DES (AZIRIDINYL-1)-3 PROPYLAMINES

La réduction catalytique en milieu basique des nitriles *1* conduit avec d'excellents rendements aux amines *2* (m = 1). La présence de base minérale (KOH) évite la formation d'amines secondaires symétriques alors que Bestian[4] en travaillant en milieu neutre en obtient 10 % (en moles). Il est à remarquer la très grande résistance à l'hydrogénolyse sur nickel de Raney des aziridines N-substituées comparée aux aziridines secondaires dont l'ouverture de cycle s'effectue à pression atmosphérique et temperature ambiante.[3] Il est aussi possible d'accéder aux amines *2* (m = 1) en réduisant les nitriles *1* par l'hydrure double d'aluminium et de lithium, mais le rendement est diminué de moitié.

La synthèse de l'(amino-2 éthyl)-1 aziridine *2i* est réalisée à partir de l'éthylènimine selon la méthode de Young[5] légèrement modifiée, mais il se forme une quantité non négligeable de trimère *2'*.

III.– N-TÉTRAHYDROPYRANNYLATION DES AMINES 2 : FORMATION DES COMPOSÉS 3

La méthode générale utilisée est la condensation des bases *2* avec le diméthylamino-2 tétrahydropyranne selon.[6] Il y a échange entre les deux amines avec déplacement de l'équilibre par élimination de l'amine la plus volatile. Dans le cas de la méthyl-2 (aziridinyl-1)-3 propylamine *2c*, la réaction est fortement ralentie vraisemblablement à cause de l'encombrement stérique provoqué par l'introduction du méthyle en position 2 au voisinage de la fonction amine primaire.[7]

Il est possible d'aboutir aux mêmes produits en partant d'hydroxy-2 tétrahydropyranne ;[8] cependant la première méthode de synthèse possède le gros avantage de fournir un composé plus pur et avec un meilleur rendement.

Les amines secondaires N-tétrahydropyrannylées formées présentent la tautomérie cycle-chaîne (schéma 2). Si les spectres infrarouges contiennent la bande moyenne résultant de la vibration de valence N—H secondaire à ~3310 cm^{-1}, il apparaît aussi un pic vers 1670 cm^{-1} qui doit être causé par la vibration de valence C=N : cette raie de faible intensité n'existe pas pour les amines tertiaires N-tétrahydropyrannylées et pour les aminoalcools *4* ; elle disparaît aussi par introduction d'un groupement méthyle en position 4 sur l'hétérocycle oxygéné : la substitution entraîne une forte stabilisation de la liaison C_α—O ce qui est conforme avec nos précédents résultats[9]. La RMN ^{1}H du produit sans solvant montre les absorptions de la forme α-aminotétrahydropyranne et celle de la forme tautomère iminoalcool (~8 %), ce qui prouve que l'échange mutuel entre les deux est très « lent » ; aux vitesses « rapides », la présence d'imine en faible proportion se traduirait par l'équivalence des déplacements chimiques des protons H^6 de l'hétérocycle oxygéné ;[9] le signal du proton « aldiminique » a une allure triplet (^{3}J ~ 4,25) et se situe à ~ 7,67 ppm du T.M.S. L'emploi simultané du tétrachlorure de carbone et de l'oxyde de deutérium permet la substitution isotopique NH/ND : il y a donc mise en équilibre rapide des protons et des deutérons. La publication récente[10] de travaux portant sur des systèmes analogues confirme l'existence de cet équilibre cycle-chaîne.

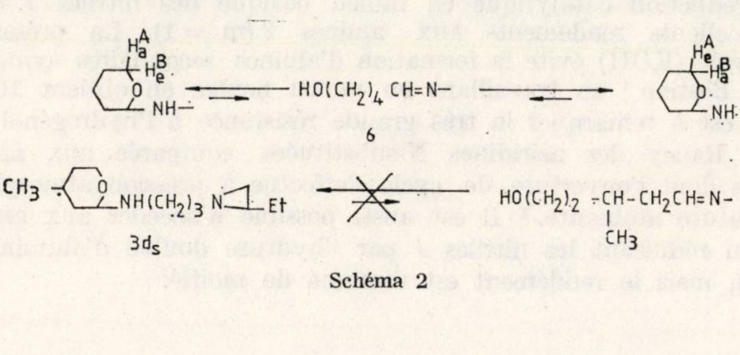

Schéma 2

L'identification de la conformation privilégiée du cycle tétrahydropyranne s'appuie sur l'examen des déplacements chimiques ; la valeur du paramètre δ mesuré sur le spectre de RMN du proton en position 2 du composé *3d* (~ 3,86), très proche de celle déterminée dans le dérivé C—4 méthylé *cis* à conformation bloquée $3d_s$ (~ 3,82) permet de conclure à une disposition préférentiellement axiale du proton anomère H^2 et donc équatoriale de NH.

La solvolyse des sels des α-aminoépoxydes complexes *3* est rapide ; toutefois elle est fortement ralentie par la méthylation du cycle tétrahydropyrannique ; il est donc probable que le mécanisme de décomposition des produits non substitués sur le cycle oxygéné procède surtout par l'intermédiaire d'un équilibre oxonium cyclique — immonium linéaire (schéma 3) sachant que la substitution renforce la liaison C_{-2}—O. On observe le même phénomène avec les amino-2 tétrahydropyrannes à fonction amine tertiaire.[11]

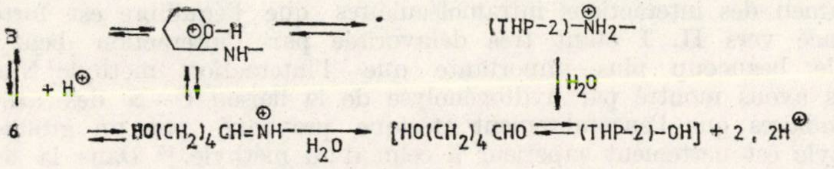

Schéma 3

IV. — RÉDUCTION DES AMINO-2 TÉTRAHYDRPYRANNES 3 EN AMINOALCOOLS 4

Elle s'effectue sur nickel de Raney en milieu alcoolique légèrement basique selon la technique de Glacet et coll.[12, 8a, 13] L'hydrogénolyse de la liaison $C_{-\alpha}$—N est peu importante, mais existe (mise en évidence d'une faible quantité d'amine *2*). La réduction par l'hydrure double d'aluminium et de lithium conduit au même échantillon d'alcool aminé mais le rendement est faible (~33 %).

Ces aminoalcools sont trop fragiles pour être déshydratés sur alumine en pipéridines et il nous a paru préférable d'employer la cyclisation de Gabriel des amines ω-halogénées : la fonction alcool primaire est facilement estérifiée par le chlorure de thionyle et la réaction d'Hofmann intramoléculaire ne présente aucune difficulté lorsque l'halogène est primaire. Dans le cas des aminoalcools simples, les rendements en pipéridines sont excellents ;[14] cependant, pour les composés *4*, la fragilité relative du cycle aziridinique dans un tel milieu réactionnel diminue les rendements en produits cyclisés *5*.

De façon générale, dans tous les composés décrits, l'inversion de l'atome d'azote engagé dans le cycle aziridine est suffisamment lente à 37° pour permettre la détection en RMN des deux invertomères. Pour les aziridines non substituées ou substituées symétriquement de part et d'autre du plan du cycle, l'inversion équilibre des invertomères de même énergie, énantiomères ou identiques entre eux et donc existent en pourcentages identiques (séries a, b, c et e). La position *syn* ou *anti* par rapport au doublet de l'azote différencie les déplacements chimiques ; le signal à champ fort est attribué au(x) proton(s) aziridiniques(s) *anti*, le signal à champ faible au(x) proton(s) *syn*.[15]

Pour les aziridines substituées différemment de part et d'autre du plan du cycle, les invertomères sont diastéréoisomères entre eux et existent en pourcentage différent. Dans la série d, des deux configurations diastéréoisomères, inverses sur l'azote (schéma 4), il est évident que la première I est défavorisée par l'interaction stérique entre les groupements quasi éclipsés N-alkyle et éthyle. Dans la série f, seule la configuration II est présente ; il y correspond des protons aziridiniques qui résonnent à champ fort ; les deux interactions quasi éclipsées du substituant à l'azote avec les substituants des carbones (eux nécessairement *cis*) rendent non viable l'invertomère I. Pour la série g, une seule configuration semble être peuplée ; sur le spectre de *1g*, nous observons deux massifs distincts pour les protons du cycle, un seul doublet pour la résonance du méthylène benzylique et un seul doublet pour les protons méthyliques plus blindés que ceux de l'isomère *1f* ; nous pouvons en conclure, ce qui est en accord avec l'examen des interactions intramoléculaires que l'équilibre est fortement déplacé vers II, I étant très défavorisée par l'interaction benzyle/N-alkyle beaucoup plus importante que l'interaction méthyle/N-alkyle. Nous avons montré par hydrogénolyse de la liaison C—N des aziridines secondaires que l'encombrement stérique provoqué par un groupement benzyle est nettement supérieur à celui d'un méthyle.[16] Dans la série h, la configuration dans laquelle le substituant N-alkyle est *cis* par rapport aux hydrogènes liés aux carbones tête de pont est figée, elle minimise les interactions stériques.

Série	α	β	γ	δ
d	C_2H_5	H	H	H
f	$C_6H_5CH_2$	CH_3	H	H
g	$C_6H_5CH_2$	H	CH_3	H
h	$-CH_2-C(CH_3)_2-CH_2-CH(CH_3)-$		H	H

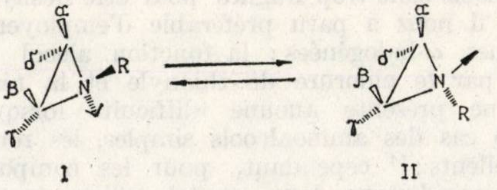

Schéma 4

PARTIE EXPÉRIMENTALE

Certains produits de réaction sont analysés par chromatographie en phase vapeur sur un appareil Perkin-Elmer type F20 comportant une colonne Carbowax 20M (15 %) — potasse (5 %) d'une longueur de 2 mètres. Les spectres I.R. ont été enregistrés sur un spectrophotomètre Perkin-ELMER modèle 21 en plaçant une fine pellicule d'échantillon liquide entre deux plaques en chlorure de sodium. La RMN ^1H est faite avec un appareil Varian A60A ; les échantillons sont dissous dans le tétrachlorure de carbone : la référence interne utilisée est le TMS et les déplacements chimiques exprimés en δ ; dans la description des spectres, les lettres s, d, t, et m signifient respectivement : singulet, doublet, triplet et multiplet.

Les dosages d'azote basique par l'acide perchlorique en milieu acétique ont été faits pour tous les produits aminés et leurs picrates (en milieu acide acétique-acétone en cas d'insolubilité prononcée). Les points de fusion instantanés ou de décomposition sont déterminés au bloc Maquenne.

L'éthylénimine, l'éthyl-2 aziridine, la diméthyl-2,2 aziridine et la méthyl-2 benzyl-3 aziridine *trans* sont préparés à partir des aminoalcools correspondants (éthanolamine, amino-2 butanol, méthyl-2 amino-2 propanol, homophénylalaninol) avec des rendements respectifs de 40, 90, 75 et 85 % selon la méthode WENKER. [17] La réduction par l'hydrure double d'aluminium et de lithium des oximes de cétones α-éthyléniques nous a permis d'accéder aux autres aziridines secondaires.

A—(Aziridinyl-1)—3 propionitriles 1 (tableaux 1 et 2)

A l'acrylonitrile en excès on ajoute l'aziridine plus ou moins rapidement selon le caractère exothermique de la réaction. L'échauffement observé, important avec l'éthylénimine, faible pour l'éthyl-2 aziridine, devient nul avec les homologues supérieurs ; il est alors nécessaire de catalyser et de réchauffer plus ou moins longtemps selon les cas. Les produits de cyanoéthylation sont isolés par distillation (tableau 3). Les spectres I.R. présentent vers 2250 $\mathrm{cm^{-1}}$ la raie de vibration de valence $\mathrm{C{\equiv}N}$ des alkylnitriles.

TABLEAU 1

Réaction de cyanoéthylation

Aziridines utilisées	mole de nitrile / mole d'aziridine	T° de réaction	Temps de réaction en h.	Catalyseur(*)	Rendement par rapport à l'aziridine (%)
Ethylénimine	1	35	12	sans	97 (a)
Ethyl-2 aziridine	1,5	80	6	avec	95
Diméthyl-2,2 aziridine	1,5	95	18	avec	91 (b)
Méthyl-2-benzyl-3 aziridine *cis*	1,5	90	5	avec	98
Méthyl-2 benzyl-3 aziridine *trans*	2	90	24	avec	100
Triméthyl-2,4,4 aza-7 bicyclo [4.1.0] heptanes *cis* et *trans*	2	95	25	avec	96

(*) On utilise 2.10^{-3} mole de $\mathrm{C_6H_5CH_2\overset{\oplus}{N}(CH_3)_3Cl^{\ominus}}$ (TMBAC) par mole d'acrylonitrile en solution dans 1 $\mathrm{cm^3}$ d'eau.

(a) litt.: 90%[4]

(b) litt.: 66%[18], 63%[19].

RMN : *1a* : 2,48, t, $\mathrm{C}H_2$ exocycliques ; 1,73 et 1,20 : m, protons aziridiniques. *1b* : 2,50, d (5,5), $\mathrm{C}H_2\mathrm{CN}$; ~1,50 : $\mathrm{C}H$; 1,70 et 1,20, protons du cycle ; 1,18, $\mathrm{C}H_3$. *1c* : 2,86, $\mathrm{C}H\mathrm{CN}$; 2,36, $\mathrm{C}H_2\mathrm{N}$; 1,74 et 1,20 : $\mathrm{C}H_2$ du cycle ; 1,33, d (~7) $\mathrm{C}H_3$. *1e* : 2,25 à 2,85, m, $\mathrm{C}H_2$ exocycliques ; 1,64, s (W1/2~3,5) $\mathrm{C}H$ cyclique ; 1,20, s, $\mathrm{C}H_3$; 1,12, s, $\mathrm{C}H_3$ et $\mathrm{C}H$ cyclique. *1f* : 7,22, $\mathrm{C_6}H_5$; 2,62, d, $\mathrm{C}H_2\mathrm{C_6H_5}$; 1,90 à 2,48, m, $\mathrm{CH_2}$ exocycliques ; ~1,20 à 1,60, m, CH aziridiniques ; 1,19, d, (4,5) $\mathrm{C}H_3$. *1g* : 7,22, $\mathrm{C_6H_5}$; 2,63, $\mathrm{C}H_2\mathrm{Ph}$, d (5,5) ; 2,1 à 2,6, $\mathrm{CH_2}$ exocycliques ; ~1,20

TABLEAU 2

Résultats des expériences avec le méthacrylonitrile et le crotonitrile

	Ethylénimine (en moles)	Catalyseur	T° et temps de réaction	Rendement %	
				par rapport au nitrile disparu	par rapport à l'aziridine disparue
Méthacrylonitrile 0,45 mole (a)	1	EtONa 1M 0,4 cm³	90 18h sous 100 kg $d'N_2$	90 résines : 2,60 g ; on récupère 17 % du nitrile de départ et 58 % de l'aziridine de départ	76
Crotonitrile 1,1 mole (b)	1	EtONa 1M 0,8cm³	80 20h	87 résines : 2,7 g ; on récupère 25% du nitrile et 22 % d'aziridine	91
	1	TMBAC 0,3g	80 60h	83 résines : 5g ; on récupère 11 % du nitrile et 3,5 % d'aziridine	84

	rapport molaire aziridine/nitrile	Rdt %
(a)	3,25	73 [20]
	1,23	41 [21]
(b)	3,1	83 [20]
	1,16	49 [21]

TABLEAU 3

Constantes physiques des nitriles de type *1*

	Eb°/mm	n_D	d_4	F picrate (°C) (*)
1a	litt[4, 23, 24]	$1,4458^{20}$	$0,955^{22}$	108
1b	litt[20]		$0,924^{20}$	144
1c	litt [20]		$0,923^{22}$	144
1d	66/2	$1,4418^{20}$	$0,903^{22}$	132
1e	91/15	$1,4440^{22}$		
1f	115/0,2	$1,5188^{20}$	$1,002^{20}$	
1g	123/0,4	$1,5208^{20}$ $1,5188^{23}$	$0,999^{23}$	
1h	91/0,8	$1,4675^{23}$	$0,927^{23}$	150

(*) Solvant : benzène ; point de décomposition pris au bloc Maquenne.

à 1,60 et 1,60 à 2 : CH aziridiniques ; 1,15, d (5,5), CH_3. *1h* : 2,10 à 2,67, m, CH_2 exocycliques ; CH_3 ax en position 4, 0,81, s (*cis*) et 0,94 (*trans*) ; CH_3 éq. en 4, 0,84, s, (*cis*) et 0,83 (*trans*) ; CH_3 pseudo-eq. en 2, 1, d (6) (*cis*) et 1,07, d (7) (*trans*).

B—Synthèse des amines 2(m=1)

Le nitrile *1* (1 mole) en solution dans 140 cm^3 de potasse éthanolique 0,95N est hydrogéné à température ambiante et sous pression (110 atm.) en présence de 14 g de catalyseur; dès que la fixation d'hydrogène a cessé, on neutralise 80 % de la potasse par addition d'HCl (concentré, filtre le NiR et le chlorure de potassium formé ; le solvant est ensuite chassé et les aziridinyl-1)-3 propylamines pures sont obtenues par distillation fractionnée avec un rendement de 95 % (tableau 4). Les spectres infra-rouge de tous ces produits présentent les bandes caractéristiques de la fonction amine primaire: 3360—3390, 3270—3300, 1590—1600 cm^{-1}.

— Synthèse de l'amine *2i* :

20 g d'éthylénimine sont portés à 100° sous azote U (30kg à 20°) en présence de 0,56 g de potassium en morceaux et agités pendant 20 heures.

Rendement en dimère : 77 % pour un coefficient de transformation de 66 %.

Rendement en trimère : 14 %.

— Etude du trimère : (aziridinyl-1)-1 diaza-3,6 hexane *2'*.

$Eb_{10} = 96°$ (litt. Eb = 220—235°[22]) ; $n_D^{20} = 1{,}4771$, $d_4^{23} = 0{,}943$.

Dosage : 1) par $HClO_4/CH_3CO_2H$: les trois azotes sont salifiés.

TABLEAU 4

Caractéristiques physiques des amines de type *2*

	Eb °/mm	n_D	d_4	F picrate (*)
2a	litt[25]		$0{,}879^{22}$	208
2b	80/34	$1{,}4543^{20}$	$0{,}885^{20}$	222
2c	65/20	$1{,}4538^{22}$	$0{,}883^{22}$	194
2d	68/18	$1{,}4488^{22}$	$0{,}884^{22}$	174—175
2e	litt[18, 19]			
2f	113/1	$1{,}5202^{20}$	$0{,}964^{20}$	154
2g	109/1	$1{,}5258^{20}$	$0{,}972^{22}$	135
2h	75/07	$1{,}4718^{22}$	$0{,}897^{22}$	211
2i	litt[4,26]			206

(*) Solvant: méthanol ou éthanol; deux moles d'acide par mole de base *2*.

N % *calc.* : 32,5 ; *tr.* : 31,5.

2) Par HCl/ isopropanol en présence d'aldéhyde salicylique : la fonction amine primaire étant transformée en fonction imine, seuls sont dosables les azotes du cycle aziridine et de l'amine secondaire.
N basique % : *calc.* : 21,68 ; *tr.* : 22,15.

3) Par $HClO_4$ en milieu CH_3COOH/Ac_2O : dans ces conditions nous n'avons plus d'azotes basiques.

Picrate : $C_{24}H_{24}N_{12}O_{21}$, M : 816,54.

F = 164 — 166° (du méthanol).

N % : *calc.* : 5,146 ; *tr.* : 5,086.

IR : 3290, 3060, 2976, 2907, 2825, 1603, 1453, 1350, 1298, 1269, 1157, 1130, 1077, 1033, 1014, 933, 925 à 770 (bandes), 760, 725.

RMN : 1,01 et 1,60 : aspect triplet, CH_2 du cycle aziridine ; 1,40 : s, NH_2 et NH ; 2,20 : t (J = 5,5 Hz), CH_2N] ; 2,38 à 2,83 : massif complexe, CH_2-N.

C—Synthèse des [(tétrahydropyrannyl-2 amino) alkyl]-1 aziridines *3* (tableau 5)

Les amines *2* sont ajoutées au diméthylamino-2 tétrahydropyranne en léger excès (5 %) ; à la température de 95°, la réaction dure deux à trois heures (rendement 94 %). Pour l'amine *2c*, où l'encombrement à l'azote est plus important, le taux de transformation est de 80 % après six heures de contact (rendement : 95 % par rapport à l'amine transformée).

TABLEAU 5

Caractéristiques physiques des amino-2 tétrahydropyrannes *3*

	Eb 0/mm	n_D	d_4
3a	79/0,4	$1{,}4772^{20}$	$0{,}977^{23}$
3b	93/0,6	$1{,}4751^{20}$	$0{,}961^{23}$
3c	83/0,4	$1{,}4742^{21}$	$0{,}961^{21}$
3d	94/0,2	$1{,}4688^{23}$	$0{,}937^{23}$
3e	95/0,4	$1{,}4715^{20}$	$0{,}944^{23}$
3f	167/0,6	$1{,}5188^{20}$	$1{,}000^{20}$
3g		$1{,}5222^{22}$	$1{,}007^{22}$
3h	122/0,4	$1{,}4818^{23}$	$0{,}955^{23}$
3i	84/2	$1{,}4755^{22}$	$0{,}987^{21}$

— Synthèse de *3d*$_s$:

Rendement : ~98 % en portant à 100° pendant 5 heures un mélange équimoléculaire de méthyl-4 diméthylamino-2 tétrahydropyranne (géométrie *cis* ~ 95 %) et d'amine *2d*.

$Eb_{0,11} = 92°$ $n_D^{23} = 1{,}4642$
N% *calc.* : 12,37 N % *tr.* : 12,36
IR : 3315 cm^{-1} : NH secondaire (vibration de valence).
3040 cm^{-1} : C—H du cycle aziridine.

RMN : (sans solvant) δ : H_a^6 3,33 ; H_a^6 ~ 3,93 ; H^2 ~ 3,82 (isomère *cis*, intensité ~ 0,8) et 4,33 (t, ε^3J ~ 7,5, isomère *trans*, intensité 0,2) ; ~pas de trace de proton « aldiminique » dans les limites de performance de l'appareil.

— Décomposition par l'acide picrique en milieu hydroalcoolique : A 0,225 g (10^{-3} mole) de base *3*d$_s$ est ajoutée 0,46 g (2. 10^{-3} mole) d'acide ; la précipitation est lente et après 24 heures nous récupérons 34 % de bipicrate identifié comme le sel de l'amine *2d* (F ~ 174°).

D — Synthèse des aminoalcools *4* (tableau 6)

Les produits *3* ont été hydrogénés en solution dans un ou deux volumes d'alcool en milieu 1N en potasse : l'hydrogénation en présence de nickel Raney est facile à 25° à la pression atmosphérique. Après fixation de l'hydrogène on ajoute prudemment la quantité d'acide chlor-

TABLEAU 6

Caractéristiques physiques des aminoalcools *4*

	Eb 0/mm	n_D^{20}	d_4	F picrate (éthanol)
4a	126/0,1	1,4785	$0{,}954^{22}$	152
4b	135/0,6	1,4770	$0{,}944^{23}$	
4c	122/0,2	$1{,}4750^{22}$	$0{,}942^{22}$	
4d	126/0,2	$1{,}4710^{23}$	$0{,}926^{23}$	109(*)
4e	138/0,6	1,4742	$0{,}930^{25}$	100
4f	174/0,1	1,5252	$0{,}990^{22}$	
4g		1,5210	$0{,}994^{22}$	
4h	141/0,1	$1{,}4838^{23}$	$0{,}940^{23}$	175
4i	113/0,6	$1{,}4762^{23}$	$0{,}961^{23}$	140

(*) dinitro-2,4 phénate ; solvant : isopropanol

TABLEAU 7

Caractéristiques physiques des pipéridines de type *5*

	Eb. °C/mm	n_D^{20}	d_4^{20}	F. picrate (CH_3OH ou C_2H_5OH)°C
5a	70/2	1,4728		147
5c	74/2,5	1,4692	$0,891^{23}$	100
5d	88/2	1,4668	0,884	153
5e	81/1,5	1,4672	0,884	175
5g	125/0,5	$1,5162^{23}$	$0,958^{23}$	149
5h	110/0,5	1,4815	0,823	190

TABLEAU 8

Déplacement chimique δ_{1_H} de quelques composés

	Série	CH_2N	$CH_2N\triangle$	CH du cycle azoté		CH_3
2	a	2,70	2,17	0,97	1,57	
(*)*3*				0,96	1,54	
(**)*4*			2,21	1,04	1,64	
5				0,93	1,57	
2	b	2,72		1,07	1,62	1,03
3				1	1,58	1,10
4				1,08	1,60	1,08
2	c	2,60	2,13	1	1,60	0,91, d, $^3J = 6$
3				1	1,60	0,95
4				1,01	1,62	0,88, d, $^3J = 6$
3	d					0,97
2	e	2,68	2,30	0,90	1,50	1,07 et 1,16
3				0,90	1,47	1,09 et 1,17
4				0,97		1,10 et 1,20
5				0,90		1,07 et 1,17
2	f(***)	2,62	2,20	1,10 – 1,65		1,20 ; d, $^3J = 4,5$
3						1,22
2	g(***)	-		1,10 – 1,90		1,12
3						1,17
4						1,20, d, $^3J = 5,5$
5						1,14
2	i	2,73	2,17	1,03	1,60	
3				1	1,60	

(*) composés *3*: δ: ~ 3,85, H_e^6, d, $^2J = |12|$; ~ 3,32, H_a^6 ; ~ 3,83, H^2

(**) composés *4*: δ: ~ 3,42, CH_2OH, t. (***) ~ 7,20: C_6H_5.

hydrique concentré nécessaire à la neutralisation de 80 % de la potasse introduite ; après le traitement habituel, on distille l'aminoalcool que l'on obtient avec un rendement de 93 %. Le spectre infrarouge présente la bande OH intense à 3280 cm^{-1}.

— Pour la cyclisation des aminoalcools *4* en pipéridines *5*, les meilleurs résultats sont obtenus pour :

— Un cycle aziridinique C-substitué au moins une fois.

— Une température d'environ —20° lors de la formation du sel d'amine ω-halogénée.

— L'emploi d'un net excès de chlorure de thionyle (trois fois la théorie), ce dernier servant à la fois comme réactif et comme solvant.

Mode opératoire :

L'aminoalcool *4* (0,03 mole), pur ou en solution concentrée dans l'éther s'il est très visqueux, est ajouté goutte à goutte au chlorure de thionyle refroidi à —20° ; l'addition terminée, on laisse revenir à l'ambiante ; on introduit 20 cm^3 de benzène, 25 cm^3 de toluène et abandonne pendant une nuit. La distillation (50°) des solvants sous vide partiel élimine le SO_2 et l'excès de $SOCl_2$; du benzène (70 cm^3) et de la lessive de soude (10 g de NaOH dans 40 g d'eau) sont ajoutés, on porte à 65° pendant 24 heures. Les rendements en produits cyclisés au départ de *4a, 4d, 4e, 4g, 4h, 4i* sont respectivement de 17, 73, 68, 70, 77 et 8 %. Les constantes physiques des pipéridines *5* sont rassemblées dans le tableau 7.

Dans le tableau 8, nous avons répertoriés les données de RMN ^{1}H de la plupart des composés préparés.

BIBLIOGRAPHIE

[1] G. Ricart, D. Couturier et C. Glacet, *Compt. rend., C*, **280**, 953 (1975).

[2] O. C. Dermer et G. E. Ham, "Ethylenimine and Other Aziridines", Academic Press, New York, 1969, p. 139.

[3] G. Ricart, *Bull. Soc. Chim. France*, **1974**, 2607 et références citées.

[4] H. Bestian, *Liebigs Ann. Chem.*, **566**, 210 (1950).

[5] J. D. Young, Dow Chemical Co., U.S. *3, 502, 654*, (1970) ; *Chem Abstr*, **73**, 14658 (1970).

[6] C. Glacet et D. Veron, *Bull. Soc. Chim. France*, **1965**, 1789.

[7] C. Glacet et D. Veron, *Compt. rend., C*, **248**, 1347 (1959).

[8] C. Glacet, *Bull. Soc. chim. France*, **1954**, 575. ^{b}C. Glacet et F. Blanchard-Bielli, *Compt. rend.*, **247**, 1467 (1958).

[9] G. Ricart, C. Glacet et D. Couturier, *Compt. rend.*, **284**, 319 (1977).

[10] S. L. Zhdanov et A. A. Potekhin, *Khim. Geterotsikl. Soedin.*, **1977**, 417 ; *Chem. Abstr.*, **87**, 39222 (1977).

[11] G. Ricart, D. Couturier et C. Glacet, résultats non publiés.

[12] C. Glacet, *Bull. Soc. Chim. France*, **1953**, 1056.

[13] G. Glacet et A. Gaumeton, *Bull. Soc. chim. France*, **1955**, 224.

[14] C. Glacet et G. Becue, *Compt. rend.*, **264**, 103 (1967).

[15a] P. Baret, H. Handel et J. L. Pierre, *Organic Magnetic Resonance*, **1974**, 35 et références citées. ^{b}H. Saitô, K. Nukada, T. Kobayashi et K. Morita, *J. Amer. Chem. Soc.*, **89**, 6605 (1967).

[16] G. Ricart, *Bull. Soc. chim. France*, **1974**, 615.

[17] H. Wenker, *J. Amer. Chem. Soc.*, **57**, 2328 (1935).

[18] D. S. Tarbell et D. K. Fukushima, *J. Amer. Chem. Soc.*, **68**, 2499 (1946).

[19] J. R. Piper, C. R. String Fellow, R. D. Elliot, J. P. Johnston, *J. Med. Chem.*, **12**, 236 (1969).

[20] D. Rosenthal, G. Brandrup, K. H. Davis et M. E. Wall, *J. Org. Chem.*, **30**, 3689 (1965).

[21] L. H. Chance, D. J. Daigle, G. L. Drake, *J. Chem. and Engineering Data*, **13**, 442 (1968).

[22] A. L. Wilson, U. S. *2, 553, 696,* (1951); *Chem. Abstr.*, **45**, 7821 (1951).

[23] O. Yoshiki, A. Toshio et K. Saburo, *Technology Reports of the Osaka University*, **17**, 541 (1967).

[24] H. L. Spell, *Analyt. Chem.*, **39**, 185 (1967).

[25] O. L. Salerni et R. N. Clarck, *J. Med. Chem.*, **9**, 778 (1966).

[26] G. D. Jones, A. Lanysjoen, M. M. C. Newmann et Y. Zomlefer, *J. Org. Chem.*, **9**, 125 (1944).

Revue Roumaine de Chimie, **25**, *3*, 393—395 (1980)

FAVORSKII REACTIONS OF α-HALO-α, β-UNSATURATED MONOCYCLIC KETONES

IBRAHIM E. KHAWAD and GEORGE M. ISKANDER,
Department of Chemistry, University of Khartoum, Sudan,

Received January 19, 1978

α, β-Unsaturated cyclenones undergo Favorskii reactions to give α-hydroxy- and α-methoxy-esters (III) and dioxan derivatives (VI), (VII) presumably arising from the corresponding epoxides e.g. (V) upon treatment with acid.

The reactions of monocyclic bromo- and chloro-ketones of the type (I) give with sodium methoxide in methanol the ring contracted saturated esters (III) — the Favorskii products, and dioxan derivatives (VI), (VII) which are dimeric forms of the unisolated epoxides (V) and ketals — the main products of competing side reactions. [1] From (II) only the unsaturated ketal, 1,1-dimethoxy-2-hydroxycyclohex-3-ene, was isolated.

As established earlier [2] for analogous bicyclic systems, the mechanism requires deconjugation of the ketone (I) to the β, γ-isomer followed by proton abstraction from the α-carbon atom, formation of the cyclopropanone intermediate [3] and its eventual cleavage to the methoxy ester (III). Unsaturated esters (IV) may be formed *in situ* as intermediates, but have never been isolated (Scheme I).

Nucleophilic attack at the CO group led to epoxides, which gave hydroxy ketals[1,3] by further reaction with alcohol. With traces of acid they readily dimerised to dioxan derivatives. Analogous findings were shown in the aliphatic [4] and alicyclic [5] series.

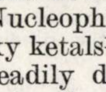

(I)

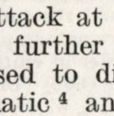

(II)

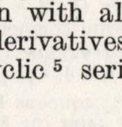

(III)

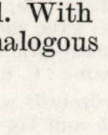

(IV)

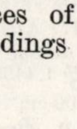

(V)

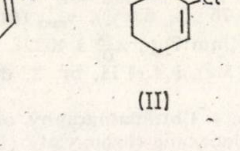

(VI)

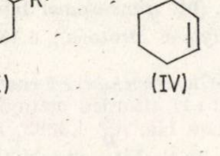

(VII)

Scheme I

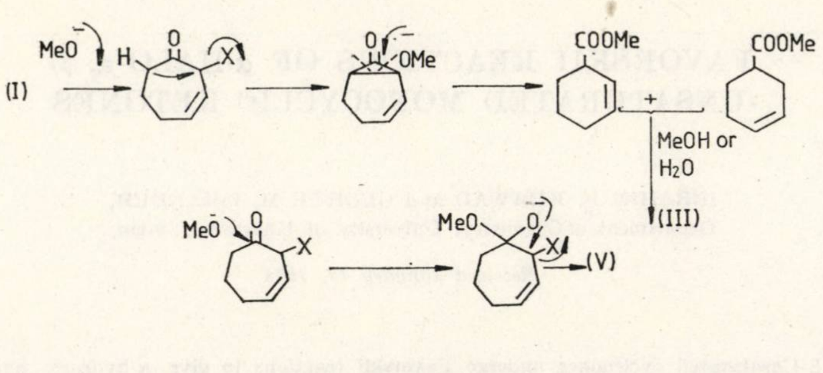

EXPERIMENTAL

I.R. and u.v. spectra were done with SP 1000 and 800 spectrophotometers. 200 Hz p.m.r. spectra were done at Harwell P.C.M.U., Oxfordshire, England. Unless otherwise stated, for chromatography the solvent system chloroform (A and petroleum ether (60—80° ; B) was used.

Preparation of the α-Halo-α, β-Unsaturated Cyclenones (I). These were prepared by the action of boiling aqueous alcoholic silver fluoroborate [5] on the corresponding dihalocarbene adducts of 1-ethoxycycloalkenes [5,6] in 60—70% yield. 6,6-Dichloro-1-ethoxybicyclo [3.1.0] hexane rearranges directly during aqueous work-up to the chloroketone (II), m.p. 71° (lit. [7] m.p. 71°), ν_{max}(Nujol) 1690 and 1630 cm $^{-1}$.

Reactions of the α-Halocyclenones with Sodium Methoxide in Methanol. To a cold solution of sodium methoxide (from 4.0 g of sodium in dry methanol, 80 ml), the unsaturated ketone (0.1 mol) in methanol (80 ml) was added dropwise with stirring and ice-cooling. The reaction mixture was left to stand in ice bath for 1 h, then at room temperature for 24 h. Methanol was evaporated *in vacuo* to a small bulk, and water (200 ml) was added. The product was extracted with methylene chloride (3X *ca.* 75 ml) which was washed with water, and dried ($MgSO_4$). Removal of the solvent afforded a brown mobile liquid, which was processed suitably. The undermentioned unsaturated ketones were reacted and the products isolated are shown. *Reaction of 2-Bromocyclohept-2-enone* (I ; R = Br) — Chromatography of the product (alumina H ; A/B, 1 : I) gave the following compounds in order of elution :

methyl 2-methoxycyclohexanecarboxylate (III ; R^1 = OMe) (14%), b.p. 56—60°/0.2 mm Hg, n_D^{25} 1.4455, (Found : C, 62.85 ; H, 9.4. C_9H_{16} requires : C, 62.8 ; H, 9.3%), ν_{max} (film) 1720, and 1100 cm^{-1}. Hydrolysis with 10% aqueous KOH afforded 2-methoxycyclohexanecarboxylic acid b.p. 50—1°/0.5 mm Hg ; n_D^{25} 1.4400 (lit. [8] b.p. 99 — 101°/17 mm Hg ; n_D^{25} 1.4442).

methyl 2-hydroxycyclohexanecarboxylate (III ; R^1 = OH) (24%), b.p. 61°/ 0.5 mm. Hg, n_D^{25} 1.4673, (Found : C, 60.4 ; H, 9.0, Calc. for $C_8H_{14}O$ C, 60.75 ; H, 8.9%), ν_{max} (film) 3500 (OH), 1710 and 1100 cm^{-1}. (lit. *trans*-isomer b.p. 116 — 17°/14 mm Hg ; n_D^{25} 1.4622), τ (CCl_4) 7.0 — 8.48 (10 H, m, methylene protons), 6,15 (3 H, s, ester Me), 5.4 (1 H, br. 3, disappeared on D_2O addition).

Reaction of 2-Chlorocyclohept-2-enone (I ; R = Cl). — Chromatography of the product (silica M.F.C. ; A/B 1 : 1) afforded methyl 2-hydroxycyclohexane-carboxylate (III ; R = OH) (14%), b.p. 40°/0.1 mm Hg, n_D^{25} 1.4893, Found : C, 63.4 ; H, 8.1. Calc. for $C_8H_{14}OC$, 60.75 ; H, 8.9%), ν_{max}(film) 3500, 1710 and 1100 cm^{-1}. It seems that this compound is an isomeric *cis-trans*-mixture as evidenced by its p.m.r. spectrum ; they are in the ratio of 1.7 : 1 respectively. τ ($CDCl_3$) 7.03 — 8.8 (10 H, m, methylene protons), 6.7 and 6.6 (2 H, 2 s, two OMe), 5.76 (1H, s, OH, *cis*-isomer), 5.70 (1H, s, OH *trans-isomer*).

The epoxide (V) was not eluted off from the column using various solvents as it seemed to have adhered irreversibly. In another experiment, the product mixture was treated with two drops of concentrated hydrochloric acid and methanol (2 ml) and afforded the lactolide *cis, cis-1,9-dimethoxy-8,16-dioxatricyclo* [$9.5 \cdot 0.0^{9,15}$] *hexadec-10-ene* (VI), needles from methanol, m.p. 228°, (Found : C, 68.5 ; H, 8.6. $C_{16}H_{24}O_4$ requires C, 68.6 ; H, 8.6 %), ν_{max}(Nujol) 1603, 1115 and 1029 cm^{-1}. τ ($CDCl_3$) 4.15 (2 H, oct. H^3 and H^{11} split by H^2 and H^{10}, $J_{3,2} = J_{11,10}$ 5 Hz), 4.55 (2 H, 2 d, H^2 and H^{10}), 5.6 (2 H, s, protons at C_7 and C_{15}), 6.80 (6 H, s, two OMe), 7.64 – 8.7 (12 H, m, methylene protons).

Reaction of 2-Chlorocyclohex-2-enone (II). — The product was chromatographed (silica M.F.C., EtOAc/$CHCl_3$; 3 : 17) to give as the only product 1,1-dimethoxy-2-hydroxycyclohex-3-ene (31 %) b.p. 53 – 4°/0.5 mm Hg, n_D^{25} 1.4775, (Found : C, 60.5 ; H, 8.9. $C_8H_7O_3$ requires C, 60.7 ; H, 8.9 %), ν_{max} (film) 3420, 1610, 1050 and 1100 cm^{-1}, τ ($CDCl_3$) 7–8.35 (5 H, m, methylene protons at C_5 and C_6), 7.5 (1 H, m, OH shielded by neighbouring OCH_3, disappeared on D_2O addition), 6.0 (1 H, m, H^2 *tert.* proton at C_2 containing OH), 4.28 1 H, d, proton at C_3, $J_{3,4}$ 7 Hz), 4.24 (1 H, d, proton at C_4, $J_{4,3}$ 7 Hz). The hydroxy ketal when treated with aqueous acetic acid hydrolysed to 2-hydroxycyclohex-3-enone, b.p. 42 – 3°/0.2 mm Hg, n_D^{25} 1.5190, ν_{max} (film) 3370, 1710 and 1600 cm^{-1}(lit.[9] b.p. 96 – 7°/25 mm Hg ; n_D^{25} 1.4995), τ($CDCl_3$) 8.0 – 9.0 (1 H, m, proton at C_5), 7.42 (1 H, m, OH, disappeared on D_2O addition), 6.0 – 6.5 (6 H, m, olefinic and methylene protons at C_4, C_5 and C_6). This compound is probably tautomeric with cyclohexane-1,2-dione giving an oxime m.p. 188° (lit.[9] m.p. 187–88°).

Reaction of 2-Bromocyclohexanone. — The product mixture, when treated with methanol and a few drops of concentrated hydrochloric acid, gave the solid lactolide *cis*, *cis*-1,8-dimethoxy-2,9-dioxa [$8.4 \cdot 0.0^{1,10}$]tetradecane (VII) (25 %), m.p. 162 – 3° (lit. [10]m.p. 165°), τ ($CDCl_3$) 7.9 – 8.75 (16 H, m, methylene protons), 6.8 (6 H, s, two OMe), 6.25 (2 H, q, protons at C_3 and C_{10} ; both split by non-equivalent vicinal methylene protons at C_4 and C_{11} respectively, $J_{3,eq.vic.} = J_{10,eq.vic.} = J_{10,ax.vic.} = 9Hz$). The methanolic filtrate upon evaporation and aqueous working up afforded 2-hydroxycyclohexanone identified from its 2,4-dinitrophenylhydrazone and semicarbazone. [11]

REFERENCES

[1] (a) R. B. Loftfield and L. Schaad, *J. Amer. Chem. Soc.*, **76**, 351 (1954).
(b) C. L. Stevens, W. Malik and P. Pratt, *ibid*, **72**, 4758 (1950).
(c) A. M. Ward, *J. Chem. Soc.*, **1929**, 1541.

[2] G. M. Iskander and I. E. Khawad, unpublished work.

[3] R. B. Loftfield, *J. Amer. Chem. Soc.*, **72**, 632 (1950) ; **73**, 4707 (1951).

[4] J. I. Temnikova and E. N. Kropacheva, *J. Gen. Chem. USSR.*, **19**, 1917 (1949).

[5] A. K. Yagoub and G. M. Iskander, *J. Chem. Soc.*, **1977**, 697.

[6] (a) A. Serini and H. Köster, *Ber. dtsch. Chem. Ges.*, **71**, 1766 (1938).
(b) H. H. Inhoffen, G. Köling, G. Koch and I. Nebel, *Chem. Ber.*, **84**, 361 (1951).

[7] M. Ohono, *Tetrahedron Letters*, **1963**, 1753.

[8] J. E. Faixt, M. A. Ferber and J. Pascual, *Anales real Soc. espñn. Fis. Quim.*, **1960**, 905 ; *Chem. Abstr.*, **55**, 2099 (1961).

[9] E. G. Rauth, G. F. Smith, C. V. Banks and H. Diehl, *J. Org. Chem.*, **10**, 199 (1945).

[10] M. Bergmann and M. M. Gierth, *Liebigs Ann. Chem.*, **1926**, 448.

[11] L. Bouveault, Chereau, *Compt. rend.*, **142**, 1086 (1906) ; A. Kötz, K. Blendermann, R. Rosenbusch and E. Sirringhans, *Liebigs Ann. Chem.*, **400**, 55 (1913).

[illegible]

[illegible]

[illegible]

[illegible]

REFERENCES

[1] (a) [illegible] J. Am. Chem. Soc. [illegible]
(b) C. L. Stevens, [illegible] *ibid.* 72, [illegible] (1950).
(c) [illegible] J. Chem. Soc. [illegible]
[2] [illegible] unpublished work.
[3] [illegible] J. Am. Chem. Soc. [illegible]
[4] [illegible] J. Org. Chem. [illegible]
[5] [illegible] J. Chem. Soc. [illegible]
[6] (a) [illegible] J. Am. Chem. Soc. [illegible]
(b) [illegible] J. Am. Chem. Soc. [illegible]
[7] [illegible] Tetrahedron Letters [illegible]
[8] [illegible]
[9] [illegible]
[10] [illegible]
[11] [illegible]

Revue Roumaine de Chimie, **25**, *3*, 397–402 (1980)

STUDIES IN INTRAMOLECULAR INTERACTION OF AROMATIC NITRO-GROUP WITH *ORTHO* SIDE-CHAIN. II[1]

FURTHER SYNTHESES OF QUINOLINEN-OXIDE DERIVATIVES

YUSUF AHMAD*, SHAMIN AHMAD SHAMSI and M. IKRAM QURESHI
Pharmaceutical and Fine Chemicals Research Division,
Pakistan Council of Scientific and Industrial Research (PCSIR)
Laboratories, Karachi–39 (Pakistan)

Received July 27, 1978

2-Chloro-3-methoxy-6-nitrobenzylidenesuccinic acid (III) reacted normally with alkali and gave 3-carboxy-5-chloro-6-methoxyquinoline-1-oxide (IVa). On the other hand, treatment of 6-nitropiperonylidenesuccinic acid (VIa) with alkali failed to give the expected 3-carboxy-6,7-methylenedioxyquinoline-1-oxide (VII ; H for Et) and instead gave intractable tar. However, ethyl ester (VIb) of VIa with MeONa or EtONa in the corresponding absolute alcohols gave 3-carboxy-7-hydroxy-6-methoxyquinoline 1-oxide (VIIIa) and 3-carboxy-6-ethoxy-7-hydroxyquinoline 1-oxide (VIIIc), respectively through an unusual opening of the methylenedioxy ring simultaneously with the ring-closure affording the expected quinoline-N-oxide.

Mechanisms for the methylenedioxy ring-opening and for the quinoline N-oxide ring closure are described.

In Part I [1] of this series intramolecular aldol type of condensation between the nitro-group and the anion generated with a base from the active methylene centre in *o*-nitroverartrylidenesuccinic acid (I) has been reported as a first example of a direct synthesis of an N-oxide of quinoline derivative (II). To test the generality of this reaction 2-chloro-3-methoxy-6-nitro-benzylidenesuccinic acid (III) has now been prepared by the nitration of 2-chloro-3-methoxybenzylidenesuccinic acid[2], which had been obtained through Stobbe's condensation [3] of 2-chloro-3-methoxy-benzaldehyde with ethyl succinate. In III the nitro-group and the active methylene are in just the right conformation to undergo the reported [1,4] reaction with alkali. And indeed 3-carboxy-5-chloro-6-methoxyquinoline -1-oxide (IVa) is formed in good yield. Compound IVa could be esterified to give the ethyl ester (IVb). The ester IVb has been doxygenated [5] with PCl_3 in chloroform to give ethyl 5-chloro-6-methoxyquinoline-3-

---

* To whom the inquiries should be addressed.

carboxylate (Vb), the hydrolysis of which gives the corresponding quinoline-3-carboxylic acid (Va).

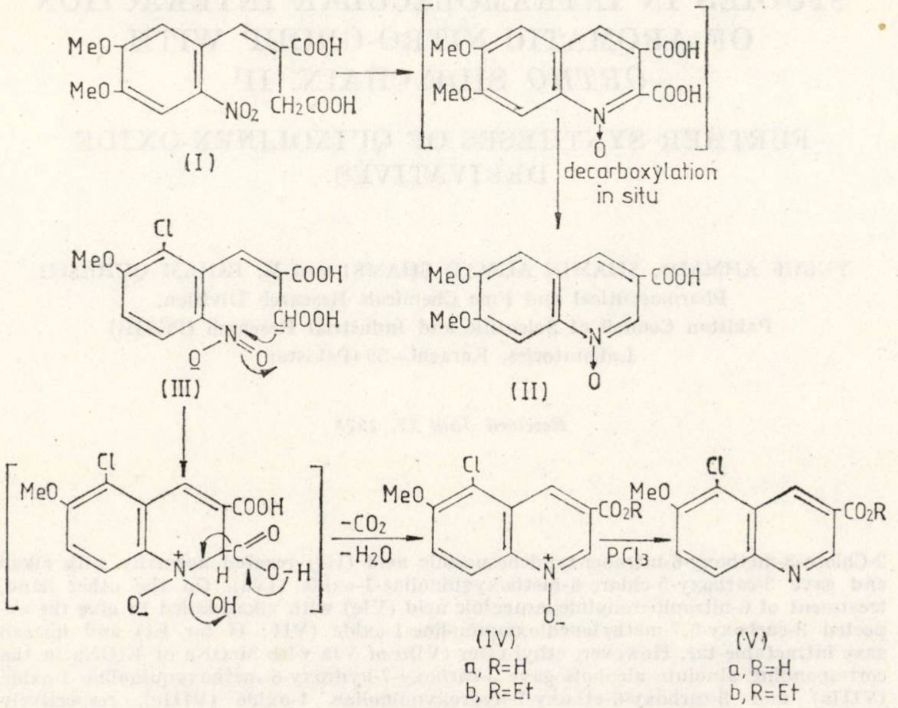
MeO
MeO
COOH
NO2 CH2COOH
(I)
MeO
MeO
COOH
COOH
N
O
decarboxylation
in situ
Cl
MeO
COOH
CHOOH
N
O
(III)
MeO
MeO
COOH
N
O
(II)
Cl
MeO
COOH
C
O
N
H
O
H
O
OH
−CO2
−H2O
Cl
MeO
CO2R
N
O
(IV)
a, R=H
b, R=Et
PCl3
Cl
MeO
CO2R
N
(V)
a, R=H
b, R=Et

Similarly, piperonal reacted with ethyl succinate through Stobbe's condensation and gave piperonylidene-succinic acid, which on nitration gave 6-nitropiperonyl-idenesuccinic acid (VIa), having the right conformation for intramolecular interaction of the nitro group with active methylene. However, VIa with alkali always gives rise to intractable tars. Its ethyl ester (VIb) when heated under reflux with dry MeONa in an excess of absolute methanol yielded a crystalline compound A($C_{11}H_9NO_5$). Similarly, with dry sodium ethoxide in absolute ethanol it afforded a different compound B($C_{12}H_{11}NO_5$).

The structure of compound A was proved to be 3-carboxy-7-hydroxy-6-methoxyquinoline 1-oxide (VIIIa) as follows:

1) The compound lacked the absorption bands for the nitro group in its IR spectrum, indicating that the nitro group in VIa had irreversibly reacted during this reaction. Its IR spectrum indicated strong carbonylic (carboxylic) and free hydroxylic (phenolic) absorption bands.

2) Its elemental analysis corresponded to $C_{11}H_9NO_5$. Its neutralization equivalent indicated it to be a monocarboxylic acid. The elemental analysis of its ethyl ester corresponded to $C_{13}H_{13}NO_5$.

3) On methylation with dimethylsulphate in dry acetone in the presence of anhydrous K_2CO_3 it afforded a compound identical (same IR

spectra ; undepressed mixed m.p) with 3-carboxy-6,7 dimethoxyquinoline-oxide, reported[1] in Part I.

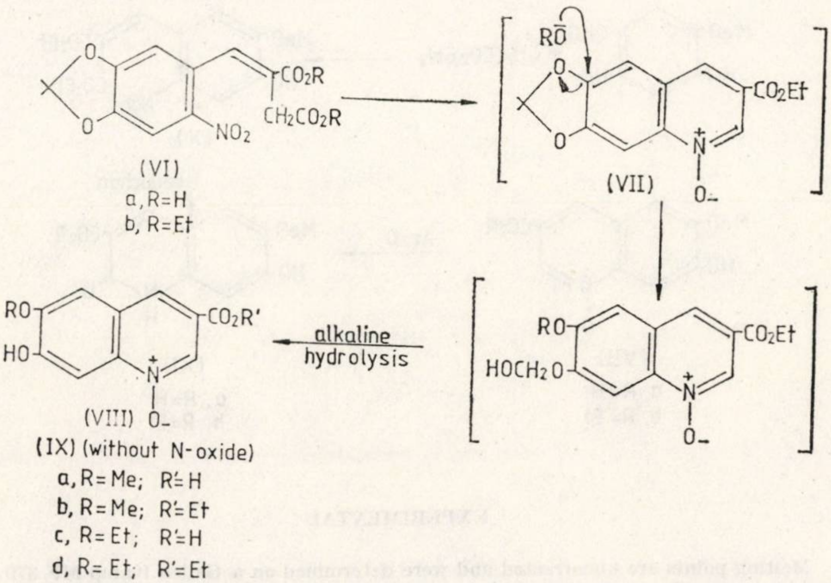

4) Apparently, during the reaction with aqueous alkali not only the ring-closure to quinoline derivative took place, but also the ring-opening of the methylenedioxy group occurred, with concomitant introduction of a methoxyl group *para* to the nitro group. At the same time, the second oxygen function appeared as free hydroxyl group, in the manner indicated above for conversion of VIb to VIIIa. It has a parallel in the reported[6] conversion of 4-nitromethylene-dioxybenzene with MeONa to 2-methoxy-5-nitrophenol and with EtONa to 2-ethoxy-5-nitrophenol; and in the conversion[7] of 6-nitropiperonal to 6-nitrovanillin in high yield.

5) In order to conclusively settle the question whether the attack of MeO^- takes place at C_6 or C_7 during the ringopening of the methylenedioxy group in VIa, the quinoline N-oxide compound was rearranged by heating it with acetic anhydride to the corresponding quinolone[8], which was synthesised unambigously by the condensation of 6-nitrovanillin with diethyl malonate, and reduction of the resulting ethyl 4-hydroxy-3-methoxy-6-nitrobenzylidene-malonate (X) to give ethyl 2,7-dihydroxy-6-methoxyquinoline-3-carboxylate[1] (XIb). Compound XIb on alkaline hydrolysis gave 2,7-dihydroxy-6-methoxyquinoline-3-carboxylic acid (XIa), as shown below :

The compound $B(C_{12}H_{11}NO_5)$ by analogy should be 3-carboxy-6-ethoxy-7-hydroxyquinoline 1-oxide (VIIIc).

The quinoline N-oxide esters VIIIb and VIIId with PCl_3 in chloroform lose normally N-oxide functions and give the corresponding deoxygenated ethyl quinoline-3-carboxylates, IXb and IXd, respectively, which on alkaline hydrolysis afforded the corresponding acids IXa and IXc.

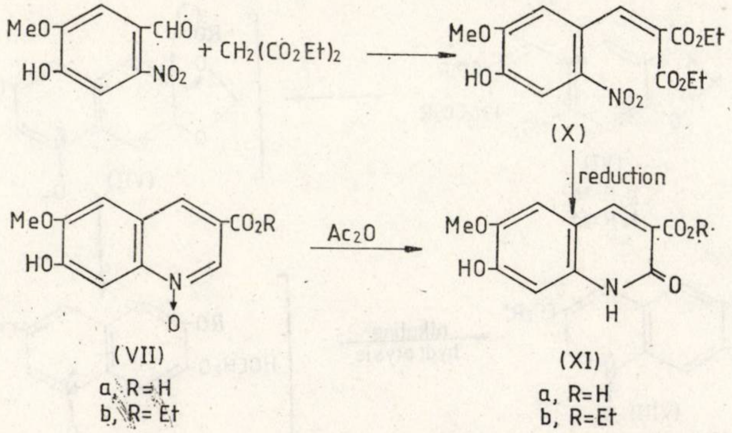

EXPERIMENTAL

Melting points are uncorrected and were determined on a Gallen Kamp MF 370 melting points apparatus. IR spectra were measured in Nujol mull using a Perkin-Elmer infrared spectrophotometer Model 137B. 2-Chloro-3-hydroxybenzaldehyde, 2-chloro-3-methoxybenzaldehyde and piperonylidenesuccinic acid were prepared by the reported methods.

2-Chloro-3-methoxybenzylidenesuccinic acid. To a solution of sodium (4.5 g) in absolute ethanol (120 ml) diethyl succinate (10 g) was added followed by 2-chloro-3-methoxybenzaldehyde (5.0 g). The mixture was heated under reflux on a water bath for 3 hrs. Alcohol was distilled off while adding water from time to time. The cooled aqueous solution was extracted with ether to remove unreacted components. Acidification of the cooled aqueous phase (after warming it to remove the remaining ether) gave a yellow semi-solid mass, which solidified when left overnight in an ice-box. It was filtered (7.0 g) and crystallized from hot water as white plates, m.p. 177—178°. Found : C, 53.39 ; H, 4.02 ; Calc. for $C_{12}H_{11}ClO_5$; C, 53.23 ; H, 4.06 %.

2-Chloro-3-methoxy-6-nitrobenzylidenesuccinic acid (III). The above acid (5.0 g) and nitric acid (d, 1.42 ; 50 ml) were heated together on a water-bath for 15—20 min. The clear solution was poured on crushed ice and the yellow precipitate thus obtained was filtered (3.5 g). Crystallization from dilute alcohol gave light yellow crystals of III, m.p. 199—200°. Found : C, 45.39 ; H, 3.36 ; Cl, 10.92 ; N, 4.74 ; Calc. for $C_{12}H_{10}ClNO_7$: C, 45.64 ; H, 3.17 ; Cl, 11.25 ; N, 4.43 %.

3-Carboxy-5-chloro-6-methoxyquinoline-1-oxide (IVb). A mixture of 2-chloro-3-methoxy-6-nitrobenzylidene succinic acid (III) (2.0 g), pyridine (20 ml) and 20 % aqueous potassium hydroxide (20 ml), was heated on water bath for 1 hr. The colour darkened. The solution, after diluting it with water, was acidified with hydrochloric acid. The light brown solid thus obtained was filtered (1.0 g) and purified by dissolving it in aqueous sodium bicarbonate solution and reprecipitating it with hydrochloric acid. Crystallization from alcohol gave dirty white needles of the *N-oxide*, IVa, m.p. 293—294°. Found : C, 51.62 ; H, 3.18 ; N, 5.45 ; Calc. for $C_{11}H_8ClNO_4$: C,52,07 ; H,3.15 ; N,5.52%.

5-Chloro-3-ethoxycarbonyl-6-methoxyquinoline-1-oxide (IVb). Through the solution of the N-oxide IVa (0.5 g) in absolute ethanol (50 ml) dry hydrogen chloride was passed for 15 min. The solution was heated under reflux on a water bath for 2 hrs. On cooling crystals of IVb separated out, which were filtered and recrystallized from dilute alcohol as white needles, m.p. 165—167°. Found. C, 55.65 ; H, 4.33 ; N, 4.83 ; Calc. for $C_{13}H_{12}ClNO_4$; C, 55.43 ; H, 4.26 ; N, 4.96 %.

Ethyl-5-chloro-6-methoxyquinoline-3-carboxylate (Vb). To a cold solution of ethyl ester IVb (1.0 g) in dry chloroform (25 ml) a solution of phosphorus trichloride (1 ml) in dry chloroform (10 ml) was added. The mixture was heated under reflux for 15 min. neutralized with cold dilute ammonia, then washed with water. The chloroform layer was collected, dried and evaporated. The residue was cooled to obtain a solid. Crystallization from dilute alcohol gave white silky needles of Vb (0.5 g), m.p. 90 — 92°. Found : C, 58.37 ; H, 4.58 ; N, 5.39 ; Calc. for $C_{13}H_{12}ClNO_3$: C, 58.75 ; H, 4.51 ; N, 5.27%.

3-Carboxy-5-chloro-6-methoxyquinoline (*Va*). Compound Vb, (0.4 g) was hydrolysed by heating it with 10% aqueous sodium hydroxide (10 ml) on a water bath for 3 hrs. The cooled solution was filtered and acidified to obtain 3-carboxy-5-chloro-6-methoxyquinoline (Va) (0.2 g). Crystallization from ethanol gave white needles, m.p. 242—244°. Found : C, 55.27 : H, 3.6 ; N, 5.51 ; Calc. for $C_{11}H_8ClNO_3$: C, 55.57 ; H, 3.36 ; N, 5.89%.

6-Nitropiperonylidenesuccinic acid (*VIa*). Nitric acid (d = 1.42, 25 ml) was added to a solution of piperonylidenesuccinic acid (5.0 g) in glacial acetic acid (50 ml) maintained at 0—5°. The mixture was stirred at room temperature for 1 hr and then poured on ice. The resulting solid (3.5 g) was collected by filtration. Crystallization from ethyl acetate and light petroleum gave yellow shining crystals of the *Nitro-acid* VIa, m.p. 181—182°. Found : C, 48.37 : H, 3.04 ; N, 4.61 ; Calc. for $C_{12}H_9NO_8$: C, 48.81 ; H, 3.05 ; N, 4.74%.

Diethyl-6-nitropiperonylidene succinate (*VIb*). Dry hydrogen chloride was passed through a solution of VIa (5.0 g) in absolute ethanol (150 ml) for 1/2 hr. The solution was heated under reflux for 2 hrs. On cooling the ethyl ester (5.0 g) separated out, which was recrystallized from ethanol to give yellow crystals of VIb, m.p. 125—126°. Found : C, 54.67 : H, 4.83 ; N, 3.96 ; Calc. for $C_{16}H_{17}NO_8$; C, 54.7 ; H, 4.84 ; N, 3.96%.

3-Carboxy-7-hydroxy-6-methoxyquinoline-1-oxide (*VIII a*). Diethyl-6-nitropiperonylidene succinate (VIb) (5.0 g) was added to a solution of sodium (16.5 g) in dry methanol (350 ml). The mixture was heated under reflux on a water bath for 16 hrs. The colour changed and finally became dark. Methanol was completely distilled off under reduced pressure and the residue was triturated with cold water. On acidification with hydrochloric acid, the brown precipitate of VIIIa (2.5 g) was obtained which was filtered. Crystallization from aqueous alcohol gave light brown crystals, m.p. 294—295°. Found : C, 54.3 ; H, 4.14 ; N, 5.73 ; Calc. for $C_{11}H_9NO_5 \cdot 1/2H_2O$: C, 54.1 ; H, 4.1, N, 5.73%.

3-Carboxy-6-ethoxy-7-hydroxyquinoline-1-oxide (*VIIIc*). Compound VIb (5.0 g) was similarly treated with sodium (16.5 g) and absolute ethanol (350 ml) to obtain the N-oxide VIIIc. Crystallization from ethanol gave light brown crystals. Recrystallization from aqueous acetic acid gave white needles, m.p. 280—282°. Found : C, 54.12, H, 4.83, N, 5.63 ; Calc. for $C_{12}H_{11}NO_5 \cdot H_2O$; C, 53.93 ; H, 4.86 ; N, 5.24%.

3-Ethoxycarbonyl-7-hydroxy-6-methoxyquinoline-1-oxide (*VIIIb*). Into a solution of VIIIa (2.0 g) in absolute ethanol (100 ml) dry hydrogen chloride was passed for 1/2 hr. The solution was heated under reflux for 2 hrs. Ethanol was completely distilled off under reduced pressure and the residue was treated with cold water. Crystallization from alcohol gave microneedles, m.p. 269°. Found : C, 59.11 ; H, 4.89 ; N, 5.26 ; Calc. for $C_{13}H_{13}NO_5$; C, 59.3 ; H, 4.94 ; N, 5.32%.

3-Ethoxycarbonyl-6-ethoxy-7-hydroxyquinoline-1-oxide (*VIIId*). Compound VIIIc (2.0 g) was similarly treated with dry hydrogen chloride to give white micro needles (from ethanol) of the ethyl ester VIIId, m.p. 243—244°. Found C, 60.5 ; H, 5.42 ; N, 5.07 ; Calc. for $C_{14}H_{15}NO_5$; C, 60.64 ; H, 5.41 ; N, 5.05%.

Ethyl-7-hydroxy-6-methoxyquinoline-3-carboxylate (*IXb*). To a cold solution of VIIIb (1.0 g) in dry chloroform (10 ml) a solution of phosphorus trichloride (1 ml) in dry chloroform (10 ml) was added. The mixture was heated under reflux for 15 hrs, then it was cooled and neutralized with cold 10% aqueous ammonia (20 ml) and shaken twice with water (20 ml). The chloroform layer was separated and dried over anhydrous sodium sulphate. Evaporation of chloroform gave ethyl-7-hydroxy-6-methoxy-quinoline-3-carboxylate (IXb) (0.6 g). Crystallization from ethanol gave white shining microneedles, m.p. 254—255°. Found : C, 62.86 ; H, 5.41 ; N, 5.47 ; Calc. for $C_{13}H_{13}NO_4$; C, 63.15 ; H, 5.3 ; N, 5.67%.

Ethyl-6-ethoxy-7-hydroxyquinoline-3-carboxylate (*IXd*). Compound IXd was prepared by a similar method, adding a solution of phosphorus trichloride (1 ml) in dry chloroform (10 ml) to a cold solution of VIIId (1.0 g) in dry chloroform (20 ml), whereby ethyl-6-ethoxy-7-hydroxyquinoline-3-carboxylate (IXd) (0.7 g) was obtained. Crystallization from ethanol gave white microneedles, m.p. 220—222°. Found : C, 64.31 ; H, 5.73 ; N, 5.22 ; Calc. for $C_{14}H_{15}NO_4$: C, 64.36 ; H, 5.74 ; N, 5.36%.

3-Carboxy-7-hydroxy-6-methoxyquinoline (*IXa*). The ester IXb (1.0 g) and 10% sodium hydroxide (10 ml) were heated together on a water bath for 2 hrs. The solution, after filtration, was made acidic with hydrochloric acid to precipitate 3-carboxy-7-hydroxy-6-methoxyquinoline IXa (0.5 g), which was crystallized from aqueous ethanol as white crystals, m.p. 268—269°. Found: C, 58.22 ; H, 4.95 ; Calc. for $C_{11}H\ NO_4 \cdot 1/2H_2O$: C, 57.89 ; H, 4.39%.

The acid IXa, when esterified with absolute ethanol and gaseous HCl, gave the parent compound IXb, identical (IR spectrum and undepressed mixed m.p.) with an authentic sample.

3-Carboxy-6-ethoxy-7-hydroxyquinoline (*IXc*). The ester IXd (0.5 g) was similarly hydrolysed by heating with 10% aqueous potassium hydroxide (10 ml) on water bath for 1 hr. Acidification with hydrochloric acid yielded IXc (0.3 g), which on crystallization from alcohol gave yellow plates, m.p. 272–273°.

The compound was repeatedly analysed, but every time it gave different results. Therefore compound IXc was esterified with absolute ethanol and gaseous HCl to give IXd, identical (IR spectrum and undepressed mixed m.p.) with an authentic specimen. This confirmed the structure of IXc.

Methylation of 3-carboxy-7-hydroxy-6-methoxyquinoline-1-oxide (*VIII a*). Dry acetone (50 ml), anhydrous sodium carbonate (2.0 g) and 3-carboxy-7-hydroxy-6-methoxyquinoline 1-oxide (VIII a) (0.5 g), were heated under reflux on a water bath. Dimethyl sulphate (2 ml) was added slowly with stirring. The mixture was further heated under reflux for 3 hrs. After removing acetone under reduced pressure the residue was dissolved in cold water. Acidification with hydrochloric acid gave a precipitate (0.4 g) which, on crystallization from alcohol, gave white microneedles, m.p. 277–280° which were identical (IR spectrum and undepressed mixed m.p.) with a sample 0f 3-carboxy-6, 7-dimethoxyquinoline 1-oxide reported in Part I.

Diethyl-4-hydroxy-3-methoxy-6-nitrobenzylidene malonate (*X*). 6-Nitrovanillin (4.5 g), diethylmalonate (6 ml), piperidine (3 ml) and pyridine (10 ml) were mixed together and left at room temperature for 7 days. The dark brown viscous liquid was then poured over ice and hydrochloric acid, and left overnight in an ice-box. The semi-solid thus obtained was filtered (4.2 g). It was purified by passing ethanolic solution through a column of silica gel (120 mesh); microneedles of X were obtained from dilute ethanol, m.p. 134–135°. Found: C, 53.15; H, 5.07; N, 4.15; Calc. for $C_{15}H_{18}NO_8$; C, 52.94; H, 5.29; N, 4.11%.

Ethyl-2,7-dihydroxy-6-methoxyquinoline-3-carboxylate (*XIb*). Compound X (2.0 g) in ethanol (150 ml) was hydrogenated using 10% Pd-C catalyst (0.5 g) (0.7 litres hydrogen absorbed in 6 hr). After filtration of the catalyst, ethanol was removed under reduced pressure and the residue was crystallized from ethanol as yellow microneedles (0.6 g), m.p. 269–270°. Found: C, 58.94: H, 4.98; N, 5.15; Calc. for $C_{13}H_{13}NO_5$; C, 59.31; H, 4.98; N, 5.32%.

2,7-Dihydroxy-6-methoxyquinoline-3-carboxylic acid (*XI a*). Hydrolysis of XIb (0.5 g) was carried out with 10% aqueous potassium hydroxide (10 ml) by heating on a water bath for 3 hrs. The cooled solution was filtered and acidified with hydrochloric acid to obtain 2,7-dihydroxy-6-methoxy-quinoline-3-carboxylic acid (XI a) (0.25 g). Crystallization from aqueous methanol gave yellow needles, m.p. 285–287°. Found: C, 54.5; H, 3.9; N, 5.55; Calc. for $C_{11}H_9NO_5 \cdot 1/2H_2O$: C, 54.1; H, 4.1; N, 5.73.

Rearrangement of 3-ethoxycarbonyl-7-hydroxy-6-methoxy quinoline-1-oxide (*VII b*) *with acetic anhydride*. Compound VII b (1.0 g) and acetic anhydride (50 ml) were heated together under reflux for 6 hrs. Acetic anhydride was distilled off under reduced pressure and the residue was triturated with cold water and the semi solid product solidified when left overnight. The solid thus obtained was filtered and dried at room temperature.

The dried solid (0.25 g) and 10% aqueous potassium hydroxide (5 ml) were heated together on water bath for 1 hr. The clear solution was cooled and, on acidification with hydrochloric acid, gave yellow precipitate (0.1 g), which on crystallization from ethanol gave yellow needles, m.p. 283–284° of a compound, identical (IR spectrum and undepressed mixed m.p.) with an authentic sample of 2,7-dihydroxy-6-methoxyquinoline-3-carboxylic acid (XI a) synthesized through the unambiguous route described above.

REFERENCES

[1] Part I: Y. Ahmad and S. A. Shamsi, *Pakistan J. Sci., Ind. Res.*, **11,** 354 (1968).

[2] N. J. Cartwright and R. D. Haworth, *J. Chem. Soc.*, **1944,** 535.

[3] H. Stobbe, *Liebigs Ann. Chem.*, **380,** 49 (1911).

[4] Y. Ahmad and S. A. Shamsi, *Bull. Chem. Soc. Japan*, **39,** 195 (1966).

[5] S. Takahashi and H. Kano, *Chem. Pharm. Bull* (*Tokyo*), **12,** 783 (1964); M. Hamana, *Yakugaku Zasshi*, **71,** 263 (1951).

[6] G. M. Robinson and R. Robinson *J. Chem. Soc.*, **1917,** 929.

[7] Y. Ahmad, S. A. Shamsi and M. I. Qureshi, *Pakistan J. Sci. Ind. Res.*, **21,** 99 (1978).

[8] E. Ochiai and T. Okamoto, *J. Pharm. Soc., Japan*, **68,** 88 (1948); E. Ochiai, *J. Org., Chem.*, **18,** 534 (1953).

Revue Roumaine de Chimie, **25**, *3*, 403—405 (1980)

DEHYDRATIONS WITH CHLOROSULFONIC ACID IN PYRIDINE. A CONVENIENT METHOD FOR THE SYNTHESIS OF AMIDES

C. I. CHIRIAC
"P. Poni" Institute of Macromolecular Chemistry
Aleea Grigore Ghica-Vodă 41A, Iași, Romania

Received December 28, 1978

By a direct condensation reaction between carboxylic acid and pyridinium salts of sulfamic acids, amides are formed in high yields. Better results are obtained in the case of aliphatic acids.

A common method of preparing N-monosubstituted amides, utilizes the reaction of primary amines with acyl chlorides. The latter compounds are often prepared by the reaction of a carboxylic acid with phosphorus trichloride or thionyl chloride. Different investigators have found that the two steps could be combined successfully into one operation. [1,2]

In a previous paper, [3] we showed that the triacylphosphites react with the amines, affording the corresponding amides in high yields.

Phosphorus compounds are well known as reagents for the synthesis of amides and polypeptides. Also, compounds with sulfur can give this type of reactions. Toluenesulfonyl chloride in pyridine [4] and methanesulfonyl chloride in pyridine, [5] were used as reagents for the synthesis of amides.

RESULTS AND DISCUSSION

By the reaction between amines and chlorosulfonic acid in pyridine there result pyridinium salts of sulfamic acid. [6,9]

The synthesis of amides starting from pyridinium salts of sulfamic acids has not been investigated. Our investigations have shown that this reagent can be used in this field.

We prepared pyridinium salts of sulfamic acids (reactive compounds), from amines and $ClSO_3H$ in solution of pyridine at 0 —10°. These compounds react with aliphatic or aromatic acids, affording the corresponding amides. For the verification of this reaction, we prepared the pure pyridinium salt of phenylsulfamic acid[10] from pyridine-sulfur trioxide[11] and aniline. This compound reacts also with benzoic acid, to give benzanilide in good yield.

The mechanism of this reaction, similar to other reactions,[8,12] is the following;

$$\underset{\text{I}}{R-NH_2}+ClSO_3H \xrightarrow{Py} \underset{\text{II}}{R-NH-SO_3^-Py^+H}+Py\cdot ClH$$

(reactive compounds)

$$II+\underset{\text{III}}{R'-COOH} \longrightarrow \underset{\text{IV}}{R'-CONH-R}+\underset{\text{V}}{SO_4^{2-}2Py^+H}$$

The presence of SO_4^{2-} ions was proved by identification and determination with $BaCl_2$.[13]

We suppose that this process involves a four-centre transition state (VI), similar to other cases;[8,14]

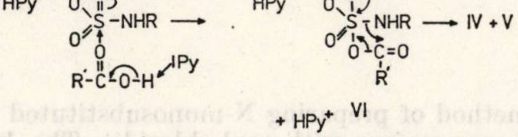

VI

This reaction is very simple. In a typical procedure, to a stirred solution of 1 mol I in dried pyridine cooled to 0° was added very slowly 1 mol + small excess of $ClSO_3H$ (the reaction is very exothermic) and then 1 mol III.

It can be seen from Table 1 that very good results were obtained in the case of aliphatic acids. In the case of aliphatic acids, a heating at 50–60° is sufficient, while for aromatic acids, a heating at reflux is necessary. A large excess of pyridine is necessary as solvent.

Table 1 shows the amides obtained in this way.

By this simple method we avoid the acyl chlorides as intermediary phase used in the classical method for the synthesis of amides.

EXPERIMENTAL

Phenylacetanilide. To a stirred solution of 1.86 g (0.02 mole) aniline in 20 ml dried pyridine cooled to 0°, 1.45 ml (0.02 ml (0.02 mole + 10% excess) $ClSO_3H$ was added very slowly. When the solution became clear (about 1 hr), 2.72g(0.02 mole) phenylacetic acid were added. The mixture was heated 4 hrs at 50–60° The obtained solution was poured into a large volume of water with ice (100–150 ml), under vigorous stirring. The product was collected by filtration, washed well with 5% NaOH (20 ml), 7% HCl (20 ml), three times with 20–30 ml H_2O and dried and were obtained 3.3g(78%) of phenylacetanilide, m.p. = =115–116°.

In similar conditions, we obtained the other amides presented in Table 1.

TABLE 1

The synthesis of amides using $ClSO_3H/Pyr$

Amine	Acid	Amides[c]		
		Yield[d] %	M.p.[e] °C	Reported m.p. °C
Aniline	Phenylacetic [a]	78	115−116	115−116
p-Toluidine	,,	84	135−136	135−136
p-Nitroaniline	,,	58 [f]	130−132	132−133
2-Naphtylamine	,,	86	164−166	165−167
Aniline	Acetic [a]	71	113−114	113−114
p-Toluidine	,,	77	149−151	150−151
p-Nitroaniline	,,	64 [f]	212−214 [f]	214−215
2-Naphtylamine	,,	73	131−133	132−133
Aniline	Benzoic [b]	61	159−161	160−162
p-Toluidine	,,	63	155−157	156−157
p-Nitroaniline	,,	40 [f]	195−196 [f]	196−197
2-Naphtylamine	,,	52 [f]	155−157 [f]	156−158
Cyclohexylamine	,,	55	146−148	147−149
Aniline	*p*-Chlorobenzoic [b]	46	192−194	193−194
p-Toluidine	,,	58	213−215	214−216
2-Naphtylamine	,,	52 [f]	204−206 [f]	206−207
p-Toluidine	*p*-Toluic [b]	68	158−160	159−160
Aniline	,,	64	143−144	144−145

a. 4 hrs at 50−60°. *b*. 1 hr at 50−60° and 4 hrs at 115−120°. *c*. The products were identified by comparing m.p. and I.R. spectra with those of authentic specimens. *d*. The yields determined by the isolation of the crude products. *e*. The melting points are given as an indication of purity. *f*. After recrystallisation.

REFERENCES

[1] T. Wieland and B. Heinke, *Liebigs Ann. Chem.*, **599,** 70 (1956) ; *Chem. Ber.*, **91,** 483 (1958).

[2] G. W. Anderson and R. W. Young, *J. Amer. Chem. Soc.*, **74,** 5304 (1952).

[3] C. I. Chiriac, *Rev. Roumaine Chim.*, **24,** 609 (1979).

[4] J. H. Brewster and C. I. Ciotti, *J. Amer. Chem. Soc.*, **77,** 6214 (1955).

[5] J. H. Looker and C. H. Hayes, *J. Amer. Chem. Soc.*, **79,** 745 (1957).

[6] P. Baumgarten, *Chem. Ber.*, **59,** 1981 (1926) ; **62,** 823 (1929).

[7] L. F. Audrieth and M. J. Butler, *Chem. Rev.*, **26,** 61 (1940) ; *J. Org. Chem.*, **9,** 91 (1944).

[8] H. O. Becker and K. F. Funk, *J. prakt. Chem.*, **14,** 55 (1961).

[9] M. L. Wolfrom and C. G. Summers, *J. Amer. Chem. Soc.*, **75,** 1519 (1953) ; **81** 1764 (1959).

[10] P. Baumgarten, *Chem. Ber.*, **59,** 1166 (1926).

[11] H. H. Sisler and L. F. Audrieth, *Inorganic Synthesis*, **2,** 173 (1946).

[12] R. N. Ring and D. Davidson, *J. Org. Chem.*, **27,** 2428 (1962).

[13] G. Ingram, "Methods of Organic Elemental Microanalysis", first edition, Chapman-Hall, London 1962, p. 238.

[14] W. Gerrard and J. A. Cade, *J. Chem. Soc.*, **1954,** 2034.

Revue Roumaine de Chimie, **25**, *3*, 407–414 (1980)

s-TRIAZOLIUM-4N-YLIDE

H.-J. TIMPE, V. SCHRÖDER und R. WORSCHECH
Technische Hochschule "Carl Schorlemmer" Leuna-Merseburg,
Sektion Chemie, DDR–42 Merseburg

Eingegangen am 2. August 1978

1-Substituierte *s*-Triazole **1** lassen sich durch Phenacylbromide, *p*-Nitrobenzylbromid und Brommalonsäurediäthylester am 4N-Atom quaternieren, Aus den Quartärsalzen **2** werden durch Zugabe von Basen *s*-Triazolium-4N-ylide **3** gebildet, die durch IR-, UV- und NMR-Spektren charakterisiert wurden. Mit Phenylisothiocyanat und Propiolsäureester reagieren die N-Ylide **3** unter Additionsreaktionen, wobei carbanion-disubstituierte N-Ylide entstehen. Die erhaltenen Ergebnisse werden mit denen der isosteren *s*-Triazol-4N-oxide und *s*-Triazol-4N-imine verglichen.

1-Substituted *s*-triazoles can be quaternized by phenacyl bromides, *p*-nitrophenylbromide and bromo diethylmalonate at the 4N-atom. *s*-Triazolium-4N-ylides are formed from the quaternary salts through the addition of bases. The former are characterized by IR-, UV- and NMR-spectra. The N-ylides react with phenyl isothiocynate and propiolic acid ester under addition reactions, which develop carbanion disubstituted N-ylides. The present results are compared with those of the isosteric *s*-triazole-4N-oxides and *s*-triazole-4N-imines.

N-Ylide sind isoster mit N-Oxiden und N-Iminen. Obwohl inzwischen eine Vielzahl von N-Yliden beschrieben worden sind, [1] gibt es vergleichsweise wenig Material über die Isosteriebeziehungen zwischen den genannten Verbindungen. Wir haben deshalb eine Reihe von *s*-Triazolium-4N-yliden hergestellt, um einige ihrer spektroskopischen und chemischen Eigenschaften mit denen der von uns bereits beschriebenen *s*-Triazol-4N-oxide [2] und *s*-Triazol-4N-imine [3–6] zu vergleichen.

Einige N-Ylide der *s*-Triazolreihe sind schon dargestellt worden[7–9], ohne daß nähere Angaben zu ihrer Charakterisierung gemacht wurden. In Analogie zu ähnlichen Fällen haben wir zur Darstellung der *s*-Triazolium-4N-ylide die Salzmethode [1] verwendet. Dazu wurden 1-substituierte *s*-Triazole **1** mit Phenacylbromiden, *p*-Nitrobenzylbromid und Brommalonsäurediäthylester zu den Quartärsalzen **2** umgesetzt; vgl. Tab. 1. Der Substitutionsort in 4-Stellung wird durch folgendes Experiment bewiesen: Die Quaternierung des 1-Benzyl- und des 4-Benzyl-*s*-triazols mit Benzylbromid liefert ein identisches Reaktionsprodukt. Ein solches Ergebnis ist nur möglich, wenn die Quaternierung von 1-substituierten *s*-Triazolen **1** in 4-Stellung und die Quaternierung von 4-substituierten *s*-Triazolen in 1-Stellung erfolgt; vgl. auch. [8–10] Die Quartärsalze **2** enthalten ein acides C—H—Proton, was durch den pK_a-Wert von 9,04 (gemessen in Wasser, t = 20°) für **2b** angezeigt wird. Damit sind die Salze **2** stärkere Säuren als

TABELLE 1

1,4-Disubstituierte *s*-Triazoliumbromide 2

Nr.	R¹	R²	R³	Ausb. (% d. Th.)	F.[a] (°C)	Summenformel	Ber. C Gef. C	H H	N N	λ_{max}[b] (lg ε)
2a	$PhCH_2$	PhCO	H	91	187	$C_{17}H_{16}BrN_3O$	57,00	4,50	11,73	247
							57,41	4,94	11,81	(4,19)
2b	CH_3	PhCO	H	83	228	$C_{11}H_{12}BrN_3O$	46,83	4,29	14,89	247
							47,00	4,41	14,10	(4,18)
2c	Ph	PhCO	H	73	158	$C_{16}H_{14}BrN_3O$	55,82	4,10	12,20	249
							55,73	4,27	12,36	(4,20)
2d	$PhCH_2$	$p-BrC_6H_4CO$	H	93	215	$C_{17}H_{15}Br_2N_3O$	46,71	3,46	9,61	262
							46,99	3,72	9,60	(4,25)
2e	CH_3	$p-BrC_6H_4CO$	H	87	222	$C_{11}H_{11}Br_2N_3O$	36,59	3,07	11,64	261
							36,75	3,05	11,83	(4,24)
2f	$PhCH_2$	$COOC_2H_5$	$COOC_2H_5$	64	133	$C_{16}H_{20}BrN_3O_4$	48,25	5,06	10,55	c)
							48,50	5,31	10,89	
2g	$PhCH_2$	$p-NO_2C_6H_4$	H	68	208	$C_{16}H_{15}BrN_4O_2$	51,22	4,03	14,93	258
							51,24	4,31	14,97	(4,02)
2h	CH_3	$p-NO_2C_6H_4$	H	62	190	$C_{10}H_{11}BrN_4O_2$	40,15	3,71	18,79	258
							39,90	3,44	18,67	(4,03)

a) umkristallisiert aus Äthanol b) aufgenommen in Methanol ; c) oberhalb 220nm nur die verbotenen Übergänge des Benzylrestes um 270nm sichtbar.

die entsprechenden Quartärsalze aus Pyridin und Phenacylbromiden.[11] Versetzt man deshalb wäßrige Lösungen der Salze **2** mit Laugen, dann entstehen die N-Ylide **3**. Für eine präparative Darstellung der N-Ylide **3a-f** hat sich die Zugabe von konz. Ammoniaklösung zu gesättigten wäßrigen Salzlösungen am besten bewährt. Verwendet man Alkalilaugen, dann entstehen nur sehr unreine N-Ylide **3**. Auf diesem Wege konnten aus den 4-*p*-Nitrobenzyl-*s*-triazoliumsalzen **2g** und **2h** keine stabilen N-Ylide gewonnen werden. Bei Laugenzugabe fallen lediglich violett gefärbte Öle aus, die sehr schnell verharzen. Schüttelt man dagegen die alkalischen Lösungen sofort mit Methylenchlorid aus, dann sind die gelösten N-Ylide **3g** und **3h** längere Zeit bei Zimmertemperatur haltbar. Aber auch die N-Ylide **3a-f** sind thermisch nicht sehr stabil. Bereits bei Zimmertemperatur tritt innerhalb weniger Tage merkliche Zersetzung ein. Deshalb ist die Reinigung der Verbindungen durch Umkristallisation mit großen Ausbeuteverlusten verbunden.

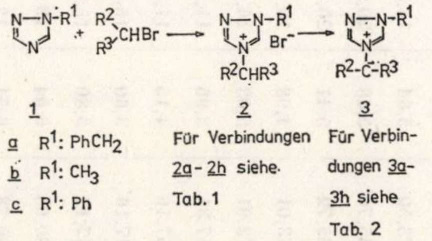
N—N-R¹
R²
R³ CHBr
Br⁻
R²CHR³
R²-C-R³
1
2
3
a R¹: PhCH₂
b R¹: CH₃
c R¹: Ph
Für Verbindungen 2a - 2h siehe Tab. 1
Für Verbindungen 3a-3h siehe Tab. 2

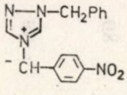
3g

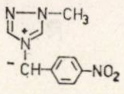
3h

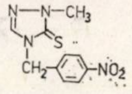
4

In den IR-Spektren der N-Ylide **3a-e** findet sich eine sehr intensive Bande bei 1590 cm^{-1}, die in den entsprechenden Quartärsalzen **2** nicht auftritt. Wir ordnen sie einer Enolatstruktur **3B** zu. Die Unterschiede zu den C=O-Schwingungen der Quartärsalze **2** betragen 100 cm^{-1} und sind damit interessanterweise völlig analog denen zwischen *s*-Triazol-4N-acyliminen und den dazu korrespondierenden Quartärsalzen [3]. Erwartete Veränderungen treten auch in den IR-Spektren des Salzes **2f** und seines N-Ylids **3f** auf. Während im Spektrum des Salzes nur eine C=O-Schwingung bei 1735 cm^{-1} vorhanden ist, enthält das Spektrum des N-Ylids wieder die starke Bande bei 1595 cm^{-1} und dazu noch eine, allerdings schwächere Bande bei 1670 cm^{-1}. Eine derartige Bandenstruktur könnte auf eine nicht völlig symmetrische Delokalisation der negativen Ladung über beide Carboxylgruppen im Sinne von **3C** hindeuten.

Das UV-Spektrum der N-Ylide **3a-e** enthält die Enolatbande bei ca. 310 nm, wie sie auch für analoge N-Ylide typisch ist;[1] vgl. Tab. 2. Demgegenüber besitzen die Quartärsalze **2** die normale Absorption für

TABELLE 2

1-Substituierte *s*-Triazolium-4N-ylide 3

Nr.	R^1	R^2	R^3	Ausb. (% d. Th.)	F.[a] (°C)	Summenformel	Ber. C Gef. C	H H	N N	λ_{max}[b] (lg ε)
3a	$PhCH_2$	PhCO	H	78	86	$C_{17}H_{15}N_3O$	73,63	5,45	15,15	321
							73,50	5,84	14,80	(3,93)
3b	CH	PhCO	H	74	89	$C_{11}H_{11}N_3O$	65,70	5,48	20,90	317
							65,72	5,41	20,79	(3,94)
3c	Ph	PhCO	H	84	119	$C_{16}H_{13}N_3O$	73,01	4,98	15,96	
							72,91	5,03	16,07	
3d	$PhCH_2$	$p-BrC_6H_4CO$	H	79	115	$C_{17}H_{14}BrN_3O$	57,31	3,96	11,78	322
							57,19	4,15	11,78	(4,02)
3e	CH_3	$p-BrC_6H_4CO$	H	80	124	$C_{11}H_{10}BrN_3O$	47,16	3,60	15,00	318
							47,17	3,80	15,18	(4,00)
3f	$PhCH_2$	$COOC_2H_5$	$COOC_2H_5$	58	187	$C_{16}H_{19}N_3O_4$	60,68	6,04	13,24	248[c]
							60,78	6,51	13,40	(4,13)
3g	$PhCH_2$	$p-NO_2C_6H_4$	H	d)						532
										(4,03)
3h	CH_3	$p-NO_2C_6H_4$	H	d)						524
										(3,98)

a) umkristallisiert aus H_2O/Ethaool (3;1): b) aufgenommen in 0,1 n Natronlauge; c) aufgenommen in Methanol: d) Verbindung nicht in Substanz isolierbar.

aromatische Ketone bei ca. 250 nm, vgl. Tab. 1. Analoge bathochrome Verschiebungen beobachtet man auch zwischen Quartärsalz **2f** und N-Ylid **3f**. Im UV-Spektrum des Quartärsalzes sind oberhalb 220 nm nur die schwachen verbotenen Übergänge des Benzylrestes sichtbar, das N-

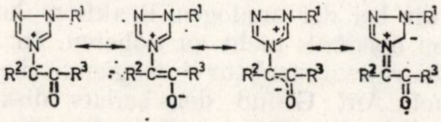

3A **3B** **3C** **3D**

Ylid **3f** besitzt dagegen einen intensiven Übergang bei 248 nm. Er liegt damit im gleichen Bereich wie bei den analogen N-Oxiden [2] und N-Iminen [3-6] und beweist somit die Gültigkeit des Isosterieprinzips für die Elektronenspektren. Infolge des dipolaren Aufbaus der N-Ylide **3** sollte der UV-Übergang eine ausgeprägte negative Solvatochromie aufweisen. [12] Unerwartet ist deshalb, daß die Lage des UV-Maximums von **3f** nur wenig vom Lösungsmittel abhängt: 248 nm in Methanol und 251 nm in Methylenchlorid.

Die *p*-Nitrophenyl-N-ylide **3g** und **3h** besitzen in Methylenchlorid einen Elektronenübergang bei 532 nm (**3g**) und 524 nm(**3h**). Das entspricht den λ_{max}-Werten von analogen N-Yliden der Imidazoline. [13]

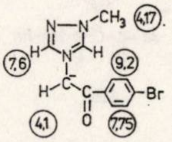

3e

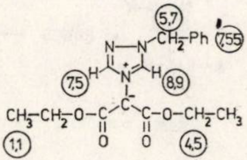

3f

Die NMR-Daten der N-Ylide sind in Schema 1 zusammengestellt. Daraus geht eindeutig hervor, daß die Protonen an C—3 und C—5 des *s*-Triazolringes sehr unterschiedlich abgeschirmt sind. Die große Differenz von ca. 1,5 ppm ist nicht durch die 1-Substitution erklärbar: im 1-Benzyl-*s*-triazol **1a** findet man nämlich die entsprechenden Signale bei 8,6 (H—3) und 8,1 ppm (H—5) und im 1-Methyl-*s*-triazol **1b** bei 8,6 (H—3) und 8,3 ppm (H—5). Die Differenzen ergeben sich eindeutig aus den Unterschieden der Elektronendichteverteilung an den beiden C-Atomen, wie sie aus den Valenzstrichformeln **3A—C** ablesbar sind. Ähnliche Spreizungen der chemischen Verschiebungen beider Protonen haben wir auch bei *s*-Triazol-4N-iminen gemessen. [3-6] Auffällig ist aber die im Vergleich zu den N-Iminen beobachtete Hochfeldverschiebung beider Signale. Offenbar spielt bei den *s*-Triazolium-4-yliden **3** die Elektronendonatorwirkung der Ylidgruppierung (vgl. Valenzstrichformel **3D**) eine gewisse Rolle, womit eine stärkere Abschirmung der beiden C-Atome verbunden wäre.

Die NMR-Signale der anderen Protonen liegen im erwarteten Bereich.

Die geringe Elektronendichte am C—5 des *s*-Triazolringes ist auch für einige Reaktionen der N-Ylide **3** verantwortlich, die sie von anderen N-Yliden [1] unterscheiden. Selbst bei Zimmertemperatur sind die N-Ylide **3a-f** gegenüber Laugen sehr labil. Dabei wird vermutlich der Triazolring gespalten, denn Produkte der Säurespaltung der N-Ylide sind nicht nachweisbar. Definierte Verbindungen der Sekundärreaktion der Ringöffnungsprodukte, die wir bei der analogen Reaktion der *s*-Triazol-4N-imine fassen konnten, waren ebenfalls nicht zu isolieren. In Analogie zu anderen Heterocyclen mit Quartärsalzstruktur [14] reagieren die Quartärsalze **2** in Pyridin mit Schwefel. Auf Grund der bereits diskutierten pK_a-Werte entsteht unter diesen Bedingungen intermediär ein N-Ylid **3**, dessen C—5-Proton am *s*-Triazolring entweder über ein nucleophiles Carben oder direkt elektrophil substituiert wird. Allerdings konnten wir nur im Falle der *p*-Nitrobenzylsalze **2g-h** definierte Endprodukte **4** isolieren; bei den Phenacyliumsalzen entsteht ein Produktgemisch, aus dem durch Kristallisation keine einheitlichen Verbindungen isolierbar waren.

Typisch für alle N-Ylide sind ihre Reaktionen mit dipolaren Reagentien, wobei die Struktur der Endprodukte stark von der Struktur des N-Ylids und den Reaktionsbedingungen abhängt. [1]

In Methylenchlorid oder Benzol reagieren die Ylide **3** sehr schnell mit Phenylisothiocyanaten. Dabei entstehen in Analogie zu ähnlichen Fällen [15] die N-Ylide **5**. Deren Struktur folgt vor allem aus den IR-Spektren, in denen eine Absorption im Carbonylgruppenbereich fehlt, die stärkste Schwingung bei 1510 cm^{-1} auftritt (assoziierte Enolatbande) und die Thioamidgruppierung durch eine Bande bei 1395 cm^{-1} angezeigt wird. Im UV-Spektrum findet sich wieder der typische Elektronenübergang der Enolatgruppe bei $\lambda = 332$ nm (lg $\varepsilon = 4{,}21$). Dieses Ergebnis steht im Gegensatz zur Reaktion der *s*-Triazol-4N-imine, die unter den gleichen Bedingungen bicyclische Produkte liefern. [16] Unübersichtlicher verläuft dagegen die Umsetzung der Ylide **3** mit Propiolsäureester in Benzol. Zwar reagieren beide Partner bei Zimmertemperatur wieder äußerst schnell, es entsteht aber ein Produktgemisch. Durch Umkristallisieren konnten daraus Ylide des Typs **6** isoliert werden, während die anderen Verbindungen sich bereits beim kurzzeitigen Erwärmen zersetzen. Die Struktur des N-Ylids **6a** wird durch die NMR-Daten ($\delta = 9{,}1$ ppm (s, 1); 7,9 ppm (s, 1); 7,7 ppm (m, 4); 7,5 ppm (d, 1); 6,05 ppm (d, 1); 4,25 ppm (s, 3); 4,1 ppm

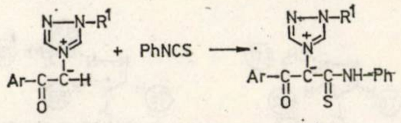

3c,e

5a,b

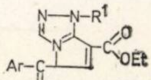

7

(q, 2); 1,2 ppm (t, 3)), das UV-Spektrum ($\lambda_{max} = 349$ nm, $\lg\varepsilon = 4{,}24$) und das IR-Spektrum (1690 und 1510 cm^{-1}) bewiesen; vgl. dazu auch analoge Daten für ein entsprechendes Ylid der Pyrazol-Reihe.[17] Auch die

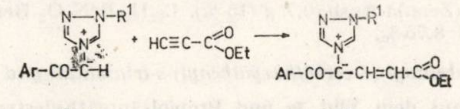

3c,e **6a,b**

Pikrylchloridprobe ist positiv. Im Reaktionsgemisch sind offensichtlich auch Produkte **7** einer Cycloadditionsreaktion vorhanden. Das folgt aus den in den IR-Spektren des Gemisches enthaltenen IR-Banden bei 1710 cm^{-1}. Die Art der Reaktionsprodukte stimmt wiederum nicht mit denen der Umsetzung von *s*-Triazol-4N-iminen und Propiolsäureestern überein. In diesem Falle wurden in hohen Ausbeuten Verbindungen isoliert, die eindeutig eine 1,3-dipolare Cycloaddition beweisen.[18]

BESCHREIBUNG DER VERSUCHE

Die Schmelzpunkte wurden auf einem Mikroheiztisch BOËTIUS bestimmt. Zur Aufnahme der NMR-Spektren mit TMS als inneren Standard diente das Gerät ZKR 60 des VEB „Carl Zeiss" Jena. Die IR-Spektren wurden mit dem Spektrophotometer UR 10 der gleichen Firma und die UV-Spektren mit dem Gerät UNICAM SP 800 aufgenonmen.

1,4-Disubstituierte s-Triazoliumsalze **2**; vgl Tab. 1

Je 0,1 Mol 1-substituiertes *s*-Triazol **1** und des betreffenden Alkylhalogenids werden in 80 ml absolutem Äthanol 5 Std. unter Rückfluß gekocht. Nach dem Abkühlen saugt man den ausgefallenen Niederschlag ab und kristallisiert aus Äthanol um.

*s-Triazolium-*4N-*Ylide* **3**; vgl. Tab. 2

Man löst 0,05 Mol Quartärsalz **2** in möglichst wenig kaltem Wasser und versetzt mit 30 ml konz. Ammoniaklösung. Der ausfallende Niederschlag wird nach kurzem Stehen abgesaugt, gut mit Wasser gewaschen und aus dem in Tab. 2 genannten Lösungsmittel umkristallisiert.

*1-Methyl-4-*p*-nitrobenzyl-s-triazol(5)thion* (**4**)

Man kocht 3 g (0,01 Mol) 1-Methyl-4-*p*-nitrobenzyl-*s*-triazoliumbromid **2h** und 0,4 g (0,013 Mol) Schwefel in 20 ml Pyridin 1 Std. unter Rückfluß. Nach dem Abkühlen wird mit Wasser verdünnt, der ausgefallene Niederschlag abgesaugt und aus Äthanol umkristallisiert. F. 160°; Ausb. 1,8 g (70 %).

$C_{10}H_{10}N_4O_2S$ Ber. C 48,01 H 4,00 N 22,39; Gef. C 48,37 H 4,17 N 22,67 %.

1-Phenyl-4-benzoyl-N'-phenylthiocarbamoyl-s-triazolium-ylid (**5a**)

2,6 g (0,01 Mol) Ylid **3c** werden in 30 ml Methylenchlorid suspendiert und unter Rühren und Wasserkühlung 1,35 g (0,01 Mol) Phenylisothiocyanat zugetropft. Dabei geht der Niederschlag in Lösung. Nach 30-minütigem Rühren dampft man i. Vak. zur Trockene und kristallisiert den Rückstand aus Äthanol/Wasser (1 : 1) um. F. 156°; Ausb. 2,8 g (70 %). $C_{23}H_{18}N_4OS$ Ber. C 69,34 H 4,54 N 14,06; Gef. C 69,42 H 4,65 N 14,10 %.

*1-Methyl-4-*p*-brombenzoyl-N'-phenylthiocarbamoyl-s-triazolium-ylid* (**5b**)

Wie vorstehend aus dem Ylid **3e** und Phenylisothiocyanat. F. 162°; Ausb. 78 %. $C_{18}H_{15}BrN_4OS$ Ber. C 52,06 H 3,64 N 25,92; Gef. C 52,06 H 3,75 N 26,15 %.

1-Benzyl-4-p-brombenzoyl-(2-carbäthoxyäthenyl)-s-triazolium-ylid **(6a)**

2,6 g (0,01 Mol) Ylid **3d** werden in 15 ml Benzol suspendiert und unter Rühren und Wasserkühlung 1,0 (0,0104 Mol) Propiolsäureäthylester zugetropft. Dabei geht der ursprüngliche Niederschlag in Lösung und es fällt nach kurzer Zeit ein neuer aus. Dieser wird abgesaugt, mit CCl_4 nachgewaschen und aus Äthanol/ Wasser (5 : 1) umkristallisiert. Dabei tritt starke Zersetzung auf. F. 143° (Zers.); Ausb. 0,7 g (15 %). $C_{22}H_{21}BrN_3O_2$ Ber. C 58,35 H 4,41 N 9,21; Gef. C. 58,71 H 4,40 N 8,75 %.

1-Methyl-4-p-brombenzoyl-(2-carbäthoxyäthenyl)-s-triazolium-ylid **(6b)**

Wie vorstehend aus dem Ylid **3e** und Propiolsäureäthylester. F. 187° (Zers.); Ausb 18 %. $C_{16}H_{16}BrN_3O_3$ Ber. C 50,81 H 4,26 N 11,11; Gef. C 50,67 H 4,30 N 10,33 %.

LITERATURVERZEICHNIS

[1] I. Zugrăvescu u. M. Petrovanu, "N-Ylid Chemistry", Mc Graw-Hill International Book Company, 1976.
[2] H. G. O. Becker, N. Sauder u. H.-J. Timpe, *J. prakt. Chem.*, **311,** 897 (1969).
[3] H. G. O. Becker, G. Görmar, H. Haufe u. H.-J. Timpe, *J. prakt. Chem.*, **314,** 101 (1972).
[4] H. G. O. Becker u. H.-J. Timpe, *J. prakt. Chem.*, **312,** 1112 (1970).
[5] H. G. O. Becker, K. Heimburger u. H.-J. Timpe, *J. prakt. Chem.*, **313,** 795 (1971).
[6] H.-J.Timpe, *Z. Chem.*, **11,** 341 (1971).
[7] H. G. O. Becker, H. D. Steinleitner u. H.-J.Timpe, *Synthesis*, **1973,** 414.
[8] V. A. Kovtunenko, L. D. Didenko u. F. S. Babichev, *Ukrain. Khim. Zhur.*, **40,** 402 (1974).
[9] M. Schulz, N. Großmann u. W. Schauer, *J. prakt. Chem.*, **318,** 586 (1976).
[10] G. F. Duffin, J. D. Kendall u. H. R. J. Waddington, *J. Chem. Soc.*, **1959,** 3799.
[11] G. Phillips u. W. Ratts, *J. Org. Chem.*, **35,** 3144 (1970).
[12] C. Reichardt, *Liebigs Ann. Chem.*, **715,** 74 (1968).
[13] T. Do Minh u. A. M. Trozolo, *J. Amer. Chem. Soc.*, **94,** 4046 (1972).
[14] H. J. Schönherr u. H. W. Wanzlick, *Liebigs Ann. Chem.*, **731,** 176 (1970).
[15] G. Surpăteanu, Thesis, University of Jassy, 1972; vgl. [1].
[16] P. Zalupsky, Privatmitteilung, 1977.
[17] V. Boekelheide u. J. E. Nottke, *J. Org. Chem.*, **34,** 4134 (1969).
[18] Y. Tamura, H. Hayashi u. M. Ikeda, *Chem. Pharm. Bull.*, **24,** 2568 (1976).

Revue Roumaine de Chimie, 25, *3*, 415–424 (1980)

REACTIONS OF SOME ARYLIDENEFURANONES

M. M. ABD ALLA, E. A. SOLIMAN and M. W. OSMAN
Faculties of Science, Zagazig and Ain Shams Universities, Cairo, Egypt

Received April 17, 1978

Hydrolysis of α-3-arylidene-5-(3,4-dichlorophenyl)-furan-3-(2*H*)-2-ones (II) and their reaction with amines and ammonium acetate has been investigated. The action of Grignard reagent and Friedel-Crafts reactions of II has been also extended and explored.

Recently, it has been reported[1] that β-3,4-dichlorobenzoylpropionic acid (I) condenses with aromatic aldehydes under Perkin conditions to give the corresponding arylidenefuranones derivatives (IIa–f).

Treatment of IIa, b and d with sodium hydroxide gave after acidification the corresponding phenacyl cinnamic acid derivatives (IIIa-c) respectively.

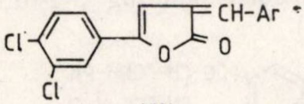

(II)

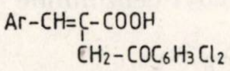

(III)

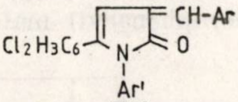

(IV)

	Ar
a,	C_6H_5
b,	$C_6H_4OCH_3(p)$
c,	$C_6H_4N(CH_3)_2-(p)$
d,	$C_6H_3O_2CH_2-3,4$
e,	$C_6H_5-CH=CH-$
f,	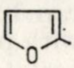

	Ar
a,	C_6H_5
b,	$C_6H_4OCH_3-(p)$
c,	$C_6H_3O_2CH_2-3,4$

	Ar	Ar'
a,	C_6H_5	C_6H_5
b,	C_6H_5	$C_6H_4CH_3-(p)$
c,	C_6H_5	$C_6H_4OCH_3-(p)$
d,	$C_6H_4OCH_3-(p)$	C_6H_5
e,	$C_6H_4OCH_3-(p)$	$C_6H_4CH_3-(p)$
f,	$C_6H_4OCH_3-(p)$	$C_6H_4OCH_3-(p)$
g,	$C_6H_3OCH_2-3,4$	$C_6H_4OCH_3-(p)$
h,	C_6H_5	$C_6H_4Cl-(o)$
i,	$C_6H_4OCH_3-(p)$	$C_6H_4Cl-(o)$

The I.R. spectra of III showed well-defined bands in the region 1700–1600 cm^{-1} characteristic of C=0 of α, β-unsaturated carboxylic acids[2a], at 1680–1660 cm^{-1} characteristic of C=0 of benzylic ketones[2b] and at 2950 cm^{-1} characteristic of –OH group[2c].

Compound IIIb can be obtained by treatment of IIb with boiling acetic anhydride.

Reaction of II with aromatic amines in the presence of acetic acid/sodium acetate gives the corresponding 4-arylidene-1-aryl-2-(3,4-dichlorophenyl)-2-pyroline-5-ones (IVa-i) by acyl-oxygen fission followed by ring closure.

The I.R. spectra of compounds IV showed well-defined bands at 1720 cm^{-1} characteristic of C=0 of α, β-unsaturated ketones and at 1590 cm^{-1} characteristic of C=C.

Similarly, when 5-(3,4-dichlorophenyl)-5-furan-3-(2*H*)-furanone (V) (prepared by cyclization of I) was treated with aniline in boiling alcohol it gave the anilide VI which was easily cyclized to 1-phenyl-2-(3,4-dichlorophenyl)-2-pyroline-5-one (VII) on treatment with acetic anhydride.

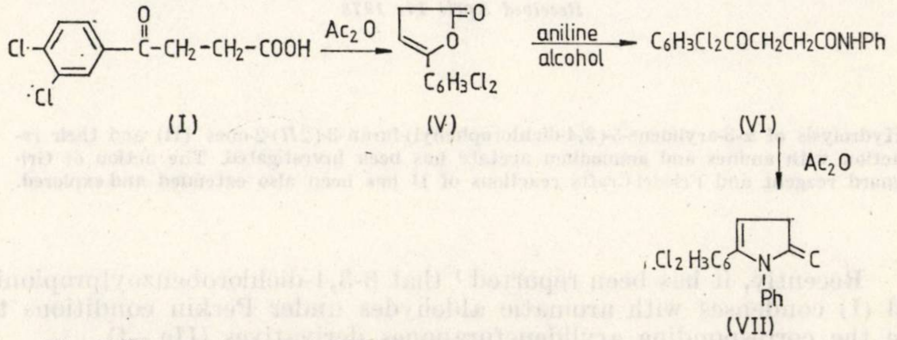
Cl
Cl
C-CH₂-CH₂-COOH
Ac₂O
O
C₆H₃Cl₂
aniline
alcohol
C₆H₃Cl₂COCH₂CH₂CONHPh
(I)
(V)
(VI)
Ac₂O
Cl₂H₃C₆
N
C
Ph
(VII)

The I.R. spectrum of VII showed a sharp band at 1715 cm^{-1} characteristic of C=C of α, β-unsaturated ketones.

However, 3-2-oxo-5-(3,4-dichlorophenyl)-3-(2*H*)-furylidene phthalide (VIII) (prepared by reaction of I with phthalic anhydride) reacts with aniline at room temperature to give the corresponding 2-2-(3,4-dichlorophenacyl) malonaniloyl-benzanilide (IX).

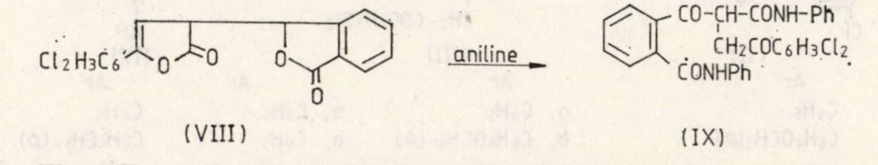
Cl₂H₃C₆
O
O
O
O
aniline
CO-CH-CONH-Ph
CH₂COC₆H₃Cl₂
CONHPh
(VIII)
(IX)

The I.R. spectrum of IX showed well-defined bands at 1660 cm^{-1} characteristic of C=O of aromatic ketones, at 1615 cm^{-1} characteristic of C=0 of the anilide [2d] and at 3250 cm^{-1} characteristic of NH group. [2e]

Similarly, on treatment of 5-(3,4-dichlorophenyl)-furan-3(2*H*)-2′-indene-1′,2′, 3′-trione (X) (prepared by reaction of VIII with phthalic anhydride in the presence of acetic anhydride and sodium acetate) with aniline at room temperature 1,3-dioxo-2-(3,4-dichlorophenyl)2-indene carboxanilide (XI) results, which can be easily cyclized in hot alcohol to give the pyrolinone derivative XII.

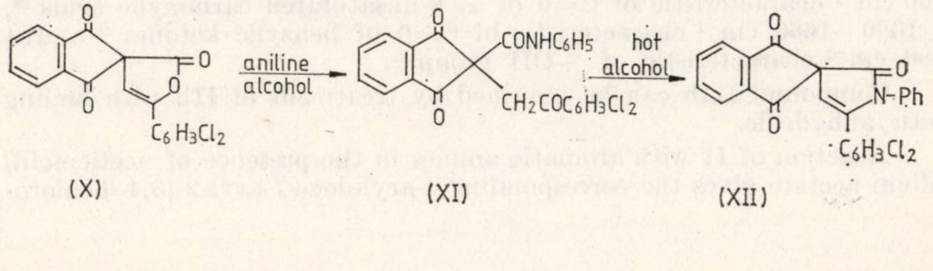
O
O
O
O
C₆H₃Cl₂
aniline
alcohol
O
CONHC₆H₅
CH₂COC₆H₃Cl₂
O
hot
alcohol
O
O
N-Ph
O
C₆H₃Cl₂
(X)
(XI)
(XII)

The I.R. spectrum of XI showed bands at 1650 cm^{-1}, 1610 cm^{-1} characteristic of C=O of the anilide and at 3250 cm^{-1} characteristic of the NH group while that of XII showed bands at 1665 cm^{-1} and 1690 cm^{-1} characteristic of C=O of pyrrolone [2f].

However, during the present investigation, it was found that IVh when allowed to react with phenylmagnesium bromide gave 1-*o*-chlorophenyl-3-(4-benzyl-4-phenyl) methyl-5-(3,4-dichlorophenyl) pyrrolin-2-one (XIII) which can be prepared authentically by reaction of IVh with anhydrous $AlCl_3$ in benzene.

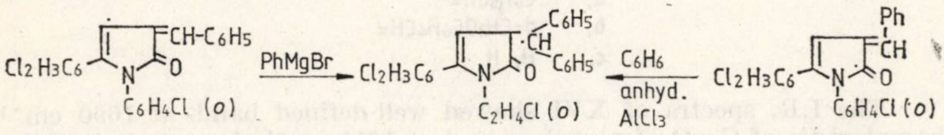

(IVh) (XIII) (IVh)

The I.R. spectrum of XIII indicated bands at 1700 cm^{-1} characteristic of C=O[2g], at 1610 cm^{-1} characteristic of C=C in ring system and the absence of —OH stretching frequency.

In the present investigation it has been found that IIa, IIb, and IId react with aliphatic amines, namely, methyl, butyl, benzyl or ethanolamine to give the corresponding N-alkyl-γ-(3,4-dichlorophenacyl) cinnamamides (XIVa-i).

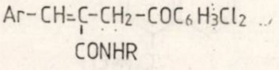

$$Ar-CH=\underset{CONHR}{C}-CH_2-COC_6H_3Cl_2$$

(XIV)

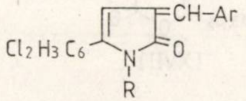

(XV)

	Ar	R
a,	C_6H_5	CH_3
b,	C_6H_5	C_4H_9
c,	C_6H_5	$C_6H_5-CH_2$
d,	C_6H_5	C_2H_5O
e,	$C_6H_4OCH_3(p)$	CH_3
f,	$C_6H_4OCH_3(p)$	C_4H_9
g,	$C_6H_4OCH_3(p)$	$C_6H_5CH_2$
h,	$C_6H_4OCH_3(p)$	C_2H_5O
i,	$C_6H_3O_2CH_2$-3,4	CH_3

	Ar	R
a,	C_6H_5	C_4H_9
b,	$C_6H_3OCH_2$ (*p*)	C_4H_9
c,	$C_6H_3OCH_2$-(3,4)	CH_3

The I.R. spectra of XIV show well-defined bands in the region of 1685—1660 cm^{-1} characteristic of C=O of aromatic ketones, at 1660 cm^{-1} 1630 cm^{-1} characteristic of C=O of amide and at 3320—3250 cm^{-1} characteristic of the NH group.

Boiling of the amides XIVb, f and i with acetic anhydride affords the corresponding 4-arylidene-1-alkyl-2 (2,3-dichlorophenyl)-2 pyrroline-5-ones (XVa-c). Compounds XVa and b can be prepared authentically via reaction of IIa and b with butylamine in the presence of acetic acid/sodium acetate mixture.

Reaction of IIa, b and V with ammonium acetate in xylene afforded 4-arylidene-2-(3,4-dichlorophenyl)-2-pyrrolin-5-ones and 2-(3,4-dichlorophenyl)-2-pyrroline-5-ones (XVI A and B), respectively.

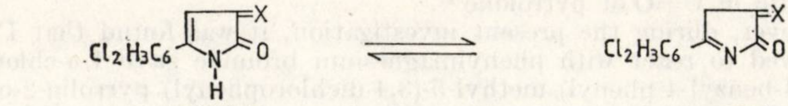
(XVI A) (XVI B)

	X
a,	$C_6H_5CH=$
b,	p-$CH_3OC_6H_4CH=$
c,	H, H

The I.R. spectra of XVI showed well-defined bands at 1690 cm^{-1} characteristic of C=O of pyrrolone and at 1615 cm^{-1} characteristic of the C=N group, and at 1610 cm^{-1} characteristic of C=C.

Compound XVIc was prepared authentically via reaction of I with ammonium acetate in boiling xylene.

As a point of interest IIa, b and d react with Grignard reagents, namely methylmagnesium iodide, ethylmagnesium iodide and phenylmagnesium bromide via 1,4-addition on the exocyclic double bond to give XVIIa-f, respectively.

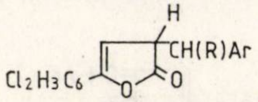
(XVII)

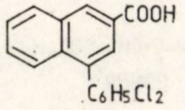
(XVIII)

	Ar	R
a,	C_6H_5	CH_3
b,	C_6H_5	C_2H_5
c,	C_6H_5	C_6H_5
d,	$C_6H_4OCH_3$	C_2H_5
e,	$C_6H_4OCH_3$	C_6H_5
f,	$C_6H_4OCH_2$-3,4	C_6H_5

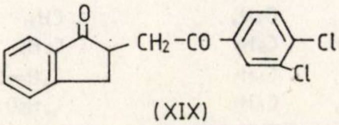
(XIX)

The I.R. spectra of compounds XVII showed well-defined bands at 1780–1760 cm^{-1} characteristic of C=O and at 1620 cm^{-1} characteristic of C=C group.

The highly conjugated carbon chain in arylidene furanones provides a third avenue for attack and this is the reactive site for the Friedel-Crafts reaction [3,4] in the reaction of γ-lactones with aromatic hydrocarbons in the presence of anhydrous $AlCl_3$ which gives naphtoic and cinnamic acid derivatives. Thus, reaction of IIa with anhydrous aluminium chloride in inert solvents, namely acetylene tetrachloride or benzene afforded 4-(3,4-dichlorophenyl)-2-naphthoic acid (XVIII) together with the corresponding 2-(3,4-dichlorophenyl)-indenone (XIX). The I.R. spectra of XVIII and XIX showed the band characteristic of C=O of carboxyl group at 1690 cm^{-1} and 1680 cm^{-1}, respectively.

On the other hand, reaction of IIa and b with reactive hydrocarbons namely *o*-chlorotoluene, anisole, toluene and chlorobenzene under Friedel-Crafts conditions, afforded butanediones XX and cinnamic acid derivatives XXI, respectively. Thus, reaction of IIa with *o*-chlorotoluene under Friedel-Crafts conditions gave the butanedione XX together with the 2-naphthoic acid XVIII.

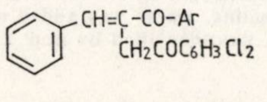

(XX)

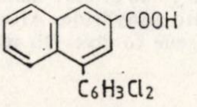

(XVIII)

The I.R. spectrum of XX showed well-defined bands at 1690 cm^{-1} characteristic of C=O of α, β-unsaturated ketone, at 1655 cm^{-1} characteristic of C=O of aryl ketone and at 1600 cm^{-1} characteristic of C=C group. The reaction of IIb with toluene or anisole, under the same conditions, gave the corresponding α-*p*-tolyl-β-(3,4-dichlorophenyl) styryl, and α-*p*-anisyl-β-(3,4-dichlorophenyl)-styryl-*p*-methoxycinnamic acids (XXIa and b), respectively.

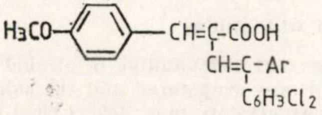

(XXI)

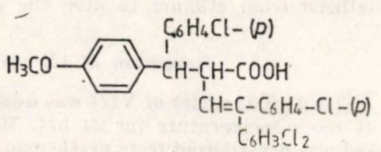

(XXII)

a, $Ar = C_6H_4-CH_3\,(p)$

b, $Ar = C_6H_4-OCH_3\,(p)$

The structure of compounds XXI was proved from the solubility in sodium bicarbonate solution and I.R. spectra which showed well-defined bands at 1700–1680 cm^{-1} characteristic of C=O of the carbonyl group and at 2980 cm^{-1} characteristic of –OH group.

Finally, the reaction of IIb with chlorobenzene under Friedel-Crafts conditions afforded XXII via alkyl-oxygen fission with further addition on the double bond.

The I.R. spectrum of XXII showed well-defined bands at 1700 cm^{-1} characteristic of C=O of the carboxyl group, at 1625 cm^{-1} characteristic of C=C and at 3420 cm characteristic of OH group.

EXPERIMENTAL

The infrared absorption spectra were determined with a Unicam SP 1200 Spectrophotometer using KBr wafer technique. All melting points are uncorrected. The characterizations of new compounds are given in Table 1.

Hydrolysis of α-3-arylidene-5-(3.4-dichlorophenyl)-furan-3(2H)-2-ones(II)

To 0.01 mole of IIa, b or d, 25 ml of 6N sodium carbonate or NaOH solution was added and the mixture was heated under reflux for 6 hrs. The reaction mixture was acidified with dilute HCl and the solid product that separated as white crystals was crystallized from benzene.

Conversion of IIIb to IIb

Compound IIIb (3.65 g, 0.01 mole) was heated on a steam bath for one hour with 10.2 ml (0.1 mole) of acetic anhydride. After cooling, water was added and the crude solid was crystallized from benzene to give IIb which was identified by m.p. 215° and mixed m.p. determinations.

Reaction of furanones II with aromatic amines. Formation of pyrrolidineones IV

To a solution of the appropriate aromatic amines (0.03 mole), furanones II (0.01 mole) in acetic acid (50 ml) and sodium acetate (0.02 mole) was added, then the solution was refluxed for 8 hrs. The mixture was poured into icewater, the solid separated was crystallized from ethanol to give IV.

Reaction of V with aniline. Formation of VI and VII via cyclization of VI

To a solution of V (2.3 g, 0.01 mole) in ethanol (0.55 ml, 0.046 g, 0.005 mole) of aniline was added and the reaction mixture was refluxed for 4 hrs then cooled. The solid separated was crystallized from ethanol to give VI. Compound VI (3.2 g ; 0.01 mole) was treated with acetic anhydride for 1 hour on steam bath then poured into water. The solid separated was crystallized from ethanol to give the pyrrolinone VII.

Formation of IX via reaction of VIII with aniline

(3.6 g ; 0.01 mole) of VIII was added to 1 ml (0.93 g ; 0.01 mole) aniline in alcohol then left at room temperature for 24 hrs. Most of the solvent was evaporated and the solid separated was crystallized from acetic acid to give IX as brown crystals, m.p. 225°, (Yield 65 %) Found : C, 66.10 ; H, 4.06 ; N, 5.20 ; $C_{30}H_{22}N_2O_4Cl_2$ requires : C, 66.05 ; H, 4.04 ; N, 5.14 %.

Formation of XI

(3.6 g ; 0.01 mole) of X were added to a solution of 1 ml (0.93 g ; 0.01 mole) of aniline in 50 ml alcohol and the reaction mixture was left overnight. The solvent was evaporated to give a solid mass which was crystallized from benzene to give XI as white crystals, m.p. 276°. (Yield 70 %). Found : C, 64.00 ; H, 3.50 ; N, 3.12 ; $C_{24}H_{15}NO_4Cl_2$ requires : C, 63.72 ; H, 3.32 ; N, 3.10%.

Conversion of XI to pyrrolidenone XII

A solution of XI (1 g ; 0.01 mole) in 50 ml alcohol was refluxed for 10 hrs then cooled after evaporation of most of the solvent. The solid separated was crystallized from acetic acid to give XII as greyish crystals, m.p. 240°, (Yield 75 %). Found : C, 66.90 ; H, 3.00 ; N, 3.05 ; $C_{25}H_{13}NO_3Cl_2$ requires : C, 67.26 ; H, 2.91 ; N, 3.14 %.

Reaction of IV with Grignard reagent

To a Grignard solution (prepared from 0.06 g atoms of magnesium and 0.6 mole of bromobenzene in 100 ml of dry ether) was added a solution of IVh (4.2 g ; 0.01 mole) in 50 ml of dry ether. The reaction mixture was heated under reflux for 2 hrs, left overnight, then decomposed by 100 ml of saturated ammonium chloride solution. The ethereal layer was dried over anhydrous sodium sulphate, evaporated, and the residue thus obtained was washed several times with petroleum ether (b. p. 40—60°), and crystallized from ethanol to give XIII as white crystals. m.p. 210° (Yield 80 %). Found : C, 69.00 ; H, 4.02 ; N, 2.80, $C_{29}H_{20}NOCl_3$ requires : C, 68.98 ; H, 3.96 ; N, 2.77 %.

Reaction of II with aliphatic amines. Formation of XIV

A solution of IIa, b or d (0.01 mole) and primary aliphatic amines, namely, methyl, buthyl benzyl or ethanol amine (0.03 mole) in 50 ml ethanol was heated under reflux for 6 hrs, The products that separated on cooling were crystallized from ethanol to give N-alkyl-α-(3,4-dichlorophenacyl) cinnamides (XIV) as white crystals.

Formation of 4-arylidene-1-alkyl-2-(3,4-dichlorophenyl)-2-pyrrolin-ones (XV)

Compound XIVb, f, or i (1 g) was added to acetic anhydride (30 ml), the reaction mixture was heated on steam bath for 6 hrs. The cold solution was poured into ice, the residue was crystallized from ethanol to give the corresponding pyrrazolinones XVa-c as pale yellow crystals.

Conversion of IIa or b to XVa or b

To a solution of IIa or b (0.01 mole) and sodium acetate (1 g ; 0.015 mole) in acetic acid (30 ml) was added butylamine (1 ml ; 0.015 mole). The reaction mixture was refluxed for 6 hrs then cooled and poured into ice. The solid separated was crystallized from ethanol to give crystals identified as XVa or b by m. p.and mixed m.p. determinations and analytical data.

Reaction of ammonium acetate with II and V. Formation of pyrrolinones XVI

A solution of IIa, b or V (0.01 mole) in xylene or acetic anhydride (50 ml) was added to ammonium acetate (5 g ; 0.065 mole), the reaction mixture was refluxed for 4 hrs, then cooled and poured into ice. The solid residue was crystallized from ethanol to give XVI.

Reaction of I with ammonium acetate. Formation of XVIc

To a solution of acid I (2.4 g ; 0.01 mole) in xylene or acetic anhydride ammonium acetate (0.04 mole) was added then the reaction mixture was refluxed for 4hrs, cooled and poured into ice. The solid residue was crystallized from ethanol to give crystals identified as XVIc by m.p. and mixed m.p. determinations and analytical data.

Reaction of XVIc with benzaldehyde and anisaldehyde. Formation of XVIa and b

To a solution of XVI c (2.2 g ; 0.01 mole) in xylene or acetic anhydride was added benzaldehyde (1 ml or 1.3 ml ; 0.01 mole), the reaction mixture was refluxed for 6 hrs, then cooled and poured into ice. The solid separated was crystallized from suitable solvent to give crystals identified as XVIa or b by m.p. and mixed m.p. determinations and analytical data.

Reaction of II with Grignard reagent. Formation of XVII

To a Grignard solution (prepared from 0.06 g atoms of magnesium and 0.06 mole methyliodide, ethyliodide or bromobenzene in 100 ml of dry ether) a solution of 0.01 mole of IIa, b or d on 50 ml of dry ether was added. The reaction mixture was heated under reflux for 2 hrs, left overnight, then decomposed by 100 ml of saturated solution of ammonium chloride. The organic layer was separated and evaporated. The residue thus obtained was washed several times with light petrol (b. p. 40—60°), then recrystallized from methanol to give XVII as colourless crystals.

Reaction of IIa under Friedel Crafts conditions. Formation of XVIII—XXII

To a mixture of aromatic hydrocarbon (100 ml) and anhydrous aluminium chloride (10 g ; 0.06 mole) a solution of IIa or b (3.1 g ; 0.02 mole) was allowed to stand overnight, then decomposed (dil. HCl) and the solvent removed by steam distillation. The solid was crystallized from a suitable solvent to give white crystals of XVIII—XXII.

TABLE 1

The characterizations of new compounds

Compd.	m.p.(°C) Yield (%)	Solvent* Colour	Formula	Analysis %		
					Found	Required
IIIa	185	B	$C_{17}H_{12}O_3Cl_2$	C	60.85	60.89
	80	White		H	3.60	3.58
IIIb	196	B	$C_{18}H_{14}O_4Cl_2$	C	59.30	59.18
	80	White		H	3.85	3.84
IIIc	204	B	$C_{18}H_{13}O_5Cl_2$	C	56.90	56.84
	74	White		H	3.41	3.42
IVa	160	E	$C_{23}H_{15}NOCl_2$	C	70.40	70.41
	85	Brown		H	3.80	3.83
				N	3.55	3.57
IVb	142	E	$C_{24}H_{17}NOCl_2$	C	70.85	70.94
	70	Yellow		H	4.01	4.19
				N	3.41	3.45
IVc	176	E	$C_{24}H_{17}NO_2Cl_2$	C	68.19	68.25
	85	Golden		H	4.10	4.03
		yellow		N	3.30	3.32
IVd	163	E	$C_{24}H_{17}NO_2Cl_2$	C	68.17	68.25
	80	Yellow		H	4.00	4.03
				N	3.35	3.32
IVe	135	E	$C_{25}H_{19}NO_2Cl_2$	C	68.75	68.81
	75	Yellowish		H	4.30	4.36
		brown		N	3.20	3.21
IVf	179	E	$C_{25}H_{19}NO_3Cl_2$	C	66.29	66.37
	85	Brown		H	4.15	4.20
				N	3.00	3.10
IVg	165	E	$C_{25}H_{17}NO_4Cl_2$	C	64.15	64.38
	75	Golden		H	3.50	3.65
		yellow		N	2.91	3.00
IVh	181	E	$C_{23}H_{14}NOCl_3$	C	64.57	64.71
	85	Golden		H	3.30	3.28
		yellow		N	3.25	3.28
IVi	184	E	$C_{24}H_{16}NO_2Cl_3$	C	63.00	63.09
	85	Golden		H	3.45	3.50
		yellow		N	3.00	3.07
VI	158	E	$C_{16}H_{13}NO_2Cl_2$	C	59.50	59.63
	80	White		H	4.00	4.04
				N	4.10	4.35
VII	185	E	$C_{16}H_{11}NOCl_2$	C	63.20	63.16
	60	Brown		H	3.69	3.62
				N	4.52	4.61
XIVa	198	E	$C_{18}H_{15}NOCl_2$	C	62.00	62.07
	90	White		H	4.58	4.31
				N	4.00	4.02

Table 1 (continued)

Compd.	m.0.(°C) Yeild %	Solvent* Colour	Formula	Analysis %		
					Found	Required
XIVb	185	E	$C_{21}H_{21}NO_2Cl_2$	C	64.50	64.62
	90	White		H	5.30	5.38
				N	3.90	3.59
XIVc	182	E	$C_{24}H_{19}NO_2Cl_2$	C	67.80	67.92
	80	White		H	4.50	4.48
				N	3.50	3.30
XIVd	181	E	$C_{19}H_{17}NO_3Cl_2$	C	60.40	60.31
	75	White		H	4.40	4.49
				N	3.71	3.70
XIVe	192	E	$C_{19}H_{17}NO_3Cl_2$	C	60.15	60.31
	85	White		H	4.50	4.49
				N	3.68	3.70
XIVf	198	E	$C_{22}H_{23}NO_3Cl_2$	C	63.00	62.86
	90	White		H	5.40	5.48
				N	3.50	3.33
XIVg	178	E	$C_{25}H_{21}NO_3Cl_2$	C	66.10	66.08
	80	White		H	4.50	4.63
				N	3.00	3.08
XIVh	160	E	$C_{20}H_{19}NO_4Cl_2$	C	59.10	58.82
	75	White		H	4.90	4.66
				N	3.80	3.43
XIVi	199	E	$C_{19}H_{15}NO_4Cl_2$	C	58.50	58.16
	80	White		H	3.75	3.83
				N	3.80	3.57
XVa	225	E	$C_{21}H_{19}NOCl_2$	C	68.00	67.74
	80	Yellow		H	5.10	5.11
				N	3.60	3.76
XVb	218	E	$C_{22}H_{21}NO_2Cl_2$	C	65.55	65.67
	80	Yellow		H	5.50	5.22
				N	3.50	3.48
XVc	220	E	$C_{19}H_{13}NO_3Cl_2$	C	61.20	60.96
	70	Yellow		H	3.40	3.48
				N	4.10	3.74
XVIa	261	A	$C_{17}H_{11}NOCl_2$	C	64.50	64.55
	80	Yellow		H	3.45	3.48
				N	4.40	4.43
XVIb	255	B	$C_{18}H_{13}NO_2Cl_2$	C	62.50	62.43
	90	Yellow		H	3.80	3.76
				N	4.00	4.05
XVIc	268	E	$C_{10}H_7NOCl_2$	C	53.00	52.63
	85	Reddish-brown		H	3.00	3.07
				N	6.00	6.14

Table 1 (continued)

Compd.	m.p. (°C) Yeld %)	Solvent* Colour	Formula	Analysis %		
					Found	Required
XVIIa	125	M	$C_{18}H_{14}O_2Cl_2$	C	64.70	64.86
	80	Colourless		H	4.20	4.20
XVIIb	248	M	$C_{19}H_{16}O_2Cl_2$	C	65.50	65.71
	75	Colourless		H	4.30	4.61
XVIIc	123	M	$C_{23}H_{16}O_2Cl_2$	C	70.10	69.87
	85	Colourless		H	4.10	4.05
XVIId	240	M	$C_{20}H_{18}O_3Cl_2$	C	63.80	63.66
	80	Colourless		H	4.90	4.77
XVIIe	113	M	$C_{24}H_{18}O_3Cl_2$	C	68.00	67.76
	85	Colourless		H	4.40	4.24
XVIIf	124	M	$C_{24}H_{16}O_4Cl_2$	C	65.80	65.60
	85	Colourless		H	3.70	3.64
XVIII	275	A	$C_{17}H_{10}O_2Cl_2$	C	64.50	64.35
	70	White		H	3.20	3.15
XIX	226	B	$C_{17}H_{10}O_2Cl_2$	C	64.60	64.35
	25	White		H	3.10	3.15
XX	268	B	$C_{24}H_{17}O_2Cl_3$	C	65.10	64.99
	50	White		H	3.80	3.83
XXIa	257	E	$C_{25}H_{20}O_3Cl_2$	C	68.50	68.34
	70	White		H	4.70	4.55
XXIb	218	A	$C_{25}H_{20}O_4Cl_2$	C	66.10	65.93
	80	White		H	4.40	4.39
XXII	260	A	$C_{30}H_{22}O_3Cl_4$	C	63.00	62.94
	75	White		H	3.80	3.85

* A = acetic acid ; B = benzene ; E = ethanol ; M = methanol

REFERENCES

[1] A. Sammour, A. F. Fahmy, M. Abd Alla and A.. A. Hamed, *Egypt J. Chem.*, **18 (b)**, 1041 (1975).

[2] L. J. Bellamy, "The Infrared Spectra of Complex Molecules", Methuen Co. London 1967; Pages a) 165; b) 134; c) 162; d) 221; e) 226; f) 148; and g) 147.

[3] R. Filler, L. H., Mark, and E. J., Piasek, *J. Org. Chem.*, **24**, 1780 (1959).

[4] R. Filler, and H. A., Leipold, *J. Org. Chem.*, **27**, 4440 (1962).

Revue Roumaine de Chimie, **25**, *3*, 425–433 (1980)

CHEMICAL MODIFICATION OF POLYMERS. II*. REACTION OF POLY(VINYL-α-CHLOROACETOPHENONE) WITH SOME HERBICIDAL SODIUM PHENOXIDES

DEMETRA DRĂGAN and A. CARPOV
"P. Poni" Institute of Macromolecular Chemistry,
Aleea Grigore Ghica Vodă 41 A, Jassy, Romania

Received March, 11, 1978

The Williamson reaction of poly(vinyl α-chloroacetophenone) with some herbicidal sodium phenoxides in dipolar aprotic solvents was investigated. Potential herbicidal polymer compositions having aryloxyalkyl aryl ketone type pendent substituents to the vinyl polymer backbone were prepared. A sequence of the relative reactivities of the tested sodium phenoxides in terms of polar and steric effects of the substituents in the ring was established. The composition of the polymers was confirmed by elemental analysis and IR spectra.

The purposeful modification of polymers by chemical reactions is proved to be a valuable route for synthesis of a large variety of biologically active polymers[1-3]. Copolymers of the desired composition can be prepared by stoichiometric control of sequential reactions.

In the previous paper of this series the Williamson reaction of some phenoxide anions with vinyl chloroacetate copolymers in dipolar aprotic solvents leading to copolymers with aryloxyalkyl carboxylic ester type moieties as pendent substituents to the polymer backbone was investigated.[4]

In an attempt to extend this reaction to other polymers bearing reactive halogen, the present paper is an account of the reaction of some of the same type phenoxide anions with poly(vinyl-α-chloroacetophenone), a much more reactive polymeric halogen derivative, leading to polymers with aryloxyalkyl aryl ketone type pendent substituents to the vinyl polymer backbone.

EXPERIMENTAL

The following herbicidal phenols were used: 2,4,5-trichlorophenol ($[H^+]_{25°} = 1.00 \times 10^{-6}$),[5] pentachlorophenol ($[H^+]_{25°} = 5.50 \times 10^{-6}$),[6] 2,6-diiodo-4-cyanophenol ($[H^+]_{25°} = 1.09 \times 10^{-4}$),[7] 2,6-dibromo-4-cyanophenol ($[H^+]_{25°} = 8.27 \times 10^{-5}$),[7] 2-sec-butyl-4,6-dinitrophenol and 2,4-dinitrophenol ($[H^+]_{25°} = 1.10 \times 10^{-4}$).[8]

The respective phenolic sodium salts were used: sodium 2,4,5-trichlorophenoxide (NaTCP), sodium pentachlorophenoxide (NaPCP), sodium 2,6-diiodo-4-cyanophenoxide (NaDICP), sodium 2,6-dibromo-4-cyanophenoxide (NaDBCP), sodium 2-sec-butyl-4,6-dinitrophenoxide (NaBDNP) and sodium 2,4-dinitrophenoxide (NaDNP). They were prepared by azeotropic removal of water from an equimolar mixture of concentrated aqueous sodium hydroxide and the respective phenol in xylene.

---

*Part I: see ref 4.

All the chemicals, except for the phenols, were of a reagent grade. The technical phenols were several times recrystalized from the appropriate solvents.

Common dipolar aprotic solvents were used: N,N-dimethyl-formamide (DMF), N-methylpyrrolidone (NMP), N,N-dimethylacetamide (DMAA), hexamethylphosphorotriamide (HMPTA) and dimethylsulphoxid (DMSO).

The catalysts used were: anhydrous sodium iodide (NaI) and triethylmethylammonium iodide (TEMAI).

The poly(vinyl α-chloroacetophenone) was prepared by Friedel-Crafts acylation of polystyrene (viscosity average molecular weight, $\bar{M}_v \cong 25{,}000$) with chloroacetyl chloride in carbon disulfide.[9] The polymer was soluble in DMP and was purified by several precipitations in water.

Anal. Calcd. for $C_{10}H_9OCl$: Cl, 19.64%; C, 66.48%; H, 4.98%;

Found: Cl, 19.10 – 19.40%; C, 67.01%; H, 5.10%.

In accordance with the above analytical data the chloroacetylated polymer is essentially a homopolymer.

All the syntheses were run in homogeneous media. Equal volumes of solutions (50 ml) of the starting polymer (14.14 moles) and of the sodium phenoxide in a slight excess (5–10%) were stirred at 25–80°, for definite time periods.

The crude polymers were purified by repeated precipitations of a DMF solution of the polymer in water and were then dried in vacuum.

The actual composition of the modified polymers was determined by elemental analysis and IR spectra.

The molar conversions of the polymers were estimated from analytical data (Cl, %; N, %) and corroborated by weight uptake measurements.

The IR spectra (KBr) were recorded on a UNICAM SP–200 spectrophotometer.

RESULTS AND DISCUSSION

The reaction of poly(vinyl α-chloroacetophenone) (I) with sodium phenoxides (II) in dipolar aprotic media is a typical Williamson reaction leading to copolymers with alkylaryl ether linkages in the side groups:

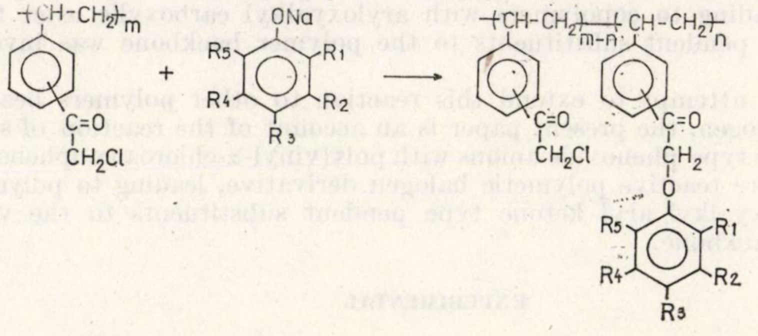

I II III

where, III–1: $R_1, R_3, R_4 = Cl$; $R_2, R_5 = H$

III–2: $R_1, R_2, R_3, R_4, R_5 = Cl$

III–3: $R_1, R_5 = I$; $R_3 = CN$; $R_2, R_4 = H$

III–4: $R_1, R_5 = Br$; $R_3 = CN$; $R_2, R_4 = H$

III–5: $R_1, R_3 = NO_2$; $R_2, R_4, R_5 = H$

III–6: $R_1 =$ sec-butyl; $R_3, R_5 = NO_2$; $R_2, R_4 = H$

The dipolar aprotic solvents used are convenient media for carrying out such O-alkylations via the homogeneous nucleophilic displacement of the reactive chlorine in the polymer with phenoxide anions. The precipitations of sodium chloride, as the substitution proceeds, exerts a strong suppression on the back reaction.

TABLE 1

Reaction with NaTCP; 6h

Code	Solvent	Temperature (°C)	Cl, % in the modified polymer	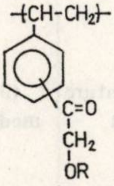 (mole, %)	Catalyst (TEMAI) molar ratio
1	HMPTA	40	25.02	36.27	
2	NMP	40	30.90	90.50	
3	DMF	40	28.89	72.50	
4	DMSO	40	29.90	83.50	
5	NMP	25	28.14	63.00	
6	NMP	25	27.19	53.00	1 :0.33

R =

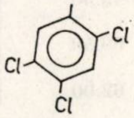

Tables 1—6 show the reaction conditions and molar conversion of the products for the six sodium phenoxides used.

The electronic and steric effects of the substituents in the phenoxide anions and also the effect of a soluble catalyst like an alkaline iodide or a tetraalkylammonium iodide in the medium were previously discussed.[4]

The amount of catalyst reported in the last column of Tables 1—6 ranges from 1 :0.16 to 1 :0.80 molar ratios of the polymeric derivative to the catalyst. Again its presence has a positive effect on the extent of reaction only in the case of the less reactive phenoxides from the series (Tables 2—6).[4]

It is believed that the local environment of the reactive center provided by the polymer itself enhances the rate of the desired reactions (O-alkylation) relative to the previously reported reaction with vinyl chloroacetate copolymers. The electronic effects ($-I$, $-E$) of the C_6H_5CO group on the carbon-chlorine bond makes the seat of the reaction, i.e. the carbon of the chloromethyl group, more positive and thus increases the attraction between this carbon atom and the attacking negative ion. The reaction moiety is also at an appreciable distance from the backbone

TABLE 2

Reaction with NaPCP ; 6h

Code	Solvent	Temperature (°C)	Cl, % in the modified polymer	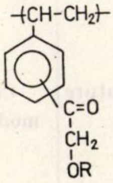 (mole, %)	Catalyst (molar ratio)	
					NaI	TEMAI
7	HMPTA	40	31.16	30.50	—	—
8	DMF	40	41.26	83.50	—	—
9	DMSO	40	36.33	52.50	—	—
10	DMSO	40	37.48	58.50	1 : 0.80	—
11	NMP	40	39.58	72.00	—	1 : 0.80
12	NMP	40	36.33	52.50	—	—
13	NMP	25	34.09	42.50	—	—
14	NMP	25	37.83	60.50	1 : 0.50	—
15	NMP	25	38.99	62.00	—	1 : 0.33

R =
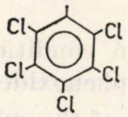

and thus the availability of the oxygen for nucleophilic displacement is greatly increased.

Therefore, the higher conversions achieved with this more activated polymeric substrate in reaction with some of the same phenoxide anions are consistent with the theoretical expectations. For instance, the phenoxides in Tables 1 and 2 can react to nearly complete conversion of the starting polymer.

The extents of reaction show the following sequence of the relative reactivity of the respective phenoxides :

NaTCP > NaPCP > NaDICP > NaDBCP > NaDNP > NaBDNP

This sequence parallels the order of the decreasing basicity of the anions except for NaDICP–NaDBCP and NaDNP–NaBDNP where an inversion is observed.

TABLE 3

Reaction with NaDICP; 6h

Code	Solvent	Temperature (°C)	N, % in the modified polymer	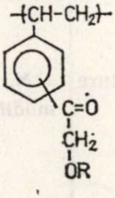 (mole, %)	Catalyst (molar ratio)	
					NaI	TEMAI
16	DMF	40	1.50	29.50	—	—
17	DMSO	40	1.70	36.12	—	—
18	NMP	40	1.62	33.35	—	—
19	HMPTA	40	1.96	46.51	—	—
20	DMAA	40	1.85	41.83	—	—
21	DMSO	40	2.54	81.49	1 : 0.80	—
22	NMP	80	2.61	91.96	—	—
23	DMSO	80	2.57	83.98	—	—
24	DMSO	25	1.90	43.91	—	1 : 0.80

R =

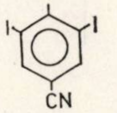

The reverse order found for the respective couples of sodium phenoxides is very likely a consequence of the joined polar and steric effects of the substituents adjacent to the phenoxydic oxygen. Specifically, the very small conversions with the NaBDNP are likely attributable to the increased steric hindrance in ether formation brought about by both the bulky sec-butyl- and nitro-substituents (R_1, R_5) from the 2,6-positions (Table 6).

The experimental data presented suggest that DMF, NMP, DMAA DMSO have quite similar effects on conversions. The small differences between them are consistent with their polarity and the corresponding electron-donor strength.[10]

With HMPTA, the most basic and the least polar solvent of the series, a competition with the phenoxides anions for the electrophilic site in the chloromethyl groups can partially take place.

TABLE 4

Reaction with NaDBCP; 6h

Code	Solvent	Temperature (°C)	N, % in the modified polymer	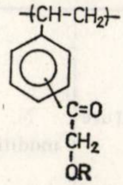 (mole, %)	Catalyst (molar ratio)	
					NAI	TEMAI
25	DMSO	40	1.79	32.62	—	—
26	DMF	40	1.50	25.50	—	—
27	NMP	40	1.70	30.30	—	—
28	HMPTA	40	1.96	37.28	—	—
29	DMAA	40	1.85	34.22	—	—
30	DMSO	40	2.38	50.79	1 : 0.80	—
31	DMF	40	2.55	57.25	—	1 : 0.16
32	DMF	40	2.70	63.52	—	1 : 0.80
33	DMF	80	2.85	70.43	—	—
34	DMSO	40	2.80	68.05	—	1 : 0.80

R = 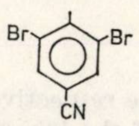

Some attempts carried out in HMPTA without a phenoxide, for 6h at 40°, led to polymers with a small content of nitrogen (0.30—0.40N, %). The occurrence of such a solvolitically substitution and the retardation of the Williamson substitution as a consequence of the relative strong nucleophilic power of the said solvent can be substantiated by the higher nitrogen contents of the polymers prepared in HMPTA using phenoxides with nitrogen substituents (Tables 3—6) and the smaller chlorine contents achieved with phenoxides having chlorine substituents (Tables 1,2).

All the chemically modified polymers are soluble in the abovementioned dipolar aprotic solvents used as reaction media, but are insoluble in water and lower alcohols. Copolymers III—2 are also soluble in chlorinated hydrocarbons.

TABLE 5

Reaction with NaDNP; 6h

Code	Solvent	Temperature (°C)	N, % in the modified polymer	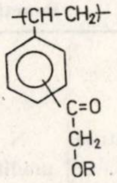 (mole, %)	Catalyst (molar ratio)	
					NaI	TEMAI
35	HMPTA	40	1.91	14.00	—	—
36	NMP	40	1.44	10.51	—	—
37	NMP	25	1.85	13.50	—	1 : 0.50
38	NMP	25	0.97	6.80	—	—
39	HMPTA	80	4.98	42.80	—	—
40	NMP	80	3.72	33.00	—	—
41	NMP	80	5.33	47.50	1 : 0.80	—
42	NMP	40	2.42	17.50	—	1 : 0.50

R = 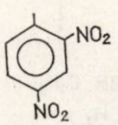

In all experiments good yields of polymers (70—90%) — which are white to light-brown powders—are obtained.

The supposed structure of copolymers III is also supported by analytical data and IR spectra.

Thus, the analytical data of some selected samples (Table 7) show a good agreement with the theoretical estimations.

The IR spectra of the starting polymers (I) and those of the chemically modified polymers (III) reveal some significant absorption bands which can be correlated with the assumed nucleophilic substitution.

Compounds I: $\nu(C-Cl)_{CH_2-Cl}$ at 715 cm^{-1}; $\nu(C=0)_{carbonyl}$ at 1680 cm^{-1}; $\nu(C=C)_{aromatic}$ at 1600 cm^{-1}; two adjacent hydrogens (aromatic 1,4-disubstitution) at 830 cm^{-1}.

Compounds III—1: $\nu(C-Cl)_{CH_2-Cl}$ at 700 cm^{-1}; $\nu(C=O)_{carbonyl}$ at 1680 cm^{-1}; $\nu(C=C)_{aromatic}$ at 1600, 1470 cm^{-1}; $\nu(C-O)_{aryl\ ether}$ at

1225 cm^{-1}, a single hydrogen at 875 cm^{-1} and two adjacent hydrogens at 830 cm^{-1} attributable to aromatic 1, 2, 4, 5 tetra- and 1′, 4′ disubstitution.

Compounds III–2 : $\nu(C-Cl)_{CH_2-Cl}$ at 680–700 cm^{-1}; $\nu(C=O)_{cardonyl}$ at 1675 cm^{-1}; $\nu(C=C)_{aromatic}$ at 1590 cm^{-1}; $\nu(C-O)_{aryl\ ether}$ at 1240 cm^{-1}; two adjacent hydrogens at 830 cm^{-1} attributable to aromatic 1,4 disubstitution.

TABLE 6

Reaction with NaBDNP; 6h

Code	Solvent	Temperature (°C)	N, % in the modified polymer	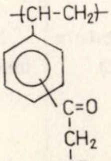 (mole, %)	Catalyst (molar ratio)	
					NaI	TEMAI
43	HMPTA	40	1.14	8.00	—	—
44	DMSO	40	1.20	8.50	—	—
45	NMP	40	1.19	8.48	1 : 0.80	—
46	NMP	40	1.09	7.60	—	—
47	NMP	60	1.37	9.20	—	1 : 0.50
48	HMPTA	80	1.77	13.30	—	—
49	NMP	80	1.24	9.00	—	—
50	NMP	80	1.40	10.00	1 : 0.80	—

R = 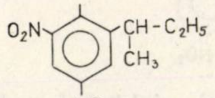

Compounds III–3 : $\nu(C-Cl)_{CH-Cl_2}$ at 690–710 cm^{-1}; $\nu(C=O)_{carbonyl}$ at 1675 cm^{-1}; $\nu(C=C)_{aromatic}$ at 1598, 1480 cm^{-1} (shoulder); $\nu(C-O)_{aryl\ ether}$ at 1240 cm^{-1}, a single hydrogen at 880 cm^{-1} and two adjacent hydrogens at 825 cm^{-1} attributable to aromatic 1, 2, 4, 6 tetra- and 1′, 4′ disubstitution; $\nu(C\equiv N)$ at 2220 cm^{-1}.

Compounds III–4 : $\nu(C-Cl)_{CH_2-Cl}$ at 690–700 cm^{-1}; $\nu(C=O)_{carbonyl}$ at 1680 cm^{-1}; $\nu(C=C)_{aromatic}$ at 1600 cm^{-1}; $\nu(C-O)_{aryl\ ether}$ at 1230cm^{-1}; a single hydrogen at 875 cm^{-1} and two adjacent hydrogens at 830 cm^{-1} attributable to aromatic 1, 2, 4, 6 tetra- and 1′, 4′ disubstitution; $\nu(C\equiv N)$ at 2230 m^{-1}.

Compounds III–5 : $\nu(C-Cl)_{CH_2-Cl}$ at 680–700 cm^{-1}; $\nu(C=O)_{carbonyl}$ at 1685 cm^{-1}; $\nu(C=C)_{aromatic}$ at 1605, 1490 cm^{-1}; $\nu(C-O)_{aryl\ ether}$ at

1230 cm^{-1}; a single hydrogen at 865 cm^{-1} and two adjacent hydrogens at 835 cm^{-1} attributable to aromatic 1, 2, 4 tri- and 1′, 4′ disubstitution; $\nu(NO_2)$ at 1345, 1530 cm^{-1}.

TABLE 7

Analytical data of some copolymers III

Code	C, %		H, %		Cl, %		N, %		Br, %		I, %	
	calcd.	found	calcd.	found	calcd.	found	calcd.	found	calcd.	found	calcd.	found
4	57.30	57.89	3.39	3.89	—	29.90	—	—	—	—	—	—
11	50.34	50.03	2.64	2.44	—	39.58	—	—	—	—	—	—
32	51.24	51.00	2.97	3.22	2.92	3.00	—	2.70	32.26	32.46	—	—
23	41.18	41.58	2.30	2.37	0.70	0.61	—	2.57	—	—	46.97	46.22
41	61.59	58.85	4.16	3.86	7.36	7.96	—	5.33	—	—	—	—
50	65.79	65.29	5.04	4.84	15.84	16.26	—	1.40	—	—	—	—

Compounds III—6 : $\nu(C-Cl)_{CH_2-Cl}$ at 710 cm^{-1}; $\nu(C=O)_{carbonyl}$ at 1680 cm^{-1}; $\nu(C=C)_{aromatic}$ at 1600 cm^{-1}; $\nu(C-O)_{aryl\ ether}$ at 1245 cm^{-1} (shoulder); a single hydrogen at 870 cm^{-1} (shoulder) and two adjacent hydrogens at 830—840 cm^{-1} attributable to aromatic 1, 2, 4, 6 tetra- and 1′, 4′, di- substitution; $\nu(NO_2)$ at 1340 cm^{-1} and 1530 cm^{-1} (shoulder).

CONCLUSIONS

The Williamson reaction of poly(vinyl α-chloroacetophenone) with some herbicidal sodium phenoxides in common dipolar aprotic solvents was investigated.

Soluble copolymers with aryloxyalkyl aryl ketone type pendent substituents to the vinyl polymer backbone which are potential herbicidal compositions can be prepared by the stoichiometric control of the extent of reaction.

A sequence of the relative reactivity of the tested sodium phenoxides was established.

The supposed structure of the copolymers was confirmed by elemental analysis and IR spectra.

REFERENCES

[1] G. G. Allan, J. F. Friedhoff, W. J. Mc Connell and J. C. Powell, *J. Macromol. Sci.-Chem.*, **A 10**, 223 (1976).
[2] R. P. Quellette and J. King, *Chem. Week*, **1976,** 27.
[3] L. G. Donaruma, "Progress in Polymer Science", vol. 4, Pergamon Press, Oxford **ed.** A. D. Jenkinsm, 1974, p. 1.
[4] D. Drăgan and A. Carpov, *Rev. Roumaine Chim.*, **25**, 285 (1980).
[5] A. Hantzsch, *Ber. dtsch. chem. Ges.*, **35,** 210 (1902).
[2] G. J. Tiessens, *Rec. Trav. chim.*, **50,** 112 (1931).
[7] B. J. Heywood, *Chem. and Ind.*, **1966,** 1946.
[8] J. M. Kolthoff, *Biochim. Z.*, **162,** 289 (1925).
[9] W. O. Kenyon and G. P. Waugh, *J. Polymer Sci.*, **32,** 83 (1958).
[12] H. Liebig, *Chem. Ztg.*, **95,** 301 (1971).

Revue Roumaine de Chimie, **25**, *3*, 435–437 (1980)

ON "A CORRECTION TECHNIQUE FOR FRACTIONATION DATA AND ITS APPLICATION TO THE FRACTIONATION OF POLYETHYLENE TEREPHTHALATE"

A. O. FULEA
Department of Physical Chemistry,
Bd. Republicii 13, Bucharest, Romania

Received December 4, 1978

It is shown that the Haseley method[1] is erroneous; a correct formula is given for the integral distribution of the molecular weight of polymers.

Haseley[1] attempted to correct the integral distribution function as obtained from fractional data by the common proceeding which presumes:

1. exactly 50% from the whole polymer weight in a fraction i has the molecular weight lower or equal with the determined average molecular weight $(\bar{M}_n)_i$;

2. the molecular weight of all polymers in the fractions 1, 2, ... $(i-1)$ is lower than $(\bar{M}_n)_i$, while in the fractions $(i+1)$, $(i+2)$ ... it is higher than $(\bar{M}_n)_i$.

In the case that the assumptions 1 and 2, hold the experimental points of the integral distribution curve are $((\bar{M}_n)_i,\ A_i)$, where:

$$A_i = \frac{1}{2} W_i + \sum_{j=1}^{i-1} W_j \tag{1}$$

$W_j =$ the weight in percents of the jth fraction.

Haseley[1] tried to consider the more general case when the assumption (2) does not hold, but, as we will show below, but he was wrong in his approach as well as in his treatment of the problem he intended to solve.

The proposal of Haseley[1] was to add a correction Δ_i to A_i, in order to get a more exact coordinate A'_i:

$$A'_i = A_i + \Delta_i$$
$$\tag{2}$$
$$\Delta_i = -\sum_{j=1}^{i-1} W_j(\bar{M} > \bar{M}_i) + \sum_{j=i}^{n} W_j(\bar{M} < \bar{M}_i)$$

where W_j is the weight in percents of subfraction j of fraction i, 100% being the weight of all fractions.

To begin with, two shortcomings of equation (2) are quite obvious. Firstly, it uses the same symbol for the weight of a fraction and for the weight of a subfraction W_j, and secondly it presumes that the subfraction $1, 2, \ldots (i-1)$ of a fraction i always have $\bar{M}_n$ lower than $(\bar{M}_n)_i$ and that the remaining subfractions have $\bar{M}_n$ higher than $(\bar{M}_n)_i$. For the sake of clearness of our discussion let us rewrite Haseley's formula, taking into account the above two points :

$$A'_i = A_i - \sum_j W_{ij}\,(\bar{M}_{ij} > \bar{M}_i) + \sum_j W_{ij}\,(\bar{M}_{ij} < \bar{M}_i) =$$

$$= \frac{1}{2}\,W_i + \sum_{j=1}^{i-1} W_j - \sum_j W_{ij}\,(\bar{M}_{ij} > \bar{M}_i) + \sum_j W_{ij}\,(\bar{M}_{ij} < \bar{M}_i)$$

where W_{ij} is the weight in percents of subfraction j of fraction i, 100% being the sum of all fractions and M_{ij} is the average molecular weight of subfraction j of fraction i.

Haseley[1] states that $W_{ij} = x_j y_j$, x_j being the weight of subfraction j in fraction i, in percents, 100% being the weight of fraction i and y_j is the weight in percents of the polymer in fraction i which has $\bar{M} > \bar{M}_i$ for the third term, or $\bar{M} < \bar{M}_i$ for the fourth term in the expression of A'_i.

In his calculations Haseley used the formula $W_{ij} = \frac{1}{100}\,x_j y_j$ taking thus into account the fact that both x_j and y_j are expressed as percents.

The formula given by Haseley[1] for W_{ij} is obviously wrong, the appropriate formula, following the definition of W_{ij}, is :

$$W_{ij} = \frac{1}{100}\,W_i x_j \tag{3}$$

Corollary the proceeding for obtaining y_j given by Haseley[1] in Figure 3[1] and used in his example of calculation in Table 3[1] has no value and should never have been given.

Finally, formula (2) is by itself wrong. Thus, if we take into account that :

$$W_i = \sum_j W_{ij}(\bar{M}_{ij} > \bar{M}_i) + \sum_j W_{ij}(\bar{M}_{ij} < \bar{M}_i) + W_{ia}(\bar{M}_{ia} = \bar{M}_i)$$

we get for A'_i :

$$A'_i = \frac{3}{2} \sum_j W_{ij}(\bar{M}_{ij} < \bar{M}_i) - \frac{1}{2} \sum_j W_{ij}\,(\bar{M}_{ij} < \bar{M}_i) +$$

$$+ \sum_{j=1}^{i-1} W_j + \frac{1}{2}\,W_{ia}\,(\bar{M}_{ia} = \bar{M}_i) \tag{4}$$

The first term in (4) shows that to A_i was added a quantity exceeding by $1/2 \sum_j W_{ij}(\bar{M}_{ij} < \bar{M}_i)$ the correction, the second term in (4) shows that a quantity exceeding by $1/2 \sum W_{ij}(\bar{M}_{ij} > \bar{M}_i)$ was subtracted from $\dot{A}_i$, while the third term shows that no correction was done for the fractions $1, 2, \ldots (i-1)$.

A straightforward proceeding is at hand if the differential distribution functions for subfractions were known:

$$A'_1 = \sum_k \sum_j W_{kj}(\bar{M}_{kj} < \bar{M}_1) + \frac{1}{2} \sum_k \sum_j W_{kj}(M_{kj} = M_1)$$

$$A'_2 = A'_1 + \sum_j \sum_k W_{kj}(\bar{M}_1 < \bar{M}_{kj} < \bar{M}_2) + \frac{1}{2} \sum_k \sum_j W_{kj}(M_{kj} = M_1) +$$

$$+ \frac{1}{2} \sum_k \sum_j W_{kj}(\bar{M}_{kj} = \bar{M}_2)$$

. . . .

$$A'_i = A'_{i-1} + \sum_k \sum_j W_{kj}(\bar{M}_{i-1} < \bar{M}_{kj} < \bar{M}_i) +$$

$$+ \frac{1}{2} \sum_k \sum_j W_{kj}(\bar{M}_{kj} = \bar{M}_{i-1}) + \frac{1}{2} \sum_k \sum_j W_{kj}(\bar{M}_{kj} = \bar{M}_i)$$

It should be also pointed out that Haseley determined the average molecular weight by measuring the viscosity, so he got $\bar{M}_v$ and not $\bar{M}_n$, as he put down in his paper.

REFERENCES

[1] E. A. Haseley, *J. Polymer. Sci.*, **4**, 309 (1959).

Revue Roumaine de Chimie, 25, 3, 439–442 (1980)

ANALYTICAL ASPECTS OF SOME ORGANIC ACIDS. II[1].

GRAVIMETRIC DETERMINATION OF THORIUM BY *o*-PHENYLENE-TRIOXYTRIACETIC ACID

SUBODH N. KAPOOR and NEERA MISRA
Chemistry Department, Lucknow University
Lucknow, India

Received October 16, 1978

o-Phenylene-trioxytriacetic acid has been found to be a selective reagent for the estimation of thorium. As little as 8.6 mg of thorium can be easily determined. The composition of the precipitate varies somewhat and direct weighing is therefore not possible. This difficulty is overcome by igniting the precipitate to its oxide ; Ni^{2+}, Ce^{3+}, Fe^{3+} Co^{2+} Be^{2+} ions do not interefere. Although Cr^{3+} ion is not precipitated in neutral or slightly acidic solutions, it contaminates the thorium precipitate, both at 0.15 N HCl and 0.35 N HCl. The amount of contamination is so small that it is removed by double precipitation.

INTRODUCTION

In a previous communication of this series,[1-14] a method for the estimation of zirconium by using *o*-phenylenetrioxytriacetic acid has already been reported. The present communication deals with the use of *o*-phenylenetrioxytriacetic acid as a new reagent for the estimation of thorium.

On the basis of systematic investigations it has been observed that *o*-phenylenetrioxytriacetic acid reagent gives a light brown curdy precipitate which is insoluble and easily washable in a hydrochloric acid medium and is in quantity up to 0.37 N HCl concentration.

EXPERIMENTAL

Reagents and Chemicals

Preparation of o-phenylenetrioxytriacetic acid

1 Mol of pyrogallol was dissolved in 7.5 M of NaOH in 120 ml of water. 3 Mol of monochloroacetic acid solution were added and mixed thoroughly. The mixed solution was refluxed on a wire gauze for 5 hours until a pasty mass was formed. The pasty mass was cooled in ice, diluted with a few ml of H_2O and acidified with HCl. The free acid was recrystallised from water.

***Reagent solution.* A 2 p.c. solution of the acid was prepared by dissolving the requisite quantity in hot water.**

Standard thorium solution. Stock solution of thorium was prepared by dissolving, a requisite quantity of Merck's G.R. grade Thorium nitrate of metal in a definite amount of water. The metal content of thorium solution was determined gravimetrically by the standard method.

Solution of other cations. Nitrates and chlorides of metals (B.D.H./A.R.) were employed in the preparation of solutions of inorganic ions and the metal contents of these stock solutions were determined by the standard methods.

Other reagents used were of A.R. grade.

Analytical Procedure

Determination of thorium. Aliquot quantities of thorium solution containing varying amounts of thorium salt (e.g. 0.0086 to 0.1064 g equivalent of thorium dioxide) were heated to boiling in a beaker. Ammonium nitrate (5 g/100 ml of soln.) was added and then a hot 2% solution of *o*-phenylenetrioxytriacetic acid was slowly added with constant stirring in slight excess. The normality of hydrochloric acid for final solution was adjusted at 0.35 N. The solution was slowly heated for a few minutes and the beaker set aside in a warm place, preferably over a water bath. The precipitate was allowed to settle and then filtered through a whatman filter paper No. 42. The precipitate was washed with a hot 0.1% solution of the above acid. It was dried and ignited to the oxide. As little as 8.6 mg of thorium dioxide gives a precipitate large enough for easy handling. A precipitate is formed even at low concentration, i.e. 4 mg, but it was too small to handle with ease. The results of estimation are given in Table 1.

TABLE 1

Determination of varying amounts of Th using *o*-phenylenetrioxytriacetic acid

Concentration of free acid=0.35 N HCl

ThO_2 taken g	ThO_2 found g	Error g
0.1064	0.1068	+0.0004
0.1026	0.1028	+0.0002
0.0916	0.0916	±0.0000
0.0800	0.0796	−0.0004
0.0712	0.0712	±0.0000
0.0634	0.0634	±0.0000
0.0412	0.0410	−0.0002
0.0356	0.0358	+0.0002
0.0210	0.0212	+0.0002
0.0086	0.0086	±0.0000

TABLE 2

Effect of H ion concentration

ThO_2 taken=0.0916g

Normality of HCl	ThO_2 found g	Error g
0.15	0.0916	±0.0000
0.20	0.0920	+0.0004
0.25	0.0922	+0.0006
0.30	0.0918	+0.0002
0.35	0.0916	±0.0000
0.37	0.0918	+0.0002
0.40	0.0910	−0.0006
0.45	0.0908	−0.0008

Effect of Hydrogen Ion Concentration

The precipitation was carried out within the range from 0.15 to 0.45 N hydrochloric acid. The thorium precipitate does not dissolve up to 0.37 N, but higher concentrations of the acid dissolve the precipitate. The effect of concentration of hydrochloric acid on thorium precipitate is shown by the results given in Table 2.

Separation from Foreign Ions

Thorium is easily separated from a large number of foreign cations, e.g. Co^{2+}, Be^{2+}, Ni^{2+}, Cr^{3+}, Ce^{3+}, Fe^{3+} by single precipitation. Although Cr^{3+} ion is coprecipitated with thorium salt, it is removed by double precipitation. The experimental results are recorded in Table 3.

TABLE 3

ThO_2 taken = 0.0916 g

Concentration of free acid = 0.15 N and 0.35 N

Concentration of HCl (N)	Absence of foreign ions		Presence of foreign ions			
	ThO_2 found g	Error g	Metal ions added	g	ThO_2 found g	Error g
0.15 N	0.0916	±0.0000	Co^{2+}	0.3662	0.0916	±0.0000
0.15 N	0.0916	±0.0000	Ni^{2+}	0.3962	0.0918	+0.0002
0.15 N	0.0916	±0.0000	Cr^{3+}(a)	0.1842	0.0920 (b)	+0.0004
0.15 N	0.0916	±0.0000	Ce^{3+}	0.3240	0.0914	−0.0002
0.15 N	0.0916	±0.0000	Fe^{3+}	0.2010	0.0916	±0.0000
0.15 N	0.0916	±0.0000	Be^{2+}	0.2926	0.0922	+0.0006
0.35 N	0.0916	±0.0000	Co^{2+}	0.3662	0.0912	−0.0004
0.35 N	0.0916	±0.0000	Ni^{2+}	0.3962	0.0914	−0.0002
0.35 N	0.0916	±0.0000	Cr^{3+}(a)	0.1842	0.0918 (b)	+0.0002
0.35 N	0.0916	±0.0000	Ce^{3+}	0.3240	0.0912	−0.0004
0.35 N	0.0916	±0.0000	Fe^{3+}	0.2010	0.0910	−0.0006
0.35 N	0.0916	±0.0000	Be^{2+}	0.2926	0.0924	−0.0008

(a) = Residue slightly coloured
(b) = Double precipitation

In order to carry out double precipitation the first precipitate was dissolved, after partial washing, on the filter paper by running it through several times with hot water. The filtrate was caught in the original beaker, the excass acid was carefully neutralised through appropriate concentration of HCl and the precipitation was repeated at 0.1 N HCl and at 0.30 N HCl.

Composition of Thorium Compound

The thorium compound of the acid was prepared by adopting the same procedure described before. The precipitate was washed with hot water several times and then with warm alcohol to remove the adhering acid. The compound was dried at 120° to a constant weight. Aliquot of the dried compound was ignited to the oxide and the results of analysis are shown in Table 4.

The samples were analysed for the percentages of carbon and hydrogen and hence the percentages of thorium were calculated. The results of analysis are shown in Table 5.

The results of analysis show that the percentage of thorium varies from 23.61 % to 23.64 % in the sample, whereas the calculated theoretical value of thorium is 23.62 which corresponds to the molecular formula $(C_{13}H_7O_7) = Th = 0. H_2O$.

ACKNOWLEDGEMENTS. Our sincerest thanks are due to Professor S. S. Tiwari, Head of the Chemistry Department, for providing research facilities and constant encouragement.

The authors' thanks are also due to U. P. State Council of Science and Technology for awarding one of us (S.N.K.) a contingency grant.

TABLE 4

Analysis of thorium compound

Amount of dried ppt g	ThO_2 obtained after ignition (g)	% Th
0.0762	0.0244	23.62
0.1015	0.0324	23.64
0.1280	0.0410	23.61

TABLE 5

Analysis of thorium compounds for the percentage of carbon and hydrogen in the samples

% Th (observed)	% Carbon	% Hydrogen	% Oxygen	% Th (Theoretical)
23.62	40.28	1.98	35.00	23.62
23.64	40.28	1.98	35.22	23.62
23.61	40.28	1.98	35.10	23.62

REFERENCES

[1] S. N. Kapoor and N. Misra, *Rev. Roumaine Chim.* (In press).

[2] L. A. Pratt and C. James, *J. Amer. Chem. Soc.*, **33,** 1330 (1911).

[3] T. O. Smith and C. James, *J. Amer. Chem. Soc.*, **34,** 281 (1912).

[4] N. Eswaranarayana and Bh. S. V. Raghav Rao, *J. Sci. Ind. Res.* (New Delhi), **13B,** 657 (1954).

[5] M. Venkataramaniah and Bh. S. V. Raghav Rao, *Analyt. Chem.*, **23,** 539 (1951); Cf. *Z. analyt. Chem.* **135,** 425 (1952).

[6] M. Venkataramaniah, Bh. S. V. Raghav Rao and C. Lakshmana Rao, *Analyt. Chem.*, **24,** 747 (1952); Cf. *Z. analyt Chem.*, **137,** 461 (1952/53).

[7] S. K. Datta; *J. Indian Chem. Soc.*, **30,** 657 (1953).

[8] S. K. Datta and G. Banerjee; *J. Indian Chem. Soc.*, **31,** 397 (1954); Cf. *Z. analyt. Chem.* **149,** 157 (1956).

[9] S. K. Datta and G. Banerjee; *J. Indian Chem. Soc.*, **31,** 773 (1954); Cf. *Z. analyt. Chem.* **149,** 158 (1956).

[10] S. K. Datta, *J. Indian Chem. Soc.*, **30,** 657 (1953).

[11] T. V. Sastri and Bh. S. V. Raghav Rao; *J. Indian Chem. Soc.*, **28,** 530 (1951).

[12] M. Venkataramaniah and Bh. S. V. Raghav Rao; *Analyt. Chem.*, **23,** 539 (1951); Cf. *Z. analyt. Chem.*, **135,** 425 (1952).

[13] S. K. Datta and G. Banerjee; *J. Indian Chem. Soc.*, **31,** 773 (1954); Cf. *Z. analyt. Chem.*, **149,** 158 (1956).

[14] C. S. Pande and T. S. Srivastava; *Z. analyt. Chem.*, **165,** 11 (1959).

Revue Roumaine de Chimie, 25, 3, 443–445 (1980)

COMPTES RENDUS

R. J. ABRAHAM and P. LOFTUS, "Proton and Carbon—13 NMR Spectroscopy. An Integrated Approach", Heyden, London, 1978, 230 p.

As stated in N. Sheppard's foreword, the modern chemist and particularly the modern organic chemist, because of the importance to him or her of both ^{1}H and ^{13}C spectra, has from now on to live with equal ease in both worlds. Owing to the historical development, ^{1}H—NMR is now familiar to every undergraduate student in chemistry, but ^{13}C—NMR has lagged behind, yet it is at least as important as the former. There exist numerous excellent textbooks on ^{1}H—NMR, but so far ^{13}C—NMR has been treated mostly for specialists. The book under discussion treats the two most important nuclei, ^{1}H and ^{13}C, as an integrated whole, not as two separate phenomena. The philosophy of the treatment was to give the precise theory of each phenomenon, and to consider the simplest example in detail, avoiding complex mathematical approaches but still illustrating basic principles and concepts.

The seven chapters of the book are entitled : Introduction and basic principles of NMR ; The chemical shift ; Spin-spin coupling ; The analysis of NMR spectra ; Pulse Fourier transform techniques ; Double resonance techniques and relaxation mechanisms ; Applications of NMR spectroscopy. A particularly attractive feature of the book are the 25 spectral problems, consisting of the molecular formula, the ^{13}C— and ^{1}H—NMR spectra (the answers, both by name and by structural formula, are given separately). A compound index (misnamed as formula index) and a subject index are appended. Each chapter is followed by a brief bibliography (Recommended Reading) consisting of a few books or reviews.

The chemical shifts are indicated both by synoptic figures and tables. Shoolery's rules for ^{1}H—NMR spectra, as well as Grant and Paul's expressions and substituent chemical shifts are presented.

The analysis of AB spin systems is detailed out very clearly on the basis of the hamiltonian and the matrix expressions ; the ABC, AB_2 and ABX systems are discussed more cursorily by providing practical examples. For the PFT techniques, the rotating frame reference system approach is used. All important and relevant topics are discussed (except for CIDNP, ENDOR, magic angle and solid state NMR) such as homo- and heteronuclear decoupling, INDOR, the nuclear Overhauser effect (NOE), gated decoupling, measurement and significance of T_1 and T_2 relaxation times, spin tickling, differential NOE, etc. The last chapter deals with isotopic (^{13}C and ^{2}H) labelling for assignments, relaxation reagents, lanthanide shift reagents, and ^{13}C—NMR elucidation of biosynthetic pathways.

It is evident, by a host of practical hints, sometimes at variance with certain textbooks (e.g. p 105 on partially decoupled spectra), that the authors have long been familiar with the field. The book is highly readable and the printing excellent. We would, however suggest, that future editions replace : dots by dashes for covalent bonds (p. 6) ; "ring rotation" by a more appropiate term in the footnote on p. 22 ; cyclopropene by cyclobutene on p. 43 ; 15.7 by 15.8 on p. 67 ; E's by F's on p. 43 ; 0.7 by 1.4 on p. 183.

The book is addressed to students of organic chemistry, but it is useful also for the teaching or research staff who are less familiar with ^{13}C—NMR. It contains in a condensed form much interesting information being therefore highly recommended.

A. T. Balaban

M. FLORESCU, "Metode ştiinţifice în dezvoltarea industriei chimice moderne" (Scientific methods in the development of modern chemical industry), Ed. Academiei RSR, Bucharest 1979, 250 p.

The book presents three principal groups of problems connected with the use of modern methods and technics, including mathematical ones, in the chemical engineering activity, in the development of a diversified chemical industry, highly efficient in itself and in the frame of the national economy.

In the first part of the work, which refers to the mathematical models of modern chemical industry processes, are presented problems concerning the types and classification of models and variables of chemical processes, the principles and the stages of analysis performed when mathematical models are elaborated, supply of calculation data for those models, the modeling principles and the application of mathematical models of unitary operations and processes, the analysis and optimisation of complex processes in the chemical industry and mathematical modeling in the chemical industry in the Socialist Republic of Romania.

The second part of the work entitled "Statistical methods in the analysis of the cybernetic system of the chemical industry", deals with a wide range of problems on the chemical industry—cybernetic system, the system theory in chemical engineering, decision optimisation in the chemical industry, indicial functions and statistical research in the chemical industry, the parameters, statistical methods and the evolution of technical-economic indicators in Romania's chemical industry and the statistical-mathematical analysis of the chemical industry development in the 1948—1975 period, extrapolated to the year 1980.

The problématique equally large of the third part of the book, entitled "The forecast in the chemical industry" discusses the opportunity of forecasting activities in this branch, marketing, forecasting methods in the chemical industry, technological and electric power supply forecasts, forecasting model and data banks, dynamic forecasting model of chemical products consumption, graph theory and its application to chemical industry forecasting, the mathematical programming by graph theory, the use of computers in forecasting the production development trends in the principal chemical domains (agrochemical, alumina and aluminium, sulphuric acid industry, sodic and chlorosodic products, carbide industry, oil processing, synthesis, petrochemical industry, plastics, chemical fibres and yarns industry, synthetical rubbers, paints and varnishes industry, inks, industries of organic pigments and drugs and so on.

The book describes the scientific methods of modeling, the cybernetic and economic analysis and prognosis in close connection with the technical and technological specificity of the chemical industry. It should be considered, from this point of view, a valuable work available to a large circle of specialists. The scientific approach by resorting to theories and methods from such sciences: as mathematics, chemical technology and cybernetics, allows a discussion of the organisational and management aspects of this complex industrial system with the view of efficiently solving their economic production problems.

The work would be useful for specialists in chemical industry technics, technology and economics, automation, informatics, management and organisation, for the teaching staff, undergraduate and graduate students, doctorands, whose interest focuses on the domains treated in the book.

D. I. Marchidan

R. M. NAUSS, "Parametric Integer Programming", University of Missouri Press, Columbia & London, 1979, 98 p.

Nauss's topic, the study of parametric integer linear programs (PILP), is a new and important one for the applied management scientist. PILP may be defined as a family of closely related integer linear programs (ILP). Nauss's work is a breakthrough, as methods for solving ILPs have only recently become efficient. In this book, the author presents a general framework for the PILP, beginning by outlining the need for PILP algorithms. He explains basic solution methodologies and states two rudimentary approaches for solving the PILP. Nauss provides proof of various theoretical properties for special parameterizations and discusses techniques for improving algorithmic efficiency. The framework concludes with an examination of the underlying factors that intimately relate to the scheduling priorities in a PILP algorithm.

Nauss studies three special PILP problem classes, including the 0—1 knapsack, generalized assignment, and capacitated facility location problems. He presents algorithms, cites computational results, and draws conclusions concerning the most efficient approaches.

In this first extensive treatment of the subject of the PILP, the author shuns the narrow viewpoint that has been employed in more limited efforts. Drawing together the research in the field, he proposes an approach to the general PILP and formulates a framework for it. In addition, he gives directions for future research.

D. I. Marchidan

L. VÁLYI, "Atom and Ion Sources", Akademiai Kiado, Budapest, 1977, 429 p.

Science and modern technology are unconceivable without atom and ion sources, starting with industrial routine techniques of layer coatings up to the analytical techniques utilizing ion or atom separations. This subject entails two main aspects, namely the theoretical framework for the working and using principles, and the effective design of these tools for concrete ends.

L. Vàlyi, of the Central Research Institute for Physics of the Hungarian Academy of Sciences, tackles these two aspects, discussing in detail many theoretical and practical problems concerning the use of particle sources. From the theoretical point of view these are reviewed, the main stages in the development of the particle beam techniques starting with the effervescent 1930's to the present time which gives the book also a historical value. The literature cited contains approximately 1500 references, many of them after 1970.

Many experimental systems liable to be suitably adjusted to a given task are discussed in detail. The rich illustrations are another asset of the book.

The Appendix (40 pages) contains 18 tables of material properties and physical quantities.

The monograph covers a large number of practical fields related to the subject of ion and atom sources such as: nuclear physics, elementary particle physics, medical research, physico-chemical methods of separation, ion implantation, etc.

Gh. Drăgan

NOTE POUR LES AUTEURS

La Revue Roumaine de Chimie publie des articles en anglais, français, russe, allemand ou espagnol. Les auteurs sont priés d'envoyer des articles et des comptes rendus inédits.

Les manuscrits seront dactylographiés à deux intervalles. La bibliographie, les tableaux et la légende des figures seront placés après le texte.

Si l'article fait partie d'une série numérotée, le titre de la partie précédente sera indiqué dans une note au bas de la première page.

Chaque article sera précédé d'un résumé comprenant quinze lignes au maximum.

Les références bibliographiques dans le texte seront faites par des exposants sans parenthèses et paraîtront comme des notes au bas de chaque page.

Les publications périodiques mentionnées dans la bibliographie seront présentées suivant les prescriptions internationales : le nom de l'auteur précédé de l'initiale du prénom, le titre du périodique abrégé conformément à « *Chemical Abstracts* » et souligné par une ligne, le numéro du tome indiqué par des chiffres arabes et souligné par deux lignes, suivi de la première page de l'article ; à la fin, l'année de la parution sera placée entre parenthèses. Le numéro de la revue ne sera pas indiqué si les pages du volume sont numérotées consécutivement.

Les textes des livres ou traités inclueront : les noms des auteurs, les initiales du prénom, le titre du livre entre guillements et sans être souligné, le numéro du tome précédé par l'abréviation « vol. » (ou « Bd. ») le numéro de l'édition, les éditions (the publisher), la localité de la parution du livre, l'année de la parution et la page de la référence précédée(s) par l'abréviation « p » (ou « S »).

Les brevets seront indiqués comme suit : L'auteur ou la firme, le pays et le numéro du brevet, la date et la revue (*Chem. Abstr.*) Par ex. : M. Jones (to Union Carbide Co.), Brit. Pat. 601 238, 2 Sept. 1959, *Chem. Abstr.*, **54**, 12808 (1960).

Les diagrammes seront tracés à l'encre de Chine sur papier calque. Les tableaux et les figures (en nombre strictement nécessaire) seront numérotés par des chiffres arabes. Les courbes dans les figures seront numérotées par des chiffres arabes et leur explication sera donnée dans la légende des figures. Prière de ne pas inscrire les mêmes données dans les tableaux et les figures. Chaque tableau aura un titre. On indiquera dans le texte la place approximative des tableaux et des figures. Les formules chimiques seront incluses dans le texte ; en outre, elle seront transcrites sur papier calque, à l'encre de Chine.

Les auteurs sont priés d'indiquer les caractères italiques (en soulignant les lettres au crayon), ainsi que tout autre caractère spécial : les préfixes *ortho*, *meta*, *para*, *cis*, *trans*, etc. seront soulignés pour indiquer leurs caractères italiques, et ne seront jamais écrits avec des majuscules.

Aucune correction à la main ne sera admise sur le manuscrit. Les corrections seront frappées à la machine. Les lettres grecques ou autres symboles spéciaux seront insérés à la main à l'encre clairement.

Le manuscrit sera signé par l'auteur.

Le colonne-titre aura 50 lettres au maximum.

L'entière responsabilité du contenu des articles appartient aux auteurs.

Pour les détails veuillez consulter la Note pour les auteurs du numéro 2/ 1980 de la Revue.

PRINTED IN ROMANIA

NOTE POUR LES AUTEURS

La Revue Roumaine de Chimie publie des articles en anglais, français, russe, allemand ou espagnol. Les auteurs sont priés d'envoyer des articles et des [illegible] résultats inédits.

Les manuscrits seront dactylographiés à deux intervalles. La bibliographie, les tableaux et la légende des figures seront placés après le texte.

Si l'article fait partie d'une série numérotée, le titre de la partie précédente sera indiqué dans une note au bas de la première page.

Chaque article sera précédé d'un résumé comprenant quinze lignes au maximum.

Les références bibliographiques dans le texte seront indiquées par des exposants sans parenthèses et [illegible] comme des notes au bas de chaque page.

Les publications périodiques mentionnées dans la bibliographie seront présentées suivant les prescriptions internationales : le nom de l'auteur [illegible] de l'initiale du prénom, le titre du périodique abrégé conformément à « Chemical Abstracts » et souligné par une ligne, le [illegible] du tome (souligné par des [illegible]) [illegible] souligné par deux lignes, suivi de la première page de l'article. Le [illegible] sera placé entre parenthèses. Le numéro de la revue ne sera pas indiqué si les pages du volume sont numérotées [illegible].

Les [illegible] des livres [illegible] comprendront : les noms [illegible] de l'initiale du prénom, le titre du livre entre guillemets [illegible] précédé par l'édition éventuelle [illegible] le numéro [illegible] les auteurs [illegible] publiés), la localité [illegible] de la parution et la [illegible] par l'abréviation « p. » ou « S. ».

Les brevets seront [illegible] volume [illegible] de la revue, la page et le numéro du brevet, la date et la revue [illegible] [illegible] [illegible] 1962, [illegible] (1960).

Les manuscrits [illegible] sur [illegible] les tableaux et les figures [illegible] seront [illegible] des chiffres [illegible] Les [illegible] les figures seront numérotés par des chiffres arabes et [illegible] dans le [illegible] Les [illegible] les mêmes [illegible] les tableaux et les figures. Chaque [illegible] un titre. On indiquera dans le texte la place approximative des tableaux et des figures. Les [illegible] bibliographiques [illegible] seront [illegible] à l'encre de Chine.

Les auteurs sont priés d'indiquer les caractères [illegible] soulignant les lettres au crayon, ainsi que tout autre caractère spécial. Les préfixes [illegible] [illegible] seront soulignés pour indiquer leur caractère italique et ne seront jamais écrits avec des majuscules.

Aucune correction à la main ne sera admise sur le manuscrit. Les corrections seront frappées à la machine. Les lettres grecques ou autres symboles spéciaux seront insérés à la main à l'encre clairement.

Le manuscrit sera signé par l'auteur.

La colonne-titre aura 50 lettres au maximum.

L'entière responsabilité du contenu des articles appartient aux auteurs.

Pour les détails veuillez consulter la « Note pour les auteurs » du numéro 2, 1980 de la Revue.

PRINTED IN ROMANIA

TRAVAUX PARUS AUX ÉDITIONS DE L'ACADÉMIE DE LA RÉPUBLIQUE SOCIALISTE DE ROUMANIE

1980 AUG 16

ELENA CEAUŞESCU, **Research work on synthesis and characterization of macromolecular compounds. Contributions**, 1974, 251 p.

CR. SIMIONESCU, VIORICA RUSAN, V. POPA, **Chimia algelor marine** (La chimie des algues marines), 1974, 212 p., 1 pl.

CONST. GH. MACAROVICI, D. MACAROVICI, **Chimia oxizilor dubli şi utilizările lor** (La chimie des oxydes doubles et leur utilisation). 1975, 195 p.

I. G. MURGULESCU, **Introducere în chimia fizică**. Vol. I, 1, **Atomi, molecule, legătură chimică** (Introduction à la chimie physique, Ier vol. 1. Atomes, molécules, liaison chimique), 1976, 560 p.

E. P. BALTĂ, E. BALTĂ, **Introduction to the physical chemistry of the vitreous state**, coédition avec Abacus Press, 1976, 287 p.

H. I. GĂLĂŢEANU, **Radiochimia aplicată. Metode şi probleme** (La radiochimie appliquée. Méthodes et problèmes), 1976, 307 p.

CONST. V. UGLEA, **Cromatografia pe gel permeabil. Noi domenii de aplicare** (La chromatographie sur gel perméable. Nouveaux domaines d'application), 1976, 123 p.

DUMITRU NEGOIU, ANGELA KRIZA, **Poluanţi anorganici în aer** (Polluants inorganiques dans l'air), 1977, 220 p.

D. PURDELA (sous la direction de), **Nomenclatura chimiei anorganice** (La nomenclature de la chimie inorganique), 1977, 153 p.

I. ZUGRĂVESCU, MAGDA PETROVANU, **N-Ylid Chemistry**, coédition avec McGraw-Hill International, 1977, 396 p,

C. DRĂGULESCU, E. PETROVICI, **Chimie structurală modernă. Chimia coordinanţei 8** (La chimie structurale moderne. La chimie de la coordinence 8), 1977, 947 p.

S. STERNBERG, FL. DANEŞ, **Termodinamica chimică aplicată** (La thermodynamique chimique appliquée), 1978, 400 p.

I. G. MURGULESCU, V. EM. SAHINI, **Introducere în chimia fizică**, Vol I, 2, **Structura şi proprietăţile moleculelor** (Introduction à la chimie physique. Ier vol. 2. La structure et les propriétés des molécules), 1978, 604 p.

ELENA CEAUŞESCU, **Participări la manifestări ştiinţifice** (Participations aux manifestations scientifiques), 1979, 208 p.

A. T. BALABAN, L. GĂLĂTEANU, G. GEORGESCU LIGIA SIMIONESCU, **Compuşi marcaţi şi radiofarmaceutici cu aplicaţii în medicina nucleară** (Composés marqués et radiopharmaceutiques à application en médecine nucléaire), 1979, 495 p.

I. G. MURGULESCU, E. SEGAL, **Introducere în chimia fizică**, vol. II. 1. **Teoria molecular cinetică a materiei** (Introduction à la chimie physique, IIe vol. 1. 5. La théorie moléculaire — cinétique de la matière), 1979, 1003 p.

I. E. TEODORESCU, MARIA FITI, **Iradierea tehnologică** (L'Irradiation technologique), 1979, 216 p.

I. P. Informaţia c. 1756

43426

Lei 25.

$ 50 (pour un abonnement annuel)

F 1103

ACADÉMIE DE LA RÉPUBLIQUE SOCIALISTE DE ROUMANIE

66

REVUE ROUMAINE DE CHIMIE

TOME 25
N° 4
Avril 1980

EDITURA ACADEMIEI REPUBLICII SOCIALISTE ROMÂNIA

Rev. Roumaine Chim.

RRCMAX, 25, 4, p. 447–616 (1980) Bucarest

ACADÉMIE DE LA RÉPUBLIQUE SOCIALISTE DE ROUMANIE

COMITÉ DE RÉDACTION

Rédacteur en chef:

I. G. MURGULESCU, membre de l'Académie de la République Socialiste de Roumanie.

Rédacteurs en chef adjoints:

A. T. BALABAN et V. EM. SAHINI, membres correspondants de l'Académie de la République Socialiste de Roumanie

Collège de rédaction:

EM. BRATU, ELENA CEAUŞESCU, ECATERINA CIORĂNESCU-NENITZESCU, C. DRĂGULESCU, CR. SIMIONESCU, membres de l'Académie de la République Socialiste de Roumanie; P. SPACU, membre correspondant de l'Académie de la République Socialiste de Roumanie; MARGARETA AVRAM, M. BANCIU, I. HAIDUC, D. I. MARCHIDAN, I. MOLDOVAN, G. NIAC et D. SĂNDULESCU

La Revue Roumaine de Chimie paraît 10 fois par an. Toute commande de l'étranger (fascicules ou abonnements) sera adressée à ILEXIM Departamentul Export-Import Presă (Revues), P.O.B. 136—137, télex 11226, Bucarest, 3, str. 13 Decembrie, Roumanie

Les manuscrits, les livres et les revues proposés en échange, ainsi que toute correspondance seront envoyés à la rédaction :

REVUE ROUMAINE DE CHIMIE

Calea Victoriei, 125, 71021 Bucarest, Roumanie, téléphone 50 76 80

EDITURA ACADEMIEI REPUBLICII SOCIALISTE ROMÂNIA
125, Calea Victoriei, 71021 Bucarest, Roumanie, téléphone 50 76 80

REVUE ROUMAINE DE CHIMIE

Tome 25, Nº 4 Avril, 1980

V. EM. SAHINI, ELENA VOLANSCHI and AURELIA MEGHEA, E.S.R. spectra and electronic structure of some diphenylamine anion-radicals . . . 449–454

EDUARDO A. CASTRO and FRANCISCO M. FERNÁNDEZ, A simple parametric procedure for saturated hydrocarbons based on the transferability of *Fock* matrix elements . . . 455–458

IOSIF ALBU and EMIL CHIFU, Interfacial tension variation in the course of liquid-liquid extraction. III. The extraction of butyric acid by different solvents 459–466

SOLOMON STERNBERG, LIUBOV SHIRSHINA and SILVIA DANEŞ, Transport of SO_4^{2-}, Cu^{2+}, H^+ ions and of water in ion exchange membranes (in French) . . . 467–473 R

M. BORÓWKO and M. JARONIEC, General formulation of adsorption from liquid mixtures on heterogeneous solid surfaces . . . 475–486

P. BUDRUGEAC, Two new kinetical derivations of the *Jovanović* isotherm for monolayer adsorption. . . . 487–491

S. M. ABD EL HALEEM and S. S. ABD EL REHIM, Corrosion behaviour of commercial Zn–Ti alloy in aqueous salt solutions. . . . 493–501 R

CONST. GH. MACAROVICI and E. CHIŞ, A new *EDTA*-Type reagent. III. Synthesis and physico-chemical study of 4, 4′ diamino-diphenylmethane-N, N′-tetraacetic acid . . . 503–511

A. C. BANCIU and V. MINCU, Electronic spectra and magnetic susceptibilities of some new tetrahedral chelate complexes with Co (d^7)-N(sp^2) bonds. II. Co(II)chelates synthesized with 1-methyl-2-carbethoxy-glyoxalanil-(1)-bromo-phenylhydrazones-(2). . . . 513–527

A. SOTO and R. CEA, Mass spectrometry of alkylated inorganic heterocycles. I. Mass spectrometry of octamethyl-cyclotetraphosphaza-tetraene and its quaternary salts with methyl and ethyl iodides (in Spanish) . . . 529–533

I. G. DINULESCU, L. ENESCU, H. L. PRASAD, AURELIA GHENCIULESCU, NICOLETA ŞTEFAN and MARGARETA AVRAM, The electrophilic addition of bromine to 9-halogeno-benzocyclobutenonorbornenes . . 535–540

GUY RICART and DANIEL COUTURIER, New synthesis of 1,5-diazobicyclo 4.4.0 decanes (in French) . . . 541–545

A. C. RĂZUŞ, ALICE MARIE GLATZ, ZS. ARVAY, F. IORDACHE and F. BADEA, The oxidation of trichloroethylene with molecular oxygen . . . 547–557 R

IBRAHIM E. KHAWAD and GEORGE M. ISKANDER, Preparation and reactions of dibromocarbene adducts of cyclohexa-1,4-dienyl-acetates and -benzoates . . . 559–562

Revue Roumaine Chim. 25, *4*, 447–616 (1980) Bucarest

A. A. EL-KHAMRY, M. A. EL-HASHASH and M. M. HABASHY, Reactions of paraconic esters isolated in the *Stobbe* condensation of *p*-bromo-, and *p*-ethylacetophenones with diethylsuccinate 563–569

VICTORIA CIURDARU, V. TAMAS and K. L. SIMPSON, 7′-benzoylamino-β-*apo*-6′-carotenoic acid and some of its derivatives via -β-*apo*-8′-carotenylidenoxazolone 571–575

M. F. EL-KASCHEF, S. M. YASSIN, M. F. ABDEL-MEGEED and F. M. ABDEL-MOTI, Heterocyclic nitrogen compounds. VI. Reaction of some 5-oxopyrazoline derivatives with hydrazine hydrate and diazoalkanes . . 577–581

K. N. RAOOT and V. G. VAIDYA, Reduction of silver(I) with cobalt(II) and manganese(II) solutions in alkaline triethanolamine medium : gravimetric estimations of silver. 583–588

R V. IOSOF and VASILICA NEACȘU, Analysis of silicate rocks by atomic absorption spectrometry 589–597

GH. MIHĂILĂ, V. ABABI and F. VITAN, Liquid–vapour equilibrium of the diisopropylether–cyclohexanone system 599–603

SPIRIDON OPREA, EMIL DUMITRIU and MIHAIL DIMA, Reactivity of acrylic monomers. II. Copolymerization of N,N-diethylacrylamide with styrene 605–610

BOOK REVIEWS 611–615

Revue Roumaine de Chimie **25**, *4*, 449–454 (1980)

E.S.R. SPECTRA AND ELECTRONIC STRUCTURE OF SOME DIPHENYLAMINE ANION-RADICALS

V. EM. SAHINI, ELENA VOLANSCHI and AURELIA MEGHEA
Department for Physical Chemistry
Polytechnic Institute-Bucharest,
Blvd Republicii 13, Romania

Received June, 29, 1979

E.S.R. and optical spectra of some nitro- and benzoyl-diphenylamine anion-radicals are presented and discussed. The influence of the acceptor substituent on the spin-density and energy-level distribution in the anion-radicals is pointed out. The experimental results are supported by the MO calculations performed.

Previous investigations [1-3] have pointed out that nitro-substitution may alter the donor character of the parent molecule, allowing the formation of anion-radicalic species. In the present paper, the results concerning the influence of the nitro- and benzoyl-substitution on another system with donor properties, diphenylamine, are presented.

EXPERIMENTAL PART

Diphenylamine (DPhA), 4-nitrodiphenylamine, N-benzoyl-diphenylamine and 4 nitro-N-benzoyl-diphenylamine were prepared and purified by standard methods.

The anion-radicals were prepared by electrochemical reduction in dimethylsulfoxide, using a method described elsewhere. [4] As supporting electrolyte, tetra-n-butylammonium perchlorate (TBAP) in concentration of 0.1 M was used.

The E.S.R. spectra were recorded on a JES-3B spectrometer, in the X-band frequency, using peroxylamine disulphonate as internal standard ($a_N = 13$ G; $g = 2.0055$).

The optical spectra of the anion-radicals were recorded during the electrolysis, on a SPECORD UV–VIS spectrophotometer, in a 1 cm-cell equipped with two platinum electrodes.

The spin-density calculations were performed by the McLachlan's approximation, on a FELIX C-256 computer, using the parameters and equations contained in table 1.

TABLE 1

Parameters and equations used in the spin-density calculations

	h_N	h_O	k_{CN}	k_{XO}	a (Gauss)
$\mathrm{C{-}N}\left\langle\begin{matrix}\mathrm{O}\\ \mathrm{O}\end{matrix}\right.$	2.2	1.4	1.2	1.67	$a_N=(99.0 \pm 10.2)\,\rho_N^\pi - 2(35.8 \pm 5.9)\rho_0^\pi$ [5]
–NH–	1.0	–	0.8	–	a) $a_N = 21\ \rho_N^\pi + 7\rho_C^\pi$ [6] b) $a_N = 19.1\ \rho_N^\pi + 9.1\ \rho_O^\pi$ [7] $a_H = \lvert 35 \rvert\ \rho_N^\pi$ [8]
C=O	–	1.5	–	1.6	$a_H = \lvert 25 \rvert\ \rho_C^\pi$

RESULTS AND DISCUSSION

The E.S.R. spectra of the anion-radicals obtained from 4-nitrodiphenylamine, N-benzoyldiphenylamine and 4-nitro-N-benzoyl diphenylamine are presented in figure 1 (a, b, c). The experimental and calculated E.S.R. parameters of the anion-radicals are collected in table 2.

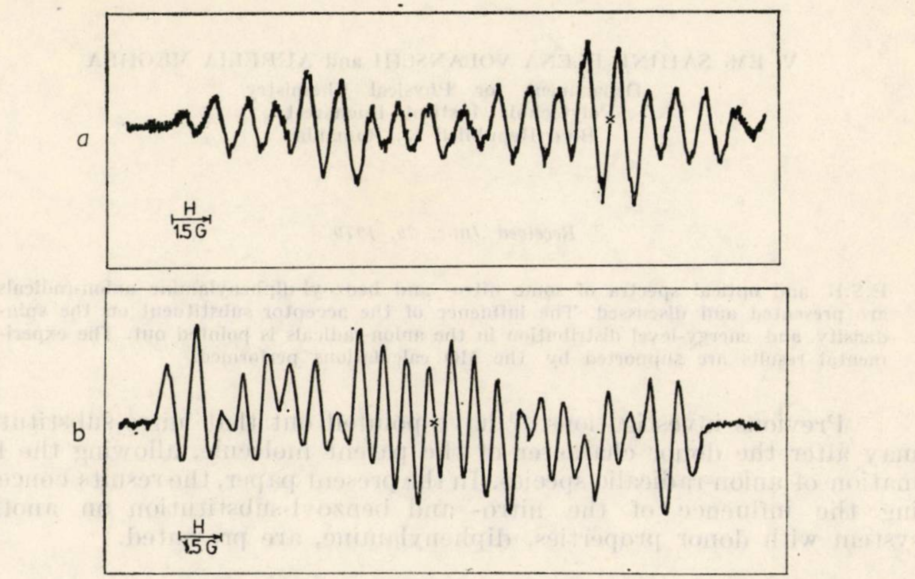

Fig. 1. — Low-field half of the E.S.R. spectrum of the anion-radicals obtained from: (a) 4-nitro DPhA; (b) -N-benzoyl DPhA; (c) 4-nitro-N-benzoyl DPhA.

Examining the data in table 2 it may be stated that the spin-distributions in the nitro containing anion-radicals (I) and (III) are simi-

TABLE 2

Experimental (Gauss) and calculated* ESR parameters of the anion-radicals

Anion-radical		$a_N^{NO_2}$	a_N	a_H^{NH}	$a_H^{2,6}$	$a_H^{3,5}$	a_H^{o}	a_H^{m}	a_H^{p}	$a_H^{2'6'}$	$a_H^{3'5'}$	$a_H^{4'}$	T.W.	L.w.	g-factor
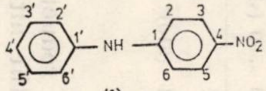 (I)	Exp.	10.50	1.15	0.82	1.00	3.60	—	—	—	<0.58	<0.58	<0.58	32.26	0.58	2.0046
	Calc.	10.69	1.29^{a}** 1.56^{b}	0.48	1.28	3.62	—	—	—	0.09	0.04	0.12			
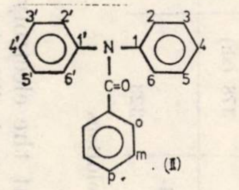 (II)	Exp.	—	1.91	—	<0.45	<0.45	4.51	1.12	5.82	<0.45	<0.45	<0.45	20.85	0.45	2.0034
	Calc.	—	2.07^{a} 2.68^{b}	—	0.16	0.07	3.76	1.09	5.98	0.16	0.07	0.32			
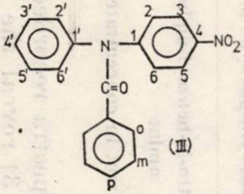 (III)	Exp.	9.40	0.82	—	1.14	3.45	<0.40	<0.40	<0.40	<0.40	<0.40	<0.40	29.61	0.40	2.0047
	Calc.	9.33	1.35^{a} 1.72^{b}	—	1.16	3.32	0.34	0.11	0.42	0.005	0.01	0.02			
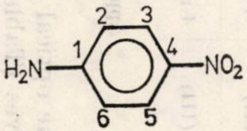 (IV)	Exp.[9] (DMF)	11.49	1.08	0.89	1.08	3.38	—	—	—	—	—	—	—	—	—

* Calculated with the parameters listed in table 1.

** Calculated with formula (a) and (b) from table 1.

lar, the hyperfine splittings of the nitro-group-containing moiety having nearly the same values as in the anion-radical of *p*-nitro-aniline (IV).

The large value of the splitting of the nitro-group nitrogen is little influenced by the extension of conjugation, decreasing only from 11.49 G in (IV) to 10.50 G in (I) and 9.40 G in (III). The proton hfs. in the second diphenylamine- or benzoyl-ring remain under the limit of resolution in the experimental spectrum.

All these facts point out a great degree of localization of the odd electron on the nitro-containing ring. A similar behaviour was noticed for the anion-radicals of 2-nitrodibenz-*p*-dioxin[2], 2-nitro-phenoxatellurine and 4-nitrodiphenylether[3], where it was stated that the central hetero-atoms could not ensure the delocalization of the odd electron on the whole molecule.

The hfs. of the anion-radical (II) reveal a quite different spin-distribution pattern, as compared to the nitro-substituted diphenylamine derivatives. This is reflected by the value of the g-factor, the greater bridge-nitrogen splitting and by the hfs. of the protons in the benzoyl ring, which are rather similar to other benzoyl-substituted heteromolecules.

It is interesting to notice that, when both reducible groups are present, as in anion-radical (III) it is the nitro, and not the benzoyl group that determines the spin-density pattern in the anion-radical.

This behaviour is well accounted for by the MO calculations and is evidenced by the variation of the spin-density on both reducible groups. Thus, in anion-radical (III) the spin-density on the carbonyl group is much smaller than in anion-radical (II) (0.0539 vs 0.3952), while the spin-density on the nitro group is comparable to that in the nitro-DPhA-anion-radical (I) (0.6013 vs. 0.6564).

TABLE 3

Electronic spectra of the diphenylamine derivatives and their anion-radicals

	Parent compound	Neutral (nm)	Anion-radical (nm)
(I)	4-nitro-diphenyl-amine	410	504 (605)*
(II)	N-benzoyldiphenyl-amine	378 (sh)	370 560 (sh)
(III)	4-nitro-N-benzoyl-diphenyl-amine	323	504 (610)*

* Apparent in concentrated solutions.

The optical spectra recorded at the electrolytic reduction of these derivatives (Table 3) reveal the same similitude of the nitrosubstituted anion-radicals (I) and (III), and the different behaviour of anion-radical (II).

The isosbestic point at 440 nm. in figure 2 evidences the reversible transformation of 4-nitro-diphenylamine in its anion-radical.

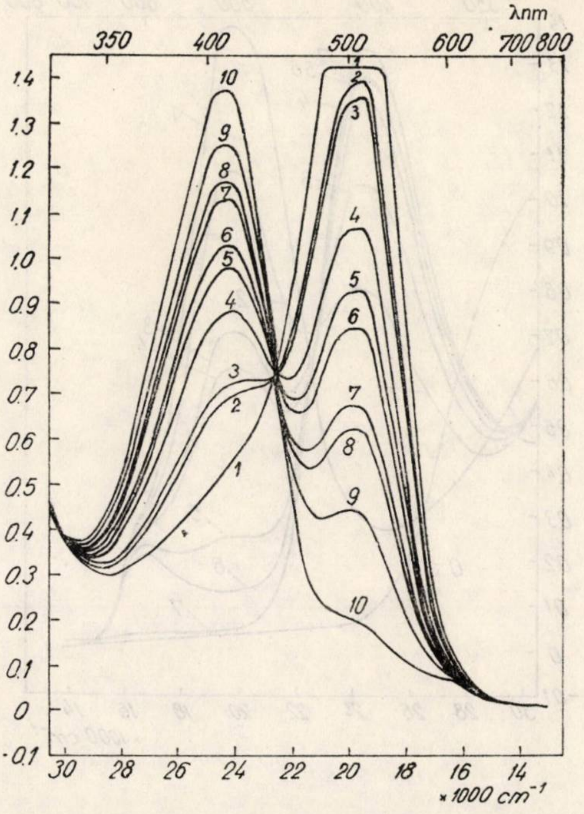

Fig. 2. — Optical spectra recorded at the decay of the electrolytically generated 4-nitro-DPhA-anion-radical.

It is to be noticed that, in the case of 4-nitro-N-benzoyl-diphenylamine a similar reversibility could not be evidenced, the decay of the anion-radical leading to the debenzoylated neutral compound, 4-nitro-diphenylamine. This is supported by the spectra recorded at the decay of anion-radical (III), (Figure 3), exhibiting the absorption peak at 410 nm, belonging to 4-nitro-diphenylamine, instead of that at 323 nm, characteristic of the parent compound (III).

It may also be stated that the second maximum in the absorption spectra of these anion-radicals is less intense and is favoured by high concentrations of parent compound. Therefore it could be due to a dimerization of the anion-radicals in solution.

In conclusion it may be stated that the nitro- or benzoyl-substitution in a donor molecule like diphenylamine brings about structural modifications, allowing the generation of anion-radicalic species in which the spin-density pattern and the energy level of the odd electron are determined by the substituent (acceptor group) and not by the bridge heteroatom.

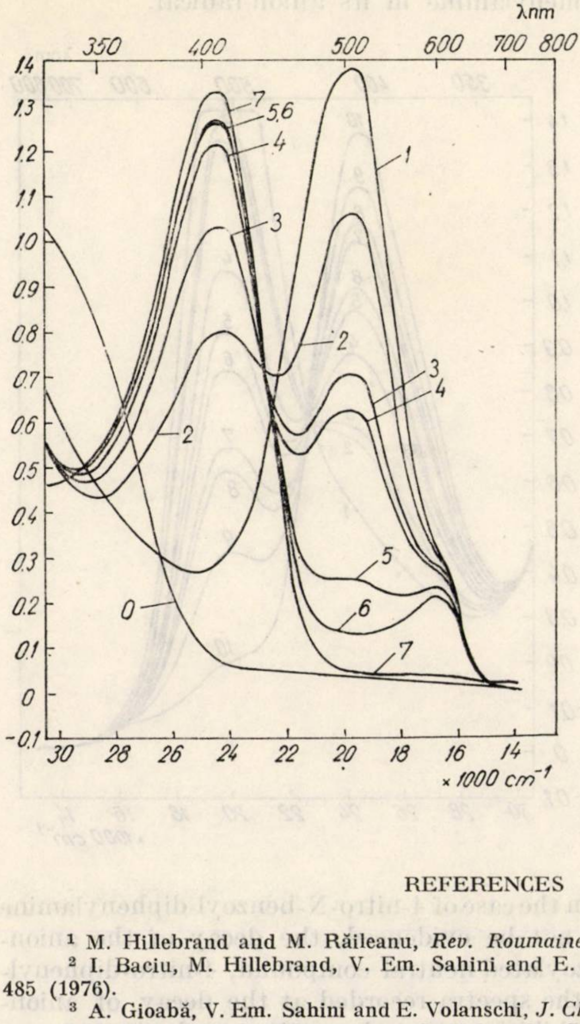

Fig. 3. — Absorption spectra of the anion-radical obtained from 4-nitro-N-benzoyl-DPhA: 0-spectrum of the parent compound; 1, spectrum of the anion-radical (III); *2–7*, spectra recorded at the decay of (III).

REFERENCES

[1] M. Hillebrand and M. Răileanu, *Rev. Roumaine Chim.*, **19**, 1227 (1974).
[2] I. Baciu, M. Hillebrand, V. Em. Sahini and E. Volanschi, *Rev. Roumaine Chim.*, **21**, 485 (1976).
[3] A. Gioabă, V. Em. Sahini and E. Volanschi, *J. Chem. Soc,. Perkin Trans. II*, **1977**, 529.
[4] E. Volanschi, C. Vlădescu and C. Volanschi, *Rev. Roumaine Chim.*, **19**, 755 (1974).
[5] P. H. Rieger and G. K. Fraenkel, *J. Chem. Phys.*, **39**, 609 (1963).
[6] R. L. Ward, *J. Amer. Chem. Soc.*, **83**, 3623 (1961); **84**, 332 (1962).
[7] J.C.M. Henning, *J. Chem. Phys.*, **44**, 2139 (1966).
[8] J. M. Lhoste and I. Tonnard, *J. Chim. phys.*, **63**, 678 (1966).
[9] R. D. Allendoerfer and P. H. Rieger, *J. Amer. Chem. Soc.*, **88**, 3711 (1966).
[10] M. Hillebrand, O. Maior, V. Em. Sahini and E. Volanschi, *Rev. Roumaine Chim.* to be published.

Revue Roumaine de Chimie, **25**, *4*, 455–458 (1980)

A SIMPLE PARAMETRIC PROCEDURE FOR SATURATED HYDROCARBONS BASED ON THE TRANSFERABILITY OF *FOCK* MATRIX ELEMENTS

EDUARDO A. CASTRO and FRANCISCO M. FERNÁNDEZ
Instituto de Investigaciones Fisicoquímicas Teóricas y Aplicadas, Sección Química Teórica Sucursal 4. Casilla de Correo 16, La Plata 1900, Argentina.

Received December 20, 1978

The *Fock* matrix elements calculated with a basis set of orthogonalized hybrid atomic orbitals are used to re-parametrize an empirical method for saturated hydrocarbons given previously. Total orbital energy is chosen so that the quantity could be approached as close as possible and constitute the test of quality for the proposed assignment. A good similarity is obtained between our results and those of the strictly *ab-initio* method.

The concept of transferability is continuously present in chemistry. Therefore we expect that a given chemical bond should be essentially the same, no matter where it is located. The functional group concept is associated with a characteristic chemical reactivity, spectral properties and so forth. The familiar notions of additivity of bond energy, bond dipole, and covalent radii reinforce our feeling that the transferability property is a natural one. There are various methods which use the transferability of Fock matrix elements to mimic *ab-initio* calculations on large molecules [1–13] in order to avoid the evaluation of electron repulsion integrals. These methods are in some respects similar to those popular semiempirical methods such as CNDO, PMO, MINDO, EHT, etc. However the methods based on the transferability property of Fock matrix elements differ from the semiempirical ones in two very important aspects: *a*) the necessary parameters are obtained directly from *ab-initio* results, and *b*) the methods aim to reproduce *ab-initio* results. Deplus *et al* have given a simple parametric procedure for saturated hydrocarbons based on the transferability of Fock matrix elements calculated with a basis set of orthogonalized hybrid atomic orbitals (OHAO). Cook [14] has pointed out that OHAO are the optimum functions to be employed in this kind of method, and moreover the values of non-diagonal terms of the Fock matrix are very low in this basis set. The comparison of molecular orbital energies and total energies for the first members of the alkane series with strictly *ab-initio* values yields satisfactory results (see Table 4 and 5 of Ref. 7) However the method presented by Deplus *et al.* is not applicable in the calculation of chemical reactivities because it assigns different parameters for chemically equivalent atoms in the construction of the synthetic Fock matrix. For example, there are two different parameters for the matrix elements between hydrogen atoms in a methyl group and their first hydrogen neighbours (see Table 3c of Ref. 7 the values for h_0^i, h_1^i, $i = 1,2$ and $h_0^1h_1^2$). In order to overcome this difficulty and make the method applicable for the calculation of chemical reactivities, we propose in this communication a re-parametrization for the construction of the synthetic Fock matrix which takes into account the "chemical equivalencies" and furthermore give results — similar to those of Deplus *et al.* Total orbital energy is taken so that the quantity should be approached as far as possible, and constitue the test of quality for the assignment proposed. The choice of this kind of test rests on the existence of good empirical relationships between SCF total molecular energies and SCF orbital energies.[15-19] Previous calculations have shown that an average error of 3% is committed with such an approximation[20] for practically all the molecules included by Snyder and Basch in their compendium of SCF wavefunctions of double zeta quality.[21] Interactions between a centre and its third neighbours are not taken into account and values less than 7×10^{-3} a.u. are put to zero. Thus, following the nomenclature of Deplus *et al.*, we get the parameters of table 1

TABLE 1

Parameters for the construction of the synthetic Fock matrix

Elements between a centre and its first neighbours	
$1sC_0\, h_1^i (i = 1, 2, 3)$	-0.0486
$1sC_0\, t_1^3$	-0.4769
$1sC_0\, t_1^i\ (i = 1, 2, 4)$	$+0.0371$
$h_0^i h_1^j\ (i, j = 1, 2, 3)$	-0.0192
$h_0^i t_1^3\ (i = 1, 2, 3)$	-0.0693
$t_0^4 t_1^3$	-0.6305
$t_0^4 t_j^i\ (i = 1, 2, 4)$	-0.0463
$t_0^i t_1^j\ (i, j = 1, 2, 3)$	$+0.0700$
Elements between a center and its second neighbours	
$1sC_0 t_2^4$	-0.0311
$t_2^4 h_2^i (i = 1, 2, 3)$	-0.0155
$t_0^4 t_2^4$	-0.0885

[1] Values in a.u. Parameters for diagonal elements and elements within a center, the same as those in Table 3 of Ref. 7.

Diagonal elements and elements within a center remained the same as those of Deplus *et al.* (Tables 3a and 3b in Ref. 7) whilst elements between a center and their first and second neighbours were modified in an average way for those cases in which chemical equivalence was required and unique values were assigned. In order to test our parametric procedure, calculations for the saturated hydrocarbons chosen in Ref. 7 were performed. Table 2 allows us to compare total molecular orbital energies obtained from the *ab-initio* calculation, the semiempirical procedure of Deplus *et al.* and our simplified method. As we can see, there exists a good similarity within the three series of values. The average errors with respect to the strictly *ab-initio* results are similar. Furthermore a smaller number of total parameters is required (24) in comparison with those of Deplus (32), which obviously simplifies the construction of the Fock synthetic matrix. From Table 2 one can see that no increase of error is expected to occur when our method is to be applied to larger molecules (errors for neopentane and cyclohexane are significatively less than those for methane and propane) and furthermore there is not any systematic error which could make our method inapplicable to larger molecules (errors are positive as well as negative).

TABLE 2

Total orbital energies of alkanes

Alkane	*ab-initio*	Deplus et al.	% error [2]	this work	% error [3]
Methane	28.3284	28.2724	0.20	28.2724	0.20
Ethane	55.3800	55.3548	0.05	55.3664	0.02
Propane	82.5676	82.4610	0.13	82.4766	0.11
Butane	109.5346	109.5648	0.03	109.5878	0.05
Isobutane	109.5590	109.5782	0.02	109.5906	0.03
Neopentane	136.7996	136.7054	0.07	136.7920	0.01
Cyclohexane	162.6381	162.6384	0.00	162.6594	0.02

[1] Values in a.u.

[2] Average error 0.07 %

[3] Average error = 0.06 %

The application of the present procedure to the calculation of chemical reactivity indices for saturated hydrocarbons and saturated periodic systems such as polyethylene is being carried in our laboratory and will be given elsewhere in a forthcoming paper.

REFERENCES

[1] R. E. Howard, M. Levy, H. Shull and S. Hagstrom, *J. Chem. Phys.*, **66**, 5181 (1978).

[2] M. Levy, W. J. Stevens, H. Shull and S. Hagstrom, *J. Chem. Phys.*, **52**, 5483 (1970); **61**, 1844 (1974).

[3] M. Levy, *J. Chem. Phys.*, **61**, 1857 (1974).

[4] R. E. Christofferson, *Adv. Quantum Chem.*, **6**, 333 (1972).

[5] G. Leroy and D. Peeters, *Theor. Chim. Acta*, **36**, 11 (1974).

[6] Ph. Degand, G. Leroy and D. Peeters, *Theor. Chim. Acta*, **30**, 243 (1973).

[7] A. Deplus, G. Leroy and D. Peeters, *Theor. Chim. Acta*, **36**, 109 (1974).

[8] M. D. Newton, F. P. Boer and W. N. Lipscomb, *J. Amer. Chem. Soc.*, **88**, 2353 (1966).

[9] J. E. Eilers and D. R. Whitman, *J. Amer. Chem. Soc.*, **95**, 2067 (1973).

[10] B. J. Duke, J. E. Eilers and B. O'Leary, *J. Chem. Soc. Faraday II*, **70**, 386 (1974).

[11] B. O'Leary, B. J. Duke and J. E. Eilers, *Adv. Quantum Chem.*, **9**, 1 (1975).

[12] G. Leory and D. Peeters, *Local. Delocal. Quantum Chem.*, **1**, 207 (1975).

[13] W. C. Herndon, *Prog. Phys. Org. Chem.*, **9**, 99 (1972).

[14] D. B. Cook, "Structures and Approximations for Electrons in Molecules", Ellis Horwood Ltd., London, 1978, p. 111.

[15] K. Ruedenberg, *J. Chem. Phys.*, **66**, 375 (1977).

[16] T. Anno and Y. Sakai, *J. Chem. Phys.*, **67**, 4771 (1977).

[17] L. J. Schaad, B. H. Robinson and B. A. Hess, *J. Chem. Phys.*, **67**, 4616 (1977).

[18] N. H. March, *J. Chem. Phys.*, **67**, 4618 (1977).

[19] P. Politzer, *J. Chem. Phys.*, **64**, 4239 (1976).

[20] E. A. Castro, *Int. J. Quantum Chem.*, (in press).

[21] L. C. Snyder and H. Basch, "Molecular Wave Functions and Properties", Wiley-Interscience, New York, 1972.

Revue Roumaine de Chimie, **25**, *4*, 459–466 (1980)

INTERFACIAL TENSION VARIATION IN THE COURSE OF LIQUID-LIQUID EXTRACTION. III[1]

THE EXTRACTION OF BUTYRIC ACID BY DIFFERENT SOLVENTS

IOSIF ALBU and EMIL CHIFU
"Babeş-Bolyai" University,
Department of Physical Chemistry, str. Arany J. nr. 11, 3400 Cluj-Napoca, România

Received April 25, 1979

Data are presented concerning the interfacial tension variation in the course of liquid-liquid extraction of butyric acid in the systems heptane/water, toluene/water and benzene/water. The results are compared with those previously obtained in the systems hexane/water and butyl acetate/water. The experimental data are discussed in the light of the thermodynamics of irreversible processes. In the case of heptane, hexane, toluene and benzene used as organic solvents, it is necessary to take into account the dimerization of the butyric acid in the oil phase, in conformity with an equation previously proposed by the authors. Only in the system butyl acetate/water the passing of the given component is simple, without the change of the molecular nature and it is governed by an equation proposed in the literature.

In the previous works [1, 2] we have studied the variation of the interfacial tension in the course of liquid-liquid extraction for some monocarboxylic aliphatic acids. The liquid-liquid systems used were hexane/water[1] and butyl acetate/water.[1, 2]

To account for the experimental data we have employed the following linear equation from the thermodynamics of irreversible processes:[3]

$$\sigma^{(e)} - \sigma = M \, \Delta\mu \tag{1}$$

where $\sigma^{(e)}$ represents the liquid/liquid interfacial tension when the distribution equilibrium is reached. σ stands for the interfacial tension at a given moment t of the extraction process — out of equilibrium — when the chemical potential difference governing the transfer of the given component from one phase into the other is $\Delta\mu$. The magnitude M is the surface transfer number, equal to the ratio of the phenomenological coefficients, L_{12}/L_{22}, which intervene in the well-known relationships

$$J_1 = L_{11}X_1 + L_{12}X_2$$
$$J_2 = L_{21}X_1 + L_{22}X_2 \tag{2}$$

between the fluxes (J_1, the substance flux; J_2 the surface flux) and the thermodynamic forces ($X_1 = \Delta\mu$, $X_2 = -(\sigma^{(e)} - \sigma)$) involved. It is obvious that at the moment when the distribution equilibrium is reached we have got in equation (1):

$$\sigma^{(e)} - \sigma = 0, \tag{3}$$

as the interfacial tension becomes constant and equal to $\sigma^{(e)}$. At the same moment

$$\Delta\mu = 0 \tag{4}$$

and the ratio of the concentrations, respectively that of the molar fractions, gets a constant value (the distribution constant).

In case that the extraction takes place in the system butyl acetate/water[1,2] the passing from one phase into another is simple, without changing the molecular nature of the involved component. Our experimental results have been satisfactorily described by the following equation proposed in the literature[4] and correspondingly derived from Eq. (1):

$$\sigma^{(e)} - \sigma = MRT \ln K \frac{M_0 d_w}{M_w d_0} - MRT \ln \frac{c_w}{c_0} \tag{5}$$

where c_0 and c_w are the molar concentrations of the transferring component in the oil, respectively the aqueous phase at the time t; M_0, M_w, d_0 and d_w are the molecular masses and the densities of the phases, R and T having their usual meanings. K is the distribution constant:

$$K = \frac{x_w^{(e)}}{x_0^{(e)}} \tag{6}$$

in which $x_0^{(e)}$ and x_w^e are the equilibrium molar fractions.

In its turn, the system hexane/water[1] gives mainly rise to the dimer forms of the above-mentioned acids in the oil phase. By adapting Eq. (1) to this situation, we have proposed[1] the following relationship which describes the interfacial tension variation with composition (c_w, c_0) in the course of the extraction:

$$\sigma^{(e)} - \sigma = MRT \ln K_D \frac{d_w}{M_w} \sqrt{\frac{1000\, M_0}{d_0}} - MRT \ln \frac{c_w}{\sqrt{c_0}} \tag{7}$$

where

$$K_D = \frac{x_w^{(e)}}{\sqrt{x_0^{(e)}}} \tag{8}$$

Eqs. (5) and (7) show both the transfer from the oil phase to the water and the inverse transfer.[1,2]

In Eqs. (5) and (7) an ideal behaviour has been ascribed to the aqueous and respectively the organic solution of the transferring component.

The equations of linear type (5) and (7) will apply in conditions not far from equilibrium. As a matter of fact, it can be noticed that for $c_w \to 0$, $\Delta\sigma \to \infty$, which has no physical meaning.[5]

We mention that though the interfacial tension plays an important role in the liquid-liquid extraction and generally in the mass transfer across interfaces, the variation of this magnitude in the course of the process has been little studied.[1-2, 4-5]

In the present work we are reporting data concerning the extraction of butyric acid in oil/water systems by making use of a larger series of oil phases (heptane, toluene and benzene); the results are compared with those previously published[1,2] where hexane and butyl acetate were utilized as oil phases.

EXPERIMENTAL

The details in working procedures have been described previously.[1,2] As a rule, in order to experimentally verify equations (5) and (7), it is necessary to simultaneously perform interfacial tension (σ, dyn/cm) and concentration (c_w; c_0, mol/l) measurements — the latter for the transferring component —, at different time intervals.

The component subjected to the transfer was introduced at first in the organic phase, at a known concentration; thus, the organic solution formed the donor phase, while the water formed the acceptor. The initial volume of each phase was of 50 ml. The concentrations in both phases were determined by titration.

The liquid-liquid interfacial tension was measured by the du Noüy method with an accuracy of ± 0.05 dyn/cm.

The parallel measurements of interfacial tension and concentration were carried on until constant values were obtained for both parameters, that is the distribution equilibrium was established.

The reagents were: butyric acid p.a. Schuchardt München, heptane VEB Laborchemie Apolda, toluene and benzene p.a. Merck. Doubly distilled water was used.

The measurements have been made at 25 ± 0.1°C.

RESULTS AND DISCUSSION

The heptane/water system

In Figures 1 and 2 we show the experimental results obtained at the transfer of butyric acid from heptane into water, for four concentration levels. Whilst in figure 1 the plotting is made in accordance with Eq. (5) which describes the simple transfer (σ vs. $\log(c_w/c_0)$), in figure 2 the data are consistent with Eq. (7) respectively with that transfer which implies dimerization in the oil phase (σ vs. $\log(c_w/\sqrt{c_0})$.

In both representations a linear variation of the interfacial tension with $\log(c_w/c_0)$ respectively $\log(c_w/\sqrt{c_0})$ can be remarked. Nevertheless, while in figure 1 the equilibrium values of the interfacial tension $\sigma^{(e)}$ are situated at quite different c_w/c_0 ratios, in figure 2 the same equilibrium values are situated at practically identical $c_w/\sqrt{c_0}$ ratios (in conformity with Eqs. (7)—(8). This state of facts offers a first indication with regard to the validity of Eq. (7) which foresees dimerization.

The identity of the slopes for the straight lines immediately follows from Eq. (7). In fact, it will be admitted above all that the surface transfer number M has a constant value for a given component transferring

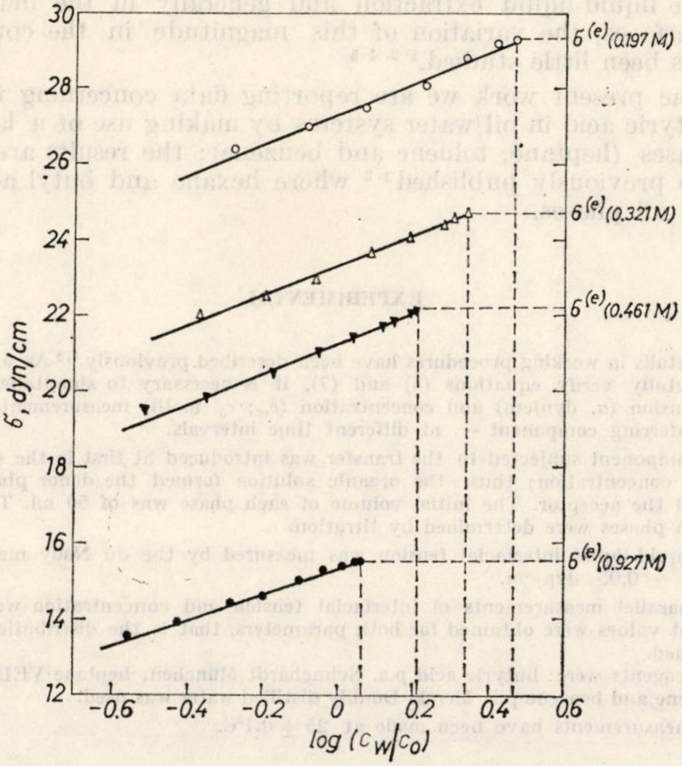

Fig. 1. — The interfacial tension (σ) as a function of $\log(c_w/c_0)$ in the course of butyric acid extraction from heptane into water. c_w and c_0 are the acid concentrations in water, respectively in heptane; $\sigma^{(e)}$ is the equilibrium interfacial tension. The initial concentrations (M) are: 0.197 (○), 0.321 (△), 0.461 (▼) and 0.927 (●).

in a certain liquid-liquid system, which seems reasonable. In this case the slope 2.3 MRT of the straight lines σ vs. $\log(c_w/\sqrt{c_0})$ is a constant. The intercepts in figure 2 are however different from a straight line to another, because, according to Eq. (7), they contain the $\sigma^{(e)}$ values which are functions of the total concentration of the transferring component.

Further on, if the $(\sigma^{(e)} - \sigma)$ values are plotted versus $\log(c_w/c_0)$ respectively $\log(c_w/\sqrt{c_0})$, a unique correlation straight line must be obtained for the simple transfer (Eq. (5)) and another one, correspondingly, for the transfer implying dimerization (Eq. (7)), independently of the concentration levels. Indeed, in accordance with Eq. (5), respectively Eq. (7), the intercepts now contain only constant values, namely the surface transfer number M and the distribution constants K — respectively K_D.

These considerations are illustrated in figures 3 and 4, respectively. It can be seen that in the $(\sigma^{(e)} - \sigma)$ vs. $\log (c_w/c_0)$ representation four different straight lines are obtained, corresponding to the four concentration levels and then Eq. (5) which admits the simple transfer of the component is not valid in the studied case (Figure 3).

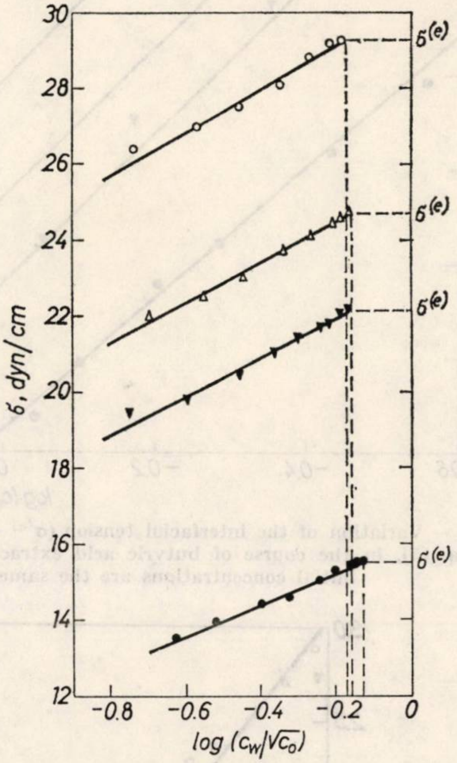

Fig. 2. — Plot of the data from Fig. 1 in σ vs. $\log(c_w/\sqrt{c_0})$ coordinates.

On the other hand, in figure 4 the experimental points corresponding to the different concentration levels satisfactorily fit a unique correlation straight line, according to Eq. (7). It results that the transfer of the butyric acid from heptane into water is described by this equation, i.e. the process develops with the dissociation of the dimeric molecules of butyric acid pre-existent in the oil phase. Similar results have been found by the authors in the system hexane/water.[1]

The systems: toluene/water and benzene/water

The processing of the experimental data, obtained at the transfer of the butyric acid from toluene into water, with the aid of Eqs. (5) and (7) respectively, led us to conclusions similar to those for the system heptane/water. In figure 5 the correlation straight line $(\sigma^{(e)} - \sigma) - \log (c_w/\sqrt{c_0})$ is directly represented for four concentration levels.

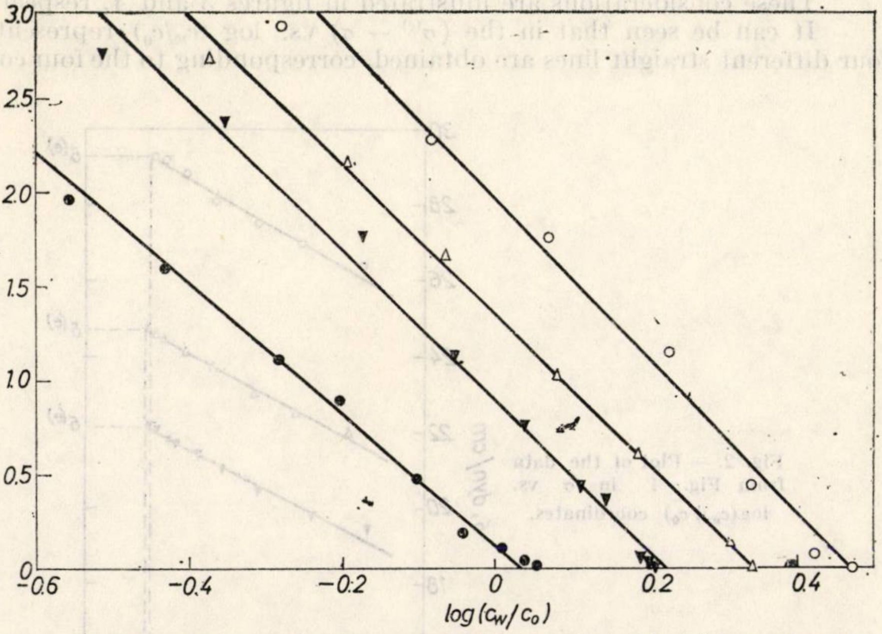

Fig. 3. — Variation of the interfacial tension ($\sigma^{(e)} - \sigma$) with log (c_w/c_0) in conformity with eq. (5), in the course of butyric acid extraction from heptane into water. The initial concentrations are the same as those in Fig. 1.

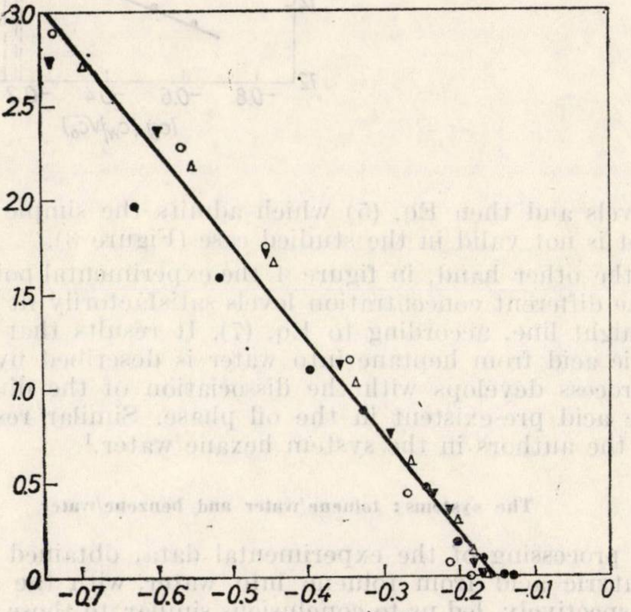

Fig. 4. — Plot of the data from Fig. 3 in ($\sigma^{(e)} - \sigma$) vs. log ($c_w/\sqrt{c_0}$) coordinates, according to eq. (7).

Data of the same type have also been obtained at the transfer of butyric acid from benzene into water, as it results from figure 6.

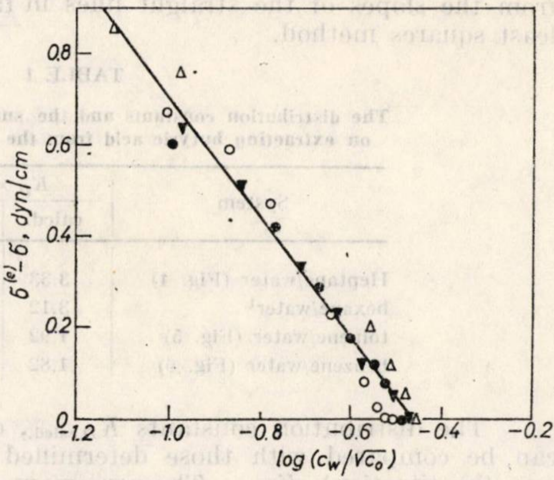

Fig. 5. — Variation of the interfacial tension ($\sigma^{(e)} - \sigma$) with log ($c_w/\sqrt{c_0}$) in accordance with eq. (7) in the course of butyric acid extraction from toluene into water. The initial concentrations (M) of the acid are: 0.197 (0), 0.333 (Δ), 0.589 (▼) and 0.985 (●)

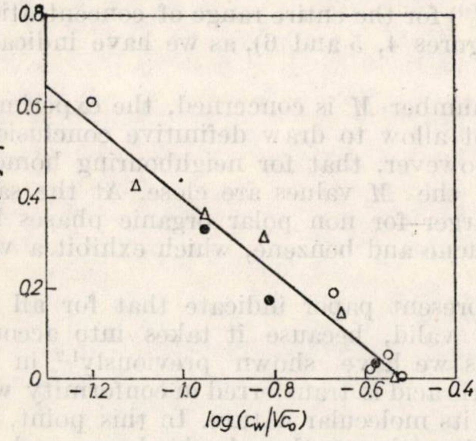

Fig. 6. — Variation of the interfacial tension ($\sigma^{(e)} - \sigma$) with log ($c_w/\sqrt{c_0}$) according to eq. (7) in the course of butyric acid extraction from benzene into water. The initial concentrations (M) of the acid are: 0.305 (0), 0.644 (Δ) and 0.888 (●).

To conclude, in the systems toluene/water and benzene/water, the extraction of butyric acid to the aqueous phase also takes place with the dissociation of the dimeric molecules existing in the oil phase as indicated by equation (7).

CONCLUSIONS

In table 1 the values of the distribution constant $K_{D,\text{calcd.}}$ and those of the surface transfer number M are listed for the extraction of butyric acid in the studied systems. For comparison, the table also contains the corresponding data, obtained at the transfer of butyric acid from hexane into water, previously published[1]. The magnitudes M and K_D have been calculated in conformity with Eq. (7), from the intercepts, respectively from the slopes of the straight lines in figures 4, 5 and 6, by using the least squares method.

TABLE 1

The distribution constants and the surface transfer numbers on extracting butyric acid from the oil phase into water

System	$K_D \times 10^2$		$M \times 10^{11}$ mol cm^{-2}
	calcd.	exp.	
Heptane/water (Fig. 4)	3.33	3.45	8.8
hexane/water[1]	3.12	3.29	9.3
toluene/water (Fig. 5)	1.92	1.92	2.3
benzene/water (Fig. 6)	1.82	2.01	1.4

The distribution constants $K_{D,\text{calcd.}}$, calculated as indicated above, can be compared with those determined in the straight experimental way (by titration), $K_{D,\text{exp.}}$ The agreement is satisfactory, within ±10 %. We mention that the $K_{D,\text{exp.}}$ values have been obtained by the processing of the equilibrium curves ($c_w^{(e)}$ vs $c_0^{(e)}$) for the entire range of concentrations investigated in the diagrams (Figures 4, 5 and 6), as we have indicated in a previous work.[1]

In what the surface transfer number M is concerned, the experimental results obtained so far do not allow to draw definitive conclusions. The data in the table suggest, however, that for neighbouring homologous substances as the oil phase, the M values are close. At the same time, the M values are much larger for non polar organic phases like heptane and hexane, than for toluene and benzene, which exhibit a very slight polarity.

The data reported in the present paper indicate that for all the studied systems equation (7) is valid, because it takes into account dimerization in the oil phase. As we have shown previously[1,2] in the system butyl acetate/water, butyric acid is transferred in conformity with Eq. (5), that is without changing its molecular nature. In this point, our data differ from those obtained by other authors,[4] who have used the same equation of the type (5) both for the simple passing and for the transfer implying molecular associations in the oil phase.

REFERENCES

[1] Part II : E. Chifu and I. Albu, *Ann. Chim.* (*Rome*), **65**, 519 (1975).

[2] E. Chifu and I. Albu, *Stud. Univ. Babeș-Bolyai, Chem.*, **19** (2), 83 (1974).

[3] A. A. Zhukhowitskii, V. A. Grigoryan and E. Mikhalik, *Doklady Akad. Nauk S.S.S.R.*, **155**, 392 (1964).

[4] G. T. Frumin, M. V. Ostrovskii and A. A. Abramzon, *Zhur. priklad. Khim.*, **40**, 1328 (1967).

[5] M. V. Ostrovskii and N. V. Golyakova, *Kolloid. Zhur.*, **37**, 584 (1975).

Revue Roumaine de Chimie, 25, 4, 467–473 (1980)

TRANSPORT DES IONS SO_4^{2-}, Cu^{2+}, H^+ ET DE L'EAU DANS LES MEMBRANES ÉCHANGEUSES D'IONS

SOLOMON STERNBERG, LIUBOV SHIRSHINA, SILVIA DANEŞ
Institut Polytechnique Bucarest Splaiul Independenţei, 313

Reçu le 24 mai 1979

On a déterminé les nombres de transport des ions SO_4^{2-}, Cu^{2+}, H^+ et le transport de l'eau pendant l'électrolyse dans deux membranes Nepton échangeuses d'ions, la A 111 PZL 183 anionique et la C61 AZL 183 cationique, en contact avec des solutions aqueuses de $CuSO_4$ ou de $CuSO_4$ et H_2SO_4 à concentration 0,1 – 2,4 n. Les membranes s'avèrent sélectives, le nombre de transport pour l'ion du même signe de charge que les groupements actifs étant petit (0,01 – 0,02) et presque indépendant de la concentration. Le transport de l'eau a lieu dans la direction du principal transporteur du courant et la dilution l'intensifie jusqu'à 50 molécules eau/ion.

The transport, numbers of SO_4^{2-}, Cu^+, H^+ ions and the transport of water on electrolysis in two Nepton A 111 PZL 183 anionic and C61 AZL 183 cationic exchange membranes were determined for aqueous $CuSO_4$ or $CuSO_4$ and H_2SO_4 0.1–2.4 m solutions. The membranes are selective; the transport number for the ion of the same sign with active groups of membranes is low (0.01 – 0.02) and nearly independent of concentration. The transport of water takes place in the direction of the main current carrier and it increases to 50 water molecules/ion when solution is diluted.

Les membranes échangeuses d'ions (MEI) ont de nombreuses applications techniques[1-3]; par exemple, la déminéralisation électrodialytique des eaux, milieu électrolyte dans les piles à combustion, etc.

L'étude des propriétés électrochimiques des MEI s'est développée aussi pendant la dernière décennie[4-8]. On a étudié surtout les solutions de chlorures des métaux alcalins et les ME de cations. L'objet du présent travail est le transport des ions Cu^{2+}, H^+, SO_4^{2-} et de l'eau autant dans les ME cationiques que dans celles anioniques.

PARTIE EXPÉRIMENTALE

L'installation utilisée (fig. 1) comprend une cellule électrochimique en U, composée de deux bras en verre (correspondant aux compartiments anodique et catodique). La MEI (anionique de type Nepton A111 PZL 183 ou cationique-Nepton C61 AZL 183 — Ionics USA — minceurs nominales 0,6 mm) est enserrée entre les flancs de deux compartiments.

L'électrolyse (galvanostatique, 4 heures, électrodes en cuivre) a été effectuée à concentrations initiales du $CuSO_4$ égales dans les solutions aqueuses des deux espaces, à savoir: 0,1 n, 0,2 n, 0,4 n, 0,8 n, 1,2 n et 2,0 n, à courant constant, respectivement 17, 17, 25, 35, 50 et 100 mA. Pour l'étude de la compétition des ions Cu^{2+} et H^+ au transport de la charge, on a électrolysé aussi une solution mixte de $CuSO_4$ (1,2 n) et H_2SO_4 (1,2 n).

L'analyse de la solution après électrolyse a été effectuée par électrogravimétrie et complexonométrie pour Cu^{2+}, tandis que la concentration des ions H^+ a été établie par acidimétrie après la déposition électrolytique du Cu. Les pesages de l'anolyte et du catholyte avant et après électrolyse ont permis d'établir les quantités des ions et de l'eau qui ont traversé la membrane.

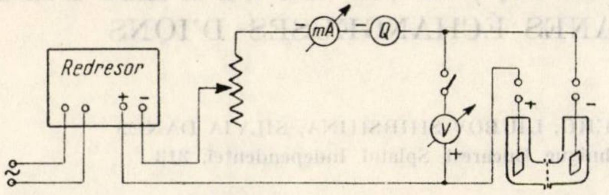

Fig. 1. — Schéma de mésure

Les courants mesurés au coulomètre, concordent assez bien avec les valeurs obtenues des variations du poids des électrodes (v. lignes 5, 6, 7 du tableau 1).

TRANSPORT DES IONS

Les nombres de transport t_i des ions $i (i = Cu^{2+}, H^+)$ peuvent être déterminés en partant des variations mesurées des quantités d'ions pendant l'électrolyse, autant dans l'anolyte :

$$t_{\mathrm{Cu}} = 1 + b\,\delta_{\mathrm{Cu},a}\,;\ t_{\mathrm{H}} = -\,b\,\delta_{\mathrm{H},a} \tag{1a}$$

que dans le catholyte :

$$t_{\mathrm{Cu}} = 1 + b\,\delta_{\mathrm{Cu},c}\,;\ t_{\mathrm{H}} = b\,\delta_{\mathrm{Cu},c} \tag{1b}$$

où b représente l'inverse de la quantité q d'électricité passée par la membrane, convertie en milliéquivalents-gramme ($b = 96{,}494/q$, avec q en coulombs) tandis que $\delta_{i,a}$ et $\delta_{i,c}$ sont les variations des quantités d'ions i pendant l'électrolyse, dans l'anolyte respectivement dans le catholyte :

$$\delta_{i,a} = n''_{i,a} - n'_{i,a}\,;\ \delta_{i,c} = n''_{i,c} - n'_{i,c} \tag{1c}$$

n'' et n' représentant la quantité finale et initiale de l'ion i ($i = H^+$ ou Cu^{2+}) en mval, dans le compartiment anodique (indice a) ou cathodique (indice c).

En principe, la somme algébrique des variations dans les deux compartiments devrait être nulle pour chaque ion ($\delta_{\mathrm{Cu},a} + \delta_{\mathrm{Cu},c} = 0$ et $\delta_{\mathrm{H},a} + \delta_{\mathrm{H},c} = 0$). Les données expérimentales (v. tableau 1) montrent toutefois des valeurs toujours négatives de ces sommes :

$$\delta_{\mathrm{Cu},a} + \delta_{\mathrm{Cu},c} = -\,p_{\mathrm{Cu}}\,;\ \delta_{\mathrm{H},a} + \delta_{\mathrm{H},c} = -\,p_{\mathrm{H}} \tag{2}$$

où p_i ($p_i > 0$) est la « perte » d'ion i des solutions pendant l'électrolyse. Il s'ensuit des nombres de transport différents, t_{ia} et t_{ic}, selon qu'on les obtient du bilan ionique selon l'anolyte (1a) ou selon le catholyte (1b) ; par exemple, pour Cu^{2+} :

$$t_{\mathrm{Cu},a} - t_{\mathrm{Cu},c} = (1 - b\,\delta_{\mathrm{Cu},a}) - (1 - b\,\delta_{\mathrm{Cu},c}) = b(\delta_{\mathrm{Cu},a} + \delta_{\mathrm{Cu},c})$$

ou, en utilisant (2) :

$$t_{\mathrm{Cu},a} - t_{\mathrm{Cu},c} = b\, p_{\mathrm{Cu}} \tag{3a}$$

ainsi que

$$t_{\mathrm{H},a} - t_{\mathrm{H},c} = b\, \mathrm{p_H} \tag{3b}$$

TABLEAU 1

Calcul des nombres de transport

Electrolyse numéro				1	2	3	
Membrane				anionique	cationique	cationique	
Concentrations initiales, mval/ml	H_2SO_4			2	0,4	1,2	
	$CuSO_4$			0	0	1,2	
Cu métal, mval	dissous, anode			14,97	3,96	7.32	
	déposé, cathode			14,95	3,96	7,37	
	déposé, coulomètre			14,95	4,04	7,31	
Cation transporté, *i*				Cu^{2+}	Cu^{2+}	Cu^{2+}	H^+
Grandeur		Symbole	Relation				
quantités en anolyte, mval	début	$n'_{i,a}$		52,82	17,82	45,30	53,23
	fin	$n''_{i,a}$		67,60	17,78	50,02	47,40
	variation	$\delta_{i,a}$	(1c)	14,78	−0,04	4,72	−5,83
quantités en catholyte mval	début	$n'_{i,c}$		51,54	12,74	46,23	54,31
	fin	$n''_{i,c}$		35,81	12,28	39,15	59,76
	variation	$\delta_{i,c}$	(1c)	−15,73	−0,46	−7,08	5,45
pertes, mval		p_i	2	0,95	0,50	2,36	0,38
nombres de transport	cation, moyenne	t_i	(4b)	−0,02	0,95	0,20	0,77
	cation, différence	Δt_i	(4c)	0,06	0,12	0,33	0,05
	anion	t_{SO_4}	(5)	1,02	0,05	0,03	

La figure 2 représente les pertes déterminées par la relation (2), en fonction de la concentration. On remarque une augmentation des pertes avec l'augmentation de la concentration, ce qui permet de les attribuer à l'adsorption des ions par la membrane, celle-là étant lavée à l'eau déionisée, après chaque électrolyse. Cette source des pertes conduit à une répartition égale entre les deux compartiments de la quantité totale perdue, puisque les concentrations des deux solutions sont restées presque égales pendant l'électrolyse, donc l'adsorption a eu lieu dans une mesure égale pour chaque compartiment. Par conséquent, les nombres de transport «vrais» seront les moyennes des valeurs obtenues selon l'anolyte (avec les relations 1a) et selon le catholyte (aux relations 1b) :

$$t_{\mathrm{Cu}} = (t_{\mathrm{Cu},a} + t_{\mathrm{Cu},c})/2\ ;\ \ t_{\mathrm{H}} = (t_{\mathrm{H},a} + t_{\mathrm{H},c})/2 \tag{4a}$$

ce qui équivaut à :

$$t_{\mathrm{Cu}} = 1 + b(\delta_{\mathrm{Cu},c} - \delta_{\mathrm{Cu},a})/2\ ; \quad t_{\mathrm{H}} = b(\delta_{\mathrm{H},c} - \delta_{\mathrm{H},a})/2 \tag{4b}$$

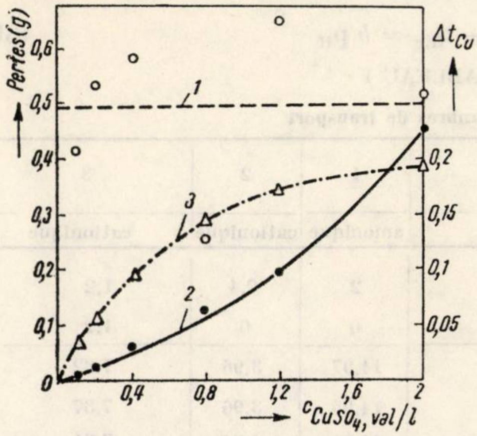

Fig. 2. — Pertes de masse et différence des nombres de transport entre les deux espaces (membrane cationique) :

1. (cercles blancs) pertes d'eau ; 2. (cercles noirs) pertes de Cu^{2+} ; 3. (triangles) Δt_{Cu}.

Le tableau 1 représente le mode de calcul pour les coefficients de transport, ainsi que pour la différence Δt_i des nombres de transport entre les deux compartiments, selon les relations (3) :

$$\Delta t_{\mathrm{Cu}} = b p_{\mathrm{Cu}}\ ; \quad \Delta t_{\mathrm{H}} = b\, p_{\mathrm{H}} \tag{4c}$$

On observe (fig. 2) que par l'augmentation de la concentration l'accroissement du Δt est moins prononcé que celui de la perte p_{Cu}, parce qu'on a choisi des valeurs q plus grandes (donc des valeurs b moindres) pour les solutions plus concentrées.

Le nombre de transport de l'anion est obtenu par les relations :

$$t_{\mathrm{SO_4}} = 1 - t_{\mathrm{Cu}} - t_{\mathrm{H}}\ ; \quad t_{\mathrm{SO_4}} = 1 - t_{\mathrm{Cu}} \tag{5}$$

en présence de H^+, respectivement en son absence.

Dans les calculs on a négligé l'effet de la diffusion (parce que la perméabilité des membranes est réduite, ainsi que les différences de concentration entre compartiments) et de la pression hydrostatique (la dénivellation n'a pas dépassé 2 cm).

Pour améliorer la précision, chaque détermination a été répétée deux ou trois fois.

TRANSPORT DE L'EAU

Soit M_w(g/mole) la masse molaire de l'eau et $E_{\mathrm{CuSO_4}}$, $E_{\mathrm{H_2SO_4}}$(g/val) les masses équivalentes (masses molaires divisées par 2) des $CuSO_4$ et H_2SO_4 Les variations δ_{wa}, δ_{wc} (mmole) des quantités d'eau dans l'anolyte et dans le catholyte sont calculables en utilisant les bilans de la masse totale par compartiments :

$$\Delta_a = M_w \delta_{wa} + E_{\mathrm{CuSO_4}} \cdot \delta_{\mathrm{Cu},a} + E_{\mathrm{H_2SO_4}} \cdot \delta_{\mathrm{H},a} \tag{6a}$$

$$\Delta_c = M_w \delta_{wc} + E_{\mathrm{CuSO_4}} \cdot \delta_{\mathrm{Cu},c} + E_{\mathrm{H_2SO_4}} \cdot \delta_{\mathrm{H},c} \tag{6b}$$

où $\delta_{i,a}$, $\delta_{i,c}(i = \text{H, Cu})$ sont les variations des quantités des ions i dans les deux espaces, tandis que Δ_a, Δ_c sont les variations du poids total de l'anolyte et du catholyte. Les données du tableau 2, qui illustre le calcul du transport de l'eau, permettent de constater que la somme des quantités d'eau dans les deux compartiments ne se conserve pas :

TABLEAU 2

Calcul du transport de l'eau

Membrane				anionique	cationique
Teneur en $CuSO_4$, mval/ml solution				0,4	2
		Symbole	Relation		
Variations de masse	anolyte, mg	Δ_a	—	−1434,4	3224,4
	catholyte, mg	Δ_c	—	702,3	−3332,7
Variations du Cu^{2+}	anolyte, mval	$\delta_{Cu,a}$	(1c)	−0,04	14,78
	catholyte, mval	$\delta_{Cu,c}$	(1c)	−0,46	15,73
Variations de l'eau	anolyte, mmole	$\delta_{w,a}$	(6a)	−79,50	113,54
	catholyte, mmole	$\delta_{w,c}$	(6b)	39,01	−114,50
Pertes d'eau, mmole		p_w	(7)	40,49	0,96
Transport d'eau, mmole		w	(8)	59,25	−114,02
Nombres d'hydratation	SO_4^{2-}	N_{SO_4}	(10a)	—	15,2
	Cu^{2+}	N_{Cu}	(10b)	29,3	—

$$\delta_{wa} + \delta_{wc} = -p_w \tag{7}$$

$p_w > 0$ représentant ainsi les « pertes » d'eau. Ces pertes s'élèvent en moyenne à 20 mmole, soit 0,5% de la masse initiale d'eau.

A l'encontre des pertes d'ions, les pertes d'eau ne dépendent pas de la concentration (v. fig. 2), ce qui justifie la supposition qu'elles sont provoquées par l'évaporation. Par conséquent, les pertes d'eau doivent être réparties également entre les deux compartiments et la quantité w (mmole) transportée de l'espace anodique dans l'espace cathodique sera :

$$w = \delta_{wc} + p_w/2 = -(\delta_{wa} + p_w/2)$$

ou, en considérant la relation (7) :

$$w = (\delta_{wc} - \delta_{wa})/2 \tag{8}$$

On a trouvé w toujours positif pour les déterminations à membrane cationique et négatif (dirigé donc du catholyte vers l'anolyte) quand on a utilisé la ME anionique ; ainsi le sens du transport de l'eau coïncide dans les deux cas avec le sens du déplacement du principal transporteur de courant. On pourrait donc supposer que l'eau traverse la membrane sous la forme de l'enveloppe d'hydratation des ions. En ce cas, w sera exprimable par les nombres apparents d'hydratation des ions, N'_i :

$$w = b(N'_{\mathrm{H}}t_{\mathrm{H}} + N'_{\mathrm{Cu}}t_{\mathrm{Cu}}/2 - N'_{\mathrm{SO_4}} \cdot t_{\mathrm{SO_4}}/2) \tag{9}$$

où les dénominateurs représentent les valences des ions. Contenant plus d'une inconnue, la relation (9) n'est pas utilisable pour la détermination simultanée des trois N'_i, tout en permettant d'obtenir des valeurs approchées, N_i, pour les nombres de transport de l'ion transporté préférentiellement (c.-à.-d. Cu^{2+} pour la ME cationique et SO_4^{2-} pour l'anionique) ; en négligeant autant le transport d'électricité que celui de l'eau par les co-ions (ions du même signe de charge que les groupements actifs de la membrane) on obtient pour les ME cationique et anionique respectivement :

$$N_{\mathrm{Cu}} = 2\,bw \tag{10a}$$

$$N_{\mathrm{SO_4}} = 2\,bw \tag{10b}$$

Pour le transport concomitant des ions Cu^{2+} et H^+, la relation (10a) conduit bien entendu à une moyenne pondérée des nombres de transport,

$$N_{\mathrm{H}}t_{\mathrm{H}} + N_{\mathrm{Cu}}t_{\mathrm{Cu}}.$$

Les résultats concernant les nombres de transport et d'hydratation sont présentés dans le tableau 3.

TABLEAU 3

Nombres de transport et d'hydratation

Membrane	Concentrations, mval/ml		Nombres de transport			Nombre de l'hydratation	
	$\mathrm{CuSO_4}$	$\mathrm{H_2SO_4}$	$\mathrm{SO_4^{2-}}$	$\mathrm{Cu^{2+}}$	$\mathrm{H^+}$	$\mathrm{SO_4^{2-}}$	$\mathrm{Cu^{2+}}$
anionique	0,1	0	0,93	0,07	—	41,0	—
,,	0,2	0	0,96	0,04	—	38,2	—
,,	0,4	0	1,02	−0,02	—	28,2	—
,,	0,8	0	0,95	0,05	—	24,8	—
,,	1,2	0	1,11	−0,11	—	23,2	—
,,	2,0	0	0,98	0,02	—	15,3	—
	moyennes		0,99	0,01			
cationique	0,1	0	0,07	0,93	—	—	47,8
,,	0,2	0	0,02	0,98	—	—	42,8
,,	0,4	0	0,05	0,95	—	—	30,6
,,	0,8	0	0,03	0,97	—	—	29,7
,,	1,2	0	0,06	0,94	—	—	28,9
,,	2,0	0	−0,11	1,11	—	—	17,5
	moyennes		0,02	0,98			
cationique	1,2	1,2	0,03	0,20	0,77	—	15,1*

*** Moyenne de Cu^{2+} et H^+**

DISCUSSION

Il s'avère que les nombres de transport du tableau 3 sont peu influencés par la concentration de la solution : dans l'intervalle 0,1—2*n*, t_i dépendent surtout du type de la membrane : $t_{SO_4} \cong 0$ et $t_{Cu} \cong 1$ pour la ME cationique, $t_{SO_4} \cong 1$ et $t_{Cu} \cong 0$ pour la ME anionique.

Pour l'électrolyte mixte $CuSO_4/H_2SO_4$, le transport de la charge à travers la membrane cationique est assuré conjointement par les cations Cu^{2+} et H^+, les derniers étant à concentration égale les principaux vecteurs du courant.

Les nombres d'hydratation du tableau 3 montrent un fort accroissement avec la diminution de la concentration, atteignant à 0,1 n des valeurs tellement hautes ($\cong 50$) qu'il faut conclure au rôle secondaire joué dans le transport de l'eau par les enveloppes d'hydratation en comparaison du rôle de l'effet électroosmotique.

BIBLIOGRAPHIE

[1] F. Helfferich, ,,Ion Exchange'', chap. 8.1., McGraw-Hill, New York, 1962.

[2] V. N. Laskorin et N. M. Smirnova, ,,Ionnobmennye menbrany i ikh primenenie'', Atomizdat, Moscou, 1961, p. 65.

[3] H. A. Liebhafsky et E. J. Cairns "Fuel Cells and Fuel Batteries", Wiley, New York, 1968.

[4] R. P. Buch "Electroanalytical Chemistry of Membranes", Ed. New York, 1977, dans *Critical Revue in Analytical Chemistry*.

[5] M. L. Rao, *J. Electrochem. Soc.*, **114**, 13 (1967).

[6] A. N. Dey, *J. Electrochem. Soc.*, **115**, 160 (1968).

[7] Y. Prigent, A. Poiteau et M. Chemla, *J. Chim. phys.*, **71**, 75 (1974).

[8] A. Poiteau, Y. Prigent et M. Chemla, *J. Chim. phys.*, **72**, 57 (1975).

Revue Roumaine de Chimie **25**, *4*, 475–486 (1980)

GENERAL FORMULATION OF ADSORPTION FROM LIQUID MIXTURES ON HETEROGENEOUS SOLID SURFACES

M. BORÓWKO and M. JARONIEC

Department of Theoretical Chemistry, Institute of Chemistry, M. Curie-Skłodowska University,
Plac M. Curie-Skłodowskiej 3, 20031 Lublin, Poland

Received November 6, 1978

A general method is described for calculating the isotherm for adsorption from nonideal multicomponent solutions on heterogeneous solid surfaces. The proposed treatment is based on the concept of generalized integral equation. The adsorption on the adsorbent surface showing patchwise and random distribution of adsorption sites is considered.

I. INTRODUCTION

The most accurate models of adsorption from liquid mixtures are those which involve the heterogeneity of the adsorbent surface and nonideality of the bulk and adsorbed phases. Hitherto, studies on liquid adsorption usually concern binary mixtures and homogeneous adsorbents (see references in the reviews[1,2]). Recently, the results have been generalized to adsorption on heterogeneous solid surfaces (see references in the review[3]). The full description of liquid adsorption, i.e., taking into account heterogeneity of the adsorbent and nonideality of both phases, has not been formulated yet. Recent results concerning the adsorption from multicomponent gas mixtures on heterogeneous solid surfaces[4-7] create new possibilities for investigations in the case of adsorption from binary and multicomponent liquid mixtures. It follows from the studies[4-8] that the topography of adsorption sites on the surface does not play any part when the adsorbed phase is assumed to be ideal; the bulk phase may be either ideal or nonideal. However, a model of nonideal adsorbed phase on a heterogeneous solid surface requires an additional assumption about topography of adsorption sites on the adsorbent surface.

The current state of theory of mixed-gas adsorption on energetically heterogeneous solid surfaces makes possible the generalization of the results concerning the adsorption from ideal and nonideal liquid mixtures on homogeneous surfaces,[9-12] to adsorption on heterogeneous adsorbents. The paper of Everett[10] is especially interesting for us, because in it the adsorption model, assuming nonideality of both phases, is considered.

Although our formulation will be based on some simplifying assumptions, it points to the fundamental problems appearing in the theory of adsorption from liquid mixtures on heterogeneous solid surfaces. This general treatment gives a simple procedure to derive equations for adsorption isotherms and thermodynamic functions, taking into account the effects of the adsorbent heterogeneity and nonideality of the bulk and adsorbed phases.

II. ADSORPTION FROM BINARY LIQUID MIXTURES ON HOMOGENEOUS SOLID SURFACES

First, we consider adsorption from binary liquid mixtures of nonelectrolytes on homogeneous solid surfaces. The assumptions underlying our approach are the following:

(a) the cell model with one molecule in each cell for both, bulk and adsorbed, phases is used;

(b) the total number of molecules in the adsorbed phase is constant;

(c) the molecular sizes of molecules of both components are equal;

(d) the interactions between both phases are neglected;

(e) the both phases are nonideal;

(f) the square-well potential for adsorbate — adsorbent interactions is applied;

(g) the potential energy of interactions between molecules in the adsorbed phase is calculated according to Lennard-Jones and Devonshire expression.[13]

For the purpose of derivation of an analytical expression for mole fractions of both components in the adsorbed phase we assume the definite solution model for the adsorbed phase; namely the Lennard-Jones and Devonshire model.[13] The same model may be assumed for the bulk solution. Since the interactions between both phases are neglected, the theoretical considerations are the same for all models of the bulk phase. Therefore, for the chemical potentials of the components in the bulk phase we employ the most general expression:

$$\mu_i^\ell = \mu_i^{0\,\ell} + k\,T \ln a_i^\ell \quad \text{for } i = 1.2 \tag{1}$$

where

$$a_i^\ell = \gamma_i^\ell\, x_i^\ell \tag{2}$$

and x_i^ℓ, γ_i^ℓ, μ_i^ℓ denote the mole fraction, the activity coefficient and the standard chemical potential of the i-th component in the bulk phase, respectively; the superscript ℓ refers to the bulk phase. Assuming the definite solution model for the bulk phase we have an analytical expression for γ_i^ℓ. Then, the relationship between x_i^σ (the mole fraction of i-th component in the adsorbed phase) and x_i^ℓ may be derived. However, using equation (1) and defining exactly the adsorbed phase, we have an analytical relationship between x_i^σ and a_i^ℓ. The analytical dependences $x_i^\sigma(a_i^\ell)$ are useful to characterize the experimental adsorption data, since the activities a_i^l (for $i = 1, 2$) may be determined independently of vapour-liquid equilibria.

The canonical partition function of the adsorbed phase satisfying the assumptions (a)—(g) may be expressed as follows :

$$Q^{NA} = Q^{IA} Q^{I} \tag{3}$$

where

$$Q^{IA} = \frac{N!}{N_1!(N - N_1)!} q_1^{N_1} q_2^{N-N_1} \tag{4}$$

and

$$Q^{I} = \exp(-E/kT) \tag{5}$$

In (3) the superscript NA refers to the adsorption model with nonideal adsorbed phase, IA refers to the ideal adsorbed phase and I refers to interactions in the adsorbed phase. Next, $N = N_1 + N_2$, N_i is the number of adsorbed molecules of the i-th component, q_i is the partition function for isolated molecule of i-th component in the adsorbed phase, E is the potential energy of interactions between molecules in the adsorbed phase, k is the Boltzman constant, and T is the absolute temperature. The function q_i is defined as :

$$q_i = J_i^{\sigma} \exp(\varepsilon_i/kT) \tag{6}$$

where J_i^{σ} is the cell partition function including internal degrees of freedom of adsorbed molecule and ε_i is the adsorption energy. The potential energy E, predicted by Lennard-Jones and Devonshire model,[13] is equal to

$$E = \frac{zN}{2}\left[(x_1)^2 u_{11} + 2x_1x_2u_{12} + (x_2)^2 u_{22}\right] \tag{7}$$

where $x_i^{\sigma} = N_i/N$, and $u_{ij}(i,j = 1,2)$ is the energy interaction between a pair of molecules $i - j$ and z is the number of nearest neighbours for a given molecule.

The function $x_1^{\sigma}(a^1)$ will be obtained by using the following equilibrium condition

$$\mu_{12}^{\sigma(NA)} = \mu_1^{\sigma(NA)} - \mu_2^{\sigma(NA)} = \mu_{12}^{1} = \mu_1^{1} - \mu_2^{1} \tag{8}$$

The difference of the chemical potentials, $\mu_{12}^{\sigma(NA)}$, obtained from (3) is equal to :

$$\mu_{12}^{\sigma(NA)} = \mu_{12}^{\sigma(IA)} + \mu_{12}^{\sigma(I)} \tag{9}$$

where

$$\mu_{12}^{\sigma(IA)} = -kT\frac{\partial \ln Q^{IA}}{\partial N_1} = kT \ln \frac{x_1^{\sigma} q_2}{x_2^{\sigma} q_1} \tag{10}$$

and

$$\mu_{12}^{\sigma(\mathrm{I})} = -kT\frac{\partial \ln Q^{\mathrm{I}}}{\partial N_1} = \omega(x_2^{\sigma} - x_1^{\sigma}) + \frac{z}{2}(u_{11} - u_{22}) \tag{11}$$

The parameter ω is defined by the following equation:

$$\omega = z\left[u_{12} - \frac{1}{2}(u_{11} + u_{22})\right] \tag{12}$$

Combining equations (8), (1), (10) and (11) we obtain the general relationship x_1^{σ} on a_1^{ℓ} for homogeneous surfaces:

$$\frac{x_1^{\sigma}}{1 - x_1^{\sigma}} = \frac{q_1}{q_2}\exp[\mu_{12}^{0.1}/kT]\exp[z(u_{22} - u_{11})/2kT] \\ \exp[-\omega(1 - 2x_1^{\sigma})/kT]\, a_{12}^{\ell} \tag{13}$$

where $a_{12}^{\ell} = a_1^{\ell}/a_2^{\ell}$.
Let us denote

$$K_{12} = \frac{q_1}{q_2}\exp[\mu_{12}^{0.1}/kT] \tag{14}$$

$$K_{12}^{\bullet} = K_{12}\exp[z(u_{11} - u_{22})/2kT] \tag{15}$$

Let us consider special cases of equation (13):
(i) adsorbate-adsorbate molecular interactions in the adsorbed phase can be neglected, i.e., $u_{11} = u_{22} = u_{12} = 0$, then $\omega = 0$ and (13) becomes:

$$\frac{x_1^{\sigma}}{1 - x_1^{\sigma}} = K_{12}\, a_{12}^{\ell} \tag{16}$$

Equation (16) has been derived by Sircar and Myers[11]. This isotherm corresponds to the adsorption model with nonideal bulk phase and ideal adsorbed phase and it is generated by the canonical function Q^{IA}. When $\gamma_i^{\mathrm{l}} = 1$ for $i = 1{,}2$ (ideal both phases) (16) reduces to the well-known relationship:

$$\frac{x_1^{\sigma}}{1 - x_1^{\sigma}} = K_{12}\, x_{12}^{\ell};\ x_{12}^{\ell} = x_1^{\ell}/x_2^{\ell} \tag{17}$$

(ii) $u_{12} = \frac{1}{2}(u_{11} + u_{22})$ and $u_{11} \neq u_{22}$, then ω is also equal to zero, but (13) becomes:

$$\frac{x_1^{\sigma}}{1 - x_1^{\sigma}} = K_{12}^{\bullet} a_{12}^{\ell} \tag{18}$$

In this case the adsorbed phase is the perfect solution.

(iii) $u_{12} \neq \frac{1}{2}(u_{11} + u_{22})$. For the case we obtain (13) which may be re-written in the slightly different form :

$$\frac{x_1^\sigma}{1 - x_1^\sigma} \exp(-\alpha\, x_1^\sigma) = K_{12}^* a_{12}^l \tag{19}$$

where

$$K_{12}^* = K_{12} \exp[z(u_{22} - u_{12})]/kT \tag{20}$$

and

$$\alpha = 2\omega/kT \tag{21}$$

The equation (19) is analogous to the Frumkin adsorption isotherm[14]. Similar expression to (18) was discussed by Everett[10]; he assumed that both regular phases interact together.

III. ADSORPTION FROM BINARY LIQUID MIXTURES ON HETEROGENEOUS SOLID SURFACES

In this section the equation (19) will be generalized to heterogeneous surfaces. First, the special cases of (19), i.e., the equations (16) and (18), will be considered. The most simple case is (16). Since in this case $Q^I = 1$ (interactions between molecules in the adsorbed phase are neglected), the topography of adsorption sites does not influence the adsorption process. Thus, equations derived on the basis of (16) are valid for adsorbents showing different distributions of adsorption sites on the surface. According to the general treatment of adsorption from binary gas mixtures,[7] each adsorption site is unambigously characterized by adsorption energies of both components. For example the adsorption sites denoted by subscript (p,r) have the adsorption energies : $\varepsilon_{1(p)}$ with respect to the 1st component and $\varepsilon_{2(r)}$ with respect to the 2nd component. The symbol $N_{(pr)}$ denotes the total number of molecules adsorbed on the adsorption sites (p,r); $N_{(pr)} = N_{1(pr)} + N_{2(pr)}$.

The canonical partition function, describing adsorption on heterogeneous surfaces at $u_{11} = u_{22} = u_{12} = 0$ is equal to :

$$Q^{\mathrm{IAH}} = \prod_{p,r} Q^{\mathrm{IA}}_{(pr)} = \\ = \prod_{p,r} \frac{N_{(pr)}!}{N_{1(pr)}!\,(N_{(pr)} - N_{1(pr)})!}\, q_{1(p)}^{N_{1(pr)}}\, q_{2(r)}^{N_{(pr)}-N_{1(pr)}} \tag{22}$$

where

$$q_{i(p)} = J_i^\sigma \exp[\varepsilon_{i(p)}/kT] \tag{23}$$

$$N = N_1 + N_2 = \sum_{p,r} N_{(pr)} \tag{24}$$

and superscript IAH refers to the ideal adsorbed phase and heterogeneous surface. We assume that constant J_i^σ is independent of the type of adsorption site ; this assumption is ussually used in the theory of adsorption on heterogeneous solid surfaces. Using standard thermodynamic transformations and the following equilibrium condition :

$$\mu_{12(pr)}^{\sigma(\mathrm{IAH})} = \mu_{12}^{1} \text{ for each } (pr) \tag{25}$$

we have

$$x_{1(pr)}^{\sigma} = \frac{K_{12(pr)} a_{12}^{\ell}}{1 + K_{12(pr)}\, a_{12}^{\ell}}\, ; \; x_{1(pr)}^{\sigma} = \frac{N_{1(pr)}}{N_{(pr)}} \tag{26}$$

The constant $K_{12(pr)}$ is analogous to that defined by (14) ; namely

$$K_{12(pr)} = \frac{q_{1(p)}}{q_{2(r)}} \exp\left[\frac{\mu_{12}^{0,1}}{kT}\right] \tag{27}$$

The mole fraction of the 1st component in the whole adsorbed phase, X_1^σ, is equal to :

$$X_1^\sigma = \frac{N_1}{N} = \sum_{p,r} f_{(pr)}\, x_{1(pr)}^{\sigma} \tag{28}$$

where

$$f_{(pr)} = N_{(pr)}/N \tag{29}$$

Replacing summation (29) by integration, we obtain the generalized integral isotherm for adsorption of binary liquid mixtures on heterogeneous solid surfaces :

$$X_1^\sigma(a_{12}^1) = \iint_{\Delta_{12}} x_1^\sigma(\varepsilon_{12}, a_{12}^{\ell}) F_{12}\,(\varepsilon_1, \varepsilon_2)\, \mathrm{d}\,\varepsilon_1\, \mathrm{d}\varepsilon_2 \tag{30}$$

where $\varepsilon_{12} = \varepsilon_1 - \varepsilon_2$; $F_{12}(\varepsilon_1\ \varepsilon_2)$ is a two-dimensional distribution function normalized to unity, which characterizes the heterogeneity of the adsorbent surface, and Δ_{12} is a two-dimensional integration region.

Using (26) for the local isotherm $x_1^\sigma(a_{12}^{\ell}, \varepsilon_{12})$ and suitable analytical expressions for $F_{12}\ (\varepsilon_1,\ \varepsilon_2)$, we can derive different equations for overall isotherm $X_1^\sigma(a_{12}^{\ell})$.

Since in liquid adsorption, the difference of adsorption energies of both components mainly influence the adsorption process, it is frequently used to characterize the adsorption sites. Introducing a new distribution $\chi_{12}(\varepsilon_{12})$, for characterizing the adsorbent heterogeneity, we obtain from (30) :

$$X_1^\sigma(a_{12}^{\ell}) = \int_{\Omega_{12}} x_1^\sigma(a_{12}^{\ell}, \varepsilon_{12})\chi_{12}(\varepsilon_{12})\, \mathrm{d}\,\varepsilon_{12} \tag{31}$$

where

$$\chi_{12}(\varepsilon_{12}) = \int_{\Delta_2} F_{12}(\varepsilon_{12} + \varepsilon_2,\ \varepsilon_2)\, d\varepsilon_2 \tag{32}$$

Equation (31) is considerably simpler than (30), and therefore is often applied to describe adsorption from liquid mixtures on heterogeneous adsorbents. [5,6]

Extension of (18) to adsorption on heterogeneous surfaces is more complicated. Equations (16) and (18) have the same form; only constants K_{12} and $K_{12}^{\bullet}$ are slightly different. Constant $K_{12}^{\bullet}$ from (18) contains additionally the term with interaction energies u_{11} and u_{22}. If the energies u_{11} and u_{22} are independent of the type of adsorption sites i.e., they are characteristic of the whole adsorbed phase, then extension of (18) to heterogeneous surfaces is identical with that presented for (16). For X_1^{σ} we obtain equations (30) and (31) with the local adsorption isotherm (18). However if energies u_{11} and u_{22} depend on the type of adsorption sites then the model of the adsorbent surface determines the type of equation describing liquid adsorption. For this case the integration with respect to energies ε_1 and ε_2 is more complicated (see (30)), because the parameters u_{11} and u_{22} are dependent on ε_1 and ε_2, respectively.

Now, we generalize equation (19) to adsorption on heterogeneous solid surfaces. First, the patchwise model of heterogeneous surface will be discussed. In this model the adsorption sites of the equal adsorption energies are assumed to be grouped together into patches. These patches are so large that the states in which two molecules adsorbed on different patches are still at interaction distances, could be neglected. The canonical partition function describing liquid adsorption (see assumptions (a)–(g)) on patchwise solid surfaces may be written as follows:

$$Q^{\mathrm{NAHP}} = \prod_{p,r} Q^{\mathrm{IA}}_{(pr)} Q^{\mathrm{I}}_{(pr)} \tag{33}$$

where

$$Q^{\mathrm{I}}_{(pr)} = \exp\left[\frac{-E_{(pr)}}{kT}\right] = \exp\left\{\frac{-zN_{(pr)}}{2kT} \times \right.$$
$$\left. \times\left[(x^{\sigma}_{1(pr)})^2 = u_{11} + 2x^{\sigma}_{1(pr)}\, x^{\sigma}_{2(pr)} u_{12} + (x^{\sigma}_{2(pr)})^2\, u_{22}\right]\right\} \tag{34}$$

and $Q^{\mathrm{IA}}_{(pr)}$ is defined by (22). However, the superscript NAHP refers to the nonideal adsorbed phase and patchwise heterogeneous surfaces.

For simplicity, we assume that u_{11} and u_{22} are independent of the type of adsorption sites. Using similar transformations as in the previous sections we have:

$$\frac{x^{\sigma}_{1(pr)}}{1 - x^{\sigma}_{1(pr)}} \exp\left(-\alpha\, x^{\sigma}_{1(pr)}\right) = K^{*}_{12(pr)} a^{\ell}_{12} \tag{35}$$

where, according to our assumption of the interaction parameters, the parameter α is characteristic of the whole adsorbent surface, whereas

$$K^*_{12(pr)} = K_{12(pr)} \exp\left[\frac{z(u_{22} - u_{12})}{kT}\right] \tag{36}$$

the constant $K_{12(pr)}$ is defined by (27).

The mole fraction X_1^σ, referring to the whole adsorbent surface, may be expressed by (30) or (31) containing the subintegral function x_1^σ obtained from (35).

Finally, we consider the liquid adsorption on surfaces showing random distribution of adsorption sites on the surface. In the random, topographical model of heterogeneous surfaces, the adsorption sites of equal energies are assumed to be distributed randomly over a heterogeneous surface.[8] In the case of surfaces with random topographical distribution of sites the function Q^I is characteristic of the whole surface, because the average interaction energy is assumed for the whole adsorbed phase (c.f. reference[15] concerning gas adsorption on heterogeneous surfaces). Thus, the canonical partition function is equal to:

$$Q^{\mathrm{NAHR}} = Q^{\mathrm{I}} \prod_{p,r} Q^{\mathrm{IA}}_{(pr)} \tag{37}$$

where Q^{IA}_{pr} is defined by (22) and

$$Q^{\mathrm{I}} = \exp\left\{\frac{-zN}{2kT}[(X_1^\sigma)^2 u_{11} + 2X_2^\sigma X_2^\sigma u_{12} + (X_2^\sigma)^2 u_{22}]\right\} \tag{38}$$

The function Q^{I} refers to the whole adsorbed phase and therefore it depends on the mole fraction X_1^σ and X_2^σ. The canonical function (37) generates the following relationship for $x^\sigma_{1(pr)}$:

$$\frac{x^\sigma_{1(pr)}}{1 - x^\sigma_{1(pr)}} \exp(-\alpha X_1^\sigma) = K^*_{12(pr)} a^\ell_{12} \tag{39}$$

Since, X_1^σ is the quantity referring to the whole adsorbent surface, (39) may be transformed into the form, which is formally identical with equation (26):

$$x^\sigma_{1(pr)} = \frac{C_{12(pr)} a^\ell_{12}}{1 + C_{12(pr)} a^\ell_{12}} \tag{40}$$

where

$$C_{12(pr)} = K^*_{12(pr)} \exp(\alpha X_1^\sigma) \tag{41}$$

Introducing (40) to equations (30) and (31) we have:

$$X_1^\sigma = \iint_{\Delta_{12}} \frac{C_{12} a^\ell_{12}}{1 + C_{12} a^\ell_{12}} F_{12}(\varepsilon_1, \varepsilon_2)\, d\varepsilon_1\, d\varepsilon_2 \tag{42}$$

and

$$X_1^{\sigma} = \int_{\Omega_{12}} \frac{C_{12} a_{12}^{\ell}}{1 + C_{12} a_{12}^{\ell}} \chi_{12}(\varepsilon_{12}) \, d\varepsilon_{12} \tag{43}$$

Equations (42) and (43) seem to be very interesting, because they are formally identical with (30) and (31) containing the subintegral function (26). The solutions of (31) for different energy distributions χ_{12} are known. [3, 16, 17] Replacing, in these solutions, the constant K_{12} by the parameter C_{12}, we obtain the solutions of (43), which describe the liquid adsorption with nonideal bulk and adsorbed phases on random heterogeneous surfaces.

IV. ADSORPTION FROM MULTICOMPONENT LIQUID MIXTURES ON HETEROGENEOUS SOLID SURFACES

Many industrial separation processes generally involve adsorption from multicomponent liquid mixtures. Further studies of these phenomena are important for many purposes including an improvement of analytical methods based on liquid/solid chromatography. Unfortunately, multicomponent liquid adsorption systems have been comparatively little investigated. A complete review of the current status of adsorption from multicomponent solutions on energetically homogeneous surfaces is given in the excellent paper of Brown and Everett.[2]

It is easy to show that the adsorption from n-component liquid mixture (the molecules of which have equal sizes) on homogeneous solid surface may be described by the following series of exchange reactions :

$$(k)^{\ell} + (n)^{\sigma} \rightleftarrows (k)^{\sigma} + (n)^{\ell} \tag{44}$$

where $k = 1, 2, .., n - 1$.
In the equilibrium it holds

$$\mu_{kn}^{\sigma(NA)} = \mu_{k}^{\sigma(NA)} - \mu_{n}^{\sigma(NA)} = \mu_{k}^{\ell} - \mu_{n}^{\ell} = \mu_{kn}^{\ell} \tag{45}$$

for $k = 1, 2, \ldots, n - 1$
The system of equations (45) is equivalent to

$$x_{k(n)}^{\sigma} / x_{n(n)}^{\sigma} = \varphi_{kn} a_{kn}^{\ell} \qquad k = 1, 2, \ldots, n - 1 \tag{46}$$

where $x_{i(n)}^{\sigma}$ is the mole fraction of the ith component in the adsorbed phase, a_i^{ℓ} is the activity of the ith component in the bulk phase, $i = 1,2, \ldots, n$ and $a_{kn}^{\ell} = a_k^{\ell}/a_n^{\ell}$. The parameter φ_{kn} from (46) depends upon a model of surface solution. It follows from (46) that the individual adsorption isotherm of the kth component has the following form :

$$x_{k(n)}^{\sigma} = \frac{\varphi_{kn} a_{kn}^{\ell}}{1 + \sum_{i=1}^{n-1} \varphi_{in} a_{in}^{\ell}} \tag{47}$$

We shall obtain an analytical form of φ_{kn} by the generalization of the method used for binary liquid mixtures.

We employ assumptions analogous to that presented in section II. Then, the canonical partition function for the multicomponent adsorbed phase may be expressed in the following form:

$$Q^{NA}_{(n)} = Q^{IA}_{(n)} Q^{I}_{(n)} \tag{48}$$

$$= \frac{N!}{\left(\prod_{i=1}^{n-1} N_i!\right)\left(N - \sum_{i=1}^{n-1} N_i\right)!} \left[\prod_{i=1}^{n-1} q_i^{N_i}\right] q_n^{N - \sum_{i=1}^{n-1} N_i} \exp\left[\frac{-E_{(n)}}{kT}\right]$$

where q_i is given by (6); N_i is the number of molecules of the ith component in the adsorbed phase, $N = \sum_{i=1}^{n} N_i$ and

$$E_{(n)} = \frac{zN}{2}\left[\sum_{i=1}^{n} (x^{\sigma}_{i(n)})^2 u_{ii} + 2 \sum_{i=1}^{n} \sum_{\substack{j=1 \\ i<j}}^{n} x^{\sigma}_{i(n)} x^{\sigma}_{j(n)} u_{ij}\right] \tag{49}$$

Similarly, as for binary mixtures we have

$$\mu^{\sigma(NA)}_{kn} = \mu^{\sigma(IA)}_{kn} + \mu^{\sigma(I)}_{kn}; \qquad k = 1, 2, \ldots, n-1 \tag{50}$$

where

$$\mu^{\sigma(IA)}_{kn} = kT \ln \frac{x^{\sigma}_{k(n)} q_n}{x^{\sigma}_{k(n)} q_k} \tag{51}$$

$$\mu^{\sigma(I)}_{kn} = z \sum_{i=1}^{n} (u_{ik} - u_{in})\, x^{\sigma}_{i(n)} \tag{52}$$

Taking (50) to (45) we obtain the adsorption isotherm (47), in which

$$\varphi_{kn} = q_{kn} \exp\left[\mu^{0,1}_{kn}/kT\right] \exp\left[-\mu^{\sigma(I)}_{kn}/kT\right] \tag{53}$$

$$= K_{kn} \exp\left[-\mu^{\sigma(I)}_{kn}/kT\right]; \quad q_{kn} = q_k/q_n$$

In the above equation the constant K_{kn} is characteristic of the following adsorption system: binary solution "k" — "n" — adsorbent. However, the term exp $(-\mu^{\sigma(I)}_{kn}/kT)$ describing interactions in the adsorbed phase, depends upon its composition and properties of the all components.

The thermodynamics of adsorption from multicomponent liquid mixtures on heterogeneous surfaces has been recently discussed by Jaroniec et al. [3] This theory is based upon the assumption of an ideal adsorbed phase.

In the case of adsorption from n-component solutions a given adsorption site is characterized by the vector $\boldsymbol{\varepsilon}_n = (\varepsilon_1, \varepsilon_2, \ldots, \varepsilon_n)$, where ε_i denotes the adsorption energy of the ith component. According to previous papers (see references in the review 3) the individual adsorption isotherm of the kth component has the form:

$$X^{\sigma}_{k(\boldsymbol{n})} = \int_{\Delta(\boldsymbol{n})} \frac{K_{kn} a^{\ell}_{kn}}{1 + \sum_{i=1}^{n} K_{in} a^{\ell}_{in}} F(\boldsymbol{\varepsilon}_n)\, \mathrm{d}\boldsymbol{\varepsilon}_n \tag{54}$$

where $F(\boldsymbol{\varepsilon}_n)$ is the n-dimensional distribution function and $\Delta(\boldsymbol{n})$ is the n-dimensional integration region. The integral (54) may be rewritten in a slightly simpler form:

$$X^{\sigma}_{k(\boldsymbol{n})} = \int_{\Delta(\boldsymbol{m})} x^{\sigma}_{1(\boldsymbol{n})}(\boldsymbol{\alpha}_m, \boldsymbol{\varepsilon}_m)\, \chi(\boldsymbol{\varepsilon}_m)\, \mathrm{d}\boldsymbol{\varepsilon}_m \tag{55}$$

where $m = n-1$, $\boldsymbol{\alpha}_m = (a_n, a_{2n}, \ldots, a_{mn})$, $\boldsymbol{\varepsilon}_m = (\varepsilon_{1n}, \varepsilon_{2n}, \ldots \varepsilon_{mn})$, and

$$\chi(\boldsymbol{\varepsilon}_m) = \int_{\Delta(n)} F(\varepsilon_{1n} + \varepsilon_n \varepsilon_{2n} + \varepsilon_n, \ldots, \varepsilon_{mn} + \varepsilon_n)\, \mathrm{d}\varepsilon_n \tag{56}$$

The subintegral function $x^{\sigma}_{1(\boldsymbol{n})}(\boldsymbol{\alpha}_m, \boldsymbol{\varepsilon}_m)$ in (55) is given by equation (47) with $\varphi_{kn} = K_{kn}$.

Now, the results of a generalization of this treatment for the adsorption with lateral interactions in the surface phase will be presented. Only the surfaces showing random distibution of adsorption sites are considered. In the same manner as in the section III, the following adsorption isotherm has been derived for adsorption from binary solutions.

$$X^{\sigma}_{k(\boldsymbol{n})} = \int_{\Delta(\boldsymbol{m})} \frac{a^{\ell}_{kn} \Phi_{kn}}{1 + \sum_{i=1}^{n-1} a^{\ell}_{in} \Phi_{in}} \chi(\boldsymbol{\varepsilon}_m)\, \mathrm{d}\boldsymbol{\varepsilon}_m \tag{57}$$

where

$$\Phi_{kn} = K_{kn} \exp\left[-\mu^{\sigma(\mathrm{I})\mathrm{HR}}_{kn}/kT\right] \tag{58}$$

and

$$\mu^{\sigma(\mathrm{I})\mathrm{HR}}_{kn} = z \sum_{i=1}^{n} (u_{ik} - u_{in})\, X^{\sigma}_{i(\boldsymbol{n})};\ k = 1, 2, \ldots, m \tag{59}$$

The equation (57) is formally analogous with (54). Thus, the solutions of (57) may be obtained by replacing the constant K_{kn} by the parameter Φ_{kn} in the solutions of the (54). The solutions of (54) are known. The generalized Dubinin-Radushkevich and Freundlich isotherms for multicomponent adsorption systems have been derived on the basis of (54) by an application of suitable distribution functions.[18]

The method discussed above affords a full description of a very complicated adsorption system : energetically heterogeneous adsorbent — nonideal multicomponent solution.

REFERENCES

[1] D. H. Everett, in "Colloid Science", Specialist Periodical Reports, vol. 1, ed. D. H. Everett, The Chemical Society, London, 1973, chap. 2.

[2] A. C. Brown and D. H. Everett, in "Colloid Science", Specialist Periodical Report vol. 2, ed. D. H. Everett, The Chemical Society, London, 1975, p. 52—100.

[3] M. Jaroniec, A. Patrykiejew and M. Borówko, "Progress in Surface and Membrane Science", 1978.

[4] M. Jaroniec, *Thin Solid Films*, **50**, 163 (1978).

[5] M. Jaroniec and W. Rudziński, *J. Catalysis Hokkaido Univ.*, **25** 197 (1977).

[6] M. Jaroniec, *Trans. Faraday Soc. II*, **74**, 1292 (1978).

[7] M. Jaroniec, *Trans. Faraday Soc. II*, **73**, 933 (1977).

[8] M. Jaroniec and M. Borówko, *J. Colloid and Interface Sci.*, **63** 362 (1978).

[9] D. H. Everett, *Trans. Faraday Soc.*, **60**, 1803 (1964).

[10] D. H. Everett, *Trans. Faraday Soc.*, **61**, 2478 (1965).

[11] S. Sircar and A. L. Myers, *J. Phys. Chem.*, **74** 2828 (1970).

[12] C. Minka and A. L. Myers, *AIChE Journal*, **19** 453 (1973).

[13] I. Prigogine, "The Molecular Theory of Solutions", North-Holland Publishing Amsterdam, 1957.

[14] A. N. Frumkin, *Trudy Khim. Inst. Karpova*, **4** 56 (1925).

[15] W. Rudziński, L. Łajtar and A. Patrykiejew, *Surface Sci.*, **67** 195 (1977).

[16] J. Ościk, A. Dabrowski, M. Jaroniec and W. Rudziński, *J. Colloid and Interface Sci*, **56** 403 (1976).

[17] J. Ościk, A. Dabrowski, S. Sokołowski and M. Jaroniec, *J. Catalysis Hokkaido Univ.*, **23** 91 (1975).

[18] M. Borówko, M. Jaroniec and W. Rudziński, *Z. phys. Chem.*, (*Leipzig*), in press.

Revue Roumaine de Chimie, **25**, *4*, 487–491(1980)

TWO NEW KINETICAL DERIVATIONS OF THE *JOVANOVIĆ* ISOTHERM FOR MONOLAYER ADSORPTION

P. BUDRUGEAC
ICECHIM, Institute of Physical Chemistry
Splaiul Independenţei 202, Bucharest 15, Romania 77208

Received June 5, 1979

Starting with several hypotheses on the gas-solid system and the adsorption phenomenon, two kinetical derivations of the Jovanović isotherm for monolayer adsorption are given. Some critical remarks on the Jovanović model and adsorption isotherm are made.

In order to derive, by kinetical method[1] and by mechanical-statistical method[2], the isotherms of monolayer and multilayer adsorption of gases on solid surfaces, the instantaneous substitution of evaporated molecules by adsorbing ones is supposed. Jovanović[3], considering this hypothesis is not plausible, derived a new isotherm for the monolayer adsorption, without lateral interactions on solid homogeneous surfaces. Jovanović[3] also, starting with this new isotherm and with BET[1] and Hüttig[4] mechanisms of multilayer adsorption, derived two new isotherms for multilayer adsorption.

Later on, the Jovanović model was extended to the case of heterogeneous surfaces,[5-7] as well as to the case of gaseous mixtures.[8-10]

Some efforts for deriving the Jovanović isotherm by mechanical-statistical method were made.[11-12]

In this paper, starting with several hypotheses on the gas-solid system and the adsorption phenomenon, two new kinetical derivations of Jovanović isotherm for monolayer adsorption will be given. These derivations will be followed by a discussion on the Jovanović model and adsorption isotherm.

1. ADSORPTION MODEL

We will suppose that the gas adsorption is reversible and takes place without lateral interactions on solid homogeneous surface. The assumption of no instantaneous substitution of evaporated molecules by adsorbing ones is made. The number of molecules which are simultaneously adsorbed or desorbed is small, but large enough to use a statistical treatment.

The gaseous phase consists of an ideal gas and the number of adsorbed molecules is negligible as compared to the number of molecules from the gaseous phase.

2. FIRST DERIVATION

This derivation, like the original Jovanović derivation[3], is based on the fact that, at equilibrium, the number of desorbed molecules in the average time of settling of a molecule on the surface is equal to the number of molecules which are adsorbed in the same time.

Let N be the number of adsorbed molecules at equilibrium.

Let us calculate the number of molecules which are desorbed in the average time of settling of a molecule on the surface (τ).

The evaporated molecules which, within the period τ, cannot be readsorbed are considered as definitely desorbed.

Let n be the number of molecules which at the moment t ($t < \tau$; $t = 0$ is the moment of the beginning of desorption) were not desorbed.

The variation, in the time dt, of the number n is given by the relationship (rate equation):

$$-\frac{\mathrm{d}n}{\mathrm{d}t} = \varphi\, n\, \sigma \tag{1}$$

where: σ is the cross section of a molecule; φ is the number of gas molecules which strike the unit area per time unit and it is given by the wellknown relation:

$$\varphi = \frac{P}{\sqrt{2\pi\, mkT}} \tag{2}$$

where: P is the gas pressure; m is the mass of a gas molecule; T is the temperature (K) and k is the Boltzmann constant.

The solution of the differential eq. (1) is:

$$n = C \exp(-\varphi\sigma t) \tag{3}$$

The constant C and the number of desorbed molecules, n_{des}, are calculated from the following obvious conditions:

$$\text{for } t = 0; \qquad n = N$$

$$\text{for } t = \tau; \qquad n = n_{\mathrm{des}} \tag{4}$$

From the relations (3) and (4) it results:

$$n_{\mathrm{des}} = N \exp(-\varphi\, \sigma\tau) \tag{5}$$

This equation is identical with the equation obtained by Jovanović[3] by many algebraic calculations.

Let us calculate the number of molecules which are adsorbed in the time τ.

Let A be the surface area of the adsorbent. The surface area accesible for the adsorption is : $A_1 = A - N\sigma$.

Let n' be the number of molecules which are adsorbed at the moment $t (t < \tau ; t = 0$ is the moment of the beginning of adsorption) on A_1. The number of molecules which will be adsorbed, beginning with the moment t, in the time dt, is given by the relation :

$$dn' = \varphi(A - N\sigma - n'\sigma)dt \tag{6}$$

The solution of the differential eq. (6) is :

$$n' = \frac{1}{\sigma}[A - N\sigma - C' \exp(-\varphi\sigma t)] \tag{7}$$

where C' is the constant of integration.

The constant C' and the number of adsorbed molecules, n_{ads}, are calculated from the following obvious conditions :

$$\begin{aligned} &\text{for } t = 0 ; \quad n' = 0 \\ &\text{for } t = \tau ; \quad n' = n_{\text{ads}} \end{aligned} \tag{8}$$

From (7) and (8) we get :

$$n_{\text{ads}} = \frac{A - N\sigma}{\sigma}[1 - \exp(-\varphi\sigma\tau)] \tag{9}$$

This equation is identical with the equation obtained by Jovanović[3] by many algebraic calculations.

At equilibrium :

$$n_{\text{des}} = n_{\text{ads}} \tag{10}$$

From the relations (5), (9) and (10) it results the Jovanović adsorption isotherm :[3]

$$N = n_m[1 - \exp(-\varphi\sigma\tau)] \tag{11}$$

where : $n_m = A/\sigma$.

Assuming that the adsorbent surface area for an adsorbed molecule is σ, it results that n_m is the maximum number of molecules in the monolayer.

3. SECOND DERIVATION

In order to derive the Jovanović isotherm it is supposed that the average number of the adsorbed molecules is equal to the number of molecules which are adsorbed on the clean surface in the average time of the settling of a molecule (τ).

The adsorption of N molecules does not take place simultaneously, but by successive adsorptions of a small number of molecules.

Let us suppose that at a given moment t ($t < \tau$; $t = 0$ is the moment of the beginning of adsorption) n molecules are adsorbed on the surface. This assumption means that the surface accesible for the following adsorptions is $(\check{A} - n\sigma)$. It follows that, beginning with the moment t, the number of molecules which will be adsorbed in the time dt is given by the relationship :

$$\mathrm{d}n = \varphi(A - n\sigma)\,\mathrm{d}t \tag{12}$$

The solution of the differential equation (12) is :

$$n = \frac{1}{\sigma}\,[A - C''\exp(-\varphi\sigma t)] \tag{13}$$

where C″ is the constant of integration.

The constant C″ and the number of adsorbed molecules at equilibrium are calculated from the following obvious conditions :

$$\begin{aligned} &\text{for } t = 0 ; \qquad n = 0 \\ &\text{for } t = \tau ; \qquad n = N \end{aligned} \tag{14}$$

From (13) and (14) it results the Jovanović adsorption isotherm :

$$N = n_m[1 - \exp(-\varphi\sigma\tau)] \tag{15}$$

4. SOME REMARKS ON THE JOVANOVIĆ ADSORPTION ISOTHERMS

It was mentioned [3] that $\exp(\varphi\sigma\tau)$ can be replaced, at low coverages, with $(1 + \varphi\sigma\tau)$ and so the Jovanović equation turns into the Langmuir equation. Vlad and Segal[10] considered that this approach is purely formal since, at low pressures, $\varphi\sigma\tau \ll 1$ and, in this case, the Jovanović equation turns into Henry adsorption equation ($N = n_m\varphi\sigma\tau$). This fact appears explicitely from our second derivation of Jovanović isotherm. Indeed, for low coverages, equation (12) becomes :

$$\mathrm{d}n = \varphi\,A\mathrm{d}t \tag{16}$$

From this equation, by the method used in § 3, it results Henry adsorption equation and not Langmuir isotherm. On the other hand, from the derivations of Langmuir isotherm,[1,2] it appears that this isotherm is valid for all coverages. Since the Jovanović and Langmuir isotherms are derived starting from different adsorption models, the transformation, in certain conditions, of Jovanović isotherm in Langmuir isotherm is purely formal.

Like in the derivation given by Jovanović[3], in our derivations any assumption on the mobility of adsorbed molecules was not made. It results that the Jovanović isotherm is valid both for localized and mobile adsorptions.

In order to compare the Jovanović isotherm with experimental isotherms, the relation of calculating the average time of settling of a molecule (τ) must be known. For adsorptions without lateral interactions (localized and mobile) the expresions of τ were derived by de Boer[13]. In these cases, it is obvious that τ does not depend on the coverage. A more complicated case is the adsorption with lateral interactions. In this case, τ depends on coverage and so the isotherm equation becomes more complicated. The assumption of lateral interactions also imposes the mechanical-statistical method for derivation of the adsorption isotherm. Unfortunately, the mechanical-statistical methods given for derivation of Jovanović isotherm [11,12] cannot be extended to the case of adsorption with lateral interactions.

5. CONCLUSIONS

Starting from the Jovanović adsorption model two new simple kinetical derivations of the Jovanović monolayer adsorption isotherm were given.

In the first derivation, the relations of n_{des} and n_{ads} given by Jovanović were derived by a new method. Using the equilibrium condition ($n_{ads} = n_{des}$), the Jovanović isotherm was obtained.

In the second derivation, the Jovanović adsorption isotherm was obtained assuming that the average number of the adsorbed molecules is equal to the number of molecules adsorbed on clean surface in the average time of settling of a molecule.

There were some remarks on the Jovanović model and adsorption isotherm.

It was shown that the transformation, in certain conditions, of Jovanović isotherm in Langmuir isotherm is purely formal.

It was mentioned that Jovanović adsorption isotherm is valid both for localized and mobile adsorptions.

Some difficulties connected with the extension of Jovanović model to the adsorptions with lateral interactions were mentioned.

REFERENCES

[1] J. H. de Boer, "The Dynamical Character of Physical Adsorption" Clarendon Press, Oxford, 1953, Ch. V.

[2] See for example : T. L. Hill, "An Introduction to Statistical Thermodynamics", Addison-Wesley Reading, Mass., 1960, Ch. 7.

[3] D. S. Jovanović, *Kolloid Z., Z. Polymers*, **235**, 1203, 1214 (1969).

[4] G. F. Hüttig, *Monatsh.*, **78**, 177 (1948).

[5] D.N.J. Misra, *J. Colloid Interface Sci.*, **43**, 85 (1973).

[6] W. Rudzinski and M. Jaroniec, *Ann. Chim. Soc. Polonorum*, **49**, 165 (1975).

[7] M. Jaroniec, *Phys. Letters.*, **59A**, 259 (1976).

[8] M. Jaroniec, *Chem. Zvesti*, **29**, 512 (1975).

[9] V. Popa and E. Segal, *Rev. Roumaine Chim.*, **21**, 977 (1976).

[10] M. Vlad and E. Segal, *Surface Sci.*, **79**, 608 (1979).

[11] M. Jaroniec, *Colloid Polymer Sci.*, **254**, 601 (1976).

[12] G. F. Cerofolini, *Z. Phys. Chem.* (*Leipzig*), **259**, 314 (1978).

[13] J. H. de Boer, *Adv. Catalysis*, **8**, 85 (1956).

Revue Roumaine de Chimie, **25**, *4*, 493–501 (1980)

CORROSION BEHAVIOUR OF COMMERCIAL Zn—Ti ALLOY IN AQUEOUS SALT SOLUTIONS

S. M. ABD EL HALEEM * and S. S. ABD EL REHIM**
* Departments of Chemistry, Faculties of Science, Zagazig
** Ain Shams Universities, Egypt

Received May 20, 1978

Variation of the potential of a commercial Zn—Ti alloy was followed in O_2-saturated and O_2-free solutions of the sodium salt of SO_4^{2-}, Cl^-, Br^-, I^-, ClO_4^-, NO_3^-, NO_2^-, CrO_4^{2-}, WO_4^{2-}, HPO_4^{2-}, and $H_2PO_4^-$ as a function of time and concentrations of these anions. In the presence and absence of oxygen, the first six anions functioned as corrosion promoters and the extent of corrosion increased with concentration. The potentials varied with concentration according to: $E = a - b \log C$, where a and b are constants. Above certain concentrations of the other anions, the potentials shifted into the noble values denoting the occurrence of inhibition or passivation.

INTRODUCTION

Several theories have been reported to explain the role of anions in promotion or stifling the corrosion of metals. Solubility of the corrosion products decides whether a given anion would act as aggressive or inhibitive.[1,2] Adsorption of the anions on the metal surface,[3-6] their ionic size and charge,[7] ion deformability,[8] and the electrostatic field sets up by the charge of the anions on the adsorption sites of the metal surface[9] are other factors which proposed to determine the role of anions on corrosion.

Brasher[10] advanced a theory in which a classification of the anions into corrosion promotors and inhibitors is given. All anions are corrosive when present in large dilution but become or tend to become inhibitive in relatively concentrated solutions. In the domain of corrosion, the potential of a number of metals in aerated solutions of different anions changes with concentration according to the relation :[10,11]

$$E = a - b \log C \qquad (1)$$

where a and b are constants. Above a certain concentration, depending on the nature of the anion, the shifts into the noble direction and inhibition of corrosion take place.

Shams El Din et al.[12,13] studied the behaviour of pure zinc in a large number of anions. Some of them behaved unifunctionally and promoted corrosion of zinc, and the steady-state potentials varied with concentration according to equation (1). Other anions behaved bifunctionally, promoting corrosion when diluted and stifling it at relatively higher concentrations.

Regarding metal alloys, little attention has been paid to their behaviour in the aqueous solutions of different anions. It is the aim of the present work to make known the variation of the potential of alloys, other than steels, in aqueous solutions. A commercial Zn—Ti alloy was chosen as the test material. This alloy is widely used in construction and industry under the name "Titan Zinc".

EXPERIMENTAL

The electrodes used throughout the work were machined from commercial Zn—Ti alloy sheets supplied by the Rhein Zinc Company (West Germany). Elemental analysis of the alloy indicated the following composition:

Ti	Cu	Si	C	Zn
1 %	0.5 %	0.05 %	2 %	the rest

The pretreatment of the electrodes involved: polishing with the finest grade emery paper, degreasing with acetone and washing with bidistilled water. The potentials of the electrode were measured in O_2-saturated and O_2-free solutions of SO_4^{2-}, Cl^-, Br^-, I^-, ClO_4^-, NO_3^-, NO_2^-, CrO_4^{2-}, WO_4^{2-}, HPO_4^{2-}, and $H_2PO_4^-$ in concentrations varying between 10^{-6} and 5 M. The anions were added in the form of their sodium salts. The electrode vessel used was made of pyrex glass and had an inlet and outlet for oxygen or nitrogen gas and contained 50 ml of test solution. Each run was performed using a newly cleaned electrode and a freshly prepared solution. Highly purified oxygen or nitrogen gas was bubbled through the solution 30 min before immersion of the electrode and during the whole time of measurements. The potentials were traced relative to S.C.E. at constant temperature 25° ± 1°, using a Philips recording potentiometer Type PO—8.

RESULTS AND DISCUSSION

1. Variation of the potential of Zn—Ti alloy in O_2-saturated solutions

The potentials of Zn—Ti alloy were followed in O_2- saturated solutions of the above-mentioned anions as a function of both time and concentration till the steady-state values were reached. In solutions of SO_4^{2-}, Cl^-, Br^-, I^-, ClO_4^- and NO_3^- ions, the steady-state potentials were approached from more negative values, and shifted into the noble direction with dilution. Figures 1 and 2 represent the variation of the potentials of Zn—Ti alloy in O_2-saturated solutions of SO_4^{2-} and Br^- ions respectively, as examples of the behaviour of this group of anions.

The curves of the type in Figures 1 and 2 clearly show that these six anions promote the corrosion of the alloy and the extent of corrosion increases with anion concentration. The steady-state potentials, in O_2-saturated 1×10^{-3} M solution of the anions of this group relative to the S.C.E. are the following:

SO_4^{2-}	— 900 mV,	I^-	— 775 mV,
Cl^-	— 815 mV,	ClO_4^-	— 750 mV,
Br^-	— 780 mV,	NO_3^-	— 565 mV.

The corrosivity of these anions decreases in the same order.

Figure 3 gives the plot of the steady-state potentials of the alloy as a function of the logarithm of molar concentration of the above six anions. Below specific concentration the electrode develops steady-state potentials which are dependent on the nature and not on the concentration of the anions. In this case, corrosion is assumed to occur at a rate equal to that of film repair by dissolved oxygen.[12] Above this specific concentration, the steady-state potentials start changing into the less noble direction and corrosion becomes the predominant reaction. The steady-state potentials vary with molar concentration of the ions in a reasonable agreement with equation (1), and invariably straight lines

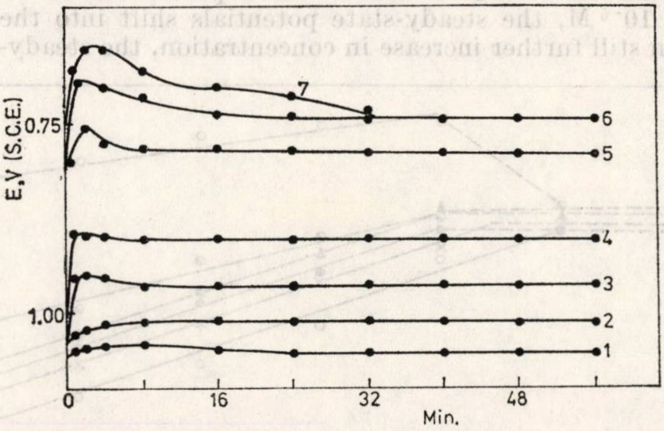

Fig. 1. — Steady-state potential *vs* time for Zn alloy in O_2-saturated Na_2SO_4 solutions: *1.* 1; *2.* 10^{-1}; *3.* 10^{-2}; *4.* 10^{-3}; *5.* 10^{-4}; *6.* 10^{-5}; *7.* 10^{-6} M.

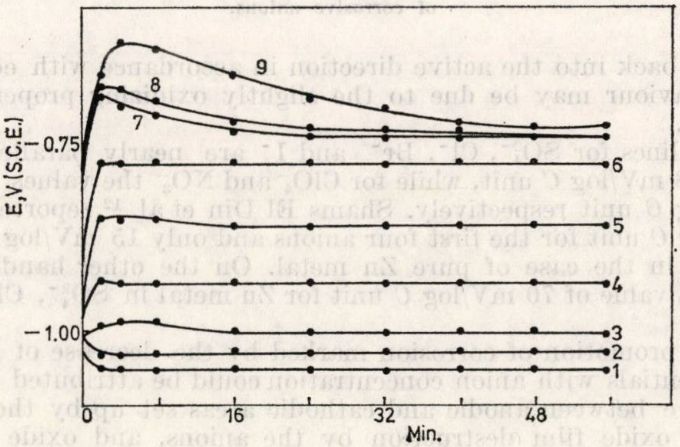

Fig. 2. — Steady-state potential *vs* time for Zn alloy in O_2-saturated NaBr solutions: *1.* 5; *2.* 3; *3.* 1; *4.* 10^{-1}; *5.* 10^{-2}; *6.* 10^{-3}; *7.* 10^{-4}; *8.* 10^{-5}; *9.* 10^{-6} M.

are obtained. It could be concluded that these six anions are unifunctionally promoting the corrosion of Zn–Ti alloy as has already been found for pure Zn metal.

The behaviour of the alloy electrode in NO_3^- solutions is of interest. Although this ion belongs to the corrosion promotors, at concentrations above 1×10^{-5} M, the steady-state potentials shift into the noble direction, but on still further increase in concentration, the steady-state potentials shift back into the active direction in accordance with equation (1). Such behaviour may be due to the slightly oxidizing properties of the NO_3^- ions.

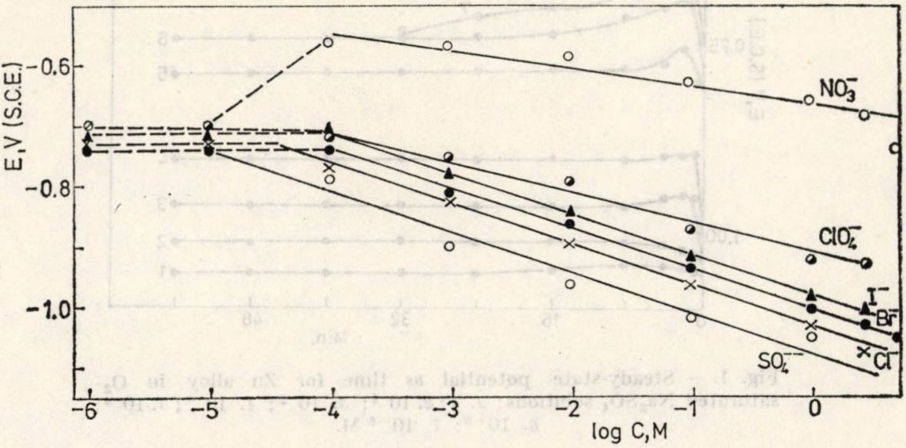

Fig. 3. — Steady-state potential *vs* log *C* for Zn alloy in O_2-saturated solutions of corrosive anions.

The lines for SO_4^{2-}, Cl^-, Br^- and I^- are nearly parallel, having a slope of 68 mV/log *C* unit, while for ClO_4^- and NO_3^- the values are 50 and 30 mV/log *C* unit respectively. Shams El Din et al.[12] reported values of 33 mV/log *C* unit for the first four anions and only 15 mV/log *C* unit for NO_3^- ions in the case of pure Zn metal. On the other hand, Brasher[11] reported a value of 70 mV/log *C* unit for Zn metal in SO_4^{2-}, Cl^- and NO_3^- solutions.

The promotion of corrosion marked by the decrease of the steady-state potentials with anion concentration could be attributed to an altered balance between anodic and cathodic areas set up by the competing action of oxide film destruction by the anions, and oxide film repair by oxygen in solution.[11] Shams El Din,[12] on the other hand, is of the opinion that the reduction of the dissolved oxygen is by far the most important cathodic reaction for corrosion in media which are saturated with oxygen. This process which is highly irreversible,[14] becomes kinetically easier as the anion concentration in solution increases. This was proved experimentally,[12] and at the same time, it was found that the ease of oxygen reduction decreases in the order $SO_4^{2-} > Cl^- > Br^- > ClO_4^- > NO_3^- > I^-$. This is in agreement with the results obtained in the present work. Therefore, in O_2-satuarated solutions, the anion which favours the reduction of oxygen, enhances the corrosion process.

Figure 4 shows the variation of the electrode potential as a function of both time and CrO_4^{2-} ion concentration in O_2-saturated solutions, as an example of the anions of the group CrO_4^{2-}, NO_2^-, WO_4^{2-}, HPO_4^- and $H_2PO_4^-$. The steady-state potentials are approached from negative values and shift into the noble direction with concentration indicating inhibition of corrosion. Figure 5 gives the plot of the steady-state potentials as a function of the logarithm of the molar concentration of these anions.

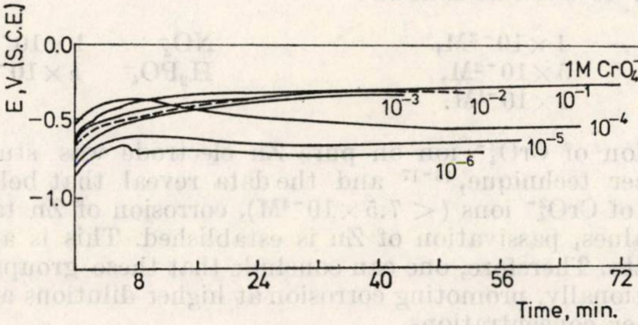

Fig. 4. — Steady-state potential *vs* time for Zn alloy in O_2-saturated Na_2CrO_4 solutions of different molarities.

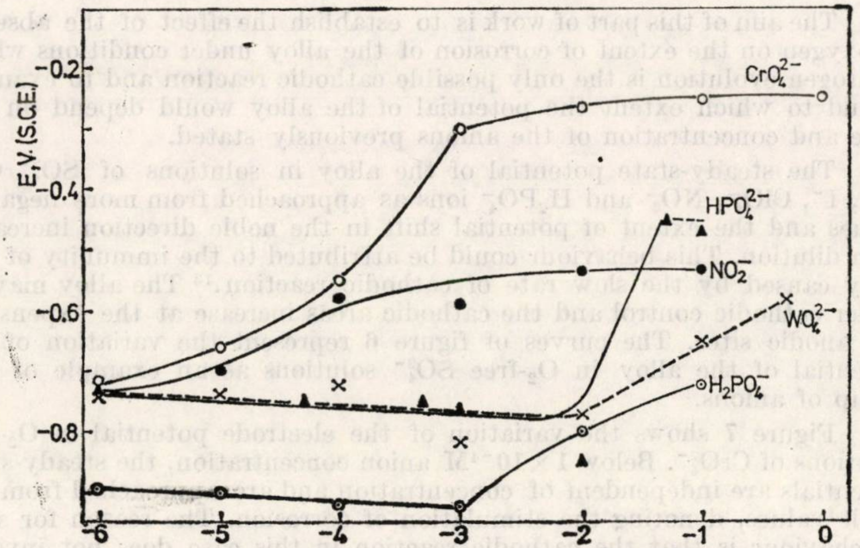

Fig. 5. — Steady-state potential *vs* log C for Zn alloy in O_2-saturated solutions of inhibitive anions.

In CrO_4^{2-} and NO_2^- solutions, the steady-state potentials change markedly into the noble direction with concentration denoting higher tendency for inhibition. Thereafter, the potentials increase slowly with further increase in concentration probably indicating the achievement of uniform passive film on the electrode surface.

On the other hand, in very dilute solutions of WO_4^{2-}, HPO_4^{2-} and $H_2PO_4^-$, the electrode develops steady-state potentials which are dependent on the type, and to a lesser extent, on the concentration of the anion. Corrosion of the alloy in these dilute solutions is suggested to occur at a rate equal to film repair by the inhibitors. Above a specific concentration, the potential shifts markedly into the noble direction, thus predominating the inhibition. The concentrations that cause marked ennobling of the potentials can be cited as follows:

CrO_4^{2-}	1×10^{-3}M,	NO_2^-	1×10^{-4} M,
HPO_4^{2-}	5×10^{-2}M,	$H_2PO_4^-$	1×10^{-2} M,
WO_4^{2-}	1×10^{-1}M.		

The action of CrO_4^{2-} ion on pure Zn electrode was studied using the radio-tracer technique,[15-17] and the data reveal that below certain concentration of CrO_4^{2-} ions ($< 7.5\times10^{-4}$M), corrosion of Zn takes place. Above this values, passivation of Zn is established. This is agreed with the present data. Therefore, one can conclude that these groups of anions behave bifunctionally, promoting corrosion at higher dilutions and inhibiting it at higher concentrations.

2. Variation of the potential of Zn–Ti alloy in O_2-free solutions

The aim of this part of work is to establish the effect of the absence of oxygen on the extent of corrosion of the alloy under conditions where hydrogen evolution is the only possible cathodic reaction and to examine if and to which extent the potential of the alloy would depend on the type and concentration of the anions previously stated.

The steady-state potential of the alloy in solutions of SO_4^{2-} Cl^-, Br^-, I^-, ClO_4^-, NO_3^- and $H_2PO_4^-$ ions as approached from more negative values and the extent of potential shift in the noble direction increased with dilution. This behaviour could be attributed to the immunity of the alloy caused by the slow rate of cathodic reaction.[13] The alloy may be under cathodic control and the cathodic areas increase at the expense of the anodic sites. The curves of figure 6 represent the variation of the potential of the alloy in O_2-free SO_4^{2-} solutions as an example of this group of anions.

Figure 7 shows the variation of the electrode potential in O_2-free solutions of CrO_4^{2-}. Below 1×10^{-4}M anion concentration, the steady-state potentials are independent of concentration and are approached from the noble values, denoting the stimulation of corrosion. The reason for such a behaviour is that the cathodic reaction in this case does not involve the discharge of hydrogen ions, but rather the reduction of Cr (VI) to Cr (III), which is thermodynamically possible.[13]

$$3\,Zn + 2\,CrO_4^{2-} + 2\,H_2O = 3\,ZnO + Cr_2O_3 + 2\,OH^- \qquad (2)$$

It is suggested that in these dilute chromate solutions, the oxide film formed is not protective. On the other hand, in more concentrated solutions, the potential of the alloy changes slowly towards the noble direction, and no steady-state values are reached during the whole span of the experiment. This could be attributed to the continuous thickening of the oxide film on the electrode surface.

632/7
0,60

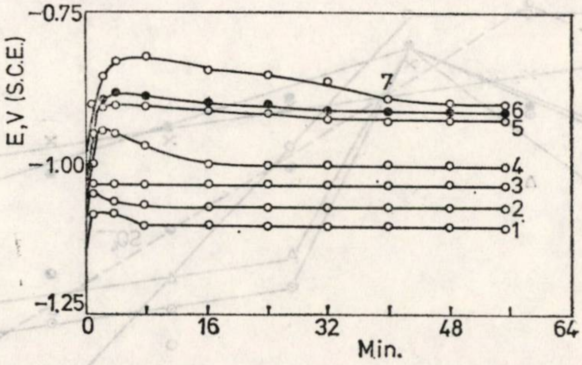

Fig. 6. — Steady-state potential *vs* time for Zn alloy in O_2-free Na_2SO_4 solutions: *1.* 1; *2.* 10^{-1}; *3.* 10^{-2}; *4.* 10^{-3}; *5.* 10^{-4}; *6.* 10^{-5}; *7.* 10^{-6} M.

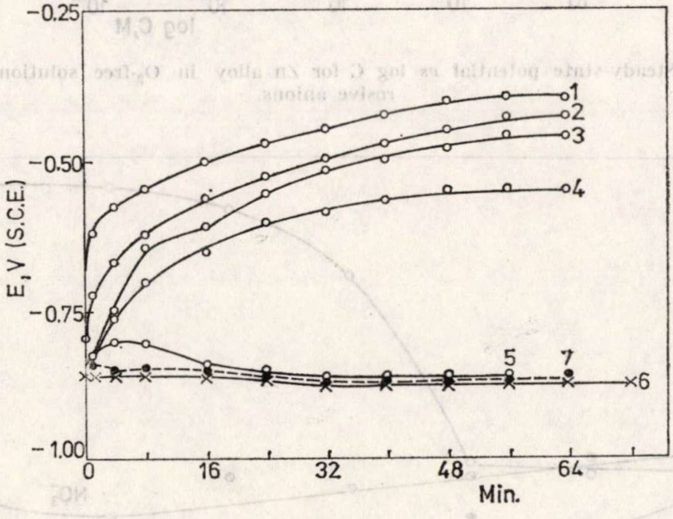

Fig. 7. — Steady-state potential *vs* time for Zn alloy in O_2-free Na_2CrO_4 solutions: *1.* 1; *2.* 10^{-1}; *3.* 10^{-2}; *4.* 10^{-3}; *5.* 10^{-4}; *6.* 10^{-5}; *7.* 10^{-6}M.

The curves in figure 8 show that below a certain concentration of SO_4^{2-}, Cl^-, Br^-, I^-, ClO_4^- and HPO_4^{2-}, the electrode develops steady-state potentials which vary with both the type and the concentration of these anions. Above this concentration, the potential decreases with concentration in accordance with equation (1). This could be explained on the basis of the effect of potential and of the specific adsorption of the anion on the rate of the cathodic hydrogen evolution.[13]

On the other hand, in the presence of CrO_4^{2-}, NO_2^-, NO_3^-, WO_4^{2-}, or $H_2PO_4^-$ ions, above a specific concentration, the steady-state potentials shift into the noble direction indicating the occurrence of inhibition or passivation as shown in figure 9.

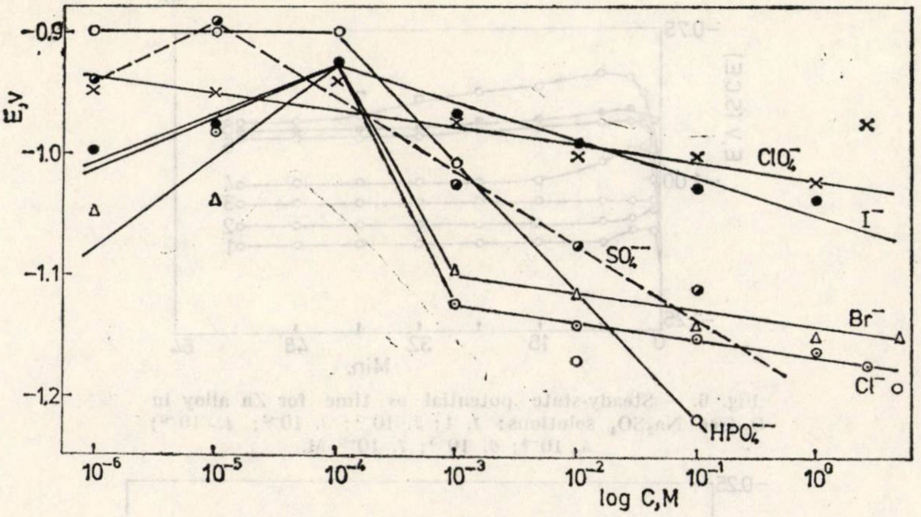

Fig. 8. — Steady-state potential *vs* log C for Zn alloy in O_2-free solutions of corrosive anions.

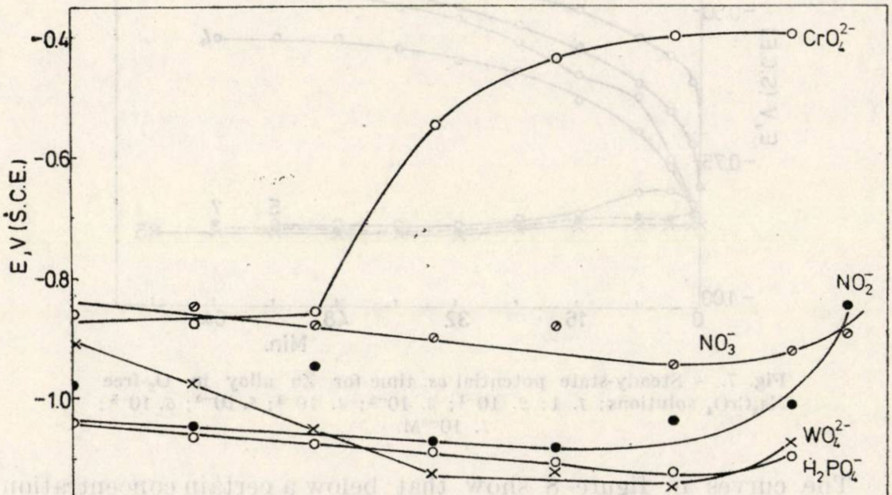

Fig. 9. — Steady-state potential *vs* log C for Zn alloy in O_2-free solutions of inhibitive anions.

REFERENCES

[1] U. R. Evans, "The Corrosion and Oxidation of Metals", Edward Arnold Ltd. London 1960, pp. 139.

[2] A. M. Azzam, S. S. Abd El Rehim and W. H. Boctor, *Acta Chim. Acad. Sci. Hung.*, **95**, 367 (1977).

[3] Seigo Matsuda and H. H. Uhlig, *J. Electrochem. Soc.*, **111**, 156 (1964).

[4] E. Mc Caffert and N. Hackerman, *J. Electrochem. Sci.*, **119**, 999 (1972).

[5] N. A. Darwish, F. Hilbert, W. J. Lorenz and H. Rosswag, *Electrochim. Acta*, **18**, 421 (1973).

[6] A. M. Shams El Din, F. M. Abd El Wahab and S. M. Abd El Haleem, *Werkstoffe u Korrosion*, **5**, 389 (1973).

[7] M. J. Pryor, *Z. Elektrochem.*, **62**, 782 (1958).

[8] R. Piontelli, *Z. Elektrochem.*, **52**, 128 (1951).

[9] G. H. Cartledge, *J. Phys. Chem.*, **60**, 32 (1952).

[10] D. M. Brasher, *Nature*, **193**, 868 (1962).

[11] D. M. Brasher, J. G. Beynon, A. D. Mercer and J. E. Rhoades-Brown, "Proceeding 2nd European Symposium Corrosion Inhibitors", Ferrara, Italy 1965, pp. 61.

[12] V. K. Gouda, M. G. Khedr and A. M. Shams El Din, *Corrosion Sci.*, **7**, 221 (1967).

[13] A. M. Shams El Din and M. G. Khedr, *Corrosion Sci.*, **12**, 393 (1972).

[14] I. M. Kolthoff and J. J. Lingane, "Polarography"' vol. 2, Interscience, London 2 nd edn., 1952, pp. 552.

[15] A. M. Shams El Din and R. H. Abu Zahra, *Naturwiss.*, **52**, 57 (1965).

[16] R. H. Abu Zahra and A. M. Shams El Din, *Corrosion Sci.*, **5**, 517 (1965).

[17] R. H. Abu Zahra, *Corrosion Sci.*, **6**, 349 (1966).

Revue Roumaine de Chimie, 25, 4, 503 – 511 (1980)

A NEW *EDTA*-TYPE REAGENT. III[1,2]

SYNTHESIS AND PHYSICO-CHEMICAL STUDY OF 4,4'-DIAMINO-DIPHENYLMETHANE-N,N'-TETRAACETIC ACID

CONST. GH. MACAROVICI * and EUGEN CHIȘ**

* Faculty of Chemical Technology, University "Babeș-Bolyai", Cluj-Napoca, Romania
** Faculty of Mathematics, Physics and Chemistry Department, University of Brașov, Romania

Received December 28, 1978

The 4,4'-diaminodiphenylmethane-N,N'-tetraacetic acid, H_4RA_4, and its sodium salts $Na_2H_2RA_4$ and Na_4RA_4, respectively, have been synthesized, where R: $= N-C_6H_4-CH_2-C_6H_4-N=$, A: $-CH_2-COO^-$. Their composition and chemical structure have been determined by using potentiometric and conductometric titration, IR spectra ; the acidity constants of the H_4RA_4 acid have been calculated.

In the previous papers we have reported the synthesis of the 4,4'-diaminodiphenylmethane-N,N'-diacetic acid, H_2RA_2, unknown in literature, of its sodium salt Na_2RA_2[1] (R : $- HN - C_6H_4-CH_2-C_6H_4- - NH -$, A : $-CH_2COO^-$) ; the determination of the acidity constants of the H_2RA_2 acid, the synthesis and properties of the corresponding salts with ions of mono- di-, tri and tetravalent metals [2].

In this paper we report the synthesis of the 4,4'-diamino-diphenylmethane-N,N'-tetraacetic acid (we note it H_4RA_4 or DFMTA) where R : $= N-C_6H_4 - CH_2-C_6H_4-N =$, A : $-CH_2COO^-$, analogous and formally close to EDTA.

EXPERIMENTAL

The synthesis of 4,4'-diaminodiphenylmethane-N,N'-tetraacetic acid, H_4RA_4, has been carried out by means of several variants, using the 4,4'-diaminodiphenylmethane as a basis and $ClCH_2COONa$, $BrCH_2COONa$, ICH_2COONa as a carboxymethylizing agent.

According to the variant considered optimum, we start with 49 g (0.25 moles) 4,4'-diaminodiphenylmethane in alcoholic solution, introduced into a three-necked round-bottomed flask with reflux refrigerator, a mechanical stirrer and a thermometer (0 – 100°) to which the amount of 49 g (0.5 moles) monochloracetic acid in aqueous solution, cold-neutralized with NaOH, is added. It is heated on a water bath, with continous stirring, by adding drop by drop NaOH, about 0.5 M, so that the pH of the composition may be maintained at about 8. After the addition of the amount of NaOH corresponding to the chlorine hydride released as a result of reaction (I):

Reaction I

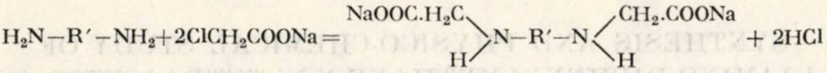

$$\mathrm{H_2N-R'-NH_2+2ClCH_2COONa=}\begin{matrix}\mathrm{NaOOC.H_2C}\\ \mathrm{H}\end{matrix}\!\!>\!\mathrm{N-R'-N}\!<\!\!\begin{matrix}\mathrm{CH_2.COONa}\\ \mathrm{H}\end{matrix}\mathrm{+\ 2HCl}$$

R′ = diphenylmethane: $-C_6H_4-CH_2-C_6H_4-$;

the composition is cooled until it reaches 30—35°, it is filtered off in order to remove the slurry, and, with continous stirring, 68.5 g (0.5 moles) monobromacetic acid, cold neutralized with NaOH, is added, in order to achieve the second step of the synthesis: the transformation of the sodium salt of the H_2RA_2 acid into a sodium salt of the H_4RA_4 acid, Na_4RA_4, respectively:

Reaction II

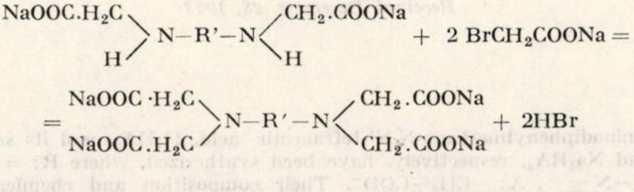

$$\begin{matrix}\mathrm{NaOOC.H_2C}\\ \mathrm{H}\end{matrix}\!\!>\!\mathrm{N-R'-N}\!<\!\!\begin{matrix}\mathrm{CH_2.COONa}\\ \mathrm{H}\end{matrix}\mathrm{+\ 2\ BrCH_2COONa=}$$

$$\mathrm{=}\begin{matrix}\mathrm{NaOOC\cdot H_2C}\\ \mathrm{NaOOC.H_2C}\end{matrix}\!\!>\!\mathrm{N-R'-N}\!<\!\!\begin{matrix}\mathrm{CH_2.COONa}\\ \mathrm{CH_2.COONa}\end{matrix}\mathrm{+\ 2HBr}$$

The pH of the reaction mixture is maintained at about 8. After the addition of NaOH (0.5M) in a quantity corresponding to HBr eliminated in the reaction and of an excess of 10—15% over the calculated stoichiometric quantity, the temperature is raised until it reaches 50—60° and it is maintained for 1—2 hours, permanently checking the pH (aprox. 8). Then the composition is cooled at 20—25° and is filtered off.

The free 4,4'-diaminodiphenylmethane-N,N'-tetraacetic acid, H_4RA_4, is obtained from the sodium salt, Na_4RA_4, in solution, by adding concentrated HCl (d = 1.19), dropwise, with continuous stirring. The H_4RA_4 acid dissociated as a result of the reaction (III),

Reaction III

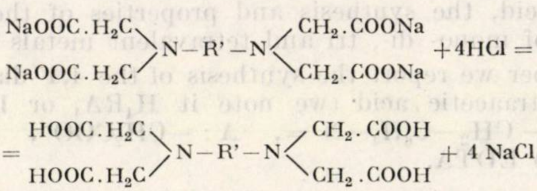

$$\begin{matrix}\mathrm{NaOOC.H_2C}\\ \mathrm{NaOOC.H_2C}\end{matrix}\!\!>\!\mathrm{N-R'-N}\!<\!\!\begin{matrix}\mathrm{CH_2.COONa}\\ \mathrm{CH_2.COONa}\end{matrix}\mathrm{+4HCl=}$$

$$\mathrm{=}\begin{matrix}\mathrm{HOOC.H_2C}\\ \mathrm{HOOC.H_2C}\end{matrix}\!\!>\!\mathrm{N-R'-N}\!<\!\!\begin{matrix}\mathrm{CH_2.COOH}\\ \mathrm{CH_2.COOH}\end{matrix}\mathrm{+4\ NaCl}$$

deposits as a white precipitate, which is filtered off and washed with cold distilled water until the Cl^- ion is completely removed. The purification of the H_4RA_4 acid is carried out by recrystallization in hot saturated aqueous solution (maximum 50°, and subsequent cooling at 10—15°). After the composition is filtered off, it is pressed between filter papers and then dried in the exicator on P_2O_5. The H_4RA_4 acid is preserved in bottles of dark colour at normal temperature and kept from contact with air.

The anhydrous H_4RA_4 acid is a non-crystalline light bluish substance (the color becomes intenser when the substance is heated or in contact with air), slightly soluble, in distilled water at low temperature (0.02%); the solubility rises very much at high temperature; at above 70°, CO_2 is released from the hot solution, resulting from decarboxylation of the acid. It is soluble in methanol, ethanol, acetic acid, mineral acids; insoluble in benzene, chloroform, dioxane, carbon tetrachloride.

The melting point of the H_4RA_4 acid is in the limits of 125—130°, after which it decomposes with a strong development of gaseous products.

The elementary analysis corresponds to the H_4RA_4 acid, $C_{21}H_{22}O_8N_2$, with molecular weight M = 430.43, satisfactorily confirmed by the method of Rast (in camphor), table 1.

To determine the structure of the synthesized acid, potentiometric and conductometric titration, IR spectra, and the acidity constants have been carried out.

TABLE 1

Elementary chemical analysis of the 4,4′-diaminodiphenylmethane-N, N'-tetraacetic acid, H_4RA_4 : $C_{21}H_{22}O_8N_2$

	% C	% H	% N	Molecular weight
Calculated :	58.60	5.15	5.51	430.43
Found :	58.63	5.77	6.26	424.26

R: $=N-C_6H_4-CH_2-C_6H_4-N=$; A: $-CH_2COO^-$;

The potentiometric titration of the H_4RA_4 acid was carried out with a Radelkis model OP 401/2 pH-meter with glass and calomel electrodes in nitrogen atmosphere, employing NaOH 0.1 N as reagent, at a constant ionic strenght 0.1 M KCl, 25° temperature.

RESULTS

The mean values obtained by the potentiometric titration of the H_4RA_4 acid with NaOH 0.1 N, on several samples taken from different charges of synthesized acid in different variants, are given in table 2.

TABLE 2

Potentiometric titration of the 4,4'-diaminodiphenylmethane-N,N'-tetraacetic acid, H_4RA_4, with NaOH 0.1 N, ionic strenght 0.1 M KCl, 25° temperature

ml NaOH added	0	1	2	3	4	4.5	5	5.5	6	7
a	0	0.2	0.4	0.6	0.8	0.9	1.0	1.1	1.2	1.4
pH	3	3.10	3.25	3.45	3.75	3.90	4.10	4.30	4.45	4.70
ml NaOH added	8	9	9.5	10	10.5	11	12	13	14	14.5
a	1.6	1.8	1.9	2.0	2.1	2.2	2.4	2.6	2.8	2.9
pH	4.95	5.15	5.20	5.30	5.35	5.45	5.7	6.00	6.40	6.65
ml NaOH added	15	15.15	16	17	18	19	19.5	20	22	24
a	3	3.1	3.2	3.4	3.6	3.8	3.9	4.0	4.4	4.8
pH	8	10.5	10.8	11.15	11.35	11.5	11.55	11.6	11.7	11.8

R: $= N-C_6H_4-CH_2-C_6H_4-N=$; A :$-CH_2COO^-$;
a = moles of base added per mole of acid.

When titrating H_4RA_4 acid with KOH, $Ba(OH)_2$, and $/N(CH_3)_4/OH$ of the same normality (0.1 N), the titration curves overlap the titration curve obtained when employing NaOH 0.1 N as reagent (Figure 1).

The data of the conductometric titration of the H_4RA_4 acid with NaOH 0.1 N obtained by means of a "Tesla" bridge under the same conditions, emphasized four inflexion points which correspond to two jumps of the potentiometric titration (Figure 2). For titration, the same amount of H_4RA_4 acid, M = 0.2152 g, M/2000 respectively, was taken every time in the same volume of solution, 100 ml, thus having the acid concentration $C_s = 0.005$ M.

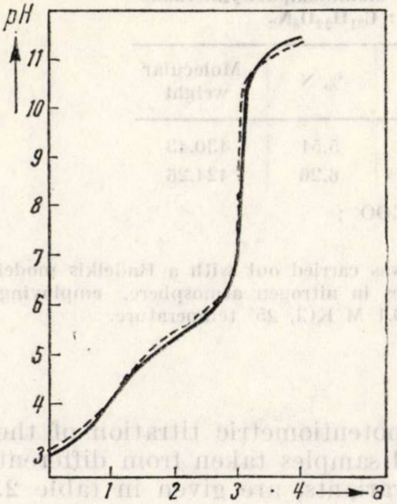

Fig. 1. — Potentiometric titration curves of the H_4RA_4 acid with:
——NaOH 0.1 N; – – – $[N(CH_3)_4]$ OH 0.1 N;
a=moles of the base added per mole acid.

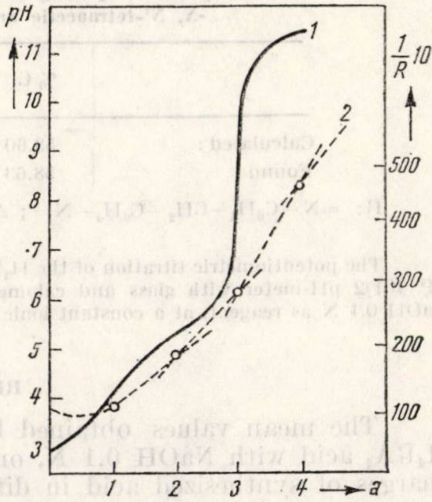

Fig. 2. — Potentiometric (*1*) and conductometric (*2*) titration curves of the H_4RA_4 acid with NaOH 0.1 N
a=moles of the base added per mole acid.

The acidity constants of the H_4RA_4 acid were calculated on the basis of potentiometric data, i.e. employing the potentiometric titration curve of the H_4RA_4 acid with NaOH 0.1 N.

For the calculation of the first two acidity constants the method described by Schwarzenbach and coworkers[3-6] for the EDTA and other aminocarboxylic acids was applied.

According to this method, starting from the dissociation equilibria of the H_4RA_4, respectively H_4R, in the first stages, we come to an equation which expresses the ratio between K_1 and K_2 in directly measurable values, C_s, a, $/H^+/$:

$$K_2\left[\frac{(2-a)\cdot C_s}{/H^+/-1}\right]-\frac{1}{K_1}\left[/H^+/\cdot(aC_s+/H^+/)\right]=(a-1)\cdot C_s+/H^+/ \qquad (1)$$

respectively:

$$K_2\left[\frac{\dfrac{(2-a)\cdot C_s}{/H^+/-1}}{(a-1)\cdot C_s+/H^+/}\right]-\frac{1}{K_1}\left[\frac{/H^+/\cdot(aC_s+/H^+/)}{(a-1)\cdot C_s+/H^+/)}\right]=1 \qquad (2)$$

If we note with :

$$x = \frac{\dfrac{(2-a)\cdot C_s}{/\mathrm{H}^+/ - 1}}{(a-1)\cdot C_s + /\mathrm{H}^+/} \quad (3) \quad \text{and} \quad y = \frac{/\mathrm{H}^+/\cdot(aC_s + /\mathrm{H}^+/)}{(a-1)\cdot C_s + /\mathrm{H}^+/} \quad (4)$$

the equation (2) can be written :

$$K_2\cdot x - \frac{1}{K_1}\cdot y = 1 \ (5), \text{ respectively, } y = K_1\cdot K_2\cdot x - K_1 \quad (6)$$

which represents a linear equation, with slope $K_1 . K_2$ and the ordinate of origin K_1, which was employed by Schwarzenbach and his coworkers$^{3-6}$ for the graphically determination of the acidity constants.

We have introduced the values of x and y by employing the potentiometric titration data of the H_4RA_4 acid with NaOH 0.1 N (Table 3)

TABLE 3

Values of x and y calculated on the basis of potentiometric titration data of the H_4RA_4 acid with NaOH 0.1 N

a	pH	H^+	x	y
0	3.00	$9.9\ 10^{-4}$	4091.419	−0.0004406104
0.2	3.10	$8.0\ 10^{-4}$	2222.222	−0.0003121951
0.4	3.25	$5.6\ 10^{-4}$	1702.008	−0.0001836559
0.6	3.45	$3.5\ 10^{-4}$	1407.249	−0.0000868421
0.8	3.75	$1.8\ 10^{-4}$	1089.845	−0.0000253608
1.0	4.10	$7.9\ 10^{-5}$	− 196.889	0.0000012682
1.2	4.45	$3.5\ 10^{-5}$	− 4899.988	0.0000091361
1.4	4.70	$2.0\ 10^{-5}$	− 14387.464	0.0000135570
1.6	4.95	$1.1\ 10^{-5}$	− 34168.926	0.0000166520
1.8	5.15	$7.1\ 10^{-6}$	− 62669.488	0.0000286538
2.0	5.30	$5.0\ 10^{-6}$	− 100049.975	0.0050050000
2.2	5.45	$3.5\ 10^{-6}$	− 155885.465	−0.0000209386
2.4	5.70	$2.0\ 10^{-6}$	−.291701.383	−0.0000069950
2.6	6.00	$9.9\ 10^{-7}$	−621630.205	−0.0000026394
2.8	6.40	$3.9\ 10^{-7}$	−1615244.461	−0.0000008954

H_4RA_4 = 4,4′-diaminodiphenylmethane-N,N′-tetraacetic acid.

in the linear regression calculation program no. 8806051 of the 324 model electronic computer, where : $y = Bx + A$, $B = K_1 \cdot K_2$ and $A = -K_1$,

$$B = \frac{\Sigma xy - \dfrac{\Sigma x \Sigma y}{N}}{\Sigma x^2 - \dfrac{(\Sigma x)^2}{N}} \qquad A = \frac{1}{N}(\Sigma y - B\Sigma x)$$

N = the number of values x or y, the pair of values xy respectively. As a result of this calculus, the following values for K_1 and K_2, pK_1 and pK_2, respectively, were obtained :

$$K_1 = 4.4966699 \cdot 10^{-4} \qquad pK_1 = 3.3471$$
$$K_2 = 1.5856089 \cdot 10^{-5} \qquad pK_2 = 4.8010$$

Applying the same calculus, using the data obtained in the potentiometric titration of EDTA, values very close to those given in literature for the first two constants [5] were obtained, thus the values determined for the first two constants of the acid synthesized by us, H_4RA_4, can be considered satisfactory (Table 4).

TABLE 4

Values of pK_1 and pK_2 for the EDTA and H_4RA_4 acid

	EDTA		H_4RA_4	
	pK_1	pK_2	pK_1	pK_2
Given in literature	1.996	2.672	—	—
Determined by us :	1.898	2.701	3.347	4.80

$R : =N-C_6H_4-CH_2-C_6H_4-N=$; $A : -CH_2COO^-$;

Being a weak acid with the acidity exponents $pK_a \geqslant 5$, pK_3 and pK_4 were determined directly from the same potentiometric titration curve (Figures 1 and 2) with a satisfactory accuracy, on the basis that the pK is equal to the pH of semiequivalence, that is :

$$pK_a = (\mathrm{pH})_{0.5\ \mathrm{Equiv.}}$$

In this way we determined the pK_3 and pK_4 values for EDTA, included in table 5, thus confirming the values pK_3 and pK_4 determined by us for the H_4RA_4 acid.

TABLE 5

Values of pK_3 and pK_4 for the EDTA and H_4RA_4 acid

	EDTA		H_4RA_4	
	pK_3	pK_4	pK_3	pK_4
Given in literature :	6.16	10.26	—	—
Determined by us :	6.16	10.30	5.70	11.15

$R : =N-C_6H_4-CH_2-C_6H_4-N=$; $A : -CH_2COO^-$;

The data obtained by us for the pK_1, pK_2, pK_3, pK_4 of the H_4RA_4 acid are enclosed between the corresponding values of different other aminopolycarboxylic acids (Table 6) found in literature.

The comparative study of the IR spectra of the H_4RA_4, H_2RA_2, acids and of the apparent substance, 4,4′-diaminodiphenylmethane, enables the observation that in the spectra no vibration corresponding to the free $-NH_2$ groups (3446, 3348, 3210, 1630 cm.$^{-1}$)[10] appears for the acids synthesized by us, H_2RA_2, and H_4RA_4. The spectra of the two acids are almost identical, with the difference that in the IR spectrum of the H_4RA_4 acid the characteristic vibrations of the free carboxylic groups are intenser and include, in addition, vibrations corresponding to the disubstituted aminoarylic group $R-N=$ (1335, 1230 cm^{-1}), table 7.

TABLE 6

pK dissociation of some aminotetracarboxylic acid

	Ethylene-diamino-tetraacetic EDTA /5/	*p*-xylene-diaminotetra-acetic /8/	Phenylene-diaminotetra-acetic /7,8/	4,4′-diamino-diphenylme-thane-N,N′-tetraacetic H_4RA_4	Ethylene-diamino-diacetic-dipropionic /9/	Ethylene-diamino-tetrapropio-nic /9/
pK_1	2.00	2.00	2.00	3.53	3.00	3.00
pK_2	2.67	2.71	2.90	4.80	3.79	3.43
pK_3	6.13	5.99	4.99	5.70	5.98	6.77
pK_4	10.26	10.88	6.04	11.15	9.83	9.60

TABLE 7

Attribution of vibrations in IR spectra of the 4,4'-diaminodiphenylmethane-N,N'-tetraacetic acid, H_4RA_4

Vibrations attributed	4,4′-diamino-diphenylme-thane	4,4′-diamino-diphenylme-thane-N,N′-diacetic acid $H_2R''A_2$	4,4′-diaminodi-phenylmethane-N,N'-tetraacetic acid H_4RA_4
ν_{as} $-NH_2$ free	3446 i	—	—
ν_s-NH_2 free	3348 i	—	—
δ $-NH_2$ free	3210 m	—	—
$\nu-CH_2-$	2885 m	2920 m	2920 m
$\nu-CH_2COOH$	—	1715 i	1720 i
$\delta-NH_2$	1630 i	—	—
$\nu_{as}-COO^-$			
$\nu_{as}-NH-CH_2COOH$	—	1615 vi	1615 vi
$\nu-C-H$	1515 wi	1515 vi	1515 vi
$\nu Ar-NH-CH_2-$			
$\nu-C-H-$aliph.	1436 m	1430 i	1430 m
$\nu-COO^-$			
$\nu-CH_2COOH$	—	1380 i	1380 vi
$\nu Ar-N=$	—	—	1335 i
$\nu-C-N$ free	1288 m	—	—
	1275 m		
$\nu-CH_2COOH$	—	1265 i	1265 i
ν $Ar-N=$	—	—	1232 i
$\nu-CH_2COOH$	—	925 m	925 i
$\nu-C_6H_4-$(phenylene)	815 i	815 i	815 i

R'' : $-HN-C_6H_4-CH_2-C_6H_4-NH-$; R' : $=N-C_6H_4-CH_2-C_6H_4-N=$;
A : $-CH_2COO^-$;
vi = very intensively ; i = intensively ; m = middle.

Taking into account the elementary analysis data of the potentiometric and conductometric titrations, the IR spectra, we can consider that the structure of the 4,4'-diaminodiphenylmethane-N,N'-tetraacetic acid, H_4RA_4, is :

Formula I

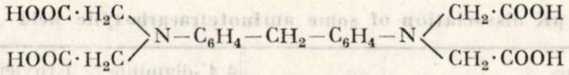

$$\begin{matrix}HOOC\cdot H_2C \\ HOOC\cdot H_2C\end{matrix}\!\!>N-C_6H_4-CH_2-C_6H_4-N<\!\!\begin{matrix}CH_2\cdot COOH \\ CH_2\cdot COOH\end{matrix}$$

4,4'-diaminodiphenylmethane-N,N'-tetraacetic acid, H_4RA_4

Preliminary attemps show that the sodium salt of this acid, $Na_2H_2RA_4.2H_2O$, which is soluble in water, can be used as a reagent in the quantitative analysis. Thus, for example, La^{3+} having a known concentration of La^{3+} (1 ml solution = 0.01715 g La) has been determined gravimetrically from a solution of $La(CH_3COO)_3\cdot 11/2\,H_2O$, by precipitation of the chelate and calcination to oxyde. (Table 8).

TABLE 8

Gravimetric determination of La^{3+} with $Na_2H_2RA_4\cdot 2H_2O$

Sample	ml solution La^{3+} salt	g La	g La_2O_3 found	% La found	% La Calculated	Difference
1	10	0.1715	0.0831	41.31	40.49	+0.82
2	15	0.2575	0.1238	41.02	40.49	+0.53
3	20	0.3430	0.1638	40.74	40.49	+0.25
4	25	0.4287	0.2051	40.80	40.49	+0.31
5	30	0.5145	0.2458	40.74	40.49	+0.25

$R : = N-C_6H_4-CH_2-C_6H_4-N= \ ; \ A : -CH_2COO^- ;$

The same element has been determined conductometrically (Table 9, Figure 3) in different samples of a solution of the same La^{3+} salt (1 ml solution = 0.0027 g La).

TABLE 9

Conductometric determination of La^{3+} from a solution $La(CH_3COO)_3$. $11/2H_2O$ (1 ml = 0.0027 g La), and using $Na_2H_2RA_4\cdot 2H_2O$, 0.002 M

Sample	ml solution La^{3+}	ml reagent solution added up to equivalence	% La content	
			calculated	Found
1	12.5	4.3	40.49	40.24
2	25	8.6	40.49	40.29

$R : = N-C_6H_4-CH_2-C_6H_4-N= \ ; \ A : -CH_2COO^- ;$

Also, some possibilities of colorimetric determination of Cu^{2+} and Co^{2+} with $Na_2H_2RA_4.2H_2O$ in solution 0.02 M have been found, on the basis of the determinations carried out by us, that is the Lambert-Beer law can be applied in this case, within the concentration limits 0.04—0.2 mg for Cu^{2+}, 0.02—1.2 mg from Co^{2+}.

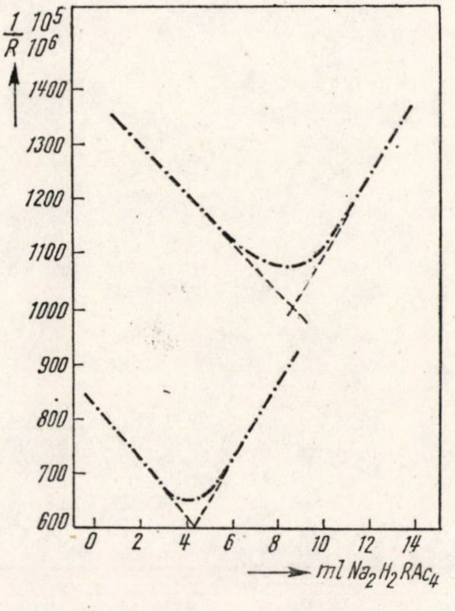

Fig. 3. — Conductometric determination of La^{3+} with $Na_2H_2RA_4.2H_2O$.

We foresee possibilities of using the same salt as well as the neutral salt $Na_4RA_4 \cdot 4H_2O$, as reagent in volumetric complexometry.

REFERENCES

[1] Part. I Const. Gh. Macarovici and E. Chiş, *Rev. Roumaine Chim.*, **19**, 1885. (1974).
[2] Part. II. Const. Ch. Macarovici and E. Chiş, *Rev. Roumaine Chim.*, **22**, 657 (1977).
[3] G. Schwarzenbach, A. Willi and O. Bach, *Helv. Chim. Acta*, **30**, 1303 (1947).
[4] G. Schwarzenbach, A. Willi and O. Bach, *Helv. Chim. Acta*, **30**, 1316 (1947).
[5] G. Schwarzenbach and H. Ackermann, *Helv. Chim. Acta*, **30**, 1798 (1947).
[6] G. Shwarzenbach and H. Ackermann, *Helv. Chim. Acta*, **31**, 1029 (1948).
[7] E. Uhling, *Z. Chem.*, **4**, 151 (1964).
[8] E. Uhling and D. Herman, *Z. anorg. Chem.*, **358**, 135 (1968).
[9] S. Chaberek and A. E. Martell, *J. Amer. Chem. Soc.*, **74**, 6228 (1952).
[10] K. Nakamoto, Y. Morimoto and A. E. Martell, *J. Amer. Chem. Soc.* **84**, 2081 (1962).

Revue Roumaine de Chimie, **25**, *4*, 513 – 527(1980)

ELECTRONIC SPECTRA AND MAGNETIC SUSCEPTIBILITIES OF SOME NEW TETRAHEDRAL CHELATE COMPLEXES WITH Co(d^7) — N(sp^2) BONDS. II[1]

Co(II) CHELATES SYNTHESIZED WITH 1-METHYL-2-CARBETHOXY-GLYOXALANIL-(1)-BROMO-PHENYLHYDRAZONES-(2)

A. C. BANCIU* and V. MINCU**

* ICECHIM — Centre of Physical Chemistry,
Bucharest, Spl. Independenţei 202, Romania
** Polytechnic Institute, Bucharest,
Bd. Republicii 13, Romania

Received December 18, 1978

The electronic spectra of some new organic ligands and the electronic spectra and magnetic susceptibilities of the Co(II) tetrahedral chelate complexes synthesized with these ligands have been studied. The complexes have identical donor atoms, of nitrogen in sp^2 hybridization. The correlation between spectral and magnetic data of the new complexes and the covalency degree of the Co(II) — N(sp^2) chemical bonds of these complexes (compared with that of other similar Co(II) complexes and correlated with the σ^+ — Brown constants of the substituent existent in these complexes) have been examined, as well as the magnitude of interactions influencing the values of magnetic susceptibilities (and moments) of the complexes (spin-orbit coupling and temperature independent paramagnetism). The magnetic data shown that both studied complexes do not present electron delocalization or ligand fields having symmetries lower than regular tetrahedral.

INTRODUCTION

Our previous papers[1-6] have described the Co(II) complexes synthesized with the new type I organic ligands, of the class of 1-methyl-2-carbethoxy-glyoxalanil-(1)-phenylhydrazones-(2) differently substituted (Y = H, CH_3, OCH_3, NO_2, Cl) at the benzene ring of the phenylhydrazone group.

Continuing these researches, the new chelate ligands Ia and Ib, and, by means of these, the corresponding new tetrahedral chelate complexes of Co(II) (*para*- and, respectively, *meta*-bromo-substituted at the benzene ring of the phenylhydrazone group) were synthesized and investigated.

The present work deals with the electronic spectra of the organic ligands and, especially, with the electronic spectra and the magnetic susceptibilities of the new Co(II) complexes. Therefore, the correlation between the spectral and magnetic data of the complexes, the calculation of the covalency degree of the Co(II)—N chemical bonds of the complexes (compared with that of other similar Co(II) complexes and correlated with the σ^+-Brown constants of the substituents existent in these complexes) and the quantitative investigation of the interactions which influence the values of the magnetic susceptibilities (and moments) of the complexes are presented.

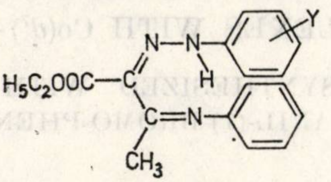

I

a: Y=p-Br ; b: Y=m-Br

EXPERIMENTAL

The new organic compounds Ia and Ib were synthesized and purified according to the method described in our previous papers.[1–5] Their analytical data, which are in good agreement with the type I formulas, are listed in table 1.

TABLE 1

1-Methyl-2-carbethoxy-glyoxalanyl-(1)-bromo-phenylhydrazones-(2). Analytical data

Coumpound	Y	C % calc. found	H % calc. found	N % calc. found	m.p. °C
Ia	p-Br	55.68 56.10	4.67 5.28	10.82 11.02	102—106
Ib	m-Br	55.68 55.90	4.67 4.99	10.82 11.10	90—94.5

The new Co(II) complexes IIa and IIb were synthesized by means of the new organic ligands Ia and Ib, respectively, as described in our previous papers. [1–5] The organic ligands Ia and Ib, respectively, were refluxed with $CoCl_2 \cdot 6H_2O$ (molar ratio $CoCl_2$: ligand = 1.20: 2) in solutions of absolute methyl alcohol, in the presence of small amounts of triethylamine. The rough complexes were repeatedly washed with a solution of 3% acetic acid (at 30—40°) and then with hot methyl alcohol. The complexes were, finally, two times recrystallized, from absolute methyl alcohol, in the presence of active charcoal and dried under vacuum, on di-P_2O_5. The analytical data of the new complexes, which are in good agreement with their type II formulas, are listed in table 2

TABLE 2

Co(II) chelates. Analytical data

Chelate	Y	Co %	C %	H %	N %	m.p. °C
		calc. found	calc. found	calc. found	calc. found	
IIa	*p*-Br	7.07 6.83	51.88 51.70	4.11 4.80	10.08 10.83	148–149
IIb	*m*-Br	7.07 6.91	51.88 51.62	4.11 4.78	10.08 10.13	137–137.5

The elemental analysis of Co, C, H and N was performed by usual micromethods.

The electronic absorption spectra were determined on a VSU-2 Carl Zeiss (Jena) spectrophotometer on solutions in absolute ethyl alcohol (compounds Ia and Ib) and in acetone (compounds IIa and IIb).

The electronic diffuse reflect ance spectra of the complexes were determined on a VSU-1 Carl Zeiss (Jena) spectrophotome ter, using MgO as standard.

The electric conductivity of the complexes was deter mined with a Radelkis OK–102/1 conductometer on solutions of absolute ethyl alcohol.

The magnetic susceptibilites were determined at room temperature, in the solid complexes, according to the Faraday method, using Hg $[Co(NCS)_4]$ as standard. The magnetic moments were calculated by formula (1),

$$\mu_{\text{eff}} = \sqrt{\frac{3k}{N\beta^2}}\sqrt{\chi'_M T} = 2.828\sqrt{\chi'_M T} \text{ B.M.} \tag{1}$$

where k is the Boltzmann constant, N is the Avogadro number, β is the Bohr magneton, T is the absolute temperature and $\chi'_M = \chi_M - \chi_M^{\text{dia}}$ is the molar susceptibility (in c.g.s. units) corrected for diamagnetism. For both complexes the diamagnetic correction was $\chi_M^{\text{dia}} = -397 \times 10^{-6}$ c.g.s.u./mole (calculated with the Pascal constants). On calculating χ_M and χ_M^{dia} the complexes were formulated as monomers, according to formulas IIa and IIb.

RESULTS AND DISCUSSIONS

To the two new Co(II) complexes a chelate tetracoordinate structure of type II has been attributed. This formula is argued by the elemental analysis (table 2), the very low values of the molar electric conductivities ($\Lambda < 2.5$ ohm^{-1} cm^2 mole), the IR spectral data (which are not herein commented) and the comparison with another similar complexes.

Each complex has a set of four identical donor atoms. These are nitrogen atoms, in sp^2 hybridization state. The Co(II) complex compound of type II which can be *ortho*-bromo-substituted at the benzene ring of the phenylhydrazone groups has not been synthesized even though the corresponding type I organic compound was easy prepared. This result is not surprising. Like bromine, all the other substituents (CH_3, OCH_3, NO_2, Cl) introduced so far in the *ortho*-position at the benzene ring of the phenylhydrazone group have sterically hindered the complexation of the transition metal ions by the organic type I compounds. Among the above-mentioned *ortho*-substituents the chlorine (van der Waals radius of 1.80 Å) also, even 20% less bulky than bromine (van der Waals radius of 1.95 Å),[7] does not allow the coordination of the metal ions.[1] The sterical

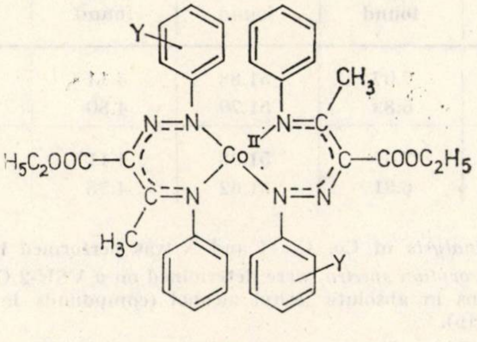

II

a: Y=*p*-Br ; b: Y=*m*-Br

hindrance of the coordination is observed only with the *ortho*-position of the mentioned substituents. This position is in the close vicinity of the nitrogen atom of the hydrazone group, to which the substituted benzene ring is bound. In the absence of sterical hindrances (all type II complexes which are *para*- or *meta*-substituted) this nitrogen atom acts as donor and forms a chemical bond with the central metal ion.

ELECTRONIC SPECTRA OF ORGANIC COMPOUNDS Ia AND Ib

The electronic spectra of the free ligands (organic compounds Ia and Ib), measured within the 220—450 nm range, on absolute ethyl alcohol solutions, are shown in figure 1.

The most intense bands ($\varepsilon_{\max} > 2.0 \times 10^4$) with maxima situated at 362 nm (compound Ia) and 355 nm (compound Ib) and extended over 400 nm represent most likely the first allowed $\Pi \rightarrow \Pi^*$ transitions in the respective organic compounds. The maxima placed at 227 nm (compound Ia) and 240 nm (compound Ib) also represent allowed $\Pi \rightarrow \Pi^*$ transitions. This last assignment is supported by the following considerations: 1. The range of wavelengths where the absorption maxima occur; 2. The high intensity of these bands, which may be compared with that of the first allowed $\Pi \rightarrow \Pi^*$ bands; 3. The shifts of these bands, in the same direction as the shifts of the first allowed $\Pi \rightarrow \Pi^*$ bands. These always hypsochromically bandshifts take place both when methyl groups are introduced in the chromophore system of the type I organic ligands and when the used solvent is varied, in the sense of increasing polarity (from *n*-hexane to ethyl alcohol).[8]

In contrast with the compounds Ia and Ib, in the spectra of almost all other type I organic compounds,[1-5] less intense shoulders, at approximately 265 nm, occur[5]. Their assignment is difficult and uncertain. They may represent shifted and intensified α benzene bands, or $n \rightarrow \sigma^*$ transitions, or $n \rightarrow \Pi^*$ transitions or forbidden $\Pi \rightarrow \Pi^*$ transitions. Such shoulders do not appear in the spectra of the herein discussed compounds Ia and Ib, being probably obscured by other more intense bands, situated at 227 nm and 240 nm, respectively.

The first allowed $\Pi \rightarrow \Pi^*$ band is more intense at the compound Ia. Assuming, reasonably, (Figure 1) that the allowed $\Pi \rightarrow \Pi^*$ bands are gaussian like, one may then calculate the oscillator strength, using the formula (2)[9]

$$f = 4.6 \times 10^{-9} \varepsilon_{\max} \delta \qquad (2)$$

where $\varepsilon_{\max}$ is the molar extinction coefficient of the band maximum and δ is the half-bandwidth (in cm^{-1}). For the first allowed $\Pi \rightarrow \Pi^*$ transition the oscillator strength is 0.53 and 0.44 for the compounds Ia and Ib, respectively. These bands also occur in the spectra of the corresponding Co(II) complexes, but shifted and intensified.

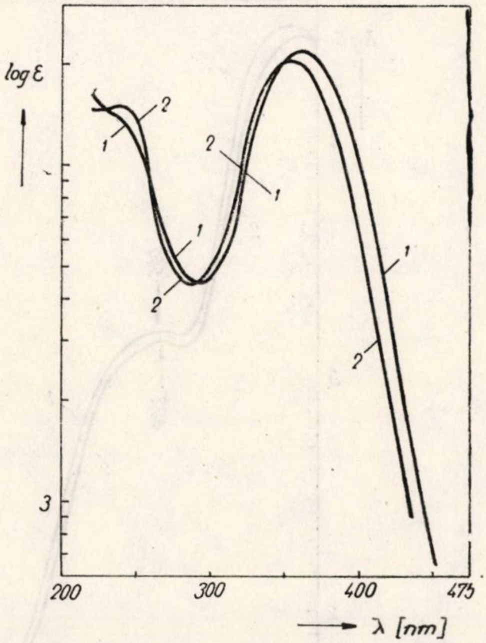

Fig. 1. — Electronic spectra of the organic compounds Ia and Ib. *1* — compound Ia; *2* — compound Ib.

ELECTRONIC SPECTRA OF THE COMPLEXES IIa AND IIb

The electronic spectra of the complexes IIa and IIb, measured within the 350—1200 nm range, on acetone solutions, are shown in figure 2.

The three bands occurring in the spectrum of each complex are of sensibly different intensities. The most intense bands with maxima situated at 378 nm (complex IIa) and 365 nm (complex IIb) represent allowed $\Pi \rightarrow \Pi^*$ transitions, belonging to the appropriate organic ligands (compounds Ia and Ib). Due to the coordination, in the spectra of the complexes these bands occur bathochromically shifted, with 16 nm (1170 cm^{-1}) for the complex IIa and with 10 nm (770 cm^{-1}) for the complex IIb, compared with the spectra of free ligands. These bands become more intense in the spectra of the corresponding complexes. If a gaussian shape (Figure 2) is assumed for these bands, the values of their oscillator strength are of 1.16 for the complex IIa and 1.24 for the complex IIb. If the *f* (oscillator strength) values for the complexes are compared with those of the free ligands, one observes that for the complex IIa

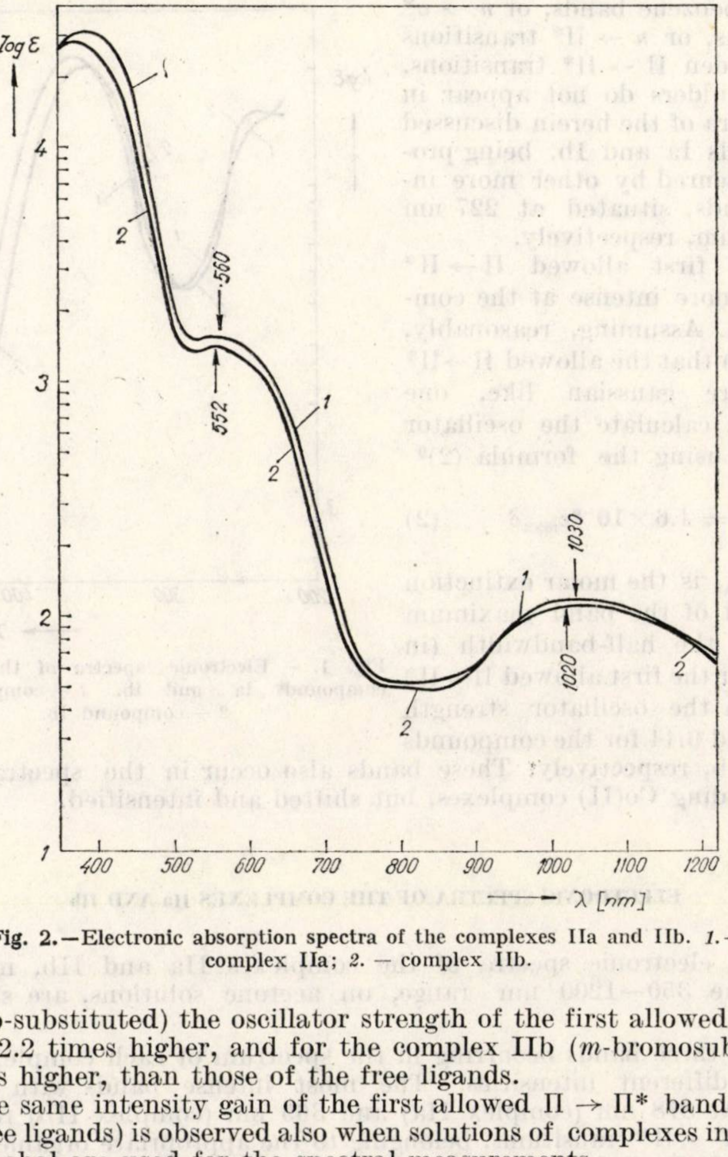

Fig. 2.—Electronic absorption spectra of the complexes IIa and IIb. *1.*— complex IIa; *2.* — complex IIb.

(*p*-bromo-substituted) the oscillator strength of the first allowed Π → Π* band is 2.2 times higher, and for the complex IIb (*m*-bromosubstituted) 2.8 times higher, than those of the free ligands.

The same intensity gain of the first allowed Π → Π* bands (proper to the free ligands) is observed also when solutions of complexes in absolute ethyl alcohol are used for the spectral measurements.

Even though the other two bands, with maxima placed at ca 550 nm ($\varepsilon_{max} > 1.4 \times 10^3$) and ca 1040 nm ($\varepsilon_{max} > 1.13 \times 10^2$), differ in their intensity, they may be both ascribed to some spin allowed *d*−*d* transitions, proper to the *d* electronic configuration of the central Co(II) ion in a tetrahedral environment. This assignment is the only able to explain reasonably these transitions, in good agreement with the type II chemical structure of tetracoordinated chelates and in good concordance with the data of paramagnetic susceptibilities measurements (see below).

The energy expressions for the spin-allowed transitions in a d^7 (T_d) electronic configuration, in the case of a weak coupling, are :[10–12]

$$ {}^4A_2(e^4t_2^3) \rightarrow {}^4T_2(e^3t_2^4) \qquad \Delta \tag{3}$$

$$ {}^4A_2(e^4t_2^3) \rightarrow {}^4T_1^a(e^3t_2^4) \qquad 1.5\Delta + 7.5B - Q \tag{4}$$

$$ {}^4A_2(e^4t_2^3) \rightarrow {}^4T_1^b(e^3t_2^4) \qquad 1.5\Delta + 7.5B + Q \tag{5}$$

where :

$$Q = \frac{1}{2}[(0.6\Delta - 15B)^2 + 0.64\Delta^2]^{1/2} \tag{6}$$

Δ is the orbital splitting parameter (the energy difference between the t_2 and e sublevels), while B is the Racah parameter for the interelectronic repulsion radial integrals ($B_{\mathrm{Co(II)}} = 980\ \mathrm{cm}^{-1}$).

The first of the indicated transitions occurs outside the measured spectral range, in the morefar infrared, at ca 4500—6500 cm.$^{-1}$ This is so since $\Delta_{T_d} = 4/9\Delta_{O_h}$ and $\Delta_{O_h} = 10000 \ldots 15000\ \mathrm{cm}^{-1}$ (relation also valid in the frame of the LCAO — MO — theory[13]).

The bands occurring in the spectra of the complexes at ca 550 nm and ca 1040 nm are due to the last two of the above indicated transitions :

$$\nu_3({}^4A_2 \rightarrow {}^4T_1^b) = 17860\ \mathrm{cm}^{-1} (560\ \mathrm{nm}) \text{ for the chelate IIa}$$

$$= 18100\ \mathrm{cm}^{-1} (552.5\ \mathrm{nm}) \text{ for the chelate IIb}$$

$$\nu_2({}^4A_2 \rightarrow {}^4T_1^a) = 9710\ \mathrm{cm}^{-1} (1030\ \mathrm{nm}) \text{ for the chelate IIa}$$

$$= 9800\ \mathrm{cm}^{-1} (1020\ \mathrm{nm}) \text{ for the chelate IIb}$$

Solving the energy expressions (4 and 5) of these transitions one obtains the values Δ and thereby the B and β values of the chelates IIa and IIb are obtained (Table 3).

TABLE 3

The ν_2, ν_3, Δ, B and β values of the new Co(II) complexes

Complex	ν_3	ν_2	Δ [cm^{-1}]	B [cm^{-1}]	β
IIa	560 nm (17860 cm^{-1})	1030 nm (9710 cm^{-1})	5475	743	0.76±0.02
IIb	552.5 nm (18100 cm^{-1})	1020 nm (9800cm^{-1})	5520	756	0.77±0.02

The determination errors for Δ, B and β were analyzed in our previous papers. [3-5] It has been shown that the highest possible experimental error, which may have the greatest influence upon the calculated value of the nephelauxetic ratio β, is the determination error of the ν_3 band maximum, at ca 550 nm. It was shown that, if the ν_3 band maximum can be located with an error of only ± 5 nm (like in the case of the above-mentioned complexes IIa and IIb), then all the cumulated errors of experimental determination of the ν_2 and ν_3 values modify, eventually, the calculated values of the nephelauxetic ratio β at most 2 units at the second decimal.

The values of the nephelauxetic ratio β for all until now synthesized[1-5] type II complexes are systematized in table 4.

TABLE 4

The values of the σ^+ — Brown constants of the substituents (Y) introduced into the type II complexes, at the benzene ring of the hydrazone group, and the values of the nephelauxetic ratio, β of the corresponding complexes

Type II complex Substituent Y	β^+ — Brown	β	References
H—	—	0.76±0.02	2
p-CH$_3$—	−0.306	0.75±0.02	3
m—CH$_3$—	−0.065	0.75±0.02	3
p—CH$_3$O—	−0.764	0.71±0.02	4
m—CH$_3$O—	+0.946	0.76±0.02	4
p—NO$_2$—	+0.777	0.81±0.04	5
m—NO$_2$—	+0.662	0.82±0.04	5
p—Cl	+0.112	0.77±0.02	1
m—Cl	+0.391	0.79±0.02	1
p—Br	+0.148	0.76±0.02	this paper
m—Br	+0.399	0.77±0.02	this paper

One may observe that the new Co(II) complexes, IIa and IIb, have, practically, the same β value as the unsubstituted type II complex. The bromine substituent fixed in the *para* or *meta* position at the benzene ring of the hydrazone group practically fails to modify the electron density at the nitrogen atom which is directly bonded to the substituted benzene ring and which asks as donor atom. Therefore, substituted in the mentioned positions the bromine fails to modify the covalency degree of the Co(II)—N chemical bonds in the type II complexes.

The strength of the electronic effects of the substituents can be measured by using the values of the σ^+ — Brown substituent constants. [14] For the substituents so far introduced in the type II complexes, the σ^+ — Brown constants are also summarized in table 4. It is observed that, among all these substituents, only the *p*-OCH$_3$ substituent and the NO$_2$ substituent (this regardless of the *para* or *meta* position) exhibit such strong electronic effects, that their σ^+ — Brown substituent constants are ***higher than 0.650, in absolute value.*** Therefore, when introduced in the type II complexes, at the benzene ring of the hydrazone group, these substituents modify the covalency degree of the metal-ligand chemical bonds to a perceptible extent (which really modifies the value of the nephelauxetic ratio β). The p-OCH_3 substituent increases the covalency degree ($\beta = 0.71 \pm 0.02$) and the NO_2 substituent decreases it[5] ($\beta \sim \sim 0.82 \pm 0.04$), regardless of the *para* or *meta* position.

It is important to mention that such a good correlation as the above mentioned one (between the β and σ^+-Brown substituent constants values) can not be found if the β values of the Co(II) complexes and the σ-Hammett values of the corresponding substituents are compared. The explanation is quite simple. For the *meta* position (which is influenced by the inductive electronic effects) the σ^+-Brown and the σ-Hammett constants take closed values.[14] For the *para* positions these constants differ sometimes very much. This is so since only the σ^+-Brown constants are sensitive to the conjugation (mesomeric) effects, which sometimes are very strong[14]. This is, for example, the pregnant case of the p-OCH_3 substituent. This increases sensitively the electronic density of the donor nitrogen atom which is directly bounded to the substituted benzene ring and increases thereby, the covalency degree of the Co(II)—N chemical bonds in the corresponding complex. In this covalency effect the preponderent role is played by the conjugation (mesomeric) effect of the p-OCH_3 substituent (σ^+-Brown constant value of -0.674). Conversely, in the *meta* position, where the conjugation (mesomeric) electronic effect is not obvious the OCH_3 substituent practically fails to influence the covalency degree of the Co(II) — N chemical bonds in the corresponding complex (which has exactly the same β value ($\beta = 0.76 \pm 0.02$) as the unsubstituted type II complex).

In a previous paper[3] has been shown that the graphical bidimensional plotting of the covalency of the tetrahedral Co(II) complexes, proposed by Cotton and Soderberg[15,16] is sometimes erroneous and other times doubtful. According to these authors the different T_d complexes of Co(II) may be represented by points, in a bidimensional graph, taking on the ordinate axis the quantity ΔB ($= B_{\text{free ion}} - B_{\text{complex ion}}$) and the quantity f_{ν_3} (the oscillator strength of the ν_3 band) on the abscissa axis. The complexes placed up to the right corner (which present concomitantly the highest ΔB and f_{ν_3} values) are the strongest covalent. We have shown that, if this graphical plotting is used, then, for a reasonable comparison, only data obtained for complexes where the electronic spectra are recorded on solutions of the same solvent should be taken. This is so since the ΔB and, especially, the f_{ν_3} values are both influenced, to a detectable extent, even by a scarce solvent effect, as that detected if the used solvent is varied to the recording of the spectra of complexes, from absolute ethyl alcohol to acetone.

For the electronic spectra of the Co(II) type II complexes measured on acetone solutions the graph of ΔB and f_{ν_3} values is represented in figure 3.

One observes that almost all complexes are comprised in the domain between $\Delta B = 200...230$ cm^{-1} and $f_{\nu_3} = 3.0 \times 10^2...3.7 \times 10^2$. Exception is made only by three type II complexes ($Y = p$-CH_3, p—OCH_3

and, respectively, m-NO_2). The p-NO_2- substituted complex cannot be exactly represented on the graph, most likely being out the above indicated domain. For the p-CH_3—substituted complex the deviation from the mentioned domain is insignificant (of only 15 cm^{-1} on the ordinate axis) being caused by the experimental errors of spectral recording of the ν_2 and ν_3 band maxima. There remain two complexes which are very different. The p-OCH_3—substituted complex (differing on ordinate by others with 40 cm^{-1}) shows a higher covalency and the m-NO_2—substituted complex (differing on ordinate by others with 35 cm^{-1}) shows lower covalency, for the Co(II)—N chemical bonds. One observes that actually in this comparison between the covalency of the Co(II) complexes the important fact is only the position of the complexes on the ordinate axis (the ΔB value). The position of the complexes on the abscisa is sometimes misleading. As an example, a more covalent complex (the p-OCH_3 — substituted) shows a lower f_{ν_3} value (2.79×10^{-2}) than a less covalent one (the p-Br-substituted, with $f_{\nu_3} = 3.57 \times 10^{-2}$). This is due to the fact that the intensities of the ν_3 bands are not only influenced by the covalency of the Co(II) — N bonds. The (partial) overlapping of the ν_3 bands (of d-d type) with more intense bands, as those proper to the free organic ligands (as for therein discussed complexes) or those of CT type, may lead to strong intensification of the ν_3 bands. This fact is sometimes more preponderant than the intensity gain caused by the increase of the covalency of the Co(II)—N chemical bonds in the complexes. In this case (of band overlapping) the f_{ν_3} values of the complexes cannot be more reasonably compared, to measure the covalency degree of the metal-ligand chemical bonds in the complexes.

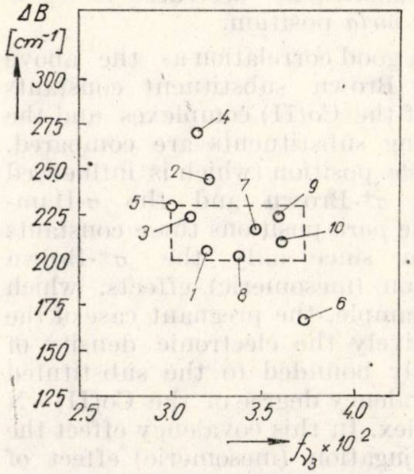

Fig. 3.—The graph of ΔB and f_{ν_3} values of the Co(II) complexes of type II. *1.* Y = H; *2.* Y = $p-CH_3$; *3.* Y = $m-CH_3$; *4.* Y = $p-OCH_3$; *5.* Y = $m-OCH_3$; *6.* Y = $m-NO_2$; *7.* Y = $p-Cl$; *8.* Y = $m-Cl$; *9.* Y = $p-Br$; *10.* Y = $m-Br$.

For this reason the simple comparison of the β values of the complexes gives logically and clearly (in good agreement with the corresponding σ^+— Brown substituent constants) more information about the covalency of the metal-ligand chemical bonds.

MAGNETIC SUSCEPTIBILITIES AND MOMENTS

The electronic diffuse reflectance spectra recorded on the solid complexes IIa and IIb agree well with their above discussed absorption spectra. This shows that both complexes, have, in solutions as well as in solid state, a tetrahedral structure for the Co(II)—N bonds.

Knowing, from the electronic spectra, the tetrahedral structure of the complexes and the value of their orbital splitting parameter Δ, the data of the magnetic susceptibility measurements, made on the solid complexes, can be well explained in the following manner.

The magnetic susceptibilities and the magnetic moments of the Co(II) tetrahedral complexes always differ from the spin-only values.[17, 18] They are (at 298 K) $\chi_M^{\text{s.o.}} = 6285 \times 10^{-6}$ c.g.s.u. and, respectively, $\mu_{\text{eff}}^{\text{s.o.}} = 3.87$ B.M.[18] The last value corresponds to the formula

$$\mu_{\text{eff}}^{\text{s.o.}} = g[S(S+1)]^{1/2}\ \text{B.M.} \tag{7}$$

where the Landè factor $g = 2$ and $S = 3/2$.

For the complexes with an A_2 ground term, such as the tetrahedral Co(II) ones, fairly exact χ_M and μ_{eff} values (i.e. close to the experimental ones) will be calculated if, besides the spin-only values, the spin-orbit coupling is considered. The latter "mixes in", to a certain extent, the energetical higher states ($^4T_2$ and $^4T_1$ in the T_d Co(II) complexes) with the A_2 ground state. Therefore, although in the complexes with A_2 ground term the orbital contribution (to the χ_M and μ_{eff} values) is, in a first approximation, totally quenched,[18] a part of it is brought back, as a result of the spin-orbit coupling.

Taking into account the influence of the spin-orbit coupling, the value of the Landè factor is given by[18, 19]

$$g = 2\left(1 - \frac{4\lambda}{\Delta}\right) \tag{8}$$

where λ is the spin-orbit coupling constant of the free ion and Δ is the orbital splitting parameter. Therefore, the magnetic moment is given by

$$\mu_{\text{eff}} = 2\left(1 - \frac{4\lambda}{\Delta}\right)[S(S+1)]^{1/2}\text{B.M.} = \left(1 - \frac{4\lambda}{\Delta}\right)\mu_{\text{eff}}^{\text{s.o.}} \tag{9}$$

and the molar magnetic susceptibility is correctly expressed by

$$\chi_M = \left(1 - \frac{4\lambda}{\Delta}\right)^2 \chi_M^{\text{s.o.}} = \left[1 - \frac{8\lambda}{\Delta} + \left(\frac{4\lambda}{\Delta}\right)^2\right]\chi_M^{\text{s.o.}} \tag{10}$$

It is to mention that, in some works[18], χ_M is calculated, taking into account the spin-orbit coupling, by means of formula

$$\chi_M = \left(1 - \frac{8\lambda}{\Delta}\right)\chi_M^{\text{s.o.}} \tag{11}$$

This expression of χ_M differs from (10) only by neglecting the square term $(4\lambda/\Delta)^2$, which is relatively small, for $\lambda \ll \Delta$. However, only the

χ_M values calculated with formula (10) may be exactly correlated (by means of formula (1)) with the μ_{eff} values calculated from formula (9).

To the value of the molar magnetic susceptibility of the T_d Co(II) complexes also contributes, to a small extent, a temperature independent paramagnetism (T.I.P.), resulted from the higher energy ligand field levels.

For complexes with an A_2 ground term the T.I.P. contribution to the χ_M value is given by[17, 18]

$$\chi_M^{\text{T.I.P.}} = \frac{8N\beta^2}{\Delta} \tag{12}$$

where N is Avogardo number, β is the Bohr magneton and the product $N\beta^2 = 0.261$ cm^{-1}.

Formula (13) permits to calculate the magnetic susceptibility of the complexes with an A_2 ground term, taking into account the spin-only value, the spin-orbit coupling and the T.I.P. contribution

$$\chi_M = \left[1 - \frac{8\lambda}{\Delta} + \left(\frac{4\lambda}{\Delta}\right)^2\right] \chi_M^{\text{s.o.}} + \frac{8N\beta^2}{\Delta} \tag{13}$$

Sometimes the magnetic susceptibility of the complexes with an A_2 ground state (as the T_dCo(II) ones) is also influenced by the electron delocalization, due to the metal-ligand chemical bond formation. The electron delocalization is expressed by the subunitary k factor, which represents the non-delocalization unit. (The value $2(1-k)$ may be, approximately, regarded as the extent to which the p_π ligand orbitals enter to the molecular orbitals for the "d" electrons of the central ion[18]).

Taking into account the spin-only value, the spin-orbit coupling and the electron delocalization, the Landè g factor is[20]

$$g = 2\left(1 - \frac{4k^2\lambda}{\Delta}\right) \tag{14}$$

and, therefore, taking into account the electron delocalization the magnetic susceptibility becomes

$$\chi_M = \left[1 - \frac{8k^2\lambda}{\Delta} + \left(\frac{4k^2\lambda}{\Delta}\right)^2\right] \chi_M^{\text{s.o.}} + \frac{8k^2N\beta^2}{\Delta} \tag{15}$$

In some papers,[18] instead of (15), is indicated the formula

$$\chi_M = \left[1 - \frac{8k^2\lambda}{\Delta}\right] \chi_M^{\text{s.o.}} + \frac{8k^2N\beta^2}{\Delta} \tag{16}$$

where the square term $(4k^2\lambda/\Delta)^2$ from (15) is neglected.

Using the formulas (15) or (16) and the experimental molar magnetic susceptibility, the k factor may be determined. The k values calculated by means of formula (16) differ at the second decimal from the values calculated using formula (15).

Knowing that $\lambda_{Co(II)} = -178\ cm^{-1}$ [11] (after [16] $\lambda_{Co(II)} = -172 cm^{-1}$) and the Δ values (determined from the electronic spectra) equal to 5475 cm^{-1} for the complex IIa and to 5520 cm^{-1} for the complex IIb, the weight of the different effects contributing to the magnetic susceptibilities (and moments) may be evaluated.

Table 5 summarizes the χ_M and μ_{eff} values calculated for the complexes IIa and IIb with the above formulas. For comparison, the same table lists the corresponding values for the well-known T_d Co(II) complex compound $Cs_2[CoCl_4]$. These last values were calculated by means of the literature data ($\lambda = -178\ cm^{-1}$ [11]; $\Delta = 3200\ cm^{-1}$ [16–18] and $\mu_{experim.} = 4.71$ B.M. at 300 K[16–18]).

TABLE 5

The χ_M and μ_{eff} values of the new Co(II) complexes IIa and IIb

Considered interactions besides the spin-only values	Formulas used for the calculation of χ_M and μ_{eff}	The new complexes IIa and IIb		The complex Cs_2CoCl_4	
		$\chi_M \times 10^6$ [c.g s.u./mole]	μ_{eff} [B.M.]	$\chi_M \times 10^6$ [c.g.s.u./mole]	μ_{eff} [B.M.]
—	(7)	6285	3.87	6285	3.87
spin-orbit coupling	(9) resp. (10) (11)	8025 7920	4.37 4.34	9390 9080	4.74 4.68
spin-orbit coupling and T.I.P.	(13) (11) and (12)	8400 8300	4.47 4.45	10040 9730	4.91 4.83
spin-orbit coupling, T.I.P and electron delocalization	experimental values (at 298 K) which may be expressed by formula (15) or (16)	8200 ± 190^a 8280 ± 190^b	$4.42 \pm 0.05^{a,c}$ $4.44 \pm 0.05^{b,c}$	9250	4.71

[a] Experimental values for the complex IIa; the experimental susceptibility is corrected for diamagnetism.

[b] Experimental values for the complex IIb; the experimental susceptibility is corrected for diamagnetism. At[a] and [b] the diamagnetic correction was $\chi_M^{dia} = -397 \times 10^{-6}$ c.g.s.u./mole.

[c] Values calculated with formula (1) by means of experimentally determined. χ_M.

One may observe that, for both type II complexes, the spin only susceptibility, of 6285×10^{-6} c.g.s.u./mole, represents ca 75 % from the experimental one. Another important contribution, of about 1740×10^{-6} c.g.s.u./mole, which represents ca 20 % from the experimental susceptibility, is the orbital contribution (as a consequence of the spin-orbit coupling). Finally, the T.I.P. term, of about 380×10^{-6}c.g.s.u./mole, contributes with up to about 5 % to the total susceptibility value. For both complexes, IIa and IIb, the T.I.P. contribution is practically equal to the diamagnetic correction (of -397×10^{-6} c.g.s.u./mole) and exceeds the limit of experimental errors (of $\pm$ 190 $\times$ 10^{-6} c.g.s.u./mole, for both complexes).

The most interesting result of the magnetic measurements is the fact that, in both complexes IIa and IIb, the electron delocalization is practically absent and no distortion from the tetrahedral structure is observed.

Indeed, by applying the equation (15), for instance, in the case of the complex IIa, we have :

$$106\,k^4 + 2014\,k^2 - 1915 = 0$$

whence the values $k^2 = 0.93$ and $k \sim 0.96$ are obtained. By applying the formula (16), which neglectes the k^4 term from (15), we have :

$$2014\,k^2 = 1915$$

and hence the values $k^2 = 0.95$ and $k \sim 0.97$ are obtained.

For the complex IIb one obtains $k^2 = 0.95$ and $k \sim 0.98$ (with formula (15)) and $k^2 = 1.00$ and $k = 1.00$ (with formula (16)).

The deviation of the calculated k values from unity is minimal and comprised within the experimental errors of determination of the magnetic susceptibility (of $\pm$ 190 $\times$ 10^{-6} c.g.s.u./mole). The electron delocalization is, therefore, practically absent in the complexes IIa and IIb. This may be directly observed from table 5, if the χ_M values are compared. The experimental χ_M values are practically equal to the χ_M values calculated from (13), where the electron delocalization is absent. Therefore, the above calculated k values, below 4 % from the maximal possible value (1.00), do not indicate a real electron delocalization.

The case of the complexes IIa and IIb differs from that represented by $Cs_2[CoCl_4]$. The experimental magnetic susceptibility of that complex, of 9250 $\times$ 10^{-6} c.g.s.u./mole, leads to the $k^2 = 0.80$ and $k = 0.90$ (with formula (15)) and $k^2 = 0.86$ and $k = 0.93$ values (with formula 16)). Such a decrease of k, between 10 % and 7 % from the maximal possible value (equal to unity, in the absence of electron delocalization) indicates that the electron delocalization may be present, to a certain extent, in this complex.

To the above calculation of the k values, using the formulas (15) and (16), it was, usually, assumed, that the decrease of the magnetic susceptibility, from the values indicated by formula (13) to the experimental determined values, is caused only by the electron delocalization. This may be, it fact, true, but, sometimes, to the decrease of the molar magnetic susceptibility value also effectively contributes the existence of ligand fields of lower symmetries than the regular octahedral (or tetrahedral) ones.[18]

It is, however, sure that, if the calculated k values are very close to unity (like in the case of the complexes IIa and IIb), in the respective complexes the electron delocalization is practically absent and no distortion from the regular octahedral (or tetrahedral) structure is observed.

The practical absence of electron delocalization in the complexes IIa and IIb (k 1.00) is not surprising. The electron delocalization depends on the π chemical bond formation between the central metal ion and ligands. In the case of the type II complexes the π chemical bonds are very weak.[2] Because of the sp^2 hybridization of the valence nitrogen orbitals, the π coordinative π bonds cannot exist in the plane of the σ bonds. The out-of-plane π bonds, theoretically possible for complexes with donor N(sp^2) atoms, appear as practically non-existent in the complexes IIa and IIb ($k \sim 1.00$).

In turn, in the case of the $Cs_2[CoCl_4]$ complex the chlorine ligands are able to form π coordinative bonds with the central metal ion. The influence of the electron delocalization on the magnetic susceptibility is still perceptible in the case of this complex ($k \sim 0.90...0.93 < 1.00$). The T.I.P. contribution to this complex is unusually high for the T_d Co(II) complexes (of about 650×10^{-6} c.g.s.u./mole).

The complexes IIa and IIb show, nevertheless, an appreciable covalency of the Co(II) — N chemical bonds. This is due to the strong σ bonds between the Co(II) ion and the N(sp^2) atoms. The value taken by the orbital splitting parameter, Δ, is unusually high for the T_d complexes of Co(II) (for the $CoCl_4^{2-}$ ion Δ is of only 3200 cm^{-1} ![18]). The high Δ value for the complexes IIa and IIb is explained by the strong σ interaction (and weak π interaction) which leads to an appreciable energy separation between the t_2 (σ antibonding) and e (π antibonding) sublevels.

REFERENCES

[1] A. C. Banciu, *Rev. Roumaine Chim.*, **23**, 707 (1978).

[2] P. Spacu, A. C. Banciu and C. I. Lepădatu, *Rev. Roumaine Chim.*, **18**, 1143 (1974).

[3] A. C. Banciu and P. Spacu, *Rev. Roumaine Chim.*, **19**, 1019 (1974).

[4] A. C. Banciu and P. Spacu, *Rev. Roumaine Chim.*, **19**, 1169 (1974).

[5] A. C. Banciu, *Rev. Roumaine Chim.*, **21**, 1487 (1976).

[6] A. C. Banciu, *Rev. Roumaine Chim.*, **22**, 1353 (1977).

[7] C. D. Nenițescu, "Chimie organică", Bucharest, 1966, vol. 1, p. 80.

[8] A. C. Banciu, Ph. D. Thesis, Polytechnic Institute Bucharest, 1974.

[9] A.B.P. Lever, "Inorganic Electronic Spectroscopy", Elsevier, Amsterdam, 1968, p. 124.

[10] Y. Tanabe and S. Sugano, *J. Phys. Soc. Japan*, **9**, 753, 766 (1954).

[11] A.B.P. Lever, *op. cit.*, Chapt. 7 and 9.

[12] E. König, *Struct. and Bonding*, **9**, 175 (1971).

[13] H. H. Schmidtke, *Z. Naturforsch.*, **19a**, 1502 (1964).

[14] F. Badea, "Mecanisme de reacție în chimia organică", Bucharest, 1971, p. 101.

[15] F. A. Cotton and R. H. Soderberg, *J. Amer. Chem. Soc.*, **84**, 872 (1962).

[16] R. L. Carlin, "Electronic Structure and Stereochemistry of Cobalt (II)", in "Transition Metal Chemistry", Marcel Dekker, New York, 1865, Vol. 1, p. 1—33.

[17] B. N. Figgis and J. Lewis, "Progress in Inorganic Chemistry", Vol. 6, Interscience, New York, 1964.

[18] B. N. Figgis, "Introduction to Ligand Fields", Interscience, New York, 1966, p. 248—310.

[19] C. J. Ballhausen, "Introduction to Ligand Field Theory", Mc. Graw-Hill, New York, 1962, p. 129.

[20] H. Watanabe, "Operator Methods in Ligand Field Theory", Prentice-Hall, Englewood Cliffs, 1966, p. 139.

Revue Roumaine de Chimie, **25**, *4*, 529–533 (1980)

ESPECTROMETRIA DE MASAS DE HETEROCICLOS INORGANICOS ALQUILADOS. I

ESPECTROMETRIA DE MASAS DE OCTAMETILCICLOTETRAFOSFAZATETRAENO Y SUS SALES CUATERNARIAS DE YODURO DE METILO Y YODURO DE ETILO*

A. SOTO y R. CEA**
Instituto de Química de la U.N.A.M., Circuito Exterior, Ciudad Universitaria, México 20, D.F.

Recibido el 27 de Setiembrie 1978

Se discute el comportamiento ante el impacto electrónico del $P_4N_4(CH_3)_8$ y de sus correspondientes sales cuaternarias con MeI y EtI. Se correlacionan las similitudes y diferencias con los espectros de masas de los halógenofosfazenos. El esquema de fragmentación se fundamenta en la estabilidad de los sistemas cíclicos P_nN_n. Con ayuda de transiciones metaestables se plantea un patrón de fragmentación.

The behaviour of $P_4N_4(CH_3)_8$ and its corresponding MeI and EtI quaternary salts upon electronic impact is studied. The corresponding Mass Spectra are correlated with those presented by the halogeno-phosphazenes. A fragmentation scheme based on the stability of the cyclic P_nN_n systems is proposed, and a fragmentation pattern based on metastable ions is established.

INTRODUCCION

Los trabajos que describen el comportamiento de los fosfazenos cíclicos hacia el impacto electrónico se han centrado fundamentalmente en los estudios de fragmentación de los halógeno[1–5] y seudohalógeno fosfazenos,[6] así como de sistemas sustituídos aril-halógenociclotrifosfazatrienos,[7–8] permitiendo correlacionar la fuerza del enlace de los grupos sustituyentes y la estabilidad del anillo P—N.

Sin embargo, el estudio de los procesos de fragmentación en espectrometría de masas de derivados alquílicos de los ciclos fosfazénicos no ha recibido atención, la única investigación al respecto corresponde al trabajo de Appel y Saleh[9] quienes obtuvieron los espectros de masas de sistemas alquilaril-ciclofosfazenos como evidencia adicional en sus determinaciones. El estudio del sistema $P_4N_4(CH_3)_8$ es de interés, ya que el sustituyente metilo puede considerarse como de muy baja electronegatividad respecto a los sustituyentes que presentan los compuestos previamente estudiados y así es posible relacionar regularidades y diferencias que presenten estos compuestos.

* Contribución No. 527 del Instituto de Química de la U.N.A.M.
** A quien deberá dirigirse la correspondencia.

La basicidad de los sistemas fosfazénicos es conocida, siendo notable la generación de sales cuaternarias $[P_4N_4(CH_3)_9]$ I y $[P_4N_4(CH_3)_8(C_2H_5)]$ I, en donde se presenta un enlace N—C. En los espectros de masas de otros ciclofosfazenos[8,9] se presentan fragmentos debidos a rearreglos hacia la formación de enlaces N—C que no están presentes originalmente. En este trabajo se estudia el comportamiento bajo el impacto electrónico de los compuestos $P_4N_4(CH_3)_8$ y de sus sales cuaternarias $[P_4N_4(CH_3)_9]$I y $[P_4N_4(CH_3)_8(C_2H_5)]$ I en los cuales el enlace N—C ya existe, con el fin de comparar los comportamientos ante el impacto electrónico de sistemas fosfazénicos con y sin enlaces N—C.

PARTE EXPERIMENTAL

El $P_4N_4(CH_3)_8$ se obtuvo mediante la amonólisis del dimetiltriclorofosforano, $(CH_3)_2PCl_3$, según la técnica descrita por Allcock.[10] El cloruro de tiofosforilo y el disulfuro de tetrametildifosfano que se emplearon fueron sintetizados por los métodos previamente informados en la literatura.[11,12] El NH_4Cl empleado en la síntesis fue reprecipitado de una solución acuosa.

Las sales cuaternarias $[P_4N_4(CH_3)_9]$I y $[P_4N_4(CH_3)_8(C_2H_5)]$I se obtuvieron por el método descrito por Searle[13] a partir del octametilciclotetrafosfazatetraeno y de los correspondientes yoduros de metilo y etilo.

Todos los espectros de masas fueron obtenidos en las mismas condiciones en un espectrómetro de masas Hitachi-Perkin Elmer RMU D6 de doble foco, operando a 70 eV con sistema de introducción directa y la cámara de ionización a 190°.

RESULTADOS Y DISCUSION

Los datos de los espectros de masas del $P_4N_4(CH_3)_8$ y de sus sales cuaternarias se presentan en la Tabla 1, así como la asignación probable a los diferentes fragmentos.

En todos los casos, el fragmento de mayor relación *m/e* corresponde a 300 que para el $P_4N_4(CH_3)_8$ se identifica con el ion molecular, pero en el caso de las sales cuaternarias corresponde al ion producido por la pérdida respectivamente del CH_3I ó C_2H_5I. Esto es consistente con la aparición en el espectro del $[P_4N_4(CH_3)_9]$I de un fragmento con una relación *m/e* de 142, correspondiente a $[CH_3I]^+$ y con un fragmento *m/e* 156 debido a $[C_2H_5]^+$ para el caso del $[P_4N_4(CH_3)_8(C_2H_5)]$I, lo cual significa que estas sales muestran un comportamiento semejante a las sales cuaternarias de nitrógeno en donde no se suelen detectar en los espectros de masas los iones moleculares.

Los espectros de masas de los tres compuestos son prácticamente idénticos, habiendo variaciones casi exclusivamente en las intensidades de los diferentes fragmentos, por lo cual la discusión siguiente será en común.

A semejanza del patrón de fragmentación de los derivados clorados y bromados, cuyos espectros de masas presentan como pico base al ion $[M-X]^+(X = Cl \text{ o } Br)$, los compuestos que nos ocupan presentan como pico base al ion $[M-CH_3]^+$. Es interesante que en le caso de los derivados fluorados el fragmento con una intensidad del 100% no corresponde

TABLA 1

Espectro de masas de derivados fosfazenicos metilados

m/e	Asignación Probable	Abundancia Relativa		
		$[PN(CH_3)_2]_4$	$[P_4N_4(CH_3)_9]I$	$[P_4N_4(CH_3)_8(C_2H_5)^1I$
300	$[P_4N_4(CH_3)_8]^+$	10.8	19.0	17.5
285	$[P_4N_4(CH_3)_7]^+$	100.0	100.0	100.0
269	$[P_4N_3(CH_3)_5(CH_2)_2]^+$	3.3	1.5	1.0
257	$[P_4N_3(CH_3)_6H]^+$	2.2	2.0	1.0
226	$[P_3N_3(CH_3)_6H]^+$	1.0	1.5	1.0
224	$[P_3N_3(CH_3)_5(CH_2)]_+$	1.0	1.0	1.0
	$[P_3N_3(CH_3)_5]^+$	23.9	15.5	15.5
210	$[P_3N_2(CH_3)_5(CH_2)]^+$			
	$[P_3N_3(CH_3)_4H]^+$	11.9	7.0	7.2
196	$[P_3N_2(CH_3)_5]^+$			
	$[P_3N_3(CH_3)_3H]^+$	3.3		
181	$[P_3N_2(CH_3)_4]^+$			
	$[P_3N_3(CH_3)_3]$	2.7	4.0	4.1
180	$[P_3N_2(CH_3)_3(CH_2)]^+$			
	$[P_3N_3(CH_3)_2H]^+$			
166	$[P_3N_2(CH_3)_3]^+$	1.0	2.0	1.0
155	$[C_2H_5I]^+$		1.5	20.6
159	$[P_2N_2(CH_3)_4]^+$	3.2	5.0	5.1
150	$[P_4N_4(CH_3)_8]^{2+}$			
142	$[CH_3I]^+$		24.0	1.5
135	$[P_2N_2(CH_3)_2]^+$	15.2	17.5	17.5
127	$[I]^+$		7.5	4.1
122	$[P_2N(CH_3)_3H]^+$	1.6	3.0	2.0
108	$[P_2N(CH_3)_2H_2]^+$	1.0		1.5
106	$[P_2N(CH_3)_2]^+$	2.7	3.0	3.9
98	$[P_3N_3(CH_3)_4H]^{2+}$			
91	$[P_2N(CH_3)]^+$	1.0	2.0	1.5
76	$[PN(CH_3)_2H]^+$	2.1	2.0	2.0
	$[PN(CH_3)H]^+$			
61	$[P(CH_3)_2]^+$	2.1	3.0	3.0
	$[P(CH_3)]^+$	1.0		
46	$[PNH]^+$			

Nota: No se presentan fragmentos con *m/e* < 46.

a $[M-F]^+$, ya que el enlace P$-$F debido a su fortaleza tiende a permanecer preferencialmente inalterado.[3]

Los productos de fragmentación del anillo son especies metiladas, supuestamente cíclicas ($P_nN_nX_{2n-y}$) di tipo P_4N_4, P_3N_3 y P_2N_2 así como especies lineales P_4N_3, P_3N_2, P_2N y PN, de acuerdo con lo postulado para las fragmentaciones de los halógenofosfazenos[2-5]. Los fragmentos con *m/e* 210, 196, 181, 180 y 166 presentan dos fórmulas posibles, especies P_3N_3 ó P_3N_2, pero se puede considerar que al menos las entidades más estables sean de tipo P_3N_3, las cuales contienen un menor número de grupos metilo, ya que se ha establecido que el enlace P—C es bastante débil, siendo por lo tanto preferencial la pérdida de grupos metilo sobre la ruptura del anillo. En las especies $P_3N_3Br_6$ donde la energía del enlace P—Br es similar a la del P—C se tiene que las especies P_3N_2 presentan una abundancia relativa baja.[4] La supuesta mayor abundancia de especies P_3N_3 sobre P_3N_2 es consistente con la presencia de transiciones metaestables que confirman procesos en los cuales hay pérdida de dos grupos metilo a partir de un mismo fragmento, adicionalmente se ha establecido que las especies supuestamente cíclicas son más estables que las lineales.[2]

Los iones metilados del tipo P_2N_2 presentan una abundancia relativa grande en relación a los sistemas halogenados, esto es probablemente debido a que el efecto inductivo de los grupos metilo estabiliza en mayor grado que los halógenos la estructura de tipo P_4 postulada por Coxon[4].

Los espectros de masas no presentan el fragmento *m/e* 225 correspondiente al trímero $[P_3N_3(CH_3)_6]^+$. Los iones doblemente cargados son poco abundantes, a diferencia de la mayoría de los sistemas fosfazénicos, y no se presentan iones triplemente cargados como los que se presentan en la mayoría de los halógenofosfazenos.

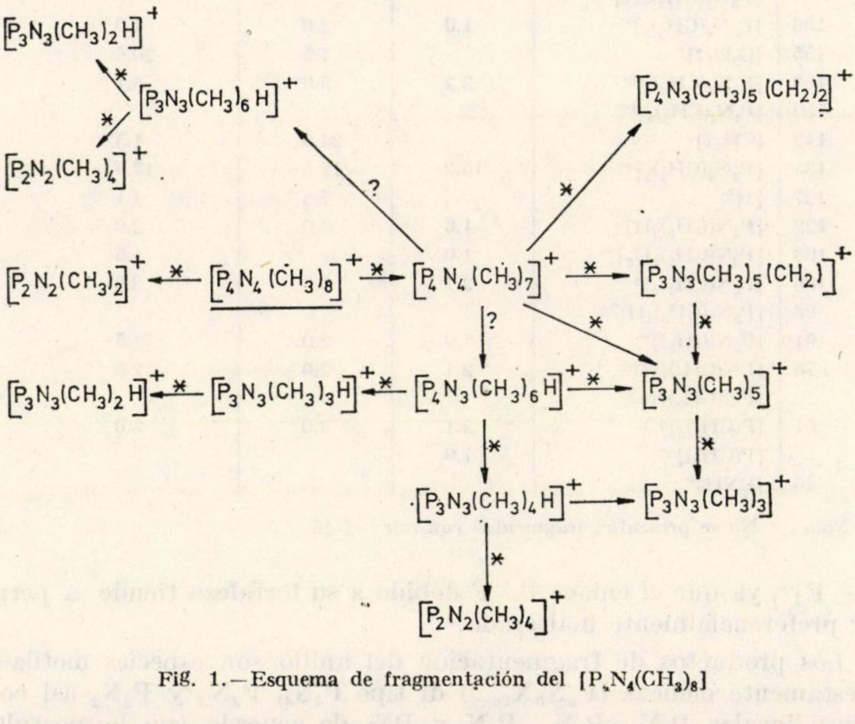

Fig. 1.—Esquema de fragmentación del $[P_4N_4(CH_3)_8]$

A diferencia de los fenilfluorofosfazenos[8] y los fenilclorofosfazenos[7] no se producen rearreglos. En los primeros se presenta un fragmento *m/e* 91 asignado al ion $[NC_6H_5]^+$, el cual supuestamente proviene de la migración de un grupo fenilo de un átomo de fósforo a uno de nitrógeno.

En interesante que en nuestro caso no se detectan fragmentos conteniendo enlace N—C provenientes de rearreglos, ni aún cuando existe originalmente como acontece en las sales cuaternarias.

Los fenilclorofosfazenos[8] y los gem-dialquil-tetrafenilciclotrifosfazatrienos[9] muestran fragmentos abundantes [Ion molecular-H]$^+$, sin embargo no se ha establecido si el hidrógeno proviene de un grupo alquílico o arílico. La ausencia de dichos fragmentos en los compuestos aquí estudiados hace suponer que dicha pérdida [M—1] proviene de los grupos arílicos.

El espectro de masas del $P_4N_4(CH_3)_8$ muestra abundantes transiciones metaestables que sugieren el esquema de fragmentación mostrado en la Fig. 1.

Agradecemos al Dr. Jacobo Gómez Lara la ayuda prestada en el desarrollo de esta investigación.

REFERENCES

[1] C. D. Schmulnbach, A. G. Cook y V. R. Miller, *Inorg. Chem.*, **7**, 2463 (1968).
[2] C. E. Brion y N. L. Paddock, *J. Chem. Soc. A*, **1968**, 388.
[3] C. E. Brion y NL. Paddock, *J. Chem. Soc. A*, **1968**, 392.
[4] G. E. Coxon, T. F. Palmer y D. B. Sowerby, *J. Chem. Soc. A*, **1967**, 1568.
[5] G. E. Coxon, T. F. Palmer y D. B. Sowerby, *J. Chem. Soc. A*, **1969**, 358.
[6] A. J. Wagner y T. Moeller, *J. Chem. Soc. A*, **1971**, 596.
[7] C. W. Allen y P. L. Toch, *J.C.S. Dalton*, **1974**, 1685.
[8] C. W. Allen y otros, *J.C.S. Dalton*, **1978**, 173.
[9] R. Appel y G. Saleh, *Chem. Ber.*, **106**, 3455 (1973).
[10] H. R. Allcock y D.B. Patterson, *Inorg. Chem.*, **16**, 197 (1977).
[11] T. Moeller, H. J. Birch y N. C. Nielsen, *Inorg. Synth.*, **4**, 71 (1953).
[12] P. J. Christen, L. M. Van der Linde y F. N. Hooge, *Rec. Trav. chim.*, **78**, 161 (1959),
[13] H. T. Searle, J. Dyson, T. N. Ranganathan y N. L. Paddock, *J.C.S. Dalton*, **1975**. 203.

Revue Roumaine de Chimie, 25, *4*, 535–540 (1980)

THE ELECTROPHILIC ADDITION OF BROMINE TO 9-HALOGENO-BENZOCYCLOBUTENONORBORNENES[1]

I. G. DINULESCU, L. ENESCU, H. L. PRASAD, AURELIA GHENCIULESCU,
NICOLETA ȘTEFAN and MARGARETA AVRAM

National Institute of Chemistry, Department of Organic Chemistry,
Spl. Independenței 202 B, 76300 Bucharest 15, Romania

Received November 8 , 1979

The addition of bromine to some 9-halogeno-benzocyclobutenonorbornenes is investigated. The reaction of the compounds with *endo* skeleton is accompanied by a skeleton rearrangement to *exo*, while that with *exo* skeleton undergoes a *trans* addition, without rearrangement.

As an extension of our studies on the behaviour of *endo* and *exo*-benzocyclobutenonorbornenes systems in reactions involving cationic intermediates[2] we report now on the synthesis of/and electrophilic bromine addition to the halogeno-alkenes **1**–**3**.

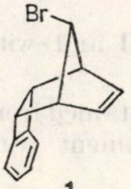

1

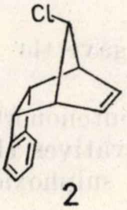

2

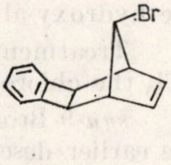

3

The *anti*-9-halogeno-alkenes **1** and **2** with *endo*-benzocyclobutenonorbornene skeleton were obtained through a several steps synthesis, following the route reported by Battiste et al.[3] with some experimental improvements.

The Diels-Alder adduct **(7)**[4] between benzocyclobutadiene **(5)** and dimethoxy-tetrachlorocyclopentadiene **(6)** was obtained according to Nenitzescu's method[5] by treating dibromobenzocyclobutene **(4)** with lithium amalgam in ethereal solution in the presence of **6.** Dehalogenation of **7** with sodium — t-butylalcohol — tetrahydrofurane, followed by hydrolysis

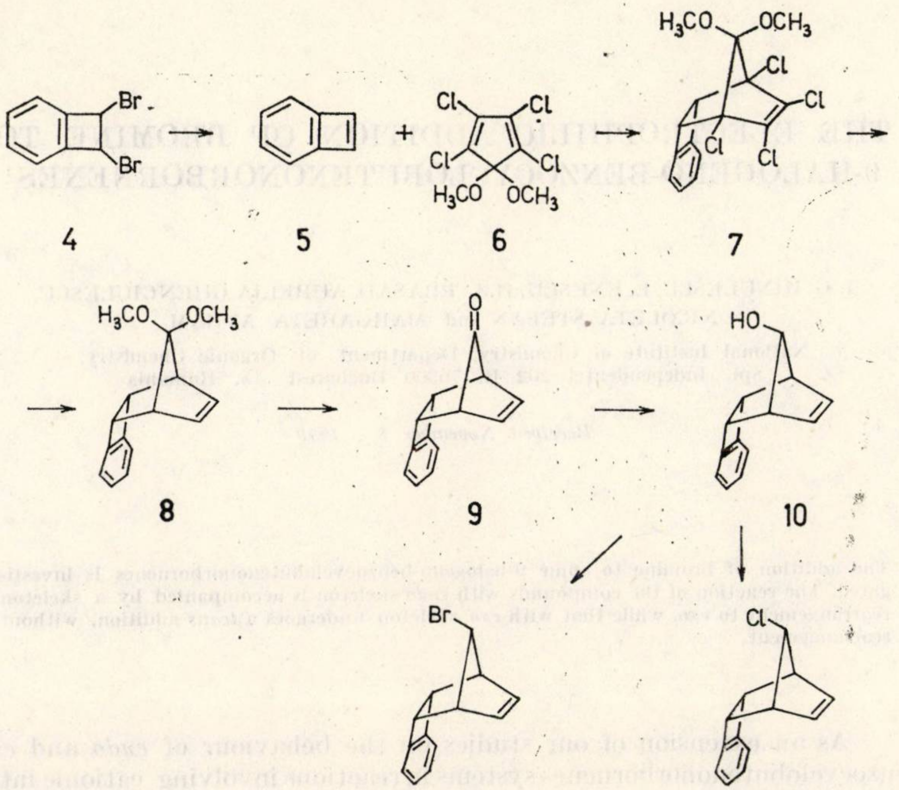
Br
Br
Cl
Cl
Cl
Cl
H₃CO
OCH₃
H₃CO
OCH₃
Cl
Cl
Cl
Cl
H₃CO
OCH₃
O
HO
Br
Cl

4 5 6 7

8 9 10

1 2

of the ketal group, yielded the keto-alkene **9**, which by reduction afforded the hydroxy-alkene **10.**[3]

Treatment of **10** with PBr_3 gave the bromo-derivative **1** and with PCl_3 the chloro-derivative **2.**

syn-9-Bromo-*exo*-benzocyclobutenonorbornene **(3)** was obtained from the earlier described dibromo-derivatives **11** and **12**[2] by treatment with potassium t-butoxide in dimethyl sulphoxide.

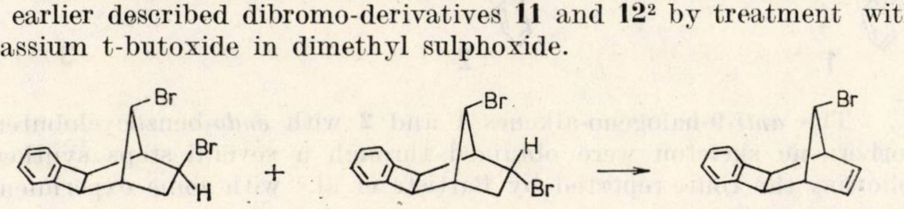
Br
Br
H
+
Br
H
Br
Br

11 12 3

The structures of the new compounds **1**–**3** were ascribed on the basis of analytical and NMR spectral data. In compounds **1** and **2** the signal of the olefinic protons appears as a sharp triplet uncoupled by long range with the H-9 proton. This feature supports the ascribed *anti*-orientation for the bromine in **1** as well as the chlorine in **2** and consequently *syn*-orientation for H-9 proton. In the 9-bromo-alkene **3** the *syn*-orientation of the bromine at C-9 is evidenced by the existence of a long range coupling between the olefinic protons and the H-9-*anti* proton by a large splitted triplet.

The reaction of *anti*-9-bromo-*endo*-benzocyclobutenonorbornene **(1)** with bromine in dichloromethane solution afforded the tribromo-derivative **13** with *exo*-benzocyclobutenonorbornene skeleton. In the same way, the reaction of *anti*-9-chloro-*endo*-alkene **2** with bromine involves a skeleton rearrangement, affording the chloro-dibromide **14.** The tribromide **13** was also obtained (in a very poor yield) from the *syn*-9-bromo-*exo*-alkene **3.** The *syn*-9-bromo-*exo*-alkene **3** was recovered unchanged from our attempts to react it with N-bromosuccinimide in acetic acid.

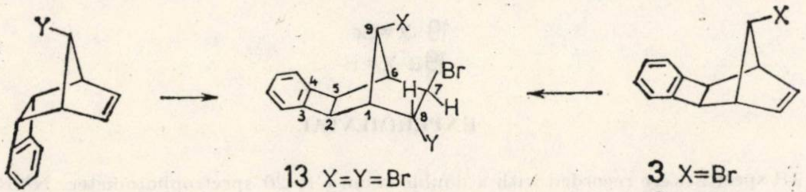

13 X=Y=Br
14 X=Br,Y=Cl

3 X=Br
3a X=H

1 Y=Br
2 Y=Cl
2a Y=H

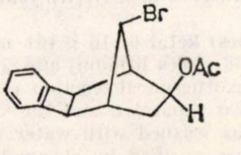

15

The obtention of *trans*-dihalogeno-derivatives **13** and **14** from **1** and **2**, respectively, with rearranged skeleton, is in accordance with the earlier observed behaviour of the parent compound **2a.** The latter, by treatment with bromine in non-polar media, gave the mixture of **11** and **12** and by solvolytic addition, the acetoxy-derivative **15**, with rearrangement from the *endo* system in the *exo* one.[2]

The different behaviour of **3** in respect of the parent compound **3a**, namely the failure to react with bromine in polar media, and the low yield in the reaction with bromine in nonpolar media, can be explained if the stereochemistry of the intermediates **16**—**18** is considered.

In **16** the *endo* attack of the bromide ion, Br^-, is hindered on sterical ground, and consequently the nonclassical ion **17** captures the nucleophile ; it is unprobable that an ion like **18** has a role in this reaction.

The behaviour of **3** seems to indicate that even the occurrence of the intermediate **19** is unfavoured on sterical ground, namely by the presence of the bulky *syn* orientated bromine atom at C-9.

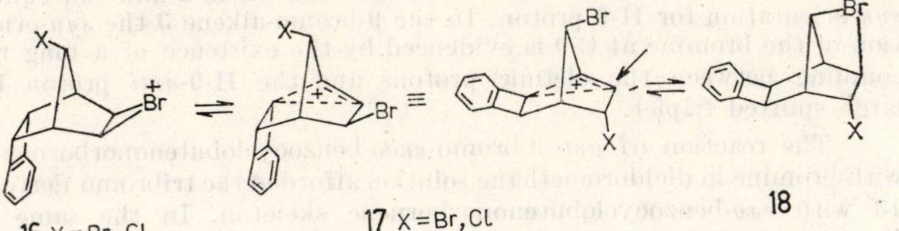

16 X = Br, Cl   17 X = Br, Cl   18

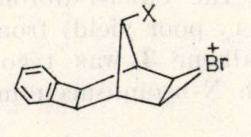

19 X = Br
19a X = H

EXPERIMENTAL

IR spectra were recorded with a double beam UR 20 spectrophotometer. NMR spectra were determined with a Varian A-60A spectrometer.

9.9-Dimethoxy-1.6.7.8-tetrachloro-*endo*-benzo[*c*]tricyclo[4.2.1.$0^{2.5}$]nona-3.7-diene (7)

A mixture of 20 g (75.8 mmoles) ketal **6**, 16 g (61 mmoles) dibromobenzocyclobutene (**4**), 540 g 0.5% lithium amalgam (0.38 moles lithium) and 250 ml anhydrous ether was stirred in a stoppered bottle. After the exothermical reaction ceased, the bottle was stirred further for 2 hours. The ethereal layer was separated and the slurry extracted for several times with ether. The organic solution was washed with water and dried. The solvent was evaporated and the crystalline residue was purified by chromatography on alumina with petroleum ether — diethyl ether 10: 1, yielding 4.5 g (25%) **7**, m.p. 130°. The spectral data and m.p. are in accordance with the earlier described compound.[4]

9.9-Dimethoxy-*endo*-benzo[*c*]tricyclo[4.2.1.$0^{2.5}$]nona-3.7-diene (8)

Into a suspension of 12 g (0.5 moles) sodium in 100 ml anhydrous tetrahydrofurane and 20 ml t-butyl alcohol, a solution of 5.0 g (13.5 mmoles) tetrachloro-adduct **7** in 75 ml tetrahydrofurane was added, and the mixture was boiled for 20 hours. The organic layer was separated and the solid residue was washed for several times with ether. After washing with water and drying, the ether was removed, yielding 2.7 — 3.0 g (87 — 96%) **8**, m.p. 78°. $C_{15}H_{16}O_2$ Calcd.: C, 78.91; H, 7.06. Found: C, 78.70; H, 7.25.

NMR spectrum (CCl_4, δ, ppm): 2.95 (m, 2H, H—1 and H—6), 3.08 — 3.18 (2s, 6H from methoxy groups,) 3,68 (m, 2H, H—2 and H—5), 5.52 (t, 2H, H—7, and H—8, $J = 2.0$ Hz), 6.60 — 7.20 (m, 4 aromatic H).

endo-Benzo[*c*]tricyclo[4.2.1.$0^{2.5}$]nona-3.7-dien-9-one (9)

A solution of 2.1 g (10 mmoles) adduct **8** in 30 ml ether was stirred with 5 ml 35%. hydrochloric acid for one hour. After working up, 1.52 g (95%) **9**, m.p. 44°, were obtained. $C_{13}H_{10}O$ Calcd.: C, 85.68; H, 5.53. Found: C, 85.40; H, 5,70.

IR spectrum (CCl_4): ν_{co} 1772 cm^{-1}.

NMR spectrum (CCl_4, δ, ppm): 3.11 (m, 2H, H—1 and H—6), 3.73 (m, 2H, H—2 and H—5), 5.97 (t, 2H, H—7 and H—8, $J = 2.0$ Hz), 6.75 — 7.38 (m, 4 aromatic H).

anti-9-Hydroxy-*endo*-benzo[*c*]tricyclo[4.2.1.$0^{2,5}$]nona-3.7-diene (10)

A solution of 0.6 g (3 mmoles) **9** in 30 ml anhydrous ether was dropped into an ethereal suspension of 0.5 g lithium aluminium hydride and the mixture was stirred at room temperature for 12 hours. After working up, 0.5 g (83%) hydroxy-alkene **10** were obtained; m.p. 139° (from diluted methanol).

$C_{13}H_{12}O$ Calcd.: C, 84.75; H, 6.57. Found: C, 84.90; H, 6.48.

IR spectrum (CCl_4): ν_{OH} 3632 cm^{-1}.

NMR spectrum ($CDCl_3$, δ, ppm): 1.94 (broad s, 1H, OH), 2.80 (m, 2H, H−1 and H−6), 3.95 (m, 2H, H−2 and H−5), 4.18 (broad s, 1H H−9), 5.60 (t, 2H, H−7 and H−8, $J = 2.0$ Hz), 6.75 − 7.35 (m, 4 aromatic H).

anti-9-Bromo-*endo*-benzo[*c*]tricyclo[4.2.1.$0^{2,5}$]nona-3.7-diene (1)

A solution of 0.50 g (2.7 mmoles) **10** in 10 ml dichloromethane was added to a solution of 1 ml phosphorous tribromide in 10 ml dichloromethane, and the mixture was left at room temperature for 24 hours. Water was added and the organic layer was washed with water until neutral and dried. After evaporation of the solvent, the residue was purified by chromatography on alumina with petroleum ether, yielding 0.48 g (71%) **1**, m.p. 66°.

$C_{13}H_{11}Br$ Calcd.: C, 63.18; H, 4.49; Br, 32.34. Found: C, 63.29; H, 4.60; Br, 32.01.

NMR spectrum (CCl_4, δ, ppm,): 3.00 (m, 2H, H−1 and H−6), 4.11 (m, 2H, H−2 and H−5), 4.28 (broad s, 1H, H−9-*syn)*, 5.65 (t, 2H, H−7 and H−8, $J = 2.0$ Hz), 6.70−7.20 (m, 4 aromatic H).

anti-9-Chloro-*endo*-benzo[*c*]tricyclo[4.2.1.$0^{2,5}$]nona-3.7-diene (2)

Working as above, but using phosphorous trichloride, the chloro-derivative **2** was obtained in 45% yield; m.p. 55°.

$C_{13}H_{11}Cl$ Calcd.: C, 77.03; H, 5.47; Cl, 17.49. Found: C, 76.76; H, 5.68; Cl, 17.64.

NMR spectrum (CCl_4, δ, ppm): 2.96 (m, 2H, H−1 and H−6), 4.06 (m, 2H, H−2 and H−5), 4.20 (broad s, 1H, H−9-*syn)*, 5.66 (t, 2H, H−7 and H−8, $J = 2.0$ Hz), 6.70−7.20 (m, 4 aromatic H).

syn-9-Bromo-*exo*-benzo[*c*]tricyclo[4.2.1.$0^{2,5}$]nona-3.7-diene (3)

The addition of bromine to *endo*-benzocyclobutenonorbornene was carried out according to the literature data[2] affording a mixture of dibromo-derivatives **11** and **12**.

Into a mixture of 5.0 g (44 mmoles) potassium t-butoxide and 100 ml anhydrous dimethyl sulphoxide, heated at 100°, 11.4 g (35 mmoles) crude dibromides **11** and **12** were added, under vigorously stirring, and the mixture was further heated at 100° for 2 hours. The cold reaction product was treated with water and extracted with dichloromethane. The organic layer was washed with water, dried and evaporated in vacuum. The brown residue (6.8 g) was chromatographied on alumina with petroleum ether, yielding 5.5 g (67%) **3**, m.p. 93−93.5° (methanol).

$C_{13}H_{11}Br$ Calcd.: C, 62.82; H, 4.44; Br, 32.32. Found: C, 62.99; H, 4.69; Br, 32.72.

NMR spectrum (CCl_4, δ, ppm): 3.03 (broad s, 2H, H−1 and H−6), 3.25 (s, 2H, H−2 and H−5), 3.56 (broad s, 1H, H−9-*anti)*, 6.20 (broad s, 2H, H−7 and H−8), 6.96 − 7.30 (m, 4 aromatic H).

Addition of bromine to *anti*-9-bromo-*endo*-alkene 1

A solution of 0.25 g (1 mmole) **1** in 20 ml dichloromethane was treated with an excess of 5% solution of bromine in dichloromethane. After 2 hours the solvent was removed, yielding 0.35 g (85%) *exo*-7-*endo*-8-*syn*-9-tribromo-*exo*-benzo[*c*]tricyclo[4.2.1.$0^{2,5}$]non-3-ene **(13)**, m.p. 141°.

$C_{13}H_{11}Br_3$ Calcd.: C, 38.37; H, 2.72; Br, 58.90. Found: C, 36,20; H, 2.94,; Br, 59.10.

NMR spectrum (CCl_4, δ, ppm): 2.76 (d, 1H, H−1, $J_{1.8} = 4.0$ Hz), 2.86 (broad s, 1H H−6), 3.46 (d, 1H, H−5, $J_{2.5} = 4.0$ Hz), 3.70 (m, 1H, H−7-*endo*, $J_{7\text{-}endo.\,8\text{-}exo} = 4.0$ Hz $J_{7\text{-}endo.\,9\text{-}anti} = 2.0$ Hz), 4.10 (d, 1H, H−2, $J_{2.5} = 4.0$ Hz), 5.15 (t, 1H, H-8-*exo*, $J_{1.8\text{-}exo} = J_{7\text{-}endo.\,8\text{-}exo} = 4.0$ Hz), 7.00−7.40 (m, 4 aromatic H).

Addition of bromine to *anti*-9-chloro-*endo*-alkene 2

A solution of 0.40 g (2 mmoles) **2** in 20 ml dichloromethane was treated with an excess of 5 % solution of bromine in dichloromethane. After working up, 0.60 g (80 %) **14** were obtained.

$C_{13}H_{11}Br_2Cl$ Calcd.: C, 43.07; H, 3.06; Hlg, 53.68. Found: C, 43.32; H, 3.24; Hlg, 53.50.

NMR spectrum (CCl_4, δ, ppm): 2.71 (d, 1H, H−1, $J_{1.8}$ = 4.0 Hz), 2.85 (s, 1H, H−6), 4.06 (d, 1H, H−2, $J_{2.5}$=4.0 Hz), 5.11 (t, 1H, H−8, $J_{1.8\text{-}exo}=J_{7\text{-}endo.\ 8\text{-}exo}$=4.0 Hz), 6.90−7.40 (m, 4 aromatic H).

Addition of bromine to *syn*-9-bromo-*exo*-alkene 3

Addition of bromine to **3** as above afforded with approximately 20 % yield the tribromo-derivative **13**, identified by its IR and NMR spectra, identical with those of the above described compound.

syn-9-Bromo-*exo*-alkene **3** was recovered unchanged on treating with an equivalent of NBS in acetic acid, in the presence of catalytic quantities of concd. sulphuric acid or anhydrous sodium acetate.

REFERENCES

[1] Part L of Investigations in the Cyclobutane Series. For Part XLIX see: A. Ghenciulescu, I. G. Dinulescu, H. L. Prasad, L. Enescu and M. Avram, *Rev. Roumaine Chim.*, **24**, 1159 (1979).

[2] a) M. Avram, I. Pogany, F. Badea, I. G. Dinulescu and C.D. Nenitzescu, *Tetrahedron Letters*, **1969**, 3851; b) M. Avram, I. Pogany, I. G. Dinulescu, F. Chiraleu and C. D. Nenitzescu, *Rev. Roumaine Chim.*, **15**, 1027 (1970); M. Avram, F. Chiraleu and I. Pogany, *Rev. Roumaine Chim.*, **15**, 1213 (1970); c) L. Enescu, H. L. Prasad, I. G. Dinulescu, A. Ghenciulescu, F. Chiraleu and M. Avram, *Rev. Roumaine Chim.*, **24**, 999 (1979).

[3] M. A. Battiste and J. W. Nebzydoski, *J. Amer. Chem. Soc.*, **92**, 4450 (1970).

[4] A. J. Boulton and J. F.W. McOmie, *J. Chem. Soc.*, **1965**, 2549.

[5] C. D. Nenitzescu, M. Avram and D. Dinu, *Chem. Ber.*, **90**, 2541 (1957).

Revue Roumaine de Chimie, 25, *4*, 541–545 (1980)

NOUVELLE SYNTHÈSE DE DIAZA-1,5 BICYCLO[4.4.0]DÉCANES

GUY RICART et DANIEL COUTURIER
Université des Sciences et Techniques de Lille
BP 36, 59650 Villeneuve d'Ascq, France

Reçu le 27 octobre 1978

Les N-(hydroxy-5 pentyl) propanediamines-1,3 primaire/secondaire et bisecondaires, chauffées sur nickel de Raney W2 se cyclisent pour donner les octahydropyrido [1,2-a] pyrimidines correspondantes. Dans les mêmes conditions, l'[(aziridinyl-1)-3 propylamino]-5 pentanol-1 fournit un mélange de diaza-1,5 et éthyl -5 diaza-1,5 bicyclo [4.4.0] décanes. L'analyse conformationnelle de ces dérivés est abordée.

Différentes méthodes de préparation des diaza-1,5 bicyclo [4.4.0] décanes sont décrites dans la littérature.[1] Le but de cette communication est de proposer et détailler une nouvelle voie d'accès à ce genre de composé bicyclique ; une présentation sommaire en a été donnée antérieurement.[2]

$HO(CH_2)_5NH(CH_2)_3NR^1R^2$

1 a: $R^1=R^2=H$
b: $R^1=C_2H_5, R^2=H$
c: $R^1, R^2=-(CH_2)_2-$

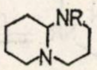

2 a: $R=H$
b: $R=C_2H_5$

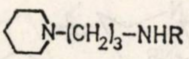

3 a: $R=H$
b: C_2H_5

Cette synthèse a pour point de départ la cyanoéthylation de l'ω-hydroxy-amylamine ; la réduction sur nickel Raney en milieu alcoolique légèrement basique transforme le nitrile en amine primaire *1a*. L'hydrogénation catalytique directe du mélange de base *1a* et d'éthanal permet d'obtenir l'amine N-éthylée *1b*. Ces diaminoalcools *1a*, *1b* se cyclisent dans le toluène à reflux en présence de nickel Raney « alcalin » pour donner respectivement les dérivés hexahydropyrimidines attendus *2a*, *2b ;* la transformation s'accompagne de la présence en faible quantité des pipéridines *3a* et *3b :* la N-aminoalkylpipéridine *3a* est facilement éliminée par réaction avec l'aldéhyde salicylique, la pipéridine *3b* avec le chlorure de benzoyle et les diaza-1,5 bicyclo [4.4.0] décanes correspondants sont alors isolés par une simple distillation.

L'((hydroxy-5 pentylamino)-3 propyl)-1 aziridine *1c*,[2a] chauffé dans le même solvant en présence du même catalyseur fournit en mélange les deux produits *2a*, *2b* dans un rapport molaire 55/45. Dans les conditions assez dures où s'effectue la réaction il y aurait hydrogénolyse du cycle aziridinique suivie d'une cyclisation immédiate des diaminoalcools *1a*, *1b* formés *in situ ;* une seconde hypothèse consiste à envisager la réaction concurrente d'hydrogénolyse de l'aziridinium issu directement de l'aminohydrine postulée au schéma 1 ou formé par addition intramoléculaire sur l'immonium intermédiaire.

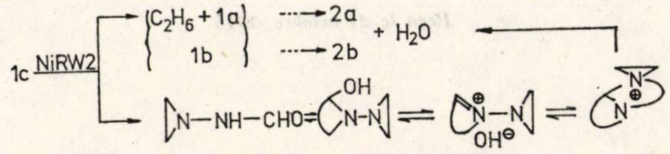

ÉTUDE DE L'ÉQUILIBRE CONFORMATIONNEL

L'analyse des spectres infra-rouge et de résonance magnétique nucléaire montre que les diaza-1,5 bicyclo [4.4.0] décanes obtenus existent essentiellement dans la conformation I (schéma 2) dans laquelle les cycles pipéridine et hexahydropyrimidine sont en jonction *trans*.

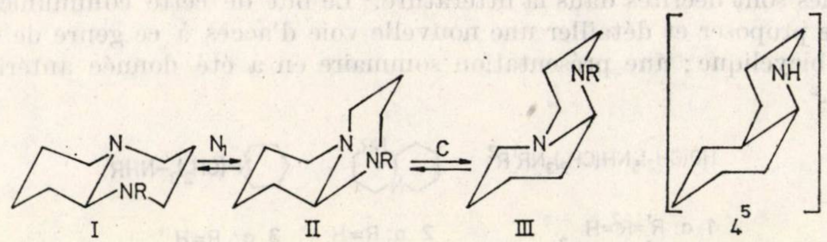

En infrarouge la présence de bandes d'absorption entre 2700 et 2800 cm^{-1}, région des bandes de Bohlmann,[3] permet en première approximation d'éliminer le conformère II pour lequel existent des effets stériques de type γ-gauche : le doublet libre d'un azote ne peut être anticoplanaire à la fois à deux protons axiaux situés en α de N ; toutefois l'application du critère de Bohlmann est ici rendue plus compliquée par la présence du deuxième atome d'azote. En RMN, l'absence de signaux pour une valeur de δ, supérieure à celle d'un proton équatorial des méthylènes en α de l'azote implique une disposition axiale du proton H_6 par rapport aux deux cycles ; en effet pour les aza-1 bicyclo [4.4.0] décanes (quinolizidines) substitués, à jonction *cis*, les quinolizidines à jonction *trans* et l'aza-2 bicyclo [4.4.0] décane *cis-4* (décahydroquinoline *cis)*, l'hydrogène porté par le carbone tête de pont lié à l'azote, résonne respectivement à

3 ; 1,7[4] et 2,65 ppm[5] ; la valeur approximative de 2,60 ppm trouvée pour le composé *2a*, très proche de celle donnée pour la décahydroquinoline *cis*, permet d'exclure la géométrie III, le remplacement du CH tête de pont par un atome d'azote, ayant son doublet libre en *cis* par rapport au proton H_6, devant provoquer un net déblindage de celui-ci et donc un glissement chimique très supérieur à 2,65 dans la conformation III.

Pour R=éthyle, on peut admettre qu'il y a nette prédominance de l'espèce R équatoriale. Crabb et Newton[6] ont montré que pour les alkyl-3 diaza-1,3 bicyclo [4.4.0] décanes non substitués, l'effet de répulsion des lobes des orbitales de l'azote d'origine polaire ("rabbit ear effect") n'était pas suffisant pour que le N-substituant éthyle adopte de façon appréciable la position axiale. Pour notre système la différence d'énergie libre entre les conformations où le groupe éthyle est en position axiale ou en orientation équatoriale est comparable à celle des diaza-1,3 bicyclo [4.4.0] décanes.

Pour R=H, nous aurions inversion de l'atome d'azote en position 5 ; la comparaison des spectres infrarouges montre que le composé *2a* absorbe moins dans la région des bandes de Bohlmann que son dérivé N-éthylé : cette différence peut provenir du dépeuplement de l'invertomère à NH axial et (ou) des liaisons C—H du méthylène du groupe N-éthyle (les amines secondaires et tertiaires ayant des hydrogènes en α absorbent la région 2700—2800 cm^{-1}.[7]

PARTIE EXPÉRIMENTALE

A) Cyclisation de l'(aziridinyl-1)-9 aza-6 nonanol-1 *(1c)* sur nickel Raney W2 dans l'éthylbenzène à reflux

Nous employons le mode opératoire décrit par Venot.[2b] Le rendement en produits *2a*, *2b* est de 30 %; leurs proportions sont évaluées par CPV analytique et par dosage protométrique; ils sont séparés par CPV sur colonne Carbowax 2OM (20 %) — potasse (5 %) d'une longueur de 6 m à la température de 180°.

B) Synthèse de l'octahydro-1,3,4,6,7,8,9,9a 2H-pyrido[1, 2-a]pyrimidine *(2a)*

1) *Synthèse du diaminoalcool 1a*

a) *Obtention du (cyano-2-éthylamino)-5 pentanol-1:* On l'obtient par addition à 10° de l'acrylonitrile (21 g) à l'hydroxy-5 pentylamine (41,5 g) en solution dans 20 ml de THF; on abandonne pendant 48 heures et élimine le solvant.

b) *Hydrogénation sur nickel Raney du produit brut de cyanoéthylation:* La réduction sous pression et en solution dans l'alcool (80 ml) en milieu N en KOH est terminée après 7 heures d'agitation à température ambiante. Le rendement est de 75 % par rapport à l'aminopentanol de départ.

(Amino-3 propylamino)-5 pentanol-1 *(1a)* : $C_8H_{20}N_2O$, M: 160, 26.
$Eb_{0,3}$: 122°; $n_D^{20} = 1,4832$; $d_4^{18}=0,964$.
N % *calculé :* 17,48; *trouvé :* 17,22.
Infrarouge (film) ν (cm^{-1}): 3250 (bande OH intense); 1610 (vibration de déformation NH_2).

2) *Cyclisation sur nickel Raney W2 dans le toluène*

Nous employons la technique précédente. Le rendement de la cyclisation est de 31 %. La N-(amino-3 propyl) pipéridine *(3a)* représente 11,5 % du mélange; les proportions relatives sont évaluées en dosant un échantillon avec une liqueur titrée d'acide chlorhydrique en solution dans l'isopropanol, car dans ces conditions un seul des deux atomes d'azote de l'octahydro 2H-pyrido[1.2-a]pyrimidine est dosable.

Le diaza-1,5 bicyclo [4.4.0] décane *(2a)* est isolé par distillation, après avoir transformé la N-(amino-3 propyl) pipéridine à l'état d'imine de l'aldéhyde salicylique.

— Diaza-1,5 bicyclo[4.4.0] décane *(2a)* : $C_8H_{16}N_2$, M :140,25.
$Eb_{2,5} = 58°$; $n_D^{20} = 1,4970$; $d_4^{19} = 0,970$.
Litt. $Eb_4 = 62-63°$[1a] ; $Eb_{11} = 85°$; $n_D^{25} = 1,4940$; [1b] $Eb_{10} = 83°$. [1c]
— Picrate : $C_{20}H_{22}N_8O_{14}$, M :598,47. N basique % : *calculé :* 4,68 ; *trouvé* 4,62 F : 165° (EtOH) litt. F = 165—166° [1c].
Monochlorhydrate : $C_8H_{17}N_2Cl$: Le chlorhydrate précipite par passage de HCl sec dans une solution éthéroalcoolique de la base *2a*. Cl % : *calculé :* 20,08 : *trouvé :* 20,30. F_{inst} : 172—175°.
IR : 3290 cm^{-1} : vibration de valence NH.
RMN (CCl_4 ; Ref. TMS) δ : 2,98 : H_e^4 ; 2,08 : s, NH (variable avec la dilution).
— N-(amino-3-propyl) pipéridine : $C_8H_{18}N_2$, M : 142,25.
$Eb_{16} = 92°$; $n_D^{20} = 1,4758$; $d_4^{18} = 0,903$. N % *calculé :* 19,69 ; *trouvé :* 19,42.
IR : 3333, 3246, 1613 cm^{-1} : vibrations NH_2.
Imine de l'aldéhyde salicylique : $C_{15}H_{22}N_2O$.
$n_D^{20} = 1,5555$. N % *calculé :* 11,37 ; *trouvé :* 11.21.
IR : 1634 cm^{-1} : C=N.
La N-(amino-3 propyl) pipéridine *(3a)* a été obtenue avec un rendement de 80 % (par rapport à la pipéridine) en employant la méthode de Whitmore et coll.[8] (condensation de la pipéridine avec l'acrylonitrile et réduction catalytique).

C) Synthèse de l'éthyl-1 heptahydro-3,4,6,7,8,9,9a 2H-pyrido[1,2-a] pyrimidine (*2b*) :

1) *Synthèse du diaminoalcool 1b*

L'acétaldéhyde (22,8 g) est ajouté lentement à l'aminoalcol *1a* (80 g) en solution dans la potasse éthanolique ; la température du milieu est maintenue vers 10° ; après hydrogénation à 20° pendant 18 heures sur nickel Raney (20 g) et sous pression (120 kg), nous obtenons l'aminoalcool *1b* avec un rendement de 70 % (évalué par rapport à l'-ω-hydroxyamylamine de départ).

2) *Cyclisation sur nickel Raney W2 dans l'éthyl benzène*

Nous récupérons avec un rendement de 51 % un mélange de composés *2b* et *3b* dans le rapport 80/20 ; ils sont séparés par chromatographie. Le dérivé bicyclique *2b* peut aussi être isolé par simple distillation après transformation de la pipéridine *3b* en N-éthyl N-(pipéridino-3 propyl) benzamide.

— Ethylamino-5 propylamino-5 pentanol-1 *(1b)* : $C_{20}H_{24}N_2O$, M : 188,32.
$Eb_{0,3} = 125°$; $n_D^{20} = 1,4790$; $d_4^{18} = 0,948$.
IR : 3270 cm^{-1} : bande OH intense.
RMN (CCl_4) δ : 3,47 : t : (5,5 Hz), CH_2O ; 2,58 ; m, CH_2N ; 2,78 : N*H* et O*H* ; 1,07 : *t*(7,5 Hz), CH_3
— Ethyl-5 diaza-1,5 bicyclo (4.4.0) décane *(2b)* : $C_{10}H_{20}N_2$, M : 168,30.
$Eb_2 = 77°$; $n_D^{20} = 1,4910$, $d_4^{19} = 0,939$.
Picrate : $C_{22}H_{26}N_8O_{14}$, M : 626,52. N basique % : *Calculé :* 4,47 ; *trouvé :* 4,42.
F = 70° (CH_3OH, Et_2O).
RMN (CCl_4) δ : 2,90 : H_e en α de N ; 2,62 : q, CH_2N exocyclique ; 0,94 : t , $^3J = 7,5$ Hz CH_3.
— N-(éthylamino-3 propyl) pipéridine : $C_{10}H_{22}N_2$, M : 170,30.
$Eb_2 = 72°$; $n_D^{20} = 1,4652$; $d_4^{18} = 0,879$.
IR : 3333 cm^{-1} : vibration de valence NH.
RMN (CCl_4) : 1,05 : t, $^3J = 7,25$ Hz, CH_3 ; 1,25 : s, N*H* ; 1,35 à 1,85 : massif complexe $4CH_2$; 2,10 à 2,85 : m, CH_2N.

Ce produit *3b* a été authentifié par comparaison avec un échantillon synthétisé à partir de la pipéridine. Le produit brut de cyanoéthylation, obtenu par condensation de 31 g de pipéridine avec 20 g d'acrylonitrile, est hydrogéné en solution dans l'alcool (50 ml) en milieu 1N en KOH : la réduction en présence de nickel Raney vers 20° à la pression de 120 kg est terminée en 4 heures ; on ajoute lentement 16 g d'acétaldéhyde en maintenant la température entre 5 et 10° ; l'addition d'aldéhyde est contrôlée par infrarouge ; l'imine formée est hydrogénée dans les mêmes conditions que précédemment ; le rendement en pipéridine *3b* évalué par rapport à la pipéridine de départ est de 60 %.

BIBLIOGRAPHIE

[1] a) T. Yamazaki, M. Nagata, H. Araki et F. Nohara, *Yakugaku Zasshi*, **88**, 212 (1968) ; *Chem. Abstr.*, **69**, 52096 (1968).
b) R. L. Peck et A. R. Day, *J. Heterocy. Chem.*, **6**, 181 (1969).
c) E. E. Mikhlina, A. D. Yanina et M. V. Rubsov, *Khim. Geterotsikl. Soedin.*, **1969**, 547 ; *Chem. Abstr,.* **71**, 124366 (1969).
d) H. Mohrle et S. Mayer, *Arch. Pharm.*, **306**, 209 (1973).
[2] a) G. Ricard, D. Couturier, et C. Glacet, *Compt. rend.*, **280**, 953 (1975).
b) A. Venot, *Bull. Soc. chim. France.*, **1972**, 4736.
[3] F. Bohlmann, *Chem. Ber.*, **91**, 2157 (1958).
[4] F. Bohlmann, D. Schumann et C. Arndt, *Tetrahedron Letters*, **1965**, 2705.
[5] H. Booth et A. H. Bostock, *Chem. Comm.* **1967**, 177.
[6] T. A. Crabb et R. F. Newton, *Tetrahedron*, **26**, 701 (1970).
[7] K. Nakanishi, T. Goto et M. Ohashi, *Bull. Chem. Soc. Japan*, **30**, 403 (1957).
[8] F. C. Whitmore, U. S. Moslaw, R. R. Adams et R. B. Taylor, *J. Amer. Chem. Soc.*, **66**, 725 (1944).

Revue Roumaine de Chimie, 25, 4, 547 – 557 (1980)

THE OXIDATION OF TRICHLOROETHYLENE WITH MOLECULAR OXYGEN

A. C. RĂZUŞ, ALICE MARIE GLATZ, ZS. ARVAY, F. IORDACHE and F. BADEA
Center of Organic Chemistry, Spl. Independenţei 202B, 78100 – Bucharest, Romania
Department of Organic Chemistry, National Chemical Institute

Received August 2, 1979

The oxidation mechanism of trichloroethylene to dichloroacetic acid chloride with molecular oxygen initiated by benzoyl peroxide and azo-bis-isobutyronitrile is discussed. The purpose of this work is to obtain better information on the epoxidation process.

INTRODUCTION

The oxidation of alkenes with molecular oxygen yields as primary oxidation product an allylhydroperoxide. At low conversions of the alkene, the hydroperoxide may be sometimes isolated in high yields, as in the case of cyclohexane[1]. However, some other alkenes, in similar oxidation processes, form epoxides as the main oxidation product. If the mechanism of the hydroperoxide formation is now known in every detail[2] the epoxide formation seems, so far as we known less understood.

Most of our knowledge of the epoxidation reaction comes from the extensive study of Mayo and coworkers.[3,4] These authors have shown that certain readily polymerizable or copolymerizable olefins, such as styrene and α-methylstyrene, may form a 1:1 copolymer of oxygen and olefin. The thermal decomposition of the copolymer yields carbonyl compounds and/or epoxides.[3,5] In the formation of the copolymer, peroxy radicals, **2**, are involved. On the other hand, peroxy radicals result either from hydroperoxides or are key intermediates in their formation. Thus, if appropiate conditions are met, both hydroperoxides and epoxides could be observed.

An experimental proof of the involvement of peroxy radicals in both types of autoxidation of alkenes was produced by Serée de Roche and Balaceanu [6]. They have studied the oxidation of cyclooctene and compared it with the oxidation of cyclohexene. Whereas the latter is oxidized to the hydroperoxide in a highly specific way (98 % selectivity), cyclooctene forms preponderently the epoxide (65 % selectivity). The reaction kinetics is similar and peroxy radicals could be detected in both processes. However, cyclohexene reacts about 8 times more rapidly than cyclooctene.

Considering these results, the oxidation of alkenes with available allylic hydrogen could be represented as follows :

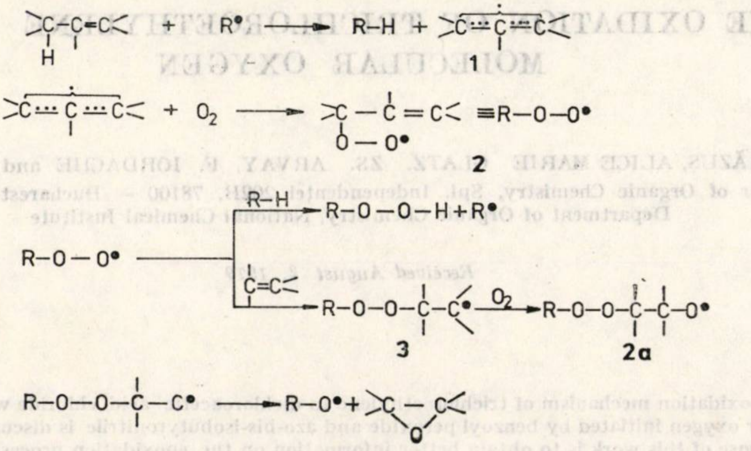

Scheme I

Actually, scheme 1 is a simplification of Mayo's copolymerization mechanism[3,4] stressing only the fact that the intermediate peroxy radicals may either yield the hydroperoxides by hydrogen abstraction or form the epoxide by addition to the double bond. Radicals **2**, **3** and **2a** are also involved in the copolymerization.

The behaviour of peroxy radicals towards double bonds has been since then, amply exemplified by other researchers.[7] Thus, the copolymerization mechanism of certain olefins with oxygen is considered to be responsible for the epoxidation reaction of alkenes with molecular oxygen.[8] Clearly, the mechanism needs the alkene to have an allylic hydrogen and does not easily explain the epoxidation of alkenes with no available allylic hydrogen. However, it has been shown recently that olefins may directly react with oxygen to form a charge-transfer complex, with the alkene as electron donor and oxygen as electron acceptor. Such complexes are precursors in the formation of polymeric peroxides of styrene (with no allylic hydrogen) and of α-methylstyrene.[9]

The formation of dichloroacetic acid chloride from trichloroethylene is a well-known industrial process.[10,11] Poluektov and coworkers[11] are, in our information, those who first studied the kinetics of trichloroethylene oxidation to dichloroacetic acid chloride. Using a radiative initiation of the process, they have found dichloroacetic acid chloride and trichloroethyleneoxide to be the main oxidation products, the epoxide being the major of the two (epoxide : chloride = 3 : 2). They conclude from the reaction kinetics that a copolymerization mechanism is also involved in trichloroethylene autoxidation, the epoxide being the autoxidation intermediate. However, they have later shown[12] that the epoxide is not thermally isomerized into the acid chloride, in the autoxidation conditions.

We have felt that the copolymerization mechanism of trichloroethylene (TCE) is not so clear-cut as it is in the other epoxidation reactions. Neither has TCE an allylic hydrogen, nor has the double bond an outstanding reactivity. Moreover, from other known reactions, TCE is rather an electrophilic alkene. Thus, it could not be expected to yield charge-transfer complexes with highly electron deficient species.

The present paper studies the autoxidation of trichloroethylene initiated by benzoyl peroxide and azo-bis-isobutyronitrile. We hoped to get some better insight into the epoxidation process by comparing two different initiators of the reaction.

RESULTS

The autoxidation reaction of TCE was performed by bubbling oxygen in a vigorously stirred solution of an initiator in TCE. Either benzoyl peroxide or azo-bis-isobutyronitrile were used. Special care was kept in order to prevent loss of volatile compounds. The reaction was studied between 64° and 84°, and was maintained during an experiment in the limits of ±1°. At regular intervals, samples were withdrawn from the reaction mixture and analyzed gas-chromathographically. Some results observed in the benzoyl peroxide initiated oxidation are given in tables 1 and 2, whereas tables 3 and 4 present the results determined in the azo-bis-isobutyronitrile initiated reaction. As shown, neglecting an initial induction period, the overall rate of TCE disappearance is best represented

TABLE 1

Trichloroethylene oxidation with oxygen ; temperature 77° ; initiator benzoyl peroxide (0.0031 M) ; oxygen : 3.6 l/h

Time (minutes)	$10^4 . k(\mathrm{min}^{-1})$	Time (minutes)	10^4 k (min^{-1})	Observations
30	24*	270	39.5	*Induction period
60	37.4*	300	41.7	
100	40.7	330	40.33	
120	40.5	360	41.0	
140	43.8	390	39.7	mean value =
160	40.7	420	40.3	41.43±2.95
180	44.7			
210	44.3			10^{-4} min^{-1}
240	41.3			

TABLE 2

Trichloroethylene oxidation with oxygen ; temperature 77° ; initiator : benzoyl peroxide (0.00207 M) ; oxygen : 3.6 l/h

Time (minutes)	$10^4 \cdot k\,(\mathrm{min}^{-1})$	Time (minutes)	$10^4 k(\mathrm{min}^{-1})$	Observations
35	12*	270	22.11	*Induction period
60	13.2*	300	22.3	
150	17.9*	330	24.2	Mean value =
180	19.3	360	23.9	$(2.33\pm0.3)10^{-3}$ min^{-1}
210	20.8	450	25.5	
240	20.6	780	22.4	

TABLE 3

Trichlorethylene oxidation with oxygen; temperature 77°; initiator: azo-bis-isobutyronitrile (0.0030 M)

Time (minutes)	$10^4\,k$ (min^{-1})	Time (minutes)	$10^4\,k$ (min^{-1})	Observations
45	36.8*	220	54.0	*Induction period
60	46.3*	240	54.8	
120	58.5	270	52.3	
140	58.8	300	49.2	
160	59.0	330	51.0	Mean value =
180	55.1	420	50.6	$(53.3 \pm 3.9)10^{-4}$ min^{-1}
200	53.6			

TABLE 4

Oxidation of trichloroethylene; temperature 77°; initiator: azo-bis-isobutyronitrile (0.0046 M)

Time (minutes)	$10^4\,k$ (min^{-1})	Time (minutes)	$10^4 k$ (min^{-1})	Observations
30	23.2*	200	65.3	*Induction period
60	42.6*	220	65.9	
80	51.9*	300	59.2	Mean value =
100	67.0	330	60.2	$10^{-4}(62.4 \pm 4.63)$ min^{-1}
120	67.5			
140	68.9			

by a first order rate equation. However, no simple relationship seems to exist between the overall reaction rate constants and the epoxide : acid chloride ratio. The ratio observed at 77° is about 1 : 31 at a low initiator concentration (0.00206 M), but 1.8 : 1 at higher concentrations (0.0161 M) of the peroxide.

A sample containing an enriched concentration of the epoxide was heated for 6 hours at 77° in the presence of benzoyl peroxide. The ratio epoxide : acid chloride was not significantly changed. In another experiment, pure dichloroacetic acid chloride was heated at 77° with benzoyl peroxide, either in an inert gas atmosphere, or in an oxygen stream. No traces of epoxide could be detected. Thus, radicals formed either through decomposition of the initiator or resulted in the oxidation process cannot isomerize the reaction product. The ratio epoxide : acid chloride is not directly affected by radical concentration.

The oxidation of TCE may also be carried out in an air stream. However, the rates are lower. Thus, in comparative experiments at 77° with benzoyl peroxide, after 420 minutes reaction time, TCE was converted into the reaction product in a 76.8% ratio if the oxidation was performed with oxygen; the similar reaction carried out with air afforded only a 28.6% conversion of the alkene.

Trichloroethylene can also be oxidized with air in the absence of any added initiator, at room temperature. After several months conservation of a pure TCE sample, only $COCl_2$ and HCl in TCE could be detected. These oxidation products (together with CO) also result in the initial stages of an initiated autoxidation of TCE. However, their formation represents less than 5% of the overall reaction and seems to take place only in the initial stages of the oxidation process. After detecting, their concentration remained unchanged throughout the reaction.

Reaction mixtures of known epoxide : acid chloride ratio, kept overnight presented a decrease in the epoxide concentration, with the corresponding increase of the acid chloride.

DISCUSSIONS

The reaction kinetics

In our information, except for the radiative initiated oxidation studied by Poluektov and coworkers,[11] no other papers have dealt with the kinetics of TCE oxidation. As in the above-mentioned work, our results agree well with a chain reaction. Thus,

— the oxidation of TCE is promoted by typical initiators, such as benzoyl peroxide and azo-bis-isobutyronitrile.

— independent of initiator nature, in all experiments we have observed an induction period ; as known,[13] the presence of an induction period in a homolytic reaction is usually characteristic of a chain process.

In our experiments, the reaction of TCE with molecular oxygen manifested a first order kinetics :

$$\text{rate} = k_{\text{obs}}[\text{TCE}] \tag{1}$$

We have not purposely studied the variation of oxygen partial pressure. However, it should be remembered that an approximately fivefold increase of the reaction rate is observed by replacing air with oxygen in the oxidation.

The rate constants are dependent upon the initiator concentration (Table 5). The dependence is fairly well represented by the simple relationship (2), usually encountered in radical initiated polymerization processes :[5,14]

$$k_{\text{obs}} = k\,[\text{Initiator}]^{1/2} \tag{2}$$

Even if not complete, our kinetic study has confirmed Poluektov and coworkers' chain mechanism. In contrast with them, we have initiated the oxidation by typical initiators, demonstrating the close behaviour of TCE oxidation with polymerization and copolymerization reactions.

The ratio epoxide : acid chloride

A fact not observed in the previous works is the somewhat puzzling dependence of the epoxide : acid chloride ratio on the initial initiator concentration. This ratio increased steeply from 1 :31 to 1 : 0.55 with an 8-fold increase of the initiator concentration.

TABLE 5

Oxidation of trichloroethylene with oxygen ; temperature : 77° ; summary of kinetic data

Initiator	Initiator concentration (M)	Observed rate constant (min^{-1})	$k'(a)10^2$
Benzoyl peroxide	0.00207	$2.33.10^{-3}$	5.12
	0.00310	$4.14.10^{-3}$	7.40
	0.00413	$3.65.10^{-3}$	5.58
	0.00540	$5.23.10^{-3}$	7.12
	0.0170	$8.34.10^{-3}$	6.57
			Mean :$(6.36 \pm 0.96)10^{-2}$
Azo-bis-iso-butyronitrile	0.00305	$5.33.10^{-3}$	9.65
	0.00460	$6.24.10^{-3}$	9.20
	0.00793	$7.13.10^{-3}$	8.09
			Mean : $(8.98 \pm 0.79)10^{-2}$

A plausible explanation is that the radicals formed in the autoxidation process may interact with the reaction products. The interpretation would thus agree with the previously demonstrated fact that, even if trichloroethyleneoxide seems to be an intermediate in dichloracetic acid chloride formation[11], it is not thermally isomerized into the acid chloride at the autoxidation temperature. Although, as the following scheme shows, radicals may be responsible for the reciprocal interconversion of the reaction products.

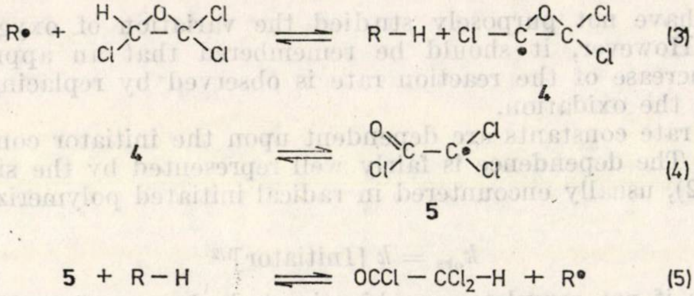

Scheme II

We were able to rule out the radical initiated interconversions by heating both the epoxide and the acid chloride with benzoyl peroxide in the autoxidation conditions. No isomerization was observed. Moreover, other epoxides heated with initiators were not converted into carbonyl compounds.[15]

However, our results have shown that by interrupting the oxidation process, even if the conversion of TCE ceases, the ratio epoxide : acid chloride continuously decreases. As the radical initiated interconversion is ruled out, we consider that the increase of the acid chloride in the reaction mixture must be due to the acid-catalyzed isomerization of the epoxide.

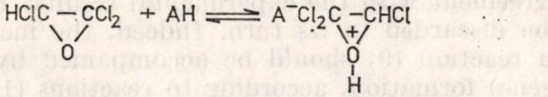
HClC — CCl₂ + AH ⇌ A⁻Cl₂C —CHCl
O
O
H

(6)

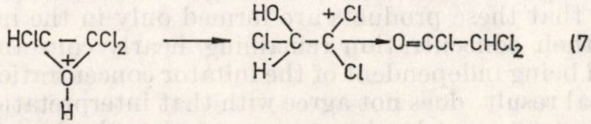
HClC — CCl₂
O
H
HO
Cl—C—C
H
Cl
O=CCl—CHCl₂

(7)

The oxidaton of TCE, as other authors have observed, produces small amounts of HCl (together with $COCl_2$ and CO). However, that small amount of HCl, even if it explains the isomerization of the epoxide into the acid chloride, does not explain the dependence of the epoxide : acid chloride ratio on the initiator concentration. Other interpretations of the results are therefore necessary.

Different routes in the decomposition of intermediate radicals

The intermediate radicals of Schemes I, II and III might have, as other heavy molecular radicals, different routes in decomposition. Thus, radicals **3**, generating the epoxide according to scheme I, may also give rise to the acid chloride. This pathway needs a radical rearrangement (8):

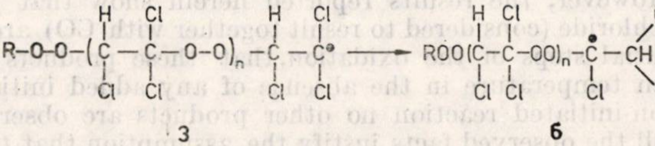
R—O—O—(C—C—O—O)ₙ—C—C•
ROO(C—C—OO)ₙ—C—CH
3
6

(8)

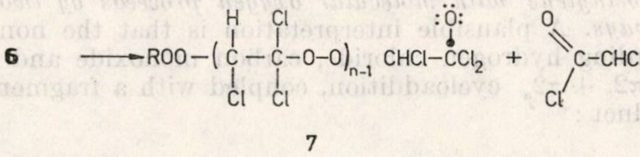
6
ROO—(C—C—O—O)ₙ₋₁ CHCl—CCl₂ + C—CHCl₂
7

(9)

The oxy radical **7** may further decompose either into another peroxy radical **2** with a lower molecular weight, or into an alcoxy radical **7** beside phosgene, carbon monoxide and hydrogen chloride:

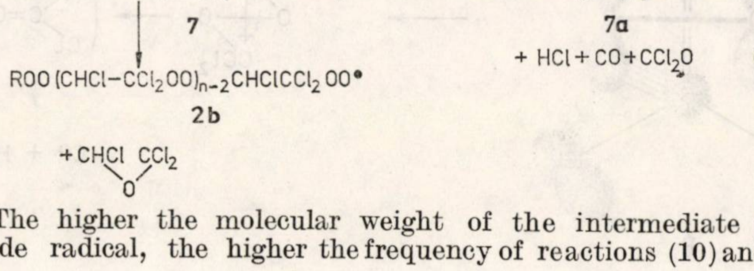
ROO—(CHCl—CCl₂OO)ₙ₋₁ CHCl—CCl₂O•
7
ROO(CHClCCl₂OO)ₙ₋₂CHCl—CCl₂O•
7a
+ HCl + CO + CCl₂O
ROO(CHCl—CCl₂OO)ₙ₋₂CHClCCl₂OO•
2b
+ CHCl CCl₂
O

(10)

The higher the molecular weight of the intermediate polymeric peroxide radical, the higher the frequency of reactions (10) and (9), producing both the acid chloride and the hydrogen chloride necessary for the isomerization of the epoxides. Thus, a low initiator concentration produces a high molecular weight polymer radical and, thus, a high amount of acid chloride, in agreement with the experimental results. However, this mechanism must be discarded in its turn. Indeed, the increase of acid chloride formed in reaction (9) should be accompanied by an increase in HCl (and phosgene) formation, according to reactions (10). However, we have shown that these products are formed only in the initial steps of the oxidation, their concentration remaining nearly constant throughout the process, and being independent of the initator concentration. Evidently, this experimental result does not agree with that interpretation. Moreover, the rearrangement (8) must be slow as compared with the epoxide formation depicted in scheme 1. An increase of radical concentration should favour the rearrangement by an intermolecular pathway. Neither that interpretation is confirmed by the results cited therein.

Different paths in oxidation

Previous observations in literature, as well as ours, indicate that TCE is oxidized in a minor extent to CO, HCl and phosgene. It was generally assumed in Mayo's copolymerization mechanism of alkene autoxidation that carbonyl compounds should accompany copolymer and epoxide formation. All secondary products observed in the autoxidation of TCE may be considered to result from common reaction intermediates (see above). However, the results reported herein show that phosgene and hydrogen chloride (considered to result together with CO) are formed only in the initial steps of the oxidation, that these products are also formed at room temperature in the absence of any added initiator and that in the non-initiated reaction no other products are observed. We consider that all the observed facts justify the assumption that *the oxidation of trichloroethylene with molecular oxygen proceeds by two different oxidation pathways*. A plausible interpretation is that the non-initiated oxidation, affording hydrogen chloride, carbon monoxide and phosgene is a concerted $\pi 2_s + \pi 2_a$ cycloaddition, coupled with a fragmentation of the resulted adduct :

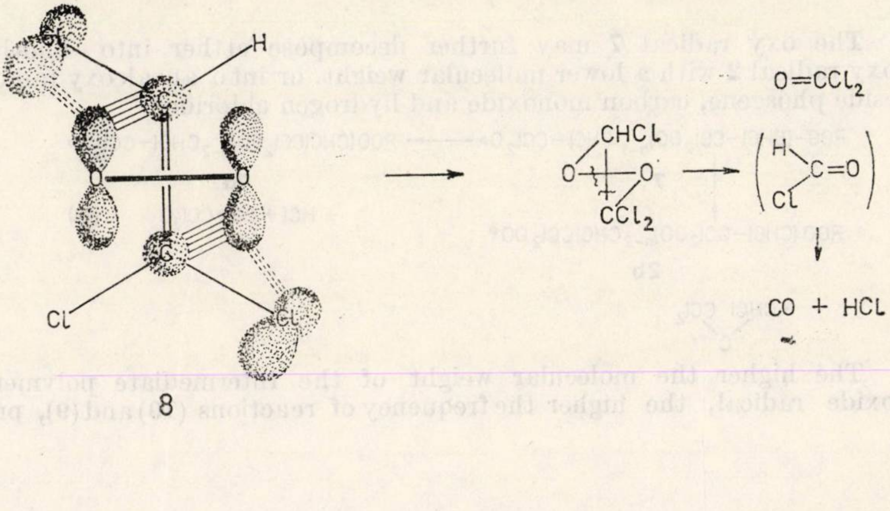

8

Indeed, the transition state **8** of the cycloaddition must be favoured by the overlap of a *p*-orbital of a chlorine atom with the *p*-orbitals of the oxygen molecule. Similar transition states, stabilized by overlap of *p*-orbitals of the atoms belonging to molecules involved in a $\pi 2_s + \pi 2_a$ cyloaddition, have been proposed in ketene additions to olefins.[17] As well-known, polar effects usually do not affect cycloaddition reactions; therefore, the poor electron-donor character of TCE cannot be an impediment in the oxidation represented by equation (11).

The competitive reaction (11) does, in our opinion, fairly well explain the data of this work. At small peroxide concentration, the initiated reaction is slow and it competes well with the non-initiated oxidaton (11). The concentration of hydrogen chloride formed in the latter reaction is sufficient to promote the isomerization of the epoxide through reactions (6) and (7). At the same time, proton, as a more powerful electrophile than oxygen, should inhibit the process (11). The observed result should be a high acid chloride ratio in the reaction mixture and a relatively constant concentration of the side-products. At higher peroxide concentrations, the epoxidation is too fast to compete with (11) and the isomerization of the epoxide. The epoxide is detected as the main reaction product; however, interrupting the reaction without working it up, it has been observed that the isomerization of the epoxide into the acid chloride proceeds even at room temperature, whereas the conversion of TCE has been completely stopped.

The nature of the initiator

By comparing the data of Table 5 it can be seen that azo-bis-isobutyronitrile is 1.5 times more efficient in promoting the oxidation of TCE than benzoyl peroxide. As the polar effects in homolytic reactions usually are small, we consider that this difference is significant and must be retraced to the initiation step.

Indeed, from the two initiating radicals studied in this work, $CN-\dot{C}(CH_3)_2$ must be more nucleophilic than phenyl radical, C_6H_5. Therefore, a faster reaction of the former radical must be anticipated in its interactions with electrophilic species. Either TCE or oxygen are electrophilic molecules, thus both (12) and (13) may occur:

$$R_N\cdot + O_2 \rightarrow R_N-O-O\cdot \qquad (12)$$

$$R_N\cdot + CHCl{=}CCl_2 \rightarrow R_N-CHCl-\dot{C}Cl_2 \qquad (13)$$

However, TCE is a poor electrophile as compared to oxygen: it generally reacts with strong nucleophiles[18] and may even react with electrophiles, such as oxygen. Therefore, it should be selective in its reactions, in agreement with the reported data. On the other hand, oxygen is a strong electrophile with less selectivity in its reactions. Our herein reported results are in agreement with reaction (12), the difference between the two initiators being too small to reflect the poor electrophilic character of TCE.

The observed reaction kinetics also agrees well with this supposition. Scheme III is an adaptation of Scheme I to our reaction, taking into account the results of this work.

Initiation :

Scheme III

$$\mathrm{In} \xrightarrow{k_d} 2\mathrm{R}\cdot \tag{14}$$

$$\mathrm{R}\cdot + \mathrm{O}_2 \xrightarrow{k_i} \mathrm{R{-}O{-}O}\cdot\ \ \mathrm{M}_2^{\cdot} \tag{15}$$

Propagation :

$$\mathrm{M}_2\cdot + \mathrm{M}_1\cdot \xrightarrow{k_{\mathrm{M}_1}} M_1\cdot \tag{16}$$

$$\mathrm{M}_1\cdot + \mathrm{O}_2 \xrightarrow{k_{\mathrm{M}_2}} \mathrm{M}_2\cdot \tag{17}$$

Termination :

$$\mathrm{M}_1 + \mathrm{M}_2^{\cdot} \xrightarrow{k_t} \mathrm{D} \tag{18}$$

$$\mathrm{D} \xrightarrow{k_D} \mathrm{P} + 2\mathrm{M}_2^{\cdot} \tag{19}$$

where :

$$\mathrm{In} = \text{initiator}\,;\ \mathrm{M}_1 = \mathrm{TCE}\,;\ \mathrm{M}_1\cdot = \mathrm{In{-}(CO{-}CHCl{-}CCl_2)_nOOCHCl\dot{C}Cl_2}$$

$$\mathrm{M}_2^{\cdot} = \mathrm{In{-}(OOCHCl{-}CCl_2)_nOOCHCl{-}CCl_2OO.}\,;\ \mathrm{P} = \text{products}$$

$$\mathrm{D{=}In{-}(OOCHCl{-}CCl_2)_n{-}O{-}O{-}(CCl_2{-}CHClOO)_p{-}In}$$

In order to observe a first order kinetics with respect only to the concentration of the oxidized alkene, oxygen concentration must be constant during the oxidation process. Our experimental conditions may determine this apparent independence of the reaction rates in respect of oxygen concentration. It is also necessary that the formation of $\mathrm{M}_1^{\cdot}$ radicals should be faster than the formation of the peroxy radicals $\mathrm{M}_2^{\cdot}$, i.e. the reaction of peroxy radicals with TCE should be faster than the reactions producing the peroxy radicals : the reactions of the intermediate radicals with oxygen (15) and (17), the decomposition of the polymeric peroxide (19). Considering the electrophilic character of the $\mathrm{R'\dot{C}Cl_2}$ radical ($= \mathrm{M}_1^{\cdot}$), this assumption seems to be a plausible approximation.

In order to result the dependence observed upon the initiator concentration, it is necessary that radicals $\mathrm{M}_2^{\cdot}$ should be produced together with the reaction products in the termination reaction. The combination of two different polymeric radicals, $\mathrm{M}_1^{\cdot}$ and $\mathrm{M}_2^{\cdot}$ (18), coupled with the decomposition of the resulted combination product D(19) may assure this condition. Indeed, a polymeric peroxide can be splitted into oxyradicals **7**. As already shown, these radicals may form epoxides and peroxy radicals.

Scheme II leads to the following rate equation :

$$\text{rate of TCE disappearance} = k_{M_1}\,(\text{const. } k_d/k_t)^{1/2}[\mathrm{M}_1]\,[\mathrm{In}]^{1/2} \tag{20}$$

Relation (20) is in perfect agreement with all our data. Further reports of our laboratories will offer other support to our reaction mechanism.

REFERENCES

[1] D. Swern, *J. Amer. Chem. Soc.*, **69**, 1692 (1947); J. Alagy, G. M. Clément and J. C. Balaceanu, *Bull. Soc. chim. France*, **1959**, 1325.

[2] C. E. Frank, Chem. Rev., *46*, 155 (1950); C. F.H. Tipper, *Quart. Rev.*, **11**, 313 (1957); C. Walling, "Free Radicals in Solution", Mc Garw Hill 1956, Chap. 18, p. 287.

[3] R. F. Mayo, *J. Amer. Chem. Soc.*, **80**, 2497 (1958).

[4] F. R. Mayo, A. A. Miller and G. A. Russel, *J. Amer. Chem. Soc.*, **80**, 2500 (1958).

[5] A. A. Miller and F. R. Mayo, *J. Amer. Chem. Soc.*, **78**, 1057 (1956); D. E. van Sickle. F. R. Mayo and R. M. Arluck, *ibid.*, **87**, 4832 (1965).

[6] I. Serée de Roch and J. C. Balaceanu, *Bull. Soc. chim. France*, **1964**, 1393.

[7] H. Hock and M. Siebert, *Chem. Ber.*, **87**, 546 (1954); J. A. Howard and K. U. Ingold, *Canad. J. chem.*, **43**, 2729 (1965); H. Tsubomura, T. Yagishita and H. Toi, *Bull. Chem. Soc. Japan.*, **46**, 3051 (1973).

[8] K. U. Ingold, *Accounts Chem. Res.*, **2**, 1 (1969).

[9] T. Kodaira, K. Hashimoto, Y. Sakanaka, *Bull. Chem. Soc. Japan*, **51**, 1487 (1978).

[10] V. A. Poluektov, I. V. Dobrov, A. V. Chertorisjky and Yu. Ya. Mekhryushev, *Khim, Prom.*, **1976**, 197, and literature quoted therein.

[11] V. A. Poluetkov and Yu. Ya. Mekhryushev, *Zhur. fiz. Khim.*, **45**, 2335 (1971).

[12] Yu. Ya. Mekhryushev and V. A. Poluektov, *Zhur fiz. Khim.*, **47**, 1695 (1973).

[13] see for example, F. Badea, "Reaction Mechanisms in Organic Chemistry", Abacus Press 1977, Tunbridge Wells, Kent, p. 544.

[14] K. Nozaki and P. D. Bartlett, *J. Amer. Chem. Soc.*, **68**, 2377 (1946).

[15] C. Condeiu, unpublished results.

[16] see for example: S. Winstein and R. B. Henderson, in "Heterocyclic Compounds", vol. 1, R. C. Elderfield, ed., J. Wiley, New York, 1950, p. 1.

[17] see for example, N. T. Anh, "Les Règles de Woodward Hoffmann", Ediscience, Paris 1970, p. 99.

[18] F. Chivu, T. Constantinescu, F. Iordache and A. Răzuş, to be published.

Relation (20) is in perfect agreement with all our data. Further reports of our laboratories will offer other support to our reaction mechanism.

REFERENCES

[1] D. Swern, J. Amer. Chem. Soc., 69, 1692 (1947); J. Alegi, C. M. Clément and J. C. Balaceanu, Bull. Soc. chim. France, 1958, 1058.

[2] C. E. Frank, Chem. Rev., 46, 155 (1950); C. F. H. Tipper, Quart. Rev., 11, 313 (1957); C. Walling, "Free Radicals in Solution", McGraw-Hill 1957, Chap. 13, p. 397.

[3] F. R. Mayo, J. Amer. Chem. Soc., 80, 2497 (1958).

[4] F. R. Mayo, A. A. Miller and G. A. Russell, J. Amer. Chem. Soc., 80, 2500 (1958).

[5] A. A. Miller and F. R. Mayo, J. Amer. Chem. Soc., 78, 1017 (1956); D. E. van Sickle, F. R. Mayo and R. M. Arluck, ibid., 87, 4832 (1965).

[6] I. Sérée de Roch and J. C. Balaceanu, Bull. Soc. chim. France, 1964, 1393.

[7] H. Hock and M. Siebert, Chem. Ber., 87, 546 (1954); J. A. Howard and K. U. Ingold, Canad. J. Chem., 43, 2729 (1965); H. Tsunooka, T. Yagishita and H. Tai, Bull. Chem. Soc. Japan, 46, 3051 (1973).

[8] K. U. Ingold, Accounts Chem. Res., 2, 1 (1969).

[9] T. Kodama, K. Hashimoto, Y. Sakanaka, Bull. Chem. Soc. Japan, 51, 1487 (1978).

[10] V. A. Poluektov, I. V. Dobrov, A. V. Chertorizhsky and Yu. Ya. Mekhryushev, Khim. Prom., 1979, 137, and literature quoted therein.

[11] V. A. Poluektov and Yu. Ya. Mekhryushev, Zhur. Fiz. Khim., 45, 2556 (1971).

[12] Yu. Ya. Mekhryushev and V. A. Poluektov, Zhur. Fiz. Khim., 47, 1659 (1973).

[13] see for example, R. Baker, "Reaction Mechanisms in Organic Chemistry", Abacus Press 1977, Tunbridge Wells, Kent, p. 594.

[14] K. Nozaki and P. D. Bartlett, J. Amer. Chem. Soc., 68, 2377 (1946).

[15] C. Gondeiu, unpublished results.

[16] see for example: S. Winstein and R. B. Henderson, in "Heterocyclic Compounds", vol. 1, R. C. Elderfield, ed., J. Wiley, New York, 1950, p. 1.

[17] see for example, N. T. Anh, "Les Règles de Woodward Hoffmann", Ediscience, Paris 1970, p. 99.

[18] F. Chiva, T. Constantinescu, E. Iordache and A. Răzuş, to be published.

Revue Roumaine de Chimie, 25, *4*, 559–562 (1980)

PREPARATION AND REACTIONS OF DIBROMOCARBENE ADDUCTS OF CYCLOHEXA-1,4-DIENYL-ACETATES AND -BENZOATES

IBRAHIM E. KHAWAD and GEORGE M. ISKANDER
Department of Chemistry, University of Khartoum, Sudan

Received February 16, 1978

Bisadducts (I ; R^1 = OAc or OCOPh) of substituted cyclohexa-1,4-dienyl acetates and -benzoates are prepared from the corresponding cyclohexa-1,4-dienol adducts[3] (I ; R^1 = = OH). Some of their reactions are described.

Cyclohexa-1,4-dienyl-acetates and -benzoates are not readily available and if obtained, might not add dibromocarbene entities so easily to give the hitherto corresponding mono- and bis-adducts.

We now report that bisdibromocarbene adducts (I ; R^1 = OAc or OCOPh) of cyclohexa-1,4-dienylacetates or -benzoates are readily obtained from Chattaway's[1] and modified Schotten-Bauman[2] esterification methods on the corresponding carbinols[3] (I ; R^1 = OH). The benzoates of the adducts (I ; R^1 = OH ; R^2 or R^3 = OMe) are hovewer, difficult to prepare and a mixture of the inseparable products was obtained the main component being the unsaturated ketone (II) possibly formed through the rearrangement of (I) in aqueous work up as previously reported.[2] Also bisadducts of enol ethers are known to be sensitive to acidic reagents and to react readily.[3]

Acetyl and benzoyl groups are found to impart remarkable stability on the hydroxy-bisadducts which otherwise undergo slow deterioration when stored in the cold for long periods.

These esters are resistant to mild aqueous or methanolic mineral acid treatment as well as to trifluoroacetic acid. However, with boiling aqueous methanolic hydrochloric acid they gave back the corresponding hydroxy-compounds together with much polymerization.

Aqueous or neat organic base has no effect, whereas aqueous or aqueous-alcoholic sodium or potassium hydroxide gave a mixture of the α,β-unsaturated ketone (II) and the corresponding Favorskii-rearranged carboxylic acids (III).

The preferential reactivity of methoxy- as opposed to alkoxycarbonylsubstituent was shown in at least one case where the bisadduct (I ; R^1 = OAc ; R^2 = H ; R^3 = OMe) gave almost exclusively the unsaturated ketone (II ; R^1 = H ; R^2 = OAc) with silver tetrafluoroborate in aqueous-alcoholic solution; whereas the analogous *para*-isomer (I; R = OAc; R^2 = OMe; R^3 = H) gave under similar conditions the phenolic ketone 4-hydroxybenzocyclobuten-1 (2H)-one (IV), presumably through the cyclo-octatetraene intermediate (V) (Scheme I).

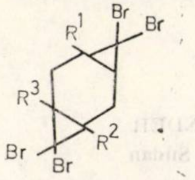
R1
Br
Br
R3
R2
Br
Br

(I) R^1 = OH; $OCOCH_3$; $OCOC_6H_5$
R^2, R^3 = H; OCH_3; CH_3
(see table 1)

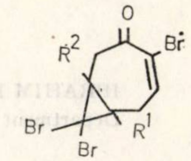
O
R2
Br
Br
R1
Br

(II) R^1, R^2 = H, CH_3
R^1, R^2 = H, OAc

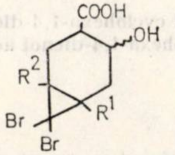
COOH
OH
R2
R1
Br
Br

(III) R^1, R^2 = H; OCH_3

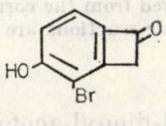

(IV)

None of the bicyclic ketone (II; R^1 = OAc; R^2 = H) could be isolated even for shorter reaction periods.

Scheme I

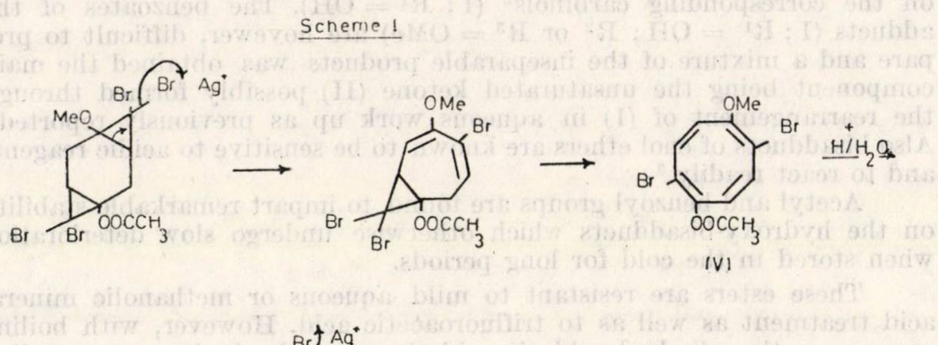
Br
Br
Ag+
MeO
Br
OOCCH3
Br
OMe
Br
Br
Br
OOCCH3
OMe
Br
Br
OOCCH3
H/H2O+
(V)
Br
Ag+
O
O
Br
(IV)

EXPERIMENTAL

I.r. and u.v. spectra were recorded with Unicam SP 1000 and SP 800 model instruments. Analyses were done at the Scandinavian Microanalytical Laboratory, Herlev, Denmark. "Petroleum" refers to the fraction b.p. 60 – 80°.

TABLE 1

Methyl and phenyl 4,4,8,8-tetrabromotricyclo [5.1.0.0^{3,5}] octanecaboxylates I (R' = OAc or OCOPh)

R_1	R_2	R_3	Yield (%)	M.P. (°C)	Formula	Analysis (%)^a C	H	Br	λ max (EtOH)/ mm (ε)	ν max/cm^{-1} (Nujol.)
OAc	CH_3	H	90	144−6	$C_{11}H_{12}Br_4O_2$	26.7(26.6)	2.4(2.4)	64.5(64.5)	210(3,500)	1750, 1100, 1080, 1030, 1015, 760
OAc	H	CH_3	92	155−58	$C_{11}H_{12}Br_4O_2$	26.8(26.6)	2.5(2.4)	64.5(64.5)	210(3,500)	1760, 1080, 1070, 1030, 1010, 750
OAc	C_2H_5	H	95	118−21	$C_{12}H_{14}Br_4O_2$	28.2(28.2)	2.8(2.75)	62.7(62.75)	210(3,800)	1752, 1165, 1100, 1040, 1030, 760
OAc	OMe	H	80	150−53	$C_{11}H_{12}Br_4O_3$	25.9(25.8)	2.4(2.3)	62.4(62.5)	209(3,300)	1750, 1150, 1090, 1060, 1030, 765
OAc	H	OMe	82	120−23	$C_{11}H_{12}Br_4O_3$	25.9(25.8)	2.4(2.3)	62.35(62.5)	209(3,200)	1760, 1130, 1080, 1040, 1030, 760
OCOPh	CH_3	H	20	176−81	$C_{16}H_{14}Br_4O_2$	34.8(34.4)	2.6(2.5)	57.1(57.35)	231(14,680)	1735, 1600, 1110, 1070, 1030, 705
OCOPh	H	CH_3	25	190−92	$C_{16}H_{14}Br_4O_2$	34.6(34.4)	2.6(2.5)	57.2(57.35)	231(16,230)	1732, 1600, 1100, 1060, 1030, 705

^{a}, Required values in parenthesis

Acetylation of Hydroxy-Bisadducts

The hydroxy-bisadduct (0.25 g) was treated with acetic anhydride (*ca.* 9 ml) containing a few drops of pyridine. The solid dissolved and the reaction mixture was left to stand at room temperaure for 48 hrs. It was then poured into ice-cold water (20 ml) and enough solid sodium bicarbonate was added so as to give a pH of 6. The separated solid was filtered, washed with water, dried any crystallized from ethanol (70—80%). I.r. spectra showed disappearance of -OH stretching band (see Table 1).

Benzoylation of the Hydroxy-Bisadducts

The hydroxy-bisadduct (0.1g) was shaken with benzoyl chloride (*ca.*, 10 ml) containing a few drops of pyridine ; aqueous sodium hydroxide promotes rearrangement of the hydroxy-compound more readily than its benzoylation. The adduct often dissolved after 1 h. The reaction mixture was left for 48 hrs at room temperature and worked-up in a manner similar to the above one. The viscous or mobile product was extracted with dichloromethane, and the extract washed with water, dried (Na_2SO_4) and evaporated *in vacuo*. Trituration of the crude product with ethanol afforded the benzoate ester (10%) which was crystallized from alcohol (see Table 1).

Reaction of the Bisadducts (I) with Silver Tetrafluoroborate in Aqueous Ethanol

The esterified bisadduct (I ; R^1= OAc or OCOPh ;3.5 g) was boiled under reflux for 13 hrs with aqueous silver ; tetrafluoroborate solution [from silver oxide, 4 mol/mol ester) and tetrafluoroboric acid (42%; *ca.*, 10 ml)]. Sodium chloride (5 g) in water (15 ml) was then added and the precipitated silver salts were filtered off and washed with small amounts of hot ethanol.

The filtrate and the washings were concentrated to ca. 20 ml and left in refrigerator over-night. The solid product was filtered, dried and crystallized from the desired solvent.

(i) The adducts (I ; R^1= OAc or OCOPh ; R^2 = CH_3 ; R^3 =H) afforded 4,8,8-tribromo--7-methylbicyclo [5.1.0] oct-4-en-3-one (II ; R^1 = CH_3 ; R^2 = H) as colourless crystals (50%) (from petroleum), identical with an authentic specimen[3] (i.r. and mixed m.p. 111°).

(ii) similarly, the adducts (I ; R^1 = OAc or OCOPh ; R^2 = H ; R^3 = CH_3) gave the unsaturated ketone 4,8,8-tribromo-1-methylbicyclo [5.1.0] oct-4-en-3-one (II ; R = H ; R^2 = = CH_3) (40—45%) (from petroleum) identical with an authentic specimen [3] (i.r. and mixed m.p. 109°).

(iii) *4,4,8,8-Tetrabromo-7-methoxy-3-methoxycarbonyltricyclo* [*5.1.0.0.*^{3,5}] *octane* (*I* ; R^1= = *OAc* ; R^2 = *OMe* ; R^3 = *H*)

The product obtained was treated with sodium carbonate solution (20%) whence it all dissolved. The alkaline extract was acidified (HCl, 2N), and the separated phenolic ketone (IV) was filtered, dried and crystallized from benzene as colourless crystals (75%) of 4-hydroxy-benzocyclobuten-1 (2H)-one m.p. 195° (lit.,[4] 195°).

Brief treatments for 3—8 hrs gave back the unconverted adduct in 60—40% yield respectively together with (IV), but nothing of the bicyclic ketone (II ; R^1 = OAc ; R^2 = H).

(iv) *4,4,8,-Tetrabromo-1-methoxy-3-methoxycarbonyltricyclo* [*5.1.0.0.*^{3,5}] *octane* (*I* ; R^1 = = *OAc* ; R^2 = *H* ; R^3 = *OMe*). Column chromatrography (silica ; ethyl acetate-petroleum, 1 :5 v/v) of the viscous oily product gave a main fraction, *4,8,8-tribromo-1-methoxycarbonylbicyclo* [*5.1.0*] *oct*-4-en-3-one (II ; R^1 = H ; R^2 = OAc) as colourless needles (25%) (from aqueous ethanol) m.p. 117—20°, R_F 0.29, (Found : C, 28.65 ; H, 2.1 ; Br, 57.4. $C_{10}H_9Br_3O_3$ requires C, 28.9 ; H, 2.15 ; Br, 57.55%), ν_{max}(Nujol) 1760 (ester CO), 1680 (conj. CO), 1590 (C=C), 1040, 1025, 1010 cm^{-1}.

REFERENCES

[1] F. D. Chattaway, *J. Chem. Soc.*, **1931**, 2495.

[2] L. Behrend and P. Roth, *Liebigs Ann. Chem.*, **1904**, 331, 361 ; H. T. Openshaw "A Laboratory Mannual of Qualitative Organic Analysis", 3rd.,edn., University Printing House, Cambridge, 1968.

[3] A. K. Yagoub and G. M. Iskander, *J. Chem. Soc. Perk. 1*, **1975**, 1043.

[4] A. J. Birch, J. M. Brown and F. Stansfield, *J. Chem. Soc.*, **1964**, 5343 ; G. M. Iskander and F. Stansfield, *J. Chem. Soc.*, **1965**, 1390.

Revue Roumaine de Chimie, 25, 4, 563–569 (1980)

REACTIONS OF PARACONIC ESTERS ISOLATED IN THE *STOBBE* CONDENSATION OF *p*-BROMO-, AND *p*-ETHYLACETOPHENONES WITH DIETHYLSUCCINATE

A. A. EL-KHAMRY, M. A. EL-HASHASH and M. M. HABASHY
Department of Chemistry, Faculty of Science, Ain Shams
University, Abbasia, Cairo, Egypt.

Received December 6, 1978

The reactions of two paraconic esters 1a and 2b (isolated in the Stobbe condensation of *p*-bromo- and *p*-ethylacetophenones with diethylsuccinate[1]) with different alkalies, amines and benzaldehyde are described.

It has been reported[2] that Stobbe condensation of succinic esters with carbonyl compounds in the presence of potassium *t*-butoxide, proceeds, *via* initial addition of the carbanion derived from succinic esters, to the carbonyl group of the second reaction component. This is followed by a cyclization step leading to the formation of an intermediate paraconic ester. This mechanism was supported by the isolation of these intermediate paraconic esters in few cases[3], particularly at shorter reaction times.[4]

In our recent investigation, the hitherto unknown compounds **1a** and **1b** were isolated (10 % yield) from the neutral fractions of the Stobbe condensation of *p*-bromo- and *p*-ethylacetophenone with diethylsuccinate under controlled conditions.

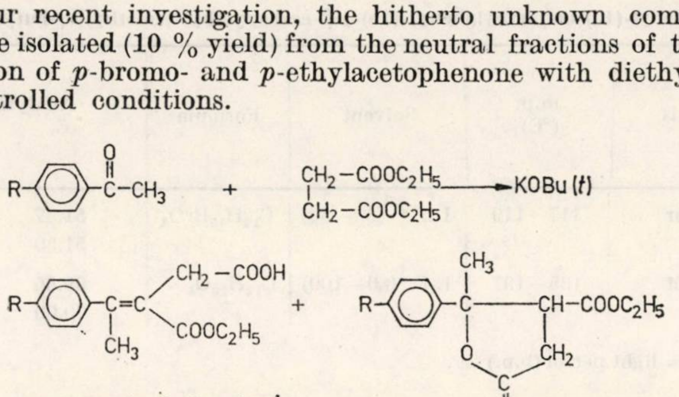
R
O
C–CH₃
+
CH₂–COOC₂H₅
CH₂–COOC₂H₅
KOBu (t)
CH₂–COOH
C=C
COOC₂H₅
CH₃
+
CH₃
CH–COOC₂H₅
O
CH₂
C
O
two isomeric half-esters¹
(1a and 1b)
a b
R= Br Et
KOBu(t), long time
high temperature

The structures of **1a** and **1b** were substantiated from the following evidences :

i) analytical data (Table 2) ; ii) their infrared spectra[5] showed absorptions attributable to ν_{max} of two carbonyl groups (Table 1) correlated with the stretching frequencies of the ester-carbonyl group and the γ-lactonic-carbonyl group, and iii) by the following reaction series which support the presence of the γ-lactonic-ester system :

TABLE 1

Infrared spectra (KBr cm^{-1}) of compounds 1–6

Compound	ν_{CO} amide	ν_{CO} acid	ν_{CO} ester	ν_{CO} lactone	ν_{NH}	ν_{OH}
1a, b			1741, 1735	1782, 1780		
2a, b		1715, 1705				3460, 3445
3a, b	1665, 1660				3350, 3345	3465, 3460
3c, d	1655, 1660				3350, 3340	3460, 3455
4a, b	1662, 1658				3340, 3350	3500, 3480
5a, b	1662, 1655			1780, 1785	3340, 3350	
5c, d	1660, 1665			1784, 1786	3348, 3360	
6a, b			1735, 1730	1785, 1790		

I) Boiling of **1a** or **1b** with a solution of potasium *t*-butoxide in *t*-butanol for long time at relatively high temperature gave an oily mixture of half-esters. Saponification of the latter gave predominantly a crystalline dibasic acid, identical (m.p., mixed m.p. and infrared spectra) with those previously obtained by saponification of the oily half-esters mixture directly resulted from the Stobbe condensation.

TABLE 2

[γ-Bromophenyl-(1a)-or-*p*-ethylphenyl-(1b)-)-β-carboxyethyl-γ-methyl]-γ-butyrolactones

Compound	R	m.p. (°C)	Solvent	Formula	Analysis (%) *Calc.* Found C,	H,
1a	Br	117–119	L.P.* (60–80)	$C_{14}H_{15}BrO_4$	51.37 51.50	4.58 4.64
1b	Et	135–137	L.P.*(80–100)	$C_{12}H_{20}O_4$	69.56 70.00	7.24 6.88

* L.P. = light petrol (b.p.)

II) Saponification of **1a** or **1b** with 10% aqueous sodium hydroxide solution gave α-*p*-bromophenyl-(**2a**)- or α-*p*-ethylphenyl -(**2b**)-α-hydroxyethylsuccinic acid.

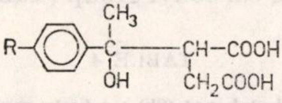

(2a and 2b)

a b

R = Br Et

The structures of **2a** and **2b** were confirmed by : analytical data (Table 3) and infrared spectra,[5] which show the expected carboxylic-carbonyl absorption of aliphatic acids, beside other absorptions (Table 1) correlated with the stretching frequency of the hydroxyl group.

TABLE 3

α-(-*p*-**Bromophenyl-(2a)-or-*p*-ethylphenyl-(2b)-α-hydroxy-ethylsuccinic acids**

Compound	R	m.p. (°C)	Solvent	Formula	Analysis (%) C,	H,	*Calc.* Found
2a	Br	208–9	Acetic acid	$C_{12}H_{13}BrO_5$	45.42 45.73	4.10 4.38	
2b	Et	197–200	Benzene/toluene	$C_{14}H_{18}O_5$	63.15 63.45	6.76 7.15	

III) Reaction of **1a or 1b** with strong nucleophiles such as hydrazine hydrate, gave α-*p*-bromophenyl-(**3a**)-or α-*p*-ethylphenyl-(**3b**)-α-hydroxyethylsuccinic dihydrazides as expected *via* the opening of the lactonic ring.[6] Similar treatment of **1a** or **1b** with phenylhydrazine gave the corresponding dihydrazides **3c** and **3d** respectively. Also the treatment of **1a** or **1b** with *o*-anisidine gave α-*p*-bromophenyl-(**4a**)-or α-*p*-ethylphenyl-(**4b**)-α-hydroxy-N-*o*-anisylethylsuccinamide. The behaviour of *o*-anisidine as a strong nucleophile can be due to the inforcement of the amino group by the (+M) effect of the methoxyl group.

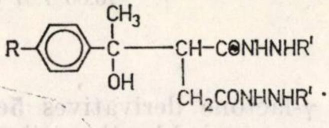

(3a--d)

a b c d

R = Br Et Br Et

R' = H H ph ph

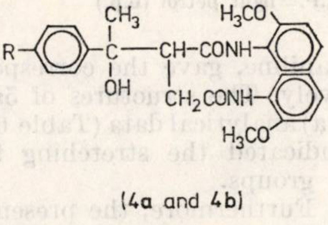

(4a and 4b)

a b

R = Br Et

The structures of compounds **3a**−**d** and **4a** and **4b** were substantiated from : a) analytical data (Tables 4 and 5) and b) the infrared spectra[5] which exhibit the stretching frequencies of the NH and the OH groups, and also those of the amide-carbonyl group (Table 1).

TABLE 4

α-(-*p*-Bromophenyl-(3a)- or-*p*-ethylphenyl-(3b)-)-α-hydroxyethyl-succinic dihydrazides and α-(-*p*-bromophenyl-(3c)-or-*p*-ethylphenyl-(3d)-)-α-hydroxyethylsuccinic phenyldihydrazides

Compound	R	R′	m.p. (°C)	Solvent	Formula	Analysis (%) *Calc.* C, H, N, Found
3a	Br	H	158−9	Ethanol	$C_{12}H_{17}BrN_4O_3$	41.73 4.92 16.23
						41.98 5.10 17.00
3b	Et	H	142	Ethanol	$C_{14}H_{22}N_4O_3$	57.14 7.47 19.00
						57.70 7.18 18.73
3c	Br	ph	271	Acetone	$C_{24}H_{25}BrN_4O_3$	57.90 5.03 11.26
						58.26 5.17 10.97
3d	Et	ph	258−60	*n*-butanol	$C_{26}H_{30}N_4O_3$	69.95 6.72 12.55
						70.04 6.13 12.87

IV) Reactions of **1a** or **1b** with relatively weak nucleophiles such as benzylamine, gave [γ-*p*-bromphenyl-(**5a**)- or -γ-ethylphenyl-(**5b**)-β-N-benzylcarboxamide-γ-methyl]-γ-butyrolactone only *via* nucleophilic attack on the ester-carbonyl group. Similar treatment of **1a** or **1b** with 2-methyl-4-chloroaniline, gave the corresponding γ-lactone derivatives **5c** and **5d** respectively. The structures of **5a**−**d** were revealed by the following evidences : a) analytical data (Table 6) and b) their infrared spectra[5] (Table 1) which indicated the stretching frequencies of ν_{CO} (lactonic), ν_{CO} (amide) and ν_{NH} groups.

TABLE 5

α-(-*p*-Bromophenyl-(4a)- or-*p*-ethylphenyl-(4b)-)-α-hydroxy-N-*o*-anisylethylsuccinamides

Compound	R	m.p. (°C)	Solvent	Formula	Analysis (%) *Calc.* C, H, N, Found
4a	Br	158	Benzene	$C_{26}H_{27}BrN_2O_5$	59.20 5.12 5.30
					58.84 5.63 5.17
4b	Et	137	L.P.*(80−100)	$C_{28}H_{32}N_2O_5$	70.58 6.72 5.89
					70.00 7.07 6.36

* L.P.=light petrol (b.p.)

V) Furthermore, the presence of an active methylene group in the isolated lactonic esters **1a** or **1b** under investigation was revealed by their condensation with benzaldehyde to give [α-benzylidene-β-carboxye-

TABLE 6

[γ-(-*p*-Bromophenyl-(5a)-or-*p*-ethylphenyl-(5b)-)-β-N-benzylcarboxamide-γ-methyl]-γ-butyrolactones and [γ-(-*p*-bromophenyl-(5c)- or -*p*-ethylphenyl-(5d)-)-γ-methyl-β-N-(2-methyl-4-chlorophenyl-carboxamide)]-γ-butyrolactones

Compound	R	Ar	m.p. (°C)	Solvent	Formula	Analysis (%) Calc. C,	H,	N, Found
5a	Br	CH_2ph	160	L.P.*(40–60)	$C_{19}H_{18}BrNO_3$	58.76	4.63	3.60
						59.02	4.32	3.20
5b	Et	CH_2ph	172	Toluene	$C_{21}H_{23}NO_3$	74.77	6.80	4.10
						75.25	7.00	4.41
5c	Br	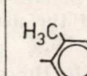	165	L.P.*(80–100)	$C_{19}H_{17}ClBrNO_3$	53.96	4.02	3.30
						54.17	4.18	3.52
5d	Et	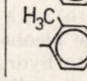	235	Toluene	$C_{21}H_{22}ClNO_3$	67.83	5.90	3.70
						67.31	6.02	3.83

* L. P. = light petrol (b.p.).

thyl-γ-*p*-bromophenyl-(**6a**)- or γ-*p*-ethylphenyl-(**6b**)-] -γ-methyl-γ-butyrolactone.

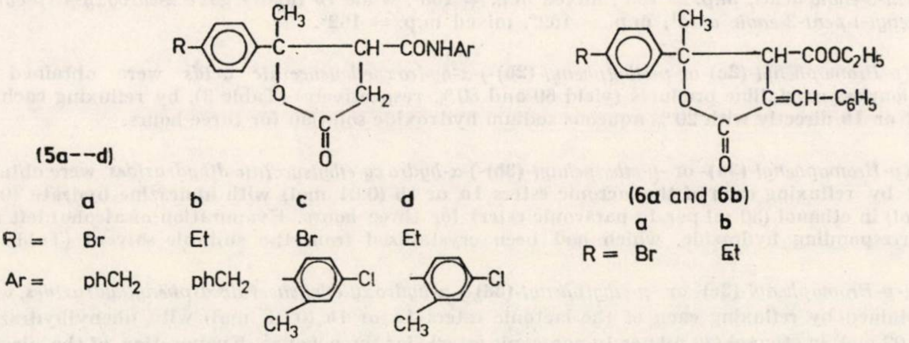

The structures of **6a** and **6b** were proved from their analytical data (Table 7) and from their infrared spectra which reflect the presence of both the ester and the lactonic-carbonyl groups (Table 1).

TABLE 7

[α-Benzylidene-β-carboxyethyl-γ-(-*p*-bromophenyl-(6a)-or-*p*-ethylphenyl-(6b)-)-γ-methyl-]-γ butyrolactones

Compound	R	m.p. (°C)	Solvent	Formula	Analysis (%) C,	H,	Calc. Found
6a	Br	162	Xylene	$C_{21}H_{19}BrO_4$	60.72	4.58	
					60.34	4.21	
6b	Et	173	Benzene/ toluene	$C_{23}H_{24}O_4$	75.82	6.59	
					76.10	6.13	

EXPERIMENTAL

Melting points are not corrected. Infrared spectra (KBr) were measured on a Perkin—Elmer Infracord 137 Spectrophotometer.

[γ-(*p-Bromophenyl-*(**1a**)-or *-p-ethylphenyl-*(**1b**)-)-β-*carboxyethyl-γ-methyl-*]-γ-*butyrolactones* (by Stobbe condensation)

A mixture of the arylmethylketone (0.1 mol) and diethylsuccinate (0.15 mol) was added in the course of 30 min, to a slightly warmed (60—70°) stirred solution of potassium *tert.* butoxide (from potassium 0.11 g atoms and 40 ml of *t*-butanol per 1g potassium) boiling and stirring being then continued for three hours. Most of the alcohol was then removed under reduced pressure, the cooled residue was acidified with dilute hydrochloric acid and the organic material was taken up in ether. Upon extraction with 10% sodium carbonate solution, the expected half-esters have been obtained after acidification. Evaporation of the neutral ethereal layer (free from acids) left a colourless solid (10% yield) ; (Table 2) **1a** or **1b**.

Conversion of **1a** and **1b** to the corresponding half-esters, and then to the corresponding dibasic acids, was carried out by boiling each of these compounds (**1a** or **1b**) with boiling (95°) stirred potassium *t*-butoxide — butanol solution for four hours. Most of the alcohol was removed under reduced pressure, the cooled residue was acidified with dilute hydrochloric acid, then the organic materials were taken up in ether. Upon extraction with 10% sodium carbonate solution and acidification of this alkaline solution with dilute hydrochloric acid, it was extracted with ether. Evaporation of the ether left in each case the oily-acidic mixture. Saponification of each of these oily mixtures was performed on boiling with 10% aqueous sodium hydroxide solution for three hours. A colourless solid compound could be isolated in each case from the corresponding oily viscous product. Compound **1a** finally gave 4-(*p-bromophenyl-*)-2-*carboxy-pent-*3-*enoic acid*[1], m.p. = 168°, mixed m.p. = 168°, while **1b** finally gave 2-*carboxy-*4-(*p-ethylphenyl-*)-*pent-*3-*enoic acid*[1], m.p. = 162°, mixed m.p. = 162°.

α-(*p-Bromophenyl-*(**2a**)-or-*p-ethylphenyl-*(**2b**)-)-α-*hydroxyethylsuccinic acids* were obtained as colourless crystalline products (yield 60 and 80% respectively) (Table 3), by refluxing each of **1a** or **1b** directly with 20% aqueous sodium hydroxide solution for three hours.

α-(*p-Bromophenyl-*(**3a**)- or *-p-ethylpehnyl-*(**3b**)-)-α-*hydroxy-ethylsuccinic dihydrazides* were obtained by refluxing each of the lactonic esters **1a** or **1b** (0.01 mol) with hydrazine hydrate (0.02 mol) in ethanol (30 ml per 1g paraconic ester) for three hours. Evaporation of alcohol left the corresponding hydrazide, which had been crystallized from the suitable solvent (Table 4).

α-(*-p-Bromophenyl-*(**3c**)- or *-p-ethylphenyl-*(**3d**)-)-α-*hydroxy-ethylsuccinic diphenylhydrazides,* were obtained by refluxing each of the lactonic esters **1a** or **1b** (0.01 mol) with phenylhydrazine (0.02 mol) in ethanol (30 ml per 1g paraconic ester) for three hours. Evaporation of the alcohol left the expected diphenylhydrazide, which had been crystallized from a proper solvent (Table 4).

α-(*-p-Bromophenyl-*(**4a**)- or (**4b**)-*p-ethylphenyl-*(**4b**)-α-*hydroxy-*N-*o-anisylethylsuccinamides,* were obtained by refluxing each of **1a** or **1b** for three hours with *o*-anisidine in ethanol (0.01 mol ester, 0.02 mol amine, and 30 ml alcohol per 1 g lactonic ester). Evaporation of the alcohol left the expected compounds, which had been crystallized from the suitable solvent (Table 5).

[γ-(*p-Bromophenyl-*(**5a**)- or *-p-ethylphenyl-*(**5b**)-)-β-N-*benzylcarboxamide-γ-methyl-*]-γ-*butyrolactones,* were obtained by refluxing **1a** or **1b** (0.01 mol) with benzylamine (0.02 mol) in ethanol (30 ml per 1g lactonic ester) for three hours. Evaporation of the alcohol left the corresponding γ-lactone derivative, which had been crystallized from the suitable solvent (Table 6).

[γ-(*p-Bromophenyl-*(**5c**)- or *-p-ethylphenyl-*(**5d**)-)-γ-*methyl-*β-N-(2-*methyl-*4-*chlorophenylcarboxamide*)-]-γ-*butyrolactones,* were obtained by refluxing each of the lactonic esters **1a** or **1b** (0.01 mol) with 2-methy-4-chloroaniline (0.02 mol) for three hours in ethanol (30 ml per 1 g ester). Evaporation of the alcohol left the expected γ-lactone derivative, which had been crystallized from a suitable solvent (Table 6).

[*α-Benzylidene-β-carboxyethyl-γ-(-p-bromophenyl-***(6a)**- or *-p-ethylphenyl-***(6b)***-γ-methyl-]-γ-butyrolactones*, were obtained by fusion the paraconic ester **1a** or **1b** (0.01 mol) with 0.5 g anhydrous $ZnCl_2$, and benzaldehyde (0.015 mol) in an oil bath at 150—160°. Upon water addition to the cooled mixture, a colourless solid precipitated which had been recrystallized from a suitable solvent (Table 7).

REFERENCES

[1] M. A. El-Hashash and A. A. El-Khamry, *Pakistan J. of Science*, **29**, 1 (1977).

[2] W. S. Johnson, J. W. Peterson and W. P. Scheinder, *J. Amer. Chem. Soc.*, **69**, 74 (1947).

[3] R. Robinson, and E. Seijo, *J. Amer. Chem. Soc.*, **44**, 582 (1941).

[4] H. Stobbe, W. Veiweg, R. Eckert, and G. Reddlien, *Liebigs Ann, Chem.*, **78**, 380 (1911).

[5] L. J. Bellamy, "The Infrared Spectra Of Complex Molecules", Wiley, New York, second ed., 1958.

[7] A. Sammour and M. A. El-Hashash, *J. prakt. Chem.*, **314**, 906 (1972).

Revue Roumaine de Chimie, **25**, *4*, 571–575 (1980)

7′-BENZOYLAMINO-β-*APO*-6′-CAROTENOIC ACID AND SOME OF ITS DERIVATIVES VIA β-*APO*-8′-CAROTENYLIDENOXAZOLONE

VICTORIA CIURDARU*, V. TAMAS * and K. L. SIMPSON **

* Department of Biochemistry, Institute of Agronomy, Str. Mănăştur 3, 3400 Cluj-Napoca, România

** Department of Food Science and Technology, University of Rhode Island, Kingston, R.I. 02881, U.S.A.

Received June 28, 1979

The nucleophilic cleavage of the β-*apo*-8′-carotenylidenoxazolone (I) ring with H_2O, MeOH, piperidine and morpholine gave the 7′-benzoylamino-β-*apo*-6′-carotenoic acid (II), its methyl ester (III), piperidide (IV) and morpholide (V) respectively. These new nitrogen containing apocarotenoidic derivatives are characterized.

Current researches show that retinoids, particularly the synthetic ones, are very promising for the prevention and reversion of neoplasms induced by chemical carcinogens or radiation.[1,2] Taking into account that the apocarotenoids are homologues of the retinoids, we thought it will be interesting to synthesize new derivatives of the series which contain structural elements potentially able to interact with some key molecules of cellular functions, in order to test their activity.

Derivatives of oxazolones have been reported to possess various therapeutic properties.[3-7]. Some oxazolones have also been reported to have pharmacodynamic activity.[7-9] Towards this end retinylidenoxazolone[10] and some apocarotenylidenoxazolones have been prepared, characterized[11] and their biological effects studied.[12]

Oxazolonic ring cleavage by nucleophilic addition at C-5[13-15] was used to synthesize the esters, piperidide and morpholide derivatives from some aromatic and aliphatic oxazolones, considering that such structures may have interesting biological properties.[16,17]

Hydrolysis, hydrazinolysis and phenylhydrazinolysis of the *all-trans* retinylidenoxazolone have been reported.[10]

This paper presents the nucleophilic cleavage of β-*apo*-8′-carotenylidenoxazolone (I) by water, methanol, piperidide and morpholine. The resulting products, 7′-bezoylamino-β-*apo*-6′-carotenoic acid (II), its methyl ester (III), piperidide (IV) and morpholide (V), respectively, contain terminal groups which might determine interesting biological effects (Scheme 1).

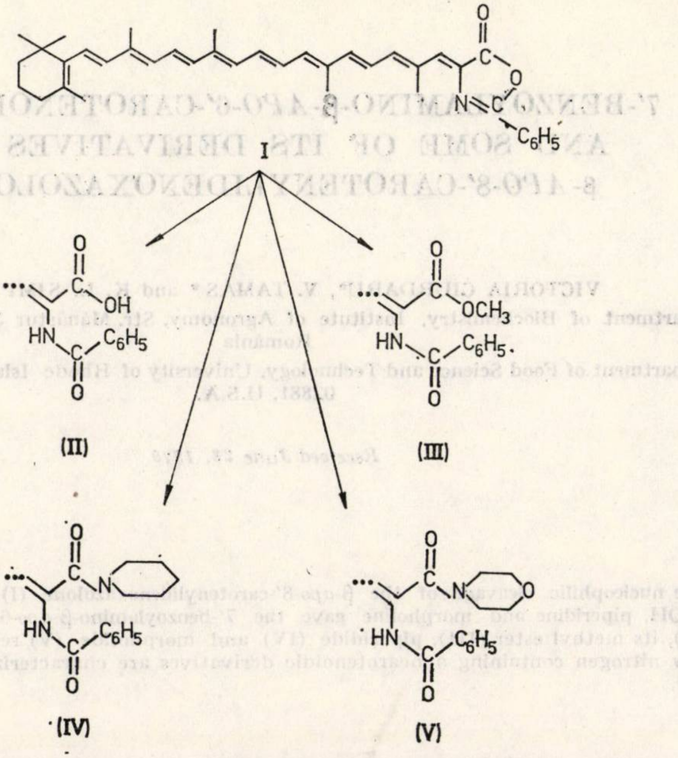

Scheme 1

RESULTS AND DISCUSSION

All the derivatives were synthesized by adding the reagents to the chloroform solution of oxazolone I, at room temperature, except the hydrolysis. In this case it was difficult to find a suitable watermiscible solvent for oxazolone I, so the reaction was performed in boiling acetone; the reaction was much slower and the yield lower. In fact the yields were not much over 80 % because of the byproducts formed.

The chromatographic control of the stability of the products II—V during purification revealed that V yields a somewhat less polar byproduct, most likely an isomer since both of them gave oxazolone I on storage in benzene solution.

The spectral data (Table 1) are in full accordance with the structure of the products.

The I.R. spectra show the strong complex bands appearing at 1660 (1680 sh) cm^{-1} (II), 1692 (1698 sh) cm^{-1} (III), 1615—1660 cm^{-1} (IV) and 1658 cm^{-1} (V) which can be assigned to the benzoylamidic $\nu_{C=O}$ groups. The I.R. spectrum of compound II shows a characteristic strong band at 1710 cm^{-1} with a shoulder at 1770 cm^{-1}. The main band corresponds to the $\nu_{C=O}$ of the dimeric form of carboxylic derivative and the shoulder to the $\nu_{C=O}$ of the monomeric form. The $\nu_{C=O}$ for the ester group in the spectrum of III appears as a peak at 1702 cm^{-1} in the complex amidic band. In the case of V there is also a band at 1615 cm^{-1} beside the benzoylamidic $\nu_{C=O}$. This band can be assignable to the morpholidic $_{C=O}$.[17] A weak and broad band around 3300 cm^{-1} appears in the spectra of all these compounds. It is characteristic of the ν_{NH}. In the spectrum of II this band is specifically broaded towards the lower frequencies and it includes also ν_{O-H}.

TABLE 1

Characteristics of the 7'-benzoylamino-β-*apo*-6'-carotenoic acid (II) and its derivatives III-V

Compound	m.p. C° (solvent)	Yield %	Visible light λ_{max}, nm	I.R. ν_{max}, cm^{-1}	MS characteristic peaks, m/e
Acid II	135–142 (benzene)	52	474	1660, 1680 sh 1710, 1770 sh 2500–3300 (very broad)	577 (M^+) 559 533 ($M-CO_2$) 105
Methyl ester III	155–160 (benzene diethyl ether)	82	484	1240 1692, 1698 sh 1702 3400 (broad)	591 (M^+) 576 ($M-CH_3$) 559 486 ($M-105$) 105
Piperidide IV	100–110 (hexane)	71	464	1615–1660 (complex) 3300 (broad)	644 (M^+) 559
Morpholide V	97–102 hexane	61	468	1615 1658 3200 (broad)	646 (M^+) 559 105

In the electronic spectra, as it was expected, the λ_{max} of compounds II–V are largely shifted towards lower wavelengths compared with λ_{max} =549 nm of the oxazolone I, due to the shortening of the conjugation in these products.

The peaks corresponding to the molecular ions are present in the mass spectra of all these compounds. A common peak of the series, m/e 559, corresponds to the molecular ion of the starting oxazolone. It can arise by a thermal reaction and/or electron impact. The compound II shows also a peak at m/e 533 and III at m/e 576, due to the $/M-CO_2/^+$ and $/M-CH_3/^+$ ions, respectively. All the mass spectra contain an intense peak corresponding to the benzoyl ion at m/e 105.

EXPERIMENTAL

Preparative TLC on silica gel G was used to isolate the products from the reaction mixture. The end point of the reaction was determined by a TLC control. Melting points (Table 1) are uncorrected. Visible light spectra were examined in $CHCl_3$ solutions with a C. Zeiss VSU-1 spectrophotometer and IR spectra were recorded on a Specord 71-IR-spectrophotometer in CCl_4 solutions except the spectrum of compound II, recorded in $CHCl_3$ solution. Mass spectra were obtained on a Varian MAT-311 spectrometer operated at 70 eV using the direct inlet system at 165—215°.

β-*Apo*-8'-carotenylidenxazolone (I) was obtained as reported[11] but purified by column chromatography, on silica gel/celite 2 :1 with chloroform as the developing solvent.

7'-Benzoylamino-β-*apo*-6'-carotenoic acid (II)

Oxazolone I (130 mg) was dissolved in refluxing acetone (500 ml) and 10% aqueous NaOH (20 ml) was added under stirring. The dark violet crystals of oxazolone were partially separated from the aqueous phase. The mixture was stirred an additional time of 8 hrs at room temperature. A 1 :1 mixture of bezene-diethyl ether was added, then acidified (AcOH) water, until the pigments passed into the upper phase. The benzene-ethereal solution was washed until neutral with water, concentrated and chromatographed. Benzene-acetone 1 :1 mixture containing traces of acetic acid was used as developing system. The red zone ($R_f =$ $= 0.33$) was eluted with a mixture of diethyl ether and aqueous acetone. The solution washed with water was evaporated to leave II as a red residue (70 mg).

7'-Benzoylamino-β-*apo*-6'-carotenoic acid methyl ester (III)

The oxazolone I (150 mg) dissolved in chloroform (50 ml) was treated with 10% methanolic NaOH solution (0.5 ml). The reaction was complete in 2 minutes. A double volume of diethyl ether was added to the reaction mixture. The solution was washed with 2% aqueous acetic acid and finally with water to a neutral pH. The solution concentrated to a minimum volume was chromatographed with chloroform as developing solvent. The main broad red zone ($R_f = 0.22$) was eluted with diethyl ether. The ethereal solution evaporated to dryness gave III (130 mg).

7'-Benzoylamino-β-*apo*-6'-carotenoic acid piperidide (IV)

The reaction of the oxazolone I(170 mg) in chloroform (50 ml) with piperidine (3 ml) was completed in ten minutes. The solution diluted with a double volume of diethyl ether was washed with water until neutral. The concentrated solution was chromatographed with chloroform-diethyl ether 2 :1 as developing system. The dark red zone ($R_f = 0.61$) eluted with diethyl ether and evaporated to dryness gave IV (140 mg).

7'-Benzoylamino-β-*apo*-6'-carotenoic acid morpholide (V)

Morpholine (5 ml) was added to a chloroform solution of oxazolone I (170 mg in 50 ml). After 1.5 hrs the reaction was incomplete but was stopped because in a preliminary experiment it was found that the reaction product V decomposed back to the oxazolone I on keeping in benzene solution for a longer time at room temperature. The reaction mixture was worked up as before and chromatographed with chloroform-diethyl ether 1 :1 mixture as developing agent. Compound V was isolated (120 mg) as above from the main red chromatographic zone ($R_f = 0.40$).

REFERENCES

[1] M. B. Sporn, N. M. Dunlop, D. L. Newton and W. R. Henderson, *Nature*, **263**, 110 (1976).

[2] L. Harisiadis, R. C. Miller, E. J. Hall and C. Borek, *Nature*, **274**, 486 (1978).

[3] L. Dall'Asta and P. Ferrario, *Helv. Chim. Acta*, **45**, 1065 (1962).

[4] B. P. Fabrichnyi, E. A. Krasnyanskaya, I. F. Shalavina and Ya. L. Gol' dfarb, *Zhur. obshchei Khim.*, **33**, 2697 (1963).

[5] T. Kametani, O. Umezawa, Y. Sato, K. Ogasawara, S. Shibuya, M. Ishiguro and D. Mizuno, *Yakugaku Zasshi*, **83**, 838 (1963) ; *Chem. Abstr.*, **60**, 446 (1964).

[6] C. Demetrescu, C. Chiriţa and V. Ion, *Chim. Ther.*, **2**, 144 (1967) ; *Chem. Abstr.*, **67**, 116696 (1967).

[7] F. D. Popp, *J. Org. Chem.*, **26**, 3020 (1961).

[8] L. Schmidt and E. Seeger, *Arzneim. Forsch.*, **6**, 22 (1956).

[9] P. K. Sharma, M. K. Menon and P. C. Dandiya, *J. Pharm. Sci.*, **53**, 1055 (1964).

[10] V. Tamas and C. Bodea, *Rev. Roumaine Chim.*, **19**, 701 (1974).

[11] V. Tamas, V. Ciurdaru and C. Bodea, *Rev. Roumaine Chim.* **18**, 1409 (1973).

[12] V. Tamas K. L. Simpson and V. Ciurdaru, Unpublished data.

[13] K. Nalepa and J. Slouka, *Monatsh.*, **98**, 412 (1967).

[14] I. Oprean, Dissertation 1968, Cluj (România).

[15] K. Nalepa and V. Bekarek, *Monatsh.*, **100**, 2004 (1969).

[16] M. Vanghelovici, I. Lupsa, C. Bilegan and A. Muste, *Studii și Cercetări Chim. Acad. R. P. România (Timișoara)*, **7**, 295 (1960).

[17] I. Lupsa, Dissertation 1973, Cluj (România).

Revue Roumaine de Chimie, **25**, *4*, 577–581 (1980)

HETEROCYCLIC NITROGEN COMPOUNDS. VI[1]

REACTION OF SOME 5-OXOPYRAZOLINE DERIVATIVES WITH HYDRAZINE HYDRATE AND DIAZOALKANES

M. F. EL-KASCHEF, S. M. YASSIN, M. F. ABDEL-MEGEED and F. M. ABDEL-MOTI
Chemistry Department, Faculty of Science, Tanta University, Tanta, A. R. Egypt

Received August 30, 1978

While hydrazine hydrate gave with compound I, in the cold, benzalazine and 1-phenyl-3-methyl-5-oxo-2-pyrazoline, it gave, on boiling, 4,4′-benzylidene-bis-(1-phenyl-3-methyl-5-oxo-2-pyrazoline IV. Hydrazine hydrate gave with compounds V or VII the reduced product, 4,4′-bis-(1-phenyl-3-methyl-5-oxo-2-pyrazoline) VI. Diazomethane was added to the exocyclic olefinic bond in both compounds I and V to give the spiroderivatives VIII and IX, respectively, while it gave methylation of the enol form in compound VII. The structures of the compounds under investigation were confirmed by IR and H-NMR spectra.

It has been shown[1], that the treatment of 4-aryl-alkylidene-1-phenyl-3-methyl-5-oxo-2-pyrazolines with hydrazine hydrate at room temperature leads to the formation of the benzalazine of the corresponding aldehyde together with 1-phenyl-3-methyl-5-oxo-2-pyrazoline. We confirmed these results and found that hydrazine hydrate reacted with 4-benzylidene-1-phenyl-3-methyl-5-oxo-2-pyrazoline I* at room temperature, affording benzalanine II together with 1-phenyl-3-methyl-5-oxo-2-pyrazoline III. This reaction when repeated by refluxing I in ethanol and hydrazine hydrate afforded 4,4′-benzylidene-bis-(1-phenyl-3-methyl-5-oxo-2-pyrazoline) IV.

It is noteworthy to mention that, the ^{1}H-NMR spectrum of compound IV reveals its plane of symmetry and therefore it gives rise to only five distinct proton resonances. The two methyl groups resonate as a six proton singlet at $\delta = 1.68$ ppm, while the two phenyl protons resonate as a ten proton multiplet centred at $\delta = 7.8$ ppm and the CH. Ph proton resonates as a five-proton singlet at $\delta = 7.2$ ppm. A typical AB_2 system was further observed in the spectrum of compound IV. Thus, the two symmetric methine protons appear as a two proton dublet centred at $\delta = 4.82$ ppm ($J = 10$ HZ) and the CH. Ph proton resonates as one proton triplet at $\delta = 4.38$ ppm ($J = 10$ HZ).

The formation of IV, could be explained by the interaction of benzalazine II or benzaldehyde hydrazone, formed as an intermediate and III. The possibility of the formation of IV as a result of the reaction of the formed intermediate III with unreacted I is improbable, since benzalazine II was not separated in this reaction under the given experimental condition.

---

* This compound was described to be formed by the reaction of ethylacetoacetate-phenylhydrazone with benzaldehyde (B. Lachowicz, *Monatsh.*, **17**, 357 (1896)., by the reaction of III with benzaldehyde (F. Stolz, *Ber. dtsch. Chem. Ges.*, **28**, 631 (1895), or by the reaction of III with benzylidene aniline. [1]

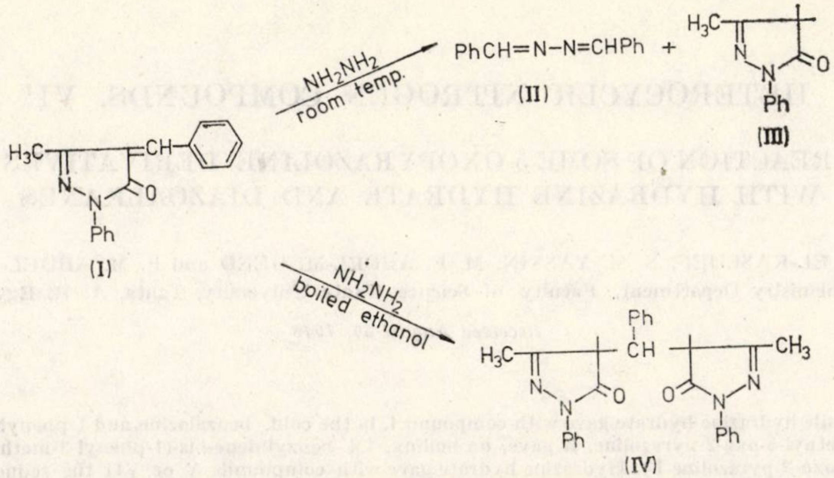

Pyrazole blue V[2] when refluxed with hydrazine hydrate in ethanol gave 4,4′-bis-(1-phenyl-3-methyl-5-oxo-2-pyrazoline) VI [3]. This implies that reduction of compound V and abstraction of hydrogen is easily accomplished.

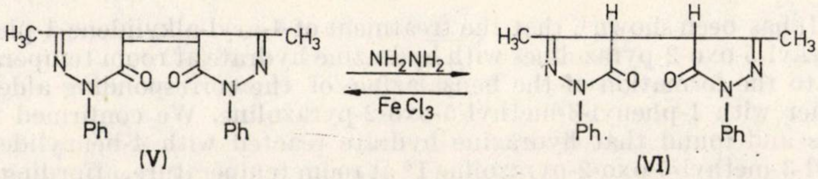

The same compound VI was also obtained by prolonged boiling of V in acetic acid or xylene. Compound VI was easily converted to V by oxidation with ferric chloride. The structures of compounds V and VI are confirmed by their ^{1}H-NMR spectra.

The spectrum of compound V comprises only two distinct proton resonances : a singlet at $\delta = 1.70$ ppm due to the six protons of the two methyl groups and a multiplet centered at $\delta = 7.76$ ppm attributed to the ten protons of the two phenyl groups. The compound VI shows three types of proton resonances, the methyl protons resonate as a six-proton singlet at $\delta = 1.68$ ppm, the phenyl protons resonate as a ten-proton multiplet centred at $\delta = 7.76$ ppm and the methine protons resonate as a two-proton singlet at $\delta = 4.20$ ppm indicating the free rotation around the C−C bond.

When rubazic acid VII was treated with hydrazine hydrate in ethanol it gave the compound VI with evolution of ammonia.

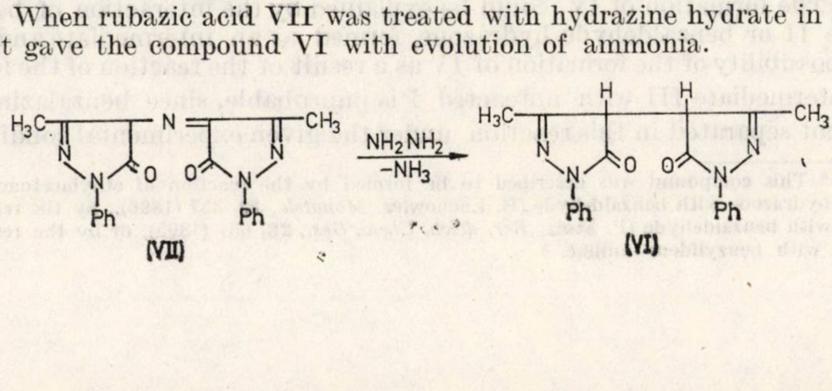

In support of this explanation could be brought the known[2] interaction of pyrazole blue V and ammonia which give rubazoic acid VII.

Diazomethane reacted with compounds I and V by addition to the exocyclic double bond to give spiro (1-phenylcyclopropane)-2,4-(1-phenyl-3-methyl-5-oxo-2-pyrazoline) VIII and dispiro (cyclopropane 1,4,4′-bis (1-phenyl-3-methyl-5-oxo-2-pyrazoline) IX, respectively.

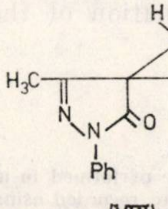

(VIII)

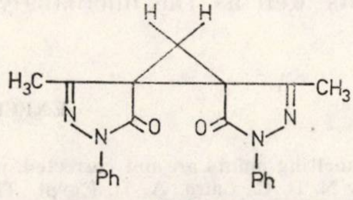

(IX)

The structures of these two compounds were supported by IR and ^{1}H-NMR spectra. The IR spectra of two compounds show the skeletal vibration of the cyclopropane ring at 1030 cm^{-1}. The ^{1}H-NMR spectrum of VIII exhibiting a singlet at $\delta = 1.74$ ppm could be attributed to three protons of the methyl group, a distinct proton resonance as a doublet centred at $\delta = 0.62$ ppm attributed to the two protons of the methylene group in cyclopropane[4]. This value was considered as an upfield shifted due to the great strain in the cyclopropane ring. Another triplet was observed at $\delta = 4.7$ ppm assigned as the proton of the methine. The aromatic region comprises two distinct signals, the first one at= 7.50 ppm as a multiplet located at $\delta = 7.76$ ppm corresponding to the five protons of N-Ph.

The ^{1}H-NMR spectrum of IX gives rise to only three types of signals indicating the symmetry in this compound. The methyl protons resonate as a six-proton singlet at $\delta = 1.74$ ppm. The methylene protons resonate as a two-proton singlet at $\delta = 0.60$ ppm and the aromatic phenyl protons resonate as a ten-proton multiplet at $\delta = 7.70$ ppm.

Further proof of the structure IX was brought by oxidation with hydrogen peroxide in acetic acid where 4-hydroxy-4′-hydroxymethyl-4,4′-bis-(1-phenyl-3-methyl-5-oxo-2-pyrazoline) X was obtained. Its IR and ^{1}H-NMR spectra are consistent with the assigned structure. The ^{1}H-NMR spectrometry could not distinguish between the two methyl groups as well as between the two phenyl groups.

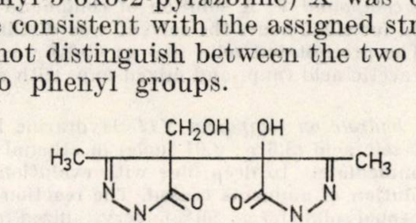

(X)

Compound VII, owing to the presence of a hydrogen atom in the vicinity of the carbonyl group, gave with diazomethane, the methyl ether of the enol form, namely 5-methoxy-5-oxo-4,4′-nitrilo-bis-(1-phenyl-3-methyl-pyrazoline) or 4-(3-methyl-5-oxo-methoxy-1-phenylpyrazol-4-yl) imino-3-methyl-1-phenyl-2-pyrazolin-5-one XI.

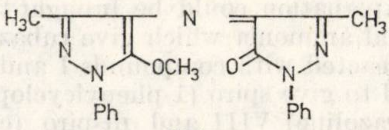

(XI)

The structure of the compound XI was confirmed by its IR and ^{1}H-NMR spectra as well as the microanalytical determination of the methoxyl group.

EXPERIMENTAL

All melting points are not corrected, microanalyses were performed in micro-analytical Laboratory N. R. C., Cairo, A. R. Egypt. The IR spectra were recorded using a PYE UNI-CAM SP. 200G. Spectrophotometer. The ^{1}H-NMR spectra* were measured using a VARIAN-A-60 MHZ Spectrometer in deuterochloroform as a solvent (40 mg/0.5 ml) unless otherwise stated and tetramethylsilane as internal reference.

Action of hydrazine hydrate on compound I. Hydrazine hydrate (5 ml; 100 %) was added to a solution of phenyl-3-methyl-5-oxo-2-pyrazoline I(2.6 g; 0.01 mole) in ethanol (20 ml). The reaction mixture was refluxed for two hours and then concentrated. The oily residue formed was separated by decantation, washed several times with water, solidified using ethanol (1.8 g; 80 %) and recrystallized from ethanol. m.p. 165. The mixed m.p. with an authentic sample of 4,4′-benzylidene-bis-(-1-phenyl-3-methyl-5-oxo-2-pyrazoline) IV showed no depression. The reaction was also carried out by mixing compound I with hydrazine hydrate and leaving at room temperature, benzaldehyde (0.50 g), m.p. and mixed m.p. with an authentic sample of benzalazine 93°[3] and 1-phenyl-3-methyl-5-oxo-2-pyrazoline (0.90 g; 53 %), m.p. and mixed m.p. with an authentic sample of 1-phenyl-3-methyl-5-oxo-2-pyrazoline 127°[2] were isolated.

Action of hydrazine hydrate on compound V. Hydrazine hydrate (5 ml; 100 %) was added to pyrazole blue V (1.7 g; 0.005 mole) suspended in ethanol (20 ml). The reaction mixture was refluxed for five hours, then cooled and filtered. The separated solid (1.5 g; 88 %) was recrystallized from glacial acetic acid, m.p. 320°. The mixed m.p. with an authentic sample of 4,4′-bis--(1-phenyl-3-methyl-5-oxo-2-pyrazoline)[2] showed no depression. This compound, when oxidized with ferric chloride solution, afforded pyrazole blue V (m.p. and mixed m.p. with an authentic sample of pyrazole blue 230°)[2].

Action of glacial acetic acid on compound V. A mixture of compound V (0.50 g; 0.00145 mole) and glacial acetic acid (20 ml) was refluxed for six hours, and then cooled. The solid precipitated (0.4 g; 80 %) was separated by filtration and crystallized from glacial acetic acid (m.p. and mixed m.p. with an authentic sample of compound VI 320°)[2].

Action of xylene on compound V. A solution of compound V (0.5 g; 0.00145 mole) in xylene (10 ml) was refluxed for eight hours the solvent was distilled off and drops of ethanol were added and heated. The precipitated solid (0.3 g; 60 %) was collected by filtration and recrystallized from glacial acetic acid (m.p. and mixed m.p. with an authentic sample of compound VI 320°)[2].

Action of hydrazine hydrate on compound VII. Hydrazine hydrate (5 ml; 100 %) was added to a solution of rubazoic acid (3.6 g; 0.01 mole) in ethanol (20 ml). The colour of the reaction mixture turned immediately to deep blue with evolution of ammonia and finally it became colourless and evolution of ammonia ceased. The reaction mixture was concentrated and boiled in water. The formed solid (1.7 g; 50 %) recrystallized from glacial acetic acid (m.p. 230°, mixed m.p. with an authentic sample of compound VI)[2] showed no depression.

Action of diazomethane on compound I. Diazomethane solution (prepared from 10 g. nitrosomethylurea in 100 ml ether) was added in 25 ml portion to a solution of compound I (2.6 g; 0.01 mole) in benzene (20 ml) and the reaction mixture was kept in refrigerator for one day and at room temperature for another day. The solvents were evaporated and the residual solid VIII (1.7 g; 63 %) recrystallized from ethanol, m.p. : 159, Found ; C, 78.0 ; H, 6.0 ; N. 10.0

---

* Chemical shifts were determined in ppm; s (singlet); d(doublet); t(triplet) and m(multiplet).

Calcd. for $C_{18}H_{16}N_2O$; C, 78.2 ; H, 5.8 ; N, 10.1 ; IR-spectrum (CCl_4) ν_{max}, 1030 and 2900 cm^{-1} (νCH_2) 1320 cm^{-1} (νCH) ; and 1720 cm^{-1} ($\nu N{=}C{=}O$) ; ^1H-NMR spectrum (CCl_4) δ : 1.74 (3H, s, CH_3) ; 3.64 (2H, d, CH_2) ; 4.7 (1H,t $-CH$) ; 7.5 (5H, m, C$-$Ph) ; 7.75 (5H, m, N$-$Ph).

Action of diazomethane on compound V. In a similar experiment as above a solution of diazomethane in ether and pyrazole blue V (3.4 g ; 0.1 mole) in ether (50 ml) was mixed. The formed solid IX (3.3 g ; 97 %) was recrystallized from ethanol, m.p. : 130 ; Found : C, 70.0 ; H, 5.3 ; N, 15.3 ; Calcd. for $C_{21}H_{18}N_4O_2$; C, 70.4 ; H, 5.1 ; N, 15.6 % ; IR-spectrum (CCl_4) : 1030 and 2900 cm^{-1} (νCH_2) ; 1720 cm^{-1} ($\nu N{=}C{=}O$) ; ^1H-NMR spectrum ($CDCl_3$) δ : 1.72 (6H,s, 2xCH_3) ; 7.78 (10H, m, 2 × N-Ph) ; 3.60 (2H, s, CH_2).

Oxidation of compound IX. Hydrogen peroxide (10 ml ; 50 vol.) was added to a solution of compound IX (1.8 g ; 0.005 mole) in glacial acetic acid (20 ml). The reaction mixture was refluxed for one hour, concentrated and then diluted with few drops of water, the precipitated solid X (1.6 g ; 82 %) was recrystallized from methanol, m.p. : 230. It did not dissolve in $NaHCO_3$ solution ; Found : C, 64.7 ; H, 4.90 ; N, 14.2 ; Calcd. for $C_{21}H_{20}N_4O_4$; C, 64.3 ; H, 5.1 ; N, 14.3 % ; IR-spectrum (Nujol mull) ν_{max}, 1700 cm^{-1} ($\nu N{=}C{=}O$) ; 3270 cm^{-1} (νOH) ; ^1H-NMR spectrum ($CDCl_3$) δ : 1.7 (3H, s, CH_3) ; 1.8 (3H, s, CH_3) ; 3.2 (1H, s, CH_2 OH) ; 3.6 (1H, s, C$-$OH) ; 4.22 (2H, s, CH_2) ; 7.70 (5H, m, N-Ph) ; 7.86 (5H, m, N-Ph).

Action of diazomethane on compound VII. Diazomethane solution in ether (prepared as described before), was added to a solution of rubazoic acid VII (3.6 g ; 0.01 mole) in benzene (50 ml) the residual solid XI (3.0 g ; 81 %) was recrystallized from methanol, m.p. : 120 ; Found : C, 67.7 ; H, 5.2 ; N, 18.8 ; Calcd. for $C_{21}H_{19}N_5O_2$: C, 67.6 ; H, 5.1 ; N, 18.8 % ; Methoxyl group (Zeisel) ; Found : 8.6 ; Calcd. : 8.3 % IR-Spectrum (CCl_4) ; 1050 cm^{-1} ($\nu O-CH_3$) ; 1195 cm^{-1} ($\nu C{=}O$) ; and 1710 cm^{-1} ($\nu N{=}C{=}O$) ; ^1H-NMR spectrum ($CDCl_3$) δ : 1.72 (3H,s, C(3) CH_3) ; 1.90 (3H, s, C(3′) CH_3) ; 2.30 (3H, s, OCH_3) ; 7.76 (5H, m, N(1) Ph) ; 8.00 (5H, m, N(1′) Ph).

Action of diphenyldiazomethane on compound V. A solution of diphenyldiazomethane (prepared from 11.8 g ; 0.06 mole of benzophenone hydrazone in 100 ml of dry benzene) was added to a solution of pyrazole blue V (3.4 g ; 0.01 mole) in dry benzene (20 ml). The reaction mixture was refluxed for four hours, and then concentrated. The residual solid VI (3.2 g ; 94 %) had an m.p. of 320 (the mixed m.p. with an authentic sample of compound VI[2] showed no depression).

REFERENCES

[1] A. Mustafa, W. Asker, A.F.A. Shalaby, Z. Selim and C. R. Daguer, *J. Org. Chem.*, **27**, 4201 (1962).

[2] L. Knorr, *Liebigs Ann. Chem.*, **238**, 137 (1887).

[3] H. R. Hatt *Organic Syntheses*, **11**, 395 (1948).

[4] "High Resolution ^1H-NMR Spectroscopy in Organic Chemistry", Varian Association, 1963.

Revue Roumaine de Chimie, **25**, *4*, 583–588 (1980)

REDUCTION OF SILVER(I) WITH COBALT (II) AND MANGANESE (II) SOLUTIONS IN ALKALINE TRIETHANOLAMINE MEDIUM: GRAVIMETRIC ESTIMATIONS OF SILVER

K. N. RAOOT* and V. G. VAIDYA
Department of Chemistry, Government College of Engineering & Technology, Raipur-492002
India

Received August, 30, 1978

Analytical investigations on the quantitative reduction of monovalent silver to the metal, separately with cobalt(II) and manganese(II) solutions in the alkaline triethanolamine medium have been carried out. The optimum conditions in terms of triethanolamine and sodium hydroxide concentrations, amount of reductants, temperature and reduction duration have been studied for the gravimetric evaluations of 10 to 100 mg of silver. Accurate and reproducible results have been recorded in the presence of Cu(II), Ni(II), Zn(II), Pb(II), Cd(II), Pd(II), Ru(III), Bi(III), Fe(III), Al(III), Sn(IV), Se(IV), Te(IV), Mo(VI) and W(VI). Pt(IV) in manganese (II) and Hg(II), Au(III), Ir(III), Rh(III) and Os(VIII) in both the reductions interfered.

Reducing power of a redox system is substantially enhanced in the presence of a complexing agent forming more stable chelate with higher valency state. Based on this fact, we employed cobalt (II) for the reductions of silver (I), gold (III) and palladium (II) in the EDTA medium.[1,2] Iron (II) in the presence of alkaline triethanolamine (TEA) has been used for the reductometric determinations of various metal irons.[3–5] In the same medium, cobalt (II) has been used for the reduction of manganese (III).[6] However, no further use of cobalt (II) or manganese (II) in TEA medium for the reduction of metal ions has been reported.

In the present paper the optimum conditions for the quantitative reduction of silver (I) with cobalt(II) as well as with manganese (I) in the alkaline TEA medium have been established and based on these, the methods for the gravimetric estimation of silver in pure solutions and in the presence of various foreign metal ions have been proposed.

EXPERIMENTAL

Silver(I) solution was prepared by dissolving 1 g silver powder (specpure, Johnson-Matthey) in minimum volume of (1 :2) HNO_3, made up to 1 litre and standardised by thiocyanate

---

*** Present address — Defence Metallurgical Research Laboratory Hyderabad — 500 258, India**

method. Cobalt(II) solution was prepared by dissolving 4.941 g $Co(NO_3)_2.6H_2O$ AR (BDH) in water and made up to 1 litre. Manganese(II) solution was prepared by dissolving 1 g of electrolytic manganese in minimum quantity of HNO_3 and made up to 1 litre. 4M sodium hydroxide solution was prepared from GR(S. Merck) pellets. Wash solution was 5% both in TEA and NaOH. All the other utilized chemicals were of analytical reagent grade.

INVESTIGATIONS

The fact that Silver(I), in the alkaline medium, is quantitatively reduced to the metal with TEA at elevated temperature was the subject matter of our recent paper.[7] However, it was also recorded, during the above study, that the rate of reduction falls down with lowering of temperature and below 10°, practically no reduction of silver(I) occurs. Ascertainment of the above fact was a prerequisite for the present work. For this, a known amount of silver(I) solution was mixed with TEA and NaOH solutions and diluted to the mark in a volumetric flask, maintaining the temperature all the while at 5°, using an ice bath. This solution and another solution containing the same amount of silver(I) in the similar volume in nitric acid medium and the matrix blank, were subjected to the atomic absorption spectrophotometric measurements. The readings recorded at the intervals of 10 minutes remained the same for both the silver solutions over a period of more than one hour. Similar observations were made during the experiments carried out at varying molarities of NaOH. Thus, it was confirmed that at the temperature around 5°, TEA has no reducing effect on silver (I) in the mediums sufficiently varying in NaOH concentrations.

The effect of TEA and NaOH on the gravimetric determinations of 25 mg of silver with cobalt(II) as well as manganese(II) were first studied in a series of experiments. It was found that a medium 0.1 to 0.5 M in TEA and also NaOH was the best suited for reduction with cobalt(II), whereas for manganese(II) reduction the optimum medium was 0.4 to 1.0 M both in TEA and NaOH. At 5° both the reductions reached the quantitative completion instantaneously.

Determination of Ag(I) in pure solution. In a 250 ml beaker, a silver(I) solution (containing 10–100 mg of silver) was taken, diluted to 50 ml and cooled to 5°. 2.5 to 12.5 ml precooled solutions of TEA and NaOH were added. Twice the stoichiometric amount of cobalt(II) solution was introduced with stirring, maintaining the total volume at 100 ml. After 5 minutes the precipitated silver metal was filtered through pulp, washed several times with washing solution and then with water. The precipitate was ignited at 600° and weighed.

In the case of reduction with manganese(II), the overall molarities of both TEA and NaOH were maintained at 0.4 to 1.0 M and manganese(II) solution was added in the same proportion as cobalt(II). The results are presented in table 1.

TABLE 1

Determination of silver in pure solution

Silver taken, mg	Found, mg with Co(II)	%Error	Found, mg with Mn(II)	% Error
10.00	9.95	−0.50	10.00	0.00
20.00	20.10	+0.50	20.10	+0.50
40.00	40.05	+0.13	39.90	−0.25
60.00	59.85	−0.25	59.90	−0.13
80.00	80.30	+0.38	80.20	+0.25
100.00	100.15	+0.15	100.25	+0.25

Effect of diverse ions. To a solution containing 20 mg silver(I) were added standardised solutions containing different amounts of foreign metal ions and after cooling to 5°, the estimation of silver was carried out in accordance with the procedure given above for pure solutions. The results of these studies are incorporated in table 2. They show that the five 5-fold excess of Cu(II), Ni(II), Pb(II), Cd(II), Zn(II), Fe(III) and Al(III) and the two fold excess of

Pd(II), Ru(III), Bi(III), Sn(IV), Se(IV), Te(IV), Mo(VI) and W(VI) had no adverse effect on either of the reductions. Pt(IV) in the case of manganese(II) reduction and Hg(II), Au(III) Ir(III), Rh(III) and Os(VIII) in both the reductions, interfere. Both the reductions remain uneffected by large quantities of chloride ions.

TABLE 2

Determination of 20.00 mg silver in the presence of foreign ions

Foreign ion, mg	Silver found (in milligrams)	
	by Co(II) reduction	by Mn(II) reduction
Cu(II), 100.6	20.05	20.10
Zn(II), 100.0	20.15	20.05
Ni(II), 100.8	19.90	20.00
Pb(II), 104.8	20.05	20.15
Cd(II), 100.8	20.05	20.20
Pd(II), 42.0	20.10	20.05
Fe(III), 106.0	20.10	20.10
Al(III), 101.0	19.95	20.15
Bi(III), 44.2	20.25	20.15
Ru(III), 43.4	20.20	20.20
Pt(IV), 40.0	20.00	—
Sn(IV), 43.5	20.05	19.95
Se(IV), 41.5	20.15	20.10
Te(IV), 40.8	20.10	20.20
Mo(VI), 44.0	20.05	19.80
W(VI), 40.0	20.05	20.10
Cl^- 282.0	20.10	20.10

RESULTS AND DISCUSSION

During the course of further studies, the optimum medium for potentiometric titration of silver (I) with cobalt(II) solution was found to consist of 0.2M TEA and 0.1M NaOH[8] and that for titration with manganese(II) solution contained 0.55 M TEA and 0.45 M NaOH[9]. The potentiometric titrations of cobalt (II) and manganese (II) with silver (I) were separately carried out in the optimum medium with respect to TEA and NaOH as shown above in the inert atmosphere using SCE-platinum electrode pair. From the potentiometric curves thus obtained, redox potentials of Co(II)/Co(III) and Mn(II)/Mn(III) couples were determined by the method followed by Conant and Feiser[10] for the determination of redox potentials of various quinones and later adopted by Rao et al.[11] for finding out the redox potential of cacotheline-reduced cacothaline system. Redox potential of Ag(I)/Ag was likewise determined in both the mediums from curves obtained by the titrations of silver (I) with Co (II) and Mn(II) solutions respectively. The formal redox potential of Co(II)/ /Co(III) couple in a medium 0.2 M in TEA and 0.1 M in NaOH was found to be + 0.13V. In a medium 0.55 M in TEA and 0.45 M NaOH the redox potential of Mn(II)/Mn(III) was estimated to be 0.23 V. The formal redox potentials of Ag(I)/Ag system in the corresponding mediums were estimated to be + 0.33 V and +0.28 V respectively. These figures show that the redox potentials of Ag(I)/Ag are substantially higher than those for Co(II)/Co(III) and Mn(II)/Mn(III) given above and hence silver (I) undergoes reduction with cobalt (II) and manganese(II) solutions. The reduction with manganese(II), however, is comparatively faster and this is supported by its negative redox potential. Lowered redox potentials in alkaline TEA medium make both cobalt(II) and manganese(II) liable for atmospheric oxidation and so their stoichiometric quantities become inadequate for the quantitative reduction of silver(I).

For ascertaining the completeness of the reduction in the selected experiments, the filtrates were quantitatively collected and made up in volumetric flasks. These solutions were aspirated in atomic absorption sphectrophotometer using silver lamp at 328.1 nm and the silver contents in the solutions were evaluated using the calibration graph of silver for the minimum permissible quantities in the identical matrix, where the reduction of silver(I) was inhibited by cooling the solutions below 5°. These investigations showed that practically no silver(I) was left unreduced and the reductions were complete and quantitative under the optimum conditions suggested. Purity of the precipitated silver metal was confirmed by subjecting the dried precipitate to X-ray diffraction studies. Samples for X-ray diffraction were made by coating the precipitate powder on a glass fibre using quickfix adhesive. The specimen diameter was 0.05 cm. The sample was rotated during 5-hour exposure employing copper radiation with nickel filter. The 'd' values with the corresponding indices measured were compared with the values given for pure silver in ASTM data card which showed that the precipitate was composed of pure silver metal with F.C.C. structure.

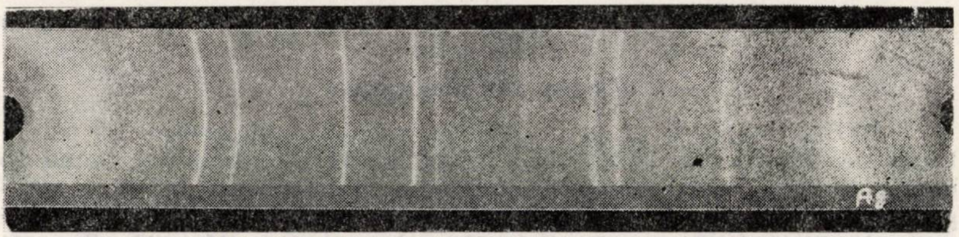

Fig. 1. — X-ray diffraction powder photograph of precipitated silver.

Various metal ions form complexes with TEA and hence there are practically no contaminations of these metal ions on the precipitated silver. This also makes the filtration and washing of the precipitate convenient and fast. The interesting feature of the present reductions is that the fairly high concentrations of chloride ions do not cause any adverse effect, since AgCl precipitated is quantitatively converted into the metal. The maximum error in the case of reductions with cobalt(II) was 1.25%, whereas that with manganese(II) solution was 1.00%. Thus the methods are comparable in accuracy with the standard methods [12] involving the use of halides, benzotriazole and reducing agents like hypophosphorous acid and ascorbic acid. Both the reductions are instantaneous, do not require any heating, offer sufficiently wide ranges of reaction conditions and thus are simpler and faster as compared to the above-referred methods. The methods can conveniently be applied to the determination of silver in its alloys.

TABLE 3

X-ray diffraction data for the precipitate

Cu K_α 2θ°	Observed "d"	ASTM, Card 4-783 "d"
38.25	2.353	2.359
44.25	2.046	2.044
64.25	1.450	1.445
77.25	1.235	1.231
81.25	1.184	1.1796
97.75	1.0225	1.0215
110.25	0.9387	0.9375
114.75	0.9145	0.9137

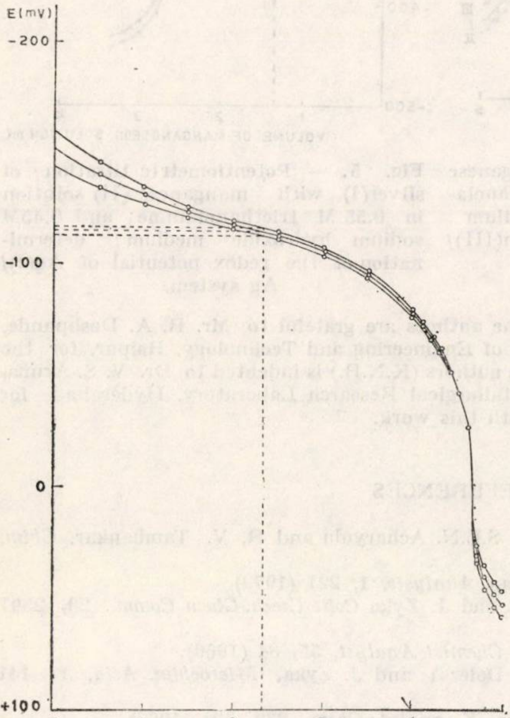

Fig. 2. — Potentiometric titration of cobalt (II) with silver(I) solution in 0.2 M triethanolamine and 0.1 M sodium hydroxide medium; determination of the redox potential of Co(III)/Co(II) couple.

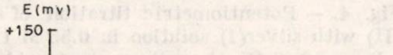

Fig. 3. — Potentiometric titration silver (I) with cobalt (II) solution in 0.2 M triethanolamine and 0.1 M sodium hydroxide medium; determination of the redox potential of Ag(I)/Ag system.

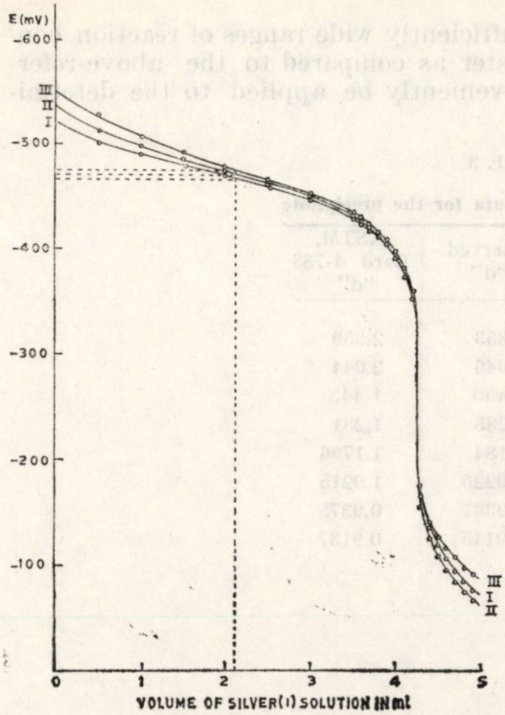

Fig. 4. — Potentiometric titration of manganese (II) with silver(I) solution in 0.55 M triethanolamine and 0.45 M sodium hydroxide medium ; determination of the redox potential of Mn(III)/Mn(II) couple.

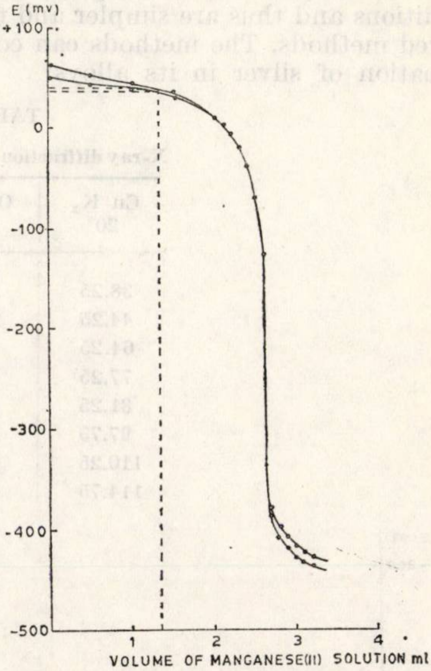

Fig. 5. — Potentiometric titration of silver(I) with manganese (II) solution in 0.55 M triethanolamine and 0.45M sodium hydroxide medium ; determination of the redox potential of Ag(I)/Ag system.

ACKNOWLEDGEMENTS. The authors are grateful to Mr. R. A. Deshpande, Principal, Government College of Engineering and Technology, Raipur, for the laboratory facilities. One of the authors (K.N.R.) is indebted to Dr. V. S. Arunachalam, Director, Defence Metallurgical Research Laboratory, Hyderabad for the permission to associate with this work.

REFERENCES

[1] S. Raoot, K. N. Raoot, B. V. Rao, S.L.N. Acharyulu and R. V. Tamhankar, *Chim. analyt.*, **53**, 584 (1971).

[2] K. N. Raoot, S. Raoot and B. V. Rao, *Aanlysis*, **1**, 221 (1972).

[3] J. Dolezal, E. Luksite, L. Rybacek and J. Zyka *Coll. Czech. Chem Comm.*, **29**, 2597 (1964).

[4] H. Alfaro, J. Dolezal and J. Zyka, *Chemist Analyst*, **55**, 84 (1966).

[5] N. A. Chugthai D. N. Sharma, J. Dolezal and J. Zyka, *Microchim. Acta*, **1**, 141 (1976).

[6] P. Blanicky, J. Dolezal and J. Zyka, *Z. analyt. Chem.*, **232**, 325 (1967).

[7] K. N. Raoot and V. G. Vaidya, *Indian J. Chem.*, **16A**, 913 (1978).

[8] K. N. Raoot and V. G. Vaidya, *Chem. Analit.*, **24**, 149 (1979).

[9] K. N. Raoot and V. G. Vaidya, *Quim. Anal.*, Under Publication.

[10] J. B. Conant and L. F. Feiser, *J. Amer. Chem. Soc.*, **46**, 1858 (1924).

[11] G. G. Rao, N. Krishnamurthy and V. N. Rao, *Talanta*, **12**, 243 (1965).

[12] K. Kodama, "Methods of Quantitative Inorganic Analysis", Interscience Publishers, New York, 1963, p. 146.

Revue Roumaine de Chimie, **25**, *4*, 589–597 (1980)

ANALYSIS OF SILICATE ROCKS BY ATOMIC ABSORPTION SPECTROMETRY

V. IOSOF and VASILICA NEACȘU

Institute of Geology and Geophysics, Street Caransebeș 1, Bucharest, Romania

Received November 27, 1978

A rapid method for the determination of major constituents in silicate rocks is described. The method is based on fusion of the sample in the presence of lithium tetraborate flux. The fusion product is dissolved in nitric acid-glycerol mixture. The resultant solution is used for the determination of SiO_2, Al_2O_3, CaO, MgO, Fe_2O_3, TiO_2, MnO by atomic absorption spectrometry, Na_2O, K_2O by flame-photometry and P_2O_5 by spectrophotometry. This method has a high accuracy, our results are in agreement with those accepted for international standards.

Many analytical schemes have been proposed since 1960, concerning both the decomposition and the determination of major constituents of the different types of rocks, soils and minerals by atomic absorption spectrometry.[1-7]

Various reagents have been used for the sample decomposition : alkaline carbonates, sodium hydroxide,[8] hydrofluoric-perchloric nitric acid mixtures, hydrofluoric acid in sealed vessels under heat and pressures.[9]

In recent years sodium tetraborate, lithium metaborate,[5] strontium metaborate,[10] lithium tetraborate,[11] lithium metaborate-tetraborate mixture[7] have been suggested as decomposition fluxes.

EXPERIMENTAL

In our method lithium tetraborate flux has been used. The silicates are converted into borates soluble in dilute acids by fusion with this flux.

Organic acids as citric acid, EDTA[12] or inorganic acids are used for dissolution of borates and borosilicates ; accordingly, we used nitric acid and added glycerol for increasing the borate solubility.[13,14]

The resulting solutions are colorless and stable and they may be preserved for a long time.

Concerning the relationship sample-flux ratio, our determinations on the acid, basic and intermediary rocks and iron rich mica minerals indicate that a 1 : 4 sample-flux ratio is the most satisfactory to produce a homogeneous glass. A reduced fusion time is characteristic of such ratio.

The most common releasing agents are lanthanum or strontium salts which suppress the chemical interferences.

Accordingly, we have used strontium nitrate in concentration of about 400 μg Sr/ml (less expensive than lanthanum salts).

For the determination of Si, Al, Ti, Ca, we have coupled this addition with a higher temperature flame obtained from acetylene and nitrous oxide mixture. The presence of lithium and strontium (elements with a low ionization potential Li = 5.39 ev ; Sr = 5.69 ev) in the solution eliminated the ionization interferences in the determination of alkali and alkaline earth elements.

The loss on ignition was determined before the decomposition and following this the sample was ground to the optimal size required for spectrometric determinations.

Similar results were obtained by using the samples dried at 105°.

Reagents and apparatus

Nitric acid, sp. gr. 1.42, $Sr(NO_3)_2$ anhydrous, $Li_2B_4O_7$ anhydrous, Glycerol anhydrous De-ionized water.

All the reagents used throughout were of analytical-reagent grade. Plastic bottles for storage.

Varian Techtron AA6- Atomic Absorption Spectrophotometer. FLAPHO 4-Flame Photometer.

Procedure

Weigh 0.1250 g of sample into a 25 ml platinum crucible and mix the sample thoroughly with 0.5000 g of $Li_2B_4O_7$.

Fuse the sample for 20 minutes at 1050° in a muffle furnace.

Place the uncovered crucible in an oxidizing atmosphere in the furnace in order to prevent the reduction of Fe, Mn, Co, Cu, Pb and their alloying with platinum. For the dissolution of the resulting melt add (into the platinum crucible) 20 ml of solution containing :

Solution A : dissolve 12.5 g $Sr(NO_3)_2$ in H_2O ; add 100 ml of concentrated HNO_3 and 300 ml glycerol and dilute to 1 liter. Store in a plastic bottle.

The borates dissolution is facilitated by stirring with the aid of a magnetic stirrer at the temperature of 60–70° for 10–30 minutes.

Transfer the solution into a 250 ml volumetric flask and dilute with distilled water.

Both the quantity of the sample and the dilution allow the direct determination of SiO_2, Al_2O_3, Fe_2O_3, CaO, MgO, TiO_2, Na_2O, K_2O, P_2O_5 from the same solution.

We used various international standards for calibration : granite GH, granite GA, basalt BR, biotit Mica-Fe, diorite DR-N (France) and granite GM, basalt BM, greisen GnA (East Germany) and their mixture in order to obtain intermediate composition.

All these reference standards with a known defined composition and almost similar to our analysed samples, eliminate the matrix effects which are very important in atomic spectrometry.

RESULTS AND DISCUSSION

Initial tests of the suggested method have been concentrated upon these international standard rocks.

The resulted contents of each element have been compared with the mean values given by Flanagan.[1]

High accuracy is provided by taking into account Pinta's[15] considerations ; he claimed that most suitable results require a number of readings for each element.

We found necessary the following readings : Si = 6 ; Al = 4 ; Ca=3 Fe = 2 ; Ti = 2 ; Mn = 2 ; Mg = 2.

TABLE 1

Instrument parameters

Element	Si	Al	Fe	Ti	Mn	Ca	Mg
Wavelength nm	251.6	309.3	372.0	364.3	279.5	422.7	285.2
Spectral band-pass nm	0.1	0.5	0.2	0.5	0.2	0.5	0.2
Lamp current mA	15	5	5	20	5	3	3
Flame	Reducing	Reducing	Oxidizing	Reducing	Oxidizing	Oxidizing	Oxidizing
Fuel	Acetylene	Acetylene	Acetylene	Acetylene	Acetylene	Acetylene	Acetylene
Oxidant	N_2O	N_2O	Air	N_2O	Air	N_2O	Air
Sensitivity µg/ml	1.5	0.75	0.55	1.4	0.021	0.013	0.003
Optimum range µg/ml	70—280	40—200	25—100	60—240	1.0—4.0	1—4	0.1—0.4
Detection limit µg/ml	0.2	0.018	0.05	0.05	0.002	0.002	0.0002

1. Silica

Silicon belongs to the group of the elements expressing low sensitivity for atomic absorption spectrophotometry.

In order to increase its accuracy, we have used a smaller spectral band pass necessary to isolate the 251.6 nm and 251.4 nm lines and to obtain a better stability of the readings.

TABLE 2

Comparative values for SiO_2 (wt. %)

Sample	Mica-Fe	Basalt BM	Granite GA	Granite GH
Literature values	34.40	49.60	69.90	75.80
$\overline{x}$, found AAS	34.49	49.75	69.72	75.57
Standard deviation	0.32	0.38	0.40	0.44
Relative deviation	0.92	0.76	0.57	0.58

Literature values given by Flanagan[1] ; $\overline{x}$ =arithmetical mean of 5 analyses. AAS = atomic absorption spectrometry.

Silicon can be determined from the lithium tetraborate fusion by colorimetric method,[7] after a preliminary depolimerization with NaF solution (SiO_2 in concentrations exceeding 200 μg/ml forms polymers which will not react with the ammonium molybdate solution).

2. Aluminium

TABLE 3

Comparative values for Al_2O_3 (wt. %)

Sample	Granite GA	Basalt BM	Diorite DR-N	Mica-Fe
Literature values	14.50	16.20	17.42	19.40
$\bar{x}$, found AAS	14.63	16.27	17.26	19.21
Standard deviation	0.15	0.14	0.18	0.22
Relative deviation	1.02	0.86	1.04	1.14

3. Iron

TABLE 4

Comparative values for Fe_2O_3 (wt. %)

Sample	Granite GH	Granite GA	Greisen GnA	Diorite DR-N
Literature values	1.34	2.83	5.84	9.91
$\bar{x}$, found AAS	1.29	2.78	5.79	9.82
Standard deviation	0.07	0.08	0.07	0.11
Relative deviation	5.42	2.87	1.20	1.12

From the main solution, Fe_2O_3 can be determined by colorimetric method using dipyridine as chromogenic agent.

4. Titanium

TABLE 5

Comparative values for TiO_2 (wt. %)

Sample	Granite GM	Diorite DR-N	Basalt BM	Mica-Fe
Literature values	0.21	1.11	1.14	2.55
$\bar{x}$, found AAS	0.22	1.12	1.13	2.53
Standard deviation	0.02	0.03	0.03	0.05
Relative deviation	9.09	2.67	2.65	1.97

In the suggested method the titanium determination by atomic absorption spectrometry is possible only for concentrations higher than 0.2 g% TiO_2. The concentrations less than 0.2 g % TiO_2 can be determined by colorimetric method with tiron (from the initial solution of lithium tetraborate).

5. Manganese

TABLE 6

Comparative values for MnO (wt. %)

Sample	Granite GA	Basalt BM	Diorite DR-N	Mica-Fe
Literature values	0.090	0.150	0.210	0.350
x̄, found AAS	0.085	0.156	0.200	0.340
Standard deviation	0.008	0.007	0.010	0.010
Relative deviation	9.41	4.48	5.00	2.90

6. Calcium

TABLE 7

Comparative values for CaO (wt. %)

Sample	Greisen GnA	Granite GA	Basalt BM	Diorite DR-N
Literature values	0.69	2.45	6.44	7.08
x̄, found AAS	0.68	2.37	6.34	7.20
Standard deviation	0.06	0.10	0.14	0.15
Relative deviation	8.82	4.21	6.34	2.08

For concentrations over 5μg/ml CaO, we have found necessary a dilution for both sample and standard with a solution of the fusion blank (in order to ensure the presence of the same concentration of lithium and strontium in the final solution which prevent the interferences).

According to various authors, rotation of the burner head is not recommended to extend the analytical range since calcium is very emissive in the flame $N_2O-C_2H_2$ at high concentrations.

In our study for the high content of calcium we extended the analytical range by rotation of the burner head and obtained a good precision.

7. Magnesium

TABLE 8

Comparative values for MgO (wt. %)

Sample	Granite GM	Granite GA	Diorite DR-N	Basalt BM
Literature values	0.38	0.95	4.50	7.46
$\bar{x}$, found AAS	0.35	0.99	4.63	7.56
Standard deviation	0.03	0.05	0.08	0.10
Relative deviation	8.57	5.05	1.72	1.32

Magnesium is a very sensitive element for the determination by atomic spectrometry.

High magnesium contents require either the sample and standard dilution or the decreasing of the sensitivity by rotation of the burner head.

8. Sodium and potassium

Sodium and potassium are determined directly from the same solution by flame-photometry.

Results are calculated from calibration curves made from international reference standards.

Working conditions

Wavelength nm : Na = 589.0 ; K = 766.5
Flame : air-propane

TABLE 9

Comparative values for Na_2O (wt. %)

Sample	Diorite DR-N	Granite GA	Granite GM	Basalt BM
Literature values	3.00	3.55	3.76	4.64
$\bar{x}$, found FP	3.02	3.47	3.77	4.57
Standard deviation	0.04	0.07	0.06	0.07
Relative deviation	1.32	2.04	1.59	1.31

FP = Flameph otometer

TABLE 10

Comparative values for K_2O (wt. %)

Sample	Basalt BM	Greisen GnA	Granite GM	Granite GH
Literature values	0.20	2.61	4.74	4.76
$\bar{x}$, found FP	0.19	2.59	4.78	4.77
Standard deviation	0.02	0.04	0.04	0.04
Relative deviation	10.52	1.54	0.84	0.84

9. Phosphorous

Colorimetric determination of phosphorus

Phosphorus is determined by colorimetric method as molybdophosphate blue complex which has an absorption maximum at 822 nm.

The interference of silicon occurring in solution is eliminated both by control of pH and by limiting the concentration of the free molybdate ions in solution.

Reagents

Ammonium molybdate solution, 5% m/V (in 0.6 M H_2SO_4);

Tartaric acid solution, 10 % m/V; acid ascorbic solution, 10 % m/V. Stock standard P_2O_5 solution : dissolve 0.18405 g K_2HPO_4, dried at 105° in blank solution (lithium tetraborate, nitric acid and glycerol) and dilute to 500 ml volumetric flask. This solution contains 300 μg/ml P_2O_5.

Working standard solution : For preparation of calibration curve, dilute 10 ml of stock solution in 200 ml volumetric flask. This contains 15 μg/ml P_2O_5.

Procedure

Transfer by pipet 10 ml aliquot of the solution (prepared as described by lithium tetraborate fusion) in a 50 ml volumetric flask. Add 10—15 ml of water, 3 ml of the tartaric acid solution, 4 ml of the ammonium molybdate solution and 7.5 ml of the ascorbic acid solution, stirring the flask after each addition of the reagents.

Preparation of standard curve

Into 50 ml volumetric flasks, measure 0 ; 1 ; 2 ; 3 ; 4 and 5 ml aliquots of the standard P_2O_5 solution (15 μg/ml). Add to each flask the corresponding fusion blank and continue with the addition of reagents as mentioned above.

Immerse the unstoppered flasks in a 37° constant temperature bath for 2 hours, remove and cool in running water. Allow to come to room temperature, dilute to volume and mix thoroughly.

Measure the absorbance at 822 nm in a 1 cm cell, using a reagent blank as the reference blank solution.

The concentration of P_2O_5, in micrograms is calculated from the standard curve.

The color of the heteropoly blue complex is stable for at least 20 hours.

The optium concentration range is 0.1—1.5 $\mu g/ml\ P_2O_5$. Observation according to Whitehead[16] and our study is : these solutions (obtained after Li-tetraborate fusion) must be kept no longer than 4 days before phosphorus determination ; otherwise lower results are obtained. The explanation of this effect has not been established experimentally.

TABLE 11

Comparative values for P_2O_5 (wt. %)

Sample	Granite GA	Mica-Fe	Basalt BR	
Literature values	0.12	0.45	1.04	
$\bar{x}$, found sf	0.13	0.42	1.04	
Standard deviation	0.01	0.02	0.02	
Relative deviation	7.69	4.76	1.92	

sf = Spectrophotometer

Separate portions of sample are used for the determinations : FeO, H_2O^-, H_2O^+, CO_2 and sulfur by the following methods :

— FeO by titration with a standard dichromate solution (using diphenylamine sulfonate indicator solution) after decomposition with HF and H_2SO_4 ;

— H_2O^- by loss of weight at 110° ; H_2O^+ by Penfield method ;
— CO_2 and sulfur by microcombustion method.

CONCLUSIONS

Our method is very simple and more rapid than the classical method for determination of those elements in silicates based on precipitations and separations which are extremly laborious.

In principle our procedure essentially involves the fusion of the sample with tetraborate flux and dissolution of the cakes obtained in dilute acid. Finally, this solution is used for the direct determinations by atomic absorption spectrometry.

This method allows the use of small samples and results indicating high precision and accuracy as listed in tables 2—11.

Interferences are eliminated by the occurrence of lithium and strontium in solution and by using standards of similar compositions to those of the analysed samples.

In this work our method has been applied for the determination of the major constituents in acid, basic, intermediary rocks and iron rich mica minerals, but can be extended to the analysis of various silicate rocks.

REFERENCES

[1] F. J. Flanagan, *Geochim. Cosmochim. Acta*, **37**, 1189 (1973).
[2] N. H. Suhr and C. O. Ingamells, *Analyt. Chem.*, **38**, 730 (1966).
[3] C. B. Belt, *Analyt. Chem.*, **39**, 676 (1967).
[4] O. K. Galle, *Appl. Spectroscopy.*, **22**, 404 (1968).
[5] J. C. Loon Van and C. M. Parrissis, *Analyst*, **94**, 1057 (1969).
[6] P. L. Boar and L. K. Ingram, *Analyst*, **95**, 124 (1970).
[7] L. Shapiro, *U.S. Geol. Surv. Bull.*, **1401**, 1 (1975).
[8] M. L. Blanchet and L. Malaprade, *Chem. Analyt.*, **49**, 11 (1967).
[9] F. J. Langmyhr and P. E. Paus, *Analyt. Chim. Acta*, **43**, 397 (1978).
[10] E. Jeanroy, *Chem. Analyt.*, **54**, 129 (1972).
[11] M. S. Wang, *Appl. Spectroscopy*, **16**, 141 (1962).
[12] K. Govindaraju, *Appl. Spectroscopy*, **24**, 8 (1970).
[13] Cl. Duval, ,,Traité de Micro-Analyse Minérale'', vol. 4 Presses Scientifiques Internationales, Paris, 1957, p. 7—16.
[14] Y. Besnus and R. Rouault, *Analusis*, **2**, 111 (1973).
[15] M. Pinta, "Spectrométrie d'absorption atomique", vol. 2, Applications à L'analyse Chimique", Masson et Cie Éditeurs, Paris, 1971, p. 315—324.
[16] D. Whitehead and S. A. Malik, *Analyst*, **101**, 485 (1976).

Revue Roumaine de Chimie, **25**, *4*, 599–603 (1980)

LIQUID-VAPOUR EQUILIBRIUM OF THE DIISOPROPYLETHER–CYCLOHEXANONE SYSTEM

GH. MIHĂILĂ, V. ABABI and F. VITAN
Department of General and Technological Chemistry, Polytechnic Institute, Splai Bahlui 71, Jassy, Romania

Received May 9, 1979

Using an apparatus with thermosiphonic mixture circulation, the liquid – vapour equilibrium data of the diisopropylether – cyclohexanone system, at atmospheric pressure, have been obtained. Composition of the two phases at equilibrium has been determined refractometrically. With the experimental data, the $t-x, y$ and $y-x$ diagrams of the system have been constructed The thermodynamic verification of the experimental data has been done by Redlich–Kister–Herington's procedure that confirmed their accuracy.

INTRODUCTION

As regards the formation of cyclohexanone, as intermediate product during caprolactum manufacture from phenol, there were made many investigations on liquid – vapour equilibrium of some systems with cyclohexanone.[1-2] Thus, there were studied the systems with cyclohexanone, having water, hexyl alcohol, cyclohexanol, toluene and cyclohexane as second component.

On the basis of some investigations,[3-4] it has been found that diisopropylether is a good extraction agent of phenol from the mixtures in which its content is low. Such a mixture is also that obtained in caprolactum manufacture. Since, after phenol extraction with this agent, the mixture contains cyclohexanone and diisopropylether too, in order to get some information on the possibility of its separation by distillation, the present paper deals with the liquid – vapour equilibrium of the diisopropylether – cyclohexanone system at 760 mm Hg.

EXPERIMENTAL

Reagents. The reagents employed for investigation of the liquid – vapour equilibrium were, first, purified by rectification. Their purity was verified by means of the refractive index at 20° and boiling point at 760 mm Hg. The values of these constants are presented in table 1. The small differences between the values of the physical properties of the purified reagents, determined experimentally and those found in literature, attest their high purity.

Apparatus. To investigate the liquid – vapour equilibrium in the binary mixture diispropylether – cyclohexanone, a Bushmakin's type apparatus was employed,[7] device that allows a continuous circulation of the liquid – vapour mixture. The boiling temperature of the mixtures was determined with a precision as high as ±0.1° ; the correction to temperature reading was done according to literature indications.[8] Pressure was maintained constant by means of an electric pressure controller.[9]

TABLE 1

Physical properties of the reagents

Reagents	Refractive index, n_D^{20}		Boiling point, °C	
	Experim.	Literat.	Experim.	Literat.
Cyclohexanone	1.4510	1.4502[5]	154.6	155.6[5]
Diisopropylether	1.3682	1.3680[6]	68.2	68.5[6]

Procedure. The diisopropylether — cyclohexanone mixtures, having different compositions, entered the apparatus successively and were heated, gradually, up to boiling temperature. Maintaining a constant pressure inside the apparatus, equal to 760 mm Hg, the boiling was conducted during 90 minutes, time long enough for the equilibrium achievement. After this time, two samples were taken out from the two phases, using some ampoules with cooling mantle. Determination of the two phases composition, at equilibrium, was done refractometrically, using an Abbé refractometer. The refractive index reading was done at a temperature of 20° kept constant by means of a thermostat. To check up if, in the mixtures having their boiling point close to that of cyclohexanone, chemical transformations do not take place, the samples were analysed chromatographically too.

For the quantitative determination of the reagents in the two phases was used a calibration curve, refractive index — composition, constructed on the basis of several diisopropylether — cyclohexanone mixtures, having known composition. The experimental data concerning the refractive index against composition of the investigated system are listed in table 2.

RESULTS

The experimental data concerning the composition of the phases and the boiling temperature of the different mixtures of diisopropylether — cyclohexanone, are summarized in table 3. The content of diisopropylether, expressed in molar percents, in the liquid phase, was noted by x_1 and, in the gaseous phase, by y_1. Together with these data, in table 3, are also given the vapour pressure of the two reagents in pure state, p_1^0 and p_2^0, activity coefficients γ_1 and γ_2, as well as $\lg \gamma_1/\gamma_2$, data needed for the thermodynamic verification of the experimental results.

Using the data presented in table 3, the $t-x,y$ diagram was constructed in figure 1, and the equilibrium diagram, $y-x$, in figure 2.

The vapour pressure of cyclohexanone, in pure state, in the temperature range in between the boiling temperatures of the two reagents, was calculated on the basis of the data found in cited literature[10]. The absence of the experimental data as regards the vapour pressure of diisopropylether at the temperatures higher than its boiling point, needed its theoretical calculation. For this purpose, the saturation pressure equation was employed, following a well-known procedure.[11]

TABLE 2

Dependence of the refractive index on composition, for the diisopropylether — cyclohexanone mixture, at 20°

Diisopropylether content, % mol	n_D^{20}
0.0	1.4510
10.0	1.4428
20.0	1.4345
30.0	1.4254
40.0	1.4170
50.0	1.4104
60.0	1.4015
70.0	1.3928
80.0	1.3845
100.0	1.3682

TABLE 3

Data of the liquid — vapour equilibrium of the diisopropylether-cyclohexanone system, at atmospheric pressure

Boiling temperature, °C	x_1, % mol	y_1, % mol	p_1^0, mm Hg	p_2^0, mm Hg	γ_1	γ_2	$\lg \frac{\gamma_1}{\gamma_2}$
154.6	0.00	0.00	—	760.00	2.2500	1.0000	0.3521
140.0	2.50	36.00	5054.00	496.93	2.1654	1.0039	1.3338
126.0	6.00	59.00	3731.60	329.00	2.0020	1.0100	0.2971
109.5	12.50	77.00	2519.27	194.69	1.8583	1.0261	0.2579
103.5	17.00	82.00	2160.74	159.05	1.6965	1.0362	0.2141
96.5	25.00	87.20	1792.26	124.60	1.4790	1.0409	0.1525
90.5	33.00	90.50	1515.94	100.32	1.3748	1.0741	0.1071
84.5	44.00	93.50	1273.21	80.19	1.2674	1.1000	0.0618
80.3	53.00	95.00	1121.84	68.24	1.2143	1.1848	0.0106
77.3	63.50	96.50	1022.40	60.67	1.1296	1.2011	−0.0266
74.7	72.00	97.50	943.47	54.82	1.0900	1.2378	−0.0552
71.5	82.00	98.50	849.72	48.06	1.0740	1.3178	−0.0888
70.0	87.60	99.00	808.97	45.19	1.0610	1.3562	−0.1066
68.2	100.00	100.00	760.00	—	1.0000	1.4500	−0.1613

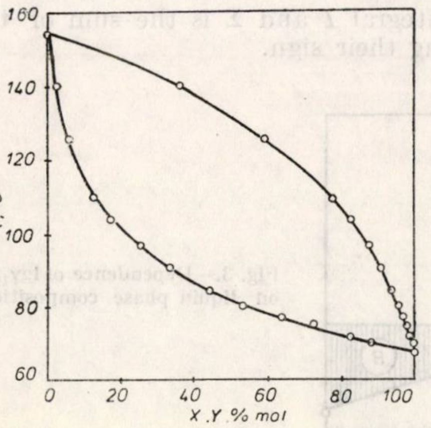

Fig. 1.— The $t-x$, y diagram at 760 mm Hg

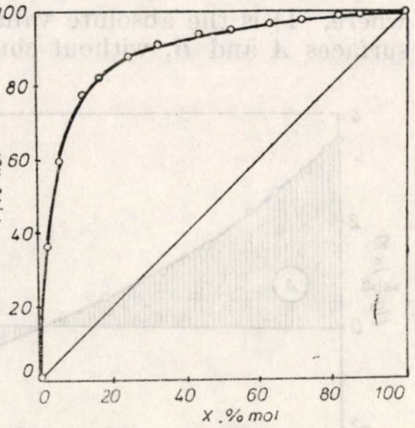

Fig. 2. — The $y-x$ diagram at 760 mmHg.

THERMODYNAMIC VERIFICATION OF THE EXPERIMENTAL DATA

The thermodynamic verification of the experimental data has been done using Redlich — Kister's method, generalized by Herington, described in detail by Hála et. al.[8]

Using the equilibrium data, determined experimentally, $\lg\gamma_1/\gamma_2$ was calculated for different values of x_1. The values of the activity coefficients, γ_1 and γ_2, have been calculated using the equation :

$$\gamma_i = \frac{P \cdot y_i}{p_i^0 \cdot x_i}$$

where P is the total pressure.

The plot, $\lg\gamma_1/\gamma_2$ versus x_1, figure 3, allowed to evaluate the integral, $I = \int_0^1 \lg \gamma_1/\gamma_2 \cdot dx$, i.e., $I = A - B = 0.0843 - 0.0355 = 0.0488$ area units.

According to Redlich — Kister's criterion, in the case of the liquid — vapour equilibrium data, determined under isothermal conditions, $I = 0$ points out the thermodynamic consistency of the data. For the equilibrium data, determined under isobaric conditions, Herington established that, if $D < J$ or, on the contrary, $D - J < 10$, the data have a good thermodynamic consistency.

Term D represents the percentage deviation, calculated using the formula :

$$D = \frac{|I| \cdot 100}{\Sigma}$$

where, $|I|$ is the absolute value of integral I and Σ is the sum of the surfaces A and B, without considering their sign.

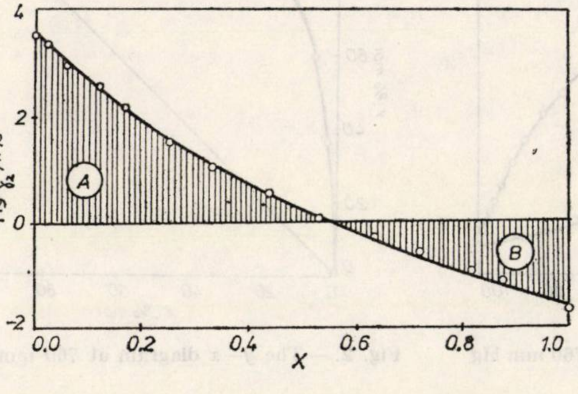

Fig. 3.—Dependence of $\lg\gamma_1/\gamma_2$ on liquid phase composition.

Term J is defined by the relation :

$$J = \frac{150 \cdot \theta}{T_{\min.}}$$

where θ is the difference between the boiling temperatures of the components and $T_{\min.}$ is the minimum boiling temperature in the system, K.

At the present system, $\Sigma = 0.1198$, $D = 40.77$ and $J = 37.96$, therefore, the conditions, $D - J = 2.81 < 10$ being fulfiled, the equilibrium experimental data are accurated enough from the thermodynamic point of view.

REFERENCES

[1] V. B. Kogan, V. M. Fridman and V. V. Kafarov, "Ravnovesie mejdu jidkosti i parom" Izdatel'stvo Nauka, Moskow — Leningrad, 1966, p. 820—822.

[2] M. P. Sukarev and R. V. Lizolova, *Zhur. priklad. Khim.*, **33**, 2786 (1960).

[3] V. Ababi and N. Naum, *Anal. Şt., Univ. "Al. I. Cuza" Iaşi*, **28**, 201 (1972).

[4] H. J. Wurm, *Chem. Ing. Tech.*, **48**, 840 (1976).

[5] * * * "Spravocinik khimika", vol. 1, Leningrad, 1962, p. 635 and 1035.

[6] S. A. Djobadze and V. A. Peremîşlin, *Gaz. promyshlenosti*, **7**, 14 (1962).

[7] I. N. Bushmakin, *Zhur. priklad. Khim.*, **32**, 812 (1959).

[8] Ed. Hála, J. Pick, V. Fried and O. Vilim, "Vapour — Liquid Equilibrium", Pergamon Press, Oxford, 1967.

[9] Gh. Mihăilă and Gh. Bendescu, *Anal. Şt., Univ. "Al. I. Cuza" Iaşi*, **11**, 99 (1965).

[10] * * * "Chemical Engineers' Handbook", Mc Graw-Hill, New York, 1950, p. 158 and 156.

[11] Em. A. Bratu, "Operaţii şi utilaje în industria chimică", vol. 1, Editura tehnică, Bucureşti, 1969, p. 111.

Revue Roumaine de Chimie, 25, 4, 605–610 (1980)

REACTIVITY OF ACRYLIC MONOMERS. II[1]

COPOLYMERIZATION OF N,N-DIETHYLACRYLAMIDE WITH STYRENE

SPIRIDON OPREA, EMIL DUMITRIU and MIHAIL DIMA

Departament of Organic Chemical Technology, Faculty of Chemical Technology,
Splai Bahlui Stinga 71, Jassy 6600, Romania

Received March, 28, 1979

The copolymerization of N,N-diethylacrylamide with styrene in dioxane solution at 60° using 2,2′-azobis (izobutironitrile) as polymerization initiator was sudied. The reactivity ratios were determined and it was stated that a penultimate effect appears in the composition range richer in styrene.

In the previous paper[1] the copolymerization of N,N-diethyl-acrylamide with methyl acrylate was studied and the reactivity ratios $r_D = 0.41$ and $r_{MA} = 0.52$ were reported; these values assume a tendency to alternate the two monomers along the copolymer chain. This tendency was confirmed by NMR analysis of copolymers in a large range of compositions of the monomer mixture.

In this paper we continue to study the behaviour of N,N-diethylacrylamide in the copolymerization process but in this case the styrene being the comonomer — a monomer with a larger possibility of conjugation than methyl acrylate.

EXPERIMENTAL

Materials

N,N-Diethylacrylamide was synthesized by the reaction of diethylamine and acryloyl chloride. A solution containing 2.1 moles of diethylamine in benzene was added dropwise with stirring, to a solution of acryloyl chloride (1 mole) at 0°. After the diethylamine hydrochloride was separated by filtration, the monomer was distilled under vacuum using Cu_2Cl_2 as inhibitor. N,N-Diethylacrylamide was purified by several rectifications on a packed column under vacuum; b.p. = 92°/4 mm Hg. Styrene used as comonomer was purified by the conventional method. 2,2′-Azobis (izobutironitrile) (AIBN) was recrystallized three times from ethanol. A stock solution of AIBN in dioxane was prepared and stored at room temperature. The solvents used were purified by usual methods.

Copolymerization

All experiments were carried out in the same manner differing only in the reaction time. Copolymerization of N,N-diethylacrylamide-styrene systems was initiated by AIBN (0.2% mole) and carried out in dioxane solution (6 mol) in sealed glass tubes at 60±0.1°. The proper time of copolymerization, i.e., the time necessary to polymerize no more than 10 % of the mixture, was found by trial and error method. After polymerization, the ampules were cooled to room temperature, and the reaction mixture was poured into light petroleum. The precipitated polymers were filtered, purified by reprecipitation and then dried at 40° under reduced pressure.

The composition of copolymers was determined by analysis of their nitrogen content by micro Kjeldahl method. The reaction conditions and results are summarized in table 1.

TABLE 1

Copolymerization of N,N-diethylacrylamide with styrene in dioxane solution at 60°

No.	Mole fraction of D in monomer feed	Mole fraction ratio of monomer mixture		*N* content of copolymer %,g	Mole fraction of *D* in copolymer	Mole fraction ratio of monomers in copolymer		Conversion %,g
		$x_D = \frac{[D]}{[S]}$	$x_S = \frac{[S]}{[D]}$			$y_D = \frac{d[D]}{d[S]}$	$y_S = \frac{d[S]}{d[D]}$	
1	0.104	0.116	8.615	2.16	0.166	0.199	5.024	7.60
2	0.199	0.248	4.025	2.92	0.228	0.295	3.386	5.56
3	0.299	0.427	2.344	3.49	0.276	0.381	2.623	5.96
4	0.407	0.686	1.457	3.86	0.307	0.443	2.257	4.80
5	0.504	1.016	0.984	4.48	0.359	0.560	1.786	4.84
6	0.595	1.469	0.681	5.15	0.419	0.721	1.387	2.90
7	0.703	2.367	0.422	6.18	0.512	1.049	0.953	4.65
8	0.802	4.051	0.247	7.11	0.599	1.494	0.699	4.57
9	0.897	8.709	0.115	8.42	0.727	2.663	0.376	3.75

RESULTS AND DISCUSSION

The data from table 1 were analysed by interception method[2] using equation 1 in order to establish the reactivity ratios :

$$r_2 = x\left[\frac{1}{y}(1 + xr_1) - 1\right] \tag{1}$$

where $x = M_1/M_2$ and $y = \mathrm{d}M_1/\mathrm{d}M_2$. It may be seen from the Mayo-Lewis plot, figure 1, that the lines corresponding to the experiments performed in dioxane cross themselves in the same area only for $0.427 < x_D < 8.709$. Evidently, in this range, the system can be adequately described by the conventional equation of composition :

$$y = x\frac{1 + r_1x}{r_2 + x} \tag{2}$$

and in this conditions the reactivity ratios have the values $r_D = 0.2$ and $r_S = 1.2$.

The Kelen-Tüdös equation[3] was applied to verify the previous observation :

$$\eta = \left(r_1 + \frac{r_2}{\alpha}\right) \xi - \frac{r_2}{\alpha} \tag{3}$$

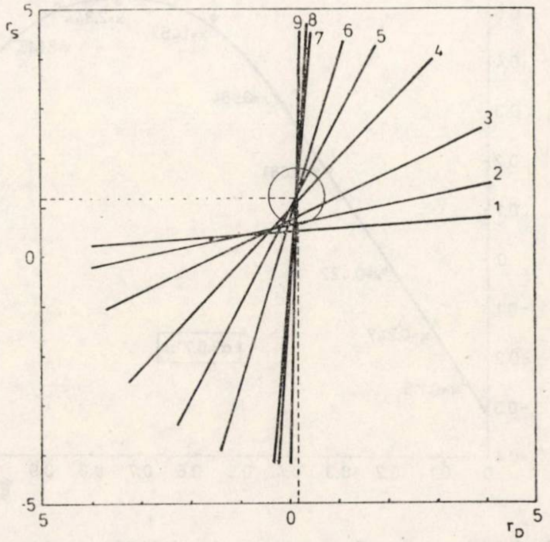

Fig. 1.—Mayo-Lewis plot for copolymerization of N,N-diethylacrylamide and styrene in dioxane at 60°. The numbers of individual straight lines correspond to the numbers of the experiments given in table 1.

where α is an equation parameter whose value is given by the relationship :

$$\alpha = \sqrt{F_m \cdot F_M}$$

and which allows a uniform and symmetrical distribution. η and ξ variables are given by the relations :

$$\xi = \frac{F}{\alpha + F}$$

and

$$\eta = \frac{G}{\alpha + F}$$

where $F = x^2/y$ and $G = (x(y-1))/y$.

As it can be seen from figure 2, because the experimental points, corresponding to the extreme composition range rich in styrene, are distributed on a curve, the validity of the terminal model is not verified for $x_S < 1.457$ and consequently it must take into account the possibility of a more complex copolymerization mechanism.

Moreover the data were analysed by Fineman-Ross method[4] using the equation :

$$\frac{G}{F} = r_1 - r_2 \frac{1}{F} \tag{4}$$

In this case, in figure 3, it may be seen that the validity of the composition equation (2) is confirmed for the range $x_S < 1.457$, when the reactivity ratios have the values $r_D = 0.204$ and $r_S = 1.15$, they

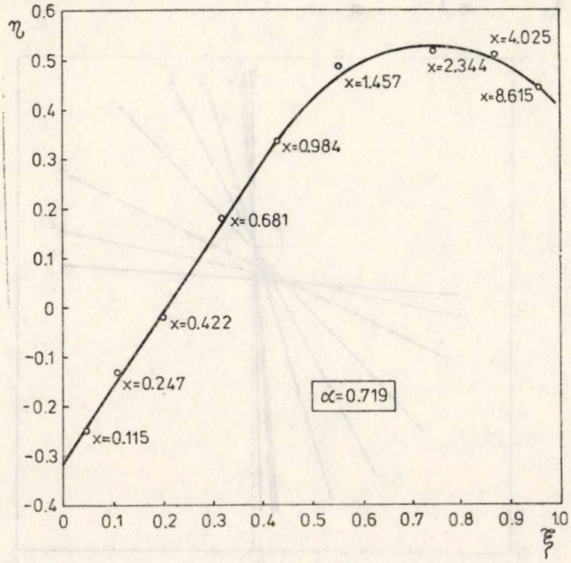

Fig. 2. — Kelen-Tüdös plot for copolymerization of N,N-diethyl-acrylamide and styrene.

being in a good agreement with the values obtained from the Mayo-Lewis plot, whereas the deviation from the straight line at the extreme composition range, for the mixtures rich in styrene, suggests a penultimate effect on the styrene-ended radicals.

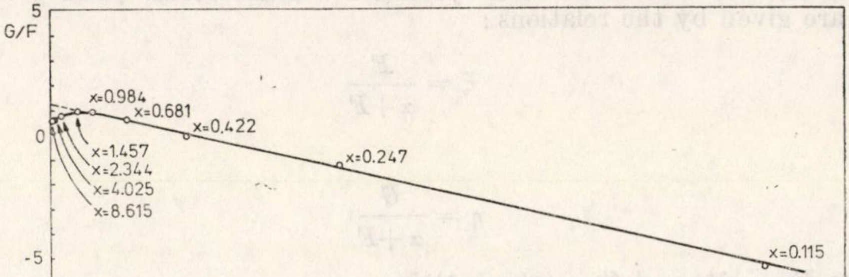

Fig. 3. — Fineman-Ross plot for copolymerization of N,N-diethylacrylamide and styrene.

The experimental data show that the consumption of N,N-diethylacrylamide rises more rapidly than it should be expected. The existence of a penultimate effect was verified by Barb method[5] which in our case, assuming that $r_{12} = r_{22}$ and having a small value while x_S a large one—

to the extreme range composition — can be simply applied by the equation :

$$r_{11} = [(y-1)/x^2\ ]\ (1/r_{21}) + [(y-2)/x] \qquad (5)$$

The graphical representation of this equation for our experimental data is given in figure 4.

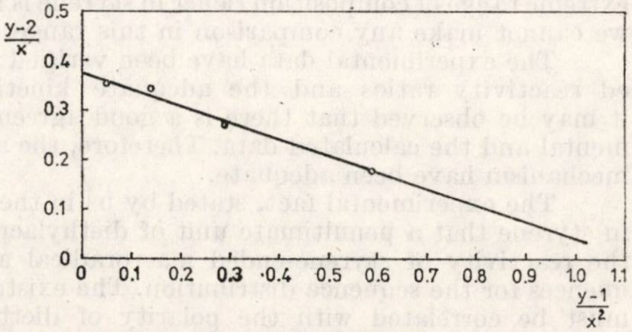

Fig. 4. — Fineman-Ross plot of the penultimate effect for styrene-ended macroradicals.

The results, graphically represented in figure 4, show a penultimate effect with $r_{SS} = 0.375$ and $r_{DS} = 2.985$, thus being in a good agreement with the experiments. Moreover, it can be stated from the same figure that it is not necessary to take into account an antepenultimate effect. The study of the other extremity of the composition range by Fineman-Ross plot with reindexed monomers has shown a linear relationship, the experimental points from the extreme range rich in diethylacrylamide

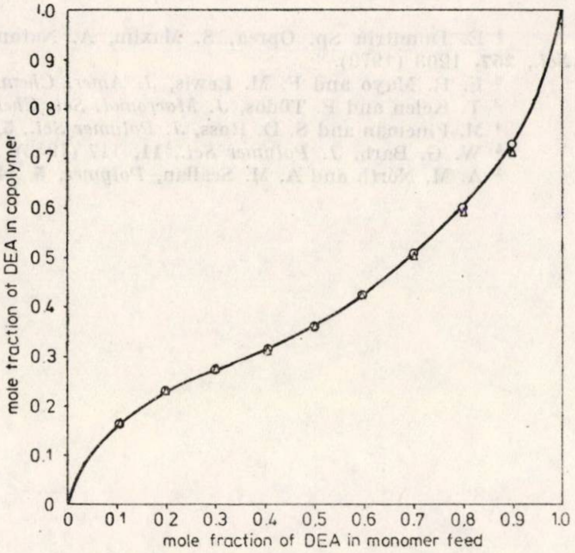

Fig. 5. — The copolymer composition against the feed composition (0)-experimental data, (Δ)-calculated data.

fitting on a straight line just like the experimental points from the central part of the composition range. The line parameters agree with the above given values for the terminal model $r_D = 0.2$ and $r_S = 1.2$ respectively.

In the case of composition range $0.427 < x_D < 8.709$ there is a good agreement between our values obtained for the system diethyl-acrylamide-styrene and the values reported $r_{amide} = 0.23$ and $r_S = 1.23$ for the system dimethylacrylamide-styrene[6]. As quoted in the paper the extreme range of composition richer in styrene is not studied and therefore, we cannot make any comparison in this range.

The experimental data have been verified on the bases of the obtained reactivity ratios and the adequate kinetic model. From figure 5 it may be observed that there is a good agreement between the experimental and the calculated data. Therefore, the assumed copolymerization mechanism have been adequate.

The experimental fact, stated by us in the composition range richer in styrene that a penultimate unit of diethylacrylamide changes strongly the reactivity of styrene-ended macroradical assumes important consequences for the sequence distribution. The existence of penultimate effect must be correlated with the polarity of diethylacrylamide too, which probably disturb the stabilization by resonance of the styrene-ended macroradical whose reactivity is modified.

REFERENCES

[1] E. Dumitriu Sp. Oprea, S. Maxim, A. Natansohn and M. Dima, *Colloid Polymer Sci.*, **257**, 1203 (1979).
[2] F. R. Mayo and F. M. Lewis, *J. Amer. Chem. Soc.*, **66**, 1594 (1944).
[3] T. Kelen and F. Tüdös, *J. Macromol. Sci. Chem.*, **A9**, 1 (1975).
[4] M. Fineman and S. D. Ross, *J. Polymer Sci.*, **5**, 259 (1950).
[5] W. G. Barb, *J. Polymer Sci.*, **11**, 117 (1953).
[2] A. M. North and A. M. Scallan, *Polymer*, **5**, 447 (1964).

COMPTES RENDUS

COULOMETRIC ANALYSIS, Edited by E. Pungor & I. Buzás. Akadémiai Kiado- Budapest, 1979. ISBN 963.05.2021.4

The book consists of a collection of plenary lectures and communications presented at "The Conference of Coulometric Analysis" held in Matrafüred, Hungary, between 17 and 19 October 1978. This conference was one of a series of similar meetings of high international prestige, organized by Prof. E. PUNGOR, member of the Academy of Science of Popular Republic of Hungary.

The eight plenary lectures present the newest aspects of theoretical and technical advances of coulometric analysis. All the lectures have emphasized the relation between the directions of progress in coulometric techniques and their possibilities of appliction to solving practical problems in analytical chemistry. Among other results the following are noteworthy : electrochemical generation of titration agents ; new aspects regarding coulometric titration in nonaqueous solvents ; applications of coulometry at controlled potential to the study of anodic oxidation in organic compounds.

The book also includes the fourteen communications given at the conference ; they cover applications of coulometry to industrial analysis, drog analysis and clinical diagnosis. These communications report methods for coulometric determination of chemical products as : sulphates, volatile thiols, chlorides in drugs, organic acids in nonaqueous solvents, dithiocarbonates, hydrazines etc. General theoretical considerations on coulometry and its applicability as research method are also given together with results on utilization of coulometry to the study of electrochemical reactions of complex combinations, numerical methods of evaluating kinetic parameters of chemical reactions associated to high potential coulometry, a procedure of accuracy evaluation in coulometric analysis, etc.

In conclusion, the book on "Coulometric Analysis" offers new aspects of coulometry and many of its applications and is therefore very useful in research laboratories and analysis laboratories in industry. It is also outstandingly useful to the faculties and students of chemistry related university departments.

C. Luca

Topics in Current Chemistry vol. 80, Springer-Verlag, Berlin, Heidelberg, New-York, 1979, 320 pag.

The 80th volume of this wellknown series is written in memory of *H. L. Meerwein* and has as main subject the carbocations. In recent years a lively controversy has centered on the classical-nonclassical ion problem. Leading investigators in this field are contributors of the book and their new developments and concepts on carbocation chemistry are presented as folows :

H. C. Brown (Purdue University, West Lafayette, Indiana USA). "Meerwein and Equilibrating Carbocations" (17 p.) The purpose of the review is to discuss the question of whether it is the Meerwein concept of equilibrating cations or the Wilson proposal of a mesomeric nonclassical cation that best corresponds to the behavior of 2-norbornyl cations. After a short history of the classical and nonclassical eras of carbocations the author presents the background of the problem referring to the relatively stable transition state responsible for the rapid equilibration of 2-norbornyl cations. Some steric arguments and facts are presented and their influence on *exo endo* rate ratio is discussed. In this conclusion the author pointed out that tertiary 2-norbornyl cation must be accepted as being essentially classical. For a more detailed discussion on the subject see also Brown H.C. with comments by Schleyer P.v.R., "The nonclassical ion problem" New York-Plenum Press 1977.

G. A. Olah (University of Southern California, Los Angeles S.U.A.) "From Boron Trifluoride to Antimony Pentafluoride in Search of Stable Carbocations" (60 p).

The starting point of this review is the review article which appeared in Angew. Chem. Ind. Ed., **12**, 173 (1973) having in mind that two distinct limiting classes of carbocations can exist : trivalent carbenium ions containing an sp^2-hybridized electron deficient carbon atom ("classical") ; and penta-(or higher) coordinated ("nonclassical") carbonium ions, which contain five (or higher) coordinated carbon atoms. The first part of the paper is devoted to the discovery and observation of stable long-lived carbocations in superacidic systems and very weakly nucleophilic solvents by NMR, IR, Raman and ESCA spectroscopy. Carbodications, heteroatom-stabilized carbocations, with halogen, oxygen, sulfur and nitrogen as heteroatoms are presented and discussed. The second part of the review has as main subject five and higher coordinated (nonclassical) carbocations as equilibrating and/or bridged carbocations.

H. Hogeveen and E.M.G.A. van Kruchten (Nijenborgh University, 9747, A. G. Groningen, The Netherlands) "Wagner-Meerwein Rearragements in Long-lived Polymethyl Substituted Bicyclo [3.2.0] heptadienyl Cations" (31 p.) In this chapter an account is given on the spectroscopic properties of the bicyclo [3.2.0] and [2.2.1] heptadienil cations, their degenerate and non-degenerate rearrangements and the influence of substituents upon stability and rearrangement. The thermodynamic ions have always turned out to have the [3.2.0] skeleton although the [221] isomers have been observed in some cases.

Wolfgang Kirmse (Ruhr Universität, Bochum, Germany), "Rearrangements of Carbocations, Stereochemistry and Mechanism" (168p). After a short introduction, carbocations in the gas phase and their thermodynamic aspects and rearrangements are examined, in keeping with the last determinations by UV, photoionization and photo-electron spectroscopy. Special atention is given to the carbocations in superacids and to the recorded methods for structural aspect studies : ^{1}H and ^{13}C-NMR, infrared, Raman and ESCA spectroscopy, including isotopic perturbation as a new tool for distinguishing between symmetrical delocalized structures and pair of rapidly equilibrating ions. In the next sections the problem of ion pairs in different solvolysis reactions is well documented and the micellar effects on nucleophilic substitution reactions and rearrangements are presented. The largest section is devoted to the bridged ions and anchimeric assistance in different reactions. Generally, the coverage of this review has been restricted to the rearrangements of carbocations which are classified as [12] sigmatropic shifts and to those aspects of mechanism which are relevant to stereochemistry.

The volume provides a comprehensive insight into carbocation chemistry for those who being contingent with the subject want to find recent accounts in the field. The readers will find therein the analysis of different opinions and theories on the subject and a lot of literature quotations. The volume also includes an author index for "Topics in Current Chemistry" vol. 26—80, namely from 1972 till now.

Flavian Cuiban

"NMR-Basic Principles and Progress". (editors P. Diehl, E. Fluck and R. Kosfeld). Vol. 16. "^{31}P and ^{13}C-NMR of Transition Metal Phosphine Complexes." P. S. Pregosin and R. W. Kunz. Springer Verlag, Berlin, Heidelberg, New York, 1979, 156 pages.

The present book was written, with the aim to demonstrate that even if the ^{1}H-NMR method has not lost its classical importance, some other equally powerful methods are available, whose potential is just being recognized. From these methods the authors have chosen the ^{31}P- and (to a lesser extend) the ^{13}C-NMR, applied to the study of transition metal complexes containing phosphine ligands. The importance of Fourier Transform methods, of the broad band ^{1}H-decoupling and of INDOR experiments in the investigation of such compounds is stressed from the beginning.

The book covers the literature for the period 1970—1977 (with 259 references).

Two important chapters present the ^{31}P-coupling constants and ^{31}P-chemical shifts of metal-phosphine complexes. Topics as "One Bond Metal-Phosphorus Coupling Constants", "Two-Bond Phosphorus-Phosphorus Coupling Constants", are included and discussed in a useful manner.

An interesting chapter of applications shows the advantages of this NMR form due to the relative spectral simplicity of most ^{31}P (^{1}H) spectra. Dynamic NMR experiments are also mentioned.

The following chapter consists in a brief survey of the ^{13}C studies of phosphorus complexes including phosphorus ligands as well as non-phosphorus ligands.

The practical utility of this book lies mainly in a detailed set of tables (56 pages) which offer the reader a very rich collection of chemical shifts and coupling constants for transition metal complexes containg phosphorus ligands.

A short index ends this interesting and useful book.

M. Banciu

W. GÜTTINGER and H. EIKEMEIER, Editors, "Structural Stability in Physics" (Springer Series in Synergetics, Volume 4), Springer-Verlag, Berlin-Heidelberg-New York, 1979, VIII + 311 pages.

As a child of our own decade, *Catastrophe Theory* has grown through the seventies showing all the excitement and torment of a child's growth in its first years of life. Born from the works of an outstanding mathematician, René Thom, it has been soon embraced as a kind of wonder kid because it promised to be a problem solver in many pending scientific fields. It became very popular not only among researchers in various branches, from exact sciences to biology to social or economic sciences, but also among laymen who thought that it offered easy solutions to many of their everyday problems.

The mathematical basis of the theory lies in the methods of establishing how the solutions to a system of equations vary when some of the parameters appearing in the equations are changed. For some such parameter perturbations the solutions have discontinuities or even singularities, jumping from one value to a significantly different one. These jumps were termed "catastrophes" even if the term may be misleading (there are also "good" jumps !). Many branches of mathematics (bifurcation theory, shock wave theory, thresholds, etc.) have contributed to setting up the main body of theorems necessary to make the catastrophe theory (CT) work, and many prominent mathematicians were, and many still are, involved in the development of the theory's apparatus.

As long as the theory had been developing on strictly mathematical grounds, the number of both adepts and critics was negligible, but the situation changed dramatically when its proponents began to look for possible applications in other branches of science. One concept largely used for a wide spectrum of applications is, e.g., the "cusp catastrophe" surface, extensively applied by another well-known mathematician, E. C. Zeeman. It was used to model phenomena as diverse as the animal aggression, stock exchange crashes, prison riots, war outbreak, propagation of nerve impulses, cell multiplication, and others. Some of the initial results of the application of the cusp surface to biologic and socio-economic problems turned out to be interesting and far-reaching and they excited the curiosity and hope of many a scientist. However, very soon they began to attract severe criticism as well, sometimes in passionate terms. Critics such as Sussman and Zahler, for instance, have got all the way to the extreme of demolishing these results point by point, and of denying the theory's possibility of describing adequately all discontinuous phenomena or the validity of its models.

It is to be noted, though, that not even the harshest critics have denied the validity of the mathematical principles of the theory, or its possible application to some physical phenomena. Outgrowing its infancy, the theory has now entered a new age by concentrating itself on precisely such phenomena and by revising and expanding its foundations.

The award of a honorary doctorate to Professor R. Thom, the founder of the theory, was a very good opportunity for several specialists gathered in 1978 at the University of Tübingen, West Germany, to discuss the state of the art and to present the latest original results. The book reviewed here is a collection of papers presented at that meeting by such researchers as E. C. Zeeman, W. Güttinger, H. Haken (founder of synergetics), R. Thom himself, and many others.

The bulk of the contributions deal with physical or chemical effects : Stable defects in ordered media (R. Thom), Structural stability in evolving flow fields (J. F. Nye), Structural stability in statistical mechanics (M. Rasetti), The 180° rule at triple points (G. Dukek), Phase diagrams and catastrophes (K. Keller *et al.*), Information measures and thermodynamic criteria of motion (F. Schlögl), Phase transitions as catastrophes (W. T. Grandy). Physicists and chemists might be interested how these familiar-sounding problems are viewed from the angle of the CT and which are the ways and means offered by it to solve them.

In contrast to earlier papers on CT applications, with their often naive approach or amateurish mathematics, the contributions published in this book look serious and well researched. They also lack the overoptimistic pitch which was so unpleasantly characteristic to older

CT papers. More experiments are proposed now by theorists and the models advanced look more realistic than before. Moreover, the papers devoted to the ways of expanding the basis and scope of the theory itself (grouped under the heading "Catastrophes in infinite dimensions") are clearly and rigorously written.

It is nevertheless surprising to find in the book no reference at all to earlier criticism of the CT, which in many cases has turned out to be justified. Neither Thom nor Zeeman, who had been the main target of this criticism, answer in any way, even marginally, the raised questions. It is however the reviewer's opinion that they have assented to these objections and their recent work, as well as the work of the other participants at the Tübingen meeting, takes them implicitly into account and tries to make the CT a really useful tool for "measuring complexity," in Thom's own words.

It is perhaps significant that the title of this collection of papers devoted to the CT is as it is—structural stability in physics. The new science has matured and its field and language has been steered to more solid and serious grounds.

Alex. Butucelea

IGOR I. SOBELMAN, "Atomic Spectra and Radiative Transitions" (Springer Series in Chemical Physics, 1), Springer-Verlag, Berlin-Heidelberg-New York, 1979, XII + 306 pages.

This is the first volume of a two-volume new book on atomic spectra. The original text, published in Russian more than 15 years ago and reissued several times, was revised and expanded for this edition. The volume reviewed herein is devoted to the theory of atomic spectra and radiative transitions. The second volume, due as No. 7 in the same Springer Series, will deal with the excitation of atoms and the spectral line broadening.

The book is mainly aimed at students of atomic structure and spectra. It adequately begins with the spectrum of hydrogen, dealing in subsequent chapters with the spectra of multielectron atoms and their systematics. The theory of atomic structure is based on Racah's techniques in the theory of angular momentum and the method of fractional parentage coefficients (Chapter 4). The *LS* and *jj* coupling schemes are dealt with in Chapter 5, the hyperfine splitting in Chapter 6, and the interaction of atoms with electric and magnetic fields in Chapters 7 and 8. The final chapter, by far the most extensive, is devoted to radiative transitions between atomic levels, including selection rules and calculation of transition probabilities. Particular attention is given to the continuous spectrum, with its related phenomena : bremsstrahlung, photocombination and photoionization. The book closes with tables of oscillator strengths and radiative transition probabilities, and with a subject index.

The book could be useful not only for understanding the atomic structure and spectra but also as a working tool to all those interested (at research level) in the application of atomic spectroscopy to plasma, laser physics, structure of small molecules, or astrophysics problems.

Alex. Butucelea

M. EIGEN and P. SCHUSTER. "The Hypercycle, a Principle of Natural Self-organization", Springer-Verlag, Berlin, 1979, 92 + VIII pp.

The book gathers a series of papers published in Die Naturwissenschaften, volumes 11 (1977), 1 and 7 (1978), and presented according to the authors' three principles : (i) hypercycles represent a natural self-organization allowing an integration and coherent evolution of a set of non-equilibrated systems ; (ii) hypercycles are a novel class of nonlinear reacting systems with unique properties, able to be described by a unified mathematical formalism, and (iii) hypercycles may be the originators in the mutant distribution of a single Darwinian quasi-species through stabilization of its diverging mutant genes, so that once nucleated they evolve to higher complexity by a process analogous to gene duplication and specialization.

This new path in the study of the non-equilibrated systems originates in Darwin's principle of natural selection, which represents the only means understood for creating information. By analyzing the conditions of hypercyclic organization, the authors reveal their equivalence to the Darwinian selection, so that while the latter considered reproduction as a kind of linear autocatalysis, the hypercycle represents the next higher level in a hierarhy of autocatalytic systems. In this context the hypercycle is defined by autocatalysis or reproduction cycles which are linked by cyclic catalysis. The authors call this process as being based on nonlinear (e.g. second or higher order) autocatalysis. This reasoning is contained in part A.

In section B a general analysis is carried out accordig to the second statement, that is hypercycles show a "regular" behaviour and can be analyzed as a particular class of reaction networks. This principle is still retained in the process of RNA phage infection, though there it applies to the closed world of the host cell.

The statement regarding the necessity of a hypercyclic organization of a primitive translation apparatus is of an "if-then" nature and does not refer to historical reality (Part C). Thus, unexpected singular events, fluctuations that do not represent any regularity of nature, might occur and then influence the historical route. Transfer RNAs as the key substances of traslation provide some information about their origin. They seem to offer a natural way by which the difficulties of a start of the nonlinear network (the nucleation problem) can be solved.

The book, written in cooperation with chemists, biochemists, biologists and physicists, provides a deeper understanding of the origin and evolution of life, and furnish the basis for many new experiments. On the other hand the enuciated statements are able to be further developed and eventually connected with nonequilibrium thermodynamics which also tried to explain some machineries of life.

Gheorghe Drăgan

A. J. CHORIN and J. E. MARSDEN, "A Mathematical Introduction to Fluid Mechanics", Universitext, Springer-Verlag, New York, 1979, 205 + V pp.

This book represents a one-quarter (i.e. very short) course in fluid mechanics taught in the Department of Mathematics of the University of California, Berkeley during the spring of 1978. The goals explained by the authors were :(i) to present some of the basic ideas of fluid mechanics in a mathematically attractive manner (not "fully rigorous") ; (ii) to present the physical background and motivation for numerical work on the Navier-Stockes equations and generally on hyperbolic systems, and (iii) to interest some of the students in this beautiful and difficult subject.

The three chapters cover these main aspects. The first chapter develops the basic equations of fluid mechanics derived from the conservation laws of mass, momentum and energy. The simplest assumptions which lead to Euler's equation for a perfect fluid are exposed in the third section to allow for viscous effects which arise from the molecular transport of momentum. The intuitive and mathematical aspects of vorticity are emphasized.

The second chapter presents a detailed study of the relationship between viscous and non-viscous flows. This study begins with inviscid irrotational flows (potential flows), continues with boundary layers which explains the main difference between slightly viscous and inviscid flows and is further developed by probabilistic methods.

The third chapter discusses the one dimensional flow for a compressible fluid and contains : weak solutions and the entropy condition for shocks ; the Riemann problem as a flow problem with particular discontinuous data, a general construction given by Glimm which uses the solution of Riemann problem to produce solutions of arbitrary problems, and finally the discussion of the flow of a gas which allows chemical energy realise.

Although the book is a good guide, we must reveal some essential lacks, such as: (i) fluid mechanics is a part of non-equilibrium thermodynamics and it is for this reason that many of the theoretical results recently obtained concerning the processes of concentration and/or heat waves could have been summarized in a useful and elegant mathematical manner, and (ii) following the same idea, the rheological models established mainly on phenomenological bases for a large domain of viscous behaviours, represent particular cases for theoretical results application, and for a better understanding of them.

Gheorghe Drăgan

lence to the Darwinian selection, so that while the latter considered reproduction as a kind of linear autocatalysis, the hypercycle represents the next higher level in a hierarchy of autocatalytic systems. In this context the hypercycle is defined by autocatalysis or reproduction cycles which are linked by cyclic catalysis. The authors call this process as being based on nonlinear (e.g. second or higher order) autocatalysis. This reasoning is contained in Part A.

In section B a general analysis is carried out according to the second statement, that is hypercycles show a "regular" behaviour and can be analyzed as a particular class of reaction networks. This principle is still retained in the process of RNA phage infection, though there it applies to the closed works of the host cell.

The statement regarding the necessity of a hypercyclic organization of a primitive translation apparatus is of an "ultimate" nature and does not refer to historical reality (Part C). Thus, unexpected singular events, fluctuations that do not represent any regularity of nature, might occur and then influence the historical route. Transfer RNAs as the key substances of translation provide some information about their origin. They seem to offer a natural way by which the difficulties of a start of the nonlinear network (the nucleation problem) can be solved.

The book, written in cooperation with chemists, biochemists, biologists and physicists, provides a deeper understanding of the origin and evolution of life, and furnish the basis for many new experiments. On the other hand the formulated statements are able to be further developed and eventually connected with nonequilibrium thermodynamics which also tried to explain some mechanisms of life.

Gheorghe Drăgan

A. J. CHORIN and J. E. MARSDEN, A Mathematical Introduction to Fluid Mechanics (Universitext), Springer-Verlag, New York, 1979, 205 + V pp.

This book represents a one-quarter (i.e. very short) course in fluid mechanics taught in the Department of Mathematics of the University of California, Berkeley during the spring of 1978. The goals explained by the authors were (i) to present some of the basic ideas of fluid mechanics in a mathematically attractive manner (not "fully rigorous"); (ii) to present the physical background and motivation for numerical work on the Navier-Stokes equations and generally on hyperbolic systems, and (iii) to interest some of the students in this beautiful and difficult subject.

The three chapters cover these main aspects. The first chapter develops the basic equations of fluid mechanics derived from the conservation laws of mass, momentum and energy. The simplest assumptions which lead to Euler's equation for a perfect fluid are relaxed in the third section to allow for viscous effects which arise from the molecular transport of momentum. The intuitive and mathematical aspects of vorticity are emphasized.

The second chapter presents a detailed study of the relationship between viscous and non-viscous flows. This study begins with inviscid irrotational flows (potential flows), continues with boundary layers which explains the main difference between slightly viscous and inviscid flows and is further developed by probabilistic methods.

The third chapter discusses the one dimensional flow for a compressible fluid and contains weak solutions and the entropy condition for shocks, the Riemann problem as a flow problem with particular discontinuous data, a general construction given by Glimm which uses the solution of Riemann problem to construct solutions of arbitrary problems and finally the discussion of the flow of a gas which undergoes chemical energy [illegible].

Although the book is a good guide, we must reveal some essential facts, such as: (i) the mechanics is a part of non-equilibrium thermodynamics and it is regrettable that only [illegible] the theoretical results recently obtained concerning the processes of concentration in shear flows could have been summarized in a short and elegant mathematical manner and (ii) following the same idea, the rheological models established mainly on phenomenological bases for a large domain of various behaviours represent particular cases for theoretical results application and for a better understanding of them.

Gheorghe Drăgan

NOTE POUR LES AUTEURS

La Revue Roumaine de Chimie publie des articles en anglais, français, russe, allemand ou espagnol. Les auteurs sont priés d'envoyer des articles et des comptes rendus inédits.

Les manuscrits seront dactylographiés à deux intervalles. La bibliographie, les tableaux et la légende des figures seront places après le texte.

Si l'article fait partie d'une série numérotée, le titre de la partie précédente sera indiqué dans une note au bas de la première page.

Chaque article sera précéde d'un résume comprenant quinze lignes au maximum.

Les références bibliographiques dans le texte seront faites par des exposants sans parenthèses et paraîtront comme des notes au bas de chaque page.

Les publications périodiques mentionnées dans la bibliographie seront présentées suivant les prescriptions internationales : le nom de l'auteur précédé de l'initiale du prénom, le titre du périodique abrégé conformément à « Chemical Abstracts » et souligné par une ligne, le numéro du tome indiqué par de chiffres arabes et souligné par deux lignes, suivi de la première page de l'article ; à la fin, l'année de la parution sera placée entre parenthèses. Le numéro de la revue ne sera pas indiqué si les pages du volume sont numérotées consécutivement

Les textes des livres ou traités incluleront le nom des auteurs, les initiales du prénom, le titre du livre entre guillemets et sans être souligné, le numéro du tome précédé par l'abréviation « vol. » (ou « Bd »), le numéro de l'édition, les éditions (the publisher), la localité de la parution du livre, l'année de la parution et la page de la référence précédée(s) par l'abréviation « p » (ou « S »).

Les brevets seront indiqués comme suit : l'auteur ou la firme, le pays et le numéro du brevet, la date et la revue (Chem. Abstr.). Par ex. : M. Jones (to Union Carbide Co), Brit. Pat. 601238, 2 Sept. 1959, *Chem. Abstr.*, **54**, 12808 (1960).

Les diagrammes seront tracés à l'encre de Chine sur papier calque. Les tableaux et les figures (en nombre strictement nécessaire) seront numérotés par des chiffres arabes. Les courbes dans les figures seront numérotées par des chiffres arabes et leur explication sera donnée dans la légende des figures. Prière de ne pas inscrire les mêmes données dans les tableaux et les figures. Chaque tableau aura un titre. On indiquera dans le texte la place approximative des tableaux et des figures. Les formules chimiques seront incluses dans le texte : en outre, elles seront transcrites sur papier calque, à l'encre de Chine.

Les auteurs sont priés d'indiquer les caractères italiques (en soulignant les lettres au crayon), ainsi que tout autre caractère spécial ; les préfixes *ortho*, *meta*, *para*, *cis*, *trans*, etc. seront soulignés pour indiquer leurs caractères italiques et ne seront jamais écrits avec des majuscules.

Aucune correction à la main ne sera admise sur le manuscrit. Les corrections seront frappées à la machine. Les lettres grecques ou autres symboles spéciaux seront insérés à la main à l'encre clairement.

Le manuscrit sera signé par l'auteur.

Le colonne-titre aura 50 lettres au maximum.

L'entière responsabilité du contenu des articles appartient aux auteurs.

Pour détails voir le n^0 2 (1980).

PRINTED IN ROMANIA

TRAVAUX PARUS AUX ÉDITIONS DE L'ACADÉMIE DE LA RÉPUBLIQUE SOCIALISTE DE ROUMANIE

A. T. BALABAN, L. GĂLĂŢEANU, G. GEORGESCU, LIGIA SIMIONESCU, **Compuşi marcaţi şi radiofarmaceutici cu aplicaţii in medicina nucleară** (Composés marqués et radiopharmaceutiques à application en médecine nucléaire), 1979, 495 p,

I. E. TEODORESCU et MARIA FITI, **Iradierea tehnologică** (L'Irradiation technologique), 216 p.

I. G. MURGULESCU, E. SEGAL, **Introducere in chimia fizică, vol. II. 1. Teoria molecular-cinetică a materiei** (Introduction à la Chimie physique. IIe vol. 1. La Théorie moléculaire-Cinétique de la matière), 1979, 1033 p.

I. G. MURGULESCU, V. EM. SAHINI, **Introducere in chimia fizică, vol. I. 2. Structura şi proprietăţile moleculelor** (Introduction à la Chimie physique. Ier vol., 2. La structure et les propriétés des molécules), 1978, 604 p.

S. STERNBERG, FL. DANEŞ, **Termodinamica chimică aplicată** (La thermodynamique chimique appliquée), 1978, 400 p.

D. PURDELA (sous la direction), **Nomenclatura chimiei anorganice** (La nomenclature de la chimie inorganique), 1977, 153 p.

C. DRĂGULESCU, E. PETROVICI, **Chimia structurală modernă. Chimia coordinanţei** 8 (La chimie structurale moderne. La Chimie de la coordinence 8), 1977, 947 p.

I. ZUGRĂVESCU, MAGDA PETROVANU, **N-ylid Chemistry**, coédition avec McGraw-Hill International Book Company, U.S.A., 1977, 396 p.

I. G. MURGULESCU, **Introducere în chimia fizică, vol. I. 1. Atomi, molecule, legătură chimică** (Introduction à la Chimie physique, Ier vol., 1. Atomes. Molécules. Liaison chimique), 1976, 560 p., 2pl.

P. BALTĂ, E. BALTĂ, **Introduction to the physical chemistry of the vitreous state**, coédition avec Abacus Press, 1976, 287 p.

M. I. GĂLĂŢEANU, **Radiochimia aplicată. Metode şi probleme** (La radiochimie appliquée. Méthodes et problèmes), 1976, 307 p.

CONST. V. UGLEA, **Cromatografia pe gel permeabil. Noi domenii de aplicare** (La chromatographie sur gel perméable. Nouveaux domaines d'application), 1976, 122 p.

GR. POPA, ŞERBAN MOLDOVEANU, **Reactivi organici în chimia analitică** (Les réactifs organiques dans la chimie analytique), 1976, 255 p.

FRANCISC A. GOTHARD, **Echilibre lichid-vapori. I. Baze teoretice şi metode de calcul** (Equilibres liquide-vapeurs. I. Bases théoriques et méthodes de calcul), 1975, 263 p., 2 pl.

CONST. GH. MACAROVICI, D. MACAROVICI, **Chimia oxizilor dubli şi utilizărilor lor** (La chimie des oxydes doubles et leur utilisation), 1975, 195 p.

M. AVRAM, **Antidăunători** (Pesticides), 1974, 496 p.

ELENA CEAUŞESCU, **Research work on synthesis and characterization of macromolecular compounds. Contributions**, 1974, 251 p.

CR. SIMIONESCU, VIORICA RUSAN, V. POPA, **Chimia algelor marine** (La chimie des algues marines), 1974, 212 p., 1 pl.

I. P. Informaţia c. 2005

43426

Lei 25.—

$50 (price per year)

F 1103 c

ACADÉMIE DE LA RÉPUBLIQUE SOCIALISTE DE ROUMANIE

REVUE ROUMAINE DE CHIMIE

BME-OMIKK Törökbálint

OF 1103

TOME 25
N° 5
Mai 1980

EDITURA ACADEMIEI REPUBLICII SOCIALISTE ROMÂNIA

Rev. Roumaine Chim.

RRCHAX, 25, 5, p. 617–760 (1980), Bucarest

ACADÉMIE DE LA RÉPUBLIQUE SOCIALISTE DE ROUMANIE

COMITÉ DE RÉDACTION

Rédacteur en chef:

I. G. MURGULESCU, membre de l'Académie de la République Socialiste de Roumanie

Rédacteurs en chef adjoints:

A. T. BALABAN et V. EM. SAHINI, membres correspondants de l'Académie de la République Socialiste de Roumanie

Collège de rédaction:

EM. BRATU, ELENA CEAUŞESCU, ECATERINA CIORĂNESCU-NENITZESCU, CR. SIMIONESCU, membres de l'Académie de la République Socialiste de Roumanie; P. SPACU, membre correspondant de l'Académie de la République Socialiste de Roumanie; MARGARETA AVRAM, M. BANCIU, I. HAIDUC, D. I. MARCHIDAN, I. MOLDOVAN, G. NIAC et D. SĂNDULESCU

La Revue Roumaine de Chimie paraît 10 fois par an. Toute commande de l'étranger pour les travaux parus aux Editions de l'Académie de la République Socialiste de Roumanie sera adressée à ILEXIM, — Departamentul Export-Import Carte (Livres)/Departamentul Export-Import Presa (Revues) P.O.B. 136—137, télex 11226, 3, str. 13 Decembrie, 70116 Bucarest, Roumanie

Les manuscrits, les livres et les revues proposés en échange, ainsi que toute correspondance seront envoyés à la rédaction :

REVUE ROUMAINE DE CHIMIE

Calea Victoriei, 125, 71021 Bucarest, Roumanie, téléphone 50 76 80

EDITURA ACADEMIEI REPUBLICII SOCIALISTE ROMÂNIA
125, Calea Victoriei, 71021 Bucarest, Roumanie, téléphone 50 76 80

DOKUMENTÁCIÓS 1983

REVUE ROUMAINE DE CHIMIE

Tome 25, N° 5 Mai, 1980

RODICA VÎLCU and ST. PERIȘANU, The ideal gas state enthalpies of formation of some monomers 619–624

MIHAELA HILLEBRAND and V. EM. SAHINI, The electronic structure of phenoxaselenine 625–630

MIHAELA HILLEBRAND and V. EM. SAHINI, Unrestricted Hartree-Fock spin densities of some heteroaromatic cation-radicals 631–634

EDUARDO A. CASTRO and FRANCISCO M. FERNÁNDEZ, An improved two-parameter Omega technique for molecular orbital calculations. I. The ITPOT method 635–641

EDUARDO A. CASTRO and FRANCISCO M. FERNÁNDEZ, An improved two-parameter Omega technique for molecular orbital calculations. II. Polyenes 643–650

VASILE MACOVEI, Spectral solvent effects in aromatic compounds solutions. VI. The solvent effects on the toluene electronic band at 2600 Å . . . 651–662

N. I. IONESCU, Kinetics of gas adsorption on heterogeneous solid surfaces 663–666

A. BREEZE, P. M. MAGEE and P.-G. PERKINS, The electronic band structure of β-PbO_2 667–672

FLORIN DANEȘ, AGNETA BÂTCĂ and SORIN M. AXINTE, Absorption of ammonia from aqueous solutions by A and X zeolites doped with transition metal ions (in French) 673–686

ROYSTON M. ROBERTS and HOFFMAN H. CHEN, The rearrangement of *sec*-butylbenzene to isobutylbenzene catalyzed by fluoroantimonic acid 687–689

TEODORA PANEA and MONICA MOLDOVAN, Oxidation of some methoxyphenothiazines by potassium dichromate in glacial acetic acid 691–695

R. K. JAIN and R. L. MITAL, Synthesis of some new polyhalogenated hydroxyphenothiazines and their alkyl and acyl derivatives 697–700

FELICIA CORNEA, D. IONESCU, MARIANA ZGLOBIU, GEORGETA BOTEZ, V. DOBRE and I. NICULESCU-DUVAZ, Potential anticancer agents. XXI. Synthesis and biological evaluation of some new triazene derivatives 701–711

Z. SIMON, S. HOLBAN, MARIA MRACEC, ANA MAURER and SEPTIMIA POLICEC, Steric optimisation by MTD of therapeutic index of n-substituted derivatives of *cis*-dichlorodiammine-platinum (II) active against ADJ/PC6A mouse plasma cell tumour 713–719

JANUSZ KYZIOŁ and JERZY TARNAWSKI, Synthesis of n-substituted derivatives of 9-aminocarbazole 721–727

Rev. Roumine Chim. **25, 5, p. 617–760 (1980) Bucarest**

IOANA DEMETRESCU and MARGARETA TOMESCU, Photochemical and thermal behaviour of acrylonitrile–butyl acrylate–vinylidene chloride terpolymer 729–733
CANDIN LITEANU, ION RÎCĂ and ELENA HOPÎRTEAN, On the determination limit 735–743
R. V. GADAG and M. R. GAJENDRAGAD, 3-Ethyl-4-benzylidene-5-mercapto-1, 2, 4-triazole as a new gravimetric reagent for the estimation of silver in salts, alloys and complexes 745–751

BOOK REVIEWS 753–759

Revue Roumaine de Chimie, **25**, *5*, 619–624 (1980)

THE IDEAL GAS STATE ENTHALPIES OF FORMATION OF SOME MONOMERS

RODICA VÎLCU and ST. PERIŞANU
Chair of Physical Chemistry, National Institute of Chemistry, 13 bd. Republicii, Bucharest, Romania

Received July, 1979

The ideal gas state enthalpies of formation of vinyl acetate, acrylic acid, ethyl acrylate and methyl methacrylate were derived from heats of combustion, hydrogenation and vaporization. The experimental enthalpies of formation in ideal gas and liquid states are compared with those calculated by means of the Allen-Skinner bond energy scheme.

1. INTRODUCTION

The heats of hydrogenation in solution of vinyl acetate, ethyl acrylate and methyl methacrylate are reported as new data. The standard state enthalpies of formation of the four monomers (including the acrylic acid, used as a standard) derived from heats of hydrogenation, are compared with those derived from heats of combustion. The experimental results for the heats of combustion and vaporization are given in this paper, or were taken from a previous one.[1]

2. EXPERIMENTAL

2.1. Materials

We have used freshly distilled monomers U.C.B. and acetic acid "Merck" of over 99% purity. The catalyst, palladium on carbon black, was prepared by the usual method, using "Merck" reagents.

The gases — hydrogen and oxygen — were over 99% pure. The benzoic acid used as a standard in combustion experiments was a "Chinoin" reagent for combustion calorimetry.

The aromatic hydrocarbons used as standards in vaporization calorimetry were p.a. grade reagents — "Reactivul".

2.2. Calorimeters

The hydrogenation calorimeter was of the Rogers-Mc. Lafferty type.[2] The tightness of the calorimeter was obtained by a black flange, with a silicon rubber gasket. This system avoided the use of a quick drying sealant, to prevent hydrogen leakage. We have used a "Fenwall" thermistor of 100 kΩ at 25° and a Wheatstone bridge to record the temperature rise on a "Graphispot II" galvanometric recorder. The samples of liquids to be hydrogenated were injected by means of an "E. Zimmerman" microsyringe of 40 μl (Fig. 1).

The vaporization calorimeter was described in a previous paper.[1]

The combustion calorimeter was a "Gallenkamp Automatic Adiabatic Bomb Calorimeter", Model 110. The samples for combustion experiments were sealed in glass ampoules and ignited electrically from a chromnickel wire, by means of a cotton fuse and a pellet of benzoic acid.

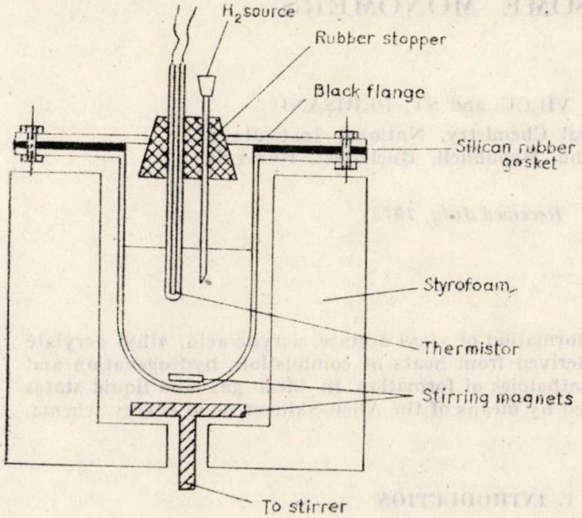

Fig. 1. — Calorimeter for hydrogenation in solution.

3. EXPERIMENTAL RESULTS

3.1. Heats of hydrogenation

Acrylic acid was used as a calorimetric standard. It is assumed to have a heat of hydrogenation of —30·35 kcal/mol. [3] The recorder scale deviation for the unknown compound relative to that of acrylic acid was used to calculate the heat of hydrogenation of the former. In all hydrogenation experiments crystalline acetic acid was used as a solvent.

Corrections were made for the heats of mixing of the hydrogenation products with the solvent, except of methyl isobutyrate.

The molar heats of hydrogenation, obtained by a simple calculation from the scale deviations, densities and molecular weights, are given in table 1. In the evaluation of the mean square deviation, we have taken

TABLE 1

The standard enthalpies of hydrogenation and formation of three monomers

Compound	$-\Delta H_h^0$ (kcal/mol)	$-\Delta H_f^0$ (kcal/mol)
Methyl methacrylate	25.9±1.2	91.40
Ethyl acrylate	32.5±1.1	88.58
Vinyl acetate	30.9±1.1	83.84

into account the uncertainty in the determination of the heat of hydrogenation of the standard too.

The heat of hydrogenation of methyl methacrylate is close to those of 2,4-dimethylpentene 1 (−26.7 kcal/mol) and 2,4,4-trimethylpentene 1 (−25.5 kcal/mol) reported by Turner et al.,[4] which correspond to the same degree of substitution of the double bond ($R_2 = CH_2$).

For ethyl acrylate, the heat of hydrogenation is more than 1 kcal/mol greater than that of the most compounds with the same type of substitution of the double bond ($RCH = CH_2$), while for vinyl acetate the corresponding value is quite normal.

3.2. Heats of combustion

The experimental data of heats of combustion for acrylic acid, vinyl acetate and methyl methacrylate are given in tables 2−4.

TABLE 2

Results of four combustion experiments for methyl methacrylate

m (sample) [g]	0.9239	0.9427	0.9041	0.9701
m (benzoic acid) [g]	0.2127	0.2391	0.2284	0.2048
m (H_2O) [g]	1	1	1	1
q (ignition) [cal]*	18.5	18.5	19.0	17.7
q (benzoic acid) [cal]	1348.8	1510.7	1443.1	1294.0
q (HNO_3) [cal]	6.0	6.0	6.0	6.0
ΔT [K]	2.826	2.887	2.816	2.918
$-\Delta U_c^\circ$ [kcal.mol^{-1}]	651.61	649.22	651.21	649.99
$-\Delta H_c^\circ$ [kcal.mol^{-1}]	652.20	650.18	651.80	650.58

Mean: Δ, H_f° ($C_5H_8O_2$, l) = −92.93 ± 0.96 kcal |mol

* Heat of combustion of cotton fuse and chromnickel wire.

TABLE 3

Results of four combustion experiments for vinyl acetate

m (sample) [g]	0.4972	0.8905	0.6170	0.7683
m (benzoic acid) [g]	0.2000	0.2061	0.2266	0.2115
m (H_2O) [g]	1	1	1	1
q (benzoic acid) [cal]	1263.6	1302.2	1431.7	1336.3
q (HNO_3) [cal]	6.0	6.0	6.0	6.0
q (ignition) [cal]	32.9	18.5	20.5	22.8
ΔT [K]	1.604	2.492	1.918	2.225
$-\Delta U_c^\circ$ [kcal. mol^{-1}]	499.51	500.53	494.94	497.79
$-\Delta H_c^\circ$ [kcal. mol^{-1}]	499.81	500.83	495.24	498.09

Mean: ΔH_f° ($C_4H_6O_2$, l) = −82.67 ± 2.45 kcal|mol

TABLE 4

Results of four combustion experiments for acrylic acid

m (sample) [g]	1.0420	1.0029	1.0849	1.0108
m (benzoic acid) [g]	0.2141	0.2277	0.2450	0.2048
m (H_2O) [g]	1	1	1	1
q (ignition) [cal]	18.5	18.5	18.5	18.5
q (benzoic acid) [cal]	1371.7	1438.6	1547.9	1293.9
q (HNO_3) [cal]	6	6	6	6
ΔT [K]	2.370	2.340	2.482	2.248
$-\Delta U_c^\circ$ [kcal.mol^{-1}]	331.14	329.15	325.86	327.80
$-\Delta H_c^\circ$ [kcal.mol^{-1}]	331.14	329.15	325.86	327.80

Mean: ΔH_f° ($C_3H_4O_2$, l) = −90.30 ± 2.22 kcal/mol

For ethyl acrylate the same data were given elsewhere. [1] The accuracy of the measurements was better than 0.3 % for all compounds under study. The limiting factor of the accuracy was the purity of reagents and of oxygen.

3.3. Heats of vaporization

We have used in these measurements a Dewar flask, stirred liquid calorimeter, which was described in another paper. [1] In the same paper the experimental results for two of the compounds under study were also reported. For other two monomers, the data of heats of vaporization are given in table 5. The experiments have been done at three temperatures

TABLE 5

The enthalpies of vaporization of vinyl acetate and acrylic acid

Compound	Vinyl acetate	Acrylic acid
Number of experiments	4	4
Sample's weight [g]	1.864	1.577
Mean temperature of experiments [°C]	52	117
Duration of one experiment [min]	16	17
Mean temperature rise (corrected)* [K]	0.486	0.758
ΔH_v (T) [kcal.mol^{-1}]	8.48±0.20	11.95±0.30
ΔH_v° [kcal.mol^{-1}]	8.88	13.70

* The temperature rise was corrected in vaporization experiments, as well as in hydrogenation experiments by means of the method of Dickinson.

(325, 345 and 390 K). The calibration at the above mentioned temperatures was made with benzene, toluene and o-xylene respectively, the calorimeter constant being comprised in this temperature range between 330 and 345 cal/K.

The standard heats of vaporization were derived from those at the temperature of the experiment, by means of the equation of Watson:

$$\Delta H_v(T_2) = \Delta H_v(T_1)\left(\frac{1 - T_{r2}}{1 - T_{r1}}\right)^{0.38}$$

T_{r1} and T_{r2} are the corresponding reduced temperatures.

4. THE ENTHALPIES OF FORMATION. DISCUSSION

In the last column of table 1, we have given the standard state enthalpies of formation of three monomers, derived from heats of hydrogenation in solution. We have used for the enthalpies of formation of ethyl acetate and methyl isobutyrate, the values recommended by Cox and Pilcher [5] and Stull, Westrum and Sinke, [6] respectively. For ethyl propionate, we have calculated the enthalpy of formation in the liquid state, by means of the Allen—Skinner bond energy scheme ($\Delta H_f^0 = -121.08$ kcal/mol). The parameters for this calculation were taken from reference. [7]

The agreement between the standard enthalpies of formation obtained from heats of hydrogenation (table 1) and combustion (tables 2—4, ΔH_f^0 for methyl methacrylate -92.93 kcal/mol [1]) is quite good, excepting the case of ethyl acrylate.

We have also calculated the ideal gas state enthalpies of formation of the four monomers, using the standard heats of vaporization of table 5. The values are listed in table 6. In the same table our data of ideal gas state enthalpies of formation derived from heats of hydrogenation and

TABLE 6

The ideal gas state enthalpies of formation of four monomers

Compound	$-\Delta H_f^0$ (g)				
	Hydrogenation in solution	Combustion	Calculated	Other authors	Selected value
Methyl methacrylate	81.82	83.35	82.03	79.12 (combustion)[8]	82.4
Ethyl acrylate	79.21	84.66	81.06	—	81.4
Vinyl acetate	74.96	73.79	74.40	75.46 (vapour phase hydrogenation)[9] 74.35 (vaporization)[10]	74.5
Acrylic acid		76.60	78.28	78.02 (hydrogenation in solution)[3]	77.5

All values in kcal/mol.

combustion are compared with those calculated, using data of other authors and by means of the Allen—Skinner bond energy scheme. We have chosen the most probable value for each compound.

For methyl methacrylate, the difference between our experimental values is within the sum of the mean square deviations. We have chosen the value —82.4 kcal/mol, close to the mean of the above-mentioned quantities and in good agreement with the calculated one. The value of von Wartenberg and Schütte[8] is the result of old determinations and is considered to be less reliable.

The greatest discrepancy between the values obtained from heats of hydrogenation and combustion is observed for ethyl acrylate. We consider the value obtained from the heat of combustion to be less reliable, because combustion was supposed to be slightly incomplete for this compound. The selected value is therefore closer to the one obtained from the heat of hydrogenation.

For vinyl acetate, all values differ from the selected one, by less than 1 kcal/mol, our experimental values being close within ± 0.6 kcal/mol to the former.

For the acrylic acid, we have chosen a value of the enthalpy of formation, closer to the value obtained from the heat hydrogenation, affected by a smaller incertitude (as is the case of ethyl acrylate). The calculated value is considered to be too great.

On the other hand, the calculated values for the three esters seem to be some tenths of kilocalories pro mole too small. Some imperfections it the application of the Allen-Skinner parameters recommended by Cox and Pilcher,[5] for carboxylic compounds, were revealed by Manson[11] too.

REFERENCES

[1] R. Vîlcu, St. Perişanu and I. Ciocăzanu, "Travaux de la 4ème Conférence Internationale de Thermodynamique Chimique", Montpellier, 1975, vol. I. p. 105.

[2] D. W. Rogers and F. J. Mc. Lafferty, *Tetrahedron*, **27**, 3765 (1971); *J. Chem. Educ.* **48**, 548 (1971).

[3] H. A. Skinner and H. Snelson, *Trans. Faraday Soc.*, **55**, 504 (1959).

[4] R. B. Turner, D. E. Nettleton and M. Perelman, *J. Amer. Chem, Soc.*, **80**, 1430 (1958).

[5] J. D. Cox and G. Pilcher, "Thermochemistry of Organic and Organometallic Compounds", Acad. Press, London, 1970.

[6] D. R. Stull, E. F. Westrum Jr. and G. C. Sinke, "The Chemical Thermodynamics of Organic Compounds", Willey, New York, 1969.

[7] R. Vîlcu and St. Perişanu, *Rev. Roumaine Chim.*, **24**, 237 (1979).

[8] H. von Wartenberg and R. Schütte, *Z. anorg. Chem*, **211**, 222 (1933).

[9] J. B. Conn, G. B. Kistiakowsky and F. A. Smith, *J. Amer, Chem. Soc.*, **61**, 1868 (1939).

[10] D. R. Stull, *Ind. Eng. Chem.*, **39**, 517 (1947).

[11] M. Manson, *J. Chem. Thermodyn.*, **4**, 865 (1972).

Revue Roumaine de Chimie, 25, 5, 625–630(1980)

THE ELECTRONIC STRUCTURE OF PHENOXASELENINE

MIHAELA HILLEBRAND and V. EM. SAHINI
Department of Physical Chemistry, Polytechnic Institute, Bucharest,
B-dul Republicii 13, Romania

Received July 20, 1979

The energy levels and the electronic transitions calculated by the SCF – CI method for phenoxaselenine are discussed in connection with phenoxathiin. The similitude in the electronic structure of both heterocycles is explained by the near equality of the F_{SS} and F_{SeSe} diagonal elements in the SCF hamiltonian, in spite of the different heteroatomic parameters used.

Several experimental data concerning the electronic spectra and the spin density distribution in the cation-radicals of some anthracene-like heterocycles point out that the substitution of the sulfur atom by selenium does not significantly perturb the electronic properties [2-3]. The same conclusion was drawn from the study of the charge-transfer complexes of phenoxathiin and phenoxaselenine with TCNE [4] and other electron acceptors.[5] As the same analogy was observed concerning the electronic spectra of phenoxathiin and phenoxaselenine, we were interested to see how a semiempirical treatment, in the frame of the PPP approximation can account for the electronic structure of phenoxaselenine and for the similitude between the sulfur and selenium heterocycles. Therefore we reanalysed the electronic spectrum of phenoxathiin and the results will be simultaneously discussed with those for phenoxaselenine.

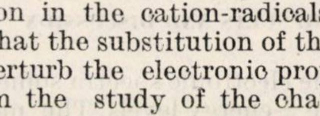

I, X=O, Y=Se; II, X=O, Y=S; III, X=Y=S; IV, X=S, Y=NH

M. O. CALCULATIONS

The calculations were performed by the SCFCI – PPP method, using a program written in Fortran IV and described elsewhere. [6] Both phenoxaselenine and phenoxathiin were considered as 16 π-electron system, with nonplanar structures. The dihedral angles were taken as

135° for phenoxaselenine and 133° for phenoxathiin. [7] For the bielectronic mono- and two-center repulsion integrals ($\gamma_{\mu\mu}$ and $\gamma_{\mu\nu}$) the Pariser-Parr [8] and, the Nishimoto-Mataga [9] approximations were adopted, respectively. To allow for the effect of the d-orbitals not taken explicitely into account, the sulfur and selenium ionization energies (W_x) were assumed adjustable entities and varied in the generally admitted range. All the geometrical and electronic parameters are contained in table 1.

TABLE 1

Bond distances (Å) and semiempirical parameters (eV)

X	r_{CX}	β_{CX}	W_X	γ_{XX}
C	1.40	-2.30	-11.16	11.13
O	1.40	-1.90	-33.00	21.52
S	1.75	-1.31 and -0.92	$(-20.00)-(-22.00)$	11.86
Se	1.87	-0.92	$(-17.40)-(-19.40)$	9.29

The configurational interaction was limited to 16 monoexcited configurations, involving the 3 highest occupied and the 4 lowest empty orbitals. The inclusions of more antiboding orbitals was required by their quasi-degenerate energy values.

RESULTS AND DISCUSSION

In order to discuss the electronic spectra some considerations must be made on the features of the π-energy levels. The molecular orbital energies and the atomic orbital coefficients, calculated for $W_{Se} = -17.40$ eV are listed in table 2. The last two rows in table 2 contain the values obtained for the orbitals influenced mostly by the change of W_{Se} to -19.40 eV, the upper limit admitted for this parameter.

The data in table 2 outline the same observations concering the MO's as for the other anthracene heteroanalogs, dibenzo-p-dioxin, phenoxathiin and thianthrene [10]. The orbitals, antisymmetric to reflection in the σ_v plane passing through the heteroatoms (C_s punctual group), are of benzenic character, having neither contribution from oxygen nor from selenium atom, and keeping the same energies for all the series. The lowest occupied orbital, $(m-1)$ is largely localized on the oxygen atom and is independent of the selenium parameter. The W_{Se} value determines somewhat different energies and especially different spatial distribution for the symmetrical orbitals, $m = 4, 7, 8$. For $W_{Se} = -17.40$ eV, the orbitals $m = 4,7$ are almost homogeneously delocalized on the whole molecule, benzenic rings and heteroatoms, while the highest occupied molecular orbital (HOMO) is approx. 70 per cent localized on the selenium atom. The decrease of W_{Se} to -19.40 eV causes a reversal of this pattern, the molecular orbital, $m = 4$, becoming localized on the selenium atom, while the other two point out a rather similar contribution from all the atomic orbitals.

The antibonding orbitals have a benzenic character, with an unsignificant contribution from the heteroatoms.

TABLE 2

The energy values (eV) and the atomic orbital coefficients for the molecular orbitals ($W_{Se} = -17.40$ eV)

m	Symm.	E	C_1	C_2	C_3	C_4	C	C_6	C_7	C_8
1	A′	−14.91	0.735	0.377	0.172	0.091	0.068	0.096	0.184	0.057
2	A″	−13.16		0.307	0.292	0.279	0.274	0.283	0.297	
3	A′	−12.47	−0.452	0.024	0.187	0.295	0.344	0.318	0.223	0.105
4	A′	−10.53	0.056	−0.024	0.303	0.360	0.096	−0.250	−0.376	0.362
5	A″	−10.30		−0.403	−0.174	0.230	0.414	0.201	−0.203	
6	A″	−10.23		−0.020	−0.364	−0.343	0.016	0.358	0.345	
7	A′	− 9.49	−0.388	0.262	0.333	−0.020	−0.342	−0.254	0.150	0.281
8	A′	− 8.14	0.186	−0.183	−0.039	0.170	0.100	−0.140	−0.140	0.860
9	A′	− 1.03	0.413	−0.189	−0.221	0.396	−0.154	−0.253		
10	A″	− 0.91		0.036	0.368	−0.333	0.040	−0.374	−0.331	
11	A′	− 0.79	0.033	−0.056	0.369	−0.325	−0.038	0.363	−0.332	0.149
12	A′	− 0.49	−0.213	0.387	−0.117	−0.261	0.410	−0.193	−0.193	0.081
13	A″	1.96		−0.266	0.284	−0.302	0.306	−0.295	0.277	
14	A′	2.21	−0.141	0.318	−0.285	−0.269	−0.265	0.272	−0.295	0.088
4	A′	−11.12*	0.042	−0.011	0.220	0.297	0.162	−0.081	−0.271	−0.720
8	A′	− 9.04*	0.376	−0.293	−0.149	0.209	0.278	−0.031	−0.298	0.470

* $W_{Se} = -19.40$ eV

The electronic spectrum of phenoxaselenine is similar to that of phenoxathiin and presents the maxima contained in table 3.

TABLE 3

Experimental and calculated energies of the electronic transitions (eV)

Molecule	$h\nu^{exp}$	$h\nu^{calc}$	M^2	Weight of the different configurations in the CI function*
Phenoxaselenine	5.25	5.28	0.3884	40.96 (7−11) ; 14.44 (5−10) ; 22.09 (6−9) ; 16 (8−12)
	5.14	5.13	1.0087	30.59 (7−10) ; 42.77 (7−9) ; 8.48 (6−12) ; 9.1 (5−11) ; 5.8 (8−10)
	4.27	4.01	0.4395	81.00 (8−10) ; 10.9 (8−9)
Phenoxathiin	5.21	5.29	0.4129	41.22 (7−11) ; 15.12 (5−10) ; 22.35 (6−9) ; 15.25 (8−12)
	5.14	5.12	1.0140	42.68 (7−9) ; 31.14 (7−10) ; 9.00 (5−11) ; 9.00 (6−12) ; 5.5 (8−10)
	4.20	3.97	0.4574	77.44 (8−10) ; 13.69 (8−9)

* The contributions below 5 per cent were not considered : (5−11) stand for $^1\chi_{5-11}$

The values $W_{Se} = -19.40$ eV and $W_S = -22.00$ eV lead to a poor agreement with the experimental values for all the electronic properties. A reasonable description of the electronic transitions is obtained for both compounds, increasing W_{Se} and W_S in the range (−18.00 eV) − (−17.40 eV), and (−20.54 eV) − (20.00 eV), respectively. The first values for each molecule determine a better agreement for the longest wavelength band, while the second ones improve the agreement for the other transitions, and in the following we prefer them. The theoretical transition energies, the transition moments and the contribution of the various configurations to the CI excited states are also given in table 3.

The only differences between the spectra of both compounds consist in a slight bathocromic shift of the longest wavelength band and in a more enhanced asymmetry of the band at 230 − 245 nm, for phenoxaselenine. This asymmetry confirms the assumption previously made for phenoxathiin on the existence in this range of two electronic transitions with very close energies. [11]

The two maxima were assigned to the transitions involving the major contributions of the $^1\chi_{7-9}$, $^1\chi_{7-10}$, and $^1\chi_{7-11}$, excited states. The small weight of the configurations implying the excitation of **HOMO** ($m = 8$), which is expected to be the most influenced by the ionization of the molecule, agrees with the unshifted position found for these bands in the cation-radicals.

The longest wavelenght bands were assigned in both molecules to transitions involving excited states with a predominant contribution of the (8−10) configurations.

This assignment explains the hypsochromic shift of this band in the series phenoxaselenine, phenoxathiin, thianthrene and phenothiazine; for all these compounds the antibonding $m=10$ orbital has the same energy and the **HOMO** ($m = 8$) is raised in this sequence in agreement with the respective ionization potential (Table 4).

TABLE 4

The longest wavelength band in the anthracene heteroanalogs (eV)

	Molecule	h_ν^{exp}	h_ν^{calc}	$E_{m=8}$	I_p^{exp}
I	Phenoxaselenine	4.27	4.01	−8.14	—
II	Phenoxathiin	4.20	3.97	−8.11	7.98
III	Thianthrene	4.12	3.86	−7.90	7.80
IV	Phenothiazine	3.87	3.68	−7.42	7.28

The charge density calculations (Table 5) point out a charge transfer character of this band from the selenium, sulfur atoms, towards the benzenic rings.

This CT − character is due to the high degree of localization of the $m = 8$ orbitals on the selenium and sulfur atoms, while the $m = 10$ orbitals present a benzenic character. As we have seen that all the antibonding

MO's are of benzenic type, for the other 8 to $8 + k (k = 1,2,3,4)$ excited states the same positivation of the heteroatoms is expected too.

Inspections of tables 3 and 5 point out that the calculated values for the electronic properties are identical for both compounds, although the geometries, the W_X and γ_{XX} values are different.

TABLE 5

Charge densities in the ground (G), SCF (8—10), and the first excited CI states: (I) = phenoxaselenine; (II)= phenoxathiin

	q	1	2	3	4	5	6	7	8
	G	1.867	1.063	1.035	1.004	1.014	1.011	1.032	1.927
I	SCF	1.833	0.974	1.169	1.086	1.006	1.132	1.122	1.188
	CI	1.815	0.991	1.196	1.038	1.025	1.164	1.065	1.300
	G	1.067	1.007	1.035	1.004	1.014	1.012	1.033	1.921
II	SCF	1.832	0.972	1.171	1.081	1.004	1.135	1.117	1.210
	CI	1.816	1.003	1.184	1.023	1.032	1.148	1.052	1.297

This case represents a good example for the remark made by some authors [12,13] referring to the decisive parameter in the semiempirical calculations.

Considering the expression of the diagonal element for the heteroatom X in the SCF hamiltonian, in which all the symbols have their usual meanings,

$$F_{XX} = W_X + 1/2\ P_{XX}\gamma_{XX} + \sum_{\mu \neq X} (P_{\mu\mu} - Z_\mu)\gamma_{\mu X}\,,$$

a simplified form $F_{XX} = W_X + \gamma_{XX}$ can be used when the ground state is characterized by a small amount of charge-transfer ($P_{XX} \simeq 2$, $P_{\mu\mu} \simeq Z_\mu$).

Taking into account for both heterocycles the charge densities in the ground state (Table 5) it can be seen that the CT amount is unsignificant and in consequence for both S and Se atoms the F_{XX} element can be approximated by the simplified formula. In this case, although different values are used for W_S, W_{Se} and γ_{SS}, γ_{SeSe}, it results that $F_{SS} = F_{SeSe} = -$ $- 8.10$ eV

This underlines that in the SCF—PPP method, the basic parameter for the heteroatoms providing two electrons to the π-system is not W_X or γ_{XX} independently, but their algebraic sum. This observation can be successfully verified for these heterocycles containing two heteroatoms because the difference between F_{oo} and F_{SeSe}, F_{SS}, respectively, does not allow a strong interaction between the two heteroatoms and the condition of a small CT is fulfilled. The equality of the F_{XX} values for both heteroatoms explains therefore the slight perturbation of the electronic structure produced by the substitution of sulfur by the selenium atom and the similar results obtained.

REFERENCES

[1] M. Hillebrand and V. Sahini, *Rev. Roumaine Chim.*, **16**, 1489 (1971).

[2] Y Matsunaga and T. Tanaka, *Bull. Chem. Soc. Japan*, **48**, 1043 (1975).

[3] M. F. Chiu and B. C. Gilbert, *J. Chem. Soc. Perkin Trans. II*, **1973**, 258.

[4] C. A. Heler, R. A. Zingaro and E. A. Meyers, *Canad. J. Chem.*, **52**, 3814 (1974).

[5] B. Hetnarschi and A. Grabowska, *Bull. Acad. polon Sci., Ser. Sci. chim.* **17**, 333 (1969).

[6] C. Bendic, M. Hillebrand and V. E. Sahini, *Rev. Roumaine Chim.*, **23**, 3 (1978).

[7] S. Hosoya, *Acta Cryst.*, **20** , 429 (1966).

[8] R. Pariser and R. G. Parr, *J. Chem. Phys.*, **21**, 767 (1953).

[9] N. Mataga and K. Nishimoto, *Z. phys. Chem. (Frankfurt)*, **13**, 140 (1957).

[10] M. Hillebrand and V. Sahini, *Rev. Roumaine Chim.*, (submitted for publication).

[11] M. Hillebrand, O. Maior, V. Sahini and E. Volanschi, *J. Chem. Soc.*, **1969**, 755.

[12] F. P. Billingsley and J. E. Bloor, *Theor. Chim. Acta*, **11**, 325 (1968).

[13] J. Koutecky, *Tetrahedron Letters*, **1968**, 1529.

Revue Roumaine de Chimie, 25, 5, 631–634 (1980)

UNRESTRICTED HARTREE-FOCK SPIN DENSITIES OF SOME HETEROAROMATIC CATION-RADICALS

MIHAELA HILLEBRAND and V. EM. SAHINI
Department of Physical Chemistry, Polytechnic Institute, Bucharest, B-dul Republicii 13, Romania

Received July 20, 1979

The main features of the spin distributions in some heteroaromatic ions, calculated by the UHF method, with and without annihilation of the quartet spin component are presented and discussed. The analysis of the spin appearing mechanisms reveals that the UHF method leads to poor results for the positions in which the SP mechanism is essential and in such cases the annihilation of the superior spin components is necessary.

The present paper deals with the UHF spin density calculations performed on the cation-radicals of 1,4-dithiin (I), 1,4-benzodithiin (II), thianthrene (III), phenoxathiin (IV) and phenoxaselenine (V), for which the experimental ESR parameters, including the hyperfine splittings from naturally occurring ^{33}S and ^{77}Se, were reported. [1,2]

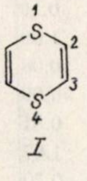

I

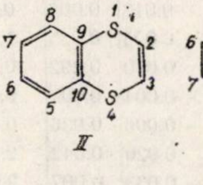

II

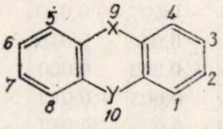

III X=S Y=S
IV X=O Y=S
V X=O Y=Se

These systems are interesting because the ^{33}S and ^{77}Se coupling constants can be used besides the proton splittings to test the validity of the M.O. calculations. Besides that, they were found to be suitable cases to discuss the effect of the annihilation of the superior spin components on the spin distribution.

M. O. CALCULATIONS

The spin densities were calculated by the semiempirical unrestricted Hartree-Fock method, both involving and not involving annihilation of the quartet spin component [3,4]. As other studies [5,6] on the neutral molecules attested the great influence of the sulfur and selenium parameters on the highest occupied molecular orbital, the most implied in the ionization process, W_S and W_{Se} were taken as empirical parameters and varied in the range of $(-20.00\ \text{eV}) - (-22.00\ \text{eV})$ and $(-17.40\ \text{eV}) - (-19.40\ \text{eV})$, respectively. Excepting a greater value for the sulfur-carbon resonance integral, i. e. $\beta_{C-S} = (-1.31\ \text{eV}$ the other parameters were taken as previously.[6] For the cation-radical (I), $\beta_{C-C} = -2.6$ eV was used to account for the smaller carbon-carbon distance (1,29 A°) in this system. For all the radicals, nonplanar geometries were assumed, with a dihedral angle of 133° – 138°.

The calculations were performed in the Felix C-256 computer, using a program described elsewhere.[7]

RESULTS AND DISCUSSION

For all the sulfur containing cation-radicals, the $W_S = -20.00$ eV value determines very large spin densities on the sulfur atoms and simultaneously too small densities on the ring positions. The spin distribution is much improved by decreasing W_S to -22.00 eV, and the resulted values are given in table 1.

TABLE 1

Spin densities and hyperfine splittings (G)

Rad.	Position	ρ_{UHF}	ρ_{aa}	$(\rho_{UHF})_{SP}$	$(\rho_{aa})_{SP}$	$(\rho)_{SD}$	$\|a_{UHF}\|$	$\|a_{aa}\|$	a_{exp}	$<S^2>$	$<S^2_{aa}>$
I	1 (S)	0.312	0.295	0.025	0.009	0.286	10.42	9.84	9.84	0.7598	0.7500
	2	0.094	0.103	−0.013	−0.004	0.107	2.54	2.78	2.82		
II	1 (S)	0.285	0.267	0.026	0.009	0.259	9.50	8.93	9.35	0.7628	0.7501
	2	0.126	0.137	−0.017	−0.006	0.143	3.39	3.70	3.30		
	5	−0.024	−0.004	−0.030	−0.010	0.006	0.65	0.11	0.20		
	6	0.039	0.031	0.012	0.004	0.027	1.05	0.84	1.05		
III	10 (S)	0.277	0.261	0.024	0.008	0.253	9.25	8.73	9.15	0.7688	0.7504
	1	−0.034	−0.007	−0.040	−0.013	0.006	0.91	0.19	0.13		
	2	0.051	0.040	0.015	0.005	0.035	1.37	1.09	1.28		
IV	10 (S)	0.322	0.302	0.030	0.010	0.292	10.75	10.08	11.91	0.7968	0.7504
	1	−0.005	0.003	−0.012	−0.004	0.007	0.14	0.09	0.26		
	2	0.018	0.030	−0.017	−0.006	0.036	0.50	0.81	0.99		
	3	0.101	0.062	0.059	0.020	0.042	2.73	1.67	2.14		
	4	−0.092	0.026	−0.098	−0.033	0.007	2.47	0.70	0.56		
V	10 (Se)	0.310	0.292	0.027	0.009	0.283	38.44	36.27	39.50	0.7992	0.7510

Inspection of table 1 reveals that the present calculations reproduce well the decrease of the sulfur spin density in the series (I) > (II) > (III), due to the extended delocalization of the odd electron on the benzene rings, as well as the greater value for (IV) as inferred from the experimental data. Concerning the sulfur spin polarization parameter, two estimations were previously made : a value of 33.4 G was found by Sullivan [1] from a McConnell type relation between the experimental splittings and McLachlan spin densities, and more recently Galasso [8] deduced a proportionality constant of 1364.47 G between the hfs. and the s – spin density on the sulfur atom calculated by the INDO method. As the present method is based on the π-approximation, we used $Q_S = 33.4$ G and the calculated splittings agree well with the experimental values, the relative deviation not exceeding 8.7 per cent.

The last row in table 1 contains the spin density on the selenium atom, calculated for $W_{Se} = -17.40$ eV.* For the ^{77}Se spin polarization parameter a single value was available, $Q_{^{77}\mathrm{Se}} = 124$ G and it leads to a calculated coupling constant matching well the value reported by Chiu and Gilbert [2].

If we consider the ring proton splittings, some discrepancies are to be noticed: the UHF values (ρ_{UHF}) reproduce correctly the experimental greatest constants in (I), (II) and (III), as well as their relative magnitude, but predict on the positions assigned to the small splittings, too large negative densities. Thus the hfs. $|a_5|$ in (II) and $|a_1|$ in (III) are found to be almost equal with $|a_6|$, respectively $|a_2|$, in spite of the significant experimental differences. A similar situation, $|a_4| \simeq |a_3|$, together with an anomalous small value for a_2, resulted for the phenoxathiin cation-radical (IV).

As the $\langle S^2 \rangle$ values in table 1 point out that the UHF function does not belong to a pure doublet state (the spin contamination increases from (I) to (V)), the UHF spin densities after the annihilation of the superior spin components (ρ_{aa}) were calculated too. Although the annihilation slightly affects, in a negative manner, the spin densities on the sulfur atom and on some ring positions, the overall spin distribution matches better the experimental one. The large negative splittings in (II), (III) and (IV) are greatly reduced, and the a_2/a_3 ratio in (IV) tends to the experimental value (1/2), although both splittings are underestimated. It may be remarked that for (IV) the agreement is poorer than for the other radicals, but some convergence difficulties were encountered, a fact already mentioned by Galasso, [9] in connection with spin density calculations by the INDO method in other sulfur heterocycles.

The remarkable effect of the annihilation for some proton splittings led us to perform an analysis of the spin appearing mechanisms. We have calculated the spin polarization (SP) and spin delocalization contributions $(\rho_{UHF})_{SP}$, $(\rho_{aa})_{SP}$, $(\rho)_{SD}$, for all the positions following the procedure given by Yonezawa :[10,11]

$$(\rho_{UHF})_{SP} = 3/2\,(\rho_{UHF} - \rho_{aa})$$

$$(\rho_{aa})_{SP} = 1/2\,(\rho_{UHF} - \rho_{aa})$$

$$(\varphi)_{SD} = \rho - (\rho)_{SP}$$

As concerns the sulfur atoms a predominant contribution of the spin delocalization mechanism (SD) is relevant, $(\rho)_{SD}$ representing 93–97 per cent from the spin density, independent of the radical or the sulfur parameter.

---

* For the phenoxaselenine cation-radical, the proton splittings are not resolved and the ^{77}Se splitting is the only experimental value available for a comparison with the theoretical data.

The SD mechanism is also essential for the positions within the dithiin nucleus (2 in (I) and in (II)) and for the positions in the benzenic cycles of (II), (III) and (IV), *para* vs. the heteroatoms. The SP contributions for these positions are very small and of different signs. The great accumulation of α spin density on the sulfur atoms determines a negative SP contribution in the dithiin ring, and a positive one for the positions *para* to the sulfur atoms in the adjacent rings. In the phenoxathiin cation-radical (IV), the same behaviour is found for position 3, while a negative SP contribution is obtained for position 2, *para* to the oxygen atom. This agrees with the result obtained if we perform a similar analysis on the spin densities reported by Ali and Wratten [12] for a related ion, the dibenzo-*p*-dioxin cation-radical, and is probably due to the presence of the oxygen atom.

The spin polarization is the determining spin appearing mechanism for all the positions *ortho* to the heteroatoms, that is, just the positions for which anomalous spin densities were obtained before annihilation. The removal of the spin contamination, also reflected by the $\langle S^2_{aa} \rangle$ values in table 1, leads to a significant decrease of $(\rho)_{SP}$ improving the agreement with the experimental values.

The role played by the annihilation of the spin quartet on the "improvement" of the spin densities is still discussed, especially in the frame of the semiempirical methods. [13,14]
The present calculations outline that the annihilation is required to obtain correct spin densities on the positions for which the main spin appearing mechanism is spin polarization.

REFERENCES

1. P. D. Sullivan, *J. Amer. Chem. Soc.*, **90**, 3618 (1968).
2. M. F. Chiu and B. C. Gilbert, *J. Chem. Soc. Perkin Trans.*, **1973**, 258.
3. A. T. Amos and J. Snyder, *J. Chem. Phys.*, **41**, 1773 (1964).
4. A. T. Amos and J. Snyder, *J. Chem. Phys.*, **42**, 3670 (1964).
5. M. Hillebrand and V. E. Sahini, *Rev. Roumaine Chim*, **25**, 625 (1980),
6. M. Hillebrand and V. E. Sahini, *Rev. Roumaine Chim*, (submitted for publication).
7. M. Hillebrand and V. E. Sahini, *Bul. Inst. Politeh. București*, **40**, 23 (1978).
8. V. Galasso, *Mol. Phys.*, **31**, 57 (1976).
9. V. Galasso, *J. Chim. phys.*, **71**, 889 (1974).
10. T. Yonezawa, H. Nakatsuji, T. Kawamura and H. Kato, *J. Chem. Phys.*, **51**, 669 (1969).
11. H. Nakatsuji, H. Kato and T. Yonezawa, *J. Chem. Phys.*, **51**, 3175 (1969).
12. M. A. Ali and R. J. Wratten, *Mol. Phys.*, **13**, 233 (1967).
13. D. Beveridge and P. A. Dobosh, *J. Chem. Phys.*, **48**, 5532 (1968).
14. J. Tino and V. Klimo, *Coll. Czech. Chem. Comm.*, **41**, 960 (1976).

Revue Roumaine de Chimie, **25**, *5*, 635 – 641 (1980)

AN IMPROVED TWO-PARAMETER OMEGA TECHNIQUE FOR MOLECULAR ORBITAL CALCULATIONS. I

THE ITPOT METHOD

EDUARDO A. CASTRO and FRANCISCO M. FERNÁNDEZ

Instituto de Investigaciones Fisicoquïmicas Teóricas y Aplicadas, Sección Química Teórica, Sucursal 4, Casilla de Correo 16, La Plata 1900,

Argentina

Received July 21, 1979

An improved Two-Parameter Omega Technique is described for the study of the physicochemical properties of aromatic systems. An exponential variation of resonance integrals β_{rs} with bond length is introduced into the calculation. Bond lengths, ionization potentials and V1 ← N transitions have been calculated and the values are in excellent agreement with the values obtained with a similar method as well as with more elaborated methods and experimental values.

INTRODUCTION

In recent years a renewed interest has emerged towards Hückel theory, specially as a guide for organic chemists in the interpretation of experiments[1]. Hess and Schaad[2] have shown that Hückel theory is as reliable as other far more sophisticated approaches for obtaining theoretical results on aromaticity. Trinajstić[3] has defined a topological resonance energy in the further development of Hückel theory, which has shown to be of great practical value for predicting the aromatic stability of an arbitrary pi-network. These and other similar results make us suspect the validity of the generally accepted statement that such a simple MO method works well due to the fortuitous cancellation of errors.

Several semi-empirical pi-electron calculations, using some variants of Pariser-Parr-Pople (PPP) [4,5] have been given for unsatured hydrocarbons.[6-16] The aim of these methods is to retain the computational simplicity of HMO type calculations[17,18] and at the same time to take into account, in an average way, the many-center integrals in the formulation of the matrix elements. The Hamiltonian matrix elements have the following general form

$$H_{rs} = H_{rs}\ (q, p, S, \lambda) \tag{1}$$

where q is the set of pi-electron densities on the picenters, p is the set of bond orders between the pi-centers, S is the set of the overlap integrals between the atomic pi-orbitals and λ denotes a set of parameters.

In one of the recently published semi-empirical methods, the so-called Two-Parameter Omega-Technique (TPOT),[16] it is shown that in order to obtain similar equation to those of the PPP in the framework of an omega-technique type method (equations of type (1)) the diagonal elements H_{rr} must depend linearly on the electron densities (q) at all centers and the off-diagonal elements H_{rs} must depend linearly on the bond orders (p). The equations obtained were

$$H_{rr} = H^0_{rr} + (1 - q_r)\,\omega\, H^0_{rs} - \sum_{\substack{s \text{ bonded} \\ \text{to } r}} (1 - q_s)\, 2\, \omega'\, H^0_{rs} \tag{2}$$

$$H_{rs} = H^0_{rs} + (1 - p_{rs})\,\omega'\, H^0_{rs} \tag{3}$$

where ω and ω' are two omega parameters with the chosen values of 1.4 and −0.6 respectively, H^0_{rr} is the reference Coulomb integral (the so-called α integral) and H^0_{rs} is the reference resonance integral (the so-called β integral). But both linear[16] and exponential[19,20,21] relations have been used to show the variation of the off-diagonal matrix elements with the bond-order (or bond distance). The following exponential relation

$$H_{rs} = H^0_{rs} \exp(0.55\, p_{rs} - 0.366) \tag{4}$$

was used by Hush and Pople[22] and Sharma et al.[11] to correlate various molecular properties with electronic structural indices.

In the present paper we have introduced the variation of the off-diagonal Hamiltonian matrix elements according to eq. (4) and for the diagonal ones we have used the formulation given by Mathur (see Eq. (7) in ref. 16). The calculations were performed on neutral, free radical and charged hydrocarbon species and the obtained results are compared with the available experimental data and the previous theoretical methods in order to establish the relevance of the present proposed method.

None of the calculated molecules required more than 10 iterations to achieve the chosen self-consistency (0.001 units in elements of the density matrix). Comparing with Mathur et al's maximum value of the required iterations (18) it can be seen that the present method is by far more rapidly convergent. No attempt was made to optimize the parameters ω and ω' in eqs (2) and (3), and values given by Mathur were used (1.4 and −0.6 respectively). In the same way, the exponential relation (4) was employed as given by the authors[21] without any optimization of the linear and independent coefficients (0.55 and 0.355, respectively). The numbering of atoms in the molecules was made similar to Mathur et al.[16] and the least squares correlation lines between theoretical and experimental quantities were determined with the help of a standard computer program.

DETAILS OF THE NUMERICAL CALCULATIONS

To allow a direct comparison, the same hydrocarbon molecules as those chosen by Mathur et al.[16] have been taken for numerical calculations. A digital computer program was written in FORTRAN IV language and it was run on an IBM/360 computer. Matrices were diagonalized by the Jacobi method[23] complemented with a subprogram necessary to order the eigenvalues in descending values. The secular equations were iterated to achieve a self-consistency of 0.001 units in the density matrix. To speed convergence three techniques were employed:

a) Ettinger's procedure[24] to modify the charge densities and bond-orders, as shown in the following equation, was used

$$\bar{D}_{ij}^{(n)} = (\bar{D}_{ij}^{(n-1)} + \bar{D}_{ij}^{(n)})/2 \qquad (5)$$

where n is the number of the iterative step and D_{ij} is an element of the density matrix (charge density or bond-order);

b) Hida's procedure[15] which uses a damping factor s in a weighted arithmetic mean of the type

$$\bar{D}_{ij}^{(n)} = (s\bar{D}_{ij}^{(n-1)} + D_{ij}^{(n)}) /(1+s) \qquad (6))$$

(we can see that Ettinger's procedure is a particular case of Hida's method);

c) A generalized geometric mean, which has the following expression

$$\bar{D}_{ij}^{(n)} = (\bar{D}_{ij}^{s(n-1)} \cdot D_{ij}^{(n)})^{1/(s+1)} \qquad (7)$$

where eq. (7) can be considered as a generalization of the averaging given by Mathur and McKennan.[25] The third method showed to be the more efficient, although the difference is not very significant with regard to Ettinger and Hida's procedures.

RESULTS AND DISCUSSION

The calculated structural indices and bond lengths for the chosen molecules are given in table 1.

In our calculation we estimated the bond lengths in conjugated hydrocarbons from an assumed linear relation between bond-order and bond length. This kind of correlation is widely used and gives results which agree with those obtained from minimization of the total molecular energy.[26]

In table 2 we give the bond lengths calculated by different authors as well as those calculated by our method, together with experimental values. To allow a direct comparison with Mathur's results, we choose the six molecules given in Table II of ref. 16.

The correlation line obtained is

$$l_{rs} = -0.21365\, p_{rs} + 1.54035\,; \;\; \mathrm{C.C.} = 0.914$$

From table 2 we can see that the ITPOT predicts bond lengths in very good agreement with experimental results and that the average deviation is less than with other methods. In particular it is interesting to note that some incorrect qualitative features given by the TPOT are improved by the ITPOT. For example, the TPOT predicts that the $C_2 - C_3$ bond in naphtalene is greater than the $C_9 - C_{10}$ bond, while the experimenta

TABLE 1

Molecular parameters calculated by the ITPOT

Atom position	Electron density	Bond	Bond order	Bond length (Å)
Benzene				
1	1.000	1—2	0.667	1.398
Fulvene				
1	0.899	1—2	0.882	1.352
2	0.984	2—3	0.331	1.470
3	1.049	3—4	0.876	1.353
4	1.010	4—5	0.374	1.460
Dimethylene-cyclobutene		1—2	0.921	1.344
1	1.000	2—3	0.248	1.487
2	1.000	2—6	0.299	1.476
3	1.000	5—6	0.881	1.352
Trimethylene-cyclopropane				
1	1.016	1—2	0.898	1.348
2	0.984	2—3	0.308	1.475
Dimethylene-cyclopropyl	Cation			
1	0.691	1—2	0.773	1.375
2	1.084	2—3	0.544	1.424
3	0.451	2—4	0.228	1.492
	Radical			
1	1.066	1—2	0.791	1.371
2	0.969	2—3	0.523	1.429
3	0.931	2—4	0.265	1.484
	Anion			
1	1.437	1—2	0.795	1.370
2	0.860	2—3	0.504	1.433
3	1.404	2—4	0.288	1.479
Butadiene				
1	1.000	1—2	0.941	1.339
2	1.000	2—3	0.338	1.468
Methylene-cyclopropene				
1	1.172	1—2	0.914	1.345
2	0.990	2—3	0.286	1.479
3	0.919	3—4	0.919	1.344
Cyclopropenyl-cation				
1	0.667	1—2	0.667	1.398
2	0.667	1—3	0.667	1.398

TABLE 2

Calculated and experimental bond lengths

Bond	Bond Order p_{rs}	Bond length (Å) l_{rs}				
		PPP[a]	SPO[a]	TPOT[b]	ITPOT[c]	Experimental values
Benzene						
1−2	0.667	1.393	1.393	1.399	1.398	1.397 [d]
Butadiene						
1−2	0.941	1.350	1.345	1.345	1.339	1.344 [e]
2−3	0.338	1.456	1.464	1.470	1.468	1.464 [e]
Trimethylene-cyclopropane						
1−2	0.898	1.349	1.346	1.351	1.348	1.343 [f]
2−3	0.307	1.463	1.469	1.473	1.475	1.453 [f]
Naphthalene						
1−2	0.756	1.373	1.396	1.378	1.379	1.363 [a]
1−9	0.533	1.421	1.426	1.428	1.426	1.421 [a]
2−3	0.564	1.416	1.422	1.424	1.420	1.415 [a]
9−10	0.553	1.403	1.396	1.413	1.422	1.418 [a]
Anthracene						
1−2	0.783	1.369	1.362	1.370	1.373	1.366 [a]
2−3	0.526	1.422	1.432	1.435	1.428	1.419 [a]
1−13	0.494	1.428	1.437	1.439	1.435	1.434 [a]
13−14	0.499	1.412	1.409	1.426	1.434	1.428 [a]
Tetracene						
1−2	0.793	1.364	1.358	1.367	1.371	1.385 [a]
2−3	0.510	1.429	1.440	1.440	1.431	1.479 [a]
1−13	0.478	1.436	1.445	1.444	1.438	1.431 [a]
13−14	0.475	1.421	1.422	1.434	1.439	1.439 [a]
12−13	0.653	1.390	1.385	1.395	1.401	1.398 [a]
12−15	0.577	1.412	1.415	1.418	1.417	1.409 [a]
15−16	0.464	1.419	1.413	1.431	1.441	1.478 [a]
Average deviation		0.0126	0.0156	0.0117	0.0102	—

[a] M. J. S. Dewar and C. J. Gleicher, *J. Amer. Chem. Soc.*, **87**, 685, 692 (1965)

[b] Ref. **16**.

[c] l_{rs}(Å) = $-\,0.21365\ p_{rs} + 1.54035$

[d] B. P. Stoicheff, *Canad. J. Phys.*, **32**, 339 (1954)

[e] A. H. Cole, G. M, Mohay and G, A. Osborne, *Spectrochim. Acta*, **23A**, 909 (1967)-

[f] E. A. Dorko, J, L. Henscher, and S. H. Bauer, *Tetrahedron*, **24**, 2425 (1968).

values prove otherwise. On the other side, the ITPOT correctly makes a prediction in accordance with the experimental results.

In tables 3 and 4 the correlation of the molecular pi-energy levels with ionization potentials and V1 ← N transitions, together with the experimental data are presented.

The correlation line obtained for ionization potentials is

$$\mathrm{IP\ (eV)} = 3.55\ m_{\gamma} + 5.70\ ;\ r = 0.999$$

TABLE 3

Ionization potential for some polyacenes (eV)

Molecule	CNDO/S2[a]	TPOT[b]	ITPOT[c]	Experimental values
Benzene	9.24	9.23	9.25	9.24
Naphthalene	8.06	8.15	8.12	8.15
Anthracene	7.40	7.44	7.41	7.40
Tetracene	7.00	6.98	6.97	7.01
Pentacene	6.74	6.65	6.67	6.64
Average deviation	0.04	0.02	0.02	

[a] See comments below Table II in Ref. 16

[b] Ref. 16, Table III

[c] $\mathrm{IP(eV)} = 3.55\ m + 5.70$

[d] N. O. Lipari and C. B. Duke, *J. Chem. Phys.*, **63**, 1768 (1975).

TABLE 4

Position of V1←N electronic transition of some polyacenes (cm^{-1})

Molecule	CNDO/S2[a]	TPOT[a]	ITPOT[b]	Experimental values
Benzene	48593	48166	48401	48400
Naphthalene	34445	35097	34726	34700
Anthracene	26235	26535	26379	26400
Tetracene	21119	20903	21079	21200
Pentacene	17708	17448	17505	17400
Average deviation	200.4	222.2	54.8	—

[a] Ref. 16, Table IV

[b] $E_{V1 \leftarrow N}\ (\mathrm{cm}^{-1}) = 21247.7\ \Delta m + 5879.7$

[c] S. C. Mathur and D. C. Singh, *Ind. J. Pure Appl. Phys.*, **8**, 788 (1970).

and the correlation line for the V1 ← N transition is

$$E_{V_1 \leftarrow N}\ (\mathrm{cm}^{-1}) = 21247 \cdot 7\, \Delta m + 5879.7\,; \quad r = 1.000$$

where m_j is the HOMO energy in units of β and $\Delta\, m$ is the difference between HOMO and LEMO in the same units. We can see again that our results are superior to those of the PPP and TPOT methods, specially the one obtained for the V1 ← N electronic transition of polyacenes.

Thus, the simple change on the off-diagonal Hamiltonian matrix elements with regard to the TPOT recipe produces superior results, although not any optimization of the necessary parameters is made. Surprisingly enough the results are also superior to the more elaborated and sophisticated SCF methods, such as PPP, CNDO/S2 and SPO. However, before a definitive conclusion on the usefulness and applicability of the ITPOT can be reached, the method will have to be applied to a wide variety of molecules and different physicochemical properties as well as to a thoroughly study of a universal set of parameters for different atoms. Currently, this investigation is being made in our laboratory.

REFERENCES

[1] C. F. Wilcox, Jr., *J. Amer. Chem. Soc.*, **91**, 2732 (1969).

[2] B. A. Hess, Jr., L. J. Schaad and C. W. Holyyoke, Jr., *Tetrahedron*, **28**, 3697 (1972). Ibid. **31**, 295 (1975); B. A. Hess, Jr., and L. J. Schaad, *J. Amer. Chem. Soc.*, **95**, 3907 (1973).

[3] N. Trinajstić, *Int. J. Quantum Chem. Symp.*, **11**, 469 (1977).

[4] J. A. Pople, *Trans. Faraday Soc.*, **49**, 1375 (1953).

[5] R. Pariser and R. G. Parr, *J. Chem. Phys.*, **21**, 446, 787 (1953).

[6] B. Krishna and S. P. Gupta, *J. Amer. Chem. Soc.*, **92**, 7247 (1970).

[7] B. Krishna and S. P. Gupta, *J. Chem. Soc.*, **A**, 123, (1971).

[8] S. P. Gupta and B. Krishna, *J. Amer. Chem. Soc.*, **94**, 57 (1972).

[9] B. Krishna, A. K. Srivastava and S. P. Gupta, *Ind. J. Pure Appl. Phys.*, **10**, 481 (1972).

[10] A. K. Srivastava and B. Krishna, *Ind. J. Pure Appl. Phys.*, **11**, 246, 354, 356 (1972)

[11] S. C. Sharma, A. K. Srivastava and B. Krishna, *JCS Faraday II*, **70**, 168, 172 (1974).

[12] E. A. Dorko, H. P. Nielsen and W. C. Bahr, *Theor. Chim. Acta*, **14**, 357 (1969).

[13] L. K. Huy and W. Forst, *Theor. Chim. Acta*, **16**, 393 (1970).

[14] W. Grundler, *Monatsh. Chem.*, **101**, 1362 (1970).

[15] M. Hida, *Mem. Fac. Techn. Tokyo Metropolitan Univ.*, **24**, 2209 (1974).

[16] S. C. Mathur, D. C. Singh, B. Kumar and S. Mitra, *Int. J. Quantum Chem.*, **11**, 759 (1977).

[17] A. Streitwieser Jr., "Molecular Orbital Theory for Organic Chemistry", Wiley, New York, 1970.

[18] E. Heilbronner and H. Bock, "Das HMO-Modell und seine Anwendung", Verlag-Chemie, Weinheim, 1968.

[19] R. S. Mulliken, C. Rieke and W. G. Brown, *J. Amer. Chem. Soc.*, **63**, 41((1949).

[20] H. C. Longuet-Higgins and L. Salem, *Proc. Roy. Soc. (London)*, **A251**, 172 (1959).

[21] G. V. Boyd and N. Singer, *Tetrahedron*, **22**, 3393 (1966).

[22] N. S. Hush and J. A. Pople, *Trans, Faraday Soc.*, **51**, 600 (1955).

[23] S. S. Kuo, "Numerical Methods and Computers", Addison-Wesley, Reading, Mass., 1965.

[24] R. Ettinger, *Tetrahedron*, **20**, 1579 (1964).

[25] S. C. Mathur and E. C. McKennan, *Int. J. Quantum Chem.* **1S**, 247 (1967).

[26] M. J. S. Dewar, "The Molecular Orbital Theory of Organic Chemistry", McGraw-Hill, New York, 1969.

Revue Roumaine de Chimie, 25, 5, 643–650 (1980)

AN IMPROVED TWO-PARAMETER OMEGA TECHNIQUE FOR MOLECULAR ORBITAL CALCULATIONS. II.*

POLYENES

EDUARDO A. CASTRO and FRANCISCO M. FERNÁNDEZ
Instituto de Investigaciones Fisicoquímicas Teóricas y Aplicadas, Sección Química Teórica, Sucursal 4, Casilla de Correo 16, La Plata 1900, *Argentina*

Received July 21, 1979

The two-parameter omega technique and the improved two-parameter omega technique are applied to various polyenes to calulate bond lengths, ionization potentials and electronic VI ←N transitions. Results are compared with available experimental data as well as with other methods. Very good correlations between theoretical and experimental values are found.

INTRODUCTION

It is worth noting that the development and parametrization of semiempirical pi-electron calculations based on MO theory is currently a rather active research area, and the results of the more recently developed methods appear to show a gradual improvement in quality. In some cases, however, the choice of the necessary parameters required to give a good agreement with experimental data is specific for a particular property or for a restricted kind of compounds, and cannot, therefore, generally be extended to a wider kind of compounds and to different properties. Recently, much attention has been paid to the omega-technique type methods[1–9] to obtain corrections for the two center two electron repulsion integrals and to get similar equations to those of the Pariser-Parr-Pople method.[10,11]

In a previous paper[12] (hereafter called I) the author and Fernández have proposed an Improved Two-Parameter Omega Technique (ITPOT) for the calculation on neutral, free radical and charged species, and the results obtained showed to be very promising for correlating experimental data and theoretical values. The ITPOT is a modification of the Two-Parameter Omega Technique (TPOT) of Mathur *et al*[9] and it showed to be of a superior quality[12].

---

*) Part I, see ref. 12.

The purpose of this paper is to apply the ITPOT and TPOT to polyenes to calculate bond lengths, ionization potentials ande electronic V1 ← N transitions, and to compare them with available experimental data as well as with other methods.

METHOD OF CALCULATION

The Hamiltonian matrix elements for the TPOT are[9]

$$H_{rr} = H^{0}_{rr} + (1 - q_r)\,\omega\, H^{0}_{rs} - \sum_{\substack{s\ \text{bonded}\\ \text{to}\ r}} (1 - q_s) 2\,\omega' H^{0}_{rs} \qquad (1)$$

$$H_{rs} = H^{0}_{rs} + (1 - p_{rs})\,\omega'\, H^{0}_{rs} \qquad (2)$$

where H^{0}_{rr} is the so-called α integral, H^{0}_{rs} is the β integral, q_r is the electronic pi charge on the r-th C atom, p_{rs} is the bond order between C_r and C_s, and ω and ω' are the two omega parameters.

For the ITPOT[12] the diagonal matrix elements are indentical to those of the TPOT, and the off-diagonal matrix elements take the following expression

$$H_{rs} = H^{0}_{rs} \exp\,(0.55\, p_{rs} - 0.366) \qquad (3)$$

The exponential relation (3) was employed by Hush and Pople[13] and Sharma *et al.*[7] to correlate electronic structural indices with molecular properties.

To speed convergence the previously described techniques[12] were employed and again the generalized geometric mean showed to the more efficient. The maximum value of the required interations was 22 for the TPOT and 14 for the ITPOT, and the chosen self-consistent upper limit was 0.001 units in elements of the density matrix. In both methods the values used for the omega parameters ω and ω' were 1.4 and -0.6 respectively and no attempt was made to optimizing them, as well as the coefficients in formula (3).

RESULTS AND DISCUSSION

The molecules studied in this work are shown in figure 1.

The calculated bond orders and bond lengths are presented in tables 1 and 2 with the corresponding values obtained by other methods and by the available experimental data.

Correlation of the molecular energy levels with ionization potentials and V1 ← N transition energies are given in tables 3 and 4 together with the experimental values for some linear polyenes.

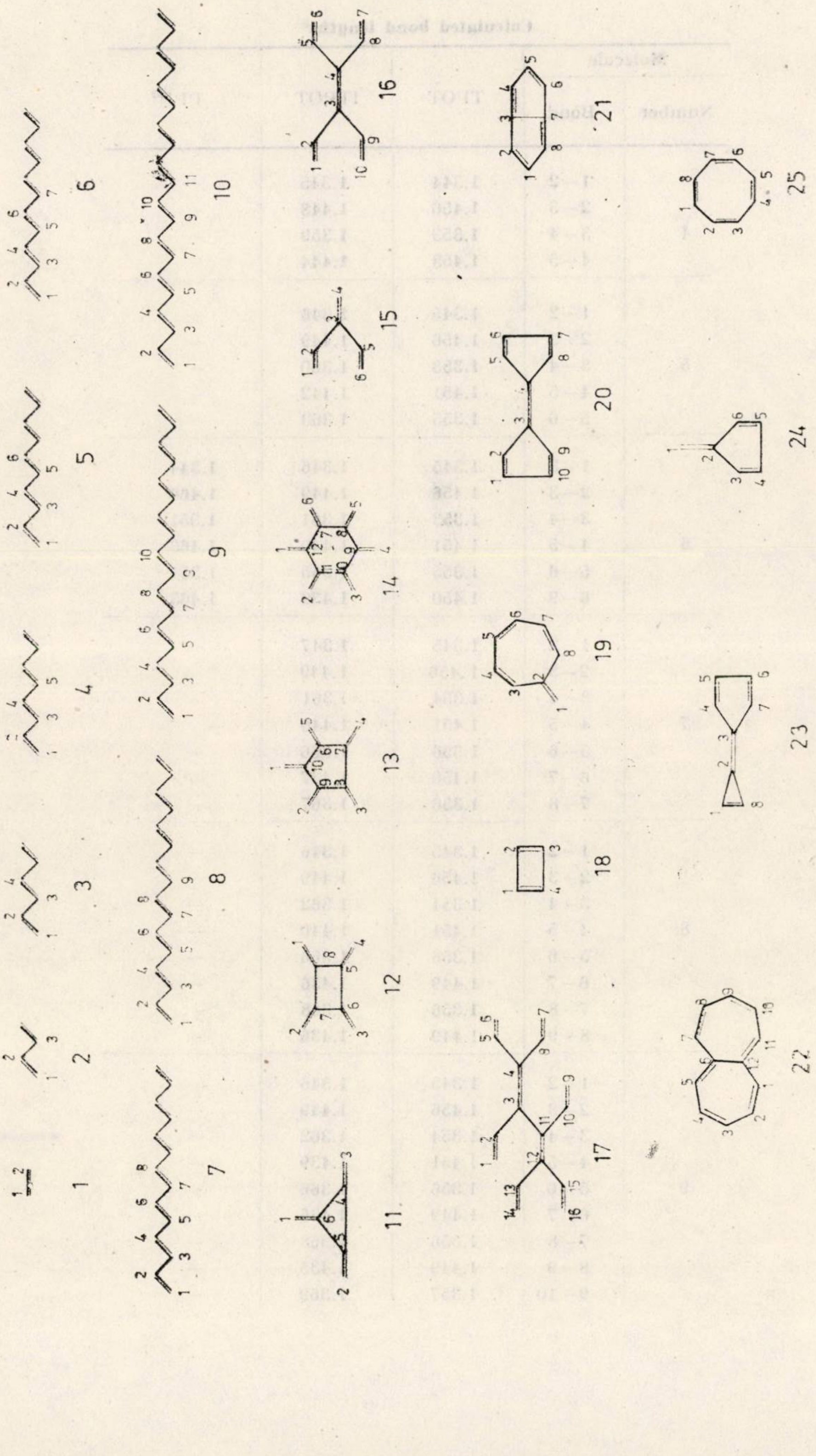
1
2
3
4
5
6
7
8
9
10
11
12
13
14
15
16
17
18
19
20
21
22
23
24
25

Fig. 1 – Numbering of molecules and of atoms in molecules.

TABLE 1

Calculated bond lengths[a]

Molecule		TPOT	ITPOT	PPP[b]
Number	Bond			
4	1−2	1.344	1.345	—
	2−3	1.456	1.448	—
	3−4	1.353	1.359	—
	4−5	1.453	1.444	—
5	1−2	1.345	1.346	—
	2−3	1.456	1.449	—
	3−4	1.353	1.360	—
	4−5	1.451	1.442	—
	5−6	1.355	1.363	—
6	1−2	1.345	1.346	1.344
	2−3	1.456	1.449	1.466
	3−4	1.353	1.361	1.351
	4−5	1.451	1.440	1.463
	5−6	1.355	1.365	1.351
	6−9	1.450	1.439	1.463
7	1−2	1.345	1.347	—
	2−3	1.456	1.449	
	3−4	1.354	1.361	—
	4−5	1.451	1.440	—
	5−6	1.356	1.366	—
	6−7	1.450	1.437	—
	7−8	1.356	1.367	—
8	1−2	1.345	1.346	—
	2−3	1.456	1.449	—
	3−4	1.354	1.362	—
	4−5	1.451	1.440	—
	5−6	1.356	1.366	—
	6−7	1.449	1.436	—
	7−8	1.356	1.368	—
	8−9	1.449	1.436	—
9	1−2	1.345	1.346	—
	2−3	1.456	1.449	—
	3−4	1.354	1.362	—
	4−5	1.451	1.439	—
	5−6	1.356	1.366	—
	6−7	1.449	1.436	—
	7−8	1.356	1.368	—
	8−9	1.449	1.435	—
	9−10	1.357	1.369	—

Table 1 (continued)

Molecule		TPOT	ITPOT	PPP^{b}
Number	Bond			
10	1 − 2	1.346	1.346	—
	2 − 3	1.456	1.449	—
	3 − 4	1.354	1.362	—
	4 − 5	1.451	1.439	—
	5 − 6	1.356	1.366	—
	6 − 7	1.449	1.436	—
	7 − 8	1.356	1.368	—
	8 − 9	1.449	1.369	—
	9 − 10	1.357		—
	10 − 11	1.449	1.434	—
12	1 − 8	1.347	1.348	—
	8 − 5	1.466	1.467	—
13	1 − 10	1.348	1.350	1.349
	10 − 6	1.464	1.464	1.471
14	1 − 12	1.348	1.350	—
	12 − 7	1.464	1.463	—
15	1 − 2	1.342	1.341	1.343
	2 − 3	1.463	1.461	1.469
	3 − 4	1.349	1.352	1.349
16	1 − 2	1.345	1.345	1.344
	2 − 3	1.457	1.453	1.466
	3 − 4	1.366	1.378	1.362
17	1 − 2	1.344	1.344	1.345
	3 − 11	1.450	1.444	1.462
	10 − 11	1.457	1.454	1.466
	11 − 12	1.369	1.383	1.363
	12 − 13	1.456	1.451	1.465
	13 − 14	1.345	1.346	1.345
18	1 − 2	1.510	1.523	1.512
	2 − 3	1.336	1.330	1.338
19	1 − 2	1.351	1.356	1.351
	2 − 3	1.459	1.456	1.467
	3 − 4	1.352	1.357	1.352
	4 − 5	1.453	1.445	1.458
	5 − 6	1.354	1.361	1.354
20	1 − 2	1.352	1.356	1.353
	2 − 3	1.457	1.455	1.465
	3 − 4	1.367	1.377	1.363
	1 − 10	1.458	1.456	1.456

Table 1 (continued)

Molecule		TPNT	ITPOT	PPP[b]
Number	Bond			
21	1−2	1.404	1.402	1.353
	2−3	1.412	1.418	1.457
	3−7	1.437	1.433	1.456
22	1−2	1.403	1.398	1.352
	2−3	1.407	1.406	1.460
	5−6	1.408	1.415	1.361
	6−12	1.451	1.440	1.463
23	1−2	1.456	1.448	1.459
	1−8	1.352	1.358	1.353
	2−3	1.367	1.384	1.369
	3−4	1.451	1.443	1.456
	4−5	1.356	1.364	1.358
	5−6	1.448	1.437	1.447

[a] All values are given in Å

[b] M. J. S. Dewar and C. de Llano, *J. Amer. Chem. Soc.*, **91** (1969) 789.

Table 2 shows that the TPOT and the ITPOT predict bond lengths not only in very good agreement with experimental results but also of a similar quality as the IMOA method; the overall results are superior to those predicated by the MINDO/3 method.

Table 3 shows an excellent correlation between HOMO for TPOT and ITPOT and the experimental ionization potentials with a mean deviation of 0.002 eV.

In table 4 we see that the ITPOT gives results which are superior to the TPOT and highely superior to other semiempirical methods. Again, the correlation between molecular energy indices ($\Delta m =$ LEMO − HOMO) and experimental values is excellent for the ITPOT and the TPOT. Both methods predict V1 ← N transition energies for linear polyenes of a remarkable quality.

As in I for neutral, free radical and charged hydrocarbon species, the performed calculations obtained show that reliable predictions can be made for various molecular properties for polyenes.

Although these results do not allow us to reach a definitive conclusion on the performance of the ITPOT and the TPOT, they are encouraging enough to continue the investigations for a wider variety of molecules as well as other molecular properties.

TABLE 2

Calculated and experimental bond lengths

Molecule		Bond length[a,e] (exper)	TPOT[b]	ITPOT[c]	IMOA[d]	MINDO/3[e]
Number	Bond					
1		1.336	1.336	1.330	1.338	1.308
2	1−2	1.342	1.343	1.342	1.340	1.330
	2−3	1.463	1.461	1.458	1.470	1.464
3	1−2	1.337	1.344	1.344	1.339	1.330
	2−3	1.458	1.457	1.452	1.456	1.462
	3−4	1.368	1.351	1.355	1.345	1.346
11	4−6	1.453	1.464	1.464	—	1.482
	1−6	1.343	1.348	1.350	—	1.321
24	2−3	1.470	1.461	1.459	1.472	1.509
	3−4	1.355	1.351	1.354	1.354	1.353
	1−2	1.349	1.350	1.353	1.342	1.339
25	1−8	1.340	1.347	1.348	1.336	1.344
	1−2	1.466	1.466	1.467	1.464	1.466
Aver. deviation		—	0.005	0.006	0.005	0.014

[a] All values are given in Å.
[b] $l_{rs}(\text{Å}) = 1.5099 - 0.1741\, p_{rs}$
[c] $l_{rs}(\text{Å}) = 1.5232 - 0.1928\, p_{rs}$.
[d] Z.B. Maksić and A. Rubcić. *J. Amer. Chem. Soc.*, **99** (1977) 4233.
[e] R. C. Bingham, M. J. S. Dewar and D. H. Lo, *J. Amer. Chem. Soc.*, **97**, 1294 (1975).

TABLE 3

Correlation of IP with E_{HOMO} for the first four linear polyenes

Molecule	IP_{exper}	IP^{b}_{TPOT}	IP^{c}_{ITPOT}
Ethylene	10.45	10.47	10.47
Butadiene	9.02	8.99	8.97
Hexatriene	8.23	8.24	8.24
Octatetraene	7.80	7.82	7.82
Average deviation	—	0.02	0.02

[a] All IP are given in eV
[b] $IP(eV) = 4.9065 + 5.5610\, E_{HOMO}$
[c] $IP(eV) = 5.7838 + 3.8975\, E_{HOMO}$

TABLE 4

Molecule	$E^{a,\,d}_{exper}$	E^{b}_{TPOT}	E^{c}_{ITPOT}	FEMO^{d}	I FEMO^{d}	HMO^{d}	HMO. 2 β^{d}_{s}
1	61500	62197	61952	51000	59000	74600	67800
2	46100	45526	45435	30600	42600	(46100)	(46100)
3	37300	37317	37393	21800	35100	33200	36200
4	32900	32558	32671	17000	31000	25900	30600
5	29900	29493	29579	13900	28300	21200	27000
6	27500	27405	27404	11800	26500	18000	24600
7	25600	25921	25798	10200	25100	15600	22900
8	24400	24790	24568	9000	24000	13800	21500
9	—	23922	23577	8100	23200	12300	20500
10	22400	23296	22801	7300	22500	11200	19700
Aver. deviation	—	415.4	291.4	1444.4	1522.2	9275.0	2975.0

[a] All energies are given in cm^{-1}

[b] $E_{V1\leftarrow N}(\mathrm{cm}^{-1}) = 50.2 + 31073.2\ (E_{LUMO} - E_{HOMO})$

[c] $E_{V1\leftarrow N}\ (\mathrm{cm}^{-1}) = 10246.1 + 21507.8\ (E_{LUMO} - E_{HOMO})$

[d] I. N. Levine, "Quantum Chemistry", Vol. I, Allyn and Bacon, 1970, p. 503.

REFERENCES

[1] B. Krishna and S. P. Gupta, *J. Amer. Chem. Soc.*, **92**, 7247 (1970).

[2] B. Krishna and S. P. Gupta, *J. Chem. Soc.* A, **1971**, 123.

[3] S. P. Gupta and B. Krishna, *J. Amer. Chem. Soc.*, **94**, 57 (1972).

[4] B. Krishna, A. K. Srivastava and S. P. Gupta, *Ind. J. Pure Appl. Phys.*, **10**, 481 (1972).

[5] A. K. Srivastava and B. Krishna, *Ind. J. Pure Appl. Phys.*, **11**, 246, 354, 356 (1972).

[6] S. P. Gupta and B. Krishna, *J. Phys. B.* **5**, 1101 (1972).

[7] S. C. Sharma, A. K. Srivastava and B. Krishna, *JCS, Faraday II*, **70**, 168, 172 (1974).

[8] E. A. Dorko, H. P. Nielsen and W. C. Bahr, *Theor. Chim. Acta*, **14**, 357 (1969).

[9] S. C. Mathur, D. C. Singh, B. Kumar and S. Mitra, *Int. J. Quantum Chem.*, **11**, 759 (1977).

[10] R. Pariser and R. G. Parr, *J. Chem. Phys.*, **21**, 446, 767 (1953).

[11] J. A. Pople, *Trans Faraday Soc.*, **49**, 1375 (1953).

[12] Part. I : E. A. Castro and F. M. Fernández, *Rev. Roumaine Chim.* **25**, 635 (1980).

[13] N. S. Hush and J. A. Pople, *Trans Faraday Soc.*, **51**, 600 (1955).

Revue Roumaine de Chimie, 25, 5, 651–662 (1980)

SPECTRAL SOLVENT EFFECTS IN AROMATIC COMPOUNDS SOLUTIONS. VI

THE SOLVENT EFFECTS ON THE TOLUENE ELECTRONIC BAND AT 2600 Å

VASILE MACOVEI
Physical Chemistry Laboratory, Faculty of Chemistry and Engineering Chemistry, Splai–Bahlui–stinga street, 71, Jassy, Romania

Received May 21, 1977
Completed September 21, 1979

The solvents influence on the position and intensity of the toluene electronic spectral band at 2600 Å is investigated, and the dipole moment of the solute molecule in the excited state is evaluated, with the aim to contribute to the elucidation of the solute-solvent interactions.

I. INTRODUCTION

In a preceding series of papers, [1–5] the solvents influence on the spectral bands of benzene, chlorobenzene, nitrobenzene, bromobenzene, and benzaldehyde was investigated to establish the behaviour differences between the benzene molecules monosubstituted with substituents of the first and second order in solution. But the formulation of some general conclusions requires the study of several molecules. Besides the monoatomic substituents, chlorine [2] and bromine, [4] a more complex substituent of the first order, as the methyl group, must be investigated. The solvents influence on the toluene electronic spectrum is thus investigated.

II. RESULTS AND DISCUSSION

The toluene molecule results from the joining of a phenyl group with a methyl group, and has a small dipole moment. [6] Toluene spectrum is expected to behave approximately similar to the benzene spectrum in solution, [1] the differences resulting from the molecular size changes, [2,3] and from the dipole moment alteration between the ground and excited states.[2–5,7]

The symmetry of toluene molecule is different from that of benzene, but the toluene spectral behaviour displays a remarkable similitude with that of the unsubstituted benzene. [8] In the ultraviolet spectral range, the monosubstituted benzene molecules, usually exhibit two bands, [9–11] out of which one, near the visible range, (neglecting the very weak band at 3400 Å) is theoretically and experimentally the most investigated, [12] and is called[9] "secondary band." This band derives from the forbidden ${}^2A_{1g} \to {}^2B_{2u}$ benzene transition, becoming the allowed ${}^1A_1 \to {}^1B_1$ transition in the toluene spectrum, on the base of the C_{2v} symmetry of the toluene molecule in the ground and in the excited states,[12] i. e. through the perturbation of the D_{6h} symmetry of benzene,[8] a fact theoretically established by Matsen.[13]

The spectral benzenoide bands shift on the benzene substitution,[9,14-16] but the problem of the transitions assignements of the monosubstituted benzenes is far from its solution.[17] Many experimental[9,10,18-23] and theoretical[14,16,24-30] works have appeared on this subject, but there are still misunderstandings concerning the characterization of the different absorption bands of the monosubstituted benzenes, whence the need of new investigations.

In the $\pi \to \pi^*$ transitions, the characteristic benzene ring vibrations are efficient, the C—C vibrations being prominent.[12] The shape of the spectrum is not considerably altered, but the origin is displaced.[31] In figure 1 some of our results are given, in a few solvents, confirming the above assertions. (The numbers in figure 1 correspond to the solvents in table 1, and the notation is preserved throughout the paper).

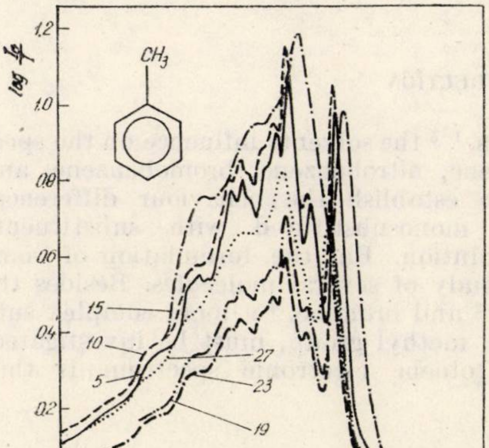

Fig. 1—The toluene spectrum in solvents : *5.* n-Heptane ; *10.* Ethanol ; *15.* Ethyl ether ; *19.* Carbon tetrachloride ; *23.* Ethyl acetate ; 27. Water.

One sees, in figure 1, the separation and the pronounced intensity of the (0,0) electrono-vibrational component, and a slight blur of the vibrational structure of the toluene spectrum. This blur is due, partly to the substitution,[32] and partly to the interactions with the solvent[1,2,8] As in the benzene case,[1] all the electrono-vibrational components in the ${}^1A_1 \to {}^1B_1$ toluene band are equally shifted in the same direction, under the solvent influence. The position of the (0,0) component may be established with an accuracy of a few cm^{-1} in the vapour spectrum, and with approximately 30 cm^{-1} in solution,[33] and thus the investigation of this component under the solvents influence is indicated. The position of the (0,0) component in the vapour spectrum of the toluene was identified [34-36] respectively, at 37 672, 37 478, and 37 484 cm^{-1}. The last value [36] was adopted as reference to establish the spectral shift, $\Delta\tilde{\nu}$(cm^{-1}), in different solvents, as seen in table 1. According to the accepted practice, [7,37,38] the absorption peak is considered as the band position. One remarks small values of the spectral shifts in water, ethyl ether, methanol, ethyl acetate, and butyl acetate. But there are great values in methylene chloride, chloroform, and particularly in carbon tetrachloride, that is approximately as in the benzene case. [1] The small dipole moment of the toluene molecule [6] causes the solvent effects in the spectrum to be dominated by the *red polarization shift.* [7] The intermolecular interactions having the major contribution to the spectral shift are the dispersion forces of the London [39] type. Then, the spectral shift in solution, $\Delta\tilde{\nu}$, must correlate lineally with the refractive index function of the solvent $f(n^2) = (n^2-1)/(2n^2+1)$, according to the expression of McRae, [40] given in equation (1) of the first paper [1] of the series. This correlation is rendered in figure 2. The representative points are oriented along a straight line, with a significant deviation in carbon tetrachloride case, and with the tendency of the straight line to cut the ordinate axis under the origin. The applicability of equation (1) from the quoted paper [1] was checked evaluating the parameter sum : (A + B) = 1742 cm^{-1}, which has the same meaning as in the preceding papers. [1,2,4,5] Using this value, the theoretical spectral shifts were estimated, and adequately registered in table 1. The correlation between the theoretical shift values and the function f(n^2) of the solvent is completely lineal, [41] with the same tendency of the straight line to cut the ordinate axis under the origin. This feature of the correlation lines for the experimental and theoretical shifts and of the f(n^2) function, as well as the points spreading in figure 2 indicate the existence of some subsidiary factors contributing to the spectral shift, [1,2,4] besides the interactions due to the dispersion forces. An important role in the spectral shift in solution has the dipole moment of the solute molecule. [1-5,7] The theoretical dipole moment of the toluene molecule [42] is 0.21 D, and is experimentally determined [43,44] as 0.39 D. The spectral shift in solution results from the difference between the solvation energies of the ground and excited

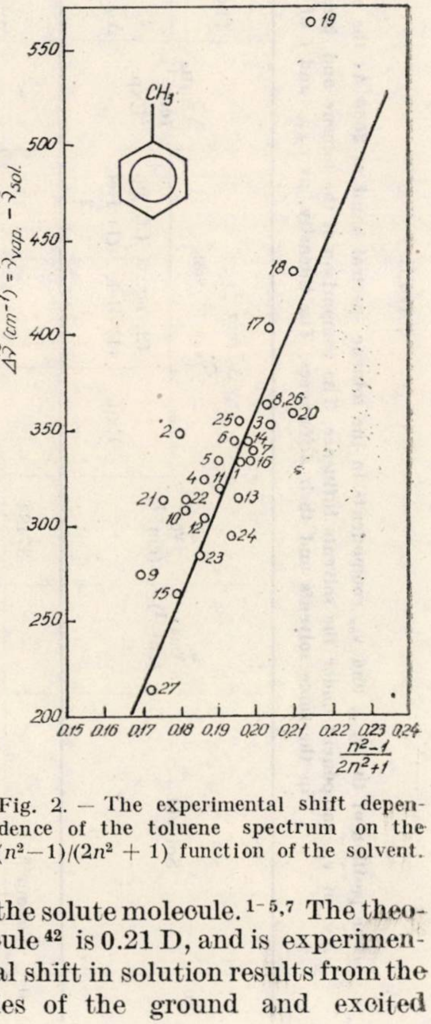

Fig. 2. — The experimental shift dependence of the toluene spectrum on the $(n^2-1)/(2n^2+1)$ function of the solvent.

TABLE 1

The position of the $\tilde{\nu}_{max}$ and $\tilde{\nu}_{00}$ components in the toluene spectral band at 2600 Å; the experimental and theoretical shifts, $\Delta\tilde{\nu}$, of $\tilde{\nu}_{00}$ component under the solvents influence. The comparison of the toluene and benzene[1] experimental spectral shifs in the same solvents and their differences. The intensity, as $\varepsilon_{max.}$ and f of the toluene band

No.	Solvent	$\tilde{\nu}_{max.}$ (cm^{-1})	$\tilde{\nu}_{00}$ (cm^{-1})	$\Delta\tilde{\nu}$ (cm^{-1}) = $\tilde{\nu}_{vap.} - \tilde{\nu}_{sol.}$			$\Delta\tilde{\nu}_{C_6H_6}$ (cm^{-1}) Exp.	The difference:	$\varepsilon_{max.}$ (l · mol^{-1} · cm^{-1})	$f \cdot 10^3$
				Exp.	Cf. eq. (1) Ref. 1	Cf. eq. (1) Ref. 2		$\Delta\tilde{\nu}_{C_7H_8} - \Delta\tilde{\nu}_{C_6H_6}$		
0	Vapour[36]	—	37484	—	—	—	—	—	—	—
1	Cyclopentane	38110	37150	334	341	365	279	55	257.20	3.14
2	n-Pentane	38105	37135	349	312	334	259	90	191.40	2.26
3	Cyclohexene	38100	37130	354	355	380	259	95	220.00	2.82
4	n-Hexane	38130	37160	324	324	347	259	65	255.70	3.05
5	n-Heptane	38140	37150	334	331	354	279	55	216.40	2.51
6	n-Octane	38100	37140	344	338	362	259	85	229.00	—
7	n-Decane	38120	37145	339	347	371	259	80	219.60	2.56
8	n-Dodecane	38085	37120	364	354	378	279	85	196.00	—
9	Methanol	38180	37210	274	294	267	219	55	235.60	2.74

10	Ethanol	38150	37175	309	315	293	259	50	228.80	3.53
11	1-Propanol	38120	37165	319	331	313	250	60	216.00	2.84
12	2-Propanol	38160	37180	304	324	300	259	45	228.00	2.75
13	1-Butanol	38125	37170	314	340	324	259	55	222.70	3.06
14	3-Methyl-1-butanol	38105	37140	344	345	332	259	85	216.00	2.49
15	Ethyl ether	38180	37220	264	310	316	239	25	199.00	2.31
16	Isoamyl ether	38125	37150	334	345	363	299	35	151.20	—
17	Methylene chloride	38045	37080	404	355	353	359	45	251.00	2.78
18	Chloroform	38025	37050	434	366	377	399	35	234.00	—
19	Carbon tetrachloride	37895	36920	564	374	400	459	105	295.00	—
20	1,2-Dichloroethane	38100	37125	359	366	363	359	0	245.00	2.86
21	Acetonitrile	38140	37170	314	305	278	239	75	172.60	2.09
22	Methyl acetate	38140	37170	314	315	312	259	55	242.00	—
23	Ethyl acetate	38180	37200	284	322	323	239	45	236.70	—
24	Butyl acetate	38160	37190	294	336	332	239	55	232.70	—
25	n–Amyl acetate	38105	37130	354	341	349	259	95	240.50	—
26	1,4-Dioxane	38105	37120	364	354	377	299	65	208.00	2.15
27	Water	38230	37270	214	298	266	179	35	—	—

states.[7] But, to the formation of the solvation energies contribute the forces due to the dispersion and dipolar interactions. These interactions are simultaneously considered in the equation of McRae,[40] given in the form of expression (1) in the second paper[2] of the series. Having the experimental shifts, $\Delta\tilde{\nu}$, in a great number of solvents it is possible to evaluate the parameter coefficients* in the last quoted equation,[2] by the least-square method,[45] the estimated values are: $(A+B+C) = 1863.92$ cm^{-1}, $E = -37.39$ cm^{-1}, and $F = -42.66$ cm^{-1}. Using these values, the spectral shifts were calculated and the obtained values are suitably listed in table 1. The comparison of the experimental and the theoretical shifts now calculated shows small values for the experimental data, exceeding the error limits of the apparatus (± 50 cm^{-1}) in the solvents: ethyl, ether and water, but greater values than those theoretically obtained in the halogenated solvents, excepting the 1,2-dischloroethane, and a very great deviation in carbon tetrachloride. These findings show that in the case of the halogenated solvents, besides the dispersion and dipolar interactions, there are auxiliary factors contributing to the spectral shift.

The interpretation of the spectral shift according to the Franck-Condon principle[7] is possible, knowing the dipole moment change in going from the ground state to the excited state. This variation may be evaluated using the explicit form of the parameter E from the equation of McRae,[40] that is the expression (2) in the preceding paper,[2] and the calculated value of this parameter. The radius of the solvent cage, a, is evaluated according to the relation (3) in the quoted paper,[2] on the base of the same considerations.[46] Having the values[44] of the molecular weight, M, and of the density, ρ (at 20°), and the value of the dipole moment[43,44] in the ground state, $M_{00} = 0.390$ D, we calculated the value of the dipole moment of the toluene molecule in the excited state: $M_{ii} = 0.788$ D. The dipole moment of the toluene increases in the excited state more than twofold. The solvation energy in the excited state is expected to be increased by the dipolar interactions, and the spectrum red shifted. But, the comparison of the spectral shifts in solutions of benzene with those of toluene shows that the last values are only a few tens of cm^{-1} greater than the spectral shifts of benzene,[1] as seen in table 1. Taking into account the molecular size of the toluene, which is greater than that of the benzene, and considering the increased dipole moment of the toluene in the excited state, we should expect much greater shifts on the red, due to the dipolar interactions. The explanation of the toluene spectral shifts, a little greater than those of benzene,[1] may be given as follows: according to the usual view, the toluene dipole moment in the ground state results from the migration of the electrons from the methyl group the benzene ring,[47] the direction of the dipole moment being $\mathrm{Me}^{\delta+} - \mathrm{Ph}^{\delta-}$. One knows that in addition to the two Kékulé structures, for toluene polar structures may be represented, involving the hyperconjugation. Since each of the three hydrogens of the methyl group may be ionic, nine ionic structures may be written down.[6] The "alternant polarization" in the benzene ring[42,47,48] contributes, also, to the formation of the dipole moment of the toluene in the ground state. Thus, the dipole moment of the toluene, in the ground state, results from a reduced transfer of the π-electrons from the methyl group in the benzene ring, and from the "alternant polarization" of the ring. The increased dipole moment in the excited state indicates that the ionic structures, with positive charges on the methyl group and with negative charges in the *ortho* and *para* positions, are preferentially stabilised, showing an increased hyperconjugation effect. But, in these structures, the formation of a double bond between the methyl group and the benzene ring results in a reduction of the molecular size. As a consequence, the solvation energy of the excited state is the result of the forces due to the dispersion and dipolar interactions, as well as of the diminution of the molecular size. The dispersive forces, together with dipolar forces augmented in the excited state because of the *orientation strain*, [7] lead to the red shift, but the decrease of the molecular size makes the solute molecule interact with a smaller number of solvent molecules, that is a reduction of the solvation energy and the spectrum is blue shifted. In this way, clearly, the toluene spectral shift cannot be much greater than the spectral shift of benzene [1] in the same solvent. The maintenance of the spectrum vibrational structure in solution is explained by the fact that even if the dipole moment in the excited states is more than twofold its value in the ground state, the absolute magnitude is not too great, and the *dipolar saturation* [7] is almost completely realised in the ground state. Then, the prominent appearance of the C—C vibrations of the benzene ring [12] indicates an unsignificant increase of the electronic charge in the benzene ring. [7]

---

* The calculation program was established at the Territorial Center of Electronic Calculus, Jassy.

The second characteristic of a spectral band supporting a strong solvent influence is the intensity, [49,50] rendered by the *molar extinction coefficients* [51] ε_ν, very useful in the fine structure analysis, as we shall see later; they are given in relation (2) of the previous paper, [1] or by the *oscillator strengths* [52] f, including the expression of *the integrated (absolute) intensity*, given in equation (4) in the above quoted paper. [1] There are in the literature [53,54] some data concerning the ε_ν and f values for the toluene band near 2600 Å, and these are given in table 2, for comparison with our results. The present results are comparable with those previously given. [53,54] In solution, the intensity of a spectral band increases under the perturbable solvent influence, [1-3] because the vibrational components in the fine structure of the weak electronic transitions behave differently regarding the intensity. [55] Indeed, the comparative vibrational analysis of our results with those previously given, [53] as in table 3, indicates the presence of new vibrational components in our data concerning the toluene spectrum, or the absence of the previous component [53] at 38,840 cm^{-1} in chloroform solution. The comparison shows, also, that our results significantly contribute to better reveal the new components in the vibrational structure, as well as their intensities, in comparison with the preceding results. [53] The appearance of the new vibrational components in the solution spectrum constitutes one of the factors which increases the intensity. [1,2,4] The toluene spectral band, at 2600 Å, has a close shape to the benzene spectral band. [1] The intensities of the electronic spectral bands of benzene and toluene should be expected to have close values. But, the only values which are close enough to those of benzene [1] are the ε_v values of the toluene, listed in table 1. In contrast, the f values, as listed in table 1 for toluene, are almost double against the benzene f values. [1] Since f represents the total electronic transition probability, [56–58] it is much increased in the toluene case, and this is due to the interaction between substituent and the benzene ring, as well as to the interaction between the solute and solvent molecules. [1,2,4] The toluene spectrum exhibits a great value of $\varepsilon_{max.}$ in carbon tetrachloride, as compared with its value in other solvents. This behaviour, together with the very great spectral shift in the same solvent requires an elucidation. According to Bayliss and Cant, [59] the efficiency of the carbon tetrachloride as a perturber, i. e. its action to shift the spectrum and to increase the intensity is remarkable for benzene and toluene, even if usually the carbon tetrachloride is considered as a "normal" solvent. The peculiarities of the toluene spectrum in carbon tetrachloride solution indicate, as in the case of the previous studied molecules, [1,2,4] the building up of a weak complex [60] between the toluene and the carbon tetrachloride molecules, with a charge transfer from the aromatic ring to the chloride atom of the carbon tetrachloride. Rao and Jatkar [61,62] considered the nature of the complexes between aromatic compounds and chlorinated solvents as being donator-accepter. Briegleb [63] claims that the spectral studies, [60] and also the freezing point studies, [64–66] are arguments in the favour of the complex formation, the aromatic compounds being the donator for the halogen atom. Furthermore, Goates et al. [67] suggest the formation of a π-bond between the benzene ring and the 3d vacant level of the chlorine atom in the carbon tetrachloride. The substituent $-CH_3$ increases the electronic density in the benzene ring, causing an augmentation of the toluene—carbon tetrachloride complex stability. The investi-

TABLE 2

Position and intensity of toluene spectral band at 2600 Å in some solvents, compared with the results from literature (in brackets)

Solvent	λ_{max} (Å)	ε_{max} ($1 \cdot mol^{-1} \cdot cm^{-1}$)	$f \cdot 10^3$
Cyclohexane	2625	220.00	2.82
	2621 (53)	266.00 (53)	3.30 (53)
n-Hexane	2623	255.70	3.05
	2619 (53)	264.00 (53)	3.30 (53)
n-Heptane	2622	216.40	2.51
	2620 (54)	250.00 (54)	—
Chloroform	2630	234.00	—
	2627 (53)	229.00 (53)	—
Carbon tetrachloride	2639	295.00	—
	2633 (53)	372.00 (53)	—

TABLE 3

Vibrational analysis of the toluene transition at 2600 Å. The $\tilde{\nu}$(cm^{-1}) and ε_ν(l . mol^{-1} · cm^{-1}) values* in some solvents, compared with the data from reference [53]

The present work		Reference[53]	
$\tilde{\nu}$	ε_ν	$\tilde{\nu}$	ε_ν
Cyclohexane			
40190 shoulder	104.40		
40020	109.40	40080	127.00
39780	108.40		
39500 inflexion	130.00		
39300	133.20	39370	185.00
39095	160.40	39120	193.00
38880 shoulder	174.00		
38565 shoulder	167.00		
38380	185.00	38440	222.00
38100	220.00	38150	266.00
37640	146.00	37725	180.00
37130	199.40	37210	247.00
n-Hexane			
41150 shoulder	73.75		
40985	78.75		
40735 shoulder	81.25	shoulder	
40465 shoulder	95.00	shoulder	
40240 shoulder	120.75	shoulder	
40050	125.00	40160	118.00
39820	124.75		
39560 shoulder	149.25	39370	180.00
39090	185.50	39120	189.00
38915 shoulder	173.25		
38390	215.00	38460	217.00
38130	255.00	38180	264.00
37655	170.75	37725	177.00
37160	238.75	37230	247.00
Ethanol			
41355 inflexion	57.80		
41205 shoulder	68.00	shoulder	
40990 shoulder	73.40	shoulder	
40790 shoulder	75.60	shoulder	
40440 inflexion	93.00		
40250 shoulder	111.40		
40075	114.60	40080	129.00
39865 shoulder	114.60		
39520 inflexion	142.00		

Table 3 (continued)

39340	160.00	39370	183.00
39105	169.20	39160	196.00
38960 shoulder	162.40		
38625 shoulder	174.00		
38410	189.00	38440	215.00
38150	228.00	38170	260.00
37710	152.40	37760	173.00
37175	208.80	37220	239.00
Chloroform			
40795 shoulder	78.00		
39860 shoulder	122.40		
38940	183.00	38980	219.00
?		38840	229.00
38025	234.00	38025	273.00
37050	194.00	37090	220.00
Carbon tetrachloride			
38820	235.50		
38310 shoulder	249.25		
37895	295.00	37980	~372.00
37600	244.50		
36920	244.50	36970	~300.00
Water			
41200 shoulder			
40260 shoulder			
40050 shoulder		Structure	
39400			
39105		indistinct	
38660 shoulder			
38230		38240	229.00
37940 inflexion			
37270		37310	197.00

* For shoulders and inflexions the values are only approximately.

gations of mesitylene[60] and hexamethylbenzene[68] complexes with the carbon tetrachloride indicate an increase of the complex strength with the augmentation of the donor ability of the aromatic ring, proving that the carbon tetrachloride behaves as an electron acceptor. The complex formation explains the great spectral shift in carbon tetrachloride, because in the excited state the molecule of the complex is much bigger, compared with the solute molecule, and determines the operation of the *packing strain*,[7] that is the solvation energy in the excited state is greater than that of the ground state, and the subsequent spectral shift on the red is added to the dispersion and dipolar effects. The molar extinction coefficients, ε_ν, of the toluene spectrum, given in table 1, are comparable with the corresponding values for the chlorobenzene [2] and bromobenzene, [4] resulting that the intensity increases in solution, and the factors determining the augmentation are the same as previously discussed. [1,2,4].

III. EXPERIMENTAL

The toluene and solvents purification is performed as previously described, [1] with the same purity criteria. The refractive indices, *n*, the dielectric constants, D, and the boiling points, b. p., of the solvents are prior given. [1] The solutions were prepared as reported, [1] the concentrations ranging between 0.04 and 0.002 M. The spectra were recorded in the same conditions [1] and with the former described spectrophotometer. [1] The position of each absorption peak and the spectral intensities are averages of at least three recordings. The integrated intensities were evaluated as reported [1].

REFERENCES

[1] V. Macovei, *Rev. Roumaine Chim.*, **20**, 1413 (1975).

[2] V. Macovei, *Rev. Roumaine Chim.*, **21**, 193 (1976).

[3] V. Macovei, *Rev. Roumaine Chim.*, **21**, 1137 (1976).

[4] V. Macovei, *Anal. Sti. Univ. "Al. I. Cuza", Iaşi. Sect. I, b*, **22**, 51 (1976).

[5] Part V: V. Macovei, *Anal. Sti. Univ. "Al. I. Cuza", Iași, Sect. I, b*, **22**, 61 (1976).

[6] C. P. Smith, "Dielectric Behaviour and Structure", McGraw-Hill, New York, 1955.

[7] N. S. Bayliss and E. G. McRae, *J. Phys. Chem.*, **58**, 1002 (1964).

[8] H. H. Jaffé and M. Orchin, "Theory and Applications of Ultraviolet Spectroscopy", Wiley, New York, 1964.

[9] L. Doub and J. M. Vandenbelt, *J. Amer. Chem. Soc.*, **69**, 2714 (1947).

[10] K. Bowden and A. E. Braude, *J. Chem. Soc.*, **1952**, 1068.

[11] M. Ballester and J. Castañer, *J. Amer. Chem. Soc.*, **82**, 4259 (1960).

[12] P. C. Upadhya, G. D. Baruah, K. N. Upadhya, and D. K. Rai, *Isr. J. Chem.*, **9**, 7 (1971).

[13] F. A. Matsen, *J. Amer. Chem. Soc.*, **72**, 5243 (1950).

[14] L. Doub and J. M. Vandenbelt, *J. Amer. Chem. Soc.*, **71**, 2414 (1949).

[15] L. Doub and J. M. Vandenbelt, *J. Amer. Chem. Soc.*, **77**, 4535 (1955).

[16] P. E. Stevenson, *J. Mol. Spectroscopy*, **15**, 220 (1965).

[17] A. Mangini, A. Trombetti, and C. Zauli, *J. Chem. Soc.*, **B 2** **1967**, 153.

[18] W. W. Robertson and F. A. Matsen, *J. Amer. Chem. Soc.*, **72**, 5248 (1950).

[19] W. W. Robertson and F. A. Matsen, *J. Amer. Chem. Soc.*, **72**, 5250 (1950).

[20] W. W. Robertson and F. A. Matsen, *J. Amer. Chem. Soc.*, **72**, 5252 (1950).

[21] J. F. Music and F. A. Matsen, *J. Amer. Chem. Soc.*, **72**, 5256 (1950).

[22] W. W. Robertson, J. F. Music, and F. A. Matsen, *J. Amer. Chem. Soc.*, **72**, 5260 (1950).

[23] A. E. Lutskii, *Zhur. obshchei Khim.*, **33**, 1601 (1963).

[24] J. R. Platt, *J. Chem. Phys.*, **19**, 101 (1951).

[25] A. Mangini and R. Paseiri, *J. Chem. Soc.*, **1952**, 1168.

[26] A. Mangini and C. Zauli, *J. Chem. Soc.*, **1956**, 4960.

[27] J. Petruska, *J. Chem. Phys.*, **34**, 1111 (1961).

[28] L. Goodman and H. Shull, *J. Chem. Phys.*, **23**, 33 (1955).

[29] L. Goodman, I. G. Ross, and H. Shull, *J. Chem. Phys.*, **26**, 474 (1957).

[30] L. Goodman and H. Shull, *J. Chem. Phys.*, **27**, 1388 (1957).

[31] N. Fuson, C. Garrigou-Lagrange, and M. L. Josien, *Spectrochim. Acta*, **16**, (1960).

[32] M. Ballester, J. Palan, and J. Riera, *J. Quant. Spectrosc., Radiant Transfer*, **4**, 819 (1964).

[33] J. Petruska, *J. Chem. Phys.*, **34**, 1120 (1961).

[34] N. Ginsburg, W. W. Robertson, and F. A. Matsen, *J. Chem. Phys.*, **14**, 511 (1946).

[35] S. Stokes, *J. Chem. Phys.*, **39**, 2309 (1963).

[36] W. J. Hammond, W. C. Price, J. P. Teegan, and A. D. Walsh, *Discuss. Faraday Soc.*, **9**, 53 (1950).

[37] W. M. Schubert, J. Robins, and J. L. Haun, *J. Amer. Chem. Soc.*, **79**, 910 (1957).

[38] W. M. Schubert, H. Steadly, and J. M. Craven, *J. Amer. Chem. Soc.*, **82**, 1353 (1960).

[39] F. London, *Z. Physik*, **63**, 245 (1930).

[40] E. G. McRae, *J. Phys. Chem.*, **61**, 562 (1957).

[41] V. Macovei, "Doctoral Thesis", Chemistry Department, The Chemistry Institute of the Polytechnical Institute, Bucharest, 1974.

[42] J. A. Pople and M. S. Gordon, *J. Amer. Chem. Soc.*, **89**, 4253 (1967).

[43] O. A. Osipov, V. J. Minkin, and A. D. Garnovskii, "Spravochinik po Dipolnym Momentam", Izd. "Vysshaia Shkola", Moskva, 1971.

[44] A. Weissberger, E. S. Proskauer, J. A. Riddick, and E. E. Toops, "Technique of Organic Chemistry; Vol. VII, Organic Solvents", 2nd ed., Interscience, New York, 1955.

[45] D. York, *Canad. J. Phys.*, **44**, 1079 (1966).

[46] M. Lamotte, G. A. Gerhold, and J. Joussot-Dubien, *J. Chim. phys.*, **67**, 2006 (1970).

[47] W. J. Hehre, L. Radom, and J. A. Pople, *J. Amer. Chem. Soc.*, **94**, 1496 (1972).

[48] W. J. Hehre and J. A. Pople, *J. Amer. Chim. Soc.*, **92**, 2191 (1970).

[49] S. E. Sheppard, *Rev. Mod. Phys.*, **14**, 303 (1942).

[50] O. P. Girin and N. G. Bakhshiev, *Uspekhi Fiz. Nauk*, **79**, 235 (1963).

[51] H. H. Willard, L. L. Merritt, Jr., and J. A. Dean, "Instrumental Methods of Analysis", 3rd ed., D. Van Nostrand, Princeton, 1960.

[52] R. S. Mulliken, *J. Chem. Phys.*, **7**, 14 (1939).

[53] N. S. Bayliss and L. Hulme, *Austral. J. Chem.*, **6**, 257 (1953).

[54] P. P. Shoryghin, V. A. Petukhov, A. H. Khomenko, and A. E. Chernyshev, *Zhur. fiz. Khim.*, **42**, 1057 (1968).

[55] A. Nakajima, *Bull. Chem. Soc. Japan*, **44**, 3272 (1971).

[56] A. Einstein, *Phys. Z.*, **18**, 121 (1917).

[57] R. Ladenburg, *Z. Physik*, **4**, 451 (1921).

[58] Ch. Füchtbauer, *Phys. Z.*, **21**, 322 (1920).

[59] N. S. Bayliss and N. W. Cant, *Spectrochim. Acta*, **18**, 1287 (1962).

[60] R. Anderson and J. M. Prausnitz, *J. Chem. Phys.*, **39**, 1225 (1963).

[61] N. S. Rao and K. K. Jatkar, *Quart. J. Ind. Inst. Sci.*, **5**, 65 (1942).

[62] N. S. Rao and K. K. Jatkar, *Quart. J. Ind. Inst. Sci.*, **6**, 1 (1943).

[63] G. Briegleb, "Elektronen-Donator-Acceptor Komplexe", Springer Verlag, Berlin, 1961.

[64] A. F. Kapustinskii and S. I. Drakin, *Izvest. Akad, Nauk S. S. S. R. Otdel. khim. Nauk*, **5**, 435 (1947).

[65] W. E. Wyatt, *Trans. Faraday Soc.*, **25**, 48 (1929).

[66] R. P. Rostogi and R. K. Nigam, *Trans. Faraday Soc.*, **55**, 2005 (1959).

[67] J. R. Goates, R. J. Sullivan, and J. B. Ott, *J. Chem. Phys.*, **63**, 589 (1954).

[68] R. F. Weimer and J. M. Prausnitz, *J. Chem. Phys.*, **42**, 3643 (1965).

Revue Roumaine de Chimie, 25, 5, 663–666 (1980)

KINETICS OF GAS ADSORPTION ON HETEROGENEOUS SOLID SURFACES

N. I. IONESCU

Center of Physical Chemistry, Splaiul Independenţei 202,
Bucharest, Romania

Received July 7, 1979

The logarithmic law used for the kinetics of gas adsorption on solid surfaces could be explained, under certain circumstances, by the existence of a surface heterogeneity.

In a previous paper [1] we have shown that the logarithmic law written in its integral form :

$$\theta = k \ln(at + 1) \tag{1}$$

where θ represents the surface coverage at the t moment and a, k are constants, can proceed also from the integration of the equation :

$$\frac{d\theta}{dt} = \frac{ak}{at + 1} \tag{2}$$

with the initial condition $\theta = 0$ for $t = 0$. In the simple [2,3] and generalized [4] model which allows for the equation (2), the surface was a homogeneous one.

In the present work we aim at studying if the existence of a surface heterogeneity [5] could justify the relationship (2) and as a consequence, the integral form of the logarithmic law.

RESULTS AND DISCUSSIONS

Let be a surface with noninteracting sites, which are not all identical. The following assumptions are taken also into consideration :

- gas adsorption is irreversible on this solid surface ;
- gas adsorption takes place at a constant pressure ;
- the activation energy of adsorption is independent of coverage ;
- all sites adsorb with the same kinetics.

In this case, the sites can be characterized by a distribution function $\varphi(E)$ of the activation energy of adsorption ; $\varphi(E)\,dE$ represents the fraction of sites with activation energy of adsorption between E and E+dE. The kinetic law of adsorption for sites having the activation energy E has the form :

$$V_a = \text{Ø}\,(\theta, \mathrm{E}) \tag{3}$$

where Ø is a certain function to be determined and θ the local coverage of the homogeneous sample considered.

Because

$$V_a = \frac{\mathrm{d}\theta}{\mathrm{d}t} \tag{4}$$

one obtains for equation (3) the form :

$$\frac{\mathrm{d}\theta}{\mathrm{d}t} = \text{Ø}(\theta, E) \tag{5}$$

which, together with the initial condition $\theta = 0$ for $t = 0$, determines the evolution law of θ, that is

$$\theta = \theta(t, E) \tag{6}$$

By means of relationship (6), equation (3) becomes :

$$V_a = \text{Ø}\,[\theta(t, E)\, E] \tag{7}$$

i. e. a function of t and E.

Because the sites are independent, the overall adsorption rate is given by

$$v_a = \int_0^{\infty} V_a(t, E)\, \varphi(E)\, \mathrm{d}E \tag{8}$$

In order to use relationship (8) it is necessary to know the functions V_a and $\varphi(E)$.

For the first-order adsorption kinetics, the usual relation

$$\text{Ø}(\theta, \mathrm{E}) = k_a\ (1 - \theta) \exp\left(-\frac{E}{kT}\right) \tag{9}$$

can be used, where k_a is a constant and the other magnitudes have their usual meanings.

By inserting equation (9) in (5) one gets :

$$\frac{\mathrm{d}\theta}{\mathrm{d}t} = k_a(1 - \theta) \exp\left(-\frac{E}{kT}\right) \tag{10}$$

which leads, by integrating with the known initial conditions to

$$1 - \theta = \exp\left[-k_a t \exp\left(-\frac{E}{kT}\right)\right] \tag{11}$$

By means of the equations (9) and (11) one obtains for the relationship (7)

$$V_a = k_a \exp\left[-k_a t \exp\left(-\frac{E}{kT}\right)\right] \exp\left(-\frac{E}{kT}\right) \tag{12}$$

In order to calculate expression (8) it is necessary to know the function φ(E). Generally, this function can be an exponential, a power or a constant.[6] As previously shown[6-9] when the distribution function of energy is a constant, one obtains a logarithmic kinetics.

Let be $\varphi(E) = \text{const}$. In this case, relationship (8) becomes :

$$v_a = \int_0^\infty k_a \exp\left[-k_a t \exp\left(-\frac{E}{kT}\right)\right] \exp\left(-\frac{E}{kT}\right) \cdot \text{const} \; \mathrm{d}E \tag{13}$$

which can be written also under the form

$$v_a = \frac{\text{const.}\, kT}{t} \int_0^\infty \exp\left[-k_a t \exp\left(-\frac{E}{kT}\right)\right] k_a t \exp\left(-\frac{E}{kT}\right) \frac{\mathrm{d}E}{kT} \tag{14}$$

which, by integrating becomes

$$v_a = \frac{\text{const}}{t} \exp\left[-k_a t \exp\left(-\frac{E}{kT}\right)\right]_0^\infty = \frac{\text{const}}{t}\,[1 - \exp(-k_a t)] \tag{15}$$

In the case $k_a t \gg 1$, the exponential can be neglected against the unity so that

$$v_a = \frac{\mathrm{d}\theta}{\mathrm{d}t} = \frac{\text{const}}{t} \tag{16}$$

i.e a (2)-type equation.

If in equation (13), φ(E) is replaced by a power or an exponential function, one obtains expressions which are not analogous with (2) and therefore can not justify a (2)-type equation.

It must be mentioned that relationship (12) has been deduced in a different way by Roginsky.[6]

In conclusion, the existence of a surface heterogeneity can be, under certain circumstances, an explanation for the existence of a logarithmic law used for the description of a gas adsorption kinetics on solid surfaces.

REFERENCES

[1] N. I. Ionescu, *Rev. Roumaine Chim.*, **24**, 399 (1979).
[2] P. T. Landsberg, *J. Chem. Phys.*, **23**, 1079 (1955).
[3] P. T. Landsberg, *J. Appl. Phys.*, **33**, 2251 (1962).
[4] N. I. Ionescu and B. Aurian-Blăjeni, *Rev. Roumaine Chim.*, **22**, 353 (1977).
[5] C. F. Cerofolini, *Z. phys. Chem. (Leipzig)*, **259**, 1020 (1978).
[6] S. S. Roginsky, "Adsorption und Katalyse an inhomogenen Oberflächen", Akademie Verlag, Berlin, 1958, p. 114.
[7] C. Aharoni and F. C. Tompkins, *Adv. Catalysis*, **21**, 1 (1970).
[8] N. I. Ionescu, *Rev. Roumaine Chim.*, **24**, 83 (1979).
[9] N. I. Ionescu, *Surf. Sci.*, **61**, 294 (1976).

Revue Roumaine de Chimie, **25**, *5* 667–672 (1980)

THE ELECTRONIC BAND STRUCTURE OF β-PbO_2

A. BREEZE, P. M. MAGEE and P. G. PERKINS*
Department of Pure and Applied Chemistry
University of Strathclyde, Glasgow G1 1XL, U. K.

Received 23, May 1979

Band-structure calculations on β-PbO_2 show that the band gap is 9.6 eV. The electronic structure is rationalised well with respect to that of lead metal and PbO. The polarity suggested is Pb(Pb) $<$ Pb(PbO) $<$ Pb(PbO_2).

There is at present some controversy over the value of the minimum band gap for β-PbO_2. Some experimentalists[1-3] place it between 1.4 and 1.85 eV, while another[4] has suggested that it occurs at 4.5 eV; however, it is uncertain whether this latter value refers to PbO_2. A semi-empirical calculation[5] using the Kohn-Korringa-Rostoker method affords a band gap of 1.6 eV at the Γ point. Since, generally, oxygen atoms inserted into a lattice of metal atoms increase the band gap by the introduction of stable bonding levels or bands, then we might expect that the band gap of PbO_2 should be higher than that of PbO, which has been calculated to lie at 4.6 eV[6]. In view of these discrepancies, we have calculated anew the electronic band structures of β-PbO_2.

The theoretical approach used was an LCAO-based method. This has been fully described[7] and input data for oxygen and lead valence orbitals have been published[6]. The method has previously been used successfully for an interpretation of the band structure and Fermi surface of metallic lead itself.[8] PbO_2 in its β-form has a tetragonal structure[9] shown in figure 1, where $a = b = 0.4931$ nm, $c = 0.3367$ nm, $u = 0.31$ nm, and $v = 0.19$ nm. Thus, along the c axis the Pb—Pb distance is slightly shorter than it is in the face-centred cubic metal itself,[8] whilst the eight Pb atoms at the corners of the cube are 0.3872 nm distant from the centre. Thus, the latter Pb atom occupies a body-centred tetragonal site and the situation is not unlike that in PbO. We might, therefore, expect to find a band structure in which there are sets of lead states interpenetrated by oxygen $2s$ and $2p$ states, the latter bonding strongly with the lead orbitals, polarising the charge and dispacing the lead states downwards (bonding) and strongly upwards (antibonding) in the energy scale.

Five unit cells, of constitution 2Pb : 4O were considered along each direction of the lattice. The resulting E(**k**) *vs* **k** band diagram, calculated from the first Brillouin zone (depicted in figure 2) along with the density-of-states and joint-density-of-states histograms, is in figure 3*a*, *b*, *c*. As can readily be seen, the lowest band gap is 9.6 eV and occurs at the Γ point. This value is very different from that from the KKR calculation but, as in the latter, the lowest energy transition is direct in nature and it involves charge transfer from the O $2p \rightarrow$ Pb $6s$ bands at the Γ point.

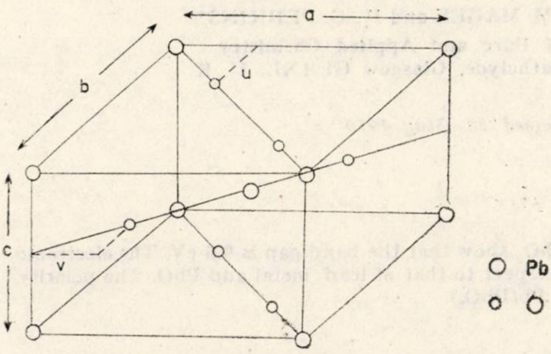

Fig. 1. — Crystal structure of β-PbO_2.

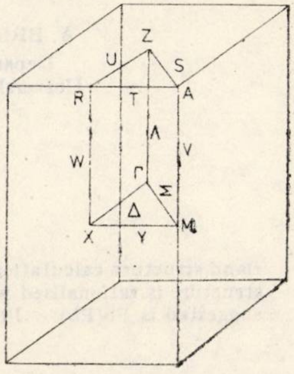

Fig. 2. — Brillouin zone for the orthorhombic lattice.

Apart from the $\Gamma - X$, $\Gamma - Z$, and $\Gamma - M$ directions, the valence bands of PbO_2 are rather flat and, in some regions (*eg* XM) are highly accidentally degenerate. The Pb $6s$ band, which occurs around -11 eV in PbO, is pushed up to around -4 eV to form the lowest conduction band. The bands of Pb $6p$ character are far less affected by the extra oxygens being displaced by ~ 2 eV upwards. This reflects the fact that the Pb $6s \rightarrow$ O $2p$ bonding is the most important stabilising factor in the system and correlates also with the stronger Pb $6s \rightarrow$ Pb $6s$ interaction which appears in PbO_2 relative to PbO because the average Pb—Pb distance is shorter in the former.

From another point of view, we might expect that the band structure for β-PbO_2 would resemble that of SiO_2, since the central atoms are from the same Periodic Group, have the same oxidation state and, essentially, the same geometry around the central atom. Figure 4 compares the valence bands for two of the principal directions in the energy space for PbO_2 and SiO_2 (β-cristobalite).[10] It can be seen immediately that the band structures are strikingly similar in both topology and energy characteristics. In fact, the chief differences occur in the lower conduction region where, for PbO_2, the $6s$ and $6p$ states reside. Thus, we would expect different photoconductance properties for PbO_2.

The density-of-states histogram exhibits four main regions lettered A, B, C, and D in the diagram (Fig. 3*b*). Region A corresponds to the O $2s$ orbitals which, as in PbO, appear around their V.S.I.P. value and show a minimal amount of curvature. Region B contains a contribution from the Pb $6s$ orbitals, as does the area under region D between -5.5 and -2.9 eV. The appearance of these orbitals at two different, well-separated energy regions is due to the strong interaction between these orbitals of the Pb atoms and both the oxygen orbitals and orbitals of other Pb atoms. The peak at C contains the O $2p$ orbitals, whose lack of curvature shows

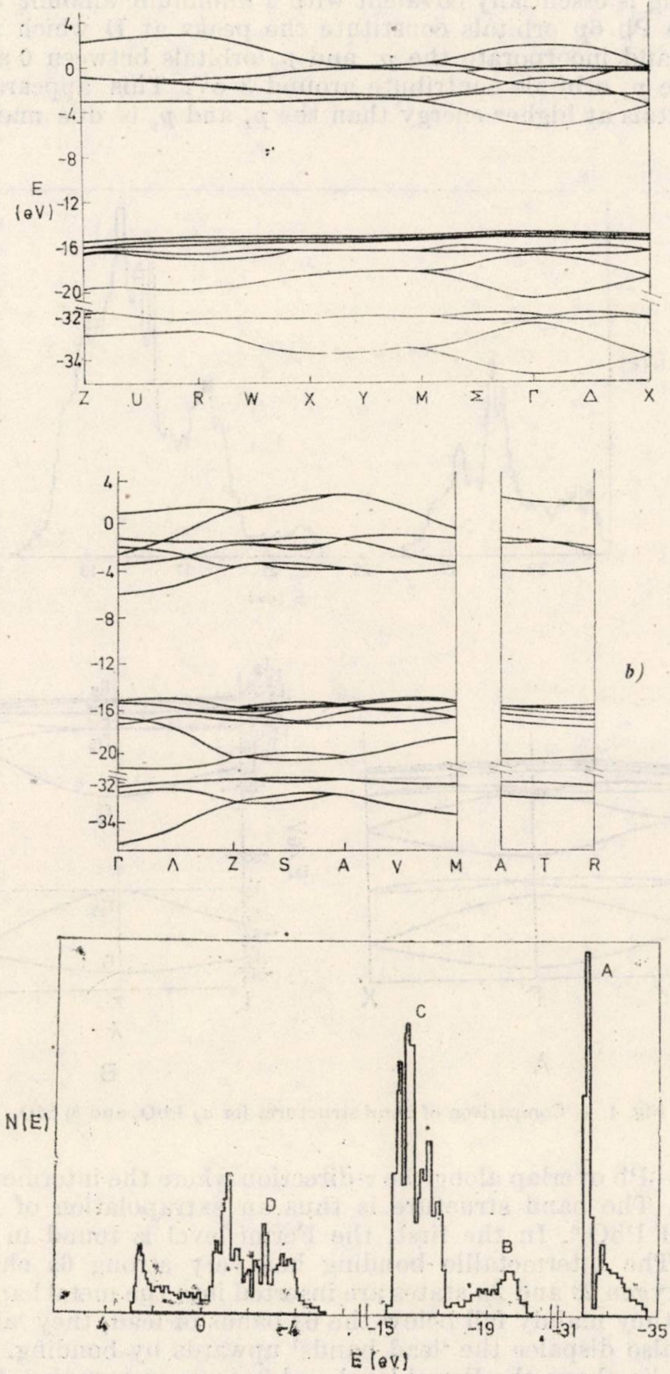

Fig. 3. — *a)* Band structure, b) Density of states and c) Joint density of states for β-PbO$_2$.

that bonding is essentially covalent with a minimum amount of delocalisation. The Pb 6*p* orbitals constitute the peaks at D which range over about 6 eV and incorporate the p_x and p_y orbitals between 0 and −3 eV, whereas the p_z orbitals contribute around 3 eV. This appearance of the Pb $6p_z$ orbitals at higher energy than the p_x and p_y is due mainly to the

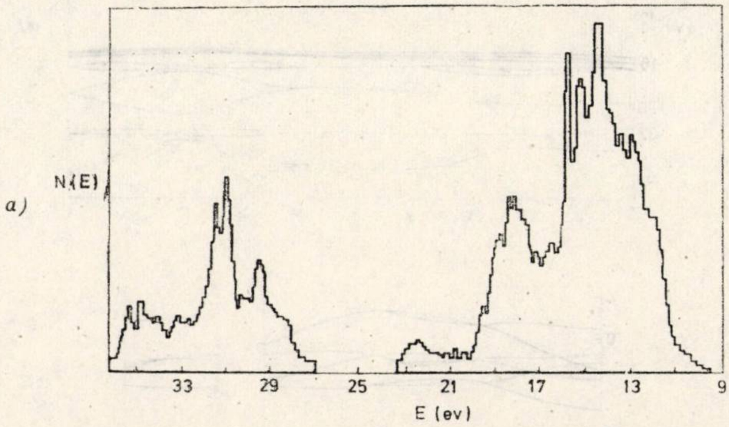

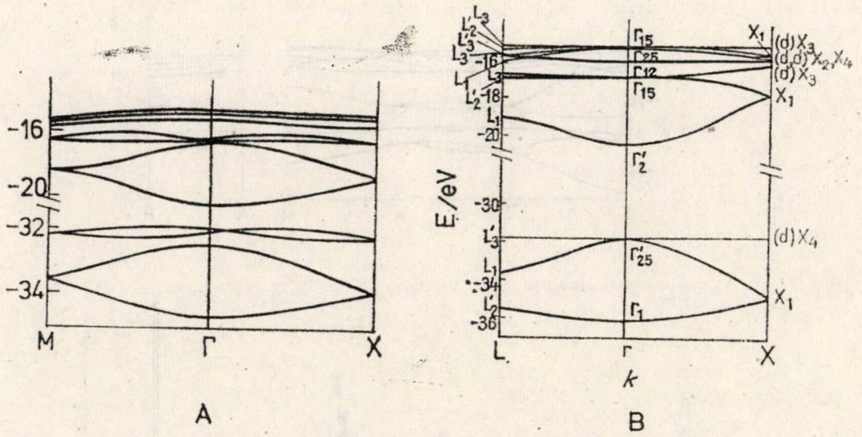

Fig. 4. — Comparison of band structures for *a)* PbO_2 and *b)* SiO_2.

greater Pb—Pb overlap along the *z*-direction where the intermetal distance is shortest. The band structure is thus an extrapolation of that of Pb metal [8] and PbO [6]. In the first, the Fermi level is found in the Pb 6*p* orbitals [8]. The intermetallic bonding has very strong 6*s* character. In PbO the oxygen 2*s* and 2*p* states are inserted into the metal band structure and, since they mainly fall below the 6*s* bands of lead, they 'absorb' electrons and also dispalce the 'lead bands' upwards by bonding. The Pb 6*p* bands then lie above the Fermi level and become unoccupied. On progressing further to β-PbO_2, even more oxygen states are inserted and both the Pb 6*s* and 6*p* states are pushed virtually completely into the conduction band. The relationship just described between Pb, PbO, and PbO_2 is best seen by reference to the band correlation diagram (Figure 5). This shows the movement of groups of levels and that Pb—O bonding becomes dominant over Pb—Pb bonding,

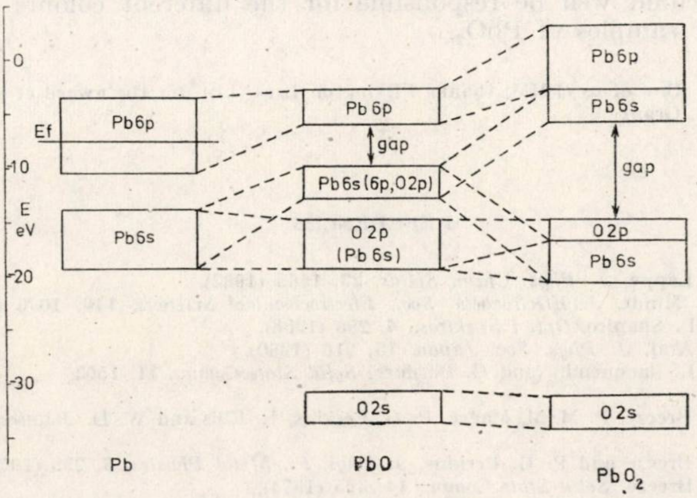

Fig. 5. — Correlation of bands for Pb, PbO, and PbO_2.

The movement of levels means that yet more electrons are displaced from lead to the oxygens. This affords a polarity order Pb(Pb) < Pb(PbO) < Pb(PbO_2). Since we regard the formal oxidation states in these systems as O, +2, and +4, then the calculations are satisfyingly consistent in this respect with chemistry.

The joint-density-of-states histogram (Fig. 3*c*) predicts that the onset of absorption should be ~ 10 eV, with a maximum at 14.5 eV due to charge transfer from the O $2p \rightarrow Pb(6p_y + 6p_z)$ bands. The smaller peak at 18.3 eV involves the O 2p → Pb $6p_z$ transitions, while the high-energy peak at ~31 eV stems from the O $2s \rightarrow Pb(6p_y + 6p_x)$ transition.

In conclusion, it remains to rationalise the band gaps of ~1.6 eV which have been found experimentally. We suggest that the materials as examined were impure, perhaps by simple contamination or, much more likely, by native impurities caused by defects. For the latter, defects in the lead lattice caused by distortions or by Pb atoms moving out of place would produce donor impurity states lying below the conduction band edge. Deficiencies in the oxygen lattice could also be responsible. It is well established that PbO_2, on heating, suffers loss of oxygen according to [11]

$$PbO_2 \rightarrow \alpha PbO_{1.66}$$

Unfortunately, the dissociation pressure for PbO_2 was not measured so it is not possible to elucidate the thermodynamics so as to find the number of oxygen vacancies at ambient temperature. However, we can calculate the effect of oxygen vacancies directly. To do this we used the 'periodic cluster' approach,[12] with four PbO_2 molecules in the cluster. Briefly, these calculations show that lead vacancies have no effect on band gap but an oxygen vacancy (in the cluster (Pb_4O_7)) introduces a filled impurity level lying ~3 eV below the conduction band. We believe it possible that a set of such oxygen vacancy levels, perhaps, numerous enough to be banded, could well be responsible for the different colours frequently found for samples of PbO_2.

One of us (PMM) thanks Pilkington Bros. Ltd. for the award of a Maintenance Grant.

REFERENCES

[1] F. Lappe, *J. Phys. Chem. Solids*, **23**, 1563 (1962).

[2] W. Mindt, *J. Electrochem. Soc., Electrochemical Sciences*, **116**, 1076 (1969).

[3] I. P. Shapiro, *Opt. i Spektros.*, **4**, 256 (1958).

[4] T. Arai, *J. Phys. Soc. Japan*, **15**, 916 (1960).

[5] J. L. Jacquemin (and G. Bordure, *Solid State Comm.*, **11**, 1563 (1972).

[6] A. Breeze, P. M. M. Magee, P. G. Perkins, E. Ellis and W. D. Johnson, *Phil. Mag.*, in Press.

[7] A. Breeze and P. G. Perkins, *J. Phys. F., Metal Physics*, **5**, 255 (1975).

[8] A. Breeze, *Solid State Comm.*, **14**, 395 (1974).

[9] A. F. Wells, "Structural Inorganic Chemistry", 3rd Edn. O.U.P., Oxford, 1962, p. 457

[10] A. Breeze and P. G. Perkins, *J. Chem. Soc., Faraday II Trans.*, **69**, 1237 (1973).

[11] G. Butler and J. L. Copp, *J. Chem. Soc.*, 1956, 725.

[12] P. G. Perkins and J. J. P. Stewart, *J. Chem. Soc., Faraday II Trans.*, submitted for publication.

Revue Roumaine de Chimie 25 5 673–686 (1980)

L'ADSORPTION DE L'AMMONIAC DES SOLUTIONS AQUEUSES PAR LES ZÉOLITHES A ET X CHARGÉS AUX IONS DES MÉTAUX TRANSITIONNELS

FLORIN DANEŞ, AGNETA BĂTCĂ et SORIN M. AXINTE
Institut Polytechnique Bucureşti, Splaiul Independenţei, 313

Reçu le 9 février 1979

On a déterminé, à 20°, les isothermes d'adsorption réelle de l'ammoniac des solutions aqueuses de concentrations 0,05–4 mol/l sur 16 adsorbants zéolithiques A et X dans les formes mixtes Na/M, au contenu différent en métaux (M) Co, Ni, Cu, Zn. Les coefficients volumiques de distribution varient entre 3,1 et 49, en augmentant quand la concentration de la solution baisse, quand on passe du zéolithe A à X et quand le degré d'échange avec M s'agrandit. La sélectivité de l'adsorption de l'ammoniac sur les diverses formes cationiques augmente aux petites concentrations dans l'ordre suivant : Ni, Co, Cu, Zn. Aux concentrations plus grandes plusieurs inversions se produisent, fonction de la nature du réseau du zéolithe et du degré d'échange ionique.

There have been determined at 20° the adsorption isotherms of ammonia from aqueous solutions with a 0.05 – 4 mol/l concentration, by 16 zeolitic A and X adsorbents in mixed forms Na/M with various contents of metals (M) Co, Ni, Cu, Zn. The range of the volumic distribution coefficient is from 3.1 to 49, increasing when the solution concentration decreases, when passing from zeolite A to X and when the loading degree with M increases. The adsorption selectivity of ammonia for different cationic forms increases at small concentrations as follows : Ni, Co, Cu, Zn, while at higher concentration inversions may appear, depending on the nature of the zeolite network and on the loading degree with M.

1. INTRODUCTION

L'ammoniac présente une forte affinité pour les zéolithes : en présence de l'ammoniac, comme en présence de l'eau (qui est aussi une substance à petite molécule polaire), l'énergie libre pour la formation du cristal de zéolithe X baisse sensiblement. [1,2] Les zéolithes sont de bons adsorbants pour l'ammoniac, du point de vue de la capacité autant que par le pouvoir de rétention. L'isotherme d'adsorption — la dépendance de la concentration de l'ammoniac dans le sorbant en fonction de la concentration c (ou la pression p) de l'ammoniac dans la phase externe fluide — a été déterminée expérimentalement surtout pour l'ammoniac pur. Les sorbants les plus étudiés à ce point de vue ont été les zéolithes Y, la sorption de l'ammoniac étant, pour ces zéolithes, une étape préliminaire de la décationisation ; il y a quand même des résultats expérimentaux pour d'autres types de zéolithes naturels — l'érionite, le gmelinite, le heulandite le lhomontite — ou synthétiques — F, L, S, T, W [3,4].

Puisque la nature du réseau zéolithique ne semble point influencer d'une manière significative l'allure de l'isotherme d'adsorption, les plus indiqués pour la rétention de l'ammoniac par adsorption seront les zéolithes synthétiques A et X, les plus disponibles et meilleur marché.

Les isothermes de la sorption de l'ammoniac à l'état pur sont étudiées pour le zéolithe A en [3,5–7] et pour le zéolithe X en [3,8–10]. On a établi que l'adsorption d'ammoniac est très intense, aux fortes valeurs des chaleurs d'adsorption [11,12] et valeurs modérées des entropies d'adsorption [13]; la première constatation indique de fortes interactions énergétiques — surtout les interactions ion/dipôle entre les cations mobiles du sorbant et l'ammoniac [14] — tandis que la deuxième correspond à un sorbate localisé. [15]

Ces deux traits caractéristiques de l'adsorption de l'ammoniac sur les zéolithes conduisent à l'idée que l'ammoniac est retenu surtout par formation des complexes des cations du zéolithe, complexes où l'ammoniac participe comme ligand. On peut donc présumer que l'ammoniac sera mieux retenu par les zéolithes en états ioniques qui correspondent aux cations qui forment des complexes amminiques d'une extrême stabilité, c'est-à-dire les ions M(II)d [7] — M(II)d [10]. A cause du bilan électrique local, les zéolithes saturés aux ions trivalents sont sensiblement instables (spécialement pour les zéolithes à grande capacité d'échange ionique, comme les A et X); c'est la raison pour laquelle la rétention de l'ammoniac sur les sorbants zéolithiques saturés avec M(III) sera diminuée. [16]

L'effet de la nature du cation mobile sur la rétention de l'ammoniac n'est pas encore systématiquement étudié; en [17] on démontre que la sorption de l'ammoniac par le zéolithe A est plus intense pour les cations bivalents que pour les monovalents et que la rétention dépend aussi du rayon ionique (la rétention étant meilleure pour les ions de petites dimensions); mais en [7] on montre que pour les zéolithes A de Co, Zn, Cd et Ni il est impossible à établir une échelle unique de l'intensité de la rétention d'ammoniac (les isothermes des différents cations s'entrecoupent). Ce phénomène peut être mis en liaison avec la présence des fortes interactions sorbate-sorbate [15] et avec l'intense hétérogénéité de la sorption d'ammoniac (manifestée par la baisse rapide de la chaleur d'adsorption [18] autant que par la diminution de l'énergie d'activation et de la conductivité électrique [19] avec l'augmentation de la quantité de l'ammoniac adsorbé), explicable par l'affaiblissement de l'interaction NH_3 — cation, pour les molécules d'ammoniac plus éloignées.

A cette interaction s'ajoute aussi l'attraction entre les protons de la molécule NH_3 et les atomes O, polarisés négativement par la carcasse aluminosilicate,[20] attraction plus faible que celle entre l'ammoniac et les cations, selon la comparaison entre l'adsorption de l'ammoniac par les aluminosilicates purs et traités au NaOH [21] ou la comparaison entre les spectres de l'ammoniac retenu par le zéolithe et par l'aérosyl.[22]

La complexité des modèles de l'interaction ammoniac-zéolithe conduit à une hétérogénéité marquée de la sorption (en [23] on établit par diffraction des rayons X la présence en NaA de quatre types de sites inéquivalents de sorption du NH_3, où l'on retient en ordre décroissant de préférence 2, 4, 8 et 12 molécules NH_3/cellule élémentaire) et qui a d'ailleurs pour conséquence la faible concordance des isothermes expérimentales de l'adsorption avec les modèles théoriques d'isothermes.[24]

La sorption d'ammoniac des mélanges présente assurément des difficultés d'interprétation encore plus grandes, étant à cause de cela peu étudiée ; le sorbate concurrent a été le n-hexane,[25] le n-décane,[26] le CO_2 [15] ou l'air.[27]

Le processus de sorption mixte est, dans tous ces cas, plus simple, parce que un seul sorbate est polaire (l'ammoniac) et il présente, donc, une affinité pour le zéolithe supérieure par rapport au composant coadsorbé.

La concurrence pour l'occupation de l'adsorbant sera tout de même intensifiée dans le cas de la rétention simultanée par le zéolithe d'un mélange des deux composants polaires, tout les deux puissement retenus, comme l'eau et l'ammoniac.

L'adsorption de l'ammoniac moléculaire du mélange avec l'eau n'a pas été encore étudiée, quoique les considérations ci-dessus démontrent son intérêt théorique.

Au point de vue pratique, la rétention du NH_3 de la solution est importante tant pour la récupération que pour la dépollution. Pour les solutions acides ou neutres, où l'ammoniac se trouve comme cation NH_4^+, le problème est résolu d'habitude en retenant l'ammoniac par échange ionique aux zéolithes ou aux résines échangeuses de cations, tandis que pour les solutions aqueuses alcalines, comme les eaux résiduelles après épuration au chaux, il n'y a pas encore de technologies convenables (on propose la rétention du NH_3 par échange des ligands sur les ions CU^{2+} fixés d'avance sur un précipité de $Zn(OH)^2$, mais ce sorbant, malgré sa grande affinité pour l'ammoniac, présente dee grands désavantages — capacité et stabilité réduites [28]).

Pour les raisons présentées ci-dessus, dans ce travail on étudie l'équilibre de l'adsorption du NH_3 (moléculaire, dissous dans l'eau) par les zéolithes A et X, chargés aux métaux transitionnels.

2. PARTIE EXPÉRIMENTALE

a) Préparation des adsorbants

On a préparé 16 adsorbants — des zéolithes A ou X, contenant des ions Na^+ conjointement aux ions des métaux transitionnels 3d de la fin de la première période longue — Co, Ni, Cu, Zn — en état bivalent, chacun pour deux degrés d'échange ionique différents.

On a obtenu les adsorbants à la température ambiante, par échange ionique entre les zéolithes A ou X dans la forme Na^+ et des solutions aqueuses de $Co(NO_3)_2$, $NiSO_4$, $CuSO_4$ et $ZnSO_4$, aux concentrations approchant 0,1 mole/l. Par la variation de la proportion zéolithe : solution (en g/l : 50 et 62 pour le zéolithe A, respectivement 23 et 50 pour le zéolithe X) on a obtenu deux degrés différents d'échange, à chaque paire zéolithe /métal transitionnel. Après l'échange ionique, les zéolithes en poudre ont été lavés à une quantité modérée d'eau et séchés à l'air.

Les zéolithes de base sont des produits commerciaux cristallins, de dimensions moyennes 2 (A) et 4 (X) µm. On n'a pas utilisé les zéolithes granulés ; les déterminations préliminaires ont démontré que la sorption du NH_3 sur ceux-ci est très lente, à la température ambiante.

Les analyses chimiques ont été effectuées sur les zéolithes de Na, pour l'humidité structurale, Al_2O_3, SiO_2 et Na_2O ; sur chaque phase solide, pour l'humidité zéolithique ; dans les solutions aqueuses Na^+/M^{++}, pour le degré d'échange.

b) L'adsorbtion de l'ammoniac

On a mis en contact sous lente agitation 25 ml solution aqueuse d'ammoniac, à concentration initiale c° variable entre 0,15 et 4,98 mol/l, avec une quantité *a* de zéolithe d'humidité connue. Les valeurs *a* et *c*° sont représentées dans le tableau 1. Après une heure de contact, on a decanté le zéolithe et on a déterminé la concentration *c* de l'ammoniac en solution. Dans des déterminations préliminaires on a établi que, après 10 minutes, le degré de réalisation de l'équilibre d'adsorption dépasse 99 %. Les concentrations c° et c ont été déterminées par titrage au HCl fixanal de 0,1 ou 1 mole/l, en présence de rouge-méthyle comme indicateur.

TABLEAU I

Conditions expérimentales d'adsorption de l'ammoniac

No.	1	2	3	4	5	6	7	8	9	10	11	12
c°, mol/l	0,150	0,200	0,400	0,500	0,850	1,030	1,280	1,900	2,55	3,10	3,75	4,98
a, g	2	1	1	1	2	1	1	2	2	2	2	2

L'adsorption *q'*, exprimée en mmol/g zéolithe en forme de pésage (c'est-à-dire en équilibre avec l'humidité atmosphérique) est calculée en utilisant les bilans d'eau et d'ammoniac.

c) Caractérisation des sorbants

Les sorbants sont cristallins et présentent une structure connue du réseau aluminosilicate.[29] La structure est caractérisée par la présence des cavités α de 10—11Å et des cavités β de 6—7 Å, en nombre égal aux premières. Pour une cavité α et une cavité β, le réseau contient 24 atomes (Al+ Si) qui présentent dans le réseau idéal une coordination tétraédrique, réalisée par l'intermédiaire des atomes O. À chaque atome Al du réseau idéal correspond un cation monovalent mobile (ou une fraction $1/z$ d'un cation de valence z). Le réseau réel contient une quantité appréciable de défauts — acidité Lewis (des atomes Al tricoordinés) et acidité Brönsted (des charges négatives de l'Al, neutralisées par des atomes H hydroxyliques). Les deux types de défauts ont comme effet une baisse de la capacité d'échange ionique ; l'acidité Brönsted correspond à l'eau structurale du zéolithe (l'eau qui se volatilise seulement à 700 — 900°, différant de l'eau zéolithique adsorbée, qui quitte le réseau à 100 — 400°). La composition du zéolithe est donc caractérisée par les paramètres suivants :

A — rapport entre le nombre d'atomes Si et Al ;

B — rapport entre le nombre de centres Lewis et d'atomes Al ;
C — rapport entre le nombre de centres Brönsted et d'atomes Al.

La capacité d'échange ionique, rapportée à un «mole conventionnel» de zéolithe (quantité qui contient $6{,}02 \times 10^{23}$ cavités α) sera :

$$Q_E = 24\,(1 - B - C)\,(1 + A)^{-1} \tag{1}$$

parce que à une cellule élémentaire correspondent 24 atomes (Al+ Si), dont 24 $A/(1+A)$ atomes Si et $24/(1+A)$ atomes Al, et puisque à chaque atome Al non défectif correspond un cation monovalent.

Soit y_i la part de la capacité d'échange ionique saturée avec les cations du type i, à charge z_i ; la quantité de cations i (mole cation/mole zéolithe) sera :

$$24(1-B-C)\,y_i/z_i(1+A)$$

et la masse moléculaire M_{zo} du zéolithe anhydre :

$$M_{zo} = 24\,[A\,M_{Si} + M_{AlO_2} - B\,M_O/2 + CM_H + (1 - B - C)\,\Sigma\, y_i E_i]/(1+A) \qquad (2)$$

où M_i sont les masses moléculaires et E_i — les masses équivalentes ($E_i = M_i/z_i$).

Notant par Q' les capacités d'échange ionique rapportées à l'unité de masse du zéolithe (mmol/g), on obtient :

$$Q'_0 = Q_{iE} \cdot 1000/M_{z0} \qquad (3\ a)$$

$$Q'_1 = Q_E \cdot 1000/M_{z1} \qquad (3\ b)$$

selon que l'on exprime la capacité pour 1 g de zéolithe anhydre, ou pour 1 g de zéolithe d'humidité donnée.

La masse moléculaire M_{z1} du zéolithe ayant l'humidité u (g eau/g zéolithe humide) sera reliée à celle du zéolithe anhydre par la relation :

$$M_{z0} = M_{z1}(1-u) \qquad (4)$$

Les grandeurs A, B, C restent invariables si l'échange ionique est effectué en solutions diluées et pas trop acides [30]. On a trouvé dans notre cas les valeurs :

$B = 0{,}01$;
$C = 0{,}02$;
$A = 1$ (zéolithe A) ;
$A = 1{,}25$ (zéolithe X).

Dans le tableau 2 on exprime les autres caractéristiques de la composition des sorbants utilisés. Pour les zéolithes X de Ni, Cu et Zn aux hauts degrés d'échange avec les ions bivalents

TABLEAU 2

Caractéristiques des sorbants utilisés

N°	Type	1 000 y			100	10	10	100	1 000	100	1 000
		Na^+	M^{++}	MOH^+	f	M_{zo}	M_{z1}	u %	Q'_0	Q'_1	z
	ANa	1000	0	0	2850	16953	21369	2066	5447	0	1945
1	ANa/Co	563	437	0	2828	17284	21665	2023	5373	235	1948
2	ANa/Co	510	490	0	2826	17323	21701	2018	5362	263	1989
3	ANa/Ni	548	452	0	2818	17287	21653	2017	5376	243	1984
4	ANa/Ni	447	553	0	2811	17362	21724	2008	5358	296	1993
5	ANa/Cu	422	578	0	2810	17544	21904	1991	5314	307	2012
6	ANa/Cu	222	778	0	2796	17749	22081	1958	5271	410	2033
7	ANa/Zn	370	630	0	2793	17665	21993	1969	5292	333	2020
8	ANa/Zn	216	784	0	2780	17826	22133	1946	5259	412	2038
	XNa	1000	0	0	3310	16671	21740	2332	4758	0	1870
9	XNa/Co	437	563	0	3282	17048	22074	2277	4634	264	1909
10	XNa/Co	341	659	0	3277	17112	22130	2268	4612	309	1916
11	XNa/Ni	299	701	0	3261	17145	22139	2256	4603	328	1917
12	XNa/Ni	180	421	399	3153	19198	24027	2010	4306	525	2075
13	XNa/Cu	254	746	0	3258	17339	22329	2235	4595	346	1935
14	XNa/Cu	152	477	381	3154	19449	24280	1998	4261	524	2098
15	XNa/Zn	153	847	0	3234	17520	22480	2207	4575	390	1949
16	XNa/Zn	92	553	355	3140	19478	24289	1981	4260	538	2100

(y_{Na} à valeur moindre), survient une hydrolyse partielle des cations des métaux transitionnels :

$$M(II)_z^{2+} + H_2O \rightarrow M(II)OH_z^+ + H_{aq}^+,$$

se formant ainsi les ions $NiOH^+$, $CuOH^+$, $ZnOH^+$.

3. LE CALCUL DE L'ISOTHERME D'ADSORPTION

On peut définir la grandeur de l'adsorption q' en rapportant la quantité de sorbate (mmol NH_3 dans la phase zéolithe) à la masse initiale du sorbant (g zéolithe en forme ionique correspondante, équilibré à l'humidité atmosphérique).

Pour la comparaison des 16 sorbants, tenant compte que la rétention du NH_3 advient surtout dans les cavités structurales (α, éventuellement α et β, d'après [13]) il convient de rapporter la quantité sorbée aux mêmes nombres des cavités zéolithiques ; l'adsorption ainsi définie, notée ici par q, est exprimée en mole NH_3/mole zéolithe ; q est relié à q' (l'adsorption de l'unité de masse) par la relation :

$$q = M_{z0}q'/1000 \tag{5}$$

La grandeur q représente le nombre de molécules NH_3 contenues dans une cavité α et dans une cavité β adjacente.

Pour le calcul des points de l'isotherme d'adsorption $q'(c)$, la version la plus simple est l'utilisation du bilan simplifié de l'ammoniac :

$$L_0(c_0 - c) = Sq'_{ap} \tag{6 a}$$

où q'_{ap} est dénommée « adsorption apparente », L est le volume initial de liquide (ml), S — la quantité de sorbant (g), c_0 et c sont les concentrations initiale et finale du NH_3 en solution (mmol/ml). Les calculs préliminaires ont montré que l'adsorption apparente est sensiblement différente par rapport à l'adsorption réelle q', qui peut être obtenue par un bilan complet de l'ammoniac :

$$L_0c_0 - (L - l)c - n_{LAV} = Sq \tag{6 b}$$

où l (ml) est la baisse de volume de la phase liquide (de façon que $L - l$ est le volume final de la solution) et n_{LAV} (en moles) est la perte d'ammoniac par vaporisation.

Les pertes par vaporisation n_{LAV} ont été calculées en partant de la valeur expérimentale de la baisse de concentration dans une expérience-témoin, sans zéolithe, effectuée dans le même récipient, au même volume de liquide et dans les mêmes conditions d'agitation que dans les déterminations d'adsorption. On a trouvé que n_{LAV} est proportionnel à la fugacité φ (torr) de l'ammoniac dans la solution :

$$n_{LAV} = k'\varphi \tag{6 c}$$

où k' est le coefficient de transfert de masse. La valeur expérimentale établie pour k' a été de 0,178 mmol/torr. La fugacité φ est une fonction de la concentration ; en employant les données de,[31] p. 1082 pour les densités, et p. 1382 pour les fugacités des solutions aqueuses d'ammoniac de molalité variable, on trouve les dépendances :

$$\widetilde{m} = c/h \tag{7 a}$$

où $\widetilde{m}$ signifie la molalité de la solution (mole NH_3/kg H_2O) et h (g/ml) est la masse d'eau dans l'unité de volume de la solution :

$$h = g_1\rho \tag{7 b}$$

où g_1 représente la fraction de poids de l'eau et ρ — la densité de la solution. A 20° les données de [31] sont représentables par les relations :

$$h = 1{,}0009 - 0{,}0246\,c + 5\cdot 10^{-5}\,c^2 \tag{8 a}$$

$$\varphi = 9{,}811\,\widetilde{m} + 0{,}348\,\widetilde{m}^2 \tag{8 b}$$

qui permettent d'exprimer — en combinaison avec les relations (6 c), (7 a) et la valeur expérimentale k' — les pertes n_{LAV} en fonction de la concentration.

La baisse l du volume de la solution pendant l'adsorption a été éliminée de la relation (6 b), en employant le bilan de masse de l'eau, en g :

$$L_0h_0 + Su_0 = (L - l)k + Su \tag{9 a}$$

où h_0 est la masse d'eau dans l'unité de volume de la solution initiale, calculable par la relation (8 a), avec remplacement de c et h par c_0 et respectivement h_0 ; u_0 — l'humidité initiale du zéolithe (g/g) et u — l'humidité finale (g H_2O/g zéolithe initial). La grandeur u n'est pas directement mesurable, mais on peut la calculer en partant de q', si l'on considère que u est fonction linéaire de la quantité d'ammoniac adsorbée :

$$u = w_M(1 - q'/q'_m)M_1/1\,000 \tag{10}$$

où q_M est la capacité d'adsorption pour l'ammoniac (mmol/g), $M_1 =$ 18,016 g/mol est la masse moléculaire de l'eau et w_M — la capacité de sorption pour l'eau, en mmol/g zéolithe (équilibré avec l'humidité atmosphérique). D'après [30], on peut calculer w_M en fonction de u_0, nommément :

$$w_M = 1000u_0/M_1k_w \tag{11}$$

la valeur k_w étant 0,86 pour le zéolithe A et 0,85 pour le zéolithe X.

On peut obtenir la capacité de sorption pour l'ammoniac, q_M, en première approximation, dans le cadre de la théorie de Gurvich [32] du remplissement volumique, en supposant que la densité de l'adsorbate soit égale à la densité du liquide, de sorte que, pour un remplissement total des cavités :

$$V_1 w_M = V_2 q'_M \tag{12}$$

où V_1 et V_2 sont les volumes molaires du H_2O et NH_3 (en état liquide) c'est-à-dire 18,03 respectivement 28,45 cm^3/mol.

En remplaçant u de (10) en (9 a) et n_{LAV} de (6 c) en (6 b), on obtient :

$$L_0 c_0 - Lc + lc - k'\varphi - Sq' = 0$$

$$L_0 h_0 - Lh + lh + Su_0 - Sw_M M_1/1000 + Sw_M q' M_1/1000\ q'_M\,;$$

d'où, par élimination de l, on obtient :

$$q' = \frac{L_0(c_0 h - ch_0)/S - k'h\varphi/S + c(M_1 w_M/1000 - u_0)}{h - M_1 c w_M/1000\ q'_M} \tag{13}$$

où h et h_0 sont fonctions de c et c_0 (relation 8 a), φ est fonction de m (relation 8 b) qui à son tour dépend de c et de h (relation 7 a), les grandeurs L_0, k' et M_1 prennent les valeurs constantes déjà citées : 25 ; 0,178 respectivement 18,016, tandis que S caractérise la détermination expérimentale (voir tableau 1).

Les grandeurs w_M, u_0 et q'_M sont caractéristiques de l'adsorbant et restent constantes pour chaque isotherme : u_0 (expérimental) et w_M (relation 11) sont présentées dans le tableau 2 et q'_M a été calculé initialement de w_M, avec la relation (12). Ensuite, puisque l'on obtient ainsi en certains cas des valeurs q plus grandes que q'_M (ce qui indique une densité supérieure pour le NH_3 adsorbé par rapport au NH_3 liquide) on a calculé q_M par passage à la limite de la relation (13 a), aux grandes concentrations :

$$q'_M = \lim_{1/c \to 0} \frac{L_1(c_0 h - ch_0) - k'h\varphi - u_0 cS}{hS}$$

Pour une augmentation de la précision de l'extrapolation, on a passé aux coordinnées Y et X, correspondant à l'isotherme de Dubinin [33] :

$$\ln q'_M = \lim_{X \to 0} Y$$

où :

$$Y = \ln\{[L_0(c_0 h - ch_0) - k'h\varphi - u_0\, cS]/hS\} \tag{14 a}$$

$$X = \ln^2(\varphi/\varphi_s) \tag{14 b}$$

où φ_s est la fugacité des vapeurs saturées de NH_3 à 20°,

$$\varphi_s = 7{,}9 \text{ atm} = 6\,000 \text{ torr}.$$

Les isothermes de sorption $q'(c)$ pour les 16 adsorbants à 20° sont représentées dans les tableaux 3 a, 3 b.

TABLEAU 3 a

Isothermes d'adsorption de l'ammoniac sur les zéolithes A

Type d'adsorbant	1	3	5	7	2	4	6	8
c	n							
0,06				47			51	57
0,08			37	52			59	66
0,1	26	13	44	58	41	18	66	75
0,12	29	15	50	63	46	21	72	82
0,15	33	18	58	70	52	24	81	91
0,2	39	24	68	82	61	33	94	105
0,25	44	29	79	92	68	39	107	118
0,3	48	34	85	101	74	45	119	130
0,4	54	44	98	118	86	59	140	151
0,5	63	53	108	132	97	73	156	169
0,6	72	63	117	143	107	93	171	180
0,8	93	82	141	160	126	125	194	200
1	121	101	163	174	148	156	212	217
1,2	144	120	181	185	164	176	224	229
1,5	175	143	207	200	188	197	245	249
2	205	177	240	224	217	227	274	280
2,5	224	209	271	248	242	250	304	296
3	240	240	294	266	263	269	332	327
4	254	270	336	298	297	298	369	360

c — concentration du NH_3 en solution aqueuse, mol/l, à l'équilibre ;
n — la quantité de NH_3 en mmol sorbée par 40 g adsorbant (en équilibre préalable avec l'humidité atmosphérique) ;
Les nombres d'ordre des adsorbants comme dans le tableau 2.

4. Résultats et discussion

Pour les raisons pratiques ce qui intéresse est surtout la capacité d'adsorption par rapport à l'unité de masse du sorbant dans sa forme usuelle (équilibré avec l'humidité atmosphérique).

Les tableaux 3 permettent la comparaison, de ce point de vue, des sélectivités des adsorbants employés. Pour faciliter la comparaison on a groupé ensemble les adsorbants préparés selon le même rapport zéolithe/solution du sel du métal transitionnel (les adsorbants nos 1, 3, 5, 7 ; 2, 4, 6, 8 ; 9, 11, 13, 15 ou 10, 12, 14, 16), quoique, dans chaque série, le degré d'échange ionique est assez variable — il augmente dans l'ordre des affinités pour le zéolithe des ions des métaux transitionnels :

$$Co < Ni < Cu < Zn \tag{15 a}$$

TABLEAU 3b

Isothermes d'adsorption de l'ammoniac sur les zéolithes X

Le type d'adsorbant	9	11	13	15	10	12	14	16
c, mol/l	*n*							
0,04								59
0,05								67
0,06			48	66	40	39	50	73
0,08	47	39	58	72	52	49	60	84
0,1	51	45	67	78	61	57	68	93
0,12	55	51	75	84	68	64	75	100
0,15	61	59	85	93	78	73	86	109
0,2	68	72	98	108	93	85	101	125
0,25	75	85	109	120	106	96	113	136
0,3	84	95	118	131	117	107	124	147
0,4	106	114	134	150	140	128	142	166
0,5	128	132	150	167	160	148	161	184
0,6	147	148	163	183	175	165	174	201
0,8	182	175	184	210	202	192	200	234
1	210	196	201	232	227	216	223	261
1,2	232	215	216	252	250	237	242	283
1,5	259	243	237	273	276	261	263	312
2	302	277	268	310	316	292	295	346
2,5	331	302	291	337	341	315	316	371
3	353	317	311	359	357	331	335	388
4	394	345	342	392	399	358	368	415

Comme traits généraux, la sélectivité de l'adsorption de l'ammoniac augmente en même temps que le contenu en cations des métaux transitionnels (comparer 1 avec 2 ; 3 avec 4, etc.) et pour le même cation elle est plus grande pour le zéolithe X que pour le zéolithe A.

Les différents éléments transitionnels présentent une sélectivité qui augmente, en général, dans l'ordre suivant :

$$Ni < Co < Cu < Zn \tag{15 b}$$

valable pour les deux réseaux et aussi pour les deux degrés d'échange, à des concentrations de NH_3 en dessous de 0,55 mol/l.

Toutefois on trouve que, par rapport à la série-standard (15 b), il y a de nombreuses inversions, pour certains domaines de concentration de l'ammoniac, comme par exemple :

1° Sur le zéolithe A, à des concentrations élevées de NH_3 (dépassant 1,3 à petits degrés d'échange et dépassant 2,3 à grands degrés d'échange), l'ion Cu retient mieux l'ammoniac par rapport au Zn ;

2° Sur le zéolithe A, à grandes concentrations de NH_3 (qui dépassent 3, aux bas contenus du cation transitionnel, et qui dépassent 0,8 aux contenus élevés), le Ni retient mieux que le Co ;

3° Sur le zéolithe X, à grandes concentrations de NH_3 (dépassant 0,85 à bas contenus et 0,55 à hauts contenus) le Co retient mieux que le Cu ;

4° Sur le zéolithe X aux petits degrés d'échange, le Ni retient mieux que le Cu, dans le cas des concentrations d'ammoniac en solution plus grandes que 1,25 mol/l ;

5° Sur les zéolithes X aux petits degrés d'échange, le Ni retient mieux que le Co, à des concentrations d'ammoniac situées entre 0,17 et 0,63 mol/l.

La variation des séries de sélectivité par rapport à la concentration, pour les deux réseaux et les deux degrés d'échange, est présentée dans le tableau 4. Dans tous les cas les formes cationiques Ni et Co retiennent moins le NH_3 que la forme Zn. L'augmentation de la concentration de la solution d'ammoniac a comme effet, au cas du zéolithe A, la hausse de la sélectivité du Cu (en comparaison du Zn) et du Ni (par rapport au Co) et au cas du zéolithe X — l'agrandissement de la sélectivité du Co et du Ni, par rapport au Cu.

TABLEAU 4

LES SÉRIES DE SÉLECTIVITÉ DE L'ADSORPTION

Le rang des cations transitinnels indique l'ordre croissant de l'adsorption de l'ammoniac
Les adsorptions comparées sont des valeurs qui se réfèrent à l'unité de masse du zéolithe, équilibré par l'humidité atmosphérique.

Réseau	Degré d'échange du Na^+ contre le cation transitionnel	c, mol/l		Rang
		de	à	
A	mince		1,3	Ni Co Cu Zn
		1,3	3,0	Ni Co Zn Cu
		3,0		Co Ni Zn Cu
	grand		0,8	Ni Co Cu Zn
		0,8	2,3	Co Ni Cu Zn
		2,3		Co Ni Zn Cu
X	mince		0,13	Ni Co Cu Zn
		0,13	0,63	Co Ni Cu Zn
		0,63	0,85	Ni Co Cu Zn
		0,85	1,25	Ni Cu Co Zn
		1,25		Cu Ni Co Zn
	grand		0,55	Ni Co Cu Zn
		0,55		Ni Cu Co Zn

La sélectivité pratique est exprimable par le coefficient de distribution D de l'ammoniac entre la phase zéolithe et la solution aqueuse, D étant défini comme le rapport des molarités de l'ammoniac dans les deux phases :

$$D = c_q/c \tag{16 a}$$

où c_q est la concentration du NH_3 adsorbé, mole/l zéolithe :

$$c_q = q' \rho_z$$

où ρ_z est la densité du zéolithe équilibré par l'humidité atmosphérique. La grandeur ρ_z a été calculée en considérant que le volume du zéolithe ne change pas à l'adsorption et que, au remplacement de Na^+ par des cations bivalents, le volume de la cellule élémentaire diminue proportionnellement au contenu de cation bivalent : c'est-à-dire pour 100% change, avec 1,5% pour le zéolithe A et avec 1% pour le zéolithe X. Dans ces conditions, en considérant les densités des formes Na^+ anhydres (A 1,54 et X 1,43 cf. [33]) et aussi leurs masses moléculaires (1695,3 A et 1667,1 g/mole X, cf. tableau 3), on obtient (ρ en g/cm³) :

$$\text{Zéolithes A : } \rho_z = 0{,}91\ M_{z1}/(1000 - 15\ y_2) \tag{17 a}$$

$$\text{Zéolithes X : } \rho_z = 0{,}82\ M_{z1}/(1000 - 10\ y_2) \tag{17 b}$$

où M_{z1} et y_2 représentent la masse moléculaire du zéolithe équilibré par l'humidité atmosphérique, respectivement le contenu de cation bivalent, les deux valeurs étant disponibles dans le tableau 2, tout comme le résultat du calcul de la densité par les relations (17).

Les coefficients de distribution obtenus des relations (16) sont présentés, pour quelques concentrations de la solution, dans le tableau 5.

TABLEAU 5

Distribution de l'ammoniac entre le zéolithe et la solution aqueuse, 20° ;
Dans le tableau — les coefficients volumiques de distribution, multipliés par 10

c, mol/l	0,1	0,2	0,4	1	2	4
Sorbant n°	10 D					
1	129	97	67	60	51	31
2	204	151	107	74	54	37
3	65	60	55	50	44	32
4	90	82	74	78	57	37
5	221	171	123	82	60	42
6	335	238	178	108	70	47
7	293	207	149	88	57	38
8	382	267	190	110	71	46
9	243	162	126	100	72	47
10	292	223	168	109	76	48
11	216	173	137	94	66	41
12	296	220	166	112	76	47
13	324	237	162	97	65	41
14	323	240	169	106	77	48
15	380	263	183	113	76	48
16	488	328	218	137	91	54

Dans ce tableau on constate que les séries de sélectivité se modifient assez peu, au remplacement des concentrations des masses par la concentration de volume dans la phase zéolithe. Le coefficient de distribution est dans tous les cas surunitaire (3,2 —48,8), ce qui montre que les zéolithes sont de bons adsorbants. Les coefficients de distribution baissent avec l'augmentation de la concentration, ce qui confirme la nature adsorptive de la rétention du NH_3 dans les zéolithes.

En même temps, avec l'agrandissement de la concentration les différences de sélectivité vont s'attenuer : le rapport entre les coefficients de distribution pour le sorbant le plus fort (no 16) et le plus faible (no 3) varie de 6,5 pour la solution 0,1 mol/l à 1,7 seulement pour la solution de 4 mol/l.

5. CONCLUSION

L'ammoniac de la solution aqueuse est fortement retenu par les zéolithes synthétiques A et X chargés de métaux transitionnels, à la température ambiante. La sélectivité augmente en même temps que le contenu de métal transitionnel, est meilleure pour les zéolithes X que pour les zéolithes A et varie par rapport à la nature du métal transitionnel : à de faibles concentrations de NH_3, la sélectivité augmente selon l'ordre : Ni, Co, Cu, Zn, correspondant à la série de la sélectivité d'échange ionique, excepté la position du Co et Ni. A de plus grandes concentrations de NH_3, l'ordre de sélectivité de la rétention de NH_3 présente de nombreuses inversions. Dans tous les cas, aux degrés supérieurs d'échange avec le métal transitionnel bivalent, le zéolithe ZnX peut être considéré comme le meilleur adsorbant parmi ceux étudiés.

BIBLIOGRAPHIE

[1] R. Barrer et G. Pratt, *J. Phys. Chem. Solids,* **12**, 130 (1959).

[2] R. Barrer, *ibid.*, **16**, 84 (1960).

[3] D. Breck, "Zeolite Molecular Sieves. Structure, Chemistry and Use", Wiley-Interscience, New York, 1974.

[4] B. Coughlan et P. Larkin, *Chem. Ind.* (*London*), **1976**, 275.

[5] D. Breck, W. Eversole, R. Milton, T. Reed et T. Thomas, *J. Amer. Chem. Soc.*, **78**, 5963 (1956).

[6] T. Peintze, K. Fiedler, H. Stach et W. Schirmer, *Monatsber. Deut. Akad. Wiss. Berlin*, **12**, 855 (1970).

[7] B. Coughlan et R. Shaw, *Proc. Roy. Irish Acad., Sect. B*, **76**, 191 (1976).

[8] R. Barrer et B. Coughlan, dans "Molecular Sieves", ed. Soc. of Chem. Ind., London, 1968, p. 233.

[9] S. S. Khvochtchev et S. P. Zhdanov, *Doklady Akad. Nauk. S.S.S.R., ser. Fiz. — Khim.*, **200**, 1156 (1971).

[10] S. S. Dyakonov, A. V. Kiselev, N. M. Kuz'menko et V. I. Lygin, *Zhur. fiz. Khim.*, **49**, 3173 (1975).

[11] R. Barrer, *J. Colloid Interface Sci.*, **21**, 415 (1966).

[12] B. V. Romanovskiy, K. V. Toptchieva, L. V. Stolyarova et A. M. Alekseev, *Kinetika i Kataliz*, **12**, 1003 (1971).

[13] R. Barrer et R. Gibbons, *Trans. Faraday Soc.*, **59**, 2569 (1963).

[14] N. N. Avgul', B. G. Aristov, A. V. Kiselev et L. Ya. Kurdyukova, *Zhur. fiz. Khim.*, **42**, 2678 (1968).

[15] B. Coughlan et R. Shaw, *Proc. Roy. Irish Acad., Sect. B*, **76**, 227 (1976).

[16] B. Coughlan et S. Kilmartin, *Trans. Faraday Soc.*, **71**, 1809 (1975).

[17] T. Peinze, K. Fiedler, H. Stach et W. Schirmer, *Monatsber. Deut. Akad. Wiss. Berlin*, **12**, 867 (1970).

[18] H. Stach, T. Peinze, K. Fiedler et W. Schirmer, *Z. Chem.*, **10**, 229 (1970).

[19] D. Stamires, *J. Chem. Phys.*, **36**, 3174 (1962).

[20] D. Yates, op. cit.,[8] p. 334.

[21] M. Malinowski, S. Malinowski et S. Krzizanowski, *J. Therm. Anal*, **10** (1), 73 (1976).

[22] A. V. Kiselev, V. I. Lygin et T. I. Titova, *Zhur. fiz. Khim.*, **38**, 2730 (1974).

[23] K. Seff, *J. Phys. Chem*, **76**, 2601 (1972).

[24] D. Bernache-Assolant et. G. Thomas, *J. Chim. phys.*, **73**, 967 (1976).

[25] M. Buclaw, V. K. Cuikina et W. Schirmer, *Z. phys. Chem. (Leipzig)*, **258**, 321 (1977).

[26] T. Peinze, M. Buclaw et W. Schirmer, *ibidem*, **258**, 533 (1977).

[27] M. D. Khadzhiev, A. I. Sidorov et N. S. Torotchechnikov, *Trudy Moskov. Khim. — Technol. Inst.*, **65**, 83 (1970).

[28] L. Smith, G. Lyerly et M. Dooley, *U. S. NTIS, PB Rep.* **1976**, PB—251418; *Chem. Abstr.*, **87**, 90314 (1977).

[29] W. Meier, op. cit.,[8] p. 10.

[30] F. Daneş, Dissertation, Martin-Luther-Univ., Halle/S. (R. D. Allemande), 1968.

[31] «Manualul Inginerului Chimist», Ed. tehnică, Bucarest, 1952.

[32] L. G. Gurvich, *Zhur. Ross. Fed. Khim. Obchtchestva*, **47**, 805 (1915).

[33] M. M. Dubinin, *Chem. Phys. Carbon*, **2**, 51 (1966).

Revue Roumaine de Chimie, 25, *5*, 687–689 (1980)

THE REARRANGEMENT OF *SEC*-BUTYLBENZENE TO ISOBUTYLBENZENE CATALYZED BY FLUOROANTIMONIC ACID[1]

ROYSTON M. ROBERTS and HOFFMAN H. CHEN
The University of Texas at Austin, Austin, Texas 78712, U.S.A.

Received May 5, 1979

The treatment of *sec*-butylbenzene with fluoroantimonic acid at 0°, 25°, and 50° is described. Rearrangement to isobutylbenzene occurred at 25° and 50° but not at 0°; transalkylation occurred at all temperatures.

The rearrangement of *sec*-butylbenzene to isobutylbenzene on heating with $AlCl_3$ was observed by Nenitzescu and coworkers[2] and shown to be reversible by Roberts and coworkers,[3] giving a pseudo-equilibrium proportion of 2 : 1 in favor of isobutylbenzene. This has been shown to be an example of a general reaction of certain alkylbenzenes when heated with $AlCl_3$ and various other Lewis acids.[4] Although the *sec*-butylbenzene—isobutylbenzene rearrangement is more facile than the automerization of isotopically-labeled *n*-propylbenzene, it is not rapid at low temperatures. When *sec*-butylbenzene was stirred with water-activated aluminum chloride at 25°–30° for 24 hr, no rearrangement occurred ; a 6-hr treatment at 50° gave 10% conversion to isobutylbenzene, and 1 hr at 100° gave the equilibrium proportion of 33% *sec*-butylbenzene : 67% isobutylbenzene.[3] Of course disproportionation to benzene and di-*sec*-butylbenzenes occurs at temperatures even as low as $-14°$.[5]

Results from a recent investigation of the dealkylation reactions of two *sec*-hexyl benzenes[6] led us to examine the effect of fluoroantimonic acid on *sec*-butyl benzene. When either 2- or 3-phenylhexane was treated with Al_2Br_6 or Al_2Br_6/HBr at temperatures from 35° to 80°, a mixture of hexane isomers was produced in yields of 19–70%. A representative reaction gave hexane, 2-methylpentane, and 3-methylpentane in the ratio 10 : 53 : 37. No other hexane isomers were detected. When 2- or 3-phenylhexane was heated for 0.5 hr at 80° with HF/SbF_5, two additional isomeric hexanes were produced, 2,3-dimethylbutane (18%) and 2,2-dimethylbutane (4%), as well as hexane (9%), 2-methylpentane (43%) and 3-methylpentane (26%). The formation of the doubly-branched hexanes by reaction of the *sec*-hexylbenzenes with HF/SbF_5, whereas reaction with Al_2Br_6 and Al_2Br_6/HBr did not produce any doubly-branched isomers, led us to test HF/SbF_5 as a catalyst for the *sec*-butylbenzene-isobutylbenzene rearrangement.

sec-Butylbenzene and HF/SbF_5 (in a molar ratio of 3 :1) were cooled to 0° and stirred together for 1 hr. After decomposition of the reaction mixture with water, the organic products were analyzed by glpc, IR spectroscopy and NMR spectroscopy and found to consist of benzene, *sec*-butylbenzene, *m*-(mainly) and *p*-di-*sec*-butylbenzene, and 1,3,5-tri-*sec*-butylbenzene.

When the reaction was repeated at 25° for 1 hr, the NMR spectra of the products showed the presence of isobutyl groups in the butylbenzene, dibutylbenzene, and tributylbenzene fractions (see Experimental section). The butylbenzene mixture was analyzed quantitatively by IR using 5% solutions in 2,2,4-trimethylpentane solutions[7] and found to consist of *sec*-butylbenzene and isobutylbenzene in a ratio of 75 : 25.

A third experiment was carried out at 50°. The butylbenzene fraction recovered consisted of *sec*-butylbenzene and isobutylbenzene in a ratio of 38 : 62, according to the IR analysis. The NMR spectra also showed the increased presence of isobutyl groups in the butyl-, dibutyl-, and tributylbenzene fractions.

It should be noted that $AlCl_3/H_2O$ produced no rearrangement of *sec*-butylbenzene in 24 hr at 25°—30°, and only 10% rearrangement was produced by this catalyst at 50° for 6 hr, whereas HF/SbF_5 is seen to produce significant rearrangement at room temperature and to give approximately the equilibrium proportion of the isometric butylbenzenes in 1 hr at 50°. The greater effectiveness of HF/SbF_5 in isomerizing *sec*-butylbenzene may be atributed to the well known ability of the SbF_6^- counterion to stabilize carbocations such as those which are involved as intermediates in this alkylbenzene rearrangement.[8]

EXPERIMENTAL

Infrared analysis was carried out on a double beam Beckmann IR-5A spectrometer. NMR spectra were recorded at 60 MHz on a Varian A60 or a Perkin-Elmer R12A instrument with TMS as internal standard. Analytical glpc identifications were made with a Wilkins Acrograph Model 600D instrument and preparative separations were made with a Varian A-700 instrument.

Fluoroantimonic acid (HF/SbF_5) was purchased from Cationics, Inc. und used as received. *sec*-Butylbenzene was Aldrich, 99+ % by glpc analysis.

Treatment of sec-Butylbenzene with Fluoroantimonic Acid

A. *Reaction at 0°C*

Fluoroantimonic acid (7.81 g, 0.0330 mol) was cooled to 0°C and pre-cooled *sec*-butylbenzene (13.4 g 0.100 mol) was added ; the mixture was stirred with a magnet capsule for 1 hr while the flask was immersed in an ice-water bath. Water (15 ml) was added to quench the reaction and the organic products were extracted into 10 ml of ether. The water layer was extracted with two 5-ml portions of ether, the combined ether solutions were washed with 5 % sodium bicarbonate solution and water, and then dried over anhydrous $MgSO_4$. The ether was evaporated and the residue was distilled through a 20—cm Vigreux column at atmospheric pressure. The following fractions were separated : (1) bp. 80—83°, 2.8 g ; (2) bp 170—177°, 3.8 g ; (3) bp 178—250°, 4.4 g ; (4) residue, 0. 4 g.

The distilled fractions were analyzed quantitatively by glpc using two 1.83 − m X 3.25 − mm columns, one containing 10 % SE-30 and the other 10 % dinonyl phthalate on Chromosorb P. The butylbenzene, dibutylbenzene, and tributylbenzene fractions were separated by preparative gas chromatography and identified by IR and NMR spectroscopy. The product distribution was as follows (wt % based on *sec*-butylbenzene starting material) : benzene (19 %) ; *sec*-butylbenzene (28 %): IR 13.15 μ ;[7] NMR (CCl_4, δ, ppm) 0.80 (t, 3H, J=7 Hz, $\gamma-CH_3$), 1.20 (d, 3H, J=7 Hz, $\beta-CH_3$), 1.48 (quintet, 2H, J=7 Hz, $\beta-CH_2$), 2.55 (sextet, 1H, $\alpha-CH$), and 7.13 (s, 5H, aromatic) ; *m*-(and *p*-)di-*sec*-butylbenzene (11 %) : IR 12.7 and 14.2μ (strong) ; NMR (CCl_4, δ, ppm) 0.82 (t, 6H, J=7 Hz, $\gamma-CH_3$'s), 1.22 (d, 6H, J=7 Hz, $\beta-CH_3$'s), 1.55 (quintet, 4H, J=7 Hz, $\beta-CH_2$'s), 2.55 (sextet, 2H, J=7 Hz, $\alpha-CH$'s), and 6.75−7.15 (m, 4H, aromatic and 1,3,5-tri-*sec*-butylbenzene (24 %) : NMR (CCl_4, δ, ppm) 0.81 (t, 9H, J=7Hz, $\gamma-CH_3$'s), 1.22 (d, 9H, J=7 Hz, β-CH_3 's), 1.52 (quintet, 6H, J=7 Hz, $\beta-CH_2$'s), 2.53 (sextet, 3H, J=7 Hz, $\alpha-CH$'s), and 6.70 (s, 3H, aromatic).

B. *Reaction at 25°*

The reaction of fluoroantimonic acid (3.28 g, 0.0139 mol) and *sec.*-butylbenzene (5.64 g, 0.0421 mol) was carried out as before except that the reactants were stirred at 25° for 1 hr. The reaction mixture was worked up as before and distilled to give the following fractions : 80−86°, 0.74 g ; (2) bp 170−178°, 3.5 g ; (3) bp 178−250°, 0.56 g ; (4) residue, 0.28 g.

Analysis of the distilled fractions as before showed the following product distribution : benzene (13 %) ; *sec*-butylbenzene and isobutylbenzene (54 %), in the ratio 75 : 25, respectively : IR 13. 15μ for *sec*-butylbenzene and 13.55μ for isobutylbenezene ; [7] *m*-(and *p*-) dibutylbenzenes (10 %) ; and 1, 3, 5-tributylbenzenes (8 %). The NMR spectra of the butyl-, dibutyl- and tributylbenzene fractions were very similar to those of the corresponding products from the reaction of 0°, but evidence of the presence of isobutyl as well as *sec*-butyl groups could be seen : the doublet for the six hydrogens on the γ-carbons at δ0.85 (J=7 Hz) and the doublet for the two hydrogens on the α-carbon at δ2.42 (J=7 Hz) of isobutylbenzene were detectable in all three spectra.

C. *Reaction at 50°*

The reaction of fluoroantimonic acid (7.81 g, 0.0330 mol) and *sec*-butylbenzene (13.4 g 0.100 mol) was carried out as before at 50° for 1 hr. The reaction mixture was worked up as before and distilled to give the following fractions : (1) bp 79−82°, 1.2 g ; (2) bp 169−172°, 3.4 g ; (3) bp 172−235°, 2.9 g ; (4) residue, 1.1 g

Analysis of the distilled fractions as before showed the following product distribution : benzene (9 %) ; *sec*-butylbenzene and isobutylbenzene (30 %), in the ratio 38 :62, respectively : IR 13.15μ and 13.55 ;[7] *m*-(and *p*-) dibutylbenzenes (11 %) and 1,3,5-tributylbenzenes (6 %). The NMR spectra of the products were similar to those from the reactions at 0° and 25°, but with increased doublet signals from the isobutyl isomers.

REFERENCES AND NOTES

[1] (a) Paper 35 in the New Friedel-Crafts Chemistry series. Paper 34 : R. M. Roberts, H. H. Chen, and B. Junhasavasdikul, *J. Org. Chem.*, **43**, 2977 (1978). (b) Generous support of this research by the Robert A. Welch Foundation is gratefully acknowledged.

[2] C. D. Nenitzescu, I. Necşoiu, A. Glatz, and M. Zalman, *Chem. Ber.*, **92**, 10 (1959).

[3] R. M. Roberts, Y. W. Han, C. H. Schmid, and D. A. Davis, *J. Amer. Chem. Soc.*, **81**, 640 (1959).

[4] (a) R. M. Roberts, *Intra-Science Chem. Rept.*, **6**, 89 (1972); (b) R. M. Roberts, A. A. Khalaf, and R. N. Greene, *J. Amer. Chem. Soc.*, **86**, 2846 (1964).

[5] R. M. Roberts, G. P. Anderson, Jr., and N. L. Doss, *J. Org. Chem.*, **33**, 4259 (1968).

[6] R. M. Roberts, H. H. Chen, and B. Junhasavasdikul, *ibid.*, **43**, 2977 (1978).

[7] The qualitative and quantitative analysis of mixtures of *sec*-butylbenzene and isobutylbenzene by IR spectroscopy is described in ref. 3.

[8] (a) D. M. Brouwer, *Rec. Trav. chim.*, **87**, 210 (1968) ; (b) D. M. Brouwer and J. M. Oelderik, *ibid.*, **87**, 721 (1968).

The distilled fractions were analyzed quantitatively by glpc using two 1.83-m × 3.25-mm columns, one containing 10% SE-30 and the other 10% dinonyl phthalate on Chromosorb P. The butylbenzenes, dibutylbenzenes, and tributylbenzene fractions were separated by preparative gas chromatography and identified by IR and NMR spectroscopy. The product distribution was as follows (wt %, based on sec-butylbenzene starting material): benzene (12%); sec-butylbenzene (28%); IR [illegible]; NMR (CCl$_4$, δ, ppm) 0.80 (t, 3H, J=7 Hz, γ-CH$_3$), 1.20 (d, 3H, J=7 Hz, β'-CH$_3$), 1.55 (quintet, 2H, J=7 Hz, β-CH$_2$), 2.53 (sextet, 1H, α-CH), and 7.13 (s, 5H, aromatic); m- and p-di-sec-butylbenzene (11%); IR [illegible] and [illegible] (strong); NMR (CCl$_4$, δ, ppm) 0.82 (t, 6H, J=7 Hz, γ-CH$_3$'s), 1.22 (d, 6H, J=7 Hz, β'-CH$_3$'s), 1.56 (quintet, 4H, J=7 Hz, β-CH$_2$'s), 2.56 (sextet, 2H, J=7 Hz, α-CH's), and 6.75–7.13 (m, 4H, aromatic); and 1,3,5-tri-sec-butylbenzene (21%); NMR (CCl$_4$, δ, ppm) 0.81 (t, 9H, J=7 Hz, γ-CH$_3$'s), 1.22 (d, 9H, J=7 Hz, β'-CH$_3$'s), 1.52 (quintet, 6H, J=7 Hz, β-CH$_2$'s), 2.53 (sextet, 3H, J=7 Hz, α-CH's), and 6.70 (s, 3H, aromatic).

B. Reaction at 25°

The reaction of trifluoromethanesulfonic acid (6.28 g, 0.0418 mol) and sec-butylbenzene (5.64 g, 0.0421 mol) was carried out as before except that the reactants were stirred at 25° for 1 hr. The reaction mixture was worked up as before and distilled to give the following fractions: (1) bp 82–86°, 0.74 g; (2) bp 170–178°, 3.5 g; (3) bp 178–220°, 0.34 g; (4) residue 0.28 g.

Analysis of the distilled fractions as before showed the following product distribution: benzene (10%); sec-butylbenzene and isobutylbenzene (35%), in the ratio 70:30, respectively (IR 13.1μ for sec-butylbenzene and 13.5μ for isobutylbenzene); m- and p-dibutylbenzenes (40%); and 1,3,5-tributylbenzenes (5%). The NMR spectra of the butyl-, dibutyl-, and tributylbenzene fractions were very similar to those of the corresponding products from the reaction at 0°, but evidence of the presence of isobutyl as well as sec-butyl groups could be seen; the doublet for the six hydrogens on the γ-carbons at 0.88 (J=7 Hz) and the doublet for the two hydrogens on the α-carbon at 2.42 (J=7 Hz) of isobutylbenzene were detectable in all these spectra.

C. Reaction at 50°

The reaction of trifluoromethanesulfonic acid (7.51 g, 0.0500 mol) and sec-butylbenzene (6.7 g, 0.050 mol) was carried out as before at 50° for 1 hr. The reaction mixture was worked up as before and distilled to give the following fractions: (1) bp 79–82°, [illegible] g; (2) bp 167–172°, 1.4 g; (3) bp 174–225°, 2.9 g; (4) residue 1.1 g.

Analysis of the distilled fractions as before showed the following product distribution: benzene (9%); sec-butylbenzene and isobutylbenzene (26%), in the ratio 38:62, respectively (IR 13.1μ and 13.35μ); m- and p-dibutylbenzenes (11%); and 1,3,5-tributylbenzenes (6%). The NMR spectra of the products were similar to those from the reactions at 0° and 25°, but with increased doublet signals from the isobutyl isomers.

REFERENCES AND NOTES

[1] (a) Paper 25 in the New Friedel-Crafts Chemistry series. Paper 24: R. M. Roberts, H. H. Chen, and K. [illegible], J. Org. Chem., 42, 3677 (1977). (b) Generous support of this research by the Robert A. Welch Foundation is gratefully acknowledged.

[2] C. D. Nenitzescu, I. Necsoiu, A. Glatz, and M. Zalman, Chem. Ber., 92, 10 (1959).

[3] R. M. Roberts, Y. W. Han, C. H. Schmid, and D. A. Davis, J. Amer. Chem. Soc., 81, 640 (1959).

[4] (a) R. M. Roberts, Intra-Science Chem. Rept., 6, [illegible] (1972); (b) R. M. Roberts, A. A. Khalaf, and R. N. Greene, J. Amer. Chem. Soc., 86, 2846 (1964).

[5] R. M. Roberts, G. P. Anderson, Jr., and N. L. Doss, J. Org. Chem., 33, 1789 (1968).

[6] R. M. Roberts, H. H. Chen, and K. [illegible], ibid., 43, 2077 (1978).

[7] The qualitative and quantitative analysis of mixtures of sec-butylbenzene and isobutylbenzene by IR spectroscopy is described in ref. 5.

[8] (a) D. M. Brouwer, Rec. Trav. chim., 87, 210 (1968); (b) D. M. Brouwer and J. M. Oelderik, ibid., 87, 721 (1968).

Revue Roumaine de Chimie, **25**, *5*, 691–695 (1980)

OXIDATION OF SOME METHOXY-PHENOTHIAZINES BY POTASSIUM DICHROMATE IN GLACIAL ACETIC ACID

TEODORA PANEA and MONICA MOLDOVAN
Institute of Chemistry, str. Donath 65–103
3400 Cluj-Napoca, Romania

Received March: 7 1978

2-Methoxy-10*H*-phenothiazine, I and 2,7-dimethoxy-10*H*-phenothiazine V are oxidized by potassium dichromate in glacial acetic acid to the corresponding 3*H*-phenothiazin-3-ones II and VI respectively. 2,3-Dimethoxy-phenothiazine yields, on oxidation by potassium dichromate in glacial acetic acid, the 3*H*-phenothiazin-3-one II, thus eliminating the 3-methoxy substituent. 2,7-Dimethoxy-3*H*-phenothiazin-3-one was reduced to 2,7-dimethoxy-3-hydroxy-10*H*-phenothiazine, VII, which was methylated to 2, 3, 7-trimethoxy-10 *H*-phenothiazine, VIII. Compounds VII and VIII are new.

INTRODUCTION

It was found [1] that several phenothiazine derivatives having methoxy substituents possess interesting physiological properties. This finding determined us to investigate the oxidation of methoxy phenothiazines by potassium dichromate in acetic acid as a starting step in introducing new methoxy substituents. The following two reaction sequences were achieved as in scheme 1.

EXPERIMENTAL

2-Methoxy-3*H*-phenothiazin-3-one (II)

To 2 g of 2-methoxy-10*H*-phenothiazine (I) in 150 ml of boiling glacial acetic acid, 4 g of potassium dichromate were added and the mixture heated to reflux for 10 minutes. The resulting red solution was poured into 500 ml of water. After cooling, the precipitate was filtered, washed with cold water and dried to yield 1.7 g of crude product. This was dissolved in toluene and passed through a column packed with silica gel. After evaporation of the solvent, 1.11 g (52.4 %) of pure II were obtained as golden-red crystals m. p. 199–200° (lit [2]. m. p. 199–200°). The compound showed the C=O stretching vibration (IR – in KBr pellet) at 1625 cm^{-1}. (Found : C, 64.02 ; H, 3.54 ; $C_{13}H_9NO_2S$ requires ; C, 64.17 ; H, 3.73 %).

2-Methoxy-3-hydroxy-10*H*-phenothiazine (III)

To 1 g of II in 100 ml of boiling glacial acetic acid small amounts of Zn powder were added until the solution became colourless (about 2 g of Zn were needed). Thereafter small por-

tions of water were added to the boiling solution, until it remained clear, and the hot mixture was filtered. On cooling, the hydroxycompound III precipitated. It was filtered, washed with cold water and dried, yield 82 % of a product with m. p. 242 – 3°, identical with that reported in the literature [2] for a product obtained by reduction with ascorbic acid in methanol. (Found : N, 5. 64 ; $C_{13}H_{11}NO_2S$ requires ; N, 5.71 %).

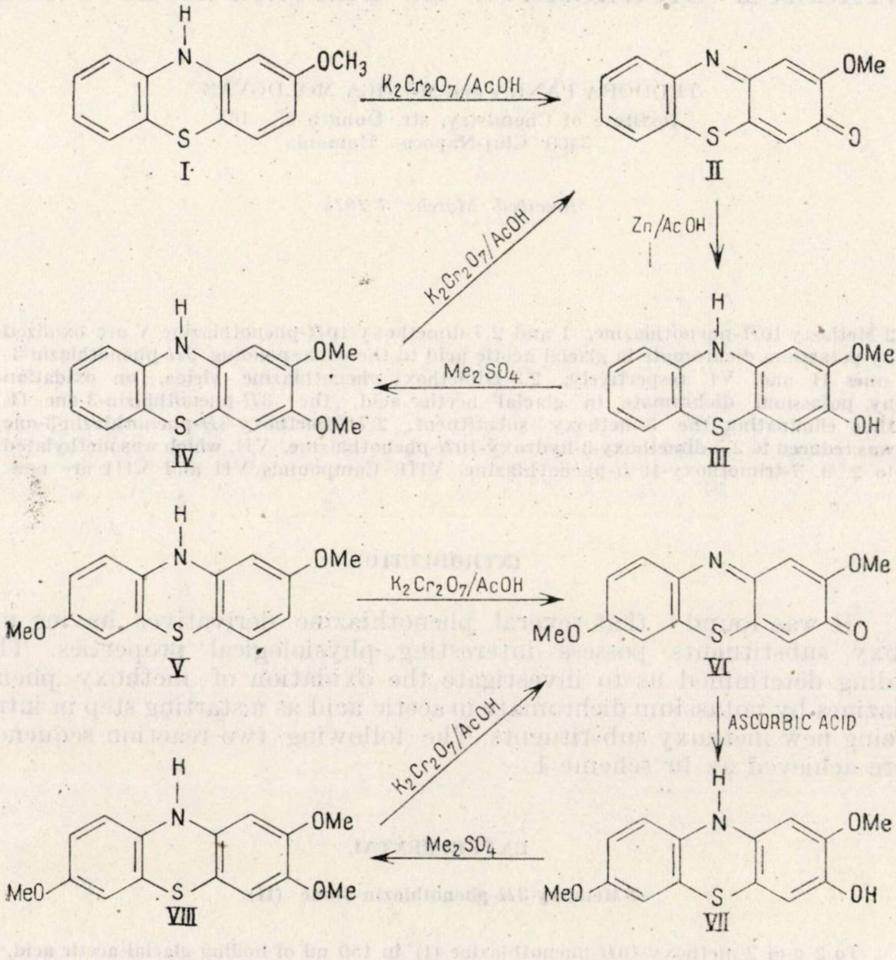
H
N
OCH3
S
I
K2Cr2O7/AcOH
N
OMe
S
O
II
Zn/AcOH
K2Cr2O7/AcOH
H
N
OMe
S
OMe
IV
Me2SO4
H
N
OMe
S
OH
III
H
N
OMe
MeO
S
V
K2Cr2O7/AcOH
N
OMe
MeO
S
O
VI
ASCORBIC ACID
K2Cr2O7/AcOH
H
N
OMe
MeO
S
OMe
VIII
Me2SO4
H
N
OMe
MeO
S
OH
VII

Scheme 1

2,3-Dimethoxy-10*H*-phenothiazine (IV)

0.5 ml of dimethylsulphate were dropped under vigorous stirring into a mixture consisting of 1 g of compound III, 40 ml acetone, 1 ml of 10 % aqueous sodium hydroxide. After 20 min stirring at room temperature the reaction mixture was poured into water. The product IV which precipitated was filtered, washed with diluted sodium hydroxide, water and dried.

m.p. = 176 – 178° (lit. [3] m.p. = 176°).

I. G. P.

Oxidation of 2,3-dimethoxy-10*H*-phenothiazine

To a boiling solution of 0.5 g of IV in 50 ml glacial acetic acid 1 g of potassium dichromate was added and the mixture refluxed for 10 minutes. It was then poured into 500 ml of water, the precipitate filtered, washed with cold water and dried. An 80% yield of the phenothiazin-3-one II (identity based on m. p., I. R., UV–VIS spectra and TLC) was thus obtained.

2,7-Dimethoxy-3*H*-phenothiazin-3-one (VI)

To a boiling solution of 1 g of V in 50 ml of glacial acetic acid 3 g of potassium dichromate were added. After further 30 s of heating the mixture was poured into water, the product filtered off, washed with water and dried. A 72% yield of VI resulted after recrystallization from toluene – ethyl acetate (1 : 1). For analyses, this product was dissolved again in toluene-ethyl acetate (1 : 1) and passed through a silica gel – packed column. Pure VI obtained this way melted at 280°, showed major IR absorption peaks at 1255 (OCH_3), 1619 (C=O str), 2845 (sym. CH str.) and 2960 cm^{-1} (asym. CH str.). (Found : C, 61.50 ; H, 4.00 ; N, 5.01 ; $C_{14}H_{11}NO_3S$ requires : C,61.54 ; H, 4.03 ; N,5.13 %).

2,7-Dimethoxy-3-hydroxy-10*H*-phenothiazine (VII)

To a boiling solution of 0.2 g VI in 15 ml ethyl alcohol 0.4 g of ascorbic acid were added. Refluxation was continued for 10 minutes, during which time the reduction was complete, as marked by a change in colour of the reaction mixture from orange-red to pale yellow. Compound VII precipitated on pouring into water ; 0.18 g of product were obtained, m. p. 290°. The surface of the crystals gradually darkened under exposure to the air. (Found : C, 61.22 ; H, 4.82 ; N, 5.02 ; $C_{14}H_{13}NO_3S$ requires : C,61.09 ; H, 4.73 ; N, 5.09 %).

2,3,7-Trimethoxy-10*H*-phenothiazine (VIII)

0.3 ml of dimethylsulphate were dropped into a mixture consisting of 0.12 g of VII, 0.3 ml of 10% aqueous sodium hydroxide and 4 ml or acetone. After 40 min. stirring at room temperature the reaction mixture was poured into water, cooled, the product filtered, washed with water and dried, obtaining 0.08 g of VIII. m.p. 143°. (Found : C,62.00 ; H, 5.09 ; N, 4.70 ; $C_{15}H_{15}NO_3S$ requires : C,62.28 ; H, 5.19 ; N, 4.84 %).

Melting points were determined in capillaries and are uncorrected. IR-Spectra were recorded in a Carl Zeiss Jena UR–10 instrument. ^1H–NMR–Spectra were obtained on a Bruker WP–60 FT–NMR spectrometer operating at 60 MHz ; the samples were dissolved in DMSO-d_6, using 4,4′-dimethyl-4-silapentane-sulfonate as internal reference.

RESULTS AND DISCUSSION

A convenient synthesis of 2-methoxy-10*H*-phenothiazine, I was previously reported by us [4]. The oxidation of this compound by potassium dichromate in glacial acetic acid seemed to us an appropiate starting step to polymethoxy-phenothiazines. Oxidation of compounds I by an analogous reactant was reported [2], but the exact structure of the reaction product was not unambigously established. Oxidation of I by potassium dichromate in glacial acetic acid yielded the quinone II, the structure of which was ascertained by the following reactions : II was reduced by zinc in acetic acid to a hydroxy compound III, identical with that obtained by the Japanese authors [2]. This hydroxy derivative was methylated by a known method [5], yielding 2,3-dimethoxy-10*H*-phenothiazine, IV, identical with an authentic sample prepared[6] by ring closure (identity based on m. p., IR spectra and TLC). Thus, we may conclude that quinone II is 2-methoxy-3*H*-phenothiazin-3-one and the hydroxy derivative III is 2-methoxy-3-hydroxy-10*H*-phenothiazine. It is most interesting that oxidation of 2,3-dimethoxy-10*H*-phenothiazine, IV with potassium dichromate in glacial acetic acid yields the same 2-methoxy-3*H*-phenothiazin-3-one, II as does 2-methoxy-10*H*-phenothiazine, I, by eliminating the 3-methoxy substituent.

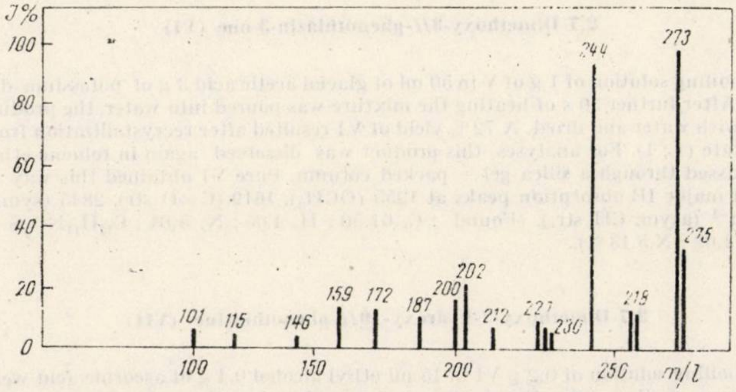

Fig. 1. — Mass spectrum of the 2,7-dimethoxy-3*H*-phenothiazin-3-one.

2,7-Dimethoxy-10*H*-phenothiazine V, synthesized by us[7] in a more convenient way than earlier methods described in the literature[3], yielded, on oxidation with potassium dichromate in glacial acetic acid, a quinone, VI. Its quinonic nature is proved by the absence of the NH stretching vibration and appearance of a strong C=O streatching band in its IR-spectrum compared to that given by compound V. Its mass spectrum (Fig. 1) shows the expected molecular ion at $m/e = 273$ and an observable $M+2$ peak due to the corresponding hydroquinone formed by reaction with the traces of water present in the spectrometer [8]. Its ^{1}H-NMR-spectrum with DSS as internal reference strongly supports the proposed structure VI, the protons in positions 6,8 and 9 afforded an ABX multiplet with the following parameters:

$\delta_{H_6} = 6.98$ ppm $\qquad J_{6-8} = 2.80$ Hz

$\delta_{H_8} = 7.10 \qquad J_{6-9} = 0.24$

$\delta_{H_9} = 7.84 \qquad J_{8-9} = 8.76$

The simulated spectrum based on this parameters had its lines $+0.22$ to -0.37 Hz in error with respect to the experimental peaks; the mean absolute error was 0.16 Hz. Protons 1 and 4 appeared as singlets at 6.78 and 6.84 ppm.

Reduction of quinone VI with ascorbic acid afforded 2,7-dimethoxy-3-hydroxy-10*H*-phenothiazine, VII, which upon methylation with dimethylsulphate yielded 2,3,7-trimethoxy-10*H*phenothiazine, VIII; none of these latter two compounds was previously reported in the literature. The obtention of VII and VIII is a further structure proof for VI; would the starting 2,7-dimethoxy-10*H*-phenothiazine, V, undergo oxidation by potassium dichromate in glacial acetic acid, at position 7, the above reaction sequence would yield compound V again.

From the data presented we may thus conclude that a methoxy substituent in position 2 of the 10*H*-phenothiazine skeleton strongly directs oxidation towards the vicinal position 3 instead of another possibility to form a p-quinonic system by oxidation at position 7. The oxidation takes place at position 3, when both positions 3 and 7 are free (compound I) or one of them is substituted by a further methoxy group (compounds IV and V). In fact, oxidation at the methoxy-substituted 3-position seems energetically preferred against the free position 7, even in the absence of the methoxy group in position 2; 3-methoxy-10*H*-phenothiazine affords [9] upon oxidation 3*H*-phenothiazin-3-one.

REFERENCES

[1] I. Ghizdavu, *Ph. D. Thesis*, Institute of Agronomy, Cluj-Napoca, Romania, 1974.

[2] S. Fujisawa and M. Kawamura, *Yakugaku Zasshi*, **86**, 541 (1966); *Chem. Abstr.* **65**, 15373 (1966).

[3] J. Schmitt, *Fr. Pat.* 1.173.121, 20 febr. 1959; *Chem. Abstr.*, **56**, 479 (1962).

[4] T. Panea, E. Broser and I. Oprean, *Claim pat. R.S.R.* No. 73727, 3 Febr. 1973.

[5] T. Panea, *Claim pat R.S.R.* No. 87010, 17 July 1976.

[6] L. Toldy, I. Tóth, M. Fekete and J. Borsy, *Acta Chim. Acad. Sci. Hung.*, **44**, 310 (1965).

[7] T. Panea, *Claim pat. R.S.R*, No. 86442, 12 June 1976.

[8] R. W. A. Oliver and R. M. Rashman, *J. Chem. Soc. B.*, **1968**, 1141.

[9] C. Bodea and M. Răileanu, *Studii și Cercetări Chim., Acad. R. S. România, Filiala Cluj*, **11**, 325 (1960); *Chem. Abstr.*, **58**, 3420 (1963).

Revue Roumaine de Chimie, 25, 5, 697–700 (1980)

SYNTHESIS OF SOME NEW POLYHALOGENATED HYDROXY-PHENOTHIAZINES AND THEIR ALKYL AND ACYL DERIVATIVES

R. K. JAIN and R. L. MITAL
Chemical Laboratories, University of Rajasthan,
Jaipur–302004, India

Received October 4, 1978

1,2,4-Trihalo-3-hydroxy-7-methyl-phenothiazines have been synthesized by condensation of zinc salt of 2-amino-5-methylbenzenethiole with chloranil or bromanil in acetone alcohol mixture and followed by reduction with sodium dithionite. Their various acylated and alkylated derivatives have been synthesized.

The wide-spread use [1–3] of phenothiazine tranquilizers has given rise to extensive investigation into synthesis of various derivatives of some polyhalogenated hydroxy-phenothiazines. Recently, Terdic and coworkers [4] have synthesized some disubstituted phenothiazine-3 ones. Synthesis of the substituted hydroxy phenothiazines [5] was initiated by condensation of zinc salt of 2-amino-5-methylbenzenethiole [6] with chloranil and bromanil [7] and followed by reduction with sodium dithionite to give 1,2,4-trichloro-3-hydroxy-7-methyl-phenothiazine [8] (I) and 1,2,4-tribromo-3-hydroxy-7 methyl-phenothiazine [8] (II).

Reaction of I and II with dimethylsulphate in refluxing acetone alcoholic potassium hydroxide solution gave 1,2,4-trihalo-3-methoxy-7-methyl-phenothiazines. Isopropyl derivatives of I and II were prepared by reaction with 2-bromopropane in acetone alcoholic potassium hydroxide solution, while the benzoylation product was obtained by reaction with benzoyl chloride in alcoholic 10% potassium hydroxide solution. Acetylation of I and II with zinc dust, acetic anhydride and pyridine medium at ambient temperature gave monoacetyl derivatives while with excess of zinc dust and refluxing for 2 hours gave diacetyl derivatives. I and II when reacted with benzylbromide in acetone and potassium carbonate (anhyd.), gave 1,2,4-trihalo-3-benzyl-7-methyl-phenothiazines.

EXPERIMENTAL *

Starting compounds

1, 2, 4-Trihalo-7-methyl-phenothiazine-3-ones. A mixture of chloranil or bromanil (0.01 mole) and zinc salt of 2-amino-5-methyl-benzene-thiol (0.005 mole) in dry ethanol (100 ml) was stirred well and heated under reflux for 3 hours. The dark red solid obtained was filtered off, washed with water, dried and crystallized from benzene to give 1,2,4-trichloro-7-methyl-phenothiazin-3-one m.p. 188° and 1,2,4-tribromo-7-methylphenothiazin-3-one m. p. 215°.

---

* All m. ps. are uncorrected.

1,2,4-Trihalo-3-hydroxy-7-methyl-phenothiazines. A mixture of 1 g of 1,2,4-trihalo-7--methyl-phenothiazine-3-one 1.5 g of sodiumdithionite, 5 ml of water and 50 ml of acetone and abs. alcohol mixture (1 :1) was heated under reflux for 2 hours and then poured into 500 ml of cold water containing 1 g sodiumdithionite. The resulting yellow solid was washed with water, dried in vacuum at 100° and crystallized from toluene to give I and II.

(I) 1,2,4-Trichloro-3-hydroxy-7-methyl-phenothiazine m. p. 140°, yield 85 %, Anal. $C_{13}H_8Cl_3NOS$ calcd. N : 4.22 %, Found N : 4.19 %.

(II) 1,2,4-Tribromo-3-hydroxy-7-methyl-phenothiazine m. p. 115°, yield 80 %, Anal. $C_{13}H_8Br_3NOS$ Calcd. N : 3.00 %, Found N : 2.99 %.

Alkyl and acyl derivatives

(III) *1,2,4-Trichloro-3-methoxy-7-methyl-phenothiazine (Scheme 2, when X = Cl)* :

To a mixture of 0.01 mole of 1,2,4-trichloro-3-hydroxy-7-methyl-phenothiazine 110 ml of 10 % ethanolic potassium hydroxide and acetone (1 : 1), 1.764 g (0.014 mole) of dimethylsulphate was added. The reaction mixture was refluxed for 5 hours and then the yellow suspension was poured into 1 litre cold water. The pale brown solid was filtered, dried in vacuo and crystallized from benzene. M.p. 118°, yield 60 %, Anal. $C_{14}H_{10}Cl_3NOS$; Calcd : N :4.04 % ; Found N : 4.00 %

(IV) *1, 2,4-Trichloro-3-isopropoxy-7-methyl-phenothiazine (Scheme 3 —when X = Cl)* was prepared by refluxing a mixture of 0.01 mole of 1,2,4-trichloro-3-hydroxy-7-methyl-phenothiazine, 0.5 g of sodium dithionite, 110 ml of 10 % ethanolic potassium hydroxide and acetone (1 : 1), to which 0.014 mole of 2-bromopropane was added. The pale yellow suspension was poured into 1 litre cold water. The brown solid was filtered, dried in vacuo and crystallized from benzene.

M. P. 129°, yield 65 %, Anal. $C_{12}H_{14}Cl_3NOS$;

Calcd : N 3.7 % ; Found : N 3.8 %.

(V) *1,2,4-Trichloro-3-acetoxy-7-methyl-phenothiazine (Scheme 4 — when X = Cl)* : 0.0038 mole of 1.2.4-trichloro-7-methyl-phenothiazine-3-one, 20 ml, acetic anhydride and 1 ml pyridine were shaken with 1 g zinc dust at room temperature for 30 minutes and then heated at 100° for 3 minutes. The pale yellow solution separated by decantation was poured into ice, the yellow solid crystallized from chloroform and recrystallized from benzene gave pale yellow crystals.

M.P. 172°, Yield 72 %, Anal. $C_{14}H_{10}Cl_3NO_2S$;

Calcd : N 3.7 % ; Found : N 3.5 %.

(VI) *1, 2,4-Trichloro-3-benzoyloxy-7-methyl-phenothiazine (Scheme 5—when X = Cl)* — was prepared from a mixture of 0.01 mole of 1,2,4-trichloro-3-hydroxy-7-methyl-phenothiazine, 0.5 g of sodium dithionite and 110 ml of 10 % ethanolic potassium hydroxide to which 0.014 mole of benzoyl chloride was added. The reaction mixture was refluxed for 4 hours, poured into cold water ; after filtration and crystallization red-brown needles were obtained.

M.P. 165°, Yield 62 %, Anal : : $C_{20}H_{12}Cl_3NO_2S$;

Calcd : N 3.2 % ; Found : N 3.1 %.

(VII) *1,2,4-Trichloro-3-acetoxy-10-acetyl-7-methyl-phenothiazine (Scheme 6 — when X = Cl)* was prepared when a mixture of (0.0038 mole) of 1,2,4-trichloro-7-metyl phenothiazine-3-one (20 ml) acetic anhydride and (1 ml) pyridine was shaken with excess of zinc dust for 45 minutes then refluxed for 2 hours. The pale-yellow solution was separated from excess zinc by decantation and then poured into ice-cold water. The yellow solid was dissolved in chloroform and the evaporation of the solvent gave yellow crystals.

M.P. 192° ; Yield 70 % ; Anal. $C_{17}H_{12}Cl_3NO_3S$;

Calcd ; N. 3.3 % ; Found : N 3.1 %.

(VIII) *1,2,4-Trichloro-3-benzyloxy-7-methyl-phenothiazine (Scheme 7—when X = Cl).* A mixture of 0.01 mole of 1,2,4-trichloro-3-hydroxy-7-methyl-phenothiazine, 0.013 mole of benzyl-bromide and 0.05 mole of potassium carbonate in 35 ml of acetone was refluxed for 6 hours. The reaction mixture was poured into ice cold water and filtered; the crystallization from benzene provided brown needles.

M.P. 300°; Yield 51 %; Anal: $C_{20}H_{14}Cl_3NOS$;
Calcd: N 3.3 %; Found: N 3.0 %.

(IX) *1,2,4-Tribromo-3-methoxy-7-methyl-phenothiazine* (*Scheme 2 — when X = Br*) was prepared similarly to (III) taking 1,2,4-tribromo-3-hydroxy-7-methyl-phenothiazine as the starting compound.

M.P. 118°; Yield 62 %; Anal: $C_{14}H_{10}Br_3NOS$;
Calcd.: N 2.90; Found: N 2.88 %.

(X) *1,2,4-Tribromo-3-isopropoxy-7-methyl-phenothiazine* (*Scheme 3 — when X = Br*) was prepared similarly to (IV) from 1,2,4-tribromo-3-hydroxy-7-methyl-phenothiazine.

M.P. 148°; Yield 60 %; Anal. $C_{16}H_{14}Br_3NOS$;
Calcd.: N 2.81 %; Found: N 2.80 %.

(XI) *1,2,4-Tribromo-3-acetoxy-7-methyl-phenothiazine* (*Scheme 4 — when X = Br*) was prepared similarly to (V) from 1,2,4-tribromo-7-methyl-phenothiazine-3-one.

M.P. 106°; Yield 73 %; Anal: $C_{15}H_{10}Br_3NO_2S$;
Calcd.: N 2.75 %; Found: N 2.73 %.

(XII) *1,2,4-Tribromo-3-benzoyloxy-7-methyl-phenothiazine* (*Scheme 5 — when X = Br*)] was prepared similarly to (VI) from 1,2,4-tribromo-3-hydroxy-7-methyl-phenothiazine.

M.P. 165°; Yield 61 %; Anal: $C_{20}H_{12}Br_3NO_2S$;
Calcd.: N. 2.45 %; Found: N 2.46 %.

SCHEME I

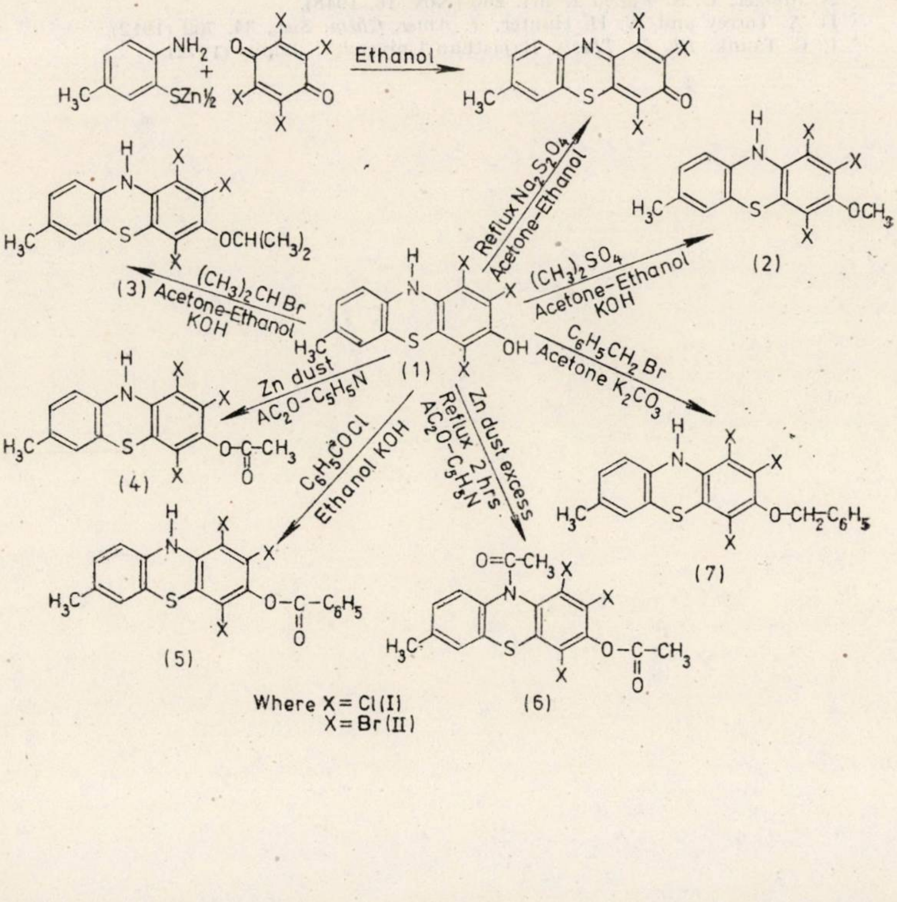
Ethanol
Reflux $Na_2S_2O_4$ Acetone-Ethanol
$(CH_3)_2SO_4$ Acetone-Ethanol KOH
$(CH_3)_2CHBr$ Acetone-Ethanol KOH
Zn dust $AC_2O-C_5H_5N$
$C_6H_5CH_2Br$ Acetone K_2CO_3
C_6H_5COCl Ethanol KOH
Reflux 2 hrs $AC_2O-C_5H_5N$ Zn dust excess
(1)
(2)
(3)
(4)
(5)
(6)
(7)
Where X = Cl(I)
X = Br(II)

(XIII) *1,2,4-Tribromo-3-acetoxy-10-acetyl-7-methyl-phenothiazine* (*Scheme 6 when X = Br*) was prepared similarly to (VII) by taking 1,2,4-tribromo-7-methyl-phenothiazine-3-one as a starting compound.

M.P. 128° ; Yield 75 % ; Anal. : $C_{17}H_{12}Br_3NO_3S$;
Calcd. : N 2.54 % ; Found : N 2.52 %.

(XIV) *1, 2,4-Tribromo-3-benzyloxy-7-methyl-phenothiazine* (*Scheme 7—when X = Br*) was prepared by taking 1,2,4-tribromo-3-hydroxy-7-methyl-phenothiazine as a starting compound and similarly to (VIII).

M.P. 130° : Yield 50 % ; Anal. : $C_{20}H_{14}Br_3NOS$,
Calcd : N 2.50 % ; Found : N 2.49 %.

All the experiments were carried out in nitrogen atmosphere.

ACKNOWLEDGEMENT. Grateful thanks to the University Grants Commission, New Delhi, India for awarding Teacher Fellowship (R.K.J.).

REFERENCES

[1] H. Goldenberg and V. Fishman, *Proc. Soc. Exptl. Biol. Med.*, **108**, 178 (1961).

[2] E. A. Nodiff, A. Saggiomo, M. Shinbo, E. Chen, H. Otomasu, Y. Kondo, T. Kikuchi, B. Verma, S. Matsuura, K. Tanabe, M. Tyagi and S. Morosawa ; *J. Medicinal Chem.*, **15**, 775 (1972).

[3] A. Moggi, *Igiene Sanita Publica* (*Rome*), **22**, 52 (1966) ; *Chem. Abstr.*, **65**, 7803 (1966).

[4] M. Terdic and I. Valter, *Liebigs Ann. Chem.*, **8**, 1285 (1978).

[5] E. A. Nodiff and M. Hausman, *J. Org. Chem.*, **31**, 625 (1966).

[6] N. Steiger, *U. S. Patent* 2, 454, 260 (Nov. 16, 1948).

[7] H. A. Torrey and W. H. Hunter, *J. Amer. Chem. Soc.*, **34**, 702 (1912).

[8] P. C. Taunk, *Ph. D. Thesis*, Rajasthan University, Jaipur (1972).

Revue Roumaine de Chimie, 25, 5, 701–711 (1980)

POTENTIAL ANTICANCER AGENTS. XXI.*

SYNTHESIS AND BIOLOGICAL EVALUATION OF SOME NEW TRIAZENE DERIVATIVES

FELICIA CORNEA**, D. IONESCU***, MARIANA ZGLOBIU, GEORGETA BOTEZ,
V. DOBRE and I. NICULESCU-DUVAZ

** Department of Organic Chemistry, The Polytechnic Institute, Bucharest, Romania
*** Oncological Institute, Bucharest, Bd. 1 May, 11 Romania

Received July 2, 1979

Thirty seven new triazenes (29 derived from 4-methyl-3-aminobenzoic acid esters and amides and 8 derived from dipeptides) were synthesized and studied. The analytical and the spectral data obtained are in good agreement with the proposed structures. Only one compound, namely *p*-(3′, 3′-dimethyl) triazenophenyl-N[α-(9-fluorenyl) acetyl]-L-alanine, ethyl-ester) exhibited a 35 % (ILS) activity against L1210 leukemia. Some compounds are moderatly active against W256 carcinosarcoma.

INTRODUCTION

The discovery of the clinical activity of 3,3,-dimethyltriazeno-4(5) imidazolyl-5(4)-carboxamide 1 (NSC 45388, DTIC etc.)[1,2] against malignant melanoma (an average of partial and complete responses of 24% in a set of 851 patients[3]) opened a new era in the triazenes study.[4–10] It was also demonstrated recently that even better results could be obtained, in this form of neoplasia using BCNU, DTIC and immunotherapy.[11]

The interest for the triazene class has recently been renewed by the observation that some of such derivatives are able to reduce, by an unknown mechanism, the number of the metastasis induced by the Lewis lung tumors in mice.[12]

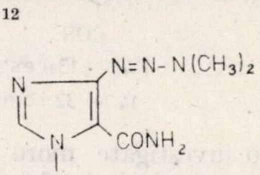

(1)

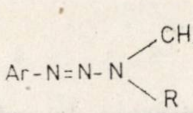

(2)

From the empiric or quantitative structure—activity correlations[12–17] which were established on a large number of triazene derivatives, the following general conclusions — not always quite concordant — could be drawn :

— the volume of R-group (general formula 2) seems to be of the main importance for the antitumoral activity. When R is a bulky group

---

[*] Preceding part, I. Niculescu-Duvăz, G. Stihi, T. Crăescu and Z. Simon, *Neoplasma*, in press.

(i.e. — *t*-butyl) all activity is lost. [15] The previous assumption that N-CH_3 group is essential for the activity was not substantiated;

— there is no special potency associated with the nature of the aromatic (heterocyclic) ring. [13, 16, 17] Electron releasing substituents acting *via* resonance effect increase the potency. [15] In this sense some favourable action of *para*-$COCH_3$ and $-CONH_2$ groups was noticed. [8] This statement is however in contrast with the findings of Connors and al., [13] who suggest that the electron releasing or withdrawing character of the substituents is of little importance for the efficiency of triazenes against TLX5 lymphoma. No positive *ortho*-effects were observed; [16–17]

— ideal lypophylicity for triazenes active against L 1210 leukemia seems to be around 1.0. [15] The value needed for activity against solid tumors is much higher [14, 16];

— according to Hansch [17] no really better compounds could be obtained in this class because no way seems to exist to dissociate the toxicity from the activity.

In order to clear up some of the before mentioned confusions and also to obtain new triazenes, the following sets of congeners were synthesized and studied:

1. derivatives of the 4-methyl-3-aminobenzoic acid. This structure proved to be an excelent carrier of the cytotoxic nitrogen mustard moiety in the case of 3,N,N-bis(2-chloroethyl)amino-4-methyl benzoic acid **3** (NSC 146.171, IOB-82) [18] of clinical use in our country. In order to asses if this property could be extended to the triazene moiety, new derivatives were prepared starting from this structure. In all compounds $\Sigma\sigma_i$ was kept constant.

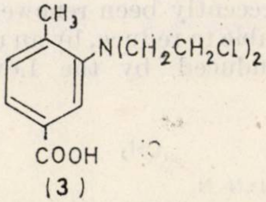

(3)

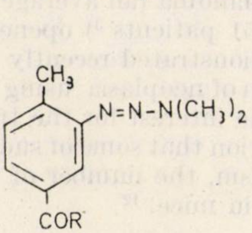

(4)-(13) esters
(14)-(32) amides

2. peptidic triazenes. In order to investigate more specific carriers for the triazene moiety some new compounds derived from peptides were prepared. Mention should be made that one of the starting peptides exhibited itself antitumor activity. [19]

RESULTS AND DISCUSSION

1. Synthesis

Two series of triazenes **4**—**13** and **14**—**32** (with $\Sigma\,\sigma_i \simeq$ ct.) were synthesized by conventional procedures starting from 3-amino-4-methylbenzoic esters and amides. The analytical data of the new compounds are given in tables 1 and 2.

TABLE 1

Analytical data of the new triazenes derived from 3-amino-4-methylbenzoic esters

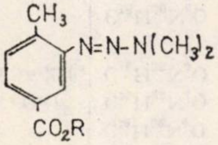

No.	R	m.p. (°C)[a]	Recrystallized from	Formula	Analytical data (%)						Yield %
					Calculated			Found			
					C	H	N	C	H	N	
4	H	132–134 (dec)	AcOEt : petrol ether	$C_{10}H_{13}N_3O_2$	57.97	6.28	20.29	58.39	6.48	20.12	85.0
5	CH_3	58–59	petrol. ether [b]	$C_{11}H_{15}N_3O_2$	59.72	6.78	19.00	59.50	7.05	19.15	84.0
6	C_2H_5	oil	distillation	$C_{12}H_{17}N_3O_2$	61.28	7.23	17.87	61.32	7.70	17.64	87.5
7	*n*-C_3H_7	oil	distillation b.p. 12 mmHg = 205–207	$C_{13}H_{1}\ N_3O_2$	62.65	7.63	16.87	62.83	7.53	17.12	82.4
8	*iso*-C_3H_7	38–39	distillation b.p. 8 mmHg = 188°	$C_{13}H_{19}N_3O_2$	62.65	7.63	16.87	63.11	7.93	17.07	86.2
9	*n*-C_4H_9	42–43	distillation	$C_{14}H_{21}N_3O_2$	63.88	7.98	15.96	64.49	8.34	16.07	84.2
10	*iso*-C_4H_7	33–34	distillation b.p. 12 mmHg = 207°	$C_{14}H_{21}N_3O_2$	63.88	7.98	15.96	64.02	8.07	15.96	70.6
11	*n*-C_5H_{11}	oil	distillation b.p. 14 mmHg = 224–227°	$C_{15}H_{23}N_3O_2$	64.98	8.30	15.16	65.10	8.72	15.10	75.3
12	*iso*-C_5H_{11}	oil	distillation b.p. 18 mmHg = 225°	$C_{15}H_{23}N_3O_2$	64.98	8.30	15.16	63.64	8.67	15.00	89.2
13	C_6H_5	102–104	petrol. ether	$C_{16}H_{23}N_3O_2$	67.85	6.00	14.84	68.18	6.42	14.90	78.0

[a] Uncorrected; [b] b·p·60 – 90°.

TABLE 2

Analytical data of the new triazenes derived from3-amino-4-methyl-benzoic amides

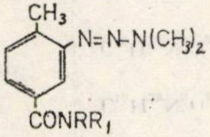

No.	R	R1	m.p. (°C)[a]	Recrystallized from	Formula	Analytical data (%)						Yield %
						Calculated			Found			
						C	H	N	C	H	N	
14	H	H	155–157	—	$C_{10}H_{14}N_4O$	58.25	6.79	27.18	58.75	7.10	29.97	92.2
15	CH_3	H	163–167	AcOEt : petrol. ether [b]	$C_{11}H_{16}N_4O$	60.00	7.27	25.45	60.38	7.49	25.21	80.3
16	C_2H_5	H	90.5–91	AcOEt : petrol. ether [b]	$C_{12}H_{18}N_4O$	61.54	7.69	23.93	61.62	7.94	23.62	76.3
17	n-C_3H_7	H	91–92	AcOEt : petrol. ether [b]	$C_{13}H_{20}N_4O$	62.90	8.07	22.58	62.88	8.34	22.45	77.6
18	i-C_3H_7	H	134–134.5	Me_2CO : petrol. ether [b]	$C_{13}H_{20}N_4O$	62.90	8.07	22.58	63.04	8.51	22.31	63.1
19	n-C_4H_9	H	58–60	AcOEt : petrol. ether [b]	$C_{14}H_{22}N_4O$	64.12	8.40	21.37	64.57	8.79	21.69	78.6
20	i-C_4H_9	H	83–85	AcOEt : petrol. ether [b]	$C_{14}H_{22}N_4O$	64.12	8.40	21.37	64.00	8.84	21.33	76.8
21	t-C_4H_9	H	120–122	—	$C_{14}H_{22}N_4O$	64.12	8.40	21.37	64.21	8.77	21.24	92.1
22	c-C_6H_{11}	H	158–159	AcOEt : petrol. ether [b]	$C_{16}H_{24}N_4O$	66.66	8.33	19.44	67.01	8.26	19.76	65.3
23	C_6H_5	H	152–154	AcOEt : petrol. ether [b]	$C_{16}H_{18}N_4O$	68.09	6.38	19.85	68.23	6.70	20.00	82.0
24	$CH_2-C_6H_5$	H	110–112	AcOEt : petrol. ether [b]	$C_{17}H_{20}N_4O$	68.92	6.76	18.92	69.24	6.89	18.71	88.6
25	CH_3	CH_3	79–80	—	$C_{12}H_{18}N_4O$	61.54	7.69	23.93	61.17	8.04	24.10	90.2
26	C_2H_5	C_2H_5	82–83	petrol. ether [b]	$C_{14}H_{22}N_4O$	64.12	8.40	21.37	64.52	8.93	21.70	72.5
27	i-C_3H_7	i-C_3H_7	87–88	Me_2CO : petrol. ether [b]	$C_{16}H_{26}N_4O$	66.21	8.96	19.37	65.81	9.33	19.10	76.6
28	n-C_4H_9	n-cC_4H_9	oil	distillation b.p. = 228, 6 mmHg	$C_{18}H_{30}N_4O$	67.92	9.43	17.61	67.52	9.80	17.24	82.9
29	i-C_4H_9	i-C_4H_9	oil	distillation	$C_{18}H_{30}N_4O$	67.92	9.43	17.61	67.63	9.80	17.71	84.8
30	c-C_6H_{11}	c-C_7H_{11}	119–120	AcOEt : petrol. ether [b]	$C_{22}H_{34}N_4O$	71.35	9.19	15.13	71.12	9.46	15.21	68.1
31	$-CH_2C_6H_5$	$-CH_2C_6H_5$	118.5–119.5	C_6H_6 : petrol. ether [b]	$C_{24}H_{26}N_4O$	74.61	6.74	14.51	74.25	7.12	14.54	74.7
32	$-(CH_2)_5-$		85–89	petrol. ether [b]	$C_{15}H_{22}N_4O$	65.69	8.03	20.44	65.85	8.21	20.24	82.0

[a] Uncorrected. [b] b. p. 60–90°,

The peptidic triazenes **35**—**41** were obtained *via* the corresponding 4-nitropeptides **33** according to the scheme I.

Scheme I

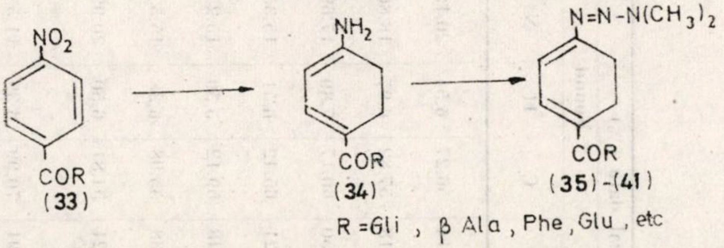
NO2
COR
(33)
NH2
COR
(34)
N=N-N(CH3)2
COR
(35)-(41)
R = Gli, β Ala, Phe, Glu, etc

The analytical data of the new peptidic triazenes were tabulated (see table 3).

By coupling of the 9-fluorenyl bromide **42** with malonic ester the 9-fluorenyl-acetic acid (**44**) was obtained during a 3-steps procedure, with an overall yield of 73%[20]. The reaction of the corresponding acid chloride **45** with 4-nitro-L-phenylalanine afforded readily the desired *p*-nitrophenyl-N[α(9-fluorenyl)acetyl]-L-alanine, ethyl-ester (**46**) (see scheme II) which was converted to the expected triazene **47** according to the general procedure.

Scheme II

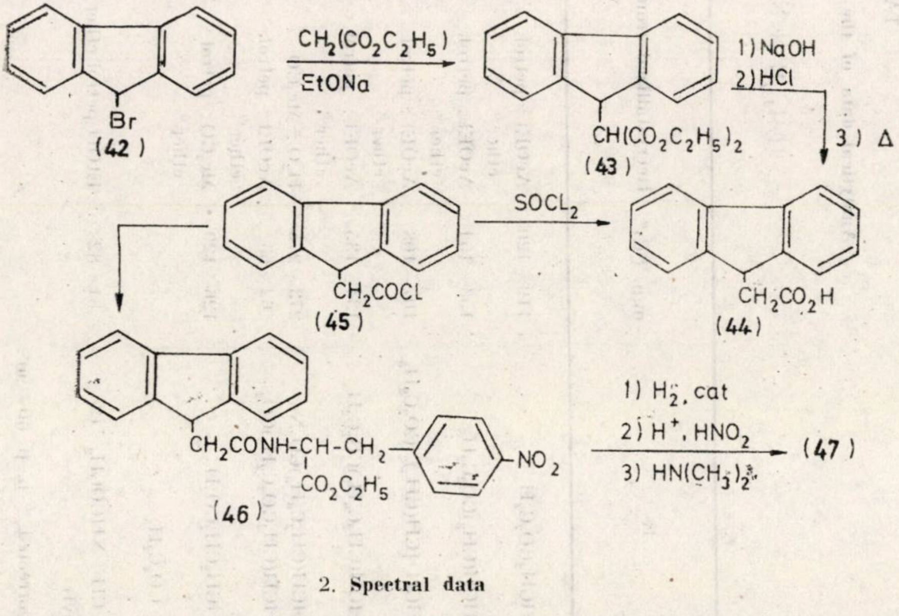
Br
(42)
CH2(CO2C2H5)
EtONa
CH(CO2C2H5)2
(43)
1) NaOH
2) HCl
3) Δ
SOCl2
CH2COCl
(45)
CH2CO2H
(44)
CH2CONH-CH-CH2
CO2C2H5
NO2
(46)
1) H2, cat
2) H+, HNO2
3) HN(CH3)2
(47)

2. **Spectral data**

Infra-red spectra. The IR spectra of the new triazenes were recorded both in KBr disks and in solution. The main characteristic absorption bands for the suggested structures are tabulated (see table 4).

TABLE 3

Analytical data of the new peptidic triazenes

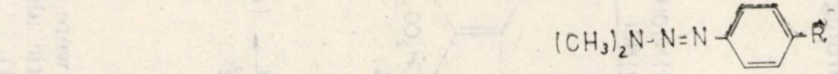

No.	R	m.p. (°C)[a]	Recrystallized from	Formula	Analytical data (%)						Yield %
					Calculated			Found			
					C	H	N	C	H	N	
35	$-CONHCH_2CO_2C_2H_5$	119–120	AcOEt : petrol. ether[b]	$C_{13}H_{18}N_4O_3$	56.12	6.47	20.14	56.27	6.54	20.15	91.3
36	$-CONHCH(CH_3)CO_2C_2H_5$	153–154	AcOEt : petrol. ether[b]	$C_{14}H_{20}N_4O_3$	57.53	6.85	19.18	57.82	6.97	18.80	89.0
37	$-CONHCH\ [CH(CH_3)_2]CO_2C_2H_5$	107–108	AcOEt : petrol. ether[b]	$C_{16}H_{24}N_4O_3$	60.00	7.50	17.50	60.17	7.89	17.69	90.7
38	$-CONHCH(CH_2C_6H_5)CO_2C_2H_5$	134–135	AcOEt : petrol. ether[b]	$C_{20}H_{24}N_4O_3$	65.22	6.52	15.21	65.42	6.51	15.35	83.3
39	$-CONHCH(CH_2C_6H_5)CO_2Na$	273–275	H_2O : Me_2CO	$C_{18}H_{19}N_4O_3Na$	59.67	5.25	15.48	59.12	5.59	15.24	75.7
40	$-CONHCH(CH_2CO_2C_2H_5)CO_2-$ $-C_2H_5$	62–63	AcOEt : petrol. ether[b]	$C_{17}H_{24}N_4O_5$	56.04	6.59	15.38	55.98	6.38	15.53	85.8
41	$-CONHCH_2CH_2CO_2H$	126–129	Me_2CO : petrol. ether[b]	$C_{12}H_{16}N_4O_3$	54.55	6.06	21.21	54.81	6.50	20.99	87.1
47	$-CH_2-\overset{\overset{CO_2C_2H_5}{\vert}}{CH}-NHCOCH_2-$(9-fluorenyl)	81–82	EtOH-petrol.ether[b]	$C_{28}H_{30}N_4O_3$	71.49	6.38	11.91	70.99	6.39	11.53	95.0

[a] Uncorrected. [b] b. p. 60–90°.

We found that the triazene moiety is always associated with the presence of a strong absorption peak located in the range of 1078–1103 cm^{-1}. This peak has been never found either at the corresponding diazonium compounds or at the hydrazines. It could be assigned to a skeleton

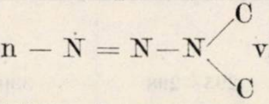

$-\dot{N}=N-N\begin{smallmatrix}C\\C\end{smallmatrix}$

vibration of the 3,3 dimethyltriazene moiety. Two additional arguments support this point of view : a) the passage from KBr to solution did not affect this band and b) the *para*-substitution with +E substituents resulted in an obviously shifting of this peak towards higher wavenumbers (see table 5).

TABLE 4

Infra-red spectra of the new triazene derivatives

Vibration type		Esters	Unsubstituted and N-monosubstituted amides	Peptides
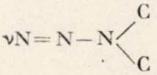 $\nu N=N-N\begin{smallmatrix}C\\C\end{smallmatrix}$		*m*-substituted 1078–1093 cm^{-1}		*p*-substituted 1087–1103 cm^{-1}
$\nu C=O$	ester	1701–1728 cm^{-1}	—	1728–1750 cm^{-1}
	amide I	—	1620–1655 cm^{-1}	1660–1664 cm^{-1}
$\nu N-H$		—	3442–3465 cm^{-1}	3439–3448 cm^{-1}

---

[a] in KBr disks or $CCl_4/CHCl_3$ solutions

U.V.Spectra. The UV spectra of the new derivatives are summarized in table 6.

Three main absoprtion bands were shown in the UV spectra of all the investigated triazenes. They were located in the following regions :

a) 225–247 nm ; primary II bands of benzenoid nature. [21]

b) 277–325 nm ; K (primary I) bands. They could be assigned to Ar–N=N structure ($\pi-\pi$ conjugation). [21–25] The bathochromic shift (and hyperchromic effect) wich occurs by passing from *m*-substituted triazenes (275–298 nm) to *p*-substituted ones (323–325 nm) with + E substituents supports this assumption. In such compounds this band masks the secondary one.

c) 316–330 nm ; secondary bands, which usually appears as shoulders or inflexions.

TABLE 5

Skeletal absorption IR bands $\left(\nu N = N - N\begin{matrix} \diagup C \\ \diagdown C \end{matrix}\right)$

in peptidic triazenes 35–41

No	Spectrum run in :	$\nu\!-\!N\!=\!N\!-\!N\begin{matrix} \diagup C \\ \diagdown C \end{matrix}$ (cm^{-1})
35	KBr	1097 vs
36	KBr	1098 s
	$CHCl_3$	1094 vs
37	KBr	1096 s
	CCl_4	1095 vs
38	KBr	1100 s
	$CHCl_3$	1094 vs
39	KBr	1087 s
40	KBr	1098 vs
	CCl_4	1089 s
41	KBr	1103 s

TABLE 6

U.V. spectra of the new triazenes

No.	Type of compounds[a]	Primary band II	K (primary I) band	Secondary band
		λ_{max} (nm) log ε	λ_{max} (nm) log ε	λ_{max} (nm) log ε
4–13	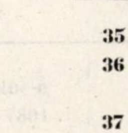 [b]	235–237 (4.10–4.19)	295–298 (4.13–4.22)	330[c] (3.92–3.97)
14–24	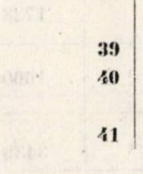	233–247 (4.11–4.23)	277–295 (4.12–4.40)	316–325 (3.89–4.06)
35–41	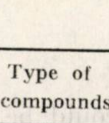	225–227 (4.02–4.07)	303–325 (4.28–4.32)	

---

[a] T = triazenic function; [b] A supplementary band appears in the 250–256 nm (4.14–4.28) range ; [c] Inflexion or shoulder.

Usually the UV spectra of trisubstituted triazenes are well accounted for by the superposition of spectra of the corresponding disubstituted compounds [26] as shown in table 7.

TABLE 7

UV spectra of some disubstituted triazenes

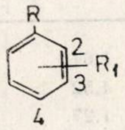

Compound		Primary band II	K (primary I) band	Secondary band
R	R_1	λ_{max} (nm) log ε	λ_{max} (nm) log ε	λ_{max}(nm) log ε
T[a]	2-CH_3	230 (4.03)	285 (4.09)	312 (4.03)
T	3-CO_2CH_3	237 (4.12)	289 (4.19)	320 (4.01)
T	3-$CONHCH_3$	238 (4.16)	290 (4.20)	318 (4.06)
CH_3	4-CO_2CH_3	206 (4.01)	238 (4.16)	268 (2.92)

[a] T=triazenic function

The hipsochromic shift exhibited by the di-N-substituted amidic triazenes (**25**—**31**) could be probably explained by the disappearance of the hydrogen bonds existing in the mono-N-substituted ones (**14**—**24**). A similar effect was noticed when the spectra of the mono-N-substituted amides were determined in *n*-hexane.

3. Biological data

The toxicity expressed as LD_{50} was determined on common mice.[27] The antitumor activity of these compounds was investigated on L 1210 leukemia and Walker 256 carcinosarcoma, according to NCI protocol. The data thus obtained were summarized in table 8.

Most of the new triazenes proved to be inactive against L 1210 leukemia, except compound **47** which exhibited moderate activity against this system. However, some of the above-mentioned compounds (**5**, **14**, **40**) exhibited significant activity against Walker 256 carcinosarcoma. A more detailed structure—activity relationship analysis of these new compounds will be reported elsewhere.

TABLE 8

Biological data of some of the new triazenes derivatives

No	LD_{50} [a]		Antitumor activity against W256 carcinosarcoma [b]	
	mg/kg b.w.	mmoles/kg b.w.	Schedule mg. subst. x no. days	TGI[c]
4	340	1.64	50 × 14	0
5	1000	4.52	200 × 14	66
14	263	1.27	50 × 14	81
22	1000	3.47	89 × 14	28
27	250	0.86	16 × 14	29
37	600	1.48	50 × 14	31
38	548	1.87	50 × 14	30
40	375	0.98	40 × 14	52
47	821	1.74	80 × 14	0

[a] on Wistar rats [b] The treatment began at the 7th day after tumor transplantation, daily administration for 14 days.
[c] TGI = (1 − T/C) 100.

EXPERIMENTAL PART

The m.p. were taken on a Franz Küster-Dresden apparatus and are uncorrected.

The UV spectra were determined with a Specord UV-VIS Carl Zeiss Jena spectrophotometer in EtOH solutions.

The IR spectra were run on a Specord 75 IR Carl Zeiss Jena spectrophotometer.

N[α-(9-Fluorenyl)acetyl] — L-p-nitrophenyl-alanine, ethyl-ester (**46**).

To a solution of 19 g (0.08 moles) of 9-fluorenylacetic acid [20] (m. p. 124—125°), in 50 ml dry $CHCl_3$, 11.5 ml (0.16 moles) of $SOCl_2$ in 25 ml $CHCl_3$ were added slowly with occasional stirring. The mixture was refluxed until no more gas was evolved and then evaporated to dryness *in vacuo* (on the water bath). The resulted pale yellow oily residue was dissolved in 50 ml anh. $CHCl_3$ and dropped under stirring to a mixture containing 23 g (0.08 moles) of ethyl-4 nitrophenyl-L-alanine ester, HCl [28], 24 ml triethyl amine and 100 ml anh. $CHCl_3$. The reaction mixture was heated at reflux for 1 hr, then cooled at 0°. The deposited solid filtered yields a part of the desired compound **46**. The filtrate, washed with a diluted HCl solution and H_2O, dried (over Na_2SO_4) and evaporated to dryness *in vacuo* afforded a second crop of compound **46**. Recrystallization of the combined two parts from MeOH : H_2O gave 27 g (84 %) of solid **46** with m.p. 186—187°.

Found : C, 70.73 ; H, 5.91 ; N, 6.37 ; Calcd. for $C_{26}H_{24}N_2O_5$: C, 70.27 ; H, 5.40 ; N, 6.30 % IR(cm^{-1}) : ν NO_2 asim and ν NO_2 sim : 1510, 1335 (KBr).

p-aminophenyl-N[α(9-fluorenyl)acetyl]-L-alanine, ethyl-ester.

16 g (0.036 moles) of the nitropeptide **46** dissolved in 50 ml MeOH were submitted to catalytic hydrogenation (over 0.5g 5 % Pd/C) at room temperature and atmospheric pressure. After the completion of the reaction the catalyst was filtered and the filtrate evaporated to dryness *in vacuo*. The oily residue thus obtained, crystallized on standing. Recrystallization from EtOH-petroleum ether (b.p. 60—90°) afforded 13 g (92 %) of a pale yellow solid m. p. = 158—159.

Found : C, 75.29 ; H, 6.64 ; N, 6.73 ; Calcd. for $C_{26}H_{26}N_2O_3$: C, 75.36 ; H, 6.28 ; N, 6.76 % IR(cm^{-1}), ν_{C-N} 1280 (KBr).

p-(3′,3′-Dimethyl)triazeno-phenyl-N[α-(9-fluorenyl) acetyl]-L-alanine, ethyl-ester (**47**).

To 10 g (0.024 moles) of previously prepared amine, dissolved in 28 ml 4N HCl, 2g of $NaNO_2$ were slowly added under stirring keeping the temperature between 0—5°. The diazonium salt solution thus obtained was dropped under vigorous stirring to a mixture containing 11 g Na_2CO_3, 10 ml dimethylamine (25 % aqueous sol.) and 50 ml H_2O. The triazene **47** (10.5 g ; 95 %) precipitated and was recrystallized from EtOH-petroleum ether (60—90°).

(For analytical data, see table 3).

AKNOWLEDGEMENT. We wish to thank Mrs Eutanța Tărnăuceanu for elemental analyses.

REFERENCES

[1] F. Y. Shealy, C. A. Krauth and J. A. Montgomery, *J. Org. Chem.*, **27**, 2150 (1962).

[2] F. Y. Shealy, J. A. Montgomery and W. R. Laster, *Biochem. Pharmacol.*, **11**, 674 (1962).

[3] R. L. Comis, *Cancer Treat. Rep.*, **60**, 165 (1976).

[4] F. Y. Shealy, *J. Pharm. Sci.*, **59**, 1533 (1970).

[5] C. S. Rondestvedt and S. J. Davis, *H. Org. Chem.*, **22**, 200 (1957).

[6] F. Y. Shealy, C. A. Krauth, C. E. Opliger, H. W. Guin and W. R. Laster, *J. Pharm. Sci.*, **60**, 1192 (1972).

[7] F. Y. Shealy and C. A. O'Dell, *J. Pharm. Sci.*, **60**, 555 (1971).

[8] Y. T. Ling, T. L. Loo, S. Vadlamudi and A. Goldin, *J. Med. Chem.*, **15**, 201 (1972).

[9] R. C. S. Audette, T. A. Connors, G. Mandel, K. Merai and W. C. J. Ross, *Biochem. Pharmacol.*, **22**, 1855 (1973).

[10] T. Giraldi, C. Nisi, T. A. Connors and P. M. Goddard, *J. Med. Chem.*, **20**, 850 (1977).

[11] J. U. Gutterman, G. M. Mavligit, R. Reed, M. A. Burgess, J. Gottlieb and E. M. Hersch, *Cancer Treat. Rep.*, **60**, 177 (1976).

[12] T. Giraldi, P. J. Haughton, D. M. Taylor and C. Nisi, *Cancer Treat. Rep.*, **62**, 721 (1978); **63**, 93 (1979).

[13] T. A. Connors, P. M. Goddard, H. Merai, W. C. J. Ross and D. E. V. Williams, *Biochem. Pharmacol.*, **25**, 241 (1976).

[14] V. A. Levin, D. Crafts. C. B. Wilson, P. Kabra, C. Hansch, E. Boldrey, J. Enot and M. Nely, *Cancer Chemoth. Rep.*, **59**, 327 (1975).

[15] W. J. Dunn III, M. J. Greenberg and S. S. Callejas, *J. Med. Chem.*, **19**, 1299 (1976).

[16] G. J. Hatheway, C. Hansch, K. H. Kim, S. R. Mildstein, C. L. Schmidt, R. N. Smith and F. R. Quinn, *J. Med. Chem.*, **21**, 563 (1978).

[17] C. Hansch, G. J. Hatheway, F. R. Quinn and N. Greenberg, *J. Med. Chem.*, **21**, 574 (1968).

[18] I. Niculescu-Duvăz, M. Ionescu, A. Cambanis, M. Vitan and V. Feyns, *J. Med. Chem.*, **11**, 500 (1968).

[19] K. Fukushima and S. Toyoshima, *Cancer Chemother. Rep.*, **59**, 309 (1975).

[20] M. Haulică and D. Stoicescu, Personal communication.

[21] C. N. R., Rao, "Ultra-Violet and Visible Spectroscopy" Butterworths, London, 1967.

[22] R. J. W. Le Févre and T. H. Liddicoet, *J. Chem. Soc.*, **1951**, 2743.

[23] P. Grammaticakis, *Bull. Soc. chim. France*, **1957**, 129.

[24] B. F. Day, T. W. Campbell and G. M. Coppinger, *J. Amer. Chem. Soc.*, **73**, 4687 (1951).

[25] P. Grammaticakis, *Compt. rend*, **245**, 1439 (1957).

[26] L. Doub and J. M. Vandenbelt, *J. Amer. Chem. Soc.*, **77**, 4535 (1955).

[27] E. Cornfield and N. Mantel, *J. Amer. Statist. Assoc.*, **45**, 181 (1950).

[28] F. Bergel and J. A. Stock, *J. Chem. Soc.*, **1954**, 2409.

Revue Roumaine de Chimie, 25, 5, 713–719 (1980)

STERIC OPTIMISATION BY MTD OF THERAPEUTIC INDEX OF N-SUBSTITUTED DERIVATIVES OF *cis*-DICHLORODIAMMINE-PLATINUM(II) ACTIVE AGAINST ADJ/PC6A MOUSE PLASMA CELL TUMOUR

Z. SIMON,* S. HOLBAN,* MARIA MRACEC,** ANA MAURER,** and
SEPTIMIA POLICEC **
* University of Timişoara, Bd. V. Pârvan, Romania
**Laboratory of Inorganic Chemistry, Chemical Research Centre, Timişoara, Bd. Mihai Viteazul 24, Romania

Received September 19, 1978

The receptor mapping by minimal steric differences is applied to a series of 26 amines in *cis*-dichlorodiammineplatinum(II) whose therapeutic indices with respect to the ADJ/PC6A tumour in mice were determined by Tobe et al. Two complexes with highly predicted therapeutic indices, one predicted with a ten time increased TI in comparison to the best compound of the series, are indicated by this procedure.

N-substituted derivatives of *cis*-dichlorodiammineplatinum (II) have been extensively studied as potential anticancer chemotherapeutics.[1-8] In a previous note [9] we tried to establish relations between the structural features of these compounds on one hand and LD_{50} values in mice, ID_{90} values against some experimental mice tumours and therapeutic indices, TI on the other hand. While both toxicity and tumour destroying ability depend (statistically significant) upon hydrophobicity and pK-values for the amines, no significant correlation was found with respect to minimal steric difference, MTD. For the 26 compounds listed in table 1, tested upon ADJ/PC6 tumour in mice, ID_{90} correlates to a significant extent only with the hydrophobicity π of the ligands. The corresponding correlational equation (with $A' = -\log ID_{90}$) is :

$$A' = -0.83 - 0.32\,\pi_i + 0.017\,pK_i\,; \quad r = 0.75 \tag{1}$$

with partial correlation coefficients $r(\pi) = -0.74$; $r(pK) = -0.23$.

The toxicity of these compounds depends also almost only upon the hydrophobicity. With $A' = -\log LD_{50}$:

$$A'' = -1.68 - 0.20\,\pi_i - 0.009\,pK_i\,; \quad r = 0.68 \tag{2}$$

$$\text{with} \quad r(\pi) = -0.68\,; \quad r(pK) = -0.32$$

The therapeutic index probably depends upon penetrability in cancer cells versus that in hematopoietic cells, and thereby upon steric features of the drug molecule. Really some dependence upon MTD was found for TI in our previous note. [9] We will therefore try to find out the optimal molecular shape for a high TI against the ADJ/PC6A tumour in mice, on hand of the receptor mapping procedure by a minimal sterical difference technique. [10-12]

*Receptor mapping**. The minimal steric difference MTD is an approximate measure for nonoverlapping volume when a molecule is superimposed upon the standard — the molecule complementary to the receptor cavity. The affinity of the molecule for the receptor is supposed to decrease in a linear manner with MTD. [10] Practically, by a maximal atom per atom superposition of the molecules one upon another, an atomic net, the hypermolecule H, is obtained; its vertices (atomic knots), j, may correspond either to the interior of the cavity (the standard parameter $\varepsilon_j = -1$), to the cavity's walls ($\varepsilon_j = +1$) or to steric irrelevant regions ($\varepsilon_j = 0$). The mean square deviation of experimental affinities vs. those calculated with MTD's is a function of the ternary ε_j-parameters for M vertices of H. The receptor is mapped by finding out the ε_j-figures which minimise the mean square deviation. The "best" molecule for the corresponding receptor will be the one with atoms as many as possible in vertices j with $\varepsilon_j = -1$ and without atoms is vertices j with $\varepsilon_j = +1$. [10-11]

EXPERIMENTAL DATA AND CONSTRUCTION OF THE HYPERMOLECULE

The amine moieties of 26 N-substituted derivatives of *cis*-dichlorodiammineplatinum (II) sinthesized by Tobe et al., screened by Connors against the ADJ/PC6A tumour in mice [3,6] are listed in table 1 together with $A_i^{\exp}$ — values, i.e. logarithms of TI values. The vertices $j(x_{ij} = 1)$ of the hypermolecule H (Fig. 1), occupied in each molecule i are also indicated as well as the MTD$_i$-figures calculated with the final, optimised map, S* (set of ε_j^*-parameters).

MTD's are calculated according to the formula:

$$\mathrm{MTD}_i = s + \sum_{j=1}^{M} \varepsilon_j x_{ij} \tag{3}$$

with s — the number of vertices with $\varepsilon_j = -1$ (corresponding to the presumed cavity, i. e. standard) in the map S*.

The hypermolecule H was constructed by searching a maximal supperposition upon the bis-cyclohexylamine complex, the one with the highest TI. We considered also that, in the aqueous surrounding, the hydrophobic moieties of the two amines within the complex will tend to associate face to face. The hypermolecule is depicted in figure 1.

---

* Some differences in terminology with respect to the previous papers [10-12] are here introduced. We use MTD for minimal steric differences, due to the topological character of our method and because MSD is of common use as abrevation for mean square deviation. Receptor map is used instead of standard and the ternary parameter figures $E_j = -1, 0$ or $+ 1$ correspond to the figures 11, 00 and 10 of the $\delta_j\gamma_j$ — doublet of note. [10]

The start map, S^0, i.e. the set of $M-\varepsilon_j^0$ values with which the optimisation procedure was started, is similar to the "best" molecule of the

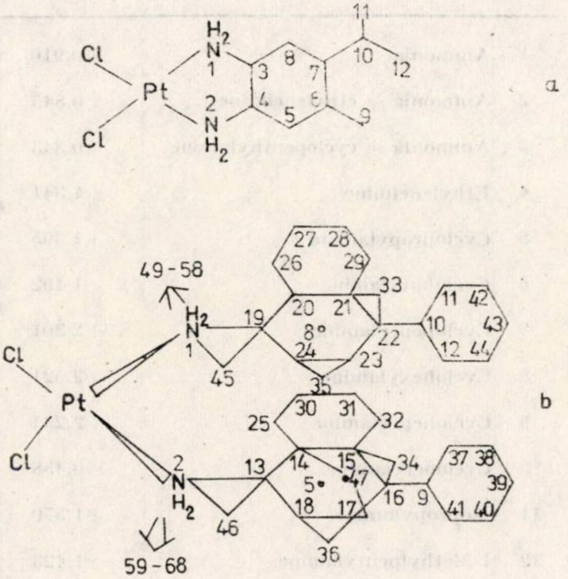

Fig. 1. — The hypermolecule H (the vertices j)
a. View perpendicular to the *cis*-$[PtCl_2(NH_2)_2R]$—plane
b. Side view.

experimental set (Table 1, $i = 8$);

$$S^0 \begin{cases} j(\varepsilon_j^0 = -1) : 1, 2, 13-24 \quad s = 14 \\ j(\varepsilon_j^0 = +1) : 3-12 \\ j(\varepsilon_j^0 = 0) : 25-68 \end{cases} \tag{4}$$

while the optimised set resulted in a computer implemented procedure was:

$$S^* \begin{cases} j(\varepsilon_j^* = -1) : 1, 2, 3, 24, 30, 32, 35\,; \ s = 7 \\ j(\varepsilon_j^* = +1) : 9-12, 25, 29, 33, 48, 59, 68 \\ j(\varepsilon_j^* = 0) : 4-8, 13-23, 26-28, 31, 36-47, 49-58, 60-67 \end{cases} \tag{5}$$

and the corresponding correlational equation was:

$$A_i^{\text{calc}} = 4.844 - 0.507\ \text{MTD}_i\,; \quad r = 0.747 \tag{6}$$

The $\Delta Y(\varepsilon_t)$ values which give an indication for the reliability of the ε_t — attributions are listed in table 2.

TAB

Therapeutic indices, TI and occupied knots $j(x_{ij} - 1)$ in

Nr.	Amine *	$A_i^{\exp}$	$j(x_j = 1)$
1	Ammonia	+0.910	1, 2
2	Ammonia + ethyleneimine	+0.845	1, 2, 19, 33
3	Ammonia + cyclopenthylamine	+0.343	1, 2, 13–15, 17, 18
4	Ethyleneimine	+1.341	1, 2, 13, 19, 45, 46
5	Cyclopropylamine	+1.395	1, 2, 13, 14, 19–20, 24
6	Cyclobutylamine	+1.492	1, 2, 5, 8, 13, 14, 18–20, 24
7	Cyclopentylamine	+2.301	1, 2, 13–15, 17–21, 23, 24
8	Cyclohexylamine	+2.521	1, 2, 13–24
9	Cycloheptylamine	+2.234	1, 2, 13–15, 19–21, 25–34
10	Cyclooctylamine	+0.458	1, 2, 13–15, 19–21, 25–36
11	Isopropylamine	+1.570	1, 2, 13, 14, 18–20, 24
12	1-Methylpentylamine	+1.423	1, 2, 9, 10, 13–16, 18–22, 24
13	2-Methylpropylamine	+1.127	1, 2, 13–15, 19–21, 25, 26
14	Cyclohexylmethylamine	+0.418	1, 2, 13–15, 19–21, 25–32
15	3-Methylbutylamine	+2.297	1, 2, 13–16, 19–22, 29, 32
16	1-Amino-4-cyclohexylbutane	0.000	1, 2, 9–12, 13–16, 19–22, 37–44
17	1-Aminoadamantane	+1.747	1, 2, 13–24, 47, 48
18	2-Aminoadamantane	+1.452	1, 2, 49–65
19	Exo-norbornylamine	0.000	1, 2, 47–55, 66–68
20	Endo-norbornylamine	0.000	1, 2, 49–68
21	4-Hydroxy-cyclohexylamine	0.000	1, 2, 9, 10, 13–24
22	4-Methyl-cyclohexylamine	+0.362	1, 2, 9, 10, 13–24
23	*o*-Phenylenediamine	+1.301	1–8
24	3-Methyl-0-phenylenediamine	+0.784	1–9
25	3,4-Dimethyl-o-phenylenediamine	+2.054	1–10
26	3-Carboxy-o-phenylenediamine	+0.295	1–8, 10–12

---

* All the compounds, except no. 2 and 3 are symmetric.

LE 1

***cis*-[Pt(II)Cl$_2$Am$_2$]; A_i^{exp} = log TI; A' = − log ID$_{90}$; A'' = − log LD$_{50}$**

MTD$_i$	A'	A''	$\pi = \pi_1 + \pi_2$	$pK = pK_1 + pK_2$
5	−0.204	−1.114	−1.80	18.60
5	−0.602	−1.147	−1.18	17.30
5	+0.301	−1.042	−0.02	19.25
5	−0.415	−1.756	−0.56	16.00
4	−0.361	−1.756	−0.24	17.32
4	−0.462	−1.954	+0.76	18.68
4	−0.380	−2.681	+1.76	19.90
4	−1.079	−3.600	+2.76	21.28
5	−0.866	−3.000	+3.76	19.98
6	−2.362	−2.820	+4.76	20.02
4	+0.046	−1.524	−0.06	21.26
6	−1.440	−2.826	+2.94	21.28
5	−0.792	−1.919	+1.30	20.86
6	−1.532	−1.950	+3.76	21.28
4	−0.763	−3.060	+2.26	21.26
8	−2.120	−2.120	+6.76	21.20
4	−1.079	−2.826	+3.58	21.28
6	−1.498	−2.950	+3.58	21.28
7	−2.800	+2.800	+6.22	21.28
7	−2.900	−2.900	+6.22	21.28
6	−3.072	−2.997	+3.76	21.28
6	−1.000	−1.362	+0.14	19.28
4	−0.380	−1.681	+0.30	9.48
5	−0.368	−1.352	+1.30	9.48
6	−0.398	−2.452	+2.30	9.48
7	−1.960	−2.255	−1.00	4.74

TABLE 2

$\Delta Y(\varepsilon_t)$ values

j	$\Delta Y(-1)$	$\Delta Y(0)$	$\Delta Y(+1)$	j	$\Delta Y(-1)$	$\Delta Y(0)$	$\Delta Y(+1)$
1,2	(0.0	0.0	0.0)	24	(0.0	1.1	5.3)
3	(0.0	1.1	4.0)	25, 26	(2.3	0.4	0.0)
4, 6, 7	(0.6	0.0	1.1)	27, 28	(0.1	0.0	1.6)
5, 8	(1.1	0.0	1.0)	29	(2.3	0.4	0.0)
9	(4.0	0.8	0.0)	30, 31	(0.0	1.6	4.9)
10	(2.9	0.3	0.0)	32	(0.0	1.1	3.1)
11, 12	(1.4	0.2	0.0)	33, 34	(1.7	0.6	0.0)
13, 14	(1.0	0.0	2.0)	35, 36	(0.0	0.5	1.4)
15	(0.3	0.0	3.1)	37−44	(0.9	0.0	0.1)
16	(0.5	0.0	2.1)	45	(0.2	0.0	0.3)
17	(1.2	0.0	1.2)	46	(0.8	0.0	0.1)
18	(1.6	0.0	1.4)	47, 48	(2.5	0.6	0.0)
19	(1.5	0.0	1.5)	49−58	(0.1	0.0	0.9)
20	(1.2	0.0	2.0)	59, 65	(3.0	1.0	0.0)
21	(0.5	0.0	2.8)	60−67	(0.1	0.1	0.0)
22	(0.5	0.0	2.1)	68	(0.1	0.0	0.1)
23	(1.1	0.0	1.0)				

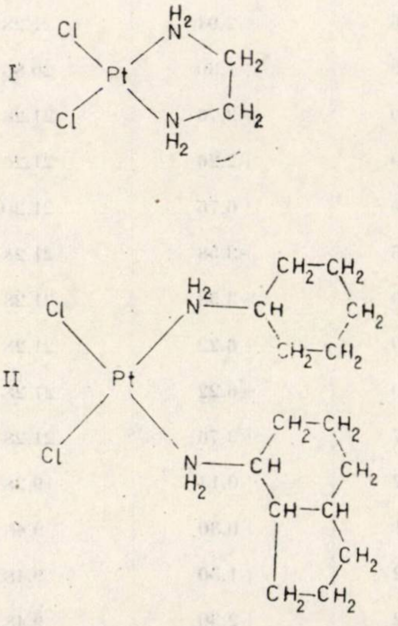
I
Cl
Cl
Pt
H2
N
N
H2
CH2
CH2
II
Cl
Cl
Pt
H2
N
CH
CH2–CH2
CH2
CH2–CH2
N
H2
CH
CH–CH2
CH2
CH–CH
CH2
CH2–CH2

Fig. 2. — Molecules with high predicted therapeutic index.

The best experimental molecule, $i = 8$, should have $\mathrm{MTD}_8 = 4$ and $A_8^{\mathrm{calc}} = 2.82$. A simple molecule, equally active, should be the ethylenediamine derivative (molecule I of figure 2, $j(x_{ij} = 1) : 1 - 4$, $\mathrm{MTD}_1 = 4$).

In fact, this compound has been considered by Rosenberg as an active antitumour complex on ground of its activity on Sarcoma 180 [1,2,4] but it doesn't belong to the series of complexes screened by Connors et al., against the ADJ/PC6A tumour. [3,6]

The complex with the highest predicted activity is the molecule II of figure 2, $j(x_{ij} = 1) : 1, 2, 13-24, 30-32$, $\mathrm{MTD}_{\mathrm{II}} = 2$, $A_i^{\mathrm{calc}} = 3.83$, i.e. a therapeutic index predicted to be about ten times higher than for the bis-cyclohexylamine complex, the most active complex of the experimentally investigated series of table 1.

The authors wish to acknowledge the generous permission given by Professor M. L. Tobe to use the experimental data of his compounds for performing this work.

REFERENCES

[1] B. Rosenberg, *Platinum Metals Rev.*, **15**, 3 (1971).

[2] B. Rosenberg, *Naturwiss.*, **60**, 399 (1973).

[3] T. A. Connors, M. Jones, W. C. J. Ross, P. D. Braddock, A. R. Khokhar, and M. L. Tobe, *Chem. Biol. Interactions*, **5**, 415 (1972).

[4] M. J. Cleare and J. D. Hoeschele, *Platinum Metals Rev.*, **17**, 2 (1973); *Bioinorg. Chem.*, **2**, 187 (1973).

[5] M. J. Cleare, *Coord. Chem. Rev.*, **12**, 349 (1974).

[6] P. D. Braddock, T. A. Connors, M. Jones, A. R. Khokhar, D. H. Melzack and M. L. Tobe, *Chem. Biol. Interactions*, **11**, 145 (1975).

[7] B. Rosenberg, *Cancer Chemother. Rep.*,, **59**, 589 (1975).

[8] R. J. Speer, H. Ridgway, L. M. Hall, D. P. Stewart, K. E. Howle, D. Z. Lieberman, A. D. Newmann and G. M. Hill, *Cancer Chemother. Rep.*, **59**, 629 (1975).

[9] Z. Simon, M. Mracec, A. Maurer, S. Policec and C. Drăgulescu, *Rev. Roumaine Biochim.*, **14**, 117 (1977).

[10] Z. Simon, A. Chiriac, I. Moţoc, S. Holban, D. Ciubotariu and Z. Szabadai, *Studia Biophysica (Berlin)*, **55**, 217 (1976).

[11] I. I. Bădilescu and Z. Simon, *Rev. Roumaine Biochim.*, **13**, 239 (1976).

[12] Z. Simon, I. I. Bădilescu and T. Racoviţan, *J. theor. Biol.*, (in press).

Revue Roumaine de Chimie, 25, 5, 721–727 (1980)

SYNTHESIS OF *N*-SUBSTITUTED DERIVATIVES OF 9-AMINOCARBAZOLE

JANUSZ KYZIOŁ and JERZY TARNAWSKI
Wyższa Szkoła Pedagogiczna, 45–052 Opole, ul. Oleska 48, Poland

Received April 23, 1979

9-Nitrosocarbazole can be obtained in a good yield when nitrosation of carbazole is performed in the mixture of ethyl ether and 50% sulfuric acid. The most convenient reducing agent for 9-aminocarbazole preparation is lithium aluminum hydride. Boron fluoride is a good catalyst for the condensation reaction of 9-aminocarbazole with carbonyl compounds. A series of diphenylenehydrazones of aromatic aldehydes and ketones was obtained. The reduction of the azomethine bond was carried out using complex hydrides in aprotic solvents.

The preparation of 9-aminocarbazole in a pure state presents some difficulties.[1] There are only a few communications about its chemical properties and its derivatives. Acylation of 9-aminocarbazole with acid chlorides and anhydrides gives stable 9-acyloaminocarbazoles.[2] The condensation with aromatic aldehydes proceeds smoothly and a series of diphenylenehydrazones is described.[3,4] The basicity and nucleophylicity of 9-aminocarbazole are low but it reacts with some reactive aryl and alkyl halides giving substitution products.[5] 9-(N-Picrylamino)-carbazole and 9-(N-triphenylmethylamino)-carbazole, obtained among others in such a way, give stable free radicals (hydrazyls) when oxidized with active lead dioxide.[6,7]

A simple method of synthesis of 9-aminocarbazole proceeds through nitrosation of carbazole and reduction of 9-nitrosoderivative. A solution of 9-nitrosocarbazole can be easily prepared when a suspension of carbazole in acetic acid is treated with sodium nitrite.[8,9] All our attemps to obtain the pure product in a good yield were unsuccessful. It is very unstable and very soluble in most organic solvents. Much better results are obtained if the reaction was performed in a mixture of ethyl ether and 50% sulfuric acid. Two moles of sodium nitrite per mole of carbazole are needed. The crude product isolated in 73–93% yield may be used for the reduction with no further purification.

The reduction of 9-nitrosocarbazole with zinc dust in a mixture of wet ethyl ether and acetic acid was firstly described by Wieland.[8] Isolation and purification of 9-aminocarbazole is laborious, the product is obtained in a poor yield, and is contaminated with carbazole. It seems that pure 9-aminocarbazole may be obtained only in an aprotic solvent. The most convenient reducing agent is lithium aluminum hydride. The reducing power of borohydrides is too low. Two moles of reducing agent per mole of 9-nitrosocarbazole guarantee high purity of the product. When only 1.5 moles $LiAlH_4$ are used the product is pink-coloured.

The condensations of 9-aminocarbazole with aromatic aldehydes were first performed by Blom in boiling ethanol solution in the presence of traces of acetic or sulfuric acid. [10] We have found that the same reaction proceeds quickly in boiling ether if catalyzed with boron trifluoride. Aromatic ketones do not react in nonpolar solvents (THF, dioxane, glyme, diglyme). The most convenient solvent is acetic acid used in a minimal amount, only enough to obtain a clear solution of substrates at temperatures between 60—70°. TLC analysis indicates that in the presence of boron, trifluoride reaction is completed after 1—2 hrs at room temperature. Benzophenone reacts slowly, and after 12 hrs the product could be isolated in 30% yield. If the reaction mixture was left for 48 hrs the yield of diphenylenehydrazone was increased to 64%. 2-Hydroxybenzophenone is unstable in the reaction conditions and the isolation of the pure product from tarry reaction mixture makes some difficulties. Condensation of 9-aminocarbazole with stable and unreactive carbonyl compounds can be performed in boiling xylene solution. All attempts to obtain rezacetophenone diphenylenehydrazone were unsuccessful. 9-Acetoamidocarbazole was the only product which could be isolated if the reaction was performed in severe conditions.

Reduction of diphenylenehydrazones of ortho-hydroxyaldehydes and ortho-hydroxyketones was performed using 1—2 moles of lithium borohydride for 1 mole of substrate. The rate of reduction is limited by the solubility of the substrate in the solvent used (THF, Et_2O). 4-Hydroxyacetophenone diphenylenehydrazone could not be reduced in such conditions and 9-(N-benzylideneamino)-carbazole reacts very slowly. When lithium aluminium hydride is used as the reducing agent, reaction proceeds very quickly and the yellow colour of the reaction mixture disappeares in 5—10 minutes. N-(9-Carbazolyl)-1,2-diphenylethanolamine was obtained in a high yield from the corresponding diphenylenehydrazone using lithium aluminium hydride. No other product was isolated. Reduction of benzophenone diphenylenehydrazone with lithium borohydride proceeds slowly and is accompanied by some side reactions. Carbazole, 9-aminocarbazole and an unidentified substance (probably benzoine diphenylenehydrazone) were detected by TLC method. A minute amount of a by-product, insoluble in *n*-heptane, was isolated from the reaction mixture. These are probably the diastereoisomers RS and SR of the main product. IR spectra indicate intramolecular hydrogen bond in N-(9-carbazolyl)-1,2-diphenylethanolamine which is impossible in the by-product because of the steric hindrance. All attemps to obtain N-(9-carbazolyl)-1-(hydroxyphenyl)-ethylamine and its 4-hydroxyphenyl isomer in a crystalline form were unsuccessful. They were isolated as colourless oils which slowly solidified to white amorphous solids. The physical properties of these compounds resembling polymers can be explained as a result of polymeric association through hydrogen bonds.

TABLE 1

Diphenylenehydrazones

Compound	Mp, °C	Yield, %	Formula	C, %		H, %	
				Calcd	Found	Calcd	Found
9-(N-Benzylideneamino) carbazole	139–40	80	$C_{19}H_{14}N_2$	84.41	84.40	5.22	5.30
9-(N-Salicylideneamino) carbazole	148–9	75	$C_{19}H_{14}N_2O$	79.69	79.49	4.93	4.94
2-Hydroxy-1-naphthaldehyde diphenylenehydrazone	246–8	80	$C_{24}H_{16}N_2O$	82.12	82.13	4.79	4.89
Acetophenone diphenylenehydrazone	133–4	80	$C_{20}H_{16}N_2$	84.47	84.30	5.67	5.76
2-Hydroxyacetophenone diphenylenehydrazone	164–5	80	$C_{20}H_{16}N_2O$	79.99	79.91	5.37	5.52
4-Hydroxyacetophenone diphenylenehydrazone	221–2	62	$C_{20}H_{16}N_2O$	79.99	79.89	5.37	5.40
Benzophenone diphenylenehydrazone	163–5	64	$C_{25}H_{18}N_2$	86.67	86.70	5.24	5.19
2-Hydroxybenzophenone diphenylenehydrazone	161–2	24	$C_{25}H_{18}N_2O$	82.85	82.90	5.00	5.12
Dibenzoyl diphenylenehydrazone	176–7	56	$C_{26}H_{18}N_2O$	83.39	83.16	4.84	4.97

TABLE 2

Diphenylenehydrazines

Compound	Mp, °C	Yield, %	Formula	C, %		H, %	
				Calcd	Found	Calcd	Found
9-(N-Benzylamino)-carbazole	120–1	89	$C_{19}H_{16}N_2$	83.80	83.70	5.92	5.87
9-N-(2-Hydroxybenzyl)-amino-carbazole	138–9	84	$C_{19}H_{16}N_2O$	79.14	79.04	5.59	5.80
9-N-(2-Hydroxynaphthyl-1-methylene)-amino-carbazole	176–7	62	$C_{23}H_{18}N_2O$	81.63	81.69	5.36	5.34
N-(9-Carbazolyl)-1-phenylethylamine	86–8	82	$C_{20}H_{18}N_2$	83.88	84.01	6.33	6.39
N-(9-Carbazolyl)-1-(2-hydroxyphenyl)-ethylamine	166–9	92	$C_{20}H_{18}N_2O$	79.44	79.52	6.00	5.91
N-(9-Carbazolyl)-1-(4-hydroxyphenyl)-ethylamine	162–5	64	$C_{20}H_{18}N_2$	79.44	79.37	6.00	6.17
N-(9-Carbazolyl)-benzhydramine	148–9	80	$C_{25}H_{20}N_2$	82.39	82.45	5.53	5.61
N-(9-Carbazolyl)-1,2-diphenylethanolamine	148–9	90	$C_{26}H_{22}N_2O$	82.51	82.38	5.86	5.82

EXPERIMENTAL

9-Nitrosocarbazole. In a 2 l reaction flask fitted with a stirrer, a reflux condenser and a separatory funnel, 50.16 g (0.30 M) of carbazole, 600 ml of ethyl ether and 150 ml of 50% sulfuric acid were placed. A solution of 41.40 g (0.6 M) of sodium nitrate in 150 ml water was added in two portions to the vigorously stirred suspension. Stirring was continued until carbazole dissolved. The organic layer was separated, dried over anhydrous sodium sulfate and concentrated to a volume of 250 ml. The solution was cooled to −20°, and the golden-yellow needles of 9-nitrosocarbazole were filtered off and dried in vacuum; yield 48.60 g (89%); mp 80—2° (lit. mp 81—2° [9]). Found: C, 73.51; H, 4.20%. Calcd for $C_{12}H_8N_2O$: C, 73.45; H, 4.11%. IR (KBr): 720, 750, 1010, 1120, 1270 (aromatic C—H deform.), 1060, 1445 (N-nitroso-group), 3060 (aromatic C—H stretch). MS, m/e: 196 (0.9, M^+), 168 (13.5), 167 (100.0), 166 (40.9), 140 (11.4), 139 (13.3), 83 (10.4), 30 (11.9).

9-Aminocarbazole. A solution of 19.62 g (0.10 M) of 9-nitrosocarbazole in 300 ml of absolute ethyl ether was gradually added to a vigorusly stirred suspension of 7.60 g (0.20 M) of lithium aluminum hydride in 500 ml of ether during one hour. This rate of addition keeps the reaction mixture gently boiling. After completion of the addition the content of the reaction vessel was stirred for 0.5 h, and then 100 ml ethanol and 25 ml of 20% aqueous potassium hydroxide solution were cautiously added. A white precipitate was filtered off and washed with two 300 ml portions of ether. The filtrate was concentrated to the volume of 500 ml. After cooling 9.08 g of 9-aminocarbazole were filtered off and dried. From the concentrated filtrate the second crop (5.98 g) of the product was isolated, mp 150—2°. After crystallization from isoöctane, 13.92 g (yield 76%) of pure 9-aminocarbazole were obtained as long, white needles, mp 151—152.5° (lit. mp 151° [10]). Found: C 79.10; H. 5.62%. Calcd for $C_{12}H_{10}N_2$: C, 79.09; H, 5.53%. IR (KBr): 715, 750 (aromatic C—H, deform.), 835, 850, 1590, 3230, 3340 (amino group), MS, m/e: 182 (3.0), 182 (21.6, M^+), 181 (8.3), 167 (11.3), 166 (12.1), 154 (2.3), 152 (2.9), 150 (5.2), 140 (7.0), 139 (6.3), 97 (12.6), 91 (23.4), 78 (100.0).

9-(N-Acetylamino)-carbazole. 9-Aminocarbazole (3.64 g — 0.02 M) and 2.1 ml (10% excess) of acetic anhydride were dissolved in 20 ml of acetic acid and refluxed for 2 hrs. From the cooled solution a crystalline solid was isolated, washed with methanol and crystallized from ethanolic solution. 9-(N-acetylamino)-carbazole (3.40 g — 77%) was obtained as transparent rods mp 256—7° (lit. mp 247° [10]). Found: C, 74.78; H, 5.46%. Calcd for $C_{14}H_{12}N_2O$: C, 74.97; H, 5.39%. IR (KBr): 750, 760 (aromatic C—H deform.) 640, 730, 1540, 1690, 3240 (amide bands), 1375, 1430, 3030 (aliphatic C—H deform. and stretching). MS, m/e: 226 (1.5), 225 (11.8), 224 (69.6 M^+), 183 (13.8), 182 (95.4), 181 (100.0), 166 (17.9), 152 (27.1), 43 (14.7). NMR (DMSO-d_6): δ, ppm, 11.29, s, 1H, (N—H), 8.16, oct. $J=7.5$ Hz, $J=1.0$ Hz, $J=0.9$ Hz, 2H (4,5-aromatic protons), 7.14—7.58, m, 6H (remaining aromatic protons), 2.23, s, 3H (acetyl group).

9-(N-Benzylideneamino)-carbazole. In 200 ml of dried ethyl ether 9.11 g (0.05 M) of 9-aminocarbazole and 5.55 ml (10% excess) of benzaldehyde were dissolved. A drop of boron fluoride etherate was added, and the mixture evaporated to dryness. The residue was crystallized twice from isoöctane yielding 10.90 g (86%) of 9-(N-benzylideneamino)-carbazole as light yellow needles mp 139—40° (lit. mp 137° [8]). IR (KBr): 725, 745, 760 (aromatic C—H deform.), 860, 1625 (azomethine group), 3050, 3060 (aromatic C—H stretch). MS, m/e: 272 (4.8), 271 (19.5), 270 (85.5, M^+), 167 (32.6), 166 (100), 140 (17.5), 104 (1.8), 103 (2.1), 77 (9.2).

9-(N-Salicylideneamino)-carbazole. The reaction was performed as above. The crude product was crystallized twice from 900 ml of ethanol, yielding 10.72 (75%) of 9-(N-salicylideneamino)-carbazole as long, light yellow needles mp 148—9° (lit. mp 147° [10]).

The solution of 10.95 g (0.06 M) of 9-aminocarbazole and 7.32 ml (0.07 M) of salicylic aldehyde in 200 ml of xylene was refluxed for 3.5 hrs. Xylene (100 ml) was distilled off and 100 ml of ethanol were added. The crude product, mp 138—40° was isolated from the cooled solution. After crystallization from ethanol, 10.30 g (yield 60%) of pure 9-(N-salicylideneamino)-carbazole were obtained; mp 148—9°. IR (KBr): 720, 745, 760 (arom. C—H deformation), 860, 1630 (azomethine group), 1270, 1320, 3095 (internally bonded O—H). MS, m/e: 287 (3.0), 286 (14.1, M^+) 182 (4.7), 167 (62.0), 166 (100.0), 140 (5.6), 139 (3.4), 120 (2.3), 116 (3.0), 115 (5.8).

2-Hydroxy-1-naphthaldehyde diphenylenehydrazone. The solution of 5.47 g (0.03 M) of 9-aminocarbazole and 5.23 g (0.03 M) of 2-naphthol-1-carboxaldehyde in 50 ml of ethyl ether deposited a yellow precipitate when refluxed for 15 min. with an addition of a drop of boron fluoride etherate. The solid was filtered, washed with ether and crystallized from 200 ml of xylene yielding 9.20 g (90%) of the product melting 243—7°. It was dissolved in 450 ml of boiling tetrahydrofuran and left for 48 hrs at a temperature of −20°. Pure 2-hydroxy-1-naphthaldehyde diphenylenehydrazone (yield 8.12 g — 80%) was obtained as a creamy, microcrystalline powder: mp 246—8°. IR (KBr): 720, 740, 750, 770, 830, 3065 (arom. C—H), 1255, 1350, 3095 (internally bonded O—H), 865, 1630 (azomethine group). MS, m/e : 337 (9.9), 336 (35.4, M^+), 167 (100.0), 166 (38.8), 140 (20.7), 139 (11.5).

Acetophenone diphenylenehydrazone. To the solution of 3.64 g (0.02 M) of 9-aminocarbazole in 30 ml of acetic acid heated to 65—70°, 2.6 ml (0.022 M) of acetophenone and a drop of boron fluoride were added. After 3 hrs in room temperature the crude product was separated as yellow rods, mp 128—9°. It was filtered, washed with cool methanol and crystallized from ethanol yielding 4.57 g (80 %) of acetophenone diphenylenehydrazone ; mp 133—4°, (lit. mp 132°[10]). IR (KBr) : 730, 750, 770 (arom. C—H), 1455, 1490, 1575, 1600 (aromatic rings stretching), 1630 (azomethine group), 1380, 1440 (methyl group). MS, m/e : 286 (2.5), 285 (3.2), 284 (100.0 M^+), 167 (27.4), 166 (63.1), 118 (86.8), 77 (68.5).

2-Hydroxyacetophenone diphenylenehydrazone. The reaction was performed in an analogous manner. The crude product, mp 161—2° was isolated in 90 % yield (5.42 g) and crystallized from the mixture of ethanol (100 ml) and a minimal amount of benzene enough to obtain a clear solution. Pure 2-hydroxyacetophenone diphenylenehydrazone (4.5 g — 80 %) was obtained as yellow prisms, mp 164—5°. IR (KBr) : 725, 750, 760 (arom. C—H), 1375, 1435 (methyl group), 1630 (azomethine group), 1235, 1340, 3090 (intramol. bonded O—H). MS, m/e : 302 (3.8), 301 (25.4) 300 (100.0, M^+), 167 (78.8), 166 (79.5), 134 (82.4), 93 (7.6) .

4-Hydroxyacetophenone diphenylenehydrazone. The crude product mp 220—1° was isolated in 78 % yield in the usual manner. After crystallization from 90 ml of ethanol 3.75 g (62 %) of pure diphenylenehydrazone were obtained as creamy yellow needles mp 221—2°. IR (KBr) : 730, 760, 830 (arom. C—H), 1380, 1435 (methyl group), 1620 (azomethine group), 1240, 1330, 3480 (O—H). MS, m/e : 302 (2.4), 301 (18.2), 300 (77.2), 167 (32.1), 166 (34.7), 134 (100.0), 93 (22.9).

Benzophenone diphenylenehydrazone. The crude product, mp 159—62° was isolated in 69 % yield from the dark brown reaction mixture after 48 hrs of standing at room temperature. It was crystallized from the mixture of toluene and ethanol 1 :1. Bright yellow prisms of benzophenone diphenylenehydrazone, mp 163—5° (dec.), were isolated in 64 % yield (4.45 g). IR (KBr) : 730, 750, 770 (arom. C—H), 1450, 1490, 1500, 1605 (arom. rings), 1630 (azomethine group). MS, m/e : 348 (2.3), 347 (21.0), 346 (76.6, M^+), 180 (100.0), 167 (21.8), 166 (21.0), 77 (88.6).

2-Hydroxyacetophenone diphenylenehydrazone. Equimolar (0.02 M) amounts of 9-aminocarbazole (3.64 g) and 2-hydroxybenzophenone (3.96 g) were dissolved in 80 ml of boiling xylene. A solution of two drops of boron fluoride — acetic acid liquid complex in 20 ml of acetic acid was added and the mixture refluxed for 2 hrs. The brown, tarry solution thus obtained was chromatographed on silicagel 60 (230 mesh. E. Merck, Darmstadt), using 50×500 mm column. Diphenylenehydrazone was eluted with a toluene — *n*-heptane 1 :1 mixture, and crystallized from *n*-heptane. The pure product, mp 161—2° was isolated in 24 % yield (1.74 g). 9-Aminocarbazole and 9-acetylaminocarbazole were also isolated and identified by their mixed mps. IR (KBr) : 725, 750, 765, 790 (arom. C—H), 1455, 1490, 1560, 1600 (arom. rings), 1625 (azomethine group), 1240, 1340, 3420 (O—H). MS, m/e : 364 (4.3), 363 (26.2), 362 (89.0, M^+), 196 (100.0), 167 (48.8), 77 (39.6).

Dibenzoyl diphenylenehydrazone. A solution of 3.64 g benzyl (0.02 M) and 3.64 g(0.02 M) of 9-aminocarbazole in 80 ml of xylene with a drop of boron fluoride etherate was refluxed for 0.5 hrs. Petroleum ether (300 ml) was added and the mixture left for crystallization. The crude product (5.10 g, mp 171—4°) was crystallized from 20 ml of butanone yielding 4.20 g (56 %) of dibenzoyl diphenylenehydrazone as orange prisms mp 176—7°. IR (KBr) : 720, 750, 790 (arom. C—H), 1445, 1480, 1560, 1595 (arom. rings), 1630 (azomethine group), 1670 (carbonyl group). MS, m/e : 376 (1.8), 375 (9.4), 374 (33.4, M^+), 166 (33.8), 105 (100.0), 103 (5.5).

9-(N-Benzylamino)-carbazole. The solution of 5.40 g (0.02 M) of 9-(N-benzylideneamino)-carbazole in 300 ml of dry ethyl ether was dropped into the stirred supension of 0.80 g (0.02 M) of lithium aluminum hydride in 150 ml of ether. The mixture was stirred and refluxed for 10 min. Ethanol (10 ml) and 10 % aqueous solution of potassiun hydroxide (5 ml) were cautiously. added. The thick paste was stirred for 10 minutes, filtered and the white precipitate washed with ether. The filtrate was evaporated to dryness and the residue crystallized from isoöctane yielding. 5.00 g (92 %) of white needles, mp 120—1°. After recrystallization 4.85 g (89 %) of 9-(N-benzylamino)-carbazole, mp 121—2°, were obtained.

In 400 ml of ethyl ether, 5.40 g (0.02 M) of 9-(N-benzylideneamino)-carbazole and 0.88 g (0.04 M) of lithium borohydride were dissolved. The solution was refluxed or 4 hrs and evaporated to dryness. The residue was washed with water and crystallized from methanol. 9-(N-Benzylamino)-carbazole, mp 117—8°, was obtained in 87% yield (4.76 g). Recrystallization from ethanol gave pure product, mp 118—20°. IR (KBr) : 720, 730, 750, 3060 (arom. C—H), 705 1500, 1320, 3300 (N—H), 2880, 3030 (alifat. C—H). MS, m/e : 274 (0.8), 273 (6.8), 272 (26.6, M^+) 182 (14.8), 181 (100.0), 166 (9.7), 91 (5.6).

9-[N-(2-Hydroxybenzyl)-amino]-carbazole. 9-(N-Salicylideneamino)-carbazole (8.58 g — — 0.03 M) and 0.87 g (0.04 M) of lithium borohydride were dissolved in 70 ml of tetrahydrofuran and refluxed for 10 min. After evaporation of the solvent the residue was washed with water and crystallized from toluene. The pure product was obtained as long, white needles, mp 138—9° ; yiled 7.28 g (84%). IR (KBr) : 730, 750, 770, 3050 (arom. C—H), 705, 1500, 3300 (N—H), 3265 (intramol. bonded O—H). MS, m/e : 289 (6.8), 288 (30.8, M^+), 182 (95.1), 181 (100.0), 166 (34.9).

9-[N-(2-Hydroxynaphthyl-1-methylene)-amino]-carbazole. The reaction was performed as above using equimolar amounts (0.02 M) of lithium borohydride. The reaction time was prolonged to 1 hr. After crystallization from ethanol, 5.25 g (77%) of the product were obtained, mp 174—7°. Recrystallization gave 4.25 g (62%) of 9-[N-(2-hydroxynaphthyl-1-methylene)-amino]-carbazole as creamy needles, mp 176—7°. IR (KBr) : 730, 760, 3070 (arom. C—H), 715, 1500, 3300 (N—H), 3400 (free O—H). MS, m/e : 183 (16.3), 182 (100.0), 166 (41.1), 156 (30.8), 128 (54.8), 127 (14.6).

N-(9-Carbazolyl)-1-phenylethylamine. Acetophenone diphenylenehydrazone (2.84 g—0.01M) and 0.40 g (0.01 M) of lithium aluminum hydride in 250 ml of ethyl ether were stirred and refluxed for 20 min. Ethanol (5 ml) and 1.5 ml of 33% aqueous potassium hydroxide were slowly added. A white precipitate was filtered off and washed with ether. The filtrate was evaporated and the residue crystallized twice from *n*-heptane. N-(Carbazoyl)-1-phenylethylamine as transparent prisms, mp 86—8° was obtained ; yield 2.35 g (82%). IR (KBr) : 730, 755, 770, 3060 (arom. C—H), 720, 1330, 1500 (N—H), 1380, 2870, 2990, 3300 (alifat. C—H). MS, m/e : 288 (1.1), 287 (5.3), 286 (22.6, M^+), 182 (37.4), 181 (100.0), 105 (21.4).

N-(9-Carbazolyl)-1-(2-hydroxyphenyl)-ethylamine. A solution of 3.00 g (0.01 M) of 2-hydroxyacetophenone diphenylenehydrazone and 0.33 g (0.015 M) of lithium borohydride in 250 ml of ethyl ether was refluxed for 10 min. Methanol (5 ml) and water (100 ml) were added to the stirred solution. The organic layer was separated, dried with anhydrous magnesium sulfate and ether evaporated to dryness. The residue was dissolved in 100 ml of *n*-heptane, boiled with charcoal, filtered and evaporated. The product was finely grounded and dried in vacuum at 80°. N-(9-Carbazolyl)-1-(2-hydroxyphenyl)-ethylamine (2.80 g, 92%) was obtained as the white amorphous solid mp 116—19°. IR (KBr) : 730, 755, 3060 (arom. C—H), 1380, 2940, 2980 (alifat. C—H). 1510 (N—H), 3265 (O—H). MS, m/e : 303 (2.3), 302 (10.3, M^+), 182 (100.0), 181 (28.6), 166 (24.0), 121 (17.5).

Diacetyl derivatives were obtained under the influence of acetic anhydride in the presence of a trace of boron trifluoride — acetic acid complex ; colourless plates, mp 144—5°. Found : C, 74.39 ; H, 5.54% . Calcd. for $C_{24}H_{22}N_2O_3$: C, 74.58 ; H, 5.74% . IR (KBr) : 730, 750, 3070 (arom. C—H), 1220, 1780 (ester group), 1690 (amide band). MS, m/e : 387 (11.0), 386 (38.5, M^+), 224 (71.3), 182 (46.9), 181 (69.4), 166 (42.1), 211 (100.0). NMR (Me_2CO-d_6) : δ, ppm, 7.90—8.12, m, 2H and 6.48—7.52, m, 10H (aromatic protons), 7.71, s, 3H (N-acetyl group), 9.08, q J=7 Hz, 1H (methine proton), 8.42, d J=7Hz, 3H (methyl group), 8.78, s, 3H (O -acetyl group).

N-(9-Carbazolyl)-1-(4-hydroxyphenyl)-ethylamine. 4-Hydroxyacetophenone diphenylenehydrazone was reduced in an analogous manner. The product was isolated as light yellow amorphous solid, mp 162—5° ; yield 64% (1.95 g). It is unstable and darkens when exposed to the air. IR (KBr) : 730, 750, 3060 (arom. C—H), 1505, 3280 (N—H), 3420 (O—H). MS. m/e : 303 (2.0), 302 (7.4, M^+), 182 (100.0), 181 (22.6), 166 (20.6), 121 (30.0).

N-(9-Carbazolyl)-benzhydramine. The reduction of 3.46 g (0.01 M) of benzophenone diphenylenehydrazone was performed in ethyl ether solution using 0.80 g (0.02 M) of lithium aluminum hydride. The mixture was stirred and refluxed for 30 minutes and worked up as usual. The crude product was crystallized twice from *n*-heptane. N-(9-Carbazolyl)-benzhydramine was obtained in 80% yield (2.79 g) as transparent rods, mp 148—9°. IR (KBr) : 730, 750, 760, 3040, 3080 (arom. C—H), 710, 1500, 3280 (N—H). MS, m/e : 350 (1.2), 349 (5.5), 348 (17.7, M^+), 182 (10.8), 181 (62.9), 167 (100.0), 166 (12.4), 165 (16.9).

N-(9-Carbazolyl)-1,2-diphenylethanolamine. Dibenzoyl diphenylenehydrazone (3.74 g — — 0.01 M) and 0.80 g (0.021 M) of lithium aluminum hydride were stirred in 300 ml of ether for 10 minutes at room temperature. A solution of 5 ml of ethanol in 20 ml of ether and 2 ml of 33% aqueous potassium hydroxide were cautiously added. A white solid was filtered off and washed with two 100 ml portions of ether. The filtrate was evaporated to dryness and the colourless, transparent oil was crystallized from 450 ml of *n*-heptane. N-(9-Carbazolyl)-1,2-diphenylethanolamine (3.42 g — 90%) was obtained as long, white needles, mp 148—9°. IR (KBr) : 730, 760 (arom. C—H deformations), 700, 1500, 3335 (N—H), 3400 (bonded O—H). MS, m/e : 380 (0.5), 379 (3.0), 378 (9.8, M^+), 272 (15.4), 271 (61.5), 182 (2.3), 181 (3.6), 166 (30.8), 167 (100.0), 140 (2.8), 139 (1.7), 105 (4.1).

Dibenzoyl diphenylenehydrazone (3.74 g — 0.01 M) and lithium borohydride (0.65 g — 0.03 M) in tetrahydrofuran (250 ml) solution were stirred and refluxed for 30 minutes. The solvent was evaporated and the residue dissolved in 100 ml of boiling ethanol. The solution when cooled to −22° deposited 0.53 g of white needles mp 165—191°. After two recrystallizations from ethanol, 0.09 g of N-(9-carbazolyl)-1-2-diphenylethanol-amine was obtained, mp 211—3°. Found : C, 82.38 ; H, 5.82% . Calcd for $C_{26}H_{22}N_2O$: C, 82.51 ; H, 5.86% . IR (KBr) : 730, 765, 3070 (arom. C—H), 705, 1500, 3315 (N—H), 3530 (free O—H). MS, m/e : 378 (3.4, M^+), 271 (22.8), 167 (100.0), 166 (61.5), 106 (32.9), 105 (43.3), 104 (30.9).
Ethanolic mother liquor was evaporated and the residue crystallized twice from *n*-heptane ; 2.15 g (57 %) of the isomer melting 148—9° was obtained.

REFERENCES

[1] W. Koga and J. P. Anselme, *J. Org. Chem.*, **33**, 3963 (1968).
[2] P. A. Smith and H. G. Pars, *J. Org. Chem.*, **24** 1325 (1959).
[3] F. D. Chataway and G. R. Clemo, *J. Chem. Soc.*, **128**, 3052 (1926).
[4] M. K. Gluzman, *Tr. Kharkov. Univ.*, **5**, 93 (1940) : *Chem. Abstr.*, **38**, 743 (1944).
[5] R. O. Matevosyan, I. J. Pospovsky and A. K. Chirkov, *Zhur. obschchei Khim.*, **30**, 3186 (1960).
[6] D. Braun and G. Peschk, *Angew. Chem.*, *Intern. Ed.*, **7**, 945 (1968).
[7] J. P. Donskikh et. al., *Zhur. org. Khim.*, **10**, 595 (1974).
[8] H. Wieland, A. Süsser and H. Fressel, *Liebigs Ann. Chem.*, **392**, 170 (1912).
[9] R. K. Eichman, W. O. Lukashevich and E. A. Silieva, *Zhur. prikład. Khim.*, **6**, 93 (1939).
[10] A. V. Blom, *Helv. Chim. Acta*, **4**, 625 (1921).

Revue Roumaine de Chimie, 25, 5, 729–733 (1980)

PHOTOCHEMICAL AND THERMAL BEHAVIOUR OF ACRYLONITRILE–BUTYL ACRYLATE–VINYLIDENE CHLORIDE TERPOLYMER

IOANA DEMETRESCU and MARGARETA TOMESCU

National Institute of Chemistry, Chair of Physical Chemistry and Electrochemical Technology,
Bucharest, Bd. Republicii 13, Romania

Received January 9, 1980

Photochemical and thermal degradation of a new copolymer[1] acrylonitrile–butyl acrylate–vinylidene chloride, prepared by radical polymerization was investigated. TG and DTA curves, UV, visible, IR spectra, molecular weight and turbidimetric curves of degradated copolymer are discussed. The experiments were performed in both argon flow and air.

INTRODUCTION

Great importance has been attached to the study of chemical transformations of polymers under the action of temperature, light and high energy radiations. It is quite probable that the properties of the polymer will change sharply as a result of degradation. Hence, it is very important to know the mechanism and pattern of degradation processes to be able to keep them under control.

There are numerous papers devoted to this problem. The present study refers to the effect of light and temperature on the new copolymer acrylonitrile (AN)–butylacrylate (BA) – vinylidene chloride (VC), and will contain a comparison between photochemical and thermal behaviour.

EXPERIMENTAL

Copolymer

The copolymer and polyacrylonitrile (PAN) used were prepared[1] in solution at 60° using 0.1% azoizobutyronitrile. Polymerization was carried out under inert atmosphere. The copolymer composition was deduced from nitrogen and chlorine analysis, using the microKjeldhal and Schöniger methods, respectively. The copolymer composition (by weight) is: AN = 70.29%, BA = 26.91% and CV = 2.80%.

Number-average molecular weight of copolymer was determined from osmotic pressure measurements of 0.2% (by weight) solutions of polymers in DMF at 30° using an automatic Hallikainen osmometer. The value was 70,000. Molecular weights of the initial and irradiated copolymer were determined also using an Ulbelhode viscosimeter.

Degradation

Photochemical irradiation was carried out on copolymer powder in quartz cells using integral light of a medium pressure mercury lamp (400 W). Cold water was circulated around the cell, keeping the temperature at about 20°. In these conditions the thermal degradation is negligible.

In order to study thermal degradation, a derivatograph MOM Budapest type Paulik-Paulik-Erdely was used. In both DTA and TG analyses the samples were heated in the same conditions.

The degradation experiments were carried out either in argon flow or in air.

Spectra

In order to get the spectra of powder samples throughout the visible and ultraviolet regions, Unicam SP 1800 with SP-890 diffuse reflectance accessory was used.

Infrared spectra were recorded using a UR–10 Karl-Zeiss Jena spectrophotometer (range 400–5000 cm^{-1}) and a Unicam SP 1000 IR spectrophotometer (range 625–3800 cm^{-1}). Spectra were recorded in KBr pellets in the same conditions and with the same polymer concentration.

Turbidimetric titration [2]

For polidispersity investigation of irradiated copolymer (at different time of irradiation) Lange turbidimeter was used. In order to get tubidimetric curves the nonsolvent addition method was chosen. In all the systems concentration of polymer was 0.02% in dimethylformamide and the nonsolvent was methylalcohol.

RESULTS AND DISCUSSION

Copolymer irradiations involve a gradual change in polymer colour from yellow to red; the same change has been observed during the thermal degradation. Consequently new bands at 285 nm and in the 420 nm region appeared which could be assigned to conjugated double bond $-C=N-C=N-$.[3] The 285 nm band can also be assigned to the carbonyl or peroxy groups,[4,5] but they are not likely to occur since the spectra of the irradiated polymer under argon flow exhibit the same absorption as the irradiated polymer in air. The 285 band can be more probable assigned to the structure formed by nitrile group oligomerization. Cyclization have been observed in both thermally degradated copolymer and polyacrylonitrile [6,7]:

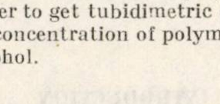

This structure is supported by infrared spectra of irradiated copolymer.

Spectra of initial and irradiated polymers at different times are presented in figure 1.

The weak 1650 cm^{-1} band is due to the isolated double bonds C=C obtained in dehydrochlorination of the vinylidene chloride units. Irradiated copolymer spectrum shows rapid chlorine disapperance (525 cm^{-1} bond) which has also been remarked at the thermal degradation.

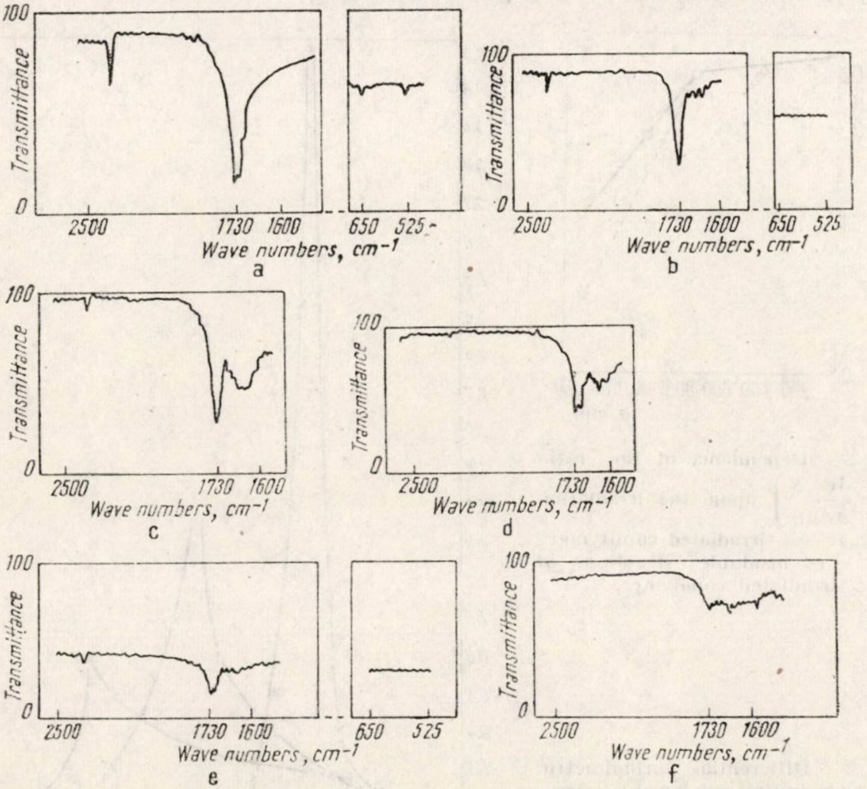

Fig. 1. — Infrared spectra of copolymer : *a*) initial copolymer ; *b*) irradiated copolymer (750 minutes) ; *c*) irradiated copolymer (1350 minutes) ; *d*) insoluble fraction (after 1350 minutes of irradiation) ; *e*) copolymer heated for 20 minutes at 200° ; *f*) copolymer heated for 20 minutes at 320°.

An analysis of IR spectra indicated that the butyl acrylate units in copolymer were only slightly affected during irradiation, while during the thermal degradation a gradual change of these units occurred. This behaviour is quite different from irradiated polybutylacrylate.[8] In the last case the degradation and crosslinking are more important than in other polyacrylates.

The spectrum of insoluble fraction in dimethylformamide (the best solvent for initial copolymer) at 1350 minutes irradiation time is shown in figure 1 d. Insoluble fraction obtained after extraction is 50.5 %. Analysis of the spectra a, b, c, d (Fig. 1) shows a rapid diminution of nitrile absorption at 2238 cm^{-1}, in insoluble fraction.

Using the standard line method arbitrarily chosen, quantitative measurement of nitrile absorption was done.

The standard line was 1730 cm^{-1} vibration, corresponding to C=O, group (because in the irradiation conditions this group is inert) and the absorption ratio $R = \frac{A_{C\equiv N}}{A_{C=O}}$ was calculated. The dependence of the ratio R upon the irradiation time is presented in figure 2.

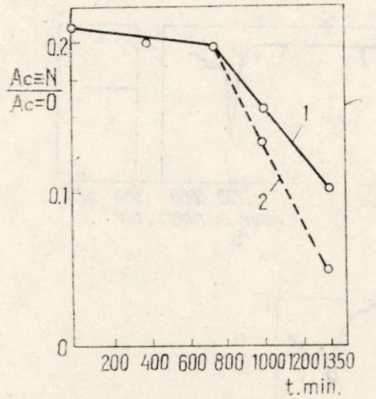

Fig. 2. — Dependence of the ratio $\left(R = \frac{A_{C\equiv N}}{A_{C=O}}\right)$ upon the irradiation time : *1.* ——— irradiated copolymer ; *2.* — — — insoluble fraction of irradiated copolymer.

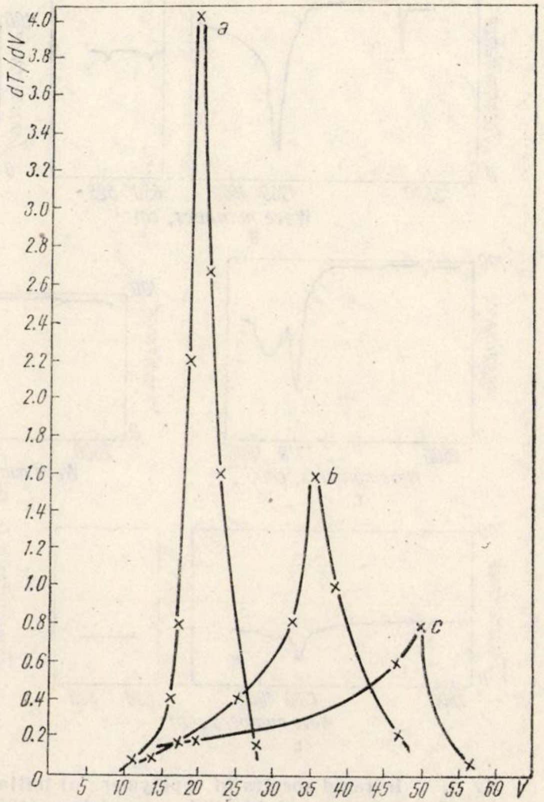

Fig. 3. — Differential turbidimetric curves : *a.* initial copolymer ; *b.* irradiated copolymer (750 minutes) ; *c.* irradiated copolymer (1350 minutes).

Spectral modifications (infrared) of irradiated copolymer, involve structural changes in copolymer. This observation is supported by a strong decrease in the solubility of the irradiated copolymer in dimethylformamide. Differential turbidimetric curves of the copolymer at different irradiation times are given in figure 3. Curve shape shows a sharp polydispersity decrease with time irradiation increase. Molecular weight is increasing at the same time. These data suggest that the nitrile groups of polyacrilonitrile can react with one another intramolecularly to form cycles :

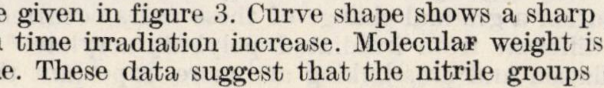

I

or intermolecularly with the formation of network structures :

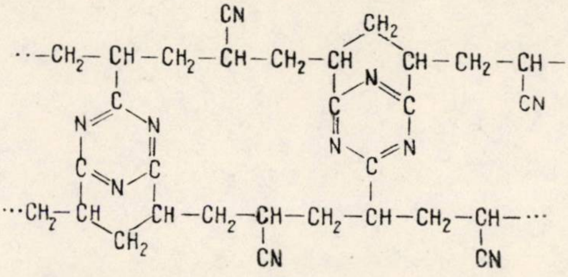

II

Intramolecular ring formation in Tager's opinion causes no loss of solubility in polymers. The fact that copolymer (or polyacrylonitrile) becomes less soluble when heated or irradiated, can be accounted for only by the formation of threedimensional networks. The products of intramolecular ring formation have elevated thermal stability.

A minor contribution in crosslinking formation is due to the intermolecular dehydrochlorination of few units of vinylidene chloride of the chain.

The structures I and II in the thermal degradation of polyacrylonitrile [8,9] and acrylic copolymers [7,10] were already established.

During the thermal degradation the cycle formation takes place around 300° while during the photochemical irradiation, intra and intermolecular cyclization takes place at room temperature, on large proportion, ar relatively short irradiation time.

CONCLUSIONS

1. The irradiation of the new AN—BA—CV copolymer under the examined conditions takes place preferentially (50.5% at 1350 minutes) through intra and intermolecular cyclization at the same time with degradation.

2. During the thermal degradation process of the same copolymer, oligomerization takes place around 300° and chain rupture appears at temperature over 460°.

3. Experimental data under argon flow in air do not indicate sensible photo-oxidative process.

REFERENCES

[1] M. Tomescu, V. Părăuşanu, M. Georgescu, S. Creţu, I. Hogea, D. Mihăiţă and E. Rizescu, RSR Patent 59.668 June, 1976.

[2] I. E. Climie and E. F. T. White, *J. Polymer. Sci.*, **47**, 149 (1960).

[3] J. Hawer and A. Maculso, *Chem. Rev.*, **64**, 473 (1964).

[4] W. H. Gibb and J. R. Mc. Callum, *European Polymer, J.*, **10**, 529 (1974).

[5] W. H. Gibb and J. R. Mc. Callum, *European Polymer J.*, **9**, 771 (1973).

[6] N. Grassie and R. Mc. Guchan, *European Polymer J.*, **6**, 1277 (1970).

[7] M. Tomescu, I. Demetrescu and E. Segal unpublished data.

[8] N. Grassie and J. R. Mc Callum, *J. Polymer. Sci.*, **A 2**, 983 (1964).

[9] A. Tager, "Physical Chemistry of Polymers" Mir Publishers, Moscow, 1972.

[10] N. Grassie and R. Mc. Guchan, *European Polymer. J.* **8**, 257 (1972).

Revue Roumaine de Chimie, 25, 5, 735–743 (1980)

ON THE DETERMINATION LIMIT

CANDIN LITEANU, ION RÎCĂ and ELENA HOPÎRTEAN

Department of Chemical Technology, University of Cluj-Napoca str. Arany János nr. 11, Cluj-Napoca, Romania

Received August 15, 1979

Considering that an information content $I_D < 1$ bit is necessarily associated to the determination limit, this value will be defined in probabilistic correlation of the fluctuations of the determination signal with the fluctuations of the detection signal. The determination limit is defined using the four–step model based on the probabilistic correlation of the fluctuations field of the determination signal with the fluctuations field of the detection signal, as well as the probabilistic correlation of the fluctuations field of the detection signal with the fluctuations field of the background signal. Hence, it results that the determination limit can be probabilistically correlated with the background fluctuations. Thus, the determination characteristic of an analytical system may be defined based on function $\bar{c}_D = f[(P_{10})_0, (P_{11})_d, (P_{10})_d, (P_{11})_D]$. Two methods for the evaluation of the determination limit are presented, namely : the procedure based on the calibration function and the frequentometric procedure.

DEFINITION OF DETERMINATION LIMIT

Since the analytical signal is a random variable, it is natural to treat chemical detection on the basis of the statistical theory of signal detection. In this way, the problem of defining and estimating the detection limit has been considered fully solved in principle.[1–5] However, the same cannot be said of the determination limit.[1,6–9]

In the case of detection, if the fluctuation field of the detection signal is probabilistically correlated with that of the background noise, the removal of one of the two equally probable alternatives (present) or (absent) will always give an information content $I_d = 1$ bit, regardless of the analytical system (method) used, according to Brillouin's formula[10] : $I_d = \log_2(P_0/P_1 = \log_2(2/1) = 1$ bit.

In the case of determination, the information content I_D is necessarily greater than 1 bit, since in this case the uncertainty eliminated is greater than one of the two alternatives : present or absent. Consequently, defining and estimating the determination limit will be based on the probabilistic correlation of the fluctuation field of the determination signal ($I_D > 1$ bit) with that of the detection signal ($I_d = 1$ bit), which is correlated in turn with that of the background ($I_b = 0$). This can be based on the four-step statistical model presented in figure 1.

All the y values in region R_1, $[y > (y_k)_d]$, can be used for detection ($I = 1$ bit) ; that is of two hypotheses $(H_0)_d$ (absent) and $(H_1)_d$ (present), the hypothesis $(H_1)_d$ is selected with true detection probability $(P_{11})_d$. The y values in region R_2, $[y > (y_k)_D]$, are used for determination ($I > 1$ bit). Therefore, to the values $y \leqslant (y_k)_D$, i. e. to the hypothesis $(H_0)_D$ (that the signal belongs only to the detection field) there is attached the probability $(P_{01})_D$ (error of the second kind) that the signal lies in the determination probability field. At the same time, for all values $y > (y_k)_D$ and hence for

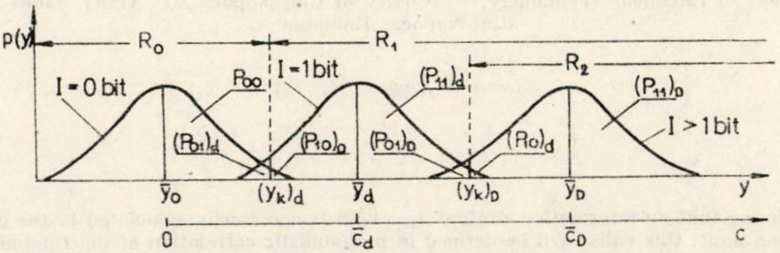

Fig. 1.— Four-step statistical model for defining of the determination limit.

hypothesis $(H_1)_D$ (that the signal belongs to the determination field), there is the true determination probability $(P_{11})_D$, and also the false determination probability $(P_{10})_d$ (error of the first kind), which corresponds to the signal being in only the detection field.

In the two-step component, detection-determination, of the four step statistical model in figure 1, it is necessary to establish the $(y_k)_D$ *determination level* in order to estimate the signal corresponding to the determination limit. To this end, as in the case of the estimation of the *detection level* ,[5] the Neyman-Pearson criterion [11] will be used, i. e. ascribing to the determination level $(y_k)_D$ a certain value of both the false determination probability $(P_{10})_d$ (error of the first kind) and of the true determination probability $(P_{11})_D$, that is a minimum value of the second kind error $(P_{01})_D$, since $(P_{11})_D + (P_{01})_D = 1$.

If the detection signal $\bar{y}_d$ is normally distributed, then normalising the function :

$$(P_{10})_d = \int_{(y_k)_D}^{\infty} p(y_d)\, dy_d \tag{1}$$

by means of_ $(z_k)_D = |\bar{y}_d - (y_k)_D|/\sigma_{y_d}$, for the determination level one obtains :

$$(y_k)_D = \bar{y}_d + (z_k)_D \sigma_{y_d} \tag{2}$$

The normal deviate values $(z_k)_D$ are obtained from table [12] for the Laplace function : $\Phi(z_k)_D = 0.5 - (P_{10})_d$.

Similarly, for the determination signal $\bar{y}_D$, normalising the function :

$$(P_{11})_D = \int_{(y_k)_D}^{\infty} p(y_D)\, dy_D \tag{3}$$

by means of the normal deviate $z_D = |(y_k)_D - \bar{y}_D|/\sigma_{y_D}$, yields

$$\bar{y}_D = (y_k)_D + z_D\sigma_{y_D} \tag{4}$$

where $\Phi(z_D) = (P_{11})_D - 0.5$.

From eqs. (2) and (4), the expression for the signal corresponding to the determination limit is obtained :

$$\bar{y}_D = \bar{y}_d + (z_k)_D\sigma_{y_D} + z_D\sigma_{y_D} \tag{5}$$

and when on the basis of the test F the hypothesis $H_0 : \sigma^2_{y_d} = \sigma^2_{y_D}$ is accepted, one obtains :

$$\bar{y}_D = \bar{y}_d + [(z_k)_D + z_D]\sigma_{y_D} \tag{6}$$

Therefore, the analytical signal corresponding to the determination limit $\bar{c}_D$ can be estimated in relation to the analytical signal corresponding to the detection limit $\bar{c}_d$.

Taking into account the relation between the background and the detection signal in the four-step statistical model in figure 1, and assuming a normal distribution of the detection signal coresponding to the detection limit and when, on the basis of the test F, the hypothesis $H_0 : \sigma^2_{y_0} = \sigma^2_{y_d}$ is accepted, one obtains :

$$\bar{y}_d = \bar{y}_0 + [(z_k)_d + z_d]\sigma_{y_d} \tag{7}$$

From eqs. (6) and (7) :

$$\bar{y}_D = \bar{y}_0 + [(z_k)_d + z_d]\sigma_{y_d} + [(z_k)_D + z_D]\sigma_{y_D} \tag{8}$$

and when on the basis of the test F the hypothesis $H_0 : \sigma^2_{y_d} = \sigma^2_{y_D}$ is accepted, one obtains :

$$\bar{y}_D = \bar{y}_0 + [(z_k)_d + z_d + (z_k)_D + z_D]\sigma_y = \bar{y}_0 + k'_D\sigma_y \tag{9}$$

whence :

$$k'_D = (\bar{y}_D - \bar{y}_0)/\sigma_y \tag{10}$$

is the *determination signal-to-noise ratio*. Therefore, the analytical signal corresponding to the determination limit, based on the four-step statistical model (figure 1), can also be estimated in relation to the background noise.

Taking, for instance, $(P_{10})_0 = (P_{10})_d = 0.025$ and $(P_{11})_d = (P_{11})_D = 0.975$, one obtains $(z_k)_d = (z_k)_D = 1.96$ and $z_d = z_D = 1.96$, so that $\bar{y}_D = \bar{y}_0 + 7.84\,\sigma_{y_D}$.

Further if the relation between signal and concentration is linear, i. e. :

$$y = \bar{y}_0 + bc \tag{11}$$

the value of the determination limit $\bar{c}_D$ can be obtained.

The determination limit is defined by that concentration value $\bar{c}_D$ *for which the determination level* $(y_k)_D$ *is associated with a false determination probability* $(P_{10})_d$ *and with a correct determination probability* $(P_{11})_D$.

Thus, the estimation of the determination limit is not based on an arbitrarily chosen value related to the relative standard deviation.[1,6,7,9]

Of the determination limit so defined, associated with the four probabilities : $(P_{10})_0$, $(P_{11})_d$, $(P_{10})_d$, $(P_{11})_D$, from equation (10), the relative standard deviation is :

$$(\text{c.v.}\,\%)_D = 100/k_D \tag{12}$$

The following relation can therefore be written :

$$\bar{c}_D = f[(P_{10})_d, (P_{11})_d, (P_{10})_d, (P_{11})_D] \tag{13}$$

and may be termed the *determination characteristic* of an analytical system by analogy with the *detection characteristic*.[4] Figure 2 shows the correspondence between the decision parameter $k_D = f[(P_{10})_d, (P_{11})_D]$ and the analytical signal $\bar{y}_D$ corresponding to the determination limit $\bar{c}_D$.

The function $(P_{11})_D = f(k_D)$ for a certain value of $(P_{10})_d$ is obtained from eq. (6) using the data from table with Laplace function $\Phi(z)$, considering $\Phi(z) = (P_{11})_D - 0.5$ for positive z and $\Phi(z) = 0.5 - (P_{11})_D$ for negative z. For instance, for $k_D = 2$ and $(P_{10})_d = 0.05$, $\Phi(z_k)_D = 0.50 - 0.05 = 0.45$, $(z_k)_D = 1.64$, $z_D = 0.36$, so $\Phi(z_D) = 0.14$, i.e. $(P_{11})_D = 0.05 + 0.14 = 0.64$.

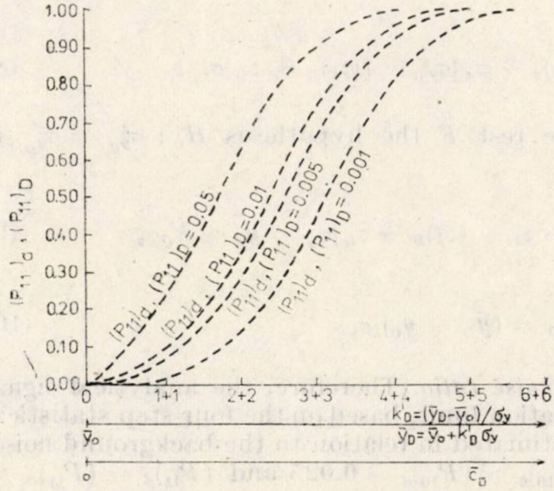

Fig. 2. — Determination characteristic for some values of false estimation probability $(P_{10})_d$, $(P_{11})_D$.

ESTIMATION OF THE DETERMINATION LIMIT

1. Estimation of the determination limit based on the calibration function $y = f(c)$

To estimate from the calibration function the analytical signal corresponding to the determination limit according to eq. (8) it is necessary to know the mean value and the standard deviation of the background fluctuations, i. e. $\bar{y}_0$ and σ_{y_0}, and the standard deviation of the analytical signal σ_y. For this purpose, the analytical signal values are recorded for a series of samples, and from the pairs of (y, c) values in the concentration range adjacent to the determination limit, one obtains by calculation (least-square methods) the calibration function (11).

In the case of a non-linear calibration function, procedures are applied to obtain a linear function having the form of eq. (11).

The confidence interval for the determination limit results, as in the case of the detection limit,[5] from the intersection of the confidence interval of the determination signal $\bar{y}_D$ with the confidence interval for the calibration function (11) delimited by two hyperbolas. An example will be given below for the estimation of the determination limit.

Each of the 5 standard steel samples with a known tungsten content was analysed for 13 times on an ARL-31000 automatic emission spectrometer. Working conditions : $\lambda_W = 2079.1$ Å, argon, intermittent arc, recording time 3 sec. Measurement results (in digits) are listed in table 1.

TABLE 1

Values of the analytical signal for tungsten (digits) for five steel standard samples recorded for 13 times each on an ARL-31,000 automatic emission spectrometer

Concentration (% W)	0.053	0.022	0.012	0.006	0.001
Digits	222	79	36	20	10
	221	75	53	12	5
	215	68	42	4	3
	223	74	53	24	8
	205	71	59	19	3
	203	83	42	24	13
	227	68	50	19	5
	197	66	59	25	0
	211	91	57	15	1
	196	71	46	20	16
	216	90	60	18	12
	226	103	55	17	2
	222	80	52	29	5
$\bar{y}$ (digits)	214.15	78.38	51.08	18.92	6.38
s_y^2	116.6	119.4	57.1	40.3	25.1
s_y	10.8	10.9	7.6	6.3	5.0

Through calculation one finds : $\bar{y}_0 = -1.8$, $b = 4026$, $s_y^2 = 94.2$, $s_y = 9.7$ so the calibration equation assumes the form :

$$y = -1.8 + 4026\ c \tag{14}$$

Taking $(P_{10})_0 = 0.025$, $(z_k)_d = 1.96$; $(P_{11})_d = 0.975$, $z_d = 1.96$; $(P_{10})_d = 0.025$, $(z_k)_D = 1.96$; $(P_{11})_D = 0.975$, $z_D = 1.96$, then, according to expression (9), one obtains $\bar{y}_D = -1.8 + (3.92 + 3.92) \times 9.7 = 74.25$

and using expression (14) it results : $\bar{c}_D = 0.0188$ % W, and using expression (7) one obtains : $\bar{y}_d = -1.8 + 3.92 + 9.7 = 36.22$ and $\bar{c}_d = 0.0094$% W.

This determination limit had been calculated from a single value $s_y = 9.7$ obtained from the calibration equation (14). For this it is necessary to verify with the test F, the approximations $\sigma_{y_0} \simeq \sigma_{y_d}$, and $\sigma_{y_d} \simeq \sigma_{y_D}$, or $s_{y_0} \simeq s_{y_d}$ and $s_{y_d} \simeq s_{y_D}$ i.e. the expression (9) which forms the basis for the calculation of the determination signal $\bar{y}_D$. For this reason it is necessary to know the relations between the estimated standard deviation s_y and the concentration in the low concentration region near the determination and detection limit, respectively :

$$s_y = f(c) \tag{15}$$

For the 5 tungsten concentration values, s_y^2 and s_y are also listed in table 1. Except for the value for $c = 0.053$% W, the function (15) assumes the form :

$$s_y = 4.6 + 279\,c \tag{16}$$

so that, considering the $\bar{c}_D$ and $\bar{c}_d$ previously calculated, we obtain : $s_{y_d} = 7.1$ and $s_{y_d}^2 = 50.4$, $s_{y_D} = 9.7$ and $s_{y_D}^2 = 94.1$, as well as $s_{y_0} = 4.6$ and $s_{y_0}^2 = 21.2$. Applying the F — test for $P = 0.95$ and $n - 1 = 13 - 1 = 12$ degrees of freedom, it results :

$$s_{y_d}^2/s_{y_0}^2 = 50.4/21.2 = 2.38 < 2.57 = F_{\text{tabular}}\,;\quad s_{y_D}^2/s_{y_d}^2 = 94.1/50.4 = 1.86 <$$
$$< 2.57 = F_{\text{tabular}}\,;\quad s_{y_D}^2/s_{y_0}^2 = 94.1/21.2 = 4.48 > 2.57 = F_{\text{tabular}}\,.$$

In conclusion, the approximations $s_{y_0} \simeq s_{y_d}$ and $s_{y_d} \simeq s_{y_D}$ are justified, but the approximation $s_{y_0} \simeq s_{y_D}$ is not. For this, the determination signal must be calculated from the expression (8) instead of (9) and we obtain $\bar{y}_D = -1.8 + 3.92 \times 7.1 + 3.92 \times 9.7 = 64.06$ and $\bar{c}_D = 0.0164$ % which is 13% smaller than the 0.0182 % previously obtained with expression (9). The result is given in figure 3.

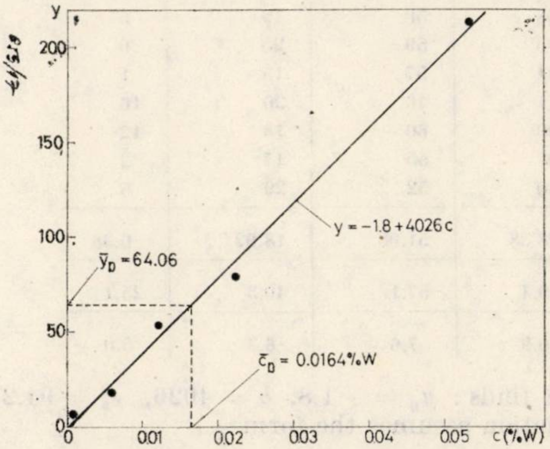

Fig. 3.— Evaluation of the determination limit from the calibration function for the experiment illustrated in table 1.

2. Frequentometric estimation of the detemination limit

As already shown, for the probability $P_{11} = n_+/n = F(c)$, where $n_+ = (n)_{y>(y_k)_D}$, all the values $y > (y_k)_D$ can be used for determination, so a non-linear calibration function can be used, i.e. :

$$F(c) = f(c) \tag{17}$$

For linearization, we pass from frequencies to variable z by means of Laplace function values : $\Phi(z) = F(c) - 0.5$ for $F(c) > 0.5$ (positive z), and $\Phi(z) = 0.5 - F(c)$ for $F(c) < 0.5$ (negative z). Thus, instead of the non-linear function (17) we obtain the linear calibration function :

$$z = \frac{c - \bar{c}}{\sigma} = a + bc \tag{18}$$

where $\bar{c}$ is the concentration value for which $F(c) = 0.5$. Under these new conditions, obviously, the z values play the role of the analytical signals, so that for $(P_{11})_D > 0.5$, $\Phi(z_D) = (P_{11})_D - 0.5$ and $z_D = a + b\bar{c}_D$. Since, according to Glivenko's theorem [13] the experimental frequencies thus obtained estimate theoretical frequencies, it is evident that the z values are also estimations, and a confidence band limited by two hyperbolas, must be associated with expression (18). An example is given below the estimation of the determination limit from the determination level $(y_k)_D$. Thus, by processing the calibration data from table 2, obtained by repeated recording of 8 steel samples with known manganese content ($c \leqslant 0.254\%$ Mn) on an ARL-31000 automatic emission spectrometer, we obtain $\bar{y}_0 = 5.0$, $b = 107.1$ and $\sigma_y = 2.1$. Taking $(P_{10})_0 = 0.025$, $(z_k)_d = 1.96$, $(P_{11})_d = 0.975$, $z_d = 0.96$, using relation (7), and assuming that $\sigma_{y_0} \simeq \sigma_y$, one obtains : $\bar{y}_d = 5.0 + 3.92 \times 2.1 = 13.23$, so that if $(P_{10})_d = 0.025$, $(z_k)_D = 1.96$, and from eq. (2), $(y_k)_D = 13.23 + 1.96 \times 2.1 = 17.44 \simeq 17$ digits. The values $F(c)$, $\Phi(z)$ and z obtained with the determination level $(y_k)_D = 17$ digits are also given in table 2.

From the data in table 2, the least-square calculation gives the calibration equation :

$$z = -5.19 + 44.03\, c \tag{19}$$

With $(P_{11})_D = 0.975$ and $z_D = 1.96$, for the determination limit we obtain $\bar{c}_D = 0.162\%$ Mn. The result is given in figure 4. Since the z_D value is related to a certain value of the true determination probability $(P_{11})_D$, the confidence interval of the determination limit is obtained as in the case of the frequentometric estimation of the detection limit [4] from the intersection of the z_D value with the two hyperbolas which delimit the confidence band of the calibration equation (18), respectively (19).

Since the calibration function $y = f(c)$, for this (table 2) is :

$$y = 5.0 + 107.1\, c \tag{20}$$

TABLE 2

Values of the analytical signal (digits) of eight standard steel samples, on an automatic emission spectrometer (ARL 31.000 type) recorded 32 times each for mangan. Working conditions : λ_{Mn} = 2639.8 Å, argon atmosphere, intermittent arc, recording time 5 sec.

Digits	Signal frequencies (number of samples)							
7	5	—	—	—	—	—	—	—
8	2	1	—	—	—	—	—	—
9	2	4	—	—	—	—	—	—
10	3	1	1	—	—	—	—	—
11	6	3	3	—	—	—	—	—
12	6	9	2	1	—	—	—	—
13	2	3	1	1	1	—	—	—
14	3	7	7	2	—	1	—	—
15	3	2	7	3	1	—	—	—
16	—	1	4	4	4	2	—	—
17	—	1	5	6	1	—	—	—
18	—	—	1	5	6	1	—	—
19	—	—	1	5	7	1	—	—
20	—	—	—	5	5	4	1	—
21	—	—	—	—	5	4	2	—
22	—	—	—	—	2	8	1	—
23	—	—	—	—	—	4	2	—
24	—	—	—	—	—	3	5	—
25	—	—	—	—	—	1	6	—
26	—	—	—	—	—	2	4	—
27	—	—	—	—	—	1	8	1
28	—	—	—	—	—	—	1	2
29	—	—	—	—	—	—	2	—
30	—	—	—	—	—	—	—	4
31	—	—	—	—	—	—	—	5
32	—	—	—	—	—	—	—	2
33	—	—	—	—	—	—	—	10
34	—	—	—	—	—	—	—	3
35	—	—	—	—	—	—	—	2
36	—	—	—	—	—	—	—	2
37	—	—	—	—	—	—	—	1
38	—	—	—	—	—	—	—	—
$\bar{y}$ (digits)	10.9	12.3	14.7	17.2	18.7	21.6	25.2	32.3
% Mn(x)	0.059	0.067	0.087	0.110	0.133	0.152	0.190	0.254
$n_+ = (n)_{y>17}$	—	—	2	15	25	29	—	—
$F(c) = n_+/n$	—	—	0.06	0.47	0.78	0.91	—	—
$\Phi(z)$	—	—	0.44	0.03	0.28	0.41	—	—
z	—	—	−1.56	−0.07	0.77	1.34	—	—

from expression (9) then for the same probabilities as in the case of frequentometric estimation, the determination signal is $\bar{y}_D = 5.0 + (3.92 + 3.92) \times \times 2.1 = 21.46$. Consequently, equation (20) for the determination limit gives $\bar{c}_D = 0.154\%$, very close to the value obtained by the frequentometric procedure.

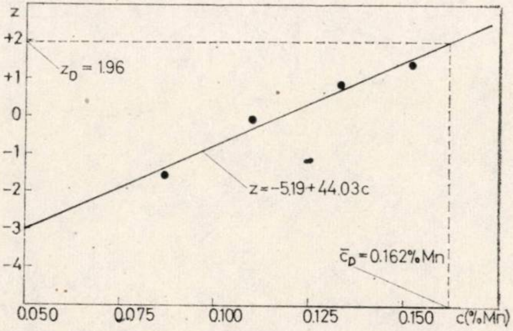

Fig. 4. — Frequentometric procedure for estimating the determination limit (data of the table 2).

REFERENCES

[1] L. A. Currie, *Analyt. Chem.* **40**, 586 (1968).

[2] V. Svoboda and R. Gerbatsch, *Z. analyt. Chem.*, **242**, 1 (1968).

[3] C. Liteanu and I. Rîcă, *Mikrochim. Acta*, **1973**, 745.

[4] C. Liteanu and I. Rîcă, *Mikrochim. Acta*, **1975**, 311.

[5] C. Liteanu and I. Rîcă, *Pure Appl. Chem.*, **44**, 535 (1975).

[6] H. Kaiser, *Spectrochim. Acta. 3*, 40 (1947); *Z. analyt. Chem.*, **209**, 15 (1965).

[7] P. B. Adams, W. O. Passmore and D. E. Campbell, "Symposium on Trace Characterization—Chemical and Physical National Bureau of Standards" (October, 1966), paper no. 14.

[8] R. Püschel, *Mikrochim. Acta, 1968*, 82.

[9] Z. Kotrba, *Chem. listy*, **70**, 71 (1976).

[10] L. Brillouin, "Scientific Uncertainity and Information". Academic Press, New York, 1964, p. 27.

[11] J. Neyman and E. S. Pearson in: C. W. Helstrom "Statistical Theory of Signal Detection", Pergamon Press, New York, 1960, p. 68.

[12] P. D. Lark, B. R. Craven and R.C.L. Bosworth, "The Handling of Chemical Data", Pergamon Press, Oxford, 1969, p. 335.

[13] B. V. Gnedenko, J. K. Beliaev and A. D. Soloviev, "Matematicheskie metody v teorii nadeshnosti", Izd. Nauka, Moskva, 1965, p. 59.

Revue Roumaine de Chimie, 25, 5, 745–751 (1980)

3-ETHYL-4-BENZYLIDENE-5-MERCAPTO-1,2,4-TRIAZOLE AS A NEW GRAVIMETRIC REAGENT FOR THE ESTIMATION OF SILVER IN SALTS, ALLOYS AND COMPLEXES

R. V. GADAG and M. R. GAJENDRAGAD*
Department of Chemistry, Karnataka Regional Engineering College, Srinivasnagar–574157, (S.K.), India

Received February 12, 1979

A rapid and accurate gravimetric method for the determination of silver using 3-ethyl-4-benzylidene-5-mercapto-1, 2, 4-triazole is proposed. The reagent precipitates silver quantitatively as a snow-white complex in ammoniacal medium. The silver complex is weighed as $(C_{11}H_{11}N_4S)Ag$ after drying at 110–130°. The separation of silver from a large number of accompanying ions using suitable masking agents is described. The method is quite suited for the analyses of silver alloys and complexes. The average relative error for the range of 20–100 mg silver is $\pm 0.12\%$ while the relative standard deviation at 40 mg level is 0.06%.

INTRODUCTION

The conventional gravimetric method of estimation of silver as silver chloride, though giving good results, requires careful control of conditions because the precipitate is photosensitive leading to negative error,[1] it disperses in the absence of electrolytes, it dissolves appreciably in excess of acids[1] and the precipitating chloride ions.[2] In addition, the method takes more time as the precipitate should be kept preferably overnight. Besides, the conversion factor (0.75263) for the metal is very high.

Keeping all these points in view, we employed in our earlier work 3-methyl-4-amino-5-mercapto-1,2,4-triazole as a gravimetric reagent for silver.[3] The reagent precipitated silver in ammoniacal medium quantitatively, the precipitate was photo-insensitive, it coagulated readily and the method was rapid (~ 2 hours). In addition the conversion factor was quite low (0.4551).

In pursuit of a still better reagent we have now used 3-ethyl-4-benzylidene-5-mercapto-1,2,4-triazole (Fig. 1, I) which also readily precipitates silver quantitatively from ammoniacal medium as snow white photo-insensitive complex. The complex is easily filterable, and it does not disperse even after repeated washings with hot water. It has high thermal stability and the conversion factor is as low as 0.31804.

---

* To whom all correspondence should be addressed.

This reagent is equally suited for the analyses of silver in complexes and alloys. Interference of the most metal ions can be overcome by using masking agents like EDTA and tartaric acid.

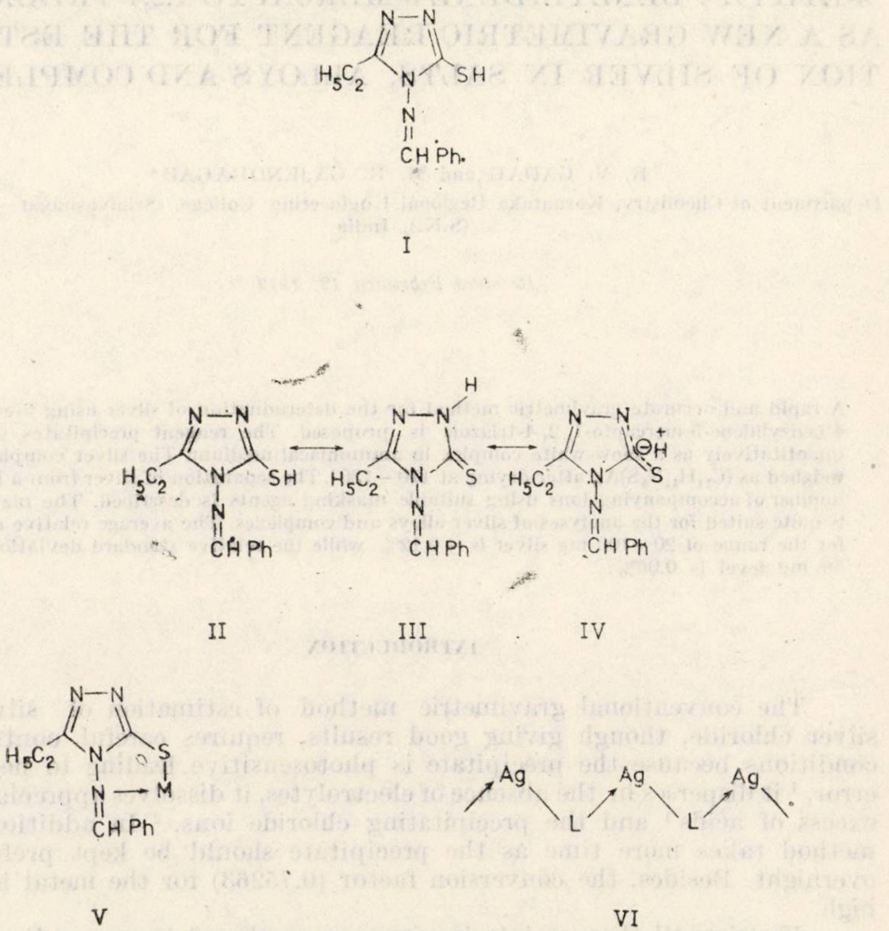

Fig. 1. — I, The reagent-3-ethyl-4-benzylidene-5-mercapto-1, 2, 4-triazole ; II, Thiol form of the reagent ; III, Thione form of the reagent ; IV, Delocalized structure (of the reagent) ; V, Bonding with silver (in the complex) ; VI, Linear polymeric structure of the silver complex.

The synthesis of the reagent, and details of gravimetric determination of silver and characterization of Ag(I) Complex are reported hereunder.

EXPERIMENTAL

Reagents

All chemicals used were of AnalaR standard or of chemically pure grade. Calibe rated Emil-Gold line pipettes were used.

Preparation of reagent

The reagent was prepared by refluxing in equimolar ratios, 28.0 g of 3-ethyl-4-amino-5-mercapto-1, 2, 4-triazole[4] and 21.0 ml of benzaldehyde in 200 ml absolute alcohol in the presence of five drops of conc. HCl for six hours. The excess of the solvent was removed by vaporization on water bath. The product was recrystallized from ethanol, when colourless crystals (m.p. 168°) were got. A twice recrystallized reagent was used for estimations.

The stock solution of silver was prepared by dissolving a known amount of standard silver in minimum amount of (1 :1) nitric acid and making up to a known volume. The silver content of the stock solution was carefully counter-checked by the chloride method.[1]

The solutions of various metal ions were prepared by dissolving either nitrates or sulphates to give concentrations of 3—4 mg/ml in distilled water containing a few drops of appropriate acids. In the case of anions, alkali salts of the respective anions were used.

Various alloys of silver with standard compositions were prepared by melting the desired amounts of the constituent metals in an electric furnace and stirring well for homogeneity. The cooled alloys were well polished, washed with water and air dried. The composition of the alloys was checked by complete analysis. Various silver complexes of substituted triazoles were prepared by adding slight excess of aqueuos (alcoholic) ligand solutions to hot ammoniacal solution of silver, digested for half an hour, centrifuged, washed with hot water, hot alcohol and ether and dried at 110—20°. The purity of the complexes was checked by elemental analysis of C, H and N on micro-scale and S and Ag on semi-micro scale.

Procedure

In a 250 ml beaker, an acidified aliquot of the stock solution containing 20—100 mg silver was diluted to about 100 ml (suitable masking agent was added in the case of foreign ions). The solution was rendered distinctly ammoniacal by adding (1 :1) ammonia. It was heated to about 80° on a water bath and a slight excess of the reagent (up to 10% excess over the molar ratio is tolerable) in the form of 1% ethanolic solution was added with constant stirring. It was kept on water bath and stirred for a few minutes whereby the complex turned snow-white and the solution became absolutely clear. After digesting for 30 minutes, it was filtered by slow suction through a previously weighed sintered-glass crucible, porosity G—4, washed repeatedly with hot water and dried at 110—130° to constant weight. The silver content was computed from the formula weight $(C_{11}H_{11}N_4S)Ag$.

Study of the effect of diverse ions

The potential interference of the foreign ions was studied by estimating silver in the presence of various ions added to the stock solution of silver. To a solution containing 43.12 mg silver were added solutions containing diverse ions, followed by 1—2 g of suitable masking agent and the silver was estimated as described above. The results are given in table 1.

Application to silver alloys and complexes

The method can be conveniently used for the rapid determination of silver in alloys and complexes also.

Procedure for silver alloys

Known amounts of the alloys were dissolved in moderately *conc.* nitric acid and diluted aliquots of these solutions were used for silver estimation by the procedure described above, using EDTA as masking agent. The results were compared with those by the chloride method to have a counter-check. The results are given in table 2.

TABLE 1

Determination of silver in the presenee of divers: ions.
Silver present in aliquot solution = 43.12 mg.

Foreign ion	Quantity of foreign ion added mg	Silver found mg	Error %
Pb (II)	50	43.22	+0.23
	100	43.25	+0.30
Cd (II)	50	43.18	+0.14
	100	43.15	+0.07
Cu (II)	50	43.12	0.0
	100	43.09	−0.07
Bi (III)	50	43.06	−0.14
	100	43.12	0.0
Hg (II)	50	43.25	+0.3
	100	43.25	+0.3
Fe (III)	50	43.18	+0.14
	100	43.25	+0.30
Al (III)	50	43.06	−0.14
	100	43.09	−0.07
Zn (II)	50	43.09	−0.07
	100	43.12	0.0
Ni (II)	50	43.06	−0.14
	100	43.18	+0.14
Co (II)	50	43.18	+0.14
	100	43.22	+0.23
Mn (II)	50	43.09	−0.07
	100	43.09	−0.07
Mg (II)	50	43.12	0.0
	100	43.09	−0.07
NO_3^-	1000	43.12	0.0
	2000	43.12	0.0
SO_4^{2-}	1000	43.06	−0.14
	2000	43.06	−0.14
EDTA	1000	43.09	−0.07
	2000	43.12	0.0
Tartrate	1000	43.00	−0.28
	2000	43.03	−0.21
Oxalate	1000	43.06	−0.14
	2000	43.00	−0.28
Citrate	1000	43.12	0.0
	2000	43.15	+0.07

TABLE 2

Determination of silver in alloys and complexes

Sample	Ag present %	Ag found %
Copper rich alloy (Ag—Cu)	9.51*	9.52
Silver rich alloy (Ag—Cu)	90.22*	90.16
Silver brazing alloy (Ag—Cu—Zn)	49.89*	49.95
$Ag(C_3H_5N_4S)$[a]	45.55	45.39
$Ag(C_2H_3N_4S_2)$[b]	42.35	42.24
$Ag(C_5H_9N_4S)$[c]	40.74	40.65
$Ag(C_{11}H_{11}N_4S)$[d]	31.8	31.67
$Ag(C_2HN_2S_3)$[e]	42.0	41.79
$Ag(C_3H_2F_3N_4S)$[f]	37.07	37.05

* Found by chloride method.

[a] Silver complex of 4-amino-3-methyl-5-mercapto-1, 2,4-triazole.

[b] Silver complex of 4-amino-3, 5-dimercapto-1,2, 4-triazole.

[c] Silver complex of 4-amino-3-propyl-5-mercapto 1, 2,4-triazole.

[d] Silver complex of 3-ethyl-4-benzylidene-5-mercapto-1,2,4-triazole.

[e] Silver complex of 2,5-dimercapto-1, 3, 5-thiadiazole.

[f] Silver complex of 3-trifluoro methyl-4-amino-5-mercapto-1,2,4-triazole.

Procedure for silver complexes

A known amount of the silver complex was heated repeatedly with conc. nitric acid and finally evaporated to dryness. The residue was dissolved in dilute nitric acid and the silver was estimated as described earlier. The results are given in table 2.

Analyses of the reagent and the silver complex

The reagent and the silver complex were analysed for C, H and N by micro methods at National Chemical Laboratory, Pune. The silver was estimated as AgCl after decomposing the complex with conc. nitric acid and the sulphur as $BaSO_4$ after alkali fusion. The results are given in table 3.

TABLE 3

Elemental analysis of the reagent and its silver complex

Compound		C, %	H, %	N, %	S, %	Ag, %
$C_{11}H_{12}N_4S$	Calcd.	56.88	5.21	24.12	13.80	—
	Found	56.79	5.28	24.12	13.65	—
$Ag(C_{11}H_{11}N_4S)$	Calcd.	38.95	3.27	16.52	9.45	31.80
	Found	38.88	3.31	16.48	9.38	31.67

RESULTS AND DISCUSSION

Accuracy and precision

In seven determinations over the range of 20 – 100 mg of silver, there was an average error of ± 0.12% and the relative standard deviation at 40.0 mg level in five determinations was 0.06%. These results show that the method is accurate and dependable.

Effect of diverse ions

The results given in table 2 show that silver can be estimated in the presence of a large number of foreign ions which do not interfere. These ions include Cu(II), Cd(II), Hg(II), Zn(II), Mn(II), Co(II), Ni(II), Pb(II), Mg(II) in the presence of EDTA and Bi(III), Pb(II), Fe(III) and Al(III), in the presence of tartrate. Anions like oxalate, tartrate, citrate, EDTA, nitrate and sulphate also do not interfere.

Characterization of the complex

TGA studies have revealed that the complex remains stable without losing any weight up to 250° and thereafter slowly loses weight. Hence, the complex can be conveniently dried at 110° – 130°.

The analytical data given in table 3 show that a 1 :1 complex is formed. The conversion factor is 0.31804.

I.R. Spectra

The ligand molecule can be expected to remain in tautomeric forms as shown in figure 1 (II and III). This is confirmed by the I. R. spectra of the ligand taken on Perkin Elmer 521 Grating Infra-red Spectrophotometer in KBr phase. Distinct bands around 3100 cm^{-1} and 2500 cm^{-1} appearing in the spectrum of the ligand can be assigned to ν (N–H) and ν(S–H) respectively. However, the band around 2500 cm^{-1} is conspicuous by its absence in the spectrum of the silver complex. This is apparently due to the deprotonation of the thiol group before complex formation. This is quite as expected from the point of charge balance. The thiol group in the ligand so deprotonated would form a bond with silver for the simple reason that $R\bar{S}$ and Ag^+ being both easily polarisable, have greater affinity towards each other. This bonding scheme is in conformity with the 'hard and soft acid base theory'.[5-8]

Further support comes to the bonding scheme proposed above from the systematic shifts in positions of thioamide bands of ligand vis-a-vis those of the complexes indicated below.

As a result of bonding through sulphur of the thiol group, the charge delocalized (Fig. 1, IV) in the ligand would get localized between C and N as shown in figure 1, V. As a result, the stretching frequency of N–H would shift towards higher wave number side while that of C−S towards lower wave number side because of increase and decrease respectively in bond order of the groups. [9] This is confirmed by the I. R. spectral data given in table 4.

TABLE 4

The positions (cm^{-1}) and assignment of the major infra red bands in the spectra of the ligand and the silver complex

Ligand	Ag (I) complex	Assignment
3075−3120 m (split band)	3040−3070	ν (N−H)
2560 W	—	ν (S−H)
1585 S	1620 S	Thioamide band (I) *
1300 S	1385 S	Thioamide band (II)**
1028 m	975 m	Thioamide band III [a]
778 S	694 S	Thioamide band IV [b]
—	375 m	ν(M−S)

* Due to δ (N−H) (major contribution) + ν(C=C) (minor contribution)

** Due to ν (C=N) (major contribution) + ν(C−N) (minor contribution)

[a] Due to ν(C−N) (major contribution) + ν(C=S) (minor contribution)

[b] Due to ν(C=S)

S = strong, m = medium, W = weak.

The complete insolubility of the complex in water leads to either a three dimensional polymeric structure or a linear polymeric structure (Fig. 1, VI). From steric considerations the linear polymeric structure seems to be more probable.

ACKNOWLEDGEMENTS. The authors are grateful to Professor K. Mahadevan, Principal and Professor T. J. Varkey, Head of the Chemistry Department, Karnataka Regional Engineering College, for providing financial assistance, laboratory facilities and all-round help.

REFERENCES

[1] A. I. Vogel, "A Text Book of Quantitative Inorganic Analysis" Longman, London, 1969 pp 460, 461, 486.

[2] R. A. Nadkarni and B. C. Haldar, *Indian J. Chem.*, **1**, 428 (1963).

[3] R. V. Gadag and M. R. Gajendragad, *Talanta*, **25**, 418 (1978).

[4] K. S. Dhaka, J. Mohan, V. K. Chadha and H. K. Pujari, *Indian J. Chem.*, **12**, 288 (1974).

[5] S. Ahriand, J. Chatt and N. R. Davies, *Quart. Rev.*, **12**, 265 (1958).

[6] R. G. Pearson, *J. Amer. Chem. Soc.*, **85**, 3533 (1963).

[7] R. G. Pearson, *Chem. Eng. News*, **43**, 90 (1965).

[8] R. G. Pearson, *Chem. Brit.*, **3**, 103 (1967).

[9] I. Suzuki, *Bull. Chem. Soc. Japan*, **35**, 1286, 1449, 1459 (1962).

Revue Roumaine de Chimie, **25**, 5, 753–759 (1980)

BOOK REVIEWS

A. CĂLUŞARU, "Electrodeposition of Metal Powders", Elsevier Scientific Publishing Company, Amsterdam 1979, 544 p. 230 figs.

This is the first extensive book dealing with the theoretical aspects, experimental research and practical production and utilisation of metal powders obtained by electrolysis of solutions and melts.

The first part consists of eleven chapters. The first one is devoted to introduce the reader into the principles and definitions of thermodynamics and electrochemical kinetics. The next chapter deals with the mechanism of crystallization. Although this subject is vast, the author approached a synthesis of the basic problems, using a high level mathematical instrument, especially for the treatment of the Ştefan type problem. The third chapter is devoted to the study of the electrocrystallization mechanism. In contrast with the general case, where the phase transition is not accompanied by chemical transformations, the electrocrystallization represents a crystallization process preceded by a charge transfer reaction at the (metal)/(electrolyte solution) interface. The crystallization overpotential is thoroughly examined, because in fact this is the electrochemical equivalent of the supersaturation. The fourth chapter is devoted to whiskers. They are basically different from dendrites but their growth occurs also along preferential directions. The main subject of the book is approached in the fifth chapter by the study of the mechanism of dendrite growth. For the case of dendrite electrocrystallization the theoretical problem is to explain the mechanism corresponding to the electrochemical processes, occurring at high overvoltages, the main condition for the dendrite growth (chapter VI). The following two chapters (VII and VIII) show the experimental results with fundamental character connected with the dendrite electrocrystallization. The characteristics and structure of electrolytic powders are presented in chapter IX. Chapters X and XI deal with some special problems related to powders obtained at low current density and the historical review of the hypothesis concerning the mechanism of powder formation. The second part, comprising 9 chapters is devoted to the obtaining of the metal powders and colloids by the electrolysis of aqueous solutions. Practically all metals which can be obtained by electrodeposition from aqueous media are considered.

The third part describes the electrodeposition of powders from melts. Since an important part of the elements cannot be obtained by electrolysis of aqueous media, the remaining alternative is the electrolysis of fused salts. The 9 chapters of this part refer to fused salts systems, working conditions and electrolysis cells in inert atmosphere. The last chapter deals with the refining of several elements in powder form by the electrolysis of the corresponding fused salt systems.

The printing of this book has turned the electrodeposition of metal powders into a new, well defined electrochemical science, having not only its own topics and field of practical applicability, but also its own theory concerning the processes occurring in the limiting current range as well. Indeed the theoretical implications of this case do not concern the interpretation of the common electrochemical processes in a such spectacular manner as in the case of the electrocrystallization of the metallic dendrites. In contrast with the polarography, whose general aim is the measurement and interpretation of the limiting currents, for the metal powders it is most important to consider the mechanism of the elementary act of the electrochemical reaction at uncommonly high overpotential. By considering a quantum model for the interpretation of the processes occurring at the limiting current, the conditions for the flow of high current density are fulfilled. The transition probability for electron transition is high and this is why the neutralization at reasonably larged distance becomes possible. In this case a quantitative theoretical deduction of the particular shape and equations of the barrier would be very complicated, without significantly affecting the results of the numerical calculations. Therefore the common transparence coefficient equation can be used as an interpolation formula in order to calculate the relationship between such parameters giving essential information on the mechanism of the electrode under reaction consideration. If the modern image of partial hydrated states of ions in the double layer, corresponding to different energy levels is considered, it has been shown that, since the discharge occurs in conditions of appreciable overpotential, generated by mass transport, the difference between the various states of partial hydration should correspond to the overvoltage associated with discharge. The limiting states are the adatom close to equilibrium, on one hand and the free hydrated atom in conditions very remote from equilibrium, on the other hand. In the intermediate states the depolarization product may be called quasifree atom.

The process *via* quasifree atoms can occur by cluster participation in the electrocrystallization, forming characteristic metal dendrites. A spectacular experimental verification of this theory was supplied by the study of powder formation as a function of electrode potential on solid electrodes and especially on the dropping mercury electrode. It has been found that while no visible change occurs on the current-voltage curve at a well defined value of the potential, dendrites are suddenly formed which can be observed and micro-photographed. Owing to hydroxide or hydrated salt precipitation, thin films are absorbed on the electrode surface and the dendrite nucleation occurs by quantum electron tunneling across the adsorbed films. Considering the above-mentioned description of the actual state of this new electrochemical science, it is possible to conclude that the electrodeposition of metal powders is satisfactory founded from both theoretical and experimental viewpoints. However the improvement of theory and also the refinement of the experimental studies remain the open problems for the further development of this new science. The book is intended for chemists and chemical engineers, physicists and metallurgical engineers, research staff and highly qualified specialists in various fields.

D. I. Marchidan

G. E. SCHULZ and R. H. SCHIRMER : "Principles of Protein Structure", Springer Verlag, New York, Heidelberg, Berlin, 1979, 314 p.

This book opens a series of Springer advanced texts in chemistry, dedicated to the needs to keep up the progress of research in fields that are rapidly changing. Among the four major types of biopolymers—nucleic acids, polysaccharides, lipid assemblies and proteins — the last are the best known through more than 70 proteins structurally well defined and analysed. These structures provide good models to get the principles of the complex protein architectures as a first step for understanding the relationship between their structure and action in an organism, very important for both scientific and practical purposes. The authors are active researchers in the field and they have accumulated a large knowledge, rendered in a very concise and attractive form in the eleven chapters of the book.

The first one (16 p.) is dedicated to the standard amino acids as basic organizational blocks of all proteins. Having unique properties each amino acid residue fulfils a certain role in a given protein and the analysis of the change frequencies during protein evolution shows some similarities among them.

In the second chapter (10 p.) structural implications of the peptide bond to protein stability and plasticity are analysed. The comparison between *cis* and *trans* peptide bonds reveals that *trans* bond is geometrically superior because it is not as restrictive as the *cis* bond.

The next chapter (10 p.) is devoted to the contribution of noncovalent forces : repulsion between nonbonded electron shells, coupling between oscillating dipoles, electrostatic attraction and repulsion of partial and/or full charges in salt bridges, and hydrogen bonds which determine protein structure as a whole. The interaction between the polypeptide chain and the aqueous environments is discussed in terms of entropies and binding energies of the constituents underlining the strong contribution of the hydrophobic forces to protein stability. All noncovalent forces are used so that the protein interior is very similar to a good crystal.

The covalent structure of protein is the content of chapter 4 (20 p.) in which the concepts of functional "domain" as autonomous region of the polypeptide chain and the structural "domain" as geometrically separate entity are regarded as the basic individual domains. The authors use the physiologically oriented definition, according to which monomers may contain more than one polypeptide chain if the polypeptide chains are linked covalently. They omit cross-links as disulfide bridge or that formed using the ε-amino group of lysine which serve mechanical as well as chemical purposes, and also the epigenetic modifications as main chain scissures or side chain modifications.

In chapter 5 (40 p) patterns of folding and association of polypeptide chains depending on the levels of structural organization are examined : amino acid sequence, secondary and supersecondary structure, structural domain, globular protein and aggregates.

A special chapter 6 is devoted to the prediction of the secondary structure from the amino acid sequence (22 p.) because it was found that some amino acids residues tend to form helices while others do not and those which do form helices in homopolymers prefer to be in helices in globular protein too. The authors classify and describe the current methods for secondary structure prediction from the sequence and for those methods based on statistical mechanics they give an introduction in the appendix of the book.

Chapter 7 (8 p) informs the reader of the models, display and documentation of protein structures, including covalent structures (amino acids sequence) and geometric structure (three-dimensional structure) and their representation.

In the following chapter 8 (16 p.) termodynamics and kinetics of polypeptide chain folding with experimental and theoretical results applying to both aspects are presented. Though the folding process of a polypeptide occurs spontaneously and it is based probably on simple physico-chemical principles it is not yet understood in detail. An exceptional effort has been made to find nuclei of the folding process which are expected to serve as scaffolds for further folding but they could not be detected till now.

A very interesting subject, the protein evolution, is discussed in chapter 9 (40 p.). The protein evolution is presented as a result of numerous natural mutations and subsequent selections (due to gene multiplication and gene fusion) which were employed to study principles of protein structures. Some aspects of speciated proteins which fulfil the same function in different organisms, and of differentiated proteins which lead to functional diversification of homologous proteins, in connection with metabolism, are analysed.

Protein-ligand interactions is the content of chapter 10 (26 p) in which some examples as ligand-binding sites of immunoglobulins, serine proteases (chymotrypsin, trypsin), haem, nucleotides, phosphorylgroups and other macromolecules (lipoproteins, glycoproteins, nucleoproteins) are described.

The last chapter (11) contains the structural basis of protein mechanism, action and function (19 p.) having as examples the proteins for which the mechanisms are known best: hemoglobin, chymotrypsin and protein of skeletal muscle.

The book contains a good subject index and about 800 references (many of them since 1978) with full title of papers which help the reader to find easily the desired details.

Emphasis mustbel aid, from the very beginning, on the special character of the book both in its content and presentation. It provides a comprehensive insight into protein for those who want to find the basic principles for the study and the investigation of the protein structure in an accessible form.

Its reading may captivate even a nonspecialist who will find many appealing problems approached in a highly original manner.

The monograph is adressed to postgraduate students preparing their doctoral thesis, to chemists and physicists interested in structural problems of protein and to researchers and specialists in industry who work in the field of organic products. It could be largely used as an auxiliary information for those dealing with the medical and pharmaceutical aspect of protein chemistry and also for those interested in the study of natural proteins.

F. Cuiban

ANDOR HAJOS, "Complex Hydrides and Related Reducing Agents in Organic Synthesis". Akademiai Kiadó, Budapest, 1979, 398 pages.

The publication of the book — dedicated to Alfred Stock — occurs soon after the centenary of the birth of this scientist who prepared for the first time the pure hydrides of boron and silicon.

The aim of the book is to present, after literature data, the achievements which appeared in the field of hydride reductions in the last 20 years (from the publication of the well-known book of N. G. Gaylord, "Reductions with Complex Metal Hydrides".)

The main chapters describe reductions with: a) Alkali metal and alkaline-earth metal hydrides (2 pages; 18 references); b) Boranes and derivatives, e. g. disiamylborane, 9-BBN, amine-boranes etc. (10 pages; 105 references); c) Aluminium hydride and its derivatives (6 pages; 86 references); d) Metal borohydrides, e. g. sodium borohydride, pure or modified with $AlCl_3$ or BF_3; sodium cyanoborohydride, sulphurated sodium borohydride etc. (32 pages; 350 references); e) Metal aluminium hydrides, e. g. $LiAlH_4$, pure or modified with $AlCl_3$, BF_3 or $CuCl_2$, lithium or sodium alkoxyaluminium hydrides etc. (84 pages; 438 references); f) Silanes, e. g. organosilanes, trichlorosilane and hexachlorodisilane (34 pages; 114 references); g) Organotin hydrides (mono- and dihydrides; 30 pages; 127 references); h) Transition metal hydrides, e. g. alkali metal tetracarbonylhydridoferates, copper hydride, hydrides of noble metals (29 pages; 101 references).

Throughout these chapters, numerous interesting examples (up to the end of 1977) are mentioned (the important reaction conditions being also included). The author underlines the main tendency in recent developments from this field, namely the control of the reducing power of hydrides by : a) synthesis of new substituted hydrides, b) utilisation of appropriate solvents and c) modification of classical hydrides with Lewis acids or metal salts.

Two short chapters present analytical procedures and technique of selective reductions with complex hydrides.

An interesting chapter (182 references) is devoted to mechanistic aspects of reductions with complex hydrides and includes problems like stereochemistry, molecular rearrangements or cleavage of molecular skeleton.

An author index (23 pages) and a detailed subject index (28 pages) end this very interesting and highly useful book, which surely would find its place in all organic laboratories.

M. Banciu

"TOPICS IN CURRENT CHEMISTRY", Volume 83, "Biochemistry", Springer Verlag, Berlin, Heidelberg, New York, 1979, 178 pages.

The book contains three chapters devoted to three modern aspects of biochemistry.

The first one, "Vitamin D and Calcium Metabolism" (65 pages, 413 references) is written by H. F. de Luca, H. E. Paaren and H. K. Schnoes. The recent discoveries which rewakened the interest of the classical organic chemists concerning the vitamin D chemistry are mentioned : the demonstration of the first active metabolites of vitamin D and the demonstration that vitamin D is a precursor of at least one steroid hormone involved in the regulation of Ca- and P-metabolism.

The recent data (1978) concerning the metabolism of vitamin D_3 are presented. The radioactive experiments as well as modern physical methods greatly aided the clarification of pathways included in vitamin D metabolism. An important part of the chapter described the enzymes which carry out the metabolism of vitamin D_3.

Another interesting part of the chapter presents the syntheses of vitamin D, following distinct side chain and A-ring modification sequences or direct modification of a pre-formed vitamin nucleus. A paragraph of structure-activity relationships is also included.

The second chapter, "Cytochrome P_{450} and Biological Hydroxylation Reactions", by V. Ullrich (37 pages, 166 references) describes some important biological reactions including "Cytochrome 450", the hemoprotein biocatalyst contained in many monooxygenases. Some data concerning the occurence and structure of this special protein are given, then the problem of electron transfer (from reduced pyridine nucleotide to the hemoprotein) and the mechanisms of heme-sulfur-dependent monooxygenases are developed.

The third chapter, "Aminoglycoside Antibiotics", by J. Reden and W. Dürkheimer (65 pages, 309 references) presents the recent achievements (since 1970) in the chemistry and biochemistry of aminoglycoside antibiotics related to Streptomicine and Gentamicine. The importance of recent physical methods of analysis in this domain is stressed from the beginning. A table containing all the important compounds and their structures seems very useful. The most developed part of the chapter is devoted to characterization and to improvement (mainly chemical modifications) of the known structures. In this connection the detailed description of the studies of modern compounds from kanamicin and gentamicin classes could be mentioned. Problems of structure-activity relationships are also included.

Being very useful for biochemists, this book could also interest a large number of medicinal chemists or even organic chemists.

M. Banciu

"TOPICS IN CURRENT CHEMISTRY", Volume 84, "Bioactive Organo-Silicon Compounds" Springer Verlag, Berlin, Heidelberg, New York, 1979, 144 pages.

The present book comprises two chapters referring to a new field of research : synthesis and biochemistry of silicon organic compounds.

The first chapter "Synthesis and Properties of Bioactive Organo-Silicon Compourds" (75 pages, 132 references) is written by R. Tacke and U. Wannagat. The physical and chemical effects of sila-substitution in organic compounds are presented in a short but comprehensive fashion. Three main research lines in bio-organosilicon chemistry are then developed, namely : a) synthesis and biological investigation of silylated derivatives of bioactive organic compounds (sulphamides, analgetics, antiseptics and even steroids such as testosterone) ; b) synthesis and biological investigation of organosilicon compounds having no organic analogues (e. g. the important class of silatranes, caged compounds with pentacoordinated silicon and tetracoordinated nitrogen) ; c) synthesis and biological investigation of organosilicon compounds, having analogous structures to well known bioactive carbon compounds. The recent achievements of this new area of synthetic chemistry (named "sila-pharmaca chemistry") are detailed in a clear and fascinating description. In all categories a very useful comparison between the carbo- and silicostructures (concerning properties and syntheses) is presented and discussed. The reader is impressed by the great number of synthesized and investigated sila-pharmaca, from which we mention only a few examples : Si-carbamates with pharmaceutical (or insecticidal) action, Si-simpathomimetic amines, tricyclic Si-containing compounds with potential psychotropic activity from the group of imipramine or promasine drugs, Si-antihistamines, Si-steroids (sila-oestradiol), etc.

The second chapter, by M. G. Voronkov, "Biological Activity of Silatranes" (55 pages, 99 references) presents the results of biological investigations of silatranes, one of the most fascinating classes of bioactive organosilicon compounds. Beside many toxicity data, the useful qualities of silatranes are presented e. g. : blood coagulation, effect on endocrine functions (androgenic, gestagenic, glucocorticoid etc.), treatment of burns, ulcers and wounds (with spectacular results discussed in details, with diagrams and photos), intensification of hair grows, antitumorous activity and immunostimmulating effect (numerous derivatives investigated with some useful results).

Another interesting topic also included refers to the effect on insects and plants (e.g. the auxin activity, comparable to indolyl acetic acid).

The apparition of a book treating such an interesting and modern aspect of pharmaceutical chemistry, will surely be favourably received by readers.

M. Banciu

KARL CAMMANN, "Working with Ion-Selective Electrodes"*, Springer-Verlag Berlin Heidelberg New York 1979, 225 pp.

The main purpose of this volume is to acquaint the large circle of people interested in specific analysis using ion-selective electrodes with its most important fundamentals and to offer practical advice for the optimum solution of the various problems which may arise.

The wide range of application, low material requirements and simplicity of the analytical procedure have not only brought ion-selective electrodes into the limelight of analytical chemistry, but have promoted their use as tools for physiologists, medical researchers, biologists, geologists, environmental protection specialists, etc. This volume should be of particular help to such people.

A brief introduction to the theoretical principles cannot be avoided if the reader is to be equipped with the understanding necessary for future development of these electrodes.

With this fundamental knowledge and a few additional types concerning practical "know-how", the innovative experimentalist should be in a position to produce functional electrodes himself. This is especially important in physiological applications, since, up to now neither suitable microelectrodes nor sensors for the important amino acids are commercially available.

The first section introduces the electrochemical nomenclature necessary for understanding the literature on ion-selective electrodes and discusses the general principles behind all electrodes like : potential-determining ions, ion-selective electrode materials, the potentiometric selectivity coefficient as a quantitative indication of the electrode selectivity, etc.

The second section is concerned with the problems which arise in any accurate electrode potential measurement in practice like : reference electrodes, the liquid junction potential, salt bridge electrolytes, etc. Here the most important reference electrodes are discussed with special reference to their use in conjuction with ion-selective electrodes. From experience, almost 75 % of all problems which arise when working with ion-selective electrodes are on account of the reference electrode.

The third section deals with individual ion-selective electrodes, principles, their properties, handling and methods of preparation, construction, characteristics. In this section, the discussion

* Translated from the German by ALBERT H. SCHROEDER

of these electrodes is not arranged according to the species detected, but rather according to the kind of construction, since from this viewpoint characteristic properties are much the same and handling procedures need only be described once for an entire series of similar electrodes.

The fourth section deals with the measuring technique with ion-selective electrodes. Here the problems of high ohmic EMF measurements such as noise level, insulation, static charging and ground loops are discussed.

The fifth section is devoted to the various evaluation methods. Here a few schemes and examples are provided to indicate the optimum practical procedures and the accuracies attainable with the various methods are discussed. For example, different ways for determination of concentration using a concentration calibration curve, a standard addition with a known slope S, a "mathematically linearized" titration curve, etc.

The last section describes special set-ups such as clinical flow-thru cells, microelectrodes for measuring intracellular ionic activities, industrial on-line techniques and the continuous environmental protection monitors. Together with the short response time (a few seconds) they are especially valuable for subsequently coupled controlling devices that can intervene with minimal delay.

This volume is not, and is not intended to be a "tables book" for specific analyses using ion-selective electrodes for two reasons : the corresponding, detailed procedures are already available from the individual electrode manufactures ; in addition, such a work would only help a relatively small group of people who hapened to be interested in the determination of the same ion in the same matrix. The reader will, however, find basic examples and suggestions throughout.

Both the qualities of contents and the graphic presentation make the book titled : "Working with Ion-Selective Electrodes", edited by Karl Cammann, a very valuable reference source for researchers who are working in fields where measuring techniques with ion selective electrodes are involved.

Iuliana Vartires

C. GH. MACAROVICI, "Analiza chimică cantitativă anorganică" (Inorganic Quantitative Chemical Analysis), Editura Academiei RSR, București 1979, 455 pp.

Chemical analysis plays an essential part in science and technology. A thorough knowledge of chemistry itself is not possible without analytical chemistry. Chemical analysis is a means used to control the results of research work and to critically appreciate them.

In addition to the classical methods of analytical chemistry (gravimetry, volumetry, etc.) instrumental methods were gradually developed. When a very high accuracy is needed (chemical survey, litigious cases, etc.) we resort to the well known verified classical methods.

The book has systematized theoretical and practical data regarding analytical chemistry, with a view to a rational understanding of the principles of the various methods and to developing the scientific thinking to the staff working in laboratories and in research. The author has pointed out that practical ability and laboratory training are essential for an analyst.

The first part of this handbook successively describes the main categories of the classical methods of analytical chemistry (gravimetry, volumetry, gas-volumetry, etc.) the different physico-chemical and physical methods, etc. This part ends with considerations concerning the statistical methods used to work up the results.

The second part of the book includes various practical methods, selected among the most accessible and most widely utilized methods for the quantitative determination of the cations and anions. Then the methods of separation are described with specific reagents, hydrolysis, distillation, extraction, chromatography, ion exchangers, etc.).

The last part of the book includes examples illustrating the course of the analysis of metals, alloys, minerals, natural waters, soils, inorganic compounds of plants, fertilizers, etc.

This handbook is a guide for students in chemistry and for all specialists working in chemical laboratories, plants and research institutes.

D. I. Marchidan

I. E. TEODORESCU and MARIA FITI, "Radiation Technology", Editura Academiei RSR, 1979, Bncureşti,

The interest in the application of ionizing radiation for industrial purposes has increased tremendously during the last decade, as evidenced by an abundant literature in this fields. Thus was created a new industry for producing devices, plants and installations used for industrial – scale applications of the ionizing radiation energy for radiation processing of food biomedical products or for automatization of various processes in chemical industry, agriculture, textile industry, water and air pollution prevention etc. Most of the work has focused firstly on the use of isotope sources, particularly cobalt, while the use of electron sources has advanced in the last decade and significant technical advances have been made in the equipment used to generate electron beams.

The monograph "Radiation Technology" written by I. E. Teodorescu and Maria Fiti concerns to the problems mentioned above and is an excellent review describing the world's technical performances in this field in an attractive, comprehensive manner. Thus the uses of large radiation sources are examined from both the technical process and plant design points of view. For the purpose of stimulating the research and development of new technologies for the chemical and textile industries and also for agriculture and food preservation, besides the already existent technologies and equipment as economically competitive, the new trends in the radiation technology are also discussed.

The contents in the seven chapters of the above mentioned monographs is well equilibrated and directed to the principal problems of radiation technology as follows :

A description of the physical grounds of irradiation technology referring to the mechanisms of radiation generation, radiation fields and electrons or photon beams and secondary effects of irradiation is given in chapter one.

The presentation in detail of the radiation source, their characteristics and the methods of technological irradiation forms the contents of chapter two. There are also characterized and described the main parameters of the radiation sources, the types of principal sources used for industrial purposes like isotopic sources, waste fuel, nuclear reactors, particle accelerators, and radiation conversion systems.

The two most important classes of industrial plants existent at present : the gamma irradiation assembly and the accelerator – based electron or Bremstrahlung (X–ray) irradiation plant are discussed in chapter three, together with the problems associated with the implementation systems, process control and radioprotection.

Chapters four to seven discuss the most significant radiation processing methods and their application in various fields of industrial and economic activities.

An important aspect concerning the theoretical basis of radiochemical synthesis and the problems referring to the radiolysis and radiation – induced chemical reactions is presented in chapter four and an evaluation of their applications is also discussed. The wide-spread applications of ionizing radiations have an increasing interest especially in chemical industry.

Thus the effects of ionizing radiations for production of synthetic polymers and their utilization for cross-linking and grafting processes are discussed in chapter five. Also the production of various plastic materials, paint and casting curing are illustrated.

In the last decade a lot of work was done and dedicated to the food preservation and sterilization by using ionizing radiations. Details on irradiation for different processes for food preservation and sterilization, radiation doses recommended and other problems concerning these processes are given in chapter six.

Several other applications of radiation technology in different areas of chemical and textile industries and some economic aspects comparing investments and production costs concerning the use of various types of radiation producing installations and plants as well a comparison between radiation processing and the so-called "classical" technologies are presented in chapter seven. The evaluation of radiation damage and hazard accompanied with the shielding calculations are also given in the last chapter.

The publication of this book in a period of the scientifical and technical revolution in our country represents not only the apparition of a scientific monograph but also a useful and practitical guide giving physical bases, nomograms and formulae necessary for the implementation of this kind of processes in industrial practice. The book is addressed to the students, engineers, research workers in chemistry, nuclear technology, scientists concerned with practical studies of environment protection, engineers in agriculture and other fields.

1983

Ioan Gălăţeanu

NOTE POUR LES AUTEURS

La Revue Roumaine de Chimie publie des articles en anglais, français, russe, allemand ou espagnol. Les auteurs sont priés d'envoyer des articles et des comptes rendus inédits.

Les manuscrits seront dactylographiés à deux intervalles. La bibliographie, les tableaux et la légende des figures seront placés après le texte.

Si l'article fait partie d'une série numérotée, le titre de la partie précédente sera indiqué dans une note au bas de la première page.

Chaque article sera précédé d'un résumé comprenant quinze lignes au maximum.

Les références bibliographiques dans le texte seront faites par des exposants sans parenthèses et paraîtront comme des notes au bas de chaque page.

Les publications périodiques mentionnées dans la bibliographie seront présentées suivant les prescriptions internationales : le nom de l'auteur précédé de l'initiale du prénom, le titre du périodique abrégé conformément à «Chemical Abstracts» et souligné par une ligne, le numéro du tome indiqué par des chiffres arabes et souligné par deux lignes, suivi de la première page de l'article ; à la fin, l'année de la parution sera placée entre parenthèses. Le numéro de la revue ne sera pas indiqué, si les pages du volume sont numérotées consécutivement.

Les textes des livres ou traités inclueront : le nom des auteurs, les initiales du prénom le titre du livre entre guillemets et sans être souligné, le numéro du tome précédé par l'abréviation «vol.» (ou «Bd.»), le numéro de l'édition, les éditions (the publisher), la localité de la parution du livre, l'année de la parution et la page de la référence précédée(s) par l'abréviation «p.» (ou «S.»).

Les brevets seront indiqués comme suit : l'auteur ou la firme, le pays et le numéro du brevet, la date et la revue (Chem. Abstr.). Par ex. : M. Jones (to Union Carbide Co), Brit. Pat. 601 238, 2 Sept. 1959, *Chem Abstr.*, **54**, 12808 (1960).

Les diagrammes seront tracés à l'encre de Chine sur papier calque. Les tableaux et les figures (en nombre strictement nécessaire) seront numérotés par des chiffres arabes. Les courbes dans les figures seront numérotés par des chiffres arabes et leur explication sera donnée dans la légende des figures. Prière de ne pas inscrire les mêmes données dans les tableaux et les figures. Chaque tableau aura un titre. On indiquera dans le texte la place approximative des tableaux et des figures. Les formules chimiques seront incluses dans le texte ; en outre elles seront transcrites sur papier calque, à l'encre de Chine.

Les auteurs sont priés d'indiquer les caractères italiques (en soulignant les lettres au crayon), ainsi que tout autre caractère spécial ; les préfixes *ortho, meta, para, cis, trans,* etc. seront soulignés pour indiquer leurs caractères italiques et ne seront jamais écrits avec des majuscules.

Aucune correction à la main ne sera admise sur le manuscrit. Les corrections seront frappées à la machine. Les lettres grecques ou autres symboles spéciaux seront insérés à la main à l'encre clairement.

Le manuscrit sera signé par l'auteur.

Le colone-titre aura 50 lettres au maximum.

L'entière responsabilité du contenu des articles appartient aux auteurs.

Pour détails voir le No 2/1980.

PRINTED IN ROMANIA

1980 JUL 14

TRAVAUX PARUS AUX ÉDITIONS DE L'ACADÉMIE DE LA RÉPUBLIQUE SOCIALISTE DE ROUMANIE

A. T. BALABAN, I. GĂLĂŢEANU, G. GEORGESCU, LIGIA SIMIONESCU, **Compuşi marcaţi şi radioformaceutici cu aplicaţii în medicina nucleară** (Composés marqués et radiopharmaceutiques à application en médecine nucléaire), 1979, 495 p.

I. G. MURGULESCU, E. SEGAL, **Introducere în chimia fizică, vol. II.1. Teoria molecular-cinetică a materiei** (Introduction à la chimie physique. IIe vol. 1. La thèorie moleculaire-cinétique de la matière), 1979, 1003 p.

I. E. TEODORESCU, M. FITI, **Iradierea tehnologică** (L'Irradiation technologique), 1979, 216 p.

S. STERNBERG, FL. DANEŞ, **Termodinamica chimică aplicată** (La thermodynamique chimique appliquée), 1978, 400 p.

I. G. MURGULESCU, V. EM. SAHINI, **Introducere în chimia fizică.** Vol. I.2. **Structura şi proprietăţile moleculelor** (Introduction à la chimie physique, Vol. I, 2. La structure et les propriétés des molécules,) 1978, 604 p.

C. DRĂGULESCU, E. PETROVICI, **Chimie structurală modernă. Chimia coordinanţei 8** (La chimie structurale moderne. La chimie de la coordinence 8), 1977, 947 p.

D. PURDELA (sous la direction de), **Nomenclatura chimiei anorganice** (La nomenclature de la chimie inorganique), 1977, 153 p.

I. ZUGRĂVESCU, MAGDA PETROVANU, **N-Ylid chemistry**, coédition avec Mc Graw-Hill International Book Company, U.S.A., 1977, 396 p. 1977, 396 p.

D. NEGOIU, ANGEL KRIZA, **Poluanţi anorganici în aer** (Polluants inorganiques dans l'air) 1977, 220 p.

I. G. MURGULESCU, **Introducere în chimia fizică. Vol. I.1. Atomi, molecule, legătură chimică** (Introduction à la chimie physique, Ier vol. I. Atomes, molécules, liaison chimique), 1976, 560 p.

E. P. BALTĂ, E. BALTĂ, **Introduction to the physical chemistry of the vitreous state**, coédition avec Abacus Press, 1976, 287 p.

I. GĂLĂŢEANU, **Radiochimia aplicată. Metode şi probleme** (La radiochimie appliquée. Méthodes et problèmes), 1976, 307 p.

CONST. V. UGLEA, **Cromatografia pe gel permeabil. Noi domenii de aplicare** (La chromatographie sur gel perméable. Nouveaux domaines d'application), 1976, 123 p.

FRANCISC A. GOTHARD, **Echilibre lichid-vapori. I. Baze teoretice şi metode de calcul** (Equilibres liquide-vapeurs, I. Bases théoriques et méthodes de calcul), 1975, 263 p., 2 pl.

CONST. GH. MACAROVICI, D. MACAROVICI, **Chimia oxizilor dubli şi utilizările lor** (La chimie des oxydes doubles et leur utilisation), 1975, 195 p.

ELENA CEAUŞESCU, **Research work on synthesis and characterization of macromolecular compounds. Contributions**, 1974, 251 p.

DUMITRU COSTACHE, **Analiza chimică prin metoda cinetică** (L'Analyse chimique par la méthode de cinétique), 1974, 251 p.

G. A. RĂDULESCU, **Proprietăţile ţiţeiurilor româneşti** (Les propriétés des pétroles roumains) 1974, 267 p., 2 pl.

CR. SIMIONESCU, VIORICA RUSAN, V. POPA, **Chimia algelor marine** (La chimie des algues marines). 1974, 212 p., 1 pl.

I. P. Informaţia c. 2063

43426

Lei 25.
$ 55 (pour un abonnement annuel)

REVUE ROUMAINE DE CHIMIE

Tome 25, N° 6 Juin, 1980

RODICA VÎLCU and ZOICA CENUȘE, Calculation of activity coefficients in the benzene-butanol systems from experimental determination of isotherms $P_{total} = f$ (composition) 763–772

RODICA VÎLCU and ZOICA CENUȘE, Association of the butanols in benzene 773–779 C

RODICA VÎLCU and ZOICA CENUȘE, Calculation of hydrogen bond energies from excess enthalpies, experimentally determined for benzene-butanol systems 781–788

B. CHATTERJEE, Relation between entropy and cohesive energy for metals 789–792

S. STERNBERG, MIHAELA DRĂGĂNOIU and A. MATEESCU, The thermodynamic activity of $ZnSO_4$ in the systems: $ZnSO_4 + H_2O$ and $ZnSO_4 + Na_2SO_4 + H_2O$ 793–798

T. C. RUGINĂ and D. P. LAZĂR, About the catalytic oxidation of ammonia 799–803 R

C. GH. MACAROVICI, J. HORÁK and CS. VÁRHELYI, On the α-dioximine complexes of transition metals. LIX. The stability of Fe(II)-and Co(II)-complexes of 1,2-cycloheptanedione dioxime and 1,2-cyclooctanedione dioxime in aqueous solutions 805–809

M. ANDRUH, C. I. LEPADATU and MARIA BREZEANU, On Uspenski's rule regarding the *cis-trans* isomerism of coordination compounds 811–813

IOAN SILAGHI-DUMITRESCU and IONEL HAIDUC, The infrared spectrum of dimethyldithiophosphinato anion $(CH_3)_2PS_2^-$. Normal coordinate analysis and Urey-Bradley force field calculation 815–821

IOAN SILAGHI-DUMITRESCU and IONEL HAIDUC, Vibrational characteristics of Ni(II) dithiophosphinato chelates. Normal coordinate analysis and Urey-Bradley force field calculation of $Ni[S_2P(CH_3)_2]_2$ 823–830

MALATESH A. PUJAR and N. S. BIRADAR, Magnetic and spectral studies of 2-substituted benzimidazole complexes of cobalt(II) . . . . 831–838 C

D. NEGOIU, J. CAMUS and N. MUREȘAN, Complex compounds of nickel involved in electron transfer processes 839–844

ANA UNGUREANU and MARIA MARC, Sulphur-containing aminoacid-metal complexes. Cobalt(II) and iron(II) complexes of cystine 845–850

M. S. SUBHANI, Effect of foreign ions on the reaction between bromide anion and persulphate anion in aqueous system . . . . 851–854 R

Revue Roumaine de Chimie, **25**, *6*, 761–908 (1980)

M. S. SUBHANI, Electrostatic contributions to the thermodynamic functions in the formation of transition state for the reaction between Br_2^- and BrO^- 855–859

M. S. SUBHANI, Study of the transition state formed between $Cu(S_2O_3)^-$ and $S_2O_8^{2-}$ anions in mixture of solvents 861–866

V. ARMEANU and SANDA VIȘAN, Spectrophotometric microdetermination of uranium with benzoin-oxime 867–874

FASIHUDDIN KAMIL, S. K. SINDHWANI and R. P. SINGH, Phenanthrenequinone monosemicarbazone as a reagent for the determination of rhodium(III) and palladium(II) 875–879

M. L. TASCON GARCIA, Chromatographic separation of golds platinum, palladium, rhodium and iridium. I. Quantitative study (in Spanish) 881–900

M. L. TASCON GARCIA, Chromatographic separation of gold platinum, palladium, rhodium and iridium. II. Quantitative study (in Spanish) . . . 901–904

BOOK REVIEWS. 905–908

Revue Roumaine de Chimie, 25, 6, 763–772 (1980)

CALCULATION OF ACTIVITY COEFFICIENTS IN THE BENZENE-BUTANOL SYSTEMS FROM EXPERIMENTAL DETERMINATION OF ISOTHERMS $P_{\text{total}} = f$(COMPOSITION)

RODICA VÎLCU and ZOICA CENUȘE
National Institute of Chemistry, Chair of Physical-Chemistry,
Bd. Republicii 13, Bucharest, Romania

Received July 2, 1979

Using a isotensioscopic method, the isothermal variation of the total pressure with composition was measured at 25, 35, 45 and 50°C in the benzene-1-butanol, benzene 2-methyl-2-propanol, benzene 2-butanol and benzene 2-methyl-2-propanol system. The fugacity coefficients of vapour phase, vapour composition at the equilibrium and activity coefficients were calculated using virial equation and consistency equation.

1. INTRODUCTION

In this work we estimated the values of activity coefficients of binary benzene – butanol systems from limited experimental data, namely that $P_{\text{total}} = f$ (composition), at 25, 35, 45 and 50°C using a static experimental method—the isotensioscopic method. A static method has been used since it is the only one with which we can obtain a real thermodynamic equilibrium and since we have been interested in calculating the excess free energies of the investigated systems.

2. EXPERIMENTAL

A. Physical properties of components

The alcohols and benzene, Merck reagents, were purified as described by Vogel[1] and Smith[2]; their purity was tested cromatographically, using a chromatograph Willy Giede. The quantity of water left in the reagents was dosed by Karl-Fischer method; this has admissible limiting values.

The physical properties of components are given in table 1.

B. Liquid — vapour equilibria

We have made use of an isotensioscopic[4] installation in order to experimentally determine $P_{\text{total}} = f(x_1)$ curves within isothermal conditions.

TABLE 1

Physical properties of pure components

Component	n_D(25°C)	ρ (g/cm³) (25°C)	T_c^3 (K)	P_c^3 (atm)	ω_H^3	Content of water (ppm)
benzene	1.4984	0.8726	562.0	48.6	—	344.8
1-butanol	1.3980	0.8068	562.9	43.6	0.252	20.4
2-methyl-1-propanol	1.3945	0.7987	549.2	42.4	0.215	40.0
2-butanol	1.3960	0.8308	535.9	41.4	0.215	37.1
2-methyl-2-propanol	1.3855 (27°C)	0.7924 (27°C)	506.2	39.2	0.201	63.2

The installation seen in figure 1 is made up of an isotensioscope set up in position *A*. A drying vessel is located in position *B*; it is filled up with active coal and silicagel, establishing connection with the environment.

Pressure gauge *C* enables the measurement of vapour pressure in the system. A phial for the sample is fixed in position *D*; it can be transferred into the isotensioscope by vacuum distillation. Flap door *E* keeps holding back, by means of freezing with carbonic snow and organic solvents (we have used carbonic snow with acetone within our measurements), or with liquid nitrogen of any vapour traces that may keep on the line of the apparatus, thus preventing the foulness of mercury in the diffusion pump *G* and of oil in the preliminary vacuum pump, *J*.

Preliminary vacuum ($5 \cdot 10^{-2}$ mmHg) was measured by means of gauge Mc. Leod, *H*, and the vacuum resulting in the diffusion pump G (10^{-4} mmHg) was measured by means of the pressure gauge Mc. Leod, *F*.

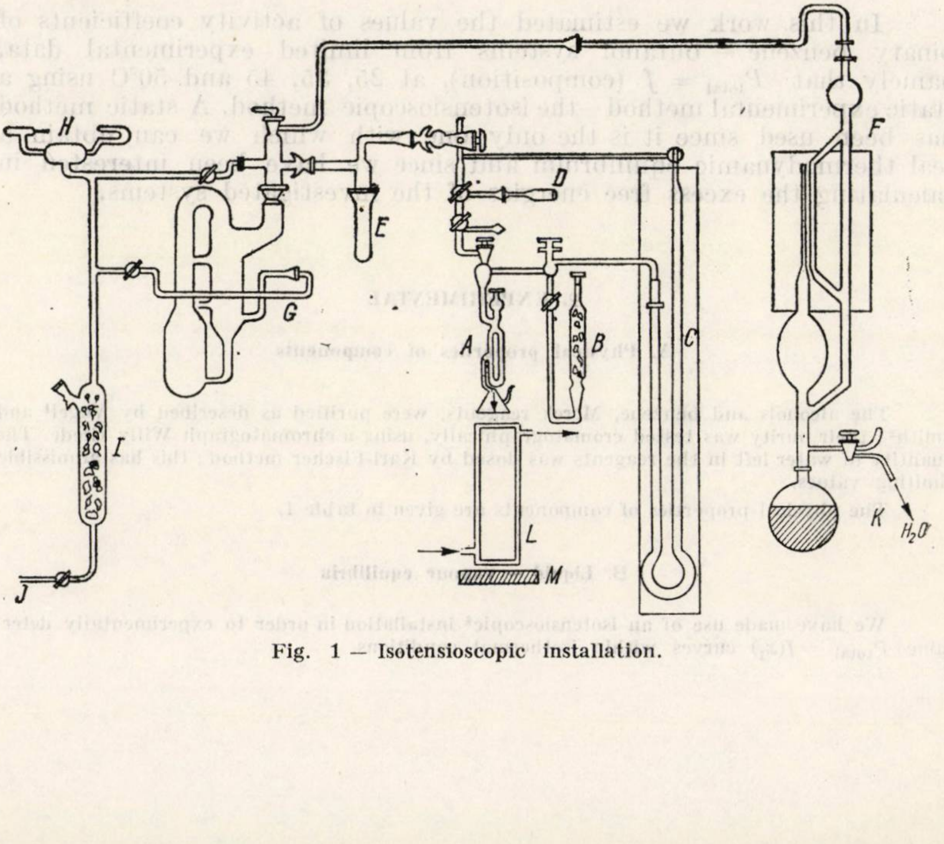

Fig. 1 — Isotensioscopic installation.

The installation also contains a thermostat L, equipped at bottom with an electromagnetic stirrer M, which enables to get settled temperature. In order to measure the vapour pressure of a system, the preliminary vacuum pump, J, is connected, which, by means of vessel I, with active coal, starts the preliminary voiding of the installation up to isotensioscope A. When a pressure of $5 \cdot 10^{-2}$ has been reached in the installation, the diffusion pump G is set working, this one achieving a vacuum of 10^{-4} mmHg within about 7—10 hours.

The following stage consists in charging the isotensioscope : first of all, the sample is introduced into the phial in position D and the isotensioscope having mercury in the two frontal arms is fixed into the installation by means of a spherical slift. Then the isotensioscope and mercury are degased by reiterated freezings and degasings ; by breaking the communication with the voiding system, the sample passes, through distillation, from phial D into the isotensioscope.

Another method consists in introducing the sample by means of a tube practised on the very isotensioscope, by opening and then closing it, in flames, after which mercury is introduced into the frontal arms. Then everything is worked as above. Having degased the isotensioscope and the system to be investigated, the vapour pressure is to be determined : with that end in view the connection is established with pressure gauge C, the isotensioscope is introduced into the thermostat L, stirrer M is started ; the precision of tempperature range is of $5 \cdot 10^{-2}$°C, being ensured by means of an ultrathermostat-type U 10.

Having obtained the equilibrium (within about 1 hour) one must read out the pressure indicated both by manometer C and by the slight uneveness of mercury in the frontal arms of the isotensioscope ; this uneveness is added or substracted to the pressure read on manometer C in accordance with its direction. The reproductibility of the measuring method of the vapour pressure by this isotensioscopic method is below 0.1%, and the precision range is of ± 0.05 mmHg.

Pressure readings were done by a precision cathetometer $5 \cdot 10^{-2}$ mmHg.

After each measurement of vapour pressure the isotensioscope was opened, the sample drawn out and analysed chromatographically in order to determine its composition. A chromatograph Willy Giede was employed making use of a 5 m column, $d = 4$ mm, carbowax 40 M as a filling material, and hydrogen as an eluent with o flow capacity of 40 ml/minute over isothermic regime of temperature (80°C).

The chromatographic value of the apparatus was determined previously ; chromatogrammes for 6 known concentrations of the systems studied have been recorded ; the average value is 1.

In table 2 there are indicated the experimental values of the vapour pressure in benzene-butanol systems.

The vapour pressure of the pure components ($x_1 = 0$ and $x_1 = 1$) in table 2 have been obtained by using the equation-type Antoine $\log P \text{ (mmHg)} = A - B / t + c$ whose constants are indicated in table 3.

In figure 2 there is represented the isothermal variation of total pressure depending on the composition in the benzene 2-butanol system.

From observing the data in table 2 as well as from the diagrams in figure 2, which are to be exemplified, it has been settled that the systems examined are real systems and not ideal ones ; they stand for the maximum azeotrope systems in $p = f(x)$ coordinates, born out by the minimum azeotrope extremes in coordinates $T = f(x)$ in Nataraj's[9] works. These azeotropes move alongside the changing of temperature towards parts with higher alcohol concentrations as far as the alcohol hydroxilic composition contributes to a hydroxilic environment.

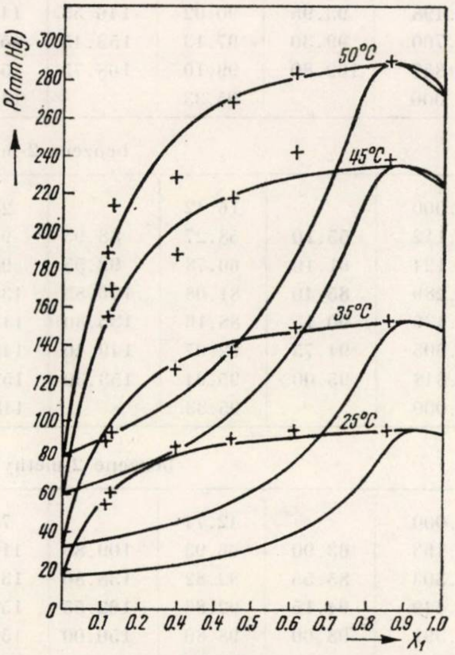

Fig. 2. — Isothermal variation (25, 35, 45 and 50°C) of the total pressure in agreement with the molar fraction of benzene in the benzene 2-butanol system

TABLE 2

Experimental and calculated out values, by Gauss, method of the isothermal variation (at 25, 35, 45 and 50°C) of total pressure with the composition in the studied systems

	25°C		35°C		45°C		50°C	
	$P_{exp.}$ (mmHg)	$P_{calc.}$ (mmHg)	$P_{exp.}$ (mmHg)	$P_{calc.}$ (mmHg)	$P_{exp.}$ (mmHg)	$P_{calc.}$ (mmHg)	$P_{exp.}$ (mmHg)	$P_{calc.}$ (mmHg)
x_1	**benzene 1-butanol system**							
0.000		8.43		15.98		28.88		38.22
0.118	54.55	54.69	90.40	85.91	142.90	131.19	174.50	160.58
0.234	69.00	73.19	109.15	114.59	162.80	174.08	196.65	212.40
0.370	89.75	83.06	138.55	130.14	195.00	197.68	227.00	241.09
0.410	81.35	84.78	135.15	132.88	213.65	201.68	240.45	246.20
0.799	94.05	92.58	149.50	145.81	230.75	221.14	284.25	269.76
1.000		95.33		148.15		223.51		271.29
	benzene 2-methyl-1-propanol system							
0.000		11.45		19.46		35.92		55.30
0.134	47.65	47.61	73.20	77.49	111.95	122.59	147.25	158.69
0.268	76.30	69.97	118.55	111.80	173.55	173.40	207.60	213.78
0.395	85.85	83.18	136.10	132.09	209.55	203.45	257.00	249.89
0.498	93.95	90.02	146.55	142.59	215.15	218.96	263.30	268.49
0.700	99.30	97.13	153.45	153.42	232.60	234.79	280.95	287.36
0.857	102.80	99.10	168.75	156.31	246.40	238.84	299.80	292.05
1.000		95.33		148.15		233.15		271.29
	benzene 2-butanol system							
0.000		16.42		28.92		59.75		79.59
0.112	55.10	58.27	88.95	95.11	150.60	150.72	187.10	187.77
0.124	61.10	60.78	92.55	98.93	168.10	156.34	212.05	194.49
0.289	85.40	81.08	126.85	130.12	186.65	202.54	226.80	250.03
0.439	90.15	88.16	135.80	141.13	216.80	218.29	267.20	269.86
0.605	94.75	92.07	149.40	147.17	240.90	227.93	291.25	289.57
0.848	95.00	95.94	153.30	152.57	237.90	234.82	298.80	288.06
1.000		95.33		148.15		233.51		271.29
	benzene 2-methyl-2-propanol system							
0.000		42.74		78.50		136.92		174.17
0.153	63.90	66.93	109.85	114.14	181.45	186.77	225.50	235.56
0.303	85.55	82.82	138.80	137.25	214.35	218.91	261.70	272.85
0.449	94.15	92.86	162.55	151.57	242.10	238.52	292.16	295.46
0.591	98.00	98.80	150.00	159.72	249.00	248.23	307.00	307.53
0.731	102.00	101.88	163.00	163.53	250.00	253.25	310.00	311.84
0.867	102.00	102.64	163.00	163.45	251.00	251.45	308.00	308.12
1.000		95.33		148.15		223.51		271.29

TABLE 3

Values of the equation Antoine[5–8] constants

Component	A	B	C
benzene	6.89745	1206.35	220
1-butanol	8.27488	1873.90	230
2-methyl-1-propanol	8.19613	1697.44	230
2-butanol	7.20428	1158.54	168
2-methyl-2-propanol	7.60339	1291.66	191

3. RESULTS

To estimate the activity coefficients, in equation (1)

$$\varphi_i \cdot y_i \cdot P = \gamma_i \cdot x_i \cdot f_i^0 \tag{1}$$

it should be calculated the fugacity coefficient, φ_i, of the gaseous phase, the molar fraction of the gaseous phase, y_i, in equilibrium with the liquid one, as well as the fugacity of reference, f_i^0, out of the isothermal experimental variation of the total pressure P, having in view the molar fraction of the liquid in equilibrium with the gaseous one.

The fugacity coefficient, φ_i, and the activity coefficient, γ_i, depend on pressure, temperature and composition and in order to simultaneously define them it is necessary that we should choose a state of reference; in the case of systems where the components are to be found in an undercritical state, the symmetric norming system is chosen for which $\lim \gamma_i \to 1$ $x_i \to 1$, the fugacity of reference being the very fugacity of pure liquid at an equilibrium temperature and pressure.

To calculate the fugacity coefficient, φ_i, it is necessary that we should know the equation of state which rules over the respective component. In the present work we have made use of the virial equation of state up to the second virial which, written for the vapour binary mixture, is :

$$\frac{PV}{RT} = 1 + \frac{y_1^2 B_{11} + 2y_1 y_2 B_{12} + y_2^2 B_{22}}{V}. \tag{2}$$

where B_{11}, B_{12}, B_{22} are temperature functions, and were determined from empirical correlation of Tsonopoulos [10].

$$\frac{B_{ii} P_{ci}}{RT_{ci}} = f^{(0)}_{(T_r)} + \omega_{H_i} \cdot f^{(1)}_{T_r} + f^{(2)}_{T_r} \tag{3}$$

where :

$$f^{(0)}_{(T_r)} = 0.1445 - \frac{0.1385}{T_r^2} - \frac{0.0121}{T_r^3} - \frac{0.000607}{T_r^8} \tag{4}$$

$$f^{(1)}_{(T_r)} = 0.0637 + \frac{0.331}{T_r^2} - \frac{0.423}{T_r^3} - \frac{0.008}{T_r^8} \tag{5}$$

$$f^{(2)}_{(T_r)} = \frac{a}{T_r^6} - \frac{b}{T_r^8} \tag{6}$$

ω_{H_i} is acentric factor of homomorph, introduced by Pitzer[11].

TABLE 4

a, b values, virial coefficients B_{ii} (ml/mol) and their variation with temperature

Component	a	b	B_{ii} (ml/mol) 25°C	35°C	45°C	50°C	square average deviation (ml/mol)
benzene	—	—	−1662	−1186	−1342	−1279	10.3 (0.8 %)
1-butanol	0.0878	0.0367	−3899	−3071	−2478	−2143	61.2 (1.6 %)
2-methyl-1-propanol	0.0878	0.0487	−4465	−3770	−2971	−2419	23.2 (1 %)
2-butanol	0.0878	0.0481	−3992	−3189	−2531	−2101	14.6 (0.5 %)
2-methyl-2-propanol	0.0878	0.0568	−2745	−2529	−1789	−1676	33.1 (1 %)

In the systems virial coefficients were calculated by means of pseudocritical parameters :

$$T_{c_{ij}} = (1 - k_{ij})\,(T_{c_i} \cdot T_{c_j})^{1/2} \tag{7}$$

$$K_{ij} = 1 - \frac{2V_{c_i} \cdot V_{c_j}}{V^2_{c_{ij}}} \cdot \frac{(I_i \cdot I_j)^{1/2}}{I_i + I_j} \tag{8}$$

$$\omega_{ij} = \frac{1}{2}(\omega_i + \omega_j). \tag{9}$$

$$P_{c_{ij}} = 4T_{c_{ij}}\left[\frac{P_{c_i} \cdot V_{c_i}}{T_{c_i}} + \frac{P_{c_j} \cdot V_{c_j}}{T_{c_j}}\right] \Big/ (V^{1/3}_{c_i} + V^{1/3}_{c_j})^3 \tag{10}$$

$$V_{c_{ij}} = \left(\frac{V^{1/3}_{c_i} + V^{1/3}_{c_j}}{2}\right)^3 \tag{11}$$

Pseudocritical parameters are indicated in table 5.

To estimate the molar fraction of vapour phase in equilibrium with the liquid one, the coexistential equation of phases was used

$$\left[\frac{y_1 \cdot y_2 \delta_{12} - v^l + x_1 B_{11} + x_2 B_{22}}{RT} + \frac{1}{P}\right] \mathrm{d}P = (y_1 - x_1)\,\mathrm{d}\ln\frac{\varphi_1(1-y_1)}{\varphi_2 \cdot y_1} + \frac{y_1 - x_1}{y_1(1-y_1)} \tag{12}$$

TABLE 5

Pseudocritical parameters

System	$K_{ij}\cdot 10^3$	$T_{c_{ij}}$	$P_{c_{ij}}$	$V_{c_{ij}}$	$\omega_{c_{ij}}$	$B_{c_{ij}}$ (ml/mol)			
		(K)	(atm)	(ml/mol)		25°C	35°C	45°C	50°C
benzene 1-butanol	2.310	560.9	46.0	241.10	0.2315	−1820	−1692	−1462	−1392
benzene 2-methyl 1-propanol	0.925	555.0	45.4	266.12	0.273	−1696	−1519	−1309	−1207
benzene 2-butanol	13.300	548.0	44.8	264.40	0.215	−1626	−1551	−1325	−1263
benzene 2-methyl 2-propanol	0.610	533.0	43.7	267.20	0.206	−1464	−1321	−1207	−1150

with : $\delta_{12} = 2B_{12} - B_{11} - B_{22}$, v^l from Rackett[12] equation, or from Gunn and Yamada[13] equation :

$$v^l = v_{\text{ref.}} \cdot z_c^{(1-T_r)^{2/7}} \tag{13}$$

$$v_{\text{ref.}} = v'_{\text{exp.}}\,[-(1 - T'_r)^{2/7}]\cdot \ln Z_e \tag{14}$$

with $z_c = 0.29056 - 0.08775\ \omega$ and V exp. an experimental value.

The molar fraction of the vapour phase in equilibrium with the liquid one was estimated using a program indicated by Prausnitz[3] with a Hewlett Packard–9100 computer and the values are presented in table 6.

In figure 3 there is represented, to exemplify, the variation of the activity coefficients of the benzene 2-butanol system function of composition and temperature.

With the methods of calculating liquid-vapour equilibria which make use of the relation based upon equation Gibbs-Duhem and upon limited experimental data, the deviation from the criterium of thermodynamic consistence is appreciated by the relation :

$$\Delta y = y_{\text{expr}} - y_{\text{calc}} \tag{16}$$

where $y_{\text{exp.}}$ = the composition of vapour phases, at equilibrium, experimentally estimated, and y_{calc} = the composition of vapour phases at equilibrium, calculated, for instance over the isothermal variation of the total pressure in reasonable agreement with the composition.

In table 7 there are presented the values Δy for the studied systems comparatively with the experimental data of Allen[14] (25°C) and Brown[15] (45°C).

TABLE 6

Molar fractions vapour phase, y_i, activity coefficients and Wilson parameters

	25°C			35°C			45°C			50°C		
X_1	y_1	γ_1	γ_2	y_1	γ_1	γ_2	y_1	γ_1	γ_2	y_1	γ_1	γ_2
benzene 1-butanol $\frac{\lambda_{12}-\lambda_{11}}{R} = 312.1$; $\frac{\lambda_{21}-\lambda_{22}}{R} = 596.2$												
0.000	—	—	—	—	—	—	—	—	—	—	—	—
0.118	0.860	4.174	1.028	0.832	4.068	1.028	0.801	3.969	1.027	0.785	3.922	1.026
0.234	0.902	2.972	1.105	0.882	2.919	1.102	0.860	2.869	1.100	0.848	2.845	1.099
0.370	0.919	2.170	1.266	0.903	2.143	1.260	0.884	2.117	1.254	0.875	2.104	1.251
0.410	0.922	2.005	1.331	0.906	1.982	1.324	0.889	1.960	1.357	0.880	1.949	1.314
0.799	0.939	1.144	3.305	0.928	1.139	3.246	0.916	1.135	3.189	0.910	1.133	3.162
1.000	—	—	—	—	—	—	—	—	—	—	—	—
benzene 2-methyl-1-propanol $\frac{\lambda_{12}-\lambda_{11}}{R} = 109.0$; $\frac{\lambda_{21}-\lambda_{22}}{R} = 1219.0$												
0.000	—	—	—	—	—	—	—	—	—	—	—	—
0.134	0.791	2.952	1.017	0.751	2.927	1.016	0.710	2.903	1.016	0.689	2.891	1.101
0.268	0.874	2.401	1.071	0.846	2.385	1.270	0.816	2.370	1.070	0.802	2.363	1.069
0.395	0.904	2.001	1.173	0.882	1.991	1.171	0.859	1.982	1.169	0.841	1.975	1.169
0.498	0.917	1.741	1.311	0.899	1.737	1.308	0.879	1.730	1.305	0.868	1.727	1.304
0.700	0.933	1.360	1.919	0.918	1.367	1.911	0.902	1.353	1.901	0.893	1.351	1.900
0.857	0.940	1.143	3.649	0.921	1.141	3.625	0.913	1.138	3.602	0.905	1.137	3.591
1.000	—	—	—	—	—	—	—	—	—	—	—	—
benzene 2-butanol $\frac{\lambda_{12}-\lambda_{11}}{R} = 309.9$; $\frac{\lambda_{21}-\lambda_{22}}{R} = 483.3$												
0.000	—	—	—	—	—	—	—	—	—	—	—	—
0.112	0.743	4.042	1.026	0.691	3.993	1.025	0.639	3.829	1.025	0.615	3.779	1.024
0.224	0.756	3.887	1.032	0.705	3.786	1.035	0.655	3.689	1.030	0.631	3.643	1.029
0.289	0.833	2.454	1.161	0.795	2.414	1.157	0.758	2.376	1.153	0.739	2.357	1.152
0.439	0.855	1.805	1.384	0.823	1.784	1.376	0.791	1.764	1.367	0.774	1.753	1.363
0.605	0.870	1.393	1.839	0.842	1.382	1.820	0.813	1.372	1.801	0.799	1.367	1.792
0.848	0.901	1.071	3.799	0.881	1.068	3.703	0.861	1.066	3.612	0.851	1.063	3.568
1.000	—	—	—	—	—	—	—	—	—	—	—	—
benzene 2-methyl-2-propanol $\frac{\lambda_{12}-\lambda_{11}}{R} = 37.3$; $\frac{\lambda_{21}-\lambda_{22}}{R} = 1024.7$												
0.000	—	—	—	—	—	—	—	—	—	—	—	—
0.153	0.452	2.074	1.014	0.409	2.058	1.014	0.374	2.023	1.011	0.353	1.999	1.013
0.303	0.618	1.777	1.062	0.576	1.763	1.062	0.537	1.740	1.060	0.519	1.725	1.059
0.449	0.705	1.534	1.161	0.668	1.523	1.161	0.634	1.508	1.151	0.617	1.499	1.153
0.591	0.761	1.336	1.350	0.729	1.328	1.349	0.699	1.319	1.340	0.685	1.314	1.333
0.731	0.804	1.178	1.731	0.777	1.172	1.727	0.752	1.167	1.707	0.740	1.165	1.692
0.867	0.851	1.059	2.688	0.831	1.056	2.649	0.812	1.054	2.590	0.840	1.053	2.554
1.000	—	—	—	—	—	—	—	—	—	—	—	—

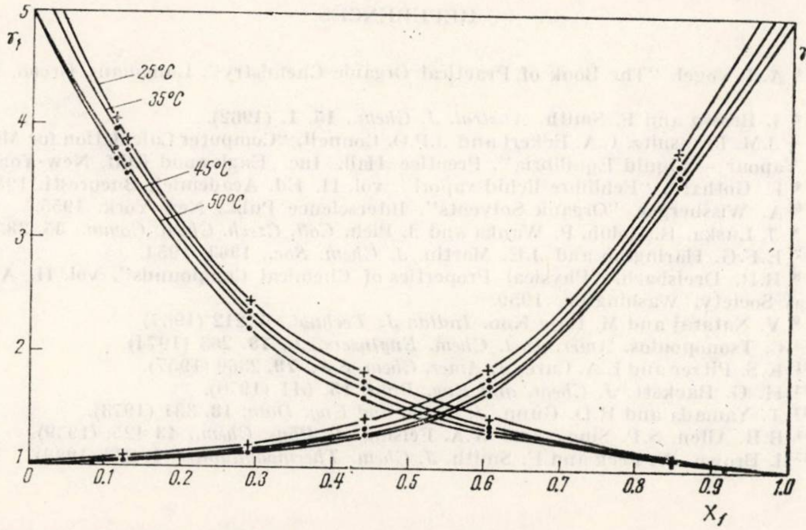

Fig. 3. — Variation of activity coefficients of the benzene 2-butanol system alongside the composition and temperature.

TABLE 7

Test of thermodynamic consistence

	Δy			Δy	
	25°C	45°C		25°C	45°C
X_1	benzene 1-butanol		benzene 2-butanol		
0.118	0.097	—	0.112	−0.073	−0.119
0.234	−0.007	—	0.124	−0.076	−0.105
0.370	−0.004	—	0.284	−0.017	−0.061
0.410	+0.005	—	0.439	−0.20	−0.051
0.799	0.013	—	0.605	−0.007	+0.011
benzene 2-methyl-1-propanol			0.848	−0.015	+0.016
0.134	−0.021	−0.040	benzene 2-methyl-2-propanol		
0.268	−0.004	−0.039	0.153	+0.008	+0.024
0.395	−0.024	−0.017	0.303	−0.003	+0.010
0.498	−0.017	−0.019	0.449	−0.027	−0.000
0.700	−0.013	−0.012	0.591	−0.021	−0.014
0.857	−0.000	+0.004	0.731	−0.015	−0.012
			0.867	−0.011	−0.008

As it is shown in table 7, the proper values calculated show average deviations under 1.5% within 0.2—0.9 molar fraction range, while for benzene 2-butanol system the deviations are above 3%. We consider, under the circumstances, that the data calculated show thermodynamic consistence.

REFERENCES

[1] A. I. Vogel, "The Book of Practical Organic Chemistry", Longmans, Green, London 1956.

[2] I. Brown and F. Smith, *Austral. J. Chem.*, **15**, 1, (1962).

[3] J.M. Prausnitz, C.A. Eckert and J.P.O.'Connell, "Computer Calculation for Multicomponent Vapour – Liquid Equilibria", Prentice Hall, Inc. Englewood Cliff, New-York, 1968.

[4] F. Gothard, "Echilibre lichid-vapori", vol. II, Ed. Academiei, Bucureşti, 1980.

[5] A. Wissberger, "Organic Solvents", Interscience Publ., New-York, 1955.

[6] J. Luska, R. Holub, P. Wanka and J. Pich, *Coll. Czech. Chem. Comm.*, **35**, 385 (1970).

[7] E.F.G. Harington and J.E. Martin, *J. Chem. Soc.*, **1963**, 1954.

[8] R.R. Dreisbach, "Physical Properties of Chemical Compounds", vol. II, American Chemical Society, Washington, 1959.

[9] V. Nataraj and M. Raje Koo, *Indian J. Technol.*, **5**, 212 (1967).

[10] C. Tsonopoulos, *Amer. Inst. Chem. Engineers.* J., **79**, 263 (1974).

[11] K.S. Pitzer and L.A. Cure, *J. Amer. Chem. Soc.*, **79**, 2369 (1957).

[12] H. G. Rackett, *J. Chem. and Eng. Data*, **15**, 511 (1970).

[13] T. Yamada and R.D. Gunn, *J. Chem. and Eng. Data*, **18**, 331 (1973).

[14] B.B. Allen, S.P. Singo, and W.A. Felsing, *J. Phys. Chem.*, **43** 425, (1939).

[15] I. Brown, W. Feck and F. Smith, *J. Chem. Thermodynamics*, **1**, 273 (1969).

Revue Roumaine de Chimie, 25, *6*, 773—779 (1980)

ASSOCIATION OF THE BUTANOLS IN BENZENE

RODICA VÎLCU and ZOICA CENUŞE
National Institute of Chemistry, Chair of Physical-Chemistry,
Bd. Republicii 13, Bucharest, Romania

Received July 2, 1979

The dielectric constants of 1-butanol, 2-methyl-1-propanol, 2-butanol and 2-methyl-2-propanol in benzene have been measured at 25°C and 40°C in the range 0—1 molar fraction. Apparent dipole moments and Kirkwood correlation factors have been evaluated. The results suggest that alcohol association is initially ($g < 1$) dominated by the formation of small, weakly polar multimers and, at $g > 1$, the small highly polar multimers predominate. Benzene has a disassociating effect, which may be compared to that produced in the pure alcohols by increased temperature.

1. INTRODUCTION

Static dielectric constants, electric dipole moment, Kirkwood correlation factor and dielectric relaxation measurements have provided useful means of examining molecular association in solution [1-2].

Most of the works have been concerned with the equilibrium constants of molecular association and with its temperature dependence.

There have been reported few works on the concentrations dependence of the intermolecular associations for alcohols in nonpolar solvents, because spectrophotometric techniques have generally been limited to alcohols, in dilute solutions.

The alcohol self association is considerably influenced by the steric environment of the hydroxyl group and by the temperature, which determines the geometry and size of the association.

In this paper we report the results of the static dielectric constants, and Kirkwood's factor for benzene-butanol systems, in which the alcohol molecular size and steric environment of the hydroxyl group are variables.

2. EXPERIMENTAL

A. Physical properties of pure substances

We have made use of butanols and benzene whose physical properties were shown previously[3].

B. Measurement method

The dielectric constants of the systems studied were measured with a dipolmeter type DM.01—W.T.W.-Wissenschaftlich — Technische Werkstatten, which is made up of two identical oscillators of high frequency (10^6 Hz). The cell for measurements is parallelly located to a high-capacity variable condenser and both of them parallel to one of the oscillators. The difference in frequency resulting from introducing a dielectric, with an unknown dielectric constant, is correspondingly transformed and applied on the vertical plate of a cathode-ray tube.

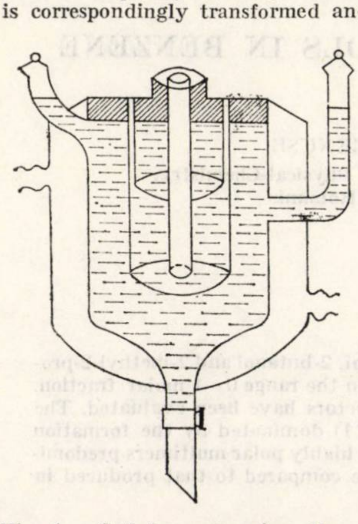

Fig. 1 — Cell for measuring dielectric constants.

The lack of equilibrium in frequency within the circuit of the two oscillators brings about the apparition of Lissajoux figures on the oscilloscope screen. The equilibrium, namely the arranging of Lissajoux figures, is achieved from a variable capacity, and the equilibrium value is read on a scale having 4500 divisions and that is why the dielectric constant is determined with high precision.

The resonance bridge used for dipole moment measurements, not having its own cell, required to make one, so that it might allow some measurements of dielectric constant under 0.1% error, within the range of dielectric constant 5—35, corresponding to the systems studied.

The cell[4] is a cylindrical condenser with symmetric field ; the outer electrode plays the part of a screen.

The graduation of the apparatus scale in dielectric constants was made with air ($\varepsilon = 1$), benzene ($\varepsilon = 2.274$), normal propyl alcohol ($\varepsilon = 20.10$), methyl alcohol ($\varepsilon = 32.63$), and nitrobenzene ($\varepsilon = 34.82$).

The dielectric constants of the benzene—butanol systems were measured at 25 ± 0.005°C and 40 ± 0.1°C.

The experimental values of the dielectric constants in the benzene — butanol system are shown in table 1.

TABLE 1

Values of dielectric constants measured for the benzene-butanol systems at 25 and 40°C

benzene 1-butanol			benzene 2-methyl-1-propanol		
X_2	25°C	40°C	X_2	25°C	40°C
0.0000	2.27	2.23	0.0000	2.27	2.23
0.1625	2.94	2.94	0.1551	3.20	2.95
0.2799	4.15	3.92	0.2862	4.25	3.62
0.4205	6.22	5.70	0.4255	6.25	5.60
0.5692	9.17	8.07	0.5653	8.95	7.80
0.7072	12.15	10.65	0.7104	12.00	10.55
0.8564	15.32	13.67	0.8831	15.50	13.60
1.0000	17.51	15.63	1.0000	17.93	15.13

benzene 2-butanol			benzene 2-methyl-2-propanol		
X_2	25°C	40°C	X_2	25°C	40°C
0.0000	2.27	2.23	0.0000	2.27	2.23
0.1389	2.77	2.39	0.1332	2.60	2.60
0.2777	3.52	3.45	0.2694	3.02	3.02
0.4184	6.40	4.52	0.4088	3.67	3.62
0.5627	7.17	6.30	0.5514	4.60	4.47
0.7070	10.15	8.67	0.6975	6.22	5.67
0.8527	13.65	11.85	0.8469	12.47	10.05
1.0000	16.56	14.16	1.0000	—	—

3. WORKING UP OF RESULTS

Calculation of Kirkwood Factor

The classical consideration of the dielectric behaviour is made by means of Clausius — Mosotti's and Debye's simple theories, which describe the dielectric behaviour of the fluid whose molecules have a permanent dipole moment and which is applied with satisfactory results to gas under low pressures, where the action of intermolecular forces is neglected.

Onsager's theory is valid to other systems as well and it settles that when a molecule with a permanent dipole moment is surrounded by others the field of this dipole polarizes the surrounding molecules as well, even if these ones have not got a permanent dipole moment. But this theory too has limits in being applied : it is supposed that every molecule occupies a spheric cavity in the dielectric and that the surrounding of each molecule is a permanent medium and no distinction is made between the interactions of the near surrounding molecules and those of the quite far ones given the central molecule. And this distinction is quite necessary in treating associated liquids and in extending treatment over liquid mixtures.

Kirkwood[5] and Frölich[6] later, desiring to explain the discrepancies between Onsager's theory and the experimental results, took from the continuous model of Onsager the area immediately surrounding the molecules so that the effect of hindering the molecular movement could be calculated from intermolecular forces at a short distance.

Kirkwood's theoretical development[7] is based on the quasi-reticular model of the liquid state, in which each molecule has a certain coordinative surrounding of the immediately neighbouring molecules. Frölich[6] suggests that the continuous liquid medium should have n^2 dielectric constants, n being the refractive index of the respective liquid, dipoles of moment $\vec{\mu}$ being fixed in this medium.

Initially inferred for a pure liquid, the equation obtained by Frölich could be applied to binary mixtures as well[8] :

$$\frac{(\varepsilon-1)(2\varepsilon+1)}{2\varepsilon}\cdot\frac{M}{d}=\left[\frac{(n_*)_1^2-1}{(n_*^2)_1+2}\cdot\frac{M_1}{d}\right]\cdot\left[\frac{\{(n_*)_1^2+2\}(2\varepsilon+1)}{\{(n_*)_1^2+2\varepsilon\}}\right]x_1+$$

$$+\left[\frac{(n_*)_2^2-1}{(n_*)_2^2+2}\cdot\frac{M_2}{d_2}\right]\cdot\left[\frac{\{(n_*)_2^2+2\}(2\varepsilon+1)}{\{(n_*)_2^2+2\varepsilon\}}\right]x_2+$$

$$+\frac{4\pi N_A}{3}\cdot\frac{g(\mu_0)_1^2}{9KT}\cdot\left[\frac{\{(n_*)_2^2+2\}(2\varepsilon+1)}{\{(n_*)_1^2+2\varepsilon\}}\right]^2 x_1 \qquad (1)$$

where ε is the dielectric constants of they system, (n_*), $(n_*)_2$ are the refractive indexes, measured at such a high frequency that they may annul the orientation polarization, g — Kirkwood correlating factor, μ_0 the molecule dipole moment of pure substance in vacuum, x_1 and x_2 the molar fractions of the two components in the respective binary system.

This equation explicitely takes into account the hindered effects of molecular rotation, due to hydrogen bonds ; the correlating parameter is a direct measure of these effects and it is function of temperature and composition. In the speciality literature there are but few works that study the variation of Kirkwood's factor alongside the concentration, over a large range of concentration.

Equation (1) worked up for calculating the apparent dipole moment of a binary system looks like:

$$\mu^2 = g\mu_0^2 = \frac{9KT(\varepsilon - \varepsilon_\infty)(2\varepsilon - \varepsilon_\infty)}{4\pi N\varepsilon(\varepsilon_\infty + 2)^2} \tag{2}$$

where K is Boltzman constant, ε_∞ is the high frequency dielectric constant which is not measured but appreciated[9] to be $\varepsilon_\infty = xn_D^2$ with $x = 1,$ 1 with alcohols and N the number of solute molecules per ml. of solution.

In table 2 there are shown the values of the refractive indicies necessary to calculate ε_∞, the values of the apparent dipole moments μ, as well as the value of Kirkwood correlative factor, g, for benzene-butanol systems.

In figure 2 there is shown the variation of Kirkwood correlative factor with the concentration and temperature (25 and 40°C) for the studied systems.

Leaving aside any association, g should be equal to the unity over the whole concentration range.

Positive deviations of g from the unity can be obtained when short distance hindered couplers favour the parallel orientation of neighbouring molecule dipoles, while negative deviations are obtained when the hindered couplers favour the antiparallel orientation as it is shown in figure 3 as well.

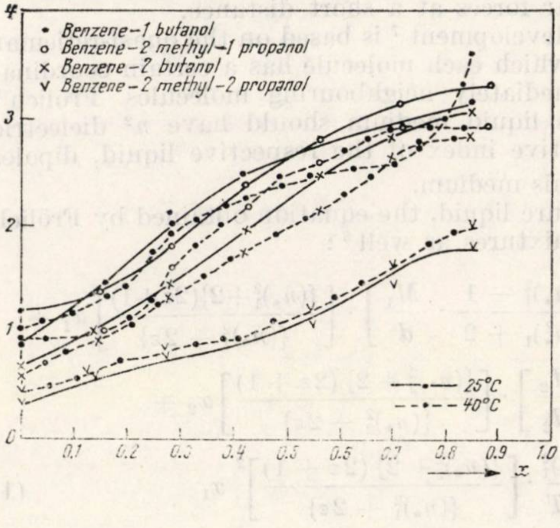

Fig. 2 — Variation of Kirkwood correlative factor with concentration for the systems: benzene 1-butanol (.), benzene 2-methyl-1-propanol (0), benzene 2-butanol (x), and benzene 2-methyl-2-propanol (v) at 25 and 40°C.

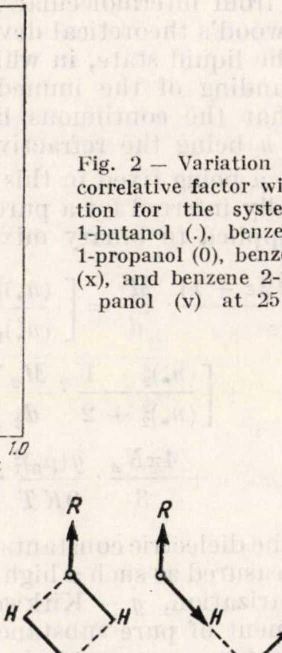

Fig. 3 — Antiparallel association ($g<1$) and parallel association ($g>1$).

TABLE 2

Molar fractions x_2, number of moles n, refractive indices n_D – experimentally determined, calculated high frequency dielectric constant ε_∞, apparent dipole moments of the solution μ and Kirkwood correlative factors g calculated for benzene-alcohol systems at 25 and 40°C.

			25°C				40°C			
	x_2	n_2	n_D	ε_∞	μ	g	n_D	ε_∞	μ	g
benzene 1-butanol	0.0000	0.0539	1.4985	2.4042	1.59	0.9286	1.4890	2.3754	1.68	1.0367
	0.1625	0.1086	1.4784	2.3319	1.98	1.4400	1.4695	2.3058	1.93	1.3682
	0.2799	0.1633	1.4560	2.2778	2.33	1.9941	1.4478	2.2556	2.26	1.8761
	0.4205	0.2168	1.4390	2.2588	2.60	2.4831	1.4320	2.2352	2.48	2.2591
	0.7072	0.2703	1.4248	2.2331	2.77	2.9083	1.4172	2.2093	2.65	2.5794
	0.8564	0.3242	1.4070	2.1776	2.93	3.1533	1.4013	2.1600	2.83	3.6522
	1.0000	—	1.3980	2.1498	—	—	1.3923	2.1323	—	—
benzene	0.0000	0.0591	1.4985	2.4159	1.78	1.1781	1.4890	2.3867	1.57	0.9164
2-methyl 1-pro-	0.1551	0.1192	1.4820	2.3685	1.90	1.3422	1.4370	2.3370	1.65	1.0122
panol	0.2862	0.1784	1.4674	2.3149	2.19	1.7832	1.4578	2.2905	2.09	1.6211
	0.4255	0.2162	1.4507	2.2721	2.55	2.1176	1.4430	2.2440	2.42	2.1774
	0.5653	0.2688	1.4372	2.2274	2.76	2.8117	1.4283	2.1993	2.64	2.5913
	0.7104	0.3236	1.4320	2.1863	2.94	3.2137	1.4140	2.1609	2.82	2.9567
	0.8831	0.3236	1.4098	2.1319	2.99	3.3239	1.4016	2.1204	2.81	2.9357
	1.0000	—	1.3945	—	—	—	1.3884	—	—	—
benzene	0.0000	0.0538	1.4985	2.4130	1.31	0.6703	1.4890	2.3835	0.18	0.6105
2-butanol	0.1389	0.1076	1.4811	2.3437	1.62	1.0255	1.4720	2.3201	1.64	1.0506
	0.2777	0.1618	1.4608	2.3032	2.36	1.4756	1.4523	2.2762	1.85	1.3369
	0.4184	0.2175	1.4470	2.2412	2.24	1.9600	1.4385	2.2149	2.12	1.7556
	0.5627	0.2718	1.4274	2.1869	2.53	2.5000	1.4190	2.1662	2.34	2.1389
	0.7070	0.3262	1.4100	2.1832	2.73	2.9112	1.4033	2.1560	2.60	2.6406
	0.8527	0.3266	1.4088	2.1437	3.07	3.1681	1.4000	2.1204	2.69	2.8266
	1.0000	—	1.3960	—	—	—	1.3884	—	—	—
benzene-2	0.0000	0.0593	1.4985	2.4107	0.91	0.3234	1.4890	2.0769	1.01	0.3984
methyl-2 propa-	0.1332	0.1187	1.4801	2.3489	1.19	0.5532	1.4700	2.3229	1.25	0.6105
nol	0.2694	0.1781	1.4613	2.2917	1.37	0.7332	1.4532	2.2692	1.40	0.7656
	0.4088	0.2374	1.4434	2.2331	1.51	0.9261	1.4363	2.2105	1.55	0.9385
	0.5514	0.2986	1.4248	2.1875	1.76	1.2100	1.4176	2.1668	1.70	1.1289
	0.6975	0.3562	1.4102	2.1486	2.06	1.6516	1.4035	2.1256	1.92	1.4400
	0.8469	—	1.3976	2.1116	2.16	1.8225	1.3901	2.0882	2.27	2.0128
	1.0000	—	1.3855	—	—	—	1.3778	—	—	—

From the study made by Dannhauser[10] on the pure butanols it has been noticed that values obtained for g decrease from normal butanol to tertiary butanol.

In the benzene solutions we have studied, as it is shown in table 2 and figure 2, the correlative factor has greater and less values than the units. So, less values of g than of the unit are obtained within the range of molecular fraction $0 < x_2 < 0.16$ for the benzene 1-butanol system, within the range $0 < x_2 < 0.22$ for the benzene 2-methyl-1-propanol system, within $0 < x_2 < 0.60$ for the benzene 2-methyl-2-propanol system. These values of g entail the formation of multimers which may be cyclic or linear dimers or trimers and whose dipole moments are much less as compared to those of the free monomers [11–14].

In figure 2 one can notice that the values of g for the benzene-2-butanol system and benzene 2-methyl-2-propanol system, within the range of concentration indicated above, are quite close to zero, supposing in this case that there are to be found little cyclic multimers [15].

Having reached the value $g = 1$, with the molar fraction shown above, it is noticed that g increases as the alcohol concentration increases. To bear up this increase there are two points of view: Dannhauser [11] and Gold [16] are for an association in linear chains, while Flechter [17] and Böttcher [18] consider that strongly polar cyclic multimers can be formed.

Within this range as well, OH groups of 2-butanol and 2-methyl-2-propanol show steric factors which are probably responsible for the more decreased concentration of the big multimers, that is for less values of g as compared to freer OH groups in the 1-butanol and 2-methyl-1-propanol.

At the same time in this range of g values there is pointed out the interaction between H atom of the hydroxylic group and π electrons of the aromatic molecules [19–20]. At a given concentration, the proportion of the associated alcohol molecules will be less in this solvent, donor of electrons, than in a relatively inert solvent like cyclohexan; the effect of dissociation worked by benzene can be compared to that worked in pure alcohols by raising temperature.

To draw a conclusion, within the range where $g > 1$, the most important species existent in benzene solutions are strongly polar little multimers, their concentration increasing from 2-methyl-2-propanol to 1-butanol. In the benzene-2-methyl-2-propanol system the prevalent kind seems to be weakly polar molecules, 2-methyl-2-propanol having the most hindered OH group, all over the concentration range.

Benzene has a dissociative effect over the aggregates made up through hydrogen bonds, which changes from 1-butanol to 2-methyl-2-propanol, but the association effect is prevalent.

These conclusions are also confirmed by the remarks made by Ibbitson and Moore [21] on the basis of some spectrophotometric IR, RMN, ultrasonic experimental determinations over the systems studied by us as well, but only in very little alcohol concentration range.

REFERENCES

[1] G.C. Piementel and A.L. Mc.Clellan, "The Hydrogen Bond", W.H. Freeman and Co., San Francisco, California, 1960.

[2] W. Dannhauser and A.F. Flueckinger, *Phys. Chem. Liq.*, **2**, 37 (1970).

[3] R. Vîlcu and Z. Cenușe, *Rev. Roumaine Chim.*, **25**, 763 (1980).

[4] A. Greff, "Ph. D. Thesis", University of Bucharest, 1973.

[5] J.G. Kirkwood, *J. Chem. Phys.*, **7**, 911, (1939).

[6] H. Frölich, *Trans. Faraday Soc.*, **44**, 238 (1948).

[7] J. G. Kirkwood, *Trans. Faraday Soc.*, **42**, 7 (1946).

[8] C. P. Smith, "Dielectric Behaviour and Structure", McGraw Hill Book Company, Inc, New York, 1955.

[9] C. E. Rayala and J. Crossby, *Canad. J. Chem.*, **49**, 3617 (1971).

[10] W. Dannhauser and L.N. Bahe, *J. Chem. Phys.*, **40**, 3058 (1964).

[11] W. Dannhauser, *J. Chem. Phys.*, **49**, 1911 (1968).

[12] H. C. Van Ness, Jon Van Winkle, H.H. Richtol and H.B. Hollinger, *J. Phys. Chem.*, **71**, 1483 (1967).

[13] J. Malecki, *J. Chem. Phys.*, **43**, 1483 (1967).

[14] J. Malecki and Z. Dopirela, *Acta Phys. Polonica*, **36**, 385, 401 and 409 (1969).

[15] G. P. Johary and W. Dannhauser, *J. Chem. Phys.*, **50**, 1862, (1969).

[16] P. J. Gold and R. L. Perrine, *J. Phys. Chem.*, **71**, 4218 (1967).

[17] A.N. Flechter and C.A. Heller, *J. Phys. Chem.*, **71**, 3742 (1967).

[18] P. Bordewijk, F. Gransch and C.J.E. Böttcher, *J. Phys. Chem.*, **73**, 3255 (1969).

[19] J. Crossley, *Canad. J. Chem.*, **49**, 712 (1971).

[20] J. Crossley and C.P. Smith, *J. Amer. Chem. Soc.*, **91**, 2482 (1969).

[21] D.A. Ibbitson and L.J. Moore, *J. Chem. Soc.*, **13**, 80 (1967).

Revue Roumaine de Chimie, **25**, *6*, 781–788 (1980)

CALCULATION OF HYDROGEN BOND ENERGIES FROM EXCESS ENTHALPIES, EXPERIMENTALLY DETERMINED FOR BENZENE-BUTANOL SYSTEMS

RODICA VÎLCU and ZOICA CENUŞE
National Institute of Chemistry, Chair of Physical-Chemistry
Bd. Republicii 13, Bucharest, Romania

Received July 2, 1979

Excess enthalpies of benzene-butanol systems are determined at 25, 40 and 50°C and correlated with excess Gibbs energy. Hydrogen bond energies of benzene-butanol systems were calculated at 25, 40 and 50°C using a reticular and group contribution model.

1. INTRODUCTION

One of the most frequently used methods for characterizing the thermodynamic behaviour of the binary systems is the multifunctional analysis by the simultaneous correlation of excess enthalpy obtained by calorimetric measurements and of Gibbs free energies, obtained from vapour pressure measurements. In the present work we focused our attention upon obtaining excess enthalpies, the correlation with free excess energy obtained from the limited determinations of the liquid-vapour equilibria and the calculation of excess entropies; we are also interested in appreciating the energy of hydrogen bonds in benzene-butanol systems using a liquid state model.

2. EXPERIMENTAL

The purity of substances for synthesizing the mixtures studied, as well as the experimental method used for obtaining excess enthalpies have been shown previously [1–2].

3. RESULTS

In table 1 there are shown the values of excess enthalpies obtained for the benzene-butanol systems.

TABLE 1

Variation of values of excess enthalpies with temperature and concentration, H^E, values of excess enthalpies driven to infinite dilution $H^E/x_1 \cdot x_2$, as well as value of Redlich—Kister parameters for benzene-butanol systems

25°C			40°C			50°C		
x_2	H^E (cal./mol)	$H^E/x_1 \cdot x_2$ (kcal/mol)	x_2	H^E (cal/mol)	$H^E/x_1 \cdot x_2$ (kcal/mol)	x_2	H^E (cal/mol)	$H^E/x_1 \cdot x_2$ (kcal/mol)
benzene 1-butanol								
0.0000		2.05	0.0000		2.39	0.0000		2.59
0.2017	217.2		0.2039	294.4		0.2115	322.3	
0.4026	264.0		0.4058	313.7		0.4170	337.2	
0.5027	248.0		0.5061	295.2		0.5177	324.0	
0.6023	206.4		0.6057	249.6		0.6168	283.7	
0.8017	111.6		0.8038	124.8		0.8111	156.5	
1.0000		0.68			0.88			1.07
C_0	978.1			1176.2			1306.8	
C_1	686.8			636.8			755.2	
C_2	393.5			366.7			519.1	
benzene 2-methyl-1-propanol								
0.0000		3.20	0.0000		3.35	0.0000		3.51
0.0997	223.4		0.1003	310.0		0.1053	260.2	
0.1994	319.2		0.2417	366.0		0.3122	372.0	
0.2992	327.0		0.5008	288.8		0.5144	307.0	
0.4991	860.3		0.7007	165.6		0.1719	182.5	
0.6993	162.0		0.8403	115.6		0.8090	140.4	
1.0000		0.98			1.06			1.11
C_0	1015.7			1123.4			1201.4	
C_1	1007.3			1119.7			1195.8	
C_2	1031.2			1078.6			1101.9	
benzene 2-butanol								
0.0000		1.65	0.0000		3.20	0.0000		3.93
0.2002	248.0		0.1007	290.4		0.2063	398.4	
0.4047	321.6		0.3011	391.2		0.4094	403.2	
0.5049	309.6		0.5011	354.0		0.5098	388.8	
0.7017	158.4		0.6010	345.6		0.6094	378.0	
0.8631	60.0		0.8007	225.6		0.8062	309.6	
1.0000		0.12			1.88			3.63
C_0	1196.9			1337.6			1560.5	
C_1	766.7			891.9			406.0	
C_2	307.9			1752.0			1805.6	

TABLE 1 (continued)

25°C			40°C			50°C		
x_2	H^E (cal./mol.)	$H^E/x_1 \cdot x_2$ (kcal/mol)	x_2	H^E (cal/mol)	$H^E/x_1 \cdot x_2$ (kcal/mol)	x_2	H^E (cal/mol)	$H^E/x_1 \cdot x_2$ (kcal/mol)
benzene 2-methyl-2-propanol								
0.0000		2.49	0.0000		2.63	0.0000		2.78
0.1990	312.0		0.2005	331.2		0.1946	338.4	
0.3984	375.6		0.4006	402.0		0.4110	417.6	
0.4984	364.8		0.5007	392.4		0.5130	408.0	
0.5985	397.9		0.6006	361.9		0.6124	374.4	
0.7991	217.4		0.8004	238.8		0.8082	316.8	
1.0000		1.50			1.68			1.95
C_0	1460.4			1569.1			1635.1	
C_1	489.7			471.0			408.0	
C_2	539.7			588.2			736.1	

It has been adopted for correlating the excess enthalpies with concentration an equation of Redlich — Kister type :

$$H^E = x_1 \cdot x_2 \sum_{i=0}^{2} C_i (x_1 - x_2)^i \tag{1}$$

the parameters of this equation up to $i = 2$ being determined by the method of the least square and shown in table 1 too.

In figure 1 it is shown, to exemplify, the variation of the excess enthalpy with temperature and concentration in the benzene 2-methyl--2-propanol system, while in figure 2, extrapolation values, $H_1^E\infty$ and $H_2^E\infty$, obtained for the same system at 25, 40 and 50° C are presented.

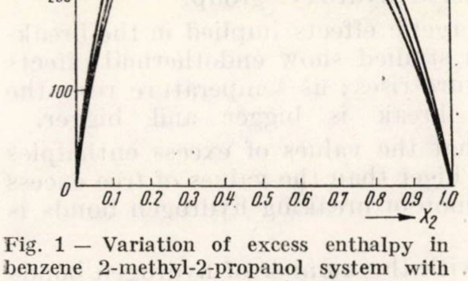

Fig. 1 — Variation of excess enthalpy in benzene 2-methyl-2-propanol system with a concentration at 25, 40 and 50°C.

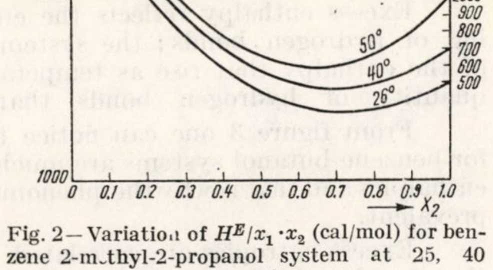

Fig. 2 — Variation of $H^E/x_1 \cdot x_2$ (cal/mol) for benzene 2-methyl-2-propanol system at 25, 40 and 50°C.

In figure 3 there are shown the values of G^E/RT previously obtained [1,2], of H^E/RT as well as the calculated values of S^E/R for the four studied systems.

As it is well known [3], alcohols are strongly associated through hydrogen bonds; the changes that occur in excess thermodynamic functions with unpolar solvents are due to hydrogen bonds and to mixing effects with solvent – dispersion forces or other specific interactions.

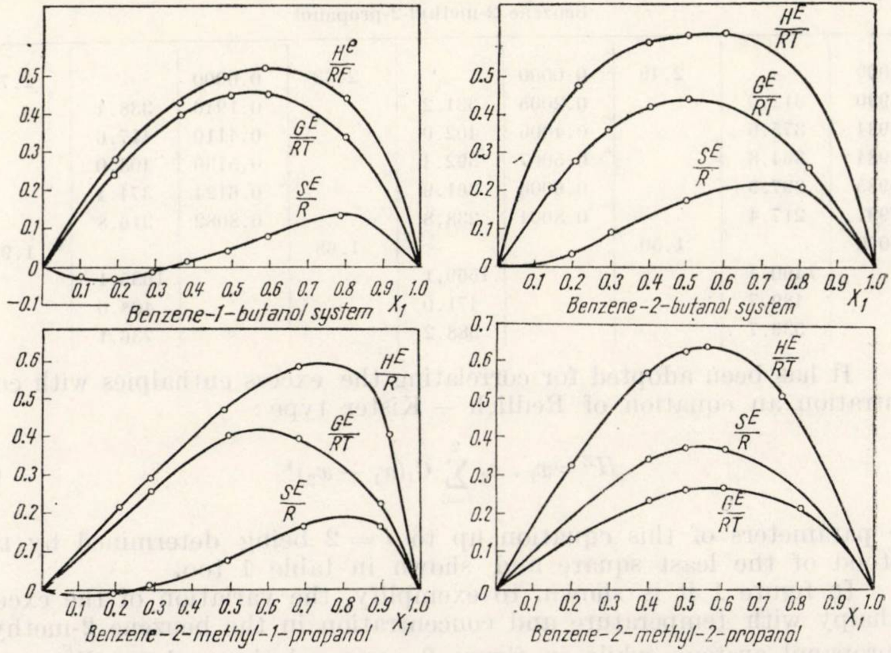

Benzene-1-butanol system

Benzene-2-butanol system

Benzene-2-methyl-1-propanol

Benzene-2-methyl-2-propanol

Fig. 3 – Adimensional free excess enthalpy G^E/RT, adimensional excess enthalpy H^E/RT, as well as adimensional excess entropy S^E/R at 25°C for benzene-butanol systems.

Free enthalpy Gibbs is correlated with the effects of forming hydrogen bonds; with the systems studied [2] the excess free energy Gibbs drops as temperature rises, so that the possibility of forming hydrogen bonds become more and more reduced as temperature rises and, at the same time, they lower from normal alcohol to tertiary butanol since this one has the most sterically hindered hydroxyl group.

Excess enthalpy reflects the energetic effects implied in the breaking of hydrogen bonds; the systems studied show endothermal effects of the enthalpy that rise as temperature rises; as temperature rises the quantity of hydrogen bonds that break is bigger and bigger.

From figure 3 one can notice that the values of excess enthalpies for benzene-butanol systems are much higer than the values of free excess enthalpies and that is why the phenomenon of breaking hydrogen bonds is prevalent.

Excess entropies are correlated with the number of hydrogen bonds that break; they generaly rise as temperature rises.

With the benzene 1-butanol systems there are also some negative values of the entropy, where the molar fraction in alcohol is very high, that is within the limits where the translation and orientation restrictions are quite big, but it becomes positive with little molar fractions in alcohol when a great number of hydrogen bonds are broken, allowing a greater freedom in orientation, but still remaining some translational restrictions.

Moreover, in benzene solutions there appear strong interactions between solvent — solvent and OH — solvent and it could explain the much more positive values of excess enthalpies and entropies in this solvent than in the cyclohexane inert.

These considerations are in reasonable agreement with the conclusions Barker[4] reached which show that in benzene solution more hydrogen bonds are broken than in hexane solutions, due to the same strong interactions between hydroxylic hydrogen and benzene.

In benzene-butanol systems where we are to consider the effects worked on thermodynamic functions by changing the structure of alcohol there also appear influences of the spatial arrangament of carbon atoms in the respective chain upon the easiness for the hydroxylic groups to draw together in order to make up hydrogen bridges, that is the so-called effect of steric hindrance.

We can appreciate from the excess enthalpies that in the 2-butanol and 2-methyl-2-propanol less hydrogen bonds are formed that in 2-methyl-1-propanol and in 1-butanol or that more hydrogen bonds in the 2-butanol and 2-methyl-2-propanol are broken at an initial dilution than in normal alcohol.

In benzene solutions the excess enthalpies for the 2-butanol and 2-methyl-2-propanol have much higher values than for normal butanol and they rise as temperature rises.

4. CALCULATION OF HYDROGEN BOND ENERGY

By virtue of those discussed above we can conclude that the excess enthalpy of a studied binary system, made up of a component that associates itself and a non-polar component is the total sum of three contributions: breaking of hydrogen bonds, dispersion effect, and specific interactions of type OH$-\pi$. If we apply these grounds to extreme dilutions, all the molar dimensions appear under the form of partial molar dimensions, that is:

$$\overline{H}_2^E\infty = \bar{h}_H^E\infty + \bar{h}_{\text{disp.}}^{E\infty} + \bar{h}_{\text{spec.}}^{E\infty} \tag{2}$$

In equation (2), in order to estimate the energy of hydrogen bond $\bar{h}_H^E\infty$, the other three quantities are to be considered $\overline{H}_2^E\infty$, $\bar{h}_{\text{disp.}}^{E\infty}$, $\bar{h}_{\text{spec.}}^{E\infty}$.

So, $\overline{H}_2^E\infty$ is estimated from the variation of $\overline{H}^E/x_1\cdot x_2=\psi(x_2)$, extrapolated to extreme dilutions, values which are to be found in table 1.

In order to achieve the contribution of the dispersion term, $h^{E\infty}_{\text{disp.}}$ we have used the method Kehiaian[5-6] applied to study some binary systems of aliphatic and aromatic hydrocarbons, a method which relies upon the reticular theory and group contribution.

Corresponding to the theory of group contribution, molecules are considered to be made up of diverse groupings or segments, and the calculations of thermodynamic properties is made on the basis of interaction between molecular surfaces of these groupings. Thus, it was considered that the groups CH_3, CH_2, CH, OH made up segments whose areas in an isolated state are equal to the unit, but whose contact areas are 0.125 (corresponding to a number of coordination of network $Z = 8$).

The expressions used for calculating the energetic contributions are those of the reticular theory of heterogeneous mixtures of Guggenheim[7] within Redlich, Derr and Pierotti's[8] approximation.

The calculating equation is:

$$F^M_V = \frac{q_1 \cdot q_2 \cdot x_1 \cdot x_2}{q_1 \cdot x_1 + q_2 x_2} \left[-\frac{1}{2} \sum_s \sum_t (\alpha_{1s} - \alpha_{2s})(\alpha_{1t} - \alpha_{2t}) \right] E^*_{st} \qquad (3)$$

where q_1, q_2 are contact surfaces of the two components of the mixture, x_1 and x_2 the molar fractions, α_{is} are fractions of species s in the molecule i, $\alpha_{is} = \frac{q_{is}}{q_i}$ and E^*_{st} the internal energy of interaction upon the area conventional unit and was estimated by Kehiaian as an adjustable parameter over the maximum of enthalpy — concentration variation: for instance, E^* alif-arom. = 199.2 cal/mol.

As the directly calculating measurement is the excess enthalpy and not the excess energy and as data necessary for transforming H^E into E^E are not available, we have considered the expression of the excess enthalpy by a similar equation to be satisfactory.

In table 2 there are shown the areas and areas fractions of the components in the systems studied.

TABLE 2

Areas and areas fractions in benzene, 1-butanol, 2-methyl-1-propanol, 2-butanol, 2-methyl-2 propanol

Component	q_i	$\alpha_{i_{\text{aliphatic}}}$	$\alpha_{i_{\text{aromatic}}}$	$\alpha_{i_{\text{hydroxyl}}}$
n-butanol	4.00	0.78125	0	0.21875
isobutanol	4.00	0.78125	0	0.21875
s-butanol	4.00	0.78125	0	0.21875
t-butanol	3.50	0.75	0	0.25
benzene	3.80	0	1	0

With 2-methyl-2-propanol, the central carbon atom is considered to be blocked off and its contact area to be zero. The benzene area is estimated by Kehiaian from the position of the maximum of the excess enthalpy curve taking into account the composition in benzene- aliphatic hydrocarbons binary systems.

The interaction enthalpy for the benzene 1-butanol, benzene 2-methyl -1-propanol and benzene 2-butanol systems has the value $h^* = 165.6$ cal/mol while for the benzene 2-methyl-2-propanol system $h^* = 159.5$ cal/mol; they have been calculated on the basis of equation (3). Changing these values in the equation equivalent to equation (3) there can be estimated the contributions of dispersion effects with excess enthalpy; by resorting to extreme dilution there can be obtained, for the three systems mentioned above, the value $\bar{h}^{E\infty}_{\text{disp.}} = 0.62$ kcal/mol, and, for the benzene 2-methyl-2-propanol system, the value $\bar{h}^{E\infty}_{\text{disp.}} = 0.53$ kcal/mol.

At last, to estimate the specific interactions $\bar{h}^{E\infty}_{\text{spec.}}$ OH$-\pi$ existent in the systems studied due to the fact that the system of electrons π in benzene acts as an accepter of protons and interferes in alcohol autoassociation, we have considered that these ones have the same value for butanols as well as for the other alcohols, as Van Ness[9] and Otterstedt and Missen[10] show, namely that: $\bar{h}^{E\infty}_{\text{spec.}} = -1.69$ kcal/mol.

Finally, the energies of hydrogen bonds shown in table 3 have been estimated.

TABLE 3

Energy of hydrogen bonds for the benzene-butanol systems at 25, 40 and 50°C

System	$\bar{h}^{E\infty}_{H}$ (kcal/mol)		
	25°C	40°C	50°C
benzene 1-butanol	6.67	5.48	4.13
benzene 2-methyl-1-propanol	5.22	4.41	4.29
benzene 2-butanol	6.30	4.35	3.84
benzene 2-methyl-2-propanol	4.13	3.97	3.82

These values are in reasonable agreement with those estimated by Pimentel[11] and Van Ness [9]. These values show that as temperature rises, the autoassociation aggregates become less and less settled, the necessary energy to destroy them being less.

The aggregates constituted in the benzene 2-methyl-2-propanol system are energetically the weakest, this being due to the approximately radial field of 2-methyl-2-propanol, to the steric hinderance of the central carbon atom.

REFERENCES

[1] Z. Cenușe, "Ph. D. Thesis", Institutul Politehnic București, București, 1976.
[2] R. Vilcu and Z. Cenușe, *Rev. Roumaine Chim.*, **21**, 343 (1976).
[3] I. Brown, W. Fock and F. Smith, *J. Chem. Thermod.*, **1**, 273 (1969).
[4] A. J. Barker, *J. Chem. Phys.*, **20**, 1526 (1952).
[5] H. V. Kehiaian, *J. Chem. Phys.*, **68**, 935 (1971).
[6] H. V. Kehiaian, K. Sonskowska and R. Hryniewicz, *J. Chem. Phys.*, **68**, 922 (1971).
[7] A. A. Guggenheim, "Mixtures", Oxford Press, 1952.
[8] O. Redlich, E.L. Derr and J. Pierotti, *J. Amer. Chem. Soc.*, **81**, 2283 (1959).
[9] C.G. Savini, D.R. Wintherholfer and H.C. Van Ness, *J. Chem. and Eng. Data*, **10**, 168 (1965).
[10] J. A. Otterstedt and R.W. Missen, *Trans. Faraday Soc.*, **58**, 879, (1962).
[11] G. C. Pimentel, "The Hydrogen Bond", W. H. Freemen and Co., San Francisco, 1960.

Revue Roumaine de Chimie, **25**, *6*, 789–792 (1980)

RELATION BETWEEN ENTROPY AND COHESIVE ENERGY FOR METALS

B. CHATTERJEE
Engelhard Industries Davis Road, Chessington Surrey KT9 1TD, United Kingdom

Received July 6, 1978

Based on theoretical considerations the entropy of metals at 298 K (S_{298}) is shown to be a logarithmic function of the cohesive energy at 0K (E_c)

$$S_{298} = 28.72\,(\log mV^{\frac{2}{3}}/E_c) + A$$

where m is the atomic weight, V is the atomic volume and A is a constant. It is assumed that the frequency of simple harmonic vibration of an atom is proportional to its characteristic Debye frequency. An analysis of the relevant data from the literature corroborates the suggested logarithmic relation.

Following the Debye model the entropy $S(JK^{-1}\,\text{mol}^{-1})$ of a metal is related inversely to the Debye temperature $\theta_D(\text{K})$ and is often defined as the measure of randomness of a system. On the other hand, one can state in an empirical way that a strong atomic binding and hence a large cohesive energy $E_c(J\,\text{mol}^{-1})$ of a metal results in large θ_D. The aim of the present paper is to establish a quantitative relation between S and E_c for metals on the basis of simple theoretical considerations. A subsequent analysis of the relevant data[1,2] supports the suggested logarithmic relation. For the present purpose, it is necessary initially to discuss the following relationships between

a) S and θ_D and

b) E_c and θ_D.

RELATION BETWEEN S AND θ_D

The major contribution to the entropy of a solid is derived from thermal vibrations of the crystal lattice. The effect of lattice vibrations on the thermodynamic functions is well known in the theories of the heat capacity of metals[3]. According to the Debye model, the vibrational entropy S of a metal is related to θ_D as

$$S = R[4D\,(\theta_D/T) - 3\ln\{1 - \exp\,(-\theta_D/T)\}] \tag{1}$$

where R is the universal constant ($8\cdot3143\ J\,K^{-1}\,\text{mol}^{-1}$) and D is the Debye function. On restricting the expansion of the function in Eq. (1)

to the first two terms only, the entropy equation for the distribution of the Debye frequencies becomes

$$S = R[4 + 3 \ln (T/\theta_D)] \tag{2}$$

RELATION BETWEEN E_c AND θ_D

A simple form of potential function in a metal is considered where all the atoms except one are fixed in their equilibrium positions. If the atom in question is regarded as oscillating in a simple harmonic motion, the vibration frequency ν of the oscillator of mass m is given by

$$\nu = (1/2\pi)\,(\alpha/m)^{\frac{1}{2}} \tag{3}$$

where α is the force constant. Following the simple theory of thermal vibrations of atoms, the force constant is determined by the second differential with respect to r of the potential energy function u at the equilibrium distance r_0 i.e. $\alpha = (\delta^2 u/\delta r^2)_{r=r_0}$. Since the potential energy function can be expanded in a Taylor series about its minimum, the total energy change of the oscillating atom and its neighbours for a displacement $\Delta r (= r - r_0)$ can be expressed as

$$u = (\alpha/2)\Delta r^2 \tag{4}$$

On substituting α of Eq. (4) into Eq. (3), one obtains

$$\nu = (1/2\pi)\,(2u/m\,\Delta r^2)^{\frac{1}{2}}$$

If it is assumed that ν is proportional to the characteristic Debye frequency $\nu_{\max}$, then the following expression would be obtained

$$\theta_D = (h\nu_{\max}/k_B)$$

$$= c(h/k_B)\,(u/2\pi^2 m\Delta r^2)^{\frac{1}{2}} \tag{5}$$

where c is a proportionality coefficient, h and k_B are the Planck and Boltzmann constants respectively. All metals crystallising in fcc, bcc and hcp lattices, can be divided into three groups according to the value of c. For the first and largest groups of the periodic table, comprising the major sub-group elements of groups 1,2 and 4, and the group 8 elements (Fe, Co, Ni, Ru and Rh), $c \simeq 1$, i.e. the characteristic frequency of the Debye theory turns out to be equal to the simple harmonic oscillation frequency for one atom given by Eq. (3). For the metals of the major sub-group 2 and some d-elements of groups 6,7 and 8, $c \simeq 1.2$, For the d-elements of sub-groups 1, 3 and 4, and also Mo and Pt, $c \simeq 0.8$.

Since the cohesive energy of a metal is considered to be made up from nearest neighbour interactions only[4], the potential energy for atoms farther away than the nearest neighbours is neglected. Thus the quantity Δr is equal to the nearest neighbour distance which is related to the lattice parameter and hence the atomic volume V (cm^3 mol^{-1}) of the crystal lattice. Thus Δr is equal to $1.09\,V^{\frac{1}{3}}$ and $1.12\,V^{\frac{1}{3}}$ for bcc and fcc lattices respectively. For a metal with N atoms per unit volume, the cohesive energy is equal to the product of N and u. Thus Eq. (5) can be written as

$$\theta_D = p(E_c/mV^{\frac{2}{3}})^{\frac{1}{2}} \tag{6}$$

where p, a constant, is approximately equal to $c(h/k_B)\ (1/2\pi^2N)^{\frac{1}{2}}$. The expression in Eq. (6) is similar to an empirical relation reported elsewhere, and is different from the well-known relation obtained from the Debye model of the lattice specific heat capacity where the energy in thermal equilibrium of a collection of oscillators of different frequencies at T is given to be equal to $9Nk_B(T^4/\theta_D^3)\int_0^{x_D} x^3\mathrm{d}x/(e^x-1)$ where $x_D = \theta_D/T$.

RELATION BETWEEN S AND E_c

On substitution of θ_D of Eq. (6) into Eq. (2), one obtains the entropy of metals at 298 K as

$$S_{298}=28.72(\log m+\log V^{\frac{2}{3}}-\log E_c)+A \tag{7}$$

where A, a constant, depends upon c and p which are functions of the characteristic frequency and the frequency of vibration respectively of the Debye model. The present work does not take into account any electronic contribution to the heat capacity and hence to the entropy of metals at 298 K. This is justifiable because of the small fraction of the electronic entropy compared to that due to the lattice vibrations at 298 K.[3,6]

In figure 1 the entropy (due to lattice vibrations) at 298 K is plotted against $(\log m + \log V^{\frac{2}{3}} - \log E_c)$ for thirty-six metals comprising simple lattice structures, namely bcc, fcc and hcp. The slope of the line agrees with the predicted value given in Eq. (7). Thus the linear relation of figure 1 corroborates the theoretical considerations used to drive Eq. (7) relating entropy with cohesive energy for metals.

The effect of temperature on the above two parameters, namely S and E_c can also be stuudied from the present quantitative relationship

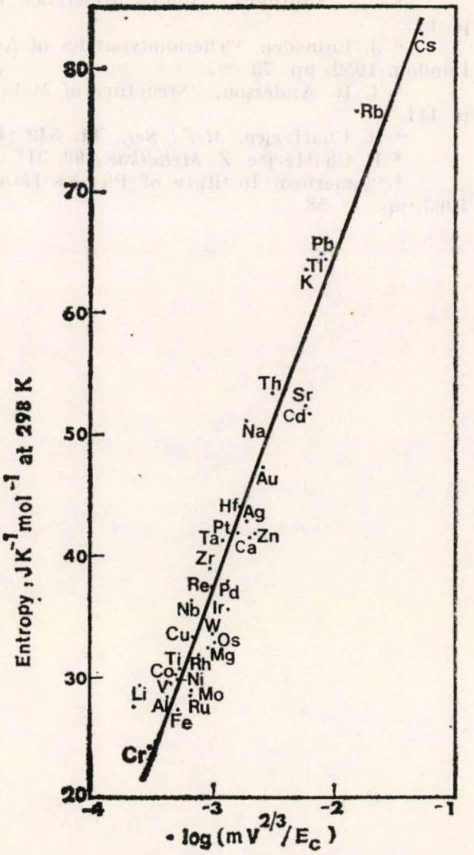

Fig. 1 — Relation between entropy and $\log\,(mV^{\frac{2}{3}}/E_c)$ for metals.

which also incorporates another temperature dependent function, namely the atomic volume. When a metal is heated up, one expects a gradual decrease in the degree of cohesion and an increase in entropy. On raising the temperature the energy of lattice vibrations i.e. internal energy E(Debye) of the atom (or molecule) would increase at the expense of the energy of cohesion. At a temperature T below the melting point, the average energy of cohesion per atom of a metal in Eq. (7) is thus to be replaced by

$$(E_c)_T = [E_c - E(\text{Debye})]/N$$

The values of E(Debye) can be evaluated from its relation with θ_D/T ratio.[7]

REFERENCES

[1] C. Kittel, "Introduction to Solid State Physics", 4th edition, Wiley, New York, 1971, p. 96.

[2] C.J. Smithells, "Metals Reference Book", 5th edition, Butterworths, Kent,1976, p. 193.

[3] J. Lumsden, "Thermodynamics of Alloys", Monograph No. 11, Institute of Metals, London, 1952, pp. 73—97.

[4] J. R. Anderson, "Structure of Metallic Catalysts", Academic Press, London, 1975, p. 111.

[5] R. Chatterjee, *Metal Sci.*, **11**, 542 (1977).

[6] B. Chatterjee, *Z. Metallkde.*, **68**, 211 (1977).

[7] "American Institute of Physics Handbook", 2nd edition McGraw-Hill, New York 1963, pp. 4—58.

Revue Roumaine de Chimie, 25, *6* 793–798 (1980)

THE THERMODYNAMIC ACTIVITY OF $ZnSO_4$ IN THE SYSTEMS : $ZnSO_4 + H_2O$ AND $ZnSO_4 + Na_2SO_4 + H_2O$

S. STERNBERG, MIHAELA DRĂGĂNOIU and A. MATEESCU

Dept. of Physical Chemistry and Electrochemistry, National Institute of Chemistry, Bucharest;
str. Polizu 1, Romania

Received June 16, 1979

The thermodynamic activity of $ZnSO_4$ has been determined in systems of binary electrolytes ($ZnSO_4 + Na_2SO_4$) using measurements of electromotive forces. The data are compared to those existing in the literature for the solutions of pure $ZnSO_4$. A more advantageous variant of the cells usually used is proposed.

The determination of the thermodynamic activity in systems of binary electrolytes is necessary in establishing some important properties like the interionic attraction, for the extension of information concerning ionic equilibria, for calculating solubilities, for calculating the degree of dissociation, a.s.o. Besides the scientific interest this problem has an incontestable practical interest because the concentrated solutions of binary electrolytes are very often used in chemical technology.

The literature in this field is still deficient regarding the problem of the determination of this thermodynamic property in systems of binary electrolytes. Most of the existing data are referring to systems of uni-univalent electrolytes, for which there is also a well-established theory of the processus[1] for the systems like HCl or HBr in solutions of alkali halides and alkali hydroxides in solutions of alkali halides. There are also data for mixed systems of alkali and alkaline-earth halides for HCl in solutions of alkaline-earth halides[1] and for some systems for 1 :2 type electrolytes,[1,2] for H_2SO_4 in alkali-sulphates solutions or 2 :2 type for the system $MgCO_3 + CaSO_4 + H_2O$. A symmetrical system of binary electrolytes recently studied is : $ZnSO_4 + CaSO_4 + H_2O$.

In this present work we set us the task of bringing some new contributions in this domain, by studying the variation of the activity coefficient of a 2 : 2 electrolyte ($ZnSO_4$) in the presence of a 1 : 2 electrolyte, with common ion (Na_2SO_4) in aqueous solutions, at the room temperature, and the determination of the $\gamma = f(m)$ dependence in such asymmetrical systems.

For the determination of the activity coefficient of $ZnSO_4$ in these systems, measurements of electromotive forces have been used. The method of the electromotive forces is advantageous to be used for measuring activities in mixed electrolyte solutions—like those studied—because of the possibility to vary the concentrations of both electrolytes as it is wished. The determination of the activity in simple $ZnSO_4$ solutions has usually been made[1] in electrochemical cells of the types:

$$Pb-Pb_xHg-PbSO_4/ZnSO_4/Zn_xHg$$

$$Hg_2SO_4-Hg/ZnSO_4/Zn_xHg$$

$$Pt-PbO_2-PbSO_4/ZnSO_4/Zn_xHg$$

EXPERIMENTAL PART

In the present work a more advantageous variant of the electrochemical cells is proposed, characterized by the simplicity of the realization and by avoiding the preparation of the metal amalgam electrodes.

The lead sulphate electrode proposed is obtained by simple immersion of an electrolytic lead plate (2 × 1 cm) in concentrated sulphuric acid for 8–10 hours. During the determinations, the so-obtained electrode has been introduced in crystals of $PbSO_4$.

Determinations have also been made using a $Pb - PbSO_4$ (crystals) electrode, without previous sulphating.

The zinc electrode used is made of electrolytical zinc wire, stripped before each series of experiments and introduced as such in the cell.

The determinations have been made with the help of the potentiometer, type R 37–1, in a cell of the type:

$$Zn/ZnSO_4/PbSO_4-Pb$$

The measured electromotive forces are reproduced in table 1, and the thermodynamic activity may be calculated with the equation:[3]

$$E = E^0 - \frac{\nu RT}{nF}\ln a_{\pm} \qquad (1)$$

in this case: $n = 2$, $\nu = 2$.

$$\text{It follows: } \ln a_{\pm} = \frac{F}{RT}(E^0 - E) = \frac{F}{RT}\Delta E \qquad (2)$$

The medium activity coefficient, whose variation we have in view, for such a system, is:

$$\gamma_{\pm} = \gamma_{+}\gamma_{-} = \frac{a_{\pm}}{[m_1(m_1+m_2)]^{1/2}} \qquad (3)$$

with: m_1 – the molality of $ZnSO_4$
m_2 – the molality of Na_2SO_4.

The fact that this electrode is proper for our purpose is proved by the values obtained for E^0 – appreciably the same for a definite mood of pretreating the electrode (Table 1). Thus, the values E^0 being practically constant, do not depend upon the concentration of SO_4^{2-} and that is why the electrode may be used for determining the thermodynamic activity.

The lead electrode without previous sulphating has also given a practically constant value for E^0 (numerically different).

In the experiments for the determination of the activities only the electrode obtained by previous sulphating has been used. It is possible to see, in table 2, that the activity coefficient γ obtained with the value $E^0 = 0.4025$ V gives a very good agreement with the data existing in the literature.[3]

The method described before has been further applied to the systems of binary electrolytes $ZnSO_4 + Na_2SO_4$ in a cell of the type:

$$Zn/ZnSO_4(m_1),\ Na_2SO_4(m_2)/PbSO_4 - Pb$$

TABLE 1

The determination of the values of E_0 in solutions of $ZnSO_4$

Concentration (mol/1000 g H_2O)	E_1(V)	E_1^0(V)	E_2(V)	E_2^0(V)
0.5	0.4920	0.4025	0.5539	0.4644
0.7	0.4845	0.4008	0.5537	0.4654
1.0	0.4840	0.4026	0.5459	0.4647
1.4	0.4770	0.4009	0.5489	0.4638
1.6	0.4785	0.4048	—	—
2.0	0.4720	0.4037	—	—
$\bar{E}^0$(V)	0.4025		0.4646	

E_1, E_1^0, $\bar{E}_1^0$ – Obtained with the lead electrode with previous sulphating

E_2, E_2^0, $\bar{E}_2^0$ – Obtained with the lead electrode without previous sulphating

TABLE 2

Comparison between γ determined and γ existing in literature

m	γ determined	γ literature
0.5	0.0620	0.0630
0.7	0.0530	0.0523
1.0	0.0422	0.0435
1.4	0.0397	0.0378
1.6	0.0369	0.0363
2.0	0.0337	0.0357

There are two possibilities to broach the problem, either to determine the activity coefficient of one electrolyte at a given concentration, in the presence of another electrolyte of variable concentration, or to measure the same extent at variable concentrations, of both electrolytes, at total constant molality (or total constant ionic strength). Different groups of determinations have been made, each of them at a given ionic strength I, and varying the proportion of the two electrolytes.

RESULTS AND DISCUSSION

The results are presented in the tables 3, 4 and 5 and in the figure 1.

In a first approximation, according to Debye-Hückel theory, the exclusive dependence on the ionic strength would have given a constant

TABLE 3

The determination of γ in solutions of $ZnSO_4 + Na_2SO_4 + H_2O$, at $I = 3$ and different proportions of the two electrolytes

Concentrations mol/1000 g H_2O	$\lvert\Delta E\rvert = -(E^0 - E)$	$a_\pm$	$\gamma\pm$
$m_1 = 0.75$ $m_2 = 0$	0.0855	0.0362	0.0482
$m_1 = 0.675$ $m_2 = 0.1$	0.0925	0.0276	0.0381
$m_1 = 0.6$ $m_2 = 0.2$	0.0941	0.0259	0.0373
$m_1 = 0.525$ $m_2 = 0.3$	0.0979	0.0224	0.0340
$m_1 = 0.45$ $m_2 = 0.4$	0.0997	0.0209	0.0337
$m_1 = 0.375$ $m_2 = 0.5$	0.1035	0.0180	0.0314
$m_1 = 0.3$ $m_2 = 0.6$	0.1095	0.0142	0.0273
$m_1 = 0.225$ $m_2 = 0.7$	0.1064	0.0160	0.0350
$m_1 = 0.15$ $m_2 = 0.8$	0.1090	0.0145	0.0384
$m_1 = 0.075$ $m_2 = 0.9$	0.1131	0.0124	0.0458

TABLE 4

The determination of γ values in solutions of $ZnSO_4 + Na_2SO_4 + H_2O$, at $I = 2.7$ and different proportions of the two electrolytes

Concentrations mol/1000 g H_2O	$\lvert\Delta E\rvert = -(E^0 - E)$	$a_\pm$	$\gamma\pm$
$m_1 = 0.675$ $m_2 = 0$	0.0835	0.0391	0.0579
$m_1 = 0.6$ $m_2 = 0.1$	0.0895	0.0310	0.0478
$m_1 = 0.525$ $m_2 = 0.2$	0.0938	0.0262	0.0424
$m_1 = 0.45$ $m_2 = 0.3$	0.0891	0.0315	0.0390
$m_1 = 0.375$ $m_2 = 0.4$	0.1045	0.0173	0.0320
$m_1 = 0.3$ $m_2 = 0.5$	0.0894	0.0311	0.0634
$m_1 = 0.225$ $m_2 = 0.6$	0.0917	0.0285	0.0661
$m_1 = 0.075$ $m_2 = 0.8$	0.0958	0.0243	0.0948

TABLE 5

The determination of γ values in solutions of $ZnSO_4 + Na_2SO_4 + H_2O$, at $I = 1.5$ and different proportions of the two electrolytes

Concentrations mol/1000 g H_2O	$\lvert\Delta E\rvert = -(E^0 - E)$	$a_\pm$	$\gamma_\pm$
$m_1 = 0.375$ $m_2 = 0$	0.0957	0.0244	0.0650
$m_1 = 0.3$ $m_2 = 0.1$	0.1012	0.198	0.0571
$m_1 = 0.225$ $m_2 = 0.2$	0.1102	0.0139	0.0449
$m_1 = 0.15$ $m_2 = 0.3$	0.1070	0.0157	0.0604
$m_1 = 0.075$ $m_2 = 0.4$	0.0993	0.0212	0.1123

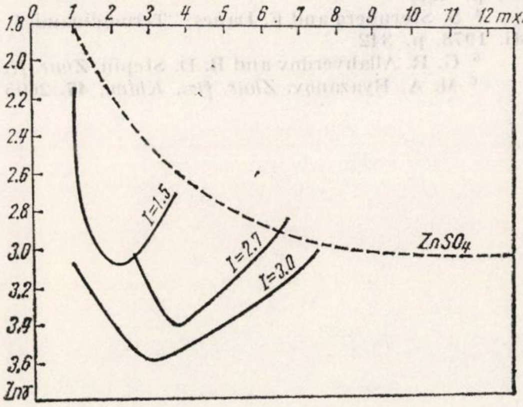

Fig. 1.—The variation $\ln \gamma\ ZnSO_4 = f(m_1)$ in solutions of $ZnSO_4 + Na_2SO_4 + H_2O$.

value γ for any ratio between the concentrations of the two electrolytes. However Harned and other authors have shown that in binary mixtures of electrolytes (e.g. the type HCl + alkali halides) it appears a relatively small effect of variations of the activity coefficient with the ratio of the two electrolytes and they have established a linear dependence $\log \gamma - I$. In the system studied by us, it also appears a variation of the coefficient of activity of $ZnSO_4$, at I = const, depending upon the ratio of the two electrolytes.

It is necessary to emphasize that these deviations have a much higher value than those mentioned by Harned and Owen for systems of 1 :1 electrolytes. The curves present also a marked minimum. This behaviour may be correlated with the thermodynamic properties of the single electrolyte $ZnSO_4 - H_2O$ (Figure 1), which presents negative exceptionally great deviations from the ideal behaviour and which could be caused by the formation of the ionic pairs.

For the behaviour of the system of binary electrolytes the following explanation is plausible : at a constant ionic strength, in the field of the great concentrations of $ZnSO_4$, deviations due to the specific interactions appear, mentioned also by other authors,[4] for mixture of electrolytes,[1,2] 1 :1. When $m_1 \to 0$ (m_2 has great values) γ_{ZnSO_4} from the mixture approaches the values from the solution of the single electrolyte, that explaining the existence of a minimum on the curves $\gamma = f(m)$.[4,5,6]

It is very probable that in the simple electrolyte, as well as in the binary electrolyte, when $m_1 \to 0$, a split, of the ionic pairs formed takes place and has as result the diminishing of the deviations from the ideal behaviour.

REFERENCES

[1] H. Harned and B. Owen, "The Physical Chemistry of Electrolytic Solutions", Third Ed., Reinhold Publishing, New York, 1958, p. 592.

[2] G. A. Motornaya and E. Ya. Ben'yash, *Zhur. fiz. Khim.*, **47**, 459 (1973).

[3] R. A. Robinson and R. H. Stokes, "Razdvory electrolitov", Inostranlitizdat, Moscowa, 1963, p. 499.

[4] S. Sternberg and F. Daneş, "Termodinamică chimică aplicată", Ed. Academiei, Bucureşti, 1978, p. 342.

[5] G. R. Allahverdov and B. D. Stepin, *Zhur. fiz. Khim.*, **47**, 386 (1973).

[6] M. A. Ryazanov, *Zhur. fiz., Khim.*, **47**, 2605 (1973).

Revue Roumaine de Chimie, 25, *6*, 799–803 (1980)

ABOUT THE CATALYTIC OXIDATION OF AMMONIA

T. C. RUGINĂ and D. P. LAZĂR

Physical Chemistry Department, Polytechnic Institute of Jassy, 71, Splai Bahlui, R-6600, Jassy, Romania

Received March 20, 1979

The investigation of the catalytic oxidation of ammonia at atmospheric pressure, in a flow system, using cobalt oxide as catalyst, evidenced a strong exothermic effect, shaped as a narrow temperature peak, whose height seems to be especially determined by the initial content of ammonia in the gaseous reaction mixture. A quite remarkable fact is the absence of any connection between the height of this temperature peak and the relative degree of ammonia conversion.

The kinetics studies on the oxidation reaction of ammonia so far accomplished have failed to give a general valid mechanism; each of these studies has proposed its own version to explain the observed phenomenology of the process and both origin and quantities of the final stable reaction products.

Regarding the non-catalysed homogeneous oxidation of ammonia, according to some studies using both shock waves and photolytic techniques in static conditions, the most important conclusion was that the oxidation process proceeds via a branched chain mechanism, an important kinetic role being attributed to the following step,

$$\dot{N}H_2 + O_2 \rightarrow \dot{N}H + H\dot{O}_2$$

Concerning the reaction mechanism, the real existence of the different elementary steps and their succession there are, however, still numerous contradictions.[1-7]

In the catalytic oxidation of ammonia it might be supposed that the NH_3/O_2 ratio, that is the chemical nature of the reaction mixture, the shape and the dimensions of the catalyst seem to control the entire process; in addition, when platinum catalyst was used, some critical phenomena were reported.[8]

EXPERIMENTAL

In the present paper, the catalytic oxidation of ammonia on a thin layer of cobalt oxide deposited on silicagel beads as solid support was investigated using a flow technique (Figure 1).

The experimental study of the catalytic oxidation of ammonia was accomplished at normal pressure and initial reactor temperatures ranging from 140°C to 450°C using ammonia : air mixtures having an ammonia content of 5.8–16.00 % (v/v).

The percentage content of ammonia gas was chromatographically monitored using a 2 m stainless steel column packed with Ethophat 60/25 (15% w/w) on Chromosorb T as support. The gaseous reaction products were, also, G.C. analysed on a 5 Å molecular sieves column.

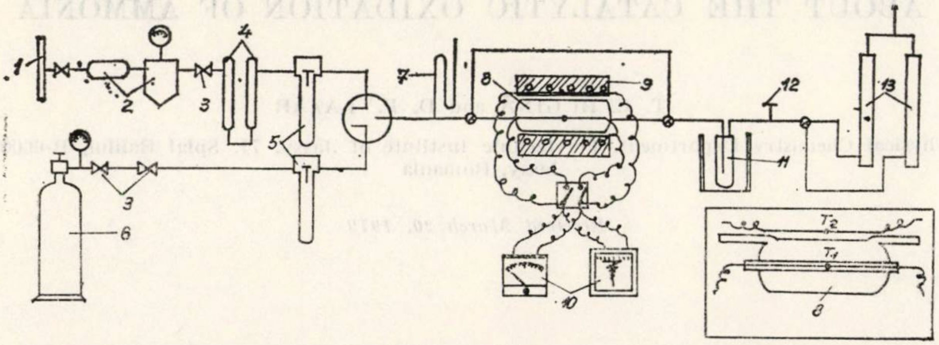

Fig. 1. — Schematic diagram of the flow equipment for the catalytic oxidation of ammonia

1. Compressed-air line; *2.* Air filters; *3.* Air valves; *4.* Purification and drying columns packed with molecular sieves and self-indicating silicagel; *5.* Flowmeters; *6.* Liquefied ammonia cylinder; *7.* Mercury manometer; *8.* Quartz reactor; *9.* Electric oven; *10.* Temperature detector and recorder; *11.* Cold trap; *12.* Sampling device for G.C. analysis; *13.* Water-cooled condensers; T_1, T_2. Thermocouplers .

RESULTS AND DISCUSSIONS

The exothermic effect of the oxidation process gave rise to a sharp temperature peak, ΔT which, depending on the experimental conditions, may exceed up to about 160°C the initial constant temperature of the reactor. At the same time, it was observed that during the establishment of the steady state of the oxidation process, the amount of the untransformed ammonia was a periodic time function.

Additionally, while flushing, after each experiment, the reactor with a pure air stream, in order to remove the substances possibly adsorbed on the catalyst surface, the temperature of the reactor increased by 10°C to 20°C over its initial temperature. It might be supposed that this effect can be considered as an experimental proof concerning a selective adsorption of ammonia on the catalyst.

The oxygen from the flushing air stream possibly reacts with this adsorbed ammonia and gradually induces its desorption. However, this desorption process seems to have a pulsatile evolution until the steady state of the main oxidation process is achieved. The maximal thermal effect ΔT, occurring during the steady state of the oxidation process, is actually defined by the temperature difference between the highest value of the temperature peak and the initial temperature of the reactor. This ΔT effect depends both on the content of ammonia in the gaseous reaction mixture and on the initial temperature of the reactor; the higher these parameters, the bigger the thermal effect is (Figures 2 and 3).

The contact time between gaseous reactants and the surface of the catalyst seems to have a less important influence on the temperature peak, and hence, the reaction mixture flow rate might affect, at the most, the relative position of the ΔT along the reactor length. However, for the same flow rate of the reaction mixture, different ΔT values have been reported, depending on the concentration of ammonia. But, as it can be observed from figure 2, there seems to be a specific behaviour of those reaction mixtures having either a higher or a lower ammonia content.

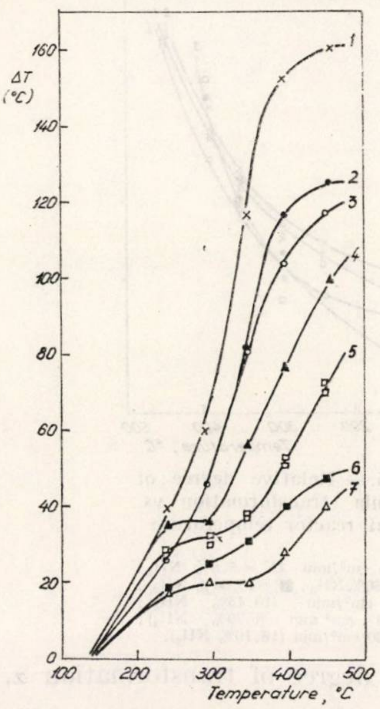

Fig. 2. — Temperature peak height against the initial temperature of the reactor

1. 3230 cm³ min (16.06% NH_3) ; *2.* 2135 cm³/min (15.80% NH_3) ; *3.* 1850 cm³/min (14.80% NH_3) ; *4.* 2135 cm³/min (11.50% NH_3) ; *5.* 1150 cm³/min (10.55% NH_3) ; *6.* 1710 cm³/min (6.79% NH_3) ; *7.* 2135 cm³/min (5.81% NH_3).

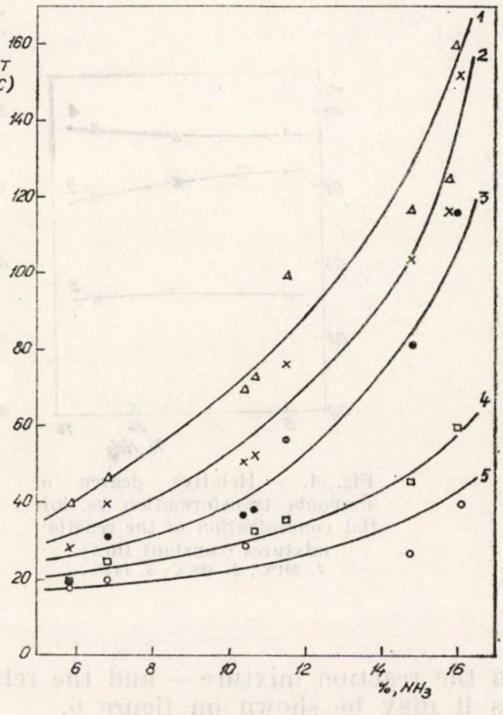

Fig. 3. — Temperature peak height as function of the initial concentration of ammonia into the reaction mixtures

1. 475° ; *2.* 391°C ; *3.* 348°C ; *4.* 290° ; *5.* 241°C.

The relative degree of transformation α — defined by the ratio between the amount of ammonia before and after oxidation process respectively — seems to primarily depend on the initial temperature of the reactor.

The modifications in the α values, due to the initial content of ammonia, are practically of small significance for the same flow rate (see Figure 4).

Even the contact time seems to be almost nonconclusive, particularly when high initial reactor temperatures were used (Figure 5), although at low initial temperatures of the reactor the influence of the flow rate may become somewhat more important.

The most striking observation to be done during the catalysed oxidation of ammonia seems to be the absence of any correlation between ΔT_{max} – which is definitely dependent on the ammonia initial content in the reaction mixture – and the relative degree of transformation α, as it may be shown on figure 6.

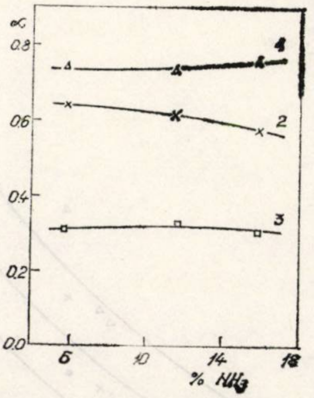

Fig. 4. – Relative degree of ammonia transformation vs. initial concentration of the reaction mixtures (constant flow)
1. 391°C; *2.* 348°C; *3.* 142°C.

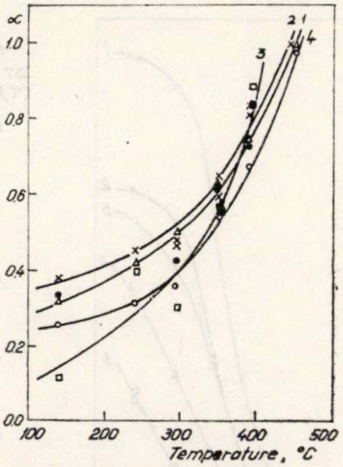

Fig. 5. – Relative degree of ammonia transformation vs. initial reactor temperature
1. 2150 cm³/min (X = 5.8% NH_3; Δ = 11.50% NH_3; ■ = 15.80% NH_3); *2.* 1210 cm³/min (10.45% NH_3); *3.* 1710 cm³ min (6.79% NH_3); *4.* 3230 cm³/min (16.10% NH_3).

Therefore, for α only, the initial temperature of the reactor seems to be a main determining factor. The same curves (Figure 6) confirm the

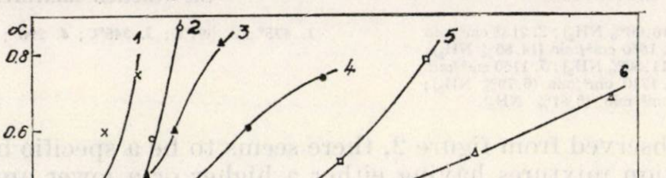

Fig. 6. – Correlation between the relative degree of ammonia transformation and the thermic effect ΔT for various flow rates and ammonia contents
1. 2150 cm³/min (5.89% NH_3); *2.* 1710 cm³/min (6.80% NH_3); *3.* 1155 cm³/min (10.45% NH_3); *4.* 2150 cm³/min (11.50 % NH_3); *5.* 1890 cm³/min (14.80% NH_3); *6.* 6320 cm³/min (16.10% NH_3).

above mentioned specific kinetic behaviour of the reaction mixtures having an ammonia content greater or smaller than 10% (in volumes).

It is, therefore, clear from the experimental data that the catalytic oxidation of ammonia evidences some characteristic features which seems to justify further more detailed examination.

REFERENCES

[1] T. Takeyama and H. Miyama, *Bull. Chem. Soc. Japan*, **30**, 1670 (1965).

[2] A. Valders and A. Van Tiggelen, *Bull. Soc. Chim. belges*, **63**, 542 (1954).

[3] D. Hussain and R.G.W. Norrish, *Proc. Roy. Soc. A.*, **273**, 245 (1965).

[4] F. W. Dalby, *Canad. J. Phys.*, **36**, 1336 (1958).

[5] A. Gerewicz and W.A. Noyes Jr., *J. Phys. Chem.*, **63**, 843 (1959).

[6] H. Gesser, *J. Amer. Chem. Soc.*, **77**, 2626 (1955).

[7] V. V. Barelko, *Kinetika i Kataliz* (preprint), March, 1971.

[8] V. V. Barelko and Iu. E. Volodin, *Kinetika i Kataliz* (preprint), U.D.K. 541. 127, July, 1974.

Revue Roumaine de Chimie, 25, *6*, 805–809 (1980)

ON THE α-DIOXIMINE COMPLEXES OF TRANSITION METALS. LIX *

THE STABILITY OF Fe(II)- AND Co(II)-COMPLEXES OF 1,2-CYCLOHEPTANEDIONE DIOXIME AND 1,2,-CYCLOOCTANEDIONE DIOXIME IN AQUEOUS SOLUTIONS

C. GH. MACAROVICI, J. HORÁK and CS. VÁRHELYI

Department of Chemical Technology, Babeș-Bolyai University, Arany János st. No. 11, Cluj-Napoca, Romania

Received May 26, 1979

The formation of the Fe(II)- and Co(II)-complexes with 1,2-cycloheptanedione dioxime and 1,2-cyclooctanedione dioxime was investigated in aqueous solutions. The stability constants of the complexes were determined at 20° and at an ionic strength of 0.1 M by potentiometric titration.

The formation, structure and stability of several transition metal complexes of dimethylglyoxime have been extensively investigated, due to their analytical importance.

The analogous complexes of other vic-dioximes, inclusing benzyldioxime, alkyl- and dialkyl glyoximes and 5–7 membered cycloalkyldione dioximes have also been studied under various experimental conditions and by different methods.[1-8]
However, experimental data concerning the formation and stability of complexes with cycloalkyldione dioximes, containing larger than seven-membered rings, have not yet been reported.

In the present paper the formation of the water-soluble Fe(II)- and Co(II)-complexes of 1,2-cycloheptanedione dioxime (Heptoxime, Heptox.H_2 : $C_7H_{12}N_2O_2$) and 1,2-cyclooctanedione dioxime (Octoxime, Octox.H_2 : $C_8H_{14}N_2O_2$) was studied by potentiometric titration with NaOH.

RESULTS AND DISCUSSION

In the aqueous solutions containing a vic-dioxime (Diox.H_2) and a divalent transition metal ion (M^{2+}) the following equilibria can be considered :

$$\mathrm{Diox.H_2} \xrightleftharpoons{K_a} \mathrm{Diox.H^-} + \mathrm{H^+} \qquad (1)$$

$$\mathrm{M^{2+}} + \mathrm{Diox.H^-} \xrightleftharpoons{K_1} \mathrm{M(Diox.H)^+} \qquad (2)$$

$$\mathrm{M(Diox.H)^+} + \mathrm{Diox.H^-} \xrightleftharpoons{K_2} \mathrm{M(Diox.H)_2} \qquad (3)$$

where K_a — the first acid dissociation constant of the dioxime, K_1 and K_2 — the stability constants of the successively appearing complex species.

The K_a values were obtained by potentiometric titrations and reported in a previous paper.[9]

The stability constants β_1 and β_2 were determined from the complex formation function[10] by using the $\bar{n}$ and $[\text{Diox.H}^-]$ values calculated from the potentiometric data and presented in tables 1 and 2.

TABLE 1

Potentiometric titration data of the system : $Diox.H_2 - Fe(ClO_4)_2 - HClO_4 - NaClO_4$ at 20° and $\mu = 0.1$ M

Heptox.H_2 ($K_a = 2.24 \times 10^{-11}$)				Octox.H_2 ($K_a = 2.88 \times 10^{-11}$)			
$C_{NaOH} \times 10^3$	pH	$\bar{n}$	$[\text{Diox.H}^-] \times 10^{10}$	$C_{NaOH} \times 10^3$	pH	$\bar{n}$	$[\text{Diox.H}^-] \times 10^{10}$
7.878	2.755	0.229	0.106	7.518	2.670	0.176	0.115
8.300	2.880	0.306	0.136	8.300	2.885	0.265	0.181
8.654	3.020	0.387	0.180	8.859	3.135	0.397	0.300
9.068	3.260	0.536	0.290	9.100	3.300	0.500	0.417
9.195	3.365	0.599	0.357	9.258	3.445	0.591	0.554
9.321	3.490	0.690	0.453	9.416	3.640	0.717	0.810
9.479	3.695	0.834	0.666	9.542	3.825	0.886	1.12
9.667	4.050	1.103	1.26	9.698	4.140	1.151	1.93
9.761	4.315	1.279	2.03	9.792	4.425	1.343	3.18
9.885	4.805	1.573	4.76	9.917	4.895	1.665	6.79

Initial concentrations : $C_{Fe^{2+}} = 4.0 \times 10^{-4}$ **M ;** $C_{Diox.H_2} = 1.0 \times 10^{-3}$ **M ;** $C_{HClO_4} = 1.04 \times 10^{-2}$ **M**

TABLE 2

Potentiometric titration data of the system : $Diox.H_2 - Co(ClO_4)_2 - HClO_4 - NaClO_4$ at 20° and $\mu = 0.1$ M

Heptox.H_2($K_a = 2.24 \times 10^{-11}$)				Octox.H_2 ($K_a = 2.88 \times 10^{-11}$)			
$C_{NaOH} \times 10^3$	pH	$\bar{n}$	$[\text{Diox.H}^-] \times 10^{10}$	$C_{NaOH} \times 10^3$	pH	$\bar{n}$	$[\text{Diox.H}^-] \times 10^{10}$
8.171	2.850	0.175	0.135	8.011	2.895	0.142	0.196
8.526	2.985	0.216	0.180	8.397	3.050	0.181	0.274
8.718	3.075	0.269	0.216	8.558	3.135	0.236	0.324
9.037	3.280	0.372	0.329	8.878	3.380	0.339	0.542
9.163	3.390	0.434	0.412	9.037	3.560	0.433	0.788
9.290	3.525	0.522	0.536	9.227	3.835	0.657	1.31
9.447	3.755	0.665	0.843	9.321	4.040	0.796	1.95
9.604	4.065	0.900	1.50	9.542	4.615	1.290	5.18
9.792	4.660	1.303	4.41	9.636	4.975	1.538	9.41
9.817	5.150	1.649	9.62	9.761	5.975	1.898	56.5

Initial concentrations : $C_{Co^{2+}} = 4.0 \times 10^{-4}$**M ;** $C_{Diox.H_2} = 1.0 \times 10^{-3}$ **M ;** $C_{HClO_4} = 1.04 \times$ $\times 10^{-2}$ **for Heptox.**H_2 **and** 1.01×10^{-2} **M for Octox.** H_2

With this end in view the relation (4) was made explicit for $N = 2$ and transformed into the form (5)

$$\bar{n} = \frac{\sum_{1}^{N} i\,\beta i\,[L^-]^i}{1+\sum_{1}^{N} i[L^-]^i} \qquad (4)$$

$$\frac{\bar{n}}{(1-\bar{n})\,[\mathrm{Diox}.\,H^-]} = \beta_2\,\frac{2-\bar{n}}{1-\bar{n}}\,[\mathrm{Diox.\,H^-}] + \beta_1 \qquad (5)$$

where $\beta_1 = K_1$ and $\beta_2 = K_1K_2$
The values

$$\frac{\bar{n}}{(1-\bar{n})\,[\mathrm{Diox.H^-}]} \text{ were plotted vs. } \frac{(2-\bar{n})}{1-\bar{n}}\,[\mathrm{Diox.H^-}]$$

For each compound 10 values included in the range of $\bar{n}$ between 0.14—1.9 were taken into account.

As seen from figures 1 and 2, a quite good linearity has been obtained.

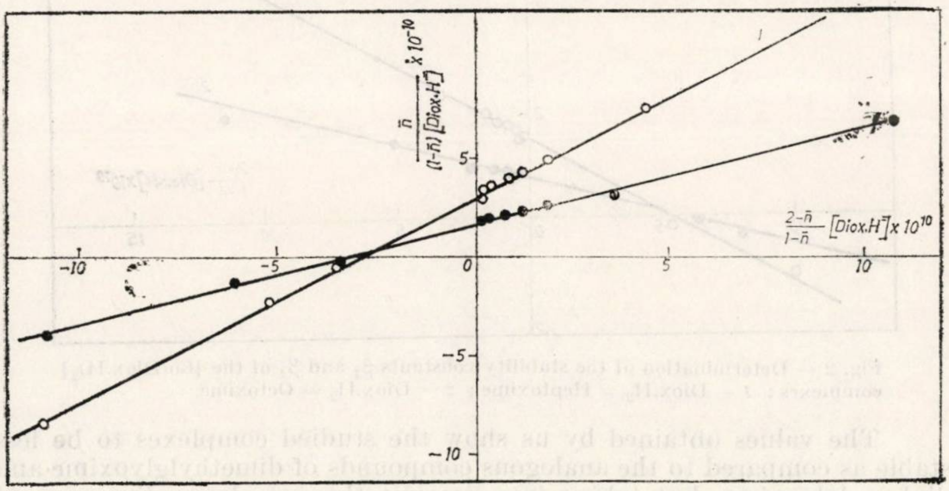

Fig. 1 — Determination of the stability constants β_1 and β_2 of the $[\mathrm{Fe(Diox.\,H)_2}]$ complexes: *1* — $\mathrm{Diox.H_2}$ = Heptoxime ; *2* — $\mathrm{Diox.H_2}$ = Octoxime.

Under these conditions, the β_1 and β_2 values were calculated from the slope and the intercept of the straight lines, by means of the least square method. The values obtained are presented in table 3.

The higher stability of both the Fe(II)- and Co(II)-complexes with heptoxime, as compared to the analogous compounds of octoxime, can be attributed to the stronger nucleophilic character of the former, which is in agreement with the lower K_a value of this dioxime.[9]

The absence of the comparing data does not allow an extensive discussion about the stability of the Fe(II) and Co(II) complexes with various vic-dioximes. Stability constants have been reported only for the Fe(II) and Co(II)-complexes of dimethylglyoxime,[1,5] diphenylglyoxime[5] and some unusual vic-dioximes[5,8] at 25°C.

TABLE 3

Stability constants of Fe(II) and Co(II) complexes of Heptox.H_2 and Octox.H_2 in aqueous solutions, at 20° and $\mu = 0.1$ M

Stability constant	F(II)		Co(II)	
	Heptox.H_2	Octox.H_2	Heptox.H_2	Octox.H_2
$\beta_1 \times 10^{-10}$	2.90 ± 0.15	1.62 ± 0.18	1.51 ± 0.10	0.742 ± 0.08
$\beta_2 \times 10^{-19}$	10.2 ± 0.30	4.97 ± 0.30	2.70 ± 0.15	1.22 ± 0.10

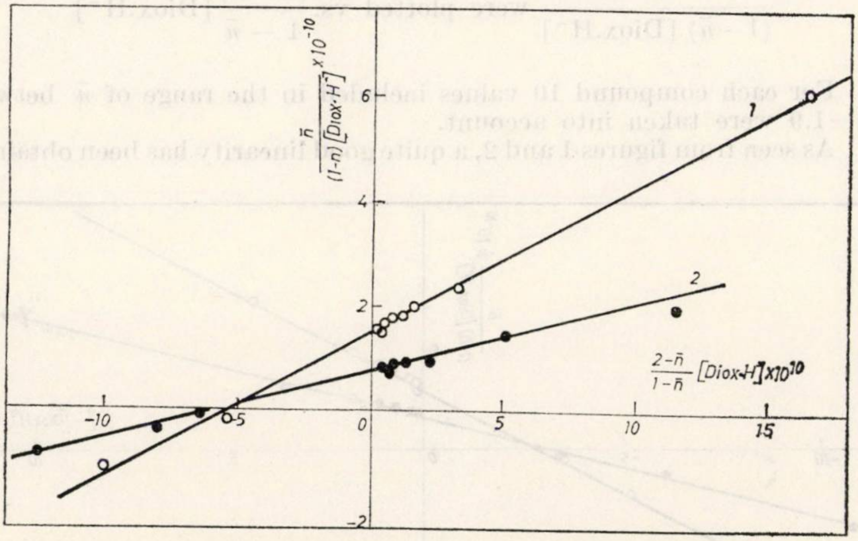

Fig. 2 — Determination of the stability constants β_1 and β_2 of the $[Co(Diox.H)_2]$ complexes : *1* — Diox.H_2 = Heptoxime ; *2* — Diox.H_2 = Octoxime.

The values obtained by us show the studied complexes to be less stable as compared to the analogous compounds of dimethylglyoxime and diphenylglyoxime, but taking into account the very large dispersion of the data reported by different authors (e.g. $\beta_2 = 21.0^5$ and 16.98^1 for the Co(II) chelate with dimethylglyoxime), this conclusion cannot be definitive.

EXPERIMENTAL

Reagents

The 1,2-cycloheptanedione dioxime and 1,2-cyclooctanedione dioxime were obtained by the oxidation of cycloheptanone and cyclooctanone with selenium dioxide in boiling absolute ethanol, followed by the oximation of the distilled 1,2-diones with an excess of hydroxylαamine hydrochloride and potassium hydroxide (molar ratio 1 : 1) in aqueous solution. The crude products were recrystallized from hot water.[11,12] Their purity was tested gravimetrically, by precipitation as $[Ni(Diox.H)_2]$ in acetate buffer solution. $Fe(ClO_4)_2$ and $Co(ClO_4)_2$ were prepared from analytical grade carbonates : $FeCO_3$ and $CoCO_3$ and $HClO_4$, respectively. The NaOH solution was obtained from solid NaOH p.a. and distilled water free of CO_2. $NaClO_4$ was used to establish a constant ionic strength of 0.1 M.

Potentiometric titrations

Samples of 25 ml containing the corresponding metal perchlorate and the vic-dioxime (mol.ratio 1 : 2.5), perchloric acid and sodium perchlorate, were titrated at $20 \pm 0.1°$ with a solution of NaOH $9.66 \cdot 10^{-2}$ M under an inert atmosphere of methane saturated with water vapors. The hydrogen ion concentration was measured with a RADELKIS-OP-205 precision pH-meter, using an OP 717-1/A type combined electrode. The rapid mixing of the solution after each addition of NaOH was assured by means of a magnetic stirrer, which was stopped during the actual pH measurements. The variation of the ionic strength of 0.1 M during the titration was negligible. The titration was performed beginning from $pH < 2$ in order to cover the whole pH range in which complex formation occurs.

Under the above described experimental conditions, the hydrolysis of the metal ion, as well as the oxidation of the free or coordinated metal are negligible.

The values of $\bar{n}$ and $[Diox.H^-]$, presented in tables 1 and 2, were calculated from the titration data using the relations

$$[\mathrm{Diox.H}^-] = \frac{K_a}{[\mathrm{H}^+]} \left(\mathrm{C}_{\mathrm{HClO}_4} + \mathrm{C}_{\mathrm{Diox.H}_2} - \mathrm{C}_{\mathrm{NaOH}} - [\mathrm{H}^+] + [\mathrm{OH}^-]\right)$$

and

$$\bar{n} = \frac{\mathrm{C}_{\mathrm{Diox.H}_2} - (1 - [\mathrm{H}^+]/K_a)\,[\mathrm{H}^+]}{\mathrm{C}_{\mathrm{M}^{2+}}}$$

REFERENCES

[*] Part LVIII. J. Zsakó, J. Horák and Cs. Várhelyi, *Monatsh. Chem.*, in press (1980).

[1] C. V. Banks and S. Anderson, *Inorg. Chem.*, **2**, 112 (1963).

[2] V. M. Peshkova and V.M. Bochkova, *Nauchn. Dokl. Vysshei Shkoly, Khim. Khim. Technol.*, **1958**, 62.

[3] V. M. Savostina, E. K. Astakhova and V. M. Peshkova, *Zhur. neorg. Khim.*, **9**, 80 (1964).

[4] V. M. Bochkova and V.M. Peshkova, *Zhur. neorg. Khim.*, **3**, 1131 (1958).

[5] K. Burger, "Coordination Chemistry : Experimental Methods", Akadémiai Kiadó, Budapest, 1973, p. 350.

[6] E. K. Astakhova, V. M. Savostina and V.M. Peshkova, *Zhur. neorg. Khim.*, **9**, 817 (1964).

[7] K. Burger and I. Ruff, *Acta Chim. Acad. Sci. Hung.*, **49**, 1 (1966).

[8] K. Burger and E. Papp-Molnár, *Magyar Kém. Folyóirat*, **73**, 77 (1967).

[9] J. Zsakó, J. Horák, Z. Finta, Cs. Várhelyi and J. Mitrache, *Mikrochim. Acta*, **1979** I., 405.

[10] J. Bjerrum, "Metal Ammine Formation in Aqueous Solution", P. Hall and Son, Copenhagen, 1941, p. 15.

[11] E. Müller and M. Bauer, *Liebigs Ann. Chem.*, **654**, 105 (1962).

[12] A. Harr, R.C. Voter and C.V. Banks, *J. Org. Chem.*, **14**, 8362 (1949).

Revue Roumaine de Chimie, 25, *6*, 811—813 (1980)

ON USPENSKI'S RULE REGARDING THE *CIS-TRANS* ISOMERISM OF COORDINATION COMPOUNDS

M. ANDRUH*, C. I. LEPADATU** and MARIA BREZEANU*

* Chemistry Institute, Laboratory of Inorganic Chemistry, 202 Splaiul Independenţei, Bucharest, Romania

** Center of Physical Chemistry — ICECHIM, 202 Splaiul Independenţei, Bucharest, Romania

Received July 2, 1979

A proof for Uspenski's rule is given by using the ligand field theory and a Gaussian-analytical form for the curves representing the $d - d$ absorption bands.

The study of the electronic spectra of the coordination compounds is a usual way to solve the geometrical isomerism. [1] This is justified by the fact that the spectral terms for a complex ion depend on the strength and symmetry of the metal-ligand chemical bonds.

Uspenski formulated many years ago an empirical rule regarding the *cis-trans* isomerism, namely, the *trans* isomer should have an absorption minimum approximately in the range where the *cis* isomer has an absorption maximum.[2] This rule is verified[3-6] by many complexes of Cr^{3+} $(3d^3)$ and $Co^{3+}(3d^6)$.

The aim of this note is to give a proof for that rule. Tables 1 and 2 give the energies of the spin allowed d-d transitions for the *cis*, *trans*-$[M(d^n)a_4b_2]$ complexes, where $n = 3, 6, 8$.

TABLE 1

Spin allowed transitions for *cis* – $[M(d^n)a_4b_2]$

Nr.	$d^3\ {}^4B_1 \rightarrow$	$d^8\ {}^5B_1 \rightarrow$	$d^6\ {}^1A_1 \rightarrow$	Transition energies
1	${}^4A_1$	${}^3A_1$	${}^1B_1$	$3/2\, e_\sigma^a + 3/2\, e_\sigma^b - 2e_\pi^a - 2e_\pi^b + W_1(d^n)$
2	${}^4A_2,\ {}^4B_2$	${}^3A_2,\ {}^3B_2$	${}^1A_2,\ {}^1B_2$	$9/4\, e_\sigma^a + 3/4\, e_\sigma^b - 3e_\pi^a - e_\pi^b + W_1(d^n)$
3	${}^4B_1$	${}^3B_1$	${}^1A_1$	$5/2\, e_\sigma^a + 1/2\, e_\sigma^b - 2e_\pi^a - 2e_\pi^b + W_2(d^n)$
4	${}^4A_2,\ {}^4B_2$	${}^3A_2,\ {}^3B_2$	${}^1A_2,\ {}^1B_2$	$7/4\, e_\sigma^a + 5/4\, e_\sigma^b - 3e_\pi^a - e_\pi^b + W_2(d^n)$
5	${}^4B_1$	${}^3B_1$	${}^1A_1$	$4e_\sigma^a + 2e_\sigma^b - 6e_\pi^a - 2e_\pi^b + W_3(d^n)$
6	${}^4A_2,\ {}^4B_2$	${}^3A_2,\ {}^3B_2$	${}^1A_2,\ {}^1B_2$	$4e_\sigma^a + 2e_\sigma^b - 5e_\pi^a - 3e_\pi^b + W_3(d^n)$

TABLE 2

Spin allowed transitions for *trans*-[M (d^n) a_4b_2]

Nr.	$d^3\ {}^4B_{1g}\rightarrow$	$d^8\ {}^3B_{1g}\rightarrow$	$d^6\ {}^1A_{1g}\rightarrow$	Transition energies
1	${}^4B_{2g}$	${}^3B_{2g}$	${}^1A_{2g}$	$3e_\sigma^a - 4e_\pi^a + W_1(d^n)$
2	${}^4E_g$	${}^3E_g$	${}^1E_g$	$3/2\ e_\sigma^a + 3/2\ e_\sigma^b - 2e_\pi^a - 2e_\pi^b + W_1(d^n)$
3	${}^4A_{2g}$	${}^3A_{2g}$	${}^1B_{2g}$	$e_\sigma^a + 2e_\sigma^b - 4e_\pi^a + W_2(d^n)$
4	${}^4E_g$	${}^3E_g$	${}^1E_g$	$5/2\ e_\sigma^a + 1/2\ e_\sigma^b - 2e_\pi^a - 2e_\pi^b + W_2(d^n)$
5	${}^4A_{2g}$	${}^3A_{2g}$	${}^1B_{2g}$	$4e_\sigma^a + 2e_\sigma^b - 4e_\pi^a - 4e_\pi^b + W_3(d^n)$
6	${}^4E_{g2}$	${}^3E_g$	${}^1E_g$	$4e_\sigma^a + 2e_\sigma^b - 6e_\pi^a - 2e_\pi^b + W_3(d^n)$

The energies of the transitions are expressed into radial parameters $e_{\sigma(\pi)}$ of the orbital energies, according to the Angular Overlap Model.[7] The quantities $W(d^n)$ represent the part of interelectronic repulsion energies, which are less sensitive than the orbital energies to the change in the spatial arrangement of the metal-ligand bonds.

The analytical expressions for $W(d^n)$'s may be found elsewhere.[1,8] The d-d transitions in *cis-trans* complexes are grouped into three domains of absorption, namely, 1 and 2 ; 3 and 4 ; 5 and 6. Assuming Gaussian-like shape for the bands[8], the analytical expression of the curves in a given absorption domain is, practically, given by :

$$\varepsilon \simeq \varepsilon_i\, e^{-\frac{\ln 2(\nu-\nu_i)^2}{\sigma_i^2}} + \varepsilon_j e^{-\frac{\ln 2(\nu-\nu_j)^2}{\sigma_j^2}}$$

where ν_i and ν_j are the absorption maxima of the two neighbour transitions, $\varepsilon_{i(j)}$ and $\sigma_{i(j)}$ being their extinction maxima and halfwidths respectively.

The minimum between the two neighbour bands is situated at that ν value which $\frac{d\varepsilon}{d\nu} = 0, \quad \frac{d^2\varepsilon}{d\nu^2} > 0$

It is not difficult to see, that $\frac{d\varepsilon}{d\nu} = 0$ for $\nu = \frac{\nu_i + \nu_j}{2}$, if $\varepsilon_i = \varepsilon_j$ and $\sigma_i = \sigma_j$.

These last conditions are satisfactorily fulfilled by the experiment.[3-5] As may be seen from tables 1 and 2,

$$\left(\frac{\nu_1 + \nu_2}{2}\right)_{trans} = (\nu_2)_{cis} ; \left(\frac{\nu_3 + \nu_4}{2}\right)_{trans} = (\nu_4)_{cis}$$

and $\left(\frac{\nu_5 + \nu_6}{2}\right)_{trans} = (\nu_6)_{cis}$ which agree with Uspenski's rule. It must be also specified that the mentioned rule refers to the $d-d$ transitions only and not to the charge-transfer ones, which are less sensitive to the changes in the spatial arrangement of the metal-ligand bonds.[1-8]

REFERENCES

[1] A. B. P. Lever, "Inorganic Electronic Spectroscopy", Elsevier, Amsterdam, 1968, chap. 7, p. 193.

[2] V. Uspenski, *Trans. Inst. Pure Chem. Reagents, U.S.S.R.*, **13**, 1 (1936).

[3] J. R. Perumareddi, *Coordination Chem. Rev.*, **4**, 73 (1969).

[4] J. R. Perumareddi, *Inorg. Chem.*, **6**, 1339 (1967).

[5] M. Linhard and M. Weigel, *Z. anorg. Chem.*, **264**, 321 (1952).

[6] S. C. Chan and C.K. Poon, *J. Chem. Soc. (A)*, **1966**, 146.

[7] C. I. Lepădatu, *Z. phys. Chem. (Frankfurt)*, **73**, 249 (1970).

[8] C. K. Jorgensen, "Absorption Spectra and Chemical Bonding in Complexes", Pergamon Press, Oxford, 1962, p. 293.

Revue Roumaine de Chimie, 25, *6*, 815–821, (1980)

THE INFRARED SPECTRUM OF DIMETHYLDITHIOPHOSPHINATO ANION $(CH_3)_2 PS_2^-$. NORMAL COORDINATE ANALYSIS AND UREY-BRADLEY FORCE FIELD CALCULATION

IOAN SILAGHI-DUMITRESCU and IONEL HAIDUC
Chemistry Department, Babeş-Bolyai University R-3400, Cluj-Napoca, Romania

Received November 27, 1979

Normal coordinate analysis was carried out for a simplified model of the $(CH_3)_2PS_2^-$ anion in the Urey-Bradley force field approximation. The force constants were refined by the least squares procedure. The best set of force constants was then used for the automatic assignment of the observed infrared active frequencies. The data show that the P–S and P–C symmetric stretching vibrations are coupled to a considerable extent. The P–S force constant in the compound investigated lies between those of $f_{P=S}$ (double bond) and f_{P-S} (single bond) suggesting π bond delocalization in the anion.

INTRODUCTION

The normal coordinate treatments reported so far for phosphorodithioic derivatives deal with their Ni(II) complexes[1,2] or $-CH_3$ esters.[3,4] Concerning the dimethyldithiophosphinato anion, Roesky, Pantzer and Goubeau[5] reported the valence force constants calculated by kinematic coupling method of Becher and Mattes.[6] Their calculation was based on six IR frequencies given by Coates and Mukherjee.[7] New spectral data are available from Cavell, Byers and Day,[8] so a reinvestigation of this anion seems worthwhile. It would be interesting to analyze in greater details the vibrations of the ligand and to compare the force constants with those obtained from the vibrational spectra of their metal complexes. In this way we can get information (via P–S bond force constant) about the charge distribution in the PS_2 group and correlate its changes with the nature of the other two groups bounded to the phosphorus atom.

As no regular dependence was observed between the values of PS_2 stretching frequencies and the masses and sizes of metal ion coordinated by this group[7–9] the changes in M–S force constants compared with those in P–S force constants would throw some light upon the strength of M–S bond in MS_2P four-membered ring.

In accordance with these, the aim of this work is to obtain a basis set of Urey-Bradley (U–B) force constants[10] of dimethyldithiophosphinato anion $(CH_3)_2PS_2^-$ and to make a rational assignment of the observed IR frequencies, based upon a normal coordinate analysis. For this purpose the sodium salt, $NaS_2P(CH_3)_2 \cdot 2H_2O$ was investigated.

SPECTRAL MEASUREMENTS AND THE PARTIAL ASSIGNMENT OF FUNDAMENTAL BANDS

IR spectra of $NaS_2P(CH_3)_2 \cdot 2H_2O$ were recorded within the 4000–400 cm^{-1} region in KBr pellets and nujol mull using a UR–20 Carl Zeiss Jena spectrophotometer. The spectrum below 400 cm^{-1} was taken from other authors.[8,11]

Since we were interested in the vibrations of the C_2PS_2 group, only the region 200–900 cm^{-1} was taken into account.

The P–C stretching frequencies are expected to occur between 620–780 cm^{-1}.[12] Our spectra exhibit three bands in this region, situated at 675, 726 and 740 cm^{-1} (Figure 1). The broad band centered at 675 cm^{-1} is absent both in the spectra of M-dimethyldithiophosphinato complexes (M = VO(II), Co(II)) of C_{2v} symmetry[13,14] and in the spectrum of $(CH_3)_2P(S)SCH_3$.[4] Both the complexes and the ester contain two bands (in the

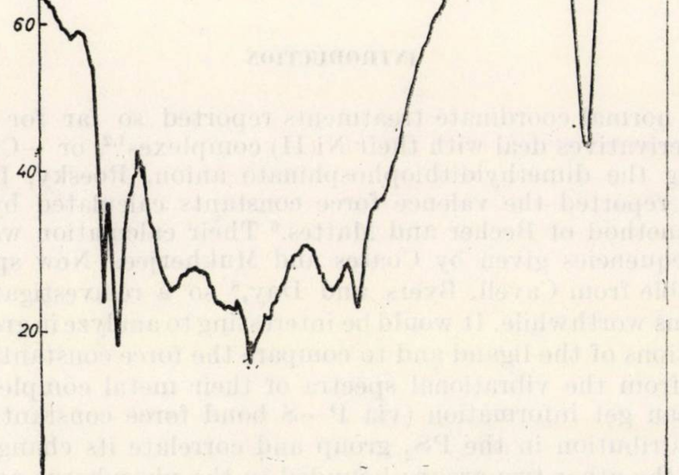

Fig. 1 – The infrared spectrum of $NaS_2P(CH_3)_2 \cdot 2H_2O$ recorded in nujol mull (800–250 cm^{-1}).

range 710 – 750 cm^{-1}) according to the selection rules of C_{2v} and C_s symmetry. These facts suggest that the 740 and 726 cm^{-1} bands might be assigned to the PC_2 vibrations.

The region characteristic of the PS_2 group frequencies is 470 – 600 cm^{-1}.[15] Both bands assigned to PS_2 vibrations in $R_2PS_2^-$ type compounds are of high intensity.[7] For this reason we have assigned the 495 cm^{-1} and 600 cm^{-1} bands to PS_2 group vibrations. The frequencies observed at 375, 280, 238 and 215 cm^{-1} were supposed to be related to the deformation modes of C_2PS_2 frame. The symmetry of the corresponding vibrations will be determined by calculations.

CALCULATIONS AND DISCUSSION OF THE RESULTS

Calculations were performed by using Shimanouchi's computer program BGLZ and LSMB,[16] modified to suit the operating system of the Felix C – 256 (Romanian made) computer, available in the Computer Center of Cluj-Napoca University.

The following approximations were made concerning the geometry of $(CH_3)_2PS_2^-$:

— the methyl groups were considered as point entities centered on C atoms with an appropriate mass;

— the P – S and P – C bond lengths were taken as 2.00 Å and 1.86 Å respectively;

— tetrahedral angles were assumed for all six bond angles.

The internal coordinate system used for the calculation of G matrix[17] elements is shown in figure 2. This model has 9 normal modes which transforms according to the symmetry species of C_{2v} point group into $4A_1 + A_2 + 2B_1 + 2B_2$. The A_1, B_1 and B_2 type vibrations are IR and Raman active, the A_2 being only Raman active.

The calculations were performed in three steps.

1) The choice of the adjustable force constants.

2) The refinement of the force constants in accordance with the results of step 1.

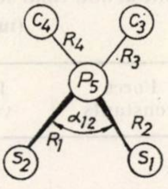

Fig. 2 – The simplified model of $(CH_3)_2PS_2^-$ and the internal coordinate system ($r_1 = \Delta R_1$; $r_2 = \Delta R_2$; $r_3 = \Delta R_3$; $r_4 = \Delta R_4$; $\alpha_1 = \Delta\alpha_{12}$; $\alpha_2 = \Delta\alpha_{13}$; $\alpha_3 = \Delta\alpha_{14}$; $\alpha_4 = \Delta\alpha_{23}$; $\alpha_5 = \Delta\alpha_{24}$; $\alpha_6 = \Delta\alpha_{34}$)

3) The solving of the secular equation $|GF_{\text{refined}} - E| = 0$ factorised, by using the symmetry coordinates obtained from the internal coordinates. Some details about these three steps are given below.

1) The eight U – B type force constants : K_{PS}, K_{PC}, H_{SPS}, H_{SPC}, H_{CPC}, $F_{S...S}$, $F_{S...C}$ and $F_{C...C}$ were classified into the k_A and k_B sets.[18]

The inspection of the eigenvalues and eigenvectors of the $\tilde{J}\ W\ J$ matrix ($J_{nm} = \partial \nu_n / \partial k_m$) shows that only K_{PS}, K_{PC}, H_{SPS}, H_{SPC}, $F_{\mathrm{S...C}}$ and H_{CPC} can be freely adjusted, i.e. the input data give sufficient information about them; they can be calculated with a rather good accuracy, so they belong to k_A set. The other two repulsive force constants $F_{\mathrm{S...S}}$ and $F_{\mathrm{C...C}}$ must be included in the k_B set, since the input data contain no information about them; they can not be determined accurately.

2) The IR observed frequencies were used to refine the six (k_A set) force constants while the k_B set force constants were kept fixed at their initial values. The weights of the observed frequencies were $1/\nu_i$ except for the only Raman active frequency for which a zero weight was taken. In the input frequencies set, the position of the A_2 — Raman active frequency was chosen in such a way, as to ensure that the calculated frequency in the last refining cycle was equal to that calculated in step three. Six refinement cycles were enough to reach the set of force constants which gives the best agreement between the observed and calculated frequencies.

TABLE 1

Observed and calculated frequencies and their relative error

Obsd.	740	726	600	497	370	280	238	—	215
Calcd.	739.7	724.8	597.0	504.0	368.8	261.4	253.5	230.9	214.7
Delta	0.3	1.2	3.0	−7.0	12.0	18.6	−15.5	—	0.3
$\Delta\nu/\nu\,\%$	0.04	0.17	0.50	−1.39	1.40	6.64	−6.51	—	0.12

Tables 1 and 2 contain the observed and calculated frequencies, the initial and final force constants, their dispersion and the P_{AB} matrix defined as $k_A = P_{AB}\ \Delta k_B$.[18] This matrix shows that the k_A set is determined with rather good accuracy; a change by 0.1 mdyne/Å in $F_{\mathrm{S...S}}$ or $F_{\mathrm{C...C}}$ would change the k_A set with small amounts varying around 0.01 mdyne/Å except for H_{SPS} which is more sensitive to changes in the k_B set (it changed by 0.05 mdyne/Å).

TABLE 2

The initial and final set of force constants and the P_{AB} matrix elements (mdyne/Å for the force constants)

Force constants	Initial values	Final values	P_{AB}	
			$F_{\mathrm{S...S}}$	$F_{\mathrm{C...C}}$
K_{PS}	2.80	2.56±0.23	0.05	−0.15
K_{PC}	3.00	2.76±0.19	0.10	0.06
H_{SPS}	0.15	0.23±0.05	−0.52	−0.01
$F_{\mathrm{S...S}}$	0.05	0.05	—	—
H_{SPC}	0.20	0.13±0.08	0.03	0.14
$F_{\mathrm{S...C}}$	0.10	0.21±0.18	0.07	−0.32
H_{CPC}	0.25	0.43±0.08	0.07	−0.45
$F_{\mathrm{C...}C}$	0.10	0.10	—	—

3) The symmetry coordinates were introduced in order to determine the correspondence of the vibrational modes with symmetry species of C_{2v} group. These symmetry coordinates are listed below :

$$A_1 : S_1 = (r_1 + r_2 + r_3 + r_4)/2$$

$$S_2 = (r_1 + r_2 - r_3 - r_4)/2$$

$$S_3 = (\alpha_1 - \alpha_6)/\sqrt{2}$$

$$S_4 = (2\alpha_1 - \alpha_2 - \alpha_3 - \alpha_4 - \alpha_5 + 2\alpha_6)/\sqrt{12}$$

$$S_5 = (\alpha_1 + \alpha_2 + \alpha_3 + \alpha_4 + \alpha_5 + \alpha_6)/\sqrt{6}$$

$$A_2 : S_6 = (\alpha_2 - \alpha_3 - \alpha_4 + \alpha_5)/2$$

$$B_1 : S_7 = (r_3 - r_4)/\sqrt{2}$$

$$S_8 = (\alpha_2 - \alpha_3 + \alpha_4 - \alpha_5)/2$$

$$B_2 : S_9 = (r_1 - r_2)/\sqrt{2}$$

$$S_{10} = (\alpha_2 + \alpha_3 - \alpha_4 - \alpha_5)/2$$

A zero frequency was obtained in the A_1 block in accordance with the S_5 redundant coordinate. In the A_2 block the calculated frequency is 230.9 cm^{-1} the same as that obtained in the refinement process (step 2) when a zero weighted frequency was intercalated between the 238 and 215 cm^{-1} observed frequencies. When the position of the zero weighted frequency in step 2 was different, its calculated values differed from those obtained in step 3. This result is, in our opinion a proof of the fact that the Raman active and IR inactive frequency must lie somewhere in the region between 238 and 215 cm^{-1}.

The potential energy distribution upon the U—B force constants (PEF) and the predicted classification of the normal vibrations according to the symmetry species of the C_{2v} point group are listed in table 3.

The band situated at 726 cm^{-1} is assigned to the symmetric P—C stretching vibration mixed to a small extent with the symmetric PS_2 stretchings and the CPC bending vibrations. The $\nu_2(A_1)$ frequency could be assigned to the PS_2 symmetric stretching. It is noteworthy the fact that this frequency depends on K_{PC}, $F_{S...C}$ and H_{CPC} more than $\nu_1(A_1)$ does on K_{PS}, $F_{S...C}$, and H_{CPC}. This is illustrated by the fact that the "extra" contributions to the potential energy of ν_2 vibrations is around 50%. The third A_1 symmetry type vibration (375 cm^{-1}) seems to be mainly related to the CPC deformation mode, accompanied by a small PS stretching. The lowest frequency from A_1 block, situated at 210 cm^{-1} corresponds to the PS_2 deformation mode. Small contribution from the PS stretching can be noticed.

There is no significant mixing within B_1 and B_2 symmetry type vibrations ; $\nu_6(B_1)$ and $\nu_8(B_2)$ are almost surely due to genuine stretching modes. The $\nu_7(B_1)$ and $\nu_9(B_2)$ frequencies are due to deformation modes of the CPS angles. The potential energy of these vibrations depends to a

TABLE 3

Potential energy distribution upon the U−B force constants

Calcd.	724.8	504.0	368.8	214.7	0.0	230.9	739.7	253.5	569.9	261.4
Obsd.	726	497	370	215	0.0	—	740	238	600	280
	ν_1	ν_2	ν_3	ν_4		ν_5	ν_6	ν_7	ν_8	ν_9
K_{P-S}	14	52	17	5					89	3
K_{P-C}	71	16					93			
H_{SPS}				72						
$F_{S...S}$				7						
H_{SPC}				9		60		59	8	54
$F_{S...C}$		12	6			40	4	41	3	43
H_{CPC}	8	12	62							
$F_{C...C}$		3	6							
Symmetry species	A_1					A_2	B_1		B_2	

great extent on H_{SPC} as well as on $F_{S...C}$, unlike the A_1 type deformation modes of the SPS and CPC angles, where the contributions from the repulsive $F_{S...S}$ and $F_{C...C}$, respectively, are not so important.

FORCE CONSTANTS

The values of some force constants available from the literature[4,5] are given in table 4, and are compared with results obtained in this work. The table contains also the phosphorus-sulfur bond order calculated by Gordy's formula :[19]

$$K = 1.67\ N_{PS}(\chi_P\ \chi_S/D^2)^{3/4} + 0.30$$

where K is the P−S bond force constant, N is the bond order, D is P−S bond length, χ_P, χ_S − the P and S atom electronegativities in Pauling's scale. The value obtained by us for the P−S force constant is somehow smaller than that calculated by Roesky, Pantzer and Goubeau.[5] As pointed out above, a feature of the symmetric PS_2 stretching vibration is its mixture to an appreciable extent with the PC_2 symmetric stretching vibration. Consequently the Becher-Mattes method[6] is not suitable in the case of dimethyldithiophosphinato anion since this method by its own nature, looks for the closest solution to the initial diagonal approximation[20] of the F matrix *i.e.* the interaction force constants are somehow underestimated. When some electron delocalization occurs, by using this method, the diagonal force constants are constrained to take greater values compared to the case when the delocalization is missing.

On the other hand our $f_{P \overset{\cdots}{-} S}$ is almost equal to the mean value of $f_{P=S}$ and f_{P-S} force constants, in agreement with the supposed π electron delocalization in the PS_2^- group. The $P \overset{\cdots}{-} S$ bond order exhibits the same behaviour ; its value is close to the mean N_{P-S} and $N_{P=S}$ from methyl ester, and is smaller than the bond order calculated with the $P \overset{\cdots}{-} S$ force constant from the reference.[5]

TABLE 4

The P—S and P—C force constants for $(CH_3)_3PS$, $(CH_3)_2P(S)SCH_3$ and $(CH_3)_2PS_2^-$

	$(CH_3)_3PS$		$(CH_3)_2PS_2CH_3$		$(CH_3)_2PS_2^-$		$(CH_3)_2PS_2^-$	
	Ref.[21]		Ref.[4]		Ref.[5]		this work	
	f_{PX}	N	f_{PX}	N	f_{PX}	N	f_{PX}	N
P=S	3.36	1.45	3.34	1.34	—	—	—	—
P—S	—	—	2.53	1.12	—	—	—	—
P...S	—	—	2.98	1.23	3.07	1.32	2.80*	1.22
P—C	3.11	—	2.97	—	3.03	—	3.08*	—

* The general valence force field's parameters were expressed in terms of the U—B type force constants.

The P—C force constant does not show considerable variations within this series of compounds, and they do not differ too much from the P—C force constant in $(CH_3)_3P$ (2.99 mdyne/Å).[22] This finding can be related to the smaller contribution of PS_2 stretching to PC_2 stretching than the contribution of PC_2 to PS_2 stretching and also to a relatively small interaction between the stretching of the PC bonds.

ACKNOWLEDGEMENT. We thank Dr. A. Butucelea (Center of Physical Chemistry, Bucharest) for useful discussions and advice, and the staff of the Computer Center of Cluj-Napoca University for competent assistance.

REFERENCES

[1] I. M. Cheremisina, L. I. Kozhevina and E.M. Yurchenko, *Zhur. strukt. Khim.*, **16** 583 (1975).

[2] W. Rudzinski, G. T. Benke and Q. Fernando, *Inorg. Chem.*, **16**, 1206 (1977).

[3] O. A. Wafa, A. Lentz and J. Goubeau, *Z. anorg. Chem.*, **380**, 128 (1971).

[4] R. Pantzer, W. Schmidt and J. Goubeau, *Z. anorg. Chem.*, **395**, 262 (1973).

[5] H. W. Roesky, R. Pantzer and J. Goubeau, *Z. anorg. Chem.*, **392**, 42 (1972).

[6] H. J. Becher and R. Mattes, *Spectrochim. Acta*, **A23**, 2449 (1967).

[7] G. E. Coates and R. N. Mukherjee, *J. Chem. Soc.*, **1964**, 1295.

[8] R. G. Cavell, W. Byers and E. D. Day, *Inorg. Chem.*, 10, 2710 (1972).

[9] W. Kuchen and H. Hertel, *Angew. Chem. Int. Ed.*, **8**, 89 (1969).

[10] T. Shimanouchi, *J. Chem. Phys.*, **17**, 245, 734, 848 (1949).

[11] We thank prof. T. A. Stephenson (Univ. of Edinburg, Scotland) for providing an infrared spectrum of the title compound down to 200 cm^{-1}.

[12] D. E. C. Corbridge, "The Infrared Spectra of Organophosphorus Compounds" in "Topics in Phosphorus Chemistry", vol. 6, Eds. M. Grayson and M. Griffith, J. Wiley, London, 1969.

[13] R. G. Cavell, E. D. Day, W. Byers and P. M. Watkins, *Inorg. Chem.*, **11**, 1951, 1598, 1759 (1972).

[14] M. L. Benett and R. H. Sumner, Univ. of Alberta, unpublished results (quoted in Ref. 13).

[15] L. C. Thomas, "Infrared Spectra of the Organophosphorus Compounds" Heyden, London, 1974.

[16] T. Shimanouchi, "Normal Coordinate Treatment of Polyatomic Molecules", Tokyo University, Tokyo, 1968.

[17] E. B. Wilson, J. C. Decius and P. C. Cross, "Molecular Vibrations — The Theory of the Infrared and Raman Vibrational Spectra", McGraw-Hill, New York, 1955.

[18] T. Shimanouchi, "The Molecular Force Field" in "Physical Chemistry, An Advanced Treatise", vol. VI (Eds. H. Eyring, D. Henderson and W. Jost), Academic Press New York 1970.

[19] W. Gordy, *J. Chem. Phys.*, **14**, 305 (1946).

[20] A. Alix and L. Bernard, *J. Mol. Structure*, **20**, 51 (1974).

[21] J. Goubeau and D. Kötgen, *Z. anorg. Chem.*, **360**, 182 (1968).

[22] H. Siebert, *Z. anorg. Chem.*, **273**, 101 (1953).

Revue Roumaine de Chimie, 25, *6*, 823–830 (1980)

VIBRATIONAL CHARACTERISTICS OF Ni(II) DITHIOPHOSPHINATO CHELATES. NORMAL COORDINATE ANALYSIS AND UREY-BRADLEY FORCE FIELD CALCULATION OF $Ni[S_2P(CH_3)_2]_2$

IOAN SILAGHI-DUMITRESCU and IONEL HAIDUC
Chemistry Department, Babeș-Bolyai University R-3400, Cluj-Napoca, Romania

Received November 27, 1979

A normal coordinate analysis of the title compound was carried out for a 1 :1 C_{2v} symmetry model in the Modified Urey-Bradley Force Field approximation. The assignment of the vibrational frequencies was made using the potential energy distribution upon force constants and the symmetry properties of the L matrix. The symmetric P—C and P—S bond stretching vibrations are coupled to a great extent, while the corresponding antisymmetric ones are almost pure P—C and P—S vibrations. The sign of the interaction force constants suggests delocalization of the π-electron density in the NiS_2P ring. The phosphorus-sulphur force constant (f_{P-S} = 2.97 mdyne/Å) is greater than f_{P-S} in the free ligand (2.80 mdyne/Å), a fact correlated with the lowering of the negative charge passing from $(CH_3)_2PSS^-$ to $[(CH_3)_2PS_2]_2Ni$, and with back donation from Nickel *3d* filled orbitals to molecular orbitals delocalized over SPS moiety.

INTRODUCTION

Nickel(II)dithiophosphato-, $[(RO)_2PS_2]_2Ni$, and dithiophosphinato-, $[R_2PS_2]_2Ni$ complexes contain a four membered NiS_2P chelate ring. Very little is known about the nature of bonding in this ring and the study of its vibrational properties may provide useful information.[1, 2] Thus, Cheremisina *et al.* [1] have correlated the stability constants with Ni—S force constant for a series of $Ni[S_2XR_2]_2$ compounds and a linear relation has been observed. Rudzinski *et al.* [2] have pointed out the importance of Ni—S force constants in predicting the correct stability of Ni(II) dithiophosphato- and xantato-chelates, compared with the Ni—S bond length, underlying the fact that the latter could lead to wrong interpretations.

It seems that force constants are more valuable characteristics in discussing the bonding properties in the NiS_2P ring than bond lengths or vibrational frequencies. With this in mind we have carried out a normal coordinate analysis on bis(dimethyldithiophosphinato)Ni(II) complex, in order to get information about the changes in the P—S and Ni—S force constants, comparatively to the corresponding dithiophosphato Ni(II) complex, studied by Rudzinski *et al.* [2]

EXPERIMENTAL

Infrared spectra were recorded using an UR 20 Carl Zeiss Jena spectrophotometer within 4000–400 cm^{-1} in KBr pellets. The 1000–200 cm^{-1} range was covered by Perkin-Elmer 621 instrument . [3]Attempts to record the Raman spectrum failed[3] because the sample decomposed under the experimental conditions (the 488 nm Ar^+ plasma line, at -196°C).[3]

BAND LOCALIZATION

The following discussion is based on an assumed C_{2v} symmetry supported by crystallographic data, [4] the methyl groups bound to the same phosphorus atom being in staggered position.

The 63 normal modes of the molecule can be divided according to the irreducible representation of the C_{2v} point group as :

$$\Gamma_{\text{total}} = 19\,A_1 + 13\,A_2 + 13\,B_1 + 18\,B_2$$

A further division is possible in terms of skeletal and $-CH_3$ vibrations. [5]

$$\Gamma_{\text{skeletal}} = 9\,A_1 + 5\,A_2 + 5\,B_1 + 8\,B_2 \quad \text{and}$$

$$\Gamma_{CH_3} = 10\,A_1 + 8\,A_2 + 8\,B_1 + 10\,B_2$$

The part of the spectrum due to CH_3 vibrations is shown in figure 1.

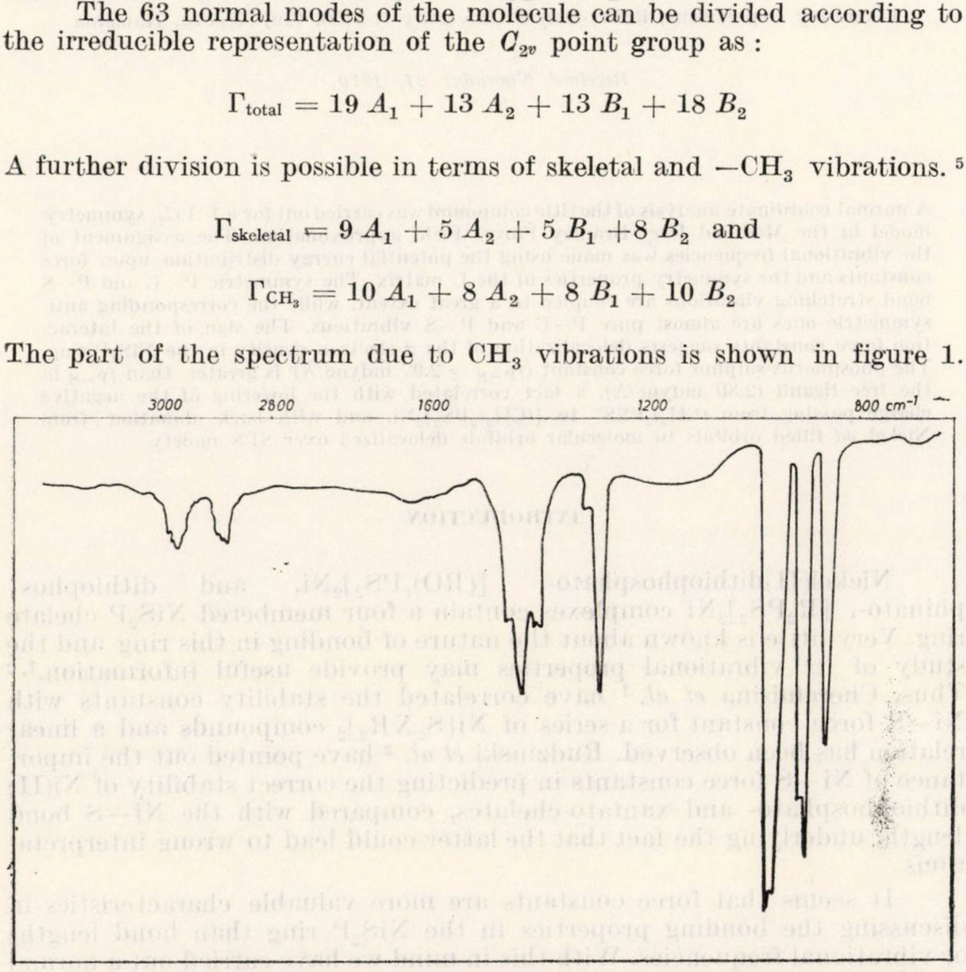

Fig. 1 – The infrared spectrum of $Ni[S_2P(CH_3)_2]_2$ in the 3000–800 cm^{-1} region.

The symmetric stretching vibration frequencies of the methyl group lie in the region 2870 ± 10 cm^{-1}.[6] Although the resolution in this part of our spectrum is not quite satisfactory, four maxima can be distinguished within 2910—2880 cm^{-1}, in accordance with the four ($2 A_1 + 2 B_2$) predicted absorptions.

The eight antisymmetric stretching frequencies of the methyl groups ($2 A_1 + 2A_2 + 2B_1 + 2B_2$) should give rise to six bands in the IR spectrum (the A_2 symmetry vibrations are not IR active). Our spectrum exhibits some maxima between 2990 and 2960 cm^{-1} but they are not resolved well enough, to make possible the comparison with the number of predicted bands.

The antisymmetric deformation frequencies of the methyl group occur in the 1470—1410 cm^{-1} region.[6] There are, all in all, eight antisymmetric deformation modes : $2A_1 + 2A_2 + 2B_1 + 2B_2$, but only six of them are infrared active. The compound investigated absorbs within 1430—1390 cm^{-1} where three maxima can be observed. Each of these three bands should have been splitted but the splitting is probably small because of the relatively heavy phosphorus atom which separates the CH_3 groups and thus reduces the coupling between the modes of the same symmetry.

The (P)—CH_3 symmetric deformation region is 1330—1280 cm^{-1}.[6] The four predicted frequencies ($2 A_1 + 2 B_2$) have only two correspondent bands in the spectrum ; no splitting can be noticed, probably because of the reason mentioned above.

The (P)—CH_3 rocking modes occur usually at about 880 cm^{-1}.[6] The four methyl groups lead to eight rocking vibrations classified as : $2 A_1 + 2 A_2 + 2 B_1 + 2B_2$ and again only six are IR active. Unlike the deformation modes, the rocking motions involve much more contribution of the P atom and the coupling of modes of the same symmetry increases. Consequently, the splitting within each band assigned to the (P)—CH_3 rocking is large enough to be felt by our apparatus, and the spectrum exhibits the pattern shown in the 960—850 cm^{-1} region.

The skeletal frequencies, formally attributed to P—S, P—C and Ni—S stretchings and the different deformations involving the angles between these bonds [7,8] are given in figure 2.

CALCULATION PROCEDURE

Calculations were performed in the Wilson GF formalism[9] using Shimanouchi's computer programs BGLZ and LSMB.[10]

If we assume a reasonably small interaction between the two dithiophosphinate ligands bound to Ni, the calculations can be simplified by treating a 1 : 1 C_{2v} symmetry planar model. This is an idealised model since X-ray structural data show that only NiS_4 moiety is planar and the NiS_2P ring is slightly distorted from planarity, namely the phosphorus atom is located out of the NiS_2 plane.[4] The methyl groups were taken as point units, a technique often used in such kind of calculations. The internal coordinates used for G matrix calculation are shown in figure 3.

There are 12 normal modes classified as $5\,A_1 + A_2 + 3B_1 + 3\,B_2$. Only the A_1, B_1 and B_2 modes are IR active, so only 11 modes are expected to be observed in IR. Since 17 internal coordinates were selected as the basis in the description of the normal modes, five redundancies have been included in the calculation and eventually, five zero frequencies were obtained.

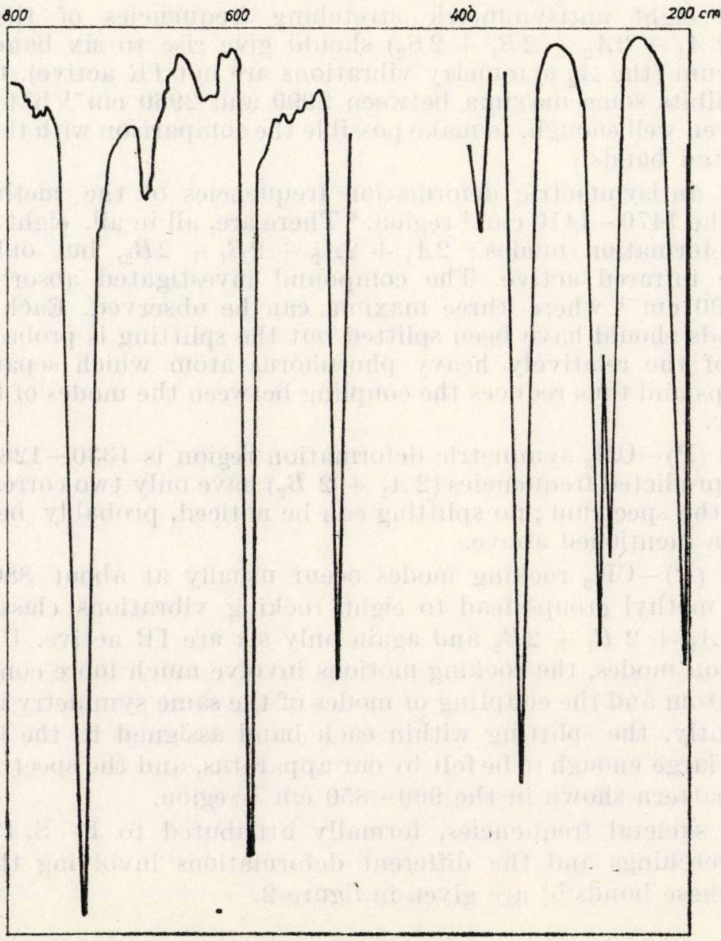

Fig. 2 — The infrared spectrum of $Ni[S_2P(CH_3)_2]_2$ in the 800—200 cm^{-1} region.

Initial F matrix elements were transferred from $[(CH_3O)_2PS_2]_2Ni$[1,2] and $(CH_3)_2PS_2^-$.[7] Since the simple Urey-Bradley force field[11] was unable to reproduce the observed spectrum with a satisfactory accuracy, some interaction constants were added, in order to improve the fitting. The observed frequencies were used for refining seven force constants. The choice of the variable force constants was made by inspecting the eigenvalues and eigenvectors of the J′ W J matrix.[10]

The refinement processes have been carried out in the following steps :

1) The choice of the variable force constants (the k_A set).

2) The adjustment of the variable force constants keeping "fixed" the k_B set.

3) Modification of the "fixed" force constants according the Jacobian matrix, in order to improve the fitting achieved in step 2.

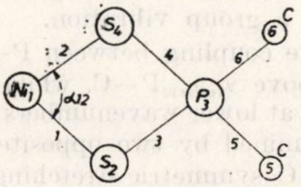

Fig. 3 — The approximate molecular model and the internal coordinate system.

4) Steps 2—3 were repeated until the best possible agreement between the observed and calculated frequencies was obtained.

RESULTS AND DISCUSSION

The assignment of the normal modes was performed by using the potential energy distribution upon the internal coordinates (PED) and upon the force constants (PEF).

Since the secular equation was not factorized using the symmetry coordinates, the labeling of the normal modes with the corresponding indices of irreducible representation was made by analysing the eigenvectors matrix *L*. The main results are summarized in table 1.

TABLE 1

Potential energy distribution

Calcd. obsd.	735.3. 736	512.5 511	387.1 385	351.4 350	261.8 271	192.0 —	731.9 732	222.0 213	44.0 —	584.4 585	280.2 280	197.0 208
K_{Ni-S}			7	46	10						91	
K_{P-S}	24	31	26							92	2	
K_{P-C}	40	45					99					
H_{SNiS}					9							
H_{SPS}	7	5	12	20	38							
H_{CPC}	11	9	28	16	10							
$F_{C...C}$		5			17							
H_{SPC}						60		59				57
$F_{S...C}$		7	4			37		38				38
$f\tau$									99			
$f_{PS,\,PC}$	8	—9										
			A_1			A_2		B_1			B_2	

Within the total symmetric vibrations set (A_1) we can notice a high degree of mixing between different internal modes. In this respect, none of the potential energy of the normal modes has a contribution higher than 50% from one of the individual force constants. Nevertheless, taking into account the higher PEF values, the assignments given in table 1 are proposed. It can be noticed that K_{P-S} contributes at least to three normal modes within this symmetry species, thus denoting the tendency of the P—S vibrations to spread over different modes rather than concentrate in a group vibration.

The coupling between P—C and P—S bond stretchings shifts ν_{sym} P—C above $\nu_{antisym}$P—C, while in the dimethyldithiophosphinato anion ν_{P-C} lies at lower wavenumbers than $\nu_{antisym}$P—C. [7] This situation could be determined by two opposite factors: *a*) the coupling between P—S and P—C symmetric stretching vibrations, resulting in a lower ν_{sym}P—S than without mixing and *b*) the strengthening of the P—S bond by $d_\pi - p_\pi$ back donation from Ni(II) *3d* filled orbitals to an unfilled molecular orbital, localised on the SPS part of the molecule, with an increase in the P—S force constant. This explains the increase in ν_{sym}P—S comparatively to the uncoordinated anion.

Since the contribution of K_{Ni-S} to other modes of A_1 symmetry is smaller than the contribution of K_{P-S} or K_{P-C}, the Ni—S stretching vibration has more pronounced group character. Based on PEF we might assign $\nu = 351$ cm^{-1} to Ni—S symmetric stretching.

There are other two A_1 symmetry normal modes, due to the CPC angle deformation ($\nu = 387$ cm^{-1}) and to NiS_2P ring deformation ($\nu = 261.8$ cm^{-1}).

The A_2 mode calculated value (192 cm^{-1}) is only Raman active and cannot be compared with the experimental value.

Concerning the B_1 and B_2 symmetry type normal modes, a high localized character can be inferred from PEF. It can be noticed the relative low value of $\nu_{antisym}$Ni—S compared to the same frequency in the Ni(II)bis(dimethyldithiophosphate). [2] This finding is probably connected with the lower Ni—S force constant in $[(CH_3)_2PS_2]_2Ni$ than in $[(CH_3O)_2PS_2]_2Ni$.

FORCE CONSTANTS

The force constants calculated in this work and the force constants of related molecules are listed in table 2.

Since a vibrational frequency is not always due to only one internal coordinate, force constants are more suitable in discussing the electronic effects accompanying the complex formation.

By passing from the free ligand $(CH_3)_2PS_2^-$ to the complex $[(CH_3)_2PS_2]_2Ni$, the P—S bond force constant increases from 2.56 mdyne/Å to 2.67 mdyne/Å (Urey-Bradley force constants). This behaviour can be related to three major causes:

a) the effect of coordination, causing a decrease in K_{P-S}

b) the effect of electronic charge — the P—S force constant increases with the decreasing negative charge on the anion.[12]

c) the effect of back donation, as mentioned above.

TABLE 2

Urey-Bradley force constants for $[(CH_3)_2PS_2]_2Ni$ and related molecules (mdyne/Å)

Force constants	$(CH_3)_2PS_2^-$	$[(CH_3O)_2PS_2]_2Ni$	$[(CH_3)_2PS_2]_2Ni$
K_{Ni-S}	—	1.20	0.91
K_{P-S}	2.56	2.80	2.67
$K_{P-C(O)}$	2.75	3.46	2.60
H_{SPS}	0.23	0.15	0.45
H_{SNiS}	—	0.30	0.10
$H_{(O)CPC(O)}$	0.25	0.39	0.39
$H_{SPC(O)}$	0.20	0.05	0.09
$F_{S...C(O)}$	0.10	0.23	0.13
$F_{S...S}$	0.05	0.05	0.03
$F_{(O)C...C(O)}$	0.10	0.40	0.10
$f_{PS,PS}$	—	—	0.05
$f_{NiS,NiS}$	—	—	0.20
$f_{PS,PC}$	—	—	−0.17
$f_{PC,PC}$	—	—	0.10
$f_{PS,CPC}$	—	—	−0.05
	Ref. 7	Ref. 2	this work

The subtle interplay of these factors leads to an overall increase in K_{P-S}. Although it is hard to discriminate the relative magnitude of these effects, the third one seems to have importance in the electron density delocalization over the whole NiS_2P ring.

It has been shown[13] that in a triatomic system $A = B - C$ a positive interaction force constant is related with a high degree of delocalization : $A \overset{\cdots}{-} B \overset{\cdots}{-} C$, while a negative value suggests a localized character of the electron density.

In the compound investigated the positive sign of $f_{NiS,NiS}$ and $f_{PS,PS}$ is in agreement with the supposed electron density delocalization in the ring.

The P—S and P—C bond orders calculated with the Gordy's formula[14] exhibit the same behavior as the corresponding force constants. Thus, N_{P-S} increases from 1.22 (free ligand) to 1.30 (in the complex investigated) and N_{P-C} decreases from 1.06 to 0.94.

It should be noticed the smaller K_{P-S} and K_{Ni-S} of the dithiophosphinato complex compared to that of the dithiophosphato complex. These differences are probably due to the different electronegativities of the substituents attached to the phosphorus atom in the two cases.[12] The lower K_{Ni-S} value in the dithiophosphinato complex is also in accordance with the position of the $(CH_3)_2PS_2^-$ anion in the nephelauxetic series,[15] denoting a lower degree of covalency in $[(CH_3)_2PS_2]_2Ni$ than in $[(CH_3O)_2PS_2]Ni$.

REFERENCES

[1] I. M. Cheremisina, L. I. Kozhevina and E. M. Yurchenko, *Zhur. strukt. Khim.*, **16**, 583 (1975).

[2] W. Rudzinski, G. T. Behnke and Q. Fernando, *Inorg. Chem.*, **16**, 1206 (1977).

[3] A. Haas, private communication.

[4] P. E. Jones, G. B. Ansell and L. Katz, *Acta Cryst.*, **B25**, 1939 (1969).

[5] L. L. Boyle, *Spectrochim. Acta*, **28A**, 1347 (1972).

[6] N. B. Colthup, L. H. Daly and S. E. Wiberley, "Introduction to Infrared and Raman Spectroscopy", Academic Press, New York, 1964.

[7] I. Silaghi-Dumitrescu and I. Haiduc, *Rev. Roumaine Chim.*, **25**, 815 (1980).

[8] R. G. Cavell, M. Byers, E. D. Day and P. M. Watkins, *Inorg. Chem.*, **11**, 1958 (1972).

[9] E. B. Wilson, J. C. Decius and P. C. Cross, "Molecular Vibrations. The Theory of the Infrared and Raman Vibrational Spectra" McGraw-Hill, New York, 1955.

[10] T. Shimanouchi, "Normal Coordinate Treatment of Polyatomic Molecules", Tokyo University, Tokyo, 1968.

[11] a) H. C. Urey and C. A. Bradley, *Phys. Rev.*, **32**, 1969 (1931).

[12] b) T. Shimanouchi, *J. Chem. Phys.*, **17**, 245, 634, 838 (1949).

[12] J. Goubeau, *Angew. Chem. Int. Ed.*, **8**, 328 (1969).

[13] K. Ohwada, *Spectrochim. Acta*, **34A**, 147 (1978).

[14] W. Gordy, *J. Chem. Phys.*, **14**, 305 (1946).

[15] M. Forster, H. Hertel and W. Kuchen, *Angew. Chem. Int. Ed.*, **9**, 811 (1970).

Revue Roumaine de Chimie, 25, 6, 831–838, (1980)

MAGNETIC AND SPECTRAL STUDIES OF 2-SUBSTITUTED BENZIMIDAZOLE COMPLEXES OF COBALT(II)

MALATESH A. PUJAR and N. S. BIRADAR*

Department of Chemistry, Karnatak University Post Graduate Centre, Gulbarga — 585 105, India

Received October 27, 1978

Cobalt(II) complexes with 2-substituted benzimidazoles have been synthesized. The complexes were characterized with the aid of chemical analysis, electrical conductance in solution, electronic and infrared spectra and magnetic susceptibilities at different temperatures (80–300K). These complexes are found to be non-electrolytes in DMSO. The electronic spectra and magnetic susceptibility data indicate distorted tetrahedral stereo-chemistry for the complexes. The various magnetic and ligand field parameters such as λ, K, g, Dq and B' values for these complexes suggest strong field in spectro-chemical and nephelauxetic series and greater orbital overlap between metal and ligand.

INTRODUCTION

Complex formation between imidazole and benzimidazole compounds and metal ions is found to be considerably interesting as it is becoming increasingly more important in molecular biology and technology.[1–4] Recently it is observed that benzimidazoles and few substituted benzimidazoles are effective inhibitors of the growth of yeasts and influenza virus.[5,6] Previous studies have shown that several complexes exist between metal ions and imidazoles and benzimidazoles.[7–10] It is also found that the substituents placed in the imidazole unit can have both a steric and an electric effect and also have an effective towards many virus inhibitors.[6,11,12] These factors encouraged us to undertake a detailed study of 2-substituted benzimidazole (A) complexes of Co(II).

I=R=H

II=R=$-CH_3$

III=R=$-CH_2-CH_3$

IV=R=$-(CH_3)_4-C_7H_5N_2$

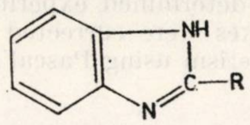

EXPERIMENTAL

The chemical used in preparing the complexes were of reagent grade. The purity of the amine and other organic compounds was checked against their m.ps or b.ps. $CoCl_2 \cdot 6H_2O$ (Riedel grade) was directly used. DMF was purified by distillation over P_2O_5 under vacuum. Distilled dried alcohol was used as a solvent.

*** Present address : Professor of Chemistry, Karnataka University, Dharwad, India**

GENERAL METHOD PREPARATION

The benzimidazole, 2-methyl and 2-ethyl benzimidazole and tetra-methylene bis benzimidazole ligands were prepared according to the modified methods described elsewhere[13]. The simple benzimidazole complex of Co(II) was prepared for comparison according to the method given by Cotton and Goodgame[7]. The following general procedure has been adopted for the preparation of 2-substituted benzimidazole complexes of Co(II).

A solution of 0.01 M $CoCl_2 \cdot 6\,H_2O$ in alcohol was treated with the appropriate amount of ligand in alcohol. To this solution a small quantity of sodium dried benzene was added. The solution was refluxed for 1—2 hours. It was then evaporated slowly. The crystals of the complexes were separated on standing, either in cold or after the addition of dried benzene or diethyl ether. The crystals were washed and dried in vacuo over P_2O_5.

The complexes were analysed for cobalt, nitrogen and chloride content by the standard method. The results of analysis are given in table 1.

PHYSICAL MEASUREMENTS

The molar conductance measurements on the complexes in DMSO at a concentration 0.5 to 1×10^{-1} M were taken with an ELICO-conductivity bridge type CM—82 having cell constant 0.829 cm^{-1}.

The electronic spectra of the complexes in DMF were obtained with Beckman DU spectrophotometer. The diffused reflectance spectral measurements in the visible region were obtained on a finally powdered sample using 8F—10 model (USSR) recording spectrophotometer. The optical grade magnesium carbonate was used as standard for high reflectance.

The IR absorption spectra (4000—650 cm^{-1}) were recorded on a Perkin-Elmer Infracord 137—B instrument using KBr pellet method.

The magnetic susceptibility of the complexes under investigation was determined at various temperatures between 85 and 300 K by the Gouy method, using $Hg[Co(CNS)_4]$ as calibrant. Temperature could be kept constant within 0.1°. Duplicate determinations were made on separately prepared samples of the complexes. The diamagnetic susceptibility of ligands was determined experimentally. The molar susceptibilities of all the comlpexes were corrected for the ligand and other constituent atoms diamagnetism using Pascal's constants for Co and Cl[14].

RESULTS AND DISCUSSION

All the benzimidazole and 2-substituted benzimidazole complexes of Co(II) under investigation are violet blue to greenish blue micro crystalline. They decompose at high temperature and are stable against light and atmosphere. They are soluble in polar solvents such as dimethyl formamide (DMI), pyridine etc. Practically all these complexes are inso-

TABLE 1

Elemental analysis, conductance and infrared spectral data of Co(II) complexes

Complex *	Colour	Cobalt %		Nitrogen %		Chloride %		Molar conductance (ohm^{-1}, cm^2 mole^{-1})	νNH (cm^{-1})	νC = N (cm^{-1})
		Obsd.	Calcd.	Obsd.	Calcd.	Obsd.	Calcd.			
1. [Co(BZD)$_2$]	Violet blue	19.89	20.11	18.99	19.2	—	—	28.10	—	1585
2. [Co(BZD)$_2$Cl$_2$]	Greenish blue	16.34	16.11	15.14	15.31	19.51	19.38	26.53	3010	1575
3. [Co(2-MeBZD)$_2$]	Blue	18.05	18.36	17.32	17.45	—	—	25.68	—	1570
4. [Co(2-Me-BZD)$_2$Cl$_2$]	Greenish blue	14.76	14.65	14.08	14.17	18.22	18.04	22.25	3100	1590
5. [Co(2-Et-BZD)$_2$Cl$_2$]	Blue	13.78	13.90	13.52	13.32	16.75	16.81	24.56	3120	1585
6. [Co(TMB-BZD)Cl$_2$]	Greenish blue	13.74	13.90	12.98	13.21	16.94	16.73	21.82	3215	1600

---

* BZD = Benzimidazole ($C_7H_6N_2$)
2-Me-BZD = 2-Methyl benzimidazole ($C_8H_8N_2$)
2-Et-BZD = 2-Ethyl benzimidazole ($C_9H_{10}N_2$)
TMB-BZD = Tetramethylene bis benzimidazole ($C_{18}H_{22}N_4$)

luble in common organic solvents such as ethanol, acetone and benzene. This limited solubility of the complexes did not permit the determination of the molecular weight of the complexes.

The elemental analysis obtained for these complexes agrees well with the formation of 1 : 2 type complexes and tetramethylene bis benzimidazole forms a complex of 1 : 1 type.

The molar conducatance of these complexes in DMSO at the concentration 10^{-3} M falls in the range 21—28 ohm^{-1} cm^2 mole^{-1} (Table 1). The values indicate that the complexes behave as non-electrolytes in DMSO[15]. The slightly high conductance observed may be due to the partial displacement of the chloro group by DMSO in the coordination sphere of the complex.

MAGNETIC PROPERTIES

A representative set of corrected molar susceptibilities at each temperature for various complexes was tabulated in table 2. The μ_{eff} values at room temperature show that the complexes are of a spin-free type and the data observed for μ_{eff} (4.1—4.5 B.M.) suggest the tetrahedral arrangement of ligand molecule around Co(II) ions[16,17]. The μ_{eff} values of these complexes indicate magnetic moments in excess of 3.88 B.M. (sole spin value for three unpaired electrons) by 0.3—0.6 B.M. The slightly higher values for the observed moment are logically due to the mixing of the ground state and higher energy terms under spin orbit coupling.

Magnetic measurements from 300 K to liquid nitrogen temperature on representative examples of the complexes under study suggest that the values of reciprocal χ_m when plotted against temperature T (K) give a linear relation in the whole temperature range. This shows that these 2-substituted benzimidazole complexes of Co(II) obey a Curie-Weiss law with small Curie-Weiss constant θ (Table 3). The magnetic moments ranging from 4.1—4.5 B.M. indicate some distortion from the ideal T_d symmetry and this observed temperature dependence is likely to arise from an antiferromagnetic interaction[18,19].

It is interesting to note that the μ_{eff} values observed for 2-substituted benzimidazole complexes of Co(II) (Table 3) are lower than those normally found for the tetrahedral complexes of Co(II), except the last complex. This may be attributed to super exchange coupling of Co(II) by means of short symmetrical N—C—N chains which form a part of a mobile π election system and also probably due to the distortion of the ideal tetrahedral symmetry T_d, which will considerably change the values of magnetic moment too[18,19].

An attempt has been made to obtain the best fit of the experimental data by plotting μ_{eff} against T with the theoretical values by using Griffith's equation[20] which has been described elsewhere[21]. Values λ (spin orbit coupling constant), Δ (splitting factor) and K (orbital reduction factor), obtained in this way are summarized in table 3 and g (Landè's splitting factor) values were calculated from the relation $g = 2\,(1 - 4\,\lambda/\Delta)$[12].

It may be noted that the values of the spin orbit coupling constant (λ) for the complexes which have been computed from magnetic susceptibility data are in the range 120—150 cm^{-1}. In every case, λ values of the complexes are lower than that of the free ion, value λ for free ion is taken [17] to be 172 cm^{-1}. The orbital reduction factor is well below unity. The calculated g values are in the range 2.1—2.3, which deviate from spin only ($g = 2.0022$). All these values λ, K, g etc., observed are in the range generally for tetrahedral Co(II) complexes and show that there is considerable orbital overlap between the ligand and the metal ion [22].

TABLE 2

Magnetic susceptibilities for the Co(II) complexes at different temperatures

Temp. (K)	$\chi M\ 10^6$ (cgs units)	μ_{eff} (B.M.)	Temp. (K)	$\chi M\ 10^6$ (cgs units)	μ_{eff} (B.M)
(1) $[Co(C_7H_5N_2)_2]$			(2) $[Co(C_7H_6N_2)_2Cl_2]$		
85.0	20620	3.75	86.0	24210	4.08
94.5	19110	3.80	92.0	23350	4.14
103.0	17960	3.85	101.5	21190	4.15
137.0	14940	4.05	113.5	19040	4.16
155.5	13480	4.09	126.0	17300	4.18
185.5	11560	4.14	146.0	15050	4.19
202.0	9631	4.23	170.0	13390	4.27
293.5	7821	4.28	201.5	11370	4.28
			239.5	9662	4.30
			297.1	7849	4.32
(3) $[Co(C_8H_7N_2)_2]$			(4) $[Co(C_8H_8N_2)_2Cl_2]$		
86.8	23520	4.04	90.0	21140	3.90
108.5	19450	4.11	105.5	18470	3.95
120.5	17620	4.12	133.5	15110	4.02
135.0	15850	4.14	151.0	13460	4.04
153.0	14070	4.15	206.0	10360	4.13
176.5	12390	4.18	248.5	8789	4.18
206.0	10690	4.20	296.7	7616	4.25
246.0	9160	4.24			
(5) $[Co(C_9H_{10}N_2)_2Cl_2]$			(6) $[Co(C_{18}H_{22}N_4)Cl_2]$		
86.0	24810	4.13	86.0	27480	4.35
96.0	22430	4.15	102.5	23330	4.37
107.5	20260	4.17	129.0	18830	4.41
119.0	18390	4.18	147.5	16420	4.40
134.5	16310	4.19	167.0	14870	4.45
153.5	14360	4.20	195.0	12860	4.48
208.0	10720	4.22	241.0	10680	4.53
249.5	9000	4.24	296.5	8636	4.52
296.0	7652	4.26			

TABLE 3

Magnetic susceptibility and absorption spectral data for Co(II) complexes

Complex	Temp. (K)	μ_{eff} (BM)	θ (K)	Δ (cm^{-1})	K	λ (cm^{-1})	g	$4A_2 \rightarrow 4T_1(P)$ ν3 (cm^{-1})	$4A_2 \rightarrow 4T_1$(F) ν2 (cm^{-1})	Calculated ν3(cm^{-1})	ν_2	$10D_q$ (cm^{-1})	B' (cm^{-1})
1.	293.5	4.28											
	155.0	4.10	−32	7255	0.83	−142	2.19	16130 15230	8570 7634 6379 6024	15620	8488	5055	596
	85.0	3.74											
2.	297.1	4.32	− 9	7406	0.80	−137	2.18	16670 15200	8929 8130 7692 6993 6123	15500	8065	4769	617
	146.0	4.20											
	86.0	4.08											
3.	296.0	4.26											
	153.0	4.15	−12	8494	0.77	−132	2.16	17860 15870	8547 7752 6540 5882	15920	8348	4939	630
	86.8	4.04											
4.	296.7	4.25											
	151.5	4.04	−16	8426	0.76	−130	2.18	18520 16050	10530 7813 7634 6836 5952	15920	8218	4832	618
	90.0	3.90											
5.	296.0	4.25											
	153.5	4.20	−10	9181	0.73	−125	2.15	17390 157900	8264 7640 6410 5950	15664	8258	4900	651
	86.0	4.13											
6.	296.5	4.52											
	167.0	4.41	−11	6262	0.87	−149	2.21	16390 15630	11240 8065 7576 6410 6024	15380	8044	4801	604
	86.0	4.30											

ELECTRONIC SPECTRA

The main bands in DMF and DMSO solutions of the complexes do not differ, in principle, from those in the solid state suggesting no significant change in sterochemistry on dissolution.

The spectra show intense multi component bands in the visible and near infrared regions, characteristic of tetrahedral Co(II) [23,24] (Table 3). A large splitting of ν_3 and ν_2 absorption region of the spectrum is observed and it has been suggested that this is caused by the distortion of the ideal tetrahedral symmetry T_d of 2-substituted benzimidazole complexes of Co(II) under study [23-25]. This finds additional support in the study of the magnetic properties of these complexes.

The single energy values from multi component bands have been selected using the method [21], and from ν_3 and ν_2 the Racah interelectronic repulsion parameter (B′) was calculated ; B for the free ion value is taken 976 cm^{-1}. [17] The observed B' is of the order of 65—75% of free ion value suggesting that there is a considerable orbital overlap. The comparison of 10 D_q values with 10 Dq values of 5100 cm^{-1} for simple benzimidazole Co(II)[7] and 5200 cm^{-1} for imidazole Co(II) [8] show that even 2-substituted benzimidazole Co(II) [8] complexes lie very high in the spectro-chemical series, in other word the ligands produce a strong ligand field towards Co(II) atom.

INFRARED SPECTRA

The range of bands observed in the region 3300—2800 cm^{-1} shows the polymeric association of benzimidazole through intermolecular hydrogen bonding [26, 27]. The bands also include the CH stretching vibration. The NH band intensity in complexes of $Co(Bzd)_2$ and $Co(2\text{-}Me\text{-}Bzd)_2$ is completely reduced and this indicates that the coordination takes place through the imino nitrogen and pyridine nitrogen of imidazole ring exhibiting tetrahedral symmetry around Co(II) atom. In other complexes this behaviour is not observed perphaps due to the more steric hidrance at the 2-position of imidazole group. Therefore these complexes show an H—N band around 3000 cm^{-1} which also indicates a shift towards lower frequency suggesting that the coordination has taken place through the unsaturated nitrogen of the imidazole ring [10]. The medium band around 1615 cm^{-1} in these complexes is assigned to the C=N stretch in view of previous assignment [8] supporting the above conclusion (Table 1).

ACKNOWLEDGEMENT. The author is grateful to Dr. V. R. Marathe and Late Prof. C. R. Kanekar, T. I. F. R., Bombay for providing facility to carry out magnetic measurements at various temperatures using Gouy balance and stimulating discussion.

REFERENCES

[1] R. J. Sundberg and R. B. Martin, *Chem. Rev.*, **74**, 471 (1974).

[2] M. N. Hughes, "The Inorganic Chemistry of Biological Processes", Wiley, London, 1972.

[3] H. Shirai, Y. Inaki and K. Takemoto, *Makromol. Chem.*, **175**, 2047 (1974).

[4] N. Sawa and M. Yasuda, *Jap. Appl.*, **73**, 25, 621 (1973) ; *Chem. Abstr.*, **81**, 28712 (1974).

[5] K. Folkers, *J. Exp. Med.*, **98**, 245 (1953).

[6] S. P. Gupta and S. Rani, *J. Indian Chem. Soc.*, **54**, 478 (1977).

[7] F. A. Cotton and M. Goodgame, *J. Amer. Chem. Soc.*, **84**, 1543 (1962).

[8] W. J. Eilbeck, F. Holmes and A. E. Underhill, *J. Chem Soc.*, *A*,. **1967**, 757.

[9] K. D. Bose and C.C. Patel, *J. Inorg. Nuclear Chem.*, **32**, 114 (1970).

[10] M. A. Pujar, A. C. Hiremath and A. S. R. Murthy, *Karnatak University J. Science*, **21**, 144 (1976).

[11] D. M. L. Goodgame, M. Goodgame and G. W. Rayner, *Inorg. Chim. Acta.*, **3**, 406 (1969).

[12] J. Reedijk, *Rec. Trav. chim.*, **91**, 1373 (1972).

[13] M. A. Pujar, Ph. D. (Thesis) Karnatak University, Dharwad (1970).

[14] B. N. Figgis and J. Lewis, "Modern Coordination Chemistry", Edited by J. Lewis and R. G. Wilkins, Interscience, New York, 1960, p. 403.

[15] J. V. Quagliano, F. Fujita, G. Franz, D. J. Phillips J. A. Walmsley, and S. Y. Tyree, *J. Amer. Chem. Soc.*, **83**, 3770 (1961).

[16] B. N. Figgis, "Introduction to Ligand Field Theory", Interscience Publishers, New York, 1966.

[17] R. L. Carlin, "Transition Metal Chemistry", Vol. 1 ; Marcel Dekker, New York, 1965, p. 1.

[18] R. A. Krause, C. Guy and M. L. Hooker, *Inorg. Chem.*, **5**, 1825 (1966).

[19] A. Earnshaw, "Introduction to Magneto Chemistry", Academic Press, London, 1968, p. 58.

[20] J. S. Griffith, "The Theory of Transition Metal Ions", Cambridge Univ. Press, London, 1961, p. 254.

[21] M. A. Pujar, V. R. Marathe and N. S. Biradar, *Indian J. Chem.*, **9**, 712 (1971).

[22] J. Owen, *Proc. Roy. Soc., (London) A*, **127**, 283 (1955).

[23] A. B. P. Lever, "Inorganic Electronic Spectroscopy", Elsevier, London, 1968.

[24] M. Goodgame, *J. Chem. Soc., A.*, **1966**, 63.

[25] D. M. L. Goodgame and M. Goodgame, *Inorg. Chem.*, **4**, 139 (1963).

[26] T. J. Lane, I. Nakagawa, J. L. Walter and A. J. Kandathi, *Inorg. Chem.*, **1**, 267 (1962).

[27] K. J. Morgan, *J. Chem. Soc., A*, **1961**, 2343.

Revue Roumaine de Chimie, 25, *6*, 839—844 (1980)

COMPLEX COMPOUNDS OF NICKEL INVOLVED IN ELECTRON TRANSFER PROCESSES

D. NEGOIU*, J. CAMUS* and N. MUREŞAN**

* National Institute of Chemistry, Faculty of Chemical Technology, 1, Polizu Street, 78126—Bucharest, Romania

** University of Craiova, Faculty of Natural Sciences 13, A. I. Cuza Street, 1100—Craiova, Romania

Received March 19, 1979

Some $[NiO_4]^z$—, $[NiN_2S_2]^z$— and $[NiO_2S_2]^z$—type complexes of nickel with quinoxalinic and naphthoquinonic ligands were synthesized. The complexes were characterized by chemical analysis, conductivity, infrared and electronic spectra, and ESR spectra. Their participation in electron transfer processes was investigated by polarography.

INTRODUCTION

During the last years, the literature has offered new data related to the complex coumponds formed between transition metals and ligands having conjugated double bonds, i.e. a system of delocalized electrons, in their molecule [1]. Most of these data deal with dithiol complexes. The chemical bond overlaps in these complexes with electron delocalization processes and this makes the oxidation state of the metal or the metal-ligand bond order difficult to define. These complexes are able to take part in monoelectronic redox reactions, giving rise to electron transfer series :

$$[M-S_4]^{2-} \rightarrow [M-S_4]^{-} \rightarrow [M-S_4]^{\circ}$$

These combinations are planar irrespective of the oxidation state of the metal.

Other four coordinated systems, having similar properties to the dithiols, were also investigated. [2-7] As a consequence of the electron transfer, the following species can be obtained in this case :

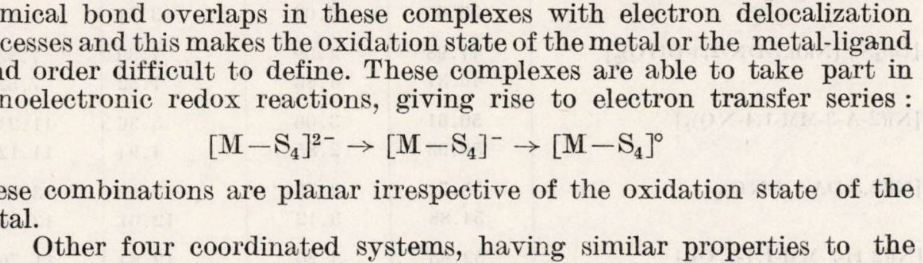

where X=Y=O ; X=Y=N ; X=O, Y=S ; and X=S, Y=N

With the view of extending these investigations to the latter systems, in this work we used quinoxalinic ligands containing X=Y=O in their *ortho* position [8,9] and naphthoquinonic ligands containing X=Y=N; X=O, Y=S; and X=S, Y=N as donor atoms.

RESULTS AND DISCUSSION

Six new complexes of the Ni(II) ion were obtained in this work with 2,3-dihydroxyquinoxaline (2,3-DHQ), 6-nitro-2,3-dihydroxyquinoxaline (6-N-2,3-DHQ), 2-amino-3-mercaptomethyl-1,4-naphthoquinone (2-A-3-MM-1,4-NQ), 2,3-diamino-1,4-naphthoquinone (2,3-DA-1,4-NQ), 2-hydroxy-3-mercaptomethyl-1,4-naphthoquinone (2-H-3-MM-1,4-NQ) and 6,7-dinitro-2,3-dihydroxyquinoxaline (6,7-DN-2,3-DHQ).

The results of the elemental chemical analysis (Table 1) and of the molar electrical conductivity measurements indicate the following formulas of the obtained complexes: [Ni(2,3-DHQ)], $[(C_4H_9)_4N]$[Ni(6-N-2,3-DHQ$)_2$], $[(C_4H_9)_4N]$[Ni(6,7-DN-2,3-DHQ$)_2$], Ni(2-A-3-MM-1,4-NQ$)_2$], [Ni(2-H-3-MM-1,4-NQ$)_2$] and [Ni(2,3-DA-1,4-NQ$)_2$].

TABLE 1

Elemental chemical analysis

Compound	Analysed element			
	C% Calcd/Found	H% Calcd/Found	N% Calcd/Found	Ni% Calcd/Found
$[Bu_4N]$ [Ni(6-N-2,3-DHQ$)_2$]	54.05	5.90	13.78	8.25
	53.65	6.02	13.51	8.91
$[Bu_4N]$ [Ni(6,7-DN-2,3-DHQ$)_2$]	47.98	4.99	7.33	7.33
	46.31	4.83	7.52	7.52
[Ni(2-A-3-MM-1,4-NQ$)_2$]	50.61	3.06	5.36	11.24
	50.93	2.85	4.94	11.12
[Ni(2,3-DA-1,4-NQ$)_2$]	55.74	2.75	12.99	13.62
	54.88	3.12	12.01	13.29
[Ni(2-H-3-MM-1,4-NQ$)_2$]	52.95	3.20	S% 12.84	11.76
	52.92	3.36	11.40	11.61

The infrared spectra show important changes between 3000 and 3500 cm^{-1}, a region comprising vibration frequencies characteristic of the —OH and —NH_2 groups, which are directly involved in the coordination process (Table 2).

The bands located at 3070 and 3300 cm^{-1}, disappear in the $[Ni-O_4(6)]^-$ — and $[Ni-O_4(6,7)]^-$ — type ([Ni(6-N-2,3-DHQ$)_2]^-$ and [Ni(6,7-DN-2,3-DHQ$)_2]^-$), nitro-substituted monoanionic complexes, but a new band, nonexisting in the spectrum of the free ligand, appears at 3400 cm^{-1} (it was assigned to unassociated OH). This indicated that the complexed ligand could partly exist in a semiquinonic type of oxidation state.

TABLE 2

IR spectra

Compound	ν_{OH}	ν_{NH}	$\nu_{C=O}$	$\nu^{ske}_{C=C}$	$\nu^{asym}_{NO_2}$	$\nu^{sym}_{NO_2}$	ν_{C-N} C=N	$\nu^{ske}_{C=C}$	ν^{benz}_{H}	ν_{2CH} rocking	ν_{4CH} rocking	$\nu_{C=S}$
[Ni(2,3-DHQ)]	—			1555 i			1260 i	1155 w 1480 i	760 m			
[Ni(6-N-2,3-DHQ)$_2$]	—			1620 w	1525 vi	1310 vi	1260 sh		750 i 760 m	835 m		
[Ni(6,7-DN-2,3-DHQ)$_2$]	—			1615 w	1520 vi	1535 vi	1260 sh	1130 w 1452 sh	730 i	850 i	760 w	
[Ni(2-H-3-MM-1,4-NQ)$_2$]	—		1660 vi 1670 vi	1590 i				1150 i 1480 w	710 vi		740 w	680 i
[Ni(2-A-3-MM-1,4-NQ)$_2$]		3310 w 3410 w	1670 i	1585 i			1278 vi	1145 w 1452 w	730 vi	865 w	758 w	670 w
[Ni(2,3-DA-1,4-NQ)$_2$]		3320 i	1665 vi	1585 i					700 vi	855 w		

vi = very iutense, i = intense, m = medium, sh = shoulder, w = weak

In the case of the [Ni—N_4] — type complex with naphthoquinonic ligands ([Ni(2,3-DA-1,4-NQ)$_2$]), the bands located at 3380 and 3470 cm^{-1}, characteristic of the primary arylamino group, disappear and a new band appears at 3320 cm^{-1}, characteristic of the N—H bond (secondary amine); this fact supports the formula advanced by Holm *et al.* [10] for this type complexes.

In the case of the [Ni-O_2S_2]° — type complex ([Ni(2-H-3-MM-1,4-NQ)$_2$]), the disappearance of the 3400 cm^{-1} vibration frequency of the O—H bond can be noticed. The strong vibration bands located at 3330 and 3442 cm^{-1} in the spectrum of the ligand are smoothed out and shifted to 3310 and 3410 cm^{-1}, respectively, in the spectrum of the [Ni—N_2S_2]° — type complex ([Ni(2-A-3-MM-1,4-NQ)$_2$]).

The electronic spectra exhibit three bands between 11,000 and 30,000 cm^{-1}. The first band is located at about 11,000 cm^{-1} and is assigned to a spin-forbidden transition. The second appears in the range 15,000—25,000 cm^{-1} and is assigned to the $^1A_{2g} \leftarrow {}^1A_{1g}$ transition. The third band appears between 23,000—30,000 cm^{-1} and is assigned to the $^1B_{1g} \leftarrow {}^1A_{1g}$ transition or to a charge transfer transition. For the Ni(II) complexes with quinoxalinic and naphthoquinonic ligands, the frequencies of these transitions are shown in table 3. The position of the second and third bands supports the square-planar conformation of these complexes, except for the dinitrosubstituted compound, in which a slight tetrahedral distortion can be noticed (Figure 1).

TABLE 3

Electronic spectra

Compound	Transition (cm^{-1})		
	ν_1	ν_2	ν_3(TS)
[Ni(6-N-2,3-DHQ)$_2$]$^-$		14500 w	24500 i
[Ni(6,7-DN-2,3-DHQ)$_2$]$^-$	13500 sh 13000 sh 10600 w	14300 w	27000 i (+NO_2)
[Ni(2,3-DA-1,4-NQ)$_2$]		20200 m	27200 shw
[Ni(2-H-3-MM-1,4-NQ)$_2$]		24500 shm	27400 shm
[Ni(2-A-3-MM-1,4-NQ)$_2$]	12500 i	20800 m	26200 shm

Strong ESR spectra were obtained for four of the nickel compounds. The complex with the unsubstituted dihydroxyquinoxaline exhibited a weak singlet, having the g factor close (2.0023) to that of the free electron which means that this compound is paramagnetic. The [Ni—N_4] — type complex has a signal with pronounced asymmetry and 3rd order anisotropy (Figure 2.3). This indicates a distortion from the square-planar conformation. The [Ni-N_2S_2] — type compound has a spectrum consisting of three components (Figure 2.2). It is suggested that the first two components (g_{II}, $g_{\perp}$) originate in the splitting of the unpaired electron in the axial symmetry field of the complex, while the third is the result of the donor-acceptor – type strong interaction between ligands and the central ion ($g_i = 2.0022$). The $[Ni-O_2S_2]^\circ$ – type complex has a weaker spectrum, having nevertheless a hyperfine structure, discernible only in less common cases (Figure 2.1). This splitting into five hyperfine components with the intensity ratio 1 : 4 : 6 : 4 : 1, is due to the interaction with four equivalent protons of the ligand. This signal supports the definition proposed by Holm *et al.* [10] for these complexes as "free radicals stabilized through cations". The ESR parameters are given in table 4.

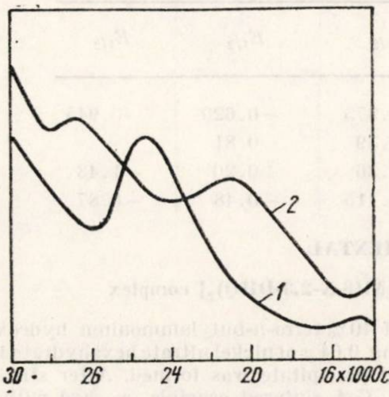

Fig. 1 – Electronic spectra:
1. $[Ni(6\text{-}N\text{-}2,3\text{-}DHQ)_2]^-$;
2. $[Ni(2\text{-}A\text{-}3\text{-}MM\text{-}1,4\text{-}NQ)_2]$

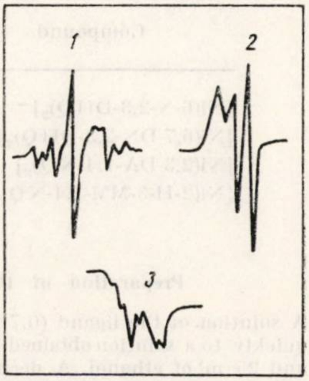

Fig. 2 – ESR spectra:
1. $[Ni(2\text{-}H\text{-}3\text{-}MM\text{-}1,4\text{-}NQ)_2]$;
2. $[Ni(2\text{-}A\text{-}3\text{-}MM\text{-}1,4\text{-}NQ)_2]$;
3. $[Ni(2,3\text{-}DA\text{-}1,4\text{-}NQ)_2]$

TABLE 4

ESR parameters

Compound	g_1 $g_{\parallel}$	g_2 $g_{\perp}$	g_3	$<g>$	g_i	A_T gauss
$[Ni(2\text{-}A\text{-}3\text{-}MM\text{-}1,4\text{-}NQ)_2]$	2.0618	2.0175	–	2.0323	2.0022	97.90
$[Ni(2\text{-}H\text{-}3\text{-}MM\text{-}1,4\text{-}NQ)_2]$	2.0058	2.0044	–	2.0049	2.0044	201.31
$[Ni(2,3\text{-}DA\text{-}1,4\text{-}NQ)_2]$	2.0767	2.0516	2.0025	2.0436		161.52

The polarographic study of the monoanionic complex combinations suggests the existence of a species with the charge $z = -2$. The neutral complexes were reduced in two steps at the dropping mercury electrode, which indicates two species with $z = -1$ and 0.

The other observed waves are due to the reduction of the ligands The data collected in connection with these complexes show that, aside from participating in electron transfer reactions, the evidenced species can also be obtained chemically, because the half-wave potentials range between +0.95 and −0.95 V, a region in which oxidizing or reducing agents do not break up the complex.

TABLE 5

Polarographic data (Volts)

Compound	$E_{1/2}$	$E_{1/2}$	$E_{1/2}$
$[Ni(6\text{-}N\text{-}2,3\text{-}DHQ)_2]^-$	−0.375	−0.620	−0.945
$[Ni(6,7\text{-}DN\text{-}2,3\text{-}DHQ)_2]^-$	−0.39	−0.81	
$[Ni(2,3\text{-}DA\text{-}1,4\text{-}NQ)_2]$	+0.36	+0.20	−1.43
$[Ni(2\text{-}H\text{-}3\text{-}MM\text{-}1,4\text{-}NQ)_2]$	−0.115	−0.48	−0.87

EXPERIMENTAL

Preparation of the $[Bu_4N]$ $[Ni(6\text{-}N\text{-}2,3\text{-}DHQ)_2]$ complex

A solution of the ligand (0.7 g in 5 ml of 40% tetra-*n*-butylammonium hydroxide) was added quickly to a solution obtained by dissolving 0.64 g of nickel nitrate hexahydrate in 5 ml of water and 25 ml of ethanol. A deep-red colored precipitate was formed. After stirring for 2 hours, the precipitate was filtered through a G-4 sintered crucible, washed with distilled water and alcohol, then dried under vacuum.

The $[Bu_4N]$ $[Ni(6,7\text{-}DN\text{-}2,3\text{-}DHQ)_2]$, $[Ni(2\text{-}A\text{-}3\text{-}MM\text{-}1,4\text{-}NQ)_2]$, $Ni(2\text{-}H\text{-}3\text{-}MM\text{-}1,4\text{-}NQ)_2]$ and $[Ni(2,3\text{-}DA\text{-}1,4\text{-}NQ)_2]$ complexes were obtained analogously.

MEASUREMENTS

The electronic spectra were recorded with a Zeiss Jena VSU-1 spectrophotometer, using spectral grade solvents and a 1.0−cm silica cell. The infrared spectra were obtained on a Zeiss Jena UR-10 spectrophotometer, the samples being pelleted in anhydrous KBr.

The polarograms were recorded with a Model 7−77−4/b Orion KTS polarograph. The half-wave potentials were measured at room temperature, using a calomel reference electrode and a dropping mercury measuring electrode 10^{-3} *M* solutions of the respective complexes were used and, as supporting electrolyte, a 0.1 *M* solution of tetra-*n*-butylammonium perchlorate.

The molar electrical conductivity of the complexes was measured on a Model OK-102/1 Radelkis conductivity-meter, the cell constant being 0.897 cm^{-1}.

The ESR spectra were recorded with an IFA Bucureşti ART−5 spectrometer, working in the X band (9060 MHz) and having a 100 kHz modulation of the magnetic field. The spectra were obtained at room temperature with a Mn^{2+} standard ($g_3 = 2.03584$, $g_4 = 1.98040$ $H_3 = 3179.5$, $H_4 = 3268.5$).

REFERENCES

[1] D. A. McCleverty, *Prog. Inorg. Chem.* **10**, 49 (1968).
[2] A. L. Balch, F. Rohrscheid and R. H. Holm, *J. Amer. Chem. Soc.*, **87**, 2301 (1965).
[3] E. I. Stiefel, J. H. Waters, E. Billig and H. B. Gray, *J. Amer. Chem. Soc.*, **87**, 3016 (1965).
[4] A. L. Balch and R. H. Holm, *J. Amer. Chem. Soc.*, **88**, 5201 (1966).
[5] R. H. Holm, A. L. Balch, A. Davison, A. H. Maki and T. E. Berry, *J. Amer. Chem. Soc.*, **89**, 2866 (1967).
[6] F. Rohrscheid, A. L. Balch and R. H. Holm, *Inorg. Chem.*, **5**, 1542 (1966).
[7] P. A. Wicklund and D. G. Brown, *Inorg. Chem.*, **2**, 396 (1976).
[8] J. Camus and D. Negoiu, *Rev. Roumaine Chim.*, **24**, 673 (1979).
[9] N. Mureşan, V. Mureşan, J. Camus and D. Negoiu, *Rev. Roumaine Chim.*, **24**, 709 (1979).
[10] A. L. Balch, I. G. Dance and R. H. Holm, *J. Amer. Chem. Soc.*, **90**, 1139 (1968).

Revue Roumaine de Chimie, 25, *6*, 845–850 (1980)

SULPHUR-CONTAINING AMINOACID-METAL COMPLEXES. COBALT(II) AND IRON(II) COMPLEXES OF CYSTINE

ANA UNGUREANU and MARIA MARC
Institute of Chemistry, R-3400 Cluj-Napoca, Donath str. 65, Romania

Received June 25, 1979

Co(II) and iron(II)-cystine complexes were prepared and investigated in solid state (infrared and diffuse reflectance spectra, magnetic moment measurements and thermal analysis).

INTRODUCTION

The ability of sulphur-containing aminoacids to form chelate compounds with a large number of metals is of particular interest for the inorganic chemistry of biological processes. The transition metal complexes of these aminoacids may serve as models for biologically important metal-containing molecules and their investigation may contribute to the understanding of redox and of other metal-protein biological processes. This explains the large number of such complexes investigated, particularly with cysteine and methionine.

Less investigated were the cystine complexes. [1–14] While this work was in progress, some cobalt-cystine complexes have been mentioned in the recent literature. [11,12] In this paper we report the isolation of Co(II) and iron(II)-cystine complexes and the results of their physico-chemical investigation.

EXPERIMENTAL

Analytical grade reagents were used for the preparation of complexes. Infrared spectra were recorded on a UR–10 Carl Zeiss Jena (DDR) spectrophotometer and diffuse reflectance spectra on a VSU C. Zeiss Jena instrument. Thermal analysis was carried out with an OD – 102 Derivatograph (MOM Budapest). Magnetic moments were determined with a Gouy balance. The metals were determined gravimetrically : cobalt(II) as a complex with α-nitroso-β-naphthol and iron as Fe_2O_3.

Preparation of the cobalt(II)-cystine complex

An amount of 1.2 g (5 mmole) L-cystine, dissolved in 100 ml NaOH 0.1 N was treated, under stirring, with small portion of a solution, containing 1.9 g (5 mmole) $CoCl_2 \cdot 6H_2O$ in

50 ml water. The solutions were stirred for one hour, when a reddish precipitate was formed. The supernatant solution had a pH value between 7–8.5. The precipitate was filtered off, washed with diluted NaOH solution (pH = 8) then with distilled water and alcohol, and dried in a desiccator, over phosphorus pentoxide. In order to avoid the contamination of the complex with cobalt hydroxide, a slight excess of cystine was used.

Analysis : Found Co 19.35, C 22.00, H 3.91, N 9.06, S 19.85 ; $C_6H_{10}CoN_2O_4S_2 \cdot H_2O$ requires : Co 18.66, C 22.84, H 3.80, N 8.88 and S 20.30%.

The analytical data support the 1 : 1 combination ratio between cobalt(II) and cystine.

Preparation of the iron(II)-cystine complex

The iron(II) complex was prepared as above, with some additional precautions, in order to avoid oxidation to iron(III). Thus, 1.2 g (5 mmole) L-cystine, dissolved in 100 ml NaOH 0.1 N, was treated with a solution obtained by dissolving 1.3 g $FeSO_4 \cdot 7H_2O$ in 50 ml degased water (by bubbling a stream of nitrogen). A protecting nitrogen atmosphere was provided throughout. An offwhite precipitate was deposited from the solution, at pH 7–8.5. The precipitate was washed with ethanol and dried in a desiccator, over phosphorus pentoxide. The precipitate was oxygen-sensitive and was readily converted to brown iron(III) hydroxide, if the contact with atmospheric oxygen was not avoided. Therefore, all operations were carried out under nitrogen. The complex is stable only in dry, solid state.

Analysis : Found Fe 18.85, C 24.03, H 3.85, N 9.40, S 20.92 ; $FeC_6H_{10}N_2O_4S_2$ requires : Fe 18.98, C 24.47, H 3.39, N 9.51 and S 21.74%.

The analytical data suggest a 1 : 1 combination ratio between iron(II) and cystine.

Both complexes were insoluble in water and common organic solvents (ethanol, acetone, chloroform, benzene). They were decomposed by alkaline solutions (pH > 10) with formation of the metal hydroxide and the alkali metal salt of cystine. Dilute acids also decomposed the complexes with formation of the respective metal salts and cystine.

Because of their insolubility, the two complexes were investigated only in solid state (infrared and diffuse reflectance spectra, magnetic moment measurements and thermal analysis). The compounds were roentgenographically amorphous.

RESULTS AND DISCUSSION

Electronic spectra and magnetic moments

Diffuse reflectance spectra and magnetic moment measurements were used to establish the coordination environment of the metal. The electronic spectrum of the cobalt(II) complex (Figure 1) exhibits a band at ~ 20 kK with a shoulder at ca 18 kK, and a weaker band at ca 8 kK.

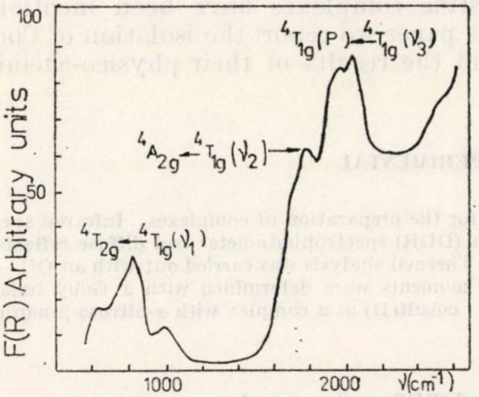

Fig. 1 — The electronic spectrum of the Co(II)-cystine complex.

These data suggest that the cobalt atom is six-coordinated, the spectrum being similar to that of $/Co(H_2O)_6/^{2+}$ and to other spectra of six-coordinated cobalt(II) complexes.[15]
According to literature data[16-21] the ν_1 band at ca 8 kK is due to a ${}^4T_{2g} \leftarrow {}^4T_{1g}$ transition, while the 20 kK band (ν_3) is due to a ${}^4T_{1g}(P) \leftarrow {}^4T_{1g}$ transition. The shoulder at ~ 18 kK may be the $\nu_2({}^4A_{2g} \leftarrow {}^4T_{1g})$ transition, which is sometimes difficult to observe.[21]

The coordination number is further confirmed by the magnetic moment $\mu = 4.8$ B.M, in agreement with literature data[22,23] which give values between 4.5 and 5.2 B.M. for six-coordinated high spin cobalt (II) complexes.

The spectrum of the iron(II)-cystine complex exhibits a broad band, between 6.5 and 8.1 kK, which shows some splitting with maxima at ca 6.5—7 kK and 7.8—8.1 kK. In agreement with literature data[24] this spectrum suggests octahedral coordination of iron(II), the absorption being due to an ${}^5E_g \leftarrow {}^5T_{2g}$ transition.

The magnetic moment found for the iron(II)-cystine complex $\mu = 5.1$ B.M. supports the octahedral coordination, since literature values for six-coordinate iron(II) complexes are in the range from 5.1 to 5.7 B.M.[22]

Infrared spectra

A comparison of the infrared spectra of complexes with those of free cystine, affords some information about the functional groups involved in coordination. The data are shown in table 1. The infrared spectral data suggest that the ligand is attached to the metal through the nitrogen atoms of the two amino groups and through the carboxylic oxygens. Thus, the absence of the cystine bands at 1500 and 1635 cm^{-1} ($\delta\ NH_3^+$) from the spectra of complexes and the splitting to the amino group stretching vibration indicate the bonding of the amino group to the metal. A shift of the ν NH bands of complexes compared with the lithium salt (in which there are free NH_2 groups)[25] supports the above conclusion.

TABLE 1

Some infrared spectral bands of cystine and its complexes (cm^{-1})

Compound	ν—COO⁻		Δν	δNH		νNH	
	sym.	asym.		sym.	asym.	sym.	asym.
Cystine	1418 s	1595 s	177	1500 s	1635 s	3030 br	
Co(II)-Cystine	1410 s	1610 s	200	absent		3280 m	3345 m
Fe(II)-Cystine	1409 s	1615 s	206	absent		3285 m	3345 m
							3365 m

The involvement of the carboxylic groups in metal bonding is suggested by the shift of ν_{asym} COO$^-$ towards higher frequencies and of ν_{sym} COO$^-$ towards lower frequencies, compared with the spectrum of free cystine. The magnitude of this shift ($\Delta\nu$) also gives some information about the strength of the M—O bond. [26,27] The spectral data can be rationalized in terms of a polymeric structure, involving bridging carboxylate groups and metal-nitrogen bonds, as shown in figure 2.

Similar structures, involving asymmetric carboxylato bridges have been previously reported for zinc and cadmium glycine complexes [28] as well as for some complexes of norleucine, methionine,[29] ethionine and S-methyl-cysteine [30] with divalent metals (Mn, Co, Ni, Cu, Zn, Cd). X-ray diffraction data on some aminoacid-metal complexes [28] have shown that these ligands may use the COO site either as monodentate or as bridging groups. When the carboxylato group is monodentate, hydrogen bonding with amine group occurs, which can be recognized in infrared spectra [29].

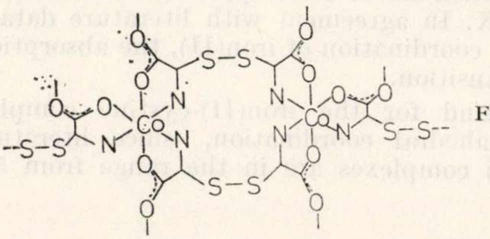

Fig. 2 — The probable structure of the Co(II)-cystine complex.

The well resolved sharp bands of NH_2 groups in the spectra of the cobalt(II) and iron(II) complexes prepared in this work, suggest the lack of hydrogen bonding, and therefore bidentate (bridging) coordination of COO groups.

It seems that the participation of the —S—S— group in coordination is unlikely, although this possibility cannot be either demonstrated or refuted on the basis of infrared spectra. This group absorbs in the range 400—700 cm^{-1} but assignments are uncertain. Some authors [29] assign a band at 540 cm^{-1}, other authors [30] at 454 cm^{-1} to this absorption. A weak band at 615 cm^{-1} is due to (—S) groups. In the IR spectra of cobalt(II) and iron(II)-cystine complexes, these bands were present and in addition, bands at 585 and 650 cm^{-1} were also observed.

Thermal decomposition

The results of the thermogravimetric analysis of the two complexes are given in tables 2 and 3.

The cobalt complex decomposes at ca 230°C and the iron complex around 180°C. The cobalt complex contains one water molecule per formula unit, which is lost before ca 150°C. The amount of oxide residues (Co_3O_4 and Fe_3O_4, respectively) is in agreement with the 1:1 metal: ligand combination ratio in the complexes investigated here.

TABLE 2

The thermal decomposition of the cobalt(II)-cystine complex

Temperature range °C	TG (% weight loss)		DTA, °C		Process
	Calcd	Found	Exothermic	Endothermic	
60–200	5.70	5.60		150	$Co.Cys.H_2O \xrightarrow[-H_2O]{} Co.Cys.$
200–320	50.12	50.0	270		$2Co.Cys. \xrightarrow{+O_2} Co_2S_3 + S + H_2O + CO_2 + NO$
			400		$S + O_2 \rightarrow SO_2$
320–960	20.35	20.50	590		$Co_2S_3 + O_2 \rightarrow Co_2(SO_4)_3$
				900	$Co_2(SO_4)_3 \rightarrow Co_3O_4 + SO_2$

TABLE 3

The thermal decomposition of the iron(II)-cystine complex

Temperature range °C	TG (% weight loss)		DTA, °C		Process
	Calcd	Found	Exothermic	Endothermic	
20–220			180–220		$Fe(II) \cdot Cys. \rightarrow Fe_2S_3 + S + H_2O + CO_2 + NO$
220–600	73.72	74.00	400		$S + O_2 \rightarrow SO_2$
			520		$Fe_2S_3 + O_2 \rightarrow Fe_2(SO_4)_3$
600–800				700	$Fe_2(SO_4)_3 \rightarrow Fe_3O_4 + SO_2$

CONCLUSIONS

L-Cystine forms six-coordinated complexes with Co(II) and Fe(II) in 1 : 1 metal-ligand combination ratio. Cystine molecule is attached to the metal through the nitrogen atoms of the two amino groups and through the carboxylic oxygens, presumably in a polymeric structure. Co(II) and Fe(II)-cystine are high spin complexes.

REFERENCES

[1] P. Rây and A. Bhaduri, *J. Indian Chem. Soc.*, **27**, 297 (1950).

[2] R. C. Wickery, *J. Chem. Soc.*, **1950**, 2058.

[3] A. Popa-Rang and R. Ralea, *Ann. Științ. Univ. "Al. I. Cuza", Iași Sect. 1C*, **10**, 145 (1964).

[4] S. N. Poddar and D. H. Biswas, *Sci. Cult (Calcutta)*, **31**, 189 (1965); *Chem. Abstr.*, **63**, 15549 (1965).

[5] A. Popa-Rang and S. Fişel, *Ann. Ştiint. Univ. "Al. I. Cuza" Iaşi Sect.* 1C, **17,** 27 (1971).

[6] H. Kahler, B. J. Lloyd and M. Eden, *J. Phys. Chem.*, **56,** 768 (1952).

[7] O. Dobozi, F. Guba and T. Mándy, *Magyar Kém. Folyóirat*, **68,** 1 (1962).

[8] C. J. Hawkins and D. D. Perrin, *Inorg. Chem.*, **2,** 843 (1963).

[9] P. Saland and K. Kloss, *Nature*, **163,** 565 (1949).

[10] V. Carassiti and L. Moggi, *Ann. Chim. (Rome)*, **50,** 602 (1960).

[11] R. J. Gale and C. A. Winkler, *Inorg. Chim. Acta*, **21,** 151 (1977).

[12] W. G. Jackson, A. M. Sargeson and P. A. Tucker, *J. Chem. Soc., Chem. Comm.*, **1977,** 199.

[13] Shiro Kominami, P. Riesz, Toshiyuki Akiyama and J. V. Silverton, *J. Phys. Chem.*, **80,** 203 (1976).

[14] H. Guntner, K. E. Schwarzhans, *Z. Naturforsch, B. Anorg. Chem., Org. Chem.*, **31** B 448 (1976).

[15] C. Y. Balhausen and C. K. Jorgensen, *Acta Chem. Scand.*, **9,** 397 (1955).

[16] A. B. P. Lever, "Inorganic Electronic Spectroscopy", Elsevier, Amsterdam 1968, p. 318.

[17] J. Ferguson, D. L. Wood and K. Knox, *J. Chem. Phys.*, **39,** 881 (1963).

[18] A. B. P. Lever, *Inorg. Chem.*, **4,** 1042 (1965).

[19] A. B. P. Lever and D. Ogden, *J. Chem. Soc. (A)*, **1967,** 2041.

[20] R. L. Carlin "Transition Metal Chemistry", vol. 1, E. Arnold and M. Dekker, New York 1965 p. 3.

[21] A. B. P. Lever, "Inorganic Electronic Spectroscopy", Elsevier, Amsterdam 1968, p. 118.

[22] M. N. Hüghes, "The Inorganic Chemistry of Biological Processes", Wiley, London 1974, p. 48.

[23] R. L. Carlin, "Transition Metal Chemistry" vol. 1, E. Arnold and M. Dekker, New York 1965, p. 21.

[24] A. B. P. Lever, "Inorganic Electronic Spectroscopy", Elsevier, Amsterdam 1968, p. 299.

[25] J. P. Casey and R. Bruce Martin, *J. Amer. Chem. Soc.*, **94,** 6141 (1972).

[26] N. Nakamoto, M. Marimoto and A. E. Martel, *J. Amer. Chem. Soc.*, **83,** 4528 (1961).

[27] L. J. Bellamy "The infra-red spectra of complex molecules", London 1960, p. 174–176.

[28] B. W. Low, F. L. Hirshfeld and F. M. Richards, *J. Amer. Chem. Soc.*, **81,** 4412 (1959).

[29] C. A. Mc Auliffe, J. V. Quagliano and L. M. Vallarino, *Inorg. Chem.*, **5,** 1996 (1966).

[30] S. E. Livingstone and J. D. Nolan, *Inorg. Chem.*, **7,** 1447 (1968).

Revue Roumaine de Chimie ,25, *6*, 851–854 (1980)

EFFECT OF FOREIGN IONS ON THE REACTION BETWEEN BROMIDE ANION AND PERSULPHATE ANION IN AQUEOUS SYSTEM

M. S. SUBHANI*

Department of Chemistry, University of Nigeria, Nsukka

Received July 2, 1977
Revised March 30, 1979

The reaction rate of the bromide and persulphate anions depends on the nature and charge of the foreign ions present in solution. According to their accelerating effect the cations form the following series : Li^+, Na^+, K^+, Cs^+, Zn^{2+} and Al^{3+} : their respective relative capacities are 1, 0, 3.0, 3, 83, 4.33, 21.66 and 31.66. The anions (PO_4^{3-}, SO_4^{2-}, Cl^-) retard the reaction as the charge on the added anions increases.

INTRODUCTION

When bromide anion reacts with persulphate anion at natural pH, the bromide ion gets oxidized by the persulphate ion, [1] according to the following mechanism

$$Sr^- + S_2O_8^{2-} \dashrightarrow BrSO_4^- + SO_4^{2-} \qquad (1)$$

$$Sr^- + BrSO_4^- \dashrightarrow Br_2 + SO_4^{2-} \qquad (2)$$

Reaction (1) is said to be the rate determining step and thus a bimolecular second order reaction.

Various workers [2,3] have carried out studies of the accelerating effect on the reaction rate between inorganic anions.

In the present work studies are made on the rate of reaction between Br^- and persulphate anions in presence of added foreign salts such as alkali chlorides, zinc chloride, aluminium chloride as well as sodium sulphate and sodium phosphate.

---

* *Present Address:* Department of Chemistry, Faculty of Science, Garyounis University, P.O. Box. 9480 Benghazi, Libya.

EXPERIMENTAL

All chemicals used were of either Analar grade or purified by recrystallization.

All solutions were prepared in triply distilled water just before the start of the experiment. UNICAM SP 500 Spectrophotometer was used for the absorption measurements as described elsewhere.[1], [4] The extinction coefficient for the bromine was determined at 50°C in solution and the value obtained was 380 5 $M^{-1}CM^2$.

A Thermostat attachment Haake Model NK22 was used to maintain a temperature of 50 ± 0.1°C throughout the experiments.

Foreign salts were introduced into the reaction mixture during the preparation of the mixture. 10^{-2} M Na_2S_2O and 5×10^{-2} M NaBr was used throughout the experiments.

RESULTS AND DISCUSSIONS

As can be seen from table 1 and figure 1 the reaction between the bromide anions and persulphate anion in aqueous solution in presence of foreign salts proceeds more rapidly, the greater the concentration of the salts and of the charge on the cation of the added salt. The slope of the straight line, shown in figure 1, was arbitrarily adopted as a measure of the accelerating capacity of a given cation. According to their accelerating capacity, the cations investigated resulted in the following series.

Added cations	d log $K/d\mu$
Li^+	0.05
Na^+	0.18
K^+	0.23
Cs^+	0.26
Zn^{2+}	1.3
Al^+	1.9

It may be assumed that the cations accelerate the reaction between the anions Br^- and $S_2O_8^{2-}$ because within the positive field it enables anions to approach one another as closely as it is necessary for the interaction.

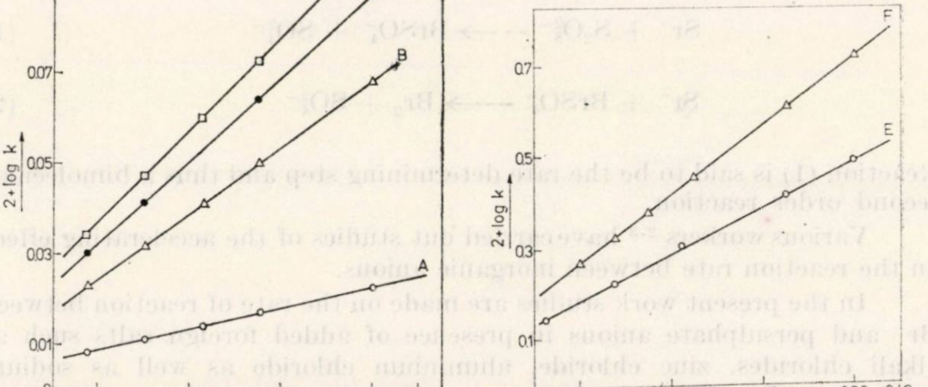

Fig. 1 — Dependence of logarithm of reaction rate constant between Br^- and $S_2O_8^{2-}$, at 50°C, on ionic strength of the solution as determined by the added salts. Effect of cations : A(Li^+), B(Na^+), C(K^+), D(Cs^+), E(Zn^{2+}), F(Al^{3+}).

This interaction is more effective the stronger the positive field of the cation.

It is necessary to take into account the fact that the result of the interaction of cations with water molecules, which has been shown above, apparently reflects the effect of hydration on the resultant field of the monovalent cations. In the case of divalent zinc and trivalent aluminium cations the effect is so large that it is customarily called as a catalytic effect.

TABLE 1

Experimental values of the specific rate constant *(k)* liter mole^{-1} sec^{-1} in presence of different cations

log *k*	Ionic strength	Cation
$\bar{2}.0228$	0.38	Li^+
$\bar{2}.0168$	0.28	Li^+
$\bar{2}.0138$	0.23	Li^+
$\bar{2}.0108$	0.18	Li^+
$\bar{2}.0078$	0.13	Li^+
$\bar{2}.0684$	0.38	Na^+
$\bar{2}.0504$	0.28	Na^+
$\bar{2}.0414$	0.23	Na^+
$\bar{2}.0324$	0.18	Na^+
$\bar{2}.0234$	0.13	Na^+
$\bar{2}.0874$	0.38	K^+
$\bar{2}.0644$	0.28	K^+
$\bar{2}.0529$	0.23	K^+
$\bar{2}.0414$	0.18	K^+
$\bar{2}.0299$	0.13	K^+
$\bar{2}.4942$	0.38	Zn^{2+}
$\bar{2}.4166$	0.32	Zn^{2+}
$\bar{2}.2990$	0.23	Zn^{2+}
$\bar{2}.2210$	0.17	Zn^{2+}
$\bar{2}.1430$	0.11	Zn^{2+}
$\bar{2}.7218$	0.38	Al^{3+}
$\bar{2}.6086$	0.32	Al^{3+}
$\bar{2}.4562$	0.24	Al^{3+}
$\bar{2}.3238$	0.17	Al^{3+}
$\bar{2}.2666$	0.14	Al^{3+}
2.0988	0.38	Cs^+
$\bar{2}.0728$	0.28	Cs^+
$\bar{2}.0598$	0.23	Cs^+
$\bar{2}.0468$	0.18	Cs^+
$\bar{2}.0338$	0.13	Cs^+

On the basis of the above assumption it would be expected that the multivalent anions should inhibit the reaction.

These expectations have indeed been confirmed by the experimental results obtained as shown in figure 2 and are summarized in table 2.

TABLE 2

Experimental values of the specific rate constant *(k)* liter mole^{-1} sec^{-1} in presence of different anions.

log *k*	Ionic strength	Anion
$\bar{2}.0494$	0.38	So_4^{2-}
$\bar{2}.0364$	0.28	So_4^{2-}
$\bar{2}.0299$	0.23	So_4^{2-}
$\bar{2}.0234$	0.18	So_4^{2-}
$\bar{2}.0169$	0.13	So_4^{2-}
$\bar{2}.0304$	0.38	Po_4^{3-}
$\bar{2}.0224$	0.28	Po_4^{3-}
$\bar{2}.0184$	0.23	Po_4^{3-}
$\bar{2}.0144$	0.18	Po_4^{3}
$\bar{2}.0104$	0.13	$Po_4^{3}-$
$\bar{2}.0684$	0.38	Cl^-
$\bar{2}.0504$	0.28	Cl^-
$\bar{2}.0414$	0.23	Cl^-
$\bar{2}.0324$	0.18	Cl^-
2.0234	0.13	Cl^-

Sodium phosphate accelerates the reaction between the bromide and phosphate anions in a noticeably smaller degree than sodium chloride; the sulphate anions occupy in this respect, an intermediate position.

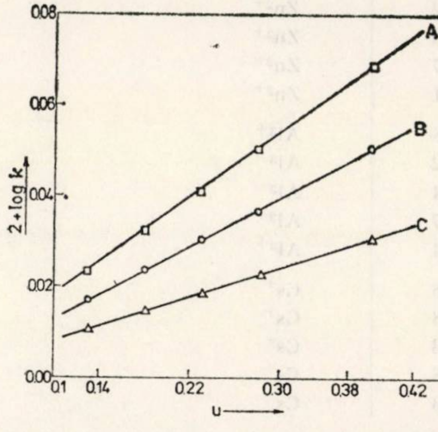

Fig. 2 — Dependence of logarithm of reaction rate constant between Br$^-$ and $S_2O_8^{2-}$, at 50°C, on ionic strength of the solution as determined by the added salts. Effect of Anions : A(Cl$^-$), B(SO_4^{2-}), C(PO_4^{3-}).

REFERENCES

1. M. S. Subhani and T. Kauser, *Pak. J. Sci. Ind. Res*; **18,** 208 (1975).
2. M. R. Kershow and J. E. Prus, *Trans. Farady Sec.*, **63,** 1198 (1967).
3. A. Indelli, V. Bartocci, F. Ferranti and M. G. Lugarelli, *J. Chem. Phys.*, **41,** 2069 (1966)
4. M. S. Subhani and M.N.H.A. Lacewala, *J. Sci. and Mathem*, **1,** 41 (1974).

Revue Roumaine de Chimie, **25**, *6*, 855–859 (1980)

ELECTROSTATIC CONTRIBUTIONS TO THE THERMODYNAMIC FUNCTIONS IN THE FORMATION OF TRANSITION STATE FOR THE REACTION BETWEEN Br_2^- AND BrO^-

M. S. SUBHANI

Department of Chemistry, University of Nigeria, Nsukka,

Received March 21 1978

Studies were carried out using different dielectric media and varying ionic strength for the reaction between Br_2^- and BrO^- in solution. From the plot of $\log k_0$ and $1/D$ the values of $r^{\neq}$ and r_{AB} were obtained for the activated complex ($Br_2 - BrO.^{2-}$) In comparison with the theoretical values the double sphere model was found to be the most suitable model for the activated state formed in this reaction. Electrostatic contributions to the changes in thermodynamic functions $\Delta G_{es}^{\neq}$, $\Delta S_{es}^{\neq}$ and $\Delta H_{es}^{\neq}$, in the formation of transition state were also evaluated.

INTRODUCTION

Various studies were carried out to observe the effect of dielectric constant and ionic strength on reaction between stable inorganic ions [1–8] and a number of models were proposed for the transition state formed during the course of reaction due to the rearrangement of the total charge of the ions on the activated complex thus formed [9–11]. Expressions relating the rate constant at zero ionic strength (k_0) to the dielectric constant (D) for a single sphere model and a double sphere model for the activated state are (1) and (2)

$$\log k_0 = \log k_i^i - \frac{e^2}{4\cdot 606\, DKT}\, \frac{(Z_A + Z_B)^2}{r^{\neq}} - \frac{Z_A^2}{r_A} - \frac{Z_B^2}{r_B} \qquad (1)$$

$$\log k_0 = \log k_i - \frac{Z_A Z_B}{2\cdot 303\, DKTr_{AB}} \qquad (2)$$

respectively.

The electrostatic contributions to the changes in free energy of activation for a single sphere and double sphere model are given in expressions (3) and (4)

$$\Delta G_{es}^{\neq} = \frac{Ne^2}{D}\, \frac{(Z_A + Z_B)^2}{r^{\neq}} - \frac{Z_A^2}{r_A} - \frac{Z_B^2}{r_B} 1 \qquad (3)$$

$$\Delta G_{es}^{\neq} = \frac{NZ_A Z_b^{e^2}}{Dr_{AB}} \qquad (4)$$

respectively.

where K_i is the rate constant at infinite dielectric constant, k the Boltzman constant, Z_A, Z_B, r_A, r_B are the charges and radii of the ions A and B, respectively and $r^{\neq}$ and r_{AB} are the radii of the activated complex in single and double sphere, respectively.

Electrostatic contributions to the entropy of activation and that of enthalpy of activation in the formation of an activated complex of a given ionic reaction can be obtained using equations (3) and (4) and the other well-established thermodynamic relationships available in the literature.

The purpose of the present work is to apply these models to the fast reaction involving ion such as BrO^- and radical anion, Br_2^-, and to establish the shape of the activated complex formed between Br_2^- and BrO^-, a second order reaction,[12] with a rate determining step

$$Br_2^- + BrO^- \longrightarrow BrO + 2Br^- \tag{5}$$

as no such studies for the fast reaction have previously been reported in literature. It was also of interest to determine electrostatic contributions to the changes in thermodynamic functions for the formation of activated state from their reactant state.

EXPERIMENTAL

All chemicals used were of analar grade and were used without further purification. Sodium hypobromite solutions were prepared by adding the required volume of bromine water to a cold solution of sodium hydroxide. This solution was freshly prepared when irradiated. All solutions were prepared in triply distilled water and saturated with Ar gas, just before irradiation, by the usual bubbling procedure described elsewhere [13].

Flash photolysis set up, used for the production of Br_2^-, was similar to that described elsewhere[14].

Kinetic spectroscopic techniques were used to study the rate of reaction at wave length 360 nm. BrO radical also absorbs at this wavelength, but the molar extinction coefficient for Br_2^- is tenfold greater[15] and a correction for the absorption due to BrO radical is applied to the observed optical density before evaluating graphically the rate constant for. the reaction between Br_2^- and BrO^-.

Dielectric constants measurements for various alcohol – water mixtures (ranging from 10% to 45%) were made by the method described elsewhere.

RESULTS AND DISCUSSIONS

The experimental values of the specific rate constant measured on flash photolysis of bromide-hypobromide system at various ionic strengths and different dielectric constants of the solutions were determined and are shown in Table 1.

The values of the specific rate constant at zero ionic strength were determined from the plots of the graph between log k and square root of ionic strength (U), at a given dielectric constant and extrapolation to zero ionic strength as established in eq (6)

$$\log k = \log k_0 + AZ_AZ_B U \tag{6}$$

TABLE 1

The values of the rate constants for the reaction of $Br_2^- + BrO^-$ at various ionic strengths and at different dielectric constants

$[BrO^-] = 10^{-4}$ M ; $[Br^-] = 10^{-4}$ M

$K \times 10^7$	μ	D	$K \times 10^7$	μ	D
7.89	0.01	79.8	7.36	0.03	65.5
8.32	0.015	79.8	8.01	0.04	65.5
8.69	0.02	79.8	8.61	0.05	65.5
9.37	0.03	79.8	4.46	0.01	56.3
9.98	0.04	79.8	4.87	0.015	56.3
10.72	0.05	79.8	5.26	0.02	56.3
6.81	0.01	72.1	5.97	0.03	56.3
7.24	0.015	72.1	6.64	0.04	56.3
7.62	0.02	72.1	7.28	0.05	56.3
8.32	0.03	72.1	3.40	0.01	49.2
8.95	0.04	72.1	3.79	0.015	49.2
9.55	0.05	72.1	4.15	0.02	49.2
5.83	0.01	65.5	4.85	0.03	49.2
6.27	0.015	65.5	5.52	0.04	49.2
6.65	0.02	65.5	6.18	0.05	49.2

where A is a constant at a given temperature and dielectric constant of the medium. The values of $\log k_0$ obtained from the intercepts of the straight lines, on plotting $\log k$ against U, on extrapolation to zero ionic strength, are shown in Table 2.

A graph was plotted between $\log k_0$ and reciprocal of dielectric constant (1/D) which resulted in a fairly good straight line (See Fig. 1), thus satisfying equations (1) and (2). From the slope of the straight line thus obtained, the values of $r^{\neq}$ and r_{AB} were evaluated using equation (1) and (2). The values are summarized in Table 3.

TABLE 2

The values of rate constants at zero ionic strength and reciprocal of dielectric constants for the reaction between

$Br_2^- + BrO^-$; $T = 298$ K

$\log k_0$	$1/D \times 10^3$
7.795	12.53
7.714	13.87
7.628	15.27
7.476	17.76
7.320	20.32

TABLE 3

The values of the radii for the activated complex formed between Br_2^- and BrO^- radiical anions and ion, respectively

	Theoretical values	Experimental values
	(A°)	(A°)
$r^{\neq}$	2.57	2.71
r_{AB}	4.085	4.05

Theoretical values of $r^{\neq}$ and r_{AB} were obtained by the method described elsewhere [3,5], using data for the various ionic radii reported in the literature [16, 17, 18].

The theoretical values of $r^{\neq}$ and r_{AB} are also shown in Table 3. A compraion between the theoretical values of $r^{\neq}$ and r_{AB} and that of experimental one (See Table 3) revealed that the shape of the activated complex formed in the reaction between Br_2^- and BrO^- most likely follows a double sphere model.

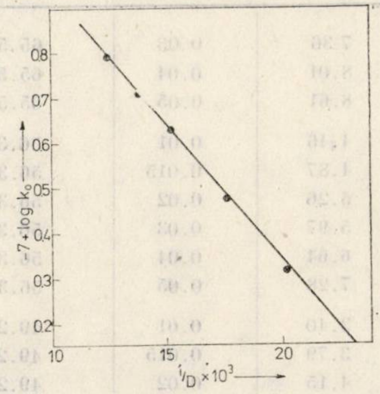

Fig. 1 — Dependence of $\log k_0$ on reciprocal of dielectric constant $(1/D)$ of the medium.

The data for r_{AB} were used to compute the electrostatic contribution to the changes in free energy of activation ($\Delta G_{es}^{\neq}$), entropy of activation ($\Delta S_{es}^{\neq}$) and enthalpy of activation ($\Delta H_{es}^{\neq}$) for the activated state formed in the course of reaction using equation (4) and other standard thermodynamic relationships reported in the literature [10]. The values are summarized in Table 4.

TABLE 4

The values of the electrostatic contributions to the changes in thermodynamic functions $\Delta G_{es}^{\neq}$, $\Delta S_{es}^{\neq}$ and $\Delta H_{es}^{\neq}$ for the formation of the transition state in the reaction between Br_2^- and BrO^-

$\Delta G_{es}^{\neq}$	$\Delta S_{es}^{\neq}$	$\Delta H_{es}^{\neq}$
XM(kcal)$^{-1}$	XMT (cal)$^{-1}$	M (cal)$^{-1}$
Theoretical values 1.019	−4.69	−378.0
Experimental values 1.028	−4.73	−381.2

The negative sign for the change in the electrostatic contribution to the entropy of activation can be interpreted in terms of the description of the initial state of reactants (ions) and that of the activated state.

The ions Br_2^- and BrO^- are shown to have single negative charge on each of them when they are at an infinite distance from each other before the reaction, whereas in the activated state the sphere is doubly negatively charged $(Br_2 - BrO)^{2-}$. The solvent molecules in the neighbourhood of these ions are acted upon by strong electrostatic forces (electrostriction). Thus more electrostriction is expected in the activated state than in the initial state of the ions, resulting a decrease in the electrostatic contribution to the entropy of activation.

REFERENCES

[1] A. A. Frost and R. G. Pearson, "Kinetics and Mechanism", 2nd ed., Wiley, New York, 1961, p. 144.

[2] D. T. Y. Chem and K. J. Laidlar, *Canad. J. Chem.*, **37,** 599 (1959).

[3] K. J. Laidlar and H. Eyring, *Ann. N. Y. Acad. Sci.*, **39,** 303 (1940).

[4] K. J. Laidlar, "Chemical Kinetics", second ed., McGraw Hill, New York, 1965, p. 221.

[5] M. S. Subhani and T. Kausar, *Pakistan J. Sci. Ind. Res.*, **18,** 208 (1975).

[6] M. S. Subhani, *Rev. Roumaine Chim.* preceding paper.

[7] M. S. Subhani and M. N. H. Lacewala, *J. Sci. Maths.*, **1,** 41 (1974).

[8] M. S. Subhani (Submitted for publication).

[9] G. Scatchard, *Chem. Rev.*, **10,** 229 (1932).

[10] K. J. Laidlar, "Chemical Kinetics", second ed., McGraw Hill, New York, 1965, p. 212, 217.

[11] E. S. Amis and J. E. Petts, *J. Amer. Chem. Soc.*, **63,** 2883 (1941).

[12] G. V. Buxton and F. S. Dainton, *Proc. Roy. Soc.*, A**304,** 427 (1968).

[13] M. S. Subhani and T. Kausar, *Rev. Roumaine Chim.* (Accepted for publication).

[14] G. V. Buxton and M. S. Subhani, *J. Chem. Soc. Faraday Trans.* **68,** 958 (1972).

[15] B. Cercek, M. Ebert, J. P. Keen and A. J. Swallow, *Science*, **145,** 919 (1964).

[16] J. Kleinberg, W. J. Argersinger and E. Griswold, "Inorganic Chemistry", D. C. Heath Co. Boston, 1965, p. 74.

[17] T. Moeler, "Inorganic Chemistry", Wiley, New York, 1965, p. 140.

[18] A. F. Kapusttnsku, *Quart. Rev.*, **10,** 283 (1956).

The ions Br_3^- and BrO^- are shown to have single negative charge on each of them when they are at an infinite distance from each other before the reaction, whereas in the activated state the sphere is doubly negatively charged $(Br_3^- - BrO)^{2-}$. The solvent molecules in the neighbourhood of these ions are acted upon by strong electrostatic forces (electrostriction). Thus more electrostriction is expected in the activated state than in the initial state of the ions, resulting a decrease in the electrostatic contribution to the entropy of activation.

REFERENCES

[1] A. A. Frost and R. G. Pearson, "Kinetics and Mechanism", 2nd ed., Wiley, New York, 1961, p. 141.
[2] D. T. Y. Chen and K. J. Laidler, *Canad. J. Chem.*, **37**, 599 (1959).
[3] K. J. Laidler and H. Eyring, *Ann. N. Y. Acad. Sci.*, **39**, 303 (1940).
[4] K. J. Laidler, "Chemical Kinetics", second ed., McGraw Hill, New York, 1965, p. 231.
[5] M. S. Subhani and T. Kausar, *Pakistan J. Sci. Ind. Res.*, **18**, 203 (1975).
[6] M. S. Subhani, *Rev. Roumaine Chim.* preceding paper.
[7] M. S. Subhani and M. N. H. Laeewala, *J. Sci. Math.*, **1**, 11 (1971).
[8] M. S. Subhani (Submitted for publication).
[9] G. Scatchard, *Chem. Rev.*, **10**, 229 (1932).
[10] K. J. Laidler, "Chemical Kinetics", second ed., McGraw Hill, New York, 1965, p. 212, 215.
[11] E. S. Amis and J. E. Potts, *J. Amer. Chem. Soc.*, **63**, 2883 (1941).
[12] G. V. Buxton and F. S. Dainton, *Proc. Roy. Soc.*, A**304**, 427 (1968).
[13] M. S. Subhani and T. Kausar, *Rev. Roumaine Chim.* (Accepted for publication).
[14] G. V. Buxton and M. S. Subhani, *J. Chem. Soc. Faraday Trans.* **68**, 958 (1972).
[15] B. Cercek, M. Ebert, J. P. Keen and A. J. Swallow, *Science*, **145**, 919 (1964).
[16] J. Kleinberg, W. J. Argersinger and E. Griswold, "Inorganic Chemistry", D.C. Heath Co. Boston, 1960, p. 74.
[17] T. Moeller, "Inorganic Chemistry", Wiley, New York, 1953, p. 140.
[18] A. P. Kapustinskii, *Quart. Rev.*, **10**, 283 (1956).

Revue Roumaine de Chimie, **25**, *6*, 861–866 (1980)

STUDY OF THE TRANSITION STATE FORMED BETWEEN $Cu(S_2O_3)^-$ AND $S_2O_8^{2-}$ ANIONS IN MIXTURE OF SOLVENTS

M. S. SUBHANI*
Department of Chemistry, University of Nigeria, Nsukka

Received July 14, 1977
Revised March 30, 1979

The effects of dielectric constant and ionic strength have been studied for the reaction between $Cu(S_2O_3)^-$ and $S_2O_8^{2-}$ in solution. From the plot of log k_0 and I/D the value of $r^{\neq}$ and r_{AB} were evaluated for the activated complex $(Cu(S_2O_3)S_2O_8)^{3-}$. In comparison with the theoretical values, the single sphere model was found to be applicable to the activated state of this reaction. Electrostatic contributions to the changes in the modynamic functions $\Delta G^{\neq}_{es}$, $\Delta S^{\neq}_{es}$ and $\Delta H^{\neq}_{es}$ for the formation of the activated state were also evaluated.

1. INTRODUCTION

Various studies have been carried out to observe the effect of dielectric constant and ionic strength on the reaction between inorganic anions [1–7] and a number of models have been proposed for the shape of the activated complex due to the rearrangement of total charge of the ions on the activated complex formed in the course of reaction [8–11].

The expressions relating the rate constants at zero ionic strength to the dielectric constant for the single and double sphere models are

$$\log_6 k_0 = \log k_i - \frac{e^2}{4.6060\ \mathrm{KT}}\left[\frac{(Z_A+Z_B)^2}{r^{\neq}} - \frac{Z_A^2}{r_A} - \frac{Z_B^2}{r_B}\right] \qquad (1)$$

$$\log k_0 = \log k_i - \frac{z_A Z_B e^2}{2.303\ DKTr} \qquad (2)$$

respectively.

The electrostatic contribution to the changes in free energy of activation for a single sphere and double sphere models are given [9]

$$\Delta G^{\neq}_{es} = \frac{Ne^2}{D}\left[\frac{(Z_A+Z_B)^2}{r^{\neq}} - \frac{Z_A^2}{r_A} - \frac{Z_B^2}{r_B}\right] \qquad (3)$$

$$\Delta G^{\neq}_{es} = \frac{NZ_A Z_B e^2}{Dr_{AB}} \qquad (4)$$

---

* *Present Address*: Department of Chemistry Faculty of Science, Garyounis University P.O. Box 9480 Benghazi, Libya.

respectively. Where k_0 is the rate constant at zero ionic strength, K_i, the rate constant at infinite dielectric constant, D, dielectric constant, K, the Boltzman constant, T, the temperature, Z_A, Z_B, r_A, r_B are the changes and radii of the ions A and B, respectively and $r^{\neq}$ and r_{AB} are the radii of the activated complex in a single and double sphere shape, respectively. The electrostatic contribution to the entropy of activation and enthalpy of activation can easily be evaluated from (3) and (4) [9].

The purpose of the present work was to investigate the shape of the activated complex formed between $Cu(S_2O_3)^-$ and $S_2O_8^{2-}$ which is a second order reaction [12] with a rate determining step

$$Cu(S_2O_3)^- + S_2O_8^{2-} \dashrightarrow$$

It was also of interest to see what is the electrostatic contribution to the changes in the thermodynamic functions for the activated state to take place.

EXPERIMENTAL

All chemicals used were of analar purity or otherwise recrystallized.

All solutions were prepared using triply distilled water.

All measurements for the residual concentration of iodine were made spectrophotometrically using UNICAM SP500 spectrophotometer.

Haake Model NK22 thermostat was used throughout the experiments to maintain the reaction mixture at 2 ± 0.05°C.

A persulphate ion concentration of 0.01 m and thiosulphate anion of 0.02 M were used in all the experiments reported.

Suitable volumes of standard solutions of reactants kept at 2°C were pipetted out and mixed together in a reaction mixture flask, previously placed in a thermostat. At the time of mixing the stop watch was started. After suitable time intervals 25 ml portion of the reaction mixture was withdrawn and transferred to a conical flask containing a known amount of alcoholic solution of idons in excess to the original concentration of S_2O^{2-} anions in the mixture. The unreacted portion of iodine was analysed spectrophotometrically at 350 nm as described elsewhere.[7]

The dielectric constants for various mixtures of solvents (water and ethanol) were measured as described elsewhere.[7]

RESULTS AND DISCUSSION

The reaction between thiosulphate and persulphate was found to be catalysed in presence of copper sulphate [12], but was still obeying first order kinetics. The catalytic effect was said to be due to the involvement of another reaction

$$Cu(S_2O_3)^- + S_2O_8^{2-} \dashrightarrow$$

which is a bimolecular reaction. Thus the rate constant for the reaction between thiosulphate anion and persulphate anion both in the presence and absence of copper sulphate were determined and are summarized in Table 1 and 2.

TABLE 1

Experimentally determined rate constant (K_{obs}) (s^{-1}) for the reaction between $S_2O_8^{2-}$ and $S_2O_3^{2-}$ in absence o copper sulphate, at various ionic strengths and different dielectric constants

$T = 275$ K, $(S_2O_3^2) = 0.02$ M
$(S_2O_8^{2-}) = 0.01$ M

$K_{obs} \times 10^5 \cdot s$	(KCl)	$\sqrt{\mu}$	D
10.91	0.12	0.46	81.2
14.10	0.12	0.46	73.9
12.82	0.12	0.46	67.2
15.85	0.12	0.46	58.9
17.34	0.12	0.46	51.1
18.92	0.12	0.46	43.7
7.83	0.095	0.43	81.2
9.98	0.095	0.43	73.9
0.02	0.095	0.43	67.2
11.22	0.095	0.43	58.9
12.46	0.095	0.43	51.1
13.98	0.095	0.43	43.7
6.98	0.08	0.41	81.2
9.12	0.08	0.41	73.9
7.92	0.08	0.41	67.2
10.21	0.08	0.41	58.9
11.52	0.08	0.41	51.1
13.09	0.08	0.41	43.7
3.93	0.04	0.36	81.2
5.42	0.04	0.36	73.9
4.60	0.04	0.36	67.2
6.17	0.04	0.36	58.9
7.27	0.04	0.36	43.7
8.39	0.04	0.36	43.7
2.67	0.025	0.34	81.2
3.53	0.025	0.34	73.9
3.08	0.025	0.34	67.2
4.23	0.025	0.34	58.9
4.98	0.025	0.34	51.1
5.83	0.025	0.34	43.7
1.53	0.0	0.30	81.2
1.83	0.0	0.30	73.9
1.06	0.0	0.30	67.2
1.98	0.0	0.30	58.
2.23	0.0	0.30	51.1
1.61	0.0	0.30	43.7

TABLE 2

Experimentally determined rate constants (K_{obs}) (s^{-1}) for the reaction between $S_2O_8^{2-}$ and $S_2O_3^{2-}$ in presence of copper sulphate at different dielectric constants and ionic strengths

$T = 275$ K, $(S_2O_3^{2-}) = 0.02$ M
$(S_2O_8^{2-} = 0.01$ M, $Cu(SO_4) = 2 \times L)^{-5}$ M

$K_{obs} \times 10^5 \cdot s$	(KCl)	$\sqrt{\mu}$	D
963.75	0.12	0.46	81.2
1237.56	0.12	0.46	73.9
1575.50	0.12	0.46	58.9
1342.00	0.12	0.46	67.2
2045.00	0.12	0.46	51.1
3100.00	0.12	0.46	43.7
835.63	0.095	0.43	81.2
1032.42	0.095	0.43	73.9
1091.58	0.095	0.43	67.2
1221.62	0.095	0.43	58.9
1495.06	0.095	0.43	51.1
2097.98	0.095	0.43	43.7
765.6	0.08	0.41	81.2
928.50	0.08	0.41	73.9
963.70	0.08	0.41	67.2
1052.00	0.08	0.41	58.9
1242.00	0.08	0.41	51.1
1658.00	0.08	0.41	43.7
596.90	0.04	0.36	81.2
697.20	0.04	0.36	73.9
672.20	0.04	0.36	67.2
679.20	0.04	0.36	73.9
672.20	0.04	0.36	67.2
697.17	0.04	0.36	58.9
723.47	0.04	0.36	51.1
840.20	0.04	0.36	43.7
542.27	0.025	0.34	81.2
601.50	0.025	0.34	73.9
584.90	0.025	0.34	67.2
574.42	0.025	0.34	58.9
588.33	0.025	0.34	51.1
645.69	0.025	0.34	43.7
407.83	0.0	0.30	81.2
441.27	0.0	0.30	73.9
395.43	0.0	0.30	67.2
356.78	0.0	0.30	58.9
322.30	0.0	0.30	51.1
303.25	0.0	0.30	43.7

The rate constant for the reaction

$$Cu(S_2O_3)^- + S_2O_8^{2-} \longrightarrow$$

was obtained from these results (Tables 1 and 2) in a similar way as described in the literature[12].

The rate constant at various dielectrics is summarized in table 3.

TABLE 3

Rate constant (K_{calc}) liter mole^{-1} s^{-1}, for the reaction between $Cu(S_2O_3)^-$ and $S_2O_8^{2-}$ at different ionic strengths and dielectric constants

$T = 275$ K, $(S_2O_3^{2-}) = 0.02$ M, $(S_2O_8^{2-}) = 0.01$ M, $(CuSo_4) = 2 \times 10^{-5}$ M

K_{calc} (l·mole^{-1},s^{-1})	$\sqrt{\mu}$	D	K_{calc}(l·mole^{-1},s^{-1})	$\sqrt{\mu}$	D
476.40	0.46	81.2	296.5	0.36	81.2
612.40	0.46	73.9	337.3	0.36	73.9
663.70	0.46	67.2	333.4	0.36	67.2
779.80	0.46	58.9	336.5	0.36	58.9
1012.00	0.46	51.1	358.1	0.36	51.1
1545.00	0.46	43.7	415.9	0.36	43.7
413.9	0.43	81.2	269.30	0.34	81.2
511.7	0.43	73.9	299.2	0.34	73.9
540.8	0.43	67.2	290.7	0.34	67.2
605.3	0.43	58.9	285.1	0.34	58.9
741.3	0.43	51.1	291.7	0.34	51.1
1042.00	0.43	43.7	319.9	0.34	43.7
379.30	0.41	81.2	203.5	0.30	81.2
460.30	0.41	73.9	218.8	0.30	73.9
477.30	0.41	67.2	196.8	0.30	67.2
520.00	0.41	58.9	177.4	0.30	58.9
615.20	0.41	51.1	160.00	0.30	51.1
822.80	0.41	43.7	150.3	0.30	43.7

The values of the rate constant (K_0) at zero ionic strenght were obtained from fairly good linear plots by plotting $\log K_{calc}$ against $\sqrt{\mu}$.

$$\log K_{calc} = \log K_0 + Z_A Z_B A \sqrt{\mu} \tag{5}$$

where A is a constant at a given temperature and dielectric constant. The values of K_0 are shown in Table 4.

A plot of log K_0 versus I/D gave a fairly good strength line (see Fig 1) and from the slope the values of $r^{\neq}$ and r_{AB} were evaluated using equations (1) and (2) for the two type of models as shown in Table 5.

TABLE 4

The values of rate constants for the reaction between $Cu(S_2O_8^{2-})$ and $S_2O_8^{2-}$ at zero ionic strength and reciprocal of the dielectric constants

log k_0	$1/D \times 10^3$
1.730	12.32
1.595	13.53
1.480	14.88
1.220	16.97
0.930	19.57
0.570	22.88

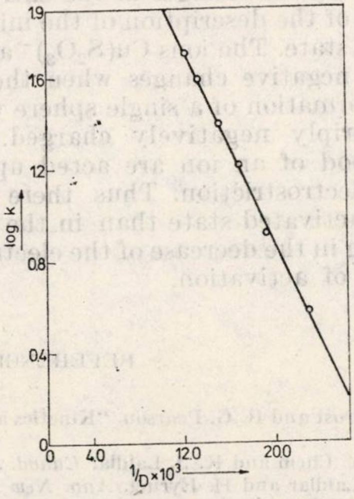

Fig. 1 — A plot of log K_0 against $1/D$ for the reaction between $Cu(S_2)_3)^-$ and $S_2O_8^{2-}$ anions in solution.

TABLE 5

Experimental and theoretical values of $r^{\neq}$ and r_{ab} for the activated state of (A) $Cu(S_2O_{3-})$ and (B) $S_2O_8^{2-}$ in the reaction between them

Radii	Experimental values A°	Theoretical values A°
$r^{\neq}$	3.33	3.29
r_{AB}	4.76	5.19

TABLE 6

Experimental and theoretical values for the electrostatic contributions to the changes in the thermodynamic functions for the activated state of the reaction between $Cu(S_2O_3)^-$ and $S_2O_8^{2-}$ anions

	Experimental values	Theoretical values
$\Delta G^{\neq}_{es}$	1746.3 cal/mole	1812 cal/mole
$\Delta S^{\neq}_{es}$	−8.033 cal/deg.mole	−8.34 cal/deg.mole
$\Delta H^{\neq}_{es}$	−463.33 cal/mole	−481.5 cal/mole

Theoretical values for $r^{\neq}$ and r_{AB} were obtained in a similar manner as described elsewhere[3,b] using data for radii for the ions obtained from the literature[6,13,14]. The values thus obtained are also shown in Table 5. In comparison with the theoretical values of $r^{\neq}$ and r_{AB} the experimental values (see Table 5) show that the activated state in this reaction follows a single sphere model.

The data for $r^{\neq}$ for the activated state were treated further to evaluate electrostatic contribution to the free energy changes ($\Delta G^{\neq}_{as}$), the changes in entropy of activation ($\Delta S^{\neq}_{es}$) and finally to the changes in enthalpy of activation ($\Delta H^{\neq}_{es}$) for the activated state using equations (3), (4) and standard thermodynamic relationships between these functions. The values are summarized in Table 6.

The physical significance of the negative change in the electrostatic contribution to the changes in the entropy of activation can be interpreted in terms of the description of the initial state of the reactants and that of activated state. The ions $Cu(S_2O_3)^-$ and $S_2O_8^{2-}$ are shown to have single and double negative changes when they are separated from each other before the formation of a single sphere where as in the activated state the sphere is triply negatively charged. The solvent molecules in the neighbourhood of an ion are acted upon by strong electrostatic forces known as electrostriction. Thus there is expected to be more electrostriction in the activated state than in the initial state of the reactant ions, this resulting in the decrease of the electrostatic contribution to the change in entropy of activation.

REFERENCES

[1] A. A. Frost and R. G. Pearson, "Kinetics and Mechanism", 2nd Ed., Wiley New York, 1961, p. 144.

[2] D. T. Y. Chem and K. J. Laidlar *Canad. J. Chem.*, **37**, 599 (1959).

[3] K. J. Laidlar and H. Eyring, *Ann. New York Acad. Sci.*, **39**, 303 (1940).

[4] K. J. Laidlar, "Chemical Kinetics" 2nd Ed., McGraw Hill New York, 1965, p. 221.

[5] M. S. Subhani and T. Kauser, *Pak. J. Sci. Ind. Research*, **18**, 208 (1975).

[6] M. S. Subhani *Rev. Roumaine Chim*, **23**, 719, (1978).

[7] M. S. Subhani and M. N. H. Lacewala, *J. Sci. Mathes*, **1**, 41 (1974).

[8] G. Scatchard, *Chem. Rev.*, **10**, 229 (1932).

[9] K. J. Laidlar, "Chemical Kinetics", 2nd Ed., McGraw Hill New York, 1965, p. 212 and p. 217.

[10] E. S. Amir and *J. E. Potts, J. Amer. Chem. SOC*, **63**, 2883 (1941).

[11] M. Born, *Z. Physik*, **1**, 45 (1920).

[12] C. V. King and O. F. Steinbach, *J. Amer. chem. Soc.*, **52**, 4779 (1930).

[13] J. Kleinberg et al., "Inorganic Chemistry", D. C. Heath and Co. Boston, 1960, p. 74.

[14] A. K. Kapustinski, *Quat. Rev.*, **10**, 283 (1956).

Revue Roumaine de Chimie **25**, *6*, 867–874 (1980)

SPECTROPHOTOMETRIC MICRODETERMINATION OF URANIUM WITH BENZOIN-OXIME

V. ARMEANU and SANDA VIȘAN
Academy of Economic Studies, Piața Română 6, București, Romania

Received September 14, 1979

The compounds formed between the benzoin-oxime and uranyl ion in three media, namely water, ethyl alcohol and ammonia (pH ~ 12.5) have been studied. The composition and stability of the compounds have been determined and corresponding structure formulas have been suggested on the basis of electronic spectra. The compound prepared in alkaline medium can be used for the spectrophotometric determination of uranium, as uranyl, with benzoin — oxime.

1. INTRODUCTION

Benzoin-oxime, Ph—CHOH—C(=NOH) Ph, is an organic reagent belonging to the class of acyloin-oximes which was used in chemical analysis for the determination of Cu (II), [1-6] Mo (VI),[1,7-10] W (VI),[1,10-12] V (V)[1,10,13] Pd(II), [14,15] Pt (IV), [14,15] Y (III), [16] La (III), [16] Ce (III), [16] Pr (III), [16] Nd (III), [16] Sm (III), [16] Gd (III), [16] Ni (II)[17].

Earlier studies available in the literature[9,11] deal with the separation methods of Mo and W, respectively from uranium, with benzoin-oxime, in strong acid solutions (HCl or H_2SO_4).

It was found that the compound formed in the reaction between benzoin-oxime and uranyl ion ($pH > 7$) is a yellow-coloured compound, slightly soluble in water, easily soluble in ethyl alcohol, methyl alcohol, acetone and 25% ammonia and can be partially extracted in chloroform, benzene, carbon tetrachloride.

The present work develops an experimental study of the uranyl-benzoin-oxime system by spectrophotometric methods.

2. REAGENTS AND EXPERIMENTAL EQUIPMENT

The benzoin-oxime and $UO_2(CH_3COO)_2 \cdot 2H_2O$ from Chinoin-Hungary and U.C.B. were used.

The spectrophotometric study was performed with Specord UV — VIS, Spekol EK—5 spectrophotometers in the ultraviolet and visible domain. A Seybold pH-meter was used to measure pH and the melting point of oxime was determined by using a Boetius apparatus.

The oxime is a white colour crystalline substance having the melting point at 153—155°C; it is soluble in ethyl alcohol and insoluble in water. The oxime solutions are subjected to change under light action and time influence (within a week). To avoid that the alcoholic solutions of oxime adulterate in time they were preserved in the dark and at low temperature, for maximum seven days.

3. RESULTS AND DISCUSSION

Electronic Band Spectra. A yellow-coloured compound formed in the reaction between benzoin-oxime and uranyl whose colour intensity is changed in various solvents and pH media. In Figure 1 are shown the uv absorption spectra of benzoin-oxime using as solvents water (1), ethyl alcohol (2) and ammonia (3); the wavelength range investigated was $\lambda = 200-400$ nm. In Figure 2 are shown the uv absorbtion spectra of the compound formed between benzoin-oxime and uranyl ion, in the same range of wavelength using the same solvents as previously and also the uv absorption spectrum of $UO_2(CH_3COO)_2$.

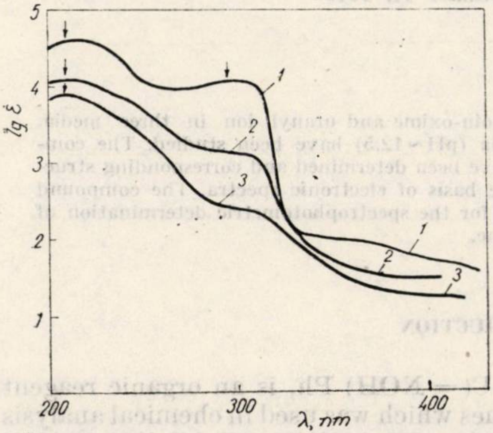

Fig. 1 — The absorption spectra of benzoin-oxime. Solvent: 1 — ammonia; 2 — ethyl alcohol; 3 — water.

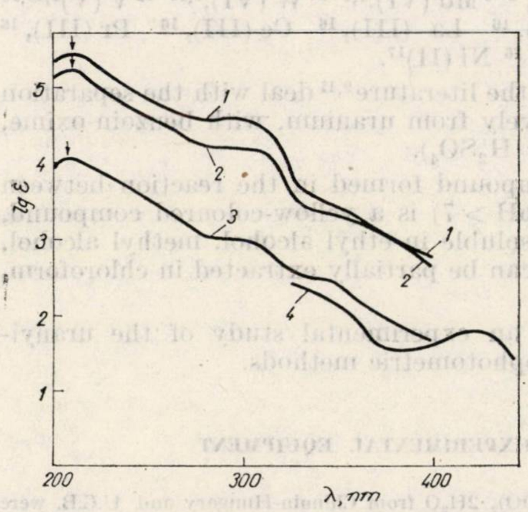

Fig. 2 — The absorption spectra of the compound formed between benzoin-oxime and uranyl. Solvent: 1 — ammonia; 2 — ethyl alcohol; 3 — water. 4 — The absorption spectrum of $UO_2(CH_3COO)_2$.

Uranyl acetate shows a wide spectral band in ultraviolet domain and a maximum, of relatively low intensity, for $\lambda = 428$ nm.

Spectral characteristics and the attribution of corresponding transitions are shown in Table 1.

TABLE 1

Spectral characteristics of benzoin-oxime and of the complex compound achieved with uranyl, in various solvent media. The spectra were recorded using corresponding solvent as reference

Transition		Oxime				Complex compound			
Solvent		*E*	*K* $\pi \rightarrow \pi^*$	*B* $\pi \rightarrow \pi^*$	*R* $n \rightarrow \pi^*$	*E*	*K* $\pi \rightarrow \pi^*$	*B* $\pi \rightarrow \pi^*$	*R* $n \rightarrow \pi^*$
Ethyl	λ	(205) max	234	294 plateaus	333	212 max	238	280 plateaus	333
Alcohol	ε	(11900)	8500	1300	80	117500	54500	14550	2550
Water	λ	207 max	238	294 plateaus	333	208 max	—	280 plateaus	333
	ε	7420	4470	270	120	11320	—	1140	320
Ammonia	λ	208 max	238	294 plateaus	333	210 max	227	296 plateaus	330
	ε	39900	28470	11570	80	179655	129000	39450	3900

The molecule of benzoin-oxime has two benzene nuclei ; therefore in ethyl alcohol, water and 25% ammonia as solvents it shows an intensive E spectrum band at $\lambda \sim 205$ nm and a *B* spectrum band, because of a $\pi \rightarrow \pi^*$ transition, with lower absorption, in $\lambda \sim 235$ nm range. *AK* (conjugated) spectrum band proves the existence of an oximino group ($: C = \ddot{N}OH$) in the benzoin-oxime molecule. The *K* band is due to the presence of a $\pi \rightarrow \pi^*$ orbital in addition and also to a *R* (radical) spectrum band due to an $n \rightarrow \pi^*$ transition. These bands result from the chromophore system existing in benzene nucleus showing the following possible bands : [18]

— E spectrum band, for $\lambda = 180-220$ nm with $\varepsilon = 2-6$ E 10^3

— K spectrum band, for $\lambda = 220-250$ nm with $\varepsilon = 3 \times 10^4$

— B spectrum band, for $\lambda = 250-290$ nm with $\varepsilon = 10^2 - 10^3$.

— R spectrum band, for $\lambda = 275 - 330$ nm with $\varepsilon = 10-100$.

Comparing Figures 1 and 2 it can be seen that, in the same solvent, the formation of a complex compound between benzoin- oxime and uranyl ion results in the displacement of *E*, *K* and *B* bands, but the more important effect conferring the colour to the complex compound, consists in its hyperchrome modification, compared with the ligand. This intensification of the bands occurs because of the strong ionization of benzoin-oxime in the presence of UO_2^{2+} ion.

Bathochromic displacements of the E band in the complex compound take place regardless of solvent nature. The K band does not appear in water as solvent, but only in ethyl alcohol and ammonia and modifications are observed compared with the ligand.

In the visible spectrum range, the curves show a shoulder around the value of $\lambda = 333$ nm, and have the same shape for all the three solvents, proving the existence of similar compounds in the three solvent media.

Further determinations were carried out at $\lambda = 340$ nm.

Extraction of the Complex Compound in Organic Solvents. A qualitative determination of the possibility to extract the complex compound formed between UO_2^{2+} ion and benzoinoxime in benzene, chloroform and carbon tetrachloride was made.

Three identical solutions were prepared consisting in 1 cm³ uranylacetate, 4.94×10^{-3} M, 1 cm³ benzoin-oxime, 5×10^{-3} M and 3 cm³ water to which 10 cm³ of benzene, chloroform and carbon tetrachloride respectively were added. The phases separated after agitation for one minute and the spectra were for both organic and aqueous phases. The complex compound was found in the organic phases and in the aqueous ones, too.

The quantity of complex compound extracted in the organic phase was calculated measuring the optical absorption of the complex compound in water (A_{water}), the complex molar absorptivity in water ($\varepsilon_{\text{water}}$) and the total concentration of the complex compound. Results are shown in Table 2.

TABLE 2

Computation of the complex compound quantity extracted with different organic solvents

Sovent	A_{water}	$\varepsilon_{\text{water}}$ l/mol·cm	Complex compound concentration in water, C_1 mol/l	Total complex compound concentration C,mol/l	Complex compound extracted quantity $\alpha = \frac{C - C_1}{C} 100$ %
Benzene	0.32	278	11.5×10^{-4}	19.76×10^{-4}	42
Carbon tetrachloride	0.31	278	11.1×10^{-4}	19.76×10^{-4}	44
Chloroform	0.27	278	9.7×10^{-4}	19.76×10^{-4}	51

Improvement of the extraction process was not found by using more concentrated oxime solutions, because of the reduced partial solubility of the oxime in water, at higher concentration. The same conclusion was reached by working in 25% ammonia (pH ~ 12.5), because of emulsification.

Influence of pH. The maximum optical absorption accurs in the range of pH = 11–12.5, achieved by adding about 15–20 cm³ 25% ammonia solution to a total volume of 25 cm³. The system α — furoinoxime — uranyl shows the same behavior.[19] Increasing pH above the value mentioned previously causes a decrease in the optical absorption.

Complex Compound Time Stability. At low concentrations (5×10^{-3} M) the complex compound formed in water is time-stable over a period of two hours; after-wards precipitation begins.

In ethyl alcohol as solvent, the complex compound is timestable about 15 hours, but optical absorption is much lower than in 25% ammonia. The highest optical absorptions are obtained preparing the complex in 25% ammonia solution, the reaction equilibrium is reached after 20 hours and the time stability is a good one.

Determining Complex Compound Composition and Stability Factor. The complex compound composition and stability factor were determined using the Asmus "straight line" method[20] which refers to complex compounds AB_n $(n \geqslant 1)$ with medium stability. Experimental conditions : $\lambda = 340$ nm, pH ~ 12,5 (solutions were completed to total volum of 25 cm^3 with 25% ammonia). Absorption values were measured half an hour after the solutions had been prepared.

The instability factor was calculated by means of the relation :

$$K^{-1} = \frac{b_0^n}{V^n \times A_0}$$

where K is the stability factor ;

b_0 is the benzoin-oxime concentration, mol/1 ;

n is the metal/ligand ratio ;

V is the total volume of the solution, cm^3 ;

A_0 is the intersection of the $1/vn = f(1/A)$ curve with the ordinate axis (v is the oxime solution volume, in cm^3, and A is the solution optical absorption).

Table 3 and Figure 3 show the work conditions and diagram used in calculating the instability factor and the stability fyctor, respectively.

In water as solvent, the time stability is very low, being limited by partial solubility of the oxime in water.

Plotted curves are linear for the metal/ligand ratio = 1, in ethyl alcohol and 25% ammonia as solvent. Therefore $n = 1$.

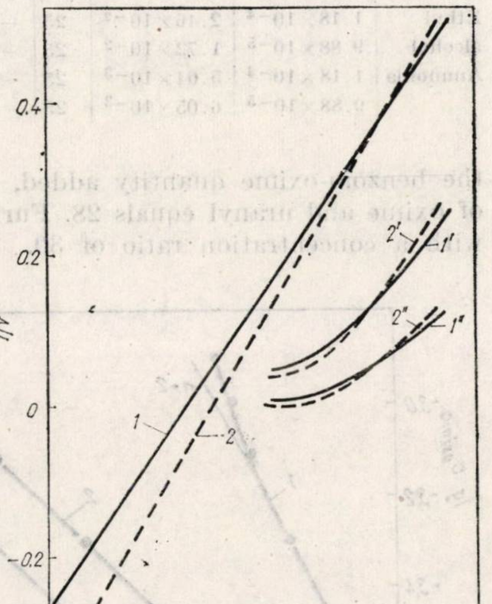

Fig. 3 — The Asmus method used in calculating the instability factor in 25% ammonia as solvent. The concentrations of the solutions : 1,1', 1'' — uranyl = 3×10^{-3} M and oxime 5.04×10^{-3} M ; 2,2', 2'' — uranyl = 2.5×10^{-3} M and oxime 6.05×10^{-3} M. $n = 1$ for the curves 1 and 2 ; n = 2 for the curves 1' and 2' ; n = 3 for the curves 1'' and 2''.

The combining metal/ligand ratio was checked, using the logarithmic method, too (Fig. 4).[21] In this way, the complex composition ($n = 1$) was confirmed.

Working with a maximum oxime concentration of 1.5×10^{-3} M it was found that in water as solvent the combining ratio is 1 : 2, as well as α – furoin-oxime – uranyl system.

The Necessary Reagent Quantity for the Complexing. For the same uranyl quantity, the solutions optical absorption varies as a function of the benzoin-oxime quantity added, until the molar concentration ratio of oxime and uranyl equals 28. Further determinations were performed with a concentration ratio of 30.

TABLE 3

Stability factor calculation using the Asmus method

Solvent	Uranyl concentration, M	Benzoin oxime concentration M	V cm^3	A_0	K^{-1}	$\overline{K}^{-1}$	$\overline{K}$
Ethyl	1.18×10^{-4}	2.46×10^{-2}	25	−0.390	2.52×10^{-3}	2.32×10^{-3}	4.3×10^{2}
alcohol	9.88×10^{-5}	1.72×10^{-2}	25	−0.325	2.12×10^{-3}		
Ammonia	1.18×10^{-4}	5.04×10^{-3}	25	−0.270	7.47×10^{-4}	7.19×10^{-4}	1.4×10^{3}
	9.88×10^{-5}	6.05×10^{-3}	25	−0.350	6.92×10^{-4}		

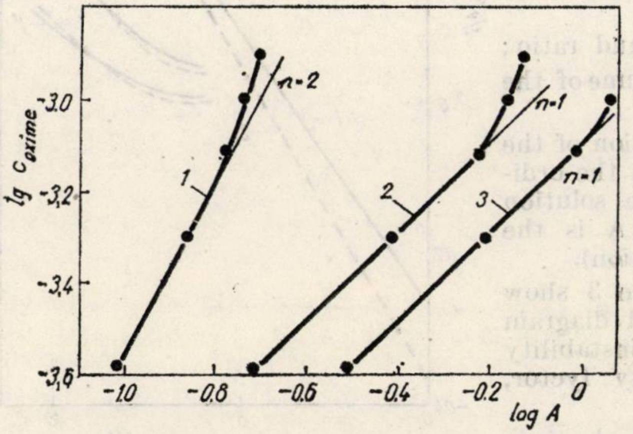

Fig. 4 – The lg concentration of oxime – lg A dependence on constant uranyl concentration. Solvents : 1 – water ; 2 – ethyl alcohol ; 3 – ammonia.

The Validity Field of the Bouguer – Lambert – Beer Law. After having fixed the experimental conditions (i.e. λ = 340 nm, pH ~ 12.5, measurements of optical absorption from half an hour after solutions were prepared, 30 times reagent quantity in excess of the oxime quantity) the validity field of the Bouguer – Lambert – Beer law was established. The optical absorption shows a linear variation as uranyl concentration increases reaching 45 μg/cm³ U (Fig. 5). To determine the calibration curve a least squares procedure was applied to values listed in Table. 4.

TABLE 4

Optical absorption variation as a function of the uranium quantity

Uranium concentration C, µg/cm	4.5	9	18	27	36	45
A	0.075	0.117	0.290	0.380	0.565	0.675

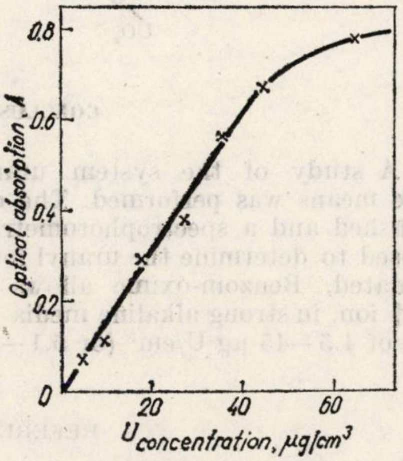

Fig. 5 — The variation of the solutions optical absorption as a function of the uranium quantity.

Summary of the calculation is shown in Table 5. The equation is:

$$C = 65.83\,(A - 0.003)\ \mu g/cm^3$$

TABLE 5

Calculation of the calibration curve

ΣA	ΣC	ΣAC	ΣC^2	$(\Sigma C)^2$
2.102	13.950	67.590	4475.25	19460.25

Experimental Method. The solution containing 100—1200 µg uranyl ions is introduced in calibrated flask of 25 cm³ adding 5 cm³ benzoin-oxime solution 3×10^{-2} M and 25% ammonia up to calibration mark. After half an hour and for λ = 340 nm, the optical absorption is determined in 1 cm thick sample boxes and in comparison with a standard sample of 5 cm³ oxime solution (3×10^{-2} M) in ethyl alcohol and 20 cm³ 25% ammonia.

Complex Compound Formula. Some complex compounds characterized by a metal/ligand ratio 1 : 1 were identified in the two investigated solvent media ; in water the metal/ligand ratio was 1 : 2. Spectral studies

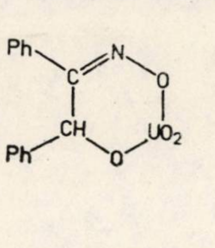

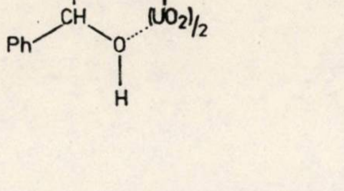

in correlation with the remarks presented above suggest the possible formation of complex compounds whose formulas were :

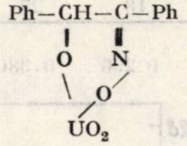

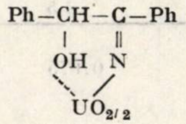

CONCLUSIONS

A study of the system uranyl-benzoin-oxime by spectrophotometric means was performed. The optical experimental conditions were established and a spectrophotometrical microdetermination method was proposed to determine the uranyl ion. The structure of the complex was formulated. Benzoin-oxime allows the determination of uranium, as uranyl ion, in strong alkaline media ($pH \sim 12.5$) and in the concentration range of $4.5-45$ μg U/cm^3 (or $5.1-51$ μ g UO_2^{2+}/cm^3).

REFERENCES

[1] K. Burger, "Organiceskie reagenty v neorganiceskom analize", Ed. Mir, Moscow, 1975.

[2] F. Feigl, G. Sicher and O. Singer, *Chem. Ber.*, **58**, 2294 (1925).

[3] I. Masayoshi and Sh. Eitaro, *J. Chem. Soc. Japan*, **64**, 46 (1943).

[4] C. Duval and Dat X. Nguyen, *Analyt. Chim. Acta*, **5**, 494 (1951).

[5] H. A. Suter and Ph. W. West, *Analyt. Chim. Acta*, **13**, 501 (1955).

[6] Chen Shou- Nan, Lee Marie C. M. and Cheng Hsiao T. D., *Hua Hsueh*, **3**, 73 (1971) ; *Chem. Abstr.*, **76**, 148426 (1972).

[7] Hutchison Dawn, *Analyst*, **97**, 118 (1972).

[8] S. W. Craven, *J. Iron Steel Inst.*, **171**, 75 (1952).

[9] Yoshinaga Oka, and Taro Yamasaki, *Nippon Genshiryoku Gakkaishi*, **3**, 110 (1961) ; *Chem. Abstr.*, **57**, 133 (1963).

[10] M. J. Hoenes and K. G. Stone, *Talanta*, **1960**, 4250.

[11] R. L. Carpenter, R. D. Gardner and W. P. Ashley, *U. S. At. Energy Comm. L. A.*, **1959**, 2270.

[12] V. Pfeifer and F. Hecht, *Z. analyt. Chem.*, **177**, 175 (1970).

[13] M. Kozlika and M. Wojtowicz, *Z. analyt. Chem.*, **257**, 191 (1971).

[14] N. K. Pshnitsyn and G. A. Nekrasova, *Izvest. Sektora Platiny i Drug. Blagorod. Metal., Inst. Obschei i Neorg. Khim.*, **30**, 59 (1955).

[15] P. K. Paria and S. K. Majumdar, *Z. analyt. Chem.*, **279**, 207 (1976).

[16] P. V. Takalkar and V. R. Rao, *J. Inorg. Nuclear Chem.*, **37**, 2103 (1975).

[17] L. Malatesta, *Gazz. chim. Ital.*, **68**, 319 (1938).

[18] S. Mager, "Analiză structurală organică", Ed. ştiinţifică şi enciclopedică, Bucureşti, 1979.

[19] V. Armeanu, S. Vişan and L. M. Băloiu, *Rev. Chim. (Bucureşti)*, **28**, 1095 (1977).

[20] E. Asmus, U. Hinz, K. Ohls and W. Richley, *Z. analyt. Chem.*, **178**, 104 (1960).

[21] H. Brent and G. French, *J. Amer. Chem. Soc.*, **63**, 568 (1941).

Revue Roumaine de Chimie, 25, *6*, 875—879 (1980)

PHENANTHRENEQUINONE MONOSEMICARBAZONE AS A REAGENT FOR THE DETERMINATION OF RHODIUM(III) AND PALLADIUM(II)

FASIHUDDIN KAMIL, S. K. SINDHWANI and R. P. SINGH
Department of Chemistry, University of Delhi, Delhi-7, India

Received May 23, 1979

The colour reactions of phenanthrenequinone monosemicarbazone (PQSC) with rhodium(III) and palladium(II) have been utilised for the spectrophotometric determination of the two metals.

Reagents used for the spectrophotometric determination of rhodium and palladium are numerous, but most of them suffer from disadvantages like interferences from other cations, poor sensitivity and poor selectivity, etc. Some of the important reagents used for the spectrophotometric determination of rhodium are tin(II) bromide,[1,2] 5-amino-2-mercaptobenzimidazole,[3] N, N′-bis(3-dimethylaminopropyl) dithiooxamide[4] and thiosalicylamide.[5] Acenaphthenequinone monoxime[6] and tropolone[7] have also been recommended and are comparable with other well-known reagents.

At one time nitrosoamines were considered to be the best reagents for the determination of palladium, *p*-nitrosodimethylaniline[1,8] and *p*-nitrosodiphenylamine[2,8] have been extensively used for the purpose. Various oximes used for the determination of palladium are dimethylglyoxime,[9,11] α-furyldioxime,[12] phenyl-α-pyridyl ketoxime,[13] methylglyoxime and salicylaldoxime.[14] 1-Nitroso-2-naphthol and 2-nitroso-1-naphthol[9,15,16] have also been recommended and the sensitivities of the two derivatives are nearly equal, but only with 2-nitroso-1-naphthol, the interference of copper, cobalt, iron and nickel can be eliminated by EDTA. The methods are free from the interference due to associated platinum metals. The sequence of addition of reagents affects the absorbance and the colour is stable only up to four hours.

The present communication describes the spectrophotometric determination of rhodium(III) and palladium(II) in pure samples and in co-existence with diverse ions.

EXPERIMENTAL

Reagents and Chemicals

A standard solution of rhodium(III) was prepared by dissolving rhodium trichloride (Johnson Matthey) in 1M hydrochloric acid. The solution was standardised gravimetrically.

A stock solution of palladium was prepared by dissolving palladium dichloride in dilute hydrochloric acid and standardised gravimetrically by precipitation with dimethylglyoxime. The solution of PQSC was prepared in ethanol.

The pH of the solutions was adjusted with acetate buffers and dilute solutions of NaOH. All other chemicals used were of analytical grade. Doubly distilled water was used throughout the work.

Absorbance measurements were carried out with a Unicam SP 600 spectrophotometer and an ECIL Expanded scale pH meter was used for measurements of pH.

Procedure for the determination of rhodium(III)

Take an aliquot amount containing 99—268 μg of rhodium and add 4 ml of 5×10^{-4}M alcoholic solution of the reagent. Adjust the pH in the range 7.2—8.8 with sodium acetate and sodium hydroxide and heat the contents for two hours on a water bath. Cool to room temperature, make up to 25.0 ml with aqueous dimethylformamide (DMF) so that the final solution is 7 :3 (DMF : water). Prepare a blank containing all components except rhodium and measure the absorbance of Rh-PQSC complex against the blank at 480 nm. From the absorbance, calculate the amount of rhodium from the calibration curve.

Procedure for the determination of palladium(II)

To a suitable aliquot containing 35.5—158.5 μg of palladium(II) add 2 ml of 5×10^{-3} M alcoholic solution of the reagent in a Pyrex stoppered bottle. Adjust the pH between 5.0—7.0 with acetate buffer and raise the volume of aqueous phase to approximately 10 ml with water and add 10 ml of chloroform. Shake the contents for a few minutes on a shaking machine and allow to stand for sometime so as to attain equilibrium. After removing the organic layer, measure the pH of the aqueous layer and it should be between 5.0—7.0. Centrifuge the separated non-aqueous layer to remove water droplets and measure the absorbance at 470 nm against a corresponding reagent blank. From the absorbance, deduce the amount of palladium.

RESULTS AND DISCUSSION

On mixing a solution of rhodium(III) with the reagent in ethanol in acidic medium, no colour formation takes place. However, on heating the contents on a water bath,a brown precipitate appears in presence of sodium acetate. The precipitate was found to be partially soluble in alcohol and chloroform, but soluble in dimethyl formamide. Increasing volumes of DMF were added and it was observed that complete dissolution of precipitate takes place in 70% DMF medium. High percentage of DMF had no effect on the absorbance. In subsequent work, the percentage of DMF was maintained at seventy. The orange brown palladium-PQSC complex was found to be soluble in chloroform, hence the determination was carried out by extracting the chelate in chloroform. The organic phase was separated, centrifuged to remove any droplets of water and the absorbance was measured. The rhodium and palladium complexes showed maximum absorbance at 480 and 470 nm, respectively. Hence, the effect of other variables was studied at these wavelengths against the corresponding reagent blanks. A study of the rate of colour development was made as very little colour is developed at room temperature in the case of rhodium. The solutions were heated on a steam bath for different intervals of time and the absorbance was measured at 480 nm. The absorbance was found to become constant after heating for about two hours. In subsequent studies, the reaction mixtures were heated for two hours. Palladium forms the complex with the reagent instantaneously at room temperature. The complexes of rhodium and palladium were found to be quite stable and no change in absorbance was observed up to 48 and 24 hours, respectively. The effect of pH on the formation of the complexes was investigated by preparing a series of solutions buffered at various pH values. The absorbances of rhodium and palladium solutions observed a constancy in the pH intervals 7.2—8.8 and 5.0—7.0. Subsequent studies were made at pH 8.0 and 6.0, respectively. Varying amounts of the reagent were added to a fixed amount of metal solution and the absorbances were measured against the corresponding reagent blanks. The results showed that at least seven and six-fold molar excess of PQSC over rhodium and palladium is required for maximum absorbance. In the course of subsequent studies, therefore, ten-fold molar excess of PQSC was used. The systems were found to follow Beer's law up to 16.46 ppm of rhodium and 19.15 ppm of palladium. The sensitivities of the colour reactions, in terms of Sandell's definition, are 0.018 μg Rh/cm^3 and 0.019 μg Pd/cm^3. The corresponding molar absorptivities for rhodium and palladium are 5550 at 480 nm and 5500 at 470 nm, respectively. The optimum ranges for the determination of rhodium and palladium, as evaluated from Ringbom plots are 3.98—10.72 and 3.55—15.85 ppm, respectively. In the determination of eight samples each containing 205.8 μg of rhodium in 25 ml solution, the mean absorbance was found to be 0.444 and in six samples each containing 106.4 μg of palladium in 10 ml solution, the mean absorbance was found to be 0.55. The standard deviation in both cases was 0.0029. Job's method of continuous variations[17,18] and mole ratio method[19] were used to ascertain the ratio of metal to reagent in the complex. Both methods indicated the formation of 1 : 3 (Rh : PQSC) and 1 : 2 (Pd : PQSC) complexes, respectively.

Effect of foreign ions

Effect of diverse ions in the determinations of rhodium and palladium was studied, following the recommended procedure. Anions were added as solutions of their sodium or potassium salts. Cations were added as solutions of their chlorides, nitrates or sulphates. Masking agents were used wherever necessary.

Cobalt(II), nickel(II), copper(II), zinc(II) and lead(II) react with PQSC at room temperature and interferences due to these ions in the determination of rhodium could be avoided by extracting them in chloroform while iron(III), osmium(VIII), iridium(III) and platinum(IV) interfered. In the determination of 8.23 ppm of rhodium, the tolerance limits (in ppm) of various ions are: Cl^- (800), Br^- (400), I^- (500), NO_3^- or F^-(1000), NO_2^- or SO_3^{2-}(125), SO_4^{2-}(900), PO_4^{3-}(175), $C_2O_4^{2-}$(300), SCN^-(400), citrate (50), tartrate (25), BO_3^{2-} (100), Zn(II) or Ba(II) (50), Cd(II) (SCN^-) (10), Hg(II) (F^-) (35), Co(II), Ni(II) or Cu(II) (100), Ag(I) (I^-) (50), Th(IV) (20), U(VI)(F^{-15}), V(V) (10), Ru(III) (2), AL(III) (15), Pb(II) (40) and Mn(II) (F^-).

Effect of diverse ions in the determination of 10.64 ppm of palladium was studied. Since osmium(VIII), iridium(III) and platinum(IV) form complexes with PQSC only on heating and further, the complexes of these platinum metals are not extractable, the determination of palladium was possible in their presence. Tolerance limits (in ppm) of various ions are given below in parentheses. Masking agents, wherever used, have been mentioned against each:

Br^-, F^-, SO_3^{2-} or ClO_4^- (1000), Cl^- (500), NO_2^- or BO_3^{2-} (200), SO_4^{2-} (900), PO_4^{3-} or citrate (300), tartrate (350), SCN^- (20), Al(III) (175), Ba(II), Ca(II) or Fe(III) (200), Sr(II) or Mg(II) (100), Hg(II) or Pb(II) (10), Ag(I) (Cl^-) (25), Zn(II), Sn(II) or Os(VIII) (20), Mn(II) (F^-) (25), Ce(IV) (15), Au(III) (5), Pt(IV) (30), U(VI) (F^-) (80), Ir(III) (35) and Ti(IV) (65). Co(II), Ni(II), Cu(II), Ru(III) and Cd(II), however, interfere seriously.

Determination of rhodium and palladium in presence of each other

Rhodium(III) reacts with PQSC at elevated temperature and the complex could not be extracted in chloroform, but was found to be soluble in DMF while palladium reacts completely with the reagent at room temperature and the complex was found to be soluble in chloroform. Based on this behaviour, palladium was extracted into chloroform before heating. The remaining aqueous solution was heated for 120 min with the ligand solution and the rhodium content determined as described in the procedure. The determination could easily be carried out in presence of five-fold molar excess of rhodium over palladium and vice-versa.

CONCLUSION

Phenanthrenequinone monosemicarbazone (PQSC) has been used as a reagent for the spectrophotometric determination of rhodium(III) and palladium(II). Optimum conditions have been investigated and molar composition of the complexes has been determined. Suitability of the methods in presence of diverse ions has been examined by the use of masking agents and the determinations of rhodium and palladium have been carried out in presence of each other.

ACKNOWLEDGEMENT. One of the authors (F.K.) gratefully acknowledges the financial assistance received from the University Grants Commission, New Delhi.

REFERENCES

[1] F. E. Beamish, "Analytical Chemistry of Noble Metals", Pergamon Press, London, 1966.

[2] E. B. Sandell, "Colorimetric Determination of Traces of Metals", Interscience, New York, 1959.

[3] J. G. Sengupta, *Talanta,* **8**, 785 (1961).

[4] F. E. Beamish and J. C. Van Loon, "Recent Advances in the Analytical Chemistry of the Noble Metals", Pergamon Press, London, 1972.

[5] K. Sur and S. C. Shome, *Analyt. Chim. Acta,* **48**, 145 (1969).

[6] S. K. Sindhwani and R. P. Singh, *Microchem. J.,* **18**, 686 (1973).

[7] G. H. Rizvi, B. P. Gupta and R. P. Singh, *Mikrochim. Acta,* **1972**, 459.

[8] J. H. Yoe and L. G. Overhober, *J. Amer. Chem. Soc.*, **61**, 2058 (1939).

[9] K. Kodama, Nagoya, *Shi Kogyo Kenkyujo Kenkyu Hokoku*, **19**, 4 (1958).

[10] V. M. Peshkova, V. I. Shlenskaya and A. I. Rashevskaya, *Izv. Sektova Plating, I.O.N. Kh. Akad. Nauk, S.S.S.R.*, **32**, 61 (1955); *Analyt. Abstr.*, **4**, 2623 (1957).

[11] *Idem, Vest. Mosk. Univ.* 9, No. 5, *Ser. Fiz. Mat. irstestven. Nauk*, No. 3, 83 (1954).

[12] O. Menis and T. C. Rains, *Analyt. Chem.*, **27**, 1932 (1955).

[13] B. Sen, *Analyt. Chem.*, **31**, 881 (1959).

[14] F. E. Beamish, *Talanta*, **12**, 743 (1965).

[15] L. E. Ross, G. Kesser and E. T. Kucera, *Analyt. Chem.*, **32**, 1367 (1960).

[16] S. Komatsu and S. Kamiyama, *Nippon Kagaku Zasshi*, **81**, 1094 (1960).

[17] P. Job, *Ann. Chim. (Ital.)*, **9**, 113 (1928).

[18] H. Irving and T. B. Pierce, *J. Chem. Soc.*, **1959**, 2565.

[19] J. H. Yoe and A. L. Jones, *Ind. Eng. Chem. Analyt. Ed.*, **16**, 111 (1944).

Revue Roumaine de Chimie, 25, 6, 881–900 (1980)

SEPARACIÓN CROMATOGRÁFICA DE ORO, PLATINO, PALADIO, RODIO E IRIDIO. I

ESTUDIO CUALITATIVO

M. L. TASCON GARCIA

Departamento de Química Analítica, Facultad de Ciencias. Univ rsidad de Valladolid,
Valladolid, España

Recibido el 21 de junio de 1979

Empleando la técnica cromatográfica ascendente y monodimensional sobre papel, se ha estudiado la separación de diferentes mezclas de los elementos oro, platino, paladio, rodio e iridio, mediante sistemas de disolventes formados por mezclas, en diversas proporciones de cetonas-ClH y alcoholes ClH, proponiéndose aquellos que conducen a una clara separación así como los detectores adecuados para la visualización. Al mismo tiempo, se ha observado la influencia que tiene sobre los desarrollos cromatográficos, la naturaleza y proporción del componente orgánico del disolvente y los límites inferiores de detección.

The separation of mixtures of gold, platinum, palladium, rhodium and iridium by ascending monodimensional chromatography technique was studied. Different mixtures of HCl-ketones and HCl-alcohols and various spraying reagents for the identification of those metals were used and the results summarized. The nature and proportion of the organic part of the solvent and the lower limits of detection have received much attention.

INTRODUCCIÓN

Este trabajo tiene por objeto la separación y estudio del comportamiento cromatográfico de diversas mezclas de los elementos oro, platino, paladio, rodio e iridio.

El análisis de los datos bibliográficos revela que la mayor parte de las investigaciones sobre la separación de dichos elementos, han sido realizadas en sistemas de cloruros.

Basándose en el estudio de la influencia de la naturaleza del disolvente orgánico (alcoholes, cetonas, esteres, mezclas de estos productos) y de la concentración de ClH en el disolvente, se recomiendan mezclas de cetonas y alcoholes con ClH en diversas proporciones, si bien la técnica cromatográfica y las dimensiones de la tira de papel son distintas.

Lederer[1] propone el sistema butanol —ClH—agua y Setty[2] trabaja con butanol saturado con ClH 0,5 N y 2 N.

Para la separación de mezclas de metales nobles que contienen iridio, Kember y Wells[3,4] utilizan butanol saturado con ClH 3 M y H_2O_2.

La influencia de la concentración de ClH en el disolvente, formado a base de butanol —ClH, es estudiada por Blasius y Fischer,[5,6] llegando a la conclusión que la composición óptima del disolvente es la de butanol —ClH 3 N y 3,5 N en proporción (7 :3).

En sistemas alcohol —ClH en proporción (1 : 1), Voicu y Nascutiu[7] estudian el comportamiento de varios elementos del grupo del platino, utilizando diversos alcoholes y ClH de 1 a 12 N.

Los disolventes de mayores pespectivas resultaron ser los compuestos por mezclas de cetonas—ClH, propuestos por Burstall[8,9] a base de metil-etil-cetona y metil-propilcetona con ClH concentrado al 30 %.

Kember y Wells[3] proponen el formado por Hexona—ClH concentrado (6 : 4), mejorándose aun las separaciones si se le añade alcohol amílico.

Debido a la gran proporción de ClH en el disolvente, la tira cromatográfica queda muy frágil, por lo que Varshal[10] impregna previamente el papel cromatográfico con ClLi y utiliza como disolvente metiletilcetona y ClH.

La separación de mezclas de metales nobles también se ha llevado a cabo mediante el método de cromatografía con inversión de fase, impregnando el soporte con trin-n-butil-fosfato[11] y utilizando como disolventes ClH, NO_3H y ClO_4H. Siguiendo este mismo procedimiento O'Langhlin[12] utiliza también tri-n-butilfosfato al 20 % en Cl_4C y como disolvente NO_3H 3 M.

Przeszlakowski,[13,14] trabaja con soportes tratados con tri-n-butilamina y tri-n-octilamina y recientemente estudia la separación de los elementos sobre papel cromatográfico impregnado con cloruro de amberlita LA- 1 en benceno y ClH 6 M como disolvente.[15]

PARTE EXPERIMENTAL

Cámaras. — Las cámaras cromatográficas son tubos de vidrio Pirex para cromatografía de 30 cm de longitud por 2,5 cm de diámetro interior, cerrados herméticamente.

Papel. — Se han empleado tiras de papel Whatman nº 3 de 19 cm de longitud por 1 cm de anchura, con señales a 10, 2,5 y 17,5 cm a partir del borde inferior, que corresponden respectivamente a la altura a la que se introduce la tira en el disolvente, lugar donde se deposita la gota de muestra y altura máxima a la que se deja llegar el disolvente en el desarrollo. Con ello tenemos un desarrollo neto de 15 cm en el sentido ascendente.

Disolventes. — Para la preparación se han utilizado reactivos "especiales para cromatografía". Las composiciones se especifican en cada caso, viniendo expresadas en la relación vol : vol, empleándose un volúmen de 3 ml por tubo, que se cambia después de cada desarrollo.

Aplicación de la muestra. — Se realiza con una microjeringa Chemetrón, depositándose 2,5 µl de la muestra. Dicha muestra se deja secar a la temperatura ambiente, antes de intropucir la tira en la cámara.

Desarrollo. — Se mantiene la tira durante 10 minutos en la cámara saturada de vapor del disolvente, antes de introducirla en el mismo. El desarrollo tiene lugar a la temperatura ambiente (15—20°C).

El cromatograma impregnado de disolvente se seca en una estufa adecuada a 50°C.

Detección. — Para localizar y visualizar los elementos, se ha realizado un estudio previo de detectores encontrándose las coloraciones que se indican en la Tabla 1.

Se proponen como idóneos :

a) La solución al 5 % de $Cl_2S_n \cdot 2H_2O$ en ClH2 N y posterior adicción sobre el cromatograma de solución acuosa al 5 % de IK

b) La solución al 0,5 % de p-nitrosodimetilanilina en alcohol absoluto y solución reguladora de pH = 2,2 (Acetato sódico 4M — ClH 4 M), mezclados en proporción 2 :1.

Preparación de soluciones. — Las soluciones patrón de los elementos se preparan a la concentración adecuada de forma que las mezclas resulten con un contenido de 10 mg/ml de oro, 12,6 mg ml de platino, 6 mg/ml de paladio, 8 mg/ml de rodio y 12, 1 mg/ml de iridio. Esta preparación se lleva a cabo de la siguiente forma :

Oro — Se disuelve una lámina de oro en agua regia, seguido de evaporación en baño de agua para eliminar el exceso de agua regia y posteriormente se diluye con agua desionizada.

TABLA 1

Coloraciones que presentan los elementos frente a diversos detectores

Detector	Oro	Platino	Paladio	Rodio	Iridio
Bencidina	verde				
Ac. Rubeánico	—	rosa fuerte	—	—	—
Cl_2S_n	negro	amarillo fuerte	azul	amarillo claro	amarillo muy débil
$Cl_2S_n + IK$	negro	marrón rojizo	gris violeta	marrón	marrón
p-nitrosodimetilanilina	gris	rojo naranja	naranja	rojo naranja	rojo naranja
2-mercaptobenzotiazol	—	—	naranja	—	—

Platino. — Se disuelve $H_2PtCl_6 \cdot 2H_2O$ en agua desionizada, ligeramente acidulada con ClH.

Paladio. — Se disuelve Cl_2Pd en agua desionizada, ligeramente acidulada con ClH.

Rodio. — Se disuelve Cl_3Rh. $3H_2O$ en agua desionizada, ligeramente acidulada con ClH.

Iridio. — Se disuelve Cl_4Ir en agua desionizada, ligeramente acidulada con ClH.

Las disoluciones de menor concentratión se preparan por dilución de las disoluciones patrón, con agua desionizada acidulada con ClH.

RESULTADOS Y DISCUSION

Se ha llevado a cabo un estudio sistemático de mezclas de oro-platino-paladio-rodio y de oro-platino-paladio-iridio, con disolventes formados por distintas cetonas —ClH concentrado, mezclados en proporción 1 : 9 hasta 9 : 1 respectivamente ; las cetonas utilizadas han sido acetona, metiletilcetona, metilpropilcetona, metilisobutilcetona, acetilacetona y acetofenona.

Igualmente se han estudiado disolventes formados por alcohol-ClH concentrado, mezclados en las mismas proporciones, siendo los alcoholes utilizados, metanol, etanol, propanol, isopropanol, butanol, isobutanol, amílico e isoamílico.

Los resultados cualitativos de los desarrollos cromatográficos se muestran en diversas gráficas en las que se pone de manifiesto la localización y la longitud de las manchas de los elementos.

Las manchas se representan por líneas rectas contínuas y las estelas mediante líneas de puntos.

Para cada uno de los disolventes, las líneas corresponden, de izquierda a derecha, al oro, platino, paladio y rodio, o bien, oro, platino, paladio e iridio respectivamente.

En las figuras 1—14 se indican los resultados correspondientes a la mezcla oro-platino-paladio-rodio.

En las figuras 15—28 se muestran los resultados obtenidos en el estudio de la mezcla oro-platino-paladio-iridio.

1) En base a los resultados obtenidos se proponen como disolventes idóneos para ambas mezclas:

a) Metilpropilcetona—ClH (7 : 3)
b) Metilisobutilcetona—ClH (7 : 3)
c) Metilisobutilcetona—ClH (8 : 2)

2) Acerca del comportamiento de los elementos según la naturaleza y proporción del componente orgánico, nos parece oportuno reseñar:

a) La separación es mejor en los sistemas cetona—ClH que en los de alcohol-ClH.

b) Dentro de cada sistema, la separación es mejor al ir aumentando la proporción de componente orgánico en el disolvente, si bien cuando ésta es muy alta dicha separación disminuye.

c) Al aumentar la cadena carbonada de la cetona y del alcohol, la separación de oro-platino-paladio aumenta, mientras que disminuye la de paladio-rodio (iridio).

d) Al iniciarse las separaciones el Rf de los elementos en orden creciente es:

$$\text{iridio} = \text{rodio} < \text{pladio} < \text{platino} < \text{oro}.$$

3) Otro factor que se ha estudiado es el límite inferior de detección de cada elemento sobre el cromatograma.

Para llevar a cabo este estudio, se desarrollan diversos cromatogramas, en los que se han depositado 2,5 µl de las mezclas de los elementos, de concentraciones inferiores y que se obtienen por sucesivas diluciones de las soluciones patrón.

Los disolventes que se utilizan son los que previamente se han considerado idóneos para la separación de los cuatro elementos de cada mezcla.

Los resultados obtenidos son: oro 1,25 µg, platino 1,58 µg, paladio 0,75 µg, rodio 0,25 µg e iridio 1,63 µg.

Para cantidades menores que las indicadas, la visualización no es buena, con los detectores que han resultado válidos para su detección.

APENDICE

Otras mezclas estudiadas.

Utilizando los mismos disolventes que se han indicado, se han estudiado mezclas binarias y ternarias de los cinco elementos llegando a unos resultados semejantes a los obtenidos con las mezclas cuaternarias, si bien el número de disolventes idóneos para su separación es mayor resultado que cabía esperar, ya que la separación de un número menor de elementos presenta generalmente menos dificultades.

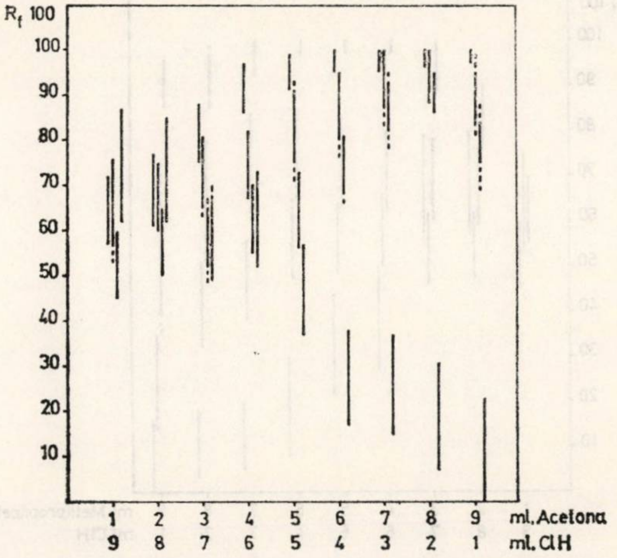

Fig. 1. — Variación del R_f con la concentración de acetona.

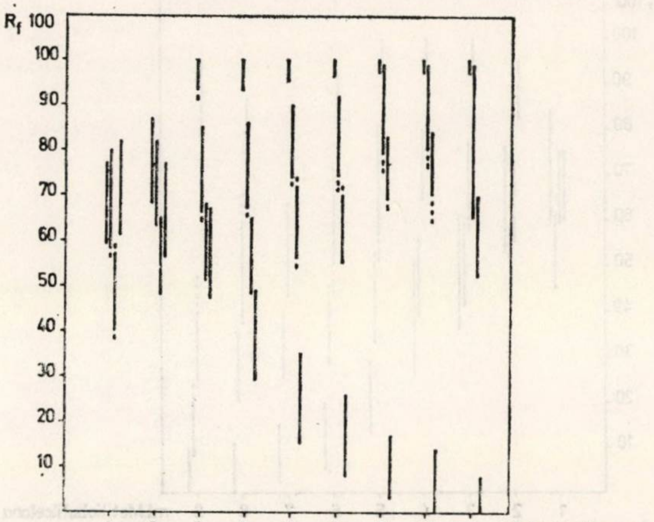

Fig. 2. — Variación del R_f con la concentración de metiletilcetona.

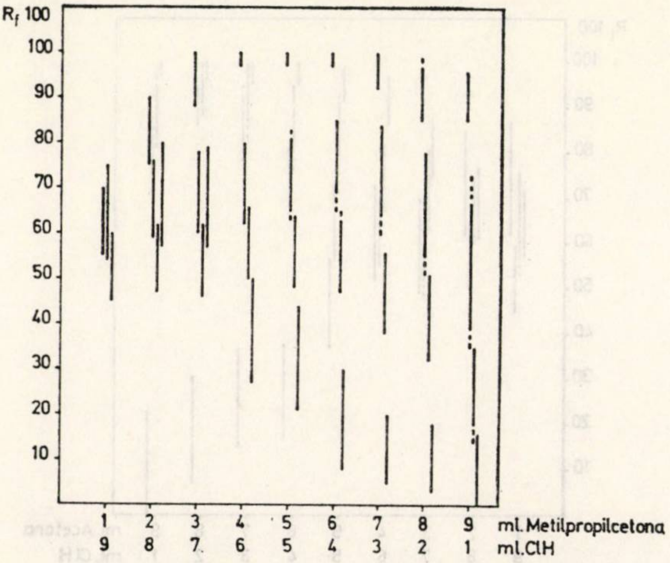

Fig. 3. — Variación del R_f con la concentración de metilpropilcetona.

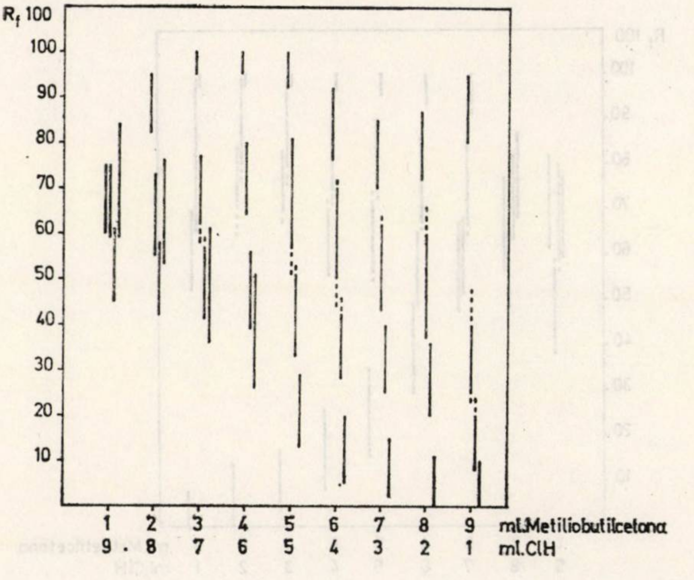

Fig. 4. — Variación del R_f con la concentración de metilisobutilcetona.

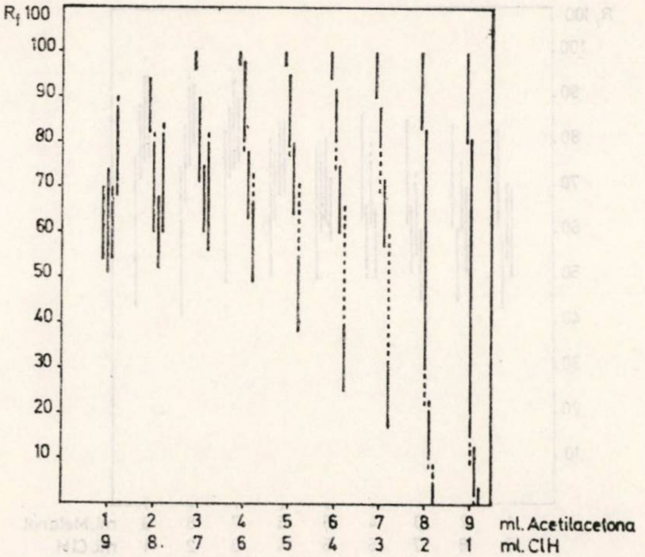

Fig. 5. — Variación del R_f con la concentración de acetilacetona.

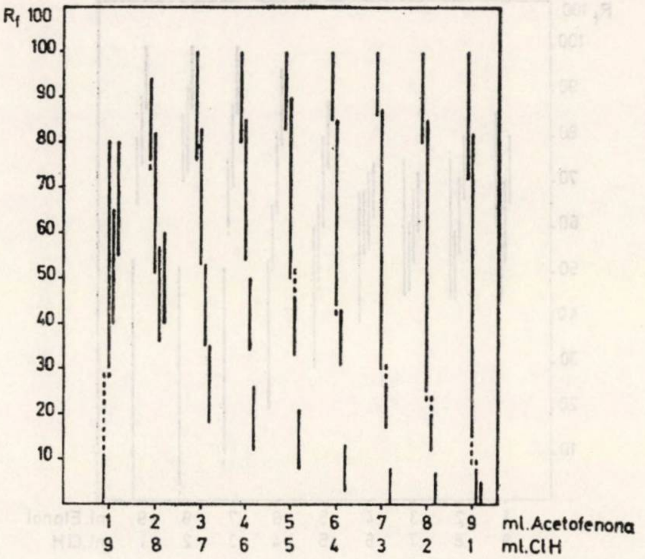

Fig. 6. — Variación del R_f con la concentración de acetofenona.

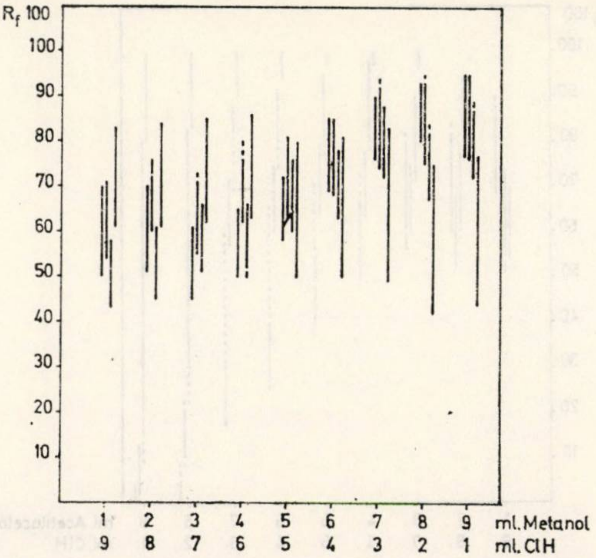

Fig. 7. — Variación del R_f con la concentración de metanol.

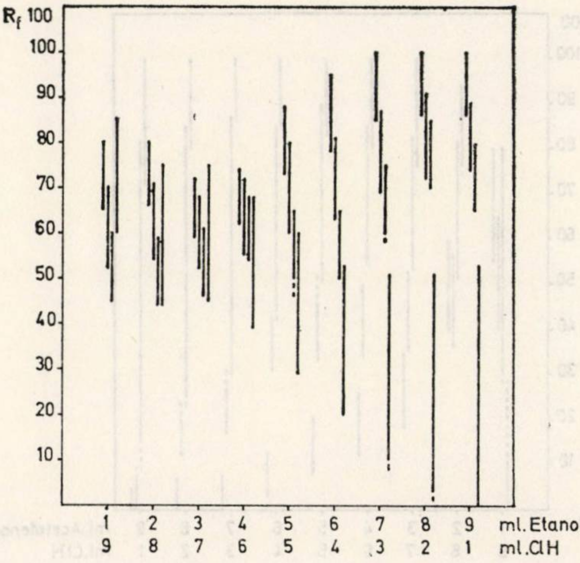

Fig. 8. — Variación del R_f con la concentración de etanol.

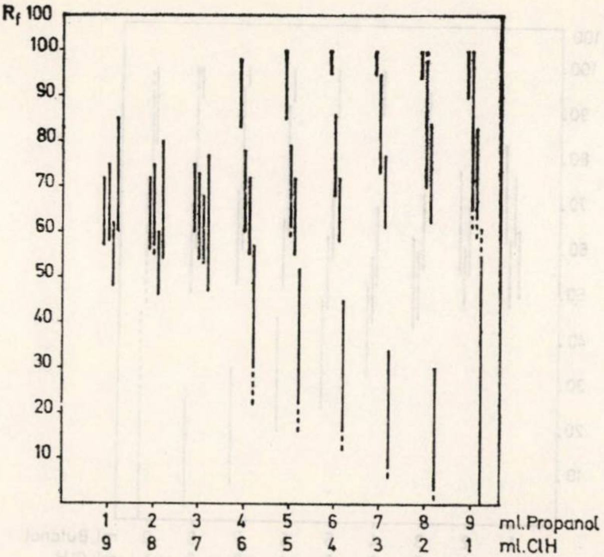

Fig. 9. — Variación del R_f con la concentración de propanol.

Fig. 10. — Variación del R_f con la concentración de isopropanol.

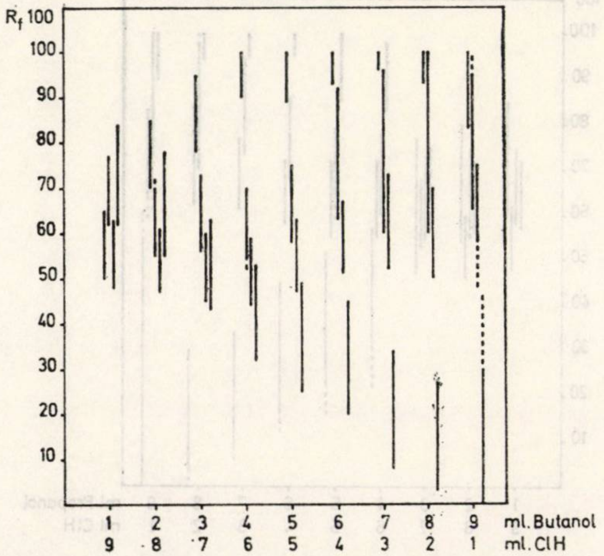

Fig. 11. — Variación del R_f con la concentración de butanol.

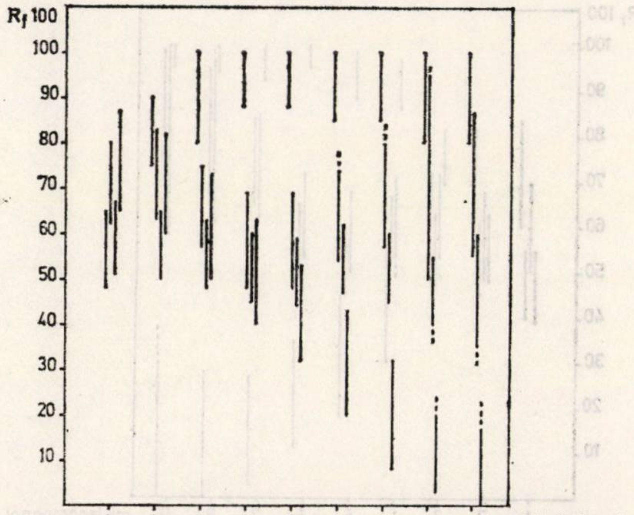

Fig. 12. — Variación del R_f con la concentración de isobutanol.

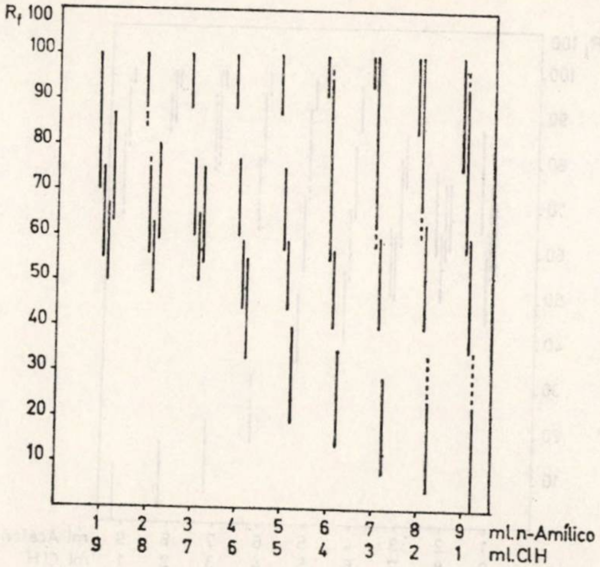

Fig. 13.— Variación del R_f con la concentración de n-amílico.

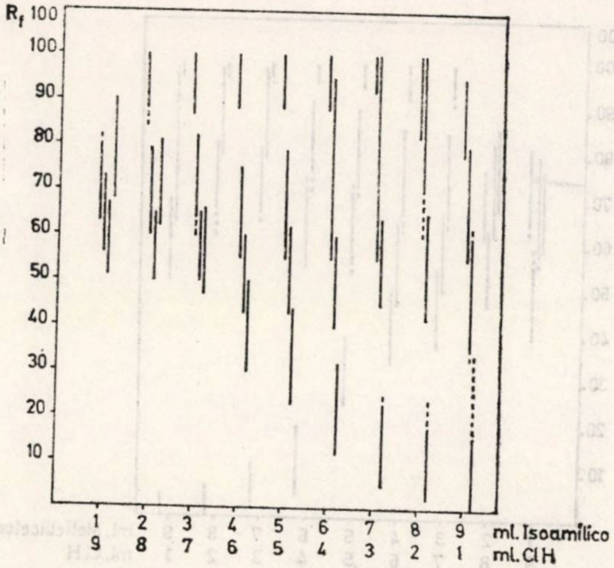

Fig. 14. — Variación del R_f con la concentración de isoamílico.

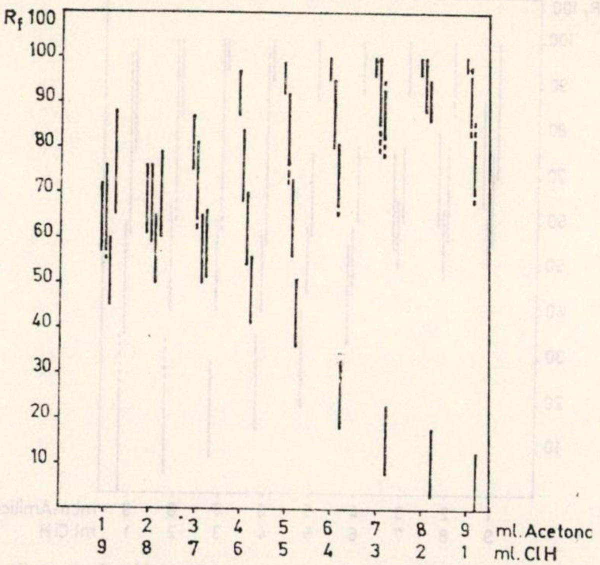

Fig. 15. — Variación del R_f con la concentración de acetona.

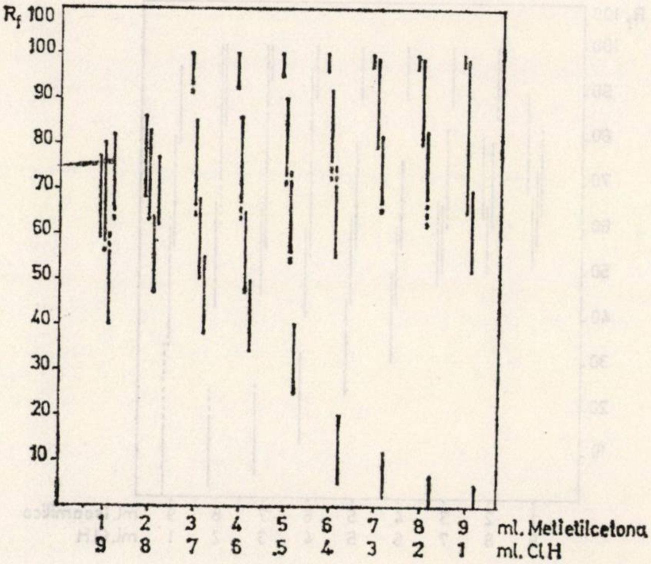

Fig. 16. — Variación del R_f con la concentración de metiletilcetona.

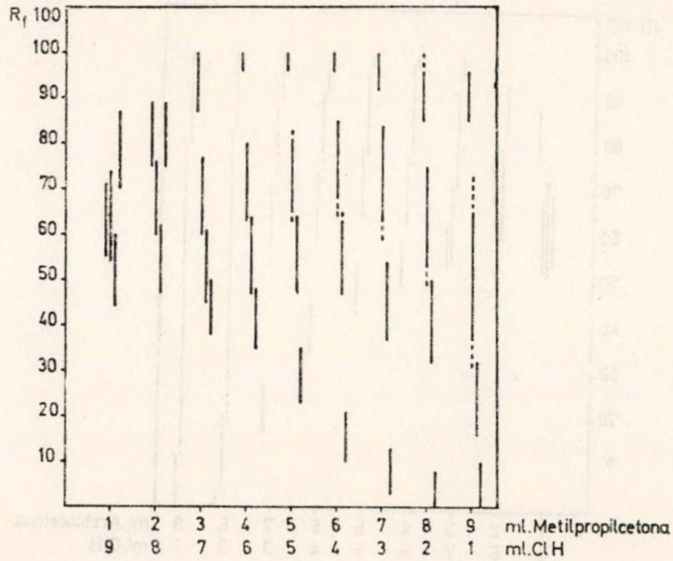

Fig. 17. — Variación del R_f con la concentración de metilpropilcetona.

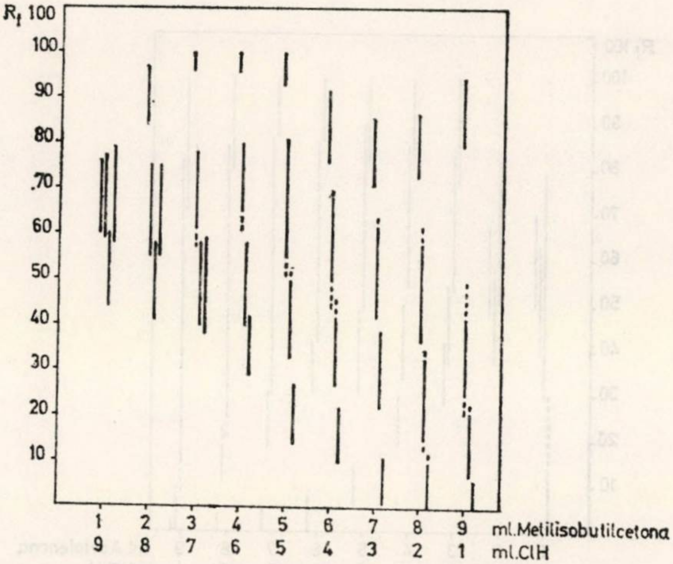

Fig. 18. — Variación del R_f con la concentración de metilisobutilcetona.

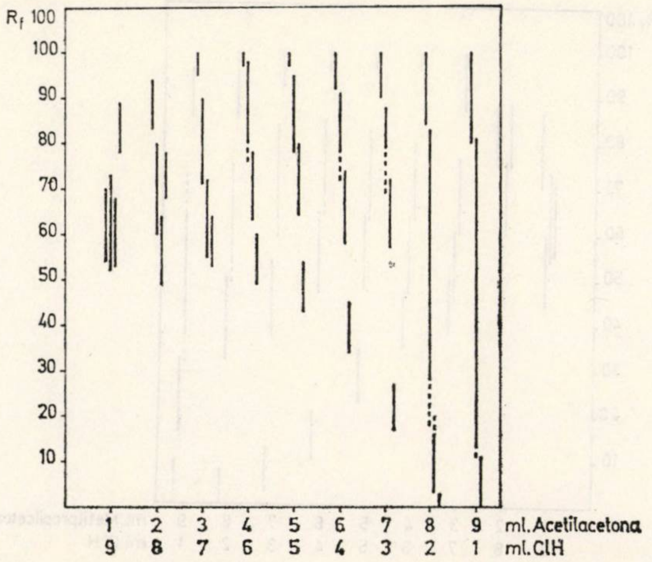

Fig. 19. — Variación del R_f con la concentración de acetilacetona.

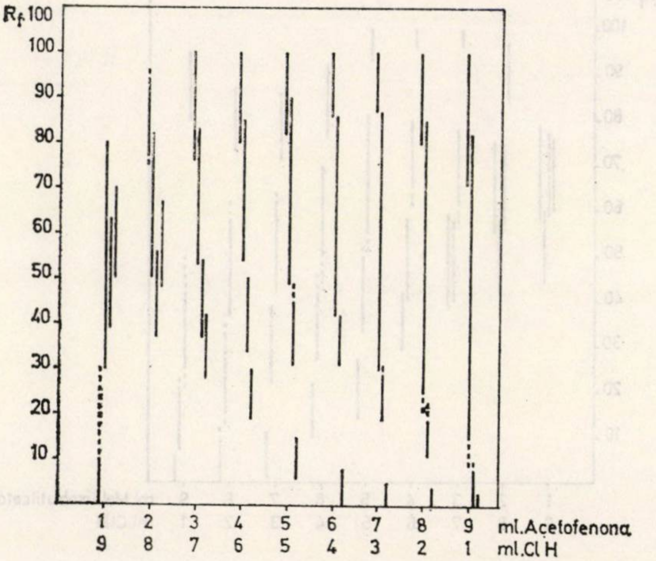

Fig. 20. — Variación del R_f con la concentración de acetofenona.

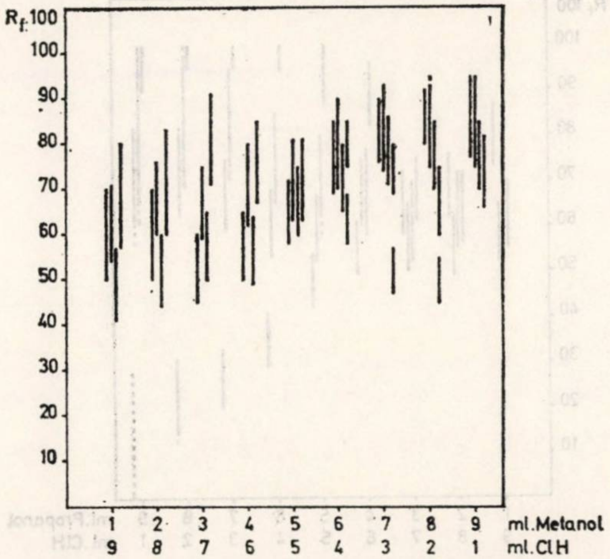

Fig. 21. — Variación del R_f con la concentración de metanol.

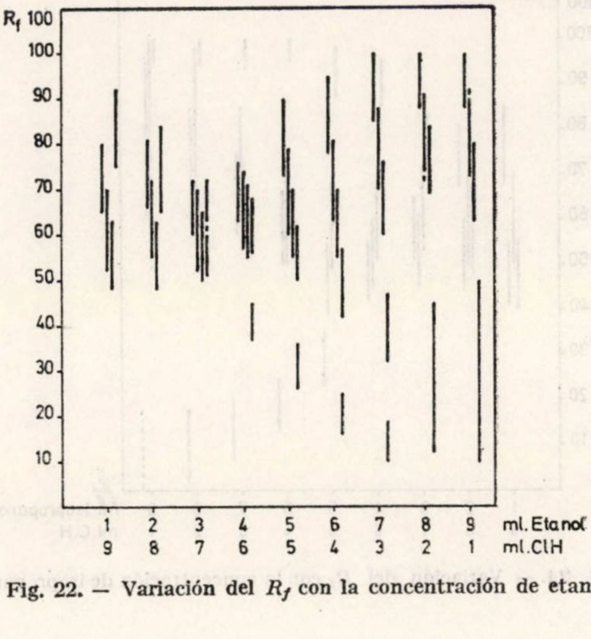

Fig. 22. — Variación del R_f con la concentración de etanol.

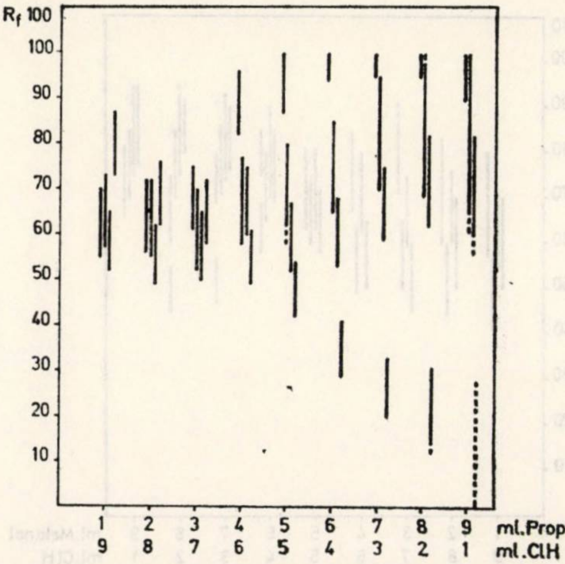

Fig. 23. — Variación del R_f con la concentración de propanol.

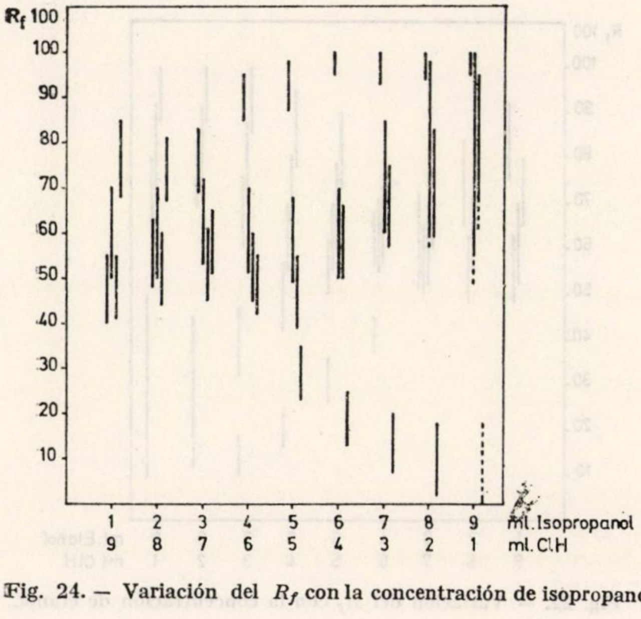

Fig. 24. — Variación del R_f con la concentración de isopropanol.

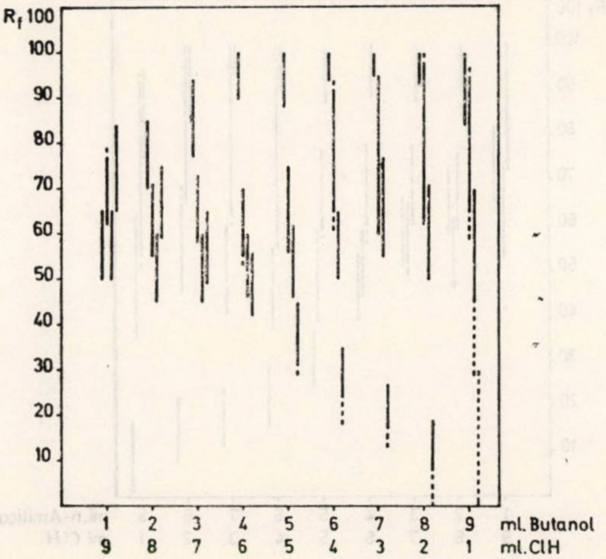

Fig. 25. — Variación del R_f con la concentración de butanol.

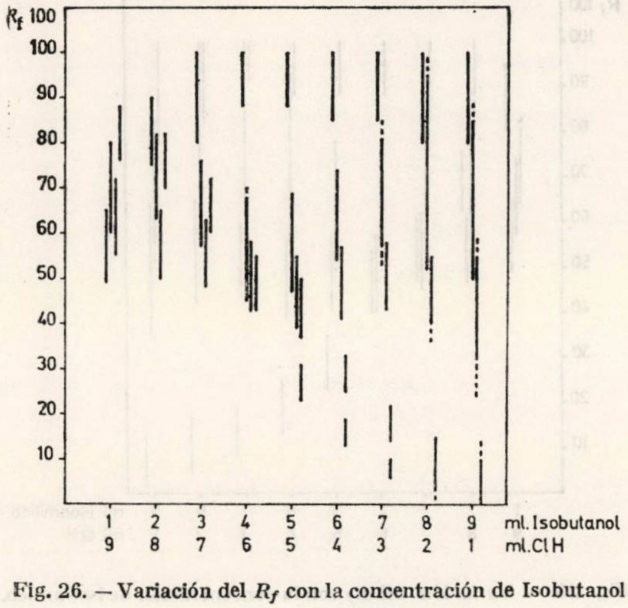

Fig. 26. — Variación del R_f con la concentración de Isobutanol.

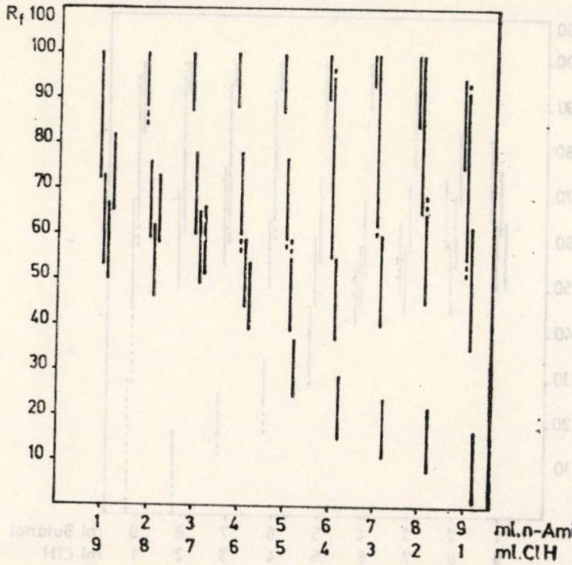

Fig. 27. — Variación del R_f con la concentración de n-amílico.

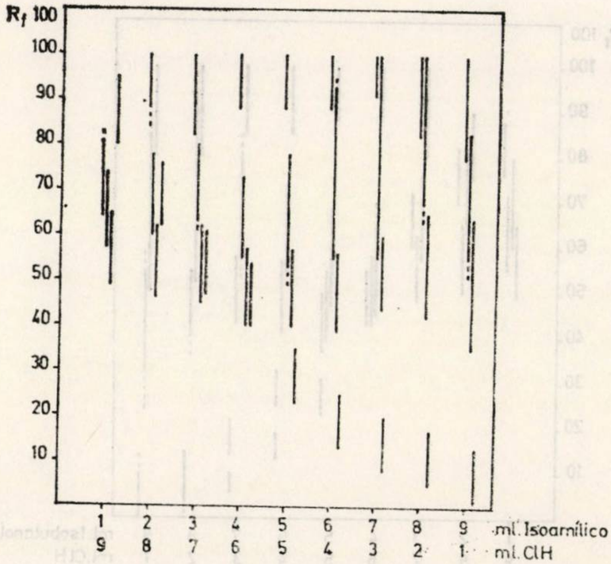

Fig. 28. — Variación del R_f con la concentración de isoamílico.

El comportamiento de estas mezclas respecto a la naturaleza y proporción del componente orgánico en el disolvente, es idéntico también al indicado para las mezclas de cuatro elementos.

También se ha llevado a cabo un estudio de la mezcla de los cinco, si bien se han utilizado otros disolventes, ya que los resultados obtenidos anteriormente, indican claramente que con disolventes formados por mezclas de cetona-ClH y alcohol-ClH en las proporciones indicadas y siguiendo la técnica utilizada, la separación de los cinco no es satisfactoria.

Asímismo, se han variado las dimensiones y naturaleza de la tira de papel cromatográfico, se ha modificado la técnica a seguir y se ha realizado cromatografía en capa fina.

A continuación se reseñan las modificaciones que se han efectuado, explicando brevemente, aquellas que nos han conducido a resultados aceptables.

1. — Desarrollos cromatográficos sobre tiras tratadas previamente
   Cloruro de Amberlita LA-1 en benceno
   Solución acuosa de ClLi al 6 %
   Solución saturada de $S_2O_8K_2$
   Solución al 20 % de tri-n-butilfosfato en Cl_4C
   Solución O'2 M de tri-n-butilamina en benceno
2. — Cromatografía ascendente sobre tiras de 3 × 22 cm con 18 cm de desarrollo neto.
3. — Cromatografía ascendente sobre tiras de papel Whatman nº1.
4. — Cromatografía descendente sobre tiras de 3 × 37 cm.
5. — Cromatografía bidimensional sobre placas de papel de 19 × 19 cm.
6. — Cromatografía en capa fina
   Sobre placas de celulosa de 500μ de espesor
   Sobre placas comerciales de silicagel con 2 mm de espesor.
7. — Cromatografía ascendente con doble desarrollo.

Utilizando como disolvente metilpropilcetona — ClH (7 : 3) se desarrolla el cromatograma en el que se ha depositado la muestra de los cinco elementos. Una vez que se ha alcanzado el límite señalado previamente, se interrumpe el mismo, se seca y se pulveriza la zona que contiene el iridio y el rodio con agua de Cl_2, con el fin de oxidar el iridio, se deja secar la tira y se vuelve a introducir en el disolvente, interrumpiendo el desarrollo cuando el frente alcanza la altura en que previamente se ha localizado el paladio.

Siguiendo este mismo procedimiento se han llevado a cabo experiencias en las que el disolvente está compuesto por butanol saturado con ClH 3 M y se pulveriza la tira con H_2O_2 de 110 vol., para lograr asímismo la oxidación del iridio.

También con este disolvente, se ha modificado el procedimiento a seguir, ya que una vez efectuado el primer desarrollo, se seca el cromatograma y se introduce nuevamente en el mismo disolvente al que se le ha añadido el H_2O_2 de 110 vol.

Los resultados obtenidos con estas experiencias y principalmente, con la indicada en último lugar, se logra una separación de los cinco elementos, si bien, debido a que el iridio y el rodio presentan coloraciones muy semejantes con los detectores válidos para estos elementos, la identificación de los mismos resulta difícil.

Por otra parte, la tira cromatográfica, sometida a este doble desarrollo se deteriora considerablemente, factor que también dificulta la identificación y diferenciación de las dos manchas.

A la vista de los resultados obtenidos, se ha considerado de mayor interés, el estudio y separación de las mezclas cuaternarias indicadas, ya que la mezcla de cinco elementos presenta serias dificultades. [16]

BIBLIOGRAFIA

[1] M. Lederer, *Nature,* **162**, 776 (1948).

[2] T. Setty, *Curr. Sci.*, **29**, 221 (1960).

[3] N. Kember y R. Wells, *Analyst*, **80**, 735 (1955).

[4] D. B. Rees-Evans, W. Ryan y R. A. Wells, *Analyst*, **83**, 356 (1958).

[5] E. Blasius y M. Fischer, *Z. anal. Chem.*, **177**, 412 (1960).

[6] E. Blasius y M. Fischer, *Z. anal. Chem.*, **178**, 28 (1960).

[7] V. Voicu y T. Nascutiu, *Studii şi Cercetări Chim. Acad. R. P. Romania Fil. Cluj*, **9**, 699 (1961).

[8] F. H. Burstall, G. R. Davies, R. P. Linstead y R. A. Wells, *Nature*, **163**, 64 (1949).

[9] F. H. Burstall, G. R. Davies, R. P. Linstead y R. A. Wells, *J. Amer. Chem. Soc.*, **72**, 516 (1950).

[10] G. M. Varshal, L. S. Shulik y V. A. Sychkova, *Zhur. anal. Khim.*, **25**, 2188 (1970).

[11] I. Akaza, T. Kiba y T. Kiba, *Bull. Chem. Soc. Japan*, **43**, 2063 (1970).

[12] J. W. O'Langhlin y C. V. Banks, *Analyt. Chem.*, **63**, 1223 (1964).

[13] S. Przeszlakowski y E. Soczewinski, *Chem. Analit.*, **11**, 898 (1966).

[14] A. Waksmundzki y S. Przeszlakowski, *Chem. Analit.*, **17**, 333 (1972).

[15] S. Przeszlakowski y A. Flieger, *J. Chromatogr.*, **81**, 129 (1973).

[16] M. L. Tascon, Tesis Doctoral, Universidad de Valladolid, 1979.

Revue Roumaine de Chimie, 25, 6, 901–904 (1980)

SEPARACIÓN CROMATOGRÁFICA DE ORO, PLATINO, PALADIO, RODIO E IRIDIO. II.

ESTUDIO CUANTITATIVO

M. L. TASCON GARCIA

Departamento de Química Analítica. Facultad de Ciencias. Universidad de Valladelid. Valladolid, España

Recibido el 21 de junio de 1979

Se ha llevado a cabo un estudio para la determinación cuantitativa de los elementos oro, platino, paladio, rodio e iridio, después de su separación cromatográfica Se propone la forma más adecuada para llevar las manchas a disolución, el método colorimétrico para determinar los elementos en la misma y el intervalo óptimo de concentración.

After chromatographic separation (reported in the Part I of this work) quantitative methods are described for the determination of gold, platinum, palladium, rhodium and iridium. The more suitable technique for the removal of the metals from the paper, the practical colorimetric method for the analytical determination and the optimous concentration range were proposed.

INTRODUCCIÓN

Con este trabajo se pretende comprobar si la separación cromatográfica de estos elementos, propuesta anteriormente[1] puede ser cuantitativa, lo que nos permitiría determinar en qué cantidad se encuentran en una muestra.

Para llevar a cabo esta determinación cuantitativa, se ha elegido la técnica colorimétrica, con el fin de llegar a unos resultados óptimos de la forma más sencilla posible, conjugando ésta con la simplicidad de la cromatografía que previamente se ha utilizado.

Ha sido muy escasa la bibliografía encontrada acerca de los procedimientos de extracción de los elementos de las zonas del cromatograma y los subsiguientes métodos de determinación cuantitativa. Así Kember y Wells[2] recomiendan para todos los elementos la elución mediante tratamiento de las zonas con soluciones de diferente composición y posteriormente determinan espectrofotometricamente el rodio y platino con Cl_2S_n, paladio con p-nitrosodimetilanilina y ácido tioglicólico y para el iridio siguen un método de microtilulación volumétrica.

Beamish[3] utiliza la combustión en seco de las zonas, disolviendo posteriormente el resíduo y determinando espectrofotométricamente el paladio con p-nitrosodimetilanilina y el platino con Cl_2S_n.

Varshal[4] propone el método espectrofotométrico para el platino y rodio con p-nitrosodimetilanilina después de extraerlos por elución y también el mismo método para el paladio con metasulfonitrofenol, después de eliminar el soporte de celulosa por incineración o por vía húmeda. Para el iridio sigue un método cinético después de que éste se ha extraido del papel por vía húmeda mediante la descomposición del mismo.[5]

PARTE EXPERIMENTAL

Aparatos y metodo general de trabajo

Los aparatos y disolventes utilizados en la separación cromatográfica se han indicado anteriormente,[1] así como la concentración y preparación de las disoluciones de los distintos elementos.

La determinación colorimétrica se lleva a cabo en un espectrofotómetro Spectronic 20 con cubetas de 1 cm de diámetro interior.

La técnica operatoria consiste en disolver las manchas de los elementos, una vez que han sido separados cromatográficamente y determinar posteriormente la cantidad presente en las mismas mediante los métodos colorimétricos elegidos.

El porcentaje de elemento se halla con ayuda de líneas de calibrado. Para la construcción de estas líneas de calibrado se utilizan cromatogramas patrón que contienen cantidades conocidas de los diferentes elementos y de los que se extraen los mismos, siguiendo el procedimiento de disolución apropiado para cada caso.

A partir de estas líneas de calibrado y siguiendo el método de Ringbom,[6] se establece el intervalo óptimo de concentración en el que el error analítico relativo es mínimo para un error fotométrico del 1 % y del 0,2 %.

DESCRIPCION Y RESULTADOS

Determinación de oro

La disolución de la mancha se lleva a cabo con agua regia y para ello se coloca la zona del cromatograma que contiene el elemento en un matraz erlenmeyer de 25 ml; se añaden 2 ml de agua regia y se calienta en baño de agua a ebullición durante 10 minutos con el fin de eliminar el agua regia. Transcurrido este tiempo se interrumpe el calentamiento y se enfría hasta temperatura ambiente, pasando a continuación la solución a un matraz aforado de 25 ml; el matraz erlenmeyer se lava dos o tres veces con pequeños volúmenes de agua.

Una vez disuelto el oro, se procede a su determinación colorimétrica siguiendo el método de la Rodamina B.[7]

Para la construcción de la línea de calibrado se han utilizado cromatogramas patrón que contienen de 2,5 µg a 30 µg de oro.

El intervalo óptimo de concentración siguiendo este procedimiento ha resultado ser de 0,45 p.p.m a 1,5 p.p.m. con un error analítico relativo de 2,88 % para un error fotométrico del 1 % (0,58 % si el error fotométrico es del 0,2 %).

Determinación de platino y rodio

Para la determinación de estos elementos se ha seguido el método de la p-nitrosodimetilanilina propuesto en la bibliografía,[4] tanto en lo que se refiere a disolución de las manchas como a método colorimétrico.

Los cromatogramas patrón utilizados para la construcción de las líneas de calibrado, contienen 1,58 μg a 25 μg de platino y de 2 μg a 20 μg de rodio.

El intervalo óptimo de concentración para el platino es de 0,11 p.p.m. a 0,39 p.p.m. con un error analítico relativo del 2,8 % para un error fotométrico del 1 % 0,56 % cuando el error fotométrico es del 0,2 %). En el caso del rodio, dicho intervalo es de 0,14 p.p.m. a 0,42 p.p.m. con un error analítico relativo del 2,8 % para el 1 % de error fotométrico (0,56 % si el error fotométrico es del 0,2 %).

Determinación de paladio

Para llevar a cabo la extracción del paladio de la tira cromatográfica, se corta la zona de la misma que contiene el elemento y se coloca en un matraz erlenmeyer de 25 ml; se añaden 1,5 ml de ClH 4 M y se calienta suavemente en baño de agua durante 10 minutos.

Transcurrido este tiempo se interrumpe el calentamiento y se enfría a temperatura ambiente.

A continuación se pasa la solución a un matraz aforado de 25 ml que contiene 1,5 ml de solución 4 M de CH_3COONa y 0,5 ml de solución de p-nitrosodimetilanilina (solución al 0,5 % de p-nitrosodimetilanilina en alcohol absoluto). El matraz erlenmeyer se lava con 4 ml de agua y succesivos volúmenes de alcohol, pasando estos volúmenes al matraz aforado que se enrasa finalmente con alcohol; transcurridos 30 minutos se mide la absorbancia a 525 nm.

La línea de calibrado se construye a partir de cromatogramas patrón que contienen de 1,5 μg a 21 μg de paladio.

La solución en blanco se prepara sometiendo al mismo tratamiento, una zona de la tira, de igual tamaño que las que contienen el paladio y que previamente se ha desarrollado con los mismos disolventes.

El intervalo óptimo de concentración es de 0,11 p.p.m. a 0,48 p.p.m., con un error analítico relativo de 2,7 % para un error fotométrico del 1 % (0,54 % cuando el error fotométrico es del 0,2 %).

Determinación de iridio

Para la determinación colorimétrica del iridio, se ha seguido el método basado en el uso de Cl_2S_n en medio BrH, [8] si bien en este caso, es necesario modificar el procedimiento, ya que previamente ha de extraerse el elemento del cromatograma. [9]

La disolución de la mancha se consigue con BrH (1 : 1)·y para ello se corta la zona del cromatograma que contiene el elemento y se coloca en un matraz erlenmeyer de 25 ml; se añaden 5 ml de BrH (d = 1,488) y 5 ml de agua y se calienta en un baño de agua en ebullición; después de 10 minutos se añaden 5 ml de solución de $Cl_2S_n \cdot 2\,H_2O$ al 25 % en BrH (d = 1,488) y se continúa el calentamiento durante 2 minutos. Transcurrido este tiempo se interrumpe este calentamiento y se enfría, hasta temperatura ambiente, en corriente de agua fría. Se filtra la solución a través de placa de vidrio filtrante y se pasa a un matraz aforado de 25 ml; se lava el matraz erlenmeyer y la placa filtrante con pequeños volúmenes de agua que se recogen en el matraz aforado y que finalmente se enrasa con agua. Transcurridos 10 minutos se mide la absorbancia a 402 nm.

La línea de calibrado se construye mediante cromatogramas patrón que contienen de 10,8 μg a 84,7 μg de iridio.

La solución en blanco se prepara sometiendo al mismo tratamiento una zona de tira cromatográfica de igual tamaño que las que contienen el iridio y que previamente se han desarrollado con los mismos disolventes.

El intervalo óptimo de concentración es de 0,79 p.p.m. a 2,9 p.p.m., con un error analítico relativo del 2,7 % para un error fotométrico del 1 % (0,54 % si el error fotométrico es del 0,2 %).

BIBLIOGRAFIA

[1] Part I: M. L. Tascon Garcia, *Rev. Roumaine Chim.* **25**, 881 (1980).

[2] N. Kember y R. Wells, *Analyst*, **80**, 735 (1955).

[3] F. H. Beamish, "The Analytical Chemistry of the Noble Metals", Pergamon Press. Oxford. 1966.

[4] G. M. Varshal, V. A. Sychkova, L. S. Shulik, R. F. Pro Pistsova y N. N. Nikol'skaya, *Zhur. anal. Khim.*, **25**, 2419 (1970).

[5] G. M. Varshal, L. P. Tikhonova, V. A. Sychkova y L. S. Shulink, *Zhur. anal. Khim.*, **25**, 2427 (1970).

[6] A. Ringbom, *Z. anal. Chem.*, **115**, 333 (1939).

[7] B. J. McNulty y L. D. Woollard, *Analyt. Chim. Acta*, **13**, 154 (1955).

[8] S. S. Berman y A. E. McBryde, *Analyst*, **81**, 566 (1956).

[9] M. L. Tascon, Tesis Doctoral, Universidad de Valladolid, 1979.

Revue Roumaine de Chimie, 25, 6, 905–908 (1980)

BOOK REVIEWS

Large Amplitude Motion in Molecules, **Volumes I and II (Topics in Current Chemistry, 81 and 82), Springer Verlag Berlin Heidelberg — New York, 1979, 180 + 184 pp.**

Structural chemistry has been traditionally concerned mostly with elucidating the conformation of quasi-rigid molecules. Large-amplitude motions have been at their best either considered separately from the small-amplitude nuclear motions, or neglected altogether as embarassing exceptions — the wrong note in the harmonious concert of the methods of treating molecular vibrations. The importance of motions such as the internal rotation, ring puckering or pyramidal inversion was early recognised, however, and these were treated properly by many workers ; Mizushima's book, for example, published a quarter of a century ago, still remains a classic for the treatment of the internal rotation.

Difficulties such as the great difference between the potentials governing small-and large-amplitude vibrations have not only prevented the emergence of a unified theory for treating both these molecular motions, but had also repercussions on the proper treatment of large-amplitude motions themselves. Lately, attempts were being made to overcome such difficulties and to consider a unique point of view in the treatment of both kinds of vibrations.

The book reviewed herein represents a collection of four extended articles which try to approach the problem of large-amplitude motions from a more encompassing point of view than in the past. The articles cover such relevant topics as the extension of group theory to non-rigid molecules, the Hamiltonian of non-rigid molecules, the electron diffraction method as a means of setting up the structure of molecules with large-amplitude motion, and the low frequency vibrations of small ring molecules.

The purpose of the theoretical contributions in the book is to offer a basis for treating the large-amplitude motions in a way as similar as possible to that already widely used for infinetisimal vibrations. Since a Hamiltonian written in a rectilinear coordinate basis, as used for rigid molecules, leads to slow convergence of the perturbation treatment when applied to non-rigid molecules, it should be necessary to find generalised coordinates which can speed up the convergence. It is the merit of the last paper in the book to have found such coordinates as natural extensions of those already standardised, as well as the compulsory transformation relations. In a similar manner proceed the authors of the other theoretical paper in the book, who extend the concept of "covering symmetry" of rigid point sets to non-rigid point sets, thus establishing the isometric group, an efficient working tool in the treatment of non-rigid molecules.

Both contributions dealing with experimental methods have the merit of being very well researched and of offering the reader a wealth of data on non-rigid molecules. The need for studying the compounds in which large-amplitude motions are present in gas phase is rightly emphasised : these motions involve low force constants and the corresponding potential function is very sensitive to the spurious intermolecular interactions which would occur in condensed phases.

Since the importance of the molecular flexibility in various chemical processes now begins to be recognised, the publication of such a book is most welcome. In fact, no interaction between molecules can be properly considered without allowing for their flexibility. For instance, such an approach would be essential in accounting for the existence of conformational option in biologically active compunds and therefore in explaining some vital phenomena or in finding more efficient drugs. On the other hand, large-amplitude vibrations make a significant contribution to the partition function of a system and therefore to the thermodynamic properties of materials. Beside such practical advantages, the study of non-rigid molecules is interesting in itself and is currently a challenge for scientists to find better ways of approaching the problem. The book may be warmly recommended to researchers as an excellent guide on these lines.

Alex. Butucelea

PH. GÜTLICH, R. LINK and A. TRAUTWEIN, *Mössbauer Spectroscopy and Transition Metal Chemistry*, Springer — Verlag, Berlin —Heidelberg — New York, 1978, 280 p.

The book authored by Prof. Philipp Gütlich and Dr. Rainer Link of Mainz University and Prof. Alfred Trautwein of Saarbrücken University, is actually an exhaustive work dedicated to the applications of the Mössbauer spectroscopy to the field of transition metal chemistry.

The material is divided into 8 chapters, differing in point of length and subject range.

The first 5 introductory chapters aim to introduce the reader into the Mössbauer spectroscopy, its theory and practice. Chapter 1 makes a short introduction (3 pages), chapter 2 (8 pages) deals with the physical grounds of the Mössbauer spectroscopy, chapter 3 (27 pages) treats the hyperfine interactions between nuclei and electronic properties such as electric and magnetic fields, chapter 4 (11 pages) contains the experimental Mössbauer techniques and chapter 5 (3 pages) mentions shortly the main mathematical methods for interpreting the Mössbauer spectra.

Chapter 6 (54 pages) treats in detail the interpretation of the Mössbauer parameters of the iron compounds. The authors emphasize the chemical information which may be obtained with the hyperfine electric and magnetic interactions, as reflected in the Mössbauer spectra. Particular emphasis is laid on the connections between chemical properties (chemical bonding and structure) and quantum chemical methods (theories) of chemical bonding. From the tremendous amount of publications regarding the^{57} Fe Mössbauer spectroscoy the authors have selected for this chapter 162 original papers.

Chapter 7 devoted to the Mössbauer active transition elements other than iron (Ni, Zn. Ru, Hf, Ta, W, Os, Ir, Pt, Au, Hg) is the most extensive part of the book (111 pages). This is so because the authors have intended this chapter to be particularly useful to all research workers who are actively concerned with Mössbauer work on non-iron transition elements. This chapter is exhaustive and 247 original papers are cited therein.

The last chapter (53 pages) aims to give to the less informed reader an idea on the various research fields where the techniques based on the Mössbauer effect play an important role (study of the solid state reactions, frozen solution studies, surface studies, metallurgical research, study of aftereffects of nuclear transformations and biological applications).

The book contains 160 figures.

The book is very interesting and useful for various researchers working in different fields (chemistry, physics, biology, metallurgy)which are not acquinted with the Mössbauer spectroscopy. It is also of especial interest for the specialists in the chemistry and physics of the transition elements as well as for those working in the Mössbauer spectroscopy of the systems (compounds and alloys) of the transition elements.

A. C. Banciu

Polymers/Properties and Applications 3, Chemistry and Application of Phenolic Resins by A.Knop and W. Scheib, Springer-Verlag, Berlin—Heidelberg — New York, 1979, XIV + 270 p.

The third volume of the Springer—Verlag series ,,Polymer/Properties and Applications'' (which continues the older one entitled ,,Chemie, Physik and Technologie der Kunststoffe in Einzeldarstellung'') published by A. Knop and W. Scheib deals with some relevant topics on the chemistry and applications of phenolic resins. The book covers a wide range of theoretical and technical aspects concerning the formation, the properties and the field of application of phenolic resins, including a number of basic references up to 1978.

After a brief presentation, in chapter 1, of the historical and economic development of phenolic resins the second chapter treats the main raw materials used for the production of phenolic resins. Owing to their importance in resin synthesis, a special attention is paid to phenols and aldehydes.

The next chapter is devoted to some characteristic aspects of the reaction mechanism. Of these, the mechanism and kinetics for phenol-formaldehyde condensation under alkaline and acidic conditions are particularly discussed. Other connected aspects such as molecular structure and reactivity of phenols as well as formaldehyde-water and formaldehyde-alcohol equilibria are also considered. The fourth chapter presents shortly the main production processes for novolaks and resols. Besides the industrial production techniques some considerations for the synthesis on laboratory scale are made. Physiologic and environmental protection are further treated in the fifth chapter. First, the action of phenols and formaldehyde on the human body are discussed, and second, attention is focused on the environmental protection including water and exhaust air treatment processes.

Analytical methods for controlling the production and final quality of the resins are presented in the following chapter ; classic and modern investigation methods for the determination of the monomer, nitrogen or water content are reported. Special emphasis is laid on the analytical characterization and structure determination by chromatrographic and spectroscopic methods. A discussion on degradation of phenolic resins (thermal degradation, oxidation reactions and degradation by high energy radiation) is found in the seventh chapter. Some aspects concerning the mechanism of degradation are included.

The next ten chapters are devoted to the most common applications of phenolic resins modified and thermal-resistant resins, composite wood materials, molding compounds, heat and sound insulation materials, industrial laminates and paper impregnation, coatings, foundry resins, abrasive materials, friction materials, resins in rubber and adhesives. A separate chapter presents some phenolic antioxidants used in resin stabilization. The final chapter contains a number of important applications of phenolic resins in carbon and graphite material production, for chemical equipment, for fibers and other fields of a wide utility. A subject index ends the book.

The work presented above has a pronounced didactic character ; it is clearly and concisely written, well structured and developed. The material is fully illustrated with diagrams, flowsheets and figures. It is supposed to be useful for students and engineers or chemists working in the polymer field as well as for other professionals connected with the resin production.

V. Drăguțan

LANDOLT-BØRNSTEIN, *Numerical Data and Functional Relationships in Science and Technology*, New Series, II/9, Magnetic Properties of Free Radicals, Part c2, Springer—Verlag, Berlin—Heidelberg—New York 1979, X + 320 p.

The present volume is a new valuable contribution to the magnetic properties of free radicals that Springer-Verlag publishes in the well-known Landolt-Börnstein series. The book tabulates the magnetic properties reported since 1964 on organic O-, P-, S-, Se-, Si-, Ge-, Sn-, Pb-, As- and Sb-centered radicals and ends the series devoted to neutral radicals.

The book contains five new chapters of volume II/9. After Fischer's general introduction, Howard presents in a first chapter (chapter 7 of volume II/9) the magnetic properties of oxy- and peroxy-alkyl radicals. Herein, successively alkoxy, peroxyalkyl and trioxy radicals are included. The peroxyalkyl are grouped in species derived from hydrocarbon compounds and from hetero-substituted hydrocarbon compounds. The second chapter (chapter 8 of volume II/9) by Uber and Stegmann tabulates the data reported for aroxyl radicals including protonated semiquinones as well. The aroxyls are divided into carbocyclic and heterocyclic compounds each of these being arranged on monocyclic and two- or three-ring condensed structures.

Phosphorus-centered organic radicals are presented in the third chapter (chapter 9 of volume II/9) by Davis and Roberts ; the reader will find the magnetic properties for phosphonyl radicals of the type $X_2P^\cdot$, phosphonyl radicals of the type $X_2P^\cdot{=}0$, phosphoranyl radicals of the type $X_4P^\cdot$ containing the phosphate radical anions and related species, phosphonium cation radicals of the type $X_3P^{\cdot+}$, phosphine dimer cation radicals of the type $X_3P{\cdot}P^+X_3$ and related species. In the next chapter (chapter 10 of volume II/9) Stegmann tabulates the published data for sulfur- and selenium-centered radicals. Besides the neutral sulfur-centered radicals cation and anion radical species are also included.

The last chapter (chapter 11 of volume II/9) by Lehning gathers the magnetic properties for Si-, Ge-, Sn-, Pb-, As- and Sb-centered radicals. The chapter offers examples of neutral radical species of the above elements containing various aliphatic and aromatic substituents.

The book covers exhaustively the literature on the subject published since 1964. It will be a valuable acquisition for all scientific libraries. Like the other already issued parts of volume II/9, the present book constitutes a valuable guide for theoretical chemists and experimental spectroscopists and chemists dealing with organic radical chemistry.

V. Drăguțan

I. G. MURGULESCU and E. SEGAL, *Introducere în chimia fizică*, (Introduction to Physical Chemistry), vol. II, 1. *Teoria molecular cinetică a materiei* (The Molecular Kinetic Theory of Matter). Ed. Academiei Republicii Socialiste România, Bucureşti, 1979, 1030 p.

Designed as an extensive several-volume work, this book by Acad. Prof. I. G. Murgulescu, is much more than just a treatise of physical chemistry ; it is a window open to physical chemistry, to basic knowledge required for smoothing out the way to handbooks, to articles in journals, to improving the qualification of those involved in any kind of chemistry. The work is to be issued in three volumes subdivided into six parts.

These volumes represent an extension and systematization of the lectures in physical chemistry given by the author, who was the brilliant head of the Physical Chemistry Chair of the Department of Chemistry, University of Bucharest, and represent almost a quarter of a century of teaching and scientific activity ; the lectures have permanently been updated with the latest achievements in the field.

The first part of volume II (in collaboration with Prof. E. Segal), presents a theoretical description of the material systems in close connection with their properties. Special emphasis is laid on the understanding of the properties of matter from the kinetic molecular standpoint.

Using the kinetic and statistical methods, the authors present the theory of gas state including ideal and real gases in equilibrium, as well as in nonequilibrium states. Much space is devoted to the general theory of the solid state. Finally, the theories of liquids and solutions systems which exhibit intermediate properties between gases and solids, are presented.

The book consists of six parts, 47 chapters, 21 appendixes and numerous references. The topic is exposed systematically to make the work accessible.

Certain prerequisite knowledge is necessary in the reader's background. He should be familiar with the general foundations of mathematics, physics and chemistry.

The book is meant to meet the requirements of students and the teaching staff interested in physical chemistry, as well as of research-workers involved in this field.

D. I. Marchida

NOTE POUR LES AUTEURS

La Revue Roumaine de Chimie publie des articles en anglais, français, russe, allemand ou espagnol. Les auteurs sont priés d'envoyer des articles et des comptes rendus inédits.

Les manuscrits seront dactylographiés à deux intervalles. La bibliographie, les tableaux et la légende des figures seront placés après le texte.

Si l'article fait partie d'une série numérotée, le titre de la partie précédente sera indiqué dans une note au bas de la première page.

Chaque article sera précédé d'un résumé comprenant quinze lignes au maximum.

Les références bibliographiques dans le texte seront faites par des exposants sans parenthèses et paraîtront à la fin de l'ouvrage.

Les publications périodiques mentionnées dans la bibliographie seront présentées suivant les prescriptions internationales : le nom de l'auteur précédé de l'initiale du prénom, le titre du périodique abrégé conformément à « Chemical Abstracts » et souligné par une ligne, le numéro du tome indiqué par des chiffres arabes et souligné par deux lignes, suivi de la première page de l'article ; à la fin, l'année de la parution sera placée entre parenthèses. Le numéro de la revue ne sera pas indiqué, si les pages du volume sont numérotées consécutivement.

Les textes des livres ou traités incluеront : le nom des auteurs, les initiales du prénom, le titre du livre entre guillemets et sans être souligné, le numéro du tome précédé par l'abréviation « vol. » (ou « Bd.) », le numéro de l'édition, les éditions (the publisher), la localité de la parution du livre, l'année de la parution et la page de la référence précédée(s) par l'abréviation «p. » (ou « S. »).

Les brevets seront indiqués comme suit : l'auteur ou la firme, le pays et le numéro du brevet, la date et la revue (Chem. Abstr.). Par ex. : M. Jones (to Union Carbide Co), Brit. Pat. 601—238, 2 Sept. 1959, *Chem Abstr.*, 54, 12808 (1970).

Les diagrammes seront tracés à l'encre de Chine sur papier calque. Les tableaux et les figures (en nombre strictement nécessaire) seront numérotés par des chiffres arabes. Les courbes dans les figures seront numérotées par des chiffres arabes et leur explication sera donnée dans la légende des figures. Prière de ne pas inscrire les mêmes données dans les tableaux et les figures. Chaque tableau aura un titre. On indiquera dans le texte la place approximative des tableaux et des figures. Les formules chimiques seront incluses dans le texte ; en outre, elles seront transcrites sur papier calque, à l'encre de Chine.

Les auteurs sont priés d'indiquer les caractères italiques (en soulignant les lettres au crayon), ainsi que tout autre caractère spécial ; les préfixes *ortho*, *meta*, *para*, *cis*, *trans*, etc. seront soulignés pour indiquer leurs caractères italiques et ne seront jamais écrits avec des majuscules.

Aucune correction à la main ne sera admise sur le manuscrit. Les corrections seront frappées à la machine. Les lettres grecques ou autres symboles spéciaux seront insérés à la main à l'encre clairement.

Le manuscrit sera signé par l'auteur.

Le colonne-titre aura 50 lettres au maximum.

L'entière responsabilité du contenu des articles appartient aux auteurs.

Pour détails voir le n° 2 (1980).

PRINTED IN ROMANIA

66

TRAVAUX PARUS AUX ÉDITIONS DE L'ACADÉMIE DE LA RÉPUBLIQUE SOCIALISTE DE ROUMANIE

ELENA CEAUŞESCU, **Polimerizarea stereospecifică a izoprenului** (La polymérisation stéréospécifique de l'isoprène), 1979, 307 p.

A. T. BALABAN, L. GĂLĂŢEANU, G. GEORGESCU, LIGIA SIMIONESCU, **Compuşi marcaţi şi radiofarmaceutici cu aplicaţii în medicina nucleară** (Composés marqués et radiopharmaceutiques à application en médecine nucléaire), 1979, 495 p.

I. G. MURGULESCU, E. SEGAL, **Introducere în chimia fizică, vol. II. 1, Teoria molecular cinetică a materiei** (Introduction à la chimie physique, IIe vol. 1. 5. La théorie moléculaire-cinétique de la matière), 1979, 1003 p.

I. E. TEODORESCU, MARIA FITI, **Iradierea tehnologică** (Irradiation technologique), 1979, 216 p.

S. STERNBERG, FL. DANEŞ, **Termodinamica chimică aplicată** (La thermodynamique chimique appliquée), 1978, 400 p.

I. G. MURGULESCU, V. EM. SAHINI, **Introducere în chimia fizică. Vol. I. 2, Structura şi proprietăţile moleculelor** (Introduction à la chimie physique, Vol. I. 2. La structure et les propriétés des molécules), 1978, 604 p.

C. DRĂGULESCU, E. PETROVICI, **Chimie structurală modernă. Chimia coordinanţei** 8 (La chimie structurale moderne. La chimie de la coordinance 8), 1977, 947 p.

D. PURDELA (sous la direction de), **Nomenclatura chimiei anorganice** (La nomenclature de la chimie inorganique), 1977, 153 p.

I. ZUGRĂVESCU, MAGDA PETROVANU, **N-ylid chemistry**, coédition avec McGraw-Hill, 1977, 396 p.

D. NEGOIU, ANGELA KRIZA, **Poluanţi anorganici în aer** (Polluants inorganiques dans l'air), 1977, 220 p.

I. G. MURGULESCU, **Introducere în chimia fizică. Vol. I. Atomi, molecule, legătură chimică** (Introduction à la Chimie Physique, Ier vol. 1. Atomes, molécules, liaison chimique), 1976, 560 p.

E. P. BALTĂ, E. BALTĂ, **Introduction to the physical chemistry of the vitreous state**, coédition avec Abacus Press, 1976, 287 p.

H. I. GĂLĂŢEANU, **Radiochimia aplicată. Metode şi probleme** (La radiochimie appliquée. Méthodes et problèmes), 1976, 307 p.

CONST. V. UGLEA, **Cromatografia pe gel permeabil. Noi domenii de aplicare** (La chromatographie sur gel perméable. Nouveaux domaines d'application), 1976, 123 p.

CONST. GH. MACAROVICI, D. MACAROVICI, **Chimia oxizilor dubli şi utilizările lor** (La chimie des oxydes doubles et leur utilisation), 1975, 195 p.

ELENA CEAUŞESCU, **Research work on synthesis and characterization of macromolecular compounds. Contributions**, 1974, 251 p.

CR. SIMIONESCU, VIORICA RUSAN, V. POPA, **Chimia algelor marine** (La chimie des algues marines), 1974, 212 p., 1 pl.

1980 NOV 17

I. P. Informaţia c. 2136

43 426

Lei 25—

$ 55 (price per year)

F 1103 04

ACADÉMIE DE LA RÉPUBLIQUE SOCIALISTE DE ROUMANIE

REVUE ROUMAINE DE CHIMIE

TOME 25
N°. 7
Juillet 1980

EDITURA ACADEMIEI REPUBLICII SOCIALISTE ROMÂNIA

Rev. Roumaine Chim.

RRCHAX, 25, 7, p. 909–1128 (1980), Bucarest

ACADÉMIE DE LA RÉPUBLIQUE SOCIALISTE DE ROUMANIE

COMITÉ DE RÉDACTION

Rédacteur en chef:

I. G. MURGULESCU, membre de l'Académie de la République Socialiste de Roumanie

Rédacteurs en chef adjoints:

A. T. BALABAN et V. EM. SAHINI, membres correspondants de l'Académie de la République Socialiste de Roumanie

Collège de rédaction:

EM. BRATU, ELENA CEAUŞESCU, ECATERINA CIORĂNESCU-NENITZESCU, CR. SIMIONESCU, membres de l'Académie de la République Socialiste de Roumanie : P. SPACU, membre correspondant de l'Académie de la République Socialiste de Roumanie : MARGARETA AVRAM M. BANCIU, I. HAIDUC, D. I. MARCHIDAN, I. MOLDOVAN, G. NIAC et D. SĂNDULESCU

La Revue Roumaine de Chimie paraît 10 fois par an. Toute commande de l'étranger pour les travaux parus aux Editions de l'Académie de la République Socialiste de Roumanie sera adressée à ILEXIM, Departamentul Export-Import Carte (Livres)/Departamentul Export-Import Presă (Revues), P.O.B. 136—137, télex 11226, 3, str. 13 Decembrie, 9517 Bucarest, 12, Roumanie

Les manuscrits, les livres et les revues proposés en échange ainsi que toute correspondance seront envoyés à la redaction :

REVUE ROUMAINE DE CHIMIE

125, Calea Victoriei, 9717 Bucarest, Roumanie, téléphone 50 76 80

EDITURA ACADEMIEI REPUBLICII SOCIALISTE ROMÂNIA

125, Calea Victoriei, 9717 Bucarest, Roumanie, téléphone 50 76 80

REVUE ROUMAINE DE CHIMIE

Tome 25, Nº 7 Juillet 1980

EDITORIAL 911–914

N. ASANDEI, M. NICU, SILVIA BRĂNIȘTEANU, VIORICA NICU, M. RUSU, MARIA LUNGU and ALMERIA NATANSOHN, Acrylonitrile-cinnamic acid copolymerization. I. Copolymer structure 915–920

R. BACALOGLU, ARIANA MORARU, MARIA NUȚIU, S. ILUC, C. CSUNDERLIK and ELENA LUNGU, Liquid Crystals. II. Synthesis of *p*-alkyl anilines for benzilidene-aniline liquid crystals (in German) . . . 921–931

V. BĂRBOIU, ALMERIA NATANSOHN, C. ANDREI and D. BLUM, ^{1}H-NMR Method for composition, branching and sequence distribution determination in ethylene-vinyl acetate copolymers 933–939

J. BENISKA, G. KYSELÁ, E. ŠTAUDNER, M. CHLUPKOVÁ, Polymerization of styrene in the presence of *tert*-butylhydroperoxide and tetramethylthiourea 941–945

JOHN C. BEVINGTON, BRIAN J. TABNER and PETRINA F. FRIDD, The reactivities of monomers towards primary radicals, studied by spin-trapping 947–952

N. COBIANU, Radical alternating copolymerization of 9-vinylcarbazole with diethyl fumarate or diethyl maleate 953–960

FELICIA CORNEA and C. STOICESCU, Complexes of pyromellitic dianhydride with pyridine derivatives 961–967

I. G. DINULESCU, I. I. POGANY, ANGELA DUMITRIU, E. G. GEORGESCU and MARGARET AVRAM, New synthesis of dibenzo $(CH)_{10}$ and tetrabenzo $(CH)_{10}$ hydrocarbons. Diels–Alder reactions of tricyclo $[4.2.2.0^{2,5}]$deca-3.7.9-triene derivatives with 9.10-dibromoanthracene . . 969–973

D. DONESCU, I. DEACONESCU, KRISTIANA GOȘA, MAGDALENA MAZĂRE and I. GAVĂT, Kinetics of emulsion polymerization of vinyl acetate in the presence of hydroxyethylcellulose 975–980

MARIA DUMITRIU, M. DĂRÂMGĂ, MARIANA PĂSTRĂVANU and TATIANA LIXANDRU, On the thermal stability of some new polyazines and polyazomethines 981–988

SEVERIAN DUMITRIU and VICTOR BULACOVSCHI, Bioactive polymers. VII. Oxydoreductases and hydrolases immobilized on cellulose derivatives . 989–994

MIHAELA HILLEBRAND and A. T. BALABAN, Unrestricted Hartree-Fock spin densities in aryl-nitroso-aminyloxides and in acyl-aryl-aminyloxides . 995–1006

A. D. JENKINS, Termination of vinyl polymerization by transition metal ions . 1007–1010

ADRIANE G. LUDWICK and C. G. OVERBERGER, Synthetic macromolecules as therapeutic agents 1011–1015

Revue Roumaine Chim. **25**, 7, 909–1128 (1980) Bucarest

F. MATEI, AL. DUCA, GH. IONESCU and M. MACOVEANU, The interpretation of the kinetic data concerning the Zn^{2+} linking and elution on ion exchange membranes 1017–1024

RODICA MICU-SEMENIUC, LUMINIŢA SILAGHI-DUMITRESCU, N. CHIRILĂ and IONEL HAIDUC, Transition metal complexes of organothiophosphorous ligands. VI. Six-coordinate adducts of nickel(II) bis(dialkylphosphorodithioate) with aromatic diamines 1025–1031

I. G. MURGULESCU, GABRIELA MINCU and ECATERINA JURCONI, Catalysis by metal cation in the oxidoreduction reaction of bisoxalatodiaquo Co(III) complex with iodide ion in acidic medium 1033–1038

SPIRIDON OPREA, EMIL DUMITRIU and LAURENŢIA STEFĂNEL, Catalysis by polymers. I. Synthesis of 3-chloro-2-hydroxypropyl acrylate using quaternized poly(dimethylamino-ethyl methacrylate) as catalyst. 1039–1043

JAN F. RABEK and BENGT RÅNBY, Polynuclear Aromatic Hydrocarbons as sensitizers of photooxidative degradation of *cis*-1,4-polybutadiene 1045–1054

V. EM. SAHINI, Ş. MOLDOVEANU and C. MIHAILCIUC, On chlorobenzamide molecular structure 1055–1057

ROLF C. SCHULZ and ERHARD JACOBI, Optical rotatory dispersion of cellulose, cellulose-nitrate and of some α-polyglucans (in German) . . . 1059–1068

R. H. SCHUSTER and ANCA NICOLAU, Effects of the medium in solvolyses of alkyl halides. IV. Hydrolysis of *t*-butyl chloride (in German) 1069–1076

B. C. SIMIONESCU, R. MORA, M. LEANCA and C. ANANIESCU, Genesis of porphyrin-like compounds under simulated abiotic conditions. A possible mechanism of their formation. 1077–1082

MIHAELA SPIRATOS, A. AIRINEI and AGLAIA CIOBANU, Coordination polymers. II. Chelated polyesters of azomethine type (in French). . . . 1083–1089

GH. SURPĂŢEANU, CRISTINA LUCHIAN, M. CONSTANTINESCU, V. BĂRBOIU, MAGDA PETROVANU, 1,2,4-Triazolium-ylides. III. The theoretical aspects on the regioselectivity in the cycloaddition reaction of the triazolium-phenacyclide to the propiolic acid esters (in French) . . . 1091–1096

KIICHI TAKEMOTO, KIKUKO KANAOKA, MIKIJI MIYATA, Synthesis of new heterocyclic monomers under simulated prebiotic conditions 1097–1100

DAN S. VASILESCU, Alternating tendency in copolymerization. III. The behaviour of the systems acrylic monomer-vinyl ether-$ZnCl_2$ 1101–1111

RODICA VÎLCU and A. CIOCHINĂ, An alternative to the transient hot-wire method for thermal conductivity measurements of fluids 1113–1122

O. VOGL and S. YOSHIDA, Synthesis and polymerization of photoactive monomers 1123–1128

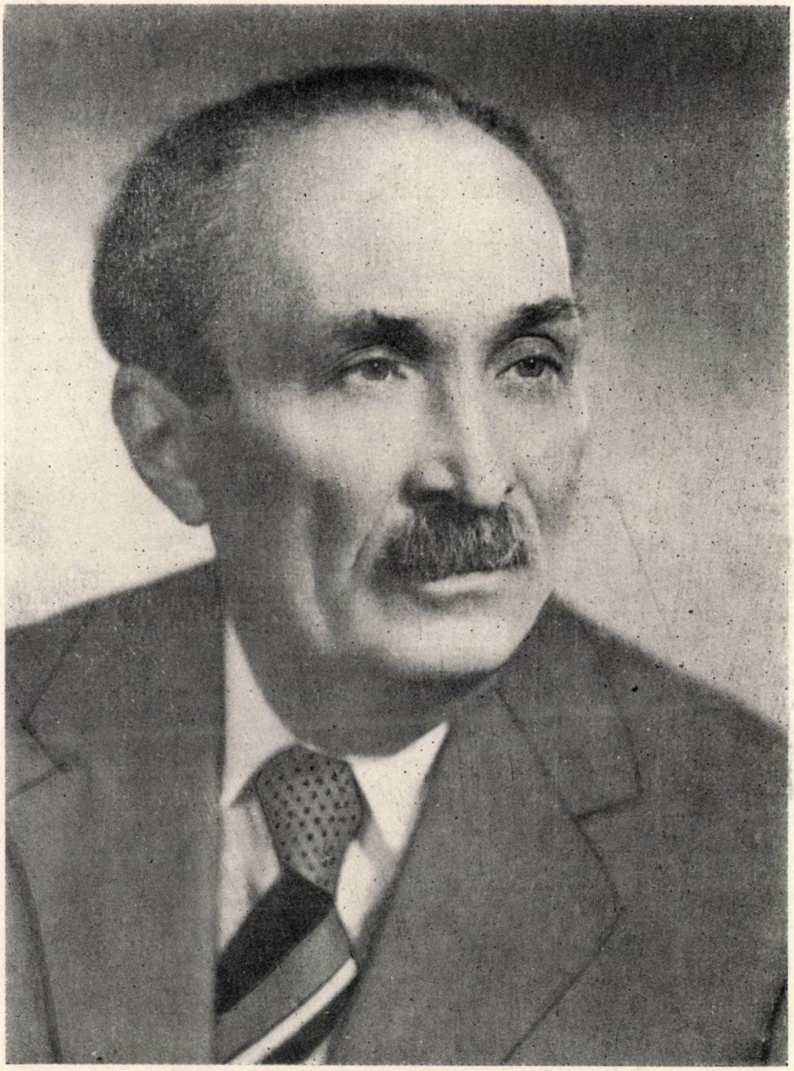

PROFESSOR CRISTOFOR I. SIMIONESCU

MEMBER OF THE ACADEMY OF THE SOCIALIST REPUBLIC OF ROMANIA

On the 17th of July, 1980, professor Cristofor I. Simionescu celebrates the 60th anniversary of his birthday.

Due to his remarkable scientific activity, his special didactic talent as well as to many-sided and continuous social activities of great responsibility, Cristofor Simionescu is an outstanding figure of a Romanian scientist and citizen, well known in his own country and abroad.

Born in 1920 in Dumbrăveni, Suceava, he attended the courses of the "Gh. Asachi" Polytechnical Institute in Iași, graduating as a chemical engineer, with "magna cum laude". Appointed as a preparative assistant, the young chemical engineer, Cristofor Simionescu passionately devoted his time to scientific and didactic activities. Over 1944—1946 he was assistant, then he started working to his doctoral thesis entitled "Contributions to knowledge of the indigeneous vegetable oils", and in 1948 he became doctor in technical sciences. Further on, he pursues the didactic hierarchy, being appointed lecturer in 1948 and professor in 1952. In 1969 he was awarded the title of Honoured Scientist, and in 1973 that of Honoured Professor.

The name of professor Cristofor Simionescu is closely related to that of the Polytechnical Institute in Iași where he has carried on his activity since the very beginning. Parallel to scientific and didactic activities, professor Simionescu has performed manifold functions of great responsibility in education. Thus, over 1949—1951 he was study director, between 1951 and 1952 a vice Rector, and since 1953 till 1976 the Rector of the Polytechnical Institute in Iași. He was a member of the High Education Commitee, General Director of the Ministry of Education (1952—1954), member of the Superior Commitee for Diplomas: now he is a member of the Superior Council of Universitary and Polytechnical Education.

The rich scientific activity of professor Simionescu, materialized in over 300 original works and 40 patents, covers various fields of great importance in the macromolecular and organic chemistry. Among these, we should first mention a field of great importance for his country, that of cellulose chemistry and related branches, the chemistry of wood, polysaccharides, paper etc. His contributions to the supermolecular structure of cellulose and to the molecular structure of lignin are well known all over the world.

As a proof of the importance of these works and the unanimous recognition of the professor Simionescu's school in this field, mention should be made of the publication of the well-known international journal "Cellulose Chemistry and Technology" in our country, journal founded in 1967 by academician Simionescu, who has been the chief editor since the very beginning.

The monographs of professor Simionescu dealing with various problems of cellulose chemistry are well known too : "The Chemistry of Wood in Romania" Ed. Academiei, 1964, "The Chemistry of Reed", Ed. Tehnică, 1966 (translated into Koreean language), "The Chemistry of Wood in Romania. Poplar and Willow" Ed. Academiei, 1973, "The Chemistry of See Weeds" Ed. Academiei, 1974.

Other major scientific contributions of professor Simionescu may be included within the large field of the macromolecular chemistry. Among these we could mention : the synthesis of new monomers, electro-initiated polymerizations, natural and synthetic polymer graftings, photo and semiconductor polymers, acetylene and ferrocene, derived polymers, small cyre-polyamides, the macrochemistry of polymers, a.s.o.

The books of professor Simionescu on these fields are well known in our country and abroad : "Mechanochemistry of Macromolecular Compounds" Ed. Tehnică, 1967, (translated into Russian), "Fractionation of Macromolecular Compounds" Ed. Academiei, 1969, as well as "A Treatise on the Chemistry of the Macromolecular Compounds" 3 volumes, Ed. Didactică și Pedagogică 1973, a book meant for the students of chemistry faculties.

Lately, professor Simionescu has tackled a new and very interesting field, that of the origin of life and of the precursors of the living matter. The original theory of professor Simionescu about the origin of life ("cold model") and the related researches (synthesis of protocells of high membrane potential from the primary atmosphere, etc.) are published in over 50 works that were the subjects of many conferences delivered at home or abroad and which are often quoted in the international literature of chemistry.

As a recognition of his important contributions to the chemical research, as well as his particular pedagogical qualities, professor Simionescu was appointed corresponding member of the Academy of Socialist Republic of Romania in 1955, and in 1963 full member of the Academy. Professor Simionescu has had important leading functions : president of the Academy Branch in Iași (1963–1974), member of the Academy

Presidium (1963 — up to the present), vice-president of the Academy (1974 — up to the present).

Professor Simionescu is the initiator and founder of the centers of research on natural and synthetic macromolecules from the Polytechnical Institute in Iași and from the Institute of Macromolecular Chemistry "Petre Poni", in Iași too. Professor Simionescu was the head of the macromolecular chemistry department (1956—1970) and since 1970 he has been its director. The important contributions of these centers of research are materialized in numerous publications and they have been presented at a large number of conferences by professor Simionescu and his collaborators at home and abroad.

Professor Simionescu passionately worked for the high level organization of many internal and international scientific manifestations, being president of the organizing commitees of six symposia on the chemistry and technology of cellulose and paper, 1961—1979, the president of the organizing commitee of the 39th International Congress of Industrial Chemistry, 1970 organized by "Société de Chimie Industrielle" — Paris, co-president of the first Romanian-American Seminar for the chemistry of polymers — Iași, 1976, co-president of the UNESCO reunion for the problems of chemical education — Louvain, 1978 and many others.

The imposing scientific activity and personality of professor Simionescu have been recognized by including him as a fellow of many foreign chemical societies (Technical Association of Pulp and Paper Industry, 1960, Association Technique de l'Industrie Papetière, 1960; Société Chimique de France, 1963; American Chemical Society, 1965, honorary member of the "Société de Chimie Industrielle", 1970; International Academy of Wood Science, 1971) by being elected a foreign member of the American Chemical Society on occasion of its centenary in 1976, by being awarded the "Diploma de Reconoscimento" of the Academy of the Republic of Cuba.

Professor Simionescu has important responsibilities as a national delegate to IUPAC (since 1967), as a member of the section of macromolecules of IUPAC (since 1969) and as the national representative in the IUPAC Commitee for Chemical Education.

Professor Simionescu carries on a complex and laborious activity as a member of the editorial commitees and advisory boards of many Romanian and foreign publications : *Celuloză și Hîrtie*, *Revista de Chimie București*, *Revue Roumaine de Chimie*, *Materiale Plastice București*, *Journal of Polymer Science*, *Faserforschung und Textiltechnik*, *European Polymer Journal*, *Polymer Bulletin*, etc.

Under the scientific guidance of professor Simionescu, 70 Romanian and foreign chemists and chemical engineers worked out their doctor's theses and researchers from various foreign countries worked under his direction. Many of the latter occupy leading places in education, industry or research.

A scientist and a citizen, professor Simionescu has carried out since his youth, parallel to the scientific activities, a manysided social-political activity. Owing to his remarkable qualities, he was elected a member of the Central Commitee of the Romanian Communist Party (at the Xth and XIth Congresses of the Romanian Communist Party), deputy in the Great National Assembly, member of the State Council, member of the Central Commision of Revision.

An aspect of the greatest importance of the activity of professor Simionescu is his work within the National Council for Science and Technology (1973—1979) and that of a member of the Executive Board (since 1973).

Continuously preoccupied by the propagation of the scientific knowledge by mass-media, he published hundreds of articles to popularize science, he published the book "Romanian Chemists" (1964), the collections of essays "Thoughts" (1978) (both in Romanian), he delivered numerous lectures.

His whole scientific, didactic, social activity has always been directed toward the benefit of the working people of his country.

For his particular achievements in his didactic, scientific and political activities, academician professor Simionescu was awarded many orders and medals of the Socialist Republic of Romania: The Star of the Socialist Republic of Romania, The Order of Work, The Order of the Scientific Merit, the Medals of the anniversaries of the Romanian Communist Party, The Order 23rd of August and many others.

On the occasion of the celebration of his 60th anniversary, the Editorial Board of our journal, his colleagues, pupils and students wish academician Cristofor Simionescu many years full of health and fruitful activity.

EDITORIAL BOARD

Revue Roumaine de Chimie, 25, 7, 915–920(1980)

Dedicated to Professor CRISTOFOR I. SIMIONESCU
on his 60th anniversary

ACRYLONITRILE-CINNAMIC ACID COPOLYMERIZATION. I.

COPOLYMER STRUCTURE

N. ASANDEI, M. NICU, SILVIA BRĂNIŞTEANU, VIORICA NICU, M. RUSU, MARIA LUNGU * and ALMERIA NATANSOHN **

* Polytechnical Institute, Dept. of Organic and Macromolecular Chemistry, Jassy, Romania

** Institute of Macromolecular Chemistry, Jassy, Romania

Received January 22, 1980

The copolymerization of acrylonitrile and cinnamic acid in water or methanol was studied; its mechanism is accurately described by a charge transfer model for low initial cinnamic acid concentrations, and by a penultimate model for higher concentrations. The copolymer composition was determined, together with some structural modifications during spinning processes, due to the spinning solution components.

1. INTRODUCTION

Cinnamic acid is a non-homopolymerizable monomer and its cost is relatively high; these are the reasons why it is not yet industrially used, although there are some literature data on its copolymers with styrene and derivatives,[1-6] acrylates,[7-9] methacrylates[10-17] and vinyl-pyridines.[6,18,19] Acrylonitrile — cinnamic acid — vinyl acetate terpolymers with less than 1% cinnamic acid in the initial mixture, were also studied.[20-23]

This work studies the mechanism of binary copolymerization of acrylonitrile with cinnamic acid and the structure of obtained copolymers. It also reveals the ways to modify the structure during the preparation of spinning solutions.

2. EXPERIMENTAL AND DISCUSSION

2.1. Cinnamic acid (CA) and acrylonitrile (AN) copolymerization

Cinnamic acid and acrylonitrile were copolymerized using the solution — suspension procedure with water or methanol as solvents. For water, the redox initiation system $K_2S_2O_8$ + + $Na_2S_2O_5$ was used, and for methanol, azoisobutyronitrile (AIBN). Initial compositions are given in table 1. The copolymers were analysed by IR and 1H-NMR spectroscopy and by nitrogen elemental analysis in order to determine their compositions (Table 1, Figure 3).

From IR spectroscopy (Figure 1), copolymer composition was determined by 700 and 2240 cm^{-1} absorption ratio, noting that the 700 cm^{-1} absorption of phenyl radical of cinnamic acid is not modified when the monomer is enchained. The calibration curve was established with polyacrylonitrile — cinnamic acid mixtures.

From NMR spectroscopy (Figure 2), the copolymer composition was determined by the ratio of signals corresponding to the CH_2 protons of acrylonitrile (2.05 ppm) and phenyl protons of cinnamic acid (7.40 ppm).

TABLE 1

Copolymerization data

Symbol	Initial mixture				Copolymer composition	
	Acrylonitrile		Cinnamic acid		Acrylonitrile	Cinnamic acid
	M_1 (% mol)	A* (mol/l)	M_2 (% mol)	B * (mol/l)	m_1(% mol)	m_2(% mol)
1051	95	12.70	5	0.14	91.5	8.5
1101	90	2.42	10	0.26	87.2	12.8
1151	85	2.16	15	0.38	83.5	16.5
1201	80	1.93	20	0.48	81.5	18.5
1251	75	1.72	25	0.57	78.7	21.3
1301	70	1.58	30	0.70	76.0	24.0
1351	65	1.36	35	0.73	73.6	26.0
1401	60	1.20	40	0.80	71.2	28.8
1451	55	1.00	45	0.87	69.0	31.0
1501	50	0.92	50	0.92	67.2	32.8

* A and B are the concentrations of the comonomers in the reaction medium.

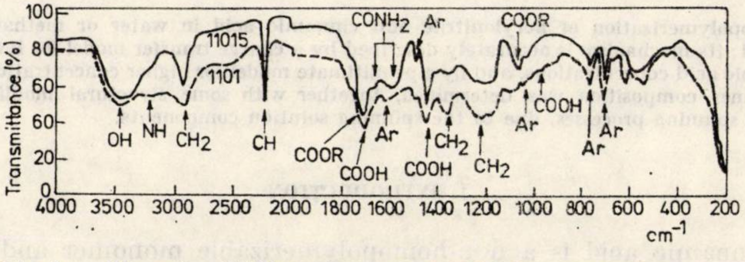

Fig. 1. — IR spectra of 1101 copolymers and of 1101 S copolymers after thermal treatment (S = solvent).

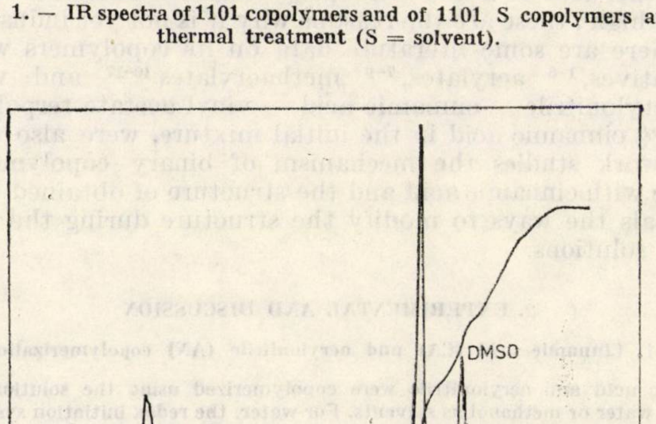

Fig. 2. — ¹H-NMR spectrum of 1401 copolymer synthesized in methanol.

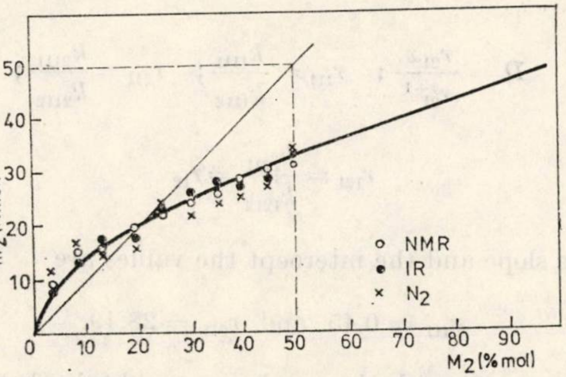

Fig. 3. – Copolymerization diagram.

2.2. Thermal treatment of spinning solutions

The synthesized copolymers were dissolved (10%) in ethylene carbonate, in order to reproduce the thermal treatement of preparation of spinning solutions. The solutions were thermostated at 80°C, 15 hours and one hour at 90°C, the copolymers were precipitated, washed with methanol and acetone, dried and reanalysed by IR and NMR spectroscopy and by nitrogen elemental analysis. Only the IR spectra evidenced structure modifications (Fig. 1).

3. COPOLYMER COMPOSITIONS

The general composition equation for the terminal model (Mayo-Lewis [24]) does not describe satisfactorily this copolymerization. This is the reason why the penultimate model described by Barb [25] is used :

$$\frac{n-2}{x}+\frac{1}{r_{21}}\cdot\frac{n-1}{x^2}=r_{11} \qquad (1)$$

where :

$$x=\frac{M_1}{M_2}; \quad n=\frac{m_1}{m_2}; \quad r_{11}=\frac{k_{111}}{k_{112}}; \quad r_{21}=\frac{k_{211}}{k_{212}}$$

and k_{111}, k_{112}, k_{211} and k_{212} are the rate constants of propagation reactions.

From the Barb diagram, the values $r_{11}=0.8$ and $r_{12}=1.5$ are obtained. These values are used to verify equation (1) (see table 2) and they satisfactorily describe the copolymerization mechanism only for initial mixtures with more than 20% cinnamic acid.

For less cinnamic acid in the initial mixture ($M_2 < 25\%$) an anti-penultimate model was tested.[24,26–28] The particular case (M_2 does not homopolymerize) gives the equation :

$$\frac{1}{x^2}\left(\frac{n-1}{D}-1\right)\frac{1}{r_{211}}+\frac{1}{x}\left(\frac{n-1}{D}-2\right)=r_{111} \qquad (2)$$

where :

$$D = \frac{r_{21}x}{r_{21}^{x+1}}\,; \quad r_{111} = \frac{k_{1111}}{k_{1112}}\,; \quad r_{211} = \frac{k_{2111}}{k_{2112}}\,;$$

$$r_{121} = \frac{k_{1211}}{k_{1212}} = r_{12}$$

From the slope and the intercept the values are

$$r_{111} = 0.45 \text{ and } r_{211} = 28.49.$$

Verifying eq. (2) with these values, one obtains better results than with eq. (1), but still unsatisfactory, especially for low initial cinnamic acid concentrations.

TABLE 2

Differences between experimental and calculated copolymer compositions ($n = n_{\text{exp.}} - n_{\text{calc.}}$)

M_2 (% mol)	5	10	15	20	25
penultimate model, eq. (1)	−5.89	−1.82	−0.88	−0.20	−0.08
antepenultimate model, eq. (2)	−0.41	−0.19	−0.01	0.07	0.02
CTC model, eq. (3)	0.16	0.17	0.00	−0.03	−0.02

The large differences between r_{11} and r_{111} and between r_{21} and r_{211}, and the fact that, for these initial mixtures, the higher differences between water and methanol — synthesized copolymer compositions are noted, suggest that charge transfer complexes (CTC) can be involved in the copolymerization mechanism.[29] A CTC can be obtained by the interaction of nitrile and phenyl groups. In this case, eq. (3) [29] must be applied :

$$\left(n - 1 - \frac{r_{1c}}{r_{1c1}}\right) \cdot B = \frac{r_{1c}}{K} - \frac{r_{1c}}{Kr_1} \cdot \frac{n-1}{x} \tag{3}$$

where :

$$x = \frac{A}{B}\,; \quad r_{1c} = \frac{k_{11}}{k_{1c1} + k_{1c2}}\,; \quad r_1 = \frac{k_{11}}{k_{12}}\,; \quad r_{1c1} = \frac{k_{11}}{k_{1c1}}$$

and K is the equilibrium constant of CTC (C) formation :

$$M_1 + M_2 \overset{K}{\rightleftarrows} [M_1M_2] \equiv C \tag{4}$$

By iterative methods eq. (3) gives :

$$\frac{r_{1c}}{r_{1c1}} = 0.9\,; \quad \frac{r_{1c}}{K} = 1.29\,; \quad \frac{r_{1c}}{Kr_1} = 0.12 \tag{5}$$

Verifying eq. (3) with the values (5), one obtains the data in table 2, from which one can conclude that, for low initial cinnamic acid concentrations, the charge transfer model characterizes better the system than the penultimate model. Also, from the values (5), one can conclude that homoaddition of AN is ten times more probable than cinnamic acid addition to the AN-ended macroradical, and that the CTC is 25 times more reactive than acrylonitrile. These facts explain the higher CA content in copolymers for lower initial concentrations, as compared with the reduced CA content in the copolymers obtained when the CA concentration in the initial mixture is higher.

4. COPOLYMER STRUCTURE

The copolymer spectra demonstrate the enchainment of the two structural units.

After thermal treatment of copolymer solutions, their structure modifies, in the IR spectrum ester and amidic groups are present, carboxyl group absorption is increased and also the number of hydrogen bonds (OH).

The amidic group appearance and the increase of carboxylic group content can be explained by the hydrolysis of nitrile groups at pH = 2—3 in the reaction medium. Because the carboxylic group absorption increases more than that of the amidic group one can suppose that amidic hydrolysis to carboxyl is faster than amidic group formation.

Ester formation is probably due to the *trans*-esterification process of ethylene carbonate with the carboxylic groups from cinnamic acid.

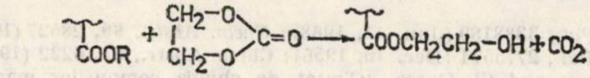

(6)

5. CONCLUSIONS

1. Cinnamic acid does not homopolymerize, but copolymerizes with acrylonitrile.

2. The copolymerization mechanism depends on the nature of the reaction solvent and on the cinnamic acid concentration; for concentrations lower than 15 % a mechanism through CTC is more probable, and for higher concentrations the penultimate model suits better the process.

3. The obtained copolymers have a statistical distribution of the structural units and do not have cinnamic acid diads.

4. When preparing the spinning solutions, cinnamic acid can react with ethylene carbonate (solvent), and small quantities of nitrile groups are hydrolysed to amidic or carboxylic groups.

5. The cinnamic acid presence in copolymers is a factor of instabilization of their solutions.

REFERENCES

[1] A. Ya. Yakubovici, V. N. Stefanowskaya and L. S. Vasiliev; USSR Pat. 251.924, Sept.-10-1969; *Chem. Abstr.*, **72**, 56287, (1970).

[2] Fuji Photo Film Co.; *Ger. Pat.*, 2358133 (Sept.-19-1974); *Chem. Abstr.*, **82**, 58499 (1975).

[3] C. A. Barson, *J. Polymer Sci.*, **62**, 128 (1962).

[4] C. A. Barson, *European Polymer J.*, **6**, 2416 (1970).

[5] C. A. Barson and M. I. Turner, *European Polymer J.*, **10**, 1053 (1974).

[6] Dunlop Rubber Co.; *Brit. Pat.*, 1055928 (January 18, 1967); *Chem. Abstr.*, **66**, 66462 (1967).

[7] Kurashiki Rayon Co.; *Fr. Pat.*, 1365521 (July 3, 1964); *Chem. Abstr.*, **62, 7947 (1965).**

[8] I. Maki, Y. Imamura and N. Yoshitada; *Japan Pat.*, 7144530 (Apr. 9, 1974); *Chem. Abstr.*, **82**, 49891 (1975).

[9] N. I. Avvakumova and E. V. Kuznetsov, *Tr. Kazan Khim. — Teknol. Inst.* **40**, (2), 125 (1969); *Chem. Abstr.*, 75, 98845 (1971).

[10] Monsanto Co.; *Fr. Pat.* 131674 (May 22, 1964); *Chem. Abstr.*, **62**, 6614 (1965).

[11] V. P. Barabanov and V. M. Tsentovski, *Izv. Vyssh. Usheb. Zaved. Khim. Khim. Tekhnol.*, **12**, 326 (1969); *Chem. Abstr.*; **71**, 3702 (1969).

[12] V. P. Barabanov and S. G. Sanikov, *Tr. Kazan. Khim. Technol. Inst.*, **34**, 235 (1965); *Chem. Abstr.*, **68**, 30093 (1968).

[13] Idem, **40**, 88 (1969); *Chem. Abstr.*, **75**, 3687 (1971).

[14] Idem, **40**, 94 (1969); *Chem. Abstr.*, **75**, 36875 (1971).

[15] C. Osada, M. Satamura and Y. Ovo; *Japan Pat.* 7310185 (February 8, 1973); *Chem. Abstr.*, **79**, 6973 (1973).

[16] Fuji Photo Film Co.; *Japan Pat.* 7483502 (Aug. 12, 1974); *Chem. Abstr.*, **82**,. 99096 (1975).

[17] A. K. Vegapova, N. I. Avvakumova and E. V. Kuznetsov, *Tr. Kazan. Khim. Tekhnol. Inst.*, **40**, 298 (1969); *Chem. Abstr.*, **75**, 36887 (1971).

[18] E. V. Kuznetsov, I. P. Prokhorova and N. I. Avvakumova; *USSR Pat.*, 203900 (Oct. 9, 1967); *Chem. Abstr.*, **69**, 3337 (1968).

[19] Academy of Sci. USSR; *USSR Pat.*, 197168 (May 13, 1967); ; *Chem. Abstr.*, **68**, 22352 (1968).

[20] K. Matsuo and S. Machida, *J. Polymer Sci.*, **A-1, 10**, 187 (1972).

[21] Monsanto Chemical Co.; *US. Pat.*, 3410835 (Nov. 12, 1968); *Chem. Abstr.*, **70**, 48544 (1969).

[22] *Idem*; *US. Pat.*, 3388189 (Jun. 11, 1968); *Chem. Abstr.*, **69**, 28527 (1968).

[23] *Idem*; *US. Pat.*, 2775574 (Dec. 15, 1956); Chem. Abstr., **51**, 6222 (1957).

[24] Cr. Simionescu and Cl. Oprea, "Tratat de chimia compușilor macromoleculari", Vol. I, Ed. did. și pedag., București, 1973, p. 509—594.

[25] W. G. Barb, *J. Polymer Sci.*, **11**, 117 (1953).

[26] A. Guyot and J. Guillot, *J. Macromol. Sci. Chem.*, **A5**, 753 (1971).

[27] *Idem;* **A5**, 1031 (1971).

[28] *Idem;* **A5**, 735 (1971).

[29] A. J. Seiner and L. H. Morton, *Macromolecules*, **4**, 308 (1971).

Revue Roumaine de Chimie, 25, 7 921–931(1980)

Zu Ehren Prof. CRISTOFOR I. SIMIONESCU
gelegentlich seines 60 Geburstags

FLÜSSIGE KRISTALLE. II[1]

SYNTHESE DER ZUR HERSTELLUNG VON BENZYLIDENANILINEN MIT FLÜSSIG-KRISTALLINER STRUKTUR GEEIGNETEN *p*-ALKYLANILINEN

R. BACALOGLU, ARIANA MORARU, MARIA NUŢIU, S. ILUC,
C. CSUNDERLIK und ELENA LUNGU
Laboratorium für Organische Chemie, Politechnisches Institut ,,Traian Vuia"
Timişoara, Bocşa Str. N° 6, Rumänian

Eingegangen am 2. Februar 1980

Die Synthesen von 4-Äthyl-, 4-n-Propyl-, 4-n-Butyl- und 4-n-Amylanilinen aus den entsprechenden Alkylbenzolen durch Acetylierung, Schmidtsche Umlagerung und Hydrolyse der so gebildeten Acetanilide werden eingehend beschrieben. Die Produkte werden anhand physikalisch-chemischer und spektroskopischer Methoden charakterisiert, und sind von entsprechender Reinheit um sich zur Synthese von flüssigen Kristallen zu eignen.

Synthesis procedures for 4-ethyl, 4-n-propyl, 4-n-butyl and 4-n-pentyl-anilines starting from corresponding alkyl benzenes trough acetylation, Schmidt transposition and hydrolysis of formed acetanilides have been described. The products have been characterized physico-chemically and spectroscopically and their purity was found satisfactory for liquid crystal syntheses.

Unter den Substanzen mit kristallin-flüssiger Struktur mit vielseitigen technischen und wissenschaftlichen Verwendungsmöglichkeiten nehmen die Benzylidenaniline eine besondere Stelle ein. Sie werden durch direkte Kondensierung von *p*-substituierten Benzaldehyden mit *p*-substituierten Anilinen erhalten, wobei diese Substituenten n-Alkyl oder n-Alkoxy sein können. Die Länge dieser Substituenten bestimmt die Orientierung dieser Moleküle und so die kristallin-flüssige Struktur [2].

Die Gewinnung der Benzaldehyde und Aniline wird aufgrund von umständlichen und in der Literatur wenig beschriebenen Methoden gewährleistet. Aus diesem Grund wurden von uns die Synthesen der *p*-substituierten Aniline von genügend hoher Reinheit zur Herstellung von Schiffschen Basen mir kristallin-flüssigen Eigenschaften, studiert.

ERGEBNISSE UND DISKUSSION

Die Synthese der *p*-n-Alkylaniline kann auf mehreren Wegen erfolgen. Eine anscheinend einfache Methode besteht aus von Reduktion gefolgter Nitrierung der Alkylbenzole. Der Nachteil dieses Syntheseweges ist, dass die Nitrierung nicht nur in *p*-Stellung stattfindet, und dass die vollständige Trennung des *o*-Isomers nicht möglich ist.[3–10]

Ein anderer Syntheseweg besteht im Acrylieren des *p*-Chlorbenzols, der Ammonolyse des gebildeten *p*-Chlorketons und der Reduktion der Carbonylgruppe. Die Acylierung des Chlorbenzols mit Säurechloriden in Gegenwart von $AlCl_3$ erfolgt mit zufriedenstellenden Ausbeuten hauptsächlich in der *p*-Stellung.[11–17] Die Ammonolyse des *p*-Chlor-Alkyl-Phenylketons wird in konzentrierter Ammoniaklösung unter Mitwirken des Kupfer (I) chlorids durchgeführt. Die Reduktion des Ketons führt zum gewünschten Produkt mit nur kleinen Ausbeuten in erster Reihe im Falle der niederen Alkylderivate.[18,19]

Die direkte Alkylierung der Aniline mit n-Alkoholen [20–24] führt mit bis zu 35%-igen Ausbeuten zu relativ komplexen Isomergemischen.

Die Umlagerung der N-n-Alkylaniline zu 4-n-Alkylanilinen, (16 Stunden bei 210° in Gegenwart von $CoCl_2$) führt zu komplizierten Gemischen von unreagierten Produkten von *ortho*- und *para*-substituierten n-Alkylanilinen die nur durch Destillation mit Drehbandsäule trennbar sind.[25,26]

Als beste Methode erwies sich die Schmidtsche Umlagerung der Alkyl-arylketone in der Gegenwart der Stickstoffwasserstoffsäure zu N-acrylierten *p*-Alkylanilinen,[27,28] gefolgt von der Hydrolyse dieser Acylanilide. Die notwendigen *p*-Alkylacetophenone werden durch Acylierung der Alkylbenzole mit Essigsäurechlorid in der Gegenwart von $AlCl_3$ gewonnen. In dieser Reaktion bildet sich fast nur der *p*-Isomer : [29]

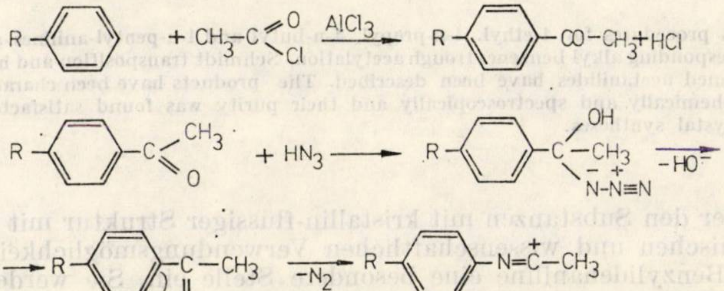

Auf diesem Weg wurden mehrere Aniline hergestellt ($R = C_nH_{2n+1}$, $n = 2, 3, 4, 5$) die anschliessend zur Synthese von Schiffschen Basen mit kristallin-flüssiger Struktur verwendet wurden.

Die in der Friedel-Crafts Alkylierung verwendeten Alkylbenzole wurden aus dem entsprechenden n-Alkylbromid und Brombenzol nach

Würtz-Fittig gewonnen. Unter den Bedingungen dieser Reaktion findet die Isomerisierung des n-Alkylrestes praktisch nicht statt.

Da in der Literatur keine Angaben über die Acylierung der uns interessierenden Alkylbenzole sowie über die Schmidt-Umlagerung und Hydrolyse der diskutierten Acetanilide zu finden waren, war es notwendig, die genauen Arbeitsbedingungen für jeden Schritt zu bestimmen. Die von uns festgelegte Arbeitsweise erlaubt die Synthese der gewünschten Produkte von hoher Reinheit mit vorzüglichen Ausbeuten (Tab. 1, 3 und 5).

In Tabelle 1 sind die Ergebnisse der *p*-Alkylacetophenonsynthesen und in Tabelle 2 sind ihre spektralen Charakteristika zusammengestellt. Aus den IR-Spektren ist zu entnehmen, dass alle erwarteten Schwingungen erscheinen. So erscheint die Valenzschwingung der C=O-Gruppe bei 1680 cm^{-1}, ein für aliphatisch-aromatische Ketone charakteristischer Wert. Die Deformationsschwingung γ_{CH} bei 830 cm^{-1} zeigt, dass die Acylierung in *p*-Stellung stattgefunden hat.[32,31] Auch die ^1H—NMR-Spektren beweisen diesen Reaktionsverlauf.

In Tabelle 3 sind die Ergebnisse der Synthesen und in Tabelle 4 die spektralen Charakteristika der *p*-Alkylacetanilide zusammengefasst. Es ist leicht ersichtlich, dass die für den aliphatischen Rest charakteristischen Banden keine bemerkenswerten Veränderungen erleiden. Die für die Amidgruppen charakteristische Banden NH und CO-Valenzschwingung sowie die mit der CN-Valenzschwingungen gekoppelten NH-Deformationen sind in den Spektren leicht identifizierbar.[31,32] Die dem *p*-substituierten Benzol charakteristischen CH-Deformationsbanden von 815—820 cm^{-1} [31,32] beweisen die Erhaltung der *p*-Substitution bei der Umlagerung der Alkylidenazide.

In den ^1H-RMN-Spektren erscheint das Wasserstoffatom der Amid-Gruppe (B in Tab. 4) bei $\tau = 1{,}75-2{,}15$ ppm, sowie die zwei Dublette bei $\tau = 2{,}62-2{,}66$ und $\tau = 2{,}95-3{,}00$, die sehr charakteristisch für die *p*-Substitution des Benzolrings sind.

In Tabelle 5 sind die Ausbeuten und die physikalischen Konstanten der *p*-Alkylaniline eingetragen.

Die in der Literatur [30] erwähnten Charakteristika des p-Äthyl- und p-Butylanilins sind in gutem Einklang mit den von uns bestimmten.

TABELLE 1

Ergebnisse der *p*-Alkylacetophenonsynthese

R	Ausbeute %	Siedepunkt °C (mm Hg) (Literatur)	n_D(°C)	d_4^{20} kg/m^3	R_M cm^3/Mol	
					exp.	ber.
CH_3-CH_2-	93	97—99(5) (113—115(11)[30])	1,5303(20,5)	988	46,356	45,62
$CH_3-(CH_2)_2-$	84	104—106(5)	1,5234(21)	980	50,528	50,36
$CH_3-(CH_2)_2-$	87	118—120(5)	1,5200(20)	942	56,799	55,05
$CH_3-(CH_2)_4-$	70	126—128(5)	1,5160(22)	914	62,779	59,785

TABELLE 2

Spektrale Charakteristika der *p*-Alkyl-acetophenone

a) IR-Spektren [32,31]

R	$\nu_{C=O}$	Aromatisches Skelett			Aliphatisches Skelett			
		$\nu_{Skelett}$	ν_{CH}	γ_{CH}	ν_{CH}	$\delta^{s}_{CH_3}$	$\delta^{as}_{CH_3}$ δ_{CH_2}	$\delta^{as}_{CH_3CO}$
CH_3-CH_2-	1680	1460 1570 1600	3000	830	2860 2950	1350	1460	1430 1405
$CH_3-CH_2-CH_2-$	1670	1450 1560 1600	2970	830	2840 2900	1350	1450	1430 1405
$CH_3-CH_2-CH_2-CH_2-$	1670	1470 1560 1600	3020	830	2880 2960	1350	1470	1435 1405
$CH_3-CH_2-CH_2-CH_2-CH_2-$	1680	1470 1560 1600	3020	810	2880 2960	1350	1470	1430 1405

b) RMN-Spektren *)

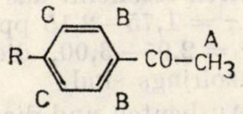

R	Chemische Verschiebung Spinkopplung (Kopplungskonstante) Zahl der Protonen							
	A	B	C	D	E	F	G	H
E D CH_3-CH_2-	7,53 S 3	2,33 d(8)2	2,82 d(8)2	7,30 cu(8)2	8,75 tr(7)3	—	—	—
E F D $CH_3-CH_2-CH_2-$	7,45** S 3	2,15 d(8)2	2,77 d(8)2	7,32** tr(7)2	9,02 tr(7)3	8,33 sx(7)2	—	—
E F G D $CH_3-CH_2-CH_2-CH_2-$	7,47** S 3	2,16 d(8)2	2,79 d(8)2	7,32** tr(7)2	9,10 tr(6)3	8,56 m, 4		
E F H G D $CH_3-CH_2-CH_2-CH_2-CH_2-$	7,45** S 3	2,15 d(8)2	2,77 d(8)2	7,32** tr(7)2	9,13 tr(7)3	8,62 m,6		

* s — Singlett, d — Dublett, tr — Triplett, cu — Quartett, sx — Sextett und m — Multiplett

** teilweise überlagert.

TABELLE 3

Ergebnisse der *p*-Alkylacetanylidsynthese

R	Ausbeute %	Schmelzpunkt °C		Umkristallisiert aus
			Lit.	
CH_3-CH_2-	73	86−88	90,1−90,7[30]	Ethanol-Wasser
$CH_3-(CH_2)_2-$	98	94−96	—	Ethanol
$CH_3-(CH_2)_3-$	74	104−105	105[30]	Ethanol
$CH_3-(CH_2)_4-$	70	101−102	—	Ethanol

TABELLE 4

Spektrale Charakteristika der *p*-Alkylacetanylide

a) IR-Spektren[32,31]

R	−NH−CO					Aromatisches Skelett			Aliphatisches Skelett			
	ν_{NH}	ν_{CO}	δ_{NH} ν_{CO}	ν_{CN} δ_{NH}	γ_{NH}	$\nu_{Skelett}$	ν_{CH}	γ_{CH}	ν_{CH}	$\delta^{s}_{CH_3}$	$\delta^{as}_{CH_3}$ δ_{CH_2}	$\delta^{as}_{CH_3CO}$
CH_3-CH_2-	3180	1660	1540	1310	750	1600 1520 1500	3050	820	2920 2850	1360 1400	1460	1440
$CH_3-CH_2-CH_2-$	3220	1660	1550	1310	750	1590 1520 1500	3100	820	2850 2920	1350 1400	1460	1430
$CH_3-CH_2-CH_2-CH_2-$	3230	1660	1550	1310	750	1590 1520 1500	3050	820	2850 2920	1360 1400	1460	1430
$CH_3-CH_2-CH_2-CH_2-CH_2-$	3240	1660	1540	1310	750	1590 1520 1500	3100	815	2850 2920	1350 1400	1460	1440

TABELLE 4

Spektrale Charakteristika der *p*-Alkylacetanylide

b) RMN Spektren

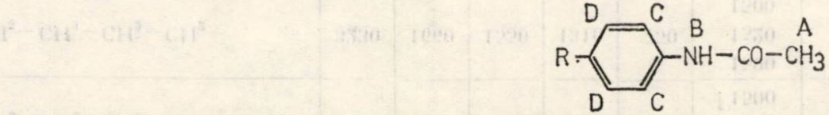

R	Chemische Verschiebung Multiplettstruktur (Kopplungskonstante, Hz) Zahl der Protonen								
	A	B	C	D	E	F	G	H	I
F E CH_3-CH_2-	7,91 s 3	1,75 s 1	2,625 d(8)2	2,95 d(8)2	7,425 cu(8)2	8,825 tr(8)3	—	—	—
F G E $CH_3-CH_2-CH_2-$	7,91 s 3	1,81 s 1	2,64 d(8)2	2,975 d(8)2	7,49 tr(7)2	9,11 tr(7)3	8,46 sx(7)2	—	—
F G H E $CH_3-CH_2-CH_2-CH_2-$	7,94 s 3	1,11 s 1	2,60 d(8)2	2,99 d(8)2	7,49 tr(7)2	9,125 tr(7)3	8,56 m,4		—
E G I H E $CH_3-CH_2-CH_2-CH_2-CH_2-$	7,91 s 3	2,15 s 1	2,66 d(8)2	2,99 d(8)2	7,49 tr(7)2	9,16 tr(7)3	8,56 m,6		

TABELLE 5

Ergebnisse der *p*-Alkylanilinsynthese

R	Ausbeute %	Siedepunkt °C (mm Hg)		n_D (°C) (Lit.)	d_4^{20} kg/m³		R_M cm³/Mol	
		Exp.	Lit.		Exp.	Lit.	exp.	ber.
CH_3-CH_2-	91	84—87(4)	92,3(10) [30]	1,5561(20) 1,5554(20) [30]	967,1	967,9 [30]	40,28	40,74
$CH_3-(CH_2)_2-$	96	102—103(5)		1,5422(25)	940		45,28	45,48
$CH_3-(CH_2)_3-$	98	100(4)	133—134(14)[30]	1,5352(22)	946	945 [30]	49,13	50,17
$CH_3-(CH_2)_4-$	97	104—106(5)		1,5324(21)	950		53,28	54,90

TABELLE 6

Spektrale Charakteristika der *p*-Alkylaniline

a) IR-Spektren [32,31]

R	Ar-NH$_2$				Aromatisches Skelett			Aliphatisches Skelett			
	ν^{s}_{NH}	ν^{as}_{NH}	δ_{NH_2}	ν_{CN}	$\nu_{Skelett}$	ν_{CH}	γ_{CH}	ν_{CH}	$\delta^{s}_{CH_3}$	$\delta^{as}_{CH_3}$ δ_{CH_2}	γ_{CH_2}
CH_3-CH_2-	3320 3400	3190	1630	1270	1450 1510 1610	3000	830	2920 2850	1370	1450	780
$CH_3-CH_2-CH_2-$	3340 3300	3180	1610	1250	1460 1495 1610	3000	800	2900 2810	1360	1460	780
$CH_3-CH_2-CH_2-CH_2-$	3380 3430	3205	1620	1270	1460 1510 1620	3000	830	2920 2850	1370	1470	750
$CH_3-CH_2-CH_2-CH_2-CH_2-$	3300 3390	3180	1610	1260	1450 1505 1610	3000	810	2920 2820	1370	1440	720

TABELLE 6

Spektrale Charakteristika der *p*-Alkylaniline
b) NMR-Spektren

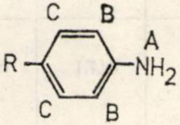

R	Chemische Verschiebung Spinkopplung (Kopplungskonstante) Zahl der Protonen							
	A	B	C	D	E	F	G	H
E D CH_3-CH_2-	6,70 s 2	3,175 d(8)2	3,6 d(8)2	7,5 cu(8)2	8,84 tr(7)3	—	—	—
E F D $CH_3-CH_2-CH_2-$	6,61 s 2	3,09 d(8)2	3,45 d(8)2	7,55 tr(8)2	9,11 tr(7)3	8,51 sx(7)4	—	—
E F G D $CH_3-CH_2-CH_2-CH_2-$	6,6 s 2	3,06 d(8)2	3,45 d(8)2	7,525 tr(7)2	9,125 tr(6)3	8,575 m,4		—
E F H G D $CH_3-CH_2-CH_2-CH_2-CH_2-$	6,65 s 2	3,06 d(8)2	3,425 d(8)2	7,51 tr(7)2	9,125 tr(6)3	8,625 m,6		

In Tabelle 6 sind die Banden der IR- und ^{1}H-NMR-Spektren der synthetisierten p-Alkylaniline aufgezählt. Die Struktur dieser primären aromatischen Amine wird durch das Verschwinden der C=O-Valenzschwingung sowie der der Amingruppe entsprechenden Banden ν_{NH}^{as} und ν_{NH}^{sim} bei 3320–3380 bzw. 3180–3200 cm^{-1} und δ_{NH_2} bei 1620–1630 cm^{-1} bewiesen.[32, 31]

In den ^{1}H-NMR-Spektren ist das Verschwinden des Singletts von $\tau = 1{,}11-2{,}15$ ppm (dem –NHCO– entsprechend) und von $\tau = 7{,}95$ (dem CH_3-CO zuzuschreiben) sowie das Erscheinen des der Aminogruppe entsprechenden Singletts von $\tau = 6{,}62$ ppm zu bemerken.

BESCHREIBUNG DER VERSUCHE

A. Synthese der *p*-Alkylacetophenone

Die Literaturdaten über die Synthese des *p*-Butylacetophenons[27] waren uns in der Synthese des *p*-Äthyl-, *p*-n-Propyl-, *p*-n-Butyl- und *p*-n-Pentylacetophenons besonders nützlich. Die Synthesen wurden in einem mit Rührer, Thermometer und Rückflusskühler vorgesehenen 21 – Dreihalskolben durchgeführt.

Der Kühler war an ein mit NaOH-Lösung gefülltes Absorbtionsgefäss angeschlossen. Als Lösungsmittel diente wasserfreies Heptan. In den Kolben werden 900 ml Heptan, 0,5 mol Alkylbenzol und 50 g (0,638 mol) Essigsäurechlorid eingeführt und auf 5°C abgekühlt. Es werden sodann 86 g (0,442 mol) $AlCl_3$ hinzugefügt.

Das Reaktionsgemisch wird unter Rühren eine Stunde bei 0–5°C, zwei Stunden bei Zimmertemperatur und anschliessend noch eine Stunde bei 60°C gehalten. Nach dem Abkühlen auf die Zimmertemperatur wird zwecks Zerstörung des Katalysators solange portionsweise Wasser hinzugefügt bis sich dieser gänzlich löst. Die organische Schicht wird abgetrennt und die wässrige Phase zweimal mit je 150 ml Heptan ausgeschüttelt. Die Heptan-Extrakte werden mit der abgetrennten organischen Schicht vereinigt, zweimal mit je 200 ml 5% NaOH-Lösung und dann zweimal mit je 200 ml Wasser gewaschen und auf $MgSO_4$ getrocknet. Nach dem Entfernen des Heptans durch Destillation wird das rohe Acetophenon durch Vakuumdestillation gereinigt. Die Ausbeute beträgt um 85% (Tab. 1).

B. Synthese der *p*-Alkylacetanilide

Die N-acylierten Derivate der *p*-Alkylaniline wurden durch die Schmidt-Umlagerung [27] der *p*-Alkylacetophenone unter Teilnahme der Stickstoffwasserstoffsäure gewonnen.

In einem wie oben beschriebenen Rundkolben werden 470 ml 40%-ige Schwefelsäure auf 10–15°C abgekühlt und mit 0,264 mol Keton versetzt. Anschliessend werden portionsweise 23,4 (0,36 mol) NaN_3 hinzugefügt, so dass die Temperatur bei 30—40°C gehalten wird und wobei auf eine nicht zu enregische Schäumung zu achten ist. Nachher wird auf 45—50°C erwärmt und noch 3—4 Stunden bei dieser Temperatur gerührt. Nach dem Abkühlen auf Zimmertemperatur wird das Reaktionsgemisch unter energischem Rühren über das vierfache Volumen Wasser geschüttet *). Das ausgefallene kristalline Reaktionsprodukt wird abgesaugt, mit Wasser gewaschen und durch Umkristallisieren aus Äthylalkohol gereinigt, wobei zu beachten ist, dass die Löslichkeit des Produktes in Alkohol mit grösserem Alkylrest beträchtlich ansteigt. Die Ausbeuten sind im allgemeinen gut (Tab. 3).

C. Hydrolyse der N-Acetylaniline

Die saure Hydrolyse der N-Acetylaniline wurde in äthanolischem Medium durchgeführt. In einem mit Rückflusskühler vorgesehenem Rundkolben werden das *p*-Alkylacetanilid, Äthanol und konzentrierte Salzsäure im molaren Verhältnis 1 : 4 : 3 eingeführt und 24—30 Stunden unter Rückfluss erwärmt. Nach dem Abkühlen wird das Reaktionsgemisch über ein 5-mal grösseres Wasservolumen geschüttet und mit 25%-iger NaOH-Lösung auf pH-Wert 8 gebracht. Das freie Amin bildet eine braune ölige Schicht, die nach dem Abtrennen mit Wasser gewaschen, auf $MgSO_4$ getrocknet und im Vakuum destilliert wird. Aus der verbliebenen Mutterlauge und aus den Waschwassern können noch kleine Aminmengen mit Dichlormethan extrahiert werden. Nach dem Verdampfen des Lösungsmittels und nach dem Waschen und Trocknen werden diese Aminmengen mit den oben erhaltenen vereinigt und destilliert.

Die Schmelzpunkte wurden mit einem Boetius-Heiztisch bestimmt. Die IR-Spektren wurden mit einem IR-Spektrographen Specord IR 71 und IR 75 (Carl Zeiss Jena) nach der flüssigen Film- oder KBr-Technik aufgezeichnet. Zur Registrierung der ^{1}H-NMR-Spektren wurde ein 80-Hz-Spektrograph (Tesla BS 487 C) beansprucht.

LITERATURVERZEICHNIS

[1] I. Mitt. R. Bacaloglu, H. Huschitt, O. Ciontea und E. Lungu, in *Bul. şt. şi tehn. al Inst. Politehn. „Traian Vuia" Timişoara* (unter Druck).

[2] H. Kelker und B. Schewele, *Angew. Chem.*, **81**, 903 (1969).

[3] R. R. Read und D. B. Mullin, *J. Amer. Chem. Soc.*, **50**, 1463 (1927); *Chem. Zentr.*, **1928**, 548.

[4] F. R. Blaum, *Pat. USA*, 2. 533. 203 (1950); *Chem. Abstr.*, **45**, 3419 f (1951).

[5] R. Sureau und R. Pernat, *Bull. Soc. Chem. France*, **1958**, 152.

[6] M. Hoya und Y. Takai, *Kagaku Zasshi*, **81**, 1629 (1961); *Chem. Abstr.*, **56**, 10006 b (1962).

[7] K. Ito, A. Komori und M. Ogawa, *Technol. Rept. Kansai. Univ.*, **5**, 31 (1963); *Chem. Abstr.*, **61**, 16191 (1964).

---

*) Die Synthese wird unter dem Abzug durchgeführt und beim Schütten des Reaktionsgemisches im Wasser wird unbedingt mit Gasmaske gearbeitet, da die sich bildende Stickstoffwasserstoffsäure äusserst giftig ist!

[8] S. I. Burnisteer und V. M. Zaiteev, *Zhur. organ. Khim.*, **1**, 502 (1965).

[9] H. Konda und S. Uyea, *Ber. dtsch. chem. Ges.*, **70**, 1091 (1937).

[10] P. N. Katschergin, *Zhur. Obshchei Khim.*, **27**, 3204 (1957).

[11] L. N. Nikolenko und K. K. Bobiewski, *Zhur. Obshchei Khim.*, **25**, 2231 (1955).

[12] R. Lang, *J. Chem. Soc.*, **1953**, 2066.

[13] A. W. Nerehan, *Ber. dtsch. chem. Ges.*, **57**, 1294 (1924).

[14] K. Komatsu, N. Kuroki und K. Konishi, *Bull. Univ. O saka. Prefect.*, **12**, 77 (1963); *Chem. Abstr.*, **60**, 8159 (1964).

[15] L. N. Nikolenko und K. K. Babiewski, *Zhur. Obshchei Khim.*, **25**, 2231 (1955).

[16] W. S. Emerson und P. M. Walters, *J. Amer. Chem. Soc.*, **60**, 2023 (1938); *Chem. Zentr.* **I** **1939**, 101.

[17] W. S. Emerson und P. M. Walters, *J. Amer. Chem. Soc.*, **77**, 1573 (1955).

[18] A. A. Balandin und A. Artomanov, *Doklady Akad. Nauk. S.S.S.R.*, **168**, 1311 (1966).

[19] K. Hoegerce und P. Butler, *Chem. Ind.*, **22**, 933 (1964).

[20] W. J. Hickinbotton, *J. Chem. Soc.*, **1927**, 64, *Chem. Zentr.*, **1927**, 1950.

[21] E. Michel, *Ber. dtsch. chem. Ges.*, **89**, 1702 (1956).

[22] F. Aslow, Pat. USA 2.533.203 (1948); *Chem. Zentr.*, **1952**, 3901.

[23] W. J. Hickinbotton, *J. Chem. Soc.*, **1934**, 1700.

[24] J. Metzger und H. Plank, *Bull. Soc. Chim. France*, **1956**, 684.

[25] W. J. Hickinbotton, *J. Chem. Soc.*, **1937**, 1119.

[26] Z. S. Gardlund, R. J. Curtis und G. W. Smith, „Liquid Crystals and Ordered Fluids", vol. 2, (Eds. J. F. Johnson und R. S. Porter), Plenum Publ. Corp., New York, S. 541.

[27] F. Knowles, *Pat. USA*, 3.689.566 (1972); *Chem. Abstr.*, **78**, 97198 (1973).

[28] J. B. Hendrickson, D. J. Cram und G. S. Hammond, „Chimie Organică", Editura Ştiinţifică şi Enciclopedică, Bucureşti, 1976, S. 741.

[29] G. Olah, „Friedel-Crafts and Related Reactions", Interscience Publishers, vol. III, J. Wiley, New York, 1964, S. 547.

[30] J. G. Grasselli und W. M. Ritchey, „Atlas of Spectral Data and Physical Constants for Organic Compounds„, vol. I—VI, CRC Press, Cleveland, Ohio, USA, 2nd Ed., 1975.

[31] M. Avram und Gh. D. Mateescu, „Spectroscopia în Infraroşu. Aplicaţii în chimia organică", Editura tehnică, Bucureşti, 1966, S. 378.

[32] N. B. Colthup, L. H. Daly und S. E. Wiberley, „Introduction to Infrared and Raman Spectroscopy", Academic Press, New York, 1975.

Revue Roumaine de Chimie, 25, 7, 933–939(1980)

Dedicated to Professor CRISTOFOR I. SIMIONESCU
on his 60th anniversary

^{1}H–NMR METHOD FOR COMPOSITION, BRANCHING AND SEQUENCE DISTRIBUTION DETERMINATION IN ETHYLENE-VINYL ACETATE COPOLYMERS

V. BĂRBOIU*, ALMERIA NATANSOHN*, C. ANDREI** and D. BLUM**
* "P. Poni" Institute of Macromolecular Chemistry, Aleea Gr. Ghica Vodă 41A, Iași, Romania
** ICECHIM – Brazi, Romania

Received October 27, 1978

Some ^{1}H-NMR spectral methods to determine the composition, branching and sequence distribution in ethylene-vinyl acetate (E-VAc) copolymers are presented. Composition and branching are determined from signal intensity ratios. Using selective amplifications of spectral signals, it is possible to measure compositions to 2–3% in weight VAc with small relative errors. Sequence distribution is determined from CH_3 signal splitting. The analysis can be made only in terms of diads.

The ethylene (E, 1) – vinyl acetate (VAc, 2) copolymers with 20–50% VAc in weight are well-known as good elastomers. Their using domain and processing properties are influenced by the chemical structure and the chain microstructure. This paper presents the possibilities to study the copolymer structure given by the high-resolution ^{1}H-NMR spectroscopy.

EXPERIMENTAL

The ^{1}H-NMR spectra were obtained at 60 MHz on a JEOL JNM-C-60 HL spectrometer. For composition determination, a.d.c. amplifier was introduced between the spectrometer output and the recorder. The amplification gain could be easily changed from 0.8 to 8.0. The ratio of the two amplification gains was exactly determined with a JEC-6 computer, being 10.0 ± 1%. This arrangement made possible to obtain different amplitudes for the integrals of spectral signals, the weak ones being increased 10 times as compared to the strong ones. Thus, the measuring precision for the weak signals improved several times, being nearly equal to that of the strong signals.

The solvents generally used were deuterochloroform, benzene and tetrachloroethylene, the last one for the copolymers with low content of VAc.

COPOLYMER COMPOSITION DETERMINATION

The ^{1}H-NMR spectrum of an E-VAc sample is presented in figure 1.

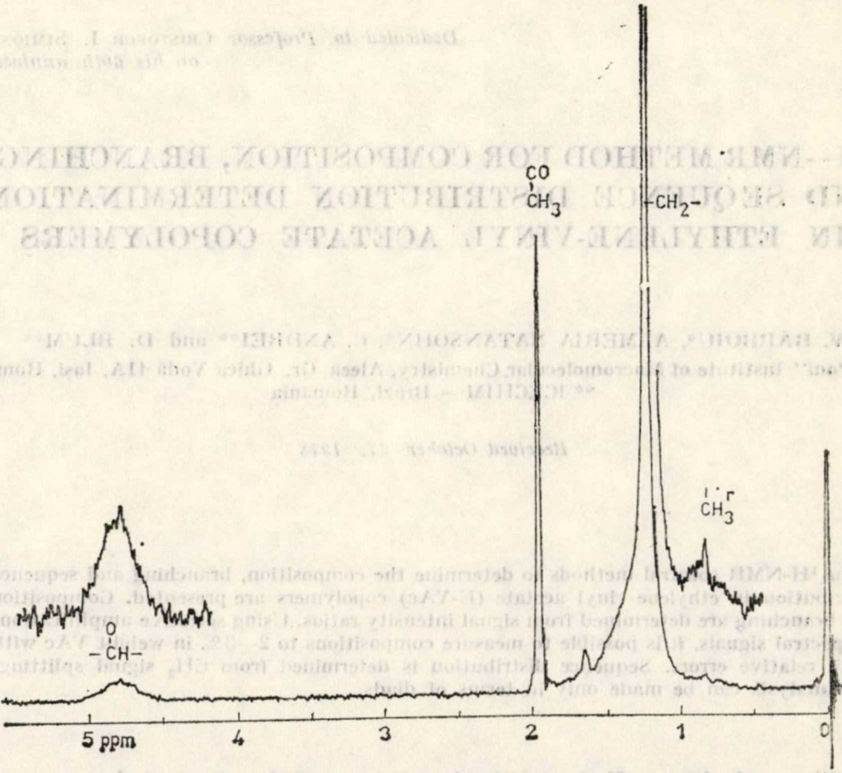

Fig. 1. — Typical ¹H-NMR spectrum for an E-VAc copolymer sample.

Assignment of signals can be made as follows :

— 4.85 ppm — CH group proton from VAc

— 2.00 ppm — CH_3 group protons from VAc

— 1.30 — 1.70 ppm — protons of CH_2 group directly bonded to a CH from VAc

— 1.20 ppm — CH_2 group from long methylenic chains

— 0.90 ppm — CH_3 group protons in branching ends.

The copolymer composition can be obtained from the ratio between integrals of the saturated region and the 4.85 ppm signal.$^{1-3}$ The main experimental difficulty arises from the poor precision in integral measurement, because the saturated region gives a much intenser signal than the CH protons from VAc.

In order to obtain a better accuracy and reproductibility, the method illustrated in figure 2 is proposed.

The CH_3 group signal from VAc structural units (2.00 ppm) is compared with the CH_2 group signal from E and VAc structural units (1.00—1.70 ppm). The spectrum is 5 times extended with precaution to prevent r.f. saturation. The integrals are recorded with a controlled amplitude ratio of 10.0 : 1, as described in the experimental part.

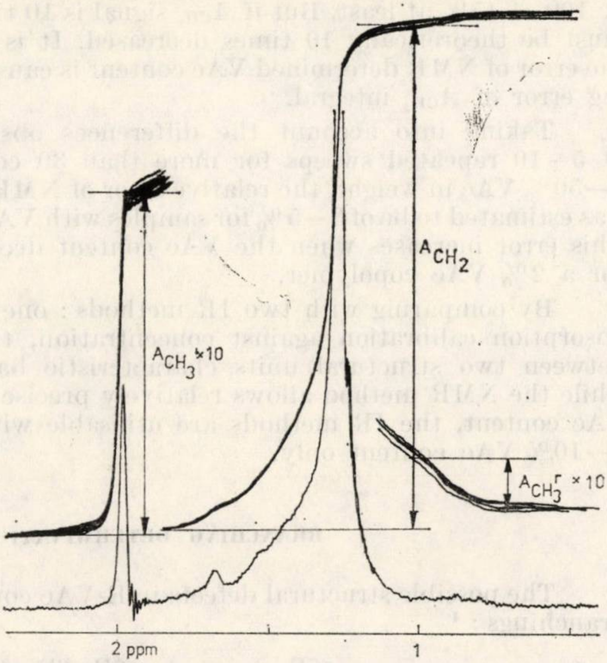

Fig. 2. — Saturated region of the spectrum for composition determination.

The VAc content can be calculated from :

$$\mathrm{VAc\,(mole\,\%)} = \frac{4A_{\mathrm{CH_3}}}{3A_{\mathrm{CH_2}} + 2A_{\mathrm{CH_3}}}\,100$$

$$\mathrm{VAc\,(weight\,\%)} = \frac{A_{\mathrm{CH_3}}}{A_{\mathrm{CH_3}} + 0.08\,(3A_{\mathrm{CH_2}} - 2A_{\mathrm{CH_3}})}\,100$$

where $A_{\mathrm{CH_3}}$ is the 2.00 ppm signal area and
$A_{\mathrm{CH_2}}$ is the 1.00—1.70 ppm signal area.

The method can be applied to the spectra obtained in $CDCl_3$, C_2Cl_4, C_6H_6 and in other solvents with no signals in 0—2.5 ppm region. In order to have a good spectrum resolution, the temperature range between 50 and 80°C can be used. The errors due to momentary fluctuations of solution state can be eliminated by 5—10 times recording of the integral spectrum and the measurement of the averaged integral value.

This method allows an important improvement of the measuring accuracy for the relative intensities of small signals, as the following example shows : The ratio between the integrals $A_{\mathrm{CH_2}}$ and $A_{\mathrm{CH_3}}$ of a 2% molar VAc copolymer should be theoretically equal to 66 : 1. As the $A_{\mathrm{CH_2}}$ integral can be adjusted to be of 150 mm the highest (for our spectrometer), the $A_{\mathrm{CH_3}}$ integral should be of 2.2 mm only. Considering that the inherent measuring error of an analytical integral is of 1 mm at least, it results that the relative error for $A_{\mathrm{CH_3}}$ is equal to (1 mm : 2.2 mm) ×

$\times$ 100 = 45 % at least. But if A_{CH_3} signal is 10 times amplified, this error must be theoretically 10 times decreased. It is important to know that the error of NMR determined VAc content is caused mainly by the measuring error of A_{CH_3} integral.

Taking into account the differences observed for A_{CH_3} integral at 5—10 repeated sweeps for more than 30 copolymer samples having 2—50 % VAc in weight, the relative error of NMR determined VAc content was estimated to be of 3—5 % for samples with VAc content more than 10 %. This error increases when the VAc content decreases, becoming of 20 % for a 2 % VAc copolymer.

By comparing with two IR methods : one based on carbonyl group absorption calibration against concentration, the other using the ratio between two structural units characteristic bands, it was found that, while the NMR method allows relatively precise determinations until 2 % VAc content, the IR methods are utilisable with similar accuracy until 8—10 % VAc content only.

BRANCHING DETERMINATION

The possible structural defects in E-VAc copolymers are the ethylene branchings : [4]

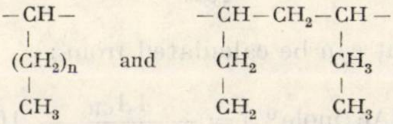

$$\begin{array}{c}-CH-\\ |\\ (CH_2)_n\\ |\\ CH_3\end{array} \quad \text{and} \quad \begin{array}{ccc}-CH- & CH_2 & -CH-\\ | & & |\\ CH_2 & & CH_3\\ | & & \\ CH_2 & & \end{array}$$

The absence of signals at 4.2 ppm and 2.1 ppm indicates that VAc structural units do not give branching :

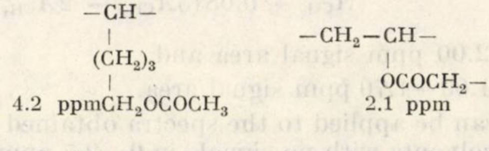

$$\begin{array}{c}-CH-\\ |\\ (CH_2)_3\\ |\\ 4.2 \text{ ppm} CH_2OCOCH_3\end{array} \qquad \begin{array}{c}-CH_2-CH-\\ |\\ OCOCH_2-\\ 2.1 \text{ ppm}\end{array}$$

The 0.90 ppm signal (Figure 1) is assigned to the CH_3 branching end groups. $A_{CH_3^r}$ being the area of this signal, the ratio of CH_3^r groups and ethylene structural units can be obtained as follows :

$$\frac{[CH_3^r]}{[CH_2CH_2]} = \frac{4}{3}\,\frac{A_{CH_3^r}}{A_{CH_2} - (2/3)\,A_{CH_3} - (1/3)\,A_{CH_3^r}}$$

The accuracy of this determination is quite low, the relative errors being about 20 % for low-branched samples.

Because the averaged length of branching cannot be determined from the ^{1}H-NMR spectra, it is impossible, also, to estimate the number of branches.

SEQUENCE DISTRIBUTION DETERMINATION

Statistical parameters of the copolymer sequence distribution are the reactivity ratios. Their values permit the sequence calculation for a sample with a known initial feed ratio. Practically, we have to know the sequence distribution without any information about the "history" of the sample, especially for industrial high-conversion copolymers. Keller[5] proposed a method to determine the run number[6] (R) by the ratio of two spectral signal areas – figure 3.

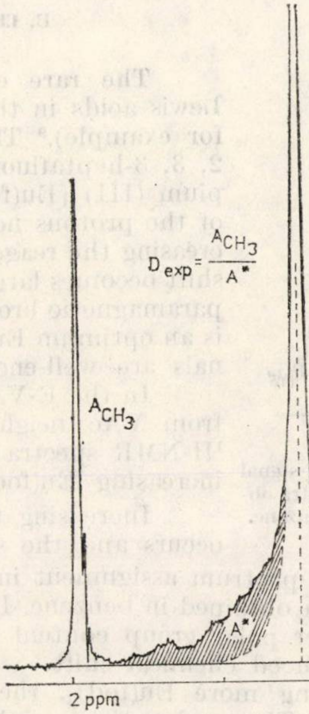

Fig. 3. — Keller method of measuring D_{exp}

If D_{exp} is determined, R is calculated according to the equation:

$$R = 3f_1 - \sqrt{9f_1^2 - 2f_1f_2((3/D_{exp}) - 2)}$$

where f_1 – ethylene structural unit molar fraction

f_2 – vinyl acetate structural unit molar fraction.

For a sample with a determined R, the average sequence length $\bar{l}_i$ and the reactivity ratios product can be calculated:

$$\bar{l}_1 = 2f_1/R \quad \bar{l}_2 = 2f_2/R$$

$$r_1r_2 = (\bar{l}_1 - 1)(\bar{l}_2 - 1)$$

These parameters give an estimation of the sequence distribution.

The main disadvantages of the Keller method are:

a. The spinning side bands of the 1.2 ppm signal cannot be entirely excluded, due to the existence of the 0.9 ppm signal arising from the ethylene branching.

b. Any imperfection of spectrum phase gives errors in measuring of A^*.

c. The CH group proton from ethylene branching resonates also in 1.30–1.70 ppm region. The attempt to eliminate this area leads to high errors, especially when branching content is low.

Taking these into account, the main source of information on sequence distribution was considered to be the CH_3 signal (2.00 ppm) splitting.

A. Spectra obtained in benzene

At 60 MHz, the spectra obtained in benzene at 70°C, and 5 times extended, present a CH_3 signal splitting as in figure 4.

This splitting is assigned to the diads:[7,8] VAc–VAc (22) and E-VAc (12) with increasing field. The ratio f_{12}/f_{22}, obtained by copying, cutting and weighing the two parts of CH_3 signal, is noted as k, and through it, the R value can be obtained as follows :

$$f_{12} = \frac{2k}{k+2} f_2 \qquad R = 100 f_{12}$$

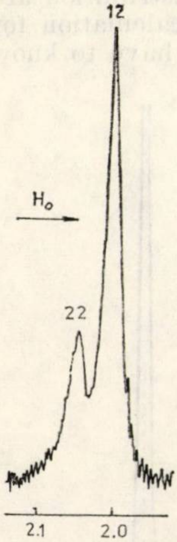

Fig. 4. — CH_3 signal from the spectra obtained in benzene.

B. Chemical shift reagent complexation

The rare earth paramagnetic complexes act as Lewis acids in the presence of basic functions (C=O for example).[9] The bulky molecule of tris(1, 1, 1, 2, 2, 3, 3-heptafluoro-7, 7-dimethyl octanedionato) europium (III) [Eu(fod)$_3$] induces a downfield chemical shift of the protons neighbouring the basic function. By increasing the reagent concentration, the induced chemical shift becomes larger, but, on the other hand, there is a paramagnetic broadening of the signals. Therefore, there is an optimum Eu(fod)$_3$ concentration for which the signals are well-enough splitted and narrow.

In the E-VAc copolymers, the CH_3 group protons from VAc neighbour the basic carbonyl group. The ^{1}H-NMR spectra in $CDCl_3$ at room temperature for two increasing Eu(fod)$_3$ concentrations are given in figure 5.

Increasing temperature, a partial decomplexation occurs and the signal becomes less splitted.

The spectrum assignment in figure 5a was made by analogy with the spectra obtained in benzene. Indeed, it seems probable that the diad with higher polar group content (22 with respect to 12) experiences a bigger induced chemical shift.

Adding more Eu(fod)$_3$, the spectrum becomes more complex — figure 5 b. The explanation can be :

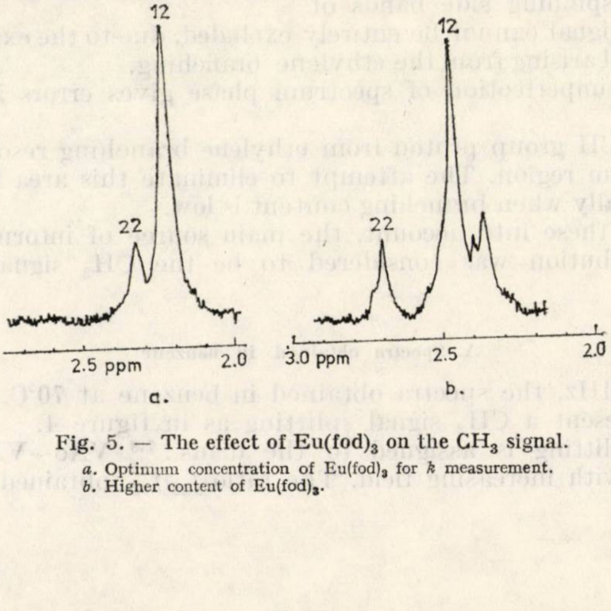

Fig. 5. — The effect of Eu(fod)$_3$ on the CH_3 signal.
a. Optimum concentration of Eu(fod)$_3$ for k measurement.
b. Higher content of Eu(fod)$_3$.

— the influence of more remote units, therefore resolving tetrad sequences,

— the configuration influence, therefore resolving sequences *and* configuration, which complicates the calculations.

Recently, it has been demonstrated that CH_3 signal splitting cannot be a configurational effect.[10] Indeed, it seems probable for configuration to affect mainly the 22 diad, and not the 12 diad which is split in the spectrum. However, triad analysis of CH_3 signal splitting is not out of discussion, due to the former results in the literature. k, f_{12} and R can be also calculated from the spectra obtained after adding $Eu(fod)_3$.

CONCLUSIONS

The high-resolution ^{1}H-NMR spectroscopy at 60 MHz gives the possibility to determine the E-VAc copolymer composition, to evaluate the branching molar percent and, through the run number, to obtain an estimation of sequence distribution in high-conversion samples.

REFERENCES

[1] R. S. Porter, S. W. Nicksic and J. F. Johnson, *Analyt. Chem.*, **35**, 1948 (1963).
[2] H. Y. Chen and M. E. Lewis, *Analyt. Chem.*, **36**, 1394 (1964).
[3] F. Keller and H. Roth, *Plaste Kaut.*, **15**, 80 (1968).
[4] M. J. Wisotsky, A. E. Kober and I. A. Zlochoner, *J. Appl. Polym. Sci.*, **15**, 1737 (1971).
[5] F. Keller, *Plaste Kaut.*, **18**, 657 (1971).
[6] H. J. Harwood and W. M. Ritchey, *J. Polym. Sci. B*, **2**, 601 (1964).
[7] T. K. Wu, *Polym. Prepr.*, **10**, 1423 (1969).
[8] T. K. Wu, *J. Polym. Sci., Polym. Phys. Ed.*, **14**, 343 (1976).
[9] R. von Ammon and R. D. Fischer, *Angew. Chem.*, **84**, 737 (1972).
[10] T. Okada and T. Ikushige, *Polym. J.*, **9**, 121 (1977).

Revue Roumaine de Chimie, 25, 7, 941–945(1980)

Dedicated to Professor CRISTOFOR I. SIMIONESFU
on his 60th anniversary

POLYMERIZATION OF STYRENE IN THE PRESENCE OF *TERT*-BUTYLHYDROPEROXIDE AND TETRAMETHYLTHIOUREA

J. BENISKA, G. KYSELÁ, E. ŠTAUDNER, M. CHLUPKOVÁ

Chemical Faculty of the Slovak Technical University, Bratislava,
Czechoslovakia

Received January 23, 1980

The study of the influence of tetramethylthiourea on the polymerization of styrene initiated by *tert*-butylhydroperoxide showed that the polymerization rate is significantly affected even at a small amount of tetramethylthiourea. Radicals able to initiate the polymerization are mainly produced during the interaction of tetramethylthiourea and *tert*-butylhydroperoxide. The experimental results are in good agreement with a mentioned simplified reaction scheme. This scheme allowed to derive the relation for the change of the polymerization rate with the tetramethylthiourea concentration and to estimate the values of the rate constant of the interaction of tetramethylthiourea and *tert*-butylhydroperoxide — k_a and of the activation energy of this reaction. The complex constants B were also estimated. The activation energy of the reinitiation reaction ($R'^{\odot} + M \xrightarrow{k_1} P^{\bullet}$) and of the transfer reaction of P · radicals on tetramethylthiourea are compared.

The study of the reactivity of sulphur and nitrogen compounds in the polymer systems showed that several of them are able to initiate the polymerization of selected vinyl monomers.[1–4] The influence of tetramethylthiuramidisulphide (TMTD) on the polymerization of styrene and methylmethacrylate was studied in details. It was found that TMTD takes place in the initiation as well as in the transfer and end reactions.

In the combination with peroxide or hydroperoxide initiators TMTD is able to form — in the dependence on the type of peroxide components — an additive, synergistic or an antagonistic initiation systems.[5]

Several other compounds with similar structures as TMTD are effective activators of the initiator systems on the base of *tert*-butylhydroperoxide (TBHP). The efficiency of those systems predominantly depends on the type of the activator used. In this paper the influence of tetramethylthiourea (TMTU) on the polymerization of styrene initiated by TBHP is studied and on the base of experimental results the mechanism of the polymerization is discussed.

EXPERIMENTAL

Styrene was purified by removing the inhibitor with 10% sodium hydroxide solution and washing with distilled water; after drying it was distilled in nitrogen.

tert-Butylhydroperoxide (TBHP) has been separated by extraction from the commercial product at low temperature with potassium hydroxide solution and regeneration by acidification in the cold with dilute sulphuric acid. The purity of TBHP, determined iodometrically, was 85.4%.

Tetramethylthiourea (TMTU) was prepared by the thermal decomposition of TMTD at atmospheric pressure. The fraction distilled at cca 245°C was separated and purified by twice repeated distillation and recrystallization from chloroform.

The polymerization was followed dilatometrically up to 8%. The molecular weights of polymers (M) were determined viscometrically using toluene as solvent at 25 ± 0.1° and were calculated using the relation[6]:

$$[\eta] = 1.7 \times 10^{-4} \times M^{0.69}$$

RESULTS AND DISCUSSION

The influence of TMTU on the polymerization of styrene initiated by TBHP at 60, 70 and 80°C was studied. The concentration of TMTU was varied over the range of 2.5×10^{-2} to 2.1×10^{-1} mole $\times$ 1^{-1} at all the following concentrations of TBHP (2.70×10^{-2}, 5.00×10^{-2} and 8.84×10^{-2} mole $\times$ 1^{-1}). The conversion curves were linear and the conversion increased with the increase of the TMTU concentration.

The dependence of the polymerization rates (R_p) on the concentration of TMTU is given in figures 1—3. From these figures it is evident that TMTU has a substantial effect on the polymerization of styrene initiated by TBHP. The polymerization rates increase even at a small amount of TMTU in the polymerization system. The relative increase of the polymerization rate increases with the increase of the total concentration of the initiation system and with the decrease of the polymerization temperature.

The effective activation energy, E_a, of the followed polymerization is not practically changed with the concentrations of TMTU and TBHP, and its value is 49.7 ± 4 kJ $\times$ mole^{-1}. This value is essentially smaller than the effective activation energy of the polymerization of styrene initiated on TBHP itself and is comparable with the activation energy for the polymerization of styrene in the presence of peroxides and tertiary amines.[7]

There was also studied the influence of TMTU on the molecular weights of the resulted polymers prepared at various temperatures and constant concentrations of TBHP and at constant temperatures and various concentrations of TBHP. From the results of this study (Table 1) it is evident that the molecular weights in all cases are falling with the raising of the concentration of TMTU, predominantly at a small concentration of TMTU.

Since TMTU itself is not able to initiate the polymerization process, on the basis of the kinetic analysis of the mentioned results we supposed that during the polymerization of styrene in the presence of TBHP and

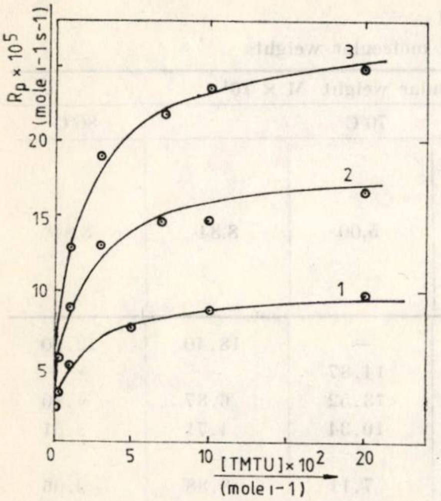

Fig. 1. — The influence of the concentration of TMTU on the polymerization rate R_p at various concentrations of TBHP at 60°C: *1* — 2.70×10^{-2}, *2* — 5.00×10^{-2}, *3* — 8.84×10^{-2} mole TBHP $\times\ l^{-1}$.

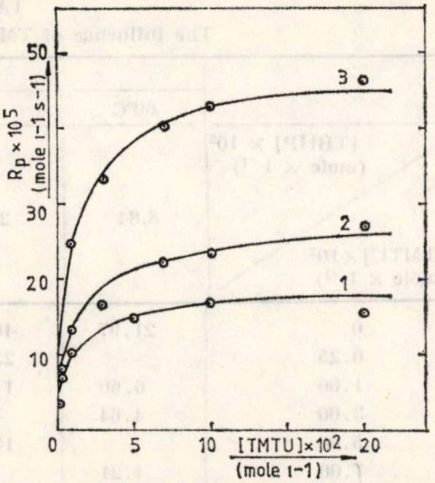

Fig. 2. — The influence of the concentration of TMTU on the polymerization rate R_p at various concentrations of TBHP at 70°C: *1* — 2.70×10^{-2}, *2* — 5.00×10^{-2}, *3* — 8.84×10^{-2} mole TBHP $\times\ l^{-1}$.

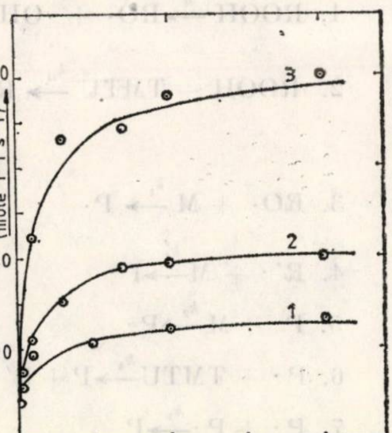

Fig. 3. — The influence of the concentration of TMTU on the polymerization rate R_p at various concentrations TBHP at 80°C: *1* — 2.70×10^{-2}, *2* — 5.00×10^{-2}, *3* — 8.84×10^{-2} mole TBHP $\times\ l^{-1}$.

TMTU the spontaneous decomposition of TBHP as well as the interaction of the components of the initiation system (the activated decomposition of TBHP) take place. This interaction is due to the formation of the radicals able to initiate the polymerization and thus able to increase the polymerization rate. The mechanism of the interaction was not studied in detail but it is possible a similar mechanism as in the case of the reaction of peroxides and tertiary amines.[7] We are also suggesting that the molecular products of the interaction are not able to react in the polymerization

TABLE 1

The influence of TMTU on molecular weights

	Molecular weight M × 10^4				
	60°C	70°C			80°C
[TBHP] × 10^2 (mole × 1^{-1}) / [TMTU] × 10^2 (mole × 1^{-1})	8.84	2.70	5.00	8.84	8.84
0	21.97	46.50	—	18.40	12.90
0.25	—	23.34	14.87	—	—
1.00	6.60	14.19	13.52	6.87	4.90
3.00	4.64	—	10.34	4.71	3.51
5.00	—	11.16	—	—	—
7.00	4.21	—	7.11	3.88	3.06
10.00	4.08	10.54	6.34	3.89	2.92
20.00	4.07	9.70	6.52	3.85	2.88

process. Accordingly the polymerization of styrene in the presence of TBHP and TMTU can be presented thus :

1. $\mathrm{ROOH} \xrightarrow{k_d} \mathrm{RO}\cdot + \cdot\mathrm{OH}$

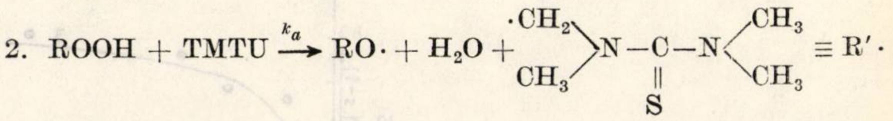

2. $\mathrm{ROOH} + \mathrm{TMTU} \xrightarrow{k_a} \mathrm{RO}\cdot + \mathrm{H_2O} + (\cdot\mathrm{CH_2})(\mathrm{CH_3})\mathrm{N{-}C({=}S){-}N(CH_3)_2} \equiv \mathrm{R}'\cdot$

3. $\mathrm{RO}\cdot + \mathrm{M} \xrightarrow{k_1} \mathrm{P}\cdot$

4. $\mathrm{R}'\cdot + \mathrm{M} \xrightarrow{k_1'} \mathrm{P}\cdot$

5. $\mathrm{P}\cdot + \mathrm{M} \xrightarrow{k_2} \mathrm{P}\cdot$

6. $\mathrm{P}\cdot + \mathrm{TMTU} \xrightarrow{k_4} \mathrm{P} + \mathrm{R}'\cdot$

7. $\mathrm{P}\cdot + \mathrm{P}\cdot \xrightarrow{k_3} \mathrm{P}$

8. $\mathrm{P}\cdot + \mathrm{R}'\cdot \xrightarrow{k_3'} \mathrm{P}$

By solving differential equations for the change of the concentration of single radicals in the stationary state and on the assumption that :

$$k_4[\mathrm{P}\cdot]\,[\mathrm{TMTU}] = k_1'[\mathrm{R}'\cdot]\,[\mathrm{M}]$$

we derived the relation :

$$R_p^2 = \frac{R^2_{p\mathrm{TBHP}} + \mathrm{A}[\mathrm{TMTU}]}{1 + 2\mathrm{B}\dfrac{[\mathrm{TMTU}]}{[\mathrm{M}]}}$$

where

$$R^2_{p\mathrm{TBHP}} = \frac{k_2^2}{k_3} k_d [\mathrm{ROOH}] [\mathrm{M}]^2$$

$$\mathrm{A} = \frac{2k_a k_2^2}{k_3} [\mathrm{ROOH}] [\mathrm{M}]^2$$

and

$$\mathrm{B} = \frac{k_3' k_4}{k_1' k_3}$$

The experimental results are in good agreement with the derived relation. They allowed to estimate the values of complex constants B and with the help of the values A using the necessary constants [7] also the values of the rate constants of the interaction of TBHP and TMTU — k_a. The estimated values of the constants B and k_a at different temperatures, showed in table 2, are the average values of B and k_a determined at various concentrations of TBHP.

TABLE 2

The values of the constants B and of the rate constants k_a

t (°C)	B	$k_a \times 10^5/1 \times \mathrm{mole}^{-1} \times \mathrm{s}^{-1}$
60	118	1.37
70	141	2.45
80	165	4.70

The constants B are relatively little changed with the temperature and the estimated activation energy E_B is 16.8 ± 2 kJ × mole^{-1}. The estimation of this energy allowed to compare the activation energy of the reinitiation (reaction 4) — E_1' and the activation energy of the transfer reaction of polymer radicals P · on TMTU (reaction 6) — E_4. We provide that E_3' is practically equal to E_3, then $E_B = E_4 - E_1'$ an dfor our case $E_4 = E_1' + 16.8$ kJ × mole^{-1}.

The estimated values of the rate constants k_a and also the activation energy of the interaction of TBHP and TMTU ($E_a = 61.1 \pm 4$ kJ × × mole^{-1}) are comparable to the published values for the induced decomposition of peroxide compounds in the presence of tertiary amines.[7]

REFERENCES

[1] J. Beniska and E. Štaudner, *J. Polym. Sci.*, **1967,** C 16, 1301.

[2] E. Štaudner and J. Beniska, *Europ. Polym. J. Supplement*, **1969,** 537.

[3] J. Beniska, *Vysokomol. Soedinenya*, **13,** 1990 (1971).

[4] E. Štaudner, G. Kyselá, J. Beniska and D. Mikolaj, *Europ. Polym. J.*, **14,** 1067 (1978).

[5] J. Beniska, E. Štaudner and G. Kyselá, *Acta Chim. Acad. Sci. Hung.*, **98,** 193 (1978).

[6] Cian-Žeň-Juan, "Opredelenie mol. vesov polimerov", I.I.L., Moskva, 1962.

[7] Ch. L. Bagdasarjan, "Teoria radikaènoj polimerizacii", IAN, S.S.S.R., Moskva, 1959.

Revue Roumaine de Chimie, 25, 7, 947–952(1980)

Dedicated to Professor CRISTOFOR I. SIMIONESCU
on his 60th anniversary

THE REACTIVITIES OF MONOMERS TOWARDS PRIMARY RADICALS, STUDIED BY SPIN-TRAPPING

JOHN C. BEVINGTON, BRIAN J. TABNER and PETRINA F. FRIDD
Department of Chemistry, The University, Lancaster, England

Received January 30, 1980

The results of experiments involving spin trapping and isotopic labelling in initiation of polymerizations are reviewed.

Much work has been done on comparisons of the reactivities of unsaturated substances towards the benzoyloxy radical.[1] The principal experimental approach has involved the use of benzoyl peroxide suitably labelled with carbon-14 or tritium, as initiator of polymerizations, followed by analysis of the resulting polymers for benzoyloxy and phenyl end-groups. The relevant reactions are

$$(C_6H_5{-}CO{-}O)_2 \rightarrow 2C_6H_5{-}CO{-}O\cdot$$

$$C_6H_5{-}CO{-}O\cdot \rightarrow C_6H_5\cdot + CO_2 \tag{1}$$

$$C_6H_5{-}CO{-}O\cdot + M \rightarrow C_6H_5{-}CO{-}O{-}M\cdot \tag{2}$$

$$C_6H_5\cdot + M \rightarrow C_6H_5{-}M\cdot \tag{3}$$

where M represents a molecule of monomer. Normally, the phenyl radicals produced in (1) are subsequently captured by monomer in (3). The value of {rate of (1)}/{rate of (2)} can therefore be found by comparison of the numbers of the two types of end-group in the polymer. Experiments are performed with various concentrations of monomer and the results are treated by the methods usually applied for study of competing processes so that the ratio k_1/k_2 can be evaluated. By working over a range of temperatures, $(E_1 - E_2)$ can be found. The reactivities of monomers towards the benzoyloxy radical are therefore compared using the dissociation (1) as the reference reaction. The treatment can be extended to copolymerizations so that it becomes possible to deal with those unsaturated substances which engage in copolymerizations but do not readily form homopolymers.

The early results have been summarized and interpreted.[2] More recent work has involved monomers such as esters of fumaric acid,[3] dienes,[4] methyl α-cyanacrylate[5] and N-vinylcarbazole[6] and also the use of doubly-labelled peroxide.[5] It has been demonstrated[7] that the ratio k_1/k_2 is sensitive to pressure.

An alternative method of working makes use of the fact that, when benzoyl peroxide at low concentrations decomposes in benzene, almost all the benzoyloxy radicals decompose according to (1). The yield of carbon dioxide is depressed if the reaction mixture also contains substances which react with the benzoyloxy radical.[8] The necessary measurements can be performed with the required accuracy using benzoyl peroxide, suitably labelled with carbon-14, and performing isotope dilution analysis for carbon dioxide. Again, standard treatments for competing reactions can lead to comparisons of the reactivities of various additives.

Experiments involving ^{14}C-benzoyl peroxide as initiator of polymerization, followed by end-group analyses of the resulting polymers, have given information on other topics including reactivities of monomers towards the phenyl radical,[9] transfer to benzoyl peroxide,[10] primary radical termination[11] and differences between the thermolysis and photolysis of the peroxide.[12,13] Studies have been made on substituted benzoyloxy radicals[14] and other radicals, such as tert. butoxy[15] and benzoyl,[16] which can dissociate to smaller radicals and stable molecules.

$$(CH_3)_3C-O\cdot \rightarrow CH_3\cdot + (CH_3)_2CO \tag{4}$$

$$C_6H_5-CO\cdot \rightarrow C_6H_5\cdot + CO$$

Isotope effects have been detected[15,17] in the dissociations (1) and (4).

It would be useful to have information on the relative reactivities of monomers towards radicals which do not dissociate further and a particularly interesting case would be the 2-cyano-2-propyl radical derived from the important initiator azobisisobutyronitrile. Various procedures have been developed and used for systems of this type; in one such study on the phenyl radical,[18] the competition between reactions (3) and (5)

$$C_6H_5\cdot + C_7H_{15}-SH \rightarrow C_6H_6 + C_7H_{15}-S\cdot \tag{5}$$

was examined by measurements of the yields of benzene in systems containing various proportions of monomer and mercaptan.

E.s.r. spectroscopy, in the form of the spin-trapping technique[19] has been used for identification of the radicals produced in systems such as mixtures of diacyl peroxides with tertiary amines.[20] The technique has also been used quantitatively for comparison of the reactivities of monomers towards certain small radicals, such as benzoylthiyl.[21] The radical is generated in a mixture of monomers containing 2-methyl-2-nitrosopropane as radical scavenger or trapping agent. The competition between the processes

$$C_6H_5-CO-S\cdot + M_a \rightarrow C_6H_5-CO-S-M_a\cdot \tag{6}$$

$$C_6H_5-CO-S\cdot + M_b \rightarrow C_6H_5-CO-S-M_b\cdot \tag{7}$$

is examined by comparing the yields of the product radicals. These products react with the trapping agent to give two types of stabilized radicals, viz. $C_6H_5-CO-S-M_a-T\cdot$ and $C_6H_5-CO-S-M_b-T\cdot$, which can be separately determined from the e.s.r. spectrum for the system. It is necessary to assume that the radicals formed in (6) and (7) are captured with equal efficiencies by the trapping agent; another difficulty might arise if some of these radicals grow before being trapped since the second monomer added to a particular radical might not be the same as the monomer already incorporated.

The spin-trapping technique has been used also with tert. butoxy radicals generated thermally at 20°C [22] in the presence of monomer, *p*.xylene and a trapping agent. The yields of radicals in the competing reactions

$$(CH_3)_3C-O\cdot + M \rightarrow (CH_3)_3C-O-M\cdot$$

$$(CH_3)_3C-O\cdot + CH_3-C_6H_4-CH_3 \rightarrow (CH_3)_3C-OH + \cdot CH_2-C_6H_4-CH_3$$

are compared by analysis of the e.s.r. spectrum corresponding to the mixture of stable radicals formed by reaction with the trapping agent. A result, perhaps with important implications, is that primary radical transfer may be very significant for monomers carrying an α-methyl group and giving rise to an allylic radical

$$(CH_3)_3C-O\cdot + CH_2=CX-CH_3 \rightarrow (CH_3)_3C-OH + CH_2=CX-CH_2\cdot$$

The spin-trapping technique has been applied [23,24] to systems involving azoisobutyronitrile but so far with only limited success.

It is clear that spin-trapping is potentially of great value for study of the details of initiation in radical polymerization and we have started a programme of research. We are considering a simple scheme based on the following reactions

$$X\cdot + T \rightarrow X-T\cdot \quad (8)$$

$$X\cdot + M \rightarrow X-M\cdot \quad (9$$

$$X-M\cdot + T \rightarrow X-M-T\cdot \quad (10)$$

where X represents the initiating radical, T the trapping agent and M the monomer. The balance between (8) and (9) is being assessed by comparing the yields of the stable radicals produced in (8) and (10). Clearly the reference reaction is (8) since this process occurs with a particular velocity constant whatever the nature of the monomer M. Some points must be made in connection with the scheme. For each monomer, a set of experiments is needed involving various values of [M]/[T]; in each set, however, only one monomer is used so avoiding complications already mentioned in connection with (6) and (7). If (9) is followed in some cases by growth reactions before the radical is trapped, the scheme is not invalidated because the stable radicals $X-M-T\cdot$, $X-M-M-T\cdot$ etc. are identical from the point of view of their e.s.r. spectra. The choice of trapping agent is critical so that reactions (8), (9) and (10) proceed at comparable rates.

One of the checks being made involves application of the procedure to various monomers with the benzoyloxy radical, since there is already an extensive collection of information on these systems. We now report the results of some preliminary experiments.

A study was made of the effects of some typical trapping agents upon the decomposition of benzoyl peroxide in dilute solution in benzene at 60°C. The peroxide was labelled with carbon-14 in the carboxyl groups and isotope dilution analyses were performed for carbon dioxide. Evidently the additives reacted readily with the benzoyloxy radical because, even at low concentrations, they depressed the yields of carbon dioxide (see Figure 1). It appears that the trapping agents had no significant effect upon the rate of decomposition of the peroxide, the half-life of roughly 70 hours (see Figure 2) being similar to that for decomposition in pure benzene.[8]

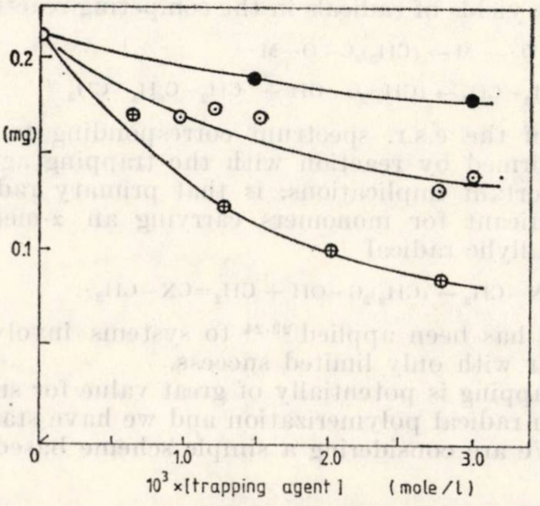

Fig. 1. — Effects of trapping agents on the yield of carbon dioxide during the decomposition of benzoyl peroxide in benzene at 60°C for 96 hours.

⊕ 2-methyl-2-nitrosopropane (BNO)
⊙ N-tert. butyl-α-phenyl nitrone (PBN)
● nitrosobenzene (NB)

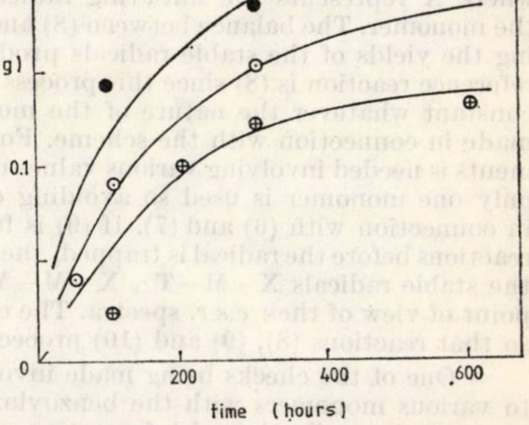

Fig. 2. — As for Figure 1 but fixed concentration of trapping agent (3×10^{-3} mole/l) and various durations of decomposition.

Benzoyl peroxide was decomposed at 60°C in benzene containing various concentrations of monomer and N-tert·butyl-α-phenyl nitrone as trapping agent [25]; the concentrations were such that few benzoyloxy radicals could have decomposed according to (1) and there was no evidence from e.s.r. spectra for the trapping of phenyl radicals. The ratios of the concentrations of the trapped radicals $C_6H_5{-}CO{-}O{-}T\cdot$ and $C_6H_5{-}CO{-}O{-}M{-}T\cdot$, see equations (8) and (10), were found from computer simulations of the observed e.s.r. spectra. If the scheme of reactions (8), (9) and (10) is applicable, then Figure 3 shows that this relationship may be satisfied with k_9/k_8 about 0.70 for *p*.methoxystyrene and about 0.02 for vinyl acetate. As expected from older results based upon (1) as the reference reaction, vinyl acetate appears to be appreciably less reactive than *p*·methoxystyrene towards the benzoyloxy radical. Exploratory experiments with other monomers have been less satisfactory, $[X{-}M{-}T\cdot]/[X{-}T\cdot]$ increasing with [M]/[T] but not strictly in accord with equation (11). Evidently further work is needed, perhaps with different trapping agents, but it seems that there may be some real value in the suggested procedure for comparing the reactivities of monomers towards primary radicals.

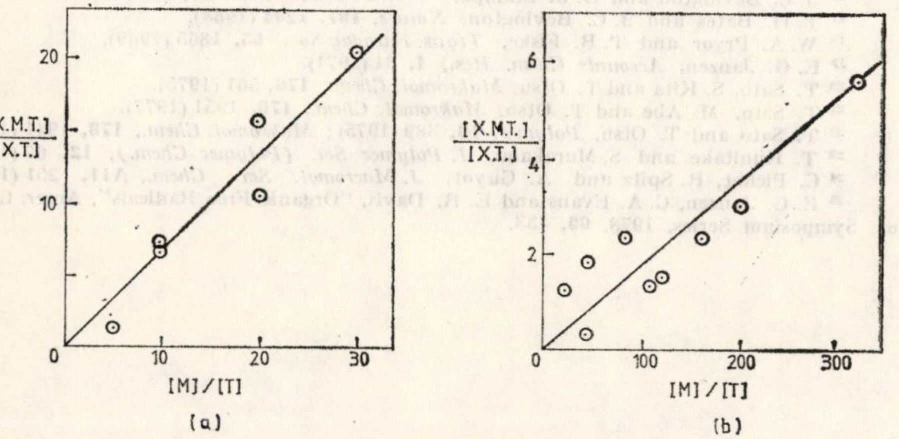

Fig. 3. — Dependence of $[C_6H_5\cdot CO\cdot O\cdot M\cdot T\cdot]/[C_6H_5\cdot CO\cdot O\cdot T\cdot]$, as found from e.s.r. spectra, on [M]/[T].
Trapping agent = BNO
(*a*) *p*.methoxystyrene (*b*) vinyl acetate.

The work referred to in this paper was performed while P.F.F. held a Research Studentship awarded by the Science Research Council.

REFERENCES

[1] J. C. Bevington and J. R. Ebdon, "Developments in Polymerization — 2", ed. R. N. Haward, Applied Science Publishers, London, 1979, Chapter 1.

[2] J. C. Bevington, "Radical Polymerization", Academic Press, London, 1961.

[3] J. C. Bevington, M. Johnson and J. P. Sheen, *European Polymer J.*, **7**, 1155 (1971).

[4] J. C. Bevington and P. K. SenGupta, *Polymer*, **15**, 467 (1974).

[5] J. C. Bevington and J. A. L. Jemmett, *J. Chem. Soc. Faraday I*, **69**, 1866 (1973).

[6] J. C. Bevington and C. J. Dyball, *J. Polymer Sci. (Polymer Chem.)*, **14**, 1819 (1976).

[7] J. C. Bevington, J. R. Suggate and K. E. Weale, *Polymer*, **18**, 749 (1977).

[8] C. A. Barson and J. C. Bevington, *Tetrahedron*, **4**, 147 (1958).

[9] J. C. Bevington and T. Ito, *Trans. Faraday Soc.*, **64**, 1329 (1968).

[10] J. C. Bevington and T. D. Lewis, *Polymer*, **1**, 1 (1960).

[11] J. K. Allen and J. C. Bevington, *Trans. Faraday Soc.*, **56**, 1762 (1960).

[12] J. C. Bevington and T. D. Lewis, *Trans. Faraday Soc.*, **54**, 1340 (1958).

[13] J. C. Bevington and P. K. SenGupta, *Polymer*, **14**, 527 (1973).

[14] see for example J. C. Bevington, J. Toole and L. Trossarelli, *Makromol. Chem.*, **32**, 57 (1959).

[15] J. K. Allen and J. C. Bevington, *Proc. Royal Society*, **262A**, 271 (1961).

[16] J. C. Bevington and D. J. Stamper, *Trans. Faraday Soc.*, **66**, 688 (1970).

[17] T. H. Bates and J. C. Bevington, *Nature*, **197**, 1294 (1963).

[18] W. A. Pryor and T. R. Fiske, *Trans. Faraday Soc.*, **65**, 1865 (1969).

[19] E. G. Janzen, *Accounts Chem. Res.*, **4**, 31 (1971).

[20] T. Sato, S. Kita and T. Otsu, *Makromol. Chem.*, **176**, 561 (1975).

[21] T. Sato, M. Abe and T. Otsu, *Makromol. Chem.*, **178**, 1951 (1977).

[22] T. Sato and T. Otsu, *Polymer*, **16**, 389 (1975) ; *Makromol. Chem.*, **178**, 1941 (1977).

[23] T. Kunitake and S. Murakami, *J. Polymer Sci. (Polymer Chem.)*, **12**, 67 (1974).

[24] C. Pichot, R. Spitz and A. Guyot, *J. Macromol. Sci., Chem.*, **A11**, 251 (1977).

[25] E. G. Janzen, C. A. Evans and E. R. Davis, "Organic Free Radicals", Amer. Chem. Soc. Symposium Series, 1978, **69**, 433.

Revue Roumaine de Chimie, 25, 7, 953–960(1980)

Dedicated to Professor CRISTOFOR I. SIMIONESCU
on his 60 th anniversary

RADICAL ALTERNATING COPOLYMERIZATION OF 9-VINYLCARBAZOLE WITH DIETHYL FUMARATE OR DIETHYL MALEATE

N. COBIANU

Department of Macromolecular Chemistry, Polytechnic Institute, Calea Victoriei 149, Bucharest, Romania

Received February 11, 1980

The alternating copolymerization of NVC and DEF or DEM has been studied. The dependence of the copolymerization rate onto monomer and initiator concentrations has been established; it shows a specific monoradical mechanism and the participation of the uncomplexed monomers along their weak charge-transfer complex in propagation reactions. The activation energy for copolymerization of the pair NVC—DEF in the presence of AIBN, has been calculated. The value found represents a proof for propagation reaction, mainly by uncomplexed monomers, in a radical mechanism. The marked alternating tendency in the chain, has been explained by the formation of dipolar resonance structure in transition state, as a result of electron transfer from the growing radical ending in NVC to DEF, or from NVC to the growing radical ending in DEF. The diffusion-controlled character of the termination reaction has been proved. By IR spectroscopic analysis of alternating copolymers, it has been shown that the termination reaction takes place mainly by recombination.

INTRODUCTION

9-Vinylcarbazole (NVC) and diethyl fumarate (DEF) form a weak charge-transfer complex; [1] in the presence of radical initiators or by photochemical initiation this pair copolymerizes in alternating manner.[1-4]

The initial rate of copolymerization of NVC—DEF [2,3] or NVC—DEM [3] increases with the molar fraction of NVC in monomer feed. Mikawa and his co-workers [2] consider that the radical ending in DEF is far less reactive than that ending in NVC. On this basis it is suggested that the reaction between radicals ending in DEF determines the rate in the termination process. On the other hand, it was shown [3] that in this radical copolymerization, the termination is diffusion-controlled.

In order to gather new experimental evidence, a detailed kinetic study was carried out.

EXPERIMENTAL

Materials

NVC used in polymer syntheses had m.p. = 64.5°C, being obtained by recrystallization from methanol.

DEF and DEM were synthetized according to literature data. [5] The reaction mixture was successively washed with water, saturated aqueous solution of Na_2CO_3, and again water, until neutral. After benzene removal, the products were distilled under vacuum ; the medium fraction was redistilled from calcium hydride. The refractive indexes of the diesters synthetized are $n_D^{20} = 1{,}4401$ (DEF) and $n_D^{20} = 1{,}4409$ (DEM).

2,2′-Azoisobutyronitrile (AIBN) was purified by recrystallization from ethanol and drying under vacuum at 25°C.

1,4-Dioxane was distilled and subsequently redistilled from sodium wire ($n_D^{20} = 1{,}4224$). Benzene and methanol were purified according to the usual procedures.

Polymerization procedure

Copolymerization reactions were carried out in glass ampoules with two reservoires.[6] The two reservoires contained the appropriate monomers as solutions in dioxane. AIBN was added (dioxane solution) in the arm of the ampoule containing diester. The ampoule content was submitted to three conventional cycles of freezing-thawing, under argon-vacuum. After the desired conversion was obtained, the polymer was precipitated in methanol, filtered and dried. The polymers submitted to some analyses were redissolved in dioxane or benzene, reprecipitated and dried in vacuum at 50°C.

Characterization of products

The copolymer composition was established by nitrogen analysis, according to semimicro Dumas method.

The intrinsic viscosities of copolymers were established on the basis of draining times. The measurements were carried out with an Ubbelohde viscometer, by using dilute polymer solutions in benzene at 25°C. The intrinsic viscosity was calculated by using the equation [4] :

$$\eta_{sp}/C = |\eta| + 0.33\,|\eta|^2 \cdot C \tag{1}$$

The average viscometric molecular weight of poly [1-(9-carbazyl)-2,3-(diethoxycarbonyl)-butane-1,4-diil] was calculated by using the equation [4] :

$$|\eta| = 1.46 \cdot 10^{-2} \cdot \overline{M}_\eta^{0.67} \tag{2}$$

For poly (NVC) the average viscometric molecular weight was calculated with Ueberreiter's [7] formula :

$$|\eta| = 3.35 \cdot 10^{-2} \cdot \overline{M}_\eta^{0.58} \tag{3}$$

at 25°C and benzene as solvent.

The viscosity of NVC and DEF in dioxane, at 25°C, was established by help of a rheoviscometer-Höppler type.

RESULTS AND DISCUSSION

1. The dependence of average viscometric molecular weight on monomer feed composition

In order to get a better comprehension of the mechanism of the alternating copolymerization of NVC with fumaric or maleic diesters it is necessary to know the law governing the dependence of molecular weight on the monomer feed composition. The molecular weight of equimolecular NVC-DEM copolymers, obtained at small conversion, varies with the monomer feed composition, as may be seen from figure 1.

An increase of copolymer molecular weight as NVC fraction in the monomer feed increases as well ($[M_1]_0 + [M_2]_0 = ct$), may be the result either of the diffusion-controlled termination reactions or of the chain transfer with the respective diester. If the second process would be negligible, then the dependence between $\overline{M}_\eta$ and the square root of viscosity of the mixture should be a linear one.

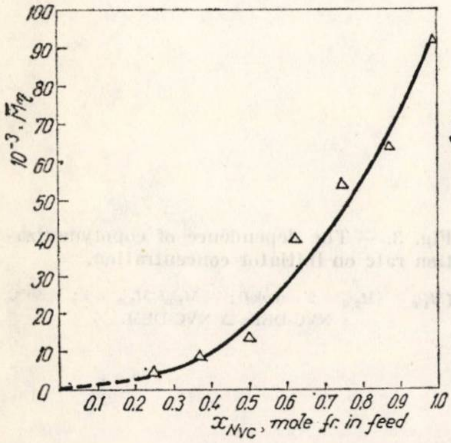

Fig. 1. — The dependence of $\overline{M}_\eta$ for the alternating copolymer NVC-DEM on monomer feed composition.

$[M_1]_0 + [M_2]_0 = 1$ mole/l; $[\text{AIBN}]_0 = 5.10^{-3}$ mole/l; 60°C.

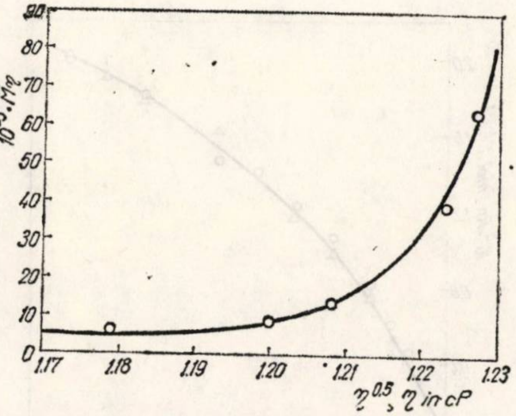

Fig. 2. — The molecular weight of the alternating copolymer NVC-DEF plotted against mixture viscosity.

On representing $\overline{M}_\eta = f(\eta)^{1/2}$ (see figure 2) it seems that both processes compete in the alteration of the average molecular weight of copolymers.

2. The influence of initiator concentration

The dependence of initial copolymerization rate on initiator concentration, for the systems NVC-DEF and NVC-DEM, is illustrated in figure 3.

By representing (on a doubly-logarithmic scale) the initial copolymerization rate as a function of [AIBN] (see figure 4), we have calculated the order of reaction with regard to initiator concentration; the data were obtained starting from an initial equimolecular monomer feed, in dioxane at 60°C we have found an order of 0.55 for the pair NVC-DEF and 0.60 for the pair NVC-DEM. The values found are quite near to that predicted by the theory (0.5) taking into account a bimolecular mechanism, in termination reaction.

The exponent for initiator concentration, higher than 0.5 could be due to the presence of some inhibitor in the system. The only impurity, able to carry out a pseudo monoradical termination, has been carbazole, present in traces in NVC (thin layer chromatography).

The fact that bimolecular termination is the most likely mechanism for the alternating copolymerization of these systems proves that, in these situations, the biradical mechanism cannot be accepted. Moreover, the thermal copolymerization of NVC with DEF or DEM did not take place, in the above-mentioned conditions,[3] this fact excluding the mechanism of cross-initiation, as well as that of spontaneous polymerization of the charge-transfer complex.

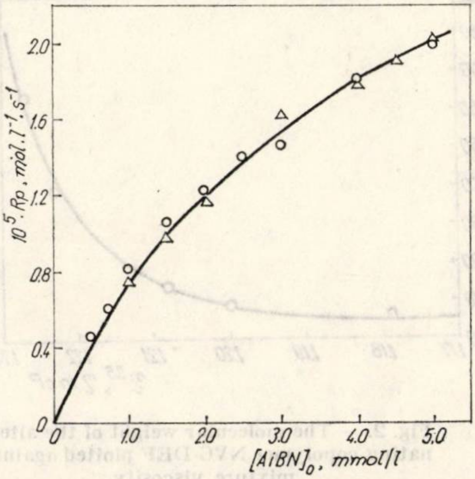

Fig. 3. — The dependence of copolymerization rate on initiator concentration.

$[M_1]_0 + [M_2]_0 = 2$ mole/l; $[M_1]_0/[M_2]_0 = 1$; 60°C
o NVC-DEF; Δ NVC-DEM.

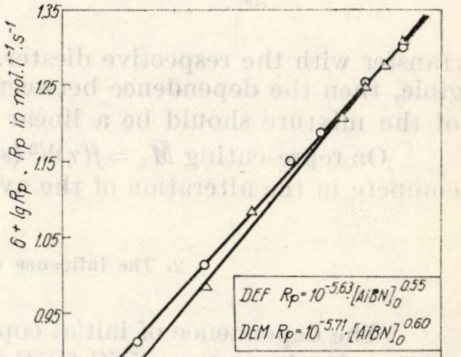

Fig. 4. — Graphical calculation of the reaction order with respect to initiator, for copolymerization of the pairs: NVC-DEF and NVC-DEM.

$[M_1]_0 + [M_2]_0 = 2$ mole/l; $x_{NVC} = 0.5$; 60°C.
o DEF; Δ DEM.

In figures 5 and 6 we have presented the dependence between the molecular weight of copolymers obtained and the initiator concentration.

The fact that the molecular weights are quite high proves that the chain transfer with dioxane is not intense.

An inverse proportionality between M_η and the square-root of initiator concentration was found for both systems.

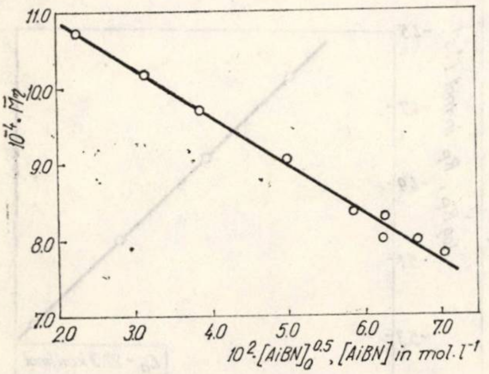

Fig. 5. — $\overline{M}_\eta = f([\text{AIBN}]_0)$ for the copolymers NVC-DEF obtained from equimolecular monomer feed.

$[M_1]_0 + [M_2]_0 = 2$ mole/l; 60°C.

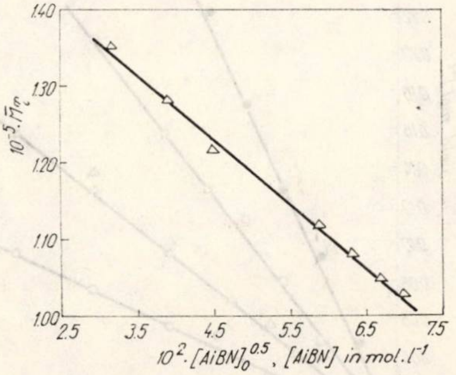

Fig. 6. — $\overline{M}_\eta = f([\text{AIBN}]_0)$ for the copolymers NVC-DEM obtained from equimolecular monomer feed.

$[M_1]_0 + [M_2]_0 = 2$ mole/l; 60°C.

3. The role of temperature

In the presence of a given electron-acceptor monomer, the higher the ionization potential of donor monomer, the easier the formation of a charge-transfer complex. The formation of a charge-transfer complex between NVC and DEF, in fundamental state, was confirmed by Mikawa and his co-workers,[1] by UV measurements. In the absence of data which would allow the determination of complex concentration, under copolymerization conditions, qualitative information regarding the propagation step may be obtained by studying the influence of temperature on reaction rate. In this respect, the value of the total activation energy may be relevant.

The conversion, as a function of reaction time and temperature, is presented in figure 7 ; figure 8 illustrates the initial copolymerization rate versus the same parameter.

The total activation energy found, calculated by usual graphic method, of 22.3 kcal/mole, is in good agreement with those reported for the alternating copolymerization of maleic anhydride with vinyl ethers, vinyl sulphides and *p*-dioxane, in the presence of AIBN,[8-9] but higher than that of the system maleic anhydride-styrene.[9] For the last system, Tsukida [9] has found $E_a = 18.6$ kcal/mole, when the solvent was THF, drawing the conclusion that the propagation via free radicals does not seem to be less important than the propagation of the charge-transfer complex.

The total activation energy in the copolymerization of NVC with DEF is in the neighbourhood of that of a usual vinyl polymerization, in the presence of radical initiators.[4] This value supports the view according to which the free radical propagation is more important than that of the charge-transfer complex. This fact may perhaps be explained by taking

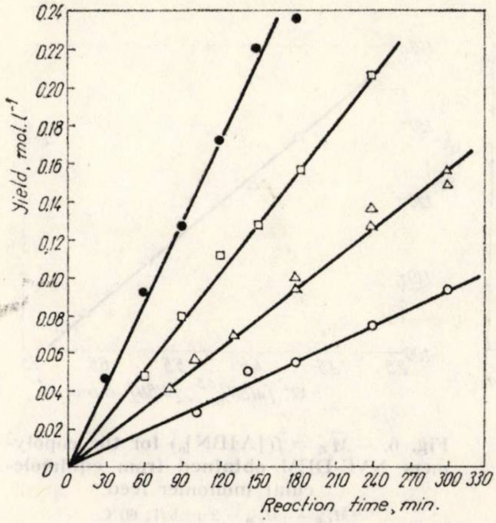

Fig. 7. — The dependence of conversion on reaction time and temperature, for the pair NVC-DEF.

$[M_1]_0 + [M_2]_0 = 1$ mole/l; $x_{NVC} = 0.5$; $[AIBN]_0 = 5 \cdot 10^{3}$ mole/l.

⊖ 55°C; △ 60°C; □ 65°C; ● 70°C.

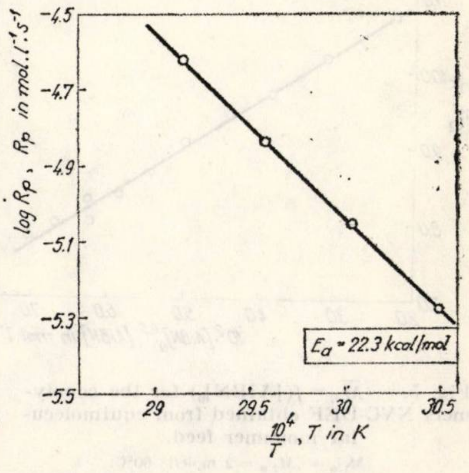

Fig. 8. — Initial reaction rate against temperature for the copolymerization of NVC-DEF.

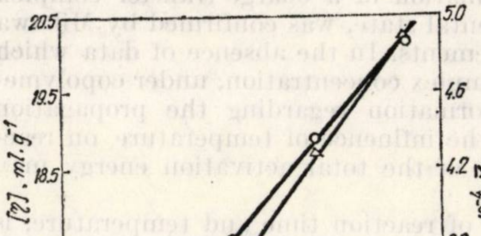

Fig. 9. — The relationship between average viscometric molecular weight and temperature for the copolymer NVC-DEF.

$[M_1]_0 + [M_2]_0 = 1$ mole/l; $[AIBN]_0 = 5 \cdot 10^{-3}$ mole/l; 60°C.

Benzene as solvent for viscometrical measurements, 25°C.

into account the extreme small concentrations of the charge-transfer complex NVC-DEF, in the studied temperature range.

In figure 9 we have presented the relation between the molecular weight of equimolecular copolymers and temperature.

4. The role of monomer concentration

Taking into account the above-presented results, we have thought interesting to study the influence of monomer concentration on initial copolymerization rate. The system investigated has been NVC-DEF, and the range of monomer concentration (dioxane as solvent) has been 0.1 – 2.0 mole/l. As it may be seen from figure 10, the copolymerization rate for a total monomer concentration of 2.0 mole/l conserves the features noticed for lower monomer concentrations in the initial system.

The linearization of the dependence of polymerization rate as a function of the product of initial monomer concentration is given in figure 11.

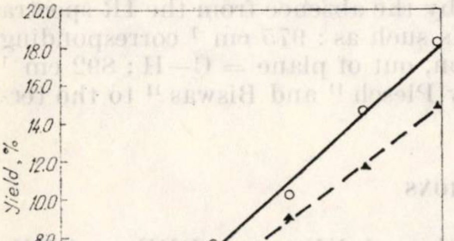

Fig. 10. — Yield versus initial monomer feed concentration for equimolecular copolymer.

⊖ — $[M_1]_0 + [M_2]_0 = 2$ mole/l; Δ- - -$[M_1]_0 +$ $+ [M_2]_0 = 1$ mole/l;
$x_{NVC} = 0.5$; $[AIBN]_0 = 5 \cdot 10^{-3}$ mole/l; 60°C.

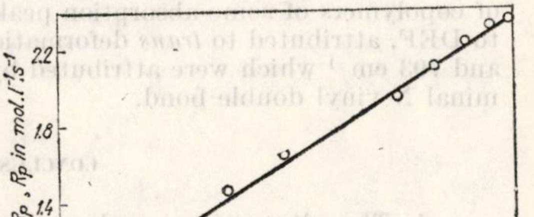

Fig. 11. — The dependence between copolymerization rate and monomer concentration for the pair NVC-DEF.

$[AIBN]_0 = 5.\ 19^{-3}$ mole/l; 60°C.

By using the data presented in this graph, the following equation was established :

$$R_{p,0} = 10^{-4.64} \cdot [M_1]_0^{0.63} \cdot [M_2]_0^{0.63} \tag{4}$$

If the formation of alternating copolymer NVC-DEF would consist only in the radical homopolymerization of the charge-transfer complex, then the polymerization rate should be proportional to complex concentration, or in other words to the product $K \cdot [M_1]_0[M_2]_0$, where K is the equilibrium constant, which characterizes the complex formation. As the experimentally measured exponent is quite remote from that predicted theoretically, it seems that the autopropagation of the charge-transfer complex may be only of minor importance. These exponent values (see equation 4) represent an indirect proof that the alternating copolymerization is not controlled by polar effects ($k_{tDD} = k_{tAA} = 0$), and in this case the expression for the rate in alternating copolymerization is :

$$R_p = \left(\frac{4k_{\mathrm{pDA}} \cdot k_{\mathrm{pAD}}}{k_{\mathrm{tAD}}} \cdot R_i\,[M_D]\cdot[M_A]\right)^{0.5} \tag{5}$$

The control by diffusion in the termination stage of the kinetic chain has been already investigated. It is quite difficult to estimate the ratio between the number of radicals disappearing by recombination and disproportionation, respectively. Starting from the curve representing the integral weight distribution,[4] we suppose that the most likely termination reaction is that of recombination.

This hypothesis is also suggested by the absence from the IR spectra of copolymers of some absorption peaks such as : 975 cm^{-1} corresponding to DEF, attributed to *trans* deformation, out of plane = C—H ; 892 cm^{-1} and 793 cm^{-1} which were attributed by Plesch [11] and Biswas [11] to the terminal N-vinyl double bond.

CONCLUSIONS

1. The alternating copolymerization of NVC and DEF or DEM, in the presence of AIBN, takes place by monoradicals.
2. The weak charge-transfer complex NVC-DEF (or NVC-DEM), in agreement with Seiner's [12] and Mikawa's [2] reports, may be considered an entity able to copolymerize. However, this complex seems to play only a minor role in initiation and propagation stages.
3. The alternating tendency along the chain seems to be due mainly to the formation of dipolar resonance structures in the transition state, as a result of electron transfer between the growing radical and co-monomer (Walling's [13] scheme), and less to the participation of the charge-transfer complex in the radical propagation, altogether with free monomers.[9]
4. The absence of ethylidenic double and terminal N-vinyl bonds in the equimolecular copolymers indicates a termination reaction by recombination.

REFERENCES

[1] M. Yoshimura, Y. Shiroto and H. Mikawa, *J. Polymer Sci., B,* **11**, 459 (1973).

[2] Y. Shirota, M. Yoshimura, A. Matsumoto and H. Mikawa, *Macromolecules,* **7**, 4 (1974).

[3] N. Cobianu, D. Thesis, Iassy, Romania, 1974.

[4] Cr. Simionescu and N. Cobianu, *European Polymer J.*, **15**, 173 (1979).

[5] A. I. Vogel, "A Text Book of Practical Organic Chemistry", 3rd Ed., Longmans Green and Co Ltd., 1956, p. 177 ; p. 389—400.

[6] T. Otsu and H. Inoue, *Makromol. Chem.*, **128**, 31 (1969).

[7] K. Ueberreiter and J. Springer, *Z. Phys. Chem.*, (Frankfurt), **36**, 299 (1963).

[8] S. Iwatsuki and Y. Yamashita, *Makromol. Chem.*, **89**, 205 (1965) ; S. Iwatsuki, M. Shin and Y. Yamashita, *Makromol. Chem.*, **102**, 232 (1967).

[9] E. Tsukida and T. Tomoto, *Makromol. Chem.*, **141**, 265 (1971).

[10] J. Pac and P. H. Plesch, *Polymer*, **8**, 237 (1967).

[11] M. Biswas and D. Chakravarty, *J. Polymer Sci., Polymer Chem. Ed.*, **11**, 7 (1973).

[12] J. A. Seiner and M. Litt, *Macromolecules*, **4**, 308 (1971).

[13] C. Walling, E. R. Briggs, K. B. Wolfstirn and F. R. Mayo, *J. Amer. Chem. Soc.*, **70**, 1537 (1948) ; C. Walling, D. Seymour and K. B. Wolfstirn, *J. Amer. Chem. Soc.*, **70**, 1544 (1948).

Revue Roumaine de Chimie, 25. 7, 961–967(1980)

Dedicated to Professor Cristofor I. Simionescu
on his 60th anniversary

COMPLEXES OF PYROMELLITIC DIANHYDRIDE WITH PYRIDINE DERIVATIVES

FELICIA CORNEA * and C. STOICESCU **
*** National Institute of Chemistry, Faculty of Technological Chemistry, Department of Organic Chemistry and Organic Technology, 202 B, Spl. Independenţei, Bucharest, Romania**
**** Pharmaceutical-Chemical Research Institute 112, Sos. Vitan, Bucharest, Romania**

Received August 4, 1979

The electron acceptor capacity of pyromellitic dianhydride (PMDA) for pyridine and some mono- or polysubstituted derivatives with electron attracting or repelling groups in the 2-, 3- or 4-position on the pyridine ring has been studied. New molecular complexes of PMDA with some pyridine derivatives in crystalline state or in solution were prepared. The resulted complexes have been characterized by chemical and spectral methods and their stability constants have been determined. On the basis of the experimental results one concludes that such complexes are of the $n \rightarrow \pi$ type. This interaction type is also supported by the behaviour of pyridine derivatives with —E type substituents, unable to form complexes, and by the correlation between the donor pK_a's and the stability constants of the complexes. A steric effect on complex formation and stability was made evident for the 2-substituted pyridines.

Pyromellitic dianhydride (PMDA) is an important raw material for the synthesis of polyamide and/or polyimide polymers. Such polymers show a remarkable thermal stability and chemical resistance at various chemicals and are therefore intended for special uses.

The synthesis of such polymers is a very interesting and important matter; hence, the cyclopolycondensation reaction of PMDA with various amines was thoroughly studied in order to extend the range of such polymers.

The ability of PMDA to behave as an electron acceptor and to form charge transfer complexes was discovered in 1926.[1] The latest studies performed on the subject emphasize the importance of the PMDA complexes both from a theoretical and practical point of view. It has been shown that PMDA-donor molecular complexes play an important role in the course of certain chemical reactions. They also enable the isolation of compounds from complex mixtures. Finally, such complexes were taken as "models" giving useful information on the study of certain biochemical systems.[2]

Thus, in the polycondensation reaction of PMDA with primary amines, Koton et al.[3,4] have made evident the initial formation of a charge transfer complex stable only at very low temperatures (about —90°C) followed by the amidation reaction. Pravednikov et al.[5,6] have obtained similar results on other PMDA-aromatic amine systems.

The processing of certain subproducts — for instance the anthracene cake resulted in coke formation — is also based on the formation of a PMDA-anthracene complex; in this way, about 80 per cent of the anthracene is recovered.[7] The isolation of pure PMDA from the complex reaction mixture produced in the oxidation of tetraalkylbenzene is also performed via complex formation, PMDA-*ortho*-xylene.[8,9]

The important role played by PMDA-donor molecular complexes in the synthesis of polyamide and polyimide polymers led to extended research in this field, by using aliphatic, aromatic and heterocycli camines as donors.[10-13]

The literature data on the formation of PMDA-pyridine complexes are highly controversial. Thus, Heaton et al.[14] did not observe a shift to visible of the λ_{max} in the UV spectra of PMDA and pyridine mixtures. They concluded that a charge transfer interaction between PMDA and pyridine did not occur and that pyridine and similar heterocyclic bases are not able to provide complex formation. However, ten years later, Zelman et al.[10] reported the isolation of a crystalline complex of PMDA with pyridine.

Taking into account the importance, from a preparative point of view, of the reaction of PMDA with heterocyclic amines and implicitly the role of the charge transfer complex within the reaction course, as well as the theoretical aspects of such complexes and finally the controversial literature data, this paper reports the results obtained in the study of the donor ability of certain heterocyclic amines from the pyridine series in the reaction with PMDA and the preparation of new molecular complexes.

RESULTS AND DISCUSSION

Pyridine and some of its derivatives may act as n- or π-type electron donors. Molecular complexes of pyridine and its derivatives with halogens (n-σ complexes),[15] as well as complexes where the given azines act as π-donors have been reported.[16] The type of the substituents and their position on the nucleus may enhance or reduce the donor ability through electronic and/or steric effects, affecting in this way the donor-acceptor interaction.

PMDA may act both as π- and n-electron acceptor. It can form $\pi - \pi^*$-type complexes with a series of donors such as mono- or polynuclear aromatics [2] or n-π^*-type complexes with certain donors such as pyridine, methylpyridines and quinolines.[11] In the latter case Chowdhury[16] has however suggested a $\pi - \pi^*$-type interaction.

We have studied the ability of complex formation by using pyridine and its mono- or polysubstituted derivatives containing either $+$E substituents: $-CH_3$, $-CH_2OH$, $-CH_2OAc$, $-X$, $-OH$, $-NH_2$, or $-$E substituents: $-CHO$, $-COOH$, $-COOR$, $-CONH_2$. The isolated complexes were investigated by chemical and spectral methods and their stability constants have been determined.

Some of the above mentioned donors form crystalline complexes which precipitate from concentrated solutions in anhydrous tetrahydrofuran (THF), dioxan or acetone. The acceptor-donor (A :D) molar ratio was determined from nitrogen elemental analysis. The results are listed in table 1, together with the corresponding melting points of the crystalline complexes, the calculated percentages of nitrogen for both A :D molar ratios = 1 :1 and 1 :2, the donor pK_a values and the stability constants of the complexes.

TABLE 1

Properties of PMDA-pyridine derivative complexes

No.	Donor	m.p.[a] °C	% N Calculated 1 : 1	% N Calculated 1 : 2	% N Found	pK_a	$K_{AD} \cdot 10^2$ (l/mole)
1	pyridine	206–212	4.70	7.43	4.76	5.17	11.90
2	2-picoline	204–208	4.50	6.91	4.74	6.02	0.42
3	3-picoline	202–206	4.50	6.91	4.30	5.68	16.46
4	4-picoline	208–210	4.50	6.91	4.47	6.04	19.64
5	2,4-lutidine	184–185	4.30	6.48	4.07	6.72	0.56
6	2-methyl-5-ethylpyridine	166–170	4.13	6.09	4.18	6.21	0.52
7	2,4,6-collidine	178–180	4.13	6.09	4.12	7.48	0.71
8	2-hydroxymethylpyridine	188–190	4.28	6.42	6.18	4.86	0.19
9	3-hydroxymethylpyridine	170–175	4.28	6.42	6.35	4.90	9.55
10	4-hydroxymethylpyridine	194–197	4.28	6.42	6.85	5.33	13.80
11	2-acetoxymethylpyridine	197–204	3.79	5.38	5.41	4.385	0.09
12	4-acetoxymethylpyridine	169–171	3.79	5.38	5.89	—	—

[a] Melting points are uncorrected. Melting occurs with decomposition.

[b] Lit.[10] 210–212°C.

We have established that the formation of crystalline complexes and their A :D molar ratio are not dependent on temperature, at least in the −15°C to +65°C temperature range. The results were the same, regardless of the solution initial concentration within the 10^{-1}M to 10 M range, or the initial ratio of the two compounds, varying from 1 :0.5 to 1 :5.

In polar solvents with higher dielectric constants, such as formamide (ε, 109.5), dimethylsulfoxide (ε, 48.9) or dimethylformamide (DMF) (ε, 36.1), the complexes were soluble. The existence of the complexes in the solution was confirmed by the similar shape of their UV spectra recorded comparatively with crystalline complexes dissolved in DMF and THF and complexes formed directly in the DMF solution.

As table 1 shows, crystalline complexes have been obtained only when pyridine, alkylpyridines, hydroxymethylpyridines and acetoxymethylpyridines were used as donors. Pyridine and alkylpyridines form complexes in 1 :1 molar ratio, whereas hydroxymethylpyridines and acetoxymethylpyridines give complexes with an A :D = 1 :2 molar ratio, whose formulae are suggested below :

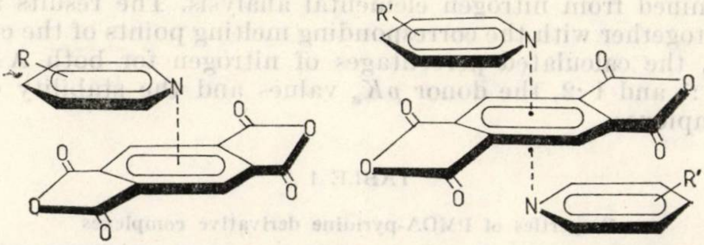

Among the other studied donors, 3-hydroxypyridine forms minute amounts of complex in a 1 :1 molar ratio. Owing to the amide structure of their predominant pyridone tautomeric forms, the 2- and 4-hydroxypyridines yield no complexes.

Neither do the halopyridines any complexes in the given reaction conditions. This is not surprising if one takes into account both the +E and —I electronic effects of the halogen substituent producing a lowering of the pyridine nitrogen atom basicity ; moreover, steric effects have to be considered in the case of the halogen atom substituted in position 2.

The 2-, 3- and 4-aminopyridines behave in a particular way. They react quickly with PMDA in solution, with heat evolution affording crystalline products with very high melting points. In the first stage, a complex is likely to be formed, not detectable in our working conditions, which is followed by an exothermal amidation reaction. Similar observations have also been reported in literature on the reaction of PMDA with aromatic primary mono- and polyamines.[3-6] The nitrogen analyses of the products from the reaction of PMDA with the three isomeric aminopyridines indicate a 1 :2 molar ratio PMDA/aminopyridine. (Calculated for $C_{10}H_2O_6 + 2\,C_5H_6N_2$, N %, 13.79 ; Found : 2-aminopyridine, 14.08, 3-aminopyridine, 13.74, 4-aminopyridine, 13.86).

Pyridine derivatives substituted with —E groups formed no complexes with PMDA, in the studied conditions.

From the above results concerning the ability of complex formation one can conclude that the type of substituents, namely their —E or +E effect, is determining for the donor ability. This conclusion is thought to prove an *n*-type donor. Therefore, pyridinecarboxaldehyde, pyridinecarboxylic acids and esters, as well as the corresponding amides are weak donors and donor-acceptor interactions with PMDA could not be made evident.

UV spectra were recorded in dioxan or THF solution for the isolated complexes listed in table 1. All compounds display similar patterns and a strong shift toward the visible region is not observed. Pure, uncomplexed PMDA shows two close $\pi_k \rightarrow \pi_k^*$ transitions at 316 and 300 nm ($\varepsilon = 2300$ and 2400, respectively). Pyridine and its derivatives show $\pi \rightarrow \pi^*$ transitions within the 255—265 nm range. However, the UV spectra of the complexes indicated a single absorption band in the $\pi \rightarrow \pi^*$ transition range, whereas the 255—265 nm bands are slightly shifted.

From the UV absorption spectra, the corresponding stability constants have been calculated, using the Benessi-Hildebrand equation[17]:

$$[A]l/\log(I_0/I) = (1/K\varepsilon_c)(1/[D]) + 1/\varepsilon_c$$

where [A] and [D] are the acceptor and donor molar concentrations, respectively, K, the stability constant, ε_c, the complex molar extinction coefficient and l, the cell width. The intercept of the curve $[A]l/\log(I_0/I)$ vs $1/[D]$ gives $1/\varepsilon_c$ and K is calculated from the slope. From the calculated values of K one concludes that the 2-substituted pyridines form less stable complexes as compared to the other derivatives.

The IR spectra have been recorded for all complexes. The changes produced in the spectra (compared to spectra of the acceptor and the corresponding donors) have been observed especially within the carbonyl frequency range of the acceptor, i.e. 1870–1735 cm^{-1}. Two strong bands at 1870 cm^{-1} ($\nu_{CO\ sym}$) and 1790 cm^{-1} ($\nu_{CO\ sym}$) are present in the uncomplexed PMDA spectrum.[18] These two bands appear much lowered in the complex spectra. Other two unsolved weak bands at 1815 cm^{-1} and 1735 cm^{-1} appear within the uncomplexed PMDA spectrum. In the complexes, the 1815 cm^{-1} band is again diminished, while the 1735 cm^{-1} one becomes strong and is shifted towards lower frequencies. Similar results for PMDA complexes with tertiary amines, i.e. shifting of the carbonyl band towards lower frequency are also reported in literature.[11]

TABLE 2

Spectral data of PMDA-pyridine derivative complexes

Donor	$\nu_{C=0}$ [cm^{-1}]	ε_c[l·cm^{-1}·mole^{-1}][a]
pyridine	1724	18900
2-picoline	1719	21400
3-picoline	1731	13600
4-picoline	1735	11500
2,4-lutidine	1727	16000
2-methyl-5-ethylpyridine	1724	17300
2,4,6-collidine	1735	12300
2-hydroxymethylpyridine	1706	27300
3-hydroxymethylpyridine	1720	23700
4-hydroxymethylpyridine	1726	16300
2-acetoxymethylpyridine	1701	29900
uncomplexed PMDA	1735	

---

[a] Calculated at $\lambda = 278$ nm

In the IR spectroscopic studies on $\pi-\sigma$ type complexes of pyridine and its derivatives with boron halides or boron hydride, changes of the absorption bands in the 1400–1600 cm^{-1} region, assigned to υ_{CC} and υ_{CN}

stretching of the pyridine nucleus are reported.[19] Since the ν_{CC} bands of the acceptor benzene ring are also found in this region, the detection of the changes produced in the donor spectrum could not be made.

Since the interaction type, namely π—π^* and n-π^* respectively, is highly important and as shown above, both types have been suggested,[16,20] we attempted to clear up this controversy.

Assuming that the ability of pyridine derivatives to behave as n-type donors may be expressed in terms of the corresponding pK_a values, a correlation between the basicity constants of the studied donors and the stability constants of the resulted complexes has been tested. We found a good agreement since the stability constants, K_{AD}, are increasing with the donor basicity (Figure 1). By plotting K_{AD} vs pK_a, two straight lines with different slopes result. One line includes pyridine and its 3- and 4-substituted derivatives and on the other line the 2-substituted pyridines are placed. The latter complexes have lower stability constants. This difference may be assigned to a steric effect, probably acting on the complex geometry and reducing the donor-acceptor interaction. This conclusion is supported by the marked difference in the behaviour of 2-substituted pyridines towards proton acids and Lewis acids,[21] also determined by the reagent bulkiness. It has been reported [22] that while 2-methylpyridine is easily protonated, its reaction with BF_3 is unfavoured by both the steric effect of the α-substituent and the electrophilic reagent bulkiness.

From figure 1 one may deduce a limiting pK_a value of the donor of about 3.9—4.0 units allowing PMDA-donor complex formation. One also notices that all those pyridine derivatives unable to be donors to PMDA in our given conditions have their pK_a's lower than the limiting experimental value.

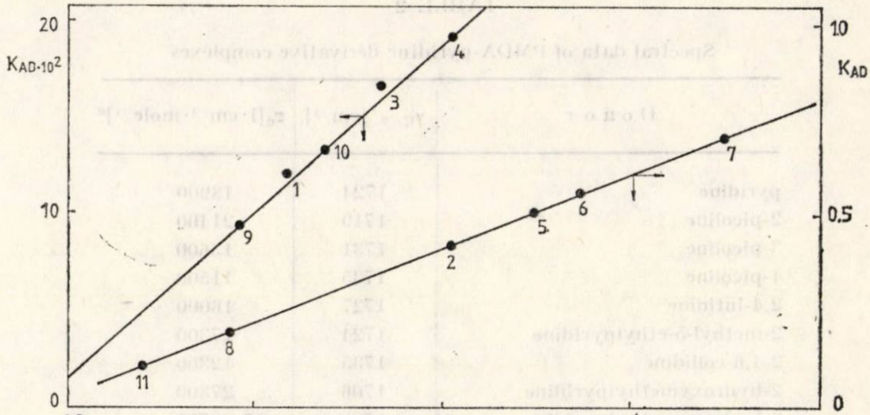

Fig. 1. — The dependence of the stability constants, K_{AD}, of the PMDA-pyridine derivative complexes on the donor pK_a's (The numbers correspond to table 1).

The above mentioned observations on the complex formation ability of pyridine and its derivatives with PMDA and the correlation with the corresponding basicity constant make us conclude that the donor-acceptor interaction is of n-π^* type in this particular case.

EXPERIMENTAL

PMDA was several times recrystallized from acetic anhydride, m. 294°C.[23]

The commercial pyridine derivatives were purified by distillation. The used solvents (THF, acetone, dioxan) have been dried by usual procedures.

The IR spectra have been recorded as KBr pellets on a UR-20 (C. Zeiss-Jena) spectrophotometer. The UV spectra have been recorded in dioxan or THF solution on a Pye-Unicam SP 1800 spectrophotometer.

REFERENCES

[1] R. Seka and H. Sedlatschek, *Monats.*, **47,** 516 (1926).

[2] R. Foster, "Organic Charge-Transfer Complexes", Academic Press, New York, 1969.

[3] K. K. Kalninsk, B. G. Belenskii, I. V. Novozhilova, V. V. Kudriavtsev and M. M. Koton, *Doklady Akad. Nauk S.S.S.R.*, **200,** 850 (1971).

[4] K. K. Kalninsk, G. I. Solovieva, B. G. Belenskii, V. V. Kudriavtsev and M. M. Koton, *Doklady Akad. Nauk S.S.S.R.*, **204,** 876 (1972).

[5] A. N. Pravednikov, I. E. Kardash, E. N. Telesov and B. V. Kotov, *Vysokomol. Soedineniya* **A, 13,** 425 (1971).

[6] A. N. Pravednikov, I. E. Kardash, N. P. Gluhaedov and A. I. Ardashnikov, *Vysokomol. Soedineniya* **A, 15,** 349 (1973).

[7] F. Casolini and A. Girelli, *Chimica e Industria*, **53,** 449 (1971).

[8] F. Caselatto and A. Girelli, *Chimica e Industria*, **55,** 779 (1973).

[9] M. Tolan, M. Corciovei, G. Barbu and G. Pop, *Rom. Pat.* 58310 (1976); *Chem. Abstr.*, **89,** 42825 (1978).

[10] M. G. Voronkov and Z. I. Zelmen, *Zhur. obshchei Khim.*, **41,** 236 (1971).

[11] A. E. Lutskii, V. V. Prezhdov and M. G. Voronkov, *Zhur. obshchei Khim.*, **41,** 292 (1971).

[12] D. F. Varfolomeev, *Doklady Neft. Khim.*, **7,** 102 (1971); *Chem. Abstr.*, **83,** 8917 (1975).

[13] M. R. Gasco, *Il Farmaco, Ed. Sci.*, **30,** 512 (1975).

[14] L. L. Ferstandig, W. G. Toland and C. D. Heaton, *J. Amer. Chem. Soc.*, **83,** 1151 (1961).

[15] S. Sorriso, G. Aloisi and S. Santini, *Z. phys. Chem. (Frankfurt)*, **94,** 117 (1975).

[16] M. Chowdhury and S. Basu, *Trans. Faraday Soc.*, **56,** 335 (1959).

[17] H. A. Benessi and J. H. Hildebrand, *J. Amer. Chem. Soc.*, **71,** 2703 (1949).

[18] F. H. Marquardt, *J. Chem. Soc. B*, **1966,** 1242.

[19] A. R. Katritzky, *J. Chem. Soc.*, **1959,** 2049.

[20] R. E. Miller and W. F. K. Wynne-Jones, *J. Chem. Soc.*, **1959,** 2375.

[21] H. C. Brown and R. H. Horowitz, *J. Amer. Chem. Soc.*, **77,** 1733 (1955).

[22] H. C. Brown and X. R. Mihm, *J. Amer. Chem. Soc.*, **77,** 1723 (1955).

[23] E. Philippi and R. Thelen, *Org. Synth., coll. vol.* **2,** 551 (1943).

Revue Roumaine de Chimie, 25, 7, 969–973(1980)

Dedicated to Professor CRISTOFOR I. SIMIONESCU
on his 60th anniversary

NEW SYNTHESIS OF DIBENZO $(CH)_{10}$ AND TETRABENZO $(CH)_{16}$ HYDROCARBONS. DIELS — ALDER REACTIONS OF TRICYCLO$[4.2.2.0^{2,5}]$ DECA-3.7.9-TRIENE DERIVATIVES WITH 9.10-DIBROMOANTHRACENE [1]

I. G. DINULESCU, I. I. POGANY, ANGELA DUMITRIU, E. G. GEORGESCU
and MARGARET AVRAM
Center of Organic Chemistry, Spl. Independenţei 202 B, 76300 Bucharest 15, Romania

Received December 13, 1979

The reaction of tricyclo$[4.2.2.0^{2,5}]$decatriene derivatives 1, 3 and 7 with dibromoanthracene (4) and some reactions of the corresponding adducts, affording to the $(CH)_{10}$ and $(CH)_{16}$ hydrocarbons 1 and 2, respectively, are described.

As part of our research aiming at the synthesis and study of the behaviour of $(CH)_n$ hydrocarbons,[2-6] we have earlier reported the synthesis of dibenzo[*g*, *i*]tricyclo$[4.2.2.0^{2,5}]$deca-3.7.9-triene (**1**),[2] the symmetrical dibenzo isomer of $(CH)_{10}$ Nenitzescu's hydrocarbon.

As a continuation of the research in this field, in this paper we present a new route for the synthesis of dibenzo $(CH)_{10}$ hydrocarbon **1**,[2,7] as well as for the synthesis of the parent compound of tetrabenzo $(CH)_{16}$ system **2**.

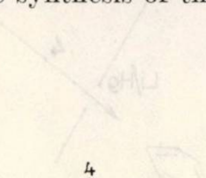

1

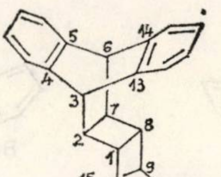

2

The strategy for the new synthesis has as background the dienophile ability of the cyclobutene ring in tricyclo$[4.2.2.0^{2,5}]$deca-3.7.9-triene (**3**) for 4 + 2 cycloaddition with reactive dienes.[8-11]

The thermal cleavages of the Alder-Rickert type of the adducts of **3** with diphenylisobenzofurane,[8] dimethyldiphenylcyclopentadienone[9,10] and dimethoxytetrachlorocyclopentadiene,[9-11] leading to polycyclic systems with cyclobutadiene[8] or cyclobutene [9-11] rings, realize in fact the transfer of the four membered ring from **3** to the diene moiety.

In the syntheses presented in chart 1, the dienic partner is 9.10-dibromoanthracene (**4**).

The heating of equimolar amounts of 7.8-dicarbomethoxy-tricyclo[4.2.2.0^{2,5}]deca-3.7.9-triene (**3**) with 9.10-dibromoanthracene (**4**)

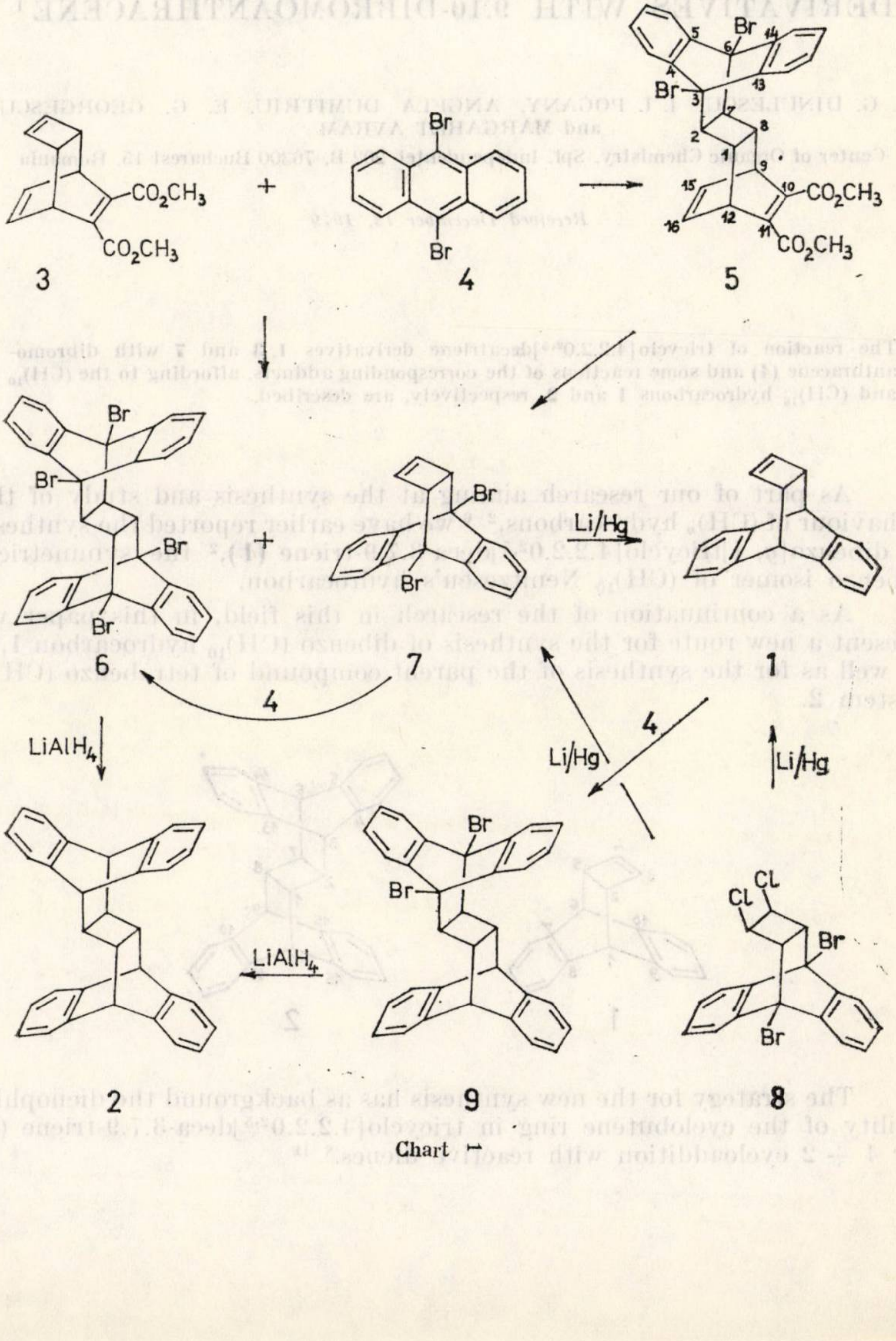

CO_2CH_3
CO_2CH_3
3
+
Br
Br
4
Br
Br
5
6
14
4
13
3
7
2
8
9
15
10
CO_2CH_3
12
16
11
CO_2CH_3
5
Br
Br
Br
Br
6
+
Br
Br
7
Li/Hg
1
4
4
LiAlH$_4$
Li/Hg
Li/Hg
Br
Br
LiAlH$_4$
Cl
Cl
Br
Br
2
9
8

Chart 1

at 120°C for 8 hours, afforded the 1 :1 Diels-Alder adduct **5**, colourless crystals, m.p. 188°C. By heating of **5** at 160°C, cleavage occurs and the dibromo-derivative **7** (m.p. 122°) together with dimethyl phthalate was obtained. Removal of the bromine atoms from **7** yielded the dibenzo $(CH)_{10}$ Nenitzescu's hydrocarbon **1**. The earlier reported [2] synthesis of **1** involves the Diels-Alder reaction of *cis*-3.4-dichlorocyclobutene with 9.10-dibromoanthracene **(4)**, followed by treatment of thus formed adduct **(8)** with lithium amalgam. It was assumed **7** as intermediate. In fact, by dehalogenation of **8** using stoechiometrical amounts of lithium amalgam, we have now isolated **7**.

It was observed that the reaction of **3** with **4**, carried out at 160°C, afforded a mixture of **7** with an insoluble compound **(6)**, m.p. $>$360°C. The analytical data of this compound correspond to the empirical formula $C_{32}H_{20}Br_4$, and subsequently supported the structure **6** of Diels-Alder adduct between **4** and **7**, the latter resulting by thermal cleavage of **5** during the heating at higher temperatures. In fact, by heating of **7** with **4** at 160°C, in *ortho*-dichlorobenzene, **6** was obtained in almost quantitative yield.

The reduction of the bromine atoms from **6** by 48 hours heating in THF, with lithium aluminium hydride, gave the tetrabenzo$(CH)_{16}$ hydrocarbon **2**, m.p. 364°C, with pentacyclo$[6 .4 .0 .2^{3\cdot 6} .2^{9\cdot 12} .0^{2\cdot 7}]$hexadeca-4 .10 .13 .15-tetraene structure.

The same tetrabenzo $(CH)_{16}$ hydrocarbon **2** was also available starting from the dibenzo $(CH)_{10}$ hydrocarbon **1**. Cycloaddition 2 + 4 between **1** and **4** occurs at 150°C, affording the dibromo-derivative **9**, which by reduction with lithium aluminium hydride yielded **2**.

Analytical data and ^{1}H-NMR spectra were in accordance with all ascribed structures.

Some characteristic features of the spectra should be evidenced.

In the spectrum of hydrocarbon **1**, the olefinic protons from cyclobutene ring (H-3 and H-4) gave a singlet at δ 5.50 ppm ; in the bromoderivative **7**, the corresponding signal is shifted down field to δ 6.01 ppm. The signal of the symmetrical benzene ring protons from **1** appears at δ 6.80 – 7.40 ppm ; in the dibromide **7**, the bridge head bromine (Br-1, Br-6) influences the chemical shift of the vicinally aromatic protons, and two A_2B_2 systems appear in the range δ 7.10 – 8.00 ppm.

Concerning the cyclobutane ring protons from the adducts **5**, **9** and hydrocarbon **2**, the spectrum evidences the great shielding of the benzene ring on the four membered ring. Thus in the spectrum of the adduct **5** two inequal shielded pairs of protons can be differentiated. The signal of H-2 and H-7 appeared at the normal value, as in other [9] adducts of **4**, at δ 2.30 ppm, while the signal of the other two protons, H-1 and H-8, strongly shielded by the benzene ring, is shifted up field, to δ 1.56 ppm ($\Delta = 0.8$ ppm).

In the compounds **9** and **2** all four cyclobutane ring protons are equally shielded, and their signals appear at δ 1.55 (in **2**) and 1.51 ppm (in **9**).

EXPERIMENTAL

IR spectra were recorded with a double beam UR 20 spectrophotometer. NMR spectra were determined with a Varian A-60A spectrometer.

Reaction of 7.8-dicarbomethoxy-tricyclo [4.2.2.0$^{2.5}$] deca-3.7.9-triene (3) with 9.10-dibromoanthracene (4)

a. A mixture of 0.70 g (2 mmoles) **4**, 0.50 g (2 mmoles) **3** and 1 ml *ortho*-dichlorobenzene was heated at 120°C for 10 hours. The reaction product was treated with 10 ml ether, filtered from any insoluble material and the solvents were removed in vacuo (60°/1 mm). The oily residue was chromatographied on alumina. Using as eluent petroleum ether, small quantities of oily material were obtained. With ether as eluent, 0.60 g (50%) **5**, m.p. 188°C (from methanol) were obtained.

$C_{28}H_{22}Br_2O_4$ Calcd. : C, 57.75 ; H, 3.80 ; Br, 27.44. Found : C, 57.18 ; H, 4.31 ; Br, 26.52.
IR (CCl_4) : ν C=O 1730 cm^{-1}.
NMR (CCl_4, δ, ppm) : 1.56 (m, 2H, H–1, H–8), 2.30 (m, 2H, H–2, H–7), 3.73 (s, 6H, two $COOCH_3$ groups), 4.08 (m, 2H, H–9, H–12), 6.45 (m, 2H, H–15, H–16), 7.25 and 7.73 (an A_2B_2 system, 8 aromatic H).

b. A mixture of 0.70 g (2 mmoles) **4** and 0.50 g (2 mmoles) **3** was heated at 160°C for 8 hours. The cooled reaction mixture was triturated with 20 ml ether and the crystals were filtered and washed with ether and methylene chloride. In this way, 0.25 g (35%) **6**, m.p. $>$ 360°C were obtained.

$C_{32}H_{20}Br_4$ Calcd. : C, 53.08 ; H, 2.78 ; Br, 44.14. Found : C, 52.75 ; H, 3.20 ; Br, 44.85.

The organic solutions were evaporated and the oily residue was chromatographied on alumina with petroleum ether, yielding 0.25 g (33%) **7**, m.p. 122°C (from methanol).

$C_{18}H_{12}Br_2$ Calcd. : C, 55.70 ; H, 3.11 ; Br, 41,18. Found : C, 54.70 ; H, 3.31 ; Br, 40.98.

NMR ($CDCl_3$, δ, ppm) : 3.43 (s, 2H, H–2, H–5), 6.01 (s, 2H, H–3, H–4), 7.16–7.33 (m, 4 aromatic H), 7.58–7.88 (m, 4 aromatic H).

Further elution with ether afforded some dimethyl phthalate, identified by IR and NMR spectra.

Thermal cleavage of the ester 5

A mixture of 0.20 g **5** and 0.3 ml *ortho*-dichlorobenzene was heated at 160°C for 8 hours. The oily reaction product was dissolved in hot methanol, and by cooling 0.11 g (85%) **7**, m.p. 122°C, were obtained. The IR and NMR spectra were identical with those of an authentic sample.

Reaction of dibromo-Nenitzescu's hydrocarbon 7 with dibromoanthracene (4)

A mixture of 38.8 mg (0.1 mmoles) **7**, 33.6 mg (0.1 mmoles) **4** and 0.3 ml *ortho*-dichlorobenzene was heated at 160°C for 3 hours. The reaction mixture was triturated with methylene chloride and the crystals were filtered, yielding 70 mg (96%) **6**, m.p. $>$ 360°.

Debromination of the dibromide 7

A mixture of 200 mg (0.5 mmoles) **7**, 10 g lithium amalgam 5% and 20 ml anhydrous ether was stirred into a stoppered flask for 24 hours. Ether was added, the mercury was filtered and washed with ether, and the ethereal solution was washed with water and dried. Evaporation of the solvent afforded 80 mg (70%) **1**, m.p. 132°C. The IR and NMR spectra were identical with those of an authentic sample ; mixed m.p. without depression.

Dechlorination of the adduct 8

A mixture of 0.45 g (1 mmole) **8**, 3.0 g lithium amalgam 5% (2 mmoles lithium) and 25 ml anhydrous ether was stirred into a stoppered flask for 24 hours. After working up as above, an oily product was obtained, from which by chromatography (petroleum ether/Al_2O_3), 70 mg (30%) **7** were isolated. The compound **7** was identified by IR and NMR spectra, identical with those of the above described product.

Reaction of dibenzo-tricyclodecatriene 1 with dibromoanthracene (4)

A mixture of 0.46 g (2 mmoles) **1**, 0.67 g (2 mmoles) **4** and 0.5 ml *ortho*-dichlorobenzene was heated at 150°C for 8 hours. The reaction product was triturated with methanol and the separated crystals filtered and purified by chromotography (petroleum ether/Al_2O_3); 0.75 g (66%) **9**, m.p. 334°C, were obtained.

$C_{32}H_{22}Br_2$ Calcd.: C, 67.87; H, 3.91; Br, 28.21. Found: C, 67.54; H, 3.65; Br, 28.05.

NMR ($CDCl_3$, δ, ppm): 1.69 (m, 2H, H−1, H−8), 2.08 (m, 2H, H−2, H−7), 4.26 (m, 2H, H−9, H−12), 6.85−7.40 (m, 12, aromatic H), 7.45−7.80 (m, 4 aromatic H).

Thermolysis of the dibromide 9

Heated over m.p., in inert atmosphere, the dibromo-derivative **9** undergoes decomposition yielding a tarry product, in which neither **4** and **1** nor **7** and anthracene, respectively, could be identified.

Tetrabenzo[d, j, m, o]pentacyclo [6.4.0.2$^{3.6}$.2$^{9.12}$.0$^{2.7}$]hexadeca-4.10.13.15-tetraene (2)

a. By dehalogenation of the dibromide **9**. A mixture of 0.25 g (0.5 mmoles) **9**, 0.25g lithium aluminium hydride and 20 ml anhydrous THF was boiled for 48 hours. After working up, 0.13 g (65%) **2**, m.p. 346°C, were obtained.

$C_{32}H_{24}$ Calcd.: C, 94.08; H, 5.92. Found: C, 94.22; H, 6.40.

NMR (CD_2Cl_2, δ, ppm): 1.55 (m, 4H, H−1, H−2, H−7, H−8), 4.21 (m, 4H, H−3, H−6, H−9, H−12), 6.80−7.40 (m, 16 aromatic H).

b. By dehalogenation of the tetrabromide **6**. In the same conditions as above, the tetrabromide **6** afforded the hydrocarbon **2** in 50% yield.

REFERENCES

[1] Part LII of "Investigations in the Cyclobutane Series". For Part LI see: O. Constantinescu-Simon, I. G. Dinulescu, F. Chiraleu and M. Avram, *Chem. Ber.*, **113**, 623 (1980).

[2] M. Avram, I. G. Dinulescu and C. D. Nenitzescu, *Liebigs Ann. Chem.*, **691**, 9 (1966).

[3] I. G. Dinulescu, M. S. Pop, F. Chiraleu, M. Avram and C. D. Nenitzescu, *Rev. Roumaine Chim.*, **19**, 1197 (1974).

[4] I. G. Dinulescu, M. S. Pop, F. Chiraleu and M. Avram, *Chem. Ber.*, **108**, 283 (1975); I. G. Dinulescu, M. S. Pop and M. Avram, *Rev. Roumaine Chim.*, **22**, 1037 (1977).

[5] L. Enescu and M. Avram, *Rev. Roumaine Chim.*, **22**, 1061 (1977).

[6] M. Elian, M. Banciu, L. Stănescu and E. Ciorănescu, *Rev. Roumanie Chim.*, **21**, 89 (1976).

[7] I. Murata, Y. Sugihara and N. Ueda, *Tetrahedron Letters*, **1973**, 1183.

[8] C. D. Nenitzescu, M. Avram, I. G. Dinulescu and G. Mateescu, *Liebigs Ann. Chem.*, **653**, 79 (1962).

[9] C. M. Anderson and J. W. McCay, *Tetrahedron Letters*, **1970**, 2735; R. N. Warrener, C. M. Anderson, J. W. McCay and N. N. Paddon-Row, *Austral. J. Chem.*, **30**, 1481 (1977).

[10] W. G. Dauben and N. L. Reitman, *J. Org. Chem.*, **40**, 835 (1975).

[11] W. G. Dauben, G. T. Rives and W. T. Zimmermann, *J. Org. Chem.*, **41**, 887 (1976).

Revue Roumaine de Chimie, 25, 7, 975–980(1980)

Dedicated to Professor CRISTOFOR I. SIMIONESCU
on his 60th anniversary

KINETICS OF EMULSION POLYMERIZATION OF VINYL ACETATE IN THE PRESENCE OF HYDROXYETHYLCELLULOSE

D. DONESCU, I. DEACONESCU, KRISTIANA GOŞA, MAGDALENA MAZĂRE and I. GAVĂT

ICECHIM — Research Center for Plastic Materials, Splaiul Independenţei no. 202, sector 6,
Bucharest — 77208, Romania

Received January 5, 1980

The influence of vinyl acetate (VAc) ,potassium persulphate (KPS) and hydroxyethylcellulose (HEC) concentrations on maximum polymerization rate ($R_{\max}$) was studied. Thus it was shown that $R_{\max} \sim |VAc|_0$ and $R_{\max} \sim |KPS|_0^{0.2} \cdot R_{\max}$ either increases or decreases with $|HEC|_0$ depending on the ratio of concentrations of protective colloid and initiator. During polymerization, grafting of VAc onto HEC occurs and graft copolymers are obtained.

I. INTRODUCTION

In previous papers [1-3] we have studied the polymerization of vinyl acetate (VAc) in the presence of poly(vinyl alcohol) and ethylene oxide—propylene oxide block copolymers. The results pointed out that in the presence of both protective colloids the polymerization rate increases with the increasing of monomer and initiator concentration. Due to the transfer reactions with protective colloid, less active centers are formed during polymerization. Therefore the maximum rate may increase or decrease with increasing concentration of protective colloid, depending on reaction conditions.

This present study investigates the kinetics of VAc polymerization in the presence of hydroxyethylcellulose (HEC) with potassium persulfate (KPS) as initiator. An important feature of this system is the fact that in the presence of KPS, HEC undergoes oxidative degradation. This reaction has previously been studied.[4]

2. EXPERIMENTAL

Polymerization and analyses were performed as shown before.[1-3] HEC employed was Hercules-Natrosol 250LR without additional purification.

3. RESULTS AND DISCUSSION

3.1. Kinetics

3.1.1. *Influence of monomer concentration*

The dependence of maximum polymerization rate (R_{max}) on initial monomer concentration is plotted in figure 1. There is a proportional increase of R_{max} with $|VAc|_0$. As in the case of poly(vinyl alcohol) or ethylene oxide-propylene oxide block copolymers, the plot is not a straight line passing through the origin.

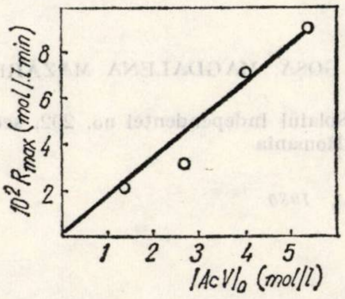

Fig. 1. — Maximum polymerization rate versus initial monomer concentration ($|HEC|_0 = 4.37 \times 10^{-2}$ mol/l ; $|K_2S_2O_8|_0 = 1.15 \times 10^{-2}$ mol/l).

The sudden increase of polymerization rate above solubility limit of VAc where emulsified monomer particles are present may have two main causes : the increase of KPS descomposition rate in the presence of existing monomer at saturation concentration in aqueous phase or the macroradicales initially formed in aqueous phase have a rich reservoir of monomer particles. The first alternative is ruled out since the decomposition rate of KPS in the presence of HEC is not affected by initial monomer concentration.

3.1.2. *Influence of initiator concentration*

The study of HEC-KPS interaction has allowed us to state that the initial decomposition rate of the initiator increases proportionally to its initial concentration. The maximum polymerization rate of VAc also increases with KPS concentration (Figure 2).

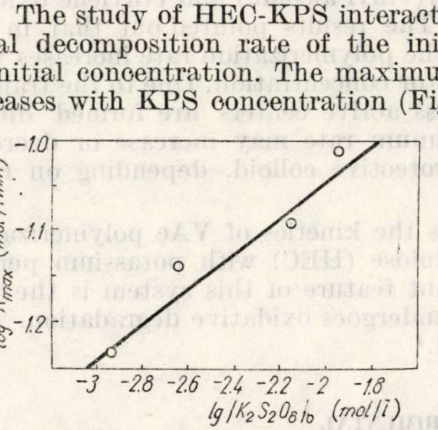

Fig. 2. — The initial initiator concentration — maximum polymerization rate correlation ($|VAc|_0 = 4.07$ mol/l ; $|HEC|_0 = 4.37 \times 10^{-2}$ mol/l).

The reaction order with respect to KPS is therefore 0.2. This is the lowest order we have found for emulsion polymerization of VAc,[1-3] lower than that for other emulsifiers.[5,6]

The results in figure 2 may be accounted for as follows : KPS forms a redox system with HEC which supplies a large number of radicals from the very first moments of polymerization. Since the initiation rate is limited by reaction conditions, the additional increase of the number of radicals formed does not affect sensitively the polymerization rate.

3.1.3. *The influence of protective colloid concentration*

The dependence of polymerization rate on colloid initial concentration is shown in figure 3.

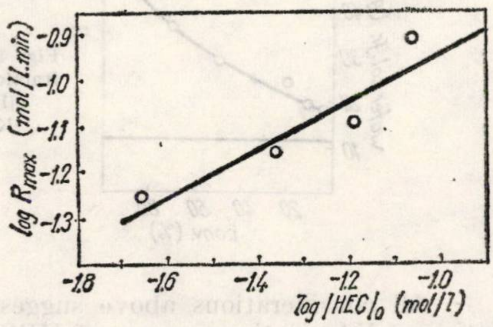

Fig. 3. — The influence of maximum HEC concentration upon maximum polymerization rate ($|VAc|_0 = 4.07$ mol/l; $|K_2S_2O_8|_0 = 1.15 \times 10^{-2}$ mol/l).

Examination of figure 3 shows that the reaction rate increases with initial HEC concentration. This increase may have the following causes : the increase of initiator decomposition rate and number of particles with the increase of $|HEC|_0$. In polymerization conditions of figure 3 the KPS decomposition rate rises as $|HEC|_0$ increases. At a $|HEC|_0/|KPS|_0$ ratio chosen the efficiency of KPS in oxidative degradation of HEC is smaller. A tenfold decrease of KPS concentration utilized in experiments whose results are given in figure 3 induces a decrease of polymerization rate with the increase of HEC concentration. In these conditions the efficiency of HEC-KPS interaction rises, which makes the percentage of the carbonyl groups formed increase. Carbonyl groups are known as strong transfer agents ; therefore they increase the transfer probability of growing macroradical.[7] On transfer to surfactant either to carbonyl group or to unaltered molecule much less reactive centers are formed. On the other hand, carbonyl groups found play the role of inhibitors for KPS decomposition reaction.[8] Therefore it turns out that similar to polymerization, in the presence of poly(vinyl alcohol) and ethylene oxide-propylene oxide block copolymers, the reaction order with respect to surfactant depends on reaction conditions.

3.2. The structure of obtained polymers

In a previous article we have shown that KPS forms with HEC a redox system which entails the increase of decomposition rate of initiator and the decrease of activation energy of this reaction.[4] The same was shown to be true in polyol-initiator systems.[9-11] The existence of a redox system proves that formation of free radicals right on HEC chain is possible.

These free radicals may act as growth centres which on VAc addition yield graft copolymers. As oxidative degradation is accompanied by the scission of the chain, free radicals are formed at the ends of HEC fragments as well. VAc addition to these radicals may cause formation of block copolymers. There are in the literature numerous works which mention the possibility that vinyl monomers are grafted on cellulose macromolecules, cellulose derivatives and starch.[12]

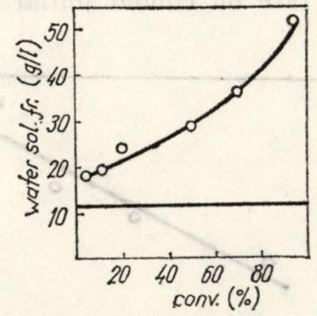

Fig. 4 — The variation of water soluble fraction concentration versus conversion ($|HEC|_0 = 4.37 \times 10^{-2}$ mol/l, $|K_2S_2O_8|_0 = 1.15 \times 10^{-2}$ mol/l).

All considerations above suggest that during emulsion polymerization of VAc in the presence of HEC, graft copolymers may be formed whose structure may be that of block copolymers.

The variation of water-soluble fraction versus conversion has shown that the fraction increases as polymerization advances (Figure 4).

This phenomenon may be explained only by the onset of VAc grafting on HEC. In water, graft copolymers of low VAc content are extracted. Grafting increases with the increasing amount of polymerized monomer.

Examination of IR spectra of water-soluble fraction shows that the 1740 cm^{-1} band (assigned to $C=O$ group) intensifies while the 1120 cm^{-1} band (assigned to $C-O-C$) fades. This behaviour may naturally point out to an increase in concentration of polyvinyl acetate against emulsifier concentration in water-soluble fraction. Unfortunately this is also the behaviour of IR spectra of HEC degraded in the presence of KPS. However one can notice that while the ratio of absorbances A_{1740} cm^{-1}/A_{1460} cm^{-1} in IR spectra taken during HEC scission rises from 0.14 to 0.42, under identical reaction condition, the same ratio for IR spectra of water-soluble fraction sampled during polymerization rises from 0.65 to 3.7. The ratio of absorbances A_{1120} cm^{-1}/A_{1460} cm^{-1} in HEC spectra decreases from 3.7 to 1.4 while the same ratio for water-soluble fractions from 11.8 to 7.5. The increase of 1740 cm^{-1} band intensity is more pronounced for water-soluble fractions than for degraded HEC samples; the A_{1740} cm^{-1}/A_{1460} cm^{-1} and A_{1120} cm^{-1}/A_{1460} cm^{-1} ratios calculated for IR spectra of the two processes are very different. These two findings have suggested that the curves of A_{1740} cm^{-1}/A_{1460} cm^{-1} and A_{1120} cm^{-1}/A_{1460} cm^{-1} ratios versus conversion (Figure 5) for water-soluble fractions originate in two parallel reactions:

— HEC oxidative degradation in the presence of KPS

— the increase of grafting of VAc onto HEC chain.

The existence of graft copolymers in the system under study is also supported by the rheological behaviour of benzene-soluble polymer fractions. The variation of intrinsic viscosity with temperature is nemonotonous,[13] as was also shown for polymerization of VAc in the presence of poly(vinyl alcohol) and ethylene oxide-propylene oxide block copolymers.

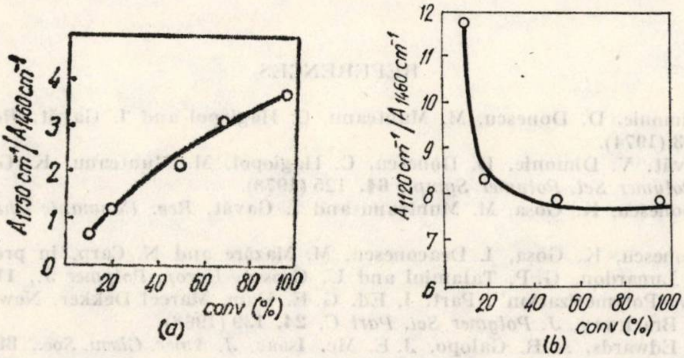

Fig. 5. — The variation of absorbance ratio (*a*, *b*) in IR spectrum of water-soluble fractions versus conversion ($|VAc|_0 = 4.07$ mol/l; $|HEC|_0 = 4.37 \times 10^{-2}$ mol/l, $|K_2S_2O_8|_0 = 1.15 \times 10^{-2}$ mol/l).

This undoubtely argues for the formation of graft copolymers which in this case may have also block copolymers structure (Figure 6).

IR spectra of benzene soluble fractions differ from those of poly(vinyl acetate). The ratio of absorbances at 1010 cm^{-1} and 1120 cm^{-1} is reversed in the former spectra comparatively with the latter. The band at 1010 cm^{-1} in the latter spectra shifts to 1020 cm^{-1} in the former ones. Moreover in the spectra of benzene-soluble fractions there is a new band at 680 cm^{-1} which is assigned to HEC. The band at 1010 cm^{-1} in poly(vinyl acetate)

Fig. 6. — The variation of intrinsic viscosity of benzene-soluble fraction versus temperature (reaction conditions as those for data in Fig. 4 ; conversion is 20 % (1) ; 97 % (2).

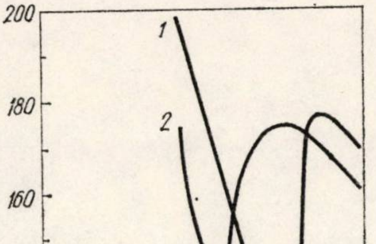

spectra is assigned to skeletal vibrations of the chain. Its shift indicates a change of macromolecular chain structure. The benzene soluble fraction contains VAc copolymers graft onto HEC of high poly(vinyl acetate) content. Enhancement of the intensity of 1020 cm^{-1} band compared to 1120 cm^{-1} is due to HEC scission.

REFERENCES

[1] V. Dimonie, D. Donescu, M. Munteanu, C. Hagiopol and I. Gavăt, *Rev. Roumaine Chim.*, **19**, 903 (1974).

[2] I. Gavăt, V. Dimonie, D. Donescu, C. Hagiopol, M. Munteanu, K. Goşa and Th. Deleanu, *J. Polymer Sci. Polymer Symp.*, **64**, 125 (1978).

[3] D. Donescu, K. Goşa, M. Munteanu and I. Gavăt, *Rev. Roumanie Chim.*, **24**, 1399 (1979).

[4] D. Donescu, K. Goşa, I. Deaconescu, M. Mazăre and N. Carp, in press.

[5] G. F. Lunardon, G. P. Talamini and U. Grosso, *Europ. Polymer J.*, **11**, 437 (1975).

[6] "Vinyl Polymerization", Part. I, Ed. G. E. Ham, Marcel Dekker, New York, 1967.

[7] C. E. Brackway, *J. Polymer Sci. Part C*, **24**, 139 (1968).

[8] J. O. Edwards, A. R. Galopo, J. E. Mc. Isaac, *J. Amer. Chem. Soc.*, **88**, 384 (1966).

[9] Y. Ikado, Y. Nishizaki and I. Sakurada, *J. Polymer Sci. Polymer Ed.*, **12**, 1829 (1974),

[10] I. Sakurada, Y. Ikado, H. Uehara, Y. Nishizaki and F. Horii, *Makromol. Chem.*, **139**, 183 (1970).

[11] J. C. Mileo and L. Nicholas, *J. Appl. Polymer Sci.*, **11**, 425 (1967).

[12] "Block and graft copolymerization" Ed. R. J. Ceresa, Wiley, London, 1976.

[13] K. Goşa and D. Donescu, *Mater. Plast.*, **15**, 88 (1978).

Revue Roumaine de Chimie, 25, 7, 981–988 (1980)

Dedicated to Professor Cristofor I. Simionescu
on his 60th anniversary

ON THE THERMAL STABILITY OF SOME NEW POLYAZINES AND POLYAZOMETHINES

MARIA DUMITRIU, M. DĂRÂNGĂ, MARIANA PĂSTRĂVANU
and TATIANA LIXANDRU
Department of Organic and Macromolecular Chemistry, Polytechnic Institute
Jassy, Calea 23 August 11, Romania

Received January, 23, 1980

The thermal stability of some new polyazines and polyazomethines was studied by thermal differential and thermogravimetric analyses. The polyazomethines were found to show a higher thermal stability than polyazines. The kinetical parameters for the thermodestruction reaction were determined by the Coats-Redfern method.

INTRODUCTION

The thermogravimetric and thermodifferential analyses are largely applied for the physico-chemical characterization of the polymers and elucidation of their structure and properties.

Among the conjugated polymers the heterochain ones show a particular thermal stability.[1–4]

In the present paper the temperature action on the polyacenaphthenequinoneazines and polyacenaphthenequinoneazomethines whose synthesis and electrophysical properties were described in previous papers[5,6] is studied.

EXPERIMENTAL

The polymers obtained by the polycondensation of acenaphtenequinone, 5-chloroacenaphthenequinone, 5-nitroacenaphthenequinone and 5,6-dinitroacenaphthenequinone with hydrazine (I) and *m*- or *p*-phenylenediamine (II) were subjected to the thermogravimetric study

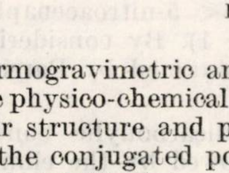

I

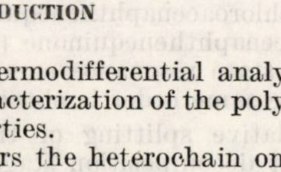

II

where :

$R_1, R_2 = H$

$R_1 = Cl, R_2 = H$

$R_1 = NO_2, R_2 = H$

$R_1, R_2 = NO_2$

$Ar = p-C_6H_4-$

$Ar = m-C_6H_4-$

The thermograms were recorded by means of a Paulik—Paulik—Erdey—MOM-Budapest derivatograph. The runs were carried out with samples of 40 mg, by heating in air, at a rate of 10°/min., within the 20—900°C range.

The energies of activation and the reaction orders for the thermodestructive processes were calculated by the Coats-Redfern method [7] and the data processed on a Felix computer.

RESULTS AND DISCUSSIONS

The thermal stabilities of the polyazines and polyazomethines were studied in comparison with those of the initial dicarbonylic components and diamines.

The processes taking place during the thermal degradation were interpreted by taking into account the maximum temperature at which the samples do not show weight losses (T_d), for the initial components and polyazines, and show weight losses of 50% for polyazomethines ($T_{0.5}$).

For the dicarbonylic components the temperature at which the thermodestruction begins increases in the following order : acenaphthenequinone < 5-chloroacenaphthenequinone < 5-nitroacenaphthenequinone < 5,6-dinitroacenaphthenequinone (Table 1). By considering the values of the ground state resonance energies obtained by Parriser-Parr-Pople calculations the same order is obtained.[8]

The oxidative splitting of the α-dicarbonylic bond takes place during the first decomposition stage followed by the elimination of the volatile components during the second stage. The increase in the stabilization energy by the introduction of the electron-withdrawing substituents results in an increased resistance to thermodestruction.

With the diaminic components two destruction stages are noticed. During the first stage the reactions take place in the liquid phase, between 120 and 280°C, leading probably to stable structures resistant up to temperatures higher than 350°C.

The polymer thermostabilities depend in a large extent on the stability of both recurring units and the bonds between them. The alternate double bond system as well as the bulky substituents conferring rigidity to the chain enhance the macromolecule thermal stability.

The polyazomethines show a higher thermal stability (Figure 1) than the polyazines, their thermal destruction beginning at 250—355°C and 220°C, respectively.

The polyazines decompose during the first stage of the thermal destruction with a sudden nitrogen elimination and formation of stable polyenes, resistant to higher temperatures, decomposing during the following thermodestruction stages.

TABLE 1

Thermal properties of dicarbonylic and diaminic compound

No. Compound	Melting point (°C)	Thermogravimetric data					
		T_d^* (°C)	Degradation steps	Temperature range (°C)	Weight losses (%)	Activation energy Kcal/mol	Reaction order
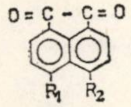							
1 $R_1=R_2=H$	262	185	I	185–420	100.0	20.5	1.1
2 $R_1=Cl$; $R_2=H$	210	195	I	195–435	91.2	18.8	1.1
			II	435–580	8.8	38.7	1.3
3 $R_1=NO_2$; $R_2=H$	180	220	I	220–394	33.5	30.1	2.0
			II	394–740	66.5	24.6	2.0
4 $R_1=NO_2$; $R_2=NO_2$	—	264	I	264–368	28.7	51.1	1.8
			II	368–693	71.3	20.9	1.8
5 $p-C_6H_4(NH_2)_2$	138	120	I	120–240	45.0	—	—
			II	345–615	50.0	—	—
6 $m-C_6H_4(NH_2)_2$	65	120	I	120–280	71.2	—	—
			II	400–600	28.8	—	—

---

* T_d = The maximum temperature at which the samples do not show weight losses.

The facile nitrogen elimination might be explained by the azo- azine tautomerism $= N - N = \rightleftharpoons - N = N -$.[9] For the polyacenaphthenequinoneazine the nitrogen removal during the first decomposition stage is confirmed by the agreement between the percentages of the weight losses and calculated nitrogen as well as by the high rate of the processes made evident by the TG and DTG curves.

The higher weight losses noticed during the first decomposition stage of the polynitroacenaphthenequinoneazine might be explained by the simultaneous elimination of some nitro groups and azinic nitrogen.

The polyazomethines (Table 3) are more stable than the polyazines, probably due to the introduction of an aryl residue between the nitrogen atoms. The *p* — substituted aromatic ring determines a slower polymer degradation than the *m* — substituted one.

The thermal stability of the polyazomethines also depends on the reaction condition (Figure 1). The decomposition temperature and the number of the decomposition stages vary with the solvent chosen as reac-

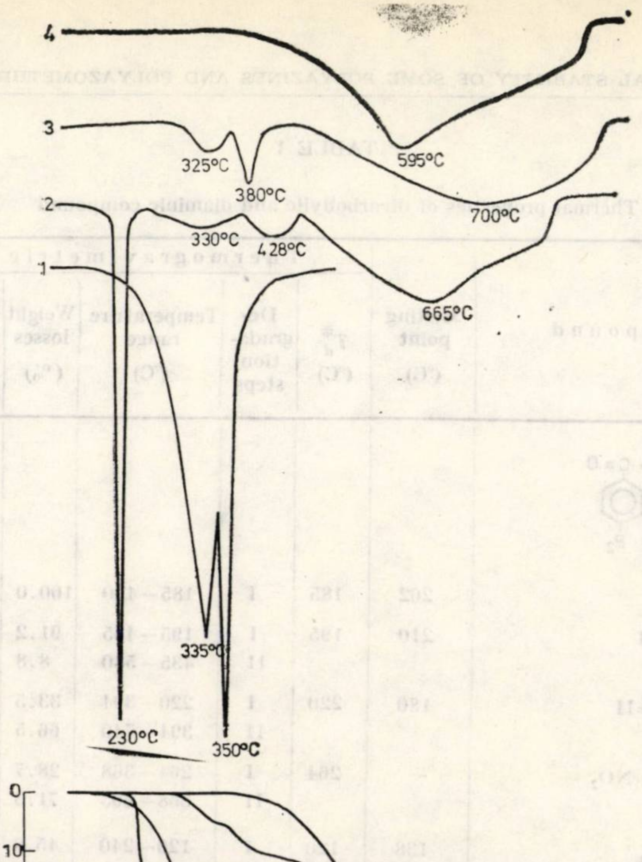

Fig. 1. — DTG and TG curves of some polymers obtained from acenaphthenequinone: *1.* acenaphthenequinone; *2.* polyazine obtained from acenaphthenequinone; *3.* polyazomethine obtained from acenaphthenequinone with *p*-phenylenediamine in acetic acid; *4.* polyazomethine obtained from acenaphthenequinone with *p*-phenylenediamine in xylene.

TABLE 2

Thermal properties of polyazines

No. POLYMER	Catalyst	Thermogravimetric data					
		T_d^* (°C)	Degradation steps	Temperature range (°C)	Weight losses (%)	Activation energy (Kcal/mol)	Reaction order
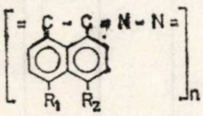							
1 $R_1=H$; $R_2=H$	—	205	I	205–256	14.0	48.0	0.0
			II	266–398	4.6	31.9	1.7
			III	398–485	6.5	72.9	2.5
			IV	485–853	71.9	24.5	1.5
2 $R_1=H$; $R_2=H$	H_2SO_4	230	I	230–300	13.5	42.7	0.2
			II	300–482	18.9	14.5	1.0
			III	482–805	67.6	27.9	1.4
3 $R_1=Cl$; $R_2=H$	—	200	I	200–325	41.6	47.6	2.3
			II	325–416	10.1	70.1	2.4
			III	448–546	15.8	—	—
			IV	546–612	11.9	—	—
			V	655–785	7.2	72.3	1.3
4 $R_1=NO_2$; $R_2=H$	—	180	I	180–248	22.8	62.6	2.1
			II	248–395	22.5	36.3	2.5
			III	418–640	48.9	—	—
5 $R_1=NO_2$; $R_2=NO_2$	—	197	I	197–405	27.2	10.4	0.5
			II	407–700	73.0	20.1	1.3
6 $R_1=NO_2$; $R_2=NO_2$	H_2SO_4	227	I	227–335	21.3	26.6	1.2
			II	335–442	17.3	—	—
			III	442–715	61.3	26.2	1.4

---

*) T_d= The maximum temperature at which the samples do not show weight losses.

tion medium. The xylene increases the destruction temperature and decreases the number of the degradation stages (Table 3).

Since the chemical and spectral analyses have made evident the presence of acetyl groups, the thermal destruction of the polyazomethines obtained in acetic acid is supposed to begin with the elimination of these groups.

The low percentage of weight losses and the values of the activation energies lying between 20.7 and 26.3 kcal/mol in the first degradation stage support this assumption. The polyazomethines obtained from dinitroace-

TABLE 3

Thermal properties of polyazomethines

No. POLYMER	Solvent	Thermogravimetric data					
		$T^*_{0.5}$ (°C)	Degradation step	Temperature range (°C)	Weight losses (%)	Activation energy (kcal/mole)	Reaction order
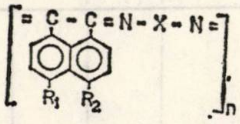							
1 $R_1=H$; $R_2=H$; $X=m-C_6H_4-$	acetic acid	550	I	272–403	8.6	25.4	1.1
			II	403–732	82.6	22.4	1.3
2 Idem	xylene	600	I	300–800	87.3	12.8	1.1
3 $R_1=H$; $R_2=H$; $X=p-C_6H_4-$	acetic acid	680	I	280–357	5.2	26.3	1.1
			II	357–410	4.7	33.6	0.0
			III	443–905	73.5	16.5	1.2
4 Idem	xylene	630	I	383–880	100.0	14.8	1.1
5 $R_1=Cl$; $R_2=H$; $X=m-C_6H_4-$	acetic acid	540	I	260–396	8.4	—	—
			II	396–730	82.8	19.6	1.5
6 Idem	xylene	570	I	315–795	92.3	15.4	1.3
7 $R_1=Cl$; $R_2=H$; $X=p-C_6H_4-$	acetic acid	590	I	224–372	12.9	23.5	1.3
			II	372–447	6.6	—	—
			III	447–807	75.3	28.3	2.3
8 Idem	xylene	605	I	332–815	95.3	14.9	1.2
9 $R_1=NO_2$; $R_2=H$; $X=m-C_6H_4-$	acetic acid	627	I	265–365	8.8	24.0	0.5
			II	365–470	9.3	58.8	2.3
			III	470–870	80.1	21.9	1.5
10 Idem	xylene	575	I	280–760	95.1	11.1	1.1
11 $R_1=NO_2$; $R_2=H$; $X=p-C_6H_4-$	acetic acid	590	I	225–390	12.0	20.7	1.6
			II	425–790	81.0	21.6	1.2
12 Idem	xylene	590	I	270–758	96.5	9.2	0.5
13 $R_1=NO_2$; $R_2=NO_2$; $X=m-C_6H_4-$	acetic acid	500	I	270–400	26.0	32.3	1.7
			II	400–680	74.0	18.7	1.1
14 Idem	xylene	540	I	220–460	27.7	12.1	1.0
			II	460–720	71.7	20.2	1.0
15 $R_1=NO_2$; $R_2=NO_2$; $X=p-C_6H_4-$	acetic acid	540	I	250–430	20.1	10.8	0.1
			II	430–726	72.4	24.5	1.7
16 Idem	xylene	585	I	230–280	4.9	8.3	2.0
			II	280–425	14.3	17.5	0.7
			III	425–820	80.8	19.3	1.5

---

*) $T_{0.5}$ = Temperature at which the samples show weight losses of 50 %.

naphthenequinone make an exception, the destructive processes of the first stage being probably in connection with the presence of nitro groups.

The data listed in table 3 show the $T_{0.5}$ to increase, with one exception, when *p*-phenylenediamine is substituted for *m*-phenylenediamine for the polymers synthesized both in acetic acid and in xylene.

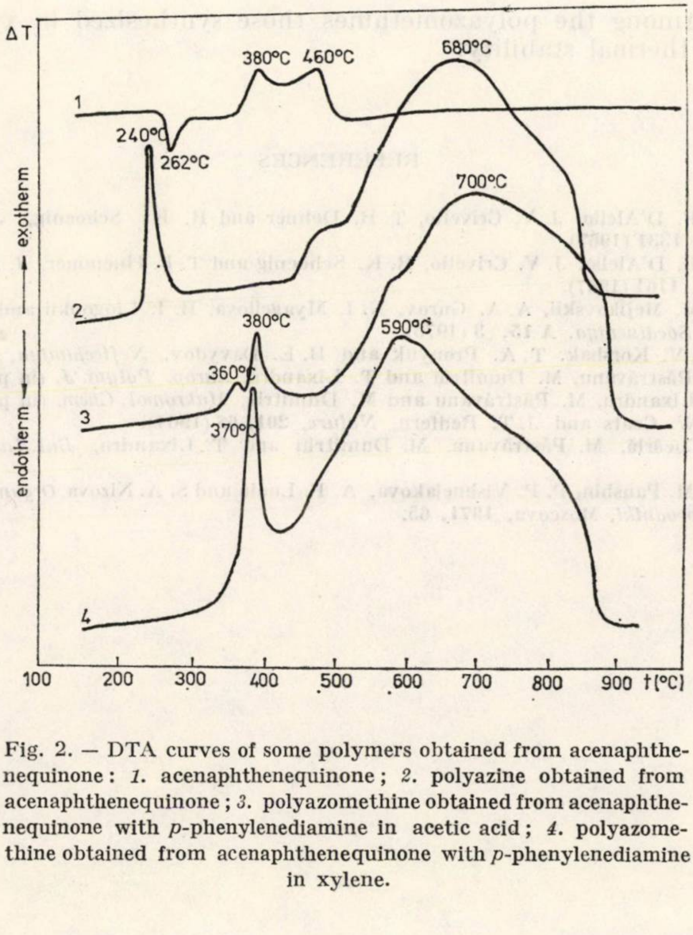

Fig. 2. — DTA curves of some polymers obtained from acenaphthenequinone: *1.* acenaphthenequinone; *2.* polyazine obtained from acenaphthenequinone; *3.* polyazomethine obtained from acenaphthenequinone with *p*-phenylenediamine in acetic acid; *4.* polyazomethine obtained from acenaphthenequinone with *p*-phenylenediamine in xylene.

Since the DTA curves denote the exothermic character of all destructive processes one may conclude that thermooxidative phenomena take place (Figure 2). All the polymers under study melt above the thermodestruction temperature, T_a. The acenaphthenequinone melts at 262°C and exhibits the first exothermic peak at 380°C. For polyazomethines this peak is located very close to 380°C, while for polyazines it appears below the melting temperature of the dicarbonylic compound, probably due to the elimination of azinic nitrogen.

CONCLUSIONS

1. The thermal properties of some polyazines and polyazomethines obtained from acenaphthenequinone and its derivatives were studied comparatively and a good thermal stability was found for the both classes of polymers.

2. The polyazomethines were found to be more stable than the polyazines.

3. Among the polyazomethines those synthesized in xylene show a higher thermal stability.

REFERENCES

[1] G. F. D'Alelio, J. V. Crivello, T. R. Dehner and R. K. Schoenig, *J. Macromol. Chem.*, **A 1,** 1331 (1967).

[2] G. F. D'Alelio, J. V. Crivello, R. K. Schoenig and T. F. Huemmer, *J. Macromol. Sci. Chem.*, **A 1,** 1161 (1967).

[3] S. M. Mejikovskii, A. A. Gurov, N. I. Myagcilova, B. I. Liogonkii and A. A. Berlin, *Vysokomol. Soedineniya*, **A 15,** 3 (1973).

[4] Yu. V. Korshak, T. A. Pronyuk and B. E. Davydov, *Neftechimiya*, **3,** 677 (1963).

[5] M. Păstrăvanu, M. Dumitriu and T. Lixandru, *Europ. Polym. J.* (in press).

[6] T. Lixandru, M. Păstrăvanu and M. Dumitriu, *Makromol. Chem.* (in press).

[7] A. W. Coats and J. T. Redfern, *Nature*, **201,** 68 (1964).

[8] I. Cocârlă, M. Păstrăvanu, M. Dumitriu and T. Lixandru, *Bul. Inst. Polit.*, Iași (in press).

[9] Ia. M. Paushin, P. P. Vishneiakova, A. F. Lunin and S. A. Nizova, *Organiceskie polimernye poluprovodniki*, Moscova, **1971,** 65.

Revue Roumaine de Chimie, 25, 7, 989–994(1980)

Dedicated to Professor CRISTOFOR I. SIMIONESCU
on his 60th anniversary

BIOACTIVE POLYMERS. VII.*
OXIDOREDUCTASES AND HYDROLASES IMMOBILIZED ON CELLULOSE DERIVATIVES

SEVERIAN DUMITRIU and VICTOR BULACOVSCHI
Polytechnic Institute of Jassy, Department of Organic and Macromolecular Chemistry,
Jassy, Romania

Received January, 23, 1980

The paper reports on the investigations undertaken to determine the coupling conditions and the retained activity of some hydrolases and oxidoreductases on cellulose derivatives. The obtained data reveal some advantages of the coupled enzymes regarding their chemical and thermal stability. The mentioned enzymes are also suitable for utilisation in continuous processes.

In the modern industry a growing number of chemical processes depends on the catalytic activity of natural enzymes. Compared with ordinary chemical catalysts, biocatalysts offer the advantage of very mild reaction conditions, high selectivity, maximum efficiency and low consumption of energy. However, the industrial use of biocatalysts is limited by the high cost of the enzymes themselves, the difficulty of separating them from the final product, their incapacity to operate in organic media or at high temperatures.

Through binding of the enzymes to insoluble matrices these limitations are somehow circumvented. Such immobilized enzymes are suitable for use in continuous processes and the obtained product is not contaminated. A further advantage is that the coupled enzymes prove to be more stable on storage or in the working conditions as compared with free enzymes.

As a consequence of the mentioned advantages in a relatively short period of time, remarkable progresses were obtained in coupling of enzymes [1–4] or, generally, of biological active products [5,6] on synthetic or natural modified polymers with high reactive groups used as supports. It is difficult for the moment to have a critical and objective appreciation of all insolubilization possibilities or of their advantages or disadvantages, but it is obvious that the covalent coupling of enzymes on solid matrices holds a distinct position. Following this procedure the risk of partial or total enzyme desactivation appears, but using a proper technique one may retain a good part of the enzymatic activity. It appears, therefore, as an imperative necessity to develop investigations both in the direction of finding the best supports and coupling conditions and in the best evaluation of the retained activity.

The present paper deals with the coupling of oxireductases and hydrolases on cellulose derivatives.

*** Previous part in ref. 10.**

1. RESULTS AND DISCUSSION

1.1. Coupling of hydrolases on cellulose derivatives

Although up to now a large number of reactive polymers has been investigated for immobilization of enzymes, the compositional and structural diversity of biologic active products makes it impossible to get an ideal support of universal applicability. Due to the various factors which influence the coupling of enzymes, each protein requires an individual solution.

The cellulose carbonate and carboxymethylcellulose acid chloride (CMC-Cl) were found to be convenient supports for the coupling of amyloglucosidase (E.C. 3 .2 .1), *alpha*-amylase (E.C. 3 .2 .1 .1) and urease (E.C. 3 .5 .1 .5).[7-10] The remarkable reactivity of functional groups allows the binding of proteins in very mild conditions which stabilize the enzyme structure and protect its enzymatic activity.

The binding ability of cellulose derivatives was strongly affected by the pH of the coupling reaction, maximum combination occurring every time in the alkaline media. Such conditions reply to the requirements for CMC-Cl and protein condensation when the alkaline pH favours the withdrawn and fixation of HCl. The cellulose carbonate showed maximum coupling activity at pH 7.8 which is explained in the following way. At lower pH values the aminogroups on the surface of the protein are protonated to a considerable extent and, therefore, they are not effective as nucleophiles. At higher pH values (pH > 8) hydrolysis of carbonate groups (by attack either by water or by hydroxide ions) occurs which competes increasingly with the attack of the nucleophilic groups on the protein molecule.[11]

The coupling mechanism in this last case can be represented as follows[12]:

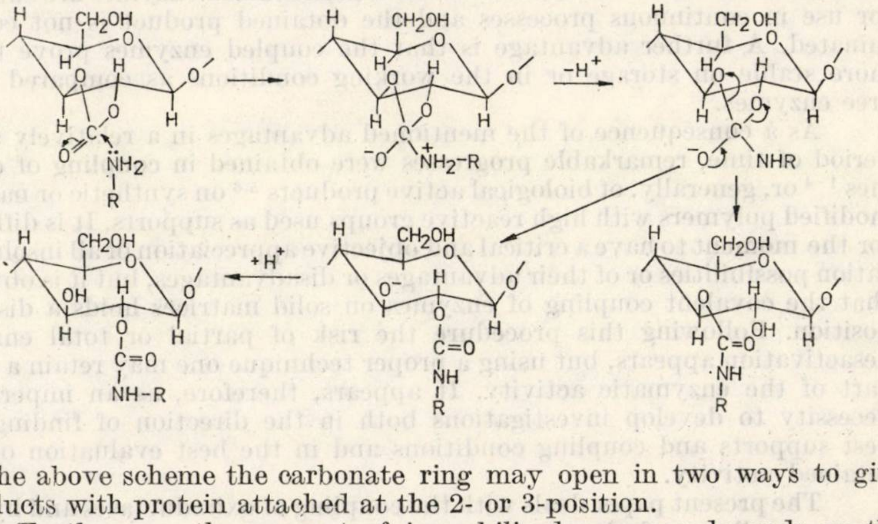

In the above scheme the carbonate ring may open in two ways to give products with protein attached at the 2- or 3-position.

Furthermore, the amount of immobilized enzymes depends on the amount and the concentration of the enzyme offered during the coupling reaction. This effect has been studied in the case of immobilization of amyloglucosidase on CMC-Cl. The obtained data (Table 1) showed that for the fixed values of pH, temperature and time, the maximum activity of the coupled product was obtained for a 1 :1 (*w*/*w*) ratio enzyme/matrix. Certainly, higher amounts of enzyme may be immobilized when higher concentrations of proteic product are used during the coupling reaction, but in this case one should account for the efficiency of the reaction.

TABLE 1

Activity of the coupled amyloglucosidase on CMC – Cl for various ratios enzyme/matrix (time = 4 h ; pH 8 ; t = 25°C ; V = 40 ml)

Enzyme / Matrix (g/g)	1.25/1	1/1	1/1.33	1/2	1/4
Activity (mg/g)	29.9	57.7	54.4	34.7	37.3

It is well known that the enzymatic activity is pH-dependent. In most cases the optimum pH of the coupled enzyme activity may differ from that of the native product. Thus, following the pH influence upon hydrolytic activity of the coupled *alpha*-amylase on CMC-Cl (Figure 1), it was found that between pH 5.8 and 8.2 a relative stabilization appears similar to the findings of the free *alpha*-amylase activated with Ca^{2+} ions.[13] A possible explanation for such a behaviour may be the stabilization of the active site and proteic chain conformations by the action of the free ionizable carboxylic groups remained on the CMC macromolecules.

Enzymes, like other proteins, are susceptible to denaturation at high temperatures. Enzymes may also increase the reaction velocity with the increase of temperature. Following the temperature profile curves for immobilized and soluble *alpha*-amylase (Figure 2), a maximum activity for both products at 38°C is observed. But, it should be mentioned that while the decreasing in activity of the former product is rapid (more than 75 % at 68°C), the coupled enzyme loses in the same conditions only aprox

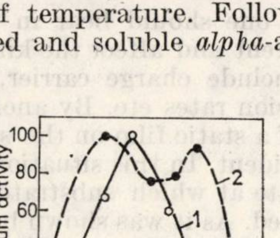

Fig. 1. — pH profiles for soluble (curve *1*)[13] and coupled *alpha*-amylase (curve *2*) in the presence of Cl^- ions (time 30 min, *t* = 38°C). Activity was ploted as percent of maximum activity at pH 5.8 for the immobilized enzyme and 6.5 for the soluble one.

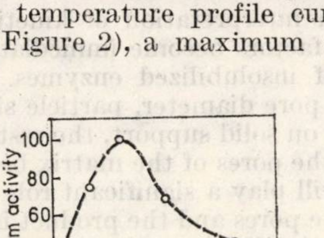

Fig. 2. — Temperature profile for the immobilized *alpha*-amylase at pH 5.8 and 30 min.

55 % from its initial activity. One may consider that the thermal denaturation of enzymes is sensibly lowered by immobilization.

Additional information concerning the coupled product stability was obtained from the pH and temperature dependence of the enzymatic activity (Figure 3). Studies on immobilized amyloglucosidase showed that its activity decreased as pH value rised (at room temperature) probably due to the destruction of the secondary structure, implicitly of the enzyme active centers.[14] A notable activity, maintained up to 15 hrs, is noticed at pH 8 and 5°C. In this case no significant losses in activity were observed even after 20 hrs. of reaction. For the same pH, at room temperature, although the activity was higher, some denaturating effects were observed.

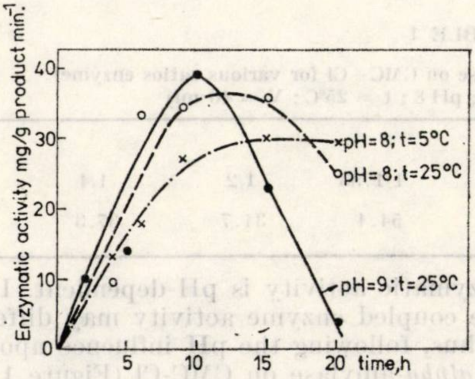

Fig. 3. — Effect of pH and temperature on activity of amyloglucosidase coupled on CMC-Cl.

In interpretation of kinetical data one should bear in mind that several factors become immediately apparent and affect the kinetic behaviour of insolubilized enzymes. These include charge carrier, substrate charge, pore diameter, particle size, diffusion rates etc. By anchoring the enzyme on solid support, the restriction of a static film on the surface and within the pores of the matrix becomes evident. In this situation diffusion effect will play a significant role in the rate at which substrate molecules enter the pores and the product is dissipated. As it was shown by different authors,[15] diffusion usually results in a change of the apparent Michaelis constants of the matrix bound enzyme as compared with the same enzyme in free solution.

In spite of the loss of mobility, attached enzymes still obey Michaelis-Menten kinetics to a first approximation, i.e. yield linear Lineweaver-Burk plots, from which it is possible to calculate apparent Michaelis constants K_M(app)(Figure 4). Thus, the Lineweaver-Burk plots for immobilized amyloglucosidase on cellulose carbonate are essentially linear, while for the coupled enzyme on CMC-Cl at various pH values (curves 2 ; 3) the linearity is maintained only for increased substrate concentrations with increased K_M. The linearity of the plots in the former case supports the assumption that immobilized amyloglucosidase molecules are located primarily on the outer cellulose carbonate surface. The diffusion of the substrate molecules to and from the surface is simplified as compared to the diffusion involved when enzymes are bound to porous supports. Here the resistance of the diffusion pathway for the substrate is defeated at increased concentrations of the substrate in the microenvironment of the enzyme. Similar results were reported by Lilly and Sharp with chymotrypsin bound to CMC.[16]

An unexpected reduced K_M value (0.13 mM) was found for the *alpha*-amylase attached to CMC-Cl. In this case one may assume that in the acidic medium (pH 5.8) the substrate molecules are positively charged by protonation while the matrix retains a negative charge. The electrostatic atraction will lead to higher concentrations of the substrate around each particle as compared to the bulk of the solution and as a consequence to lowering of K_M value.

Diffusion of the substrate molecules should be taken into account also in the case of reactions catalysed by urease fixed on CMC-Cl. The difference between the substrate concentration around the particles and in bulk of the solution explains probably the increasing of the Michaelis constant ($K_M = 15.7$ mM) as compared with the value corresponding to the free enzyme.

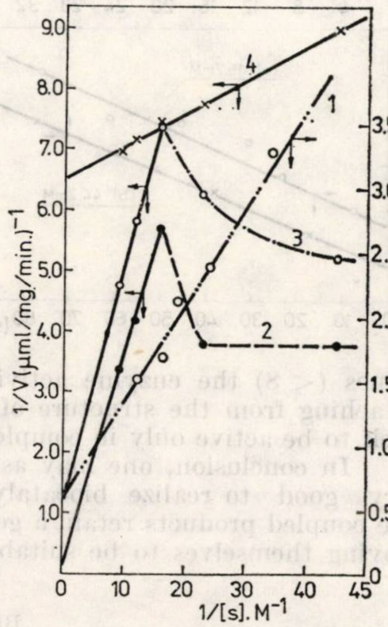

Fig. 4. — Lineweaver-Burk plots for *alpha*-amylase (1, pH 5.8) and amyloglucosidase immobilized on CMC-Cl pH 8 (2), pH 9 (3) and on cellulose carbonate at pH 8(4).

2. Coupling of enzymes from oxidoreductases class

For the immobilization of an oxidoreductase, namely alcoholdehydrogenase (ADH), the *p*-aminobenzoylcellulose was selected as inert support. In this case we considered the possibility of coupling the biologically active product through the aromatic moieties from its structure, protecting in this way the active sites of the enzyme.

In order to establish the best coupling conditions a second order central composed rotable design was undertaken.[17] Statistical analysis of the experimental data outlined the optimum values of pH, time and coupling temperature to be at 8.3 ; 3.5 hrs, respectively 12.5°C.

It is worth mentioning that the basic conditions are electrostatically favorable for diazonium coupling since the diazonium salts have a full ionic positive charge whereas the ADH is expected to be negatively charged under these conditions.

The kinetics of matrix-bound ADH showed that Michaelis-Menten relation is also respected (Figure 5), but the K_M was found to be high (44.2 mM). Diffusion effects do not explain satisfactory the increase of the K_M, thus we should consider that the conformational modifications of the active site may affect the kinetic behaviour of the enzyme. As it is well known, the ADH molecule is built up from 4 protomers bound together through a Zn atom and 4 coenzyme molecules.[18] In the coupling process the chemical bound is possible to appear only at one protomer and the quaternary structure is destroyed. In fact, at lower coupling pH values (< 8) the enzyme activity is very decreased, due probably to detaching from the structure of the nonbound protomers. ADH proves itself to be active only in complete structural composition.

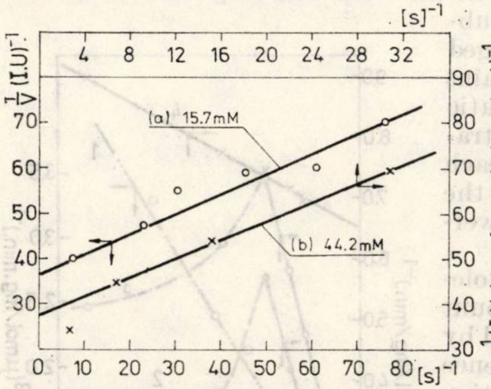

Fig. 5. — Lineweaver-Burk plots for urease immobilized on CMC-Cl (*a*) and for ADH coupled on *p*-aminobenzoyl-cellulose (*b*).

In conclusion, one may assert that enzymes on inert supports are very good to realize biocatalysts eventually for industrial use also. The coupled products retain a good stability and a considerable activity, proving themselves to be suitable for use in continuous processes.

REFERENCES

[1] I. Chibata, *Pure and Appl. Chem.*, **50**, 667 (1978).
[2] G. Manecke and H. G. Vogt, *Pure and Appl. Chem.*, **50**, 655 (1978).
[3] N. Weliky, H. H. Weetall, R. V. Gilden, and D. H. Campbell, *Immunochemistry*, **1**, 219 (1964).
[4] Yu-Yen Linko, P. Saarinen and M. Links, *Biotechn. Bioeng.*, **17**, 153 (1975).
[5] Cr. Simionescu, S. Dumitriu and R. Butnaru *Cellulose Chem. Technol.*, **8**, 393 (1974).
[6] L. Sundberg, J. Poroth and K. Aspberg, *Biochim. Biophys. Acta*, **221**, 394 (1970).
[7] Cr. Simionescu, S. Dumitriu, R. Butnaru and V. Bulacovschi, "IUPAC International Symp. Macromolec. Chem.", Vol. II, 1—12, p. 370 Madrid, Spain, 1974.
[8] Cr. Simionescu, S. Dumitriu, V. Bulacovschi and V. I. Popa, "17th Microsymposium on Macromolecules, Medical Polymers — Prague", August 15—18, 1977, C36, 1—3.
[9] Cr. Simionescu, S. Dumitriu, V. Bulacovschi and V. I. Popa, *Cellulose Chem. Technol.*, **12**, 253 (1978).
[10] S. Dumitriu, V. Bulacovschi, D. Constantinescu and A. Rugină, *Cellulose Chem. Technol.*, **13**, 391 (1979).
[11] S. A. Barker, S. H. Doss, C. J. Gray, J. F. Kennedy, M. Stacey and T. H. Yeo, *Carbohyd. Res.*, **20**, 1 (1971).
[12] J. F. Kennedy and A. Rosevear, *J. C. S. Perkin* I, **1974**, 757.
[13] E. H. Fischer and E. A. Stein, "The Enzymes" 2nd Ed, vol. 4, p. 333, 1960.
[14] G. O. Hustad, T. Richardson and N. F. Olson, *J. Dairy Sci.*, **56**, 1118 (1973).
[15] W. E. Hornby, M. Lilly and E. M. Crook, *Biochem. J.*, **107**, 669 (1968).
[16] D. M. Lilly and A. K. Sharp, *Chem. Eng. (London)*, **215**, CE 12 (1968).
[17] W. G. Cochran and G. M. Cox, "Experimental Designs", Wiley, New York, 1968, p. 350.
[18] J. R. Kagi and B. L. Vallee, *J. Biol. Chem.*, **235**, 3188 (1960).

Revue Roumaine de Chimie, 25, 7, 995–1006(1980)

Dedicated to Professor CRISTOFOR I. SIMIONESCU
on his 60th anniversary

UNRESTRICTED HARTREE-FOCK SPIN DENSITIES IN ARYL-NITROSO-AMINYLOXIDES AND IN ACYL-ARYL-AMINYLOXIDES

MIHAELA HILLEBRAND[a] and A. T. BALABAN[b]

[a] Department of Physical Chemistry, The Polytechnic, Bucharest, Roumania
[b] Department of Organic Chemistry, The Polytechnic, Bucharest, Roumania

Received December 4, 1979

Unrestricted Hartree-Fock and McLachlan spin densities were calculated for *p*-substituted aryl-nitroso-aminyloxides and acyl-aryl-aminyloxides in E and Z conformations. Correlations with experimental coupling constants indicate satisfactory agreement between UHF spin densities and experimental data.

INTRODUCTION

Push-pull free radicals predicted theoretically by Dewar [1] to possess enhanced stability relative to symmetrically substituted systems were first investigated experimentally in the case of aminyls.[2-10] Persistent aminyls were obtained when steric shielding was also present, even in the absence of aromatic delocalization.[10] The extreme persistence of DPPH and related hydrazyls was interpreted as being due to a combination of strong electronic push-pull effects, steric shielding and aromatic delocalization.[2-4]

More recently, Katritzky proposed the term *merostabilization* for this push-pull effect in free radicals,[11] while Viehe advanced the term *capto-dative* which presents the obvious advantage that it can be used as an adjective.[12] Persistent capto-dative carbon free radicals were recently obtained.[12-15]

By contrast, capto-dative aminyloxides (nitroxides) do not seem to have additional stabilization; since several such aminyloxides with acyl,[16,17] arenesulphonyl,[18] or nitroso groups[18-20] as acceptors and aryl groups as donors were prepared in our laboratory, we undertook the present theoretical study, in an effort for rationalizing observed hyperfine coupling constants and for obtaining information on conformations. Unrestricted

Hartree-Fock (UHF) spin distributions were calculated for a series of aryl-aminyloxides I where R is nitroso or acyl.

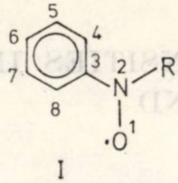

I

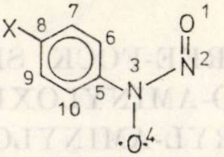

a, X = H
b, X = NO_2
c, X = OCH_3

II

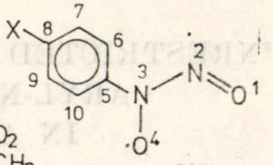

III

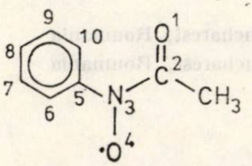

IV

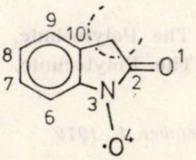

V

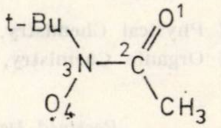

VI

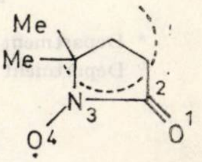

VII

The calculations were directed at finding the variations of coupling constants a_N, a_H on varying R in I (NO, $COCH_3$), on varying the *para*-substituent X in II or III for acceptor (NO_2) and donor groups (OCH_3), and finally on varying the E/Z geometry (II *versus* III); the conformation of aryl-nitroso-nitroxides may be either with the two oxygens *anti* (E) as in II, or *syn* (Z) as in III, and so far there are no experimental arguments for one conformation or the other. By contrast, in the case of analogous acyclic acyl-aryl-aminyloxides IV, the coupling constant a_N indicates the E conformation, since the related cyclic aminyloxide V has an appreciably smaller a_N value owing to its constrained Z conformation.[16,17] In addition to calculations for systems II—V, in order to check the parametrization, we report calculated results for systems devoid of aryl groups, namely the acyl-aminyl-oxide VI (acetyl-*t*-butyl-aminyloxide, E conformer) and VII (5,5-dimethyl-2-pyrrolidone-N-aminyloxide, frozen Z conformation).[20-22]

CALCULATIONS

Calculations were performed using the UHF method with the annihilation of the superior spin component. The computer program based on Amos and Snyder's equations [23] was written in FORTRAN IV.[24] Bielectronic bicentric repulsion integrals were evaluated by applying the Nishimoto-Mataga [25] and the Pariser-Parr methods.[26] Ionization potentials of valence states were taken from usual tables; for taking into account electronegativity differences, in some cases a variation of ±1 eV relative to the standard values was introduced. Integrals of β_{ij} type were initially calculated considering their dependence on overlap integrals S_{ij}, and then corrected for obtaining an optimal fit with experimental data. The highest difference between the initial and the corrected β_{ij} value appeared for β_{NO} (final corrected value -1.6 eV).

For the N-nitroso group two models were used, namely the usual sp^2-hybridized model in which the N—O group participates with two π-electrons, and Julg's model [27] with sp-hybridized nitrogen and four π-electron participation. For nitro and methoxy groups, conjugative-inductive models were used,[28] and for the *t*-butyl groups an inductive model was employed.

SPIN POLARIZATION PARAMETERS

From calculated spin densities, the proton hyperfine coupling constants were obtained by the McConnell relation with $Q_{\mathrm{H}}^{\mathrm{CH}}$ equal to $|2.7|$ mT. For the nitrogen atoms in aminyloxides, Ayscough and Sargent recomended [29] the values $Q_{\mathrm{N}}^{\mathrm{N}} = 2.42$ mT and $Q_{\mathrm{O}}^{\mathrm{N}} = -0.36$ mT, while Kikuchi and Someno [30] use values $Q_{\mathrm{N}}^{\mathrm{N}} = 3.05$ mT and $Q_{\mathrm{O}}^{\mathrm{N}} = -1.36$ mT. Aurich et al.[31] determined the spin polarization parameters $Q_{\mathrm{N}}^{\mathrm{N}}$ and $Q_{\mathrm{O}}^{\mathrm{O}}$ by following the variation of hyperfine splitting constants a_{N} and $a_{17_{\mathrm{O}}}$ against changing solvent polarities, and assuming a simple McConnell-type dependence a_{N} *vs.* ρ_{N} and a_{O} *vs.* ρ_{O}. The value thus obtained, $Q_{\mathrm{N}} = 3.31$ mT leads to reasonable splitting constants using McLachlan calculations. Since this value is too large to be used in UHF calculations of spin density and the previous values given for $Q_{\mathrm{O}}^{\mathrm{N}}$ differ too much, we estimated $Q_{\mathrm{N}}^{\mathrm{N}}$ and $Q_{\mathrm{O}}^{\mathrm{N}}$ by the method of multiple correlation; from the spin densities calculated for compounds listed in Table 1 the values which were obtained are $Q_{\mathrm{N}}^{\mathrm{N}} = 2.152$ mT, $Q_{\mathrm{O}}^{\mathrm{N}} = -0.332$ mT.

These values are close to the values proposed by Ayscough and Sargent [29] and will therefore be used subsequently in the present paper for calculating a_{N} values in aryl-N-nitroso-nitroxides. For the nitrogen coupling constant of the nitroso group, we used a McConnell formula with $Q_{\mathrm{N}}^{\mathrm{NO}} = 3.0$ mT, since literature data are scarce and they refer mainly to anion-radicals possessing nitroso groups.

AMINYLOXIDES DEVOID OF NITROSO GROUPS

When using bielectronic-bicentric repulsion integrals obtained by the Nishimoto-Mataga (NM) procedure,[25] irrespective of the parametrization, unsatisfactory agreement with experimental coupling constants was obtained, namely a calculated ratio $\rho_{ortho}/\rho_{meta} \simeq 1.4$ (experimentally this ratio is closer to 3) and a low spin density on the nitrogen atom of the aminyloxide group. This procedure for evaluating the γ matrix maintains the 'spin contamination' even after the application of annihilation methods, as shown by the values $\langle S_{aa}^2 \rangle \simeq 1.1$, and this explains the unsatisfactory results. Ladik et al.[32] also mention the poor results on using the Nishimoto-Mataga procedure; they propose an adjustment $\gamma = k\gamma_{\mathrm{NM}}$ with $k = 1.5$ for optimizing the spin densities calculated for haloderivatives of *t*-butyl-phenyl-aminyloxide.

Better results can be obtained by calculating the interelectronic repulsion matrix by the Pariser-Parr procedure.[26] Since this procedure

TABLE 1

Calculated spin densities ρ, and calculated and experimental hyperfine coupling constants for aminyloxides I (R = H), IV—VII used for obtaining spin polarization parameters

Radical	Position	ρ_{calc}	$\lvert a_{calc} \rvert$(mT)	$\lvert a_{exp} \rvert$(mT)	Ref.
I	O	0.373	—	—	
(R=H)	N	0.475	0.896	0.904	
	H	—	1.226	1.196	
	4(*o*)	0.091	0.246	0.296	30
	5(*m*)	−0.028	0.076	0.096	
	6(*p*)	0.071	0.192	0.296	
IV	O	0.433	—	—	
	N	0.402	0.721	0.720	
	6(*o*)	0.062	0.167	0.147	16
	7(*m*)	−0.022	0.059	0.062	
	8(*p*)	0.050	0.135	0.147	
V	O	0.497	—	—	
	N	0.334	0.554	0.550−0.580	
	6(*o*)	0.066	0.178	0.190−0.260	16
	7(*m*)	−0.023	0.062	0.050−0.070	
	8(*p*)	0.053	0.143	0.190−0.260	
VI	O	0.505	—	—	
	N	0.444	0.788	0.780	21
VII	O	0.559	—	—	21
	N	0.388	0.650	0.650	

$$a_N = 2.152\ \rho_N^\pi - 0.332\ \rho_0$$
$$a_H^{NH} = |2.75|\rho_N^\pi$$
$$a_H = |2.70|\ \rho_C^\pi$$

leads to larger values for repulsion integrals, it is expected (as discussed by Tino and Klimo [33]) to determine a lower contribution of higher spin components in the UHF function. The larger values thus obtained are close to those resulted from the Ladik et al.'s approach.[32]

For radicals **I**, IV and V (Table 1) the semiempirical parameters of the aminyloxide group were : $W_N = -28.7$ eV, $W_O = -17.7$ eV and $\beta_{NO} = -1.6$ eV, while for VI and VII, devoid of aryl groups, $W_N = -28.3$ eV. Since for compound **I** the hyperfine coupling constants indicate strong delocalization involving the phenyl ring, we selected $\beta_{N-Ph} = -2.8$ eV.

The results of our calculations agree with Kikuchi and Someno's results obtained through the UHF$_{aa}$ method[34] for the spin distribution in the benzene ring, but our calculations would indicate a reversal of the relative spin densities ρ_N and ρ_O in the aminyloxide group, similar to data obtained by McLachlan[30;35] calculations. The calculated ρ_N agrees excellent with the experiment. The spin density ratio *ortho/meta* is in agreement with experimental data (both densities are underestimated). The couplings *ortho/para* which experimentally appear equivalent under normal resolution are calculated to be different with a smaller *para* spin density.

The acyl-aminyloxides IV–VII are calculated to possess markedly higher a_N couplings in the E conformation (IV, VI) than in the Z conformation of the cyclic systems V, VII, in agreement with the experiment. The presence of aryl groups lowers the coupling constants to a smaller extent than the preceding effect of stereoisomerism.

For the cyclic aromatic acyl-nitroxide V, the calculation neglects the interaction with the five-membered ring; experimentally, as seen from Table 1 on varying the structure, the effect on a_N is low ($\Delta a_N = 0.03$ mT, i.e. 6%) but the a_H values are affected much more i.e. 25–30% of the a_H value. It is noteworthy that a negative spin density on the carbon atom of the carbonyl group was found for acyl-aminyloxides, in agreement with literature data.[36]

The difference between the a_N splittings in the E (IV) and Z(V) forms was rationalized by the larger dipole repulsion in the latter conformation between the carbonyl and aminyloxide dipoles; as a result the contribution of the second resonance structure with dipolar aminyloxide groups (VIII B)

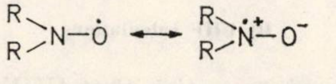

VIIIA VIIIB

is decreased in conformation Z, leading to an increased contribution of the second resonance structure with low a_N coupling. Indeed Table 2 indicates that the E conformation has a higher polarity than the Z conformation for acyl-aminyloxides.

In conclusion, the data from Table 1 show that a correct spin distribution can be calculated for the above series without modifying the

TABLE 2

Charge distributions in acetyl-phenyl-aminyloxides IV and V

Radical	q_N	$q_O^{(N-O)}$	q_C	$q_O^{(C-O)}$	Δq_N	$\Delta q_O^{(N-O)}$	Δq_C	$\Delta q_O^{(C-O)}$
IV(E)	1.399	1.564	0.619	1.455	0.600	−0.564	0.381	−0.455
V(Z)	1.443	1.482	0.667	1.404	0.557	−0.482	0.333	−0.404

parameters both for aminyloxides with nonpolar substituents (I) and with polar substituents (IV–VII) in various geometries.

AMINYLOXIDES WITH NITROSO GROUPS

A) McLachlan calculations

In order to obtain preliminary information on the spin distribution in radical II, McLachlan spin density calculations were performed. The large number of semiempirical parameters, namely eight, did not allow an exhaustive study of all the possible combinations of these parameters. The results obtained for several sets of parameters are listed in Table 3. For the aminyloxide group we used initially the parameters proposed by Someno et al.[30,35] for the radical I. As seen in Table 3, the spin density calculated for the aminyloxide group is too low in comparison with that found for radical I in contradiction with experimental data; secondly, the spin density on the nitroso nitrogen is practically zero. On attempting to improve this latter spin density, i.e. to obtain $\rho_{\mathrm{N}}^{\mathrm{N=O}} \cong 0.07-0.08$ by the increase of the k_{NO} value, the other spin densities $\rho_{\mathrm{N}}^{\mathrm{N-O}}$ and $\rho_{\mathrm{H}}^{\mathrm{ring}}$ become less satisfactory. This unfavourable effect of the new k_{NO} value on the ring and aminyloxide group spin densities can be corrected using simultaneously a larger value for the coulombian parameter of the oxygen atom.

Despite all these attempts, we failed in obtaining a satisfactory overall agreement between the calculated splittings and the experimental data; the $a_{\mathrm{N}}^{\mathrm{NO}}$ value in II remains smaller than in I.

B) UHF calculations

It was seen in a previous section that UHF calculations for aminyloxides devoid of nitroso groups led to a satisfactory consistent picture. On attempting to include into this series the aryl-N-nitroso-aminyloxides II or III, we stumbled on difficulties, therefore we shall discuss two models (two *versus* four π-electrons) for the nitroso group.

With the previous parameters for the aminyloxide group, and with parameters for the nitroso group corresponding to the structure $\dot{\mathrm{N}}-\dot{\mathrm{O}}$, the spin distribution calculated for radicals II (E) and III (Z), X=H, has the following salient features:

— A low spin density on the aminyloxide nitrogen, in disagreement with experimental data which show a higher a_{N} value in aryl-nitroso-nitroxides than in alkyl-aryl-aminyloxides.

— Low spin densities in the aryl ring ($a_{\mathrm{H}_{o,p}} \simeq 0.16$ mT).

— A negative spin density on the nitroso nitrogen.

The only parameters which influence positively the coupling constants are W_{N} and W_{O}; with the values for these parameters of -27.70 and -18.70 eV, respectively, corresponding to a higher positivation of nitrogen and a negativation of oxygen, the spin density on the nitroso oxygen is too high relative to the aminyloxide oxygen (0.38 and 0.16, respectively);

TABLE 3

McLachlan spin densities calculated for radicals I and (II−III) using different parameters for the aminyloxide group and experimental splittings (mT) ; $h_O(N{=}O) = 1.3$; $h_N(N{=}O) = 0.8$; $k_{NO}(N{=}O) = 1.3$; $h_N(N{-}O) = 1.5$

Radical		h_O	k_{NO}	k_{CN}	k_{NN}	N(N−O)	O(N−O)	N(N=O)	O(N=O)	ρ_{ortho}	ρ_{meta}	ρ_{para}
I R = H	ρ_{calc}	1.3	0.7	—	—	0.442	0.327	—	—	0.129	−0.058	−0.114
	a_{exp}	—	—	—	—	0.900	—	—	—	0.296	0.097	0.296
II−III	ρ_{calc}	1.3	0.7	1.1	0.9	0.265	0.288	0.004	0.162	0.106	−0.043	0.131
		1.3	1.0	1.0	0.7	0.282	0.450	0.036	0.138	0.071	−0.035	0.062
		1.3	1.2	1.1	0.7	0.239	0.433	0.070	0.158	0.073	−0.033	0.063
		1.4	1.0	1.1	0.7	0.303	0.358	0.029	0.141	0.103	−0.049	0.098
		1.4	1.2	1.1	0.7	0.265	0.387	0.061	0.157	0.083	−0.035	0.075
	a_{exp}	—	—	—	—	1.000	—	0.350	—	0.275	0.096	0.275

however, even with these extreme values, the spin density obtained for aminyloxide nitrogen is not higher than on the phenyl-aminyloxide I, R=H. Table 4 presents the results obtained for an intermediate situation, with $W_N = -28.70$ eV as in the other radicals but with $W_O = -18.70$ eV. A comparison of the spin densities for the two conformers (II and III) indicates that only the nitroso nitrogen is affected by the conformational change. In order to explain this influence, the contribution of the two mechanisms was calculated using Yonezawa's formulas [37,38] (spin polarization SP; spin delocalization SD):

$$(\rho_{aa})_{\mathrm{SP}} = 3(\rho_{\mathrm{UHF}} - \rho_{aa})/2$$

$$(\rho_{aa})_{\mathrm{SD}} = \rho_{aa} - (\rho_{aa})_{\mathrm{SP}}$$

Inspection of these values shows that for the nitroso nitrogen, the dominating mechanism for the apparition of spin density is the spin polarization. This may be explained by the vicinity of two positions with high α spin density, namely the nitroso oxygen and the aminyloxide nitrogen.

The two conformers II and III differ in their interaction between the nitroso oxygen and *ortho* position of the benzene ring as indicated in Table 5. Thus between the two oxygen and carbon atoms having α spin density, in the Z form (III) a repulsive interaction of 3.45 eV appears, whereas in the E form (II) the interaction is 5.60 eV. As a consequence, an opposite polarization (β) appears leading to an increase of β charge density on the nitroso oxygen, therefore a decrease of β charge density on the nitroso nitrogen.

From the four resonance structures of aryl-N-nitroso-aminyloxide, the forms XC and D are characteristic for the action of the nitroso group. Table 4 indicates indeed an increased polarity of the aminyloxide bond relative to other compounds.

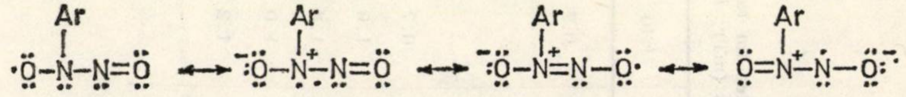

XA XB XC XD

The model which considers that the nitroso group contributes four electrons to the delocalized systems,[27] and which is less currently used, agrees with experimental data without raising the value of the oxygen parameter, which is, as in the other normal compounds, $W_O - 17.70$ eV. The aminyloxide nitrogen hyperfine splitting constant calculated with this model agrees perfectly with the experimental value, unlike the preceding case. The a_H splitting constants are practically unmodified and the only significant difference appears for the spin density on the nitroso

TABLE 4

Spin densities ρ, charge densities q, and hyperfine coupling constants a for N-nitroso-phenyl-aminyloxide in Z and E conformations (III and II, respectively, with X=H), and for the related compound IX[19]

Position	$\rho_{UHF.aa}$		$(\rho_{aa})_{SP}$		$(\rho_{aa})_{SD}$		q		$\lvert a_{calc}\rvert$(mT)		$\lvert a_{exp}\rvert$ (mT)	
	(E)	(Z)	(E)	(Z)	(E)	(Z)	(E)	(Z)	(E)	(Z)	II, III	IX
O(N=O)	0.296	0.320	0.087	0.097	0.209	0.223	1.199	1.122	—	—	—	—
N(N=O)	−0.076	−0.101	−0.116	−0.132	0.040	0.031	0.933	0.988	0.220	0.300	0.350	0.375
N(N−O)	0.403	0.406	0.027	0.029	0.376	0.376	1.214	1.226	0.800	0.800	1.000	1.020
O(N−O)	0.209	0.230	0.011	0.012	0.198	0.218	1.750	1.729	—	—	—	—
6(*o*)	0.090	0.085	0.033	0.034	0.053	0.046	0.970	0.998	0.243	0.229	0.275	0.253
7(*m*)	0.031	0.031	−0.033	−0.032	0.003	0.003	0.995	0.989	0.084	0.084	0.090	—
8(*p*)	0.075	0.070	0.036	0.035	0.037	0.035	0.933	0.941	0.202	0.189	0.275	0.213

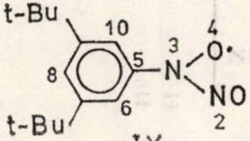

IX

TABLE 5

Charge densities of α and β spin on the nitroso group and *ortho* carbon atoms in the two conformers of phenyl-nitroso-aminyloxide

Conformer	Position	O(N=O)	N(N=O)	*ortho*
E(II)	q_α	0.833	0.313	0.565
	q_β	0.366	0.620	0.405
Z(III)	q_α	0.821	0.314	0.574
	q_β	0.301	0.674	0.424

nitrogen, for which a positive value is obtained, and for the nitroso oxygen which possesses a very low spin density.

Table 6 indicates also the hyperfine splitting constants obtained by this model for *para*-substituted N-nitroso-phenyl-aminyloxides either

TABLE 6

Spin densities ρ and hyperfine coupling constants a, in aryl-nitroso-nitroxides, obtained by Julg's model [27] without discriminating between rotamers II or III

X	Position	ρ	$\lvert a_{calc}\rvert$ (mT)	$\lvert a_{exp}\rvert$ (mT)
H	O (N=O)	0.011	—	—
IIa	N (N=O)	0.099	0.297	0.350
	N (N–O)	0.500	1.000	1.000
	O (N–O)	0.239	—	—
	6 (*o*)	0.090	0.243	0.275
	7 (*m*)	−0.027	0.073	0.090
	8 (*p*)	0.069	0.186	0.275
OCH_3	O (N=O)	0.010	—	—
IIb	N (N=O)	0.098	0.294	0.343
	N (N–O)	0.515	1.035	1.030
	O (N–O)	0.221	—	—
	6 (*o*)	0.088	0.238	0.343
	7 (*m*)	−0.023	0.062	—
NO_2	O (N=O)	0.014	—	—
IIc	N (N=O)	0.107	0.321	0.245
	N (N–O)	0.431	0.840	0.900
	O (N–O)	0.300	—	—
	6 (*o*)	0.084	0.227	0.245
	7 (*m*)	−0.020	0.054	0.081
	N (NO_2)*	−0.004	0.092	0.160
	O (NO_2)	0.007		

---

* $a_{NO_2} = 9.9\rho_N^\pi - 3.55\ \Sigma\rho_O^\pi$

with a donor (OCH_3) or with an acceptor substituent (NO_2). The trend of the calculated splitting constants for the aminyloxide nitrogen is correct (the substitution affects strongly the spin density of the aminyloxide oxygen too, but in the absence of ^{17}O labelling this spin density cannot be compared with an experimental value). However, the calculated spin densities on the nitroso nitrogen, on the hydrogens and on the *p*-nitro group are less satisfactory.

CONCLUSION

The spin density calculations performed explain the variation of the a_N values for all radicals which were studied. A particular problem is raised by the N-nitroso-aminyloxides. The possible explanation for the larger a_N value than that in radical **I**, consisting in a sterical effect, does not account for the observed facts. Though a sterical shielding around the aminyloxide group could cause a decrease in the π conjugation between the ring and the nitrogen atom, hence a higher localization of the odd electron on this nitrogen, all the theoretical models based on this idea led to a reduction of a_{N}^{NO} in **II** relative to **I**. An adequate spin density pattern for radical **II** was obtained only when we considered an increase in the ionization potential of the oxygen atom. Although Julg's model has seldom been applied, we consider that in our case it can be favoured owing to the proximity of the nitroso group to a strongly positivated position (the aminyloxide nitrogen).

REFERENCES

[1] M. J. S. Dewar, *J. Amer. Chem. Soc.*, **74,** 3353 (1952).

[2] Review : A. T. Balaban, *Rev. Roumaine Chim.*, **16,** 725 (1971).

[3] A. T. Balaban, P. T. Frangopol, M. Mărculescu and I. Bally, *Tetrahedron*, **13,** 258 (1961).

[4] A. T. Balaban, M. Mărculescu, I. Pascaru, M. Rotaru, A. Valeriu and M. Weiner, *Z. phys. Chem. (Leipzig)*, **219,** 285 (1962).

[5] A. T. Balaban, P. T. Frangopol, M. Frangopol and N. Negoiţă, *Tetrahedron*, **23,** 4661 (1967).

[6] N. Negoiţă, R. Baican and A. T. Balaban, *Tetrahedron*, **30,** 73 (1974).

[7] R. Istrăţoiu, I. Pascaru and A. T. Balaban, *Z. Naturforsch.* **28b,** 543 (1973).

[8] N. Negoiţă, R. Baican and A. T. Balaban, *Tetrahedron Letters*, **1973,** 1877.

[9] A. T. Balaban, N. Negoiţă and R. Baican, *Chem. Phys. Letters*, **24,** 30 (1974).

[10] A. T. Balaban and R. Istrăţoiu, *Tetrahedron Letters*, **1973,** 1879.

[11] R. W. Baldock, P. Hudson, A. R. Katritzky and F. Soti, *J. Chem. Soc. Perkin I*, **1974,** 1422 ; A. R. Katritzky and F. Soti, *ibid.* **1974,** 1427 ; *Heterocycles*, **1,** 67 (1973).

[12] L. Stella, Z. Janousek, R. Merenyi and H. G. Viehe, *Angew. Chem.*, **90,** 741 (1978) ; *Angew. Chem. Int. Ed. Engl.*, **17,** 691 (1978).

[13] H. G. Aurich, E. Deuschle and W. Weiss, *J. Chem. Research, (S)*, **1977,** 301 ; *(M)*, **1977,** 3457.

[14] Z. Janousek, F. Huys, L. René, M. Masquelier, L. Stella, R. Merenyi and H. G. Viehe, *Angew. Chem.*, **91,** 651 (1979) ; *Angew. Chem. Int. Ed. Engl.*, **18,** 616 (1979) ; H. G. Viehe, R. Merenyi,, L. Stella and Z. Janousek in press.

[15] L. de Vries, *J. Org. Chem.*. **38,** 2604, 4357 (1973) ; *J. Amer. Chem. Soc.*, **99,** 1982 (1977) ; **100,** 926 (1978) ; T. H. Koch, *J. Amer. Chem. Soc.*, **101,** 2750 (1979) ; N. E. Heimar, *J. Org. Chem.*, **42,** 3767 (1967).

[16] A. T. Balaban, I. Pascaru and F. Cuiban, *J. Magnetic Resonance.* **7,** 241 (1972).

[17] A. T. Balaban, H. G. Aurich, J. Trosken, E. Brugger, D. Döpp and K. H. Sailer, *Tetrahedron*, **30,** 739 (1974).

[18] A. T. Balaban and N. Negoiţă, *Rev. Roumaine Chim.*, **17,** 1227 (1972) ; A. T. Balaban, N. Negoiţă and I. Pascaru, *ibid.*, **16,** 721 (1971).

[19] M. T. Căproiu, N. Negoiţă and A. T. Balaban, *Tetrahedron Letters*, **1977,** 1825.

[20] A. T. Balaban, N. Negoiţă and R. Baican, *J. Magnetic Resonance*, **9,** 1 (1973).

[21] A. Mackor, T. A. J. W. Wajer and T. J. de Boer, *Tetrahedron*, **24,** 1623 (1968).

[22] H. G. Aurich, J. Trosken and H. Forster, *Angew. Chem.*, **83,** 892 (1971).

[23] A. T. Amos and J. Snyder, *J. Chem. Phys.*, **41,** 1773 (1964) ; **42,** 3670(1964).

[24] M. Hillebrand and V. E. Sahini, *Bull. Inst. Politechnic Bucureşti, Seria Chimie—Metalurgie*, **40,** 23 (1978).

[25] M. Mataga and K. Nishimoto, *Z. phys. Chem.*, **13,** 140 (1957).

[26] R. Pariser and R. Parr, *J. Chem. Phys.*, **21,** 767 (1953).

[27] A. Julg, "Chimie Quantique", chapter 5, Dunod, Paris, 1967.

[28] N. Singer and P. R. Whittingten, *Tetrahedron*, **26,** 3731 (1970).

[29] P. B. Ayscough and F. B. Sargent, *J. Chem. Soc. B.*, **1966,** 907.

[30] O. Kikuchi and K. Someno, *Bull. Chem. Soc. Japan*, **40,** 2549 (1967).

[31] H. G. Aurich and H. Czepluch, *Tetrahedron Letters*, **1978,** 1187 ; H. G. Aurich, H. Czepluch and K. Hahn, *ibid.*, **1977,** 4373 ; H. G. Aurich, K. Hahn, K. Stork and W. Weiss, *Tetrahedron*, **33,** 969 (1977).

[32] J. Ladik, G. Biczo, I. Kande and L. Sumegi, *Acta Chimica Acad. Scient. Hung.*, **61,** 381 (1969).

[33] J. Tino and V. Klimo, *Coll. Czech. Chem. Comm.*, **41,** 960 (1976).

[34] O. Kikuchi, *Bull. Chem. Soc. Japan*, **42,** 2881 (1969).

[35] T. Nishikawa and K. Someno, *Bull. Chem. Soc. Japan*, **47,** 1472 (1974).

[36] T. J. Jenkins, M. J. Perkins and B. Terem, *Tetrahedron Letters*, **1978,** 2925.

[37] T. Yonezawa, H. Nakatsuji, T. Kawamura and H. Kato, *J. Chem. Phys.*, **51,** 669 (1969).

[38] H. Nakatsuji, H. Kato and T. Yonezawa, *J. Chem. Phys.*, **51,** 3175 (1969).

Revue Roumaine de Chimie, 25, 7, 1007—1010(1980)

Dedicated to Professor CRISTOFOR I. SIMIONESCU
on his 60th anniversary

TERMINATION OF VINYL POLYMERIZATION BY TRANSITION METAL IONS

A.D. JENKINS
School of Molecular Sciences
University of Sussex, Brighton BN1 9QJ, Sussex, England

Received January 23, 1980

A short review is presented, summarizing the current state of knowledge regarding the participation of the ions of transition metals in high oxidation states in termination reactions with the radicals present in the polymerizations of several vinyl monomers.

One of the earliest methods to be suggested for the polymerization of vinyl monomers on a large scale was by application of redox initiation systems in aqueous media.[1] The polymerization of acrylonitrile lends itself to such a technique because of the relatively high solubility of this monomer in water.

Among the available redox radical-generating systems, the Fenton reagent's combination of ferrous salt and hydrogen peroxide proved popular, no doubt because its component chemicals were cheap, readily available and free from serious toxic or other hazard. In the presence of normal concentrations of monomer, the only significant reaction of this system [2] is

$$Fe^{2+} + H_2O_2 \rightarrow Fe^{3+} + OH^- + \cdot OH$$

A little later, transition metal salts also attracted attention as a result of their suitability for use as photosensitizers of polymerization in aqueous media,[3-6] such systems being very valuable for kinetic studies of the detailed mechanism of polymerization reactions. Although useful for investigations of aqueous reactions, the very limited solubility of vinyl monomers in water restricts the utility of this technique in revealing the fine details of the chemistry of polymerization processes : the heterogeneity of such systems intrinsically complicates the kinetics [7] and it destroys constancy of rate of photo-initiation.

For these reasons, and also to permit comparative studies to be made of a wide variety of monomers in uniformly homogeneous conditions, attention was also directed to studies in solvents which had the ability to maintain initiator, monomer, polymer and salt in solution. The medium employed has mostly been N, N-dimethylformamide (DMF)[8-10] but a few studies in dimethylsulphoxide (DMSO) have also been made.[11]

In DMF, photo-initiation with sensitization by, for example, iron (III) salts is also a useful technique but, as in aqueous solution, the reaction may be complicated by participation of Fe^{3+} in termination processes.[12] These latter reactions are of particular interest, qualitatively because they offer a simple means for the control of rate and degree of polymerization (In favourable cases, a useful way of stabilizing a monomer during storage, one which admits of simple monomer purification by distillation) and quantitatively because they constitute an unusual type of process for the study of the influence of substituents on polymer radicals on reactivity. Such studies have been of interest since the advent of the Q-e scheme [13,14] and, more especially, in the light of the Patterns of Reactivity interpretation.[15-18]

If the Fe(III) species is used as an example, the reaction scheme for a polymerization initiated by thermal decomposition of an initiator C, incorporating termination between polymer radicals and Fe(III) ions, must, at a minimum, comprise the following reactions, where R and X represent, respectively, primary and polymer radicals, M denotes monomer, and cognizance is taken of the wastage of a fraction of the initiator by decomposition *via* routes which do not produce useful radicals, k being the specific velocity constant for overall initiator decomposition and k_i the specific velocity constant for the reaction producing primary radicals.

$$C \xrightarrow{k_i} 2R \tag{1 a}$$

$$C \xrightarrow{(k-k_i)} \text{inert products} \tag{1b}$$

$$R + M \longrightarrow X_1 \tag{2}$$

$$X_n + M \xrightarrow{k_p} X_{n+1} \tag{3}$$

$$X_n + X_n \xrightarrow{k_t} \text{polymer} \tag{4}$$

$$X_n + \text{Fe(III)} \xrightarrow{k_s} \text{polymer} + \text{Fe(II)} \tag{5}$$

With methyl acrylate, methyl methacrylate, acrylonitrile or methacrylonitrile as monomer, the Fe (III) species, in the form of added $FeCl_3$, acts as an ideal retarder [8,12] to the point where, at relatively high concentrations ($[FeCl_3] \sim 10^{-3}$, $[C] \sim 10^{-2}$M), reaction (5) overwhelms (4). This has two important kinetic consequences : (a) every primary radical used in reaction (2) ultimately generates Fe(II). This provides a most useful method [12] for the determination of the rate of initiation by simple analysis for Fe(II). (b) The rate of reaction (w) corresponds to the equation

$$w = \frac{k_p\,[M]\,I}{k_s[\text{Fe(III)}]}$$

where $I = 2k_i\,[C]$. The rate is then directly proportional to [C] and inversely proportional to [Fe(III)].

With styrene or vinyl acetate as the monomer, polymerization is inhibited[8,12]; the reaction with styrene has been studied in some detail and a new method for the determination of k_5 from an analysis of the reaction immediately following the end of the inhibition period has been described.[12]

The only other terminating species to have been examined in any detail is Cu(II).[9,19–23] For the most part, the reaction is parallel to that of Fe(III) but the reactivity of Cu(II) is at a markedly higher level, as a very rough guide, some 50 times greater. In consequence, the reactions of all six monomers mentioned above are inhibited if $[C] \sim 10^{-2}$, $[\mathrm{Cu(II)}] \sim \sim 10^{-3}$M. It has been possible to obtain k_5 values for all the monomers listed, with the exception of vinyl acetate, but in the case of two of them, acrylonitrile[20,23] and methyl acrylate,[23] a new kinetic feature is apparent in that the steady rate achieved after the acceleration at the end of the inhibition period is less than would be expected, even when allowance is made for depletion of inhibitor during the time which has elapsed up to the point at which a steady rate is attained. Furthermore, the higher the initial concentration of Cu(II), the lower is the ultimate steady rate.

The only explanation of this phenomenon seems to be that the product of reaction between polymer radicals and Cu(II), presumably Cu(I), is a retarder so one must, in these cases, add to the appropriate form of equation (5)

$$X_n + \mathrm{Cu(II)} \xrightarrow{k_5} \text{polymer} + \mathrm{Cu(I)}$$

a further reaction

$$X_n + \mathrm{Cu(I)} \xrightarrow{k_6} \text{polymer}. \qquad (6)$$

With the inclusion of this process, the full reaction scheme is essentially that proposed by Bengough and Fairservice.[20]

It is essential to note the identity of the anion component of the transition metal salt. It appears that Fe(III) or Cu(II) is most effective in the form of chloride or bromide, but that other anions considerably lower reactivity[23,24]; there is some evidence from aqueous systems that the bromide is far more effective than the chloride (cf. reference [24]) and in this case sulphate, nitrate and acetate are inert.[25]

In view of this influence of anion, it is important to ensure that the interpretation of all the results above in terms of reaction with the metal component is valid. Accordingly, a study of the effect of a simple main group salt, lithium cholride, on the polymerization of acrylonitrile in DMF was made.[26] It was found that both lithium and chloride ions can complex with and modify the reactivity of the polyacrylonitrile radicals but that the effect of the chloride ion would be absolutely negligible at the concentrations employed in the work with Fe(III) and Cu(II) salts.

Despite this latter result, it is necessary to consider carefully the true nature of the species present in solutions of these salts in DMF. Dass and George[10,11,27,28] have made a detailed examination of these systems from which it is clear that the species present when $FeCl_3$ is dissolved in DMF include $\mathrm{Fe(DMF)_6^{3+}}$, $\mathrm{Fe(DMF)_5Cl^{2+}}$, $\mathrm{Fe(DMF)_4Cl_2^+}$ and $\mathrm{FeCl_4^-}$, of which the last three all react rapidly with polystyryl radicals. DMSO is a stronger ligand for Fe^{3+} than is DMF, and in DMSO as solvent the situation is broadly similar but $Fe(DMSO)_4Cl_2^+$ is not observed to exist.

When polymerization reactions are performed in the presence of $FeCl_3$ and with various added amounts of LiCl, it is found that the greater the LiCl concentration, the more sharp is the transition between inhibition and steady rate. Since an abrupt discontinuity corresponds to $k_5 = \infty$, it is clear that the effective value of k_5 is increased by the addition of lithium chloride, and, since k_5 for $Fe(DMF)_5Cl^{2+}$, $Fe(DMF)_4Cl_2^+$ and $FeCl_4^-$ are not vastly different from one another but all much greater than that for $Fe(DMF)_6^{3+}$, it must be concluded that, in the absence of LiCl, a substantial proportion of the Fe(III) is in the form of $Fe(DMF)_6^{3+}$.

Further studies of these interesting systems are in progress; some preliminary results with $NiCl_2$ show that Ni(II) can also take part in reactions similar to (5) but at a much reduced rate compared to Fe(III) or Cu(II).[29]

In the field of vinyl polymerization in the presence of metal salts, as in so many other areas of polymer science, Academician Professor Cristofor Simionescu was one of the first to contribute, and the present author is delighted to pay tribute to his personal friend and respected colleague on his 60th anniversary.

REFERENCES

[1] R. G. R. Bacon, *Quart. Rev.*, **9**, 287 (1955).
[2] J. G. Baxendale, M. G. Evans and J. H. Kilham, *Trans. Faraday Soc.*, **42**, 668 (1946).
[3] M. G. Evans, M. Santappa and N. Uri, *J. Polymer Sci.*, **7**, 243 (1951).
[4] F. S. Dainton and D. G. L. James, *Disc. Faraday Soc.*, **14**, 244 (1953).
[5] F. S. Dainton, P. H. Seaman, D. G. L. James and R. S. Eaton, *J. Polymer Sci.*, **34**, 209 (1959).
[6] C. Simionescu, D. Feldman and S. Oprea, *J. App. Polymer Sci.*, **8**, 447 (1964).
[7] C. H. Bamford and A. D. Jenkins, *Proc. Roy. Soc.*, **A216**, 515 (1953).
[8] C. H. Bamford, A. D. Jenkins and R. Johnston, *J. Polymer Sci.*, **29**, 355 (1958).
[9] W. I. Bengough and W. H. Fairservice, *Trans. Faraday Soc.*, **61**, 1206 (1965).
[10] N. N. Dass and M. H. George, *J. Polymer Sci. (B)*, **5**, 1119 (1967).
[11] N. N. Dass and M. H. George, *European Polymer J.*, **6**, 897 (1970).
[12] C. H. Bamford, A. D. Jenkins and R. Johnston, *Proc. Roy. Soc.*, **A239**, 214 (1957).
[13] T. Alfrey and C. C. Price, *J. Polymer Sci.*, **2**, 101 (1947).
[14] C. C. Price, *J. Polymer Sci.*, **3**, 772 (1948).
[15] C. H. Bamford, A. D. Jenkins and R. Johnston, *Trans. Faraday Soc.*, **55**, 418 (1959).
[16] C. H. Bamford and A. D. Jenkins, *J. Polymer Sci.*, **53**, 149 (1961).
[17] C. H. Bamford and A. D. Jenkins, *Trans. Faraday Soc.*, **59**, 530 (1963).
[18] A. D. Jenkins, Chapter 4 in "Reactivity, Mechanism and Structure in Polymer Chemistry", ed. A. D. Jenkins and A. Ledwith Wiley, London, 1974.
[19] W. I. Bengough and I. C. Ross, *Trans. Faraday Soc.*, **62**, 2251 (1966).
[20] W. I. Bengough and W. H. Fairservice, *Trans. Faraday Soc.*, **63**, 382 (1967).
[21] W. I. Bengough and T. O'Neill, *Trans. Faraday Soc.*, **64**, 1014 (1968).
[22] W. I. Bengough and T. O'Neill, *Trans. Faraday Soc.*, **64**, 2415 (1960).
[23] N. C. Billingham, A. J. Chapman and A. D. Jenkins, *J. Polymer Sci.*, in press.
[24] E. R. Entwistle, *Trans. Faraday Soc.*, **56**, 284 (1960).
[25] M. Watanabe and H. Kiuchi, *J. Polymer Sci.*, **58**, 103 (1962).
[26] C. H. Bamford, A. D. Jenkins and R. Johnston, *Proc. Roy. Soc.*, **A241**, 364 (1957).
[27] N. N. Dass and M. H. George, *J. Polymer Sci. (A—1)*, **7**, 269 (1969).
[28] N. N. Dass and M. H. George, *European Polymer J.*, **7**, 1185 (1971).
[29] N. C. Billingham, A. D. Jenkins and B. H. Mustafa, unpublished results.

Revue Roumaine de Chimie, 25, 7, 1011–1015(1980)

Dedicated to Professor CRISTOFOR I. SIMIONESCU
on his 60th anniversary

SYNTHETIC MACROMOLECULES AS THERAPEUTIC AGENTS

ADRIANE G. LUDWICK[a] and C. G. OVERBERGER
Department of Chemistry and the Macromolecular Research Center
The University of Michigan, Ann Arbor, Michigan 48109, USA

Received January 23, 1980

Potentially therapeutic compounds synthesized in our laboratory are discussed. Copolymers of maleic acid with vinylimidazoles or vinyl-2-pyrrolidone; terpolymers of maleic acid, vinylimidazoles and vinylpyrrolidone; branched and linear polyethylenimine polymers to which amino acids and/or nucleic acid bases have been grafted; polymers of 2-amino-2-methylpropylacrylamide with amino acid grafts and analogously grafted copolymers of the acrylamide with N-vinylimidazole or N-vinylpyrrolidone have been screened against L-1210 lymphoid or P388 lymphocyte leukemia. Less than ten percent of these polymers showed significant activity. A detailed, systematic study of the biological activity of such polymers is desirable.

The use of synthetic macromolecules as therapeutic agents is a promising area. As an example, poly(9-vinyladenine) and related nucleic acid base substituted polyvinyl compounds have been tested for biological activity.[1–4] Poly(9-vinyladenine) has been shown to selectively inhibit the replication of exogenous murine leukemia virus in primary mouse embryo cells. However, it does not effect the induction of endogenous murine leukemia virus by 5-iodo-2′-deoxyuridine nor the replication of lytic RNA viruses. Most recently it has been shown to interfere with the replication of Friend leukemia virus in mice. The mechanism of action was shown not to be through enhancement of the host immune response system nor through interferon induction. Instead, the inhibition by these electroneutral polymers is deduced to be caused by direct inhibition of some important early step in the viral replication mechanism.

The biological activity of the maleic anhydride-divinyl ether copolymer systems (pyran-type systems) has been studied even more extensively.[5] Pyran-type systems have been shown to be effective against a number of murine leukemias as well as solid tumors. The toxicity of the systems is directly proportional to molecular weight. Hence considerable work has been concerned with the therapeutic value of various molecular weight fractions. A molecular weight of 15,000 appears to be the toxicity limit.

---

[a] Permanent address: Department of Chemistry, Tuskegee Institute, Alabama 36088, USA.

The mechanism of action of these polyanions is probably analogous to that of another class of polyanions, the polynucleotides (*e.g.*, polyadenylic acid). They affect the immune response system of the host and are interferon inducers. Hence their role as therapeutic agents could well become complementary to that of the polyvinyl nucleotides.

In our laboratory, we have achieved the synthesis of a number of potentially therapeutic compounds. Most of these have been initially screened at the National Cancer Institute in Bethesda, Maryland USA. From this a small number have been judged as potentially active. However, no detailed biological study of our compounds has been made to date.

Initial work involved the copolymers of maleic acid with vinylimidazoles or vinyl-2-pyrrolidone. Terpolymers of maleic acid, vinylimidazoles and vinylpyrrolidone were also prepared (Figure 1).[6] These polymers (**1** a-c and **2** a, b) have shown only insignificant activity when screened against L-1210 lymphoid leukemia and no activity against human epidermoid carcinoma in a cell culture test. In a test to determine if this type of polymer would inhibit the reverse transcriptase of murine leukemia virus, a 1 : 1 copolymer of 1-methyl-5-vinyl-imidazole and 4(5)-vinylimidazole was found to be as good an inhibitor as poly-(9-vinylpurine) and about one order less effective than poly(N-vinylimidazole).[7]

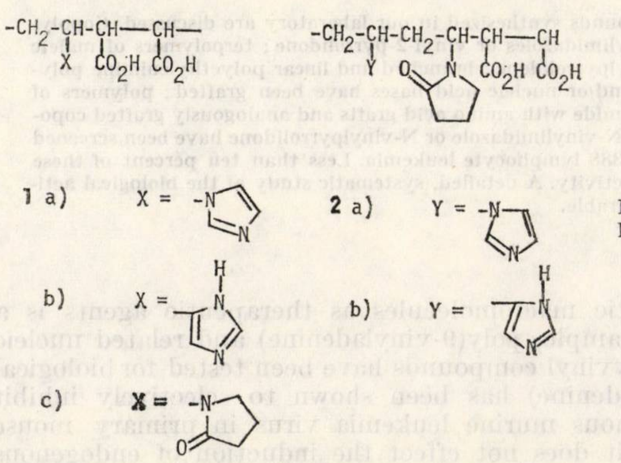

Fig. 1. — Copolymers and terpolymers of maleic acid, vinylimidazoles and vinylpyrrolidone.

The success of T. D. Perrine in an examination of his compounds for antitumor activity directly influenced the work of our laboratory. The Sloan-Kettering Institute for Cancer Research found his terpolymer of N-vinylpyrrolidone, maleic anhydride and *para*-acetoxystyrene with monomeric grafts of L-serine and L-histidine to inhibit Ehrlich ascites tumor very effectively. An analogous result was found for a branched polyethylenimine of unknown molecular weight with monomeric grafts of L-serine and L-histidine.[8] Both these polymers were found to have negligible toxicity. The terpolymer without grafts was also found to be non-toxic. However, the branched polyethylenimine without grafts was determined to be quite toxic.

Since these results, we have undertaken the examination of a number of branched and linear polyethylenimine polymers to which amino acids [9] and/or nucleic acid bases [10] have been grafted (Tables 1 and 2). Of the forty-eight compounds listed, five were found to have activity during initial screening: **11, 32, 47, 48** and **49**. Compound **11** showed activity against L-1210 lymphoid leukemia. Compounds **32, 47, 48** and **49** were active against P388 lymphocyte leukemia. However, slight variations in testing rendered their activity insignificant. For example, **47, 48** and **49** were active when the hosts were a BDF$_1$ strain of mice. Changing to a CDF$_1$ strain resulted in insignificant activity. No further testing has been done yet on these compounds.

TABLE 1

Polyethylenimine (PEI) Polymers with Amino Acid Nucleic Acid Base Grafts

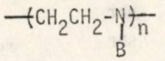

$$-\!\left(CH_2CH_2-\underset{B}{N}\right)_n\!-$$

Compound No.	PEI Backbone, n	Graft [a] B
3	45 (linear)	asp(NH$_2$)
4	80 (linear)	asp(NH$_2$)
5	815 (branched)	asp(NH$_2$)
6	1725 (branched)	asp(NH$_2$)
7	45 (linear)	[asp(NH$_2$)]$_5$
8	80 (linear)	[asp(NH$_2$)]$_5$
9	45 (linear)	asp
10	80 (linear)	asp
11	815 (branched)	asp
12	1725 (branched)	asp
13	45 (linear)	(asp)$_5$
14	80 (linear)	(asp)$_5$
15	45 (linear)	ser
16	80 (linear)	ser
17	815 (branched)	ser
18	1725 (branched)	ser
19	45 (linear)	(ser)$_5$
20	80 (linear)	(ser)$_5$
21	815 (branched)	(ser)$_5$
22	1725 (branched)	(ser)$_5$
23	45 (linear)	his
24	80 (linear)	his
25	815 (branched)	his
26	1725 (branched)	his
27	45 (linear)	(his)$_5$
28	80 (linear)	(his)$_5$
29	815 (branched)	(his)$_5$
30	1725 (branched)	(his)$_5$
31	60 (linear)	Ad
32	40 (branched)	Ad
33	815 (branched)	Ad
34	1725 (branched)	Ad
35	60 (linear)	Th
36	40 (branched)	Th
37	815 (branched)	Th
38	1725 (branched)	Th
39	60 (linear)	ala-Ad
40	60 (linear)	ala-Th
41	60 (linear)	asp-Ad
42	60 (linear)	asp-Th
43	60 (linear)	ser-Ad
44	60 (linear)	ser-Th
45	60 (linear)	his-Ad
46	60 (linear)	his-Th

[a] asp(NH$_2$): L-asparagine; asp = L-aspartic acid; ser = L-serine; his = L-histidine; Ad = adenine; Th = thymine.

TABLE 2

Polyethylenimine (PEI) copolymers with amino acid grafts

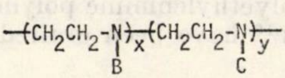

$$-\!\!\left(CH_2CH_2\text{-}\underset{B}{N}\right)_x\!\!-\!\!\left(CH_2CH_2\text{-}\underset{C}{N}\right)_y\!\!-$$

Compound No.	PEI Backbone		Graft [a]	
	x	y	b	c
47	22	22	his	ser
48	40	40	his	ser
49	410	410	his	ser
50	860	860	his	ser

[a] His = L-histidine; ser = L-serine.

Polymers of 2-amino-2-methylpropylacrylamide (**51**) with aspartic acid or serine grafts and copolymers of **51** with N-vinylimidazole or

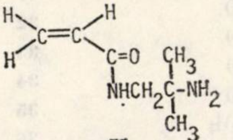

51

N-vinylpyrrolidone have been synthesized.[11] Both copolymers also had aspartic acid or serine grafts. None of these compounds showed significant activity when tested against L-1210 lymphoid leukemia.

Most recently we have examined a linear polyethylenimine system with a chiral nucleic acid base graft (**52**).[12] Spectroscopic studies (UV, CD) indicate

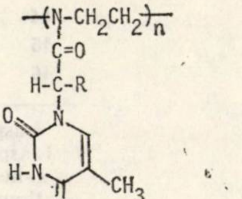

52 a) R = CH_3

b) R = $(CH_3)_2CH$

52a is helical with significant base stacking. The racemic adenine graft corresponding to **52a** has also been synthesized. Significant hypochromicity (45%) relative to a model compound has been measured for this compound in aqueous solution. Currently work is under way to synthesize **52b** and the corresponding adenine graft. The bulkier isopropyl group should further restrict rotation about the $-\underset{\underset{O}{\|}}{C}-CHR-$ bond, thereby increasing the population of the conformation in which base stacking occurs. Additionally, the synthesis of the guanine and uracil grafts of **52a** is in progress. These compounds will be submitted for testing against encephalomyocarditis virus and Moloney leukemia virus as well as to determine if they inhibit the influenza virion-associated transcriptase or exhibit cytotoxicity in L-cells.[13]

In addition to these examples cited from our laboratory, the literature indicates many analogous systems. For example, recent reviews on nucleic acid models[14,15] show the diversity as well as the immense number of such compounds. Remarkably only a small percentage of this type of compound has apparently been systematically tested for biological activity. It would seem worthwhile to repeat the sentiments of the Russian reviewers,[14] as well as the Pithas,[1,4] that such a study is necessary if one is to learn what parts of the system are desirable or not. While the possibility of a "magic bullet" macromolecule is perhaps remote, much untried ammunition is available.

ACKNOWLEDGEMENTS. One of us (AGL) is indebted to the National Institutes of Health (Grant 1 F34 GMO6579—01) and the National Science Foundation (Grant SPI 78—19121) for financial support while on leave from Tuskegee Institute. The paper is submitted on the occasion of the 60th birthday of Professor Simionescu.

REFERENCES

[1] J. Pitha, *Polymer*, **18**, 425 (1977) and references cited therein.

[2] J. Pitha, S. H. Wilson, and P. M. Pitha, *Biochem. Biophys. Res. Commun.*, **81**, 217 (1978).

[3] V. E. Vengris, P. M. Pitha, L. L. Sensenbrenner, and J. Pitha, *Mol. Pharmacol.*, **14**, 271 (1978).

[4] P. M. Pitha and J. Pitha, *Pharmac. Ther. A*, **2**, 247 (1978).

[5] M. A. Chirigos, Ed., "Proceedings of the Fourth Conference on Immune Modulation and Control of Neoplasia by Adjuvant Therapy, Division of Cancer Cause and Prevention", National Cancer Institute, March 29—31, 1978, Bethesda, Maryland USA, as reported in *Cancer Treat. Rep.*, **62**, 1791 (1978).

[6] C. Messing and C. G. Overberger, unpublished results ; see C. G. Overberger and Y. Kawakami, *Y. Polym. Sci., Polym. Chem. Ed.*, **16**, 1237, 1249 (1978) for details on the syntheses of poly(vinylimidazoles).

[7] J. Pitha, National Institutes of Health, private communication, December 5, 1975.

[8] T. D. Perrine, National Institutes of Health, private communications, December 3, 1969 and January 19, 1970.

[9] K. W. Dixon, Ph. D. Dissertation, The University of Michigan, Ann Arbor, Michigan USA, 1974.

[10] C. G. Overberger and Y. Inaki, *J. Polym. Sci., Polym. Chem. Ed.*, **17**, 1739—1758 (1979) and C. G. Overberger, Y. Inaki, and Y. Nambu, *J. Polym. Sci., Polym. Chem. Ed.*, **17**, 1759 (1979).

[11] M. S. Chi and C. G. Overberger, unpublished results.

[12] Y. Morishima and C. G. Overberger, *J. Macromol. Sci.-Chem.*, **1979**, 573 ; C. G. Overberger, Y. Inaki, and Y. Morishima, *Polymer Preprints*, **20**, (1979). C. G. Overberger and Y. Morishima, *J. Polym. Sci., Polym. Chem. Ed.*, in press.

[13] N. Stebbing, Searle Research Laboratories, private communication, October 30, 1979.

[14] Z. A. Shomshtein and S. A. Giller, *Chem. Heterocyclic Comp.*, **12**, 27 (1976).

[15] S. Hoffmann, *Z. Chem.*, **19**, 241 (1979).

Revue Roumaine de Chimie, 25, 7, 1017–1024(1980)

Dedicated to Professor CRISTOFOR I. SIMIONESCU
on his 60th anniversary

THE INTERPRETATION OF THE KINETIC DATA CONCERNING THE Zn^{2+} LINKING AND ELUTION ON ION EXCHANGE MEMBRANES

F. MATEI, AL. DUCA, GH. IONESCU and M. MACOVEANU

Department of Analytical Chemistry, Department of Physical Chemistry and Department of Chemical Engineering, Polytechnic Institute Iași, 71 Splai Bahlui, Romania

Received January 22, 1980

By using the diffusion theory through the liquid film which is formed at the solution/ions exchange membranes contact, the equations of the linking degree-time and elution degree-time functions have been deduced. These equations, settled in linear coordinates, have been used for the interpretation of the kinetic data regarding the Zn^{2+} linking and elution both from sulphuric acid solutions and with sulphuric acid solutions of optimal concentrations, respectively. To calculate the linking and elution degree at a given moment by these equations, a computer programme has been prepared.

1. INTRODUCTION

The use of the ion exchange membranes in the processes of separation and concentration of small amounts of electrolytes or non-electrolytes and their analytical aspects have been dwelled on in several studies.[1–7]

A number of important theoretical and experimental studies have been dedicated both to the physico-chemical processes from the ion exchange membranes and to the determination of the characteristics for these processes. As far back as 1956 Schlögl [8] classified the theories concerning the ion exchange membranes properties in three groups, function of the physical and mathematical model, on the basis of which these theories have been devised (see also [9]). The mentioned theories are concerned with the equilibrium of ion exchange on ion exchange membranes,[3] with substance transfer through ion exchange membranes [10–17] and with membrane potential.[18–21] Obviously, there is not any distinct boundary between these three domains, but a certain interconnection.

The linking and elution of ions on ion exchange membranes, which do not imply the ions crossing through the membrane, are, however, compound processes. The linking process implies the ion diffusion through solution towards the ion exchange membranes, the crossing of the Nernst diffusion layer, the carrying on diffusion through the ion exchange membranes (through the gel phase), and the ion exchange reaction. In the elution process the same ion travels through the way inversely. Following the general principle of electroneutrality of the ion exchange process, simultaneously with the ion flow which attaches or eludes there exists a flow of the opposite ions.

In a concrete case, the overall rate of the linking and elution process, respectively, can be decided by the rate of one of the above mentioned stages.

Previous studies [9,22] established that the kinetics of the ion exchange is controlled by the diffusion stages, namely, by the diffusion through the Nernst layer if the ions have a small radius and valence, by dilute solution, by relatively small flow or stirring rate both of this solution and of the diffusion through the gel phase if the ions are voluminous and polyvalent, by turbulent state of flow by nonaqueous solvents.[23]

In the paper [7] the behaviour of the Zn^{2+} and Co^{2+} ions in the linking and elution processes on C-10 Permaplex and C-20 Zerolit ion exchange membranes has been studied with the view of both their separation and their concentration in some eluents. The used experimental conditions make us suppose, from a kinetic point of view, that both the linking process on ion exchange membranes and the elution process have the rate determinated by the exterior diffusion (film diffusion).

2. THE KINETIC EQUATION OF THE EXTERIOR DIFFUSION PROCESS

The section of the concentration variation of the ion which attaches to the exchange membrane is shown in figure 1, where:

c = ion concentration in solution at the t moment;

c' = ion concentration at the film/membrane interface;

c_e = ion equilibrium concentration in the solid phase at film/membrane interface;

s = ion concentration in membrane at the t moment;

s_0 = initial ion concentration in membrane;

s_e = ion equilibrium concentration in membrane.

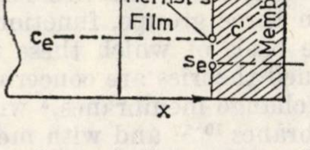

Fig. 1. — The variation of the ion concentrations through the ions exchange membrane.

The flux of the conveyed ion on an x direction perpendicular to the membrane, for the process of the exterior diffusion in the case of the admission of a linear concentration gradient in film, is given by the equation:

$$-\frac{dc}{dt} = \frac{D}{\delta}\,\frac{dc}{dx} = k(c - c') \qquad (1)$$

For the calculation of the c' value accepted as a mean concentration of the equilibrium composition in the membrane phase at the t moment [24] we have to know the isotherm of the ion exchange equilibrium. The determination of such an isotherm is a difficult problem requiring the knowledge of the activities of the ions which are changing both in the liquid and in the solid phase. To avoid such difficulties, some experimental ways which had to allow the substitution of the c' value have been suggested. One of these experimental ways consists in the use of some solution/membrane systems in which an insignificant increase in the concentration of the membrane has to correspond to an important decrease in the concentration in solution. Such systems correspond in fact to the content of the separation and concentration process by ion exchange membranes. As a result, c' will practically be considered a constant,, equal to the concentration of the equilibrium composition in the solide phase c_e. Thus the equation (1) becomes :

$$-\frac{dc}{dt} = k(c - c_e) \tag{2}$$

We can see from figure 1 that $s_e < c_e$. This inequality makes the difference $c_e - s_e$ (although small in the given experimental conditions) provide a concentration gradient of the ion which attaches to the ion exchange membranes, a gradient necessary to the diffusion of this ion from the membrane surface to its interior.

By integrating the equation (2), we get the following solution :

$$\ln (c - c_e) = - k \cdot t + q \tag{3}$$

By subtracting the expresion $\ln (c_0 - c_e)$ from both members of the equation (3), we obtain :

$$\ln \frac{c - c_e}{c_0 - c_e} = - k \cdot t + q - \ln (c_0 - c_e) \tag{4}$$

(c_0 = initial concentration in solution of the ion which attaches to the ions exchange membranes).

If c_0 is added to and subtracted from the numerator of the fraction, then the equation (4) can be modified as follows :

$$\ln \left(\frac{c - c_0}{c_0 - c_e} + 1 \right) = - k \cdot t + q - \ln(c_0 - c_e) \tag{5}$$

Defining the linking degree of the ion on the ion exchange membranes as the ratio $(c_0 - c)/(c_0 - c_e) = F$ and introducing the notation $p = q - \ln (c_0 - c_e)$, then the equation (5) becomes :

$$\ln \frac{1}{1 - F} = k \cdot t - p \tag{6}$$

To check the equation (6), we have to use, from the reference,[7] some experimental data concerning the Zn^{2+} linking from the solution of sulphuric acid on ions exchange membranes; these data are noted in table 1 and are graphically shown in figure 2.

TABLE 1

Experimental data regarding the Zn^{2+} linking

a) $c(H_2SO_4) = (0.1 \ldots 0.2)$ mol. l^{-1}

t, min.	0	15	30	60	120	180	200...∞
$\%Zn^{2+} = c$	$c_0 = 100$	39	26	15	7	3.6	$3 \ldots c_e = 2$
$\ln \frac{1\ 1}{1-F}$	—	0.974	1.407	2.020	2.976	4.115	4.585...∞

b) $c(H_2SO_4) = 0.5$ mol. l^{-1}

t, min.	0	30	60	90	180	250...∞
$\%Zn^{2+} = c$	$c_0 = 100$	85	79	74	63	60...55
$\ln \frac{1}{1-F}$	—	0.405	0.629	0.862	1.500	2.197...∞

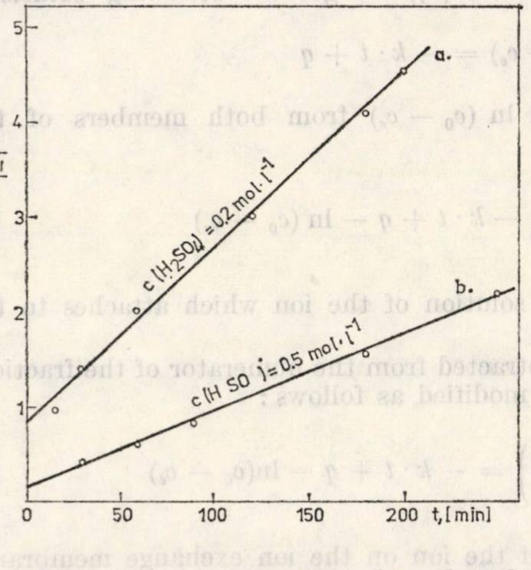

Fig. 2. — The linear diagram for the verification of the equation (6′).

It can be seen from these data that the equation (6) is independently checked of the concentration of the solvent from which the Zn^{2+} linking is made. The linking degree decreases with the increase of the concentration of the sulphuric acid. On a larger ion concentration domain, namely $0.2 \ldots 2)$ mol $\cdot$ l^{-1}, the linking rate ($d\,\%\,Zn^{2+}/dt$), as a function of the acid concentration and at a constant time, is presented in figure 3; it can be seen from here that Zn^{2+} ($c_0 = 10^{-3}$ mol · l^{-1}) does not practically attach to the ions exchange membranes used, starting with an acid concentration of approximately 2 mol · l^{-1}.

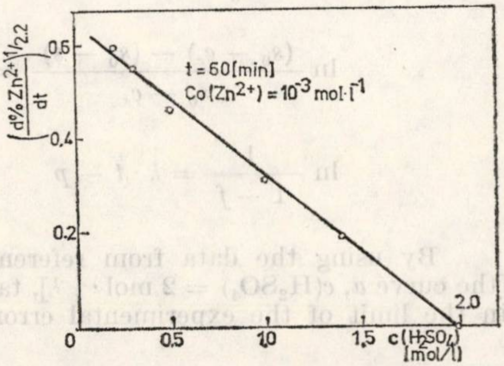

Fig. 3. — The linear diagram of the function linking rate-acid concentration.

The linearizing of this function is based on the consecutive processing of the experimental data and not on the theoretical considerations.

The $F(t)$ function is relatively complicated. To calculate the linking degree at a given moment, the equation of the straight line $\ln 1/(1 - F)$ — time has been obtained by statistical processing of the data from table 1, for the case "a" favorable to the Zn^{2+} linking. The equation is of the (6′) form, where t is to be considered in minutes:

$$\ln \frac{1}{1 - F} = 0.7906 + 1.873 \cdot 10^{-2} \cdot t \tag{6′}$$

For the elution process, taking also into account the exterior diffusion as a limitative rate process, the differential equation has the form:

$$-\frac{\mathrm{d}s}{\mathrm{d}t} = k(s - c_e) \tag{7}$$

Because $s = s_0 - c$, we get $-\,\mathrm{d}s\,\mathrm{d}t = +\,\mathrm{d}c\,\mathrm{d}t$ and, thus, the equation (7) becomes:

$$\frac{\mathrm{d}c}{\mathrm{d}t} = k(s_0 - c - c_e) \tag{8}$$

By separating the variables and by integrating, the following solution is obtained:

$$\ln(s_0 - c_e) - c = -k \cdot t + q \tag{9}$$

Defining the elution degree by the expression $f = (s_0 - s)/(s_0 - c_e) = c/(s_0 - c_e)$ and subtracting the expression $\ln(s_0 - c_e)$ from both members of the equation (9), we get :

$$\ln \frac{(s_0 - c_e) - c}{s_0 - c_e} = -k \cdot t + q - \ln(s_0 - c_e)$$

$$\ln \frac{(s_0 - c_e) - (s_0 - s)}{s_0 - c_e} = -k \cdot t + p$$

$$\ln \frac{1}{1 - f} = k \cdot t - p \qquad (10)$$

By using the data from reference [7] concerning the Zn^{2+} elution [the curve a, $c(H_2SO_4) = 2\ \mathrm{mol} \cdot \mathrm{l}^{-1}$], table 2, the equation (10) is checked in the limit of the experimental errors, figure 4.

TABLE 2

Experimental data regarding the Zn^{2+} elution

t, min.	30	60	120	180	240	280
$\%Zn^{2+} = c$	34	37.5	41	44	46	47
$\ln \frac{1}{1-f}$	1.139	1.386	1.715	2.120	2.526	2.813

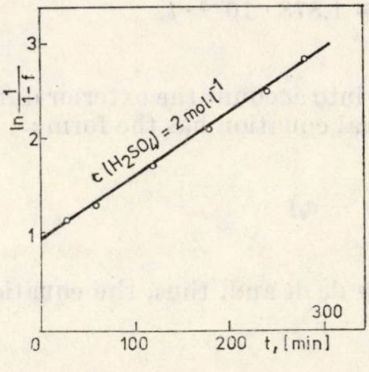

Fig. 4. — The linear diagram for the verification of the equation (10′).

To calculate the elution degree at a given moment for this favorable case, the equation of the straight line from figure 4 has been written by statistical processing of the data from table 2. The equation is of the form (10′), where t will be considered in minutes :

$$\ln \frac{1}{1 - f} = 0.939 + 6.641 \cdot 10^{-3} \cdot t \qquad (10')$$

As the functions $F(t)$, $f(t)$ are relatively complicated, to easily calculate the linking or the elution degree at a given moment a computer programme has been established, which is common to both functions (6′) and (10′), figure 5.

4. PROGRAMME (FORTRAN 4, FELIX-256)

```
DOUBLE PRECISION T, T1, T2, DT, A1, A2, F1, F2. DEXP
DATA T1, T2, DT/15.D0, 245.D0, 5.D0/
T=T1
1 A1=DEXP(0.7906D0 + 0.01873D0 T)
IF(A1.EQ.1.D0) GO TO 2
F1=1.D0-1.D0/A1
GO TO 3
2 F1=1.D75
3 A2=DEXP(0.939D0 + 0.006641D0 T)
  IF(A2.EQ.1.D0) GO TO 4
F2=1.D0-1.D0/A2
GO TO 5
4 F2=1.D75
5 PRINT 6, T, F1, F2
6 FORMAT (10X, 'T', 23X, 'F1'- 23X, 'F2', //F11.1.2D25.12)
T=T+DT
IF(T.LE.T2) GO TO 1
STOP
END
```

Notations in the Computer Programme

F1=F (the linkind degree).

F2=f (the elution degree).

$$A1 = \frac{1}{1 - F}.$$

$$A2 = \frac{1}{1 - f}.$$

Fig. 5. — Listing of the computer programme (FORTRAN 4).

3. CONCLUSIONS

By using the diffusion theory through the liquid film which is formed at the solution ion exchange membranes contact, the equations of the linking degree-time and elution degree-time functions have been deduced. These equations, arranged in linear coordinates, have been used for the interpretation of the kinetic data regarding the Zn^{2+} linking and elution both from sulphuric acid solutions and with sulphuric acid solutions of optimal concentrations established in reference,[7] respectively.

By statistically processing of the experimental data the equations of the two obtained linear functions have been established. To calculate the linking and elution degree at a given moment by these equations, a computer programme has been suggested, as the functions $F(t)$ and $f(t)$, respectively, are relatively complicated.

REFERENCES

[1] E. Gluckauf and P. G. Kitt, *J. Appl. Chem.*, **6**, 511 (1956).

[2] J. Blaedel and J. T. Haupert, *Analyt. Chem.*, **38**, 1305 (1966).

[3] J. Blaedel and L. E. Christensen, *Analyt. Chem.*, **38**, 305 (1966).

[4] J. Blaedel and L. E. Christensen, *Analyt. Chem.*, **39**, 1262 (1967).

[5] E. Sëléghy and Y. Prigent, *Bull. Soc. chim. France*, 1968, 2245.

[6] N. I. Isaev and E. M. Malinovskaia, *Zhur. fiz. khim.*, **43**, 1742 (1969).

[7] A. Duca and F. Matei, "Lucrările celei de a III-a conferințe naționale de chimie analitică", vol. IV, Brașov (Romania), sept. 1971.

[8] R. Schlögl, *Discuss. Faraday Soc.*, **71**, 46 (1956).

[9] F. Helferich, "Ionity", Izd. Inostr. Lit., Moskva 1962, p. 304; p. 237.

[10] N. Lakshminarayanaiah, *Chem. Rev.*, **65**, 492 (1965).

[11] A. V. Gordievskii, *Zhur. fiz. khim.*, **40**, 1806 (1966).

[12] R. Yamate, *Bul. Chem. Soc. Japan.*, **42**, 2741 (1969).

[13] C. R. Srivastava, *Indian J. Chem.*, **7**, 1025 (1969).

[14] J. Blaedel, *Analyt. Chem.*, **41**, 583 (1969).

[15] P. Langer, Angew. Chem., 81, 56 (1969).

[16] H. B. J. George, *J. Electrochem. Soc.*, **117**, 892 (1970).

[17] W. E. Marf, *Analyt. Chem.*, **48**, 1031 (1976).

[18] Y. Kobatake, *Jap. Phys. Chem.*, **69**, 3981 (1965).

[19] Y. Kobatake, *Jap. Phys. Chem.*, **70**, 1187 (1966).

[20] B. P. Nikolskii, *Doklady Akad. Nauk S.S.S.R.*, **194**, 377 (1970).

[21] R. Jerome, *Ind. chim. belge*, **36**, 578 (1971).

[22] M. A. Peterson and H. P. Gregor, *J. Electrochem. Soc.*, **106**, 1051 (1959).

[23] J. A. Kitchener, "Novye problemy sovremennoi electrokhimii", Izd. Inostr. Lit., Moskva 1962, p. 150–162.

[24] I. A. Legencenko, N. P. Hromova and M. E. Korttelli, *Ukrain. khim. Zhur.*, **9**, 913 (1959).

Revue Roumaine de Chimie, 25, 7, 1025–1031(1980)

Dedicated to Professor CRISTOFOR I. SIMIONESCU
on his 60th anniversary

TRANSITION METAL COMPLEXES OF ORGANOTHIOPHOSPHORUS LIGANDS. VI *

SIX-COORDINATE ADDUCTS OF NICKEL (II) BIS(DIALKYLPHOSPHORODITHIOATE) WITH AROMATIC DIAMINES

RODICA MICU-SEMENIUC, LUMINIȚA SILAGHI-DUMITRESCU,
N. CHIRILĂ and IONEL HAIDUC **
Chemistry Department, Babeș-Bolyai University
R-3400 Cluj-Napoca, România

Received January 23, 1980

Nickel(II) bis(dialkyldithiophosphates) (alkyl = methyl, ethyl, *n*-propyl and *n*-butyl) form several types of six-coordinate adducts with aromatic primary diamines (*ortho*- and *para*-diaminobiphenyl (*o, o'*-DABP and *p,p'*-DABP) ; *ortho*- and *para*-phenylenediamine (*o*- and *p*-PHDA) and 2,7-diaminofluorene (2,7-DAF)). The compounds were characterized by elemental analysis, electronic and infrared spectra and magnetic moments. Evidence for both NiS_2N_4 and NiS_4N_2 chromophores, with a high degree of covalence, has been obtained.

INTRODUCTION

In recent years we have been interested in dithiophosphoric acids and their transition-metal salts, particularly nickel chelates and their amine adducts.[1-7] Spectroscopic investigation and some X-ray molecular structure determinations of these compounds revealed some interesting features, *e.g.* the non-equivalence of Ni–S and P–S bonds in the same molecule.[2,4,6]

Another point of interest is the influence of organic groups upon the coordination of sulfur to metal in transition metal-derivatives of phosphorodithioic acids. Therefore we investigated both alkyl- and aryl-phosphorodithioates.

We now report some adducts of Ni(II) bis(dialkylphosphorodithioates) (alkyl = methyl (Me) ; ethyl (Et) ; *n*-propyl (Pr) and *n*-butyl (Bu), prepared and investigated in order to compare their properties and structure with the adducts of Ni(II) bis(diphenylphosphorodithioate) reported so far.[3]

The amine used as ligands were *ortho*, *ortho'*- and *para*, *para'*-diaminobiphenyl (*o*, *o'*-DABP and *p*, *p'*-DABP) ; *ortho*- and *para*-phenylenediamine (*o*-PHDA and *p*-PHDA) and 2,7-diaminofluorene (2,7-DAF).

EXPERIMENTAL

The reagents used were of analytical grade purity. Dialkyl-phosphorodithioic acids $(RO)_2P(S)SH$ and their Ni(II) salts have been prepared according to the literature.[3,7-9]

---

* See reference 7 for previous part in the series.

** Author to whom the correspondence should be addressed.

TABLE 1

Elemental analysis and some properties of the adducts

No.	Compound	Elemental Analysis						Colour	M.P.°C	μ_{eff} (BM)
		% Ni found	% Ni calcd	% P found	% P calcd	% N found	% N calcd			
1	Ni(Medtp)$_2$. *o, o'*-DABP	10.21	10.54	11.16	11.12	4.82	5.04	light green	118	
2	Ni(Etdtp)$_2$. *o, o'*-DABP	8.98	9.57	10.57	10.10	4.82	4.56	green	117	
3	Ni(Prdtp)$_2$. *o, o'*-DABP	8.36	8.77	9.24	9.26	4.43	4.20	green	120	2.89
4	Ni(Budtp)$_2$. *o, o'*-DABP	7.82	8.09	8.22	8.54	3.65	3.87	green	105	
5	Ni(Medtp)$_2$. *p, p'*-DABP	10.15	10.54	10.82	11.12	5.17	5.04	yellow green	104	
6	Ni(Etdtp)$_2$. *p, p'*-DABP	9.53	9.57	10.46	10.10	4.77	4.56	yellow-green	105	
7	Ni(Prdtp)$_2$. *p, p'*-DABP	8.32	8.77	9.24	9.26	4.35	4.20	yellow	dc	3.12
8	Ni(Budtp)$_2$. *p, p'*-DABP	7.83	8.09	8.14	8.54	4.02	3.87	yellow	107—109	
9	Ni(Medtp)$_2$. 2,7-DAF	10.35	10.32	10.22	10.88	4.68	4.82	beige	dc	
10	Ni(Etdtp)$_2$. 2,7-DAF	8.82	9.39	9.53	9.91	4.62	4.39	beige	dc	
11	Ni(Prdtp)$_2$. 2,7-DAF	8.07	8.82	8.75	9.09	3.72	4.04	yellow-green	110	3.18
12	Ni(Budtp)$_2$. 2,7-DAF	7.83	7.96	8.15	8.40	3.92	3.74	beige	140	
13	Ni(Medtp)$_2$. *p*-PHDA	12.10	12.20	12.47	12.87	5.34	5.55	dark-green	133—134	
14	Ni(Etdtp)$_2$. *p*-PHDA	10.88	10.93	11.14	11.53	4.65	4.98	light-green	151	
15	Ni(Prdtp)$_2$. *p*-PHDA	9.84	9.92	10.03	10.44	4.67	4·54	green	117	3.20

TABLE 1 (continued)

No.	Compound	Elemental Analysis			Colour	M.P.°C	μ_{eff} (BM)
		% Ni found	% P found	% N found			
		calcd	calcd	calcd			
16	Ni(Budtp)$_2$. *p*-PHDA	8.80	9.03	4.36	green	110	
		9.04	9.54	4.16			
17	Ni(Medtp)$_2$. *o*-PHDA	12.10	12.32	5.74	green	143	
		12.20	12.87	5.55			
18	Ni(Etdtp)$_2$. *o*-PHDA	10.72	10.82	5.22	green	141	
		10.93	11.53	4.98			
19	Ni(Prdtp)$_2$. *o*-PHDA	9.25	10.13	4.82	green	153	2.98
		9.92	10.44	4.54			
20	Ni(Budtp)$_2$. *o*-PHDA	8.73	9.16	4.42	green	135–136	
		9.04	9.54	4.16			
21	Ni(Medtp)$_2$. 2-*o*-PHDA	10.46	10.61	8.51	mauve	150	
		9.96	10.51	8.78			
22	Ni(Etdtp)$_2$. 2 *o*-PHDA	8.95	9.96	8.32	mauve	175	
		9.10	9.60	8.07			
23	Ni(Prdtp)$_2$. 2 *o*-PHDA	7.92	8.70	7.32	mauve	157	3.03
		8.37	8.83	7.48			
24	Ni(Budtp)$_2$. 2 *o*-PHDA	7.50	7.85	7.62	mauve	138	
		7.75	8.18	7.96			

Infrared spectra were recorded in KBr pellets on a UR-20 Carl Zeiss-Jena spectrophotometer and electronic spectra (diffuse reflectance and absorption) on a VSU-2G Carl Zeiss-Jena instrument. Magnetic moments were determined on a Faraday balance at room temperature and were corrected for the diamagnetism of ligands.

The metal content was determined as Ni(II) bis(dimethyl-glyoximate) and phosphorus as ammonium 12-molybdophosphate (gravimetrically). The nitrogen content was found by combustion.

Except for the green adducts with *o*-PHDA, the compounds were prepared by mixing the reagents in calculated amounts, as required by 1 Ni : 1 L and 1 Ni : 2 L molar ratios, in diethyl-ether or/and acetone. The adducts of Ni[(C$_4$H$_9$O)$_2$PS$_2$]$_2$ were at first stage, separated as green viscous gums. After repeated recrystallizations from petroleum ether and diethyl ether, microcrystalline products were obtained. The solution as filtered, washed with diethyl ether or ethanol and dried in air. The synthesis of *o*-PHDA adducts yields two different compounds: a green one (1 Ni : 1 L ratio) and a pink-purple one (1 Ni : 2 L ratio) (see Table 1), unlike Ni(II) bis(diphenylphosphorodithioate) adducts with *o*-PHDA where two isomers were obtained.[3]

Using anhydrous diethylether (dried over sodium) and fresh Ni(II) bis(dialkyldithiophosphate), the green adducts were obtained. The pink-purple compounds were obtained using the above mentioned method.

All compounds prepared, with some of their properties and analytical data are listed in Table 1.

RESULTS AND DISCUSSION

The reaction of Ni(II) bis(dialkylphosphorodithioates) with aromatic diamines yields adducts with 1 Ni : 1 L and 1 Ni : 2 L molar ratios. Electronic spectra and magnetic moments discussed below show that all of them contain six-coordinate nickel(II) ion. When *ortho-* and *para-*diamines are used as reagents, the structure and consequently the chromophores of six-coordinated adducts may not be the same. The ligands with amino group in *para*-positions (*p*, *p*′-DABP, *p*-PHDA and 2,7-DAF) cannot coordinate both nitrogen atoms to the same metal atom, therefore, the adducts have probably a polymeric structure, similar to other known adducts with the same diamines.[3,10] In these compounds the diamines form bridges between the nickel atoms. The *ortho*-diamines form a *cis*-type adducts, as shown before for the Ni(II)-bis(diphenylphosphorodithioate) adducts with such diamines.[3]

The adducts are not very stable towards dissociation, in marked contrast to the same amine-adducts of Ni(II) bis(diphenylphosphorodithioate), handled in our laboratory. They often dissociate on evaporation of their solutions, with release of amine and free Ni(II) bis(dialkylphosphorodithioate).

The electronic spectra of these adducts exhibit three bands in visible region, expected for an octahedral configuration of Ni(II) ion : $\nu_1({}^3T_{2g}(F) \leftarrow {}^3A_{2g}(F))$; $\nu_2({}^3T_{1g}(F) \leftarrow {}^3A_{2g}(F))$ and $\nu_3({}^3T_{1g}(P) \leftarrow {}^3A_{2g}(F))$. The energy of these transitions is listed in table 2. The third band situated at wave numbers higher than 20,000 cm^{-1} occurs sometimes as a shoulder on a charge transfer band, which is expected to appear at wave numbers higher than 25,000 cm^{-1}. For some of the adducts this band is well resolved and can be undoubtedly assigned to the ν_3 transition. From the electronic

TABLE 2

Electronic spectra of Ni(II) bis (dialkylphosphorodithioato)adducts (cm^{-1})

Compound	ν_1	ν_2	ν_3	B′	10 Dq	β
Ni(Medtp)$_2$. *o*, *o*′-DABP	10 800	15 000	24 000	770	11 088	0.72
Ni(Medtp)$_2$. *p*, *p*′-DABP		13 800	24 800	930	9 950	0.89
Ni(Etdtp)$_2$. *p*, *p*′-DABP	8 930	14 300	23 800	880	10 560	0.83
Ni(Prdtp)$_2$. *p*, *p*′-DABP		14 500	24 000	830	10 855	0.78
Ni(Etdtp)$_2$. 2,7-DAF	9 200	14 500	23 100	890	9 800	0.84
Ni(Medtp)$_2$. *p*-PHDA	9 090	14 300	26 400	990	8 910	0.86
Ni(Etdtp)$_2$. *p*-PHDA	9 500	14 800	25 400	873	9 340	0.82
Ni(Prdtp)$_2$. *p*-PHDA	9 808	16 000	26 800	817	9 700	0.79
Ni(Medtp)$_2$. *o*-PHDA		14 800	24 500	835	10 020	0.78
Ni(Etdtp)$_2$. *o*-PHDA	11 800	15 200	24 600	783	11 200	0.74
	11 000	15 000	24 000	768	11 059	0.72
Ni(Prdtp)$_2$. *o*-PHDA	10 715	17 000	27 800	885	12 740	0.83
Ni(Etdtp)$_2$. 2 *o*-PHDA						

spectral data, the Racah parameter B′, the covalency factor β and 10 Dq parameter were calculated (Table 2) with the aid of a graphical method.[11] The values found are in the same range as for the other similar adducts with related ligands.[3,9,10] The value of the nephelauxetic parameter β decreases for Ni $[(RO)_2PS_2]_2$. L from R = methyl to R = propyl, and 10 Dq increases in the same way.

For $Ni(Etdtp)_2 \cdot 2$ *o*-PHDA the β parameter is 0.83 larger than in the 1 Ni : 1 L ratio adducts with the same amine (0.78—0.72) supporting the presence of the NiS_2N_4 chromophore in the first compound and the NiS_4N_2 chromophore in the second ones.

The *magnetic moments* are in agreement with electronic spectra: the values of μ_{eff} are close to the spin-only value (see Table 1) suggesting that the ground state of six-coordinated Ni(II) ion is a $^3A_{2g}$ one. The values obtained are in the same range as for the other similar adducts from Ni(II) bis(dialkyl- and diarylphosphorodithioates).[3,5,9,12]

The values of magnetic moments obtained for some compounds (R = propyl) (see Table 1) lie in the range 2.89—3.0 BM for the adducts with *ortho*-substituted amines (1 Ni : 1 L ratio, the *cis* form of the adducts) and in the range 3.0—3.20 BM with *para*-substituted amines (the *trans* form of the adducts).

The infrared spectra were recorded for two ranges: 700—400 cm^{-1} and 3400—3000 cm^{-1}, corresponding to the stretching frequencies of PS_2 groups and $-NH_2$ groups, respectively.

In the range of PS_2 stretching vibrations two main bands assigned to $\nu_{as}(PS_2)$ and $\nu_s(PS_2)$] frequencies were found. The values are located around 670 cm^{-1} and 550 cm^{-1}, respectively. They are situated at energies higher than the same bands in the parent Ni(II) bis(dialkylphosphorodithioates)[12,13] (see Table 3), due to an increase of electronic density around the central ion, by formation of the adducts.

On the other hand it can be seen that the stretching vibration frequencies of this group $\nu_s(PS_2)$ increase with the increase of the number of the carbon atoms in the alkyl group, except for the *n*-butyl derivatives. These results are in agreement with the influence of *R* groups upon the electronic structure of O, O-dialkylphosphorodithioic esters, evidenced by CNDO/2 calculations.[14]

Concerning the stretching vibrations of the NH_2 groups, it can be noticed that their frequencies are shifted to lower energies, compared to the free ligands. Consequently, all $-NH_2$ groups appear to be bonded to nickel. The compounds with *para*-amino-derivatives contain a NiS_4N_2 chromophore, with the nitrogen atom in *trans*-position; the diamine forms a bridge between two metal atoms (structure I). The *ortho*-derivatives form compounds of *cis*-type when the combination ratio is 1 Ni : 1 L (structure II). The spectra of the compounds with *o*-PHDA (1 Ni : 2 L ratio) exhibit two types of bands in the $\nu(NH_2)$ range, both being shifted to lower values of frequencies; consequently all NH_2 groups are bonded.

TABLE 3

Infrared spectra of the synthesised compounds (cm^{-1})

Compound	$\nu_{as}(PS_2)$	$\nu_s(PS_2)$	$\nu_{as}(NH_2)$	$\nu_s(NH_2)$
o, o′-DABP	—	—	3380	3270
Ni(Medtp)$_2$. *o, o′*-DABP	670	535	3320	3250
Ni(Etdtp)$_2$. *o, o′*-DABP	665	555	3330	3250
Ni(Prdtp)$_2$. *o, o′*-DABP	665	570	3320	3250
Ni(Budtp)$_2$. *o, o′*-DABP	665	570	3310	3250
p, p′-DABP	—	—	3390	3280
Ni(Medtp)$_2$. *p, p′*-DABP	680	540	3320	3280
Ni(Etdtp)$_2$. *p, p′*-DABP	670	555	3346	3270
Ni(Prdtp)$_2$. *p, p′*-DABP	670	555	3348	3240
Ni(Budtp)$_2$. *p, p′*-DABP	682	555	3330	3220
2,7-DAF	—	—	3380	3305
Ni(Medtp)$_2$. 2,7-DAF	675	540	3350	3280
Ni(Etdtp)$_2$. 2,7-DAF	680	555	3345	3250
Ni(Prdtp)$_2$. 2,7-DAF	680	560	3300	3210
Ni(Budtp)$_2$. 2,7-DAF	682	560	3300	3260
p-PHDA	—	—	3433	3345
Ni(Medtp)$_2$. *p*-PHDA	680	535	3330	3275
Ni(Etdtp)$_2$. *p*-PHDA	670	550	3350	3295
Ni(Prdtp)$_2$. *p*-PHDA	680	575	3330	3260
Ni(Budtp)$_2$. *p*-PHDA	670	570	3330	3255
o-PHDA	—	—	3400	3325
Ni(Medtp)$_2$. *o*-PHDA	690	540	3330	3280
Ni(Etdtp)$_2$. *o*-PHDA	680	555	3320	3220
Ni(Prdtp)$_2$. *o*-PHDA	675	570	3330	3200
Ni(Budtp)$_2$. *o*-PHDA	685	560	3215	3100
Ni(Medtp)$_2$. 2 *o*-PHDA	683	550	3330 3270	3270 3214
Ni(Etdtp)$_2$. 2 *o*-PHDA	682	555	3346 3220	3220 3100
Ni(Prdtp)$_2$. 2 *o*-PHDA	675	570	3320 3230	3190 3100
Ni(Budtp)$_2$. 2 *o*-PHDA	677	560	3310 3290	3290 3200
Ni(Medtp)$_2$	648	524	—	—
Ni(Etdtp)$_2$	644	551	—	—
Ni(Prdtp)$_2$	645	545	—	—
Ni(Budtp)$_2$	660	575	—	—

This is consistent with a probable structure with monodentate phosphorodithioato ligands, containing the NiS_2N_4 chromophore (structure III).

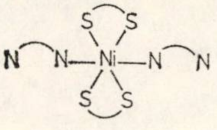

I

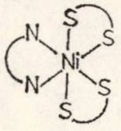

II

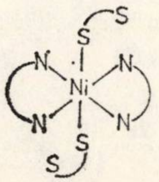

III

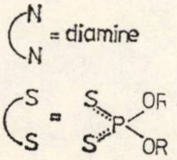

REFERENCES

[1] I. Haiduc and M. Curtui, *Syn. React. Inorg. Metal-Org. Chem.*, **6,** 125 (1976).

[2] D. B. Sowerby and I. Haiduc, *Inorg. Chim. Acta*, **17,** L15 (1976).

[3] R. Micu-Semeniuc, L. Dumitrescu-Silaghi and I. Haiduc, *Inorg. Chim. Acta*, **17,** 5 (1976).

[4] D. B. Sowerby and I. Haiduc, *Inorg. Nucl. Chem. Letters*, **12,** 791 (1976).

[5] R. Constantinescu, F. Martinaş and I. Haiduc, *Inorg. Chim. Acta*, **19,** 105 (1976).

[6] S. P. Bone, D. B. Sowerby, R. Constantinescu and I. Haiduc, *J. Chem. Research (S)*, **1979,** 69.

[7] R. Micu-Semeniuc, L. Dumitrescu-Silaghi and I. Haiduc, *Inorg. Chim. Acta*, **33,** 281 (1979).

[8] "Methoden der Organischen Chemie", Houben-Weyl, XII/2, Georg Thieme Verlag, Stuttgart, 1964, p. 85.

[9] J. R. Wasson, G. M. Volterman and J. H. Stoklosa, *Fortschr. Chem. Forsch.*, **35,** 65 (1973), and references therein.

[10] R. Micu-Semeniuc, C. Opriş and I. Haiduc, in press.

[11] A. B. P. Lever, "Inorganic Electronic Spectroscopy", Elsevier Amsterdam, 1968.

[12] S. E. Livingstone and J. Mikkelson, *Inorg. Chem.*, **9,** 2545 (1970).

[13] N. Nanjo and T. Yamasaki, *J. Inorg. Nucl. Chem.*, **32,** 2411 (1970).

[14] I. Silaghi-Dumitrescu and I. Haiduc, *Rev. Roumaine Chim.*, **25,** 815 (1980).

Revue Roumaine de Chimie, 25, 7, 1033—1038 (1980)

Dedicated to Professor Cristofor I. Simionescu
on his 60th anniversary

CATALYSIS BY METAL CATION IN THE OXIDOREDUCTION REACTION OF BISOXALATODIAQUO Co(III) COMPLEX WITH IODIDE ION IN ACIDIC MEDIUM

I. G. MURGULESCU, GABRIELA MINCU and ECATERINA JURCONI
Institute of Chemistry, Department of Physical Chemistry, Bd. Republicii 13, Bucharest, Romania

Received November 16, 1979

The kinetics and mechanism of the oxidoreduction reaction of bisoxalatodiaquo Co(III) complex with iodide ion in acidic medium were investigated at different inert salt concentrations. According to the proposed mechanism, a catalytic action of the alkaline cations was revealed.

Our preceding papers in this series [1,2] dealt with the kinetics and mechanism of the bisoxalatodiaquo Co(III) complex oxidoreduction reaction with iodide ion in acidic medium.

The present paper deals with the salt effects on the reaction rate.

EXPERIMENTAL

The procedure (clock method) was described in a previous paper.[2] All the experiments were performed at constant concentration of hydrogen ion ($1.04 \cdot 10^{-1}$M), iodide ion ($2.09 \cdot 10^{-1}$M) and complex salt ($5.22 \cdot 10^{-3}$M), varying the added salt concentration. The bisoxalatodiaquo complex was obtained in acidic medium from Durrant's salt, prepared as indicated in literature.[3] The alkaline salts were of analytical reagent grade "Anala R".

RESULTS

The experiments were performed in NaCl, KCl, RbCl, CsCl and KNO_3 media. The kinetics data verified a first order law in respect to the complex concentration, as can be seen in figure 1.

The rate constants obtained at different inert salt concentrations are listed in table 1.

By analysing these data one observes that the rate constant increases with the increase of added salt concentration and also in the series from Na^+ to Cs^+. The rate constants determined in chloride media are larger than in the nitrate media. In all cases the observed rate constants of the

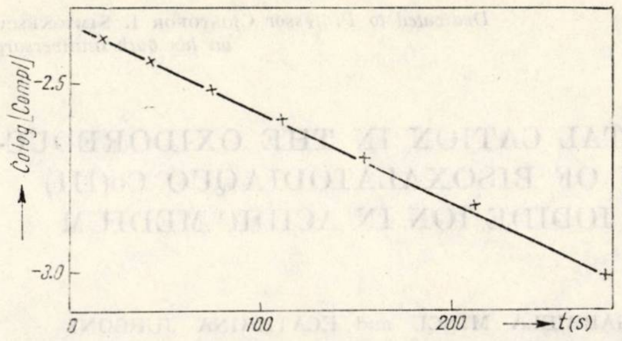

Fig. 1. – Typical first order dependence ($C_{complex} = 5.22 \cdot 10^{-3}$ M, $C_{acid} = 0.104$ M; $C_{I^-} = 0.209$ M, $C_{K}^{+} = 0.3$ M, temp. = 19.5°C).

oxidoreduction reaction between the complex ion $[Co(C_2O_4)_2(H_2O)_2]^-$ and I^- in the presence of added salts are larger than in their absence (k in the absence of the salts is $3.82 \cdot 10^{-3}$ sec^{-1}).

TABLE 1

Rate constants at different concentrations of alkaline cations

c_{salt} (M)	$k \cdot 10^3 (s^{-1})$				
	NaCl	KCl	RbCl	CsCl	$NaNO_3$
0.10	4.10	4.37	4.50	4.58	4.65
0.20	4.55	4.92	5.14	6.13	5.13
0.30	4.68	5.23	5.91	6.50	5.55
0.50	5.69	6.66	7.53	8.06	5.73
0.70	6.45	8.01	8.56	9.86	6.36
1.00	7.00	8.89	10.76		7.14
1.25	8.24	10.36			
1.50	9.39	11.80			

DISCUSSION

The experimental results presented above are obtained at high hydrogen ion concentrations using a large excess of iodide ion. Under these conditions we selected from the mechanism proposed in the previous paper [2] the sequences involved in the acid catalysed domain, like these:

$$\text{(a)}\quad [Co(C_2O_4)_2(H_2O)_2]^- + H_3O^+ \underset{k_1'}{\overset{k_1}{\rightleftharpoons}} [Co(C_2O_4)\,(HC_2O_4)(H_2O)_3] \quad \text{rapid}$$

$$\text{b)}\quad [Co(C_2H_4)\,(HC_2O_4)\,(H_2O)_3] + I^- \xrightarrow{k_2} [Co(C_2O_4)\,(HC_2O_4)\,(H_2O)_3I]^- \quad \text{slow}$$

$$\text{(c)}\quad [Co(C_2H_4)(HC_2O_4)(H_2O)_3I]^- \xrightarrow{k_3} CoC_2O_4 + HC_2O_4^- + 1/2I_2 + 3H_2O \quad \text{rapid}$$

The first step of this reaction mechanism is the protonation preequilibrium, followed by the rate determining step consisting in the formation of the seven-coordinated intermediate. The last rapid step leads to the reaction products.

According to the suggested mechanism, the differential kinetic equation of the oxidoreduction reaction is :

$$-\frac{\mathrm{d}C_D}{\mathrm{d}t} = k_1 C_D C_{H_3O} - k_1' C_{DH} \tag{1}$$

where : C_D = concentration of the bisoxalatodiaquo Co(III) complex
C_{DH} = concentration of the protonated complex

By applying the stationary state approximation to the intermediates *DH* and *DI* (where *DI* is the seven-coordinated intermediate), we found finally :

$$-\frac{\mathrm{d}C_D}{\mathrm{d}t} = k_{\text{obs}} C_{\text{H}_3\text{O}} C_I C_D \tag{2}$$

The expression (2) is in good agreement with the first-order dependence in respect of the Co(III) complex, hydrogen and iodide ion concentrations revealed from our experimental data. In the equation (2) :

$$k_{\text{obs}} = K_1 k_2 \tag{3}$$

where K_1 is the protonation preequilibrium constant and k_2 is the first order constant of the rate determining step in acidic medium. The expressions (2) and (3) confirm the catalytic action of H^+ ion.

Taking into account the simplified reaction mechanism, we explained the salt effects on the oxidoreduction reaction in two ways : on the basis of ion-pair formation, or in terms of the salt influence on the activity coefficients for the ground and transition states.[4-6]

The kinetic way of ion-pair detection consists in a plot of rate constants *versus* salt concentrations ; this plot leads to a constant value of k for high salt concentrations. These plots may show an increase or decrease of the rate constant with added salt as the ion-pair reacts faster or slower than the free ion. In our case, the accelerating alkaline salts show no saturation of the effect within the investigated concentration range. This fact does not exclude completely the presence of ion-pairs. By reason of solubility we cannot increase the added salt concentration more than 1.5 M and consequently the saturation effects were not observed.

The influence of added salt on the investigated reaction can be also discussed in terms of the salt influence on the activity coefficients of the ground and transition states. In this treatment the salts are assumed to be completely dissociated and ion-pairing is not considered. Our reaction system is complicated ; it consists of the complex salt and the added electrolytes (HCl, KI, alkaline salts, etc.). For such mixtures it is necessary to know the dependence of the activity coefficients of the species in respect to the ionic strength of the medium. Since there are difficulties in establishing a quantitative relation, we give first a qualitative explanation of the salt effect on the reaction rate.

The reaction mechanism presented above may be illustrated in figure 2.

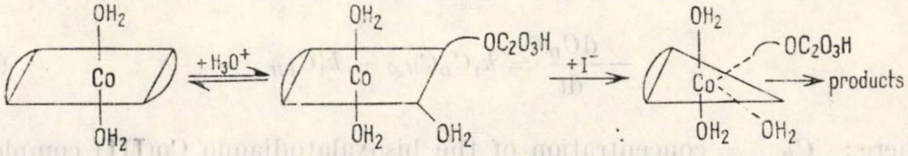

Fig. 2. — Scheme of the reaction mechanism.

The first step is a rapid bimolecular collision which leads to the appearance of the protonated complex, with an oxalic group detached from a coordination site, followed by the slow attack of I^- leading to a seven-coordinated intermediate, characterized by the stretching of the metal — (oxalic) oxygen bond. In the last step the electron transfer between Co(III) and I^- occurs yielding to the final products. The salt effects on the total reaction are expressed in the absolute rate theory by the introduction of activity coefficients for the ground and transition states :

$$R = k_{\mathrm{obs}} \cdot [\text{complex}] \tag{4}$$

$$\log k_{\mathrm{obs}} = \log k_0 + \log (f_{\mathrm{ground}}/f_{\mathrm{transition}}) \tag{5}$$

Using for the activity coefficients the equation of Debye—Hückel[7] :

$$\log f_{\pm} = -\frac{AZ_{+}Z_{-}I^{1/2}}{1 + B\mathring{a}I^{1/2}} \tag{6}$$

the difference of the $\mathring{a}$ values can be estimated for the ground and transition states, which is rather difficult. Assuming for the mechanism in question that the change in the $\mathring{a}$ parameter is due only to the stretching of the metal — (oxalic) oxygen bond in the transition state, an increase of the activity coefficient for the transition state is expected leading to a deceleration of the reaction. This is, indeed, opposite to the experimental facts and it pleads for a more elaborate mechanism of the reaction.

An alternative mechanism presented in figure 2 consists in an ion-pair catalysed dechelation. This mechanism involves, as figure 3 shows, an ion-pair preequilibrium between the complex ion and the cation of the added salt.

The ion-pair complex is assumed to react faster than the free complex. This is possibly due to a special interaction between the metal cation and the oxalic ligand, which results in a labilization of the oxalic ligand. This facilitates the penetration of a water molecule (H_3O^+ ion) and then of an iodide ion in the coordination sphere of the complex leading to the seven-coordinated intermediate formation. The oxalate dechelation should only occur when the catalysing metal competes successfully with the attraction force exerted by the central cobalt ion. The smallest (in terms of crystallographic radii) alkali ions (Li^+, Na^+) form the ion pairs less probably than the largest ones (Cs^+, Rb^+), due to the size of the hydration spheres. Therefore, the rate constants determined for a sodium cation medium must be smaller than for a cesium cation medium, which has been confirmed experimentaly (Table 1).

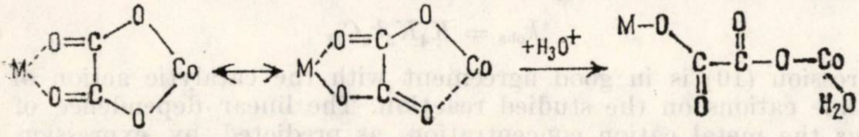

Fig. 3. — Scheme of the mechanism of an ion-pair catalysed dechelation.

The mechanism of an ion-pair catalysed dechelation can be represented by the following scheme:

$$\text{(d)}\quad [Co(C_2O_4)_2(H_2O)_2]^- + M^+ \underset{k'_4}{\overset{k_4}{\rightleftharpoons}} [Co(C_2O_4)(H_2O)_2(OC_2O_3M)] \qquad \text{rapid}$$

$$\text{(e)}\quad [Co(C_2O_4)(H_2O)_2(OC_2O_3M)] + H_3O^+ \underset{k'_5}{\overset{k_5}{\rightleftharpoons}} [Co(C_2O_4)(H_2O)_2(OC_2O_3M)(H_3O)]^+ \qquad \text{rapid}$$

$$\text{(f)}\quad [Co(C_2O_4)(H_2O)_2(OC_2O_3M)(H_3O)]^+ + I^- \xrightarrow{k_6} [Co(C_2C_4)(H_2O)_3(OC_2O_3H)I]^- + M^+ \qquad \text{slow}$$

$$\text{(g)}\quad [Co(C_2O_4)(H_2O)_3(OC_2O_3H)I]^- \xrightarrow{k_7} CoC_2O_4 + HC_2O_4^- + 3\,H_2O + 1/2I_2 \qquad \text{rapid}$$

The first step (d) of this reaction mechanism is the ion-pair formation, the second (e) is the protonation preequilibrium, followed by the rate-determining step (f). The last step, an intramolecular charge transfer, leads to the reactions products.

The differential kinetic equation of the oxidoreduction reaction is:

$$-\frac{\mathrm{d}C_D}{\mathrm{d}t} = k_4 \cdot C_D C_M - k'_4 C_{DM} \qquad (7)$$

where: C_D = concentration of the bisoxalatodiaquo Co(III) complex
C_{DM} = concentration of the ion pair

By applying the stationary state approximation to the intermediate *DM*, DHM (the protonated complex) and DI(the seven-coordinated intermediate), we found finally:

$$-\frac{\mathrm{d}C_D}{\mathrm{d}t} = K_4 K_5 k_6 C_{H_3O} C_M C_I C_D \qquad (8)$$

This equation confirms our experimental results i.e., the first order with respect to Co(III) complex, hydrogen, iodide and metalic ion concentrations.

The equation (8) can be written as follows:

$$-\frac{\mathrm{d}C_D}{\mathrm{d}t} = k_{\mathrm{obs}} \cdot C_{\mathrm{H_3O}} \cdot C_I C_D \tag{9}$$

which is similar to the expression (2). In this case:

$$k_{\mathrm{obs}} = K_4 K_5 k_6 C_M \tag{10}$$

Expression (10) is in good agreement with the catalytic action of the alkaline cations on the studied reaction. The linear dependence of k_{obs} *versus* the metal cation concentration, as predicted by expression (10) was verified by our data (Figure 4).

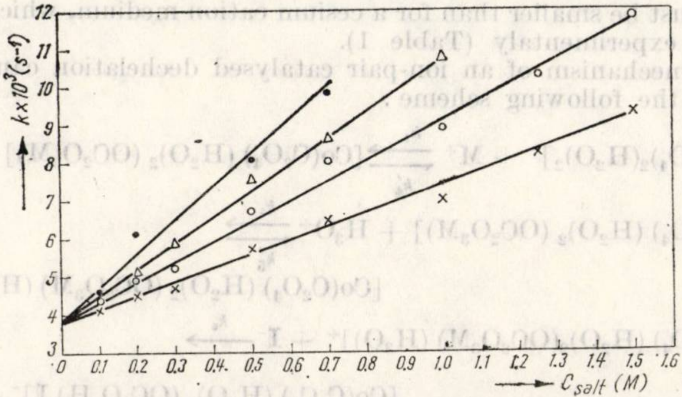

Fig. 4. — Variation of the rate constant with the metal cation concentration (temp. = 19.5°C).

Concerning the anion effect on the reaction rate, we observed that the rate constants for the nitrate media are smaller than for the chloride media. This can be explained by the reduction of the possibility of the potassium ion attack in the nitrate media in comparison with the chloride media. The nitrate anion is large and "negatively hydrated", therefore the electric field in its neighborhood exerts a greater orientation effect upon the potassium ion as against the hydrated chloride ion.

In conclusion, the present study reveals the catalytic action of the monovalent cations on the oxidoreduction reaction of bisoxalatodiaquo Co(III) complex with iodide ion in acidic medium, supporting the previously proposed reaction mechanism.

REFERENCES

[1] G. Mincu, *Studii și Cercetări Chim., Acad. R. S. România*, **20,** 533 (1972).
[2] I. G. Murgulescu and G. Mincu, *Rev. Roumaine Chim.*, **23,** 471 (1978).
[3] R. G. Durrant, *J. Chem. Soc.*, **1905,** 176.
[4] H. Kelm, Thesis, (1965).
[5] T. Oncescu and E. Jurconi, *Rev. Roumaine Chim.*, **22,** 69 (1979).
[6] T. Oncescu and E. Jurconi, *Rev. Roumaine Chim.*, **22,** 1471 (1977).
[7] P. Debye and E. Hückel, *Phys. Z.*, **24,** 185 (1923).

Revue Roumaine de Chimie, 25, 7, 1039–1043 (1980)

Dedicated to Professor CRISTOFOR I. SIMIONESCU
on his 60th anniversary

CATALYSIS BY POLYMERS. I.

SYNTHESIS OF 3-CHLORO-2-HYDROXYPROPYL ACRYLATE USING QUATERNIZED POLY(DIMETHYL-AMINO-ETHYL METHACRYLATE) AS CATALYST

SPIRIDON OPREA, EMIL DUMITRIU and LAURENŢIA ŞTEFĂNEL
Department of Organic Chemical Technology, Faculty of Chemical Technology,
Bahlui Stînga Street 71, Jassy 6600, Romania

Received January 25, 1980

Quaternized poly(dimethylaminoethyl methacrylate) has been tested as catalyst in the esterification of acrylic acid with epichlorohydrin. The influence of concentration of catalyst, temperature and mole ratio of the reactants on the conversion of acrylic acid has been investigated. The results obtained demonstrate an important catalytic activity of the polymer.

The catalysis of the reactions of micromolecular compounds by synthetic macromolecules is another field of catalysis which has obtained very interesting and spectacular achievements in the last years. The interest shown for such processes is determined by two main aspects: 1) the analogies which may be drawn between the processes catalysed by synthetic macromolecules and enzymatic processes, and 2) the high catalytic activities of macromolecules as compared to their micromolecular analogues.

The analysis of the data from literature indicates that most research works on catalysis by synthetic linear macromolecules (or unreticuled polymers) have been effected in the field of solvolytic reactions. For such reactions has been found, as pointed out by Overberger and Smith,[1] that some polymers may show, to a certain extent, a behaviour which is similar to the enzymatic systems (specificity of substrate hydrolysis, higher reactivities than the corresponding monomeric systems, saturation phenomena, competitive inhibition by compounds similar to the substrate etc.), although these polymers lack the tertiary and secondary structures of enzymes.

Among the polymers used, in the solvolytic studies may be indicated: poly(acrylic acid),[2] poly(4-vinylpyridine),[3] poly 4(5-vinylimidazole,[4,5] copolymers of vinylimidazoles with acrylic acid, *p*-vinylphenol,[6] *N*-vinylpyrrolidone, acrylamide [7] etc. Certainly the solvolytic studies have shown an interest especially due to the analogies with enzymatic processes, but in the field of catalysis by synthetic macromolecules there are other types of reactions which show both theoretical and practical interest. Thus, in the field of esterification reactions the studies realized are centered exclusively on catalysis by ion exchange resins which are insoluble in the reaction mixture. Evidently, the study of the esterification reaction catalysed by synthetic polymers in homogeneous system may present very interesting aspects.

The aim of this paper is to study the catalytic effects of the quaternized poly(dimethylaminoethyl methacrylate) on the esterification of acrylic acid with epichlorohydrin. Since the polymer obtained by quaternization of poly(dimethylamino-ethyl methacrylate) with methyl iodide:

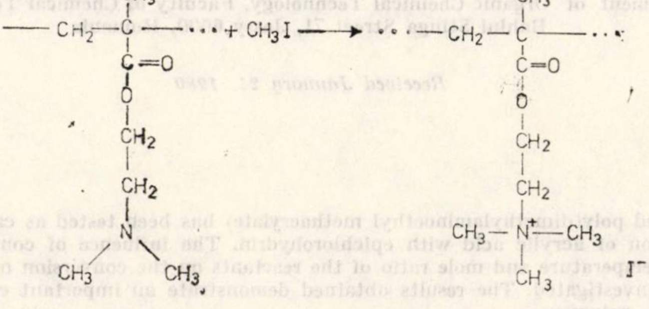

is perfectly soluble in the reaction medium, the esterification can be carried out in a homogeneous system. It should be mentioned that this polymer was used for the first time for such catalytic reactions.

EXPERIMENTAL

Materials

Epichlorohydrin (1-chloro-2,3-epoxypropane) was dried over anhydrous $CaCl_2$, then purified by distillation under vacuum. The middle fraction was collected; b.p. = 116°C, $n_D^{20} = 1.4375$, $d^{25} = 1.183$.

Acrylic acid, Merck reagent, was distilled under vacuum and the middle fraction was collected. The product was stabilized with 200 ppm hydroquinone.

Catalyst

Dimethylaminoethyl methacrylate was purified by rectification on a packed column under vacuum. The monomer, freshly distilled, b.p. = 69°C/10 mm Hg, $n_D^{25} = 1.4376$, was polymerized in dioxane solution at 60°C using 2,2′-azobis (isobutironitrile) as initiator. The polymer was isolated by precipitation in light petroleum. The purification of the polymer was made by several reprecipitations from the dioxane-light petroleum system (solvent and nonsolvent), after which the polymer was dried under vacuum at 60°C for 48 h.

The quaternization of amino groups in the side chains was realized by methyl iodide. Poly(dimethylaminoethyl methacrylate) was dissolved in methanol (10% concentration), then the methyl iodide was added in excess over the amino group, with stirring. While the quaternization proceeds the modified polymer separates as precipitate. Finally the precipitated polymer was filtered and washed with methanol in order to remove the methyl iodide. The advanced purification of polymer was made by several reprecipitations from the water-acetone system (solvent and nonsolvent). The degree of quaternization was determined by potentiometric titration of iodide ion with 0.05 N $AgNO_3$. The results of analysis has shown a 89.5 % quaternization, therefore the quaternized poly(dimethylaminoethyl methacrylate) was in fact a copolymer with 89.5 % quaternized units.

Catalytic esterification

In order to study the esterification reaction the ampoules technique was used. Since the preliminary tests have indicated that the esterification reaction between acrylic acid and epichlorohydrin takes place at the ambient temperature at a negligible rate, it was possible to prepare the stock solutions of the two reagents at the desired molar ratio and catalyst concentration. The initial acidity was determined by titration of acrylic acid with 0.5 N NaOH solution. Then, about 6 ml of reaction mixture are introduced in each ampoule and the sealed ampoules are placed in the thermostat. At the proper intervals of time the ampoules are taken from the bath and cooled, then the acidity is determined by titration.

RESULTS AND DISCUSSION

Evidently, the first stage of our study consisted in testing the catalytic activity of the polymer and in establishing the level of catalytic concentration at which the reaction rate is acceptable. On the basis of preliminary tests it was chosen as reaction temperature 55°C, for all experiments in which the influence of the amount of catalyst was studied.

As it may be observed from figure 1 the concentration of catalyst influences to an appreciable extent the conversion of acrylic acid to ester. The reaction rate in the absence of catalyst is so small that for the first 300 minutes the experimental points fit on a straight line which overlaps on abscissa, while for the lowest level of concentration of used catalyst, line (1), it can ascertain a significant rise of reaction rate thus the conversion reaches about 7 % for 300 minutes. When the catalyst concentration rises to 5 and 10 %, the lines (2) and (3), the rate of reaction still increases.

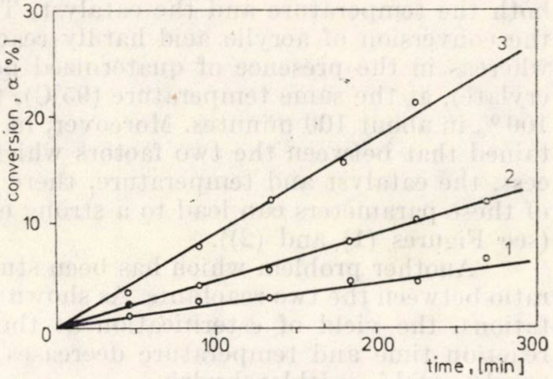

Fig. 1. — Influence of catalytic concentration on the acrylic acid conversion; reaction temperature 55°C, molar ratio 1.1, catalytic concentration (1) 2.5 %, (2) 5 % and (3) 10 %.

Another important observation in figure 1 is the similarity between the values of catalytic concentration ratio and slope ratio. This fact shows that at least in the range of small catalytic concentrations, at 55°C, there is a linear relationship between the concentration of catalyst and the catalytic effect.

Further, admitting the catalytic concentration of 10 % as convenient level for our measurements, the effect of temperature was studied.

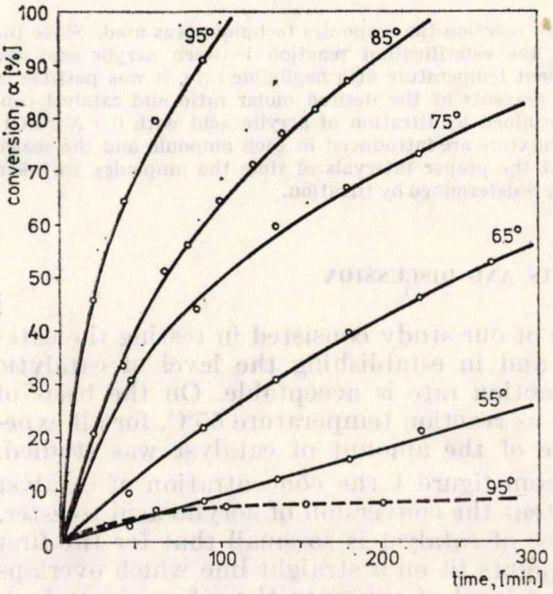

Fig. 2. — Conversion of acid against time at different reaction temperatures; molar ratio 1.1, catalytic concentration 10%

It can be clearly observed from figure 2 the noteworthy effect of both the temperature and the catalyst. Thus, in the absence of catalyst the conversion of acrylic acid hardly reaches 8 % in about 200 minutes, whereas in the presence of quaternized poly(dimethylaminoethyl methacrylate), at the same temperature (95°C), the conversion of acid is almost 100 % in about 100 minutes. Moreover, in the same figure it can be ascertained that between the two factors which influence the rate of the process, the catalyst and temperature, there is a strong interaction; neither of these parameters can lead to a strong effect as when they act together (see Figures (1) and (2)).

Another problem which has been studied was the influence of molar ratio between the two reactants. As shown in figure 3, in spite of the expectations, the yield of esterification at the same catalytic concentration, reaction time and temperature decreases with the rising of molar ratio acrylic acid : epichlorohydrin.

Certainly, the major problem which appears in this system consists in the manner of action of the quaternized poly(dimethylaminoethyl methacrylate) as catalyst. Generally, the polymeric catalyst can act in two ways:

a) the polymer has usually the catalytic centers in the side chains which act in the same manner as micromolecular analogues but it acts with other magnitude due to polymeric effect, and

b) the catalytic effect is due to the change of the distribution of reactants in the reaction medium by the possibility of polymers to concentrate one or both reactants on its surface.

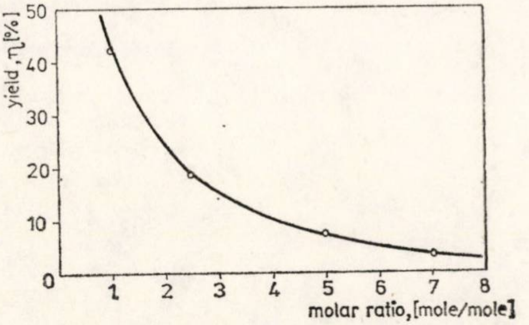

Fig. 3. — Yield against the molar ratio between acrylic acid and epichlorohydrin; reaction temperature 75°C catalytic concentration 10% and reaction time 1.5 h.

In the second case it is more difficult to demonstrate the action of the polymer. However, in our situation, the second case is more probable. We can assume that our polymer having quaternary ammonium groups concentrates the acid on its surface and facilitates the dissociation of acrylic acid. A very interesting fact is that the polymer is more soluble in the reaction mixture than in the acrylic acid (epichlorohydrin does not dissolve the quaternized polymer). Moreover, the ester formed acts as a solvent for the catalyst. These observations lead us to the hypothesis that at least one of the reagents is concentrated on the surface of the quaternized poly(dimethylaminoethyl methacrylate).

REFERENCES

[1] C. G. Overberger and T. W. Smith in "Reactions on Polymers", edited by J. A. Moore, D. Reidel Publishing Co., Dordrecht-Holland/Boston — U.S.A., 1973, p. 1.

[2] H. Morawetz and J. A. Shafer, *J. Phys. Chem.*, **67,** 1293 (1963).

[3] R. L. Letsinger and T. J. Savereide, *J. Amer. Chem. Soc.*, **84,** 3122 (1962).

[4] C. G. Overberger, T. St. Pierre, N. Vorcheimer, J. Lee and S. Yaroslavsky, *J. Amer. Chem. Soc.*, **87,** 296 (1965).

[5] C. G. Overberger, R. Corett, J. C. Salamone and S. Yaroslavsky, *Macromolecules*, **1,** 331 (1968).

[6] C. G. Overberger and H. Maki, *Macromolecules*, **3,** 214, 220 (1970).

[7] T. Kunitake and S. Shinkai, *J. Amer. Chem. Soc.*, **93,** 4247, 4256 (1971).

Revue Roumaine de Chimie, 25, 7, 1045–1054(1980)

Dedicated to Professor CRISTOFOR I. SIMIONESCU
on his 60th anniversary

POLYNUCLEAR AROMATIC HYDROCARBONS AS SENSITIZERS OF PHOTOOXIDATIVE DEGRADATION OF *cis*-1,4-POLYBUTADIENE

JAN F. RABEK and BENGT RÅNBY
Department of Polymer Technology, The Royal Institute of Technology
Stockholm, Sweden

Received January, 23, 1980

Polynuclear aromatic hydrocarbons (PAH) are present in polluted air in industrial and urban areas. In this paper three PAH such as anthracene, 9,10-dimethylanthracene and 9,10-diphenylanthracene, are shown to be effective sensitizers of photooxidative degradation of *cis*-1,4-polybutadiene. Both singlet oxygen and free radical mechanisms of oxidation are involved. The presence of PAH in polluted ai is one of several possible contributors to accelerated ageing of rubber materials.

INTRODUCTION

Research during the last decade has demonstrated the ubiquity of polynuclear aromatic hydrocarbons (PAH) as pollutants in the atmosphere, which is a result of increasing industrial and urban development and growing consumption of fossil fuels. The total concentration of PAH in rural areas and in industrial areas differ much, eg. naphthalene 70–350 ng/1000 m^3, anthracene 10–140 ng/1000 m^3 and diphenylanthracene 50–4400 ng/1000 m^3. PAH are present in polluted air adsorbed onto airborne particulate matter [1-6] and can easily be adsorbed on polymer surfaces.[7-9] Several previously published papers show that PAH may sensitize photooxidative degradation of polymers like polyolefins,[7-11] polystyrene,[12-14] poly(vinyl chloride),[15] polymethacrylates[16-20] and poly(vinyl acetate).[20] In our previously published results on singlet oxidation of polymers,[21] we have preliminary reported that anthracene accelerates photodegradation of polydienes. In this paper a more detailed study of the photosensitizing effect on anthracene derivatives on photooxidation of *cis*-1,4-polybutadiene is presented.

EXPERIMENTAL

Commercial *cis*-1,4-polybutadiene (PB) (Ameripol CB 220 from Goodrich Chemical Co.,) was purified by dissolving in benzene (analytically pure grade) and precipitation with ethanol under N_2. This procedure was repeated.

Anthracene (I) (Merck, Germany), 9,10-dimethylanthracene (II) (ICN-K & K Lab. Inc. USA) and 9,10-diphenylantracene (III) (ICN-K & K Lab. Inc. USA) were used without additional purification.

IR spectra of PB were obtained from films cast from 1 wt-% benzene solution on NaCl plate using a Perkin-Elmer 257 IR spectrometer.

Oxygen absorption was measured by a micromanometric method.[22] After each period of irradiation, the cell containing sample and the micromanometer were conditioned to room temperature (18°C) for 24 hrs.

Chain scission $S = (\overline{M}_{v0}/\overline{M}_{vt} - 1)$ was estimated from viscometric measurements of PB solutions in benzene at 32°C using an Ubbelohde viscometer. The $\overline{M}_v$ values were calculated from the Mark-Houwink-Sakurada relation $[\eta] = 14.5 \times 10^{-5}\, \overline{M}_v^{0.76}$.[23]

RESULTS AND DISCUSSION

Three polynuclear aromatic hydrocarbons (PAH) : anthracene (I), 9,10-dimethylanthracene (II) and 9,10-diphenylanthracene (III) were chosen for a study of the sensitizing effect on photo-oxidative degradation of *cis*-1,4-polybutadiene (PB). The three compounds I, II and III have very strong absorption in the region 250—300 nm and considerably weaker in the region 300—380 nm (Table 1). For that reason and also in order to avoid direct photodegradation of PB by light in the region 250—300 nm, we made all experiments with light of $\lambda > 310$ nm (using Schott Filter OG-310) which is not very harmful for PB.

The IR spectra of PB obtained after light irradiation (> 315 nm) in the presence of I, II and III (10^{-3}M) are almost identical with those of PB UV irradiated (250—400 nm) in air. The IR spectra show (Figure 1) :

(i) Formation of a strong absorption band in the range 3300—3600 cm^{-1} characteristic for hydroperoxy (OOH) and/or hydroxy (OH) groups. The OOH band can be partially removed by heating the sample in vacuum to 180°C (thermal decomposition of OOH groups). This indicates that the absorption band of hydroxy (OH) groups (3440—3450 cm^{-1}) is overlapped by the stronger absorption band of hydroperoxy (OOH) groups. It was also possible to remove hydroperoxy (OOH) groups by exposing the sample for 24 hrs to SO_2 (1 atm) (increase of SO_2 pressure gives better results). By this method the hydroperoxide (OOH) groups react selectively with SO_2 to form alkyl hydrogen sulphate :[24]

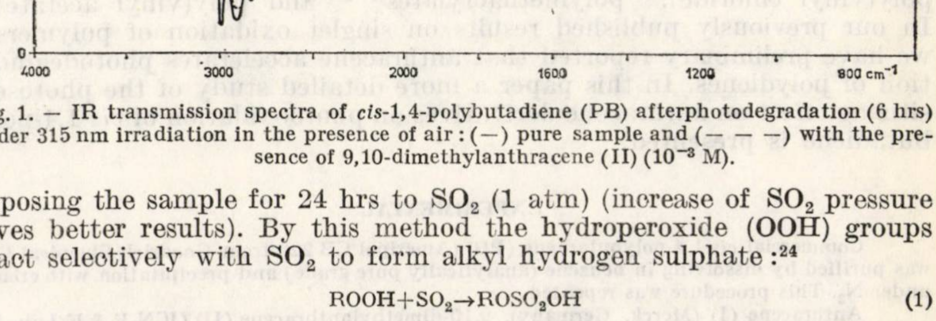

Fig. 1. — IR transmission spectra of *cis*-1,4-polybutadiene (PB) afterphotodegradation (6 hrs) under 315 nm irradiation in the presence of air : (—) pure sample and (— — —) with the presence of 9,10-dimethylanthracene (II) (10^{-3} M).

$$ROOH + SO_2 \rightarrow ROSO_2OH \tag{1}$$

After SO_2 treatment, the sample shows a residual band of hydroxy (OH) groups. The intensity of this band is approximately the same as that obtained after thermal decomposition of OOH groups.

(ii) Increase of absorption in the region 2720 cm^{-1} due to the CH stretching in aldehyde groups (CHO).

(iii) Formation of a strong absorption band at 1610–1740 cm^{-1} with a maximum at 1715 cm^{-1}, characteristic of CO stretching of different keton and/or aldehyde groups. This range is also characteristic for carboxylic acid groups at 1705 cm^{-1} which probably do not form during the oxidation of PB. The intensity of the peak at 1715 cm^{-1} increases with increasing time of irradiation.

(iv) Increase of absorption in the region 1200–800 cm^{-1}. Some assignments of particular peaks in this regions are made : peak at 1310 cm^{-1} (CH of *cis*-CH=CH), 990 cm^{-1} (CH out of plane of *cis*-CH=CH) and 910 cm^{-1} (CH_2 out of plane of CH_2=CH). It is generally accepted that increasing absorption in the range 1150–1000 cm^{-1} is due to C—O vibrations.

The IR spectra of PB irradiated in the presence of I, II or III show a possible *cis-trans* isomerization of PB (decrease of an absorption peak at 990 cm^{-1} (*cis*) and formation of a new peak at 965 cm^{-1} (CH out of plane of *trans*-CH=CH)).

(v) Decrease of the peak at 745 cm^{-1} assigned to *cis*-CH=CH.

The kinetics of oxygen consumption (Figure 2) measured by the micromanometric method shows that the rates of PB oxidation in the presence of the different PAN (10^{-3}M) are in the order II III I. The kinetic curves in figure 2 show accumulated oxygen consumption by PB and PAH. The PAH compounds are photooxidized to 9,10-endoperoxides. Because of the low concentration of added PAH (10^{-3}M) the amount of oxygen consumed by these additives is negligible in comparison with oxygen consumed by PB. Steric hinderance at 9,10 positions of anthracene, prevents II and III photodimerization, which is a competitive process to the formation of endoperoxides for I.[25–27] Photo-dimer of I is stable toward UV light irradiation, whereas endoperoxides of I, II and III can be completely or partially destroyed by light (depending on wavelength) with the formation of alkoxy bi-radicals produced by a cleavage of the 9,10-endoperoxide bond and different amounts of anthraquinone.[10] It was reported that singlet oxygen ($^1O_2$) is formed during photodecomposition of endoperoxides.[28–30] Subsequently a reaction occurs between the excited triplet

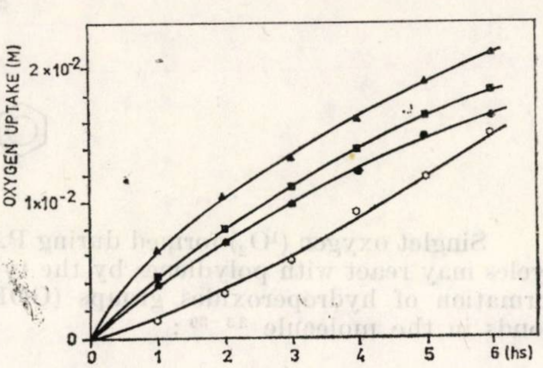

Fig. 2. — Kinetics of oxygen consumption of *cis*-1,4-polybutadiene (PB) during 315 nm irradiation in pure oxygen : (o) pure sample and in the presence of (10^{-3} M) ; (●) anthracene (I) ; (▲) 9,10-dimethylanthracene (II) and (■) 9,10-diphenylanthracene (III).

state of PAH and molecular oxygen with formation of $^1O_2$ by an energy transfer mechanism. $^1O_2$ reacts immediately with PAH molecule to give endoperoxide,[31,32] which is further decomposed with generation of $^1O_2$ or formation of alkoxy biradicals :

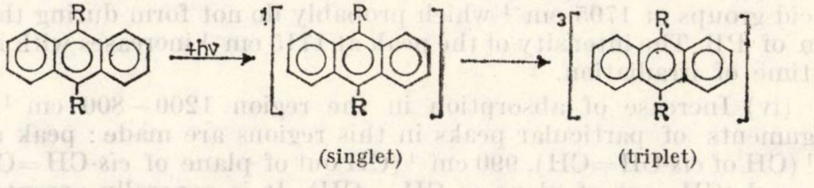
R
R
+hν
1
R
R
(singlet)
3
R
R
(triplet)

(2)

where R : H, CH_3 or C_6H_5.

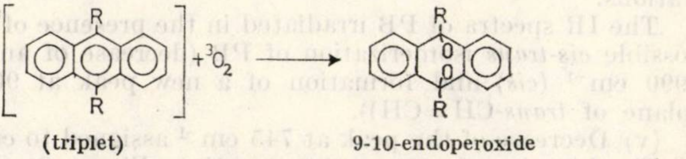
3
R
R
(triplet)
+$^3O_2$
R
O
O
R
9-10-endoperoxide

(3)

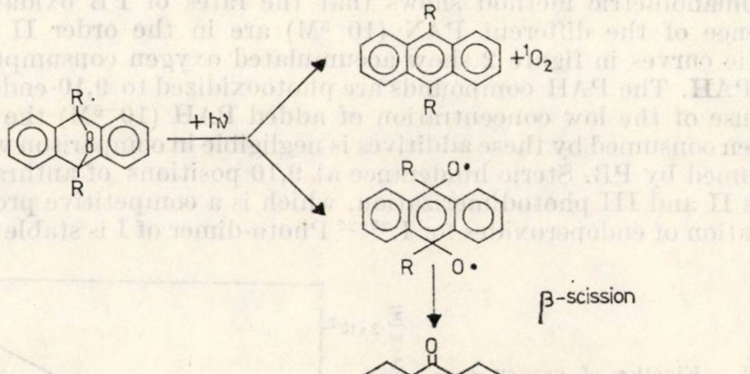
R
R
+$^1O_2$
R
O
O
R
+hν
R
O•
R
O•
β-scission
O
O
+2R•

(4)

(5)

(6)

Singlet oxygen ($^1O_2$) formed during PAH photooxidation in different cycles may react with polydienes by the typical "ene" type reaction with formation of hydroperoxides groups (OOH) and a shift of the double bonds in the molecule [33-39] :

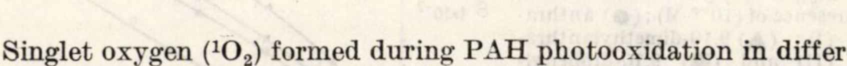

$$-CH_2-CH{=}CH-CH_2- + {}^1O_2 \rightarrow -CH{=}CH-\overset{\overset{\large OOH}{|}}{C}H-CH_2- \qquad (7)$$

Hydroperoxide groups can also be formed in a parallel reaction by a free radical oxidation mechanism. Alkoxy biradicals of PAH (·R·) (cf. reaction 5) formed from photolysis of 9,10-endoperoxide may abstract hydrogen from a methylene group of PB. As a result of this reaction a polymer allyl radical (I) is formed:

$$-CH_2-CH=CH-CH_2- + \cdot R\cdot \rightarrow -CH_2-CH=\underset{(I)}{\dot{C}H}- + \cdot RH \qquad (8)$$

Polymer allyl radicals (I) react immediately with molecular oxygen to form polymer peroxyradicals (II):

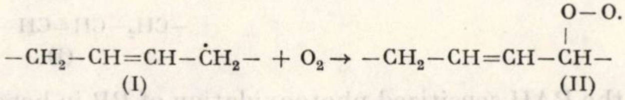
(9)

$$\underset{(I)}{-CH_2-CH=CH-\dot{C}H_2-} + O_2 \rightarrow \underset{(II)}{-CH_2-CH=CH-\overset{\overset{O-O.}{|}}{CH}-} \qquad (9)$$

Polymer peroxy radical (II) may further abstract hydrogen from the neighbouring or the same macromolecule to form hydroperoxide groups:

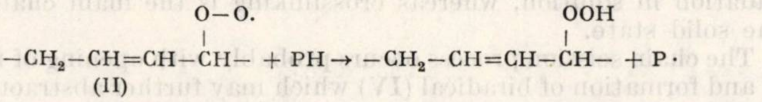
(10)

$$\underset{(II)}{-CH_2-CH=CH-\overset{\overset{O-O.}{|}}{CH}-} + PH \rightarrow -CH_2-CH=CH-\overset{\overset{OOH}{|}}{CH}- + P\cdot \qquad (10)$$

where PH is the polymer molecule.

During irradiation the concentration of hydroperoxy groups reaches a certain level (Figure 3) and stays constant during continued irradiation. The quanta in the UV light used for irradiation (310–400 nm) have sufficient energy to cleave the RO–OH bond (bond energy 42 kcal/mole).[40] Because the first excited state of hydroperoxides is dissociative, it is not possible to stop the photolysis of these groups. It occurs by a well known

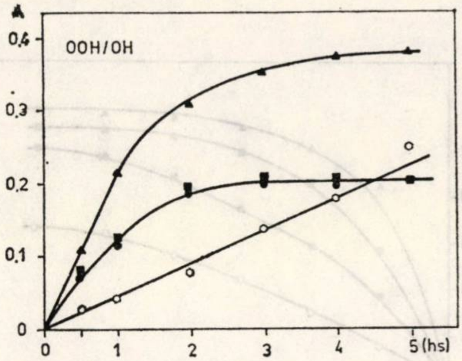

Fig. 3. — Kinetics of chain scission (S) *versus* time of exposure to 315 nm irradiation of *cis*-1,4-polybutadiene (PB) in the presence of air: (○) pure sample and in the presence of (10^{-3}): (●) anthracene (I); (▲) 9,10-dimethylanthracene (II) and (■) 9,10-diphenylanthracene (III).

mechanism in which polymer alkoxyradicals (III) and hydroxy radicals are formed:

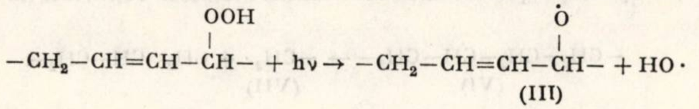
(11)

$$-CH_2-CH=CH-\overset{\overset{OOH}{|}}{CH}- + h\nu \rightarrow \underset{(III)}{-CH_2-CH=CH-\overset{\overset{\dot{O}}{|}}{CH}-} + HO\cdot \qquad (11)$$

Polymer alkoxyradical (III) can abstract hydrogen from the same or neighbouring macromolecule to produce hydroxy groups and new polymer allyl radicals (I):

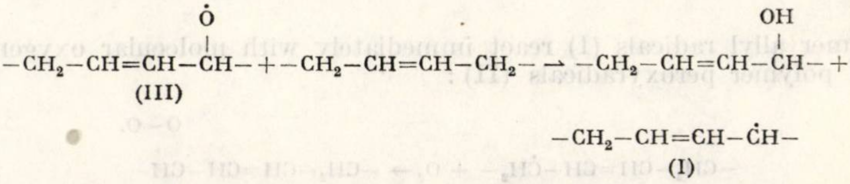

$$\underset{(III)}{-CH_2-CH=CH-\overset{\dot{O}}{CH}-} + -CH_2-CH=CH-CH_2- \rightarrow -CH_2-CH=CH-\overset{OH}{CH}- + \underset{(I)}{-CH_2-CH=CH-\dot{C}H-} \tag{12}$$

During the PAH sensitized photooxidation of PB in benzene solution a chain scission reaction of polymer molecules is observed (Fig. 4). This process occurs by a free radical mechanism and is independent of the oxidation by $^1O_2$ which occurs parallely. Crosslinking does not occur during degradation in solution, whereas crosslinking is the main chain reaction in the solid state.

The chain scission process occurs probably with opening of the double bond and formation of biradical (IV) which may further abstract hydrogen from the same or neighbouring macromolecule and form two radicals (I) and (V):

$$-CH_2-CH=CH-CH_2- \xrightarrow{+h\nu} \underset{(V)}{-CH_2-\dot{C}H-\dot{C}H-CH_2-} \tag{13}$$

$$\underset{(V)}{-CH_2-\dot{C}H-\dot{C}H-CH_2-} + -\dot{C}H_2-CH=CH-CH_2- \rightarrow \underset{(I)}{-CH_2-CH=CH-\dot{C}H-} + \underset{(VI)}{-CH_2-CH_2-\dot{C}H-CH_2-} \tag{14}$$

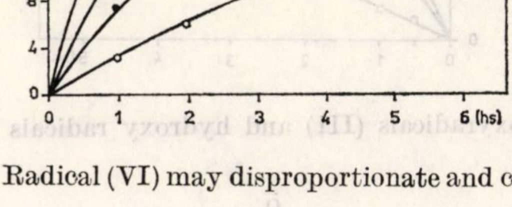

Fig. 4. — Kinetics of formation of OOH(OH) groups at 3345 cm^{-1} in *cis*-1,4-polybutadiene (PB) in the presence of air: (○) pure sample and in the presence of (10^{-3} M): (●) anthracene (I); (▲) 9,10-dimethylanthracene (II) and (■) 9,10-diphenylanthracene (III).

Radical (VI) may disproportionate and chain scission reaction is observed:

$$\underset{(VI)}{-CH_2-CH_2-\dot{C}H-CH_2-} \rightarrow -CH_2\cdot + \underset{(VII)}{CH_2=CH-CH_2-} \tag{15}$$

In this way are formed vinyl end groups which may react with singlet oxygen :

$$CH_2{=}CH{-}CH_2{-} + {}^1O_2 \rightarrow HOOH{-}CH_2{-}CH{=}CH{-} \qquad (16)$$

The crosslinking process occurs by the recombination of different types of polymer radicals such as (I)—(VII). It can also be considered another mechanism in which alkoxy biradical of PAH (·R·) may react with two polymer radicals, forming a bridge between them :

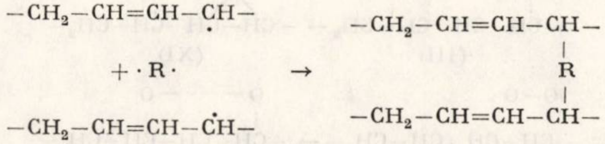

$$\begin{array}{l} -CH_2-CH=CH-\dot{C}H- \\ \qquad\qquad + \cdot R \cdot \\ -CH_2-CH=CH-\dot{C}H- \end{array} \rightarrow \begin{array}{c} -CH_2-CH=CH-CH- \\ | \\ R \\ | \\ -CH_2-CH=CH-CH- \end{array} \qquad (17)$$

Various types of free radicals are intermediates in the complex mechanism in which different groups such as OOH, OH, CHO, CO, —O— or —O—O— are formed along a polymer chain or at its ends. Below are presented some of possible mechanisms in which different oxygen containing groups can be formed.

Polymer end free radical (VII) formed in disproportionation reaction (15) reacts further with molecular oxygen to give polymer end peroxy radical (VIII) :

$$\underset{(VII)}{-CH_2\cdot} + O_2 \rightarrow \underset{(VIII)}{-CH_2-OO\cdot} \qquad (18)$$

which abstracts hydrogen from the same or neighbouring macromolecule to form hydroperoxide end groups :

$$\underset{(VIII)}{-CH_2-OO\cdot} + PH \rightarrow -CH_2-OOH + P\cdot \qquad (19)$$

The hydroperoxide groups thus produced can be further photolyzed under UV light to produce end polymer oxy radicals (IX) and hydroxy radicals :

$$-CH_2-OOH + h\nu \rightarrow \underset{(IX)}{-CH_2-O\cdot} + \cdot OH \qquad (20)$$

This radical after abstraction of hydrogen from the same or neighbouring macromolecule forms end hydroxygroups :

$$\underset{(IX)}{-CH_2-O\cdot} + PH \rightarrow -CH_2-OH + P\cdot \qquad (21)$$

The similar mechanism can be considered for the formation of OOH and OH groups along the backbone chain : (reactions 9—12).

The polymer oxy radical (X) which can be formed from the radical (VI) by the analogical reaction like 9—12 may disproportionate with formation of aldehyde end group and of an end free radical (VII) by the mechanism :

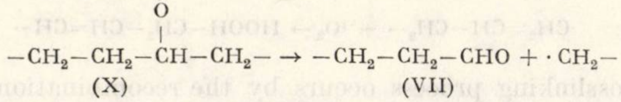

$$\underset{(\mathrm{X})}{-\mathrm{CH_2-CH_2-}\overset{\dot{\mathrm{O}}}{\overset{|}{\mathrm{CH}}}\mathrm{-CH_2-}} \rightarrow \underset{(\mathrm{VII})}{-\mathrm{CH_2-CH_2-CHO} + \cdot\mathrm{CH_2}-} \qquad (22)$$

There are also several possibilities for the formation of —O— and —O—O— groups during free radical oxidative degradation of PB :

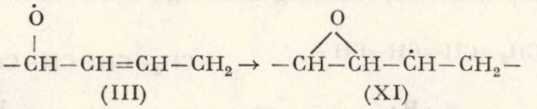

$$\underset{(\mathrm{III})}{-\overset{\dot{\mathrm{O}}}{\overset{|}{\mathrm{CH}}}\mathrm{-CH{=}CH-CH_2}} \rightarrow \underset{(\mathrm{XI})}{-\overset{\mathrm{O}}{\overbrace{\mathrm{CH-CH}}}\mathrm{-\dot{C}H-CH_2-}} \qquad (23)$$

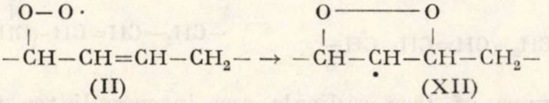

$$\underset{(\mathrm{II})}{-\overset{\mathrm{O-O\cdot}}{\overset{|}{\mathrm{CH}}}\mathrm{-CH{=}CH-CH_2-}} \rightarrow \underset{(\mathrm{XII})}{-\overset{\mathrm{O}\text{———}\mathrm{O}}{\overbrace{\mathrm{CH-\underset{\bullet}{CH}-CH}}}\mathrm{-CH_2-}} \qquad (24)$$

Many of polymer oxy- and peroxy radicals (II, III, and other possible types) may participate in the crosslinking processes with formation of oxy- and peroxy-bridges :

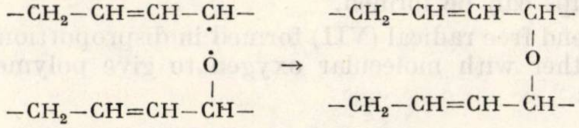

$$\begin{array}{c} -\mathrm{CH_2-CH{=}CH-\underset{\bullet}{CH}-} \\ \dot{\mathrm{O}} \\ | \\ -\mathrm{CH_2-CH{=}CH-CH-} \end{array} \rightarrow \begin{array}{c} -\mathrm{CH_2-CH{=}CH-CH-} \\ | \\ \mathrm{O} \\ | \\ -\mathrm{CH_2-CH{=}CH-CH-} \end{array} \qquad (25)$$

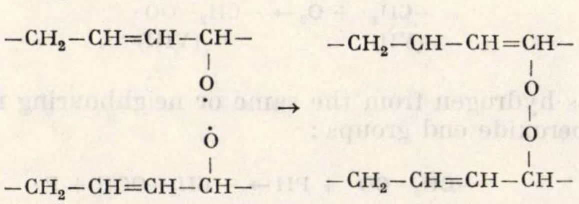

$$\begin{array}{c} -\mathrm{CH_2-CH{=}CH-CH-} \\ | \\ \dot{\mathrm{O}} \\ \\ \dot{\mathrm{O}} \\ | \\ -\mathrm{CH_2-CH{=}CH-CH-} \end{array} \rightarrow \begin{array}{c} -\mathrm{CH_2-CH-CH{=}CH-} \\ | \\ \mathrm{O} \\ | \\ \mathrm{O} \\ | \\ -\mathrm{CH_2-CH{=}CH-CH-} \end{array} \qquad (26)$$

All these reactions (7)—(22) show that mechanism of the free radical (and singlet oxygen) oxidation is rather a very complicated process, because many different types of free radicals are involved in it. Many of these free radicals were identified by ESR spectroscopy.[41]

A *cis-trans* isomerization reaction observed during the UV irradiation of PB occurs by a mechanism in which the double bond is opened and a biradical (V) (reaction 13) is formed. A new double bond formed after rotation of macromolecule fragment around $-\dot{C}-\dot{C}-$ bond should be preferentially *trans* (considering the lower energy level of *trans* form) :

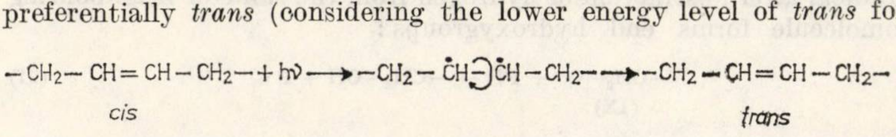

$$\underset{cis}{-\mathrm{CH_2-CH{=}CH-CH_2-}} + h\nu \longrightarrow -\mathrm{CH_2-\dot{C}H{\frown}\dot{C}H-CH_2-} \longrightarrow \underset{trans}{-\mathrm{CH_2-CH{=}CH-CH_2-}} \qquad (27)$$

A detailed study of IR spectra supports the above presented mechanism for oxidative degradation of PB :

Formation of hydroxy (OH) groups — IR band with max at 3440—3450 cm^{-1} (Fig. 1 and Fig. 3).

Formation of hydroperoxide groups (OOH)— IR band with max at 3440—3450 cm^{-1} (Fig. 1 and Fig. 3).

Formation of aldehyde(ketone)(CHO(CO)) groups — IR bands at 2720 cm^{-1} and 1610—1740 cm^{-1} (Fig. 1 and Fig. 5).

Formation of —O—(—O—O—) groups — IR band not well defined, but formation of this group can be supported by observed increase of IR spectrum in the range 1400—800 cm^{-1} (Fig. 1).

Cis-trans isomerization — IR bands at 990 cm^{-1} (*cis*) (decreasing) and 965 cm^{-1} (*trans*)(increasing)(Fig. 1).

Kinetic measurements of the formation HOO(HO)band at 3345 cm^{-1} (Fig. 3) and CHO(CO)band at 1715 cm^{-1} (Figure 5) show that PAH compounds sensitize oxidation in the order II > I ~ III.

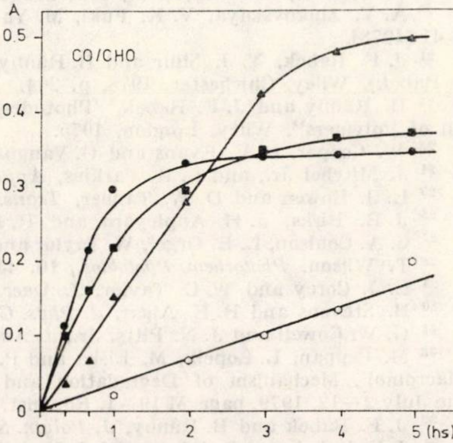

Fig. 5. — Kinetics of formation of CO(CHO) groups at 1717 cm^{-1} in *cis*-1,4-polybutadiene (PB) in the presence of air : (○) pure sample and in the presence of (10^{-3} M) : (●) anthracene (I); (▲) 9,10-dimethylanthracene (II) and (■) 9,10-diphenylanthracene (III).

Considering the role of PAH in the photo-oxidative degradation of PB, we may conclude that both mechanisms singlet oxygen and free radical oxidation occur simultaneously and cannot be separated from one another.

The mechanism is complicated because PAH endoperoxides and even quinone formed can effectively sensitize the oxidation process. The quinone was previously reported to sensitize the photo-oxidation of polypropylene,[42,43] polystyrene [44] and *cis*-1,4-polyisoprene [45,46] by free radical mechanism. The presence of PAH in polluted air may be responsible for one of many possible ways of accelerated ageing of rubber materials.

These investigations are part of a research program on photooxidation and photostabilization of polymers supported by the Swedish Board for Technical Development (STU) and is a project in the NORDFORSK program on singlet oxygen.

REFERENCES

[1] M. A. Fox and S. W. Staley, *Analyt. Chem.*, **48**, 972 (1976).
[2] R. J. Gordon, *Environm. Sci. Technol.*, **10**, 370 (1976).
[3] R. C. Pierce and M. Katz, *Environm. Sci. Technol.*, **9**, 347 (1975).

[4] M. Dong, D. C. Locke and E. Ferrand, *Analyt. Chem.*, **48**, 368 (1976).

[5] A. M. Krustlovic, D. M. Rosie and P. R. Brown, *Analyt. Chem.*, **48**, 1383 (1976).

[6] A. M. Krustlovic, D. M. Rosie and P. R. Brown, *Intern. Lab.*, **1977**, 11.

[7] D. J. Carlsson and D. M. Wiles, *J. Polym. Sci.*, **B11**, 759 (1973).

[8] R. H. Partridge, *J. Chem. Phys.*, **45**, 1679 (1966).

[9] A. P. Pivovarov, Y. V. Gak and A. Lukovnikov, *Vysokomol. Soedin.*, **A13**, 2110 (1971).

[10] J. Aspler, D. J. Carlsson and D. M. Wiles, *Macromolecules*, **9**, 691 (1976).

[11] D. J. Carlsson, A. Garton and D. M. Wiles, *Macromolecules*, **9**, 695 (1976).

[12] G. Rämme and J. F. Rabek, *Europ. Polym. J.*, **13**, 855 (1977).

[13] M. Nowakowska, *Makromol. Chem.*, **179**, 2953, 2959 (1978).

[14] G. Beggiato, P. Bortolus, S. Gardini, F. Minto and G. Pezzin, *Chim. Ind.*, **60**, 10(1978).

[15] E. D. Owen and J. I. Williams, *J. Polym. Sci.*, *A1*, **11**, 905 (1973).

[16] H. Mönig and H. Kriegel, "Proc. 3rd Intern. Congress on Photobiology", (Ed. B. C. Christensen and B. Buchman) Elsevier, Amsterdam, 1961, p. 618.

[17] H. Mönig and H. Kriegel, *Z. Naturforsch.*, **15b**, 333 (1960).

[18] H. Mönig and H. Kriegel, *Biophysik*, **2**, 22 (1964).

[19] H. Siewert, *Z. Naturforsch.*, **19b**, 806 (1964).

[20] A. V. Zinkovskaya, V. K. Fuki, M. Ya. Melnikov and V. N. Foch, *J. Polym. Sci.*, **B16**, 41 (1978).

[21] J. F. Rabek, Y. J. Shur and B. Rånby, in "Singlet Oxygen" (Eds. B. Rånby and J. F. Rabek), Wiley, Chichester, 1978, p. 264.

[22] B. Rånby and J. F. Rabek, "Photodegradation, Photo-Oxidation and Photostabilization of Polymers", Wiley, London, 1975.

[23] W. Cooper, D. E. Evans and G. Vaughan, *J. Polym. Sci.*, **59**, 241 (1962).

[24] J. Mitchel Jr., and L. R. Parkins, *Appl. Polym. Symp.*, **4**, 167 (1967).

[25] E. J. Bowen and D. W. Tanner, *Trans. Faraday Soc.*, **51**, 475 (1955).

[26] J. B. Birks, J. H. Appleyard and R. Pope, *Photochem. Photobiol.*, **2**, 493 (1963).

[27] C. A. Coulson, L. E. Orgel, W. Taylor and J. Weiss, *J. Chem. Soc.*, **1955**, 2961.

[28] T. Wilson, *Photochem. Photobiol.*, **10**, 441 (1969).

[29] E. J. Corey and W. C. Taylor, *J. Amer. Chem. Soc.*, **86**, 3881 (1964).

[30] B. Stevens and B. E. Algar, *J. Phys. Chem.*, **72**, 3468 (1968).

[31] G. W. Cowell and J. N. Pitts, Jr., *J. Amer. Chem. Soc.*, **90**, 1106 (1968).

[32] M. Čeppan, L. Lopčik, M. Liška and P. Pelikan", Proc. of 19th Prague Microsymp. on Macromol., Mechanism of Degradation and Stabilization of Hydrocarbon Polymers". Prague July 2—12, 1979, page M 19—1, Ed. Inst. of Macromol. Chem. Prague, 1979.

[33] J. F. Rabek and B. Rånby, *J. Polym. Sci.*, *A1*, **14**, 1463 (1976).

[34] J. F. Rabek and B. Rånby, *Photochem. Photobiol.*, **28**, 557 (1978).

[35] J. F. Rabek and B. Rånby, *Photochem. Photobiol.*, **30**, 133 (1979).

[36] J. F. Rabek and B. Rånby, *J. Appl. Polym. Sci.*, **23**, 2481 (1979).

[37] M. A. Golub, R. V. Gemmer and M. C. Rosenberg, *Adv. Chem.* Ser., No. 129, 11 (1978).

[38] M. A. Golub, M. C. Rosenberg and R. V. Gemmer, *Rubber Chem. Technol.*, **50**, 704 (1977).

[39] H. C. Ng and J. E. Guillet, *Macromolecules*, **11**, 929 (1978).

[40] S. W. Benson, *J. Chem. Educ.*, **42**, 502 (1965).

[41] B. Rånby and J. F. Rabek, "ESR Spectroscopy in Polymer Research", Springer Verlag, Berlin, 1977.

[42] D. J. Harper and J. F. McKellar, *Chem. Ind. (London)*, **21**, 848 (1972).

[43] M. Kitano, Jap. Pat. 71 24796 (1971) ; *Chem. Abstr.*, **77**, 20740 (1972).

[44] J. F. Rabek and B. Rånby, *J. Polym. Sci.*, *A1*, **12**, 295 (1974).

[45] J. F. Rabek in "23rd IUPAC Congress", Boston, 1971, Ed. Butterworths, London, Vol. 8, p. 29.

[46] J. F. Rabek, *Chemia Stosow.*, **11**, 89 (1967) (In Polish).

Revue Roumaine de Chimie, 25, 7, 1055–1057 (1980)

Dedicated to Professor CRISTOFOR I. SIMIONESCU
on his 60th anniversary

ON CHLOROBENZAMIDE MOLECULAR STRUCTURE

V. E. SAHINI, Ş. MOLDOVEANU and C. MIHAILCIUC
National Institute of Chemistry,
Bd. Republicii 13, Bucharest, Romania

Received January 10, 1980

The results of EHT and point charge computations for *ortho*- and *para*-chlorobenzamide are reported, and evidence for nonplanarity of the *ortho*-isomer is justified.

In our search for molecular structure — biological effects relationship of some benzamide derivatives, we studied theoretically the non-planarity of *ortho*- and *para*-chlorobenzamide using [1-3] the Extended Hückel Molecular Orbital Theory (EHT) followed by an electrostatic point-charge correction.

1. METHODS OF COMPUTATION

The EHT MO's were computed using a modified variant of the original EHT program with the parametrization listed in table 1. In both molecules studied, some angles and interatomic distances being considered as constants (those related to the benzenic ring and the amidic radical), the only one structural parameter to be examined is the dihedral angle between the aromatic ring and the plane defined by the amidic group; the following bond lengths (in Å) were used in our computation (we note by C′ a benzenic carbon atom) : C′—C′ : 1.39 ; C′—H : 1.09 ; C′—C : 1.52 ; C=O : 1.22 ; C—N : 1.34 ; C′—Cl : 1.65 and N—H : 1.02. Except the follow-

TABLE 1

Atomic	Orbital	Slater exponent	Ionisation potential (eV)
H	1s	1.2	13.6
C	2s	1.625	21.4
C	2p	1.625	11.4
N	2s	1.95	26.0
H	2p	1.95	13.4
O	2s	2.275	32.3
O	2p	2.275	14.8
Cl	3s	2.033	30.0
Cl	3p	2.033	14.5

ing angles : C′CO : 118° ; C′CN : 117° ; OCN : 123° and CNH : 107°, all the remainder angles were considered as having a value of 120°. For the *ortho*-isomer, the zero value of the dihedral angle corresponds to the oxygen atom of the amidic group on the side of the chlorine atom. The computation was performed with a 10° step for the 0°—180° range of *ortho*-isomer and 0°—90° for the *para*-isomer.

TABLE 3

Angle	Energy (eV)
0°	−955.3452
5°	−955.3716
10°	−955.3520
20°	−955.3447
30°	−955.3462
40°	−955.3203
50°	−955.1626
60°	−955.2358
70°	−955.2290
80°	−955.2090
90°	−955.1860

A correction suggested in order to diminish the too large covalent character of the bonds, as introduced by EHT, is the point-charge approximation, used in our computation in the case of the relatively strong electrostatic interactions between the amidic group and *ortho*-chlorine atom.[4-7]

2. RESULTS AND DISCUSSIONS

The energy values obtained for *ortho*-chlorobenzamide using both EHT and point-charge methods are listed in table 2. Two minima of energy are evidenced at 120° and 60° using EHT method and a minimum at 100° using point-charge method. It follows that for the molecular structure of *ortho*-chlorobenzamide our results suggest the existence of a 60°—80° dihedral angle with the nitrogen atom on the

TABLE 2

Angle	Energy (eV) point charge	Energy (eV) EHT
0°	−17.2525	−954.9682
10°	−17.2721	−954.9956
20°	−17.3384	−955.0629
30°	−17.4307	−955.1396
40°	−17.5577	−955.1709
50°	−17.6444	−955.2099
60°	−17.7376	−955.1948
70°	−17.8027	−955.1831
80°	−17.8340	−955.1787
90°	−17.8377	−955.1831
100°	−17.8417	−955.1733
110°	−17.8016	−955.1743
120°	−17.7610	−955.1949
130°	−17.6677	−955.1831
140°	−17.5494	−955.0508
150°	−17.4178	−954.8318
160°	−17.3280	−954.6718
170°	−17.2703	−954.4756
180°	−17.2611	−954.4838

side of the chlorine atom. The obtained rotation barrier, approximately 0.82 eV, represents a too high value to allow the interconversion between the two conformers at normal temperature.

The results of the EHT computation for the *para*-chlorobenzamide are listed in table 3. It follows that the molecule is nearly planar (in this case some computations were performed at intermediate angles between 0° and 10°), a very small dihedral angle (5°) being found to correspond to a minimum; it reflects probably a weak steric interaction between the NH_2 group and the *ortho*-hydrogen atom. The distance between the chlorine atom and the amidic group is too large in this isomer to assume an important electrostatic interaction; then a point charge correction is without significance. The rotation barrier, estimated at nearly 0.21 eV, is fully compatible with similar values obtained both experimentally and theoretically for many other molecules.

As a final point, we note that in the case of *para*-chlorobenzamide, an estimation of the dipole moment was obtained using the atomic charges resulted from EHT computation. Taking into account a value of 0.43 as a recommended [2] correction for the charge, the computed dipole moment is 3.17 D, in a satisfactory agreement with different experimental results : 3.38 D; 3.43 D and 3.73 D, obtained by Bates and Hobbs[8].

REFERENCES

[1] R. Hoffmann, *J. Chem. Phys.*, **39**, 1397 (1963).

[2] A. Botrel and C. R. Guerillot, *J. Chim. physique*, **71**, 974 (1974).

[3] K. Ruedenberg, *J. Chem. Phys.*, **66**, 375 (1977).

[4] H. Fischer and H. Kollmar, *Theor. Chim. Acta*, **16**, 163 (1970).

[5] M. J. S. Dewar and H. D. Lo, *J. Amer. Chem. Soc.*, **92**, 7201 (1971).

[6] S. Moldoveanu and A. Savin "Aplicaţii în chimie ale metodelor semiempirice de orbitali moleculari", Ed. Academiei, Bucharest (1980).

[7] R. S. Mulliken, *J. chim. physique*, **46**, 497, 675 (1949).

[8] W. W. Bates and M. E. Hobbs, *J. Amer. Chem. Soc.*, **73**, 2151 (1951); **74**, 746 (1952).

Revue Roumaine de Chimie, 25, 7, 1059–1068 (1980)

Dem vielseitigen Forscher, Herrn Professor Dr. Cristofor I. Simionescu,
mit den besten Grüßen und Glückwünschen zum 60. Geburtstag gewidmet

OPTISCHE ROTATIONSDISPERSION VON CELLULOSE, CELLULOSE-NITRAT UND EINIGEN α-POLYGLUCANEN

ROLF C. SCHULZ und ERHARD JACOBI
Institut für Organische Chemie, Universität Mainz, D-6500 Mainz,
Federal Republic of Germany

Eingegangen am 30. Januar 1980

ORD- und CD-Messungen an Cellulose waren bisher nur nach Überfuhrung in lösliche Derivate möglich. Nach Untersuchungen von Johnson und Swenson bildet Cellulose in Dimethylsulfoxid-Paraformaldehyd-Mischungen beim Erwärmen farblose, klare Lösungen. In der vorliegenden Arbeit wird festgestellt, daß diese Lösungen zur Messung der Rotationsdispersion verschiedener Cellulose-Proben geeignet sind. Man erhält glatte ORD-Kurven mit kleinen positiven Drehwerten zwischen 600 und 350 nm und zunehmenden negativen Werten unterhalb 320 nm. Die Kurven lassen sich nicht durch eine Yang-Doty-Gleichung linearisieren. Durch Vergleich mit α-Polyglucanen wird festgestellt, daß die Methylolierung während des Lösungsvorgangs keinen Einfluß auf die Drehwerte hat. Außerdem wurden die chiroptischen Eigenschaften von Cellulose-Nitraten bestimmt.

Till now optical rotatory dispersion (ORD) and circular dichroism (CD) of cellulose have been measured only for soluble derivatives. According to investigations from Johnson and Swenson, cellulose on heating in a mixture of dimethylsulfoxide and paraformaldehyde gives clear and colourless solutions. The present paper demonstrates that these cellulose solutions are suitable for ORD measurements. The plain CRD curves show small positive values between 600 and 350 nm and increasingly negative values at wavelengths less than 320 nm. These curves cannot be accomodated by the Yang-Doty-equation. Comparison with α-polyglucans showed that the methylolation during the solution process has no influence on the optical rotation. The chiroptical properties of cellulose nitrate were also investigated.

EINLEITUNG

Die Messung der optischen Rotationsdispersion (ORD) und des Circulardichroismus (CD) wurde im Laufe der letzten Jahre in sehr zahlreichen Untersuchungen zur Strukturaufklärung von Polypeptiden und Nucleinsäuren eingesetzt. Demgegenüber gibt es viel weniger Arbeiten, in denen diese Methoden auf Polysaccharide angewandt werden, da diese oberhalb von 180 nm keine Chromophore enthalten und daher meist glatte ORD-Kurven liefern[1,2,11] und außerdem, wie im Falle der Cellulose. Probleme bezüglich geeigneter Lösungsmittel auftreten. Wie wir in früheren Publikationen zeigen konnten, führen Wechselwirkungen zwischen Amylose und Jod,[3,4] Azofarbstoffen[5,6] oder Schwermetallsalzen[7] zu anormalen ORD-Kurven und Cotton-Effekten, aus denen Rückschlüsse auf Zusammensetzung und Struktur der Addukte und Komplexe möglich sind. Entsprechende Untersuchungen an Cellulose scheitern an der Unlöslichkeit dieses Polysaccharids. Es gelingt zwar, Cellulose durch Veresterung oder Verätherung in Derivate zu überführen, die nicht nur löslich sind, sondern auch für ORD-Messungen geeignete Chromophore enthalten ;[8] allerdings kann man hieraus keine Rückschlüsse auf die Rotationsdispersion der unsubstituierten Cellulose ziehen, da die chemische Modifizierung auch die Sekundärstruktur des Polysaccharids verändert. Das gleiche gilt für Drehwerte von Cellulose, gelöst in Schwermetallkomplex-Lösungen wie Cuoxam, Cadoxen usw.[7]. Kürzlich beschrieben Johnson et al,[9] und Swenson,[10] daß Cellulose beim Erwärmen in einer Mischung aus Dimethylsulfoxid und Paraformaldehyd klare, farblose Lösungen bildet. Man nimmt an, daß eine Methylolierung der primären OH-Gruppe am C_6-Atom der Glucosebausteine stattfindet[9] ; da diese Reaktion vermutlich aber kaum Einfluß auf die Drehwerte hat, erschien dieses Lösungsmittel für ORD-Messungen an Cellulose besonders geeignet. Im folgenden wird über die Rotatiosndispersion von Cellulose und verschiedenen α-Polyglucanen in Dimethylsulfoxid-Formaldehyd (DMSO/CH_2O) berichtet.

ERGEBNISSE UND DISKUSSION

Für die Untersuchungen wurden Cellulose-Proben mit verschiedenen Polymerisationsgraden (DP) und unterschiedlicher Kristallinität verwendet (siehe Tab. 1).

TAB. 1

Verwendete Cellulose-Proben

	Probenbezeichnung	DP	Röntgenkristallinität*)
Baumwoll-Linters	Cell-L	1250	70 %
Mikrokristalline Cellulose	MKC	166	78 %
Regenerat-Cellulose	Cell-R	230	40 %
Sulfit-Zellstoff	Cell-N	820	65 %

*) nach Firmenangaben

Der Lösungsvorgang ist im experimentellen Teil beschrieben. Bei dieser Arbeitsweise waren alle Proben, unabhängig vom DP und der Kristallinität, gut löslich ; es entstanden nach ca. 3 min. klare, farblose Lösungen, die nur noch geringe Anteile von nicht abgebautem Paraformaldehyd enthielten. Lediglich bei Sulfit-Zellstoffen blieb auch nach verlängerter Lösedauer bzw. nochmaliger Zugabe von Paraformaldehyd noch Ungelöstes zurück. Die Filtrate dieser sehr viskosen Ansätze waren leicht gelb gefärbt. Das abweichende Verhalten ist sicherlich auf unterschiedliche Restgehalte an Lignin und Fremdzuckerbestandteilen zurückzuführen. Da solche Lösungen für ORD-Messungen ungeeignet sind, wurden die Sulfit-Zellstoffe nicht weiter untersucht.

In Abb. 1 ist die ORD-Kurse einer 1% igen Lösung von Cell-L in DMSO/CH_2O gezeigt. Für die anderen Cellulose-Proben ergeben sich innerhalb der Fehlerbreite die gleichen Kurven. Sie zeigen im Wellenlängenbereich von 600–350 nm positive Drehwerte mit $[\alpha] < +10$ Grd ·ml/g ·dm ; zwischen 310 und 330 nm erfolgt ein Vorzeichenwechsel, und die Drehwerte nehmen mit abnehmender Wellenlänge zu. Bei 260 nm beträgt der spez. Drehwert $[\alpha] = -45$ Grd ·ml/g ·dm. Wegen der Absorption des DMSO is hier die Grenze des Meßbereichs erreicht. Erwartungsgemäß liegt eine glatte Rotatiosdispersion ohne Cotton-Effekte vor, da weder Cellulose noch Methylol-Cellulose in diesem Bereich absorbieren. Die in Frage kommenden Chromophore des Glucosebausteines zeigen Cotton-Effekte erst um bzw. unterhalb von 180 nm [2,11,12] und haben deshalb keinen Einfluß auf den Verlauf der ORD-Kurve, die somit die sogenannte Grundrotation darstellen sollte.

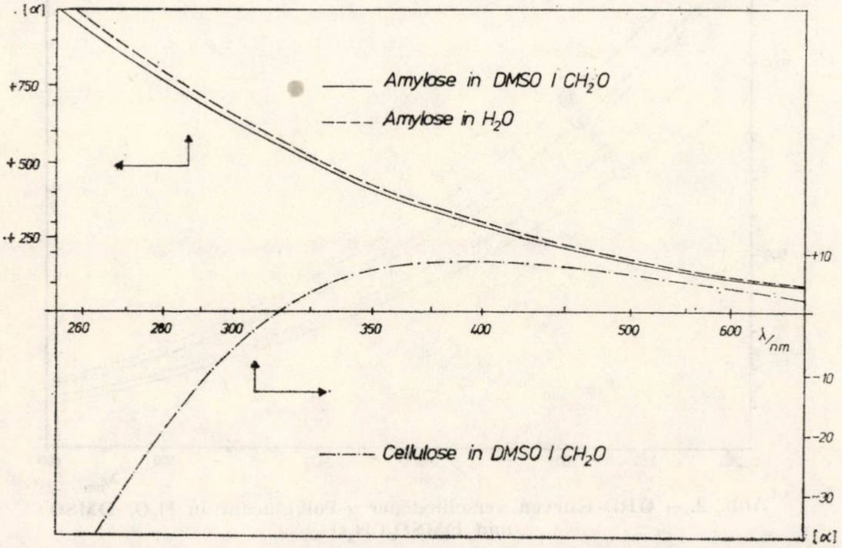

Abb. 1. – ORD-Kurven von Amylose und Cellulose in DMSO/CH_2O und H_2O.

Um zu prüfen, ob das Lösungsmittel DMSO/CH_2O einen Einfluß auf das chiroptische Verhalten der Cellulose hat, wurden einige Polysaccharide zum Vergleich herangezogen, die sowohl in H_2O als auch in DMSO und DMSO/CH_2O löslich sind. Als besonders geeignet erschienen die α-Polyglucane Amylose, Amylopektin, Glykogen sowie α- und β-Schardinger-Dextrin. Der Lösevorgang mit DMSO/CH_2O wurde unter den gleichen Bedingungen wie bei den Cellulose-Proben durchgeführt. Es wurde nicht untersucht, ob und in welcher Position die Methylolierung stattfindet. Aus dem wesentlich schnelleren Verlauf des Lösens in DMSO/CH_2O (im Vergleich zu H_2O und DMSO) kann geschlossen werden, daß hier eine der Cellulose analoge Reaktion erfolgt. Obwohl nicht ohne weiteres davon ausgegangen werden kann, daß bei allen hier verwendeten α-Polyglucanen ebenfalls vorwiegend die Hydroxylgruppe am achiralen C_6 reargiert, sollte dennoch aus diesen Messungen hervorgehen, ob die Methylolgruppe auf das chiroptische Verhalten einen Einfluß hat. Die ORD-Kurven der verschiedenen in H_2O, DMSO und DMSO/CH_2O gelösten Polysaccharide sind in Abb. 2 dargestellt.

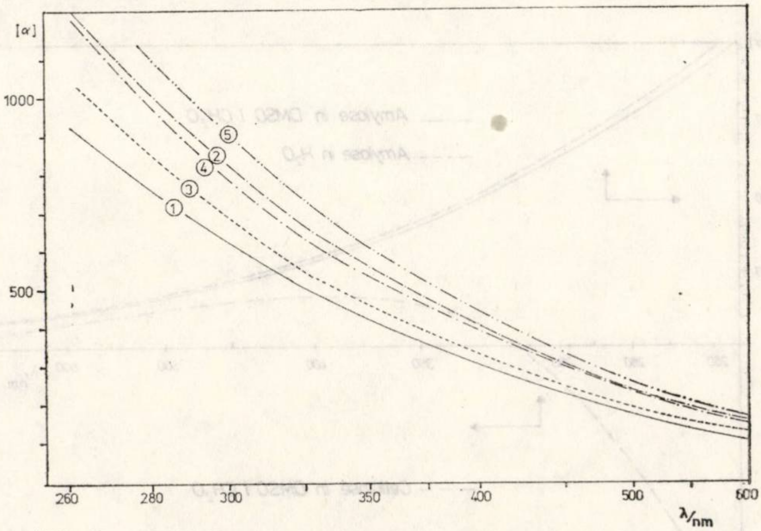

Abb. 2. — ORD-Kurven verschiedener α-Polyglucane in H_2O, DMSO und DMSO/CH_2O.

1 Amylose (in H_2O oder DMSO oder DMSO/CH_2O);
2 Amylopektin (in H_2O oder DMSO oder DMSO/CH_2O);
3 α- und ß-Schardinger-Dextrin (in H_2O oder DMSO oder DMSO/CH_2O);
4 Glykogen (in H_2O oder DMSO);
5 Glykogen (in DMSO/CH_2O).

Sie verlaufen erwartungsgemäß im positiven Bereich, wobei die Drehwerte nach kurzen Wellenlängen hin zunehmen. Wie eine Auftragung der nach Yang-Doty modifizierten eintermigen Drude-Gleichung (Gl. 1) eindeutig zeigt, handelt es sich bei

$$[\alpha]\cdot\lambda^2 = [\alpha]\cdot\lambda_0^2 + A \qquad \text{(Gl. 1)}$$

mit $[\alpha]$: spez. Drehung Grd ml/g dm
λ : Wellenlänge in nm
A : Rotationskonstante
λ_0 : Dispersionskonstante

allen α-Polyglucanen um normale ORD-Kurven. Die aus den jeweiligen Geradensteigungen erhältlichen Dispersions-konstanten λ_0 stimmen untereinander sehr gut überein und werden durch die bisher in der Literatur [13] angegebenen Werte von $\lambda_0 = 140-160$ nm bestätigt. Es ergeben sich für Amylose, Amylopektin, Glakogen : $\lambda_0 = 158$ nm ; für α- und β-Schardinger-Dextrin : $\lambda_0 = 160$ nm.

Für die vorliegende Problemstellung ist besonders wichtig, daß die ORD-Kurven der in H_2O gelösten Polysaccharide mit denen in DMSO und DMSO/CH_2O praktisch identisch sind. Lediglich beim Glykogen sind die Drehwerte in DMSO/CH_2O etwas größer als in H_2O oder DMSO. Die Übereinstimmung in der Dispersionskonstante λ_0 macht jedoch deutlich, daß auch hier keine grundsätzliche Veränderung der Kurvenform vorliegt.

Es kann also davon ausgegangen werden, daß durch das Lösungsmittel-system DMSO/CH_2O und die damit bewirkte Methylolierung keine entscheidenden chiroptischen Veränderungen gegenüber den unsubstituierten Polysacchariden erfolgt und daher auch die ORD-Kurven der verschiedenen Cellulosen als charakterisch für die unsubstituierte Cellulose angesehen werden können.

Vergleicht man nun die ORD-Kurven der α-Polyglucane mit denen von Cellulose, so fällt auf, daß die spez. Drehwerte der Cellulose weitgehend im negativen Gebiet verlaufen und dem absoluten Betrag nach um ein bis zwei Zehnerpotenzen kleiner sind. Dies ist um so bemerkenswerter, als man nach der vorliegenden Literatur sowohl bei den α-Polyglucanen [14] als auch bei dem starren Cellulose-Molekül [15] eine helicale und somit chirale Sekundärstruktur im betrachteten Lösungsmittel ausschließen kann

Die stark unterschiedlichen Drehwerte der Lösungen von Amylose, Amylopektin und Glykogen einerseits sowie von Cellulose andererseits sollten also vorwiegend auf dem einzigen grundlegenden Unterschied beruhen, nämlich auf der Konfiguration am C_1-Atom des Anhydroglucoserestes. Darüber hinaus kann gesagt werden, daß das asymmetrische C_1-Atom betragsmäßig den größten Beitrag zum Gesamtdrehwert liefert. Dies steht in Einklang mit Untersuchungen von Listowski et al.[16]

Die in DMSO/CH_2O beobachteten Unterschiede zwischen Amylose und Cellulose werden auch für andere Derivate der beiden Polysaccharide festgestellt. Während 2,3,6-Tris(0-trimethylsilyl)-, Trimethyl-sowie Triacetylamylose,[17] in $CHCl_3$ gelöst, jeweils Drehwerte zeigen, die denen der unsubstituierten Amylose in H_2O entsprechen, werden für die analogen Celluloseverbindungen [17–19,29] negative $[\alpha]$-Werte gemessen. Lediglich diejenigen Derivate zeigen ein hiervon abweichendes Verhalten, bei denen Substituenten eingeführt wurden, die im zugänglichen Meßbereich absorbieren und deren ORD-Kurven deshalb Cotton-Effekte aufweisen.[17]

Solche Chromophore scheinen auch der Grund dafür zu sein, daß z.B. Cellulose-Nitrat (Abb. 4) und Tribenzoylcellulose wenn auch kleine, so doch positive $[\alpha]_D$-Werte zeigen, während viele andere Cellulosederivate negative Drehwerte besitzen. So zeigen Cellulose-Xanthate,[20] die erwähnten 2,3,6-Tris(O-trimethylsilyl)- und Trimethylcellulose [17] sowie sämtliche untersuchten Tricarbonsäureester der Cellulose [21,29] negative $[\alpha]_D$ Werte.

Neben Vorzeichen und Größe der Drehwerte sollte aber auch der Verlauf der in Abb. 1 gezeigten ORD-Kurve Beachtung finden. Im Gegensatz zu den α-Polyglucanen ergibt die Rotationsdispersion der Celluloselösung bei einer Auftragung nach Gl. 1 keine Gerade (Abb. 3).

Im allgemeinen treten Abweichungen von der eintermigen Drude-Gleichung auf im Bereich einer Cotton-Bande oder bei helicalen Sekundärstrukturen. Wie bereits erwähnt, trifft hier beides nicht zu.

Für ein von der eintermigen Drude-Gleichung abweichendes Verhalten von Cellulosederivaten finden sich in der Literatur verschiedene Erklärungen; Buntjakov und Averyanova [22] schreiben das komplexe Verhalten von Cellulose-Acetaten den verschiedenen Asymmetriezentren zu, die mit unterschiedlichen Vorzeichen und unterschiedlicher Stärke zur Rotation beitragen.

Spezielle Ordnungszustände machen Neely [23] sowie Treiber und Nadziakiewicz [20] für das komplexe Verhalten der Lösungen von Methylcellulose bzw. Viskose verantwortlich.

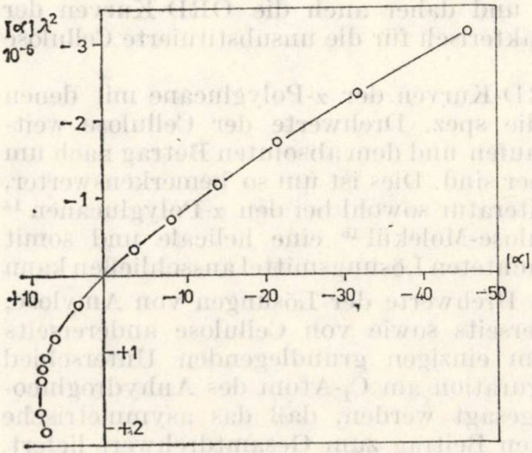

Abb. 3. — Auftragung der ORD-Kurve von Cellulose in DMSO/CH_2O (aus Abb. 1) nach der Yang-Doty-Gleichung (Gl. 1).

In diesem Zusammenhang seien auch die Untersuchungen von Fort, Moore und Tidswell [24] erwähnt, die die Änderung von $[\alpha]_D$ für Cellulose-Acetat in verschiedenen basischen Lösungsmitteln auf die Stärke der spezifischen Wechselwirkung des Polymeren mit dem Lösungsmittel zurückführen. Auch Buntjakov und Averyanova [22] erklären den Lösungsmitteleinfluß auf die ORD-Kurven von Cellulose-Acetat mit der Fähigkeit dieser Lösungsmittel, mit den Hydroxyl-gruppen der nicht vollständig acetylierten Cellulose eine Wechselwirkugehen.

Für das Lösungsmittel DMSO/CH_2O wäre Ahnliches durchaus denkbar, da die Lösewirkung dieses Systems nicht zuletzt auf einer solchen Wechselwirkung des DMSO mit den verschiedenen Hydroxylgruppen beruht.

Die komplexen ORD-Kurven der Methylol-Cellulose könnten aber auch durch ein zur Viskose analoges Verhalten erklärt werden. Treiber und Nadziakiewicz [20] beobachteten nämlich die erwähnten Abweichungen von der Drude-Gleichung im besonderen bei hohen Viskosekonzentrationen (2,1 und 7,8 %).

Da 1 % ige Lösungen aller Cellulose-Proben in DMSO/CH_2O hohe Viskositäten haben, sind hier besondere Ordnungszustände nicht auszuschließen. Es wäre interessant, die ORD-Kurven von Cellulose in DMSO/CH_2O über einen größeren Konzentrationsbereich zu untersuchen. Leider läßt sich aber die Konzentration nicht ausreichend variieren. Einerseits sind die 1 % igen Lösungen schon so viskos, daß höhere Kontentrationen nicht mehr zu handhaben sind ; andererseits sind die Meßeffekte bei geringeren Konzentrationen mit den zur Verfügung stehenden Spektral polarimetern zu klein. Daher waren Messungen an den für dieses Problem besonders aufschlußreichen verdünnten Cellulose-Lösungen nicht mehr mit ausreichender Genauigkeit möglich. In diesem Zusammenhang sei auch auf kürzlich publizierte Untersuchungen von E. und R. Gruber [25] hingewiesen, die aus Lichtstreuungs- und Viskositätsmessungen an Cellulose in DMSO/CH_2O auf das Vorhandensein von übermolekularen Aggregaten schließen. Eigene Viskositätsmessungen an verschiedenen Cellulose-Proben deuten ebenfalls darauf hin, daß das Lösungsmittelsystem DMSO/CH_2O nicht so problemlos ist, wie von den Autoren [9,11] bisher angonommen. So konnte die von Sweson [10] für dieses System aufgestellte Staudinger-Kuhn-Mark-Houwink-Gleichung nicht bestätigt werden.

Zur Bestimmung des Polymerisationsgrades (DP) der verwendeten Proben wurden diese daher nach bekannter Methode [26] in die Cellulose-Nitrate überführt und nach Lösen in Athylacetat viskosimetriert. Die so erhaltenen DP sind in Tab. 1 angegeben. Obwohl Cellulose-Nitrate ausführlich untersucht wurden, enthält die Literatur, außer einigen Angaben über $[\alpha]$ -Werte, nur wenige Daten über chiroptische Eigenschaften.[27] Es lag daher nahe, im Rahmen dieser Arbeit auch die optische Aktivität von Cellulose-Nitrat zu untersuchen. Es zeigte sich, daß die ORD- und CD-Kurven aller gemessenen Proben bei N-Gehalten zwischen 11,0 und 12,8% innerhalb der Meßgenauigkeit von $\pm 5\%$ übereinstimmen. Eine in diesen Grenzen für die verschiedenen Cellulose-Nitrate gültige ORD-bzw. CD-Kurve ist in Abb. 4 gezeigt. Die ORD-Kurve beginnt im langwelligen Bereich bei positiven Drehwerten, die den $[\alpha]_D$-Werten der o. a. Autoren [27] entsprechen. Der Verlauf der Kurve mit einem „Gipfel" bei 290 nm zeigt einen positiven Cotton-Effekt an, wie sich dies auch durch die CD-Spektren bestätigen ließ ($[\alpha]_{290} = +315$ Grd $\cdot$ml$\cdot$g$^{-1}\cdot$dm^{-1}).

Das „Tal" der ORD-Kurve konnte nicht mehr erfaßt werden, da ebenso wie beim CD das Spektrum nach der kurzwelligen Seite durch die Absorption des Lösungsmittels Äthylacetat bei ca. 250 nm begrenzt wird. Die CD-Messungen ergaben für sämtliche Proben einen gleichen Kurvenverlauf mit einem molaren dichroitischen Absorptionskoeffizienten bei 264 nm von $\Delta\varepsilon_{\max} = +0{,}51 \pm 0{,}04$.

In Abb. 4 ist neben der optischen Rotationsdispersion und dem Circular-Dichroismus auch das UV-Spektrum von Cellulose-Nitrat (in Äthylacetat) gezeigt sowie die ORD-Kurve für Methylol-Cellulose, die als die sog. Grundrotation für Cellulose angesehen werden kann. Es wird deutlich, daß zum einen der Schnittpunkt zwischen der Grundrotation und der anormalen ORD-Kurve mit dem Wendepunkt dieser Kurve übereinstimmt und zum anderen in diesem Bereich von 263 bis 265 nm auch das Maximum der CD-Kurve liegt. Da das Auftreten eines Cotton-Effektes immer mit einer Absorption verbunden ist, kann die CD-Bande bei 264 nm der im UV-Spektrum nur schwach erkennbaren Schulter in gleicher spektraler Lage zugeordnet werden.

Der Dissymmetriefaktor bei dieser Wellenlänge liegt mit $g_{264} = \Delta\varepsilon/\varepsilon = 1{,}0 \cdot 10^{-2}$ in der erwarteten Größenordnung für inhärent dissymmetrische Chromophore [28].

In diesem Zusammenhang erscheint es interessant, die Verknüpfung von CD und ORD etwas näher zu betrachten, indem man die über das Kronig-Kramer-Theorem abgeleitete Beziehung zwischen der Molekular-

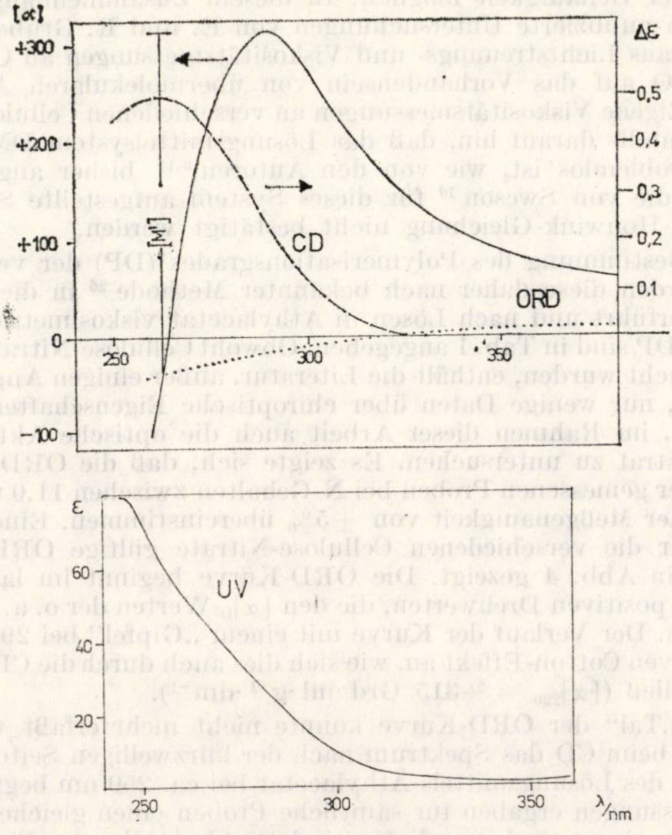

Abb. 4. — *oben*

ORD von Cellulose-Nitrat ($c = 1$ g/100 ml); Schichtdicke: 0,5 cm.
ORD von Cell-L in DMSO/CH_2O (aus Abb. 1) $[M'] = 50\,a$ (siehe Gl. 2)
$[\alpha]$ = spezifische Drehung in Grd. ml. g^{-1}. dm^{-1}.
CD von Cellulose-Nitrat
$\Delta\varepsilon$ = molarer dichroitischer Absorptionskoeffizient in 1. mol^{-1}. cm^{-1}.

unten

UV-Spektrum von Cellulose-Nitrat
= molarer Absorptionskoeffizient in 1. mol^{-1}. cm^{-1}.

amplitude a der ORD-Kurve und dem molaren dichroitischen Absorptionskoeffizienten $\Delta\varepsilon_{max}$ anwendet.

$$a = 40{,}28 \cdot \Delta\varepsilon \qquad \text{(Gl. 2)}$$

mit $a = \dfrac{[M]_1 - [M]_2}{100}$; $[M]_1$: molekulare Drehung beim Gipfel

$[M]_2$: molekulare Drehung beim Tal

Da bei der ORD-Kurve nur der Gipfel erfaßt werden konnte, wurde näherungsweise $a = 2[M']/100$ gesetzt, wobei $[M']$ den Betrag der molekularen

Drehung zwischen Gipfel und Schnittpunkt der Grundrotations-Kurve mit der anormalen ORD-Kurve bei etwa 264 nm darstellt (s. Abb. 4).

Danach erhält man für $[M'] = 1055$ * und für die Molekularamplitude $a = 21{,}1$ Grd $\cdot$cm^2 $\cdot$decimol^{-1}. Nach Gl. 2 kann nun mit $\Delta\varepsilon = 0{,}51$ l $\cdot$mol^{-1} $\cdot$cm^{-1} die Molekularamplitude berechnet werden :

$$a = 40{,}28 \cdot 0{,}51 = 20{,}5 \text{ Grd} \cdot \text{cm}^2 \cdot \text{decimol}^{-1}$$

Wie man sieht, zeigen die experimentelle und die berechnete Molekularamplitude innerhalb der Fehlerbreite gute Übereinstimmung ; vor allem, wenn man berücksichtigt, daß Gl. 2, genau genommen, nur für den $n \rightarrow \pi^*$-Übergang einer Carbonylgruppe in einem gesättigten Keton gilt und für andere Chromophore nur näherungsweise Gültigkeit hat.

EXPERIMENTELLER TEIL

In Anlehnung an die Vorschriften von Johnson et al.[9] bzw. Swenson[10] wurde zur Herstellung einer 1 %igen Lösung folgendermaßen vorgegangen : 0,1 g Cellulose und 0,5 g Paraformaldehyd werden bei Raumtemperatur zusammen mit 10 ml DMSO in ein Reagenzglas gegeben, das weitgehend in in Siliconölbad (135—140°C) eingetaucht wird. Unter kräftigem Rühren (Magnetrührer) steigt die Temperature nach 3 min. auf ca. 120°C wobei eine starke Formaldehydentwicklung einsetzt. Nach weiteren 3 min. ist die Temperatur von ca. 130°C erreicht, die dann bis zum Ende der vollständigen Gasentwicklung und dem Erreichen einer klaren Lösung nur noch gering ansteigt.

Anschließend wird zur Abtrennung von geringen ungelösten Rückständen über eine G4-Fritte abgesaugt und die Lösung bei leichtem Unterdruck im Exsiccator abkühlen lassen. Die ungelösten Rückstände bestehen vorwiegend aus Paraformaldehyd.

LITERATUR

[1] V. S. R. Rao und J. F. Foster, *Biopolymers*, **1**, 527 (1963).

[2] R. W. Woody, *J. Polym. Sci.-Macromol. Rev.*, **12**, 302 (1977).

[3] R. C. Schulz, R. Wolf und H. Mayerhöfer, *Kolloid-Z. Z. Polymere* **227**, 65 (1968).

[4] B. Pfannemüller, H. Mayerhöfer und R. C. Schulz, *Makromol. Chem.*, **121**, 147 (1969) ; *Biopolymers*, **10**, 243 (1971).

[5] H. M. Bössler und R. C. Schulz, *Kolloid-Z. Z. Polymere*, **238**, 578 (1970).

[6] J. Adriani Trisnadi, H. M. Nössler und R. C. Schulz, *Colloid Polym. Sic.*, **252**, 222 (1974).

[7] H. M. Bössler und R. C. Schulz, *Makromol. Chem.*, **135**, 87 (1970).

[8] H. Bittiger und G. Keillich, *Angew. Chem.*, **81**, 336 (1969).

[9] D. C. Johnson, M. D. Nicholson und F. C. Haigh, *Appl. Polym. Symp.*, **28**, 931 (1976) ; M. D. Nicholson und D. C. Johnson, *Cellulose Chem. Techn.*, **11**, 349 (1977).

[10] H. A. Swenson, *Appl. Polym. Symp.*, **28**, 945 (1976).

[11] R. G. Nelson und W. C. Johnson Jr., *J. Amer. Chem. Soc.*, **94**, 3343 (1972).

[12] D. G. Lewis und W. C. Johnson Jr., *Biopolymers*, **17**, 1439 (1978).

[13] J. Szejtli und S. Augustat, *Stärke*, **18**, 38 (1966) ; J. Szejtli, M. Richter und S. Augustat, *Biopolymers*, **5**, 5 (1967) ; M. Richetr, S. Augustat und E. Schierbaum, ,,Ausgewählte Methoden der Stärkechemie'', Wissenschaftl. Verlagsges., Stuttgart 1968 ; R. M. Purvinas und H. F. Zobel, *Carbohydrate Res.*, **10**, 129 (1969) ; F. R. Dintzis und R. Tobin, *Biopolymers*, **7**, 581 (1969).

---

*) In Abb. 4 wurde sowohl beim molaren Circulardichronismus $\Delta\varepsilon$, der molekularen bzw. mittleren grundmolaren Drehung $[M']$ als auch beim molaren Extinktionskoeffizienten ε mit einem mittleren Grundmolgewich für die Cellulose-Nitrate von $M_g = 297$ gerechnet, obwohl die untersuchten Nitrate nur einen N-Gehalt von 11,0—12,8 % hatten, was einem Substitutionsgrad von DS = 2,0—2,5 pro Glucoseeinheit entspricht.

[14] W. Banks und C. T. Greenwood, *Stärke*, **23**, 300 (1971).

[15] K. E. Goebel, C. E. Harvie und D. A. Brant, *Appl. Polym. Symp.*, **28**, 671 (1976) ; H. A. Swenson, *Appl. Polym. Symp.*, **28**, 945 (1976).

[16] I. Listowsky, G. Avigard und S. Englard, *J. Am. Chem. Soc.*, **87**, 1765 (1965) ; I. Listowsky und S. Englard, *Biochem. Biophys. Res. Commun.*, **30**, 329 (1968).

[17] H. Bittiger und G. Keilich, *Biopolymers*, **7**, 539 (1969).

[18] A. S. Duntjakov und V. M. Averyanova, *J. Polym. Sci.*, *C* **38**, 109 (1972).

[19] K. Hess, ,,Die Chemie der Cellulose und ihrer Begleiter", Akademie-Verlag, Leipzig, 1928, S. 594.
W. B. Neely, *Nature*, **185**, 159 (1960).

[20] E. Treiber und H. C. Nadziakiewicz, *J. Polym. Sci.*, *C* **2**, 357 (1963).

[21] C. J. Malm, J. W. Mench, D. L. Kendall und G. D. Hiatt, *Ind. Eng. Chem.*, **43**, 688 (1951).

[22] A. S. Buntjakov und V. M. Averyanova, *J. Polymer Sci.*, *C* **38**, 109 (1972).

[23] W. B. Neely, *Nature*, **185**, 159 (1960).

[24] R. J. Fort, W. R. Moore, B. M. Tidswell, *Chem. Ind. (London)*, **1964**, 108.

[25] E. Gruber und R. Gruber, *Cellulose Chem. Tech.*, **12**, 345 (1978).

[26] G. V. Schulz, M. Marx-Figini, *Makromol. Chem.*, **31**, 140 (1959 ; *Makromol. Chem.*, **52**, 133 (1962) ; *Makromol. Chem.*, **54**, 102 (1962).

[27] L. Vignon, *Bull. Soc. chim. France*, **31**, 107 (1904) ; H. von Mosenthal, *Angew. Chem.*, **20**, 1970 (1907).

[28] P. Crabbé, ,,Optical Rotatory Dispersion and Circular Dichronism in Organic Chemistry", Holden-Day, San Francisco 1965.

[29] S. Mukherjee, R. H. Marchessault und A. Sarko, *Biopolymers*, **11**, 291 (1972).

Revue Roumaine de Chimie, 25, 7, 1069–1076 (1980)

Zu Ehren Prof. Cristofor I. Simionescu
gelegentlich seines 60 Geburstags

MEDIUMEINFLÜSSE BEI DER SOLVOLYSE VON ALKYLHALOGENIDEN. IV[1]

HYDROLYSE VON *t*-BUTYLCHLORID

R. H. SCHUSTER und ANCA NICOLAU
Zentrum für physikalische Chemie ICECHIM Bukarest, Splaiul Independenţei 202, Bukarest

Eingegangen am 4. August 1979

Die Temperaturabhängigkeit der Reaktionsgeschwindigkeitskonstanten der Hydrolyse von *t*-Butylchlorid in Wasser wurde im Bereich 278,26–323,16 K untersucht. Aus der systematischen Abweichung der Ergebnisse von einem der Arrhenius-Gleichung entsprechenden Verhalten wurde ein polynomialer Korrekturfaktor des Präexponentialfaktors berechnet. Die somit korrigierte Arrheniusgleichung erlaubt eine genaue Beschreibung der Temperaturabhängigkeit der Reaktionsgeschwindigkeitskonstanten für die untersuchte Reaktion. Bei konstanten Präexponentialfaktor ergibt sich aus den experimentellen Ergebnissen eine temperaturabhängige Aktivierungsenergie, der ein $\Delta C_p \neq$ Wert von $-$ 88 cal.K^{-1} entspricht. Die erhaltenen Ergebnisse werden als Lösungsmitteleffekte diskutiert.

The temperature dependence of the rate constants for hydrolysis of *t*-buthylchloride in water was investigated in the temperature range 278.26–323.16 K. A polynomial correction to the preexponential factor of Arrhenius equation was calculated for the systematical deviation of the experimental data. The corrected Arrhenius-equation described the temperature dependence of reaction rates within the experimental errors. Keeping constant the preexponential factor, the activation energy is temperature dependent; the slope corresponds to a value of $\Delta C_p \neq = -$ 88 cal.K^{-1}. The experimental results are discussed as solvent effects.

Die Hydrolyse von Alkyhalogeniden und im Besonderen von *t*-Butylchlorid (*t*-BuCl) ist öfter in einer Reihe von wässerigen binären Gemischen [2] und seltener in reinem Wasser [3,4] untersucht worden. Kinetische Untersuchungen lassen sich bei Solvolysen in hochwässerigen Lösungsmitteln zufriedenstellend mittels elektrischen Leitfähigkeitsmessungen [5,6] durchführen, wobei genau bestimmte Reaktionsgeschwindigkeitskonstanten (RGK) im Falle von Hydrolysereaktionen prägnante temperaturabhängige Lösungsmitteleffekte anzeigen können. Im Folgenden soll auf die Temperaturabhängigkeit der RGK bei der Hydrolyse von *t*-BuCl näher eingegangen werden.

EXPERIMENTELLES

Reagenzien : *t*-BuCl (BDH) wurde über wasserfreiem K_2CO_3 destilliert und anschliessend in wasserfreiem Aceton zu einer Standardlösung gelösst, die, wie Kontrolleitfähigkeitsmessungen ergaben, längere Zeit stabil blieb.

Wasser mit einer spezifischen Leitfähigkeit von 0,5—0,8 μS wurde aus destilliertem Wasser über eine Ionenaustauschersäule von 1000 mm × 40 mm, mit einer Durchlaufgeschwindigkeit von 100 ml. Min^{-1}, hergestellt. Dabei wurden die ersten 800 ml entfernt und erst der Rest zum Reinigen und Abfüllen der Messzelle verwendet. Der Behälter für Leitfähigkeitswasser wurde unter einer CO_2-freien Stickstoffatmosphäre abgefüllt.

Versuchsanordnung : Die verwendete Messzelle (50 ml Volumen) (Abbildung 1) ist mit einem Kapillarinjektionsstutzen (1) versehen. Die Flüssigkeit in der Messzelle wurde mit einem magnetischen Rührer (2), der mit einem Ring versehen war um eine geringe Reibung und eine gute Führung zu gewährleisten, kräftig angerüht, wobei die in die Innenwände der Zelle praktizierten Dornen (3) sowie auch die Elektrodenhalterungen (4) und das Thermometer (5) eine Wirbelströmung gewährleisten.

Durch den konischen Glassprofen (6), dem die Elektrodenhalterung (4) ange-schweisst ist, kann die mit Leitfähigkeitswasser angefüllte Messzelle so verschlossen werden, dass das überschüssige Wasservolumen herausgedrängt wird, wodurch dass in der Messzelle vorhandene Gasvolumen möglichst klein gehalten wird, so dass eine Verflüchtigung des *t*-BuCl auf ein Minimum herabgesetzt ist.

Mittels zwei in Serie geschalteter Thermostaten (U—10, VEB Prüfgerätewerk Medingen-Dresden — DDR) konnten die Temperaturschwankungen in der Messzelle auf ± 0,02° reduziert werden.

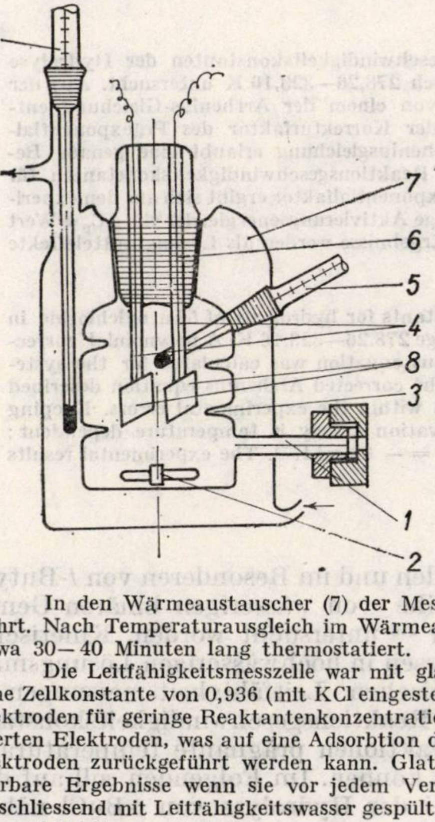

Abb. 1. — Schematische Darstellung der Messzelle : *1* — Kapillarinjektionsstutzen ; *2* — Magnetrührer ; *3* — Dornen ; *4* — Elektrodenhalterung ; *5* — Präzisionsthermometer ; *6* — Konischer Glasspfropfen ; *7* — Wärmeaustauscher ; *8* — Platinelektroden ; *9* — Thermometer.

In den Wärmeaustauscher (7) der Messzelle wurde ein zweites Thermometer (9) eingeführt. Nach Temperaturausgleich im Wärmeaustauscher und Messzelle, wurde zusätzlich noch etwa 30—40 Minuten lang thermostatiert.

Die Leitfähigkeitsmesszelle war mit glatten Platinelektroden (8) ausgestattet und hatte eine Zellkonstante von 0,936 (mit KCl eingestellt), da die mit Platinschwarz überzogenen Platinelektroden für geringe Reaktantenkonzentrationen kleinere RGK-Werte ergaben als mit unplatinierten Elektroden, was auf eine Adsorbtion des Elektrolyten an den porösen schwarzen Platinelektroden zurückgeführt werden kann. Glatte Platinelektroden zeigen dagegen gut reproduzierbare Ergebnisse wenn sie vor jedem Versucht mit heisser Salpetersäuere behandelt und anschliessend mit Leitfähigkeitswasser gespült werden. Die erhaltenen Leitfähigkeitswerte waren bis auf 0,1 % reproduzierbar.

Die Messzelle aus Borosilikatglass wurde vor jedem Versuch gespült ausgedampft und anschliessend mit einem warmen CO_2-freien Stickstoffstrom getrocknet. Unter einem CO_2-freien Stickstoffstrom wurde die Messzelle auch mit Leitfähigkeitswasser angefüllt. Lag die anschliessend gemessene spezifische Leitfähigkeit über 1 μ S wurde die gesammte Messzelle geleert und von neuem gereinigt. Wird die Messzelle etwa 10—15 s lang geöffnet, so steigt die Leitfähigkeit des Wassers etwa 0,5—1 % an, was sich als bedeutungslos erweisst, da die Leitfätigkeitsmessungen des Lösungsmittels im Falle von Lösungen starker Säuern vernachlässigt werden kann, falls CO_2 die einzige Verunreinigung im Lösungsmittel ist.

Um die Vermischzeit zu vermindern wurde die Spitze der Hamiltonspritze so verformt, dass die Flüssigkeit unter einem grossen Winkel ausgespritzt wurde.

Die Leitfähigkeitsmessungen wurden mit einem Radelkis Konduktivimeter (Type OK—102) vorgenommen, dessen Anzeigezeit für den ganzen Skalenbereich 0,1 s, bzw bis zur mittleren Halbwertskonzentration etwa 0,03—0,05 s betrug. Der bei den Versuchen durch Einspritzen der Reaktanten, Vermischen und Anzeige bedingte Zeitfehler konnte ermittelt werden, indem 0,05 ml Salzsäure (0,05 n) unter heftigem Rühren in die Messzelle eingespritzt wurden. Unter Verwendung eines an das Konduktivimeter angeschlossenen Schnellschreiber, wurden im Mittel 0,11 s bis zum volständigen Ausschlang gemessen.

Da der Widerstand, R_x (oder die Leitfähigkeit $1/R_x$), einer Lösung durch eine allgemeine Gleichung der Form:

$$A/R_x = C - BC^\alpha$$

wiedergegeben werden kann, wo A, B Konstanten sind, C die Molkonzentration bedeutet, denen die Werte $B < 1$, $\alpha > 1$ bzw. $C = 10^{-4}—10^{-2}$ Mol. 1^{-1} zukommen, kann die Beziehung durch eine Gerade:

$$1/R_x = C/A$$

angenähert werden, wobei maximal ein Fehler von 0,2 % auftritt.[2] Die Reaktionszeit wurde auf 0,05 s genau bestimmt. Bei allen ausgeführten Versuchen war keine Olefinausbeute zu beobachten.

Kinetische Messungen: In die vorbereitete Messzelle wurde mit einer Hamiltonspritze (1 ml), deren Nadel 8 cm lang war, 0,05—0,1 ml *t*-BuCl in Aceton-Standardlösung in die turbulent durchgerühte Flüssigkeit so schnell als möglich eingespritzt.

Während des Reaktionsablaufes wurde ein Anwachsen der RGK beobachtet. Bis zu Umsätzen von 20—30 %, war dieser Anstieg nicht linear, wonach sich mit guter Annäherung eine lineare RGK-Zeit Beziehung ergab. Für RGK-Bestimmungen wurden die Messungen im linearen Bereich ausgeführt und die erhaltenen Werte nach der Methode der kleinsten Quadrate auf unendliche Verdünnung des gebildeten Elektrolyten ($t = 0$) extrapoliert. Versuche mit verschiedenen Messzellen zeigten, dass die erhaltenen extrapolierten RGK-Werte nicht von den Aussmassen der Zelle oder den Reaktantenkonzentrationen abhängen. Bei niederer Temperaturen wurden mindestens fünf Versuche durchgeführt, während bei höheren Temperaturen 15—20 Versuche nötig waren um statistisch gesicherte Werte zu erhalten, wobei auch die Standardfehler, σ, für die extrapolierten RGK (k_{ex}) berechnet wurden. Da, bei ansteigenden RGK, die für verschiedene Zeitpunkte erhaltenen Werte einen Mittelwert haben, der von dem Zeitbereich in dem die Messungen durchgeführt wurden abhängt, sei darauf hingewiesen dass die Extrapolierung der RGK Werte auf $t = 0$ reelle und reproduzierbare Werte ergibt.

ERGEBNISSE UND DISKUSSION

Die kinetischen Messungen wurden im Temperaturbereich 278,26—323,16 K bei neunzehn verschiedenen Temperaturen durchgeführt. Im Verlauf der Versuche erschien die Notwendigkeit systematische Fehler, wie z.B. die Verflüchtigung von *t*-BuCl in den Gasraum der Messzelle auszuschliessen. In Tabelle 1 sind die extrapolierten k_{ex} mit den jeweiligen Standardfehlern (k_{ex}), neben den berechneten RGK-Werten (k_{ber} und k_{korr}) für den untersuchten Temperaturbereich angegeben.

TABELLE 1

Extrapolierte Reaktionsgeschwindigkeitskonstanten und Standardabweichungen, sowie die nach Gleichung (1) und (3) berechnete Reaktionsgeschwindigkeitskonstanten für die Hydrolyse von *t*-Butylchlorid

T(K)	$k_{ex}(s^{-1}) \times 10^5$	$\pm\sigma\,(s^{-1}) \times 10^5$	$k_{ber}(s^{-1}) \times 10^5$	$\frac{\Delta k}{k_{ber}} \times 100$	$k_{korr}(s^{-1}) \times 10^5$	$\frac{\Delta k'}{k_{korr}} \times 100$
278,26	156,6	4,1	167,1	−6,28	156,1	+0,32
280,46	221,4	5,2	232,4	−4,73	222,4	−0,44
282,96	324,2	7,2	335,9	−3,48	329,2	−1,5
285,61	493,3	9,4	492,8	+0,10	493,3	0,0
288,26	727,0	13	717,9	+1,26	731,4	−0,6
291,16	1114	18	1075	+3,62	1111	+0,27
293,36	1508	24	1452	+3,85	1514	−0,39
295,46	2027	24	1928	+5,13	2022	+0,24
298,16	2911	34	2759	+5,50	2907	+0,13
301,16	4299	56	4077	+5,22	4301	−0,04
303,46	5766	69	5472	+5,37	5761	+0,08
304,26	6352	68	6055	+4,90	6373	−0,03
307,86	9818	140	9489	+3,46	9883	−0,06
309,96	12555	240	12272	+2,26	12670	−0,94
313,26	18540	430	18250	+1,58	18510	+0,16
315,67	24410	680	24530	−0,48	24460	−0,83
318,36	32280	740	33190	−2,74	32380	−0,30
320,86	41850	1400	44180	−5,27	42060	−0,49
323,16	53070	2000	57260	−7,31	53110	−0,07

Die k_{ex}-Werte steigen ungefähr $3 \cdot 10^2$ mal im untersuchten Temperaturbereich an, was jedoch im Vergleich zu der lösungsmittelbedingten Steigerung der RGK-Werte gering ist. So ist z.B. die RGK bei 298,16 K in Wasser etwa $5 \cdot 10^5$ mal grösser als im Aceton-Wasser Gemisch mit $X_{H_2O} = 0{,}311$.[7]

Werden aber z.B. die k_{ex} Werte für *t*-BuCl mit den entsprechenden Werten für *iso*-Propylchlorid (*i*-PrCl)[8] bei verschiedenen Temperaturen verglichen, so erhält man folgendes Bild:

T (K)	291,16	298,16	318,36
$\frac{k_{t-\mathrm{BuCl}}}{k_{i-\mathrm{PrCl}}}$	$1{,}5 \cdot 10^5$	$1{,}3 \cdot 10^5$	$9{,}3 \cdot 10^4$

Somit scheint der Einfluss der α-Methylierung bei der Hydrolyse von Alkylhalogeniden temperaturabhängig.

Die prozentuellen Fehler (ε) liegen zu Beginn und Ende des untersuchten Temperaturbereiches zwischen 0,2–0,6% und zeigen wie aus Abbildung 2 hervorgeht in Abhängigkeit von ln k_{ex} ein breites flaches Minimum das $\varepsilon = 0{,}2\%$ nicht übersteigt.

Die Temperaturabhängigkeit der RGK kann in erster Annäherung durch die Arrhenius-Gleichung:

$$k_{ber} = (2{,}92 \pm 0{,}49)10^{15} \exp\left(-\frac{23220 \pm 210}{RT}\right) \tag{1}$$

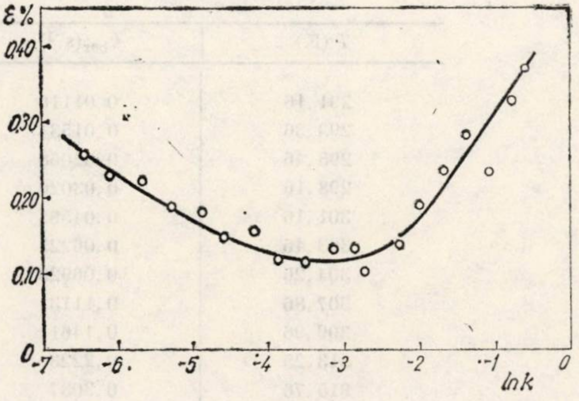

Abb. 2. – Änderung der prozentuellen Fehler (ε) in Abhängigkeit von ln k_{ex}.

ausgedrückt werden, wobei sowohl der präexponentielle Faktor, als auch die Arrhenius-Aktivierungsenergie in dem für die Hydrolyse von Alkylderivaten normalen Bereich liegen.

Die relativen Abweichungen $(k_{ex} - k_{ber})/k_{ber}$, der k_{ex}-Werte von den berechneten RGK, k_{ber}, zeigen aber eine systematische Abweichung wie aus Tabelle 1 ersichtlich ist und übersteigen die experimentelle Fehlergrenze im Mittel um eine Grössenordnung. Die Temperaturabhängigkeit dieser relativen Abweichung kann durch Gleichung (2) dargestellt werden:

$$\text{Ø}(T) = -\,2{,}4659 \cdot 10^{-4} T^2 + 0{,}148157\ T - 22{,}1988 \tag{2}$$

Wird diese Gleichung als Korrekturfaktor in die Arrhenius-Gleichung (1) eingeführt, ergibt sich:

$$k_{korr} = \mathrm{A}/1 + \text{Ø}(T)/\exp(-E_a/RT) \tag{3}$$

wobei die nach Gleichung (3) berechneten RGK mit k_{ex} innerhalb der experimentellen Fehlergrenze gut übereinstimmen. Somit kann die Temperaturabhängigkeit von k_{ex} durch Gleichung (3) zufriedenstellend dargestellt werden. Die analytische Form von Ø (T) zeigt an, dass die gefundennen k_{ex} Werte in Abhängigkeit der Temperatur weniger ansteigen als aufgrund einer rein exponentiellen Gleichung zu erwarten ist. So lautet für die ersten untersuchten Temperaturen die Arrhenius-Gleichung:

$$k = 2{,}91 \cdot 10^{16} \exp(-24580/\mathrm{RT}) \tag{4}$$

Da die k_{ex} Werte mit ansteigenden Temperaturen stetig kleiner werden als die nach Gleichung (4) berechneten, beträgt bei 323,16 K die Abweichung schon 28% (Tabelle 2).

TABELLE 2

Vergleich der experimentell bestimmten mit der nach Arrheniusgleichung (4) berechneten RGK

T (K)	$k_{\text{ber}}(\text{s}^{-1})$	$(k_{ex} - k_{\text{ber}})/k_{\text{ber}}$
291,16	0,01116	0,019
293,36	0,01534	0,017
295,46	0,02068	0,02
298,16	0,03020	0,036
301,16	0,04563	0,057
303,46	0,06225	0,074
304,26	0,06928	0,084
307,86	0,1113	0,11
309,96	0,1461	0,14
313,25	0,2223	0,16
315,76	0,3037	0,19
318,36	0,4180	0,22
320,86	0,5655	0,25
323,16	0,7434	0,28

Das beobachtete Verhalten kann durch ein temperaturabhängiges Verhalten der Aktivierungsparameter erklärt werden. Aus den k_{ex} für je zwei benachbarte Temperaturen wurde die Aktivierungsenergie berechnet.[9] In Abbildung 3 ist der eindeutig abfallende Trend der, im Mittel auf ±190 cal·Mol^{-1} bestimmten, Aktivierungsenergie zu bemerken.

Die Gleichung für die Temperaturabhängigkeit der Aktivierungsenergie lautet:

$$E_a = 50190 - 90{,}3\ T \tag{5}$$

wobei der von uns erhaltenen Wert für dE/dT von 90,3 cal·K^{-1} oder entsprechend $\Delta C_p^{\neq} = -88{,}4$ cal·K^{-1} höher liegt, als die in der Literatur angegebenen Daten.[2] Wir nehmen an, dass unser $\Delta C_p^{\neq}$ Wert sowohl durch den grossen Temperaturbereich, wie auch den kleinen Fehlerbereich ($\varepsilon = 0{,}2\%$) bei der RGK-Bestimmung gesichert ist.

Wie aus Abbildung 3 ersichtlich ist, hat die berechnete Aktivierungsenergie[9] durchwegs positive Werte und fällt eindeutig gegen höhere Temperaturen ab, wobei die erhaltenen Werte in dem für SN_1 Reaktionen bekannten Bereich liegen. Die Temperaturabhängigkeit der Aktivierungsentropie kann durch die Gleichung (6) angenähert werden:

$$\Delta S^{\neq} = 92{,}8 - 0{,}275\ T \tag{6}$$

Sowohl die negative Aktivierungswärmekapazität, als auch die positive Aktivierungsentropie lassen sich aufgrund der Modelle von wässerigen Nichtelektrolytlösungen erklären.[10,11] Wasser besteht aus Molekülclustern die infolge von Wasserstoffbrückenbindungen mit 4, 3, 2 oder 1 benachbarten Wassermolekülen in tridimensionale Strukturen eingegliedert sind und aus ungebundenen Wassermolekülen. Mit Temperaturanstieg wird der Molbruch gebundener Wassermoleküle kleiner. Man nimmt nun an, dass beim Lösen eines Nichtelektrolyten, z.B. *t*-BuCl, in Wasser durch das grosse Volumen desselben die Wassermoleküle exoterm in eine höher geordnete und gleichzeitig kompaktere Struktur hineingedrängt werden, wodurch der Anteil gebundener Wassermoleküle in der ersten und zweiten Solvatationssphäre ansteigt. Dieser Vorgang bedingt aber einen Abfall der Enthalpie und Entropie des Grundzustandes im Vergleich zu dem einer hypothetischen Gasreaktion. Die schwache Polarisierbarkeit des *t*-BuCl Radikals bewirkt dass beim Lösen schwache *t*-BuCl-Wasser Wechselwirkungen auftreten, die wieder einen negativen Beitrag zur Solvatationsentropie liefern. Die Überlagerung beider Vorgänge mit gegensätzlichem Effekt bewirkt insgesammt sowohl einen negativen Beitrag zur Solvatationsenthalpie als auch zur Solvatationsentropie. Der Grundzustand wird daher im Vergleich zu einer hypothetischen Gasreaktion durch eine negative Solvatationsenthalpie als auch – entropie gekennzeichnet. Durch Einwirken des Kräftefeldes der Solvatationssphäre wird der Grundzustand des *t*-BuCl stetig gegen den Übergangszustand hin ionisiert. Das Auftreten von partiellen elektrischen Ladungen im Übergangszustand, bewirkt aber gleichzeitig eine Zerstörung der Struktur der Solvatationssphäre und eine

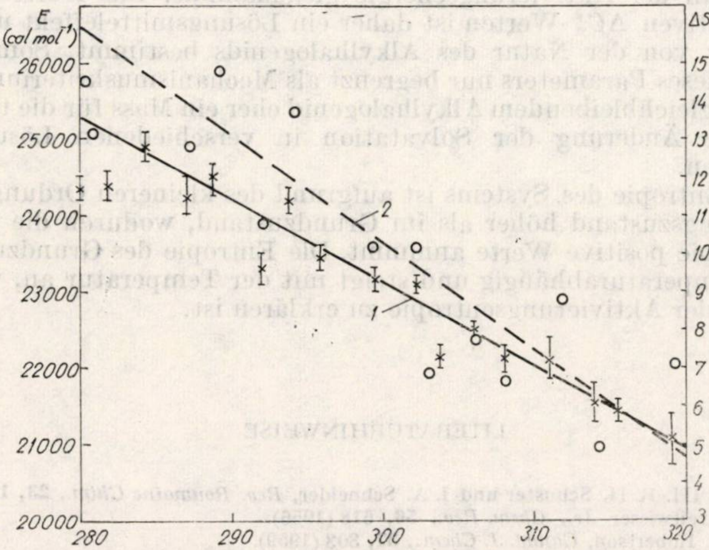

Abb. 3. — Temperaturabhängigkeit der Aktivierungsenergie 1. (x—x—) und Aktiviersungsentropie 2. (o—o—o—o).

Reorganisation durch Ion-Dipol Kräfte. Mit ansteigender Temperatur wird nun die zur Zerstörung nötige Energie kleiner da der Anteil der in eine geordnete Struktur eingebauten Wassermoleküle in der Solvatationssphäre kleiner ist. Wird angenommen, dass der Übergangszustand sich dann ausbildet, wenn die Energie der restlichen Wasser-Wasser Wechselwirkungen gleich der der Wasser-Ionenpaar Wechselwirkungen ist,[12] wird mit ansteigender Temperatur der Übergangszustand leichter erreicht, was schliesslich einem Abfall der Aktivierungsenergie gleichkommt. Das Auftreten von hohen negativen $\Delta C_p^{\neq}$ Werten ist daher ein Lösungsmitteleffekt und wird quantitativ von der Natur des Alkylhalogenids bestimmt. Somit kann der Wert dieses Parameters nur begrenzt als Mechanismuskriterium gelten und ist bei gleichbleibendem Alkylhalogenid eher ein Mass für die temperaturbedingte Änderung der Solvatation in verschiedenen Lösungsmittelgemischen.

Die Entropie des Systems ist aufgrund des kleineren Ordungsgrades im Übergangszustand höher als im Grundzustand, wodurch die Aktivierungsentropie positive Werte annimmt. Die Entropie des Grundzustandes ist aber temperaturabhängig und steigt mit der Temperatur an, wodurch ein Abfall der Aktivierungsentropie zu erklären ist.

LITERATURHINWEISE

[1] Mitt. III. R. H. Schuster und I. A. Schneider, *Rev. Roumaine Chim.*, **23**, 1203 (1978).
[2] A. Streitwieser Jr., *Chem. Rev.*, **56**, 618 (1956).
[3] R. E. Robertson, *Canad. J. Chem.*, **37**, 803 (1959).
[4] E. A. Moelwyn-Hughes, *J. Chem. Soc.*, **1962**, 4301.
[5] R. E. Robertson, *Canad. J. Chem.*, **33**, 1536 (1955).
[6] B. L. Murr Jr. und H. J. Shiner Jr., *J. Amer. Chem. Soc.*, **84**, 4672 (1962).
[7] R. H. Schuster und I. A. Schneider, *Rev. Roumaine Chim.*, **22**, 1, 103 (1977).
[8] I. A. Schneider und R. H. Schuster, *Z. Chem.*, **20**, 63 (1980).
[9] L. L. Schaleger und F. A. Long, „Advances in Physikall Organic Chemistry", vol. 1 ed. V. Gold, Acad. Press, London, 1963.
[10] H. S. Frank und W. Y. Wenn, *Discuss Faraday Soc.*, **24**, 133 (1957).
[11] G. Nemethy und H. Scheraga, *J. Chem. Phys.*, **36**, 12, 3382 (1963).
[12] K. T. Leffek, R. E. Robertson und S. Sugamori, *J. Amer. Chem. Soc.*, **87**, 2097 (1965).

Revue Roumaine de Chimie, 25, 7, 1077–1082(1980)

Dedicated to Professor CRISTOFOR I. SIMIONESCU
on his 60th anniversary

GENESIS OF PORPHYRIN-LIKE COMPOUNDS UNDER SIMULATED ABIOTIC CONDITIONS. A POSSIBLE MECHANISM OF THEIR FORMATION

B. C. SIMIONESCU, R. MORA *, M. LEANCA and C. ANANIESCU
Department of Organic and Macromolecular Chemistry, Polytechnic Institute, 6600 Jassy, Romania

Received January 23, 1980

Investigations concerning the synthesis of porphyrin-like compounds from methane, ammonia and water vapour were carried out using high frequency discharges as energy source. The analytical criteria established for the identification of porphyrins in terrestrial and extraterrestrial samples (spectrophotometry, spectrofluorimetry, metal complexing, demetallation, remetallation and solvent partition) showed that porphyrin-like pigments were formed in this way. Experimental data suggest the possibility of their appearance from pyrrole and formaldehyde.

INTRODUCTION

During the recent years, many investigators have devoted their efforts to a new kind of experimental activity bearing on chemical evolution, protobiochemistry, primordial biogenesis, or, simply, on studies on the origin of life.

In some previously published papers, a research group led by C. I. Simionescu presented certain aspects of an original conception (the "cold theory"[1,2]) on the synthesis of living matter precursors and the emergence of life. Experimental data, obtained according to the "cold theory", confirmed the starting theoretical hypothesis. The primeval atmosphere of the earth was simulated using a mixture of methane, ammonia and water vapour and high frequency electrical discharge was taken as energy source In the discharge products, along with simple organic compounds,[3] amino acids,[4] purinic and pirimidinic bases,[5] sugars,[6] hydrocarbons,[3] fatty acids,[7] nucleosides,[8] polymeric structures [1,9] (peptide-like, lipid-like, polysaccharide-like) and porphyrin-like pigments[10] were identified.

Porphyrins (or porphyrin-like compounds) have a significant importance during the transition period of the primeval reducing atmosphere

---

[*] Present address: Institute for Cellular Biology and Pathology, 8, Hașdeu street, 70646 Bucharest, Romania.

of the earth to an oxidative one. Initially, they could perform effective catalysis of certain reactions, the chemical energy thus released being further used to satisfy the energy requirements of the first living entities. The incorporation of porphyrins into the early organisms determined more and more effective participation as sensitizers of photoreactions to obtain chemical energy. The processes providing the useful energy for organisms developed in time, evolving into contemporary bioenergetic processes. Nowadays, porphyrins are involved in two essential processes of life, with major bioenergetical functions — photosynthesis and cellular respiration.[2]

These statements justify the great interest in search for the appearing mode, evolution and role of porphyrinic pigments during the chemical and subsequent biological evolution.

We have already reported the abiogenesis of porphyrins [10] and of metalloporphyrins [11] and advanced the possibility of their formation from pyrrole (Py) and formaldehyde (FA). The present paper presents some data to support this hypothesis.

EXPERIMENTAL

Experiments intending to simulate the primitive conditions of the earth were performed under flow conditions, using an apparatus described elsewhere.[12] Different gaseous mixtures — CH_4 (2—7 Torr), NH_3 (2—7 Torr), H_2O (0.03—0.005 ml/h) were exposed to electrical discharges generated by two external electrodes coupled to a high frequency generator (electrical tension between the electrodes — 12 kV, discharge frequency — 1.66 MHz, power — 40 W). The reaction products were collected in a vessel cooled by liquid nitrogen. In some experiments water soluble salts of some metallic cations were added in the collecting vessel.

The reaction products were reduced to dryness, extracted with benzene — methanol 9/1 *v/v*, and the soluble part was transferred to *n*-heptane and chromatographed on silica gel. Chromatographic fractions were obtained with *n*-heptane, *n*-heptane — benzene 1/1 *v/v*, benzene, benzene — methanol 99/1, 98/2, 95/5, 90/10 *v/v* and methanol. The eluates were analysed by absorption and fluorescence spectrophotometry, metal complexing, demetallation, remetallation and solvent partition.

A second set of experiments was performed starting from Py and FA which were condensed at room temperature, in aqueous solutions, in the presence or in the absence of metallic salts (0.4 ml Py, 1.2 ml FA 40 % in volume, in water, in 100 ml distilled water, with or without 40 mg metal). In some cases a peridotite rock (containing Fe_2O_3 9.31 %, FeO 2.90 %, MgO 33.17 %, etc.) was introduced instead of the metallic salt. The formation of tetrapyrrolic compounds was followed by absorption spectrophotometry.

RESULTS AND DISCUSSIONS

Following the column chromatography, absorption signals in the Soret region (significant for porphyrin analysis) were observed for *n*-heptane (380 nm), *n*-heptane—benzene (380 nm), benzene (390 nm) and benzene—methanol 99/1 *v/v* (390 nm) eluates. The bulk of porphyrins, obtained in the presence of metallic salts or in their absence, was eluted by benzene—methanol 99/1 *v/v* mixture. The absorption spectra of this fraction showed four distinct non-Soret maxima at 505, 545,590 and 615 nm, attributed to free-base prophyrin-like pigments, obtained in the absence of metals (see Figure 1, curve 1), and two non-Soret maxima (at 505 and 570 nm, for instance, for zinc-porphyrins) attributed to metalloporphyrins obtained in the presence of metals (see Figure 1, curve 2).

Typical emission and excitation fluorescence spectra for free-base porphyrins isolated from the discharge products are presented in figure 2.

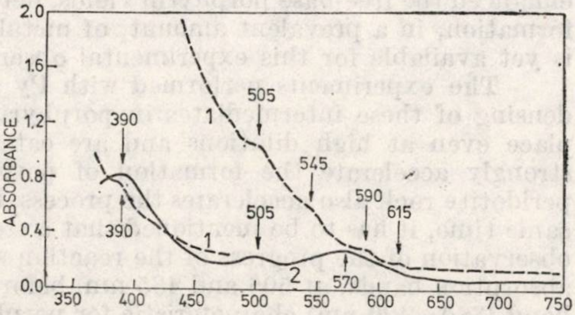

Fig. 1. — Absorption spectra of abiotically synthesized porphyrins (1) and of zinc-porphyrin complex (2).

Figure 3 shows fluorescence spectra (excitation) of porphyrinic pigments obtained in the absence of metallic salt (curve 1), in the absence of the salt, but complexed with zinc after the chromatographic separation

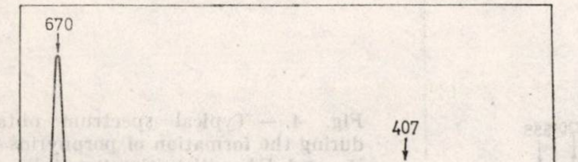

Fig. 2. — Typical fluorescence of free-base porphyrins isolated from the discharge products (*n*-heptane eluate).

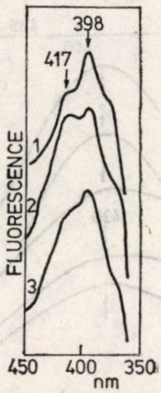

Fig. 3. — Excitation spectra of porphyrins obtained in the absence of metallic salts (1), complexed with zinc after the chromatographic separation (2), and obtained in the presence of zinc acetate (3).

(curve 2), and in the presence of zinc acetate introduced in the collecting vessel before the abiotic synthesis (curve 3).

In all abiotic experiments a mixture of probably very different substituted porphyrin-like pigments was obtained. The presence of water soluble salts of some metallic cations in the collecting vessel considerably enhanced the free-base porphyrin yields, determining at the same time the formation, in a prevalent amount, of metalloporphyrins. No explanation is yet available for this experimental observation.

The experiments performed with Py and FA proved the easy condensing of these intermediates in porphyrinic rings. The reactions take place even at high dilutions and are catalysed by metallic ions which strongly accelerate the formation of porphyrins. The presence of the peridotite rock also accelerates the process, but in a smaller extent. At the same time, it has to be mentioned that a step by step spectrophotometric observation of the progress of the reaction showed the appearance of two absorption bands, at 505 and 435 nm, before the appearance of the Soret band (380—420 nm) characteristic for porphyrins (see Figure 4, curve 1). These two peaks diminish in time for the benefit of the absorption bands of porphyrins. The complete separation, by extraction with benzene of tetrapyrrolic compounds obtained both in the presence or in the absence of metallic salts, from the reaction mixture (see Figure 4, curve 2) showed

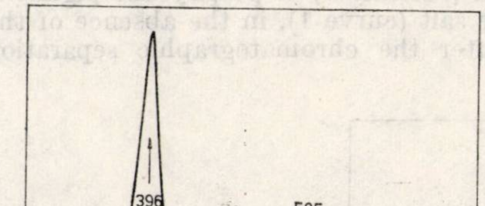

Fig. 4. — Typical spectrum obtained during the formation of porphyrins from Py and FA with/without metallic salts (1); Cu-porphyrins separated from Py—FA — Cu acetate synthesis (2); (3)—(8) — the organic eluates of discharge pigments : 3) benzene-methanol 99/1 *v/v*, and (4) benzene, no metal in the synthesis; (5) benzene — methanol 98/2 *v/v*, iron in the synthesis; (6) benzene, magnesium in the synthesis; (7) benzene, zinc in the synthesis; (8) benzene, copper in the synthesis.

that new amounts of porphyrins were formed, the process being preceded by a new diminishing of the 505 and 435 nm bands. This observation confirms that intermediate compounds are yielded from Py and FA and that porphyrins arise in time from these compounds.

The reaction between Py and FA was also followed by ^{1}H-NMR spectroscopy, the spectra being registered at different reaction times. The ^{1}H-NMR spectrum of Py consists in two main signals at 6.1 ppm (protons 3 and 4) and 6.7 ppm (protons 2 and 5). During the reaction, a decrease of 6.7 ppm signal, assigned to the substitution of 2 and 5 protons, was observed. The substitution rate was followed by the ratio of 6.7 ppm to 6.1 ppm signal integrals. At the same time, at higher field (5.3 ppm) a signal appeared and increased. This signal is assigned to the protons in the structures which cannot be distinguished. Both structures exist in the porphyrinic ring.

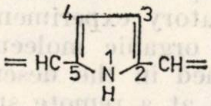

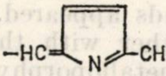

The olefinic protons attached to the Py molecule are not bonded to an oxygen atom, because an aldehydic substituent induces a shift of the third (or/and the fourth) proton to lower fields (about 6.9 ppm) and no signals appear in this region. Also, saturated structures such as

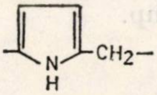

should give signals corresponding to CH_2 protons in the saturated region of the spectrum ; these are absent, too.

Even if the spectra were registered in D_2O, due to the intense signal of water protons which lie in the proximity of the 5.3 ppm signal, the intermediate structures could not be measured and clearly identified.

The abiotic experiments simulating the primeval conditions of the earth revealed the possibility of porphyrins appearance in the earliest stages of molecular evolution. Nevertheless, many chromatographic eluates obtained according to the separation scheme of the discharge pigments showed absorption shoulders at 435 and/or 505 nm (see Figure 4, curves 3–8).

The benzene eluates were usually accompanied by a pronounced peak at 435 nm. These absorptions could be due to precursors of porphyrins. But, since they appear also in experiments performed with Py and FA, it is reasonable to consider that abiotic porphyrins are yielded from the same compounds. In addition, excellent yields of FA as well as smaller amounts of Py were identified by gas chromatography in the reaction products resulted by submitting a mixture of methane, ammonia and water vapour to electrical discharges (a Porapak QS column was used for FA and a Chromosorb–Propylene glycol 5% one for Py).

It has to be also mentioned that thermal condensation under geologically simulated conditions of these two compounds into porphyrinic pigments, in the presence of minerals, was achieved by Hodgson and Baker,[13] who reproduced a previous experiment of Krasnovsky.[14]

Last but not least, the conclusion concerning the possible emergence of porphyrins, in abiotic conditions, from Py and FA formed from gaseous mixtures exposed to electrical discharges is supported by the fact that it comes from more than twenty abiotic experiments performed in the presence or absence of metals, the appearance of the 435 and/or 505 nm shoulders in eluates being a general feature.

CONCLUSIONS

Even if it is hard to establish exactly at what moment the porphyrin-like compounds appeared, the laboratory experiments suggest their abiogenesis together with the simplest organic molecules. The rather high yields of metalloporphyrins obtained in the described conditions led to the idea of their intervention even at a remote stage of chemical evolution.

As concerns the mechanism of reactions involved in their prebiotic synthesis, it is not dependent on the very complex enzymatic biological steps by which porphyrins are synthesized in living organisms. Their emergence could be due to the spontaneous condensation (catalysed or not by metallic cations) of Py and FA, components which were present in the so-called primordial soup.

REFERENCES

[1] C. I. Simionescu, F. Deneş and I. Negulescu, *J. Polym. Sci., Polym. Symp.*, **64,** 281 (1978).

[2] C. I. Simionescu, R. Mora and B. C. Simionescu, *Bioelectrochem. Bioenerg.*, **5,** 1 (1978).

[3] C. I. Simionescu, S. Dumitriu, V. Bulacovschi, V. I. Popa and B. C. Simionescu, *Rev. Roumaine Chim.*, **23,** 89 (1978).

[4] C. I. Simionescu, R. Mora, N. Olaru and E. Ioanid, *Compt. rend., Série C,* **282,** 679 (1976).

[5] C. I. Simionescu, T. Lixandru, C. Gorea and V. Gorduza, *Compt. rend., Série C,* **280,** 683 (1975).

[6] C. I. Simionescu, S. Dumitriu, V. Bulacovschi and V. I. Popa, Cellulose Chem. Technol. **12,** 585 (1978).

[7] B. C. Simionescu, M. Leancă, R. Mora, D. Mancaş and C. I. Simionescu, *Rev. Roumaine Chim.*, **24,** 1521 (1979).

[8] C. I. Simionescu, T. Lixandru, V. Gorduza and C. Gorea, *Origins of Life*, **8,** 237 (1977).

[9] C. I. Simionescu, M. Totolin and F. Deneş, *Biosystems,* **8,** 153 (1976).

[10] C. I. Simionescu, B. C. Simionescu, R. Mora and M. Leancă, *Origins of Life*, **9,** 103 (1978).

[11] C. I. Simionescu, B. C. Simionescu, R. Mora, M. Leancă and M. Vasilescu, *Compt. rend., Série D,* **286,** 1021 (1978).

[12] C. I. Simionescu, B. C. Simionescu, R. Mora, M. Leancă and E. Ioanid, *Compt. rend., Série C,* **284,** 743 (1977).

[13] G. W. Hodgson and B. L. Baker, *Nature (London)*, **216,** 29 (1967).

[14] A. A. Krasnovsky and A. V. Umrikhina, "Molecular Evolution, Prebiological and Biological", D. L. Rohlfing and A. I. Oparin (Editors), Plenum Press, New York, 1972, p. 141.

Revue Roumaine de Chimie, 25, 7, 1083—1089 (1980)

Hommage au Professeur Cristofor I. Simionescu
à l'occasion de son 60e anniversaire

POLYMÈRES DE COORDINATION. II [1]

POLYESTERS CHÉLATÉS DU TYPE AZOMÉTHINIQUE

MIHAELA SPIRATOS, A. AIRINEI et AGLAIA CIOBANU
Institut de Chimie Macromoléculaire « P. Poni », 41 A, Aleea Gr. Ghica Vodă, 6600 Iaşi, Roumanie

Reçu le 3 janvier 1979

On a synthétisé des polyesters à partir des bis(dihydroxy-2,4 benzaldéhyde) éthylènediimine nickel, bis(dihydroxy-2,4 acétophénone) éthylènediimine nickel et cuivre, bis(dihydroxy-2,4 acétophénoneimine) nickel et bis(dihydroxy-2,4 benzophénone) éthylènediimine nickel et des chlorures acides aromatiques, par polycondensation interfaciale. Pour caractériser les polymères on a utilisé l'analyse élémentaire et thermogravimétrique et la spectroscopie infrarouge.

Ni(II) and Cu(II) chelate polymers of bis(2,4-dihydroxybenzaldehyde) ethylenediimine, bis(2,4-dihydroxyacetophenone) ethylenediimine, bis(2,4-dihydroxyacetophenoneimine) and bis(2,4-dihydroxybenzophenone) ethylenediimine and aromatic acid chlorides have been synthesized by interfacial polycondensation. The polymers were characterized by elemental analysis, thermogravimetric analysis, magnetic properties and infrared spectroscopy.

Les polymères de coordination tiennent une place intermédiaire entre les composés organiques et les composés inorganiques purs, ainsi leur étude pourrait conduire à l'obtention de polymères à stabilité thermique et à propriétés mécaniques supérieures.

On connaît la possibilité d'obtenir des polyesters à partir des complexes bisphénoliques et des chlorures acides aromatiques par polycondensation interfaciale.[1,2]

Dans le présent travail nous avons étudié les conditions de synthèse et certaines caractéristiques physico-chimiques des polyesters obtenus à partir de bis(dihydroxy-2,4 benzaldéhyde)éthylènediimine nickel, bis(dihydroxy-2,4 acétophénone)éthylènediimine nickel et cuivre, bis(dihydroxy-2,4 benzophénone) éthylènediimine nickel et bis(dihydroxy-2,4 acétophénoneimine)nickel avec des chlorures acides aromatiques dans un système consistant en deux phases. Ces polyesters correspondent aux formules générales suivantes :

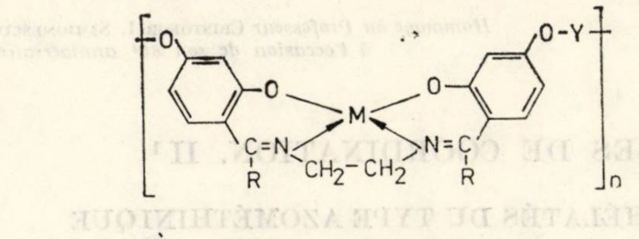

où

$R = -H \quad , \quad M = Ni^{2+}$

$R = -CH_3 \quad , \quad M = Ni^{2+}$

$R = -CH_3 \quad , \quad M = Cu^{2+}$

$R = -C_6H_5 , \quad M = Ni^{2+}$

Ia,IIa,IIIa,IVa :

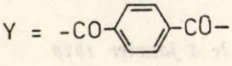

Ib,IIb,IIIb,IVb :

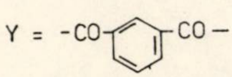

Ic,IIc,IIIc,IVc :

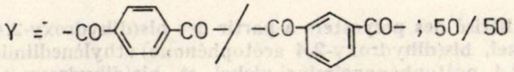

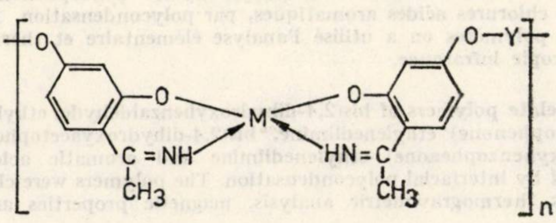

où

Va :

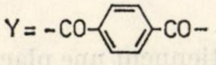

Vb :

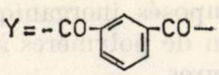

Vc :

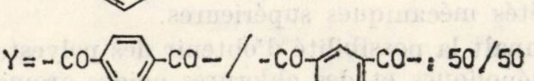

Les homopolymères ainsi que les copolymères ont été préparés de cette même manière.

PARTIE EXPÉRIMENTALE

Les bis(dihydroxy-2,4 benzaldéhyde) éthylènediimine nickel (I), bis(dihydroxy-2,4 benzophénone)éthylènediimine nickel (IV) et bis(dihydroxy-2,4 acétophénoneimine)nickel (V) ont été préparés selon les méthodes décrites dans la littérature. [3]

Les bis(dihydroxy-2,4 acétophénone)éthylènediimine nickel (II) et bis(dihydroxy-2,4 acétophénone) éthylènediimine cuivre (III) ont été obtenues par la méthode suivante : on ajoute 0,1 mole d'acétate de nickel ou de cuivre dans 10 ml d'eau à 0,1 mole de bis(dihydroxy-2,4

TABLEAU 1

Analyse élémentaire et caractéristiques magnétiques des composés étudiés

Composé	C %		H %		N %		M %		Caractéristiques magnétiques
	calculé	*trouvé*	*calculé*	*trouvé*	*calculé*	*trouvé*	*calculé*	*trouvé*	
I	51,24	50,87	4,26	4,79	7,47	7,46	14,95	15,66	diamagnétique
$\mathrm{I_a}$	59,17	58,10	3,28	4,24	5,75	5,44	12,05	10,54	diamagnétique
$\mathrm{I_b}$	59,17	58,08	3,28	4,01	5,75	5,37	12,05	11,73	diamagnétique
$\mathrm{I_c}$	59,17	57,44	3,28	3,75	5,75	4,99	12,05	11,03	diamagnétique
II	50,77	51,07	4,22	4,87	6,57	6,20	14,93	15,17	diamagnétique
$\mathrm{II_a}$	60,05	57,42	3,80	4,40	5,38	4,62	12,22	11,39	diamagnétique
$\mathrm{II_b}$	60,05	56,73	3,80	4,39	5,38	5,26	12,22	10,86	diamagnétique
$\mathrm{II_c}$	60,05	57,58	3,80	4,53	5,38	4,20	12,22	10,41	diamagnétique
III	56,14	57,12	4,67	5,11	7,27	6,63	15,25	14,88	paramagnétique
$\mathrm{III_a}$	60,61	60,43	3,88	4,43	5,43	5.13	11,20	10,51	paramagnétique
$\mathrm{III_b}$	60,61	58,31	3,88	4,31	5,43	5.25	11,20	9,92	paramagnétique
$\mathrm{III_c}$	60,61	57,24	3,88	4,45	5,43	5,49	11,20	9,60	paramagnétique
IV	66,05	65,86	4,32	4,18	5,51	5,85	11,54	11,58	diamagnétique
$\mathrm{IV_a}$	67,63	66,72	3,75	2,98	4,38	3,95	9.19	8,50	diamagnétique
$\mathrm{IV_b}$	67,63	66,87	3,75	3,10	4,38	4,10	9,19	8,45	diamagnétique
$\mathrm{IV_c}$	67,63	66,57	3,75	3,05	4,38	3,80	9,19	8,75	diamagnétique
V	53,56	53,96	4,45	4,05	7,79	7,84	16,31	15,52	paramagnétique
$\mathrm{V_a}$	58,90	57,77	3,68	4,15	5,72	4,93	12,00	11,43	paramagnétique
$\mathrm{V_b}$	58,90	57,46	3,68	4,57	5,72	5,31	12,00	11,55	paramagnétique
$\mathrm{V_c}$	58,90	56,69	3,68	3,88	5,72	4,78	12,00	11,51	paramagnétique

acétophénone) éthylènediimine dissous dans 200 ml de méthanol. Après trois heures de chauffage, un précipité apparait qui a été filtré et purifié par dissolution en hydroxyde de sodium 0,1 N et reprécipitation avec bioxyde de carbone. Dans le tableau 1 sont présentés les résultats de l'analyse élémentaire.

La synthèse des polymères à partir du bis(dihydroxy-2,4-acétophénoneimine) nickel (V) a été présentée antérieurement.[4]

Les polymères obtenus des chélatés I—IV ont été préparés par polycondensation interfaciale. Toutes les réactions de polymérisation ont été conduites selon la méthode décrite par Eareckson.[5] Ainsi, $8{,}33 \cdot 10^{-3}$ mole de sel complexe, dans une solution d'hydroxyde de sodium ($1{,}67 \cdot 10^{-2}$ mole) réagit avec $8{,}33 \cdot 10^{-3}$ mole de chlorure acide (le chlorure de l'acide téréphtalique, le chlorure de l'acide isophtalique ou leur mélange) en dichlorméthane, en présence de sulfate de lauryle sodium, comme agent de dispersion. Les réactants sont agités énergiquement, ensuite les polymères sont isolés par précipitation en acétone et purifiés par extractions répétées avec méthanol et éthanol.

Les résultats de l'analyse élémentaire et les caractéristiques magnétiques des composés étudiés sont présents dans le tableau 1.

Les spectres infrarouges ont été enregistrés avec un spectrophotomètre Perkin-Elmer, modèle 577 sur des pastilles à KBr. Les spectres électroniques de réflexion ont été enregistrés à l'aide d'un spectrophotomètre Unicam SP-800 B, à la température ambiante, en utilisant comme matériel de référence l'oxyde de magnésium. Les propriétés magnétiques ont été déterminées avec une balance Gouy dans un champ magnétique non homogène. Les thermogrammes ont été enregistrés avec un dérivatographe MOM-Budapest type Paulik-Paulik-Erdey, en l'air, la vitesse de chauffage étant de 9°C/mn.

RÉSULTATS ET DISCUSSION

La formation des polymères chélatés a lieu par la réaction entre le sel de sodium du chélate (en solution aqueuse) et le dichlorure acide respectif avec élimination de chlorure de sodium selon le schéma de réaction suivant :

$$C_{16}H_{12}O_4N_2MNa_2 + C_8H_4Cl_2O_8 \xrightarrow[-NaCl]{5-8\ \text{min.}} -(C_{24}H_{16}O_6N_2M)_{\overline{n}}$$

Les polymères obtenus se présentent sous la forme de poudres colorées, infusibles et insolubles dans les dissolvants communs. Les mesurages magnétiques (tableau 1) montrent que tous les polymères à nickel sont diamagnétiques, à l'exception des polymères obtenus du bis(dihydroxy-2,4 acétophénoneimine)nickel (V_a, V_b, V_c). Les polymères résultant du bis(dihydroxy-2,4 acétophénone)éthylène-diimine cuivre sont paramagnétiques. Le paramagnétisme des polymères obtenus des bis(dihydroxy-2,4 acétophénoneimine)nickel et bis-(dihydroxy-2,4 acétophénone)éthylènediimine cuivre est le résultat d'une configuration octaédrique réalisée par l'atome de nickel et cuivre en liant deux molécules d'eau,[6] confirmée par l'analyse élémentaire et l'analyse thermogravimétrique.

Les spectres électroniques de réflexion indiquent une configuration plane-quadratique des polymères III_a, III_b, III_c, mise en évidence par la bande d'absorption de la 540—550 nm[7,8] et une configuration octaédrique légèrement distorse pour les polymères V_a, V_b, V_c, confirmée par la présence des bandes d'absorption de 410, 550—750 nm.[9]

Dans les polymères I_a, I_b, I_c et II_a, II_b, II_c l'atome de nickel est hexacoordiné par la liaison de deux molecules d'eau. La présence des ligands non équivalents produit une puissante distorsion de la symétrie octaédrique conduisant à des composés tétragonaux, diamagnétiques, mise en évidence par la bande d'absorption de 550—750 nm.[10-13]

Les polymères IV_a, IV_b, IV_c, dont l'atome de nickel est tétracoordiné sont diamagnétique et tétragonaux. Le comportement différent de ces composés est dû à l'absence de l'eau de coordination chez l'atome centrale, à cause des empêchements stériques déterminés par la présence du cycle éthylènediiminique et du radical phényle.[14]

La stabilité thermique des chélatés et des polymères a été déterminée en mesurant la perte en poids. La perte en poids sur les thermogrammes représente la volatilisation de l'eau de coordination qui a lieu entre 100—200°C. Le pourcentage de l'eau dans les polymères déterminé thermogravimétriquement est en concordance avec les valeurs trouvées sur l'unité structurale de polymère par l'analyse élémentaire. Après la perte de l'eau sur chaque thermogramme apparaît une pente escarpée, ce qui indique la perte rapide en poids due à la combustion complète du matériel organique.

En analysant les données obtenues, on constate que les polymères qui contiennent l'atome de nickel, II_a, II_b, II_c, sont plus stables (figure 2) que ceux contenant du cuivre, III_a, III_b, III_c, (figure 3). Dans la série des polymères à nickel on observe une décroissance de la stabilité thermique en fonction de la nature du substituent chez l'atome de carbone azométhinique, dans l'ordre suivant : $-H > -C_6H_5 > -CH_3$, due probablement au cumul des effets inductifs et électromères exercés par le substituent (figures 1, 4, 2).

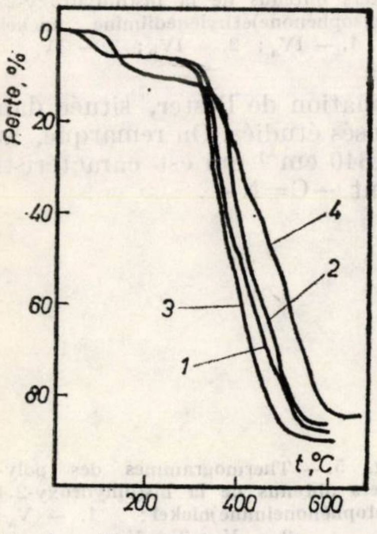

Fig. 1. — Thermogrammes des polyesters obtenus de la bis(dihydroxy-2,4 benzaldéhyde)éthylènediimine nickel : 1, — I_a ; 2, — I_b ; 3, — I_c ; 4, — I.

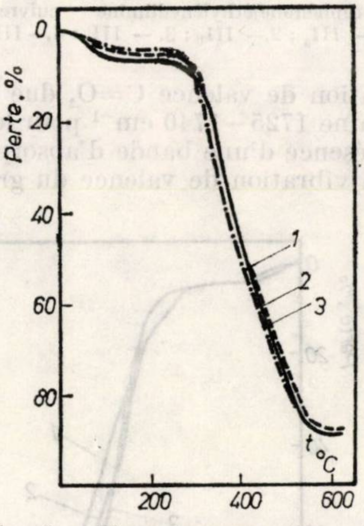

Fig. 2. — Thermogrammes des polyesters obtenus de la bis(dihydroxy-2,4 acétophénone)éthylènediimine nickel : 1, — II_a ; 2, — II_c ; 3, — II_b.

On confirme, aussi, la stabilité thermique plus grande des combinaisons dont l'ion central participe à la formation de plusieurs cycles (figures 2, 4, 5).

Les spectres d'absorption en infrarouge indiquent que la réaction de condensation entre les groupes —OH phénolique et le chlorure acide déterminent l'apparition d'une bande d'absorption caractéristique de la vibration de valence C=O, due à la formation de l'ester, située dans le domaine 1725—1740 cm^{-1} pour les composés étudiés. On remarque, aussi, la présence d'une bande d'absorption à 1640 cm^{-1} qui est caractéristique de la vibration de valence du groupement —C=N—.

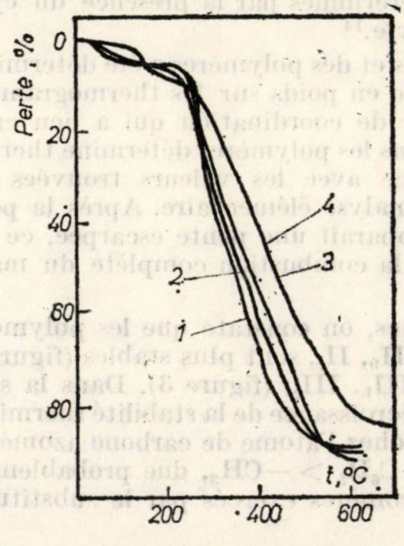

Fig. 3. — Thermogrammes des polyesters obtenus de la bis(dihydroxy-2,4 acétophénone)éthylènediimine cuivre : 1, — III_a ; 2,— III_b ; 3, — III_c ; 4,— III.

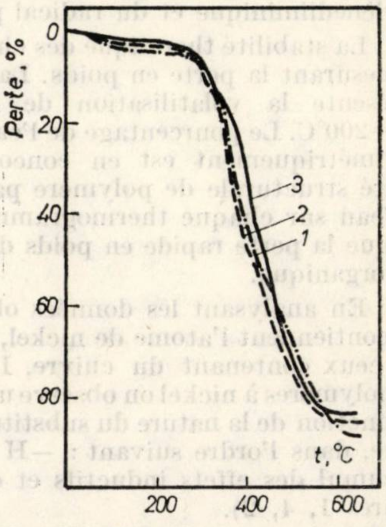

Fig. 4. — Thermogrammes des polyesters obtenus de la bis(dihydroxy-2,4 benzophénone)éthylènediimine nickel : 1, — IV_a ; 2, — IV_b ; 3, — IV_c.

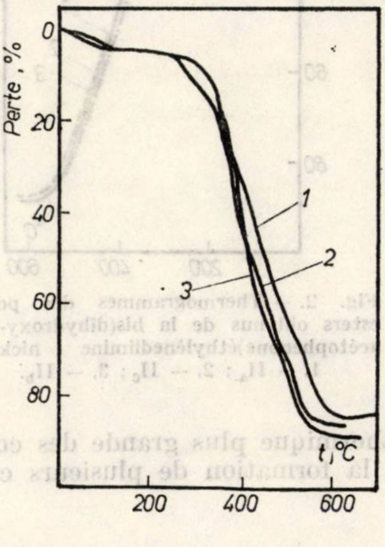

Fig. 5. — Thermogrammes des polyesters obtenus de la bis(dihydroxy-2,4 acétophénoneimine)nickel : 1, — V_a ; 2, — V_b ; 3 — V_c.

L'insolubilité, les résultats obtenus à l'analyse élémentaire et les spectres d'absorption en infrarouge prouvent la structure polymérique de ces combinaisons.

BIBLIOGRAPHIE

[1] M. Spiratos, A. Airinei et M. Bostan, *Mater. Plast.*, **16**, 137 (1979).
[2] L. V. Interrante et J. C. Bailar, Jr., *Inorg. Chem.*, **3**, 1339 (1964).
[3] P. Pfeiffer, E. Breith, E. Lübbe et T. Tsumaki, *Liebigs Ann. Chem.*, **503**, 84 (1933).
[4] M. Marcu et M. Spiratos, Brevet Rom. 63.915 (1978).
[5] W. M. Eareckson, *J. Polymer Sci.*, **40**, 399 (1959).
[6] E. A. Tomic, *J. Appl. Polymer Sci.*, **9**, 3745 (1965).
[7] R. K. Kohli et P. K. Bhattacharya, *Bull. Chem. Soc. Japan*, **49**, 2872 (1976).
[8] B. T. Thaker et P. K. Bhattacharya, *Bull. Chem. Soc. Japan*, **49**, 2845 (1976).
[9] R. S. Drago, "Physical Methods in Inorganic Chemistry", Reinhold Publishing Corporation, New York, 1965, p. 81, 177.
[10] C. C. Ballhausen et A. D. Liehr, *J. Amer. Chem. Soc.*, **81**, 538 (1958).
[11] G. Maki, *J. Chem. Phys.*, **29**, 162 (1959).
[12] D. M. L. Goodgame, M. Goodgame, M. A. Hitchman et M. J. Weeks, *J. Chem. Soc.*, **1966**, 1769.
[13] F. A. Cotton et R. H. Holm, *J. Amer. Chem. Soc.*, **82**, 2979 (1960).
[14] J. Lewis et R. A. Walton, *J. Chem. Soc.*, **1966**, 1559.

Revue Roumaine de Chimie, 25, 7, 1091–1096 (1980)

Hommage au Professeur Cristofor I. Simionescu
à l'occasion de son 60e anniversaire

1,2,4-TRIAZOLIUM-YLURES. III[1]

ASPECTS THÉORIQUES SUR LA RÉGIOSÉLECTIVITÉ DANS LA RÉACTION DE CYCLOADDITION DU TRIAZOLIUM-PHÉNACYLURE SUR LES ESTERS DE L'ACIDE PROPIOLIQUE

GH. SURPĂȚEANU *, CRISTINA LUCHIAN *, M. CONSTANTINESCU **, V. BĂRBOIU *** et MAGDA PETROVANU *

* Institut Polytechnique « Gh. Asachi », Laboratoire de Chimie Organique, Jassy, 11, str. 23 August, Roumanie
** Centre de Calcul de l'Université « Al. I. Cuza », Jassy
*** Institut de Chimie Macromoléculaire « P. Poni », Jassy, 41 A, Aleea Ghica Vodă, Roumanie

Reçu le 29 novembre 1979

Une interprétation théorique des résultats concernant la réaction du triazolium-phénacylure avec le propiolate d'éthyle est proposée. Cette interprétation est fondée sur l'utilisation de la théorie des orbitales moléculaires de frontière dans le cadre de la théorie des perturbations du second ordre. Les résultats obtenus plaident en faveur d'un sens de l'addition du dipôle sur le dipolarophile inverse à celui indiqué par les facteurs électroniques.

A theoretical explanation of the results concerning the reaction between triazolium-pheacylide with ethyl propiolate is proposed. The explanation is based on the use of the frontier molecular orbital theory in the second order perturbation method. The obtained theoretical results indicate that the sense of the addition of the dipole on the dipolarophile is contrary to that indicated by the electronic factors.

I. INTRODUCTION

Il est connu que la cycloaddition 1,3 dipolaire aux alcynes constitue une excellente voie d'accès aux hétérocycles à cinq chaînons. Parmi d'autres dipôles 1,3 étudiés dans les réactions avec les alcynes on peut citer les cycloimmonium-ylures,[2] qui admettent à côté des structures Ia stabilisées par un « octet », des structures Ib dipolaires 1,3 (« sextet sans double liaison »).

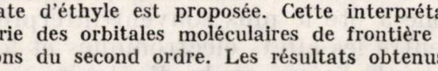

I

(R = COC_6H_5 ; CN ; $COCH_3$ .... etc.)

On trouve dans la littérature de nombreux exemples d'adduits cycliques de structures pyrroliques de type III, IV et V obtenus dans les additions des cycloïmmonium-ylures aux alcynes.[3]

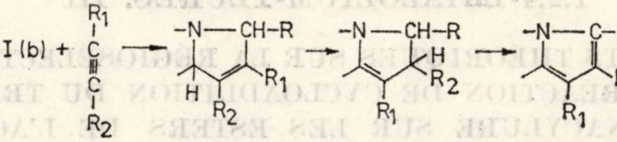

II III IV V

$R_1 = R_2 = CO_2Me$

$R_1 = H$; $R_2 = CO_2Et$

Les réactions de cycloadditions 1,3 dipolaires sont généralement rapides, quantitatives et souvent univoques avec les acétylènes symétriques. Les alcynes disubstitués disymétriques sont presque toujours le siège d'un double sens d'addition, le produit majoritaire dépendant de la substitution de l'alcyne ainsi que de la nature et de la substitution du dipôle.

Le mécanisme de la cycloaddition 1,3 dipolaire aux alcynes n'est pas entièrement élucidé. Le problème non résolu le plus important dans ce domaine est le phénomène d'orientation, ou autrement dit, la régiosélectivité. Ce phénomène a été le plus souvent interprété en tenant compte de la compétition entre les effets électroniques et les effets stériques des substituants de la triple liaison et du dipôle.

En discutant la réactivité du phénylazide vis-à-vis de divers dipolarophiles Sustman a montré, pour la première foie, l'intérêt de l'énergie des orbitales frontières lors de la cycloaddition 1,3 dipolaire.[4]

La théorie des perturbations du second ordre est fondée sur l'utilisation, dans le cadre de la théorie des perturbations, des interactions secondaires au niveau des orbitales frontières HO (plus haute orbitale moléculaire occupée) et BV (plus basse orbitale moléculaire vacante) des deux réactifs. Cette théorie des orbitales moléculaires frontières permet, dans beaucoup de cas, de déterminer la régiosélectivité de la cycloaddition.[5,6] Comme on le sait, dans une réaction possible selon une certaine voie de réaction, les coefficients orbitales qui interréagissent sont de même signe. Dans le cas où cette première condition est remplie par plusieurs paires d'orbitales, les paires qui impliquent des orbitales atomiques possédant les valeurs absolues les plus proches seront favorisées.[7,8]

II. RÉSULTATS ET DISCUSSIONS

Pour l'étude de la régiosélectivité de la réaction de cycloaddition 1,3 dipolaire entre le 4-phényle-1,2,4-triazolium-phénacylure et le propiolate d'éthyle nous avons eu recours à la méthode CNDO/2.

Les géométries des molécules considérées en vue du calcul des orbitales moléculaires d'après la méthode CNDO/2 sont présentées dans les figures 1 et 2.

Nous soulignons le fait que dans le cas du triazolium-ylure les atomes de carbone, arbitrairement notés par 1 et 3, sont coplanaires. La distance entre l'atome d'azote et l'atome de carbone ylurique est d'environ 1,43 Å. La géométrie du reste de phénacyle est presque la même utilisée dans les travaux antérieurs.[9,10] Les angles de valence au niveau du carbone ylurique sont de 120° (fig. 1) :

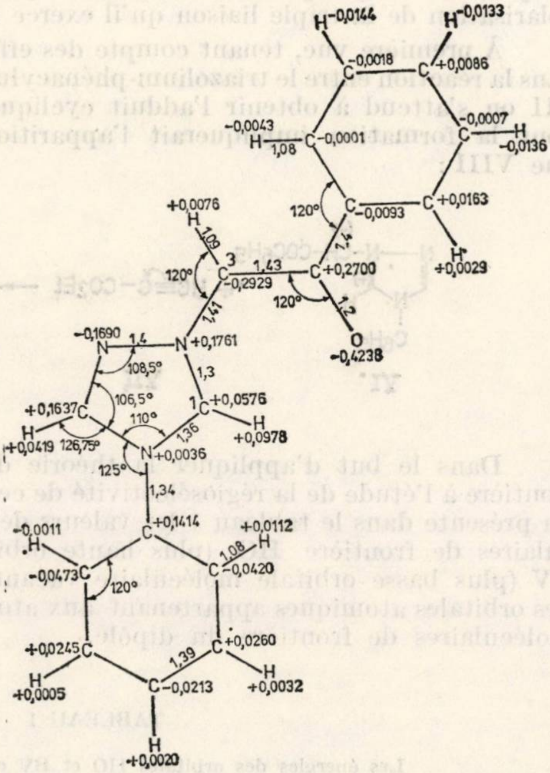
-0,0144
-0,0133
-0,0018
+0,0086
-0,0043
1,08
-0,0001
-0,0007
-0,0136
120°
-0,0093
+0,0163
+0,0076
1,09
1,4
3
120°
1,43
-0,2929
+0,2700
+0,0029
120°
1,2
1,41
-0,4238
-0,1690
1,4
+0,1761
108,5°
1,3
106,5°
1
+0,0576
+0,1637
110°
+0,0978
+0,0419
126,75°
1,36
+0,0036
125°
1,34
+0,1414
-0,0011
+0,0112
1,08
-0,0473
-0,0420
120°
+0,0245
1,39
+0,0260
+0,0005
-0,0213
+0,0032
+0,0020

Fig. 1. — La géométrie et les charges atomiques totales de la molécule de 4-phényle-1,2,4-triazolium-phénacylure.

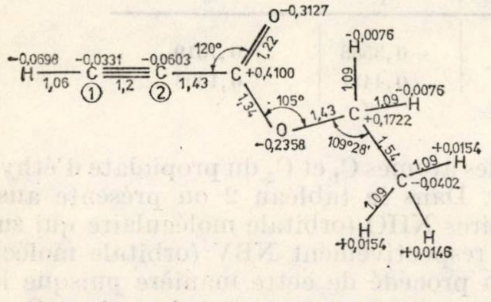
-0,3127
-0,0698
-0,0331
-0,0603
120°
1,22
1,06
①
1,2
②
1,43
+0,4100
-0,0076
1,09
-0,0076
1,34
105°
1,43
1,09
+0,1722
-0,2358
109°28′
1,54
+0,0154
1,09
-0,0402
1,09
+0,0154
+0,0146

Fig. 2. — La géométrie et les charges atomiques totales de la molécule de propiolate d'éthyle.

La molécule de propiolate d'éthyle est linéaire au niveau de la triple liaison. Les distances et les angles entre les atomes composants sont ceux standardisés pour les états d'hybridation des atomes respectifs,[11] (fig. 2) :

Dans les figures 1 et 2 on présente les valeurs des charges atomiques totales. Tenant compte des signes de ces charges sur les atomes 1 et 3 (fig. 1) la structure de résonance Ib représenterait le mieux le dipôle ylurique 1,3. Dans le cas du propiolate d'éthyle la situation est complètement différente, car les deux atomes de carbone 1 et 2 possèdent des charges négatives. Habituellement on accepte que le groupement carbéthoxylique (CO_2Et) est un groupement électron-accepteur ce qui explique l'effet de polarisation de la triple liaison qu'il exerce selon la formule VII.

À première vue, tenant compte des effets électroniques et stériques dans la réaction entre le triazolium-phénacylure VI et le propiolate d'éthyle VII on s'attend à obtenir l'adduit cyclique VIII ou d'autres produits dont la formation impliquerait l'apparition d'un intermédiaire cyclique VIII :

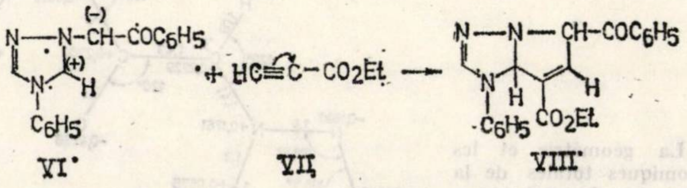

Dans le but d'appliquer la théorie des orbitales moléculaires de frontière à l'étude de la régiosélectivité de cette réaction de cycloaddition, on présente dans le tableau 1 les valeurs des énergies des orbitales moléculaires de frontière HO (plus haute orbitale moléculaire occupée) et BV (plus basse orbitale moléculaire vacante), ainsi que les coefficients des orbitales atomiques appartenant aux atomes C_1 et C_3 dans les orbitales moléculaires de frontière du dipôle.

TABLEAU 1

Les énergies des orbitales HO et BV et les coefficients des orbitales atomiques des atomes C_1 et C_3 pour l'ylure VI

Orbitale	Énergie (eV)	C_1	C_3
HO	−8,28	−0,3583	0,7019
BV	2,22	0,4411	0,1008

Les mêmes coefficients pour les atomes C_1 et C_2 du propiolate d'éthyle sont présentés dans le tableau 2. Dans le tableau 2 on présente aussi les énergies des orbitales moléculaires NHO (orbitale moléculaire qui suit après l'orbitale moléculaire HO), respectivement NBV (orbitale moléculaire qui suit l'orbitale BV). On a procédé de cette manière puisque les coefficients des orbitales atomiques appartenant aux atomes C_1 et C_2 de l'orbitale HO sont nuls (0) et ne peuvent pas être utilisés pour représenter les voies de réactions.

TABLEAU 2

Les énergies des orbitales HO, NHO, BV et NBV et les coefficients des orbitales atomiques des atomes C_1 et C_2 pour le propiolate d'éthyle

Orbitale	Energie (eV)	C_1	C_2
HO	−14,10	0	0
NHO	−14,30	0,2677	0,1922
BV	3,40	−0,5074	0,3004
NBV	6,15	0	0

A l'aide des résultats des calculs qui sont donnés dans les tableaux 1 et 2 on peut construire les diagrammes présentés dans les fig. 3 et 4 :

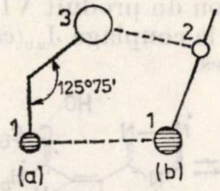

Fig. 3. — Les coefficients des orbitales atomiques des atomes C_1 et C_3 de l'orbitale HO du triazolium-ylure VI (a) et des atomes C_1 et C_2 de l'orbitale BV du propiolate d'éthyle (b). $\Delta E = 11{,}68$ eV. ○ = orbitale avec le signe (+) ; ● = orbitale avec le signe (−).

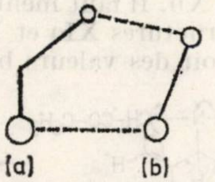

Fig. 4. — Les coefficients des orbitales atomiques des atomes C_1 et C_3 de l'orbitale BV du triazolium-ylure VI (a) et des atomes C_1 et C_2 de l'orbitale NHO du propiolate d'éthyle (b). $\Delta E = 16{,}52$eV. ○ = orbitale avec le signe (+) ; ● = orbitale avec le signe (−).

Les deux diagrammes indiquent que la réaction de cycloaddition découle dans le sens montré par le schéma suivant :

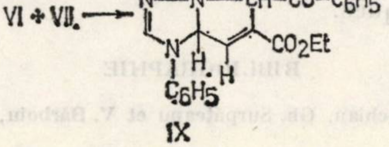

IX

Comme on le voit, la formation de l'adduit cyclique devrait se produire par suite d'une cycloaddition inverse à celle présentée pour le produit VIII.

Si l'on tient compte des différences d'énergie entre les orbitales impliquées dans les voies de réaction représentées dans les figures 3 et 4, respectivement 11,68 et 16,52 eV, le schéma réactionnel présenté dans la figure 3 est favorisée énergétiquement. On peut affirmer que cette réaction de cycloaddition est HO contrôlée [7] par rapport à l'ylure.

Pratiquement, dans la réaction entre le 4-phényle-1,2,4-triazolium-phénacylure VI généré *in situ* à partir du sel de cycloimmonium et de la triéthylamine et le propiolate d'éthyle, en solution chloroformique on obtient le produit X. Ce dernier se forme par suite de l'ouverture de l'adduit cyclique IX selon le schéma réactionnel suivant :

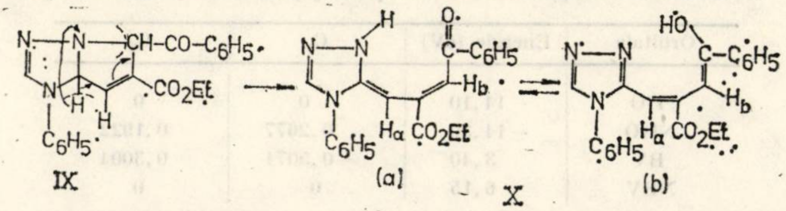

Le principal argument en faveur de la formation des produits X réside dans la valeur basse de 1,6 Hz du couplage J_{ab} constatée dans le spectre ^{1}H-RMN du produit Xa pur, obtenu en milieu d'acétone deutériée. Dans le chloroforme deutérié on constate la présence des deux formes Xa et Xb. Il faut mentionner que la scission du produit VIII conduirait aux structures XIa et XIb dans lesquelles le couplage J_{ab}(*cis* ou *trans*) devrait avoir des valeurs beaucoup plus élevées.

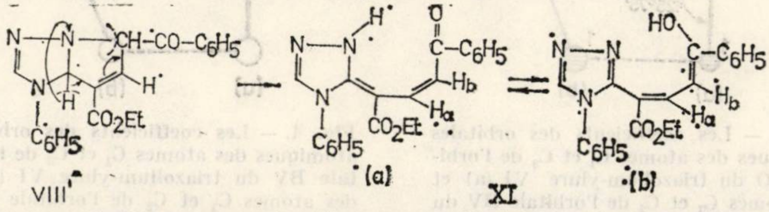

En conclusion, on peut affirmer que l'addition du triazolium-phéncylure VI au propiolate d'éthyle est HO contrôlée par rapport à l'ylure (au dipôle 1,3) ; dans ce cas l'adduit cyclique intermédiaire conduit, par suite d'une scission du cycle, aux produits X. Il résulte que le sens de l'addition est inverse à celui dicté par la polarisation attendue de la triple liaison, selon l'influence du groupement carbéthoxylique électron-accepteur. Les données de la littérature indiquent[12] l'existence de cycloadditions similaires qui ont lieu dans le sens inverse de celui prévu par les influences électroniques et stériques.

BIBLIOGRAPHIE

[1] M. Petrovanu, C. Luchian, Gh. Surpăţeanu et V. Bărboiu, *Rev. Roumaine Chim.*, **24**, 1053 (1979), IIe partie.

[2] R. Huisgen, *Angew. Chem.*, Internat. Edit., **2**, 565 (1963).

[3] I. Zugrăvescu et M. Petrovanu, « N-Ylide Chemistry », McGraw-Hill, London, 1976.

[4] R. Sustman, *Tetrahedron Letters*, **1971**, 2717.

[5] K. H. Houk, J. Sims, R. E. Duke, R. W. Storzier et John K. George, *J. Amer. Chem. Soc.*, **95**, 7289 (1973).

[6] K. H. Houk, J. Sims, C. R. Watts et J. Luskus, *J. Amer. Chem. Soc.*, **95**, 7301 (1973).

[7] J. Fleming, « Frontier Orbitals and Organic Chemical Reactions », Wiley, London, 1976.

[8] G. Klopman, « Chemical Reactivity and Reaction Paths », Wiley, London, 1974.

[9] I. Zugrăvescu, M. Constantinescu, Gh. Surpăţeanu, A. Lablache-Combier et L. Devos, *Rev. Roumaine Chim.*, **24**, 1089 (1979).

[10] Gh. Surpăţeanu, M. Constantinescu, I. Zugrăvescu, A. Lablache-Combier et L. Devos, *Rev. Roumaine Phys.* (sous presse).

[11] J. S. Rollett, *Acta Cryst.*, **8**, 487 (1955).

[12] K. Bunge, R. Huisgen, R. Raab et H. I. Sturm, *Chem. Ber.*, **105**, 1307 (1973).

Revue Roumaine de Chimie, 25, 7, 1097–1100 (1980)

Dedicated to Professor Cristofor I. Simionescu
on his 60th anniversary

SYNTHESIS OF NEW HETEROCYCLIC MONOMERS UNDER SIMULATED PREBIOTIC CONDITIONS

KIICHI TAKEMOTO, KIKUKO KANAOKA and MIKIJI MIYATA
Department of Petroleum Chemistry, Faculty of Engineering,
Osaka University, Suita, Osaka, Japan

Received January 23, 1980

A series of thiazolidine and relating heterocyclic derivatives was prepared by one-step reaction from unsaturated dicarboxylic acids including maleic and acetylene-dicarboxylic acids and thiourea in aqueous phosphoric and polyphosphoric acid solutions. By the reaction of 2,4-dioxothiazolidine-5-acetic acid thus prepared with *p*-aminostyrene in the presence of dicyclohexylcarbodiimide, a new monomer was obtained conveniently under mild conditions.

INTRODUCTION

The synthesis of various organic compounds under possible prebiotic conditions has recently received much attention. On this line, we are also concerned with the synthesis of heterocyclic compounds by the reaction of unsaturated carboxylic acids including maleic, acrylic, methacrylic and sorbic acid with urea and thiourea in the presence of phosphoric and polyphosphoric acids.[1–3] Among them, one-step synthesis of rather complicated heterocycles, the analogs of which have similar structures to those found in natural compounds, appears to be particularly of interest. Thus, we reported a synthesis of 2,4-dioxothiazolidine-5-acetic acid (I) from maleic acid and thiourea in a 86% yield.[2] The present paper deals with a further study on the synthesis of the heterocyclic compound in question, and on the new polymerizable monomer synthesis starting from this compound.

RESULTS AND DISCUSSION

The reaction of maleic acid with thiourea was carried out first at 50°C, in aqueous phosphoric acid solution. Different from the case of reactions of a series of acrylic acid derivatives with urea and thiourea, which afforded exclusively six-membered heterocycles (Eq. 1),[2] the reaction of maleic acid with thiourea gave a five-membered compound (II). When the reaction was performed at an elevated temperature as high as 195°C for 45 min. or, when compound II was kept at the same temperature for 20 min., compound I was obtained in a high yield (Eq. 2). The reaction was found to proceed also smoothly in 50% aqueous polyphosphoric acid solution. It proceeded even at room temperature and gave an almost quantitative yield

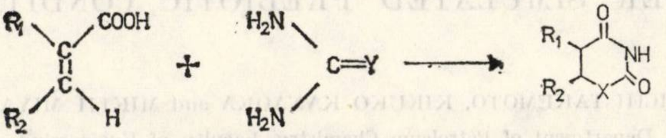
R₁
COOH
C
C
R₂
H
+
H₂N
C=Y
H₂N
O
R₁
NH
R₂
X
O

(Eq. 1)

$R_1 = H, CH_3$
$R_2 = H, CH_3, C_6H_5, CH_3CH=CH-$
$Y=O \ (X=NH)$
$Y=S(X=S)$

after several days. Under these conditions, however, the products proved not to be of six-membered structure, as could be expected. Similar results were obtained by the reaction of fumaric acid and thiourea.

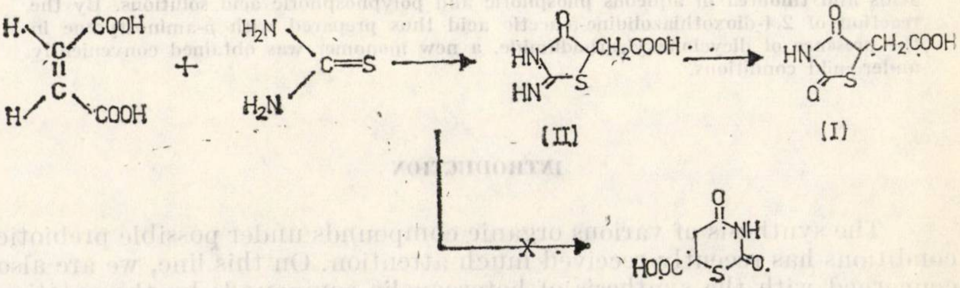
H
COOH
C
C
H
COOH
+
H₂N
C=S
H₂N
O
HN
CH₂COOH
HN
S
(II)
O
HN
CH₂COOH
O
S
(I)
X
O
NH
HOOC
S
O

(Eq. 2)

The compounds obtained were identified as being those synthesized earlier by the other usual organic syntheses.$^{4-8}$

In a similar way, acetylene dicarboxylic acid was allowed to react with thiourea at room temperature to give five-membered compound (III), which is further converted to (IV) at an elevated temperature of 140°C:

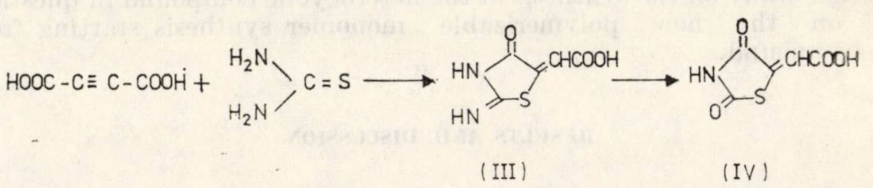
HOOC-C≡C-COOH +
H₂N
C=S
H₂N
O
HN
CHCOOH
S
HN
(III)
O
HN
CHCOOH
S
O
(IV)

(3)

Acetylene dicarboxylic acid reacts also with urea at 60°C to afford a dioxo five-membered compound (V) directly, without forming the corresponding iminooxo compound:

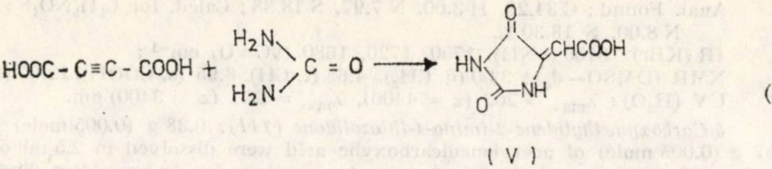

(4)

It was thus concluded that the unsaturated dicarboxylic compounds discussed here react with urea and thiourea exclusively to give five-membered ones, contrary to the case of the reaction with monocarboxylic acids which afford six-membered compounds.[2] The reaction mechanism should contain dehydration condensation as well as successive cycloaddition to give compounds with five-membered structure. At the step of the cycloaddition, dicarboxylic acids prefer the pathway which results in the five-membered ring closure.

The heterocyclic acid prepared (I) was further allowed to react with *p*-aminostyrene in the presence of dicyclohexylcarbodiimide (DCC). The reaction proceeded rather smoothly at 0°C to give a vinyl compound (VI). Similarly, the heterocyclic acid(II) was found to react also with *p*-aminostyrene, affording 2-imino-4-oxathiazolidine-5-acetic acid-4′-vinylanilide (VI)

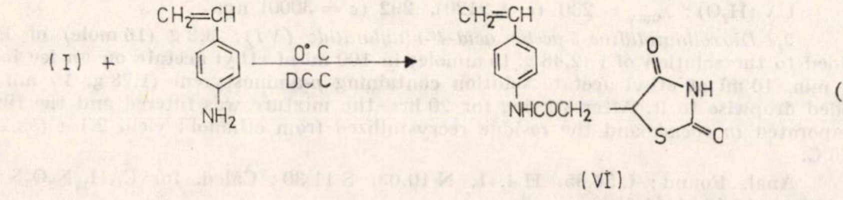

(5)

The vinyl compound VI can be polymerized with a free radical initiator. A detailed study on the polymerization of these monomers is now in progress.

EXPERIMENTAL

2-Imino-4-oxothiazolidine-5-acetic acid (II): 1.52 g (0.02 mole) of thiourea and 2.32 g (0.02 mole) of maleic acid were dissolved in 10 ml of aqueous phosphoric acid solution, and kept at 50°C for 24 hrs. In the case of 50 % aqueous polyphosphoric acid solution, the reaction mixture was kept at 100°C for 1 hr. The reaction mixture was diluted with 30 ml of water, and then left overnight. The crystals obtained were recrystallized from water: yield 2.60 g (74.7 %) in the former case, m.p. 269°C (dec.) (lit. [6] 252−253° C (dec.)).

Anal. Found; C 34.32, H 3.39, N 16.21, S 18.54; Calcd. for $C_5H_6N_2O_3S$; C 34.47, H 3.48, N 16.09, S 18.41 %.

IR (KBr): 3200 (νNH), 1700, 1680 (νC=O), 1600 (νC=N) cm^{-1};

NMR (DMSO-d_6): 2.62 (d−d, H_a), 3.05 (d−d, H_b), 4.30 (d−d, H_c), 8.75 (broad, COOH), 10.55 (broad, NH) ppm; $J_{ab} = 16.4$, $J_{ac}=10.4$, $J_{bc} = 3.8$ cps;

UV (H_2O): $\lambda_{max} = 224$ ($\varepsilon = 7840$), $\lambda_{max} = 252$ ($\varepsilon = 6800$) nm.

2,4-dioxothiazolidine-5-acetic acid (I): 3.48 g (0.02 mole) of II were heated in 10 ml of phosphoric acid solution at 195°C for 20 min. The mixture was diluted with 30 ml of water and stood overnight. The crystalline product was recrystallized from water: yield 2.70 g (77.2 %), mp. 173−175°C (lit.[6] 168°C).

Anal. Found ; C 34.28, H 3.00, N 7.97, S 18.38 ; Calcd. for $C_5H_5NO_4S$; C 34.28, H 2.88, N 8.00, S 18.30 %.

IR (KBr) : 3150 (νNH), 1750, 1720, 1680 (νC=O) cm^{-1} ;

NMR (DMSO$-d_6$) : 3.00 (d, CH_2), 4.65 (t, CH), 8.95 (s, COOH), 12.97 (broad, NH)ppm ;

UV (H_2O) : λ_{max} = 203 (ε = 4400), λ_{max} = 231 (ε = 3400) nm.

5-Carboxymethylidene-2-imino-4-thiazolidone (III): 0.38 g (0.005 mole) of thiourea and 0.57 g (0.005 mole) of acetylenedicarboxylic acid were dissolved in 2.5 ml of aqueous phosphoric acid solution and stirred at room temperature for 16 hrs. After dilution with 7.5 ml of water, the crystals obtained were recrystallized from water : yield 0.78 g (91 %), m.p. 284°C (dec.).

Anal. Found ; C 34.65, H 2.11, N 16.11 ; Calcd. for $C_5H_4N_2O_3S$: C 34.88, H 2.35, N 16.27 %.

IR (KBr) : 3260 (νNH), 1660 (νC=O) cm^{-1} ;

NMR (DMSO$-d_6$) : 6.60 (s, CH), 9.35, 9.0$-$12.3 (2NH, COOH) ppm.

5-Carboxymethylidene-1,3-thiazolidine-2,4-dione (IV): 0.86 g (0.005 mole) of III were heated in 2 ml phosphoric acid solution at 140°C for 20 min. After dilution with 5 ml of water, the product was recrystallized from water : yield 0.34 g (42.7 %), m.p. 255°C (lit.[6] 252$-$253°C (dec.)).

IR (KBr) : 3220 (νNH), 1760, 1660 (νC=O) cm^{-1} ;

NMR (DMSO$-d_6$) : 6.73 (s, CH), 12.02 (broad, NH, COOH) ppm ;

UV (H_2O) : λ_{max} = 232 (ε = 7600), 301 (ε = 8400) nm.

5-Carboxymethylidene hydantoin (V): 0.6 g (0.01 mole) of urea and 1.14 g (0.01 mole) of acetylenedicarboxylic acid in 5 ml of phosphoric acid solution were stirred at 60°C for 48 hrs. After dilution with 15 ml of water, the product was recrystallized from water : yield 0.74 g (42.6 %), mp. 325°C (lit.[9] over 400°C, lit.[10] 360°C).

IR (KBr) : 3200 (νNH), 1780, 1730 (νC=O), 1675 (ab-unsaturated C=O) cm^{-1} ;

UV (H_2O) : λ_{max} = 230 (ε = 2120), 292 (ε = 3000) nm.

2,4-Dioxothiazolidine-5-acetic acid-4′-vinylanilide (VI): 3.3 g (16 mole) of DCC were added to the solution of I (2.48 g, 15 mmole) in 100 ml of ethyl acetate on an ice bath. After 30 min. 10 ml of ethyl acetate solution containing *p*-aminostyrene (1.78 g, 15 mmole) were added dropwise to it. After stirring for 20 hrs, the mixture was filtered and the filtrate was evaporated *in vacuo*, and the residue recrystallized from ethanol : yield 2.1 g (53.2 %), m.p. 216°C.

Anal. Found ; C 56.55, H 4.41, N 10.03, S 11.30 ; Calcd. for $C_{13}H_{12}N_2O_3S$; C 56.50, H 4.39, N 10.14, S 11.60 %.

IR (KBr) : 3310 (νNH), 1780, 1710, 1680 (νC=O), 1610 (νC=C), 1550, 1530 (δNH), 1000, 920 (δCH_{vinyl}) cm^{-1} ;

NMR (DMSO$-d_6$): 3.11 (m, CHCO), 4.66 (m, 5H), 5.11, 5.72, 6.61 (d$-$d, vinyl), 7.39 (d, aromatic), 10.06 (s, NHCO), 11.80 (s, NH) ppm ;

UV (MeOH) : λ_{max} = 212 (ε = 19500), 275 (ε = 23000) nm.

The synthesis of 2-imino-4-oxothiazolidine-5-acetic acid-4′-vinylanilide (VII) was made in a similar way as VI.

REFERENCES

[1] K. Takemoto and Y. Yamamoto, *Synthesis*, **1971**, 154.
[2] K. Takemoto, H. Tahara, Y. Inaki, and N. Ueda, *Chem. Lett.*, **1972**, 767.
[3] M. Otsuru, Y. Inaki, K. Kondo, and K. Takemoto, *Techn. Repts. Osaka Univ.*, **24**, 873 (1974).
[4] R. Tambach, *Liebigs Ann. Chem.*, **280**, 233 (1894).
[5] H. Nagase, *Chem. Pharm. Bull.*, **21**, 270 (1973).
[6] R. Deghenghi and G. Daneault, *Canad. J. Chem.*, **38**, 1255 (1960).
[7] R. Andreasch, *Monatsh.*, **16**, 789 (1895).
[8] J. F. Nyc and H. K. Mitchell, *J. Amer. Chem. Soc.*, **69**, 1382 (1947).
[9] K. Moriyama, *Yakugaku Zasshi*, **83**, 169 (1963).
[10] C. O'Murchu, *Chimia*, **29**, 508 (1975).

Revue Roumaine de Chimie, 25, 7, 1101–1111(1980)

Dedicated to Professor CRISTOFOR I. SIMIONESCU
on his 60th anniversary

ALTERNATING TENDENCY IN COPOLYMERIZATION. III[1]

THE BEHAVIOUR OF THE SYSTEMS ACRYLIC MONOMER-VINYL ETHER-$ZnCl_2$

DAN SORIN VASILESCU
Laboratory of Macromolecular Chemistry, Polytechnical Institute,
Calea Victoriei 149, Bucharest, Romania

Received January 15, 1980

The homopolymerization reaction of various vinyl ethers in the presence of the complex acrylonitrile-zinc chloride was studied. Kinetic measurements were possible by using an appropriate polymerization technique. The reaction path is determined by the mixing conditions. An initiation mechanism was suggested in order to explain the kinetic features.

1. INTRODUCTION

The regulated copolymerizations in the presence of metal salts have some common features, regardless of the nature of a particular system :

— Polar monomers (group A) having nitrile or ester groups form strong coordinate bonds with metal salts or Lewis acids ; the metal (Al, Zn, Sn) being electron deficient and the nitrile or ester group having a pair of non-bonded electrons, the resulting complex is a stable one. When an electron donor monomer (group B) is mixed with the complex, equimolecular copolymers with an alternating structure are formed, over a wide range of monomer feed compositions. Their composition (1 :1) differs dramatically from that obtained as a result of a usual free radical copolymerization. In a previous paper,[1] we have reported the main features in the radical copolymerization of acrylic monomers (group A) with butyl vinyl ethers (group B), in the absence of metal salts.

— The copolymerization may be initiated by UV rays, AIBN, peroxides etc., but in several systems "spontaneous" copolymerizations were reported in the absence of any initiator. However, the addition of radical initiator may increase the rate of copolymerization, without altering the alternating character of the reaction.

— Hirooka [2,3] reported that no charge transfer occurred when the regulated copolymerization took place in the presence of carbon tetrachloride ; in some systems [3] the copolymerization process is not altered by hydroquinone, but in others hydroquinone acts as a strong retarder.

— Monomers which usually do not polymerize by free radicals (α-methyl styrene, 2-butene, isobutene etc.) can yield alternating copolymers in the presence of acrylic monomers and metal salts.

All these features are in many respects similar to those of the alternating radical copolymerization, in the absence of metal salts.[4] Some of them might be explained by the laws governing the radical copolymerization, but many other completly new aspects require a "nonclassical" interpretation (such as the homopolymerization of charge transfer complexes)

It is already agreed that complexed radicals exist in some reactions, including polymerization processes. Comprehensive papers on this subject [5,6,7] gathered experimental facts substantiating this idea, which was used by Yabumoto and Zubov [8-13] to develop the theory of favoured cross-propagation in regulated copolymerization. Nevertheless, the supporters of this scheme failed to give a clear explanation for the mechanism of initiation. It is perhaps ironical that Golubev et al.[12] and Hirai and his co-workers,[14] both using ESR measurements, arrived at opposite conclusions.

On the other hand, charge transfer complexes are not a novelty. In the field of polymer chemistry their existence was demonstrated for ionic polymerizations and for some copolymerization processes. Sille and his co-workers [15] have brought convincing proof about charge transfer complexes in copolymerizations involving vinylidene cyanide.

In recent years several authors have reported that in the regulated copolymerization in the presence of metal salts, besides the alternating copolymer, some cationically formed polymers (from the monomers belonging to the group B) also appeared. We have previously mentioned one of Zubov's works [9] in which the cationic polymerization of styrene in the presence of methyl methacrylate and aluminium halides was reported. Gaylord [16] described the formation of poly-α-methyl styrene in admixture with the alternating copolymer acrylonitrile-α-methyl styrene.

The occurrence of the cationic polymerization of monomers from the group B in the presence of complexed acrylic monomers depends on the structure of the electron donor monomers (group B). Yamada and Yamagita [17] have prepared the acrylonitrile-ethyl aluminium dichloride complex and tried to copolymerize it with various monomers; isobutyl vinyl ether and α-methyl styrene undergo cationic polymerization, while isoprene, butadiene and styrene form alternating copolymers.

The present work started from the idea that the cationic polymerization of donor monomers in the presence of complexed acrylic monomers has the same causes as the alternating copolymerization. Consequently, we approached the study of the systems of the type acrylonitrile-$ZnCl_2$-vinyl ethers.

2. EXPERIMENTAL

2.1. Materials

Acrylonitrile was purified according to the usual methods and dried over calcium hydride; after the final fractionation, the pure monomer was stored over calcium hydride in vacuum.

The butyl and isobutyl vinyl ethers (BVE and IBVE) and 2-chloroethyl vinyl ether (CEVE) were washed four times with water in order to remove traces of alcohol and dried overnight with potassium hydroxide. The vinyl ethers were fractionally distilled from freshly extruded sodium wire; BVE were stored over sodium wire in vacuum, while CEVE was kept over calcium hydride.

The solvents were purified by distillation from appropriate drying agents.

Methanol and petroleum spirit — reagent grade — were used without further purifications.

Since zinc chloride is a very hygroscopic material and traces of water may be cocatalysts in the cationic polymerization, $ZnCl_2$ reagent grade was dried and sublimed in vacuum.

2.2. The complex acrylonitrile —$ZnCl_2$

The desired amount of zinc chloride was sublimed in a conventional-type sublimator; the sublimator was opened in a dry-box filled with dry argon. $ZnCl_2$ was subsequently transferred into preweighed ampoules; this operation was carried out in the same dry-box. The ampoule was put on the vacuum line and the desired amounts of acrylonitrile (AN) and solvent were distilled into the ampoule; the mixture was degassed by conventional freezing, evacuation and thawing cycles. After four cycles the ampoule was sealed off and put in a shaking machine until zinc chloride was completely dissolved in AN. Ampoules containing the complex AN-$ZnCl_2$ were subsequently connected to vessels into which other monomers could be distilled.

2.3. Dilatometric measurements in the system AN-$ZnCl_2$-IBVE

The operation of filling the ampoules with monomers, solvents etc. was carried out on a vacuum line in the usual manner. The typical apparatus used in kinetic measurements consisted of double ampoules separated by a break seal; the ampoule A is the one presented in figure 1, containing $ZnCl_2$ and AN. A previously calibrated dilatometer ($2\ cm^2$ capacity approximately and capillary of 1 mm internal diameter-Veridia tubing) was connected to the ampoule B. The installation was put on a vacuum line; the necessary amounts of monomer and solvent were calculated as a function of the initial weight of $ZnCl_2$.

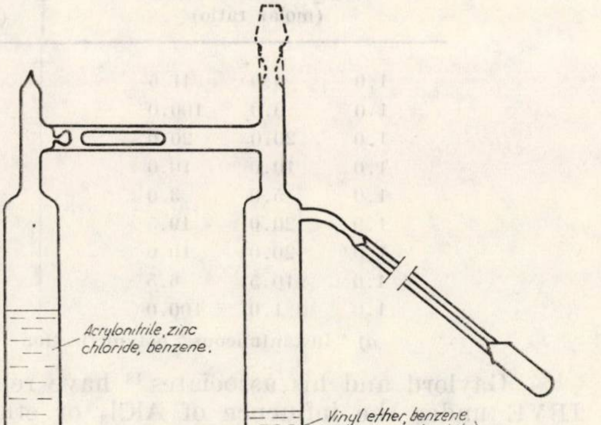
Acrylonitrile, zinc chloride, benzene.
Vinyl ether, benzene (styrene, acrylonitrile)
A
B

Fig. 1. — Installation for investigation of polymerization of vinyl ethers under the influence of AN-$ZnCl_2$ complex.

All the above described operations were carried out in sodium light, in order to eliminate possible photoreactions. The polymerization reaction starts at the very moment of mixing the two solutions, from the ampoules A and B respectively. The system was cooled down at 10°C before mixing the reactants, as the reaction was investigated at 25°C. The mixing operation was followed by rapid filling of the dilatometer to a suitable level. The dilatometer was sealed off from the rest of system and quickly placed in a thermostat; as will be shown later, the order of mixing has a crucial importance. The operations described above may last maximum 10 minutes; we have taken into account this period and we have extrapolated the recorded contraction-time data for the time "zero" (the moment of mixing). The reaction mixture remained in ampoules was also put in the thermostat, for the same period as the dilatometer; the gravimetrically established conversions were finally compared.

2.4. Composition and structure of products

The composition of copolymers was established by elemental analysis (C, H, N, Cl and ash); copolymers of high AN content, generally infusible, were reprecipitated before being submitted to analysis in order to obtain finely powdered products. Confirmation of their structure was obtained from their IR (usually KBr pellets) and NMR (60 MHz, external TMS, 0 – 10 ppm) spectra.

3. RESULTS AND DISCUSSION

As was shown earlier [1] in the systems acrylonitrile-vinyl ether in the presence of radical initiators the only product of the reaction is the copolymer; the formation of poly-vinyl ether was not noticed.

Zinc chloride is a weak Lewis acid and initiates the cationic polymerization of isobutyl vinyl ether (IBVE), even in the presence of acrylonitrile. $ZnCl_2$ is not soluble in vinyl ethers; if zinc chloride was purified and dried as described, the polymerization reaction was slow (see table 1); it also seems reasonable to assume a heterogeneous mechanism of initiation, since apparently the change in the IBVE/$ZnCl_2$ ratio (from 41.6 to 100) does not sensibly affect the yield.

TABLE 1

Homopolymerization of IBVE catalyzed by the AN-$ZnCl_2$ complex: "instantaneous" and "slow" reactions at 25°C

$ZnCl_2$: AN : IBVE (molar ratio)			Time (hours)	Conversion (%)
1.0	0.0	41.6	24	21.3
1.0	0.0	100.0	24	23.6
1.0	20.0	20.0	a)	27.8
1.0	10.0	10.0	a)	74.2
1.0	5.0	3.0	a)	48.6
1.0	20.0	19.5	18	4.6
1.0	20.0	10.0	24	0.5
1.0	10.5	6.5	24	27.0
1.0	1.0	100.0	24	53.9

a) "Instantaneous" polymerization

Gaylord and his associates [18] have reported the polymerization of IBVE under the influence of $AlCl_3$ or ethyl aluminium sesquichloride (EASC) in the presence of equimolecular amounts of acrylic monomers or their saturated analogues as reaction media; they have suggested that the etherates of $AlCl_3$ or EASC, formed with IBVE, initiate the cationic polymerization, as aluminium compounds complex more easily with ethereal oxygen than with the nitrile group.

Our results (Table 1) make us hardly agree with the possibility of a direct complexing of $ZnCl_2$ to IBVE, as zinc chloride is insoluble in IBVE; in the presence of acrylonitrile, $ZnCl_2$ was entirely dissolved and a homogeneous solution resulted. We found that the order of mixing is the main factor which determines the reaction path. If a vinyl ether is poured over the AN-$ZnCl_2$ mixture, an "instantaneous" polymerization takes place, the poly-vinyl ether being the only product. It is important to notice that the yield is around 50%; subsequently the polymerization continues but with a considerably smaller rate. On the other hand, the conversion obtained as a result of the "instantaneous" polymerization is not a reproducible value, as it depends on the mixing conditions. The experimental evidence suggests that the rate of the chemical process (homopolymerization) may be far higher than that of the physical one (mixing). When the homogeneity of the mixture has been realized, the reaction takes place slowly, since acrylonitrile appears to be a retardant. This assertion is also sustained by the fact that when acrylonitrile was shared from the beginning between the ampoules (60 % from the total AN amount in ampoule A to dissolve $ZnCl_2$ and 40 % in ampoule B for preventing IBVE from an early polymerization) and mixing was carried out by pouring the contents of ampoule A over B, the polymerization took place rather slowly from the commencement (Table 1). All the kinetic measurements which are described farther, were made by using this technique.

In our systems $ZnCl_2$ had been complexed to AN (ampoule A) prior mixing with IBVE (ampoule B). The striking kinetic feature of the systems studied by us is the relatively low homopolymerization rate in view of the high propagation rate coefficient, characteristic of vinyl ethers at room temperature.[19] When stabilized cations, even in small concentrations are used to initiate the polymerization of vinyl ethers,[20] the reaction reaches high yields in a few seconds.

In the system AN-$ZnCl_2$-IBVE although the homopolymerization rate for IBVE is considerable, especially in the initial stages, it is nevertheless much smaller than that previously observed,[20] suggesting a slow initiation step.

In order to elucidate the nature of the initiation mechanism, we have to identify the real initiator and subsequently to establish how the initiation act takes place.

In our view, the actual initiator is the complex AN-$ZnCl_2$, since acrylonitrile alone does not induce the homopolymerization of BVE[1] and on the other hand $ZnCl_2$ produces only small amounts of poly-IBVE, likely by a heterogeneous catalysis.

The following mechanisms may be possible :

— Acrylonitrile dissolves the salt and acts as a cocatalyst, eventually giving a proton to the vinyl ether.

— A charge-transfer complex between AN-$ZnCl_2$ and IBVE is formed and the resulting radical-cation initiates the polymerization of IBVE ; the experimental facts seem to indicate that the second proposal may be correct, since the first mechanism should imply a higher initiation rate.

Several workers have stressed [14,21-27] that in the An-$ZnCl_2$—S (S = styrene) or related systems, the initiation step might consist in forming a charge transfer complex between the acrylic monomer (complexed to the Lewis acid) and the electron donor monomer.

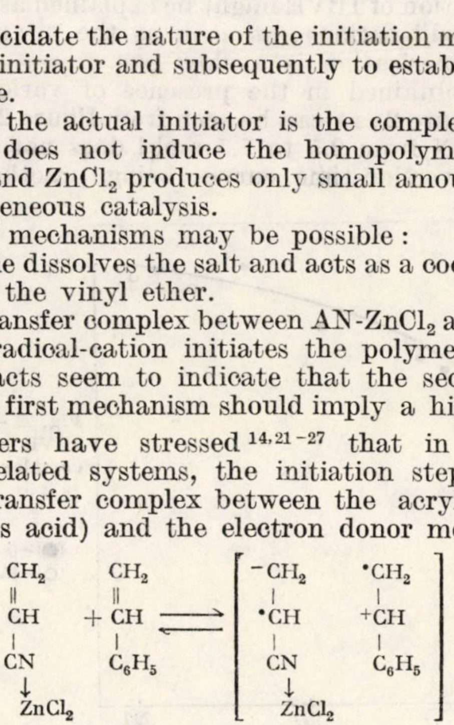

$$\underset{\text{I}}{CH_2{=}CH{-}CN \rightarrow ZnCl_2} + \underset{\text{II}}{CH_2{=}CH{-}C_6H_5} \rightleftharpoons \underset{\text{III}}{\left[\,{}^{-}CH_2{-}{}^{\bullet}CH{-}CN \rightarrow ZnCl_2 \qquad {}^{\bullet}CH_2{-}{}^{+}CH{-}C_6H_5\,\right]} \tag{1}$$

I II III

We think that a similar explanation could be given for the AN-$ZnCl_2$-IBVE (IV—V) system ; the radical-cation (VII) might initiate the cationic polymerization of IBVE.

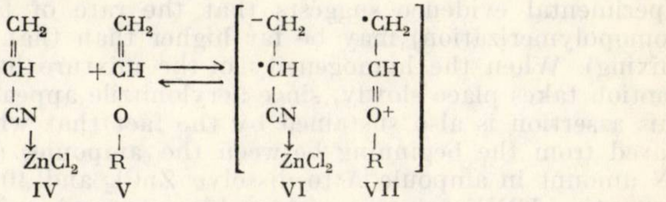

$$\begin{array}{c} CH_2 \\ \| \\ CH \\ | \\ CN \\ \downarrow \\ ZnCl_2 \\ \mathrm{IV} \end{array} + \begin{array}{c} CH_2 \\ \| \\ CH \\ | \\ O \\ | \\ R \\ \mathrm{V} \end{array} \rightleftharpoons \left[\begin{array}{c} -CH_2 \\ | \\ \cdot CH \\ | \\ CN \\ \downarrow \\ ZnCl_2 \\ \mathrm{VI} \end{array} \quad \begin{array}{c} \cdot CH_2 \\ | \\ CH \\ \| \\ O^+ \\ | \\ R \\ \mathrm{VII} \end{array} \right] \qquad (2)$$

Since initiation is the slow step, it seems reasonable to assume that the concentration of (VII) should be very small ; as (VII) is consumed in the initiation of the polymerization process, new radical-cations may be formed from the proposed equilibrium reaction. In this way the long time for which the polymerization lasts can receive a plausible explanation.

The preliminary tests (Table 1) showed that the excess of AN behaved as a retarder. This fact could be understood if taking into account that the growing end is not a free cation, but it is coordinated to acrylonitrile ; for instance, the structure (VIII) is a possible one.

$$-C^+ \leftarrow :N{\equiv}C-CH{=}CH_2 \qquad \mathrm{(VIII)}$$

It is also conceivable that the radical anion (VI) is in the neighbourhood of the growing end, acting as a "gegen ion". In this way the spontaneous polymerization of IBVE might be explained as a rapid propagation through "unshielded" cations ; as soon as the mixture becomes homogeneous, the polymerization is a slow one.

The results obtained in the presence of various amounts of AN are presented in figure 2 ; as can be seen from figure 2, the increase in the concentration of AN from 2.5 to 7.5 mol/l does not change the reaction rate, the two conversion-time curves being practically identical.

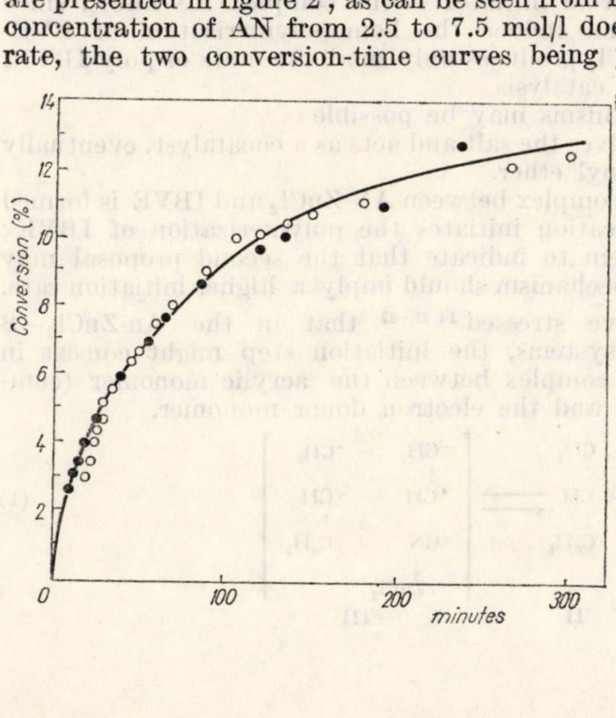

Fig. 2. — Homopolymerization of IBVE under the influence of the complex AN-$ZnCl_2$; [IBVE] = = 2.5 mol/l ; solvent-benzene ; $t = 25°C$.

(●) – [AN] = 2.5 mol/l, AN/$ZnCl_2$ = 5

(○) – [AN] = 7.5 mol/l; AN/$ZnCl_2$ = 15

It is likely that by using an excess of AN the presence of traces of water would not matter too much. However, even if the water content is relatively small (curve 1 — figure 3), the homopolymerization rate is higher than that for the same process, measured under "standard" conditions (curve 2 — figure 3). As was previously shown,[28] the presence of water, especially at very small concentrations is a very controversial problem in the sphere of cationic polymerization. In the experimental part we have described the "standard" procedure for purification and drying of $ZnCl_2$, monomers and benzene. Instead of measuring the small but unknown level of water in our systems, which would have been a laborious and perhaps unreliable operation, we have approached this problem by introducing known amounts of water into the system. This was done by shaking pure benzene with water for 24 hours and subsequently leaving the mixture for several days in order to obtain a complete separation of the two layers. The upper layer was considered to be water-saturated benzene; the concentration of water is given [29] as 0.06 g H_2O for 100 g benzene at 25°C. Using this benzene, instead of the dry one, the concentration of water reached 0.017 mol/l.

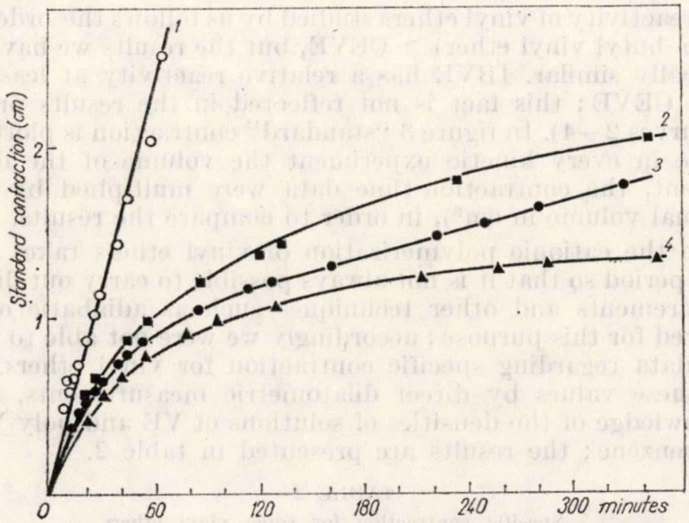

Fig. 3. — Homopolymerization of various vinyl ethers (VE) under the influence of the complex AN-$ZnCl_2$; $[AN]/[ZnCl_2] = 5$; $[AN] = 2.5$ mol/l ; $[VE] = 2.5$ mol/l ; solvent-benzene ; $t = 25$°C. *1.* VE = IBVE and $[H_2O] = 0.017$ mol/l ; *2.* VE = IBVE ; *3.* VE = NBVE ; *4.* VE=CEVE.

As previously described, the polymerization of vinyl ethers begins at the very moment of mixing the VE with the complex AN-$ZnCl_2$. The operations of mixing, filling the dilatometer etc. may last maximum ten minutes; consequently the first recording does not coincide with the real time "zero". As the contraction-time data were extrapolated for the time "zero", a comparison between the homopolymerization rate of IBVE in the presence of water and in "standard" conditions is not relevant in the initial period; nevertheless, for the later stages it becomes clear that the polymerization of IBVE takes place two-three times faster in the presence of water ($IBVE/H_2O = 147$) than in "standard" conditions (Figure 3). Our experimental precautions allowed us to obtain reproducible results; it may be concluded that the actual concentration of water was, in all the experiments, below a certain level from which it would have become significant from the kinetic viewpoint.

The reactivity of vinyl ethers studied by us follows the order IBVE > > NBVE(*n*-butyl vinyl ether) > CEVE, but the results we have obtained are practically similar. IBVE has a relative reactivity at least 25 times more than CEVE; this fact is not reflected in the results presented in figure 3 (curves 2—4). In figure 3 "standard" contraction is plotted against time. Since in every kinetic experiment the volume of the dilatometer was different, the contraction-time data were multiplied by the factor ($2\ cm^3$/actual volume in cm^3), in order to compare the results.

Often the cationic polymerization of vinyl ethers takes place in a very short period so that it is not always possible to carry out dilatometric rate measurements and other techniques such as adiabatic calorimetry are employed for this purpose; accordingly we were not able to find in the literature data regarding specific contraction for vinyl ethers. We have obtained these values by direct dilatometric measurements, as well as from a knowledge of the densities of solutions of VE and poly-VE respectively in benzene; the results are presented in table 2.

TABLE 2

Specific contraction for some vinyl ethers

Monomer	Specific contraction (%)
iso-butyl vinyl ether	17.1
n-butyl vinyl ether	18.1
2-chloroethyl vinyl ether	17.6

In the AN-$ZnCl_2$-IBVE system the formation of any AN-IBVE copolymer was not noticed, the only product being poly-IBVE. It is not consistent with the experimental evidence to say that there are two competitive reactions (homopolymerization and copolymerization) of which the first takes place with a much higher rate, since after 24 hours there remained an important proportion of unreacted vinyl ether.

It appears from figure 4 that as the IBVE concentration increases for the initial stage of the reaction, a first order dependence with respect to monomer concentration is found; in the later stage the polymerization rate is maintained practically constant.

CEVE exhibits a similar behaviour (Figure 5); nevertheless in this case the formation of some traces of benzene-insoluble polymer were noticed as well. For instance, under the conditions corresponding to curve 2 (Figure 5) after 24 hours, the yields of poly-CEVE and AN-CEVE copolymer respectively are 14% (of the initial CEVE) and 0.7% (with regard to both monomers). The AN-CEVE is richer in AN units (75% approximately) although in the initial monomer feed the concentrations of AN and CEVE were equal (2.5 mol/l).

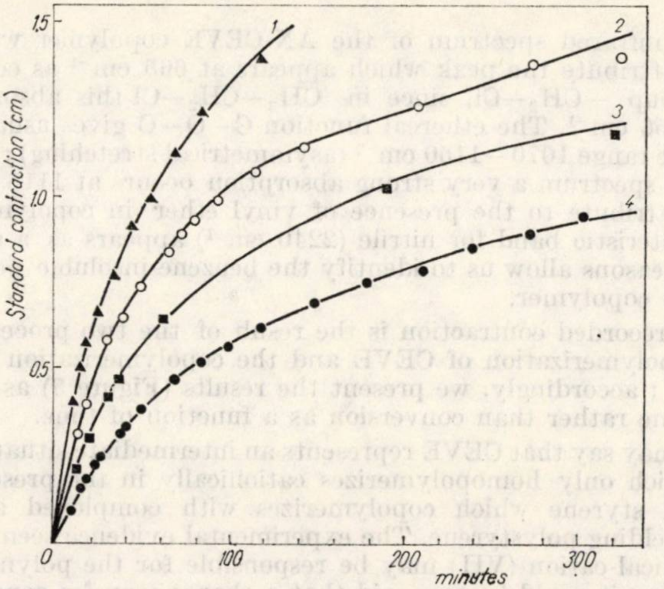

Fig. 4. — The influence of the concentration of IBVE on the homopolymerization rate ; [AN] = 2.5 mol/l ; [AN]/[ZnCl$_2$] = 5 ; solvent-benzene ; t = 25°. *1.* [IBVE] = 2.5 mol/l ; *2.* [IBVE] = = 2.0 mol/l ; *3.* [IBVE] = 1.5 mol/l ; *4.* [IBVE] = 1.0 mol/l.

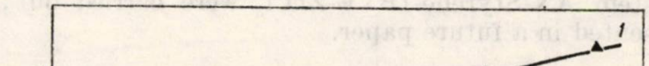

Fig. 5. — The polymerization of 2-chloroethyl vinyl ether under the influence of the AN-ZnCl$_2$ complex ; [AN] = 2.5 mol/l ; [AN]/[ZnCl$_2$] = 5 ; solvent — benzene ; t = 25°. *1.* [CEVE] = = 3.5 mol/l ; *2.* [CEVE] = 2.5 mol/l ; *3.* [CEVE] = 1.5 mol/l.

The infrared spectrum of the AN-CEVE copolymer was recorded. We may attribute the peak which appears at 665 cm^{-1} as corresponding to the group $-CH_2-Cl$, since in CH_3-CH_2-Cl this absorption takes place at 656 cm^{-1}. The ethereal function $C-O-C$ gives usually a strong peak in the range 1070—1150 cm^{-1} (asymmetrical stretching); in the above mentioned spectrum a very strong absorption occurs at 1118 cm^{-1}, which we may attribute to the presence of vinyl ether in copolymer. Finally, the characteristic band for nitrile (2240 cm^{-1}) appears as a strong peak. All these reasons allow us to identify the benzene-insoluble polymer as an AN-CEVE copolymer.

The recorded contraction is the result of the two processes, namely the homopolymerization of CEVE and the copolymerization of the pair AN-CEVE; accordingly, we present the results (Figure 5) as contraction against time rather than conversion as a function of time.

We may say that CEVE represents an intermediate situation between IBVE, which only homopolymerizes cationically in the presence of AN-$ZnCl_2$ and styrene which copolymerizes with complexed acrylonitrile, without yielding polystyrene. The experimental evidence seems to suggest that a radical-cation (VII) may be responsible for the polymerization of vinyl ethers; it could be also said that a charge transfer complex similar to (VI—VII) is the initiator of free radical copolymerization of AN and CEVE.

In order to gather further evidence for this idea, experiments involving the system AN-Styrene-IBVE-$ZnCl_2$ were carried out; the results will be presented in a future paper.

REFERENCES

[1] Part. I: D. S. Vasilescu, *Rev. Roumaine Chim.*, **19**, 1393 (1974); Part. II: *Rev. Roumaine Chim.*, **19**, 1637 (1974).

[2] M. Hirooka, 23rd Congress of IUPAC, Boston, *Macromol. Preprint*, **1**, 311 (1971).

[3] M. Hirooka, *J. Polymer Sci.*, *B*, **10**, 171 (1972).

[4] O. F. Solomon and D. S. Vasilescu, *Materiale Plastice (Bucureşti)*, **7**, 112, 159, 215 (1970).

[5] C. H. Bamford, "Radical Intermediates in Polymerization Processes", in "Molecular Behaviour and the Development of Polymeric Materials", (A. Ledwith and A. M. North editors), Chapman and Hall, London, 1974.

[6] C. H. Bamford and G. C. Eastmond, *Pure Appl. Chem.*, **12**, 183 (1966).

[7] C. H. Bamford, *Pure Appl. Chem.*, **15**, 333 (1967).

[8] S. Yabumoto, K. Ishii and K. Arita, *J. Polymer Sci.*, A—1, **7**, 1577 (1969); **8**, 295 (1970).

[9] V. P. Zubov, L. I. Valuev, V. A. Kabanov and V. A. Kargin, *J. Polymer Sci.*, A—1, **9**, 833 (1971).

[10] Yu. D. Semchinov, A. V. Ryabov, N. L. Khratova and Ye. N. Milchenko, *Vysokomol. Soedineniya*, A, **15**, 451 (1973).

[11] V.I. Zubov and V. A. Kabanov, *Vysokomol. Soedineniya*, A, **14**, 5 (1972).

[12] V. B. Golubev, V. P. Zubov, G. S. Georgiev, I. L. Stoyachenko and V. A. Kabanov, *J. Polymer Sci.*, A—1, **11**, 2463 (1973).

[13] G. S. Georgiev, A. M. Caplan, V. P. Zubov, V. B. Golubev, I. M. Barkalov and V. A. Kabanov, *Vysokomol. Soedineniya*, A, **14**, 177 (1972).

[14] H. Hirai and M. Komiyama, *J. Polymer Sci.*, A—1, **13,** 2419 (1975).

[15] J. K. Sille, N. Oguni, D. C. Chung, R. F. Tarvin, S. Aoki and M. Kamachi, *J. Macromol. Sci. (Chem.)*, A, **9,** 745 (1975).

[16] N. G. Gaylord, B. Patnaik and A. Takahashi, *J. Polymer Sci.*, **8,** 809 (1970).

[17] A. Yamada and M. Yamagita, *J. Polymer Sci.*, B, **10,** 91 (1972).

[18] N. G. Gaylord, A. B. Deshpande and S. S. Dixit, *J. Polymer Sci.*, B, **13,** 79 (1975).

[19] A. Ledwith, *Makromol. Chem.*, **175,** 1117 (1974).

[20] A. D. Ledwith, E. Lockett and D. C. Sherrington, *Polymer*, **16,** 31 (1975).

[21] S. Pasynkiewicz, T. Diem, W. Kuran and K. Kolbrecka, *Makromol. Chem.*, **156,** 251 (1972).

[22] N. G. Gaylord and A. Takahashi, *J. Polymer Sci.*, B, **17,** 443 (1969).

[23] Y. Koma, S. Kondo and K. Iimura, *J. Polymer Sci.*, B, **12,** 153 (1974).

[24] J. K. Hecht, *J. Polymer Sci.*, A—1, **8,** 2181 (1970).

[25] S. Pasynkiewicz, T. Diem and A. Korol, *Makromol. Chem.*, **137,** 61 (1970).

[26] F. Shepherd and H. J. Harwood, *J. Polymer Sci.*, B, **10,** 799 (1972).

[27] W. Kuran, S. Pasynkiewicz and Z. Florjańczyc, *Makromol. Chem.*, **154,** 71 (1972).

[28] P. Sigwalt, *Makromol. Chem.*, **175,** 1017 (1974).

[29] A. Seidell, "Solubilities of organic compounds", Van Nostrand, London, 1941.

Revue Roumaine de Chimie, 25, 7, 1113–1122 (1980)

Dedicated to Professor Cristofor I. Simionescu
on his 60th anniversary

AN ALTERNATIVE TO THE TRANSIENT HOT-WIRE METHOD FOR THERMAL CONDUCTIVITY MEASUREMENTS OF FLUIDS

RODICA VÎLCU * and A. CIOCHINĂ **

* Polytechnical Institute, Department of Physical Chemistry, Bd. Republicii 13, Bucharest, Romania

** ICECHIM, Centre of Physical Chemistry, Spl. Independenţei, 202, Bucharest, Romania

Received February 5, 1980

The paper describes an instrument to measure the thermal conductivity of liquids in an absolute way. The apparatus works on the hot-wire principle with a platinum wire, and operates in the transient condition. Determinations consist in principle in measuring the times at which the hot wire attains two preset temperature values. Results on toluene are given. The reproducibility of the apparatus is 1 %, the accuracy being estimated at 7 %.

1. INTRODUCTION

Practical problems concerning the design, accomplishment and the correct and economical performing of heat transfer processes require the values of the thermal conductivity and thermal diffusivity of the materials taken into account in the heat balance. Data on the thermal conductivity of fluids are rather scarce and agreement between reported results has often been poor. The scatter in the data on a number of common fluids extends over 10 or 20 % and agreement within a few per cent must be regarded as indicative of careful work.[1,2] A need for more precise data to help the establishing standards for thermal conductivity measurements and to solve the heat transfer problems occurring in modern technology appears.

In principle, the transient line source technique for thermal conductivity measurement consists in recording the temperature rise of a fine, steadily heated vertical wire immersed in the test fluid. The hot wire acts both as an electrical heating element and a resistance thermometer.

This method is certainly more advantageous than the steady state hot-wire method[1,3–5]: small-volume, low-diameter cell; only two or four electrical connexions have to be brought out of the cell; the geometrical requirements of the cell are simple; the geometrical factor of the cell consists simply in a single length, which is more easily obtained to a high accuracy than the geometrical factors of steady state cells. The most serious sources of error in fluid thermal conductivity measurements are generally heat transfer by radiation and convection. In the steady-state method these effects can be eliminated or shown to be negligible by repeated determinations in which the temperature drop across the fluid layer, or the layer thickness is varied. The transient method yields information about the presence of such parasitic phenomena in the course of experiments lasting only several seconds. Unavoidable heat losses (at the ends and by potential leads) are much smaller in the transient method,measurements are shown to be unaffected by a constant thermal resistance at the wire-fluid interface, and the short duration of the experiment minimises the development of concentration gradients by thermal diffusion in fluid mixtures or in fluids which are unstable in time. By the transient method one can obtain data in conditions which are fundamentally different from those of the steady state method,[6-8] and the agreement between data obtained by different methods gives a test of consistency of the techniques.

2. THEORETICAL PRINCIPLES OF THE METHOD

In the transient, hot-wire method, the thermal conductivity of the fluid is determined by observing the rate at which the temperature of a thin wire increases with time after a step pulse of constant electric power applied to it. The wire approximates a line source of constant heat flux, q, per unit length, which generates into the fluid a time increasing radial field of temperature of cylindrical symmetry. After a time t_A from the start of the step-pulse ($t = 0$), the product between the time and the rate of temperature rise in wire is inversely proportional to the fluid thermal conductivity λ. For $t \geqslant t_A$, the temperature increase $\theta\ (r_1,\ t)$ at the wire of radius r_1 itself is described by the formula[9] :

$$\theta(r_1,\ t) = \frac{q}{4\pi\lambda} \ln \frac{4at}{r_1^2 \cdot C} \tag{1}$$

where $a = \lambda/(\rho c_p)$ is the thermal diffusivity of the fluid ; ρ and c_p are the density and the specific heat at constant pressure ; $C = e^{\gamma} = 1.781$, where $\gamma = 0.5772\ldots$ is Euler's constant. The temperature increase of the wire can be measured by monitoring the resistance R of the wire after a calibration $R(T)$, where T is the temperature.

The increase in temperature described by eq. (1) gives a straight line $\theta(r_1,\ t)$ versus ($\ln t$) and the slope p of this line is inversely proportional to the thermal conductivity. This straight-line relation will be observed only between times t_A and t_B, $t_A \leqslant t \leqslant t_B$, systematic deviations occurring both for short ($t < t_A$) and long ($t > t_B$) times. The time t_A depends on geometrical and physical constants of the wire, and t_B is a limiting time for natural convection and wall cell effects. By measuring $\theta(r_1,\ t)$ at two times t_1 and t_2 within this interval, the termal conductivity of the fluid is obtained from eq. (1) as follows :

$$\lambda = \frac{q}{4\pi}\,\frac{\ln t_2 - \ln t_1}{\theta(r_1,\ t_2) - \theta(r_1,\ t_1)} \tag{2}$$

provided that $r_1^2/(4\ at)$ is sufficiently small in the range t_1 to t_2. This method gives directly the value of the thermal conductivity and not the thermal diffusivity, as is the general case of transient methods. By measuring the increase of temperature of the wire at two different times, the wire diameter is not required in calculations. The detailed analysis of the theory of the method and of the corrections will be given in subsequent papers.

3. THE PRINCIPLE AND BLOCK DIAGRAM OF THE APPARATUS

The apparatus made[10] for thermal conductivity measurements in fluids measures the time t in which the wire temperature reaches a preset threshold and the slope of the curve θ *versus* t between the moments t and $t + \mathrm{d}t$ (Fig. 1).

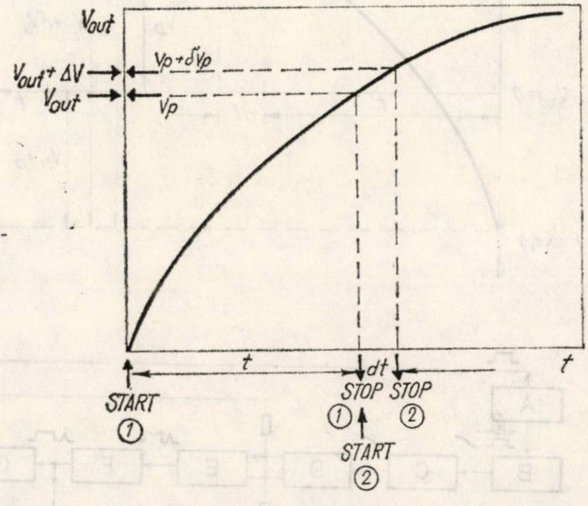

Fig. 1. — The principle of the measuring method.

The wire is connected into a Wheatstone bridge, maintained initially ($t = 0$) at balance. A preset constant current step pulse of finite duration (3 s) is applied at time $t = 0^+$ on the bridge input from a constant current generator. The current is so chosen as to lead to a small temperature increase of the wire (0.5 — 2 K), so that the change in the electrical resistance can be assumed linearly with respect to temperature. The output signal of the bridge is amplified by a differential amplifier with gain A and single ended output. By using a potentiometer, the amplifier output $V_{\mathrm{out},\,0}$ can be scaled within a range of several volts. The output signal of the amplifier, V_{out}, goes to input of voltage comparator with preset (but adjustable) threshold V_p. Two time intervals are measured with the aid of digital counters which are triggered by the voltage comparator: the time between $t = 0$ when the step heating pulse is started to the bridge input (START the first counter) and up to the moment t when $V_{\mathrm{out}} = V_p$ (STOP the first counter and START the second counter); the time interval dt between t and $t + \mathrm{d}t$ when the signal at the comparator input $V_{\mathrm{out}} + \Delta V$ becomes equal to a new threshold value $V_p + \delta V_p$ (STOP the second counter) The instantaneous increase of the threshold to the (preset and adjustable) value $V_p + \delta V_p$ is triggered by the comparator. In order to obtain the curve θ *versus* t and also the slope p of the curve at various points (i.e. different times), successive pulses are applied thus changing the threshold values V_p by displacing $V_{\text{out,o}}$ while the threshold level V_D of the comparator is constant (Fig. 2). The block diagram of the apparatus is given in figure 3.

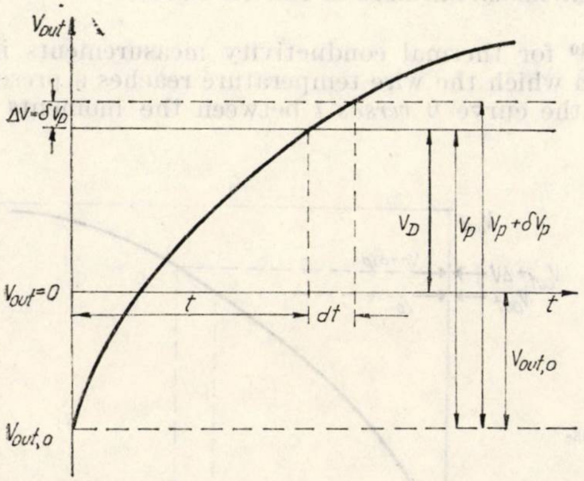

Fig. 2. — Temperature recording principles.

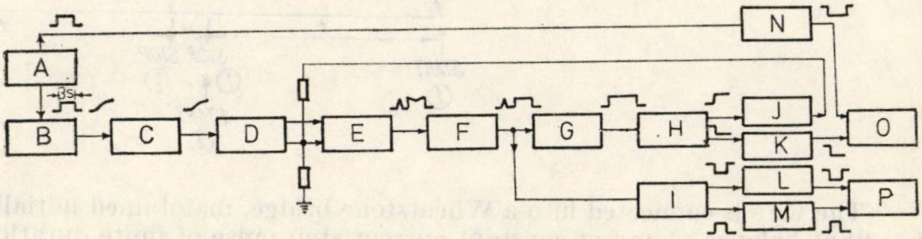

Fig. 3. — Block diagram of the apparatus :

A — pulse generator ; B — Wheatstone bridge ; C — differential amplifier ; D — output follower ; E — comparator ; F — Schmitt trigger ; G — monostable ; H — bistable 1 ; I — bistable 2 ; J — follower ΔV ; K — follower STOP t ; L — follower START dt ; M — follower STOP dt ; N — inverter START t ; O — counter t ; P — counter dt.

4. THE CELL

The measuring cell (glass or metal, inner diameter of 1—2 cm for liquids and 4—5 cm for gases) contains the investigated fluid. The transducer made of platinum wire (diameter d_1 about 0.02 mm and length L about 0.6 m) connected at the ends on thick copper leads is immersed into the fluid. The ensemble is maintained at the temperature T (in a thermostat).

5. THE CALCULATION FORMULA

From eq. (2) one obtains:

$$\lambda = \frac{q}{4\pi}\,\frac{\ln(t+\mathrm{d}t)-\ln t}{\theta(r_1, t+\mathrm{d}t)-\theta(r_1, t)} = \frac{q}{4\pi}\,\frac{\Delta(\ln t)}{\Delta\theta} \tag{3}$$

or

$$\lambda = \frac{q}{4\pi}\,\frac{\Delta(\ln t)}{\Delta R_1}\,\frac{\Delta R_1}{\Delta\theta} \tag{4}$$

where q is constant heat flux per unit length of the wire, and ΔR_1 an increase of the resistance corresponding to a temperature rise $\Delta\theta$. For small $\Delta\theta$ one has $\Delta R_1/\Delta\theta = \mathrm{d}R/\mathrm{d}\theta =$ constant.

$$\Delta R_1 = \frac{\Delta V_1}{I_1} - \frac{V_1}{I_1^2}(\Delta I_1)$$

where ΔV_1 is the voltage increase on the wire corresponding to ΔR_1, I_1 is the constant heating current of the wire and V_1 is the voltage on the wire ends. As the wire is supplied from a fast response constant current generator: $\Delta R_1 = \Delta V_1/I_1$.

$$I_1 = \frac{V_1}{R}\,; \quad q = \frac{V_1 I_1}{L} = \frac{V_1^2}{RL}\,; \quad \frac{\mathrm{d}R}{R(\mathrm{d}\theta)} = \alpha$$

where R is the resistance of the wire of length L at time $t = 0$ and temperature T, and α is the temperature coefficient of the resistance of the wire.

It results:

$$\lambda = \frac{V_1 I_1^2}{4\pi L}\,\frac{\Delta(\ln t)}{\Delta V_1}\,\frac{\mathrm{d}R}{\mathrm{d}\theta} \tag{5}$$

For a Wheatstone bridge with all the arms equal, the bridge output ΔV is correlated to the signal ΔV_1 as follows:

$$\Delta V = \frac{\Delta V_1}{2} A$$

where A is the gain of the amplifier. Eq. (5) becomes:

$$\lambda = \frac{V_1^3 \alpha A}{8\pi RL}\,\frac{\Delta(\ln t)}{\Delta V} \tag{6}$$

a)
$$\delta V_p = \Delta V << V_p$$

$$\lim_{\Delta V \to 0} \frac{\mathrm{d}(\ln t)}{\Delta V} = \frac{\mathrm{d}}{\mathrm{d}t}(\ln t)\,\frac{\mathrm{d}t}{\Delta V} = \frac{1}{t}\,\frac{\mathrm{d}t}{\Delta V}$$

$$\lambda = \frac{V_1^3 \alpha A}{8\pi R L(\Delta V)}\,\frac{\mathrm{d}t}{t} \tag{7}$$

b)
$$\delta V_p = \Delta V < V_p$$

$$\ln(t + \mathrm{d}t) - \ln t = \ln\left(1 + \frac{\mathrm{d}t}{t}\right)$$

$$\lambda = \frac{V_1^3 \alpha A}{8\pi R L(\Delta V)} \ln\left(1 + \frac{\mathrm{d}t}{t}\right) \tag{8}$$

6. THE ESTIMATION OF INSTRUMENTAL ERRORS

Designating by δ the error associated to a measured quantity, we have:

a)
$$\varepsilon = \frac{\delta_\lambda}{\lambda} = \left[\left(\frac{3\delta_{V_1}}{V_1}\right)^2 + \left(\frac{\delta_\alpha}{\alpha}\right)^2 + \left(\frac{\delta_A}{A}\right)^2 + \left(\frac{\delta_L}{L}\right)^2 + \right.$$
$$\left. + \left(\frac{\delta_R}{R}\right)^2 + \left(\frac{\delta_{\Delta V}}{\Delta V}\right)^2 + \left(\frac{\delta_t}{t}\right)^2 + \left(\frac{\delta_{\mathrm{d}t}}{\mathrm{d}t}\right)^2\right]^{1/2} \tag{9}$$

$$\varepsilon = (\varepsilon_1 + \varepsilon_2)^{1/2}$$

where ε_1 is the sum of the first six terms in the bracket.

b)
$$\varepsilon = \frac{\delta_\lambda}{\lambda} = \left\{\varepsilon_1 + \frac{1}{\left[\ln\left(1 + \frac{\mathrm{d}t}{t}\right)\right]^2}\left[\left(\frac{\delta_{t+\mathrm{d}t}}{t + \mathrm{d}t}\right)^2 + \left(\frac{\delta_t}{t}\right)^2\right]\right\}^{1/2} \tag{10}$$

The error of the counters is smaller than 0.1 % so that ε_2 can be neglected; hence the total error ε is decided by the value of ε_1. In both cases ε_1 is at most equal to:

$$\varepsilon_1 = [(2 \cdot 10^{-2})^2 + (1 \cdot 10^{-2})^2 + (6 \cdot 10^{-2})^2 + (1 \cdot 10^{-3})^2 +$$
$$+ (2 \cdot 10^{-3})^2 + (2 \cdot 10^{-3})^2]^{1/2}$$

$$\varepsilon_1 \leqslant 6.4\,\%$$

The determining terms in ε_1 are V_1 (dynamic measurement on a digital voltmeter) and A (instability and partial distorsions of the transient signal, and also differences between A values measured in static and dynamic regime).

7. EXPERIMENTAL RESULTS

The apparatus has been tested on gases and organic liquids (argon, nitrogen, hydrogen, benzene, toluene, carbon tetrachloride) which have known thermal conductivities with an accuracy of 1.5–3%. Determinations of thermal conductivity of gases have not been successful. For liquids, the obtained results enable an interpretation both from the point of view of the theory of the method and for the evaluatin of the precision of the apparatus.

A part of the results obtained on toluene ("Reactivul" p.a. reagent grade) are given in table 1. The platinum wire constants are : $L = 0.636$ m, $\alpha = 3.38 \cdot 10^{-3}$ $(\mathrm{K})^{-1}$ and $2r_1 \simeq 0.02$ mm. The gain of the amplifier was $A = 268$. Data are calculated using eq. (8). In tables [1,2,11,12] the mean value of the thermal conductivity for toluene at $T = 298.15$ K is $\lambda = 0.133 \pm 3\%$ W/(mK), as results from table 2.

From the values given in table 1 for $\Delta V = 25, 50, 60$ mV it results that :

— at short and long times, one obtains systematic deviations for the thermal conductivity values, which are consistent with the theory of the transient hot-wire method ;

— in the range of validity of eq. (1), the reproducibility of calculated λ is better than 1% ;

— all the calculated values of λ are higher than the reference value ;

— one can also notice that the less ΔV, the smaller the calculated value of λ :

$$\bar{\lambda} = 0.142 \text{ W/(m K) for } \overline{\Delta V} = 25.65 \text{ mV}$$

$$\bar{\lambda} = 0.145 \text{ W/(m K) for } \overline{\Delta V} = 50.42 \text{ mV}$$

$$\bar{\lambda} = 0.148 \text{ W/(m K) for } \overline{\Delta V} = 60.17 \text{ mV}$$

Determinations carried out with $\Delta V < 20$ mV have not been reproducible, due to electrical instabilities of the apparatus, noises superimposed on the signal and small ratio between the window of the threshold level of ΔV and ΔV.

The influence of the time t_A can be evaluated from the relative error ε_A of the slope at different times :

$$\varepsilon_A = \frac{\delta_p}{p} = \frac{r_1^2}{2at}\left[1 + \left(1 - \frac{\rho_1 c_1}{\rho c_p}\right)\left(\ln\frac{4at}{r_1^2 C} - 1\right)\right] \tag{11}$$

TABLE 1

Experimentally determined thermal conductivity of toluene

T (K)	R (Ω)	V_1 (V)	ΔV (mV)	$10^3\ t$ (s)	$10^3\ (dt)$ (s)	λ W/(m K)
296.8	183.7	4.50	25.70	622.58	91.597	0.147
296.8	183.7		25.70	407.71	57.827	0.142
296.6	183.6		25.67	355.33	49.766	0.140
296.4	183.5		25.66	331.07	49.242	0.146
297.7	184.4		25.52	245.67	32.230	0.133
296.0	183.3	4.10	49.99	1.776	1.050	0.198
297.2	184.0		50.51	4.426	2.025	0.159
295.5	183.2		49.99	7.126	3.002	0.149
297.2	184.0		50.52	9.340	4.002	0.150
296.2	183.4		49.99	11.405	4.650	0.146
297.5	184.2		50.45	14.703	5.882	0.142
297.0	183.9		50.55	16.790	6.899	0.145
297.2	184.0		50.57	17.490	7.198	0.145
297.2	184.0		50.58	22.961	9.521	0.146
297.5	184.2		50.46	24.985	10.242	0.145
297.1	183.9		50.53	30.270	12.436	0.145
297.2	184.0		50.61	32.154	12.909	0.142
297.2	184.0		50.62	40.999	16.719	0.144
297.6	184.3		50.48	44.559	18.095	0.143
297.5	184.2		50.47	54.444	22.423	0.145
297.0	183.9		50.51	57.580	24.060	0.147
297.2	184.0		50.57	75.715	30.667	0.143
297.2	184.0		50.57	81.563	34.064	0.147
297.3	184.1		50.57	94.037	38.841	0.145
297.6	184.3		50.57	111.84	46.589	0.146
297.2	184.0		50.42	118.29	47.670	0.143
296.2	183.4		49.96	155.29	63.644	0.147
297.4	184.1		50.44	175.64	71.738	0.144
297.6	184.3		50.53	189.37	78.123	0.145
296.5	183.6		49.94	204.41	83.149	0.146
296.7	183.7		50.44	363.62	153.68	0.148
296.2	183.4		49.92	403.93	166.69	0.148
295.5	182.9		50.40	665.17	283.47	0.150
296.0	183.3		49.62	799.61	345.31	0.155
296.3	183.4		49.92	849.12	359.42	0.150
296.0	183.3		50.03	911.08	397.52	0.154
296.2	183.4		49.92	1336.4	557.24	0.152
296.2	183.4	4.10	60.17	45.200	23.586	0.148
296.0	183.3		60.17	71.141	36.816	0.148
296.2	183.4		60.17	140.39	72.018	0.147
296.2	183.4		60.17	266.83	138.66	0.149
296.3	183.4		60.17	425.26	222.63	0.150
295.5	182.9		60.02	1051.7	560.18	0.151

TABLE 2

Toluene thermal conductivity table data

reference [1]		reference [2]		reference [11]		reference [12]	
T (K)	λ (W/(mK))	T (K)	λ (W/(mK))	T (K)	λ (W/(mK))	T (K)	λ (W/(mK))
298.02	0.1311	294.15	0.1295	293.15	0.135	290	0.1366
298.05	0.1316	297.15	0.127	303.15	0.132	300	0.1340
298.09	0.1326	297.55	0.1444				
		298.15	0.1326				
			0.1291				
			0.1331				
			0.1365				
			0.1335				

where ρ_1, c_1 are the density and specific heat of the wire (platinum). With $r_1 = 10^{-5}$ m and $\rho_1 c_1 = 2.86 \cdot 10^6$ J/(m^{3}K), the error ε_A has been calculated at various times for argon and toluene as standard fluids [11,12] (Table 3).

TABLE 3

The relative error ε_A of the slope

t_A (s)	ε_A (%) argon $\rho = 1.60$ kg/m^3; $c_p = 520$ J/(kg. K) $a = 2 \cdot 10^{-5}$ m^2/s	ε_A (%) toluene $\rho = 860$ kg/m^3; $c_p = 1700$ J/(kg. K) $a = 0.9 \cdot 10^{-7}$ m^2/s
0.005		-2.8
0.01		-5.1
0.05		-2.7
0.1	-83.5	-1.7
0.5		-0.5
1	-10.3	-0.3

For the set of values from table 1, the best reproducibility is found for $15 < t < 200$ ms. The average error of the slope in this time range is $\bar{\varepsilon}_A = -2.2\%$, so that the thermal conductivity values are overestimated by 2.2%. The mean experimental value, $\bar{\lambda} = 0.145$ W/(m K) is corrected to $\bar{\lambda}_c = 0.142$ W/(m K), leaving an error of $+6.8\%$ with respect to the reference value.

The critical time t_B associated to the start of natural convection is estimated from:

$$\frac{g\beta r_1^3}{\nu a}\,\frac{q}{4\pi\lambda}\ln\frac{4at_B}{r_1^2 C}\left(\sqrt{\frac{4at_B}{r_1^2 C}}-1\right)^3 < 1000 \qquad (12)$$

where $g = 9.81$ m/s^2 is the acceleration of gravity, β is the volumetric expansion coefficient of the fluid and ν the kinematic viscosity of the fluid.

For argon $\beta = 3.45 \cdot 10^{-3}$ $(K)^{-1}$ and $\nu = 1.35 \cdot 10^{-5}$ m^2/s; for toluene $\beta = 1.09 \cdot 10^{-3}$ $(K)^{-1}$ and $\nu = 7 \cdot 10^{-7}$ m^2/s. In both cases $q = 4.1^2/(184 \cdot 0.636) = 0.15$ W/m.

We obtain $t_B < 0.4$ s for argon and $t_B < 4$ s for toluene. Though these figures are only estimations ($\pm 10\%$), they do explain the impossibility of effectuating measurements on gases. In order to diminish t_A, one must diminish the wire diameter, and in order to increase t_B one must diminish q.

The study effectuated on this first apparatus has been very useful for the following reasons : the performances and possibilities of the apparatus have been experimentally tested ; the theory of the method has been developed in all details and the limitations of using exclusively the linear law $\theta(r_1, t)$ *versus* ($\ln t$) have been pointed out ; a more advantageous design of a new apparatus has been found.

The apparatus and the experimental procedure presented above lead to values of thermal conductivity for liquids with an accuracy of 7%.

REFERENCES

[1] E. McLaughlin and J. F. T. Pittman, *Phil. Trans. Roy. Soc., London*, **270**, 557 (1971).

[2] D. T. Jamieson, J. B. Irving and J. S. Tudhope, "Liquid Thermal Conductivity A Data Survey to 1973", N.E.L., Edinburgh, 1975.

[3] "Thermal Conductivity", ed. R.P. Tye, vol. II, Academic Press, London, 1969.

[4] N. V. Tsederberg, "Thermal Conductivity of Gases and Liquids", Edward Arnold Ltd., London, 1965.

[5] A. Missenard, "Conductivité thermique des solides, liquides, gaz et leur mélanges", Eyrolles, Paris, 1965.

[6] R. Vîlcu and A. Ciochină, *Rev. Roumaine Chim.*, **17**, 1679 (1972).

[7] R. Vîlcu and A. Ciochină, *Studii și Cercetări de Chimie, Acad. R.S.R.*, **21**, 571 (1973).

[8] R. Vîlcu and A. Ciochină, *Studii și Cercetări de Chimie, Acad. R.S.R.*, **21**, 643 (1973).

[9] H. S. Carslaw and J. C. Jaeger, "Conduction of Heat in Solids", Clarendon Press, Oxford, 1959.

[10] I. Constantinescu, T. O. N. Moisin and L. P. Dumitrescu, Romanian Patent No. 64025 (1975).

[11] N. B. Vargaftik, "Spravochnik po teplofizicheskim svoistvam gazov i zhidkostei", Nauka, Moscova, 1972.

[12] Y. S. Touloukian, P. E. Liley and S. C. Saxena, "Thermophysical Properties of Matter", vol. 3, TPRC Data Series, Plenum Press, New York, 1970.

Revue Roumaine de Chimie, 25, 7, 1123–1128 (1980)

This paper is dedicated to Professor Cr. I. Simionescu
on the occasion of his 60th. birthday,
with warmest personal wishes

SYNTHESIS AND POLYMERIZATION OF PHOTOACTIVE MONOMERS

O. VOGL and S. YOSHIDA
Polymer Science and Engineering Department,
University of Massachusetts,
Amherst, Massachusetts 01003

Received January 23, 1980

INTRODUCTION

Absorbed energy from solar radiation can cause photochemical reactions in polymers, such as chain cleavage, crosslinking and the formation of functional groups. Plastics are generally protected from solar radiation by addition of UV absorbers. The UV absorber must be effective over a long period of time and must not be volatile or be leached out. Normal UV stabilizers may be lost due to exudation, on extraction in use or by volatilization during fabrication. Mobility and compatibility as a function of molecular weight, size and kind of the stabilizers has been studied. In more recent years an interest in having these stabilizers in a compatible form or even in a high molecular weight form has received increased interest.[1]

The advantage of using polymeric UV stabilizers for the protection of polymers is most evident in samples with high surface area to volume ratio where low molecular weight stabilizers are more susceptible to loss of stabilizers of low molecular weight. Although it was initially believed that the low molecular weight stabilizer together with the appropriate compatibilizing group, was sufficient or even advantageous for the protection of the polymers, especially since the stabilizer is primarily present and consequently effective in the amorphous fraction of the polymer, more recent experiments on grafted stabilizers on rubbers have shown that UV stabilizing groups could be incorporated into the polymer and did not diminish the effectivity of the UV stabilizer. There are five typical UV absorbing groups that have greatest importance in UV stabilization; they are salicylate esters, 2-hydroxybenzophenones, α-cyano-β-phenylcinnamate esters, 4-aminobenzoate esters and 2-hydroxyphenylbenzotriazoles.

Most attempts in the past have been concerned with the preparation of monomeric UV stabilizer by a relatively simple reaction on already formed stabilizers.[2] Examples are the reaction of methacroyl chloride with 2-hydroxybenzophenone derivatives or salicylates [3] to form methacrylate esters or the condensation of 2-hydroxybenzophenone derivatives with allyl bromide to from ring substituted allyl 2-hydroxybenzophenone derivatives, which is a commercially available "polymerizable" UV stabilizer.[2] Radical polymerization of allyl derivatives of UV absorbers has been achieved only with a considerable amount of difficulty and consequently these compounds were not generally useful. In the salicylic acid series, vinyl salicylate [4] has recently been reported and also vinyl N,N-diaminobenzoate [5] has been synthesized.

Esters of α-cyano-β-phenylcinnamic acid have been used in the past as UV stabilizers especially when UV absorbers with free phenolic —OH groups were undersirable.[6,7] In some cases, α-cyano-β-phenylcinnamate esters were found to be quite volatile and significant losses were noticed during fabrication. Conseqxently, bis-esters of glycols, such as that of 1,10-decane diol and α-cyano-β-phenylcinnamic acid were prepared.[8] The most important routes for the synthetic attempts to prepare polymerizable monomer from 2-hydroxylbenzophenones utilized the 4-hydroxyl group of 2,4-dihydroxybenzophenone [2] and acrylates, methacrylates and unsaturated epoxides have been synthesized. Attempts have also been made to prepare 2-hydroxy or 2,4-dihydroxy derivatives of 4′-vinylbenzophenone by dealkylating the corresponding methoxy derivatives.[9]

The most important class of ultraviolet absorbing compounds belongs to the class of (2-hydroxyphenyl)benzotriazoles ; this group in the molecule is of special interest since it provides the most effective UV stabilizing group.[10] In the past, a number of substituted 2-(2-hydroxyphenyl)benzotriazoles [2-(2-H-benzotriazole-2-yl)-phenols] were prepared [11] ; some of these compounds have also been attached to polymeric carriers.[12] 2-(2-Hydroxyphenyl)benzotriazole derivatives with long side chains for improved compatibility have also been prepared [13] and efforts were made to synthesize polymerizable 2-hydroxyphenyl-benzotriazoles. These compounds have as polymerizable groups, methacryloylamine, and acryloylamino-, acryloxy, vinylsulfonyl- and vinyloxy- groups.[14]

Some years ago we undertook an extensive study of the synthesis of polymerizable UV absorbers, and set as our goal the synthesis of a number of methyl vinylsalicylates [15-21] (I), 2,4-dihydroxy-4′-vinylbenzophenone [22,23] (II), a vinyl derivative of ethyl α-cyano-β-phenylcinnamate [24,25] (III), and various isomers of 2-vinyl(2-hydroxyphenyl)benzotriazoles [26] (IV) ; in this paper we would like to summarize the successful syntheses of these compounds.

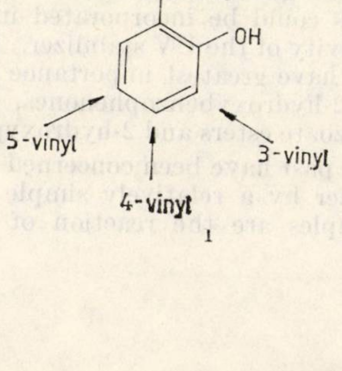

I

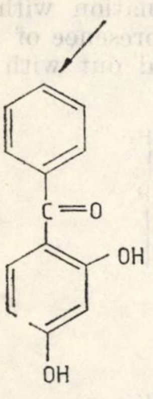

II

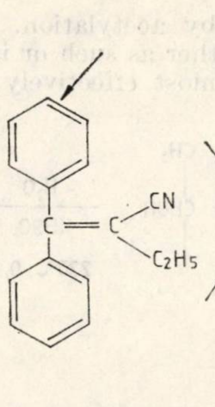

III

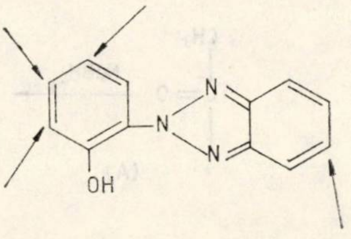

IV

RESULTS AND DISCUSSION

We have chosen to synthesize photoactive monomers which have the vinyl group attached to the benzene ring of the UV absorbers. This gave the UV absorber a polymerizability similar to that of styrene or its derivatives. Indeed, the results of our work have shown that such stabilizers can be polymerized with styrenes, dienes, acrylic, and methacrylic acid derivatives, if AIBN was used as the radical initiator. Since most UV absorbers, to be effective, must have a hydroxyl group in the molecule, our original concern was that the free hydroxyl group would interfere with the polymerization; this, however, was only the case if reactive alkyl or aryl radicals are used as the initiating species or if oxygen radicals are involved in some point of the polymerization. Normal radical polymerization of resonance stabilized monomers with AIBN have now shown to be readily polymerized in the presence of free phenolic OH groups.

The synthesis of styrene derivatives is normally carried out by two classical ways. The first method consists of the dehydration of either the 1-hydroxy- or the 2-hydroxyethyl group substituted on the benzene ring (A). The 1-hydroxyethyl group is easily introduced by Friedel-Crafts acetylation with acetyl chloride or by Fries rearrangement of an O-acetyl group; the acetyl group is then appropriately reduced usually with a $NaBH_4$. The dehydration of the hydroxy ethyl groups requires that the product formed has sufficient volatility; the dehydration is carried out under reduced pressure and the vinyl compound immediately removed from the reaction. The formation of the vinyl group of styrenes from the primary or secondary alcohol gives a very pure product since the separation of the vinyl compound from the alcoholic product is very efficient. The second method for the preparation of styrene derivatives has as its starting material an ethyl benzene derivative (B) which must be properly prepared for the subsequent bromination with N-bromosuccinimide (NBS); for example, active groups such as free phenolic-OH groups must be protected and deactivated by acetylation. Bromination with NBS in CCl_4 is carried out directly either as such or in the presence of AIBN. Dehydrobromination has been most effectively carried out with Bu_3N

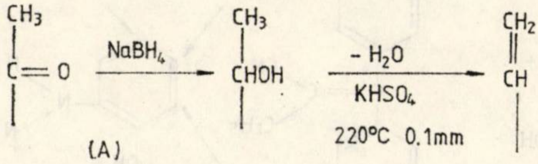

(A)

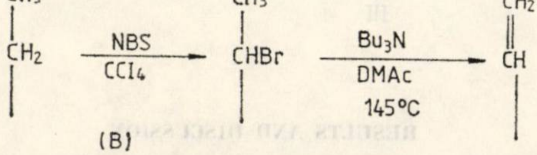

(B)

in DMAc at 145°C or with Et_3N in CH_3CN at the boiling point. All other techniques have proven to be inferior. This route has as a great disadvantage, the fact that dehydrobromination must be quantitative, even at the expense of yield reducing side reactions since impurities containing aliphatic C—Br bonds act as chain transfer agents in radical polymerization and may cause lowering of the molecular weight of the polymer.

Four structural isomers of methyl vinylsalicylate exist, three of which, methyl 3-vinylsalicylate, methyl 4-vinylsalicylate and methyl 5-vinylsalicylate are relatively easily accessible for synthesis. Methyl 5-vinylsalicylate was synthesized in a five-step reaction in an overall yield of 60 % from methyl salicylate. Methyl salicylate was acetylated in the position *para* to the phenolic OH group by a modified Friedel-Crafts reaction or by a Fries rearrangement of methyl 5-acetylsalicylate. The acetyl group of methyl 5-acetylsalicylate was reduced with $NaBH_4$ to the 1-hydroxyethyl group which was then dehydrated with $KHSO_4$ at 225°C and 0.1 mm. A mixture of methyl 5-vinylsalicylate and methyl 5-vinylacetylsalicylate was obtained which could be transformed into methyl 5-vinylsalicylate with sodium methoxide and methano (see also ref.[27]).

The synthesis of methyl 5-vinylsalicylate used the dehydration of the 1-hydroxyethyl compound. For the syntheses of all other vinylsalicylic acid isomers but also of the other photoactive monomers, bromination with NBS followed by dehydrobromination was used for the formation of the vinyl group of the styrene derivative.

Methyl 3-vinylsalicylate was prepared in more than 40 % overall yield from 2-ethylphenol. This compound was treated with CO_2 and K_2CO_3 at 175°C (Kolbe-Schmitt reaction) and gave 3-ethylsalicylic acid. Esterification was accomplished with methanol and sulfuric acid, the methyl 3-ethylsalicylate was acetylated with acetic anhydride and brominated with NBS in the presence of a small amount of AIBN in CCl_4 solution and gave an almost quantitative yield of the 1-bromoethyl compound without side products. Dehydrobromination with acetonitrile and triethylamine yielded methyl 3-vinylsalicylate.

Methyl 4-vinylsalicylate was synthesized from 4-ethylphenol. Carbonation, esterification, acetylation, bromination and dehydrobromination with Bu_3N in DMAc gave a nearly 50 % overall yield of the desired methyl 4-vinylsalicylate.

The synthesis of 2,4-dihydroxy-4′-vinylbenzophenone, another powerful UV absorber, was an important challenge and was finally accomplished in an overall yield of 15 % from 4-ethylbenzoic acid. Condensation with resorcinol in the presence of BF_3 gave 2,4-dihydroxy-4′-ethylbenzophenone which was acetylated and brominated with NBS in the presence of AIBN. The 4′-(1-bromoethyl)-compound was dehydrobrominated with Bu_3N in DMAc and hydrolyzed with sodium dicarbonate in aqueous methanol.

Ethyl 4-vinyl-α-cyano-β-phenylcinnamate was synthesized in a sequence of five reaction steps in an overall yield of 20 % also from 4-ethylbenzoic acid. The acid chloride of 4-ethylbenzoic acid was allowed to react with benzene and $AlCl_3$ in a Friedel-Crafts reaction and gave 4-ethylbenzophenone in high yield. Knoevenagel reaction of this compound with cyanoacetate yielded ethyl 4-ethyl-α-cyano-β-phenylcinnamate. The bromination at the methylene group of the ethyl side chain was accomplished in 100 % yield with NBS and the bromination product was dehydrobrominated with Bu_3N in DMAc. As an asymmetric, tetrasubstituted ethylene, methyl 4-vinyl-α-cyano-β-phenylcinnamate consists of a mixture of the two geometric isomers which were identified but not separated.

2-(5-Vinyl-2-hydroxyphenol)benzotriazole was synthesized in six steps with an overall yield of approximately 20 % from *o*-nitroanine. This compound was diazotized and coupled with 4-ethylphenol; the nitro group was reduced with Zn powder in NaOH. During this reaction ring closure to the benzotriazole ring system was also accomplished. In preparation for the bromination with NBS, the compound had to be acetylated with acetic anhydride in order to prevent ring bromination. In this specific case, the bromination with NBS was relatively slow, but the 1-bromoethyl compound was ultimately obtained in quantitative yield; dehydrobromination with Bu_3N in DMAc followed by hydrolysis with NaOH gave 2-(5-vinyl-2-hydroxylphenol)benzotriazole. Advances in the syntheses of the 3-vinyl- and 4-vinyl- compounds have been considerable and attempts for the preparation of 2-hydroxylphenoltriazole with a vinyl group in the benzene ring of the benzotriazole system are underway. The arrows in equation 2 indicate our synthesis strategy to introduce vinyl groups as substituents in four classes of photoactive monomers, and what we have accomplished.

Each of these photoactive monomers described in this paper have been homopolymerized with AIBN as the initiator and copolymerized with at least styrene and methyl methacrylates; in some selected cases, our monomers have been copolymerized with a number of addition monomers. Studies are now underway to utilize our photoactive monomers for further copolymerization studies and for grafting reactions.

REFERENCES

[1] D. Bailey and O. Vogl, *J. Macromol. Sci., Reviews,* **C14(2)**, 267 (1976).

[2] S. Tocker, *Makromol. Chem.*, **101**, 23 (1967).

[3] J. Fertig, A. I. Goldberg and M. Scoultchi, *J. Appl. Polym. Sci.*, **10**, 663 (1966).

[4] G. Heublein, B. Heublein, B. Heyroth and E. Brendel, *Z. Chem.*, **19(3)**, 104 (1979).

[5] H. Hopff and H. Lussi, *Makromol. Chem.*, **18/19**, 227 (1956).

[6] A. F. Strobel and S. C. Catino, *Belg. Pat.*, 619, 809 (1962) ; *Chem. Abstr.*, **58**, P13853 (1963).

[7] D. P. Carlson, U.S. Pat. 3, 081, 280 (1963) ; *Chem. Abstr.*, **58**, P11539 (1963).

[8] D. P. Carlson and M. Esayian, French Pat. 1, 381, 743 (1964) ; *Chem. Abstr.*, **62**, 11975 (1965).

[9] C. Pinazzi and A. Fernandez, *Makromol. Chem.*, **167**, 147 (1973).

[10] H. Heller, E. Keller, H. Gysling and F. Minderman, U.S. Pat. 3, 004, 896 (1961) ; *Chem. Abstr.*, **57**, 9860 (1962).

[11] L. Balaban, J. Borkovec and D. Rysavy, Czechoslovakian Pat. 108, 792 (1963) ; *Chem. Abstr.*, **61**, 3267 (1964).

[12] J. P. Millionis and W. B. Hardy, U.S. Pat. 3, 072, 548 (1963) ; *Chem. Abstr.*, **59**, 11503 (1963).

[13] J. P. Millionis, W. B. Hardy and W. F. Baitinger, U.S. Pat. 3, 159, 646 (1964) ; *Chem. Abstr.*, **62**, 7951 (1965).

[14] H. Heller, J. Rody and E. Keller, U.S. Pat. 3, 399, 173 (1965) ; *Chem. Abstr.*, **69**, 87597 (1968).

[15] D. Tirrell, D. Bailey and O. Vogl, *Polymer Preprints, ACS Division of Polymer Chemistry*, **18**(1), 542 (1977).

[16] D. Tirrell and O. Vogl, "Abstrs. of Papers", Seventh NERM, # 312, Albany (1976).

[17] D. Bailey, D. Tirrell and O. Vogl, *J. Polym. Sci., Polym. Chem. Ed.*, **14**, 2725 (1976).

[18] D. Bailey, D. Tirrell and O. Vogl, *J. Macromol. Sci., Chem.*, **A12(5)**, 661 (1978).

[19] M. Iwasaki, S. Blanks, D. Tirrell and O. Vogl, "Abstr. of Papers, 20th. Canadian High Polymer Forum", # 15, 1979 (Quebec).

[20] D. Tirell and O. Vogl, *Makromol. Chem.*, in press.

[21] M. Iwasaki, D. Tirrell and O. Vogl, *J. Polym. Sci., Polym. Chem. Ed.*, in press.

[22] D. Tirrell, O. Bailey, C. Pinazzi and O. Vogl, *Macromolecules*, **11(2)**, 312 (1978).

[23] O. Vogl, *Pure and Applied Chem.*, in press.

[24] Y. Sumida, S. Yoshida and O. Vogl, *Polymer Preprints, ACS Division of Polymer Chemistry*, **21(1)**, 1980.

[25] Y. Sumida and O. Vogl, *Polymer (London)*, in press.

[26] S. Yoshida and O. Vogl, *Polymer Preprints, ACS Division of Polymer Chemistry*, **21(1)**, 1980.

[27] H. Carlson, *Z. Chem.*, **18(3)**, 95 (1978).

ORSZÁGOS DOKUMENTÁCIÓS 1983

NOTE POUR LES AUTEURS

La Revue Roumaine de Chimie publie des articles en anglais, français, russe, allemand ou espagnol. Les auteurs sont priés d'envoyer des articles et de comptes rendus inédits.

Les manuscrits seront dactylographiés à deux intervalles. La bibliographie, les tableaux et la légende des figures seront placés après le texte.

Si l'article fait partie d'une série numérotée, le titre de la partie précédente sera indiqué dans une note au bas de la première page.

Chaque article sera précédé d'un résumé comprenant quinze lignes au maximum.

Les références bibliographiques dans le texte seront faites par des exposants sans paranthèses et paraîtront comme des notes au bas de chaque page.

Les publications périodiques mentionnées dans la bibliographie seront présentées suivant les prescriptions internationales : le nom de l'auteur précédé de l'initiale du prénom, le titre du périodique abrégé conformément à « Chemical Abstracts » et souligné par une ligne, le numéro du tome indiqué par des chiffres arabes et souligné par deux lignes, suivi de la première page de l'article : à la fin, l'année de la parution sera placée entre parenthèses. Le numéro de la revue ne sera pas indiqué si les pages du volume sont numérotées consécutivement.

Les textes des livres ou traités incluëront : les noms des auteurs, les initiales du prénom, le titre du livre entre guillemets et sans être souligné, le numéro du tome précédé par l'abréviation « vol. » (ou « Bd. »), le numéro de l'édition, les éditions (the publisher), la localité de la parution du livre, l'année de la parution et la page de la référence précédée(s) par l'abréviation « p » (ou « S »).

Les brevets seront indiqués comme suit : L'auteur ou la firme, le pays et le numéro du brevet, la date et la revue (Chem. Abstr.) Par ex. : M. Jones (to Union Carbide Co.), Brit. Pat. 601 238, 2 Sept. 1959, *Chem. Abstr.*, **54**, 12808 (1960).

Les diagrammes seront tracés à l'encre de Chine sur papier calque. Les tableaux et les figures (en nombre strictement nécessaire) seront numérotés par des chiffres arabes. Les courbes dans les figures seront numérotées par des chiffres arabes et leur explication sera donnée dans la légende des figures. Prière de ne pas inscrire les mêmes données dans les tableaux et les figures. Chaque tableau aura un titre. On indiquera dans le texte la place approximative des tableaux et des figures. Les formules chimiques seront incluses dans le texte : en outre, elle seront transcrites sur papier calque, à l'encre de Chine.

Les auteurs sont priés d'indiquer les caractères italiques (en soulignant les lettres au crayon), ainsi que tout autre caractère spécial : les préfixes *ortho, meta, para, cis, trans,* etc. seront soulignés pour indiquer leurs caractères italiques, et ne seront jamais écrits avec des majuscules.

Aucune correction à la main ne sera admise sur le manuscrit. Les corrections seront frappées à la machine. Les lettres grecques ou autres symboles spéciaux seront insérés à la main à l'encre clairement.

Le manuscrit sera signé par l'auteur.

Le colonne-titre aura 50 lettres au maximum.

L'entière responsabilité du contenu des articles appartient aux auteurs.

Pour détails voir le No 2/1980.

PRINTED IN ROMANIA

TRAVAUX PARUS AUX ÉDITIONS DE L'ACADÉMIE DE LA RÉPUBLIQUE SOCIALISTE DE ROUMANIE

1980 NOV 17

ELENA CEAUŞESCU, **Polimerizarea stereospecifică a izoprenului** (La polymérisation stéréospécifique de l'isoprène), 1979, 307.

A. T. BALABAN, L. GĂLĂŢEANU, G. GEORGESCU, LIGIA SIMIONESCU, **Compuşi marcaţi şi radiofarmaceutici cu aplicaţii în medicina nucleară** (Composés marqués et radio-pharmaceutiques à application en médecine nucléaire), 1979, 495 p.

I. G. MURGULESCU, E. SEGAL, **Introducere în chimia fizică**, vol. II. 1. **Teoria molecular cinetică a materiei** (Introduction à la chimie physique, IIe vol. 1. La théorie moléculaire-cinétique de la matière), 1979, 1003 p.

I. E. TEODORESCU, MARIA FITI, **Iradierea tehnologică** (Irradiation technologique), 1979 216 p.

S. STERNBERG, FL. DANEŞ, **Termodinamica chimică aplicată** (La thermodynamique chimique appliquée), 1978, 400 p.

I. G. MURGULESCU, V. EM. SAHINI, **Introducere în chimia fizică, Vol. I, 2. Structura şi proprietăţile moleculelor** (Introduction à la chimie physique, Ier vol. 2. La structure et les propriétés des molécules), 1978, 604 p.

C. DRĂGULESCU, E. PETROVICI **Chimie structurală modernă, Chimia coordinanţei 8** (La chimie structurale moderne. La chimie de la coordinence 8), 1977, 947 p.

D. PURDELA (sous la direction de), **Nomenclatura chimiei anorganice** (La nomenclature de la chimie inorganique), 1977, 153 p.

I. ZUGRĂVESCU, MAGDA PETROVANU, **N-ylid chemistry**, coédition avec McGraw-Hill, 1977, 396 p.

D. NEGOIU, ANGELA KRIZA, **Poluanţi anorganici în aer** (Polluants inorganiques dans l'air), 1977, 220 p.

I. G. MURGULESCU, **Introducere în chimia fizică. Vol. I. Atomi, molecule, legătură chimică** (Introduction à la Chimie Physique, Ier vol. 1. Atomes, molécules, liaison chimique), 1976, 460 p.

E. P. BALTĂ, E. BALTĂ, **Introduction to the physical chemistry of the vitreous state**, coédition avec Abacus Press, 1976, 287 p.

M. I. GĂLĂŢEANU, **Radiochimia aplicată. Metode şi probleme** (La radiochimie appliquée. Méthodes et problèmes), 1976, 307 p.

CONST. V. UGLEA, **Cromatografia pe gel permeabil. Noi domenii de aplicare** (La chromatographie sur gel perméable. Nouveaux domaines d'application), 1976, 123 p.

FRANCISC GOTHARD, **Echilibre lichid-vapori. I. Baze teoretice şi metode de calcul** (Equilibres liquide-vapeurs. I. Bases théoriques et méthodes de calcul), 1975, 263 p., 2 pl.

CONST. GH. MACAROVICI, D. MACAROVICI, **Chimia oxizilor dubli şi utilizările lor** (La chimie des oxydes doubles et leur utilisation), 1975, 195 p.

ELENA CEAUŞESCU, **Research work on synthesis and characterization of macromolecular compounds. Contributions**, 1974, 251 p.

CR. SIMIONESCU, VIORICA RUSAN, V. POPA, **Chimia algelor marine** (La chimie des algues marines), 1974, 212 p., 1 pl.

I. P. Informaţia c. 2230

43 426

Lei 25. —

50 (price per year)

F 1103

6 b

ACADÉMIE DE LA RÉPUBLIQUE SOCIALISTE DE ROUMANIE

R

REVUE ROUMAINE DE CHIMIE

TOME 25
N° 8
Août 1980

EDITURA ACADEMIEI REPUBLICII SOCIALISTE ROMÂNIA

Rev. Roumaine Chim.

RRCHAX, 25, 8, p. 1129–1284 (1980), Bucarest

ACADÉMIE DE LA RÉPUBLIQUE SOCIALISTE DE ROUMANIE

COMITÉ DE RÉDACTION

Rédacteur en chef :

I. G. MURGULESCU, membre de l'Académie de la République Socialiste de Roumanie

Rédacteurs en chef adjoints :

A. T. BALABAN et V. EM. SAHINI, membres correspondants de l'Académie de la République Socialiste de Roumanie

Collège de rédaction :

EM. BRATU, ELENA CEAUŞESCU, ECATERINA CIORĂNESCU-NENITZESCU, CR. SIMIONESCU, membres de l'Académie de la République Socialiste de Roumanie ; P. SPACU, membre correspondant de l'Académie de la République Socialiste de Roumanie ; MARGARETA AVRAM, M. BANCIU, I. HAIDUC, D. I. MARCHIDAN, I. MOLDOVAN, G. NIAC et D. SĂNDULESCU

La Revue Roumaine de Chimie paraît 10 fois par an. Toute commande de l'étranger pour les travaux parus aux Editions de l'Académie de la République Socialiste de Roumanie sera adressée à ILEXIM, Departamentul Export-Import Carte (Livres)/Departamentul Export-Import Presă (Revues), P.O.B. 136—137, télex 11226, 3, str. 13 Decembrie, 79517 Bucarest 12, Roumanie

Les manuscrits, les livres et les revues proposés en échange ainsi que toute correspondance seront envoyés à la rédaction :

REVUE ROUMAINE DE CHIMIE

125, Calea Victoriei, 79717 Bucarest, Roumanie, téléphone 50 76 80

EDITURA ACADEMIEI REPUBLICII SOCIALISTE ROMÂNIA
125, Calea Victoriei, 79717 Bucarest, Roumanie, téléphone 50 76 80

ORSZÁGOS MŰSZAKI KÖNYVTÁR ÉS DOKUMENTÁCIÓS KÖZP.

REVUE ROUMAINE DE CHIMIE

Tome 25, Nº 8 Août, 1980

RODICA VÎLCU and ELENA DIMITRIU, The propagation of ultrasound in n-alkanes 1131–1138

G. CHANDRA and S. N. SRIVASTAVA, Investigation of the kinetics and mechanism of silver (I) ion catalysed oxidation of d,l (α) valine by peroxydisulphate. 1139–1148

G. CHANDRA and S. N. SRIVASTAVA, Kinetics of the glycine oxidation by peroxydisulphate. 1149–1158

I. BRAŞOVEANU, S. I. BLEJOIU, A. SZABO, P. ROTARU and I. V. NICOLESCU, Structural strains appearing in the high temperature shift conversion Fe–Cr catalyst 1159–1169

N. CALU, N. FOCA and M. LUCHIAN, Kinetic data on the formation and thermal decomposition of the $[Pd(p\text{-}ON-C_6H_4-N(CH_3)_2)_2Cl_2]\cdot H_2O$ complex 1171–1175

EWA KULIG, DANUTA CZAKIS-SULIKOWSKA and RYSZARD WOJTAŠ, Investigation of lead (II) complexes. III. Simple and mixed complexes of lead (II) with some anions of aliphatic acids in aqueous solution . . . 1177–1185

MARIA POPESCU and DOREL CRIŞAN, Study on structure and properties of some triazenic complexes of mercury 1187–1195

A. E. MAHGOUB and M. M. SHOUKRY, Palladium (II) chelate of phenylazobenzaldoxime 1197–1200

AL. CECAL, Complexes of Th (IV) and U (VI) with pyrocatechol, pirocatecholdisulfonic acid and chromatropic acid (in German) 1201–1211

VIORICA BACIU and ALEXANDRU T. BALABAN, Chemical graphs. XXXIX. Valence isomers of monodehydro-[*n*]annulenes 1213–1220

M. BANCIU, RODICA VLAD, PHAN LE THUY and C. DRĂGHICI, Solvolysis of 7 (γ-tosyloxypropyl)-7H-dibenzo [a, e] cycloheptene, 5(β-tosyloxyethyl)- and 5 (γ-tosyloxypropyl)-5H-dibenzo [a, c] cycloheptene 1221–1228

I. A. SILBERG and M. V. DIUDEA, Phenazathionium cations. I. The dual mechanistic behaviour of phenazathionium cations and its implications in the reaction of $NaNO_2$ with halogenophenothiazines 1229–1238

I. A. SILBERG and M. V. DIUDEA, Phenazathionium cations. II. The accessibility of positions 1 (9) in nucleophilic substitutions involving phenazathionium cations 1239–1244

V. PĂRĂUŞAN, M. TRIFAN and R. AVRAM, n-Dodecylnitrile oxidation in liquid phase with molecular oxygen. III. Composition of acid mixtures 1245–1248

Revue Roumaine Chim. 25, *8*, 1129–1284 (1980) Bucarest

GH. C. CONSTANTINESCU, Influence of substituents on the analytical and extractive properties of organic reagents in their reaction with Au (III). I. Influence of methoxy substituents (in German) 1249–1258

GH. C. CONSTANTINESCU and CECILIA CONSTANTINESCU, Influence of substituents on the analytical and extractive properties of organic reagents in their reaction with Au (III). II. Influence of methoxy substituents (in German) 1259–1267

LUMINIȚA VLĂDESCU and DĂNUȚA VOICU, Utilisation of sodium hydroxide in separation of tin with ion exchange resins. II. Cation exchange separations 1269–1274

BOOK REVIEWS 1275–1284

Revue Roumaine de Chimie 25, *8*, 1131–1138(1980)

THE PROPAGATION OF ULTRASOUND IN n-ALKANES

RODICA VÎLCU*, ELENA DIMITRIU**

* The National Institute of Chemistry, Chair of Physical Chemistry and Electrochemical Technology, 13, Bd. Republicii, Bucharest, Romania

** ICEFIZ, Institute of Physics and Technology of Materials, Măgurele, Bucharest, Romania

Received February 11, 1980

From the experimental data for the propagation velocities of ultrasounds obtained with a device based on the diffraction of light, the covolume, the effective molecular radius and the free volume of n-pentane, n-hexane, n-heptane, n-octane and n-nonane were calculated. The results were correlated to the molecular structure of n-alkanes.

INTRODUCTION

The value of the propagation velocity of ultrasounds provides important data concerning the properties of the medium they cross. Most of the works dealing with this topic refer to the relations between the ultrasound propagation velocity and the adiabatic compressibility, the molecular velocity, the molecular adiabatic compressibility.[1]

The purpose of this work is the calculation of the covolume from the Van der Waals equation of state according to the propagation velocity of ultrasounds in n-alkanes.

Assuming that in these liquids the molecules would be assimilated with non-polar hard spheres, the effective molecular radii and the free volumes in liquids have been calculated. The results were correlated to the molecular structure of n-alkanes.

EXPERIMENTAL PART

The propagation velocity of ultrasounds in n-pentane, n-hexane, n-heptane, n-octane, n-nonane at the temperature of 298.15 K was calculated. The experimental installation makes use of a device based on the diffraction effect of light, when crosses perpendicularly an ultrasonic network. It was described in a previous work. [2]

The propagation velocity of ultrasounds is connected with the gap, d, between the diffraction maxima of an order of magnitude ±1, being expressed by the relation :

$$c = \frac{\lambda \nu f}{d}$$

where $\lambda = 546.1$ nm is the wavelength of the monocromatic light ; the frequency $\nu = 15.6$M.Hz ; $f = 0.60$ m stands for the focal distance of the lens of the device. The frequency was measured with the help of a Tesla absorption Wavemeter and the temperature was measured with a ±0.02°C precision thermocouple.

RESULTS AND COMMENTARY

The properties of liquids may be described both by means of theories of statistical mechanics and with the help of approximate methods. From the approximate methods, equations of the Van der Waals type are used, as in :

$$\frac{PV}{RT}=\Phi(y)-\frac{a}{RTV} \tag{2}$$

where y stands for the ratio between the covolume, b, and the total volume V and a is a constant of characteristic attraction. In the initial Van der Waals theory, $\Phi(y)$ was :

$$\Phi(y)=(1-4y)^{-1}$$

$$y=\frac{b}{4V} \tag{3}$$

while recent theories give other expressions for $\Phi(y)$, the best of them being that of Carnahan and Stirling [3]

$$\Phi(y)=(1+y+y^2-y^3)/(1-y)^3$$

$$y=\frac{\pi N\sigma^3}{6V} \tag{4}$$

where N is the total number of molecules in the system ; σ is the diameter of the hard sphere. The covolume and the constant of attraction are usually obtained from gas — liquid critical data, but these refer only to conditions which are different from the normal state of liquid, therefore the values will not be the best. In order to avoid such errors, Shaafs [4] provides a relation between the propagation velocity of ultrasound and the covolume :

$$b=\frac{M}{\rho}\left\{1-\frac{RT}{Mc^2}\left[1+\frac{Mc^2}{3RT}\right)^{1/2}-1\Big]\Big]\right\} \tag{5}$$

(c = the ultrasound velocity, M = the molecular weight of the liquid, ρ = the density).

Considering a model of liquid made up of non-polar hard spheres molecules, we may calculate the effective molecular radius, r_m, according to the covolume, with the relation :

$$b=4V_m$$

$$=\frac{16}{3}\pi r_m^3 N_A$$

(V_m = geometrical volume of the molecules, N_A = the Avogadro number) and V_f = the free volume of the liquid :

$$V_f = \frac{4}{3}\ \pi N_A \left(\frac{V_a}{Y}\right)^3 \tag{7}$$

where V_a is the available molar volume, Y = the total molecular surface per mol.

The total molecular surface is :

$$Y = (36\pi N_A V_m^2)^{1/3} \tag{8}$$

and the available molar volume is expressed according to the experimental molar volume, V, and the collision factor, S, as :

$$V_a = V - SV_m \tag{9}$$

Taking into consideration the fact that the molecules in real liquids are not hard spheres, the collision factor will not have the value 4, but it will have to be calculated from the experimental data. Shaafs [5] expresses the collision factor depending on the velocity of ultrasounds as in :

$$c = \frac{c_\infty S V_m}{V} \tag{10}$$

$c_\infty = 1600\,\mathrm{ms}^{-1}$ is the propagation velocity of ultrasounds at a very high frequency.

From the relations (5), (8) — (10) we may infer for the free volume the expression :

$$V_f = \frac{16V}{27\,b^2}\left(1 - \frac{c}{c_\infty}\right) \tag{11}$$

The data in Table 1 contain the propagation velocities of ultrasounds for n-alkanes at a temperature of 298.15 K and at a frequency of 15.6 MHz, obtained experimentally. For these values the covolume, b, the effective molecular radius, r_m, and the free volumes were calculated, by relations (5), (6), (10) and (11).

Using the values for the propagation velocities of ultrasounds in n-hexane, n-heptane, n-octane and n-nonane, from the already existent specialized literature[6], b, r_m, and V_f were calculated in the same way for the temperatures of 293.15 K, 313.15 K, 333.15 K.

The variation of the covolume with the propagation velocity of ultrasounds at the given temperatures is presented in figure 1. A growth of the covolume with the increase of the velocity of n-alkanes is noticed.

For the same n-alkane a growth of the covolume with the growth of the temperature is observed. The obtained isotherms have the same aspect.

The effective molecular radius goes up in the same manner, the slope of the isotherms being the same. As in the case of the covolume variation with the increase of the temperature, the values of molecular effective radius grow (see Figure 2).

TABLE 1

Properties for n-alkanes at 293.15 K

	c $m \cdot s^{-1}$	$b \times 10^6$ m^3	r_m nm	$V_f \times 10^6$ m^3
n-pentane	992.9	114.86	0.225	3.75
n-hexane	1056.8*	130.38**	0.234	3.04
n-heptane	1101.9	146.51	0.243***	2.63
n-octane	1140.2	162.49	0.252	2.29
n-nonane	1182.0	178.63	0.260	1.89

* 1050 $m.s^{-1}$, [7]
** 121.8 cm^3, [8]
***0.234 nm, [9]

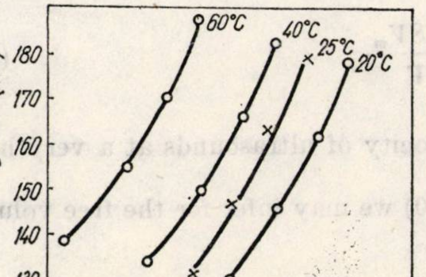

Fig. 1. — Plot of the covolume *vs.* the propagation velocity of ultrasound : x — experimental data ; O— calculated from existent velocity data.[6]

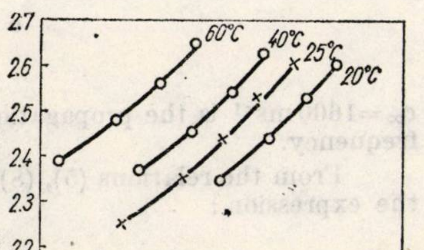

Fig. 2. — The variation of the effective molecular radius *vs.* velocity : x — experimental data ; O— calculated from existent velocity data.[6]

The variation of the free volume of n-alkanes with the propagation velocity of ultrasounds and with the temperature is shown in figure 3. The free volume decreases with the increase of the velocity for all studied temperatures. The decrease of the free volume is more marked at 333.15K. The aspect of the curves is the same at 293.15 K, 298.15 K, 313.15 K. The change of the slope of the last isotherm, as compared to the other temperatures is due to the fact that at 333.15 K n-hexane is very close by the critical temperature ($T_{c,\ \mathrm{hex}} = 341.95$ K) and it has a behaviour similar to a gas.

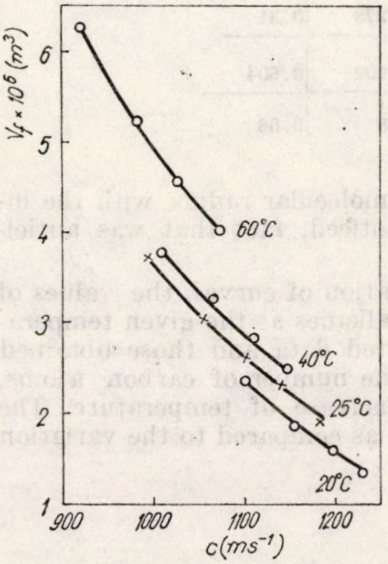

Fig. 3. — Plot of the free volume *vs.* velocity : x — experimental data ; O — calculated from the existent velocity data. [6]

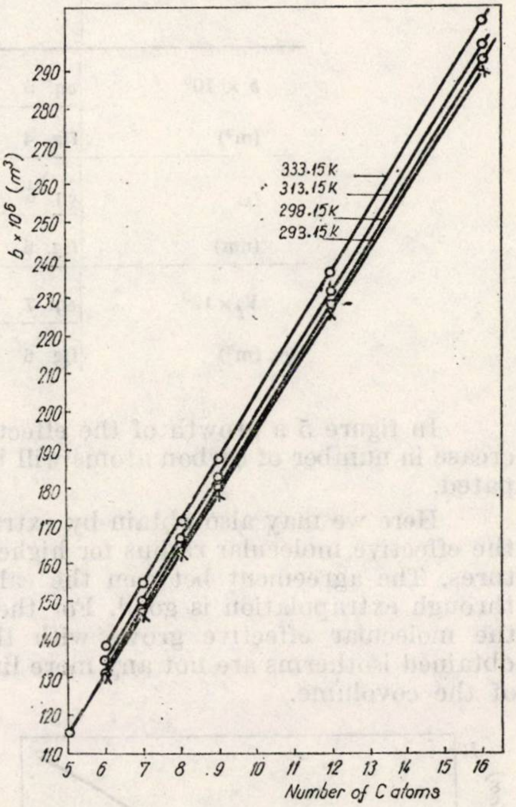

Fig. 4. — Plot of the covolume *vs.* the number of carbon atoms : x — experimental data ; O — calculated from existent velocity data. [6]

Figures 4—6 present the variation of the covolume, of the effective molecular radius and of the free volume of saturated hydrocarbons at 293.15 K, 298.15 K, 313.15 K, 333.15 K.

Analysing the isoterms in figure 4, a growth of the covolume with the increase of the number of carbon atoms is to be noticed. Thus, by taking into consideration the linear variation, we obtain, by extrapolation, the covolume values for higher hydrocarbons. For instance, for dodecane at 293.15 K, $b = 226 \times 10^{-6} \mathrm{m}^3$ and for hexadecane, at the same temperature, $b = 290 \times 10^{-6} \mathrm{m}^3$.

These values from extrapolation are in agrement with those calculated from relation (6) according to the ultrasound propagation velocity data existent in literature, [6] as we can see from table 2.

TABLE 2

Properties of n-dodecane and n-hexadecane at 293.15 K

		n-dodecane	n-hexadecane
$b \times 10^6$	eq. 5	227.41	291.43
(m^3)	fig. 4	226	290
r_m	eq. 6	0.282	0.306
(nm)	fig. 5	0.278	0.31
$V_f \times 10^6$	eq. 7	0.902	0.604
(m^3)	fig. 6	0.8	0.68

In figure 5 a growth of the effective molecular radius with the increase in number of carbon atoms will be noticed, fact that was anticipated.

Here we may also obtain by extrapolation of curves, the values of the effective molecular radius for higher n-alkanes at the given temperatures. The agreement between the calculated data and those obtained through extrapolation is good. For the same number of carbon atoms, the molecular effective grows with the increase of temperature. The obtained isotherms are not any more linear as compared to the variation of the covolume.

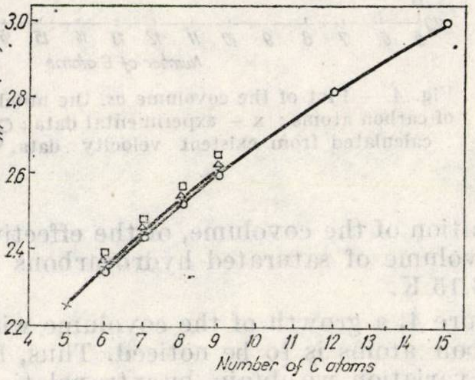

Fig. 5. — The variation of the effective molecular radius *vs.* the number of carbon atoms : x — experimental data ; O — calculated from existent velocity data at 293.15 K, △ — at 313.15 K, □ — at 333.15 K.

It is known[10] that the chains of n-alkanes in solid state, display a zigzag shape, the carbon atoms occurring on the same plane. The valence angles are approximately those of a regular tetrahedron (109°35′). In crystals, the molecules are placed parallelly as close as possible. In melted state, owing to the free rotation of the bound $>C-C<$ the molecules may take any shape, oscillating between the shape described above and that of a spiral. It seems that even in liquid state the zigzag shape, with lower potential energy is more stable than the second shape. In saturated alkanes the length of the hydrocarbon chain may be calculated additively in terms of the distances $>C-C<$ (equal to 0.254 nm) and $>C-H$ (equal to 0.154 nm) and the valence angles. If we compare the chain length of each n-alkane, which is calculated by addition, with the double effective molecular radius, inferred from formula (5) we shall discover that the latter is smaller, the differences growing for higher n-alkanes. This difference has a few causes, of which we give the following :

a) In the present paper we have started from the hypothesis for the sake of simplicity, that the model of liquid made up of non-polar hard spheric molecules is valid, which does no longer apply to higher hydrocarbons.

b) When the ultrasounds cross the liquid, the energy of the thermal agitation of molecules increases. This fact probably calls forth the appearance of a larger number of spinal-shaped molecules, as compared to those existing in the system unaffected by ultrasound propagation. As a consequence to this fact, the effective molecular radius, which was calculated in the present paper, is smaller than the one calculated additively.

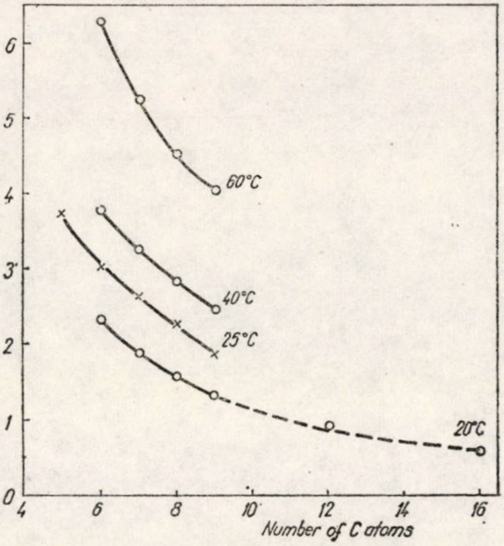

Fig. 6. — Plot of the free volume *vs.* the number of carbon atoms : x — experimental data ; O— calculated from existent velocity data.[6]

Figure 6 shows the variation of the free volumes according to the number of carbon atoms. At the same temperature, the free volume decreases, fact that was anticipated, considering the growth of the dimensions of the molecules. With the temperature rise, the free volume of every n-alkane grows. Due to the thermal agitation, the intermolecular distance being longer, the fluid displays a behaviour which is more similar to that of a gas. The greatest value of the free volume for n-hexane at 333.15 K is observed, because at this temperature the n-hexane is near to the critical temperature. Actually, this behaviour may be also inferred from the fact that, while the temperature rises, the propagation velocity of the ultrasounds decreases.

The free volume of higher n-alkanes may be obtained through the extrapolation of the isotherms in figure 6, the values being in agreement with the ones calculated from relation (7).

Table 2 shows these values inferred from extrapolation and the calculated values for n-dodecane and n-hexadecane.

REFERENCES

[1] W. Van Dael "Experimental Thermodynamics of Nonreacting Fluids", Vol. II, Chapt. 11 (Editors B. Le Neindre and B. Vodar), Butterworths, London, 1975.

[2] R. Vîlcu, E. Dimitriu and V. Dima, *Rev. Roumaine Chim.*, **24**, 1247 (1979).

[3] R. H. Stokes and K. N. Marsh, *Ann. Ref. Phys. Chem.*, **23**, 65 (1972).

[4] von W. Shaafs, *Acustica*, **33**, 272 (1957).

[5] von W. Shaafs, *Acustica*, **30**, 275 (1974).

[6] J. W. M. Boelhouwer, *Physica*, **34**, 484 (1967).

[7] W. J. Snyder and J. R. Snyder, *J. Chem. Eng. Data*, **19**, 270 (1974).

[8] P. N. Gupta and S. C. Sinka, *Acustica*, **25**, 147 (1971).

[9] G. W. Marks, *J. Acoust. Soc. Amer.*, **27**, 680 (1955).

[10] C. D. Nenițescu, "Chimie organică", vol. I, Ed. didactică și pedagogică, București, 1966.

Revue Roumaine de Chimie 25, *8*, 1139–1148 (1980)

INVESTIGATION OF THE KINETICS AND MECHANISM OF SILVER (I) ION CATALYS OXIDATION OF d,l(α) VALINE BY PEROXYDISULPHATE

G. CHANDRA and S. N. SRIVASTAVA
Chemistry Department, Agra College, Agra, India

Received March 4, 1978

Kinetics of d,l (α) valine oxidation by peroxydisulphate catalysed by silver ion has been studied in aqueous solution. The reaction is found to be of first order in peroxydisulphate and independent of valine concentration. The reaction rate is linearly related to the concentration of silver ion. A negative salt effect is observed but there is no regular variation of specific rate with ionic strength. However, cations inhibit the reaction and the order of decrease in the rate constant is $K^+ > Na^+ > NH_4^+$. At last in order to account for these observed facts a suitable chain mechanism has been proposed and the following rate laws have been deduced :

$$-\,d\,(S_2O_8^{2-})/\,dt = (k' + k''\,(Ag^+))\,(S_2O_8^{2-})\ \text{(at higher temp.)}$$

$$-\,d\,(S_2O_8^{2-})/\,dt = k''(Ag^+)\,(S_2O_8^{2-})\ \text{(at lower temp.)}$$

INTRODUCTION

Peroxydisulphate ion has been well known for its oxidising properties in aqueous solution. Non-catalysed oxidations involving this ion are generally slow [1] and, therefore, silver ion has been used as a catalyst. The kinetic studies on the oxidation of a variety of substrates both inorganic and organic by peroxydisulphate were reviewed by House, [2] who revealed that only a few kinetic investigations had been made with organic nitrogen compounds and peroxydisulphate. [3-6] Silver catalysed oxidation of glycine and alanine by peroxydisulphate ion is being investigated in this laboratory [7,8] in order to get a better insight of the mechanism of the oxidation. The oxidation of valine by chromic acid in sulphuric acid solution, MnO_2 and MnO_4 solutions (acidic, alkaline and neutral) has been studied by some investigators. [9-11] In the present communication, the kinetics of the d, l (α) valine oxidation by peroxydisulphate ion in the presence of silver (I) as catalyst has been investigated.

EXPERIMENTAL

Materials : (i) An aqueous solution of potassium peroxydisulphate was prepared freshly before every run from Merck sample of G.R. grade by dissolving the exact weight in the required volume ; (ii) aqueous solution of d, l (α) valine and $AgNO_3$ were always prepared from AnalaR BDH sample by direct weighing; (iii) all other reagents were of analytical grade; (iv) bidistilled water from all pyrex glass apparatus was employed for preparing the solution and dilution where necessary. The reaction vessels were of pyrex glass and were coated on the outside with Japan black to exclude photochemical discrepancies.

Procedure : Measured quantities of solutions of valine and silver nitrate were kept in a thermostat maintained at the temperature of experiment (35°C with an accuracy of ±0.1°C). The reaction was started by the required volume of peroxydisulphate solution in the reaction vessel. The progress of the reaction was followed by estimating the amount of unconsumed peroxydisulphate with time iodometrically by slightly modified method of Bartlett and Cotman[12] adopted by Saxena and Singhal.[13]

RESULTS

Stoichiometry

Reaction mixture with excess of potassium peroxydisulphate was maintained at 35°C. The remaining persulphate was estimated by the method described earlier. Decomposition of peroxydisulphate by silver (I) ion was also taken into consideration. The amounts of the peroxydisulphate consumed by valine are shown below, in table 1.

TABLE 1

The amount of peroxydisulphate consumed by valine
$AgNO_3 = 0.0005$ M, Temperature = 35°C

Initial $[S_2O_8^{2-}]$ (M)	$[S_2O_8^{2-}]$ decomposed (M)	$[S_2O_8^{2-}]$ decomposed (M)	$[S_2O_8^{2-}]$ consumed by valine (M)
0.0150	0.0115	0.0021	0.0094
0.0175	0.0120	0.0025	0.0095

It is evident from the above table that the equimolecular consumption of valine and peroxydisulphate takes place. This leads to the following stoichiometry :

$$S_2O_8^{2-} + (CH_3)_2CH-CH(NH_2)COO^- + H_2O \xrightarrow{Ag^+}$$

$$(CH_3)_2CH-CHO + NH_3 + CO_2 + HSO_4^- + SO_4^{2-}$$

Kinetics

Kinetics of the reaction was studied at 35°C employing concentrations of the reactants ($S_2O_8^{2-}$ and valine) in stoichiometric proportions (1 : 1 mole). The results are given in table 2.

Fairly constant values of specific rates are obtained with equimolecular concentrations of valine and $S_2O_8^{2-}$ suggests that the overall order of the reaction is one at constant silver ion concentration.

Standard deviation from the mean value was calculated for the values given in table 2 and it was found to be ± 0.083. Throughout the paper the mean values of rate constants are given. The standard deviations (σ) were calculated for all such cases. The lower and upper limits of σ for $10^3 k$ values are ± 0.043 and ± 0.085.

TABLE 2

First order dependence of silver catalysed valine peroxydisulphate reaction

$K_2S_2O_8 = 0.01$ M, Valine = 0.01 M, $AgNO_3 = 0.0005$ M, Temperature = 35°C

Time (min.)	30	60	90	120	150	180
$10^3k/2.303$ (min. $^{-1}$)	3.45	3.48	3.29	3.43	3.45	3.54

Peroxydisulphate dependence

To evaluate the order of the reaction with respect to oxidant, the reaction was carried out at different concentrations of peroxydisulphate. The reaction followed first order disappearance in $S_2O_8^{2-}$ and the log $a/a-x$

TABLE 3

Peroxydisulphate dependence

Valine = 0.01 M, $AgNO_3 = 0.0005$ M, Temperature = 35°C

$[S_2O^{2-}]$ (M)	0.005	0.01	0.0125	0.015	0.0175
$k \times 10^3$(min^{-1})	9.71	7.94	7.38	6.93	6.61

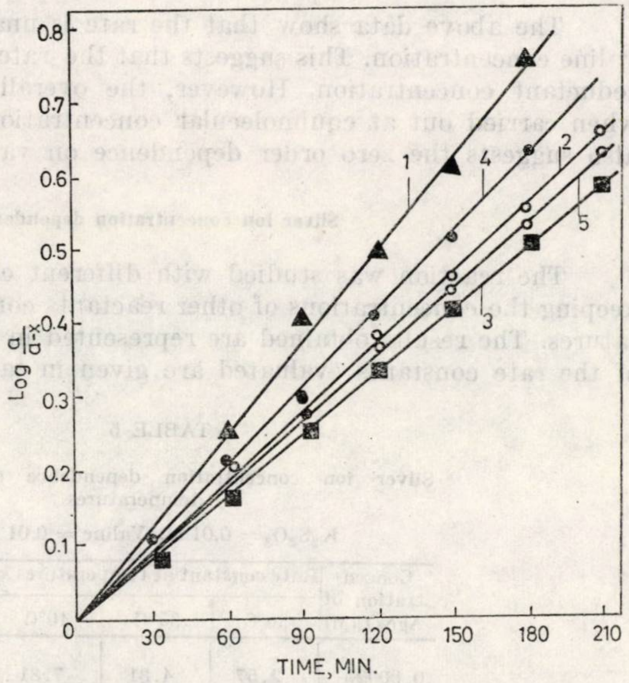

Fig. 1. — Plot of log $a/a-x$ *vs.* time, valine = 0.01 M, $AgNO_3 = 0.0005$ M, Temperature = 35°C :

1. $K_2S_2O_8 = 0.005$ M,
2. $K_2S_2O_8 = 0.0125$ M,
3. $K_2S_2O_8 = 0.0175$ M,
4. $K_2S_2O_8 = 0.01$ M,
5. $K_2S_2O_8 = 0.015$ M.

vs. time plots were linear up to 80% of the reaction (Fig. 1). The rate constants have been calculated from the slopes of these straight lines. Table 3 summarizes the results obtained.

It is evident from the above table that the rate constant decreases with an increase in the concentration of peroxydisulphate. The decrease in the rate constant is attributed partly to the increase in the ionic strength by addition of $S_2O_8^{2-}$ ions and partly to the inhibitory action of K^+ ion,[12, 14–16] which is a common feature of peroxydisulphate oxidations. It will be confirmed later from salt effect studies that both of the factors (ionic strength and K^+ ion inhibition) are responsible for the decrease in rate constant.

d, l (α) Valine dependence

The rate constants corresponding to different initial concentrations of valine are summarized below in table 4.

TABLE 4

d, l (α) Valine dependence

$K_2S_2O_8$ = 0.01 M, $AgNO_3$ = 0.0005 M, Temperature = 35°C

(Valine) M	0.005	0.01	0.015	0.02	0.025
$k \times 10^3 (\text{min}^{-1})$	7.85	7.93	7.95	8.08	8.13

The above data show that the rate is unaffected by a change in valine concentration. This suggests that the rate law is zero order in the reductant concentration. However, the overall reaction is first order when carried out at equimolecular concentration of the reactants. This also suggests the zero order dependence on valine concentration.

Silver ion concentration dependence

The reaction was studied with different concentrations of $AgNO_3$ keeping the concentrations of other reactants constant at various temperatures. The results obtained are represented in figure 2 and the values of the rate constants evaluated are given in table 5.

TABLE 5

Silver ion concentration dependence at various temperatures

$K_2S_2O_8$ = 0.01 M, Valine = 0.01 M.

Concentration of $AgNO_3$(M)	Rate constant at temperatures $k \times 10 \text{min.}^{-1}$			
	30°C	35°C	40°C	45°C
0.00025	2.57	4.81	7.81	11.88
0.0005	5.34	7.94	12.55	21.51
0.0010	9.57	16.03	21.26	35.34
0.0015	14.06	23.42	31.99	51.38

A close scrutiny of the above table reveals that at lower temperatures, on increasing the concentration of $AgNO_3$ twofold, the rate constants are almost doubled showing first order dependence on silver ion concentration and the reaction obeys a rate expression of the form

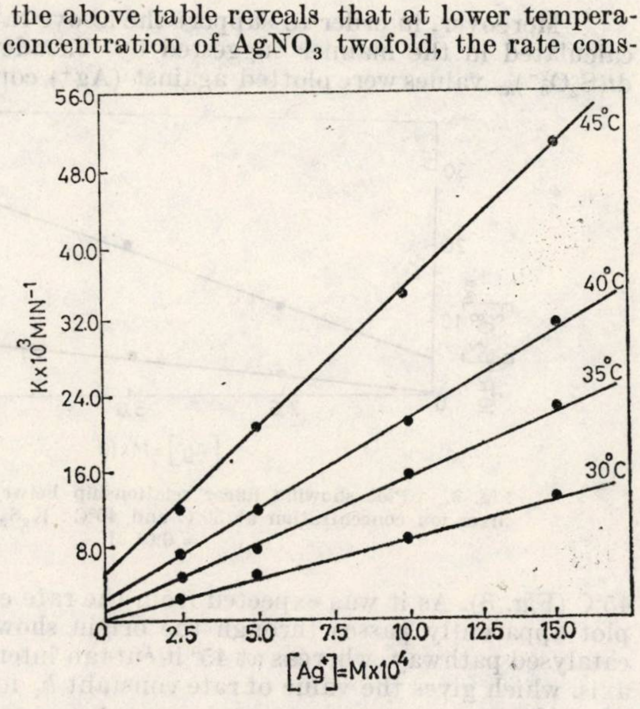

Fig. 2. — Plot showing linear relationship between rate constant (k) and silver ion concentrations at four different temperatures : $K_2S_2O_8 = 0.01$ M, Valine $= 0.01$ M.

$$\mathrm{d}x/\mathrm{d}t = k_2[\mathrm{Ag}^+]\,[\mathrm{S_2O_8^{2-}}]$$

$$\text{where } k_{\text{obs.}} = k_2[\mathrm{Ag}^+]$$

whereas at higher temperatures this does not hold good, and a plot of rate constant *vs.* silver ion concentration gives straight lines which do not pass through origin (Fig. 2). This clearly indicates that the observed rate constant can be written as

$$k_{\text{obs.}} = k_1 + k_2(\mathrm{Ag}^+)$$

This shows that though at higher temperatures, the order with respect to silver ion concentration is equal to one, nevertheless, a non-catalysed oxidation of valine is also taking place simultaneously. Thus, the observed rate constant is linearly related to silver ion concentration. In this case the reaction obeys a rate expression of the form

$$\mathrm{d}x/\mathrm{d}t = k_1 + k_2\,[\mathrm{Ag}^+]\,[\mathrm{S_2O_8^{2-}}]$$

where k_1 and k_2 are the rate constants for noncatalysed and catalysed pathways.

Moreover, in order to support the above rate laws dx/dt values were calculated in the manner suggested by Vasudeva and Wasif[17] and $dx/dt(S_2O_8^{2-})_{av}$ values were plotted against (Ag^+) concentrations for 30°C and 45°C (Fig. 3). As it was expected from the rate expressions at 30°C, linear plot apparently passes through the origin showing the absence of noncatalysed pathway, whereas at 45° it cuts an intercept on the $dx/dt(S_2O_8^{2-})_{av}$ axis, which gives the value of rate constant k_1 for noncatalysed pathway of oxidation.

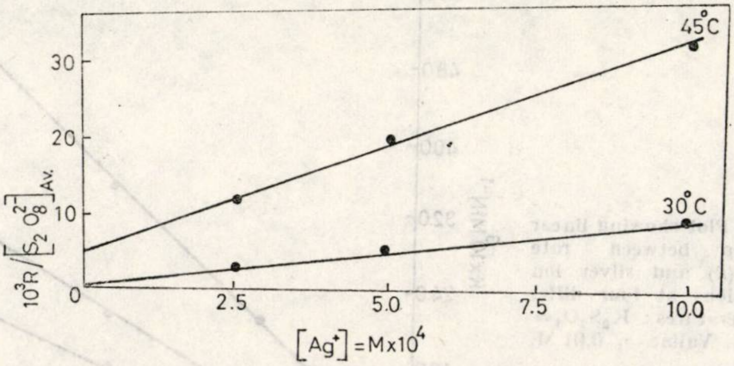

Fig. 3. — Plot showing linear relationship between $R/[S_2O_8^{2-}]_{av}$ and silver ion concentration at 30°C and 45°C : $K_2S_2O_8 = 0.01$ M, Valine $= 0.01$ M.

Temperature dependence

The rate constants k_1 and k_2 for noncatalysed pathway and catalysed pathway have been calculated separately for four different temperatures from the intercepts and slopes of the lines in figure 2. The values calculated from figure 3 are in agreement with the values obtained from figure 2. It was observed that at 30° the rate constant for noncatalysed pathways tends to zero. The catalysed oxidation of valine is associated with a low value of energy of activation, 14.72 kcal and negative value of $\Delta S^{\neq}(-16.0$ E.U.). This low value of $E^{\neq}$ and the negative $\Delta S^{\neq}$ value suggest that the rate determining stage(s) is probably between two oppositely charged ions[18] *viz.* $Ag^+ + S_2O_8^{2-}$.

Effect of neutral salts

The effect of different neutral salts on the reaction rate has been suggested and it was observed that the rate constant decreases with increasing ionic strength *e.g.* by adding 0.01, 0.02 and 0.03 M NH_4NO_3 in the reaction mixture containing $K_2S_2O_8 =$ valine $= 0.01$ M and $AgNO_3 = 0.0005$ M at 35° ; the rate constants obtained were 7.70, 7.41 and 7.15 × $\times 10^{-3}$ min^{-1}, respectively. But a close scrutiny reveals that the decrease in the rate constant is not strictly dependent on the increase in ionic strength for 0.03 M NH_4NO_3, 0.03 M $NaNO_3$ and 0.01 M K_2SO_4 contribute the same ionic strength ($\mu = 0.03$) but the rate constants were found

7.15, 6.98 and 6.31×10^{-3} min^{-1}. Therefore, a pronounced specific effect of the ions is there, and the order in which the cations inhibit the reaction is $K^+ > Na^+ > NH_4^+$.

This further confirms the results obtained with varying concentrations of $S_2O_8^{2-}$ *i.e.* the decrease in the rate constant by increasing $S_2O_8^{2-}$ concentration is due to the increase in ionic strength and inhibitory action of K^+.

Effect of Nitrogen gas

The reaction has been studied in the environment of nitrogen. For this the nitrogen gas is bubbled through the reaction mixture containing $K_2S_2O_8$ = valine = 0.01 M, $AgNO_3$ = 0.0005 M at 35°C, with a uniform rate. The value of the rate constant was found 10.24×10^{-3} min^{-1} which is about 28% higher than the value obtained under similar conditions in the air.

Identification of *iso*-butaldehyde

The main reaction product, *iso*-butaldehyde has been identified in the reaction mixture by preparing its 2 : 4 dinitro phenylhydrazone and determining its m.p. which is found to be 186°C (Lit. m.p. 187°C).

DISCUSSION

In silver ion catalysed oxidations by peroxydisulphate, the catalytic activity of silver ion is due to the formation of higher valent silver species. Some visual observations were made on mixing peroxydisulphate and silver nitrate solutions. A black suspension is produced, which increases with time and is proportional to the concentrations of $AgNO_3$ and peroxydisulphate. Malaguti [22] concluded, based on his experiments, that this suspension is a compound of bivalent silver. In the present investigation no such black suspension was obtained because the concentration of silver used was too low. The following scheme has been proposed for the oxidation of valine by peroxydisulphate catalysed by silver ion:

The first step involves the homolytic fission of peroxydisulphate ion (at higher temperature, 35—45°C) into two sulphate free radical ions [12].

$$S_2O_8^{2-} \xrightarrow{k_1} 2SO_4^{\cdot -} \qquad (1)$$

The formation of $SO_4^{\cdot -}$ also takes place by the equation

$$S_2O_8^{2-} + Ag^+ \xrightarrow{k_2} SO_4^{\cdot -} + SO_4^{2-} + Ag^{2+} \qquad (2)$$

The sulphate free radical ion further reacts with silver ion to generate higher valent silver [20]

$$SO_4^{\cdot -} + Ag^+ \xrightarrow{k_3} Ag^{2+} + SO_4^{2-} \qquad (3)$$

The higher valent silver species attacks the reductant molecules to yield products as follows :

$$(CH_3)_2CH\cdot CHNH_2COO^- + Ag^{2+} \xrightarrow{k_4} (CH_3)_2CH\cdot CHNH_2COO\cdot + Ag^+ \tag{4}$$

$$(CH_3)_2CH\cdot CHNH_2COO\cdot \xrightarrow{k_5} (CH_3)_2\dot{C}H\cdot CHNH_2 + CO_2 \tag{5}$$

$$(CH_3)_2CH\cdot \dot{C}HNH_2 + H_2O + O_2 \xrightarrow{k_6} NH_3 + (CH_3)_2CH{-}CHO + HO_2 \tag{6}$$

This peroxo radical further reacts with $S_2O_8^{2-}$ as follows :

$$S_2O_8^{2-} + HO_2 \xrightarrow{k_7} HSO_4^- + SO_4^{\cdot -} + O_2 \tag{7}$$

and the chain terminating step can be given by the equation

$$SO_4^{\cdot -} + HO_2 \xrightarrow{k_8} HSO_4^- + O_2 \tag{8}$$

From the foregoing mechanism the rate law is given by the equation

$$-d(S_2O_8^{2-})/dt = k_1(S_2O_8^{2-}) + k_2(S_2O_8^{2-})(Ag^+) + + k_7[S_2O_8^{2-}][HO_2] \tag{9}$$

Making the usual steady state assumptions that the change rate of free radical concentration is zero, the following equation can be obtained

$$(HO_2) = -k_1/4k_7 + 1/k_7(k_2k_3k_7/k_6)^{\frac{1}{2}} \left\{([Ag^+] + k_1/4k_2)^2 + + \frac{k_1^2(k_2k_8 - k_3k_7)}{16k_2k_3k_7}\right\}^{\frac{1}{2}} \tag{10}$$

k_1, the thermal decomposition of $S_2O_8^{2-}$, is very small and the difference $(k_2k_8 - k_3k_7)$ is also small quantity, the last term of the above equation can be neglected, thus

$$[HO_2] = -k_1/4k_7 + 1/4k_2(k_2k_3k_7/k_8)^{\frac{1}{2}}[Ag^+] + k_1/4k_2k_7(k_2k_3k_7/k_8)^{\frac{1}{2}} \tag{11}$$

This value of $[HO_2]$ is fed into the equation (9) to obtain the final expression

$$-d/t[S_2O_8^{2-}] = (k_1/4k_2(k_2k_3k_7/k_8)^{\frac{1}{2}} + 3k_1/4)[S_2O_8^{2-}] + (k_2 + (k_2k_3k_7/k_8)^{\frac{1}{2}})[Ag^+][S_2O_8^{2-}] \tag{12}$$

Which is of the form

$$-\,d[S_2O_8^{2-}]/dt = \{k' + k''[Ag^+]\}\,[S_2O_8^{2-}] \qquad (13)$$

where $k_{obs.} = k' + k''[Ag^+]$

However, at low temperature the initial step ($S_2O_8^{2-} \xrightarrow{k_1} 2SO_4^{\cdot-}$) can be omitted and in that case the rate expression will take the form

$$-d[S_2O_8^{2-}]/dt = (k_2 + k_7(k_2k_3k_7/k_8)^{\frac{1}{2}})[Ag^+][S_2O_8^{2-}] \qquad (14)$$

These rate expressions (13) and (14) satisfactorily explain the observed kinetics of the oxidation reaction. Expression (14) explains the first order kinetics in peroxydisulphate, first order in silver ion concentration and independent of valine concentration at low temperature, whereas expression (13) explains the first order dependence of $S_2O_8^{2-}$, linear relationship between Ag^+ and rate constant and zero order dependence of valine.

It has been observed that in the absence of reductant (valine) silver ion decomposes peroxydisulphate very slowly. The rate constant for decomposition of 0.01 M $S_2O_8^{2-}$ in the presence of 0.0005 M $AgNO_3$ at 35°C is 0.95×10^{-3} min^{-1}, whereas in the presence of valine (0.01 M) the rate constant is found to be 7.94×10^{-3} min^{-1}. This increase in reaction rate is due to the further decomposition of $S_2O_8^{2-}$ by HO_2 radical produced by adding reductant. This supports the reaction sequence (7) of the proposed mechanism. This is further supported by the fact that in the environment of N_2 the specific reaction rate is increased by 28 %. Because in the absence of air (O_2) $H^{\cdot}$ free atom cannot react with oxygen to yield HO_2 radicals and, therefore, equation (7) and (8) take the form:

$$S_2O_8^{2-} + H^{\cdot} \xrightarrow{k_7'} SO_4^{\cdot-} + HSO_4^-$$

$$SO_4^{\cdot-} + H^{\cdot} \xrightarrow{k_8'} HSO_4^-$$

These k_7' and k_8' are certainly different from k_7 and k_8 and thus the observed rate constants in air and N_2 environment are different.

ACKNOWLEDGEMENT. Thanks are due to Council of Scientific and Industrial Research, New Delhi, India for the award of a Senior Research Fellowship to one of the authors (G.C.)

REFERENCES

[1] H. Marshall, *J. Chem. Soc.*, **59**, 771 (1891).

[2] D. A. House, *Chem. Rev.*, **62**, 185 (1962).

[3] N. M. Beilerian, *Trudy Erevan. Gosudarst. Univ. Ser. Khim. Nauk*, **60**, 143 (1957); *Chem. Abstr.*, **53**, 11081 (1959).

[4] N. M. Beilerian, *Doklady Akad. Nauk Arm. S.S.R.*, **30**, 225 (1960).

[5] M. C. Agarwal and S. P. Mushran, *J. Indian Chem. Soc.* **42**, 629 (1965).

[6] J. P. Whalley, H. G. V. Evans and C. A. Winkler, *Canad. J. Chem.*, **34** 1154, (1956).

[7] G. Chandra and S. N. Srivastava, *Bull. Chem. Soc. Japan*, **44**, 3000 (1971).

[8] G. Chandra and S. N. Srivastava, *J. Inorg. Nuclear Chem.*, **34**, 197 (1972).

[9] J. Garia-Blanco and A. M. Pascual-Leone, *Rev. Espan. Fisol*, **11**, 143 (1955); *Chem. Abstr.*, **50**, 4701 (1956).

[10] M. Z. Barakat, M. E. Abdal-Wahab and M. M. Etstarm, *J. Chem. Soc.* **1956**, 4685.

[11] O. G. Pokrovskaya, *Izvest. Siber. Otdel Akad. Nauk. S.S.SR.* **8**, 50 (1959).

[12] P. D. Bartlett and J. D. Cotman, *J. Amer. Chem. Soc.*, **71**, 1419 (1949).

[13] L. K. Sexena and C. P. Singhal, *Agra Univ. J. Sci.*, **6**, 43 (1957).

[14] R. L. Eager and C. A. Winkler, *Canad. J. Res.*, **26B**, 527 (1948).

[15] S. P. Srivastava and S. Ghosh, *Z. phys. Chem.*, **202**, 198 (1953).

[16] Y. K. Gupta and S. Ghosh *J. Inorg. Nuclear Chem.*, **11**, 62 (1959).

[17] W. C. Vasudeva and S. Wasif, *J. Chem. Soc.*, **B, 1970**, 960.

[18] L. R. Subbraman and M. Santappa, *Z. phys. Chem.*, **48**, 172 (1966).

[19] A. Malaguti, *Analyt. Chem.*, **42**, 138 (1952).

[20] D. Benson, "Mechanism of Inorganic Reactions in Solution", McGraw-Hill, London, 1968, p. 193.

Revue Roumaine de Chimie 25, 8, 1149–1158 (1980)

KINETICS OF GLYCINE OXIDATION BY PEROXYDISULPHATE

G. CHANDRA and S. N. SRIVASTAVA
Chemistry Department, Agra College, Agra, India

Received May 3, 1978

A kinetic study of the oxidation of glycine by peroxydisulphate has been made. The rate has been measured by estimating the remaining peroxydisulphate iodometrically. The data follow the rate expression

$$-\,d[S_2O_8^{2-}]/dt = k_1[S_2O_8^{2-}] + k_2[S_2O_8^{2-}]\,[\text{glycine}]^0$$

where k_1 is the rate constant for the thermal decomposition of peroxydisulphate and k_2 is the rate constant for the bimolecular reaction between peroxydisulphate and glycine. k_1 being very small in comparison to k_2 the first term of the expression can be neglected and, therefore, the rate expression reduces to

$$-\,d[S_2O_8^{2-}]/dt = k_2[S_2O_8^{2-}]\,[\text{glycine}]^0$$

A chain mechanism was proposed whose initiating step is the decomposition of peroxydisulphate. Allyl acetate inhibited the reaction whereas increased area/ volume ratio and the gases CO_2 and N_2 accelerated the rate of the reaction. A negative salt effect was observed and it was concluded that the ions exerted an inhibitory action. Energy and entropy of activation were found to be 26.35 kcal and $^+6.31$ e.u. respectively.

INTRODUCTION

Redox reactions involving peroxydisulphate ions, both catalysed and uncatalysed were previously studied by many investigators. [1] Three types of silver catalysed oxidations were reported. The oxidation of vanadyl, [2] chromium, [3] cerious ions [4] and acetone [5] is slow. Oxidation of ammonium ion [6] is moderately fast and the oxalate ion [7] oxidation is about 400–4000 times faster than others. And therefore, the studies with the acid containing this ion and with other carboxalic acids were made by some investigators *e.g.* the oxidation of oxalic acid and formic acid was studied by Srivastava and Ghosh [8-10] and Saxena and Singhal.[11, 12] Later Kumar and Saxena [13] investigated the kinetics of α-amino acetic acid (glycine) by peroxydisulphate. Silver catalysed oxidation of glycine [14] has already been reported by the authors and a chain mechanism has been proposed. In general, most of the uncatalysed reactions are slow at room temperature and almost all the oxidations described above are first order in peroxydisulphate and independent of the concentration of the reducing agent.

The present investigation has been undertaken with a view to study the kinetics of the reaction and to suggest a mechanism for the reaction which explains the increased rate in the decomposition of peroxydisulphate by the addition of glycine as the mechanism suggested by the previous investigators[13] does not explain this fact.

EXPERIMENTAL

All chemicals were of B.D.H.A.R. quality or E. Merck G.R. quality and the vessels for storing redistilled water, preparing solutions and reaction vessels were of Jena glass and pyrex glass. The reaction vessels were coated outside with japan black to exclude any photochemical effect.

Stock solutions of glycine were prepared by dissolving the exact weight of glycine in bidistilled water and the strength was checked by Sorensen formal method. Peroxydisulphate solution was always prepared fresh by direct weighing.

The calculated volume of glycine solution in a reaction vessel was placed in a thermostat at 45°. The desired volume of the peroxydisulphate solution was then transferred to the reaction vessel by means of a pipette and quickly shaken. The peroxydisulphate solution was not normally preheated to thermostat temperature before addition lest it should decompose. However, the variation in the temperature of the reaction mixture thus caused is insignificant as reported by Allen.[15] Five millilitres of the reaction mixture were pipetted out at suitable intervals of time and the concentration of the unreacted peroxydisulphate was determined by the slightly modified method[13] of Bartlett and Cotman.[16]

STOICHIOMETRY

The stoichiometry of the reaction was studied by taking peroxydisulphate solutions in excess in the reaction mixture containing glycine (0.01 M) at 45°C. The progress of the reaction was checked by pipetting out 5 ml of aliquote portion after certain time intervals and calculating the rate constant in each case. Completion of the reaction was indicated by sudden decrease in the rate constant because after total consumption of glycine the decomposition rate of peroxydisulphate would be practically ceased. The amount of the peroxydisulphate consumed by 0.01 M glycine is shown in table 1.

TABLE 1

Amount of the peroxydisulphate consumed by 0.01 M glycine. $CH_2NH_2COOH = 0.01$ M, temperature = 45°C*

$[S_2O_8^{2-}]_0$ moles/l	Unreacted $[S_2O_8^{2-}]$ moles/l	$[S_2O_8^{2-}]$ consumed moles/l
0.0125	0.0022	0.0103
0.0150	0.0048	0.0102
0.0175	0.0074	0.0101
0.0200	0.0104	0.0096

* The thermal decomposition of peroxydisulphate is neglected at this temperature.

Table 1 shows that the equimolecular consumption of peroxydisulphate and glycine takes place and, therefore, the stoichiometric equation is :

$$CH_2NH_2COO^- + S_2O_8^{2-} + H_2O = HCHO + NH_3 + CO_2 + HSO_4^- + SO_4^{2-}$$

EFFECT OF CHANGING THE CONCENTRATION OF REACTANTS

Table 2 gives the result of a representative experiment where the first order constant has been calculated from the relation $k = 2.303/t$ $(\log (a/a-x))$, a and $a-x$ being the concentrations of peroxydisulphate initially and after time t.

TABLE 2

First order dependence of glycine-peroxydisulphate reaction $K_2S_2O_8 = 0.01$ M $CH_2NH_2COOH = 0.01$ M, temperature = 45° C

Time in minutes	$a - x$ ml. of $Na_2S_2O_3$	Conc. $C \times 10^3$ moles/l	$k/2.303 \times 10^3$ min.$^{-1}$
0	11.40	10.000	—
30	8.50	7.456	4.25*
60	5.40	4.737	5.41
90	3.70	3.246	5.43
120	2.45	2.149	5.56
150	1.70	1.491	5.51
180	1.15	1.009	5.59
210	0.80	0.701	5.49
* neglected		mean	5.50

$k = 12.67 \times 10^{-3}$ min.$^{-1}$

The reaction has been carried out with varying concentrations of peroxydisulphate and with 0.01 M glycine at 45°C. The plots of log C *vs.* time (Fig. 1) (Where C is the concentration of peroxydisulphate in moles/l,

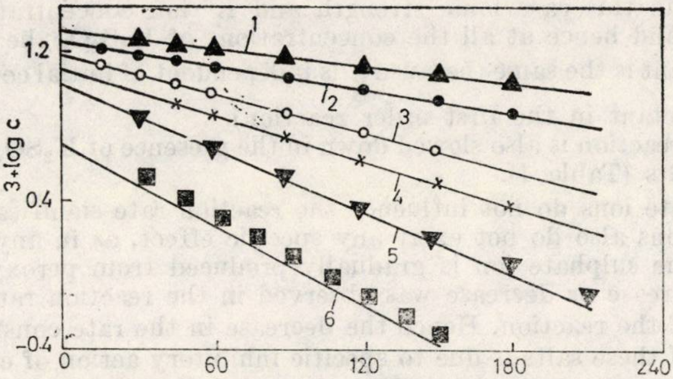

Fig. 1. — Plot of log C *vs.* time, $CH_2CH_2COOH = 0.01$ M. Temperature = 45°C. *1.* $K_2S_2O_8 = 0.02$ M, *2.* $K_2S_2O_8 = 0.0175$ M, *3.* $K_2S_2O_8 = 0.015$ M, *4.* $K_2S_2O_8 = 0.0125$ M, *5.* $K_2S_2O_8 = 0.01$ M, *6.* $K_2S_2O_8 = 0.005$ M.

at different time intervals) were drawn in each case and the linear relationship between log *C* and time suggested the first order dependence of reaction rate in peroxydisulphate concentration. The values of the rate constant calculated for different concentrations of peroxydisulphate and glycine are given in table 3.

TABLE 3

Effect of peroxydisulphate and glycine concentration on reaction rate

$K_2S_2O_8$ moles/l	CH_2NH_2COOH moles/l	$k \times 10^3$ min^{-1}
0.0050	0.0100	16.14
0.0100	0.0100	12.67
0.0125	0.0100	9.33
0.0150	0.0100	7.90
0.0175	0.0100	4.79
0.0200	0.0100	3.71
0.0200	0.0075	12.23
0.0100	0.0150	12.41
0.0100	0.0200	12.57
0.0100	0.0250	12.39

The rate constant decrease with the increase in the peroxydisulphate concentration is due to the inhibition by potassium ions, which seems to be a characteristic of most peroxydisulphate reactions. [9, 11, 17]

This fact is supported by plotting $[S_2O_8^{2-}]_t$ moles/l against time (Fig. 2). It can be seen that $t_{\frac{1}{2}}$ remains the same as peroxydisulphate concentration changes from 0.01 M to 0.005 M in the course of the reaction. This also confirms the first order disappearance of peroxydisulphate. Moreover in this case ionic strength and K^+ ion concentration remain the same and hence at all the concentrations of $K_2S_2O_8$ the first order rate constant is the same (because $t_{\frac{1}{2}}$ is independent of initial concentration of the reactant in the first order reaction).

The reaction is also slowed down in the presence of K_2SO_4 and other neutral salts (Table 4).

Nitrate ions do not influence the reaction rate significantly [18] and sulphate ions also do not exert any specific effect, as in any particular reaction the sulphate ion is gradually produced from peroxydisulphate but no increase or decrease was observed in the reaction rate with the progress of the reaction. Hence the decrease in the rate constant in the presence of these salts is due to specific inhibitory action of cations, and therefore, no conclusion regarding the salt effect could be drawn *e.g.* ionic strength contributed by 2×10^{-3} M K_2SO_4 and 1×10^{-3}M $Al(NO_3)_3$ are the same but the *k* values obtained are 9.43×10^{-3} min.$^{-1}$ and 11.97×10^{-3} min.$^{-1}$

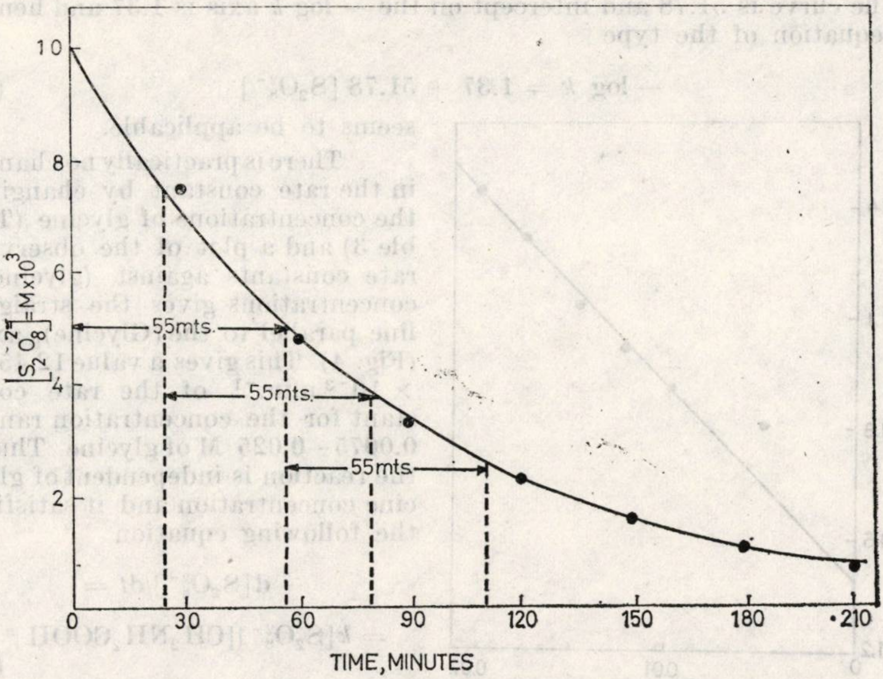

Fig. 2. — Plot of $[S_2O_8^{2-}]_t$ *vs.* time, CH_2NH_2COOH = 0.01 M. Temperature = 45°C.

The relationship between $-\log k$ and $[S_2O_8^{2-}]_0$ is linear (Fig. 3), where k is observed first order rate constant for glycine oxidation and $[S_2O_8^{2-}]_0$ is the initial concentration of peroxydisulphate. The slope

TABLE 4

Effect of neutral salts on reaction rate

$K_2S_2O_8$ = 0.01 M, CH_2NH_2COOH = 0.01 M, temperature = 45°C

Neutral salt	Concentration M × 10^3	Ionic strength contributed × 10^3	Rate Constant $k \times 10^3$ min.$^{-1}$
NH_4NO_3	1.0	1.0	12.41
	2.0	2.0	12.00
	4.0	4.0	11.13
$NaNO_3$	1.0	1.0	12.23
	2.0	2.0	11.98
	4.0	4.0	10.87
K_2SO_4	1.0	3.0	10.01
	2.0	6.0	9.43
	4.0	12.0	8.01
$Al(NO_3)_3$	1.0	6.0	11.97
	2.0	12.0	11.40
	4.0	24.0	10.26

of the curve is 51.78 and intercept on the $-\log k$ axis is 1.37 and hence an equation of the type

$$-\log k = 1.37 + 51.78\,[S_2O_8^{2-}] \tag{1}$$

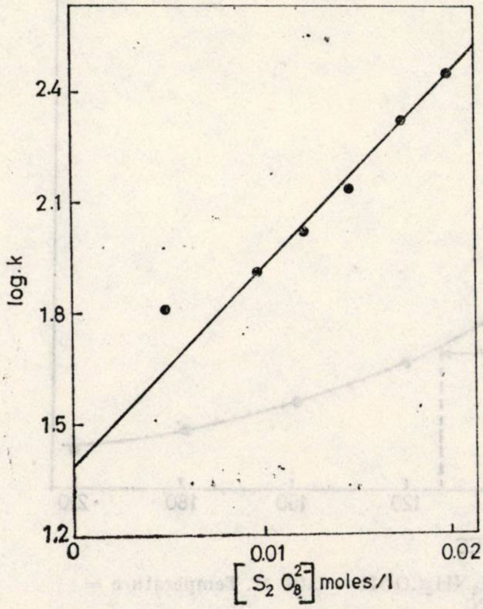

Fig. 3. — Plot of $-\log k$ vs. $[S_2O_8^{2-}]_0$, $CH_2NH_2COOH = 0.01$ M. Temperature = 45°C.

seems to be applicable.

There is practically no change in the rate constant by changing the concentrations of glycine (Table 3) and a plot of the observed rate constants against $(\text{glycine})_0$ concentrations gives the straight line parallel to the $(\text{Glycine})_0$ axis (Fig. 4). This gives a value 12.45×10^{-3} min.$^{-1}$ of the rate constant for the concentration range 0.0075—0.025 M of glycine. Thus, the reaction is independent of glycine concentration and it satisfies the following equation

$$-d[S_2O_8^{2-}]/dt = k[S_2O_8^{2-}][CH_2NH_2COOH]^0 \tag{2}$$

where k is the observed rate constant and is made up of two terms i.e. thermal decomposition of peroxydisulphate alone and the bimolecular reaction between glycine and peroxydisulphate, therefore

$$k = k_1 + k_2 \quad [\text{glycine}]^n \tag{3}$$

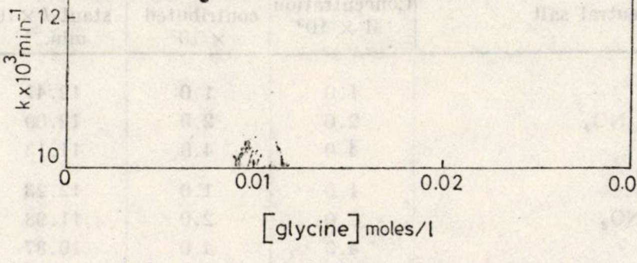

Fig. 4. — Plot of rate constant vs. glycine concentration. $K_2S_2O_8 = 0.01$ M, temperature = 45°C.

Since the order of the reaction with respect to glycine is zero the above equation reduces to

$$k = k_1 + k_2 \tag{4}$$

Introducing this value of k into the rate expression, we obtain

$$-\,\mathrm{d}[S_2O_8^{2-}]/\mathrm{d}t = k_1[S_2O_8^{2-}] + k_2[S_2O_8^{2-}]\quad (\text{glycine})^0 \qquad (5)$$

In the present reaction k_1, the rate constant for thermal decomposition of peroxydisulphate can be neglected as the oxidation of glycine by peroxydisulphate is much faster (the rate constant for thermal decomposition of 0.01 M peroxydisulphate is 0.3593×10^{-3} min.$^{-1}$ at 55°C whereas in the presence of 0.01 M glycine it increases to the value $45.60 \times \times 10^{-3}$ min.$^{-1}$) and, therefore, $k_2 = k$ (observed rate constant). Hence final rate expression can be written as

$$-\,\mathrm{d}[S_2O_8^{2-}]/\mathrm{d}t = k_2[S_2O_8^{2-}]\quad [\text{glycine}]^0 \qquad (6)$$

CALCULATION OF *E*, *A*, AND ΔS

In order to evaluate the frequency factor and the entropy of activation, the energy of activation was calculated from measurements at temperature range 40—55°C with 0.01 M potassium peroxydisulphate and glycine each. The values are given in table 5.

TABLE 5

Activation parameters for glycine — peroxydisulphate reaction $K_2S_2O_8 = 0.01$ M, $CH_2NH_2COOH = 0.01$ M

Temperature	$k \times 10^3$ min.$^{-1}$	Temp. coeff.	E kcal.	$A \times 10^{-14}$ s^{-1}	ΔS e.u.
40	6.62			1.595	6.39
45	12.67	3.61	25.98	1.530	6.28
50	23.91	3.60	26.73	1.550	6.28
55	45.60			1.588	6.29
		Mean	26.35	1.566	6.31

The mean value of frequency factor is 1.6×10^{14} and hence a general expression for the rate constant is given by

$$k = 1.6 \times 10^{14} \exp.\ (-26350/RT) \qquad (7)$$

EFFECT OF INCREASED SURFACE AND ALLYL ACETATE

The rate of the reaction was enhanced by increasing the area/volume ratio by adding glass beads and $BaSO_4$. The rate of the reaction is increased with 3—20% by the added surface. On the other hand a few reactions were studied in the presence of allyl acetate and it was found that the reaction is considerably slowed down. These observations led to the conclusion that the reaction follows a chain path.

EFFECT OF GASES

The gases (N_2, CO_2 and O_2) were bubbled through the reaction mixture at a uniform rate and the first order rate constants were calculated in each case. The results are given in table 6.

TABLE 6

Effects of gases

$K_2S_2O_8 = 0.01$ M, $CH_2NH_2COOH = 0.01$ M, temperature = 45°C

Gas	Air	Nitrogen	Carbon-di-oxide	Oxygen
$k \times 10^{-3}$ min.$^{-1}$	12.67	13.88	13.79	12.59

Nitrogen and carbon dioxide exert an accelerating influence on the velocity of the reaction whereas oxygen affects a little decrease in the rate constant.

IDENTIFICATION OF THE REACTION PRODUCT

The main reaction product, formaldehyde, was not detected in the reaction mixture in the absence of an alkali, probably due to the reason that formaldehyde reacts with ammonia (a byproduct of the reaction). However, in the presence of 0.01 N NaOH the formaldehyde was identified in the reaction mixture by taking 2 ml of it and adding equal volume of chromotropic acid in the test tube. The mixture was heated for ten minutes. A violet colour indicated the presence of formaldehyde. It was further confirmed by preparing 2 : 4 dinitro phenyl hydrazone and determining the melting point which was found to be 165°C (Lit. val. 166°C).

DISCUSSION

The reaction is first order in peroxydisulphate concentration and independent of glycine concentration. This feature is not uncommon in peroxydisulphate since this was reported in connection with the reaction of peroxydisulphate with oxalate, formate and aldehyde substrates. Further on, the chain mechanism should be operative for the reaction as the observation with increased surface area and allyl acetate suggests.

It has been discussed earlier that the thermal decomposition of peroxydisulphate occurs with the progress of the reaction between $S_2O_8^{2-}$ and glycine. This leads to the suggestion of equation (5) for the rate law. The following general plan represents the glycine peroxydisulphate reaction :

glycine + peroxydisulphate ⟨ Path I : Thermal decomposition of $S_2O_8^{2-}$
Path II : Oxidation of glycine

The following chain mechanism has been proposed to account for the observations.

The chain initiation is ascribed to the thermal decomposition of peroxydisulphate ion which undergoes homolytic fission to produce two sulphate radical ions as shown below:

Initiation:

$$S_2O_8^{2-} \xrightarrow{k_1} 2SO_4^{\cdot -} \tag{I}$$

Propagation:

$$SO_4^{\cdot -} + H_2O \xrightarrow{k_2} HSO_4^- + OH\cdot \tag{II}$$

$$CH_2NH_2COO^- + OH\cdot \xrightarrow{k_3} CH_2NH_2COO\cdot + OH^- \tag{III}$$

$$CH_2NH_2COO\cdot \xrightarrow{k_4} \dot{C}H_2NH_2 + CO_2 \tag{IV}$$

$$\dot{C}H_2NH_2 + H_2O + O_2 \xrightarrow{k_5} HCHO + NH_3 + HO_2 \tag{V}$$

$$S_2O_8^{2-} + HO_2 \xrightarrow{k_6} SO_4^{\cdot -} + HSO_4^- + O_2 \tag{VI}$$

Termination:

$$SO_4^{\cdot -} + HO_2 \xrightarrow{k_7} HSO_4^- + O_2 \tag{VII}$$

From the foregoing mechanism the rate law is given by the expression

$$-\,d[S_2O_8^{2-}]/dt = k_1[S_2O_8^{2-}] + k_6[HO_2][S_2O_8^{2-}] \tag{VIII}$$

Applying the steady state assumptions, the following expression was obtained

$$[HO_2] = -k_1/4k_6 \pm \frac{1}{\frac{1}{2}k_6}\left(k_1^2/4 + 4k_1k_2k_6[H_2O]/2k_7\right)^{\frac{1}{2}} \tag{IX}$$

Since the value of $[HO_2]$ cannot be negative, the negative root was not considered.

This value of $[HO_2]$ is fed into the equation (VIII) to get the final rate expression (X)

$$-d[S_2O_8^{2-}]/dt = k_1[S_2O_8^{2-}] + k'k_6[S_2O_8^{2-}] \tag{X}$$

where $k' = -k_1/2 + (k_1^2/4 + 4k_1k_2k_6/2k_7 \times [H_2O])^{\frac{1}{2}}/2k_6$

k_1 = rate constant for thermal decomposition of peroxydisulphate $k'k_6$ = rate constant for bimolecular reaction between glycine and peroxydisulphate.

Therefore, the observed rate constant $k = k_1 + k'k_6$

As it was experimentally found, the reaction is much faster than the thermal decomposition of peroxydisulphate alone, k_1 can be ignored and thus $k = k'k_6$
The rate expression (X) reduces to

$$-\,\mathrm{d}[\mathrm{S_2O_8^{2-}}]/\mathrm{d}t = k'k_6[\mathrm{S_2O_8^{2-}}] \qquad \text{(XI)}$$

The above rate expression explains the observed first order kinetics in peroxydisulphate and increase in the rate of disappearance of peroxydisulphate in the presence of glycine. It also satisfies the observed zero order dependence of reaction rate on glycine concentration. The reaction sequence given by equation (VI) finds support from the observed increase in the rate constant in nitrogen and carbon dioxide environment, because in such an atmosphere the formation of peroxo radical will not take place and the equations (VI) and (VII) will take the form .

$$\mathrm{S_2O_8^{2-}} + \mathrm{H}\cdot \xrightarrow{k_6'} \mathrm{HSO_4^-} + \mathrm{SO_4^{\cdot -}} \qquad \text{(XII)}$$

$$\mathrm{SO_4^{\cdot -}} + \mathrm{H}\cdot \xrightarrow{k_7'} \mathrm{HSO_4^-} \qquad \text{(XIII)}$$

The k_0' and k_7' are different from k_6 and k_7.

ACKNOWLEDGEMENT. Thanks are due to Council of Scientific and Industrial Research, Rafi Marg, New Delhi for the award of a CSIR Senior Research Fellowship to one of the authors (G.C.).

REFERENCES

[1] D. A. House, *Chem. Rev.*, **62**, 185 (1962).
[2] D. M. Yost and W. Claussen, *J. Amer. Chem. Soc.*, **53**, 3349 (1931).
[3] D. M. Yost, *J. Amer. Chem. Soc.*, **48**, 152 (1926).
[4] W. H. Cone, *J. Amer. Chem. Soc.*, **67**, 78 (1945).
[5] E. Bekier and W. Kijowski, *Rocznicki Chem.*, **15**, 136 (1937).
[6] C. V. King, *J. Amer. Chem. Soc.*, **50**, 2080 (1928).
[7] Y. K. Gupta and S. Ghosh, *J. Inorg. Nuclear Chem.*, **11**, 320 (1959).
[8] S. P. Srivastava and S. Ghosh, *Z. phys. Chem.*, **207**, 161 (1957).
[9] S. P. Srivastava and S. Ghosh, *Z. phys. Chem.*, **211**, 148 (1959).
[10] S. P. Srivastava and S. Ghosh, *Z. phys. Chem.*, **205**, 332 (1956).
[11] L. I. Saxena and C. P. Singhal, *Agra Univ. J. Res. (Sci.)*, **6**, 43 (1957).
[12] L. K. Saxena and C. P. Singhal, *Z. phys. Chem.*, **211**, 168 (1959).
[13] K. Kumar and L. K. Saxena, *J. Indian Chem. Soc.*, **47**, 435 (1970).
[14] G. Chandra and S. N. Srivastava, *Bull. Chem. Soc. Japan*, **44**, 3000 (1971).
[15] T. L. Allen, *J. Amer. Chem. Soc.*, **73**, 3589 (1951).
[16] P. D. Bartlett and J. D. Cotman, *J. Amer. Chem. Soc.*, **71**, 1419 (1949).
[17] A. Kailan and L. Olbrich, *Monatsch*, **47**, 449 (1927).
[18] M. C. Agarwal and S. P. Mushran, *Chem. Analit.*, **50**, 310 (1968).

Revue Roumaine de Chimie, 25, 8, 1159–1169 (1980)

STRUCTURAL STRAINS APPEARING IN THE HIGH TEMPERATURE SHIFT CONVERSION Fe–Cr CATALYST

I. BRAȘOVEANU *, S. I. BLEJOIU ** , A. SZABO ***,
P. ROTARU * and I. V. NICOLESCU ***

* — Research Center for Chemical Fertilizers, Craiova, Romania
** — Chemical Works, Craiova, Romania
*** — National Institute of Chemistry, Bucharest, Romania

Received October 19, 1977
Revised June 23, 1979

The modification of the textural properties, mechanical strengths, and of the remanent stresses depending on the tabletting pressure has been investigated. The appearance and the increase of remanent stresses have been related to the data concerning the mechanical strength and the pore structure of the catalyst tablets. From these relations, the limit pressure for tabletting this catalyst has been established.

1. INTRODUCTION

Research workers have studied the way in which the strains induced by different techniques in polycrystalline materials cause modifications in the catalytic activity of these materials for the specific catalytic processes. Thus, plastic deformation of copper and metallic nickel led to the rise of activity of these metals, [1] and the decomposition rate of oxygenated water on the surface of some platinum foils was obviously correlated with the processing by the platinum, cold deformation. [2] The examination, by means of X-ray of the cold processed platinum, showed a significant breadth of the diffraction peaks, but the authors restricted their work to the phenomenon existence only.

In the paper [3] it has been noticed that the compression strength of the tableted catalysts for the high temperature shift conversion depends significantly on the conditions in which the tabletting is made. The low value of the mechanical strength of the industrial tablets is explained by the strong deformation that takes place on the shock pressing, causing the appearance of the stresses in the obtained tablets.

In a more recent paper, [4] the study of the tabletting condition influence on the mechanical strength for the same catalyst is taken back and the appearance of the internal stresses in tablets is pointed out, especially in the case of tabletting high pressures.

Investigation of tabletting pressure influence on the catalytic activity, pore structure, and diffusional properties, also on the mechanical strength of the Fe — Cr shift conversion catalyst tablets has determined the best tabletting pressure.[5]

In the present paper, the induced remanent stresses on tabletting the material studied in ref.[5] have been determined, and the appearance and the rising of the remanent stresses have been correlated with the data concerning mechanical strength and the porous structure of the tablets.

2. EXPERIMENTAL

The used experimental techniques

The apparent densities of the tablets were calculated from the data obtained by weighing on the precision balance and by measuring the sizes with the micrometer.

The true density has been measured by pycnometer and the surface area has been determined by the BET method from the nitrogen adsorption at the liquid nitrogen temperature.

The pores volume measurement has been made by the penetration method of the mercury under pressure, with a Carlo-Erba porosimeter, 70 H type, range 37 500 — 75 000 Å.

The mechanical strengths on axial and radial compressions have been determined on a Wolpert apparatus, ZR 60/300 type.

The thermodifferential and thermogravimetric analyses was accomplished on a 1128 B70 SETARAM type thermobalance.

The rate of the temperature rising was 7° C/min and the speed of sheet, 0.0025 cm/s. The thermall analysis in the 20—800°C range was made.

The phase composition analysis was made by X-Ray diffraction method. For recording was used a PW 1410 Philips diffractometer with vertical goniometer. The tube had a copper anode which has been operated at 24 mA and 40 kV. The radiation was monochromatized by a bent — crystal monochromator situated in the diffracted beam. The exploration speed was 1/8° C(20), and the moving speed of the sheet, 5 mm/min.

The experimental techniques utilised for determination of the remanent stresses cannot be separately treated from the description and the interpretation of the respective phenomena, thus these techniques will be treated later in this paper.

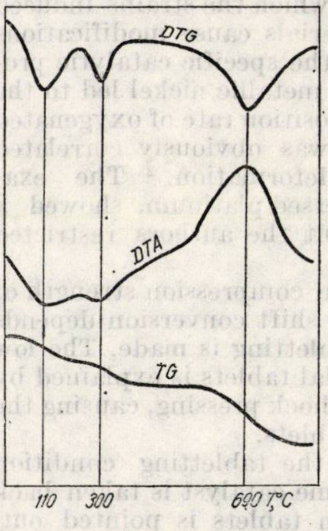

Fig. 1. — The TG, DTA and DTG curves for the material utilized in the determination of remanent stresses.

The description of the material for study

The material used for estimating the remanent stresses was obtained from ferrous sulphate, ammonium carbonate and chromium trioxide, by precipitation filtration, washing, kneading, drying and calcination.[6]

— *Chemical composition* (wt %):

Fe_2O_3	81.50
Cr_2O_3	8.15
Graphite	3.50

— *Thermic analysis.* Material loss weight in the 20 — 800°C range was 10%, graphite contribution being 3.5%.

The TG, DTA and DTG curves are shown in figure 1 and indicate two endothermic effects at 110 and respectively at 300°C and one exothermic effect at 680°C, belonging to graphite burning.

— *Surface area* : 50 m²/g.

— *True density* : 4.35 g/cm³.

— *Qualitative phase analysis.* The diffraction pattern obtained from the studied material contained crystalline phase α-Fe_2O_3 only (Figure 2).

Sample preparation

For tabletting a 20 tf laboratory hydraulic press and the instrument described in figure 3 were used. Cylindric tablets, 13 mm diameter and 0.5 g weight, for 14 tabletting pressures in the 1—14 kbars range were obtained. For each tablet the pressure was maintained for 2 minutes. The rise and the relaxation of the pressure were made gradually.

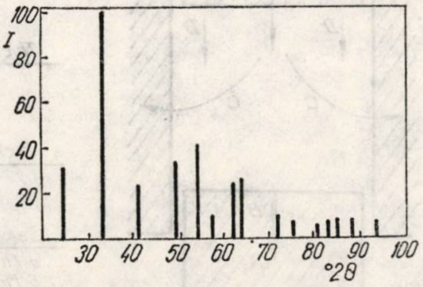

Fig. 2.—Schematical X-ray diffraction pattern for the studied material.

The determination of the remanent stresses induced by tabletting

Remanent stresses present a system of stresses which may occur in a solid when this is not subjected by an external force. They are also named internal residual stresses. Remanent stresses occur whenever a body acquires uneven plastic deformation. [7]

The force system produced by remanent stresses must be in a static equilibrium, that is the total force which acts upon a certain plane from body and in the total moment must be zero. When the force system produced by the remanent stresses goes out of equilibrium, that is when the total force is not zero, the influence of this phenomenon on the mechanical properties of a material appears by an increased dimensional unstability. This is the case of the frequent fracture of catalyst tablets when by tabletting remanent stresses are induced.

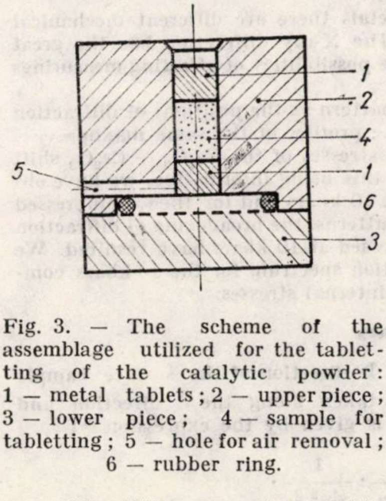

Fig. 3. — The scheme of the assemblage utilized for the tabletting of the catalytic powder: 1 — metal tablets ; 2 — upper piece ; 3 — lower piece ; 4 — sample for tabletting ; 5 — hole for air removal ; 6 — rubber ring.

It is important to distinguish between macrostresses and microstresses. Remanent macrostresses vary continuously in the whole volum of the body and act upon zones of great dimensions comparing with atomic dimensions. Microstresses act on zones containing a few cells, although their effect may include more than one crystallite.

For understanding of the occurring phenomenon of remanent stresses in catalyst tablets, let us study in brief the obtaining principle of tablets in an industrial tabletting press. [8] The tabletting includes the powder compression, thus obtaining adequate bonds between grains to acquire a structure of preestablished form and dimensions. The compression is made with different types of mechanical equipment, which have all, three basic elements : dies, action and reaction punches·

The "C" component of total force "A", transmitted by action punch is absorbed by matrix walls, and the "D" component is canceled by friction effects, therefore the efficient compression force on the powder is the resulting "B" only (Figure 4).

Because of such an inhomogeneous distribution, different density areas appear in the interior of tablet.

The stages of tabletting process may be outlined as in figure 5. [8]

Depending on powder properties, the stage can proceed continuously (elastic deformation and plastic deformation), or discontinuously, because of fracture and breaking of grains. In the first case, therefore, the efficient pressure "B" rises continuously, and in the second, deviations can occur. Internal stresses in catalyst tablets appear in the deformation stage, but only when this is plastic or proceeds with breaking of grains. Owing to the rapidity of proceeding of the tabletting stages, and because of the inhomogeneous force distribution inside the tablets the plastic deformations may be nonuniform, this being a necessary and sufficient condition for internal residual stresses occurring.

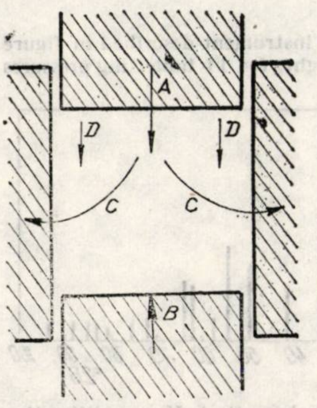

Fig. 4. — Force distribution during tabletting.

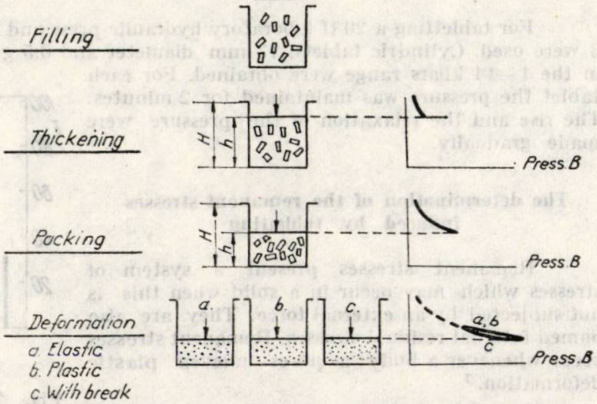

Fig. 5. — Schematic representation of the fundamental phases of tabletting process and of the corresponding behaviour of pressure.

The measurement of the remanent stresses cannot be directly made, but one calculates them using the measurement of remanent deformation.

For determination of the remanent stresses in metals there are different mechanical methods, and also the X-ray diffraction method.[7,9,10] The X-ray diffraction has the great advantage to be a nondestructive method, because of the possibilities of effecting measurings for the stressed material only.

The macrostresses appear in the X-ray diffraction pattern as the positions of diffraction maxima shift, and microstresses determine changes in the profiles of the same maxima.

We have applied this method to estimate remanent stresses of the $Fe_2O_3 - Cr_2O_3$ shift conversion catalyst tablets. Making the first experiment, this being informative, we have obtained the diffraction patterns for the catalyst tableted at 10 kbars and for the uncompressed catalyst. Comparatively examinating the both diffraction patterns, the broadening of diffraction maxima and shift of their positions for the sample compressed at 10 kbars have resulted. We have correlated the modifications appeared in the diffraction spectrum for the 10 kbars compressed catalyst with the existence in tablets of residual internal stresses.

Estimation of macrostresses

Let the stress σ_Φ be desired at point 0 in the Φ direction of the surface sample (Fig. 6).[7,10] It can be obtained from diffraction patterns taken along the Z direction and along the ψ direction. In this case the value of σ_Φ stress is given by the expression[10]:

$$\sigma_\Phi = (2\theta_\perp - 2\theta_\psi) \cdot \frac{\operatorname{ctg}\theta}{2} \cdot \frac{E}{1+\nu} \cdot \frac{1}{\sin^2\psi},$$

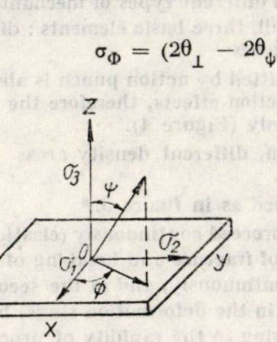

Fig. 6. — Angular relations for determination of the stress component in the Φ direction from the sample surface.

where $2\theta_{\perp}$ is the Bragg angle value for $\psi = 0$ (obtained when the incident X-ray beam is perpendicular to the plane surface of the sample), $2\theta_{\psi}$ is the Bragg angle value for the same crystalline plane *(hkl)*, but obtained in an assemblage in which the incident beam makes an angle ψ with the normal to the plane surface of the sample, E is Young's modulus, and ν, Poisson's constant.

In determination of the remanent macrostresses by this method there is some lack of exactness, because of the Young's modulus E and of the Poisson's constant ν values, that vary appreciably in function of the crystallographic direction. Since the method is based on the measurement of the reduction or elongation of the net in certain crystallographic directions, appears the question if one can use average values for E and ν, experimentally determined or existing in literature. The most research workers who have used X-ray based methods for remanent stress determination have considered that the use of average values for E and ν don't introduce great errors. [7] For this reason, we introduce E, ν, ctg θ and $\sin^2 \psi$ into the constant K, and we will rewrite the previous expression as :

$$\sigma_{\Phi} = K\,(2\theta_{\perp} - 2\theta_{\psi}) = K.\Delta(2\theta)$$

Thus, we will estimate σ_{Φ} in arbitrary units, which can be properly used for determination of the remanant macrostresses appearance and of their evolution during the tabletting pressure increase.

For accurate determination of the diffraction maxima position we have utilised the method of the parabola fitted to three points. [11] In accordance with this method, the position of maxima is obtained by :

$$2\theta_p = x_1 + \frac{c}{2} \cdot \frac{3a + b}{a + b}$$

The data belonging to this expression have the meaning in figure 7.

To ensure a great accuracy for measurements, we utilised CrK$_{\alpha}$ radiation and diffraction maximum (218) for crystalline α-Fe$_2$O$_3$ phase, corresponding to the (2θ) diffraction angle 148.85°. The two assemblage geometries for the same sample (Fig. 8), [10] corresponded to $\psi = 0$ and $\psi = 45°$ angles. For the two assemblage geometries we utilised a special equipment which allows the change of the ψ angle from 0 to 60°. The determinations were made with a PW 1410 Philips diffractometer ; high voltage and anodic tube power were ultrastabilized. For the signal detecting, a proportional counter connected with an analysis system of pulses distribution by extent was used. The diffraction maximum form was determined making measurements at 0.02° (2θ) interval. In the selected positions for maxima determinations by "parabola fitted to three points" method, recordings at 200 000 pulses were made. The operation conditions for the X-ray tube were : high voltage 28 kV, anodic power 20 mA. For the incident beam to enter the samples sizes, a X-ray slit of 1°, and a receiving slit of 1/2° were used. The radiation was monochromatized by a bent-crystal monochromator situated in the diffracted beam.

Estimation of microstrains

For estimation of microstrains occurred in the catalyst tablets during the tabletting operation, we utilized the integral breadth method elaborated by Williamson and Hall. [12]

From the analysed diffraction maxima we have used the component K$_{\alpha_1}$ only, which we have sepparated from observed profiles of the maxima by Rachinger method. [13] The values of the integral breadth were obtained dividing the profile area by its maximum height.

The correction for elimination of the instrument broadening was made with the expression. [12]

$$\beta^* = \beta^*_M - \frac{(\beta_i^M)^2}{\beta^*_M},$$

where β^*_c is the integral breadth, corrected by subtracting the instrument broadening, β^*_i and β^*_M are integral breadths for a standard sample and respectively for studied material sample.

β_i^* and β_M^* have resulted from, expressions :

$$\beta_i^* = \beta_i \frac{\cos\theta}{\lambda}, \quad \beta_M^* = \beta_M \frac{\cos\theta}{\lambda},$$

where β_i and β_M are the integral breadths measured.

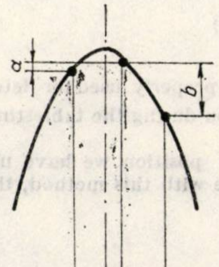

Fig. 7. – The meaning of the quantities a, b, c and x_1 for the determination of diffraction maxima position by "parabola fitted to three points" method.

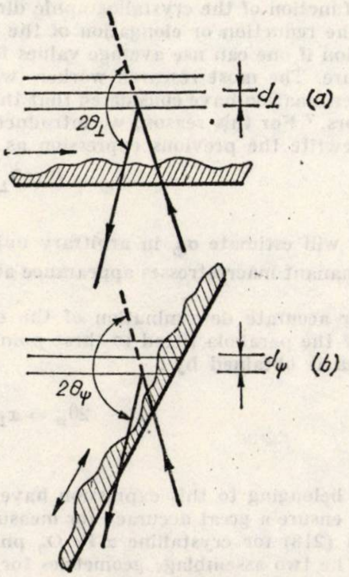

Fig. 8. – The two assemblage geometries of the sample for the incident beam. *a*) The measurement of the parallel planes to the sample surface. *b*) The measurement of the planes which make an angle ψ to the sample surface ; $d_\perp$ – interplanar spacing of planes parallel to sample surface ; d_ψ – interplanar spacing for the same planes, but which make an angle ψ to the sample surface.

The selected standard sample was α-Fe_2O_3 calcined for 40 hours at 900°C, which has given a diffraction pattern with very narrow maxima.

In accordance with Williamson and Hall's method,[12] the contribution of the crystallite sizes and of the microstrains to the integral breadth β_c^*, may be separated using the expression :

$$\beta_c^* = \frac{1}{D} + 2\varepsilon \frac{2\sin\theta}{\lambda},$$

where D is the crystallite size, and ε, microstrains. Representing graphically the straight lines $\beta_c^* = f\left(\frac{2\sin\theta}{\lambda}\right)$ for two different orders of one reflection, the slopes of the straight lines give the 2ε values, out of which results ε, microstrains, and the cuttings on the *y* axis give the 1/D values, wherefrom we can calculate the average sizes of the crystallites (Figures 9–12).

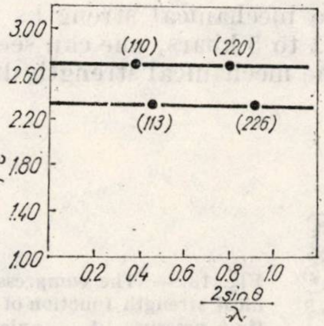

Fig. 9. — Graphic representation of the function $\beta_c^* = f\left(\frac{2\sin\theta}{\lambda}\right)$ for the tabletting pressure 1 kbars.

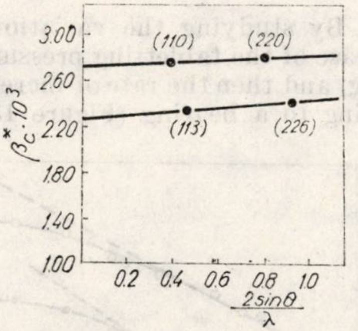

Fig. 10. — Graphic representation of the function $\beta_c^* = f\left(\frac{2\sin\theta}{\lambda}\right)$ for the tabletting pressure 7 kbars.

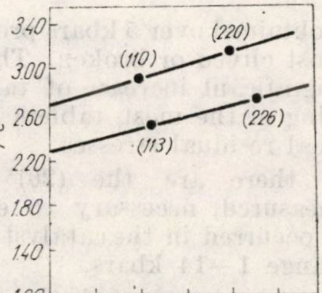

Fig. 11. — Graphic representation of the function $\beta_c^* = f\left(\frac{2\sin\theta}{\lambda}\right)$ for the tabletting pressure 10 kbars.

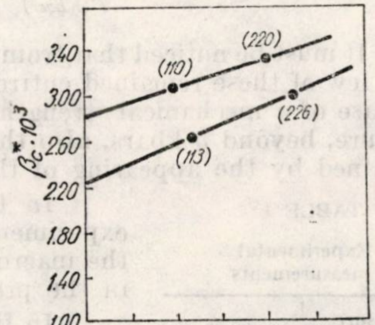

Fig. 12. — Graphic representation of the function $\beta_c^* = f\left(\frac{2\sin\theta}{\lambda}\right)$ for the tabletting pressure 12 kbars.

To determine these quantities we have utilized the pairs of reflections (110) — (220) and (113) — (226). The indexation was made in the hexagonal system, and therefore we can apply the Warren theory,[14] which shows that the reflection breadth for which $h - k = 3N$ (N being 0, 1, 2, 3) is not changed by packing defects, therefore the last expression gives crystallite sizes and microstrains.

Selected diffraction maxima for the determination of microstrains were obtained with the same X-ray apparatus as for macrostresses determination, but CuK$_\alpha$ radiation was used. The high voltage was 40 kV, and anodic power 24 mA, X-ray slit 1°, and receiving slit 1/4°. The exploration of the maxima (110) — (220) and (113) — (226) was made accumulating an exact number of pulses (10 000), thus being assured a statistical error of 1 % for the counting rate for the entire profile of the maxima. From these data the integral intensities, maxima heights were obtained and from their ratios the integral breadths.

3. RESULTS AND COMMENTS

By studying the variations of the mechanical strengths with the increase of the tabletting pressure from 1 to 5 kbars, one can see a linear rising, and then the rate of increase of the mechanical strength diminishes tending to a bearing (Figure 13).

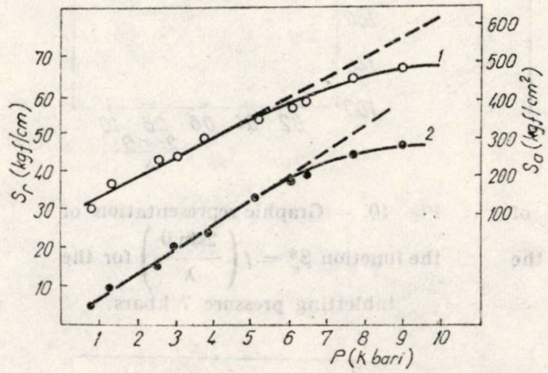

Fig. 13. — The compression mechanical strength function of the tabletting pressure 1 — axial compression mechanical strength, 2 — radial compression strengths.

It must be noticed that from tablets obtained over 5 kbars pressures, very few of these remained entire, the most clived or broken. The small increase of a mechanical strength for a significant increase of tabletting pressure, beyond 5 kbars, also the breaking of the most tablets may be explained by the appearing of the internal residual stresses.

TABLE 1

Experimental measurements

Pressure (kbars)	2θ(°)
1	+0.011
2	+0.013
3	−0.015
4	+0.012
5	−0.02
6	+0.012
7	−0.018
8	−0.028
9	−0.035
10	−0.034
11	−0.045
12	−0.054
13	−0.072
14	−0.069

In table 1 there are the (2θ)° shifts, experimentally measured, necessary to evaluate the macrostresses occurred in the catalyst tablets, in the pressure range 1—14 kbars.

In figure 14 were represented the macrostresses (expressed in arbitrary σ units), *versus* applied pressure. Examining figure 14 one can observe that the macrostresses have a low value in all range 1—5 kbars.

The pressure of 5 kbars marks a sudden increase of macrostresses, this increase continues to 14 kbars, the limit of study pressures. In the 6—14 kbars range, the increase of the macrostresses is linear.

In table 2 there are listed microstrain values, calculated for the reflexions (110) and (113), for four values of the tabletting pressure. One can see that at 7 kbars the microstrains have measurable values and they increase with the increase of the tabletting pressure.

TABLE 2

Microstrains values

Pressure (kbars)	$\varepsilon_{(110)} \cdot 10^{-3}$	$\varepsilon_{(113)} \cdot 10^{-3}$
1	0	0
7	0.04	0.07
10	0.32	0.28
12	0.34	0.44

The appearance of the remanent stresses coincides with the change of the pore structure in the micropores and of the average radius pores range, that is the relative contribution of average radius pores decreases, and, in the same manner, the contribution of the micropores increases (Figure 15).

The appearance of the remanent stresses coincides, also, with changes in the variation rate of the apparent densities, of the total pore volume and of the average pore radius, the variation of those quantities tending to a bearing when the tabletting pressure exceeds 6 kbars (Figure 16).

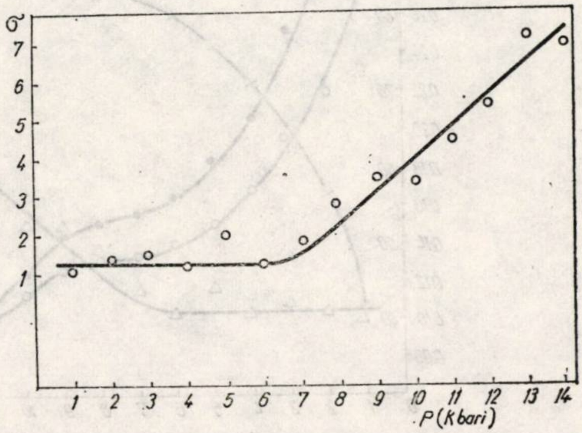

Fig. 14. — The function of the remanent macrostresses (expressed in arbitrary σ units) of the tabletting applied pressure.

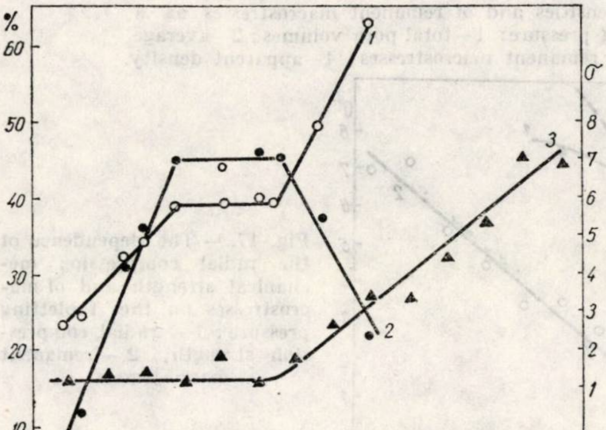

Fig. 15. — The variations of the relative contributions of the pores with 37—100 Å (1) and 100—200 Å (2) radius and of the macrostresses (3), as a function of the tabletting pressure.

Mechanical strengths increase linearly to 6 kbars, pressure which marks the sudden increase of remanent stresses, then the increase rate of the mechanical strengths decreases, tending to a bearing (Figure 17).

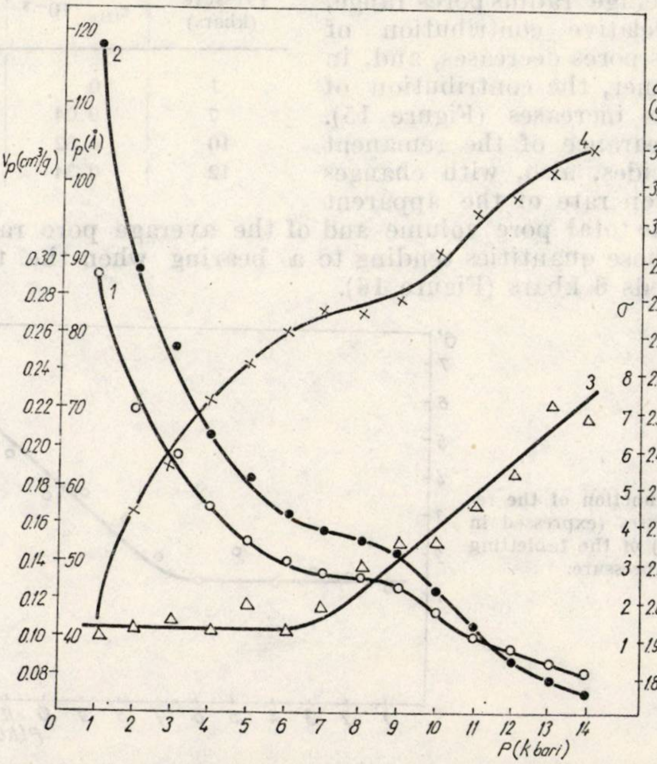

Fig. 16. — The variations of pore volumes, of average radius of pores, of apparent densities and of remanent macrostresses as a function of tabletting pressure: 1—total pore volumes; 2—average radius of pores; 3 — remanent macrostresses; 4—apparent density.

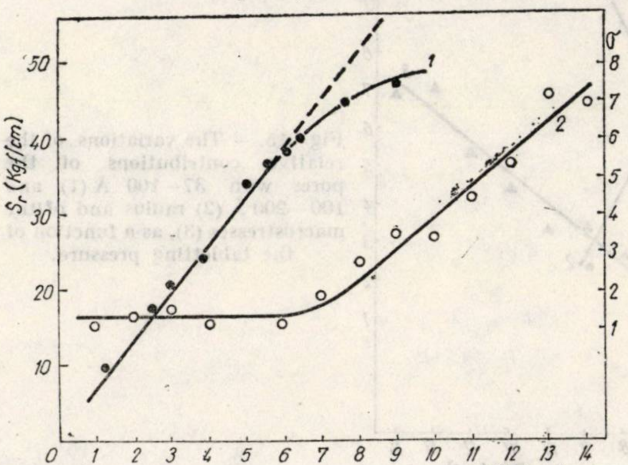

Fig. 17. — The dependence of the radial compression mechanical strength and of macrostresses on the tabletting pressure: 1 — radial compression strength, 2 — remanent macrostresses.

4. CONCLUSIONS

Analysing the change of the textural properties, mechanical strengths and remanent stresses as a function of the tabletting pressure, it was established that the upper limit pressure on tabletting of the $Fe_2O_3 - Cr_2O_3$ shift conversion catalyst is 5 kbars. The best tabletting pressure was previously established, 3 kbars, analysing also the diffusional properties and the catalytic activity of this catalyst. [5]

REFERENCES

[1] I. Uhara, S. Kishimoto, T. Hikino, Y. Kageyama, H. Haonada and Y. Nuonata, *J. Phys. Chem.*, **67**, 996 (1963).

[2] K. B. Keating, A. G. Rozner and J. L. Youngblood, *J. Catal.*, **4**, 608 (1965).

[3] E. L. Furen, D. V. Gernet and T. A. Semenova, *Khim. Prom.*, **4**, 285 (1972).

[4] E. L. Furen, D. V. Gernet and T. A. Semenova, *Katal. Katal.* **13**, 107 (1975).

[5] S. I. Blejoiu, A. Szabo, P. Rotaru, I. Brașoveanu and I. V. Nicolescu, *Rev. Chim. (București)*, **29**, 933 (1978).

[6] Brevet Romania, 60169 (1976).

[7] G. E. Dieter, "Metalurgie mecanică", Ed. Tehnică, București, 1970.

[8] F. Traina and N. Pernicone, "Catalysis Symposium", Milan, 1969.

[9] H. P. Klug and L. D. Alexander "X-Ray Diffraction Procedures", Wiley, New York, 1966.

[10] D. P. Koistinen, E. R. Marburger and M. Semchyshen, SAE Technical Report TR-182, "The Measurement of Stress by X-Ray", SAE Inc., New York, 1960.

[11] A. L. Christenson, D. P. Koistinen, R. E. Marburger, M. Semchyshen and W. P. Ewans, "The Measurement of Stress by X-Ray", SAE Handbook Supplement, SAE Inc., New York, 1960.

[12] G. K. Williamson and W. H. Hall, *Acta Met.*, **1**, 22 (1953).

[13] W. A. Rachinger, *J. Sci. Instr.*, **25**, 254 (1948).

[14] B. E. Waren, "X-Ray Diffraction", Addison-Wesley, Massachussetts, 1969.

Revue Roumaine de Chimie 25, 8, 1171–1175 (1980)

KINETIC DATA ON THE FORMATION AND THERMAL DECOMPOSITION OF THE [Pd (p-ON$-C_6H_4-N(CH_3)_2)_2$ Cl_2]$\cdot H_2O$ COMPLEX

N. CALU, N. FOCA and M. LUCHIAN

Department of Inorganic Chemistry, Polytechnical Institute,
Iassy, Splai Bahlui 71, Romania

Received February 22, 1977
Revised January 24, 1980

The formation reaction of the [Pd (p-ON-$C_6H_4-N(CH_3)_2)_2Cl_2$]. H_2O complex, performed in 90% ethanol at the temperature of 23°C, has an overall second order kinetics with the rate constant of 33.6 l. mol^{-1}. s^{-1} and an activation energy of 21.4 kcal mol^{-1}. The thermal decomposition of this complex under heating rate of 12.4°C/min exhibits several distinct stages. During the first stage (~100°C), a mole of water is removed for each mole of complex ; during the second stage (190°C) the decomposition develops explosively, going on the third stage when the rest bonded by palladium, is released. Kinetical parameters of the third decomposition stage of the complex are $n=0$ and $E=52$ kcal. mol^{-1} for the heating rate 2.4C°/min.

In the $PdCl_2$-p-nitrosodimethylaniline system, having the molar ratio equal to 1 : 2, [Pd (p-ON-($C_6H_4 - N(CH_3)_2Cl_2$] $\cdot H_2O$* complex occurs.[1,2]

At room temperature, during a time of the order of tens of minutes, the formation of this complex takes place. At its end in the solution ~ 1.10^{-4} M, the complex mentioned above crystallizes.

Further on, some data concerning the overall kinetics of the reaction in the $PdCl_2$-p-nitrosodimethylaniline system as well as the thermal decomposition of PdL_2Cl_2 complex are reported.

EXPERIMENTAL

The whole kinetics of the reaction between $PdCl_2$ and p-nitrosodimethylaniline, in 90% ethylic alcohol medium, was investigated spectrophotometrically. The reaction order was established using the differential method. The complex PdL_2Cl_2 was separated from solution by both crystallization and extraction with benzene, chloroform or carbontetrachloride. Its elementary analysis was in good agreement with the respective chemical formula.

The thermal analysis of the complex, PdL_2Cl_2, was carried out on a Paulik-Paulik-Erdey, MOM-Budapest derivatograph, under heating rate of 12.4°C/ min and 2.4°C/ min.

Powder of α-Al_2O_3 preliminary calcinated at 1000°C for several hours, was used as reference inert material. The same material was used as support for analysing sample degradation.

*** Further on, this complex is symbolized as PdL_2Cl_2.**

RESULTS AND DISCUSSION

a. General kinetics of the reaction in the $PdCl_2$—p-nitrosodimethylaniline system

General kinetics of the reaction between $PdCl_2$ and *p*-nitrosodimethylaniline with the molar ratio equal to 1 : 2 has been studied on the basis of absorption bands with their λ_{max} equal to 222 and 276 nm proper to this system.[2]

The concentration of reactants and product at any instant has been computed using Beer-Lambert's law in the form:

$$A = d \sum C_i \cdot \varepsilon_i$$

where, A is the solution absorbance, d is the thickness of sample layer and ε_i is the molar absorption coefficient of "i" species having the concentration $C_i \cdot A$ and ε_i refer to a given wavelength.

The estimating equations have been established according to the following observation:

The overall reaction can be writen as follows:

$$PdCl_2 + 2L \rightleftharpoons PdL_2Cl_2$$

1. At the beginning of the reaction:**

$$A_{Pd(II)+L} = A_{Pd(II)} + A_L = d \cdot C_{Pd(II)} \, (\varepsilon_{Pd(II)} + 2\varepsilon_L) \, ;$$

where $C_{Pd(II)} = 1.10^{-4}M$.

2. At the end of the reaction:

$$A_C = dC_C \cdot \varepsilon_C \, ; \quad \text{where} \quad C_C = 1.10^{-4}\,M$$

3. At any instant of the reaction:

$$A_{Pd(II)+L+C} = x.d.C_{Pd(II)} \, (\varepsilon_{Pd(II)} + 2\varepsilon_L) + y.d.C_C \, \varepsilon_C$$

For the two wavelengths, 222 and 276 nm, the following equations come out:

$$A'/d = x \cdot C_{Pd(II)} \, (\varepsilon'_{Pd(II)} + 2\varepsilon'_L) + y \cdot C_C \cdot \varepsilon'_C$$

$$A''/d = x \cdot C_{Pd(II)} \, (\varepsilon''_{Pd(II)} + 2\varepsilon''_L + y \cdot C_C \cdot \varepsilon''_C$$

The obtained kinetic parameters are listed in table 1. They are reproduced up to a conversion degree of. 0.74.

TABLE 1

The data regarding the entire kinetics of the reaction in the $PdCl_2$—*p*-nitrosodimethylaniline (1 : 2) system

Temperature °C	The reaction order	Reaction constant rate l. mol $^{-1}$. s $^{-1}$	Activation energy kcal. mol $^{-1}$	Preexponential factor
16		8.804		
23	II	33.656	21.378	$22.131.10^{17}$
26		36.566		
34		86.634		

** The indexes Pd (II), L and C attached to absorbance A, molar coefficient and concentration C represent $PdCl_2$, *p*-nitrosodimethylaniline and the complex formed reaction, respectively.

b. Derivatographical analysis

From the thermograms recorded in the air, represented in figures 1 and 2, it has been found out that the thermal decomposition reaction under heating rate of 12.4°C/min. takes place in four distinct stages within the temperature range of 200—525°C, while under heating rate of 2.4°C/min., within the same temperature range, the decomposition develops in three steps among which a stability interval is recorded.

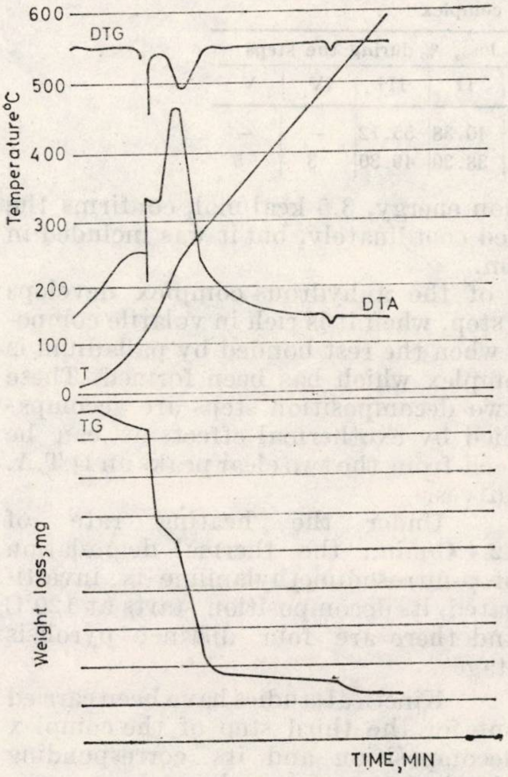

Fig. 1. — Thermogram of $PdL_2Cl_2 . H_2O$ complex in the air ; heating rate = 12.4°/min.

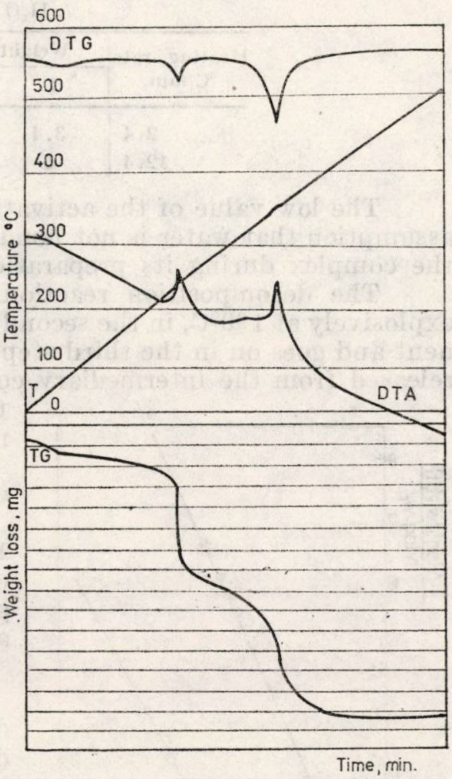

Fig. 2. — Thermogram of $PdL_2Cl_2 . H_2O$ complex in the air ; heating rate = 2.4°/min.

Since within the temperature range mentioned above, there are not occurring all decomposition steps, we conclude that the decomposition mechanisms are different [3]. The residue from thermal decomposition of the complex being palladium, there is a good agreement between its value established theoretically (21.5%) and experimentally (21%).

The thermogravimetrical data for each step of degradation of the complex are listed in table 2.

In the first step the removal of one molecule of water takes place ; it starts in the low temperature range, under 100°C, and is accompanied by a weight loss of several percents.

The water removal takes place prior to the real decomposition as can be seen from the steep beginning of the "S" shape T.G. curve, which corresponds to the start of the D.T.G. and D.T.A. curves too.

TABLE 2

The thermogravimetrical data concerning the $PdL_2Cl_2 \cdot H_2O$ complex

Heating rate °C/min.	Weight loss, % during the steps				
	I	II	III	IV	V
2.4	3.4	40.38	55.12	—	—
12.4	5	38.30	49.30	3	5

The low value of the activation energy, 3.5 kcal/mol, confirms the assumption that water is not bonded coordinately, but it was included in the complex during its preparation.

The decomposition reaction of the anhydrous complex develops explosively at 190°C, in the second step, when it is rich in volatile component and goes on in the third step when the rest bonded by palladium is released from the intermediary complex which has been formed. These two decomposition steps are accompanied by exothermal effects as can be seen from the two clear peaks on D.T.A. curves.

Under the heating rate of 12.4°C/min., the thermal degradation of *p*-nitrosodimethylaniline is investigated, its decomposition starts at 120°C and there are four distinct pyrolisis stages.

Kinetical studies have been carried out for the third step of the complex decomposition and its corresponding kinetical parameters have been estimated using Freeman-Carroll's procedure. [4] Their values are summarized in table 3.

TABLE 3

The kinetical parameters of the $PdL_2Cl_2 \cdot H_2O$ complex decomposition on the third step

Heating rate, °C/min.	n	E, kcal/mol
2.4	0	52.0

In figure 3 Freeman-Carroll's straight lines of the two different heating shifts for the third decomposition step are represented.

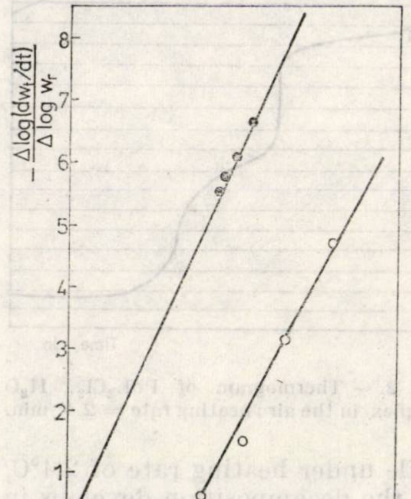

Fig. 3. — Freeman — Carroll plot for $PdL_2Cl_2 \cdot H_2O$; heating rate : ● — 2.4°C/min. o — 12.4°C/min.

This decomposition step under low heating rate, takes place in diffusional regime (n=O). On the basis of both analytical data and IR spectra of each decomposition step, recorded in solid state, for thermal decomposition of complex under heating rate of 2.4°/min., the following scheme can be admitted :

$$PdL_2Cl_2H_2O \xrightarrow{-H_2O} \ldots PdL_2Cl_2 \xrightarrow[-2/3L]{} \ldots PdL1/3Cl_2 \xrightarrow[-1/3L]{-Cl_2} \ldots Pd$$

These investigations pointed out that the decomposition reaction is a complex process with the formation of certain intermediates. [5]

REFERENCES

[1] N. Calu and N. Foca, *Bul. Inst. Politehnic Iași.*, **XXV (XXIX)**, *1–2, SII*, 9(1979).
[2] N. Calu, N. Foca and M. Luchian, *Rev. Roumaine Chim.*, **23**, 551 (1977).
[3] N. Hurduc, L. Odochian and I. A. Schneider, *J. Thermal Analysis*, **6**, 17 (1974).
[4] E. S. Freeman and B. Carroll, *J. Phys Chem.*, **62**, 394 (1958).
[5] I. G. Murgulescu, E. Segal and D. Fătu, *Rev. Roumaine Chim.*, **11**, 291 (1966).

Revue Roumaine de Chimie 25, 8, 1177–1185 (1980)

INVESTIGATION OF LEAD (II) COMPLEXES. III.[1]

SIMPLE AND MIXED COMPLEXES OF LEAD(II) WITH SOME ANIONS OF ALIPHATIC ACIDS IN AQUEOUS SOLUTION

EWA KULIG, DANUTA CZAKIS – SULIKOWSKA * and
RYSZARD WOJTAŠ

Department of Technical Chemistry, Polytechnical University,
25–314 Kielce, Poland

* Institute of General Chemistry, Polytechnical University, 90–924 Łódź, Poland

Received November 7, 1978

Formation of complexes of the PbL and PbL_2 type where $L = CH_2ClCOO^-$, CH_2BrCOO^-, CH_2JCOO^-, $CH_2 = CHCOO^-$, $^-OCO-CH_2-CHOH-COO^-$, $Pb(CHOH)_2\ (COO)_2$ was studied by the potentiometric method. The processes of mixed complexes formation : PbOxL type ($L = CH_2ClCOO^-$, CH_2BrCOO^-, $Ox = C_2O_4^{--}$) and PbJ_2L ($L = CH_2OHCOO^-$, $CH_3CH_2COO^-$, $CH_3CHOHCOO^-$) were investigated by the solubility method. Stability constants of those complexes in aqueous solutions were determined.

INTRODUCTION

Lead (II) shows a great tendency to form complexes with anions of aliphatic acids. Formation of simple lead (II) complexes having the general formula PbL_n ($n = 1-3$) was studied with the anions : formate, acetate and butyrate[2]; propionate [2,3]; glycolate and lactate [4]; β-hydroxybutyrate [5]; malonate and succinate [6]; maleate [7]; malate [8] and tartrate.[9]

Mixed complexes of lead (II), of PbOxL type, are also described, with anions : formate and acetate [10]; lactate [11]; propionate, malonate, succinate, malate and tartrate [12]; glycolate, acrylate, butyrate, β-hydroxybutyrate and maleate. [1]

The aim of the investigation was to determine the composition and stability constants of the simple complexes of the PbL_n type ($L = CH_2ClCOO^-$, CH_2BrCOO^-, CH_2JCOO^-, $CH_2 = CHCOO^-$, $^-OCO\text{-}CH_2 - CHOH - COO^-(CHOH)_2\ (COO)_2^{--}$) and of the mixed complexes of the PbOxL type ($L = CH_2ClCOO^-$, CH_2BrCOO^-; $Ox = C_2O_4^{--}$) and PbJ_2L type ($L = CH_2OHCOO^-$, $CH_3CH_2COO^-$, $CH_3CHOHCOO^-$). The influence of the ligand basicity and some substituents (Cl, Br, J, OH) in the chain of aliphatic acid on the stability of complexes being formed in the aqueous solution was considered.

EXPERIMENTAL

Reagents and investigation method

Reagents : $Pb(NO_3)_2$, $H_2C_2O_4$, NaOH, $CH_2ClCOOH$, $CH_2BrCOOH$, $(CHOH)_2\ (COONa)_2$, Hg, PbJ_2, Pb — p.p.a. — POCh Gliwice, $HClO_4$ — AnalaR England, $CH_2OHCOONa$, $CH_3CHOHCOONa$, CH_2JCOOH — FLUKA AG, CH_3CH_2COOH — REACHIM USSR, $CH_2CHOH(COOH)_2$ — KOCH-LIGHT England, $CH_2{=}CHCOOH$ — UCB Belgium. Propionic acid was purified through distillation. Ligands in the solid state were purified through crystallization from bidistilled water. Lead oxalate was obtained in a way already described. [13] Solution of $Pb(ClO_4)_2$ was prepared by diluting lead carbonate in a definite quantity of 12 m $HClO_4$. The lead (II) content in such solution was determined by titration with a sodium versenate against eriochromic black. [13] Initial solutions $CH_2OHCOONa$, $CH_3CHOHCOONa$, $(CHOH)_2\ (COONa)_2$ were acidified by perchloric acid up to $pH \approx 4.5$, whereas solutions $CH_2ClCOONa$, $CH_2BrCOONa$, $CH_2JCOONa$, CH_3CH_2COONa, $CH_2{=}CHCOONa$, $CH_2CHOH\ (COONa)_2$ were prepared from respective acids (their concentration being known) by neutralization with sodium hydroxide up to $pH \approx 4.5$ and by dilution with water till a definite volume was reached. Concentrations of the above-mentioned solutions were determined alkalimetrically. [14] All measurements were made in a solution with constant ionic strength $\mu = 2.1\ (NaClO_4)$ at temperature 20°C ± 1°C at $pH \approx 4.5$. Only the system $Pb(ClO_4)_2 - (CHOH)_2\,(COONa)_2 - H_2O$ was investigated at temperature 30 °C ± 1°C.

Potentiometric method. The process of simple complex formation was investigated by the potentiometric method. For this purpose electromotive force of the cell was measured :

$$\begin{array}{l|l|c|l|l} & 3 \times 10^{-3}\ \dfrac{m}{dm^3}\ Pb^{2+}(c^0_{Pb^{2+}}) & & 2.0\,\dfrac{m}{dm^3}\ NaClO_4 & \text{saturated} \\ Pb/\,Hg/ & x\,\dfrac{m}{dm^3}\ NaL\ (Na_2L) & 2.1\,\dfrac{m}{dm^3}\ NaClO_4 & 0.1\,\dfrac{m}{dm^3}\ NaCl & \text{calomel} \\ & (2.1 - x(3x) - 3c^0_{Pb^{2+}})\ \dfrac{m}{dm^3}\ NaClO_4 & & & \text{electrode} \end{array} \tag{1}$$

SEM measurements of the cell were performed in the direct current compensator KM 145 with the use of a mirror galvanometer. Lead (II) amalgam saturated in the nitrogen atmosphere was used as the indicator electrode. [15] The reference electrode was a calomel one. Potentiometric measurements were performed in the range of ligand concentrations $0.03 - 0.44\ m/dm^3$. Oxygen — free atmosphere was maintained by passing dry and oxygen-free nitrogen through the investigated systems. The concentrations of hydrogen ions in the equilibrium state was measured by an N—512 type pH-meter. The function of complexation $\varphi = \dfrac{c^0_{Pb^{2+}}}{[Pb^{2+}]}$ was determined from the measurements of the electromotive force by means of the following dependence

$$\triangle E = \frac{RT}{nF} \ln \frac{c^0_{Pb^{2+}}}{[Pb^{2+}]} \tag{2}$$

Hence :

$$\log \varphi = 0.0344\ \triangle E \qquad \text{(at. temp. 20°C)} \tag{3}$$

$$\log \varphi = 0.0332\ \triangle E \qquad \text{(at temp. 30°C)} \tag{4}$$

The composition of the forming complexes was determined by plotting a dependence between $\log \dfrac{[PbL_n]}{[Pb^{2+}]}$ and the equilibrium concentration of ligand. [16,17] The slopes of the respective straight lines correspond with the number of ligand molecules included in the composition of the complex. The concentration of lead ions in the equilibrium state was determined from the dependence $\varphi = \frac{c^0_{Pb^{2+}}}{[Pb^{2+}]}$; and the concentration of the complex PbL_n — from the equation

$$c^0_{Pb^{++}} = [PbL_n] + [Pb^{2+}] \tag{5}$$

The equilibrium concentration of ligand [L] for uni- and bivalent anions was calculated from the following formulae, respectively:

$$[L] = \frac{K/c_0 - n\,[PbL_n]/}{K + [H^+]} \tag{6}$$

$$[L] = \frac{K_1 K_2/c_0 - n[PbL_n]/}{K_1 K_2 + K_1[H^+] + [H^+]^2} \tag{7}$$

where: c_0 — initial concentration of ligand; $[H^+]$ — concentration of hydrogen ions in the equilibrium state; in the first approximation it was assumed $n = 1$. Dissociation constants K, K_1 and K_2 for acids: $CH_2CLCOOH$ $K = 1.40 \times 10^{-3}$, $CH_2BrCOOH$ $K = 1.26 \times 10^{-3}$, CH_2JCOOH $K = 6.70 \times 10^{-4}$, $CH_2{=}CHCOOH$ $K = 5.53 \times 10^{-5}$, $CH_2CHOH(COOH)_2$ $K_1 = 3.90 \times 10^{-4}$, $K_2 = 7.80 \times 10^{-6}$, $(CHOH)_2\ (COOH)_2$ $K_1 = 1.04 \times 10^{-3}$, $K_2 = 4.56 \times 10^{-5}$.[18] Stability constants of the forming complexes, PbL_n type were determined by the Leden method by means of the equation[19]

$$\varphi = \frac{c^0_{Pb^{++}}}{[Pb^{++}]} = 1 + \beta_1[L] + \beta_2[L]^2 + \ldots + \beta_n[L]^n \tag{8}$$

Solubility method. It was found that oxalate insoluble in water, and lead iodide likewise, dissolve in aqueous solutions of the investigated ligands. Therefore, the solubility method was employed in the investigation of mixed complexes, PbOxL type ($L = CH_2ClCOO^-$, CH_2BrCOO^-) and PbJ_2L type ($L = CH_2OHCOO^-$, $CH_3CH_2COO^-$, $CH_3CHOHCOO^-$). The solubility measurements were performed in the range of ligand concentrations 0.1 — 1.0 m/dm^3 in the case of PbOx and in the range of ligand concentration 0.15 — 1.5 m/dm^3 for PbJ_2. The investigation technique by the solubility method was described in the previous paper.[12] The Pb (II) concentration in saturated solutions was determined by the complexometric method.[13] It was found that anions of the investigated organic acids do not interfere with determination of lead (II) by the complexometric method. From the solubility of PbOx in aqueous solution of NaL stability, constants of mixed complexes were determined by means of Leden equation[19]

$$\psi = \frac{S}{I_r} = \beta_1 + \beta_{2m}[L] + \ldots + \beta_{nm}[L]^{n=1} \tag{9}$$

where: β_1; β_{2m}; β_{nm} — stability constants of complexes PbOx, PbOxL, $PbOxL_{n-1}$ ($L = CH_2ClCOO^-$, CH_2BrCOO^-), S — solubility of PbOx in the solutions of NaL in m/dm^3, $I_r = 8.3 \times 10^{-12}$ — solubility ratio of PbOx.[20] For systems $PbJ_{2(so)}$ — $NaL(Na_2L)$ — H_2O Leden function can be expressed by the formula:

$$\psi = \frac{S}{I_r} = A + {}_{3m}[L] + \beta_{4m}[L]^2 \tag{10}$$

where:

S — solubility of PbJ_2 in the solutions of respective ligands

I_r — 1.05×10^{-9} — solubility ratio of PbJ_2[21]

A — value qualifying the participation of complexes PbJ^+, PbJ_2, PbJ_3^- in Leden function[22]

β_{3m}, β_{4m} — stability constants of PbJ_2L, PbJ_2L_2 complexes

Equilibrium concentrations of ligands were calculated from equations (6) or (7) assuming: $[PbL_n] = S$; $n=1$ and for $CH_2OHCOOH$ − $K = 1.48\times10^{-4}$, CH_3CH_2COOH − $K=1.34\times10^{-5}$, $CH_3CHOHCOOH$ − $K = 1.37 \times 10^{-4}$.

RESULTS AND DISCUSSION

Complexes of lead (II) of the PbL_n type

On the basis of the results of potentiometric measurements the composition and stability constants of forming complexes of lead (II) have been determined in the systems: $Pb(ClO_4)_2 - NaL(Na_2L) - H_2O$. The composition of the complexes has been determined graphically from the plot of the dependence $\log \dfrac{[PbL_n]}{[Pb^{++}]} = f/\log\,[L]/$.

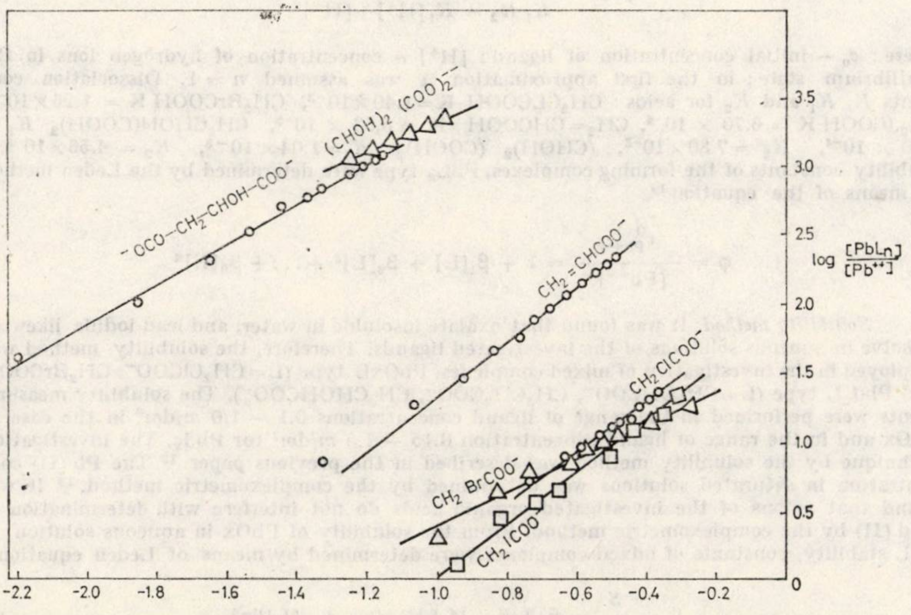

Fig. 1. — Determination of the composition of complexes being formed in the systems: $Pb(ClO_4)_2 - NaL(Na_2L) - H_2O$

The values of tangents of the slope of straight lines (CH_2ClCOO^- — tgα ≈ 1.7; CH_2BrCOO^- — tgα ≈ 1.25; CH_2JCOO^-—tgα ≈ 1.8; $CH_2{=}CHCOO^-$ — tg α ≈ 2.0; $^-OCO-CH_2-CHOH-COO^-$ tg α ≈ 1.42; $(CHOH)_2(COO)_2^{--}$ — tgα ≈ 1.0) indicate the formation of compounds of PbL and PbL_2 types in the investigated range of ligand concentration. The values of stability constants of the complexes have been determined from the dependence (8) by the graphic and numeric method. The calculation was performed in the electronic digital computer ODRA 1325 by the method of least squares. For example, the course of the Leden function for one of the investigated systems is shown in figure 2.

The obtained values of the stability constants of the complexes PbL and PbL_2 are presented in Table 1.

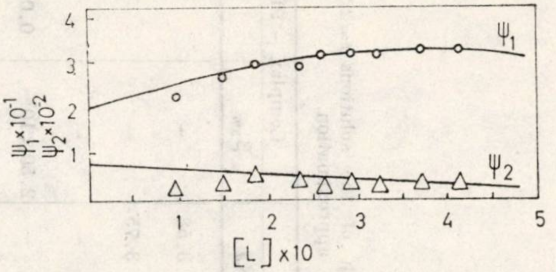

Fig. 2. — A plot of Leden function for the system: $Pb(ClO_4)_2 - CH_2BrCOONa - H_2O$

Curves: $\psi_1 = \frac{\varphi - 1}{[CH_2BrCOO^-]}$; $\psi_2 = \frac{\psi_1 - \beta_1}{[CH_2BrCOO^-]}$

Mixed complexes of lead (II) of the PbOxL and PbJ_2L type

Stability constants of simple complexes PbOx and PbJ_2 are markedly greater in comparison to the stability of simple complexes of lead (II) with the investigated ligands ($\beta_{PbOx,\ PbJ_2} > \beta_{PbL_2}$). [21] Therefore, it may be assumed that in the studied systems addition reactions occur according to the following equations

$$PbOx_{(so)} + L \rightleftharpoons PbOxL$$

or (11)

$$PbJ_{2(so)} + L \rightleftharpoons PbJ_2L$$

Stability constants of the forming mixed complexes have been determined by the numeric method by means of the equations (9) and (10). The following equations of the solubility curves have been obtained: PbOx (12) and (13), PbJ_2 ((14) — (16)) in the solutions NaL (Na_2L)

$$\psi = \frac{S}{I_r} = 2.79 \times 10^7 + 7.01 \times 10^7 [CH_2ClCOO^-]; \ \triangle = 0.002 \times 10^7 \qquad (12)$$

$$\psi = \frac{S}{I_r} = 4.54 \times 10^7 + 8.97 \times 10^7 [CH_2BrCOO^-]; \ \triangle = 0.006 \times 10^7 \qquad (13)$$

$$\psi = \frac{S}{I_r} = 3.96 \times 10^6 + 2.50 \times 10^7 [CH_2OHCOO^-]; \ \triangle = 0.010 \times 10^6 \qquad (14)$$

$$\psi = \frac{S}{I_r} = 6.15 \times 10^6 + 3.90 \times 10^7 [CH_3CH_2COO^-]; \ \triangle = 0.020 \times 10^6 \qquad (15)$$

$$\psi = \frac{S}{I_r} = 5.49 \times 10^6 + 1.97 \times 10^7 [CH_3CHOHCOO^-]; \ \triangle = 0.004 \times 10^6 \qquad (16)$$

$\triangle$ — average error of the approximation by the method of least squares.

TABLE

Stability constants of complexes PbL_n, $PbOxL$, PbJ_2L at temperature 20°C ± 1°C and ionic strength of the solutions $\mu = 2.1$; pK_d — exponent of co-ordinative disproportionation constants ; $\triangle$ — average error of the approximation.

Ligand	Complex — PbL_n			Complex — $PbOxL$			Complex — PbJ_2L	
	β_1	β_2	$\triangle$	β_{2m}	$\triangle$	pK_d	β_{3m}	$\triangle$
CH_2ClCOO^-	8.26	100.00	0.010×10^2	7.01×10^7	0.003×10^7	3.58	—	—
CH_2BrCOO^-	20.00	70.80	0.008×10^2	8.97×10^7	0.006×10^7	3.75	—	—
CH_2JCOO^-	5.00	55.00	0.010×10^2	—	—	—	—	—
CH_2OHCOO^-	—	—	—	—	—	—	2.50×10^7	0.001×10^7
$CH_3CH_2COO^-$	—	—	—	—	—	—	3.90×10^7	0.002×10^7
$CH_3CHOHCOO^-$	—	—	—	—	—	—	1.97×10^7	0.004×10^6
$CH_2{=}CHCOO^-$	94.00	9.40×10^2	0.010×10^2	—	—	—	—	—
$CH_2CHOH/COO/_2^{--}$	5.86×10^3	1.61×10^5	0.008×10^5	—	—	—	—	—
$/CHOH/_2/COO/_2^{--}$	1.92×10^4	—	0.020×10^4	—	—	—	—	—

Figure 3 shows the course of Leden functions for the system : $PbC_2O_{4(so)} - CH_2ClCOONa - H_2O$.

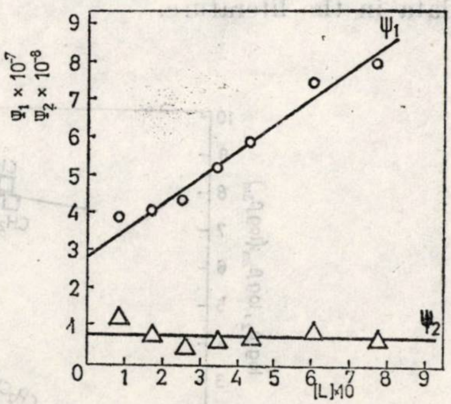

Fig. 3. — A plot of Leden function for the system : $PbC_2O_{4(so)} - CH_2ClCOONa - H_2O$

Curves : $\psi_1 = \frac{S}{I_r}$; $\psi_2 = \frac{\psi_1 - \beta_1}{[CH_2ClCOO^-]}$

Equilibrium constants (K_d) of the co-ordinative disproportionation reaction have been calculated. The results are shown in the Table.

Taking into account the complex forming properties of the investigated ligands one can distinguish two groups of compounds : complexes with carboxyl acids and complexes with hydroxyacids. In both groups an increase in the stability of the complexes can be observed together with the increase in pK (pK_2) of the respective acid — figure 4. The increased stability of hydroxycomplexes can be accounted for by the participation of hydroxyl groups in the process of complex formation. On the other hand, the presence of halogen atoms in the chain of aliphatic acid causes decrease of stability of simple complexes, in the same manner as in analogous Sn/II/ complexes.[23]

$$\begin{array}{llll} & Pb(CH_2OHCOO)_2 > & Pb(CH_3COO)_2 > & Pb(CH_2ClCOO)_2 > \\ \log\beta_2 & 3.24^4 & 3.13^2 & 2.00 \\ & > Pb(CH_2BrCOO)_2 > & Pb(CH_2JCOO)_2 & \\ \log\beta_2 & 1.85 & 1.74 & \end{array}$$

Lead (II) behaves as A type acceptor in relation to halogen derivative ligands of acetic acids.

While considering the stability of complexes PbOxL ($L = CH_2ClCOO^-$, CH_2BrCOO^-) and PbJ_2L ($L = CH_2OHCOO^-$, $CH_3CH_2COO^-$, $CH_3CHOHCOO^-$), it was found that they have markedly greater stability than that in simple complexes PbL and PbL_2 ; at the same time PbOxL complexes are more stable than the respective PbJ_2L complexes. An increase in stability is due to the increase of the co-ordination number ; and in the case of PbOxL, it is due, too, to the chelate effect, previously observed in $MeOxL_n$ complexes (where : $Me - Sn^{++}$; Pb^{++} ; Zn^{++} ; Cd^{++} ; Ag^+).[10,13,24] The positive value of pK_d for complexes $PbOx(CH_2ClCOO)^-$, PbOx $(CH_2BrCOO)^-$ indicates that they are stable in aqueous solutions. For the remaining mixed complexes of lead (II) co-ordinative disproportionation constants have not been calculated because of lack of available data in the literature.

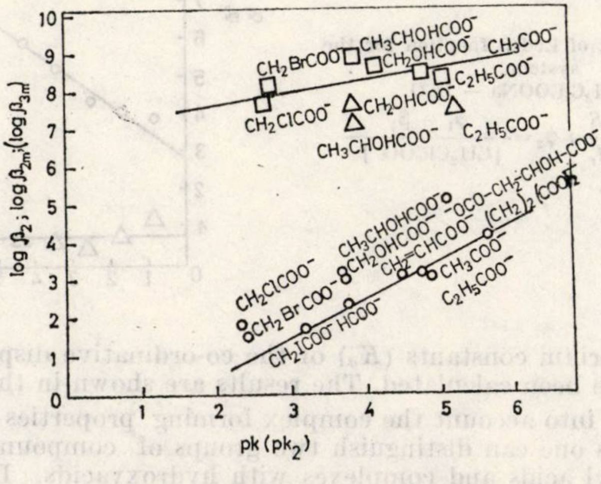

Fig. 4.—Dependence of log β_2 (○) ; log β_{2m}(□) ; log β_{3m}(△) of pK (pK_2)

○ — PbL_2 (L = $HCOO^-$,[2] CH_3COO^-,[2] $C_2H_5COO^-$,[2] CH_2OHCOO^-,[4] $CH_3CHOHCOO^-$,[4] $(CH_2)_2(COO)_2^{\,-}$[6])

□ — PbOxL (L = CH_2OHCOO^-,[1] CH_3COO^-,[10] $CH_3CHOHCOO^-$,[11] $C_2H_5COO^-$[12])

△ — PbJ_2L(L = CH_2OHCOO^-, $C_2H_5COO^-$, $CH_3CHOHCOO^-$)

REFERENCES

[1] E. Kulig and R. Wojtaś, *Zesz. Nauk. Politechniki Świętokrzyskiej* "Chemia", **7,** 5, (1978).

[2] N. P. Samsonova, T. T. Adger, E. A. Sinyacova, V. G. Sharynova and V. A. Fedorov, *Koordinatsionnaya khimiya*, **1**, 1691 (1975).

[3] B. Lenarcik and Z. Warnke, *Roczniki Chem.*, **43**, 1329 (1969).

[4] A. Basiński and Z. Warnke, *ibid.*, **39,** 1769 (1965).

[5] Z. Warnke and A. Basiński, *ibid.*, **41**, 13 (1967).

[6] A. Hamman, Ake Olin and P. Svanström, *Acta Chem. Scand.*, **A 31**, 384 (1977).

[7] Ake Olin and P. Svanström, *ibid.*, **A 29**, 849 (1975).

[8] V. Toiuzovskii, B. Yurdanoviskii and D. Nikolovska, *Godishen Zb. Prirodno-mat. fak., Univ. Skopjii*, **22,** 185 (1972).

[9] A. Pavlonova and C. Demiiancik, *M. N. Kh.*, **14,** 459 (1969).

[10] B. Kuźnik and D. M. Czakis-Sulikowska, *Zesz. Nauk. Politechniki Łódzkiej*, **29,** 5(1974).

[11] B. Kuźnik, *Polish J. Chem.*, **52,** 3 (1978).

[12] E. Kulig, R. Wojtaś and D. M. Czakis-Sulikowska, *Roczniki Chem.*, **51**, 1235 (1977).

[13] B. Kuźnik and D. M. Czakis-Sulikowska, *ibid.*, **45**, 959 (1971).

[14] I. N. Kal'tgof and V. A. Stenger, *Obemmyi analiz.*, **2**, 189 (1952).

[15] M. T. Kozlovskii, "Ruut'i amal'gamaty v elektrohimicheskih metodoh analiza" Alma Ata, 1965.

[16] A. M. Golub and O. T. Biluk, *M. N. Kh.*, **2**, 2723 (1957).

[17] A. M. Golub and S. D. Ivanenko, *M. N. Kh.*, **3**, 333 (1958).

[18] Collected work: "Poradnik fizykochemiczny", PWN, Warszawa, 1974.

[19] J. Leden, *Z. phys. Chem.*, **A 188**, 160 (1941).

[20] Yu. Yu. Lur'e, "Spravochnik po analiticheskoi himii", Izd. "Mir", Moscow, 1967.

[21] K. B. Yatsimirskii and A. A. Shutov, *M. N. Kh.*, **27**, 792 (1953).

[22] B. A. Fedorov, N. P. Samsonova and V. E. Mironov, *M. N. Kh.*, **7**, 1301 (1972)

[23] R. Wojtaś, *Roczniki Chem.*, **50**, 619 (1976).

[24] R. Wojtaś and D. M. Czakis-Sulikowska, *Zesz. Nauk. Kielecko-Radomskiej Wyższej Szkoły Inżynierskiej "Chemia"*, **2**, 5, 25 (1970).

Revue Roumaine de Chimie, 25, *8*, 1187–1195 (1980)

STUDY ON STRUCTURE AND PROPERTIES OF SOME TRIAZENIC COMPLEXES OF MERCURY

MARIA POPESCU* and DOREL CRIȘAN **
*** Institute of Constructions, Bucharest, Romania**
**** Center of Physical Chemistry, Bucarest, Romania**

Received June 5, 1979

The paper deals with the solubility products and the extraction constants of five Hg triazenic complexes determined with ^{203}Hg, IR spectra with the main characteristic vibrations, and X-ray diffraction data. The reagents were used in the determination of mercury traces in various matrixes at pH = 6.5. Hg (II) forms complexes of HgR_2 type.

The diazoamino (triazenic) compounds contain the —N=NH— group, they form stable complex compounds with Hg (II), Hg_2 (II) enabling the quantitative determination of mercury with a good selectivity.

By spectrophotometric studies, we found that Hg (II) forms complexes of the type

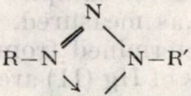

soluble in organic solvents with the stability constants of the order 10^{10} both in aqueous and organic phase. [1,2]

The high selectivity of the reaction at a neutral pH enabled the determination of mercury traces in waste [3] and mineral [4] waters.

The structure of triazenic compounds is much discussed in literature, assuming various formulations with monomer, dimer and polymer structure [5–8] depending on the nature of the anion linked to mercury. [9,10]

In our spectrophotometric studies we used the following triazenic reagents: diazoaminobenzene (DAB) *p*-nitro-diazoamino-benzene (NDAB), *p*, *p'*-dinitrodiazoaminobenzene (DNDAB), *p*-nitrophenyldiazoamino-azobenzene or Cadion A (CA) and *p*-nitronaphthyldiazoaminoazobenzene or Cadion 2B (C2B).

The Hg (II) complexes with these reagents have sufficient thermal stability to be used in gravimetric determinations. [2]

In this paper we present the solubility products, the extraction constants in various solvents, the elemental analysis, IR spectra and X-ray diffraction spectra of the Hg complexes with the above-mentioned reagents.

EXPERIMENTAL

Reagents and instruments

— solution of ^{203}Hg acetate containing 186 μg Hg (II)/ ml of specific activity $\lambda_s = 95.7$ millicuries/g ;

— solutions of reagents in EtOH : DAB 0.05% ; CA and C2B 0.015% ; in nitrobenzene NDAB 0.020 % and DNDAB 0.025% ;

— buffer solution of 2M sodium acetate to maintain a constant pH of 6.5.

The radiometric measurements were carried out on an impulse counter NP40 made in Czechoslovakia.

IR spectra were recorded with a Perkin Elmer Spectrophotometer 621 and for molecular weight determination a Knauer Dampfdruck-Osmometer was used.

The X-ray diffraction determinations were performed on an HZG—3 diffractometer with a proportional counter type VAZ—522 and a TUR—M62 generator.

All radiometric determinations were carried out in a medium of 0.2 ionic strength.

The X-ray diffraction patterns were recorded under the following conditions : Cuk α radiation ; Ni filter ; counter speed 0.5°C/ min ; paper speed 600 mm/h ; the tube is supplied at 40 kV and 35 mA and the proportional counter at 1650 V, with the threshold voltage of 1.4 V ; counter slit 0.6 mm ; impulse scale 1.8×10^5 impulses/ min.

RESULTS AND DISCUSSIONS

Determination of solubility products

The ^{203}Hg complexes of the above-mentioned reagents were obtained using ^{203}Hg acetate in excess to the reagent. The excess of mercury was removed quantitatively by washing with water, and then the quantitative removal of ^{203}Hg excess was checked radiometrically.

An amount of 2 ml of the respective solvent and an excess of each ^{203}Hg (II) complex in solid state are introduced in 3 ml stoppered test tubes. The tubes were mechanically stirred for half an hour, then centrifugated and thermostated at 25°C. Samples of 1 ml were taken from each test tube and the activity was measured. Table 1 shows the solubility products of the complexes determined from the activity of the solutions.

The triazenic complexes of Hg (II) are found to be sparingly soluble in water and acetone. The low solubility of these complexes generally reduces the possibility of instrumental investigation of their structure, therefore the determination of molecular weight was effected only for DAB-Hg (II) complex, its solubility in C_6H_6 being sufficient for the determination (Table 3).

Determination of extraction constants of Hg (II) triazenic complexes in various organic solvents

A solution containing 8 ml water, 1 ml buffer solution of 2M sodium acetate, then 0.5 ml ^{203} Hg solution and different quantities of reagent (Table 2) were introduced in 50 ml separatory funnels. Then, the activity was measured for 1 ml solution of aqueous phase and 1 ml solution of organic phase. The values obtained were used in the determination of Hg (II) distribution ratio in the two phases and the values of the distribution ratio were used in the determination of the extraction constants. [11]

The relatively low values of the distribution ratio may be due to Hg (II) disproportion in mercury acetate in aqueous solution at pH = = 6.5 as well as to the blocking of mercury under the form of $HgOH^+$, $Hg(OH)_2$.

TABLE 1

Solubility products of Hg (II) triazenic complexes in various solvents

R	R	Solvent	P_s	R	R'	Solvent	P_s
C_6H_5	C_6H_5	H_2O	7.68×10^{-18}	$O_2N-C_6H_4$	$C_6H_4-N=N-C_6H_5$	H_2O	1.24×10^{-18}
		CH_3OH	1.27×10^{-12}			CH_3OH	1.25×10^{-13}
		C_2H_5OH	6.26×10^{-15}			C_2H_5OH	9.18×10^{-15}
		C_3H_7OH	1.09×10^{-13}			C_3H_7OH	2.39×10^{-14}
		$CH_3-CO-CH_3$	6.81×10^{-11}			CH_3COCH_3	7.97×10^{-11}
		$CH_3CO-C_2H_5$	7.06×10^{-11}			$CH_3COC_2H_5$	2.71×10^{-11}
		$CHCl_3$	2.04×10^{-16}			CCl_4	7.96×10^{-16}
						CS_2	8.38×10^{-14}
$O_2N-C_6H_4$	C_6H_5	H_2O	4.46×10^{-17}	$O_2N-C_{10}H_6$	$C_6H_4-N=N-C_6H_5$	H_2O	2.51×10^{-17}
		CH_3OH	9.79×10^{-12}			CH_3OH	3.63×10^{-13}
		C_2H_5OH	9.39×10^{-14}			C_2H_5OH	1.21×10^{-15}
		C_3H_7OH	2.33×10^{-13}			C_3H_7OH	7.64×10^{-14}
		CH_3COCH_3	1.45×10^{-10}			CH_3COCH_3	9.20×10^{-12}
		$CH_3COC_2H_5$	2.93×10^{-10}			$CH_3COC_2H_5$	2.84×10^{-12}
		CCl_4	1.34×10^{-14}			CCl_4	2.30×10^{-16}
		CS_2	1.57×10^{-13}				
$O_2N-C_6H_4$	$C_6H_4-NO_2$	H_2O	5.56×10^{-17}				
		CH_3OH	3.34×10^{-14}				
		C_2H_5OH	1.37×10^{-16}				
		C_3H_7OH	1.42×10^{-15}				
		CH_3COCH_3	8.46×10^{-12}				
		$CH_3COC_2H_5$	1.19×10^{-11}				
		C_6H_6	3.55×10^{-18}				
		$C_6H_5-CH_3$	8.17×10^{-15}				
		$C_6H_4-(CH_3)_2$	2.22×10^{-14}				
		CCl_4	2.22×10^{-19}				
		$CHCl_3$	9.28×10^{-17}				
		CS_2	7.27×10^{-16}				

TABLE 2

The distribution ratio and percentage extraction for $[Hg] = 4.65 \times 10^{-5}$ and different amounts of reagent in various solvents

R	R′	Solvent	$[HA] \times 10^{+5}$	D	E%	log K
C_6H_5	C_6H_5	C_6H_6	3.1	59.33	98.35	−4.21
			0.93	4.16	80.63	−4.31
			0.31	0.39	28.45	−4.38
		$C_6H_5-CH_3$	3.1	103.08	99.04	−3.96
		$p-C_6H_4-(CH_3)_2$	3.1	81.82	98.79	−4.07
		$C_6H_5-NO_2$	3.1	60.88	98.38	−4.20
		CCl_4	3.1	87.95	98.87	−4.04
		$CHCl_3$	3.1	0.08	7.42	−7.08
		CS_2	3.1	79.20	98.75	−4.08
$O_2N-C_6H_4$	C_6H_5	C_6H_6	2.48	29.50	96.72	−4.32
		$C_6H_5-CH_3$	2.48	40.47	97.59	−4.18
		$p-C_6H_4-(CH_3)_2$	2.48	61.51	98.40	−3.99
		$C_6H_5-NO_2$	1.24	23.05	95.84	−3.82
			0.209	0.497	33.21	−3.94
			0.1045	0.32	24.27	−3.53
		$CHCl_3$	2.48	0.68	40.64	−5.95
$O_2N-C_6H_4$	$C_6H_4-NO_2$	$C_6H_5-NO_2$	2.09	53.9	98.18	−3.91
			0.627	3.108	75.66	−4.10
			0.209	0.486	32.69	−3.95
$O_2N-C_6H_4$	$C_6H_4-N=N-C_6H_5$	C_6H_6	1.73	55.74	98.23	−3.73
			0.867	21.17	95.49	−3.55
			0.0867	0.129	42.76	−3.76
		$C_6H_5-CH_3$	1.73	65.67	98.50	−3.65
		$p-C_6H_4-(CH_3)_2$	1.73	160.44	99.38	−3.27
		$C_6H_5-NO_2$	1.73	25.28	96.19	−4.07
		$CHCl_3$	1.73	73.95	98.6	−3.60
$O_2N-C_{10}H_6$	$C_6H_4-N=N-C_6H_5$	C_6H_6	1.51	4.54	81.95	−4.70
			0.755	0.698	41.117	−4.91
			0.453	0.355	26.24	−4.76
		$C_6H_5-CH_3$	1.51	5.08	83.55	−4.65
		$p-C_6H_4-(CH_3)_2$	1.51	15.07	93.78	−4.18
		$C_6H_5-NO_2$	1.51	8.97	89.97	−4.40
		$CHCl_3$	1.51	2.85	74.05	−4.90
		CS_2	1.51	48.06	97.96	−3.67

TABLE 3

Elemental analysis of Hg (II) triazenic complexes

Complex	C% calc.	C% found	H% calc.	H% found	Hg% calc.	Hg% found	M	Formula
Hg-DAB	48.56	47.36	3.37	3.58	33.78	32.7	610	$C_{24}H_{20}N_6Hg$
Hg-NDAB	42.22	42.91	2.64	2.70	29.32	28.5	603	$C_{24}H_{18}N_8O_4Hg$
Hg-DNDAB	37.30	37.63	2.07	2.16	25.90	26.1		$C_{24}H_{16}N_{10}O_8Hg$
Hg-Ca	48.54	46.39	2.92	2.76	22.47	23.1		$C_{36}H_{26}N_{12}O_4Hg$
Hg-C2B	53.33	52.20	3.03	2.96	20.20	19.80		$C_{44}H_{30}N_{12}O_4Hg$

Elemental analysis

The elemental analysis (Table 3) of the complexes supports the formulation given earlier.

Hg (II) was determined spectrophotometrically with dithizon. The values of molecular weight for the DAB complex demonstrate the monomer structure in agreement with an earlier literature report. [8]

IR spectra

The characteristic vibration bands of N—H bond appear at 3185—3280 cm^{-1} and at 1520 cm^{-1} in the triazenic reagents. [12,13,7]

The characteristic band of N—H bond disappear in Hg (II) complexes and those characteristic of C_6H_5—N=bond are shifted with $\Delta\nu =$ $= 25-45$ cm^{-1} (Table 4). [7]

TABLE 4

Main vibrations in IR for triazenic reagents and their Hg (II) complexes

Substance	νN—H cm^{-1}		νN—Hg cm^{-1}	ν C—H—N= cm^{-1}					
						Δ ν			Δ ν
DAB	1520	3185		1235		25	1320		45
Hg-DAB			480		1210			1275	
NDAB	1520	3275		1240		50	1320		40
Hg-NDAB			470		1190			1280	
DNDAB	1520	3280		1230		20	1315		35
Hg-DNDAB			490		1210			1280	
CA	1520	3270		1240		20	1320		40
Hg-CA			470		1220			1280	
C2B	1520	3270		1230		20	1310		25
Hg-C2B			485		1210			1285	

For the Hg (II) complexes, a widening of the band in the range 1295—1345 cm^{-1} was found, as well as the appearance of a new band due to N—Hg bond in the range of 470—490 cm^{-1}. In literature, [13] the vibration of N—Hg bond is given in a wider range 400—700 cm^{-1}.

The diffraction data presented in table 5 confirm that the complexes are well defined compounds. No lines belonging to the reagent or $HgCl_2$ were identified which demonstrates their purity.

TABLE 5

Main diffraction lines for the triazenic reagents and their Hg(II)-complexes

DAB		Hg-DAB		NDAB		Hg-NDAB		$HgCl_2$(ASTM 4−331)	
d (Å)	I_{obs}	d (Å)	I_{obs}	d (Å)	I_{obs}	d (Å)	I_{obs}	d (Å)	I_{obs}
		16.2	46	19.4	82				
		9.4	39			13.6	65		
9.1	100					11.9	15		
		8.11	100			11.3	65		
7.7	26					8.5	44		
6.57	29					7.7	100		
		6.15	29			6.86	27		
5.79	21					6.67	15		
5.63	83					6.16	74		
				6.10	37				
5.19	28			5.64	96				
		5.03	20			5.61	53		
5.01	45	4.72	25	5.41	14	5.47	76		
4.56	100					5.34	34		
		4.54	8	4.92	37	4.93	14	4.35	100
						4.81	29		
				4.74	11			4.10	38
		4.08	8			4.65	20		
4.02	21					4.55	24		
		3.89	15	4.49	12				
3.83	45					4.27	21		
		3.80	44			4.02	16		
3.58	41			3.93	13	3.94	17		
		3.55	8			3.70	22		
		3.50	8	3.68	10				
3.41	72					3.62	24		
3.38	69					3.458	8	3.38	31
		3.367	12			3.424	12		
3.31	10			3.414	100				
						3.321	71		
						3.227	19	3.188	11
		3.166	18			3.204	25		
		3.097	15			3.166	39		
3.076	47			3.108	56				
				3.035	19				
3.035	100					2.99	15	3.033	21
						2.813	13	2.986	48
2.976	60					2.723	18		
						2.606	13		
		2.913	12						

TABLE 5 *(continued)*

DAB		Hg-DAB		NDAB		Hg-NDAB		$HgCl_2$(ASTM 4-331)	
d (Å)	I_{obs}	*d* (Å)	I_{obs}	*d* (Å)	I_{obs}	*d* (Å)	I_{obs}	*d* (Å)	I_{obs}
2.820	19								
2.777	14					2.297	14		
		2.782	19			2.171	10		
						2.08	10	2.707	36
2.505	9								
								2.42	14
		2.40	8						
2.277	10							2.132	9
								2.065	13
2.016	15							2.004	16
1.997	10							1.940	11
1.857	9							1.902	8

CA		Hg−CA		DNDAB		Hg-DNDAB		C2B		Hg-C2B	
d (Å)	I_{obs}	*d* (Å)	I_{obs}	*d*(Å)	I_{obs}	*d* (Å)	I_{obs}	*d* (Å)	I_{obs}	*d* (Å)	I_{obs}
26.9	100										
				13.7	13						
		17.4	73			12.4	67	17.7	19		
		9.7	100	9.6	14					15.5	66
9.1	44							13.8	28		
		8.8	62			7.6	37			13.5	100
		7.6	59			7.1	26			10.9	27
6.89	13			6.85	10	6.87	27	10.6	8		
6.15	24					6.19	100	10.0	13		
		6.02	80	6.06	100					9.6	15
5.61	60					6.00	18	8.8	30		
		5.55	95			5.79	47	7.75	9	7.8	27
5.15	56	5.17	35	5.56	70			7.43	10		
						5.26	30	6.92	32		
4.57	12									6.75	27
						4.89	46	6.63	17		
				4.81	11					6.51	78

TABLE 5 *(continued)*

CA		Hg−CA		DNDAB		Hg-DNDAB		C2B		Hg-C2B	
d (Å)	I_{obs}	*d* (Å)	I_{obs}	*d* (Å)	I_{obs}	*d* (Å)	I_{obs}	*d* (Å)	I_{obs}	*d* (Å)	I_{obs}
3.99	9					4.78	20	5.90	100		
				4.53	54					5.36	11
3.65	36					4.40	15			5.25	21
3.53	22							5.14	48		
3.348	79					4.14	31			5.11	22
		3.173	97			3.88	12				
3.133	38			3.74	49					4.68	15
3.058	14							4.53	39		
2.926	10					3.56	11			4.12	50
						3.52	10	3.99	15		
						3.463	28			3.93	26
				3.376	16	3.378	29	3.84	30		
						3.278	83	3.76	16		
						3.220	24			3.65	19
				3.204	88	3.195	24	3.63	65		
				3.131	8					3.59	18
						3.095	30	3.512	72		
				3.01	10			3.366	78	3.371	26
				3.015	13			3.259	27		
						2.976	18	3.227	40	3.236	20
						2.912	13	3.168	17	3.166	38
						2.839	18	3.003	13		
						2·553	16	2.897	10	2.976	15
						2.493	16	2.820	36	2.751	16
						2.391	10	1.994	24	2.72	16
						2.307	9			2.656	12
						2.154	10			2.456	10

REFERENCES

[1] Gr. Popa, A. F. Dăneţ and M. Popescu, *Talanta*, **25**, 546 (1978).

[2] M. Popescu and D. N. Todor, *Rev. Chim. (Bucureşti)*, **10**, 987 (1978).

[3] Gr. Popa and M. Popescu, Paper presented at the "National Congress of Chemistry" Bucharest, 1978.

[4] M. Popescu and D. N. Todor, *Rev. Chim. (Bucureşti)*, **12**, 1182 (1978).

[5] C. M. Harris, F. B. Hoskins and R. L. Martin, *J. Chem. Soc*, **1959**, 3728.

[6] A. P. Terent'ev, E. G. Rukhadze and T. V. Ershova, *Doklady Akad. Nauk S.S.S.R.*, **163**, 606 (1966).

[7] T. V. Ershova, E. G. Rukhadze and A. P. Terent'ev, *Zhur. obshchei Khim.*, **39**, 59 (1969).

[8] A. P. Terent'ev, T. V. Ershova and E. G. Rukhadze, *Zhur. obshchei Khim.*, **36**, 1046 (1966).

[9] C. M. Knowles and G. W. Watt, *J. Amer. Chem. Soc.*, **64**, 935 (1942).

[10] K. L. Mandal, *Science and Culture*, **6**, 59 (1940).

[11] J. Stary and K. Kratzer, *Analyt. Chim. Acta*, **40**, 93 (1968).

[12] K. Nakamoto, "Infrared Spectra of Inorganic and Coordinative Compounds", Wiley, New York, 1968.

[13] K. Brodersen, *Chem. Ber.*, **89**, 1487 (1956).

[14] W. Klemperer and L. Lindeman, *J. Chem. Phys.*, **25**, 397 (1956).

Revue Roumaine de Chimie **25**, *8* 1197–1200 (1980)

PALLADIUM (II) CHELATE OF PHENYLAZOBENZALDOXIME

A. E. MAHGOUB and M. M. SHOUKRY
Chemistry Department, Faculty of Science, Cairo University
Giza, A. R. Egypt

Received March 18, 1978

Palladium (II) complex of phenylazobenzaldoxime was synthesised and investigated. Analytical data proved the formation of the monoligated complex species. Electrolytic conductance and magnetic measurements suggest the formation of binuclear molecules, the dimerisation occurring through chlorine bridges. Spectral data shed some light on the structure of the metal chelate ring.

INTRODUCTION

Phenylazobenzaldoxime (I) was reported [1-4] to form stable chelates with various metal ions. Compound (I) was used successfully as analytical reagent for cobalt (II) [5] and palladium (II).[6]

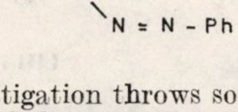

$$Ph-C(=N-OH)-N=N-Ph$$

(I)

The present investigation throws some light on the structure of the palladium (II) chelate of phenylazobenzaldoxime, on the basis of physico-chemical studies, including electrolytic conductance, magnetic and spectral measurements.

EXPERIMENTAL

Palladium (II) chloride was a BDH product. Phenylazobenzaldoxime was prepared by nitrosation of benzaldehyde phenylhydrazone, according to the experimental conditions described by Bamberger and Pamsel [7].

The palladium complex was prepared in the 1 : 1 ratio (metal ion : ligand). It was precipitated on direct mixing of ethanolic solutions of palladium (II) chloride (0.01 mole) with the ligand (0.01 mole). The complex was filtered and washed thoroughly with ethanol-water mixture (1 ; 1). The palladium complex gave satisfactory elemental analysis data for a monoligated complex.

Analytical data

$C_{13}H_{11}N_3OClPd$

Found : C, 42.72 ; H, 2.50 ; N, 11.70 ; Cl, 9.40% ;

Calcd : C, 42.64 ; H, 2.73 ; N, 11.48 ; Cl, 9.70%

Colour : Purple & Shape : Powder & Solubility ; Soluble in most organic solvents.

The electrolytic conductance was measured at $25 \pm 0.02°C$, for 10^{-3} M complex solution in N,N dimethylformamide (DMF). The instrument used was a conductivity meter, model LBR, produced by WTW, Germany.

Electronic absorption spectra, in dioxan, were taken on a Beckman Dkl recording spectrophotometer. The IR spectra were recorded in KBr pellets with a Pye Unicum SP 1100 spectrometer.

Magnetic susceptibility of the solid complex was measured using Gouy's powder method [8]. $CuSO_4 . 5H_2O$ was used as a calibrant. The Gouy tube was 13 cm long and 4 mm in diameter, with a flat bottom. All measurements were performed at room temperature (300 K) at varying magnetic field strength.

RESULTS AND DISCUSSION

Complex formation between palladium (II) and phenylazobenzaldoxime was previously investigated in solution.[6] These studies indicate the formation of only one stable complex species of stoichiometric ratio 1 : 1. The structure of the palladium complex was further investigated in the light of the results obtained from electrolytic conductance, spectral and magnetic characteristics of the solid complex.

The electrolytic conductance in N, N dimethylformamide (DMF), corrected for solvent effect, ($\Lambda_M = 2.5$ ohm^{-1} cm^2 mole^{-1}; concentration $= 10^{-3}$ M) indicates a complex of nonelectrolytic nature [9]. However, the monomeric form of the complex (II) should be a 1 : 1 charged electrolyte. For this reason the dimeric species (III) and not (II) is suggested. Such a view is in agreement with the reported molecular weight data [4].

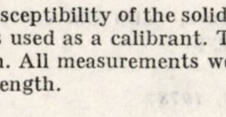

(II)

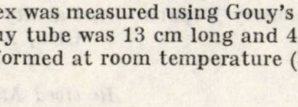

(III)

The magnetic susceptibility measurement indicates that the palladium complex is diamagnetic ($X_M = -417 \times 10^{-6}$ e.m. U. mole^{-1}) as expected for a d^8 system, the coordination being essentially square planar around the palladium atom. [10] The diamagnetism of the complex sugests that the dimerisation takes place through the chlorine bridge (III), as the direct metal-metal interaction would lead to unpairing of some of the *d* electrons giving rise to a paramagnetic effect, which is not observed.

The electronic absorption spectrum, in the visible range, of palladium complex shows two maxima at 550 nm ($\varepsilon = 3600$) and 460 nm ($\varepsilon = 1500$) which are presumably assigned [11] as of $1A_{1g} \rightarrow 1A_{2g}$ and $1A_{1g} \rightarrow$ $\rightarrow 1B_{1g}$ transitions, respectively. These strong maxima are CT bands. Such a pattern is comparable to that observed in the spectra of square planar halo-complexes [12–15] of palladium (II). The presence of an arylazo-group in the palladium complex was deduced from the uv spectra of the ligand and its palladium complex. The spectrum of the ligand exhibits a transition at 295 nm, with $\log \varepsilon = 4.18$, which is characteristic of azo-compounds.[16] For azobenzene it is at 281 nm ($\varepsilon = 5260$) for *cis*[17] and at 319 nm ($\varepsilon = 19500$) for *trans*[18]-isomers. The transition is presumably of the $\pi - \pi^*$ type, and is red shifted, to 310 nm, with $\log \varepsilon = 4.39$, in the complex spectrum. This is expected since the energy level separation in the complex will be lower than that in the free ligand.

The IR spectrum of the ligand exhibits an intense band in the 3000–3400 cm^{-1}region, presumably due to the OH group stretching. The latter band has disappeared in the IR spectrum of the palladium complex. This indicates that the oxime proton is released in the formation of the complex. The chelate ring can be one of the following:

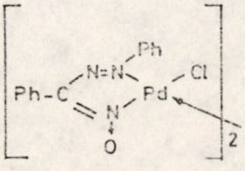

IV

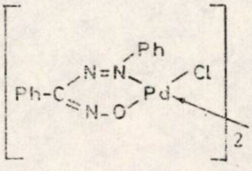

V

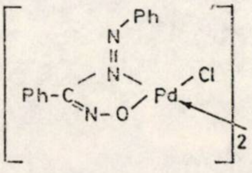

VI

Kalia *et. al.*[4] favour the five-membered formulation (IV) on the basis of the IR spectrum in the range 1000–1300 cm^{-1}, however, the molecule studied has a complicated IR pattern in this range, and the assignement of the bands is uncertain. In our opinion, since the oxime proton is released during the complex formation a bond between oxygen and palladium seems likely. Therefore, one of the structures V and VI is more reasonable. A choice between five- and six-membered formulations (V, VI) requires further studies. However by reason of their close analogy with metal complexes of the *o*-hydroxyazo-compounds[19], structure V may be considered to be the most probable.

REFERENCES

[1] K. C. Kalia and A. Chakravorty, *Inorg. Chem.*, **7,** 2016 (1968).

[2] A. E. Mahgoub, A. S. Shawali and M. M. Shoukry, *Gazz. Chim. Ital.*, **107,** 387 (1977)

[3] L. Malatesta and R. Pizzoti, *Gazz. Chim. Ital.*, **67,** 141 (1946).

[4] K. C. Kalia and A. Chakravorty, *Inorg. Chem.*, **8,** 2586 (1969).

[5] A. E. Mahgoub, A. S. Shawali and M. M. Shoukry, *Z. anal. Chem.*, **284,** 205 (1977).

[6] A. E. Mahgoub, N. A. Darwish and M. M. Shoukry, *Analyst*, **103,** 879 (1978).

[7] E. Bamberger and W. Pamsel, *Ber. dtsch. Chem. Ges.*, **36,** 53 (1903).

[8] A. Earnshaw, "Introduction to Magnetochemistry" Academic Press, New York, 1968, p. 84.

[9] G. Macotrigiano, R. Battistuzzi and G. Peyronel, *J. Inorg. Nuclear Chem.*, **35,** 2265 (1973).

[10] V. I. Belova, *Izvest. Sektora Platiny i Drug. Blagorod. Metal., Inst. Obshchei i Neorg. Khim., Akad. Nauk S.S.S.R.*, **31**, 39 (1955) ; *Chem. Abstr*, **50**, 15148 (1956).

[11] H. L. Ray, K. B. Pandeya and R. P. Singh, *Indian J. Chem.*, **12**, 532 (1974).

[12] H. B. Gray and C. J. Balhausen, *J. Amer. Chem. Soc.*, **85**, 260 (1963).

[13] J. Chott, G. A. Gamlen and L. E. Orgel, *J. Chem. Soc.*, **1958**, 486.

[14] S. Yamada, *J. Amer. Chem. Soc.*, **73**, 1182 (1951).

[15] C. M. Harris, S. E. Livingstone and I. H. Reece, *J. Chem. Soc.*, 1505, (1959).

[16] A. Burawoy, *J. Chem. Soc.*, **1937**, 1865.

[17] H. Suzuki, "Electronic Absorption Spectra and Geometry of Organic Molecules", Academic Press, New York, 1967.

[18] K. C. Kalia and A. Chakravorty, *J. Org. Chem.*, **35**, 2231 (1970).

[19] M. Elkins and L. Hunter, *J. Chem. Soc.*, **1935**, 1598.

Revue Roumaine de Chimie **25**, *8*, 1201–1211 (1980)

Th (IV) UND U (VI) KOMPLEXVERBINDUNGEN MIT PYROCATECHIN, PYROCATECHINDISULFONSAURE UND CHROMOTROPSAURE

AL. CECAL
Fakultät für Chemische Technologie des Polytechnischen Instituts, Splai Bahlui–71, Iaşi, Rumänien

Eingegangen am 27 Juni, 1978

In dieser Arbeit wurden Komplexverbindungen von Th^{4+} und UO_2^{2+} Ionen mit Pyrocatechin, (Brenzcatechin) Pyrocatechindisulfonsäure und Chromotropsäure hergestellt und spektrofotometrisch das Metall-Ligand Kombinationsverhältnis und die Stabilitätskonstanten bei verschiedenen Temperaturen bestimmt. Ausserdem wurden die Gibbs Energien, die Bildungsenthalpien und -entropien berechnet und daraus der Typ der Komplexverbindungen abgeleitet. Zusätzlich wurde der Medium Effekt (Wasser-Äthanol) auf die UO_2^{2+} Komplexverbindungen untersucht.

Complex compounds of Th^{4+} and UO_2^{2+} ions with pyrocatechol, pyrocatechol-disulfonic acid and chromotropic acid were prepared. By means of spectrophotometric methods there were established both the metal -ligand combination ratios and the stability constants at various temperatures. The values of the Gibbs free energy, formation enthalpy and – entropy, were calculated, from which the conclusions about the type of the prepared complex compounds were drawn. The medium effect (water-ethanol) on the UO_2^{2+} complex compounds was also studied.

EINFÜHRUNG

Bis jetzt wurden mehre Arbeiten die sich mit der Synthese und thermodynamischen Charakterisierung einiger Komplexverbindungen von Th^{4+} und UO_2^{2+} Ionen mit organischen Liganden beschäftigen, publiziert. Die Herstellung von UO_2^{2+} und ins besondere von Th^{4+} Komplexverbindungen mit solchen Liganden ist in Lösung und unter bestimmten Bedingungen sehr schwierig, da sich "polynuclear compounds" bilden können.[1–2] Trotz dieser Schwerigkeiten wurden einige Th^{4+} und UO_2^{2+} Komplexverbindungen mit organischen Liganden wie 8-Hydroxyquinolin und seinen Derivaten,[3–6] Beta-Diketonen,[7–9] organische mono- und polybasische Säuren[10–17] hergestellt.

In dieser Arbeit wird nun ein Vergleichstudium der thermodynamischen Parameter von Th^{4+} und UO_2^{2+} Komplexverbindungen mit Pyrocatechin, Pyrocatechindisulfonsäure und Chromotropsäure ausgeführt. Obwohl UO_2^{2+} Komplexverbindungen mit Pyrocatechin und Pyrocatechindisulfonsäure als Festkörper[18–21] bekannt sind, wurden diese in die Untersuchungen mit übernommen um diese Verbindungen thermodynamisch (in Lösung) zu charakterisieren und den Medium Effekt zu analysieren, wobei ein spektrofotometrisches Verfahren verwendet worden ist.

EXPERIMENTELLER TEIL

Das spektrofotometrische Studium der Metall-Ligand Kombinationsverhältnisse für Th^{4+} und UO_2^{2+} Komplexverbindungen mit Pyrocatechin, Pyrocatechindisulfonsäure und Chromotropsäure wurde nach Job [22], dem Molenbruch [23] und Neigungsverhältnis [24] durchgeführt.

Es wurden zuerst wässerige Lösungen gleiche Molarität von Liganden und den anorganischen Salzen Th $(NO_3)_4 \cdot 6H_2O$ und $UO_2(NO^3)_2 \cdot 6H_2O$ vorbereitet und die Spektren mit einem Cary—14 Spektrofotometer gemessen. Von diesen Ausgangslösungen wurden dem verschiedenen Proben in denen sich das Metall-Ligand Verhältnis entsprechen der Messmethode geändert wurde, hergestellt.

Für jede Probe ist die Absorptionskoeffizienten bei der charakteristischen Wellenlänge gemessen worden. Nach dem das optimalen Metall-Ligand Verhältnis ermittelt worden war, wurden spektrofotometrisch auch die Stabilitätskonstanten bei 4 verschiedenen temperaturen nach Nagakura [25–26] bestimmt.

Im Falle der UO_2^{2+} Komplexverbindungen wurde dieselbe Methode auch für die Bestimmung der Stabilitätskonstanten in verschiedenen Wasser Äthanol Mischungen verwendet, um den Medium Effekt auf der Bildung solchen Verbindungen zu untersuchen.

ERGEBNISSE UND DISKUSSION

In der Tabelle 1 ist eine Zusammenfassung der Spektrofotometrischen Daten der einzelnen Reaktanten und der entsprechenden Komplexverbindungen wiedergegeben.

Zur Bestimmung dem Metall-Ligand Kombinationsverhältnis wurden jedes mal je 2 unterschiedliche Methoden verwendet: für die Th^{4+} Komplexverbindungen mit Pyrocatechin, Pyrocatechindisulfonsäure und Chromotropsäure Methoden nach Job und das Molenbruchverhältnis, für UO_2^{2+} Komplexverbindungen mit den selben Liganden, nach Job und das Neigungsverhältnis (Tabelle 2—5).

Wie aus den Tabellen II—V ersichtlich, ist für beide Ionen das optimale 1 : 1 Metall-Ligand Verhältnis in der wässerigen Phase erreicht worden.

Um die Stabilitätskonstanten (K) nach Nagakura zu berechnen, wurde die Absorptionskoeffizienten bei 4 verschiedenen Temperaturen für 1 : 1 und 5 : 1 Metall-Ligand Verhältnisse (Tabelle 6) gemessen. Mit Hilfe der Stabilitätskonstanten wurden danach die Gibbs-Energien berechnet:

$$\Delta G = -RT \ln K \tag{1}$$

und durch graphische Darstellung :$\Delta G = f(T)$, oder nach

$$\Delta G = \Delta H - T\Delta S \tag{2}$$

TABELLE 1

Charakteristiche spektrofotometrische Daten für die untersuchten Verbindungen

Substanz	λ (A°)	ε (L/Mol. cm)
$Th(NO_3)_4 . 6H_2O$	3025	$2,28 . 10^1$
$UO_2(NO_3)_2 . 6H_2O$	3635	1,68
	3703	1,40
	4052	5,08
	4161	5,88
	4275	5,09
Pyrocatechin	2725	$1,55 . 10^2$
Pyrocatechindisulfonsäure	2341	$5,54 . 10^4$
	2923	$2,81 . 10^4$
Chromotropsäure	3310	$1,48 . 10^4$
	3487	$2,31 . 10^4$
Pyrocatechin-Th^{4+} (1 : 1)	2798	$3,26 . 10^3$
Pyrocatechindisulfonsäure-Th^{4+} (1 : 1)	3085	$5,00 . 10^3$
	3209	$8,51 . 10^3$
Chromotropsäure-Th^{4+}(1 : 1)	3475	$1,69 . 10^4$
	3630	$8,00 . 10^4$
Pyrocatechin-UO_2^{2+} (1 : 1)	3615	7,80
	3628	7,73
	3937	8,21
	4040	9,18
	4140	8,26
Pyrocatechindisulfonsäure-UO_2^{2+}(1 : 1)	3726	$2,34 . 10^2$
Chromotropsaure-UO_2^{2+} (1 : 1)	3150	$1,34 . 10^4$
	3329	$1,84 . 10^4$
	3486	$2,47 . 10^4$
	3601	$5,02 . 10^4$

konnten die Bildungsenthalpien und — entropien (ΔH und ΔS) der obenerwähnten Komplexverbindungen bestimmt werden.

Die thermodynamische Daten sind in Tabelle 7 wiedergegeben.

Die Bildungsenthalpien und -entropien der Komplexverbindungen führen zu wichtige Angaben über die Komplexverbindungen.[27-29] Weisen die Enthalpien und Entropien positive Werte auf, so kann angenommen werden, dass die Hydratations (-Solvatations) Hülle um die Ionen zerstört ist, so dass das komplexierende Metallion weniger Transitions und -Rotationsfreigrade in vergleich zu dem Anfangszustand braucht. Somit

TABELLE 2

Die Bestimmung des Th^{4+} Ligand Verhältnisses nach Job

Ligand	ml. Ligand	ml. Th^{4+}	λ (Å)	E (Mol. cm/L)
Pyrocatechin	9	1	2798	0,65
	7	3	,,	0,98
	5	5	,,	1,27
	3	7	,,	0,38
	1	9	,,	0,06
Pyrocatechindisulfonsäure	1	9	3085	0,03
	3	7	,,	0,33
	5	5	,,	0,66
	7	3	,,	0,54
	9	1	,,	0,10
Chromotropsäure	9	1	3630	0,21
	7	3	,,	0,35
	5	5	,,	0,78
	3	7	,,	0,60
	1	9	,,	0,23

TABELLE 3

Methode nach Job zur Bestimmung des Metall-Ligand Verhältnisses für UO_2^{2+}

Ligand	ml. Ligand	ml. UO_2^{2+}	λ (Å)	E (Mol. cm/L)
Pyrocatechin	9	1	4040	0,61
	7	3	,,	0,82
	5	5	,,	0,89
	3	7	,,	0,76
	1	9	,,	0,23
Pyrocatechindisulfonsäure	9	1	3726	0,71
	7,5	2,5	,,	1,12
	6,5	3,5	,,	1,37
	5	5	,,	1,58
	3	7	,,	1,29
Chromotropsäure	1	9	3601	0,46
	3	7	,,	0,86
	5	5	,,	0,97
	7	3	,,	0,83
	9	1	,,	0,57

TABELLE 4

Bestimmung des Th^{4+} -Ligand Kombinationsverhältnisses nach der Molenbruch Methode.

Ligand	ml. Ligand	ml. Th^{4+}	λ (Å)	E (Mol. cm/L)
Pyrocatechin	1	0,5	2798	0,62
	1	1	,,	0,66
	1	2	,,	0,70
	1	3	,,	0,72
	1	4	,,	0,74
	0,5	1	2798	0,25
	1	1	,,	0,66
	2	1	,,	0,80
	3	1	,,	1,03
Pyrocatechindisulfonsäure	1	0,5	3085	0,27
	1	1	,,	0,47
	1	2	,,	0,48
	1	3	,,	0,48
	1	4	,,	0,50
	0,5	1	3085	0,16
	1	1	,,	0,47
	2	1	,,	0,53
	3	1	,,	0,56
Chromotropsäure	0,5	2	3630	0,45
	1	2	,,	0,99
	2	2	,,	1,10
	3	2	,,	1,14
	4	2	,,	1,15
	1	0,5	3630	0,48
	1	1	,,	1,11
	1	2	,,	1,16
	1	3	,,	1,16
	1	4	,,	1,17

kann die allgemeine “inner Sphären” Struktur : [(Metall-Ligand)-Wesser] oder [(Metall-Ligand)-Lösungsmittel] angenommen werden. [30]

Abschliessend der Medium Effekt auf die Bildung von UO_2^{2+} Komplexverbindungen mit Pyrocatechin, Pyrocatechindisulfonsäure und Chromotropsäure in verschiedenen Wasser-Äthanol Mischungen verfolgt. Dazu wurde die Absorbtionskoeffizienten der Liganden und für 1 : 1 und 5 : 1 Metall-Ligand Verhältnisse gemessen. Da für die einzelnen Liganden (Tabelle 8) ein klaren Unterschied zwischen der Absorbtionswerten in

TABELLE 5

Neigungsverhältnismethode zur Bestimmung des UO_2^{2+}-Ligand Kombinationsverhältnisses

Ligand	ml. Ligand	ml. UO_2^{2+}	λ (Å)	E (Mol. cm/L)
Pyrocatechin	0,5	4	4040	0,19
	1	4	,,	0,25
	2	4	,,	0,42
	4	4	,,	0,69
	6	4	,,	0,81
	8	4	,,	0,88
	4	0,5	4040	0,24
	4	1	,,	0,33
	4	2	,,	0,46
	4	4	,,	0,67
	4	6	,,	0,79
	4	8	,,	0,85
Pyrocatechindisulfonsäure	1	1	3726	0,22
	1	2	,,	0,36
	1	3	,,	0,44
	1	4	,,	0,50
	1	5	,,	0,55
	0,5	1	3726	0,14
	1	1	,,	0,22
	2	1	,,	0,39
	3	1	,,	0,50
	4	1	,,	0,53
	5	1	,,	0,65
Chromotropsäure	1	1	3601	0,18
	1	2	,,	0,26
	1	3	,,	0,33
	1	4	,,	0,37
	1	15	,,	0,49
	0,5	1	3601	0,09
	1	1	,,	0,19
	2	1	,,	0,22
	3	1	,,	0,31
	4	1	,,	0,37

den verschiedenen Wasser-Äthanol Mischungen beobachtet wurde, kann man annehmen, dass für den Medium Effekt die Gleichung :

$$\log_m \gamma_L = \log \frac{E_W}{E_S} \tag{3}$$

TABELLE 6

Temperatureinfluss auf die Extinktion (E) für zwei verschiedenen Metall-Ligand Verhältnisse

Komplexverbindung	λ (A°)	C (Mol/L)	E (Mol. cm/L)			
			12,7°C	20,1°C	33,5°C	45,3°C
Pyrocatechin-Th^{4+}	2798	8.10^{-5}				
1 : 1			0,39	0,40	0,41	0,42
1 : 5			0,41	0,42	0,44	0,45
Pyrocatechindisulfonsäure-Th^{4+}	3085	1.10^{-4}				
1 : 1			0,67	0,68	0,69	0,71
1 : 5			0,69	0,71	0,72	0,74
Chromotropsäure-Th^{4+}	3630	4.10^{-5}				
1 : 1			0,17	0,17	0,18	0,19
1 : 5,5			0,08	0,10	0,11	0,12
Pyrocatechin-UO_2^{2+}	4040	6.10^{-3}				
1 : 1			0,13	0,13	0,14	0,15
1 : 5			0,20	0,22	0,23	0,24
Pyrocatechindisulfonsäure-UO_2^{2+}	3726	1.10^{-3}				
1 : 1			0,31	0,34	0,38	0,41
1 : 5			0,61	0,65	0,71	0,76
Chromotropsäure-UO_2^{2+}	3601	4.10^{-5}				
1 : 1			0,07	0,11	0,15	0,18
1 : 5			0,21	0,23	0,25	0,29

* Anfangskonzentration der beiden Substanzen

gültig ist. Hier bedeuten E_W und E_S die Absorptionskoeffizienten der Liganden in Wasser und in Wasser-Äthanol Lösungen.

In der oben angeführten Gleichung entspricht :

$$E = f\,([C_L]) \tag{4}$$

und so

$$\log_m \gamma_L = \log \frac{[C_L]_W}{[C_L]_S} \tag{5}$$

Aus Tabelle 8 kann man ersehen dass bei einer steigender Äthanol Konzentration, der Medium Effekt bei Pyrocatechin zunimmt, wogegen er für die anderen organischen Liganden abnimmt. Das kann durch dis grössere Affinität der $-$ SO_3H Gruppe gegenüber Wasser als für Äthanol erklärt werden.

Für die UO_2^{2+} Komplexverbindungen mit Pyrocatechin, Pyrocatechindisulfonsäure und Chromotropsäure wurden für jede Wasser-Äthanol

TABELLE 7

Thermodynamische Daten für die untersuchten Komplexverbindungen von Th^{4+} und UO_2^{2+}

Komplexverbindung	12,7°C		20,1°C		33,5°C		45,3°C		Δ H (Kca/Mol)	Δ S (Ca/Mol.g)
	log K	Δ G*	log K	Δ G	log K	Δ G	log K	Δ G		
Pyrocatechin-Th^{4+}	5,34	7,09	5,45	7,27	5,57	7,78	5,77	8,37	2,22	33,25
Pyrocatechindisulfonsäure-Th^{4+}	5,10	6,64	5,16	6,89	5,25	7,34	5,35	7,73	3,10	34,14
Chromotropsäure-Th^{4+}	4,85	6,32	4,91	6,57	4,95	6,91	4,98	7,22	3,58	34,28
Pyrocatechin-UO_2^{2+}	2,07	2,70	2,10	2,81	2,20	3,07	2,14	3,11	1,96	15,31
Pyrocatechindisulfonsäure-UO_2^{2+}	2,75	3,58	2,84	3,79	2,85	3,99	2,86	4,15	2,25	20,96
Chromotropsäure-UO_2^{2+}	3,74	4,87	4,26	5,69	4,30	6,01	4,55	6,60	6,25	39,31

* ΔG wurde in kcal/Mol gemessen

TABELLE 8

Medium Effekt in verschiedenen Wasser-Äthanol Mischungen

Ligand	Wasser-Äthanol (ml)	E (Mol.cm/L	$\log_m \gamma_L$
Pyrocatechin	25 : 0	1,52	—
	20 : 5	1,54	−0,002
	15 : 10	1,59	−0,021
	10 : 15	1,63	−0,031
	5 : 20	1,66	−0,036
	2 : 23	1,76	−0,064
Pyrocatechindisulfonsäure	25 : 0	0,71	—
	20 : 5	0,68	0,019
	15 : 10	0,66	0,028
	10 : 15	0,67	0,025
	5 : 20	0,70	0,006
	1 : 24	0,71	0,002
Chromotropsäure	25 : 0	0,86	—
	20 : 5	0,85	0,003
	15 : 10	0,83	0,011
	10 : 15	0,85	0,004
	5 : 20	0,86	0,001
	1 : 24	0,92	−0,032

Mischung die Stabilitätskonstanten nach Nagakura berechnet, wobei der Medium Effekt auf die Bildung der UO_2^{2+} Komplexverbindungen nach Gleichung abgeleitet wurde:

$$M^{n+} + nL^- \rightleftharpoons ML_n$$

$$K = \frac{[ML_n]}{[M^{n+}][L^-]^n} \tag{6}$$

$$\log_m \gamma_{ML_n} = \log \frac{K_W}{K_S} + \log {}_m\gamma_{M^{n+}} + n \log_m \gamma_{L^-} \tag{7}$$

Hier bedeuten K_W und K_S die gemessenen Stabilitätskonstanten in Wasser und in Wasser-Äthanol Mischungen. Die experimentällen Ergebnisse sind in den Tabellen 9 und 10 aufgeführt.

TABELLE 9

Abhängigkeit der Stabilitätskonstanten von Wasser-Äthanol Mischungen für die UO_2^{2+} Komplexverbindungen

Komplexverbindung	Wasser-Äthanol (ml)	UO_2^{2+}-Ligand Verhältnis	$E_{20,1\,°C}$ (Mol. cm/L)	log K
Pyrocatechin-UO_2^{2+}	50 : 0	1 : 1	0,13	2,11
		5 : 1	0,22	
	45 : 5	1 : 1	0,16	2,17
		5 : 1	0,26	
	35 : 15	1 : 1	0,17	2,18
		5 : 1	0,27	
	24 : 26	1 : 1	0,19	2,20
		5 : 1	0,28	
Pyrocatechindisulfonsäure-UO_2^{2+}	50 : 0	1 : 1	0,33	2,84
		5 : 1	0,65	
	45 : 5	1 : 1	0,40	2,90
		5 : 1	0,72	
	35 : 15	1 : 1	0,49	2,92
		5 : 1	0,85	
	24 : 26	1 : 1	0,64	2,95
		5 : 1	0,99	
	12 : 38	1 : 1	0,76	3,09
		5 : 1	1,35	
Chromtropsäure-UO_2^{2+}	50 : 0	1 : 1	0,14	4,26
		5 : 1	0,23	
	45 : 5	1 : 1	0,23	4,59
		5 : 1	0,34	
	35 : 15	1 : 1	0,18	4,66
		5 : 1	0,25	
	24 : 26	1 : 1	0,15	4,81
		5 : 1	0,25	
	12 : 38	1 : 1	0,11	4,98
		5 : 1	0,14	

TABELLE 10

Wasser-Äthanol Medium Effekt auf UO_2^{2+} Komplexverbindungen

Komplexverbindung	Wasser-Äthanol (ml)	Molenbruch (x_S)	$\log \frac{K_W}{K_S}$	$\log_m \gamma_{UO_2^{2+}}$	$n \log_m \gamma_{L^-}$	$\log_m \gamma_{UO_2^{2+}-nL^-}$
Pyrocatechin-UO_2^{2+}	50 : 0	—	—	—	—	—
	45 : 5	0,03	0,06	−0,64	−0,015	0,31
	35 : 15	0,11	0,07	−0,77	−0,007	0,19
	24 : 26	0,25	0,09	0,72	−0,025	1,66
Pyrocatechindisulfonsäure-UO_2^{2+}	50 : 0	—	—	—	—	—
	45 : 5	0,03	0,06	−0,64	0,012	0,35
	35 : 15	0,11	0,10	−0,77	0,024	0,29
	24 : 26	0,25	0,12	0,72	0,28	1,71
	12 : 38	0,49	0,25	2,99	0,011	3,91
Chromotropsäure-UO_2^{2+}	50 : 0	—	—	—	—	—
	45 : 5	0,03	0,33	−0,64	0,035	0,30
	35 : 15	0,11	0,40	−0,77	0,009	0,15
	24 : 26	0,25	0,55	0,72	0,01	1,62
	12 : 38	0,49	0,72	2,99	0,015	3,84

Werden die schwachen Abweichungen der Stabilitätskonstanten Verhältnisse $\log K_W/K_S$ gegenüber verschiedenen Wasser-Äthanol Mischungen berücksichtigt, so kann die oben angeführte Hypotese unterstützt werden, wonach sich die Lösungsmittel — oder Wassermoleküle ausserhalb der inneren Sphäre befindet. Bei Änderung des Wasser-Äthanol verhältnisses wird die Komplexverbindung nur schwach beeinflusst und daher kann man vermuten, dass die Ligandenposition sich zwischen Metall und Lösungsmittel — oder Wassermoleküle befindet.

Der Autor dankt Herrn Prof. Dr. H. -J. Born aus dem Institut für Radiochemie der Technischen Universität München für die grosszügige Förderung dieser Arbeit und der "Alexander von Humboldt" Stiftung aus Bonn-Bad Godesberg (BRD) für ihre Hilfe und Unterstützung.

LITERATUR

[1] S. Hietanen, *Acta Chim. Scand.*, **8**, 1926 (1954).

[2] J. J. Katz und G. T. Seaborg, "The Chemistry of the Actinide Elements" Methuen Co. Ltd, London, 1957.

[3] R. L. Frank, G. R. Clark und J. N. Coker, *J. Amer. Chem. Soc.*, **72**, 1827 (1950).

[4] T. Moeller und M. V. Ramaniah, *J. Amer. Chem. Soc.*, **76**, 2022 (1954).

[5] J. Szöcke, *Acta Phys. Phys. Chem. Szeged*, **5**, 51 (1959).

[6] E. Bullwinkel und P. Noppe, *J. Amer. Chem. Soc*, **80**, 2955 (1958).

[7] D. Dyrssen, *Svensk. Kem. Tid.*, **68**, 212 (1953).

[8] M. S. Subramanian und V. K. Manchanda, *J. Inorg. Nuclear Chem.*, **33**, 3001 (1971).

[9] B. I. Kim, C. Miyake und S. Imoto, *J. Inorg. Nuclear Chem.*, **77**, 963 (1975).

[10] B. Hök-Bernström, *Acta Chem. Scand.*, **10**, 174 (1956).

[11] D. Nebel und G. Urban, *Z. phys. Chem. (Leipzig)*, **233**, 73 (1966).

[12] G. Courtois, *Bull. Soc. chim. France*, **33**, 1762 (1923).

[13] O. Inghilleri und G. Gori, *Atti. Accad. Fisicritici Siena*, **1**, 506 (1901).

[14] N. C. Li und I. M. White, *J. Inorg. Nuclear Chem.*, **16**, 131 (1960).

[15] M. Bobtelsky und B. Graus, *Bull. Soc. chim. France*, **1953**, 382.

[16] I. I. Chernyaev, "Complex Compounds of Uranium", Israel Program for Scientific Translations, Jerusalem, 1966.

[17] M. J. Cabell, *Analyst*, **77**, 859 (1952).

[18] A. Müller, *Z. anorg. Chem.*, **109**, 235 (1920).

[19] L. Fernandes, *Gazz. chim. Ital*, **55**, 424 (1925).

[20] L. Fernandes, *Gazz. chim. Ital.*, **56**, 412 (1926).

[21] B. Sarma und G. P. Savariar, *J. Sci. Ind. Research*, **16—B**, 80 (1957).

[22] P. Job, *Ann. Chim. Phys.*, **9**, 113 (1928).

[23] J. H. Yoe und A. L. Jones, *Ind. Eng. Chem. Anal. Educ.*, **16**, 111 (1944).

[24] A. E. Harvey und D. L. Manning, *J. Amer. Chem. Soc.*, **72**, 4488 (1950).

[25] S. Nagakura, *J. Amer. Chem. Soc.*, **76**, 3570 (1954).

[26] S. Nagakura, *J. Amer. Chem. Soc.*, **80**, 520 (1958).

[27] M. Bobtelsky und B. Graus, *J. Amer. Chem. Soc.*, **76**, 1536 (1952).

[28] C. Keller, "The Chemistry of the Transuranium Elements", Verlag Chemie GmbH, Weinheim, 1971.

[29] A. D. Jones und G. R. Choppin, in "Actinides Reviews" Edited by A. H. W. Aten jr. and J. Kooi, Elsevier Publ. Comp., Amsterdam, 1969.

[30] J. I. Kim, H. Duschner, T. Hashimoto, "Preferential Solvatations of Single Ions", Preprint.

Revue Roumaine de Chimie **25**, *8*, 1213–1220 (1980)

CHEMICAL GRAPHS. XXXIX[1]

VALENCE ISOMERS OF MONODEHYDRO-[*n*]ANNULENES

VIORICA BACIU[a] and ALEXANDRU T. BALABAN*[,b]
[a]Geological Prospecting Enterprise for Solid Minerals,
Bucharest, Romania.
[b]Department of Organic Chemistry, The Polytechnic, Bucharest, Romania

An algorithm is developed for obtaining the structures of all valence isomers of monodehydro-[*n*]annulenes, $C_2(CH)_{n-2}$ for $n = 4, 6, 8$, and 10. Benzocyclobutadiene ** is an example for $n = 8$, and naphthalene for $n = 10$. Drawings are presented for graphs $C_2(CH)_{n-2}$ with $n = 4$ and 6, but the numbers for $n = 8$ and 10 are too large so that the respective drawings are available on request.

INTRODUCTION

Previous papers in this series have introduced a new, graph-theoretical, definition of valence isomerism (see below), and have presented procedures (algorithms) for obtaining the structure and numbers of valence isomers of [*n*] annulenes (*n*-valenes, connected cubic multigraphs on *n* vertices) with $n = 4-10$[2,3] and 12,[4] benzo-*n*-valenes with $n = 4$, 6, 8 and 10,[5] and homovalenes with 3, 5, 7 and 9 carbon atoms,[6a] and the benzoderivatives of homovalenes.[6b] Structures of homovalenes with 11 carbon atoms were determined and are available on request. The numbers of general cubic graphs for $n = 4-12$ were calculated[7] by means of a computer program for implementing the formula[8] giving the numbers of general cubic graphs on *n* points

$$Z\,(S_n[S_3]) \cap Z\,(S_{3n/2}[S_2])$$

and subtracting the number of disconnected graphs. The values thus found for $n = 4-12$ are exactly those obtained earlier by means of the recurrence algorithm.[2,3]

---

* To whom correspondence should be addressed.

** We prefer this name to the *Chem. Abstr.* name of benzocyclobutene.

Valence isomers of hydrocarbons are defined as hydrogen-depleted graphs which have the same partition of vertex degrees. For example n-valenes or valence isomers of $[n]$annulenes are those isomers of hydrocarbons C_nH_n whose constitutional hydrogen-depleted graphs are cubic graphs, i.e. all vertices have degree three, so that the formula of n-valenes is $(CH)_n$.

The present paper discusses valence isomers of dehydroannulenes, i.e. hydrocarbons which have two hydrogens less than valenes with the same number of carbon atoms. Several important compounds belong to this class : just as benzene $(CH)_6$ is the most important annulene, naphthalene $C_2(CH)_8$ is the simplest condensed benzenoid hydrocarbon. Naphthalene $C_2(CH)_8$ is a valence isomer of dehydro-[10]annulene. At one time one of us had believed on the basis of using ^{14}C-labelling experiments[9] that naphthalene underwent in the presence of aluminium chloride a degenerate rearrangement (automerization) which reshuffled its carbon atoms ; this was, however, soon proved to be based on erroneous experimental data when ^{14}C was replaced by ^{13}C (probably owing to unfortunate fortuitous radiochemical impurities in the experiments using ^{14}C). [10,11] Recently, however, Scott has shown [12] that naphthalene does automerize thermally at 1035°C, scrambling the α and β carbon atoms. The mechanism advanced for this automerization also accomodates the unexplained isomerization of azulene to naphthalene, and involves strained unstable valence isomers (azulene is also a valence isomer of naphthalene and dehydro- [10] annulene) in a symmetry allowed process :

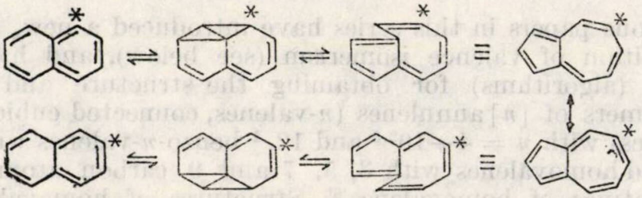

Scheme 1. Proposed [12] mechanism for the automerization of naphthalene above 1000°C involving valence isomerization to azulene and to a strained valence isomer with a bicyclobutane subgraph.

More recent data produced by Alder and coworkers on the basis of thermolysis of ^2H-, ^{13}C- and methyl-labelled azulene and of benzo[*f*]-azulene (the latter gives phenanthrene and not anthracene as expected) indicated, however, that free radicals are more likely intermediates ; the mechanism proposed involves spiranic radicals which rearrange by "methylene walks". [13-15] A different mechanism was suggested by Wentrup and Becker [16] who obtained naphthalene and azulene on pyrolyzing 4-cinnamylidene-3-methylisoxazol-5(4*H*)-one at 700°C in vacuum : the intermediate vinylidene (formed by splitting acetonitrile and carbon dioxide) rearranges to two valence isomers of naphthalene, one with tɹidle bond which was stable enough to be isolated in low amounts, and a postulated one.

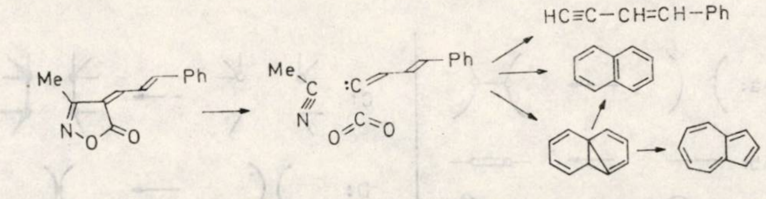

Scheme 2. Proposed[16] mechanism for the formation of naphthalene and azulene from cinnamylidene-methylisoxazolone.

The formation of azulene and naphthalene derivatives in the pyrolysis of phenylacetylene derivatives was observed by Brown.[17]

We decided therefore to analyze the manifold of valence isomers of dehydro-[*n*] annulenes with $n = 4, 6, 8$, and 10 carbon atoms ; their hydrogen-depleted formulas are connected multigraphs with two vertices of degree four and $n-2$ vertices of degree three. *

VALENCE ISOMERS OF MONODEHYDRO-[*n*]ANNULENES

We developed a constructive algorithm for obtaining the required connected multigraphs with two vertices of degree four and $n-2$ vertices of degree three. It is based on the following recurrence relations (Fig. 1) :

A. In a connected or disconnected general multigraph with two vertices of degree four and $n-4$ vertices of degree three we create two new vertices of degree three, either (a) inter-edge, or (b) intra-edge ; as a particular application of the latter operation, we form a cyclopropenyl subgraph from a loop of a general graph (c). This procedure was described earlier.[2,3]

B. In a connected or disconnected cubic (trivalent) multigraph with *n* vertices, we join two vertices by a new edge. In this case, the two newly formed vertices of degree four are adjacent.

C. In a connected or disconnected multigraph with two vertices of degree two and $n-2$ vertices of degree three, each vertex of degree two is joined by a new edge to a vertex of degree three.

D. In a connected or disconnected multigraph with one vertex of degree four and $n-2$ vertices of degree three, we create one new vertex of degree four at the crosspoint of two edges.

---

* Graph-theoretical terminology : Simple graphs have neither loops nor multiple edges. Connected graphs are those where there is a path linking any pair of points (vertices). In multigraphs two adjacent vertices may be joined by more than one edge (multiple bond). In general graphs, a vertex may be connected to itself by a loop which is counted twice in the degree of that vertex. The degree of a vertex is the number of lines (edges) meeting in that vertex. Planar graphs may be written on a plane so that no two edges cross. All vertices of a regular graph have the same degree ; a regular graph (or multigraph) of degree three is called cubic, or trivalent, graph (multigraph).

E. In a connected or disconnected multigraph with one vertex of degree two, one vertex of degree four, and $n-2$ vertices of degree three, we join the vertex of degree two to a vertex of degree three.

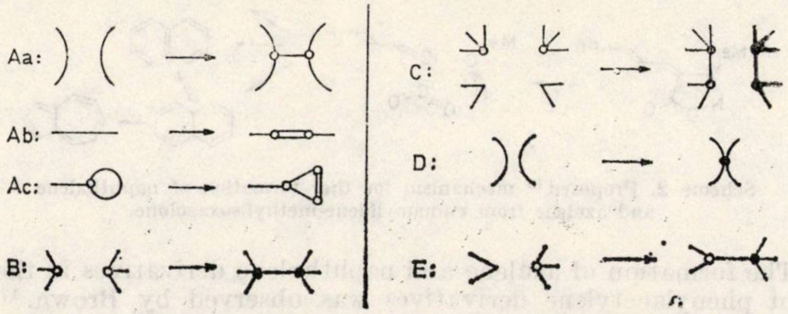

Fig. 1. — Operations used in constructing valence isomers of $C_2(CH)_{n-2}$; white points denote vertices of degree three, black points of degree four, and kinks denote points of degree two.

The lists of connected cubic multigraphs with 4, 6, 8, and 10 vertices, [2] of connected cubic general graphs with the same number of vertices, [3] of planar connected cubic multigraphs with 12 vertices, [4] and of connected multigraphs with vertices of degrees four or less and the total number of vertices smaller than six, [18] are published. To obtain disconnected graphs one has to combine (up to isomorphism) smaller connected graphs in pairs, triples, etc.

After performing on each graph all possible operations A—E in all possible combinations of vertices/ edges, one has to remove all chemically irrelevant graphs. Those graphs which have to be discarded are, in order :

(1) graphs which are isomorphic with graphs already obtained ;

(2) disconnected graphs, multigraphs or general graphs ;

(3) loop-graphs, i.e. all general graphs possessing one or more loops ;

(4) non-planar graphs or multigraphs.

Indeed, disconnected graphs have only been of interest in chemistry for bond and electron (be)-matrices and synthetic strategy planning, [19] not for structural investigations as in the present context ; loop-graphs have only found applications for symbolising (through the loop and its adjacent vertex) a heteroatom, with the restriction that graphs with geminal loops are chemically irrelevant. Finally, all constitutional formulas so far known correspond to planar graphs in which vertices symbolize atoms, and edges symbolize covalent bonds ; usually, hydrogen and other univalent atoms are omitted leading to hydrogen-depleted formulas (multigraphs).

In practice, it has proved sufficient to employ operations A, C, D ; operation D is in fact a check-up for completeness of the procedure.

In order to perform the discarding operations (1)—(4) the following procedures were applied :

For (1), when the number of vertices is lower than six, it is necessary to group the connected multigraphs corresponding to $C_2(CH)_{n-2}$

according to easily recognized structural characteristics. As in earlier publications, these parameters will be in order : the number β of double bonds, or circuits with two vertices (with the convention that a triple band is counted as two double bonds) ; the number *t* of circuits with three vertices ; and the number *q* of circuits with four vertices. For a given *n* value, each graph is coded by four digits, denoting in order β, *t*, *q*, and a serial number *s* which is 1, unless two or more graphs have identical triples for β, *t*, and *q* ; in this case *s* is 1, 2, . . . ordered according to the following criteria (similarly to criteria used earlier [5]) in the given order of priority :

— the smaller number of 5-circuits, 6-circuits, etc. ;

— with the double bond(s) in smaller rings ;

— with the double bonds at the smaller distance (for two double bonds, this gives the order : triple bond > cumulated > conjugated > isolated double bonds ; the first such pair prevails) ;

— with a larger number of double bonds at smaller distances (by distance here and in the preceding criterion we mean topological distance) ;

— with vertices of highest degree at smaller distance ;

— with vertices of highest degree bonded by more edges.

This grouping facilitates the recognition of isomorphic multigraphs.

For (2) and (3), disconnected or loop-graphs are easily recognized and discarded.

For (4), non-planar graphs have, according to the well-known Kuratowsky theorem, either a complete K_5 subgraph, or a bipartite $K_{3.3}$ subgraph. Therefore if one eliminates in the construction non-planar starting graphs, a large portion of non-planar graphs are also eliminated ; there remain, however, non-planar graphs obtained from planar graphs on the basis of the construction procedures A—E, which have to be discarded as chemically irrelevant. In the following figures all graphs will be drawn so that planar graphs are shown without crossing edges. Examples of non-planar graphs are the two possible non-planar graphs with 6 vertices corresponding to $C_2(CH)_4$: the first is a simple graph, the second is a multigraph, and both have the dotted line in addition to $K_{3.3}$.

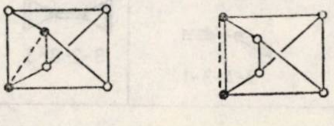

$2_4 4_3$-0-3-9-1 $2_4 4_3$-1-0-9-1

Scheme 3. The two possible non-planar graphs with six vertices corresponding to $C_2(CH)_4$; they differ only by the position of the broken edge. The two black points have degree four, the four white points (vertices) have degree three.

The planar graphs (connected multigraphs) $C_2(CH)_{n-2}$ for $n = 4$ and 6 are presented in Fig. 2 with the notation giving under each graph, in order, β—*t*—*q*—*s*. Actually, these four numbers should every time be preceded by $(n-2)_3 2_4$ indicating that from the n vertices, $n-2$ have degree three, and two vertices have degree four ;[18] however, for the simplification of Fig. 2 these indications are given only once, in the column under n. For $n = 8$ and 10 the numbers of such graphs are too large, as seen from Table 1, therefore the drawing of these latter graphs is available on request. A comparison between the total numbers of graphs shows that when n increases by 2 the total numbers of graphs from Table 1 increases approximately by an order of magnitude, and that the ratio between successive total numbers increases with increasing n.

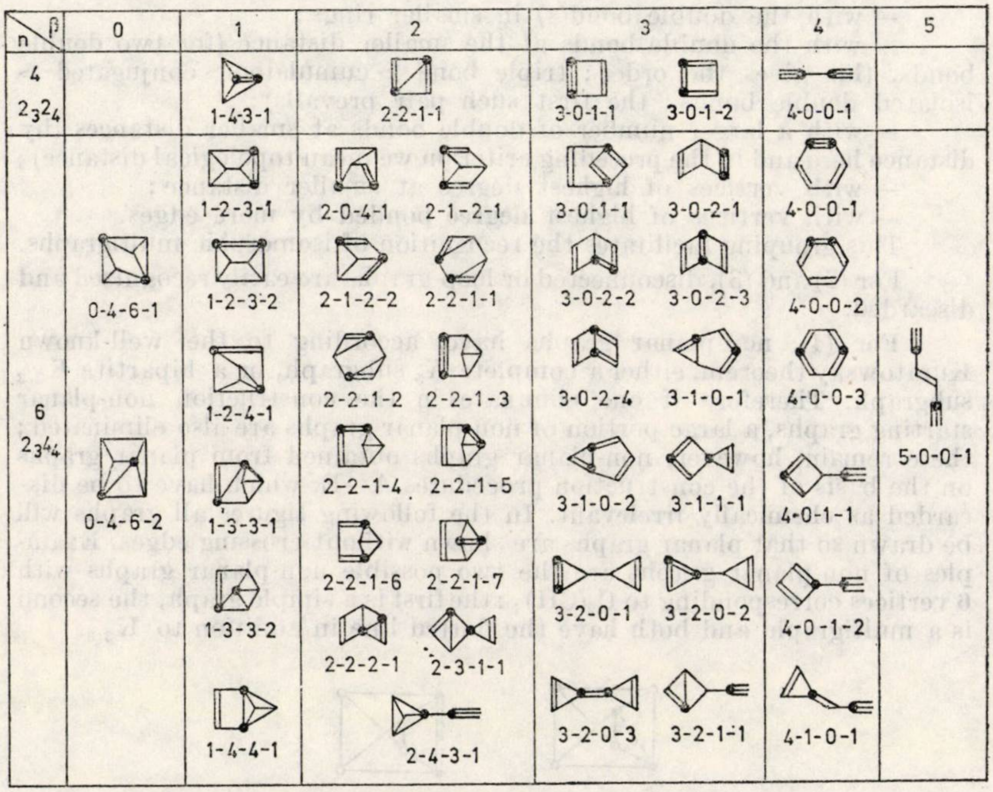
n
β
0
1
2
3
4
5
4
2₃2₄
1-4-3-1
2-2-1-1
3-0-1-1
3-0-1-2
4-0-0-1
6
2₃4₄
1-2-3-1
2-0-4-1
2-1-2-1
3-0-1-1
3-0-2-1
4-0-0-1
0-4-6-1
1-2-3-2
2-1-2-2
2-2-1-1
3-0-2-2
3-0-2-3
4-0-0-2
1-2-4-1
2-2-1-2
2-2-1-3
3-0-2-4
3-1-0-1
4-0-0-3
5-0-0-1
0-4-6-2
1-3-3-1
2-2-1-4
2-2-1-5
3-1-0-2
3-1-1-1
4-0-1-1
1-3-3-2
2-2-1-6
2-2-1-7
3-2-0-1
3-2-0-2
4-0-1-2
2-2-2-1
2-3-1-1
1-4-4-1
2-4-3-1
3-2-0-3
3-2-1-1
4-1-0-1

Fig. 2. — Planar connected multigraphs corresponding to valence isomers of monodehydro-[n] annulenes $C_2(CH)_{n-2}$ for $n = 4$ and 6. The two black points have in each case degree four, the remaining $n-2$ points have degree three.

Of course, only a relatively small fraction of those planar connected multigraphs can correspond to stable chemical compounds, namely : those devoid of triple bonds or of cumulated double bonds in smaller rings than C_8, those obeying Bredt's rule (though this requirement is less stringent than the preceding one), [20] those which do not possess tetrahedrane skeletons (though tetra-t-butyl-tetrahedrane is stable) [21] or cyclobutadiene moieties (though some stable cyclobutadienes are known either with

TABLE 1

Numbers of planar connected multigraphs $C_2(CH)_{n-2}$ with β double bonds

β / Vertices *n*	0	1	2	3	4	5	6	7	Total
4	0	1	1	2	1	—	—	—	5
6	2	6	13	12	6	1	—	—	40
8	16	57	108	104	57	12	1	—	355
10	139	611	1211	1094	588	170	24	1	3838

t-butyl groups, or with push-pull effects, or with larger annelated rings).[22] Thus from Fig. 1, for $n = 4$ only butadiyne (diacetylene) 4—0—0—1 is stable, and for $n = 6$ only graphs 3—2—0—3, 4—1—0—1 and 5—0—0—1 should correspond to stable molecules; in addition, *ortho*- (4—0—0—1 ↔ ↔4—0—0—2), *meta*- (3—1—0—1) and *para*-benzyne (3—0—2—3 and 3—0—2—4 are also resonant structures) have been studied chemically as reactive intermediates.[23] It is questionable whether formula 4—0—0—3 for $n = 6$ is also a resonant structure of *para*-benzyne. For explaining rearrangements or automerizations (topomerizations)[24] a certain degree of instability is acceptable for intermediates.

REFERENCES

[1] Preceding part, A. T. Balaban, *Math. Chem.*, **8**, 159 (1980).

[2] A. T. Balaban, *Rev. Roumaine Chim.* **11,** 1097 (1966); erratum *ibid.* **12,** No. 1, last page (1967).

[3] A. T. Balaban, *Rev. Roumaine Chim.* **15,** 463 (1970); **19,** 1323 (1974).

[4] A. T. Balaban, *Rev. Roumaine Chim.*, **17,** 865 (1972).

[5] A. T. Balaban, *Rev. Roumaine Chim.*, **19,** 1185 (1974).

[6a] A. T. Balaban, *Rev. Roumaine Chim.*, **19,** 1611 (1974); erratum *ibid.* **23,** 311 (1978).

[6b] A. T. Balaban, *Rev. Roumaine Chim.*, **22,** 987 (1977).

[7] A. T. Balaban, I. Moţoc, and R. Vancea, to appear.

[8] F. Harary and E. M. Palmer, "Graphical Enumeration", Academic Press, New York, 1973, p. 174.

[9] A. T. Balaban, D. Fărcaşiu, and C. Măntescu, *J. Amer. Chem. Soc.*, **89,** 1958 (1967); A. T. Balaban and D. Fărcaşiu, *Tetrahedron Letters*, **1968,** 1273.

[10] A. T. Balaban, D. Fărcaşiu, V. A. Koptyug, I. S. Isaev, M. I. Gorfinkel and A. I. Rezvukhin, *Tetrahedron Letters*, **1968,** 4757.

[11] H. A. Staab and M. Haenel, *Chem. Ber.*, **103,** 1095 (1970); *Angew. Chem.*, **80,** 567 (1968).

[12] L. T. Scott and G. K. Agopian, *J. Amer. Chem. Soc.*, **99,** 4506 (1977).

[13] R. W. Alder and G. Whittaker, *J. Chem. Soc. Perkin Trans.* 2, **1975,** 714.

[14] R. W. Alder and C. Wilshire, *J. Chem. Soc. Perkin Trans.* 2, **1975,** 1464;

[15] R. W. Alder, R. W. Whiteside, G. Whittaker and C. Wilshire, *J. Amer. Chem. Soc.*, **101,** 629 (1979).

[16] J. Becker, C. Wentrup, E. Katz and K, — P. Zeller, *J. Amer. Chem. Soc.*, **102,** 5110 (1980).

[17] R. F. C. Brown, F. W. Eastwood, and F. P. Jackman, *Austral. J. Chem.*, **30,** 1757 1977); **31,** 979 (1978); G. J. Baxter and R. F. C. Brown, *ibid.*, **31,** 327 (1978).

[18] A. T. Balaban, *Rev. Roumaine Chim.*, **18**, 635 (1973) ; erratum, *ibid.* **19**, No. 2, 338 (1974).

[19] J. Dugundji, P. Gillespie, D. Marquarding, I. Ugi and F. Ramirez, in "Chemical Applications of Graph Theory" (editor A. T. Balaban), Academic Press, London, 1976, p. 107 ; I. Ugi, J. Bauer, J. Brandt, J. Friedrich, J. Gasteiger, J. Jochum and W. Schubert, *Angew. Chem.*, **91**, 99 (1979).

[20] G. Köbrich, *Angew. Chem., Internat. Ed. Engl.*, **12**, 464 (1973).

[21] G. Maier, S. Pfriem, U. Schäfer and R. Matusch, *Angew. Chem.*, **90**, 552 (1978).

[22] G. Maier, *Angew. Chem.*, **86**, 491 (1974) ; *Angew. Chem. Internat. Ed. Engl.*, **13**, 425 (1974).

[23] R. H. Levin, in "Reactive Intermediates" (editors M. Jones, Jr. and R. A. Moss), Wiley, New York, 1978.

[24] G. Binsch, E. L. Eliel and H. Kessler, *Angew. Chem. Internat. Ed. Engl.*, **10**, 570 (1971).

Revue Roumaine de Chimie 25, *8*, 1221–1228 (1980)

SOLVOLYSIS OF 7(γ-TOSYLOXYPROPYL)-7H-DIBENZO [a, e] CYCLOHEPTENE, 5(β-TOSYLOXYETHYL)-AND 5 (γ-TOSYLOXYPROPYL)-5H-DIBENZO [a, c] CYCLOHEPTENE

M. BANCIU,[a] RODICA VLAD,[a] PHAN LE THUY[a] and C. DRĂGHICI[b]
[a] Laboratory of Organic Chemistry — TCH ; Polytechnic Institute
76206 — Bucharest — 16, Romania
[b] Centre of Organic Chemistry, Bucharest, Romania

Received March 4, 1980

The title tosylates 4, 5 and 6 were synthesized starting from 7*H*-dibenzo[*a*, *e*]cyclohepten-7-yl-acetic acid (7a) and 5*H*-dibenzo[*a*, *c*]cyclohepten-5-yl-acetic acid (9a) respectively. The kinetic data as well as the structures of solvolysis products of 4, 5 and 4 in acetic acid, trifluoroacetic acid and trifluoroethanol indicated the lack of double bond participation. An explanation for this behaviour is suggested.

1. INTRODUCTION

In the earlier papers from this laboratory the effect of the side-chain elongation on the degree of double bond participation in solvolyses of tosylates with a 7*H*-dibenzo [*a*, *e*] cycloheptene skeleton was investigated.[1, 2]

The acetolyses of the tosylate **2** gave rise[1] to about 85% bridged products in comparison to only 6.5—8.5% products of double bond participation observed in acetolyses of **1**.[2] The kinetic determinations showed that the acetolysis rate constant[3] of the tosylate **2** is seven times greater[4] than that of the tosylate **1** (table 1) and 15 times greater than the rate constant of the saturated analogue **3**.

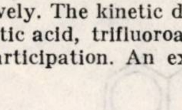

1

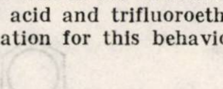

2

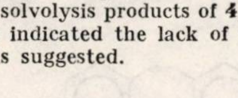

3

In the present paper we report the results obtained from the solvolyses of the tosylate **4**, the next higher homologue of **2**, as well as of the tosylates **5** and **6**, isomeric with **2** and **4**, respectively.

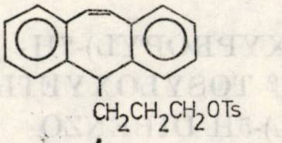

4

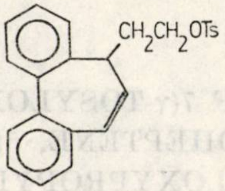

5

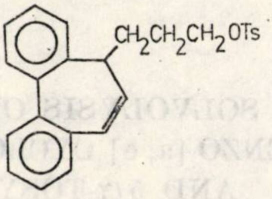

6

Examination of molecular models as well as other investigations from this laboratory concerning related dibenzo[*a*, *c*]cycloheptene derivatives have shown [5] that, at least in the case of tosylate **6**, the participation of the double bond is possible.

2. SYNTHESIS

The tosylate **4** was synthesized by an Arndt-Eistert homologation of the known [1,6] acid **7a** through the acid chloride **7b** [7] and diazoketone **7c**. [7] Reduction of the obtained ester **8a** with $LiAlH_4$ afforded the alcohol **8b** *)[8] from which the tosylate **4***)[8b,c] was then obtained in the usual manner.

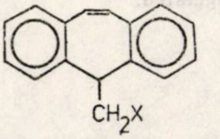

7

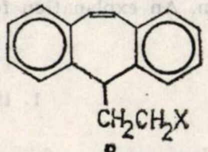

8

a : $X = COOH$
b : $X = COCl$
c : $X = COCHN_2$

a : $X = COOCH_3$
b : $X = CH_2OH$
c : $X = Br$

d : $X = CN$
e : $X = COOH$
f : $X = COOC_2H_5$

Analogous results were obtained starting from the previously synthesized [9] bromide **8c**. Treatment with potassium cyanide and subsequent hydrolysis of the nitrile **7d** *)[8d] afforded the acid **8e** *)[8d]. The corresponding ester **8f** [8d,10] was converted through conventional reactions mentioned above into the tosylate **4**.

Tosylates **5** and **6** were synthesized starting from the unsaturated acid **9a**, obtained in this laboratory in connection with other investigations.[5] The tosylate **6** was synthesized from **9a**, by usual reactions through the ester **9b** and the alcohol **9c**.

On the other hand, the same acid **9a** was converted into the acid chloride, [5] then into the corresponding diazoketone.[5] The Wolff rearrangement of this diazoketone in ethanol in the presence of Ag_2O afforded the ester **10a** with a three carbon side chain, which was further successively converted into the alcohol **10b** and the tosylate **6**.

---

*) product mentioned in the patent literature but not characterized.

The IR and ^1H—NMR spectra (see Experimental) of all the above new compounds confirm their structures.

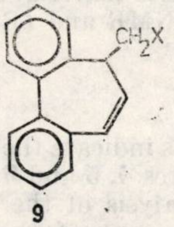

9

a : X = COOH
b : X = $COOCH_3$
c : X = CH_2OH

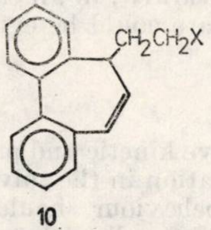

10

a : X = $COOC_2H_5$
b : X = CH_2OH

3. RESULTS

The rate constants of unbuffered acetolyses of tosylates **4**, **5** and **6** at 110°C (see table 1) are of the same order of magnitude as the rate constant of the saturated tosylate **3**, suggesting the absence of double bond participation.

TABLE 1

Rate constants for acetolysis at 110°C of some dibenzo[a, e]—and dibenzo [a, c]cycloheptene tosylates

Tosylate	k.$10^5(s^{-1})$	Relative rate
2[a]	20.4	15.2
3[a]	1.34	1
1[b]	3.18	2.37
4	1.64	1.22
5	0.71	0.53
6	2.3	1.74

[a] Ref. 3, [b] Ref. 4

The preparative acetolyses of the tosylates **4**, **5** and **6** at reflux in the presence of sodium acetate, afforded, in the mentioned order, 79%, 90% and 98% of the starting acetate (or alcohol, after reduction with $LiAlH_4$ of the crude reaction mixture) along with numerous minor compounds (in the cases of tosylates **4** and **5**) which could not be identified or separated.

In order to favour the participation of the double bond, the solvolyses of the investigated tosylates were carried out in less nucleophilic solvents, namely trifluoroacetic acid and trifluoroethanol.

The buffered trifluoroacetolyses of the three tosylates **4**, **5** and **6** at reflux or at room temperature yielded only polymeric material. Even on quenching the solvolysis mixture after a short reaction time, the products contain polymers along with the starting material.

Trifluoroethanolyses of the same tosylates (performed at reflux) proceed very slowly; in all cases only polymeric material along with the starting tosylate could be evidenced by ^1H-NMR and IR spectroscopy.

4. DISCUSSION

The above kinetic and preparative results indicate the lack of double bond participation in the solvolyses of tosylates **4**, **5** and **6**. The explanation of this behaviour should include an analysis of the factors which usually determine the involvement of the double bond during solvolyses, namley: (i) a convenient distance between the ionising centre and double bond; (ii) an efficient overlap between π orbitals and the vacant p orbital (enthalpic condition) and (iii) the abundance (population) of the most suitable conformation for double bond participation (entropic condition).

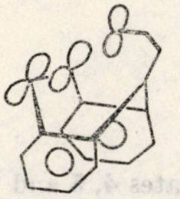
11

The inspection of Dreiding stereomodels of the tosylate **4** indicate that the first two from the above conditions are fulfilled. In one of the two possible conformers, **11**, *) the cationic centre could approach to a favourable distance (1.54 Å or less) the double bond, preserving at the same time the parallelism of the lone p orbital with the π orbitals. The lack of double bond participation seems to be due in this case to the existence of a large number of conformations of the three carbon side-chain, which considerably lowers the activation entropy. The important double bond participation shown [1] in the acetolyses of the lower homologue **2** results, very probably, from a more favourable entropic factor (two — membered in comparison with three — membered side chain).

In the case of the tosylate **6** with a dibenzo[a, c]cycloheptene skeleton, the molecular models reveal that a favourable geometry for double bond participation could be attained in both possible conformations (**12A** and **12B**). When the parallelism of the interacting orbitals was achieved, a distance of about 1.55 Å was calculated between C^+ and C^6 in **12A** and also between C^+ and C^7 in **12B**.

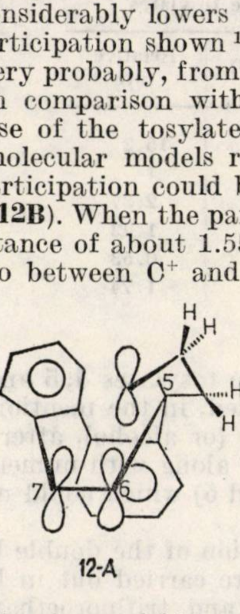

12-A

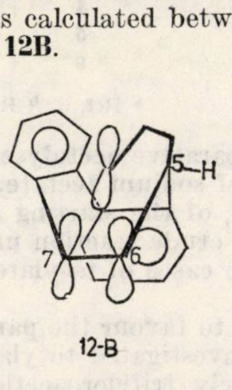

12-B

---

*) The second conformer of **4** is unsuitable to double bond participation, but could be converted into the first one through ring inversion, which could occur easy in solvolysis conditions.

Here again the large number of conformations of the three-membered side-chain seems to diminish the probability of approach between the cationic centre and the double bond at a C—C bond distance.

The absence of double bond participation was also shown[11] for the cyclopentenyl nosylate **13** with a three — membered side-chain, in spite of the strong participation exhibited by the lower homologue **14**,[12] where all the requirements for double bond assistance are attained.

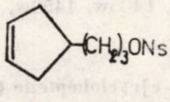

13

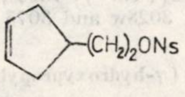

14

The solvolytic behaviour of the lower homologue of **6**, namely the tosylate **5**, markedly differs from that of the isomeric tosylate **2** with a dibenzo [*a*, *e*] cycloheptene skeleton. In this case the explanation seems to be mainly of steric origin. Owing to geometric reasons the vacant orbital from the β-carbon atom in the side-chain cannot approach sufficiently the π orbitals of the middle-ring double bond in order to form a new bond. The examination of Dreiding models shows that in either of the two possible conformations of the dibenzocycloheptene skeleton (**15A**, **15B**) the minimal distance between the cationic centre and the carbon atoms of the double bond ($C^+ \ldots C^6$ in **15A** and $C^+ \ldots C^7$ in **15B**) is about 2.3—2.4 Å (when the interacting orbitals are parallel to each other) in comparison with 1.55 Å in the tosylate **2**.

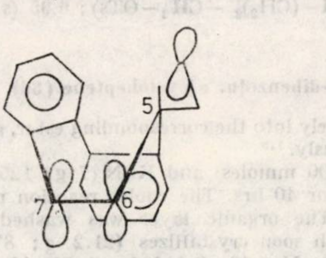

15-A

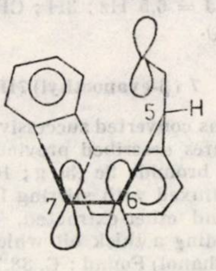

15-B

From the above results it follows that the double bond does not participate during the solvolyses of the investigated tosylates, owing to the unfavourable geometry in the case of **5** and to unfavourable entropic factors in the cases of **4** and **6**.

EXPERIMENTAL

Melting points are uncorrected. IR spectra were recorded with a C. Zeiss Jena UR—20 spectrometer. ^1H-NMR-Spectra were registered on a Varian A-60A spectrometer using TMS as internal standard.

For kinetic determinations the ampoule technique was used. The liberated *p*-toluenesulfonic acid formed in the acetolyses was determined after addition of a known excess of 0.05 M NaOAc/AcOH solution, by titration with a 0.05 M $HClO_4$/AcOH solution in the presence of crystal-violet. The concentrations of the tosylate solutions were 10^{-2} M.

Methyl 7H-dibenzo[a, e]cyclohepten-7-yl propionate (8a)

The acid **7a**[1] was converted into the acid chloride **7b** and diazoketone **7c** as previously described.[7] Into a stirred solution of crude diazoketone **7c** (1 g; 3.64 mmoles) in 20 ml anhydrous methanol, warmed at 50°C, Ag_2O (about 0,8 g; freshly prepared and dried) was added in small portions. The addition of Ag_2O was continued until no evolution of gases was observed when a sample of reaction mixture was treated with conc. HCl (about 8 hrs.). After filtration the solvent was removed *in vacuo*, affording the crude ester **8a** (0.9 g; 90%). *The ester* **8a**, m.p. 195–7° (from methanol). Found: C, 81.94; H, 6.33. Calcd. for $C_{19}H_{18}O_2$: C, 81.99; H, 6.50%.

IR spectrum (CCl_4; cm^{-1}): 1090s, 1170w, 1188w, 1405w, 1452w, 1465w, 1495w, 1725s, 2825w, 2852w, 2930w, 3028w and 3075 w.

7 (γ-hydroxypropyl) 7H-dibenzo[a, e]cycloheptene (8b)

Over a stirred suspension of $LiAlH_4$ (0.21 g; 5.5 mmoles) in 20 ml anhydrous ether a solution of the ester **8a** (1.53 g; 5.5 mmoles) in 50 ml anhydrous ether was dropped during 1 hr. The reaction mixture was refluxed for 10 hrs then left overnight. The usual work-up afforded the alcohol **8b** (1.35 g; 98%) as a pale yellow oil which could be crystallized by addition of a few drops of cyclohexane. *The alcohol* **8b**, m.p. 46–48°C (from cyclohexane).

IR spectrum (CCl_4; cm^{-1}): 946w, 1032m, 1060s, 1115w, 1165w, 1440m, 1460m, 1495s, 2877s, 2945s, 3022s, 3071m, 3180–3550 large, and 3636w.

^{1}H-NMR spectrum (CCl_4; δppm): 0.8–1.95 (m; 4H; $CH_2-CH_2-CH_2OH$); 2.6 (s; 1H; OH); 3.27 (t; J = 6.5 Hz; 2H; CH_2-OH); 3.86 (t; J = 8 Hz; 1H; $CH-CH_2$); 6.90 (s; 2H; $H^{3,4}$); 7.1–7.5 (m; 8H; H_{arom}).

The alcohol **8b** was also obtained by $LiAlH_4$ reduction of the ethyl ester **8f** *(vide infra)*.

7 (γ-tosyloxypropyl) 7H-dibenzo [a, e] cycloheptene (4), was obtained as a pale yellow oil, on treatment of the alcohol **8b** with *p*-toluenesulfochloride in pyridine (60% yield).

IR spectrum (CS_2; CCl_4; cm^{-1}): 557s, 667s, 765vs, 786vs, 798vs, 940s, 1102m, 1180vs, 1192vs, 1376vs, 1440m, 1465m, 1498m, 1605w, 2930m, 2965m, 3030m and 3075m.

^{1}H-NMR spectrum ($CDCl_3$; δ ppm): 1.1–2.1 (m; 4H; $CH_2-CH_2-CH_2-$); 2.42 (s; 3H; CH_3); 3.90 (t; J = 6.5 Hz; 3H; $CH-(CH_2)_2-CH_2-OTs$); 6.95 (s; 2H; $H^{3,4}$); 7.1–8.0 (m; 12H; H_{arom}).

7 (β-cyanoethyl) 7H-dibenzo[a, e]cycloheptene (8d)

The acid **7a** was converted successively into the corresponding ester, alcohol and bromide **8c** after the procedures described previously.[1,9]

A solution of bromide **8c** (30 g; 100 mmoles) and KCN (7 g; 125 mmoles) in 150 ml 95% ethanol was refluxed with stirring for 40 hrs. The cooled reaction mixture was diluted with 250 ml water and ether-extracted. The organic layer was washed with water, dried and evaporated affording a thick oil which soon crystallizes (21.2 g; 87%). *The nitrile* **8d**, m.p. 104–7° (from ethanol) Found: C, 88.1; H, 6.48; Calcd. for $C_{18}H_{15}N$: C, 88.1; H, 6.16%.

IR spectrum (CCl_4; cm^{-1}): 1090s, 1122 m, 1462m, 1508m, 2248w, 2872s, 2935s, 2980s, 3028s, and 3075m.

7H-dibenzo[a, e]cyclohepten-7-yl propionic acid (8e)

A solution of nitrile **8d** (7.5 g; 30.5 mmoles) and KOH (5.5 g; 97.5 mmoles) in 30 ml methanol : water mixture (5 : 1) was refluxed for 8 hrs. The cooled reaction mixture was diluted with water (50 ml) and ether-extracted. The aqueous layer was boiled with Norit, filtered, cooled and acidified with dil. HCl, affording the acid **8e** (6.3 g; 78%). *The acid* **8e**, m.p. 175–8° (from ethanol). Found: C, 82.0; H, 6.33; Calcd. for $C_{18}H_{16}O_2$: C, 81.79; H, 6.10%.

IR spectrum (KBr; cm^{-1}): 767s, 801s, 1206m, 1220m, 1242m, 1266m, 1296m, 1306m, 1436m, 1495m, 1700vs and 2300–3400 large.

^{1}H-NMR spectrum ($CDCl_3$; δ ppm): 2.0–2.2 (m; 4H; CH_2-CH_2-); 4.1 (m; 1H; $CH-CH_2-$); 7.03 (s; 2H; $H^{3,4}$); 7.2–7.7 (m; 8H; H_{arom}); 10.6 (s; 1H; COOH).

Ethyl 7H-dibenzo [a, e] cyclohepten–7–yl–propionate (8f), was obtained in 98% yield on refluxing the acid **8e** with ethanol and conc. H_2SO_4 for 20 hrs. *The ester* **8f**, m.p. 47–50°C (lit[10] b.p./1 mm 185–190°).

IR spectrum (CCl_4 ; (cm^{-1}) : 1045m, 1160vs, 1185vs, 1195vs, 1218s, 1240s, 1375s, 1440m, 1465m, 1495m, 1735vs, 2935m, 2985s, 3025s and 3070m.

^1H-NMR spectrum (CCl_4 ; δ ppm) : 1.21 (t ; J = 7Hz ; 3H ; CH_3-CH_2-) 1.85 – 2.1 (m ; 4H ; $-CH_2-CH_2-$) ; 4.02 (q ; J = 7 Hz ; 2H ; CH_2-CH_3) ; 4.06 (m ; 1H ; $CH-CH_2-$) ; 6.90 (s ; 2H ; $H^{3,4}$) ; 7.1–7.5 (m ; 8H ; H_{arom}).

Methyl 5H-dibenzo [a, c]cyclohepten-5-yl acetate (9b) was obtained as a pale yellow oil, in 87% yield, on refluxing (7 hrs) the acid **9a** [5] with methanol previously saturated with anhydrous gaseous HCl. A pure sample of **9b** was obtained by column chromatography on alumina of the crude ester, on elution with ethyl ether : petroleum ether (2: 8) mixture. Found : C, 81.26 ; H, 5.92 ; Calcd. for $C_{18}H_{16}O_2$: C, 81.79 ; H, 6.11%.

IR spectrum (CS_2 ; CCl_4 ; cm^{-1}) : 738m, 751s, 766s, 785s, 1166s, 1742vs, 2955m, 3029 m and 3068 m.

^1H-NMR spectrum (CCl_4 ; δ ppm) : 2.0–4.2 (m, 3H ; $CH-CH_2$) ; 3.51 (s ; 3H ; COO CH_3) ; 5.98 (m, 1H ; H^6) ; 6.53 (d ; J = 10 Hz ; 1H ; H^7) ; 7.0–7.8 (m ; 8H ; H_{arom})

5 (β-hidroxyethyl)-5H-dibenzo[a, c]cycloheptene (9c) was obtained as a pale yellow oil in 97% yield, through $LiAlH_4$ reduction of the ester **9b** in the manner described above for **8b**.

IR spectrum (CS_2 ; CCl_4 ; cm^{-1}) : 732s, 756vs, 785vs, 790vs, 1051s, 2879s, 2936s, 3026s, 3065s, 3200–3500 large and 3635m.

^1H-NMR spectrum (CCl_4 ; δ ppm) : 1.9–3.8 (m ; 6H ; $CH-(CH_2)_2OH$) ; 6.0 (m ; 1H ; H^6) ; 6.54 (d ; J = 10 Hz ; 1H ; H^7) ; 7.1–7.9 (m, 8H, H_{arom}).

5 (β-acetoxyethyl) 5H-dibenzo [a, c]cycloheptene, was obtained as an uncoloured oil from the alcohol **9c** and acetic anhydride in pyridine.

IR spectrum (CS_2 ; CCl_4 ; cm^{-1}) : 736s, 756vs, 773s, 788s, 1236vs, 1740vs, 2858w, 2936m, 2959m, 3026m and 3066m.

^1H-NMR spectrum (CCl_4 ; δ ppm) : 1.8–3 (m, 3H ; $CH-CH_2$) ; 1.95 (s ; 3H ; $COCH_3$) ; 4.10 (m ; 2H ; CH_2O) ; 5.98 (m ; 1H ; H^6) ; 6.58 (d ; J = 10 Hz ; 1H ; H^7) ; 7.1–7.8 (m ; 8H ; H_{arom}).

5 (β-tosyloxyethyl)5H-dibenzo[a, c]cycloheptene (5) was obtained as a pale yellow oil from the alcohol **9c** and *p*-toluensulfonyl chloride in pyridine (80% yield).

IR spectrum (CS_2; CCl_4 ; cm^{-1}) : 727s, 756vs, 775vs, 790vs, 1176vs, 1187vs, 1370vs, 2910 m, 3024m and 3064m.

^1H-NMR spectrum (CCl_4 ; δ ppm) : 1.9–4.2 (m ; 5H ; $-CH-(CH_2)_2$) ; 2.31 (s ; 3H ; CH_3) ; 5.90 (m ; 1H ; H^6) ; 6.48 (d ; J = 10 Hz ; 1H ; H^7) ; 7.0–7.8 (m ; 12H ; H_{arom}).

Ethyl 5H-dibenzo[a, c]cyclohepten-5-yl propionate (10a)

The acid **9a**[5] was converted into the acid chloride, then into the corresponding diazoketone after the described procedures.[5]

The ester **10a** was obtained as a yellow oil in 95% yield from the diazoketone in the manner described above for **8a**.

IR spectrum (CS_2 ; CCl_4 ; cm^{-1}) : 736vs, 756vs, 773vs, 790vs, 1190s, 1231s, 1734vs, 2878w, 2935m, 2985m, 3026m and 3061m.

^1H-NMR spectrum (CCl_4 ; δ ppm) : 1.20 (t ; J = 7 Hz ; 3H ; CH_3) ; 1.7–3.2 (m ; 5H ; $-CH-CH_2)_2$; 4.11 (q ; J = 7 Hz ; 2H ; CH_2-CH_3) ; 5.97 (m ; 1H ; H^6) ; 6.61 (d ; J = 10 Hz ; 1H ; H^7) ; 7.1–7.8 (m, 8H ; H_{arom}).

5 (γ-tosyloxypropyl) 5H-dibenzo [a, c] cycloheptene (6) was obtained as a pale yellow oil, on treatment of the alcohol **10b** with *p*-toluenesulfonyl chloride in pyridine (75% yield).

IR spectrum (CCl_4 ; cm^{-1}) : 1060m, 1180vs, 1192vs, 1380s, 1440s, 1490s, 2868s, 2920s, 3020s and 3070m.

^1H-NMR spectrum CCl_4 ; δ ppm) : 1.2–2.8 (m ; 5H ; $-CH(CH_2)_2$) ; 2.29 (s ; 3H ; CH_3) ; 3.95 (m ; 2H ; CH_2O) ; 5.90 (m ; 1H ; H^6) ; 6.54 (d ; J = 10 Hz ; 1H ; H^7) ; 7.1–8.0 (m ; 12H ; H_{arom}).

Acetolysis of tosylate 4. A solution of tosylate 4 (3.5 g ; 8.65 mmoles) in 175 ml anhydrous acetic acid buffered with NaOAc (1.3 g ; 15.8 mmoles) was refluxed for 90 hrs. After dilution with cold water the reaction mixture was neutralized with solid Na_2CO_3 then ether extracted. The organic layer was washed, dried and evaporated *in vacuo* affording a yellow oil (2.5 g ; 98%) which was subsequently reduced with $LiAlH_4$ (0.8 g ; 21 mmoles) in 75 ml anhydrous ether. The usual work-up (decomposition with cold 10% H_2SO_4 solution ; extraction and evaporation of the solvent) afforded a thick yellow oil (1.8 g ; 85 %) whose v.p.c. analysis indicated the presence of 79 % unrearranged alcohol **8b**, beside five minor components reaching : 32. ; 3.7 ; 6.0 ; 5.0 and 3.1 % (in order of elution) which were not further investigated.

Acetolysis of tosylate **5**. A solution of tosylate **5** (1.5 g ; 3.85 mmoles) in 30 ml anhydrous acetic acid (with or without added NaOAc buffer, 0.33 g ; 4 mmoles) was refluxed for 70 hrs. After dilution with cold water the reaction mixture was neutralized with solid Na_2CO_3 then ether extracted. The organic layer was washed, dried and evaporated *in vacuo* affording a yellow oil (1 g ; 93 %) whose IR, ^{1}H—NMR and v.p.c. analysis indicated the presence of 90 % unrearranged acetate beside different minor components.

Acetolysis of tosylate **6**. A solution of tosylate **6** (1.25 g; 3.1 mmoles) and anhydrous NaOAc (0.28 g ; 3.4 mmoles) in 30 ml anhydrous acetic acid was refluxed for 24 hrs. The reaction mixture was then worked-up and reduced with $LiAlH_4$ (0.15 g ; 3.95 mmoles) as described for tosylate **4** *(vide supra)*. The IR, ^{1}H—NMR, and v.p.c. analysis of the product (0.7 g ; 95 %, yellow oil) indicated the presence of the slightly impurified alcohol **10b**.

Trifluoroethanolyses of tosylates **4**, **5** *and* **6**. A solution of tosylate **4**, **5** or **6** (0.5 g) in 10 ml trifluoroethanol was refluxed for 96 hrs (for **4**) ; 126 hrs (for **5**) or 34 hrs (for **6**), then poured into 20 ml cold water. The reaction mixture was ether extracted (some polymeric material remains insoluble), the organic layer was washed with water, dried and evaporated affording an oily residue, whose ^{1}H—NMR and IR — spectra indicated the presence of the slightly impurified starting tosylate.

Trifluoroacetolyses of tosylates **4**, **5** *and* **6**. Solutions of tosylates **4**, **5** or **6** (0.5 g) and sodium trifluoroacetate (1.1 equivalents) in anhydrous trifluoroacetic acid (20 ml) were maintained : a) 310 hrs at room temp. followed by 6 hrs at 60°C (for tosylate **4**) b) 385 hrs at room temp. or 5 hrs at reflux (for tosylate **5**) c) 144 hrs at room temp. (for tosylate **6**). The red-black reaction mixtures afforded, after usual work-up, only untractable polymeric material. În the case of tosylate **4** IR and ^{1}H—NMR spectra indicated the presence of unreacted tosylate in significant amounts.

ACKNOWLEDGEMENTS. We wish to thank Miss Ligia Stănescu for v.p.c. analyses.

REFERENCES

[1] E. Ciorănescu, M. Banciu, R. Jelescu, M. Rentzea, M. Elian and C. D. Nenitzescu *Tetrahedron Letters*, **1969**, 1871 ; *Rev. Roumaine Chim.*, **14**, 911 (1969).

[2] E. Ciorănescu, A. Bucur, F. Badea, M. Rentzea and C. D. Nenitzescu, *Tetrahedron, Letters*, **1969**, 1867.

[3] M. Voicu and F. Badea, *Rev. Roumaine Chim.*, **14**, 929 (1969).

[4] E. Ciorănescu, A. Bucur, M. Elian, M. Banciu, M. Voicu and C. D. Nenitzescu, *Rev. Roumaine Chim.*, **10**, 161 (1965).

[5] E. Ciorănescu and co-workers, to be published.

[6] C. van der Stelt, A. Haasjes, H. M. Tersteege and W. T. Nauta, *Rec. Trav. chim.*, **84**, 1466 (1965).

[7] M. Banciu, M. Elian, E. Ciorănescu and C. D. Nenitzescu, *Tetrahedron Letters*, **1972**, 2573 ; M. Elian, M. Banciu, L. Stănescu and E. Ciorănescu, *Rev. Roumaine Chim.*, **21, 89** (1976).

[8]a. N. L. Wendler and D. Taub, *Belg. pat.*, 633597 (1963) ; *Chem. Abstr.*, **61**, 1816 (1964) ; b) N. Wendler, *Belg. pat.*, 633316 (1963) ; *Chem. Abstr.*, **60**, 15806 (1964) ; c) N. Wendler, *U. S. pat.*, 3332977 (1967) ; *Chem. Abstr.*, **69**, 18935 (1968) ; d) M. Tishler, *Belg. pat.*, 635014 (1964) ; *Chem. Abstr.*, **61**, 13260 (1964).

[9] M. Banciu, F. Badea, R. Jelescu and E. Ciorănescu, *Rev. Roumaine Chim.*, **20**, 121 (1975).

[10] F. J. Villani, *U. S. pat.*, 3409640 (1964) ; *Chem. Abstr.*, **70**, 68009 (1969).

[11] P. D. Bartlett, W. S. Trahanowski, D. A. Bolon and G. H. Schmidt, *J. Amer. Chem. Soc.*, **87**, 1314 (1965).

[12] P. D. Bartlett and S. Bank, *J. Amer. Chem. Soc.*, **83**, 2591 (1961) ; R. G. Lawton, *ibid*, **83**, 2399 (1961).

Revue Roumaine de Chimie, 25, *8*, 1229–1238 (1980)

PHENAZATHIONIUM CATIONS. I

THE DUAL MECHANISTIC BEHAVIOUR OF PHENAZATHIONIUM CATIONS AND ITS IMPLICATIONS IN THE REACTION OF $NaNO_2$ WITH HALOGENOPHENOTHIAZINES

IOAN A. SILBERG and MIRCEA V. DIUDEA
Institute of Chemistry, R–3400 Cluj-Napoca, str. Donath 65–103, Romania

Received January 20, 1977
Revised January 24, 1980

The factors determining the behaviour of phenazathionium cations in reactions with nucleophiles are discussed, pointing out that, as a rule, there is a formation of S-derivatives under kinetically controlled conditions, and of C-substituted phenothiazines in thermodynamically controlled processes. It is shown that by reacting halogenophenothiazines with $NaNO_2$ in the presence of CH_3COOH the replacement of halogens by nitro groups takes place, and that, unlike literature data, nitrosulfoxides are also obtainable.

The chemistry of phenothiazine is dominated by two major trends, consequences of the specific electrono-structural features of this heterocycle : its propensity to donate electrons, yielding oxidized cationic and radicalic species of unusual stability, and the prevailing influence of the nitrogen atom in establishing the electron densities and the order of reactivity of the different positions of the ring. [1] The decisive part played by the nitrogen atom is particularly conspicuous in the states immediately preceding substitution reactions, as shown by theoretical [2] and experimental [1] data. Among the latter, a special place is occupied by nitration reactions, which, together with halogenations [1,3] substantially contributed to the elucidation of the basic lines of phenothiazine chemistry. Since many theoretical facets of the nitration of phenothiazines are to be found in the literature only in an implicit form, and without correlation with other authors' results, we found it of interest to carry out a short comparative analysis of the existing data on these topics, in order to arrive at new generalizing conclusions, and to outline the preparative prospects of this reaction.

The introduction of nitro groups into the phenothiazine ring has been carried out almost exclusively by means of two reagents, namely nitric acid and sodium nitrite in acid media. The highest number of nitro groups directly attached to the phenothiazine ring is encountered in tetranitroderivatives, substances synthesized only by using nitric acid under severe conditions. [1,4–8] The nitro groups enter positions 1, 3, 7 and

9 (*ortho*- and *para*- with respect to the ring nitrogen) in all compounds with firmly established structures (cf. however [9,10]). The nitration with HNO_3 is always accompanied by oxidation of the sulfide linkage, under formation of 5-oxides and sometimes even 5,5-dioxides; [9,12] it is also noteworthy that nitric acid is able to convert into nitroderivatives not only phenothiazines, but also their 5-oxides and 5,5-dioxides.

The nitrating action exerted on phenothiazines by sodium nitrite in the presence of carboxylic acids (usually acetic acid) displays at least three specific features, according to the existing data: [1,6,13–17] (i) nitro groups can be introduced only in positions 3 and 7; (ii) one can nitrate only phenothiazines, not their 5-oxides or 5,5-dioxides; and (iii) the reaction leads only to nitrophenothiazines unoxidized at the sulfide bridge. All the above data strongly suggest important mechanistic differences between these two reactions.

As far as the nitric acid nitration of phenothiazine is concerned, this reaction [1,4–8,11,18–22] shows all of the specific features of an electrophilic substitution, which can be a direct nitration (with NO_2^+ as an electrophilic agent) or may proceed as well *via* a nitrosation, as in the case of other reactive aromatic compounds. If one may consider, with unsubstituted phenothiazine and some of its derivatives, a nucleophilic mechanism of the type presented below, this is absolutely out of question with phenothiazine-5,5-dioxides. The course of the reaction and the accessibility of positions 1 and 9 on treatment with nitric acid prompted us to extend the validity of the conclusions drawn from experiments on 5,5-dioxides over other types of phenothiazines.

SCHEME 1

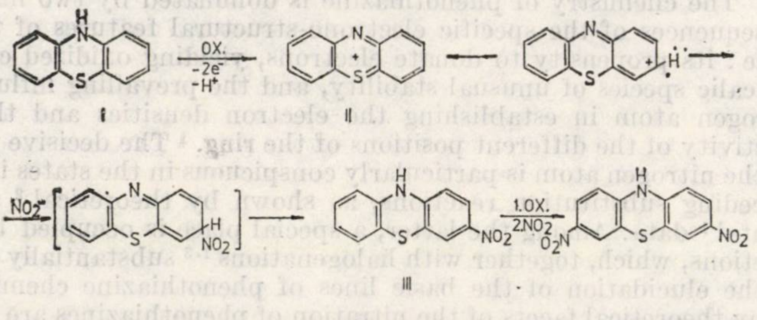

There are, in exchange, well-grounded reasons, both theoretical and experimental, to favour a nucleophilic mechanism for the nitrations with $NaNO_2$ in acid media. The $C-NO_2$ bonds should appear, according to such a mechanism, by the attack of NO_2^- anions on the doubly oxidized species, the phenazathionium cations T^+ (II), [1]* formed by electron transfer from the phenothiazine derivative to the nitric oxides present in the system (Scheme 1).

The nitric oxides are able to bring about the conversion of the nitroderivative thus formed into a T^+ cation, in spite of the considerable increase of phenothiazine redox potential induced by the introduction of a nitro group (over 900 mV).[23] Consequently, there is no difficulty in explaining the current occurrence of 3,7-dinitrophenothiazine in this process.[6,13,14] Other aspects of this problem will be discussed below.

---

* We use in this and the following paper this abbreviation which should not be mistaken for tritium.

Direct experimental evidence supporting this interpretation has recently been reported by Daneke and Wanzlick,[24] who obtained 3-nitrophenothiazine (III) by treating with $NaNO_2$ the T^+ cation generated independently (oxidation of unsubstituted phenothiazine with $FeCl_3$ in methanol, buffered with potassium acetate).

This nucleophilic mechanism of $NaNO_2$ nitration of phenothiazines coherently explains all the distinctive features of the reaction. The clear-cut difference between positions 3 (7) and 1 (9) stems from the well-established energetical prevailing of *para- vs. ortho*-quinonoid systems; thus, species with positive charge at C—1(9) have a lower contribution (see IIb and IIc). The attack of NO_2^- anions (as well as that of other nucleophilic reagents) will take place almost exclusively at positions 3 and 7 (Scheme 2).

SCHEME 2

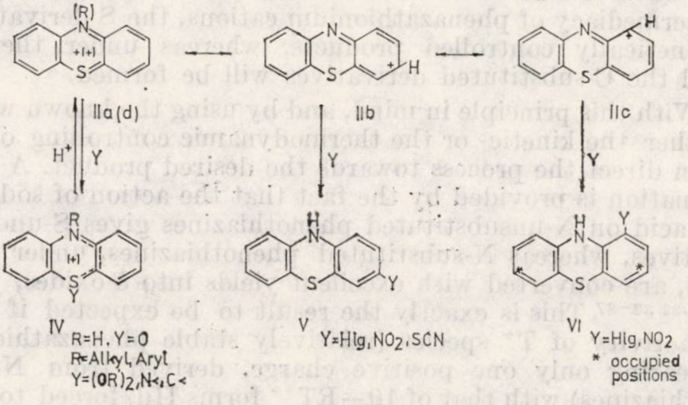

The fact that, according to literature data, the $NaNO_2/RCO_2H$ system does not nitrate the S-oxidized forms of phenothiazine,[1,6,13,17] correlates directly with the already mentioned impossibility of realizing sufficiently high concentrations of T^+ species in carboxylic acid media; in the case of 5,5-dioxides, the formation of such species — and hence the nucleophilic attack of the reagent — is definitely ruled out.

Finally, the appearance of nitrophenothiazines with unoxidized sulfide linkages in $NaNO_2$ nitrations represents one of the facets of the dual chemical behaviour of phenazathionium cations, as summarized in Scheme 2. The attack of the nucleophilic reagent can be directed either to the sulfur atom, as in IIa (d) (to yield IV), or to carbon atoms from positions 3 (7) and 1 (9), as in IIb and IIc (to produce V and VI respectively). The degree of positive charge localization in the central ring is very important (as shown, for instance, by a comparison with the unpaired spin density distribution in the molecule of the cation-radical $S^{+}\cdot$)[25] so that the primary attack of nucleophiles will be always directed towards sulfur in the first place. Until very recently, the only products (IV), isolated from such reactions were the sulfoxides, [1,26] that is, the newly formed S—Y bonds displayed enough covalent character only when Y=O. During the last few years, the S-derivatives became a relatively well-represented class of compounds, with the advent of alkoxy-sulfuranes $[Y=(OR)_2]$, [27] sulfilimines (Y=NR), [28–30] S-pyridinium derivatives (Y= pyridine) [31] and oxoalkylsulfonium compounds (Y=COR). [32] The S—Y bonds are subject to dissociation upon protonation, which will induce the reverse process, leading back to T^+ (or RT^{++}) cations. [26,32] On the contrary, the attack at carbon will take place much more slowly, due to a markedly smaller positivation as compared with the sulfur atom; the reaction is also slowed down by the prototropism which is required for restoring the aromaticity of the substituted ring (see Scheme 1). In exchange, this process leads to the formation of stable covalences with a large variety of Y^- (or Y :) reagents (as in V and, as will be shown below, in VI); the substitution at carbon appears this way as a slower, but a much more irreversible reaction.

These considerations, directly derived from experimental data, lead to the obvious conclusions that in the case of reactions proceeding by the intermediacy of phenazathionium cations, the S-derivatives represent the kinetically controlled products, whereas under thermodynamical control the C-substituted derivatives will be formed.

With this principle in mind, and by using the known ways of favouring either the kinetic- or the thermodynamic controlling of the reaction, one can direct the process towards the desired product. A simple, direct confirmation is provided by the fact that the action of sodium nitrite in acetic acid on N-unsubstituted phenothiazines gives S-unoxidized nitroderivatives, whereas N-substituted phenothiazines, under the same conditions, are converted with excellent yields into 5-oxides, without nitration. [19,22,33–37] This is exactly the result to be expected if one compares the reactivity of T^+ species (relatively stable phenazathionium cations IIa, bearing only one positive charge, derived from N-unsubstituted phenothiazines) with that of $10-RT^{++}$ forms IId, forced to accommodate two positive charges, since there is no possibility, in their case, to expel a proton. The formation of 10-substituted-phenothiazine-5-oxides, result of the kinetically controlled reaction, represents the stabilisation pathway of these highly reactive cations, even in the case of anodic oxidations carried out in carefully dehydrated media. [37] The preparation of thermodynamically favoured products is feasible only at low pH, when there is an efficient conversion of the 5-oxide back into the cation; a typical example is offered by the "reductive halogenation", the treatment of phenothiazin-, and 10-R-phenothiazin-5-oxides with hydracids to yield C-haloderivatives.[1]

On the contrary, the more stable T^+ cations can be relatively easily intercepted by nitrite anions, giving 3,7-dinitrophenothiazines.

Another example, illustrating also the part played by the reactivity of the nucleophile, is to be found in the chemical behaviour of 3-nitrophenothiazines. These compounds gave, on oxidation, 5-oxides and not phenothiazones [38]; the substantial raise in reactivity as a result of destabilizing the positive charge by the strong electron-withdrawing substituent, strategically located in the molecule, brings in the forefront, again, the product formed in the kinetically controlled process. On the other hand, at the $NaNO_2/RCO_2H$ nitrations, the 3-nitro-T^+ species are efficiently attacked by NO_2^- anions, yielding 3,7-dinitrophenothiazine. This points out the difference in reactivity between NO_2^- and H_2O, the latter being the reagent which could lead to the formation of phenothiazones.

An even finer demarkation of the effect of substituents is observed in the reaction of $K_2Cr_2O_7$ with 3-nitro-7-chlorophenothiazine [38] and with 2-nitro-7-chlorophenothiazine. [39] In the first case one obtains the sulfoxide, whereas in the second 2-nitro-7H-phenothiazin-7-one is formed; the influences exerted by nitro groups from positions 2 and 3 are situated just on the opposite sides of the diffuse frontier separating kinetically- and thermodynamically controlled processes.

The above quoted facts are clearly stressing out the validity of the central tenet of this paper, namely, that there is no rigid barrier between the two kinds of reactions (formation of S- and C-derivatives); each can be brought in a prevailing situation, given the right conditions. It becomes thus obvious that the synthesis of phenothiazones, bearing nitro groups located *ortho-* and *para-* to the nitrogen heteroatom, as well as other related nucleophilic substitutions, must be feasible if sufficiently high concentrations of cationic species are maintained in the system, and adequately reactive nucleophiles are used. *

From the practical point of view, these considerations are thus demonstrating the existence of quite a number of still unexplored synthetical prospects in this field. For instance, provided very high concentrations of T^+ cations, under thermodynamically controlled conditions, one can attack even positions 1 and 9 (see Scheme 2), a less favoured, but by no means excluded, process. The moderation of pH may bring, on the other hand, even sodium nitrite nitrations under conditions partly, or entirely controlled by kinetic factors, thus leading to S-oxidized nitrophenothiazines. The series of practically useful indications which can be derived for future work in this field from the general image of T^+ chemical behaviour, outlined above, is, of course, not confined to those already listed, and they are being put to work in our current investigations.

We intend to present, also, in this paper, two preparative aspects, which are new with respect to the state-of-the-art in phenothiazine chemistry: the possibility of replacing not only hydrogen-, but also halogen atoms from positions 3 and 7 by nitro groups during $NaNO_2/RCO_2H$ nitrations, and the preparation of nitrophenothiazin-5-oxides by means of the same reaction.

The halogen atoms, directly attached to the phenothiazine ring, show, as expected, a low mobility. There are however, reports on replacing these atoms by other groups, [1] and we will quote here only two such reactions, namely the conversion of halogenophenothiazines into phenothiazones under the action of $K_2Cr_2O_7$ in glacial acetic acid, [38-47] and the preparation of 3,7-dinitro-phenothiazin-5,5-dioxides from bromophenothiazines and bromophenothiazin-5,5-dioxides, by means of concentrated nitric acid. [11] In the first case, we witness a nucleofugal displacement of a halogenide ion (Cl^- or Br^-) from the phenazathionium cation by a water molecule; the second case is a typical electrophilic substitution (other examples, see [48,49]). It is to be noted that during these HNO_3 nitrations, nitro groups replace only the bromine atoms, and only if these are located at the positions with maximum electron density, *para* to nitrogen. As expected for reactions not involving phenazathionium cations, nitro groups cannot replace bromine atoms from positions 1 and 9, but can enter these positions when free (e.g., in 3,7-dibromo-5,5-dioxide).

---

* While preparing this manuscript, the smooth conversion of 3-nitro- and of octachlorophenothiazine-5-oxides into the corresponding phenothiazones was performed in our laboratory by heating with carboxylic acid anhydrides, thus confirming this prediction.

Aiming at demonstrating the structures of some new halogenoderivatives [50] and at enriching knowledge on the reactions proceeding through the intermediacy of phenazathionium cations, we subjected a series of chloro- and bromophenothiazines to the action of sodium nitrite in the presence of acetic acid. We preferred dimethylformamide as a reaction medium, [51] because this solvent is particularly favourable for reactions involving polar intermediates, but similar results could be obtained in other solvents, e.g. $CHCl_3$.

We found thus that nitro groups replace chlorine and bromine atoms from positions 3 and 7, in yields sometimes exceeding 85%, positions 1 and 9 remaining unaffected, even when free. As a function of the excess of reagent, reaction time and nature of the substituents preexistent on the ring, one can obtain mono- or dinitro-derivatives, unlike the classical case of the substitution of hydrogen atoms from positions 3 (7), when 3,7-dinitrophenothiazines were constantly obtained. We could easily note that phenothiazines with one free 3(7) position react much more readily, and stopping the reaction at the stage of 3-nitro-7-halogeno-derivative is considerably less difficult.

The elimination of halide anions was proved qualitatively and quantitatively, by precipitation with $AgNO_3$. In the conversion of 3,7-dichlorophenothiazine into 3,7-dinitrophenothiazine, we found in the solution 85% of the chlorine present in the starting compound.

On the other hand, with tetrachloro- and tetrabromo-phenothiazine, the reaction is much slower, owing to the poorer solubility and the higher redox potential of these compounds, but we could isolate—from the reaction mixture, by column chromatography, along with mono- (VII) and dinitro-halogeno-phenothiazines (IX), — a series of nitro-halogeno-sulfoxides (VIII and X). The latter accounted for over 90% of the crude reaction product. The formation of nitrosulfoxides by sodium nitrite nitrations has not yet been reported in the literature.

The raise of the redox potential and the destabilization of the phenazathionium cations by the introduction of halogen atoms in positions 1 and 9 lead, as predicted by theoretical considerations, to the switching from a thermodynamically controlled reaction (formation of S-unoxidized 3,7-dinitrophenothiazine from 3,7-dihalogeno-derivatives) to a reaction yielding kinetically controlled products (formation of nitro-halogeno-phenothiazin-5-oxides from tetrahalogeno-phenothiazines). These results clearly illustrate the possibility of conducting the reaction of phenazathionium cations to different directions, by using the theoretical indications.

The reactions investigated in this paper are summarized in Scheme 3. Considering the complexity of the redox processes occurring in these

SCHEME 3

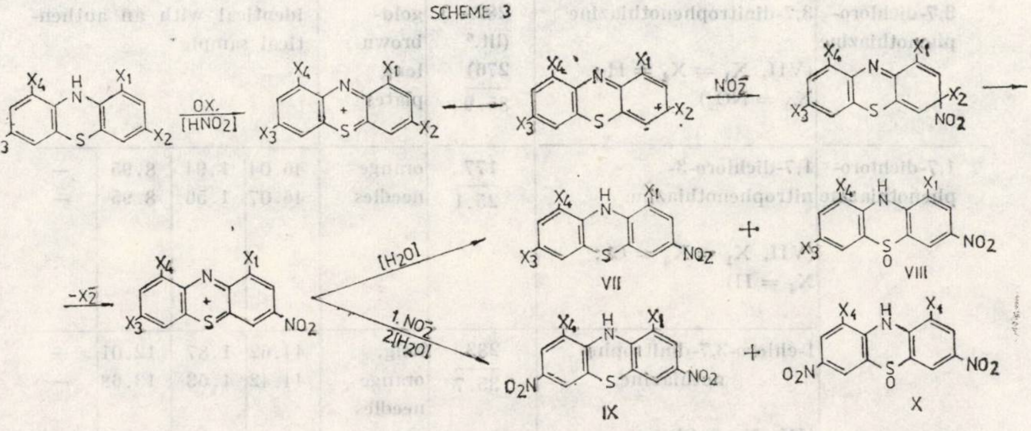

systems, as well as in many others, involving phenazathionium cations, the ratio of reduced and oxidized forms cannot be derived from simple stoichiometric equations; consequently this scheme is to be understood strictly in qualitative terms, without implying determined proportions between nitro-halogeno-phenothiazines and the corresponding sulfoxides.

With the only exception of 3,7-dinitrophenothiazine, the substances prepared in this work are new compounds.

Subsequent papers will be devoted to the investigations of nucleophilic substitutions at C—1 (9) and to other aspects of the chemistry of phenazathionium cations.

EXPERIMENTAL

Melting points are uncorrected. Mass-spectra were recorded on a MAT-Atlas 311, Bremen, and the elemental analyses were carried out by the Analytical laboratory of the Institute.

The action of $NaNO_2$ on halogenophenothiazines (general procedure)

A dilute solution of halogenophenothiazine in dimethylformamide was treated with excess solid $NaNO_2$, and glacial acetic acid was added to the mixture. The reaction requires from 0.5 hrs to several hours at room temperature or on a water bath, as a function of the structure of the initial compound, being the longer, the higher the number of halogen atoms. The reaction mixture was poured into water and filtered. The precipitate was dissolved in warm benzene or toluene, and chromatographed on Al_2O_3, eluent benzene or toluene. The results are summarized in the Table.

TABLE

Products obtained by the action of $NaNO_2$ on halophenothiazines

Starting compound	Product (VII–X)	m.p. °C yield %	Appearance	Analyses % calculated % found C	H	N	Halg
3,7-dichlorophenothiazine	3,7-dinitrophenothiazine (VII, $X_1 = X_4 = H$; $X_3 = NO_2$)	282–3 (lit.[6] 276) 85.9	gold-brown long plates	identical with an authentical sample [6]			
1,7-dichlorophenothiazine	1,7-dichloro-3-nitrophenothiazine (VII, $X_1 = X_3 = Cl$; $X_4 = H$)	177 25.1	orange needles	46.04 46.07	1.94 1.56	8.95 8.95	— —
	1-chloro-3,7-dinitrophenothiazine (IX, $X_1 = Cl$; $X_4 = H$)	283 35.7	long, orange needles	44.62 44.42	1.87 1.53	12.01 13.68	— —
1,3,7,9-tetrachlorophenothiazine	1,7,9-trichloro-3-nitrophenothiazine (VII, $X_1 = X_3 = X_4 = Cl$)	193 traces	light orange needles	characterized by mass spectrum: $M^+ = 346$, 3 chlorine atoms (isotopic peaks distribution)			
	1,9-dichloro-3,7-dinitrophenothiazine (IX, $X_1 = X_4 = Cl$)	258 traces	deep orange needles	characterized by mass spectrum: $M^+ = 357$, 2 chlorine atoms (isotopic peaks distribution)			
	1,7,9-trichloro-3-nitrophenothiazin-5-oxide (VIII, $X_1 = X_3 = X_4 = Cl$)	202 (decompn.) 91.4	yellow needles	— —	— —	— —	29.29 29.01
	1,9-dichloro-3,7-dinitrophenothiazin-5-oxide (X, $X_1 = X_4 = Cl$)	228 (decompn.) 87.2	light orange needles	— —	— —	11.23 11.41	18.95 18.62
1,3,7,9-tetrabromophenothiazine	1,9-dibromo-3,7-dinitrophenothiazin-5-oxide (X, $X_1 = X_4 = Br$)	263 63.7	light orange needles	31.13 31.54	1.09 1.09	—	—

3,7-Dinitrophenothiazine (VII, $X_1 = X_4 = H$, $X_3 = NO_2$)

A mixture of 1 g 3,7-dichlorophenothiazine and 3 g $NaNO_2$ in 100 ml DMF was treated under stirring with acetic acid until the evolution of nitrous gases subsided. After 15 min standing, the crystalline precipitate was filtered off, washed with a small amount of DMF, then with acetone to yield 0.92 g (85.98 %) 3,7-dinitrophenothiazine VII, $X_1=X_4=H$, $X_3=NO_2$), brown-gold crystals, m.p. 282—3°C (lit. m.p. 276°C); IR and TLC identical with those of an authentic sample.

REFERENCES

[1] C. Bodea and I. A. Silberg, *Adv. Heterocycl. Chem.*, **9**, 322 (1968); A. R. Katritzky and A. J. Boulton, ed. Academic Press, New York.

[2] H. H. Mantsch and J. Dehler, *Canad. J. Chem.*, **47**, 3173 (1969).

[3] I. A. Silberg, Doctorate Dissertation, Institute of Chemistry, Cluj, 1970.

[4] Ch. Monard, H. Ficheroulle and R. Fournier, *Mem. Poudres*, **34**, 179 (1952).

[5] K. Toei, *Nippon Kagaku Zasshi*, **76**, 1083 (1955); *Chem. Abstr.*, **51**, 11913 (1957).

[6] C. Bodea and M. Răileanu, *Studii și Cercetări Chim. Acad. R.P.R. Fil. Cluj*, **8**, 303 (1957).

[7] K. Toei, *Nippon Kagaku Zasshi*, **77**, 1270 (1956); *Chem. Abstr.*, **52**, 961 (1958).

[8] A. Turcu and M. Răileanu, *Rev. Roumaine Chim.*, **14**, 1579 (1969).

[9] T. Urbansky, K. Szycz-Lewanska and P. Kalinowsky, *Bull. Wojskowej Akad. Tech.* **7**, 56 (1957); *Chem. Abstr.*, **53**, 5269 (1959).

[10] T. Urbansky, K. Szycz-Lewanska and P. Kalinowsky, *Bull. Acad. Polon. Sci., Ser. Sci. Chim., Geol., Geograph.*, **7**, 147 (1959).

[11] C. Bodea, V. Fărcășan and I. Oprean, *Zhur. obshchei Khim.*, **34**, 2369 (1964).

[12] C. Bodea, V. Fărcășan and T. Panea, *Rev. Roumaine Chim.*, **11**, 239 (1966).

[13] R. Havemann, H. Pietsch and H. Reiche, *Z. Wiss. Phot., Photophys. Photochem.*, **58**, 3 (1964).

[14] F. Kehrmann and O. Nossenko, *Ber. dtsch. chem. Ges.*, **46**, 2809 (1913).

[15] F. Kehrmann and F. Ringer, *Ber. dtsch. chem. Ges.*, **46**, 3014 (1913).

[16] M. Răileanu, I. Radulian and S. Florea, *Rev. Roumaine Chim.*, **11**, 1411 (1966).

[17] M. Răileanu and A. Turcu, *Rev. Roumaine Chim.*, **11**, 1423 (1966).

[18] F. Kehrmann and P. Zybs, *Ber. dtsch. chem. Ges.*, **52**, 132 (1919).

[19] D. Simov and L. Kamenova, *God. Sofii. Univ. Khim. Fak.*, **58**, 207 (1963—64); *Chem. Abstr.*, **65**, 5457 (1967).

[20] J. H. Driscoll (Monsanto Research Co.) U. S. P., 3, 334, 092; *Chem. Abstr.*, **68**, 59594 (1968).

[21] I. M. Roushadi and S. Rida, *Sci. Pharm. Proc. 25th*, **1**, 191 (1965); *Chem. Abstr.*, 70, 11654 (1969).

[22] D. Simov, Iv. Taulov and St. Tomov, *God. Sofii. Univ. Khim. Fak.*, **61**, 183 (1966—67); *Chem. Abstr.*, **72**, 3448 (1970).

[23] J. Cymerman-Craig and M. E. Tate, *Progr. Drug. Res.*, **3**, 84 (1961).

[24] J. Daneke and W. H. Wanzlick, *Liebigs Ann. Chem.*, **740**, 52 (1970).

[25] J. M. Lhoste and F. Tonnard, *J. Chim. Phys. Physicochim. Biol.*, **63**, 678 (1966).

[26] H. J. Shine and E. E. Mach, *J. Org. Chem.*, **30**, 2130 (1965).

[27] E. F. Perozzi and J. C. Martin, *J. Org. Chem.*, **42**, 3222 (1977).

[28] K. Bandlish-Baldev, A. G. Padilla and H. J. Shine, *J. Org. Chem.*, **40**, 2590 (1975).

[29] J. J. Shah, *J. Tenn. Acad. Sci.*, **52**, 19 (1977).

[30] H. J. Shine and K. Kiongtae, *Tetrahedron Letters*, 99 (1974).

[31] J. F. Evans, J. R. Lenhard and H. N. Blount, *J. Org. Chem.*, **42**, 983 (1977).

[32] A. G. Padilla, K. Bandlish-Baldev and H. J. Shine, *J. Org. Chem.*, **42**, 1833 (1977).

[33] D. Simov-Antonov, *Compt. rend. Acad. bulg. Sci.*, **10**, 21 (1957); *Chem. Abstr.* **52**, 6357 (1958).

[34] D. Simov-Antonov, *Izv. Khim. Inst. Bulgar. Akad. Nauk*, **5**, 51 (1957); *Chem. Abstr*. **55**, 16556 (1961).

[35] D. Simov and S. Fakirov, *God. Sofii. Univ. Khim. Fak.*, **56**, 111 (1963); *Chem. Abstr.*, **61**, **9493** (1964).

[36] K. Bandlish-Baldev, K. Kiongtae and H. J. Shine, *J. Heterocycl. Chem.*, **14,** 209 (1977).
[37] J. P. Billon, *Ann. Chim. (France)*, **7,** 183 (1962).
[38] C. Bodea and M. Răileanu, *Liebigs Ann. Chem.*, **620,** 88 (1959).
[39] T. Panea, C. Bodea and V. Fărcășan, *Rev. Roumaine Chim.*, **16,** 759 (1971).
[40] C. Bodea and M. Răileanu, *Liebigs Ann. Chem.*, **631,** 194 (1960).
[41] C. Bodea and I. A. Silberg, *Rev. Chim. Acad. R.P.R.*, **7,** 683 (1962).
[42] C. Bodea and M. Răileanu, *Liebigs Ann. Chem.*, **614,** 171 (1958).
[43] C. Bodea and V. Fărcășan, *Studii și Cercetări Chim. Acad. R.P.R. Fil. Cluj*, **11,** 121 (1960).
[44] C. Bodea and M. Răileanu, *Zhur. obschchei Khim.*, **30,** 1131 (1960).
[45] C. Bodea, M. Terdic and I. A. Silberg, *Liebigs Ann. Chem.*, **673,** 113 (1964).
[46] C. Bodea, V. Fărcășan and T. Panea, *Agressologie*, **9,** 77 (1968).
[47] C. Bodea and M. Terdic, *Rev. Roumaine Chim.*, **13,** 1235 (1968).
[48] D. V. Nightingale, *Chem. Rev.*, **40,** 117 (1947).
[49] C. Bodea, M. Terdic and E. Broser, *Liebigs Ann. Chem.*, **715,** 122 (1968).
[50] I. A. Silberg, V. Fărcășan and M. V. Diudea, *J. prakt. Chem.*, **318,** 353 (1976).
[51] Gh. Rusu, Doctorate Dissertation, Institute of Chemistry, Cluj-Napoca, 1978.

Revue Roumaine de Chimie 25, *8*, 1239–1244 (1980)

PHENAZATHIONIUM CATIONS. II[1]

THE ACCESSIBILITY OF POSITIONS 1(9) IN NUCLEOPHILIC SUBSTITUTIONS INVOLVING PHENAZATHIONIUM CATIONS

I. A. SILBERG and M. V. DIUDEA
Institute of Chemistry, R–3400, Cluj-Napoca, Str. Donath 65–103,
Romania

Received January 20, 1977
Revised January 24, 1980

The possibility of introducing substituents into positions 1 (9) of phenazathionium cations by nucleophilic substitutions, carried out under conditions allowing the formation of thermodynamically controlled products, is demonstrated. 1,3,7-Trinitrophenothiazine was thus obtained, and an easier way to prepare 1,3,7,9-tetrahalophenothiazines was described. The sodium nitrite – acetic acid reagent for generation of phenazathionium cations was also used in an improved synthesis of 3,7-disubstituted phenothiazines.

In the previous paper of this series [1] we reported the nitration of phenothiazine and of its halogenated derivatives by using sodium nitrite-acetic acid-dimethylformamide systems. We pointed out that chlorine and bromine atoms from positions 3 and 7 can be replaced by nitro groups under relatively mild conditions (room temperature or heating on a steam bath) and that this reaction consists of the nucleophilic attack of NO_2^- anions (supplied by excess $NaNO_2$) on the oxidized cationic T^+ species[2] formed by the interaction of phenothiazine with nitrogen oxides generated in the system. On the basis of these experimental facts and of pertinent literature data the general conclusion was formulated that the evolution of systems containing phenothiazines, oxidants and nucleophilic reagents can be directed towards the selective formation of the desired product, by creating conditions which ensure the control of either kinetics or thermodynamic factors ; S-derivatives (see [1]) are obtained in the former case and C-substituted (usually 3- or 7- substituted) species in the latter.

The above statement enabled us to put forward the hypothesis that positions 1 and 9, usually not affected during nucleophilic substitutions carried out on phenazathionium cations (because such substitutions require energetically unfavourable *ortho*-quinoid transition states or intermediates) could become accessible for these substitutions under conditions allowing the formation of thermodynamically controlled products. The major requirement for performing such reactions would be the use of high concentrations of both T^+ species and of the nucleophilic reagents ; the reactivity of the latter must also be high enough to compete with 5-oxidation.

We were encouraged by the observation that there is a distinct trend towards polysubstitution in such reactions, as indicated by the preferential formation of 3,7-disubstituted products even under conditions which should lead to monosubstituted products ; the destabilization of the T^+ cation by unsymmetrical substitution with electron-withdrawing groups represents the theoretical reason for this phenomenon.

Another reaction which might be related to those carried out in our investigations is represented by the formation of 1, 3, 7, 9-tetrachlorophenothiazine on treating 3,7-dichloro-10-methyl-phenothiazin-5-oxide with hydrochloric acid.[3] However, in this, as well as in other "reductive halogenation" reactions,[2] the mechanism is rather controversial and the intermediacy of T^+ species was questioned.

The present paper reports a series of reactions which confirm our hypothesis and illustrate the possibility of introducing substituents on the phenothiazine ring in position 1 (9) by nucleophilic substitutions occurring in phenothiazine — oxidant — nucleophile — systems for which only reactions leading to 3- or 3,7-disubstituted derivatives have been reported so far.

Thus, by treating phenothiazine (I) with sodium nitrite in the presence of hydrochloric acid or hydrobromic acid in acetic acid, we obtained fair yields of 1, 3, 7, 9-tetrahalophenothiazines (II, III). It is noteworthy that the nitration reaction is practically absent under these conditions, a fact which points out the role of the concentrations of the active species corresponding to both the substrate and reagents in ensuring a thermodynamical control on the evolution of the reaction (by the intermediacy of the mass law). The overcoming of the resistance of T^+ cations against substituting the 1(9) positions requires conditions which are so energetic, that it is no more possible to differentiate these two positions, and tetrahalo-derivatives are directly obtained.

SCHEME 1

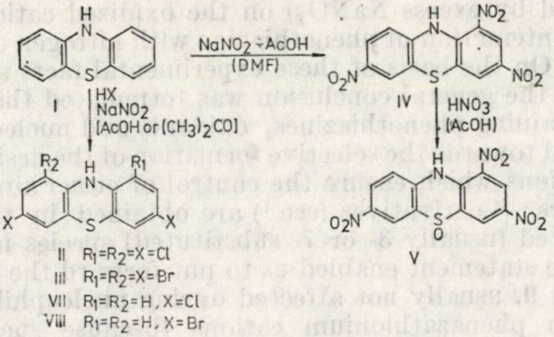

In connection with the above mentioned reactions one may consider the possibility that the polyhaloderivatives (most of them ill-defined as individual compounds) obtained during pioneering work in phenothiazine chemistry by Unger and Hoffmann [4] acting with nitrous gases and hydracids on phenothiazine, were, at least partly, formed by processes related to those herewith reported.

The rapid and easy preparation of tetrachlorophenothiazine (starting material for phenothiazones and other compounds) by the procedure described in this paper shows distinct practical advantages in comparison with the method making use of chlorination in nitrobenzene.[5]

As far as the introduction of other substituents in position 1(9) of phenothiazine by the above described method is concerned, a particular interest is presented by the nitration, a reaction which, according to the existing data, was subject to certain limitations. Thus, the obtaining of nitroderivatives not oxidized at sulfur was possible only up to the level of 3,7-dinitroderivative (by the reaction of phenothiazine with sodium nitrite in chloroform[6] or dimethylformamide[7] in the presence of carboxylic acids). The higher substituted nitrophenothiazines were accessible exclusively as sulfoxides (by the reaction with nitric acid, see[1] and references therein).

Our previous investigations[1] already extended these limits, by showing that the $NaNO_2$ — acetic acid reagent can be used for obtaining nitro-5-oxides as well, at least in case of di- and tetra-halophenothiazines which generate T^+ species with relatively high redox potentials. However nitrophenothiazines with more than two nitro groups could not be obtained with this reagent, either at room temperature, or on the water bath.

In exchange, by treating phenothiazine with a rather large excess of sodium nitrite in refluxing dimethylformamide, in the presence of acetic acid (caution ! violent reaction with abundant foaming may occur) we succeeded in both surpassing the disubstitution step and avoiding the 5-oxidation ; 1, 3, 7-trinitrophenothiazine was thus obtained.

1, 3, 7-Trinitrophenothiazine (IV), was also obtained by Kehrmann[8] but in an essentially different way, namely, by nitrating 1, 3-dinitrophenothiazine in position 7 — a normal substitution reaction for a phenothiazine derivative with a free position *para* to nitrogen.

In the orientation of this reaction, a decisive part was played by the high temperature, the large concentration of NO_2^- anions and the fact that the latter were not solvated by aprotic dipolar solvent. The formation of the kinetically controlled product, the sulfoxide, was practically suppressed.

The introduction of a fourth nitro group is hindered to such extent by electronic factors, that even formation of the 5-oxide is more favorable than continuation of substitution, and traces of 1, 3, 7-trinitro-phenothiazin-5-oxide (V) began to appear on prolonging the reaction. For preparative purposes, V (a new compound) was obtained by the classical procedure,[6] with nitric acid in acetic acid.

The nitration reaction was the only observed process when, in an attempt to generalize the above reaction, we tried to introduce chlorine or bromine atoms on the phenothiazine ring by using sodium halides as sources for X^- ions. Most probably, the failure of this reaction was due to the poor solubility of NaX in the reaction medium, the X^- anions being thus present at a much too low concentration to enable them to compete with the reactive NO_2^- anions.

On the contrary, 3, 7-bis- (thiocyano)-phenothiazine (VI) was obtained under much more advantageous conditions and in a better yield

($> 70\%$) than the ones reported in the literature,[9] when we treated phenothiazine with potassium thiocyanate in the presence of sodium nitrite and acetic acid. Attempts to introduce more than two SCN- groups on the phenothiazine ring failed so far, owing to the relatively low reactivity of SCN^- anions under the given conditions; this is supported by the finding[9] that 3-(thiocyano)-phenothiazine can be relatively easily prepared, a rare instance when a substitution reaction on the phenothiazine nucleus can be stopped at the stage of monosubstitution.

SCHEME 2

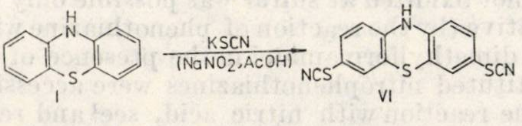

We developed also an advantageous procedure for obtaining 3,7-dihalo-phenothiazines, by carrying out the $NaNO_2 - HX$ — acetic acid halogenations under less severe acidic conditions. Thus, 3,7-dichlorophenothiazine (VII) (35% yield) and 3, 7-dibromophenothiazine (VIII) (36% yield) were obtained by using much more available and easier handled reagents and conditions with respect to those recommended by the literature.[10-13]

EXPERIMENTAL

Melting points were taken on a Boetius device and are uncorrected. The IR-spectra were recorded in KBr pellets on a double-beam IR—10 Carl Zeiss Jena spectrophotometer.

1,3,7,9-Tetrachlorophenothiazine (II). A suspension of 2 g I in 100 ml glacial acetic acid and 50 ml concentrated hydrochloric acid was treated dropwise under stirring during 5 min. with a solution of 4 g sodium nitrite in 20 ml water. The reaction mixture became dark-red; white crystals separated over night, which were filtered off, washed with water, then with acetone until the filtrate was practically colourless. After drying, the crystalline material was recrystallized from nitrobenzene to yield 2.2 g (65.2%) II, m.p. 237—8° (lit.[5] capillary m.p. 235°C); no depression of the m.p. on admixture of an authentical sample.[5]

1,3,7,9-Tetrabromophenothiazine (III). This compound was prepared following the same procedure as indicated above for II, by replacing HCl with 40% HBr (50 ml). Recrystallization from nitrobenzene of the crude product gave 1.4 g (27.1%) III, m.p. 271°C (lit.[12] m.p. 272—3°C); no depression of the m.p. on admixture of an authentical sample.[12]

3,7-bis-(Thiocyano)-phenothiazine (VI). A suspension of 2 g I and 14 g KSCN in 100 ml acetic acid was treated under stirring with a solution of 4 g $NaNO_2$ in 20 ml water, the mustard-coloured mixture kept overnight, filtered, and the precipitate washed with water. A recrystallization from acetic acid yields 2.3 g (73.1%) VI, m.p. 191°C (lit.[9] m.p. 193—5°); no depression on admixture of an authentical sample.[9]

1,3,7-Trinitrophenothiazine (IV). A solution of 5 g I in 100 ml N,N-dimethylformamide (DMF) was mixed with 30 g solid $NaNO_2$ and treated dropwise under gentle heating with 50 ml acetic acid. After a mild reflux, a rather violent reaction occurs and the mixture forms a foaming cake (caution!). After adding 100 ml DMF and 10 min. refluxing, the reaction mass was poured into water and 10 g crude, brick-red product, was obtained. On recrystallization from aniline, 1.7 g (23%) 3,7-dinitrophenothiazine was separated. The aniline mother liqueurs were steam-distilled, the remaining suspension extracted with toluene and the solution chromatographied on alumina. The first fraction yielded 1.23 g (14.7%) long brown-gold crystals of IV, m.p. 223°C Boetius), (lit.[8] m.p. 214°C), IR :1335, 1505, 3280 cm^{-1}.

$C_{12}H_6O_6N_4S$, N%, Calcd. : 16.76, Found : 16.70.

1,3,7-Trinitrophenothiazine-5-oxide (V). A suspension of 0.2 g IV in 50 ml acetic acid was treated dropwise with a 1: 1 mixture of HNO_3 (d=1.40) and acetic acid, until the red colour turned orange-yellow. After addition of excess water, the product was extracted in toluene. The organic layer was evaporated to a small volume when orange-yellow crystals separated. On recrystallization from nitrobenzene, 0.1 g (48%) small yellow plates of V, m.p. 278°C, were obtained. IR : 1050, 1340, 1500, 3260 (broad) cm^{-1}.

$C_{12}H_6O_7N_4S$, N%, Calcd. : 16.00, Found : 16.34.

3,7-Dichlorophenothiazine (VII). A solution of 4 g I in 35 ml acetone was treated under stirring with 60 ml concd. HCl, then with 3.5 g $NaNO_2$ dissolved in a minimum amount of water. After 15 min. the evolution of nitrous gases subsided, the brown-violet precipitate was filtered off and washed with water then with warm acetone. The acetone solution was diluted with excess water, the precipitate was filtered off, washed with water and dried, to yield 5.5 g crude product. The recrystallization from benzene gave 1.9 g (35.2%) VII, m.p. 231°C (lit.[11], capillary m.p. 227°C), identical with an authentical sample.[11]

3,7-Dibromophenothiazine (VIII). From 2 g I, 30 ml. concd. HBr and 2 g $NaNO_2$, according to the procedure described above for VII. On recrystallization of the crude product from toluene, 1.3 g (36.2%) VIII, m.p. 193°C was obtained. A second recrystallization from toluene raises the m.p. to 202—3°C (lit.[13] m.p. 193°C, then 206—7°C), identical with an authentic sample.[13]

REFERENCES

[1] I. A. Silberg and M. V. Diudea, *Rev. Roumaine Chim.*, preceding paper.

[2] C. Bodea and K. A. Silberg, *Adv. Heterocycl. Chem.*, **9**, 322 (1968).

[3] A. C. Schmalz and A. Burger. *J. Amer. Chem. Soc.*, **76**, 5455 (1954).

[4] O. Unger and K. A. Hoffmann, *Ber. dtsch. chem. Ges.*, **29** II, 1364 (1896).

[5] C. Bodea and M. Răileanu, *Liebigs Ann. Chem.*, **620**, 88 (1959).

[6] C. Bodea and M. Răileanu, *Studii și Cercetări Chim. Acad. R.P.R. Fil. Cluj*, **8**, 303 (1957).

[7] Gh. Rusu, Doctorate Dissertation, Institute of Chemistry, Cluj-Napoca, 1978.

[8] F. Kehrmann and F. Ringer, *Ber. dtsch. chem. Ges.*, **46**, 3014 (1913).

[9] C. Bodea and M. Terdic, *Studii și cercetări Chim. Acad. R.S.R. Fil Cluj*, **12**, 309 (1961).

[10] C. Bodea and M. Răileanu, *Studii și Cercetări Chim. Acad. R.S.R. Fil. Cluj*, **9**, 159 (1958).

[11] M. Shell and M. Rupprecht, German Patent, 938, 669 ; *Chem. Abstr.*, **53**, 8173 (1959).

[12] C. Bodea and M. Răileanu, *Liebigs Ann. Chem.*, **631**, 194 (1960).

[13] C. Bodea and M. Terdic, *Studii și Cercetări Chim. Acad. R.S.R. Fil. Cluj*, **14**, 165 (1963).

Revue Roumaine de Chimie 25, *8*, 1245–1248 (1980)

n-DODECYLNITRILE OXIDATION IN LIQUID PHASE WITH MOLECULAR OXYGEN. III[1]

COMPOSITION OF ACID MIXTURES

V. PĂRĂUŞAN, M. TRIFAN and R. AVRAM

Academy of Economic Sciences, Bucharest, Romania
The Polytechnic, Laboratory of Organic Technology, Bucharest, Romania

Received October 27, 1978

Acid mixtures separated from the autoxidation reaction mass were analyzed and their compositions were determined.

INTRODUCTION

Advanced degradation in oxidation reactions is known to be generated chiefly by severe working conditions ; the harder the working conditions and the greater the number of different functional groups in the initial product, the more complex the reaction mixtures.

Owing to their complexity, some oxidation reactions among which that of n-alkylnitriles, have been studied to a lesser extent. n-Dodecylnitrile oxidation in liquid phase may give rise to complex mixtures whose separation, purification and identification become very difficult. The study of these complicated reactions has been facilitated by the advanced methods of analysis (chromatography, spectrometry etc.) which offered the possibility of detailed investigation.

Some aspects concerning n-dodecylnitrile oxidation in liquid phase have been mentioned in earlier papers.[1,2]

Few publications refer to n-alkylnitrile oxidation. The behaviour of some nitriles (aliphatic and aromatic) in biological oxidation reactions has been studied mainly on samples in which they were to be found in non-purified waters [3] or in the presence of certain mineral salt solutions. [4] Cyanic hydroperoxides (aliphatic, aromatic) have been obtained by the oxidation of some nitriles with oxygen, under specific conditions. [5]

EXPERIMENTAL

n-Dodecylnitrile was oxidized in liquid phase with molecular oxygen in the presence of cobalt naphthenate in an apparatus whose scheme has already been described. [1]

The oxidation products obtained by catalytic oxidation of n-dodecylnitrile with molecular oxygen were separated (Figure 1) and processed for chromatography. About 5 ml of the potassium salt products, separated as shown in Figure 1, were acidulated with lutidinic acid in order to release the acid compounds. Lutidinic acid is widely used owing to the good results obtained in the identification of acid compounds with 2–12 carbon atoms in their molecule. Chromatographic determinations were carried out in a Carlo Erba 2407 T preparatory chromatograph, supplied with a computer and recording device.

The determinations were done under the following conditions:
– flame ionization detection (FID);
– temperature programmed regime at an increase rate 6°/minute;
– temperature of columns: initial 80°C, final 220°C;
– injection temperature 250°C
– carrier gas: nitrogen;

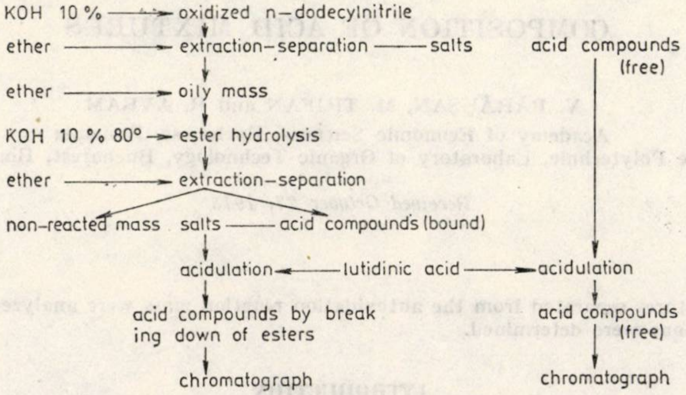
KOH 10 %
oxidized n–dodecylnitrile
ether
extraction–separation
salts
acid compounds (free)
ether
oily mass
KOH 10 % 80°
ester hydrolysis
ether
extraction–separation
non-reacted mass
salts
acid compounds (bound)
acidulation
lutidinic acid
acidulation
acid compounds by breaking down of esters
acid compounds (free)
chromatograph
chromatograph

Fig. 1. – Processing of oxidized n-dodecylnitrile for chromatographic analysis.

– gas output: $Q_{\text{nitrogen}} = 50$ ml/minute, $Q_{\text{hydrogen}} = 25$ ml/minute $Q_{\text{air}} = 250$ ml/minute;
– stainless steel columns with $\Phi_e = 4$ mm, $\Phi_i = 2$ mm, length $= 2$ m;
– supporting mass: Cromosorb W 60/80 mesh, washed with acid;
– distribution liquid, 10%: Carbowax 20^{M} plus terephthalic acid.

RESULTS AND DISCUSSION

The process of n-dodecylnitrile oxidation with molecular oxygen in liquid phase and in the presence of cobalt naphthenate, produces in the reaction mass free acids and cyanoacids and also acids and cyanoacids bound in the form of esters. Treatment of the oxidized mass with potassium hydroxide according to the acidity index plus a 5% excess, separation of the acid compound potassium salts, their release with lutidinic acid and chromatographic separation, showed the prevalence of free acids with 4, 5 and 6 carbon atoms in the reaction mass (Figure 2). The predominant cyanoacids released by the oxidized reaction mass, were the cyanoacids with 5, 6, 7 and 10 carbon atoms (Figure 3).

As already mentioned, during the oxidation process of n-dodecylnitrile, esters are also formed; hydrolysis of the latter results in their component acids and cyanoacids. The esters formed in the oxidized mass were hydrolyzed at 80°C with potassium hydroxide. The quantity of potassium hydroxide corresponded to the saponification index with 5% excess. The results obtained by chromatography of the acid compounds, components of the esters formed, are presented in figure 4.

From these data it may be seen that acids having 4 and 11 carbon atoms are prevalent in the composition of esters. As regards the cyanoacids formed and bound in esters, an appreciable amount of components with 9 carbon atoms are to be found in the mixtures (Figure 5). Analysis

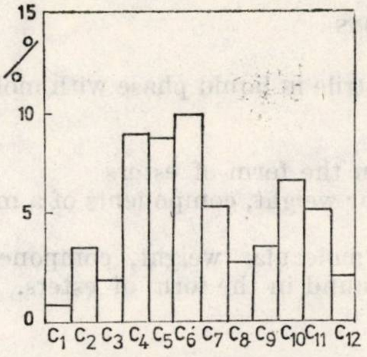

Fig. 2. — Composition of free acids resulting from n-dodecylnitrile oxidation with oxygen.

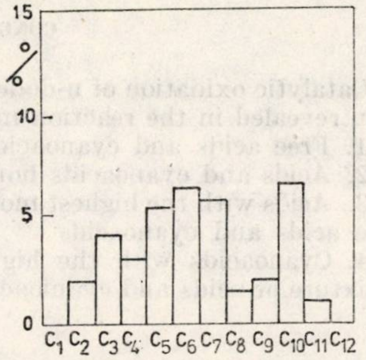

Fig. 3. — Composition of free cyanoacids resulting from n-dodecylnitrile oxidation with oxygen.

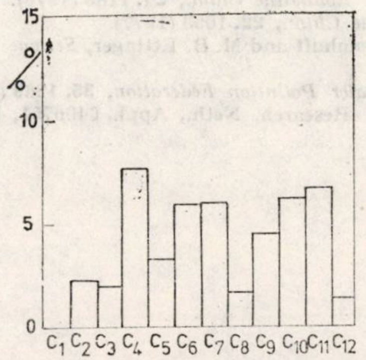

Fig. 4. — Composition of acids bound in the form of esters resulting from n-dodecylnitrile oxidation with oxygen.

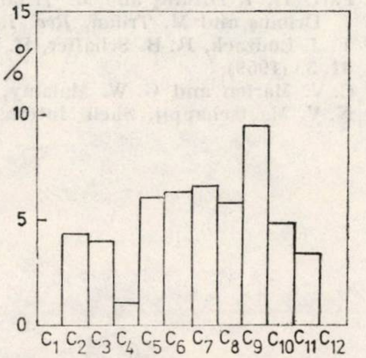

Fig. 5. — Composition of cyanoacids bound in the form of esters resulting from n-dodecylnitrile oxidation with oxygen.

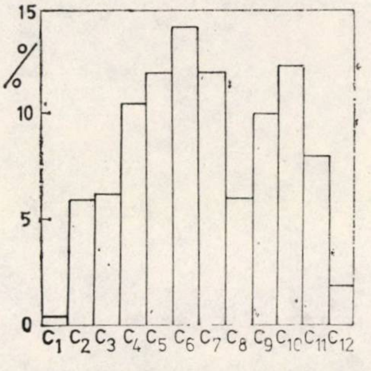

Fig. 6. — Composition of acids and cyanoacids resulting from n-dodecylnitrile oxidation with molecular oxygen.

of the compounds with an acid character formed during the oxidation of n-dodecylnitrile, shows that n-dodecylnitrile oxidation with molecular oxygen in the presence of cobalt naphthenate, results in acid compounds (acids and cyanoacids) in the following order : $C_6 > C_{10} > C_7 > C_5 > C_4 > C_9 > C_{11} > C_3 > C_8 > C_2 > C_{12} > C_1$ (Figure 6).

CONCLUSIONS

Catalytic oxidation of n-dodecylnitrile in liquid phase with molecular oxygen revealed in the reaction mass :

1. Free acids and cyanoacids
2. Acids and cyanoacids bound in the form of esters
3. Acids with the highest molecular weight, components of a mixture of free acids and cyanoacids
4. Cyanoacids with the highest molecular weight, components of the mixture of acids and cyanioacids bound in the form of esters.

REFERENCES

[1] Part. II, I. Drimuş and M. Trifan, *Rev. Roumaine Chim.*, **24,** 1185 (1979).

[2] I. Drimuş and M. Trifan, *Rev. Roumaine Chim.*, **22,** 1053 (1977).

[3] F. J. Ludzack, R. B. Schaffer, R. N. Bloomhuff and M. B. Ettinger, *Sewage and Ind. Wastes*, **31**, 33 (1959).

[4] C. V. Marion and G. W. Malamy, *J. Water Pollution Federation*, **35,** 1269 (1963).

[5] N. V. Maatschappij, Shell International Research, Neth., Appl. 6406751, Dec, 16, 1965.

Revue Roumaine de Chimie **25**, *8*, 1249—1258 (1980)

EINFLUSS DER SUBSTITUENTEN AUF DIE ANALYTISCHEN UND EXTRAKTIVEN EIGENSCHAFTEN VON ORGANISCHEN REAGENZIEN IN DER REAKTION MIT Au (III)

1. Mitt. EINFLUSS DER METHOXYL-SUBSTITUENTEN

GHEORGHE C. CONSTANTINESCU
Polytechnische Hochschule Bukarest, Polizustr. 1, Rumänien

Eingegangen am 20 Februar 1979

In der vorliegenden Arbeit wurden die Reaktionen zwischen dem Komplexanion $[AuCl_4]^-$ und *ortho-* bzw. *para*-Anisgrün studiert. Die vom Verfasser dargestellten Farbstoffe sind aus der diamminotriphenylmetanischen Klasse, Derivaten des Malachitgrüns, mit OCH_3-Gruppen in *ortho-* oder *para*-Stellung. Sie bilden mit $[AuCl_4]^-$ in Wasser unlösliche, in organischen Lösungsmitteln aber löslische Verbindungen, die dann in Benzol extrahiert werden. Die organischen Extrakte sind spektrophotometrisch und konduktometrisch untersucht. Außerdem wurden die Verbindungen aus Wasserlösung ausgefällt und der Elementer- bzw IR-Spektralanalyse unterworfen. Es werden auch die Grundbedingungen für die Anwendung der Reaktionen zur Goldbestimmung festgestellt. Das ganze Studium ist im Vergleich zu unsubstituiertem Malachitgrün durchgeführt worden.

The reaction of the basic reagents *ortho-* and *para-* Anisgrün with the complex anion $[AuCl_4]^-$ is studied. The obtained combinations were extracted in benzene. The benzenic extracts have some good spectrophotometric properties, obey the Lambert-Beer law between 2.0—10.0 μg Au/ml for *(ortho-* Anisgrün — $AuCl_4^-$) with $\varepsilon = 37\,000$, and 1.0—12.0 μg Au/ml for *(para-* Anisgrün$^+$ $AuCl_4^-$) with $\varepsilon = 55\,000$.

Malachitgrün, ein Farbstoff der dyaminotriphenylmetanischen Klasse, vermag im sauren Milieu mit Komplexanionen verschiedene Verbindungen vom Typ der Ionischen Assoziation zu bilden. Solche in Wasser unlösliche Verbindungen kristalisieren bei Zimmertemperatur. Da sie aber in organischen Lösungamitteln leicht löslich sind und die auf diese Weise gewonnenen Extrakte bestimmte spektrophotometrische Eigenschaften besitzen, können sie zur Trennung der Metallionen und zu deren Bestimmung angewendet werden.

Die Reaktion zwischen Malachitgrün unde $[AuCl_4]^-$ ist weniger empfindlich [1], deshalb haben wir Malachitgründerivaten unter Benutzung von Substituenten — OCH_3 — NO_2 oder-Cl in *ortho-* oder *para*-Stellung hergestellt. Die Erklärung des Substituenteneinflusses auf die Selektivität und Empfindlichkeit der Reaktionen vermutet die Kentnisse über die eigenstellten Gleichgewichte im homogenen oder heterogenen System sowie die Eigenschaften der gebildeten Komplexverbindungen und deren wasser- oder organischen Lösungen.

In dieser Arbeit werden die Synthesen der basischen Farbstoffen *ortho-* und *para-*Anisgrün, die Ergebnisse der Forschungen bezüglich der Bildungareaktion der Ionischen Assoziationen zwischen $[AuCl_4]^-$ und der Kationen der Farbstoffe, sowie auch die Struktur und einige Eigenschaften der erhaltenen Verbindungen im Vergleich zu dem Farbstoff Malachitgrün dargestellt.

VERSUCHSTEIL

Synthese der Farbstoffe. (*ortho-*Anisgrün z. B. ist der Handelsname der chlorid von *p-*dimethylamminobenzol-*o-*metoxylbenzol-*p-*chinondimethylimmoniumethan). Die verwendeten Farbstoffe wurden durch Kondensierung von Benzolaldehyde bzw. von *ortho-* und *para-*Metoxybenzaldehyde (Anisaldehyde) mit Dimethylanilin gewonnen [2]. Die durch Erhitzung auf dem Wasserbad erhaltene dickflüssige Masse ist mit Wasserdampf angetrieben. Der zurückgebliebene Rückstand ist in Äthylalkohol aufgelöst, woraus die Leukobasis wieder ausgefällt wird. Durch Oxydation mit Bleidioxyd erhält man das entsprächende Carbinol, welches mit Salzsäure die Verbindungen mit folgender Struktur bildet.

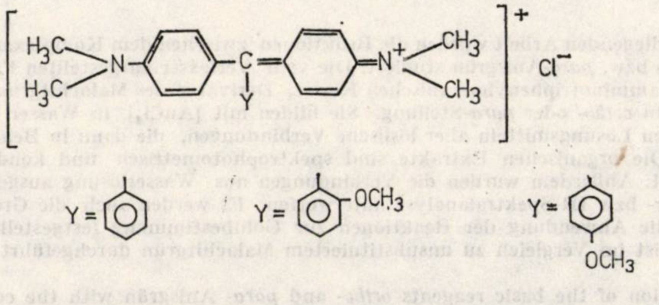

Die Reinigung der Farbstoffe erfolgte durch wiederholte Umkristallisation, wonach die Reinhart durch die Kaliumdichromatmethode bestimmt wurde [3]. Die Papierchromatogramen zeigten einheitliche Zusammensetzung.

Reagenzien und Lösungen

— Die wässriege Lösung des Au (III) wurde durch die Auflösung des H $[AuCl_4]$ (Merck) unter Zuführung einer bestimmter Menge Salzsäure hergestellt. Es wird eine Eichlösung vorbereitet, die 197 µg Au/ml enthält. Der Titer dieser Lösung wurde durch die jodometrische Methode bestimmt [4]. Die in dieser Arbeit benutzten Lösungen sind durch angemessene Verdünnungen vorbereitet.

— Man verwendet 1.10^{-3} m Wasserlösungen bezogen auf die 100 % ige Reinheit der Farbstoffen ;

— 6 n Salzsäurelösung

— Benzol p.a.

— Wasserlösungen von Nitraten, Sulfaten und/ oder Chloriden verschiedener Kationen,

Extraktion der Komplexe

Die 1.10^{-4} m Lösung von Au (III) in Volumina von 0,1 — 2 ml werden in einen Scheidetrichter oder Meßkolben von 50 ml mit 6 n Salzsäure (1ml), destilliertem Wasser und 1.10^{-3} m Reagenzlösung bis zum Volumen von 10 ml gefürt. Man fügt 10 ml organisches Lösungsmittel hinzu und schüttelt 2 Minuten lang am Schüttelapparat. In ähnlicher Weise werden auch die Kontrollproben vorbereitet. Man mißt die Extinktionen der gefärbten organischen Phase bei den entsprächenden Wellenlängen in 1 cm dicken Küvetten.

ERGEBNISSE UND DISKUSSIONEN

Synthese der Komplexe

Um das Kombinationsverhältnis des Komplexanions mit den untersuchten Reagenzien im festen Zustand festzulegen, wurden 0,025 g Au (III) in 10 ml Wasser und Salzsäure bis zu der optimalen Normalität gelöst und mit etwa 0,60 g in 25 ml gelöster Farbstof gemischt. Es erscheint ein grünblauer Niederschalg, der durch Filtrierung unter Wakuum getrennt und mit Wasser gewaschen wurde. Die Verbindungen wurden bezüglich des Gehaltes an Gold [4] an Stickstoff und an Chlor [5,6] analysiert. Die erhaltenen Ergebnisse sind in Tabelle 1 eingetragen, woraus hervorgeht, daß das molarische Kombinationsverhältniss Metall-Farbstoff 1 : 1 ist.

TABELLE 1

Elementaranalyse der Komplexverbindungen

Verbindung	Gold		Stickstoff		Chlor	
	Berechnet %	Gefunden %	Berechnet %	Gefunden %	Berechnet %	Gefunden %
Malachitgrün$^+$ $[AuCl_4]^-$	29,49	29,38	4,19	4,24	21,25	21,18
(*ortho*-Anisgrün$^+$ $[AuCl_4]^-$	28,22	28,28	4,25	4,21	20,31	20,26
(*para*-Anisgrün$^+$ $[AuCl_4]^-$	28,22	28,81	4,25	4,06	20,31	20,60

IR-Spektren

Diese Spektren werden in einem Bereich von 420—3800 cm^{-1} erforscht (UR—10 — Karl Zeiss — Jena). Bei Vergleichung der IR Spektren der reinen Farbstoffen mit denen der entsprächenden Goldkomplexverbindungen wurde festgestellt, daß sich die Lagen und die Größen der Vibrationsbänder nach der Reaktion nicht verändert haben, ein Hinweis dafür, daß sich die Komplexe mit Ladungsübertragung bildeten. Die charakterischen Vibrationen der Bindung C—N (1400 cm^{-1}), C—C (1600 cm^{-1}) C—H (1000 cm^{-1}) in den Spektren der Komplexe sind gewöhnlich etwas verschoden gegen kleinere Frequenzen wegen der Ausdehnung dieser Bindungen nach der Komplexierung. Die Bindungen des Goldes konnten nicht hervorgehoben werden, weil die betreffenden Vibrationen unter 400 cm^{-1} erscheinen und dieser Bereich mit dem verwendeten Apparat nicht erforscht wurde.

Thermischer Abbau

Der thermooxydative Abbau von reinen Farbstoffen und deren mit $[AuCl_4]^-$ hergestellten Komplexverbindungen erfolgte thermogravimetrisch [7] in einem Temperaturintervall von 20—900° mit einem Gerät von Typ MOM Budapest, Erwärmungsgeschwindigkeit 9° min in 100 min. In Abbildung 1 geben wir als Beispiel die Derivatogramen vom Farbstoff *ortho*-Anisgrün und deren Komplexverbindung mit $[AuCl_4]^-$ wieder.

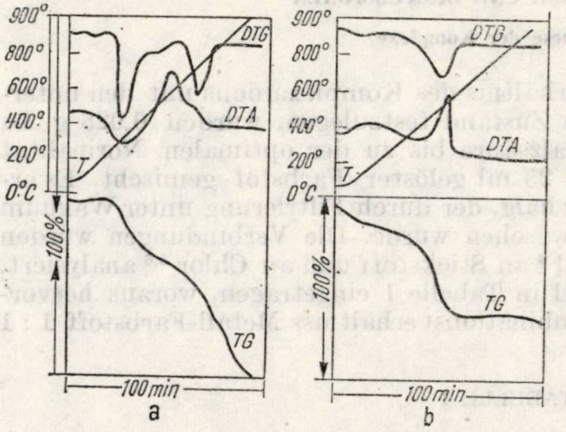

Abb. 1. — Derivatogramen von *ortho*-Anisgrün (1a) und von (*ortho*-Anisgrün$^+$ $[AuCl_4]^-$) (1b).

Der Farbstoff ist bis cca 620° in drei Stufen abgebaut. Die DTA-Kurve gibt uns Informationen über den thermischen Effekt jeder Abbaustufe. Die ersten drei Stufen zeigen einen schwachen endothermischen Effekt und die dritte Stufe von 350—620°, einen ausgeprägten exothermischen Effekt, als Folge der oxydation von Abbauprodukten.

Der Abbau von Komplexverbindung zeigt ein ähnliches Verhalten aber mit anderen Gewichtsverlusten für jede Stufe (Abbildung 1b).

Bis 580° zeigt die Verbindung einen sehr schwachen Abbau und ab 580° weist die Entwicklung einen exothermischen Effekt auf, welcher zu Goldtrioxyd führt. Die Komplexverbindung ist temperaturbeständiger als der Farbstoff. Der Rückstand, in Gewichtsprozenten zu Einwaage, stimmt mit der berechneten Zusammensetzung der Elementaranalyse überein. Bis cca. 100° können die Verluste von 4% als Wasserverlust betrachtet werden.

Eigenschaften der organischen Lösung von Komplexen
Verteilungsqoeffizient

Um den Verteilungsqoeffizient des Metalls zwischen den beiden Phasen festzulegen, kam eine spektrophotometrische Methode zur Anwendung. [8] Die Komplexverbindungen wurden unter optimalischen Bedindungen hergestellt und in Benzol extrahiert. Die beiden Phasen wurden getrennt dann jede mit konzentrierter Schwefelsäure und Wasserstoffsperoxyd behandelt. Die auf diese Weise gelösten Goldmengen wurden in beiden Fällen durch Rodamin B in Gegenwart von Salzsäure bestimmt [9]. Die Ergebnisse sind in der Tabelle 2 eingentregen.

Eine zufriedene Extraktion stellt man bei der Verwendung von *para*-Anisgrün und *ortho*-Anisgrün gefolgt von Malachitgrün fest.

TABELLE 2

Verteillungsqoeffizent (q) und Extraktibilität der Komplexe (E)

Reagenz	q	E %
(Malachitgrün$^+$ $[AuCl_4]^-$	5,29	84,20
(*ortho*-Anisgrün$^+$ $[AuCl_4]^-$	8,51	89,73
(*para*-Anisgrün$^+$ $[AuCl_4]^-$	8,68	90,36

$$q = \frac{\mu g \text{ Au/ml organische Phase}}{\mu g \text{ Au/ml wässrige Phase}}$$

$$E\,\% = \frac{100\ q}{q + \frac{V_{H_2O}}{V_{Benzol}}}$$

Wahl des Lösungsmittels

Es wurden folgende Lösungsmittel erprobt: Benzol, Toluol, und Gemische von Benzol mit kleinen Mengen von Aceton, Cyklohexanon, Methyläthylketon, Alkohole oder Äther, die sich in ähnlichen Arbeiten wirksam zeigten. Die Ergebnisse sind in Tabelle 3 eingetragen. In unseren Forschungen wurde dann nur das Benzol verwendet, weil dieses Lösungsmittel kein freier Farbstoff mitextrahiert. Die Kontrollproben waren farblos.

TABELLE 3

Wahl der Lösungsmittel

Lösungsmittel	E_{1max}		
	Malachitgrün$^+$ $[AuCl_4]^-$	(ortho Anisgrün$^+$ $[AuCl_4]^-$)	(para-Anisgrün$^+$ $[AuCl_4]^-$)
Benzol	0,34	0,69	0,71
Benzol-Äther 2 : 1	0,14	0,16	0,17
Benzol-Methanol 2 : 1	0,20	0,12	0,12
Benzol-Äthanol 2 : 1	0,16	0,18	0,18
Benzol-Cyklohexanol 2 : 1	0,24	0,20	0,24
Benzol-Methyläthylketon 4 : 1	0,28	0,38	0,42
Benzol-Methyläthylketon 6 : 1	0,35	0,52	0,54
Benzol-Methyläthylketon 8 : 1	0,38	0,73	0,77
Benzol-Aceton 3 : 1	0,16	0,28	0,30
Benzol-Cyklohexanon 3 : 1	0,20	0,40	0,42

Absorptionsspektren im sichtbaren Bereich

Bei Bestimmung der elektronischen Absorptionsspektren von wässrigen Lösungen der Reagenzien (Abbildung 2) wird festgestellt, daß das Spektrum von Malachitgrün ein Absorptionsmaximum bei 620 nm hat und die des substituierten Malachitgrüns Absorptionsmaxima bei 606 nm haben. Diese Tatsachen stimmten mit den von Dewar festgestellten [10,11] überein, u.z. daß die elektronenabstrossenden Substituenten einen hypsochromischen Effekt zur Folge haben. Die mit Au (III) in 10 ml Benzol erhaltenen Verbindungen weisen alle batochromische Verschiebung der elektronischen Absorbptionsmaxima im Vergleich zu den wässrigen Lösungen der reinen Farbstoffen hin.

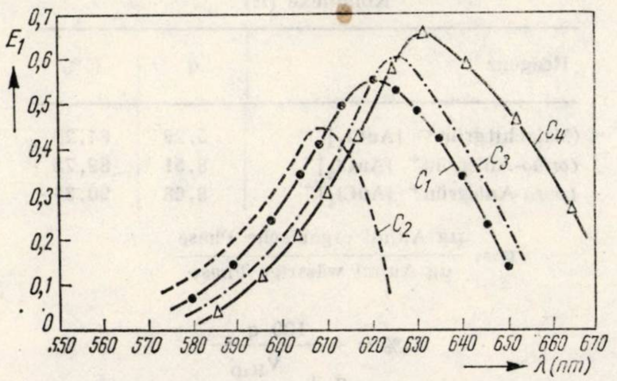

Abb. 2. — Absorptionsspektren im eichtbaren Bereich : C_1 — Malachitgrün ; C_2 — (Malachitgrün $^+[AuCl_4]^-$; C_3 — (*ortho*-Anisgrün $^+AuCl_4^-$) ; C_4 — *para*- Anisgrün $^+[AuCl_4]^-$).

Lösungsacidität

Alle studierte Reaktionen laufen im Medium von Salzsäure ab. Bei 0,3 n für Malachitgrün erhält man die maximale Absorbanz. Es ist wichtig, daß der substituierte Malachitgrün weniger ausgeprägte Abhängigkeit von der Lösungsazidität als Malachitgrün selbst aufweisen, d.h. man kann die Reaktion in größeren pH-Intervallen mit Erhaltung der optimalischen Bedingungen aus führen. In der Abbildung 3 ist es deutlich zu ersehen.

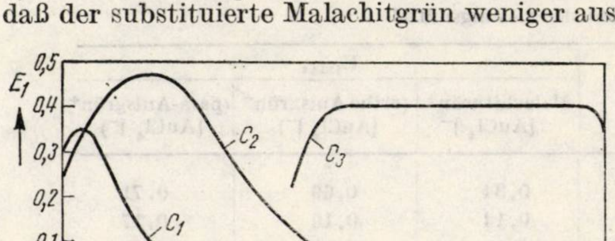

Abb. 3. — Eifluse der Lösungsazidität auf die Extraktbilität von Komplexen : C_1 — (Malachitgrün $^+[AuCl_4]^-$; C_2 — (*ortho*-Anisgrün $^+[AuCl_4]^-$) ; C_3 — (*para*-Anisgrün $[AuCl_4]^-$).

Die Abhängigkeit der Komplexbildung von der Acidität der wässrigen Phase könnte man durch das Vorhandensein von Farbstoffskation in monomeren Form erklären. Bei niedrigeren bzw höheren pH-Werte können polymere Formen der Kationen eintretten [12].

Die Reagenzkonzentration

Bei Veränderung der Farbstoffmenge von 0,5–5,0 ml 1.10^{-3}m (um das eingestellte Gleichgewicht nach rechte zu verschieben) wurde eine Erhöhung der Extinktion bis zu einer bestimmter Konzentration festgestellt, nach der sie konstant bleiben. Die bestmögliche Konzentration, in Abbildung 4 ersichtlich, ist für die Komplexe mit Malachitgrün bei $1{,}6.10^{-4}$m, für die mit *ortho*-Anisgrün bei 3.10^{-4}m, für die mit *para*-Nitralgrün bei $1{,}5.10^{-4}$m zu 10 ml wässriger Lösung.

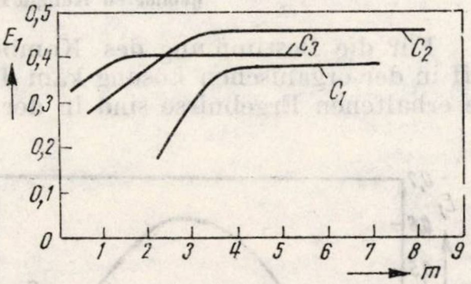

Abb. 4. — Reagenzkonzentration : C_1 — (Malachitgrün $^{+}[AuCl_4]^{-}$) ; C_2— (*ortho*- Anisgrün $^{+}[AuCl_4]^{-}$) ; C_3 — (*para*- Anisgrün $^{+}[AuCl_4]^{-}$).

Eichkurven

Das Studium der Absorptionsvariation in Abhängigkeit der Konzentration von Gold hat gezeigt, daß das Lambert-Beer'sche Gesetz zwischen den in der Tabelle 4 eingeordneten Grenzen gültig sei :

TABELLE 4

Gültigkeitsgrenzen des Lambert-Beer'schen Gesetzes

Verbindung	µg Au/ml		
	min	max	ε
(Malachitgrün^{+} $[AuCl_4]^{-}$)	10,0	100	5 700
(*ortho*-Anisgrün^{+} $[AuCl_4]^{-}$)	2,0	10	37 500
(*para*-Anisgrün^{+} $[AuCl_4]^{-}$)	1,0	12	55 000

Die Beständigkeit der Lösungen von Komplexverbindungen beträgt :
— 1/2 Stunde für das Komplex mit Malachitgrün
— 48 Stunden für das Komplex mit orto-Anisgrün
— 24 Stunden für das Komplex mit para-Anisgrün

Es ist auch wichtig, daß bei der Zufügung von 1 ml gesättigter Lösung von Ammoniumchlorid die Extinctionen unverändert bleiben.

Die Eichkurven wurdem durch Verbesserung der Versuchsdaten mit Hilfe der Methode kleinster Quatrate erhalten. Durch die statistische Bearbeitung der Ergebnisse (Warscheinlichkeit 0,95) wird ersichtlich, daß die relative Abweichung zwischen ±2,3% wechselt. Die Sensibilität der Reaktion ist größer bei der Anwendung substituierter Malachitgrün, unabhängig von der Substituentenstellung. Bei dem Vergleich der Substituenten miteinander, stellt man fest, daß die *para-* der *ortho-*Stellung überlegen zu sein scheint.

Studium der Zusammensetzung in organischer Lösung gebildeten Komplexverbindungen

Für die Bestimmung des Kombinationsverhältnisses Metall-Farbstoff in der organischen Lösung kam die Methode Job [13] zur Anwendung. Die erhaltenen Ergebnisse sind in der Abbildung 5 darges dargestellt.

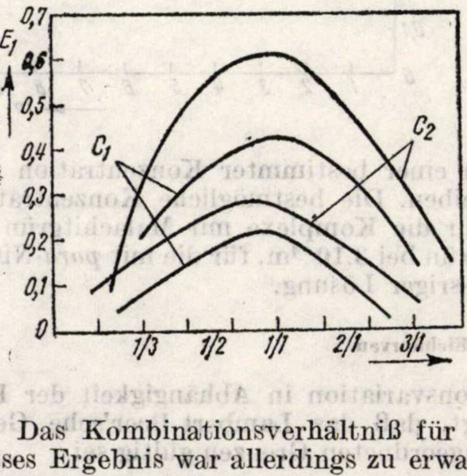

Abb. 5. — Zusammensetzung der gelösten Komplexverbindungen C_1 — (Malachitgrün $^+[AuCl_4]^-$); C_2 — (*ortho*-Anisgrün $^+[AuCl_4]^-$).

Das Kombinationsverhältniß für alle drei Verbindungen ist 1 : 1. Diesses Ergebnis war allerdings zu erwarten, da die Reaktionen im pH-Bereich durchgeführt werden, in dem der Farbstoff hauptsächlich als Kation in monomerer Form vorliegt.

Instabilitätskonstanten

Aus der Versuchsdaten (Abbildung 6), sind die Instabilitätskonstanten errechnet [13] und es wurde für das zwischen Au (III) und Malachitgrün gebildete Komplex $K_i = 0{,}4 \cdot 10^{-4}$, für das mit *ortho*-Anisgrün gebildete $K_i = 2{,}0.10^{-4}$ und für das mit *para*-Anisgrün gebildete K_i — $2{,}8.10^{-4}$ gefunden. Die erhaltenen Ergebnisse zeigen, daß sich durch Fällung hauptsächlich Komplexverbindungen vom Typ $(R^+[AuCl_4]^-)$ bildeten :

$$H^+[AuCl_4]^- + R^+Cl^- = (R^+[AuCl_4]^-) + H^+Cl^-$$

Es ist aber Möglich, daß in der Lösung auch andere in Gleichgewicht befindenden Arten existieren.

Konduktivitätsbestimmungen

Die Bestimmung der Konduktivität wurde unter Verwendung organischer Lösungen der Komplexverbindungen im Vergleich zu der Kontrollprobe und zu reinem Benzol durchgeführt. Ein Megaohmmeter vom Typ Tetralin Statron (DDR) kam zur Anwendung. Die Ergebnisse sind in der Tabelle 5 wiedergegeben.

TABELLE 5

Konduktivität von Benzollösungen der Komplexe

	$\rho = \frac{1}{R}$ (Ω.cm)	$\gamma = \frac{1}{\rho}$ ($\Omega^{-1}cm^{-1}$)
Benzol	$0,82.10^{11}$	$1,22.10^{-11}$
kontrolle	$0,33.10^{8}$	$3,0.10^{-8}$
(Malachitgrün$^+$ [$AuCl_4$]	$0,148.10^{7}$	$6,8.10^{-7}$
(*ortho*-Anisgrün$^+$ [$AuCl_4$]	$0,23.10^{7}$	$0,46.10^{-7}$
(*para*-Anisgrün$^+$ [$AuCl_4$]	$0,83.10^{7}$	$1,25.10^{-7}$

Der Konduktivitätsunterschied zwischen Benzol und der Kontrolprobe wird wohl der Gegenwart von in Benzol gelösten Wasser und Säuremengen, als Folge der Mischung beider Phasen zugeschrieben. In Vergleich zur Kontrolle steigt die Konduktivität gelösten Komplexverbindungen etwa mit einer Grössenordnung, was auf eine gewisse Ionisierung hindeutet. Als Ursache vermuten wir auch das in Benzol gelöste Wasser.

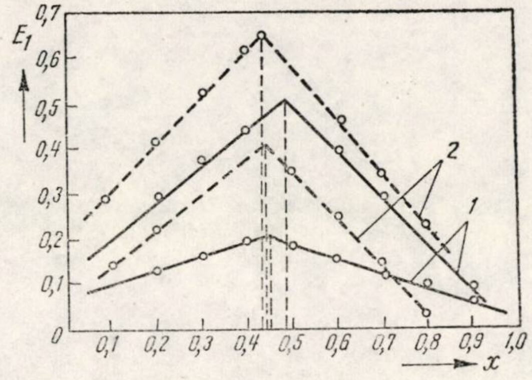

Abb. 6. — Annäherung der Instabilitätskonstanten : 1 — (*ortho*-Anisgrün $^+[AuCl_4]^-$) ; 2 — (*para*-Anisgrün $^+[AuCl_4]^-$).

Einfluβ fremder Ionen

Es wurde die Interferenz jener Ionen geprüfft, die gewöhnlich in verschiedene Materialien Gold begleiten und ähnliche Verbindungen bilden, so wie Indium, Gallium, Eisen, Antimonium, Vanadin, Thallium, Germanium, Molibden, Cupfer, Cadmium, Zinn, Cobalt, Nickel. Die Reaktionen sind in folgender Reihenfolgen von den fremden Ionen gestört :

Malachitgrün	Tl > In > Ga > Bi > Sb > Fe > Ge
ortho-Anisgrün	Tl > Sb > Bi > Ga > Fe
para-Anisgrün	Tl > Ga > Sb > Bi > In > Fe

Die anderen geprüfften Elementen stören die Reaktionen nicht.

LITERATURANGABEN

[1] Gh. Constantinescu, *Rev. Roumaine Chim.*, **20**, 1267 (1975).

[2] H. Sanielevici und L. Floru, "Sinteza intermediarilor aromatici şi a coloranţilor", Ed. II, Bucureşti 1971, S. 277.

[3] R. P. Lastovski und Io. I. Vainstein, „Tehniceskii analiz v proizvodstve promejutocinich i Crasitelei" Gosudarstvenoe naucino tehniceskoe izdatelistvo himiceskoi literaturi, Moskva, 1958.

[4] A. Chow und F. E. Beamish, *Talanta*, **10**, 883 (1963).

[5] I. S. Lealicov, "Metode fizico-chimice de analiză", Editura Tehnică, Bucureşti, 1961.

[6] N. H. Furman, "Standard Methods of Chemical Analysis" Ed. II Van Nostrand, New York, 1962–1963.

[7] O. Vicol, A. Biro und I. Schneider, *Thermal Anal.*, **1**, 435 (1969).

[8] S. Fisel, "Chimie analitică cantitativă", Bucureşti, 1973, S. 294.

[9] J. H. Yoe und A. E. Harvey, *J. Amer. Chem. Soc.*, **70**, 648 (1948).

[10] M. J. S. Dewar, *J. Amer. Chem. Soc.*, **74**, 3341, 3357 (1952).

[13] M. J. S. Dewar, *J. Chem. Soc.*, **1950**, 2327 ; **1954**, 2134.

[12] O. F. Ginsburg und C. M. Zavlin, *Zhur. obshchei Khim.*, **32**, 3559 (1962).

[13] P. Job, *Ann. Chim. (France)*, **9**, 113 (1928).

Revue Roumaine de Chimie 25, *8*, 1259–1267 (1980)

EINFLUSS DER SUBSTITUENTEN AUF DIE ANALYTISCHEN UND EXTRAKTIVEN EIGENSCHAFTEN VON ORGANISCHEN REAGENZIEN IN DER REAKTION MIT Au (III)

2. Mitt[1] EINFLUSS DER NITRO-SUBSTITUENTEN

GHEORGHE C. CONSTANTINESCU und CECILIA CONSTANTINESCU
Polytechnische Hochschule Bukarest, Polizu str. 1, Rumänien

Eingegangen am 20 Februar 1979

In der vorliegenden Arbeit wurden die Reaktionen zwischen dem Komplexanion $[AuCl_4]^-$ und dem *ortho-* bzw *para*-Nitralgrün studiert. Die gewonnenen Farbstoffe bilden mit $[AuCl_4]^-$ in Wasser unlösliche, in organischen Lösungsmitteln aber löslische Verbindungen, die dann in Benzol extrahiert werden. Die organischen Extrakte sind spektrophotometrisch und konduktometrisch untersucht. Außerdem wurden die Verbindungen aus Wasserlösung ausgefällt und der Elementar – bzw. IR-Spektralanalyse unterworfen. Es wurden auch die Grundbedingungen für die Anwendung der Reaktionen zur Goldbestimmung festgestellt. Die studierten Farbstoffe zählen zwischen den besten Reagenzien zur spektrophotometrischen Goldbestimmung und können auch für die Extraktion des Goldes aus verschiedenen Vorkommen verwendet werden.

The reaction of the basic reagents *ortho-* and *para*-Nitralgrün with the complex anion $[AuCl_4]$ is studied. The obtained combinations were extracted in benzene. The benzenic extracts have very good spectrophotometric properties, respect Lambert-Beer law between 0,6–10,0 μg Au/ml for *ortho*-Nitralgrün$^+$ $[AuCl_4^-]$ with $\varepsilon = 81\,000$ and 0,2–8.0 μg Au/ml for (para-Nitralgrün$^+$ $AuCl_4^-$) with $\varepsilon = 100\,000$. The sensibility of the reactions is very good.

In einer anderen Arbeit [1] haben wir die Ergebnisse unserer Forschungen bezüglich der Bildung von Komplexverbindungen zwischen Malachitgrün und dem selben mit Metoxylgruppen in *ortho-* und *para*-Sellung substituierten Farbstoff veröffentlicht.

Wir kamen zu dem Schluss, daß der substituierte Malachitgrün günstigere Reaktionsbedingungen als Malachitgrün selbst zu schaffen vermag. Wenn *ortho*-bzw. *para*-Anisgrün, Farbstoffe die elektronenabstossenden Gruppen als Substituent enthalten, dem Malachitgrün in der Reaktion mit $[AuCl_4]^-$ überlegen worden waren, dann war es zu erwarten, daß das Studium der Reaktionen mit Malachitgründerivaten, die elektronenziehenden Gruppen als Substituent haben und deren Elektronen an den chinoiden System des Farbstoffes beteiligt sein können zu noch interessanten Ergebnisse führen sollten. Wir konnten tatsächlich feststellen, daß solche Farbstoffe wie die *ortho-* und *para*-Nitralgrün einige der empfinlichsten Reagenzien zur spektrophotometrischen Goldbestimmung wie Methylviolett, Rodamin B oder Viktoria Reinblau BO ausgleichen.

In dieser Arbeit werden die Synthesen der basischen Farbstoffen *ortho*- und *para*-Nitralgrün, die Ergebnisse der Forschungen bezüglich der Bildungsreaktion der Ionischen Assoziationen zwischen $[AuCl_4]^-$ und der Kationen der Farbstoffe, sowie auch die Struktur und einige Eigenschaften der erhaltenen Verbindungen im Vergleich zu dem Farbstoff Malachitgrün dargestellt.

VERSUCHSTEIL

Synthese der Farbstoffe. (*Ortho*-Nitralgrün ist der Handelsname der chlorid von *p*-dimethylamminobenzol-*o*-nitrobenzol-*p*-chinondimethylammonium-methan). Die verwendeten Farbstoffe wurden durch Kondensierung von *ortho*- bzw *para*-Nitrobenzaldehyde mit Dimethylanilin gewonnen [2]. Die durch Erhitzung auf dem Wasserbad erhaltene dickflüssige Masse ist mit Wasserdampf angetrieben. Der zurückgebliebene Rückstand ist in Äthylalkohol aufgelöst, woraus die Leukobasis wieder ausgefällt wird. Durch Oxydation mit Bleidioxyd erhält man das entsprechende Carbinol, welches mit Salzsäure die Verbindung mit folgender Struktur bildet :

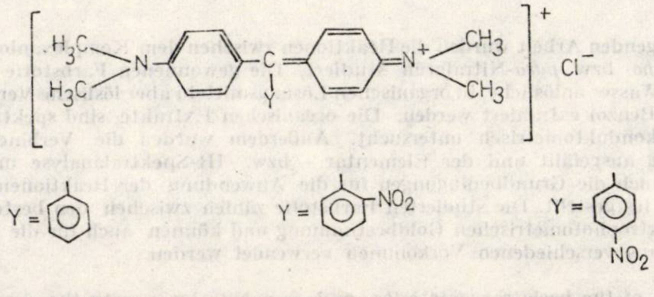

Malachitgrün *ortho*- Nitralgrün *para*-Nitralgrün

Die Reinigung der Farbstoffe erfolgte durch wiederholte Umkristallisation, wonach die Reinhart durch die Kaliumdichromatmethode bestimmt wurde [3]. Die Papierchromatogramen zeigten einheitliche Zusammensetzung.

Reagenzien und Lösungen

Die wägriege Lösung des Au (III) wurde durch die Auflösung des $H[AuCl_4]$ (Merck) unter Zuführung einer bestimmten Menge Salzsäure hergestellt. Es wird eine Eichlösung vorbereitet, die 197 g Au/ml enthält. Der Titer dieser Lösung wurde durch die jodometrische Methode bestimmt [4]. Die in dieser Arbeit benutzten Lösungen sind durch angemessene Verdünnungen vorbereitet.

— Man verwendet $1 . 10^{-3}$ m Wasserlösungen bezogen auf die 100% ige Reinheit der Farbstoffen ;

— 6 n Salzsäurelösung

— Benzol p.a.

— Wasserlösungen von Nitraten, Sulfaten und/ oder Chloriden verschiedener Kationen

Extraction der Komplexe

Die $1 . 10^{-4}$ m Lösung von Au (III) in Volumina von 0,1—2 ml werden in einen Scheidetrichter oder Meßkolben von 50 ml mit 6 n-en Salzsäure (1 ml), destilliertem Wasser und 1.10^{-3} m Reagenzlösung bis zum Volumen von 10 ml geführt. Man fügt 10 ml organisches Lösungsmittel hinzu und schüttelt 2 Minuten lang am Schüttelapparat. In ähnlicher Weise werden auch die Kontrollproben vorbereitet. Man mißt die Extinktionen der gefärbten organischen. Phase bei den entsprechenden Wellenlängen in 1 cm dicken Küvetten.

ERGEBNISSE UND DISKUSSIONEN

Synthese der Komplexe

Um das Kombinationaverhältnis des Komplexanions mit den untersuchten Reagenzien im festen Zustand festzulegen, wurden 0,25 g Au (III) in 10 ml Wasser und Salzsaure bis zu der optimalen Normalität gelöst und mit etwa 0,50 g in 10 ml gelöster Farbstoff gemischt. Es erscheint ein grünblauer Niederschlag, der durch Filtrierung unter Wakuum getrennt und mit Wasser gewaschen wurde. Die Verbindungen wurden bezüglich des Gehaltes an Gold [4] an Stickstoff und an Chlor [5,6] analysiert. Die erhaltenen Ergebnisse sind in Tabelle 1 eingetragen, woraus hervorgeht, daß das molarische Kombinationsverhältniss Metall-Farbstoff 1 : 1 ist.

TABELLE 1

Elementaranalyse der Komplexe

Verbindung		Gold		Stickstoff		Chlor	
Name	Substituent	berechnet	gefunden	berechnet	gefunden	berechnet	gefunden
Malachit-grün	y = 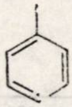	29,49	29,38	4,19	4,24	21,25	21,28
ortho-Nitral-grün$^+$[AuCl$_4$]$^-$	y = 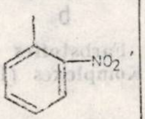	27,63	26,91	5,89	5,73	19,77	19,14
para-Nitral-grün$^+$[AuCl$_4$]$^-$	y = 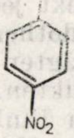	27,63	27,04	5,89	5,79	19,77	19,20

Die IR-Spektren

Diese Spektren wurden in einem Bereich von 400—4000 cm^{-1} erforscht. Bei Vergleichung der IR Spektren der reinen Farbstoffen mit denen der entsprächenden Goldkomplexverbindungen wurde festgestellt, daß sich die Lagen und die Größen der Vibrationsbänder nach der Reaktion nicht verändert haben, ein Hinweis dafür, daß sich die Komplexe mit Ladungsübertragung bildeten. Die charakteristischen Vibrationen der Bindung C—N (1400 cm^{-1}), C—C (1600 cm^{-1}) C—H (1000 cm^{-1}) in den Spektren der Komplexe sind gewöhnlich etwas verschoben gegen kleinere Frequenzen wegen der Ausdehnung dieser Bindungen nach der Komplexierung. Die Bindungen des Goldes konnten nicht hervorgehoben werden, weil die betreffenden Vibrationen unter 400 cm^{-1} erscheinen und dieser Bereich mit dem verwendeten Apparat nicht erforscht wurde.

Thermischer Abbau

Der thermooxydative Abbau von reinen Farbstoffen und deren mit $[AuCl_4]^-$ hergestellten Komplexverbindungen erfolgte thermogravimetrisch [7] in einem Temperaturintervall von 20—900° mit einem Gerät von Typ MOM Budapest, Erwärmungsgeschwindigkeit 9°/min în 100 min. In Abbildung 1 geben wir als Beispiel die Derivatogramen vom Farbstoff *orto*-Nitralgrün und deren Komplexverbindung mit $[AuCl_4]^-$ wieder.

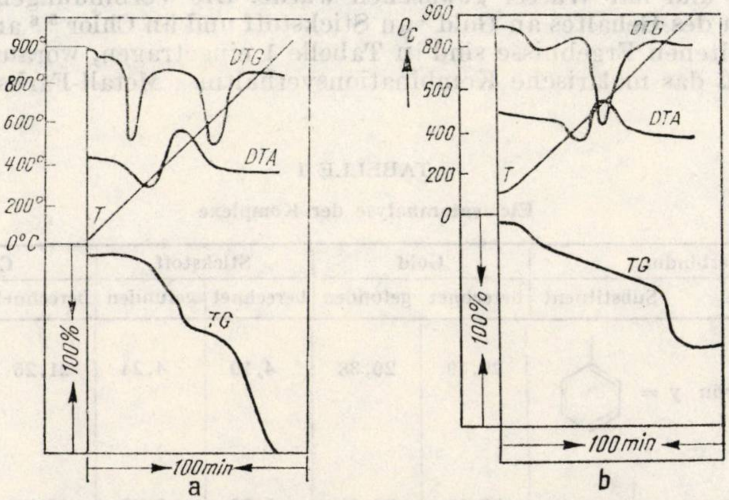

Abb. 1a und 1b. — Derivatogramen des freien Farbstoffes (1a) und des mit *ortho*- Nitralgrün gewonnenen Komplexes (1b).

Der Farbstoff ist bis 610° in vier Stufen abgebaut. Die DTA-Kurve gibt uns Informationen über den thermischen Effekt jeder Abbaustufe. Die ersten drei Stufen zeigen einen schwachen endothermischen Effekt und die vierte Stufe von 450—610°C, einen ausgeprägten exothermischen Effekt, als Folge der oxydation von Abbauprodukten.

Der Abbau von Komplexverbindung zeigt ein ähnliches Verhalten aber mit anderen Gewichtsverlusten für jede Stufe (Abbildung 1).

Bis 480° zeigt die Verbindung einen sehr schwachen Abbau und ab 480° die Entwicklung einen exothermischen Effekt auf, welcher zu Goldtrioxyd führt. Die Komplexverbindung ist temperaturbeständiger als der Farbstoff. Der Rückstand, in Gewichtsprozenten zu Einwaage, stimmt mit der berechneten Zusammensetzung der Elementaranalyse überein. Bis cca. 100° können die Verluste von 4% als Wasserverlust betrachtet werden.

Eigenschaften der organischen Lösung von Komplexen
Verteilungsqoeffizient

Um den Verteilungsqoeffizient des Metalls zwischen den beiden Phasen festzulegen, kam eine spektrophotometrische Methode zur Anwendung. [8] Die Komplexverbindungen wurden unter optimalischen Bedingungen hergestellt und in Benzol extrahiert. Die beiden Phasen wurden getrennt dann jede mit konzentrierter Schwefelsäure und Wasserstoffperoxyd behandelt. Die auf diese Weise gelösten Goldmengen wurden in beiden Fällen durch Rodamin B in Gegenwart von Salzsäure bestimmt [9]. Die Ergebnisse sind in die Tabelle 2 eingetragen.

TABELLE 2

Verteilungsqoeffizient (q) und Extraktibilität der Komplexe (E)

Verbindung Name	q	%E
Malachitgrün $^+[AuCl_4]^-$	5,29	84,20
ortho-Nitralgrün $^+[AuCl_4]^-$	11,01	98,21
ortho-Nitralgrün $^+[AuCl_4]^-$	11,00	98,00

Eine bessere Extraktion stellt man bei der Verwendung von *para*-Nitralgrün gefolgt von *orto*-Nitralgrün fest.

Die Wahl des Lösungsmittels

Es wurden folgende Lösungsmittel er robt : Benzol, Toluol, unde Gemische von Benzol mit kleinen Mengen von Aceton, Cyklohexanon, Methyläthylketon, Alkohole oder Äther, die sich in ähnlichen Arbeiten wirksam zeigten. Die Ergebnisse sind in Tabelle 3 eingetragen. In unseren Forschungen wurde dann nur das Benzol verwendet, weil dieses Lösungsmittel kein freier Farbstoff mitextrahiert. Die Kontrollproben waren farblos.

TABELLE 3

Wahl des Losüngsmittels

Lösungsmittel	$E_{1\,max}$		
	(Malachgr.$^+$ $[AuCl_4]^-$	(*ortho*-Nitr.$^+$ $[AuCl_4]^-$)	(*para*-Nitr.$^+$ $[AuCl_4]^-$)
Benzol	0,34	0,82	0,84
Benzol-Äther 2 : 1	0,14	0,08	0,10
Benzol-Methanol 2 : 1	0,20	0,23	0,21
Benzol-Äthanol 2 : 1	0,16	0,28	0,25
Benzol-Cyklohexanol 2 : 1	0,24	0,31	0,32
BenzolA-ceton 3 : 1	0,12	0,26	0,25
Benzol-Cyklohexanon 3 : 1	0,16	0,42	0,44
Benzol-Methyläthylketon 4 : 1	0,28	0,63	0,70
Benzol-Methyläthylketon 6 : 1	0,35	0,70	0,74
Benzol-Methyläthalketon 8 : 1	0,38	0,88	0,90

Absorptionsspektren im sichtbaren Bereich

Bei Bestimmung der elektrischen Absorptionsspektren von wäßrigen Lösungen der Reagenzien (Abbildung 2) wird festgestellt, daß das Spektrum von Malachitgrün ein Absorptionsmaximum bei 620 nm hat. Da die

Spektren von substituierten Malachitgrün Absorptionsmaxima bei 635 nm (*ortho*-Nitralgrün) und 640 nm (*para*-Nitralgrün) haben, stimmten diese Tatsachen mit den von Dewar festgestellten[10,11] überein, u.z. daß die elektronenanziehenden Substituenten einen batochromischen Effekt zur Folge haben. Die mit Au (III) in 10 ml Benzol erhaltenen Verbindungen weisen alle batochromische Verschiebung der elektronischen Absorptionsmaxima im Vergleich zu den wäßrigen Lösungen der reinen Farbstoffen hin.

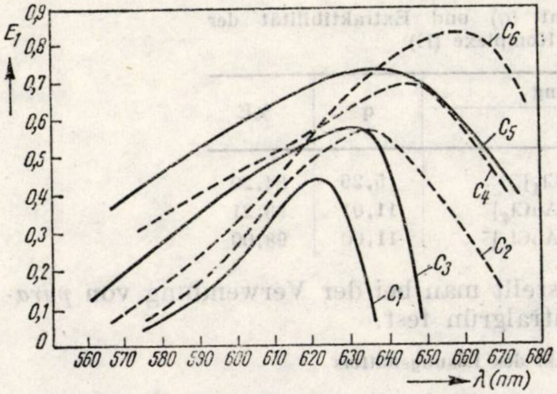

Abb. 2. — Absorptionsspektren im sichtbaren Bereich C_1 — Malachitgrün/ Wasser ; C_2 — (Malachitgrün $[AuCl_4]^-$/ Benzol ; C_3 — *ortho*-Nitralgrün/ Wasser ; C_4 — (*ortho*-Nitralgrün$^+$ $[AuCl_4]$ / Benzol ; C_5 — *para*-Nitralgrün/ Wasser ; C_6 — (*para*-Nitralgrün$^+$ $[AuCl_4]^-$)/ Benzol.

Lösungsacidität

Alle studierte Reaktionen laufen im Medium von Salzsäure ab. Bei 0,3 n für Malachitgrün erhält man die maximale Absorbanz. Es ist wichtig, daß der substituierte Malachitgrün weniger ausgeprägte Abhängigkeit von der Lösungsazidität als Malachitgrün selbst aufweisen, d.h. man kann die Reaktion in größeren pH-Intervallen mit Behaltung der optimalischen Bedingungen ausführen. In der Abbildung 3 ist es deutlich zu ersehen.

Die Abhängigkeit der Komplexbildung von der Acidität der wäßrigen Phase könnte man durch das Vorhandensein von Farbstoffskation in monomeren Form erklären. Bei niedrigeren bzw höheren pH-Werte können polymere Formen der Kationen eintretten[12].

Die Reagenzkonzentration

Bei Veränderung der Farbstoffmenge von 0,5—5,0 ml 1.10^{-3} m (um das eingestellte Gleichgewicht nach rechts zu verschieben) wurde eine Erhöhung der Extinktion bis zu einer bestimmter Konzentration festgestellt, nach der sie konstant bleibt. Die bestmögliche Konzentration, in Abbildung 4 ersichtlich, ist für die Komplexe mit Malachitgrün bei $1,6.10^{-4}$ m für die mit *ortho*-Nitralgrün bei 3.10^{-4} m für die mit *para*-Nitralgrün auch bei 3.10^{-4} m zu 10 ml wässriger Lösung.

Eichkurven

Das Studium der Absorbtionsvariation in Abhängigkeit der Konzentration von Gold hat gezeigt, daß das Lambert-Beer'sche Gesetz zwischen den in der Tabelle 4 eingeordneten Grenzen gültig sei:

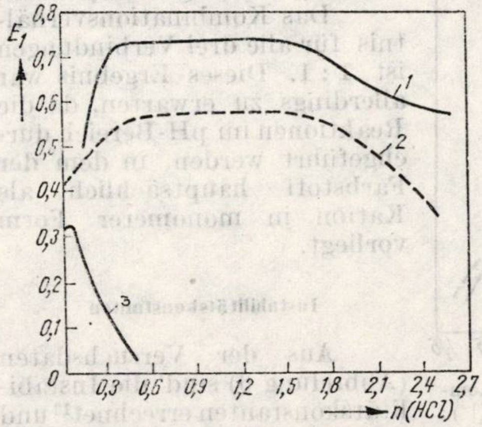

Abb. 3. — Einfluss der Lösungsacidität auf die Extraktibilität der Komplexe C_1 — (*ortho*-Nitralgrün$^+$ $[AuCl_4]^-$); C_2 — (*para*-Nitralgrün$^-$ $[AuCl_4]^+$); C_3 — (Malachitgrün $[AuCl_4]^-$).

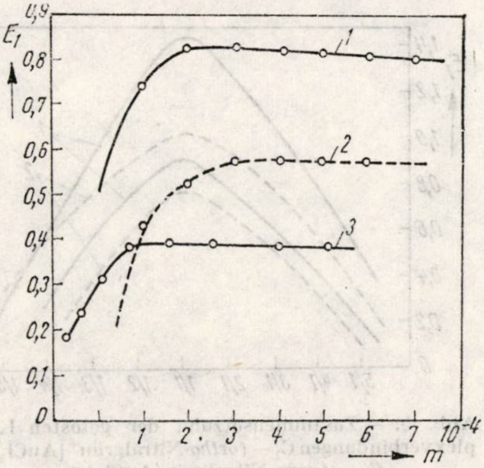

Abb. 4. — Reagenzkonzentration C_1 — *ortho* Nitralgrün; C_2 — *para*-Nitralgrün; C_3 — Malachitgrün.

Die Beständigkeit der Komplexverbindungen beträgt:

— 1/2 Stunde für das Komplex mit Malachitgrün
— 48 Stunden für das Komplex mit *ortho*-Nitralgrün
— 4 Stunden für das Komplex mit *para*-Nitralgrün

TABELLE 4

Grenzen des Lambert-Beer'schen Gesetzes

Verbindung	µg/Au/ml	ε
(Malachitgrün $AuCl_4^-$])	10,0—100	5.700
(*ortho*-Nitralgrün [$AuCl_4^-$)	0,6—10	81.000
(*para*-Nitralgrün $AuCl_4^-$)	0,2—8	100.000

Die Eichkurven wurden durch Verbesserung der Versuchsdaten mit Hilfe der Methode kleinster Quadrate erhalten. Durch die statistische Bearbeitung der Ergebnisse (Warscheinlichkeit 0,95) wird ersichtlich, daß die relative Abweichung zwischen ± 2,3% wechselt. Die Sensibilität der Reaktion ist größer bei der Anwendung substituierter Malachitgrün, unabhängig von der Substituentenstellung. Bei dem Vergleich der Substituenten miteinander, stellt man fest, daß die *para*- der *ortho*-Stellung überlegen zu sein scheint.

Studium der Zusammensetzung in organischer Lösung gebildeten Komplexverbindungen

Für die Bestimmung des Kombinationsverhältnisses Metall-Farbstoff in der organischen Lösung kam die Methode Job[13] zur Anwendung. Die erhaltenen Ergebnisse sind in der Abbildung 5 dargestellt.

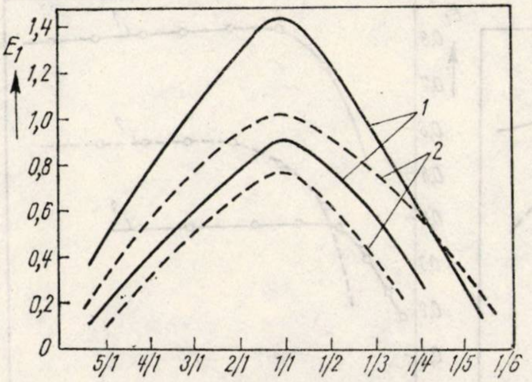

Abb. 5. — Zusammensetzung der gelösten Komplexverbindungen C_1— (*ortho*-Nitralgrün$^+$ [$AuCl_4$]$^-$) ; C_2 — (*para* Nitralgrün [$AuCl_4$]$^-$.

Das Kombinationsverhältnis für alle drei Verbindungen ist 1 : 1. Dieses Ergebnis war allerdings zu erwarten, da die Reaktionen im pH-Bereich durchgeführt werden, in dem der Farbstoff hauptsächlich als Kation in monomerer Form vorliegt.

Instabilitätskonstanten

Aus der Versuchsdaten (Abbildung 6) sind die Instabilitätskonstanten errechnet[13] und es wurde für das zwischen Au (III) und Malachitgrün gebildete Komplex $K_i = 0{,}4 . 10^{-4}$, für das mit *ortho*-Nitralgrün gebildete $K_i = 1{,}2 . 10^{-5}$ und für das mit *para*-Nitralgrün gebildete $K_i = 9{,}8 . 10^{-6}$ gefunden. Die erhaltenen Ergebnisse zeigen, daß dich durch Fällung hauptsächlich Komplexverbindungen vom Typ ($R^+[AuCl_4]^-$) bildeten :

$$H^+[AuCl_4]^- + R^+Cl^- = (R^+[AuCl_4]^-) + H^+Cl^-$$

Es ist aber Möglich, daß in der Lösung auch andere in Gleichgewicht befindenden Arten existieren.

Konduktivitätsbestimmungen

Die Bestimmung der Konduktivität wurde unter Verwendung organischer Lösungen der Komplexverbindungen im Vergleich zu der Kontrollprobe und zu reinem Benzol durchgeführt. Ein Megaohmmeter vom Typ Tetralin Statron (DDR) kam zur Anwendung. Die Ergebnisse sind in der Tabelle 5 wiedergegeben.

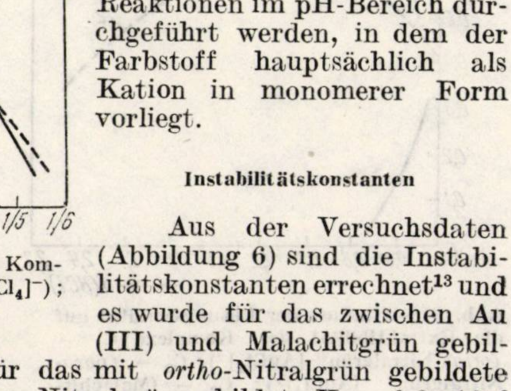

Abb. 6. — Annäherung der Instabilitätskonstanten C_1— (*ortho* Nitralgrün$^+$ [$AuCl_4^-$] ; C_2 — (*para* Nitralgrün$^+$ [$AuCl_4$]$^-$).

Der Konduktivitätsunterschied zwischen Benzol und der Kontrolprobe wird wohl der Gegenwart von in Benzol gelösten Wasser und Säuremengen, als Folge der Michung beider Phasen zugeschrieben. Im

Vergleich zur Kontrolle steigt die Konduktivität der gelösten Komplexverbindungen etwa mit einer Grössenordnung, was auf eine gewisse Ionisierung hindeutet. Als Ursache vermuten wir auch das in Benzol gelöste Wasser.

TABELLE 5

Konduktivität von Benzollösungen der Komplexe

Verbindung	$\rho = \frac{1}{R}$ (Ω cm)	$\gamma = \frac{1}{\rho}$ (Ω^{-1} cm^{-1})
Benzol	$0,82 . 10^{11}$	$1,22 . 10^{-11}$
Iontrolle	$0,148 . 10^{8}$	$3,0 . 10^{-8}$
(Malachitgrün^{+}[AuCl$_4$]$^{-}$)	$0,148 . 10^{7}$	$6,8 . 10^{-7}$
(*ortho*-Nitralgrün^{+}[AuCl$_4$]$^{-}$)	$0,338 . 10^{7}$	$3,0 . 10^{-7}$
(*para*-Nitralgrün^{+}[AuCl$_4$]$^{-}$)	$0,675 . 10^{7}$	$1,5 . 10^{-7}$

Einfluß fremder Ionen

Es wurde die Interferenz jener Ionen geprüfft, die gewöhnlich in verschiedenen Materialien Gold begleiten und ähnliche Verbindungen bilden, so wie Indium, Gallium, Eisen, Antimonium, Vanadin, Thallium, Germanium, Molibden, Cupfer, Cadmium, Zinn, Cobalt, Nickel. Die Reaktionen sind in folgender Reihenfolgen von den fremden Ionen gestört :

Malachitgrün	Tl > In > Ga > Bi > Sb > Fe > Ge
ortho-Nitralgrün	Tl > Sb > In > Ga > Bi > Fe
para-Nitralgrün	Tl > Ga > Sb > Bi > In > Fe

Die anderen geprüfften Elementen stören die Reaktionen nicht.

LITERATURANGABEN

[1] Gh. Constantinescu, *Rev. Roumaine Chim.*, **20**, 1267 (1975).

[2] H. Sanielevici und L. Floru, "Sinteza intermediarilor aromatici şi a coloranţilor", Ed II, Bucureşti, 1971, S. 277.

[3] R. P. Lastovski und Io. I. Vainstein, "Tehniceskii analiz v proizvodstve promejutocinîch Crasitelei" Gosudarstvenoe naucino tehniceskoe izdatelistvo himiceskoi literaturî, Moskva, 1958.

[4] A. Chow und F. E. Beamish, *Talanta*, **10**, 883 (1963).

[5] I. S. Lealicov, "Metode fizico-chimice de analiză", Editura tehnică Bucureşti, 1961.

[6] N. H. Furman, "Standard Methods of Chemical Analysis", Ed. II, Van Nostrand, New York, 1962–1963.

[7] O. Vicol, A. Biro, und I. Schneider, *Thermal Anal.*, **1**, 435 (1969).

[8] S. Fisel, "Chimie analitică cantitativă", Bucureşti, 1973, p. 294.

[9] J. H. Yoe und A. E. Harvey, *J. Amer. Chem. Soc.*, **70**, 648 (1948).

[10] M. J. S. Dewar, *J. Amer. Chem. Soc.*, **74**, 3341, 3357 (1952).

[11] M. J. S. Dewar, *J. Chem. Soc.*, **1950**, 2327 ; **1954**, 2134.

[12] O. F. Ginsburg und C. M. Zavlin, Zhur. *Obshchei Khim* **32**, 3559 (1962).

[13] P. Job, *Ann. Chim. (France)*, **9**, 113 (1928).

Revue Roumaine de Chimie 25, *8*, 1269–1274 (1980)

UTILIZATION OF SODIUM HYDROXIDE IN SEPARATION OF TIN WITH ION EXCHANGE RESINS. II[1]

CATION EXCHANGE SEPARATIONS

LUMINIŢA VLĂDESCU and DĂNUŢA VOICU
National Institute of Chemistry, Laboratory of Analytical Chemistry, Splaiul Independenţei No 202, Bucharest, Romania

Received November 8, 1979

In the present work the cation exchange behaviour of As (V, III), Sn (IV), Ti (IV), Zr (IV), Sb (III), Bi (III), Fe (III, II), Cu (II) and Pb (II) in the presence of NaOH, under the optimal conditions established for the elution of Sn (II) from a cationite, was investigated. The results have underlain the devising of a method for the separation of tin from impurifying elements.

As (V, III), Sb (V, III), Ti (IV), Zr (IV), Bi (III), Fe (III, II), Cu (II) and Pb (II) are among the elements most frequently found together with tin in its natural and synthetic compounds. As the ions of these elements interfere in quantitative determination of tin, analytical separation procedures have to be developed.

In this work, the employing of sodium hydroxide as elution agent in separation of interfering elements from tin on cation exchange resins is proposed.

Therefore, the cation exchange behaviour of As (V, III), Sn (IV), Ti (IV), Zr (IV), Sb (III), Bi (III), Fe (III, II), Cu (II) and Pb (II) in the presence of NaOH, under the conditions established, in the first part of this work,[1] as optimal for the elution of tin (II) from a cationite, was investigated.

The results have underlain the devising of a method for the separation and concentration of tin.

EXPERIMENTAL

Merck I strongly acid cation exchange resin was employed. The following reagents were also utilized : tin (II) chloride p.a. and technical grade, and tin (IV) chloride, antimony (III) chloride, copper arsenite, sodium arseniate, bismuth nitrate, Mohr salt, iron (III) chloride, lead (II) nitrate, NaOH, HCl, $KBrO_3$, Xylenol Orange, KSCN, α, α′-dipyridyl, ascorbic acid, Pyrocatechine Violet, EDTA, NH_3, all p.a. grade.

The quantitative determination of studied elements was achieved as follows : Sn (II), Sb (III) and As (III) by volumetric method with potassium bromate ;[2] Sn (IV), Fe (III), Fe (II), Ti (IV) Zr (IV) and Cu (II) spectrophotometrically with colour reagents e.g. : Xylenol Orange, [3] KSCN, [4] α, α′-dipyridyl, [5] ascorbic acid, [6] Pyrocatechine Violet [7] and NH_3, respectively ; Pb (II) and Bi (III) volumetrically with EDTA. [2]

The working procedure was described earlier. [1]

RESULTS AND DISCUSSION

To establish the working parameters which allow separation of tin from interfering elements, the cation exchange behaviour of Sn (IV), As(V, III), Ti(IV), Zr(IV), Sb(III), Bi(III), Fe(III, II), Cu(II) and Pb(II) was studied.

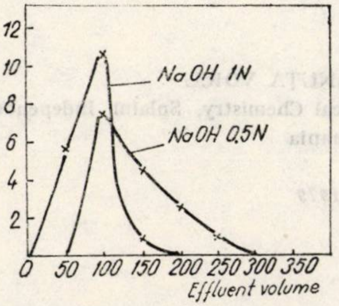

Fig. 1. — The influence of NaOH concentration on the elution of Sn (IV) from a cation exchange resin.

The elution curves of tin(IV) shown in figure 1 exhibit the same dependence of elution on NaOH concentration, found for tin (II), [1] however Sn(IV) leaves the column faster than Sn (II).

Since under working conditions As(V) and As (III) are found as AsO_4^{3-} and AsO_3^{3-} anions, they are not retained by a cation exchange resin and all are found in the effluent on column washing with distilled water (Figure 2a).

Figure 2 b shows that Pb (II) is eluted from cationite with 1N NaOH, while Ti (IV), Zr (IV), Bi (III), Cu (II), Fe (III) and Fe (II) stay over in the resin.

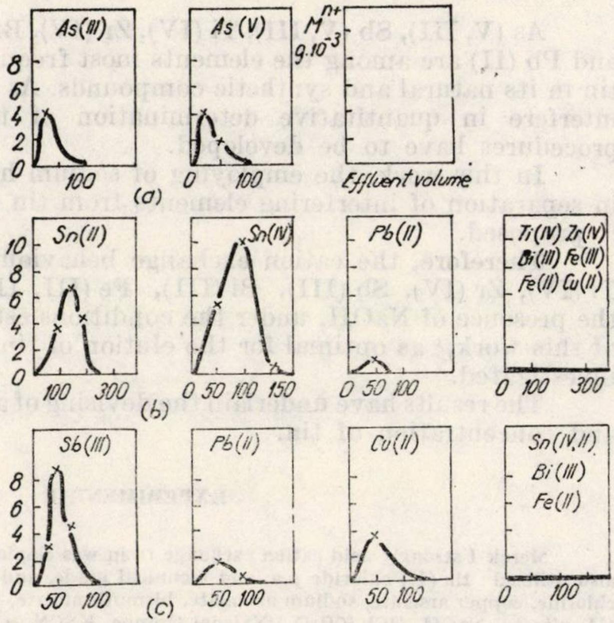

Fig. 2. — The cation exchange behaviour of Sn (IV), As (V, III), Zr (IV), Sb (III), Bi (III), Fe (III, II), Cu (II) and Pb (II). Elluent : a) H_2O ; b) 1N NaOH ; c) tartaric acid.

Further on, given the possibility of employing 2 % tartaric acid for selective elution of antimony (III) retained together with Sn (II) on a cation exchange resin, the influence of this reagent upon cation exchange behaviour of studied elements was approached.

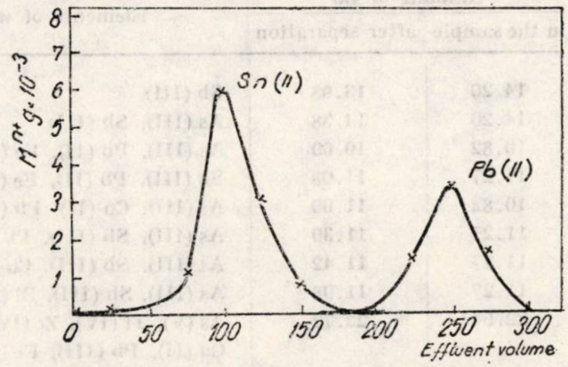

Fig. 3. — Elution curves: Sn (II) — Pb (II) separation.

According to figure 2c Sb (III), Pb (II), Cu (II), and Fe (III) may be eluted with 2% tartaric acid solution, while Bi (III), Sn (II), Sn (IV) and Fe (II) stay in the resin.

The analysis of results shows that tin may be separated from the studied elements by retaining the sample's cations in a cation exchange resin, elution of As (V) and As (III) with distilled water and elution of Sb (III), Bi (III), Fe (III), Cu (II) and Pb (II) with 2% tartaric acid. Tin is finally eluted with 1N NaOH and quantitatively determined in the effluent.

The analysis of samples that do not contain antimony, does no longer require utilization of tartaric acid. Thus, in such cases, separation of arsenic by washing the column with distilled water, is followed by elution of tin with 1N NaOH ; all the other cations remain attached to the resin.

Although lead (II) leaves the column on elution with 1N NaOH, in the presence of tin its elution is delayed (Figure 3). This behaviour allows separation of the two elements by subsequent elution with 1N NaOH.

APPLICATIONS

The results presented above have been applied to separation of synthetic mixtures of : Sn (II, IV), Sb (III) ; Sn (II), As (III), Pb (II), Fe (II) ; Sn (II, IV), As (V, III), Cu (II), Pb (II), Fe (II) ; Sn (II, IV), As (III), Sb (III), Cu (II), Pb (II), Fe (II) ; Sn (IV), As (V), Ti (IV), Zr (IV), Bi (III), Cu (II), Fe (III) ; Sn (II, IV), As (III, V), Ti (IV), Zr (IV), Sb (III), Bi (III), Cu (II), Pb (II), Fe (II, III).

Data in table 1 show a good agreement between the amounts of tin taken in the sample and those determined after separation.

Figures 4 a, b, c present the elution curves obtained for several of the mixtures separated.

TABLE 1

The results for separation of tin from various elements

Amount of tin		Elements of which tin has been separated
in the sample	after separation	
14.20	13.98	Sb (III)
14.20	14.38	As (III), Sb (III)
10.82	10.60	As (III), Pb (II), Fe (II)
11.27	11.08	Sb (III), Pb (II), Fe (II)
10.82	11.00	As (III), Cu (II), Pb (II), Fe (II)
11.27	11.30	As (III), Sb (III), Pb (II), Fe (II)
11.27	11.42	As (III), Sb (III), Cu (II), Pb (II), Fe (II)
11.27	11.08	As (III), Sb (III), Bi (III), Fe (III), Cu (II), Pb (II), Fe (II)
22.54	22.72	As (V), Ti (IV), Zr (IV), As (III), Sb (III), Bi (III), Fe (III), Cu (II), Pb (III), Fe (II)

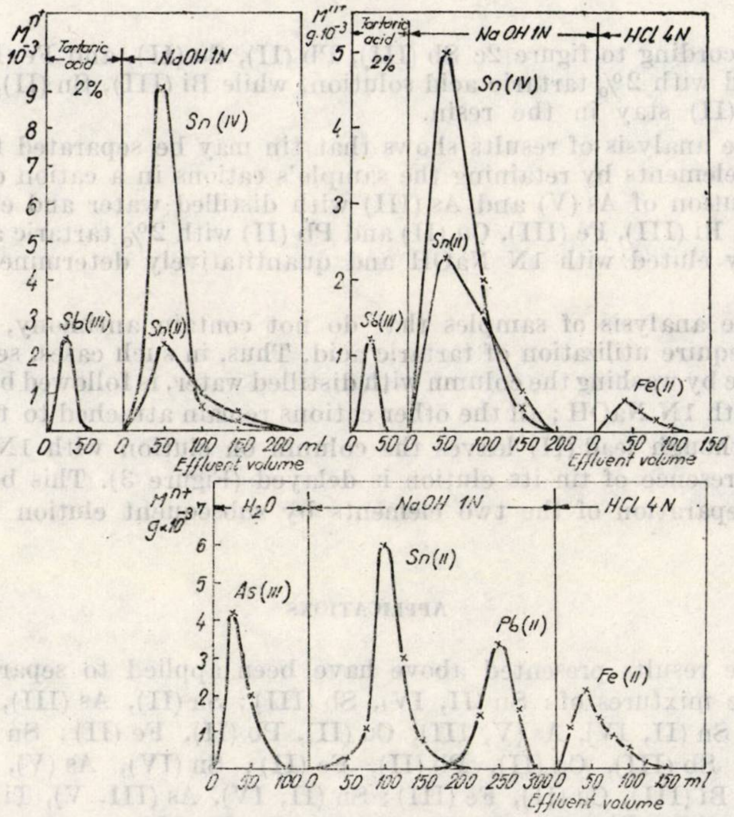

Fig. 4. — Elution curves : a) Separation Sb (III) — Sn (II, IV) ; b) Separation Sb (III) — Sn (II, IV) — Fe (II) ; c) Separation As (III) — Sn (II) — Pb (II) — Fe (II).

The separation method was then applied to the analysis of some bronzes. The results in table 2 show a good agreement between the content

TABLE 3

The results of application of the method to purification and analysis of tin's compounds

Sample		Determined after separation												Content according to analysis bulletin (%)				
Subst.	g	Sn		$SnCl_2 \cdot 2H_2O$		Pb		Fe		As		Sb			Pb	Fe	As	Sb
		g	%	g	%	g	%	g	%	g	%	g	%					
$SnCl_2 \cdot 2H_2O$	0.50015	0.2514		0.4780	95.57	0.0020	0.40							min. 95 % $SnCl_2 \cdot 2H_2O$	0.04	0.1	0.0004	
	1.5217	0.7987		1.5183	99.77	0.0063	0.35	0.00017	0.01									
Sn metallic	0.5935	0.5923	99,8			0.00030	0.05	0.00021	0.036	0.00018	0.02	0.0006	0.1	99.75 %Sn	0.06	0.04	0.015	0.1
	0.5970	0.5820	97,5			0.0119	2	0.00107	0.18	0.0015	0.25	0.0041	0.7	98 % sn.	1.7	0.15	0.2	0.6

determined by application of the method discussed here and that indicated in the analysis bulletin of the bronzes in question.

TABLE 2

The results of application of the method to tin determination in bronzes

Type of bronze		Bz 6	Bz × Pb 15	Bz 14T
Content Sn %	Determined	5.35	9.43	9.55
	According to Romanian Standard	6±1	10	10

The separation procedure advanced here was also applied to purification and analysis of some tin salts, which were either "Reactivul" reagents, or were obtained in the laboratory, starting up with metallic tin of various purities. The percent contents of tin and impurities determined after separation, were within the limits specified in the analysis bulletins of products under study (Table 3).

CONCLUSIONS

Tin may be separated from elements that accompany it in metallic tin and natural and synthetic compounds, by utilization of cation exchange resins and sodium hydroxide, as elution agent; when antimony is present, 2% tartaric acid has to be employed.

The method allows :

a. separation of tin from As (V, III), Ti (IV), Zr (IV), Sb (III), Bi (III), Fe (III, II), Pb (II), Cu (II);

b. quantitative determination of tin (II) by titration with potassium bromate (the most widely employed method recommended by Romanian Standard Association, applies only in the absence of As (III) and Sb (III));

c. quantitative determination of tin (IV) with Xylenol Orange (the most confortable and sensitive spectrophotometric method, which requires alkali stante solutions and the absence of Sb, Cu, Zr, Bi, Fe);

d. purification of tin (II, IV) salts.

The separation method advanced here, requires only simple equipment and cheap reagents, it is rapid and quantitative.

REFERENCES

[1] L. Vlădescu and D. Voicu, *Rev. Roumaine Chim.*, **25,** 267 (1980).

[2] C. Liteanu, "Chimie analitică cantitativă — Volumetria", Editura didactică şi pedagogică, Bucureşti, 1969.

[3] N. V. Danilova, *Zavodskaya Lab.*, **29,** 407 (1963).

[4] M. Zimmermann, "Photometric Metal and Water Analysis", W.V.C., M.B.H., Stuttgart, 1962, section B—b 6/1 (61).

[5] G. T. Woods and M. G. Mellon, *Ind. Eng. Chem., Analyt. Ed.*, **13,** 551 (1941).

[6] J. Korkisch, *Z. Analyt. Chem.*, **178,** 39 (1960).

[7] J. P. Young, J. R. French and J. C. White, *Analyt. Chem.*, **30,** 422 (1958).

Revue Roumaine de Chimie **25**, *8*, 1275–1284 (1980)

COMPTES RENDUS

ELENA CEAUŞESCU, "Polimerizarea stereospecifică a izoprenului" (Stereospecific polymerization of isoprene), Editura Academiei, Bucureşti, 1979, 306 p.

Publication of the work of Dr. eng. Elena Ceauşescu, member of the Academy of the Socialist Republic of Romania : *Stereospecific polymerization of isoprene* by Editura Academiei S. R. Romania represents an outstanding editorial event. It is an exceptional achievement by the importance of its theme – beloging to a forefront area in the chemistry of macromolecular compounds – by the original way in which the subject is broached and by the results presented, to the benefit of science and technology. As known, the sources of the chemistry of synthetic polymers are to be found in the attempts made to understand the role and structure of the giant molecules generated by nature and which govern the essential processes of life. During the last three decades, penetration with skill and courage into these secrets, unravelling with the mind's eyes and the tools of research of the order within matter, offered unforeseen possibilities for synthetic chemistry, for theoretical investigations, and for progress in the practical applications of industry. The architecture of most macromolecular compounds of natural origin is complicated and its re-edification by catalytic processes raises deep-rooted problems that involve all the basic domains of chemistry. This is the framework of Acad. Dr. Elena Ceauşescu's book, the fruit of almost two decades of persevering scientific activity, conveying to the field the virtues of novelty, of fine discrimination in the experimental approach, of consistent progress from theoretical bases to practical finalization, with sobriety and rigorous accuracy. The beginnings of the chemistry and technology of synthetic macromolecular compounds with elastomer properties in our country are linked with the name of Acad. Dr. Elena Ceauşescu. She chose as subject for her doctoral thesis the synthesis of *cis*-1,4-polyisoprenic rubber with a structure and properties very close to those of natural rubber, used for the manufacture of tyres and other technical articles. The first part of the present work dwells on the stereospecific polymerization of isoprene and represents in essence her doctoral dissertation (sustained in 1967). It is difficult in a presentation of Acad. Dr. eng. Elena Ceauşescu's work addressed to a more general public, to penetrate into the core of the subject and at the same time to avoid as much as possible the special chemical vocabulary. This is the reason for which we have tried to emphasize the author's original contribution, the scientific and engineering progress marked by the publication of this work, avoiding a rigid scientific approach and all-inclusive analysis.

Polyisoprene rubber is synthesized by a chemical process that results in a regular spatial structure. This process, called *stereospecific polymerization* was first carried out as the result of the discovery of a catalytic process (trialkylaluminium and titanium tetrachloride) by K. Ziegler, promoted by G. Natta for obtaining polypropylene and other polyolefins ; these organometallic complexes have opened new vistas in modern macromolecular chemistry. Stereoselective catalysis, applied to the synthesis of polymers, offers wide possibilities for the synthesis of macromolecular edifices with a high crystalline content and a structure close to that of natural compounds. It stands to reason that by their properties these new polymers compete with nature.

In an ample, systematical and critical analysis – in the first four theoretical chapters (of part I) – of the dimensions of stereospecific catalysis, of the mechanisms of synthesis and kinetics of polymerization, Acad. Elena Ceauşescu *discusses her own selective and original experimental approach* for obtaining a new rubber with attributes nearer to those of natural rubber, starting from isoprene.

The experimental technique is impressive by the exceptional accuracy applied in the purification of the reactants (monomer, solvents, catalytic systems, inert gas).

This part of the book has a substantial analytical content, dealing with the chemical treatment, distillation and percolation through molecular sieves, procedures that result in marked purification and optimal conditions of the synthetic process. The study of stereospecific polymerization of isoprene with heterogenous catalytic systems, promoted by the wish to set to value a petroleum fraction with a low isoprene content (up to 25%) and to investigate the optimum Al/Ti ratio — have necessitated an important quota of inventiveness. Chapter II in the experimental part of the doctoral thesis concentrates the essence of the strategy chosen by the author for polymerization of a low concentration isoprene, with a view to synthesizing a qualitatively superior elastomer. This elastomer is further studied by up-to-date methods, determining its microstructure, crystallinity pshysico-chemical and mechanical characteristics.

This procedure for the polymerization of isoprene at a concentration of approximately 25% with heterogeneous catalytic systems — dealt with in the first part of the book — has resisted owing to its originality to the impact of time, maintaining both its theoretical and applicative validity.

The second part of Acad. Elena Ceaușescu's work systematizes the theoretical and practical data obtained following the optimization of the basic parameters and detection of the finer processes upon which the kinetics and mechanism of the system depend. These results refer to the performed Ziegler-Natta catalytical systems, to stereospecific polymerization with these compounds, to deactivation of the catalyst and stabilization of the polymer, to removal of the solvent from the polyisoprene solution and characterization of the rubber by nuclear magnetic resonance and electronic microscopy. This part of the book — the result of a series of investigations after completion of the doctoral thesis — likewise displays dialectic unity between method and scope, internal logic, the ability to select the best approach in highly complex chemical processes and the firmness of the final arguments.

Although Acad. Elena Ceaușescu's work comprises two distinct parts, subordinated to the evolution in time of the problem studied, they are unified and form a single body, fed by the sap of the same thought and sustained by the vigour of the same aim : *to produce on industrial scale a polyisoprenic rubber, by a Romanian procedure* under advantageous economic conditions, from an indigenous source (C_5 fraction of gasoline obtained by pyrolysis).

The bibliography, which anchors the book in the soil of universal knowledge in this domain, is particularly vast, summing up 635 references to the original literature.

As already mentioned, the publication — in a clear condensed form, at a high theoretical and applicative level, of Acad. Dr. eng. Elena Ceaușescu's book *Stereospecific polymerization of isoprene* is not only an editorial event but also an incentive for further original, scientific and technical research work in Romania. It has the significance of a stirring appeal — enhanced by the personal example of the author — and is addressed to all scientists, encouraging them to serve by their tenacious, fruitful work the progress of Romanian economy, to tackle themes courageously, from the most advanced positions of contemporary thought, consequently subordinated to the fundamental aim of the party policy : the genera welfare of the people.

Highly commended as a reference book in the chemistry of synthetic polymers by al group of well known Romanian chemists, among whom the late member of the Romanian Academy C. D. Nenițescu — a scientific referee of the author's doctoral thesis — and praised by numerous international scientists, some of whom Nobel Prize winners, Acad. Dr. eng. Elena Ceaușescu's work — also including her doctoral thesis — is recommended as model for scientific research. It leads the reader from the original idea to the producing plant with skill and deep interest proving the author's receptivity to new ideas, capacity of analysis and synthesis, creative spirit and a deep engagement in long-term achievements.

The Publishing House of Academy of the Socialist Republic of Romania, consistent with its tradition of promoting the values of national science and culture, presents in excellent graphical conditions the work whose author — a member of the Romanian Academy — has endeavoured and has fully succeeded in enriching the inheritance of Romanian and world chemistry with contributions that do credit to Romanian scientific and engineering achievements and mobilize all available forces and means for the progress of society.

Acad. Cristofor Simionescu

R. A. Y. JONES, "Physical and Mechanistic Organic Chemistry", Cambridge University Press, Cambridge, 1979, 357 pp, 8.50 pounds (paperback) or 25.00 pounds (hard-cover edition).

In the series "Cambridge Texts in Chemistry and Biochemistry" addressed to advanced undergraduate or graduate students, the book of Dr. Richard A. Y. Jones is a welcome addition. Its contents place it in the class of monographs on physical organic chemistry, yet the spirit is rather different — as mentioned in the introduction and the first chapter, nowadays organic chemistry can no longer be learned by rote, and the understanding of reaction mechanisms not only helps the didactic process and satisfies the natural curiosity, but it also enables the chemist to predict new reactions and to improve the yield of known reactions. The odissey of the von Richter reaction serves for illustrating how difficult it is sometimes to obtain a correct representation of a reaction mechanism.

The book consists of two parts and is divided into fifteen chapters. The first part describes the theories and techniques of physical organic chemistry. It has the following chapters :

1. Structure and mechanism ;
2. Kinetic studies ;
3. Linear free energy relationships ;
4. Acids and bases ;
5. The reaction medium ;
6. Molecular orbital methods.

The second part presents the mechanisms of some of the most important reaction types, indicating both the methods used for establishing these mechanisms, and the factors influencing the mechanisms. The chapters in this part are :

7. Aliphatic nucleophilic substitution ;
8. Elimination reactions ;
9. Addition to carbon-carbon double bonds ;
10. Aromatic electrophilic substitution ;
11. Addition to the carbonyl group and related reactions ;
12. The hydrolysis of carboxylic esters ;
13. Aromatic nucleophilic substitution ;
14. Molecular rearrangements ;
15. Pericyclic reactions.

The book is an outstanding modern treatment of theoretical and mechanistic organic chemistry. It presupposes familiarity with elementary organic chemistry and is accessible to advanced undergraduates. It is highly readable, abundantly illustrated with clearly-drawn formulas, figures, tables and diagrams. All data are in SI units.

Each chapter is concluded with recommended books and reviews for further reading, and a general list of references (indexed using A. R. Katritzky's system) is appended at the end of the book. A subject index concludes the book.

As mentioned in the author's preface, a book of this length cannot be comprehensive so that many important areas of chemistry have to be omitted ; the heterolytic and homogeneous reactions have been emphasized at the expense of the homolytic and heterogeneous reactions. Yet it is remarkable how the books succeeds in reviewing almost the whole of present-day mechanistic organic chemistry. Both libraries and individuals will profit from this highly recommendable book.

A. T. Balaban

"THE PERMUTATION GROUP IN PHYSICS AND CHEMISTRY" (ed. J. Hinze), *Lecture Notes in Chemistry*, vol. 12, Springer Verlag, Berlin, 1979, 230 pp.

The proceedings of a symposium held in July 1978 at the Centre of Interdisciplinary Studies of the University of Bielefeld, Federal Republic of Germany, have been gathered in one volume.

The first lectures by A. Kerber, entitled "Counting Isomers and Such" treats in a generalized approach the isomer counting problem. The lemmas of Burnside and de Bruijn yield the tools for calculations. The famous Pólya theorem is shown to be one particular case ($i = 1$) of equivalence relations "$\sim_i$", where $i=1, 2, 3$. The lecture is concluded by a unified treatment of the Redfield and Pólya theories, making use of matrices and wreath products, so that Redfield's "cap-operation" is explained as a corollary of Kerber's unified treatment.

The next two lectures are by J. G. Nourse : "Application of the Permutation Group to Stereoisomer Generation for Computer Assisted Structure Elucidation" and "Applications of the Permutation Group in Dynamic Stereochemistry". The first lecture discusses stereoisomer counting by using the Configuration Symmetry Group which is a subgroup of the wreath product group $S_n[S_2]$; the second one discusses homomorphisms of groups referring to reaction graphs such as the R.S. Berry pseudorotation of five-coordinate phosphorus compounds. It has an annex giving correspondences between chemical concepts and permutation group structures such as cosets (corresponding to maximally substituted isomers), double cosets (corresponding to isomers with some identical substituents), unions of double cosets (corresponding to isomerization modes), etc.

Some of the papers deal with purely physical applications of permutation groups : boson polynomials in U (n), Racah algebra, etc. Some other papers treat molecular symmetry groups for rigid and non-rigid molecules. R. S. Berry's paper is entitled "Symmetry and Thermodynamics from Structured Molecules to Liquid Drops".

We shall conclude this review by highlighting the last three of the 13 papers contained in the book : T. H. Seligman (Double Cosets and the Evaluation of Matrix Elements), J. S. Frame (Properties of Double Cosets with Applications to Theoretical Chemistry) and A. Dress (The Chirality Algebra ; some comments concerning mathematical aspects of the Roch/ Schönhofer chirality theory). In these papers the double cosets and the chirality functions introduced by Ernst Ruch and his coworkers are discussed and presented in a slightly different manner from that originally introduced by Ruch and his school, in order to make these concepts more familiar to chemists and mathematicians.

The collection of papers is of primary interest to chemists, physicists and mathematicians interested in modern interdisciplinary approaches involving permutation groups.

A. T. Balaban

E. G. ROZANTSEV and V. D. SHOLLE, "Organic Chemistry of Free Radicals" (in Russian), Khimiya Publ. House, Moscow, 1979, 343 pp.

As the authors state in their preface, more than ten years have elapsed since the most successful book in this field has appeared : A. R. Forrester, J. M. Hay and R. H. Thomson's "Organic Chemistry of Stable Free Radicals", Academic Press, London, 1968. Many new methods have appeared in the meantime, such as the two remarkable techniques which have many biochemical applications : spin labelling and spin trapping. The authors have contributed themselves appreciably to the enrichment of the field. It is well known that the chemistry of aminyloxides (nitroxides, nitroxyls, aminoxyls) which lie at the basis of the two above-mentioned techniques, has received the present upstart owing mainly to the Soviet school led by Prof. E. G. Rozantsev and to the French school led by Prof. A. Rassat. Also, Prof. Rozantsev's earlier book "Free Nitroxyl Radicals", Plenum Press, New York, London, 1970 is well-known. Together with his junior collaborator, Dr. V. D. Sholle, Professor Rozantsev has written a comprehensive review on synthetical aspects of aminyloxides *(Synthesis*, **1971**, 190, 404).

The seven chapters of the present book and the corresponding numbers of pages (in brackets) are : 1. Free Radicals ; general character (91) ; 2. Carbon radicals (30) ; 3. Aroxyl radicals (42) ; 4. Nitroxyl and alkylideneiminoxyl radicals (76) ; 5. Aminyl radicals (26) ; 6. Hydrazyl and hydrazidyl radicals (42) ; 7. Other classes of organic radicals (28). Each chapter is accompanied by 100–200 literature references (excepting chapter 5 which has 464 references) totalling more than one thousand quotations, which aim (as the authors state in their preface) to cover mainly the last two decades, without repeating references previously quoted in other books or of historical interest only.

As seen from the above table of contents, by its coverage the present book is closer to Forrester-Hay-Thomson's book than to any other monograph in this field, with the difference (purposely stressed by the authors in selecting their title) that the present book covers all free radicals, not only the stable ones, as Forrester- Hay-Thomson's book. Indeed the titles of the two books differ only by the absence of the word "stable" from the title of the book analyzed here. It should be mentioned in passing that the Russian text makes no distinction between "stable" and "persistent" as was advocated by K.U. Ingold and his school in recent years.

The main theme of the book is indeed the organic chemistry of free radicals, manifested in methods for obtaining free radicals, and in their reactions. These reactions may involve the unpaired electron (recombination, disproportionation, oxidation, reduction, addition) or may not (as exemplified for nitroxyl radicals, including many data from the laboratory of the authors of this book). Frequently throughout the book, brief preparative indications are inserted with pertinent literature data.

The first chapter discusses in general methods for producing free radicals, their properties, and methods for identifying and detecting both stable and reactive free radicals. The last chapter includes phosphorus, sulphur and selenium radicals, as well as radicals of elements from the third and fourth group of the periodic system which were not included in previous chapters.

By the author's own statement, it was impossible to unify all the existing nomenclature for free radicals (an example is provided by the four names existing for aminyloxides ; another example is provided by the name "hydrazidyls" suggested by Neugebauer and adopted in this book, as a generic term including verdazyls, tetrazolyls and tetraaza-pentadienyls). However the authors have tried to be consistent throughout the book.

The authors have included useful information for the numerous applications of free radicals in chemistry (chain reactions, photochemical initiation, polymerization, analytical chemistry, inhibitors and stabilizers), biology, physics (quantum generators, magnetometers radiation dosimeters).

The book is necessary to all those interested in the field and is useful to students and research workers in related areas such as biochemistry and biophysics.

Alexandru T. Balaban

GABOR A. SOMORJAI and MICHAEL A. VAN HOVE, "Adsorbed monolayers on solid surfaces", Springer-Verlag, Berlin, Heidelberg, New York, 1979, 146 pp.

"Structure and Bonding" is issued at irregular intervals according to the material received. In the 38th volume, titled "Adsorbed Monolayers on Solid Surfaces", there are reviewed the various experimental parameters that can be used to characterize the adsorbate layer in the sub-monolayer to few-monolayer range. The authors discuss the principles of ordering the adsorbate layer, since one of the most exciting observations of low energy electron diffraction studies is the predominance of ordering within these layers. They list the ordered adsorbate layer structures and summarize what can be learned about the nature of their bonding from the available structural data. Separately, this will be done for the many (~ 1000) surfaces whose two-dimensional unit cells are known in terms of shape, size and orientation, and for the fewer (~ 100) surfaces for which additionally the contents of the unit cell are known (adsorption site, bond lengths, etc.). Many types of adsorption will be covered, including atomic and molecular adsorption, co-adsorption, metallic adsorbates, nonmetallic adsorbates and organic adsorbates.

The present volume is remarkably valuable, because under the usual environmental conditions (about one atmosphere and 300 K and in the presence of oxygen, nitrogen, water vapor and assorted hydrocarbons) all solid surfaces are covered with a monolayer of adsorbate and the build-up of multiple adsorbate layers is often detectable. The constant presence of the adsorbate layer influences all the chemical, mechanical and electronic surface properties. Adhesion, lubrication, the onset of chemical corrosion or photoconductivity are just a few of the many macroscopic surface processes that are controlled by the various properties of a monolayer of adsorbates.

The volume is organised in seven chapters.

After the first chapter, the introduction, the second chapter presents principles of monolayer adsorption. In the authors' opinion, two macroscopic, experimentally measurable parameters, θ (the coverage) and ΔH_{ads} (the heat of adsorption), usually well characterize the adsorbed monolayer and the form of their interdependence often reveals the nature of bonding in the adsorbed layer. The third chapter deals with the principles of ordering of adsorbed monolayers. Problems like causes of ordering, the degree of ordering, the effect of different parameters (temperature, surface, irregularities, etc.) on the ordering of adsorbed monolayers, unit cell notations, unit cell, etc. are well illustrated.

The fourth chapter presents methods of structure analysis. In this chapter are reviewed the various experimental techniques used to study the arrangement of atoms and molecules at surfaces. First there are discussed the basic aspects of the sample preparation, since this is a particularly critical step in surface studies. Then there are discussed the principles involved in the measurements of surface specific physical quantities. Since each of the many techniques of surface analysis is sensitive to a few particular aspects of the surface (such as relative atomic position, electronic levels, chemical composition, binding energies and vibration frequencies) these techniques are classified according to the surface characteristic that they are most sensitive to.

The fifth chapter is concerned with the ordering of adsorbates. In this section is presented a comprehensive tabulation of the observed ordered structures for any adsorbate on any substrate. For most of these cases the surface structure has not been analyzed beyond the implications of the unit cell shape, size and orientation. Many of these structures are good candidates for a structural analysis of the binding sites, bond lengths and bond angles. It is hoped that the list of geometrically analyzed structures (discussed in detail in Sects. VI and VII) will grow rapidly so as to present an expanding base for the extraction of fundamental laws governing the adsorption phenomenon.

Chapter 6 is devoted to the surface crystallography of ordered monolayers of atoms. Since the substrate on which adsorbates are deposited greatly influences the behaviour of those adsorbates it is important to first examine the substrates themselves. We must distinguish between the clean surface and the same when covered with adsorbates, because adsorbantes are capable of modifying the geometric (and electronic) structure of the substrate. To enable a convenient comparison, Table 6.1 combines the structures known to us for both clean and adsorbate covered surface, as far as they have been determined with a reasonable degree of precision and reliability by the various surface crystallographic techniques mentioned in chapter IV.

The seventh chapter presents surface crystallography of ordered multi-atomic and molecular monolayers.

The study of the structure of multi-atomic and molecular adsorbates is in its very early stages, but more and more efforts are devoted to it because of its obvious importance in catalysis and other fields. The techniques of investigation used are primarily LEED, photoemission and high resolution electron energy loss spectroscopy. The detailed adsorption geometry has been analyzed so far for a few cases of co-adsorption of atoms and a few adsorbed molecules. The ordering characteristics of molecular monolayers have been investigated for a number of small molecules and a sizable family of larger organic molecules. Remarkable is the arrangement of the tables (chapters V and VI) which facilitates the easy finding of the data needed and up to date references in that field.

Both the qualities of contents and the graphic presentation make the 38th volume of ,'Structure and Bonding'' titled : ''Adsorbed Monolayers on Solid Surfaces'', by Gabor A. Somorjai and Michael A. Van Hove, a very valuable reference source for researchers who are working in fields where adsorption and catalysis are involved.

Iuliana Vartires

T. KREMMER and L. BOROSS, ''Gel Chromatography. Theory, Methodology, Applications'', Akadémiai Kiadó, Budapest, 1979, 300 pp.

This volume is a revised English version of the original hungarian ''Gélkromatográfia'', Müszaki Könyvkiadó, Budapest. The book offers a full review of a rapidly progressing new area of liquid chromatography which spread about in many branches of chemistry such as organic chemistry, polymers and especially biochemistry. The book gives information concerning the theoretical development of the method, presents the main practical techniques used in gel chromatography and illustrates the vast possibilities of application for the separation of natural and synthetic compounds.

In the first part Kremmer treats the basic limits of the theory of gel chromatography. Herein, the author discusses several aspects concerning the fundamentals of gel chromatography including gel formation, the structure of gels, gel-forming substances and their production. A special emphasis is laid on the volumetric and kinetic theories of gel chromatography based on the analogy with the non-miscible polymer solutions and the osmotic properties of the gels. Some essential problems as the volumetric distribution of the gel bed, steric-volumetric theory of gel chromatography, volumetric equations of gel chromatography, geometric model of molecular exclusion are further touched on. After a detailed consideration of the kinetic theories of gel chromatography some thermodynamic aspects are finally pointed out.

The second part, also by Kremmer, is devoted to the practical techniques of gel chromatography. The author describes the preparation and treatment of gels, equipment, the common and special devices used in the column and thin-layer gel chromatography. The preparative (batch) procedures of gel chromatography are also dealt with.

In the third part Boross gives typical examples for the practical use of gel chromatography. The author illustrates the application of gel chromatography for the separation of proteins, peptides and amino acids, purification and characterization of nucleic acids, fractionation and separation of oligosaccharides and polysaccharides as well as separation and characterization of synthetic polymers. The extension of gel chromatography to the separation and purification of small-molecule organic compounds are exemplified for aliphatic and aromatic hydrocarbons, organic acids, alcohols and ethers, phenols and organic bases. In addition, the application of gel chromatography for analysis of inorganic ions is illustrated.

A bibliographic section and subject index end the book.

In summary, the volume is logically written and assembled containing a vast amount of material well structured and presented. The book may serve as an introductory text as well as a comprehensive monograph on the subject. The reader will find in it many theoretical incursions along with practical information. The material will be useful for researchers working in synthetic and analytical areas of organic chemistry, macromolecular chemistry and biochemistry and for all those interested in methods of separation of natural or synthetic compounds.

V. Drăguţan

"APPLICATION OF ZEOLITES IN CATALYSIS", G. K. Boreskov and Kh. M. Minachev (editors), Akadémiai Kiadó, Budapest, 1979, 180 pp.

Zeolites are synthetic aluminosilicates with a three-dimensional structure which gained a major importance in the last decades as industrial catalysts. The book "Application of Zeolites in Catalysis", edited by Boreskov and Minachev, presents several original contributions of the well-known soviet scientists reported at the 1st All-Union Conference on Zeolite Catalysis held in March 1976 in Novosibirsk, USSR. The most important topics refer to organic synthesis with zeolites, catalytic and acid-base properties of zeolite systems, factors determining the activity and selectivity of zeolites in cracking processes, the role of transition metals on zeolite catalysis, structure investigation of zeolites by spectroscopic methods and diffusion processes in zeolite catalysts.

In the first paper Minachev presents some relevant applications of zeolites for organic reactions among which hydrocarbon conversion and monomer synthesis became widespread processes of great utility. The second paper of Mirsky and coworkers deals with the properties and characteristics of soviet zeolite-containing catalysts used for the cracking of petroleum fractions. In the third paper Topchieva discusses the catalytic and acid-base properties of zeolite systems.

A subsequent report by Dorogochinski and coworkers is devoted to factors determinig the activity and selectivity of zeolite-containing cracking catalysts. In this report the reader will find a significant amount of original data published by the authors concerning the activity and selectivity of various faujasites and catalysts prepared on their base. Another review of Ione, Kuznetsov and Romannikov deals with the effect the state of transition elements in the zeolite framework exerts on the catalytic properties of Y-zeolites. Herein, results available in the literature and data obtained at the Institute of the Siberian Branch of the USSR Academy of Sciences are surveyed. A large space is further devoted to the investigation of the state of cations in zeolites by spectroscopic techniques in the work of Anufrienko et al. These authors have studied the electronic state of the Cu^{2+} and Ni^{2+} ions in Y-zeolites as well as the relationship between the distribution of these ions and the ion-exchange conditions.

The investigation of the nature of the bond between Ni, Co, Cr and the zeolite framework by X-ray photoelectron spectroscopy (XPS) is the subject of the next paper by Minachev. The author evidences the influence of pretreatments of zeolite catalysts on the valence and physical state of the above mentioned elements.

The last report by Dubinin and coworkers focuses on diffusion processes in biporous adsorbents and catalysts. In this interesting paper the authors provide theoretical considerations exemplified on practical models. The knowledge of the diffusion mechanism of the reactant molecules in the intracrystalline zeolite channels constitutes a subject that remains to be studied in details in the near future. The elucidation of this mechanism is important for the correct interpretation of the catalytic data and for further improvement of zeolite catalysts.

As a welcome addition to the rich literature on zeolite catalysis the volume provides a significant amount of original data published by the soviet scientists working in the area. The edition of the volume is somewhat delayed though its content is still of interest. The material compiled in the book will be useful for scientists and technical staff working in heterogenous catalytic processes, in organic chemistry and petrochemistry. The volume will also be a good reference source for students and researchers interested in catalysis over zeolites.

V. Drăguţan

"LIGHT TRANSDUCING MEMBRANES – STRUCTURE, FUNCTION AND EVOLUTION", Edited by David W. Deamer, Academic Press, New York, San Francisco, London, 1978, xiv + 358 p.

The book under review contains 19 papers presented at the joint Australian – American Seminar on the Evolution of Light-Trapping Biological Systems held in Honolulu, Hawaii, during December 1977. It was designed to focus on structural, functional and evolutionary aspects of light energy transduction by membranes, including also an evolutionary perspective.

It has to be mentioned that research in the field (or in neighbouring domains) was growing these last years, a great number of books being published since 1970 (see, for instance, *Perspectives in Membrane Biology*, edited by Sergio Estrada – O. and Carlos Gitler, Academic Press, New York, San Francisco, London, 1974, xvi + 659 p., or *Molecular Dynamics in Biological Membranes*, by Milton H. Saier, Jr. and Charles D. Stiles, Springer-Verlag, New York, Heidelberg, Berlin, 1975, 129 p., etc.).

The volume edited by David W. Deamer includes four subtopical areas, as follows :

— The chemical evolution of biomolecules on the primitive earth (3 papers), of special interest for those working in primordial biogenesis, exploring the problems concerning the evolution of membrane-related biomolecules, the formation of lipid bilayer structures and the mechanisms available for light energy transduction in early stages of chemical evolution ;

— Self-assembling membrane systems (3 papers), investigating the mechanisms by which ions, lipids and proteins interact in membraneous systems, also bearing on chemical evolution ;

— Bacterial light transducing systems (6 papers), considering the importance of some bacterial membranes as reconstituted light transducing systems, of interest for those involved in current bioenergetic research, and presenting (in two papers) relevant aspects of mitochondrial energy transduction ;

— Analysis of contemporary light transducing systems (7 papers), dealing with the progress in analysing mechanisms by which intact bacteria and chloroplasts interact with light energy.

As it can be seen, the book is focused on different structural and functional aspects of membraneous evolution. One of the participants, Dr. F. A. Smith, summarized the seminar as follows :

"We wonder how cells came to be"
Said scientists at Waikiki.
"We think the solution
Was slow evolution
In hot, salty, lipid-rich sea !"

On the whole, *Light Transducing Membranes* succeeds in highlighting numerous very interesting and complex problems ; the papers are signed by outstanding specialists currently doing research on the specific topics being covered. Provided with new and interesting results, summing a large information, the book is addressed to all research chemists and biologists who wish to keep abreast of advances in the chemistry and biochemistry of membranes, in the role they played during the prebiological evolution and in the mechanisms of light energy transduction in photoactive membranes. Highly recommended.

Bogdan C. Simionescu

YOSHIHIKO SAITO, "Inorganic Molecular Dissymmetry" (Inorganic Chemistry Concepts Series, No. 4), Springer-Verlag, Berlin-Heidelberg-New York, 1979, IX + 167 pages.

Dissymmetry, though unappealing from an aesthetic point of view, is nevertheless a fact which has to be faced by those investigating molecular structure and its connection with materials' properties. Several thousand of chemical species are known today whose molecules lack an improper rotation axis, thus making the molecule unsuperposable upon its mirror image, and optically active. In fact the very existence and role of left- and right-handed molecules is still a fundamental question of life research and any new advance in the study of their appearance and behaviour would greatly contribute to clearing up some of the most basic problems of the living matter.

Handedness (or chirality) is not, however, restricted to organic substances. This is a phenomenon also met in inorganic systems, mostly in complexes and chelates. The existence of two optical isomers of the $[Co(ethylenediamine)_2NH_3Cl]Cl_2$ salt was signaled by Alfred Werner as early as 1911 and many other complexes which reveal such isomerism have since been discovered. One basic problem with such complexes has been the determination of their *absolute* conformation, i.e. of the exact three-dimensional structure of all the isomers. The book reviewed herein has as its subject matter a description of all the methods used today to this aim — anomalous X-ray scattering (that is at wavelengths near the metal's absorption edges), anomalous neutron diffraction, conformational analysis, electron density distribution measurements, and circular dichroism.

All these methods are detailed and the text can be read even by those who are not familiar with their principle or use. Professor Saito's style is very neat and the richness of examples given in each case reflects his own major original contributions to the understanding of the optically active compounds.

Rodica Grigorovici

A. J. SWALLOW, "Reactions of Free Radicals Produced from Organic Compounds in Aqueou Solution by Means of Radiation (Progress in Reaction kinetics)", editors : K. R. Jenning and R. B. Cundall, vol. 9, number 3/4), Pergamon Press, Oxford, New York, 1978, 167 p

The study of organic free radicals is of importance for a large variety of subjects ranging from management of energy resources to cancer research. Of even a greater interest is the understanding of the reactions of the radicals in aqueous environments, not matter they are produced by photolysis, the use of transition metal ions and hydrogen peroxide or irradiation with fast electrons or X- or γ-rays. Research using the radiation method is in full flood and the growing interest in reaction kinetics is documented by the continually increasing volume of publications on the subject.

The aim of *Progress in Reaction Kinetics*, appearing in Pergamon Press, is to provide articles of lasting value that will become established as reference articles in a particular field.

Reaction of Free Radicals Produced from Organic Compounds in Aqueous Solution by Means of Radiation follows an earlier paper published by the same author, which had dealt with work published during the period October 1969 to September 1971 (A. J. SWALLOW, *MPT International Review of Science, Organic Chemistry*, Series One, 10, 263, 1973) and covers original work published during the period October 1971 to December 1976. The paper under review excludes data concerning work on macromolecular free radicals and radicals in the frozen state.

The material is divided into twenty-two main parts, namely *Introduction, Hydrocarbons, Halides, Alcohols, Ethers, Carbonyl Compounds, Phosphate Esters, Carbohydrates, Carboxylic Acids and Esters, Amines, Pyrrole and Derivatives, Amides, Nitriles, Phenol and Derivatives, Sulphur Compounds, Pyrimidines, Imidazoles, Purines, Pyridine and Derivatives, Compounds Containing the Pyrazine Ring, Nitro Compounds and Other Nitrogen-Containing Compounds* and is based on 372 references. As it can be seen, each section contains results concerning a particular class of chemicals, results generally summarized in tables.

All the material is provided in as condensed and rapidly reviewable form as possible. It reflects modern significant research accomplishments in the field and is a valuable information source both for those working in the domain and for those which have not expert knowledge.

The quality of the paper and illustrations, the clear printing, increase the value of the book.

Bogdan C. Simionescu

NOTE POUR LES AUTEURS

La Revue Roumaine de Chimie publie des articles en anglais, français, russe, allemand ou espagnol. Les auteurs sont priés d'envoyer des articles et des comptes rendus inédits.

Les manuscrits seront dactylographiés à deux intervalles. La bibliographie, les tableaux et la légende des figures seront placés après le texte.

Si l'article fait partie d'une série numérotée, le titre de la partie précédente sera indiqué dans une note au bas de la première page.

Chaque article sera précédé d'un résumé comprenant quinze lignes au maximum.

Les références bibliographiques dans le texte seront faites par des exposants sans parenthèses et paraîtront à la fin de l'ouvrage.

Les publications périodiques mentionnées dans la bibliographie seront présentées suivant les prescriptions internationales : le nom de l'auteur précédé de l'initiale du prénom, le titre du périodique abrégé conformément à «Chemical Abstracts» et souligné par une ligne, le numéro du tome, indiqué par des chiffres arabes et souligné par deux lignes, suivi de la première page de l'article ; à la fin, l'année de la parution sera placée entre parenthèses. Le numéro de la revue ne sera pas indiqué si les pages du volume sont numérotées consécutivement. Pour les revues dont les tomes ne sont pas numérotés (par ex. Bull. Soc. Chim. France, etc), l'année de la parution soulignée par deux lignes précèdera l'indication de la page.

Les textes des livres incluеront : les noms des auteurs, les initiales du prénom, le titre du livre entre guillements et sans être souligné, le numéro du tome précédé par l'abréviation « vol. » (ou « Bd. »), le numéro de l'édition, les éditions (the publisher), la localité de la parution et la page de la référence précédée par l'abréviation « p ». (ou « S. »).

Les brevets seront indiqués comme suit : l'auteur ou la firme, le pays et le numéro du brevet, la date et la revue (Chem. Abstr.). Par ex. M. Jones (to Union Carbide co.), Brit. Pat. 601 238, 2 sept. 1959, Chem. Abstr., 54, 12808 (1960).

Si la référence n'a pas été lue en original, on indiquera aussi la revue de références consultée.

Les diagrammes seront tracés à l'encre de Chine sur papier calque. Les tableaux et les figures (en nombre strictement nécessaire) seront numérotés par des chiffres arabes et leur explication sera donnée dans la légende des figures. Prière de ne pas inscrire les mêmes données dans les tableaux et dans les figures. Chaque tableau aura un titre. On indiquera dans le texte la place approxi- mative des tableaux et des figures. Les formules chimiques seront incluses dans le texte ; en outre, elles seront transcrites sur papier calque, à l'encre de Chine.

Les auteurs sont priés d'indiquer les caractères italiques (en soulignant les lettres au crayon), ainsi que tout autre caractère spécial ; les préfixes *ortho, meta, para, cis, trans*, etc. seront soulignés pour indiquer leurs caractères italiques et ne seront jamais écrits avec des majuscules.

Aucune correction à la main ne sera admise sur le manuscrit. Les corrections seront frappées à la machine. Les lettres grecques ou d'autres symboles spéciaux seront insérés à la main à l'encre clairement.

Le manuscrit sera signé par l'auteur.

Le colonne-titre aura 50 lettres au maximum.

L'entière responsabilité du contenu des articles appartient aux auteurs.

Pour détails voir le n° 2 (1980).

PRINTED IN ROMANIA

TRAVAUX PARUS AUX EDITIONS DE L'ACADÉMIE DE LA RÉPUBLIQUE SOCIALISTE DE ROUMANIE

ELENA CEAUŞESCU, **Polimerizarea stereospecifică a izoprenului** (La polymérisation stéréospecifique de l'isopréne), 1979, 307 p.

A. T. BALABAN, I. GĂLĂŢEANU, G. GEORGESCU, LIGIA SIMIONESCU, **Compuşi marcaţi şi radiofarmaceutici cu aplicaţii în medicina nucleară** (Composés marqués et radiopharmaceutiques à application en médecine nucléaire), 1979, 495 p.

I. G. MURGULESCU, E. SEGAL, **Introducere în chimia fizică**, vol. II. 1, **Teoria molecular cinetică a materiei** (Introduction à la chimie physique, IIe vol. 1. La théorie moléculaire-cinétique de la matière), 1979, 1003 p.

I. E. TEODORESCU, MARIA FITI, **Iradierea tehnologică** (L'Irradiation technologique), 1979, 216 p.

S. STERNBERG, FL. DANEŞ, **Termodinamica chimică aplicată** (La thermodynamique chimique appliquée), 1978, 400 p.

I. G. MURGULESCU, V. EM. SAHINI, **Introducere în chimia fizică**. Vol. 1.2. **Structura şi proprietăţile moleculelor** (Introduction à la chimie physique, Vol. I, 2. La structure et les propriétés des molécules), 1978, 604 p.

C. DRĂGULESCU, E. PETROVICI, **Chimie structurală modernă. Chimia coordinanţei** 8 (La chimie structurale moderne. La chimie de la coordinance 8). 1977, 947 p.

D. PURDELA (sous la direction de), **Nomenclatura chimiei anorganice** (La nomenclature de la chimie inorganique), 1977, 153 p.

I. ZUGRĂVESCU, MAGDA PETROVANU, **N-ylid chemistry**, 1977, 396 p.

D. NEGOIU, ANGELA KRIZA, **Poluanţi anorganici în aer** (Polluants inorganiques dans l'air), 1977, 220 p.

I. G. MURGULESCU, **Introducere în chimia fizică. Vol. I. Atomi, molecule, legătură chimică** (Introduction à la Chimie Physique, 1er vol. 1. Atomes, molécules, liaison chimique), 1976, 560 p.

E. P. BALTĂ, E. BALTĂ, **Introduction to the physical chemistry of the vitreous state**, coédition avec Abacus Press, 1976, 287 p.

H. I. GĂLĂŢEANU, **Radiochimia aplicată. Metode şi probleme** (La radiochimie appliquée. Méthodes et problèmes), 1976, 307 p.

CONST. V. UGLEA, **Cromatografia pe gel permeabil. Noi domenii de aplicare** (La chromatographie sur gel perméable. Nouveaux domaines d'application), 1978, 123 p.

CONST. GH. MACAROVICI, D. MACAROVICI, **Chimia oxizilor dubli şi utilizările lor** (La chimie des oxydes doubles et leur utilisation), 1975, 195 p.

ELENA CEAUŞESCU, **Research work on synthesis and characterization of macromolecular compounds. Contributions**, 1974, 251 p.

CR. SIMIONESCU, VIORICA RUSAN, V. POPA, **Chimia algelor marine** (La chimie des algues marines), 1974, 212 p., 1 pl.

1980 NOV 15

I. P. INFORMAŢIA c. 2302

43 426

Lei 25

55 $ (pour un abonnement annuel)

F1103

REFERÁLVA

R

ACADÉMIE DE LA RÉPUBLIQUE SOCIALISTE DE ROUMANIE

REVUE ROUMAINE DE CHIMIE

TOME 25

N°s 11–12

Novembre—Décembre 1980

EDITURA ACADEMIEI REPUBLICII SOCIALISTE ROMÂNIA

| Rev. Roumaine Chim. | RRCPAX, 25, *11–12*, p. 1447–1614(1980), Bucarest

ACADÉMIE DE LA RÉPUBLIQUE SOCIALISTE DE ROUMANIE

COMITÉ DE RÉDACTION

Rédacteur en chef :

I. G. MURGULESCU, membre de l'Académie de la République Socialiste de Roumanie.

Rédacteurs en chef adjoints :

A. T. BALABAN et V. EM. SAHINI, membres correspondants de l'Académie de la République Socialiste de Roumanie

Collège de rédaction :

EM. BRATU, ELENA CEAUŞESCU, ECATERINA CIORĂNESCU-NENITZESCU, CR. SIMIONESCU, membres de l'Académie de la République Socialiste de Roumanie ; P. SPACU, membre correspondant de l'Académie de la République Socialiste de Roumanie ; MARGARETA AVRAM M. BANCIU, I. HAIDUC, D. I. MARCHIDAN, I. MOLDOVAN, G. NIAC et S. SĂNDULESCU

La Revue Roumaine de Chimie paraît 10 fois par an. Toute commande de l'étranger (fascicules ou abonnements) sera adressée à ILEXIM Departamentul Export-Import Presă (Revues), P.O.B. 136–137, télex 11226, 79517 Bucarest, 3, str. 13 Decembrie, Roumanie

Les manuscrits, les livres et les revues proposés en échange, ainsi que toute correspondance seront envoyés à la rédaction :

REVUE ROUMAINE DE CHIMIE

125, Calea Victoriei, 79717 Bucarest, Roumanie, téléphone 50 76 80

EDITURA ACADEMIEI REPUBLICII SOCIALISTE ROMANIA

125, Calea Victoriei, 79717 Bucarest, Roumanie, téléphone 50 76 80

REVUE ROUMAINE DE CHIMIE

ORSZÁGOS MŰSZAKI KÖNYVTÁR ÉS DOKUMENTÁCIÓS KÖZPONT 1981

Tome 25, N°s 11–12 Novembre—Décembre 1980

EMIL CHIFU and IOAN STAN, Model for the undeformable free drop acted by interfacial tension gradients 1449–1459

S. NARASIMHA MURTHY, Effects of couple stresses on the dispersion of a solute with simultaneous chemical reaction 1461–1468

GH. SINGUREL, Study of the hydrogen bond in the mandelic and 4-chloromandelic acids 1469–1475

A. N. ABD EL-RAHMAN and M. H. ABDALLA, Calculations of the change in the geometrical structure of $Cl_2C=S$ during the $^1A_2 \rightarrow ^1A_1$ electronic transition 1477–1483

D. BARB, L. DIAMANDESCU, V. ZNAMIROVSCHI, D. CIURCHEA and R. SEMENIUC, Mössbauer spectroscopy investigations of iron in some pentacoordinate complexes . . . . 1485–1487 R

RODICA MICU-SEMENIUC, CRISTINA OPRIŞ and IONEL HAIDUC, Transition metal complexes of organothiophosphorus ligands. VII. Amine adducts of Di(α-and β-naphthyl) phosphorodithioato nickel (II) 1489–1498

J. ZSAKÓ, Some problems of deriving stability costants of ML_2 type complexes from spectrophotometric data 1499–1504

ANTONIE DINCULESCU and ALEXANDRU T. BALABAN, Reactions of pyrylium salts with nucleophiles. XIV. New pyridinium salts with potential biological activity . . . . 1505–1528 C

L. ALBERT, B. TÖKÉS and F. HODOŞAN, Mechanism and kinetics of the electroreduction of sterol nitrates 1529–1534

Y. M. ISSA, A. M. HINDAWEY, R. M. ISSA and A.M.G. NASSAR, A comparative study of the infrared spectra of charge transfer compounds of aniline derivatives with 3,5-dinitrosalicylic acid 1535–1541

F. M. ALBERT, MARIA GIURGINCA, AURELIA MEGHEA and G. IVAN, Basicity constants of some N,N'-disubstituted *p*-phenylenediamines . . . 1543–1548

M. M. ABD ALLA, E. A. SOLIMAN, A. A. HAMED and M. W. OSMAN, Some reactions of β-3,4-dichlorobenzoylpropionic acid 1549–1560

CECILIA CONSTANTINESCU and GH. C. CONSTANTINESCU, Spectrophotometric determination of thallium with Astrazone Red Violet 3R (in French) 1561–1565

Rev. Roumaine Chim. **25**, *11–12*, 1447–1614 (1980) Bucarest

R

M. S. SUBHANI and S. F. LODHI, A mechanism for the photolytic decomposition of hypobromite in aqueous solution at 365 nm, 313 nm and 253.7 nm . . 1567–1578

M. S. SUBHANI, The study of the transition state involves electrostatic contributions to the thermodynamic functions for the reaction between two IO^- ions 1579–1583

BOOK REVIEWS 1585–1587

AUTHOR INDEX 1589–1604

SUBJECT INDEX 1605–1614

Revue Roumaine de Chimie, **25**, *11–12*, 1449–1459 (1980)

MODEL FOR THE UNDEFORMABLE FREE DROP ACTED BY INTERFACIAL TENSION GRADIENTS

EMIL CHIFU* and IOAN STAN**
Departments of *Physical Chemistry and
**** Differential Equations and Mechanics, Babeş-Bolyai University, 3400 Cluj-Napoca, Romania**

Received April 14, 1980

A hydrodynamic theoretical model is proposed for an undeformable drop at neutral buoyancy or at zero gravity. If interfacial tension gradients act on its surface, the drop, initially motionless, undergoes a translational movement. This displacement represents a direct consequence of the surface flow i.e. of the Marangoni effect.

Drops submerged in an unmiscible liquid undergo complicated motions when interfacial tension gradients arise on their surface. Earlier studies referring to the pulsations of pendant drops[1–5] or to the "interfacial activity" of free drops[6–7] have mentioned this phenomenon.

Recent investigations are also concerned with the chemical and hydrodynamic instability of fluid interfaces, present in the Prigogine-Glansdorff-type "dissipative structures", where the interfacial tension is the coupling parameter between the chemical and the hydrodynamic processes.[8–20]

The phenomena generated by interfacial tension gradients have raised a special interest in problems of mass transfer through fluid interfaces [19–20] as well as in the modelling of certain deformation processes or movements at the biosurface level [8–11; 14; 21]. After all, because the surface (interfacial) tension plays an important role in the behaviour of the liquids at zero gravity, [22–28] we think that the phenomena determined by the above-mentioned gradients will be revealed in space experiments as well.

In this paper a theoretical hydrodynamic model is presented for a submerged free drop, initially motionless. Further on it is subjected to the action of interfacial tension gradients on account of which it undergoes a translational motion. This translation of the drop is thought of as a direct consequence of the surface flow (the Marangoni effect), which in turn is caused by the interfacial tension gradients.

We point out that, unlike other recent investigations, dealing with interfacial turbulence, described by perturbation equations,[8–20] our model assumes that the interfacial tension gradients give rise to a flow governed by laminar hydrodynamic equations.

Let us then consider a drop L' of the radius a submerged in an unmiscible liquid L (Fig. 1). The force $\vec{F}$ which acts on the volume unit of the drop,

$$\vec{F} = (\rho' - \rho)\vec{g}$$

will be cancelled, either when the densities of the two liquids become equal ($\rho' = \rho$), or in the absence of gravity ($\vec{g} = 0$).

We consider such a drop as a "free" one, namely having no initial motion (buoyancy).

Suppose that the initial liquid/liquid interfacial tension is σ_0. In the point P_1 (Fig. 1) on the surface of the drop the interfacial tension is lowered to σ_1 by injecting a surface-active substance, while at the opposite "pole" P_0 it remains at its initial value σ_0. An interfacial tension difference $\sigma_0 - \sigma_1$ arises along the drop meridians.

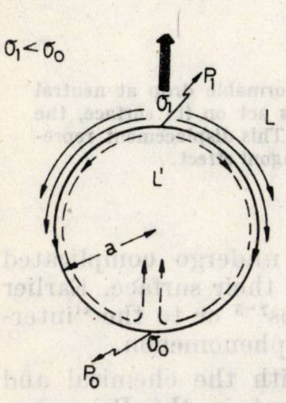

Fig. 1. — The model for the translational motion of an undeformable free drop under the action of the surface flow.

From the complex processes appearing as a consequence of this difference, the following are the most likely to be considered :

— the translational displacement of the drop and its possible rotation ;

— the deformation and the oscillation of the drop, the occurrence of waves on its surface ;

— circulatory streams of liquid.

By observing such processes, Valentine and co-workers[6-7] have estimated the order of magnitude of the dissipated energy corresponding to the different forms of "movement" of the drop. Still they consider that the solving of the equations of motion of the fluid is too an intricate question.

We mention that there is no rigorous and complete theory elaborated till now for the phenomena generated by the interfacial tension gradients on a free drop.

With the aim of solving this problem, we think that a quantitative treatment must take into account, above all, the Marangoni effect — respectivelly the surface flow.[29-42] It is surprising that the quoted authors[6-7] do not explicitly specify this process among the above-enumerated phenomena, although it represents the most direct result of the interfacial tension gradients.

Coming back to Fig. 1, we see that, under the action of the $\sigma_0 - \sigma_1$ interfacial tension difference, a flow occurs on the very surface of the drop L'. Simultaneously, the movement of a liquid layer L will take place following the arrows outside the drop, and streams of liquid arise inside the drop L' (see the dotted arrows) ; the last two processes are explained by the lack of sliding between the proper surface of the drop, acted by the interfacial tension gradient and the two bulk liquids (L and L').

Due to the surface flow which draws the external liquid, hydrodynamic pressure forces act upon the drop. Their resultant determines the translational movement of the entire drop in a direction joining the point of maximum to that of minimum interfacial tension (see Fig. 1, the upward arrow).

Other processes (deformation, oscillation, surface waves etc.) undergone by the drop on account of the interfacial tension gradients will not be considered in the present work; in other words the drop is thought of as undeformable in the first approximation. Actually, this state will come into being at small interfacial tension gradients and large viscosities of the liquid L' which makes up the drop ^{41}.

THE GOVERNING EQUATIONS

We suppose that:

— the liquids L and L' are viscous and incompressible;

— the physical parameters (density ρ, ρ'; viscosity $\nu = \frac{\mu}{\rho}$ $\nu' = \frac{\mu'}{\rho'}$; temperature T, T') are constants;

— the volume force $(\rho - \rho')\vec{g}$ acting on the drop is cancelled, as supposed in the model;

— the flow caused by the interfacial tension gradient along the drop meridians is, in the first approximation, steady;

— the Reynolds number R is small;

— the Bond number Bo and the Weber number We are both small which means that the interfacial tension σ will be dominant in determining the liquid flow.

The equations governing the flow are the continuity and the Navier-Stokes equations.

The continuity equations are

$$\operatorname{div} \vec{v} = 0 \tag{1a}$$

$$\operatorname{div} \vec{v}' = 0 \tag{1b}$$

where $\vec{v}$, $\vec{v}'$ are the velocities of the liquids outside and inside the drop.

The Navier-Stokes equations for the steady motion are

$$(\vec{v} \cdot \nabla)\vec{v} = -\frac{1}{\rho} \operatorname{grad} p + \nu\Delta\vec{v} \tag{2a}$$

$$(\vec{v}' \cdot \nabla)\vec{v}' = -\frac{1}{\rho'} \operatorname{grad} p' + \nu\Delta v' \tag{2b}$$

where p and p' are the pressures outside and inside the drop.

Because the convective term $(\vec{v}\cdot\nabla)\,\vec{v}$ is of the order $\frac{v^2}{a}$ and the viscosity term $\nu\Delta\vec{v}$ is of the order $\frac{\nu v}{a^2}$, the ratio of the first term to the second is the Reynolds number. For small Reynolds numbers we can neglect the convective term and the flow equations (2) become

$$\operatorname{grad} p = \mu\Delta\vec{v} \tag{3a}$$

$$\operatorname{grad} p' = \mu'\Delta\vec{v}\,' \tag{3b}$$

The symmetry of the problem suggests a system of spherical coordinates $(r,\ \theta,\ \varphi)$ with the origin placed at the drop centre and the symmetrical axis Oz passing through the sphere in the point of minimum interfacial tension (Fig. 2).

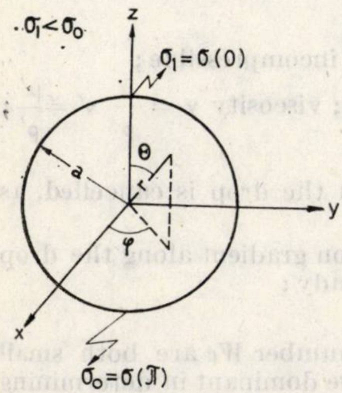

Fig. 2. — The system of spherical coordinates $r,\ \theta,\ \varphi$.

Since the motion of the liquid is symmetrical with respect to the Oz axis the velocities of the inner and outer liquid flows are not functions of the angle φ; they are functions only of r and θ, $v_r(r,\ \theta)$, $v_\theta(r,\ \theta)$, $v_r'(r,\theta)$, $v_\theta'(r,\ \theta)$.

The Navier-Stokes equations in spherical coordinates have the form [42]

$$\frac{\partial p}{\partial r} = \mu\left(\frac{\partial^2 v_r}{\partial r^2} + \frac{1}{r^2}\frac{\partial^2 v_r}{\partial\theta^2} + \frac{2}{r}\frac{\partial v_r}{\partial r} + \frac{\operatorname{ctg}\theta}{r^2}\frac{\partial v_r}{\partial\theta} - \frac{2}{r^2}\frac{\partial v_\theta}{\partial\theta} - \frac{2v_r}{r^2} - \frac{2\operatorname{ctg}\theta}{r^2}v_\theta\right) \tag{4a}$$

$$\frac{1}{r}\frac{\partial p}{\partial\theta} = \mu\left(\frac{\partial^2 v_\theta}{\partial r^2} + \frac{1}{r^2}\frac{\partial^2 v_\theta}{\partial\theta^2} + \frac{2}{r}\frac{\partial v_\theta}{\partial r} + \frac{\operatorname{ctg}\theta}{r^2}\frac{\partial v_\theta}{\partial\theta} + \frac{2}{r^2}\frac{\partial v_r}{\partial\theta} - \frac{v_\theta}{r^2\sin^2\theta}\right) \tag{4b}$$

and the continuity equation has the form

$$\frac{\partial v_r}{\partial r} + \frac{1}{r}\frac{\partial v_\theta}{\partial\theta} + \frac{2v_r}{r} + \frac{v_\theta\operatorname{ctg}\theta}{r} = 0 \tag{4c}$$

The equations for the inner liquid motion have similar forms.

BOUNDARY CONDITIONS

In order to find the distributions of the velocities $\vec{v}$ and $\vec{v}\,'$ and of the pressures p and p', the system of equations (4) must be solved taking the appropiate boundary conditions into consideration.

The velocities of the inner and outer liquids must satisfy the following conditions:

— the outer velocity must be zero far from the drop

$$v_r = v_\theta = 0 \qquad \text{for } r \to \infty\,; \tag{5a}$$

— the normal components of the inner and outer velocities must be zero on the surface of the undeformable drop

$$v_r = v'_r = 0 \qquad \text{at } r = a\,; \tag{5b}$$

— the tangential velocity components of the two liquids at the interface must be continuous

$$v_\theta = v'_\theta \qquad \text{at } r = a\,; \tag{5c}$$

— the velocity components within the drop must remain finite at all points, particularly at the centre of the drop

$$v'_r,\ v'_\theta \quad \text{finite at } r = 0 \tag{5d}$$

In addition to these kinematic conditions a dynamic condition must also be fulfilled at the interface. When the interfacial tension σ of the liquid-liquid system varies from point to point, a tangential force arises on the liquid surface. The tangential force is directed from points of lesser to points of greater interfacial tension. This force per unit of liquid surface area is given by[42-43]

$$\vec{p}_t = \operatorname{grad} \sigma$$

and is directed tangentially to the interface.

The condition of continuity of the tangential components p_{r_θ}, p'_{r_θ} of the stress tensor becomes

$$p_{r_\theta} + p_t = p'_{r_\theta}$$

or in spherical coordinates, on the surface of the drop, it can be written in the form

$$\mu\left(\frac{1}{r}\frac{\partial v_r}{\partial \theta} + \frac{\partial v_\theta}{\partial r} - \frac{v_\theta}{r}\right)_{r=a} + \frac{1}{a}\frac{\partial \sigma}{\partial \theta} = \mu'\left(\frac{1}{r}\frac{\partial v'_r}{\partial \theta} + \frac{\partial v'_\theta}{\partial r} - \frac{v'_\theta}{r}\right)_{r=a} \tag{5e}$$

SOLUTIONS OF THE BULK AND SURFACE FLOW EQUATIONS

The form of the solution can be obtained if we notice that the surface flow gives rise to a stream of liquid directed to the drop along the *Oz* axis. This stream arises as a consequence of the continual replacement of that liquid layer which had been displaced by the surface flow, a ventilation effect, as can be seen in Fig. 3. The profile of the flow in Fig. 3 indicates that a solution of the equations (4) should be sought in the form [42]

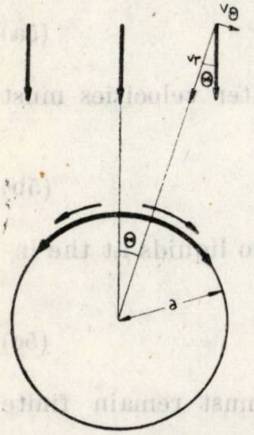

Fig. 3. — The surface flow and the current directed to the drop (ventilation effect).

$$v_r = f(r)\cos\theta,\ v_\theta = g(r)\sin\theta,\ p = \mu h(r)\cos\theta \tag{6a}$$

and similarly

$$v'_r = f'(r)\cos\theta,\ v'_\theta = g'(r)\sin\theta,\ p' = \mu' h'(r)\cos\theta \tag{6b}$$

By substituting these solutions into equations (4) we find

$$\frac{\mathrm{d}^2 f}{\mathrm{d}r^2} + \frac{2}{r}\frac{\mathrm{d}f}{\mathrm{d}r} - \frac{4(f+g)}{r^2} = \frac{\mathrm{d}h}{\mathrm{d}r} \tag{7a}$$

$$\frac{\mathrm{d}^2 g}{\mathrm{d}r^2} + \frac{2}{r}\frac{\mathrm{d}g}{\mathrm{d}r} - \frac{2(f+g)}{r^2} = -\frac{h}{r} \tag{7b}$$

$$\frac{\mathrm{d}f}{\mathrm{d}r} + \frac{2(f+g)}{r} = 0 \tag{7c}$$

and a similar system of linear, ordinary differential equations for the inner liquid flow.

After classical manipulation we obtain for $f(r)$, $g(r)$ and $h(r)$

$$f = \frac{b_1}{r^3} + \frac{b_2}{r} + b_3 + a_1 r^2$$

$$g = \frac{b_1}{2r^3} - \frac{b_2}{2r} - b_3 - 2a_1 r^2$$

$$h = \frac{b_2}{r} + 10\, a_1 r$$

By substituting the above-determined values of f, g, and h into (6) and taking into consideration (5a) and (5d) we obtain for the outer liquid motion

$$v_r = \left(\frac{b_2}{r} + \frac{b_1}{r^3}\right)\cos\theta \tag{8a}$$

$$v_\theta = \left(\frac{b_1}{2r^3} - \frac{b_2}{2r}\right)\sin\theta \tag{8b}$$

$$p = \mu\left(\frac{b_2}{r^2}\right)\cos\theta \tag{8c}$$

and

$$v'_r = (a_1 r^2 + a_2) \cos\theta \tag{9a}$$

$$v'_\theta = -(2a_1 r^2 + a_2) \sin\theta \tag{9b}$$

$$p' = 10\, \mu' a_1 r \cos\theta \tag{9c}$$

for the inner liquid motion.

The four unknowns a_1, a_2, b_1, b_2 will be determined from the boundary conditions (5). We have from (5b) and (5c)

$$a_1 = -\frac{b_1}{a^5}, \quad a_2 = \frac{b_1}{a^3}, \quad b_2 = -\frac{b_1}{a^2} \tag{10}$$

which give, from (5e)

$$\frac{d\sigma}{d\theta} = \frac{3b_1}{a^3}(\mu + \mu') \sin\theta \tag{11}$$

In order to find the dependence of the constant b_1 on the interfacial tension σ at the maximum and minimum of the σ, we integrate (11) after θ, over the interval $5 \leqslant \theta \leqslant \pi$. We obtain

$$b_1 = \frac{\sigma_0 - \sigma_1}{6(\mu + \mu')} a^3 \tag{12}$$

where $\sigma_1 = \sigma(0)$ and $\sigma_0 = \sigma(\pi)$ (see fig. 2).

With (10) and (12) the velocities and pressures for the outer flow are

$$v_r = \frac{(\sigma_0 - \sigma_1) a^3}{6(\mu + \mu')} \left(\frac{1}{r^3} - \frac{1}{a^2 r} \right) \cos\theta \tag{13a}$$

$$v_\theta = \frac{(\sigma_0 - \sigma_1) a^3}{6(\mu + \mu')} \left(\frac{1}{2r^3} + \frac{1}{2a^2 r} \right) \sin\theta \tag{13b}$$

$$p = -\frac{\mu(\sigma_0 - \sigma_1) a}{6r^2(\mu + \mu')} \cos\theta \tag{13c}$$

and for the inner flow

$$v'_r = \frac{\sigma_0 - \sigma_1}{6(\mu + \mu')} \left(1 - \frac{r^2}{a^2} \right) \cos\theta \tag{14a}$$

$$v'_\theta = -\frac{\sigma_0 - \sigma_1}{6(\mu + \mu')} \left(1 - \frac{2r^2}{a^2} \right) \sin\theta \tag{14b}$$

$$p' = -\frac{5\mu'(\sigma_0 - \sigma_1)}{3a^2(\mu + \mu')} r \cos\theta. \tag{14c}$$

The liquid on the surface of the drop moves at the velocity

$$(v_\theta)_{r=a} = \frac{\sigma_0 - \sigma_1}{6(\mu + \mu')} \sin\theta. \tag{15}$$

where the magnitude of the velocity at the drop "equator" is

$$v_0 = \frac{\sigma_0 - \sigma_1}{6(\mu + \mu')} \tag{16}$$

In order to have a picture of the studied phenomenon in Fig. 4 we plot the transversal velocity as a function of the distance r, in conformity with Eqs. (13b) and (14b), for two interfacial tension differences

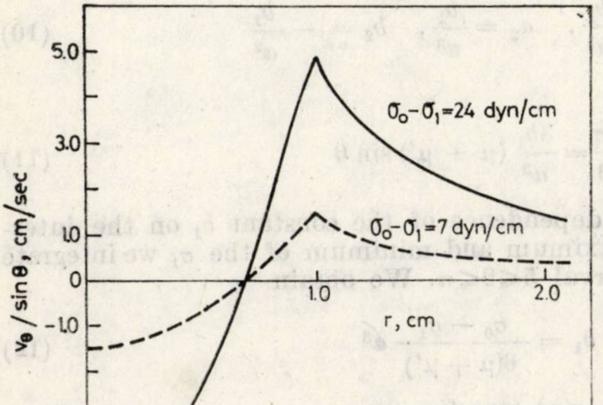

Fig. 4. — Plots of transversal velocity $v_\theta/\sin\theta$ as a function of the distance r for two interfacial tension differences (Eqs. (13b) and (14b)); $\mu_1 + \mu' = 0.813$ poise, $a = 0.98$ cm.

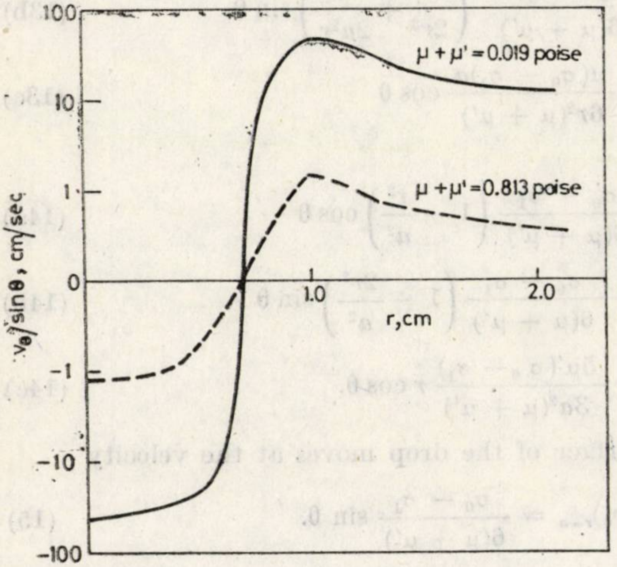

Fig. 5. — Transversal velocity $v_\theta/\sin\theta$ vs. the distance r for two liquid viscosities sums; $\sigma_0 - \sigma_1 = 7$ dyn/cm; $a = 0.98$ cm.

$(\sigma_0 - \sigma_1)$, at constant values of the viscosity $(\mu + \mu')$ and of the drop radius a. Then, in Fig. 5, we represent two curves calculated for different $(\mu + \mu')$ values. One finds that the maximum flow velocity is reached on the drop surface $(r = a)$.

As far as the flow on the very surface of the drop is concerned a term corresponding to the surface viscosity could be introduced. Our preliminary calculations show that in Eqs (13–16) the surface viscosity[31] arises as a correction term which can be neglected in the case of sufficiently large drops.

The adsorption and diffusion phenomena have not been considered yet as we suppose that they are fast enough in comparison to the surface flow. The interference of such processes will be thought of later.

Our first experiments[41] performed on practically undeformable drops of paraffin oil submerged in ethanol-water or methanol-water mixtures and using n – or isopropanol as a surfactant agree with Eqs. (15–16). The flow velocities on the surface of the drop, of the order of 1–2 cm.s^{-1}, lead to Reynolds numbers smaller than unity; so that the premises lying at the basis of our hydrodynamic model are plausibile.

MOTION OF TRANSLATION OF THE DROP

In the following we attempt to calculate the translation velocity of the entire drop (Fig. 1). As the preliminary experimental measurements[41] of this translation velocity led to Reynolds numbers situated between 10 and 60, the direct integration of the hydrodynamic equations was not done and we followed a different way.

Indeed, in conformity with the model of a surface flow involving the draw of the outer liquid L (Fig. 1), forces of hydrodynamic pressure act on the drop L'. By taking into account the symmetry of the surface flow, it follows that the resultant F_a of the forces is orientated to the positive sense of the Oz axis (Fig. 2). The propulsive force F_a determines in this way the translational motion of the drop as a whole along the positive Oz axis.

The force F_a arising as a consequence of the flow of the liquid L around the drop L' will be of the form[43]

$$F_a = \iint_S (p_{rr} \cos\theta - p_{r_\theta} \sin\theta)\, ds$$

or, because $ds = 2\pi a^2 \sin\theta\, d\theta$,

$$F_a = \int_0^\pi (p_{rr} \cos\theta - p_{r_\theta} \sin\theta)\, 2\pi a^2 \sin\theta\, d\theta \tag{17}$$

The normal and tangential components of the viscous stress tensor are

$$p_{rr} = -p + 2\mu \frac{\partial v_r}{\partial r} \tag{18a}$$

$$p_{r\theta} = \mu\left(\frac{1}{r}\frac{\partial v_r}{\partial \theta} + \frac{\partial v_\theta}{\partial r} - \frac{v_\theta}{r}\right) \tag{18b}$$

On the drop surface, because for $r = a$, $v_r = 0$, $\dfrac{\partial v_r}{\partial r} = \dfrac{\partial v_r}{\partial \theta} = 0$, from (13c) an (13b) we find

$$p_{rr} = \frac{\mu(\sigma_0 - \sigma_1)}{6a(\mu + \mu')}\cos\theta \tag{19a}$$

$$p_{r\theta} = \frac{\mu(\sigma_0 - \sigma_1)}{2a(\mu + \mu')}\sin\theta. \tag{19b}$$

Evaluation of Eq. (17) with the values of p_{rr} and $p_{r\theta}$ given by Eqs (19) leads to

$$F_a = \frac{14\pi\mu a(\sigma_0 - \sigma_1)}{9(\mu + \mu')}. \tag{20}$$

It will be admitted that the entire energy corresponding to the force F_a (Eq. 20) is transformed into kinetic energy. In other words, the force F_a causes the translational motion of the drop along the positive Oz axis (Fig. 2). Thus, it works as a motive force directly proportional to the interfacial tension difference.

The drag force F_r which is opposed to the displacement of the spherical drop will be of the following form [42, 44]

$$F_r = \frac{1}{2}\pi a^2 \rho\, u^2 C_d \tag{21}$$

where u is the displacement velocity and C_d the drag coefficient depending on the Reynolds number. For Reynolds number lower than 300 the C_d coefficient corresponding to the liquid drop is the same as for a solid sphere of equal radius and it can be obtained by interpolation from curves of the $R = R(C_d)$ dependence.[44]

By equalling the force in Eqs (20) and (21) we obtain the translational velocity

$$u = \sqrt{\frac{28\,\mu(\sigma_0 - \sigma_1)}{9\rho a C_d(\mu + \mu')}} \tag{22}$$

It is obvious that Eq. (22) describes only the initial velocity of the drop. This movement will then be damped out due to the vanishing of the interfacial tension gradient by the very process of surface flow and also because of the friction with the viscous medium. The overall phenomenon has a transient character.

In conclusion, in our hydrodynamic model, the translation of the free or imponderable — initially motionless — drop, whose surface is acted by interfacial tension gradients, is explained by the surface flow processes. This fact has not been described in literature as yet.

REFERENCES

[1] J. B. Lewis and H.R.C. Pratt, *Nature*, **171**, 1155 (1953).

[2] D. A. Haydon, *Nature*, **176**, 839 (1955).

[3] D. A. Haydon, *Proc. Roy. Soc.*, **A243**, 483 (1958).

[4] J. T. Davies and D. A. Haydon, *Proc. Roy. Soc.*, **A243**, 492 (1958).

[5] H. Grothuis and F. J. Zuiderweg, *Chem. Eng. Sci.*, **12**, 288 (1960).

[6] R. S. Valentine and W. J. Heideger, *Ind. Eng. Chem. Fundamentals*, **2**, 242 (1963).

[7] R. S. Valentine, N.F. Sather and W. J. Heideger, *Chem. Eng. Sci.*, **20**, 719 (1965).

[8] A. Steinchen-Sanfeld and A. Sanfeld, *Chem. Phys.*, **1**, 156 (1973).

[9] A. Steinchen and A. Sanfeld, in "Chemie, physikalische Chemie und Anwendungstechnik der grenzflächnaktiven Stofe", Carl Hansen Verlag, München, 1973, p. 139.

[10] F. Deyhimi and A. Sanfeld, *Compt. rend.*, **279**, D-437 (1974).

[11] A. Sanfeld and A. Steinchen, *Biophys. Chem.*, **3**, 99 (1975).

[12] M. Hennenberg, T. S. Sørensen, A. Steinchen-Sanfeld and A. Sanfeld *J. Chim. Phys.*, **72**, 1202 (1975).

[13] P. Joos and M. van Bockstaele, *Anales Quim.*, **71**, 889 (1975).

[14] T. S. Sørensen, M. Hennenberg, A. Steinchen and A. Sanfeld, *J. Colloid Interface Sci.*, **56**, 191 (1976).

[15] T. S. Sørensen, M. Hennenberg and A. Sanfeld, *J. Colloid Interface Sci.*, **61**, 62 (1977).

[16] M. Hennenberg, T. S. Sørensen and A. Sanfeld, *J.C.S. Faraday II*, **73**, 48 (1977).

[17] T. S. Sørensen, F. Y. Hansen, J. Nielsen and M. Hennenberg, *J.C.S. Faraday II*, **73**, 1589 (1977).

[18] T. S. Sørensen, M. Hennenberg and F. Y. Hansen, *J.C.S. Faraday II*, **74**, 1005 (1978).

[19] M. Hennenberg, P. M. Bisch, M. Vignes-Adler and A. Sanfeld, *J. Colloid Interface Sci.*, **69**, 128 (1979).

[20] M. Hennenberg, T. S. Sørensen, F. Y. Hansen and A. Sanfeld, in "Colloid and Surface Science", Vol. III, Academic Press, New York 1976, p. 165.

[21] M. Dupeyrat and E. Nakache, *Bioelectrochemistry and Bioenergetics*, **5**, 134 (1978).

[22] E. W. Otto, *Chem. Engng. Progr. Symp.* Ser. **62**, 158 (1966).

[23] E. T. Benedikt, *ARS Journal*, **29**, 150 (1959).

[24] T. Li, *J. Chem. Phys.*, **36**, 2369 (1962).

[25] H. L. Paynter, *AIAA Journal*, **2**, 1627 (1964).

[26] V. B. Zenkovici, *Teplofiz. Vys. Temperatur.*, **2**, 230 (1964).

[27] V. N. Serebryakov, *Kosm. Issled.*, **4**, 713 (1966).

[28] J. G. Seebold, M. P. Hollister and H. M. Satterlee, *J. Spacecraft*, **4**, 101 (1967).

[29] C. V. Sternling and L. E. Scriven, *A.I. Ch. E. Journal*, **5**, 514 (1959).

[30] L. E. Scriven and C. V. Sternling, *Nature*, **187**, 186 (1960).

[31] L. E. Scriven, *Chem. Eng. Sci.*, **12**, 98 (1960).

[32] E. Chifu and I. Cadariu, *Stud. Univ. Babeș-Bolyai Chem.*, **6** (2) 19(1961).

[33] E. Chifu, *Stud. Univ. Babeș-Bolyai Chem.*, **8**(1) 49 (1963).

[34] E. Chifu and L. Oniciu, *Stud. Univ. Babeș-Bolyai Chem.*, **9**(1) 95 (1964).

[35] R. Deutsch and E. Chifu, *Stud. Univ. Babeș-Bolyai Chem.*, **9** (1) 101(1964).

[36] E. Chifu, *Stud. Univ. Babeș-Bolyai Chem.*, **10**, (2) 85 (1965).

[37] R. Deutsch, P. Sandru and E. Chifu, *Stud. Univ. Babeș-Bolyai Chem.*, **10** (2) 91 (1965).

[38] R. Deutsch, H. Szöcs and E. Chifu, *Stud. Univ. Babeș-Bolyai Chem.*, **10** (2) 99 (1965).

[39] E. Chifu and R. Deutsch, *Rev. Roumaine Chim.*, **11**, 873 (1966).

[40] E. Chifu and I. Albu, *Stud. Univ. Babeș-Bolyai Chem.*, **13**(1) 99 (1968).

[41] E. Chifu, I. Stan, Z. Finta and E. Gavrilă, *Rev. Chim.*, (București) **31**, 765(1980).

[42] V. G. Levich, "Physicochemical Hydrodynamics", Prentice Hall, New Jersey, 1962, chap. VII—VIII.

[43] L. Landau and E. Lifschitz, "Mécanique des fluides", Editions Mir, Moscou, 1971, chap. III and VII.

[44] H. Schlichting, "Boundary Layer Theory", McGraw-Hill, New York, 1960, chap. I.

Revue Roumaine de Chimie, 25, *11–12*, 1461–1468 (1980)

EFFECTS OF COUPLE STRESSES ON THE DISPERSION OF A SOLUTE WITH SIMULTANEOUS CHEMICAL REACTION

S. NARASIMHA MURTHY

Department of Mathematics, College of Science, University of Mosul, Mosul, Iraq

Received April 12, 1976
Revised March 11, 1980

In this paper, the effects of couple stress parameter and the first order irreversible chemical reaction on the dispersion of a solute in a solvent is studied by using Taylor's analysis. In the case of diffusion with a homogeneous first order reaction, we find that the effective dispersion coefficient decreases with increase in the couple stress parameter. However, for large values of it the diffusion is not affected. In the case of diffusion combined with the homogeneous and heterogeneous reaction, the increase in the wall catalytic parameter together with the couple stress parameter also causes a decrease in the effective Taylor's dispersion coefficient. The above analysis suggests that couple stresses in a solvent can regulate the rate of diffusion.

INTRODUCTION

The dispersion of a soluble matter in an incompressible viscous fluid flowing in a circular pipe under laminar conditions was discussed by Taylor.[1-3] He found that relative to a plane moving with the mean speed of the flow, the solute is dispersed with an apparent diffusion coefficient $R^2\bar{V}_x^2/48\,D$. Here, R, V and D are the radius of the pipe, the average velocity, and the molecular diffusion coefficient respectively. Aris [4] extended this study and established that the rate of growth of the variance of the solute distribution is proportional to the sum of molecular diffusion coefficient and Taylor's coefficient. Fan and Hwang [5] extended to include dispersion in a non-Newtonian fluid, the fluid considered being the power-law type due to Ostwald-de-waele. Recently, Ghoshal [6] extended the analysis to investigate dispersion of solute in Eyring and Reiner-Philoppoff fluids.

An analysis of the dispersion of a solute in a channel flow of a fluid with couple stresses has been done by Soundalgekar. [7]He showed that whenever the couple stress parameter is less than 20, they are more effective in reducing the rate of dispersion.

Although a good deal of work has been done on dispersion of solute in Newtonian and non-Newtonian fluids, the study of the effect of chemical reaction on it has not received due attention. Only recently, Gupta and Gupta,[8] Narasimha Murthy and Krishna Murthy [9] studied the case of dispersion of a solute in a Newtonian fluid for the case of non-magnetic field and with magnetic field in the presence of a first order chemical reaction, respectively. The aim of the present investigation is to discuss the effects of couple stresses in fluids on the dispersion of a solute in a channel flow in the presence of an irreversible first order chemical reaction. The problem of chemical reaction in non-Newtonian fluids is encountered in such industrial processes as the hydrogenation of unsaturated macromolecules as pointed out by Mihail.[10]

2. DIFFUSION WITH A HOMOGENEOUS FIRST ORDER REACTION

Consider the dispersion of a solute in the laminar flow of a viscous fluid between two parallel plates, $y = \pm h$. The expression for the velocity in fully developed flow as derived by Stokes [11] is

$$u_x(y) = \frac{-h^2 p'}{2\mu}\left[1 - \left(\frac{y}{h}\right)^2 - \frac{2}{\alpha^3}\left(1 - \frac{\cosh\left(\frac{\alpha y}{h}\right)}{\cosh\alpha}\right)\right]. \tag{1}$$

Here, p' is the pressure gradient along the plates, μ is the viscosity, $\alpha = \frac{h}{\lambda}$, $\lambda = \left(\frac{\eta}{\mu}\right)^{\frac{1}{2}}$, η is a material constant with dimensions MLT^{-1}. For a particular fluid, the parameter α depends upon the value of h.

The average velocity from (1) is

$$\overline{\mathcal{U}} = \frac{-h^2 p'}{2\mu}\left[\frac{2}{3} - \frac{2}{\alpha^2}\left(1 - \frac{\tanh\alpha}{\alpha}\right)\right]. \tag{2}$$

If a solute diffuses in the fully developed flow and simultaneously undergoes a first order irreversible chemical reaction under isothermal conditions, then the concentration of the solute satisfies the following equation:

$$\frac{\partial c}{\partial t} + \mathcal{U}_x \frac{\partial c}{\partial x} = D\left(\frac{\partial^2 c}{\partial x^2} + \frac{\partial^2 c}{\partial y^2}\right) - k_1 c. \tag{3}$$

The last term on the R.H.S of (3) accounts for a first order chemical reaction and D, the molecular diffusion coefficient assumed constant.

We now consider the convection across a plane moving with the mean speed of the flow. Then, relative to this plane, the fluid velocity is:

$$\mathcal{V}_x = \mathcal{U}_x - \bar{u} = -\frac{h^2 p'}{2\mu}\left[\frac{1}{3} - \left(\frac{y}{h}\right)^2 - \frac{2}{\alpha^3}\left(\frac{\tanh\alpha}{\alpha} - \frac{\cosh\left(\frac{\alpha y}{h}\right)}{\cosh\alpha}\right)\right]. \tag{4}$$

Equation (3), after assuming that,

$$\frac{\partial^2 c}{\partial x^2} \ll \frac{\partial^2 c}{\partial y^2}$$

and using (4) and the following dimensionless quantities :

$$\xi = \frac{x - \bar{u}t}{L}, \quad \eta = \frac{y}{h}, \quad \theta = \frac{t}{\bar{t}}, \quad \bar{t} = \frac{L}{\mathcal{U}} \tag{5}$$

reduces to

$$\frac{\partial^2 c}{\partial \eta^2} = \frac{h^2}{DL} \mathcal{V}_x \frac{\partial c}{\partial \xi} + k_1 \frac{h^2}{D} c. \tag{6}$$

If Taylor's limiting conditions are valid in the present investigation, then partial equilibrium may be assumed in any cross-section of the channel. Equation for c then will be :

$$\frac{\partial^2 c}{\partial \eta^2} - r^2 c = \frac{h^2}{DL} \mathcal{V}_x \frac{\partial c}{\partial \xi}, \tag{7}$$

where, $r = h\left(\frac{k_1}{D}\right)^{\frac{1}{2}}$, the homogeneous reaction rate parameter.

The dimensionless form of (4) is :

$$\mathcal{V}_x = z\left[\frac{1}{3} - \eta^2 - \frac{2}{\alpha^2}\left(\frac{\tanh \alpha}{\alpha} - \frac{\cosh \alpha' \eta}{\cosh \alpha}\right)\right], \tag{8}$$

where, $z = -\frac{h^2 p'}{2\mu}$, $\alpha = \frac{h}{\lambda}$, the couple stress parameter.

Assuming $\frac{\partial c}{\partial \xi}$ to be independent of η at any cross-section, equation (7) may be integrated to obtain the variation of c with η. The boundary conditions which express zero mass transport at the walls and the symmetry of the concentration profile, about the central line of the channel, are :

$$\begin{aligned} \frac{\partial c}{\partial \eta} &= 0 \quad \text{at} \quad \eta = 1 \\ \frac{\partial c}{\partial \eta} &= 0 \quad \text{at} \quad n = 0. \end{aligned} \tag{9}$$

The variation of c is given by :

$$C = \frac{Zh^2}{DL} \frac{\partial c}{\partial \xi}\left[\frac{2 + r^2\eta^2}{r^4} - \frac{1}{3r^2} + \frac{2}{\alpha^2}\left\{\frac{\tanh \alpha}{\alpha r^2} + \frac{\cosh \alpha r \eta}{\cosh \alpha(\alpha^2 - r^2)}\right\} - \right.$$
$$\left. - \frac{2\cosh r\eta}{r \sinh r}\left(\frac{1}{r^2} + \frac{\tanh \alpha}{\alpha(\alpha^2 - r^2)}\right)\right]. \tag{10}$$

The volumetric rate at which the solute is transported across a section of the channel of unit breadth in non-dimensional form is :

$$Q = \int_{-1}^{1} c \mathcal{V}_x \, \mathrm{d}\eta. \tag{11}$$

Inserting for c from (10), and $\mathcal{V}_x$ from (8), and integrating, we get

$$Q = \frac{h^7 (P')^2}{4DL\,\mu^2}\,\frac{\partial c}{\partial \xi}\,F(\alpha, r); \tag{12}$$

where,

$$\begin{aligned} F(\alpha, r) = \Bigg[& -\frac{2}{45 r^2} + \frac{\tanh\alpha\,(2r^2-\alpha^2)}{3\alpha^3 r^2(\alpha^2 - r^2)} - \frac{2\tanh^2\alpha}{\alpha^2(\alpha^2 - r^2)} \\ & + \frac{1}{\alpha r}\left\{\frac{1}{r^2} + \frac{\tanh\alpha}{\alpha(\alpha^2 - r^2)}\right\}\left\{\frac{2\tanh\alpha}{\alpha^2 r} - \frac{\sinh\alpha}{3\sinh r}\right\} \\ & + \frac{1}{\alpha}\left\{\frac{\sinh\alpha}{\alpha^2}(2+\alpha^2) - \cosh\alpha\right\}\left\{\frac{(\alpha^2 - 2r^2)}{\alpha^2 r^2(\alpha^2 - r^2)\cosh\alpha} + \right. \\ & \left. + \frac{1}{r\sinh r}\left(\frac{1}{r^2} + \frac{\tanh\alpha}{\alpha(\alpha^2 - r^2)}\right)\right\} - \frac{1}{2\alpha^3}\{\sinh 2\alpha + 2\alpha\} \\ & \left\{-\frac{1}{\alpha^2\cosh^2\alpha\,(\alpha^2 - r^2)} + \frac{1}{r^3\sinh r\cosh\alpha} + \frac{\tanh\alpha}{\alpha r\sinh r\cosh\alpha(\alpha^2 - r^2)}\right\}\Bigg] \end{aligned} \tag{13}$$

In passing we note that for $r = 0$, we get back the equation (13) of Soundalgekar.[7]

On comparing equation (12) with Fick's law of diffusion, we find that the solute is dispersed relative to a plane moving with the mean speed of the flow with an effective dispersion coefficient D^* given by:

$$D^* = \frac{h^6 (p')^2}{D\mu^2}\,F(\alpha, r), \tag{14}$$

where $F(\alpha, r)$ is defined by equation (13).

The numerical values of $F\,(\alpha, r)$ for different values of α and r are plotted in figures 1 and 2.

From Figure 1, it can be seen that for a fixed value of homogeneous reaction rate, the effective dispersion coefficient decreases with increase in the couple stress parameter. We also observe that for large values of α, the Taylor diffusion coefficient is not affected by the couple stress parameter. Figure 2 shows that for a fixed value of couple stress parameter, the Taylor diffusion coefficient decreases with homogeneous reaction rate parameter r. This is due to the fact that as the reaction rate increases, a more and more amount of solute undergoes chemical reaction.

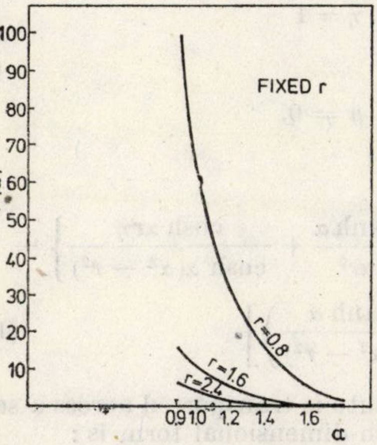

Fig. 1. — Variation of effective dispersion coefficient against heterogeneous reaction.

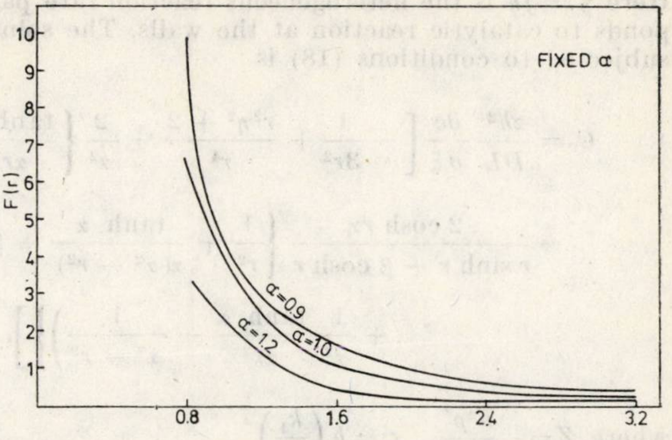

Fig. 2. — Variation of effective dispersion coefficient against couple stress parameter.

3. DIFFUSION WITH THE COMBINED HOMOGENEOUS AND HETEROGENEOUS REACTION

We now discuss the problem of diffusion in a channel with first order irreversible chemical reaction taking place both in the bulk of the liquid and at the walls which are assumed to be catalytic to reaction.

In this case the diffusion equation

$$\frac{\partial c}{\partial t} + \mathcal{U}_x \frac{\partial c}{\partial x} = D \frac{\partial^2 c}{\partial y^2} - k_1 c, \tag{15}$$

subjected to the following boundary conditions:

$$\begin{aligned} \frac{\partial c}{\partial y} + fc = 0 \quad \text{at} \quad y = h \\ \frac{\partial c}{\partial y} - fc = 0 \quad \text{at} \quad y = -h \end{aligned} \tag{16}$$

is to be solved.

Again, introducing the dimensionless quantities as in (5) and assuming the limiting conditions of Taylor, the diffusion equation is

$$- k_1 \frac{\mathrm{d}^2}{D} c + \frac{\partial^2 c}{\partial \eta^2} = \frac{h^2}{DL} \mathcal{U}_x \frac{\partial c}{\partial \xi} \tag{17}$$

with boundary conditions

$$\begin{aligned} \frac{\partial c}{\partial \eta} + \beta c = 0 \quad \text{at} \quad \eta = 1 \\ \frac{\partial c}{\partial \eta} - \beta c = 0 \quad \text{at} \quad \eta = -1 \end{aligned} \tag{18}$$

Here $\beta = fh$ is the heterogeneous reaction rate parameter which corresponds to catalytic reaction at the walls. The solution of equation (17) subjected to conditions (18) is

$$C = \frac{zh^2}{DL}\frac{\partial c}{\partial \xi}\Bigg[-\frac{1}{3r^2} + \frac{r^2\eta^2+2}{r^4} + \frac{2}{\alpha^2}\left\{\frac{\tanh\alpha}{\alpha r^2} + \frac{\cosh\alpha\eta}{(\alpha^2-r^2)}\right\}$$

$$-\frac{2\cosh r\eta}{r\sinh r + \beta\cosh r}\Bigg\{\frac{1}{r^2} + \frac{\tanh\alpha}{\alpha(\alpha^2-r^2)} + \beta\Bigg(\frac{1}{r^4} + \frac{1}{3r^2} +$$

$$+\frac{1}{\alpha^2}\cdot\frac{\tanh\alpha}{\alpha r^2} + \frac{1}{\alpha^2-r^2}\Bigg)\Bigg\}\Bigg], \tag{19}$$

where $Z = -\dfrac{h^2p'}{2\mu}$, $r = h\left(\dfrac{k_1}{D}\right)^{\frac{1}{2}}$.

The volumetric rate at which the solute is transported across a section of the channel of unit breadth is:

$$Q = \int_{-1}^{1} c\mathcal{U}_x \, d\eta. \tag{20}$$

Using expression for C from (19) and u_x from (1) we obtain

$$Q = \frac{4z^2h^2}{DL}\frac{\partial c}{\partial \xi}G(\alpha, \beta, r). \tag{21}$$

Here

$$G(\alpha, \beta, r) = \Bigg[-\frac{2}{45r^2} + \frac{\tanh\alpha}{3\alpha^2(\alpha^2-r^2)} + \frac{1}{r\sinh r + \beta\cosh r}$$

$$\left\{\frac{1}{r^2} + \frac{\tanh\alpha}{\alpha(\alpha^2-r^2)} + \beta\left(\frac{1}{r^4} + \frac{1}{3r^2} + \frac{1}{\alpha^2}\frac{\tanh\alpha}{\alpha r^2} + \frac{1}{\alpha^2-r^2}\right)\right\}$$

$$\Bigg\{-\frac{\sinh r}{3r} + \frac{1}{\alpha}\sinh\alpha\left(1+\frac{2}{\alpha^2}\right) - \cosh\alpha + \frac{1}{\alpha^4}\Bigg(\frac{2\tanh\alpha\sinh r}{\alpha r}$$

$$-\frac{1}{\cosh\alpha}\frac{\sinh(\alpha+r)}{(\alpha+r)} + \frac{\sinh(\alpha-r)}{2(\alpha-r)} + \frac{\sinh(r-\alpha)}{2(r-\alpha)}\Bigg)\Bigg\}$$

$$-\frac{1}{\alpha^3(\alpha^2-r^2)\cosh\alpha}\left\{\sinh\alpha\left(1+\frac{2}{\alpha^2}\right) - \cosh\alpha\right\}$$

$$-\frac{1}{\alpha^2r^2}\left(\frac{1}{3}+\frac{2}{\alpha^2}\right)\frac{\tanh\alpha}{\alpha} + \frac{1}{\alpha^3r^4\cosh\alpha}$$

$$\left\{r^2 \sinh \alpha \left(1 + \frac{2}{\alpha^2}\right) - \cosh \alpha + 2\sinh \alpha\right\}$$

$$+ \frac{1}{\alpha^4(\alpha^2 - r^2)} \left\{\frac{2\tanh^2 \alpha}{\alpha^2} + \frac{1}{\cosh^2\alpha}\left(1 + \frac{\sinh 2\alpha}{2\alpha}\right)\right\}\Bigg]. \tag{22}$$

We note that for $\beta = 0$, we get equation (12).

On comparing (21) with Fick's law of diffusion we find that the solute is dispersed relative to a plane moving with the mean speed of the flow with an effective dispersion coefficient D^* given by:

$$D^* = \frac{h^5(p')^2}{D\mu^2} G(\alpha, \beta, r) \tag{23}$$

where $G(\alpha, \beta, r)$ is given by (22).
The values of $\bar{x}\, G(\alpha, \beta, r)$ for fixed values of γ and β are plotted in Figures 3 and 4.

As it can be seen, for a fixed value of homogeneous reaction rate, the effective dispersion coefficient decreases with increase in the heterogeneous reaction rate and couple stresses. Figure 4 shows the variation of effective dispersion coefficient against the couple stress parameter for fixed values of heterogeneous reaction rate. Again, we notice that the dispersion coefficient decreases with increase in the couple stress parameter and heterogeneous reaction rate. In other words, the combined effect of couple stresses and the heterogeneous reaction is to decrease the effective dispersion coefficient.

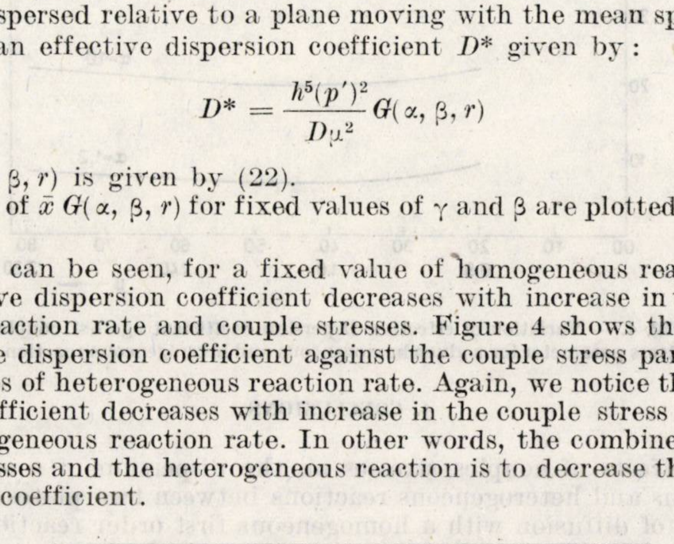

Fig. 3. — Variation of effective dispersion coefficient against homogeneous reaction.

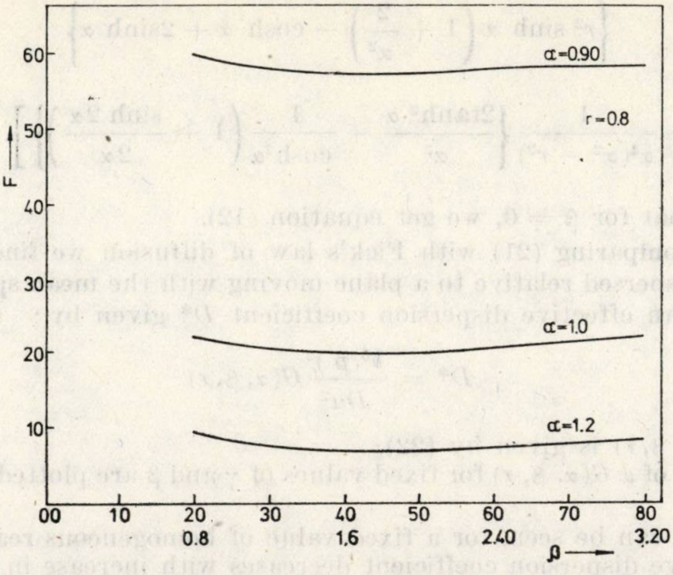

Fig. 4. — Variation of effective dispersion coefficient against couple stress parameter for a given homogeneous and heterogeneous reaction.

4. CONCLUSIONS

The effects of couples stresses on the dispersion of a solute with homogeneous and heterogeneous reactions between two plates is studied. In the case of diffusion with a homogeneous first order reaction, we find that the effective dispersion coefficient decreases with increase in the couple stress parameter. However, for large values of couple stress parameter, the diffusion is not affected. In the case of diffusion combined with the homogeneous and heterogeneous reaction, the increase in the wall catalytic parameter together with the couple stress paramater also causes a decrease in the effective Taylor's coefficient. The above analysis suggests that the couple stresses in a solvent can regulate the rate of diffusion.

REFERENCES

[1] G. I. Taylor, *Proc. Roy. Soc.*, **A219**, 186 (1953).
[2] G. I. Taylor, *Proc. Roy. Soc.*, **A223**, 446 (1954).
[3] G. I. Taylor, *Proc. Roy. Soc.*, **A225**, 473 (1954).
[4] R. Aris, *Proc. Roy. Soc.*, **A235**, 67 (1956).
[5] L. T. Fan and W. S. Hwang, *Proc. Roy. Soc.*, **A283**, 576 (1965).
[6] S. Ghoshal, *Chem. Eng. Sci.*, **26**, 185 (1971).
[7] V. M. Soundalgekar, *Phys. Fluids.*, **14**, 19 (1971).
[8] P. S. Gupta and A. S. Gupta *Proc. Roy. Soc.*, **A330**, 59 (1972).
[9] S. Narasimha Murthy and M. R. Krishna Murthy, *Ind. J. Phys.*, **48**, 634 (1974).
[10] R. Mihail, *Chem. Eng. Sci.*, **26**, 2117 (1971).
[11] V. M. Stokes, *Phys. Fluids*, **9**, 1709 (1966).

Revue Roumaine de Chimie, 25, *11–12*, 1469–1475 (1980)

STUDY OF THE HYDROGEN BOND IN THE MANDELIC AND 4-CHLOROMANDELIC ACIDS

GH. SINGUREL
Spectroscopy Laboratory, "Al. I. Cuza" University, Iaşi, Calea 23 August 11, Romania

Received March 5, 1979

From the data on the modifications of the $C=O$ and OH valency oscillation bands, the interaction of the mandelic and 4-chloromandelic acids, respectively, with proton acceptor or donor solvents in ternary mixtures was studied. The energy of the hydrogen bonds occurring between the dimerized molecules of these acids was determined.

The IR spectral study of the mandelic (**M**) acid and some of its derivatives in the valency oscillation region of $C=O$ and OH bonds showed an intramolecular hydrogen bond between hydroxyl group and the oxygen atom of the *cis*-carboxyl structure in respect to the $C-O$ bond.[1] In this paper the results of the study of interactions between the molecules of the **M** acid and **4-Cl M** acid, respectively, and the molecules of some proton acceptor or donor compounds are presented.

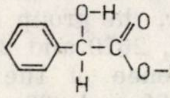

(M)

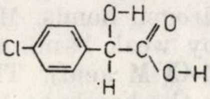

(4-Cl M)

EXPERIMENTAL

IR spectra of the M and 4-Cl M acids, both in KBr pellets and solution were recorded with a UR-20 "C. Zeiss-Jena" spectrometer, using NaCl prism in the 1600–1800 cm^{-1} range, and LiF one in 3400–3600 cm^{-1} range. The frequencies observed were calibrated against those of a standard polystyrene film. The spectral slit width calculated was 4 cm^{-1} at the wave number of 1700 cm^{-1} and 2.5 cm^{-1} at 3500 cm^{-1}.

Both for binding energy determination and for spectra recording in ternary mixtures, NaCl-window cells, 5 mm in thickness, were used. Also, in the case of the binary mixtures the 0.1 mm in thickeness cells were used.

In order to determine the energy of the hydrogen bond, the NaCl window cells, 5 mm in thickness, containing the acid solution in CCl_4 were thermostated, the solution temperature being maintained during the measurements in the limits of 1°C. The integral intensity was measured in the temperature range of 295–353 K. The spectra were directly recorded in extinction using the N1 B102a recorder of the UR-20 spectrometer. In order to separate the two bands in the $C=O$ valency oscillation range, which are used in the binding energy calculus, their shapes were symmetrically considered. The separated area of the bands was measured

with a planimeter. The experimental data processing indicated an error in the binding energy of 1 kcal/mol.

The interaction of M and 4-Cl M acids, respectively, which various proton acceptors or donors was studied in ternary mixtures of CCl_4, investigated acid and proton acceptor or donor compound. To establish certain details of the interactions which appear in the ternary mixtures, the IR spectrum in the C=O and OH range, using a differential method,[2] was recorded. The cell with the ternary mixture was placed in the measurement beam, and the cell with the solution of the same acid concentration in CCl_4 was introduced in the reference beam. The unbalance between the radiation flux of the two beams is determined by interactions occurring in the ternary mixture between the acid and the proton acceptor or donor compounds. The method can be applied only in the case of proton acceptor or donor compounds which have no bands in the analysed range.

RESULTS AND DISCUSSION

IR spectrum in KBr pellets. Spectra have bands which are characteristic of the molecules associated by means of the carboxyl group. The valency C=O oscillation of the **M** acid has two peaks at 1715 cm^{-1} and 1730 cm^{-1}. That of the **4-Cl M** acid occurs at 1728 cm^{-1} and shows a shoulder at 1692 cm^{-1}. This structure of the C=O band, as has been first noticed by Davies and Sutherland,[3] can be explained supposing that the molecules of these compounds occur in the form of dimers of the type:

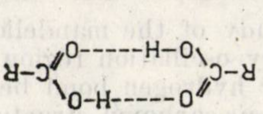

(1)

The existence of dimers is revealed also by the behaviour of the OH group oscillations. The IR spectrum of both acids shows a very intense and wide absorption range between 2400 and 3200 cm^{-1}, which seems to be formed of two bands. This range is assigned to the OH group of molecules connected by hydrogen bonds. Moreover, the group of linked molecules is characterized by weak bands at 2630, 2670 and 2815 cm^{-1} (**M** acid) and 2600 cm^{-1} (**4-Cl M** acid). The presence of the dimerized form is confirmed also by the bands at 1380, 1300 and 890 cm^{-1} of the **M** acid and at 1410, 1325 and 912 cm^{-1} of the **4-Cl M** acid, which are characteristic of the dimerized carboxyl group.[4]

The **M** acid shows a very intense band at 3400 cm^{-1}, while the **4-Cl M** acid has the same intense band at 3410 cm^{-1}. If we consider that the molecules in the solid state are completely dimerized, these bands could be assigned to the hydroxyl group.

IR spectrum in CCl_4. Both compounds have two bands in the range of C=O oscillations at 1718 and 1762 cm^{-1}. The study of the dependence of band intensity on concentration has pointed out that the 1718 cm^{-1} band belongs to the dimer and the 1762 cm^{-1} one belongs to the monomer (Fig. 1a). As concentration increases, the intensity of the dimer band increases more quickly than that of the monomer band. Figure 2 shows this dependence in the case of the **4-Cl M** acid. Even for very low concentrations, dimer formations do not completely disappear, but their number is smaller than that of the monomers.

In CCl_4, in the range of the OH valence oscillations, there occurs a band which shows asymmetry towards large wave numbers (Fig. 3a).

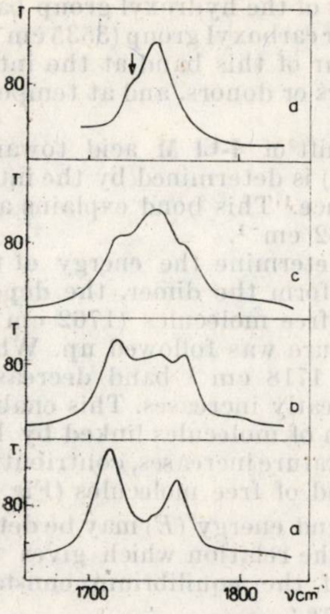

Fig. 1. — a) The range of C═O oscillations of the 4-Cl M acid in CCl_4 ($C \sim 5\times10^{-4}$ mol/l); b), c) The same oscillation range when dioxane is added ($C \sim 5\times10^{-3}$, respectively, $\sim 10^{-2}$ mol/l; d) The C═O oscillation of the 4-Cl M acid in dioxane.

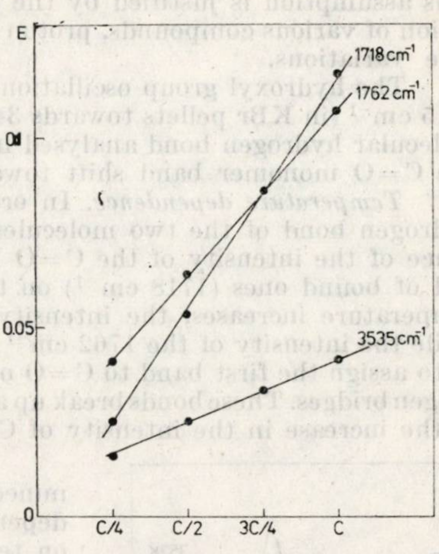

Fig. 2. — The extinction of C═O bands from 1718 and 1762 cm^{-1} and OH 3535 cm^{-1} vs. concentration.

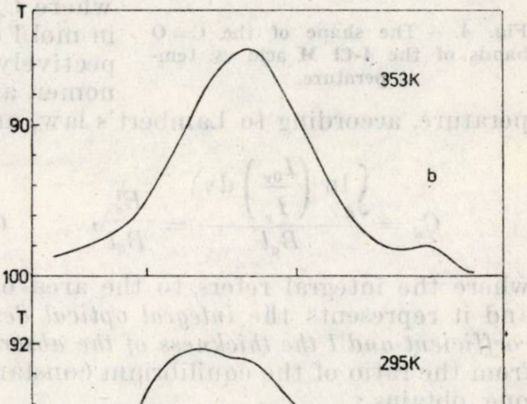

Fig. 3. — a) The OH oscillation range of the 4-Cl M acid in CCl_4 at 295 K; b) at 353 K.

Asymmetry is determined by the overlapping of the hydroxyl group band ($3515 cm^{-1}$) and of the OH band of the monomer carboxyl group ($3535\ cm^{-1}$). This assumption is justified by the behaviour of this band at the interaction of various compounds, proton acceptors or donors, and at temperature variations.

The hydroxyl group oscillation band shift of **4-Cl M** acid towards $3515\ cm^{-1}$ (in KBr pellets towards $3410\ cm^{-1}$) is determined by the intramolecular hydrogen bond analysed in reference.[1] This bond explains also the $C=O$ monomer band shift towards $1762\ cm^{-1}$.

Temperature dependence. In order to determine the energy of the hydrogen bond of the two molecules which form the dimer, the dependence of the intensity of the $C=O$ band of free molecules ($1762\ cm^{-1}$), and of bound ones ($1718\ cm^{-1}$) on temperature was followed up. When temperature increases, the intensity of the $1718\ cm^{-1}$ band decreases, while the intensity of the $1762\ cm^{-1}$ band greatly increases. This enables us to assign the first band to $C=O$ oscillation of molecules linked by hydrogen bridges. These bonds break up as temperature increases, contributing to the increase in the intensity of $C=O$ band of free molecules (Fig. 4).

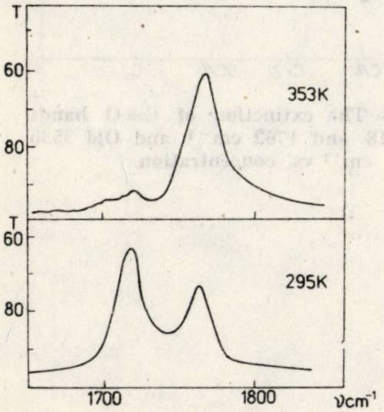

Fig. 4. — The shape of the $C=O$ bands of the **4-Cl M** acid vs. temperature.

The bound energy (E) may be determined using the relation which gives the dependence of the equilibrium constant on temperature:

$$K = \text{const} \times \exp\,(-E/RT) \qquad (2)$$

Supposing that dimers are formed according to scheme (1), the equilibrium constant for a determined temperature is given by the relation:

$$K = \frac{C_d}{(C - C_d)^2} = \frac{C_d}{C_m^2} \qquad (3)$$

where C_d and C_m are the concentrations in mol/l of the dimer and monomer, respectively. The concentrations of the monomer and dimer, for a determined temperature, according to Lambert's law, are given by the relation [2]:

$$C_d = \frac{\int_d \ln\left(\frac{I_{0\nu}}{I_\nu}\right) d\nu}{B_d l} = \frac{E_d^i}{B_d l}, \qquad C_m = \frac{\int_m \ln\left(\frac{I_{0\nu}}{I_\nu}\right) d\nu}{B_m l} = \frac{E_m^i}{B_m l} \qquad (4)$$

where the integral refers to the area of the dimer or monomer bands and it represents the *integral optical density, B is the integral absorption coefficient and l the thickness of the absorbing layer*. With these notations, from the ratio of the equilibrium constants at two different temperatures one obtains:

$$2.303\,\mathrm{R}\,\lg\left[\frac{E_{d1}^i}{E_{d2}^i}\left(\frac{E_{m2}^i}{E_{m1}^i}\right)^2\right] = -E\left(\frac{1}{T_1} - \frac{1}{T_2}\right) \qquad (5)$$

Using the measurement data relation (5) was plotted, and the bound energy was determined from the slope of the straight line (Fig. 5). The bound energy of the molecules of the **4-Cl M** acid, supposed to be associated according to scheme (1), is of (10 ± 1) kcal/mol. The same value was also obtained for the molecules of the **M** acid.

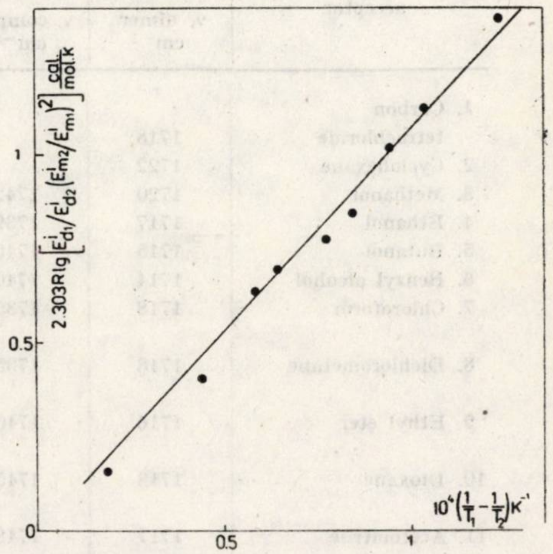

Fig. 5. — The integral extinction of C=O bands of the **4-Cl M** acid vs. temperature.

As temperature rises, the shape of the band from the range of OH valency oscillations of both compounds is modified. The intensity of the shoulder at 3535 cm^{-1} becomes higher (Fig. 3b), confirming the fact that it belongs to the OH oscillation of the carboxyl group of the monomers.

Interactions with proton acceptors and donors. The modifications produced by the third component on the C=O and OH bands of the carboxyl and hydroxyl groups of the **M** and **4-Cl M** acids have been studied. Both acids have the same behaviour and, therefore, the results obtained are presented only for the interaction with the **4-Cl M** acid. The proton donor and acceptor compounds listed in table 1 were used as third component. Table 1 includes the wave numbers of the bands of the **4-Cl M** monomer, dimer and complex in the ternary mixture, as well as the position of the C=O band of the acid in binary mixtures of various solvents.

When a proton acceptor compound is added to a binary mixture, with the equilibrium described by (1), the equilibrium is changed owing to the occurrence of a complex of the form[4]:

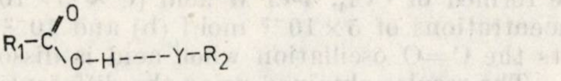

$$R_1-C\overset{\displaystyle\nearrow O}{\underset{\displaystyle\searrow O-H----Y-R_2}{}} \qquad (6)$$

The formation of the complex is revealed in the IR spectrum by occurrence of a new band, whose wave number is placed between the monomer

TABLE 1

The wave numbers of the dimer, complex and monomer of the **4-Cl M** acid in ternary mixtures and the wave numbers of the complex in binary mixtures

Proton donor or proton acceptor	Ternary mixture			Binary mixture
	ν, dimer cm^{-1}	ν, complex cm^{-1}	ν, monomer cm^{-1}	ν, complex cm^{-1}
1. Carbon tetrachloride	1718		1762	
2. Cyclohexane	1722		1762	
3. Methanol	1720	1742	1765	
4. Ethanol	1717	1739	1763	
5. Butanol	1715	1740	1761	
6. Benzyl alcohol	1714	1740	1762	
7. Chloroform	1718	1735	1762	1714 1725
8. Dichlorometane	1718	1735	1761	1722 1752
9. Ethyl eter	1716	1740	1766	1733sh 1742
10. Dioxane	1718	1745	1762	1725sh 1743
11. Acetonitrile	1717	1748	1764	1727sh 1750
12. Acrylonitrile	1717	1748	1761	1727sh 1748
13. Benzonitrile	1715	1747	1760	1727sh 1745
14. Pyridine	1716	1700 1735	1765	1712 1725
15. γ-Picoline	1718	1703 1735	1764	1710 1725
16. Dimethyl sulfoxide (DMSO)	1725	1710 1735	1765	1712 1727

sh-shoulder

and the dimer ones. The absorption intensity in this band increases when the concentration of the third component increases. At the same time, one can notice a decrease in the absorption intensity of the monomers and dimers. Also, with the temperature increase, the intensity of this band decreases owing to the hydrogen bond breaking up. Figure 1 b, c show the aspect of the C=O valency oscillation range in the ternary mixture formed of CCl_4, **4-Cl M** acid ($C \sim 5\times10^{-4}$ mol/l) and dioxane for concentrations of 5×10^{-3} mol/l (b) and 10^{-2} nol/l (c). Figure 1d represents the C=O oscillation when acid is dissolved into dioxane.

The results obtained using the differential method are in agreement with those given in table 1. At the same time, in the case of DMSO, in addition to the band at 1735 cm^{-1} assigned to the complex of type (6), there also occurs a band at 1710 cm^{-1}. The intensity of this new band depends, like the intensity of the 1735 cm^{-1} band, on the DMSO concentration in the ternary mixture. It is possible that this band belongs to the complex formed as a result of the breaking up of the intramolecular hydrogen bond, between one acid molecule and two DMSO ones linked by the two OH acid groups :

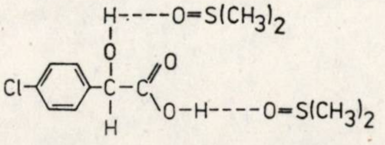

(7)

The same behaviour is noticed also when pyridine or γ-picoline is added as the third component : besides the 1735 cm^{-1} band there occurs a supplementary band at 1700 cm^{-1}. As is shown in table 1, in addition to the main peak, there also occurs a secondary peak or a shoulder when acids are dissolved in the solvents presented there. It is possible that the secondary peak may be determined by the formation of complexes of type (7).

As for the 3530 cm^{-1} band, considered to be formed by the overlapping of the OH band of the hydroxyl group and of the OH band of the carboxyl group, the results obtained in ternary mixtures support this supposition. As the concentration of the proton acceptor compound increases, there occurs the decrease in the intensity of the shoulder at 3535 cm^{-1} The band disappears at direct dissolving in the proton acceptor solvent, because the association occurs both at the OH bond of the carboxyl group and the hydroxyl group. In the ternary mixtures with pyridine or γ-picoline, with increasing concentration, the decrease of the band intensity is accompanied by its shift towards 3500 cm^{-1}.

If the third component respresents a proton donor, the occurrence of a new band is also observed, which may be assigned to a complex of the form[4] :

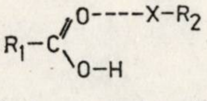

(8)

The position of the band of the complex formed is given in table 1. In this case, using the differential method, it has been noticed that the band at 3530 cm^{-1} is not affected.

ACKNOWLEDGEMENT. The author wish to thank Prof. Dr. docent C. Mihul and Dr. V. Pop for the critical reading of the manuscript and many helpful discussions.

REFERENCES

[1] N. Mori, Y. Asano, T. Irie and Y. Tsuzuki, *Bull. Chem. Soc. Japan*, **42**, 482 (1969).
[2] I. Kössler, "Methoden der Infrarot-Spektroskopie in der chemischen Analyse", Akademische Verla gsgesellschaft, Leipizig, 1961, p. 127–132, 190–198.
[3] M. M. Davies and G.B.B.M. Sutherland, *J. Chem. Phys.*, **6**, 755 (1938).
[4] M. Avram, "Spectroscopia în infraroșu. Aplicații în chimia organică", Ed. Tehnică, București, 1966, p. 446–456.

Revue Roumaine de Chimie, 25, 11–12, 1477–1483 (1980)

CALCULATIONS OF THE CHANGE IN THE GEOMETRICAL STRUCTURE OF $Cl_2C=S$ DURING THE $^1A_2 \longrightarrow {}^1A_1$ ELECTRONIC TRANSITION

A. N. ABD EL-RAHMAN and M. H. ABDALLA
Faculty of Science, Zagazig Univ., Egypt

Received May 23, 1979

The polydimensional Frank-Condon principle was applied in order to calculate the change in the geometrical structure of Cl_2 C= S during the $^1A_2 \rightarrow {}^1A_1$ electronic transition. The measured displacements in the normal coordinate were transformed into the internal coordinate. A calculated change in the C= S bond-length of 0.17 ± 0.017 A°, – 0.023 ± 0.0008 A° in the C–Cl bond length and a deformation of 3.65° ± 0.96° in the angle Cl–C–Cl were evaluated.

INTRODUCTION

The geometrical structure of an excited electronic state of a molecule differs from that of the ground state. From microwave and infrared spectra the structure of the ground state is known in the case of many simple polyatomic molecules, but structures are known only for a few molecules in their excited states.

The recent development in the evaluation of the structure of the molecules in their excited electronic states has been made by using the Frank-Condon principle.

According to this principle, the intensity distribution in a progression of bands depends on the change of the geometrical structure during the electronic transition. It is therefore expected that measurements of band intensitites could permit the calculation of this change in the structure.

Craig [1] has obtained the increase in C–C bond of benzene. Hunt [2] has given a method of calculating the change in the case of the aromatic hydrocarbons. Fujimura [3] determined the electronically excited states of conjugated molecules.

Fewer quantitative calculations have been made by using the polydimensional Frank-Condon principle in the case of polyatomic molecules.

Coon[4] has applied the method to triatomic molecules. Moule[5] has evaluated the electronic structure of formaldehyde.

In the present work the change in the geometry of thiocarbonyl chloride in the $^1A_2 \rightarrow {}^1A_1$ transition is calculated by applying the polydimensional Frank-Condon principle.

The fluorescence spectra were determined by Brand[6] who used Ar laser as a source of excitation. His measured intensities in the case of the total symmetrical modes of vibration are given in table 1.

The geometrical structure of the ground state has been determined by Carpenter[7] by using micro-wave spectroscopy.

TABLE 1

Intensities of a selected set of lines and their assignments

Intensity		Assignment		
		ν_1''	ν_2''	ν_3''
209	16	0	0	1
497	3	0	1	0
582	14	0	0	2
788	2	0	1	1
870	2	0	0	3
1134	12	1	0	0
2259	7	2	0	0
2750	8	2	1	0
3252	4	2	2	0
3376	5	3	0	0
4370	3	3	2	0

THE FRANK-CONDON RELATIONS

The interpretation of the intensity distribution in a progression of bands goes back to the original work of Frank[8] and the quantum mechanical interpretation which was made by Condon.[9] There is also a number of articles where the theory is illustrated (4, 5). In these literature data there are some useful relations which connect the ratios of the overlap integrals $R(v_i', v_i'')$ and the displacement d (in the normal coordinates). From these relations the displacements for different transitions can be given as follows:

$$d = \frac{R_{(1,\,0)}}{R_{(0,\,0)}}\left(\frac{\nu' + \nu''}{\nu''}\right)\left(\frac{h}{8\pi^2 c\,\nu'}\right)^{1/2} \tag{1}$$

$$d^2 = \frac{(\nu''/\nu')^2 + 2\,(1 + \nu''/\nu')^2\,\dfrac{R_{(2,\,0)}}{R_{(0,\,0)}} - 1}{\nu''^2/\nu'^2(8\pi^2 c\nu'/h)} \tag{2}$$

$$d^2 = \frac{\sqrt{6}\,(1 + \nu''/\nu')^2\,\dfrac{R_{(3,\,0)}}{R_{(1,\,0)}} + 3\,(\nu''^2/\nu'^2 - 1)}{\nu''^2/\nu'^2(8\pi^2 c\nu'/h)} \tag{3}$$

and

$$d = \sqrt{2}\left[\frac{(1 + \nu''/\nu')}{\nu''/\nu'}\,\frac{R_{(2,\,0)}}{R_{(1,\,0)}} + \frac{\nu''/\nu' - 1}{2(\nu''/\nu')}\,\frac{R_{(2,\,0)}}{R_{(1,\,0)}}\right](8\pi^2 c\nu'/h)^{-1/2} \tag{4}$$

where ν' and ν'' are the frequencies of the excited and the ground state measured in cm^{-1}.

The relation between the squares of the overlap integrals and the intensity of lines, in emission and absorption, was given by McCoy[10] as :

$$I_n/I_0 = \nu_n/\nu_0\left(\frac{R_n}{R_0}\right)^2 \ldots \text{absorption} \tag{5}$$

$$I_n/I_0 = (\nu_n/\nu_0)^4\ (R_n/R_0)^2 \ldots \text{emission} \tag{6}$$

where $\nu_n = (\nu_0 \pm n\nu)$ and ν is the frequency of the vibration in cm^{-1}.

RELATION BETWEEN THE NORMAL AND INTERNAL COORDINATES

The calculated displacement, in the normal coordinates, is meaningless from the physical point of view. So, the internal coordinates (bond lengths and angles) are used instead of it.

The relation connects the change in the normal coordinates (displacement without any rotation) and can be given as :

$$Q' = Q'' - d$$

where Q' and Q'' are the normal coordinates of the ground and excited state respectively.

The L matrix connects the internal symmetry coordinates S_i to the normal coordinates Q, by :

$$S'' = L''\,Q'',\ S' = L'\,Q'$$

$$\Delta L'^{-1}\,S' = L''^{-1}\,S'' - d$$

and

$$S' = L'(L'')^{-1}\,S'' - L'd$$

When the normal coordinates are taken to be parallel in the two states, then $L' = L''$

$$\Delta S' = S'' - L'd,\ S'' - S' = L'd$$

(i.e.) $\Delta S = L'd$ or $\Delta S = L''d$

Since the transformation matrix L and its transpose L^* are connected to the G matrix by :

$$LG^{-1}L^* = 1$$

and when the G matrix is chosen to be diagonal, the L matrix and its transpose must be diagonal too and the expression is obtained as follows :

$$L_i = G_i^{1/2} \quad \text{for } i = 1,\ 2,$$

$$\Delta S = G_i^{1/2}\,d \tag{7}$$

In the case of the totally symmetrical vibration the relations between the symmetry coordinates S_i and the internal coordinates R_i (for the

Y molecules) are given by Shimanouchi;[11]

$$S_1 = \frac{1}{\sqrt{2}} (R_1 + R_2) \tag{8}$$

$$S_2 = R_3 \tag{9}$$

$$S_3 = \frac{1}{\sqrt{6}} (2R_4 - R_5 - R_6) \tag{10}$$

where R_1 and R_2 correspond to the stretching of the two C—Cl bonds while R_3 corresponds to C = S stretching. R_4, R_5 and R_6 are respectively the ⌜Cl, C Cl_2 and ⌜S C Cl_1 and ⌜S C Cl_2.

If the molecule is supposed to be planar, the change in $(R_5 + R_6)$ is equal to the change in R_4 and in the opposite direction.

$$\Delta S_3 = \frac{1}{\sqrt{6}} (3R_4) \tag{11}$$

G matrix: As previously shown, the determination of the *G* matrix has a great importance in carrying on the transformation between normal and internal coordinate.

A model for the *Y* planar molecules was assumed to have a suitable set of cartesian displacement coordinates. A scheme was found and applied to solve this model — and determine the *G* matrix. This scheme is similar to that given by Brand [12] in the case of triatomic molecules. The resulting value of the *G* matrix in our case is given as:

$$G = \begin{bmatrix} 1/2(\mu_2+\mu_3)+\mu_1(1+\cos\alpha) & -\sqrt{2}\,\mu_1 \cos 1/2\alpha & -\sqrt{3}\mu_1 p_2(1+\cos\alpha) \\ -\sqrt{2}\mu_1 \cos 1/2\,\alpha & \mu_1 + \mu_4 & \sqrt{6}(\mu_1-\mu_4)p_2 \cos 1/2\alpha \\ -\sqrt{3}\,\mu_1 p_2(1+\cos\alpha) & \sqrt{6}(\mu_1-\mu_4)\,p_2 \cos 1/2\alpha & \frac{3}{2}\,p_2^2(\mu_2+\mu_3+2(\mu_1+\mu_4) \\ & & (1+\cos\alpha) \end{bmatrix}$$

where μ_1, μ_2, μ_3, μ_4 are the reciprocal masses of the atoms C, Cl, Cl, and S. p_2 is the reciprocal of the bond length (C—Cl) and α is the Cl C Cl angle.

RESULTS AND DISCUSSION

In the determination of the excited state structure the ground state structure must be known. Their values are given in table 4. Also, the assignment of the totally symmetric modes of vibrations and the intensities of the selected bands are listed in table 1.

As equation 6 applied to the data given in table 1 the squares of the overlap integrals of some relative transitions are evaluated. The ratios of the determined overlap integrals were substituted in eqs. 1—4 and the displacements are evaluated in table 2 where the intensity of a pair of

TABLE 2

Displacements measured in the normal coordinates

Band A	Band B	$d \times 10^{-20}$ $gm^{1/2}$ cm	$\bar{d}$	S.D.
(2, 0, 0)	(1, 0, 0)	0.4160861		
(2, 1, 0)	(0, 1, 0)	0.5545683	d_1 = 0.4862699	±0.0483126
(3, 0, 0)	(1, 0, 0)	0.488155		
(2, 2, 0)	(2, 0, 0)	0.512026		
(2, 1, 0)	(2, 0, 0)	0.5301334	d_2 = 0.5248254	±0.0119947
(3, 2, 0)	(3, 0, 0)	0.5343886		
(2, 2, 0)	(2, 1, 0)	0.5227537		
(0, 0, 2)	(0, 0, 1)	0.5268265		
(0, 1, 1)	(0, 1, 0)	0.8903528	d_3 = 0.6869296	±0.1855944
(0, 0, 3)	(0, 0, 1)	0.6426095		

S.D. = Standard deviation

bands different only in their ν_i assignments leads to displacement d_1 . . . etc.

To illustrate the applicable of the Frank-Condon principle the intensity of the 0 → 0 transition was considered theoretically equal to 10 units. A set of calculated band intensities and that measured by Brand [6] against the frequencies (cm^{-1}) are shown in figure 1. Both curves have the same shape with slight difference in the intensities indicating that the proposed value of the 0 → 0 transition is somewhat greater than its actual value.

In order to evaluate the change in the structure in the internal coordinates (bond lengths and angles) instead of the previously calculated ones in the normal coordinates the transformation procedure must be applied.

A convenient simplification is obtained by neglecting the off diagonal elements of the *G* matrix. In this event the 1st mode of vibration would be a pure C—Cl stretching, the 2nd mode would be a pure C=S stretching and the third one a pure Cl C Cl deformation. This simplification gives a result which is approximately the same as in applying the one-dimensional Frank-Condon principle.

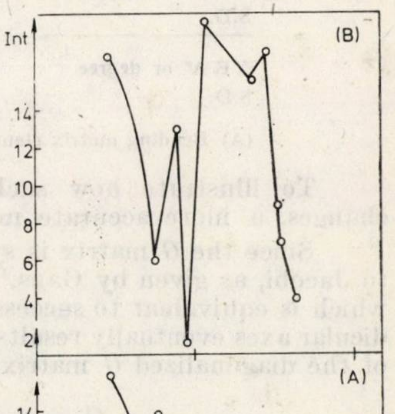

Fig. 1. — The relation between the observed intensities (A) and the calculated ones (B) against frequencies.

In table 3 the diagonal elements of the G matrix are given each for the corresponding mode of vibration.

Substituting in eq. 7 the calculated changes are measured in the symmetry coordinates. The last step is achieved by applying eqs. 8–11 and consequently the measured changes in symmetry coordinates are obtained in internal coordinates.

TABLE 3

Change in the geometrical structure measured in the different coördinates

Mode	C= S	C−Cl	⌜Cl−C−Cl
	ν_2	ν_1	ν_3
ν'' $X\,(^1A_1)$	1139	503.5	288
ν' $A\,(^1A_2)$	907.4	480	245
$d \times 10^{-20}$ gm$^{1/2}$ cm	0.4862699	0.5248554	0.6869296
S.D.	±0.0483126	±0.0119947	±0.1855944
$G \times 10^{22}$ gm^{-1} (A)	6.9	4.925	15.8
Δ S A° or degree	0.127	0.1165	8.976
S.D.	±0.0107	±0.00266	±2.44
Δ R A° or degree	0.127	0.0824	7.33°
S.D.	±0.0107	±0.00188	±1.99°

(A) Bending matrix element scaled by the factor R(C−Cl).

To illustrate how such a simplification affects the calculated changes, a more accurate method was applied.

Since the G matrix is symmetric, the commonly used method due to Jacobi, as given by Gans,[13] was used. This orthogonal transformation which is equivalent to successive rotations about three mutually perpendicular axes eventually results in a diagonal matrix. The numerical values of the diagonalized G matrix were found to be

$$G_{\text{diag.}} \simeq [1.587 \quad 12.757 \quad 3.69]$$

The change in the internal coordinate using both the accurate and the approximate methods are given in table 4, in addition to the calculated values of the change in the internal coordinates for the same molecule as given by Brand [14] and Lombardi. [15]

The sign of the change in the internal coordinate is indeterminate because the elements are derived from the square roots of the G matrix and also, from the square roots of the relative Frank-Condon factors and hence eight possible sign combinations may be obtained. Perhaps the most difficult aspect of a polydimensional Frank-Condon calculation is the selection of the correct combination, since the choice must be based on information drawn from a variety of outside sources. Here in our case, since the thiophosgene is chemically analogous to formaldehyde the set

TABLE 4

Structural parameters of thiophosgene in the ground and excited state

Method	Mode		
	C=S	C−Cl	⌜Cl−C−Cl
1. Ground state	1.601	1.7286	111.19°
2. Excited state			
a. Approximate method	+0.127	−0.041	+7.33°
	±0.0107	±0.0009	±1.99°
b. Accurate method	+0.17	−0.023	+3.65°
(Jacobi)	±0.017	±0.0008	±0.96°
c. Brand et al.	+0.1	+0.022	+8°
d. Lombardi	+0.1	−0.01	+1°

(+ − +) was selected similar to that given by Moule[5] in the case of formaldehyde.

The data given in table 4 indicate that our calculated results by the simplification method are comparable to those given by Brand[14] using also Frank-Condon principle. On the other hand, the results obtained after applying the Jacobi refine method are nearly those given by Lombardi[15] using the analysis of rotational structure. He based his calculations on assuming that the change in the C=S band to be equal to that given by Brand. This may indicate the reason why his results did not coincide with ours.

ACKNOWLEDGEMENT. The authors wish to express their gratitude to Prof. Dr. M. I. Nasser "National Research Center, Cairo, Egypt" for his valuable discussions and suggestions.

REFERENCES

[1] D. P. Craig, *J. Chem. Soc.*, **1950**, 2146.

[2] G. R. Hunt, E. F. McCoy, and I. G. Ross, *Austral J. Chem.*, **18**, 591 (1962).

[3] Y. Fujimura, and H. Ymaguchi, *Bull. Chem. Soc. Japan*, **46**, 2034 (1973).

[4] J. B. Coon, R. E. Dewandes, and C. M. Loyed, *J. Mol. Spec.*, **8**, 285 (1962).

[5] D. C. Moule, Edited by J. R. Buring, "Vibration Spectra and Structure", Vol. 6, 1977, p. 228.

[6] J.C .D. Brand, J. L. Hardwick, and K. E. Teo, *J. Mol. Spec.*, **57**, 215 (1975).

[7] J. H.Carpenter, D. F. Rimmer, J. G. Smith, and D. H. Whiffen, *J. Chem. Soc. Faraday Transact.*, **2**, 1752 (1975).

[8] J. Frank, *Trans. Farad. Soc.*, **21**, 536 (1925).

[9] E. U. Condon, *Phys. Rev.*, **32**, 858 (1928).

[10] E. F. McCoy, and L. G. Ross, *Austral. J. Chem.*, **15**, 573 (1962).

[11] T. Shimanouchi, and I. Suzuki, *J. Chem. Phys.*, **42**, 296 (1965).

[12] J.C.D. Brand, and J. C. Spenkman, "Molecular Stucture, The Physical Approach", Edward Arnold, London, 1975.

[13] P. Gans, "Vibrating Molecules", Chapman & Hall, London, 1971.

[14] J.C.D. Brand, J.H. Callomon, D.C. Moule, J. Tyrrell, and T. H. Goodwin, *Trans. Faraday. Soc.*, **61**, 2356 (1965).

[15] G. R. Lombardi, *J. Chem. Phys.*, **52**, 6126 (1970).

Revue Roumaine de Chimie, **25**, *11–12*, 1485–1487 (1980)

MÖSSBAUER SPECTROSCOPY INVESTIGATIONS OF IRON IN SOME PENTACOORDINATE COMPLEXES

D. BARB *, L. DIAMANDESCU *, V. ZNAMIROVSCHI **, D. CIURCHEA **, R. SEMENIUC**

* Institute of Physics and Technology of Materials P.O. Box 5207, Bucharest, Romania
** Faculty of Physics, Babeş-Bolyai University Cluj-Napoca, Romania

Received October 17, 1979

Several iron pentacoordinate complexes were studied by means of Mössbauer spectroscopy. Taking into account the isomer shift values, the covalency degree was evaluated for the investigated complexes. A possible explanation of covalency degree found in the studied complexes is proposed.

The isomer shift, the quadrupole splitting and the magnetic splitting derived from Mössbauer spectra may provide information about the valency states, the nature of chemical bonding, the origin of hyperfine magnetic fields at the Mössbauer nucleus.

In this paper we present some preliminary results obtained in the study of some pentacoordinate complexes by means of Mössbauer spectroscopy.

The following complexes were investigated :

dipyridinium iron (III) pentachloride . . .$(pyH)_2^+(FeCl)^{--}$
β – methyl dipicolinium iron (III) pentachloride. . .$(\beta picH)_2^+(FeCl_5)^{--}$
γ – methyl dipicolinium iron (III) pentachloride. . .$(\gamma picH)_2^+(FeCl_5)^{--}$

The first complex was synthesized in 1974 by Sharma,[1] the other two were prepared by us following the same method (the organic base, pyridine or picoline, was treated with concentrated HCl and then refluxed, for three hours, with $FeCl_3$).

Elementary analysis, made by classical methods, leads to the following results for $(\beta\text{-picH})_2\,FeCl_2$: % Fe calculated 13.31 and found 13.52 ; % Cl calculated 42.32 and found 42.51 ; % N calculated 6.67 and found 6.41 ; m.p. °C = 114–116. For $(\gamma\text{-picH})_2\,FeCl_5$: % Fe calculated 13.31 and found 13.61 ; % Cl calculated 42.32 and found 42.72 ; % N calculated 6.67 and found 6.45 ; m.p. °C = 115–117.

The Mössbauer spectra were measured with an ELRON type Mössbauer spectrometer using a 10 mCi $^{57}Co(Cu)$ source. The spectrometer calibration was performed in a constant acceleration mode using a mixture of Fe_2O_3 and sodium nitroprusside. The experimental spectra were fitted by means of a FORTRAN IV program on an IBM 370/135 type computer. All

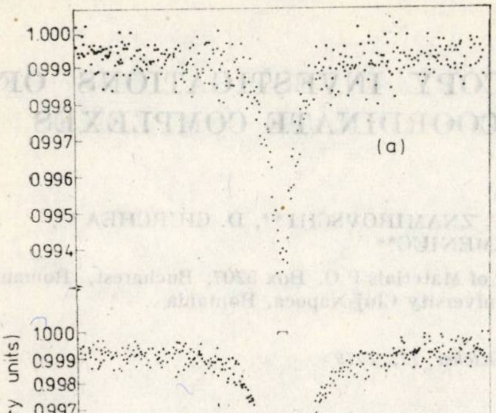

Fig. 1. — Mössbauer spectra of the investigated samples: a) $(pyH)_2^+(FeCl_5)^{--}$ b) $(\beta\, picH)_2^+(FeCl_5)^{--}$ c) $(\gamma\, picH)_2^+(FeCl_5)^{--}$

complexes were measured at room temperature. In figure 1 the Mössbauer spectra of the above mentioned complexes are shown. The parameters obtained after the computer analysis are included in table 1. The isomer shift is reported relative to Fe in Cu source. One can observe the absence of magnetic hyperfine splitting for all three spectra. In the case of $(pyH)_2^+(FeCl_5)^{--}$ complex the quadrupole splitting and the isomer shift are equal to zero, indicating a spherical symmetry in the Fe^{3+} environment. For the other two compounds the isomer shift is negative, indicating an increase of the electronic charge density at the Mössbauer nucleus.

Using M. O. data, Danon[2] studied the dependence of the isomer shift on covalency degree for some iron complexes. From his graphs we have appreciated the covalency degree[2,5] of our complexes as follows:

a) $(pyH)_2^+(FeCl_5)^{--}$ 42%

b) $(\beta picH)_2^+(FeCl_5)^{--}$ 50%

c) $(\gamma picH)_2^+(FeCl_5)^{--}$ 52%

This increase of covalency degree might be due to the methyl group (present in the last two compounds) by creating a polarisation of π cloud electrons of pyridinium ion to nitrogen atom. This leads to a decrease of the ionic character of chemical bonding between

TABLE 1

Mössbauer parameters of the investigated samples

Sample	Isomer shift (mm/s)	Quadrupolar splitting (mm/s)	Effect (%)	Line width (mm/s)
$(pyH)_2^+(FeCl_5)^{--}$	-0.000 ± 0.001	0.000 ± 0.002	0.71 ± 0.03	0.303 ± 0.011
$(\beta picH)_2^+(FeCl_5)^{--}$	-0.098 ± 0.005	0.196 ± 0.004	1.01 ± 0.04	0.308 ± 0.005
$(\gamma picH)_2^+(FeCl_5)^{--}$	-1.104 ± 0.024	0.174 ± 0.002	0.62 ± 0.01	0.280 ± 0.001

$(FeCl_5)^{--}$ and 12 $(picH)^+$ ions ; that means an increase of covalency degree between these two ions.

For the last two compounds the quadrupole splitting is different from zero, being characteristic for the Fe^{3+} in a non-spherical symmetry.

In the case of pentacoordinate compounds MX_5, the five donor atoms can lead to the D_{3h} or C_{4v} symmetry .[4] From Furlani's [4] calculations the D_{3h} symmetry seems to be the most probable one in the case of $(FeCl_5)^{--}$ ion.

Taking into account the small value of $10Dq$ for Cl^- ion it results a high spin state for the iron ion in these compounds. This assumption was confirmed by EPR measurements. Further studies are in progress.

REFERENCES

[1] R. K. Sharma and N. Kumar, *J. Inorg. Nuclear Chem.*, **36**, 1172 (1974).

[2] J. Danon, "Applications of the Mössbauer Spectroscopy in Chemistry and Solid State Physics", Int. At. En. Agency, Vienna, 1966, p. 89.

[3] D. Barb, "Efectul Mössbauer și aplicațiile sale", Editura Academiei, București, 1972.

[4] C. Furlani, *Coord. Chem.*, **3**, 141 (1968).

Revue Roumaine de Chimie, 25, *11–12*, 1489–1498 (1980)

TRANSITION METAL COMPLEXES OF ORGANOTHIO-PHOSPHORUS LIGANDS. VII[a]

AMINE ADDUCTS OF DI(α- AND β-NAPHTHYL)PHOSPHORODITHIOATO NICKEL (II)

RODICA MICU-SEMENIUC, CRISTINA OPRIŞ and IONEL HAIDUC *
Chemistry Department, Babeş-Bolyai University R-3400 Cluj-Napoca, Romania

Received February 14, 1980

Nickel(II)bis di(α- and β-naphthyl)phosphorodithioates form six-coordinate adducts with several amines (pyridine, picolines, 2,2'- and 4,4'-dipyridyl, *o*-phenantroline, ethylenediamine, propylenediamine, *o*- and *p*-phenylenediamine and benzidine). While pyridine and the picolines form *trans*-octahedral complexes, the diamines exhibit a more diversified behaviour. Thus, 2,2'-dipyridyl, *o*-phenantroline, ethylenediamine, propylenediamine and *o*-phenylenediamine coordinate as bidentate ligands, thereby forcing the phosphorodithioato ligand to liberate some of the coordination sites at nickel and to become monodentate or even anionic.

INTRODUCTION

Transition metal complexes of phosphorodithioic acids[1] focused uninterupted interest in recent years. Particularly, the formation of six- and five-coordinate adducts and some structural peculiarities (e.g. the non-equivalence of Ni-S and P–S bonds in some phosphorodithioatonickel(II)-amine adducts[2–5]) are points of special interest. The **O,O-*dialkyl*** esters of phosphorodithioic acids, their transition metal complexes and their adducts with various donors, have been widely investigated in the literature (see [1] and references cited therein). Much less effort was spent for the investigation of the **O,O-*diaryl*** esters and their complexes. Thus, A. I. Busev et al.[6] reported the formation of pyridine adducts of $M[S_2P(OPh)_2]_2$ complexes, where $M = Co(II), Ni(II), Zn(II)$ and $Cd(II)$, but these authors suggested that the diphenylphosphorodithioato group is anionic. A more detailed study of the bis(diphenylphosphorodithioato) nickel(II) with a series of amines [7,8] showed that the $(PhO)_2PS_2$ groups are coordinated to nickel(II) either as mono- or bidentate ligands.

In this work we report the results of the investigation of some O,O-bis(α- and β-dinaphthylphosphorodithioato)nickel(II) amine adducts.

---

[a] Part VI : R. Micu-Semeniuc, L. Dumitrescu-Silaghi, N. Chirilă and I. Haiduc, *Rev. Roumaine Chim.*, **25,** 1025 (1980).

* Author to whom all the correspondence should be addressed.

The phosphorodithioic acid O-,O-di(α- and β-naphthyl)-esters and their nickel(II) complexes have been described in the literature.[9-11] Amine adducts of these complexes have not been reported so far.

EXPERIMENTAL

REAGENTS AND PROCEDURES

The chemicals used were of reagent grade purity and were used as received from commercial sources, except for the O,O-di(α- and β-naphthyl)esters of the phosphorodithioic acid, which were prepared according to the literature.[9-11] The adducts prepared have been characterized by elemental analysis, electronic and infrared spectra. The nickel content was determined as Ni(II) dimethylglyoximate, phosphorus as ammonium 12-molybdophosphate (gravimetrically) and the nitrogen by combustion. Some of the adducts exhibit a remarkable stability. For their decomposition and solubilization of nickel(II) ions it was necessary to use strongly oxidizing concentrated acid mixtures ($HClO_4 + H_2SO_4 + HNO_3$ or $HNO_3 + H_2SO_4$) or either ammonium persulfate or ammonium hydrogen sulfate melts. During this treatment the metal was partly oxidized to Ni(III), resulting in the negative errors. The electronic spectra were recorded on a Specord UV—VIS Carl Zeiss Jena, DDR instrument and the infrared spectra on a UR-20 Carl Zeiss Jena, DDR spectrophotometer (in the range 4,000—400 cm^{-1}).

PREPARATION OF THE ADDUCTS

The adducts were prepared by the reaction of bis(di-α- and β-naphthyl)phosphorodithioato nickel(II), abbreviated Ni(α-dtp)$_2$ and Ni(β-dtp)$_2$, and a series of organic bases, containing either the $-NH_2$ group or tertiary nitrogen, including pyridine (py), 2-, 3- and 4-methylpyridines (2-, 3- and 4-pic), 2,2′-and 4,4′-dipyridyl (2,2′-and 4,4′-dipy), 1,10-phenantroline (phen). *iso*-butylamine (*i*-bu), 1,2-ethylenediamine (enda), 1,3-propanediamine (pnda), *ortho*- and *para*-phenylenediamine (*o*- and *p*-PHDA) and benzidine (bzd).

The adducts were prepared by one of the two following procedures:

(a) mixing of solutions containing stoichiometrically equivalent amounts of reagents in 1 Ni : 2 L molar ratio (L = organic ligand), in various solvents (method A); and

(b) grinding together stoichiometric amounts of the reagents, in solid state, without solvent, followed by the extraction of the complex with anhydrous ether or petroleum ether and acetone (method B).

In some cases the adducts obtained by method *A* were semisolids or viscous oils, which solidified on treatment with small amounts of water or petroleum ether. The conditions used for each compound are listed in table 1. Analytical data for the compounds prepared are given in table 2.

RESULTS AND DISCUSSION

The compounds prepared in this work are listed in table 1. The usual combination ratios Ni(dtp)$_2$: L are 1 : 2 for monofunctional and some of difunctional amines, but compounds with ratio Ni(dtp)$_2$: L = 1 : 1 were obtained for L = 4,4′-dipy (compound **13**), phen (compound **15**), *p*-PHDA (compound **21**) and bzd (compound **23**). In one case a 1 : 3 compound Ni (β-dtp)$_2$ .2,2'-dipy$_3$ (compound **11**) has been obtained. With *o*-PHDA only the adduct with Ni(α-dtp)$_2$ could be isolated (compound **20**), and with bzd only the adduct with Ni(β-dtp)$_2$ (compound **23**). It should be mentioned that with phen and *p*-PHDA, the combination ratios with Ni(α- and β-dtp)$_2$ are different (compare compounds **14**—**15** and

TABLE 1

Preparation of bis(di-α-and β-naphthyl)phosphorodithioato nickel(II) — amine adducts

No.	Compound	Reagents used (method)[a]	Form of separation[b]	Solvent[c]	Colour of the comp.	MP °C (dc)[d]
1	2	3	4	5	6	7
1.	Ni(α-dtp)$_2$.py$_2$	I+py(A)	ws	CHCl$_3$—PE	green	(185) 198
2.	Ni(β-dtp)$_2$.py$_2$	II+py(A)	pp	CHCl$_3$	green	(180) 205—207
3.	Ni(α-dtp)$_2$.2-pic$_2$	I+2-pic(A)	ws	CHCl$_3$—PE	brown	(185)
4.	Ni(β-dtp)$_2$.2-pic$_2$	II+2-pic(A)	pp	CNCl$_3$—PE	yellow	109—111
5.	Ni(α-dtp)$_2$.3-pic$_2$	I+3-pic(A)	ws	CHCl$_3$-ether	green	(220)
6.	Ni(β-dtp)$_2$.3-pic$_2$	II+3-pic(A)	pp	CHCl$_3$	green	(200)
7.	Ni(α-dtp)$_2$.4-pic$_2$	I+4-pic(A)	ws	CHCl$_3$-acetone	green	(225)
8.	Ni(β-dtp)$_2$.4-pic$_2$	II+4-pic(A)	pp	CHCl$_3$	green	224 (212)
9.	Ni(α-dtp)$_2$.2,2′-dipy$_2$	I+2,2′-dipy(B)	ws	acetone PE	beige	115—117
10.	Ni(β-dtp)$_2$.2,2′-dipy$_2$	II+2,2′-dipy(A)	pp[e]	CHCl$_3$-ether	green	(190)
11.	Ni(β-dtp)$_2$.2,2′-dipy$_3$	same	ws	ether	pink	182
12.	Ni(α-dtp)$_2$.4,4′-dipy$_2$	I+4,4′-dipy(B)	pp	ether	green	(215) 247
13.	Ni(β-dtp)$_2$.4,4′-dipy	II+4,4′-dipy(A)	pp	CHCl$_3$	green	(250—256)
14.	Ni(α-dtp)$_2$.phen$_2$	I+phen (B)	pp	PE	beige	135
15.	Ni(β-dtp)$_2$.phen	II+phen(A)	ws[f]	CHCl$_3$—PE	green	(200)
16.	Ni(α-dtp)$_2$.*i*-bu$_2$	I+*i*-bu (A)	pp	ether	green	175—180
17.	Ni(α-dtp)$_2$.enda$_2$	I+enda(A)	pp	ether	pink	199 (205)
18.	Ni(β-dtp)$_2$.enda$_2$	II+enda(A)	ws	water	mauve	135—140
19.	Ni(β-dtp)$_2$.pnda$_2$	II+pnda(A)	ws	CHCl$_3$—water	mauve	
20.	Ni(α-dtp)$_2$.*o*-PHDA$_2$	I+*o*-PHDA(A)	ws	acetone-water	green	145
21.	Ni(α-dtp)$_2$.*p*-PHDA	I+*p*-PHDA(B)	pp	ether	green	170
22.	Ni(β-dtp)$_2$.*p*-PHDA$_2$	II+*p*-PHDA(A)	ws	CHCl$_3$—PE	green	94
23.	Ni(α-dtp)$_2$.bzd	I+bzd(B)	pp	ether	green	(112) 125

a) I=Ni[S$_2$P(OC$_{10}$H$_7$—α)$_2$]$_2$; II = Ni[S$_2$P(OC$_{10}$H$_7$—β)$_2$]$_2$
A and B are the two preparation methods

b) pp=precipitate ; ws=waxy semisolid

c) Solvent used for extraction or treatment of the waxy semisolids ; PE=petroleum ether

d) Decomposition temperatures are given in parentheses

e) A green chloroformic solution and a pink waxy solid were obtained simultaneously.

f) The green chloroformic solution transformed into a green waxy solid from which the adduct can be extracted with petroleum ether.

21—22). These apparent irregularities cannot be explained in a straightforward manner at this stage.

The compounds listed in table 1 are fairly stable and can be stored for long time without any apparent decomposition. They are soluble in chloroform and in some other common organic solvents. The adducts

TABLE 2

Results of elemental analysis

No.	Compound	Composition					
		%Ni		%P		%N	
		Found	calcd.	found	calcd	found	calcd
1.	Ni(α-dtp)$_2$.py$_2$	5.42	5.99	6.49	6.34	2.96	2.86
2.	Ni(β-dtp)$_2$.py$_2$	5.34	5.99	6.21	6.34	2.72	2.86
3.	Ni(α-dtp)$_2$.2-pic$_2$	5.65	5.83	6.03	6.16	2.53	2.78
4.	Ni(β-dtp)$_2$.2-pic$_2$	5.52	5.83	6.39	6.16	2.43	2.78
5.	Ni(α-dtp)$_2$.3-pic$_2$	5.74	5.83	5.78	6.16	2.52	2.78
6.	Ni(β-dtp)$_2$.3-pic$_2$	5.25	5.83	6.34	6.16	2.56	2.78
7.	Ni(α-dtp)$_2$.4-pic$_2$	5.95	5.83	6.20	6.16	2.90	2.78
8.	Ni(β-dtp)$_2$.4-pic$_2$	5.69	5.83	5.97	6.16	3.01	2.78
9.	Ni(α-dtp)$_2$.2,2′-dipy$_2$	4.82	5.16	5.18	5.47	4.70	4.94
10.	Ni(β-dtp)$_2$.2,2′-dipy$_2$	5.32	5.16	5.32	5.47	4.81	4.94
11.	Ni(β-dtp)$_2$.2,2′-dipy$_2$	4.34	4.55	4.39	4.78	—	
12.	Ni(α-dtp)$_2$.4,4′-dipy$_2$	4.87	5.16	5.03	5.47	4.88	4.94
13.	Ni(β-dtp)$_2$.4,4′-dipy	5.52	6.01	5.98	6.34	3.01	2.86
14.	Ni(α-dtp)$_2$.phen$_2$	4.45	4.82	4.93	5.09	4.80	4.74

TABLE 2 (continued)

No.	Compound	Composition					
		%Ni		%P		% N	
		found	calcd	found	calcd	found	calcd
15.	$\mathrm{Ni(\beta\text{-}dtp)_2\cdot phen}$	5.43	5.75	6.12	6.08	3.01	2.80
16.	$\mathrm{Ni(\alpha\text{-}dtp)_2\cdot}\,i\text{-}\mathrm{bu_2}$	5.60	6.07	6.03	6.41	2.85	2.89
17.	$\mathrm{Ni(\alpha\text{-}dtp)_2\cdot enda_2}$	5.85	6.24	6.23	6.59	5.75	5.95
18.	$\mathrm{Ni(\beta\text{-}dtp)_2\cdot enda_2}$	5.92	6.24	6.31	6.59	6.25	5.95
19.	$\mathrm{Ni(\beta\text{-}dtp)_2\cdot pnda_2}$	5.95	6.05	6.35	6.40	5.60	5.78
20.	$\mathrm{Ni(\alpha\text{-}dtp)_2\cdot}\,o\text{-}\mathrm{PHDA_2}$	4.98	5.66	5.53	5.98	5.65	5.40
21.	$\mathrm{Ni(\alpha\text{-}dtp)_2\cdot}\,p\text{-}\mathrm{PHDA}$	5.80	6.30	6.23	6.60	3.28	3.01
22.	$\mathrm{Ni(\beta\text{-}dtp)_2\cdot}\,p\text{-}\mathrm{PHDA_2}$	5.48	5.66	5.66	5.98	5.68	5.40
23.	$\mathrm{Ni(\alpha\text{-}dtp)_2\cdot bzd}$	5.32	5.86	5.82	6.17	3.02	2.79

containing polycyclic ligands with tertiary nitrogen are less soluble than those containing primary amino groups. Some of them exhibit well-defined melting points, while others decompose before melting (see Table 1).

The electronic spectra of the adducts differ significantly from those of the parent Ni(II)phosphorodithioates [11] because of the changes in the local symmetry of the central atom, by coordination of the organic bases (Table 3). Thus, the pyridine and 2-, 3- and 4-methylpyridine adducts exhibit two bands in the visible range of the spectrum and these are assigned to the ν_2 and ν_3 transitions of the nickel(II) ion (Table 3). With the aid of the graphical method[12] the parameters Dq, B' and β were calculated from the spectra. Since the band due to the first transition (ν_1) could not be recorded with our equipment, by the calculation of the 10 Dq parameter, an estimation of the crystal field strength around the Ni(II) is, however, possible indirectly.

TABLE 3

Electronic spectra and ligand field parameters of the adducts (cm^{-1})

Compound [a)]	${}^3T_{1g}(F) \leftarrow$ $\leftarrow {}^3A_{2g}(F)$ ν_2	${}^3T_{1g}(P) \leftarrow$ $\leftarrow {}^3A_{2g}(F)$ ν_3	B'	Dq	β
1. Ni(α-dtp)$_2$.py$_2$	13,300	22,000	702	842	0.66
2. Ni(β-dtp)$_2$.py$_2$	13,400	22,000	698	851	0.66
3. Ni(α-dtp)$_2$.2-pic$_2$	13,000	21,200	658	822	0.63
4. Ni(β-dtp)$_2$.2-pic$_2$	13,000	21,500	686	823	0.65
5. Ni(α-dtp)$_2$.3-pic$_2$	13,300	22,000	702	842	0.66
6. Ni(β-dtp)$_2$.3-pic$_2$	13,300	22,000	702	842	0.66
7. Ni(α-dtp)$_2$.4-pic$_2$	13,300	22,000	702	842	0.66
8. Ni(β-dtp)$_2$.4-pic$_2$	13,400	22,000	698	851	0.66
16. Ni(α-dtp)$_2$.*i*-bu$_2$	13,000	22,000	746	820	0.72

a) The numbering of the compounds is the same as in tables 1 and 2.

The data in table 3 show that the crystal field parameter is in the range 8,200 – 8,500 cm^{-1}, where the first transition is expected. The interelectronic repulsion parameter B' has much lower value than in the free ion, thus suggesting an appreciable degree of covalent bonding in the adducts (the β values lie between 0.66 and 0.72).

The coordination of the phosphorodithioato groups is also confirmed by the UV spectra of the adducts. The charge transfer bands of the free acids (O,O(α- and β-dinaphthylphosphorodithioic)) occur at the following positions in the spectrum (kK):

$(\alpha\text{-}C_{10}H_7O)_2P(S)SH$: 30.8 32.9 34.5.

$(\beta\text{-}C_{10}H_7O)_2P(S)SH$: 31.4 32.0 32.9 34.8 sh 36.0 and 37.4 sh.

In the adducts the intensity of these bands is enhanced and shifted towards higher energies. Thus, the 34.5 kK band of di-α-naphthylphosphorodithioic acid appears in the adducts at 34.5 – 35.5 kK. Two additional bands occur at 36.2 and 37.9 kK. In the adducts derived from di-β-naphthylphosphorodithioic acid the first three bands of the acid are combined into a single, broader band, located at 31.2 – 31.5 kK; the shoulder at 37.4 kK becomes an intense band and new shoulders appear on the absorption curve in the range 38.0 – 39.0 kK.

The infrared spectra of the adducts exhibit also obvious changes compared with the parent nickel(II) phosphorodithioates. The changes in the frequency range due to $\nu(PS_2)$ can give some information about the coordination of the phosphorodithioate ligand. In addition, the infrared spectra of the adducts containing primary amino groups, give information about the coordination of the NH_2 groups. The results are summarized in tables 4 and 5.

In the adducts the $\nu_{as}(PS_2)$ is shifted towards higher energies, as a result of weakening the Ni-S bond and strengthening the P – S bond. In the range of $\nu_s(PS_2)$ a doublet is observed, which is similarly shifted towards higher wave numbers (Table 4). The data suggest *bidentate* coordination of the phosphorodithioato ligands, with the formation of a

NiS_4N_2 chromophore, in the adducts of Ni(α-dtp)$_2$ with pyridine, 2-, 3- and 4-methylpyridines and 4,4′-dipyridyl. In the adduct with 2,2′- dipyridyl the phosphorodithioato group should be *monodentate*, with the formation of a NiS_2N_4 chromophore, since the organic base forms five-membered chelate ring. The *o*-phenanthroline adduct (compound **14**) exhibits an increased number of bands in this range, suggesting that the phosphorodithioato ligands are bonded in different ways (Table 4): one of them is bidentate and maintains the NiS_2P four-membered chelate ring, while the second is in anionic form and not directly attached to nickel. The chromophore is also NiS_2N_4.

In the adducts obtained from Ni(β-dtp)$_2$ (Table 4) the $\nu_{as}(PS_2)$ bands are shifted towards higher values than in the parent complex, but these shifts are smaller than for the adducts derived from Ni(α-dtp)$_2$. The pyridine, 2-, 3- and 4-methylpyridine derivatives behave similarly to those obtained from Ni(α-dtp)$_2$, discussed above. The adduct containing two molecules of 2,2'-dipyridyl (compound **10**) behaves differently: the first phosphorodithioato ligand is bidentate, while the second is anionic and not coordinated; the chromophore is NiS_2N_4. In the adduct Ni(β-dtp)$_2$. 2,2'-dipy$_3$ (compound **11**) both phosphorodithioato groups are anionic, and the compound should be written as [Ni(2,2′-dipy)$_3$](β-dtp)$_2$.

In Ni (β-dtp)$_2$ .4,4′-dipy (compound **13**), containing only one molecule of organic ligand, both phosphorodithioato groups are bidentate and the chromophore is NiS_4N_2; this compound is probably a polymer (*A*), while the *o*-phenantroline adduct is a six-coordinate monomer (*B*):

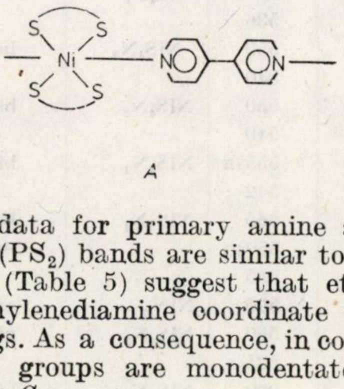

A

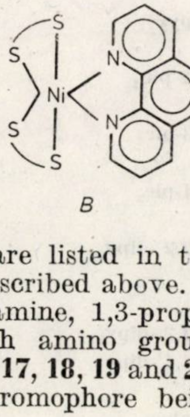

B

The data for primary amine adducts are listed in table 5. The shifts of ν (PS$_2$) bands are similar to those described above. The values of ν(NH$_2$) (Table 5) suggest that ethylenediamine, 1,3-propanediamine and *o*-phenylenediamine coordinate with both amino groups forming chelate rings. As a consequence, in compounds **17, 18, 19** and **20** phosphorodithioato groups are monodentate, the chromophore being NiS_2N_4, as shown in *C*:

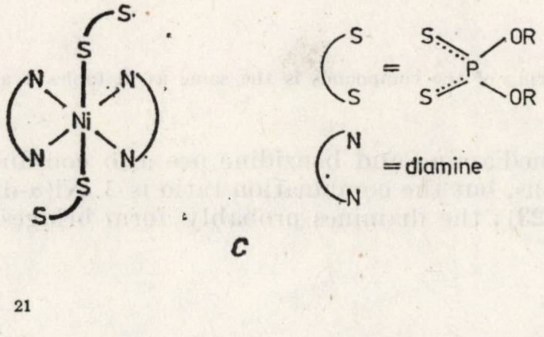

C

TABLE 4

Infrared spectra in the range of $\nu(PS_2)$ frequencies of the adducts with tertiary amines (cm^{-1})

Compound[a]	$\nu_{as}(PS_2)$	$\nu_s(PS_2)$	Chromophore	Bonding of the dtp ligand
Ni(α-dtp)₂(ref. 11)	660	525	NiS_4	bidentate
1. Ni(α-dtp)$_2$·py$_2$	680	575 548	NiS_4N_2	,,
3. Ni(α-dtp)$_2$.2-pic$_2$	682	575 545	NiS_4N_2	,,
5. Ni(α-dtp)$_2$.3-pic$_2$	686	575 560	NiS_4N_2	,,
7. Ni(α-dtp)$_2$.4-pic$_2$	686	575 550	NiS_4N_2	,,
9. Ni(α-dtp)$_2$.2,2′-dipy$_2$	687	575 550sh	NiS_2N_4	monodentate
12. Ni(α-dtp)$_2$.4,4′-dipy$_2$	685	575	NiS_4N_2	bidentate
14. Ni(α-dtp)$_2$·phen$_2$	686 670	574 550 530	NiS_2N_4	bidentate + anionic
Ni(β-dtp)₂(ref. 11)	665	545	NiS_4	bidentate
2. Ni(β-dtp)$_2$·py$_2$	676	555 536	NiS_4N_2	bidentate
4. Ni(β-dtp)$_2$.2-pic$_2$	675	550 540	NiS_4N_2	bidentate
6. Ni(β-dtp)$_2$.3-pic$_2$	674	550 540sh	NiS_4N_2	bidentate
8. Ni(β-dtp)$_2$.4-pic$_2$	670	555sh 542	NiS_4N_2	bidentate
10. Ni(β-dtp)$_2$.2,2′-dipy$_2$	685 670	565 550sh 535	NiS_2N_4	bidentate + anionic
11. Ni(β-dtp)$_2$.2,2′-dipy$_3$	685	565	NiN_6	anionic
13. Ni(β-dtp)$_2$.4,4′-dipy	671	560 535	NiS_4N_2	bidentate
15. Ni(β-dtp)$_2$·phen	670	560 540	NiS_4N_2	bidentate

---

[a] The numbering of the compounds is the same as in tables 1 and 2.

p-Phenylenediamine and benzidine are also coordinated with both nitrogen functions, but the combination ratio is 1 Ni(α-dtp)$_2$: 1 L (compounds **21** and **23**) ; the diamines probably form bridges in a polymeric structure (*D*) :

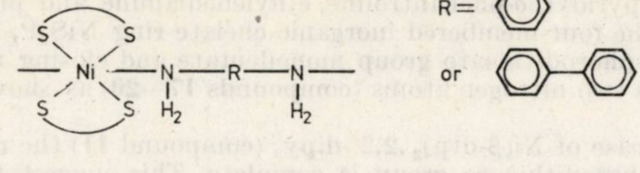

D

In the adduct Ni(β-dtp)$_2$.*p*-PHDA$_2$ (compound **22**) each diamine molecule is bonded to nickel only through one amine group, while the second one remains free (structure *E*); this is clearly suggested by the presence of four ν(NH$_2$) bands in the infrared spectrum, as expected for the presence of two nonequivalent amine groups (Table 5).

TABLE 5

Infrared spectra of primary amine adducts (cm^{-1})

Compound[a]	$\nu_{as}(PS_2)$	$\nu_s(PS_2)$	$\nu_a(NH_2)$	$\nu_s(NH_2)$	Observations	
					Chromoph.	Ligand
17. Ni(α-dtp)$_2$.enda$_2$	685	570	3315	3260	NiS_2N_4	monodentate
18. Ni(β-dtp)$_2$.enda$_2$	675	572	3320	3278	NiS_2N_4	monodentate
19. Ni(β-dtp)$_2$.pnda$_2$	675	562	3300	3250	NiS_2N_4	monodentate
20. Ni(α-dtp)$_2$.*o*-phda$_2$	685	575 549	3280	3200	NiS_2N_4	monodentate
21. Ni(α-dtp)$_2$.*p*-PHDA	682	575 547	3340	3275	NiS_4N_2	bidentate
22. Ni(β-dtp)$_2$.*p*-PHDA	670	561			NiS_4N_2	bidentate
			3380	3300sh		free NH$_2$
			3340	3230		bonded NH$_2$
23. Ni(α-dtp)$_2$.bzd	685	575 550	3325	3215	NiS_4N_2	bidentate

a) The numbering of the compounds is the same as in tables 1 and 2.

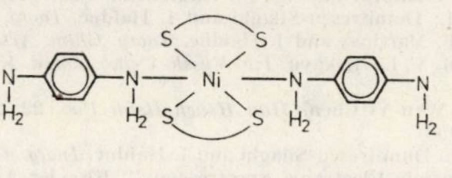

E

The results of the present investigation reveal some interesting features, regarding the competition between the phosphorodithioato liagand and the amine for metal sites : the monofunctional amines, even strong donor (pyridine, 2-, 3- and 4-methylpyridines) fulfil the coordination number of nickel(II) to six, without replacing the phosphorodithioato ligand, the latter remaining bidentate (and chelate-forming). The diamines, with strong donor ability, enhanced by the ability to close chelate rings (2,2'-dipyridyl, *o*-phenantroline, ethylenediamine and propylenediamine) open the four-membered inorganic chelate ring NiS_2P, thus rendering the phosphorodithioato group monodentate and closing new chelate rings through two nitrogen atoms (compounds **17**—**20**) as shown in structure *C*.

In the case of $Ni(\beta\text{-dtp})_2.2,2'\text{-dipy}_3$ (compound **11**) the replacement of the phosphorodithioato group is complete. This suggests that chelating diamines have a slightly higher coordination ability towards nickel atom than the phosphorodithioato groups. It would be of interest to investigate if, and under what conditions, one can obtain with these diamines all the members of the potential adduct series, including compounds in which the phosphorodithioato group is bidentate $Ni(dtp)_2$. diamine, monodentate $Ni(dtp)_2.diamine_2$ and ionic $[Ni(diamine)_3]$ $(dtp)_2$. Our experience shows that the stoichiometric ratio between the parent phosphorodithioate and diamine is not the only factor which determines the composition of the adduct, and therefore, the type of coordination of the phosphorodithioato ligands. We pursue this matter in our current research program.

The monodentate behaviour of phosphorodithioato ligands, revealed in this and previous works from this laboratory[7,8] and first established by X-ray diffraction in only one compound (namely $Ni[S_2P(OEt)_2]_2.1,9$-dimethylphenanthroline[2]) is worth emphasizing since the phosphorodithioato groups exhibit a strong tendency to form chelate rings and in the great majority of the transition metal complexes known these ligands are bidentate.

REFERENCES

[1] J. R. Wasson, G. H. Volterman and H.J. Stoklosa, *Fortschr. Chem. Forsch.*, **35**, 65 (1973).

[2] P. S. Shetty and Q. Fernando, *J. Amer. Chem. Soc.*, **92**, 3964 (1970).

[3] D. B. Sowerby and I. Haiduc, *Inorg. Chim. Acta*, **17**, L15—L16 (1976).

[4] D.B. Sowerby and I. Haiduc, *Inorg. Nucl. Chem. Letters.*, **12**, 791 (1976).

[5] S. P. Bone, D.B. Sowerby, R. Constantinescu and I. Haiduc, *J. Chem. Research* (*S*), **1979**, 69.

[6] A. I. Busev, M. I. Ivaniutin and M. F. Turchinski, *Vest. Moskov. Univ.*, **2**, 177 (1957).

[7] R. Micu-Semeniuc, L. Dumitrescu-Silaghi and I. Haiduc, *Inorg. Chim. Acta*, **17**, 5 (1976).

[8] R. Constantinescu, F. Martinaş and I. Haiduc, *Inorg. Chim. Acta*, **19**, 105 (1976).

[9] I.P. Komkov and M. V. Levitskaya, *Izv. Vyssh. Ucheb. Zaved. Khim. Khim. Tekhnol.*, **10**, 1014 (1967).

[10] Ping-Fang Hu and Wan-Yi Chen, *Hua Hsüch Hsöh Pao*, **22**, 215 (1956), through *Chem. Abstr.*, **52**, 7186 (1958).

[11] R. Micu-Semeniuc, L. Dumitrescu-Silaghi and I. Haiduc, *Inorg. Chim. Acta*, **33**, 281 (1979).

[12] A.B.P. Lever, "Inorganic Electronic Spectroscopy", Elsevier Amsterdam, 1968.

Revue Roumaine de Chimie, **25**, *11–12*, 1499–1504 (1980)

SOME PROBLEMS OF DERIVING STABILITY CONSTANTS OF ML_2 TYPE COMPLEXES FROM SPECTROPHOTOMETRIC DATA

J. ZSAKÓ
Faculty of Chemical Technology, "Babeş-Bolyai" University, str. Arany János 11, 3400
Cluj-Napoca, Romania

Received August 8, 1979

An approximation method is proposed which allows the determination of the overall stability constant β_2 by using the absorption A of the solution, its limiting value A_∞ at high ligand excess and formula (4). The range of β_2 and of the first stability constant K_1 is determined as function of the overall metal concentration cM (Fig. 5) in which β_2 can be derived with an error less than 10%.

INTRODUCTION

The absorption A of an ideal solution in which ML_2 type complex is formed, characterized by the successive stability constants K_1 and K_2, can be given as

$$A = \frac{\varepsilon_0 + \varepsilon_1 K_1[\mathrm{L}] + \varepsilon_2 K_1 K_2[\mathrm{L}]^2}{1 + K_1[\mathrm{L}] + K_1 K_1[\mathrm{L}]^2}\, dc_M + \varepsilon_L d[L] \qquad (1)$$

where ε_0, ε_1, ε_2, and ε_L stand for the molar absorptivity of the species M, ML, ML_2 and L respectively, d for the cell length, c_M for the overall metal concentration : $c_M = [\mathrm{M}] + [\mathrm{ML}] + [\mathrm{ML}_2]$, and [L] for the free ligand concentration.

Relation (1) contains 7 unknown magnitudes, *viz.* K_1, K_2, ε_0, ε_1, ε_2, ε_L and [L], from which ε_0 and ε_L can be measured without difficulty. In the case of sufficiently stable complexes ε_2 can be derived too, from the limiting value A_∞ of the absorption at high ligand concentrations.

Since generally 5 magnitudes are unknown, Thamer[1] proposes to measure A at 5 different ligand concentrations and to derive these magnitudes from the 5 relations (1) obtained. Although this procedure is correct from mathematical point of view, it is unrealistic, requiring experimental data of practically not available high precision. Otherwise it can give even negative stability constants or absorptivities.

The extrapolation methods, like that of Yatsimirsky,[2,3] imply in most cases a non linear extrapolation, which makes the results rather uncertain and frequently this procedure cannot be applied at all.

The dilution method[4] can be used only if $K_1 \approx 0$ and even if the overall stability constant $\beta_2 = K_1K_2$ is small.

The method of corresponding solutions[5,6] has also a very limited applicability.

APPROXIMATION METHOD OF DERIVING β_2

Let us consider $\varepsilon_0 = \varepsilon_L = 0$ and $\varepsilon_1 < \varepsilon_2$. (If $\varepsilon_0 \neq 0$ and/or $\varepsilon_L \neq 0$, the same method can be used for the corrected absorption values, obtained by subtracting the approximate value of the absorption of the free M and of the free L). In the first approximation the concentration of the species ML can be neglected and relation (1) becomes

$$A = \frac{\varepsilon_2\beta_2[\mathrm{L}]^2}{1 + \beta_2[\mathrm{L}]^2}\, dc_M \tag{2}$$

By defining the degree of formation of ML_2 as

$$\alpha = \frac{[\mathrm{ML}_2]}{c_M} \tag{3}$$

its value can be approximated as $\alpha = A/A_\infty$.

In this approximation one can derive the stability constant β_2 from the absorption values by means of the following relation

$$\beta_2 = \frac{\alpha\, c_M}{(1-\alpha)c_M(c_L - 2\alpha c_M)^2} = \frac{A\, A_\infty^2}{c_M^2(A_\infty - A)\,(rA_\infty - 2A)^2} \tag{4}$$

where c_L stands for the analytical concentration of the ligand and r for the ratio c_L/c_M.

Obviously, this relation can give reliable results only if K_1 is sufficiently small as compared to β_2.

In the present paper we studied the conditions of the applicability of the formula (4). In this purpose the maximum values of K_1 and β_2 have been derived (as function of c_M), which still allow the determination of β_2 with an error not exceeding 10%.

COMPLEXES WITH $K_1 = 0$

In this case relation (4) is rigorously valid and its application is limited on the one hand by the complete transformation of M into ML_2 in the case of very stable complexes, and on the other hand, by the impossibility to determine A_∞ if the complex is not stable enough.

In order to obtain a clear picture, we have calculated the ratios r at which the degree of formation of $ML_2(\alpha)$ attains the values 0.3, 0.5, 0.7 and 0.9, by varying systematically β_2 and c_M. Calculations have been performed by means of a programmable minicalculator Texas Instruments SR 56. These calculations showed the existence of a univoque relation between r and the magnitude $c_M\sqrt{\beta_2}$ and allowed the construction of the diagram given in figure 1.

As seen from figure 1, at $\log c_M\sqrt{\beta_2} = 2$ the ratio r becomes independent of the stability of the complex and it is almost constant even beginning from $\log c_M\sqrt{\beta_2}=1$. This means that practically the spectrophotometric method and relation (4) can be used only if

$$\beta_2 < 10^2 c_M^{-2}$$

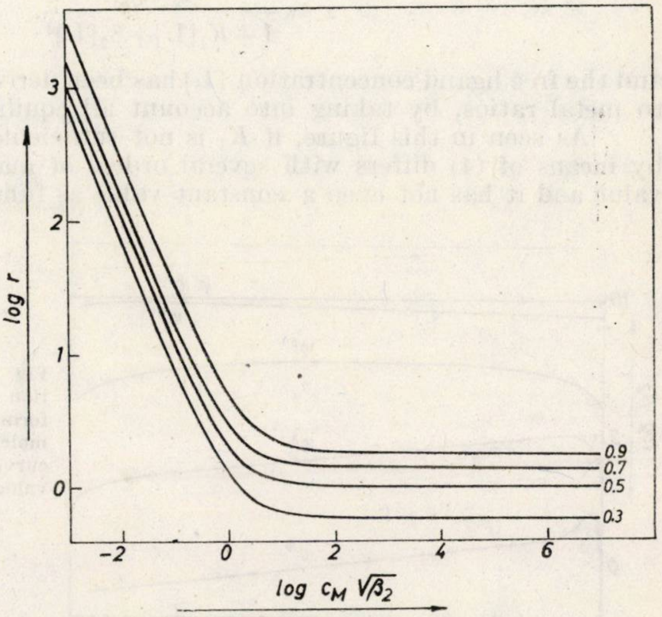

Fig. 1. — The ratio ligand to metal at which the degree of formation of $ML_2(\alpha)$ attains the value indicated beneath the curves.

and in the best case up to $10^4 c_M^{-2}$, but in the region

$$10^2 c_M^{-2} < \beta_2 < 10^4 c_M^{-2}$$

results might be rather unsure and very scattered.

Since the absorption measurements are possible very seldom in solutions with $c_M < 10^{-5}$ mole/l, the upper limit of β_2 which can be derived spectrophotometrically is of about $10^{12} \ldots 10^{14}$.

The lower limit of β_2 depends much on the solubility of the ligand. Generally, this does not exceed 1 mole l. Consequently, the maximum possible value of r will be equal to c_M^{-1}. Our calculations showed that A_∞ can be determined, even by extrapolation, only if $\beta_2 > 30$, irrespective of the metal concentration, up to $c_M \approx 10^{-1}$ mole/l.

If $\beta_2 < 30$, A_∞ cannot be determined, but other spectrophotometric methods can be used, like the dilution method.[4]

In conclusion, the stability constant can be derived from experimental data by means of (4) only if

$$30 < \beta_2 < 10^2 c_M^{-2} \tag{5}$$

COMPLEXES WITH $K_1 \neq 0$

The finite concentration of ML can modify sensibly the β_2 value calculated by means of (4), even if $\varepsilon_1 \approx 0$. In order to illustrate the influence of K_1, we give the β_2 values calculated by means of (4), using the theoretical A and A_∞ values, obtained for $c_M = 10^{-4}$ mole/l, $\beta_2 = 10^{10}$. In figure 2 these β_2 values are given as function of α for several K_1 values. The degree of formation α has been calculated by using the formula

$$\alpha = \frac{\beta_2[\mathrm{L}]^2}{1+K_1[\mathrm{L}]+\beta_2[\mathrm{L}]^2}.$$

and the free ligand concentration [L] has been derived for different ligand to metal ratios, by taking into account all equilibria.

As seen in this figure, if K_1 is not sufficiently small, β_2 calculated by means of (4) differs with several orders of magnitude from the real value and it has not even a constant value as function of α.

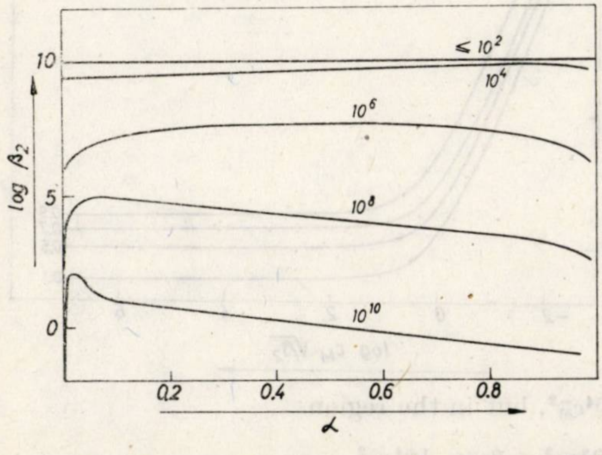

Fig. 2. — log β_2 values as function of α, calculated by means of formula (4) in the case of 10^{-4} mole/l solutions. $\beta_2 = 10^{10}$. The curves correspond to different K_1 values, indicated above each curve.

Further on, the ratio r has been calculated at which $\alpha = 0.9$ in solutions with $c_M = 10^{-4}$ mole/l. A separate curve is obtained for each β_2 value as function of the ratio β_2/K_1. Several curves of this type are presented in figure 3.

Practically, the utilization of formula (4) is possible only on the horizontal portion of the curves. At higher c_M concentrations the region of the applicability of (4) is even much less, as seen from figure 4, representing the ratio r at which $\alpha = 0.9$ in solutions with $c_M = 10^{-1}$ mole/l.

Finally, a correlation has been sought between β_2, c_M and the maximum value of K_1 which allows the determination of β_2 by means of formula (4). For this purpose theoretical r values have been calculated (for some $\beta_2 - c_M$ pairs and different K_1 values) at which α has the following values: 0.3, 0.4, 0.5, 0.6, 0.7, 0.8 and 0.9. In the calculation of A the condition $\varepsilon_1 = 0$ has been used. On the basis of these r data and by means of formula (4), β_2 values have been derived for the above α values and their arithmetical mean $\overline{\beta_2}$ have been calculated. The

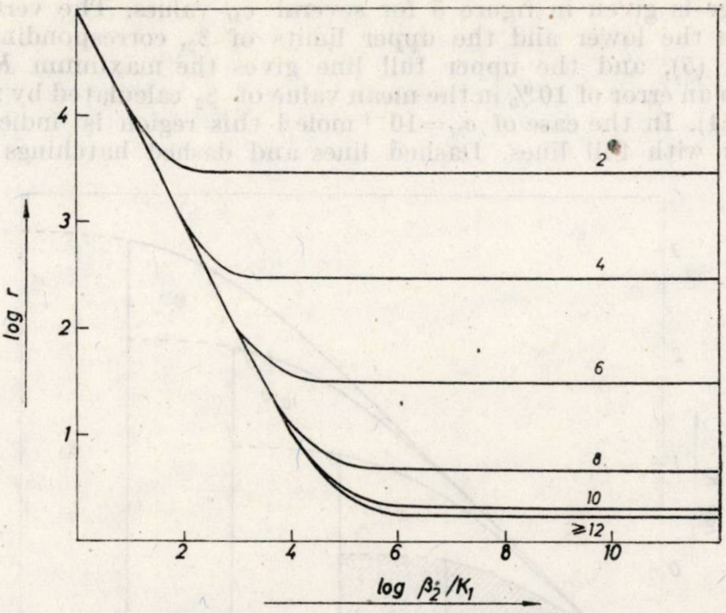

Fig. 3. — log r values at which $\alpha = 0.9$ in solutions with $c_M = 10^{-4}$ mole/l. Figures beneath the curves represent log β_2.

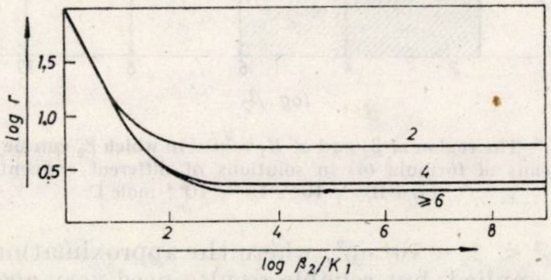

Fig. 4. — log r values at which $\alpha = 0.9$ in solutions with $c_M = 10^{-1}$ mole/l. Figures beneath the curves represent log β_2.

TABLE 1

The maximum K_1 value allowing the calculation of β_2 by means of formula (4) with an error less than 10%

$\log c_M \sqrt{\beta_2}$	$\log K_1 c_M$
−4	−5.135
−3	−4.135
−2	−3.138
−1	−2.158
0	−1.319
1	−0.936
2	−0.870

presumed K_1 value has been varied systematically until $\overline{\beta}_2$ became equal to 0.9 of the real β_2 value. It is worth mentioning that results are very little influenced by the absorption of ML. Errors are even less if $0 < \varepsilon_1 < 0.3\ \varepsilon_2$.

This study allowed us to obtain a univoque correlation between β_2, c_M and this maximum K_1 value. This correlation can be expressed by a single curve in the co-ordinates $\log c_M \sqrt{\beta_2} - \log K_1 c_M$. Several points of this curve are given in table 1.

On the basis of this correlation one can find easily the range of applicability of formula (4) and of the approximation method proposed.

This range is given in figure 5 for several c_M values. The vertical full lines give the lower and the upper limits of β_2, corresponding to the condition (5), and the upper full line gives the maximum K_1 value, leading to an error of 10 % in the mean value of β_2 calculated by means of formula (4). In the case of $c_M = 10^{-1}$ mole/l this region is indicated by hatchings with full lines. Dashed lines and dashed hatchings indicate the region $10^2 c_M^{-2} < \beta_2 < 10^4 c_M^{-2}$, where the approximation method proposed can be still applied, but reliable results need very accurate absorption data.

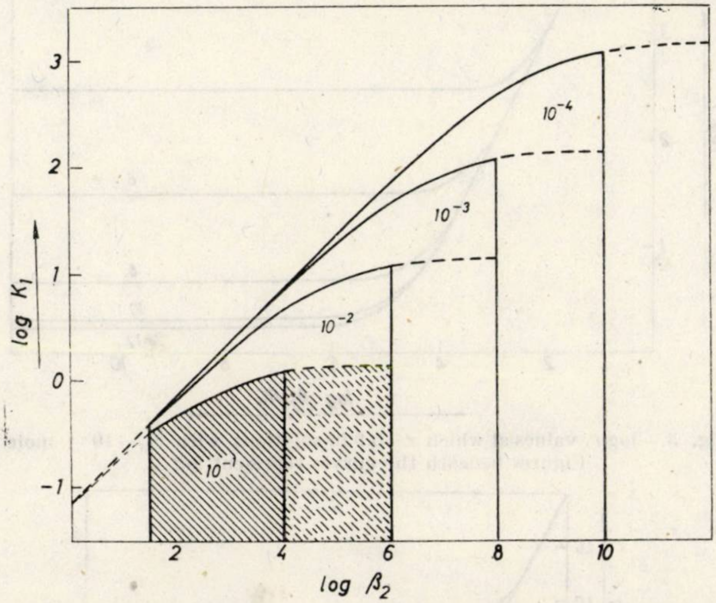

Fig. 5. — The region of β_2 and of K_1 values in which β_2 can be derived by means of formula (4) in solutions of different concentrations. $c_M = 10^{-1}, 10^{-2}, 10^{-3}, 10^{-4}$ mole/l.

REFERENCES

[1] B. J. Thamer, *J. Phys. Chem.*, **59**, 450 (1955).
[2] K. B. Yatsimirsky, *Zhur. neorg. Khim.*, **1**, 2306 (1956).
[3] J. Zsakó, *Rev. Roumaine Chim.*, **11**, 315 (1966).
[4] G. Cilento and D. L. Sanioto, *Z. phys. Chem. (Leipzig)*, **223**, 333 (1963).
[5] J. Bjerrum, *J. Kgl. Dansk. Vid. Selsk. Mat.-Fys. Medd.*, **21** (4), 1 (1944).
[6] H. Irving and D. P. Mellor, *J. Chem. Soc.*, **1955**, 3957.

Revue Roumaine de Chimie, 25, *11–12*, 1505–1528 (1980)

REACTIONS OF PYRYLIUM SALTS WITH NUCLEOPHILES. XIV.[1]

NEW PYRIDINIUM SALTS WITH POTENTIAL BIOLOGICAL ACTIVITY

ANTONIE DINCULESCU[a] and ALEXANDRU T. BALABAN[b,*]

[a] Institute of Chemical-Pharmaceutical Research, Bucharest, Romania

[b] The Polytechnic, Department of Organic Chemistry, Bucharest, Romania

Received April 25, 1980

Pyrylium salts 9a–c yield new pyridinium salts on treatment with functionalised primary amines: ethanolamine, 2-haloethylamines, allylamine, 2-arylethylamines, benzylamines, arylamines, 1,ω-diamines, 1,ω-aminocarboxylic acids or their derivatives. The pyridinium salts thus obtained may undergo various reactions such as esterification of hydroxy group, dehydrohalogenation yielding N-vinylpyridinium salts, halogen addition to double bonds, etc. Some of the pyridinium salts present biological activity.

1. INTRODUCTION

The formation of pyridinium salts **7** from pyrylium salts **1** and primary amines $R-NH_2$ takes place in mild conditions and gives excellent yields.[2]

Some limitations are imposed on the basicity of the amine (too high basicities in aqueous solution lead to pseudobase formation, too low basicities and nucleophilicities prevent the reaction) and on the steric requirements (with t-butylamine the ring-opened intermediate **6** does not cyclize,[2] while some primary amines with the NH_2 group attached to a secondary carbon react with pyrylium salts possessing an α-standing methyl group ($R' = CH_3$) by an alternative ring closure leading to aniline derivatives **8**).[3]

The reaction mechanism is the following:[2,4]

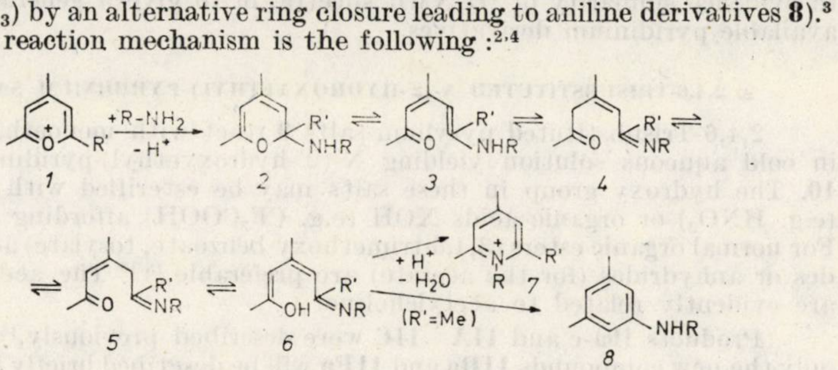

---

* To receive any correspondence.

α-Addition of the nucleophile leads to a valence-tautomeric system **2**–**3** by a thermally-allowed electrocyclic process, and then by prototropy to the imino-enol **6**, which usually may be evidenced as a transient intermediate, but in some cases (R = t-Bu) is stable. Tautomeric forms **3**–**5** are also possible.

Since Baeyer and Piccard's discovery in 1910,[5,6] this reaction has been repeatedly employed for obtaining difficultly accessible pyridinium salts.[7] Thus Dimroth and Reichardt obtained from 2,4,6-triphenylpyrylium and *p*-aminophenol an N-pyridinium phenol-betaine presenting an unprecedented solvatochromy;[8-10] Van Allan and Reynolds starting from pyranylidene-bisiminium salts obtained an interesting series of copyrinium salts;[11] from appropriate asymmetrically substituted pyrylium salts and anilines, atropisomeric N-arylpyridinium salts were prepared.[12] Also, from 2,4,6-trimethylpyrylium perchlorate and primary aromatic amines, numerous N-aryl-2,4,6-trimethylpyridinium cations were obtained, whose ^{1}H-NMR spectra provide a method for assessing quantitatively the aromaticity of the N-aryl group through the shielding of α-methyl groups relative to the chemical shift of the γ-methyl;[1,13] from the same pyrylium perchlorate and primary amines whose NH_2 group is attached to a secondary carbon atom, N-alkyl-2,4-6-trimethylpyridinium salts were prepared which evidence by dynamic ^{1}H-NMR and ^{13}C-NMR spectroscopy measurable rotation barriers around the $\overset{+}{N}(sp^2)-C(sp^3)$ bond.[14]

Starting from the observation that many biologically active compounds contain quaternary nitrogen(s), the present paper reports the synthesis of pyridinium salts whose N-substituents are similar to currently used drugs and pharmaceuticals. They differ from the latter through one of the following features exemplified in Scheme 1 : (i) they have pyridinium instead of trialkylamonium quaternary groups; (ii) they have substituents on the pyridinium ring which differ from those of the drugs; (iii) instead of primary amino groups they have substituted pyridinium rings.

This paper presents only the chemical aspects; biological aspects will be presented in a separate paper.

Some of the compounds presented in the following tables have been described earlier;[1,15] if they are included here, this is only in order to evidence similarity of ^{1}H-NMR spectra, or to give a general view on available pyridinium derivatives.

2. 2,4,6-TRISUBSTITUTED N-(2′-HYDROXYETHYL)-PYRIDINIUM SALTS

2,4,6-Trisubstituted pyrylium salts **9** react with monoethanolamine in cold aqueous solution yielding N-(2′-hydroxyethyl)-pyridinium salts **10**. The hydroxy group in these salts may be esterified with inorganic (e.g. HNO_3) or organic acids XOH (e.g. CF_3COOH) affording esters **11**. For normal organic esters (3,4,5-trimethoxy-benzoate, tosylate) acid chlorides or anhydrides (for the acetate) are preferable.[15,16] The acetates **11A** are evidently related to acetylcholine.

Products **10a-c** and **11A**–**11C** were described previously,[15] therefore only the new compounds **11Da** and **11Ea** will be described briefly in the following.

Scheme 1. Comparison between structures with known physiological activity and newly synthesised compounds (Py^+ stands for a 2,4,6-trisubstituted pyridinium ring linked to the remainder of the molecule through the quaternary nitrogen atom).

Type	Known structures	New products
i	Choline $HO-CH_2-CH_2-\overset{+}{N}Me_3$	$HO-CH_2-CH_2-Py^+$
	Acetylcholine $AcO-CH_2-CH_2-\overset{+}{N}Me_3$	$AcO-CH_2-CH_2-Py^+$
	Methonium salts $Me_3\overset{+}{N}-(CH_2)_n-\overset{+}{N}Me_3$	$Py^+-(CH_2)_n-Py^+$
ii	"Amprolium" (coccidiostatic) 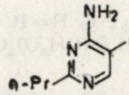	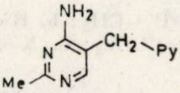
	Aminoacids $HOOC-(CH_2)_n-NH_2$	$HOOC-(CH_2)_n-Py^+$
	2-Arylethylamines $Ar-CH_2-CH_2-NH_2$	$Ar-CH_2-CH_2-Py^+$
	Anestesine $p\text{-}EtOOC-C_6H_4-NH_2$	$p\text{-}EtOOC-C_6H_4-Py^+$
	p-Aminohippuric acid $p\text{-}HOOC-CH_2-NH-CO-C_6H_4-NH_2$	$p\text{-}HOOC-CH_2-NH-CO-C_6H_4-Py^+$
	"Mafenide" (sulfonamide) $p\text{-}H_2N-SO_2-C_6H_4-CH_2-NH_2$	$p\text{-}H_2N-SO_2-C_6H_4-CH_2-Py^+$
iii	Aminoantipyrine 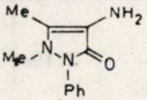	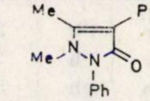
	Histamine 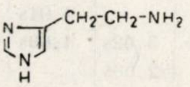	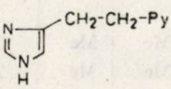
	Tryptamine 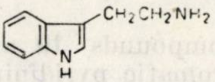	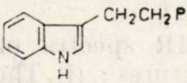
	6-Aminopenicillanic acid 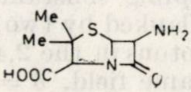	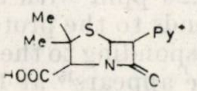 a

---

[a] Will be reported in a future paper

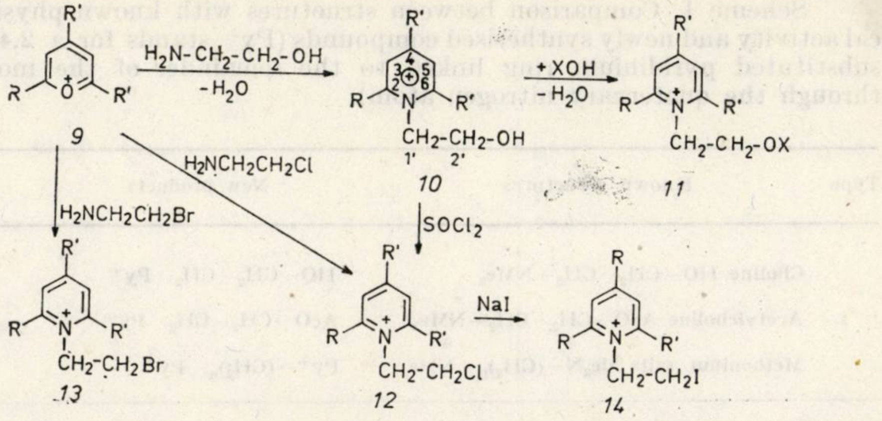

a, $R=R'=CH_3$; b, $R=CH_3$, $R'=C_6H_5$; c, $R=R'=C_6H_5$*
A, $X=COCH_3$; B, $X=COCF_3$; C, X=Ts; D, $X=3,4,5\text{-}(CH_3O)_3C_6H_2-CO$; E, $X=NO_2$

The trimethoxybenzoate **11Da** was obtained on heating the N-hydroxyethyl-pyridinium salt **10a** with 3,4,5-trimethoxybenzoyl chloride at 100–110°C. The nitrate **11Ea** was obtained from **10a** with fuming nitric acid at room temperature; this nitrate explodes powerfully on heating.

TABLE 1

^1H–NMR Spectra (δ, ppm) of pyridinium salts **10** and **11**, in trifluoroacetic acid.

No.	X	R	R′	2(6)–CH_3	4–CH_3	X–CH_3	1′–CH_2	2′–CH_2	3–CH	5-CH
10b	H	Me	Ph	3.13s	—	—	4.97t	4.04t	7.99d	8.15d
11Ab	$COCH_3$	Me	Ph	3.17s	—	2.19s	5.08t	4.51t	8.02d	8.22d
11Bb	$COCF_3$	Me	Ph	3.14s	—	—	5.16t	4.66t	8.01d	8.20d
11Cb	Ts	Me	Ph	3.10s	—	2.47s	5.08t	4.35t	7.98d	8.14d
11Da	3,4,5-$(MeO)_3$-C_6H_2–CO	Me	Me	3.03s	3.62s	4.04s 4.09s	5.05s		7.61s[a]	
11Ea	NO_2	Me	Me	2.94s	2.60s	—	5.00s		7.60s	

[a] The aroyl *ortho*-protons resonate at δ = 7.45s ppm.

The ^1H-NMR spectra of compounds **10** and **11** (Table 1) have the following features: (i) The aromatic pyridinium β-proton peaks in the asymmetrically substituted compounds **b** appear as two doublets at δ 8.00 and 8.20 ppm with a coupling constant J = 3 Hz. The latter doublet corresponds to the proton 5 flanked by two phenyl groups; indeed, the singlet corresponding to the β-protons in the 2,4,6-triphenyl-substituted compounds **c** appears[15] at the same field, δ = 8.20 ppm. (ii) In the aroyl-derivatives **11Da**, the β-pyridinium protons appear at lower field

---

* These structural abbreviations will be conserved throughout this paper: **a** stands for 2,4,6-trimethyl-, **b** for 2-methyl-4,6-diphenyl-, and **c** for 2,4,6-triphenyl-.

(δ 7.61 ppm) than the aroyl protons (δ 7.45 ppm), in agreement with the relative electronic densities. (iii) The 2′-methylene protons are strongly influenced by the nature of the functional group bonded to the same carbon. The deshielding effect increases in the series $\mathrm{OH} < \mathrm{OAc} < \mathrm{OCOCF_3} < \mathrm{ONO_2} < \mathrm{OCOAr}$ (cf. also ref.[15]). Thus the last two compounds **11Ea** and **11Da** have one practically degenerate peak for all methylene protons. (iv) For the ^{1}H-NMR peak of the 1′-methylene protons see chapter 10.

3. 2,4,6-TRISUBSTITUTED N-(2′-HALOETHYL)- AND -(2′,3′-DIHALOPROPYL)-PYRIDINIUM SALTS

As mentioned earlier,[15] pyrylium perchlorates **9** react with 2-chloroethylamine yielding 2,4,6-trisubstituted N-(2′-haloethyl)-pyridinium salts **12**. Later experiments showed that the same compounds **12** may be obtained from the 2′-hydroxyethyl-pyridinium salts **10** on treatment with thionyl chloride.[17] Similarly, pyrylium salts **9** and 2-bromoethylamine afford N-(2′-bromoethyl)-pyridinium salts **13**, while the N-(2′-iodoethyl)-pyridinium salts **14** were prepared from the chloroethyl-derivatives **12** and sodium iodide by a Finkelstein reaction.[18]

In the course of the latter reaction, an anion exchange takes place at the same time yielding the pyridinium iodide **14a** which, however, is readily converted by perchloric acid into the corresponding perchlorate **14a**.

On addition of bromine to N-allyl-2-methyl-4,6-diphenylpyrylium sulfoacetate **15** (readily obtained from allylamine and 2-methyl-4,6-diphenylpyrylium sulfoacetate[15,19]), 2-methyl-4,6-diphenyl-(2′,3′-dibromopropyl)-pyridinium bromide was obtained, which is readily converted by perchloric acid into the corresponding perchlorate **16b**.

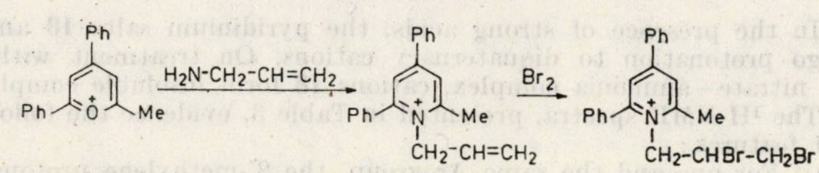

9b *15* *16*

The ^{1}H-NMR spectra (Table 2) evidence a gradual deshielding of the 2′-methylene protons bonded to the same carbon in the series $\mathrm{I} < \mathrm{Br} < \mathrm{Cl}$ in agreement with the known effect of halogen atoms. The vicinal coupling constants for the two methylene groups (A_2B_2 system) are about 6 Hz for all compounds in Tables 1 and 2 which present the two distorted triplets. In the ^{1}H-NMR spectrum of **16b**, both methylene groups bonded to the asymmetric carbon atom appear magnetically nonequivalent (chemical shift non-equivalent).

TABLE 2

^{1}H–NMR Spectra (δ, ppm) of pyridinium salts **12–16**, in trifluoroacetic acid

No.	Hal	R	R′	$2(6)-CH_3$	$4-CH_3$	$1'-CH_2$	$2'(3')-CH_2$	$3-CH$	$5-CH$
12a[a]	Cl	Me	Me	2.93s	2.61s	4.97t	4.04t	7.61s	
12b	Cl	Me	Ph	3.15s	–	5.03t	3.74t	8.02d	8.22d
13a	Br	Me	Me	2.93s	2.62s	4.98t	3.82t	7.65s	
14a	I	Me	Me	2.93s	2.62s	4.89t	3.54t	7.63s	
16b	Br_2	Me	Ph	3 22s	–	5 33dt	3.67dt	8 07d	8.23d[b]

[a] From ref.[15] and included for comparison.
[b] A multiplet at $\delta = 4.25$ is due to the CHBr proton.

4. 2,4,6-TRISUBSTITUTED N-(2′-ARYLETHYL)-PYRIDINIUM SALTS

Pyrylium salts **9** react with 2-phenylethylamine, histamine or tryptamine yielding 2,4,6-trisubstituted N-(2′-arylethyl)-pyridinium salts **17**–**19**, whose structure bears similarities with biologically active compounds such as serotonine, histidine, tryptophane, etc.[20,21]

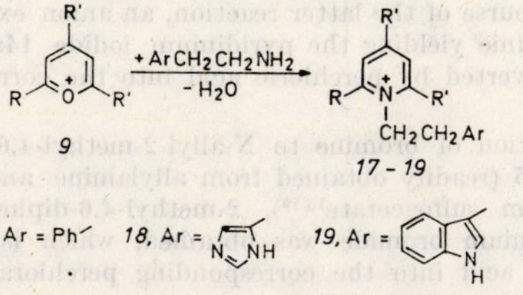

In the presence of strong acids, the pyridinium salts **18** and **19** undergo protonation to diquaternary cations. On treatment with the silver nitrate–ammonia complex, cations **18** form insoluble complexes.

The ^{1}H-NMR spectra, presented in Table 3, evidence the following salient features:

(i) For one and the same Ar group, the 2′-methylene protons are shielded proportionally to the number of α-phenyl groups bonded in positions 2 or 6 to the pyridinium moiety.

(ii) The α-methyl protons bonded in positions 2 or 6 to the pyridinium moiety in **17** and **19** are shielded relative to compounds in Tables 1 and 2, owing to the ring current in the 2′-aryl group. (The shielding exerted by the protonated imidazole ring is much lower).

(iii) Vice-versa, in pyridinium salts obtained from histamine, the α-standing phenyl groups in **18a** and **18c** shield the 2″ and 4″(5″) protons (the histidinic 2″-proton appears at lower field since it is bonded to a carbon placed between two nitrogen atoms).

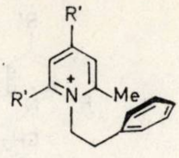

17, 19

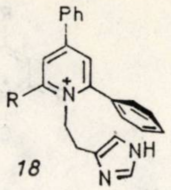

18

TABLE 3

^{1}H–NMR Spectra (δ, ppm) of pyridinium salts 17–19, in trifluoroacetic acid

No.	R	R′	2(6)–CH_3	4–CH_3	1′–CH_2	2′ CH_2	3–CH	5–CH	2″–CH	4″(5″)–CH
17a	Me	Me	2.70s	2.56s	4.76t	3.20t	7.50s		—	—
17b	Me	Ph	3.01s	—	4.81t	3.03t	7.90d	8.10d	—	—
17c	Ph	Ph	—	—	4.82t	2.95t	8.07s		—	—
18a	Me	Me	2.94s	2.63s	4.90t	3.55t	7.60s		8.90s	7.60s
18b	Me	Ph	3.17s	—	5.06t	3.43t	8.08d	8.21d	8.65s	7.09s
18c	Ph	Ph	—	—	5.10t	3.17t	8.21s		8.53s	6.83s
19a	Me	Me	2.65s	2.55s	4.74t	3.30t	7.40s		[a]	[a]
19b	Me	Ph	3.05s	—	4.92t	3.22t	7.90d	8.15d	[a]	[a]
19c	Ph	Ph	—	—	4.99t	2.92t	8.15s		[a]	[a]

[a] Submerged under phenyl multiplet

5. 2,4,6-TRISUBSTITUTED N-(ARYLMETHYL)-PYRIDINIUM SALTS

Benzylamine and other arylmethylamines such as ring-substituted benzylamines, 5-aminomethylpyrimidines or 4-aminomethylthiazole convert pyrylium salts **9** into N-(arylmethyl)-pyridinium salts **20**–**23**.[22,23] Some of these are structurally similar to known agents useful in the treatment of coccidiosis (a common and widespread poultry disease) e.g. "Amprolium" i.e. N-(2′-propyl-4′-amino-5′-pyrimidinylmethyl)-2-picolinium chloride hydrochloride.[24]

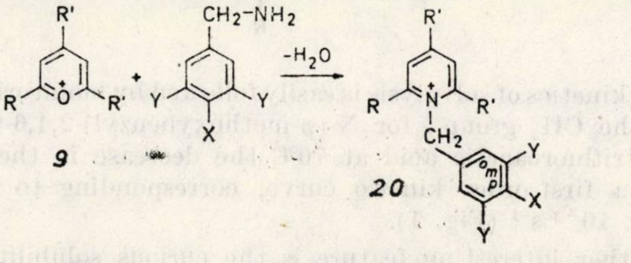

20 A, X = H, Y = H
B, X = Me, Y = H
C, X = OMe, Y = H

20 D, NO_2 Y = H
E, X = SO_2NH_2, Y = H
F, X = OMe, Y = OMe

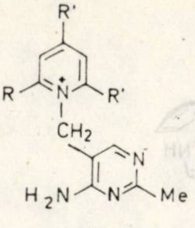

21

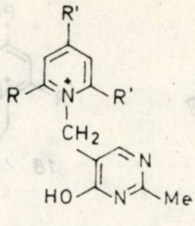

22

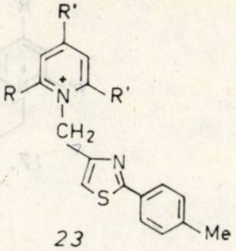

23

A characteristic reaction of these compounds, especially with 2,4,6-triarylsubstituents, is the solvolysis on heating in various solvents, first observed for N-methyl-2,4,6-triphenylpyridinium halides,[25] then developed into a powerful synthetical method by Katritzky.[26] In the present cases the ability of triphenylpyridine to act as a leaving group is enhanced by the conjugative stabilization in the benzyl cation formed (or partially formed in the transition state) as the second fragment.

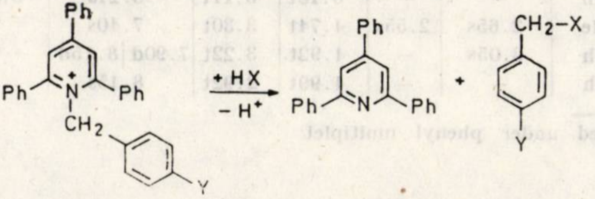

The overall reaction consists actually in replacing a primary amino group in R-NH_2 by a substituent X originating in the reagent (solvent) HX, using as driving force the increasing aromaticity in the series pyrylium — pyridinium — pyridine.

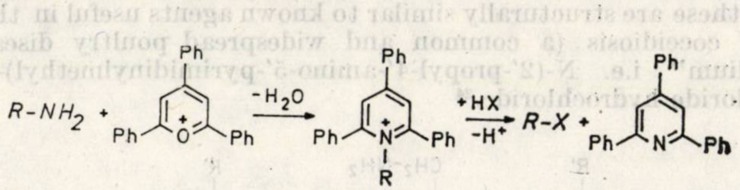

The kinetics of solvolysis is easily followed by monitoring the ^{1}H-NMR peak of the CH_2 group: for N-(*p*-methoxybenzyl)-2,4,6-triphenylpyridinium in trifluoroacetic acid at 70°C the decrease in the integral curve leads to a first-order kinetic curve, corresponding to a reaction rate $k = 2.4 \times 10^{-3}$ s^{-1} (Fig. 1).

Another interesting feature is the curious solubility variation for the pyridinium perchlorate **21a** in the mixed solvent system water—acetone: although the solubility is low in both solvents when pure (under

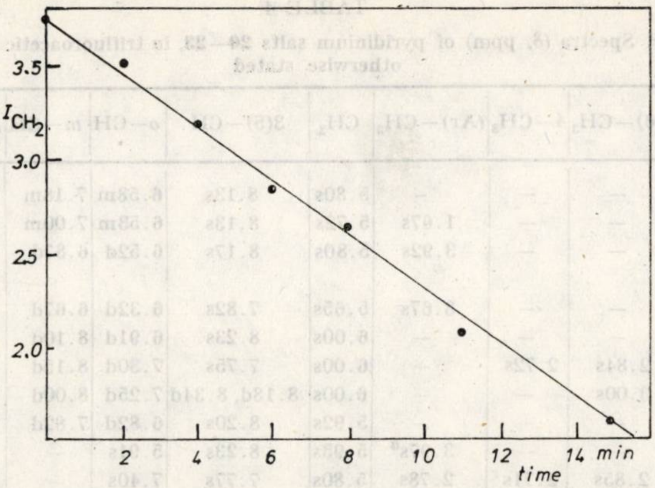

Fig. 1. — Kinetic plot of the intensity (integral curve) of the CH_2 peak in the ^{1}H-NMR spectrum of **20Cc** in trifluoroacetic acid at 70°C *versus* time.

10 g/l), in an equivolumetric mixture the solubility reaches 218 g/l at room temperature (Fig. 2). Covalent hydration[27] may be involved.

The ^{1}H-NMR spectra (Table 4) evidence that : (i) the *para*-substituent in N-benzylpyridinium salts influences the chemical shift of the CH_2 protons. A Hammett plot of δ (CH_2) *versus* σ_{para} [28,29]evidences a linear correlation excepting the value for the methoxy group (Fig. 3).

(ii) In the *para*-substituted benzyl-derivatives **20c** having α-phenyl substituents, the *ortho*-protons are shielded appreciably more than the *meta*-protons ; the difference between the corresponding chemical shifts $\Delta\delta$ ($m-o$) presents an excellent correlation *versus* σ_{para} (Fig. 4).

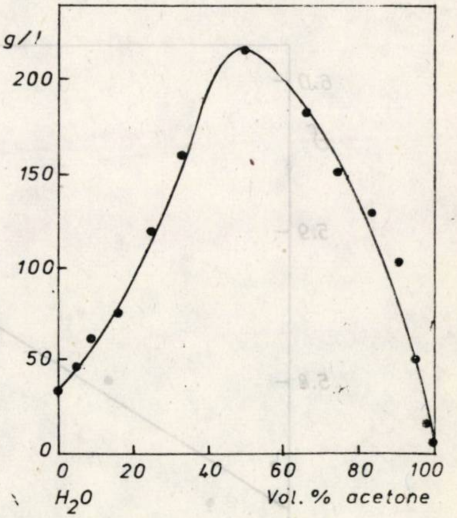

Fig. 2. — Solubility of **21a** in a solvent mixture of water—acetone at room temperature (25°C).

6. N-(ω-CARBOXY-POLYMETHYLENE)-PYRIDINIUM SALTS

The reaction of pyrylium salts with glycine was described earlier.[30] Other α-aminoacids were also reported to react with pyrylium salts.[31,32] We now report the reaction with ethyl α-aminoacetate (glycine ester),

TABLE 4

^{1}H–NMR Spectra (δ, ppm) of pyridinium salts **20**–**23**, in trifluoroacetic acid, unless otherwise stated

No.	R	R′	2(6)–CH_3	4–CH_3	(Ar)–CH_3	CH_2	3(5)–CH	o–CH	m–CH	Δδ(m–o)	σ_p
20Ac	Ph	Ph	—	—	–	5.80s	8.13s	6.58m	7.18m	0.60	0
20Bc	Ph	Ph	—	—	1.67s	5.72s	8.13s	6.53m	7.00m	0.47	−0.170
20Cc	Ph	Ph	—	—	3.92s	5.80s	8.17s	6.52d	6.87d	0.35	−0.268
(idem, in $CDCl_3$)			—	—	3.67s	5.65s	7.82s	6.32d	6.67d	0.35	−0.268
20Dc	Ph	Ph	—	—	—	6.00s	8.23s	6.91d	8.10d	1.19	0.778
20Ea	Me	Me	2.84s	2.72s	—	6.00s	7.75s	7.30d	8.15d	—	—
20Eb	Me	Ph	3.00s	—	—	6.00s	8.18d, 8.34d	7.25d	8.00d	—	—
20Ec	Ph	Ph	—	—	—	5.92s	8.20s	6.82d	7.82d	1.00	0.570
20Fc	Ph	Ph	—	—	3.97s^a	5.95s	8.23s	5.91s	—	—	—
21a	Me	Me	2.85s	2.71s	2.78s	5.80s	7.77s	7.40s	—	—	—
22a	Me	Me	2.91s	2.69s	3.00s	5.80s	7.72s	7.85s	—	—	—
23c	Ph	Ph	—	—	2.52s	6.18s	8.27s	—	—	—	—

---

^{a} The *meta*-methoxy protons resonate at δ 3.78s ppm.

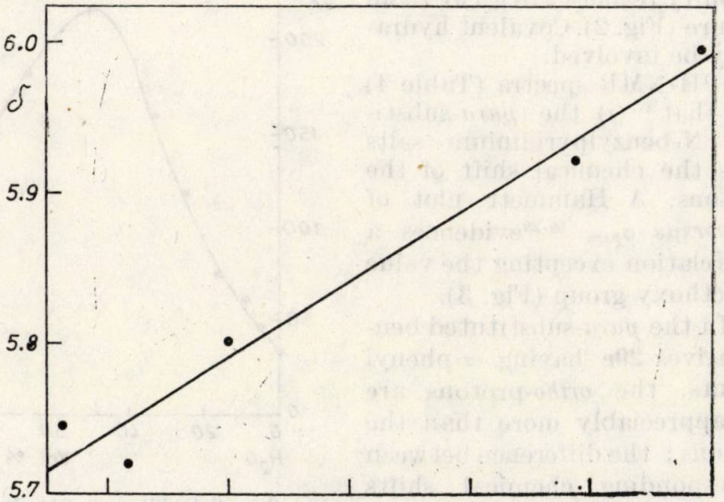

Fig. 3. — Hammett plot *versus* σ_{para} of the chemical shift for the CH_2 group in N-benzylpyridinium salts **20** bearing various substituents in the *para*-position of the benzyl group (^{1}H-NMR spectra in trifluoroacetic acid at 38°C).

β-alanine, γ-aminobutyric and ε-aminocapronic acids affording pyridinium salts **24**–**27**. Since the ester is much more basic than the betainic free acids, the reaction proceeds much more readily with the ester.

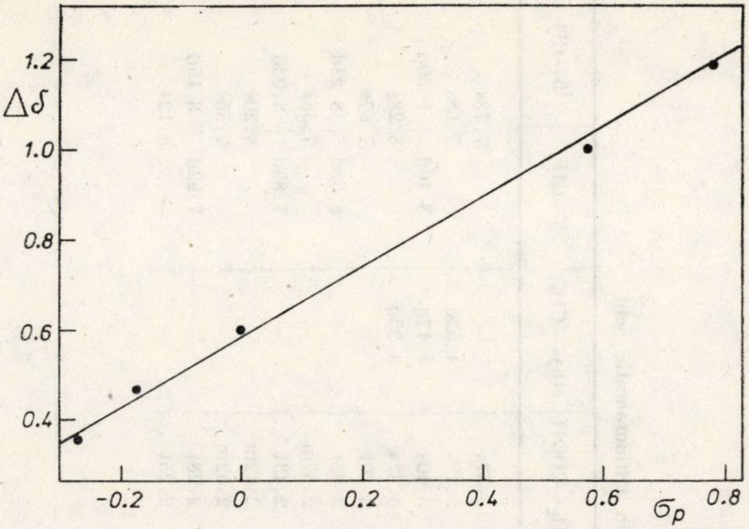

Fig. 4. — Hammett plot *versus* σ_{para} of the difference Δδ between the chemical shifts of *meta* and *ortho* aromatic protons in the *p*-substituted benzyl group.

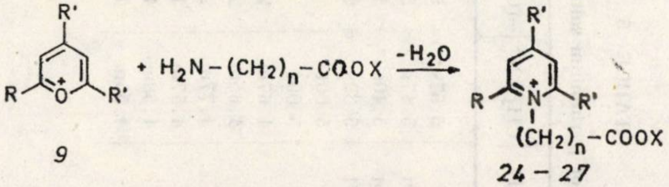

24A, n = 1, X = H
24B, n = 1, X = Et
25 , n = 2, X = H
26 , n = 3, X = H
27 , n = 5, X = H

The ^{1}H-NMR spectra (Table 5) evidence the strong deshielding exerted by the pyridinium and the carboxy groups on the ends of the polymethylene chain.

7. N-(ω-AMINOPOLYMETHYLENE)-PYRIDINIUM AND N,N'-POLYMETHYLENE-BIS-PYRIDINIUM SALTS

The biological activities of methonium salts $[Me_3\overset{+}{N}-(CH_2)_n-\overset{+}{N}Me_3]\,2X^-$ (currare-like or blocking agents, according to the value of n) and of bis-pyridinium salts (herbicides) are known. We investigated [33] the reaction of pyrylium salts **9** with 1,ω-polymethylenediamines $H_2N-(CH_2)_n-NH_2$ (where n = 2, 4, 6 or 8) which leads to N,N'-polymethylene-bis-pyridinium salts **29** under usual conditions.

TABLE 5

^{1}H−NMR Spectra (δ, ppm) of pyridinium salts **24**−**27**, in trifluoroacetic acid

No.	R	R′	2(6)−CH_3	4−CH_3	ethyl−CH_3	CH_2−N^+	−$(CH_2)_{n-2}$−	CH_2−COOH	ethyl−CH_2	3−CH	5−CH
24Aa[a]	Me	Me	2.88s	2.68s	—	5.57s =	5.57s =	5.57s	—	7.73s	
24Ba	Me	Me	2.82s	2.65s	1.40t	5.47s =	5.47s =	5.47s	4.52q	7.68s	
24Bb	Me	Ph	3.02s	—	1.35t	5.40s =	5.40s =	5.40s	4.47q	8.10d	8.30d
24Bc	Ph	Ph	—	—	1.17t	5.32s =	5.32s =	5.32s	4.23q	8.28s	
25a[a]	Me	Me	2.97s	2.63s	—	5.00t	—	3.20t	—	7.67s	
25b	Me	Ph	3.13s	—	—	5.00t	—	3.03t	—	8.03d	8.23d
26a	Me	Me	2.95s	2.62s	—	4.67m	2.33m	2.67m	—	7.58s	
26b	Me	Ph	3.12s	—	—	4.65m	2.17m	2.43t	—	7.83d	8.03d
26c	Ph	Ph	—	—	—	4.77m	2.12m	2.12m	—	8.20s	
27a	Me	Me	2.87s	2.57s	—	4.57m	1.80m	2.52m	—	7.55s	
27b	Me	Ph	3.10s	—	—	4.58m	1.50m	2.28t	—	7.92d	8.15d
27c	Ph	Ph	—	—	—	4.55m	1.38m	2.25t	—	8.12s	

[a] Ref. 30

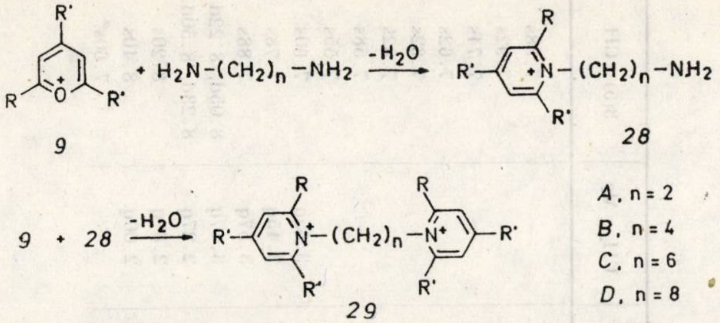
R'
R
R'
+ H2N-(CH2)n-NH2
-H2O
R
R'
N-(CH2)n-NH2
R'
9
28
9 + 28
-H2O
R
R
R'
N-(CH2)n-N
R'
R'
R'
29
A, n = 2
B, n = 4
C, n = 6
D, n = 8

However, if the reaction is performed with excess amine under high dilution, N-(ω-aminopolymethylene)-pyridinium salts **28** are obtained, which are intermediates in the preceding reaction. Evidently, if one group of the diamine is tertiary, as in the case of N,N′-diethyl-ethylenediamine, the reaction stops at the monopyridinium salt stage **30**.

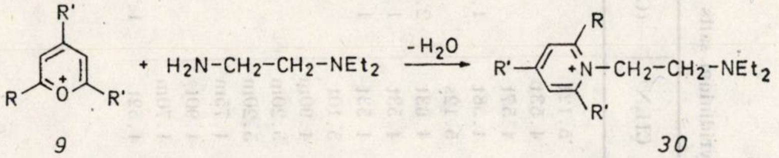
R'
R
R'
+ H2N-CH2-CH2-NEt2
-H2O
R
R'
N-CH2-CH2-NEt2
R'
9
30

Owing to the basicity of the amino nitrogen, a mono- and a di-perchlorate of cations **28** and **30** may be isolated. Since compounds **28** have a free primary amino group, they can undergo various reactions at this group, e.g. aroylation with 3,4,5-trimethoxybenzoyl chloride leading to amide **31**.

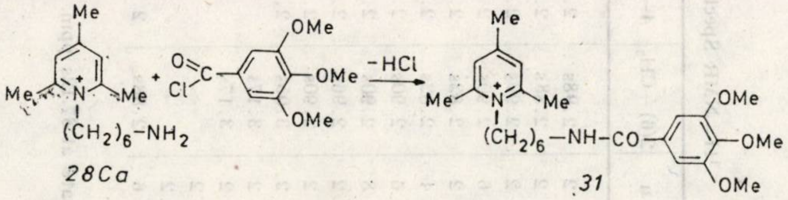
Me
Me
Me
(CH2)6-NH2
28Ca
+
O
C
Cl
OMe
OMe
OMe
-HCl
Me
Me
Me
(CH2)6-NH-CO
OMe
OMe
OMe
31

The ^{1}H-NMR spectra presented in Table 6, have the following salient features:

(i) The methyl group in γ-position of the pyridinium nuclei appears at remarkably constant field.

(ii) For bis-pyridinium salts **29**, the longer the polymethylene chain, the higher the field where $^+N-CH_2$ and other methylene protons resonate, because the influence of the second pyridinium ring is felt less and less.

(iii) In compounds **28** the amino group is protonated in trifluoroacetic acid so that the adjacent methylene protons appear at lower field than in dimethylsulfoxide-d_6 where the NH_2 group stays as such.

(iv) In compounds **30**, with increasing number of α-phenyl groups, the ethyl protons become more and more shielded owing to the ring current.

TABLE 6

^1H-NMR Spectra (δ, ppm) of pyridinium salts **28–31**.

No.	Solvent	R	R′	n	$2(6)-CH_3$	$4-CH_3$	other CH_3	CH_2N^+	$-(CH_2)_{n-2}$	CH_2N	CH_2-Me	$3(5)-CH$
28Aa	CF_3COOH	Me	Me	2	2.98s	2.62s	—	5.12t	—	3.97t	—	7.58s
28Aa	CD_3SOCD_3	Me	Me	2	2.88s	2.53s	—	4.53t	—	3.04t	—	7.92s
28Aa	CD_3CN	Me	Me	2	2.90s	2.58s	—	4.57t	—	3.18t	—	7.74s
28Ca	CF_3COOH	Me	Me	6	2.90s	2.62s	—	4.58t	1.78m	3.38t	—	7.62s
29Aa	,,	Me	Me	2	2.83s	2.57s	—	5.12s	—	—	—	7.62s
29Ba	,,	Me	Me	4	2.83s	2.57s	—	4.63t	2.20m	—	—	7.62s
29Ca	,,	Me	Me	6	2.90s	2.58s	—	4.53t	1.83m	—	—	7.58s
29Da	,,	Me	Me	8	2.90s	2.58s	—	4.53t	1.60m	—	—	7.55s
30a	,,	Me	Me	2	2.96s	2.60s	1.54t	5.10t	—	3.82m	3.65q	7.60s
30a	CD_3CN	Me	Me	2	2.90s	2.58s	1.37t	4.90m	—	3.50m	3.45q	7.78s
30a	CD_3COCD_3	Me	Me	2	3.05s	2.61s	1.43t	5.20m	—	3.87m	3.57q	7.88s
30b	CF_3COOH	Me	Ph	2	3.17s	—	1.20t	5.20m	—	3.55m	3.17q	8.05d, 8.22d
30b	CD_3COCD_3	Me	Ph	2	3.17s	—	0.76t	4.75m	—	2.80m	2.27q	8.23d, 8.50d
30c	CF_3COOH	Ph	Ph	2	—	—	0.97t	4.90t	—	3.40m	2.87q	8.20s
30c	CD_3COCD_3	Ph	Ph	2	—	—	0.51t	4.70m	—	2.57m	2.00q	8.40s
31a	CF_3COOH	Me	Me	6	2.88s	2.60s	2.42s	4.52t	1.73m	3.55m	—	7.60s[a]

[a] The aroyl *ortho*-protons resonate at δ7.12s ppm.

(v) Compounds **28** and **30** are protonated at the amino nitrogen in trifluoroacetic acid, but in acetone-d_6, dimethylsulfoxide-d_6 or in acetonitrile-d_3 they have a free amino group. The difference between these two groups of solvents is felt mainly at the protons bonded to the carbons directly adjacent to the amino nitrogen. However, as seen from the table 6, there exist smaller differences even between the spectra determined in D_3C-CN and $(D_3C)_2CO$ for the same compound.

8. N-ARYLPYRIDINIUM SALTS

On reacting pyrylium salts **9** with primary aromatic amines, both carbocyclic and heterocyclic, a host of N-aryl-2,4,6-trisubstituted pyridinium salts were obtained, some of them derived from biologically active amines like anestesine, antipyrine, *p*-aminohippuric acid, etc. Some of these products have been described earlier,[1,34] so that they will not be further discussed here except for mentioning that 2,4,6-trimethyl-N-aryl-pyridinium can be used for establishing by ^{1}H-NMR spectra the presence and magnitude of a ring current in the N-aryl group.[13]

Owing to their reduced basicity (and to steric hindrance for *ortho*-substituted arylamines), aromatic amines react more sluggishly with pyrylium salts than aliphatic amines : it is necessary to heat the reagents in ethanol under reflux, and in some cases without solvent in the molten amine to higher temperatures (up to 150°C).[1]

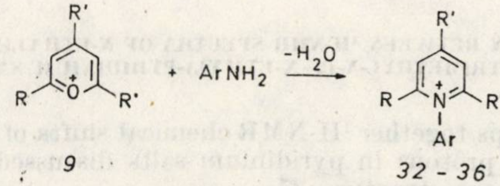

32, benzene derivatives
33, naphthalene derivatives
34, pyridine derivatives
35, thiazole derivatives
36, benzimidazole derivatives

The ^{1}H-NMR spectra of N-aryl-2,4,6-trimethylpyridinium salts are presented in Table 7. The assignments are straightforward. The occurrence of α-methyl protons at higher field than the γ-methyl protons, opposite to the relative position of these peaks in all other compounds discussed so far, is explained by the ring current in the N-aryl ring which is almost orthogonal to the pyridinium ring ; this allows a measurement of the ring current as reported separately.[13]

TABLE 7

^{1}H–NMR spectra (δ, ppm) of pyridinium salts **30–34**, in trifluoroacetic acid

No.	Ar (with positions of substituents on Ar)	2(6)–CH_3	4-CH_3	(Ar)–CH_3	3(5)–CH
32A	C_6H_4Cl (2′)	2.52s	2.80s	—	7.88s
32B$_1$	C_6H_4F (2′)	2.53s	2.77s	—	7.83s
32B$_2$	C_6H_4F (4′)	2.52s	2.75s	—	7.78s
32C	C_6H_3ClF (3′, 4′)	2.56s	2.77s	—	7.85s
32D$_1$	$C_6H_4CF_3$ (2′)	2.52s	2.78s	—	7.83s
32D$_2$	$C_6H_4CF_3$ (3′)	2.52s	2.77s	—	7.83s
32E$_1$	$C_6H_4CH_3$ (2′)	2.43s	2.75s	2.07s	7.77s
32E$_2$	$C_6H_4CH_3$ (3′)	2.50s	2.73s	2.58s	7.77s
32F$_1$	$C_6H_3(CH_3)_2$ (2′, 3′)	2.44s	2.77s	1.95s, 2.52s	7.80s
32F$_2$	$C_6H_3(CH_3)_2$ (3′, 4′)	2.49s	2.71s	2.49s	7.73s
32F$_3$	$C_6H_3(CH_3)_2$ (2′,6′)	2.43s	2.78s	2.04s	7.88s
32G	$C_6H_2(CH_3)_3$ (2′, 4′, 6′)	2.43s	2.78s	1.98s, 2.50s	7.90s
32H	$C_6H_4OCH_3$ (4′)	2.50s	2.71s	4.08s	7.75s
32I	$C_6H_4N(CH_3)_2$ (4′)	2.50s	2.75s	3.68d	7.82s
32J	$C_6H_4COOCH_3$ (2′)	2.42s	2.73s	3.97s	7.73s
33A	1′-naphthyl	2.43s	2.86s	—	7.93s
33B	2′-naphthyl	2.54s	2.78s	—	7.83s
33C	1′-(8′-amino)-naphthyl	2.57s	2.83s	—	7.98s
34A	2′-pyridyl	2.56s	2.80s	—	7.87s
34B	4′-pyridyl	2.57s	2.78s	—	7.83s
35	2′-thiazolyl	2.61s	2.78s	—	7.83s
36	2′-benzimidazolyl	2.78s	2.90s	—	8.02s

9. COMPARISON BETWEEN ^{1}H-NMR SPECTRA OF N-ETHYLENE PEAKS IN 2,4,6-TRIMETHYL-N-(2′-X-ETHYL)-PYRIDINIUM SALTS

Table 8 groups together ^{1}H-NMR chemical shifts of the N-methylene and X-methylene protons in pyridinium salts discussed in earlier paragraphs which possess structure **37**.

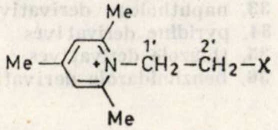

37

It can be seen that when the 2,4,6-substituents are maintained constant, i.e. methyls, the N-(1′)-methylene protons appear in a narrow range (δ = 4.74 – 5.12 ppm); however, the X-(2′)-methylene protons vary considerably on varying the nature of the X group (δ = 3.00–5.12 ppm). To compare this variation with literature data,[35] we selected as reference compounds the n-propyl derivatives with the same X group, i.e. $CH_3-CH_2-CH_2-X$. The column labelled Δ in Table 8 indicates the difference between the chemical shifts of the $X-CH_2$ methylene protons in the pyridinium and n-propyl compounds. It can be seen that an approximately constant difference $\Delta = 0.6-0.9$ ppm is found in all compounds with the exception of the amino and halogen derivatives X = Cl, Br, I, where this difference is smaller (0.57 ; 0.47 ; and 0.38 ppm, respectively). This constancy is an indication for the correctness of the assignments in the ^{1}H-NMR spectra of these compounds.

TABLE 8

^{1}H$-$NMR chemical shifts (δ, ppm) of methylene protons in pyridinium salts **37**

No.	X	$\overset{+}{N}-CH_2$	$X-CH_2$	Solvent	$X-CH_2-Et$[35]	Δ
10a	OH	4.89	4.40	CF_3COOH	3.49	0.91
11Aa	OAc	4.92	4.83	,,	3.98	0.85
11Ba	$OCOCF_3$	5.02	4.98	,,	—	—
11Ca	OTs	4.99	4.67	,,	3.94	0.73
11Da	$OCOC_6H_2(OMe)_3$	5.05	5.05	,,	4.25	0.80
11Ea	NO_2	5.00	5.00	,,	4.28	0.72
12a	Cl	4.97	4.04	,,	3.47	0.57
13a	Br	4.98	3.82	,,	3.35	0.47
14a	I	4.89	3.54	,,	3.16	0.38
17a	Ph	4.76	3.20	,,	2.59	0.61
18a	Imidazolyl	4.90	3.55	,,	—	—
19a	β-Indolyl	4.74	3.30	,,	—	—
25a	COOH	5.00	3.20	,,	2.31	0.89
26a	CH_2COOH	4.67	2.33	,,	—	—
27a	$CH_2CH_2CH_2COOH$	4.57	1.80	,,	—	—
28A′a	NH_2	4.53	3.04	CD_3SOCD_3	2.61	0.43
28A″a	$\overset{+}{N}H_3$	5.12	3.97	CF_3COOH	—	—
28Ca	$(CH_2)_4\overset{+}{N}H_3$	4.58	1.78	,,	—	—
29Aa	Me_3Py^{+}[a]	5.12	5.12	,,	—	—
30′a	NEt_2	4.90	3.60	CD_3CN	—	—
30″a	$\overset{+}{N}HEt_2$	5.10	3.88	CF_3COOH	—	—

---

[a] X = 1-substituted 2,4,6-trimethylpyridinium.

A conclusive proof for the correctness of the assignment for 1′- and 2′-CH_2 signals was provided by ^{1}H-NMR spectra recorded in the presence of lanthanide shift reagents : the upfield shifts caused by $Pr(fod)_3$ in acetonitrile-d_3 (the solubility in less polar solvents was too low) for the 2′-hydroxyethyl-2,4,6-trimethylpyridinium perchlorate and the downfield shifts caused by $Eu(dpm)_3$ for the 2′-aminoethyl-2,4,6-trimethylpyridinium perchlorate in the same solvent decrease in both cases in the order : $2'-CH_2 > 1'-CH_2 >$

$>2-CH_3>3-H>4-CH_3$ (Figures 5 and 6), exactly according to the increasing distances between the respective protons and the coordinating group (OH and NH_2, respectively). The NH_2 protons in the second case have the highest slope, since they are close to the coordinating group; in the first case, the OH proton does not appear in the usual range. Owing to the high polarity of the solvent, the lanthanide-induced shifts are not meaningful in themselves since the solvent also coordinates with the shift reagent, but the trend is quite clear from figures 5 and 6.

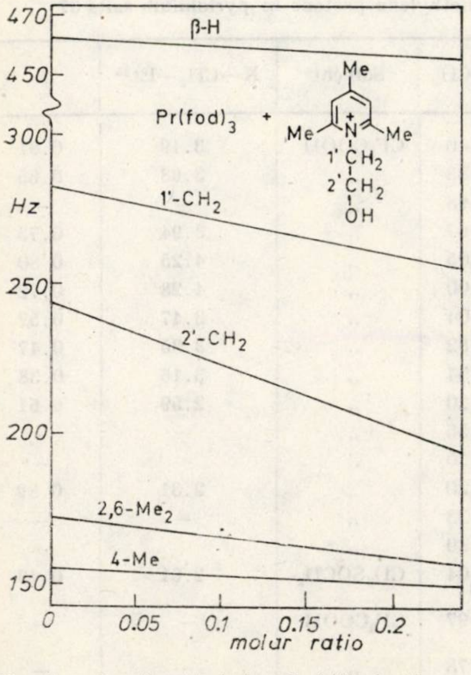

Fig. 5. — Lanthanide-induced shifts in the ^1H-NMR spectrum of **10a** in the presence (fod)$_3$ in acetonitrile-d$_3$.

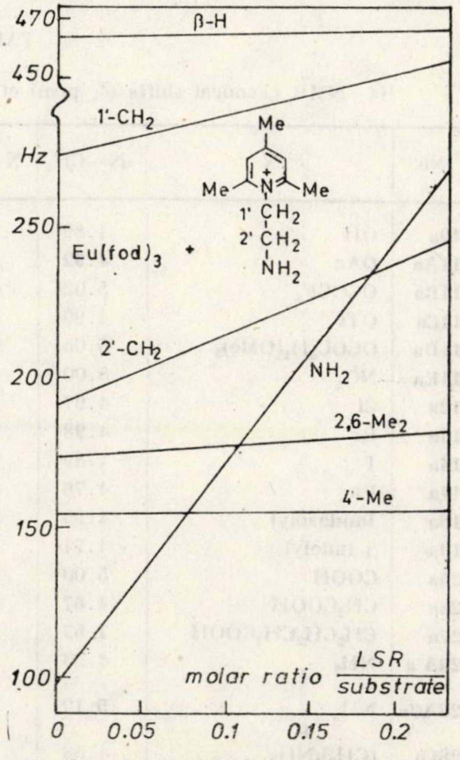

Fig. 6. — Lanthanide-induced shifts in the ^1H-NMR spectrum of **28Aa** in acetonitrile-d$_3$ in the presence of Eu(fod)$_3$.

10. EXPERIMENTAL PART

N-(2'-Hydroxyethyl)-2,4,6-trimethylpyridinium perchlorate (**10a**) was prepared from the pyrylium salt **9a** and monoethanolamine as described earlier.[15] Its *3,4,5-trimethoxybenzoate* (**11Da**) was prepared by melting at 80°C 12 g (52 mmol) 3,4,5-trimethoxybenzoyl chloride and introducing 8 g (30 mmol) of the above perchlorate **10a**. The heating was continued for 15 minutes at 100—110°C. After cooling at 70°C, sufficient benzene was added to remove all unreacted acid chloride, and the residue was washed on the Buchner funnel with warm benzene. The residue was recrystallized from ethanol yielding white crystals m.p. 162°C, in 73% yield. Found: N, 3.16; Cl, 7.92%. $C_{20}H_{26}NO_5^+ClO_4^-$ requires N, 3.04; Cl, 7.70%.

The *nitrate* (**11Ea**) was prepared by dissolving 2 g perchlorate **10a** in 2 ml fuming nitric acid (d = 1.52 g/ml). After standing for one hour at room temperature, the mixture was poured with mixing into 50 ml isopropanol, then 50 ml ether was added. The product was filtered off after 30 minutes, white needles **m.p. 162°C,** 95% yield. Found: N, 9.25; Cl, 11.62%. $C_{10}H_{15}N_2O_3^+\ ClO_4^-$ requires N, 9.01; **Cl, 11.40%.**

N-(2′-Bromoethyl)-2,4,6-trimethylpyridinium ***perchlorate*** (**13a**). 2-Bromoethylamine hydrobromide (15 g, 75 mmol) in 50 ml water was neutralised with 15% aqueous sodium hydroxide to pH 7. The resulted solution was added dropwise into a suspension of 11 g (50 mmol) of 2,4,6-trimethylpyrylium perchlorate in 100 ml water, maintaining the pH value between 7.0 and 6.5 by simultaneous addition of 15% aqueous sodium hydroxide. Then the mixture was stirred for another half-hour at room temperature, and the lower oily layer was separated. On digesting this layer with about 1 ml ethanol, the product crystallised and was triturated with ether. For purification it was recrystallised from ethanol, white crystals with m.p. 101°C, 69% yield. Found: N, 4.50; Br, 24.10%. $C_{10}H_{15}BrN^+ClO_4^-$ requires: N, 4.26; Br, 24.30%.

N-(2′-Iodoethyl)-2,4,6-trimethylpyridinium iodide and perchlorate (**14Aa**). N-(2′-Chloroethyl)-2,4,6-trimethylpyridinium perchlorate (**12a**), 12 g (42 mmol), was dissolved in 25 ml acetone. A solution of 9 g (60 mmol) of sodium iodide in 50 ml acetone was added, and the mixture was refluxed for six hours. The precipitated sodium chloride was filtered off, the solution was purified with carbon black, and the product was precipitated by adding 1—2 ml ether. After recrystallisation from isopropanol, the iodide **14a**, white crystals with m.p. 163°, was obtained in 85% yield. Found: N, 3.20; I, 64.0%. $C_{10}H_{15}IN^+I^-$ requires: N, 3.47; I, 63.0%. For obtaining the corresponding *perchlorate* **14a**, the iodide was dissolved in isopropanol, and a slight excess of 70% perchloric acid was added, when the perchlorate was obtained as white crystals with m.p. 138°C in 98% yield relatively to the iodide. Found: N, 3.50; I, 33.1%. $C_{10}H_{15}IN^+ClO_4^-$ requires: N, 3.73; I, 33.8%.

N-(2′,3′-Dibromopropyl)-2-methyl-4,6-diphenylpyridinium tribromide and perchlorate (**16Ab** and **16Bb**). 2-Methyl-4,6-diphenylpyrylium sulfoacetate (18 g, 40 mmol) suspended in 200 ml methanol was treated with 10 ml allylamine. The resulted clear red solution was evaporated leaving a dark red oil. This was dissolved in 100 ml chloroform and bromine was added (50 mmol), refluxing for three minutes. After cooling, 200 ml ether was added, the lower layer was separated and shaken several times with ether for removing unreacted bromine. After redissolving in a small volume of chloroform, methanol was added when N-(2′, 3′-dibromopropyl)-2-methyl-4,6-diphenylpyridinium tribromide precipitated, yellow crystals with m.p. 126°C, in 92% yield. Found: N, 2.30; Br, 59.00%. $C_{21}H_{20}N_2Br_2N^+Br_3^-$ requires: N, 2.04; Br, 58.31%.

For obtaining the corresponding *perchlorate*, the tribromide was dissolved in chloroform, excess 70% perchloric acid and enough methanol for obtaining a clear solution were added. On dilution with ether, the white perchlorate m.p. 223°C precipitated in 90% yield. Found: N, 2.50%. $C_{21}H_{20}Br_2N^+ClO_4^-$ requires: N, 2.57%.

N-(2′-Phenylethyl)-pyridinium perchlorates (**17**). The pyrylium perchlorate (50 mmol) suspended in 100 ml dioxan was treated with 10 ml 2-phenylethylamine at room temperature with stirring for one hour. Then 200 ml ether was added to the resulted clear solution, when the product precipitated. After filtration and washing with ether, the product was recrystallised from ethanol.

17a, m.p. 181°C, yield 78%. Found: N, 4.30; Cl, 10.85%. $C_{16}H_{20}N^+ClO_4^-$ requires: N, 4.17; Cl, 10.87%.

17b, m.p. 186°C, yield 90%. Found: N, 2.98; Cl, 7.72%. $C_{26}H_{24}N^+ClO_4^-$ requires: N, 3.10; Cl, 7.87%.

17c, m.p. 277°C, yield 86%. Found: N, 2.70; Cl, 6.80%. $C_{31}H_{26}N^+ClO_4^-$ requires: N, 2.75; Cl, 6.90%.

N-2′-(4″-Imidazolylethyl)-pyridinium salts (**18**). A solution of sodium methoxide was prepared from 0.3 g sodium and 20 ml methanol. Then 1.4 g of histamine dihydrochloride was added, and after 10 minutes' stirring at room temperature the precipitated sodium chloride was filtered off. Into the filtered solution, 70 mmoles of pyrylium salt were introduced. After 2 hrs' stirring at room temperature, a double volume of ether was added. The precipitated products were recrystallized from 75% aqueous ethanol.

18a, m.p. 165°, yield 65%. Found: N, 13.10; Cl, 11.15%. $C_{13}H_{19}N_3^+ClO_4^-$ requires: N, 13.30; Cl, 11.22%.

18b, m.p. 180°, yield 76%. Found: N, 9.80; Cl, 8.20%. $C_{23}H_{23}N_3^+ClO_4^-$ requires: N, 9.55; Cl, 8.06%.

18c, m.p. 225°, yield 58 %. Found: N, 8.42; Cl, 7.00 %. $C_{28}H_{25}N_3^+ClO_4^-$ requires: N, 8.30; Cl, 7.06 %.

N-2'-(3''-Indolylethyl)-perchlorates (**19**). A solution of sodium methoxide was prepared from 0.25 g sodium and 50 ml methanol. Then 2 g (10 mmol) tryptamine hydrochloride was added and stirred for ten minutes at room temperature. The resulted solution was introduced dropwise into a suspension of 10 mmoles pyrylium salt in 100 ml methanol. After two hours' stirring at room temperature, the clear solution was diluted with a double volume of ether, the product was filtered off and recrystallized from acetone: isopropanol (2:1).

19a, m.p. 254°, yield 73 %. Found: N, 7.50; Cl, 9.77 %. $C_{18}H_{21}N_2^+ClO_4^-$ requires: N, 7.68; Cl, 9.70 %.

19b, m.p. 285°, yield 62 %. Found: N, 5.83; Cl, 7.42 % $C_{28}H_{25}N_2^+ClO_4^-$ requires: N, 5.75; Cl, 7.29 %.

19c, m.p. 208°, yield 68 %. Found: N, 5.12; Cl, 6.50 %. $C_{33}H_{27}N_2^+ClO_4^-$ requires: N, 5.08; Cl, 6.44 %.

Substituted N-benzylpyridinium perchlorates (**20**). Pyrylium perchlorates (20 mmoles) were suspended in 50 ml alcohol (MeOH, EtOH, i-PrOH), dioxan or acetonitrile and were treated dropwise with a solution of 30 mmoles benzylamine in the same solvent (also 50 ml solution). If a clear solution results after one hour's stirring at room temperature, ether is added to crystallize the product; in other cases, the pyrylium salt goes rapidly into solution and the pyridinium salt crystallizes spontaneously from the solvent without adding ether. Table 9 summarizes the properties of the products.

TABLE 9

No.	Formula	%N		%Cl		M.p. °C	Yield %
		Found	Calc.	Found	Calc.		
20Ac	$C_{30}H_{24}N^+ClO_4^-$	2.65	2.82	7.20	7.15	195	85
20Bc	$C_{31}H_{26}N^+ClO_4^-$	2.49	2.73	6.80	6.90	145	48
20Cc	$C_{31}H_{26}NO^+ClO_4^-$	2.64	2.65	6.62	6.83	120	90
20Dc	$C_{30}H_{23}N_2O_2^+ClO_4^-$	4.90	5.16	6.50	6.53	148	86
20Ea	$C_{15}H_{19}N_2O_2S^+ClO_4^-$	7.00	7.16	9.05	9.07	193	79
20Eb	$C_{25}H_{23}N_2O_2S^+ClO_4^-$	5.20	5.40	7.01	6.88	247	78
20Ec	$C_{30}H_{25}N_2O_2S^+ClO_4^-$	5.00	4.86	6.40	6.14	112	52
20Fc	$C_{33}H_{30}NO_3^+ClO_4^-$	2.30	2.38	6.14	6.07	141	41

N-(5'-Pyrimidinylmethyl)-2,4,6-trimethylpyridinium perchlorates (**21 a** and **22 a**). 2,4,6-Trimethylpyrylium perchlorate (0.1 mol) was suspended in 50 ml water, then the substituted 5-aminomethylpyrimidine was added in small portions under stirring until the pH reached 7.0 when the solution became clear. After 15—30 minutes' standing at room temperature, the product crystallized.

21a, m.p. 163°, yield 85 %. Found: N, 15.51; Cl, 9.90 %. $C_{14}H_{19}N_4^+ClO_4^-H_2O$ requires: N, 15.53; Cl, 9.83 %.

22a, m.p. 218°, yield 80 %. Found: N, 12.30; Cl, 10.36 %. $C_{14}H_{18}N_3O^+ClO_4^-$ requires: N, 12.20; Cl, 10.30 %.

N-(2'-p-Tolyl-4'-thiazolylmethyl)-2,4,6-triphenylpyridinium perchlorate (**23c**). 2-(*p*-Tolyl)-4-aminomethyl-thiazole dihydrochloride (4 g, 15 mmol) was dissolved in 40 ml absolute ethanol and neutralised with the stoichiometric amount of sodium ethoxide. After addition of 80 ml dry ether and filtration, the solution was treated with 4 g (10 mmol) of 2,4,6-triphenylpyrylium perchlorate. After one hour's stirring at room temperature, the resulted red solution was evaporated to dryness. The residue was washed with ether, and recrystallized from ethanol with decolorizing carbon, yielding white crystals with m.p. 140°C in 63 % yield. Found: N, 4.52; Cl, 5.80; S, 5.15 %. $C_{34}H_{27}N_2S^+ClO_4^-$ requires: N, 4.70; Cl, 5.96; S, 5.38 %.

N-(ω-Carbethoxymethylene)-pyridinium perchlorates (**24B**). A solution of sodium ethoxide freshly prepared from 1 g sodium and 100 ml absolute ethanol was mixed with an ethanolic solution of 40 mmol ethyl aminoacetate hydrochloride. The precipitated sodium chloride was filtered off and 25 mmoles of pyrylium salt were added. After one hour's stirring at room temperature, an equal volume of ether was added. The product was filtered off and recrystallized from isopropyl alcohol.

24Ba, m.p. 150°C, yield 85%. Found: N, 4.25; Cl, 11.30%. $C_{12}H_{18}NO_2^+ClO_4^-$ requires: N, 4.54; Cl, 11.52%.

24Bb, m.p. 189°C, yield 83%. Found: N, 3.10; Cl, 8.16%. $C_{22}H_{22}NO_2^+ClO_4^-$ requires: N, 3.24; Cl, 8.22%.

24Bc, m.p. 142°C, yield 91%. Found: N, 3.00; Cl, 7.00%. $C_{27}H_{24}NO_2^+ClO_4^-$ requires: N, 2.83; Cl, 7.19%.

N-(ω-Carboxy-polymethylene)-pyridinium perchlorates (**25**—**27**). A solution of 40 mmoles aminoacid and 20 mmoles pyrylium perchlorate in 100 ml water or ethanol was refluxed for 15—20 minutes. Decolorizing carbon was added and the filtered solution was concentrated to a third of the initial volume. The product crystallized or was precipitated by adding ether into the ethanolic solution, or isopropanol into the aqueous solution. Table 10 summarizes the properties of the products.

N-(ω-Aminopolymethylene)-pyridinium perchlorates (**28**). A saturated solution of 50 mmol pyrylium salt in methanol was added at room temperature into a solution of 200 mmol 1,ω-polymethylenediamine in 250 ml methanol. The resulted solution was decolorized with animal carbon and evaporated under vacuum. The remaining oil crystallized on refluxing with 50 ml isopropanol. For obtaining the diperchlorate **28A″a**, a slight excess of 77% perchloric acid was added to the oil before refluxing in isopropyl alcohol.

TABLE 10

No.	Formula	%N		%Cl		M.p. °C	Yield %
		Found	Calc.	Found	Calc.		
25b	$C_{21}H_{20}NO_2^+ClO_4^-$	3.50	3.36	8.28	8.51	203	78
26a	$C_{12}H_{18}NO_2^+ClO_4^-$	4.32	4.54	11.66	11.52	75	86
26b	$C_{22}H_{22}NO_2^+ClO_4^-$	3.50	3.24	8.00	8.22	233	82
26c	$C_{27}H_{24}NO_2^+ClO_4^-$	2 95	2.83	6.96	7.19	210[a]	88
27a	$C_{14}H_{22}NO_2^+ClO_4^-$	4.45	4.17	10.18	10.56	120	80
27b	$C_{24}H_{26}NO_2^+ClO_4^-$	3 00	3.04	7.55	7.72	99	89
27c	$C_{29}H_{28}NO_2^+ClO_4^-$	2.95	2.68	6.66	6.80	145	83

[a] Lit.[36] m.p. 215°C

28A′a, m.p. 98°C, yield 65%. Found: N, 10.51; Cl, 13.10%. $C_{10}H_{17}N_2^+ClO_4^-$ requires: N, 10.56; Cl, 13.40%.

28A″a, m.p. 110°C, yield 53%. Found: N, 7.82; Cl, 19.10%. $C_{10}H_{18}N_2^{2+}Cl_2O_8^{2-}$ requires: N, 7.69; Cl, 19.40%.

28Ca, m.p. 147°C, yield 72%. Found: N, 8.60; Cl, 11.30%. $C_{14}H_{25}N_2^+ClO_4^-$ requires: N, 8.70; Cl, 11.10%.

N,N′-(1, ω-Polymethylene)-bis-pyridinium perchlorates (**29**). A suspension of 220 mmoles pyrylium salt in 100 ml water or ethanol was treated under stirring with 100 mmoles 1, ω-polymethylenediamine. The dark solution was stirred for one hour at room temperature, during which the product crystallized and the solution became lighter-coloured. After another hour's stirring the product was filtered off and recrystallized from water or 50% ethanol. Table 11 presents the properties of the products.

TABLE 11

No.	Formula	%N		%Cl		M.p. °C	Yield %
		Found	Calc.	Found	Calc.		
29Aa	$C_{18}H_{26}N_2^{2+}Cl_2O_8^{2-}$	6.01	5.96	15.00	15.10	298	87
29Ba	$C_{20}H_{30}N_2^{2+}Cl_2O_8^{2-}$	5.70	5.65	14.10	14.30	268	91
29Ca	$C_{22}H_{34}N_2^{2+}Cl_2O_8^{2-}$	5.30	5.34	13.30	13.50	267	93
29Da	$C_{24}H_{38}N_2^{2+}Cl_2O_8^{2-}$	5.10	5.07	12.65	12.80	281	80

N-(2′-Diethylaminoethyl)-pyridinium perchlorates (**30**). A solution of 50 mmol pyrylium salt and 10 ml (70 mmol) N,N-diethyl-ethylenediamine in 100 ml methanol was stirred at room temperature for one hour, decolorized with carbon powder, concentrated to one third of its initial volume, and precipitated with ether. For obtaining diperchlorates, perchloric acid was introduced before adding ether. The products were recrystallized from methanol and their properties are indicated in Table 12.

TABLE 12

No.	Formula	%N		%Cl		M.p. °C	Yield %
		Found	Calc.	Found	Calc.		
30a′	$C_{14}H_{26}N_2^{2+}Cl_2O_8^{2-}$	6.82	6.65	17.00	16.90	195	83
30a″	$C_{14}H_{25}N_2^+ClO_4^-$	8.90	8.73	10.86	11.10	184	81
30b	$C_{24}H_{29}N_2^+ClO_4^-$	6.45	6.29	7.70	7.90	135	88
30c	$C_{29}H_{31}N_2^+ClO_4^-$	5.39	5.52	6.60	6.90	166	86

Amide of 3,4,5-trimethoxybenzoic acid with N-(6′-aminohexamethylene)-2,4,6-trimethylpyridinium perchlorate (**31a**). A suspension of 2.5 g (10 mmol) N-(6′-aminohexamethylene)-2,4,6-trimethylpyridinium perchlorate in 20 ml chloroform was treated with 3 g 3,4,5-trimethoxybenzoyl chloride under reflux for 10 minutes. After cooling, the product was filtered off and washed with ether for removing unreacted acid chloride. White crystals with m.p. 248°C. Found: N, 5.60; Cl, 7.00%. $C_{24}H_{35}N_2O_4^+ClO_4^-$ requires: N, 5.44; Cl, 6.92%.

N-Aryl-2,4,6-trimethylpyridinium perchlorates (**32**—**36**). The preparation was carried in some cases (i) on refluxing in ethanol or acetic acid, while other amines (ii) required a higher reaction temperature (in the molten amine without a solvent).

(i) In the former case, 20 mmol pyrylium salt and 40 mmol arylamine were refluxed for 10—20 minutes in ethanol or acetic acid. Decolorizing carbon was added and after another 5 minutes' refluxation the solution was filtered and concentrated to one third of its initial volume. The product was precipitated by adding ether and was recrystallized from isopropanol containing 1—2 drops of 70% perchloric acid. Table 13 presents the properties of the products.

TABLE 13

No.	Formula	%N		%Cl		M.p. °C	Yield %
		Found	Calc.	Found	Calc.		
32A	$C_{14}H_{15}ClN^+ClO_4^-$	3.98	4.20	21.50	21.32	165	76
32B$_1$	$C_{14}H_{15}FN^+ClO_4^-$	4.70	4.43	—	—	134	85
32B$_2$	,,	4.66	4.43	—	—	118	82
32C	$C_{14}H_{14}ClFN^+ClO_4^-$	4.15	3.98	—	—	161	73
32D$_1$	$C_{15}H_{15}F_3N^+ClO_4^-$	4.00	3.82	—	—	181	69
32D$_2$	,,	3.95	3.82	—	—	178	71
32H	$C_{15}H_{18}NO^+ClO_4^-$	4.10	4.27	10.75	10.82	104	89
33A	$C_{18}H_{18}N^+ClO_4^-$	4.26	4.02	10.06	10.20	215	92
33C	$C_{18}H_{19}N_2^+ClO_4^-$	7.90	7.71	10.00	9.78	230	85
34A	$C_{13}H_{15}N_2^+ClO_4^-$	9.50	9.36	12.05	11.87	92	57
35	$C_{11}H_{13}N_2S^+ClO_4^-$	9.00	9.18	11.55	11.64	175	86
36	$C_{15}H_{16}N_3^+ClO_4^-$	12.68	12.43	10.73	10.50	134	83

(ii) In the latter case, the pyrylium perchlorate (20 mmol) was introduced into the molten amine in excess (100 mmol) and heated for 5 minutes at 120—150°C with a thermometer introduced into the stirred melt. After cooling, the product was triturated with 50 ml isopropanol, the insoluble solid was filtered off and recrystallized from water or from isopropanol. Table 14 summarizes the properties of the products.

TABLE 14

No.	Formula	%N Found	%N Calc.	%Cl Found	%Cl Calc.	M.p. °C	Yield %
32E₁	$C_{15}H_{18}N^+ClO_4^-$	4.65	4.49	11.45	11.38	175	75
32E₂	,,	4.52	4.49	11.16	11.38	139	88
32F₁	$C_{16}H_{20}N^+ClO_4^-$	4.55	4.29	10.76	10.89	210	81
32F₂	,,	4.15	4.29	10.68	10.89	150	87
32F₃	,,	4.48	4.29	11.00	10.89	148	74
32G	$C_{17}H_{22}N^+ClO_4^-$	3.95	4.12	10.65	10.44	164	69
32I	$C_{16}H_{22}N_2^{2+}Cl_2O_8^{2-}$	6.51	6.53	8.00	8.03	274	94
32J	$C_{16}H_{18}NO_2^+ClO_4^-$	4.10	3.93	9.82	9.97	190	82

ACKNOWLEDGEMENT. Thanks are expressed to Mr. Filip Chiraleu for the ^1H-NMR spectra, to Mr. Constantin Drăghici for the lanthanide shift measurements, and to Mrs. Cornelia Ioan for elemental analyses.

REFERENCES

1. Preceding part, A. Dinculescu, H. N. Koutrakis and A. T. Balaban, *Rev. Roumaine Chim.*, **24**, 439 (1979).
2. A. T. Balaban and C. Toma, *Tetrahedron*, Suppl. **7**, 1 (1966).
3. C. Toma and A. T. Balaban, *Tetrahedron*, Suppl. **7**, 9 (1966).
4. A. T. Balaban and W. Silhan, *Tetrahedron*, **26**, 743 (1970).
5. A. Baeyer and T. Piccard, *Liebigs Ann. Chem.*, **384**, 208 (1911).
6. A. Baeyer, *Ber. dtsch. chem. Ges.*, **43**, 2337 (1910).
7. A. Dinculescu, *Ph. D. Thesis*, Bucharest, 1979.
8. K. Dimroth, Ch. Reichardt, Th. Liepmann and F. Bohlmann, *Liebigs Ann. Chem.*, **661**, 1 (1963).
9. K. Dimroth, Ch. Reichardt and A. Schweig, *Liebigs Ann. Chem.*, **669**, 95 (1963).
10. K. Dimroth and Ch. Reichardt, *Liebigs Ann. Chem.*, **727**, 93 (1969).
11. J. H. Van Allan, G. A. Reynolds, D. P. Maier and S. Chie Chang, *J. Heterocyclic Chem.*, **9**, 1229 (1972).
12. C. Uncuţa and A. T. Balaban, *Rev. Roumaine Chim.*, **21**, 251 (1976).
13. A. T. Balaban, A. Dinculescu, H. N. Koutrakis and F. Chiraleu, *Tetrahedron Letters*, **1979**, 437.
14. A. T. Balaban, C. Uncuţa, A. Dinculescu, M. Elian and F. Chiraleu, *Tetrahedron Letters*, **1980**, 1553.
15. A. R. Katritzky, J. B. Bapat, R. M. Claramunt, F. S. Yates, A. Dinculescu, A. T. Balaban and F. Chiraleu, *J. Chem. Research*, (M) 4783 (1978); (S) 395 (1978).
16. A. Dinculescu and A. T. Balaban, *Roumanian Patent*, 72 174 (1978).
17. A. Dinculescu and A. T. Balaban, *Roumanian Patent*, 71 871 (1978).
18. A. Dinculescu and A. T. Balaban, *Roumanian Patent*, 73 505 (1978).
19. A. Dinculescu and A. T. Balaban, *Roumanian Patent*, 71 869 (1978).
20. A. Dinculescu and A. T. Balaban, *Roumanian Patent*, 72 175 (1978).
21. A. Dinculescu and A. T. Balaban, *Roumanian Patent*, 73 503 (1978).
22. A. Dinculescu and A. T. Balaban, *Roumanian Patent*, 71 870 (1978).
23. A. Dinculescu, S. Cilianu and C. Drăghici, *Roumanian Patent*, 69 761 (1977).

[24] A. Dinculescu and Gh. Andreescu, *Roumanian Patent*, 55 461 (1972).

[25] A. B. Susan and A. T. Balaban, *Rev. Roumaine Chim.*, **14**, 111 (1969).

[26] J. B. Bapat, R. J. Blade, A. J. Boulton, J. Epsztajn, A. R. Katritzky, J. Lewis, P. Melina-Buendia, Pai-Lin-Nic and C. A. Romsdon, *Tetrahedron Letters*, **1976**, 2691.

[27] A. Albert and W. L. Armarego, *Adv. Heterocyclic Chem.*, **4**, 1 (1965).

[28] A. A. Bothner-By and R. E. Glick, *J. Amer. Chem. Soc.*, **78**, 1071 (1956).

[29] P. L. Corio and B. P. Doiley, *J. Amer. Chem. Soc.*, **78**, 3043 (1956).

[30] C. Toma and A. T. Balaban, *Tetrahedron*, Suppl. **7**, 27 (1966).

[31] Yu. A. Zhdanov, G. N. Dorofeenko and A. N. Narkevich, *Zhur. Obshchei Khim.*, **33**, 2418 (1963).

[32] M. N. O'Leary and G. A. Samberg, *J. Amer. Chem. Soc.*, **93**, 3530 (1971).

[33] A. Dinculescu, A. T. Balaban and E. Stepan, *Roumanian Patent*, 73 504 (1978).

[34] R. Neidlein and P. Witerzens, *Monatsh. Chem.*, **106**, 643 (1975).

[35] E. Pretsch, T. Clerc, J. Seibl, and W. Simon "Tabellen zur Strukturaufklärung Organischer Verbindungen", Springer, Berlin, 1976.

[36] E. A. Zvezdina, M. P. Zhdanov, V. A. Bren' and G. N. Dorofeenko, *Khim. Get. Soed.*, **1978**, 944.

Revue Roumaine de Chimie, 25, *11–12*, 1529–1534 (1980)

MECHANISM AND KINETICS OF THE ELECTROREDUCTION OF STEROL NITRATES

L. ALBERT[a], B. TÖKÉS[a] and F. HODOŞAN[b]

[a] Institute of Medicine and Pharmacy, Tîrgu Mureş, Str. Gh. Marinescu 38, Romania
[b] Institute of Chemistry, Cluj-Napoca, Str. Donath 65, Romania

Received July 11, 1979

Sterol nitrates are reduced polarographically by O—N bond cleavage to the parent sterols and nitric acid. The reaction proceeds through an irreversible one-step transfer of two electrons.

The preparative importance[1] and the remarkable biological activities[2] of sterol nitrates prompted us to investigate certain analytical problems related to this class of compounds which were completely neglected hitherto. The easiness with which the nitrate group can be reduced on the dropping mercury electrode[3] directed our attention to the polarographic analysis.[4] To what extent the results obtained with simple nitrate esters[5–7] are applicable to the more complex steroid compounds constituted the first problem which was posed. In order to answer this question we investigated four sterol nitrates, namely 17 β-nitroxy-5α-androstan-3-one (I), 3β-nitroxy-5α-androstan-17-one (II), 3α-nitroxy-5α-androstan-17-one (III) and 5α-nitroxy-androstan-17-one (IV), focusing our attention upon the mechanism and kinetic aspects of the electroreduction; the results obtained are reported in this paper.

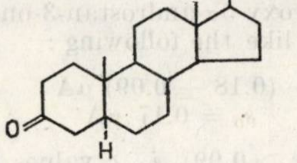

I

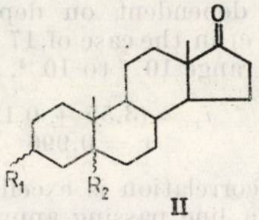

II

II. $R_1 = \beta-ONO_2$ $R_2 = \alpha-H$
III. $R_1 = \alpha-ONO_2$ $R_2 = \beta-H$
IV. $R_1 = H$ $R_2 = \alpha-ONO_2$

In a second series of measurements carried out on a larger number of sterol nitrates, we studied the relations between certain structural (especially steric) factors and the polarogrpahic behaviour; these data will be published later.

EXPERIMENTAL

Materials. Ethanol, LiCl, Britton-Robinson buffer ($pH = 5.72$), Triton X−100 (octylphenol polyethoxylate) were of analytical grade. The sterol nitrates I−IV were synthesized by the authors, their purity checked by thin layer chromatography.

Apparatus. The measurements were carried out with a model LP−55A Heyrovsky polarograph, fitted with an EZ-2 recorder, as well as with a Radelkis model OH−110 polarograph. For electrolysis an H-form polarographic cell was used, and that in a Höppler constant temperature bath; the temperature was controlled to ±0.05°C.

The dropping mercury electrode had the following parameters (in distilled water, at 0.00 V, and $T = 298$ K): $m = 2.48$ mg s^{-1}, $t_1 = 3.15$ s, $K = m^{2/3} \cdot t^{1/6} = 2.21$ $mg^{2/3} \cdot s^{-1/2}$. All half-wave potentials were referred to the saturated calomel electrode (S.C.E.). The number of electrons involved in the reduction was determined using microcells of 0.4 and 0.6 ml, and a rapid dropping capillary in order to reduce the electrolysis time.

Methods. Depolarizer solutions of 10^{-2} to 10^{-4} M in 70% ethanol were used. Lithium chloride 0.1 M and Britton-Robinson buffer respectively, were used as supporting electrolytes. Dissolved oxygen was removed from all the solutions by means of pure methane just prior to polarographic examination. Methane was purified by passing through the following solutions: a) H_2SO_4 conc., b) 20 ml of 10% $CdCl_2$ + 25 ml of Na_2CO_3 1N + 35 ml of water, c) 12 g of pyrogallol in 80 ml of 20% KOH, d) a solution identical with that used as supporting electrolyte in the corresponding polarographic examination.[8] The recording rate was 1.66 mV/s. The investigations were performed in a temperature range of 298 to 323 K. The height of the mercury reservoir (h) varied between 30−80 cm. Triton X-100 was used as suppressor of maxima.

RESULTS AND DISCUSSION

The detailed mechanism of an electrode reaction is characterized by a series of factors namely: the transport of particles to the electrode surface, the chemical processes preceding the strictly speaking electrode process, the orientation of molecules during electrode reaction, the steps of global process, as well as their rate, the structure of the transition states, the chemical reactions occurring after the electrode reaction, and the transport of products from the electrode surface. These details can be understood using various "diagnostical" criteria whereby considering the influence of various factors upon the electrode process.

The character of depolarizer transport at the mercury electrode surface has been stated by examining the intensity variation of the limiting current dependent on depolarizer concentration. The correlation equation ($\bar{i}_1$, c) in the case of 17 β-nitroxy-5α-androstan-3-one (I), in the concentation range 10^{-2} to 10^{-4}, looks like the following:

$$\bar{i}_1 = (3.55 \pm 0.12)\ c - (0.18 \pm 0.09)\ \mu A$$
$$r = 0.996 \qquad s_0 = 0.17\ \mu A$$

Linear correlation is excellent ($r > 0.99$), $\bar{i}_1$, c values being distributed along a line passing approximately through the origin. By compounds II−IV only the numerical coefficients of the correlation equation are changed, while existing further on an excellent linearity. These data demonstrate the diffusion character of the polarographic current. The value of the diffusion coefficient, as resulting from the correlation equation (i_1, c), is located in the range 1.17 to 4.62×10^{-6} $cm^2\ s^{-1}$.

The diffusion character of the current is emphasized also by the dependence of current intensity from mercury column pressure, that is by the parameters of the regression line ($\lg \bar{i}_1$, $\lg h$). Here is the correlation equation for nitrate **I**:

$$\lg \bar{i}_1 = (0.52 \pm 0.03) \lg h - (0.12 \pm 0.06)$$
$$r = 0.991 \qquad s_0 = \pm 0.013$$

where h represents the mercury column height in cm. From this correlation equation results $i_1 = kh^{1/2}$ in excellent agreement with Ilkovic's equation. As to the other compounds studied, we obtained practically identical results.

The height of polarographic steps for sterol nitrates increased with increasing *temperature*. The value of temperature coefficient was found in the range of 1.52 to 1.97 % K, thus suggesting the current process, as controlling factor. This conclusion is confirmed also by the energies of activation in the transport process as resulted from the equation[9]:

$$\lg \frac{\bar{i}_1}{m^{2/3} . t_1^{1/6}} = \lg 607 \text{ n.c.} D^{1/2} - \frac{1/2\, E_{tr}}{2/3 RT}$$

E_{tr} values were calculated from the parameters of the correlation equations $\left(\lg \bar{i}_1, \frac{1}{T}\right)$ (the variation of parameters m and t_1 in a relatively narrow temperature range can be ignored). The following correlation equations have been used:

Compound **I**:

$$\lg \bar{i}_1 = -(0.581 \pm 0.032)\, 10^3 \frac{1}{T} + (2.08 \pm 0.01)$$
$$r = -0.982 \qquad s_0 = \pm 0.003$$

Compound **II**:

$$\lg \bar{i}_1 = -(0.842 \pm 0.050)\, 10^3 \frac{1}{T} + (3.36 \pm 0.27)$$
$$r = -0.991 \qquad s_0 = \pm 0.013$$

Compound **III**:

$$\lg \bar{i}_1 = -(0.601 \pm 0.145)\, 10^3 \frac{1}{T} + (2.57 \pm 0.48)$$
$$r = -0.900 \qquad s_0 = \pm 0.032$$

Compound **IV**:

$$\lg \bar{i}_1 = -(0.810 \pm 0.072)\, 10^3 \frac{1}{T} + (3.22 \pm 0.24)$$
$$r = -0.922 \qquad s_0 = \pm 0.016$$

The values of the energy of activation of the transport process, as calculated from the equations above, were found in the limits 5.3 to 7.7 kcal/mol, a range agreeing with transport by diffusion.

The *electron transfer* was established by a method of polarographic microcoulometry.[10] The average values obtained could be found between the limits 1.87 and 2.05, respectively, thus being evident that during the electroreduction of sterol nitrates two electrons are transferred to the depolarizer. During coulometrical examination, one could notice that the height of polarographic steps decreases in time, however without appearing the appropiate anode step, thus meaning *irreversible character* of the electron transfer. The linearity of function (pK, E) as resulted from Meites and Israel's

$$k = \left[\frac{i/i_a}{1 - i/i_a}\right]^{0.9163} \cdot \frac{1}{1.349}\sqrt{\frac{D}{t_1}}$$

equation[11] shows that both electrons are accepted in the same step (Fig. 1).

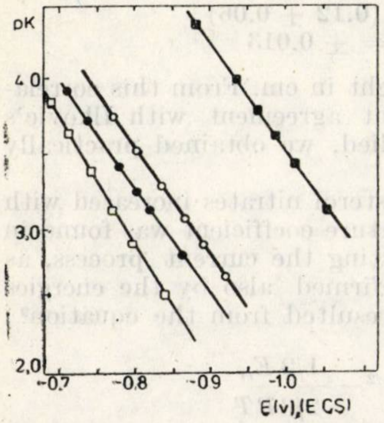

Fig. 1.—Dependence of pK value on potential (E) during the electroduction of sterol nitrates I—IV

The correlation equations presenting this dependence are the following:

Compound I:

$$E = -(0.121 \pm 0.004)\lg\frac{i}{i_a - i} - (4.122 \pm 0.0012)$$

$$r = -0.999 \qquad s_0 = \pm 0.004\ \mathrm{V}$$

Compound II:

$$E = -(0.122 \pm 0.005)\lg\frac{i}{i_a - i} - (4.728 \pm 0.001)$$

$$r = -0.997 \qquad s_0 = \pm 0.005\ \mathrm{V}$$

Compound III:

$$E = -(0.113 \pm 0.032)\lg\frac{i}{i_a - i} - (4.840 \pm 0.014)$$

$$r = -0.997 \qquad s_0 = \pm 0.011\ \mathrm{V}$$

Compound IV:

$$E = -(0.121 \pm 0.005)\lg\frac{i}{i_a - i} - (4.120 \pm 0.013)$$

$$r = -0.997 \qquad s_0 = \pm 0.011\ \mathrm{V}$$

The values of transfer coefficient (α) vary from 0.15 to 0.60. The half-wave potential varies with the depolarizer concentration, whereby it is evident that the electrode process has a *global kinetic order* higher than 1. Consequently, participation of a second component from the solution (e.g. H^+ ions) can be assumed.

By comparing the polarograms of sterol nitrates measured in broad pH ranges, at constant ion strength, one could state that their half-wave potentials are practically independent of pH.

This means that the protons do not participate at the potential determining step but they can interfere in another step of the electrochemical reaction. This assumption has been checked by the method of "latent limiting currents"[12] and by calculating the *number of protons* involved in the global reaction (q). This value of q results from the equation:

$$q = 2\left[1 - \frac{\Sigma i}{i_{\mathrm{RONO_2}}}\right],$$ being equal to 1.2, as seen in figure 2.

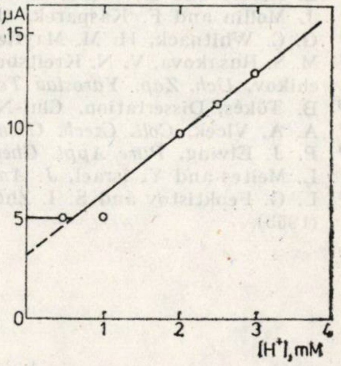

Fig. 2. — Determination of coefficient p by the electroreduction of 17β-nitroxy-5α-androstan-3-one (I).

According to the experimental data obtained we suppose two possible mechanisms of the rection:

1. $R-O-NO_2+2e^- \rightarrow RO^- + NO_2^-$

$$RO^- + H_3O^+ \rightarrow R-OH + H_2O$$

$$NO_2^- + H_3O^+ \rightarrow HNO_2 + H_2O$$

2. $R-O-NO_2+2e^- \rightarrow R^- + NO_3^-$

$$R^- + H_3O^+ \rightarrow R-H + H_2O$$

For being able to choose the actual mechanism, preparative electrolyses of the compounds studied were performed. These were carried out at constant cathodic potential corresponding to the limiting current, thus providing conditions identical with those of the polarographic examinations. Starting with a known concentration c_0 of the depolarizer, registering *versus* time the limiting current intensity, on the basis of the proportionality between i_d and c, we calculated the concentration of depolarizer as well as of the supposed reaction products at the end of electrolysis. The presence of sterols and NO_2^- ions could be identified. Sterols $(R-OH)$ were identified by thin layer chromatography and found to be identical with the starting alcohols from which the nitrate esters have been prepared. The NO_2^- amounts, determined photometrically according to Griess-Ilosvay reaction, were proved to be 68 to 79% of the calculated values. No $R-H$ type compound could be identified. These data agree also with the value higher than 1 of coefficient q, and can be explained by the dissociation of nitrous acid taking place in diluted solutions ($K_a = 6.10^{-4}$, at 273 K).

The results obtained demonstrate that sterol nitrates are polarographically reduced according to mechanism 1.

REFERENCES

[1] I. Tănăsescu, F. Hodoşan, and I. Jude, papers quoted in C. Djerassi, "Steroid Reactions", Holden-Day, San Francisco, 1963, pp. 75, 410.

[2] F. Hodoşan, D. Breazu, B. Cuparencu, L. Jude, O. Mantsch and N. Sterescu, *Arzneim. Forsch.*, **19,** 684 (1969) ; F. P. Hodoşan, D. Breazu, B. Cuparencu, I. Jude, O. Mantsch and H. Sterescu, *Rom. Pat. 52, 205,* 8 Sept. 1969 ; *Chem. Abstr.*, **75**, 77155 (1971) ; G. R. Wendt, and K. W. Ledig, *U.S. Pat. 3, 352, 891,* 14 Nov. 1967 ; *Chem. Abstr.*, **69** 19404 (1968).

[3] F. Kaufman, H. J. Cook and S. M. Davis, *J. Amer. Chem. Soc.*, **74**, 4997 (1952).

[4] L. Albert and B. Tökés, *Revista Medicală*, **19**, 152 (1973).

[5] J. Mollin and F. Kasparek, *Coll. Czech. Chem. Comm.*, **26**, 2438 (1961).

[6] G. C. Whitnack, H. M. Mayfield and E. S. C. Ganz, *Analyt. Chem.*, **35**, 403 (1963).

[7] M. S. Rusakova, V. N. Kreitsberg, V. A. Podgorova, E. P. Shuyrikov and B. F. Ustavshchikov, *Uch. Zap. Yaroslav Tehnol. Inst.*, **19**, 70 (1970) ; *Chem. Abstr.*, **77**, 47621 (1972).

[8] B. Tökés, Dissertation, Cluj-Napoca, 1971.

[9] A. A. Vlcek, *Coll. Czech. Chem. Comm.*, **24**, 2538 (1959).

[10] P. J. Elving, *Pure Appl. Chem.*, **15**, 297 (1967).

[11] L. Meites and Y. Israel, *J. Amer. Chem. Sco.*, **83**, 4903 (1961).

[12] L. G. Feoktistov and S. I. Zhdanov, *Izvest. Akad. Nauk S.S.S.R., Otdel. khim. Nauk*, **45** (1963).

Revue Roumaine de Chimie, 25, *11–12*, 1535–1541 (1980)

A COMPARATIVE STUDY OF THE INFRARED SPECTRA OF CHARGE TRANSFER COMPOUNDS OF ANILINE DERIVATIVES WITH 3,5-DINITROSALICYLIC ACID

Y.M. ISSA *, A.M. HINDAWEY, R.M. ISSA ** and A.M.G. NASSAR
Chemistry Department, Faculty of Science, Alexandria University
(* Cairo University, ** Tanta University) A.R. Egypt

Received November 17, 1978

Charge transfer compounds of substituted anilines as donors with 3,5-dinitrosalicylic acid as acceptor are prepared from ethanol or benzene solvents. The infrared spectra of the compounds obtained were recorded and compared with those of the constituents. This comparison revealed that the compounds prepared from ethanol belong to proton transfer type, whereas those obtained from benzene are either charge transfer complexes for very weak basic amines or proton transfer type for strong or moderate basic ones.

INTRODUCTION

In previous articles, we reported on the charge transfer compounds of aromatic amines with some trinitrobenzene derivatives[1–3] and 3,5-dinitrobenzoic acid.[4] In these studies it was pointed out that the reaction products depend on both the basicity of the aromatic amine and the acidity of the nitro compound. The success of the reaction with 3,5-dinitrobenzoic acid revealed that the existence of the three nitro groups is not essential. Thus, the presence of two nitro groups would be sufficient to give the aromatic ring a good acceptor character. To test this point, the reaction of 2,4-dinitrophenol with aniline derivatives was investigated.[5] The results proved that 2,4-dinitrophenol is quite comparable in its behaviour with picric acid, though it formed compounds with salt character with strongly basic aniline derivatives only.

3,5-Dinitrosalicylic acid **(1)** combines the structure of both 2,4-dinitrophenol **(2)** and 3,5-dinitrobenzoic acid **(3)**, also its structure resembles that of picric acid **(4)** in which case a nitro is displaced by the carboxylic group.

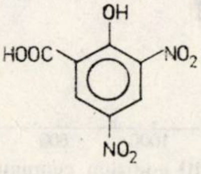

1

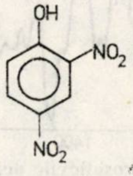

2

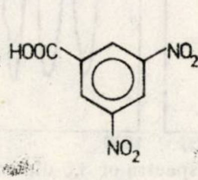

3

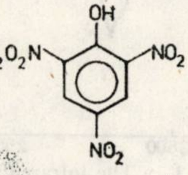

4

Based on these relations in structure the charge transfer compounds of aniline derivatives with 3,5-dinitrosalicylic acid are prepared and studied by IR-spectroscopy, the results obtained with 3,5-dinitrosalicylic acid are compared with those obtained in the previous studies.[6]

EXPERIMENTAL

The compounds used in the present investigation were pure laboratory grade BDH products. The charge transfer compounds were prepared by mixing a hot solution of the 3,5-dinitrosalicylic acid (0.01 mole in the least amount of absolute ethanol) with a similar one containing the aniline derivative. The addition compounds separated were recrystallized from ethanol, then their melting points were determined.

The infrared spectra of the compounds were recorded on a Unicam SP 1000 infrared spectrophotometer using the KBr disc technique.

RESULTS AND DISCUSSION

A clear understanding of the interaction between aniline derivatives and 3,5-dinitrosalicylic acid **(1)** requires a previous assignment of the bands in the infrared spectrum of the acceptor especially those corresponding to groups liable to suffer some changes.

(I) THE IR-SPECTRUM OF 3,5-DINITROSALICYLIC ACID

The infrared spectrum of **(1)** displays two bands at 3570 and 3460 cm^{-1} corresponding to the ν(OH) stretching vibration of the COOH group (Fig. 1, Table 1). The stretching vibration of the phenolic OH-group

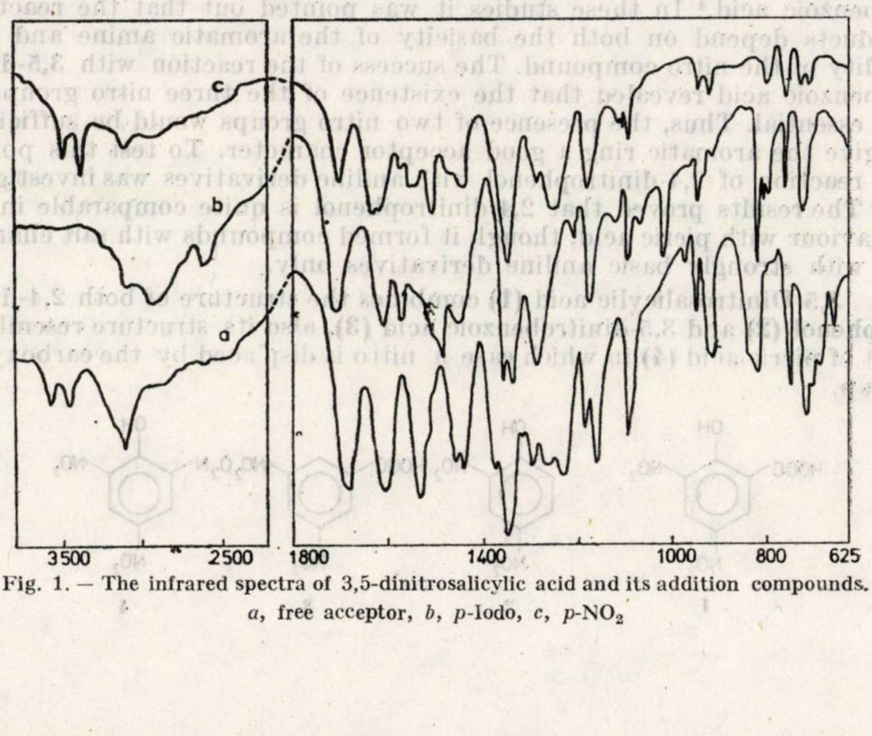

Fig. 1. — The infrared spectra of 3,5-dinitrosalicylic acid and its addition compounds. *a*, free acceptor, *b*, *p*-Iodo, *c*, *p*-NO$_2$

TABLE 1

Important bands in the IR-spectra of charge transfer complexes of 3,5-dinitrosalicylic acid with aniline derivatives

Substituent	Type	Colour	Solvent	m.p. °C	pK_a	ν(OH)	ν(C=O)	NO_2 asym.	NO_2 sym.	γ(CH)
free acceptor						3570, 3460 3100	1700 1675	1540, 1530	1345, 1335	925, 825
H	P.T.	Y	E, B	180		3180	1700	1535, 1525	1355, 1336	918, 812
p-OCH$_3$	P.T.	G.Y.	E, B	140	5.34	3180	1710	1530, 1516	1345, 1335	920, 813
m-OCH$_3$	P.T.	G.Y.	E, B	190	4.23	3230	1710	1540, 1525	1350, 1330	910, 813
o-OCH$_3$	P.T.	G.Y.	E, B	173	4.51	3230	1715	1535, 1525	1340, 1335	908, 808
p-OH	P.T.	G.Y.	E, B	180	5.51	3270	1700	1530	1350, 1330	920, 815
m-OH	P.T.	G.Y.	E	190	4.12	3200	1710	1540, 1520	1350, 1330	910, 813
o-OH	C.T.	R.b.	E, B	160	4.72	3420, 3170	1695	1530	1343	920, 815
p-CH$_3$	P.T.	Y	E, B	169	5.08	3150	1710	1540, 1525	1350, 1335	918, 813
m-CH$_3$	P.T.	Y	E, B	190	4.73	3230	1700	1530, 1520	1340, 1325	923, 815
o-CH$_3$	P.T.	Y	E, B	190	4.45	3150	1710	1525, 1515sh	1350, 1335	910, 810
p-I	P.T.	Y	E	170	— —	3220	1700	1540, 1520	1340, 1330	905, 810
p-Br	P.T.	Y	E, B	190	3.86	3250	1705	1530, 1520	1350, 1330	920, 815
m-Br	P.T.	Y	E, B		3.58	3240	1690	1540, 1520	1340, 1330	920, 810
p-Cl	P.T.	G.Y.	E, B	195	4.15	3190	1705	1540, 1525	1350, 1335	—, 818
m-Cl	P.T.	G.Y.	E, B	170	3.46	3230	1690	1545, 1540	1333, 1330	910, 815
o-Cl	P.T.	G.Y.	E, B	158	2.65	3100	1700	1550, 1535	1350, 1335	905, 810
p-COOH	P.T.	O.Y.	E		2.50	3220	1700	1535, 1520	1353, 1330	—, 810
p-COOH	C.T.	O.b.	B			3480, 3200	1695	1550, 1540	1350, 1325	915, 810
m-COOH	P.T.	G.Y.	E	198	2.04	3200	1700	1530, 1520	1355, 1335	910, 813
m-COOH	P.T.	p.b.	B			3200	1710	1535 1520	1355 1325	915 810
o-COOH	P.T.	Y	E, B	160	2.11	3350sh	1695	1535, 1520	1335sh, 1325	910, 810
p-NO$_2$	P.T.	O	E, B	160	2.03	3200	1690	1535, 1520	1340, 1330	920, 815
m-NO$_2$	P.T.	Y	E, B	154	2.45	3300	1700	1540, 1530	1340, 1325	913, 815
o-NO$_2$	C.T.	O	E, B	118	0.06	3480, 3200	1695	1550, 1540	1350, 1345	912, 815
p-COCH$_3$	P.T.	O.Y.	E, B	140	— — —	3200	1700	1530, 1520	1350, 1325	915, 810

P.T. = proton transfer, C.T. = charge transfer, E = ethanol, B = benzene, Y = yellow, G = green, R = red, b = brown, O = orange, p = pale.

leads to a broad intense band near 3100 cm^{-1} overlapped with the ν(CH) bands of the benzene ring. The existence of two bands for the ν(OH) of the COOH-group indicates the existence of two forms for this group, a free and bonded one. The appearance and position of the ν(OH) band of the phenolic OH-group is quite comparable with that of 2,4-dinitrophenol or picric acid. Thus, the phenolic OH group would be involved in an intramolecular hydrogen bonding with the NO_2 group in *o*-position to it. The bonding between the various groups may be formulated as follows :

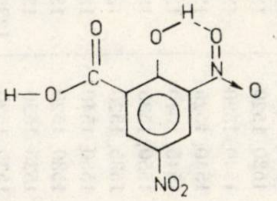

1a

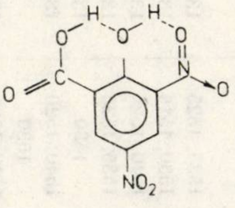

1b

The C = O bands near 1700 and 1675 cm^{-1} as well as the NO_2-bands at 1540, 1530 (asym.) and 1345, 1335 (sym.) cm^{-1} are broadened. The presence of two bands for each vibrational motion denotes that the C = O and NO_2-group have different energy states corresponding to the free and the hydrogen bonded groups.

The deformation vibration of the phenolic OH-group leads to an intense band at 1370 cm^{-1} while the C—OH stretching mode gives the band at 1175 cm^{-1}; both types of vibrations are coupled together and hence the two bands would be characteristic of the phenolic OH-group.[7] The bands at 3570 and 3460 cm^{-1} can be assigned to the vibration of the carboxyl OH-group. Support for the assignment is joined by comparing the IR-spectrum of 3,5-dinitrosalicylic acid with those of 2,4-dinitrophenol and 3,5-dinitrobenzoic acid.

(II) SPECTRA OF THE CHARGE TRANSFER COMPLEXES

On comparing the IR-spectra of the charge transfer compounds with those of their constituents, the following changes can be readily observed.

(i) Compounds prepared from ethanol

For aniline derivatives not containing the NO_2 group, the spectra of the addition compounds do not show the bands due to the stretching vibration of the NH_2- or the phenolic OH- group. Thus, the spectral region above 3000 cm^{-1} displays the bands assigned to ν(OH) of the aromatic ring, as well as a broad band due to a hydrogen bonded OH-group of (1) within the 3180—3350 cm^{-1} range. The spectra are also characterized by a group of interacting intense bands within the 3200—2500 cm^{-1} range. These latter bands can be assigned to the stretching vibration of the $-N^+H_3$-group which results from a proton transfer from the acceptor molecule **(1)** to the aniline derivative.[8,9]

The proton transfer from **(1)** to the aniline derivative would take place from either the phenolic or carboxylic group whereby the phenate or carboxylate ion is formed. The existence of the addition compounds reveals that the carboxyl group still retains its identity in the addition compounds. Thus it can be concluded that the proton of the phenolic group would be that participating in the formation of the addition compounds. This is supported by the disappearance of the two bands at 1370 and 1175 cm^{-1} corresponding to δ(OH) and ν(C–OH) of the phenolic group. The negative charge left on the phenate ion interacts strongly with the carboxyl OH-group forming a strong intramolecular hydrogen bonding. The formation of the proton transfer compound in this case can be formulated as follows :

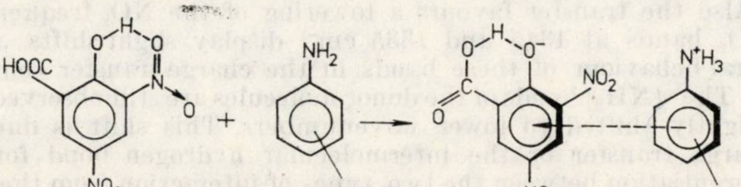

Substantial support for the suggested structure is attained by considering the spectral shifts due to the formation of the addition compound. The splitting of the C=O and NO_2 bands appearing in the spectrum of **(1)**, is no more clear in the spectra of the addition compounds. This denotes that the carboxyl group exhibits one probable structure in which the OH-group is involved in a strong hydrogen bonding. Also the two NO_2-groups would have almost the same energy as a result of the destruction of the intramolecular hydrogen bonding between the NO_2-group in position 3 and the phenolic OH-group. The NO_2-bands are shifted to higher or lower wavenumbers which is characteristic of compounds of the salt type.[2,8]

The γ(CH) bands of **(1)** are shifted to lower wavenumbers indicating that the aromatic ring functioned as an acceptor for the negative charge from the ring of the aniline derivative. The band at 825 cm^{-1} interacts with other bands on the lower frequency side.

For the amine component, the bands corresponding to NH_2-deformation vibrations are no more observed in the spectra of the P. T. compound.

Instead of these the bands due to the N^+H_3 structure are observed.

Accordingly, the spectral changes observed reveal that the interaction between **(1)** and the aniline derivatives under investigation involves a proton transfer from the phenolic group of 3,5-dinitrosalicylic acid to the aniline derivative,.

(ii) Compounds of the charge transfer complex type

These compounds are obtained from benzene in the case of *o*-NO_2 and *p*-COOH aniline derivatives and *o*-NO_2 from ethanol. These have orange, red or brown colours. The main spectral shifts can be given as follows :

(1) The γ(CH) bands of the acceptor part at 925 and 825 cm^{-1} are shifted to lower wavenumbers where the γ(CH) of the donor molecule

are generally shifted to higher wavenumbers. This behaviour is common among C.T. complexes and reveals the $\pi-\pi^*$ interaction in which an electron is transferred from the highly filled π-orbital of the donor molecule to a vacant orbital of the acceptor molecule.[10]

(2) The asym. NO_2 bands of the acceptor at 1540 and 1530 cm^{-1} retain their original appearance (being splitted to two bands) but shifted to higher or lower wavenumbers. The shift to high wavenumbers is common of compounds involving $n-\pi^*$ transition i.e. where an n-electron is transferred from the NH_2-groups to a vacant π^*-orbital on the NO_2-group, which affords a higher band order for the N=O linkage. On the other hand, the shift of the NO_2-bands to lower wavenumbers occurs when the NH_2 group forms an intermolecular hydrogen bonding with the NO_2 group. Also the transfer favours a lowering of the NO_2-frequency. The sym. NO_2 bands at 1345 and 1335 cm^{-1} display slight shifts which is the general behaviour of these bands in the charge transfer compounds.

(3) The $\nu(NH_2)$ bands of the donor molecules are still observed though being slightly shifted to lower wavenumbers. This shift is due to the n-π^* charge transfer or the intermolecular hydrogen bond formation. The differentiation between the two types of interaction from the behaviour of the bands alone is not possible but the shifts of the NO_2 bands should also be considered.

(4) The ν(OH) bands are still observed but are shifted to lower wavenumbers indicating a stronger intermolecular hydrogen bonding which results from the increased electron density on the ring of the donor in the C.T. complex. The ν(OH) bands of the COOH groups are turned to a single band at lower wavenumbers indicating that the possible isomeric form in the free 3,5-dinitrosalicylic acid and in the C.T. complex is that the carboxylic OH group would be involved in an intramolecular hydrogen bonding with the phenolic group.

(5) The C = O group displays a single band at 1695 cm^1 which is shifted to higher wavenumbers compared to the free acceptor. This reveals that the mesomeric interaction between the C= O and carboxylic OH group is lowered due to the participation of the latter in the intermolecular hydrogen bonding.

Based on the behaviour of the different bands the C.T. compounds can be classified into ; (a) compounds involving n-π^* in addition to the $\pi-\pi^*$ interaction, and (b) compounds comprising intermolecular hydrogen bonding besides the $\pi-\pi^*$ transfer. The structure of the charge transfer complexes can be formulated as follows :

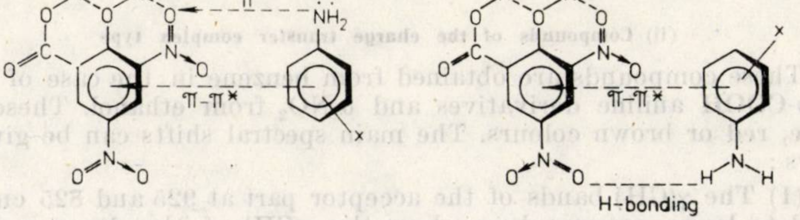

REFERENCES

[1] R. M. Issa and M. M. El-Essawey, *Z. phys. Chem. (Leipzig)*, **253**, 96 (1973).
[2] A. M. Hindawey, A. M. G. Nassar and R. M. Issa, *Acta Chim. Acad. Sci. Hung.*, **88**, 341 (1976).
[3] A. M. G. Nassar and A. M. Hindawey, *Egypt. J. Chem.*, **19**, 257 (1976).
[4] A. M. Hindawey, A. M. G. Nassar and R. M. Issa, *Acta Chim. Acad. Sci. Hung.*, **92**, 263 (1977).
[5] Y. M. Issa, A. M. Hindawey, A.M.G. Nassar and R. M. Issa, in press.
[6] R. Mecke and G. Rossmy, *Z. Elektrochem.*, **59**, 866 (1955).
[7] R. D. Kross and V. A. Fassel, *J. Amer. Chem. Soc.*, **79**, 38 (1956).
[8] G. Briegleb and H. Delle, *Z. Elektrochem.*, **64**, 347 (1960); *Z. phys. Chem. (Frankfurt)*, **24**, 359 (1960).
[9] J. Bellanato, *Spectrochim. Acta*, **16**, 1344 (1960).
[10] G. Briegleb, "Elektron-Donator Komplexe", Springer Verlag, Berlin, 1961.

Revue Roumaine de Chimie, 25, *11–12*, 1543–1548 (1980)

BASICITY CONSTANTS OF SOME *N,N'*-DISUBSTITUTED *p*-PHENYLENEDIAMINES*)

F. M. ALBERT,[a] MARIA GIURGINCA,[b] AURELIA MEGHEA[a] and G. IVAN[b]
[a] National Institute of Chemistry, R-78126 Bucharest, Romania
[b] Research Institute for Rubber and Plastics Processing R-75651 Bucharest, Romania

Received August 21, 1979

Basicity constants were determined spectroscopically for fourteen N, N'-disubstituted *p*-phenylenediamines used as stabilizers in the rubber industry. Some correlations of basicity constants and other physical chemical characteristics are also discussed.

Previously published results on structural, spectroscopic and complexing properties of N,N'-disubstituted *p*-phenylenediamines [1,2] are completed in the present paper in an attempt to provide a better support to explain antioxidant and antiozonant properties of some *p*-phenylenediamine derivatives of interest in the rubber industry.

In spite of the fact that substituted anilines are well studied in respect to dissociation equilibria of conjugated acids and, in general, for thermodynamical properties, data on basicity constants of aromatic diamines available in literature are limited only to unsubstituted derivatives of benzidine,[3,4] and to phenylenediamine isomers.[4–7]

EXPERIMENTAL

Substances used in the present work (Table 1) were of quality *p.a.* or were purified in our laboratory. Sample A14 was examined as a mixture of isomers.

Solutions were prepared with the concentration 10^{-3} mol.

Spectra were recorded on a Specord UV–VIS spectrophotometer (VEB Carl Zeiss, German Democratic Republic) in the range 200–850 nm, at 25°C.

pH measurements were accomplished by an A74 pH-meter (INM, Romania).

Evaluation procedures. Calculations of basicity constants were based on determination of conjugated species participating in acid-base equilibrium for the two protonation steps :

$$B + H^+ \rightleftarrows BH^+ \tag{1}$$

$$BH^+ + H^+ \rightleftarrows BH_2^{++} \tag{2}$$

Dissociation constants of the conjugated acids were computed by the relation :

$$pKa_1 = \mathrm{pH} - \log\frac{[B]}{[BH^+]} + \log \gamma_{BH^+} \tag{3}$$

where the last term, with correction purpose, could be neglected since diluted solutions of diamines were used. [8]

---

*) **Presented at National Congress of Chemistry, Bucharest 1978**

The ratio of the concentrations of the conjugated pairs were estimated by measurement of optical density of free base (D_B), and of protonated forms (D_{BH^+} ; $D_{BH_2^{+}+}$), and of an equilibrium mixture of the three species (D), hence

$$\frac{[B]}{[BH^+]} = \frac{D - D_{BH^+}}{D_B - D} \tag{4}$$

TABLE 1

NN'-disubstituted *p*-phenylenediamines

A_1	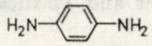
A_2	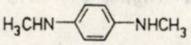 H₃CHN NHCH₃
A_3	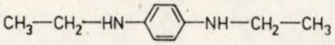 CH₃—CH₂—HN NH—CH₂—CH₃
A_4	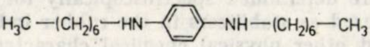 H₃C—(CH₂)₆—HN NH—(CH₂)₆—CH₃
A_5	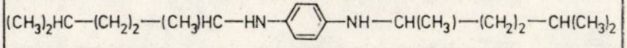 (CH₃)₂HC—(CH₂)₂—(CH₃)HC—HN NH—CH(CH₃)—(CH₂)₂—CH(CH₃)₂
A_6	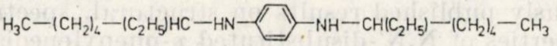 H₃C—(CH₂)₄—(C₂H₅)HC—HN NH—CH(C₂H₅)—(CH₂)₄—CH₃
A_7	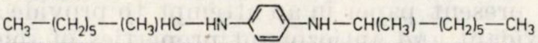 CH₃—(CH₂)₅—(CH₃)HC—HN NH—CH(CH₃)—(CH₂)₅—CH₃
A_8	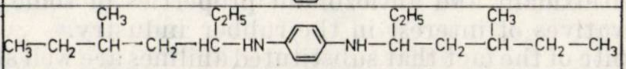 CH₃ C₂H₅ C₂H₅ CH₃ CH₃—CH₂—CH—CH₂—HC—HN NH—CH—CH₂—CH—CH₂—CH₃
A_9	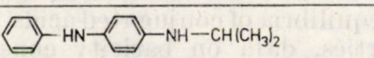 HN NH—CH(CH₃)₂
A_{10}	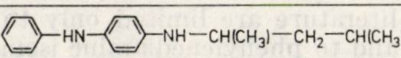 HN NH—CH(CH₃)—CH₂—CH(CH₃)₂
A_{11}	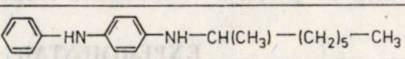 HN NH—CH(CH₃)—(CH₂)₅—CH₃
A_{12}	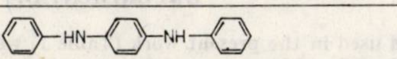
A_{13}	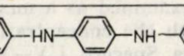
A_{14}	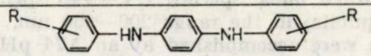
A_{15}	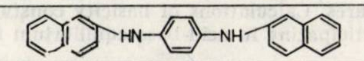

Spectrophotometric measurements were accomplished in aqueous media using solutions with various pH values. Depending on the necessary domain of pH, determined by the basic strength of the amines, the actual value was determined by different ways :

(a) for the domain of pH from 2 to 8, series of buffer solutions with known pH were used[9] ;

(b) for the domain of pH from .9 to 3.5, the acidity of medium was modified by adding diluted HCl solutions [10] and checking by pH-meter ;

(c) for every weak bases, with *p*Ka < 0, in domain of the Hammett acidities, sulfuric acid solutions with known acidity function (H_0) were used. [5,11] For this situation, relation (3) becomes :

$$pKa = H_0 - \log \frac{[B]}{[BH]^+} \tag{5}$$

Experimental results were processed graphically or analytically, using for each case two or three methods in order to compare and to establish the most accurate value of pKa.

Analytical computation was based on the method developed by Albert and Sergeant, [12] using for N, N′-dialkyl-*p*-phenylenediamines **(A1 to A8)** series of buffer solutions, for determination of both protonation constants, and hydrochloric acid solutions for the second constant. The results obtained are presented in table 2.

TABLE 2

Acidity constants of N, N′-dialkyl-*p*-phenylenediamines

Amines	Method with buffer solutions				Method with HCl solutions
	Analytical evaluation		Graphical evaluation		Analytical evaluation
	pKa_1	pKa_2	pKa_1	pKa_2	pKa_2
A1*⁾	6.10	3.20	6.15	3.15	2.55
A2	6.45	3.60	6.30	3.45	2.51
A3	6.36	3.13	6.25	3.30	2.48
A4	6.80	2.65	6.76	2.55	2.49
A5	6.75	2.45	6.60	2.60	2.81
A6	6.80	3.50	6.60	3.60	3.30
A7	6.35	2.00	6.30	1.92	1.88
A8	6.25	2.20	6.30	2.25	2.37

*⁾ For *p*-phenylenediamine the following *pKa* values were already published : $pKa_1 = 6.23$ and $pKa_2 = 3.29$ reported by [3,4] ; $pKa_1 = 6.16$ and $pKa_2 = 2.67$ reported by. [6]

For alkyl-aryl- and diaryldisubstituted *p*-phenylenediamines **(A9 to A15)**, evaluation of first protonation step was accomplished using hydrochloric acid solutions with known pH, and for the second step, situated in the range of Hammett acidities, sulfuric acid solutions with known H_0 were used.

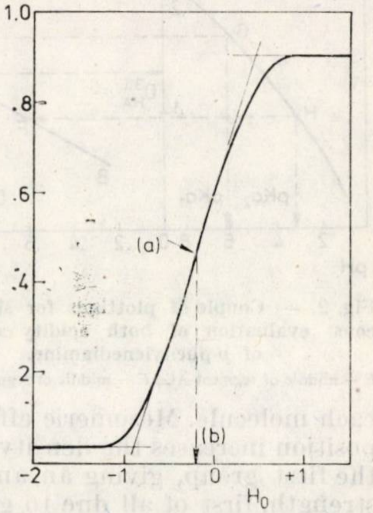

Fig. 1. — Plotting of D as a function of H_0 for N-isopropyl-N′-phenyl-’*p*-phenylenediamine **(A9)**.

(a) — the middle of straight part of the plotting;
(b) — $pKa_2 = -0.25$

Results of analytical computations were verified by graphical evaluation for amines **A9** to **A15** by plotting D as a function of pH in accordance with equation (3) for the first protonation step, and consequently by plotting D as a function of H_0 in accordance with equation (5) for the second protonation step (as illustrated in Figure 1). The results obtained by both computation ways are grouped in table 3 where the good agreement of the results of the different methods may be observed.

Since values of pKa_2 for amines **A1** to **A8**, obtained by graphical evaluation of the measurements conducted in hydrochloric acid, are in a less good concordance with analytical estimation from measurements with buffer solutions, these experimental results were processed also by another graphical method [8] illustrated in figure 2 for *p*-phenylenediamine.

The method consists of a couple of plottings where the left part represents the dependence of optical density of a given band on pH *i.e.* $D^{320} = f(pH)$, and the right part represents the correlation of the two absorption bands, *i.e.* $D^{310} = f(D^{245})$. This graphi-

TABLE 3

Acidity constants of N-alkyl-N′-aryl-*p*-phenylenediamines and of N, N′-diaryl-*p*-phenylenediamines

Amines	pKa_1 determined in HCl solutions		pKa_2 determined in H_2SO_4 solutions	
	Graphical evaluation $D = f(pH)$	Analytical evaluation	Graphical evaluation $D = f(H_0)$	Analytical evaluation
4-Amino-diphenylamine	2.80	2.85	.78	.80
A9	2.10	1.90	−0.25	−0.26
A10	1.02	1.02	−0.30	−0.30
A11	1.22	1.22	−0.37	−0.36
A12	2.11	2.10	−0.20	−0.22
A13	2.02	2.03	−0.65	−0.62
A14	1.87	1.98	−0.65	−0.65
A15	2.24	2.25	−1.12	−1.15

cal method allows simultaneous evaluation of the two acidity constants from the same experimental data, leading to results in close agreement with the analytical results as presented in table 2.

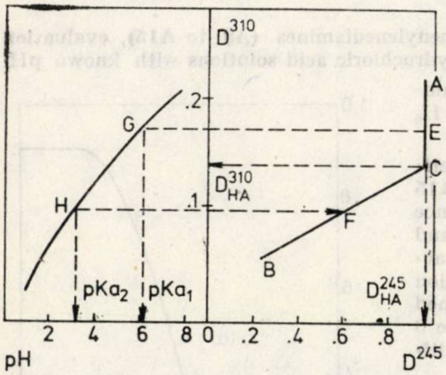

Fig. 2. — Couple of plottings for simultaneous evaluation of both acidity constants of *p*-phenylenediamine.

E — middle of segment AC; *F* — middle of segment CB.

RESULTS AND DISCUSSIONS

The first term of the studied series, *p*-phenylenediamine, could be considered as a *p*-substituted aniline. Introduction of the second amino group leads to alteration of *pKa* value of the aniline ($pKa = 4.6$)[13,14] as presented in table 2. These modifications are due to electron donor effect of the NH_2 group which contributes to increase of *pKa* value. For the particular case of *p*-phenylenediamine, pKa, values are increased also by a statistic factor as there are two proton accepting positions for each molecule. Mesomeric effect of the two NH_2 groups situated in *para* position increases the density of electrons on both groups. Protonation of the first group, giving an ammonium group $-NH_3^+$ diminishes the base strength, first of all due to group interaction, but rather large difference between the two pKa values ($\Delta pKa \cong 3$) suggests that the preponderant effect is the inductive one.[13]

In comparison with *p*-phenylenediamine, N,N′-dialkyl-*p*-phenylenediamines (**A2** to **A8**) exhibit slightly increased *pKa* values which should be attributed to the hyperconjugation effect of alkyl groups leading to increase of charge density on nitrogen atom, in agreement with previously reported data.[1] Results of the present work allows the observation that length and branching of the alkyl radical seem to have not a great influence on the first protonation constant. This affirmation could not be extended on the second *pKa* value, while this seems to be affected by the length of alkyl substituent (e.g. for **A4**) as well as by a sterical effect for *iso*-alkyl substituents. The highest pKa_2 value found for A6 should be explained by a favourable position of ethyl radical against nitrogen atom and thus it contributes to the increase of the base strength.[13,15]

The group of amines from **A9** to **A14** can be considered also as derivatives of 4-aminodiphenylamine alkylated or arylated at 4-amino group; this approach of discussion allows to emphasize the influence of the substituents on basicity constants.

Table 3 presents the basicity constants for N-alkyl-N′-aryl-*p*-phenylenediamines and for N,N′-diaryl-*p*-phenylenediamines. In comparison with the *p*-phenylenediamine itself, amines **A9** to **A15** exhibit an appreciable decrease of basicity constant which could be attributed mainly to an intense conjugation effect extended on the whole molecule; in this extended system, lone pair electrons of nitrogen participate by hybridization, and π-p-π conjugation is realized with *p* component of hybridized *n*-orbital.[16]

Amines **A9** to **A11** with *iso*-alkyl substituents at 4-amino group exhibit lower values of basicity constants in comparison with 4-aminodiphenylamine giving evidence of a steric effect of *iso*-alkyl groups unfavourably positioned against the basic center. This steric hindrance is more marked for voluminous *iso*-alkyls, as for amines **A10** and **A11**; the expected weak inductive effect observable for amines **9A** and **A12** is overlapped here by the more powerful steric effect.

In the case of amines **A13** to **A15**, the more extended conjugation determined the decrease of the basicity constants, particularly for the second protonation step.

Amine **A14** was studied as a mixture of isomers. It has a pKa_1 value little lower in comparison with amine **A13** and this difference could be explained by preponderance of *ortho*- substituted isomer that induces a supplemental steric hindrance on amino goup.

REFERENCES

[1] M. Giurginca, A. Meghea and G. Ivan, *Rev. Chim. (București)*, **27**, 470 (1976).

[2] F. M. Albert, M. Giurginca, A. Meghea and G. Ivan, Paper presented at National Congress of Chemistry, Bucharest 1978.

[3] R. Kuhn and F. Zumstein, *Ber. dtsch. chem. Ges.*, **59**, 488 (1926).

[4] R. Kuhn and A. Wasserman, *Helv. Chim. Acta*, **11**, 1 (1928).

[5] F. G. Manrique, A. Mederos, A. R. Gonzáles, A. Hardisson and Y. G. Smeyers, *Quimica (Madrid)*, **69**, 305 (1973).

[6] J. M. Vandenbelt, C. Henrich and S. G. Vanden, *Analyt. Chem.*, **26**, 726 (1954).

[7] N. F. Hall, *J. Amer. Chem. Soc.*, **52**, 5115 (1930).

[8] I. Ya. Berstein and Yu. L. Kaminsky, "Spektrofotometricheskii analiz v organicheskoĭ khimii", Khimiia, Leningrad 1975, p. 144.

[9] J. P. Elving, J. M. Markowitz and J. Rosenthal, *Analyt. Chem.*, **28**, 1179 (1956).

[10] C. Luca, "pH-ul şi aplicaţiile lui", Editura tehnică, Bucharest 1964, p. 54.

[11] P. Vetešnik, *Coll. Czech. Chem. Comm.*, **33**, 556 (1968).

[12] A. Albert and E. R. Sergeant, "Ionization Constants of Acids and Bases", Russian translation, Khimiia, Moscow 1964, p. 67.

[13] J. W. Smith, "Basicity and Complex Formation", Chapter 4 in "The Chemistry of Amino Group" by S. Patai (Editor), Interscience, New York 1968, p. 161.

[14] A. Meghea, M. Vlad, T. Moldovan and A. Stefan, *Rev. Chim. (Bucureşti)*, **26**, 329 (1975).

[15] D. D. Perrin and J. Clark, *Quart. Rev.*, **18**, 295 (1964).

[16] O. V. Sverdlova, "Elektronnye spektry v organicheskoĭ khimii", Khimiia, Leningrad 1973, p. 144.

Revue Roumaine de Chimie, **25**, *11–12*, 1549–1560 (1980)

SOME REACTIONS OF β-3,4-DICHLOROBENZOYL-PROPIONIC ACID

M.M. ABD ALLA, E. A. SOLIMAN, A. A. HAMED and M. W. OSMAN
Faculties of Sciences, Zagazig and Ain Shams Universities,
Cairo, Egypt

Received May 26, 1979

Condensation of β-3,4-dichlorobenzoylpropionic acid (I) with aromatic aldehydes, isatine, phthalic anhydride, 3-nitrophthalic anhydride and cyclohexanone under Perkin conditions afforded the furanone derivatives II, IV, V. The condensation of I with ketones in the presence of ammonium acetate in boiling xyline has been explored and extended. The action of hydrazine on the above products has been also studied.

In continuation of our recent study,[1] β-3,4-dichlorobenzoyl-propionic acid (I) was condensed with aromatic aldehydes namely, benzaldehyde, anisaldehyde, *p*-dimethylaminobenzaldehyde, piperonal, cinnamaldehyde and furfural under Perkin conditions. The products were the corresponding α-3-arylidene -5,3,4-dichlorophenylfuran-3(2H)-2-ones (IIa-f).

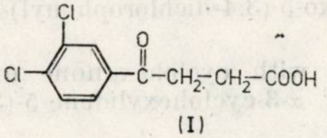
(I)

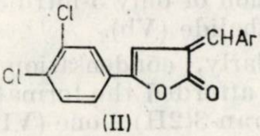

(II)

a, Ar $= C_6H_5$; b, Ar $= C_6H_4\,OCH_3(p-)$; c, Ar $= C_6H_4N(CH_3)_2(p-)$

d, $C_6H_3O_2CH_2-34$; e, $C_6H_5-CH=CH$; f, 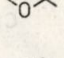

Compound IIb can be prepared authentically by condensation of 5-(3,4-dichlorophenyl)-5-furan-3-(2H)-one (III) (prepared via cyclisation of I with anisaldehyde).

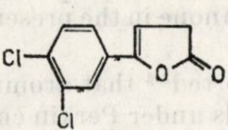
III

Condensation of I with isatine under the same conditions gives 3-[2-oxo-5-(3,4-dichlorophenyl)-3-(2H)-furylidene]-2-indolinone (IV).

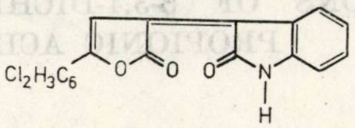

(IV)

Compound IV can be prepared authentically via condensation of III with isatine under the same conditions.

On the other hand, condensation of I with phthalic anhydride under the same conditions, afforded the formation of two products : 3-[2-oxo-5-(3,4-dichlorophenyl)-3(2H)-furylidene] phthalide (Va) resulted from the condensation of the carbonyl group of the anhydride, and 5-(3,4-dichlorophenyl)-[furan-3(2H), 2,4-inden]-1′, 2′, 3′-trione (VI) resulted from the condensation at the anhydride oxygen with α-CH_2 of the acid I.

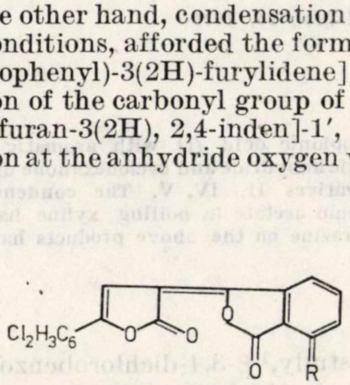

(V)

a, R = H ; b, R = NO_2

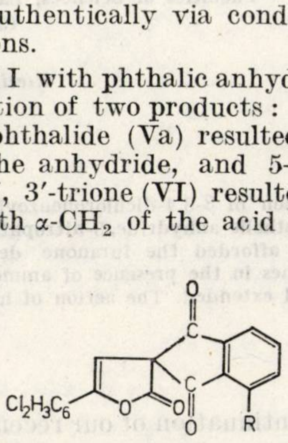

(VI)

However, condensation of I with 3-nitrophthalic anhydride afforded the formation of only 3-nitro-3-[2-oxo-5-(3,4-dichlorophenyl)-3 (2H)-furylidene] phthalide (Vb).

Similarly, condensation of I with cyclohexanone under Perkin conditions afforded the formation of α-3-cyclohexylidene-5-(3,4-dichlorophenyl) furan-3(2H)-2-one (VII).

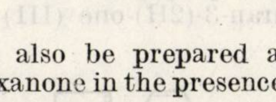

(VII)

Compound VII can also be prepared authentically via condensation of III with cyclohexanone in the presence of acetic anhydride and sodium acetate.

It was previously reported[3,4] that aromatic or aliphatic ketones fail to condense with γ-keto acids under Perkin condensations in the presence of acetic anhydride and sodium acetate.

In the present investigation it has been observed that all attempts to separate any solid product by condensation of I with ketones in the presence of acetic anhydride and sodium acetate failed.

TABLE 1

Condensation products II—VII

Compd	Sol-vent*	Colour	m.p. (°C) yield (%)	Formula	Analysis %	
					Found	Required
IIa	B	Yellow	220 85	$C_{17}H_{10}O_2Cl_2$	C 64.32 H 3.10	64.35 3.15
IIb	B	Yellow	215 85	$C_{18}H_{12}O_3Cl_2$	C 62.20 H 3.50	62.25 3.46
IIc	B	Red	240 75	$C_{19}H_{15}NO_2Cl_2$	C 63.00 H 4.20 N 3.80	63.33 4.17 3.89
IId	B	Yellow	238 70	$C_{18}H_{10}O_4Cl_2$	C 59.50 H 2.70	59.83 2.77
IIe	B	Yellow	215 70	$C_{19}H_{12}O_2Cl_2$	C 66.10 H 3.20	66.47 3.49
IIf	B	Yellowish	200 65	$C_{15}H_8O_3Cl_2$	C 58.65 H 2.60	58.63 2.61
IV	B	Red	236	$C_{18}H_9NO_3Cl_2$	C 60.10 H 2.50 N 3.85	60.34 2.51 3.91
Va	B	Brown	255 20	$C_{18}H_8O_4Cl_2$	C 60.20 H 2.25	60.18 2.23
VI	B	Brown	267 70	$C_{18}H_8O_4Cl_2$	C 60.10 H 2.20	60.18 2.23
Vb	A	Brown	257 85	$C_{18}H_7NO_6Cl_2$	C 53.60 H 1.75 N 3.40	53.46 1.53 3.47
VII	E	Red	185 80	$C_{16}H_{14}O_2Cl_2$	C 62.20 H 4.50	62.14 4.53

* A — acetic acid B — benzene E — ethanol

On the other hand, if ammonium acetate in boiling xylene is used instead of sodium acetate/acetic anhydride, solid products can be sepa-

TABLE 2

Products of condensation with ketones cyclohexanones and isatine VIII—XI

Compd	Sol-vent*	Colour.	M.p.(°C) yield (%)	Formula	Analysis %	
					Found	Required
VIIIa	B	Greenish-yellow	198 90	$C_{14}H_{13}NOCl_2$	C 59.70 H 4.60 N 5.00	59.57 4.61 4.96
VIIIb	B	Yellow	221 90	$C_{18}H_{13}NOCl_2$	C 65.10 H 3.90 H 4.20	65.45 3.94 4.24
VIIIc	B	Orange	245 85	$C_{23}H_{14}NOCl_2$	C 70.20 H 3.85 N 3.60	70.41 3.83 3.57
VIIId	B	Colourless	215 75	$C_{24}H_{15}NO_2Cl_2$	C 68.51 H 3.60 N 3.20	68.57 3.57 3.33
VIIIe	B	Brown	202 60	$C_{14}H_{11}NO_2Cl_2$	C 56.50 H 3.61 N 4.71	56.76 3.72 4.73
X	E	Yellow	225 70	$C_{16}H_{15}NOCl_2$	C 62.31 H 4.69 N 4.50	62.33 4.90 4.57
XI	B	Colourless	278 85	$C_{18}H_{10}N_2O_2Cl_2$	C 60.52 H 2.80 N 7.86	60.50 2.80 7.84

* B = benzene E = ethanol

TABLE 3

β-3,4-Dichlorophenacylcinnamic acid hydrazide derivatives (XIIa, b)

Compd	M.p. (°C)	Yield (%)	Formula	Analysis (%)	
				Found	Required
XIIa	174	80	$C_{17}H_{14}N_2O_2Cl_2$	C 58.50 H 4.55 N 8.00	58.45 4.61 8.02
XIIb	230	85	$C_{18}H_{16}N_2O_3Cl_2$	C 56.80 H 4.10 N 7.30	56.99 4.22 7.38

TABLE 4

4-Arylidene-1,4-dihydro-6-(3,4-dichlorophenyl)-3 (2H)-pyridazinones (XIVa-c)

Compd	Colour	M.p. (°C)	Yield (%)	Formula	Analysis (%) Found	Analysis (%) Required
XIVa	white	208	85	$C_{17}H_{12}N_2OCl_2$	C 61.50 H 3.50 N 8.50	61.63 3.63 8.46
XIVb	Pale yellow	175	85	$C_{19}H_{14}N_2OCl_2$	C 63.60 H 3.90 N 8.00	63.85 3.92 7.84
XIVe	Pale yellow	161	80	$C_{15}H_{10}N_2O_2Cl_2$	C 56.70 H 3.00 N 9.00	56.67 3.12 8.72

TABLE 5

Phenylhydrazine adducts (XXI, XXII)

Compd	M.p. (°C)	Yield (%)	Formula	Analysis (%) Found	Analysis (%) Required
XXI	174	75	$C_{30}H_{24}N_4O_4Cl_2$	C 62.50 H 4.30 N 10.10	62.61 4.17 9.74
XXII	180	80	$C_{24}H_{16}N_2O_4Cl_2$	C 61.50 H 3.50 N 6.10	61.67 3.45 5.99

rated. Thus, condensation of I with ketones, namely ethyl methyl ketone, acetophenone, benzophenone, benzyl or diacetyl, in boiling xylene in the presence of ammonium acetate yielded the corresponding α-arylidene or alkylidene-γ-(3,4-dichlorophenyl)-$\Delta^{\beta,\gamma}$-pyrrolidenone (VIIIa-e).

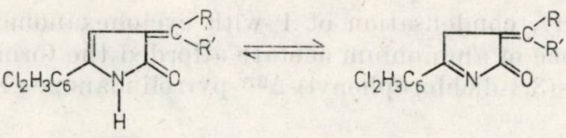
(VIII)

a, $R=C_2H_5$; $R'=CH_3$; b, $R=CH_3$, $R'=C_6H_5$; c, $R=C_6H_5$ $R'=C_6H_5$

d, $R=C_6H_5$ $R'=C_6H_5-CO-$; e, $R=CH_3$, $R'=CH_3-CO-$

Also compound VIIIb can be prepared authentically via condensation of pyrrolidenone IX (obtained by treating the acid I with ammonium acetate in acetic anhydride) with acetophenone.

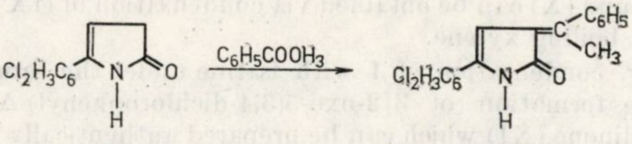
(IX) (VIII b)

TABLE 6

^{1}H-NMR spectral data

Compd. No.	τ	No. of protons	Solvent	System
IV	2.0−3.5(m)	7	$CDCl_3$	Ar protons
	4 (s)			NH
	6.4 (s)			HC=C cyclic
VIIIa	7.5 (s)	3	$DMSO_4$	CH_3
	8 (t)	3		CH_2-CH_3
	7.3 (q)	2		CH_2-CH_3
	2.0−3.4(m)	3		Ar protons
	4.1 (s)	1		NH
	6.4 (s)	1		C=CH cyclic
VIIIc	1.8−3 (m)	13	$CDCl_3$	aromatic protons
	4.2 (s)	1		NH
	6.3 (s)	1		CH=cyclic
XI	1.8−3 (m)	7	$CDCl_3$	Ar protons
	3.8 (s)			2(NH) groups
	6.4 (s)			HC=
XV	2−3.5(m)	11	DMSO-d_6	Ar protons
	3.8 (s)	1		NH
	6.8 (s)	1		CH=cyclic
	6.5 (s)	1		ArCH=
	4.7 (s)	2		$O-CH_2-O$

Similarly, condensation of I with cyclohexanone in boiling xylene in the presence of ammonium acetate afforded the formation of α-cyclohexylidene-γ-(3,4-dichlorophenyl)-$\Delta^{\beta,\gamma}$-pyrrolindanone (X).

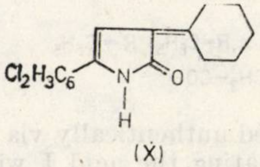

(X)

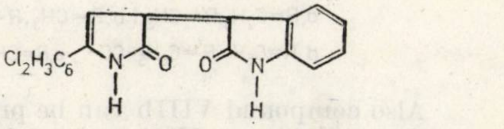

(XI)

Compound (X) can be obtained via condensation of (IX) with cyclohexanone in boiling xylene.

Finally, condensation of I with isatine under the same conditions afforded the formation of 3[2-oxo-5(3,4-dichlorophenyl)-$\Delta^{\beta,\gamma}$-pyrrolidenone]-2-indolinone (XI) which can be prepared authentically via reaction of the furanone IV with ammonium acetate.

TABLE 7

IR Spectra

Compd No.	cm^{-1}	Attribution
II	1725—1750	α, β-unsaturated-γ-lactones [2a]
	1680—1620	C=C in ring system [2b]
	1680—1640	C=C of α, β-unsaturated ketones [2c]
IV	1775	C=O of γ-lactone
	1690	C=C cyclic
	1600	α, β-unsaturated ketone
V	1870—1775	γ-lactone
	1725—1640	C=C cyclic
	1670—1580	C=C α, β-unsaturated system
VI	1780	α, β-unsaturated-γ-lactone
	1650	C=C cyclic
	1760	C=O cyclic dione system [2d]
VII	1775	C=O α, β-unsaturated-γ-lactone
	1610	C=C α, β-unsaturated ketone
VIII	1690—1670	α, β-unsaturated ketones
	1610—1590	C=N [2e]
	3495—3490	NH [2f]
X	1680	C=O α, β-unsaturated ketone
	3250	NH
XI	1700	C=O cyclic imide [2g]
	1580	C=N cyclic [2h]
	3400	NH broad band
XII	1660	C=O amide
	1710—1690	C=C aryl ketone
	3300—3200	NH group
XIII	1700	aryl ketone
	1670	C=O of amide
	1610	C=N
	3300	NH
XIV	1720—1650	C=O
	1640—1600	C=N
	2850	NH
XV	1690	C=O
	1600	C=C
	3320	NH

Table 7 (continued)

Compd. No.	cm^{-1}	Attribution
XVI	1690	C=O aryl ketone
	1650	C=O amide
	3100	NH
XVIII	1690	aryl ketone
	1670	C=O amide
	1610	C=N
	3250	NH
XIX	1670	C=O
	3260	NH
XX	1700	C=O
	3200	NH
XXI	1670	C=O aryl ketones
	1620	C=O amide
	3300	NH

ACTION OF HYDRAZINES

In the present investigation it has been found that IIa and IIb react with hydrazine hydrate in ethanol at room temperature to give α-(3,4-dichlorophenacyl) cinnamic acid hydrazide (XIIa and b) via acyl-oxygen cleavage of the furanone ring.

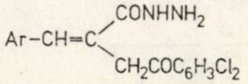

$\mathrm{Ar{-}CH{=}C}\begin{matrix}\diagup \mathrm{CONHNH_2}\\ \diagdown \mathrm{CH_2COC_6H_3Cl_2}\end{matrix}$

(XII)

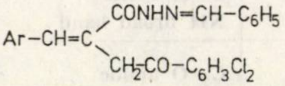

$\mathrm{Ar{-}CH{=}C}\begin{matrix}\diagup \mathrm{CONHN{=}CH{-}C_6H_5}\\ \diagdown \mathrm{CH_2{-}CO{-}C_6H_3Cl_2}\end{matrix}$

(XIII)

a, Ar=C_6H_5 ; b, Ar = $C_6H_4OCH_3p^-$

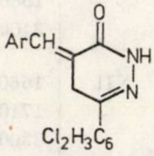

(XIV)

a, Ar=C_6H_5 ; b, Ar=C_6H_5–CH=CH

e, 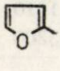

Condensation of XIIb with benzaldehyde gives α-(3,4-dichlorophenanyl) cinnamic acid benzylidene hydrazide (XIII).

Ring closure of XIIa in hot alcohol gives a substance which was found to be identical with XIVa (from melting point and mixed m.p. determinations).

Similarly, treatment of IId with phenylhydrazine in hot alcohol gave 4-piperonylidene-1,4-dihydro-6-(3,4-dichlorophenyl)-1-phenyl-3(2H)-pyridazinone (XV).

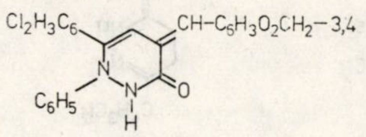
Cl₂H₃C₆
CH–C₆H₃O₂CH₂–3,4
N
N
C₆H₅
H
O

(XV)

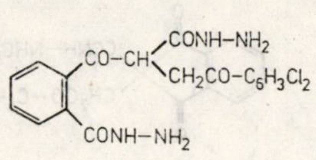
CONH–NH₂
CO–CH
CH₂CO–C₆H₃Cl₂
CONH–NH₂

(XVI)

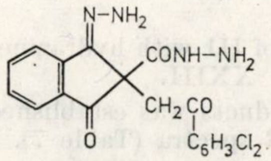
N–NH₂
CONH–NH₂
CH₂CO
O
C₆H₃Cl₂

(XVII)

As a point of interest, condensation of Va or VI with hydrazine hydrate or phenylhydrazine in ethanol at room temperature afforded the formation of 2-carbonyl-α(3,4-dichlorophenacyl)-hydrocinnamic acid dihydrazide (XVI) and of 1,3-dioxo-2-(3,4-dichlorophenacyl)-2-indan carboxylic acid hydrazide-1-hydrazone (XVII), respectively.

Condensation of XVII with benzaldehyde afforded the formation of 1,3-dioxo-2-(3,4-dichlorobenzoyl)-2-indan carboxylic acid benzylidene hydrazide-1-hydrazone (XVIII).

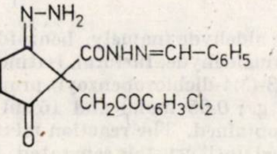
N–NH₂
CONHN=CH–C₆H₅
CH₂COC₆H₃Cl₂
O

(XVIII)

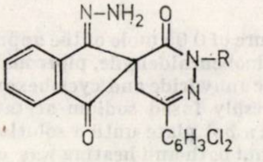
N–NH₂
O
N–R
N
O
C₆H₃Cl₂

(XIX) R=H
(XX) R=COCH₃

Heating VI with hydrazine hydrate in boiling alcohol affords 1′, 2′-dihydro-6-(3,4-dichlorophenacyl)-[indan-2,4-(3′*H*)-pyridazine]-1,3,3′-trione-1-hydrazone (XIX).

Condensation of VI with hydrazine hydrate in boiling acetic acid gives XIX beside the acetyl derivative XX.

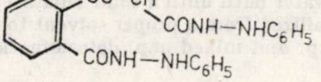
CH₂COC₆H₃Cl₂
CO–CH
CONH–NHC₆H₅
CONH–NHC₆H₅

(XXI)

On the other hand condensation of Va with phenylhydrazine in ethanol gave 2-carbonyl-α-(3,4-dichlorophenacyl)-hydrocinnamic acid dihydrazide (XXI).

Similarly, reaction of VI with phenylhydrazine gave 1,3-dioxo-2-(3,4-dichlorophenacyl)-2-indan carboxylic acid N-phenylhydrazide (XXII).

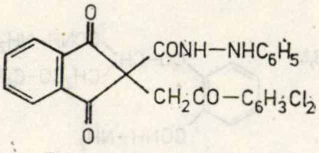

(XXII)

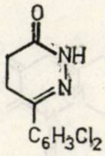

(XXIII)

Also, condensation of III with hydrazine hydrate in boiling ethanol afforded the formation of XXIII.

Structure of the adducts was established on the basis of ^1H-NMR spectra (Table 6) and IR spectra (Table 7).

EXPERIMENTAL

The NMR spectra were carried out using a Jeol-JNM-FX100 Fourier Transformer NMR spectrometer, Norway; the IR spectra were obtained with a Unicam SP 1200 Spectrophotomer using KBr wafer technique. All melting points are uncorrected.

CONDENSATION OF I WITH ALDEHYDES, ISATIN, PHTHALIC ANHYDRIDE, NITROPHTHALIC ANHYDRIDE AND CYCLOHEXANONE

A mixture of 0.05 mole of the appropriate aldehyde (namely, benzaldehyde, anisaldehyde *p*-dimethylaminobenzaldehyde, piperonal, cinnamaldehyde, furfural, isatine, phthalic anhydride, 3-nitrophthalic anhydride and cyclohexanone), β-(3,4-dichlorobenzoyl)-propionic acid (I) (13 g. ; 0.05 mole), freshly fused sodium acetate (4.6 g. ; 0.05 mole) and 16 ml of acetic anhydride was heated on a hot plate until a solution was obtained. The reaction mixture was then transferred to a steam bath and heating was continued until crystals separated. The reaction mixture was then poured into water, the solid product obtained was filtered off, washed with water and finally recrystallized from a proper solvent to give the corresponding compounds II—VII. The detailed results are listed in table 1.

FORMATION OF IIb, IV AND VII VIA CONDENSATION OF III WITH ANISALDEHYDE, ISATINE OR CYCLOHEXANONE

A mixture of 1 g of III (formed via cyclization of I (13 g) in acetic anhydride (16 ml) and crystallised from benzene-light petrol (b.p. 80—100°C) as brown crystals m.p. 136°C (yield 45%) was added to (0.01 mole) of anisaldehyde, isatine or cyclohexanone in the presence of 0.05 g of sodium acetate on a water bath until a solid separated. The mixure was poured into water and the solid was recrystallized from a proper solvent to give a product identified to be IIb, IV or VII by means of m.p. and mixed m.p. determinations.

FORMATION OF VIII—XI VIA CONDENSATION OF I W KETONES, CYCLOHEXANONE AND ISATINE

A mixture of acid I(0.01 mole), ammonium acetate (4 g ; 0.04 mole) and ketone (0.01 mole) namely, methyl ethyl ketone, acetophenone, benzophenone, benzyl, diacetyl cyclohexanone or isatine was refluxed in acetic anhydride or xylene (50 ml) for 10 hrs. The reaction mixture was poured into ice, the solid separated after treatment with light petrol was crystallized from a proper solvent to give VIII—XI. The detailed results are listed in table 2.

FORMATION OF VIIIb VIA CONDENSATION OF II WITH ACETOPHENONE

A mixture of pyrrolidenone II (prepared via cyclization of acid I in the presence of ammonium acetate (0.01 mole) and 15 ml acetic anhydride or xylene and crystallized from ethanol as reddish brown crystals, m.p. 268°C yield 60 %, and acetophenone (1.2 g. ; 0.01 mole) was refluxed in acetic anhydride or xylene for 10 hrs. The reaction mixture was poured into ice and the solid separated after treatment with petrol was recrystallized from benzene to give a compound identified to be VIIIb by means of m.p. and mixed m.p. determinations.

ACTION OF HYDRAZINE HYDRATE ON II

A solution of IIa or IIb (0.01 mole) and hydrazine hydrate (0.05 mole) in 30 ml of ethanol was left at room temperature for 24 hrs, then most of the solvent was evaporated and the solid separated was crystallized from ethanol to give XIIa, b as white crystals. The detailed results are listed in table 3.

CONDENSATION OF XIIb WITH BENZALDEHYDE

A solution of XIb (1 g. ; 0.003 mol) in 30 ml alcohol was treated with benzaldehyde (1.2 ml 0.01 mole) and the reaction mixture was refluxed for 6 hrs, then most of the solution was evaporated to give XIII, m.p. 166°C (yield 80 %) ; Found : C, 64.20 ; H, 4.50 ; N, 6.00 ; $C_{25}H_{20}N_2O_3Cl_2$ requires : C, 64.24 ; H, 4.28 ; N, 5.99.

ACTION OF HYDRAZINE HYDRATE OR II

To a solution of IIa, IIe or IIf (0.01 mole) in 50 ml ethanol hydrazine (0.05 mole), was added, the reaction mixture was refluxed for 4 hrs, then most of the solvent evaporated and the solid separated was crystallized from methanol to give XIV-a-c. The results are listed in table 4.

CONVERSION OF XIIIa TO XIVa

A solution of XIIa (1 g ; 0.003 mole) in 30 ml of ethanol was heated under reflux for. 10 hrs, then cooled and the solid separated was identified to be XIVa by m.p. and mixed m.p determinations.

ACTION OF PHENYLHYDRAZINE ON IId

To a solution of IId (3.5 g. ; 0.01 mole) in 50 ml ethanol, phenylhydrazine (0.05 mole) was added, the reaction mixture was refluxed for 10 hrs, then most of the solvent evaporated, the solid separated was crystallized from methanol to give XV as yellowish green crystals m.p. 183°C (yield 85 %). Found : C, 63.80 ; H, 3.10 ; N, 6.35 ; $C_{24}H_{16}N_2O_3Cl$ requires : C, 63.86 ; H, 3.55 ; N, 6.21 %.

ACTION OF HYDRAZINE HYDRATE ON

To a solution of Va (3.6 g ; 0.01 mole) in 30 ml ethanol hydrazine hydrate (0.05 mole) was added, the reaction mixture was left overnight and then usually worked-up to give XVII as white crystals, m.p. 300°C (yield 80 %). Found : C, 53.50 ; H, 3.50 ; N, 14.10 ; $C_{18}H_{14}N_4O_3Cl_2$ requires ; C, 53.33 ; H, 3.46 ; N, 13.83 %.

ACTION OF BENZALDEHYDE ON XII

(1g. ; 0.005 mole) of III was added to benzaldehyde (0.1 mole) in 50 ml of ethanol and the reaction mixture was refluxed for 6 hrs, then the solid separated was crystallized from alcohol to give XVIII, m.p. 300°C (yield 85 %), Found : C, 61.00 ; H, 3.70 ; N, 11.40 ; $C_{25}H_{18}N_4O_3Cl_2$ requires : C, 60.85 ; H, 3.65 ; N, 11.36 %.

FORMATION OF HYDRAZONE XIX

(3.6 g. ; 0.01 mole) of VI in 50 ml ethanol was added to hydrazine hydrate (1.5 ml : 0.05 mole), the mixture was refluxed for 6 hrs, then worked-up as usual to give XIX, which was crystallized from acetic acid as white crystals, m.p. 300°C (yield 75 %) : Found : C, 56.10 ; H, 3.20 ; N, 14.50 ; $C_{18}H_{12}N_4O_2Cl_2$ requires : C, 55.81 ; H, 3.10 ; N, 14.47 %.

CYCLIZATION OF XVII

(1 g : 0.003 mole) of XVII in 50 ml of ethanol was refluxed for 10 hrs, then the solid was crystallized to give XIX which was identified by m.p. and mixed m.p. determinations.

REACTION OF VI WITH HYDRAZINE HYDRATE IN BOILING ACETIC ACID

(3.6 g. ; 0.01 mole) of VI in 50 ml of acetic acid was added to hydrazine hydrate (1.5 ml ; 0.05 mole) and the mixture was refluxed for 6 hrs, then most of the solvent was evaporated. The oil which separated was triturated with alcohol to give XIX which was identified by m.p. and mixed m.p. together with its acetyl derivative XX m.p. 300°C as white crystals from ethanol (yield 70 %) ; Found : C, 56.20 ; H, 3.40 ; N, 13.20 ; $C_{20}H_{14}N_4O_3Cl_2$ requires : C, 55.94 ; H, 3.26 ; N, 13.05 %.

ACTION OF PHENYLHYDRAZINE ON Va OR VI

To a solution of Va or VI (3.6 g. ; 0.01 mole) in 30 ml ethanol phenylhydrazine (2.5g ; 0.05 mole) was added, the reaction mixture was left overnight then most of the solvent evaporated and the solid mass separated after treatment with light petrol was crystallized from ethanol to give the hydrazides XXI, XXII as white crystals. The results are listed in table 5.

ACTION OF HYDRAZINE HYDRATE ON III

To a solution of III (2.3 g ; 0.01 mole) in 30 ml of ethanol, hydrazine hydrate (1 g ; 0.05 mole), was added, the reaction mixture was refluxed for 6 hrs. After evaporation of most of the solvent, the remained solid was recrystallized from ethanol to give colourless crystals, m.p. 157°C (yield 80 %) ; Found : C, 49.40 ; H, 3.30 ; N, 11.50 ; $C_{10}H_8N_2OCl_2$ requires : C. 49.38 ; H, 3.29 ; N, 11.52 %.

REFERENCES

[1] A. Sammour, A. F. Fahmy, M. M. Abd Alla and A. A. Hamed, *Egypt. J. Chem.*, **18b**, 1041 (1975).

[2] L. J. Bellamy, "The Infrared Spectra of Complex Molecules" Methuen Co. London, pages a) (186), b) (71), c) (39), d) (141), e) (177), f) (249), g) (205), h) (270).

[3] R. Filler, and H. A. Leipold, *J. Org. Chem.*, **27**, 4440 (1962).

[4] Shyamsunder Rao, Y., *Chem. Rev.*, **64**, 353 (1964).

Revue Roumaine de Chimie, 25, *11–12*, 1561–1565 (1980)

DOSAGE SPECTROPHOTOMÉTRIQUE DU THALLIUM AVEC ASTRAZON ROUGE VIOLET 3R

CECILIA CONSTANTINESCU et GH. C. CONSTANTINESCU
Institut Polytechnique
str. Polizu Nº 1, Bucarest, Roumanie

Reçu le 22 jauvier 1980

The reaction of Astrazon Rouge-Violet 3R basic reagent with the complexanion $[TlBr_4]^-$ is studied. The combination obtained was extracted in benzene (extractibility above 91%). The benzenic extracts have good spectrophotometric properties, obey Lambert-Beer law between 0.1–1.4 µgTl/ml. The sensibility of the reaction is good, $\varepsilon = 86\,000$. By elimination of the interferences, the studied reactive is used for the determination of the teaps of Tl(III) in minerals.

Dans un milieu aqueux fortement acide, l'anion tétrabromothallique réagit avec le cation du colorant basique Astrazon Rouge Violet 3 R, en formant des combinaisons pratiquement insolubles dans l'eau et légèrement solubles dans des solvants organiques comme le benzène. Les meilleures conditions d'obtention et d'extraction du composé ont été étudiées, ainsi que l'étude spectrophotométriques des équilibres formés. A partir de ces données on a établi une nouvelle méthode de dosage du Thallium qui a été ensuite appliquée sur trois matériaux contenant du Thallium : cadmium technique, concentré de pyrite et poussière du filtre électrique, d'une installation de fabrication de l'acide sulfurique.

Le comportement des colorants basiques indoliques en solution aqueuse acide en comparaison des colorants triphénylméthaniques les indiquent capables de former avec des anions complexes telles que $[TlBr_4]^-$ par exemple, des associations ioniques qui sont pratiquement insolubles dans l'eau.[1-3]

Les techniques modernes de séparation des métaux sont aussi fondées sur la formation des complexes métal-organiques séparés ensuite par précipitation ou extraction liquide-liquide.

L'efficacité du traitement est largement influencé par le choix du colorant, dont la réactivité encore imparfaitement connue dépend de sa structure.

Nous avons particulièrement étudié la réaction entre $[TlBr_4]^-$ et le cation du colorant Astrazon Rouge Violet 3 R en milieu aqueux et les équilibres d'extraction avec benzène de la combinaison fermée.

On a visé deux applications pratiques importantes : l'extraction du métal et le dosage quantitatif de l'anion complexe.

Les conditions de réaction, surtout le pH de la solution aqueuse, la forme cationique du colorant dans la solution aqueuse, la composition du composé obtenu, ainsi que les paramètres de l'extraction à des solvants organiques sont les problèmes qui doient être d'abord étudiés.

PARTIE EXPÉRIMENTALE

Le colorant Astrazon Rouge Violet 3 R produit par la Firme Bayer AG est entièrement soluble dans l'eau froide donnant une solution rouge. En présence d'acide bromhydrique le colorant libre n'est pas extractible par benzène. Les solutions aqueuses du colorant ont un maximum d'absorption à 550 nm. On a utilisé des solutions 1.10^{-3} M.

La solution d'étalonnage qui contient du $H[TlBr_4]$ a été préparée à partir du $Tl\,NO_3$ par oxydation avec l'eau de brome en présence d'acide bromhydrique.

Pour l'extraction on a utilisé des ampoules à décanter ou des Erlens à 50 ml et le volume de la solution aqueuse égal à celui du benzène : 10 ml à 10 ml. L'équilibre entre les deux phases liquides est atteint après une agitation énergique pendant 1–2 minutes. Les essais à blanc (sans $(H^+[Tl\,Br_4]^-)$ sont préparés de la même manière.

Pour établir le coefficient de distribution à l'équilibre on a conduit les extractions de la manière décrite ci-dessus en déterminant les quantités de Thallium dans la solution benzénique et la solution aqueuse (porté au sec en ajoutant du H_2SO_4 conc. et du H_2O_2 30%). Pour comparaison on a choisi la méthode spectrophotométrique du dosage à Méthylviolet).[4] Les résultats sont présenté dans le tableau 1, où $D = \dfrac{\mu g\ \mathrm{Tl\ (phase\ organ)}}{\mu g\ \mathrm{Tl\ (phase\ aqueuse)}}$

et $C = C_0 \dfrac{1}{1 + D}$ C_0 = concentration du Tl dans la solution benzénique.

Le dosage spectrophotométrique a été fait à 575 nm, longueur d'onde à laquelle la solution benzénique possède un maximum (comme ou peut voir sur la figure 1), en utilisant des appareils du type Spekol et VSU–2P–Carl Zeiss Jena RDA, cuve de 1 cm.

TABLEAU 1

Coefficient de distribution D et l'extractibilité du complexe

Combinaison	D	E % par une extraction
(Méthyl violet)$^+$ $[Tl\,Br_4]^-$	11,12	98,0 %
(Violet Rouge Astraton) $[Tl\,Br_4]^-$	10,50	91,0 %

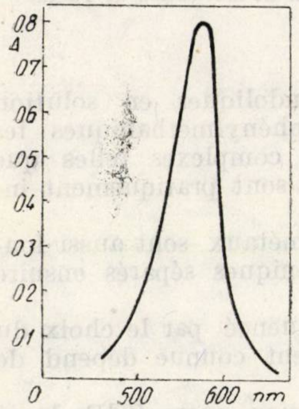

Fig. 1. — Spectre d'absorption du composé.

L'équilibre d'extraction dépend du pH de la solution aqueuse et de la concentration du réactif complexant. Sur la figure 2 on voit que l'acidité optimale est située entre 0,34–0,62 n (HBr) et de a figure 3 il résulte que la concentration du réactif dans la solution aqueuse doit être presque 100 fois plus grande que celle du Thallium pour que l'équilibre :

$$H\,[TlBr_4] + (\mathrm{Astrazon})^+Cl^- \rightleftharpoons (\mathrm{Astrazon}^+[TlBr_4]^-) + H^+Br^-$$ soit déplacé à droite.

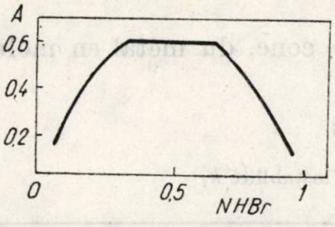

Fig. 2. — Acidité de la solution.

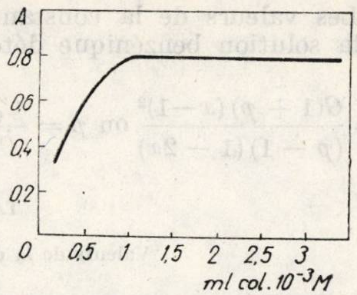

Fig. 3. — Concentration du colorant.

L'étude des limites dans lesquelles la loi de Lambert-Beer est valable et les valeurs du coefficient molaire d'extinction sont présentées dans le tableau 2 et sur la figure 4.

TABLEAU 2

Limites de l'applicabilité de la loi de Lambert Beer et le coefficient molaire d'extinction

Combinaison	μgTl ml^{-1}	ε
Astrazen Rouge Violet 3 R)$^{+}$ [TlBr$_4$]$^{-}$	0,1—1,4	86.000

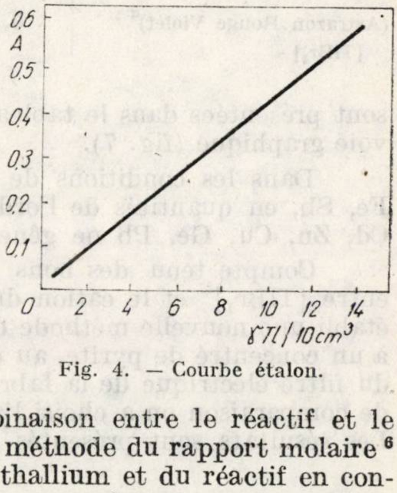

Fig. 4. — Courbe étalon.

La stabilité des solutions organiques est très bonne : en présence de l'air et de la lumière, les solutions présentent après une semaine les mêmes caractéristiques spectrophotométriques.

On a déterminé le rapport de combinaison entre le réactif et le thallium par la méthode de Job [5] et par la méthode du rapport molaire [6] en choisissant des solutions isomolaires de thallium et du réactif en concentration de 1.10^{-4} et de 2.10^{-4} m et on a trouvé toujours un rapport molaire de 1 : 1 (figures 5 et 6).

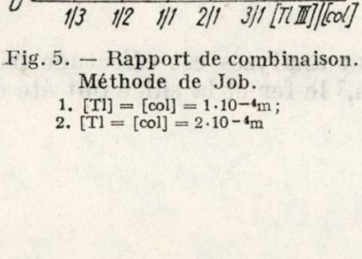

Fig. 5. — Rapport de combinaison. Méthode de Job.
1. $[Tl] = [col] = 1\cdot10^{-4}$m ;
2. $[Tl = [col] = 2\cdot10^{-4}$m

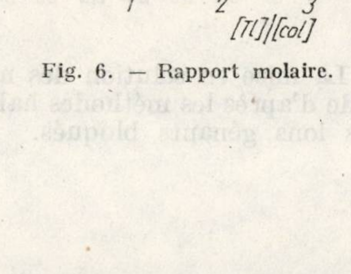

Fig. 6. — Rapport molaire.

Les valeurs de la constante d'instabilité de l'association ionique dans la solution benzénique déterminées par la méthode de Job[5] selon

$$k = \frac{G(1+p)(x-1)^2}{(p-1)(1-2x)} \text{ ou } p = \frac{C_{\text{réactif}}}{C_{\text{métal}}} \quad C = \text{conc. du métal en mole}\cdot 1^{-1}$$

TABLEAU 3

Valeurs de la constante d'instabilité k_i

	x_{max}	$p=\frac{C'}{C}$	C_{Tl} (mol.1^{-1})	C_{CO1} (mol. 1^{-1})	k_i
(Astrazon Rouge Violet)$^+$ $[TlBr_4]^-$	0,43	4	2.10^{-5}	8.10^{-5}	$6,1.10^{-5}$
(Astrazon Rouge Violet)$^+$ $[TlBr_4]$	0,48	2	1.10^{-4}	2.10^{-4}	$6,0.10^{-5}$

sont présentées dans le tableau 3 et les valeurs de x ont été établies par voie graphique (fig. 7).

Dans les conditions de travail interfèrent seulement Ga, Au, In, Fe, Sb, en quantités de l'ordre Tl/métal = 1 : 10. Des éléments comme Cd, Zn, Cu, Ge, Pb ne gênent pas.

Compte tenu des bons résultats de l'étude concernant la réaction entre $[TlBr_4]^-$ et le cation du colorant Astrazon Rouge Violet 3R on a établi une nouvelle méthode de dosage du thallium que l'on a appliquée à un concentré de pyrite, au cadmium technique ainsi qu' à la poussière du filtre électrique de la fabrication d'acide sulfurique. Comme méthode de comparaison on a choisi l'absorptiométrie avec le violet de méthyle.[4] Les résultats sont présentés dans le tableau 4.

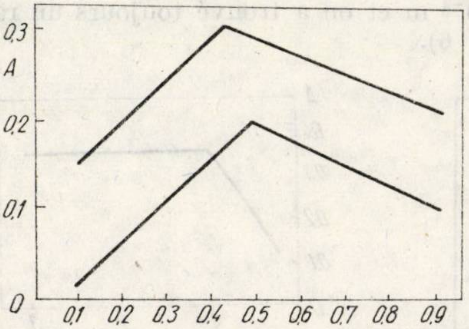

Fig. 7.— Approximation de la constante d'instabilité.

La mise en solution des matériaux analysés est effectuée par voie humide d'après les méthodes habituelles,[7] le fer et la silice ont été écartés et les ions gênants bloqués.

TABLEAU 4

Dosage du Thallium

	Tl contenu en (g)	Méthode avec Violet de méthyle	Méthode avec Astrazon Rouge Violet 3 R
Concentré de pyrrite	1,00	0,0131 %	0,0132 %
	0,50	0,0132 %	0,0130 %
Cadmium technique	1,00	0,0450 %	0,043 %
	0,50	0,0445 %	0,044 %
Poussière du filtre électrique	1,00	0,0031 %	0,0030 %
	0,50	0,0032 %	0,00285 %

BIBLIOGRAPHIE

[1] N. T. Voskresenskaia, *Thur. analit. Khim.*, **11**, 585 (1956).

[2] C. Constantinescu, *Rev. Chim. (București)*, **2**, 165 (1972).

[3] C. Constantinescu et Gh. C. Constantinescu, *Rev. Roumaine Chim.*, **21**, 391 (1976).

[4] H. Onishi, *Mikrochim. Acta*, **9** (1959).

[5] P. Job, *Ann. Chim. (France)*, **9**, 113 (1928).

[6] A. Demetrescu, A. Tutoveanu et A. Ionescu, « Analiza tehnică a minereurilor », Ed. tehnică București, 1966.

[7] E. A. Alexeevski et R. K. Golț, « Analiza cantitativă », Ed. tehnică, București, 1955, p. 440, 530.

Revue Roumaine de Chimie, 25, *11–12*, 1567–1578 (1980)

A MECHANISM FOR THE PHOTOLYTIC DECOMPOSITION OF HYPOBROMITE IN AQUEOUS SOLUTION AT 365 NM 313 NM AND 253.7 NM

M.S. SUBHANI* and S. F. LODHI
Department of Chemistry, University of Nigeria, Nsukka, Nigeria

Received July 11, 1978

Photochemical studies on the decomposition of hypobromite ion in aqueous solution were carried out using steady state and flash photolysis techniques. At 365 nm the primary photolytic processes were found to be

$$BrO^- \xrightarrow{h\nu} Br^- + O[^3P] \qquad (a)$$

$$BrO^- \xrightarrow{h\nu} Br + O^- \qquad (b)$$

and $\Phi_a = 0.318 \pm 0.02$ and $\Phi_b = 0.09 \pm 0.015$. At 313 nm and 253.7 nm in addition to primary photolytic processes (a) and (b) another primary photolytic process (c)

$$BrO^- \xrightarrow{h\nu} Br^- + O(^1D) \qquad (c)$$

was also observed to occur and the quantum yields are $\Phi_a = 0.089 \pm 0.014$, $\Phi_b = 0.155 \pm$ ± 0.015 and $\Phi_c = 0.026 \pm 0.015$ at 313 nm and $\Phi_a = 0.084 \pm 0.018$, $\Phi_b = 0.326 \pm$ ± 0.016 and $\Phi_c = 0.150 \pm 0.018$ at 253.7 nm. It was also observed that $O(^3P)$ reacts with BrO^- and BrO^-2 by abstraction of O as well as by addition. A complete mechanism for the photochemical decomposition of BrO^- ion is proposed at all the three wavelengths.

INTRODUCTION

The photochemical decomposition of oxyanions of halogens in aqueous solution has been the subject of a number of investigations.[1–10] Flash photolysis studies were also carried out [7, 8, 11] and some primary photolytic processes were reported for the photochemical decomposition but as yet no overall mechanism for the photolytic decomposition of hypobromite ion in aqueous solution has been completely understood. The purpose of this paper is to present a complete photochemical mechanism for the decomposition of BrO^- and to evaluate primary quantum yields for all the primary photolytic processes involved.

EXPERIMENTAL

All solutions were prepared in triply distilled water just before irradiation. All the chemicals used were of analaR grade and were used without further purifications. Sodium hypobromite solutions were prepared by adding the required volume of bromine water to a cold solution of sodium hydroxide. These solutions were freshly prepared when required in triply distilled water. Flash photolysis set up was similar to that described elsewhere.[12]

Steady state photolysis was carried out using reaction cells 6 cm in diameter, 2.5 cm deep quartz cylinder having optically flat faces and was sealed to a 100 ml pyrex bulb carrying a side arm to allow solution to be degassed on a vacuum line by the freeze-pump-thaw method.

Light of wavelength 253.7 nm was obtained from a mercury resonance lamp (Hanovia) through a constant voltage transformer. The lamp was used in conjunction with a water filter (2.5 cm deep) to exclude light of wavelength 184.9 nm. Under these conditions 96% of actinic effects are due to light of wavelength 253.7 nm.Light of wavelength 313 nm and 365 nm was obtained by isolating the appropriate lines of the mercury arc. The source was a medium pressure 250 W arc lamp (G. E.C.) operated from the main through a choke. The folowing filter combinations were used to isolate the required wavelengths : (a) 313 nm, 0.02% K_2CrO_4 solution (2 cm) + OX7 filter glass (Chance-Pilkington) ; (b) 365 nm, OX1 + OV1 filter glasses (Chance-Pilkington).

The light intensity was measured using a ferrioxalate actinometer,[13] the yield of ferrous ion being determined spectrophotometrically as the *o*-phenanthroline complex. All experiments were carried out at room temperature (25 ± 0.5°C).

ANALYSIS :

Gaseous products such as oxygen were analyzed using chromatographic technique by Pye 101 series chromatograph.

Hypobromite was determined spectrophotometrically taking BrO^- at 331 nm as 326 M^{-1} cm^{-1}. Mixtures of hypobromite, bromite and bromate were analyzed by the following methods :

(a) Hypobromite + bromite

An aliquot of the solution was added to sufficient potassium iodide solution buffered at pH 4 with potassium hydrogen phthalate so that the final solution contained 10^{-1}MI^-. Under these conditions only BrO^- and BrO_2^- oxidized I^-. The amount of tri-iodide ion produced was measured spectrophotometrically at 350 nm with I_3^- = 25700 M^{-1} cm^{-1}.

(b) Bromite ion

An aliquot of the solution was added to potasium iodide solution as in (a) followed by dilute sulphuric acid to make the hydrogen ion concentration 0.2 N. Under these conditions all the three anions oxidize iodide. In all cases test solutions were measured against reagents blanks.

RESULTS

(a) On flash photolysis oxygenated solution of 2×10^{-4}M BrO^- at pH 9.8 and at pH 12.1 the spectra of two transient-species identified as O_3 and O_3^- were reported in the literature.[14,15,16] Since these species are known to be produced by reactions (1) and (2) :

$$O(^3P) + O_2 \rightarrow O_3 \qquad (1)$$

$$O^- + O_2 \rightarrow O_3^- \qquad (2)$$

it was concluded that $O(^3P)$ and O^- were products of photodecomposition of hypobromite ion by reactions (3) and (4)

$$BrO^- \xrightarrow{h\nu} Br^- + O(^3P) \qquad (3)$$

$$BrO^- \xrightarrow{h\nu} Br + O^- \qquad (4)$$

This is in agreement with the results reported in the literature.[11] When light of wavelength less than 300 nm was removed by interposing pyrex glass filter between the lamp and the cell, the yield of O_3^- relative to O_3 was found to be reduced (see table 1),

TABLE 1

Yield of O_3 and O_3^- radical anion from the flash photolysis of oxygenated hypobromite solutions
Flash energy=585 J
$[BrO^-] - 1.5 \times 10^{-4}$ M

λ(nm)	pH	$(O_3)10^6$/M	$(O_3^-)10^6$/M
> 300	9.8	0.49	—
⩽ 300	12.1	—	0.34
Full range	9.8	0.98	—
Full range	12.1	—	1.21

indicating that the primary process (3) was more important at larger wavelengths. The yield of O_3 produced at pH 9.

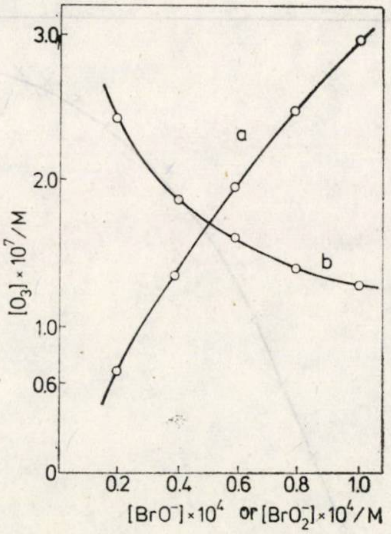

Fig. 1. — Dependence of O_3 yield on (*a*) $[BrO^-]$ and (*b*) $[BrO_2^-]$ in the presence of 10^{-4} M$[BrO^-]$. Full curves are calculated from (*a*) equation (12) (*b*) equation (13) (see text).

The yields of O_3 produced at pH 9.8 at different BrO^- in the absence of BrO_2^-, and at different BrO_2^- in the presence of 10^{-4} M BrO_2^- are shown in figure 1. In these determinations the flash energy was kept constant and photolyzing light was restricted to wavelengths above 300 nm. Under these conditions the amount of light absorbed was directly proportional to BrO^- in the absence of BrO_2^-, and a negligible amount was absorbed by BrO_2^- when present. The decrease in ozone yield per unit amount of light absorbed as BrO^- or BrO_2^- increased thus confirming that each of these ions competed with O_2 for $O(^3P)$ atoms.

On flash photolysis argon saturated solution of 10^{-4}M BrO^- ion a transient species with max = 360 nm was identified as $BrO^\bullet$ from its absorption spectrum and kinetics reported in the literature.[17]The transient species is most likely to be produced by the reactions

$$BrO^- + {}^{\bullet}OH \rightarrow BrO^{\bullet} + OH^- \quad (5)$$

$$BrO^- + O^- \rightarrow BrO^{\bullet} + O^{2-} \quad (6)$$

In all these experiments a combination of an interference filter having maximum transmission at 250 nm and a bandwidth of 2.5 nm, and a Ni–Co solution filter[6] was used to minimize photolysis of the solution by the analysing light.

It was found that the rate of decay of O_3 was too slow to be measured and appeared to be unaffected by changes in the concentration of BrO^- and BrO_2^- ions, which suggests that O_3 reacts slowly, or not at all, with either of these ions.

No absorption due to O_3 was observed on flash photolysis of argon saturated BrO^- 10^{-4}M solution at pH 9.8.

(b) In the steady state photolysis the quantum yields for the products and the disappearance of BrO_2^- was a major oxygen containing product at 365 nm similar to that of ClO^- ion[5,6]; its yield is zero at 313 nm and 253.7 nm.

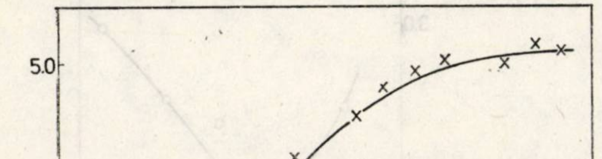

Fig. 2. — Variation of yield of $[BrO_2^-]$ with the amount of light absorbed in photolysis at 365 nm. Full curve for $[BrO_2^-]$ yield is calculated from equation (32) (see text).

At 365 nm all the yields were proportional to the amount of light absorbed up to 1.0×10^{21} quanta 1^{-1}, but at higher doses $\Phi(BrO^-)$ decreased by about 15 % and $\Phi(BrO_2)$ was found to be decreasing continuously.

The quantum yields listed in table 2 are obtained from the initial slopes of the yield-dose plots. At 313 nm and 253.7 nm all the yields were proportional to the amount of light absorbed. The material balance equation in terms of oxygen contents is (7):

$$\Phi(\mathrm{BrO^-}) = 2\Phi(\mathrm{BrO_2^-}) + 2\Phi(\mathrm{O})_2 + 3\Phi(\mathrm{BrO_3^-}) \qquad (7)$$

and the data shown in tbale 2 satisfy this relationship quite closely, indicating that no other oxygen containing product is formed.

The yield of bromide ion was not measured and was obtained from the difference between $\Phi(-\mathrm{BrO^-})$ and $\Phi(\mathrm{BrO_2^-}) + \Phi(\mathrm{BrO_3^-})$. The change in light intensity and the presence of N_2O or air had no effect on the rate of photolysis of BrO^- but added BrO_2^- had a marked effect on the yields at 313 nm and 253.7 nm, as shown in table 3.

TABLE 2

Product yields and disappearance yield for the steady state photolysis of hypobromite ion in aqueous solution

λ (nm)		365	313	253.7
pH		12.1	12.1	12.1
$[\mathrm{BrO^-}]$/M		$(0.8-1)10^{-3}$	$(0.5-1)10^{-3}$	0.8×10^{-3}
$\Phi(-\mathrm{BrO^-})$	Experimental	0.70 ±0.02	0.47 ±0.01	0.88±0.02
	Calculated	0.727±0.05	0.486±0.05	0.93±0.08
$\Phi(\mathrm{BrO_2^-})$	Experimental	0.18 ±0.005	0.0	0.0
	Calculated	———	———	———
$\Phi(\mathrm{O_2})$	Experimental	0.05 ±0.008	0.075±0.005	0.19±0.006
	Calculated	———	———	———
$\Phi(\mathrm{BrO_3^-})$	Experimental	0.09 ±0.01	0.095±0.01	0.16±0.01
	Calculated	——	——	——
$\Phi(\mathrm{Br^-})$	Experimental*	0.43 ±0.04	0.375±0.03	0.72±0.03
	Calculated	0.45 ±0.05	0.372±0.045	0.81±0.04

---

* Calculated from $\Phi(\mathrm{BrO^-}) - \Phi(\mathrm{BrO_2^-}) = \Phi(\mathrm{BrO_3^-})$

The effect was to reduce $\Phi(-\mathrm{BrO^-})$ and $\Phi(\mathrm{O_2})$ and to increase $\Phi(\mathrm{BrO_3^-})$ and BrO_2^- was destroyed. When $\mathrm{BrO_2^-} = 3\times10^{-5}$M, $\Phi(-\mathrm{BrO_2^-})$ decreased. These effects are qualitatively similar to those reported for the radiolysis of BrO^- in the presence of BrO_2^- in aqueous solution.[18] The data shown in table 2 show a good material balance in terms of equation (8)

$$\Phi(-\mathrm{BrO^-}) + 2\Phi(-\mathrm{BrO_2^-}) = 3\Phi(\mathrm{BrO_3^-}) + 2\Phi(\mathrm{O_2}) \qquad (8)$$

$\Phi(\mathrm{Br^-})$ was calculated from the difference between $\Phi(-\mathrm{BrO^-}) + \Phi(-\mathrm{BrO_2^-})$ and $\Phi(\mathrm{BrO_3^-})$.

TABLE 3

Product yields and disappearance yield for the photolysis of hypobromite ion in the presence of bromite ion

pH		12.1	12.1
$(BrO^-)/M$		2×10^{-3}	
$(BrO^-)/M$		10^{-4}	
λ (nm)		313	253.7
$\Phi(-BrO^-)$	Experimental	0.38 ± 0.008	0.70 ± 0.01
	Calculated	0.362 ± 0.032	0.72 ± 0.041
$\Phi(-BrO_2^-)$		0.075 ± 0.010	0.24 ± 0.008
$\Phi(O_2)$		0.042 ± 0.012	0.16 ± 0.017
$\Phi(BrO_3^-)$		0.155 ± 0.007	0.31 ± 0.008
$\Phi(Br^-)$	Experimental*	0.30 ± 0.02	0.63 ± 0.02
	Calculated	0.289 ± 0.041	0.651 ± 0.019

---

* Calculated from $\Phi(-BrO^-)+\Phi(BrO_2^-)-\Phi(BrO_3^-)$

No N_2 gas was found to be produced when N_2O saturated solution of BrO^- was photolyzed at 365 nm, 313 nm and 253.7 nm.

DISCUSSIONS

The data shown in figure 1 indicate that both BrO^- and BrO_2^- compete with O_2 for $O(^3P)$ atom. The competition reactions are (1), (9) and (10) and the yield of O_3 is given by eq. 11

$$O(^3P) + O_2 \rightarrow O_3 \tag{1}$$

$$O(^3P) + BrO^- \rightarrow \text{Products} \tag{9}$$

$$O(^3P) + BrO_2^- \rightarrow \text{Products} \tag{10}$$

$$1/\Phi(O_3) = 1/\Phi(O)\, 1+\left(\frac{k_9[BrO^-] + k_{10}[BrO_2^-]}{k_1[O_2])}\right) \tag{11}$$

Although $\Phi(O)$ is not known, it will be proportional to $[BrO^-]$ under the experimental conditions employed, and therefore when $[BrO^-] = 0$, k_9/k_1 can be evaluated from eq. (12) by measuring the yield of O_3 at different $[BrO^-]$ and taking the ratio of any two values.

$$\frac{[O_3]_1[BrO^-]_2}{[O_3]_2[BrO^-]_1} = \frac{1+\dfrac{k_9}{k_{10}}\dfrac{[BrO^-]_2}{[O_2]}}{1+\dfrac{k_9}{k_{10}}\dfrac{[BrO^-]_1}{[O_2]_1}} \tag{12}$$

Similarly when BrO_2^- is present and the concentration of BrO^- is kept constant the expression becomes (13)

$$\frac{(O_3)_1}{(O_3)_2} = \frac{1 + \dfrac{k_9[BrO^-] + k_{10}[BrO_2^-]_2}{k_1[O_2]}}{1 + \dfrac{k_9[BrO^-] + k_{10}[BrO_2^-]_1}{k_1[O_2]}} \qquad (13)$$

The best fits of data in figure 1 are obtained with $k_9/k_1 = 3.12$ and $k_{10}/k_1 = 17.2$ and are shown by the full line in figure 1. Reaction (1) is efficient since the formation of O_3 was complete at the end of the flash. The earliest measurements were made at 60 s after the start of the flash. Taking $[O_3] = 1.3\times10^{-3}M$ the k_i was estimated to be at least $5\times10^7 M^{-1}s^{-1}$. Since k_{10} will not exceed the diffusion controlled limit of about 2×10^{10} $M^{-1}s^{-1}$, k_1 will have the upper limit of $10^9 M^{-1}s^{-1}$.

The origin of O^- producing O_3^- may be either the primary process (4) or (14)

$$BrO^- \xrightarrow{h\nu} BrO^\bullet + e^-_{aq} \qquad (14)$$

$$e^-_{aq} + BrO^- \rightarrow Br^- + O^- \qquad (15)$$

Reaction (15) is very rapid;[19] the absence of any effect of N_2O on the rate of photolysis of BrO^- and considerations of low energy absorption band,[7] all lead to the conclusion that process (14) does not occur to a significant extent. Process (4) is the only source for the O^- radical anion. It has been pointed out in the literature [20] that there is no evidence till now to distinguish between (4) and (16)

$$BrO^-H_2O \xrightarrow{h\nu} Br + {}^\bullet OH + OH^- \qquad (16)$$

However the equilibrium between $^\bullet OH$ and $^\bullet O^-$ is rapid [21]

$$^\bullet OH + OH^- \rightleftharpoons O^- + H_2O \qquad (17)$$

so that whether (4) or (15) occurs the overall result is the same. The bromine atoms produced in reaction (4) are expected to oxidize BrO^- to BrO as the electron affinity of Br exceeds that of BrO [22] and the subsequent reactions of BrO are expected to be the same as suggested in the radiation chemistry of BrO^- ion.[19,23] The overall mechanism for the photolytic decomposition of BrO^- following the primary process (4) is

$$BrO^- \xrightarrow{h\nu} Br + O^- \qquad (4)$$

$$^\bullet OH + OH^- \rightleftharpoons O^- + H_2O \qquad (17)$$

$$^{\bullet}OH + BrO^- \rightarrow BrO^{\bullet} + OH^- \tag{5}$$

$$O^- + BrO^- \rightarrow BrO^{\bullet} + O^- \tag{6}$$

$$Br + BrO^- \rightarrow Br^- + BrO^{\bullet} \tag{18}$$

$$2BrO \rightleftharpoons Br_2O_2 \tag{19}$$

$$Br_2O_2 + H_2O \rightarrow BrO^- + BrO_2^- + 2H^- \tag{20}$$

$$Br_2O_2 + H_2O \rightarrow BrO^- + Br^- + O_2 + 2H^+ \tag{21}$$

$$Br_2O_2 + 2BrO_2^- \rightarrow 2BrO^- + 2BrO_2 \tag{22}$$

$$2BrO_2 \rightleftharpoons Br_2O_4 \tag{23}$$

$$Br_2O_4 + H_2O \rightarrow BrO_3^- + BrO_2^- + 2H^+ \tag{24}$$

The final products are BrO_3^-, O_2 and Br^-.

(i) Photodecomposition at 365 nm.

During the early stages of photolysis when $[BrO^-] = [BrO_2^-]$ reaction (10) can be regarded as negligible and insufficient energy is available or the process (25)

$$BrO^- \xrightarrow{h\nu} Br^- + O(^1D) \tag{25}$$

to occur. The products O_2, BrO_3^-, BrO_2^- and Br^- must result from the occurrence of reactions (3) and (4). Reaction (4) followed by 17—24 accounts for BrO_3^- but not for O_2 since reaction (21) will be completely suppressed when BrO_2^- 3×10^{-5}M, a condition which is achieved when less than 2 % BrO^- has been decomposed. Thus reaction (9) is the source for both O_2 and BrO_2^-. In this case $O(^3P)$ should add or abstract oxygen in the reaction with BrO^-

$$O(^3P) + BrO^- \rightarrow BrO_2^- \tag{9(a)}$$

$$O(^2P) + BrO^- \rightarrow Br^- + O_2 \tag{9(b)}$$

The quantum yields for the destruction of BrO^- and the formation of products are predicted in terms of the quantum yields for the primary processes (3) and (4) by the relationships (26—30)

$$\Phi(-BrO) = 2\Phi_3 + \Phi_4 \tag{26}$$

$$\Phi(BrO_2^-) = (k_{9a}/k_9)\Phi_3 - \Phi_4 \tag{27}$$

$$\Phi(O_2) = (k_{9b}/k_9)\,\Phi_3 \tag{28}$$

$$\Phi(BrO_3^-) = \Phi_4 \tag{29}$$

$$\Phi(Br^-) = \Phi_3(1 + k_{9b}/k_9) + \Phi_4 \tag{30}$$

Substitution of the data from table 2 in equatinos (27 to 29) gives $k_{9b}/k_9 = 0.18 + 0.06$ and values of Φ_3 and Φ_4 are shown in table 4.

TABLE 4

Primary quantum yields Φ_3, Φ_4 and Φ_{25} for the primary photochemical processes

$$BrO^- \xrightarrow{h\nu} Br^- + O(^3P)$$

$$BrO^- \xrightarrow{h\nu} Br + O^-$$

$$BrO^- \xrightarrow{h\nu} Br^- + O(^1D)$$

λ (nm)	365	313	253.7
Φ_3	0.318 ± 0.02	0.089 ± 0.014	0.081 ± 0.018
Φ_4	0.09 ± 0.15	0.155 ± 0.015	0.325 ± 0.016
Φ_{25}	0	0.026 ± 0.015	0.150 ± 0.018

Using these data in equations (26) and (30) we calculated $\Phi(-BrO^-) = 0.727 \pm 0.05$ and $\Phi(Br^-) = 0.45 \pm 0.05$ in fair agreement with the experimental values.

As the concentration of BrO_2^- increases, reaction (10) will begin to compete with (9) which accounts for the decrease in yield of BrC_2^- as the extent of photodecomposition of BrO^- increases, A similar reaction to that for ClO_2^{-3} must be taking place

$$O(^3P) + BrO_2^- \rightarrow BrO_3^- \tag{10a}$$

$$O(^3P) + BrO_2^- \rightarrow O_2 + Br^- + O(^3P) \tag{10b}$$

The data obtained and presented [24] substantiate the mechanism for reaction (10) which shows that $k_{1cb}/k_{1ca} = 1.6 \pm 0.22$.

When reaction (10) is included in the mechanism, equation (27) becomes (31) and expression relating (BrO_2^-) to the amount of light is (32).

$$\Phi(BrO_2^-) = \Phi_3\left(\frac{1-2.5xR}{1+6+xR}\right) - \Phi_4 \tag{31}$$

$$(BrO_2^-) = \Phi_3\left(\int_0^{I_a} \frac{1-2.5xR}{1+y+xR}\, dI_a\right) - \Phi_4 I_a \tag{32}$$

where $x = k_{1ca}/k_9$, $y = k_{9b}/k_{9a}$ and $R = BrO_2^-/BrO^-$

Equation (32) was used to fit the calculated yield of BrO_2^- to the data in figure 2, and a best and a satisfactory fit was obtained with $\Phi_3 = 0.318$, $\Phi_4 = 0.09$, $k_{1ca}/k_9 = 2.4$.

Thus the complete mechanism can be written as follows :

$$\mathrm{BrO^-} + h\nu \begin{array}{ll} \nearrow \mathrm{Br^-} + \mathrm{O(^3P)} & (3)\\ \rightarrow \mathrm{Br} + \mathrm{O^-} & (4)\\ \searrow \mathrm{Br} + \mathrm{O(^1D)} & (25)\end{array}$$

$$\mathrm{O(^3P)} + \mathrm{BrO^-} \begin{array}{ll} \nearrow \mathrm{BrO_2^-} & 9(\mathrm{a})\\ \searrow \mathrm{Br^-} + \mathrm{O_2} & 9(\mathrm{b})\end{array}$$

$$\mathrm{O(^3P)} + \mathrm{BrO_2^-} \begin{array}{ll} \nearrow \mathrm{BrO_3^-} & (10\mathrm{a})\\ \searrow \mathrm{Br^-} + \mathrm{O_2} + \mathrm{O[^3P]} & (10\mathrm{b})\end{array}$$

$$\mathrm{OH} + \mathrm{BrO^-} \rightarrow \mathrm{BrO} + \mathrm{OH^-} \tag{5}$$

$$\mathrm{O^-} + \mathrm{BrO^-} \rightarrow \mathrm{BrO} + \mathrm{O^{2-}} \tag{6}$$

$$2\mathrm{BrO}\cdot \rightleftharpoons \mathrm{Br_2O_4} \tag{19}$$

$$\mathrm{Br_2O_2} + \mathrm{H_2O} \rightarrow \mathrm{BrO^-} + \mathrm{BrO_2^-} + 2\mathrm{H^+} \tag{20}$$

$$\mathrm{Br_2O_2} + \mathrm{H_2O} \rightarrow \mathrm{Br^-} + \mathrm{O_2} + \mathrm{BrO^-} + 2\mathrm{H^+} \tag{21}$$

$$\mathrm{Br_2O_2} + 2\mathrm{BrO_2^-} \rightarrow 2\mathrm{BrO_2} + 2\mathrm{BrO^-} \tag{22}$$

$$2\mathrm{BrO_2} \rightleftharpoons \mathrm{Br_2O_4} \tag{23}$$

$$\mathrm{Br_2O_4} + \mathrm{H_2O} \rightarrow \mathrm{BrO_3^-} + \mathrm{BrO_3^-} + \mathrm{BrO_2^-} + 2\mathrm{H^+} \tag{24}$$

(ii) Photodecomposition at 313 and 253.7 nm.

At these wavelengths $\mathrm{BrO_2^-}$ ion was no longer among the observed products. This clearly suggests that $\Phi_4 = \Phi_3$ so that any $\mathrm{BrO_2^+}$ ion produced by reaction (9a) is destroyed by reaction (22).

This is further supported by the observations that added $\mathrm{BrO_2^-}$ is destroyed, and also the yields of $\mathrm{O_3}$ and $\mathrm{O_3^-}$ measured in the flash photolysis experiments also indicate that $\Phi_4 = \Phi_1$ at shorter wavelength (see table 1).

In the absence of added bromite the ion oxygen will be produced by reaction (21) as well as (9b). If $\mathrm{O(^1D)}$ are produced at these wavelengths they will also lead to oxygen through the following reactions :

$$\mathrm{O(^1D)} + \mathrm{H_2O} \rightarrow \mathrm{H_2O_2} \tag{33}$$

$$\mathrm{H_2O_2} + \mathrm{BrO^-} \rightarrow \mathrm{Br^-} + \mathrm{O_2} + \mathrm{H_2O} \tag{34}$$

Reaction (34) is well known and there is good evidence that reaction (33) represents the fate of $\mathrm{O(^1D)}$ in dilute aqueous solution.[15,17] In the presence of added bromite, reactions (20) and (21) are suppressed but the yields of O_2, although lowered, are appreciable since O_2 will result from reaction (10b) when BrO_2^- is present but the ratio BrO^-/BrO_2^- was such that no more than 10% of $O(^3P)$ will have reacted with O_3. The yield of O_2 produced by reactions (9 b) and (10b) will be small and it seems likely that primary process (25) accounts for some of the observed yields.

The expressions relating the measured quantum yields to primary yields Φ_3, Φ_4 and Φ_{25} are

$$\Phi(-BrO^-) = \Phi_3\left\{1 + \left(1 + k_{10a}\frac{[BrO_2^-]}{k_9[BrO^-]}\right)^{-1}\right\} + \Phi_4 + 2\Phi_{25} \quad (35)$$

$$\Phi(-BrO_2^-) = \Phi_4 - \Phi_3\{2k_9[BrO^- - 1]/k_9[BrO^-]+k_{10b}[BrO_2^-]\} \quad (36)$$

$$\Phi(O_2) = \Phi_3\left(\frac{(k_{9b}[BrO^-] + k_{10b}[BrO_2^-]}{k_9[BrO^-] + k_{10a}[BrO_2^-]}\right) + \Phi_4 \quad (37)$$

$$\Phi(BrO_3^-) = \Phi_3\left(1 + \frac{k_9[BrO^-]}{k_{10a}[BrO_2^-]}\right)^{-1} + \Phi_4 \quad (38)$$

$$\Phi(Br^-) = \Phi_3\left(1 + \frac{(k_{9b}[BrO^-] + k_{10b}[BrO_2^-])}{(k_9[BrO^-] + k_{10a}[BrO_2^-])}\right) + \Phi_4 + 2\Phi_{25} \quad (39)$$

Taking $[BrO^-]/[BrO_2^-] = 20$, the ratio of the values used during experiments $k_{10b}/k_{10a} = 1.6 \pm 0.22$; $k_{10}/k_9 = 5.5$ and $k_{9b}/k_{9a} = 0.18 \pm 0.06$, and substituting these values and data from table 3 in equations (36–38), the values of Φ_3, Φ_4 and Φ_{25} shown in table 4 are given. The values of $\Phi[Br^-]$ and $\Phi[BrO^-]$ were calculated from equations when the experimental and calculated values provide strong support for the proposed mechanism.

In the absence of added bromite reactions, (20) and (21) will occur but reaction (10) will not take place, and equations (35 to 39) are replaced by equations (40 to 43):

$$\Phi(BrO^-) = 2\Phi_3 + \Phi_4(1 + a + b) + 2\Phi_{25} \quad (40)$$

$$\Phi(O_2) = \Phi_3/(1 + k_{9b}) + b\Phi_4 + \Phi_{25} \quad (41)$$

$$\Phi(BrO_3^-) = \Phi_4(1 - a - b) \quad (42)$$

$$\Phi(Br^-) = \Phi_3(1 + k_{9b}/k_9) + \Phi_4(1 + b) + 2\Phi_{25} \quad (43)$$

where

$$a = k_{20}/k_{20} + k_{21} + k_{22}/k_{24}[BrO_2^-]_s$$

$$b = k_{2k}/k_{20} + k_{21} + k_{22}/k_{24}[BrO_3^-]_s$$

where $[BrO_2^-]_s$ is the stationary concentration of bromite ion. It is not possible to evaluate primary quantum yields from these equations but they can be used to calculate quantities on the left hand side provided

a and b are known. The data obtained by the radiolysis of BrO^- solutions,[18,19,13] $a/b = 2.11 \pm 0.12$ and $k_{22}/k_{20} = (1.6 \pm 0.22) \times 10^5 M^{-1}$. On solving equation (41) for (b) using appropriate data from tables (2) and (4) and taking $k_{9b}/k_{9a} = 0.18 \pm 0.06$, the valuse of a and b are calculated at 313 nm and 253.7 nm as shown in table 5.

TABLE 5

Values calculated for a and b at wavelengths 313 nm and 253.7 nm

λ (nm)	313	253.7
a	0.42 ± 0.18	0.29 ± 0.09
b	0.23 ± 0.098	0.16 ± 0.03

Substitution of these values and those of Φ_3, Φ_4 and Φ_{25} in equations (40), (42) and (43) gives the calculated yields of $\Phi(-BrO^-)$, $\Phi(BrO_3^-)$ and $\Phi(Br^-)$ shown in table 2. The agreement is good in all the cases which provide a further support for the proposed mechanism. In principle the magnitude of $[BrO_2^-]_s$ can be evaluated from the expressions for a and b given above but unfortunately the uncertainties in the values in the parameters made precise calculations meaningless. However, it is clear from these values that $[BrO_2^-]$ is of the order of 10^{-6}M, a concentration which is not detectable by the analytical techniques employed.

REFERENCES

[1] A. J. Allmand, P. W. Cunliffe and R. E. Maddison, *J. Chem. Soc.*, **1925**, 882.

[2] A. J. Allmand, P. W. Cunliffe and R. E. Maddison, *J. Chem. Soc.*, **1927**, 655.

[3] A. J. Allmand and W. W. Weblo, *Z. phys. Chim.*, **A131**, 189, (1928).

[4] K. W. Young and A. J. Allmand, *Canad. J. Chem.*, **27B**, 318, (1949).

[5] G. V. Buxton and R. J. Williams, *Proc. Chem. Soc.*, **1962**, 141.

[6] A. Prokopckas, J. Janickis and M. Salkauskas, *Lietuvous T. S. E. Mokslu Akad Darbai Ser*, **B 3(38)**, 49 (1964).

[7] M. J. Blandamen and M. F. Fox, *Chem. Rev.*, **70**, 59 (1970).

[8] M. S. Subhani and G. V. Buxton, *J. Chem. Soc. Trans Faraday* 1, **68**, 958 (1972).

[9] O. Amichai and A. Tneinin, *Chem. Phys. Let.*, **3**, 611 (1969).

[10] O. Amichai and A. Theinin, *J. Phys. Chem.*, **74**, 830 (1970).

[11] O. Amichai, G. Czapski and A. Tneinin, *Israel J. Chem.*, **7**, 351 (1969).

[12] M. S. Subhani, *Rev. Roumaine Chim.* (accepted for publication).

[13] C. G. Hatchard and C. A. Parker, (a) *Proc. Roy. Soc.*, **A220**, 104 (1953); (b) *Proc. Roy. Soc.*, **A235**, 518 (1956).

[14] C. H. Cheek and J. Linnenbom, *J. Phys. Chem.*, **67**, 1856 (1963).

[15] H. Taubc, *Trans. Faraday Soc.*, **53**, 656 (1957).

[16] G. Czapski and L. M. Dorfman, *J. Phys. Chem.*, **68**, 1169 (1964).

[17] F. S. Dainton and P. Fowles, *Proc. Roy. Soc.*, **A287**, 295 (1965).

[18] G. V. Buxton and F. S. Dainton, *Proc. Roy. Soc.*, **A304**, 441 (1968).

[19] G. V. Buxton and F. S. Dainton, *Proc. Roy Soc.*, **A304**, 427 (1968).

[20] A. Tneinin, *Israel J. Chem.*, **8**, 103 (1970).

[21] G. V. Buxton, *Trans. Faraday Soc.*, **66**, 1656 (1970).

[22] V. I. Vedeneyev, L. V. Gwruich, V. N. Konratyev, A. V. Meduodeu and Ye. L. Frankevich, "Bond Energies, Ionization Potentials and Electron Affinities", Arnold, London, 1966.

[23] M. S. Subhani and A. Frank (Submitted for publication). *J. Nig. Chem. Soc.*

[24] M. S. Subhani (Submitted for publication). *J. Nig. Chem. Soc.*

Revue Roumaine de Chimie, 25, *11–12*, 1579–1583 (1980)

THE STUDY OF THE TRANSITION STATE INVOLVES ELECTROSTATIC CONTRIBUTIONS TO THE THERMODYNAMIC FUNCTIONS FOR THE REACTION BETWEEN TWO IO^- IONS

M. S. SUBHANI*

Department of Chemistry, University of Nigeria, Nsukka, Nigeria

Received September 23, 1978

Investigations were carried out using different dielectric media and various ionic strengths for the reaction between IO^- and IO^- in solution. From the plot of log K_0 and 1/D the values of $r^{\neq}$ and r_{AB} were obtained for the activated couple ($IO^- - IO^-$). On comparison with the theoretical results for the radii the double sphere model was found to be the most suitable model for the activated state formed in the reaction. Electrostatic contributions to the changes in thermodynamic functions $\Delta G^{\neq}_{es}$, $\Delta S^{\neq}_{es}$ and $\Delta H^{\neq}_{es}$ in the formation of transition state were also evaluated.

INTRODUCTION

Various studies have been carried out to see the effect of dielectric constant and ionic strength on the reaction between stable inorganic ions.[1-8] A number of models have been proposed for the transition state formed during the course of reaction due to the rearrangement of the total charge of the reactants on the activated complex formed.[9,10,11] Expressions relating the rate constant at zero ionic strength (k_0) to the dielectric constant(D) for a single sphere model and that of double sphere model are as follows:

$$\log k_0 = \log k_i = \frac{e^2}{4.606\,DKT}\left(\frac{(Z_A + Z_B)^2}{r^{\neq}} - \frac{Z_A^2}{r_A} - \frac{Z_B^2}{r_B}\right) \qquad (1)$$

$$\log k_0 = \log k_i - \frac{Z_A Z_B e^2}{2.303 DKT r_{AB}} \qquad (2)$$

The electrostatic contributions to the thermodynamic functions such as free energy of activation in a single and a double sphere model are given in the literature[10,11] as in equations (3) and (4)

---

* Faculty of Science, Garyounis University, Post Box, 9480, Benghazi, Libya.

$$G^{\neq}_{es} = \frac{Ne^2}{D}\left(\frac{(Z_A + Z_B)^2}{r^{\neq}} - \frac{Z_A^2}{r_A} - \frac{Z_B^2}{r_B}\right) \tag{3}$$

$$G^{\neq}_{es} = \frac{NZ_AZ_Be^2}{Dr_{AB}} \tag{4}$$

respectively, where k_i, the rate constant at infinite dielectric constant, k, the Bollzman constant, Z_A, Z_B, r_A and r_B are the charges and radii of ions A and B respectively. $r^{\neq}$ and r_{AB} are the radii of the activated complex in single and double sphere models respectively. Electrostatic contributions to entropy of activation or enthalpy of activation can be calculated using equations (3) and (4) and other standard thermodynamic relationships reported in the literature.[10] In the present paper the work which is carried out on reaction between IO^- and IO^- is presented. This reaction is found to be of the second order and the rate determining step can be written as reported in the literature.[12]

$$IO^- + IO^- \rightarrow IO_2^- + I^- \tag{5}$$

EXPERIMENTAL

All chemicals used were of analaR grade and were used without further purification. Dilute solution of NaIO (10^{-3} M to 10^{-4} M) were prepared by rapidly dissolving solid I_2 in solution containing 10^{-1}M NaOH. All solutions were prepared in triply distilled water just before the experiment and were saturated with Ar gas by the usual bubbling procedure described elsewhere.[13] All measurements were made at (2 ± 0.1)°C. UNICAM SP 500 spectrophotometer with thermostat attachment was used for the optical density measurement at different time intervals. The measurements were made at $\lambda = 365$ nm where IO^- in solution has maximum absorption. A series of absorption spectra were run using media of various dielectric constants to get the correct molar absorption coefficients used for the calculations of rate constant. Dielectric constant measurements for various systems (10 % to 45 % mixtures of alcohol/water) were made by the method described elsewhere.

RESULTS AND DISCUSSIONS

The values observed for the rate constant measured spectrophotometrically for the reaction between two IO^- using alkaline solution at different ionic strengths and varying dielectric constant are shown in table 1.

From the rate constant observed for reaction (5) the values for the specific rate constant at zero ionic strength (k_0) were determined from the plots of graph between log k and square root of ionic strength (M) at a given dielectric constant. The intercept at zero ionic strength obtained on extra-polation gives the value of log k_0 as expected from equation (6)

$$\log k = \log k_0 + AZ_AZ_B \tag{6}$$

TABLE 1

The values observed for the rate constants (k) of the reaction between IO^- and IO^- at various ionic strengths and different dielectric constants in solution.
$T = 275$ K
$[IO^-] = 10^{-3}$ M
k × 10^{-3}

$(M^{-1} s^{-1})$	μ	D
7.31	0.1	80.2
10.33	0.2	80.2
13.49	0.3	80.2
16.90	0.4	80.2
20.61	0.5	80.2
29.04	0.6	80.2
7.06	0.1	73.9
10.59	0.2	73.9
14.16	0.3	73.9
18.24	0.4	73.9
22.86	0.5	73.9
33.57	0.6	73.9
6.84	0.1	67.2
10.74	0.2	67.2
15.21	0.3	67.2
20.37	0.4	67.2
26.42	0.5	67.2
41.30	0.6	67.2
6.59	0.1	58.9
11.43	0.2	58.9
17.46	0.3	58.9
24.95	0.4	58.9
34.28	0.5	58.9
58.88	0.6	58.9
6.41	0.1	51.1
12.65	0.2	51.1
21.38	0.3	51.1
33.19	0.4	51.1
49.09	0.5	51.1
95.94	0.6	51.1

TABLE 2

The values obtained for the rate constant at zero ionic strength (k_0) for the reaction between IO^- and IO^- as a function of the reciprocal of the dielectric constant (1/D)
T = 275°/C

Log k_0	1/D × 10^3
$\bar{3}.50$	12.469
$\bar{3}.44$	13.53
$\bar{3}.36$	14.880
$\bar{3}.24$	16.978
$\bar{3}.09$	19.569

TABLE 3

The values for the radii of the activated complex formed between IO^- and IO^- ions.

	Theoretical values (A°)	Expermental values (A°)
$r^{\neq}$	2.94	3.036
r_{AB}	4.69	4.64

where A is a constant at a given temperature and dielectric constant of the system.

The values of log k_0 thus obtained are shown in table 2.

A graph was plotted between log k_0 and reciprocal of dielectric constant (1/D); a fairly good straight line was obtained (See figure 1) which satisfies equations (1) and (2). From the slope of the straight line the values of $r^{\neq}$ and r_{AB} were evaluated graphically using equations (1) and (2). The values are given in table 3.

Theoretical values for $r^{\neq}$ and r_{AB} were obtained by the method described in the literature,[3,5] using data for the various ionic radii reported in the literature.[14,16] The values are given in table 3. The comparison of the theoretical values of $r^{\neq}$ and r_{AB} with those of the experimentally obtained values (see table 3) shows that the most probable shape of. the activated complex formed in the reaction is of double sphere type

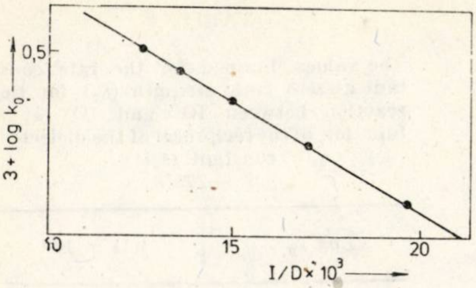

Fig. 1.—Dependence of log k_0 on reciprocal of dielectric constant (1/D) of the medium.

The data obtained for r_{AB} were further used to calculate electrostatic contributions to the changes in the free energy of activation ($\Delta G^{\neq}_{es}$), entropy of activation ($\Delta S^{\neq}_{es}$) and enthalpy of activation ($\Delta H^{\neq}_{es}$) for the activated state formed during the course of reaction. The values are summarized in table 4.

TABLE 4

The values for the electrostatic contributions to the changes in the thermodynamic functions $\Delta G^{\neq}_{es}$, $\Delta S^{\neq}_{es}$ and $\Delta H^{\neq}_{es}$ for the formation of the transition state in the reaction between IO^- and IO^- ions.

	$\Delta G^{\neq}_{es}$ XM(cal)$^{-1}$	$\Delta S^{\neq}_{es}$ XMT(cal)$^{-1}$	$\Delta H^{\neq}_{es}$ M(cal)$^{-1}$
Theoretical values	887.7	−4.083	−329
Experimental values	897.2	−4.127	−332.7

The negative sign and magnitude for the change in electrostatic contributions to the entropy of activation can be interpreted in terms of the description of the initial state of reactants and that in the activated state. Both IO^- and IO^- are singly negatively charged spheres before the start of the reaction when they are regarded at infinite distance from each other. In the activated state the sphere is doubly negatively charged $(IO - IO)^{2-}$. Thus solvent molecules in the neighbourhood of these ions are acted upon by electrostrictions. More electrostriction is expected in the initial state of the reactants. This results in decrease in electrostatic contributions to the entropy of activation.

REFERENCES

[1] A. A. Frost and R. G. Pearson, "Kinetics and Mechanism", 2nd Ed. Wiley, New York, 1961, p. 74.

[2] D.T.Y. Chem and K. J. Laidlar, *Canad. J. Chem.*, **37**, 599 (1959).

[3] K. J. Laidlar and H. Enring, *Ann. New York Acad. Sci.*, **39**, 303 (1940).
[4] K. J. Laidlar, "Chemical Kinetics", 2nd Ed., McGraw Hil!, New York, 1965, p. 221.
[5] M. S. Subhani and T. Kausar, *Pak. J. Sci. Ind. Research* **18**, 208 (1975).
[6] M. S. Subhani, *Rev. Roumaine Chim.*, in press.
[7] M. S. Subhani and M. N. H. Lacewala, *J. Sci Mathes*, **1**, 41, (1974).
[8] M. S. Subhani (Submitted for publication). *Pak. J. Sci. Ind. Research.*
[9] G. Scatchard, *Chem. Rev.* **10**, 229 (1932).
[10] K. J. Laidlar, "Chemical Kinetics", 2nd Ed., McGraw Hill, New York, 1965, p. 212 and p. 217.
[11] E. S. Amis and J. E. Petts, *J. Amer. Chem. Soc.*, **63**, 2883 (1941).
[12] O. Haimovich and A. Treinin, *J. Phys. Chem.*, **71**, 1941 (1967).
[13] M. S. Subhani and T. Kauser, *Rev. Roumaine Chim.*, (Accepted for publication).
[14] J. Kleinberg, W. J. Argersinger and E. Griswold, "Inorganic Chemistry", D. C. Heath Co., Boston, 1965, p. 74.
[15] T. Moeler, "Inorganic Chemistry", Wiley, New York, 1965, p. 140.
[16] A. F. Kapustinsku, *Quart Rev.*, **10**, 283 (1956).

Revue Roumaine de Chimie, **25**, *11–12*, 1585–1587 (1980)

COMPTES RENDUS

A. VERTES, L. KORECZ and K. BURGER, "MÖSSBAUER SPECTROSCOPY", Akadémiai Kiadó, Budapest, 1979, 432 pp.

The book analyzed here is not only a new review on a rapidly developing field, but it has a distinctive coverage of an area which is not presented in depth in other books : a whole section, the third (114 pages), is devoted to the Mössbauer effect in frozen solutions. It is known that the recoil-free nuclear resonance absorption (Mössbauer effect) takes place with measurable probability only in solids. It was Dézsi's systematic work which drew the attention to the possibilities offered by this technique ; the authors of the present monograph have been active personally in research involving frozen solutions. Though two of them are chemists and one is a physicist, they have produced together a valuable monograph. Professor Vértes has published several papers together with I. Dézsi.

The first part treats the physical bases of Mössbauer spectroscopy. The second part is entitled "The application of Mössbauer spectroscopy in inorganic chemistry". The third part, on the Mössbauer effect in solutions has already been mentioned. The fourth part is entitled "Application of the Mössbauer spectroscopy in biological research". The fifth part is entitled "Metallurgical studies". The book is concluded by an author index and by a short subject index.

The whole book is a valuable collection of information. Through the inclusion of data on metalloproteins and on organometallic complexes, it also gives interesting data on organic structures incorporating Mössbauer nuclei. The English translation and the printing conditions are excellent. The book is an invaluable addition to libraries of universities and institutes where the Mössbauer effect is used.

A. T. Balaban

"Topics in Current Chemistry". Volume 86. "Spectroscopy", Springer Verlag, Berlin, Heidelberg, New York, 1979, 294 pages.

The book contains four contributions, two of them concerning far-UV spectroscopy and the other two concerning photoelectron spectroscopy.

The first chapter "Photochemistry and Spectroscopy of Simple Polyatomic Molecules" (90 pages, 371 references) is written by M.N.R. Ashfold, M.T. Macpherson and J.P. Simons. The authors begin with the interesting observation that "the distinction between the UV and vacuum-UV regions is essentially terrestrial, arising from the unique planetary atmosphere we still (thankfully) enjoy", and show further the interest of the vacuum-UV spectroscopy which explores the energy range from the intravalency shell transitions to photoionization limit. After a description of the nature of molecular electronic states populated in the vacuum-UV, including the influence of the molecular core and concluding that the "characterization of the lower lying states of polyatomic molecules populated by absorption in vacuum-UV region is no easy task", various applications are presented. The authors offer not an exhaustive review but a detailed description of some representative simple polyatomic molecules e.g. H_2O ; D_2O ; H_2Se ; H_2Se ; NH_3 ; ND_3 ; HCN ; CO_2 ; COS ; $BrCN$; $(CN)_2$; CH_3CN ; CH_3NC etc. In each case data concerning the spectroscopy and the photochemistry of the analysed compound are given in an effort to correlate the above both domains "in order to penetrate the elusive secrets of photodissociative state". The review contains numerous vacuum-UV spectra (not easy to find together elsewhere) beside different electronic state correlation diagrams whose utility and limitations are stressed for every example.

The second chapter "Far — Ultraviolet Absorption Spectra of Organic Molecules" (47 pages, 180 references), is written by Camille Sandorfy, a well-known authority in the domain of UV spectroscopy. As indicated in the introduction, this chapter "is not a review but a presentation meant to provoke discussions". The author succeeded in description — in a few number of pages — of the present state of far-UV spectroscopy as well as of its future trends ("towards a Rydberg chemistry"). The presentation is made in a fascinating way, captivating the reader from the very beginning to the last line. The simple style, the numerous questions proposed and solved in a clear way, the continuous underlining of the characteristic features of the Rydberg transitions in opposition to the valence-shell ones are only some of the qualities of this chapter. The second part of the chapter presents in the same style four groups of far-UV spectra : σ-electron spectra (parrafins, fluorocarbons, silanes), lone-pair spectra (halides and oxo-compounds), π-electron spectra (ethylene and butadiene) and C = C, C = N, C = O spectra. Throughout this part the junction of molecular spectroscopy and photochemical behaviour is stressed, following the belief of the writer that "the ultimate goal of electronic spectroscopy is photochemistry".

The third chapter "Some Aspects of the Photoelectron Spectroscopy of Organic Sulfur Compounds", by R. Gleiter and J. Spanget — Larsen (56 pages ; 132 references), and the fourth one "Photoelectron Spectra and Bonding in Small Ring Hydrocarbons" by R. Gleiter (88 pages ; 127 references) present the most important achievements obtained in the title domains during the last ten years.

In both chapters a nearly similar presentation is adopted. After a concise and instructive introduction concerning the principles of PE spectroscopy and underlining the importance of Koopman theorem, different representative groups of compounds are discussed.

In chapter three the saturated sulfides (hydrogen sulfides, alkyl sulfides, spirocompounds and disulfides), unsaturated sulfides (aryl-alkyl-sulfides and π-systems), thiocarbonyls and polyvalent sulfur compounds are treated considering briefly the application of band shape and intensity criteria in the assignment of PE bands to molecular states.

In the fourth chapter the attention is focussed towards cyclopropane rings (e.g. simple cyclopropane, vinylcyclopropanes, bi- and tri-cyclopropyl derivatives etc.), cyclobutane rings (cyclobutane, vinylcyclobutane, bicyclohexanes and tricyclooctanes), bicyclobutanes, cubanes and tetrahedrane. In spite of the known limitation of PE spectroscopy to small molecules, the present reviews describe numerous "big" molecules, steadily relating them to other simpler analogs, following the idea that the above limitations "could be partly surmonted by studying a series of closely related compounds". Numerous examples from the authors' laboratory are included.

A very useful table with PE spectral data and references (for 110 sulfur compounds and 204 cyclic hydrocarbons) ends each of these chapters.

Throughout these reviews the sober, elevated, didactical presentation of the material, characteristic features of papers and lectures of professor Rolf Gleiter (who recently visited our country), is apparent.

We highly recommend this book useful to every chemist interested in spectroscopy.

M. Banciu

Ö. GAÁL, G.A. MEDGYESI and L. VERECZKEY, "*Electrophoresis in the Separation of Biological Molecules*" Akadémiai Kiadó, Budapest, 1980, 422 pages.

This new book concerning electrophoresis reviews the methodology of electro-migration techniques and presents applications from the field of biological macromolecules.

The first part (181 pages) is dedicated to theoretical and technical bases of electrophoretic methods. The authors realized that : "for the user of our book, a critical assessment of the advantages and disadvantages of the individual methods would be of greater practical value than a mere collection of laboratory recipes". Consequently, the authors describe the three fundamentally types of electrophoresis, namely : moving boundary electrophoresis, zone electrophoresis and steady state electrophoresis, presenting in detail some important and recent techniques e.g. electrophoresis in polyacrylamide gels, isoelectric focusing and isotachophoresis. In these paragraphs, beside theoretical aspects, numerous practical problems concerning apparatus and technique are given. A lot of useful figures, schemes and diagrams completes the text written in a clear and didactic style.

In the second part a discussion concerning the electrophoresis of proteins is presented in some detail (144 pages). A special attention is accorded to important problems of the field such as : separation of proteins according to molecular size and estimation of molecular weights, immunoelectrophoresis, staining of proteins, detection of proteins by enzymatic activity. Numerous interesting and modern examples of electrophoretic separation of proteins are given (e.g. nuclear proteins, haemoglobins, serum proteins etc.).

The third part (24 pages) and the fourth one (5 pages) offer a presentation of electrophoresis of nucleic acids and polynucleotides respectively of glycosaminoglycans.

The entire applicative part of the book (part II, III and IV) succeeded in the demonstration that the properties of a given group of macromolecules greatly influence the applicability of the separation technique.

A rich reference list and a subject index end this interesting book.

We warmly recommend this book, which would be useful to all chemists, biochemists and analysts working in this domain.

M. Banciu

FRANCO A. GIANTURCO, "The Transfer of Molecular Energies by Collision : Recent Quantum Treatments" (Lecture Notes in Chemistry Series, No. 11), Springer-Verlag, Berlin-Heidelberg-New York, 1979, VIII + 327 pages.

The Springer "Lecture Notes in Chemistry" series, of which the reviewed book is the eleventh, publishes preliminary drafts of original papers or monographs, lectures on a new field, or reports of meetings (if these are devoted to a single topic). Timeliness of a manuscript is therefore regarded by the editors as more important than its form, which may be unfinished or tentative. Prompt publication ensures a swift dissemination among researchers of any new knowledge in frontier domains of chemistry. Usefulness of such a publication procedure could hardly be overemphasised.

This book, which is an edited version of the lectures given by Dr. Gianturco at the University of Genoa in the late 70s, intends to present the theoretical and computational methods used in the treatment of energy transfer taking place during molecular collisions.

Understanding how chemistry works at a microscopic level has been an ultimate scope of chemical research, mainly dealt with by physical chemistry and chemical physics. Among the phenomena for which such a "translation" into physical terms is mostly sought, those involving the transformation of a certain kind of molecular energy into another kind or its transfer from or to the environment are extremely important because they lie at the core of chemical reactions.

The author chooses to treat and solve the problem by remaining entirely within the boundaries of quantum mechanics. Such a rigorous approach has the obvious drawback of driving the student to no practical conclusion in the case of real systems. The author is thus compelled to resort to the simplest type of collisional energy transfer, that involving conversion of the translational energy of an atom or of a small molecule into the internal rotational and vibrational energies of a diatomic molecule. This situation, though oversimplified, covers nonetheless the various events happening during a chemical reaction. Even thus restricted, the problem does not become manageable but with the price of a series of further simplifications, such as the neglect of any external radiative field, fully accounted for in the book. The working formalism is crisply introduced, then the treatment of inelastic collisions and the calculation of cross sections are dealt with. A survey of the numerical methods for solving the coupled equations is also offered. Finally, some rotovibrational relaxation models are presented for simple gases such as the H_2—He or CO—He systems. With a view to the reader who might wish to get more deeply into the subject matter, a long list of references follows each chapter.

Even if the procedure proposed by Dr. Gianturco cannot be effective for more complex systems, it is certainly useful as an introduction to the quantum-mechanical treatment of the collisional energy transfer in gases and indeed as a valuable example of a rigorous approach of a quantum chemistry problem.

Alex. Butucelea

INDEX DES AUTEURS

A

ABABI V., voir MIHĂILĂ GH. 599

ABD ALLA M. M. and E. A. SOLIMAN, A. A. HAMED, M. W. OSMAN, Some reactions of β-3, 4-dichlorobenzoylpropionic acid 1549

ABD ALLA M. M. and E. A. SOLIMAN, M. W. OSMAN, Reactions of some arylidenefuranones 415

ABD EL HALEEM S. M. and S. S. ABD EL REHIM, Corrosion behaviour of commercial Zn-Ti alloy in aqueous salt solutions 493

ABD EL-RAHMAN A. N. and H. M. ABDALLA, Calculations of the change in the geometrical structure of $Cl_2C=S$ during the $1_{A_2} \rightarrow 1_{A_1}$ electronic transition 1477

ABD EL REHIM S. S., voir ABD EL HALEEM S. M. 493

ABDALLA M. and M. A. SALEM, A. HATABA, Base catalysed cycloaddition of acetylacetone to *p*-dimethylaminochalcone and diarylideneacetone 1335

ABDALLA M. and M. A. SALEM, A. HATABA, Some reactions of 6-acetyl-3,5-diarylcyclohex-2-enones 1341

ABDALLA M. H., voir ABD EL-RAHMAN A. N. 1477

ABDEL-HAMID M. M., voir OMARA M. M. 253

ABDEL-HAY F. I., voir OMARA M. M. 253

ABDEL-MEGEED M. F., voir EL-KASCHEF M. F. 577

ABDEL-MOTI F. M., voir EL-KASCHEF M. F. 577

AFIFY A. A., voir FAHMY A. F. 125

AHMAD Y. and S. A. SHAMSI, M. I. QURESHI, Studies in intramolecular interaction of aromatic nitro-group with *ortho* side-chain. II. Further syntheses of quinoline N-oxide derivatives 397

AIRINEI A., voir SPIRATOS M. 1083

ALBERT F. M. and M. GIURGINCA, A. MEGHEA, G. IVAN, Basicity constants of some N, N′-disubstituted *p*-phenylenediamines 1543

ALBERT L. and B. TŐKÉS, F. HODOȘAN, Mechanism and kinetics of the electroreduction of sterol nitrates 1529

ALBU I. and E. CHIFU, Interfacial tension variation in the course of liquid-liquid extraction. III. The extraction of butyric acid by different solvents 459

ANANIESCU C., voir SIMIONESCU B. C. 1077

ANDREI C., voir BĂRBOIU V. 933

ANDRUH M. and C. I. LEPĂDATU, M. BREZEANU, On Uspenski's rule regarding the *cis-trans* isomerism of coordination compounds 811

ARMEANU V. and S. VIȘAN, Spectrophotometric microdetermination of uranium with benzoin-oxime 867

ARVAY ZS., voir RĂZUȘ A. C. 547

ASANDEI N. and M. NICU, S. BRĂNIȘTEANU, V. NICU, M. RUSU, M. LUNGU, A. NATANSOHN, Acrylonitrile-cinnamic acid copolymerization. I. Copolymer structure 915

ATANASIU ION Prof. (*in memoriam*) 3

AVRAM M., voir DINULESCU I. G. 535

— , voir DINULESCU I. G. 969

AVRAM R., voir PĂRĂUȘAN V. 1245

AXINTE S. M., voir DANEȘ F. 673

B

BACALOGLU R. and A. MORARU, M. NUŢIU, S. ILUC, C. CSUNDERLIK, E. LUNGU, Liquid crystals. II. Synthesis of *p*-alkyl anilines for benzilideneaniline liquid crystals (in German) 921

BACIU V. and A. T. BALABAN, Chemical graphs. XXXIX. Valence isomers of monodehydro-[*n*[annulenes 1213

BADAWI M., voir OMARA M. M. 253

BADEA F., voir RĂZUŞ A. C. 547

BĂDILESCU I. I., voir CARAGHEORGHEOPOL A. 307

BAHADUR P., voir VARMA R. P. 201

BALABAN A. T., voir BACIU V. 1213

— and M. T. CĂPROIU, N. NEGOIŢĂ, Factors affecting stability and equilibria of free radicals. X. 1-Cyano-2, 2-bis-(3′, 5′-di-t-butylphenyl)-hydrazyl 1327

— , voir DINCULESCU A. 1505

— , voir HILLEBRAND M. 995

BANCIU A. C. and V. MINCU, Electronic spectra and magnetic susceptibilities of some new tetrahedral chelate complexes with Co(d^2)-N(sp^2) bonds. II. Co(II) chelates synthesized with 1-methyl-2-carbethoxy-glyoxalanil-(1)-bromo-phenylhydrazones-(2) 513

BANCIU M. and R. VLAD, PHAN LE THUY, C. DRĂGHICI, Solvolysis of 7(γ-tosyloxypropyl)-7H-dibenzo[a, e]cycloheptene, 5(β-tosyloxyethyl)- and 5(γ-tosyloxypropyl)-5H-dibenzo[a, c]cycloheptene 1221

BARB D. and L. DIAMANDESCU, V. ZNAMIROVSCHI, D. CIURCHEA and R. SEMENIUC, Mössbauer spectroscopy investigations of iron in some pentacoordinate complexes 1485

BĂRBOIU V. and A. NATANSOHN, C. ANDREI, D. BLUM, ^{1}H-NMR method for composition, branching and sequence distribution determination in ethylene-vinyl acetate copolymers 933

— , voir SURPĂŢEANU GH. 1091

BARBU S. and C. GH. MACAROVICI, Complex combinations of thiocarbohydrazine of isonicotinealdehyde and thiphene-2-carbaldehyde (in French) 339

— and C. GH. MACAROVICI, Metallic complexes of nicotinealdehyde-thiocarbohydrazone (in French) 207

BÂTCĂ A., voir DANEŞ F. 673

BAWDEN M. G., voir KHAN S. A. 1433

BENISKA J. and G. KYSELÁ, E. ŠTAUNDER, M. CHLUPKOVÁ, Polymerization of styrene in the presence of *tert*-butylhydroperoxide and tetramethylthiourea 941

BEVINGTON J. C. and B. J. TABNER, P. F. FRIDD, The reactivities of monomers towards primary radicals, studied by spin-trapping 947

BÎLBĂ D., voir FIŞEL S. 1405

BIRADAR N. S., voir PUJAR M. A. 831

BLEJOIU S. I., voir BRAŞOVEANU I. 1159

BLUM D., voir BĂRBOIU V. 933

BODEA C., voir OŞIANU D. 261

BODOR A. and L. FEY, D. BREAZU, Studies on the oxime formation of steroid ketones with O-substituted hydroxylamines 1367

BOEŞTEANU N., voir SÂRBU C. 245

BOOK REVIEWS, 165, 166, 167, 167, 168, 169, 169, 170, 171, 171 ; 301, 301, 302, 302 ; 443, 443, 444, 445 ; 611, 611, 612, 613, 614, 614, 615 ; 753, 754, 755, 756, 756, 757, 758, 759 ; 905, 906, 906, 907, 908 ; 1275, 1277, 1278, 1278, 1279, 1280, 1281, 1282, 1283, 1283 ; 1443, 1443, 1444. . . . .

BORÓWKO M. and M. JARONIEC, General formulation of adsorption from liquid mixtures on heterogeneous solid surfaces 475

BOTEZ G., voir CORNEA F. 701

BRĂNIȘTEANU S., voir ASANDEI N. 915

BRAȘOVEANU I. and S. I. BLEJOIU, A. SZABO, P. ROTARU, I. V. NICOLESCU, Structural strains appearing in the high temperature shift conversion Fe-Cr catalyst 1159

BREAZU D., voir BODOR A. 1367

BREZEANU M., voir ANDRUH M. 811

BREEZE A. and P. M. MAGEE, P. G. PERKINS, The electronic band structure of β-PbO_2 667

BUDRUGEAC P., Two new kinetical derivations of the Jovanović isotherm for monolayer adsorption 487

BULACOVSCHI V., voir DUMITRIU S. 989

C

CĂLDĂRARU H., voir CARAGHEORGHEOPOL A. 307

CALU N. and N. FOCA, M. LUCHIAN, Kinetic data on the formation and thermal decomposition of the $[Pd(p\text{-}ON-C_6H_4-N(CH_3)_2)_2Cl_2]\ H_2O$ complex. 1171

CAMUS J., voir NEGOIU D. 223

— , voir NEGOIU D. 349

— , voir NEGOIU D. 839

CĂPROIU M. T., voir BALABAN A. T. 1327

CARAGHEORGHEOPOL A. and H. CĂLDĂRARU, I. I. BĂDILESCU, V. E. SAHINI, An electron spin resonance study of the iminoxy radicals of 1-benzoxepin-5-one derivatives 307

CARPOV A., voir DRĂGAN D. 285

— , voir DRĂGAN D. 425

CASTRO E. A., Application of an approximate calculation for the total energy of the hydrogen molecule-ion 41

— and F. M. FERNÁNDEZ, A simple parametric procedure for saturated hydrocarbon based on the transferability of Fock matrix elements 455

— and F. M. FERNÁNDEZ, An improved two-parameter Omega technique for molecular orbital calculations. I. The ITPOT method 635

— and F. M. FERNÁNDEZ, An improved two-parameter Omega technique for molecular orbital calculations. II. Polyenes. 643

— and A. H. JUBERT, RRKM calculation of the unimolecular decomposition of trifluoromethyl hypofluorite. 75

CEA R., voir SOTO A. 529

CECAL AL., Complexes of Th(IV) and U(VI) with pyrocatechol, pyrocatecholdisulfonic acid and chromatropic acid (in German) 1201

— , Selective solvation of ion exchangers of type R_4Th and R_2UO_2 in water-organic solvent mixtures (in French) 1397

CENUȘE Z., voir VÎLCU R. 763

— , voir VÎLCU R. 773

— , voir VÎLCU R. 781

CHAKRABORTY A. Kr., voir PAL P. 81

CHANDRA G. and S. N. SRIVASTAVA, Investigation of the kinetics and mechanism of silver(I) ion catalysed oxidation of d, l(α) valine by peroxydisulphate. 1139

— and S. N. SRIVASTAVA, Kinetics of the oxidation of glycine by peroxydisulphate 1149

CHATTERJEE B., Relation between entropy and cohesive energy for metals . . . 789

CHEN H. H., voir ROBERTS R. M. 687

CHIFU E., voir ALBU I. 459

— and I. STAN, Model for the undeformable free drop acted by interfacial tension gradient. 1449

— , voir TOMOAIA-COTIŞEL M. 175

CHIRALEU F., voir IOVU M. 1383

CHIRIAC C. I., Dehydrations with chlorosulfonic acid in pyridine. A convenient method for the synthesis of amides 403

CHIRILĂ N., voir MICU-SEMENIUC R. 1025

CHIŞ E., voir MACAROVICI C. GH. 95

— , voir MACAROVICI C. GH. 503

CHLUPKOVÁ M., voir BENISKA J. 941

CIOBANU A., voir SPIRATOS M. 1083

CIOCHINĂ A., voir VÎLCU R.. 1113

CIURCHEA D., voir BARB D. 1485

CIURDARU V. and V. TAMAŞ, K. L. SIMPSON, 7′-Benzoylamino-β-*apo*-6′-carotenic acid and some of its derivatives via -β-*apo*-8′-carotenylidenoxazolone. 571

COBIANU N., Radical alternating copolymerization of 9-vinylcarbazole with diethyl fumarate or diethyl maleate 953

COMĂNIŢĂ E., voir HAOUAM A. 1389

CONSTANTINESCU C., voir CONSTANTINESCU GH. C. 1259

— and GH. C. CONSTANTINESCU, Separation by extraction and spectrophotometric determination of T1(III) with basic dyes (in German) 1411

— and GH. C. CONSTANTINESCU, Spectrophotometric determination of rhenium with Astrazon blue G (in French). 1421

— and GH. C. CONSTANTINESCU, Spectrophotometric determination of thallium with Astrazone Red Violet 3R (in French). 1561

CONSTANTINESCU GH. C., Influence of substituents on the analytical and extractive properties of organic reagents in their reaction with Au(III). I. Influence of methoxy substituents (in German) 1249

— , voir CONSTANTINESCU C. 1411

— , voir CONSTANTINESCU C. 1421

— , voir CONSTANTINESCU C. 1561

— and C. CONSTANTINESCU, Influence of substituents on the analytical and extractive properties of organic reagents in their reaction with Au(III). II. Influence of methoxy substituents (in German). 1259

CONSTANTINESCU M., voir SURPĂŢEANU GH. 1091

CONŢESCU CR., voir VASS M. I. 55

CORNEA F. and D. IONESCU, M. ZGLOBIU, G. BOTEZ, V. DOBRE, I. NICULESCU-DUVĂZ, Potential anticancer agents. XXI. Synthesis and biological evaluation of some new triazene derivatives 701

CORNEA F. and C. STOICESCU, Complexes of pyromellitic dianhydride with pyridine derivatives 961

COUTURIER D., voir RICART G. 541

CRIȘAN D., voir POPESCU M. 1187
CSUNDERLIK C., voir BACALOGLU R. 921
CSUNDERLIK C., voir IORGA I. 1351
CZAKIS-SULIKOWSKA D., voir KULIG E. 1177

D

DANEȘ F. and BÂTCĂ A., S. M. AXINTE, Absorption of ammonia from aqueous solutions by A and X zeolites doped with transition metal ions (in French) 673
DĂNEȚ A., voir POPA GR. 1427
DANEȘ S., voir STERNBERG S. 467
DĂRÎNGĂ M., voir DUMITRIU M. 981
DAYAL R., voir VARMA R. P. 201
DEACONESCU I., voir DONESCU D. 975
DEMETRESCU I. and M. TOMESCU, Photochemical and thermal behaviour of acrylonitrile-butyl acrylate-vinylidene chloride terpolymer 729
DIAMANDESCU L., voir BARB D. 1485
DIMA M., voir OPREA S. 605
DIMITRIU E., voir VÎLCU R. 1131
DIMOFTE L., voir ONCESCU T. 15
— , voir ONCESCU T. 23
DINCULESCU A. and A. T. BALABAN, Reactions of pyrylium salts with nucleophiles. XIV. New pyridinium salts with potential biological activity 1505
DINULESCU I. G. and L. ENESCU, H. L. PRASHAD, A. GHENCIULESCU, N. ȘTEFAN, M. AVRAM, The electrophilic addition of bromine to 9-halogenobenzocyclobutenonorbornenes 535
— and I. I. POGANY, A. DUMITRIU, E. G. GEORGESCU, M. AVRAM, New synthesis of dibenzo (CH)$_{10}$ and tetra-benzo (CH)$_{10}$ hydrocarbons. Diels-Alder reactions of tricyclo [4.2.2.0^{2,5}[deca-3.7.9-triene derivatives with 9.10-dibromoanthracene 969
DIUDEA M. V., voir SILBERG I. A. 1229
— , voir SILBERG I. A. 1239
DOBRE V., voir CORNEA F. 701
DONESCU A., voir WEINBERG J. 189
DONESCU D. and I. DEACONESCU, K. GOȘA, M. MAZĂRE, I. GAVĂT, Kinetics of emulsion polymerization of vinyl acetate in the presence of hydroxyethylcellulose 975
DOROBANȚU M., voir SOLACOLU S. 111
DRĂGAN D. and A. CARPOV, Chemical modification of polymers. I. Reaction of vinyl chloracetate copolymers with some herbicidal sodium phenoxides 285
— and A. CARPOV, Chemical modification of polymers. II. Reaction of poly(vinyl α-chloroacetophenone) with some herbicidal sodium phenoxides 425
DRĂGAN S., voir PETRARIU I. 145
DRĂGĂNOIU M., voir STERNBERG S. 793
DRĂGHICI C., voir BANCIU M. 1221
DUCA AL., voir MATEI F. 1017
DUMITRIU A., voir DINULESCU I. G. 969
DUMITRU E., voir OPREA S. 605
— E., voir OPREA S. 1039

DUMITRIU M. and M. DĂRÂNGĂ, M. PĂSTRĂVANU, T. LIXANDRU, On the thermal stability of some new polyazines and polyazomethines 981

DUMITRIU S. and V. BULACOVSCHI, Bioactive polymers. VIII. Oxydoreductases and hydrolases immobilized on cellulose derivatives 989

E

EDITORIAL 911

EL-BARBARY A. A., voir OMARA M. M. 253

EL FADLY A. A. and V. MATEI, V. VÎNTU, Kinetic studies of alkyl carboxylic acid esters pyrolysis 1311

EL KADY M. Y., voir FAHMY A. F. 125

— , voir MOHAMED M. M. 237

EL-KASCHEF M. F. and S. M. YASSIN, M. F. ABBEL-MEGEED, F. M. ABDEL-MOTI, Heterocyclic nitrogen compounds. VI. Reaction of some 5-oxopyrazoline derivatives with hydrazine hydrate and diazoalkanes 577

EL-KHAMRY A. A. and M. M. EL-HASHASH, M. M. HABASHY, Reactions of paraconic esters isolated in the Stobbe condensation of *p*-bromo- and *p*-ethylacetophenones with diethylsuccinate 563

ELHASHASH M. A., voir ELKADY M. 1361

— , voir EL-KHAMRY A. A. 563

— , voir FAHMY A. F. 125

— , voir MOHAMED M. M. 237

— , voir SAYED G. H. 1375

ELKADY M. and M. A. ELHASHASH, G. H. SAYED, M. M. MOHAMED, Some reactions of β-aroylacrylic acids 1361

— , voir SAYED G. H. 1375

ENESCU L., voir DINULESCU I. G. 535

F

FAHMY A. F. and M. M. MOHAMED, A. A. AFIFY, M. Y. EL KADY, M. A. EL HASHASH, Base-catalyzed Michael addition of active methylene compounds on arylidene malonates and arylidene barbituric acids 125

FERNÁNDEZ F. M., voir CASTRO E. A. 455

— , voir CASTRO E. A. 635

— , voir CASTRO E. A. 643

FEY L., voir BODOR A. 1367

FIŞEL S. and D. BÎLBĂ, Some considerations on the sorption mechanism of Al^{3+} on cellulose phosphate 1405

FOCA N., voir CALU N. 1171

FRIDD P. F., voir BEVINGTON J. C. 947

FULEA A. O., On "A correction technique for fractionation data and its application to the fractionation of polyethylene terephthalate" 435

G

GADAG R. V. and M. R. GAJENDRAGAD, 3-Ethyl-4-benzylidene-5-mercapto-1, 2, 4-triazole as a new gravimetric reagent for the estimation of silver in salts, alloys and complexes 745

GAJENDRAGAD M. R., voir GADAG R. V. 745

GAVĂT I., voir DONESCU D. 975

GEORGESCU E. G., voir DINULESCU I. G. 969

GHENCIULESCU A., voir I. G. DINULESCU 535

GIRGIS M. M. and D. P. LAZĂR, Catalytic oxidation of ammonia. I. Low temperature oxidation on an iron-chromium catalyst 1293

GIURGINCA M., voir ALBERT F. M. 1542

GLATZ A. M., voir RĂZUȘ A. C. 547

GOCAN S. and C. KONNERT, Resolution in thin-layer chromatography with orthogonal temperatures gradient in S-chamber (in German) 273

GOȘA K., voir DONESCU D. 975

GOȘA V., voir SCHUSTER R. H. 1301

GRIGORAȘ S. and A. MEDEȘAN, I. RUSU, Ș. MOLDOVEANU, A theoretical study of the hydration and hydration effects on some substituted benzoic acid molecules. II. The calculation of the substituent effect by semiempirical MO methods 67

H

HABASHY M. M., voir EL-KHAMRY A. A. 563

HAIDUC I., voir MICU-SEMENIUC R. 1025

— , voir MICU-SEMENIUC R. 1489

— , voir SILAGHI-DUMITRESCU I. 815

— , voir SILAGHI-DUMITRESCU I. 823

HAMED A. A., voir ABD ALLA M. M. 1549

HAOUAM A. and G. SURPĂȚEANU, E. COMĂNIȚĂ, CR. SIMIONESCU, Experimental and theoretical study on the polymerization of N-pentenylcarbazole (NPC) 1389

HASSAN M. A., voir MOHAMED M. M. 237

HATABA A., voir ABDALLA M. 1335

— , voir ABDALLA M. 1341

HILLEBRAND M. and A. T. BALABAN, Unrestricted Hartree-Fock spin densities in aryl-nitroso-aminyloxides and in acyl-aryl-aminyloxides 995

— and V. EM. SAHINI, The electronic structure of phenoxaselenine 625

— and V. EM. SAHINI, Unrestricted Hartree-Fock spin densities of some heteroaromatic cation-radicals 631

HINDAWEY A. M., voir ISSA Y. M. 1535

HODOȘAN F., voir ALBERT L. 1529

HOLBAN S., voir SIMON Z. 713

HOPÎRTEAN E., voir LITEANU C. 735

HORÁK J., voir MACAROVICI C. GH. 805

HURWITZ H., voir VLĂDESCU L. 135

I

ILUC S., voir BACALOGLU R. 921

IOAN C., voir SÂRBU C. 245

IONESCU D., voir CORNEA F. 701

IONESCU GH., voir MATEI F. 1017

IONESCU M., voir SÂRBU C. 245

IONESCU N. I., Kinetics of gas adsorption on heterogeneous solid surfaces 663

— , voir SCHUSTER R. H. 1301

IORDACHE F., voir RĂZUȘ A. C. 547

IORGA I. and C. CSUNDERLIK, M. SAFTA, G. OSTROGOVICH, Studies on the field of 1.3.5-triazines. XVIII. b. The protons-deuterons exchange rate at the methyl-groups of 2.4.6-trimethyl-1.3.5.-triazine in D$_2$O and in the presence of DO$^-$-ions (in German) 1351

IOSOF V. and V. NEACȘU, Analysis of silicate rocks by atomic absorption spectrometry 589

IOVU M. and F. CHIRALEU, E. VASILESCU, Observations on the IR and ^{1}H-NMR spectra of some asymmetric ethers 1383

ISKANDER G. M., voir KHAWAD I. E. 393

— , voir KHAWAD I. E. 559

— , voir KHAWAD I. E. 1321

ISSA R. M., voir ISSA Y. M. 1535

ISSA Y. M. and A. M. HINDAWEY, R. M. ISSA, A. M. G. NASSAR, A comparative study of the infrared spectra of change transfer compounds of aniline derivatives with 3,5-dinitrosalicylic acid 1535

IVAN G., voir ALBERT F. M. 1543

J

JACOBI E., voir SCHULZ R. C. 1059

JAIN R. K. and R. L. MITAL, Synthesis of some new polyhalogenated hydroxyphenothiazines and their alkyl and acyl derivatives 697

JARONIEC M., voir BORÓWKO M. 475

JENKINS A. D., Termination of vinyl polymerization by transition metal ions 1007

OHRI K. N. and K. A. VENUGOPALAN, Thermogravimetric investigation of the decomposition of certain metal dithiocarbamates 215

JUBERT A. H., voir CASTRO E. A. 75

JULEAN I., voir NIMARĂ A. 231

JURCONI E., voir MURGULESCU I. G. 1033

K

KAKKAR K. K., voir RUPAINWAR D. C. 295

KAMIL F. and S. K. SINDHWANI, R. P. SINGH, Phenanthrenequinone monosemicarbazone as a reagent for the determination of rhodium(III) and palladium(II) 875

KANAOKA K., voir TAKEMOTO K. 1097

KAPOOR S. N. and N. MISRA, Analytical aspects of some organic acids. II. Gravimetric determination of thorium by *o*-phenylene trioxytriacetic acid 439

KHAN I. A., voir SULTANA N. 105

KHAN S. A. and M. STONE, M. G. BAWDEN, A rapid improved colorimetric method for the microdetermination of boron in silicate rocks and minerals by use of carminic acid 1433

KHAWAD I. E. and G. M. ISKANDER, Favorskii reactions of α-halo-α, β-unsaturated monocyclic ketones 393

— and G. M. ISKANDER, Favorskii rearrangements of 4, 8, 8-tribromobicyclo-[5.1.0] oct-4-en-3-ones 1321

— and G. M. ISKANDER, Preparation and reactions of dibromocarbene adducts of cyclohexa-1, 4-dienyl-acetates and -benzoates 559

KONNERT C., voir GOCAN L. 273

KULIG E. and D. CZAKIS-SULIKOWSKA, R. WOJTAŠ, Investigation of lead(II) complexes. III. Simple and mixed complexes of lead(II) with some anions of aliphatic acids in aqueous solution 1177

KYSELÁ G., voir BENISKA J. 941

KYZIOŁ J. and J. TARNAWSKI, Synthesis of n-substituted derivatives of 9-aminocarbazole 721

L

LAL K., Complexes of copper(II), nickel(II), cobalt(II), iron(II) and manganese(II) with Schiff bases derived from sulphamethoxypyridazine 355

LAZĂR D. P., voir GIRGIS M. M. 1293

— , voir RUGINĂ T. C. 799

LĂZĂRESCU G., voir LĂZĂRESCU V. 1287

LĂZĂRESCU V. and G. LĂZĂRESCU, A new approach for Tafel approximation in metallic electrodeposition 1287

LEANCA M., voir SIMIONESCU B. C. 1077

LEPĂDATU C. I., voir ANDRUH M. 811

LITEANU C. and I. RÎCĂ, E. HOPÎRTEAN, On the determination limit 735

LIXANDRU T., voir DUMITRIU M. 981

— , voir SIMIONESCU CR. 277

LODHI S. F., voir SUBHANI M. S. 1567

LUCHIAN C., voir SURPĂŢEANU GH. 1091

LUCHIAN M., voir CALU N. 1171

LUDWICK A. G. and C. G. OVERBERGER, Synthetic macromolecules as therapeutic agents 1011

LUNGU E., voir BACALOGLU R. 921

LUNGU M., voir ASANDEI N. 915

M

MACAROVICI C. GH., voir BARBU S. 207

— , voir BARBU S. 339

— and E. CHIŞ, A new EDTA-Type reagent. III. Synthesis and physico-chemical study of 4, 4′-diamino-diphenylmethane-N, N′-tetraacetic acid 503

— and E. CHIŞ, Synthesis and physico-chemical investigation of neutral salts of 4, 4′-diaminodiphenylmethane-N, N′-tetraacetic acid with mono-, di-, tri- and tetravalent metal ions (in German) 95

— and J. HORÁK, CS. VÁRHELYI, On the α-dioximine complexes of transition metals. LIX. The stability of Fe(II)- and Co(II)-complexes of 1, 2-cycloheptanedione dioxime and 1, 2-cyclooctanedione dioxime in aqueous solutions . . . 805

MACOVEANU M., voir MATEI F. 1017

MACOVEI V., Spectral solvent effects in aromatic compounds solutions. VI. The solvent effects on the toluene electronic band at 2600 Å 651

MAGEE P. M., voir BREEZE A. 667

MAHGOUB A. E. and M. M. SHOUKRY, Palladium(II) chelate of phenylazobenzaldoxime 1197

MARC M., voir UNGUREANU A. 845

MARCHIDAN S. and I. VARTIRES, N. D. TOTIR, Determination of trace quantities of the group V-A elements by anodic stripping voltammetry. I. Trace analysis of arsenic 33

MĂRCULEŢIU V., voir TOMOAIA-COTIŞEL M. 175

MATEESCU A., voir STERNBERG S. 793

MATEI F. and AL. DUCA, GH. IONESCU, M. MACOVEANU, The interpretation of the kinetic data concerning the Zn^{2+} linking and education on ion exchange membranes 1017

MATEI V., voir EL FADLY A. A. 1311
MAURER A., voir SIMON Z. 713
MAZĂRE M., voir DONESCU D. 975
MAZILU I., voir SIMIONESCU CR. 277
MEDEŞAN A., voir GRIGORAŞ S. 67
MEGHEA A., voir ALBERT F. M. 1543
— , voir SAHINI V. EM. 449
MICU-SEMENIUC R. and L. SILAGHI-DUMITRESCU, N. CHIRILĂ, I. HAIDUC Transition metal complexes of organo-thiophosphorus ligands. VI. Six-coordinate adducts of nickel(II) bis(dialkylphosphorodithioate) with aromatic diamines. 1025
MIHĂILĂ GH. and V. ABABI, F. VITAN, Liquid-vapour equilibrium of the diisopropylether-cyclohexanone system 599
MIHAILCIUC C., voir SAHINI V. EM. 1055
MINCU G., voir MURGULESCU I. G. 1033
MINCU V., voir BANCIU A. C. 513
MISRA N., voir KAPOOR S. N. 439
MITAL R. L., voir JAIN R. K. 697
MIYATA M., voir TAKEMOTO K. 1097
MOHAMED M. M., voir ELKADY M. 1361
— , voir FAHMY A. F. 125
— and M. A. EL HASHASH, M. Y. EL KADY, M. A. HASSAN Some reactions with arylidene malonic acid and diethyl arylidene malonate 237
MOLDOVAN M., voir PANEA T. 691
MOLDOVEANU Ş., voir GRIGORAŞ S. 67
— , voir SAHINI V. EM. 1055
MORA R., voir SIMIONESCU B. C. 1077
MORARU A., voir BACALOGLU R. 921
MOROŞANU C.-E. and E. SEGAL, Deposition kinetics of Si_2N_4 films by the radiofrequency glow discharge and low pressure CVD methods 315
— and E. SEGAL, Kinetics of silicon nitride deposition on silicon from N-Gas. 181
— and E. SEGAL, Nondestructive thickness determination of silicon nitride films deposited on silicon 47
MRACEC M., voir SIMON Z. 713
MUREŞAN N., voir NEGOIU D. 349
— , voir NEGOIU D. 839
MURGULESCU I. G. and G. MINCU, E. JURCONI, Catalysis by metal cation in the oxidoreduction reaction of bisoxalatodiaquo Co(III) complex with iodide ion in acidic medium 1033
MURTHY S. N., Effects of couple stresses on the dispersion of a solute with simultaneous chemical reaction 1461

N

NĂFORNIŢĂ C., voir TUDOSE R. Z. 155
NAQVI S. R. R., voir SULTANA N. 105
NASSAR A. M. G., voir ISSA Y. M. 1535
NATANSOHN A., voir ASANDEI N. 915
— , voir BĂRBOIU V. 933
NEACŞU V., voir IOSOF V. 589
NEGOIŢĂ N., voir BALABAN A. T. 1327

NEGOIU D. and J. CAMUS, Electron transfer reactions in some complex compounds of Hg(II), Co(II) and Cu(I) with quinoxalinic and naphtoquinonic ligands. . . . 223
— and J. CAMUS, N. MUREŞAN, Electron transfer in some vanadium complexes with quinoxalinic and naphtoquinonic ligands 349
— and J. CAMUS, N. MUREŞAN, Complex compounds of nickel involved in electron transfer processes 839
NEGRIŢESCU S., voir SÂRBU C. 245
NICOARĂ E., voir OŞIANU D. 261
NICOLAU A., voir SCHUSTER R. H. 1069
NICOLESCU I. V., voir BRAŞOVEANU I. 1159
NICU M., voir ASANDEI N. 915
NICU V., voir ASANDEI N. 915
NICULESCU-DUVĂZ I., voir CORNEA F. 701
NIMARĂ A. and I. JULEAN, Basic salts of bismuth. I. Formation and properties of the basic bismuth chlorates 231
NUŢIU M., voir BACALOGLU R. 921

O

OANCEA D., voir SCHUSTER R. H. 1301
OLTEANU M., voir WEINBERG J. 189
OMARA M. M. and F. I. ABDEL-HAY, A. A. EL BARBARY, M. BADAWI, M. M. ABDEL HAMID, Organophosphorus derivatives of expected biological activity. I. Reaction of phenols with N-aryl-hexachlorocyclodiphosphazanes 253
ONCESCU T. and L. DIMOFTE, Kinetics and mechanisms of the reaction between 5-chloro-2-pentanone and diethylamine. I. Solvent effect 15
— and L. DIMOFTE, Kinetics and mechanism of the reaction between 5-chloro-2-pentanone and diethylamine. II. Influence of the nucleophilic reagents. . . . 23
OPREA S. and E. DUMITRIU, M. DIMA, Reactivity of acrylic monomers. II. Copolymerization of N, N-diethylacrylamide with styrene 605
— and E. DUMITRIU, L. ŞTEFĂNEL, Catalysis by polymers. I. Synthesis of 3-chloro-2-hydroxypropyl acrylate using quaternized poly(dimethylaminoethyl methacrylate) as catalyst 1039
OPRIŞ C., voir SEMENIUC-MICU R. 1489
OŞIANU D. and E. NICOARĂ, C. BODEA, Inchain epoxides of carotenoids VII. Astacene 9, 10- and 11, 12-epoxides 261
OSMAN M. W., voir ABD ALLA M. M. 415
— , voir ABD ALLA M. M. 1549
OSTROGOVICH G., voir IORGA I. 1351
OVERBERGER C. G., voir LUDWICK A. G. 1011

P

PAL P. and A. KR. CHAKRABORTY, Investigation of some thermodynamical properties of 2-1 electrolytes in solution 81
PANEA T. and M. MOLDOVAN, Oxidation of some methoxyphenothiazines by potassium dichromate in glacial acetic acid 691
PĂRĂUŞAN V. and M. TRIFAN, R. AVRAM, n-Dodecylnitrile oxidation in liquid phase with molecular oxygen. III. Composition of acid mixtures 1245
PERIŞANU ŞT., voir VÎLCU R. 619
PERKINS P. G., voir BREEZE A. 667
PĂSTRĂVANU M., voir DUMITRIU M. 981

PETRARIU I. and M. ROTARU, S. DRĂGAN, Quaternary ammonium polyelectrolytes. II. Quaternization reaction of some tertiary amines with chloromethylated polystyrene 145

PETROVANU M., voir SURPĂŢEANU GH. 1091

PHAN LE THUY, voir BANCIU M. 1221

POGANY I. I., voir DINULESCU I.G. 969

POLICEC S., voir SIMON Z. 713

POPA GR. and M. POPESCU, A. DĂNEŢ, Spectrophotometric determination of Hg(II) in industrial caustic soda, waste water from chloro alkali industry and acetaldehyde production with diazoamino reagents 1427

POPA M. V., voir RADOVICI O. 87

POPESCU D., voir SCHUSTER R. H. 1301

POPESCU M. and D. CRIŞAN, Study on structure and properties of some triazenic complexes of mercury 1187

— , voir POPA GR. 1427

PRASHAD J., Comparative studies of Corona pressure effect. Joshi effect and thermionic analogue of Joshi effect in argon under semi-ozonizer discharge 323

PRASHAD H. L., voir DINULESCU I. G. 535

PUJAR M. A. and N. S. BIRADAR, Magnetic and spectral studies of 2-substituted benzimidazole complexes of cobalt(III) 831

Q

QURESHI M. I., voir AHMAD Y. 397

R

RABEK J. F. and B. RÅNBY, Polynuclear aromatic hydrocarbons as sensitizers of photooxidative degradation of *cis*-1, 4-polybutadiene 1045

RADOVICI O. and M. V. POPA, The influence of the structure and the type of alloy on stress corrosion cracking in hydrochloric acid solutions. 87

RĂDULESCU N., voir SÂRBU C. 245

RÅNBY B., voir RABEK J. F. 1045

RAOOT K. N. and V. G. VAIDYA, Reduction of silver(I) with cobalt(II) and manganese (II) solutions in alkaline triethanolamine medium : gravimetric estimations of silver 583

RĂZUŞ A. C. and A. M. GLATZ, ZS. ARVAY, F. IORDACHE, F. BADEA, The oxidation of trichlorethylene with molecular oxygen. 547

RÎCĂ I., voir LITEANU C. 735

RICART G., Synthesis of [(5-hydroxypentylamino)-1-n-alkyl]-aziridines (in French). . 379

— and D. COUTURIER, New synthesis of 1, 5-diazobicyclo-4.4.0 decanes (in French) 541

ROBERTS R. M. and H. H. CHEN, The rearrangement of *sec*-butyl-benzene to isobutylbenzene catalyzed by fluoroantimonic acid 687

ROTARU M., voir PETRARIU I. 145

ROTARU P., voir BRAŞOVEANU I. 1159

RUGINĂ T. C. and D. P. LAZĂR, About the catalytic oxidation of ammonia. 799

RUPAINWAR D. C. and K. K. KAKKAR, A modified reversion technique for the spectrophotometric determination of thallium. 295

RUSU I., voir GRIGORAŞ S. 67

RUSU M., voir ASANDEI N. 915

S

SAFTA M., voir IORGA I. 1351

SAHINI V. EM., voir CARAGHEORGHEOPOL A. 307

— , voir HILLEBRAND M. 625

— , voir HILLEBRAND M. 631

— and Ş. MOLDOVEANU, C. MIHAILCIUC, On chlorobenzamide molecular structure 1055

— and E. VOLANSCHI, A. MEGHEA, E.S.R. spectra and electronic structure of some diphenylamine anion-radicals 449

— , voir WEINBERG J. 9

SALEM M. A., voir ABDALLA M. 1335

— , voir ABDALLA M. 1341

SÂRBU C. and N. RĂDULESCU, M. IONESCU, S. NEGRIŢESCU, C. IOAN, N. BOEŞTEANU, M. SIMIONOVICI, New indole derivatives with biological activity 245

SAYED G. H., voir ELKADY M. 1361

— and M. ELKADY, M. A. ELHASHASH, Study on 4-aryl-6-(3′, 4′-dichlorophenyl)-2, 3, 4, 5-tetrahydropyridazin-3-ones and 4-aryl-3-mercapto-6-(3′, 4′-dichlorophenyl)-2, 3-dihydropyridazine 1375

SCHRÖDER V., voir TIMPE H.-J.. 407

SCHULZ R. C. and E. JACOBI, Optical rotatory dispersion of cellulose, cellulose-nitrate and of some α-polyglucans (in German) 1059

SCHUSTER R. H. and N. I. IONESCU, D. OANCEA, D. POPESCU, V. GOŞA, Some aspects of the explosion of mixtures between vinylacetylene and air (in German) 1301

— and A. NICOLAU, Effects of the medium in solvolyses of alkyl halides. IV. Hydrolysis of *t*-butyl chloride (in German) 1069

SEGAL E., voir MOROŞANU C.-E. 47

— , voir MOROŞANU C.-E. 181

— , voir MOROŞANU C.-E. 315

SEMENIUC R., voir BARB D. 1485

SEMENIUC-MICU R. and C. OPRIŞ, I. HAIDUC, Transition metal complexes of organothiophosphorus ligands. VII. Amine adducts of di(α- and β-naphthyl) phosphorodithioato nickel (II) . . . .

SHAMSI S. A., voir AHMAD Y. 397

SHIRSHINA L., voir STERNBERG S. 467

SHOUKRY M. M., voir MAHGOUB A. E.. 1197

SILAGHI-DUMITRESCU I. and I. HAIDUC, The infrared spectrum of dimethyldithiophosphinato anion $(CH_3)_2PS_2^-$. Normal coordinate analysis and Urey-Bradley force field calculation 815

— and I. HAIDUC, Vibrational characteristics of Ni (II) dithiophosphinato chelates. Normal coordinate analysis and Urey-Bradley force field calculation of Ni $[S_2P(CH_3)_2]_2$ 823

SILAGHI-DUMITRESCU L., voir MICU-SEMENIUC R. 1025

SILBERG I. A. and M. V. DIUDEA, Phenazathionium cations. I. The dual mechanistic behaviour of phenazathionium cations and its implications in the reaction of $NaNO_2$ with halogenophenothiazines 1229

— and M. V. DIUDEA, Phenazathionium cations. II. The accessibility of positions 1 (9) in nucleophilic substitutions involving phenazathionium cations 1239

SIMIONESCU B. C. and R. MORA, M. LEANCA, C. ANANIESCU, Genesis of porphyrin-like compounds under simulated abiotic conditions. A possible mechanism of their formation 1077

SIMIONESCU CR., voir HAOUAM A. 1389

— and I. MAZILU, L. TĂTARU, T. LIXANDRU, Ferrocene polymers as polymerization initiators. II. Polymerization of some *p*-alkylated chloroformylated vinyl monomers 277

SIMIONOVICI M., voir SÂRBU C. 245

SIMON Z. and S. HOLBAN, M. MRACEC, A. MAURER, S. POLICEC, Steric optimisation by MTD of therapeutic index of n-substituted derivatives of *cis*-dichlorodiammine-platinum (II) active against ADJ/PC6A mouse plasma cell tumor . 713

SIMPSON K. L., voir CIURDARU V. 571

SINDHWANI S. K., voir KAMIL F. 875

SINGH R. P., voir KAMIL F. 875

SINGUREL GH., Study of the hydrogen bond in the mandelic and 4-chloromandelic acids 1469

SOLACOLU S. and M. ZAHARESCU, M. DOROBANȚU, Thermal phase equilibria in the system BaO—ZnO—Fe$_2$O$_3$ with application on magnetoceramics. 111

SOLIMAN E. A., voir ABD ALLA M. M. 415

— , voir ABD ALLA M. M. 1549

SOTO A. and R. CEA, Mass spectrometry of alkylated inorganic heterocycles. I Mass spectrometry of octamethyl-cyclotetraphosphazatetraene and its quaternary salts with methyl and ethyl iodides (in Spanish) 529

SPIRATOS M. and A. AIRINEI, A. CIOBANU, Coordination polymers. II. Chelated polyesters of azomethine type (in French) 1083

SRIVASTAVA S. N., voir CHANDRA G. 1139

— , voir CHANDRA G. 1149

STAN I., voir CHIFU E. 1449

ŠTAUDNER E., voir BENISKA J. 941

ȘTEFAN N., voir DINULESCU I. G. 535

ȘTEFĂNEL L., voir OPREA S. 1039

STERNBERG S. and M. DRĂGĂNOIU, A. MATEESCU, The thermodynamic activity of ZnSO$_4$ in the systems : ZnSO$_4$ + H$_2$O and ZnSO$_4$ + Na$_2$SO$_4$ + H$_2$O 793

— and L. SHIRSHINA, S. DANEȘ, Transport of SO$_4^{2-}$, Cu^{2+}, H$^+$ ions and of water in ion exchange membranes (in French) 467

STOICESCU C., voir CORNEA F. 961

STONE M., voir KHAN S. A. 1433

SUBHANI M. S., An investigation of the reaction between tellurite and chlorite ions in solution 327

— , Effect of foreign ions on the reaction between bromide anion and persulphate anion in aqueous system 851

— , Electrostatic contributions to the thermodynamic functions in the formation of transition state for the reaction between Br$_2^-$ and BrO$^-$ 855

— , Study of the transition state formed between Cu(S$_2$O$_3$)$^-$ and S$_2$O$_8^{2-}$ anions in mixture of solvents 861

— , The effect of the solvent and ionic strength on the kinetics of reaction between I$_2^-$ and IO$^-$ 195

— , The study of the transition state involves electrostatic contributions to the thermodynamic functions for the reaction between two IO$^-$ ions 1579

— , Thermochemical studies on solutions of monobromo-dibromo- and tri-bromoacetic acids in water and chloroform 333
— Thermodynamic stability constants and other related thermodynamic properties for Cu(II)-PMBP complex 121
— and S. F. LODHI, A mechanism for the photolytic decomposition of hypobromite in aqueous solution at 365 nm, 313 nm and 253.7 nm 1567
SULTANA N. and I. A. KHAN, S. R. R. NAQVI, Chemical and spectroscopic properties of silver-phosphine complexes containing oxine 105
SURPĂŢEANU GH., voir HAOUAM A. 1389
— and C. LUCHIAN, M. CONSTANTINESCU, V. BĂRBOIU, M. PETROVANU, 1,2,4-Triazolium-ylides. III. The theoretical aspects on the regioselectivity in the cycloaddition reaction of the triazolium-phenacyclide to the propiolic acid esters (in French) 1091
SZABO A., voir BRAŞOVEANU I. 1159

T

TABNER B. J. voir BEVINGTON J. C. 947
TAKEMOTO K. and K. KANAOKA, M. MIYATA, Synthesis of new heterocyclic monomers under simulated prebiotic conditions 1097
TĂMAŞ V., voir TOMOAIA-COTIŞEL M. 175
— , voir CIURDARU V. 571
TARNAWSKI J., voir KYZIOŁ J. 721
TASCON GARCIA M. L., Chromatographic separation of gold, platinum, palladium, rhodium and iridium. I. Qualitative study 881
— , Chromatographic separation of gold, platinum, palladium, rhodium and iridium. II. Quantitative study 901
TĂTARU L., voir SIMIONESCU CR. 277
TIMPE H.-J., and V. SCHRÖDER, R. WORSCHECH, *s*-Triazolium-4N-ylide 407
TŐKÉS B., voir ALBERT L. 1529
TOMESCU M., voir DEMETRESCU I. 729
TOMOAIA-COTIŞEL M. and E. CHIFU, V. TĂMAŞ, V. MĂRCULEŢIU, Behaviour of some apocarotenoid derivatives at the air/water interface 175
TOTIR N. D., voir MARCHIDAN S. 33
TRIFAN M., voir PĂRĂUŞAN V. 1245
TUDOSE R. Z. and C. NĂFORNIŢĂ, An experimental study of liquid flow in thin films on inclined plates at angles greater than 90° 155

U

UNGUREANU A. and M. MARC, Sulphur-containing aminoacid-metal complexes. Cobalt (II) and iron (II) complexes of cystine 845

V

VĂCĂRESCU D., Contributions to the chemistry of quaternary ammonium complexes. N-Cetyl-β-picolinium salts of halogen- and thiocyanate complex ions of Zn (II) and Cd (II) 361
— , Study of some N-cetyl-β-picolinium halogen and thiocyanatomercurates (II) . . 371
VAIDYA V. G., voir RAOOT K. N. 583
VÂNTU V., voir EL FADLY A. A. 1311
VÁRHELYI CS., voir MACAROVICI C. GH. 805

VARMA R. P. and P. BAHADUR, R. DAYAL, Conductivity studies of alkaline earth metal soaps in methanol 201

VARTIRES I., voir MARCHIDAN S. 32

VASILESCU D.S., Alternating tendency in copolymerization. III. The behaviour of the systems acrylic monomer-vinyl ether-$ZnCl_2$ 1101

VASILESCU E., voir IOVU M. 1383

VASS M. I. and CR. CONȚESCU, Studies of alloy formation and surface properties in Ni—Cu systems 55

VENUGOPALAN K. A., voir JOHRI K. N. 215

VÎLCU R. and Z. CENUȘE, Calculation of activity coefficients in the benzene-butanol systems from experimental determination of isotherms $P_{total} = f$ (composition) 763

— and Z. CENUȘE, Association of the butanols in benzene 773

— and Z. CENUȘE, Calculation of hydrogen bond energies from excess enthalpies, experimentally determined for benzene-butanol systems 781

— and A. CIOCHINĂ, An alternative to the transient hot-wire method for thermal conductivity measurements of fluids 1113

— and E. DIMITRIU, The propagation of ultrasound in n-alkanes 1131

— and ȘT. PERIȘANU, The ideal gas state enthalpies of formation of some monomers 619

VIȘAN S., voir ARMEANU V. 867

VITAN F., voir MIHĂILĂ GH. 599

VLAD R., voir BANCIU M. 1221

VLĂDESCU L. and H. HURWITZ, On the combined ion exchange system-solvents extraction. II. A theoretical approach (in French) 135

— and D. VOICU, Utilization of sodium hydroxide in separation of tin (II) with ion exchange resins. I. Cation-exchange behavior of tin (II) 267

— and D. VOICU, Utilziation of sodium hydroxide in separation of tin with ion exchange resins. II. Cation exchange separations 1269

VOGL O. and S. YOSHIDA, Synthesis and polymerization of photoactive monomers . 1123

VOICU D., voir VLĂDESCU L. 267

— , voir VLĂDESCU L. 1269

VOLANSCHI E., voir SAHINI V. EM. 449

W

WEINBERG J. and A. DONESCU, M. OLTEANU, Decomposition mechanism of sodium merthiolate in aqueous solutions at various pH values 189

— and V. EM. SAHINI, Xylidine isomers. VI. CNDO calculations on 2,4- and 2,5-xylidine 9

WOJTAŠ R., voir KULIG E. 1177

WORSCHECH R., voir TIMPE H.-J. 407

Z

ZAHARESCU M., voir SOLACOLU S. 111

ZGLOBIU M., voir CORNEA F. 701

ZNAMIROVSCHI V., voir BARB D. 1485

ZSAKÓ J., Some problems of deriving stability constants of ML_2 type complexes from spectrophotometric data 1499

Y

YASSIN S. M., voir EL-KASCHEF M. F. 577

YOSHIDA S., voir VOGL O. 1123

INDEX DES SUJETS

6-Acetyl-3,5-diarylcyclohex-2-enones, Some reactions of —, M. ABDALLA, M. A. SALEM and A. HATABA 1341

Acrylic monomers. II. Copolymerization of N,N-diethylacrylamide with styrene, Reactivity of —, S. OPREA, E. DUMITRIU and M. DIMA 605

Acrylonitrile-butyl acrylate-vinylidene chloride terpolymer, Photochemical and thermal behaviour of —, I. DEMETRESCU and M. TOMESCU 729

Acrylonitrile-cinnamic acid copolymerization. I. Copolymer structure, N. ASANDEI, M. NICU, S. BRĂNIȘTEANU, V. NICU, M. RUSU, M. LUNGU and A. NATANSOHN 915

Activity coefficients in the benzene-butanol systems from experimental determination of isotherms $P_{\text{total}} = f$ (composition), Calculation of —, R. VÎLCU and Z. CENUȘE 763

Adsorption from liquid mixtures on heterogeneous solid surfaces, General formulation of —, M. BORÓWKO and M. JARONIEC 475

Adsorption on heterogeneous solid surfaces, Kinetics of gas —, N. I. IONESCU 663

Alkyl carboxylic acid esters pyrolysis, Kinetic studies of —, A. A. EL FADLY, V. MATEI and V. VÂNTU 1311

9-Aminocarbazole, Synthesis of *n*-substituted derivatives of —, J. KYZIOŁ and J. TARNAWSKI 721

Aniline derivatives with 3,5-dinitrosalicylic acid, A comparative study of the infrared spectra of charge transfer compounds of —, Y. M. ISSA, A. M. HINDAWEY, R. M. ISSA and A. M. G. NASSAR 1535

Anodic stripping voltammetry. I. Trace analysis of arsenic, Determination of trace quantities of the group V—A elements by —, S. MARCHIDAN, I. VARTIRES and N. D. TOTIR 33

Apocarotenoid derivatives at the air/water interface, Behaviour of some —, M. TOMOAIA-COTIȘEL, E. CHIFU, V. TĂMAȘ and V. MĂRCULEȚIU 175

β-Aroylacrylic acids, Some reactions of —, M. ELKADY, M. A. ELHASHASH, G. H. SAYED and M. M. MOHAMED 1361

4-Aryl-6-(3′-4′-dichlorophenyl)-2,3,4,5-tetrahydropyridazin-3-ones and 4-aryl-3-mercapto-6-(3′, 4′-dichlorophenyl)-2,3-dihydropyridazine, Study on —, G. H. SAYED, M. ELKADY and M. A. ELHASHASH 1375

Arylidene malonic acid and diethyl arylidene malonate, Some reactions with —, M. M. MOHAMED, M. A. EL HASHASH, M. Y. EL KADY, M. A. HASSAN 237

Arylidenefuranones, Reactions of some —, M. M. ABD ALLA, E. A. SOLIMAN and M. W. OSMAN 415

Aziridines, Synthesis of [(5-Hydroxypentylamino)-1-n-Alkyl] — (in French), — G. RICART 379

Base-catalyzed Michael addition of active methylene compounds on arylidene malonates and arylidene barbituric acids, A. F. FAHMY, M. M. MOHAMED, A. A. AFIFY, M. Y. EL KADY and M. M. EL HASHASH 125

Basicity constants of some N,N′-disubstituted *p*-phenylenediamines, F. M. ALBERT, M. GIURGINCA, A. MEGHEA and G. IVAN 1543

Benzimidazole complexes of cobalt (II), Magnetic and spectral studies of 2-substituted —, M. A. PUJAR and N. S. BIRADAR 831

7′-Benzoyliamino-β-*azo*-6′-carotenoic acid and some of its derivatives via β-*apo*-8′-carotenylidenoxazolone, V. CIURDARU, V. TĂMAS and K. L. SIMPSON 571

Bioactive polymers. VII. Oxydoreductases and hydrolases immobilized on cellulose derivatives, S. DUMITRIU and V. BULACOVSCHI 989

Bismuth. I. Formation and properties of the basic bismuth chlorates, Basic salts of —, A. NIMARĂ and I. JULEAN 231

Bisoxalatodiaquo Co (III) complex with iodide ion in acidic medium, Catalysis by metal cation in the oxidoreduction reaction of —, I. G. MURGULESCU, G. MINCU and E. JURCONI 1033

Boron in silicate rock and minerals by use of carminic acid, A rapid improved colorimetric method for the microdetermination of —, S. A. KHAN, M. STONE and M. G. BAWDEN 1433

Bromide anion and persulphate anion in aqueous system, Effect of foreign ions on the reaction between —, M. S. SUBHANI 851

Butanols in benzene, Association of the —, R. VÎLCU and Z. CENUȘE 773

Carotenoids. VII. Astacene 9,10- and 11,12-epoxides, Inchain epoxides of —, D. OȘIANU, E. NICOARĂ and C. BODEA 261

Catalysis by polymers. I. Synthesis of 3-chloro-2-hydroxypropyl acrylate using quaternized poly(dimethylamino-ethyl methacrylate) as catalyst, S. OPREA, E. DUMITRU and L. ȘTEFĂNEL 1039

Catalytic oxidation of ammonia, About the —, T. C. RUGINĂ and D. P. LAZĂR 799

Catalytic oxidation of ammonia. I. Low temperature oxidation on an iron-chromium catalyst, M. M. GIRGIS and D. P. LAZĂR 1293

Cellulose phosphate, Some considerations on the sorption mechanism of Al^{3+} on —, S. FIȘEL and D. BÎLBĂ 1405

Chemical graphs. XXXIX. Valence isomers of monodehydro-[n] annulenes, V. BACIU and A. T. BALABAN 1213

Chlorobenzamide molecular structure, On —, V. E. SAHINI, Ș. MOLDOVEANU and C. MIHAILCIUC 1055

Chromatographic separation of gold, platinum, palladium, rhodium and iridium. I. Qualitative study (in Spanish), M. L. TASCON GARCIA 881

Chromatographic separation of gold, platinum, palladium, rhodium and iridium. II. Quantitative study (in Spanish), M. L. TASCON GARCIA 901

Complexes of Th(IV) and U(VI) with pyrocatechol, pyrocatecholdisulfonic acid and chromatropic acid (in German), AL. CECAL 1201

Conductivity studies of alkaline earth metal soaps in methanol, R. P. VARMA, P. BAHADUR and R. DAYAL 201

Coordination compounds, On Uspenski's rule regarding the *cis-trans* isomerism of —, M. ANDRUH C. I. LEPĂDATU and M. BREZEANU 811

Coordination polymers. II. Chelated polyesters of azomethine type (in French), M. SPIRATOS, A. AIRINEI and A. CIOBANU 1083

Copolymerization. III. The behaviour of the systems acrylic monomer-vinyl ether-$ZnCl_2$, Alternating tendency in —, D. S. VASILESCU 1101

Copper(II) nickel(II), cobalt(II), iron(II) and manganese(II) with Schiff bases derived from sulphamethoxypyridazine, Complexes of —, KEEMTI LAL 355

Corrosion behaviour of commercial Zn—Ti alloy in aqueous salt solutions, S. M. ABD EL HALEEM and S. S. ABD EL REHIM 493

Cycloaddition of acetylacetone to *p*-dimethylaminochalcone and diarylideneacetone, Base catalysed —, M. ABDALLA, M. A. SALEM and A. HATABA 1335

Cyclohexa-1,4-dienyl-acetates and — benzoates, Preparation and reactions of dibromocarbene adducts of —, I. E. KHAWAD and G. M. ISKANDER 559

Dehydrations with chlorosulfonic acid in pyridine. A convenient method for the synthesis of amides, C. I. CHIRIAC 403

Determination limit, On the — C. LITEANU, I. RÎCĂ and E. HOPÎRTEAN 735

1,5-Diazabicyclo 4.4.0 decanes (in French), G. RICART and D. COUTURIER 541

Dibenzo$(CH)_{10}$ and tetrabenzo$(CH)_{10}$ hydrocarbons. Diels-Alder reactions of tricyclo $[4.2.2.0^{2,5}]$deca-3.7.9-triene derivatives with 9.10-dibromoanthracene, New synthesis of —, I. G. DINULESCU, I. I. POGANY, A. DUMITRIU, E. G. GEORGESCU and M. AVRAM 969

β-3,4-Dichlorobenzoylpropionic acid, Some reactions of —, M. M. ABD ALLA, E. A. SOLIMAN, A. A. HAMED and M. W. OSMAN 1549

Diisopropylether-cyclohexanone system, Liquid-vapour equilibrium of the —, GH. MIHĂILĂ, V. ABABI and F. VITAN 599

Dimethyldithiophosphinato anion $(CH_3)_2PS_2^-$, Normal coordinate analysis and Urey-Bradley force field calculation, The infrared spectrum of —, I. SILAGHI-DUMITRESCU and I. HAIDUC 815

Diphenylamine anion-radicals, E. S. R. spectra and electronic structure of some —, V. EM. SAHINI, E. VOLANSCHI and A. MEGHEA 449

Dispersion of a solute with simultaneous chemical reaction, Effects of couple stresses on the —, S. NARASIMHA MURTHY 1461

n-Dodecylnitrile oxidation in liquid phase with molecular oxygen. III. Composition of acid mixtures, V. PĂRĂUŞAN, M. TRIFAN and R. AVRAM 1245

Editorial 911

EDTA-Type reagent. III. Synthesis and physico-chemical study of 4,4′-diamino-diphenylmethane-N,N′-tetraacetic acid, A new, CONST. GH. MACAROVICI and E. CHIŞ 503

Effect of the solvent and ionic strentgh on the kinetics of reaction between I_2^- and IO^-, The —, M. S. SUBHANI 195

Electron transfer reactions in some complex compounds of Hg(II), Co(II) and Cu(I) with quinoxalinic and naphtoquinonic ligands, D. NEGOIU and P. CAMUS . . . 223

Electronic band structure of β-PbO_2, The —, A. BREEZE, P. M. MAGEE and P. G. PERKINS 667

Electrophilic addition of bromine to 9-halogeno-benzocyclobutenonorbornenes, The —, I. G. DINULESCU, L. ENESCU, H. L. PRASAD ,A .GHENCIULESCU, N. STEFAN and M. AVRAM 535

Electrostatic contributions to the thermodynamic functions in the formation of transition state for the reaction between Br_2^- and BrO^-, M. S. SUBHANI 855

Enthalpies of formation of some monomers, The ideal gas state —, R. VÎLCU and ŞT. PERIŞANU 619

Entropy and cohesive energy for metals, Relation between —, B. CHATTERJEE . . 789

Ethers, Observations on the IR and ^1H-NMR spectra of some asymmetric —, M. IOVU, F. CHIRALEU and E. VASILESCU 1383

Ethylene-vinyl acetate copolymers, ^1H-NMR method for composition branching and sequence distribution determination in —, V. BĂRBOIU, A. NATANSOHN, C. ANDREI and D. BLUM 933

Explosion of mixture between vinylacetylene and air, Some aspects of the — (in German), R. H. SCHUSTER, N. I. IONESCU, D. OANCEA, D. POPESCU and V. GOŞA 1301

Favorskii rearrangements of 4,8,8-tribromobicyclo[5.1.0]oct-4-en-3-ones, I. E. KHAWAD and G. M. ISKANDER 1321

Ferrocene polymers as polymerization initatiors. II. Polymerization of some-*p*-alkylated chloroformylated vinyl monomers, CR. SIMIONESCU, I. MAZILU, L. TĂTARU and T. LIXANDRU 277

Fractionation of polyethylene terephthalate, On "A correction technique for fractionation, — A. O. FULEA 435

Free radicals. X. 1-Cyano-2,2-bis-(3′,5′-di-t-butylphenyl)-hydrazyl, Factors affecting stability and equilibria of —, A. T. BALABAN, M. T. CĂPROIU and N. NEGOIŢĂ 1327

Geometrical structure of $Cl_2C=S$ during the $^1A_2 \rightarrow {}^1A_1$ electronic transition, Calculations of the change in the —, A. N. ABD EL-RAHMAN and M. H. ABDALLA 1477

Glycine by peroxydisulphate, Kinetics of the oxidation of —, G. CHANDRA and S. N. SRIVASTAVA 1149

Heteroaromatic cation-radicals, Unrestricted Hartree-Fock spin densities of some π, M. HILLEBRAND and V. EM. SAHINI 631

Heterocyclic monomers under simulated prebiotic conditions, Synthesis of new —, K. TAKEMOTO, K. KANAOKA and M. MIYATA 1097

Heterocyclic nitrogen compounds. VI. Reaction of some 5-oxopyrazoline derivatives with hydazine hydrate and diazoalkanes, M. F. EL-KASHEF, S. M. YASSIN, M. F. ABDEL-MEGEED and F. M. ABDEL-MOTI 577

Hg(II) in industrial caustic soda, waste water from chloro alkali industry and acetaldehyde production with diazamino reagents, Spectrophotometric determination of —, GR. POPA, M. POPESCU and A. DĂNEŢ 1 427

Hydration and hydration effects on some substituted benzoic acid molecules. II. The calculation of the substituent effect by semiempirical MO methods, A theoretical study of the —, S. GRIGORAŞ, A. MEDEŞAN, I. RUSU and Ş. MOLDOVEANU 67

Hydrocarbons based on the transferability of Fock matrix elements, A simple parametric procedure for saturated —, E. A. CASTRO and F. M. FERNÁNDEZ 455

Hydrogen bond energies from excess enthalpies, experimentally determined for benzene-butanol systems, Calculation of —, R. VÎLCU and Z. CENUŞE 781

Hydrogen molecule-ion, Application of an approximate calculation for the total energy of the —, E. A. CASTRO 41

Hydroxyphenothiazines and their alkyl and acyl derivatives, Synthesis of some new polyhalogenated —, R. K. JAIN and R. L. MITAL 697

Iminoxy radicals of 1-benzoxepin-5-one derivatives, An electron spin resonance study of the —, A. ÇARAGHEORGHEOPOL, M. CĂLDĂRARU, I. I. BĂDILESCU and V. E. SAHINI 307

Indole derivatives with biological activity, New —, C. SÂRBU, N. RĂDULESCU, M. IONESCU, S. NEGRIŢESCU, C. IOAN, N. BOEŞTEANU and M. SIMIONOVICI 245

Interfacial tension gradients, Model for the undeformable free drop acted by —, E. CHIFU and I. STAN 1 449

Interfacial tension variation in the course of liquid-liquid extraction. III. The extraction of butyric acid by different solvents, I. ALBU and E. CHIFU 459

Intramolecular interaction of aromatic nitro-group with *ortho* side-chain. II. Further syntheses of quinoline N-oxide derivatives. Studies in —, Y. AHMAD, S. A. SHAMSI and M. I. QURESHI 397

Ion exchange membranes, The interpretation of the kinetic data concerning the Zn^{2+} linking and elution on —, F. MATEI, AL. DUCA, GH. IONESCU and M. MACOVEANU 1 017

Ion exchange membranes, Transport of SO_4^{2-}, Cu^{2+}, H^+ ions and of water in — (in French), S. STERNBERG, L. SHIRSHINA and S. DANEȘ 467

Ion exchange system-solvents extraction. II. A theoretical approach, On the combined— (in French), L. VLĂDESCU and H. HURWITZ 135

Ion exchangers of type R_4Th and R_2UO_2 in water-organic solvent mixtures, Selective solvation of — (in French), AL. CECAL 1 397

Isobutylbenzene catalyzed by fluoroantimonic acid, The rearrangement of *sec*-butylbenzene to —, R. M. ROBERTS and H. H. CHEN. 687

Joshi effect and thermionic analogue of Joshi effect in argon under semi-ozonizer discharge, Comparative studies of corona pressure effect, J. PRASHAD 323

Kinetics and mechanism of the reaction between 5-chloro-2-pentanone and diethylamine. I. Solvent effect, T. ONCESCU and L. DIMOFTE 15

Kinetics and mechanism of the reaction between 5-chloro-2-pentanone and diethylamine. II. Influence of the nucleophilic reagents, T. ONCESCU and L. DIMOFTE . . . 23

Lead (II) complexes. III. Simple and mixed complexes of lead (II) with some anions of aliphatic acids in aqueous solution, Investigation of —, E. KULIG, D. CZAKIS-SULIKOWSKA and R. WOJTAŠ 1 177

Liquid crystals. II. Synthesis of *p*-alkyl anilines for benzilidene-aniline liquid crystals (in German), R. BACALOGLU, A. MORARU, M. NUȚIU, S. ILUC, C. CSUNDERLIK and E. LUNGU 921

Liquid flow in thin films on inclined plates at angles greater than 90°, An experimental study of —, R. Z. TUDOSE and C. NĂFORNIȚĂ 155

Macromolecules as therapeutic agents, Synthetic —, A. C. LUDWICK and C. G. OVERBERGER 1 011

Mandelic and 4-chloromandelic acids, Study of the hydrogen bond in the —, GH. SINGUREL 1 469

Mass spectrometry of alkylated inorganic heterocycles I. Mass spectrometry of octamethylcyclotetraphosphaza-tetraene and its quaternary salts with methyl and ethyl iodides (in Spanish), A. SOTO and R. CEA 529

Metal ions, Synthesis and physico-chemical investigation of neutral salts of 4,4′-diaminodiphenylmethane-N,N′-tetraacetic acid with mono-, di-, tri- and tetravalent— (in German), C. GH. MACAROVICI and E. CHIȘ 95

Metallic complexes of nicotinealdehyde-thiocarbohydrazone (in French), S. BARBU and C. GH. MACAROVICI. 207

Metallic electrodeposition, A new approach for Tafel approximation in —, V. LĂZĂRESCU and G. LĂZĂRESCU 1 287

Methoxyphenothiazines by potassium dichromate in glacial acetic acid, Oxidation of some —, T. PANEA and M. MOLDOVAN 691

Molecular orbital calculations. I. The ITPOT method, An improved two-parameter Omega technique for —, E. A. CASTRO and F. M. FERNÁNDEZ 635

Molecular orbital calculations. II. Polyenes, An improved two-parameter Omega technique for —, E. A. CASTRO and F. M. FERNÁNDEZ 643

Monocyclic ketones, Favorskiĭ reactions of α-halo-α, β-unsaturated —, I. E. KHAWAD and G. M. ISKANDER 393

Monolayer adsorption, Two new kinetical derivations of the Jovanović isotherm for —, P. BUDRUGEAC 487

Monomers towards primary radicals, studied by spin-trapping, The reactivities of —, J. C. BEVINGTON, B. J. TABNER and P. F. FRIDD 947

N-cetyl-β-picolinium halogen and thiocyanatomercurates (II), Study of some —, D. VĂCĂRESCU 371

Ni(II) dithiophosphinato chelates. Normal coordinate analysis and Urey-Bradley force field calculation of $Ni[S_2P(CH_3)_2]_2$, Vibrational characteristics of —, I. SILAGHI-DUMITRESCU and I. HAIDUC 823

Nickel involved in electron transfer processes, Complex compounds of —, D. NEGOIU, J. CAMUS and N. MUREȘAN 839

Optical rotatory dispersion of cellulose, cellulose-nitrate and of some α-polyglucans (in German), R. C. SCHULZ and E. JACOBI 1 059

Organic acids. II. Gravimetric determination of thorium by *o*-phenylene trioxytriacetic acid, Analytical aspects of some —, S. N. KAPOOR and N. MISRA . . . 439

Organic reagents in their reaction with Au(III). I. Influence of methoxy substituents, Influence of substituents on the analytical and extractive properties of — (in German), GH. C. CONSTANTINESCU 1 249

Organic reagents in their reaction with Au(III). II. Influence of methoxy substituents, Influence of substituents on the analytical and extractive properties of — (in German), GH. C. CONSTANTINESCU and C. CONSTANTINESCU 1 259

Organophosphorus derivatives of expected biological activity. I. Reaction of phenols with N-arylhexachlorocyclodiphosphazanes, M. M. OMARA, F. I. ABDEL-HAY, EL-BARBARY, M. BADAWI and M. M. ABDEL HAMID 253

Organothiophosphorus ligands. VII. Amine adducts of di (α- and β-napththyl) phosphorodithioato nickel (II), Transition metal complex of —, R. MICU-SEMENIUC, C. OPRIȘ and I. HAIDUC 1 489

Palladium(II) chelates of phenylazobenzaldoxime, A. E. MAHGOUB and M. M. SHOUKRY 1 197

Paraconic esters isolated in the Stobbe condensation of *p*-bromo-, and *p*-ethylacetophenones with diethylsuccinate, Reactions of —, A. A. EL-KHAMRY, M. A. EL-HASHASH and M. M. HABASHY 563

Pentacoordinate complexes, Mössbauer spectroscopy investigation of iron in some —, D. BARB, L. DIAMANDESCU, V. ZNAMIROVSCHI, D. CIURCHEA and R. SEMENIUC 1 485

Phenanthrenequinone monosemicarbazone as a reagent for the determination of rhodium(III) and palladium (II), F. KAMIL, S. K. SINDHWANI and R. P. SINGH 875

Phenazathionium cations. I. The dual mechanistic behaviour of phenazathionium cations and its implications in the reaction of $NaNO_2$ with halogenophenothiazines, I. A. SILBERG and M. V. DIUDEA 1 229

Phenazathionium cations. II. The accessibility of positions 1 (9) in nucleophilic substitutions involving phenazathionium cations, I. A. SILBERG and M. V. DIUDEA 1 239

Phenoxaselenine, The electronic structure of —, M. HILLEBRAND and V. EM. SAHINI 625

Photolytic decomposition of hypobromite in aqueous solution at 365 nm, 313 nm and 253.7 nm, A mechanism for the —, M. S. SUBHANI and S. F. LODHI 1 567

Polyazines and polyazomethines, On the thermal stability of some new —, M. DUMITRIU, M. DĂRÂNGĂ, M. PĂSTRĂVANU and T. LIXANDRU 981

Polymerization of *N*-pentenylcarbazole (NPC), Experimental and theoretical study on the —, A. HAOUAM, G. SURPĂŢEANU, E. COMĂNIŢĂ and CR. SIMIONESCU 1 389

Polymerization of photoactive monomers, Synthesis and —, O. VOGL and S. YOSHIDA 1 123

Polymers. I. Reaction of vinyl chloroacetate copolymers with some herbicidal sodium phenoxides, Chemical modification of —, D. DRĂGAN and A. CARPOV . . 285

Polymers. II. Reaction of poly(vinyl α-chloroacetophenone) with some herbicidal sodium phenoxides, Chemical modification of —, D. DRĂGAN and A. CARPOV . . . 425

Polynuclear aromatic hydrocarbons as sensitizers of photooxidative degradation of *cis*-1,4-polybutadiene, J. F. RÅBEK and B. RÅNBY 1 045

Porphyrin-like compounds under simulated abiotic conditions. A possible mechanism of their formation, Genesis of —, B. C. SIMIONESCU, R. MORA, M. LEANCA and C. ANANIESCU 1 077

Pyromellitic dianhydride with pyridine derivatives, Complexes of —, F. CORNEA and C. STOICESCU 961

Pyrylium salts with nucleophiles. XIV. New pyridinium salts with potential biological activity, Reactions of —, A. DINCULESCU and A. T. BALABAN 1 505

Quaternary ammonium complexes. N-Cetyl-β-picolinium salts of halogen- and thiocyanate complex ions of Zn(II) and Cd(II), Contributions to the chemistry of —, D. VĂCĂRESCU 361

Quaternary ammonium polyelectrolytes. II. Quaternization reaction of some tertiary amines with chloromethylated polyetyrene, I. PETRARIU, M. ROTARU and S. DRĂGAN 145

Radical alternating copolymerization of 9-vinylcarbazole with diethyl fumarate or diethyl maleate, N. COBIANU 953

Radiofrequency glow discharge and low pressure CVD methods. Deposition kinetics of Si_2N_4 films by the —, C. E. MOROŞANU and E. SEGAL 315

Rhenium with Astrazone Blue G, Spectrophotometric determination of — (in French), C. CONSTANTINESCU and GH. C. CONSTANTINESCU 1 421

Silicate rocks by atomic absorption spectrometry, Analysis of —, V. IOSOF and V. NEACŞU 589

Silicon nitride deposition on silicon from N-Gas, Kinetics of —, C. E. MOROŞANU and E. SEGAL 181

Silicon nitride films deposited on silicon, Nondestructive thickness determination of —, C. E. MOROŞAN and E. SEGAL 47

Silver in salts, alloys and complexes, 3-Ethyl-4-benzylidene-5-mercapto-1,2,4-triazole as a new gravimetric reagent for the estimation of —, R. V. GADAG and M. R. GAJENDRAGAD 745

Silver-phosphine complexes containing oxine, Chemical and spectroscopic properties of —, N. SULTANA, I. A. KHAN and S. R. R. NAQVI 105

Silver(I) with cobalt(II) and manganese(II) solutions in alkaline triethanolamine medium ; gravimetric estimations of silver, Reduction of —, K. N. RAOOT and V. G. VAIDYA 583

Sodium merthiolate in aqueous solutions at various pH values, Decomposition mechanism of —, J. WEINBERG, A. DONESCU and M. OLTEANU 189

Solvolyses of alkyl halides. IV. Hydrolysis of *t*-butyl chloride, Effects of the medium — (in German), R. H. SCHUSTER and A. NICOLAU 1 069

Solvolysis of 7(γ-tosyloxypropyl)-7H-dibenzo[a, e]cycloheptene, 5(β-tosyloxyethyl)- and 5(γ-tosyloxypropyl)-5H-dibenzo[a, c] cycloheptene, M. BANCIU, R. VLAD, PHAN LE THUY and C. DRĂGHICI 1 221

Spectral solvent effects in aromatic compounds solutions .VI. The solvent effects on the toluene electronic band at 2 600 Å, V. MACOVEI 651

Stability constants of ML_2 type complexes from spectrophotometric data, Some problems of deriving —, J. ZSAKÓ 1 499

Steric optimisation by MTD of therapeutic index of n-substituted derivatives of *cis*-dichlorodiammine-platinum(II) active against ADJ/PC6A mouse plasma cell tumour, Z. SIMON, S. HOLBAN, M. MRACEC, A. MAURER and S. POLICEC 713

Steroid ketones with O-substituted hydroxylamines, Studies on the oxime formation of —, A. BODOR, L. FEY and D. BREAZU 1 367

Sterol nitrates, Mechanism and kinetics of the electroreduction of —, L. ALBERT, B. TŐKÉS and F. HODOŞAN 1 529

Stress corrosion cracking in hydrochloric acid solutions, The influence of the structure and the type of alloy on —, O. RADOVICI and M. V. POPA 87

Structural strains appearing in the high temperature shift conversion Fe-Cr catalyst, I. BRAŞOVEANU, S. I. BLEJOIU, A. SZABO, P. ROTARU and I. V. NICOLESCU 1 159

Styrene in the presence of *tert*-butylhydroperoxide and tetramethyl-thiourea, Polymerization of —, J. BENISKA, G. KYSELÁ, E. ŠTAUDNER and M. CHLUPKOVÁ 941

Sulphur-containing aminoacid-metal complexes. Cobalt(II) and iron(II) complexes of cystine, A. UNGUREANU and M. MARC 845

Surface properties in Ni-Cu systems, Studies of alloy formation and —, M. I. VASS and CR. CONŢESCU 55

Tellurite and chlorite ions in solution, An investigation of the reaction between —, M. S. SUBHANI 327

Tetrahedral chelate complexes with Co(d^7)-N(sp^2) bonds. II. Co(II) chelates synthesized with 1-methyl-2-carbethoxy-glyoxalanil-(1)-bromo-phenylhydrazones-(2), Electronic spectra and magnetic susceptibilities of some new —, A. C. BANCIU and V. MINCU 513

Thallium, A modified reversion technique for the spectrophotometric determination of —, D. C. RUPAINWAR and K. K. KAKKAR 295

Thallium with Astrazone Red Violet 3R, Spectrophotometric determination of — (in French), C. CONSTANTINESCU and GH. C. CONSTANTINESCU 1 561

Thermal conductivity measurements of fluids, An alternative to the transient hot-wire method for —, R. VÎLCU and A. CIOCHINA 1 113

Thermal decomposition of the $[Pd(p\text{-}ON-C_6H_4-N(CH_3)_2)_2Cl_2]\cdot H_2O$ complex, Kinetic data on the formation and —, N. CALU, N. FOCA and M. LUCHIAN 1 171

Thermal phase equilibria in the system $BaO-ZnO-Fe_2O_3$ with application to magnetoceramics, S. SOLACOLU, M. ZAHARESCU and M. DOROBANŢU 111

Thermochemical studies on solutions of monobromo-, dibromo- and tribromo-acetic acids in water and chloroform, M. S. SUBHANI 333

Thermodynamic activity of $ZnSO_4$ in the systems : $ZnSO_4 + H_2O$ and $ZnSO_4 + Na_2SO_4 + H_2O$, The —, S. STERNBERG, M. DRĂGĂNOIU and A. MATEESCU . . 793

Thermodynamic functions for the reaction between two IO^- ions, The study of the transition state involves electrostatic contributions to the —, M. S. SUBHANI 1 579

Thermodynamic stability constants and other related thermodynamic properties for Cu(II)-PMBP complex, M. S. SUBHANI 121

Thermodynamical properties of 2—1 electrolytes in solution, Investigation of some —, P. PAL and A. KR. CHAKRABORTY 81

Thermogravimetric investigation on the decomposition of certain metal dithiocarbamates, K. N. JOHRI and K. A. VENUGOPALAN 215

Thin-layer chromatography with orthogonal temperatures gradient in S-chamber, Resolution in — (in German), S. GOCAN and C. KONNERT 273

Thiocarbohydrazine of isonicotinealdehyde and thiphene-2-carbaldehyde, Complex combinations of —(in French), S. BARBU and CONST. GH. MACAROVICI 339

Tin(II) with ion exchange resins. I. Cation-exchange behavior of tin(II), Utilisation of sodium hydroxide in separation of —, L. VLĂDESCU and D. VOICU 267

Tin with ion exchange resins. II. Cation exchange separations, Utilisation of sodium hydroxide in separation of —, L. VLĂDESCU and D. VOICU 1 269

Tl(III) with basic dyes, Separation by extraction and spectrophotometric determination of — (in German), C. CONSTANTINESCU and GH. C. CONSTANTINESCU 1 411

Transition metal complexes of organo-thiophosphorous ligands. VI. Six-coordinate adducts of nickel(II) bis (dialkylphosphorodihioate) with aromatic diamines, R. MICU-SEMENIUC, L. SILAGHI-DUMITRESCU, N. CHIRILĂ and I. HAIDUC 1 025

Transition metals. LIX. The stability of Fe(II)- and Co(II)-complexes of 1,2-cycloheptanedione dioxime and 1,2-cyclooctanedione dioxime in aqueous solutions, On the α-dioximine complexes of —, C. GH. MACAROVICI, J. HORÁK and CS. VÁRHELYI 805

Transition state formed between $Cu(S_2O_3)^-$ and $S_2O_8^{2-}$ anions in mixture of solvents, Study of the —, M. S. SUBHANI 861

Triazene derivatives, Potential anticancer agents. XXI. Synthesis and biological evaluation of some new-, F. CORNEA, D. IONESCU, M. ZGLOBIU, G. BOTEZ, V. DOBRE and I. NICULESCU-DUVAZ 701

Triazenic complexes of mercury, Study on structure and properties of some —, M. POPESCU and D. CRIȘAN 1 187

1,3,5-Triazines. XVIII.b. The protons-deuterons exchange rate at the methyl-groups of 2.4.6 trimethyl-1.3.5-triazine in D_2O and in the presence of DO^- ions. Studies on the field of — (in German), I. IORGA, C. CSUNDERLIK, M. SAFTA and G. OSTROGOVICH 1 351

s-Triazolium-4N-ylide (in German), H. J. TIMPE, V. SCHRÖDER and R. WORSCHECH 407

1,2,4-Triazolium-ylides. III. The theoretical aspects on the regioselectivity in the cycloaddition reaction of the triazolium-phenacyclide to the propiolic acid esters (in French), GH. SURPĂȚEANU, C. LUCHIAN, M. CONSTANTINESCU, V. BĂRBOIU and M. PETROVANU 1 091

Trichloroethylene with molecular oxygen, The oxidation of —, A. C. RĂZUȘ, A. M. GLATZ, ZS. ARVAY, F. IORDACHE and F. BADEA 547

Trifluoromethyl hypofluorite, RRKM calculation of the unimolecular decomposition of —, E. A. CASTRO and A. H. JUBERT 75

Ultrasound in n-alkanes, The propagation of —, R. VÎLCU and E. DIMITRIU 1 131

Unrestricted Hartree-Fock spin densities in aryl-nitroso-aminyl-oxides and in acyl-aryl-aminyloxides, M. HILLEBRAND and A. T. BALABAN 995

Uranium with benzoin-oxime, Spectrophotometric microdetermination of —, V. ARMEANU and S. VIŞAN 867

Valine by peroxydisulphate, Investigation of the kinetics and mechanism of silver (I) ion catalysed oxidation of d, l(α) —, G. CHANDRA and S. N. SRIVASTAVA 1 139

Vanadium complexes with quinoxalinic and naphtoquinonic ligands, Electron transfer in some —, D. NEGOIU, J. CAMUS and N. MUREŞAN 349

Vinyl acetate in the presence of hydroxyethylcellulose, Kinetics of emulsion polymerization of —, D. DONESCU, I. DEACONESCU, K. GOŞA, M. MAZĂRE and I. GAVĂT 975

Vinyl polymerization by transition metal ions, Termination of —, A. D. JENKINS 1 007

Zeolites doped with transition metal ions, Absorption of ammonia from aqueous solutions by A and X — (in French), F. DANEŞ, A. BÂTCĂ and S. M. AXINTE 673

Xylidine isomers. VI. CNDO calculations on 2,4- and 2,6-xylidine, J. WEINBERG and V. EM. SAHINI 9

ORSZÁGOS MŰSZAKI KÖNYVTÁR ÉS DOKUMENTÁCIÓS KÖZPONT 1883

NOTE POUR LES AUTEURS

La Revue Roumaine de Chimie publie des articles en anglais, français, russe, allemand ou espagnol. Les auteurs sont priés d'envoyer des articles et des comptes rendus inédits.

Les manuscrits seront dactylographiés à deux intervalles. La bibliographie, les tableaux et la légende des figures seront placés après le texte.

Si l'article fait partie d'une série numérotée, le titre de la partie précédente sera indiqué dans une note au bas de la première page.

Chaque article sera précédé d'un résumé comprenant quinze lignes au maximum.

Les références bibliographiques dans le texte seront faits par des exposants sans parenthèses et paraîtront à la fin de l'ouvrage.

Les publications périodique mentionnées dans la bibliographie seront présentées suivant les prescriptions internationales : le nom de l'auteur précédé de l'initiale du prénom, le titre du périodique abrégé conformément à « Chemical Abstracts » et souligné par une ligne, le numéro du tome indiqué par des chiffres arabes et souligné par deux lignes, suivi de la première page de l'article ; à la fin, l'année de la parution sera placé entre parenthèses. Le numéro de la revue ne sera pas indiqué si les pages du volume sont numérotées consécutivement.

Les textes des livres ou traités inclueront le noms des auteurs, les initiales du prénom, le titre du livre entre guillemets et dans être souligné, le numéro de tome précédé par l'abréviation « vol. » (ou « Bd. »), le numéro de l'édition, les éditions (the publisher), la localité de la parution du livre, l'année de la parution et la page de la référence précédée(s) par l'abréviation « p. » (ou « S. »).

Les brevets seront indiqués comme suit : l'auteur ou la firme, le pays et le numéro du brevet, la date et la revue (Chem. Abstr.). Par ex. : M. Jones (to Union Carbide Co), Brit. Pat. 601 238, 2 Sept. 1959, *Chem. Abstr.*, **54**, 12808 (1960).

Les diagrammes seront tracés à l'encre de Chine sur papier calque. Les tableaux et les figures (en nombre strictement nécessaire) seront, numérotés par des chiffres arabes. Les courbes dans les figures seront numérotées par des chiffres arabes et leur explication sera donnée dans la légende des figures. Prière de ne pas inscrire les mêmes données dans les tableaux et les figures. Chaque tableau aura un titre. On indiquera dans le texte la place aproximative des tableaux et des figures. Les formules chimiques seront icluses dans le texte ; en outre, elle seront transcrites sur papier calque, à l'encre de Chine.

Les auteurs sont priés d'indiquer les caractères italiques (en soulignant les lettres au crayon), ainsi que tout autre caractère spécial ; les préfixes *ortho, meta, para, cis, trans* etc. seront soulignés pour indiquer leurs caractères italiques et ne seront jamais écrits avec des majuscles.

Aucune correction à la main ne sera admise sur le manuscrit. Les corrections seront frappées à la machine. Les lettres grecques ou autres symboles spéciaux seront insérés à la main à l'encre clairement.

Le manuscrit sera signé par l'auteur.

Le colonne-titre aura 50 lettres au maximum.

L'entière responsabilité du contenu des articles appartient aux auteurs.

PRINTED IN ROMANIA

1981 MAR 11

TRAVAUX PARUS AUX ÉDITIONS DE L'ACADÉMIE DE LA RÉPUBLIQUE SOCIALISTE DE ROUMANIE

ELENA CEAUȘESCU, **Polimerizarea stereospecifică a izoprenului** (La polymérisation stéréospecifique de l'isoprène), 1979, 307 p.

CR. SIMIONESCU, VALERIA GORDUZA, **Polimeri biocompatibili și biologic activi** (Polymèrs biocompatibles et biologiquement actifs), 1980, 479 p.

MIHAIL FLORESCU, **Metode științifice în dezvoltarea industriei chimice moderne** (Méthodes scientifiques dans le développement de l'industrie chimique moderne), 1979, 256 p.

CONST. GH. MACAROVICI, **Analiza chimică cantitativă anorganică** (L'Analyse chimique quantitative inorganique), 1979, 457 p.

Ș. MOLDOVEANU et A. SAVIN, **Aplicații în chimie ale metodelor semiempirice de orbitali moleculari.** (Applications en chimie des méthodes semi-empiriques d'orbitaux moléculaires), 1980, 286 p.

A. T. BALABAN, I. GĂLĂȚEANU, G. GEORGESCU, LIGIA SIMIONESCU, **Compuși marcați și radiofarmaceutici cu aplicații în medicina nucleară** (Composés marqués et radiopharmaceutiques à application en médecine nucléaire), 1979, 495 p.

I. E. TEODORESCU et MARIA FITI, **Iradierea tehnologică** (L'Irradiation technologique), 1979, 216 p.

I. G. MURGULESCU, E. SEGAL, **Introducere în chimia fizică, vol. II. 1. Teoria molecular-cinetică a materiei** (Introduction à la chimie physique. IIe vol. 1. La Théorie moléculaire-cinetique de la matière), 1979, 1036 p.

I. G. MURGULESCU, V. EM. SAHINI, **Introducere în chimia fizică, vol. I. 2. Structura și proprietățile moleculelor** (Introduction à la chimie physique. Ier vol. 2. La structure et les propriétés des molécules), 1978, 604 p.

S. STERNBERG, FL. DANEȘ, **Termodinamica chimică aplicată** (La thermodynamique chimique appliquée), 1978, 400 p.

D. PURDELA (sous la direction), **Nomenclatura chimiei anorganice** (La nomenclature de la chimie inorganique), 1977, 153 p.

C. DRĂGULESCU, E. PETROVICI, **Chimia structurală modernă. Chimia coordinanței 8** (La chimie structurale moderne. La chimie de la coordinence 8), 1977, 917 p.

I. ZUGRĂVESCU, MAGDA PETROVANU, **N-ylid chemistry**, coédition avec McGraw-Hill International Book Company, U.S.A., 1977, 396 p.

I. G. MURGULESCU, **Introducere în chimia fizică, vol. I. 1. Atomi, molecule, legătură chimică** (Introduction à la chimie physique, Ier vol. 1. Atomes. Molécules, liaison chimique), 1976, 560 p. 2 pl.

P. BALTĂ, E. BALTĂ, **Introduction to the physical chemistry of the vitreous state**, coédition avec Abacus Press, 1976, 287 p.

I. GĂLĂȚEANU, **Radiochimia aplicată. Metode și probleme** (La radiochimie appliquée. Méthodes et problèmes), 1976, 307 p.

CONST. V. UGLEA, **Cromatografia pe gel permeabil. Noi domenii de aplicare** (La chromatographie sur gel perméable. Nouveaux domaines d'application), 1976, 122 p.

CONST. GH. MACAROVICI, D. MACAROVICI, **Chimia oxizilor dubli și utilizările lor** (La chimie des oxydes doubles et leur utilisation), 1975, 195 p.

ELENA CEAUȘESCU, **Research work on synthesis and characterization of macromolecular compounds. Contributions**, 1974, 251 p.

CR. SIMIONESCU, VIORICA RUSAN, V. POPA, **Chimia algelor marine** (La chimie des algues marines), 1974, 212 p., 1 pl.

Lei 25.—

. P. Informația c. 2449

43426

$ 55 (price per year)